ARTIFICIAL HEART PROGRAM CONFERENCE

Proceedings
June 9-13, 1969
Washington, D.C.

U.S. DEPARTMENT OF HEALTH, EDUCATION, AND WELFARE
Public Health Service National Institutes of Health

WITHDRAWN
from
LIBRARY
NATIONAL INSTITUTES OF HEA

ARTIFICIAL HEART PROGRAM CONFERENCE

NATIONAL HEART INSTITUTE
ARTIFICIAL HEART PROGRAM

Frank W. Hastings, M.D., Chief
Lowell T. Harmison, Ph. D., Assistant Chief

PROCEEDINGS
Washington, D.C., June 9–13, 1969
Edited by Ruth Johnsson Hegyeli, M.D.

For sale by the Superintendent of Documents, U.S. Government Printing Office
Washington, D.C. 20402 - Price $10.00

RD598
A791
1969
c.2

PREFACE

This document contains the Proceedings of the first Artificial Heart Conference sponsored by the Artificial Heart Program, National Heart Institute, National Institutes of Health. The Conference was held in Washington, D. C., June 9-13, 1969, and was attended by more than 750 scientists and developers from the United States and abroad.

The objectives of the Conference were: (1) to advance liaisons between the scientific and technologic disciplines interested in contributing to the further development of cardiovascular assist and replacement devices; (2) to make public the knowledge and information accumulated by the Artificial Heart Program contractors; and (3) to facilitate personal contact and exchange of information among the scientists working in the area.

It is hoped that the information assembled here will serve the purpose of the researchers as well as that of the developers. A conscious effort has been made to present not only the positive results of current research and development efforts, but also to identify areas where negative results, failures, or problems have been encountered. Thus these Proceedings will serve to inform the reader not only of the achievements which have been made but also to give him an opportunity to learn from the mistakes that inevitably must occur in this kind of research and development effort. This negative information is presented with the intent that other investigators will be made aware of those approaches which have already been explored but found to be unproductive.

In order to promote the free flow of information and ideas, each presentation at the Conference was followed by a ten-minute discussion period, during which both the contractors of the Artificial Heart Program as well as other participants had the opportunity to address questions to the speaker. This resulted in a vigorous exchange of information on the detailed nature and requirements of cardiac devices. Hopefully, these discussions and the personal contacts which were made will help dispel any conflicts and obstruction to flow of information which might occur in interdisciplinary research as a result of individual rivalries and professional pride.

The aim of this document is to serve as a challenge to new and creative thinking on how to achieve a reduction of death and disability through the use of cardiac devices. It is hoped that the Proceedings will provide a framework upon which to build a greater understanding of the basic technological problems that must be solved, and that they will encourage imagination that will provide a forward look and a perceptive concern for the obstacles and opportunities that exist in the research and development efforts from an academic, industrial and Government point of view.

These Proceedings report, with only minor editorial revision, the ninety-two papers that were presented by the contractors, along with the discussion that each paper evolved. The material is presented in the order of the presentations of the papers at the Conference. In some cases, due to the limited time available for the oral presentation, the papers present in more detail the information that could only be presented in capsule form at the Conference. It is hoped that the longer version will provide a more complete understanding of the work discussed. The hours of intensive work and deliberation, as well as the research work itself, that have been condensed in this report are presented to the reader in the hope that they will provide guidance to those people involved in new efforts in the field of cardiovascular devices. We would like to acknowledge and thank all those who have participated either directly or indirectly in the Conference.

F.W.H.

TABLE OF CONTENTS

INTRODUCTION

PAGE

Chapter 1
THE ARTIFICIAL HEART PROGRAM.
L. T. Harmison and F. W. Hastings 1

SECTION I. DEVELOPMENT OF MATERIALS FOR USE IN CIRCULATORY ASSIST DEVICES

Introduction 17

Chapter 2
DEVELOPMENT OF MATERIALS FOR USE IN CIRCULATORY ASSIST DEVICES
G. A. Grode, R. D. Falb, and S. J. Anderson,
Battelle Memorial Institute, Columbus Laboratories, Columbus, Ohio 19

Chapter 3
THE HEPARINIZATION OF SILICONE RUBBER USING AMINOORGANOSILANE COUPLING AGENTS.
Robert L. Merker, Liberty J. Eylash, Susan H. Mayhew and Jean Y. C. Wang,
Carnegie-Mellon University, Mellon Institute, Pittsburgh, Pennsylvania 29

Chapter 4
DEVELOPMENT OF BLOOD COMPATIBLE SILICONE ELASTOMERS
Martin C. Musolf, Verne D. Hulce, and Virgil L. Metevia
Dow Corning Corporation, Midland, Michigan 41

Chapter 5
COMPATIBILITY OF CARBON AND BLOOD
L. D. LaGrange, V. L. Gott, J. C. Bokros and M. D. Ramos
Gulf General Atomic, San Diego, California 47

Chapter 6
MATERIALS AND COMPONENTS FOR CIRCULATORY ASSIST DEVICES
I. O. Salyer and W. E. Weesner
Monsanto Research Corporation, Dayton Laboratory, Dayton, Ohio 59

Chapter 7
ANIONIC CELLULOSE: A POTENTIAL BLOOD COMPATIBLE MATERIAL
Robert G. Nemchin,
Melpar, Inc., Falls Church, Virginia 71

Chapter 8
POLYELECTROLYTE COMPLEXES AS ANTITHROMBOGENIC MATERIALS
H. J. Bixler, R. A. Cross and D. W. Marshall
Amicon Corporation, Lexington, Massachusetts 79

Chapter 9
HYDROGELS AS NON-THROMBOGENIC SURFACES
B. David Halpern, Hsiung Cheng, Shen-yen Kuo and Herman Greenberg
Polysciences, Inc., Warrington, Pennsylvania 87

Chapter 10
STUDIES RELATIVE TO MATERIALS SUITABLE FOR USE IN ARTIFICIAL HEARTS
P. Murphy, A. Lacroix, and S. Merchant
Thermo Electron Corp., Waltham, Massachusetts and W. Bernhard
Children's Hospital Medical Center, Boston, Massachusetts 99

Chapter 11
THE EFFECT OF CHEMICAL STRUCTURE AND SURFACE PROPERTIES OF SYNTHETIC POLYMERS ON THE COAGULATION OF BLOOD
Donald J. Lyman, John L. Brash and Karen G. Klein
Stanford Research Institute, Menlo Park, California 113

Chapter 12
POLYMERIC MATERIALS FOR CIRCULATORY ASSIST DEVICES
Joseph S. Byck, Sui-Wu Chow, Leonhard J. Gonsior, Walter A. Miller,
William P. Mulvaney, Lloyd M. Robeson and Mark A. Spivack
Union Carbide Corporation, Bound Brook, New Jersey 123

Chapter 13
BLOCK COPOLYMERS FOR USE IN BLOOD PUMPS AND OXYGENATORS: PREPARATION AND CHARACTERIZATION
Eugene T. Bishop and William P. O'Neill
Shell Development Company, Emeryville, California 133

Chapter 14
DEVELOPMENT OF MATERIALS FOR ARTIFICIAL HEARTS AND BLOOD OXYGENATORS
Henry Lee, Donald G. Stoffey, and Frank Abroson
The Epoxylite Corporation, South El Monte, California 143

Chapter 15
RESEARCH ON MATERIALS COMPATIBLE WITH BLOOD
E. S. Nuwayser
Monsanto Co., Everett, Massachusetts 153

Chapter 16
RECONSTRUCTION OF DIFFERENTIATED TISSUE LAYERS FROM DISSOCIATED CELLS: USE OF TISSUE CULTURE TECHNIQUES TO DEVELOP NON-THROMBOGENIC AUTOLOGOUS CELL SURFACES FOR USE AS CARDIAC LININGS
Leonard Schutz, Clifford Grobstein, Ruth Grobstein, Brian S. Bull,
and Nina S. Braunwald.
University of California, San Diego, California 169

SECTION II. ANALYSIS OF THE EFFECTS OF MATERIALS ON BLOOD AND TISSUES

Introduction 179

Chapter 17
THE IN VIVO SCREENING OF POTENTIAL THROMBORESISTANT MATERIALS
Vincent L. Gott, Manuel D. Ramos, Faysal B. Najjar, James L. Allen and Karl E. Becker
Johns Hopkins University School of Medicine, Baltimore, Maryland 181

Chapter 18
BLOOD COMPATIBILITY OF SOME POLYMERIC AND NONPOLYMERIC MATERIALS: IN VITRO AND EX VIVO STUDIES
R. G. Mason, N. F. Rodman, D. E. Scarborough, L. D. Ikenberry
University of North Carolina, Chapel Hill, North Carolina, Duke University, Durham, North Carolina, and Research Triangle Institute, Research Triangel, North Carolina 193

Chapter 19
FURTHER STUDIES OF THE INTERACTION OF BLOOD AND TISSUE CELLS WITH ARTIFICIAL HEART IMPLANT CANDIDATE MATERIALS IN VITRO
Ruth Johnsson-Hegyeli, Richard Gallagher and L. P. Peterson
Battelle Memorial Institute, Columbus Laboratories, Columbus, Ohio 203

Chapter 20
STUDIES ON THE COMPATIBILITY OF VARIOUS PLASTICS WITH THE PROTEINS IN HUMAN PLASMA
Seymour P. Halbert, Milton Anken and Alexis E. Ushakoff
Cordis Laboratories, Miami, Florida 223

Chapter 21
ANALYSIS AND MEASUREMENT OF THE EFFECTS OF MATERIALS ON BLOOD
B. Kusserow, R. Larrow and J. Nichols
University of Vermont, Burlington, Vermont 233

Chapter 22
NEW APPROACHES IN THE SELECTION OF MATERIALS COMPATIBLE WITH BLOOD
P. N. Sawyer and S. Srinivasan
Electrochem. and Biophy. Lab., Dept. of Surg., SUNY, Downstate Med. Center, Brooklyn, New York .. 243

Chapter 23
IMMUNOGENIC EFFECTS OF MATERIALS ON PLASMA PROTEINS
Ivan J. Stern, Andreas A. Kapsalis and Barbara L. Neil
Travenol Laboratories, In., Morton Grove, Illinois 259

SECTION III. BLOOD FLOW THROUGH PUMPS AND VALVES

Introduction 269

Chapter 24
THROMBUS FORMATION ON ARTIFICIAL SURFACES
H. E. Petschek and P. N. Madras
Avco Everett Research Laboratory, Everett, Massachusetts 271

Chapter 25
RED CELL BEHAVIOR NEAR WALLS
P. L. Blackshear, Jr., K. H. Keller, R. J. Goldstein, F. D. Dorman, M. Rosenberg, J. White,
K. Kihara, M. Bess, S. Deneroff, M. Gupta, D. Kreid, M. Kammin, and M. Larherbaum
University of Minnesota, Minneapolis, Minnesota 291

Chapter 26
STUDIES OF BLOOD FLOW IN AND ADJACENT TO BLOOD PUMPS
S. M. Scala, N. R. Kuchar, M. P. Sherman and P. Gordon
General Electric Co., Philadelphia, Pennsylvania and L. U. Lilleleht,
University of Virginia, Charlottesville, Virginia 309

SECTION IV. CARDIAC CONTROL PARAMETERS

Introduction 325

Chapter 27
CARDIAC CONTROL: HEART RATE OPEN LOOP RESPONSE.
E. Dong, H. Glaze, E. Stinson, C. Weaver
Stanford University Medical Center, Stanford, California 327

SECTION V. OXYGENATOR DEVELOPMENT

Introduction 337

Chapter 28
BLOOD OXYGENATOR WITH PREFORMED, MEMBRANE-LINED, CAPILLARY CHANNELS
Philip Dantowitz and Alex Borsanyi
Monsanto Research Corporation, Everett, Massachusetts 339

Chapter 29
DEVELOPMENT OF A CAPILLARY MEMBRANE BLOOD OXYGENATOR
Richard P. deFilippi, Frederick C. Tompkins, James H. Porter and Grady W. Harris
Abcor, Incorporated, Cambridge, Massachusetts 347

Chapter 30
HOLLOW FIBERS FOR USE IN MEMBRANE OXYGENATORS
B. J. Lipps, W. E. Skiens, E. A. McLain and P. D. Oja
Dow Chemical Company, Walnut Creek, California 357

Chapter 31
A HOLLOW FILAMENT FABRIC BLOOD OXYGENATOR
T. Leigh Williams, Ph.D., Lewis H. Bosher, M.D., Teruhisa Nakamura, M.D.
Medical College of Virginia, Richmond, Virginia 365

Chapter 32
DEVELOPMENT OF CAPILLARY NETWORK MEMBRANE OXYGENATORS
Ray L. Hauser, David H. Thompson
Hauser Research and Engineering Company, Boulder, Colorado and
John A. Jacobey, Denver, Colorado 373

Chapter 33
DEVELOPMENT OF A LIQUID-LIQUID BLOOD OXYGENATOR
Richard P. deFilippi, Richard M. Anderson, James H. Porter and Grady W. Harris
Abcor, Incorporated, Cambridge, Massachusetts and
Yukihiko Nose, Cleveland Clinic, Cleveland, Ohio 381

Chapter 34
DEVELOPMENT OF A COUETTE OXYGENATOR
Kenneth H. Keller
University of Minnesota, Minneapolis, Minnesota 393

Chapter 35
DESIGN AND FABRICATION OF BLOOD OXYGENATOR FOR CIRCULATORY ASSIST DEVICES
E. Converse Peirce II, M.D.,
Emory University School of Medicine, Atlanta, Georgia and
W. F. Mathewson, Jr., Ph.D., General Electric Company, Schenectady, New York 405

Chapter 36
PROGRESS IN THE TESTING AND DEVELOPMENT OF PRACTICAL FLAT PLATE MEMBRANE OXYGENATORS FOR CARIO-PULMONARY ASSIST
A. J. Lande, R. N. Tiedemann, V. A. Subramanian, S. J. Fillmore and C. W. Lillehei
Cornell University Medical College, New York, New York 417

Chapter 37
DEVELOPMENTS TO IMPROVE THE BRAMSON MEMBRANE OXYGENATOR
Robert C. Eberhart, Myer L. Coval
Institute of Medical Sciences, San Francisco, California 431

Chapter 38
DEVELOPMENT OF A TIDAL-FLOW OXYGENATOR
Edward F. Leonard and Robert M. Koffsky
Artificial Organs Research Laboratory, Columbia University, New York 445

Chapter 39
SPIRAL COIL BLOOD OXYGENATOR
Kenneth Abel,
Litton Industries, Minneapolis, Minnesota 451

SECTION VI. CIRCULATORY ASSIST DEVICES

Introduction 455

Chapter 40
EVALUATION OF THE ANSTADT VENTRICULAR ASSIST DEVICE IN ACUTE AND CHRONIC STUDIES
E. T., Tragus, H. W. Wallace, J. Marchesini, M. Bendon, P. Jennings,
W. Zerby, R. Thorn, and W. S. Blakemore
University of Pennsylvania, Philadelphia, Pennsylvania 457

Chapter 41
NEW MODIFICATIONS FOR MECHANICAL VENTRICULAR ASSIST (MVA)
David B. Skinner, Mary Dutka, Alfio Raciti, Peter Schiff, George L. Anstadt
The Johns Hopkins University School of Medicine, Baltimore, Maryland 475

Chapter 42
COMBINED PERIPHERAL AND THORACIC MODALITIES OF SYNCHRONOUS EXTERNAL PRESSURE ASSIST
William C. Birtwell, Fabio Giron and Harry S. Soroff
Tufts-New England Medical Center Hospitals, Boston, Massachusetts 483

Chapter 43
SEQUENCED EXTERNAL PULSATION IN THE THERAPY OF CARDIOGENIC SHOCK
L. S. Cohen, J. H. Mitchell, C. B. Mullins, and D. C. Porterfield
The University of Texas, Southwestern Medical School at Dallas, Dallas, Texas and
Hamilton Standard Division of United Aircraft Corporation, Farmington, Connecticut 495

Chapter 44
FLUID MECHANICS OF INTRA-AORTIC BALLOON COUNTERPULSATION
Ascher H. Shapiro, Michel Y. Jaffrin, Colin Clark, V. Sreedhara Murthy, Thomas A. McMahon
Fluid Mechanics Laboratory, Department of Mechanical Engineering, Massachusetts Institute of Technology, Cambridge, Massachusetts 505

Chapter 45
DEVELOPMENT OF AN INTRA-AORTIC BALLOON ASSIST DEVICE
B. G. Brown, W. D. Gondle, D. L. Trump, M. D. Ramos and V. L. Gott
Johns Hopkins University, Baltimore, Maryland and
J. M. Evans and G E. McGinnis, Westinghouse Electric Corporation, Pittsburgh, Pennsylvania . 515

Chapter 46
LEFT HEART ASSIST DEVICES
Tetsuzo Akutsu, Hiroyuki Takagi, Hisateru Takano and Charles A. Farish
University of Mississippi Medical Center, Jackson, Mississippi 529

Chapter 47
THE IN-SERIES SUBCUTANEOUS EXTERIORIZED PUMPING VENTRICLE WITH POSITIVE ACTING VALVE
Fabio Giron, William C. Birtwell and Harry S. Soroff
Tufts-New England Medical Center Hospitals, Boston, Massachusetts 541

Chapter 48
DEVELOPMENT AND INITIAL PHYSIOLOGICAL EVALUATION OF THE COPULSATION TECHNIQUE FOR CIRCULATORY ASSIST
B. L. Hochman, Hamilton Standard, Farmington, Connecticut
T. Sato, Yale University, New Haven, Connecticut
W. L. Sugg, Southwest Medical School, Dallas, Texas 551

Chapter 49
DEVELOPMENT AND EVALUATION OF A LEFT VENTRICULAR-AORTIC ASSIST DEVICE
W. F. Bernhard, C. G. LaFarge
Surgical Research Laboratory, Children's Hospital, Boston, Massachusetts and
T. D. Robinson, Thermo-Electron Corporation, Waltham, Massachusetts 559

Chapter 50
TOTAL HEART REPLACEMENT DEVICE AND ITS CONTROL AND DRIVING SYSTEM
Tetsuzo Akutsu, Hiroyuki Takagi, Hisateru Takano, and Charles A. Farish
University of Mississippi Medical Center, Jackson, Mississippi 581

SECTION VII. PHYSIOLOGIC EFFECTS OF CIRCULATORY ASSIST DEVICES IN ANIMALS

Introduction 591

Chapter 51
CONTINUING EVALUATION OF THE BAYLOR LEFT VENTRICULAR BYPASS DEVICE
Eugene F. Bernstein, Michael A. Shea and D. A. Spyker
University of Minnesota, Minneapolis, Minnesota 593

Chapter 52
A PHYSIOLOGIC EVALUATION OF THE BAYLOR LEFT VENTRICULAR BYPASS
C. G. LaFarge, W. F. Bernhard, Surgical Research Laboratory, Children's Hospital, Boston, Massachusetts
and T. C. Robinson, Thermo Electron Corporation, Waltham, Massachusetts 619

Chapter 53
INTRA-AORTIC BALLOON PUMPING AT DIFFERENT LEVELS OF EXPERIMENTAL ACUTE LEFT VENTRICULAR FAILURE (IABP)
Mario Feola, J. H. Kennedy, Nils A. Norman, Otto Haiderer
Cleveland Metropolitan General Hospital, Case Western Reserve University, Cleveland Ohio 637

Chapter 54
PHYSIOLOGIC EFFECTS AND ENGINEERING EVALUATION OF INTRA-AORTIC BALLOONS AND CONTROL CONSOLES
F. T. Galysh, A. S. Patel and C. Y. Lin
Travenol Labs., Inc., Morton Grove, Illinois 659

Chapter 55
DEVELOPMENT OF FABRICATION TECHNOLOGY FOR CIRCULATORY ASSIST DEVICES
John Sprung, Western Gear Corp., South Gate, California 679

Chapter 56
A NEW ANIMAL MODEL - MYOCARDIAL INFARCTION
W. Elzinga, W. Kaufman, D. Upright and D. Powell
Hittman Associates, Inc., Columbia, Maryland 689

Chapter 57
A STUDY OF THE VASCULATURE OF THE OVINE THORAX AND ASSOCIATED STRUCTURES
W. D. Anderson
University of Minnesota, Minneapolis, Minnesota 701

SECTION VIII. INSTRUMENTATION APPLICABLE TO ARTIFICIAL HEART DEVELOPMENT AND USE

Introduction 723

Chapter 58
DEVELOPMENT OF A CONTINUOUS BLOOD po_2 MEASURING SYSTEM
Philip Reichner, Yehuda Tamari and G. E. McGinnis
Westinghouse Electric Corporation, Pittsburgh, Pennsylvania 725

Chapter 59
INSTRUMENTATION FOR ANALYSIS OF BLOOD LACTATE AND PYRUVATE
David L. Williams and Alfred R. Doig
Monsanto Co., Everett, Massachusetts 733

Chapter 60
CHRONICALLY IMPLANTABLE PRESSURE TRANSDUCERS
P. R. Perino
Statham Instruments, Inc., Oxnard, California 739

Chapter 61
MINIATURE PRESSURE TRANSDUCERS
M. Kienitz, T. S. Finnegan and F. Sutter
Corbin-Farnsworth, Smith Kline Instrument Inc., Palo Alto, California 747

Chapter 62
IMPROVED DIAGNOSTIC ACCURACY IN ACUTE MYOCARDIAL INFARCTION WITH MULTI-CHANNEL ELECTROCARDIOGRAPHIC DATA ACQUISITION AND ANALYSIS
Joel H. Cyprus, Texas Instruments, Houston, Texas and
C. Gunnar Blomqvist, A. Ben C. Dowdy, Stanley Lightfoot and Robert S. Putnam
Southwestern Medical School, Dallas, Texas 755

Chapter 63
IMPLANTABLE IMPERMEABLE ENCAPSULANTS FOR ARTIFICIAL ORGANS
Carl C. Enger and Frederick W. Rhinelander
Case Western Reserve University, Cleveland, Ohio 765

Chapter 64
ENCAPSULATION PROCEDURES TO ISOLATE COMPONENTS FROM BODY FLUIDS
Charles R. Nichols
Hydrospace Research Corporation, Rockville, Maryland 773

Chapter 65
DEVELOPMENT OF IMPROVED ENCAPSULATION MATERIALS FOR IMPLANTATION
Henry Lee, Arthur L. Cupples, Kris Neville, Gordon W. Culp and R. J. Schubert
The Epoxylite Corporation, South El Monte, California 777

SECTION IX. PERCUTANEOUS LEADS

Introduction 791

Chapter 66
DEVELOPMENT OF SATISFACTORY LONG-TERM PERCUTANEOUS LEADS
Henry Lee, David E. Ocumpaugh, Gordon W. Culp and Arthur L. Cupples
The Epoxylite Corporation, South El Monte, California 793

Chapter 67
BIOLOGICALLY COMPATIBLE POLYELECTROLYTE COMPLEX HYDROGELS FOR USE AS TISSUE/LEAD ADHESIVES FOR LONG-TERM PERCUTANEOUS LEADS
Edward Friedman, Lita Nelsen, and Harris J. Bixler
Amicon Corporation, Lexington, Massachusetts 809

SECTION X. BIOLOGICAL FUEL CELLS

Introduction 815

Chapter 68
FEASIBILITY STUDIES - IMPLANTABLE BIOLOGICAL FUEL CELL
J. S. Batzold and M. Beltzer
Government Research Laboratory, Esso Research and Engineering Company, Linden, New Jersey .. 817

Chapter 69
OXYGEN REDUCTION ON GOLD-PALLADIUM ALLOYS IN NEUTRAL MEDIA
J. H. Fishman and J. F. Henry
Leesona Moos Laboratories, Great Neck, New York 825

Chapter 70
ANODIC OXIDATION OF GLUCOSE
Jose Giner and Paul Malachesky
Tyco Laboratories, Inc., Waltham, Massachusetts 839

Chapter 71
SEARCH FOR A SPECIFIC CATALYST FOR ELECTROCHEMICAL OXYGEN REDUCTION IN NEUTRAL NaCl SOLUTION
A. Kozawa, V. E. Zilionis, R. J. Brodd, and R. A. Powers
Union Carbide Corporation Consumer Products Division, Para Technical Center, Cleveland, Ohio 849

Chapter 72
ON THE DESIGN OF CATALYSTS FOR BIOLOGICAL FUEL CELLS
Carlo V. Bocciarelli
Pennsylvania Research Associates, Philadelphia, Pennsylvania 861

Chapter 73
IMPLANTABLE FUEL CELL FOR AN ARTIFICIAL HEART
R. F. Drake
Monsanto Research Corporation, Boston Lab., Everett, Massachusetts 869

SECTION XI. EFFECTS OF ADDITIONAL ENDOGENOUS HEAT

Introduction 881

Chapter 74
STUDIES ON THE EFFECTS OF ADDED ENDOGENOUS HEAT AND ON HEAT EXCHANGER DESIGNS
Murlin F. Gillis and Paul C. Walkup
Battelle Memorial Institute, Pacific Northwest Laboratories, Richland, Washington 883

Chapter 75
STUDIES OF THE EFFECTS OF ADDITIONAL ENDOGENOUS HEAT
Robert O. Rawson
John B. Pierce Foundation Laboratory, New Haven, Connecticut 893

Chapter 76
EFFECTS OF INTRACORPOREAL HEAT AND RADIATION ON DOGS
J. Norman, C. Pegg, G. Sandberg, R. Lee
Sears Surgical Research Laboratory, Boston 901

SECTION XII. IMPLANTABLE ENERGY SYSTEMS

Introduction 913

Chapter 77
POWER TRANSFORMER FOR MECHANICAL HEARTS
A. I. Thumim, G. E. Reed, F. J. Lupo, G. H. Myers and L. Cortes
New York University, New York, New York 915

Chapter 78
SKIN TRANSFORMER AND POWER CONDITIONING COMPONENTS
Peter M. Newgard and George J. Eilers
Stanford Research Institute, Menlo Park, California 927

Chapter 79
ENERGY TRANSMISSION THROUGH THE INTACT SKIN
Lawrence A. Heimlich and Fritz H. Christiansen
Biomedical Systems Department, Hamilton Standard, Division of United Aircraft
Farmington, Connecticut; T. Sato M.D. Yale University, New Haven, Connecticut 937

Chapter 80
IMPLANTABLE ENERGY SYSTEM FOR A CARDIAC ASSIST DEVICE
Jack Chambers
Statham Instruments, Inc., Oxnard, California 945

Chapter 81
DEVELOPMENT OF AN ELECTROHYDRAULIC ENERGY SOURCE TO POWER AND CONTROL CIRCULATORY ASSIST DEVICES
Neil J. Griffith and Winton H. Burns
Indiana University, Medical Center 953

Chapter 82
ELECTROMAGNETIC IMPLANTABLE ENERGY CONVERSION SYSTEMS
J. W. Christie, Ph.D. and G. M. Benson, Ph.D.
ERG Inc., Oakland, California 969

Chapter 83
DEVELOPMENT OF A PIEZOELECTRIC DRIVER FOR AN ARTIFICIAL LEFT VENTRICLE
P. C. Smiley, C. G. O'Neill, W. W. Olander and J. C. Creighton
Physics International Co., San Leandro, California 981

Chapter 84
PIEZOELECTRIC IMPLANTABLE ENERGY CONVERTERS
G. M. Benson, and J. W. Christie
ERG, Inc., Oakland, California 993

Chapter 85
HIGH FREQUENCY PIEZOELECTRIC MOTOR PUMP FOR IMPLANTED ENERGY CONVERSION
L. A. Heimlich, P. D. Knerr, B. Hanson, R. Colville and H. Chalifoux
Biomedical Systems Department, Hamilton Standard Div. of United Aircraft Corp.
Farmington, Connecticut 1011

Chapter 86
INTERNAL ENERGY STORAGE FOR CIRCULATORY ASSIST DEVICES
R. P. Hamlen, E. G. Siwek, G. Rampel, and L. D. Wechsler
General Electric Research and Development Center, Schenectady, New York 1017

Chapter 87
DEVELOPMENT OF AN ELECTRICAL ENERGY STORAGE SYSTEM FOR USE WITH A CIRCULATORY ASSIST DEVICE
Ralph A. Miller, Edward J. Glanfield,
General Electric Company, Valley Forge Space Technology Center
King of Prussia, Pennsylvania 1027

Chapter 88
DEVELOPMENT OF A HEAT SOURCE FOR AN IMPLANTABLE CIRCULATORY SUPPORT POWER SUPPLY
Maurice Bleustein and Fred N. Huffman
Thermo Electron Corporation, Waltham, Massachusetts 1037

Chapter 89
DEVELOPMENT OF THE THERMOCOMPRESSOR AS THE POWER SOURCE FOR AN ARTIFICIAL HEART
William R. Martini
McDonnell Douglas Corporation, Donald W. Douglas Laboratories, Richland, Washington 1053

Chapter 90
DEVELOPMENT OF A MODIFIED STIRLING CYCLE HEART ENGINE
Keith E. Buck
Aerojet-General Corporation, San Ramon, California 1069

Chapter 91
DEVELOPMENT STATUS OF AN IMPLANTABLE RANKINE-CYCLE CIRCULATORY SUPPORT SYSTEM
F. N. Huffman, T. C. Robinson, and S. S. Kitrilakis
Thermo Electron Corporation, Waltham, Massachusetts 1083

Chapter 92
ALL FLUID CONTROL SYSTEM TO COUPLE A STIRLING ENGINE GAS COMPRESSOR TO LEFT VENTRICULAR ASSIST DEVICE
G. H. Peterson, A. G. Kessler, G. H. Thorne, R. R. Clark and O. L. Wood
Fluidonics Research Laboratory, Salt Lake City, Utah 1093

FILMS SHOWN AT CONFERENCE 1109

INDEX OF CONTRACTORS 1110

REGISTRANTS 1111

ARTIFICIAL HEART PROGRAM PERSONNEL 1123

OUTLINE OF RESEARCH CONTRACTS PROCEDURES 1124

TECHNICAL REPORTS ON CONTRACTS OF THE ARTIFICIAL HEART PROGRAM AVAILABLE IN THE CLEARINGHOUSE FOR FEDERAL SCIENTIFIC AND TECHNICAL INFORMATION 1125

CHAPTER 1

ARTIFICIAL HEART PROGRAM

Lowell T. Harmison, Ph.D., and Frank W. Hastings, M.D.

Artificial Heart Program
National Heart Institute
Bethesda, Maryland

BACKGROUND

Why is there a need for the development of Artificial Hearts and Mechanical Assist Devices? This question is partially answered by considering the Public Health data and statistics on heart disease. According to some of the latest statistics, coronary heart disease alone accounts for approximately 500,000 of the 1,000,000 cardiovascular deaths occurring in the United States within the period of one year. These statistics place heart disease in the position of leading cause of death, responsible for approximately 54 percent of all deaths, as compared with cancer, the next common cause, at approximately 16 percent. Mortality statistics, of course, provide only a partial picture of the total impact that coronary disease has on individuals, families, and society as a whole. A consideration of the magnitude of the cardiovascular disease problem must also take into account morbidity statistics and the patient population in various stages of transition from the suspect stage to that of definite heart disease. Data compiled between 1960 and 1962 by the National Health Survey indicate that 14,621,000 Americans, aged 18-79, have definite heart disease. An additional 12,979,000 have "suspect heart disease," i.e., findings on physical examination that suggest the presence of heart disease, but too inconclusive to confirm the diagnosis. Approximately 25 percent of American adults have definite or suspect heart disease. Approximately two million of these patients are seriously handicapped by their disease. It has been found that many of these patients with diseased hearts are otherwise healthy and could be benefited by a temporary or permanent replacement heart or assist device if these were available. In addition, the potential uses for such devices, when fully developed and available on short-term notice, are not going to be limited to cardiovascular patients. These devices might also be lifesaving in many other conditions where cardiac or cardiopulmonary failure is not normally considered the primary, but rather the secondary, cause of death and thus does not appear in the usual mortality statistics. It is obvious, therefore, that the need for development of effective, safe and readily available temporary and permanent cardiovascular assist and replacement devices is central to the health of the nation as well as a challenge to our technology.

Limitations of Current Therapeutic Approaches.

Educational and scientific programs aimed at the prevention of cardiovascular disease are being pursued by the medical community, the Government, and the lay public. In spite of these efforts at prevention, the number of patients with cardiovascular disease continues to increase. The nature and magnitude of the problem certainly requires national emphasis, both from a therapeutic and a preventive standpoint. Because of the acuteness of the final cardiovascular episode, and the generally long time constants needed for preventive measures to take effect, there is a need for new and more effective therapeutic approaches to deal with the problem at hand.

Basically, there are only three current therapeutic techniques for the treatment of patients with heart disease. These are chemotherapy, surgery, and mechanical intervention. The role and value of each of these stands unquestioned. Each approach has its unique advantages and limitations in relation to the specific disability being treated. The effectiveness of these measures, whether applied singly or collectively, is limited not by the existing technology which could be applied to the problem, but by the existing state of development. Despite successes in cardiac therapy and increasing progress in patient management, it is generally recognized that the results of research and development efforts are relatively limited and definitely inadequate to cope with cardiovascular disease. This lag in research and development has occurred in spite of the increased involvement of applied and physical scientists in the biological and medical research areas in recent years. It should, however, be pointed out that these activities in the past have principally involved only the academic sector of the respective disciplines, and the expertise of the scientific-industrial communities has remained essentially untapped. It is clear that these groups do possess in large measure the necessary capability to solve certain critical problems in cardiovascular device development. Yet, their involvement has been insufficient to permit their effective sensing of what the critical needs and requirements are in order to apply this expertise to the problems to be solved.

Feasibility of Mechanical Intervention and Artificial Circulation.

The subject of the feasibility of mechanical intervention and artificial circulation has been thoroughly explored during the last three decades. These studies have yielded devices such as the pump oxygenator that can take over the integral function of the heart and lungs for a limited period of time, as well as a number of other experimental devices designed to assist the circulation or replace the heart function for short periods of time. Certainly, developments in cardiopulmonary bypass, improved techniques of physiological monitoring, advances in diagnostic techniques, supportive care and cardiac pacing, etc., have been major achievements in medicine, achievements that have extended the therapeutic frontier of cardiac therapy. The success and utility of such devices has been clearly demonstrated and forms the basis for current open heart surgery, which has prolonged the useful lives of many persons. This mechanical system has extended the time limitations of cardiac corrective surgery from minutes to several hours, thereby making it feasible for the cardiac surgeon to undertake complex repairs not within reach before the introduction of the mechanical device. This success has been achieved even though the mode of operation of these devices creates conditions which are quite different from the states encountered in the undisturbed organism. Certainly, these non-physiological conditions can be tolerated for a limited period of time. In addition, it should also be pointed out that in the several cases of independent applications of mechanical devices to support inadequate circulation in humans, the experimenters believe that survival would not have been achieved without mechanical intervention. With these applications and along with animal blood pump research extending back several decades, it is apparent that there is little need for concern over the feasibility of mechanical intervention and support of circulation in humans. In fact, one might view temporary and permanent assist or total replacement of cardiac function as merely extensions in time of application of acute devices. This does not mean that all the problems that exist at the research and development level of these devices have been solved. On the contrary, there are specific biological and engineering problems which must be solved for each type of device before it is ready for use in humans.

PROGRAM

Formulation.

With a growing awareness of the medical problem and with the conviction that new knowledge and approaches to deal with the problem could be accelerated, the National Advisory Heart Council requested the National Heart Institute to explore the feasibility of establishing a program for developing mechanical devices that might assist or replace a failing heart. In 1964, the Artificial Heart Program was established by the National Heart Institute to focus upon the role of cardiac prostheses and supporting techniques. It was organized to bring together the national effort in an attempt to: (1) unify the isolated elements of existing research and to further develop these; (2) mount a direct attack upon heart disease by providing the patient and the medical care community with new therapeutic tools to support and augment current chemotherapy and heart surgery methodology. Possibly no other single program identified today encompasses such a spectrum of disciplines. It is challenged to assimilate the fundamental knowledge that has been gained in many research laboratories over the years, to define the problem in solvable terms, to establish requirements for therapeutic devices, to catalyze development of devices for diverse cardiovascular disorders, and to recycle these devices as necessary to evolve approaches that will afford practical relief from disability and untimely death from heart disease.

The mission of the Artificial Heart Program is illustrated in Figure 1.

ARTIFICIAL HEART PROGRAM

MISSION

TO REDUCE DEATH AND DISABILITY FROM HEART DISEASE THROUGH THE DEVELOPMENT AND USE OF A VARIETY OF THERAPEUTICALLY EFFECTIVE, SAFE, AND RELIABLE CARDIAC ASSIST AND TOTAL REPLACEMENT SYSTEMS.

FIGURE 1.

The philosophy of the Artificial Heart Program is to stress rehabilitation rather than mere prolongation of life. In planning the achievement of this goal, the Program has recognized the need for a graded series of devices, designed to meet the varying needs of different classes of heart disease patients. The effects that the availability of circulatory assist devices and total heart replacement would have on the mortality and morbidity statistics of cardiovascular diseases are difficult to estimate, since the total number of potential candidate patients for such intervention has not been clearly determined. Also, statistics have nevery really been gathered in a form that would permit the answering of these critical questions. This stems from the lack of firm figures on the number of patients in different categories of heart disease. Over 100,000 heart disease patients a year who die in hospitals are under the age of 65 and do not have any concomitant disease such as cancer, advanced diabetes, senility, or mental illness. Another 250,000 individuals fitting this description are over the age of 65, raising the total number to approximately 350,000. Since these individuals reach medical care and do not have serious concomitant diseases, it would be difficult to justify that any of these should be excluded as candidates for cardiovascular assist devices. It will not be evident how many individuals would require each type of device until their effectiveness and reliability have been assessed. Since the disease process is progressive, the more patients that are kept alive with heart assist devices, the more will eventually require total heart replacement. Also, it is anticipated that the demand for the assist device will be reduced when it is realized that the mechanical portion of the permanent device is the same as that of the total heart replacement, and that the assist device is subject to the low reliability of the diseased natural heart. Thus, the total heart replacement will probably be demanded by an increasing number of patients, which may well be in the neighborhood of 200,000. Any program assumption that ignores this probably increasing demand, or imagines that physicians will withhold this mode of therapy from patients above a certain age, would only result in disastrous logistic problems at a later date.

In addition, the assumption is made that a patient is not a candidate for one of these devices until he is almost taking his last breath. One piece of information which we have learned from heart transplantation patients is that they are not willing to wait until they are taking their last breath before some type of assistance is initiated. Thus, at one time there were in excess of 100 patients waiting around in motels near a transplant center in the United States hoping to receive a heart transplant. These patients were not on their death beds, yet they were willing to wait for an approach which at the current time would seem to have very low reliability even for a period of six months. It, therefore, appears obvious that many of the patients now dying before they reach a hospital after many attacks and considerable disability would not wait that long before seeking help. About all we can say is that the number of patients who need and desire some form of circulatory assist or total support is very large and, in some respects, potentially frighteningly large.

Another fact to be considered is the financial burden that current management of cardiovascular diseases imposes on the economy of the country. The Federal Government now spends more than 300 million dollars a year for Social Security benefits alone to individuals under the age of 65 who are permanently and totally disabled as a result of heart disease. Any significant increase in this number would result in an expenditure by the Government far in excess of the 8 million dollar research and development funds now allocated for the concurrent development of cardiac assist and total replacement devices in the Artificial Heart Program. Of these individuals dying under the age of 65, approximately one half die from myocardial infarction (heart attack). It may be expected that, in the future, the successful development and widespread application of circulatory assist and total replacement devices, in parallel with measures of prevention, will have as dramatic an impact upon American mortality and life expectancy statistics as did the advent of antibiotics.

Objectives.

With the criterion of patient salvage and rehabilitation, the Artificial Heart Program has recognized the need for specific objectives (Figure 2.). These objectives include: (1) emergency assist systems and techniques which involve the development of therapeutic approaches applicable outside as well as within the hospital for the emergency treatment of cardiac arrhythmias and cardiogenic shock. The purpose of these systems is to increase the number of critically ill patients reaching the hospital for more definitive care and to improve emergency treatment within medical facilities; (2) temporary cardiac assist systems, both implanted and external, that are directed at the short-term treatment of cardiovascular insufficiency of diverse etiologies, with prominent examples being acute myocardial infarction and cardiac defects. In clinical applications, these may be employed without previous mechanical assistance or their application may follow the prior use of emergency support devices. They may also provide circulatory assist support for periods of several days to several weeks, until the clinical condition has been reversed or stabilized, or until more effective treatment can be instituted; (3) permanently implanted assist systems that are an extension of the concept of temporary cardiac assist, aimed at taking over a physiologically significant portion of the heart's workload for the remainder of the patient's life; and (4) total heart replacement systems, which involve the transfer of all blood pumping activity of both ventricles to a permanently implanted total artificial heart.

Why these objectives and not more limited ones? From our studies to date, it has become apparent that artificial heart devices could offer a mode of therapy for a large percentage of patients dying from heart disease, assuming, of course, that other disease states are not overriding. However, if we were to develop heart assist devices that do not fully rehabilitate the patient or at least get him on his feet and, hopefully, back to work, then a far greater health problem would be created than would be solved by the mere prolongation of the life of an invalid

PROGRAM OBJECTIVES

- EMERGENCY ASSIST SYSTEMS AND TECHNIQUES
- TEMPORARY CARDIAC ASSIST SYSTEMS AND TECHNIQUES – IMPLANTED AND NON-IMPLANTED
- PERMANENTLY IMPLANTED ASSIST SYSTEMS
- TOTAL HEART REPLACEMENT SYSTEMS

FIGURE 2.

patient. It is imperative, therefore, that ultimate rehabilitative artificial heart devices must be developed concurrently with temporary assists that chain the patient to his bed or to an immobile machine and delay the moment of death indefinitely or until the machine is turned off. It has been the contention of the Artificial Heart Program since its inception that it would be a grave mistake to develop heart assist devices without the parallel development of emergency systems and totally implantable artificial hearts. If this development were realized without devices or only partially effective devices for each category, the impact on society would be far reaching and tragic. It is obvious that a complete family of devices and supportive techniques must be developed to provide the medical care community with the necessary choices to treat diverse disease states in a manner which is tailored to the needs of individual patients. Therefore, any series of devices must minimally provide for: (1) decreasing the number of patients dying before reaching definitive care in a hospital; (2) supporting the biological heart through a period of convalescence either after a heart attack or after surgery; (3) sustaining the heart following the convalescent period under conditions where the biological heart is viable but incapable of satisfying the physiological demands; and (4) replacing the heart when it is incapable of maintaining even minimal physiologic demands. While the development of a complete family of devices was initially envisioned and planned, Artificial Heart Program priorities and budget restrictions have resulted in emphasis on only one family of devices, namely cardiac assist devices. Until recently, the Program was not permitted to develop total artificial heart replacement devices.

Assessment of Technologies.

In order to achieve these objectives, the Artificial Heart Program Office first undertook to assess the exact needs for research and development. Specifically, information was sought in the following areas: (1) identification of the exact problems to be solved in the areas where technology already existed; (2) stating these problems in solvable terms; and (3) what problems would seem to be more difficult to solve and how should one go about solving these. The Program Office, therefore, sponsored initial feasibility studies designed to define the basic requirements for treatment of heart disease patients, to sense the scientific and technological problems, to estimate current and future technologies and to translate the findings into research and development programs. The specific steps involved are summarized in Figure 3.

The feasibility studies were carried out by a number of medical schools, universities, industrial and research institutes with very different backgrounds in performing such studies. Specifically, the Program Office was interested to: (1) determine as exactly as possible what the needs were for different types of devices, including emergency devices, which could be used by laymen, temporary devices for cardiac assistance, permanent cardiac assist devices and total heart

PROGRAM DEFINITION STEPS

- ASSESSMENT OF NEED FOR ARTIFICIAL SYSTEMS
- CHARACTERIZATION OF THE BIOMEDICAL AND TECHNOLOGICAL PROBLEMS
- SURVEY OF APPLICABLE TECHNOLOGY
- ESTIMATE OF FUTURE EXTENSIONS OF TECHNOLOGY
- DETERMINATION OF KEY TECHNICAL DEVELOPMENT PROBLEMS
- ASSESSMENT OF RESOURCES
- DETERMINATION OF PERFORMANCE CRITERIA AND DEVELOPMENT REQUIREMENTS

FIGURE 3.

replacement; (2) determine as clearly as possible the biological as well as the engineering requirements and problems associated with all types of devices; (3) explore the state-of-the-art in each of the areas that would be involved, not only hardware but software; (4) estimate what the future state-of-the-art might be, considering the extensions in the state of technology predicted to take place over the next five to fifteen years; (5) identify the areas which would require additional stimulation through Artificial Heart Program funding in order to bring the level of technology up to a point which would permit utilization in a timely manner; (6) make an assessment of available resources and identify the non-hardware aspects of a development program if a full systems approach were to be applied to the problem and to identify responsibilities, both in the areas of medical, engineering, and lay communities; and (7) investigate and develop a number of possible plans for accomplishing the total Program goal.

The analysis of the above tasks and the possible approaches suggested by the different investigators provided much information on the nature and complexity of the varying biological and engineering problems broadly associated with the development requirements for artificial heart devices. These basic studies were very valuable to the Program. Some of the critical technical and non-technical problems in the development of a variety of artificial heart devices are identified in Figure 4. In particular, these efforts identified the critical importance of the blood/materials problems, the importance of proteins, platelets, erythrocytes, leukocytes, and other elements of the blood, the need for definition of physiologic control and regulation mechanisms of the cardiovascular system relative to assist and artificial heart devices, the importance of developing energy systems that would provide satisfactory physiologic output and yet be compatible with the physiologic environment, and the development of diagnostic instrumentation as well as instrumentation for control systems for assist devices. A major emphasis was placed upon the importance of identifying the significant legal and ethical problems involved in developing and providing artificial heart devices. Also other software aspects of the Program were highlighted as critical elements involving such areas as medical personnel training efforts, the survey of facilities and sufficient backup support to insure that devices, when available, could be effectively implanted. There was considerable encouragement to establish a series of diagnostic procedures that would help identify cardiac patients as well as to develop new and more effective techniques for improved monitoring and diagnostic work-up for patients having devices implanted.

SOME OF THE TECHNICAL AND NON-TECHNICAL PROBLEMS OF DEVELOPMENT AND APPLICATION

- BLOOD/MATERIALS
- BLOOD PUMPS AND CONTROLS
- ENERGY SYSTEMS
- PHYSIOLOGICAL EFFECTS
- INSTRUMENTATION
- BLOOD OXYGENATORS
- ENDOGENOUS HEAT
- PERCUTANEOUS LEADS
- BLOOD FLOW
- RELIABILITY AND MAINTAINABILITY
- SAFETY
- PATIENT DIAGNOSIS (PATIENT SUITABILITY)
- ANATOMY (SPACE, SUPPORT, WEIGHT)
- FACILITIES, PERSONNEL, EQUIPMENT
- MORAL AND ETHICAL CONSIDERATIONS
- LEGAL CONSIDERATIONS
- SOCIAL AND PSYCHOLOGICAL FACTORS
- ECONOMICS

FIGURE 4.

Management Approach.

Modified Systems Approach. In seeking solutions to the identified technological problems, the Artificial Heart Program decided to follow a modified systems approach rather than the conventional step-by-step approach which is more customary in most developments in the medical field. The systems analysis approach may be defined as a cycle of: (1) defining objectives; (2) designing alternative systems to achieve those objectives; (3) evaluating the alternatives in terms of their effectiveness and costs; (4) questioning the objectives and other assumptions underlying the analysis; (5) opening new alternatives; (6) establishing new objectives; and (7) repeating these steps as many times as necessary in order to achieve the final goal. In this approach, competing parallel programs and systems are explored and adopted or discarded on the basis of their contribution to the goals and subgoals to be accomplished, as well as their effects on the total mission. Balance within a given subsystem and within the entire system is sought, always with a single overriding objective -- that of achieving the mission.

The fairly standardized systems approaches developed and utilized in the aerospace and defense industries have been modified by the Artificial Heart Program to fit biomedical problems and the constraints peculiar to this field of development. This involves a continuous process of defining and redefining how techniques of systems management can most effectively be applied to the development of cardiovascular devices. The Program is structured so as to permit technology to be rapidly translated into workable and practical devices to be used by the physician in a relatively straightforward manner, while at the same time allowing for research to proceed in certain critical areas of Program needs. The research efforts of the Program are carefully programmed so as to take into consideration current states-of-the-art within the pertinent technologies, and the information gaps that need to be closed in order to arrive at a proper framework for effective further development. These background research projects provide the basic knowledge necessary for the specifications and subsequent development of hardware, as well as the development of the technology required to effectively diagnose the patients and implement the developed technology for use in patients.

Because of the very nature of the systems to be developed, the Artificial Heart Program systems approach is unique in several important respects. First, it is necessary to define what we mean by a system in this context. A particular system consists of the following subsystems: the specific cardiovascular device to be developed; the engineering analyses of the device; the animal evaluation; the clinical trials; the method(s) for applying the device; the necessary knowledge for applying the device; the attending physician; and the sick patient. There are a great number of complete families of such biomedical systems, each with a large number of variables that might interact. The modified systems approach for biological development differs from that of the aerospace/defense oriented systems in other respects as well. As principally utilized, the aerospace/defense systems have primarily involved major hardware development programs utilizing only the physical sciences and engineering technologies. These, in turn, have been based, to a significant degree, upon several decades of proven theory and technology in physics and engineering. This extensive theoretical and technical background has permitted a high degree of quantification of the various tasks required to perform these major and complex systems activities. However, probably the single most important fact responsible for the success of these systems is that the Government essentially is the originator, the supplier of resources, as well as the ultimate user of the development end-products, exclusive of spin-off technologies. This, in itself, forms a closed type of system from specifications to development, production, and ultimate application. Such a system forms a closed loop which is in distinct contradiction, or opposite in direction, to a biomedical open system which must be designed for the patient and society. In a medical system, one is dealing with such complex and partially unknown variables as a sick, responding living organism, families of devices of partially defined hardware and technologies, unknown variables of application, and limitations of attending medical staff, with the ultimate success of the total systems approach being gauged by the degree of clinical improvement achieved in individual patients. The different etiologies of cardiovascular diseases, the wide variability of patient response, the broad and often diverse backgrounds of physicians, and the involvement of very complex technologies derived from the scientific and industrial communities, formulate the open-ended system. When compared with the ever converging systems evolved in the past in such programs as the Manhattan Project, the Fleet Ballistics Missile Program, the Nuclear Submarine Program and others, the modified biomedical systems approach employed by the Artificial Heart Program is seen to be far more complex, and to consist of diverging as well as converging variables, making previous straightforward systems development approaches inadequate in several areas. In order to permit the development of effective systems for solving problems in medicine, the effectiveness of the system cannot be based on any single subsystem or part of that system. Instead, the effectiveness must be based upon what the overall combined system does, both in terms of adequacies and inadequacies. This requires not only that a subsystem perform as required, but that the interdependencies of the subsystems are adequate as well. The biomedical systems approach must also take into account that much of current medical knowledge is based on empiricism rather than on exact scientific data. Significant modification of the systems development approach is necessary in order to allow for this variable.

There are many additional reasons for the Artificial Heart Program decision to follow the modified systems approach for the development of cardiovascular devices. One of these is economic in nature. As mentioned earlier, the United States Government currently spends in excess of 300 million dollars each year for Social Security payments to individuals who are disabled as a result of heart disease. This fact is one of the most compelling reasons for following the systems, rather than the more conventional step-by-step, approach. A step-by-step approach would significantly increase the number of cardiac cripples. If the Program were to follow such an approach (as has been suggested by many), developing first a device with an external power source which would not allow ambulation, this would result in significant increase in the number of bedridden patients in and out of hospitals, thereby greatly increasing the burden imposed on the economy of the nation, as well as accomplishing little of real value to the patients. If, after this first device were developed, a portable external power source were developed, this would allow for ambulation, but not rehabilitation; and if, after that, a device that allowed for full rehabilitation were developed, the entire length and cost of the Artificial Heart Program would be increased significantly and the total expenditures in Social Security benefits would far outweigh a research and development program based upon a concomitant systems approach.

In addition, the modified systems approach as adapted by the Program involves a team effort designed to provide for a continuous involvement as opposed to a fragmented one so that all members of the team become involved in a continuous process, not having only specific immediate objectives, but responsibility that extends from their initial selection and involvement through to the completion of the objectives for their part in the overall system. It is the contention of the Program that in this manner inevitable problems of communication are minimized and motivation and commitment enhanced not only at higher management levels, but also at the scientific and technical working levels. This approach provides the basic framework for integrating the efforts of the various disciplines of the team, i.e., the hardware development, the biological and technological research, and clinical evaluation, in order to complete development and to accomplish the Program objectives of bringing a therapeutic device to the patient. It is felt that by securing a high degree of personal involvement, scientific challenge, and responsibility for total developmental efforts, effective relationships between the physical science and engineering community and the medical community can be successfully developed. As illustrated in Figure 5, the Program involves researchers, developers, testers and evaluators, clinicians, the medical care community, requiring the sensitive interaction of different disciplines, such as medical, scientific, engineering, management, legal, social, etc., and diverse institutions with different philosophies and modes of operation, e.g., universities, hospitals, industries, and research institutes.

The team approach can provide for the necessary emphasis to cut across traditional functional lines of departments and divisions in each of the various areas of research, development, production and manufacturing that are involved in satisfactorily carrying out the systems development approach. This approach provides for the early sensing of engineering and medical problems that need to be solved within the current development efforts, as well as the identification of new areas in need of exploration and development. The team provides a coherent organization promoting responsibility in carrying out the research and development efforts, timely sensing of the

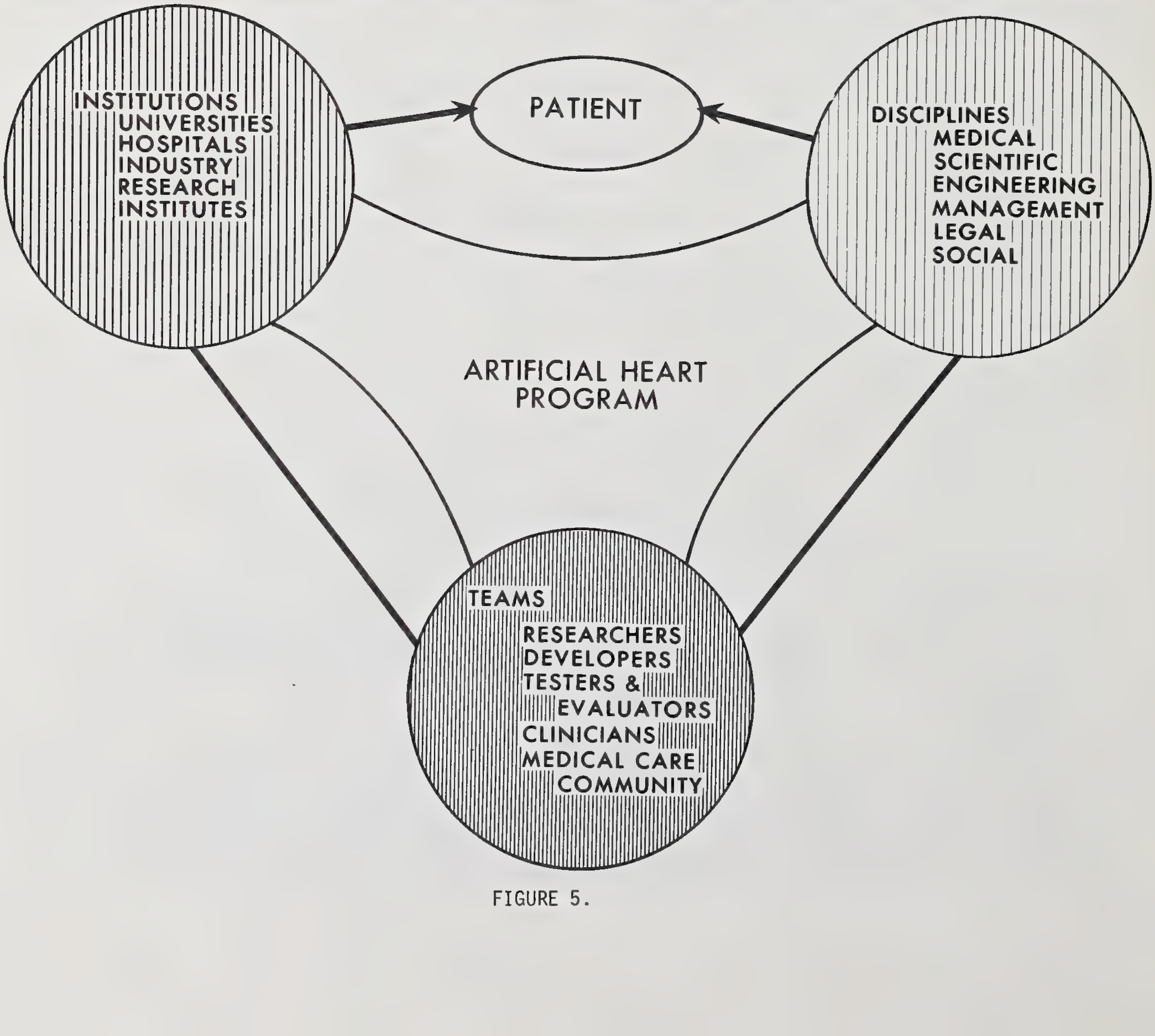

FIGURE 5.

potential utility of a device, extensive testing to permit early transition from the laboratory prototype stage to the development state. It considers factors such as the cost and manufacturing problems involved in converting the device into a reproducible item with adequate performance characteristics and satisfactory reliability within the economic constraints imposed by the requirement that its cost should be within the reach of the physician and his patient. The involvement through the team approach provides for a continuous, rather than discontinuous, path even in those cases where discrete developments are undertaken by groups separated widely both in space and time.

Responsibilities are effectively fostered by the team approach. Communication gaps and commitment vacuums tend to lessen with the joint involvement by different team members in achieving a common goal. The common tendency for different scientific and technological disciplines to use languages, attitudes or techniques unique to their own areas of specialization are minimized. This encourages better understanding, interaction, and involvement. These activities combine to provide for more innovative problem solving cycles all the way from the research level through to the final production levels.

Developmental Approach. To cope with the identified problems, the Artificial Heart Program implemented three basic and interrelated thrusts directed toward the mission as illustrated in Figure 6. The thrusts are organized so as to make possible the identification and utilization of the results of two decades of basic research, and to insure that new knowledge and techniques, when available, are applied to the problems of artificial heart development.

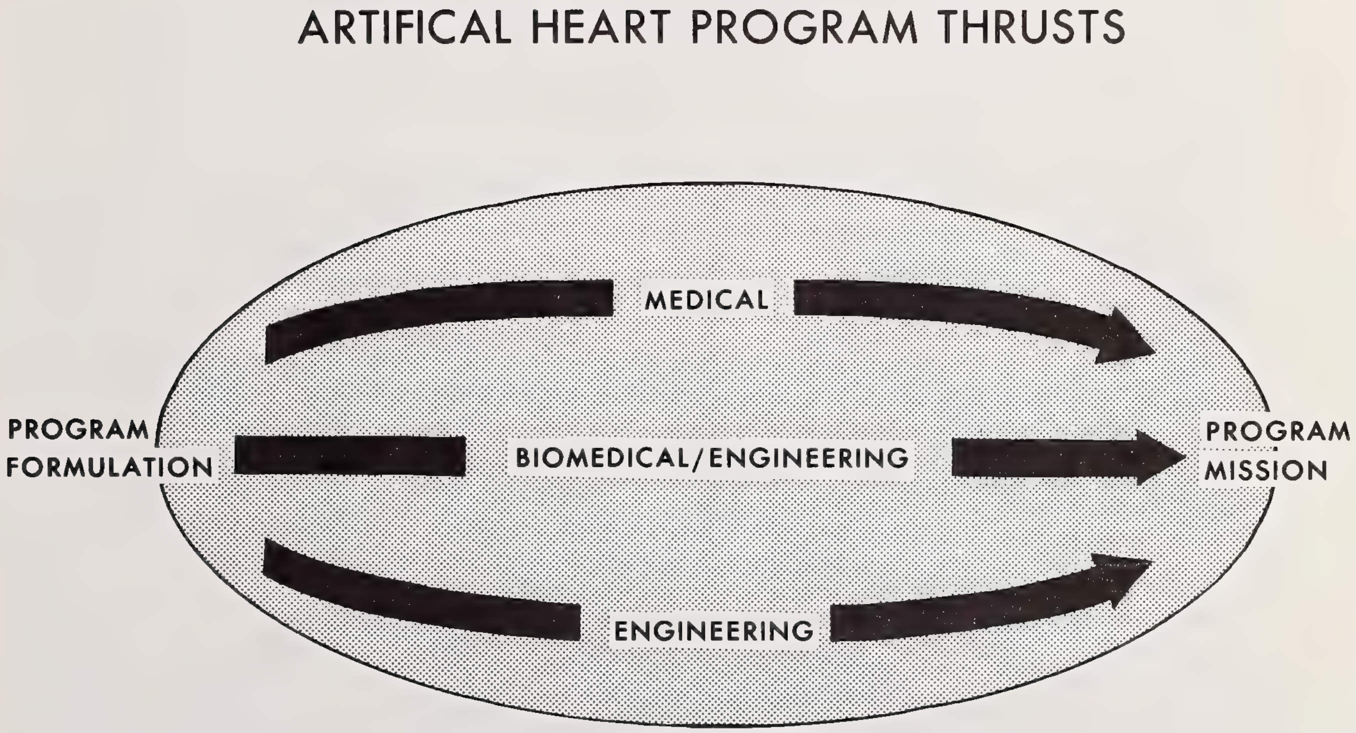

FIGURE 6.

The overall development approach involves three major approaches illustrated in Figure 7. They are: (1) a non-hardware approach involving the biological and technological research and clinical evaluation; (2) test and evaluation; and (3) the hardware approach.

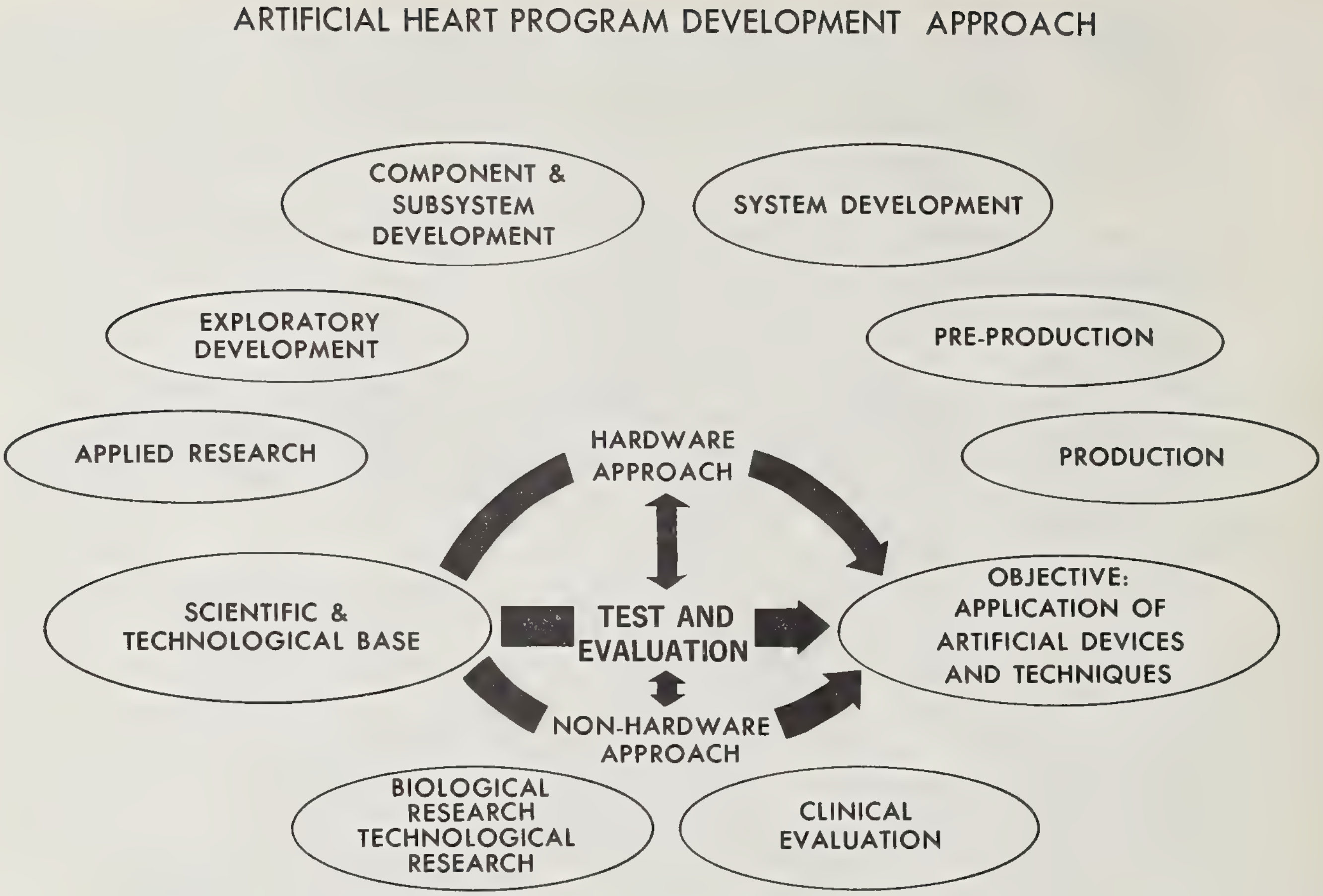
ARTIFICIAL HEART PROGRAM DEVELOPMENT APPROACH
COMPONENT & SUBSYSTEM DEVELOPMENT
SYSTEM DEVELOPMENT
EXPLORATORY DEVELOPMENT
PRE-PRODUCTION
APPLIED RESEARCH
HARDWARE APPROACH
PRODUCTION
SCIENTIFIC & TECHNOLOGICAL BASE
TEST AND EVALUATION
OBJECTIVE: APPLICATION OF ARTIFICIAL DEVICES AND TECHNIQUES
NON-HARDWARE APPROACH
BIOLOGICAL RESEARCH TECHNOLOGICAL RESEARCH
CLINICAL EVALUATION

FIGURE 7.

Artificial Heart Program studies to date have been in line with the developmental approach adopted at the inception of the Program. The various subsystems that make up the variety of artificial heart devices, the facilities, and other resources required for their implementation were defined; for example, various types of blood pumps, different energy sources, different approaches to biocompatible materials, physiologic controls, diagnostic instrumentation, monitoring before and after surgery, and long-term follow-up care, etc. Work is proceeding concurrently on each of these subsystems. Within each area, a number of different approaches are being followed. Approaches that appear to be more promising are continued, while those less so are discontinued. The advantages and disadvantages of each are compared with a view to how they would tie in with the advantages and disadvantages of other related subsystems. This is referred to as "trade-off analyses." Among the identified subsystems are several of a non-hardware nature -- for example, the acceptability of devices by the medical community, the patient, and society; social and ethical problems; etc. Due to a lack of funds, work on these important subsystems has not yet been implemented.

One of the major problems in developing devices in medicine is the fact that specific criteria or specifications cannot be given for the optimal type of device. A set of specifications which would be satisfactory for one group of patients would be unsatisfactory for another. The research and development effort has been designed along the various paths outlined above to identify the various components that might be utilized in a variety of these systems, and the variety within a particular type such as the permanently implantable assist devices. These involve trade-offs in materials, the type of blood pump, energy, converter, blood flow patterns, controls, etc., which are required for artificial heart and circulatory assist devices. The goal is to develop these devices to the point where their trade-offs can be effectively identified and then to select the most satisfactory combination of the components to yield devices that have a very high probability of success. This is not simply a matter of hardware development as some people have stated. The objective of this Program is not just to develop pieces of hardware, but to insure that these developments have taken into consideration pertinent physiological, biological, engineering factors and the constraints of the medical care community. This is necessary in order to provide patients with devices that will give practical relief from death and disability from heart disease. Simply developing a piece of hardware which is adequate to do the job is not enough. With concurrent problems only partially identified, such an approach would undoubtedly prove impractical in that the device might not be acceptable to the biological environment when finally tested. Thus, the process of device development might have to be repeated several times in order to get a workable device.

Transition Phase.

Beyond the research and system definition phases, there are a number of pertinent factors influencing the availability of devices to the medical care community and to the patient. The development costs are expected to be relatively high because of the parallel approaches required and because of the continuously evolving specifications. Potential commercial considerations which need to be faced will involve market size and complexity, profit potentials, as well as many other associated factors. The degree of involvement of industry and Government in the research and development stages as well as in the transition stage from research and development to initial production as well as to final production, product transition phase, and the marketing stages, will influence the rate of progress to a great extent. Questions regarding background rights, proprietary data, and patents will need to be effectively resolved to promote involvement by all groups concerned. Other factors which will need consideration are the complexity of applications involving the medical community, system and component standards, to assure the desired quality and reliability for effective and safe devices. These will include factors such as facilities, personnel, etc., for practical systems diagnosis, maintenance and repair, as well as many other technical, managerial, legal, ethical and social considerations. Future work is planned in each of these areas.

One area scheduled for immediate future emphasis by the Program is that of device evaluation, preclinical studies, and clinical trials. Developers, Government agencies, and the scientific community are currently examining their respective roles in this area. Questions as to how devices should be evaluated, by whom, and whether or not they should be certified, are being considered.

The Program Office believes that it is imperative that devices or components satisfy rigid biological and engineering criteria before they can be considered for clinical trials. At present, there is a tendency to move too quickly from the laboratory to the clinical situation. This step is often taken before (1) there is sufficient laboratory evidence that the heart, other vital organs, and/or the body as a whole can be helped through the use of the device; (2) adequate criteria have been developed for patient selection and specific indications for the particular mode of therapy have been identified; and (3) adequate monitoring techniques have been developed which will permit evaluation of the device and comparison with other forms of therapy.

Thus, history of medical device development to date has followed a somewhat fragmented course with many missing links in communication between engineers and physicians. Secondly, it has represented principally the efforts of only one of these groups. One might characterize this approach in the following manner: an ingenious, enterprising physician working with a group of technicians or engineers would develop a device and try it in animals. If some animals live, the physician would then frequently try the device in humans and, if some humans live, the clinical trials would be continued. These trials would then be pursued by the individual physician and possibly by a few others for a number of years until investigators would perform some objective critical clinical trials and publish their results in the medical literature. After some period of time, the medical community would finally decide whether to accept this new mode of therapy. In the meantime, many patients have been subjected to a potentially dangerous mode of therapy, while countless others may have been deprived of a possibly effective therapeutic device.

An analysis of past development of devices has shown that the longest time-lag for utilization of devices is between its clinical trial and its acceptance by the medical community and by the lay public. This is a big problem in device development, one of patient protection, all factors considered, as well as the problem of having devices adequately evaluated so that the medical community can have some assurance that the device is really safe, reliable and effective. In the past, some devices have never reached the public because they have never been properly evaluated.

It is the plan of the Program Office to make sure that all components, materials, and devices developed under the Artificial Heart Program are adequately and systematically tested before being considered for clinical use. The Program is, therefore, setting up Test and Evaluation Centers that will provide testing and evaluation under controlled conditions. The principal purpose of the Test and Evaluation Facility is to provide data and information on the devices, and also to assure the developer that the product is safe and reliable, and that representatives of the scientific community and the Government are satisfied that those attempts that seem appropriate in evaluating the device have been tried. This will help to insure that the patient can be provided with this device if it is found satisfactory. If the device is found unsatisfactory, the developer might continue the development of the device or explore its effectiveness in alternate areas of application.

The protocols for the Test and Evaluation Facilities will be established as a result of interactions of a Special Task Force with the Artificial Heart Program Office, along with inputs from the developer and from the testing facility itself. The Special Task Force is composed of knowledgeable scientists representing the biological, engineering, clinical and systems management disciplines. It is an attempt to get the scientific community more involved in the actual evaluation of devices in the future. It is hoped that this task force will serve as an example of how the involvement of informed scientists can serve to give quality and flexibility to and speed up the device evaluation process. The devices will be thoroughly evaluated by competent and objective groups that have no part in the development of the particular device. These evaluations will be in addition to the evaluations provided by the developer himself. The test and evaluation process will start with engineering and animal test and evaluation; then, if the device appears satisfactory, it will continue into the clinical phase. This phase will cover its effectiveness in humans, the indications and contraindications for its use, and problems relating to the various pathological conditions that will be met. There will be a continuous feedback of information to the developer so that improvements can be made in the device, as necessary. It is hoped that, in this manner, devices of an optimal design can become available to the general patient population far quicker than is customary at present.

These efforts by the Artificial Heart Program are designed to involve the scientific and industrial communities in establishing the standards, specifications, and criteria necessary for continued device development and application. This is advanced thinking and requires that one project oneself many years into the future to face the questions of what does a physician need to know about the device in order to apply it, not only what he needs to know, but what will he have on hand to make an assessment of the information that is at his disposal in order to decide whether it is a mode of therapy for this particular patient.

Contracts Management.

Management of the Artificial Heart Program follows systems techniques modified to fit biomedical problems. The networks are developed along two basic orientations: research-oriented networks and technologically oriented networks. This is done in order to provide flexibility in research while retaining guidance toward specific objectives. This minimizes the problems encountered in applying rigid networks with specific time and cost to completion as used in non-research efforts. Time-oriented sequential networks are developed for the major technology areas, in terms of subsystems and systems, in order to identify requirements, goals, and critical areas of the Program. These program network plans and the overall priorities and resources of the Artificial Heart Program are then utilized in formulating overall program plans for the development of therapeutic devices. A schematic of the planning cycle and the relationship of areas of the Program are illustrated in Figure 8.

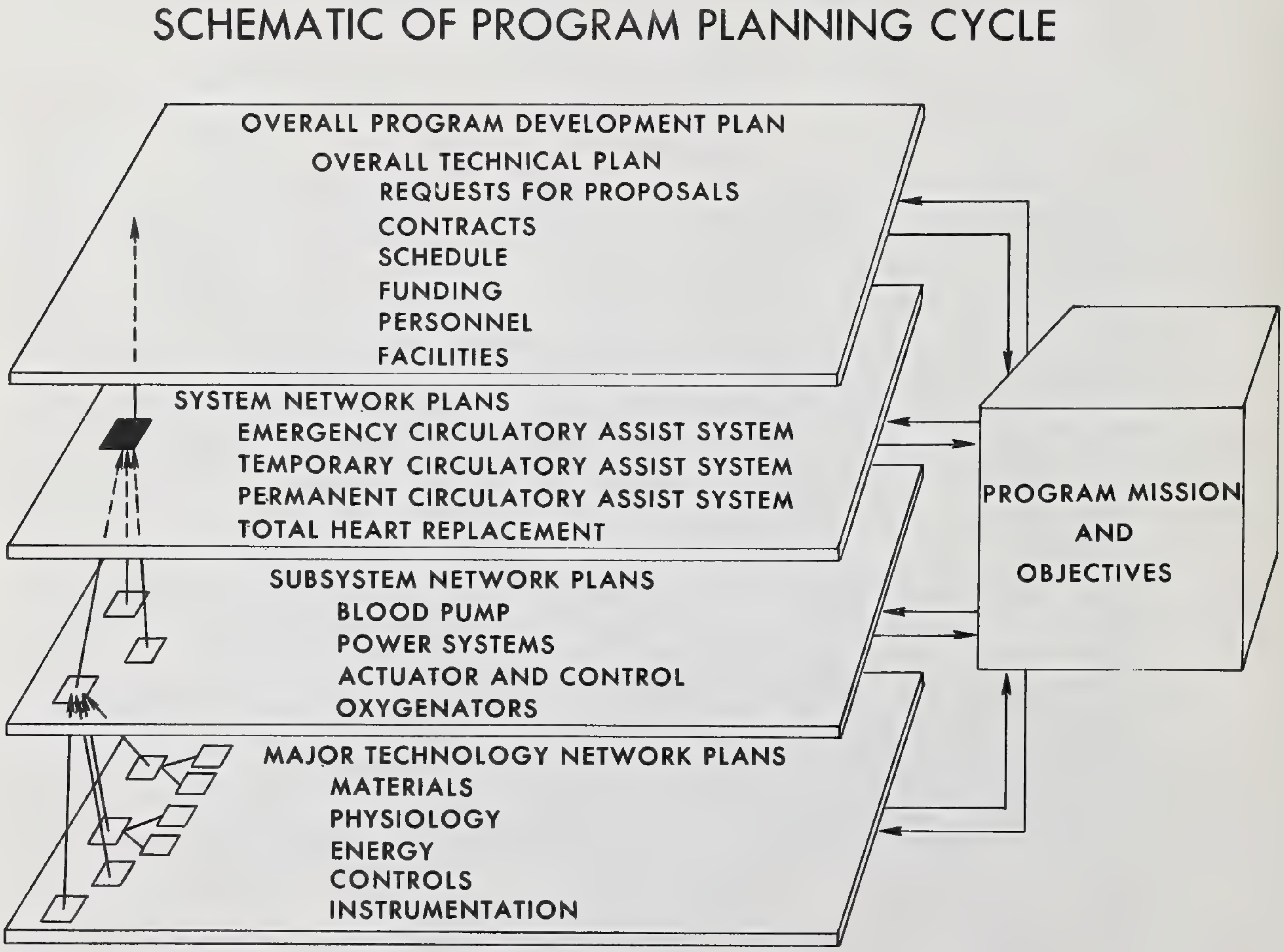

FIGURE 8.

As an example, we would like to consider the blood/materials area. The approach involves the definition of requirements such as those indicated in Figure 9. The network plan is then formulated on the basis of these intermediate objectives and represented in a hierarchy of phases and steps down to individual programs to achieve the objectives of the blood/materials program.

FACTORS BASIC TO MATERIALS DEVELOPMENT AND TESTING PLAN DEVELOPMENT

- BLOOD/MATERIAL COMPATIBILITY – CELLULAR AND NON-CELLULAR
- TISSUE/MATERIAL COMPATIBILITY – METABOLIC PROCESSES, CARCINOGENIC OR HYPERSENSITIVE ALLERGIC REACTIONS
- STABILITY IN BIOLOGICAL ENVIRONMENT
- ADEQUATE PHYSICAL, MECHANICAL & CHEMICAL PROPERTIES
- FABRICATION CONSIDERATIONS
- STERILIZATION AND HANDLING CONSIDERATIONS
- REPRODUCIBILITY – PURITY
- ACUTE AND CHRONIC BIOLOGICAL EFFECTS
- STANDARDIZATION OF TESTS

FIGURE 9.

Each contract is planned and managed in accordance with the technical requirements of the Program, the personnel and type of organization, and the relationship of the specific program to the overall Artificial Heart Program. A development plan is worked out by the contractor in conjunction with the Artificial Heart Program Office to identify key elements and to show how all activities of the contract will be performed. This is charted within the Program Office and used as a basis for monitoring and guiding the Program. The management center of the Artificial Heart Program is shown in Figures 10, 11 and 12. The program plan puts the objectives of the Program in specific terms and tasks, and not in generalities. This permits realistic utilization of both time and monies in the performance of the Program. The preparation of these plans takes into consideration the variable nature of the problems involved and the type of research and development to be performed. For example, a plan for developing an electronic drive system for a circulatory assist device is very different from a plan for developing a material that is to be compatible with blood. These differences are recognized, as well as the differences within the organizations that are to perform the work.

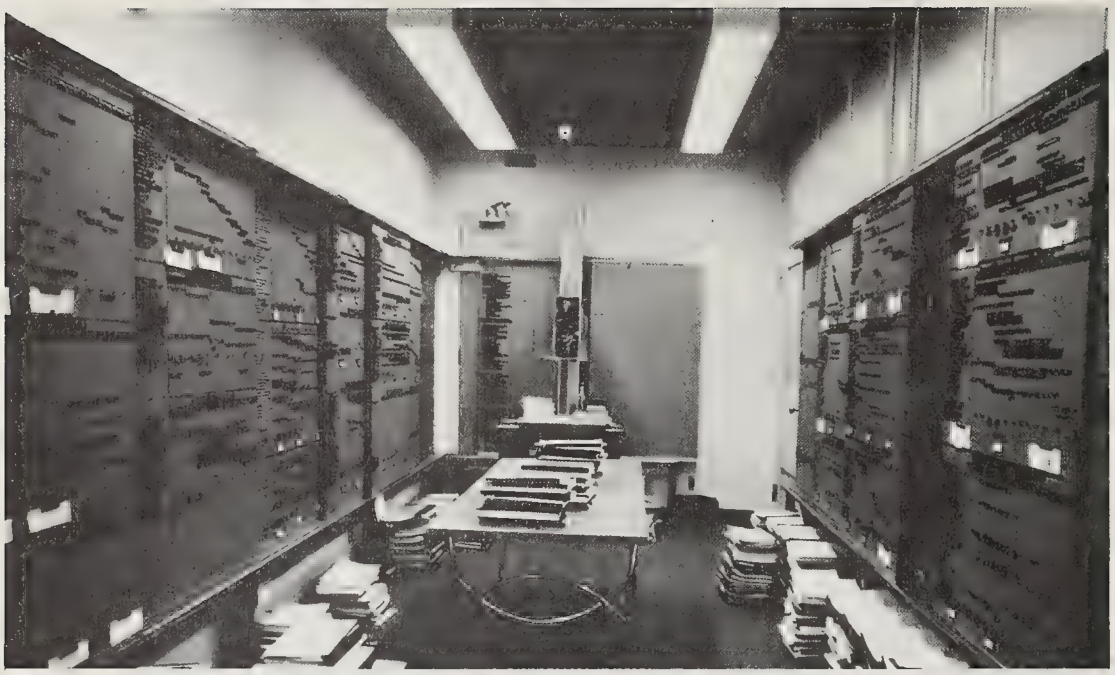

FIGURE 10. MANAGEMENT CENTER OF THE ARTIFICIAL HEART PROGRAM

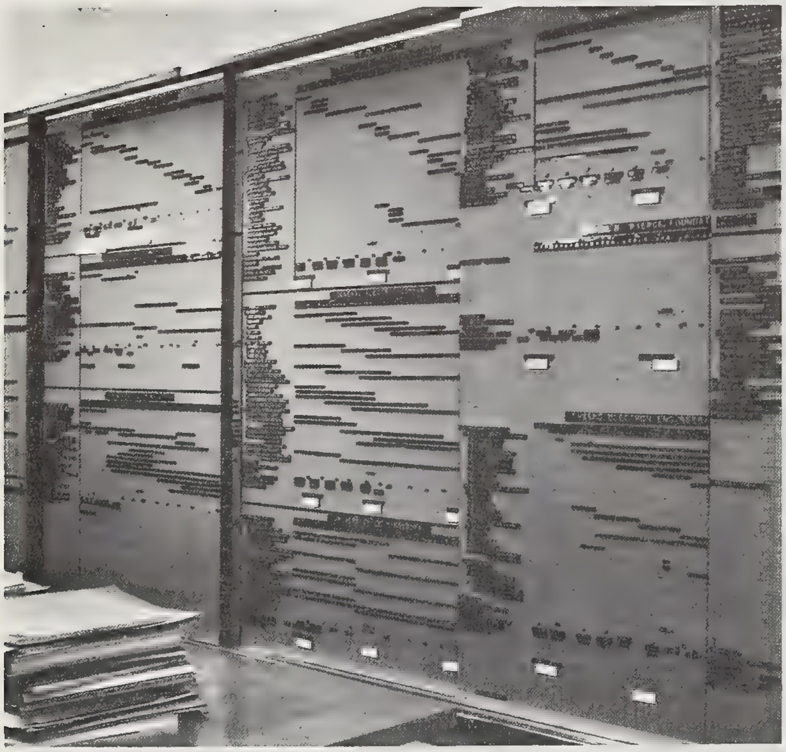

FIGURE 11. CLOSER VIEW OF PLANNING CHARTS IN THE MANAGEMENT CENTER

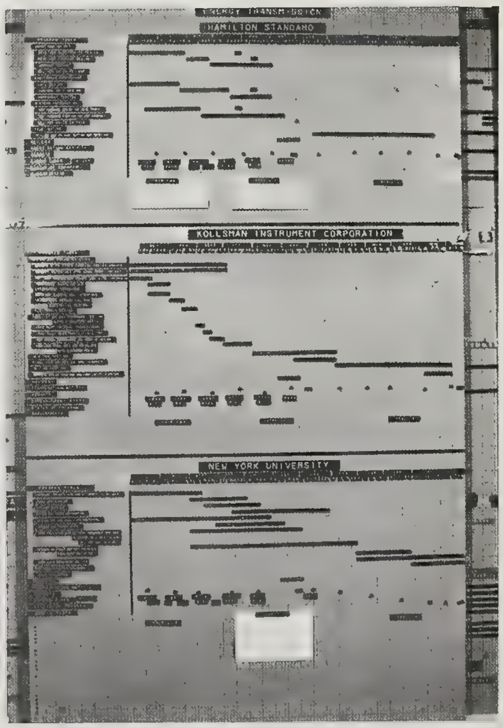

FIGURE 12. EXAMPLES OF CONTRACT PLANS

SUMMARY

In summary, having highlighted the background, the mission, the objectives, and management approach of the Artificial Heart Program, we would now like to identify the technical elements of the current Program (Figure 13). They are: Development of Materials for Use in Circulatory Assist Devices, Analysis of the Effects of Materials on Blood, Blood Flow through Pumps and Valves, Cardiac Control Parameters, Oxygenator Development, Circulatory Assist Devices, Physiologic Effects of Assist Devices in Animals, Instrumentation Applicable to Artificial Heart Development and Utilization, Development and Use of Percutaneous Leads, Biological Fuel Cells, Effects of Additional Endogenous Heat, Implantable Energy Systems, and Test and Evaluation Facilities.

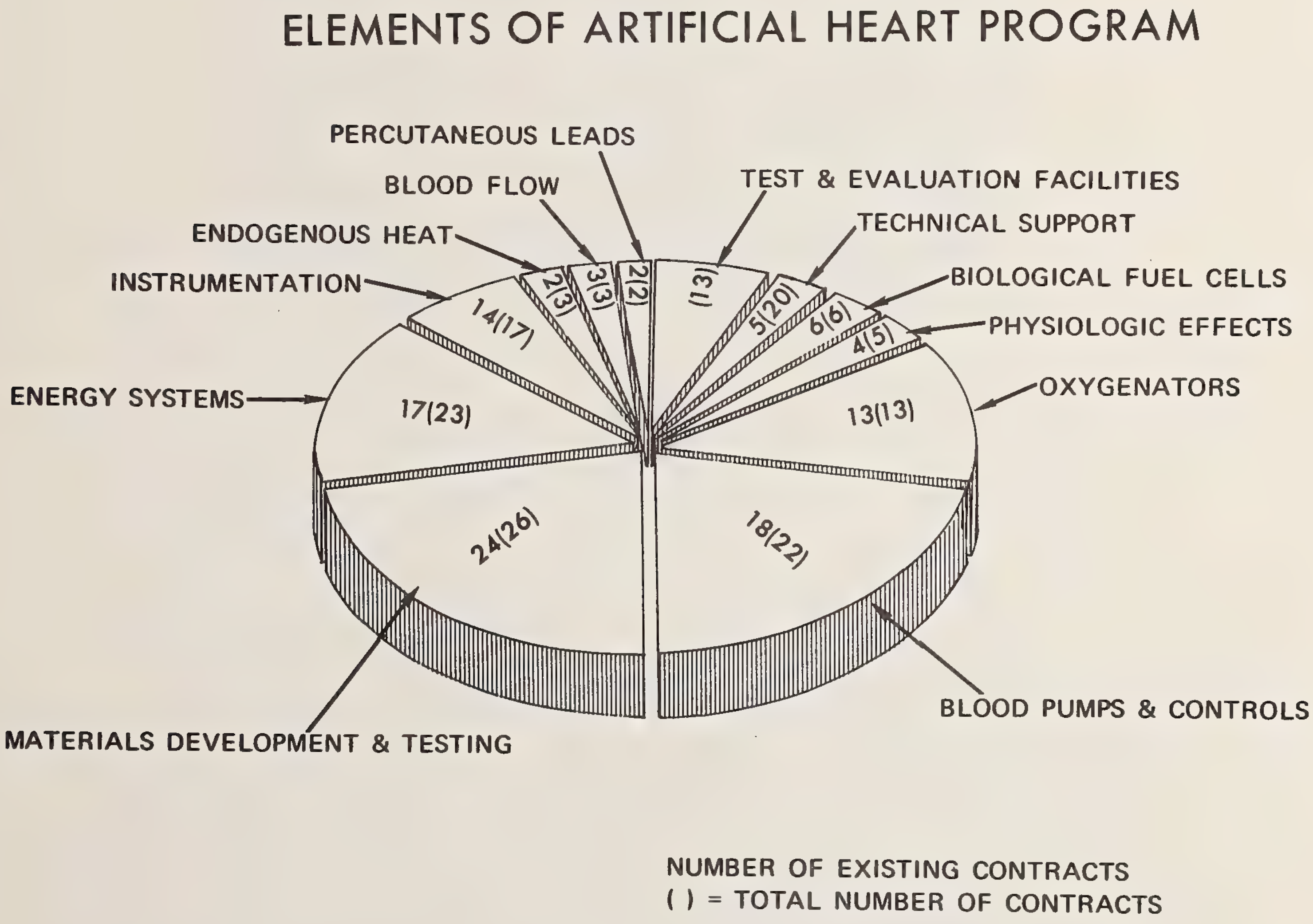

FIGURE 13.

The Artificial Heart Program is a team approach, involving diverse disciplines and institutions with a mission. The requirements and challenges for the biological and medical professions, the engineering and physical science professions, industry and Government in developing and applying practical modes of therapy to minimize disability and to reduce untimely death due to heart disease are formidable. It is our hope that the following presentations and discussions will be stimulating, as well as challenging, to you in these regards. These papers center upon specific research and development projects of the Program and not upon complete systems.

SECTION I

DEVELOPMENT OF MATERIALS FOR USE IN CIRCULATORY ASSIST DEVICES

Chairmen: Frank W. Hastings, M.D.
Lowell T. Harmison, Ph.D.
Anthony M. Bruno, M.D.

INTRODUCTION

One of the critical problems still confronting the Artificial Heart Program is the unavailability of materials (for both short-term and long-term use) which are completely compatible with blood. In addition to the need for such materials for blood pumps, there is a similar need for such materials which also have optimal O_2 and CO_2 transport properties for use in blood oxygenators. Some new surfaces appear promising; however, even these represent improvements in only limited aspects of blood compatibility. Most of the promising surfaces may not be as permanent as would be required for long-term assist devices. The Artificial Heart Program is now supporting a number of approaches to this materials problem, including developing more permanent heparin surfaces, bonded enzymes, specially prepared graphite surfaces, modified cellulose surfaces, endothelial surfaces, polymers with "permanent" negative surface charges, hydrogels with and without ionically charged surfaces, new and more compatible silicones, and other polymer configurations.

CHAPTER 2

DEVELOPMENT OF MATERIALS FOR USE IN CIRCULATORY ASSIST DEVICES

G. Grode, R. Falb and S. Anderson

Battelle Memorial Institute, Columbus, Ohio

Objectives of this research program are: modification of materials to produce nonthrombogenic surfaces and study of the basic interactions occurring at the blood/foreign surface interface. Work has been carried out on the modification of synthetic polymers by the chemical attachment of heparin to their surfaces. Techniques developed include both ionic and covalent bonding of heparin to a wide variety of polymers including all of those currently used for prosthetic devices. A rapid and simple method for ionic bonding of heparin using water-insoluble quaternary ammonium salts has been developed and results show excellent in vitro and in vivo performance. The stability of heparin to elution by simulated plasma indicates good potential for use in short-term applications. Heparin has been covalently bonded to silicone rubber by means of a cyanuric chloride intermediate and this product has an even greater resistance to elution. Products of this type are suggested for long-term applications of nonthrombogenic materials. Studies of the blood/foreign surface interface have been carried out to elucidate the requirements of a nonthrombogenic surface. The basic interactions of blood components such as lipids, lipoproteins, proteins, coagulation factors and formed elements with heparinized and control surfaces have been investigated. Heparinized surfaces prepared by means of water insoluble quaternary salts interact strongly with lipid and lipoprotein components upon initial contact, but after equilibration no further interaction occurs.

Clotting factor interactions and platelet viability vary with the chemical nature of the contacted surface. Surfaces have been prepared containing the following functional groups: hydroxyl, sulfate ester, sulfhydryl, carboxylic acid, amino, sulfamido, and quaternary ammonium salts. In addition, polyamino acid chains were grafted to surfaces. The relationship of these various chemical moieties to interactions with the hematological system is now being studied.

INTRODUCTION

The objectives of the research work at Battelle on biocompatible materials have been in two main areas.

These are:

1. The development of blood-compatible polymers
2. The investigation of blood/foreign-surface interface interactions.

Work directed toward the first objective has emphasized the development of materials that do not activate the clotting mechanism. The current effort is based on four years of experience and study in a continuing program with the National Heart Institute. We have found that appropriate surface heparinization treatments can make a large number of materials nonthrombogenic. Two methods are used presently in our research on surface heparinization. One of these methods uses electrostatic or ionic forces to bind heparin to the surfaces of products that are expected to be suitable for most short-term applications. The other introduces a covalent bond between the heparin and the substrate polymer. Covalent bonds are expected to provide a more stable heparin layer on materials suitable for long-term applications.

The investigations on interactions at the blood/foreign surface interface (coagulation, protein absorption, lipid and lipoprotein interactions, cell adsorption and rupture, and changes in enzyme and clotting factors) have furnished insight into the basic coagulation phenomena as related to heparinization requirements.

EXPERIMENTAL

Facile Method for the Attachment of Heparin by TDMAC Impregnation Process

Much of the laboratory work on heparinization methods has been concentrated on the development of rapid and facile techniques which would be applicable to a large number of materials and design configurations. This work has resulted in a very simple method in which heparin can be ionically bonded to a surface using a water-insoluble quaternary ammonium salt. Heparinization of a water insoluble surface may be accomplished by steeping the material in a solution of the quarternary ammonium salt (tridodecylmethyl ammonium chloride (TDMAC)), followed by exposure to a heparin solution. This technique is applicable to the types of materials shown in Table 1.

TABLE 1

MATERIALS TREATED USING TDMAC/HEPARIN

- Silicone Rubber
- Polyurethane
- Polypropylene
- Polyethylene
- Glass
- Acrylic
- Polyvinyl Chloride
- Polycarbonate
- Mylar
- Teflon
- Aluminum

This process makes possible the heparinization of a broad range (Table 2) of prosthetic vascular devices and their auxiliaries.

TABLE 2

DEVICES TREATED USING TDMAC/HEPARIN

- Vineberg tubes
- Gott rings
- Silicone rubber tubing
- Heart valves
- Catheters
- Blood pump
- Shunts
- Capillary tubing
- Oxygenator membrane
- Heat exchangers
- Manifold bags
- Heart assist device

Environmental stability of the heparin-bonded surfaces was measured *in vitro* by the exposure of S^{35} heparin-treated surfaces to physiological saline solution and bovine plasma. Table 3 lists some representative results.

TABLE 3

STABILITY OF TDMAC/HEPARIN SURFACES TO EXPOSURE OF SALINE AND BOVINE PLASMA

Material	Material Originally Bound, A	Heparin Retention, %	
		After 100 hr in saline	After 3 hr in plasma
Silicone rubber	2,200	91	--
Polyurethane	18,600	100	98
Polyethylene	2,500	100	94
Polyvinyl chloride	2,500	100	95

In vitro stability was also measured by impregnating a finely ground material with a radioactive TDMAC/heparin, and then packing this in a column thermostated at 37 C and passing plasma over its surface. The effluent was collected in small fractions of 3-4 ml and analyzed for radioactivity. A sketch of the apparatus used in this technique is shown in Figure 1. The fractions were also analyzed for changes occurring in blood component levels and these data are reported subsequently. Figure 2 illustrates a typical stability determination. As indicated, small quantities of heparin were removed (2-4 µg/ml); however, this did not constitute an anticoagulant level of heparin (approximately 25 µg/ml). The graph also shows an increase which has been observed repeatedly in eluted heparin in the initial saline fractions following the plasma flow. To determine if the loss was due to heparin removal alone, or was caused by the displacement of a heparin-TDMAC complex, C^{14} labeled TDMAC was prepared. The data indicated that the complex was removed in small quantities. Removal essentially stopped when saline followed the flowing plasma; however, if 4 N sodium chloride was used, substantial quantities were again eluted. Since one might expect removal of heparin and not TDMAC by increased ionic strength, these data suggest that TDMAC is present on these surfaces in combination with a substance which gives it increased solubility at higher ionic strengths. The identity of this substance, which could be a protein, is being investigated by isolation and characterization of the complex.

In vitro and *in vivo* compatibilities were obtained on materials impregnated by the above techniques. *In vitro* tests consisted of the exposure of whole human blood to the heparinized material in a modified Lee-White clotting test until the blood clots or for a period of one hour. If no clots formed during the one-hour period, a small amount of thromboplastin was added and the time to a clot was noted. Clot formation in 30 to 60 seconds indicated that no appreciable quantity of heparin had been leached during the exposure. The impregnation technique consistently produced materials which did not cause whole human recalcified blood to clot during the initial test hour. Clots were produced in approximately 45 seconds after the addition of thromboplastin, indicating the materials were not nonthrombogenic by the mechanism of heparin leaching.

The in vivo compatibility was evaluated by a number of independent laboratories and is summarized in Tables 4 and 5. Table 4 shows the results obtained by Dr. Vincent Gott at Johns Hopkins Medical Center which indicate no thrombus formation in both short-and long-term tests.

TABLE 4. IN VIVO COMPATIBILITY

ACUTE					CHRONIC				
MATERIAL	DATE OF IMPLANT	STERILIZATION	AMOUNT OF THROMBUS IN LUMEN	COMMENTS	MATERIAL	DATE OF IMPLANT	STERILIZATION	AMOUNT OF THROMBUS IN LUMEN	COMMENTS
Silicone TDMAC heparin	11/2/67	TDMAC	○	Clear	Silicone TDMAC heparin	11/10/67	TDMAC	○	Sacrificed after two weeks-clear
"	"	"	○	"	"	11/28/67	"	○	"
"	11/6/67	"	○	"	"	"	"	○	"
					"	11/30/67	"	○	"
					"	1/19/68	"	○	"

TABLE 5

IN VIVO TESTS RUN AT COLLABORATING INSTITUTES

Institute	Material	Results
University of Colorado	Tubing	Control organized thrombus tests, no evidence of clot
University of Miami	Vena caval umbrellas	3 umbrellas - 2 patent, 1 thrombosed within 2 weeks
Harvard Medical School	Femoral tubing artery to vein shunt	Nonthrombogenic in 24 hr. test
Thermo Electron Corp.	Stainless steel heat exchangers	Thrombosed within 2 weeks
Johns Hopkins	Catheters	No clots-animals maintained one month

Tables 4 and 5 indicate the good potential of this system for use in short-term nonthrombogenic material preparation. This simple impregnation process essentially meets the objective of this research for a simple, efficacious method of producing nonthrombogenic materials for short-term applications.

Other Water Insoluble Quaternary Ammonium Salts.

In the process of the development of the TDMAC impregnation procedure other quaternary ammonium salts have been investigated to insure that optimum results were being obtained. Table 6 lists quaternary ammonium compounds that were prepared and evaluated for thrombogenicity.

The benzyl and ethyl-difunctional material has appreciable water solubility so that further investigations have been ruled out. The studies on the tetradodecyl and pentyldifunctional salts are still being pursued, and these materials appear to have characteristics distinctly different from the TDMAC products. These characteristics will be discussed further in a later section of this report.

Heparin-Complexing Plasticizers.

As an alternative method for heparinization of selected polymer systems, work has been conducted on the use of heparin-complexing plasticizers. The advantage of this approach is that the nonthrombogenic heparin complex would be present throughout the bulk of the polymer, and thus surface erosion would not expose unheparinized sites. To be useful, the plasticizer should be compatible with the plastic and should not degrade any desirable mechanical properties. In past reports we have described the use of hydrin rubber and TDMAC as plasticizers for polyvinylchloride, silicone rubber, and natural rubber. However, these materials did not contain heparin throughout their bulk.

Two potential heparin-complexing plasticizers which have been under preliminary examination are the complex of TDMAC/heparin and a compound prepared by reacting tridodecylamine with dichloroethyl phthalate. The phthalate ester quaternary ammonium salt was appreciably water soluble and this characteristic made it unsuitable for use as a plasticizer. The TDMAC/heparin complex gave a material which had a complete range of solubilities; that is, portions were soluble in petroleum ether, toluene, alcohol, and water. Attempts are under way to isolate the various fractions and incorporate the oil-soluble materials in polymers.

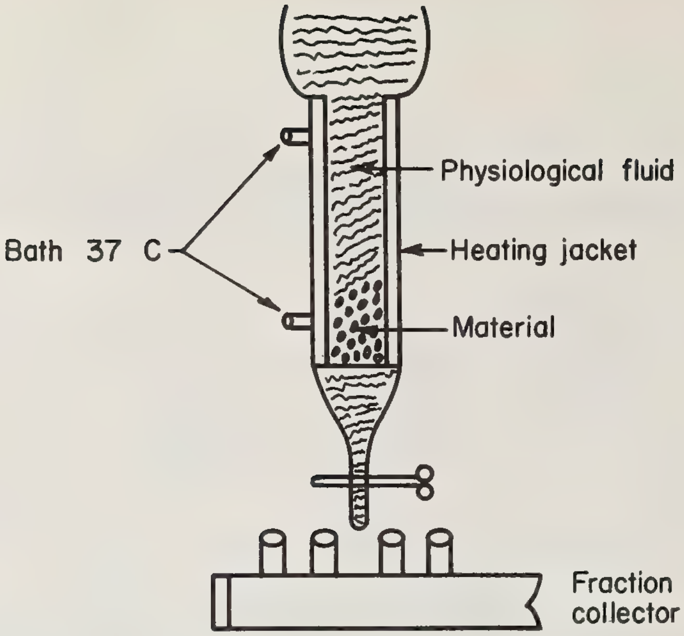

FIGURE 1. SKETCH OF COLUMN EXPOSURE TECHNIQUE

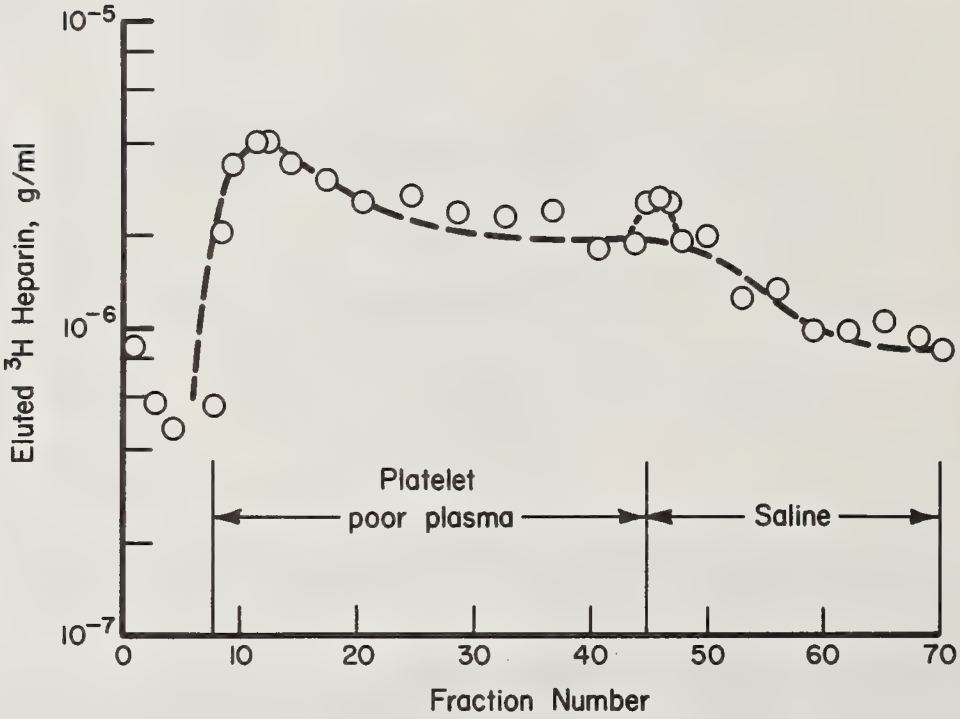

FIGURE 2. ELUTION OF HEPARIN FROM A TDMAC IMPREGNATED SILICONE RUBBER SURFACE

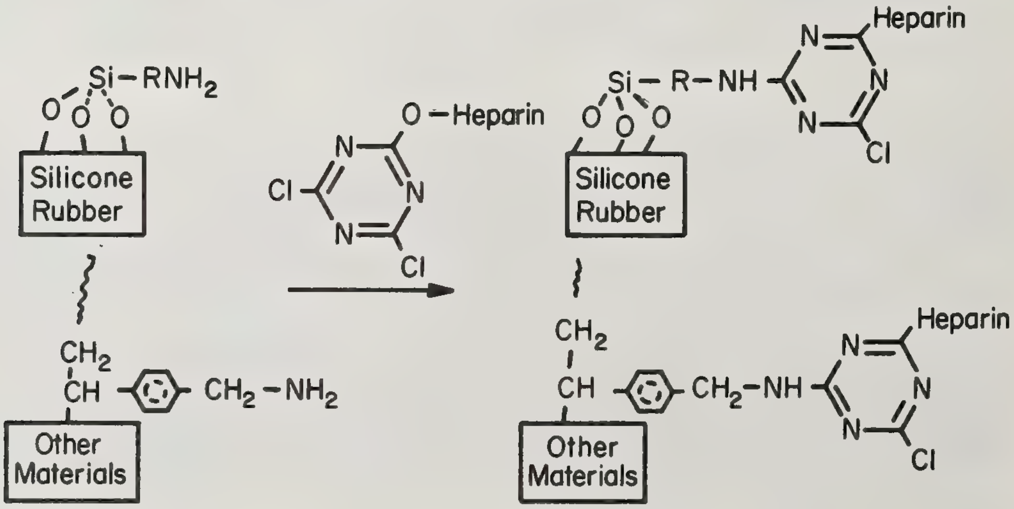

FIGURE 3. COVALENTLY BONDED HEPARIN (CYANURIC CHLORIDE ADDUCT)

TABLE 6

STRUCTURAL ELEMENTS OF VARIOUS QUATERNARY AMMONIUM COMPOUNDS

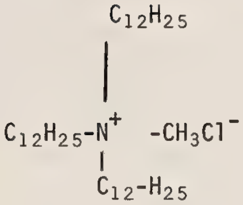

$$C_{12}H_{25}-\overset{C_{12}H_{25}}{\underset{C_{12}-H_{25}}{N^+}}\ -CH_3Cl^-$$

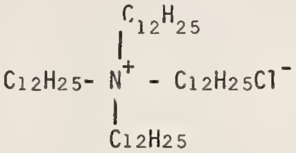

$$C_{12}H_{25}-\overset{C_{12}H_{25}}{\underset{C_{12}H_{25}}{N^+}}-C_{12}H_{25}Cl^-$$

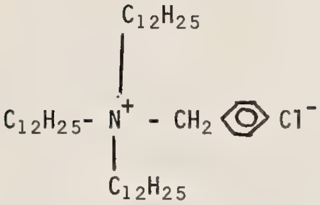

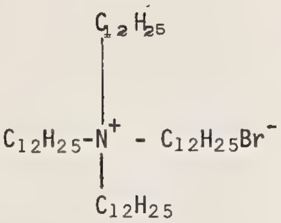

$$C_{12}H_{25}-\overset{C_{12}H_{25}}{\underset{C_{12}H_{25}}{N^+}}-C_{12}H_{25}Br^-$$

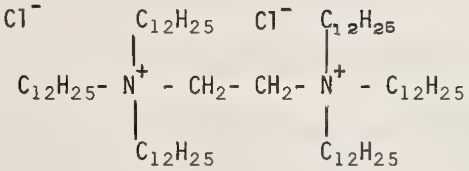

$$\overset{Cl^-}{}\ C_{12}H_{25}-\overset{C_{12}H_{25}}{\underset{C_{12}H_{25}}{N^+}}-CH_2-CH_2-\overset{Cl^-\ C_{12}H_{25}}{\underset{C_{12}H_{25}}{N^+}}-C_{12}H_{25}$$

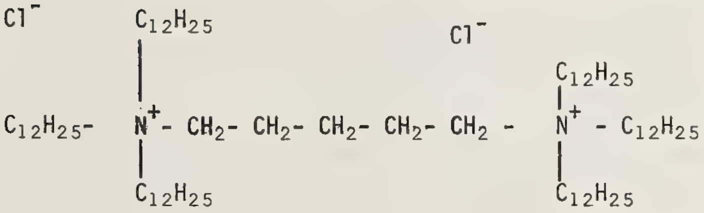

$$\overset{Cl^-}{}\ C_{12}H_{25}-\overset{C_{12}H_{25}}{\underset{C_{12}H_{25}}{N^+}}-CH_2-CH_2-CH_2-CH_2-CH_2-\overset{Cl^-\ C_{12}H_{25}}{\underset{C_{12}H_{25}}{N^+}}-C_{12}H_{25}$$

Covalently Bonded Heparin

Work is continuing on methods of attaching heparin to polymeric surfaces by means of covalent bonds. Because of the more permanent nature of covalent bonds compared to ionic bonds, we feel that this approach may impart greater stability to heparinized materials.

To effect covalent attachment of heparin, heparin derivatives have been synthetized which can subsequently react with functional groups on polymer surfaces. The most successful of the derivatives has been the heparin/cyanuric chloride adduct. This compound, when prepared in an aqueous environment at 4 C utilizing sodium bicarbonate as the acid acceptor, retained approximately 80-90 percent of its original biological activity.

The heparin/cyanuric chloride adduct was then reacted with polymeric materials containing reactive amine groups at the surface. The amine groups were introduced to the plastic surfaces in two ways. First, silicone rubber was reacted with y-aminopropyltriethoxy silane through the displacement of ethoxy groups of the silane by hydroxyl groups present in the filler. The second method, which is applicable to practically all polymers, used high-energy radiation to graft polystyrene to the surface. This modified surface was then chloromethylated and subsequently treated with alcoholic solutions of ammonia to produce a surface containing reactive benzylamine groups. These schemes of heparin attachment are illustrated in Figure 3.

The amine-bearing surfaces reacted optimally with the heparin adduct at 37 C in the presence of sodium bicarbonate as an acid acceptor. Table 7 illustrates the heparin bonding capacity and stability of this system. The surfaces of bonded heparin-cyanuric chloride adduct were nonthrombogenic as tested by a modified Lee-White coagulation test. The silicone rubber surfaces also had good *in vitro* stability to an environment of flowing saline. At present, the relatively low stability of the bonded layer on the polypropylene samples is not well understood. Electrostatic binding of heparin by amine groups of modified silicone rubber is effective in producing a heparinized surface which resists displacement by saline.

The results also dramatically illustrate the difference between covalently bonded and ionic bonded heparin when exposed to 4 N sodium chloride. Heparin covalently bonded to silicone rubber was not displaced by the high salt concentration, whereas 45 percent of the ionically bonded heparin was removed.

TABLE 7

EVALUATION OF CYANURIC CHLORIDE/HEPARIN ADDUCT ATTACHMENT

Attachment Conditions [a]	Material [b]	Initial A [c]	Heparin Adduct Retention, % After 100 hr. Exposure to Flowing Saline [d]	Heparin Adduct Retention, % After 4 hr. Exposure to 4 N Sodium Chloride [e]
Heparin adduct	Polypropylene	600	60	--
	(benzylamine)	900	--	55
Heparin control	Polypropylene	600	80	--
	(benzylamine)	400	--	50
Heparin adduct	Silicone rubber	4700	100	--
	(γ-propylamino silane)	9100	--	97
Heparin control	Silicone rubber	500	91	--
	(γ-propylamino silane)	400	--	55

[a] Conditions were identical; however, pure heparin was used in the control case and the heparin/cyanuric chloride adduct was used in the other.

[b] Material modified as discussed in text to produce surface amine groups.

[c] Measured using S^{35} labeled heparin.

[d] Material placed in circulating bath thermostated at 37 C and arranged so that the surface area of the material was exposed to the flowing saline.

[e] Material exposed to 4 N NaCl in a 37 C thermostated cell.

Work is proceeding on these products and *in vivo* performance data are being obtained.

Blood/Foreign Surface Interface Studies.

In an effort to better understand the mechanism of coagulation and thereby be able to prepare more compatible materials, work has gone forward on the study of interactions between blood elements and the foreign surface interface.

During the last six months, a series of experiments designed to study the effects of surface exposure on blood proteins, lipids, lipoproteins and formed elements has been under way. To simulate conditions of blood flowing past a relatively large surface area, plasma was eluted through various materials in the form of finely divided particles packed in a column (Figure 1). Initially, saline was passed over the surface followed by either platelet-rich or platelet-poor plasma, and finally saline. This sequence eliminated any artifacts due to a plasma-air interface. The column was thermostated at 37°C and the effluent collected in successive fractions of approximately 4 cc. Each fraction was exposed to at least 500 cm^2 surface area (assuming the particles to be spherical). The particles in most cases are microscopically rough so that the true surface area was actually greater. The fractions were then analyzed for specific components.

Lipid and Lipoprotein Interactions. Interactions of lipids and lipoproteins with various treated surfaces were studied in detail because of effects detected earlier in initial plasma fractions contacting surfaces modified with TDMAC prior to heparinization.

Figure 4 illustrates some typical quantitative data obtained. As seen from the figure, fairly gross interactions are evident in the initial fractions of platelet-poor plasma eluted from the column. As is readily seen from this graph, the greatest interactions occurred with surfaces which contained high concentrations of pure TDMAC. The heparinization of these surfaces lowered the adverse interactions substantially. Washing the heparinized surfaces with a solvent for TDMAC lowered these adverse effects even further. Lipoprotein interactions followed this same course although quantitation of this is not yet complete. It should be noted that the removal of lipids and lipoproteins occurred in the initial fractions and that the levels returned to normal in the later fractions. Thus, the removal was not continuous but occurred only until equilibration was reached.

It was interesting to note that tetradodecylammonium bromide (TDAB), produced no detectable adverse interactions. No explanation for this behavior is immediately available and work is continuing on this promising heparin binding agent.

Platelet Interactions. The effect of various surfaces on platelet aggregation was also investigated because of the importance of platelet interactions in the initial stages of coagulation. As shown in Figure 5, aggregation was most severe when platelets were exposed to surfaces containing excesses of TDMAC. The areas under the various curves are in general proportional to the amount of platelet aggregation. The greater aggregation in the later fractions of plasma contacting a washed TDMAC/heparin surface appears anomalous. These data concur with those of other workers in the area[1] and indicate that the greater the number of free quaternary ammonium sites present at the surface the greater the amount of aggregation. However, these results do not indicate the quantities of adsorbed platelets. Platelets were adsorbed in all cases and quantitation of the data shows again that excess TDMAC should be removed to obtain minimum adsorption. Acid phosphatase and platelet

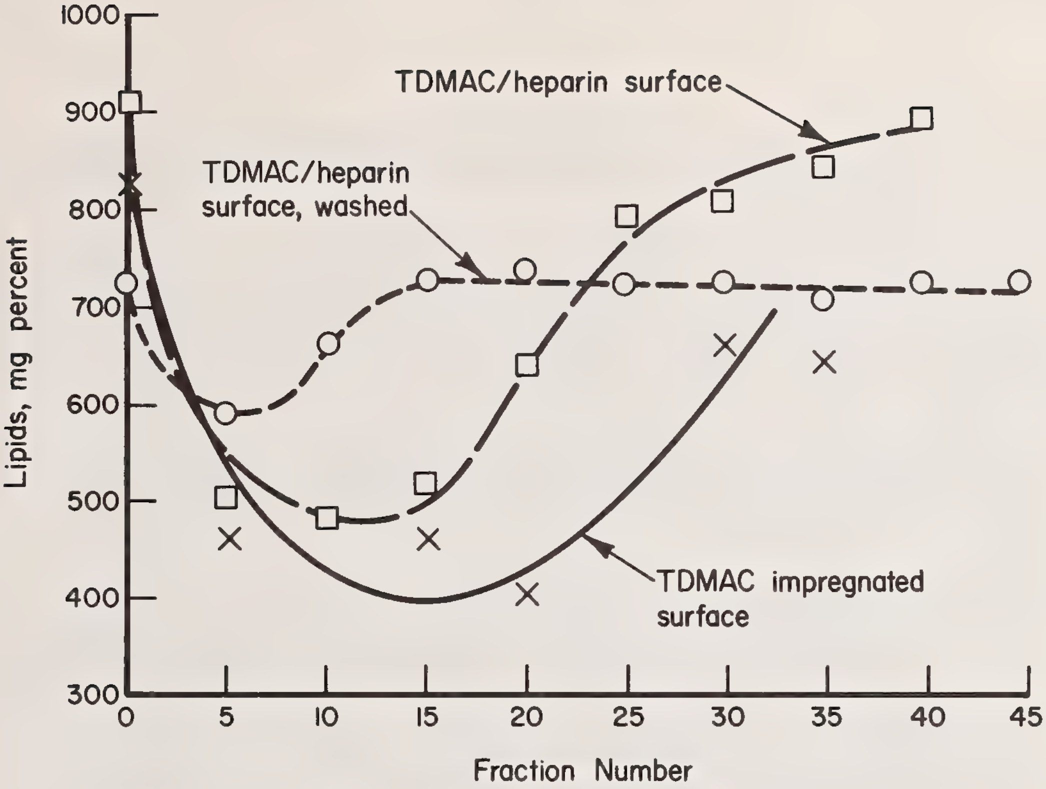

FIGURE 4. EFFECT OF TDMAC SURFACE CONTACT ON PLASMA LIPID LEVELS

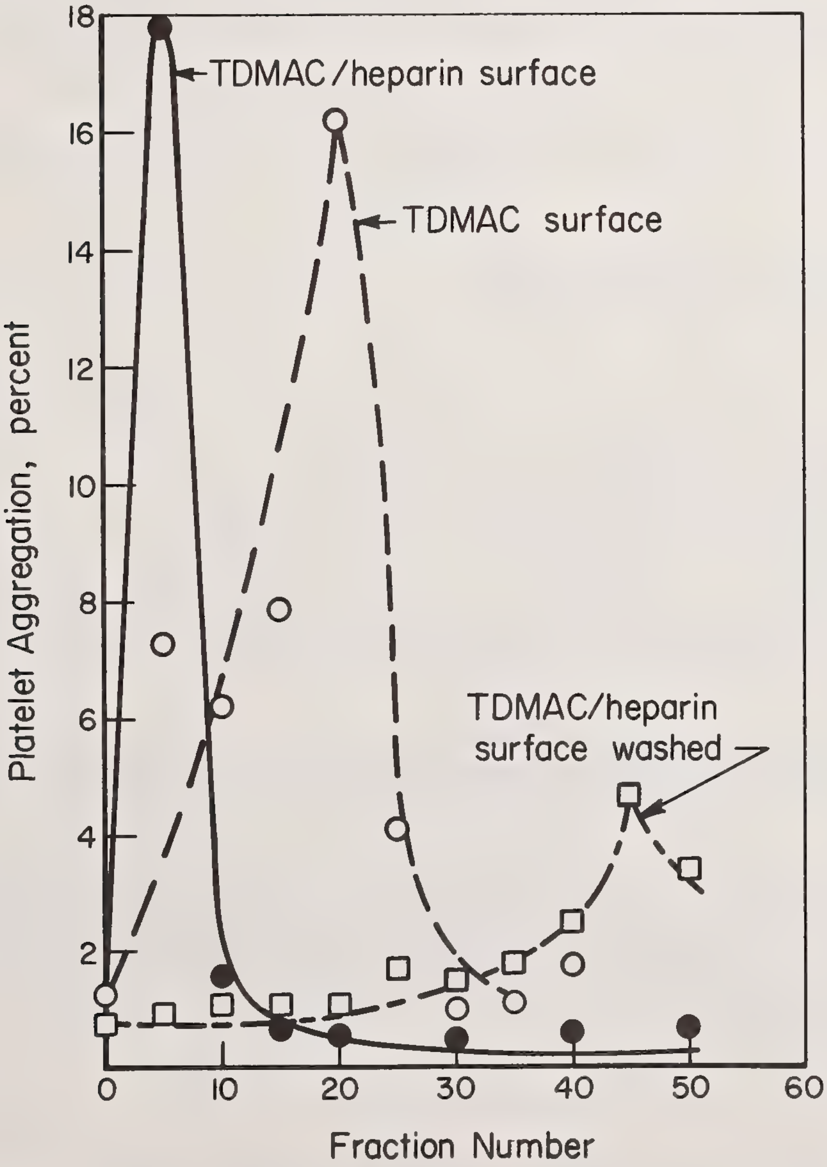

FIGURE 5. PLATELET AGGREGATION OF SELECTED PLASMA FRACTIONS SUBSEQUENT TO EXPOSURE

factor III levels were measured in the various fractions and taken as an indication of platelet rupture. The data indicate that even though adsorption did occur, apparently no appreciable amount of platelet rupture took place.

Clotting Factor-Protein Interactions. In addition to the studies on lipid, lipoprotein, and platelet interactions, clotting factor levels of plasma contacted with these various surfaces were analyzed. Preliminary data indicated certain differences in the interactions occurring at the surface of glass and at a TDMAC surface. Prothrombin (PT) and partial thromboplastin times (PTT) were used as initial screening tests to detect deficiencies of clotting factors in plasma subsequent to surface contact. Extended PT times indicate deficiencies of Factors X, VII, V, II, and I, while extended PTT times are due to any of the above factor deficiencies, plus deficiencies of Factors XII, XI, IX, and VIII.

Glass effectively removed one or more of Factors XII, XI, IX, or VIII, but did not affect the other factors. TDMAC surfaces on the other hand affected some additional factor(s). As indicated, all of these surfaces affect the intrinsic clotting pathway (PTT times) but not the extrinsic pathway (PT times). Work is now proceeding on determinations of specific factors for these various plasma fractions.

In addition to the work on the TDMAC surfaces, a detailed study on the effect of surface chemistry on the interaction with blood proteins, coagulation factors, and formed elements was undertaken during the last six months. This study has been approached through the attachment of a wide variety of functional groups onto the surface of crosslinked polystyrene beads. The functional groups being studied are hydroxyl, sulfate ester, sulfhydryl, carboxylic acid, amino, sulfamido, and quaternary ammonium salts. In addition, surface functional groups will be produced by the "grafting" of polypeptide chains prepared by the exposure of amino acid N-carboxyanhydrides to aminated polystyrene surfaces. The amino acids include glutamic and aspartic acids, lysine, tyrosine, serine, phenylalanine, and leucine. The beads containing the functional groups are to be packed into a column for elution with platelet-rich plasma. Eluted fractions will then be analyzed for platelet counts, platelet clumping, clotting factor levels, and levels of specific proteins.

Preliminary data from surfaces containing sulfonic acid, nitro, or amine functional groups showed significant differences in the type and extent of interaction. The sulfonated surfaces produced plasma fractions which were deficient in clotting Factors XII, XI, and IX. These factors unchanged in fractions which contacted the nitrated or amine-bearing surfaces. Initial data on interactions of the nitro and amine surfaces with platelets also indicated significant differences between these two surfaces. The aminated surfaces caused some platelet rupture, whereas the nitrated surface did not as evidenced by acid phosphatase levels. Work is continuing with these systems.

REFERENCE

1. Wilner, G. D., Nossel, H. L. and LeRoy, E. C., Aggregation of Platelets by Collagen, The Journ. of Clin. Invest, 47, 2616-2629 (1968).

DISCUSSION

DR. KELLER: The first question is that when you saw the lipids disappearing, did you find that the entire lipoprotein disappears or simply that the lipid released from the protein complex disappears?

MR. GRODE: The lipoprotein as a whole disappears.

DR. KELLER: I see; the protein presumably is also leaving the suspension?

MR. GRODE: That's right. The interactions are almost identical with the lipid interaction, and they quickly return to normal after a short period of time.

DR. KELLER: The second question was that it seemed that the layers were many molecules thick, certainly thicker than the heparin, and I was wondering what your model is of the covalent bonding process that makes it consistent with the many layers of heparin layed down on the surface over the quaternary amines.

MR. GRODE: I don't think I can really explain that. We see the same thing with the ionically bonded heparin. We know that it takes approximately 21 moles of quaternary ammonium salt for every tetrasaccharide unit of heparin. At least that's what we have available on the surface; and we haven't done these tests on the covalent bonding system yet. That's one of the things we hope to do in the future.

DR. GILLIS: Were you using human blood?

MR. GRODE: Yes, it was human blood.

DR. MITZ: I have two questions. One question is on your covalent bonding. Did you have a control without the heparin?

MR. GRODE: Without the heparin? No.

DR. MITZ: The second question is, in your system for studying the effects of the interaction with the blood, did you protect the container in any way?

MR. GRODE: The containers were siliconized.

DR. FOUNTAIN: Do you have any explanation for the failure to obtain antithrombogenic surfaces for such functionalities as the diazonium salt or azide or the H-CO group?

MR. GRODE: We have obtained nonthrombogenic surfaces in these cases; however, we have not been able to reproducibly obtain them every time we try.

DR. FOUNTAIN: Is this a function of uniformity of functionalization of the surface?

MR. GRODE: I think this is a function of the difficulty of attaching heparin by these techniques. Uniformity may also be a problem.

DR. BYCK: Have you ever measured the pH of the fractions which you collect with your column technique?

MR. GRODE: No, we have not.

UNIDENTIFIED DISCUSSANT: Is your work including the diffusional resistance of gases through these platelet surfaces?

MR. GRODE: Not through the platelet surfaces. We run these tests on the heparinized surfaces and on control surfaces to see if any changes occur, but not against the surfaces after they have been contacted by plasma.

UNIDENTIFIED DISCUSSANT: You do have some data though that shows the change in the gas diffusion rate?

MR. GRODE: Yes, we do. On the heparinized surfaces as against the control surfaces.

MR. SALYER: I have two questions. One of them is: Isn't the impregnation procedure with the quaternary amine critical? Second: Isn't this very similar to the process developed, I believe, in Sweden, University of Stockholm, about three years ago, on which, I think, they have some patents pending?

MR. GRODE: The technique in Sweden uses a water soluble quaternary ammonium salt. This is completely water insoluble. What was the first question again?

MR. SALYER: Isn't the impregnation procedure critical?

MR. GRODE: We have found that you can treat many materials in the same manner and it doesn't appear to be very critical.

DR. SRINIVASAN: What evidence did you have in your second method of preparation for covalent bonding? Could it still be an ionic bonding, because there are quite a number of ionic groups present?

MR. GRODE: The exposure to 4N sodium chloride as we showed indicates that a definite covalent bond has been formed.

CHAPTER 3

THE HEPARINIZATION OF SILICONE RUBBER USING AMINOORGANOSILANE COUPLING AGENTS

R. L. Merker, L. J. Elyash, S. H. Mayhew and J. Y. C. Wang

Carnegie-Mellon University, Mellon Institute, Pittsburgh, Pennsylvania

The major goal of the research described in this paper was to improve the surface characteristics of silicone polymers in the body environment with particular emphasis on achieving a higher degree of nonthrombogenicity. In the first phase of this investigation, finely divided silicas were successfully heparinized utilizing aminoorganosilanes as coupling agents. The incorporation of these heparinized silicas as fillers into polymeric systems such as room temperature vulcanizable silicone rubbers and polystyrene led to only modest improvement in surface characteristics based on Lee-White blood clotting times. This suggests an insufficient concentration of heparin available at the polymer-blood interface. The second phase of this research concerned the heparinization of vulcanized silicone rubber already containing finely divided silica as a reinforcing agent. Utilizing this approach, surfaces possessing greatly enhanced nonthrombogenic character were reproducibly obtained.

INTRODUCTION

The ideal material for use in artificial hearts or circulatory assist devices, in addition to having satisfactory physical and mechanical properties, should not cause clotting or hemolysis and should not affect the blood, body tissue, or body reactions in any harmful way. Also, the material itself must be resistant to attack by blood, body tissue, enzymes, etc. No single material possessing all these attributes has yet been found.

One of the more satisfactory materials known to date is silicone rubber. It is completely acceptable to the body and is chemically inert in the body environment. In certain applications, it is unsatisfactory since it promotes the clotting of blood.

The major goal of the research described in this paper was to improve the surface characteristics of silicone polymers in the body environment with particular emphasis on achieving a higher degree of nonthrombogenicity.

DISCUSSION

The improvement in thrombogenic character, possible through surface treatment done, has been dramatically illustrated by the observation that if certain plastics are coated with colloidal graphite then treated with benzalkonium chloride (a cationic surface active agent), and finally with heparin[1,2], surfaces are obtained which no longer induce clotting even in trials of a year's duration. Unfortunately, the technique so far has failed with three important polymers, silicone rubber, Teflon, and polyethylene because these will not bind the collodial graphite.

An alternative approach to overcome the difficulties encountered in the treatment of silicone rubber surfaces with the graphite - benzalkonium - heparin system is indicated. In addition to the polysiloxane polymer, most commercial silicone rubbers contain extensive quantities (ca. 26% by wt.) of very finely divided silica as a reinforcing agent. Such silicas, depending on methods of preparation and pre-treatment history, have surfaces which are hydroxylated to varying degrees. The presence of free surface hydroxyl groups, the very high surface area, and the large amounts which may be employed in composite formulations, lend attraction to the alteration of silicone rubber through chemisorption of appropriate materials at reactive hydroxyl sites on the silica surface.

One of the more promising classes of chemisorbing agents is the aminoalkylsilanes[3,4,5,6]. In an earlier phase of this investigation, finely divided silicas were successfully heparinized as shown in Figure 1. The incorporation of these heparinized silicas as fillers into room temperature vulcanizable silicone rubbers led to only modest improvement in surface characteristics based on Lee-White blood clotting times. This suggests an insufficient concentration of heparin at the polymer-blood interface. An extension of this earlier research led to the successful heparinization of high temperature vulcanized silicone rubber by a solvent swelling technique. Utilizing this approach, nonthrombogenic surfaces have been obtained reproducibly by the methods developed.

EXPERIMENTAL WORK AND RESULTS

Reaction of Silica with 3-Aminopropyltriethoxysilane.

In a flask equipped with a stirrer and reflux condenser were added 3 gm of silica (Quso F-22), 1.5 gm of 3-aminopropyltriethoxysilane (APTES) and 60 ml of benzene. The mixture was refluxed for 5 hours. At the end of reflux, benzene and the ethanol formed through reaction of APTES with the silica were partially removed by distillation. Fresh benzene was added to the mixture twice during this procedure to ensure complete removal of the ethanol. To the cooled solution was added 50 ml of methanol. This mixture was poured into 150 ml of water and the benzene layer was separated from the aqueous layer. The silica was centrifuged from the aqueous layer, washed three times with water and dried to constant weight. The results of treating silica by this or slightly modified procedures are shown in Table 1.

TABLE 1

SILICA WITH 3-AMINOPROPYLTRIETHOXYSILANE (APTES)

Designation	Starting Materials		Solvent[a]	Temp.	Time	Yield of Treated Silica	Analysis[b]			Ratio[c]	% APTES[d] Employed
	SiO_2(g)	APTES(g)	ml		(hr.)	(g)	C%	H%	N%	N/C	On Surface
SiO_2[e]/APTES[f]/1	3.0	1.5	60	Reflux	5	2.8	4.85	1.78	1.87	0.386	75.0
SiO_2/APTES/2	3.0	1.0	60	"	"	2.34	3.95	1.84	1.36	0.344	84.8
SiO_2/APTES/3	3.0	3.0	60	"	"	2.67	3.35	1.85	1.45	0.403	30.8
SiO_2/APTES/4	10.0	5.0	200	"	7	12.2	3.33	1.80	1.25	0.334	51.06
SiO_2/APTES/5	3.0	10.0	20	R.T.	4 days	2.95	5.11	3.65	1.83	0.358	-----

Remarks:
- a Benzene
- b All analyses in this report were conducted by Galbraith Laboratories, Knoxville, Tennessee.
- c Theoretical ratio of N/C for the structure, $(NH_2-(CH_2)_3-)$ = 0.388.
- d $\frac{\text{amt. APTES on silica}}{\text{amt. APTES used}} \times 100$
- e Quso F-22, pH 5, particle size 12 millimicrons, surface area 325 square meters per gram. (Philadelphia Quartz Company)
- f Peninsular Chem. Research, Inc.

The analytical results clearly indicate the presence of a bound layer of the aminopropylsilane moiety on the silica surface. The nitrogen/carbon ratio found agrees reasonably well with the theoretical nitrogen/carbon ratio in the aminopropyltrisiloxane structure. As expected, when a constant amount of silica was treated with increasing amounts of aminopropyltriethoxysilane, the ratio of material bound on the silica surface to that used in the treatment decreased. This is merely a reflection of the constant number of active sites available for chemisorption.

Heparinization of 3-Aminopropyltriethoxysilane Treated Silica.

The treated silica was added to a methanol-water mixture in a flask equipped with reflux condenser and magnetic stirrer. The mixture was stirred for one-half hour and then dilute hydrochloric acid was slowly added. This mixture was stirred at room temperature for 4 hours. At the end of this period, aqueous heparin sodium solution was added slowly and stirring was continued for another 17 hours. The heparinized silica was centrifuged from the methanol-water mixture, washed thoroughly three times by water and dried to constant weight. In experiments conducted in the same manner with the exception that no treated silica was present, no hydrolyzed sodium heparinate was recovered.

Similar procedures were used for all the heparinization reactions described in Table 2. The analytical data provides ample evidence for the effectiveness of the methods employed for binding heparin to finely divided silica. Based on sulfur analysis, it was found that very little heparin was bound to untreated silica. Somewhat more heparin was bound to silica which had been treated with aminopropyltriethoxysilane. Finally, maximum heparin binding was achieved using silica with aminopropyltriethoxysilane and hydrochloric acid.

Since the use of these heparinized silicas in composite formulations with silicone rubber and a number of other polymeric materials led to only a modest improvement in thrombogenic character - probably as a result of particle encapsulation by polymer matrix - other approaches employing the same reaction scheme were investigated.

Heparinization of Vulcanized Silicone Rubber by the Solvent Swelling Technique.

The solvent swelling technique for the heparinization of silicone rubber is portrayed schematically in Figure 2 and the experimental conditions are summarized in Table 3.

The Lee-White blood-clotting tubes for this study were fabricated from Silastic 372 (Dow Corning) which contains finely divided SiO_2 as a reinforcing agent. The tubes were vulcanized at 300°F for ½ hr. and cured at 400°F for 4 hours. After these treatments, all sample tubes were extracted with benzene for about two hours for removal of soluble compounds, then dried to constant weight. The weight lost in benzene extraction was around 2.2%. The extracted tubes were reacted with a 3-aminopropyltriethoxysilane solution in benzene (5 g/100 ml) about one hour. After this reaction period, samples were dried at room temperature and reduced pressure to constant weight.

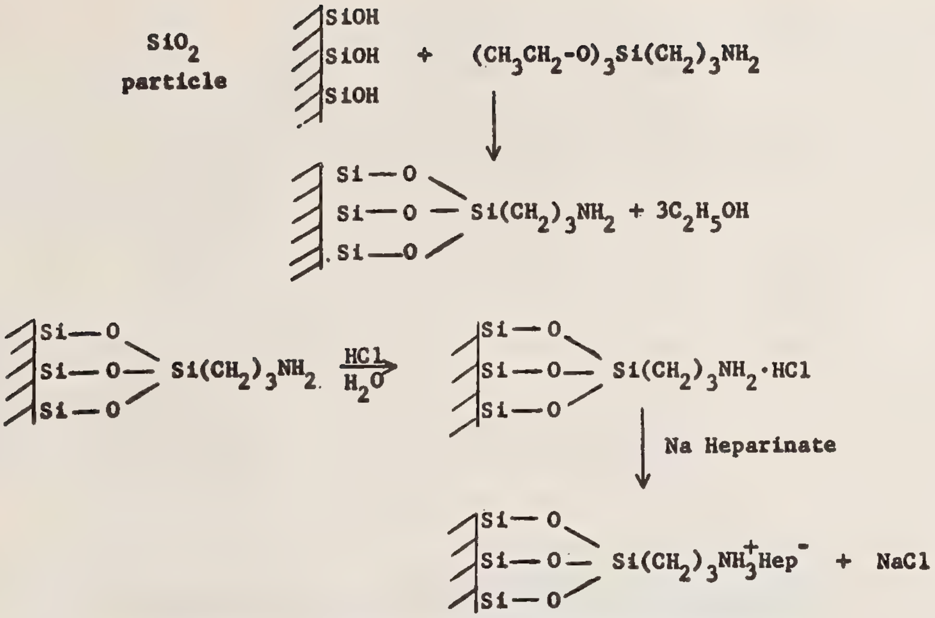
SiO_2 particle
SiOH
SiOH
SiOH
+
$(CH_3CH_2\text{-}O)_3Si(CH_2)_3NH_2$
Si—O
Si—O
Si—O
$Si(CH_2)_3NH_2$ + $3C_2H_5OH$
$Si(CH_2)_3NH_2$
HCl
H_2O
$Si(CH_2)_3NH_2 \cdot HCl$
Na Heparinate
$Si(CH_2)_3NH_3^+Hep^-$ + NaCl

FIGURE 1. HEPARINIZATION OF FINELY DIVIDED SILICA

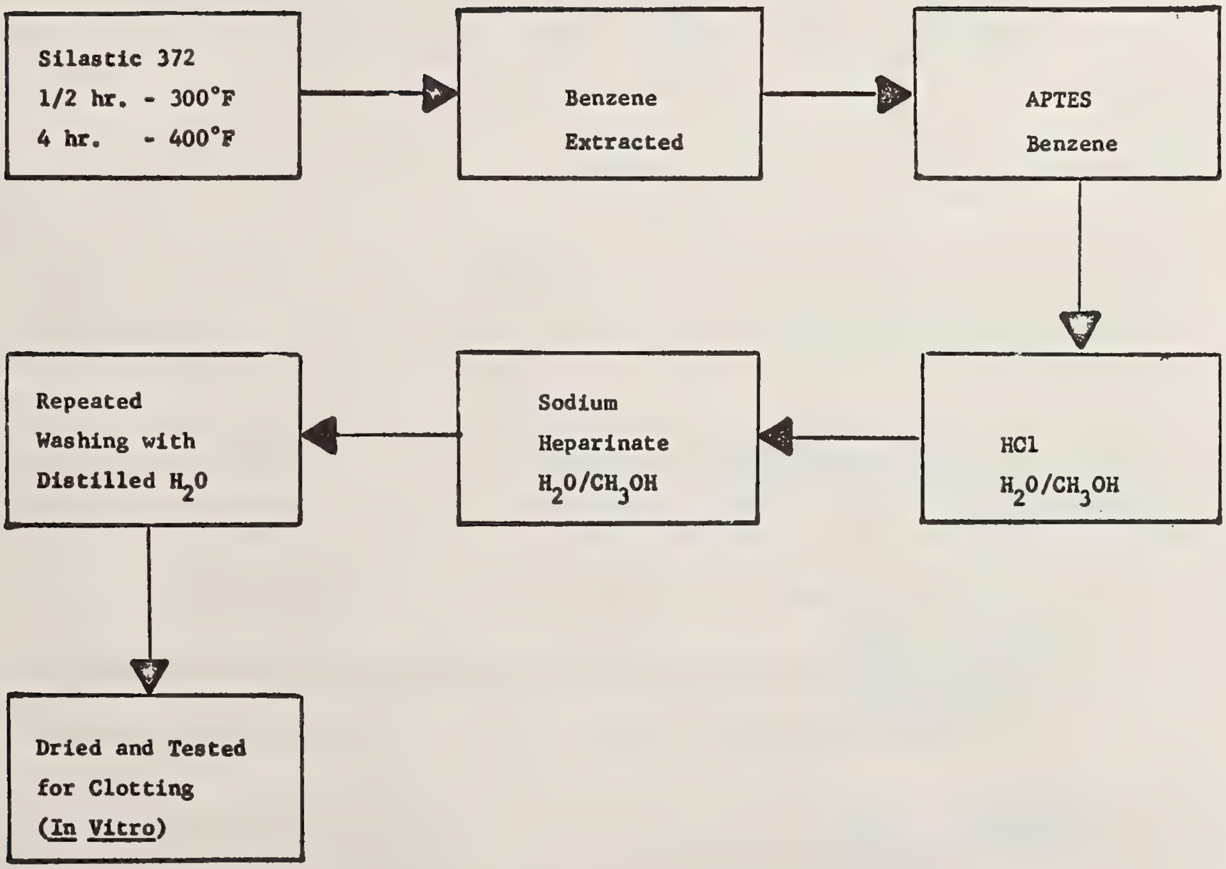

FIGURE 2. HEPARINIZATION OF SILICONE RUBBER BY THE SOLVENT SWELLING TECHNIQUE

TABLE 2

HEPARINIZATION OF VARIOUS SILICAS [a]

Designation	Starting Materials: Silica (g)	Starting Materials: HCl^d (g)	Starting Materials: Hep. Sod. (mg)	Solvent $MeOH/H_2O$ (ml)	Time (hr): HCl	Time (hr): Hep. Sod.	Analysis %: C	Analysis %: H	Analysis %: N	Analysis %: S^f	$Ratio^h$: N/C	$Ratio^h$: S/C	$Ratio^h$: S/N
SiO_2/Hep. Sod./1[b]	SiO_2 1.0	---	200	30/10	---	3da	0.38	0.97	---	0.07	---	---	---
SiO_2/APTES/ Hep. Sod./1[c]	SiO_2/APTES/2 1.0	---	280	40/1	---	1da	4.23	1.80	1.23	0.58	---	---	---
SiO_2/APTES/HCl/ Hep. Sod./1	SiO_2/APTES/1 1.0	0.17	700	30/10	4	17	7.14	2.31	1.48	1.78	0.207	0.249	1.20
SiO_2/APTES/HCl/ Hep. Sod./2	SiO_2/APTES/2 1.0	0.15	280	20/10[e]	4½	21	6.07	1.76	1.19	2.42	0.196	0.398	2.03
SiO_2/APTES/HCl/ Hep. Sod./3	SiO_2/APTES/4 5.0	0.552	2050	130/60	7	18	5.48	1.97	1.20	1.70	0.221	0.313	1.416[i]

Remarks:
- a All reactions at room temperature.
- b Untreated silica reacted with Heparin Sodium
- c Treated silica reacted with Heparin Sodium without prior reaction with HCl
- d 38% HCl, excess 10% over that calc. for free -- NH_2
- e Mixed solvents: Acetone/MeOH/H_2O = 40/20/10ml
- f %S in Heparin Moiety ($C_{24}H_{31}O_{35}S_5N_2$) = 14.98%
- h Theoretical ratio: N/C = 0.209; S/C = 0.342; S/N = 1.632
- i Cl% = 0.09

TABLE 3

HEPARINIZATION OF SILICONE RUBBER BY SOLVENT SWELLING TECHNIQUE

	$Benzene^a$: Time (hr)	$Benzene^a$: Conc. (ml)	APTES/Benzene: Time (hr)	APTES/Benzene: Conc. (g/ml)	$HCL/H_2O-MeOH^b$: Time (hr)	$HCL/H_2O-MeOH^b$: Conc. (g/ml)	Hep. Sod./$H_2O-MeOH^b$: Time (hr)	Hep. Sod./$H_2O-MeOH^b$: Conc. (g/ml)	$Clotting^e$ Time
ST/4	2	300							
4-1									6.0-6.5 min.
4-2			1	5/100					5.0-5.5 min.
4-3-1			1	5/100	2	0.85/80	21	1/60[c]	> 1 hr.
4-3-2			1		2		21		> 1 hr.
4-3-3			1		2		21		> 1 hr.
4-4-1			1	5/100	2	0.85/80	21	1/45[c]	12.0-13.0 min.
4-4-2			1		2		21		> 1 hr.
4-4-3			1		2		21		> 1 hr.
4-5-1			1	5/100	2	0.85/80	21	1/75[c]	> 1 hr.
4-5-2			1		2		21		> 1 hr.
4-5-3			1		2		21		> 1 hr.
ST/5[d]	2	200							
5-1-1							21	0.6/50	5.5-6.0 min.
5-1-2							21		6.0-6.5 min.

- a All sample tubes immersed in benzene solvent
- b H_2O-Methanol ratio = 1-3
- c H_2O-Methanol = 1-2
- d Series 5-1-1 and 5-1-2 treated with Heparin sodium solution directly, without prior salt formation
- e Mod. Prothrombin time for all samples of >1 hr. clotting time was less than 30 sec.

In Vitro Testing.

Blood Clotting Determination. Human donor ACD blood of Type O and Rh positive was used throughout the testing. Each unit of blood was checked for prothrombin time on whole blood and plasma as well as clotting time against standard surfaces. In all cases, 75 mm x 12 mm test tubes were used as test containers for modified Lee-White clotting time determinations. Bath temperature was kept at 37°C ± 0.1° and tubes tilted manually every 30 seconds. Table 4 shows the clot times obtained for recalcified ACD blood against "standard" surfaces.

When blood did not clot in a tube at the end of an hour, rabbit brain thromboplastin (DADE) was added and clotting time noted. If the blood subsequently clotted within 30 seconds, it was assumed that no heparin had been released into the blood. Clotting times of more than one hour are not believed to be significant.

TABLE 4

MODIFIED LEE-WHITE CLOTTING TIMES OF STANDARD SURFACES

Material	Clot Time
Glass	1.5-2.0 min
Polyethylene	6.0-6.5 min
Polystyrene	5.5-6.0 min
Silicone Rubber (Silastic 372)	6.0-6.5 min

TABLE 5

MECHANICAL PROPERTIES OF SILASTIC 372 BEFORE AND AFTER HEPARINIZATION

	Tensile[a] Strength lbs./sq. in.	Elong. At Break, %	Hardness Shore A
Silastic 372	1200	500	58
Silastic 372 APTES/2 hrs. HCl/NaHep.	1000	250	77
Silastic 372 APTES/6 hrs. HCl/NaHep.	700	200	--

[a] Sample (Test Section) 0.03" x 0.125" x 1"
RAM speed - 20"/min.

Other In Vitro Tests. Silicone rubber heparinized as described in Table 3 has been shown by the Cordis Corporation to have no adverse effects on the plasma proteins. Other *in vitro* tests are in progress.

Physical Properties.

The effects of the solvent swelling method for heparinizing silicone rubber on some of the mechanical properties of Silastic 372 are shown in Table 5. While some sacrifice in mechanical properties is clearly evident, it is not severe enough to preclude the solvent swelling technique as an effective method for producing nonthrombogenic surfaces on silicone rubber.

Sterilization of Heparinized Silicone Rubber.

Because sodium heparinate is sensitive to moderately elevated temperatures, articles containing it cannot be sterilized by heat. However, sterilization can be accomplished with ethylene oxide. Modified Silastic 372 was, therefore, exposed to the action of ethylene oxide contained in a proprietary formulation (CRY-OXCIDE) of 11 wt.% of ethylene oxide in a carrier. Exposure time was 4 hours to sterilant followed by at least 24 hours equilibration time with ambient air. The blood clot times in Table 6 indicate no change in clotting time.

TABLE 6

EFFECT OF ETHYLENE OXIDE STERILIZATION ON CLOTTING TIME FOR MODIFIED SILICONE RUBBER

Material and Treatment	Clotting time	
	Exposed to Sterilant	No Exposure
Silastic 372/APTES/NaHep[a]	> 1 hr.	> 1 hr.

[a] Aminopropyltriethoxysilane-Sodium Heparinate

In Vivo Testing

Gott Implant Rings in Dogs. Gott implant rings fabricated from Silastic 372 treated with aminopropyltriethoxysilane and sodium heparinate as described in Table 3 were sent to Dr. V. L. Gott at the Johns Hopkins Hospital for *in vivo* testing. The results of both acute and chronic tests are presented in Table 7. In the acute tests (2 hours) two of the rings were completely clear while the third contained a minute fibrin deposit, thus indicating that this material possessed rather good nonthrombogenic properties. The chronic tests (2 weeks) yielded two rings which were not thrombosed, one with a very small thrombus and two which were nearly completely thrombosed. It is tempting to conclude that slow leaching of the heparin from the silicone rubber leads to the thrombosed condition of the rings. However, this does not explain the nearly nonthrombosed condition of the remaining three rings where leaching could reasonably be expected to have occurred to an equal extent. Thus, the addition of γ-aminopropyltriethoxysilane to silicone rubber by the solvent swelling technique and subsequent heparinization leads to a silicone rubber surface possessing a high degree of nonthrombogenic character as indicated from *in vitro* blood clotting tests and acute *in vivo* tests. Chronic *in vivo* tests suggest either some loss of thromboresistance with time in the body environment or that some quality control standards need to be established in heparinization techniques.

TABLE 7

In Vivo Tests (Gott Implant Rings) of Silicone Rubber Heparinized with Aminopropyltriethoxysilane as a Coupling Agent

ACUTE							CHRONIC						
Material	Date of Implant	Sterilization	Spec. Treat	At. ☐	○	Comments	Material	Date of Implant	Sterilization	Spec. Treat	At. ☐	○	Comments
SILASTIC 372	3.29.68	GAS	Heparinized	☐	○	Tiny Fibrin	SILASTIC 372	4.26.68	GAS	Heparinized	☐	○	Sacrificed After Two Weeks
"	"	"	"	☐	○	CLEAR	"	"	"	"	☐	○	"
"	"	"	"	☐	○	"	"	5.2.68	"	"	☐	○	"
							"	5.3.68	"	"	▣	◉	"
							"	"	"	"	▣	◉	"

Chronic Analgesia By Silicone Rubber Diffusion. A number of silicone rubber arterial-venous shunts furnished by the Holter Company were heparinized by the methods outlined in Table 3. These were sent to Dr. Judah Folkman of Harvard Medical School for *in vivo* evaluation in dogs. Dr. Folkman has been studying the slow diffusion of anesthetics through such shunts for several years.[7] Such diffusion (methoxyflurane) through short shunts produces intense analgesia for long periods of time. The animal is awake and alert but feels no pain. A photograph of the shunt inserted from the carotid artery to the jugular vein in the neck is shown in Figure 3. The small glass cylinder around the silicone rubber tubing is filled with methoxyflurane which slowly diffuses into the circulating blood inside the tubing. A more detailed photograph of the shunt is shown in Figure 4. A standard silicone rubber shunt will remain in a dog for about one day, but if anesthetic is added it will clot in 1 to 2 hours. These data are quite reliable since approximately 65 dogs have been tested.[7] Systematic heparinization of the dogs led to bleeding and when the heparin level was reduced to a lower level, blood clotted in the shunts.

The shunts heparinized by the solvent swelling technique have been evaluated in a number of dogs. The shunts remained open for over a week with continuous diffusion of anesthetic. Clotting times, platelet counts, white blood cell count, blood electrolytes, liver chemistries and renal chemistries remained normal. One animal was sacrificed at the end of a week and histological sections of tissues revealed no abnormalities. In one animal, the tubing was clamped for forty minutes, and clotting occurred while the anesthetic was still diffusing in. However, it was a completely different type of clot than had been observed previously. It was soft and could be easily flushed from the tubing to re-establish normal blood flow when the clamp was removed. A silicone rubber shunt heparinized by the solvent swelling technique has also been implanted in the wrist of a human patient with equally gratifying results.

TABLE 8

PREPARATION OF AMINOORGANOSILICON COMPOUNDS

Product	Reactants	Product B.P.	%C		%H		%N		%Si		%I	
			Actual	Theor.	Actual	Theor.	Actual	Theor.	Actual	Theor.	Actual	Theor.
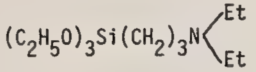 $(C_2H_5O)_3Si(CH_2)_3N\begin{matrix}Et\\Et\end{matrix}$	$CH_2 = CHCH_2N(C_2H_5)_2$ $(C_2H_5O)_3SiH$	57°C/0.02 mm	56.89	56.32	11.21	11.19	5.62	5.05	11.16	10.11	--	--
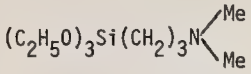 $(C_2H_5O)_3Si(CH_2)_3N\begin{matrix}Me\\Me\end{matrix}$	$CH_2 = CHCH_2N(CH_3)_2$ $(C_2H_5O)_3SiH$	45°C/0.25 mm	53.01	52.79	10.84	10.64	11.25	11.04	5.62	5.60	--	--
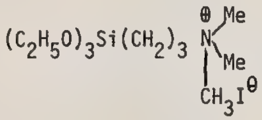 $(C_2H_5O)_3Si(CH_2)_3\overset{\oplus}{N}\begin{matrix}Me\\Me\\CH_3I^{\ominus}\end{matrix}$	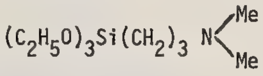 $(C_2H_5O)_3Si(CH_2)_3N\begin{matrix}Me\\Me\end{matrix}$ CH_3I	m.p. 100°C	36.73	36.83	7.73	7.67	3.59	3.58	7.36	7.16	32.62	32.48
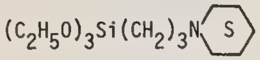	$(C_2H_5O)_3SiH$ 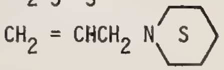	75°C/0.004 mm	58.15	58.13	10.85	10.73	5.00	4.84	9.53	9.69	--	--
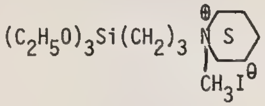	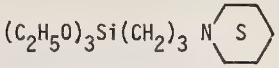 CH_3I	m.p. 65°C	41.51	41.78	7.98	7.89	3.19	3.25	6.76	6.50	29.47	29.45
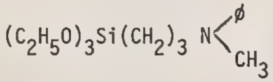 $(C_2H_5O)_3Si(CH_2)_3N\begin{matrix}\phi\\CH_3\end{matrix}$	$(C_2H_5O)_3SiH$ 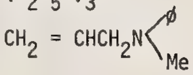 $CH_2 = CHCH_2N\begin{matrix}\phi\\Me\end{matrix}$	130°/0.004 mm	61.99	61.73	9.56	9.32	4.56	4.50	9.33	9.00	--	--
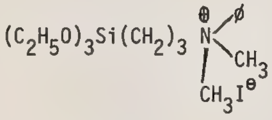 $(C_2H_5O)_3Si(CH_2)_3\overset{\oplus}{N}\begin{matrix}\phi\\CH_3\\CH_3I^{\ominus}\end{matrix}$	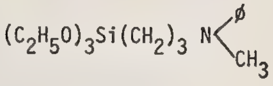 $(C_2H_5O)_3Si(CH_2)_3N\begin{matrix}\phi\\CH_3\end{matrix}$ CH_3I	m.p. 72°C	44.93	45.04	7.03	7.07	2.95	3.09	6.42	6.18	28.29	28.02

Treatment of Silicone Rubber with Other Aminoorganosilanes.

Synthesis of Aminoorganosilicon Compounds. Four tertiary aminoorganosilicon compounds were synthesized utilizing an addition-type reaction: (1) N-(dimethyl)-γaminopropyltriethoxysilane, (2) 1-Triethoxysilyl-piperidine, (3) N-ϕ-N-methyl-γ-aminopropyltriethoxysilane, and (4) N-(diethyl)-γ-aminopropyltriethoxysilane. The reaction conditions for the first three have been reported previously. The last compound, a new compound, was prepared in a similar manner, using 0.8 ml of a solution of 1.04 gm $H_2PtCl_6 \cdot 6H_2O$ in 10 ml iso-propanol and reacting the mixture at a temperature of 115-120°C for 4 hr. See Table 8.

Synthesis of Quaternary Salts. Quaternary salts of the first three compounds mentioned above were prepared as previously reported. A solid product was formed in all three cases. The quaternary salts were soluble in benzene and insoluble in cyclohexane and heptane (Table 8).

Treatment of Silicone Rubber with Aminoorganosilicon Compounds.

Using the solvent swelling technique, Silastic tubes were treated with the compounds synthesized (mentioned above). For each compound, one tube was treated with the animoorganosilicon compound and another tube with the same compound followed by acidification and treatment with heparin sodium. The results of the Lee-White clotting tests are listed in Table 9. Previous results obtained with γ-aminopropyltriethoxysilane and N-bis(beta-hydroxyethyl)-γ-aminopropyltriethoxysilane have been included for comparison. The results clearly indicate that under the conditions employed, treatment of silicone rubber with γ-aminopropyltriethoxysilane and subsequent heparinization yields a much higher degree of nonthrombogenicity than with the other amines and quaternary salts investigated. An explanation for this is not immediately apparent, but is of sufficient importance for further improvement in the solvent swelling technique to merit further study. The results obtained previously and shown in Table 9 for N-bis(beta-hydroxyethyl)-γ-aminopropyltriethoxysilane (A-1111) indicate this compound possesses considerable antithrombogenic activity. Surprisingly, subsequent heparinization of silicone rubbers so treated does not enhance their nonthrombogenic nature but detracts from it. This is just the reverse of the situation encountered for aminopropyltriethoxysilane. Since A-1111 is distributed throughout the bulk of the silicone rubber and since it is covalently bonded to the silica surfaces, leaching into the blood or tissue should be minimal. *In vivo* tests carried out by Dr. Gott showed this compound to possess significant thromboresistance. As can be seen in Table 10, all three of the two hour implants displayed small thrombi, but three out of five chronic implants were virtually free of any thrombus.

Methods for Optimizing Solvent Swelling Treatment.

Heparin Distribution. An autoradiographic technique was used to determine the distribution of heparin on a silicone rubber surface treated with γ-aminopropyltriethoxysilane by the solvent swelling method and subsequently heparinized. Ten percent of S^{35} labeled heparin was substituted for the regular heparin used in the treatment. Silastic 372 sheets treated in this manner were placed between two sheets of Ilford G X-Ray film and allowed to remain in close contact for periods ranging from 2 to 7 days. The film was then developed with the result that blackening of the film occurred where S^{35} labeled heparin was present, Figure 5. Data obtained using a beta counter reveal there is about 18 μg of heparin per cm^2 of surface.

The above operation was repeated after briskly scrubbing a strip 1/2" wide with several pieces of rough cotton cloth. The second film (Figure 6) now shows that a major part of the coating has been removed but that there is still some darkening of the film - indicating residual heparin. Based on the radiographs, it is apparent that even greater nonthrombogenicity of silicone rubber can be achieved if (1) the heparin distribution over the surface were more uniform and (2) a deeper penetration of heparin into the bulk of the rubber were obtained. Referring to Figure 2, it is rather obvious that if the acidification of the free amine and subsequent heparinization of the amine salt could be carried out in a solvent which swelled silicone rubber, these goals should be attainable.

Recent work toward these objectives is extremely promising. The reaction of ammonium chloride with γ-aminopropyltriethoxysilane to yield the corresponding hydrochloride quantitatively is depicted below.

$$(C_2H_5O)_3Si(CH_2)_3NH_2 + NH_4Cl \xrightarrow[EtOH]{Refluxing} (C_2H_5O)_3Si(CH_2)_3\overset{+}{N}H_3Cl^- + NH_3\uparrow$$

The crystalline product is extremely soluble in benzene and since benzene is the solvent of choice for the solvent-swelling technique for the heparinization of silicone rubber, the acidification step can be eliminated.

Tridodecylmethylammonium chloride (TDMAC) was prepared according to the method of Dr. Richard Falb of Battelle Memorial Institute.

$$(C_{12}H_{25})_3N + CH_3Cl \longrightarrow (C_{12}H_{25})_3\overset{+}{N}(Ch_3)Cl^-$$

Tridodecylmethylammonium heparinate was subsequently prepared by methods developed in this laboratory although it has been previously reported by Falb et al.

$$X(C_{12}H_{25})_3\overset{+}{N}(CH_3)Cl^- + Na_x Hep^- —— [(C_{12}H_{25})_3\overset{+}{N}(CH_3)]_x Hep^- + xNaCl$$

Sodium heparin in 1/3 H_2O/MeOH was added to a well stirred solution of TDMAC in the same solvent. A precipitate formed immediately, was collected, purified, and identified as TDMA heparin by IR spectra and elemental analysis. Assuming a five to one stoichiometry for TDMAC to heparin, the experimental percent and calculated percent agree fairly well.

Element	Calculated %	Experimental %
C	66.8	66.9
H	11.3	12.1
N	2.6	2.5
S	4.3	3.7
O	14.9	(14.9)
Cl	--	None

TABLE 9

CLOTTING TIMES FOR SILICONE RUBBER TREATED BY SOLVENT SWELLING TECHNIQUE WITH AMINOORGANOSILANES

	Aminoorganosilane Used for Treatment (1.5 g/30 ml ϕH)	Lee-White Clotting Times
1.	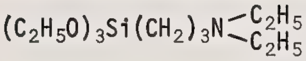 $(C_2H_5O)_3Si(CH_2)_3N\begin{smallmatrix}C_2H_5\\C_2H_5\end{smallmatrix}$	10.0-11.0 min.
	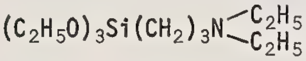 $(C_2H_5O)_3Si(CH_2)_3N\begin{smallmatrix}C_2H_5\\C_2H_5\end{smallmatrix}$ + Na^+Hep^-	6.5-7.0 min.
2.	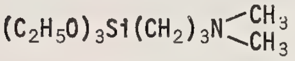 $(C_2H_5O)_3Si(CH_2)_3N\begin{smallmatrix}CH_3\\CH_3\end{smallmatrix}$	7.0-7.5 min.
	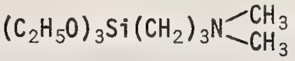 $(C_2H_5O)_3Si(CH_2)_3N\begin{smallmatrix}CH_3\\CH_3\end{smallmatrix}$ + Na^+Hep^-	15 min.
3.	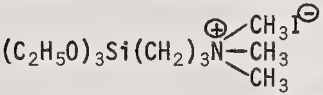 $(C_2H_5O)_3Si(CH_2)_3\overset{\oplus}{N}\begin{smallmatrix}CH_3I^{\ominus}\\CH_3\\CH_3\end{smallmatrix}$	7.0-8.0 min.
	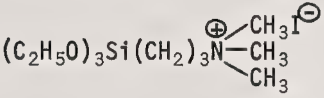 $(C_2H_5O)_3Si(CH_2)_3\overset{\oplus}{N}\begin{smallmatrix}CH_3I^{\ominus}\\CH_3\\CH_3\end{smallmatrix}$ + Na^+Hep^-	8.5-9.0 min.
4.	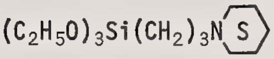	6.0-6.5 min.
	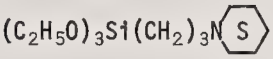 + Na^+Hep^-	4.5-5.0 min.
5.	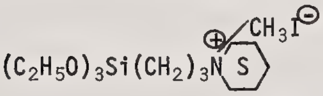	--
	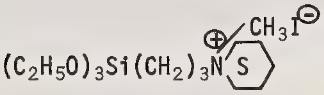 + Na^+Hep^-	--
6.	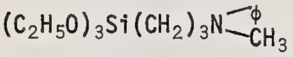 $(C_2H_5O)_3Si(CH_2)_3N\begin{smallmatrix}\phi\\CH_3\end{smallmatrix}$	8.5-9.0 min.
	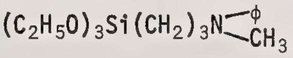 $(C_2H_5O)_3Si(CH_2)_3N\begin{smallmatrix}\phi\\CH_3\end{smallmatrix}$ + Na^+Hep^-	5.0-5.3 min.
7.	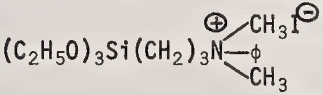 $(C_2H_5O)_3Si(CH_2)_3\overset{\oplus}{N}\begin{smallmatrix}CH_3I^{\ominus}\\\phi\\CH_3\end{smallmatrix}$	--
	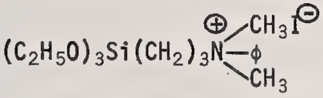 $(C_2H_5O)_3Si(CH_2)_3\overset{\oplus}{N}\begin{smallmatrix}CH_3I^{\ominus}\\\phi\\CH_3\end{smallmatrix}$ + Na^+Hep^-	--
8.	$(C_2H_5O)_3Si(CH_2)_3NH_2$ + Na^+Hep^-	>1 hr.
9.	$(C_2H_5O)_3Si(CH_2)_2N(CH_2CH_2OH)_2$ ----	26 min.
10.	$(C_2H_5O)_3Si(CH_2)_2N(CH_2CH_2OH)_2$ + Na^+Hep^-	6.0 min.

TABLE 10

In Vivo Tests (Gott Implant Rings) of Silicone Rubber Treated with N-bis(beta-hydroxyethyl)-γ-Aminopropyltriethoxysilane

ACUTE							CHRONIC						
SILASTIC ST-18	11-25-68	GAS	A-1111*	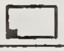	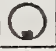		SILASTIC ST-18	11-29-68	GAS	A-1111*	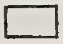	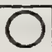	
"	11-26-68	"	"	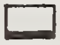			"	11-29-68	"	"	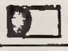	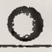	DIED AFTER 24 HRS.
"	11-26-68	"	"	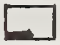			"	11-29-68	"	"	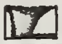		DIED AFTER 3 DAYS
							"	12-6-68	"	"	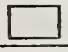	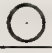	
							"	12-6-68	"	"	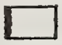		

* N-bis (B-hydroxyethyl) γ-aminopropyltriethoxysilane

TDMA heparin is soluble in benzene and forms a clear polymeric film when cast from this solution. Thus it now appears possible to also perform the heparinization step in benzene solution.

$$_{3/2}OSi(CH_2)_3\overset{+}{N}H_3Cl^- + (C_{12}H_{25})_3\overset{+}{N}(CH_3)Hep^- \longrightarrow {}_{3/2}OSi(CH_2)_3\overset{+}{N}H_3Hep^- + (C_{12}H_{25})_3\overset{+}{N}(CH_3)Cl^-$$

The excess TDMA heparin and formed TDMAC can be readily removed by solvent extraction.

CONCLUSIONS

(1) The heparinization of silicone rubber utilizing γ-aminopropyltriethoxysilane as a coupling agent yields a surface possessing a high degree of nonthrombogenicity based on both *in vitro* and *in vivo* tests.

(2) A number of other aminoorganosilanes used as coupling agents for heparin in silicone rubber offered from little to only modest improvement in nonthrombogenic character based on *in vitro* tests.

(3) The addition of N-bis(beta-hydroxyethyl)-γ-aminopropyltriethoxysilane to silicone rubber leads to a covalently bound surface having significant thromboresistance based on both *in vitro* and *in vivo* tests.

REFERENCES

1. Gott, Vincent L., et al., Trans. Am. Soc. Art. Int. Organs. X, 213 (1964).
2. Leininger, R. I., et al., Ibid., 237 (1964).
3. Chuiko, A. A., Tertykh, V. A., Plavnik, G. E. and Neimark, I. E., Colloid J. (USSR) (English Translation) 27, 770 (1965).
4. Chuiko, A. A., Pavlik, G. E. and Neimark, I. E., Dopovidi Akad. Nauk Ukr. SSR (2), 230-4 (1963); C. A., 59, 12836 (1963).
5. Tertykh, V. A., Burushkina, T. N. and Chuiko, A. A., Modifikatsiya Svoistv Polimerov i Polymernykh Materialov, Akad. Nauk Ukr. SSR, Resp., Mezhvedomstv Sb., 1965, p. 85-95.
6. Wolf, F., Beyer, H. and Hadicke, U., J. Prakt. Chem. 24 (3-4), 158-63 (1964).
7. Folkman, Judah, Reiling, W. and Williams, G., "Chronic Analgesia by Silicone Rubber Diffusion" to be published.

DISCUSSION

DR. GILLIS: Did I understand correctly that in the in vivo preparation of the AV shunt clotting was apparently induced by anesthesia?

DR. MERKER: Yes. This is with the untreated silicone rubber. This was Dr. Folkman's work. The AV shunt would remain open for approximately 24 hours in the absence of perfusing anesthetic. But it would clot within an hour when the anesthetic was introduced into the shunt.

DR. GILLIS: This did not occur in the treated AV shunts?

DR. MERKER: No. They remained open for over a week.

DR. GILLIS: Yes.

DR. HASTINGS: Any other questions?

DR. HERSH: Would you describe again the benzene soluble heparin complex you formed?

DR. MERKER: Did you want to know about the preparation?

DR. HERSH: Yes.

DR. MERKER: Well, it is an ionic complex. In the repeating unit of heparin on the average there are five sodium atoms, and what we have done is merely to replace the five sodium atoms with the tridodecylammonium which makes it soluble in organic solvents whereas the sodium salt is only soluble in water.

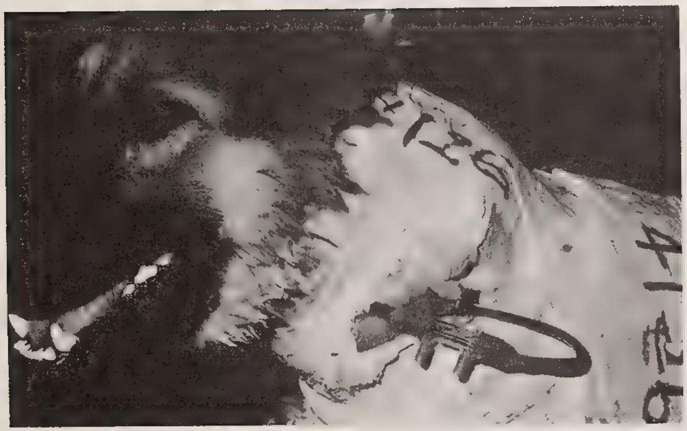

FIGURE 3. CHRONIC ANALGESIA BY SILICONE RUBBER DIFFUSION

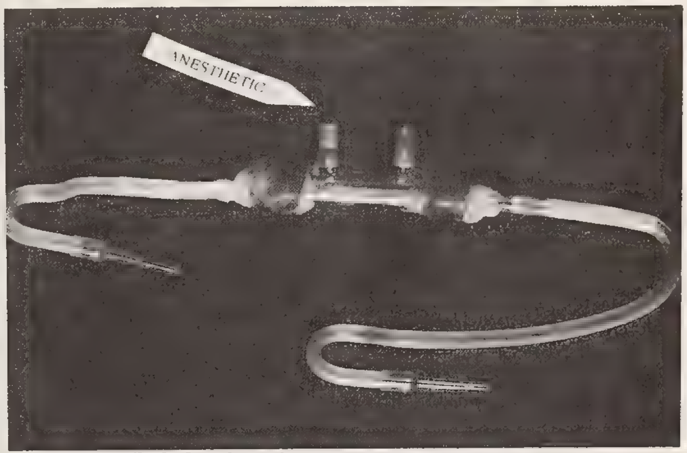

FIGURE 4. ARTERIAL-VENOUS SHUNT

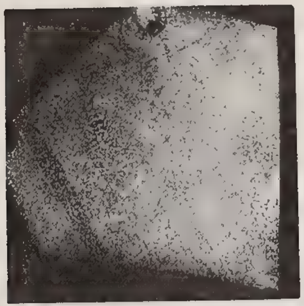

FIGURE 5. DISTRIBUTION OF HEPARIN ON SILICONE RUBBER SURFACE

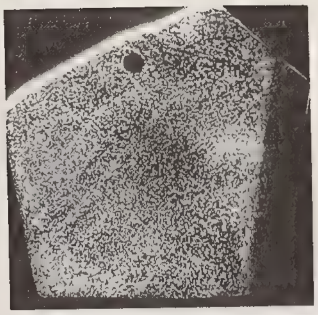

FIGURE 6. REMOVAL OF HEPARIN FROM SILICONE RUBBER SURFACE BY ABRASION

CHAPTER 4

DEVELOPMENT OF BLOOD COMPATIBLE SILICONE ELASTOMERS

M.C. Musolf, V.L. Metevia, and V.D. Hulce

Dow Corning Corporation, Midland, Michigan

A study was made to improve the fabrication and surgical handling properties of our potentially non-thrombogenic silicone elastomers. High durometer elastomers and shelf stable non-vulcanized elastomer stocks were prepared. Thermoplastic silicone elastomers were prepared and evaluated. A study of the influence of the low molecular weight polymeric contaminants in elastomers upon the surface properties is in progress. Hydrophobicity of a trifluoropropylmethylsiloxane containing elastomer was insensitive to both postcuring at 200°C and solvent extraction while a dimethylsiloxane containing elastomer became more hydrophobic after either postcuring or solvent extraction. The influence of these variables upon the vena cava ring test has not been obtained. The *in vivo* testing was carried out by the vena cava ring method. Three promising trifluoropropylmethylpolysiloxane containing elastomers were implanted for chronic 2 week periods. The results continue to indicate that these elastomers can possess non-thrombogenic characteristics. The high durometer elastomer, RB-1622, containing fluoroalkyl functionality was shown to be thrombotic. This is the first trifluoropropylmethylsiloxane to exhibit thrombogenic characteristics. One thermoplastic elastomer containing a 50/50 mole ratio of tetramethylsilphenylene/dimethylsiloxane was found to be quite non-thrombogenic while another with a 75/25 mole ratio was very thrombotic. Oxygen and carbon dioxide gas transmission measurements were made on 18 silicone elastomers. Parts molded from two promising silicone elastomers were submitted to four NHI sponsored contractors for testing.

EXPERIMENTAL

Elastomer Preparation.

The elastomers discussed in this paper were prepared using standard processing techniques. They were silica filled, peroxide, vulcanized, and postcured for 4 hours at 200°C. The three thermoplastic silicones were prepared in benzene solvent by the base catalyzed condensation of $HOMe_2Si$ ⌬ $SiMe_2OH$ with $HO(Me_2SiO)_{40}H$ according to the procedures described in US 3,202,634.

Gas Transport Measurements.

The gas permeation cell which was used for gas permeability studies is the "Dow Gas Transmission Cell". This instrument was developed by Brown and Sauber[1] and is now the accepted ASTM standard[2] for measuring gas transmission rates of plastic film and rubber sheeting.

The ASTM recommends that the gas transmission rate be calculated rather than the permeability unless the thickness-to-gas transmission rate relationship has been pre-determined for the membrane-to-gas combination. It has been found in this laboratory and by Galletti, Snider and Silbert-Aidan[3] that the gas transmission rate of non-reactive gases is a linear function of the reciprocal of the thickness of siloxane films. Thus the gas transmission rates have been normalized to unit thickness to obtain the permeability.

The calculations were done by the method of Paul and DiBenedetto[4]. The permeation rates which were calculated by this method were the same as those of the ASTM method, but in addition this method also allows the calculation of the diffusion coefficient and the solubility of the gas in the membrane. This method requires calculation of a correction for the fact that the pressure on the downstream side of the membrane is allowed to increase instead of remaining negligible as in the classical apparatus for which the calculations of Daynes[5] could be used. The required calculations have thus become tedious enough that a computer program has been written for the IBM 360.

The samples were molded into flat sheets, 40 mils thick, postcured 3 hours at 200°C, and then cut into 4 inch discs.

RESULTS AND DISCUSSION

It was observed from earlier contract effort that silicone elastomers containing carboxyl functionality were very thrombotic and possessed no advantage over a standard dimethylpolysiloxane elastomer. Dimethylsiloxane elastomers containing phenylmethylsiloxane and diphenylsiloxane functionality displayed marginal thromboresistance and were not considered for further study. Silicone elastomers containing a high molecular weight homopolymer of trifluoroprophymethylsiloxane (frequently written $\{TFPMeSiO\}_x$) or blends of this polymer with a high molecular weight homopolymer of dimethylsiloxane (written $\{Me_2SiO\}_x$) were found, however, to exhibit significant thrombo-resistance by both the inferior vena cava ring test and the right atrial sword implant test. It was therefore felt important to investigate the trifluoropropylmethylsiloxane-dimethylsiloxane elastomeric system in more detail.

The existing fluoroalkyl containing elastomers were found to have poor shelf stability as noted by their becoming hard and unmillable (crepe hardening). Formulation changes involving filler loading, crosslink density, and low molecular weight processing aids were studied. Two series of elastomers resulted. In the first series the levels of the low molecular weight processing fluids were increased. This eliminated crepe hardening but did not provide the needed hardness (durometer) of the elastomers. A comparison of the mechanical properties of the original elastomers, RB-1326 through RB-1413, with those for the corresponding first elastomer modifications (RB-1519 through RB-1525) is shown in Table 1.

TABLE 1

COMPARISON OF THE PROPERTIES OF THE ORIGINAL ELASTOMERS TO THE CORRESPONDING MODIFIED ELASTOMERS

Elastomer[a] Code No.	High Polymer Composition Mole, Ratio $(\mathrm{TFPMeSiO})_x/(\mathrm{Me_2SiO})_x$	Mechanical Properties Duro-meter	Ten.Str. psi	% Elong.	Tear pli
RB-1326	100/0	36	1,650	460	
RB-1519	100/0	47	1,460	530	158
RB-1327	65/35	44	1,420	520	
RB-1520	65/35	49	1,370	560	206
RB-1328	38/62	51	1,380	480	
RB-1521	38/62	53	980	500	214
RB-1329	38/62	50	1,210	470	
RB-1522	38/62	55	800	450	92
RB-1330	19/81	50	1,130	350	
RB-1523	19/81	57	890	460	80
RB-1413	0/100	33	1,466	950	239
RB-1525	0/100	47	1,020	260	67

a. Elastomers coded RB-1326through RB-1413 are the original formulations; RB-1519 through RB-1525 are the first formulation modifications.

In the second series, elastomers were made higher in durometer by increasing the filler loading, the crosslink density, and the level of the processing aids. The properties in Table 2 show that these elastomers are significantly harder and from preliminary data they also appear to have much better surgical handling properties. This increase in durometer, however, was accomplished at the expense of tensile strength, elongation, and tear strength which noticeably decreased in value.

Included in the second series (Table 2) are elastomers which were formulated to evaluate the influence of low molecular weight processing aids upon thrombogenicity. Elastomers of the $(\mathrm{TFPMeSio})_x/(\mathrm{Me_2SiO})_x$ polymer system were prepared with a low molecular weight $(\mathrm{Me_2SiO})_x$ processing additive, with a low molecular weight $(\mathrm{TFPMeSiO})_x$ additive, or with both additives. In one case a dimethylpolysiloxane elastomer was made with no processing additives.

At this time only one of these elastomers (RB-1622, Table 2) has been evaluated by the inferior vena cava ring test. Here three acute two hour ring implants were highly thrombosed. This is the only example to date of a $(\mathrm{TFPMeSiO})_x$ containing elastomer which was thrombotic. The main difference between this elastomer and the corresponding original nonthrombogenic elastomer (RB-1328) is the includion of the $(\mathrm{Me_2SiO})_x$ processing additive and the increase in filler. The pending vena cava ring results from the other elastomers should help to describe the contributions. which the processing aids have on the overall thromboresistance of this system of elastomers.

It is known that many silicone elastomers will swell when immersed in solvents such as toluene or methylisobutylketone (MIBK). During this swelling process low molecular weight siloxane contaminates and catalyst by-products can dissolve in the solvent and be removed from the elastomer. Through such an extraction process (48 hours in MIBK) two elastomers, a homopolymer of $(\mathrm{TFPMeSiO})_x$ RB-1519 and a blend polymer of $(\mathrm{TFPMeSiO})_x$ and $(\mathrm{Me_2SiO})_x$, RB-1622, were found to have weight losses of 3.1% and 4.1% respectively. Thus the silicone elastomers involved in this contract work can be "purified" to some degree by extraction.

TABLE 2

PROPERTIES OF HIGH DUROMETER ELASTOMERS

Elastomer Code No.	High Polymer Composition Mole Ratio $\{TFPMeSiO\}_x/\{Me_2SiO\}_x$	Processing Aids		Mechanical Properties			
		$\{Me_2SiO\}_x$	$\{TFPMeSiO\}_x$	Durometer	Ten. Str. psi	% Elong	Tear pli
RB-1687	100/0	---	yes	64	1,290	220	95
RB-1686	100/0	yes	---	71	1,020	210	90
RB-1685	65/35	---	yes	70	1,050	170	87
RB-1622	38/62	yes	yes	75	950	250	97
RB-1684	38/62	---	yes	76	910	130	69
RB-1682	0/100	yes	---	68	750	130	49
RB-1688	0/100	---	yes	72	840	120	54
RB-1681	0/100	---	---	56	750	390	71

Using this extraction technique two thrombus initiating elastomers, a homopolymer of $\{Me_2SiO\}_x$ (RB-1682) and RB-1622 described above, were molded into rings and then extracted 48 hours in a soxhlet extractor. These extracted rings have been sent to Dr. Gott for evaluation but have not been tested as yet. The results from these rings should also help to describe the relationship between the low molecular weight contaminates and the thromboresistance of candidate elastomers.

Thermoplastic Silicones.

The preparation of thermoplastic silicones was undertaken so that an alternate method of fabricating silicone elastomers could be studied. The approach taken was to build crystallinity into dimethylpolysiloxane by incorporating in it the crystalline tetramethylsilphenylene, Me_2Si ⬡ $SiMe_2O$, unit. Three such thermoplastic block copolymers were prepared which contained 25, 50, and 75 mole percent of the tetramethylsilphenylene structure. Two of these materials were molded into vena cava rings and were evaluated by Dr. Gott. A sample containing 75% tetramethylsilphenylene was observed to be very thrombotic, while the material containing 50% tetramethylsilphenylene was found to be quite thromboresistant. These 2 hour acute implants for the 50% sample were sufficiently encouraging that chronic 2 week implants are being planned. The material containing 25% tetramethylsilphenylene could not be compression molded into satisfactory vena cava rings, thus it was not evaluated *in vivo*.

Gas Transport Evaluations of Silicone Elastomers

The permeability, diffusivity, and solubility of gases in dimethylsiloxane and trifluoropropylmethylsiloxane rubbers have been measured previous to this study. Dimethylsiloxane has been investigated extensively both in the literature and in this laboratory. Trifluoropropylmethylsiloxane has had only a few published papers on its permeability. No measurements on copolymers or on mechanical mixtures of siloxane polymers have been done.

Oxygen and carbon dioxide gas transport measurements were made on the series of silicone elastomers which have been studied under this contract. These data appear in Table 3. It can be readily seen that additions of the less permeable trifluoropropylmethylsiloxane or $\{Me_2Si$ ⬡ $SiMe_2O\}_x$ reduce the permeability of dimethylpolysiloxane. When permeability and diffusivity are plotted against elastomer composition the values are observed to deviate markedly from a linear correlation. The addition of the less permeable polymers reduces the permeability and diffusivity more than would be expected, while the solubility of the gas differs very little from what would be expected. Since the equation relating permeability, diffusivity, and solubility is $P = (D)(S)$, it is seen that what is occurring in these rubbers is that the less permeable rubber makes it harder for the gas molecules to diffuse through the mixed rubbers.

In Vivo Testing

The inferior vena cava ring test as performed by Dr. Gott and coworkers has been used in this contract effort as the method of evaluating candidate elastomers for thromboresistance. A summary of the results of this work appears in Table 4.

TABLE 3

GAS TRANSPORT MEASUREMENTS FOR SILICONE ELASTOMERS

Elastomer Code No.	High Polymer Composition (Mole Ratio)		Oxygen			Carbon Dioxide		
			$P \times 10^9$	$D \times 10^6$	$S \times 10^4$	$P \times 10^9$	$D \times 10^6$	$S \times 10^4$
RB-1519	$(\mathrm{TFPMeSiO})_x/$ $(\mathrm{Me_2SiO})_x$	100/0	9.75	3.80	25.7	48.0	2.63	185
RB-1520	$(\mathrm{TFPMeSiO})_x/$ $(\mathrm{Me_2SiO})_x$	65/35	13.1	5.40	24.2	66.9	3.48	196
RB-1521	$(\mathrm{TFPMeSiO})_x/$ $(\mathrm{Me_2SiO})_x$	38/62	23.1	7.98	28.9	109	6.49	172
RB-1522	$(\mathrm{TFPMeSiO})_x/$ $(\mathrm{Me_2SiO})_x$	38/62	23.4	8.90	26.1	111	5.87	193
RB-1622	$(\mathrm{TFPMeSiO})_x/$ $(\mathrm{Me_2SiO})_x$	38/62	21.0	8.31	25.2	108	5.70	191
RB-1523	$(\mathrm{TFPMeSiO})_x/$ $(\mathrm{Me_2SiO})_x$	19/81	39.6	12.0	33.0	185	11.2	163
RB-1524	$(\mathrm{TFPMeSiO})_x/$ $(\mathrm{Me_2SiO})_x$	38/62	33.6	10.8	30.9	148	9.16	164
RB-1525	$(\mathrm{Me_2SiO})_x$	0/100	57.0	18.3	31.2	253	17.6	145
RB-1413	$(\mathrm{Me_2SiO})_x$	0/100	54.5	17.4	31.6	285	13.6	216
RB-1541	$(\mathrm{Me_2Si}$ ⌬ $\mathrm{xSiMe_2O})_x/$ $(\mathrm{Me_2SiO})_x$	25/75	26.8	15.5	17.3	156	14.5	100
RB-1542	$(\mathrm{Me_2Si}$ ⌬ $\mathrm{xSiMe_2O})_x/$ $(\mathrm{Me_2SiO})_x$	50/50	8.36	7.29	11.5	23.0	4.75	44.5
RB-1543	$(\mathrm{Me_2Si}$ ⌬ $\mathrm{xSiMe_2O})_x/$ $(\mathrm{Me_2SiO})_x$	75/25	2.00	1.79	11.2	11.4	1.67	68.3

Units

P = Permeability = $(\text{cm}^3 \text{ gas})(\text{cm})/\text{cm}^2$ sec. cm Hg

D = Diffusivity = cm^2/ses.

S = Solubility = $(\text{cm}^3 \text{ gas})/(\text{cm}^3 \text{ rubber})$ cm Hg

TABLE 4

SUMMARY OF VENA CAVA RING TESTS

Elastomer Code No.	High Polymer Composition (Mole Ratio)		Degree of Thrombus Formation View of Atrial End							
			2 Hour Results			2 Week Results				
RB-1326	$(\mathrm{TFPMeSiO})_x$	100	○	○	◒	○	◯	●	●	
RB-1327	$(\mathrm{TFPMeSiO})_x/(\mathrm{Me_2SiO})_x$	65/35	○							
RB-1328	$(\mathrm{TFPMeSiO})_x/(\mathrm{Me_2SiO})_x$	38/62	○	○	○	○	○	○	◯	●
RB-1329	$(\mathrm{TFPMeSiO})_x/(\mathrm{Me_2SiO})_x$	38/62	○	◯	○	◒	○			
RB-1330	$(\mathrm{TFPMeSiO})_x/(\mathrm{Me_2SiO})_x$	19/81	○							
RB-1331	$(\mathrm{TFPMeSiO})_x/(\mathrm{Me_2SiO})_x$	38/62	○	○	●					
RB-1622	$(\mathrm{TFPMeSiO})_x/(\mathrm{Me_2SiO})_x$	38/62	●	●	●					
RB-1413	$(\mathrm{Me_2SiO})_x$	100	●	●	●					
RB-1332	$(\mathrm{Me_2SiO})_x$	100	○	○	●					
RB-1542	Silphenylene/$\mathrm{Me_2SiO}$	50/50	○	◒	◒					
RB-1543	Silphenylene/$\mathrm{Me_2SiO}$	75/25	●	●	●					

Three of the six promising $\{TFPMeSiO\}_x$ containing elastomers were evaluated in the chronic 2 week implantation test. Of the 11 rings implanted 5 were thrombus free, 3 had minor thrombus formations and 3 were occluded. These chronic data continue to show that the $\{TFPMeSiO\}_x$ elastomers exhibit thromboresistance. The vena cava results for the two thermoplastic silicones and the high durometer $TFPMeSiO/Me_2SiO$ elastomer (RB-1622) were discussed earlier.

Sample Preparation for Outside Contract Evaluation

Elastomeric samples were fabricated and sent to five NHI sponsored testing laboratories. These laboratories are as follows:

Dr. Ruth Johnsson Hegyeli - Battelle Memorial Institute
Dr. Randolph Mason - University of North Carolina
Dr. Harry Petschek - Avco Everett
Dr. Seymour Halbert - Cordis Corporation
Dr. Ivan Stern - Travenol Laboratories

The results from these evaluations are incomplete at this time and will be reported at a later date. Preliminary data from Dr. Mason has indicated that elastomers RB-1519, a $\{TFPMeSiO\}_x$ homopolymer and RB-1622, a blend of $\{TFPMeSiO\}_x$ and $\{Me_2SiO\}_x$, produced slight to moderate damage to blood platelets. Sample RB-1622, however, had good overall blood compatibility characteristics.

SUMMARY

The in vivo evaluation of the trifluoropropylmethylpolysiloxane/dimethylpolysiloxane elastomeric system by Dr. Gott's chronic two week ring implant test continues to indicate that this system can exhibit significant thromboresistance . Formulation changes have led to an elastomer with improved higher durometer and improved surgical handling properties. Studies are in progress which are directed toward determining the influence of elastomer processing additives upon the blood compatibility of the candidate silicone elastomers. Also in progress is a study to determine to what extent solvent extracting cured silicone elastomers has upon blood compatibility.

Two thermoplastic silicones were prepared from block copolymers of $\{Me_2Si\text{⬡}SiMe_2O\}_x/\{Me2SiO\}_x$ and then evaluated by Dr. Gott's ring test. One of these materials was very thrombotic while the other showed good thromboresistance, during the two hour acute test. Chronic two week tests will be carried out on the latter polymer.

Carbon dioxide and oxygen gas transport measurements were made for several candidate silicone elastomers. These measurements showed that the incorporation of trifluoropropylmethylsiloxane or $\{Me_2Si\text{⬡}SiMe_2O\}_x$ polymers into the basic dimethylsiloxane system reduced the permeability and diffusivity of the dimethylpolysiloxane elastomer.

ACKNOWLEDGEMENTS

The authors would like to acknowledge the assistance of Dr. V. L. Gott and coworkers who evaluated all the candidate silicone elastomers by means of their in vivo inferior vena cava ring test.

REFERENCES

1. Brown, W. E., and Sauber, W. J. Gas Transmission by Plastic Films , Modern Plastics, August, 1959, p. 107.
2. ASTM Standard D-1434-63. Gas Transmission Rate of Plastic Film and Sheeting , ASTM Standards, Pt. 27, 444, (1966).
3. Galletti, P. M., Snider, M. T., and Silbert-Aidan, D. Gas Permeability of Plastic Membranes for Artificial Lungs , Medical Research Engineering, 5, No. 2, 20-23, (1966).
4. Paul, D. R., and DiBenedetto, A. T. Diffusion in Amorphous Polymers , J. Poly. Sci. C (10) 17 (1965).
5. Daynes, H. A. Process of Diffusion Through a Rubber Membrane , Proc. Roy. Soc. (London), 97A, 286-307, (1920).

DISCUSSION

MR. SALYER: I get the impression that the processing additive you describe is actually responsible for some of the thromboresistance you have observed? What is the material?

MR. MUSOLF: The material which you refer to is a trifluropropylmethylsiloxane fluid similar in structure to the base polymer used in the elastomer.

MR. NEMCHIN: I noticed that you had a carboxylated siloxane compound in the diagram in your first figure. Do you have any *in vitro* and *in vivo* data on this compound?

MR. MUSOLF: Yes. This evaluation was done in the earlier contract work. The particular silicone elastomer contained a high molecular weight carboxylated siloxane which was blended with a high molecular weight polydimethylsiloxane. The *in vivo* evaluation of this material by means of the Gott ring test showed it to be quite thrombogenic.

CHAPTER 5

COMPATIBILITY OF CARBON AND BLOOD

L. D. LaGrange, V. L. Gott, J. C. Bokros, and M. D. Ramos

Gulf General Atomic, San Diego, California

The objective of this program has been to determine the relationships between the crystal structure, surface topography and surface chemistry of a variety of different carbonaceous materials and their compatibility with blood. Past work has shown that certain outgassed and smooth surfaces of isotropic carbons deposited at low temperatures (LTI carbons) have significant thromboresistant properties which are independent of the usual pretreatments with benzalkonium chloride and heparin. One aspect of the current work has involved developing methods to firmly bond heparin covalently to these surfaces and thus provide added active suppression of coagulation initiation at the blood-carbon interface. Several schemes to achieve a covalent linkage between carbon and heparin without destroying the anticoagulation activity of the bonded heparin have been tried but none have been successful. In vivo results from tests at the Johns Hopkins Hospital during the current contract year have shown that porous carbon Gott rings are quite thrombogenic if they are implanted without pretreatment but are significantly thromboresistant if pretreated in such a way that the benzalkonium-heparin complex is formed and held within the accessible porosity. In vivo tests also show that as-deposited outgassed coatings with a preponderance of layer faces at the blood-carbon interface are more thromboresistant than isotropic coatings. This suggests a new approach that may be used to further enhance the already thromboresistant polished and outgassed LTI surfaces. In vivo elutriation results in canine vena cavae for a variety of carbon surface treated with radioactive (S-35) heparin indicate rapid elutriation of most of the heparin initially sorbed but continued significant thromboresistance for periods extending beyond one month. Four heparinized porous graphite rings and four polished LTI carbon coated rings are still implanted. Examples of carbon coatings on devices will be presented.

INTRODUCTION

For the past 2 years Gulf General Atomic has been studying the factors that are important to the compatibility of carbon and blood. The program plan is given in Figure 1. The work has been aimed at determining the relationships between the crystal structure, surface topography, and surface chemistry of a variety of carbonaceous materials and their compatibility with blood. The sorptivity of heparin has been investigated using radioactive tracer techniques, and retentivity of sorbed heparin has been determined using a variety of elutriation methods. In addition, specimens of specially prepared carbon surfaces have been supplied to other laboratories supported by the Artificial Heart Program for specific investigations into blood-carbon interactions. These laboratories include the Battelle Memorial Institute (BMI), Travenol Laboratories, Inc., Cordis Corporation, the University of New York, and the University of North Carolina. Reference may be made to the presentations made by these groups at this conference for details of their procedures and observations.

Although a wide variety of carbonaceous materials has been investigated, special emphasis has been given to a family of materials called Pyrolite* carbons, which were originally developed for applications on nuclear fuel. These materials are deposited from gaseous environments in such a way that their microstructures do not contain growth features. Pyrolite coatings in their pure form have fracture strengths in excess of 50,000 psi, and alloyed varieties are much stronger. Their ability to sustain elastic strains of from 1 to 2% make them much tougher, for example, than glassy or vitreous carbon.

RESULTS

The results from the first year of the program have been documented in two publications.[1,2] A detailed discussion of the crystal structure and surface topography of carbon and the methods used in their characterization is given in the first reference. The most important conclusions are summarized schematically in Figures 2 through 4.

Results for smooth isotropic carbons deposited at low temperature (LTI Pyrolite carbons) and cleaned by outgassing are given in Figure 2. One of the most interesting and important conclusions has been that polished and clean LTI carbons are thromboresistant. These carbons are

---

*A trademark of Gulf General Atomic.

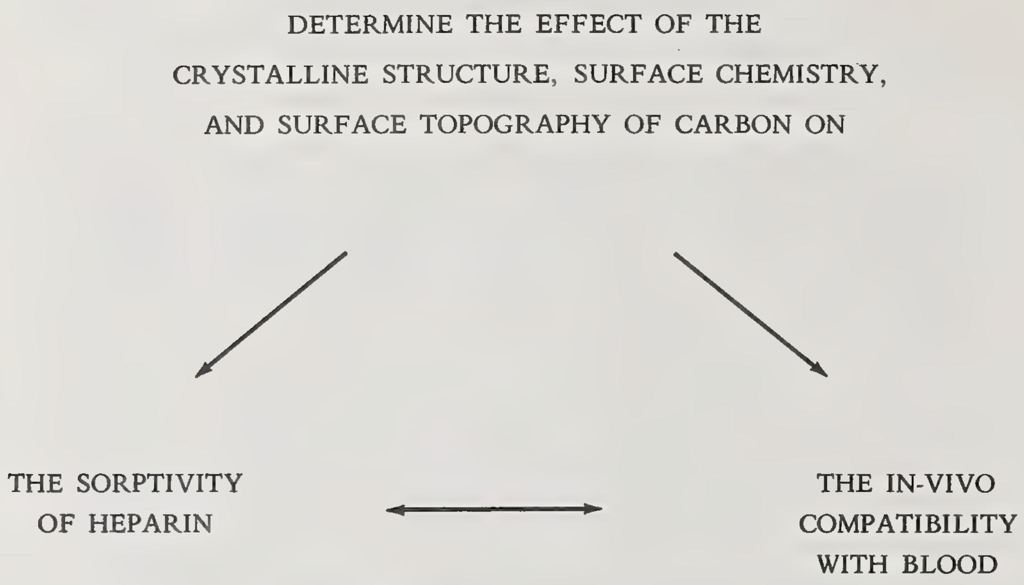
DETERMINE THE EFFECT OF THE
CRYSTALLINE STRUCTURE, SURFACE CHEMISTRY,
AND SURFACE TOPOGRAPHY OF CARBON ON
THE SORPTIVITY OF HEPARIN
THE IN-VIVO COMPATIBILITY WITH BLOOD

FIGURE 1. SCHEMATIC DIAGRAM OF PROGRAM RESEARCH OBJECTIVES

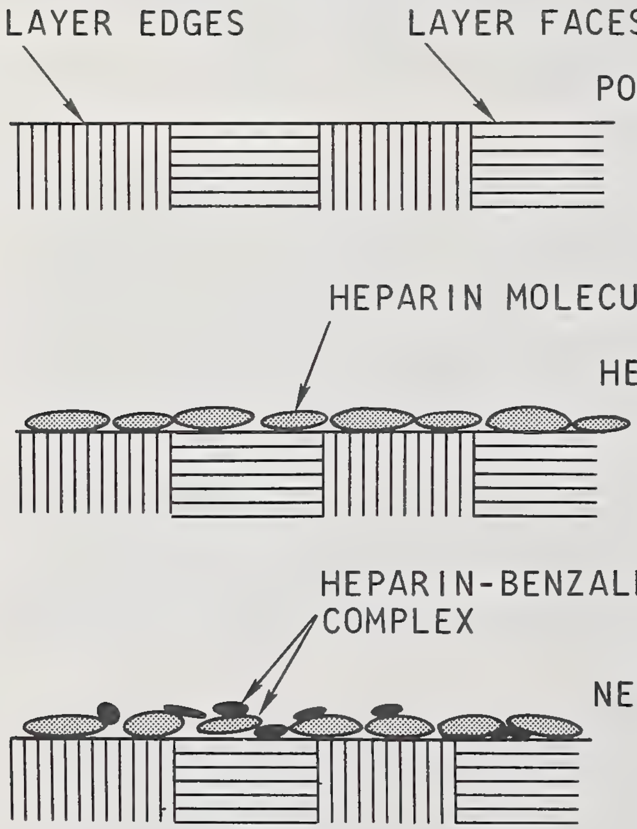

POLISHED, CLEAN ISOTROPIC CARBONS DEPOSITED AT LOW TEMPERATURES (LTI CARBONS) ARE THROMBORESISTANT.

HEPARIN IS ADSORBED ON LTI CARBON SURFACES AS A MONOLAYER; THE ADSORPTION IS NOT DEPENDENT ON CRYSTAL STRUCTURE AND DOES NOT IMPROVE THE THROMBORESISTANCE.

NEITHER HEPARIN ADSORPTION NOR IN-VIVO THROMBORESISTANCE OF LTI CARBON IS ENHANCED BY THE PRESENCE OF BENZALKONIUM CHLORIDE.

FIGURE 2. RESULTS FOR CLEAN, SMOOTH LTI CARBON SURFACES

impermeable and the heparin is adsorbed on them (as on other smooth carbon surfaces) as a monolayer. It has been found that the adsorption is not crystallographically selective and, interestingly, adsorbed heparin on the surface of LTI carbons does not improve their thromboresistance. Furthermore, neither the heparin adsorption nor the in vivo thromboresistance of LTI carbon is enhanced by the presence of benzalkonium chloride.

Results for smooth LTI carbon surfaces contaminated with oxygen are summarized in Figure 3. These data indicate that chemisorbed oxygen (hydrophilic sites) on LTI carbon surfaces markedly reduces their thromboresistance. Chemisorbed oxygen does not influence the amount of heparin that can be adsorbed on LTI carbon surfaces, and adsorbed heparin on oxidized surfaces does not improve the in vivo thromboresistance.

The conclusions obtained from studies of rough and porous carbon surfaces are displayed in Figure 4. Rough, unpolished LTI carbon surfaces are less thromboresistant than polished surfaces, and adsorbed heparin does not improve the thromboresistance of unpolished surfaces. Heparin sorption on surfaces with deep, accessible porosity is greatly increased by a surface pretreatment with benzalkonium chloride. This increase is due to the precipitation of the water-insoluble quaternary ammonium salt of heparin in the pores. These very rough carbon surfaces are only thromboresistant when the heparin-benzalkonium complex is sorbed in the porosity. From the sorption characteristics of Dag surfaces, it has been concluded that they are surfaces on which there is deep, accessible porosity.

A large fraction of the heparin sorbed on all the carbon surfaces that were studied is elutriated by brief washing in plasma; however, a small residue persists for very long times. This long time persistence suggests that some heparin on the surface is sealed in place by a layer of material adsorbed from the plasma.

Because of the rapid loss of heparin from smooth surfaces, the current effort is directed toward developing methods by which heparin is firmly attached to carbon by covalent bonding. Figure 5 outlines the steps that have been used in the treatments designed to achieve covalent bonding of heparin to LTI carbon. The carbon surfaces are first treated to attach a reactive functional group. There is evidence that this group must be attached via a chain a few carbon bonds long to avoid steric hindrance during subsequent heparin bonding reactions. Heparin is converted from the sodium salt to the benzalkonium salt and taken into solution in pyridine for use either in the bonding reaction or in the preparation of derivatives reactive toward the carbon surface functionality. The effectiveness of the various reaction sequences attempted has been evaluated by counting the beta activity of the S^{35} tracer in the heparin after washing the treated carbon in a sodium lauryl sulfate detergent solution.

Examples of some of the carbon surface preparations that have failed to promote bonding are oxidation (both chemical and anodic), heat- and peroxide-promoted bonding of maleic anhydride, and radiation-induced bonding of glutaric acid.

A reaction sequence described in Figure 5, which involves sulfonation followed by potassium cyanide fusion to replace the sulfonic acid group with a nitrile and hydrolysis of the nitrile to yield a carboxy group, has been successful in bonding heparin to LTI carbon surfaces. In this scheme the neutralized carboxylic acid is reacted with epichlorohydrin to yield the glycidyl ester. Heparin in pyridine solution is prepared for the bonding reaction by esterification with glutaric anhydride to yield heparin acid glutarate. The labile hydrogen on the free carboxy group of glutaric acid is reactive toward the epoxy ring of the glycidyl ester and can be expected to yield, upon contact, heparin bonded to the carbon surface through a series of ester linkages. Heparin surface concentrations of 2 to 3 micrograms/cm^2 after 24 hours of detergent wash have been achieved, and the surface concentration has persisted at the level of 0.6 to 1 microgram/cm^2 after 500 hours of washing. Procedures that will consistently yield high surface concentrations of heparin are being optimized.

In vivo tests were carried out to determine the influence of crystallite size, accessible surface porosity, orientation of the carbon layers at the surface, and alloying elements on the thromboresistance of carbonaceous materials. The results are listed in Tables 1 through 5.

The data in Table 1 compare the thromboresistance of two impermeable isotropic pyrolytic carbons. One material (the LTI carbon) was deposited at low temperature (less than 1500°C) and, accordingly, has a small crystallite size (30 A). The other material (the HTI carbon) was deposited at high temperature and has a larger crystallite size (140 A). Each material was polished and outgassed prior to the test. Some rings were tested with either a benzalkonium chloride-heparin treatment or a treatment with heparin alone; others were implanted without heparinization. The data indicate that both materials are quite thromboresistant; the LTI carbons may be somewhat better. There is no strong dependence of the thromboresistance on crystallite size in the range 30 to 140 A.

Data for two porous materials are presented in Table 2. The data for the Poco graphite indicate that porous graphite implanted without heparinization is thrombogenic. The data for a porous HTI carbon indicate that a pretreatment with benzalkonium chloride and heparin provides for excellent thromboresistance in a 2-hour test, but some thrombus was formed in rings implanted for the 2-week test period. As mentioned previously, the increase of the thromboresistance of porous carbons by a prior heparinization treatment is thought to be due to the formation and entrapment of the insoluble benzalkonium-heparin complex in the porosity that is accessible from the surface.

TABLE 1

IN-VIVO RESULTS FOR RINGS COATED WITH IMPERMEABLE, POLISHED AND OUTGASSED LTI AND HTI CARBONS THAT WERE TESTED IN CANINE VENAE CAVAE

TREATMENT BEFORE IMPLANTATION	THROMBUS IN LUMEN AT END OF TEST(a)			
	LTI CARBON		HTI CARBON	
	2-HR TEST	14-DAY TEST	2-HR TEST	14-DAY TEST
BENZALKONIUM CHLORIDE-HEPARIN	◒ ○ ○ ○ ○	● ◕ ○ ○ ○	◒ ◒ ◌	(b)(c) ● ● ○ ○ ○
HEPARIN	◒ ◒ ○ ○ ○	● ◒ ○ ○ ○	◒ ◒ ○	● ○ ○ ○
NONE	◒ ◒ ○ ○ ○	◒ ○ ○ ○ ○	◒ ◌ ◌	

(a) ◒ BLACKENED AREA DEPICTS THROMBUS FORMED IN RING DURING TEST
(b) DIED AFTER 3 DAYS
(c) DIED AFTER 10 DAYS

TABLE 2

IN-VIVO RESULTS FOR RINGS COATED WITH OUTGASSED, POROUS HTI CARBON AND RINGS OF OUTGASSED, POROUS POCO AXZ GRAPHITE. RINGS WERE TESTED IN CANINE VENAE CAVAE

TREATMENT BEFORE IMPLANTATION	THROMBUS IN LUMEN AT END OF TEST(a)		
	POCO AXZ GRAPHITE	POROUS HTI CARBON	
	2-HR TEST	2-HR TEST	14-DAY TEST
BENZALKONIUM CHLORIDE-HEPARIN		○ ○ ○	● ◒ ◒ ◒ ○
NONE	● ◒ ○		

(a) ◒ BLACKENED AREA DEPICTS THROMBUS FORMED IN RING DURING TEST

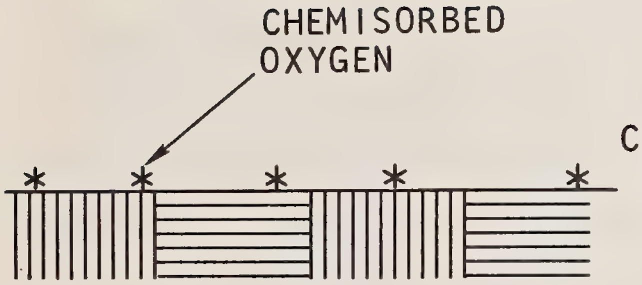

CHEMISORBED OXYGEN ON LTI CARBON SURFACES REDUCES THEIR THROMBORESISTANCE.

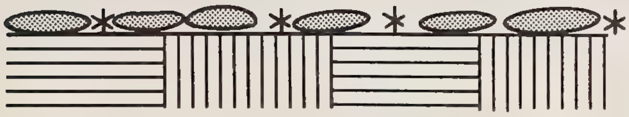

HEPARIN ADSORPTION ON LTI CARBON SURFACES IS NOT INFLUENCED BY CHEMISORBED OXYGEN, AND ADSORBED HEPARIN ON OXIDIZED SURFACES DOES NOT IMPROVE THEIR THROMBORESISTANCE.

FIGURE 3. RESULTS FOR SMOOTH LTI CARBON SURFACES CONTAMINATED WITH OXYGEN

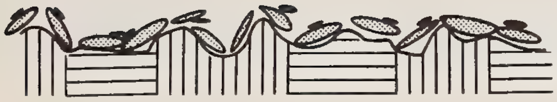

SURFACE ROUGHNESS DECREASES THE THROMBORESISTANCE OF LTI CARBON SURFACES; ADSORBED HEPARIN (OR HEPARIN-BENZALKONIUM COMPLEX) DOES NOT INCREASE THEIR THROMBORESISTANCE.

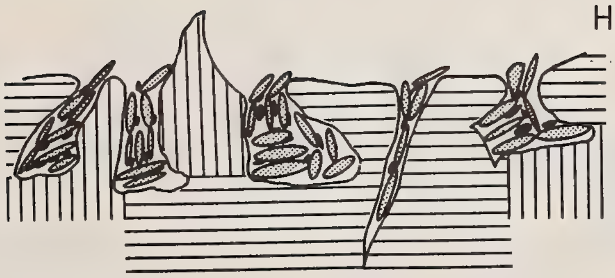

HEPARIN SORPTION ON CARBON SURFACES WITH DEEP ACCESSIBLE POROSITY IS MARKEDLY IMPROVED BY A PRETREATMENT WITH BENZALKONIUM CHLORIDE. SURFACES LIKE THIS ARE ONLY THROMBORESISTANT WHEN THE HEPARIN-BENZALKONIUM COMPLEX IS SORBED IN THE POROSITY.

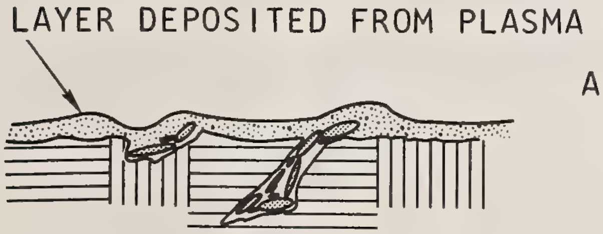

A LARGE FRACTION OF THE HEPARIN SORBED ON CARBON SURFACES IS ELUTRIATED RAPIDLY IN PLASMA, BUT A SMALL RESIDUAL AMOUNT PERSISTS.

FIGURE 4. RESULTS FOR ROUGH AND POROUS CARBON SURFACES

TABLE 3

IN-VIVO RESULTS FOR RINGS COATED WITH IMPERMEABLE, AS-DEPOSITED AND OUTGASSED SURFACES OF ISOTROPIC (LTI) AND ANISOTROPIC (HTL) CARBON THAT WERE TESTED IN CANINE VENAE CAVAE

TREATMENT BEFORE IMPLANTATION	THROMBUS IN LUMEN AT END OF TEST[a]			
	LTI SURFACE		HTL SURFACE	
	2-HR TEST	14-DAY TEST	2-HR TEST	14-DAY TEST
BENZALKONIUM CHLORIDE-HEPARIN	●●◒◒○○○	(b)(b)(c)(d) ●●◒◒○	●○○	
HEPARIN			○○○	◒○○○○
NONE	●◒◒○○		◒◒◌	

(a) ◒ BLACKENED AREA DEPICTS THROMBUS FORMED IN RING DURING TEST

(b) DIED AFTER 2 DAYS

(c) DIED AFTER 12 DAYS

(d) DIED AFTER 7 DAYS

TABLE 4

RESULTS OF POLISHED PYROLITE RING TESTS IN CANINE VENAE CAVAE

TREATMENT BEFORE IMPLANTATION	AMOUNT OF THROMBUS IN LUMEN			
	UNALLOYED PYROLITE		ALLOYED PYROLITE	
	2 HOUR TEST	14 DAY TEST	2 HOUR TEST	14 DAY TEST
BENZALKONIUM CHLORIDE-HEPARIN	◒○○○○	●●○○○	◒◒◒○○	◒◒○○○
HEPARIN	◒○◒○○	●○◒○○	TESTS ANTICIPATED	
NONE	◒○◒○○	○◒○○○	TESTS ANTICIPATED	

◒ BLACKENED AREA DEPICTS THROMBUS IN RING, AT END OF TEST.

In order to compare the thromboresistance of an isotropic carbon surface with that of a surface on which there is a preponderance of c-faces exposed to the blood at the interface, a graded structure was prepared (Figure 6). Because of the incompatibility of the thermal expansion coefficients of isotropic substrate graphites and highly anisotropic pyrolytic carbon, it was necessary to first deposit an isotropic carbon layer and then change the pyrolysis conditions gradually so that only a thin, anisotropic outer layer was formed. The outer layer is called an HTL carbon. Data for rings coated with the composite carbon (HTI graded to HTL) are compared in Table 3 with data for the isotropic LTI carbon. Both materials were tested in the unpolished, but outgassed, condition. Although the data are not extensive, the data from the 2-week tests indicate that the oriented HTL surface layer is more thromboresistant than an isotropic surface. Accordingly, additional work is anticipated in which stronger, low-temperature laminar (LTL) surfaces will be studied. Comparison of the data in Tables 1 and 3 suggests that polished LTI surfaces may be more thromboresistant than any surface tested thus far.

Because the valve components of an artificial heart will be required to operate many hundreds of millions of times during their lifetime, and for certain designs very little wear can be tolerated, a new family of alloyed pyrolytic carbons with improved wear resistance has been developed.* In vivo compatibility of one of these new materials alloyed with Si is compared in Table 4 with that of polished LTI carbon with similar crystal structure but without an alloying addition. The data show that the alloyed Pyrolite carbon is as thromboresistant as the unalloyed material.

The data in Table 4 suggested that SiC might have antithrombogenic properties. Therefore, several rings coated with pure SiC were tested. The results in Table 5 indicate that SiC is itself thrombogenic. Even though SiC is thrombogenic, when it is dispersed as submicron particles in a carbon matrix, the thromboresistance of the carbon is not impaired.

In addition to the conventional vena cava ring tests described above, a second series of experiments has been carried out to determine the rate of heparin elutriation from various heparinized carbon surfaces. The results for material treated with heparin by soaking for 20 hours in benzalkonium chloride (1:750), drying, and then vacuum impregnating in heparin (10 mg/ml) are listed in Table 6. The data show a rapid elutriation to a low level, which persists for long periods of time. These data are to serve as controls for anticipated in vivo tests of surfaces prepared by covalently bonding heparin to carbon.

TABLE 5

IN-VIVO RESULTS FOR RINGS COATED WITH IMPERMEABLE, POLISHED, SILICON-CARBIDE DOPED LTI CARBON AND RINGS COATED WITH PURE SILICON CARBIDE THAT WERE TESTED IN CANINE VENAE CAVAE. RINGS WERE SOAKED IN BENZALKONIUM CHLORIDE (1:750) FOR 60 MIN AND HEPARIN (10 MG/ML) FOR 60 MIN BEFORE INPLANTATION

DURATION OF TEST	THROMBUS IN LUMEN AT END OF TEST(a)	
	PURE SiC	SiC-DOPED LTI CARBON
2-HR TEST		◒ ◒ ◒ ○ ○
14-DAY TEST	(b) (b) ● ● ●	◒ ◒ ○ ○ ○

(a) ◒ BLACKENED AREA DEPICTS THROMBUS FORMED IN RING DURING TEST
(b) DIED AFTER 24 HR

---

*Alloyed Pyrolite carbons were developed in a program supported by Gulf General Atomic.

TABLE 6

HEPARIN SURFACE CONCENTRATION ON INSIDE OF RINGS BEFORE AND AFTER IMPLANT IN CANINE VENAE CAVAE

Material	Specimen No.	Implant Time	Heparin Surface Concentration ($\mu g/cm^2$) Before	After	
Dag 154 on polycarbonate (Type W)	1	4 hr	5.1	0.36	○
	4	4 hr	12.0	0.75	●
	2	24 hr	5.4	0.39	○
	3	24 hr	7.6	0.51	○
	5	1 day(a)	4.1	0.65	●
LTI 3534-115 as-deposited (Type X)	2	1 hr(a)	2.2	0.99	●
	1	4 hr	2.9	2.6	⊙
	3	1 week	2.1	0.49	○
	4	2 weeks	2.2	0.63	○
	5	1 month	3.2	3.6	○
LTI 3534-115 polished (Type Y)	1	4 hr	1.0	0.55	⊙
	2	24 hr	0.84	0.15	◌
	3	1 week	0.79	0.23	⊙
	4	2 weeks	1.4	0.70	○
	5	1 month	1.3	0.59	◒
	6	1 month	0.79	0.45	○
Poco Type AXZ porous graphite (Type Z)	1	4 hr	39.8	2.2	⊙
	3	4 hr	19.6	3.1	○
	4	1 week	24.5	0.59	○
	5	2 weeks	19.6	0.64	○
	6	1 month	33.0	0.48	○

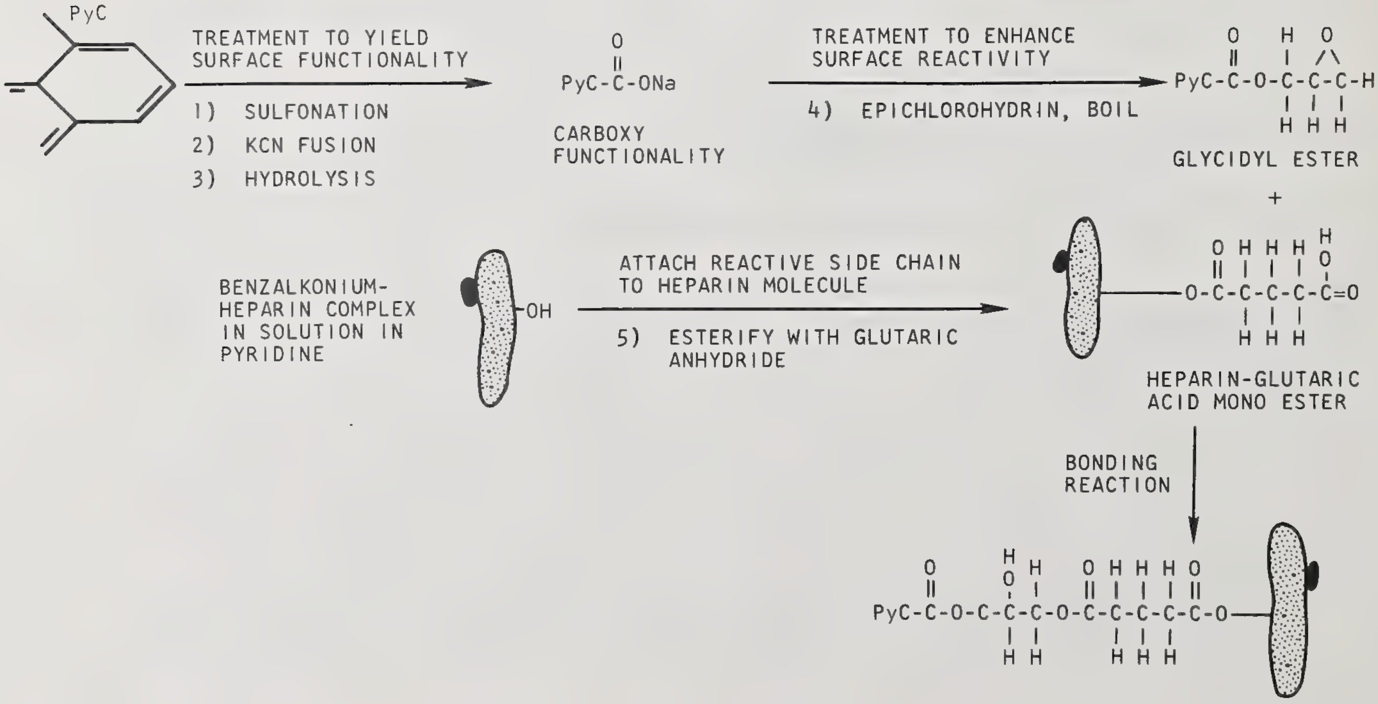
PyC
TREATMENT TO YIELD SURFACE FUNCTIONALITY
1) SULFONATION
2) KCN FUSION
3) HYDROLYSIS
PyC-C-ONa
CARBOXY FUNCTIONALITY
TREATMENT TO ENHANCE SURFACE REACTIVITY
4) EPICHLOROHYDRIN, BOIL
PyC-C-O-C-C-C-H
GLYCIDYL ESTER
+
BENZALKONIUM-HEPARIN COMPLEX IN SOLUTION IN PYRIDINE
OH
ATTACH REACTIVE SIDE CHAIN TO HEPARIN MOLECULE
5) ESTERIFY WITH GLUTARIC ANHYDRIDE
O-C-C-C-C-C=O
HEPARIN-GLUTARIC ACID MONO ESTER
BONDING REACTION
PyC-C-O-C-C-C-O-C-C-C-C-C-O

FIGURE 5. OUTLINE OF PROCEDURE FOR COVALENTLY BONDING HEPARIN TO PYROLYTIC CARBON SURFACE

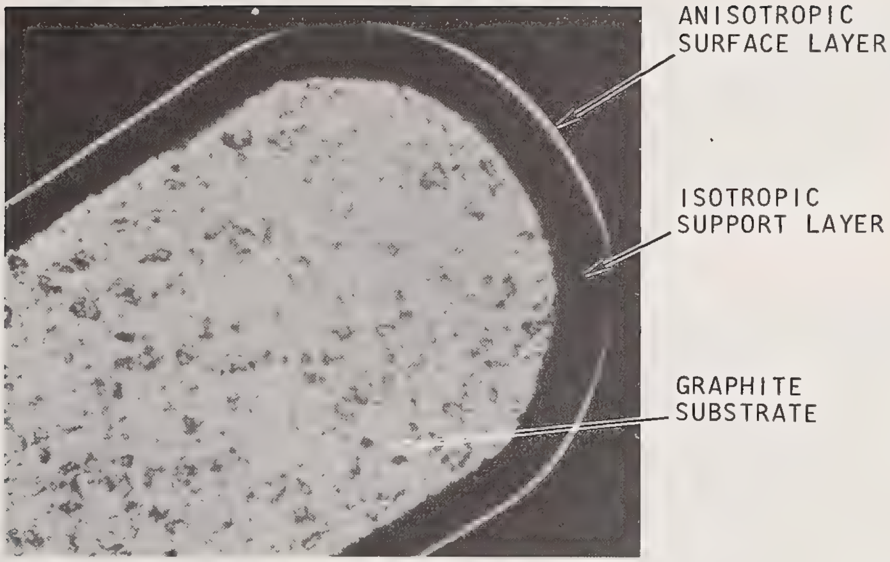

FIGURE 6. PHOTOMICROGRAPH OF SECTION THROUGH GRAPHITE SUBSTRATE DISK THAT HAD BEEN COATED WITH A COMPOSITE LAYER, INNER PORTION OF COMPOSITE IS ISOTROPIC. OUTER PORTION WAS GRADED TO A HIGHLY ORIENTED SURFACE LAYER. (50x ORIGINAL MAGIFICATION)

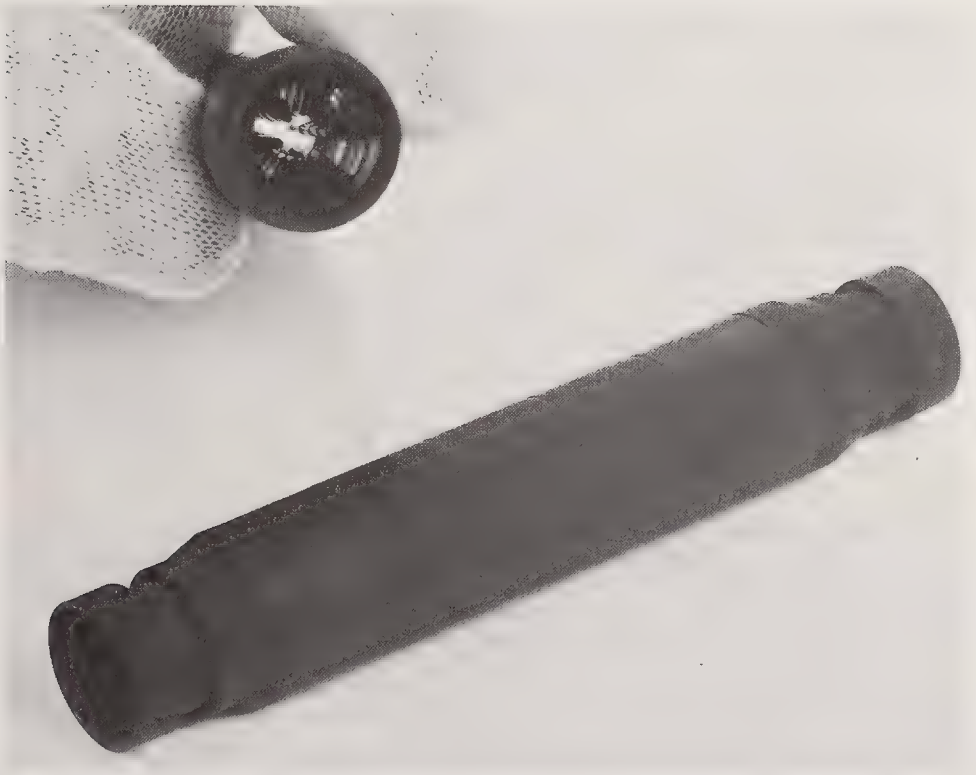

FIGURE 7. BLOOD HEAT EXCHANGER FOR NHI ENDOGENOUS HEAT PROGRAM

In addition to the in vivo vena cava ring tests, in vitro blood compatibility tests have been carried out at BMI in Columbus (R. I. Johnsson Hegyeli) and at the University of North Carolina (R. G. Mason). Reference may be made to the papers presented at this conference by Johnsson-Hegyeli and Mason for details of their experimental procedures and a complete documentation of their results. A qualitative summary of their procedures and general observations is given in Table 7.

TABLE 7

SUMMARY OF CARBON-BLOOD COMPATIBILITY TESTS

Investigator	Test Method	Summary of Observations
Johnsson Hegyeli (BMI)	Incubation in platelet-rich plasma for 1 hour at 37°C	Slight to massive cell adherence depending on sterilization procedure.
Johnsson Hegyeli (BMI)	Exposure to ACD red cross blood for 1 hour at 37°C	Slight to moderate adherence of formed blood elements. Clean, polished nonsterilized surfaces showed least adherence.
Johnsson Hegyeli (BMI)	Tissue culture studies	Plain carbon surfaces without BH supported growth of normal tissue cells. Carbon surfaces treated with BH caused complete destruction of cells.
Mason (Univ. of N.C.)	Stypven time, partial thromboplastin time, hemoglobin and adenine nucleotide release	Compatibility of clean, polished carbon surfaces was similar to silicone-coated glass.

The BMI results indicate that certain sterilization procedures result in surfaces to which cells and other formed blood elements adhere. The best surfaces as far as cell adherence is concerned were polished and cleaned but not sterilized before testing. Heating in vacuum caused cell adherence. Accordingly, in future tests surfaces sterilized by high-energy electrons will be studied.

Tissue culture studies carried out by Johnsson Hegyeli indicate that most of the clean carbon surfaces support the growth of normal tissue cells. Carbon surfaces treated with benzalkonium chloride and heparin caused complete destruction of cells.

The data of Mason and his colleagues indicate that carbon surfaces are comparable to siliconized glass in activating the clotting sequence. Similarly, the hemolysis caused by the carbon surfaces was not greater than that caused by siliconized glass. Since all of Mason's tests were carried out so that during the tests the blood was exposed to siliconized glass as well as carbon, it may be concluded that, in these tests, carbon is at least as compatible with blood as siliconized glass.

The heat exchanger shown in Figure 7 is an example of an application of LTI carbon in the Artificial Heart Program. The device was used at the Battelle Northwest Laboratories to experimentally determine the effects caused by transferring endogenously generated heat to blood.[3] The device was implanted in the thoracic aorta of a pig; the pig received no anticoagulants. In spite of the fact that the surfaces were not polished and that there were deep cul-de-sacs between the internal fins, the device was completely free of thrombus when it was retrieved on the twenty-fourth day of implantation.

A second heat exchanger was similarly implanted in a pig. The time of implantation at this writing was 11 weeks. For 8 of these 11 weeks, 60 watts of heat were transferred to the blood. In vivo measurements of the temperature of the heat exchanger suggest that it was remaining clean.[4]

SUMMARY

Many of the relationships between the crystal structure, surface topography, and surface chemistry of a variety of carbonaceous materials and their compatibility with blood have been defined. One of the most important results has been that certain outgassed and smooth isotropic carbons deposited at low temperatures (LTI carbons) have significant thromboresistant properties without pretreatment with benzalkonium chloride and heparin.

Methods to bond heparin covalently to carbon surfaces are being sought. Several schemes to achieve a covalent linkage between carbon and heparin have been tried; one has been successful.

In vivo test results have shown that porous carbon rings are thrombogenic if they are implanted without pretreatment but are thromboresistant if pretreated in such a way that the benzalkonium-heparin complex is formed and held within the accessible porosity. In vivo tests also show that coatings with a preponderance of layer faces at the blood-carbon interface are more thromboresistant than isotropic coatings.

In vivo elutriation test results for a variety of carbon surfaces treated with radioactive (S-35) heparin indicate rapid elutriation of most of the heparin but continued thromboresistance for periods extending beyond 1 month.

ACKNOWLEDGEMENTS

The authors gratefully acknowledge the experimental assistance of W. H. Ellis, F. J. Gagnon, L. J. Noble, C. D. Whiting, and K. I. McDonald. The *in vitro* blood compatibility studies carried out at BMI under the direction of R. I. Johnsson Hegyeli, M.D., and those carried out at the University of North Carolina by R. G. Mason, M.D., Ph.D., and his colleagues; and the sorption studies at Gulf General Atomic were all sponsored by the Artificial Heart Contract Program under the direction of Frank Hastings, M.D., and the Biomaterials Development Program under the direction of L. T. Harmison, Ph.D., under Contracts Ph-43-67-1411 and Ph-43-68-84.

REFERENCES

1. Bokros, J. C., V. L. Gott, L. D. LaGrange, M. M. Fadali, K. D. Vos, and M. D. Ramos, "Correlations Between the Blood Compatibility and Heparin Sorptivity for an Impermeable, Isotropic Pyrolytic Carbon," *J. Biomed. Mater. Res.* (to be published). Also Gulf General Atomic Report GA-9050, October 31, 1968.
2. Bokros, J. C., V. L. Gott, L. D. LaGrange, M. M. Fadali, K. D. Vos, and M. D. Ramos, "Heparin Sorptivity and Blood Compatibility of Carbon Surfaces," *J. Biomed. Mater. Res.* (to be published). Also Gulf General Atomic Report GA-9300, March 17, 1969.
3. Gillis, M. F., P. C. Walkup, and M. T. Karagianes, "Second 12 Month Technical Progress Report on A Study of the Effect of Additional Endogenous Heat Relating to the Artificial Heart," Battelle Northwest Laboratories Report to the National Institutes of Health, Report PB-180941, December 30, 1968.
4. Gillis, M. F., and P. C. Walkup, paper presented at the Artificial Heart Program Contractors Meeting, Washington, D.C., June 9-13, 1969.

DISCUSSION

DR. WAKABAYASHI: We have developed a nonthrombogenic film coating which consists of Estane, PVC and Dag "154". These three ingredients are dissolved in tetrahydrofuran. We can coat a variety of materials by simply dipping them into the solution for one or two seconds. This coating shows excellent nonthrombogenecity.

DR. KENNEDY: I rise to compliment the authors on this interesting piece of work. I wonder if you could tell us, please, the method by which oxygen bonding was achieved in your carbon prostheses. Secondly, is this something which can occur under physiological conditions? In other words, does it require a chemical treatment or can this occur in the body?

DR. LaGRANGE: I assume you refer to the attempt to put hydrophilic sites on the carbon. This was done at 450° centigrade for many hours in very dry oxygen, i.e., not under physiological conditions. I think that it will not occur in the body.

DR. FOUNTAIN: How were your carbons deposited, both high and low temperature carbons?

DR. LaGRANGE: The low temperature isotropic carbons are deposited below 1500° centigrade. They have a crystallite size of about 30 angstrom units. The high temperature isotropic carbons are deposited above 1500° and have a crystallite size of about 140 angstrom units. In a figure which was not shown in the oral presentation, the thrombogenicity and the absorption of heparin on these two crystallite sizes were compared. Essentially, there was no appreciable difference in the absorption of heparin, nor in the thrombogenicity. Both were equally nonthrombogenic.

DR. FOUNTAIN: Have you ever attempted deposition of carbon under conditions which result in the deposition of indigent carbon, similar to experiments that Skell did (P.S. Skell and L.D. Wescott, J.Am.Chem.Soc. 85, 1023, 1963)? In his experiments Skell applied a high potential under high vacuum to the carbon, and actually boiled off such species as C_2 and C_3, presumably leaving compatible species at the surface of the carbon. It seems to me that these carbene and dicarbene species would make very excellent indigent functionalities for attachment of heparin.

DR. LaGRANGE: None of this work was done by that technique; for it grew out of the development of nuclear fuel particle coatings. This was done by fluidized bed. However, it sounds like an interesting thing. Can he put these coatings on nonrefractory surfaces for instance?

DR. FOUNTAIN: Skell can trap these in glassy matrices and look at their chemistry quite easily. He has been able to show that these C_2 and C_3 species can react with such compounds as frozen olefins and frozen alcohols, and I imagine it would be a very easy experiment. I think one could deposit these coatings on graphite at low temperature from the vapor stage or one could use the surface from which these species were boiled off.

DR. KOLFF: I have just been a guest of a Mr. Benson in Los Angeles. This gentlemen has had a carbon button implanted in his arm for many weeks without any evidence of tissue reaction. I bring this up because it demonstrates the very good compatibility of carbon with tissues. I realize that the presentation deals with the interaction between carbon and blood but it is, of course, important that the compatibility of tissue and carbon seems to be excellent, as well.

DR. HALBERT: Did you have an opportunity to examine the _in vivo_ implants to see if there had been any attachment or growth of endothelial cells on their inner surfaces?

DR. LaGRANGE: I am not sure whether we had the opportunity or not. The _in vivo_ implants were returned to our laboratory for sulphur 35 count. They had been taken out of the animals and then rinsed off. We did not examine them microscopically.

CHAPTER 6

MATERIALS AND COMPONENTS FOR CIRCULATORY ASSIST DEVICES

I. O. Salyer and W. E. Weesner

Monsanto Research Corporation, Dayton Laboratory, Dayton, Ohio

Tissue- and blood-compatible polymer systems are desired. We have previously described epoxy resins with heparin uniformly distributed throughout. In vivo test data confirm that these materials have excellent anticlotting activity. Compositions with 3 and 7 parts of heparin/100 parts of resin (phr) have passed the chronic 2-week test. Strength and toughness of these products have been improved by curing with "Ajicure", a cyclic ether amine. Epoxy compositions with heparin ionically-coupled to the surface, in addition to the heparin throughout, are being tested. Samples of heparin-containing epoxy polymers are being prepared for evaluation by nine other contractors.

A study of polymers that do not contain heparin was continued. Epoxy resins containing Santomerse SX (an alkylbenzene sulfonate), Pluronic F-68 (a nonionic detergent), EN-1661L (from Endo Laboratories) and vinylpyridine/ethyl acrylate copolymer showed no anticlotting activity in in vitro tests. The first three samples were tested in vivo and the products with EN-1661L and Pluronic F-68 had moderate anticlotting activity in the acute, 2-hour test Hydrophilic polyurethanes with high swelling indices in water had no activity in in vitro tests, but may show activity in in vivo tests.

Scanning electron microscope studies were made on various heparin-containing and heparin-free epoxy polymers. An unheparinized, rigid epoxy had some deposits, assumed to be proteins, after 2-hours exposure to recalcified blood bank blood. A flexible epoxy containing 8 phr of heparin had a heavier surface deposit after 24 hours in a dog's vena cava than did a similar sample after 2 weeks. The former was completely thrombosed, the latter clot-free.

INTRODUCTION

The research we are reporting here was performed at the Dayton Laboratory of Monsanto Research Corporation under the National Heart Institute Contract PH 43-66-975.

This work is well into its third year. A brief review of the results obtained demonstrates that our major objectives have been largely achieved. At the end of the first year's work (Table 1) we had prepared and examined by in vitro and in vivo testing a series of materials covering a range of polarities (hydrolyzed ethylene/vinyl acetate copolymers of varying vinyl alcohol content), a series varying in negative surface charge (hydrolyzed ethylene/methyl acrylate copolymers of varying acrylic acid content), a polarity range-surface charge series (hydrolyzed ethylene/vinyl acetate/methacrylic acid terpolymer), as well as a representative series of rigid and flexible thermosetting and thermoplastic polymers and plastics.

TABLE 1

STATUS — JULY 1967

PREPARATION AND IN VITRO TESTING COMPLETED ON:

- POLARITY RANGE SERIES
- SURFACE CHARGE SERIES
- POLARITY RANGE-SURFACE CHARGE SERIES
- INITIAL EPOXY-HEPARIN MIXTURES

IN VITRO CLOT TESTS DEVELOPED

DIRECT FROM VEIN TEST DEVICE CONSTRUCTED & EVALUATED

A modified Lee-White in vitro clot test using blood bank blood was standardized for screening polymer compositions. It was statistically established that the test gave reproducible and significant data.

A device for drawing blood directly from the vein of a donor into a closed sphere/tube constructed of the polymer under investigation was also developed and evaluated during the first year's work.

An important finding from the first year's research was that, in the absence of adverse extractable impurities or degradation products, all the organic polymers tested (including the medical grade silicones) had essentially the same blood clotting characteristics in vitro (modified Lee-White test with recalcified blood bank blood) and in vivo (rings implanted in the vena cava of dogs). These results led us to the conclusion that implant surfaces must be modified in some way so as to mimic the intima of the natural blood vessels and positively inhibit clotting at blood/material interfaces. Consequently, near the end of the first year, we began investigation of incorporating heparin into epoxy and urethane polymers by methods calculated to obtain long lasting or permanent thromboresistance in the implant material.

Our accomplishments during the second year of this contract are summarized in Table 2.

TABLE 2

STATUS — JULY 1968

HEPARIN-CONTAINING POLYMERS IMPROVED

- EPOXIES, URETHANES AND POLYMERIC QUATERNARIES PASS 2-HOUR ACUTE IN VIVO TEST
- EPOXIES, POLYMERIC QUATERNARIES PASS 2-WEEK CHRONIC IN VIVO TEST

HEPARIN-FREE SYSTEMS WITH ANTICLOTTING ACTIVITY PREPARED

- EPOXIES WITH SANTOMERSE SX ADDED
- ETHYLENE/VINYL TRIFLUOROACETATE (E/VTA)
- ETHYLENE/VINYL PENTAFLUOROPROPIONATE

SCANNING ELECTRON MICROSCOPE STUDIES IN PROGRESS

A variety of polymer systems with heparin uniformly reacted and distributed throughout the bulk polymer were made and evaluated in in vitro and in vivo tests. Epoxy polymers, polyurethanes, and quaternized styrene/2-methyl-5-vinylpyridine containing up to 3 percent heparin all passed Dr. Gott's 2-hour, acute in vivo test in dogs. The epoxy and polymeric quaternary systems also passed the 2-week, chronic in vivo test in dogs. Correlation was poor, however, between anticlotting activity and heparin content, indicating uncontrolled variables were present.

The scope of our work was broadened to include samples that did not contain heparin. Epoxy polymers with Santomerse SX*, low surface energy ethylene/vinyl trifluoroacetate and ethylene/vinyl penta-fluoropropionate copolymers were prepared and evaluated. The sample with Santomerse SX did show slight activity in in vitro studies, however, none of these materials showed sufficient activity in 2-hour in vivo tests to warrant further study. Work was initiated to study surface roughness of various polymer specimens with the scanning electron microscope and to correlate these results with anticlotting activity.

CURRENT RESEARCH PROGRAM

Our current program, which we will report in greater detail, includes four major areas or tasks as shown in Table 3.

We have continued our development of heparinized epoxies and urethanes to include synthesis of a series of products ranging from soft rubbers to semi-rigid and very rigid materials. The effects of higher concentrations of heparin were studied, as well as evaluation of the effects of sterilization procedures. Study was initiated on several new heparin free systems, some of which have shown pronounced antithrombogenic activity. Additional work has been done with the scanning electron microscope to evaluate the effects of blood exposure on heparinized and unheparinized surfaces. An appreciable percentage of our current effort has been spent in preparing samples of our heparin-containing epoxy polymers for study and evaluation by other contractors.

Heparin Containing Polymers.

Table 4 presents the types of heparin-containing epoxy polymers we have examined in detail. Further improvements have been made in epoxy polymers containing heparin uniformly incorporated throughout the bulk of the polymer. To make this system even more effective in thromboresistance, we have combined the heparin throughout approach with an ionically-coupled heparin surface treatment.

---

*Santomerse is a registered trademark of Monsanto Company

TABLE 3

CURRENT PROGRAM

PREPARE NONTHROMBOGENIC POLYMERS
    HEPARIN CONTAINING
    HEPARIN FREE
ESTABLISH UTILITY
    VIA IN VITRO TESTS
    VIA IN VIVO TESTS
PREPARE SAMPLES FOR OTHER CONTRACTORS
CONTINUE SCANNING ELECTRON MICROSCOPE STUDIES

TABLE 4

HEPARIN-CONTAINING EPOXY POLYMERS STUDIED

HEPARIN INCORPORATED THROUGHOUT POLYMER

HEPARIN INCORPORATED THROUGHOUT POLYMER AND IONICALLY-COUPLED ON SURFACE

CURED WITH DIETHYLENETRIAMINE

CURED WITH AJICURE AMINES

Adequate strength, toughness, and flexibility are as important as anticlotting activity in materials to be implanted. Variations in epoxy monomer composition and in amine curing agents were studied to improve these toughness properties of heparinized epoxies.

Table 5 outlines the method used to incorporate heparin into the epoxy polymer system.

TABLE 5

FLEXIBLE EPOXY POLYMERS

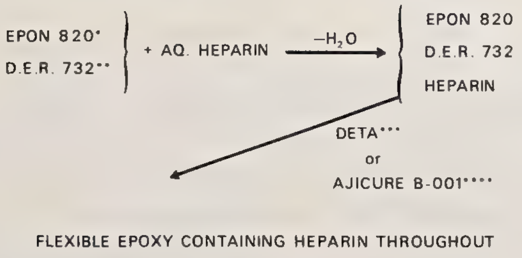

*Diglycidyl ether of bisphenol-A

**Diglycidyl ether of propylene glycol

***Diethylenetriamine

****Aliphatic cyclic ether amine

Removal of water under vacuum and moderate heat from a solution of epoxy resins and aqueous heparin leaves the resin with heparin partly reacted and uniformly distributed throughout the polymer system. Amine curing with DETA has been used in the past to provide the finished product. "Ajicure" amines from Ajinomoto Company are now preferred because of the increased strength and toughness they impart.

Table 6 presents a typical formulation for a rigid, a semi-flexible, and a flexible epoxy polymer containing heparin. The Epon 820 provides the rigidizing component and the DER 732 the flexibilizing portion of the copolymer. The Ajicure curing agent imparts some added flexibility to the product in addition to markedly increasing strength and toughness.

TABLE 6

TYPICAL EPOXY FORMULATIONS

	RIGID	FLEXIBLE
EPON 820	65–100	40–60
D.E.R. 732	35–0	60–40
DETA*	6–11	7–9
or AJICURE B-001*	50	50
HEPARIN*	2–8	2–8

*Parts per 100 parts of resin

A new type of heparinized epoxy is described in Table 7. Here we start with an amine-cured polymer already containing heparin reacted and dispersed through the entire mass. The amine sites at the surface are then quaternized by soaking the molded polymer in a solution of benzyl chloride and hexane. After quaternization, the sample is then soaked in a solution of heparin in water and methanol. This process provides heparin ionically coupled on the surface for rapid-acting anti-clotting activity, with the heparin distributed throughout the bulk of the polymer providing a reservoir for long lasting activity.

TABLE 7

SURFACE HEPARINIZED EPOXY POLYMERS

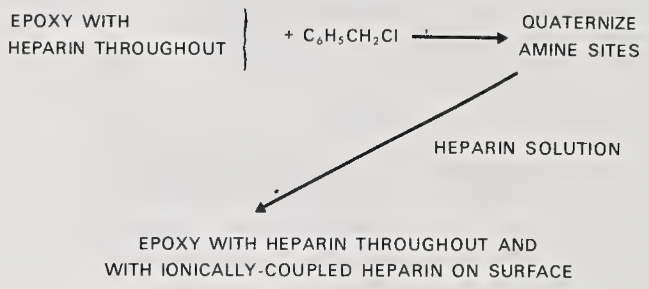

Some *in vivo* results obtained by Dr. Gott on heparin-containing epoxy polymers are shown in the next several figures (1 through 4). Ethylene oxide is used to sterilize these rings before implantation. During the past six months it has been conclusively demonstrated that ethylene oxide-sterilized rings, unless degassed thoroughly, promote clot formation in the 2-week chronic test. The absence of degassing caused many of our previous heparinized epoxy samples to perform poorly in this test. The samples shown in Figure 1 were degassed 48 hours at ambient conditions. As illustrated the results are very good. At 3 phr of heparin, two rings were completely clear and one had a tiny thrombus. At 7 phr of heparin, four rings were completely clear and one had a tiny thrombus. These rigid epoxy materials were cured with diethylenetriamine.

Figure 2 presents *in vivo* results on flexible epoxy polymers, also cured with diethylenetriamine. These 2-week, *chronic* tests again demonstrate the excellent results obtained when the cylinders are sterilized with ethylene oxide and adequately degassed. With 7 phr of heparin, a tiny thrombus was present in one ring out of four. With 8 phr of heparin, all four rings were completely clear of clots.

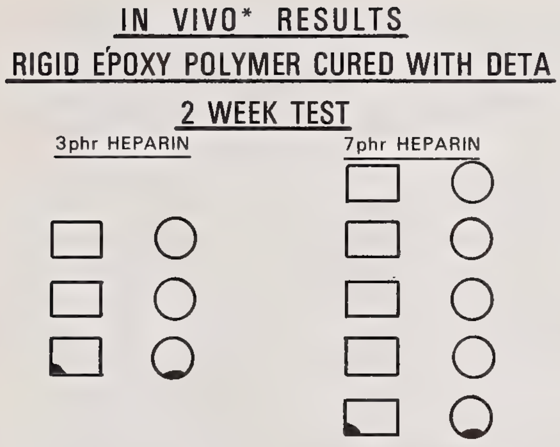

*Dr. V.L. GOTT, JOHNS HOPKINS UNIVERSITY

FIGURE 1.

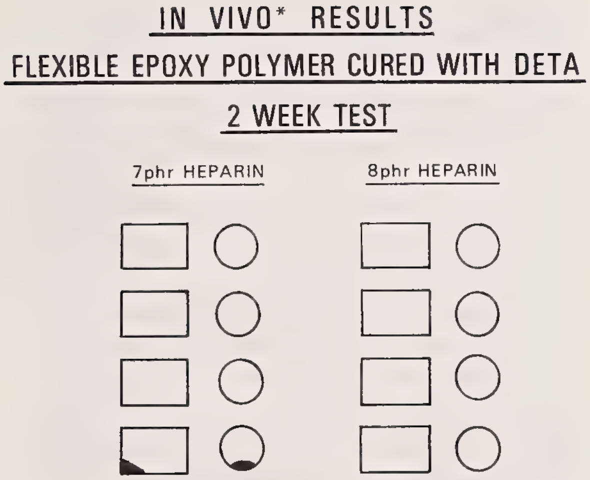

*Dr. V.L. GOTT, JOHNS HOPKINS UNIVERSITY

FIGURE 2.

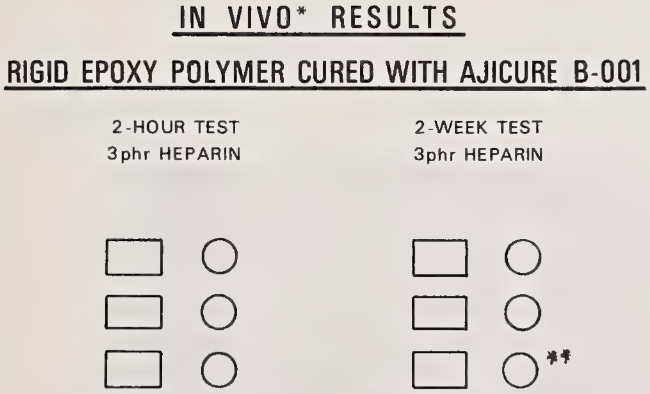

*Dr. V.L. GOTT, JOHNS HOPKINS UNIVERSITY
** DOG DIED IN 8 DAYS, RING CLEAN

FIGURE 3.

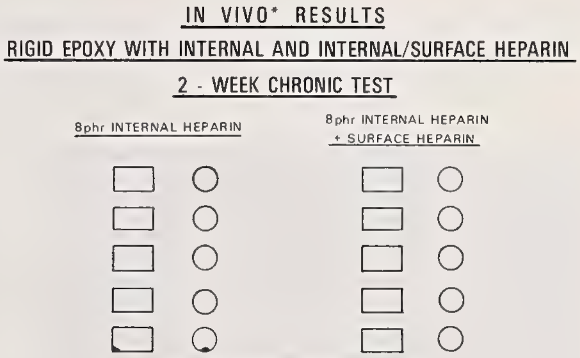
IN VIVO* RESULTS
RIGID EPOXY WITH INTERNAL AND INTERNAL/SURFACE HEPARIN
2 - WEEK CHRONIC TEST
8phr INTERNAL HEPARIN
8phr INTERNAL HEPARIN + SURFACE HEPARIN

*Dr V L GOTT, JOHNS HOPKINS UNIVERSITY

FIGURE 4.

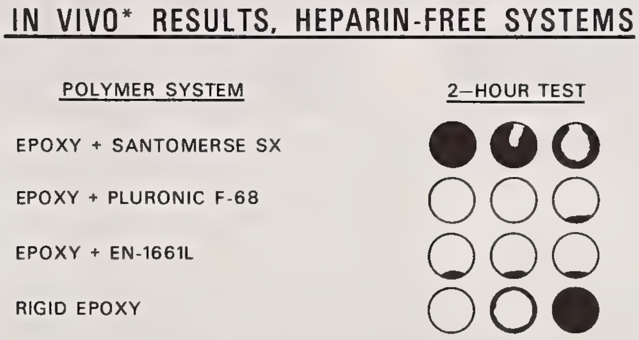

*Dr. V.L. GOTT, JOHNS HOPKINS UNIVERSITY

FIGURE 5.

Figure 3 illustrates in vivo results obtained on heparin-containing epoxy polymers cured with Ajicure B-001. With 3 phr of heparin, three rings were completely clear in the 2-hour, acute test. In chronic, 2-week tests, three rings also remained completely clean. The Ajicure-cured samples are much tougher and stronger for a given flexibility and appear to be very promising systems for construction of implantable prostheses.

Evaluation tests of these heparinized materials on a separate contract for the National Institute of Arthritis and Metabolic Diseases has shown that cannula tips remain patent for up to 7 months or longer without clot formation.

Figure 4 compares data obtained on an epoxy polymer containing 8 phr of internally incorporated heparin with the same heparin-containing polymer having added ionically-bonded surface heparin. As indicated, both materials did extremely well in the chronic 2-week test with only one small bit of thrombus in one of 5 rings in the internally heparinized material, and none in 5 rings of the combined internal and external heparinized rings. The slight improvement noted in the combined internal/external heparinized ring is not deemed sufficient to establish the merit of this system. However, the combination approach is believed to provide some added protection for patient safety.

Heparin-free Polymers.

Heparin-free systems for obtaining nonthrombogenic activity were also studied. Table 8 summarizes the products prepared. Flexible epoxy polymers with Santomerse SX* and Pluronic F-68* added, rigid epoxy polymers with EN-1661L*, hydrophilic polyurethanes, and vinylpyridine/ethyl acrylate copolymers were examined.

TABLE 8

HEPARIN-FREE SYSTEMS STUDIED

FLEXIBLE EPOXY + SANTOMERSE SX*
FLEXIBLE EPOXY + PLURONIC F-68**
RIGID EPOXY + EN-1661L***
HYDROPHILIC POLYURETHANES
VINYLPYRIDINE/ETHYL ACRYLATE COPOLYMER

*SODIUM ALKYLBENZENE SULFONATE
**NON-IONIC DETERGENT
***FROM ENDO LABORATORIES

Table 9 illustrates the preparation of flexible epoxy polymers containing three of the additives identified on the previous slide at concentrations of 2-5 phr. The procedure for incorporating these additives is the same as that used in incorporating heparin into epoxy polymers. In in vitro blood clot tests, only the sample containing Santomerse SX showed increased thromboresistance.

TABLE 9

HEPARIN-FREE FLEXIBLE EPOXY POLYMERS

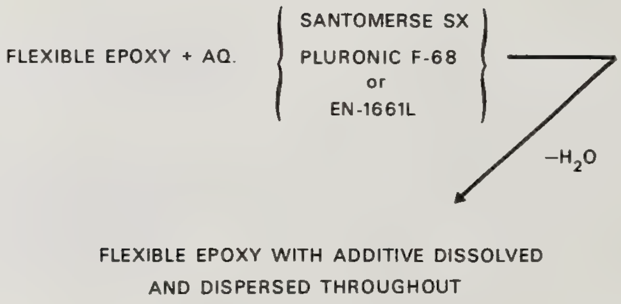

---

*Santomerse SX - dodecylbenzene sulfonate
Pluronic F-68 - copolymer of PO/EO 20/80, mol. wt. 1750
EN-1661L - 1,1' - tetramethylene bis-1,2,3,4-tetrahydro-6,7- dimethoxyisoquinoline.

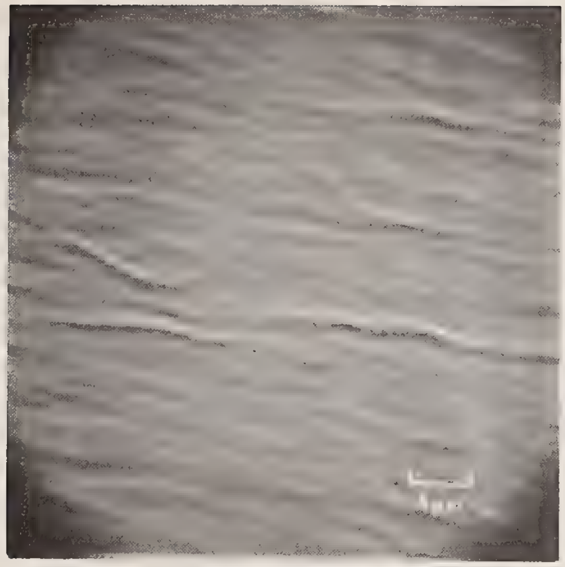

FIGURE 6. ROUGH AREA. RIGID EPOXY WITHOUT HEPARIN (CONTROL)

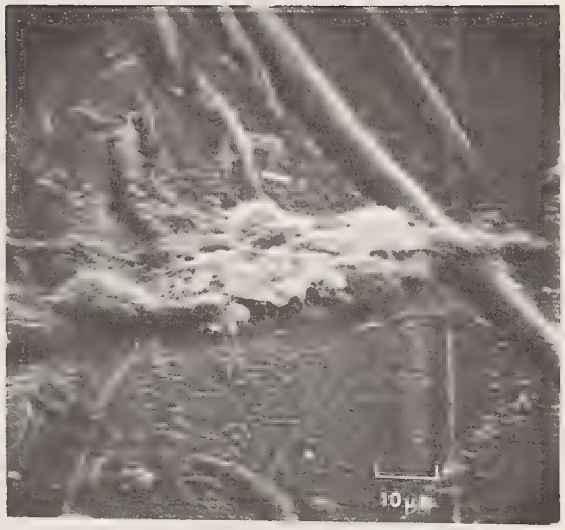

FIGURE 7. RIGID EPOXY WITHOUT HEPARIN EXPOSED TO BLOOD BANK BLOOD FOR 2 HOURS

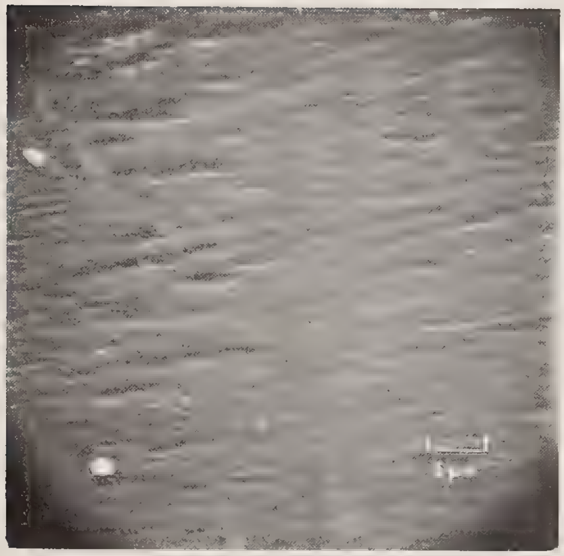

FIGURE 8. SMOOTH AREA. FLEXIBLE EPOXY WITH 8 PHR HEPARIN (CONTROL)

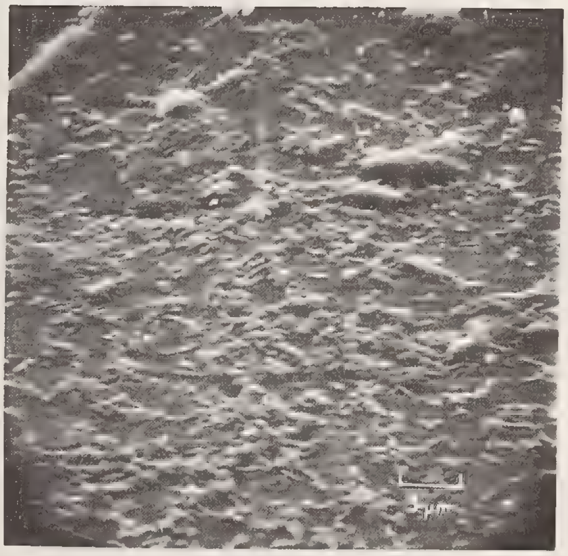

FIGURE 9. FLEXIBLE EPOXY WITH 8 PHR HEPARIN AFTER 24 HOURS IN VENA CAVA OF DOG

Figure 5 presents the in vivo results obtained by Dr. Gott on these three heparin-free systems. As shown, the Santomerse SX system performed very poorly in the 2-hour acute test. Both the sample with Pluronic F-68 and EN-1661L showed sufficient activity in the 2-hour test to warrant additional testing in the chronic 2-week test. The rigid epoxy with no additives present had slight thromboresistance. Recent chronic test results received from Dr. Gott have shown the Pluronic modified rings have excellent thromboresistance with 5 rings out of 5 being completely clear of thrombus.

Another nonheparin approach, hydrophilic polyurethanes, was investigated because it was felt a swellable, wettable, slick surface might reduce the tendency for platelets to adhere, and thereby help prevent initiation of the clotting mechanism. Table 10 illustrates the preparation of this type of material. Carbowax 600 and varying amounts of CP-260 were reacted with tolylene diisocyanate. The degree of swelling in saline solution increased as the concentration of the CP-260 (a trifunctional crosslinking agent) decreased. As the degree of swelling increases, the strength properties decrease. Therefore, a strong, highly swollen material can probably be best obtained as a thin coating, firmly attached to a more hydrophobic backing. An increase in swelling index did not provide greater thromboresistance in in vitro blood clotting tests. However, materials of this kind must be examined in in vivo studies before a decision on their utility can be made.

TABLE 10

HYDROPHILIC POLYURETHANES

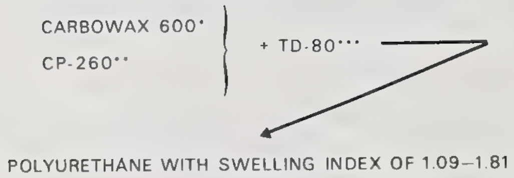

*Polyethylene glycol, mol. wt.~600

**Tris (hydroxypropyl) glycerine

***Tolylene diisocyanate

Another heparin-free polymer system that we believe merits study is the vinylpyridine/ethyl acrylate copolymer shown in Table 11. This is a versatile material since it can be hydrolyzed to form a polyampholyte containing both amine and potassium carboxylate groups. Alternately the copolymer can be quaternized to form a quaternary; or hydrolyzed and quaternized to provide a polymer with quaternary and carboxylate groups. These studies were completed through the formation of the quaternized copolymer. In vitro blood clot tests showed improvement in thromboresistance in some samples. Hydrolysis studies and in vivo tests are scheduled.

TABLE 11

VINYLPYRIDINE/ETHYL ACRYLATE COPOLYMER

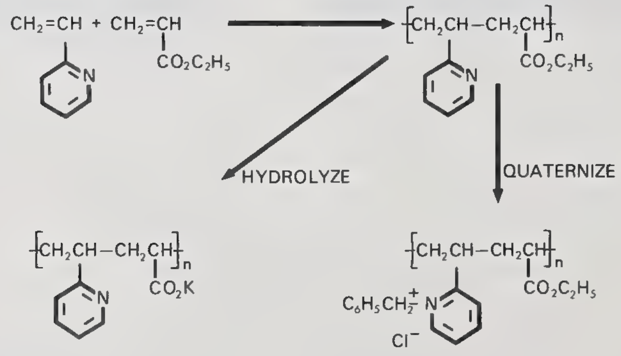

The hydrophobic/hydrophilic balance in this interesting series of polyampholytes can be adjusted by incorporating a third hydrocarbon type monomer such as ethylene. Terpolymers of ethylene/vinylpyridine/methyl acrylate have been synthesized but not yet evaluated.

Scanning Electron Microscopy.

The third task of the current program involved the use of the scanning electron microscope to study the surface characteristics of various candidate polymers at high magnification (e.g., 2,000 diameters). It should be emphasized that this was of necessity a minor portion of our program and was intended to establish the utility of this instrument for evaluating surface effects. The polymers examined included rigid and flexible epoxy polymers, with and without heparin, exposed and unexposed to blood. In view of the considerable promise of the heparinized epoxy system in both *in vitro* and *in vivo* tests, several electron scanning microscope pictures were made of these surfaces and some of these are shown in the following figures.

Figure 6 is a micrograph of the surface of a rigid epoxy polymer that contains no heparin and has not contacted blood. Figure 7 shows this same rigid epoxy, without heparin, after exposure to recalcified citrated blood bank blood for 2 hours at 37°C. Although this picture is magnified less than the preceding one, it is apparent that an appreciable amount of material has been deposited on the surface. The next figure (Figure 8) shows the surface of a flexible epoxy with 8 phr of heparin incorporated throughout. Figure 9 shows how the surface character changes on exposure to dog's blood for 24 hours in the vena cava. This particular specimen was nearly thrombosed in this time, probably due to inadequate degassing after sterilization. The surface is nearly completely covered with adsorbed material.

The final figure in this series (Figure 10) depicts the surface of an identical ring of flexible epoxy of 8 phr heparin implanted for 2 weeks in the vena cava of a dog. This sample was clot-free after the 2-week period. The amount of surface deposits is much less than was evident on the slide of heparinized material which thrombosed. Our conclusions from this study are that in samples exposed to blood, heparinized or not, the scanning electron microscope could be valuable in showing something of the nature and the amount of deposits that result. Detailed examination and identification of the deposits would be desirable.

Preparation of Samples for Other Contractors.

As the fourth task in the current contract, we were requested to prepare samples of our most promising material for evaluation by other contractors. The list of contractors and the type of sample required are shown in Table 12. The samples submitted to these contractors were semi-flexible epoxy polymers containing 3 and 7 parts of heparin per 100 parts of resin (phr) and a control containing no heparin. As illustrated, a rather wide variety of shapes and types of castings and coatings were required to complete this assignment. The fabrication of intraaortic balloons and the left ventricles as requested by NIH is now in progress. Preparation of all of the other test samples has been completed.

TABLE 12

EVALUATION SAMPLES FROM HEPARINIZED EPOXIES

Samples	Company
Discs	Battelle
Rings	Johns Hopkins
Paddles, coated tubes	U. North Carolina
Coated cover glasses	Avco Everett
Pellets	Cordis Corp.
Rings, tubes	State University of New York
Balloons with catheter	N.I.H.
Left ventricle	N.I.H.
Microspheres	Travenol Lab.

Some of the first results of these evaluations by other contractors are just beginning to be received. Dr. R. G. Mason at the University of North Carolina reported that in contrast to other surface heparinized materials, he was unable to remove the heparin from our products by his usual extraction procedures. In his letter to us on April 4, he stated: "In short, we are unable to test the heparinized materials without resorting to an elaborate, time consuming, sterile leaching process. These materials appear to release heparin slowly whether by design or otherwise."

FUTURE RESEARCH PLANS

Our plans for continuing research and development on thromboresistant materials, components, and designs for circulatory assist polymers are summarized below:

1. We expect to complete *in vivo* tests of blood compatibility on heparinized flexible and rigid epoxy polymers.
2. We shall complete the preparation of test specimens for evaluation by other contractors plus the balloons and ventricles for the National Heart Institute.
3. We shall also continue studies to develop nonthrombogenic polymer systems that do not contain heparin.

DISCUSSION

MR. GRODE: Several years ago we showed at Battelle that epoxy resins cured with amines could ionically couple heparin, and I was wondering if you had any data which indicate that in fact you have covalently bonded heparin in your system?

MR. SALYER: I think you are right. It could happen, since heparin contains hydroxyl to solubilize it. We have done some work to obtain data to support this, but as yet this has not been completed. I think what I stated was that we felt certain that a good deal of chemical reaction does occur in terms of covalent bonding. The ionic bond is formed when you have the amine groups quaternized. I don't know what you would get if the amines are not quaternized. Ionic coupling would certainly be less.

DR. FOURT: On your last scanning electron microscope photograph, would you know whether there are any topographical indications related to the direction of the flow of blood across the specimen?

MR. SALYER: You mean, were the particles oriented in the direction of the flow of blood?

DR. FOURT: Correct.

MR. SALYER: I don't remember the figure that well. The photograph showed the ring after it had been sliced open down the equator. I suspect that the ring was oriented from top to bottom, i.e., the direction of blood flow would have been from the top to the bottom of the figure as shown in the slide. I think this is correct, but I am not sure. Did you notice any significant difference in the figure?

DR. FOURT: Well, of course, that all depends upon the orientation of the picture. But I was thinking of Dr. Dutton's and other people's studies, on which we will hear some more, of deposition in the presence of flow.

MR. SALYER: I didn't notice any strong orientation of the small rods in the photograph.

DR. LEONARD: Is Pluronic a nonionic detergent?

MR. SALYER: Yes. I think I indicated the composition. It is a copolymer. Incidentally, a series of these Pluronics are available, containing ethylene oxide and propylene oxide in various ratios and molecular weights. You can get a whole spectrum of these. This Pluronic F-68 is a 20/80 copolymer of propylene oxide/ethylene oxide. The molecular weight of the propylene oxide segment is about 1750, and the molecular weight of the final copolymer about 8,000.

DR. LEONARD: Is the copolymer a polyether?

MR. SALYER: Yes, it is a hydroxyl-terminated polyether.

DR. LEONARD: May I ask, what was the rationale for trying it?

MR. SALYER: What was the rationale for trying it? I saw a publication where this pluronic material had been used on a patient that was on the heart-lung bypass. Much less hemolysis and degradation of blood was noticed when they introduced a small amount of pluronic. Therefore, it seemed like a good thing to try. The second part of the rationale, is that we always felt that a balance of hydrophilic/hydrophobic properties at the blood/material interface might be important. We still do. For instance, this is the rationale for the polyurethane series, as well.

DR. LEONARD: May I have one other question? Does the pluronic chelate calcium, or does it combine with calcium at all?

MR. SALYER: I sure wouldn't expect it to, since similar materials do not. It is a very simple detergent. As I said it is a polyether, and not an unusual one. In fact, these pluronics are also used as components in conventional urethanes.

DR. NOSE: About two years ago at the Gordon Research Conference, I advocated to Mr. Salyer the use of the nonionic pluronic detergent series to make the blood contacting materials soapy. Then platelets and proteins will not attach to the surface of the materials. I am very glad that Mr. Salyer proved that possibility and I would like to ask one question: There are a great number of pluronic series. Did you ever use materials other than Pluronic F-68?

MR. SALYER: Sometimes the test of a good idea is whether or not someone else has already thought of it. But the exact composition is critical, and we now have a series of these nonionic surfactants under investigation. I think this is a very promising approach, for two reasons: 1. The pluronic can be used as an additive directly, and be effective. 2. More importantly, I see a very clear route to incorporating these monomers directly into either the urethane or the epoxy polymers.

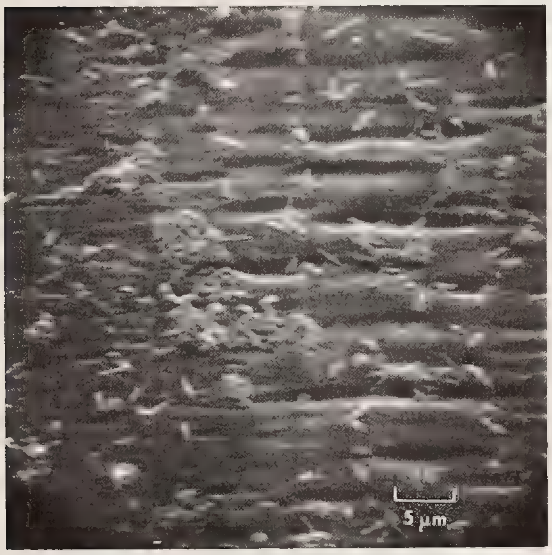

FIGURE 10. FLEXIBLE EPOXY WITH 8 PHR HEPARIN AFTER 2 WEEKS IN VENA CAVA OF DOG.

CHAPTER 7

ANIONIC CELLULOSE: A POTENTIAL BLOOD COMPATIBLE MATERIAL

R.G. Nemchin, A.R. Patel, H.I. Able, L. Sims and D.M. Speaker

Melpar, Inc., Falls Church, Virginia

The selection of the natural polymer, cellulose, was influenced by the consideration that the intimal surface is partly composed of polysacharides bearing an electrical potential. Our early studies demonstrated that chemically modified celluloses were thromboresistant *in vitro* and showed promise *in vivo*. The degree of thromboresistance depended on the type and distribution of the modifying functional group; anionic celluloses (phosphate, sulfonate, carboxymethyl) were essentially blood compatible, while cationic celluloses (diethylaminoethyl, quaternary ammonium) were not. If the degree of cellulose functional group substitution was greater than 0.10 (i.e., one group per 10 glucose residues) significant thromboresistance was observed. The weakly acidic carboxymethyl group was the most effective. Recent structure-function studies with carboxymethyl cellulose (CMC) and structurally related derivatives (oxy-, α - propionate-, esterified CMC) show a direct relationship between D. S. and *in vitro* thromboresistance and solubility. This relationship holds for both the oxycelluloses and the CMC, but not for the other derivatives. In fact, chemical modification (e.g. esterification) of the carboxymethyl moiety did not result in thromboresistance. In the case of the effective materials, thromboresistance was not due to slowly solubilized CMC acting as an anticoagulant, but to the fixed carboxymethyl surface groups. Our findings suggest that: (1) a minimum number of active groups along the polymer chain is required; (2) the surface should be hydrophilic; (3) thromboresistance is related to substitutent configuration; (4) thromboresistance is not a direct function of increasing acidity (negativity). Our studies also indicate that, under physiological conditions, significant quantities of calcium ions do not bind to surface carboxyl groups. The mechanical properties of CMC materials are greatly improved by cross-linking with diisocyanates or compounding with a secondary polymer such as polyvinyl alcohol.

INTRODUCTION

Our research has been directed toward two principal goals: (1) the development of a practical cellulosic material which is compatible with blood and (2) an understanding of the fundamental structure-function relationships of such blood compatible materials.

Our earlier studies[1] were largely concerned with evaluating the blood compatibility properties of celluloses which had been chemically modified so that the different types of modifying functional groups conferred surface charges of varied intensities and polarities. In these studies we showed that the degree of *in vitro* clot resistance depended upon the type and distribution of the modifying functional group. The anionic celluloses such as carboxylate, phosphate, and sulfonate were essentially nonclotting *in vitro*, non-hemolytic and non-adsorptive toward the soluble and formed elements of blood, while the cationic celluloses such as diethylaminoethyl and quaternary ammonium were not. The most consistent results were obtained with highly substituted cellulose derivatives. This suggested the importance of a minimum density of surface functional groups in order to obtain a thromboresistant surface.

As a result of these studies, we focused our attention on the highly substituted carboxymethyl celluloses as the most promising derivatives for more detailed study. This study was designed to determine the physical and chemical properties of this material as they relate to polymeric structure and thromboresistance both *in vitro* and *in vivo* and to optimize the desired mechanical properties for useful application. The results lend support to the hypothesis that a material which chemically resembles the primary constituents of the vascular intima should be inherently non-thrombogenic.[2]

STRUCTURE-FUNCTION STUDIES (IN VITRO)

The structure-function studies were aimed at correlating *in vitro* clot resistivity with cellulose functional group structure.

Effect on Cellulose Substituent (Functional Group) on Clot Resistance.

The particular cellulose derivatives examined were selected because they represent structural analogs of the anionic derivative, carboxymethyl cellulose. The choice of functional groups took into account the presence or absence of ionic charge, degree of acidity (negativity), substituent chain length, and hydrophilic or hydrophobic character of the substituent.

The degree of substitution was, in each case, greater than 0.2,i.e.,there was, on the average, at least one functional group for every 5 glucose residues in the cellulose polymer chain. The degree of substitution was determined by potentiometric titration. In vitro clotting tests were performed according to the modified Lee-White method. The highly substituted celluloses, though initially water soluble, form insoluble films upon drying, chiefly through internal hydrogen bonding and this is the form in which they were tested. A summary of the results with several films of each type is presented in Table 1.

TABLE 1

RELATIONSHIP BETWEEN CELLULOSE FUNCTIONAL GROUP STRUCTURE AND IN VITRO CLOT RESISTANCE

Cellulose Derivative	Structure	Clotting Time (Min.)[a]
Anionic		
carboxymethyl-	$-O-CH_2COOH$	> 60
oxy[b] -	-COOH	> 60
carboxyethyl-	$-O-CH_2CH_2COOH$	22 ± 2
α -propionate-	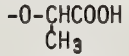 $-O-\underset{CH_3}{CH}COOH$	14 ± 2
sulfonate-	$-O-SO_3H$	45 ± 5
Nonionic		
hydroxyethyl-	$-O-CH_2CH_2COH$	8 ± 2
hydroxypropyl-	$-O-CH_2CH_2CH_2OH$	6 ± 1
Ester		
carboxymethyl	$-O-CH_2COOCH_3$	10 ± 1
acetate	$-OOCCH_3$	6 ± 2
Hydrazide		
carboxymethyl	$-O-CH_2CONHNH_2$	27 ± 2
Glass (Control)		7 ± 1

a Clotting tests were limited to 60 minutes duration after addition of 0.75 ml of 0.1 M $CaCl_2$ to 5 ml of fresh ACD blood.

b Oxycellulose is natural wood or cotton cellulose in which the primary (C_6) alcohol units have been oxidized to carboxylic acid groups.

The data show that, although many of the cellulose derivatives are generically similar to the carboxymethyl cellulose, not all result in an in vitro clot resistant surface. The results obtained with the nonionic and esterified cellulose derivatives demonstrate the importance of the negatively charged equivalent structure. However, not all of the anionic celluloses were clot resistant to the same degree.

For example, increasing the length of the cellulose carboxymethyl side-group by the addition of a single carbon (carboxyethyl: CH_2CH_2COOH), or by the introduction of an iso-substituted moiety (α -propionic: $-CH(CH_3)COOH$), does not result in a clot resistant material. Clot resistance thus appears to be sensitive to the type of cellulose substituent as well as to charge.

Esterified carboxymethyl cellulose and cellulose acetate are less hydrophilic (as determined by contact angle measurements and solubility studies) than the anionic celluloses and are correspondingly less clot resistant as well. With the exception of these derivatives, all the others form very hydrophilic surfaces. Clearly, a hydrophilic surface, while necessary, is not alone a sufficient condition for non-clotting in vitro.

Effect of Degree of Substitution (D.S.) on Clot Resistance.

In order to establish the importance of maintaining a minimum density of ionic surface groups to obtain a clot resistant material, a series of carboxymethyl derivatives differing only in the degree of substitution, (ranging from 0.02 to 1.1) were synthesized and examined with regard to their clot resistance (Table 2).

TABLE 2

IN VITRO CLOTTING TIMES OF CARBOXYMETHYL CELLULOSE FILMS OF DIFFERENT DEGREES OF SUBSTITUTION (D.S.) [a]

Preparation No. Cell-O-CH_2COOH	% Solubility in Water (25°C)	D.S. (water soluble fraction)	Clotting Time [b,c] (Min)
5	1.2	0.02	12
3	7.0	0.06	13
1	28.6	0.11	No Clotting
8	83.0	0.28	"
4	90.1	0.31	"
2	95.0	0.63	"
12	96.0	0.65	"
6	100.0	1.1	"

[a] Clotting tests performed on insolubilized films of the initially water-soluble fraction.

[b] Clotting tests limited to 30 minutes after addition of 0.75 ml of 0.1 M $CaCl_2$ to 5 ml fresh ACD blood.

[c] The clotting time of blood on glass surfaces was 7-8 minutes.

The experiments correlating CMC at different D.S. values with clot resistance indicate a clear requirement for a minimum number of carboxymethyl groups along the polymer chain: the CMC should have at least a D.S. = 0.1 to 0.2, i.e., one anionic group per 10 or 5 glucose residues, to demonstrate significant clot resistance. It is therefore essential that the density of anionic groups be sufficiently high to increase the probability that a uniform distribution of charged groups over the blood-contacting surface is ensured.

The solubility behavior of the modified CMC raised the question that the observed clot resistance of insolubilized CMC films might be due to partial solubility of the surface of the film in the blood, the mode of action being in much the same fashion as the soluble anticoagulant, heparin. To test this, CMC was added to ACD blood so that the CMC concentration ranged from 1 microgram to 100 mg per ml of blood to which $CaCl_2$ was subsequently added and the clotting times recorded.

In all cases, the clotting times were the same as the controls (~ 9 min). These results indicated that the clot resistant behavior of the HCMC films is not due to solubilization of the film surface by the blood, nor can it act in the soluble form as an anti-coagulant at these concentrations.

Cellulose Functional Group Acidity and Clot Resistance.

In vitro clot resistance does not appear to be a simple linear function of the degree of acidity (negativity) of the modifying moiety (Table 3).

TABLE 3

CELLULOSE SUBSTITUENT ACIDITY (NEGATIVITY) AND IN VITRO CLOT RESISTANCE

Derivative	pK	Clotting Time (Min.)[a]
Cellulose	5.9	12
CMC-hydrazide	5.2	25
CMC	3.5	No Clotting
Cellulose ethylsulfonate	2.2	40
Cellulose sulfate	1.8	45

[a] Clotting time determinations were terminated 60 minutes following recalcification.

These results suggest that there may be some optimal range which is consistent with minimal deleterious interaction with blood. We have not yet completed the correlation of pK values with zeta potentials, but it is interesting to note that the zeta potential in Ringer's solution for CMC film is -4 to -7 mv and that for cellulose sulfate is approximately -15 mv.

Binding of Calcium by Carboxymethyl Cellulose.

The question has been raised as to whether carboxylated polymers as blood contacting materials are effective because of the possibility of extensive Ca^{++} binding. Such bound Ca^{++} is supposedly prevented from serving as a cofactor in the clotting process, the carboxylated polymer acting as a chelating agent. Any material which would irreversibly sequester considerable quantities of cofactors, such as Ca^{++}, may well impair the normal clotting mechanism in blood subsequent to contact with such a material.

Since carboxymethyl cellulose (CMC) behaves as a weakly acidic cation exchanger, several experiments were performed to answer the following questions: (1) Does CMC bind Ca^{++}, (2) If so, to what extent,and (3) is the binding reversible under physiological conditions? Although it is not possible to describe these experiments in detail here, the following example illustrates the phenomenon.

It is well known that the basic dye methylene blue, reacts with free cellulose carboxyl groups, the latter being the sodium salt or the free acid. The dye can thus be used to simply demonstrate the binding of calcium by CMC when a section of HCMC film is soaked in a $CaCl_2$ solution. If the film is subsequently transferred to a solution of methylene blue, very little dye is bound to the film, i.e., dye binding to the carboxyl groups is blocked by the presence of calcium. If a section of CMC film is soaked in a solution containing both $CaCl_2$ and NaCl in physiological concentrations, and then transferred to the methylene blue solution, a large amount of dye is taken up by the film.

This experiment shows that calcium can bind to CMC. However, it binds the ion only in the absence of sodium ions. From other types of experiments we have found that under these conditions the calcium ion binds stoichiometrically, i.e.,one calcium ion occupies two carboxyl sites on CMC.[4] However, in the presence of physiological concentrations of NaCl, calcium does not sensibly bind to CMC. The results suggest that the CMC is in a system of dynamic equilibrium with the low molecular weight (and possibly the macromolecular) solutes of blood.

These studies provide guidelines for the selection of an optimal blood compatible cellulose material. The carboxylated celluloses were shown to be clot resistant *in vitro* and promising *in vivo*.[5] Our earlier findings that platelet counts were undisturbed after contact with carboxymethyl cellulose have been confirmed by interference microscopy.[6] These results further supported the conclusion that carboxylated cellulose may be in a state of reversible equilibrium with the formed elements of blood.

MATERIALS DEVELOPMENT

Meaningful application of this material to the needs of the Artificial Heart Program can require either rigid or flexible forms.

The carboxymethyl cellulose may be prepared in three forms: (1) coatings, (2) films and (3) rigid forms, each with its own particular set of mechanical properties. Consequently, a constrained set of applications exists for each form.

In order to impart a wider range of desirable mechanical properties (and potential applications) to the CMC (for example, increased flexibility and tear strength) and to meet the configuration requirements of the materials evaluators, three basic approaches were explored.

One approach consisted of depositing the substituted cellulose, as a coating, on a substrate having the desirable mechanical properties. In the second approach, we used cross-linking agents to modify the inherent mechanical properties of the CMC. In the third approach, we formulated a composite with a chemically related secondary polymer possessing improved mechanical properties.

Carboxymethyl Cellulose Coatings (HCMC) and Films.

It may be recalled that the initially water soluble Na-CMC can be converted to the free acid by ion-exchange techniques. Water insoluble, isotropic films can thus be prepared with this material by casting the films and air drying. The insolubility is due to the formation of hydrogen bonded crystallites into a lattice structure upon drying. The crystalline regions are essentially inaccessible to solvent molecules.

Films cast from aqueous solutions of carboxymethyl cellulose have the following chacteristics (Table 4) when tested according to ASTM procedures.

It can be seen that, although the tensile strength of these cellulose films is high, the tear strength is poor. Also, the elongation and flexural properties are not satisfactory for certain applications. Since carboxymethyl cellulose is not thermoplastic nor thermosetting it cannot be handled by the usual forming techniques such as molding, extruding, etc., but smooth, continuous coatings may be deposited on hydrophilic surfaces.

Coatings of HCMC on surfaces which maximize interfacial bonding are consistently clot resistant *in vitro* and show moderate thromboresistance in acute *in vivo* experiments. Previously, polycarbonate rings were used as the rigid substrate for the *in vivo* testing of HCMC coatings. The polycarbonate ring does not permit optimal coating because its surface is hydrophobic and coating discontinuities easily occur. Consequently, the results were not consistent from ring to ring, i.e.,some rings were completely free of thrombi while others were thrombosed. We concluded that the achievement of consistently thromboresistant surfaces *in vivo* for our material depends on minimizing both surface roughness of the substrate material and coating discontinuities.

TABLE 4

PHYSICAL AND CHEMICAL PROPERTIES OF INSOLUBILIZED CARBOXYMETHYL CELLULOSE FILMS (HCMC)(D.S.=0.8)

Physical Properties	ASTM	
Tensile Strength, psi	D882	5000-7000
Elongation, %	D882	15-25
Tear Strength, gm/mil	D689	0.5-2.0
Flex Strength	D643	Fair
Heat Seal Range		Not Sealable
Water Absorption (24 hrs)	D570	High
Water Vapor Permeability	E96	High
Chemical Resistance		
Strong Acids	D543 or D1239	Poor
Strong Alkali		Poor
Organic Solvents		Excellent

More recently, a hydrophilic material was selected for coating with HCMC. This material is a commercially obtained vulcanized cellulose tubing (Forbon) from which vena cava rings were machined. The vulcanized cellulose material, by itself, is not clot resistant in vitro or in vivo. These rings were coated with the HCMC formulation. The coatings on this material appeared to be firmly adherent.

Acute in vivo testing of these HCMC coated rings demonstrated moderate thromboresistance. Again, the results were not consistent; some rings were wholly free of thrombus, while others showed evidence of limited thrombus formation at the atrial end of the ring. In view of the fact that the rings were streamlined, the inconsistencies may be due to the nature of the substrate surface. Since the substrate material imbibes the HCMC to some extent, multiple coatings (more than 3 to 4 coatings) appear to be essential and currently are being examined. In addition, the fibrous character of the substrate surface imposes a roughness which, we believe, may be a potential cause of turbulence.

Cross-Linked Carboxymethyl Cellulose (CUFAB).

A preparation that looks promising according to the in vivo results is the urea-formaldehyde butanol cross-linked CMC. This formulation which we call CUFAB, was prepared in order to fabricate vena cava implant rings (Gott rings) of the CMC itself as opposed to using it as a coating. During the chemical reaction the cellulose becomes cross-linked at the hydroxyl groups leaving the carboxyl groups free.

The final product is obtained as a water-insoluble material which may be compression molded and then machined into rings. This material can be autoclaved without evidence of degradation. CUFAB was nonclotting in vitro and the in vivo implants remained patent during the 2-hour acute test period. Exposure of CUFAB to blood in vitro for one week did not appear to alter its mechanical properties. There was no perceptible swelling, as is common with unmodified celluloses. For these preparations, highly substituted CMC (D.S.=1) was used. In contrast, rings of CUFAB, prepared from CMC with a D.S.=0.07, were not thromboresistant in vivo. This result is consistent with the in vitro results mentioned previously, i.e., a minimal number of anionic surface groups must be exposed to the blood for the material to demonstrate clot resistance. The CUFAB, however, is extremely friable and difficult to machine. Also the preparations are non-flexible and CMC film, because of its crystalline character, is also not sufficiently flexible in itself to meet the many applications that absolutely require flexible material.

Carboxymethyl Cellulose Polyvinyl Alcohol Composites.

Our approach to this requirement has been to use a secondary polymer in admixture with CMC. The purpose was to confer upon the latter the desirable tensile and tear strengths and properties of the secondary polymer while still retaining the intrinsic clot resistive behavior of the CMC. For this secondary polymer, we chose polyvinyl alcohol (PVA).

Like cellulose, PVA is a polyhydric alcohol. Ordinarily water-soluble, PVA can be insolubilized by chemical or thermal cross-linking. Thermal cross-linking (diether linkage) results in a water-insoluble, though hydrophilic, film which is both tough and flexible. The flexibility is enhanced when the film is wet.

These PVA films by themselves are not clot resistant in vitro. In these preliminary studies mixtures of PVA with HCMC in various proportions were examined with regard to the clot-resistant behavior and mechanical properties of the composites. In some instances, polyvinyl methyl ether/maleic anhydride (PVMMA) was added to the PVA to facilitate cross-linking. In vitro clotting tests were conducted in the usual manner (modified Lee-White). The results thus far are shown in the next table (Table 5).

TABLE 5

IN VITRO CLOTTING PROPERTIES OF PVA-HCMC COMPOSITE FILMS [a]

Preparation	Composition PVA/HCMC (W/W)	Clotting Time (Min.) [b]
PVA	100%	6
PVA/PVMMA [c]	10/1	14
PVA-PVMMA/HCMC [c]	1/2	No Clotting
PVA-PVMMA/HCMC [c]	3/1	No Clotting
PVA-PVMMA/HCMC [c]	5/1	4
PVA/HCMC	1/1	No Clotting
PVA/HCMC	3/1	20
PVA/HCMC	5/1	8

a Films were cast from a water solution and thermally cross-linked (with and without PVMMA).
b Clotting tests were limited to 60 minutes (37°C).
c PVMMA (polyvinyl methyl ether/maleic anhydride). Concentrations were maintained at 10% of the PVA concentration.

The table shows that PVA-HCMC films are clot resistant *in vitro* if blended in certain proportions.

The striking enhancement in flexibility of the HCMC films, when PVA is incorporated into the formulation, is reflected in the next table (Table 6).

TABLE 6

MECHANICAL PROPERTIES OF ISOTROPIC PVA-HCMC COMPOSITE FILMS [a,b]

	HCMC	PVA	PVA/HCMC (3/1)
Tensile Strength, psi	5000-7000	1000-5000	5500-7200
Elongation to Break, %	15-25	600	200
Elastic Recovery (100 cycles),			
at 25% elongation, %	30	100	100
at 50% elongation, %	-	90	99

a All measurements were performed on 10 mil thick films at 100% relative humidity with an Instron testing machine.
b Films were cast from aqueous solution, air dried at 25°C, cured at 115°C for 3 hours, treated with 0.1N HCl and washed in water until neutral. Films were stored at 4°C and 90% humidity until tested.

From the above data it is quite clear that a significant degree of elasticity is imparted to the HCMC by forming a composite with PVA. This "rubberized" cellulose has, at this time, undergone more than 60,000 successive twist and stretch (~ 12% elongation) cycles at 37°C in physiological saline solution without obvious impairment of tensile or flex properties. Of particular significance is the fact that at 25% elongation (approximately 2 times greater than that experienced by a CAD bladder) stretch recovery is virtually complete with no evidence of permanent set.

DISCUSSION AND CONCLUSIONS

It is inferred that for thromboresistance to be observed, the cellulose must contain substituents which (1) confer a moderate negative charge to the polymer, such charges being uniformly distributed over the surface; (2) provide a hydrophilic surface;and (3) are present in sufficiently high density along the polymer chain. It is also shown that CMC cannot serve as a blood soluble anticoagulant and that it does not bind sufficient calcium to interfere with the clotting process by calcium sequestration.

Several approaches have been explored in order to impart a wider spectrum of desirable mechanical properties to the cellulose without sacrificing the thromboresistant properties. The CUFAB is a water-insoluble material which can be compressed into rigid forms and has been found to be non-thrombogenic in vivo. However, this formulation is not easily cast into mechanically durable films and has not been extensively tested. The incorporation of PVA into the CMC formulation strikingly improves the mechanical properties of HCMC films as well as providing an in vitro non-clotting surface.

We have successfully treated cellulose acetate surfaces so that the acetate groups have been replaced with carboxymethyl groups. In addition, carboxymethylated PVA surfaces have also been successfully prepared. These materials are currently undergoing fabrication into the forms necessary for in vivo evaluation.

REFERENCES

1. Nemchin, R. G., Evaluation of Biopolymers as Blood-Compatible Materials, Annual Report, December 1968, Contract PH-43-67-1413.
2. Lyman, D. J., W. M. Muir, and I. J. Lee, Trans. Amer. Soc. Artif. Intern. Org., 11:301 (1965).
3. Srinivasan, S., and P. N. Sawyer, New Approaches in the Selection of Materials Compatible with Blood, Annual Report, 1968, Contract PH-43-68-75.
4. Tarkow, H., Abstracts, 156th National Meeting of the American Chemical Society, Sept. 1968.
5. Gott, V. L., Personal Communication.
6. Johnsson-Hegyeli, R., Personal Communication.

DISCUSSION

DR. HERSH: I am interested in the correlation you showed between pK's and clotting time. Are these actually measured pK's of the modified cellulose material, or are you assuming a pK for the group you have attached?

MR. NEMCHIN: No, these are actually measured pK values. They are done by potentiometric titration. The example, which we showed on the slide was that of carboxymethyl cellulose which has a pK of about 3.5. If I were to quote literature values, an analogous structure to this carboxymethyl functional group is acetic acid which has a pK of 4.7. So we can see that the carboxyl group in carboxymethyl cellulose (CMC) has a lower pK value.

MR. WALKUP: In your clotting studies did you expose your CMC membranes to calcium prior to doing the clotting time?

MR. NEMCHIN: We did this in last year's study. We found out it did not effect the clotting time values.

MR. BELLAMY: Does wetness have any effect on the strength of material? Must it be maintained in a wet condition?

MR. NEMCHIN: Which material are you referring to, Sir?

MR. BELLAMY: The last material that you discussed (PVA/HCMC).

MR. NEMCHIN: It is preferable to keep it wet. It does change on drying out, and becomes tougher, less rubbery and more plastic.

MR. STERN: Returning again to the pK value and the hydrazide, isn't the pK value for the hydrazide a pK_B value? If so, it is a positively charged residue instead of an anion.

MR. NEMCHIN: The hydrazide is a weak acid.

DR. KOLFF: Cellulose used to be in the realm of the artificial kidney people, and I see that Dr. Hastings is now trespassing into the artificial kidney field, and I am all in favor of it. I would like to ask the speaker, did I understand during his lecture that at a certain moment and for a certain substance he said that a change toward the negative of the surface potential resulted in longer clotting times? If that is so, is there some contradiction to point 4 in your abstract where you said that thromboresistance is not a direct function of increasing acidity?

MR. NEMCHIN: That only refers to the fact that the pK goes through a maximum. As we increase the acidity of the substance, we don't necessarily get a non-thrombogenic surface. The best results, at least in our system, is with the CMC which is a moderately acidic derivative. The sulphate or sulphonate derivatives did not give us as long a clotting time nor did the weakly acidic derivatives.

DR. KOLFF: Did you have a certain substance in which an optimum of negative surface potential gave you a longer clotting time?

MR. NEMCHIN: At least, within our system this seems to be the case. Whether this will hold for other types of surfaces, I don't know. Since cellulose is a natural polymer it might have peculiar characteristics which will not hold for synthetic polymers.

DR. SPAET: In evaluating prolonged clotting times, did you at any time transfer blood that did not clot in your experiments to a glass surface to show that it then clotted rapidly; indicating whether or not methyl cellulose which is a well known absorbent of clotting factors, might have removed some essential clotting components?

MR. NEMCHIN: No, but we had done this early last year when we were first looking at carboxymethyl cellulose. We then removed the blood from the test system, put it in glass, and it clotted normally.

DR. FALB: I wonder why you get the relationship between pK and clotting because pK's are down around 3 and 4 and 5. At the pH of blood, which is 7.4, you are going to have these groups essentially 100% ionized irrespective of the pK. They are going to have a negative charge at this pH, since their pK's are removed from the pH of the solution by several orders of magnitude. I don't see the basis for the relationship.

MR. NEMCHIN: We're just referring to pK as a method of distinguishing between a weakly acidic or anionic derivative and a strongly anionic derivative. Of course, confirmation will come with the determination of zeta potentials for each of these derivatives.

CHAPTER 8

POLYELECTROLYTE COMPLEXES AS ANTITHROMBOGENIC MATERIALS

H.J. Bixler, R.A. Cross and D.W. Marshall

Amicon Corporation, Lexington, Mass.

Amicon Corporation has been under contract to the NHI since July 1, 1966 to evaluate polyelectrolyte complexes ("Ioplex") as antithrombogenic materials. During previous contracts it was demonstrated by in vivo tests that a slightly anionic form of Ioplex was antithrombogenic. The present program at Amicon (since July 1, 1968) has been directed toward the furthur characterization of these materials. Sufficient tests have been completed to indicate a possible correlation between the polyanionic density and the thromboresistant characteristics. Further work to confirm this correlation is being undertaken. Reinforcement of the polyelectrolyte complexes has been accomplished by the use of polyester or special glass fabrics so that a range of strengths and stiffness can be made available. Attempts to improve the physical properties of the polymer by altering its basic structure have resulted in new materials which also exhibit antithrombogenic properties and may offer certain advantages over current systems. Techniques for fabricating both reinforced and unreinforced Ioplex shapes have been investigated and the necessary sterilization procedures developed. A primer has been developed for those substrates where adhesion is a problem. Special solvent systems are also being developed to facilitate the coating of sensitive substrates. Several forms of the resins have been supplied to other NHI contractors for evaluation.

INTRODUCTION

Since mid-1966 Amicon Corporation has been under contract to the National Heart Institute to evaluate polyelectrolyte complexes (Ioplex) as antithrombogenic materials for possible use in an artificial heart. During contracts prior to the present reporting period which began July 1, 1968, Amicon has demonstrated by in vivo tests performed by Dr. Vincent Gott, Johns Hopkins Hospital, that a slightly anionic form of Ioplex is essentially antithrombogenic. These tests were performed by inserting small rings, 9 mm long by 8 mm I.D., into the vena cava of dogs for periods of either two hours or two weeks (promising materials received the longer times), sacrificing the animal, and examining the rings for clots. The anionic complex which has shown the best results to date is Ioplex with 0.5 milliequivalents of anionic excess, and a gel water content of 40-50 percent. This material has been found to be almost completely antithrombogenic.

The present program is concerned with the further characterization of Ioplex resins. The basic resin, Ioplex 101, is a complex of poly(vinyl benzyltrimethylammonium chloride) and poly (styrene sulfonate). The ionic charge inherent in this material can be varied from cationic to anionic by adjusting the stoichiometry of the components. The investigation of the antithrombogenic properties of various ionic excesses is continuing; however, sufficient data have been gathered to indicate that the density of sulfonate groups might control antithrombogenic behavior. If the density of the anion does indeed control the polymer's in vivo behavior, then it should be possible to predict the thrombogenic behavior of other polyelectrolyte complexes.

In order to perform a useful function in the body any material even if antithrombogenic, must be able to withstand the mechanical forces imposed on it. A number of reinforcements for Ioplex have been investigated with particular success obtained from the use of lightweight fabrics including those made from glass, Dacron, carbon, and Nomex nylon. A major limitation in the reinforcement and adhesion of Ioplex resins has been the effects on the substrate of the acidic solution from which the resin is deposited. The aforementioned reinforcements are acid resistant, but such substrates as ordinary nylon-6,6 is not. For the protection of sensitive reinforcements or substrates, work on the use of non-acidic electrolytes for shielding solvents has been undertaken. These solvents contain a salt instead of the usual acid, and certain formulations show considerable promise. Improvement of the physical properties of polyelectrolyte complexes may also be accomplished by altering the basic structure of the polymer chain. At least one of these modified complexes has some antithrombogenic behavior and offers some advantages physically as well.

A significant proportion of Amicon's program with the National Heart Institute involves the preparation of samples for other NHI contractors. These samples are important for they not only yield information that may be difficult for Amicon to provide, but comments of the independent investigator can point to the direction that further research should take to provide the most fruitful returns. These samples have ranged from finely divided Ioplex powders to coated slides for blood impingement studies. Techniques to fabricate both these and many other shapes from reinforced and unreinforced Ioplexes have been developed along with the necessary sterilization techniques. Hence, we feel that these polyelectrolyte complexes will be quite valuable in the construction of artificial heart components.

RESULTS

Development of Polyelectrolyte Complexes

The basic polyelectrolyte complex on which most of Amicon's previous data has been gathered is an ionic hydrogel formed from the coreaction of poly(vinyl benzyltrimethylammonium chloride) with sodium polystyrene sulfonate, Ioplex 101. A theoretical schematic of the structure of this polymer is shown in Figure 1. It is doubtful that the chains are aligned as nicely as in the schematic, the probability being that the chains are twisted and the charges are more diffuse. An excess of one charge over the other is obtained by simply changing the ratio of one component to the other. When this was done and rings were submitted to Dr. Vincent Gott of Johns Hopkins Hospital for *in vivo* testing, it was found that a complex with 0.5 meq. excess, based on the dry weight of the resin, with a 40-55 percent water content was essentially antithrombogenic. Water content of these materials can be varied within limits by adjusting electrolyte concentration in the carrying (shielding) solvent used to deposit these materials. A series of Ioplexes of minimum water content with various ionic excesses has been made with the results shown in Figure 2. From this plot we can see the maximum charge density is at approximately 1.2 meq. excess anion per gram of dry resin. The best antithrombogenic material, however, has been shown to be at a portion of 0.5 meq. on the same curve. It appears that charge density alone is not responsible for antithrombogenic behavior. If, however, the density of sulfonate groups in the wet resin versus the milliequivalents of charge on the dry resin is plotted, as is done in Figure 3, we see that the maximum occurs in the correct position. The position of the other points on the curve seems to agree with the degree of antithrombogenic behavior as determined from the Gott tests. Thus it appears that the clotting tendency of Ioplex 101 is a function of sulfonate density.

A second polyelectrolyte complex has been developed based on the reaction between poly(diallyldimethyl ammonium chloride) and sodium polystyrene sulfonate. This material, Ioplex 103, Figure 4, exhibits many of the properties of Ioplex 101 but has a higher temperature resistance and may be able to be steam sterilized. Initial *in vivo* tests have proved promising and further work with this resin is continuing. To choose the best material for testing, a graph similar to Figure 3 was made and a point near the maximum picked. Specimens with ionic densities displaced from the maximums are being made to see if the sulfonate ion density controls the antithrombogenic behavior in the same manner as it does with Ioplex 101.

When a polyelectrolyte complex was made by replacing polystyrene sulfonate with styrene maleic anhydride, an initially promising material resulted. The polymer could be cast from a single solvent, dimethyl sulfoxide, and would therefore be less likely to damage acid sensitive substrates. However, when placed in animals the complex softened and began to dissolve. It was found that the material was sensitive to alkaline conditions and was stable only at an acidic pH. Work on this material was discontinued.

Reinforcement of Polyelectrolyte Complexes

For some internal body components Ioplex would have to withstand rather severe mechanical strains. The Ioplex can, of course, be coated on many stronger materials; however, this may not be necessary since methods of reinforcing the polymer have been developed. The first attempts to reinforce polyelectrolyte complexes involved the use of chopped fibers. One quarter inch glass fibers were added to the resin solution but were found to be very difficult to disperse and ineffective reinforcement. Similar problems arose when Dacron flock or tow was used in place of the glass. Particulate fillers in the form of treated clays were also used, but adhesion seemed very poor and film properties were degraded.

Several varieties of woven fabrics have proven to be excellent reinforcements. A fine square woven cloth, 1 mil thick, Type 104 glass cloth, when impregnated with Ioplex, is strong and retains most of the flexibility of the unreinforced material. A photograph of this material is shown in Figure 5. Each fiber which makes up the yarn from which the Type 104 cloth is woven is about 10 microns in diameter and it is likely that the reinforcement of the Ioplex occurs because of a mechanical interlocking with these fine fibers. The tensile strength of Ioplex 101 can be increased from 600 psi to approximately 1,200 psi with this reinforcement. Thickness of the composite has been varied from 2 mils to 10 mils. A stronger and stiffer composite can be made by replacing the light glass cloth with a heavier material such as Volan A treated Type 181 cloth. This is a satin weave cloth which is rather densely woven and is more difficult to penetrate with the Ioplex solution. Peel strength is as good as it is for the Type 104 glass with the Ioplex failing in both cases rather than the bond. Both Type 104 and Type 181 glass cloths are made by the J. P. Stevens Co. of New York, New York. Various surface finishes for the glass are available. Untreated or greige goods come with the original starch sizing which is used to facilitate weaving. Other finishes include the silanes and Volan finishes which are used to improve bonding to various resins and are not water soluble as are the starches. Most of our work involves the Volan A finished fabrics.

Other types of fabric reinforcements have also given good results. Pluton B, an 85-90 percent carbon cloth manufactured by 3-M Company, has been impregnated with Ioplex 101 to give a flexible (though not as flexible as the 104 glass) composite. The carbon reinforced material is particularly interesting in that carbon alone has exhibited some antithrombogenic properties. There are a variety of both carbon and graphite cloths available of variable carbon contents and with minor metallic impurities. Peel strength of the Ioplex on Pluton B is good with the Ioplex failing. The method of testing for peel strength is being investigated as problems of distortion, particularly with the

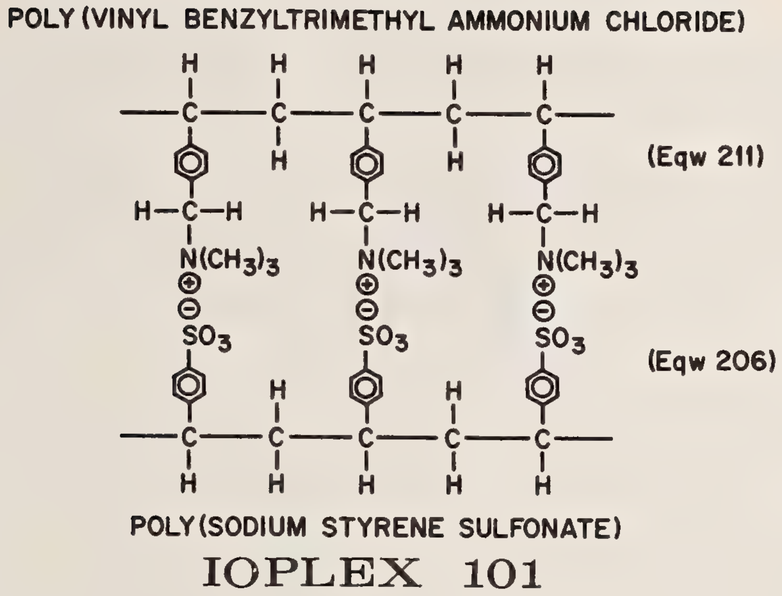
POLY (VINYL BENZYLTRIMETHYL AMMONIUM CHLORIDE)
(Eqw 211)
H—C—H
N(CH3)3
SO3
(Eqw 206)
POLY (SODIUM STYRENE SULFONATE)
IOPLEX 101

FIGURE 1.

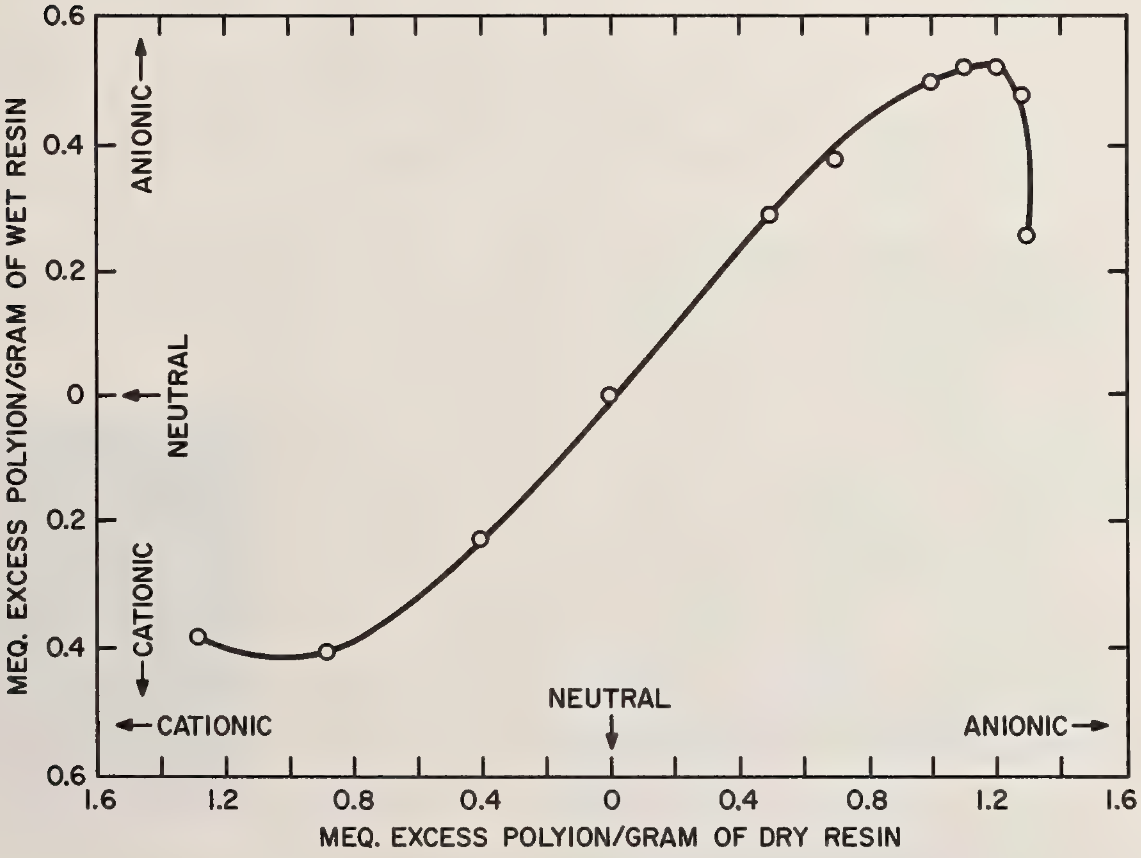

FIGURE 2. MEQ. EXCESS POLYION/GRAM OF WET RESIN VERSUS MEQ. EXCESS POLYION/GRAM OF DRY RESIN

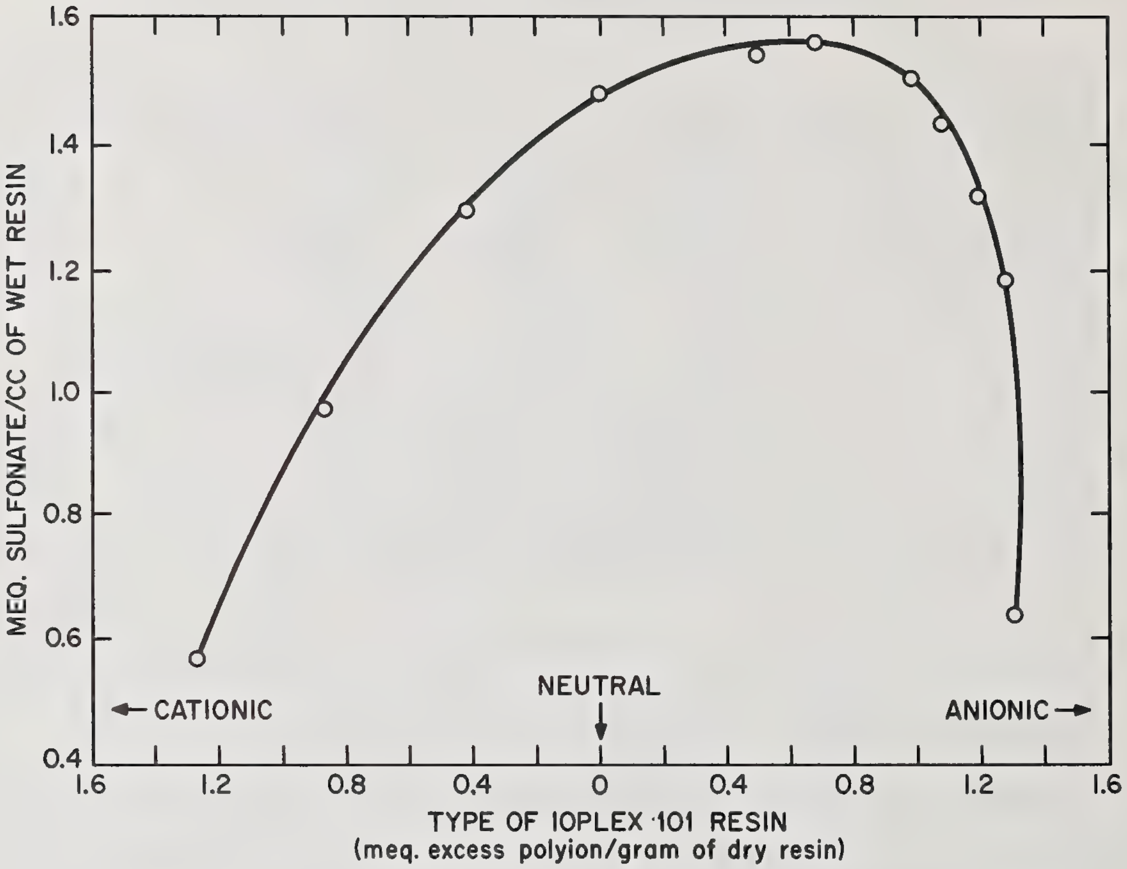

FIGURE 3. MEQ. SULFONATE/CC OF WET RESIN VERSUS TYPE OF IOPLEX 101 RESIN

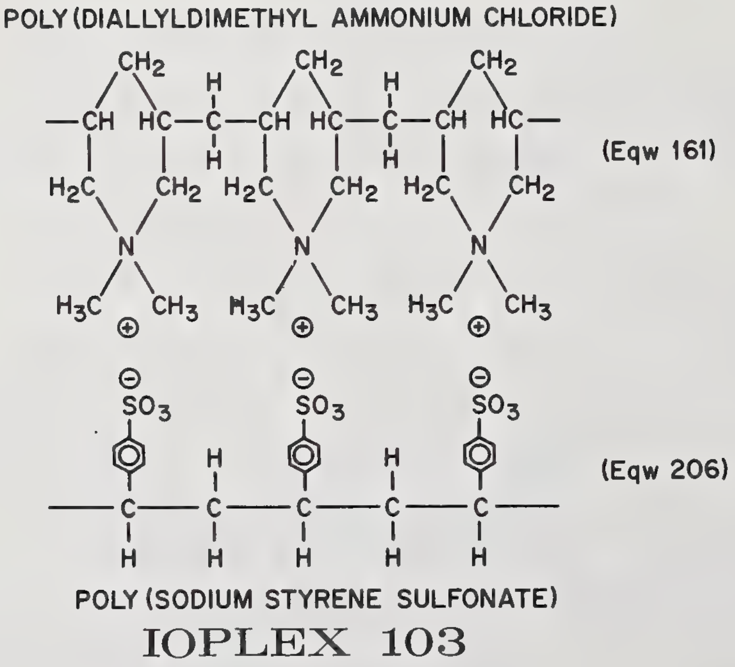
POLY(DIALLYLDIMETHYL AMMONIUM CHLORIDE)
(Eqw 161)
(Eqw 206)
POLY(SODIUM STYRENE SULFONATE)
IOPLEX 103

FIGURE 4.

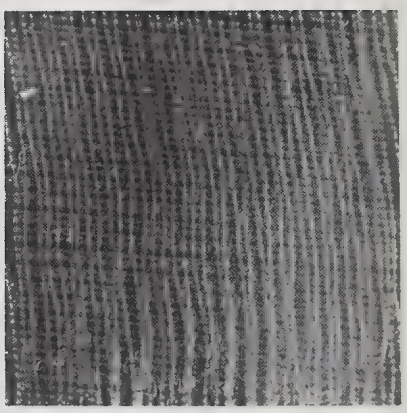

FIGURE 5. TYPE 104 GLASS CLOTH IMPREGNATED WITH IOPLEX

lighter glass fabrics, makes it difficult to get quantitative data. Poor peel strength does show up in the normal 180° peel test, however, as samples made with a Nomex nylon fabric failed by having the Ioplex peel cleanly off the surface of the fabric.

A lightweight Dacron fabric from J. P. Stevens Co., Style 39839-455, has been impregnated with Ioplex 101 along with a Dacron velour, Type 6107, from U. S. Catheter and Instrument Corp. The velour was relatively easy to coat although considerable resin was needed as the thickness of the composite was almost 80 mils. This resulted in a stiff, cardboard-like composite. Thinner velours would be correspondingly more flexible. Some difficulty in coating the lightweight fabric was encountered as it did not appear to be wet readily by the Ioplex solution. A second fabric, Style 38325, which is somewhat heavier and had less of a "glossy" appearance seemed better in this respect.

Tensile strengths for the reinforced Ioplexes tested to date are shown in Table 1.

TABLE 1

TENSILE STRENGTH OF IOPLEX 101 COMPOSITES

Material	Tensile[a] Strength psi	No. Tests	Comments
Ioplex 101 Type 104 Glass Cloth	1,200	7	Some failures at grips. Generally a tear would start and slowly propagate across width of specimen.
Ioplex 101 Pluton B Carbon Cloth	1,200	5	Good failures with the exception of 1 specimen which failed in grip
Ioplex 101 Type 181 Glass Cloth	4,020	5	Cloth distorted and most specimens failed in shear
Ioplex 101 Unreinforced	380	5	Generally good except a few tearing type failures

---

[a] All except the unreinforced Ioplex tested with a 6-inch gauge length and a crosshead speed of 10 inches/min. Unreinforced Ioplex 101 had a 4-inch gauge length. In general, smaller gauge lengths gave higher results.

It should be noted that most of the values do not depict the true tensile strength, but are undoubtedly low since the composite failed by shear. That is, the cloth distorted within the Ioplex till the fibers could pull past one another and slide out of the Ioplex with a minimum number of fibers breaking or in some cases a tear would start on one side of the tensile specimen and slowly progress across its width. The type of failure for each specimen is noted in the table.

Fabrication

Techniques have been clearly developed for coating Ioplex resins on various substrates as well as for fabricating reinforced and unreinforced Ioplex structures. Figures 6 and 7 are photographs of several Ioplex items. Included are Dacron reinforced tubes for arteries, unreinforced tubes, and unreinforced catheter tips, and a 181 glass-reinforced Ioplex 101 sheet. Figure 8 is an all-Ioplex catheter. These are only a few of the types of items that can presently be constructed.

Ioplex coatings can be adhered to many surfaces by the use of an epoxy primer. Adhesion to substrates such as silicon rubber can be achieved by bonding a Dacron velour to the rubber using a fluorosilicone adhesive such as Dow Corning's Silastic 733, and priming the rubber with Dow Corning's A-7094 primer. The Ioplex can then be easily adhered to the velour to form a rubber-backed reinforced Ioplex. The ordinary medical grade silicone adhesive cannot be used to bond the velour to the rubber since it is attacked by the shielding solvent of the Ioplex solution. Non-acidic Ioplex solutions are being developed so that sensitive substrates may be coated. Thin coatings using either $CaCl_2$ or $CaBr_2$ to replace the acid have been successful although layers greater than about 1 mil sometimes result in precipitation of the salts. Work is continuing in this area.

Sterilization

Ioplex may be sterilized by treating with a strong hydrochloric acid solution by using the following procedure:

a. Soak Ioplex sample for 1 hour in 1 part concentrated hydrochloric acid to 2 parts water
b. Leach until approximately neutral in several changes of sterile saline.
c. Soak in approximately 0.1 normal NaOH (sterile) for an hour.
d. Leach until approximately neutral in sterile saline.
e. Soak in sterile saline overnight.

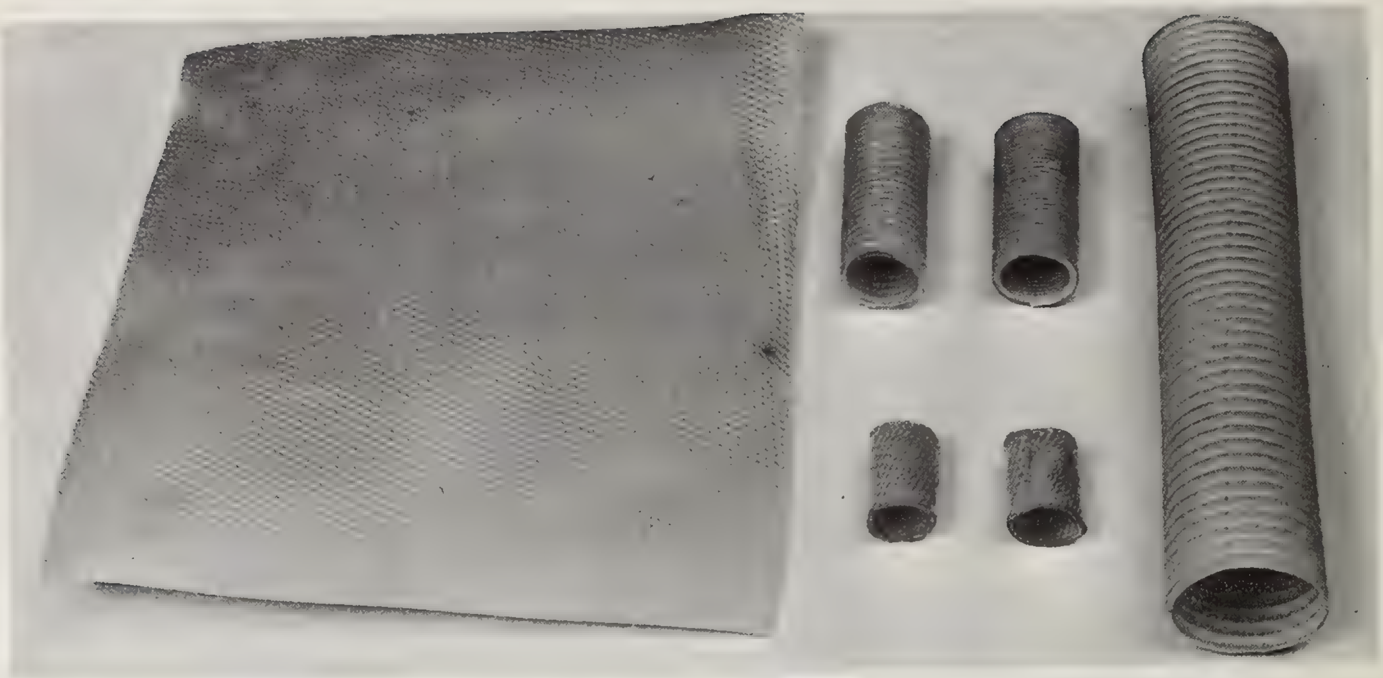

FIGURE 6. DEVICES MADE FROM IOPLEX REINFORCED WITH DACRON OR 181 GLASS

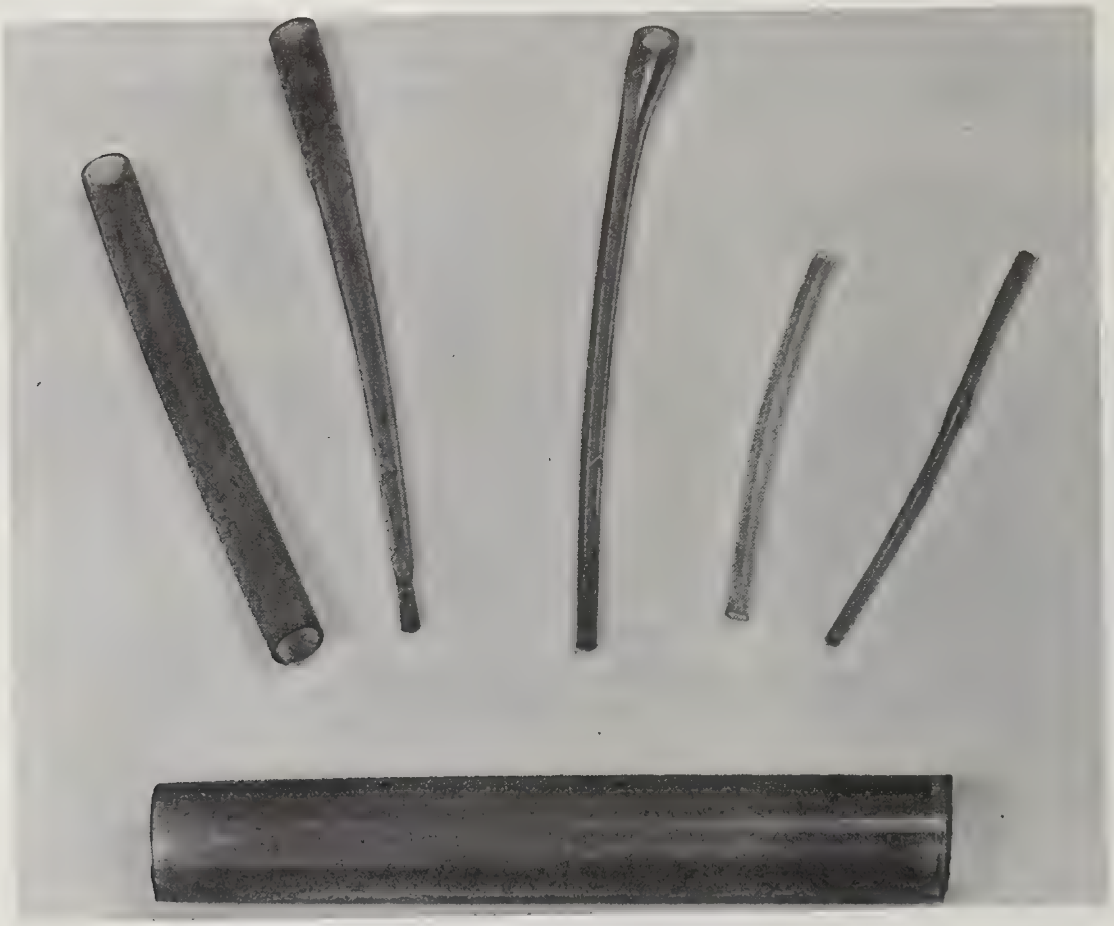

FIGURE 7. DEVICES MADE FROM IOPLEX

It was found necessary to include step c so that the rings would be slightly alkaline after leaching. If the pH of the rings was below 7.0, in vivo tests resulted in clotting. However, as long as the pH was above 7 the material was satisfactory. The above procedure is rather long and tedious and better methods are being investigated. Formalin sterilization has not been successful as removal of the formalin is difficult, and if any traces remain clotting occurs.

Glycerol can reversibly replace the gel water of Ioplex. This is done by simply immersing the Ioplex object in a glycerol bath; re-immersion in water replaces the glycerol without significantly changing the dimensional stability of the Ioplex. Removal of the water in this manner may allow ethylene oxide sterilization. Once sterilized the glycerol can be replaced by sterile water.

Electron bombardment is probably the simplest method of sterilizing the Ioplex resins. The object to be sterilized can be placed in a polythylene bag with a small amount of water, placed in an electron generator and irradiated with 3 megarads of energy. This is sufficient for sterilization and the object is already packaged and ready for shipment. A great number of objects can be sterilized in a short period of time in this manner, although it is expensive if only a few items are to be sterilized.

Results of In Vivo Tests.

Dr. Vincent L. Gott (of Johns Hopkins Hospital, Baltimore, Maryland) has developed an in vivo screening test for anti-thrombogenic behavior which is increasingly being used as a standard test for screening the antithrombogenic behavior of a wide range of materials. In his test, small cylinders, with approximately 8 mm inside diameter, and about 9 mm length, are placed in the canine thoracic inferior vena cava. In the acute studies performed as preliminary screening tests, the test dogs are sacrificed after two hours, and the rings examined for the presence of clots. On tests performed on a wide range of unheparinized conventional polymers--with both high and low surface energies--the rings were found substantially clotted after two hours, indicating the severity of the test.

Chronic (2 week) tests are run on materials which reproducibly remain unclotted in the 2-hour tests. Materials which remain unclotted for two weeks are considered most likely to have antithrombogenic activity sufficient for practical applications. The significance of these tests is enhanced by the fact that dogs are known to be hypercoagulable, so that any materials which survive in the dog, would be expected to survive in the human.

Tables 2 and 3 summarize some of the in vivo test results obtained by Dr. Gott on Ioplex resins.

TABLE 2

RING TYPE	IONIC STRUCTURE	H_2O CONTENT	2 WEEK IMPLANT RESULTS				
I. MODERATELY ANIONIC	0.5 MEQ. ANIONIC EXCESS	55%	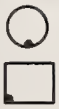	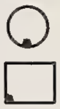	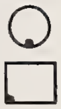	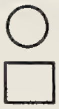	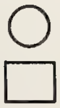

LEGEND:

SIDE VIEW

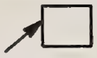

atrial end

END VIEW

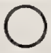

atrial end

(Dark Areas Denote Clotting)

TABLE 3

RING TYPE	IONIC STRUCTURE	H_2O CONTENT	2 HOUR IMPLANT RESULTS		
I. MODERATELY ANIONIC	0.5 MEQ. EXCESS POLYANION PER DRY GRAM OF RESIN	55% (WET BASIS)	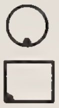	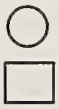	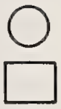
II. HIGHLY ANIONIC	1.3 MEQ. ANIONIC EXCESS	80%	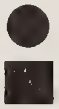	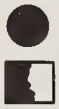	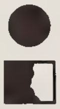
III. NEUTRAL	NEUTRAL	50%	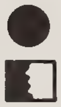	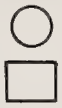	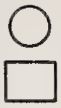
IV. MODERATELY CATIONIC	0.86 MEQ. CATIONIC EXCESS	67%	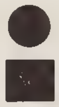	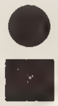	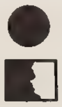

The 0.5 milli-equivalent excess anion resin has by far the best results, although the neutral material also shows some promise. It is interesting to note that even in those tests where a small clot did form on the 0.5 meq. material, that it did not propagate. Most other materials, once the clot has formed, become completely occluded or nearly so.

Some new formulations involving high water content Ioplex 101 and Ioplex 103 have also shown thromboresistance. Two rings of Ioplex 103 which had 33 percent water and 0.15 anionic excess were implanted and showed a small thrombus on the atrial outflow lip of the ring. The small 1 mm thick ring of thrombus was limited to the lower half of the outflow lip. Three rings of Ioplex 101 with 65 percent water and 0.5 anionic excess were also implanted. One had a tiny amount of thrombus on the atrial outflow lip; a second had the atrial one-half occluded and the third ring had a thrombus occluding just the terminal 1.5 mm outflow end of the ring. Three rings of Ioplex 101 with 65 percent water and 0.83 anionic excess were implanted. Two of these rings had a very small amount of thrombus on the floor of the ring, but a third was almost occluded when viewed both on end and laterally. Dr. Gott reported that he had considerable trouble implanting all these rings since they deformed very easily and handled similar to very wet cardboard. They could not be reformed to a round shape after deformation and this probably accounts for the variation between samples. New samples are being prepared for Dr. Gott, and those Ioplex formulations which are too flexible for his tests are being reinforced to provide the additional stiffness he needs.

CONCLUSIONS

1. Ioplex 101 with 0.5 milliequivalents excess anion is essentially nonthrombogenic, and it appears at least for Ioplex 101 that the degree of antithrombogenic behavior is related to the sulfonate ion density.
2. Ioplex based on the reaction between sodium polystyrene sulfonate and poly(diallyl dimethyl ammonium chloride), Ioplex 103, also shows some antithrombogenic behavior.
3. Ioplex reinforced with light or heavy glass fabric, carbon cloth, Dacron cloth, and Nomex nylon cloth can be used successfully to fabricate both cylindrical and flat shapes.
4. Ioplex can be bonded to many substrates using an epoxy based primer.
5. Fluorosilicone adhesives can be used to bond surfaces that will be exposed to the acidic Ioplex shielding solvent.
6. Ioplex may be sterilized by electron bombardment or a strongly acidic wash. To retain the antithrombogenic properties of Ioplex if the acidic bath is used, the Ioplex must be neutralized to a slightly basic pH.
7. The ability to reinforce Ioplex will allow the higher water content and soften polyelectrolyte complexes to be evaluated for antithrombogenic properties in *in vivo* testing.

DISCUSSION

DR. KUSSEROW: I have two questions. One relates to the mechanical characteristics of the film. Have you observed any incidents of loosening, flaking, or dislodgement of the Ioplex, not from the supporting material, but from the bulk of the Ioplex itself? Secondly, a question relating to another area. The Ioplex molecular aggregates are fairly large. Do you feel confident that a complex of this size (in an *in vivo* situation) would not ultimately elicit some sort of an immune or antibody response?

MR. MARSHALL: Materials have now been implanted in muscle tissue for about two years without causing any problems. We are still investigating this area, however. The point you made about Ioplex separating from itself is well taken. This can occur if one uses certain methods of sterilization. For instance, if you try to heat sterilize these materials, they will essentially fall apart within a short period of time. The gel structure cannot withstand sterilization temperatures. This is about the only instance we have found where the Ioplex separates from itself unless the material has been allowed to dry out.

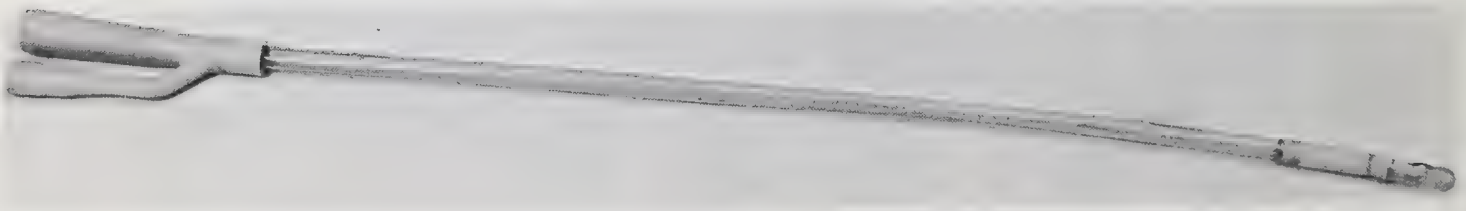

FIGURE 8. AN ALL-IOPLEX CATHETER

CHAPTER 9

HYDROGELS AS NON-THROMBOGENIC SURFACES

B. D. Halpern, H. Cheng, S. Kuo and H. Greenberg

Polysciences, Inc., Warrington, Pennsylvania

A number of synthetic hydrogels which approximate some of the physical characteristics of tissue have been investigated as non-thrombogenic surfaces. Parameters that were studied in relation to clotting behavior include nature of polymer backbone, gel solids, % cross-linker, gel osmolality, heparin in gel, pH, and various ionic and non-ionic functional groups pendant on the polymer backbone. At 20% polyacrylamide solids, significant anti-thrombogenic character is found. For non-purified acrylamide, Lee-White times of approximately 45 minutes were found whereas greater than 24 hours resulted for purified acrylamide. Basic or acidic comonomers in low mole % resulted in very significant improvement in clotting time. Dimethylaminoethylmethacrylate with unpurified acrylamide was the best of a number of weak base monomers studied, showing clotting times greater than 24 hours. Strongly cationic comonomers were not effective. Anionic comonomer (β-sulfoethylmethacrylic acid) was better than the unpurified acrylamide control. A simple electrostatic model which takes into account the ionic double layer of the blood platelets may relate to this improved performance. By using UV instead of redox-persulfate as an initiator, much tougher gels resulted. Other bis-acrylamide cross-linkers formed from 1,6-, 1,10-, and 1,18-diamines also gave tough gels as would be expected from their larger chain separation. Simple shapes such as tubes, bags, discs, films and the like can be fabricated from methylene bis-acrylamide and acrylamide gels even though they are the weakest of all tested. Toughness of gels is markedly improved by re-enforcing with textile fabric thus allowing the construction of prosthetic devices. Preliminary data from other NIH investigators who have tested our fabricated gels, supports our data that these synthetic hydrogels show promise as non-thrombogenic interface materials for cardiac devices.

RATIONALE

Blood is normally rapidly damaged when it comes in contact with surfaces "foreign" to itself.[1] The design of a synthetic surface, which is both antithrombogenic and nonhemolytic to blood, is essential for the successful, long-term implantation of prostheses, such as artificial hearts. We have found that some non-ionic and ionic hydrogels of synthetic cross-linked polymers show substantially reduced clotting tendency *in vitro* when measured by Lee-White clotting tests at 25 C. It is thought that the initial step in the blood-clotting sequence of Macfarlane is the result of the adsorption of some factor from the blood onto the "foreign" surface. This view of a solid surface must be compatible with the known fact that the direct introduction of soluble polymer molecules into the blood, such as polyvinyl pyrrolidone, polyvinyl pyridine N-oxide and dextran do not clot blood although they are, in the Macfarlane sense, "foreign surfaces." We think that the dimensions of these soluble polymers in relation to blood components are not large enough to allow bridging and organization into clots, and therefore they cannot result in large fixed clots.

The rationale on which our work with synthetic hydrogels is based assumes that a highly hydrated surface is only a partial surface and will also be less receptive to adsorption of blood elements and therefore more antithrombogenic. Synthetic hydrogels also allow easy alteration of the ionic nature of that surface by judicious use of monomers and comonomers. Our normal body tissues may be envisioned as a collagenous gel system in which water is largely contained within the gel network of the tissue protein. The presence of heparin polymer molecule on the tissue surface does not substantially alter this gel model concept since heparin undoubtedly exists in the water phase as a highly hydrated molecule. (Our work on the covalent bonding of heparin to a polymer surface to produce non-clotting surfaces will not be given here as it has been recently reported elsewhere.[2]) The low solids hydrogel surface, which are reported here, may be analogous to normal tissue in that it, too, does not present a continuous surface. Continuous surfaces offer more numerous sites for adhesion where the organization of blood components to a clot may, therefore, more readily occur. A hydrogel surface is also more energy absorbing because of its hydrated character. In conditions of hydraulic shear, hemolytic damage due to impact at a blood interface should less readily occur; thus resulting in less leakage of clotting enzymes into blood from cells or platelets.

RESULTS

The blood tests were conducted in standard size Lee-White clotting tubes on uniform fresh, whole blood samples. The clotting times of the whole blood in glass varied from 11.5 to 13 minutes depending on the day of trial and the volunteer donor. All blood samples were taken by a double syringe technique to minimize trauma effects due to needle puncture. The gel tubes were formed by casting against a flame polished Teflon mold.

Basic Materials.

Most of our hydrogels contained acrylamide with or without various modifying ionic comonomers. Cross-linking was achieved by methylene-bis-acrylamide (MBA) or its higher homologues. Initiation of polymerization was achieved with an ammonium persulfate-dimethylaminopropionitrile redox system.

Homopolymer Acrylamide Gels. The effect of solids, cross-link density saline, pH. Gels with less than 10 percent solids were too limp to allow handling. Gels greater than 60 percent solids exothermed in our mold so that voids in the gel structure occurred. In the range of 10-53 percent acrylamide solids containing 0.1 percent MBA, we observed Lee-White clotting times of 25-45 minutes. The glass controls had approximately 12-minute clotting times. The gels with lower solids showed slightly lower clotting times. It was necessary to adjust the pH of the water phase to 7.4 and to make the solution 0.85 percent saline, otherwise lower clotting times occurred and in addition severe hemolysis of the blood was noted. When this improvement was made, the clotting times improved to a maximum of 56 minutes. These times are essentially identical with clotting times of 60 minutes reported by others for ethylene glycol monomethacrylate gels.[3] Quintuplicate checks of clotting time at a given set of conditions showed variations of ± 8 minutes of the average time, and therefore caution must be used in categorically stating a trend exists. The data summarized above are shown in Table 1.

TABLE 1

ACRYLAMIDE GELS

Composition	Variation of Cross-Linking Agent and Total Solids	Lee-White (Av. of 5)
Acrylamide 10%	M.B.A. .2%	45 Min.
" 20%	" "	47 Min.
" 30%	" "	41 Min.
" 40%	" "	37 Min.
" 50%	" "	50 Min.
" 10%	" .1%	56 Min.
" 20%	" "	48 Min.
" 30%	" "	45 Min.
" 40%	" "	45 Min.
" 50%	" "	47 Min.
"	HMBA	35 Min.
"	HMBMA	30 Min.

MBA = methylene-bis-acrylamide
HMBA = hexamethylene-bis-acrylamide
HMBMA = hexamethylene-bis-methacrylamide
All gels at 0.85% NaCl and phosphate buffered to pH 7.38

For all these trials we used only singly recrystallized acrylamide. When we triply recrystallized the acrylamide and methylene-bis-acrylamide, clotting times in excess of 24 hours were repeatedly observed. The impurities in acrylamide were found to be beta-sulfatopropionamide, acrylic acid and nitrilotrispropionamide (Table 2). When they and persulfate were added back to the highly purified monomer solution in amounts of 0.01 to 1.0 percent, the clotting times fell back to less than 42 minutes. The purified acrylamide controls were always still over 24 hours. In general, we have found that any diffusable, non-physiological small molecule can be potentially troublesome by provoking the clotting sequence. In some of our recent work of preparation of prototype constructions for evaluation by other contractors, we have learned to polymerize our gels solely with UV light and persulfate catalyst and thus have eliminated some of the residual catalyst fragments resulting from our redox system. As yet, these have not been evaluated in *in vitro* blood tests.

Varying the concentration of the methylene-bis-acrylamide cross-linker from 0.1 percent to 5.0 percent, caused only minor changes in clotting time with no discernible trend related to the percent of cross-linker. When we substituted a higher homologue, namely hexamethylene-bis-acrylamide, the clotting times were also about 35 minutes. The corresponding methacrylamides were slightly shorter in clotting time. The tear resistance and rubbery character of the hydrogels were substantially improved when the chain extended cross-linkers were used. These properties are of

TABLE 2

LEE-WHITE CLOTTING TEST FOR IMPURE POLYACRYLAMIDE HYDROGELS

Impurity	Impurities Tested	Lee-White Clotting Time (min.)
Ammonium persulfate	-1%[a]	29
	-1%	31
	-.1%	38
	-.1%	35
	-.01%	34
	-.01%	36
p-sulfatopropionamide	-1%	35
	-1%	32
	-.1%	37
	-.1%	42
	-.01%	35
	-.01%	36
Nitrilotrispropionamide	-1%	35
	-1%	38
	-.1%	38
	-.1%	35
	-.01%	33
	-.01%	42

[a] Weight/wt. (Acrylamide)
Crosslinking used: .1% methylenebisacrylamide, 10% acrylamide
Redox catalyst system: .85 gm NaCl added per 100 ml monomer solution
Monomer solution buffered to pH 7.38
Purified acrylamide control 24 hours clotting time. Glass clotting time 12 minutes.

value in fabrication of special shapes required by our contract. The 1,6 diamine yielded cross-linkers which were water soluble but the 1,10 and 1,18 diamines yielded cross-linkers, which were not water soluble, and special solution casting methods were needed to prepare gels. In general residual solvents caused more rapid clotting (Table 3).

TABLE 3

EFFECT OF SOLVENTS FOR LEE-WHITE CLOTTING TEST

Solvent System	Lee-White Clotting Time
Methanol 10%	65 min.
DMF 10%	4 hrs.
Dioxane 10%	4 hrs.
Ethyleneglycol 10%	55 min.
Tetrahydrofuran 10%	7 hrs.

OBSERVATIONS: 97-31-5 Some hemolysis; slight darkening of blood after 3 hours.
96-6-5 Some color change after 4 hours; no hemolysis evident.
Footnote: pH 7.36, 0.85% saline, Redox catalyst.
All hydrogels 1% DMAEMA; 10% acrylamide; 0.05% MBA

This is consistent with previous study that residual diffusable monomer impurities caused poor clotting times. Ethylene glycol and methanol were responsible for relatively low clotting times, whereas tetrahydrofuran and dimethylformamide had a less deleterious effect. This may be because the alcohols are more easily oxidized by blood components.

Acrylamide-Dimethylaminoethyl Methacrylate Hydrogels and Other Weak Base Gels.

Dimethylaminoethyl methacrylate is a weakly basic monomer. Hydrogels containing 10 percent of singly recrystallized acrylamide solids of which 10 percent was the amino methacrylate consistently showed greater than 24 hours clotting time. These gels seemed very sensitive to total solids for the clotting times fell to 78 and 55 minutes as the total solids were raised to 30 and 40 percent respectively. The use of hexamethylene-bis-acrylamide as a replacement for methylene-bis-acrylamide did not drop the clotting time below the 24 hours previously observed if solids were 10 percent (Table 4).

TABLE 4

DIMETHYLAMINOETHYL METHACRYLATE-ACRYLAMIDE HYDROGELS

Relation of Clotting Time to Composition

Monomer Composition	Lee-White Clotting Time (Av. of 5)
DMAEMA 0.5% Acrylamide 5%	24 hrs.
DMAEMA 1% Acrylamide 10%	24 hrs.
DMAEMA 1% Acrylamide 20%	78 min.
DMAEMA 1% Acrylamide 30%	55 min.
DMAEMA 1% Acrylamide 40%	80 min.
DMAEMA 2.5% Acrylamide 10%	17 hrs.

If the cross-linker (MBA) was raised above 0.3 percent in this weakly basic gel, we now found a drop from 24 hours to less than one hour in clotting time (Table 5). With homopolymer acrylamide gels, we did not see this great difference in clotting time, but this series had clotting times of less than an hour and may not have been sensitive to such variations.

TABLE 5

EFFECT OF MBA CONCENTRATION ON LEE-WHITE CLOTTING TIME

MBA Concentration	Lee-White Clotting Time
0.02%	3 hrs.
0.05%	4 hrs.
0.10%	24 hrs.
0.30%	24 hrs.
0.60%	55 min.
0.90%	15 min.
1.20%[a]	35 min.

OBSERVATIONS: a. Dimethylaminoethylmethacrylate
100-95-5 Color change at 80 minutes; blood is darker. Hemolysis is not apparent.
90-17-5 No color change. Very little surface wetting after 1-1/2 hours.
90-41-5 Very little effect on blood. Firm clots.
Footnote: pH 7.38, 0.85% NaCl, Room temperature
Redox catalyst. All monomer concentration 1% DMAEMA; 10% Acrylamide.

We found that other N-alkyl aminoethyl methacrylates were particularly useful as comonomers in extending Lee-White clotting times (Table 6). The monomers studied were dimethylaminoethyl methacrylate, diethylaminoethyl methacrylate and t-butylaminoethyl methacrylate and 2(-1-aziridinyl) ethyl methacrylate. The dimethylaminoethyl methacrylate and the aziridinyl methacrylate were very good and showed no clotting after 200 minutes at which time the test was stopped. The aziridinyl methacrylate is similar to the dimethyl compound except the ring is closed through the carbons on the substituted methyls.

We also studied anionic comonomers with acrylamide (Table 7). Acrylic and methacrylic acid showed relatively poor Lee-White clotting times, probably due to the fact that we did not buffer the gels and pH was very low. A single attempt to make a polyampholyte gave an inconclusive result. Likewise, 2-sulfoethyl methacrylate, a strong acid monomer, causes relatively rapid clotting. This monomer was likewise not controlled in pH, and we knew from previous data that low pH caused poor clotting times. A strongly cationic monomer, 2-hydroxy-3-methacryloxypropyl trimethyl ammonium chloride (G-Mac) showed some slight improvement but still not of the same order of magnitude as the 24-hour times of our best samples.

We also looked at another non-ionic monomer, 2-hydroxyethyl methacrylate (glycol methacrylate). This showed good extension of the Lee-White clotting time. We did not extensively study this as we got some homopolymer glycol dimethacrylate in the gel making it hard to see through. This small amount of ethylene glycol dimethacrylate resulted from self trans-esterification as we tried to clean up the mono-methacrylate monomer. Clear gels can be obtained, as we know from Refojo's work

TABLE 6

LEE-WHITE CLOTTING TEST FOR ALKYLAMINOMETHACRYLATE

Sample Number	Monomer Composition	Monomer Ratio	Lee-White Clotting Time
75-1-5	DMAEMA 5% AM 13%	1:6	>200 min.
74-4-5	DMAEMA 10% AM 17%	1:3	>200 min.
77-7-5	DMAEMA 5% AM 13%	1:7	100 min.
77-8-5	DMAEMA 10% AM 17%	1:4	75 min.
76-2-5	TBAEMA 5% AM 13%	1:7	146 min.
76-9-5	TBAEMA 10% AM 17%	1:4	74 min.
88-2-5	IMEMA 1%[a]	1:22	>200 min.

AM: acrylamide DMAEMA: dimethylaminoethylmethacrylate
TBAEMA: t-butylaminoethylmethacrylate IMEMA: Iminolmethacrylate
a. 10% acrylamide solution was used for making hydrogel.
Footnote: Redox catalyst, 0.85% NaCl, pH 7.38, glass control clotting time 12 minutes.

TABLE 7

LEE-WHITE CLOTTING TEST FOR VARIOUS IONIC AND NON-IONIC MONOMERS

Monomer Composition	MBA Concentration	Lee-White Clotting Time
Acrylic acid 15%	2.5%	25 min.
Methacrylic acid 15%	1.5%	40 min.
Acrylic acid 5% DMAEMA 10%	1.0%	26 min.
Styrene sulfonate 10% Acrylamide 15%	1.0%	77 min.
SEMA 36%	1.0%	27 min.
SEMA 36% Acrylamide 11%	1.0%	34-1/2 min.
G-MAC 10% Acrylamide 15%	1.0%	50 min.
Glycol M.A. 30%	-	125 min.
Thiogel 5%	-	22 min.
Gelatin 15%	-	18 min.

DMAEMA: dimethylaminoethylmethacrylate
SEMA: 2-sulfoethylmethacrylate sodium salt
G-MAC: 2-hydroxy-3-methacryloloxypropyltrimethylammonium chloride

on this hydrogel in opthalmic systems.[4] Thiogel and gelatin, which are natural proteins, gave very poor clotting results. When we used the sodium salt of 2-sulfoethyl methacrylate, much improved clotting behavior resulted (Table 8). At 20 percent mole ratio of this comonomer, the Lee-White

TABLE 8

LEE-WHITE CLOTTING TEST FOR 2-SULFOETHYLMETHACRYLATE SODIUM SALT-ACRYLAMIDE COPOLYMER HYDROGEL

Sample Number	Monomer Composition	Concentration of Acrylamide Solution	Monomer Ratio	Glass Clotting Time	Lee-White Clotting Time
5-1-109	Acrylamide - SEMA	10%	5:1	12 min.	>180 min.
5-13-109	"	"	10:1	12 min.	133 min.
5-8-109	"	"	15:1	12 min.	66 min.
5-16-109	"	"	20:1	12 min.	54 min.

Note: The clotting time is the average of quintuplicate tests.
Hydrogels were prepared by adding 1% catalyst, 0.1% MBA, 0.85% NaCl and buffering to pH 7.38 at room temperature.

clotting times were greater than three hours. As the mole percent of Na-SEMA dropped, so did the clotting times. We were using unpurified acrylamide in these trials.

We examined the effect of other weakly basic monomers in the series (Table 9), 2-vinyl, 4-vinyl and 2-methyl 5-vinyl pyridine. The 4-vinyl pyridine copolymer was outstandingly better. The reason for this may be due to its higher basicity or more likely that, in the polymer, the pendant nitrogen group is more accessible to blood components (Table 10).

TABLE 9

EFFECT OF PYRIDINE DERIVATIVE MONOMER ON LEE-WHITE CLOTTING TEST

Monomer Concentration	Lee-White Clotting Time
2-vinyl pyridine 5% acrylamide 32%	40 min.
4-vinyl-pyridine 5% acrylamide 39%	105 min.
2-methyl-5-vinyl pyridine 5% acrylamide 39%	77 min.
N-vinyl-2 pyrrolidone acrylamide 18%	47 min.

Footnote: pH 7.38, 0.85% NaCl, Redox catalyst
Acrylamide not purified

TABLE 10

CHEMICAL STRUCTURE AND PHYSICAL PROPERTIES OF VINYLPYRIDINE MONOMER

2-Vinylpyridine	4-Vinylpyridine	2-Methyl-5-Vinylpyridine
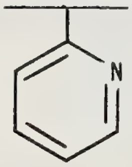	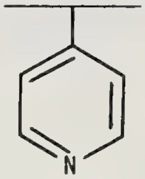	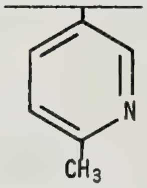
pH:[a] 9.89	pH:[a] 10.08	pH:[a] 8.52
b.p.: 110°C (150 mmHg)	b.p.: 121°C (150 mmHg)	b.p.: 133°C (150 mmHg)

a. This indicates the pH of the monomer solution in the case of 1:10 molar ratio for vinylpyridine to acrylamide.

The mechanism of action of weakly basic groups is unclear. They may have a shielding ionic action on the double layer around blood platelets, or they may bind heparin from the blood. We should also be aware that sulfate polymer end groups can result in polymerization and the weak base may serve to bind these sites.

At about this time, we became aware of the fact that singly recrystallized acrylamide was still relatively impure. When we triply recrystallized acrylamide and methylene-bis-acrylamide and repeated the 2- and 4-vinyl pyridine series, we got improvements in Lee-White clotting times (Table 11) from less than 100 minutes to over 480 minutes.

A N-vinyl pyrrolidone polymer studied in this series showed only average performance. We were not able to get full polymerization, and we may have had residual monomer in the gel. The literature on blood plasma extenders would indicate that good blood compatibility should be obtained.

The Effect of Heparin in Gel.

In view of the known anti-thrombogenic character of heparin, we studied the effect of heparin polymerized *in situ* into the gel and heparin adsorbed on the surface of the gel (Table 12). The clotting times of the tubes containing either adsorbed or caged heparin were not significantly better than control tubes which contained no heparin. In fact, a number of control tubes at 20 percent gel concentration had clotting time equivalent to the best of the heparinized series. The redox catalyst system may be in some way injurious to the heparin or the heparin may be too firmly caged in the gel network and, hence, unavailable to the blood elements. We did not do any leaching studies to confirm this.

Effect of Soluble Polymers on Clotting.

We were interested to see if there was any relationship of molecular weight of soluble polymers to clotting behavior of fresh whole blood. A series of eight polyacrylamides varying in

TABLE 11

LEE-WHITE CLOTTING TEST FOR VINYLPYRIDINE-ACRYLAMIDE AND VINYLPYRROLIDONE-ACRYLAMIDE COPOLYMER HYDROGEL

Monomer Composition	Lee-White Clotting Time
4-vinylpyridine: Acrylamide (purif.)	480 min.
"	480 min.
"	480 min.
2-vinylpyridine: Acrylamide (purif.)	113 min.
"	270 min.
"	121 min.
vinylpyrrolidone: Acrylamide (purif.)	117 min.
"	81 min.
"	160 min.

Note: The clotting time is the average of quintuplicate tests. Hydrogels were prepared by adding 1% catalyst, 0.1% MBA, 0.1% NaCl and buffering to pH 7.38 at room temperature (vinylpyrrolidone), 70°C oven (vinylpyridine).

TABLE 12

EFFECT OF HEPARIN IN ACRYLAMIDE GEL

	HEPARIN COMPOSITION		
Sample Number	Combined Unit ml. of total monomer solution	Absorbed Unit ml. of heparin solution	Clotting Time (min.)
31	1	-	26.0
32	10	-	30.5
33	50	-	30.0
34	100	-	42.0
35	-	1	32.0
36	-	10	32.0
37	-	50	23.0
38	-	100	24.0

All gels 20% acrylamide, 0.2% MBA, Glass clotting time 11.5

molecular weight from 7,000 to 2,000,000 were tested in vitro by adding 1 ml of fresh whole blood to 5 ml of 1 percent polymer in 0.85% saline. The clotting time varied from 2.5 to 6.0 hours. The delayed clotting may simply be related to dilution of the blood. We noticed no significant relation in clotting time as a function of molecular weight of the polymer in solution. The hematology technician did report that the higher molecular weight polymer seemed to thicken the blood more rapidly prior to clotting. When the same test was run with sodium polystyrene sulfonate of 40,000, 50,000 and 4,000,000 molecular weight, the blood seemed to thicken almost as soon as it hit the solution of polymer.

If the mode of addition were reversed and now we added 5 drops of polymer solution to 1 ml of whole blood, the clotting in the polyacrylamide series occurred within 5-10 minutes. With sodium polystyrene sulfonate, no clots were noted after 24 hours although the high molecular weight sample appeared to thicken the blood. No clear cut conclusion was possible. The anomalous results occurring with inversion of addition are not explained at this time. It is obvious that solution polymers do, indeed, behave very differently than solid polymers when in contact with blood. Our trials probably had too high a concentration of polymer for the available blood. If time permits, we intend to reexamine this. It would be most desirable to make in vivo trials in animals.

Hydration Character of Gels.

In conjunction with the problems of improving the fabrication of our gels, some miscellaneous data on swelling of polyacrylamide gels was obtained. The swelling rates are obviously related to the degree and the nature of the cross-linking. As shown in Figure 1, the degree of swelling increased from an equilibrium value of 90 percent to 260 percent when methylene-bis-acrylamide was replaced by 1,6-hexamethylene-bis-methacrylamide. Even at 260 percent, the gel had not equilibrated after 14 days of soaking. When actual prostheses are made, we shall be able to use higher solids gels than 10 percent and 20 percent since they will further hydrate when implanted. In Figure 2 we can see that at high concentrations of cross-linker (1 percent), we obtained much the same swelling behavior for the methylene-bis-acrylamide as we did for the 1,6 cross-linker.

conc. of acrylamide: 10%
saline content : 85%

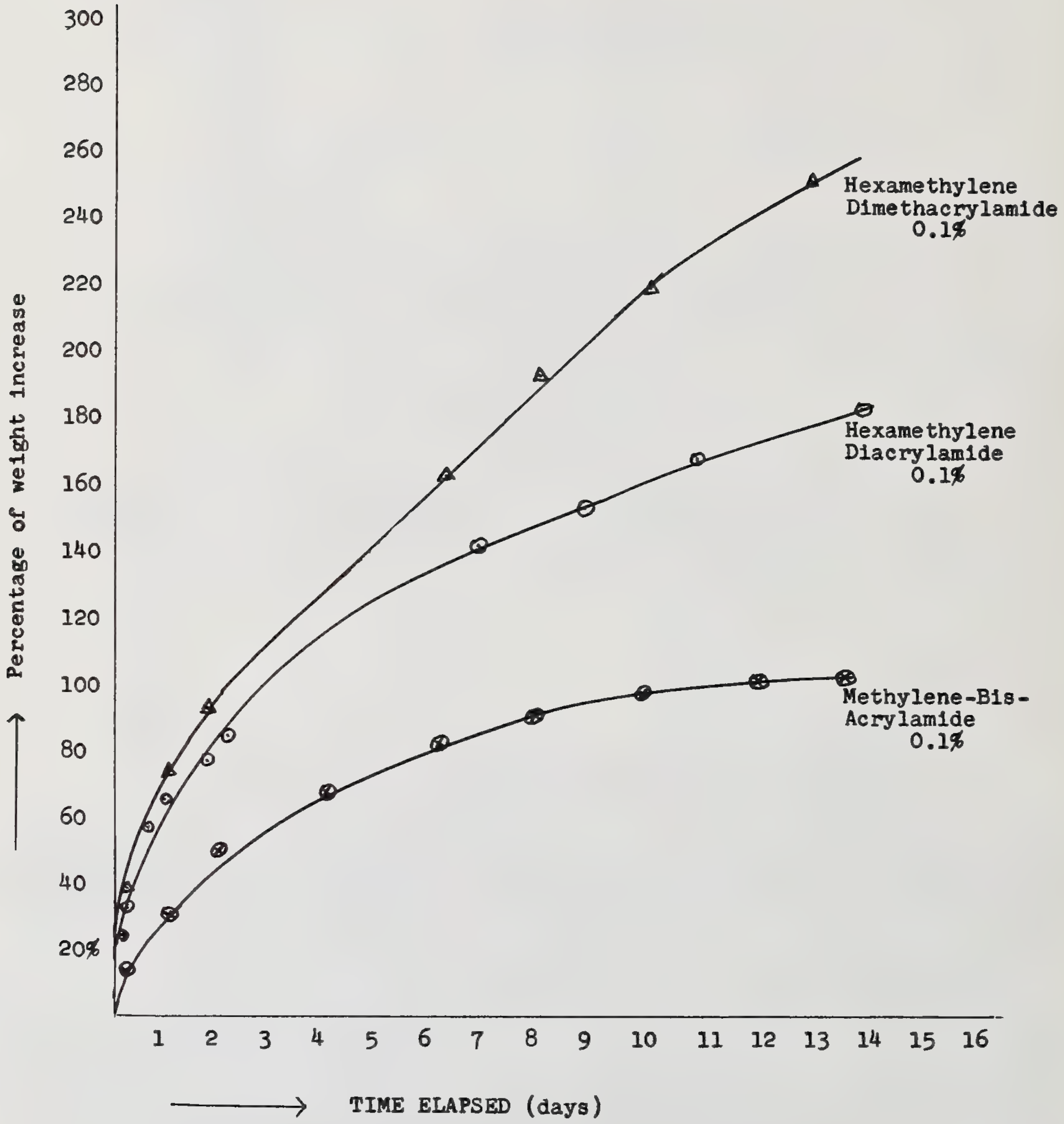

FIGURE 1. SWELLING OF ACRYLAMIDE HYDROGEL IN WATER

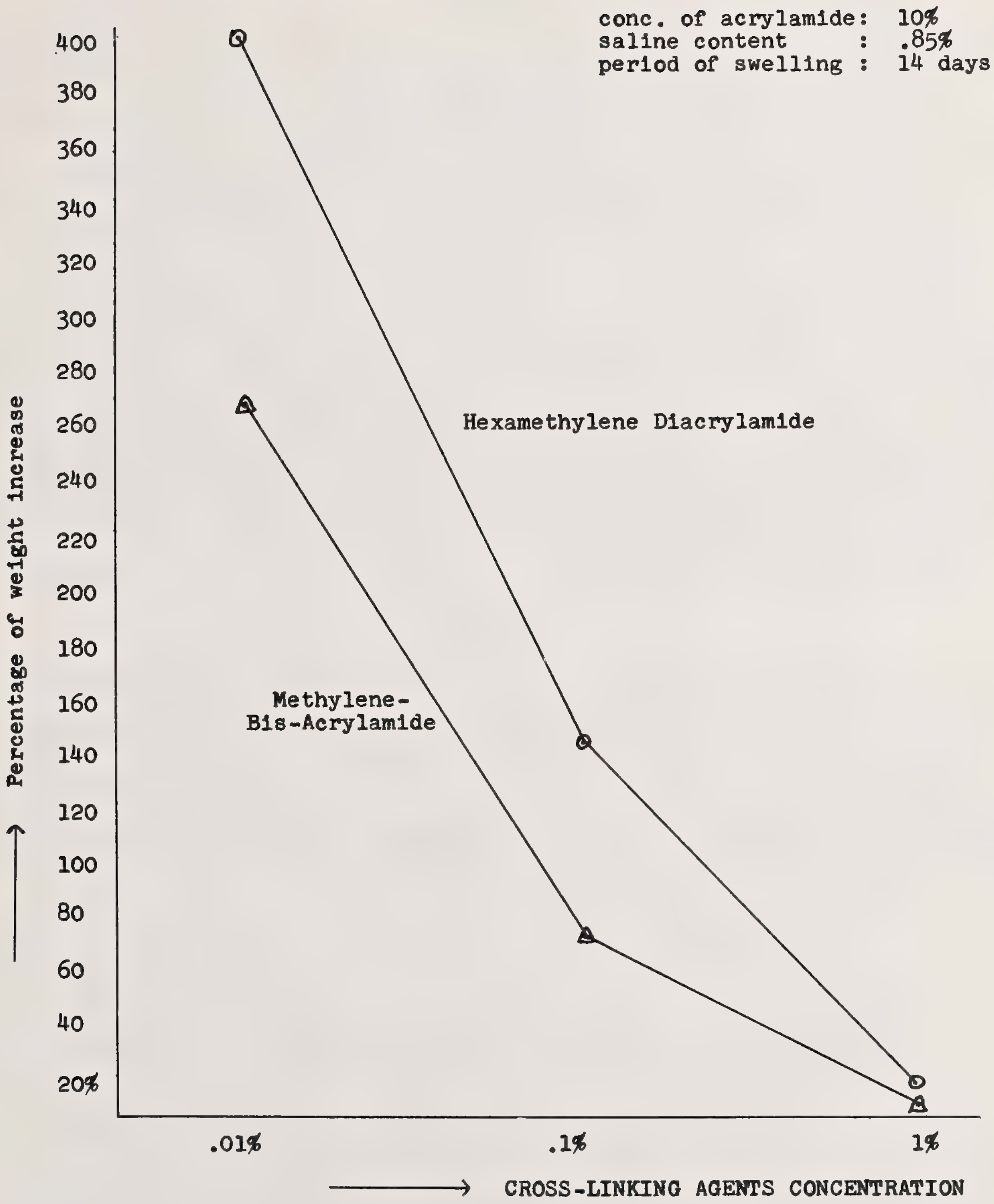

FIGURE 2. SWELLING OF ACRYLAMIDE GEL IN WATER

APPLICATIONS

A number of gel systems consistently showed very high clotting times. The four best gels were selected for fabrication into specific shapes as requested by the National Heart Institute. These hydrogels were all 20 percent solids and 0.1 percent MBA. They included purified acrylamide and its copolymers with dimethylaminoethyl methacrylate, sodium sulfatoethyl methacrylate and 4-vinyl pyridine. The fabrication of the gels can be achieved in a variety of ways. Shapes, such as tubes, discs, films, bags and fine particle spherical beads, have been reasonably readily achieved through the use of appropriate molds. In their unsupported and hydrated form, the gels at 20 percent solids are very flexible, but are also subject to tear. At 50 percent solids, they are very tough. The use of longer chain cross-linking agents, such as 1,6 hexamethylenediacrylamides or U.V. polymerization also permit tougher gels. Since none of our blood data has been obtained using these newer systems we did not fabricate our gels from these improved formulations for submission to other N.H.I. contractors.

By casting the monomers onto supporting textile mesh or by impregnation of textile velours, we have obtained materials with good tear strength, higher flexibility, high tensile strength and increased modulus. We are currently planning to coat the velour lining on a Statham heart pump. Coatings on metal, glass and other polymer surfaces have also been made. If the gels are fully dehydrated, they are very horny in character and may be machined into specific shapes. Upon rehydration, they again swell to the desired shape. Sterilization is achieved by boiling in water or by short autoclaving. The residual persulfate and dimethylaminopropionitrile catalyst fragment are easily extracted by such treatment. Some tests at the Manhattan Eye Hospital indicate these residual catalyst fragments cause corneal reaction in the eye of rabbits. By simple extraction, we hope to eliminate this. Ultimately, we expect to obtain thin hydrogel coatings by grafting the gel to the desired surface by direct polymerization from a monomer or by chemical reaction of a preformed polymer having the proper hydrophilic character.

Preliminary results from four other N.H.I. laboratories, testing our gels, confirm our own *in vitro* results concerning the promising anti-clotting character of our gels.

REFERENCES

1. Macfarlane, R. J., An enzyme cascade in the blood clotting and its function as a biochemical amplifier, *Nature* *202*, 498 (1964).
2. Halpern, B. D. and Shibakawa, R., Heparin Covalently bonded to polymer surface in interaction of liquids at solid surfaces, *Advance in Chemistry Series* *87*, American Chemical Society, R. F. Gould, editor.
3. Levowitz, B. S., et al, Biologic compatibility and applications of Hydron, *Trans. Am. Soc. Artificial Internal Organs* *14*, 82 (1968).
4. Refojo, M. F., and Yasuda, H., Hydrogels from 2-hydroxyethyl methacrylate and propylene glycol monoacrylate, *J. Appl. Polym.*, *Sci.* *9*, 2425, (1965).

DISCUSSION

DR. HASTINGS: I would like to ask a couple of questions. Did you equilibrate these gels with calcium ion, and did you check your clotting times by pouring the blood into a glass control after your tests?

DR. HALPERN: In answer to the first question, when we first obtained the improved clotting results, we thought that possibly we were sequestering some of the calcium ions from the whole blood. We did make some tests where we took aliquots of calcium ion and attempted to see if they became bound to the gel after 4 to 5 hours soaking. We did not find any migration of calcium ions from the solution nor into the acrylamide gel. In answer to the second question, we did not remove the blood from our gel test for subsequent blood clotting tests in plain glass tubes.

DR. BYCK: Could you compare the mechanical strengths of your materials with those of the Amicon Ioplex resins?

DR. HALPERN. We have not compared them. On the basis of water content I would assume they would be the same or better. This is just a qualitative evaluation. We have fewer effective cross links and we may, therefore, have higher strength, but we would have to make comparison to be sure.

DR. BYCK: Where you have used these materials on various textile substrates, are you able to get good adhesion between the hydrogels and hydrophobic surfaces?

DR. HALPERN: I don't know whether one can say that we obtain adhesion, in the sense of true adhesive bonding.

DR. BYCK; Was the bonding which you obtained useful in a practical, operational sense?

DR. HALPERN: Yes. In a practical operational sense we do get adhesion, because what happens is that the monomer permeates the structure of the textile or mesh and joins to itself. It is firmly bonded so that one can do considerable mechanical work with it.

DR. O'NEILL: Could you describe or give a reference to the double syringe blood sampling technique?

DR. HALPERN: There is some suspicion that trauma to the blood cells occurs when the needle is first inserted during venepuncture and that this trauma releases some of the clotting factors. To control this experimental variable the first barrel of blood collected is discarded. An additional sample of blood is then collected in a second syringe connected to the same needle. Presumably, any released tissue juices and clotting factors will be removed in the blood in the first syringe which is discarded.

DR. FALB: One of the things that all of us working on materials are particularly interested in is the effect of surface functional groups. It seems to me that the only evidence that basic groups are compatible is your report on the diethylaminoethylmethacrylate. I am wondering how you would differentiate this basic material from all the other materials containing amine groups which seem to be very compatible with blood. Is there some principle which differentiates the diethylaminoethylmethacrylates?

DR. HALPERN: We have an unproven theory - rationale, if you will - that would account for the seemingly contradictory observations that sometimes the cationic groups and, in other cases, the anionic groups are beneficial. I think that if you use a strongly basic group like a quaternary ammonium group, this is sufficiently strong that you can strip away the double layer of cations that surround a platelet in the blood, thus attracting the platelet to this positive surface. In the case of a weakly basic material such as dimethylaminoethylmethacrylate, the charge is not sufficiently strong that it can detach the double layer that is around the platelet and we get mutual repulsion. In the case of the anionic groups, these will not attract the negative platelet even though protected by its double layer. It seems, therefore, to me that you have to rationalize the effect of different ionic groups on the basis of the strength of the particular ionic species that you are talking about. What we have here is just some clotting tests. As many of you here will recognize, when you exceed one hour of clotting time, many questions are raised. We are only reporting the test data as received from the hematology technician.

DR. FALB: Do you think it is possible that the basic group may be hydrolyzing since it is somewhat easily hydrolyzable, and that you could be losing it at the surface?

DR. HALPERN: It may be possible. I don't really think it occurs because it is firmly bound into the polymer chain. The backbone of the polymer is an acrylic chain and it is known that acrylic emulsions do not easily hydrolyze. Moreover, we keep all our gel systems at pH 7.5 because we found that this gave optimum clotting performance. The rate of hydrolysis at this pH, I expect, is extremely low, if any.

DR. FALB: The rate of hydrolysis of methyl groups of methacrylate esters is low, but those of amine-containing esters are higher because of internal catalysis. Hydrolysis occurs with little effort.

DR. HALPERN: That is quite possible. We found much the same values of prolonged clotting times with vinyl pyridine polymers and these cannot hydrolyze. While they weren't as good as the diethylaminoethylmethacrylate, they were still in the range of 6 and 7 hours.

DR. HASTINGS: Any other discussion?

MR. SALYER: I was just going to make one observation about the multiple syringe technique. We have used this multiple syringe technique too in the sphere tube test, you may remember in the first year of our contract research. We usually filled five or six tubes from the arm of the donor, with some help in holding the syringe steady and the needle in the arm, while we were changing. I cannot say that we noticed any significant difference between the clotting characteristics of the first tube (which we know contained the tissue juices) and the subsequent ones.

DR. HASTINGS: One short question.

UNIDENTIFIED DISCUSSANT: In your studies have you been able to determine whether or not there is any adsorption of plasma on the hydrogels?

DR. HALPERN. We have not done this. There has been some work done by Dr. Johnsson-Hegyeli, Dr. Mason and the people at the Cordis Corporation. I think this will be reported later. However, the results have not yet come back to us. Tentatively I believe there is less adsorption of the plasma protein onto our particular surfaces. I think there is also another reason that is clearly a mechanical one that should be considered in plasma adsorption. We were initially concerned about the nature of our surface. We found, for example, that when we make these test cells, we must cast them against a Teflon mold. We found that when we flame-polished the Teflon plug and thereby sintered it, we had a smoother surface and improved our results substantially. The adsorption of plasma proteins, I feel reasonably sure in my own mind, is very much related to the total amount of surface that is exposed, and often the surface irregularities are far greater than one would normally assume. In one of the previous question periods, someone wondered why the heparin forms a thick layer rather than a monolayer. The surfaces are often not absolutely planar but very irregular. We did some electron micrographs of Gott GBH type surfaces and found that they are extremely irregular, having approximately 100 times the surface area you would normally expect on a planar surface. I feel sure that this affects plasma adsorption also, just as it does the layering of heparin.

DR. CULP. I would just like to put in a helpful hint. At Epoxylite we are making Gott test tubes exactly the way you are making them and in order to prevent contamination of the Teflon mandrels, we have put them on a lathe and used another piece of Teflon to burnish the surfaces. It smears the projecting particles down into the grooves, making a very, very shiny surface.

DR. HALPERN: That is interesting. Perhaps we will be able to try that.

CHAPTER 10

STUDIES RELATIVE TO MATERIALS SUITABLE FOR USE IN ARTIFICIAL HEARTS

P. Murphy, A. Lacroix, and S. Merchant

Thermo Electron Corporation, Massachusetts

and

W. Bernhard

Children's Hospital Medical Center, Boston, Massachusetts

It has been the objective of this program to examine the role of electrical effects at polymer surfaces on the initiation of thrombosis, and to improve the thrombus resistance of selected polymers by means of persistent electrical polarization. Parallel efforts have been carried out on the characterization of surface properties related to the electret state in polymers, on the stability of the electret state under simulated blood pumping conditions, and on in vitro and in vivo blood compatibility experiments. Polarization stability following immersion and flexing in saline has been reasonably good for the four polymers studied. Charge-strain measurements on polymer electrets have shown that variations in surface charge produced by pump flexing will be small. In vitro blood compatibility has been explored using both a modified Lee-White clotting test and a platelet adsorption experiment. No significant difference in clotting time was found for polarized samples; however, those with negative charge did adsorb fewer platelets. A series of in vivo studies has been carried out using right atrial flags of polyvinylidene chloride and vena cava rings of Teflon, Hypalon, and Hypalon/2% polysulfonate. In all cases, negatively polarized samples showed improved blood compatibility. About 2/3 of the negatively charged atrial flags showed little or no thrombus, while 2/3 of the positively charged flags showed severe thrombus. Of 22 negative ring implants, 16 showed little or no thrombus. For the rings with moderate to heavy thrombus, a correlation with anomalous contact angle or low charge was found in 4 of 6 cases.

INTRODUCTION

Thermo Electron has been working under contract to the National Heart Institute for the last three years on the development of blood compatible materials. It has been the objective of this program to examine the role of electrical effects at polymer surfaces on the initiation of thrombosis, and to improve the thrombus resistance of selected polymers by means of persistent electrical polarization. Parallel efforts have been carried out on the characterization of surface properties related to the electret state in polymers, on the stability of the electret state under simulated blood pumping conditions, and on in vitro and in vivo blood compatibility experiments.

For those who have not previously followed this work, I will describe briefly the electret phenomena, and then report our recent results, including data on the magnitude and distribution of charge in several polymers, and on the changes in polymer surface energy produced by electrification. The effect of simulated pump flexing on both the transient surface charge and the long-term stability of polarization will be discussed. Finally, blood compatibility experiments with electrified materials will be covered. These experiments include in vitro platelet-surface studies, and in vivo atrial tab implants and vena caval ring implants.

CHARACTERIZATION OF ELECTRET SURFACE

Electrets are often thought of as electrical analogues of permanent magnets. By definition, an electret is an insulator having persistent, internal, electric polarization. The electric field associated with the polarization is utilized generally by electromechanical transducers operating in air. In an aqueous solution, such as blood, no field can be maintained for more than an instant because mobile ions will screen the charge. An electret is not a battery and, thus, cannot supply the energy to maintain a field in the presence of mobile ions. Hence, the effects of the electret state on blood coagulation must relate to the electrical double layer at the blood-electret interface and its modification by surface charge and orientation.

Figure 1 shows schematically the typical electret polarization. Two types of polarization of opposite sign are shown. The first is related to conventional dielectric absorption and is called heterocharge; it is usually thought to be a volume dipolar orientation. However, space charge can also be present. The second type of polarization is homocharge; it is composed of an ionic sheath near the surface which is produced by air breakdown and charge injection during polarization. Electrets are made simply by heating and cooling a dielectric in an electric field. However, the polarization can be varied greatly by the conditions of polarization and the properties of the material.

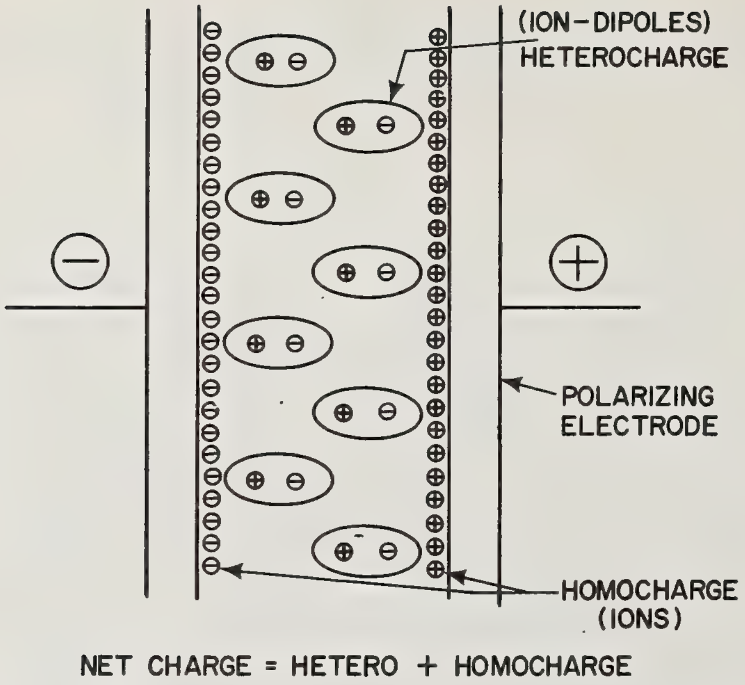

FIGURE 1. SCHEMATIC REPRESENTATION OF CHARGE DISTRIBUTION IN ELECTRETS

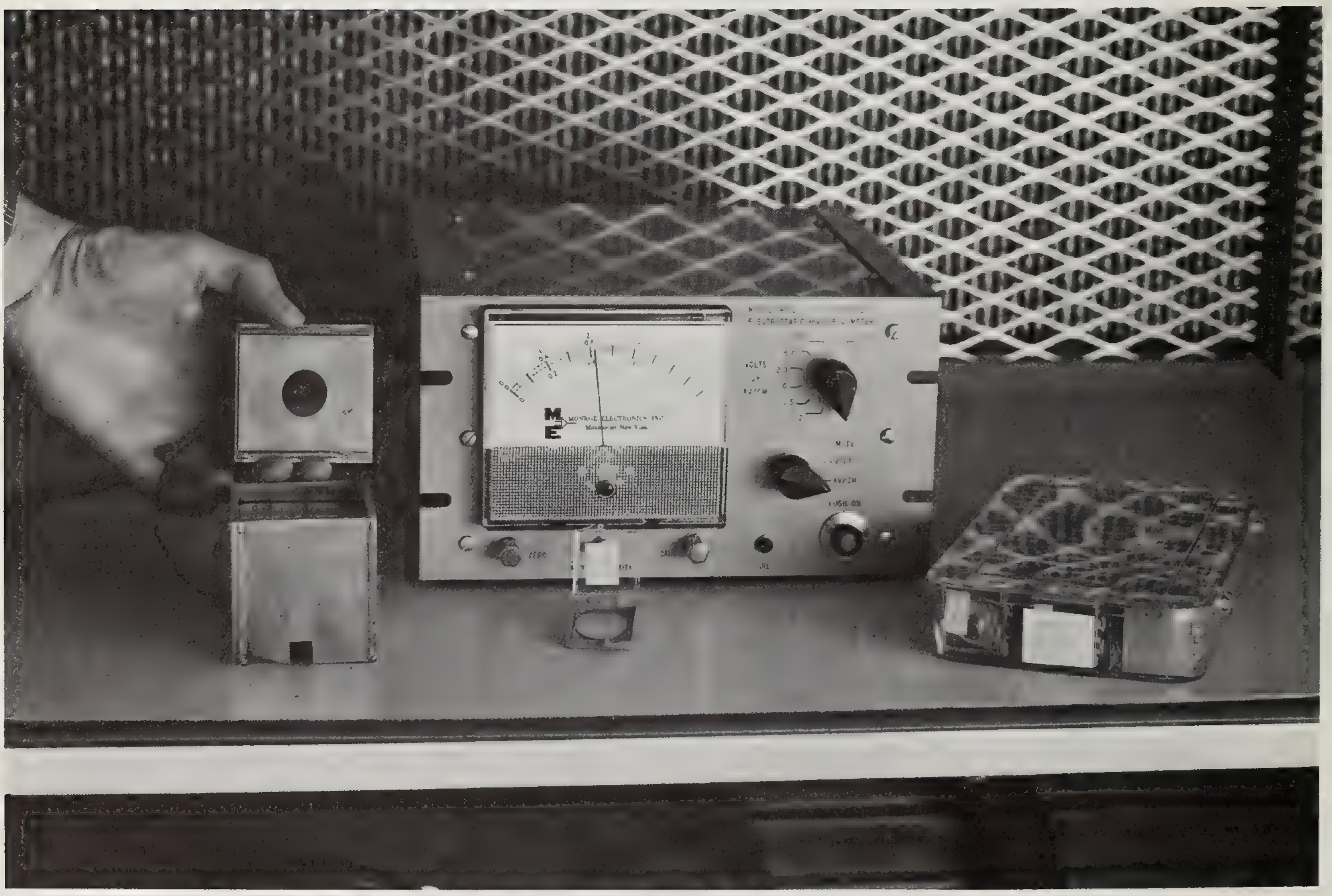

FIGURE 2. NET CHARGE MEASUREMENT BY NULL VOLTAGE TECHNIQUE

Charge Measurement.

We usually make two types of charge measurements on electrets; the first is shown in Figure 2. This is a measurement of net charge, or the algebraic sum of heterocharge and homocharge. Since it measures charge difference, it is inadequate by itself for characterizing the charge. However, it is historically the earliest electret charge measurement and using the new vibrating probe electrometer shown in Figure 2, it is simple, accurate and nondestructive. It fails to give the true value of net charge on occasions when an adsorbed water film shields the charge; we will describe a few such instances.

Another measurement involves reheating the electret, while it is short-circuited through an electrometer, and measuring the release of residual charge. This is a more difficult measurement to make, as the discharge curves are often complex, and it is a destructive measurement. Figure 3 shows typical data obtained in a depolarization experiment. Several identical samples are usually run simultaneously, since there is considerable data scatter. The figure shows current and temperature for two samples of Kel-F as a function of time. This particular curve was taken during studies on electret flexing and is typical of the more complex, double-peaked curves. The charges are obtained from the area under the curves; heterocharge gives positive peaks, homocharge negative. In spite of the difficulties, this measurement provides the best characterization of charge.

Some typical values of charge are shown in Table 1.

TABLE 1

CHARACTERIZATION OF ELECTRET CHARGE FOR THIN POLYMER FILMS

(Typical Values of Charge Density in esu/cm^2)
(1 μcoul = 3,000 esu)

Polymer	Net Charge (measured)	Net Charge (calculated)	Heterocharge (measured)	Homocharge (measured)	Homocharge (calculated)
PVLC	(-) 10		(+)1000-5000		(-)1000-5000[a]
PCTFE	(-) 30		(+)20-80		(-)50-110
PFEP	(-) 30		(+)10-20		(-)40-50
PFEP (ionized gas)	(-) 70	-90	Small	-90[a]	
Hypalon	0-1		(-)1000-5000[a]		(+)0-5000
Hypalon (ionized gas)	0-1	(-)500-1000	Small	-500-1000[a]	
Urethane	0-1		(-)1000		(+)0-1000

a Charge values typical of implanted specimens

These data were obtained in our laboratories during the last two years and are not published elsewhere. As shown in the table PVLC electrets have very large and nearly equal values of both heterocharge and homocharge, so the net charge is small. On the other hand, Teflon and Kel-F-type materials give rather small values of internal polarization, but they can maintain a rather large difference or net charge. Normally, the depolarization measurement gives the heterocharge only; however, in two cases, homocharge curves were found. For the Teflon electrets polarized with a gas contact, we measured nearly the full homocharge as a net charge; rings prepared in this manner showed good blood compatibility. Hypalon is rather interesting in that the net charge is always near zero, even though a large homocharge located near the surface may be present. Since the surface is slightly hydrophilic, we believe this behavior results from an adsorbed film of water screening the net charge. Similar behavior with water adsorption has been observed with the other materials following immersion in water; i.e., the net charge increases slowly with time as the water film desorbs. The data on urethane are preliminary. As a matter of comparison with respect to charge densities, we may note that the surface charge of cells is usually in the neighborhood of (-) 1 μcoul/cm^2 or (-)3000 esu/cm^2.

Electrokinetic measurements have been made on occasion; however, we have not completed a systematic study at this date. This work will be reported in the future.

Charge Distribution.

While electret science has not progressed to the point where charge can be related to individual ions and molecular dipoles, we have speculated on probable configurations. These are shown in Figures 4 and 5.

Figure 4 shows Teflon with the usual excess homocharge. The homocharge is produced by injection of electrons and inert gas ions which probably transfer their charge to the fluorocarbon chains. The charge is located both on and near the surface; presumably, most of it is a few molecular diameters from the surface. The heterocharge is small and produced by impurities and polar chain terminations on the fluorocarbon molecules.

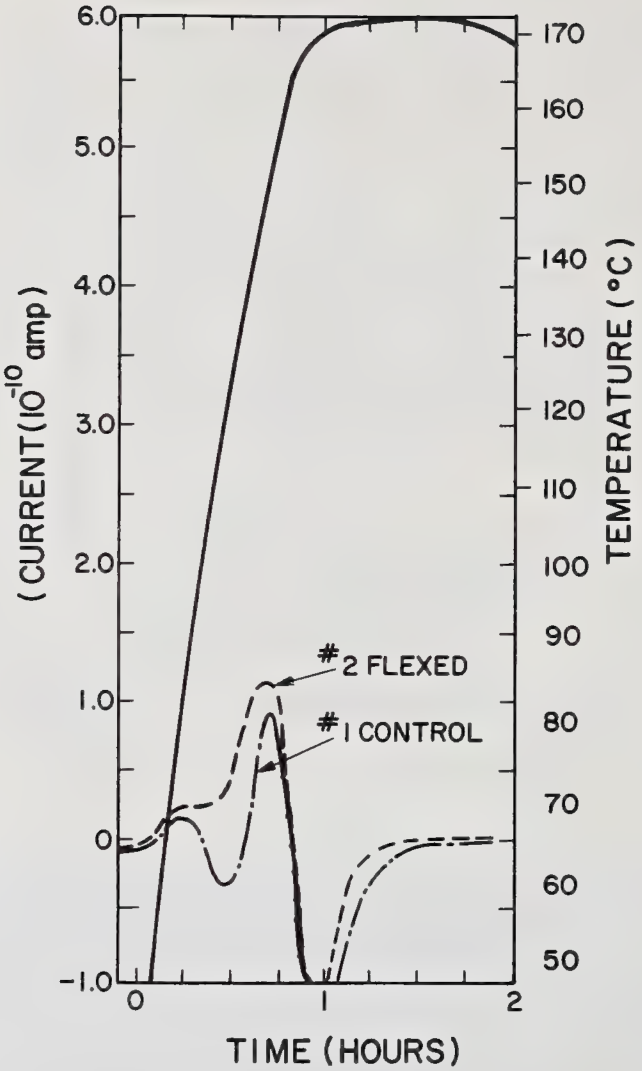

FIGURE 3. THERMAL DISCHARGE CURVES FOR INTERNAL POLARIZATION OF KEL-F

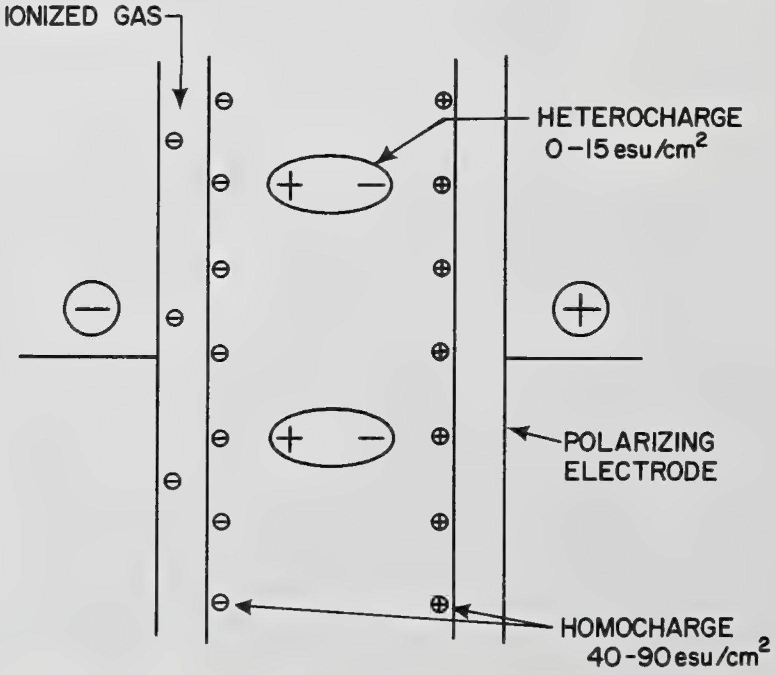

FIGURE 4. SCHEMATIC CHARGE DISTRIBUTION IN FEP TEFLON ELECTRETS

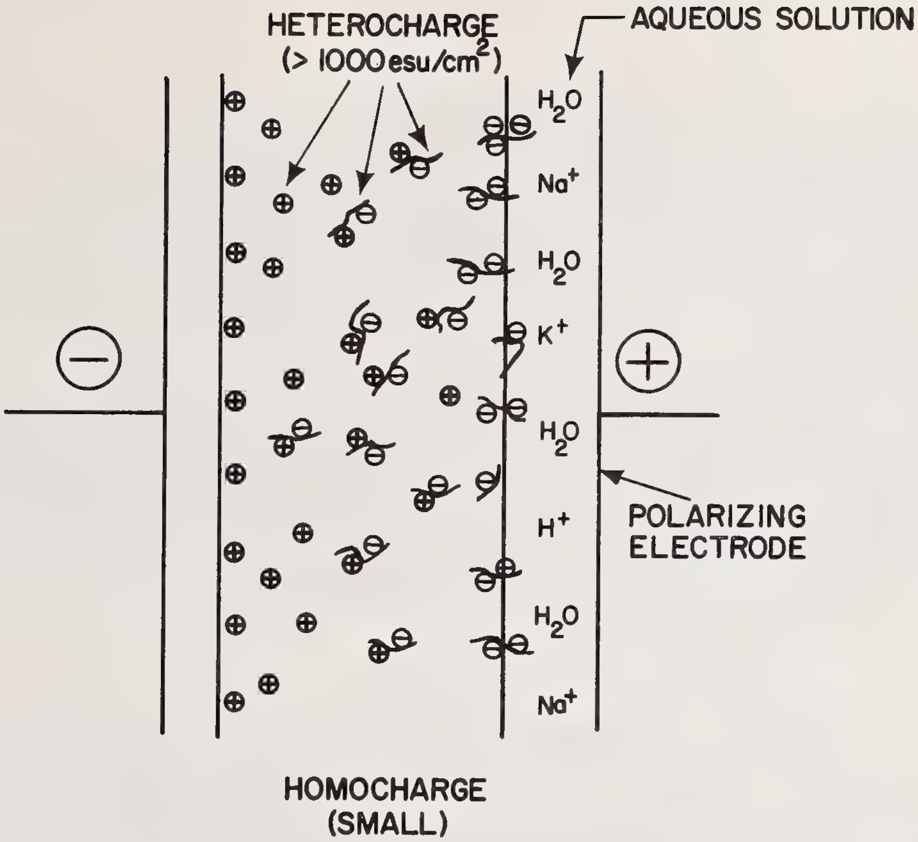

FIGURE 5. SCHEMATIC CHARGE DISTRIBUTION IN HYPALON AND HYPALON-PSS ELECTRETS

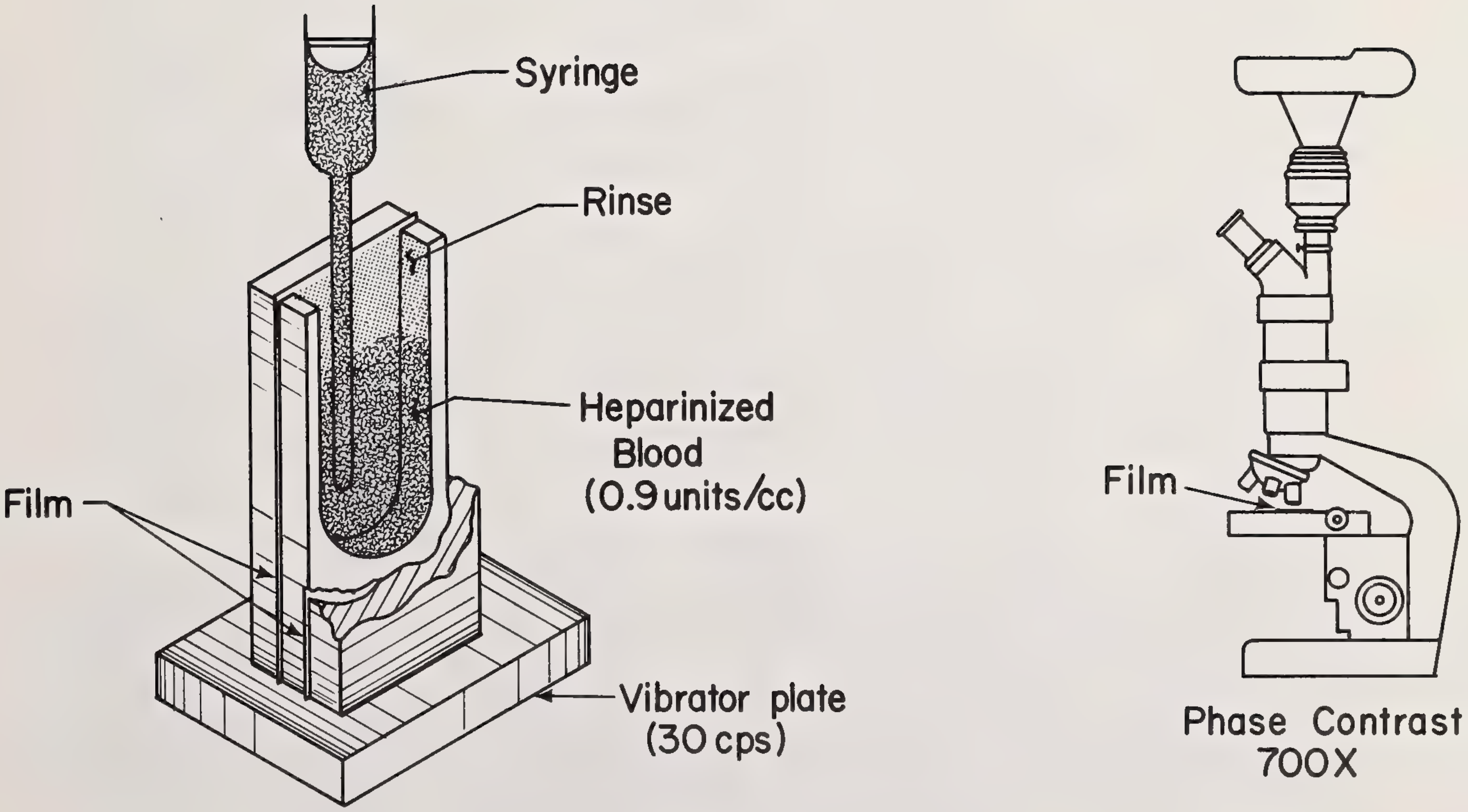

FIGURE 6. PLATELET SURFACE STUDIES

We envision a rather different structure for Hypalon and polystyrene sulfonate-doped Hypalon electrets, as shown in Figure 5. These materials have a number of known ionic groups which should be oriented during polarization. For example, the polystyrene sulfonate groups drift toward the positive pole during polarization, while counter-ions drift in the opposite direction. Heat applied during polarization actuates a free radical cross-linking agent which helps to freeze the configuration. This differs slightly from the more common polarization in which the reduction in temperature alone freezes in the configuration. You will note that a heterocharge is formed here, and that an aqueous solution contacts the surface during polarization. Electrets formed in this manner have performed quite well *in vivo*, as we will describe shortly.

Contact Angle.

The surfaces of polymers used in charge studies and in blood compatibility studies are characterized by a contact angle measurement using a drop of water. We find this measurement valuable as a control for surface uniformity, reproducibility, and freedom from contamination. Some correlations of contact angle change with polarization and with blood compatibility also have been observed. We have made occasional measurements of critical surface tension using a series of homologous organic liquids, and have found changes in surface tension similar to changes in the water contact angle. This has added to our confidence in the contact angle measurement.

Table 2 shows some typical data on contact angle and change in angle on polarization.

TABLE 2

EFFECT OF ELECTRIFICATION ON CONTACT ANGLE OF POLYMERS

Charge	Contact Angle	Polymer	Charge	Contact Angle
Ionized Gas Electrode		PVLC I-8	Metal Electrode	
0	25° ± 2°	θ film = 85°	0	84° - 86°
(+)(-)	20° - 60°		(+)(-)	72° - 82°
Ionized Gas Electrode		PFEP	Metal Electrode	
0	107° ± 2°	θ film = 107°	0	107°
(+)	101° - 103°		(-)	105° - 106°
Ionized Gas Electrode		PCTFE	Metal Electrode	
0	94°	θ film = 96°	0	96°
(+)	76° - 90°		(-)	80° - 93°
Ionized Gas Electrode		Hypalon	Aqueous Electrode	
0	89° - 90°	θ film = 89°	0	86° - 91°
(-)	88° - 89°		(-)	82° - 86°
Ionized Gas Electrode		Hypalon-PSS	Aqueous Electrode	
0	93° - 98°	θ film = 93°	0	86° - 96°
(-)	93° - 98°		(-)	67° - 76°

For PVLC, a decrease of 3-6° usually accompanied polarization with metal electrodes, while gas contact caused large and erratic decreases in polarization whether or not the film was being polarized. Presumably, the changes are due to an increase of surface chlorine and chloride. Polarized Teflon shows small changes in contact angle while Kel-F shows a somewhat greater change. Hypalon shows a considerably greater change when an aqueous contact is used instead of the ionized gas contact. It is rather surprising that the addition of a few percent polystyrene sulfonate increases the contact angle. For this material, the angle is unchanged on exposure to an ionized gas contact. However, polarization with the aqueous contact causes a very large decrease in contact angle. This large decrease is compatible with the orientation shown in the previous figure.

FLEXING AND CHARGE-STRAIN MEASUREMENTS

It would be desirable to apply the materials under development especially to blood pump bladders since these present a very large area of foreign surface to the blood. In this application, one should know how prolonged flexing will affect the surface properties. Therefore, we have studied the effect of flexing on two surface electrical properties, electret charge stability, and possible transient piezoelectric or charge-strain effects.

Flexing Studies.

One might expect continual flexing or electrolytic effects to accelerate the rate of charge decay and surface disorientation. To explore this possibility, we have carried out a series of experiments in which polarized films were flexed hydraulically with a saline solution at 2 cycles per second and 3 psi pressure to simulate an assist pump. Although a simple technique to monitor charge stability is not readily available, we have employed the thermodepolarization measurement to estimate the polarization remaining in flexed and nonflexed control samples. Tests are run with pairs of test and control films. The two films are polarized together, one flexed and the other stored in a dessicator for a period of 1 to 15 days, and the polarization remaining in each measured. Typical depolarization curves were shown previously in Figure 3. Some of the data obtained are summarized in Table 3.

TABLE 3

CHARGE STABILITY FOLLOWING SIMULATED PUMP FLEXING OF ELECTRET FILMS

Material	Flex Period (cycles x 10^6)	Polarization	Measured Charge Release	
			Flexed (esu/cm^2)	Control (esu/cm^2)
PVLC	0.17	Hetero	4050	5500
"	0.17	Hetero	6500	5500
"	1.9	Hetero	1160	900
"	2.2	Hetero	1000	1200
PFEP	0.53	Homo	180	180
PCTFE (Cast)	0.17	Hetero	22	10
"	0.88	Hetero	22	27
		Homo	12	10
PCTFE (Extruded)	0.17	Hetero	3	20
"	0.13	Hetero	7	14
		Homo	8	9
Hypalon	0.72	Homo	510	490
"	0.72	Homo	920	1000

Tests on the four materials can be summarized as follows: (1) For polyvinylidene chloride electrets, within the precision of measurement, there is no difference in the heterocharge of flexed and control samples. The flexing periods extended to 2.2 million cycles. (2) For FEP Teflon electrified with an ionized gas contact to give a large homocharge, flexing had no effect on the charge. (3) There was no measurable effect of flexing on electrified, cast Kel-F film; on the other hand, the heterocharge of Kel-F was reduced substantially for samples of extruded, oriented film. Two peaks corresponding to the heterocharge and homocharge were often given by Kel-F; the homocharge peak was not affected by flexing in either type of film. (4) Finally, Hypalon rubber electrets with homocharge appeared to be unaffected by flexing. In conclusion, it appears that, with the possible exception of Kel-F, pump flexing should not affect the electret polarization.

Charge-Strain Measurements.

To explore piezoelectric or charge-strain effects, we have assembled a measuring device to monitor net surface charge in air while the films are stressed under extension at 4.5 psi. A summary of results is shown in Table 4.

TABLE 4

VARIATION OF NULL VOLTAGE FOR ELECTRET FILMS ON SIMULATED PUMP EXTENSION

Material	Dominant Polarization	ΔV_{null} at 4.5 psi extension
PVLC	None	± 0.01 V
PVLC	Hetero	-0.1 to +0.5 V
PFEP	None	+3 to +5 V
PFEP	Hetero	25 V
PFEP	Homo	50 V
PCTFE	None	+0.1 to +0.2 V
PCTFE	Hetero	16 V
PCTFE	Homo	50 V
Hypalon	None	±4 V

In general, we believe the changes in surface charge produced by strain to be negligible for both unpolarized film and electrets. For unpolarized film, the changes in null voltage under strain varied from about 0.01 volt for PVLC to 4 volts for Teflon and Hypalon. For electrets, the values were considerably greater, varying from a fraction of a volt for PVLC to 20-50 volts for Teflon and Kel-F. The voltage swings increased with electret null voltage, but at no time did the change exceed 5-10 percent of the total null voltage. In most instances, the voltage increased and decreased in proportion to strain. However, in some cases, a voltage hysteresis was apparent. On the basis of these measurements, we doubt that pump flexing will produce an electropositive surface which could cause blood damage.

IN VITRO EXPERIMENTS

A series of platelet-surface studies has been carried out with polarized and nonpolarized polymers in both film and ring form. The fixture used in the film experiments is shown in Figure 6. Two films or coatings to be compared are placed on opposite sides of the cell, which is then filled with Ringer's solution. Ringer's was selected for priming and displacing blood after experiments with several other media. The priming solution is displaced with freshly-drawn, heparinized blood (0.9 units heparin/cm^3) in such a manner that blood-air interfaces are avoided. The cell is agitated for one minute to provide mixing; then the blood is displaced by Ringer's solution. The films are removed and examined for adherent platelets using phase contrast at 700X.

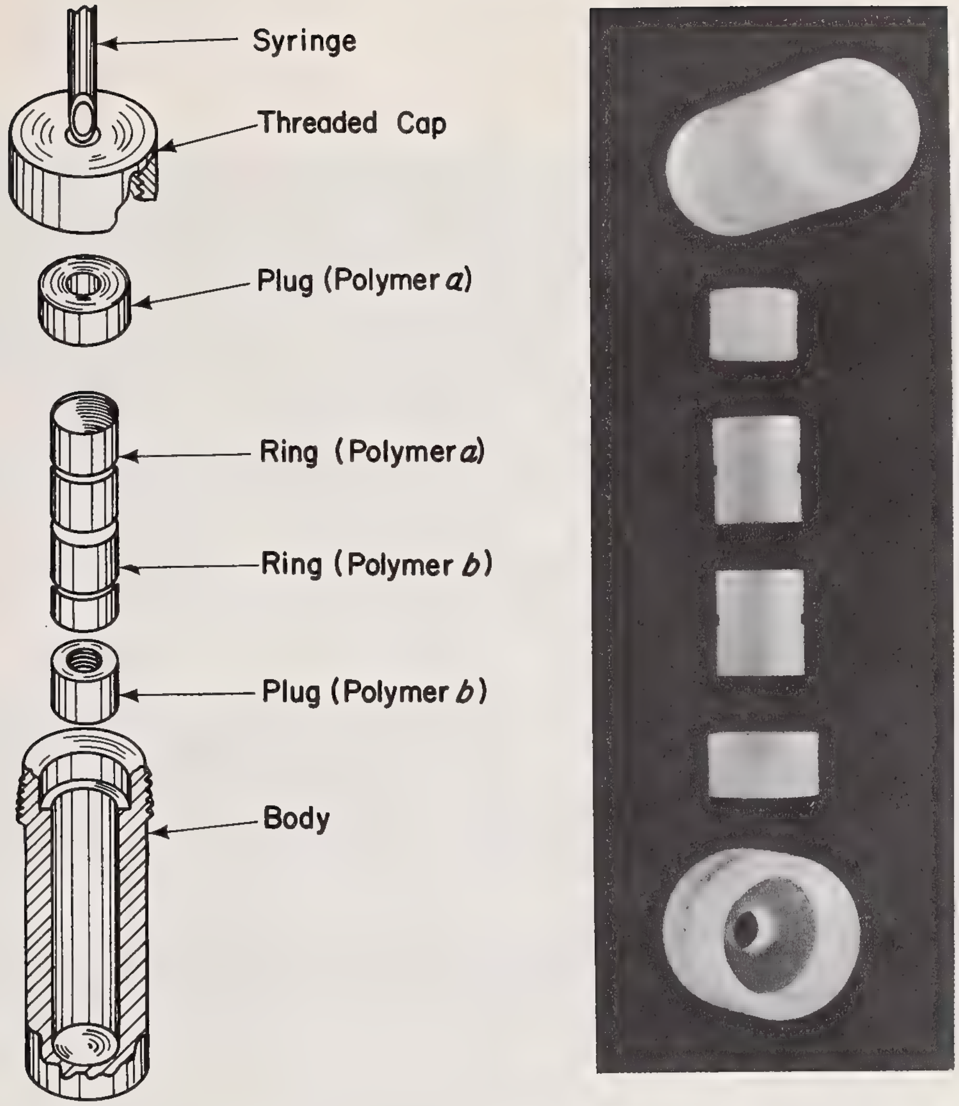

a. Exploded View

b. Components

FIGURE 7. APPARATUS FOR IN VITRO TESTING OF RINGS

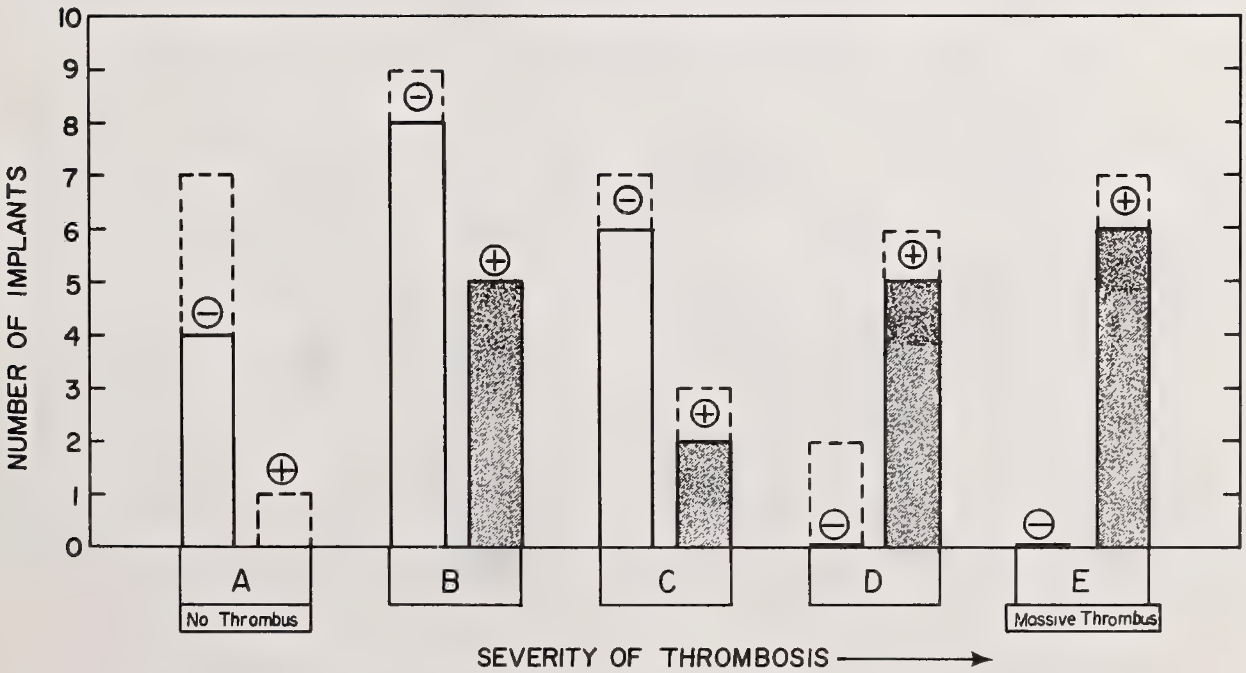

FIGURE 8. SUMMARY OF IN VIVO COMPATIBILITY STUDIES WITH PVLC ELECTRETS

Unpolarized films of Teflon, Kel-F, and cross-linked Hypalon all showed a rather light deposit of platelets of about the same density. Considerably greater platelet adhesion was found for uncross-linked Hypalon. Platelets were generally adsorbed at scratches and imperfections. For polarized samples of Kel-F film, greater platelet adhesion was found on a positive surface than on an uncharged surface, which in turn had more platelets than a negative surface.

Experiments were also carried out with rings of the type implanted in the vena cava. The apparatus shown in Figure 7 was employed. The same priming and rinsing procedures were followed. Rings were cut in half and stained (Wright's procedure) after exposure to blood. Unpolarized Kel-F rings showed considerably greater adhesion of platelets and cellular elements than Teflon rings. Hence, an alternate source of Kel-F was sought for the fabrication of vena caval rings. Negatively-polarized Teflon rings with 5 esu/cm^2 homocharge showed considerably fewer adherent platelets than uncharged rings. Polarized rings with smaller negative charge (1/4 esu/cm^2) had the same platelet deposit as nonpolarized rings. Thus, in general, the negative surfaces appeared to adsorb fewer platelets.

A variety of samples of polarized and nonpolarized surfaces has been supplied to other contractors for *in vitro* studies. We do not have the results of this work at present.

IN VIVO EXPERIMENTS

Right Atrial Tab Implants.

We carried out a series of *in vivo* tab implants during the first and second year of this program and the results have been discussed previously. However, for those who have not read our previous presentation, Figure 8 shows a summary of these experiments. Implants were usually located in the right atrium and were left in place for 1 to 30 days. Two tabs of polyvinylidene chloride (usually positively and negatively charged) were placed about 2 cm apart. On removal, the tabs were graded for thrombus starting from A for no thrombus to E for massive thrombus. It will be noted that negative tabs were relatively free of thrombus, while positive tabs were thrombosed.

Vena Caval Ring Implants.

During the past year, we have fabricated a series of vena caval rings which have been evaluated by Dr. Gott. Rings of Teflon were fabricated by machining, and rings of Hypalon and Hypalon-2% polystyrene sulfonate were prepared by coating on a metal substrate. The polarizing conditions and *in vivo* results for Teflon rings are shown in Table 5.

TABLE 5

SUMMARY OF ACUTE IN VIVO BLOOD COMPATIBILITY TEST OF NEGATIVELY POLARIZED VENA CAVA RINGS

Lot Number	Material	Date of Implant	Ring Number	Contact During Polarization	Thrombus at 2 hr		Contact Angle			V_{null}
							θ_o	θ_{pol}	$\Delta\theta$	
3	Hypalon 45	11/18/68	4	Aqueous	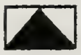	●	82°	89°	+7	-2.0
		11/19/68	5	Aqueous	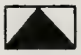	●	86°	84°	-2	-1.5
		11/20/68	6	Aqueous	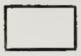	○	91°	86°	-5	-1.5
		11/21/68	7	Aqueous	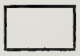	○	90°	82°	-8	-1.0
		11/21/68	8	Aqueous	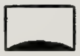	○	84°	92°	+8	-2.5
4	Hypalon 45X	11/26/68	10	Aqueous	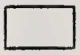	○	86°	88°	+2	-2.5
		11/26/68	11	Aqueous	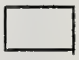	○	91°	94°	+3	-2.5
		11/27/68	12	Aqueous	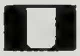	●	92°	95°	+3	-2.0
5	Hypalon 45X		4	Ionized Gas	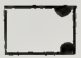		90°	88°	-2	-2.0
			5	Ionized Gas	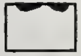		89°	89°	0	-2.0
			6	Ionized Gas	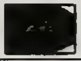		77°	99°	+22	-2.0

All rings were polarized with an ionized gas contact to give a negative homocharge. The -1200 null voltage corresponds to -24 esu/cm^2 net charge. It will be noted that all three of the rings with high negative charge were relatively free of thrombus. Ring No. 1 with the thin covering of thrombus had a considerably lower charge; in addition, the contact angle increased substantially after polarization. Contact angle changes do show a preliminary correlation with blood compatibility. Large increases in contact angle (decreases in surface tension) seem to be undesirable and decreases desirable.

The performance of Hypalon-coated rings is shown in Table 6.

TABLE 6

SUMMARY OF ACUTE IN VIVO BLOOD COMPATIBILITY TEST OF NEGATIVELY POLARIZED VENA CAVA RINGS

Lot Number	Material	Date of Implant	Ring Number	Contact During Polarization	Thrombus at 2 hr		Contact Angle θ_o	θ_{pol}	$\Delta\theta$
6	Hypalon 30X/ 2% PSSA	3/3/69	3	Aqueous	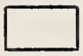	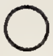	96°	69°	-27
		3/3/69	4	Aqueous	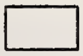	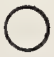	86°	67°	-19
		3/4/69	5	Aqueous	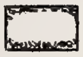	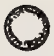	88°	76°	-12
7	Hypalon 30X/ 2% PSSA	3/14/69	2	Ionized Gas	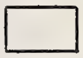	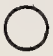	93°	95°	+2
		3/13/69	8	Ionized Gas	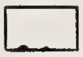	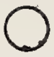	95°	92°	-3
		3/14/69	10	Ionized Gas	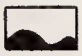	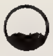	98°	98°	0
		3/13/69	11	Ionized Gas	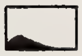	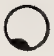	97°	98°	+1

You will note that about two-thirds of the rings were relatively free of thrombus after two-hour implants. Cross-linking had no obvious effect. Surprisingly, surfaces contacted with water or ionized gas during polarization performed the same. Measurement of net charge has little value for Hypalon, since an adsorbed water film screens the surface. It should be noted that ring 5-6 had a large increase in contact angle and thrombosed; ring 3-4 performed likewise. The other two occluded rings did not show anomalous increases in contact angle.

The performance of polystyrene sulfonate-doped Hypalon rings is shown in Table 7.

TABLE 7

SUMMARY OF ACUTE IN VIVO BLOOD COMPATIBILITY TEST OF NEGATIVELY POLARIZED VENA CAVA RINGS

Lot Number	Material	Date of Implant	Ring Number	Contact During Polarization	Thrombus at 2 hr		Contact Angle θ_o	θ_{pol}	$\Delta\theta$	V_{null}
8	Teflon	3/4/69	1	Ionized Gas	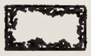	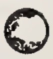	81°	92°	+11	- 400
		3/4/69	2	Ionized Gas	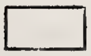	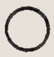	94°	93°	- 1	-1200
		3/5/69	3	Ionized Gas	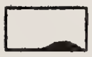	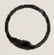	101°	102°	+ 1	-1200
		3/5/69	4	Ionized Gas	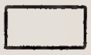	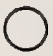	100°	100°	0	-1200

The polyelectrolyte was oriented and cross-linked during polarization to give a negative surface. These rings performed better in general than the plain Hypalon rings, since none was completely occluded. We believe the aqueous contact to be preferable for polarization, although one ring did show substantial thrombus. It should be noted that this ring had a contact angle about 8° higher than the other two, which remained free of thrombus.

We believe this surface to be especially promising for use in a pump bladder on the basis of its good blood compatibility and elastic properties. Encouraged by these experiments with elastomers, we are currently carrying out work on polyurethanes and other materials. We would like to conclude by noting that the electrical treatment of elastomers for pump bladders is a very practical approach, since the surfaces do not seem to be prone to leaching or failure of a coating, and the mechanical properties are not compromised.

DISCUSSION

MR. FOUNTAIN: Can you give some theoretical indication of what type of functionality makes good electrets?

DR. MURPHY: In order to produce an electret, one needs an electrical asymmetry in the molecules. In other words, polar molecules. This covers just about anything in a practical sense because even Teflon, which is basically non-polar, has polar end groups. They can be oriented and maintained in a fixed position. For this particular application we believe the orientational effects are quite important, i.e., we believe that the ability to orient a negatively charged unit is important. For example, with polystyrene sulfonate we are able, at least using an aqueous contact in polarization, to orient the negative groups to the surface, while in other cases where you don't carry out such treatment, the negative groups are randomly oriented.

MR. FOUNTAIN: Is there some threshold of, say, polarizability or net dipole moment below which an electret can be produced? I am thinking particularly of the classic electret experiments with canarba wax. These are very long chain acid and alcohol waxes with a very small net dipole moment, and yet they form excellent electrets.

DR. MURPHY: I would say that Teflon has an even smaller dipole moment so it is not strictly the dipole moment that is important here. It really depends on what your application is. If you want to make an electret for a transducer, I think you'd apply a different philosophy than if you want to make one for a blood compatible surface. A transducer should have very high resistivity, for example, because you want to have a material where the net charge or the charge measured by a vibrating capacitor is very high. On the other hand, we don't believe that the net charge is so important for the materials immersed in solution, because mobile ions will come to the surface and neutralize any net charge immediately when the surface is immersed in an aqueous solution. Therefore, we looked rather for a material which has appropriate polar units which we can orient on the surface.

MR. FOUNTAIN: Would you then expect that a material capable of chelating ions, e.g., positive ions, and forming an electrostatic double layer would make a good electret?

DR. MURPHY: Did you say chelating ions?

MR. FOUNTAIN: Yes, such as calcium and magnesium ions, and thereby absorbing anions to form a double layer, perhaps the chelate itself would also be capable of accepting electrons, say from a plate. If one could obtain a chelate of a polycharged metal, where one could then reduce the valence state of say a plus three transition metal that would chelate, into a plus two or plus one state, would you speculate that perhaps one might be very successful in forming electrets?

DR. MURPHY: I'm afraid I really don't have a feeling for such a system. I think that in general a system where you can achieve a fair separation of charges, such as in the ionic sulfonate or carboxyl polymer systems where you can really drift the ions apart, you can also get the orientation, but I think if you want to freeze an orientation you can't freeze a simple molecular dipole, i.e., a simple dipole of a small molecule. You can, however, freeze a polymer chain which consists of a number of carbon units. This can be frozen by entangling it in the polymer network or by actually bonding it by crosslinking. But simple molecular dipoles cannot be frozen at ambient temperatures.

DR. BYCK: You indicated that in the case of your halocarbon polymers heterocharge could be attributed either to the presence of impurities or to polar end groups. Does this mean that you've pretty much ruled out the participation of oriented carbon halogen bond dipoles?

DR. MURPHY: As I just said I don't think a simple bond as such can be permanently oriented. I think that the carbon halogen bonds may be oriented in groups or domains, i.e., you may have more domains oriented in one direction as opposed to another.

DR. BYCK: Might there be restricted rotation to give orientation in one direction?

DR. MURPHY: Yes, if there is restricted rotation of domains. However, I would anticipate that a more probable explanation could be developed simply from the number of end groups and impurities present.

DR. BYCK: Have you ever done any studies with other halocarbons where you related the magnitude of restricted rotation as a function of the size of the halogen to its ability to form electrets?

DR. MURPHY: No studies of this sort have been performed. The only studies related to halogens have been carried out on alkali metal halides. There are some very complete studies of this sort where different impurity sites related to the halogen vacancies have been related to electret behavior. In these cases, the size of the halogen is important. However, in this case, it's a matter of ionic movement rather than dipolar.

MR. PURDY: If instead of an electret you were to substitute another mechanism by which you could provide an electrostatic field, would you have the same effect *in vivo* as you would with the electret in the material?

DR. MURPHY: As I described in my presentation, the electret is not a battery as such, and therefore does not maintain an electrostatic field. If you apply a bias using electrodes, you will have electrolysis and continuous movement of ions as well as chemical reactions. An electret is different in the sense that it is a static system, so I can't think of another effective way to simulate electrets.

MR. PURDY: Well, if you could provide a high resistance to charge flow, would you not inhibit the thrombosis; or is the effect some chemical occurrence at the interface between the blood and the material surface?

DR. MURPHY: Well, we believe that it is an interface effect, simply because you cannot maintain a field for any distance beyond the double layer thickness. This double layer may be 10 or 20 angstroms and we believe it is a field effect within that limit. We have attempted to simulate an electret with a film in series with a battery but we don't consider the attempt very successful.

CHAPTER 11

THE EFFECT OF CHEMICAL STRUCTURE AND SURFACE PROPERTIES OF SYNTHETIC POLYMERS ON THE COAGULATION OF BLOOD

D.J. Lyman*, J.L. Brash, and K.G. Klein

Stanford Research Institute, Menlo Park, Calif.

Previously we showed that in static systems, individual plasma proteins are physically adsorbed in globular form to a variety of neutral hydrophobic polymer surfaces, forming compact monolayers. It appears as though in a mixture (such as in blood) proteins would be adsorbed in proportion to their collision frequency with the surface, i.e., to their concentration. In flow systems, adsorption is affected by the nature of the flow; in laminar flow, adsorption is similar to that observed for static systems, while in turbulent flow, adsorption can be delayed or even prevented. Studies on the interaction of platelets with polymers show that platelet adsorption does decrease with decreasing critical surface tension of the polymer surface. The lower energy surfaces, and thereby the surfaces with lower platelet adsorption, are the less thrombogenic. Polymer surfaces that have been precoated with a plasma protein monolayer - - a layer in which our studies have indicated the protein to be in its native globular state - - showed marked reduction in platelet adsorption, with average number of platelets adsorbed per 20,000μ^2 approaching zero. These data indicate that platelet-polymer interaction is the initiating step in *in vivo* clotting on neutral, hydrophobic polymer surfaces. A variety of new segmented urethane elastomers have been prepared as potential candidates for intra-aortic balloons. These materials show low platelet adsorption and can be prepared with a variety of mechanical properties.

INTRODUCTION AND GOALS

The mechanism of foreign surface-induced blood coagulation has been actively investigated for many years, and these studies have added greatly to the understanding of the various processes involved in clotting. However, there is a lack of fundamental information necessary for the development of non-thrombogenic materials. Therefore, the goal of this program is to gain an understanding of the adverse interactions occurring between blood and foreign materials, in particular synthetic polymers.

RESEARCH PROGRESS

Infrared Studies of Protein Adsorption

In initial studies,[1] it was hypothesized that for neutral hydrophobic surfaces, thrombogenicity should decrease as the surface energy decreases. Examination of literature data as well as new data generated by us gave support to this hypothesis.

Since it is expected that surface energy would be directly related to adsorptivity it could be deduced that thrombogenicity is in turn also related to adsorptivity. Further, since proteins are the most abundant constituent of blood excluding the cells, it might be reasonable to suppose that coagulation is initiated by adsorption of some protein. This is, of course, the basis of the various proposed contact activation mechanisms for clotting. These mechanisms would appear to be well established for the *ex vivo* clotting of blood in contact with glass.[2]

In order to explore these mechanisms further, we began a study of the adsorption of plasma constituents from solution to polymer surfaces using infrared internal reflection spectroscopy.[3] The results for individual plasma proteins (albumin, γ-globulin, fibrinogen) indicated that these proteins are physically adsorbed on a variety of neutral hydrophobic polymer surfaces.

From quantitative spectral measurements it was deduced that compact monomolecular layers are formed in which the proteins retain their native globular form. There is no evidence of dimensional denaturation such as is generally assumed to take place at the air-water interface.[4] Due to the similarity of the infrared spectra of different proteins the technique cannot be used to study competitive adsorption from mixtures. However, since all proteins studied behave the same we assume that in a mixture proteins would be adsorbed in proportion to their collision frequency with the surface, i.e., to their concentration. In addition, since adsorption is similar on surfaces having a wide range of surface energy, the contact activation theory as applied to these materials would seem to be in some doubt.

In order to achieve a closer approach to potential "in use" conditions we undertook a study of these same protein-polymer surface systems under conditions of flow.

Measurements were made under both turbulent and laminar flow conditions in channels of different geometry. Most of the work was carried out with Silastic and polyethylene substrates and serum albumin solutions.

---

*Present address: University of Utah, Division of Materials Science and Engineering, and Division of Artificial Organs, Salt Lake City, Utah, 84112.

For the polyethylene-albumin system (Figure 1), adsorption in laminar flow is virtually identical to that observed under static conditions: adsorption reaches saturation within a few minutes and remains at this "monolayer" level with perhaps a slight increase after 200 minutes. In turbulent flow conditions adsorption reaches multilayer proportions within 15 minutes, the surface concentration being about 10 times that in the monolayer. Solution optical rotation measurements were also carried out as a means of observing corresponding solution denaturation. It was found that substantial increases in levorotation occurred in both laminar and turbulent conditions but in the latter the rate was about twice as fast. No significant differences could be observed in the first 5 hours of flow where the adsorption is different for the two types of flow.

For the Silastic-albumin system (Figure 2) laminar flow adsorption and changes in rotation are virtually identical to those for polyethylene-albumin. However, in turbulent flow, it would appear that adsorption is negligible up to at least 5 hours. Thereafter the data are somewhat contradictory and no definite conclusions can be drawn at this time. The fact that there is no adsorption in the initial stages of turbulent flow would suggest that denaturation of the solution cannot be attributed to an adsorption-denaturation-desorption sequence and is probably a phenomenon independent of the surface. By analogy, we may speculate that this is also true for polyethylene. In that system, however, or any system where adsorption does occur the adsorbed layer could still be continuously exchanging with molecules in solution, since, if no surface denaturation occurs, there will be zero net effect on the solution.

In laminar flow conditions, which have a more direct bearing on blood circulation, both adsorption and solution denaturation occur in the two systems we have studied. The denaturation is slower than for turbulent flow and by analogy is also presumably independent of the surface.

Electron Microscopy of Proteins on Surfaces

Both static and flow adsorption studies using the infrared reflection technique suggest that no dimensional denaturation of proteins occurs on polymer surfaces. However, these infrared studies indicate only the average behavior of the surface over a relatively large area whereas it may well be that due to the enzyme amplifier nature of the coagulation scheme[5] a few isolated events are the critical ones in terms of initiation of clotting. Such events would not be revealed by the infrared technique, but might show up in direct visualization such as with the electron microscope.

Difficulties were encountered in applying shadow replication procedures (developed earlier for polished silica surfaces) to hydrophobic polymer surfaces. The surfaces revealed considerable structure and shadow grain was coarse to the point of obscuring any protein forms which might be present.

Limited success has been achieved for γ-globulin adsorbed on Silastic, polyethylene, and Teflon FEP with a staining technique using phosphotungstic acid. With a few fairly minor differences these substrates behaved similarly. The protein appeared to cover the surface in a loose lace-like network with retention of native form within the lace. The lace density varied from surface to surface as did the time to achieve an "equilibrium" coverage.

The distribution of protein on these surfaces is certainly different from that observed on silica, though both do show "spherical segments" which have the dimensions of the native protein. This distribution is also somewhat at odds with deductions from the infrared data, though the latter data cannot distinguish between different distributions of protein as long as the surface concentration remains the same.

Adsorption of Phospholipids

Phospholipids are known to play an essential role in clotting and are required in the activation of Factors VIII and V. They are present in normal plasma at a concentration of around 200 mg % and, of course, are released by damaged platelets in hemostasis. It seemed important, therefore, to consider the behavior of phospholipids at polymer surfaces.

The infrared reflection spectroscopy technique proved feasible for study of phospholipids but due to the lower molecular weight and lower extinction coefficient of the observed band the sensitivity was much reduced.

The results of static adsorption experiments with animal lecithin on a variety of hydrophobic polymer surfaces show that although there is a small but definite interaction with polyethylene and polystyrene, there is none with the lower energy surfaces, silastic and Teflon FEP. This suggests that a minimum surface energy may be necessary for the adsorption of phospholipids, with the critical value somewhere between 32 ergs/cm^2 (polyethylene, 32, and polystyrene, 33) and 20 ergs/cm^2 (Teflon FEP, 18, and Silastic, 20). The surface concentration on polyethylene and polystyrene corresponds approximately to a monolayer of micelles.

In laminar flow conditions polyethylene was found to adsorb up to five times as much phospholipid as in the static experiments for 2-hour exposures (Table 1). This could be explained either by a change in configuration of micelles within a monolayer or by the onset of multilayer formation. It is not clear, however, why there should be this marked difference between static and flow conditions.

TABLE 1

SURFACE CONCENTRATION($\mu g/cm^2$) OF PHOSPHOLIPIDS ADSORBED TO POLYETHYLENE, SUSPENSIONS (200 mg %) ARE IN LAMINAR FLOW AT 100 ML/MIN THROUGH A BABB GRIMSRUD CELL

		15 min	30 min	45 min	1 hr	2 hr	2 hr static
Ether Solution Suspensions	Lecithin	0.82	1.63	1.47	1.96	2.61	0
	Cephalin	1.58	2.12	3.8	4.67	4.56	0
Mechanical Suspensions	Syn. Lecithin	1.7	2.4	2.2	3.1		
	Lecithin	0.87	1.8	2.28	3.86	4.89	1.0
	Cephalin	1.63	2.94	2.17	3.19	6.0	0.76

Protein Interaction with Hydrophilic Materials

Preliminary work has begun on the adsorption of plasma proteins on hydrophilic materials, using cellulose (Cuprophane) as the substrate since the infrared technique can be used by measuring the amide II band at 6.5 μ. Studies have been made with albumin, γ-globulin, and fibrinogen. Each system has been investigated by measuring adsorption as a function of time at a fixed protein concentration and as a function of protein concentration at a fixed time. Equilibration appears to take place around the same value for each approach, with albumin equilibrating at a concentration of 0.5 $\mu g/cm^2$ apparent surface area and γ-globulin at 0.4 $\mu g/cm^2$. Fibrinogen adsorption is negligible, indicating a decreasing adsorptivity with increase in molecular size. These concentrations are to be compared to values of about 1.0 $\mu g/cm^2$ for these proteins on hydrophobic surfaces. Whether this is an indication of a real difference in adsorption is difficult to assess at this time, since the actual surface area of the swollen material is unknown. However, there is a real difference in the ease of desorption between hydrophobic surfaces and the hydrophilic Cuprophane surface. Overnight (and possibly shorter) immersion of the cellulose-protein complex in distilled water returns the spectrum to its original form. On the other hand, protein can never be completely removed from a hydrophobic surface.

Interaction of Platelets with Polymer Surfaces

Since the overall goal of our studies is to gain an understanding of the adverse *in vivo* interactions that occur when blood comes in contact with polymers, we must consider the interactions of the cellular elements as well as the interaction of plasma constituents. The role of platelets is of particular importance in the study of *in vivo* thrombus formation. Our preliminary studies[6] showed heavy platelet adsorption resulting from a denatured protein layer deposition formed by the movement of the polymer surface through an air/blood interface. To avoid this a closed (flow-through) cell was developed in which the blood displaces buffered saline from the prefilled cell, thus preventing the formation of an air interface.[6]

The platelet adsorption characteristics of a variety of uncharged, hydrophobic polymers have been determined using this closed (flow-through) cell technique (Table 2).

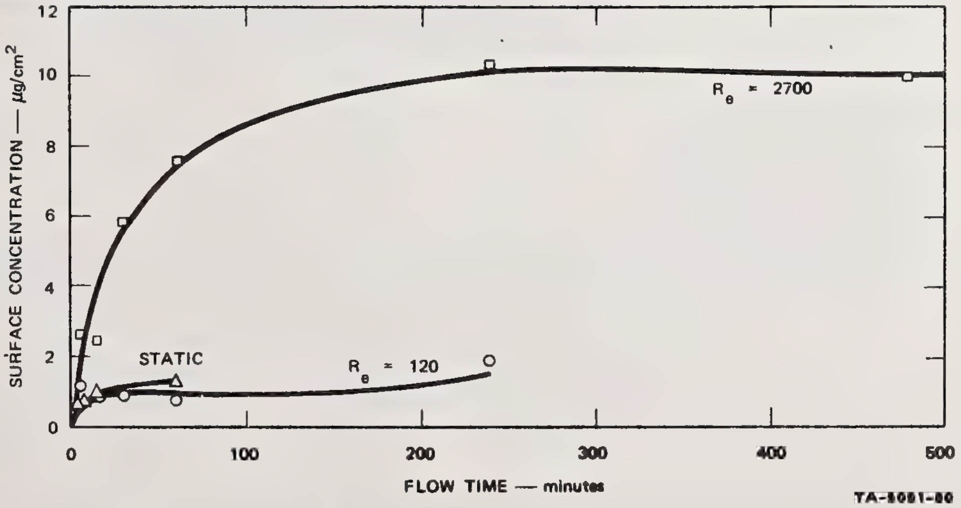

FIGURE 1. ADSORPTION OF ALBUMIN TO POLYETHYLENE SURFACES IN FLOW SYSTEMS

TABLE 2

ADSORPTION OF PLATELETS FROM WHOLE BLOOD TO VARIOUS POLYMER SURFACES [a]

Polymer	Critical Surface Tension dynes/cm	Average Platelet Adsorption, per 20,000 μ^2
Poly-1,1-dihydroperfluoroacrylate	16.5	1.6
Polytetrafluoroethylene	18.5	4.6
Fluorinated ethylene/propylene copolymer	20.0	5.4
Polydimethyl siloxane	21.0	4.6
Polybutyl acrylate	22.0	1.7
Polypropylene	30.0	8.9
Polyethylene	31.0	15.3
Polystyrene	36.0	11.3
Polyvinyl chloride	39.0	17.1
Poly(ethylene 4,4′-methylene diphenylene-urethane)	39.3	11.3
Polynonamethylene adipamide	40.0	16.7
Poly(4,4′-isopropylidene diphenylene carbonate)	42.5	15.5
Polyethylene terephthalate	43.0	16.1

a. Flow time 1 minute using closed (flow-through) cell.

A plot of platelet adsorptivity versus critical surface tension shows a qualitative similarity to the relationships demonstrated earlier between critical surface tension and surface thrombogenicity as measured by partial thromboplastin time and between critical surface tension and *in vivo* surface thrombogenicity.

It was of interest to note that when an air bubble was inadvertently introduced into the cell, heavier than normal platelet adsorption occurred, again indicating the damaging effects of a blood/air interface.

These observations led us to examine the effect of a native protein layer on platelet adsorption, since it was felt that such a surface should be less damaging to platelets. A series of polymer surfaces were coated (from solution) with adsorbed monolayers of albumin, fibrinogen, and γ-globulin, and their platelet adsorption characteristics were determined. The results (Table 3) indicate that when a polymer is precoated with a native protein layer, fewer platelets are adsorbed than on the pure polymer surface, or on a denatured protein surface such as that formed at an air/blood interface.

TABLE 3

ADSORPTION OF PLATELETS FROM WHOLE BLOOD TO VARIOUS PROTEIN-COATED POLYMER SURFACES

	Protein Coating			
Substrate	Albumin	γ-Globulin	Fibrinogen	Plasma
Polyethylene	0.1	0.5	0.6	0.5
Polytetrafluoroethylene	-	0.6	0.7	0.7
Fluorinated ethylene/ propylene copolymer	0.5	0.4	0.9	0.5
Polydimethylsiloxane	0.1	0.5	0.4	-
Poly(4,4′-isopropylidene diphenylene carbonate	-	-	-	0.5

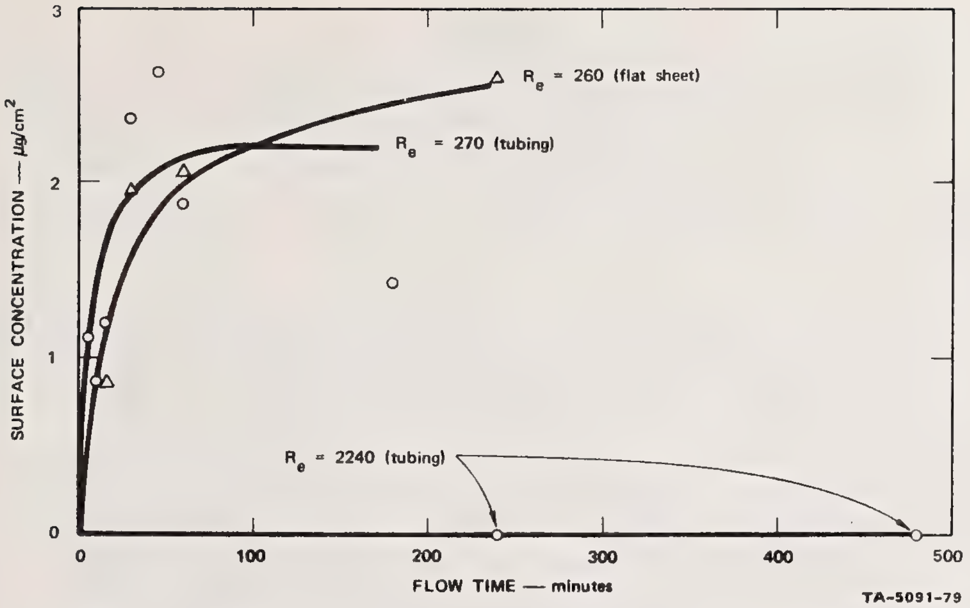

FIGURE 2. ADSORPTION OF ALBUMIN TO SILASTIC SURFACES IN FLOW SYSTEMS

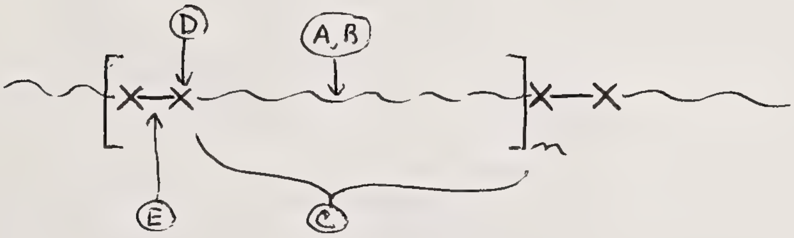

FIGURE 3. SCHEMATIC OF BLOCK COPOLYURETHANE ELASTOMER

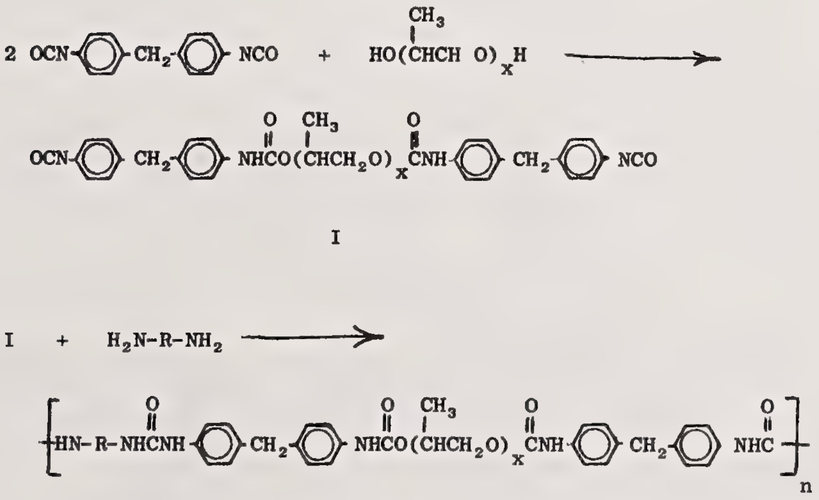
2 OCN-⬡-CH₂-⬡-NCO + HO(CHCH O)ₓH
OCN-⬡-CH₂-⬡-NHCO(CHCH₂O)ₓCNH-⬡-CH₂-⬡-NCO
I
I + H₂N-R-NH₂
HN-R-NHCNH-⬡-CH₂-⬡-NHCO(CHCH₂O)ₓCNH-⬡-CH₂-⬡-NHC
n

FIGURE 4. SYNTHESIS OF BLOCK COPOLYURETHANE ELASTOMER

This is not unexpected since, if these proteins are truly native, their interaction with platelets should be no different than that in blood itself. The similarity in adsorption of platelets to the various albumin-coated surfaces (average platelet count was 0.2 per 20,000 μ^2), the various γ-globulin-coated surfaces (0.5) and the various fibrinogen-coated surfaces (0.7) would indicate essentially complete masking of the substrate and would suggest that such adsorption is due either to impurities in the plasma protein coating (other plasma constituents, denatured proteins, or coating imperfections), or to the nature of the surface resulting from these closely packed arrays. The fact that platelet adsorption is essentially zero when the surface is coated with protein by our standard adsorption technique, whereas it is high when a blood/air interface is present, provides additional evidence that proteins adsorbed to a polymer surface in the absence of an air interface are not denatured.

White cells often attacked the protein coatings (especially albumin and γ-globulin) and platelets were often found clumped around the white cells. To minimize this effect, the polymer surfaces were coated with the donor's own plasma, then the films were exposed to their whole blood in the closed (flow-through) cell. As expected, fewer white cells adsorbed and those that did were in good condition and not lysed. Platelet adsorption on these plasma-coated surfaces averaged 0.6 platelets per 20,000 μ^2 area.

It was also of interest to see whether or not platelet adsorption on the protein-coated surfaces would increase with longer exposure times. From experiments with a fluorinated ethylene/propylene copolymer coated with albumin, it would seem as though the adsorption does not increase with time. The average number of plates adsorbed was 0.2 per 20,000 μ^2 for times ranging from 30 seconds to 3 minutes on the albumin-coated surfaces, while for the uncoated polymer surface, the number of platelets increased from 2.6 per 20,000 μ^2 at 30 seconds exposure to over 18 per 20,000 μ^2 at 3 minutes.

It would appear, therefore, that coating uncharged, hydrophobic polymer surfaces with a native layer of a plasma protein might represent an approach to achieving a nonthrombogenic surface. Of the proteins studied, albumin appears to be the most effective coating material.

Elastomeric Copolyurethane Materials

The increased interest in intra-aortic balloon devices has focused attention on the need for improved elastomeric materials for fabrication of the balloons. Several commercial materials, such as the Lycra and Estane urethane elastomers, have shown some promise. It was of interest then to investigate this generic type of polymer in more detail to determine if an improved balloon elastomer could be developed.

These urethane elastomers (shown schematically in Figure 3) are essentially block copolymers composed of flexible blocks, or macrosegments, coupled by relatively non-flexible segments. The blocks tend to aggregate into discrete phase-domains and as a result, the crystallization of the stiff, or "hard," segments act as non-covalently bonded crosslinks. Since the properties of a polymeric material are basically determined by the structural features of the polymer chains, it is necessary to consider the contribution of both the flexible segments and the non-flexible segments to the overall elastomeric properties. For example, the properties of the flexible block may be altered by: varying the type of macrosegment (A) used, i.e., polyether, polyester, polyhydrocarbon, etc.; varying the molecular weight, or chain length (B), of that segment; or by varying the structural arrangement of the overall flexible block, or macrodiisocyanate (C), i.e., a mono-type, a dimer-type, etc. The properties of the non-flexible segment may be changed by varying the type of diisocyanate (D) used and by varying the type of coupling molecule (E), usually a diamine, used to chain extend the macrodiisocyanate.

Linear elastic copolyurethanes of this generic type can be prepared by a modified solution polymerization technique.[7] In this modification, the diisocyanate and polyether (such as polypropylene glycol) are first reacted in solution (dimethyl sulfoxide), to give a macrodiisocyanate (Figure 4), then the reaction mixture cooled, and a diamine added to couple these macrodiisocyanate segments together, forming a viscous solution of high molecular weight polymer.

The coupling reaction occurs readily at 10-30 C when hydrazine and aliphatic diamines are used. When aromatic diamines are used, higher temperatures (50 C) are needed.

These linear polymers can be isolated, and redissolved in urethane solvents such as N,N-dimethylformamide and dimethyl sulfoxide, and the viscous solution cast on glass plates or over mandrels to get the desired fabricated form.

A series of copolyether-urethanes of this type, in which the polypropylene glycol, molecular weight 1000 and 2000, was capped with methylene bis(4-phenylisocyanate) and then chain extended with hydrazine, ethylene-diamine, and hexamethylenediamine, have been prepared and cast into films. All of these materials are elastomeric. Their physical properties are shown in Table 4, and compared to an Estane sample being used for preliminary balloon fabrication studies.

TABLE 4

PHYSICAL AND MECHANICAL PROPERTIES OF BLOCK COPOLYETHER-URETHANES (a)

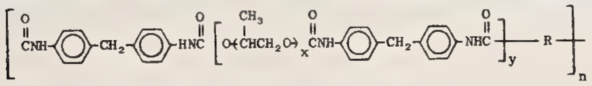

Structure			Initial Modulus, psi	Recovery Time from 200% E, sec	Average number of platelets adsorbed[d] per 20,000 μ^2
R	Mol. wt. $(\overset{CH_3}{CH}CH_2O)_x$	Y			
-HNNH-	1000	1	-	-	-
$-NH(CH_2)_2NH-$	1000	1	3570	60	0.4
$-NH(CH_2)_6NH-$	1000	1	2330	60	0.2 (0.1-0.4)
-HNNH-	1000	2	375	15	0.5 (0.4-0.6)
$-NH(CH_2)_2NH-$	1000	2	1140	60	0.4 (0.4-0.4)
$-NH(CH_2)_6NH-$	1000	2	945	60	0.2 (0.0-0.4)
-HNNH-	2000	1	481	10	0.4 (0.3-0.4)
$-NH(CH_2)_2NH-$	2000	1	-	-	-
$-NH(CH_2)_6NH-$	2000	1	1656	60	0.7
-HNNH-	2000	2	244	Immediate	0.1 (0.0-0.2)
$-NH(CH_2)_2NH-$	2000	2	-	-	-
$-NH(CH_2)_6NH-$	2000	2	-	-	-
Western Gear Estane sample			5900	Partial recovery in 15 minutes	0.5 (0.0-1.0)

In terms of the initial modulus, calculated as the slope of the sigma (stress) versus lambda (1 + strain) curve, it appears that the ethylene diamine coupled structures are better than the hexamethylene diamine structures which are, in turn, better than the hydrazine coupled structures; similarly, the 1000 mono structures > 2000 mono structures > 1000 dimer structures > 2000 dimer structures. However, while the initial moduli of these samples are still not as good as the Estane material, their stress recovery is much better. As an approach to improve the initial moduli, additional samples of this series in which the polypropylene glycol molecular weight is 440, and samples in which the chain extender is p-phenylene diamine are in preparation.

Platelet adsorption studies on these materials using our closed (flow-through) cell show that all of these surfaces have platelet adsorption less than one per 20,000 μ^2. (Table 4) Thus, these surfaces are more similar to the protein monolayer surfaces (platelet adsorption $\ll 1$) than to the hydrophobic polyurethane surfaces (platelet adsorption $\sim$ 15-20). This would suggest that the "hard" urethane segment domains are in a morphological configuration which effectively masks their influence. Since it is possible to vary the physical and mechanical properties of these elastomers by altering the structure of the constituents and the overall organization of the block copolyurethane, it should be possible to tailor-make copolyether-urethanes having specific end use requirements for intra-aortic balloons.

REFERENCES

1. D. J. Lyman, W. M. Muir, I. J. Lee, Trans. Amer. Soc. Artif. Int. Organs 11, 301 (1965).
2. R. G. MacFarlane, Thromb. Diath. Haemorrhag. Suppl. 17, 45 (1964).
3. J. L. Brash and D. J. Lyman, J. Biomed. Maters. Res., in press.
4. E. Gorter and F. Grendel, Proc. Koninkl. Ned. Akad. Wetenschap. 29, 1262 (1926); 32, 770 (1929).
5. H. C. Hemker, P. W. Hemker, and E. A. Loeliger, Thromb. Diathes. Haemorrh. 13, 155 (1964).
6. D. J. Lyman, J. L. Brash, S. W. Chaikin, K. G. Klein, and M. Carini, Trans. Amer. Soc. Artif. Int. Organs 14, 250 (1968).
7. D. J. Lyman, J. Polymer Sci. 45, 49 (1960).

DISCUSSION

DR. BLACKSHEAR: In your slides of the kinetics of protein deposition, there appeared to be a time interval before you reach some sort of steady state of concentration. This seems rather slow to be diffusion controlled. Had you looked into whether this is a process limited by diffusion or whether some reaction took place that admitted additional protein on the surface?

DR. LYMAN: No. This has to be done in our next studies. I feel that it is a diffusion limited process.

DR. BLACKSHEAR: You noted that when a bubble was introduced into the test cell, you noticed a large increase in platelet deposition; were the platelets present at the time the bubble was introduced?

DR. LYMAN: In general, the bubble was at the interface between the blood and the buffered saline filling solution.

DR. BLACKSHEAR: Was it at the head of the blood?

DR. LYMAN: Yes.

DR. BLACKSHEAR: Then, platelets were present on one side?

DR. LYMAN: Yes.

DR. SPAET: I wonder if you could characterize the blood that is passing through your test cells?

DR. LYMAN: It is human venous blood drawn from the cuboidal vein, passing directly through our closed (flow-through) cell.

MRS. ANDERSON: I was wondering why you have been using whole blood for these protein adsorption studies rather than platelet rich plasma. Is it not possible that you are getting some red cell damage and the subsequent release of ADP from the red cell aggregation followed by platelet aggregation and/or adsorption? My question is why not use platelet-rich plasma for these protein adsorption studies rather than whole blood?

DR. LYMAN: From some of our discussions, we felt that the platelets in platelet-rich plasma may not be in the same condition as they are in the whole blood. It is possible that red cell contact could leave behind some debris on which the platelets would stick. Since the system is flowing, I do not think that ADP release from the red cells would have much effect on platelet adsorption.

MRS. ANDERSON: My other question is that I believe that at one point in your presentation you used the term "platelet damage". Are you using the terms "platelet adsorption" and "platelet aggregation" interchangeably? The reason I ask this is that our studies in the last few years have shown that you can have considerable platelet adsorption on surfaces without subsequent platelet damage or rupture. Having determined Stypven clotting times for platelet factor III, and platelet acid phosphatase, we find that the platelets are essentially undamaged even though they have been adsorbed. Have you measured the platelet aggregation and/or platelet damage?

DR. LYMAN: The number of platelets being adsorbed on our surfaces is very small compared to the total number of platelets in the flowing blood. As a result, I do not think we would be able to detect some of these factors released from the platelets. On some of these surfaces we may well have platelet adsorption with no accompanying damage.

UNIDENTIFIED DISCUSSANT: Did you notice any correlation between the concentration of the protein solution used for adsorption and the structure of the monolayer?

DR. LYMAN: No, we have done the experiments at different solution concentrations, and at various adsorption times, and we approach the same equilibrium structure.

UNIDENTIFIED DISCUSSANT: We have found that there is considerable denaturation on adsorption from very diluted solutions.

DR. LYMAN: Onto what surface?

UNIDENTIFIED DISCUSSANT: On polystyrene.

DR. LYMAN: No, I'd say we have found no difference in our experiments.

DR. PETSCHEK: I am rather surprised at the platelet concentrations that you obtain on your surfaces. In our experiments, we find numbers more in the order of a thousand per 20 thousand square microns on a variety of material surfaces. I was wondering whether there were any surfaces that did show an increased adherence of platelets, or if you have any idea why there is a difference between our results and yours?

DR. LYMAN: When we have an air interface present or when we put a denatured protein layer on a surface, we do get the higher values, though not quite approaching the values that you mentioned. There is another difference between your work and our work which is that we apparently obtain platelet adsorption by 30 seconds, (which is the fastest we can do our experiments), and possibly earlier while you see no platelet adsorption in your experiments before one minute. Do you have any explanation for that?

DR. PETSCHEK: With polyurethane between 30 and 50 seconds elapse before platelets begin to settle on the surface. Our experiment does not have an air interface. I do not believe, however, that this is the explanation. It may be that the differences in flow rate and flow configuration are significant factors.

DR. LYMAN: It might also be that the difference in turbulence between the two test systems might be an accentuating factor accounting for some of the observed differences.

CHAPTER 12

POLYMERIC MATERIALS FOR CIRCULATORY ASSIST DEVICES

J. S. Byck, S. Chow, L. J. Gonsior, W. A. Miller, W. P. Mulvaney,
L. M. Robeson, and M. A. Spivak

Union Carbide Corporation, Bound Brook, N. J.

As part of a program of polymer synthesis, an attempt has been made to develop a mechanically useful peptide-like polymer by block copolymerization of poly(amino acids) with polysiloxanes. Recent experiments have shown that difunctional hydroxyl terminated poly(γ-benzyl L-glutamate) oligomers can be prepared and then coupled with suitably terminated silicones to produce promising block copolymers. In a second phase of the program, the factors influencing polyelectrolyte blood compatibility are being studied by systematic synthesis of several families of carboxylic and sulfonic acid substituted copolymers. Much of this work has involved ethylene/acrylate copolymers, with particular emphasis on their partially neutralized Li, Na, K, Mg, and Ca ionomers. A high pressure aqueous emulsion polymerization route to the analogous ethylene/vinyl sulfonate polyelectrolyte system has been developed, as has a route to the more water sensitive vinyl acetate/crotonate copolymer system. Attention has also been given to the problem of developing a polymeric material which can be rendered compatible by growth and anchoring of an exceedingly thin nondegenerating neointima. Fabrication of such an experimental material has been accomplished by using an immiscible polymer fibrillation technique to generate polypropylene fibers in the 1μ diameter range, and then forming them into ultrathin nonwoven networks as thin as 2μ. The grossamer networks can be reinforced and bonded to a nonporous support by vapor deposition of a several thousand angstrom conformal coating of a Parylene polymer.

During the last year, the Polymer Research and Development Laboratories of Union Carbide Corporation have been conducting a three part research program directed at development of improved polymeric materials for use in circulatory assist devices.

AMINO ACID-CONTAINING BLOCK COPOLYMERS

One of two polymer synthesis projects in this program has been an investigation of modified synthetic polypeptides prepared by block copolymerization of poly(amino acids) with conventional synthetic polymers. Other than the research by Lyman and coworkers[1] involving sarcosine/urethane copolymers, this broad class of macromolecules has not received significant attention. Block copolymers are, of course, distinguished by the fact that they consist of discrete, extended homopolymer segments which may alternate repeatedly in a single copolymer chain to form $(AB)_n$ block copolymers, or may only repeat once or twice to form AB or ABA block copolymers (Figure 1). During the current stage of this investigation, attention has been given to poly(L-glutamic acid) and poly (γ-benzyl L-glutamate) as the peptide "A" blocks and polysiloxanes (silicones) as the "B" blocks.

As in all block copolymerizations, preparation of silicone/poly(amino acid) copolymers has involved two major problems. These are:

1. Preparation of appropriate block segments or "oligomers" having reactive functional groups at the ends of the oligomer chain; and
2. Utilization of proper chemical techniques to couple functionalized oligomers to yield high molecular weight block copolymers.

In the current program, it has been necessary to primarily focus attention on synthesis of hydroxyl-terminated difunctional poly(amino acid) oligomers.

As might be expected, the well known polymerization of amino acid N-carboxy anhydrides has been employed as the oligomer-forming reaction (Figure 2). This has permitted introduction of hydroxyl functionality at the C-terminal position of the poly (amino acid) by a simple and straight forward procedure. Since N-carboxy anhydrides are characteristically polymerized to moderate molecular weights by primary amine initiation, it is possible to initiate polymerization of γ-benzyl L-glutamate N-carboxy anhydride with hydroxyl substituted primary amines--such as ethanolamine or para-aminophenol--and, thus, to directly obtain mono-hydroxy-functional oligomers. It is also necessary, however, to introduce a small quantity of phenylalanine N-carboxy anhydride near the end of the polymerization reaction to produce phenylalanyl terminated polypeptides. This is done to prevent cyclization of the N-terminal benzyl glutamate residue, which is a slow side reaction that otherwise would render the N-terminal position unreactive. These polymers have primary amino groups at the N-terminal position, and must therefore, be converted to difunctional oligomers in a second reaction (Figure 3). Introduction of hydroxyl groups in place of the amino moieties in the monofunctional oligomer mixture is best carried out by a simple end-capping reaction. This is accomplished by reacting the mono-hydroxyfunctional materials with an excess of ε-caprolactone at elevated temperatures. The resulting ring-opening reaction yields ε-hydroxyamide terminated oligomers which are difunctional. In general, it is observed that conversion of 100% of the oligomers

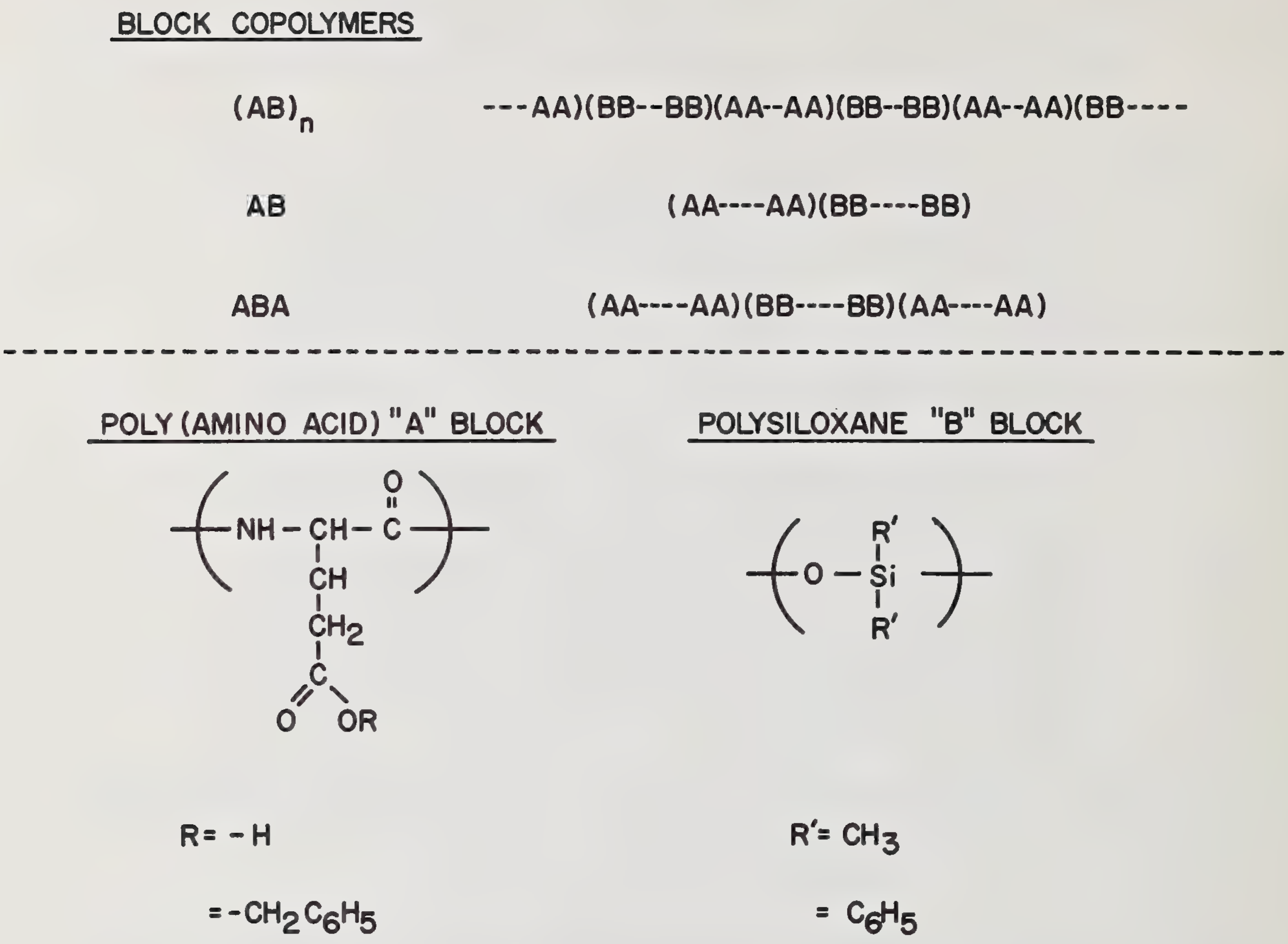

FIGURE 1. BLOCK COPOLYMERS

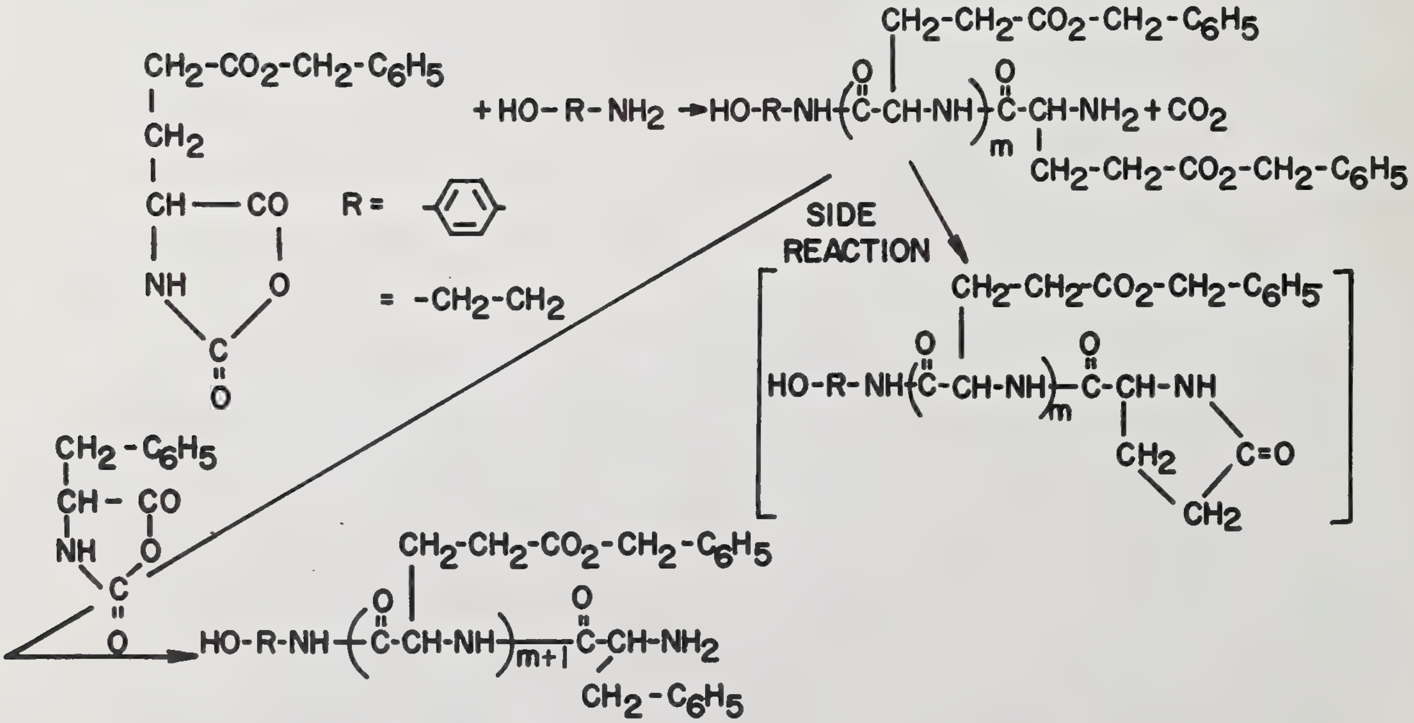

FIGURE 2. POLYMERIZATION OF AMINO ACID N-CARBOXY ANHYDRIDES

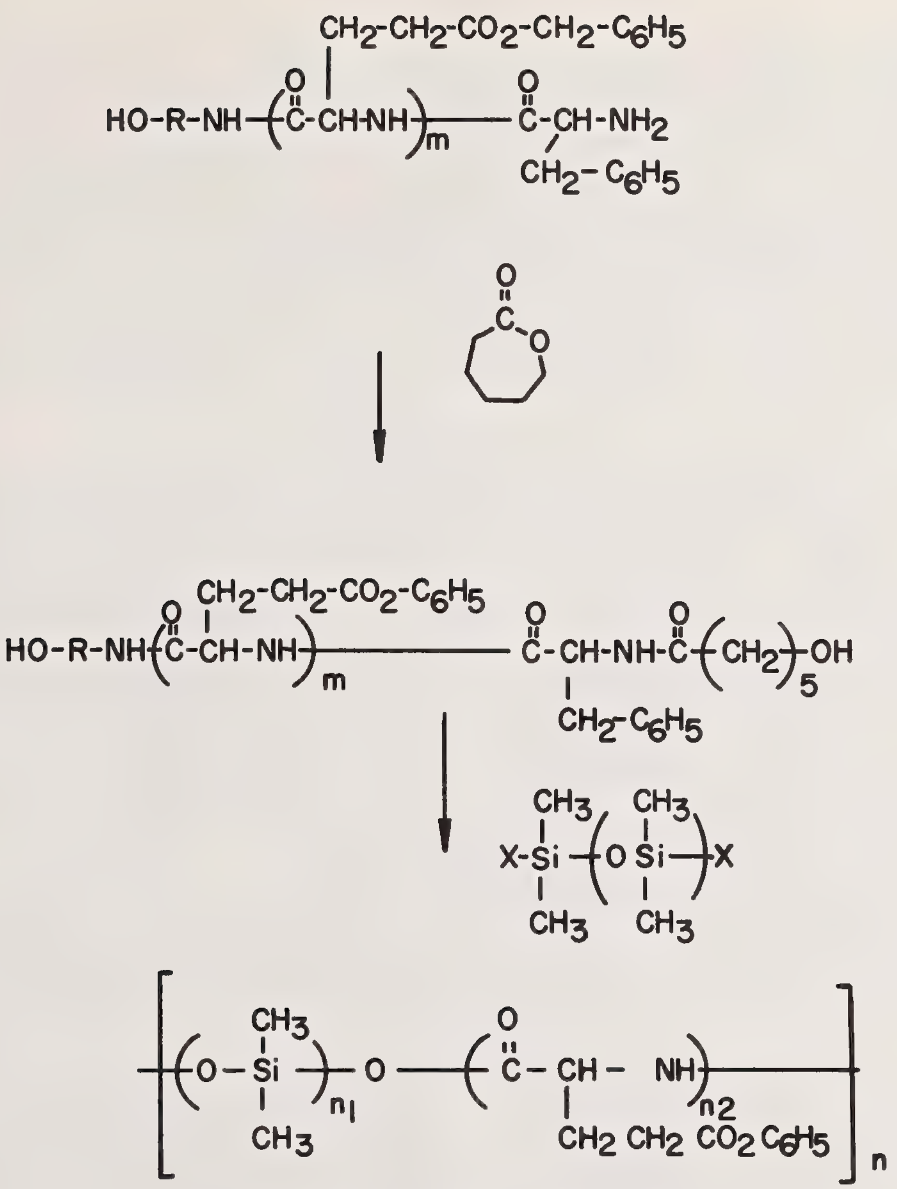

FIGURE 3. CONVERSION TO DIFUNCTIONAL OLIGOMERS

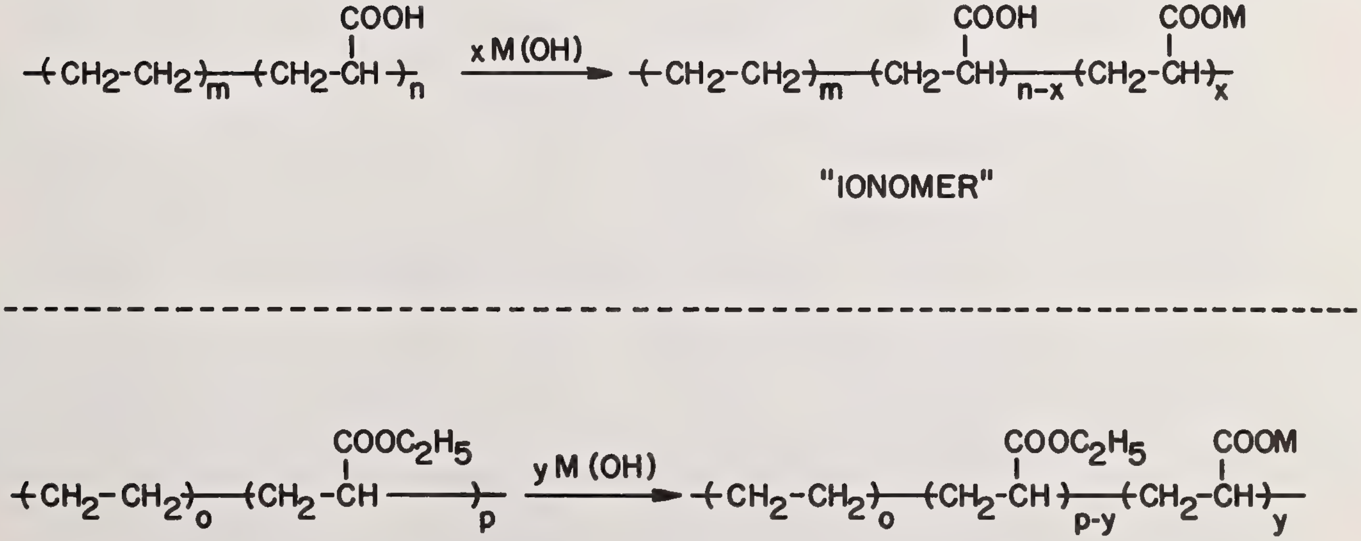

FIGURE 4. ETHYLENE/ACRYLATE RANDOM COPOLYMER FAMILY OF ANIONIC POLYELECTROLYTES

to the difunctional form is not possible, but that >90% conversion can be routinely accomplished. It also appears that more than one lactone molecule can react to extend the copolymer chain with short polylactone segments, but these never account for more than ~5% of the total polymer.

Using this multistep synthetic procedure, it has been possible to prepare poly(γ-benzyl L-glutamate) oligomers ranging in molecular weight from five to eighty thousand. Block copolymerizations have been carried out by coupling poly(amino acid) oligomers of approximately 8,000 molecular weight with 5,400 average molecular weight oligomeric poly(dimethylsiloxanes). This reaction, which must be carried out at elevated temperatures, yields stiff and relatively nonwettable $(AB)_n$ block copolymers, which have been shown by solution viscosity measurements to be of only moderate molecular weight. ABA copolymers have also been prepared by condensation of 77,000 average molecular weight monofunctional amino acid oligomers with 20,900 m.w. polysiloxanes. Although experiments are continuing which are directed at increasing molecular weight and improving mechanical performance, blood compatibility evaluations are also being initiated at this time.

POLYELECTROLYTES

The second synthetic project is an investigation which will hopefully shed new light on the blood compatibility of anionic polyelectrolytes. The primary objective of this study is synthesis and evaluation of novel mechanically useful vinyl addition polymers containing pendant carboxylate or sulfonate groups. In order to proceed sensibly with such a study, however, it has first been necessary to characterize the possible role in blood compatibility of certain general parameters of polyelectrolyte chemistry. This is being accomplished through systematic studies employing the already familiar ethylene/acrylate random copolymer family of anionic polyelectrolytes (Figure 4). These include ethylene/acrylic acid copolymers; the corresponding partially neutralized ethylene/acrylate polyelectrolyte salts or "ionomers"; and the corresponding ionomers prepared from ethylene/ethyl acrylate copolymers, in which no unneutralized carboxyl groups are present.

Clearly, the achievement of blood compatibility in a polymer will depend primarily upon the chemical nature of its component elements. In the case of polyelectrolytes, however, there are additional secondary factors which may play a role. Significant parameters include the following:

1. Total concentration of acidic groups;
2. Ratio of neutralized to unneutralized groups; and
3. Nature of the positively charged counterion.

Control of these parameters is certainly not a sufficient condition for blood compatibility. Their importance cannot be minimized, however, since inadequate regulation of such factors may obscure the compatibility of otherwise promising polymer compositions. This is best understood by briefly examining chemical reactions involved in the complex equilibration of polyelectrolytes with physiological fluids and the resulting short-term perturbations in solution pH and soluble electrolyte balance.

In the example (Figure 5) the polyelectrolyte is present as its partially neutralized monovalent metal salt. Its composition is characterized by "w" (the carboxyl concentration) and "x" (the carboxylate salt concentration). The pH of the medium which is exposed to the polymer is determined by "a" and "b" (the hydronium and hydroxyl ion concentrations) and the electrolyte balance is indicated by the remaining ion concentrations, only two of which are shown. In a highly neutralized ionomer system, dissociation of the salt to carboxylate anion and alkali metal cation (Reaction 1) should be favorable, with resulting increase in the concentration of the cation in the immediate vicinity of the polymer surface. A second effect will be equilibration of the undissociated and ionized forms of the carboxylic acid (Reactions 2, 5), which shifts the hydronium ion concentration and thus might be expected to produce an abnormal pH near the surface. There may also be an equilibrium involving the carboxylate anion and soluble divalent cations (Reactions 3, 4) to form partially dissociating alkaline earth salts, thus depleting the local concentration of ions such as magnesium or calcium. In a similar fashion, a polyelectrolyte salt which had been prepared by neutralization with an alkaline earth hydroxide would participate in the same equilibria (Reactions 3, 4) to increase the concentration of that ion.

In order to assess the role of these chemical changes in blood compatibility, a carefully selected series of ethylene/acrylate copolymers and ionomers was prepared and is now being evaluated (Table 1). The composition parameters include carboxyl content varied in the ratio 1:1.5:2; comparison of unneutralized copolymers with ~1/3 and ~2/3 neutralized ionomers; and preparation of ionomers having lithium, sodium, potassium, magnesium, and calcium as the metallic counterions. Ethylene/ethyl acrylate copolymers and saponified ionomers were similarly prepared. Evaluation data are still too incomplete to permit derivation of meaningful correlations. It is becoming clear, however, that these parameters do have a measurable effect.

While studies with the ethylene/acrylate copolymers have been continuing, attention has also been given to the problem of synthesizing two other families of anionic copolymers having related structures. In one case (Figure 6), vinyl sulfonic acid has been employed in place of acrylic acid as a comonomer with ethylene. Comparison of the resulting ethylene/vinyl sulfonate copolymers with the corresponding acrylic acid copolymers will permit identification of enhanced compatibility which might result from the presence of sulfonic acid groups. Preparation of these copolymers is carried out by copolymerization of sodium vinyl sulfonate in aqueous emulsion at ethylene pressures exceeding 15,000 psi. Although the polymerization is difficult to control, it is possible to obtain ethylene/sodium vinyl sulfonate copolymers free from homopolymer impurities. These copolymers can

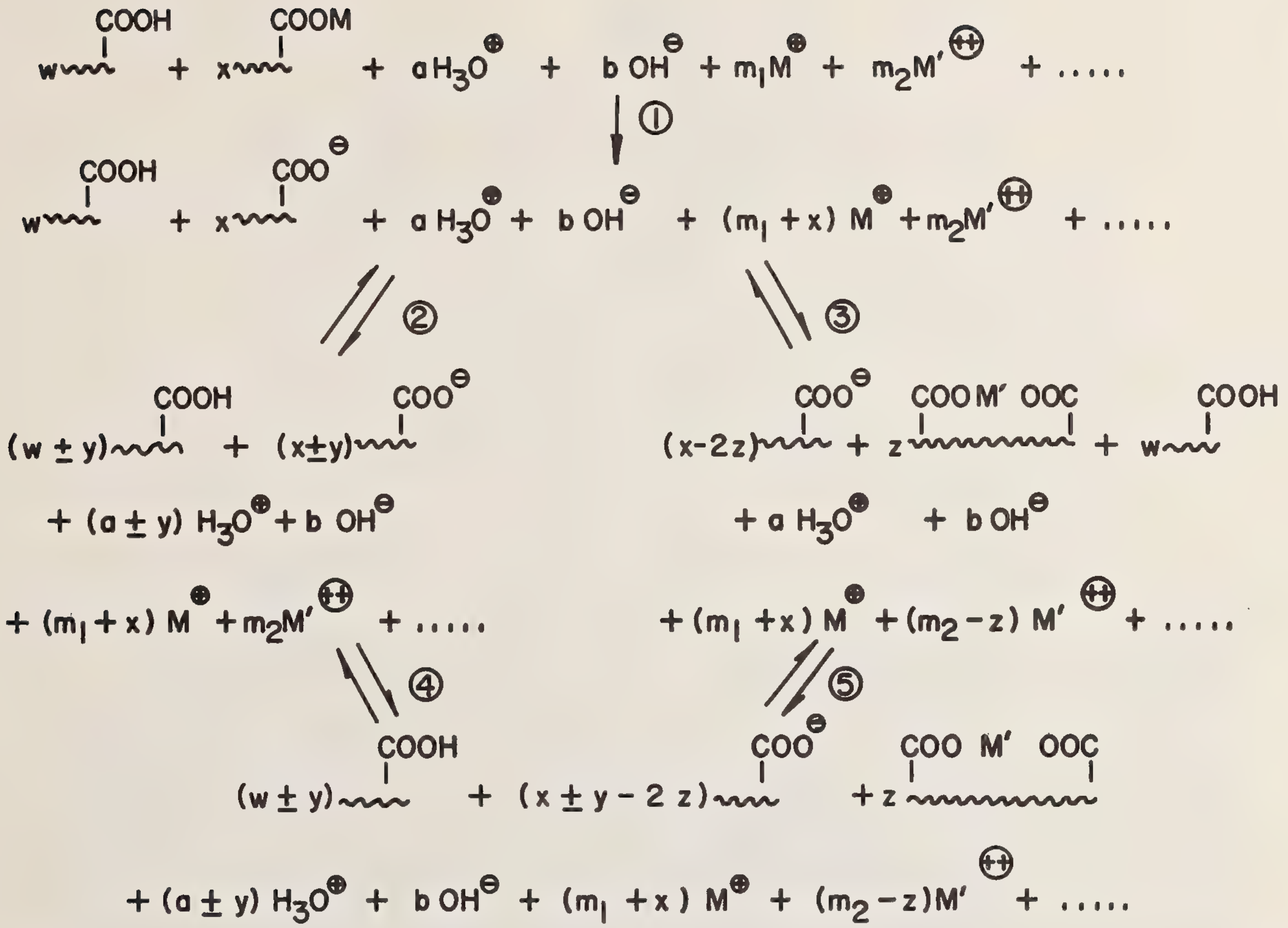

FIGURE 5. CHEMICAL REACTIONS INVOLVED IN EQUILIBRATION OF POLYELECTROLYTES WITH PHYSIOLOGICAL FLUIDS

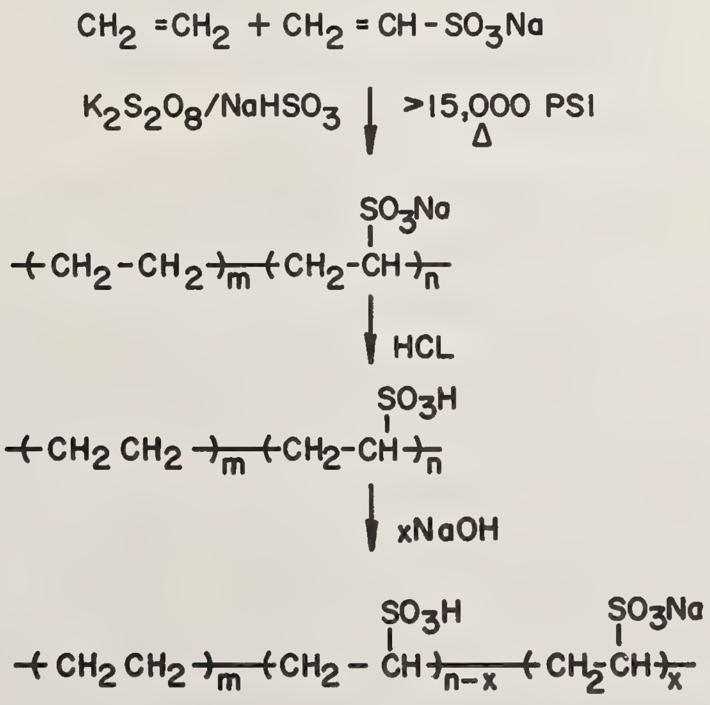

FIGURE 6. PREPARATION OF ETHYLENE/VINYL SULFONATE COPOLYMERS

TABLE 1

NEUTRALIZED ETHYLENE/ACRYLIC ACID COPOLYMERS

	%Acrylic Acid	%Neutralization	Metallic Cation				
			Li^+	Na^+	K^+	Mg^{++}	Ca^{++}
1.	9.8	0					
2.	9.8	29.5		X			
3.	9.8	71		X			
4.	14.7	0					
5.	14.7	32		X			
6.	14.7	62		X			
7.	19.2	0					
8.	19.2	27	X				
9.	19.2	28		X			
10.	19.2	24			X		
11.	19.2	27				X	
12.	19.2	26.5					X
13.	19.2	65	X				
14.	19.2	61		X			
15.	19.2	40.5			X		
16.	19.2	61.5				X	
17.	19.2	61.5					X

be acidified to vinyl sulfonic acid copolymers. The latter can be partially neutralized to ionomers by back titration with base.

Current efforts (Figure 7) are also directed at preparation of carboxyl-containing vinyl acetate copolymers, which would serve as highly hydrophilic analogues of the ethylene/acrylate series. Since vinyl acetate and acrylic acid differ widely in their reactivities as vinyl monomers, the desired polymers were synthesized by copolymerization of vinyl acetate with crotonic acid. Polymers of this type have now been prepared having crotonic acid concentrations ranging from 3% to 25%. These are all water swellable polymers which are insoluble in water. It is also possible to prepare water soluble polymers by neutralization to the sodium ionomers or by methanolysis to the vinyl alcohol/crotonic acid copolymer form. Blood compatibility studies employing ethylene/vinyl sulfonate, vinyl acetate/crotonate, and vinyl alcohol/crotonate copolymers are now or soon will be underway

ULTRATHIN FIBER SUBSTRATE FOR TISSUE CULTURE

The third and final segment of this program has been a problem in polymer fabrication, rather than polymer synthesis. The objective of this effort is development of a fibrous material which can be rendered compatible by permanent ingrowth and anchoring of healthy tissue. The material being sought, however, differs from conventional porous prostheses in that it should be extremely thin in order to promote development of a thin, nondegenerating neointima. The target values for these experiments were, therefore, established as follows:

1.	Fiber network thickness	≤ 10 microns
2.	Fiber diameter	≃ 1 micron or less

Clearly, these dimensions exclude the possibility of employing conventional fiber spinning and mechanical weaving or knitting techniques, and presumably require the use of a non-woven random fiber material. Furthermore, it was assumed that this material would be employed as a penetrable fiber network bonded to the surface of nonporous substrates.

Ultrafine plastic fibers are produced by a technique based on coextrusion of incompatible polymer mixtures (Figure 8).[2] Two immiscible thermoplastics--in this case, polypropylene and a suitable acrylic resin--are mechanically worked in the molten state to form a suspension of mutually insoluble polymer droplets which are ~10μ in diameter. Extrusion of such a mixture results in formation of a polymer composite consisting of individual rod-like fibers of the two polymers aligned in the extrusion direction. After stretch orientation to further attenuate and strengthen the fibers, the mixture can be extracted with an appropriate solvent to remove one polymer component. In this case, the acrylic resin is removed to produce ultrafine polypropylene fibers having diameters in the range 0.05-1μ. Fibers prepared by this technique have been shown by electron microscopy (75,000X) to be uniform in diameter and essentially circular in cross section.

The fiber composites can, of course, be extruded in a variety of shapes. As was indicated at the previous Contractors' Conference, however, formation of ultrathin nonwoven fine fiber networks is greatly facilitated by extrusion of thin flat films or tapes in which the fibers are oriented in a single direction. These tapes maintain much of their integrity even after the extraction step. Conversion to an ultrathin random network is, therefore, accomplished by stretching the wet extracted tape in the direction perpendicular to that of the fibers. This produces four separate effects. The fibers lose their parallel orientation to create the random network; the area of the fiber mat increases; the thickness of the fiber mat decreases; and the fiber density is reduced

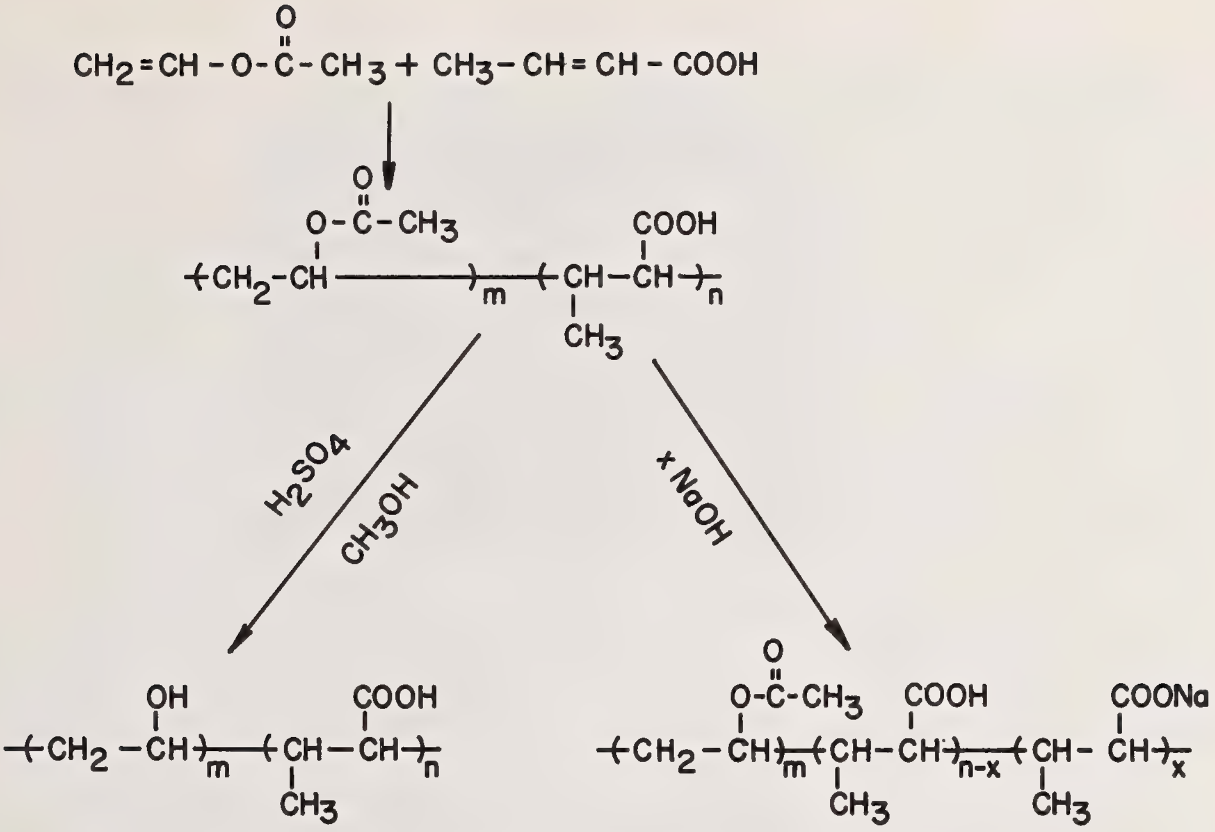

FIGURE 7. PREPARATION OF CARBOXYL-CONTAINING VINYL ACETATE COPOLYMERS

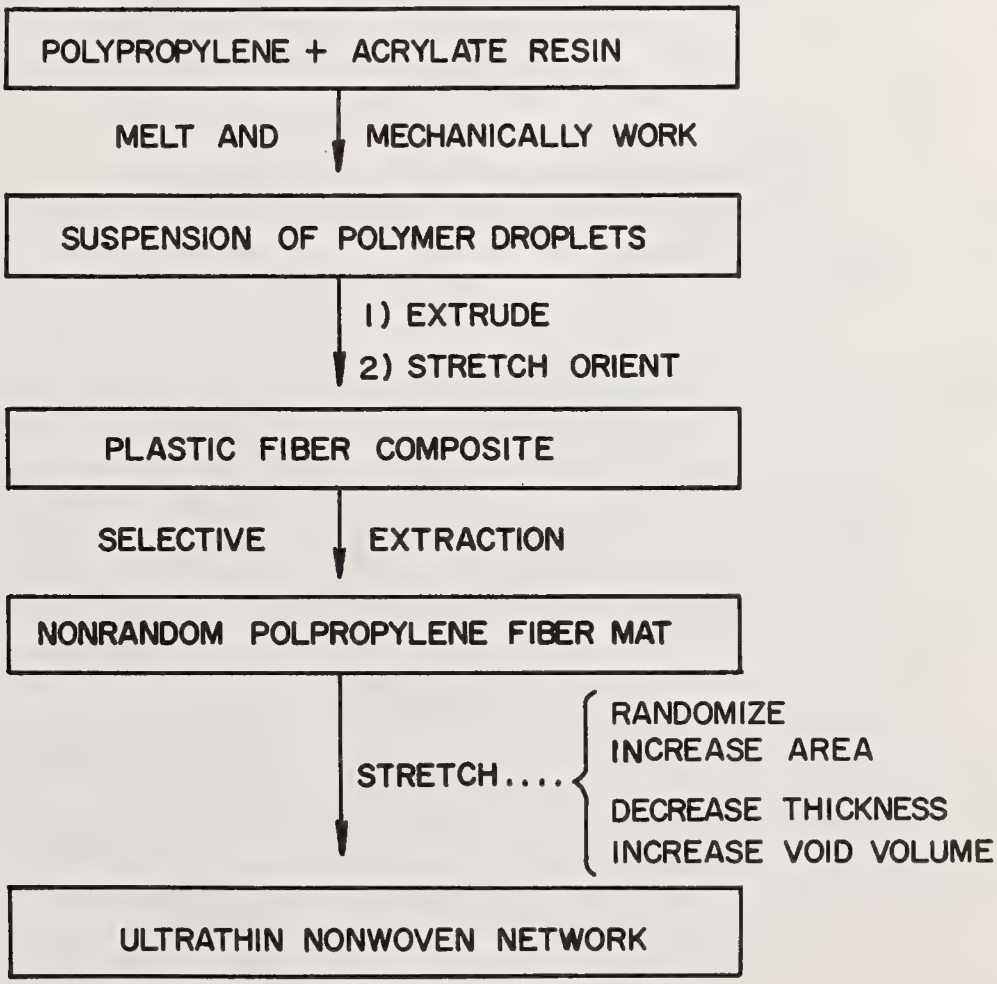
POLYPROPYLENE + ACRYLATE RESIN
MELT AND MECHANICALLY WORK
SUSPENSION OF POLYMER DROPLETS
1) EXTRUDE
2) STRETCH ORIENT
PLASTIC FIBER COMPOSITE
SELECTIVE EXTRACTION
NONRANDOM POLPROPYLENE FIBER MAT
STRETCH....
RANDOMIZE
INCREASE AREA
DECREASE THICKNESS
INCREASE VOID VOLUME
ULTRATHIN NONWOVEN NETWORK

FIGURE 8. PREPARATION OF ULTRAFINE PLASTIC FIBERS

(void volume of the network increases). Using this technique, it has been found that there is little difficulty in achieving the 10μ target value for mat thickness. It is possible, in fact, to produce fiber mats thinner than 2μ (Figure 9), which can be employed singly or in multiple layers. The void volumes of these networks vary within the range 40-80%, but the variation within an individual sample does not appear to be greater than ±10%.

The remaining step in fabrication of an ultrathin fine fiber tissue substrate is anchoring of the gossamer-like fiber network to the nonporous supporting material. This must be accomplished, of course, without significantly reducing the void volume of the network or otherwise disturbing its microporous character. This delicate task requires the use of unusual polymers known as Parylenes. The term "Parylene" is the generic name for the poly(para-xylylene) polymer series developed in our laboratories. In addition to their excellent chemical and thermal stability, these polymers owe their uniqueness to the process by which they are formed (Figure 10) and to the resultant nature of Parylene thin films. In this process, the reactive monomer species is generated thermally in the vapor phase and polymerizes only after condensation onto a cool surface. In this way, a continuous adherent coating is formed which precisely replicates the contours of the surface. The capabilities of this process permit formation of pin-hole free films as thin as 250Å. It was, therefore, anticipated that vapor deposition of a Parylene onto a supported fiber network would result in formation of a conformal coating on each individual fiber and on the supporting substrate (Figure 11).[3] This should result in fiber-to-substrate bonds, and also in fiber-to-fiber bonds which would reinforce the network.

Experiments with Parylene C indicate that Parylene deposition has exactly the effect anticipated. Under appropriate conditions, there is excellent bonding to glass and polypropylene substrates. The reinforcing effect, as indicated by increased abrasion resistance, is also immediately apparent. Photomicrographs at 285X clearly indicate that the Parylene coating is of a conformal nature without bridging of the fibers except at crossing points (Figure 12). The porosity of the networks is additionally confirmed by permeability measurements. In the photomicrograph, a thick Parylene coating has been used to make it clearly visible. However, a coating as thin as 1000 Å is sufficient to produce the desired bonding and reinforcement.

One particularly challenging problem has been application of fine fiber networks to the interior surfaces of cylindrical nonporous tubes having dimensions appropriate for use as vascular prostheses. This can now be accomplished by a multistep process (Table 2) in which the wet fiber web is first applied to a Teflon wrapped mandrel and is then transferred to the substrate tube.

TABLE 2

PREPARATION OF FINE FIBER NETWORKS

1. Application of thin Teflon film to mandrel;
2. Deposition of fiber web onto surface of Teflon film;
3. Removal of film and web from mandrel;
4. Insertion of collapsed film and web into treated tube;
5. Reinsertion of mandrel to expand film and web to bring web into uniform contact with wall of tube;
6. Removal of mandrel;
7. Removal of Teflon film, with transfer of web to tube;
8. Deposition of Parylene.

Needless to say, this is a very delicate procedure which requires considerable manual dexterity and much practice before it becomes possible to produce linings which are free from blisters and wrinkles. It has now been shown that 3" long tubes can be produced which are as narrow as 3/16" i.d. (<5mm.).

Recent experiments indicate that the fine fiber networks are also potentially useful as unsupported porous materials. They can, for example, be lap wound into multilayer porous tubes having walls only ~0.0005" thick. These tubes are suprisingly strong, even when not coated with Parylene. In flat sheet form, single layers of the ultrathin porous web can be handled fairly easily if suitably supported at the edges. Preliminary biological experiments indicate that human tissue cells are able to grow on and into both Parylene-coated and uncoated fiber webs. These results are reported elsewhere.[4,5]

REFERENCES

1. Lyman, D. J., J. L. Brash, R. D. Hamilton, B. K. Fritzinger, C. L. Stephens, and B. H. Loo, "New Synthetic Membranes for the Dialysis of Blood", PB 179172, May 1968.
2. Merriam, C. N., and W. A. Miller, U. S. 3,099,067, July 30, 1963.
3. Loeb, W. E., F. R. Tittmann and M. Goldin, U. S. 3,429,739, February 25, 1969.
4. Schutz, L., C. Grobstein, R. Grobstein, B. S. Bull and N. S. Braunwald, Proceedings of this Conference.
5. Johnsson-Hegyeli, R. and R. Gallagher, Proceedings of this Conference.

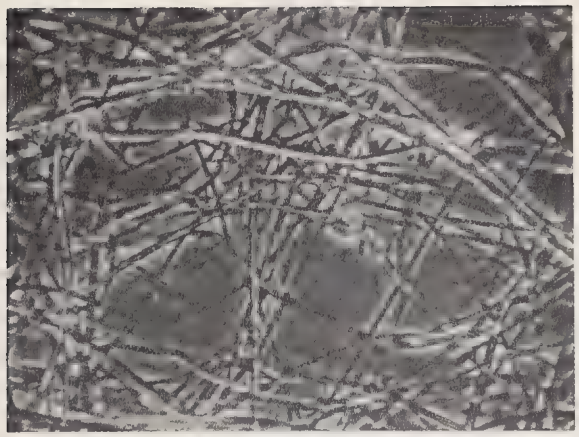

FIGURE 9. POLYPROPYLENE FIBER WEB (1000x ORIGINAL MAGNIFICATION)

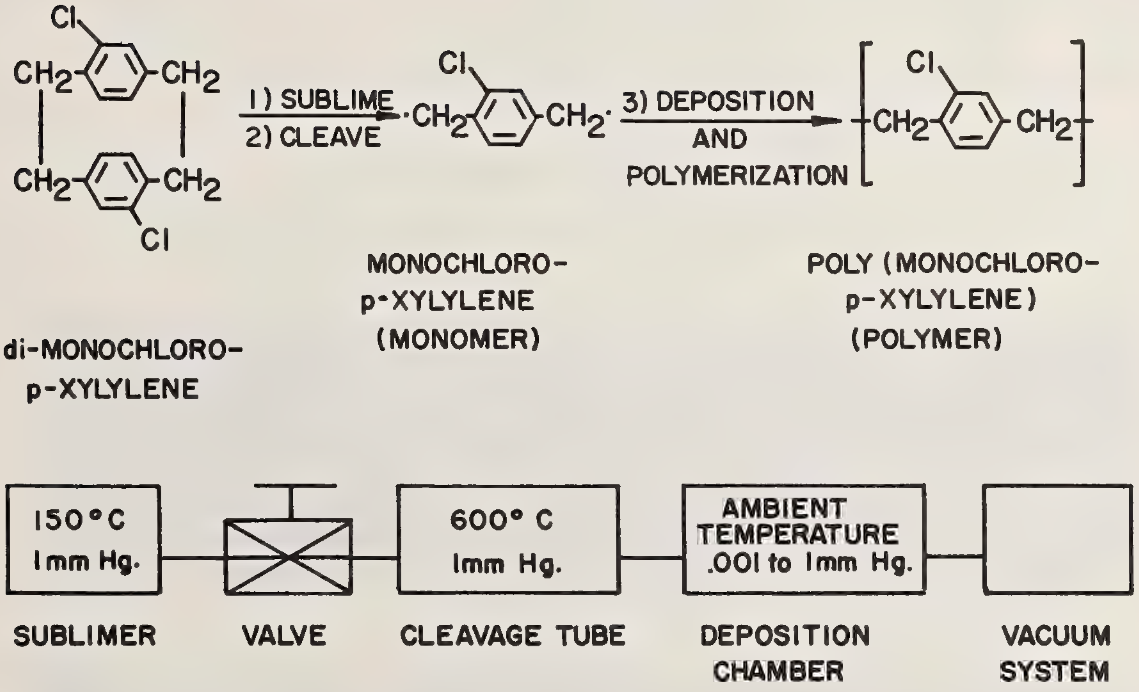

FIGURE 10. PREPARATION OF PARYLENES

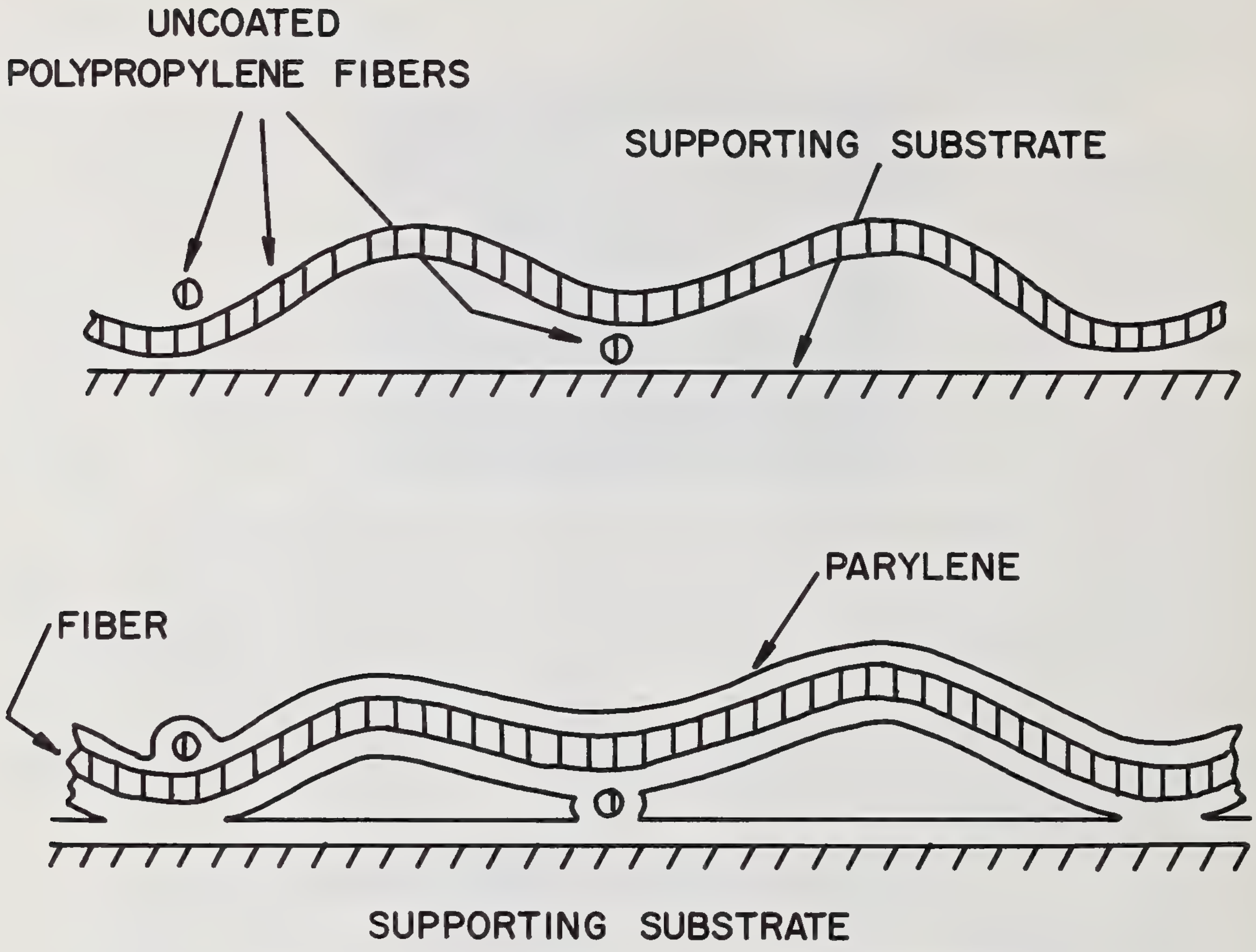

FIGURE 11. PARYLENE DEPOSITION ONTO A SUPPORTED FIBER NETWORK

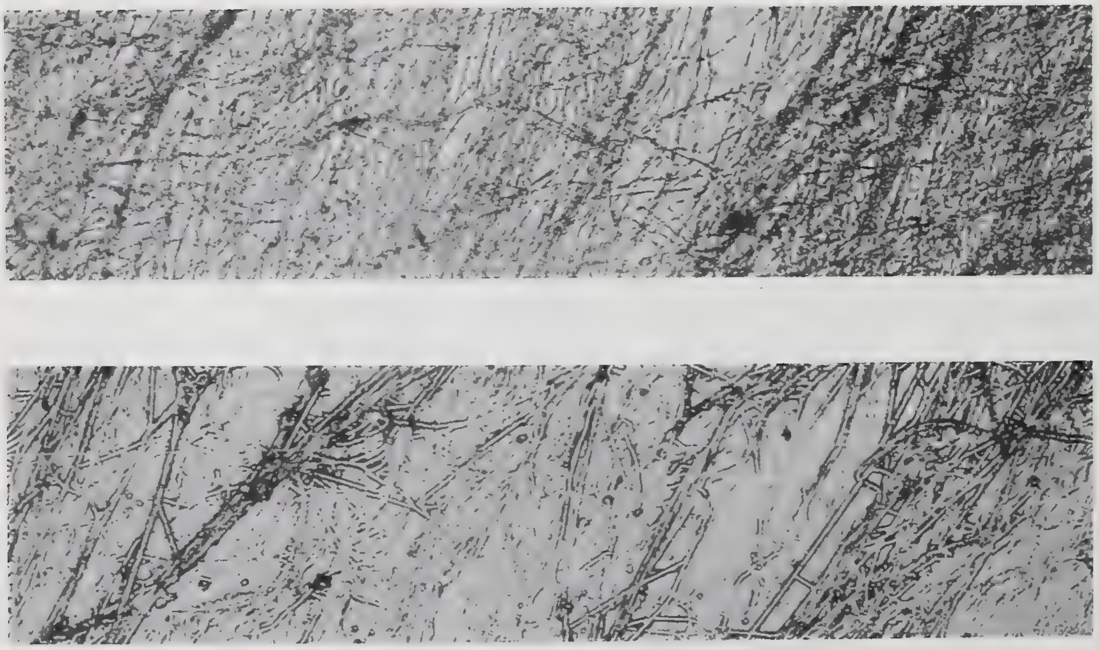

FIGURE 12. PHOTOMICROGRAPHS OF UNCOATED AND PARYLENE COATED FIBER WEBS (285x ORIGINAL MAGNIFICATION)

CHAPTER 13

BLOCK COPOLYMERS FOR USE IN BLOOD PUMPS AND OXYGENATORS: PREPARATION AND CHARACTERIZATION

E.T. Bishop and W.P. O'Neill

Shell Development Company, Emeryville, California

The objective of the present program is to prepare segmented copolymers with potential for use in contact with blood. We have employed techniques of block copolymerization and chemical derivatization to synthesize new elastomeric substances which may be useful in cardio-vascular assist devices. Two general types of block copolymers have been prepared: 1) hydrophobic, saturated hydrocarbon materials, and 2) materials containing polar groups in order to make them hydrophilic and anionic. In the former class, two segmented hydrocarbon polymers with thermoplastic elastomer properties (polyvinylcyclohexane-ethylene/propylene copolymer-polyvinylcyclohexane and polystyrene-ethylene/propylene copolymer-polystyrene) have been prepared and provided to biomedical evaluators in the Artificial Heart Program. Because there is strong evidence in the literature that hydrocarbon polymers may be suitable, at best, only for short-term applications in contact with the blood stream, we have synthesized a series of novel block copolymers containing pendant polar groups. Since thermoplastic elastomers derive their mechanical properties from the spontaneous and reversible formation of hard plastic domains in a continuous rubbery matrix, we have attempted to introduce polar functionality exclusively in the segments which form the rubber phase. By performing various derivatization reactions on the block copolymer polystyrene-polyisoprene-polystyrene, we have prepared and characterized materials with useful concentrations of hydroxyl, carboxylate sulfate and sulfonate groups in the continuous phase. Evaluation and comparison of this homologous series in contact with the blood is under way.

INTRODUCTION

The objective of the present program is to prepare segmented copolymers with potential for use in contact with blood. The techniques of block copolymerization and subsequent chemical derivatization reactions are being employed to synthesize a family of novel elastomeric substances which may prove useful for constructing cardio-vascular devices.

The literature suggests that two types of materials have potential utility in contact with blood. First there are those materials, like paraffin and silicone, which show little tendency to aggravate the clotting mechanism. These substances are generally characterized by inertness, low surface energy and amorphous microstructure. A second class consists of materials which actually inhibit coagulation. Included in this class are the natural anticoagulant heparin, synthetic anticoagulants and the blood vessel lining. Generally these materials are hydrophilic salts of polymeric strong acids. Prosthetic materials of the first class may be suitable for temporary assist devices, but they would be subject to coagulation induced by constriction of flow. Materials of the second type, which actively resist coagulation, would be far more trustworthy for long term implantation. Block copolymers can be made hydrophobic or hydrophilic, neutral or charged; therefore members of both classes may be accessible by this route.

BLOCK COPOLYMER BACKGROUND

The virtue of block copolymerization is that a variety of mechanical properties can be "built-into" the macromolecular structure of a block polymer. The most interesting property attainable is that characteristic of a soft, strong, highly elastic rubber. Such a material might be useful in a variety of cardio-vascular devices. Certain block polymers occupy a unique position among polymeric materials (Table 1). Conventional elastomers require vulcanizing and reinforcing additives to produce dimensional stability and strength. Such additives form permanent cross-links between molecules; they also can create toxicity problems. Vulcanizing and the change of properties with the state of cure can also be troublesome. A system which depends on chemical reactions at or after the fabrication stage is inherently less reliable than one in which the properties result directly from the structure of stable and tractable macromolecules.

TABLE 1

CLASSIFICATIONS OF POLYMERS

	THERMOSETTING (COVALENT CROSS-LINKING)	THERMOPLASTIC (ENTANGLEMENT AND CRYSTALLINITY)
Rigid	Epoxy Resins	Polystyrene
	Condensation Resins: Phenol or Urea-formaldehyde resins	Polyvinyl Chloride
	Hard Rubber	Polypropylene
Flexible	Reinforced and/or Highly Vulcanized Rubbers	Polyethylene Ethylene-vinylacetate Copolymers Plasticized Polyvinylchloride
Elastomeric	Vulcanized Rubbers Cured Silicones and Polyurethanes	THERMOPLASTIC ELASTOMERS

Segmented copolymers - depending on the nature of the segments, their size and sequence - may range in mechanical properties from limp, snappy rubbers to hard, glassy plastics.

Our own interests focus on soft rubbery materials derived from hydrocarbon block copolymers. These are known generically as thermoplastic elastomers. They possess the mechanical properties of cross-linked elastomers along with the solubility and moldability advantages of thermoplastics. A series of thermoplastic elastomers are marketed by Shell Chemical Company under the trade name KRATON®. While these commercial products are not involved in the present work, the principles governing their behavior are being applied in the preparation of biomedical materials. Thermoplastic elastomers have been discussed in detail in several publications. [1-5]

The unique combination of properties characteristic of thermoplastic elastomers, occurs because incompatible polymeric segments have been joined together into the same molecule. Since the two types of polymeric segments are immiscible, two phases occur. Further the segments have been joined together in such a manner that two plastic segments are linked by an elastomer segment. At the service temperature the end segments are below their glass transition and the center segment is above its glass transition.

The block copolymers of polystyrene and polybutadiene provide a well characterized illustration of these points. Polybutadiene itself is a viscous liquid; however, when it is vulcanized and reinforced with a particulate filler, it becomes strong and elastic. Polystyrene is a brittle glass at room temperature. These two polymers are incompatible, that is the free energy of mixing is positive. When the segmented structure polystyrene-polybutadiene-polystyrene is constructed, the segments remain incompatible and two phases occur. As depicted in Figure 1, the polystyrene segments accumulate in microregions, with an optimum diameter of about 300 Å, scattered throughout a polybutadiene matrix. The plastic phase regions are referred to as domains. The polystyrene domains effectively immobilize the ends of the polybutadiene chains. In this respect the domains act as multifunctional cross-links in a manner analogous to the role of reinforcing agents in other elastomers. The naturally occurring chain entanglements in the polybutadiene phase are thus entrapped by the restriction of the chain ends at the domain interfaces. These topologically trapped entanglements act like conventional tetra-functional cross-links in a vulcanized rubber. As a result polystyrene-polybutadiene-polystyrene displays high strength and elastic elongation characteristic of a cross-linked rubber. Nevertheless it is soluble in a number of organic solvents and forms a viscous melt at 125-150°C.

That the sequence plastic segment-elastomer segment-plastic segment (or ABA) is essential for elastomeric characteristics is illustrated in Table 2, where the tensile properties of a polystyrene-polybutadiene-polystyrene (SBS) copolymer are compared with a polybutadiene-polystyrene-polybutadiene (BSB) copolymer. The SBS has the strength and elasticity characteristic of a cross-linked reinforced elastomer, while the BSB is quite weak. The composition and molecular weights are identical, only the sequence is different.

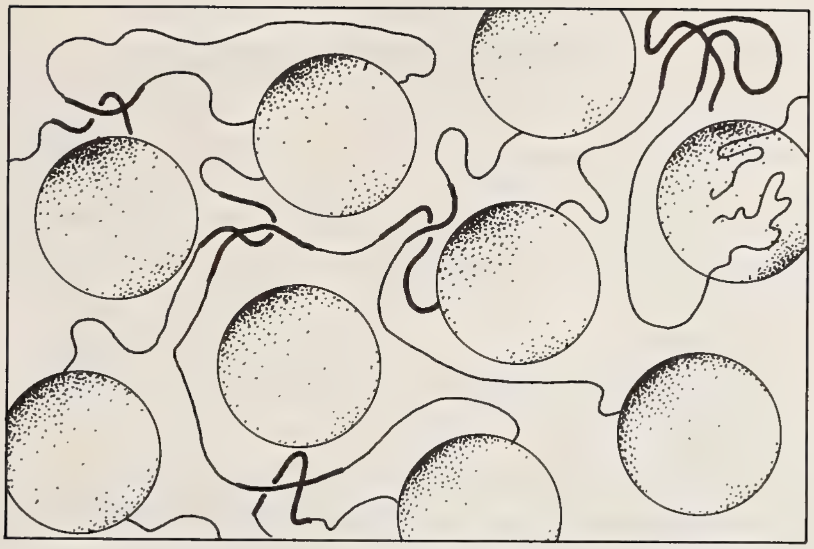

FIGURE 1. MODEL OF AN A-B-A BLOCK POLYMER WITH 25% END BLOCK

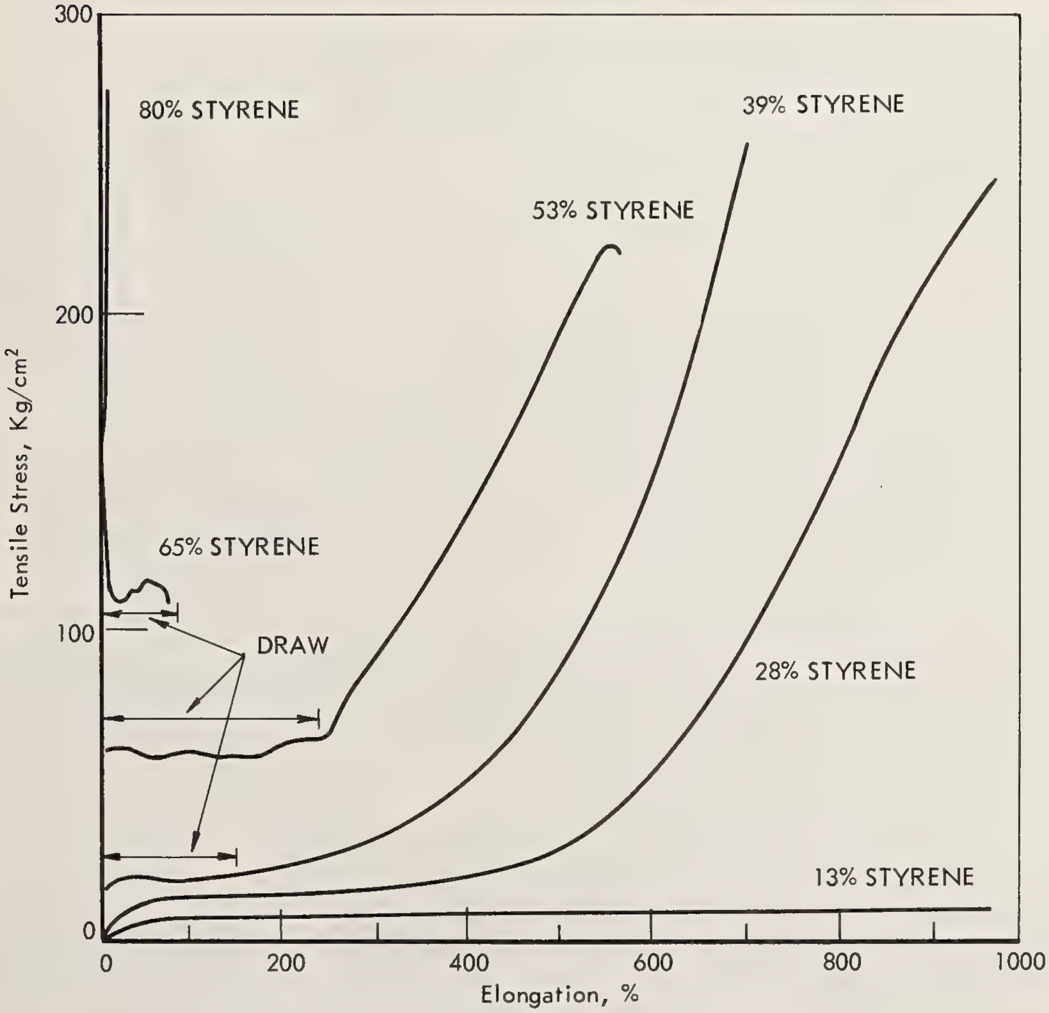

FIGURE 2. SBS POLYMERS OF VARIOUS STYRENE CONTENTS

TABLE 2

COMPARISON OF SBS AND BSB POLYMERS

Composition		
Segmental Molecular Weights	10S-52B-10S	28B-20.5S-28B
Styrene Content (%)	27.5	27
Total Molecular Weight	73,000	76,000
Mechanical Properties		
100% Modulus, psi	240	70
Extension at Break (%)	860	120
Ultimate Tensile Strength, psi	4060	70
Shore A Hardness	65	17

The mechanical properties of a plastic-elastic-plastic copolymer are not significantly affected by the size of the elastomer segment because the density of entanglement cross-links is determined by the flexibility, that is the structure, not the molecular weight of the elastomer. Examples of this fact are shown in Table 3 where the mechanical properties of three SBS polymers with 27% polystyrene are compared. Unlike the mechanical properties, however, the viscosity increases markedly with increasing molecular weight.

TABLE 3

MOLECULAR WEIGHT CHANGES WITH CONSTANT PLASTIC CONTENT IN SBS

MW x 10^{-3}	10-52-10	14-74-14	20-110-20
Total MW x 10^{-3}	73	102	150
Styrene, %	27.5	27.5	26.5
Tensile Strength, psi	3950	4050	3600
Elongation at Break, %	860	820	850
Modulus at 300%	300	430	300

If one holds molecular weight constant and varies the proportions of the segments, powerful effects are seen (Figure 2). Here are depicted the stress-strain curves for a series of polymers all of 80,000 total molecular weight. The polymer with small styrene segments behaves like uncured polybutadiene, which has no strength. When the styrene content is increased to 27%, the behavior is like that of a vulcanized elastomer. At higher styrene contents the polymers exhibit plastic yield phenomena with drawing and then undergo elastic extension. Above 75% styrene content, SBS polymers do not draw but break at about the same elongation as pure polystyrene. Block copolymers containing more than one-third plastic content may have a continuous plastic phase, as well as a continuous elastomer phase. It is such a continuous plastic phase which produces the high initial modulus and plastic yield. During the drawing a phase change may occur to a state where discrete plastic regions are suspended in a continuous elastic matrix, and typically elastic behavior is then found.

The properties of a block copolymer material are influenced by a great many variables including the chemical nature of the monomer units in each segment, and the number, size and sequence of the segments. When considered along with the other parameters available for all polymer synthesis, these present a powerful array of tools for building a polymer to perform a specific job. But first one must know what is required and be able to describe it in terms which can be related to molecular structure. It should be noted at this point that while the authors are concerned with hydrocarbon block polymer derivatives, several other block polymer systems including polyurethanes [6,7] and certain silicone rubbers [8] are being investigated by other groups.

Before a device can be developed for a particular cardio-vascular application one must know: 1) what chemical compositions can be tolerated in the physiological environment of the application, and 2) what are the mechanical requirements of the application. Subsequently one must consider how a given device can be made from suitable materials in a convenient and reproducible fashion. Most of the work to date has been directed toward defining which block copolymers are sufficiently compatible with blood.

SATURATED HYDROCARBON BLOCK COPOLYMERS

The unsaturated hydrocarbon block copolymers do not possess the biological inertness and chemical stability required for surgical applications. Copolymers containing only saturated hydocarbon elastomer segments were therefore selected as a promising base material. As a model we chose a polymer with elastomer segments corresponding to ethylene/propylene copolymer rubber and end segments of polyvinylcyclohexane. Samples were prepared in a high state of purity for biomedical evaluation by treatment with activated alumina and silica gel followed by Millipore filtration. This polymer is extremely strong, elastic, glass clear and inert. It is soluble in cyclohexane, toluene, etc., but unaffected in aqueous media. The mechanical properties are summarized in Table 4 along with values for medical grade silicone rubber in order to put the data in perspective. This polymer is only a representative of a family with similar composition.

TABLE 4

MECHANICAL PROPERTIES OF BIOMEDICAL ELASTOMERS

	BM-1 Block Copolymer	Silastic 328 (Dow Corning) Reinforced Silicone Rubber
Tensile strength	4500 psi	650 psi
Modulus at 100% Elongation	275 psi	650 psi
Elongation at Break	700%	150%
Hardness, Shore A	64	50

The current biomedical data on this polymer are summarized in Table 5. Static clotting tests were conducted according to the Lee-White procedures with freshly drawn canine blood. The clotting time averaged 7.5 min for BM-1 compared to 6.9 min for silicone coated glass and 3.3 min for glass itself. The silicone treatment (Clay-Adam's Siliclad) was used to coat the syringe and needle for all of the tests. It is perhaps significant that the clots in the BM-1 and silicone coated tubes were non-adherent, which is interpreted to mean that coagulation was initiated, not at the interface with the polymer, but in the bulk of the blood, perhaps by platelets damaged when the blood samples were drawn.

TABLE 5

BIOMEDICAL EVALUATIONS OF BM-1
(VINYLCYCLOHEXANE, ETHYLENE/PROPYLENE BLOCK COPOLYMER)

Tests	Results
Lee-White Clotting (Hine Laboratories, San Francisco)	7.5 ± 1.5 min vs 6.9 ± 0.6 min for Siliclad and 3.3 ± 0.8 min for glass
Platelet Adsorption (D.J. Lyman, Stanford Research)	4 platelets per 20,000μ^2
Platelet Aggregation and Rupture, Hemolysis Prothrombin Activation (R.G. Mason, U. North Carolina)	"Good" rating
Ex-vivo Coagulation (P. Madras, Avco-Everett Corp.)	No coagulation up to 90 minutes

Dr. Lyman at Stanford Reasearch Institute has examined samples of BM-1 and found platelet adsorption of about 4 platelets per unit area such as he finds for other hydrocarbon polymers. Dr. Mason at the University of North Carolina reports that the adsorbed platelets apparently are not significantly damaged. He found slight evidence of activation of the clotting mechanism, but overall he ranks the polymer high among the materials he has rated. Dr. Madras of Avco-Everett found very favorable performance with BM-1 in his ex-vivo flow test. He observed no platelet agglomeration or coagulation over periods as long as 90 minutes. Samples of BM-1 are undergoing further tests by other contractors. At present it appears that material of this general structure may be suitable at least for temporary assist type devices. Since the polymer tested is representative of a group of materials of similar composition, additional samples which differ in plastic block content have been prepared. Table 6 summarizes the range of properties practically attainable with this basic structure without additives.

TABLE 6

MECHANICAL PROPERTY RANGE OF BM-1 TYPE POLYMERS

Tensile Strength	5000 psi	3500 psi
Modulus at 10%	150 psi	50 psi
Modulus at 30%	225 psi	75 psi
Modulus at 100%	300 psi	150 psi
Modulus at 300%	400 psi	175 psi
Elongation at Break	700%	1600%
Hardness, Shore A	65	40

The soft polymer is extremely strong; the actual stress sustained before breaking is well in excess of 10,000 psi. Stiffening the polymer by increasing the plastic block content gives rise to the plastic yield phenomenon mentioned earlier due to the appearance of a continuous plastic phase at plastic contents near 30%. This results in set after deformation. For applications which require higher modulus with no plastic yield, it will be necessary to introduce reinforcing fillers in the elastomer phase or to provide an additional source of cross-linking, for example by high energy irradiation.

A few tests have been made on a polymer, BM-4, which has the same elastomer segment as BM-1, but in which the plastic segments are polystyrene. It was anticipated that there would be little difference in the surface properties of the two polymers, since the identical elastomer forms the continuous phase in both cases and the dissimilar plastic domains are buried in that elastomer matrix. That this is the case is born out by the measurement of identical critical surface tensions for the two polymers. This is in contrast to their solubility characteristics which are quite different. The biomedical evaluators have found BM-1 and BM-4 to be nearly identical in contact with blood, although BM-1 may be slightly better with respect to platelet aggregation. The significance of these results is that the nature of the end segments can be varied to achieve particular mechanical or processing advantages without affecting the biomedical properties.

POLAR BLOCK COPOLYMER DERIVATIVES

Assuming that hydrocarbon polymers will not suffice for long-term implantation and that anticoagulant properties must be built into a material for such an application, the synthesis of hydrophilic block copolymers was undertaken. An interesting new family of ionic hydrophilic block copolymers is receiving special attention.

Since the rubber mid-segment of a thermoplastic elastomer forms the continuous matrix which the blood "sees", for functional groups to be effective they must be placed in that phase. The addition of polar groups to an elastomer commonly raises its glass-transition temperature making it less of a rubber. This effect may be counteracted by swelling the polymer with a plasticizer. Water can act as a plasticizer in hydrophilic polymers. Obviously plasticization could be deleterious if it occurred in the rigid plastic phase of a block polymer. Thus derivitization reactions must be selective for the elastomer segments.

Epoxidation of an unsaturated elastomer segment as shown in Figure 3 followed by ring opening to the glycol proceeded well at low concentrations of epoxide groups. However, when this approach was extended to try to produce vicinal glycol groups on half of the isoprene units of a polystyrene-polyisoprene-polystyrene block copolymer, a reaction (Figure 4) which forms cyclic ethers was favored. The polymers obtained were not very hydrophilic. They absorb only 5%w of water and show elastic properties only when they are swollen with alcohols. Hydroboration (Figure 5) was applied to quantitatively introduce one hydroxyl per double bond on a polystyrene-polyisoprene-polystyrene block copolymer. Again the product was only moderately hydrophilic (approximately 10%w water absorption).

In hopes of imitating the negative ionic charge of natural anticoagulant polymers, several routes to block copolymers containing anionic sites throughout the elastomer phases were examined. A couple of reactions for introducing weak carboxylic acid groups were screened but they were incapable of adding more than a few carboxyl groups to the elastomer segment without simultaneously attacking the plastic segments. Because of the success in preparing sulfonated block polymers, the work on carboxylated derivatives has not been pursued.

Most sulfonation reaction conditions will produce sulfonic acid sites in both the plastic and elastomer phases. For example, sulfochlorination of the saturated block polymer of polyvinylcyclohexane and ethylene/propylene produces sulfonation in both phases of the polymer. Such a polymer becomes weak in an aqueous environment due to swelling of the plastic domains. Sulfur trioxide or chlorosulfonic acid will attack polystyrene as well as unsaturated elastomers. However,

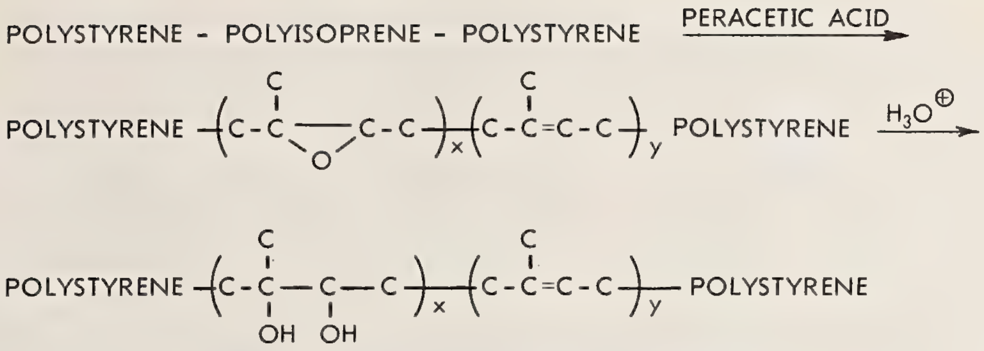

FIGURE 3. HYDROXYLATION VIA EPOXIDATION OF SIS

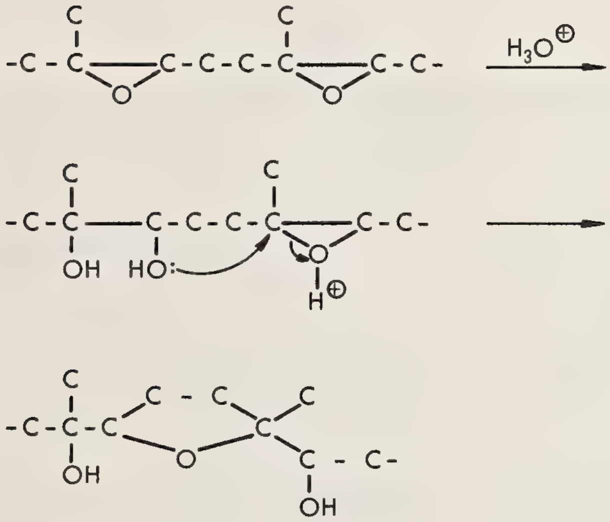

FIGURE 4. CYCLIZATION DURING HYDROLYSIS OF EPOXIDIZED SIS

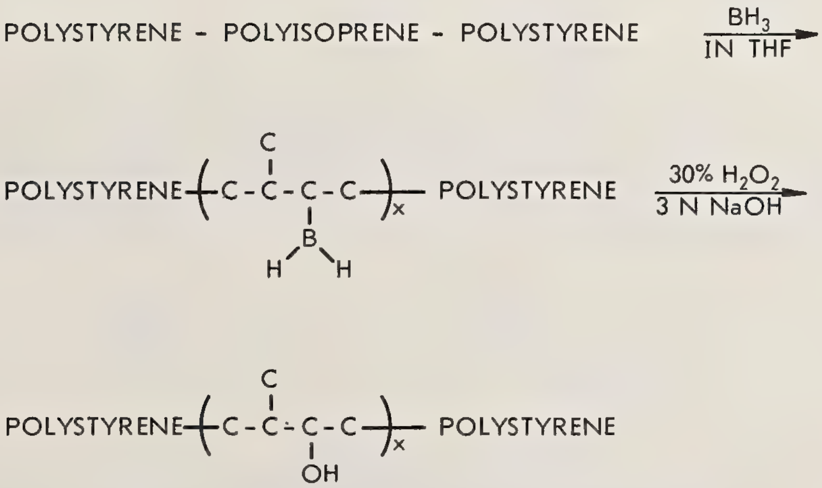

FIGURE 5. HYDROXYLATION VIA HYDROBORATION OF SIS

complexes of chlorosulfonic acid with ethers are mild sulfonating agents which do not react with aromatic rings. Using such a complex we were able to sulfonate most of the hydroxyls in the block polymer alcohol prepared via the hydroboration reaction described earlier. The reaction is outlined in Figure 6. The effect was quite dramatic, water swelling increased from 10%w to greater than 1000%w. Naturally such a highly swollen polymer is quite weak. It was found that the same complexes would directly sulfonate the olefinic center segment of a polystyrene-polyisoprene-polystyrene block copolymer without affecting the polystyrene portion (Figure 7). Spectral evidence supports the assignment of a β,γ-unsaturated sulfonic acid structure to the product. Such a carbonbound sulfonic acid should be more stable toward hydrolysis than the half-ester sulfate prepared from the polymeric alcohol. However, these polymers are subject to acid catalyzed oxidation and special isolation procedures had to be developed to prevent degradation.

Conversion of approximately 20% of the carbon-carbon double bonds in the elastomer segment of a polystyrene-polyisoprene-polystyrene copolymer gave a polymer which swelled more than 10 times its volume in water. However, as Figure 8 shows the swelling is markedly decreased in the presence of salt to about 100% in physiological saline. Nevertheless, 100% swelling is still so much that the polymer will not adhere to glass adequately for testing under most procedures.

As a matter of convenience, therefore, the initial biomedical tests were conducted on a sulfonated SIS containing only one-third as many acid sites as the one just discussed. The pertinent data are summarized in Table 7. This polymer swells to about 20% in physiological saline.

TABLE 7

BIOMEDICAL EVALUATIONS OF BM-15 (SULFONATED SIS)

Tests	Results
Lee-White Clotting (Hine Laboratories, San Francisco)	8.4 ± 1.0 min vs 6.9 ± 0.6 min for Siliclad and 3.3 ± 0.8 min for glass
Platelet Aggregation and Rupture, Hemolysis, Prothrombin Activation (R.G. Mason, U. North Carolina)	More thrombogenic than the hydrocarbon block polymers; Discolored plasma
Ex-Vivo Coagulation (P. Madras, Avco-Everett Corp.)	Thrombus formed in folds caused by swelling of polymer

Under the Lee-White test conditions, the sulfonated SIS averaged 8.4 min for clotting. This compared favorably with the siliconized glass, 6.9 min. Unfortunately, Dr. Mason and Dr. Madras report that this polymer is not as promising in their tests as were the hydrocarbon block polymers. More highly sulfonated and stabilized samples are currently being tested. The sulfates are also being prepared in forms suitable for biomedical evaluation.

With respect to the role of surface energy and wetting phenomena, it was somewhat surprising to learn that the critical surface tensions for wetting the sulfonated polymers is typical of hydrocarbons (31 dynes/cm^2). The interaction with water is one of hydration not wetting.

A highly sulfonated block polymer (2 meq/g cation exchange capacity) film at equilibrium in Ringer's isotonic solution is actually 57% water. The tensile properties of this water swollen film are shown in Table 8. The properties of a typical medical grade reinforced silicone rubber, which of course is not hydrophilic, are shown for comparison. Even in this highly swollen state, the mechanical properties of the sulfonated polymer are attractive. The composition of the sulfonated block polymer is by no means optimized.

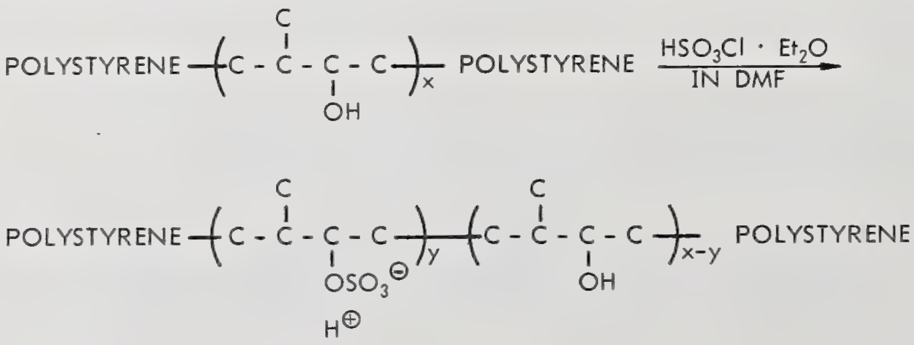

FIGURE 6. SULFONATION OF HYDROXYLATED SIS

TABLE 8

PROPERTIES OF A SULFONATED SIS SWOLLEN WITH RINGER'S SOLUTION

	BM-15	Silastic 382 (ex Dow Corning)
Acid Eq/100 g dry wt.	0.21	-
Water Content in Ringer's	57%	<1%
Tensile Strength, psi	750	650
Modulus, 100%	500	650
Elongation at Break	200	150
Hardness, Shore A	40	50

In summary, it appears that saturated block copolymers may be useful at least for temporary cardio-vascular assist devices. Sulfonation of block copolymers offers a hope of producing an anticoagulant surface by direct synthesis. The time has come to identify the precise mechanical requirements of particular applications in which the soft, rubbery, strong qualities of our thermoplastic elastomers can be useful.

ACKNOWLEDGEMENT

Many individuals in the Shell organization have contributed in one way or another to this work. We especially wish to acknowledge the contributions of W.V. Turner and D.E. Winkler.

REFERENCES

1. G. Holden, E.T. Bishop and N.R. Legge, "Thermoplastic Elastomers", The Proceedings of the International Rubber Conference, May 1967, p. 287.
2. E.T. Bishop and S. Davison, "Network Characteristics of the Thermoplastic Elastomers", Journal of Polymer Science, C26, 1969, p. 59.
3. D.J. Meier,"Theory of Domain Formation in Block Copolymers", Journal of Polymer Science, C26, 1969, p. 81.
4. J.T. Bailey, E.T. Bishop, W.R. Hendricks, G. Holden and M.R. Legge, "Thermoplastic Elastomers, Physical Properties and Applications", Rubber Age, Oct. 1966, p. 69.
5. M. Vlig, "Physico-Chemical Aspects of Three Block Copolymers", Journal of the IRL, August 1968, p. 182.
6. D.J. Lyman and B.H. Loo, "Copolyether-Urethane Membrane Systems", Journal of Biomedical Materials Research, March 1967, p. 17.
7. J.W. Boretos and W.S. Pierce, "Segmented Polyurethane: A Polyether System", Journal of Biomedical Materials Research, March 1968, p. 121.
8. R.L. Merker, M.J. Scott and G.G. Haberland, "Random and Block Copolymers of Poly(tetramethyl-p-Silphenylene-Siloxane) and Polydimethyl-siloxane", Journal of Polymer Science, A2, 1964, p. 31.

DISCUSSION

DR. HALPERN: The problem of obtaining ready hydration in your block polymer is somewhat analogous to that of hydration of fully hydrolyzed polyvinyl alcohol . This is difficult to hydrate because of hydrogen bonding. In the block segments where the hydroborated butadiene is then hydroxylated, you do have a chance for hydroxyl interaction, and you therefore can obtain a high degree of hydrogen bonding. Would it not be better if you made a random copolymer of styrene and butadiene which would avoid this kind of hydrogen bonding since there would be less order in the chain?

DR. O'NEILL: We can see no evidence of crystallinity, although I am sure there is very strong hydrogen bonding. You are quite right, any polar polymer, once it has been dried, is very hard to reswell with water.

MR. PURDY: Could you give us some information on the fatigue characteristics of your material compared to that of silicone rubbers? For example, could you hypothesize it to go to 10^{10} cycles at 500 psi or something like that?

DR. O'NEILL: I have no specific information on the fatigue properties of these polymers, but on the basis of experience with our commercial polymers of related structures, I would anticipate the flex characteristics to be superior to silicone rubbers.

MR. PURDY: Could you estimate what you think a good number might be?

DR. O'NEILL: In order to establish the fatigue characteristics, you would, of course, have to specify the size and shape of your specimen and the test conditions used. Therefore, I cannot come up with a number right now.

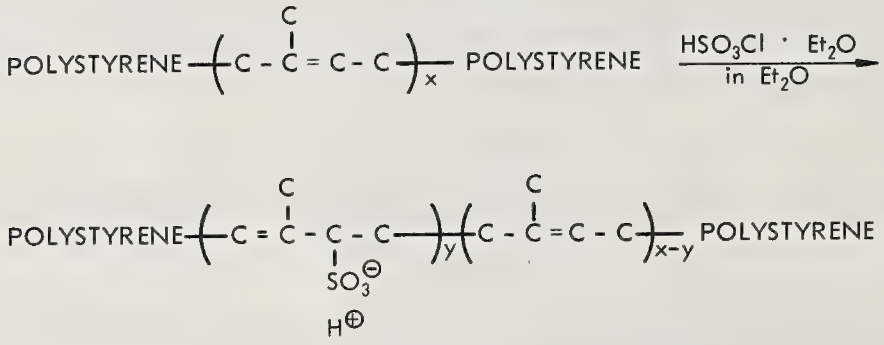

FIGURE 7. SULFONATION OF OLEFIN SEGMENT OF SIS

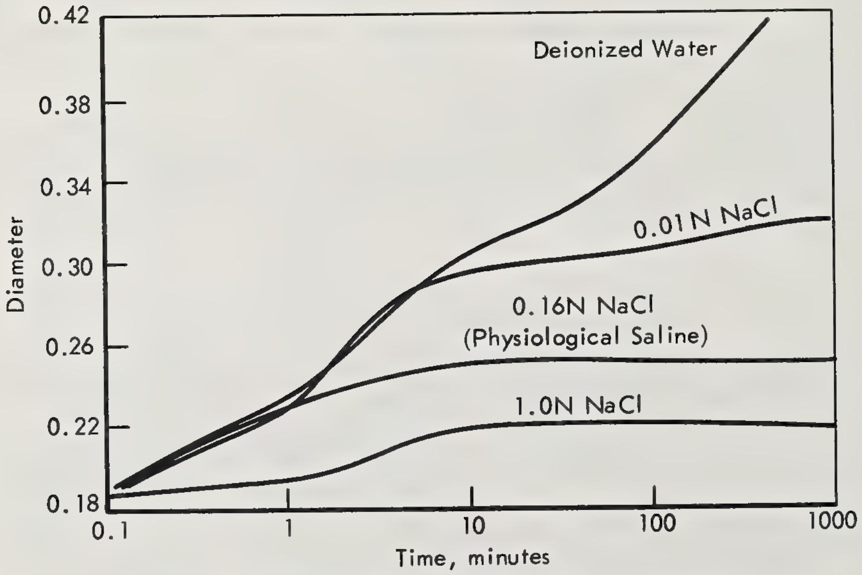

FIGURE 8. SWELLING OF SULFONATED SIS IN AQUEOUS MEDIA

CHAPTER 14

DEVELOPMENT OF MATERIALS FOR ARTIFICIAL HEARTS AND BLOOD OXYGENATORS

H. Lee, D.G. Stoffey, and F. Abroson

The Epoxylite Corporation, South El Monte, Calif.

The purpose of this research is to develop a solid-walled vascular prosthesis which contains an inner, blood-contact layer of covalently bonded cholesterol and sialic acid, that may simulate the environment of the natural intima, and a soft outer layer of a flexible plastic for tissue compatibility. Films and test tubes of polyvinyl alcohol (PVA) have been prepared for use as substrates for the attachment of cholesterol and sialic acid half esters. Six diacid chlorides 6 to 22 carbons long have been prepared and purified for use in the synthesis of the half esters. The cholesterol half esters of succinic, glutaric, adipic, and dodecanedioic acids have been prepared. Methods to obtain the half esters in high purity have been developed. PVA films and test tubes have been lightly and heavily esterified by stearic acid, by the adipic acid monocholesterol ester (AAME), and by a combination of AAME and dodecanedioic acid monosialic acid ester (DAMSE). The infrared spectra of untreated PVA films and esterified PVA films have been taken by both the transmission and frustrated multiple internal reflectance modes. These surfaces have also been examined by scanning electron microscopy. The blood clotting times of the synthesized surfaces as well as glass, siliconized glass, heparinized glass and parylene have been taken. PVA, stearated PVA, and PVA lightly esterified with AAME have clotting times in the range of most other plastic surfaces. PVA heavily esterified with AAME and PVA esterified with both AAME and DAMSE have clotting times in the range of siliconized glass. The possibility of using solutions of commercially available spandex materials for the outer layer of our artificial circulatory implant was studied. Two materials, Lycra T-126 and Roylar A-850, offer promise. Tensile bars of these two materials were made and tested. Also tensile bars were implanted in dogs for long term compatibility studies. The synthesis of more soluble spandex materials has been started.

INTRODUCTION

In the past many different types of surfaces have been tested for compatibility with blood. In each case, the main emphasis has been placed on one particular property of the surfaces being tested, i.e., the degree of smoothness, wettability, electrical character or chemical composition. Although different advances have been made towards producing surfaces which are non-clotting, it is not unexpected that generally useful blood-compatible materials have not yet been prepared. In general, the materials used have been both foreign to the circulatory system and much harder than tissue. The long-term implants now in use in the circulatory system are loosely woven fabrics which become covered with a pseudo-intima and thereby isolated from contact with blood, or are made of silicone rubber or Stellite metal and depend upon high blood flow rates and anticoagulant therapy to prevent thrombus formation. Little effort has been devoted to producing synthetic surfaces that approximate the vascular system.

In our research, we have made the first step towards the production of a synthetic blood conduit which resembles natural tissue. We have produced a three-layered structural member which has an elastic, load-bearing outer layer of spandex rubber, a softer, hydrophilic middle layer of polyurethane and an inner layer of highly hydrophilic polyvinyl alcohol (PVA) (Figure 1). This PVA layer has been esterified first by half cholesterol esters of dicarboxylic acids (Figure 2) and next by the half sialic (N-acetylneuraminic) acid ester of a longer chain dicarboxylic acid (Figure 3). The chemically modified surface has then been treated with a tissue culture medium which contains salts and proteins found in the blood (Figure 4).

We reasoned that cholesterol esters naturally occur in the blood and are often found in high concentration in such areas as atherosclerotic plaques without the blood being directly affected in a chemical sense by these deposits. We included the N-acetylneuraminic esters because sialic acids are naturally occurring constituents of cell membranes and give our blood-contact layer areas of high polarity and an anionic character similar to cell membranes.

Since any foreign material which comes into contact with blood is coated with proteins and the necessary balancing ions within seconds, we pretreat our surfaces with a mixture of physiological salt and blood proteins to produce the adsorbed layer before contact with blood to eliminate the possibility that the large, local change in concentration of the blood components caused by the introduction of the virgin material might trigger clotting in some manner.

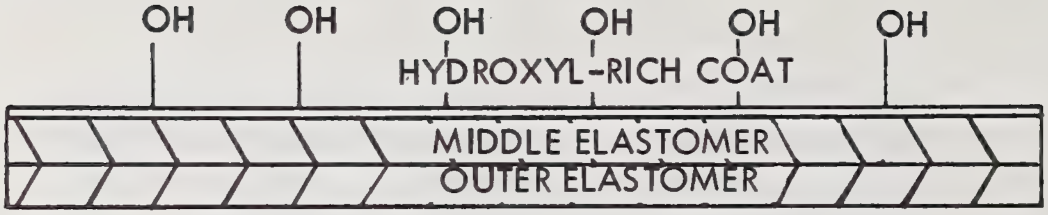

FIGURE 1. STRUCTURAL LAYERS OF THE ARTIFICIAL INTIMA

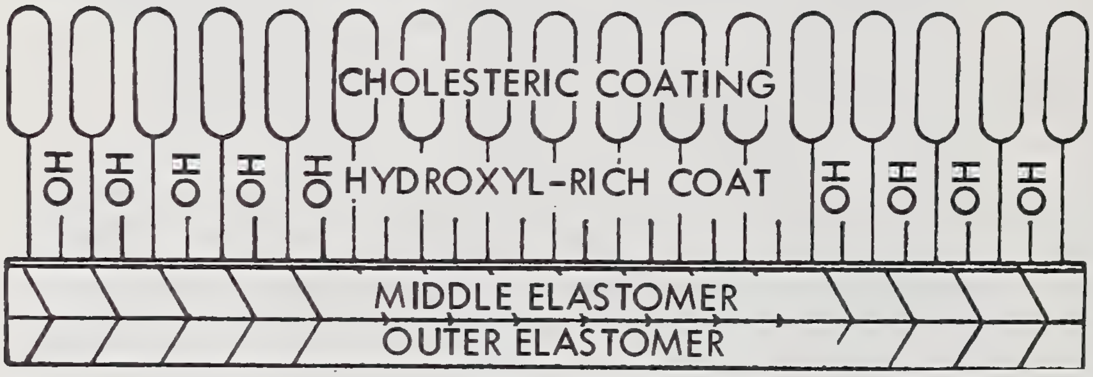

FIGURE 2. ARTIFICIAL INTIMA PARTIALLY ESTERIFIED BY A HALF CHOLESTEROL ESTER OF A DIACID

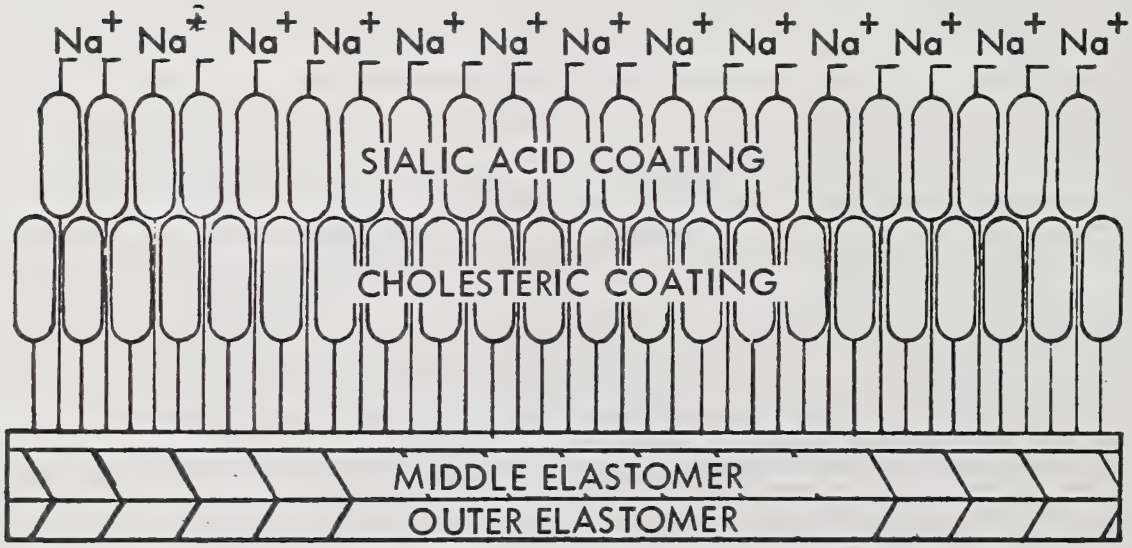

FIGURE 3. ARTIFICIAL INTIMA ESTERIFIED BY A HALF CHOLESTEROL ESTER OF A DIACID AND BY SIALIC ACID HALF ESTER OF A DIACID

EXPERIMENTS

Polyvinyl Alcohol Films and Test Tubes.

Polyvinyl alcohol is available as a free-flowing dry powder and is soluble in water. Solutions containing up to 30% solids are pourable at room temperature. At 100 C solutions containing 40% solids are usable. In our work, 10% solutions are used to make cast films, and 30% solutions to prepare test tubes.

Ten mil cast films are prepared by pouring the solution on a flat glass plate and drying it in a forced air oven. Such films are used to test new reaction conditions and check for reaction by spectroscopic or radiotracer techniques.

In order to have test tubes with an inner PVA surface, we first tried to line test tubes with this polymer. The polymer, however, does not adhere to the glass and in most cases pulls away from the test tube wall while drying. We then tried a Teflon mandrel dipped in a hot 30% PVA solution (Figure 5). This PVA layer is stabilized and dried by immersion in a stirred acetone bath (Figure 6). Baking in the oven removes any remaining water.

The Teflon mandrel had a high polish at the start, but became roughened after being used a few times, at which point, small specks of Teflon could be seen on the inside surfaces of the PVA tubes. Because of this problem, we went to polished stainless steel mandrels. The tubes produced from these mandrels are very smooth and clear (Figure 7). The tubes are removed from the mandrel by cooling to -120 C, at which temperature, they can be pulled off.

Cholesterol Half Esters of Dicarboxylic Acids.

A series of cholesterol half esters (CHE) of dicarboxylic acids of different lengths were needed to esterify the PVA surfaces. The half esters are most easily prepared from cholesterol and the cyclic anhydrides when available. The acid chlorides are used for adipic and longer chain acids. Table 1 lists the diacids and the chain lengths that we have used.

TABLE 1

LENGTH OF DICARBOXYLIC ACIDS - $HO_2C(CH_2)_nCO_2H$

N	Acid	Length, Å
2	Succinic	4
3	Glutaric	7
4	Adipic	9
8	Sebacic	14
10	Dodecanedioic	16
12	Tetradecanedioic	18
14	Hexadecanedioic	21
20	Docosanedioic	29

Succinic and glutaric anhydrides are allowed to react with equal molar amounts of cholesterol and a drop of pyridine in refluxing toluene. The extent of the reaction is checked by the disappearance of the anhydride bands in the infrared. When the reactions are complete and the mixtures allowed to cool to room temperature, the products crystallize out as white solids.

The longer-chain CHEs are prepared from a two-fold excess of the diacid chloride over cholesterol. Triethylamine is used to take up the hydrogen chloride released and to speed up the reaction. Dry acetone is used as the solvent. When the reaction is complete, the mixture is poured into water to dissolve the amine hydrochloride and to hydrolyze the remaining acid chloride groups. The solids are treated with hot toluene which dissolves the esters but not the unreacted diacids. When cooled to -20 C, the product crystallizes out. This material is then recrystallized from dioxane to give CHE of high purity.

Polyvinyl Alcohol Surfaces Esterified by CHE.

Polyvinyl alcohol films or test tubes to be esterified are dried for 20 hours at 110 C. Stoichiometric amounts of thionyl chloride are added to a 10% solution of the CHE in dry benzene, followed by equal molar amounts of triethylamine. This mixture is then brought into contact with the PVA surfaces to be esterified. The system is then heated at 70 C for three hours. The PVA darkens (Figure 8). The degree of darkening agrees well with the hydrophobic character of the surface. Very light colored surfaces are wetted easily and become swollen with water; medium colored surfaces are wetted but do not swell; dark colored surfaces are not wetted. The infrared spectra of these surfaces show decreased amounts of hydroxyl groups and the presence of ester bonds.

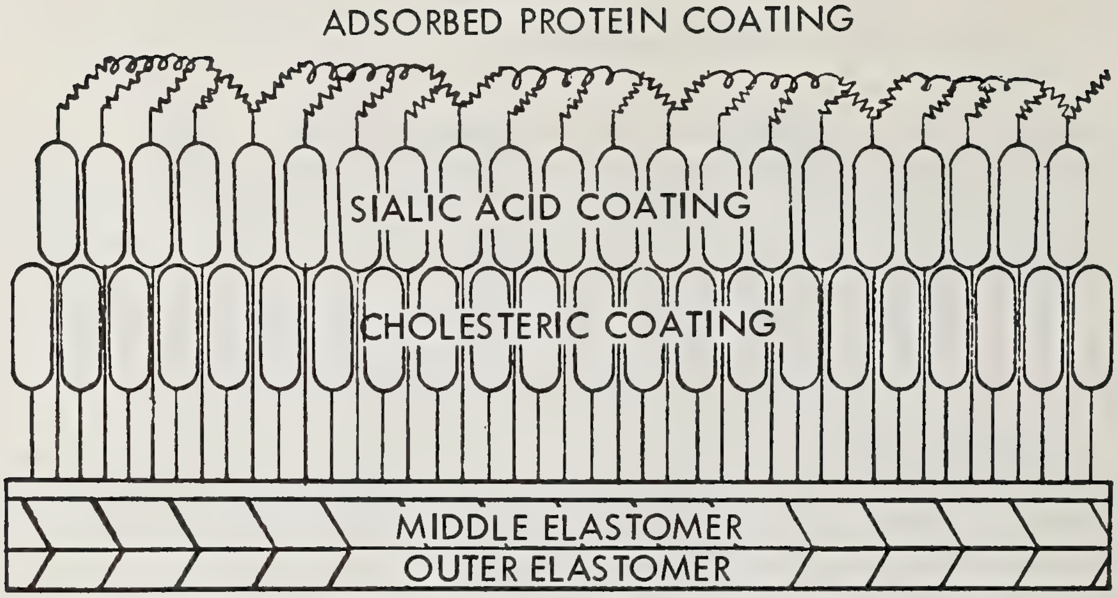

FIGURE 4. ESTERIFIED SURFACE OF THE ARTIFICIAL INTIMA WITH ADSORBED PROTEIN COAT

FIGURE 5. TEFLON MANDREL BEING DIPPED INTO A HOT 30% AQUEOUS PVA SOLUTION

FIGURE 6. PVA COATED MANDREL IN ACETONE DRYING BATH

FIGURE 7. COMPARISION OF PVA TEST TUBES PREPARED ON MANDRELS OF TEFLON (TOP) AND STAINLESS STEEL (BOTTOM)

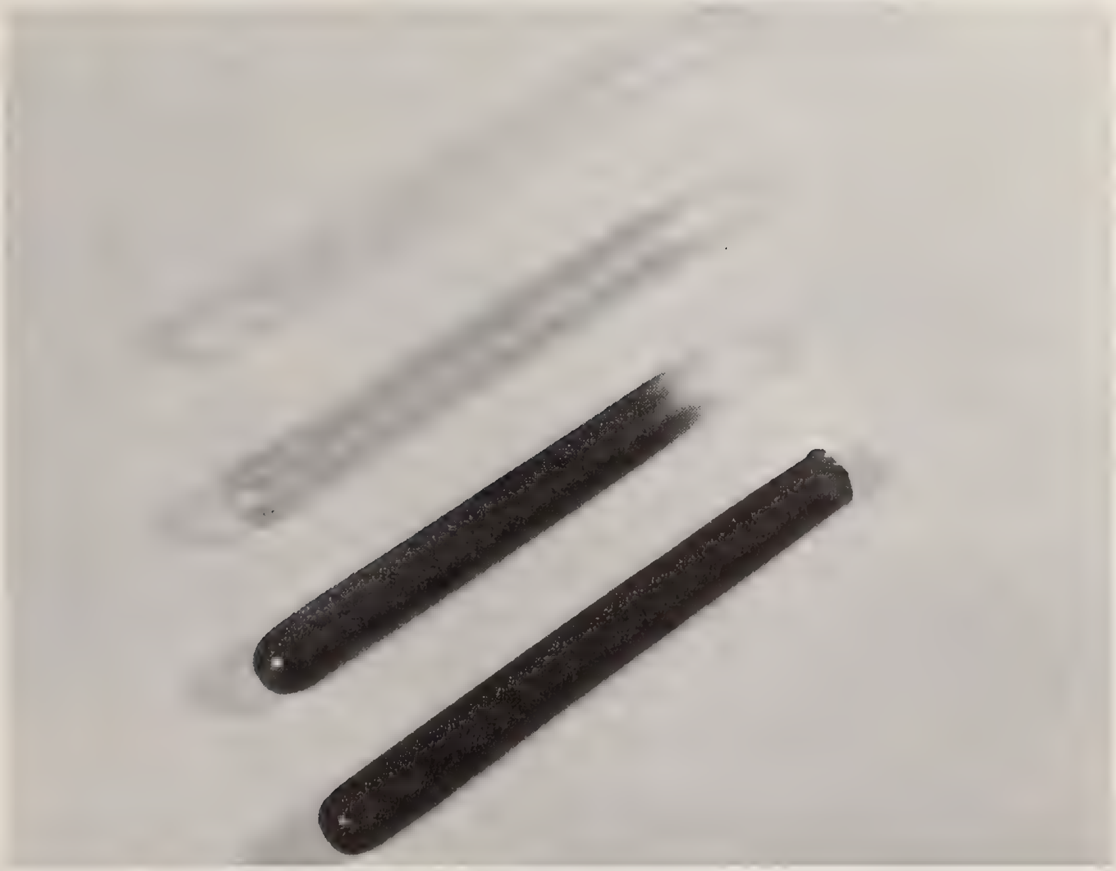

FIGURE 8. PVA TEST TUBES FROM TOP TO BOTTOM: UNTREATED PVA; ESTERIFIED WITH ACID-HALF CHOLESTEROL ESTER; LIGHTLY ESTERIFIED WITH STEARIC ACID; HEAVILY ESTERIFIED WITH STEARIC ACID.

Polyvinyl Alcohol Surfaces Esterified with CHE and Sialic Acid Half Esters.

As the degree of esterification of the PVA surfaces by the CHE increases, the remaining available hydroxyl groups become fewer and more isolated. A stage is reached when diacid chlorides are able to react at one end only because the other end is no longer able to find another unreacted hydroxyl. In practice this type of reaction can be made to take place almost exclusively if most of the hydroxyl groups have been esterified by monofunctional acid already. But, of course, it is not possible to have a surface where all the diacid chlorides react only at one end.

The medium-colored CHE-esterified surfaces are usually used for attachment of the sialic acid. These surfaces are first allowed to react with equal molar amounts of a very long diacid chloride, i.e., docosanedioyl chloride, and triethylamine in dry benzene at 70 C for 20 hours. The reagent is then removed from the surface and then the surface is washed with dry solvent. Next a dry dimethylacetamide (DMAC) solution of the sialic acid (Figure 9) and pyridine is added, and this heated at 70 C for three hours. The reagents are again removed. The surfaces are finally washed with DMAC to remove any remaining reagent.

Blood Clotting Times of Surfaces.

The blood clotting times of our different surfaces are measured by the Lee-White method. Two ml. of freshly drawn blood taken with a siliconized syringe and needle is added to a standard size test tube, the inner wall being made of the material being tested. Three test tubes are used for each material. The first tube of each test set is tipped every 30 seconds until the blood no longer flows when the tube is given a light tap. The next tube of that set is then so tested and so on. The time at which the blood in the third tube no longer flows is taken as the clotting time of that material. Table 2 summarizes the clotting times of the different surfaces tested in our program.

TABLE 2

BLOOD CLOTTING TIMES AT 24 C

Type of Surface	Human Blood	Canine Blood
Glass	15.5 Min.	8.5 - 13.5 Min.
" Siliconized		48
" Heparinized		31
PVA	23.5	
" Lightly Stearylated	10.5	
" Heavily Stearylated	27.0	
" Adipochlosterolated		18
" " Dark		38.5
" " Light		12
" " Sialic Acid		42.5
" " and Dodecanedioyl-Cholesterolated		61

Large differences with the same surface by this test are possible, as seen from the two clotting times for glass using canine blood. However, the very long clotting times for the darkly esterified PVA and the PVA esterified with CHE of adipic acid and SAHE of docosanedioic acid were measured in the same group of clotting times in which glass gave six minutes. Therefore, the 42.5 min. value for the mixed esterified surface is very good indeed.

Spandex Type Polyurethane.

The outer layer of our composite blood conduit replacement is composed of a spandex material. We have been making this layer out of DuPont's Lycra. As a structural material for this use, Lycra has very good physical properties. However, it has one very large drawback. It is very insoluble. When dissolved even in hot dimethylacetamide, the best solvent for the material, the solution becomes colloidal upon cooling. DMAC is quite hygroscopic and small amounts of water cause the room temperature colloidal solution to break and the Lycra separates out. The remaining wet solvent presents a major problem when dip coating parts. A second coat of the spandex solution will not adhere to the first coat until all of the wet solvent has been removed. This makes the process of fabricating a multi-dipped part very time-consuming. New, more soluble spandex materials are being investigated.

Samples of a number of commercially available spandex materials have been obtained as possible candidates for the outer layer of our composite system. The physical properties of these materials have been measured and are listed in Table 3.

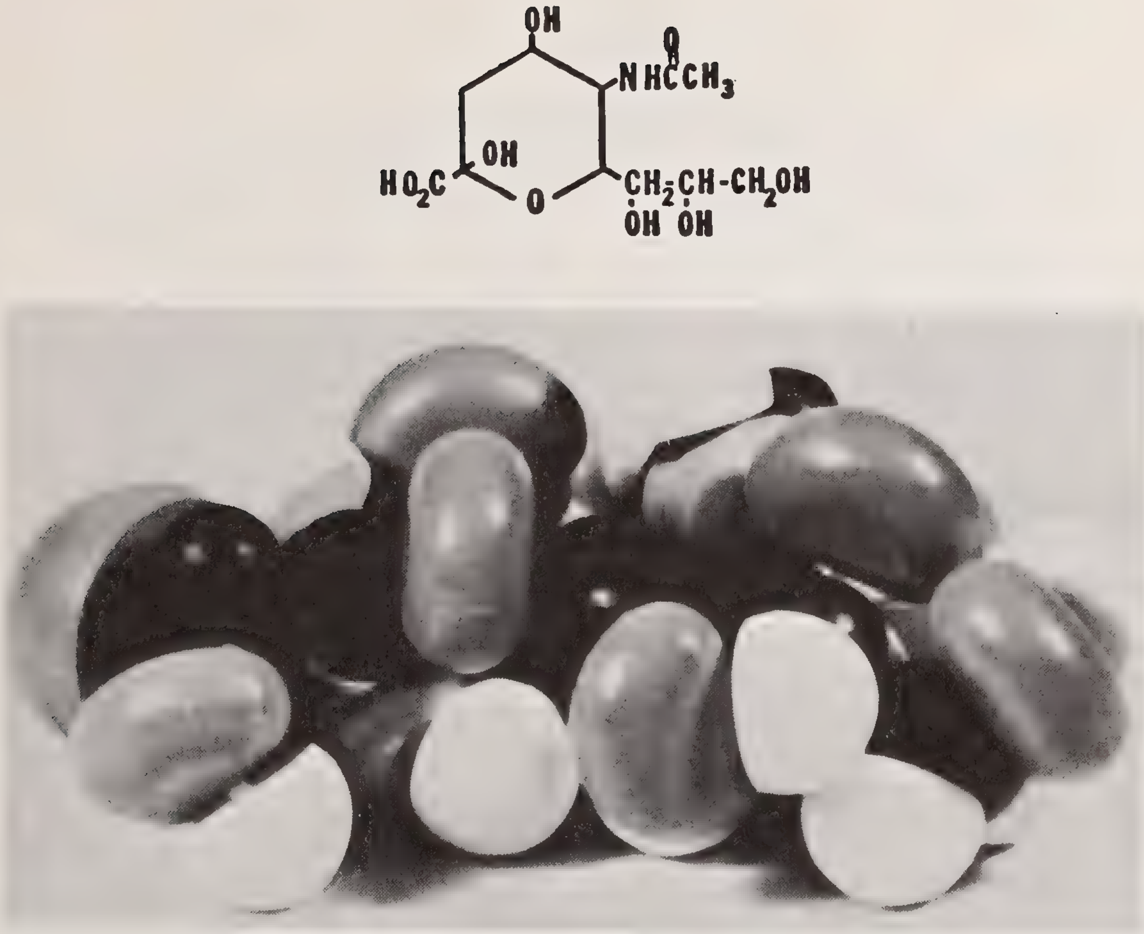

FIGURE 9. N-ACETYLNEURAMINIC ACID (SIALIC ACID)

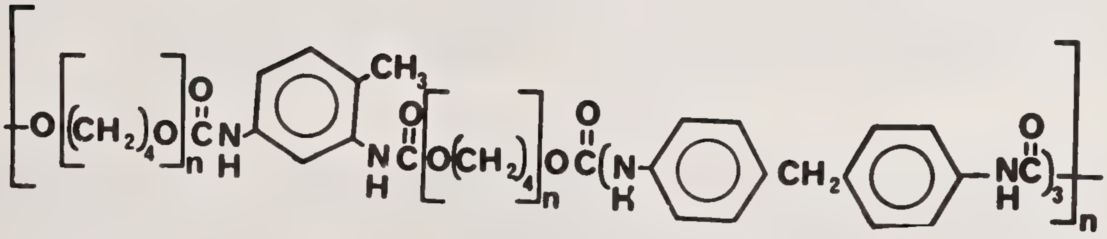

LYCRA SPANDEX

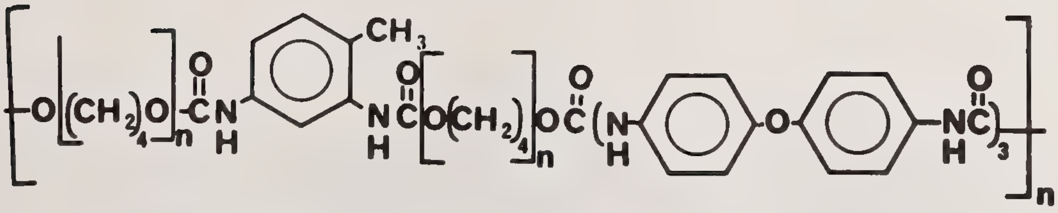

PHENYL ETHER BASED SPANDEX

FIGURE 10. LYCRA AND PHENYL-ETHER BASED SPANDEXES

TABLE 3

PROPERTIES OF SPANDEX MATERIALS

Spandex Material	Type of Flexible Chain	Hardness, Shore A	Tensile Strength, PSI	Elongation, %	Elastic Recovery, %	Stress Decay, %	Tear Strength	Water Sorption %	Viscosity in DMAC 20% sol.
Epoxylite 753	Polyether	72	5390	705	93/95.5	6.5	437	2.42	3650
Epoxylite 754	Polyether	91	7750	725	86/94	18.2	607	1.47	1740
Epoxylite 762	Polybutadiene	87	1460	283	94/97	-	126	0.93	Not Soluble
Estane 5707	Polyester	90	8040	634	80.5/85	-	197	-	3300
Estane 5710	Polyester	65/70	3944	830	93/98	11.8	681	-	3500
Glaspan S-1	Polyester	-	-	-	-	-	-	-	Not Soluble
Rucothane CO-67	Polyester	80	5545	801	90/92	14.4	391	-	-
Rucothane CO-68	Polyester	83	4222	740	82/94	13.0	382	-	-
Rucothane CO-75	Polyester	80	2269	502	94/96	19.2	338	-	-
Rucothane P-49	Polyester	-	-	-	-	-	-	-	120
Rucothane P-53	Polyester	60/70	536	427	88/92	25.8	211	-	176
Adiprene L-100, MOCA	Polyether	85	3375	395	88.5/92	8.5	374	-	Not Soluble
Adiprene L-100, ODA	Polyether	80	4772	577	93/95.5	-	287	-	Gelled
Adiprene L-100, CPE	Polyether	90	7280	500	-	-	471	-	Gelled

Lycra still seems to have the best all around physical properties although Epoxylite 754 has better strength, and Epoxylite 762 had the best stability in aqueous environments. The 762 actually has greatly improved physical properties after being in boiling water for 30 days. Other spandex materials will be compared as samples are obtained.

Currently we are working on preparing a spandex material based upon phenyl ether rather than diphenyl methyl (Figure 10). In our case, oxydianiline is used in place of methylene bisaniline, and bis(4-cyanatophenyl) ether is used in place of bis(4-cyanatophenyl) methane. We feel that the oxygen atom in place of the methylene group will give the polymer increased solubility. Other polymers which have phenyl ether groupings have greater solubilities than their hydrocarbon analogs.

CONCLUSION

At this stage of our work, we have been able to obtain surfaces esterified with cholesterol and N-acetylneuraminic acid. These surfaces have blood clotting times as long as siliconized glass. Since these clotting times were obtained on the first few surfaces prepared, we have high confidence that the clotting times will be even longer as we perfect our system. Part of our work planned is based upon studies using radioactive cholesterol to gain further insight into the conditions necessary to obtain the best surfaces reproducibly. Gott rings of the best surfaces are being prepared for *in vivo* studies.

DISCUSSION

MR. STERN: Do you have some reason for using sialic acid, i.e., has it been demonstrated to be important in the anti-clotting mechanisms?

DR. STOFFEY: No. As far as I know, this is the first use of sialic acid in a blood clotting reaction, but it is among the saccharides that are found in natural cell constituents, especially in the cell membranes. In fact, it appears to be the principal material which imparts a negative charge to the surface of various cells. Also, chemically, it is not really too far removed from materials such as heparin or other saccharides that serve the function of preventing clotting.

MR. STERN: It has been my experience that it is very hard to obtain sialic acid. Who is your supplier of sialic acid?

DR. STOFFEY: There are several places where it can be obtained. One has a double German name, which I cannot recall off hand. I will send you their catalogue. The sialic acid is not cheap, but it is not so bad since you are only putting a few micrograms per unit area on the surface. Thus, the cost per square centimeter is certainly quite small.

DR. CORCORAN: Is this composite system, using layers of cholesterol and sialic acid esters stable in the physiological environment?

DR. STOFFEY: This we have not yet tested. As we prepare our different surfaces to the best of our ability and construct a pseudo-endothelial cell membrane and surface, we will characterize our surfaces to a greater extent and determine just how stable these materials are to attach *in vivo*. We believe that the ester bonds attaching these materials to the surface of the synthetic polymer are sufficiently different from those in the physiological system that they won't be easily attacked by enzymes or that the prosthesis will be used in locations where ester-breaking enzymes will not be present.

CHAPTER 15

RESEARCH ON MATERIALS COMPATIBLE WITH BLOOD

E.S. Nuwayser, S. Bonacci, J. Knudsen, R. Tuelings, S. Davis

Monsanto Co., Everett, Mass.

The objective of this program is to develop textile structures for preparing composite materials with a surface of micro-cellular anchoring devices (micro CAD) having a "pile" height of 15-30 microns. The devices will be used to anchor fibroblastic and endothelial cells to form a "living" surface similar to that present on the intimal wall of the adult normal artery. The approaches which have been investigated for preparing the textile structures include nonwoven fabrics, flocked surfaces, knitted and woven fabrics, textured surfaces, polyblend fibers, and core wrap yarns. Sheets and tubes were fabricated from these structures and submitted for animal evaluation. They were made from nylon, polyester, carbon and silicone rubber, and were prepared in "pile" heights ranging from 15-400 microns. Methods for determining the entrapment of fetal calf fibroblasts by the surfaces were studied. Those based on counting the number of cells present under fabric loops were found to be unsatisfactory. A chemical method for determining the degree of attachment and mechanical entrapment of the cells is being evaluated. The relationship between cell adhesion and the chemical nature of the surface is also under investigation.

OBJECTIVE

The objective of this program is to develop surfaces with mechanical microdevices capable of anchoring viable fibroblastic and endothelial cells for use in living impermeable vascular grafts, heart-assist and other implantable devices.

These structures are referred to as microcellular anchoring devices (micro CAD), and possess a 15-30 micron pile height (Figure 1).

The devices will be used to anchor a layer of fibroblastic cells and endothelial cells to produce a "living" surface which simulates the intima of the normal adult human artery. This, hopefully, will present to the blood a surface that is passive, not "foreign" and therefore completely and truly compatible with it. The selection of 15-30 micron pile height is based on studies by Robertson (1965) who studied the transfer of nutrients from the blood stream into the arterial wall. He detected their presence to a distance of 100 microns from the endothelium.

During the first year of the program, we succeeded in developing several structures which satisfy the suggested 15-30 micron mat height. In our studies we have made extensive use of nylon 6-6, yarns and fabrics for preparing mechanical models of the microcellular anchoring surfaces. Nylon was selected as a model biomaterial because of its high tensile strength and availability in "microdenier" filaments. It has been established, however, that nylon is quickly degraded in the body and therefore is not a useful polymer for prolonged implantation.

In addition to investigating new structures, during this year we have initiated programs for the evaluation of the surfaces, *in vitro* and *in vivo*, both at our laboratories and in collaboration with other investigators affiliated with the National Heart Institute.

FRACTIONAL DENIER YARNS

Fractional denier fibers made by melt spinning of nylon and polyester were prepared by extrapolation of conventional spinning technology. In addition, by employing a proprietary solution spinning process patented by Monsanto, we were able to prepare 0.5 dpf samples of acrylic fibers with excellent physical properties from four different polymer compositions. These include fibers made from an acrylonitrile/vinyl acetate copolymer containing about 94% acrylonitrile, an acrylonitrile/acrylic acid copolymer containing about 10% acrylic acid, a polyblend of acrylonitrile copolymers containing about 6% vinyl pyridine groups, and an acrylonitrile/methyl vinyl pyridine copolymer containing about 7% MVP (Table 1).

These copolymers were selected on the basis of availability, ease of preparation, and fiber forming characteristics. Pure polyacrylonitrile is relatively insoluble and difficult to spin. It requires high solution temperatures and is usually degraded and discolored during the prolonged heating required to make spinning solutions. The vinyl acetate copolymer containing 6% vinyl acetate is typical of the copolymers used to prepare commercial acrylic fibers. It is readily soluble, spins well, and gives high quality fiber. Vinyl acetate was selected since it copolymerizes readily with acrylonitrile, but does not introduce easily reacted acid or basic groups. The level of addition (6% by weight) is sufficient to impart improved spinning performance without affecting the basic mechanical properties of PAN.

To prepare the copolymer containing acid groups we selected acrylic acid for our comonomer since it is easily copolymerized, readily available, and imparts a reasonably strong acidic group which is readily reacted with any basic material. The level of addition (~10% by weight) was

TABLE 1

PROPERTIES OF MICRODENIER YARNS

Sample	Polymer	Denier Per Filament	Tenacity gpd(a)	Elongation	Filament Diameter (microns)
1N	Nylon	1			12.8
1PE	Polyethylene Terephthalate	0.9			10.7
1A	Acrylonitrile-Vinyl Acetate 94/6	0.54	3.64	17%	11.8
1AC-b-Sample 1	Acrylonitrile-Acrylic Acid 90/10	0.51	3.7	20%	6.4
1AC-a-Sample 1	Acrylonitrile-Methylvinyl Pyridine-93/6 Vinyl Acetate	0.49	3.6	17%	8.6
1AC-a-Sample 2	Acrylonitrile-Methyl Vinyl Pyridine 93/7	0.63	5.22	8%	8.6
1PVF	Polyvinyledene Fluoride	0.69	2.38	17-18%	6.4

(a) gpd = grams per denier

selected to provide a reasonable number of acid groups in the fiber without imparting excessive water sensitivity. The comonomer selected to prepare fibers containing basic sites was 2-methyl, 5-vinyl pyridine (MVP). This material copolymerizes readily with acrylonitrile and causes fewer problems in handling and spinning than vinyl pyridine. MVP copolymers are sufficiently basic to complex readily with any strong or weak acidic group. We prepared two copolymers with MVP. The first was blended with AN/VA copolymer to give about 6% MVP in the blend prior to spinning. This polyblend was prepared in anticipation of spinning problems with the 93/7 copolymer. As expected, the 93/7 material did not spin well, but a small amount of fiber (sample 1AC-a2) was made. The polyblend spun well (sample 1AC-a1).

We also attempted to prepare fractional denier polyvinylidene fluoride fibers by our patented process. Although our initial attempt was unsuccessful we were able, on the second try, to get small quantities of fiber for evaluation.

For the development of textured flocks, two microdenier yarns were prepared: a textured nylon with 10.7 micron filament diameter, and a textured acrylic with 6.4 micron filament diameter.

Fractional denier yarns will be used for the development of flocks and fabrics. In addition they are useful for studying the effect of chemical structure on cell entrapment.

DEVELOPMENT OF MICROFLOCK FILAMENTS

One of the objectives is the development of microflock filaments (25-50 microns) for direct flocking onto devices. It is true that the process of negative flocking has achieved a mat height of 15-20 microns. However, negative flocking is currently useful for flat sheets, which in turn must be bonded to the device. If the device happens to be flat, then no problem exists. However, if the device is curved (as it usually is in the case of devices) bonding the sheets will require butting two edges together, leaving seams of unflocked adhesive.

Two approaches were evaluated for the development of microflock filaments. In the first the flocked surface of the device was treated with a solvent selective for the polymer used in the flock filaments. This approach had limited success mainly because of difficulty in controlling the dissolution rate of the flock filaments.

In a second approach, we mounted the filaments in Versamid 940. The block was then mounted on a Reichert Microtome and sliced at intervals of 50 microns thickness. The Versamid was then extracted with a solvent and the microflock fiber was washed and dried. This procedure produced the desired microfiber flocks. However, it was slow, and the yields were very low. An automatic microtome will improve yields considerably. Figure 2 illustrates the fibers obtained by this process using nylon filaments.

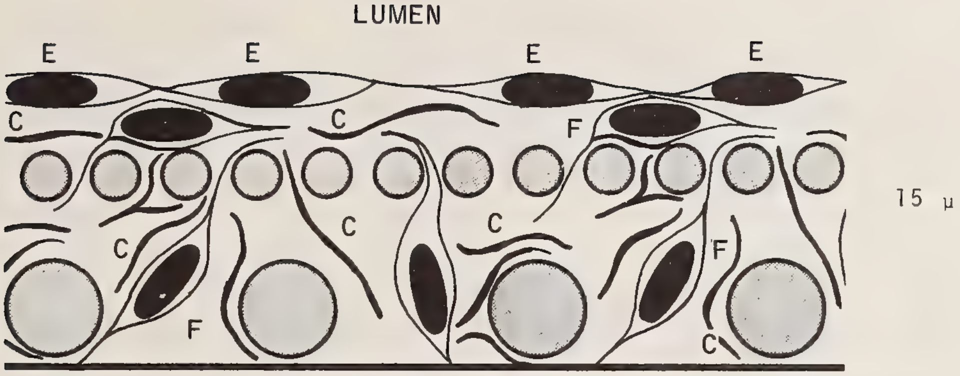

FIGURE 1. SCHEMATIC REPRESENTATION OF GROWTH OF CULTURED TISSUE IN MICRO-CAD

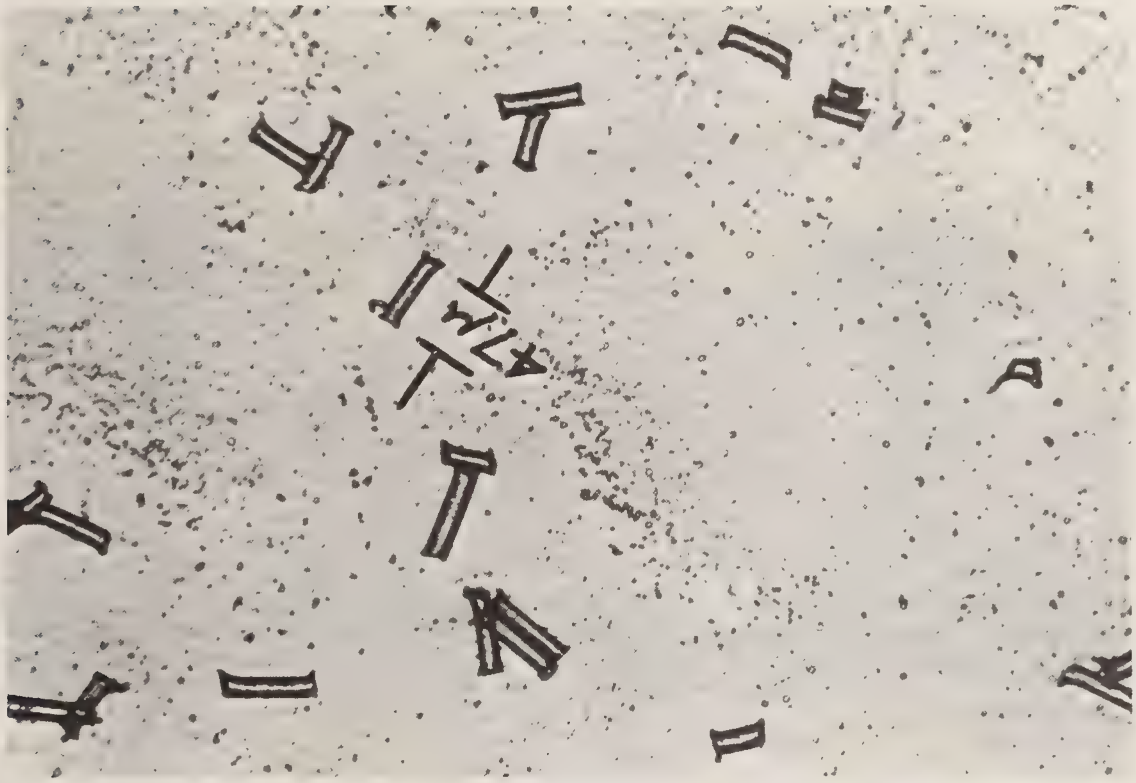

FIGURE 2. NYLON MICROFLOCK PREPARED BY MICROTOMING A SKEIN OF NYLON YARN IN VERSAMID

NEGATIVE FLOCKING

A new process which we labelled negative flocking was developed last year to obtain flocked surfaces 15-20 microns high. The principle of the method is illustrated in Figure 3.

A layer of soluble adhesive is first cast on a glass plate to a thickness of 15-30 microns. The fiber is then flocked through this layer onto the glass plate. After removing excess flock, medical grade Silastic Adhesive Type A is cast on the flocked surface. When the Silastic adhesive is cured, the first layer of adhesive is removed from the glass and the flocked fiber by treatment with acetone, a solvent in which the Silastic and the nylon fiber are insoluble.

In the preparation of negatively flocked surfaces, a film of Fuller's Adhesive W-3999 was used to control the final height of the flock mat. To improve the control of this height, we studied the influence of adhesive dilution in water on the degree of film shrinkage. To ascertain a reproducible result, films were cast in thicknesses of 50, 75, 100 and 125 microns. The adhesive was diluted with water to a maximum concentration of 50%. After drying, we measured the thickness of an enlarged section of the film under the microscope. The results are summarized in the curve shown in Figure 4.

These data show that the undiluted film shrank by 67%. Addition of only 15% water raised the degree of shrinkage to 80%. Although the 50% dilution produced films less than 10 microns thick, the solution was very fluid. The solution did not have enough viscosity to maintain a uniform film on glass; hence, we could not prepare a uniformly thin film for our flocking experiments. Similar results were obtained with the 35% dilution. For this reason, the 25% dilution seems to offer the best compromise of viscosity and film shear.

Using a 25% water concentration, a 50μ film (the lower limit of our casting blade) was cast, flocked with nylon yarn, and allowed to dry. After preparation of the negative flock, the final mat height obtained was 15 microns. This, then, becomes the lower limit of the present system. If a surface of lower mat height is desirable by this technique, it will be necessary to use a precision casting method capable of fabricating films thinner than 50 microns.

The degree of flock penetration into the adhesive was determined by flocking into films of the adhesive varying from 89 to 294 microns. The results which are shown in Table 2 indicated that the flock penetrated to a maximum depth of 50 microns.

TABLE 2

RELATION BETWEEN ADHESIVE THICKNESS (FULLER'S W-3999) AND FREE FLOCK BY NEGATIVE FLOCKING

Thickness of Adhesive Applied (microns)	Theoretical Thickness of Adhesive After 60% Shrink (microns)	Actual Free Flock (microns)
294	100	59
266	90	48
234	80	39
200	70	62
178	60	54
147	50	62
117	40	54
89	30	45
	Average	53 microns

In order to prepare a 100-micron flock mat, a new approach was used. The fibers were first flocked on contact paper by electrostatic deposition. A thin layer of Dow Corning 360 medical fluid (silicone) was spread over the flock to a height of 100 microns. On top of this was spread a 1:1 dilution in heptane of Type A medical adhesive. After curing for 48 hours, the composite was washed in acetone.

PORELOCK STRUCTURES

A novel approach for modifying the cell entrapment properties of flocked surfaces involves coating the flock with a very thin porous film. This structure, which is a composite of a porous film and flock, was called Porelock. Two major problems have to be solved before a satisfactory surface is obtained: very thin foam films must be developed, and the film must be bonded to the tips of the flock filaments on the surface of the device.

The development of very thin sheets of open cell foam in itself should be very rewarding. The effect of several parameters on cell size and type of foam (open vs. closed) was studied using Dow Corning Silastic S-5370RTV Silicone Rubber Foam. The studies were made on very thin films. Limited success was obtained with films of foam below 25 microns in thickness. Best results were produced by coagulation of the polymer film after bonding to the Silastic base. Pore size varied between 1-30 microns; the majority falling around 15 microns. The structure is illustrated in the

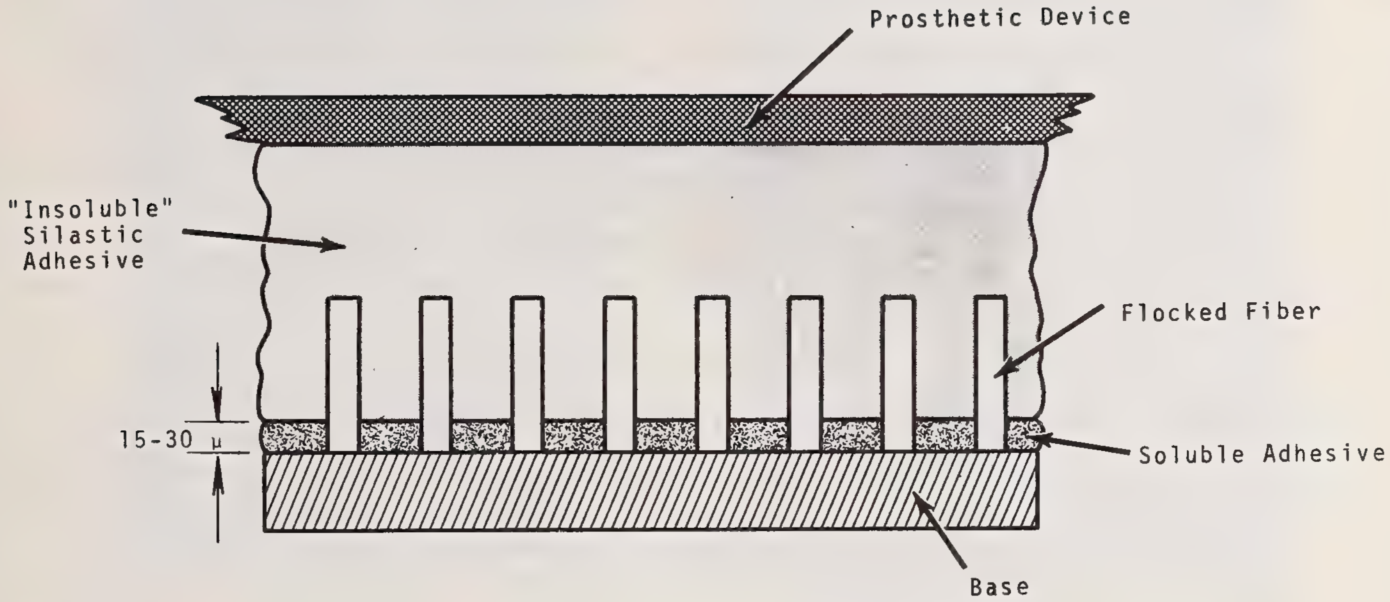

FIGURE 3. PROCESS OF NEGATIVE SURFACE FLOCKING

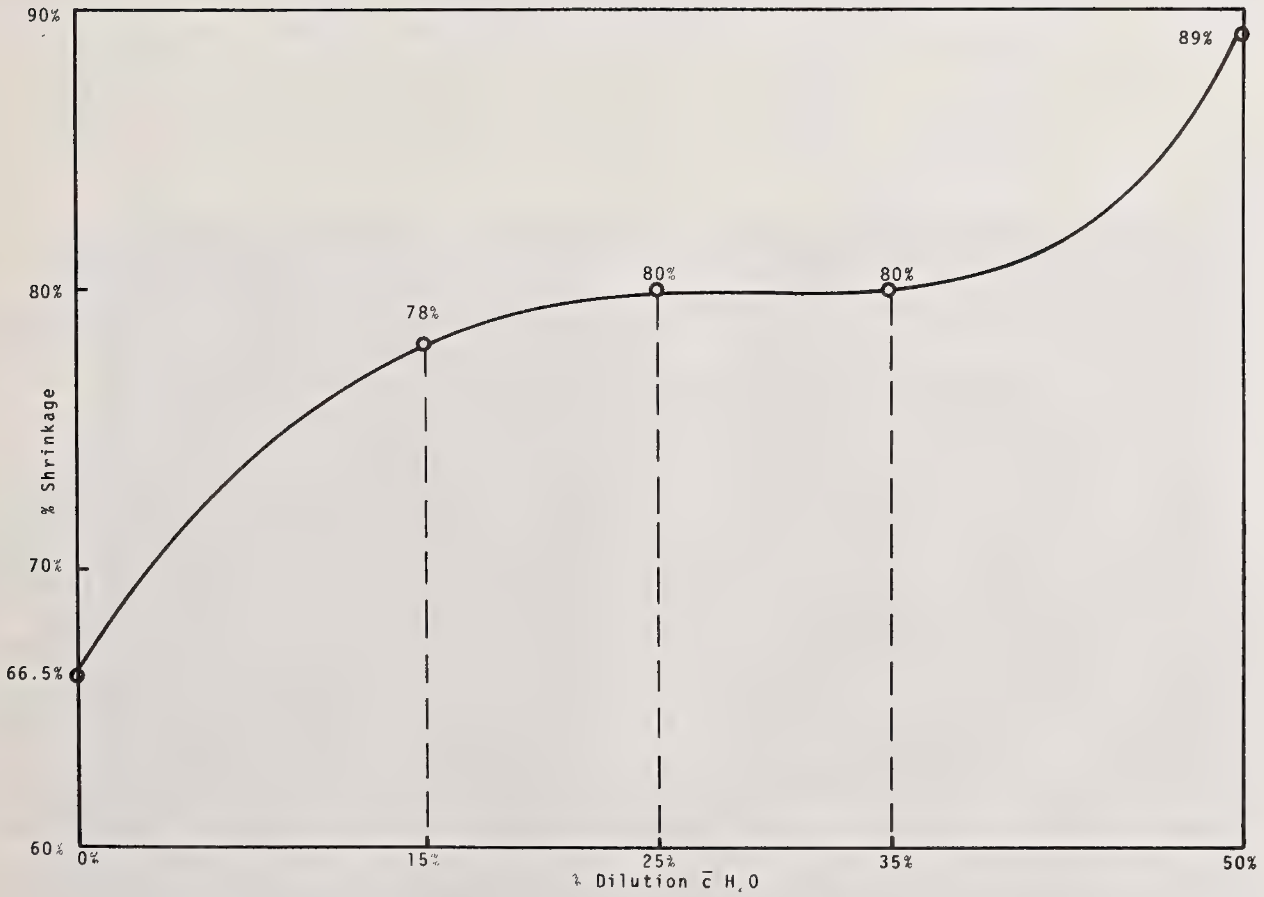

FIGURE 4. EFFECT OF WATER CONCENTRATION ON SHRINKAGE OF FULLER'S W-3999 ADHESIVE

electron scan photographs shown in Figures 5 and 6. A close examination of this surface indicates the presence of small connecting cells between the larger cells. This makes this type of structure very attractive for anchoring cells and for supplying nutrition to them from three directions.

Even more attractive than the above structure, is the potential it offers in the development of the Porelock structure. Such a structure would indeed represent the ideal surface for anchoring cells without inhibiting their survival and growth.

Although bonding a porous film to flocked surfaces seems at first to be an insurmountable problem, especially at the micron levels of interest, the problem becomes much simpler if such a film is produced in situ from the flock itself. Thus, if the flock tips are allowed to form a film, and then the film is coagulated with a nonsolvent, a Porelock structure would result.

Initial experiments to test this approach were made with nylon flock. The results which are shown in Figure 7 are very promising. The 100X magnified photograph shows a porous film of nylon coating the tips of the nylon flock.

MICRODENIER NONWOVEN FABRICS

A new batch of nonwoven fabric was prepared from nylon 6-6 microdenier web, by a method described in last year's report. This sample weighed nearly 0.045 oz/yd^2, and is the lightest web we could make. The fabric proved to be too light and too delicate to handle, and presented difficulties in bonding to Silastic. Fabrics weighing 0.06 oz/yd^2 proved to be easier to handle and have been prepared in 25 microns thickness.

The technology developed for preparation of nylon microfibers from formic acid solution followed by deposition on a moving belt was modified and adapted to allow preparation of microdenier nonwovens from acrylic polymers.

We encountered several problems in preparing the acrylic webs. Microfiber formation proved to be difficult except at relatively low polymer concentrations which in turn brought about problems in solvent evaporation. We found it difficult to prevent the microfibers from fusing, clumping, or redissolving during the heating required for solvent removal. The key difference in behavior between nylon and acrylic polymers is that nylon precipitates rapidly from formic acid solution in crystalline form above a maximum concentration and does not easily redissolve whereas the acrylics simply form more and more viscous solutions as the solvent is removed. In addition, formic acid is much more volatile than the acrylic solvent (BP ~100° vs 165°C). As a result of these problems we were able to prepare only small quantities of acrylic microdenier nonwovens.

The material was spun from dimethylacetamide solvent. The thickness of the web was about 15 microns and the weight 0.035 oz/yd^2. The polymer used for this preparation was 7.4% vinyl acetate and 92.6% acrylonitrile. We found this material to be highly electrostatic and to require preconditioning in a humid atmosphere. Filament diameter range is from 0.5 to 4.3 microns (Figure 8).

Another microdenier acrylic web was prepared in a density of 0.5 oz/yd^2. The fabric, however, was too thick to use in preparing 20-micron surfaces. Filament diameters range from 0.5 to 8 microns.

Efforts to prepare microdenier nonwovens from polyvinylidene fluoride were not successful. The same problems found with acrylic polymers were encountered to such a degree that web formation was not possible.

Microdenier nonwoven production from polyester has not been attempted. We have been unable to find volatile polyester solvents which will permit microfiber formation.

YARNS AND FABRICS FROM MIXED POLYMER MELTS

The general process scheme for the preparation of polyblend yarns is outlined in Figure 9. The polymer blend is melted in a screw extruder, then passed through a metering pump and sand filter to the spinnerette. Intermixing of the two polymers during extrusion is a crucial step in the process because this largely determines the number and size distribution of in situ microfibers formed when the yarn is post-drawn. The problem lies in determining the proper combination of extrustion conditions which will provide smooth spinning performance coupled with the right degree of intermixing (Figure 10).

Efforts originally planned in this area included melt spinning of nylon/polystyrene melt blends to produce nylon microdenier fibers in a removable polystyrene matrix; these were attempted with some success.

Extrusion of the blend was readily accomplished and nylon microfiber formation in the polystyrene matrix was excellent. However, due to the wide divergence of melting points (nylon 265°C, polystyrene ~150°C) we had serious difficulties with filaments fusing. In spite of these problems, a small amount of yarn was collected (Figure 11). Attempts to knit and weave this yarn have not been very successful due to the brittle nature of the polystyrene matrix. Successful spinning has been achieved with the polyester/nylon system, and samples of polyblend yarn were prepared from a blend of 20% polyester in 80% nylon matrix. Preliminary tests indicated the nylon is readily removed to give very light thin structures of polyester microfibers. However, these microfibers were excessively short and poorly formed. Fabrics knitted from the polyblend yarn lost their integrity after removal of the nylon matrix.

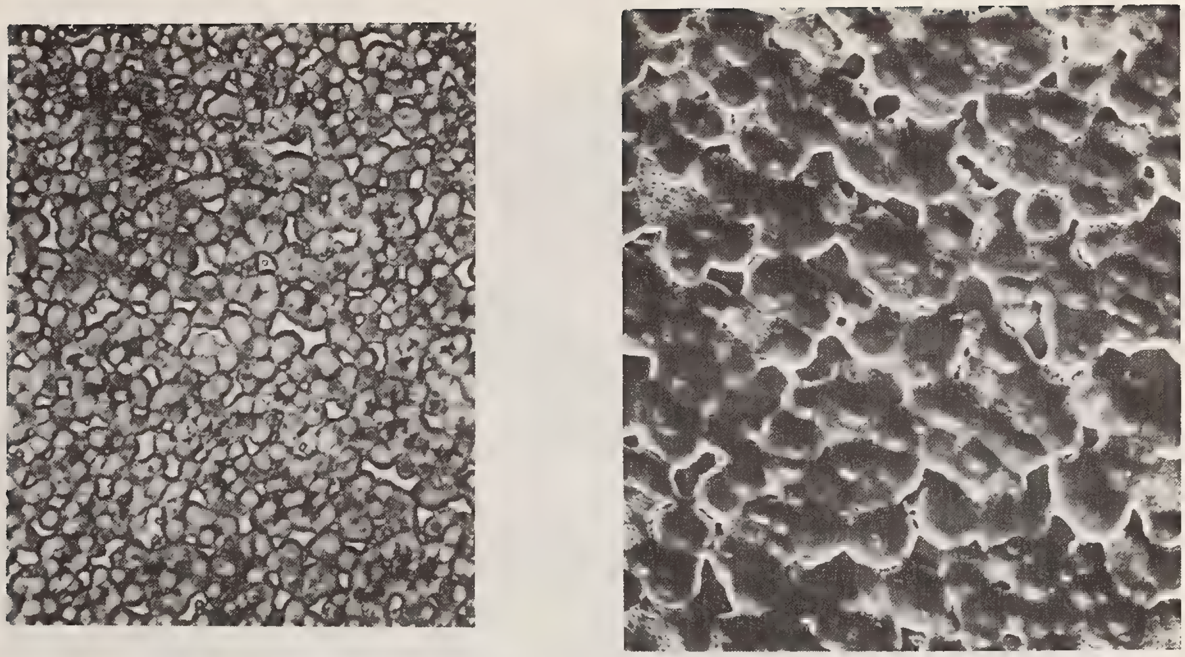

FIGURE 5. SURFACE MICROGRAPHS OF 25 MICRON MICROPOROUS NYLON FILM
A. OPTICAL MICROSCOPE AT 125x ORIGINAL MAGNIFICATION
B. ELECTRON SCAN MICROSCOPE AT 400x ORIGINAL MAGNIFICATION

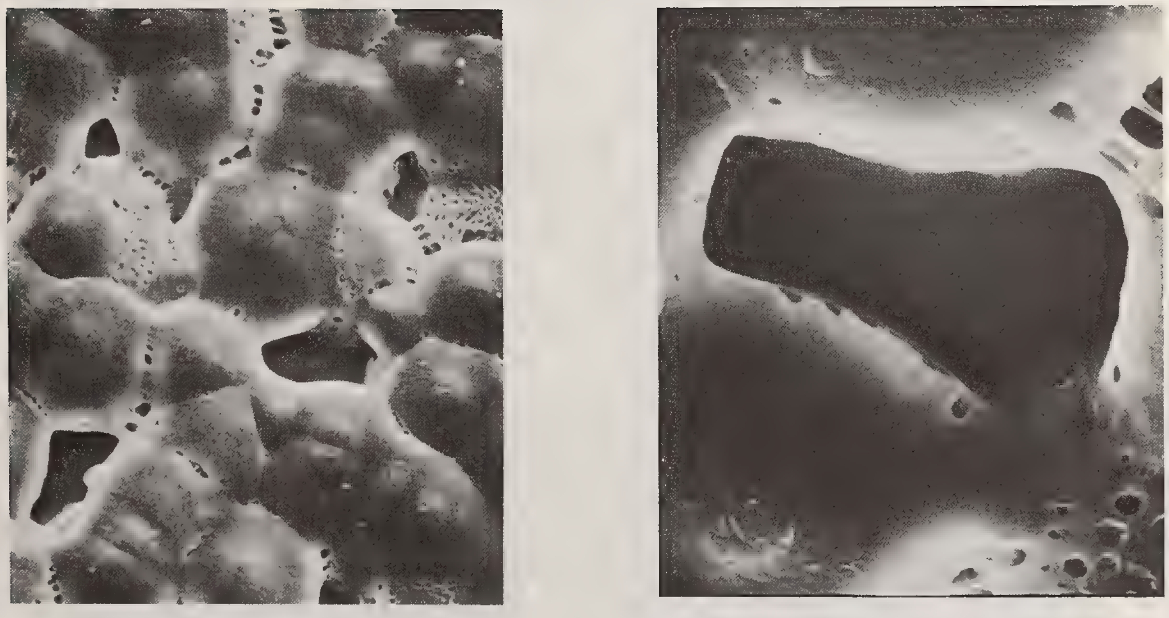

FIGURE 6. ELECTRON SCAN MICROGRAPHS OF 25 MICROPOROUS NYLON FILM BONDED TO SILASTIC
A. 1400x ORIGINAL MAGNIFICATION
B. 4000x ORIGINAL MAGNIFICATION

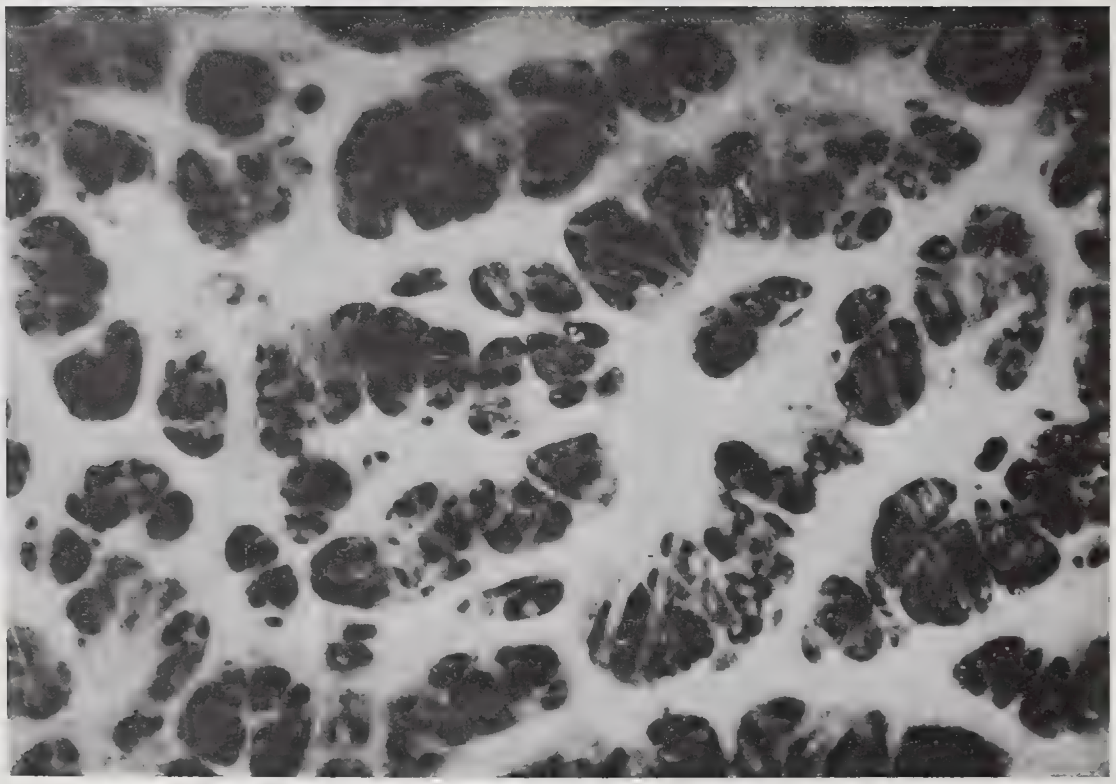

FIGURE 7. SURFACE MICROGRAPH OF NYLON PORELOCK STRUCTURE AT 100x MAGNIFICATION SHOWING THE POROUS FILM COATING ON THE FLOCKED SURFACE

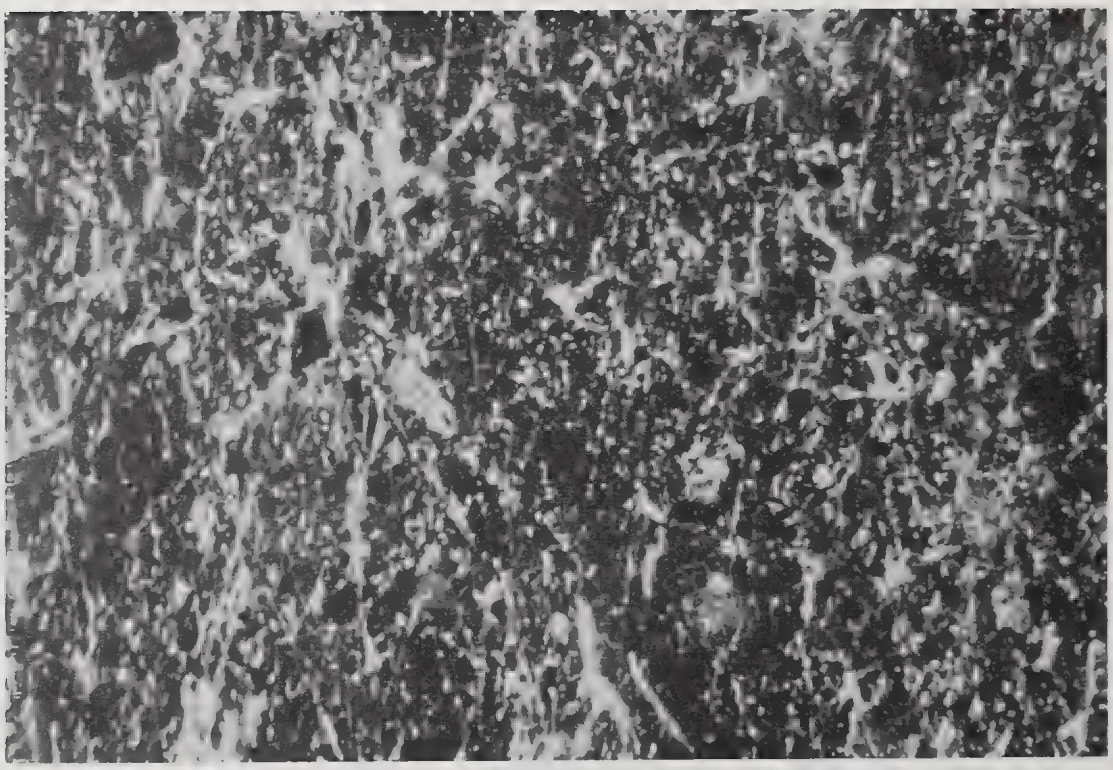

FIGURE 8. ACRILAN-SILICONE RUBBER COMPOSITE (60x ORIGINAL MAGNIFICATION) FILAMENT DIAMETER 0.5 - 4.3 MICRONS

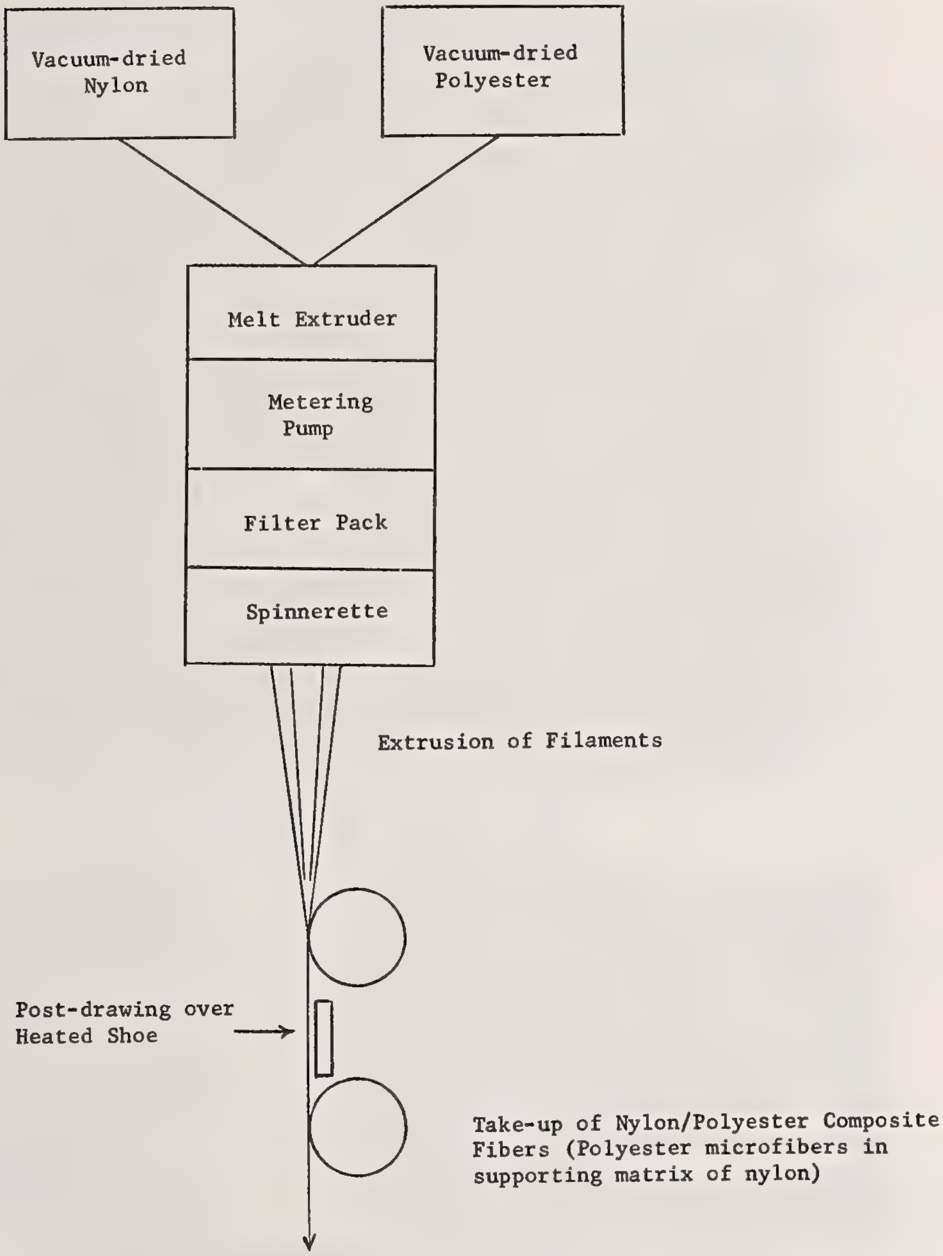
Vacuum-dried Nylon
Vacuum-dried Polyester
Melt Extruder
Metering Pump
Filter Pack
Spinnerette
Extrusion of Filaments
Post-drawing over Heated Shoe
Take-up of Nylon/Polyester Composite Fibers (Polyester microfibers in supporting matrix of nylon)

FIGURE 9. PROCESS FOR SPINNING NYLON/POLYESTER IN COMPOSITE FIBERS

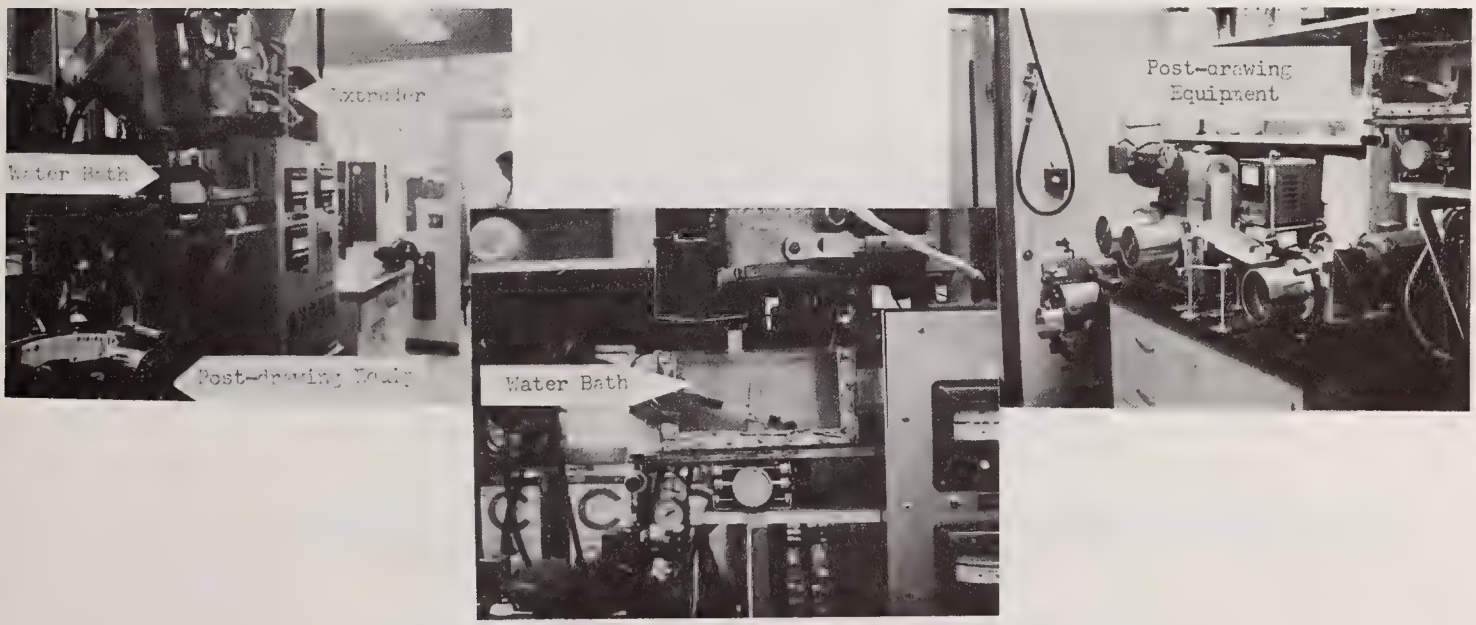

FIGURE 10. EQUIPMENT USED IN SPINNING NYLON/POLYPROPYLENE RIBBON

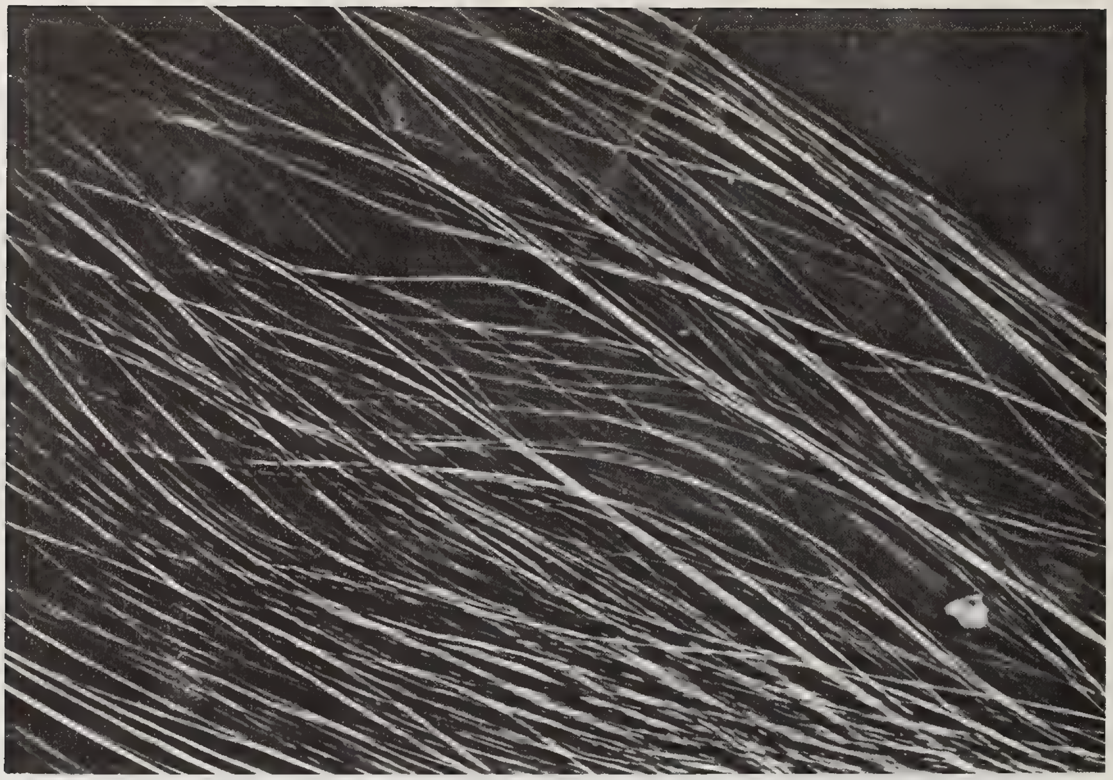

FIGURE 11. SAMPLE 456407: NYLON MICROFIBERS AFTER POLYSTYRENE MATRIX REMOVAL (135x ORIGINAL MAGNIFICATION)

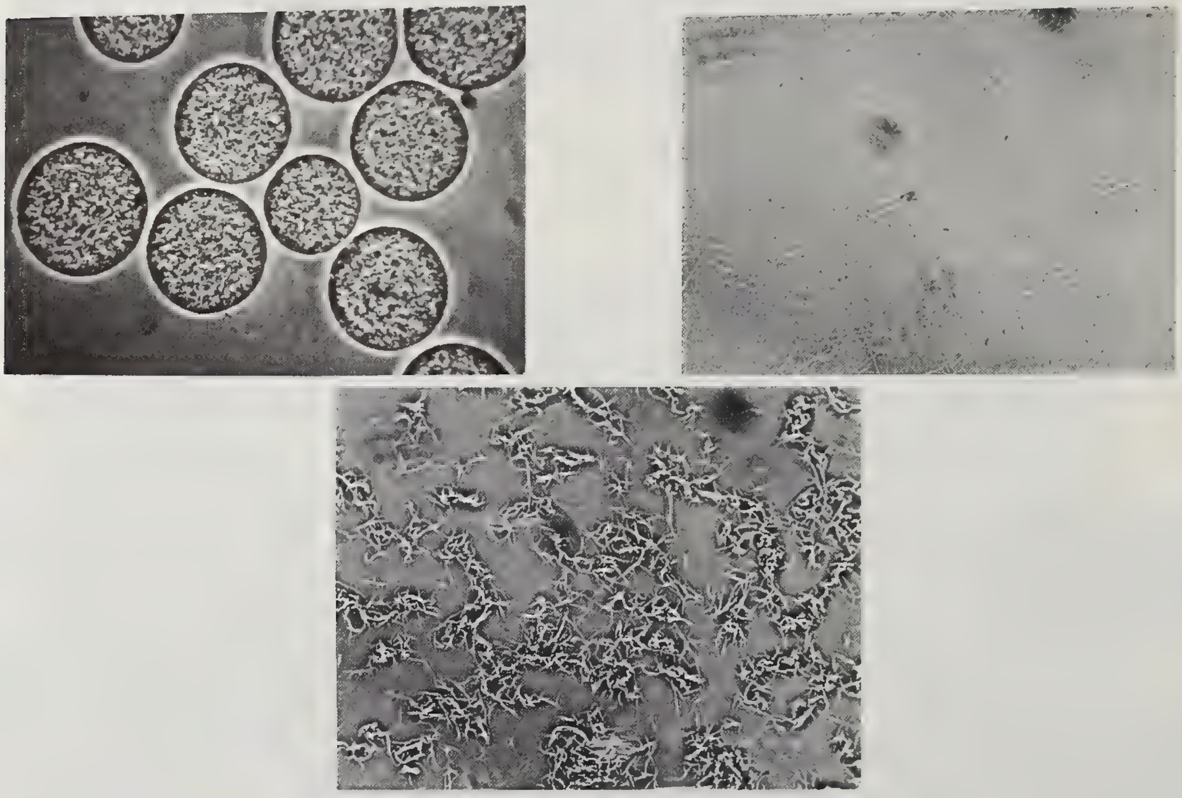

FIGURE 12. NYLON/POLYESTER FIBERS

A. CROSS-SECTIONS OF YARN SAMPLE 702816-1 (800x ORIGINAL MAGNIFICATION) 80% NYLON/20% POLYESTER. THE POLYESTER COMPONENT (LIGHT PHASE) IS WELL DISPERSED THROUGH THE NYLON MATRIX

B. PHOTOMICROGRAPH OF POLYESTER MICROFIBERS ISOLATED FROM YARN 702816-1 BEFORE POST-DRAWING (135x ORIGINAL MAGNIFICATION).

C. PHOTOMICROGRAPH OF POLYESTER MICROFIBERS ISOLATED FROM YARN 702816-1 AFTER 2.9x POST-DRAWING (135x ORIGINAL MAGNIFICATION). NOTE THE LENGTH AND FINENESS OF THE MICROFIBERS IN CONTRAST TO FIGURE B.

An experimental program was undertaken aimed at making a yarn with longer microfibers suitable for weaving and knitting. Thirty extrusion experiments were carried out in a systematic investigation of the variables. Trials were attempted at nylon/polyester blend ratios ranging from 80/20 to 50/50 by weight, with extruder temperature settings adjusted as deemed necessary. The degree of mixing of the blended polymer components was varied by using two types of extruders, one equipped with a conventional screw for handling nylon and the other with a screw designed especially for blending. In addition each of these extruders was operated using (a) standard filter packs filled with 40-mesh sand, (b) filter packs containing half the usual amount of sand and (c) with no filter at all.

The experimental results were for the most part disappointing. Nylon/polyester spinning was generally difficult, and in the trials where it was possible to collect fiber samples, the denier uniformity was poor and draw ratio low. We were unsuccessful in obtaining nylon/polyester yarn of adequate quality or in sufficient quantity for weaving (Figure 12).

We believed at first that over-mixing of the polymer blend during extrusion might have been responsible for the poor spinning performance of the nylon/polyester polyblends. However, the observed facts have led to a different hypothesis, namely that the polyester component was probably degraded during extrusion, either by hydrolysis or as a result of chemical reaction with the nylon (ester-amide interchange). Good IS microfiber formation was, in fact, demonstrated with our extrusion equipment when polypropylene was substituted for the polyester component, so mixing conditions in the extruder seem to have been just about right. However, the finished yarns were highly variable in denier and contained many broken filaments, thus making them unsuitable for weaving.

A modified procedure was used for spinning nylon/polypropylene ribbon. A blend of 80% nylon-20% polypropylene was extruded. The microfibers formed are shown in Figure 13. We are currently evaluating the preparation of woven fabrics from this ribbon.

Mixed polymer systems were also used to prepare nonwoven fabrics. A nylon/polyester fabric is shown in Figure 14. Figure 15 shows the same fabric after washing the nylon matrix. Little change in yarn dimensions was noted due to dumping of the filaments during the washing process. The structure, however, is very attractive for cell entrapment.

IN VIVO EVALUATION

We submitted to the program office for evaluation in animals, 216 samples consisting of sheets and tubes. Surfaces prepared included flocks, nonwovens, wovens and textured Silastic. The samples were composed of nylon, Dacron, carbon and Silastic rubber. These are shown in Table 3.

TABLE 3

LIST OF MICROCELLULAR ANCHORING DEVICES SUBMITTED TO NHI

		Mat Height(μ)	Sheets 4" x 4"	Sheets Total	Tubes 3/4" x 3"	Tubes Total
I.	Nonwoven Fabric					
	A. Nylon	15	12		4	
		30	12			
		50	12	36		12
II.	Flock					
	A. Nylon	20	8		4	
		50	12		4	
		100	12		4	12
		400	12	44		
	B. Dacron	20	8		4	
		50	8		4	
		100	8	24	4	12
	C. Carbon	20	8		4	
		50	8		4	
		100	8	24	4	12
III.	Textured Silastic	10	8	8	-	
IV.	Woven Fabric					
	A. Nylon	80	12		4	
		120	12	24	4	8
	TOTAL			160		56

CELL ENTRAPMENT

The objective of the in vitro cell studies is to determine whether the surfaces are capable of fibroblast entrapment and will permit cell growth. We are currently attempting to answer the first question.

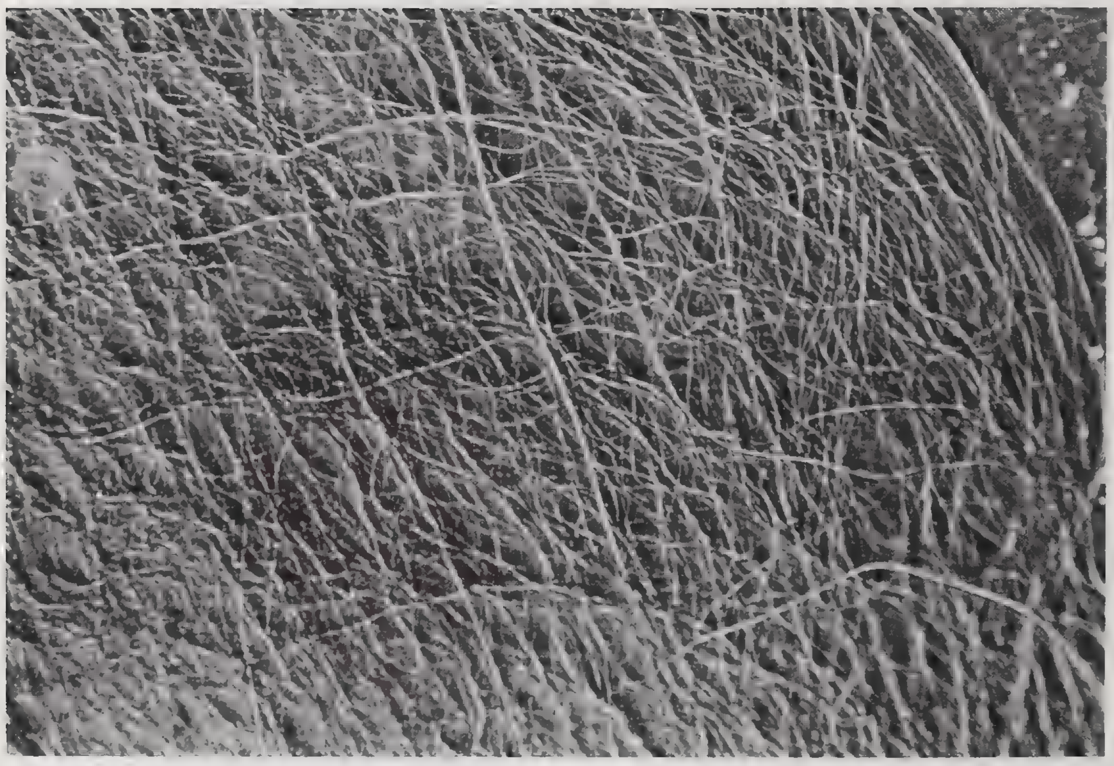

FIGURE 13. PHOTOMICROGRAPH OF POLYPROPYLENE MICROFIBERS ISOLATED FROM RIBBON SAMPLE 702829-1

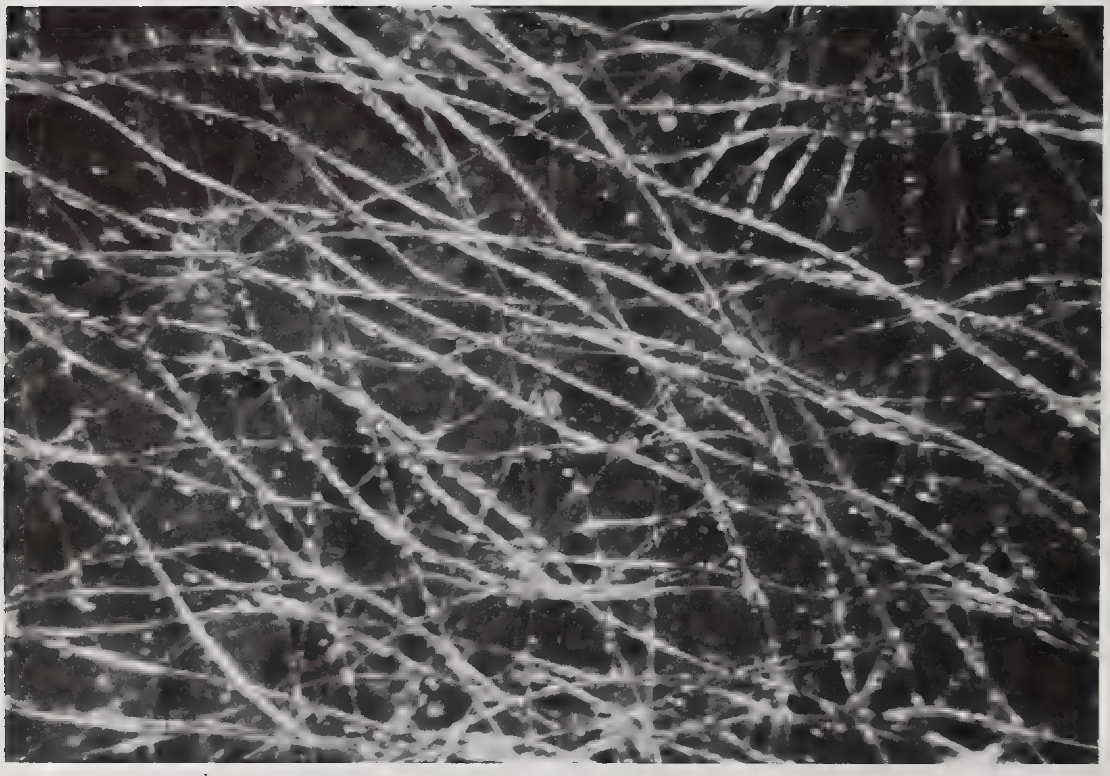

FIGURE 14. NYLON/POLYESTER POLYBLEND NONWOVEN FABRIC (30x ORIGINAL MAGNIFICATION)

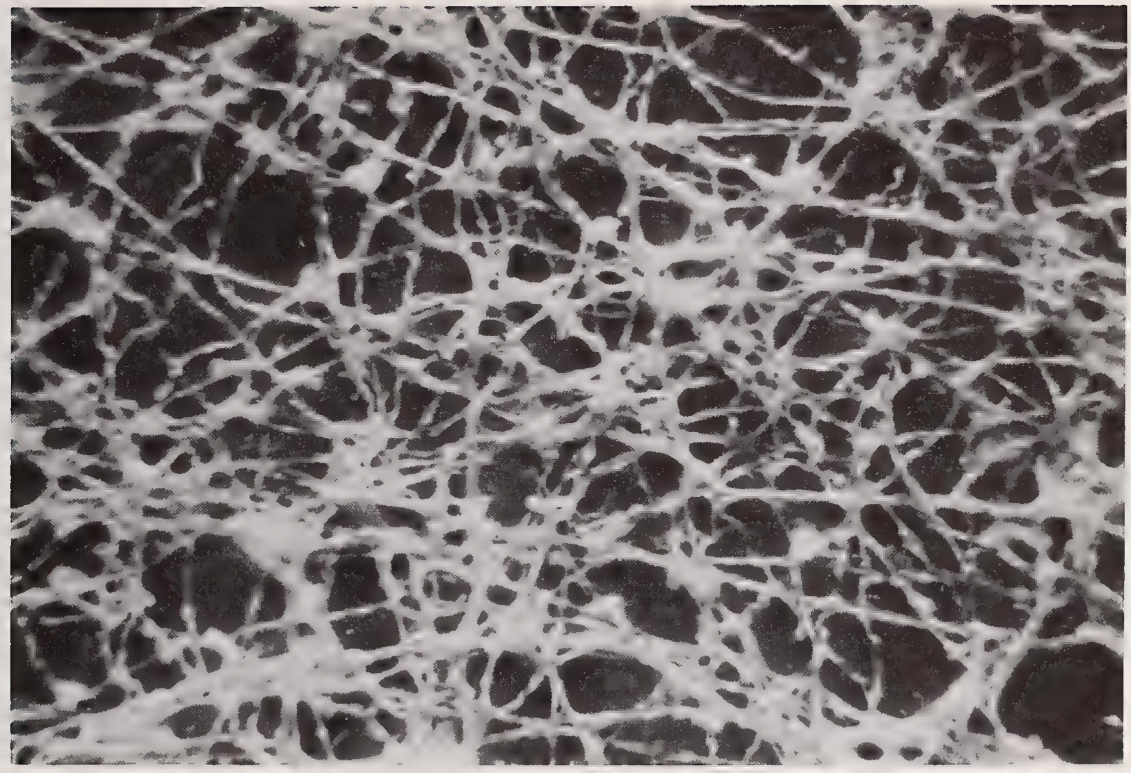

FIGURE 15. NYLON/POLYESTER POLYBLEND NONWOVEN FABRIC AFTER EXTRACTION OF THE NYLON MATRIX WITH FORMIC ACID (30x ORIGINAL MAGNIFICATION)

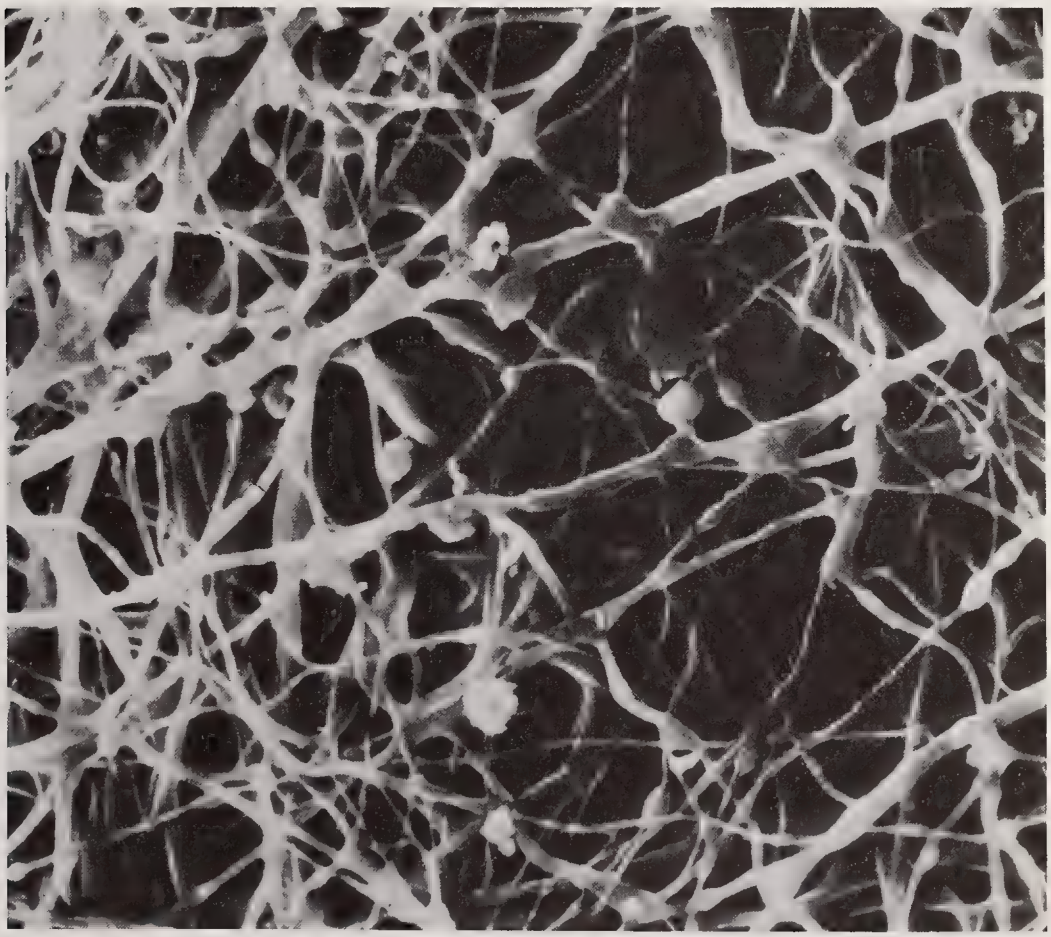

FIGURE 16. CALF FETAL FIBROBLASTS ON NONWOVEN NYLON FABRIC (450x ORIGINAL MAGNIFICATION)

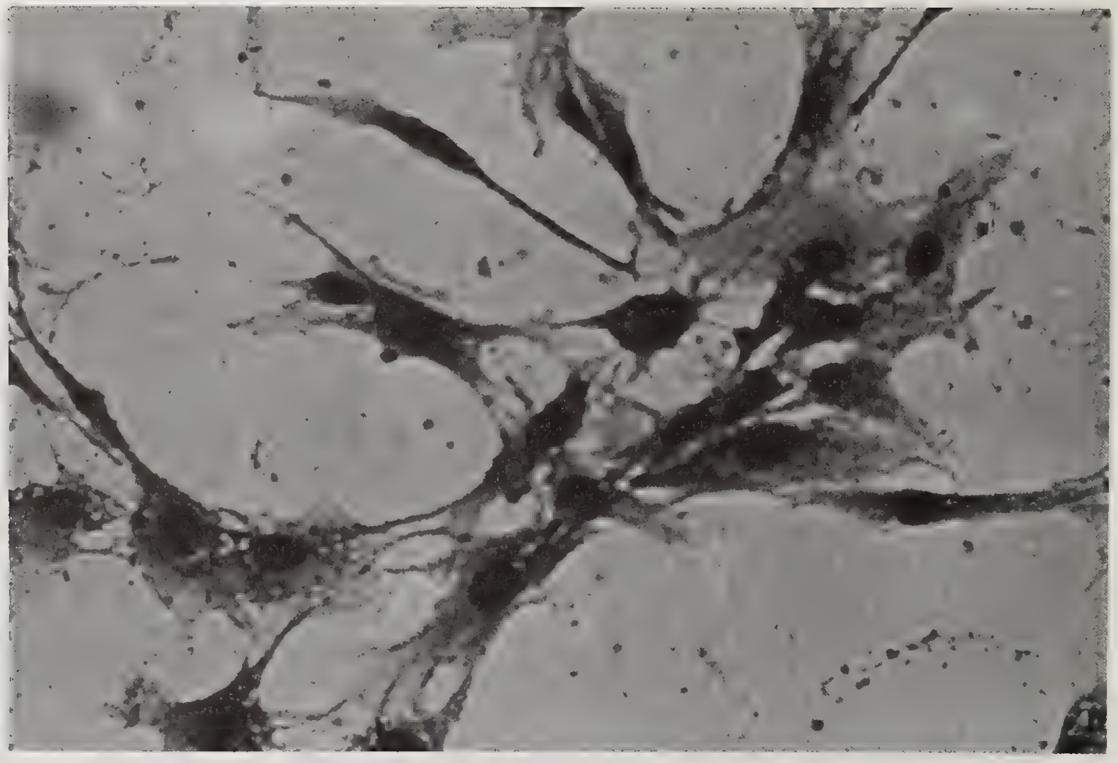

FIGURE 17. CALF FIBROBLAST CELLS ON FALCON DISH - CONTROL CULTURE (200x ORIGINAL MAGNIFICATION)

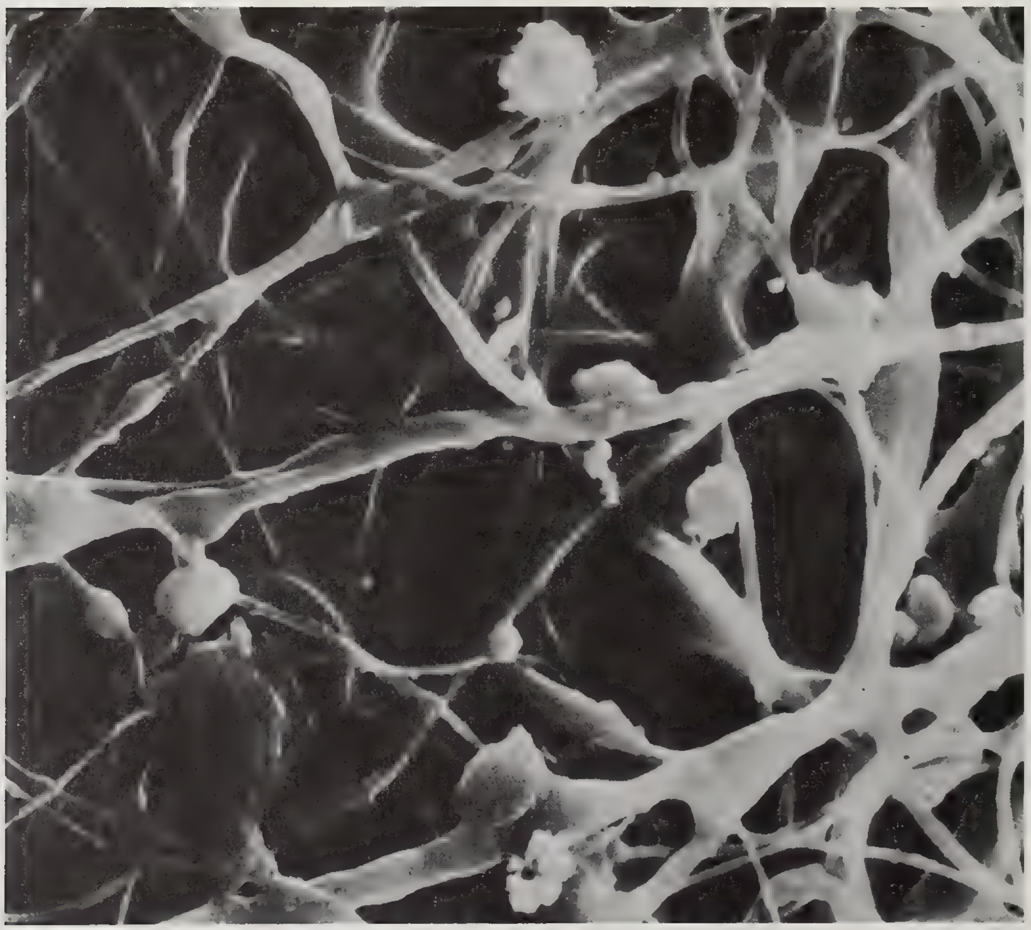

FIGURE 18. CALF FETAL FIBROBLASTS ON NONWOVEN NYLON FABRIC (800x ORIGINAL MAGNIFICATION)

For these studies, cell suspensions of calf fibroblasts (fetal 2-1/2 to 3 months) were obtained from Doctor W. Bernhard at Children's Hospital Medical Center in Boston. When fibroblasts are in suspension, they do not possess the same morphology as when they are attached to a surface. In suspension they are spherical and look like tiny balls (Figure 16). The average diameter of these cells is 10 microns. When cells come in contact with a surface, they attach to the surface with pseudopods and spread out to 20-30 microns in width and 40-60 microns in length (Figure 17).

Initially, attempts were made to develop a method for qualitative determination of cell entrapment on the surface by applying the original definition of cell entrapment as the number of cells present under a fabric loop. However, major problems arose when attempting to qualitate our results, namely:

1. Difficulty in determining whether a cell was located above or below a fabric loop;
2. Difficulty in selecting representative areas from the fabric surface which will yield a meaningful value;
3. Difficulty in counting the cells present on a surface with a complex three dimensional configuration.

This is illustrated in Figure 18. The fact that a cell is present under a loop does not necessarily mean that its location has been permanently fixed by that loop and that it will not wander around to an area where no loops are present. Furthermore, the fact that a cell is located on a filament does not preclude the possibility that it is attached to the filament by wrapping its pseudopods around that filament either mechanically or through a chemical bond.

For this reason we believe that a "dynamic" system in which all "unattached" cells are removed by washing the surface will give, with proper controls, more meaningful values for comparing the cell retaining ability of the various mechanical structures developed. The cells retained are a function of the mechanical as well as the chemical nature of the surface. The chemical composition of the surface is that due to the chemical nature of the base material (in this case Silastic) and the chemical nature of the fabric. Any effect due to the Silastic can be reduced with proper controls (e.g., Silastic base with no fabric).

We therefore propose to explore a method which will differentiate between mechanically and chemically attached cells. In this method, the cells are applied to the surface by a standard technique. They are then thoroughly washed in isotonic saline to remove all loose cells. After this, the surface is treated with a solution of trypsin in order to loosen all chemically attached cells. Trypsin is universally accepted as the enzyme of choice for detachment of fibroblastic cells from the surface. Any cells remaining in the fabric mesh after this treatment are then assumed to be held by mechanical configurations of the surface rather than its chemical structure.

By using proper controls and determining the total number of cells present in the sample at each stage, it should be possible to obtain more meaningful values for cell entrapment.

We are currently evaluating this approach using the measurement of DNA concentration in the sample for determination of the number of cells present on the surface. This is being done using a specially designed cell chamber which can take 4 surfaces at the same time including controls (Figure 19).

REFERENCE

Robertson, A. L., (1965) Clev. Clin. Quart. 32, 99.

DISCUSSION

DR. BYCK: Do you observe any relationship between the adherence of cells to the web and the wettability of the polymer from which the fiber is formed?

DR. NUWAYSER: We have not reached that stage yet.

MR. PURDY: You specifically excluded silica fibers. Was there any reason for that in your examination?

DR. NUWAYSER: We have not at all considered them right from the start. Did I make a statement to the effect that I did not wish to use them?

MR. PURDY: No, I just noticed that you had excluded them from your study, and I wondered why. Silica fibers are obtainable in sizes down to about two microns in diameter.

DR. NUWAYSER: I wasn't aware of this.

DR. BRUCK: I would like to ask you a question about nylons. Nylons generally belong to a class of polyamides, including 6-nylons, 6-6 nylons, and others. I assume that you use 6-6 nylon, is that right? Have you tried other nylons?

DR. NUWAYSER: No, we have not.

DR. BRUCK: For instance, more hydrophobic ones.

DR. NUWAYSER: No, we haven't. We have limited our work to the 6-6 and, as I said in the beginning, we have utilized the nylon as a model material for developing the very fine microfilaments. We are aware of the fact that nylon is not the best material for implantation.

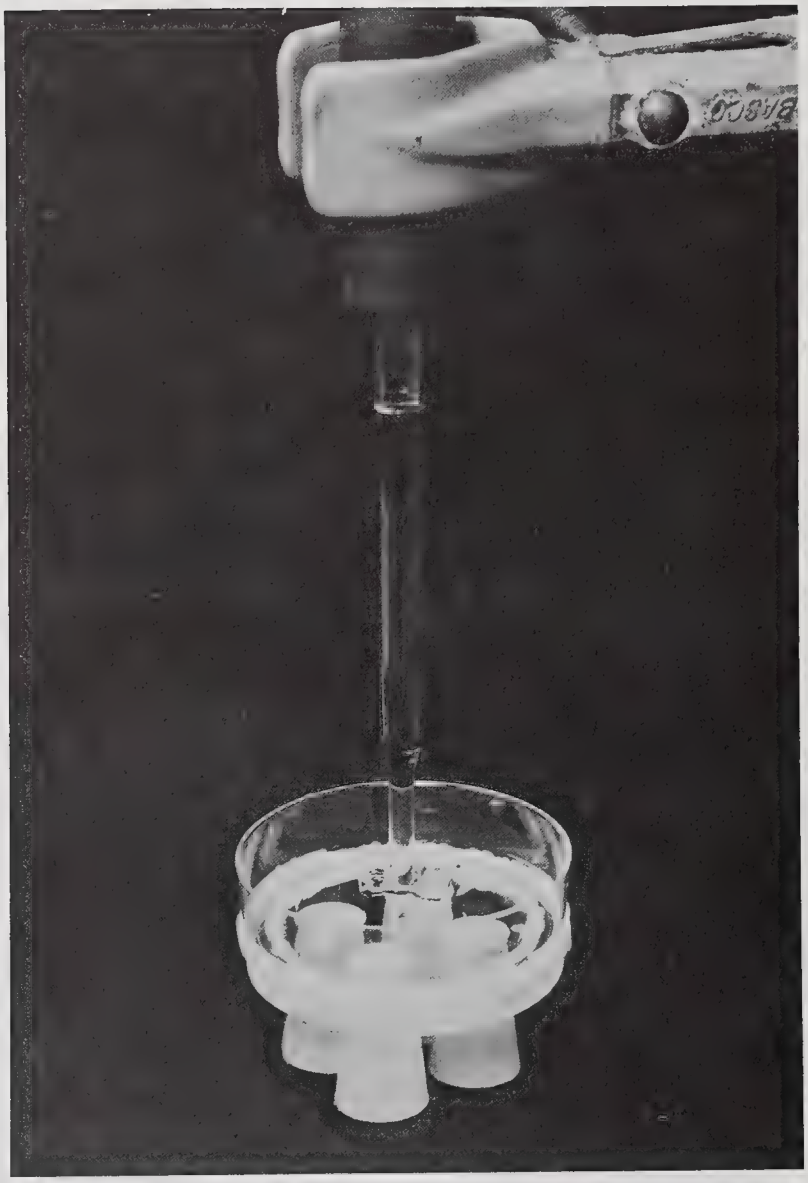

FIGURE 19. CHAMBER FOR CELL ENTRAPMENT STUDIES

CHAPTER 16

RECONSTRUCTION OF DIFFERENTIATED TISSUE LAYERS FROM DISSOCIATED CELLS: USE OF TISSUE CULTURE TECHNIQUES TO DEVELOP NONTHROMBOGENIC AUTOLOGOUS CELL SURFACES FOR USE AS CARDIAC LININGS

L. Schutz, C. Grobstein, R. Grobstein, B. Bull* and N. Braunwald

University of California, San Diego, California

Thrombosis of circulatory assist devices and incorporated prosthetic valves currently constitutes a major problem which has not been solved by the administration of anticoagulants. A useful lead to overcome this problem has been developed; the lining of all the exposed portions with a porous fabric results in the deposition of an autologous tissue lining which appears to be highly resistant to thrombosis. It has previously been demonstrated that encouragement of the development of such autologous tissue layers on fabric linings covering these prosthetic devices is a fruitful approach to the development of surfaces which are resistant to thrombosis when used in the cardiovascular system. However, their development takes over a month to be completed in experimental animals and is certain to take longer in humans. In order for the autologous surfaces to afford maximal protection when used to line the artificial heart and similar prosthetic devices, the development of the tissue must be complete either at the time of implantation in the body or soon after. In the present study methods of preforming or accelerating these linings in the Tissue Culture Laboratory are being explored. In order to achieve this goal fabric lattices are being seeded with cells from autologous endocardium, endothelium, circulating leukocytes, bone marrow, skin, or blood vessel adventitia, and then are grown in tissue culture prior to reimplantation in the body.

INTRODUCTION

Although great strides have been made in the development of an artificial heart, problems resulting from the blood material interface remain formidable. Thrombosis of circulatory assist devices and incorporated prosthetic valves currently constitutes a major problem which has not been solved by the administration of anticoagulants. A useful lead to overcome this problem has been developed; the lining of all the exposed portions with a porous fabric results in the deposition of an autologous tissue lining which appears to be highly resistant to thrombosis. It has previously been demonstrated that encouragement of the development of such autologous tissue layers on fabric linings covering these prosthetic devices is a fruitful approach to the development of surfaces which are resistant to thrombosis when used in the cardiovascular system.[1] However, their development takes over a month to be completed in experimental animals and is certain to take longer in humans. In order for the autologous surfaces to afford maximal protection when used to line the artificial heart and similar prosthetic devices, the development of the tissue must be complete either at the time of implantation in the body or soon after. In addition, it must be more than simple sheets of cells. It must be a completely differentiated tissue capable of long term survival; otherwise, it may be vulnerable to ultimate degenerative changes in the body associated with inadequate nourishment.

The research objective of the present study centers about the development of in vitro methods of performing or accelerating these linings in the Tissue Culture Laboratory. In order to achieve this goal, fabric lattices have been seeded with a variety of cells which are then grown in tissue culture prior to reimplantation in the body.

METHODS

Growth of Embryonic Cells on a Fabric Lattice.

At the beginning of this effort it was apparent that there was a large body of past experience dealing with the growth of embryonic tissues in the Tissue Culture Laboratory. On the other hand, experience with adult mammalian cell lines was rather more limited. Therefore, initial experiments in the Tissue Culture Laboratory were directed towards studying the behavior of primary cultures of embryonic origin with known growth characteristics on porous fabric surfaces in order to see what kind of cell layers would develop under the most advantageous circumstances. It was appreciated that in general embryonic tissues grow much more rapidly than adult tissues.

In the initial set of experiments, 13 day mouse embryonic salivary glands, either whole glands or mesenchyme alone, were utilized as the cell source for seeding the fabrics. The culture medium included: 10% Embryo Juice, 10% Horse Serum, and Eagles' Medium.

The fabrics used in these preliminary experiments were made of 60 denier Dacron or 70 denier polypropylene fibers in a porous construction, materials previously demonstrated to encourage autologous tissue linings with satisfactory histological characteristics in vivo in experimental animals in our laboratory. The embryonic cells were seeded on small pieces of fabric which had been coated with a chicken plasma clot. These cultures were then allowed to grow from one to two weeks in incubators humidified and gassed with 5% CO_2-95% air at 37°C. The medium was changed every other day. When good growth was evident, the cultures were terminated. Histological sections of the specimens were made and indicated that the embryonic salivary gland tissue spread out well over the surface of the fabric during this period of time,completely enclosing the synthetic threads of the fibers (Figure 1). The layers which developed were quite thin, extending only several micra beyond the individual fabric lattice itself. In many areas the cells on the surface had a somewhat flattened appearance. After one to two weeks in culture, the cells tended to completely replace the plasma clot probably due to fibrinolytic activity.

---

*Loma Linda University, Loma Linda, Calif.

Studies were then initiated to determine if adult cells obtained from a canine population could be made to cover the fabrics in a fashion similar to that observed when embryonic cells were used. Initially, endothelium, skin, and bone marrow were selected for testing. Ease of procurement from the donor was a consideration in choosing a cell source. Our initial experience with endothelium suggested that cell proliferation of endothelial cells appeared to be extremely slow. On the other hand, cell growth was somewhat more rapid when skin and bone marrow were used. The following method was employed in the case of bone marrow. Sternal marrow was removed under sterile conditions and chopped with scissors into tiny fragments. The free cells were washed from the osseous material with Puck's Saline G. A small piece of fabric was mounted on a small, plexiglass "O" ring, 75 micra in thickness, having an OD of 0.95 cm. and an ID of 0.65 cm. with MF cement (Millipore Corporation). The fabrics employed at this stage included a smooth, porous Dacron fabric knit; a 70 denier monofilament, porous polypropylene fabric; and a"Flufon" Dacron, a texturized yarn, multi-strand fiber. The medium, which was changed every other day, consisted of Puck's Growth Medium with 15% autologous canine serum obtained from the same dog which supplied the bone marrow cells. On histological examination of the fabrics seeded with bone marrow after one month's growth in tissue culture, the individual fibers of the fabric were covered in some areas by thin layers of tissue which completely encapsulated the fabric (Figure 2). In other areas cellular proliferation was more sparse.

As this phase of the work progressed, it became apparent that it was going to be difficult to get sufficient numbers of the cells to adhere to the fabrics being used to assure adequate seeding initially. Yet in order to get rapid coverage of any fabric with tissue, it is essential to get a high concentration of the cells to adhere to its surface. The higher the concentration of the cells which remain in close proximity to the threads, the more rapidly complete covering of the fabric will be achieved. It was observed during the course of our early experiments that many of the cells slid off the ultra-smooth surfaces of the synthetic polymer threads and fell between the pores of the fabric to the culture dish below. This was somewhat less of a problem if the rougher, multi-strand, texturized Dacron yarn was used than if fabrics made up of smooth yarn were utilized. The rougher the fiber surface, the more likely it was to trap an increased number of cells.

An effort was made to try to improve the adherence of an increased number of cells to the fabric surfaces initially using other techniques. These included the use of natural plasma clot or artificial fibrinogen clots to coat the individual fibers in order to provide surfaces more conducive to cell adherence. Alternately, the cells were dispersed in a plasma clot prior to application to the fabric so that they would be entrapped once the clot solidified. Although both of these approaches did tend to get more cells to remain in the vicinity of the threads until growth was initiated, they also introduced certain disadvantages. It seemed likely that while viable, stable living cell surfaces might be antithrombogenic, any residual plasma or fibrinogen clot left on the surface at the time of introduction into the bloodstream might tend to be thrombogenic. In other words, it would be desirable to have all of the clot replaced by cells prior to implantation.

Tubular Fabrics.

The configurations of artificial heart devices are such that many of their internal surfaces will have tubular or eccentric forms. Therefore, experiments were designed to see if it was possible to develop viable linings in tissue culture on surfaces having irregular shapes. Initially, 60 denier Dacron fabric in tubular form was used as a testing model. The fabric was placed over plastic rods made of polyethylene. These, in turn, were placed in a specially designed plexiglass suspension block which fit within a petri dish (Figure 3). The cells were then applied on the fabric over or within a clot using either a micropipet or a sterile paint brush. Histological examination of the layers which developed indicated that cellular growth on the tubes was roughly comparable to that seen on the flat fabric surfaces at equivalent time intervals.

At this point it seemed desirable to evaluate the behavior *in vivo* of some of the cellular layers which had been developed in the tissue culture laboratory. A simple testing device was employed. This device consisted of a simple fabric covered platinum iridium probe. This, in turn, was seeded with autologous bone marrow cells donated either from the animal in which the probe was subsequently to be implanted or from a non-related donor. The probes were placed initially in the *in vitro* culture environment and implanted in the left atria of the animals after three to four

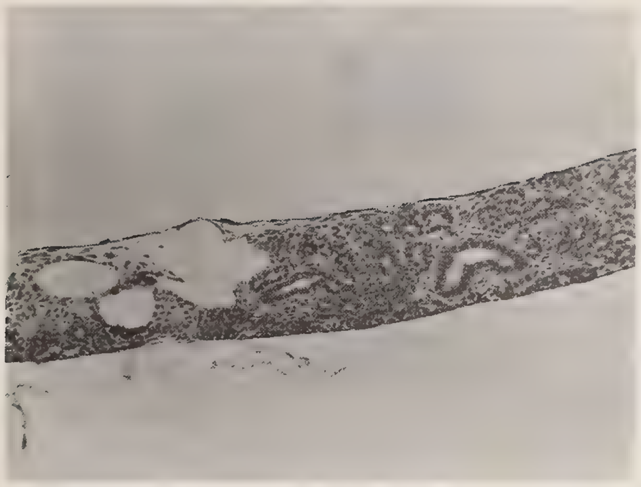

FIGURE 1. HISTOLOGICAL APPEARANCE OF WHOLE SALIVARY GLAND FROM 13 DAY MOUSE EMBRYO WHICH HAS BEEN PLACED ON A PIECE OF DACRON FABRIC AFTER TWO WEEKS GROWTH IN TISSUE CULTURE. THE TRANSPARENT CIRCULAR AREAS REPRESENT THE DACRON FIBERS. THE FABRIC IS WELL INFILTRATED BY THE TISSUE LAYER, AND THE PLASMA CLOT HAS DISAPPEARED. (100x ORIGINAL MAGNIFICATION).

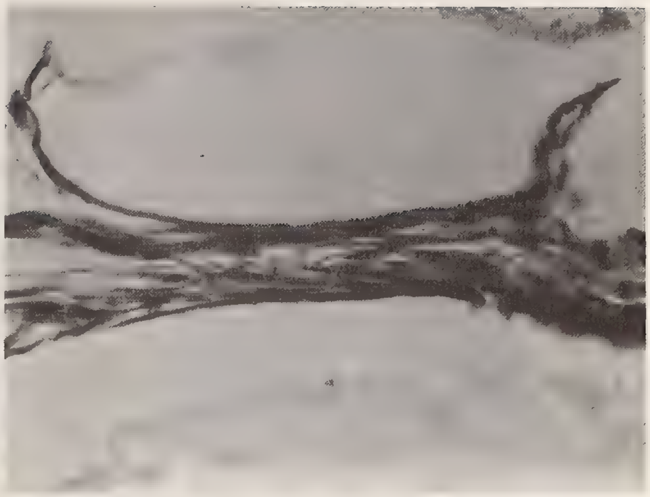

FIGURE 2. HISTOLOGICAL APPEARANCE OF DACRON FABRIC AFTER ONE MONTH OF GROWTH IN TISSUE CULTURE FOLLOWING SEEDING WITH CANINE BONE MARROW CELLS. IN MANY AREAS THE INDIVIDUAL FIBERS OF THE FABRIC (CIRCULAR SPACES) ARE COVERED BY THIN LAYERS OF TISSUE WHICH COMPLETELY ENCAPSULATE THE FABRIC. (400x ORIGINAL MAGIFICATION).

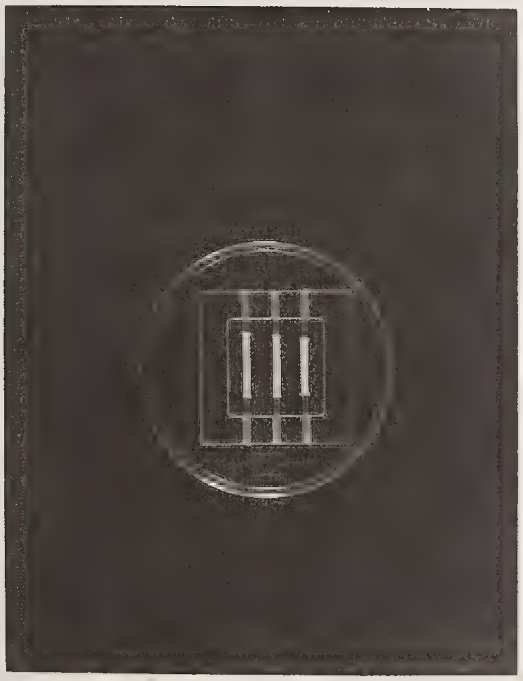

FIGURE 3. TESTING CHAMBER DEVELOPED TO GROW CELLS ON TUBULAR FABRIC CONFIGURATIONS IN TISSUE CULTURE

weeks of growth in tissue culture. A similar unit had previously been tested in the circulatory system of dogs in our laboratories and has been found to be a useful tool for evaluating the antithrombogenic characteristics of autogenous tissue coverings developed in the bloodstream.[3]

Gross examination at the time of sacrifice one week postoperatively revealed that there was a greater amount of thrombotic deposit present on the probes which had been placed in the tissue culture environment than was evident on a control series of bare fabric probes (Figure 4). Histological examination of the fabric on the probes at the end of this time indicated that there was a thin layer of tissue growing on the outer surface of the fabric, 1 to 4 cell layers deep over approximately half of the circumference of the tubular fabric. Apparently, even after several weeks in tissue culture, cell proliferation of adult bone marrow cells was not always prolific enough to ensure complete encapsulation of all of the fabric threads. Analysis of the data suggested that some of the constituents of the tissue culture media might be thrombogenic in themselves, since in some areas where proliferating cells did not surround the threads, increased thrombotic deposits were seen. Therefore, studies aimed at determining the thrombogenic characteristics of some of the constituents of the tissue culture media used to promote cell growth as well as the canine plasma clot used as an adhesive to hold the canine cells to the fabric were initiated. The data suggested that the plasma clot made from canine plasma, as well as certain components of the tissue culture media itself, often provided surfaces which tended to encourage increased thrombotic deposit in vivo in the absence of living cells.

A review of the data from many of our past experiments suggested that, in general, the rate of proliferation of adult canine cells was far too slow to be ideal for the development of cardiac linings. This was especially the case if large surface areas were involved. It was often observed that even after several weeks growth in vitro, areas of the fabric were not infiltrated by cells using techniques presently available to us. Therefore, it was decided to carry out a series of experiments using fetal canine tissue obtained by caesarean section from pregnant dogs for seeding the fabric lattices instead of autologous adult canine cells. Fetal tissue classically grows much more rapidly in tissue culture. It was hoped that it would be possible to more completely encapsulate all of the fabric lattice with a richer layer of cells in a much shorter time if fetal cells were used rather than to rely on the antithrombogenic protective effect of the very thin coat of cells which only partially covered the probes even after a month's growth in tissue culture when cells derived from adult mammalian donors were used to coat the fabrics.

When fetal cells were substituted for adult ones, it was consistently observed that the rate of cell proliferation was much more rapid. Under conditions virtually identical to those used when employing canine adult bone marrow cells to cover a fabric surface, the coverings could be developed in less than half the time. Therefore, use of the fetal cells achieved much more complete covering of a given fabric surface in a given period of time.

Once again the cell layers were tested for their antithrombogenic potential in vivo. After 7 to 9 days growth in tissue culture, the probes covered with the developing embryonic canine tissue layer were placed in the left atria of dogs for one week. Gross pathological examination once again indicated that the probes were fairly consistently covered with a thrombotic deposit which was greater than that seen in controls. On histologic examination the embryonic tissue culture layers developed in the in vitro environment were extremely thick.

Improved Fabric Lattices.

Analysis of the studies performed in the tissue culture laboratory suggested that the commercially manufactured materials which are currently available for developing the tissue layers were far from ideal. Often the fabrics were too thick, and the threads tended to be too smooth. As a result, the cells adhered poorly or not at all to the individual fibers at the time of initial seeding. When some of the newer materials developed to serve as heart linings under separate NIH contracts were made available to us for testing, a program was initiated in our laboratory in an effort to try to characterize the nature of some of these newer synthetic fabrics and to study their behavior in the presence of proliferating cells.

The scanning electron microscope permits examination of a material at extremely high magnification, and this instrument was utilized to examine the topography of these new materials in some detail (Figure 5). The fabrics examined included flock dacron, nylon and carbon, texturized Silastic, non-woven nylons, and woven nylon fabrics with mat heights in the range of 15 to 400 micra. All fibers were attached to a solid Silastic backing.

In order to study the interaction of living cells to these fabrics, tissue culture techniques were used. It was appreciated as a result of work carried out in our laboratory earlier in the year that the rate of growth of cells obtained from adult donors was extremely slow in tissue culture. Therefore, fetal cells were preferentially selected for testing in the initial sets of experiments. Cells derived from both fetal avian (chick) donors as well as fetal mammalian (canine) donors were used in order to study the relationship between cellular ingrowth and the fabric lattice. Embryos were finely macerated and trypsinized for ten minutes at 37°C. At the end of 24 hours in the case of chick cells, and one week when canine cells were used, the cells were subcultured onto various fabrics.

The fabrics were cut into disc shapes (approximately 2 cm. in diameter) with a punch, and placed, rubberized side down, into the petri dishes. An 0.5cc. aliquot of resuspended cells was placed on each fabric disc, and the cells were allowed to settle for 30 minutes before an additional 5.0cc. of Eagle's or Puck's medium was added. The dishes were incubated for three days to six days at 37°C. in an atmosphere containing five parts per hundred of carbon dioxide. At the end of this

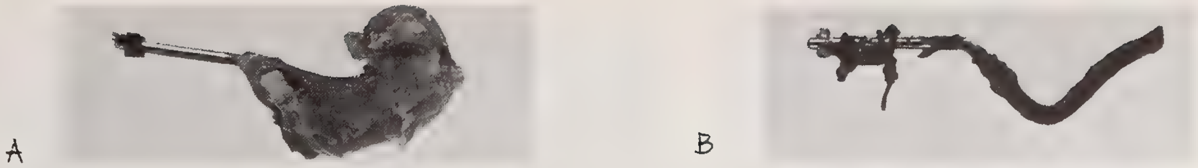

FIGURE 4. A. GROSS APPEARANCE OF FABRIC COVERED PROBE FROM AN ANIMAL ONE WEEK AFTER IMPLANTATION IN THE LEFT ATRIUM. THE PROBE HAD PREVIOUSLY BEEN SEEDED WITH ADULT CANINE BONE MARROW CELLS AND PLACED IN TISSUE CULTURE FOR 24 DAYS PRIOR TO INSERTION IN THE HEART

B. APPEARANCE OF BARE FABRIC COVERED PROBE IN A CONTROL ANIMAL WHICH HAD BEEN IMPLANTED IN THE LEFT ATRIUM FOR ONE WEEK.

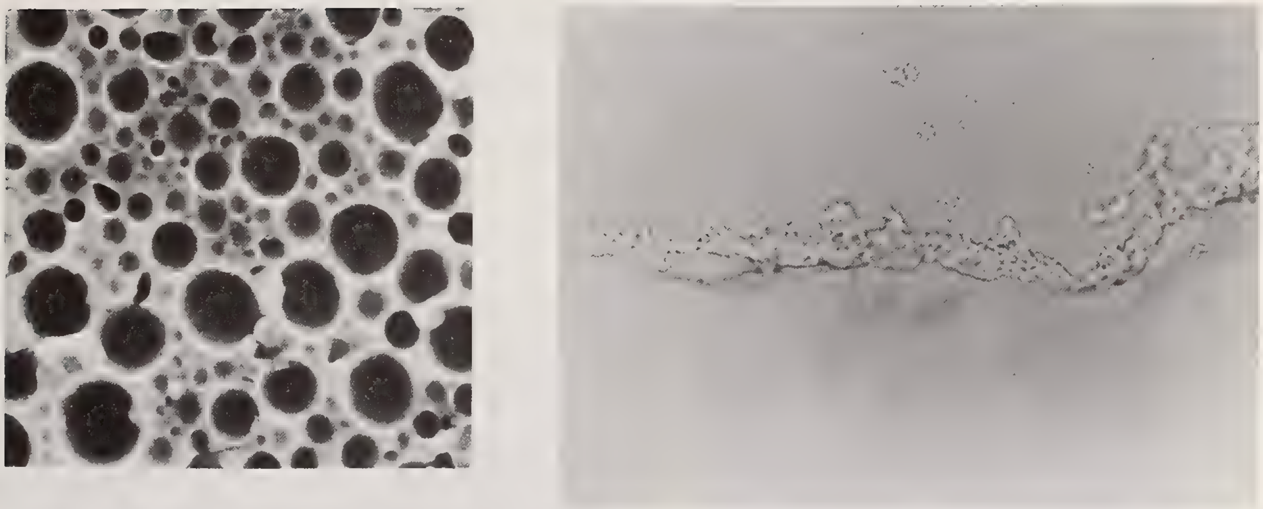

FIGURE 5. A. APPEARANCE OF TEXTURIZED SILASTIC MATERIAL 15±5µ UNDER THE SCANNING ELECTRON MICROSCOPE (7000x ORIGINAL MAGNIFICATION)

B. HISTOLOGICAL APPEARANCE OF TEXTURIZED SILASTIC MATERIAL 15±5µ UNDER THE SCANNING ELECTRON MICROSCOPE (7000x ORIGINAL MAGNIFICATION)

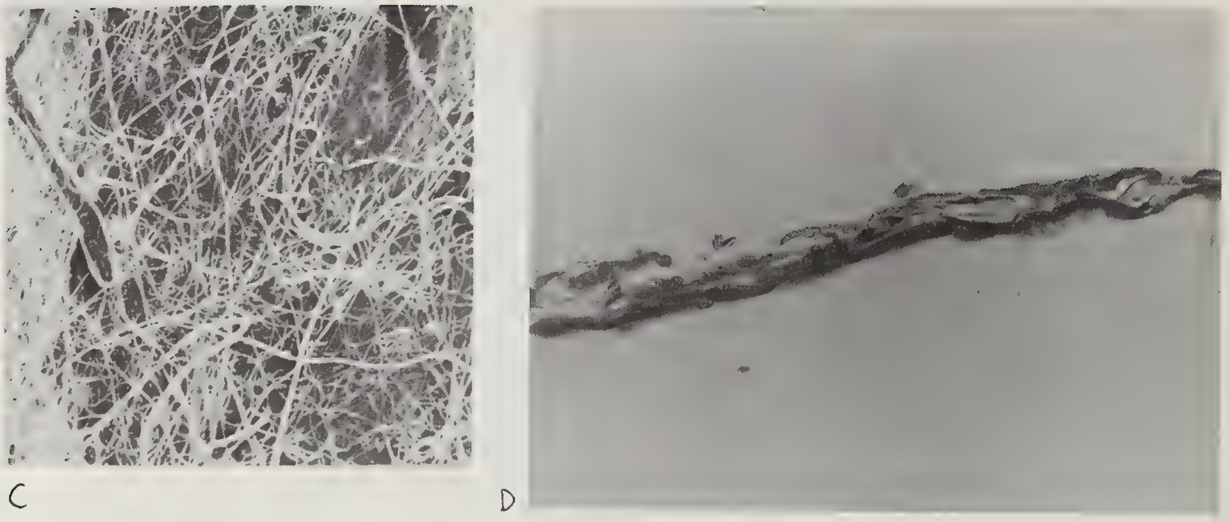

FIGURE 5. C. APPEARANCE OF NON-WOVEN NYLON 50±15μ UNDER THE SCANNING ELECTRON MICROSCOPE (1200x ORIGINAL MAGNIFICATION)

D. HISTOLOGICAL APPEARANCE OF NON-WOVEN NYLON MATERIAL 50±15μ SEEDED WITH FETAL AVIAN CELLS. CELLULAR INFILTRATION AROUND INDIVIDUAL FIBERS IS EVIDENT (425x ORIGINAL MAGNIFICATION)

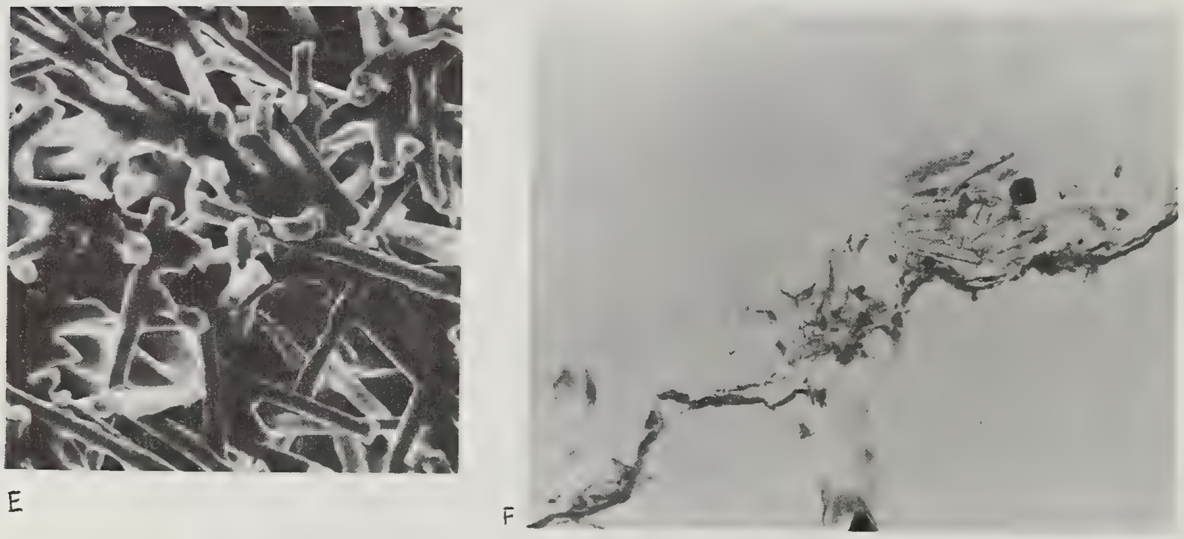

FIGURE 5. E. APPEARANCE OF FLOCK DACRON MATERIAL 100±20μ UNDER THE SCANNING ELECTRON MICROSCOPE (1200x ORIGINAL MAGNIFICATION)

F. HISTOLOGICAL SECTION OF FLOCK DACRON MATERIAL 100±20μ SEEDED WITH FETAL AVIAN CELLS (200x ORIGINAL MAGNIFICATION). CELLULAR COVERING ON SURFACE IS EVIDENT period the fabrics were removed, placed in small vials, fixed with Bouin's solution, and prepared for histological examination.

Histological examination of the specimens was complicated by the fact that it was very difficult to section the Silastic backings. However, on a comparative basis, some conclusions could be drawn. The nylon flock Silastic materials showed very poor union of the tissue to the underlying prosthetic material. Similar findings were noted on the textured Silastic surface, but it must be admitted that the trauma of tissue preparation may have separated the cell layer from the surface of both of these types of materials. Intermediate results were obtained using the various nylon and dacron flock materials. The size of the flocked particles was very large in relationship to the cells growing around them, and the quality of the support offered by the flocked surface would appear to be very focal in nature. Still, the flocked surfaces were able to maintain intact or relatively intact, cell layers throughout the trauma of processing; and judging from the surface as seen in the scanning electron microscope, the chances of a viable tissue layer adhering to this type of surface should be fairly good. Even better in terms of ability to hold and support a thin and delicate layer of tissue culture grown cells were the nylon velours of varying mat heights and the woven nylon fabric. Of the two, the woven nylon fabric appeared histologically to be guilty of over-support in that there were large masses of nylon fibers which could conceivably pinch off supporting blood vessels. The thicker nylon velours, i.e., the non-woven nylons, however, appeared to be the most ideal of all the materials studied in this group. They were able to provide fairly uniform support for a very delicate monolayer of cells as evidenced by the preservation of such cell layers through the trauma of tissue processing. The roughened backing of the Silastic might offer some added advantage if nutrient blood vessels could be encouraged to infiltrate beneath the outer cell layer and fill the crevices.

DISCUSSION

Analysis of the data accrued thus far indicates that it is possible to use tissue culture techniques to develop cell linings on fabric lattices using adult mammalian cells. While these tissue layers resemble those grown in vivo qualitatively, quantitatively they tend to be quite scanty when compared to similar layers developed naturally inside the body at equivalent periods of time and which have been shown to be nonthrombogenic.[1,3] When fetal cells are substituted for adult cells in vitro, the rate of growth is much more rapid. Yet, thus far in our experience, neither the use of adult autologous cells nor the use of the more prolific fetal cells has insured that the artifically produced surfaces are sufficiently nonthrombogenic when returned to the bloodstream. It is possible that the limitations thus far are those imposed by the state of refinement of the techniques which we are using. The cell layers developed when adult cells are used often have areas of exposed plasma clot. The cell layers developed when embryonic cells are used are quite thick, and perhaps all of the cells on the surfaces are not adequately nourished upon transplantation to the host. The death of even a few cells would release thromboplastin, and thus, in turn, would certainly lead to increased platelet fibrin deposit. Perhaps if any practical benefit is to be derived from the overall approach, it will be necessary to combine the use of pharmacological agents with the use of the cellular linings in the early postoperative period to allow the transplanted cells and host to come into nutritional equilibrium.

SUMMARY

Employing modifications of standard tissue culture techniques, it is possible to grow adult and fetal mammalian cells successfully on fabric lattices in tissue culture. Thus far, bone marrow appears to be one favorable source of cells for routinely achieving reliable cell growth. Other cells, such as blood vessel and skin fibroblasts obtained from the dog, can also be made to grow using similar techniques. However, preliminary results indicate that the rate of multiplication with any adult cells is relatively slow in the first several weeks, and that using methods presently available it may take up to a month or more to achieve complete encapsulation of many of the fabrics. It would be preferable to find a cell source for seeding which would achieve more rapid covering of the fabrics. Fetal cells are one such source, but if they are used, it is impossible to develop autologous linings; and one would have to face the risk ultimately of incurring the rejection phenomena.

If these tissue culture techniques are to become practical, it will be necessary to find better ways to encourage cellular adherence to fabric surfaces. The modification of the physical surface characteristics of the individual synthetic fibers, as well as their construction into fabric supports which tend to increase their overall roughness so as to trap more cells at the time of initial seeding, might help to achieve this goal. Some of the new fabrics being developed under the Artificial Heart Program show promise of providing such improved lattice surfaces for the development of proliferating cell layers.

REFERENCES

1. Braunwald, N. S. and Bonchek, L. I.: Prevention of thrombus formation on rigid prosthetic heart valves by ingrowth of autogenous tissue. J. Thorac. Cardiovasc. Surg. 54:630, 1967

2. Bull, B., Fuchs, J. C. A., and Braunwald, N. S.: Mechanism of formation of tissue layers on the fabric lattice covering intravascular prosthetic devices. Surgery 65:640, 1969.
3. Bonchek, L. I., Fuchs, J. C. A., and Braunwald, N. S.: A simplified method for the study of thrombus formation on intravascular prostheses. J. Surg. Res. 9:229, 1969.
4. Ghidoni, J. J., Liotta, D., Hall, C. W., O'Neal, R. M., and DeBakey, M. E.: Production of cellular linings in impermeable velour-lined cardiovascular prosthesis: Growth from implanted tissue fragments. Surgery 65:70, 1969.

DISCUSSION

DR. BRAUNWALD: Are there any questions?

DR. WAKABAYASHI: I have some fear about your technique. Once we culture normal cells in tissue culture media they often show atypical mitoses and we cannot differentiate these cells from malignant cells. I am worrying about the potential carcinogenicity of cells grown on artificial material surfaces.

DR. BRAUNWALD: Naturally, whenever one tackles any problem, one worries about cancer, but we decided to use a more positive approach. We decided to first see if we could develop linings which were nonthrombogenic, and worry about carcinogenesis at a later date, once we achieved our primary goal. I think that it remains a theoretical possibility, on the other hand it may never materialize.

DR. BYCK: I would like to pose essentially the same question that I asked of Dr. Nuwayser. The fiber systems with which he is working and those which we described earlier today generally involve reasonably hydrophobic fiber systems. We have recently observed, however, that Parylene coated fibers can be rendered considerably more hydrophilic. Whereas these fibers originally have contact angles on the order of 120°, these can be reduced to below 60° by various radiation treatments. I was wondering whether this sort of change might not be as important to initial cell adhesion as roughening of fibers which are already quite fine relative to the dimensions of the cells.

DR. BRAUNWALD: I think that now we have a model which can help us to answer some of these questions. I think we are now ready to obtain some of these newer materials and begin to examine them. I think that in time we may be able to get some of these answers.

DR. KOLFF: I thought this was a highly original presentation, and it is always a delight to hear Nina Braunwald and from that point of view we should perhaps have more women in the program. The use of heparin-coated fibers might perhaps be considered. In the old book by E. Jospes in Sweden entitled "Heparin", he shows some pictures where there is strong indication that heparin is present in wound healing and activates the growth of fibroblasts. Therefore, heparin might serve a dual purpose if you incorporated it here or grafted it to your fibers. It would prevent clotting and might accelerate cellular growth. Also, I would like to ask you, have you ever considered the return to foam which you used many years ago?

DR. BRAUNWALD: To return to foam?

DR. KOLFF: Yes, foam.

DR. BRAUNWALD: Yes. Dr. Kolff is referring to the fact that we started out ten years or more ago with polyurethane foams to get open cell surfaces, and I suppose that in a sense this texturized silastic is a kind of foam. The cell entrapment that we observed with this silastic which had a foam-like configuration was not particularly good, but this may have been due to the fact that it was silastic. We certainly would be interested in exploring the possibility that a heparin coating would improve cell adhesion. We would like to find any tool that would make the cells stick better.

MR. HARTH: I was interested in your platinum iridium probe. Did you notice any cellular reactions to the material in this probe?

DR. BRAUNWALD: If we used a bare probe without any fabric which was our original control for the fabric covering experiments, then we got increased platelet fibrin deposition on the uncovered plain probe.

MR. HARTH: Do you know the composition of the probe?

DR. BRAUNWALD: Beyond platinum iridium? No.

DR. KUSSEROW: If one reviews the current literature in this area, one is struck by the fact that it is becoming quite fashionable to seed various substrate materials with fetal cells. This is done despite the well known, historically established fact that the fetal cell represents an allograft, tissue which the host in its normal state will recognize as non-self. Dr. Braunwald has alluded to this fact. My question is, have you in any of the in vivo experiments noted any evidence of fetal cell rejection, such as necrosis or possibly the appearance of serum antibodies?

DR. BRAUNWALD: We have not noticed this in the in vitro work, but it is becoming somewhat evident to us that in the in vivo work there is a much higher degree of acute inflammatory cell infiltration on those probes in which fetal cells rather than adult cells were used.

DR. KUSSEROW: As a further question, I would be interested in some sort of a statement from one of the investigators in the field, perhaps yourself, with regard to the rationale for using fetal cells at all, if we know from past experience that they will ultimately succumb to immune rejection. It is realized that they do proliferate more quickly.

DR. BRAUNWALD: Well, I think that first of all I might say we have battled the problem of the slow growth of adult cells over most of the past year because we would prefer to develop autologous cell linings. We only considered fetal cells to try to help us in answering a particular question a little more quickly. We would anticipate that within the first week the rejection problem should not be overly severe and we wanted to see if we could use the fetal cell preparations to answer a specific question for us, i.e., if we could once get a really luxurious cell covering on these probes, would they be less thrombogenic. If we could accomplish this then it would be worthwhile to go back to the adult cells and try to improve our tissue culture environment in order to achieve more prolific growth of adult cells. It was for that reason that we looked at this fetal cell model.

DR. HALBERT: It is well known, of course, that the interior of blood vessels is composed of a specialized type of cell, the endothelial cell, and I wonder if it might not be worthwhile, even though it would take a longer period of time, to try to get endothelial cells to grow on these implants?

DR. BRAUNWALD: We would think so. Time did not permit us to present all of our data. However, being very familiar with the work of Abel Lazareni Robinson, who did so much work with endothelial cells in tissue culture, we spent several of the early weeks and months of this year trying to get endothelial cells to grow in vitro. We used cross sectional pieces of blood vessels in order to try to encourage the intimal cells to proliferate. We were able to confirm data which seem to indicate that if for some reason adult cells are slow to grow in tissue culture, one of the slowest of adult cells is the endothelial cell. We have not given up, but this is an extremely slow growing cell in vitro.

DR. SPAET: Presumably the cell that you are growing in vitro is a fibroblast. Is that right?

DR. BRAUNWALD: Probably. We have the feeling that all tissue explants cultured in vitro end up as fibroblast cultures. But this is difficult to confirm.

DR. SPAET: Yes. Now when the fibroblast performs its function, it makes collagen, and collagen is perhaps the most thrombogenic material that I am aware of.

DR. BRAUNWALD: Well, this takes us back to the findings in our past in vivo work using colonies of both dogs and calves. Some of these animals have been surviving up to three years now. These in vivo developed tissue linings have had collagen demonstrated in them under the electron microscope, yet they remain non-thrombogenic up to three years. Perhaps collagen within a viable tissue layer is not thrombogenic. Histologically, the cells seen on the outer layers of the tissues which develop in the blood stream look flattened. They resemble endothelial cells, but they may in fact be only flattened fibroblasts. The collagen is buried within the layer.

DR. RODMAN: Dr. Braunwald, knowing that the collagenous covering that you have on your materials is very thrombogenic, it occurred to me as this last interchange was going on, that it might be possible to treat this material with collagenase. Thereby, the surface might be changed just enough that it might not be thrombogenic. This is turn might avoid the deposition of thrombi for a time period long enough for the endothelial cells to proliferate on the material surface in the in vivo experiments?

DR. BRAUNWALD: Well, I think that we have to understand what leads to the development of these layers in vivo. This was something we did not appreciate early in our work but only more recently as we looked at the developing layers under the electron microscope. If one presents to the blood stream a surface which is completely nonthrombogenic, whether it be a solid or a fabric lattice, then these cell layers will probably never develop in vivo. These layers are able to develop in the body using controlled thrombosis, if you will. For some reason, the lattice fabric configuration allows the deposition of just a little bit of platelet fibrin material. The organization of this very thin layer of platelet fibrin material in the body leads to the development of a tissue lining. If it never deposited at all it could never organize. You would be no better off than with the bare metal.

DR. RODMAN: Then, what do you think if you get a thin layer? What is it that inhibits it from becoming a thicker layer?

DR. BRAUNWALD: I don't know. We have thought about this mystery for a long time and we cannot come up with an answer. It seems as if the platelet fibrin deposit sends out some message, perhaps chemical, which limits the extent of the deposit. It may relate in part to the velocity of the blood flow past the surface. The more turbulence, the less the velocity of flow, the thicker will be the platelet fibrin layer that will deposit on any given fabric. In the case of well designed heart valves at least the velocity seems to be adequate so that the deposit accumulates to about a micron or so beyond the outer fabric thread.

DR. HALPERN: One of the means of obtaining a more textured surface to provide lodgement sites for your growing cells might be to include a submicron particulate material in your fibers which can be then swollen and subsequently leached. This has been done with polyethylene into which starch has been milled. The starch is swollen in boiling water, and then removed by acid hydrolysis or treatment with amylase.

DR. BRAUNWALD: What we hope, in fact, is that other contractors will come forward with the perfect fabric.

DR. RUTSTEIN: Have you tried using any spun glass fabric? It is well known that multiple layers of cells, including human ones, can be grown very easily on glass.

DR. BRAUNWALD: No, we have not tried that.

SECTION II

ANALYSIS OF THE EFFECTS OF MATERIALS ON BLOOD

Chairmen: Anthony M. Bruno, M.D.
Lowell T. Harmison, Ph.D.

INTRODUCTION

The materials testing activities of the Artificial Heart Program are designed to permit timely evaluation of materials in order that they are not prematurely used or inadvertently rejected because of the lack of knowledge concerning their *in vitro* or *in vivo* performance. The long life and high reliability requirements of the final intra-thoracic prosthesis require extensive physical, mechanical, and biological evaluations to eliminate harmful iatrogenic effects on blood and tissues. During the past year, seven contractors have directed their efforts toward biological evaluations of the output of the various materials and device developers, while two contractors have been primarily concerned with studies of the physical and mechanical properties of materials and finished devices.

CHAPTER 17

THE IN VIVO SCREENING OF POTENTIAL THROMBORESISTANT MATERIALS

V.L. Gott, M.D. Ramos, F.B. Najjar, J.L. Allen and K.E. Becker

Johns Hopkins University School of Medicine
Baltimore, Maryland

The primary purpose of this study has been to screen potentially thromboresistant materials which have been developed by research groups supported by the Artificial Heart Program. In our laboratory there has been continued evaluation of different types of in vivo screening techniques and after considerable experience with "flags", "swords" and vena cava rings, it appears that the latter test device still provides the most consistent information with regard to material thromboresistance. Materials have been evaluated from twelve different materials contractors. Extremely encouraging results have been obtained. In order to provide a more severe screening test, the authors have been studying caval implant rings with various internal channel configurations to provide a controlled degree of turbulence. The altered configuration has been mainly in the form of a very low circumferential curbstone in the middle of the ring. Even with heparinized surfaces, this type of turbulence has provided highly enhanced thrombogenesis. The studies leading to the development of the turbulent ring appear to have considerable application in the design of all types of intravascular prosthetic devices. In an attempt to better understand the thromboresistant mechanism of the heparinized surface, studies have been carried out in our laboratory on the binding of heparin to serum proteins using starch block and acrylamide gel electrophoresis. As of this time, it appears that the heparin is binding primarily with a single protein in the alpha-2 region.

INTRODUCTION

It is generally agreed that the most significant problem to be solved in the development of an artificial heart is that of providing biomaterials that are completely compatible with blood. The Artificial Heart Program*, therefore, is supporting a number of research groups in the search for suitable materials for the various cardiac assist and replacement devices currently under development. With the great number of new materials and surfaces being developed by these research groups, it is imperative to provide various screening techniques in order to select those materials that appear most promising. It had been hoped that some of the simple in vitro clotting tests could serve this purpose, however, for the most part, these procedures have not been reliable in predicting how the material or surface will perform when actually placed in the blood stream.

In this report, the authors will present their current thoughts on the various types of in vivo test devices for the screening of biomaterials. Also, a brief summary will be presented of in vivo test results of materials received from several research groups supported by the Artificial Heart Program. Since over 500 separate in vivo implant studies were performed during the past twelve months in the evaluation of materials from ten different research groups, specific results for each material cannot be provided in this short report. These in vivo test results, however, will be included in the reports from each of the biomaterials contractors at this Symposium and also in the principal investigator's six month technical reports prepared for the Artificial Heart Program.

It would appear that materials which have been evaluated in our laboratory from the ten research groups fall primarily into three categories and we will summarize some of the favorable and unfavorable characteristics of the materials in each of these categories.

In our attempt to develop a more satisfactory in vivo test prosthesis for the screening of new biomaterials, we have been investigating the role of turbulence in thrombus formation. As might be expected, a minimal amount of turbulence can greatly enhance the process of thrombosis. Our attempt to develop an intravascular test prosthesis that would provide a small amount of controlled turbulence, not only will provide a more severe test-bed for the better biomaterials that are currently being developed, but also possibly have application in the design of prosthetic devices for cardiac assist or cardiac replacement.

Finally, in an attempt to better understand the thromboresistant mechanism of heparinized surfaces, studies have been carried out in our laboratory during the past contract year on the binding of heparin to serum proteins using starch block and acrylamide gel electrophoresis. The preliminary results of these studies will be presented.

IN VIVO TEST DEVICES FOR THE SCREENING OF BIOMATERIALS

Many types of prosthetic devices have been devised and used in the past by a number of investigators in order to screen different biomaterials. These test devices can be placed either in the

---

From the Departments of Surgery and Medicine, The Johns Hopkins University School of Medicine, Baltimore, Maryland, 21205. Supported by Contract PH 43-68-84 from the Artificial Heart Program of the National Heart Institute.

arterial circuit or in the veno-arterial system. The latter test-bed has ordinarily been selected because it provides a much more severe test of thromboresistance than the arterial circuit with its high streaming velocity. We have had experience with a number of in vivo test devices over the past nine years and find there are advantages and disadvantages to each of these test units. Our laboratory, along with a number of other research groups, has tested atrial "flags" and rigid atrial probes or "swords".[1,2] The placement of flags of flexible materials and swords in the right atrium is a relatively simple surgical procedure; however, the results have not been found to be consistent enough from preparation to preparation to be of significant value. The inconsistency of the results arises mainly from the unpredictable fibrinolytic activity in the experimental animal. It is possible to have a significant thrombus on a right atrial prosthesis at four hours and yet at 24 hours this thrombus can be completely lysed[3]. This same criticism of the right atrial flag and right atrial sword would apply to the right atrial "button" device that has been used extensively by other investigators. After nine years of laboratory experience with various in vivo test devices, we feel that the inferior vena cava prosthetic ring provides the most consistently reliable results in the evaluation of new biomaterials. This is a very severe test, for ordinarily all plain, unaltered polymers and unaltered metals will be the site of severe thrombus after a two-hour vena cava ring implant study[4]. Materials that remain free of thrombus after a two-hour implantation in the vena cava appear to have significant thromboresistance and in our standard test, those materials that pass the two-hour evaluation, then are implanted as test rings for two weeks. It appears that fibrinolysis is not such a critical factor in the ring test particularly after the prosthetic ring is completely occluded with thrombus.

The standard vena cava ring which we would prefer to use and which has been utilized in most of the screening studies discussed later in this report is 9 mm. long, has an OD of 8 mm. and an ID of 7 mm. This wall thickness of 1/2 mm. is suitable for a rigid material, however, for some of the flexible elastomers, it is necessary to increase the wall thickness very slightly. It is imperative that the leading and trailing edges of the ring be properly streamlined, for as will be apparent in a later section of this report, even minimal turbulence can significantly alter the thromboresistant properties of a test device.

MATERIALS UNDERGOING IN VIVO EVALUATION DURING THE CURRENT CONTRACT PERIOD

During the past twelve months, materials have been received from ten research groups that are supported by contracts from the Artificial Heart Program. These materials, for the most part, can be placed into three different categories, as indicated in Figures 1, 2, and 3. It is not our intention to present in detail the chemical makeup of these surfaces for that information is being presented in each of the individual reports from the contract groups. We would like at this time merely to categorize these materials and present in a simple form the basic chemical nature of the surfaces. The order of listing of the categories and the materials in the categories is not of significance and is only arranged in this sequence to permit a more logical presentation.

Category I includes two types of materials which provide heparinized surfaces. As is indicated in Figure 1, a number of flexible and rigid polymers and silicone rubber materials have been prepared with a heparinized surface by the investigators at Battelle Memorial Laboratories. The cationic surfactant, TDMAC (tri-dodecyl methyl ammonium chloride) is carried into the material by a solvent which then evaporates and permits the electrochemical binding of heparin. The investigators from Monsanto Research Corporation have prepared heparinized polymers by adding up to eight parts per hundred of heparin to the bulk polymer. They have also been able to provide additional surface heparin in other biomaterial preparations by quaternizing surface amines in these materials prior to additional heparin exposure.

The largest group of materials falls into Category II, which provide surfaces with ionic radicals or imposed electrical charges. The first three materials depicted in Category II present anionic radicals which provide an electro-negative surface effect. The Amicon research group has achieved this by combining an excess of polyanionic resin with a polycationic resin. The Melpar research group have altered cellulosic materials in such a way as to provide a significant number of carboxyl radicals on the surface. The investigators at the United States Army Biomechanical Laboratory have utilized an anionic surfactant to stabilize droplets of acrylic monomer, thus coating the acrylate with negative charges. Thermo Electron investigators have developed electret materials with an imposed negative charge on the surface of the biomaterial. This can be achieved on inert materials such as Teflon by a charge-injection of the material so that there are negative ionic groups located both on the surface and immediately beneath the surface. Also, in the case of substances such as Hypalon rubber, the material can be "doped" with sulfonated polymers which can be oriented on the surface by a "heterocharge". The negatively charged polymer particles are attracted to the surface by the electrical field activity and then the material can be cross-linked by heat to "freeze" this oriented configuration. At the Mellon Institute, silicone rubber has been treated with N-bis (β hydroxyethyl)Γ-aminopropyltriethoxysilane, (Union Carbide's A-1111) to, in turn, provide a surface with excess positive charges. In this case, the Mellon investigators were attempting to simulate the chemical nature of polybrene which is a substance used to counteract heparin, but when utilized in high concentrations has anticoagulant properties.

I HEPARINIZED SURFACES

RESEARCH GROUPS	BASIC MATERIALS	SURFACE CHEMISTRY
1. BATTELLE LABORATORIES	MOST POLYMERS AND SILICONE RUBBER	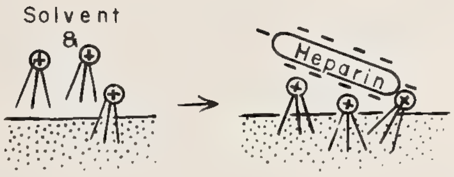
2. MONSANTO RESEARCH CORP.	EPOXY PLASTIC	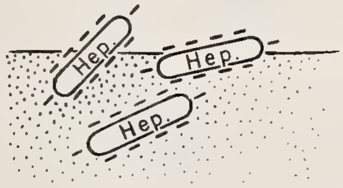

FIGURE 1.

II SURFACES WITH IONIC RADICALS OR IMPOSED ELECTRICAL CHARGES

RESEARCH GROUPS	BASIC MATERIALS	SURFACE CHEMISTRY
1. AMICON, CORP.	CATIONIC POLYMER PLUS EXCESS ANIONIC POLYMER	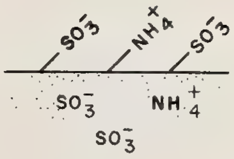 SO_3^- NH_4^+ SO_3^- SO_3^- NH_4^+ SO_3^-
2. U.S. ARMY BIOMECHANICS LABORATORY	ACRYLIC MONOMERS PLUS ANIONIC DETERGENT	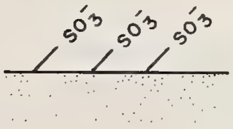
3. MELPAR, INC.	CELLULOSE	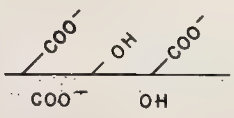
4. THERMO-ELECTRON CORP.	ELECTRETS	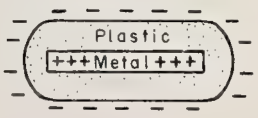
5. MELLON INSTITUTE	SILICONE RUBBER	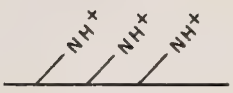

FIGURE 2.

III SURFACES OF RELATIVELY INERT MATERIALS

	RESEARCH GROUPS	BASIC MATERIALS	SURFACE CHEMISTRY
1.	GULF GENERAL ATOMIC, INC.	L.T.I. PYROLYTIC CARBON	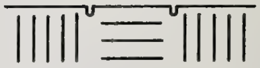
2.	DENVER RESEARCH INSTITUTE	ALBUMINATED POLYSTYRENE	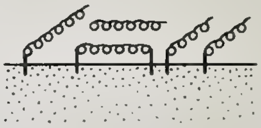
3.	DOW CORNING CORP.	SILICONE RUBBER	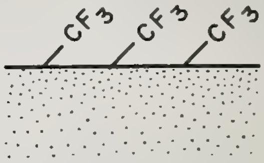

FIGURE 3.

RESULTS OF NONTURBULENT & TURBULENT FLOW IN I.V.C. RINGS

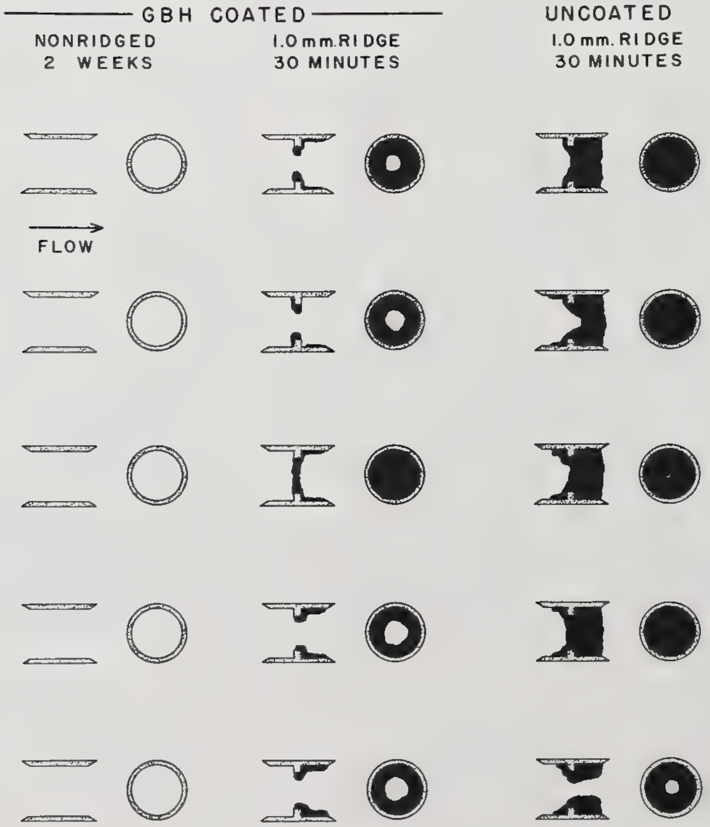

FIGURE 4.

Category III includes surfaces that are of a relatively inert material. In the case of these materials, it is hoped that thromboresistance can be achieved by providing a surface that is chemically inert and compatible with the contacting blood. The low temperature isotropic (LTI) pyrolytic carbons were initially studied by the investigators from Gulf General Atomic, Inc. because of properties possibly similar to the graphite in the GBH surface[5]. It was determined, however, that these nonporous carbons could not bind significant quantities of benzalkonium and heparin, but that in spite of this, they offered significant thromboresistance as outgassed plain carbon surfaces. These investigators have also been able to develop carbon materials that will bind significant quantities of benzalkonium and heparin by providing a more porous carbon surface. The albuminated surface from Denver Research Institute has been developed on polystyrene after a chloromethylation procedure is carried out on the polymer. This appears to provide a protein surface with minimal denaturization and with significant thromboresistance. The silicone rubber materials from the Dow Corning Corporation likewise provide a relatively inert surface with CF_3 groups as depicted in Figure 3.

Since it appears that in the development of an artificial heart or a cardiac assist device, it will be particularly important to have flexible materials that are thromboresistant, the majority of the materials from the ten research groups are nonrigid. The solid carbon materials from Gulf General Atomic, Inc., are, of course, rigid materials and the materials from the other nine contractors can be provided in varying degrees of flexibility.

It is encouraging that all of these materials have demonstrated significant thromboresistance when evaluated as vena cava test rings in our laboratory. Some of the surfaces appear to have, at this stage of development, more significant thromboresistance than others. This is particularly true when comparing materials within Category II, although some of the differences in thromboresistance in the materials in Category II are probably related to the presence of microscopic fissures and cracks in some of the surfaces.

As of this date, materials in Categories I & III have, with reasonable consistency, given satisfactory results in the two-week vena cava implant test. In Category II, three of the materials have satisfactorily passed the two-hour implant test and have performed satisfactorily in most cases in the two-week implant studies. Materials from Thermo Electron and Melpar have been under evaluation for a shorter period of time and have not yet been submitted to two-week implantation studies.

It is significant that all these materials appear to be providing encouraging results from the standpoint of thromboresistance. It appears that, at this early date, there may be some favorable factors and some factors that are not so favorable in considering these different types of surfaces. In Table 1, the authors list a few favorable and unfavorable factors that may be applicable to these materials.

TABLE 1

FAVORABLE AND UNFAVORABLE FACTORS REGARDING BIOMATERIALS

Heparinized (Category I)		Non-Heparinized (Categories II & III)	
Pro	Con	Pro	Con
1. Seem to have more initial thromboresistance.	1. Heparin might be gradually depleted from surface.	1. May have a more stable surface over long periods of implantation.	1. Hydrated and protein coated surfaces cannot dry out during insertion of prosthesis.
	2. Heparinized materials seem to bind greater quantities of lipid. This might weaken material if it was not initially rugged.		2. Some of these same coatings are difficult to bond to underlying materials.

At this time, the materials can be considered in Table 1 as either heparinized (Category I) or non-heparinized (Categories II & III). The relative thromboresistance of these materials as indicated in Table 1 can only be hypothesized at this time and additional studies will have to be carried out to finally determine the degree of thromboresistance over prolonged periods of implantation. Also, no firm statement can be made with regard to lipid binding by heparinized materials, but this is something that will have to be carefully considered as further studies are carried out. It is true, however, that greater care has to be taken in working with devices coated with protein or high water-content surfaces for these ordinarily should not dry out and by the same token, sterilization of these types of surfaces can be more difficult, at least at this stage of development.

Simplified sterilization techniques are important in the use of complicated prosthetic devices and it became apparent during the evaluation of several of these materials that some standard sterilization techniques can adversely affect the thromboresistant properties of the material. This appears to be particularly true in the use of gas sterilization with ethylene oxide. It was found that in the sterilization of the heparinized epoxy materials from the Monsanto Research Corporation, that it was imperative to provide at least 48 hours degassing in order to achieve maximal thromboresistance of the material. Lesser periods of degassing definitely had subtle adverse influence on thromboresistance and this was apparent only after implanting these materials for two-week periods.

STUDIES ON CONTROLLED TURBULENCE AND THROMBOSIS

Since there are a number of materials and surfaces with significant thromboresistance that are now capable of remaining free of thrombus during the two-week standard caval implant test, the authors have been interested for the past several months in developing a more severe test of thromboresistance. It appears that one way of greatly enhancing thrombogenesis within a prosthetic device is to provide a small degree of turbulent flow. Virtually all cardiac assist devices and artificial heart units under development will have some degree of turbulent flow and so this is a factor that must be considered in the evaluation of potentially thromboresistant materials.

In order to achieve varying degrees of controlled turbulence, our research group has worked with the basic caval test ring and merely added a circumferential ridge or "curbstone" in the middle of the ring. This ridge in each case has been 1 mm. wide and of varying height. In Figure 4, the results of five such rings designed for the study of controlled turbulence are depicted. These rings with a 1 mm. high ridge were coated with graphite, benzalkonium and heparin and implanted for 30 minutes in the canine vena cavae. The amount of thrombus that developed in these turbulent rings was quite significant when compared to five non-ridged rings coated with GBH. Actually, a high percentage of the latter GBH rings with nonturbulent flow are free of thrombus even after two years of caval placement. Five control ridged-rings of uncoated Lexan are also depicted. Previously published data on streamlined uncoated Lexan rings revealed complete thrombosis in each of these rings within a two-hour period.

GBH-coated rings have also been constructed with ridges 0.5, 0.6, and 0.75 mm. high. These studies have been carried out by one of the coauthors and will be reported in detail in the near future*. Thrombosis does not ordinarily occur on a GBH ring implanted for 30 minutes with an 0.5 mm. high ridge, but does occur in rings having an 0.6 mm. high ridge. The thrombosis that occurs almost always starts on the exposed corner of the leading edge of the ridge. The thrombus as viewed under a microscope at this site is always a platelet thrombus and then as time progresses a stagnant red cell thrombus forms behind this platelet thrombus.

As of this date, a specific design for a ring with controlled turbulence has not been selected but after further studies are carried out it may be that some of the materials with more outstanding thromboresistance should be submitted to this type of test with controlled turbulence. In addition, the results from these studies with turbulent rings should have significant relevance in the design of many types of intravascular prosthetic devices.

STUDIES ON THE BINDING OF HEPARIN TO SERUM PROTEINS

The authors have had a long-standing interest in the thromboresistance provided by heparinized surfaces and a small part of our contract effort has been devoted to the clarification of the mechanism of action of this type of surface.

In the past, two possible mechanisms of thromboresistance have been suggested for heparinized surfaces: 1) direct action of heparin in binding cofactors necessary in the clotting mechanism; or 2) indirect action of heparin by binding a number of proteins and thereby producing a "passavated-surface" of unaltered protein which would make the prosthetic surface inaccessible for activation of the thrombotic process. It has been further hypothesized that heparin might specifically bind to one or several serum proteins and that the characterization and isolation of these proteins might be useful in constructing thromboresistant surfaces. Thus, this study was undertaken to elucidate the mechanism of heparin-serum protein binding under physiologic conditions, and to identify proteins to which heparin selectively binds.

Initial evidence for the binding of heparin to serum proteins was obtained by starch block electrophoresis using a tritiated heparin-whole serum mixture and suitable controls. Comparison of protein and radioisotope distributions indicated that heparin did complex with serum proteins and that, of the bound heparin, approximately 2.7 per cent was in the gamma region, 5.6 per cent in the beta region, 54.3 per cent in the alpha-2 region, and 37.4 per cent in the alpha-1 albumin region (Figure 5).

In order to study further the binding of heparin in the alpha-2 region, analytical acrylamide gel electrophoresis was performed on whole serum and on alpha-2 fractions isolated by starch block electrophoresis. Definite binding of tritiated heparin in the slow alpha-2 region was demonstrated in these studies. Attempts at quantitation of the amount of bound heparin versus free heparin revealed that approximately five to ten per cent of the total heparin content was bound.

In order to assess further heparin binding to alpha globulins, the alpha globulin region in the acrylamide gels which demonstrated heparin activity was eluted, purified by re-electrophoresis on acrylamide gels, and concentrated. When this purified preparation of alpha globulins was incubated with tritiated heparin and again electrophoresed, enhanced binding of heparin was demonstrated. These purified alpha-2 proteins were further studied by surcrose density gradient ultracentrifugation which demonstrated a single sharp peak migrating in a position similar to that of albumin. In order to identify specifically the purified alpha-2 proteins, immunoelectrophoresis and Ouchterlony immunodiffusion were employed. Immunoelectrophoresis using anti-whole serum demonstrated a single protein migrating slightly anodely from the origin. When this alpha-2 preparation was developed against specific antisera for proteins in the alpha-2 region on Ouchterlony plates, the preparation did not show any major precipitin bands, but did show several minor bands. However, when the alpha-2 preparation was developed against anti-whole serum on Ouchterlony plates, a single major precipitin band and several minor bands were produced. Furthermore, the purified protein did not stain with the Oil Red O stain for lipoproteins.

---

*This work on the development of rings with controlled turbulent flow has been supported by USPHS Grant No. HE-9997.

Thus, this study has demonstrated selective binding of tritiated heparin to a protein migrating in the alpha-2 region. This protein has not as yet been identified by antisera of known specificity, but this protein does demonstrate a strong precipitin band when developed against anti-whole serum.

It should be mentioned that many different proteins migrate electrophoretically in the alpha-2 region; among these proteins are clotting factors V, X, and prothrombin as well as heparin cofactor. Our data does not allow us to determine whether or not our isolated protein is one of the above mentioned proteins, but is hoped that the isolation of a protein(s) to which heparin binds selectively will be useful in determining the mechanism of thromboresistance with heparin-coated materials. It is further speculated that this purified protein might be used to coat heparinized surfaces and thereby enhance the thromboresistance of these materials.

CONCLUSIONS

1. Current materials submitted by biomaterial contractors for in vivo evaluation can be placed in three categories. These include: heparinized surfaces; surfaces with ionic radicals or imposed electrical charges; and surfaces of relatively inert materials.
2. Materials in all three of these categories have demonstrated significant thromboresistance when submitted to the standard caval ring implant test.
3. Standard caval rings with a small circumferential ridge to provide minimal turbulence are much more thrombogenic even when coated with heparin.
4. Electrophoretic studies with tritiated heparin reveal selective binding to a protein migrating in the alpha-2 region.

REFERENCES

1. Valiathan, S., Whiffen, J.D., Weldon, C.S., and Gott, V.L.: Endocardial prosthetic junction thrombosis - an experimental study of the etiological factors. Trans. Amer. Soc. Artif. Intern. Organs, 12:174, 1966.
2. Gott, V.L., Ameli, M.M., Whiffen, J.D., Leininger, R.I., and Falb, R.D.: Newer thromboresistant surfaces: Evaluation with a new in-vivo technique. Surg. Clinics on N. Amer., 47:1443, 1967.
3. Jacobs, L.A., Klopp, E., and Gott, V.L.: Studies on the fibrinolytic removal of thrombus from prosthetic surfaces. Trans. Amer. Soc. Artif. Int. Organs, XIV:63, 1968.
4. Gott, V.L., Koepke, D.E., Daggett, R.L., Zarnstorff, W., Young, W.P.: The coating of intravascular prostheses with colloidal graphite - the relative importance of electrical change in the prevention of clot formations. Surg. 50:382, 1961.
5. Gott, V.L., Whiffen, J.D., and Dutton, R.C., Heparin bonding on colloidal graphite surfaces. Science, 142:1297, 1963.

DISCUSSION

DR. BLACKSHEAR: Could you tell us, when the ridge was not thrombogenic, was it right at the front end or was it behind the little wedge that you have on each of your other vena caval rings?

DR. GOTT: No. Perry, it was right at the front end, and when it was the typical square ridge we saw the same degree of thrombus as when the step was in the middle of the ring. When we rounded that off slightly we found that there was no thrombus there by the end of 30 minutes. We have not proceeded further.

DR. BLACKSHEAR: Then as far as the front of the step is concerned, it has changed from a one millimeter step to a two or three millimeter step?

DR. GOTT: The overall width is the same.

DR. BLACKSHEAR: Then the change from the vena cava diameter to the edge of the step is now two millimeters.

DR. GOTT: Yes, since we have not changed the diameter of the ring.

DR. BLACKSHEAR: One other thing. You mentioned that this was, in effect, turbulence. Do you have information to show what the turbulence, or the velocity fluctuations look like?

DR. GOTT: No, we don't. The thrombus was not where we would have anticipated its location. We think it is actually at a point of maximal shear and I would appreciate your thoughts on this. Mr. Topaz, who is here, has very neatly recorded this with some wind tunnel studies showing the buildup of the chemical agents he uses in his system right on the leading corner of the ridge. It appears, I think, that this is the area of maximal shear.

MR. SCHIPPER: I wonder whether you still have any heparin on the ridge in your GBH surface. Have you ever done any studies with labeled heparin?

DR. GOTT: We have not. We will have to do this, but I would anticipate that at thirty minutes we would still have a significant amount of heparin there. Dr. Whiffen and a number of others here have done a number of studies with radioactive heparin and, as you know, there is a considerable loss in the first 24 hours, but you still retain 10 to 15 percent of it by one year. This would be an interesting thing to determine.

DR. ROTH: I was going to ask about the flow patterns, but you have answered that question. However, I would like to suggest that this structure is very similar to the geometry of orifice type flowmeters, which have been used particularly in the hydrocarbon field in petroleum refineries for many years. One of the problems with them is that there are carbon deposits and other general filth in the petroleum product. The build up of contaminants along the edge of the orifice affects the calibration. There must be a tremendous amount of literature that might be helpful to you in this work.

DR. LAGERGREN: May I ask you how many rings do you put in the same dog?

DR. GOTT: We put only one ring. We used to try years ago to insert multiple rings for two hours and we found that there was too much trauma in the vena cava. It is true that with these 30-minute tests with the ridged rings we will typically put in three successive rings.

DR. LAGERGREN: I think these experimental conditions are not equivalent to the clinical situation in cardiovascular operations when you have a heparinized patient. In these animals you have a greater release of prothrombin if you have more rings and prolonged experiments. You have therefore different experimental conditions at the end of the operation than you had in the beginning.

DR. GOTT: Yes. We have never in the last five years implanted more than one ring in the 2-hour study; we always used one ring in one dog.

DR. LEONARD: Dr. Gott, suppose that you put a crimp in the inferior vena cava similar to the one millimeter ridge that you had in your rings. Would you get thrombosis in this case as well?

DR. GOTT: I don't think so, Dr. Leonard. I could be wrong, but I just cannot imagine this kind of thrombus beginning on intima.

DR. LEONARD: So you are indicating that if we truly had a nonthrombogenic surface that this would be thromboresistant independent of crimps or smoothness and geometry.

DR. GOTT: That's right.

DR. NUWAYSER: Dr. Gott, what is the smallest diameter tube that you have been able to use with a graphite benzalkonium heparin coating which is still nonthrombogenic?

DR. GOTT: We have selected this particular vena cava ring with a 7 mm I.D. and except for putting in some 4 mm GBH coated dacron grafts in the carotid artery, we have not worked with smaller diameter devices.

DR. NUWAYSER. Do you think there is a relation between the diameter of the ridge or the distance between the ridge and the ring for this thrombus formation?

DR. GOTT: The distance?

DR. NUWAYSER: You are actually physically reducing the size of the tube.

DR. GOTT: Yes.

DR. NUWAYSER: And therefore, since you say that you went down to about 3 or 4 millimeters, what is the actual distance then.

DR. GOTT: Yes, we are reducing an internal diameter of 7 millimeters down to 5 millimeters at the site of the circumferential ridge.

DR. NUWAYSER: Would that be the critical point then?

DR. GOTT: Yes, that is possible.

DR. TOPAZ: Dr. Gott, let me clear up one thing. The original ridges were so specified that the flow area would be one half of the original flow area of the ring. This would essentially make the fluid velocity twice that at the entrance of the ring. With a square edge orifice, as has been mentioned, you have separation at that leading edge which gives a circular eddy. The unforeseen fault in this is that when you round the edge according to the rounded orifice flowmeter theory, you are supposed to get smooth flow through the constriction. A thrombus is generated one-half way up the ridge when the ridge is in the middle of the test ring. You have an effect of the leading edge of the rigid ring in the soft vena cava which gives you a trail of thrombogenic factors which impacts approximately .65 millimeters up from the edge of the flow channel. When you go to the front edge of the ring you get streamlined flow completely through the nozzle with no problems of thrombosis. With square edge orifices of 1 mm height you still get separation as the flow tries to make the turn; and the flow channels are one half of the main flow channel to give twice the average flow velocities.

DR. NUWAYSER: If you use a tube which is the same diameter as that one half that you mentioned, would you still get a clot?

DR. TOPAZ: No.

DR. SILVAY: In your tests are you using the same sizes of rings in all cases or are you using different sizes depending upon the size of the vena cava of the animal?

DR. GOTT: We use a standard ring in a standard size dog. We select an animal of about 17 lbs. so that the ring fits snugly in the vena cava. We also put an external wrap around the vena cava so there is no cul de sac between the vein wall and the ring.

DR. SILVAY: Are there some differences in regard to implantation of rings into the superior vena cava as opposed to the suprarenal or infrarenal inferior vena cava?

DR. GOTT: We have settled on the inferior vena caval site. We worked with the superior cava at an earlier time. We did not notice any great difference between the superior cava and the inferior vena cava tests.

DR. SILVAY: How is it possible to observe the embolization in your screening tests? Have you developed some technique for post mortem identification of thrombi in the lungs or in other organs?

DR. GOTT: We do a post mortem and have not noted embolization. There is a possibility that we may have some embolization, but we feel this has not been a significant problem.

MR. SALYER: Dr. Gott, I just wanted to know how the Pluronic rings rate in your tests, which category they will be placed in, and your judgement as to their potential, pro and con.

DR. GOTT: Yes, it was so recent we could not include it. I think it is a non-ionic detergent. I would include it in the group of inert surfaces. Certainly, at this point, the Pluronic surface looks quite good. I would say that the results are very encouraging and very promising.

MR. SAWYER: Aren't you, by removing the curbstone from the center of the tube to the edge of the tube, introducing a change in the experiment which may be critical? For instance, when you go from the vena cava to the tube, you go into a situation where you produce changes in capacitance, permeability, and all the other events that occur as you go from a porous vena cava to a totally nonporous tube. You've also introduced turbulence and to a certain degree, an obstruction at that point and this is probably more difficult to ascertain. I wanted to ask you and Steve both if perhaps this is not already a critical experiment and whether you could perhaps use a light microscope to determine whether they have different characteristics, at the leading edge where you have a tendency to junctional thrombus formation and in the center where you have a different type of thrombus formation.

DR. GOTT: Phil, the thrombus we see when the curbstone is on the leading edge is not a junctional thrombus. It does not occur at the junction between the vena cava and the prosthesis. It starts up there on the leading corner of the square 1 mm ridge and will then occlude the orifice. Frequently the thrombus will not even get down to the intersection of the ring and vena cava.

DR. SAWYER: In other words, it never goes over the edge of the lip. It never fills in the cul de sac behind the curbstone.

DR. GOTT: Yes, it can fill the stagnant area behind the ridge if given enough time, but ordinarily the thrombus will fill the orifice first and after that you get a stasis thrombus downstream.

DR. SAWYER: That is a very interesting problem.

DR. LUDWIN: My question concerns the repeatability of your results from the dog to dog. In other words, how consistently will the results reappear in a series of dogs using the same type ring?

DR. GOTT: I think you can say that they are quite reproducible. We couldn't give you any definite data after implanting one ring for two hours, but I think after we've implanted three rings or five rings for two hours, or five rings for two weeks, we can; the results are reproducible enough that we can be fairly definite as to the thromboresistance. We have found the results are really quite reproducible with this method of testing.

DR. KANTROWITZ: Dr. Gott, I am wondering whether or not this is too severe a test perhaps. Wouldn't it be worthwhile to try to reproduce this geometry with a viable lining of veins? I would be surprised if it didn't clot.

DR. GOTT: Well, it may be too severe, but we have so many materials now that pass our two week implantation test that we are really at a point where we would like to futher categorize the comparative thromboresistance of these materials. We thought that by going to this turbulent test might be helpful in this respect. We felt also that this test might be helpful in designing AV fistulas, AV shunts and similar configurations. We were surprised to see the position of the thrombus in the ridged ring.

DR. KANTROWITZ: Is it possible to construct this kind of geometry with a vein?

DR. GOTT: I think it is very difficult because of the thickness of the vein wall.

DR. KANTROWITZ: Yes and you'd get a very smooth topography. You would not get sharp corners which I think is very critical.

DR. GOTT: Yes.

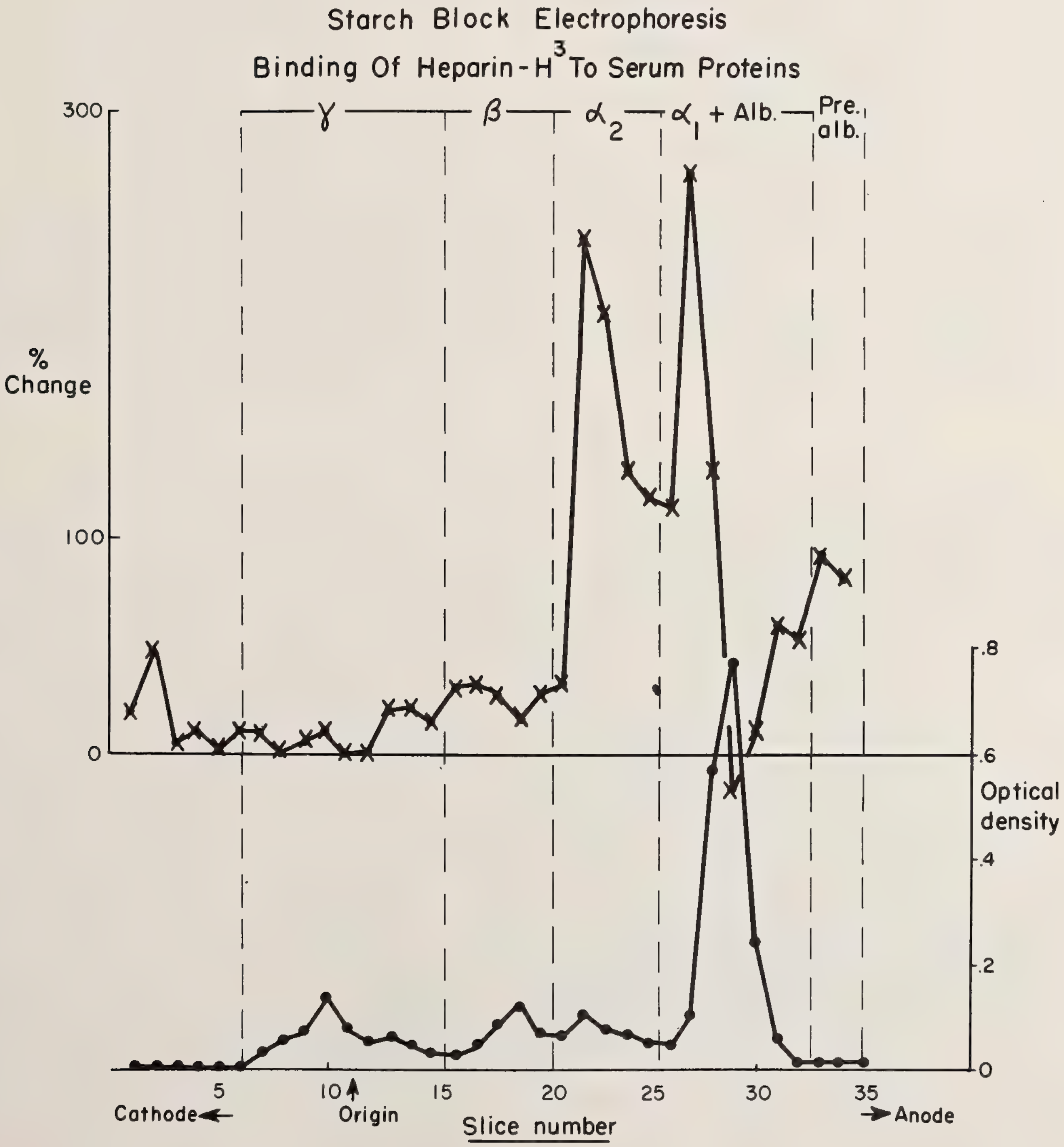

FIGURE 5.

CHAPTER 18

BLOOD COMPATIBILITY OF SOME POLYMERIC AND NONPOLYMERIC MATERIALS

R. G. Mason, N.F. Rodman, D.E. Scarborough and
L.D. Ikenberry

University of North Carolina, Chapel Hill, N.C.

Blood compatibility studies have been conducted in one in vitro and two different ex vivo test systems on fifteen polymeric and three nonpolymeric meterials. Following exposure of test materials to native blood for 10 min., tests were performed to determine the degree of damage to platelets and erythrocytes and the degree of activation of the coagulation system. Test materials are listed in order of decreasing compatibility with blood: collagen, L-1624 (3M Co.), poly(dichloro para xylylene), carbon-graphite, poly(methyl acrylate), poly(vinyl chloride) chlorinated, heparinized hydrin rubber, poly(methyl methacrylate) isotactic, balata rubber, poly(methyl methacrylate), poly(hydroxypropyl methacrylate), hevea rubber, and poly(oxymethylene). Scanning electron microscopic studies of some test materials were conducted following exposure of the material to blood. It is tentatively concluded that type and number of surface reactive groups correlates poorly with observed blood compatibility while surface roughness and presence of impurities in test materials tend to decrease the degree of blood compatibility.

The aim for the work performed during the second year of our contract was to examine in vitro and ex vivo the blood compatibility characteristics of a large number of materials. These test materials were supplied to us by Dr. Ikenberry, our subcontractor, and by a number of contractors in the Artificial Heart Program. In previous work we have surveyed 58 different materials for blood compatibility in an in vitro test system. Seventeen of the materials found to be most compatible with blood in this test system were re-examined in three different test systems. These test systems consisted of a modification of the previously used in vitro system, an adaptation of Dr. Don Lyman's ex vivo system, and an ex vivo system of our own design. In addition, using these three test systems, we examined the blood compatibility characteristics of a number of materials supplied to us by other contractors.

METHODS AND MATERIALS

The three test systems permit us to examine materials possessing a wide range of chemicophysical properties. The paddles and tube test system is illustrated in Figure 1. Blood is drawn without anticoagulant into a silicone-coated glass syringe and quickly transferred to the tube which is either coated internally with test material or composed wholly of test material. A paddle, either coated with test material or composed of it, stirs the blood at 60 RPM for 10 minutes at which point sufficient 3.2% sodium citrate is added to the blood to prevent further clotting. This anticoagulated blood is certrifuged at 4°C in prechilled silicone-coated glass tubes to remove the cellular elements, and the plasma is saved for testing. The paddle and tube system is an in vitro system possessing the possible disadvantage of a blood-air interface.

The modified Lyman cell test system, or test cell I, is illustrated in Figure 2. Standard microscope slides covered with test material or slabs of test material of similar size and shape, form two of the walls of the silicone-coated glass cell. Within the cell is a free-falling silicone-coated glass plate which acts as a mixer. The cell and attached silastic rubber tubes are filled with normal saline and then connected to a needle inserted in a vein. Blood displaces the saline in the cell with practically no mixing of the blood and saline layers. Once filled with blood, the cell is disconnected from the lead-in tube and inverted manually every 10 seconds for 10 minutes. Following the 10 minute period of exposure of native blood to test material, the blood is drained into a prechilled silicone-coated glass tube containing an appropriate quantity of 3.2% sodium citrate and centrifuged to remove cellular elements.

The construction of an ex vivo test cell of our own design is illustrated in Figure 3. This cell, referred to as test cell II, consists of two sheets of test material separated by a 3mm-thick silastic rubber gasket through which are inserted two 16 gauge silicone-coated needles. The cell is filled with saline and subsequently with blood in the same manner as test cell I. Since there is no mixing plate in test cell II, the cell is left undisturbed during the 10 minute interval of exposure of test material to native blood. Following exposure of blood to test material, the blood is anticoagulated and the cellular elements removed by centrifugation.

Four tests or assays are performed upon plasma from blood which has been exposed to test material. These are presented in Table 1.

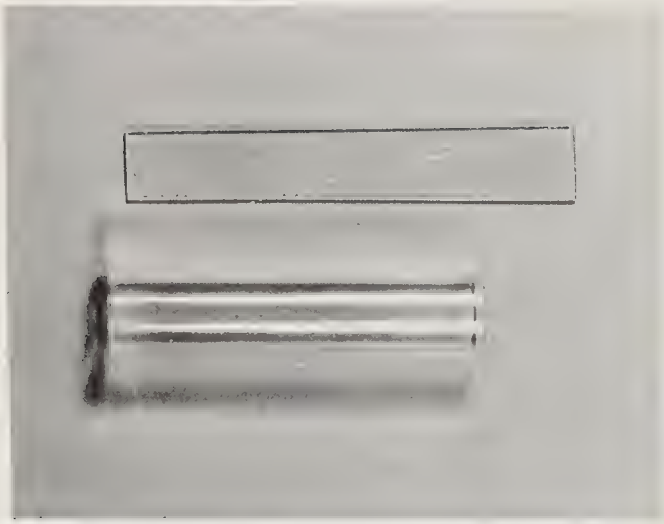

FIGURE 1. THE PADDLE AND TUBE TEST SYSTEM (SEE TEXT)

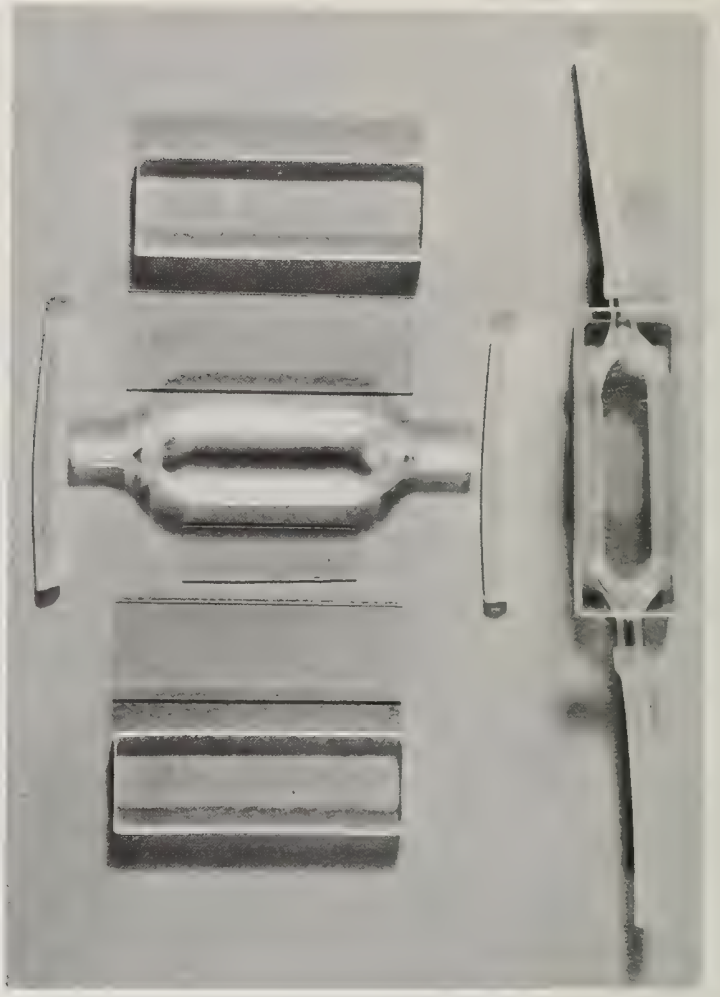

FIGURE 2. THE TEST CELL I SYSTEM (SEE TEXT)

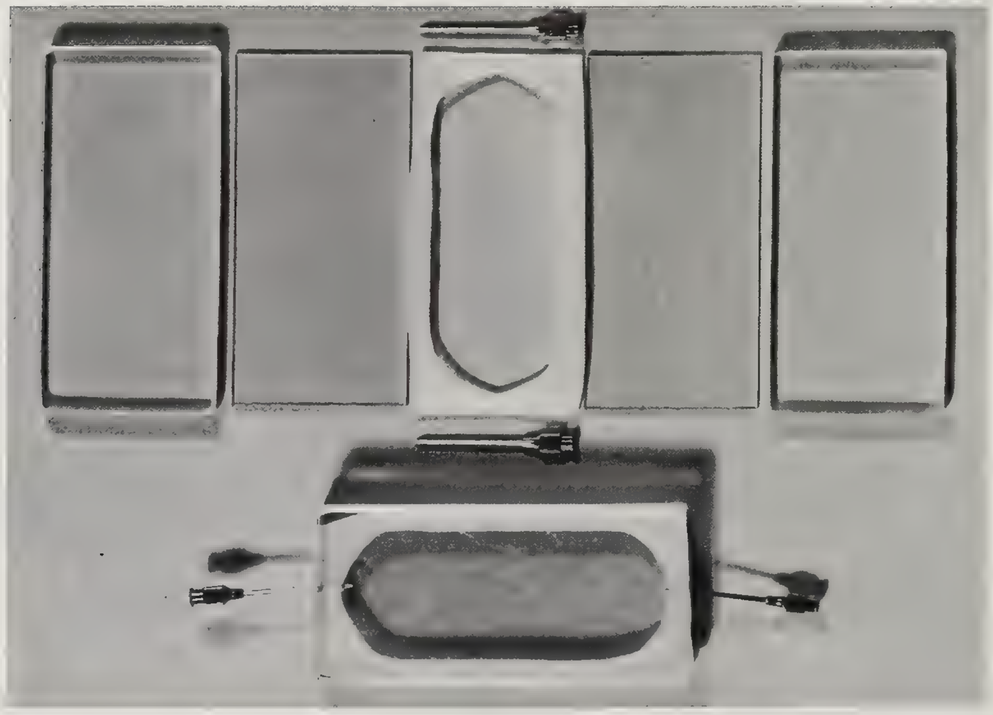

FIGURE 3. THE TEST CELL II SYSTEM (SEE TEXT)

TABLE 1

ASSAYS PERFORMED ON CITRATED PLASMA

1. Stypven Time Test (ST)
   Indicates release of platelet factor 3.
2. Partial Thromboplastin Time Test (PTT)
   Indicates activation of the blood coagulation sequences.
3. Hemoglobin Assay (Hb)
   Indicates rupture of red blood cells.
4. Adenosine Triphosphate (ATP) Assay
   Indicates cellular damage, especially to platelets.

The Stypven time is a coagulation test which gives an indication of the amount of thromboplastic material released from cellular elements, predominantly platelets. This test gives a measure of the damage inflicted upon platelets by contact with a foreign surface. The partial thromboplastin time test (PTT) gives a measure of the degree of activation of the coagulation mechanism brought about by contact of blood with the test material. The assay for hemoglobin quantitates the amount of hemoglobin released from damaged erythrocytes; these values have been negligible for most test materials. The assay for adenosine triphosphate (ATP) is sensitive to nanomole quantities of ATP. ATP is released from damaged cells including platelets. In general, shortened Stypven time values, indicating damage to platelets with release of the thromboplastic platelet factor 3, are accompanied by elevated values for ATP release.

Assay values are expressed as % of the value obtained in the same assay using blood exposed only to silicone-coated glass. In this way, silicone-coated glass serves as the standard surface to which test surfaces are compared.

RESULTS

A comparison of values obtained in different test systems with two of the test materials is presented in Table 2.

TABLE 2

COMPARISON OF BLOOD COMPATIBILITY CHARACTERISTICS OF TWO MATERIALS

Test Material	Test System	Stypven Time	Partial Thromboplastin Time	Hemoglobin Release	ATP Release
Collagen	PT	102	102	145	34
	TCII	103	98	84	11
PCTFE	TCI	99	28	162	106
	TCII	98	39	73	120

PCTFE = poly (chlorotrifluoro ethylene)
PT = paddle and tube
TC = test cell

Collagen, which appears to have better blood compatibility characteristics than does silicone-coated glass, gives nearly identical ST values in paddle and tube and test cell II systems. The PTT values obtained with collagen in the two systems are close but not identical. ATP values agree with ST values in each case. Poly (chlorotrifluoro ethylene), on the other hand, has relatively poor blood compatibility characteristics. In the paddle and tube system blood clotted in tubes coated with this polymer in less than 10 minutes. The ST values indicate little damage to platelets, but the PTT values show that marked activation of coagulation has taken place. With both collagen and poly (chlorotrifluoro ethylene), hemolysis was insignificant.

A composite ranking in order of decreasing compatibility with blood was made for materials examined in the paddle and tube and test cell II systems. This was accomplished by ranking each material according to decreasing ST and PTT values for each test system. The ranked materials were then given consecutive rank numbers. The sum of the rank number for the ST and PTT values was the composite rank number for that material. Essentially this is an arbitrary method of ranking test materials by their ST and PTT values. It provides a useful means of comparing the performance of test materials in the two test systems.

The composite ranking of test materials according to their performance in the paddle and tube system is shown in Table 3.

TABLE 3

COMPOSITE RANKING OF MATERIALS: PADDLE AND TUBE TEST SYSTEM

Collagen Poly (methyl methacrylate) isotactic Poly (vinyl chloride) chlorinated
Hydrin rubber heparinized
Carbon-graphite
Poly (hydroxypropyl methacrylate)
Poly (methyl methacrylate)
Poly (styrene)-poly (vinyl pyridine) graft
Poly (dichloropara xylylene)
Balata rubber Hevea rubber
Poly (vinyl chloride)
L-1624
Poly (methyl acrylate)
Stainless steel
Hydrin rubber Poly (chlorotrifluoro ethylene)

Materials grouped by a bracket had identical composite rank numbers. As in previous work, collagen, several methacrylates, carbon-graphite, heparinized Hydrin rubber, and chlorinated poly (vinyl chloride) ranked high in blood compatibility. We could detect no release of heparin from heparinized Hydrin rubber into plasma, but minute quantities can affect test values. Stainless steel, nonheparinized Hydrin rubber, and poly (chlorotrifluoro ethylene) had low blood compatibility rankings.

The composite ranking of test materials in test cell II system is shown in Table 4.

TABLE 4

COMPOSITE RANKING OF MATERIALS: TEST CELL II

Collagen
Poly (methyl methacrylate)
Hevea rubber
Poly (dichloropara xylylene)
Poly (vinyl chloride) chlorinated
Poly (styrene)-poly (vinyl pyridine) graft
Poly (hydroxypropyl methacrylate)
Poly (chlorotrifluoro ethylene)
L-1624
Stainless steel
Hydrin rubber

Carbon-graphite, heparinized Hydrin rubber, and isotactic poly (methyl methacrylate) were not tested in this system. Collagen and chlorinated poly (vinyl chloride) still rank high, while stainless steel and Hydrin rubber rank low in blood compatibility.

Table 5 gives an overall ranking of test materials obtained by combining the composite ranking values for each material in each of the three test systems. It can be seen that heparinized Hydrin rubber, collagen,.isotactic poly (methyl methacrylate), chlorinated poly (vinyl chloride), and carbon-graphite lead the list in compatibility with blood. This data agrees well with that from the previous year's work and indicates that the different test systems produce nearly comparable results.

Four of the test materials were examined by scanning electron microscopy following the 10 minute period of exposure to blood. Figure 4 shows the finely granular surface of collagen upon which rest individual and aggregated platelets, erythrocytes, and a few fibrin strands.

The surface of isotactic poly (methyl methacrylate) is shown in Figure 5 and appears moderately irregular with numerous small craters. Upon this surface are individual and aggregated platelets but neither erythrocytes nor fibrin are demonstrated.

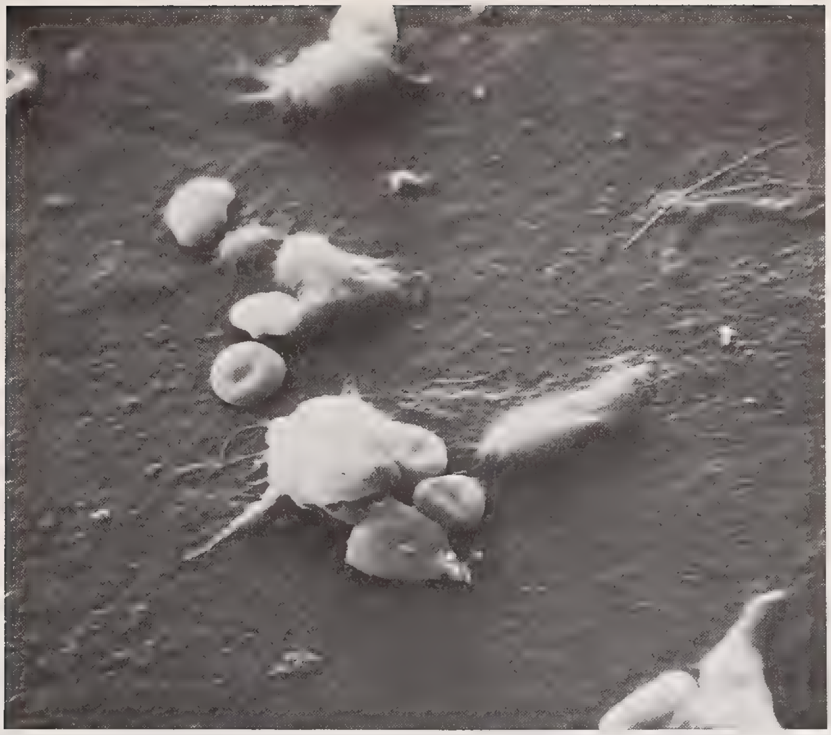

FIGURE 4. SCANNING ELECTRON MICROGRAPH OF COLLAGEN SURFACE FOLLOWING EXPOSURE TO NATIVE BLOOD FOR 10 MINUTES (SEE TEXT). ORIGINAL MAGNIFICATION 1500x.

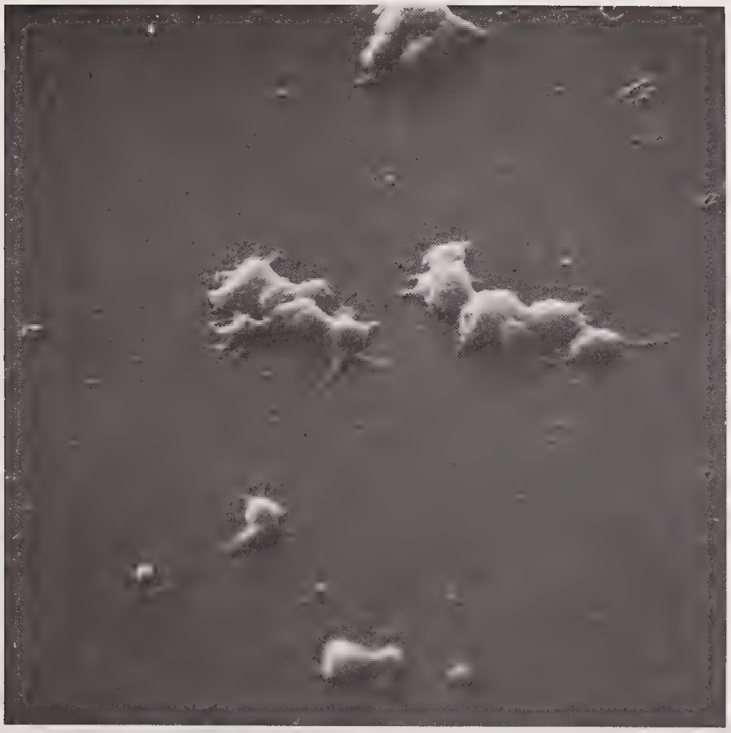

FIGURE 5. SCANNING ELECTRON MICROGRAPH OF POLY(METHYL METHACRYLATE) SURFACE FOLLOWING EXPOSURE TO NATIVE BLOOD FOR 10 MINUTES (SEE TEXT). ORIGINAL MAGNIFICATION 2500x.

TABLE 5

OVERALL RANKING OF TEST MATERIALS FOR ALL THREE TEST SYSTEMS

Hydrin rubber, heparinized
Collagen
Poly (methyl methacrylate) isotactic
Poly (vinyl chloride) chlorinated
Carbon-graphite
Poly (methyl methacrylate)
Hevea rubber
Poly (methyl acrylate)
Balata rubber
Poly (dichloropara xylylene)
Poly (styrene) - poly (vinyl pyridine) graft
Poly (hydroxypropyl methacrylate)
Poly (vinyl chloride)
Poly (chlorotrifluro ethylene)
L-1624
Stainless steel

The surface of balata rubber is somewhat irregular as is shown in Figure 6. Numerous individual and aggregated platelets are adherent to this surface, and pseudopod formation is marked. This finding is surprising since the ST value for balata rubber indicated little damage to platelets; however, it is of interest that in this case the ATP value indicated moderate platelet damage. Perhaps certain surfaces can produce differential release of platelet factor 3 and ATP. This electron micrograph was taken at roughly one-half the magnification used for Figures 5 and 7 making it appear that there are larger numbers of adherent platelets than is really the case.

Figure 7 shows the softly undulating, finely granular surface of L-1624. Single and aggregated platelets with numerous pseudopods are adherent to the surface. The remaining adherent cellular elements appear to be either leukocytes or markedly distorted erythrocytes. The crack is an artifact which occurred during examination of the specimen in the scanning electron microscope.

In excess of 45 materials submitted by other contractors were examined for compatibility with blood. Participants in this program are listed in Table 6.

TABLE 6

CONTRACTORS SUBMITTING MATERIALS FOR BLOOD COMPATIBILITY EVALUATION

Amicon	3
Battelle	2
Dow Chemical	3
Dow Corning	2
Gulf General Atomic	2
Medical College of Virginia	2
Monsanto	3
Polysciences	1
Shell	3
Thermo Electron	2
Union Carbide	24++

Each material, except those submitted by Union Carbide, was examined in one or more of our three test systems. Choice of the test system was dictated by materials submitted and by some of their physical properties such as hardness and roughness. Materials were tested in all three test systems whenever possible. Contractors were unable to supply materials in certain forms in several cases and technical problems precluded testing of a few submitted materials.

Presentation of an overall ranking of test materials obtained by combining the composite ranking values for each material in each of the test systems appears to be the fairest method. Presentation of composite rankings for each of the three test systems would be unfair to contractors whose material could not be tested in a particular system. The overall ranking of test materials is presented in Table 7.

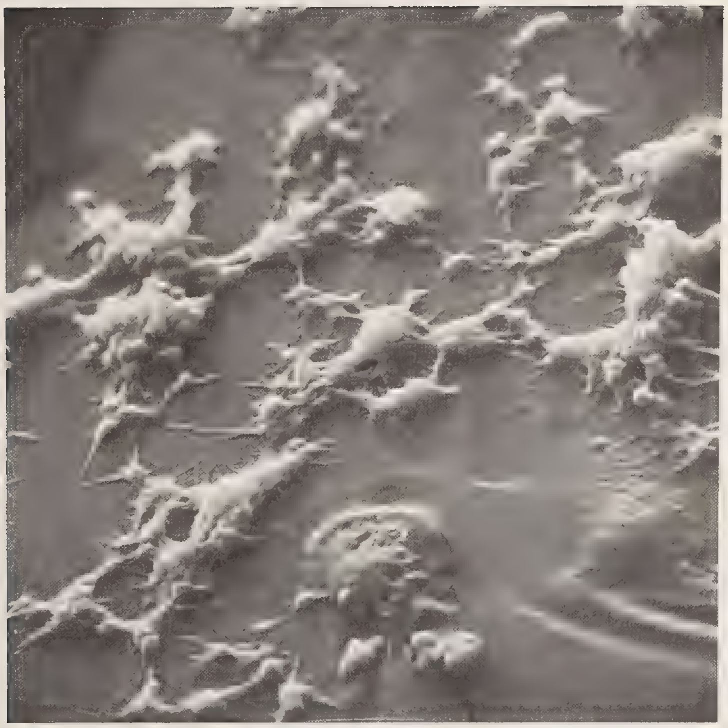

FIGURE 6. SCANNING ELECTRON MICROGRAPH OF BALATA RUBBER SURFACE FOLLOWING EXPOSURE TO NATIVE BLOOD FOR 10 MINUTES (SEE TEXT). ORIGINAL MAGNIFICATION 1475x.

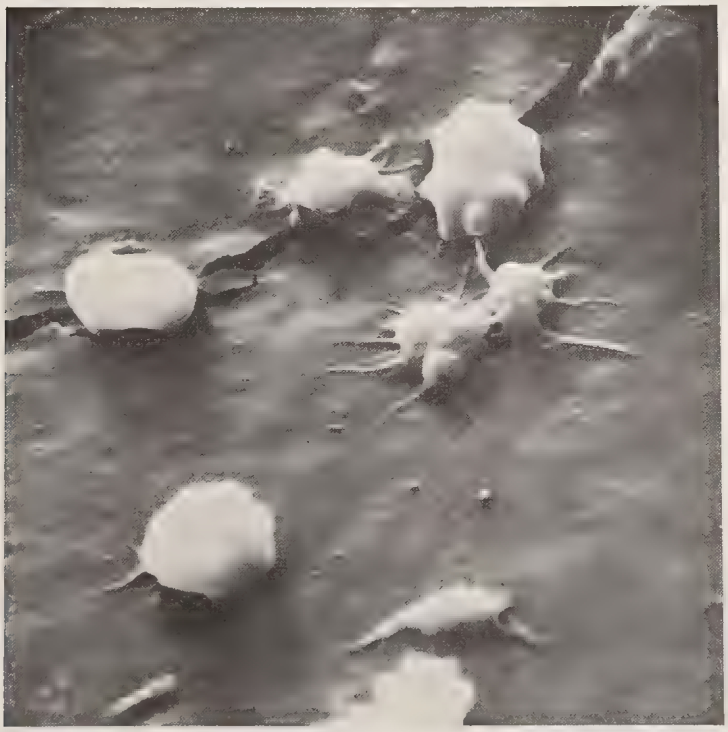

FIGURE 7. SCANNING ELECTRON MICROGRAPH OF L-1624 SURFACE FOLLOWING EXPOSURE TO NATIVE BLOOD FOR 10 MINUTES (SEE TEXT). ORIGINAL MAGNIFICATION 2800x.

TABLE 7

OVERALL RANKING OF TEST MATERIALS FOR ALL THREE TEST SYSTEMS

Battelle, heparinized
Medical College of Virginia, MEM
Amicon, neutral
Dow Corning, 1622
Shell, BM 1
Gulf General Atomic, 103
Amicon, A
Gulf General Atomic, 95
Medical College of Virginia, TPX
Polysciences
Dow Chemical, C
Shell, BM 4
Amicon, C
Dow Corning, 1519
Shell, BM 15
Dow Chemical, B
Dow Chemical, A

Inclusion of the heparinized Battelle product in this list is probably unfair since some heparin was shown to have gone into solution in the plasma by thrombin time tests. Of the remaining test materials, only Dow Chemical A, B, and C, Dow Corning 1519, and Medical College of Virginia TPX were inferior to silicone-coated glass in one or both of the assays. Conversely, only Medical College of Virginia MEM was superior to silicone-coated glass in both assays. The remaining materials were superior to silicone-coated glass in one of the two assays but inferior to it in the other assay.

FUTURE WORK

We plan to test a number of new materials in the coming months including surfaces with varying mixtures of positive and negative charges and with varying mixtures of hydrophilic and hydrophobic groups. In addition, we shall most likely continue to evaluate materials from other contractors on a limited basis.

DISCUSSION

Several conclusions can be drawn from our work of the past two years. First, it is possible to test materials for blood compatibility in *in vitro* and *ex vivo* test systems and obtain reproducible results, only if great care is taken in preparation of materials and selection of blood donors. Secondly, from the results obtained from the wide spectrum of materials we have tested, we can only conclude that chemical properties of materials alone do not determine blood compatibility. Physical properties such as roughness as well as one or more as yet undetermined properties contribute, at least in part, to the effects a surface has on the cellular elements and coagulation mechanism of blood.

DISCUSSION

DR. BLACKSHEAR: Did you ever try any tests in which you preceded the introduction of blood by a short space of time in which plasma was introduced into the cells first?

DR. MASON: No, we have not done that yet.

MR. SALYER: I have to ask, since you included our materials and didn't comment on them. I read a little bit of your quotation from your letter this morning, but I think people might be interested. You did not rank them.

DR. MASON: We did not include your material in the slides because we were essentially unable to test it. The amount of heparin which leaked out completely ruined our assays.

DR. HERSH: This may be a very naive question but I just wondered, is there a correlation between your composite ranking of materials with some of the results Dr. Gott has obtained in his 2 hour or 2 week tests?

DR. MASON: We have not as yet been able to make this correlation. We certainly want to very much, and we are hoping that as soon as more of the data is in we will be able to do this. We have tested these materials on a blind basis in almost every case, and that's the reason for some of the rather bizarre names that were given to them, such as ABC. This is the way they were sent to us and, in certain cases, we had no idea what these materials were. In other cases, we were informed after the testing what they were. It is hoped that at the end of this contract year we can compare the results we get with the results that other people get. We are very interested to see how it stacks up.

DR. KELLER: I was wondering, since you mentioned the results of your hemoglobin assays and presumably inferred, or I assumed you were inferring, that the damage to red blood cells was minimal: Is there any evidence that cells have hit the surface, any of your surfaces, and then left the surface? The picture showed many cells on the surface, but because of the very low shears at which you were operating, I was curious as to whether you think that you are getting contacts which result in a cell hitting a surface and subsequently leaving it.

DR. MASON: We have not tested for this as yet. However, the work in the next three months will include some studies in which we will try to take samples at varying periods of time and see if we can detect loss of cells from the surface.

UNIDENTIFIED DISCUSSANT: Do the electron micrographs give any indication whether the fibrin forms before platelets adhere or aggregate or could the primary event be platelet aggregation followed by fibrin formation?

DR. MASON: Dr. Rodman will answer that.

DR. RODMAN: The scanning electron micrographs don't help on this. However, we have done some transmission electron microscopic work, and it seems likely that the platelets adhere first. In fact, they are below the red cells when the two of them are present together. The platelets are closer to the adsorbed protein layer than the red cells. The adsorbed protein layer appears to be there before the fibrin forms.

UNIDENTIFIED DISCUSSANT: Have any experiments been done with platelet free material to see if fibrin forms in the absence of platelets?

DR. MASON: We have not done that.

MR. NEMCHIN: I'd like to pose a question with regards to your test system. Have you experienced any cavitation phenomena in your system? The reason I ask is that the high energies involved in cavitation phenomena might impose an unusually severe stress on the blood.

DR. MASON: What do you mean by cavitation?

MR. NEMCHIN: Bubble formation in the clots accompanied by the release of energy.

DR. MASON: No, we have not. At least we have not detected it.

MR. PURDY: Have you separated the surface roughness variable in your experiments. For example, I noticed that the materials appeared to have a very smooth surface and you did have a comment that stainless steel had a low rating? I wondered if possibly it might be the fact that the surface roughness of the stainless was high that influenced the results which you obtained?

DR. MASON: It certainly contributed. The stainless steel was not as smooth as many of the materials we have tested. It was not as rough, however, as some of the other materials such as certain rubbers.

MR. PURDY: Are you planning to try to observe the effect of surface roughness in part of your experimentation?

DR. MASON: We hope to do this in the next year of work, because we have noticed that it does seem to affect the results.

MR. PURDY: Are you also going to include materials such as pure titanium and titanium aluminum vanadium materials?

DR. MASON: We have no plans to test those.

MR. PURDY: Is there a reason for that? For excluding those materials which are supposedly very resistant to thrombosis?

DR. MASON: No, it is simply that we have just never thought of including them.

MR. RATNER: Have you looked at all at protein adsorption on any parts of your equipment, on the paddles or in the cells perhaps?

DR. MASON: We are very much aware that this is taking place and as Dr. Rodman mentioned in some of the transmission electron microscopic studies, you can see a layer of adsorbed material form on the surface of the material. It forms on almost every material that we have examined and we are aware that this is taking place. We are much interested in it and hope to put a large part of our effort next year into working with this.

CHAPTER 19

FURTHER STUDIES OF THE INTERACTION OF BLOOD AND TISSUE CELLS WITH ARTIFICIAL HEART IMPLANT CANDIDATE MATERIALS IN VITRO

R. J. Hegyeli, R. Gallagher, and L. K. Peterson

Battelle Memorial Institute, Columbus Laboratories

Columbus, Ohio

The planned development of cardiovascular implant materials will to a great extent depend upon an increased understanding of the basic processes and problems encountered when biological tissues and implant materials are allowed to interact. The aim of this project is to contribute to the development of new biocompatible materials. The objectives are: (1) Cell culture studies with prosthetic materials. (2) Further development of and testing with a dynamic test system. (3) Investigation of other contractors' materials. (4) Use of scanning electron microscopy to further elucidate certain cell/material interactions. The experimental techniques have been described in previous publications. All of these investigations involve direct visualization of blood/materials or tissue cells/materials interfaces. The choice of materials to be studied has been guided by the decision of the Artificial Heart Program Office. Thirteen contractors are providing materials for study. The biological evaluation of these new materials confirms the experimental results reported last year of the importance of sterilization and storage methods in modifying the adherence of formed blood elements to the surface of the materials. Several new observations which may be of practical importance to the development and evaluation of prosthetic materials were made, i.e., (1) Human cells were found to react differently to certain materials than did animal cells. In one case human cells were able to grow on a material which caused complete destruction of animal cells. (2) The treatment necessary to render a material nonthrombogenic sometimes results in a surface which is highly toxic to tissue cells. These results emphasize the importance of (1) including a human test system for preclinical testing and (2) evaluation of biotoxicity in parallel with nonthrombogenicity so that toxic contaminants can be identified and eliminated early during the development of a new material.

INTRODUCTION

An implanted device intended to become a permanent functional part of the human body may be considered a potentially hazardous bulk pharmaceutical. It is the purpose of this research program to contribute to the development of reliable and meaningful biological specifications, contributing to the human safety of biomedical materials. The successful achievement of this goal would serve as a useful guide for future development of prosthetic materials designed specifically for biomedical applications.

In the two years during which we have had the privilege to examine candidate materials developed by fifteen collaborating Artificial Heart Program contractors we have seen significant advances in materials development. The materials investigated during last year's contract represented only one of the three possible avenues for the development of improved cardiovascular tissue replacements (Wesolowski, 1962). The materials submitted during this year's contract (Table 1) on the other hand, represent the two main approaches, namely:

(1) The concept of a prosthesis (suggested designation: "homoprosthesis") composed entirely of a more or less homogeneous mass of foreign material, the surface of which is rendered smooth and antithrombogenic so as to be suitable for continuous, direct contact with flowing blood in humans.

(2) The concept of a prosthesis (suggested designation: "heteroprosthesis") composed of a mixture of foreign inert material and living tissue, existing in the body as a unit. In this case the material acts only as a porous or fibrous scaffold into which tissue cells are made to migrate *in vitro* or *in vivo*. The scaffold can be made flexible, semi-rigid, or rigid as the need may be. Once the surface of such a "heteroprosthesis" becomes completely covered with cells, it has been found to possess antithrombogenic properties similar to those of normal endothelial-lined cardiovascular surfaces (Ghidoni, et al, 1968). Thus, almost any candidate material can be considered for "heteroprosthesis" use, as long as it is compatible with human body cells and cellular products. The "heteroprosthesis" has a third advantage in that it is self-renewing, allowing the natural life processes of cell death and cell division to proceed in response to the continuous high rate of wear and tear within the cardiovascular system. Nutrition to the cells within a "heteroprosthesis" is superior to that provided cells which manage to survive on a "homoprosthesis" surface. In the first case nutrition is acquired directly from the blood flowing by it; in the second case, further nutrition is derived from the ingrowth of blood

TABLE 1

CANDIDATE MATERIALS EVALUATED OR SCHEDULED FOR EVALUATION

Different types of carbon surfaces; heparinized and untreated
Silicone rubber; heparinized (TDMAC technique) and untreated
Polypropylene; heparinized (TDMAC technique) and untreated
Hydrin rubber; heparinized (TDMAC technique) and untreated
Teflon; heparinized (TDMAC technique) and untreated
Polyvinylchloride; heparinized (polyurethane technique) and untreated
Silicone rubber; heparinized (polyurethane technique) and untreated
Teflon; heparinized (polyurethane technique) and untreated
Polypropylene; heparinized (polyurethane technique) and untreated
Methyl methacrylate; heparinized (polyurethane technique) and untreated
Experimental fiber mats for tissue ingrowth
Blood oxygenator membrane following *in vivo* use
Hydron
Electrified Hypalon
Carboxymethyl cellulose formulations
Silicone fluoroalkyl formulations
Semiflexible epoxy; heparinized and untreated
Carnegie Mellon heparinized polymer surfaces
Polyacrylamide formulations
Hydrocarbon elastomers

vessels through the porosities of the material, if these are of sufficient size. Lack of this second source of nutrition has been demonstrated to be a factor contributing to long-term failures in human vascular prosthetic grafts (Wesolowski, 1964).

The third concept of a compound cardiovascular replacement (Wesolowski, 1959) consisting of both permanent and absorbable components has not yet been investigated during this program. However, it would be a logical extension of the "heteroprosthesis" concept. Partially or completely resorbable "heteroprostheses" of different sizes and shapes might have great future potential, particularly in pediatric cardiovascular reconstructive surgery. It should become possible, in the future, to program the interlocking of, the gradual resorption of, and physiological excretion of the reinforcing foreign material scaffold in such a manner as to allow the continuous growth and increase in size of the "heteroprosthesis" to proceed in pace with the increasing age and size of the child.

The current research project is concerned with an investigation of two of the main biological problems of importance in the development of prosthetic cardiovascular devices in humans:

(1) Interactions at the interface between the candidate material and human blood
(2) The interaction between the candidate material and the human tissue cells.

RESEARCH PROGRESS

According to the approved program plan, the experimental work on the current year's research contract was divided into four tasks to be pursued over a period of 15 months:

Task 1. Cell culture studies with prosthetic materials
Task 2. Further development of and testing with a dynamic test system introduced during last year's contract
Task 3. Investigation of other contractors' materials
Task 4. Nominal use of scanning electron microscopy to further investigate certain cell/materials interactions.

The subtasks in each category are identified in Table 2.

This paper summarizes the research progress made during the first ten months of the project. Figures 1 through 24 show photographs illustrating some of the more important observations during the project, grouped together according to candidate material and type of study. The work is proceeding according to the approved program schedule. The reporting of the work has followed the requested schedule of a six month's technical report on December 28, 1968, and monthly interim progress reports. Collaboration has been initiated with other contractors as indicated in Table 3.

Experimental Work.

The following materials research and development tasks were performed:

Task 1. Cell Culture Studies with Prosthetic Materials. The most logical approach to the bioassay of candidate implant materials or finished devices is, of course, the holistic or whole organism approach. However, since ethical considerations preclude the use of humans for such experiments, the predictive value for humans of whole organism experiments ultimately depends upon how closely the physiology, diet, and life pattern of the experimental test animal approaches that of human beings.

TABLE 2. MAJOR AND INTERMEDIATE EVENTS

TASK 1

CELL CULTURE STUDIES

- Photography of Prosthetic Surface Before and After Cell Growth
- Human Cell Cultures Grown on Prosthetic Surfaces
- Photography of Cell-Prosthetic Surface Interaction
- Parallel Implant Degradation Studies of Selected Implants
- Limited Carcinogenesis Studies of Selected Implants

TASK 2

DEVELOPMENT OF DYNAMIC TEST SYSTEM

- Optimization of Dynamic Test System
- Photography of Movement of Formed Blood Elements in Relation to Inner Wall of Tubing Made From Prosthetic Material
- Destruction of Platelets in Relation to Surface Topography
- Parallel Plasma Enzyme Degradation Studies

TASK 3

EVALUATION OF OTHER CONTRACTORS' MATERIALS BY TECHNIQUES DEVELOPED DURING LAST YEAR

- Prosthetic Surface Before Exposure to Blood
- Following *In Vivo* Exposure
- Following Exposure to Whole Blood *In Vitro*
- Following Exposure to Platelet-Rich Plasma *In Vitro*
- Evaluation in Dynamic Test System (If Requested)
- Cell Culture Biocompatibility Studies (If Requested)

TASK 4

SCANNING ELECTRON MICROSCOPY IN PARALLEL WITH REFLECTED LIGHT INTERFERENCE MICROSCOPY

- Examination of Selected Untreated Surfaces
- Examination of Selected Blood/Materials Interfaces
- Examination of Selected Tissue Cell/Materials Interfaces

TABLE 3

COLLABORATION WITH OTHER MEMBERS IN THE ARTIFICIAL HEART PROGRAM (IN PROGRESS OR SCHEDULED)

Investigator	Institution
Dr. J. C. Bokros	Gulf General Atomic, Inc. San Diego, California
Dr. R. D. Falb	Battelle Memorial Institute Columbus, Ohio
Dr. J. S. Byck	Union Carbide Corporation Bound Brook, New Jersey
Dr. A. Lande	Cornell Medical School New York, New York
Dr. F. E. Gould	Hydron Laboratories New Brunswick, New Jersey
Dr. Preston V. Murphy	Thermo Electron Corporation Waltham, Massachusetts
Mr. Robert Nemchin	Melpar, Inc. Falls Church, Virginia
Dr. M. Musolf	Dow Corning Corporation Midland, Michigan
Mr. I. Salyer	Monsanto Research Corporation Dayton, Ohio
Mr. R. L. Merker	Carnegie Mellon University Pittsburgh, Pennsylvania
Dr. Herman Greenberg	Polysciences, Inc. Rydal, Pennsylvania
Dr. W. P. O'Neill	Shell Development Company Emeryville, California
Mrs. Lita Nelson	Amicon Corporation Lexington, Massachusetts
Dr. Paul Predecki	Denver Research Institute University of Denver Denver, Colorado
Dr. Henry L. Lee, Jr.	Epoxylite Corporation Research Development Center S. El Monte, California

The fundamental concept and design of the current contract experiments makes use of a second approach to a bioassay system of a certain predictive value for humans. This approach is that of observing the interaction between different types of tissue cells and the candidate materials under carefully controlled experimental conditions in vitro. The tissue culture technique offers the advantage that human cells rather than animals can be used for the bioassay experiments. Also, the cells can be chosen for close correspondence with the intended implant site, e.g., bone cells for the bioassay of orthopedic implant materials, and aortic cells for aortic implant materials. Tissue culture studies of implant materials can give indications both of the degeneration of a candidate material in a biological environment, and its acceptance by different types of body cells. A fourth advantage is that tissue culture is rapid and can give indication of compatibility within a matter of days rather than months. The tissue culture technique used for the current contract studies is a new one, particularly suited for the study of implant candidate materials. It differs from previous methods in that the cells are grown directly on the surface of the implant being evaluated. The cells are thus in as intimate contact with the candidate material as they could be in the body. It was hypothesized that cells grown in direct contact with the candidate material might accelerate the deterioration (if any) of the implant, resulting in a more rapid release of toxic products if present. Such studies might therefore yield information qualitatively and quantitatively different from that obtained by previous indirect cell culture methods.

1. Materials and Methods. The materials evaluated by tissue culture and their conditions of evaluation are listed in Table 4.

TABLE 4

IN VITRO BIOCOMPATIBILITY STUDIES

Sterilized Prosthetic Material	Before Cell Growth	Establishment of Cell Cultures	Photography	Analysis of Cell Cultures for Growth Compared to that on Glass
Silicone Rubber	o(a)	o	o	o
Hydrin Rubber	o	o	o	o
Polypropylene	o	o	o	o
Teflon	o	o	o	o
Carbon Preparations	o	o	o	o
Hydron Preparations	o	o	o	o
Polypropylene microfiber Preparations	o	o	o	o

(a) Photographic Documentation

The technique for the cell culture experiments was the same as that used during last year's contract.[1] The method employed is particularly well suited for the preliminary bioassay screening of a variety of materials intended for use in the human body environment. The cells are grown directly on the surface of the implant candidate material, and the interaction between the living human cells and the material observed and photographed by means of a new microscopic technique.

Earlier cell toxicity experiments of implant materials were performed in the following manner:

a. Tissue culture cells were grown on a glass surface in a plasma clot, as a monolayer, in a hanging drop, or in an agar medium.
b. The test material was either introduced into the tissue culture chamber in the shape of a disk and deposited onto the already formed layer of cells, or introduced as a suspension in the nutrient culture medium after the cells had become established.
c. The toxicity or biocompatibility of the material was established either by measuring the zone of growth inhibition around the material disk, or by observing the signs of toxicity evident in the cell culture as a whole, as measured in terms of decreased rate of growth.

The results of these studies showed that this indirect technique to determine the toxicity did not predict the in vivo performance in humans in all cases.

A more recent method[2] which has shown very good correlation with in vivo results is carried out in the following manner:

a. The test material coupon is allowed to interact with the nutrient tissue culture medium for a given period of time at 37 C.
b. The nutrient medium which has interacted with the test material is then used for tissue cultures grown on glass coverslips in a conventional manner.
c. The degree of toxicity of the implant material to tissue cells is measured by the degree of growth inhibition induced.

In addition to making possible a study of the tissue culture cells directly on the candidate material surface, the tissue culture technique used in the current contract experiments incorporates features of both of these alternate experimental approaches: (1) The placing of the implant test coupon on top of a standard glass coverslip before inoculating the test tube with human cells makes it possible to study and compare the growth of the cells both on the implant surface itself and on the glass coverslip next to it, in one and the same test tube, and (2) The test coupon is incubated in the nutrient medium throughout the experiment.

While the direct interaction between the cells and the implant material is important, the research program incorporates a second feature previously ignored in tissue culture studies of implant materials, i.e., documentation of the implant material before, during, and after exposure to the sheet of cells grown in intimate contact with its surface.

The details of the cell culture procedures were given on Page 26 of the Annual Technical Report for the period June 29, 1967, to June 28, 1968. L-929 mouse fibroblast cells, Wish human amnion cells, and human aortic cells were used.

The photographic documentation of the cell-materials interfaces was accomplished by means of reflected light interference microscopy according to a technique developed at Battelle.[3,4]

This technique makes possible the microscopic photography of surfaces of opaque and transparent materials in three-dimensional color without pretreatment of the surface in any way. There is no need for replica preparation, vacuum deposition of carbon, or metal coating of the specimens. The possibility of direct documentation of the wet surface is of particular value in the case of those candidate surfaces which crack on drying. It also makes possible the photography of living tissue and blood cells growing directly on or adhering to opaque implant surfaces. The cell-prosthetic interface can thus be studied without the introduction of artifacts such as the inadvertent falling off of cells from the implant surface during the procedures of preparation of the specimen for microscopy.

The experimental record for each implant material consisted of one or all of the following:

a. Photographs of living cells growing on the candidate material
b. Cultures fixed in electron microscopic fixatives adapted from Sabatini, Bensch, and Burnett, 1963, for reflected light interference microscopy later
c. Cultures prepared for scanning electron microscopy examination

This information was analyzed for:

a. Evidence of cytotoxicity
    - changes in the cytoplasm of the cells; vacuoles, pseudopodic activity as compared with cells grown in glass control cultures
    - changes in the nucleus and nucleoli
b. Rate of growth as compared to that on glass
c. Morphology of the cells and the cell colonies.

Since several of the implant candidate materials examined during last year's contract did not show any signs of toxicity under these conditions of evaluation, it appears that the biological endpoint to aim for in the tissue culture studies should be complete lack of toxicity or growth retardation of human cells by the implant candidate material. The currently used tissue culture technique and analysis is simple yet sufficiently sensitive to make this distinction. It can be expected that in the future, a number of candidate materials will meet this criterion of cellular biocompatibility. It will then be logical to carry the tissue culture analysis still further in comparing the relative merits of the different materials. This can be done through studies of the DNA, RNA, and protein synthesis of the cells on the candidate materials surfaces.

2. Results.

Battelle Heparinized Surfaces. Eight types of autoclave-sterilized heparinized and unheparinized Battelle polymer surfaces were used as substrates for Wish human amnion cells grown directly on their surfaces. The interaction of the cells with the surfaces was studied and photographed by means of reflected light interference microscopy. It was noted that the TDMAC heparinized surfaces had a different range of cellular reactivity than did the Battelle styrene-grafted heparinized surfaces examined during the 1967 contract period (Table 5). For example, Wish human amnion cells grew on styrene-grafted heparinized silicone rubber (1967 evaluation) whereas they did not grow on the new TDMAC heparinized silicone rubber surfaces (1968 evaluation).

TABLE 5

BIOASSAY OF SURFACE COMPATIBILITY FOR CELL GROWTH - BATTELLE HEPARINIZED MATERIALS

Test Year	Rubber Substrate	Surface Layer	Growth of Cells	
			L-929	Wish
1967	Silicone	Hep. (Styrene grafted)	+	+
		None	+	+
1967	Hydrin	Hep. (Styrene grafted)	0	n.a.
		None	0	n.a.
1968	Silicone	Hep. (TDMAC method)	n.a.	0
		None	+	+
1968	Hydrin	Hep. (TDMAC method)	n.a.	+
		None	0	+

n.a. - Data not available

Secondly, in the case of Hydrin rubber, the 1967 evaluation carried out with L-929 mouse cells, showed complete absence of cell growth in replicate experiments with both styrene-grafted heparinized and unheparinized surfaces. It was therefore a surprise to find that the human Wish amnion cells grew well on the 1968 Hydrin surfaces.

The tissue culture studies were therefore repeated in 1968, with L-929 mouse fibroblast cells which did not grow on the previous samples of Hydrin rubber. The rationale for these studies was the hope that they would indicate whether the results with the Wish human cells in 1968 are due to an improvement in the Hydrin rubber used for the experiments, or whether the Wish human cells respond to Hydrin rubber in a way which is different from that of L-929 mouse cells. Representative experimental photographs of these experiments are shown in Figures 1 - 6. These repeat studies in 1968 confirmed the 1967 results in that there was a complete lack of growth of the mouse cells on the Hydrin rubber and an almost complete lack of growth of mouse cells on the adjacent glass cover-slip surrounding the Hydrin rubber patch in the experimental test tube. Figure 1 shows Wish human amnion cells growing at a normal rate on Hydrin rubber. The results of these experiments demonstrate that the Wish human amnion cells have a different reactivity to the Hydrin rubber than do the L-929 mouse cells.

Since there was such a marked difference between the apparent response of the mouse cells versus the human cells in the case of Hydrin rubber, representative specimens from these experiments were chosen for further study by scanning electron microscopy. These studies are reported under Task 4. Further experiments will be needed to establish whether the observed difference in reactivity between human and mouse cells has its basis in species specificity, or whether it is related to the type of tissue cell used.

Gulf General Atomic Carbon Surfaces. Tissue culture studies on these carbon surfaces were completed. They were performed on samples from the same lot number as that used for the blood compatibility studies reported later on. The carbon surfaces were used as substrates for Wish human amnion cells according to procedures described earlier. The results of these studies are summarized in Table 6.

TABLE 6. GULF GENERAL ATOMIC MATERIALS: SUMMARY OF TISSUE CULTURE COMPATIBILITY STUDIES

Type of Carbon	Surface Preparation	Sterilization at GGA	Treatment at BMI Before Use in Test	Results of Tissue Culture Test		
				Growth Rate	Cell Colony Appearance	Cellular Morphology
Silicon doped LTI	Polished one side through 1μ diamond	Shipped in 1:750 benzalkonium chloride	Soak 1 hour in 10 mg/ml heparin; rinsed in normal saline; steam autoclaved	Complete destruction of the cells		
Silicon doped LTI	Polished one side through 1μ diamond	None	Steam autoclaved	About 50% of controls	Round, discrete; tendency to curl around edges	Normal appearance
Silcon doped LTI	Polished one side through 1μ diamond	Steam autoclaved 250 F for 20 min at 230 psi steam	Resterilized by steam autoclaving prior to use	About 50% of controls	Round, discrete	Normal appearance
LTI Carbon	Polished one side through 1μ diamond	Shipped in 1:750 benzalkonium chloride	Soak 1 hour in 10 mg/ml heparin; rinsed in normal saline; steam autoclaved	Complete destruction of the cells		
LTI Carbon	Polished one side through 1μ diamond	None	Steam autoclaved	About 50% of controls	Round, discrete	Normal appearance
LTI Carbon	Polished one side through 1μ diamond	Steam autoclaved 250 F for 20 min at 230 psi steam	Resterilized by steam autoclaving prior to use	About 50% of controls	Round, discrete	Normal appearance
LTI Carbon	Polished one side through 1μ diamond	Heated at 130 C for 12 hours in vacuum	Steam autoclaving	Less than 50% of controls	Round, balled up, discrete	Normal appearance
LTI Carbon	Polished one side through 1μ diamond	Heated to 900 C for 1 hour in vacuum	Steam autoclaving	Slight reduction	Irregularly shaped; confluent	Normal appearance
CONTROL GLASS SURFACE -Bellco tissue culture glass	--	--	Steam autoclaving	CONTROL	Irregularly shaped; confluent	Normal appearance

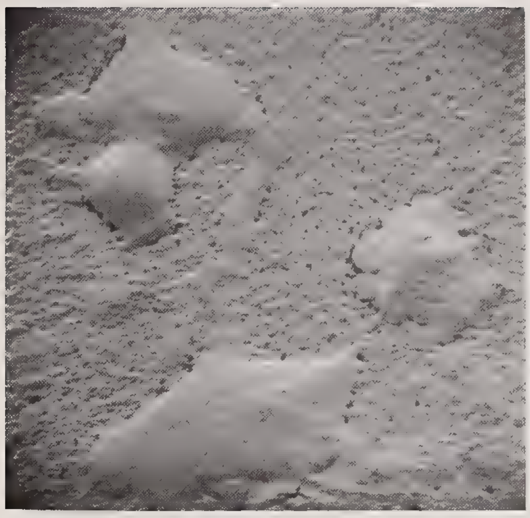

FIGURE 1.
CANDIDATE MATERIAL: HYDRIN RUBBER #3. SURFACE TREATMENT: NONE. STERILIZATION: WET AUTOCLAVING. USED FOR CELL CULTURE: WISH HUMAN AMNION CELLS. GROWTH AGE OF CULTURE: 72 HOURS. PHOTOGRAPHED BY SCANNING ELECTRON MICROSCOPY. APPROX. 1000x MAGNIFICATION. EXPERIMENTAL FINDINGS: THE CELLS APPEAR VERY TIGHTLY ATTACHED TO THE HYDRIN RUBBER.

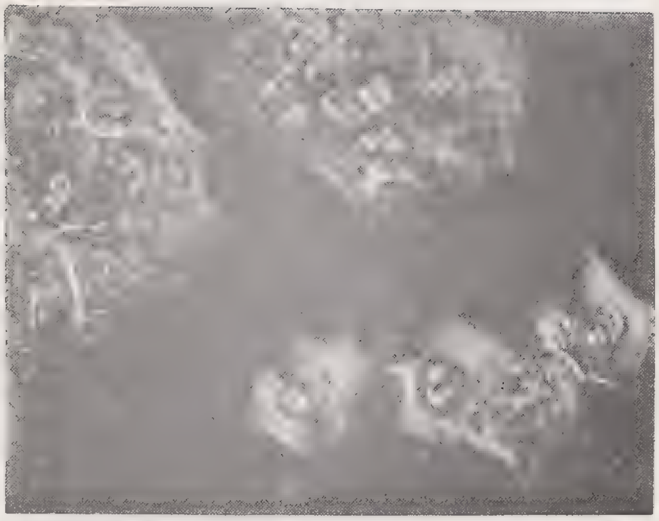

FIGURE 2.
CONTROL TISSUE CULTURE FOR MATERIAL IN FIGURE 1. MATERIAL: BOROSILICATE TISSUE CULTURE GLASS SURFACE PLACED ADJACENT TO AND PARTIALLY UNDERNEATH THE HYDRIN RUBBER SEEN IN FIGURE 1. STERILE PREPARATION. CELLS: WISH HUMAN AMNION. GROWTH AGE OF CULTURE: 72 HOURS. REFLECTED LIGHT INTERFERENCE MICROSCOPY. APPROX. 500x MAGNIFICATION. EXPERIMENTAL FINDINGS: THERE IS NO INDICATION OF RETARDATION OF GROWTH NOR OF ABNORMAL CELLULAR MORPHOLOGY DUE TO SUBSTANCES WHICH MAY HAVE BEEN RELEASED INTO THE TISSUE CULTURE MEDIUM FROM THE SAMPLE COUPON OF HYDRIN RUBBER CONTAINED IN THE SAME TEST TUBE. THE CELLS COMPARE WELL WITH THOSE GROWN ON GLASS IN TUBES NOT CONTAINING THE CANDIDATE MATERIAL.

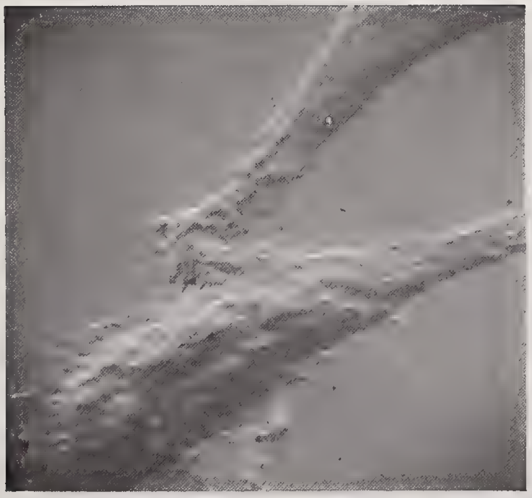

FIGURE 3.
CONTROL TISSUE CULTURE FOR MATERIAL IN FIGURES 5 AND 6. MATERIAL: BOROSILICATE TISSUE CULTURE GLASS. STERILE PREPARATION. CELLS:L-929 MOUSE FIBROBLASTS. GROWTH AGE OF CULTURE: 72 HOURS. SCANNING ELECTRON MICROSCOPY. APPROX. 2000x MAGNIFICATION. EXPERIMENTAL FINDINGS: IN ADDITION TO THE LONG, NARROW PROTOPLASMIC EXTENSIONS WHICH COULD BE SEEN BY LIGHT MICROSCOPY THE CELLS ARE SEEN TO BE INTERCONNECTED BY MANY VERY FINE FIBRILS.

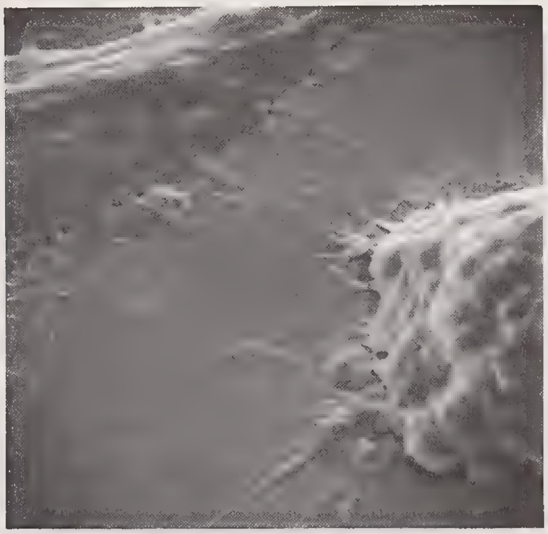

FIGURE 4.
CONTROL TISSUE CULTURE FOR MATERIAL IN FIGURES 5 AND 6. MATERIAL: BOROSILICATE TISSUE CULTURE GLASS. STERILE PREPARATION. CELLS: L-929 MOUSE FIBROBLASTS. GROWTH AGE OF CULTURE: 72 HOURS. SCANNING ELECTRON MICROSCOPY. APPROX. 5000x MAGNIFICATION. EXPERIMENTAL FINDINGS: THIS PICTURE SHOWS THE FINE FIBRILLAR INTERCELLULAR CONNECTIONS EVEN MORE CLEARLY THAN IN FIGURE 3.

FIGURE 5.
CANDIDATE MATERIAL: HYDRIN RUBBER #3 (SAME LOT NO. AS THAT USED IN EXPERIMENTS ILLUSTRATED IN FIGURE 1). SURFACE TREATMENT: NONE. STERILIZATION: WET AUTOCLAVING. USED FOR CELL CULTURE. CELLS: L-929 MOUSE FIBROBLASTS. GROWTH AGE OF CULTURE: 72 HOURS. REFLECTED LIGHT INTERFERENCE MICROSCOPY. APPROX. 500x MAGNIFICATION. EXPERIMENTAL FINDINGS: THERE IS A COMPLETE LACK OF GROWTH OF THE MOUSE CELLS ON THE SAME TYPE OF CANDIDATE MATERIAL WHICH WAS SHOWN IN FIGURE 1 TO BE ADEQUATE FOR THE SUPPORT OF HUMAN CELLS.

FIGURE 6.
CANDIDATE MATERIAL: SAME AS IN FIGURE 5. SURFACE TREATMENT AND BIOLOGICAL EXPOSURE: SAME AS IN FIGURE 5. SCANNING ELECTRON MICROSCOPY. APPROX. 1000x MAGNIFICATION. EXPERIMANTAL FINDINGS: SCANNING ELECTRON MICROSCOPIC EXAMINATION CONFIRMED THE LACK OF ANY INTACT MOUSE CELLS ON THE HYDRIN RUBBER SURFACE.

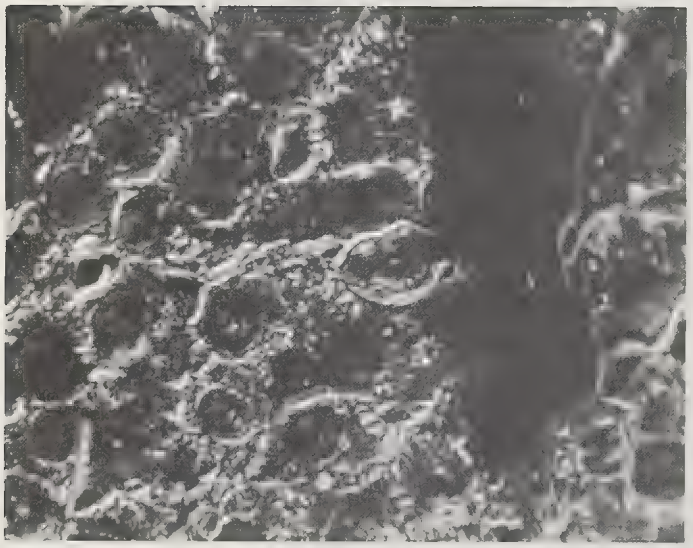

FIGURE 7.
CONTROL TISSUE CULTURE FOR MATERIALS IN FIGURES 8 AND 9. MATERIAL: BOROSILICATE TISSUE CULTURE GLASS SURFACE. STEAM AUTOCLAVED. CELLS: WISH HUMAN AMNION. GROWTH AGE OF CULTURE: 72 HOURS. FIXATION: SABATINI-BENSCH. REFLECTED LIGHT INTERFERENCE MICROSCOPY. APPROXIMATELY 600x MAGNIFICATION.

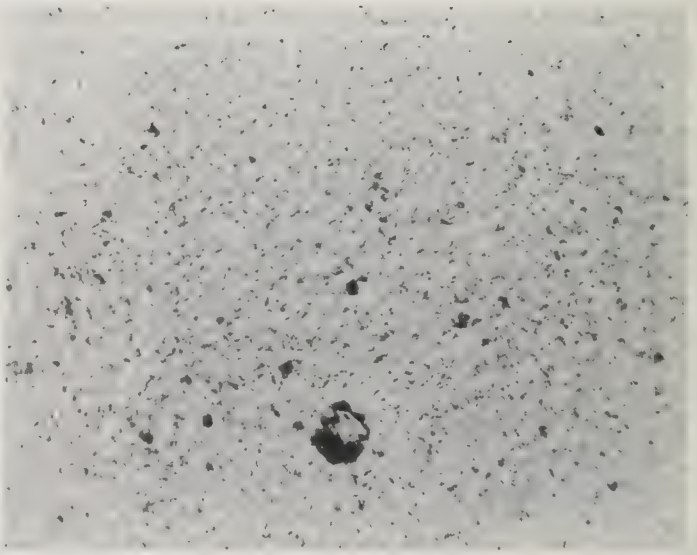

FIGURE 8.
CANDIDATE MATERIAL: LTI CARBON. POLISHED ONE SIDE THROUGH 1μ DIAMOND. SHIPPED IN 1:750 BENZALKONIUM CHLORIDE. SOAKED 1 HOUR IN 10 MG/ML HEPARIN; RINSED; STEAM AUTOCLAVED. CELLS: WISH HUMAN AMNION. GROWTH AGE OF CULTURE: 72 HOURS. FIXATION: SABATINI-BENSCH. REFLECTED LIGHT INTERFERENCE MICROSCOPY. APPROXIMATELY 600x MAGNIFICATION. THE PHOTOGRAPH SHOWS A COMPLETE ABSENCE OF CELLS ON THIS SURFACE.

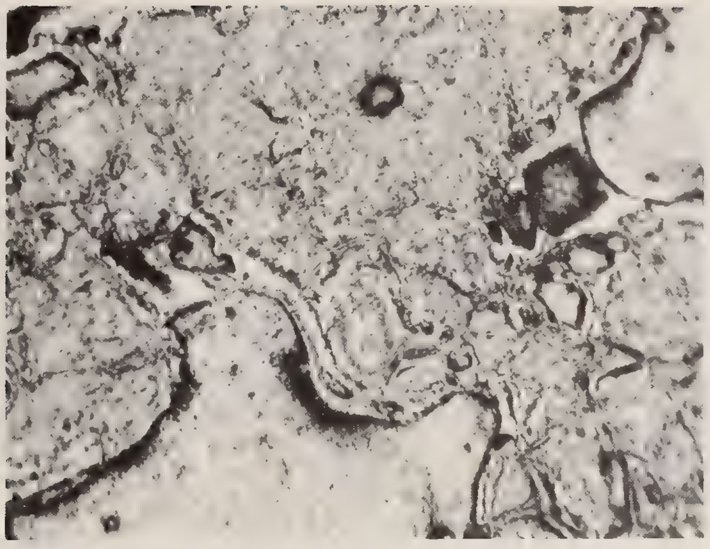

FIGURE 9.
CANDIDATE MATERIAL: LTI CARBON. POLISHED ONE SIDE THROUGH 1 μ DIAMOND. HEATED TO 900 C FOR 1 HOUR IN VACUUM AT GGA; STEAM AUTOCLAVED AT BATTELLE. CELLS: WISH HUMAN AMNION. GROWTH AGE OF CULTURE: 72 HOURS. 72 HOURS. FIXATION: SABATINI-BENSCH. REFLECTED LIGHT INTERFERENCE MICROSCOPY. APPROXIMATELY 600x MAGNIFICATION. THE PHOTOGRAPH SHOWS AN IRREGULARLY SHAPED, ALMOST CONFLUENT SHEET OF CELLS COVERING THE GREATER PORTION OF THE SURFACE: THE GROWTH RATE OF THE CELLS ON THIS CANDIDATE MATERIAL WAS ONLY SLIGHTLY LESS THAN THAT OF CONTROL CULTURES ON GLASS.

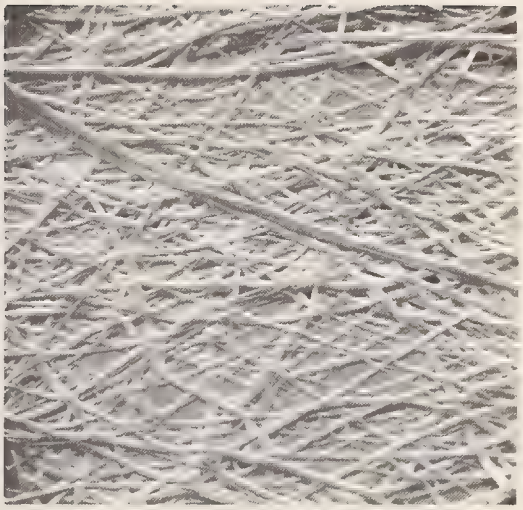

FIGURE 10.
CANDIDATE MATERIAL: UNION CARBIDE POLYPROPYLENE FIBER MATS (9079-11C SERIES). SURFACE TREATMENT: 4100 A PARYLENE COATING. SCANNING ELECTRON MICROSCOPY. 1000x MAGNIFICATION.

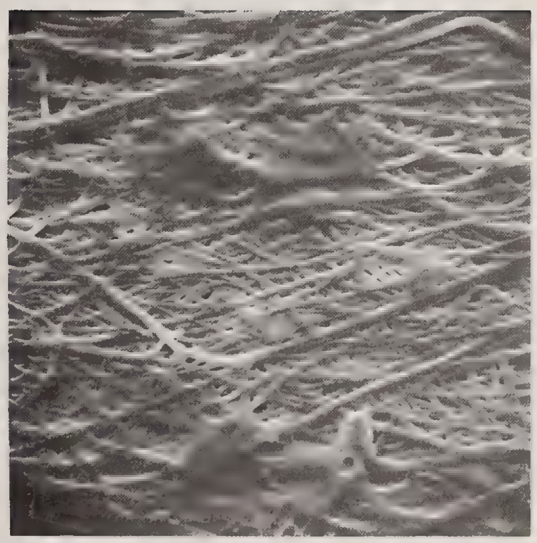

FIGURE 11.
CANDIDATE MATERIAL: SAME AS IN FIGURE 10. SURFACE TREATMENT: SAME AS IN FIGURE 10. STERILIZATION: AUTOCLAVING. USED FOR CELL CULTURE. CELLS: WISH HUMAN AMNION. GROWTH AGE OF CULTURE: 72 HOURS. SCANNING ELECTRON MICROSCOPY. 1000x MAGNIFICATION.

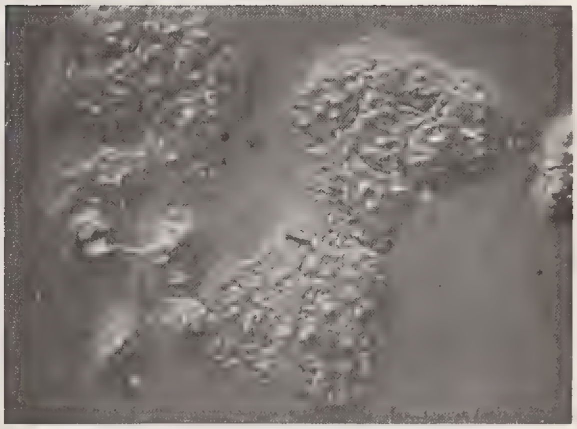

FIGURE 12.
CONTROL TISSUE CULTURE FOR MATERIAL IN FIGURE 13. MATERIAL: BOROSILICATE TISSUE CULTURE GLASS. STERILE PREPARATION. CELLS: WISH HUMAN AMNION. GROWTH AGE OF CULTURE: 72 HOURS. FIXATION: SABATINI-BENSCH. REFLECTED LIGHT INTERFERENCE MICROSCOPY. APPROX. 500x MAGNIFICATION.

As can be seen from the table both the plain carbon surfaces and the silicon doped carbon surfaces are able to support the growth of tissue culture cells in direct contact with the surface. On the other hand, a complete destruction of the tissue cells occurred on carefully rinsed benzalkonium-heparin treated carbon surfaces, tested in parallel. This was the case both with the heparinized silicon-doped carbon surfaces as well as with the nonsilicon treated carbons. Of the eight carbon formulations evaluated, the LTI carbon which had been heated to 900 C for 1 hour in vacuum was the only carbon surface which supported the growth of human cells at a rate similar to that which is achieved on parallel tissue-culture-glass control surfaces. Examples of the photographic documentation of these experiments are shown in Figures 7 through 9.

Hydron Surfaces. Two types of Hydron surfaces were received from Dr. F. E. Gould, Hydron Laboratories, New Brunswick, New Jersey:

HL-11-178	Modified Hydron film
HL-11-194	Unmodified Hydron film

The tissue culture studies of these materials were completed. It was found that the unmodified Hydron surfaces were highly compatible with human cells, and supported the growth of these cells at a rate comparable to that achieved on glass control coverslips. Steam autoclaved samples of the modified HL-11-178 Hydron material did not support any growth of cells, however. The reason for this might be that these samples had an acidifying effect on the tissue culture growth medium. Since these particular candidate materials are able to withstand boiling, it is possible that this toxic effect might be eliminated in future experiments by boiling the samples prior to the biocompatibility studies.

Union Carbide Microfiber Mats for "Heteroprostheses." At the request of the Program Office, cell culture studies with the microfiber materials, received from Union Carbide were performed in preparation for the extensive studies of microfibers to be initiated on May 1, 1969, under the amended contract. Three sets of glass slides coated with micron-range-diameter polypropylene fibers were used for these experiments. The difference between the sets is in the Parylene coating. Set 9079-11A is uncoated; set 9079-11B has a 3400 Å coating; and set 9079-11C has a 4100 Å coating. These microfiber specimens were used as substrates for tissue cultures. The cultures were studied and photographed by reflected light interference microscopy. It was found that the visualization of living cells within the fibermat was difficult in the case of fibers coated with Parylene.

Further studies with fixed tissue cell preparations, reflected light interference microscopy, and scanning electron microscopy were therefore made. These experiments showed that all three types of fibermats were able to support the growth of the Wish human amnion cells. Further details of the SEM studies are given under Task 4. Examples of the photographic documentation of these experiments are shown in Figures 10 through 13.

Aortic Cells. Tissue cells derived from human aorta were obtained from the Flow Laboratories. These cells originated from the cell strain described by Behbehani et al.[5]

While possessing the advantage of closer correspondence to the intended implant site of artificial heart candidate materials, the aortic cells have at least two practical drawbacks as compared with the other heteroploid cell strains used in previous experiments during the current research project:

(1) These human cells, as with other cells with a diploid chromosome number, can only be carried in vitro for a limited period of time of about 30 passages before becoming senescent and starting to degenerate. However, the cell strain can be maintained for longer periods of time by careful culturing and by preparing large numbers of stock cultures, followed by subsequent storage of the cells in liquid nitrogen. The cells can then be revived from their frozen state as the experimental requirements dictate.

(2) Compared with the other cells used in previous studies, the aortic cells grow very slowly in tissue culture. Whereas, the Wish human amnion cells can be split 1:10 or 1:20 every 7 days of culture, the aortic cells can only be split in the ratio 1:2 in the same period of time. Therefore, it can be expected that the bioassay of materials by means of aortic cell cultures will require a correspondingly longer experimental period than is the case with the Wish human amnion cells which require a period of 3 days.

Attempts are being made to grow these cells in the quantities needed for the bioassay experiments.

Carcinogenesis Studies. Most immediate failures of cardiovascular "homoprosthesis" materials are related to problems in the category of blood compatibility. As better materials are made available, and as the "heteroprosthesis" concept finds increased acceptance, it will become increasingly important to develop biological criteria which will aid in predicting the probable long-term performance of these materials in the human body. One such criterion which one would hope for is their lack of carcinogenicity to human tissue cells.

Tissue culture carcinogenesis studies have been initiated during the current contract period. The results of these studies will not be available until the completion of the contract period. The technology developed during the current program offers three advantages over previous carcinogenesis studies related to materials:

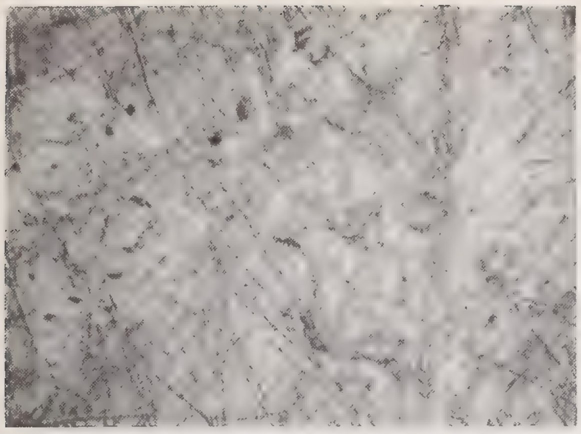

FIGURE 13.
CANDIDATE MATERIAL: UNION CARBIDE POLYPROPYLENE FIBER MATS (9079-11A SERIES). SURFACE TREATMENT: NONE. STERILIZATION: AUTOCLAVING. USED FOR CELL CULTURE. CELLS: WISH HUMAN AMNION. GROWTH AGE OF CULTURE: 72 HOURS. FIXATION: SABATINI-BENSCH. REFLECTED LIGHT INTERFERENCE MICROSCOPY. APPROX. 500x MAGNIFICATION.

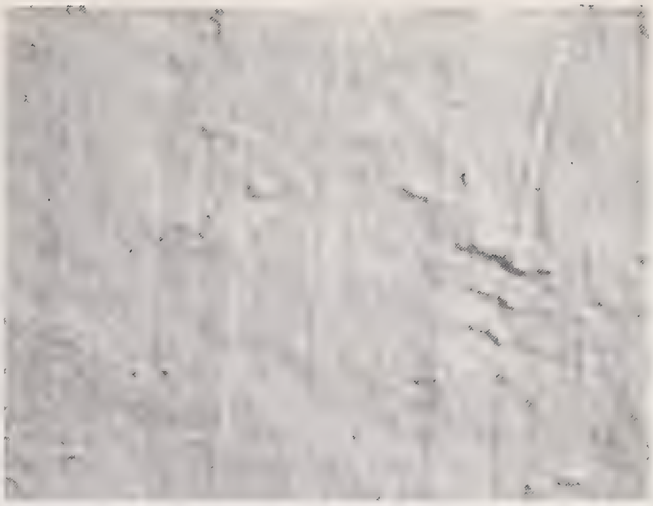

FIGURE 14.
CANDIDATE MATERIAL: SILICONE RUBBER, DOW-CORNING SILASTIC 372. SURFACE TREATMENT: WET AUTOCLAVED FOR 15 MIN. AT 15 LBS PRESSURE; RINSED WITH NORMAL SALINE. EXPOSURE TO BIOLOGICAL ENVIRONMENT: IN CONTACT WITH STERILE TISSUE CULTURE NUTRIENT MEDIUM AT 37 C FOR 3 DAYS. FIXED WITH SABATINI-BENSCH FIXATIVE AS WOULD BE USED FOR TISSUE CULTURE CELLS GROWN ON THE CANDIDATE MATERIAL. PHOTOGRAPHED BY REFLECTED LIGHT INTERFERENCE MICROSCOPY. APPROXIMATELY 500x MAGNIFICATION. EXPERIMENTAL FINDINGS: NO MICROSCOPICALLY DETECTABLE CHANGE IN THE CANDIDATE MATERIAL (AT THIS LEVEL OF MAGNIFICATION) ON STERILIZATION.

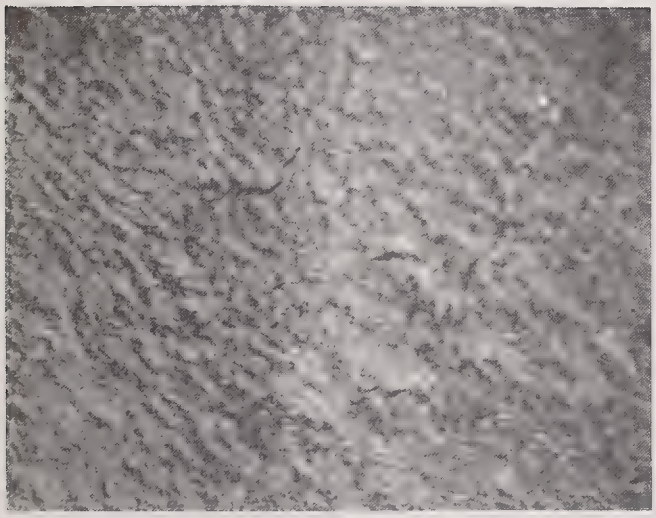

FIGURE 15.
CANDIDATE MATERIAL: SILICONE RUBBER, DOW-CORNING SILASTIC 372. SURFACE TREATMENT: HEPARINIZED BY BATTELLE TDMAC TECHNIQUE. STERILIZATION: WET AUTOCLAVED FOR 15 MINUTES AT 15 LBS. PRESSURE; RINSED WITH NORMAL SALINE. PHOTOGRAPHED BY REFLECTED LIGHT INTERFERENCE MICROSCOPY. APPROX. 500x MAGNIFICATION. EXPERIMENTAL FINDINGS: THE TREATED SURFACE BECOMES MORE GRANULAR ON AUTOCLAVING, AND THE CRACKS SEEN IN THE NONSTERILE SPECIMEN ALMOST DISAPPEAR.

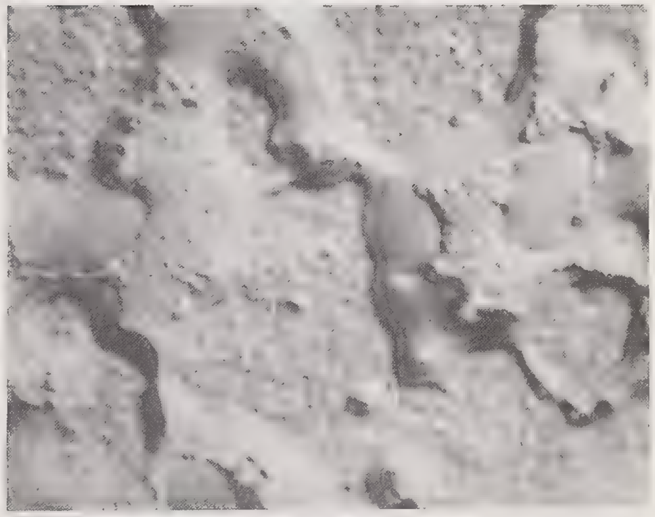

FIGURE 16.
CANDIDATE MATERIAL: SILICONE RUBBER, DOW-CORNING SILASTIC 372. SURFACE TREATMENT: SAME AS IN FIGURE 15. STERILIZATION: SAME AS IN FIGURE 14. EXPOSURE TO BIOLOGICAL ENVIRONMENT: SAME AS IN FIGURE 14. PHOTOGRAPHED BY REFLECTED LIGHT INTERFERENCE MICROSCOPY. APPROX. 500x MAGNIFICATION. EXPERIMENTAL FINDINGS: CONTRARY TO THE CASE WITH THE UNTREATED SILICONE RUBBER, ILLUSTRATED IN FIGURE 14, THE HEPARINIZED SILICONE RUBBER UNDERGOES TOPOGRAPHICAL CHANGES DUE TO THE ABOVE SERIES OF TREATMENTS.

(1) The tissue cells can be grown in direct contact with the implant material
(2) Changes in the appearance and growth pattern can be recorded by time-lapse photography of the cell-materials interphase
(3) Human tissue cells of various types can be used.

It is therefore proposed that, in those cases where the results of the short-term tissue culture studies suggest the need for further investigation, tissue culture carcinogenesis studies be initiated as directed by the Program Office. While carcinogenesis in vivo in humans is estimated to occur over a period of 15 to 30 years, the in vitro process in human cells usually takes less than one year, making this investigation feasible in the evaluation of long-term candidate implant materials.

Implant Degradation Studies. The following studies have been initiated on representative implants before and after exposure to the in vitro environment with and without the presence of cells:

(1) Microscopic examination and photography of the surface by reflected light interference microscopy and/or scanning electron microscopy. Examples of these studies are shown in Figures 14 to 16.
(2) Tensile strength measurements. The results of these studies will be available at a later date.

Task 2. Dynamic Test System.

Since many of the most promising materials so far tested during this project are not transparent or available in the form of films, attempts are being made to develop a dynamic system which will allow the reflected light interference photography of the surface interaction from above, rather than by transmitting light through a more or less optically clear polymer membrane viewed from below.

The efforts during the current project year are being concentrated in two areas:
(1) Optimization of the unit
(2) Testing of additional candidate materials.

Biochemical studies of protein denaturation and enzyme inactivation will be carried out in parallel with the cellular studies. This task is still in progress and has not been completed.

1. Materials and Methods. The materials used for these experiments to date have been Silastic tubing 602-265 with an inside diameter of 0.062". The experimental samples were heparinized according to the Battelle TDMAC technique. The initial experiments were carried out according to the procedure developed during last year's contract for dynamic in vitro testing of artificial heart implant materials in contact with blood. This procedure was described on Page 31 of the Annual Technical Report on last year's project. Before adding the blood, the tubing was rinsed carefully with filtered normal saline to remove loose particles which might interfere with the experiment.

Also, because of the uneven character of the test surfaces and consequent difficulty in identifying platelets against such a test surface, certain later experiments were carried out in a simple dynamic system consisting of a loop of tubing made of the candidate material through which blood was allowed to flow for a period of time. At the end of the period, the tubing was gently rinsed with normal saline, and the tubing opened up and examined microscopically for presence of adhering formed blood elements.

2. Results. The TDMAC heparinization technique resulted in a surface roughness considerably higher than a similar surface, heparinized according to the earlier styrene radiation-grafting procedure. Also, in certain cases, the roughness and topography of the TDMAC heparinized surfaces was such as to interfere with the visualization of deposited platelets in the dynamic test system. While some TDMAC surfaces caused clearly visible deposition of platelets, others did not appear to do so. In the latter, it was not possible to determine with confidence whether this apparent lack of platelets was indeed due to nonadhesion of platelets or only to the inability to visualize them against an uneven surface with a granularity of the same order as platelets.

In an attempt to resolve this question, different lots of TDMAC heparinized tubing and patches were examined in parallel with unheparinized silicone rubber tubing and patches, both in the dynamic test system and in the stationary test system developed during the last year's program. It was found that the microscopic appearance as well as cellular adherence to the TDMAC heparinized surfaces varied considerably from lot to lot. Thus, one lot was found to be very coarse in texture at a magnification of 500 times, covered with a choppy, streaky surface coating, irregularly distributed across the silicone rubber surface. These surfaces caused marked and patchy adherence of platelets and red blood cells when tested in a stationary system. Another lot of TDMAC heparinized surfaces was finely granular in texture and covered with many irregular protrusions between two and five microns across. These surfaces caused a decreased adherence of platelets from platelet-rich plasma as compared with untreated silicone rubber. However, this decreased platelet adhesion was associated with an increased adherence of white blood cells upon exposure to whole blood.

Like the cellular biocompatibility described above, the interaction of the TDMAC heparinized surfaces with blood in vitro also appears to be different from that previously observed with the styrene-grafted heparinized surfaces. While the reproducibility from sample to sample is still low, a new pattern of non-adhesiveness of platelets is emerging, as opposed to the marked platelet-adhesiveness to the styrene-grafted heparinized surfaces.

Task 3. Investigation of Other Contractors' Materials.

The current research program has provided for increased evaluation of other contractors' materials as directed by the Artificial Heart Program Office. Nine groups of materials have been investigated during this report period. They are: (1) Heparinized and nonheparinized carbon surfaces developed by Gulf General Atomic, Inc., (2) Polymer surfaces heparinized according to the TDMAC method developed at Battelle's Columbus Laboratories under another contract, (3) Experimental fiber mats from Union Carbide Company, (4) Hypalon coverslips from Thermo Electron, Inc., (5) Heparinized polyurethane-treated polymer surfaces from Battelle's Columbus Laboratories, (6) Carboxymethylcellulose surfaces from Melpar, Inc., (7) Oxygenator membrane surfaces from Cornell Medical School, (8) Hydron surfaces from Hydron Laboratories, and (9) Ten formulations of ethylene/ethyl acrylate polyelectrolytes from Union Carbide Company. In addition to the cellular compatibility studies reported above, the following studies have been completed to date:

Photographic Documentation of Prosthetic Materials Before and After Contact with Blood In Vitro and In Vivo. The rationale behind these experiments is that the differential adherence of blood formed elements to the surface of a foreign material varies with and is characteristic for each material. This differential adherence is one index of the blood compatibility of the surface.

1. Materials and Methods. All the materials listed above, with the exception of the microfiber materials, have been or are in the process of evaluation. The technique and procedures for these experiments were described in detail on Page 5 of the Annual Technical report on last year's contract.

2. Results.

Battelle TDMAC Heparinized Surfaces. Photographic documentation of TDMAC heparinized silicone rubber surfaces were carried out in static *in vitro* tests:

a. Before and after alcohol and wet autoclave sterilization
b. Alcohol and wet autoclave sterilized surfaces before and after exposure to whole blood for one hour at 37 C in humidified air in incubator
c. Alcohol and wet autoclave sterilized surfaces before and after exposure to gravity-sedimented, platelet-rich plasma for one hour at 37 C in humidified air in an incubator.

As noted above under the dynamic experiments, these new type heparinized surfaces differed markedly from those heparinized according to the styrene-grafting technique which were examined during last year's contract period. This difference is evident both with respect to microscopic topography and biological reactivity as illustrated in Figures 14 to 16. The lack of uniformity in microscopic topography and biological reactivity, particularly in the earlier lots of these new surfaces appears to be related to the amount of the TDMAC technique reagents still present on the surface at the time of heparinization. With more careful rinsing of the surfaces prior to heparinization, they became less erratic in appearance and interaction with blood.

Gulf General Atomic Carbon Surfaces. An inverse relationship between crystallinity and platelet adhesion was noted during last year's contract in the case of the carbon surfaces submitted by Gulf General Atomic, Inc. At the December, 1967, Artificial Heart Contractors' Meeting, Dr. Bokros described the low temperature isotropic (LTI) carbons as being poorly crystalline in structure with no preferred orientation, whereas the high temperature isotropic (HTI) samples were shown to be turbostratic carbons with a two-dimensional crystalline structure. The crystalline HTI carbon surfaces showed minimal adhesion of platelets whereas the poorly crystalline LTI surfaces induced marked adhesion of platelets and also of red blood cells. It is of interest to note here that the DAG 154 Graphite-Benzalkonium-Heparin surfaces which were shown to cause little or no adhesion of platelets (last year's contract) also have a crystalline carbon phase, in this case three-dimensional in nature.

The Gulf General Atomic surfaces submitted during this contract period were all LTI carbon surfaces. They represented different types of surface treatments and techniques of sterilization as listed in Table 6. The following types of studies were carried out in static *in vitro* tests:

a. Reflected light interference microscopy of the test specimens before and after exposure to whole blood for one hour at 37 C in humidified air in incubator
b. Reflected light interference microscopy of the test specimens before and after exposure to gravity-sedimented, platelet-rich plasma for one hour at 37 C in humidified air in an incubator
c. Scanning electron microscopy of selected blood/implant interfaces - reported later under Task 4.

Representative photographs are shown in Figures 17 - 20.

In general, the Gulf General Atomic surfaces submitted were found to be very smooth, and similar in microtopography at 500 times magnification. In agreement with our studies of these materials during last year's contract, all the LTI surfaces submitted were found to attract platelets to varying degrees. The silicon-doped LTI, before sterilization or heparinization, induced the least degree of platelet adhesion, and also did not promote the aggregation of platelets. Based upon our previous experience with other candidate materials, the even deposition of single platelets *in vitro*, such as in this case, has correlated well with good *in vivo* performance. Generally speaking, with the exception of the specimens sterilized by dry heat, none of the LTI specimens induced marked aggregation of platelets. A detailed report of these studies has been forwarded to the Gulf General Atomic Company.

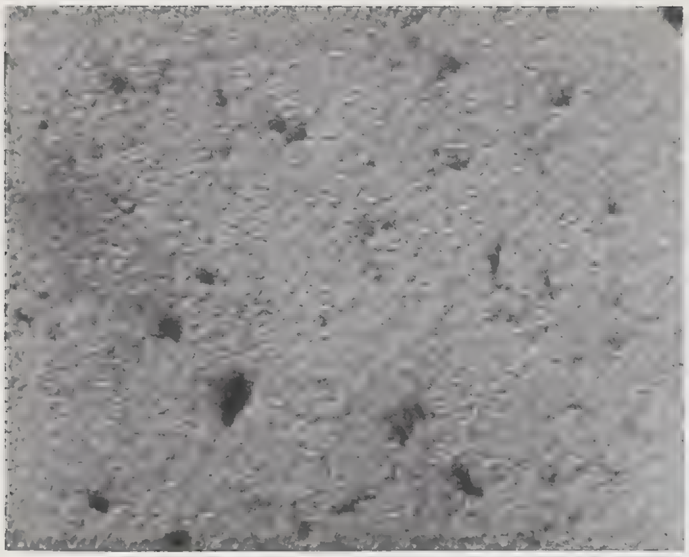

FIGURE 17.
CANDIDATE MATERIAL: LTI CARBON. GULF GENERAL ATOMIC NO. 4344-75. SURFACE PREPARATION: ONE SIDE POLISHED THROUGH 1µ DIAMOND. STERILIZATION TREATMENT: STEAM-AUTOCLAVED AT GULF GENERAL ATOMIC AT 250 F FOR 20 MINUTES AT 230 PSI STEAM. PHOTOGRAPHED BY REFLECTED LIGHT INTERFERENCE MICROSCOPY. APPROX. 500x MAGNIFICATION.

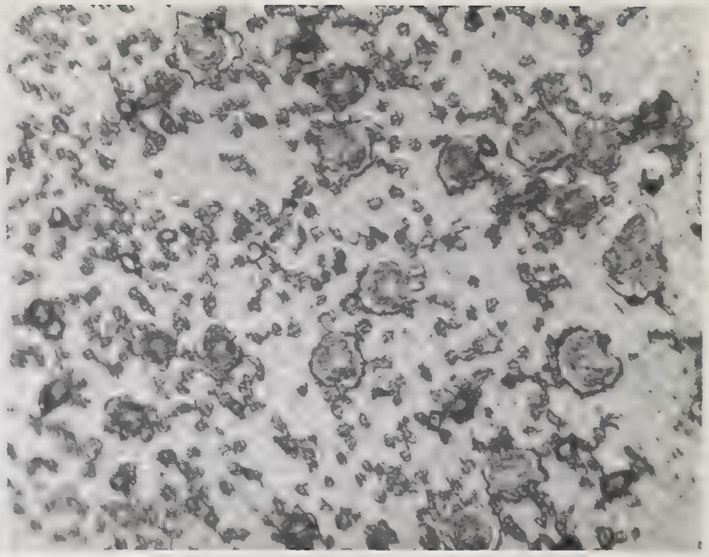

FIGURE 18.
CANDIDATE MATERIAL: LTI CARBON. GULF GENERAL ATOMIC NO. 4344-75. SURFACE PREPARATION: ONE SIDE POLISHED THROUGH 1µ DIAMOND. STERILIZATION TREATMENT: NONE. EXPOSED TO PLATELET-RICH PLASMA PREPARED FROM BMI DONOR BLOOD NO. 94, COLLECTED AT UNIVERSITY HOSPITAL IN RED CROSS BAG. THE PLASMA-MATERIAL INTERFACE WAS PHOTOGRAPHED FOLLOWING FIXATION WITH SABATINI-BENSCH FIXATIVE. PHOTOGRAPHED BY REFLECTED LIGHT INTERFERENCE MICROSCOPY. APPROX. 500x MAGNIFICATION. EXPERIMENTAL FINDINGS: MODERATE ADHERENCE OF MOSTLY SINGLE PLATELETS AND OCCASIONAL LEUKOCYTES AND ERYTHROCYTES.

FIGURE 19.
CANDIDATE MATERIAL: SAME AS IN FIGURE 18. STERILIZATION TREATMENT: NONE. EXPOSURE TO PLASMA: SAME AS IN FIGURE 18. PHOTOGRAPHED BY SCANNING ELECTRON MICROSCOPY. APPROX. 1000x MAGNIFICATION. EXPERIMENTAL FINDINGS: MANY DEFORMED, FLATTENED, SINGLE PLATELETS STRETCHED OUT ON THE SURFACE OF THE CANDIDATE MATERIAL. ALSO SHOWN ARE "FOOTPRINTS" OF BOTH ERYTHROCYTES AND PLATELETS WHICH HAD BECOME DISLODGED FROM THE SURFACE DURING THE PREPARATION OF THE SPECIMEN FOR SCANNING ELECTRON MICROSCOPY. THE SPATTER SURROUNDING THE ONE ERYTHROCYTE REMAINING SUGGESTS THAT A VIGOROUS INTERACTION OCCURRED ON CONTACT BETWEEN THE MATERIAL AND THE HUMAN BLOOD.

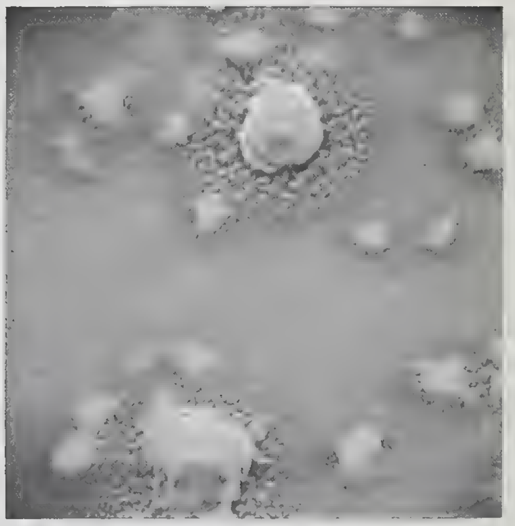

FIGURE 20.
CANDIDATE MATERIAL: SAME AS IN FIGURE 18. TREATMENT: SAME AS IN FIGURE 19. PHOTOGRAPHED BY SCANNING ELECTRON MICROSCOPY. APPROX. 2000x MAGNIFICATION. EXPERIMENTAL FINDINGS: THIS PICTURE CLEARLY SHOWS THE MARKED SPATTER SURROUNDING TWO ERYTHROCYTES WHICH BECOME ADHERENT TO THE SURFACE. TO A LESSER DEGREE THIS SPATTERING EFFECT IS SEEN WITH THE PLATELETS AS WELL.

Monsanto Research Corporation (Dayton) Materials. Valuable further information was received concerning the commercial polymers submitted by the Monsanto Research Corporation (Dayton) for blood compatibility studies during the first year of this contract. The information consisted of data regarding the sample number, source, chemical composition, crystallinity, type of manufacturing process, clotting test results, and molding conditions of each polymer. On comparing this information with the results of our blood compatibility studies, it became apparent that the crystallinity of this particular series of materials appeared to correlate inversely with the *in vitro* platelet adsorption to the untreated, unsterilized, saline-rinsed surfaces. Thus, there was no or negligible platelet adhesion to highly crystalline (80-90 percent according to the Monsanto information sheet) materials such as polyethylene (low pressure) and to polypropylene (isotactic). On the other hand, there was marked platelet adhesion to noncrystalline materials (0 percent according to the Monsanto information sheet) as polystyrene (atactic) and styrene/acrylonitrile copolymer (72/28). It must be noted, however, that there are also compositional differences which may be of greater importance. A similar inverse relationship between the crystallinity and platelet adhesion was noted earlier in the report in the case of carbon surfaces submitted by Gulf General Atomic.

Blood Oxygenator Membranes. Blood oxygenator membranes were received from Dr. A. J. Lande of the New York Hospital-Cornell Medical Center. A pilot study was performed demonstrating the feasibility and usefulness of studying these membranes by means of the techniques developed at Battelle during the current contract. Photographic documentation of the blood-membrane interaction was carried out following successful use *in vivo*. A marked adherence of irregularly distributed cellular aggregates, primarily of red blood cells was noted.

Task 4. Scanning Electron Microscopy.

From studies conducted by means of reflected light microscopy during last year's contract, it appeared that the technique of scanning electron microscopy might be valuable in further establishing the suitability of a candidate material which has already passed other *in vivo* and *in vitro* tests.

1. Materials and Methods. The specimens used for these experiments were of four kinds: (1) Silicone rubber before and after different techniques of sterilization, (2) Hydrin rubber surfaces before and after tissue culture on the surfaces, (3) Gulf General Atomic surfaces before and after interaction with whole blood and platelet-rich plasma, and (4) Union Carbide polypropylene microfibers before and after cell culture.

A Cambridge "Stereoscan" scanning electron microscope (SEM) was used for these investigations. These studies were carried out with the assistance of Mr. E. Muenze.

It was found that the techniques and fixation methods developed by Dr. A. Hegyeli during last year's contract for the preservation of the blood/materials and the tissue cells/materials interface were immediately applicable to the above program. By fixing the tissue cells with this technique prior to vacuum evaporation of gold onto the surface of the cells/materials interface, it was possible to arrive at a preparation nearly identical to that observed in the living cell cultures as photographed by reflected light interference microscopy. The sample preparation was monitored by reflected light interference microscopy of the specimens before and after exposure in the SEM.

2. Results.

Silicone Rubber Under Different Conditions of Sterilization. Figures 21 to 24 show examples of these experiments. They depict the interaction of platelet-rich plasma with silicone rubber prepared in different ways. The scanning electron microscope pictures show clearly the marked aggregation of platelets which occurs on the autoclaved surface as compared with the untreated surface. It also shows differences between the two surfaces in the deposition of noncellular material. These differences could not be resolved by the reflected light interference microscopy.

Hydrin Rubber Surfaces Before and After Tissue Culture. Figures 1, 2, 3 and 4 show examples of these experiments. Wish human amnion cells are seen to grow well on the Hydrin rubber while there is complete absence of growth of the L-929 mouse cells on the same surfaces. Scanning electron microscopy further revealed that the occasional cells which were seen on the coverslip surrounding the Hydrin rubber coupon in the L-929 cultures were actually disintegrated ghost cells. This could not be resolved with light microscopy.

Gulf General Atomic Surfaces Before and After Interaction with Whole Blood and Platelet-Rich Plasma. Figures 19 and 20 show examples of these experiments. The photographs show the very violent interaction between platelets and non-sterile LTI carbon surfaces resulting in changes in size and shape of the platelets, and also other formed blood elements. There was adherence of formed blood elements to autoclaved LTI carbon surfaces, and also a tendency for the platelets to aggregate. Higher magnification demonstrated, as was also the case with the silicone rubber surfaces, that the autoclaved surface induces a marked build-up of noncellular material as well, and that the formed blood elements adhere to this noncellular material by means of processes of varying sizes and shapes. The silicon-doped LTI carbon which had been treated with benzalkonium chloride and heparinized, induced a very even adherence of mostly single platelets to the entire surface. Additional observations are noted in the description of the figures.

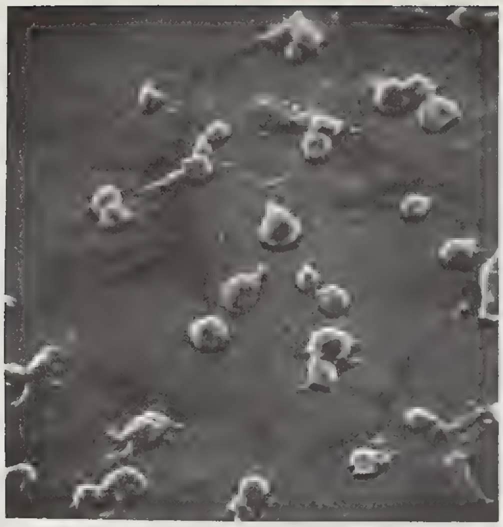

FIGURE 21.
CANDIDATE MATERIAL: SILICONE RUBBER, DOW-CORNING SILASTIC 372. SURFACE TREATMENT: "STERILIZED" IN 70 PERCENT ETHANOL FOR ONE-HALF HOUR; RINSED WITH NORMAL SALINE. EXPOSURE TO BIOLOGICAL ENVIRONMENT: IN CONTACT WITH PRP (BMI DONOR BLOOD NO. 83) FOR ONE HOUR AT 37 C. PHOTOGRAPHED BY SCANNING ELECTRON MICROSCOPY. APPROXIMATELY 2000x MAGNIFICATION. EXPERIMENTAL FINDINGS: THIS PICTURE SHOWS THE DEPOSITION OF INTACT PLATELETS ON TOP OF A FLAKY SHEET OF WHAT APPEARS TO BE DEGRANULATED, FLATTENED PLATELETS. EACH FLAKE CONSISTS OF AN IRREGULARLY SHAPED FLAT AREA (7 TO 10 IN DIAMETER), SURROUNDING A CENTRAL GRANULAR AREA (4 TO 5 MICRONS IN DIAMETER). THE PLATELETS ARE DEPOSITED SINGLY OR IN CLUSTERS OF TWO OR THREE. THE EDGES OF THE FLAKES HAVE A TENDENCY TO OVERLAP OR PILE UP.

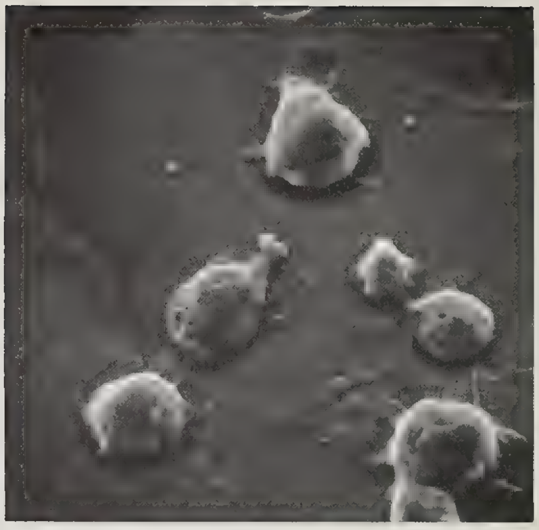

FIGURE 22.
CANDIDATE MATERIAL: SAME AS IN FIGURE 21. TREATMENT: SAME AS IN FIGURE 21. PHOTOGRAPHED BY SCANNING ELECTRON MICROSCOPY. APPROX. 5000x MAGNIFICATION. EXPERIMENTAL FINDINGS: THIS PICTURE SHOWS THAT SOME OF THE INTACT PLATELETS ARE CONNECTED WITH VERY FINE FIBRILS.

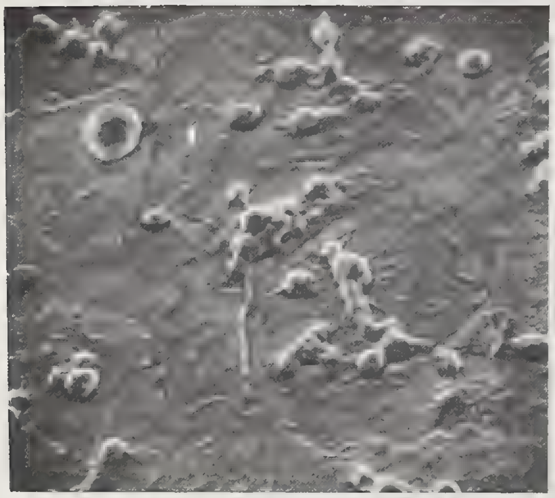

FIGURE 23.
CANDIDATE MATERIAL: SAME AS IN FIGURE 21. SURFACE TREATMENT: WET AUTOCLAVED FOR 15 MINUTES AT 15 LBS PRESSURE; RINSED WITH NORMAL SALINE. EXPOSURE TO BIOLOGICAL ENVIRONMENT: SAME AS IN FIGURE 21. PHOTOGRAPHED BY SCANNING ELECTRON MICROSCOPY. APPROX. 2000x MAGNIFICATION. EXPERIMENTAL FINDINGS: THIS PICTURE SHOWS THE DEPOSITION OF PLATELETS ON TOP OF A SHEET OF VERY IRREGULAR NONCELLULAR MATERIAL ON THE SURFACE OF THE POLYMER. THE PLATELETS ARE AGGREGATED IN CLUSTERS OR CHAINS, AND SINGLE PLATELETS ARE RARE. THE BOUNDARIES OF THE FLAKY MATERIAL UNDERNEATH THE PLATELETS APPEAR LESS DISTINCT THAN IN FIGURES 21 AND 22. ALSO, THERE IS NO PROMINENT OVERLAP OF THE FLAKES.

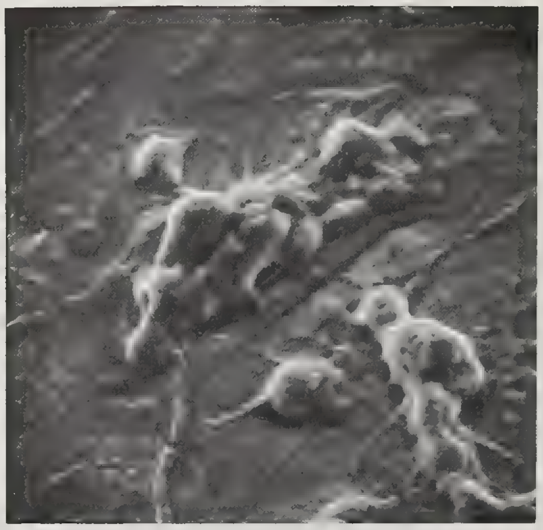

FIGURE 24.
CANDIDATE MATERIAL: SAME AS IN FIGURE 21. TREATMENT: SAME AS IN FIGURE 23. PHOTOGRAPHED BY SCANNING ELECTRON MICROSCOPY. APPROX. 5000x MAGNIFICATION. EXPERIMENTAL FINDINGS: THIS PICTURE SHOWS THAT THE PLATELETS ARE PREDOMINANTLY DENDRITIC IN FORM AND THAT A NETWORK OF DENDRITES ARE SEEN TO BE COVERING THE FLAKY MATERIAL DESCRIBED IN FIGURES 21 AND 22.

Union Carbide Microfiber Mats for "Heteroprosthesis." All three types of microfibers allowed the growth of the human tissue cells. Further experiments will be necessary to determine whether there are differences in the rate of growth on the different fiber mats. The cells were difficult to make out on the 9079-11C polypropylene fibers with 4100 Å coating since they sink into the fiber mat as they grow. Control specimens examined in parallel included nonsterile fiber mats, sterilized fiber mats, and sterile fiber mats exposed to nutrient tissue culture medium only. Figures 10 and 11 show photographs of these studies.

DISCUSSION AND RECOMMENDATIONS

Since an implant is essentially a tissue substitute, any foreign material being considered as a potential human prosthesis must meet a number of very critical requirements which were enumerated in last year's presentation (Tables 7 and 8).

TABLE 7

EFFECTS OF MATERIALS ON RECIPIENT - DESIRED CHARACTERISTICS

1. Not toxic
2. No inflammatory response
3. No allergic effect
4. Not carcinogenic
5. No other adverse effects on cells or body fluids

TABLE 8

DESIRED MATERIALS CHARACTERISTICS

1. Can be reproducibly obtained
2. Can be fabricated into the desired shape without being degraded or adversely changed
3. Will have the needed chemical, physical and mechanical properties to perform its function
4. Can be sterilized without change in properties or shape
5. Will not have its properties adversely altered by the biological environment
6. Will not dissolve and migrate to distant body sites and tissues

As yet, none of the materials submitted for evaluation during this research project meets all of these criteria. The development of nonreactive, nontoxic materials which are also resistant to attack by the biological environment is therefore needed. The rationale of the current research program is that the planned development of such materials will to a great extent depend upon an increased understanding of the basic processes and problems encountered when biological tissue and implant candidate materials are allowed to interact.

The biological evaluation of these new candidate materials has further confirmed the experimental observations reported during last year's contract regarding the importance of sterility of the candidate material surface, the method of sterilization, and the method of storage, in determining the adherence of formed blood elements to the surface of the materials. Several new observations which may be of practical importance in the development and evaluation of prosthetic materials for cardiovascular use were made:

(1) Observed species difference in tissue compatibility. Human cells were found to react differently to some candidate materials than did animal cells.

(2) Growth of human cells within microfiber materials. Human tissue cells were able to survive and multiply within the meshwork provided by microfiber materials prepared from different sizes and types of synthetic fiber.

(3) Nonthrombogenicity versus tissue cell compatibility. In several cases nonthrombogenicity of a candidate material was found to be accompanied by lack of cellular compatibility. Thus, the treatment necessary to achieve nonthrombogenicity sometimes results in a surface which is highly toxic to tissue cells.

(4) Deposition of formed blood elements on blood oxygenator membranes in vivo. Blood oxygenator membranes used in dogs in vivo were found to become coated with a varying thickness of erythrocytes and aggregated platelets. This observation emphasizes the need for the development of membranes which do not promote such adherence and the resultant physical impairment in the free gaseous exchange across the membrane.

(5) Crystallinity versus platelet adherence. A possible relationship between crystallinity and platelet adherence was observed in the case of two groups of materials.

(6) Unsuitability of steam autoclaving for sterilization of certain candidate materials. Steam autoclaving was found to result in increased adherence and aggregation of platelets and also of

intercellular material to certain candidate surfaces. Thus, there is a need for the development of more satisfactory methods of sterilization which will not impair the blood compatible properties which have been induced in the candidate material surface in order to make it suitable for use in the human cardiovascular system.

(7) *Scanning electron microscopy studies.* Scanning electron microscopy was found to be a valuable tool in resolving certain differences in the blood/materials and tissue cell/materials interface in those cases where light microscopic examination showed only minor differences. Differences in the deposition of intercellular material were observed by this means.

The technical progress during the current contract is significant in that it points out several ways that the bioassay specificity, and the materials development and preparation can be improved. The results suggest the following recommendations for future studies:

(1) A human test system is important for preclinical bioassays of implant candidate materials
(2) A planned study would be justified to determine whether the apparent relationship between adherence of blood cells to candidate material surfaces and the crystallinity of the material can be exploited in developing new candidate materials
(3) The use of scanning electron microscopy serves to increase the bioassay specificity
(4) The biotoxicity of surfaces should be evaluated in parallel with nonthrombogenicity studies so that toxic contaminants can be eliminated early during the development of new surfaces
(5) Sterilization techniques other than autoclaving are needed to preserve the integrity of the carefully developed nonthrombogenic solid surface
(6) *In vitro* biodegradation studies for prolonged periods of time
(7) *In vitro* carcinogenesis studies using human cells
(8) *The need* for documentation of the comparative rates of cellular adherence and aggregation to blood oxygenator membranes used *in vivo*, and ways of controlling this deposition to the degree that it does not interfere with *free* gaseous exchange across the membrane.

During the course of this contract, it has become increasingly apparent that the designation of many of the new artificial heart materials as promising is not based upon demonstrated prolongation of clotting *in vitro*. In fact, in many cases there is no record of any clotting assay ever having been performed. Therefore, at the specific request of a collaborating contractor, and with the approval of the Program Office, arrangements have been made recently to have these clotting assays performed at Battelle in parallel with the other biocompatibility studies, starting May 1, 1969. For a period of nine months, starting May 1, 1969, we will also initiate a concentrated effort directed toward the evaluation of new families of microfiber materials to be used in "heteroprosthesis" cardiovascular applications. We anticipate such a program will prove highly productive and of great value to the future of implant surgery in general, and the Artificial Heart Program in particular.

The consideration of microfiber textures for long-term cardiovascular implant materials rather than solid surfaces appears particularly appropriate in the light of the clinical experience reported from various centers at the Second National Conference on Prosthetic Valves.[6] It was reported at this conference that the most promising innovation in valve design was the introduction of cloth encapsulation of the valve to reduce embolization. Emboli have been the most frequent complication of artificial valves despite extensive use of anticoagulants. In fact, the high incidence of thrombo-embolism associated with the artificial implants has been the principal argument advanced in favor of using valve homografts. The incidence of thrombo-embolic complications in Dr. Starr's own series of patients receiving a mitral valve has been 61 percent. This incidence dropped to 7 percent with the introduction of a cloth-covered seat.

REFERENCES

1. Johnsson, R., and A. F. Hegyeli, Ann. N.Y.A.S., 146 (1), 66-76, 1968.
2. Robinson, W. A., and B. Eiseman, The Lancet, II, 1014, 1968.
3. Johnsson, R. I., and A. F. Hegyeli, Ann. N.Y.A.S., 146 (11), 67-76, 1968.
4. Hegyeli, A. F., and R. I. Johnsson-Hegyeli, Nature, 213, 471, 1967.
5. Behbehani, A. M., J. L. Melnick, and M. E. DeBakey, "Continuous Cell Strains Derived from Human Atheromatous Lesions and Their Viral Susceptibility," Proc. Soc. Exp. Biol. Med., 118, 759, 1965.
6. Medical News, J. Am. Med. Assoc., 205 (3), 28, 1968.
7. Ghidoni, J. J., D. Liotta, C. W. Hall, R. M. O'Neal, and M. E. DeBakey, Trans. Amer. Soc. Artif. Int. Organs, 14 (1968).
8. Mustard, J. F., Exp. and Mil. Path. 7, 366 (1967).
9. Nematollahi, J., W. L. Guess, and J. Autian, J. Pharm. Scie., 56 (11), 1446 (1967).
10. Oppenheimer, B. S., E. T. Oppenheimer, and A. P. Stout, Proc. Soc. Exper. Biol. Med., 67, 33 (1948).
11. Oppenheimer, E. T., M. Willhite, A. P. Stout, I. Danishefsky, and M. M. Fishman, Cancer Res., 24, 519 (1964).
12. Raykhlin, N. T., and A. F. Kogan, Problems in Oncology, 7 (9) (1961).
13. Robinson, W. A., and B. Eiseman, The Lancet, II, 1014 (1968).
14. Wesolowski, S. A., "Evaluation of Tissue and Prosthetic Vascular Grafts." Springfield, Illinois. Charles C. Thomas Company (1962).

DISCUSSION

DR. NUWAYSER: You showed in your figures flattened tissue cells on various fiber substrates. How thick, on the average, would these cells be?

DR. JOHNSSON-HEGYELI: This would vary in different regions of the cell and with different types of surfaces. On a perfectly flat surface a cell typically assumes a fried egg appearance, with the central portion being the nucleus. This part of the cell may be about 1 micron in thickness under these conditions.

DR. NUWAYSER: How can this be in agreement with the known fact that a round cell has a diameter of about 10 microns?

DR. JOHNSSON-HEGYELI: These facts are in agreement. A cell in suspension assumes a spherical form, while the shape of a cell deposited or growing on a planar or fiber surface conforms to the topography of the surface and may become very thin and flattened out.

DR. SCOTT: Do primate cells, e.g., from monkeys, react to implant materials in a way similar to human cells? Also, do you ascribe the observed difference in response between mouse fibroblast cells and human amnion cells to a species difference, or to a difference in cell type?

DR. JOHNSSON-HEGYELI: We have not tested primate cells. Further experiments are needed to establish whether the observed difference in response between mouse and human cells is due to a species difference. Many reports of differences in response between cells from different species to a given toxic agent have been reported in the literature, however.

CHAPTER 20

STUDIES ON THE COMPATIBILITY OF VARIOUS PLASTICS WITH THE PROTEINS IN HUMAN PLASMA*

S. P. Halbert, M. Anken and A. E. Ushakoff

Cordis Laboratories, Miami, Florida

The effects of various implantable materials on plasma protein have been further investigated in a specially devised experimental system, using a large number of specific parameters for evidence of denaturation. Although silicone rubber was compatible with plasma, silicone rubber which had been heparinized by means of quaternary ammonium salts produced profound turbidity of this plasma. Polyurethane similarly heparinized produced the same effects. These were found to be due almost exclusively to denaturation of the lipoproteins. The liberated cholesterol was absorbed to a considerable extent onto the treated plastics. Further study demonstrated that it was not the heparin on the surface of the plastic, but the quaternary ammonium salt which brought about the destructive changes. Silicone rubber heparinized by a different technic (via an aminoorganosilane covalently bonded to the silica particles) was inert to plasma proteins. Epoxy resin and heparinized epoxy resins brought about changes in certain enzymes, and in some plasma proteins detectable by "disc" electrophoresis. The proteins involved in the latter have not yet been identified. A carbon surface, polycarbonate, and several acrylamide surfaces proved relatively inert toward plasma proteins.

The increasing use of plastics in modern surgery, particularly cardio-vascular surgery, has raised important questions about their compatibility with the constituents of blood. Much research emphasis has centered around thrombo-embolic phenomena, or on damage to formed elements by such plastic devices.[1] In addition, some concern has been expressed about the potential denaturation of the plasma proteins by implantable materials.[2,3] The effects of direct contact of plasma with various plastic surfaces in an experimentally isolated situation has been the subject of investigation in our laboratory.[4] The present report is concerned with denaturation detected in human plasma as a result of its exposure to heparinized plastic surfaces.

MATERIALS AND METHODS

The system used for the assay of the effects of plastics on plasma proteins and plasma enzymes has been described in detail elsewhere.[4] It utilized a multi-chambered receptacle made of silicone rubber (Dow-Corning Corporation, Midland, Michigan), which allowed plasma samples to be obtained from blood which was not in contact with any other surface throughout the experiment. Silicone rubber, in previous as well as in the present experiments, was found to have no significant effects on human plasma proteins and enzymes under these conditions. Blood was drawn from adult male donors into the main chamber of the receptacle, which contained sodium citrate as anticoagulant. After centrifugation of the plasma within the main chamber, approximately equal amounts of plasma (35-40 ml) were forced into the side chambers, one of them containing a large surface of the plastic material under consideration, in granular form. The latter was sifted through 20 mesh and was retained by 40 mesh stainless steel screens. The test chambers were incubated at 37°C so that the granules were in constant motion; and samples of plasma were removed at 0, 24 and 48 hours. The samples were assayed for changes in plasma protein concentrations and for changes in enzyme activities. The following were studied.

Plasma Proteins. Transferrin ceruloplasmin, fibrinogen, immunoglobulins A, M, and G, pre-albumin, albumin, alpha and beta lipoproteins, alpha-1-acid glycoprotein, beta-2-glycoprotein, alpha-1-antitrypsin, haptoglobin, hemopexin, β_{1c}/β_{1a} globulin, and alpha-2-macroglobulin. The radial immunodiffusion method[5] used for their quantitative assay, as well as the method used for calcium replacement clotting times were identical to those previously employed.[4]

Plasma Enzymes. The methods for the determination of the activities of the following enzymes were also described earlier.[4] The following were studied: glutamic-pyruvic and glutamic-oxalacetic transaminases, isocitric and lactic dehydrogenases, cholinesterase, amylase, acid and alkaline phosphatases and lipoprotein lipase. Cholesterol was determined in the plasma, in extracts of plasma sediments, and in extracts of the plastic material under test, using the acetic anhydride-sulfuric acid procedure.[6] The lipids were extracted with a 1:1 ethyl alcohol-acetone mixture from the drained but unwashed granules.

---

*This investigation was supported by the National Heart Institute under Contract No. PH43-66-980.

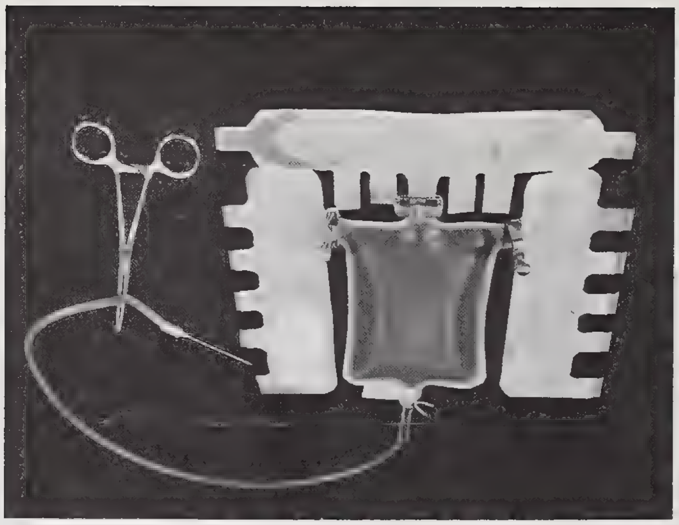

FIGURE 1. SYSTEM USED FOR TESTING PLASTIC MATERIALS WITH PLASMA.

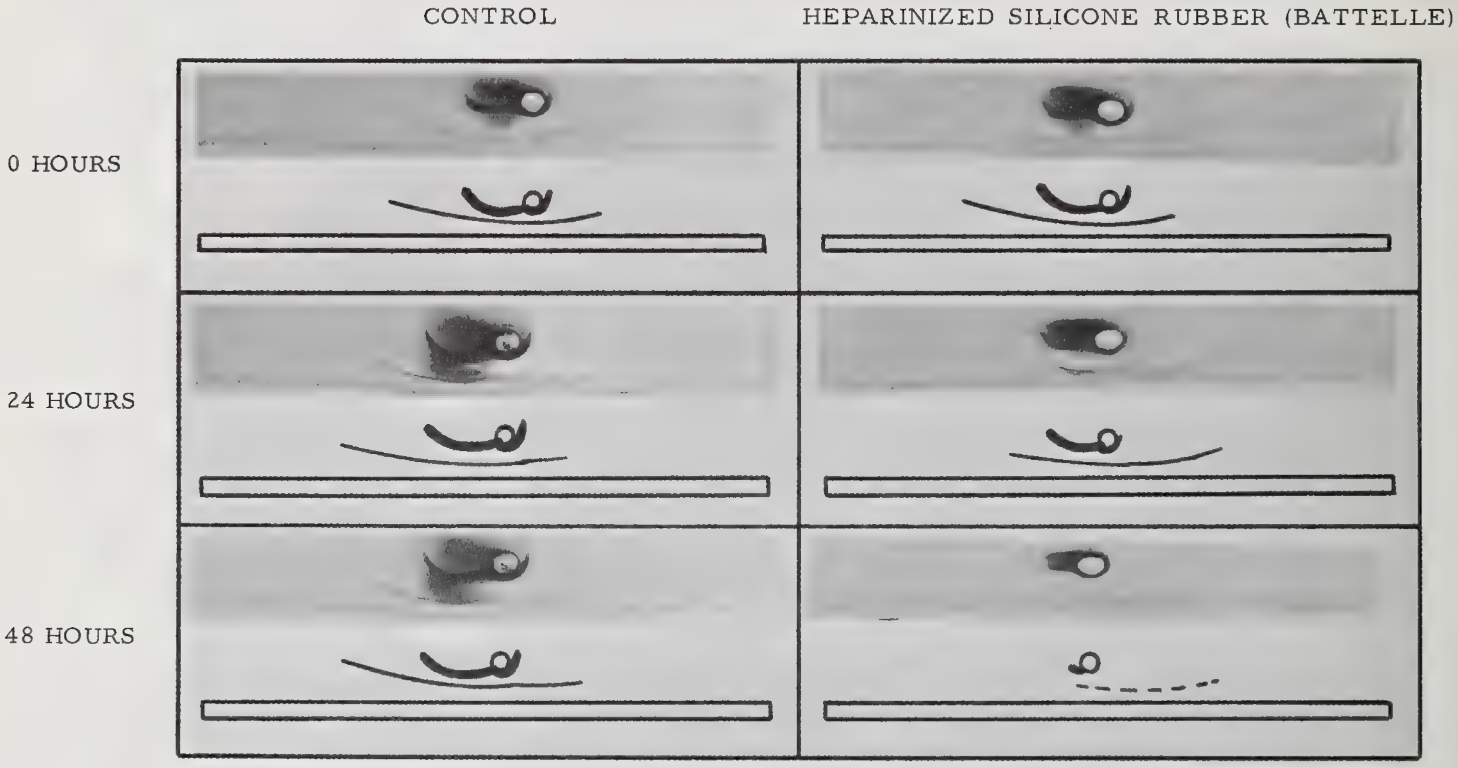

FIGURE 2. IMMUNOELECTROPHORETIC PATTERNS OF PLASMA STAINED FOR LIPOPROTEINS. HORSE ANTISERUM TO NORMAL HUMAN SERUM IN TRENCH. WHEN STAINED FOR PROTEIN, THESE SLIDES WOULD REVEAL AT LEAST 20 IMMUNE SYSTEMS.

PLASTICS STUDIED

Silicone Rubber Preparations.

1. Silicone rubber, Silastic 372, obtained from Dow-Corning Corporation (Midland, Michigan).
2. Silicone rubber, Silastic 372, heparinized by the Battelle Memorial Institute (Columbus, Ohio), according to the procedure described by Falb.[7] The final product contained 2.5 μg of bonded heparin per cm^2. The ionic binding was achieved with the quaternary ammonium salt, tridodecylmethylammonium chloride (TDMAC).
3. Silicone rubber, Silastic 372, was heparinized at the Carnegie-Mellon Institute (Pittsburgh, Pa.) by ionic bonds to the silica particles in the plastic, via an amino organosilane complex. The concentration of heparin per cm^2 is not known.[8] Control experiments were performed with plain silicone rubber plus added soluble heparin, as well as with silicone rubber preparations treated with the TDMAC alone.
4. Segmented polyurethane, DuPont de Nemours (Wilmington, Del.).
5. Segmented polyurethane heparinized by the Battelle Memorial Institute, using TDMAC as the intermediate bonding agent.

RESULTS

In confirmation of earlier investigations, plasma exposed to a large silicone rubber surface did not show significant differences in any of the measured parameters from those seen in the 37°C controls. Increases in the beta lipoprotein measurements, and in the amylase activities were seen in the controls, as well as in the test mixtures. The other plasma protein concentrations and enzyme activities remained unaffected by their exposure to silicone rubber, and the clarity of the plasma samples was unimpaired. Plasma clotting times were slightly prolonged within the 48 hour period studied (Tables 1, 2, 3 show representative values).

TABLE 1

PLASMA PROTEIN CONCENTRATIONS AFTER EXPOSURE OF PLASMA TO VARIOUS PLASTICS

Plastic	Plasma Protein	Sample	Relative Concentration in Plasma[a] After		
			0 HOURS	24 HOURS	48 HOURS
Silicone Rubber	βlipoprotein	4°C Control	4,200	4,200	4,200
		37°C Control	5,200	7,000	7,300
		37°C Exposed	3,575	7,000	7,850
Heparinized Silicone Rubber	$\alpha_1$lipoprotein	37°C Control	3,900	3,900	3,900
		37°C Battelle	3,900	undetectable	undetectable
		37°C Carnegie-Mellon	5,300	3,950	3,900
	βlipoprotein	37°C Control	3,600	5,700	7,800
		37°C Battelle	2,000	undetectable	undetectable
		37°C Carnegie-Mellon	4,100	5,000	6,300
	Fibrinogen	37°C Control	800	870	1,300
		37°C Battelle	585	undetectable	undetectable
		37°C Carnegie-Mellon	1,000	1,300	1,300
	$\alpha_1$anti-trypsin	37°C Control	4,400	4,000	4,300
		37°C Battelle	4,200	1,450	1,410
		37°C Carnegie-Mellon	3,950	3,750	4,000
Segmented Polyurethane	βlipoprotein	37°C Control	5,700	8,200	14,000
		37°C Exposed	5,700	7,350	10,350
Heparinized Segmented Polyurethane	$\alpha_1$lipoprotein	37°C Control	5,350	3,250	3,900
		37°C Battelle	5,800	3,900	440
	βlipoprotein	37°C Control	6,000	5,600	7,760
		37°C Battelle	4,800	3,075	1,725
	Fibrinogen	37°C Control	940	965	940
		37°C Battelle	755	800	735
	$\alpha_1$anti-trypsin	37°C Control	4,700	5,200	5,000
		37°C Battelle	3,500	3,700	3,950

[a] The values for βlipoprotein, $\alpha_1$lipoprotein and $\alpha_1$anti-trypsin are based on standard curves obtained with a single lot of lyophilized normal human plasma. In the case of fibrinogen, the figures represent absolute concentrations (mg/100 ml) using standard curves obtained with highly purified fibrinogen.

The following number of experiments were carried out with each material: Silicone rubber (4); Heparinized Silicone Rubber, Battelle (4); Heparinized Silicone Rubber, Carnegie-Mellon (3); Segmented Polyurethane (2); Heparinized Segmented Polyurethane, (2).

TABLE 2

PLASMA ENZYME ACTIVITIES AFTER EXPOSURE OF PLASMAS TO VARIOUS PLASTICS

Enzyme	Plastic	Enzyme Activities in Arbitrary Units		
		0 HOURS	24 HOURS	48 HOURS
Acid Phosphatase	Control	19	21	27
	Silicone Rubber	16	16	20
	Control	50	40	40
	Hep. Sil. Rubb. Battelle	62	30	3
Cholinesterase	Control	78	75	75
	Silicone Rubber	76	69	68
	Control	98	98	100
	Hep. Sil. Rubb. Battelle	90	40	34
Lactic Dehydrogenase	Control	180	210	225
	Silicone Rubber	180	210	195
	Control	240	260	270
	Hep. Sil. Rubb. Battelle	240	270	250
Glutamic-Oxalacetic Transaminase	Control	9	9	9
	Silicone Rubber	9	7	8
	Control	14	14	13
	Hep. Sil. Rubb. Battelle	12	14	9

TABLE 3

CALCIUM REPLACEMENT CLOTTING TIMES AFTER EXPOSURE TO VARIOUS PLASTICS

Plastic	Plasma Incubation Time (Hours)	Clotting Times in Minutes		
		4°C Control	37°C Control	37°C Exposed
Silicone Rubber	0	9	11	9
	24	14	15	13
	48	14	26	23
Silicone Rubber Heparinized by Battelle	0	6	7	6
	24	7	16	>24 hrs.
	48	10	>24 hrs.	>24 hrs.
Silicone Rubber Heparinized by Carnegie-Mellon	0	--	6	14
	24	--	68	>24 hrs.
	48	--	>24 hrs.	>24 hrs.
Segmented Polyurethane	0	--	8	13
	24	--	16	26
	48	--	35	52
Segmented Polyurethane Heparinized by Battelle	0	--	9	11
	24	--	24	35
	48	--	158	>24 hrs.
Silicone Rubber Tridodecylmethyl Ammonium Chloride Treated	0	--	8	13
	24	--	21	>24 hrs.
	48	--	104	>24 hrs.

Silicone Rubber Heparinized by Battelle.

Exposure of plasma to this plastic resulted in appreciable turbidity at 24 hours, which increased considerably by 48 hours. Concomitantly, the concentrations of the alpha and beta lipoproteins dropped strikingly, and often became undetectable (Table 1). The disappearance of these two lipoproteins was confirmed by disc acrylamide gel electrophoresis. With one batch of such heparinized silicone rubber, the fibrinogen and alpha-1-antitrypsin also decreased. None of the other plasma protein concentrations measured were affected, however.

Of the enzymes studied, a consistent, but small decrease in cholinesterase occurred following exposure to the heparinized sample. In most of the experiments, the acid phosphatase also decreased somewhat, but the other enzymes were not regularly affected (Table 2). In no instance was lipoprotein lipase activity detected before or after exposure to any of the plastics.

In some cases, the turbid plasma resulting from treatment with the heparinized surface demonstrated a substantial flotation layer after low speed centrifugation. This was never observed in the plasmas exposed to plain silicone rubber.

The heparinized silicone rubber granules became increasingly yellow during their contact with plasma, and the 48 hour exposed plasma was considerably depleted or devoid of cholesterol (Table 4).

TABLE 4

CHOLESTEROL CONCENTRATIONS IN PLASMA, IN EXTRACTS OF CENTRIFUGED SEDIMENTS AND IN EXTRACTS OF HEPARINIZED TEST GRANULES

			Total Amount of Cholesterol in mg			
Plastic		Plasma Incubation Time (hours) @ 37°C	Plasma	Sediment Centrifuged from Plasma	Test Granules	Flotation Layer
Plain		0	94.6	ND[a]	ND	--[b]
Silicone Rubber		24	90.8	ND	ND	--
		48	95.2	ND	4.2	--
Silicone Rubber		0	66.3	0	ND	--
Heparinized	Lot #1	24	54.8	0	ND	--
by Battelle		48	16.5	1.0	13.3	9.0
		0	73.5	0.9	ND	--
	Lot #2	24	14.1	1.2	ND	--
		48	2.6	1.8	71.0	--
Silicone Rubber		0	70.1	0.4	ND	--
Heparinized by		24	70.1	0.4	ND	--
Carnegie-Mellon		48	71.0	0.4	6.5	--
Plain Segmented		0	67.6	ND	ND	--
Polyurethane		24	66.2	ND	ND	--
		48	63.7	ND	ND	--
Segmented		0	69.9	0	ND	--
Polyurethane		24	64.2	0	ND	--
Heparinized		48	50.2	0.4	4.4	8.2
by Battelle						

a ND - not done

b -- not available

A large portion of the cholesterol which had disappeared from the plasma could be detected in extracts of the granules. A portion of the cholesterol could also be found in the flotation layers and in the plasma sediments following centrifugation. As shown in Table 4, with one lot of heparinized rubber, no flotation layers were observed, and in these cases, the yield of cholesterol from the extracted granules was considerably greater. The "disappearance" of the plasma cholesterol was paralleled by the above mentioned loss of the beta and alpha-1-lipoproteins.

The exposed plasma samples often failed to clot after replacement of the calcium ions (Table 3).

Silicone Rubber Heparinized by Carnegie-Mellon.

Plasma exposed to the Carnegie-Mellon heparinized silicone rubber remained clear, and failed to show any significant changes in the concentrations of the 17 proteins measured. Similarly, the enzyme activities of such exposed plasma samples did not differ appreciably from the 37°C values. There was no loss of cholesterol from the plasma, although some uptake by the granules was observed (Table 4). The small quantities of cholesterol adherent to the particles of this material and plain silicone rubber may have been due in part to the fact that these were extracted without washing.

Segmented Polyurethane.

Exposure of plasma to segmented polyurethane led to a slight prolongation of its clotting time (Table 3). None of the plasma proteins were significantly altered; nor, with the exception of a possible decrease in isocitric and lactic dehydrogenase activities, were any enzymes affected. The plasma throughout its exposure to this plastic material remained clear.

Segmented Polyurethane Heparinized by Battelle.

Plasma also became increasingly turbid during its exposure to the heparinized polyurethane. The alpha and beta lipoproteins were significantly reduced in the 48 hour exposed samples (Table 1). There was an appreciable decrease in the plasma cholesterol concentration after 48 hours, and a significant portion of this cholesterol was extractable from the flotation layer (Table 5). Plasma exposed to heparinized polyurethane became non-clotting at 48 hours (Table 3). The other proteins and enzymes were not affected.

Experiments with Component Constituents.

Tests were conducted to determine which of the constituents of the treated plastics might have caused the observed denaturations. In order to determine whether leached heparin could possibly account for these changes, plasma was collected in plain silicone rubber, in which the citrate anticoagulant contained heparin to give a final concentration of 100 μg/ml in the plasma. Such plasma, when exposed to plain silicone rubber granules did not become turbid, and did not show any reduction in the lipoprotein concentrations. The plasma proteins and enzyme activities measured were also not affected.

On the other hand, exposure of plasma to tridodecylmethylammonium chloride treated silicone rubber granules resulted in all of the changes produced by the Battelle heparinized plastics (Tables 6 & 7). The samples became quite turbid; the lipoproteins decreased strikingly, and the granules became deep yellow, with high concentrations of extractable cholesterol. In addition, it was of interest that the calcium replacement clotting times of such plasmas were indefinitely prolonged after 24 and 48 hours of exposure (Table 3).

TABLE 5

CHOLESTEROL CONCENTRATIONS IN PLASMA, IN EXTRACTS OF CENTRIFUGED SEDIMENTS AND IN EXTRACTS OF TEST GRANULES AFTER EXPOSURE TO SILICONE RUBBER COATED WITH TDMAC

	Incubation Time (hours) @ 37°C	Total Amount of Cholesterol in mg		
		Plasma	Sediment Centrifuged from Plasma	Test Powder
	0	72	0.5	--
Control	24	72	0.4	--
	48	71	0.4	--
Silicone Rubber	0	69	0.5	--
Coated with	24	9	3.5	--
TDMAC	48	3	4.1	44.0

TABLE 6

THE EFFECT OF TDMAC COATED SILICONE RUBBER ON PLASMA LIPOPROTEINS

Proteins	Sample	mg/100 ml of plasma after 0 HOURS	24 HOURS	48 HOURS
βLipoprotein	37°C Control	5,200	5,200	7,400
	37°C Exposed	3,125	undetectable	undetectable
α_1Lipoprotein	37°C Control	8,350	5,700	5,700
	37°C Exposed	7,250	undetectable	undetectable

DISCUSSION

Under the experimental conditions used here, medical grade silicone rubber and segmented polyurethane have been found to be rather inert toward the plasma proteins and plasma enzymes studied. However, when silicone rubber and segmented polyurethane were heparinized by means of a quaternary ammonium salt, important alterations in some protein constituents of exposed plasma were detected. The plasma exposed to such heparinized plastics became milky in appearance, while the granular plastics turned distinctly yellow. Removal of the insoluble phase from the turbid plasma often left a liquid phase which was almost completely colorless. In some experiments, low speed centrifugation resulted in a large flotation layer of lipid-like material, which contained considerable quantities of cholesterol. A substantial decrease in plasma cholesterol after 48 hours was always observed. The cholesterol which was lost from the plasma could in large measure be recovered from extracts of the test granules, the plasma sediment and the flotation layer. In those instances where there was no visible flotation layer, the bulk of the recovered cholesterol was derived from the plastic granules. Immunodiffusion assays of the exposed plasma indicated that the cholesterol was derived from denatured alpha and beta lipoproteins, since these were consistently reduced to low or undetectable levels at 24 hours and after. Acrylamide gel disc electrophoresis confirmed the disappearance of both of the lipoproteins.

Analysis of the factors involved in the observed changes, clearly pointed to the quaternary ammonium salt as the responsible agent. Addition of soluble heparin to plasma exposed to plain silicone rubber, did not reveal in any evident protein denaturation. Lipoprotein lipase activity was never detected in any of these samples. However, all of the alterations observed were duplicated by exposure of plasma to rubber particles treated with the water insoluble quaternary salt. The precise mechanisms involved are not clear, but it may be pointed out that quaternary ammonium salts, as well as heparin, have been known for some time[9,10] to cause precipitation of plasma lipoproteins.

None of the plasma protein denaturing effects noted with the Battelle-TDMAC-heparinized silicone rubber powder were observed with the Carnegie-Mellon preparation. There were also no significant changes in plasma enzyme activities due to this plastic. It thus seems possible to prepare an antithrombogenic surface without affecting the integrity of the plasma proteins investigated.

In considering the relevance of these observations to clinical problems, it is worth pointing out that progressive changes have sometimes been reported in the silicone rubber balls of artificial heart valves. They can become yellow over a period of time and recent studies have demonstrated that this may be associated with an accumulation of cholesterol and other extractable lipids.[11,12,13,14] It is conceivable that a deposition of these fats may result in deterioration of their physical properties and their subsequent mechanical failure. It has been suggested that the biochemical changes precede the physical alterations.[11] The lipids in the silicone rubber of heart valves may be derived from plasma lipoproteins or erythrocytes in vivo since it is well known that hemolytic anemias are rather common in patients with such prostheses. Under any circumstances, additional evaluations would be indicated before treating such silicone rubber balls with quaternary ammonium salts for anti-thrombogenic purposes, in view of the above studies which suggest that the deposition of lipids can be significantly increased in the presence of TDMAC.

SUMMARY

Silicone rubber or polyurethane surfaces which have been heparinized by means of ionic bonding with a quaternary ammonium salt caused significant denaturation of the lipoproteins in plasma. A considerable amount of the plasma cholesterol could be extracted from the plastic granules. The factor responsible for this denaturation appeared to be the quaternary ammonium salt used to complex the heparin. Heparinized silicone rubber prepared by a different chemical process was inert with regard to the plasma protein parameters investigated. The possible relation of these findings to certain degenerative changes noted in silicone rubber heart valves are briefly discussed.

REFERENCES

1. Gott, V. L., Whiffen J. D., Dutton R. C., Leininger R. I., and Young W. P. Biophysical Studies on Various Graphite - Benzalkonium - Heparin Surfaces. In Biophysical Mechanisms in Vascular Homeostasis and Intravascular Thrombosis, Sawyer P. N. ed.: 197-305, Appleton - Century-Crafts, New York, N.Y.
2. Lee, W. H. Jr., Krumhaar D., Fonkalsrud E. W., Schjeide O. A., Maloney J. V. Jr. Denaturation of Plasma Proteins as a Cause of Morbidity and Death after Intracardiac Operations, Surgery 50: 29-39, 1961.
3. Haberman, S., Guess W. L., Rowan D. F., Bowman R. O., and Bower R. K. Effects of Plastics and their Additives on Human Serum Proteins, Antibodies and Developing Chick Embryos. SPE Journal 24:62-69, 1968.
4. Halbert S. P., Ushakoff A. E. and Anken M. In manuscript.
5. Fahey J. H. and McKelvey E. M. Quantitative Denaturation of Serum Immunoglobulins in Antibody Agar-Plates. J. Immunology 94:84-90, 1965.
6. Abell, E. Simple Rapid Technic for Serum Total Cholesterol. Amer. J. Med. Tech., 25:65-66, 1959.
7. Falb, R. D. Personal communication.
8. Merker R. L. Personal communication.
9. Takruri H. and Ecanow B. Interactions of Surfactants with Lipoproteins. Journal Pharmaceutical Sciences, 35:979-981, 1966.
10. Burstein M. and Morfin R. Precipitation des Lipoproteines Seriques en Presence de Detergents Anioniques et de Protamine, ou de Detergents Cationiques et d'Heparine. Revue Francaise d'Etudes Cliniques et Biologiques 13:274-277, 1968.
11. Pierie W. R., Hancock W. D., Koorajian S. and Starr A. Materials and Heart Valve Prostheses. Annals N. Y. Academy of Sciences, 146:345-359, 1968.
12. Garcia M. D., Clarysse A. M., Alexander C. S., Sako Y. and Swaim W. R. Hemolytic Anemia Due to Progressive Enlargement of Silastic Ball Component of Aortic Prosthesis. Circulation 38: 505-513, 1968.
13. Braley S. The Silicones as Subdermal Engineering Materials. Annals N. Y. Academy of Sciences, 146:148-157, 1968.
14. Smeloff E. A. and McHenry M. M. Fatal Ball Variance: A Complication of Full-Orifice Prosthetic Heart Valves (abstract). Circulation 38:VI-181, Suppl. 6, 1968.

DISCUSSION

MRS. NELSEN: In a number of your anionic polymers, in the absence of any gross changes, you did get slight prolongations of clotting time. Could this be due to chelation of calcium ions by the anionic groups? Is the effect of that order?

DR. HALBERT: Well, in carrying out the clotting time tests we replace an overabundance of calcium in the samples. After the samples are withdrawn from the test system, we replace the calcium ions so that the clotting sequence can be activated.

MRS. NELSEN: Clotting times are usually pretty sensitive to calcium levels and will be prolonged if you either have a little bit too much or a little bit too little calcium.

DR. HALBERT: It is conceivable that we were putting in a little too much. But we have judged on the basis of comparision with 37 degree controls. These are always the baseline for the significance of all these observations.

MR. GRODE: I think that Dr. Halbert should be commended for the excellent work he did in studying the interactions of proteins with the TDMAC surfaces. I think that for the benefit of those who did not hear the talk earlier this morning, it should be pointed out that when one runs these tests in a manner such that physiological conditions are more closely simulated where you are getting flow of new plasma over the surface, these protein interactions are only initial interactions and they quickly stop.

DR. HALBERT: We have not conducted any tests to explore this possibility. These have been single samples as you have indicated but we have seen some instances where the changes in plasma proteins have not been maximum at 24 hours but they have gone on to become even greater at 48 hours.

MR. GRODE: These are essentially static conditions. Is that right?

DR. CORDIS: No, they are not. The test system is maintained in constant, gentle motion causing the test samples in the form of granules to flow through the plasma.

MR. GRODE: However, it is the same blood which is used for the 24 or 48 hours and the process is essentially a batch process.

DR. HALBERT: Dr. Falb suggested sometime ago a test which we have not yet done; and that is to take the exposed granules and subject them to a fresh sample of plasma. This is something we certainly should do.

DR. KENNEDY: I would like to compliment you on the quality of the material which you have presented. Can you share with us any data you have on changes in the stress-fatigue characteristics or structural changes in the polyurethane when lipid adsorption was noted?

DR. HALBERT: I am afraid we have no information concerning that, but we are intrigued by the fact that the artificial heart valves that have now been used for some years, and which have been implanted for long periods of time have walls made of silicone rubber. There is accumulating evidence that these do become yellow with age, that the yellow color is due to an accumulation of lipid, and that this discoloration seems to be associated with the deterioration of the biological properties. It is certainly something that should be investigated.

DR. BYCK: This seems to be a remarkably ambitious testing program. Can you give us any estimate of how much calendar time and how much manpower is required for the study of a single polymer?

DR. HALBERT: We have simplified the testing by removing 4 degree control samples which we used to do. We now feel that this is not necessary. The only relevant controls are 37 degree controls. We have also simplified the system by using only silicone rubber units, since it is apparent that silicone rubber seems to be inert to all of these parameters, as you have seen in my presentation. We can do two experiments with all these parameters in a month, i.e. we can examine two materials in duplicate in one month.

DR. BYCK: In looking at your slides showing adsorption on to the heparinized silicone versus unheparinized silicone, I noticed a marked difference in sample volume. Does this reflect swelling of the heparin treated polymers or are these just differences in densities of the polymers?

DR. HALBERT: In clinical volume?

DR. BYCK: You showed two test tubes, one showed the yellow coloration as a result of adsorption.

DR. HALBERT: Oh no, the two test tubes were simply filled with unequal aliquots from the test bags.

MR. SALYER: I was very pleased to hear for the first time tonight about the excellent results you have had with the heparinized epoxies and their general inertness. I have just one comment on the experiment and it is this: You are talking about idealizing it by getting away from the silicone bag. You know, the only way I could think of to do it would be to make the bag also out of the material under test and this might be more difficult but at least you would have eliminated one variable.

DR. HALBERT: There is no question about that. As we reported at previous meetings we started this program out by doing exactly that. And the studies with heparinized silicone rubber with quaternary salt were done in complete units made of this material. The experiments on polyurethane were done in the same way. The experiments with Teflon were done the same way with slightly different units. But we compared the results obtained in silicone rubber bags with those results obtained in units made entirely satisfied that the current procedure is a sound one and a feasible shortcut.

DR. EVANS: We have implanted a small series of polyurethane samples, both heparinized and unheparinized, in animals and while the heparinized samples did indeed turn bright yellow we have observed no changes in mechanical strength for a period of 14 days.

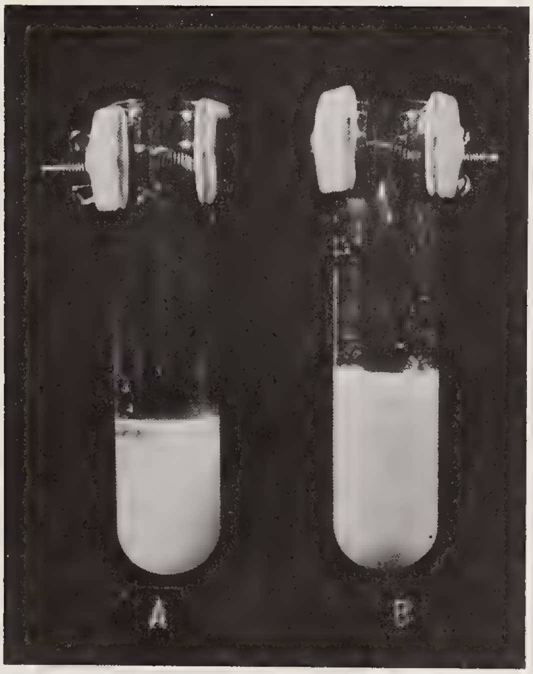

PLAIN SILICONE RUBBER   BATTELLE TDMAC HEPARINIZED SILICONE RUBBER

FIGURE 3. THE EFFECT OF A 48-HOUR EXPOSURE OF HUMAN PLASMA TO PLAIN SILICONE RUBBER GRANULES (TUBE A) AND TO QUATERNARY AMMONIUM SALT (TDMAC) AND TO QUATERNARY AMMONIUM SALT (TDMAC) HEPARINIZED SILICONE RUBBER GRANULES (TUBE B).

CHAPTER 21

ANALYSIS AND MEASUREMENT OF THE EFFECTS OF MATERIALS ON BLOOD

B. Kusserow, R. Larrow and J. Nichols

University of Vermont, Burlington, Vermont

I. IN VIVO EMBOLUS TEST SYSTEM. Two approaches have been utilized in an attempt to develop a sensitive tissue indicator of embolic and thrombotic episodes occurring at the surface of prosthetic intravascular implants. One technique involved supplementation of the currently used caval ring implant system (in dogs) by experimental alteration of the pulmonary circulation in such fashion (unilateral bronchial artery ablation and contralateral pulmonary artery ligation) that the lung became increasingly susceptible to infarction subsequent to the lodgment of embolic particles in the pulmonary arterial bed. The resulting infarct serves as a permanent tissue marker of the embolic event. The surgical procedure did not of itself cause spontaneous infarction. Intravenous injections of particulate autologous blood clot, however, produced identifiable pulmonary infarcts. A second method utilizes the renal vascular bed and parenchyma as biologic indicators of embolic events. Ligation of the abdominal aorta below the origin of the renal arteries is accompanied by insertion of a ring of test material immediately above the origin of these vessels. Under these circumstances blood flowing through the test ring must course through the kidneys (organs which are highly susceptible to infarction). The injection of particles of autologous blood clot into the aorta immediately above the origin of the renal vessels in dogs so prepared resulted in the development of numerous renal infarcts.

II. TRAUMA-INDUCED, REGRESSIVE LEUKOCYTE ALTERATIONS. A number of *in vitro* perfusions (duration 16 hrs.) were carried out to assess the effects of prolonged blood pumping upon leukocytes specifically. The circuit consisted of a roller pump coupled to a loop of plastic (polyvinyl chloride) tubing. Findings in summary form are as follows: (1) distinct decreases in leukocyte oxygen utilization were noted in pumped samples, (2) cytologic aberrations were observed in pumped leukocytes and (3) non-granulocytic leukocytes were relatively decreased in differential counts after pumping.

IN VIVO EMBOLUS TEST SYSTEM

The occurrence of thrombo-embolic phenomena represents a serious and not infrequent consequence of the exposure of blood to surfaces other than the intact vascular intima. Indeed the problem of thrombosis and embolism, occurring at the blood contacting surfaces of circulatory assist devices remains entrenched as a yet incompletely surmounted obstacle to the safe and prolonged use of circulatory assist devices. Very considerable progress has, however, been made in the fabrication of synthetic and biologic nonthrombogenic surfaces, and it is to be anticipated that further improvement will ensue. In this regard,it is apparent that there is a need for a sensitive *in vivo* test system to critically assess a given synthetic or biologic surface with respect to its thrombogenic and embolic propensities. Efforts to establish such a test system were accordingly initiated inasmuch as there is currently no established *in vivo* test system known to the writers which will critically detect or demonstrate the occurrence of *both* surface thrombosis and embolization from a prosthetic device or test surface implanted into or coupled with the vascular system. The now well established inferior vena cava and right atrium implant systems[1] represent excellent and most useful techniques for the detection of thrombotic material actually present on the surface of the implant, but are somewhat less optimally suited to demonstrate the prior occurrence of lesser embolic phenomena with certainty. This is largely due to the fact that emboli originating in either the vena cava or right atrium from the surface of a prosthetic implant are carried to the lungs. There they disappear with considerable rapidity[2], due presumably in part to the destructive action of the fibrinolytic system of the animal. While it is true that relatively large embolic masses may remain and can be detected at autopsy, it is quite likely that many smaller (and especially minute) emboli will entirely escape detection. In this regard it is also to be noted that although small emboli may be of lesser consequence in the pulmonary circulation, even minute emboli may be lethal or seriously injurious within the systemic arterial system. Clinical experience with artificial heart valves and cardiac patches has well demonstrated this danger. Furthermore, since the large majority of circulatory assist devices will be positioned in the systemic rather than in the pulmonary circulation, the problem of embolization, regardless of particle size becomes of special significance. Indeed, the safety of any circulatory assist device is open to serious question until it has been conclusively demonstrated that its blood contacting surfaces do not cause embolic episodes. Thus the observation by itself that the blood contacting surfaces of a device are free of thrombi in no way rules out the possibility of one or more previous episodes of thrombosis with subsequent dislodgement of thrombus and embolization. The inferior vena cava and right atrium implant systems thus are felt to represent very necessary and useful, but not entirely sufficient, test conditions to document rigorously the safety of an intravascular prosthetic device. This is especially true of a device intended for indefinite or long-term implantation.

Three approaches were utilized to develop a sensitive tissue indicator of both thrombotic and embolic phenomena occurring at the surface of an intravascular prosthetic device. Two approaches involved modification of the pulmonary circulation in such fashion that the lung became increasingly susceptible to infarction subsequent to the lodgement of embolic particles in the pulmonary arterial bed. The resulting infarct thus served as a more or less permanent tissue marker of the embolic event. The third approach involved utilization of the renal vascular bed and renal parenchyma as biologic indicators of embolic events.

Unilateral Pulmonary Vein Ligation

This approach involves supplementation of the vena cava or right atrium implant systems by experimental alteration of the pulmonary venous circulation in such fashion that emboli arising from a caval or atrial implant will result in pulmonary infarcts. The latter then represent more or less durable tissue markers of the embolic episodes. Normal lungs possessing an intact pulmonary and bronchial circulation are remarkably resistant to infarction in consequence of their dual blood supply, and the concomitant action of the fibrinolytic system[2,3]. It is well known on both clinical and experimental grounds, however, that passively congested lungs are considerably more susceptible to embolic infarction than normal lungs[3]. It was consequently planned to precondition the pulmonary circulation in test animals by experimental ligation of all pulmonary veins to one lung, a maneuver which of itself does not cause infarction[4], but which renders the lung more susceptible to infarction by emboli[3]. Some pulmonary arterial flow continues to the ligated lung. Indeed, after a period of three to five months the blood flow through a lung deprived of its pulmonary venous outflow channels may attain values ranging between 8 and 20 percent of that expected, were the pulmonary venous drainage intact[5]. Venous exit is via bronchial veins which become markedly enlarged following pulmonary venous ligation.

Experimental Methods and Results

Left pulmonary vein ligations (intra-pericardial) were carried out under sterile technique in a series of six dogs. Two of these animals were followed postoperatively for periods of nine and sixteen days respectively and were then sacrificed. Each animal was anticoagulated with intravenous heparin immediately prior to sacrifice. Autopsy studies indicated that such unilateral ligation of pulmonary veins will of itself not induce spontaneous pulmonary arterial thrombosis or infarction.

The remaining group of four dogs were also subjected to unilateral pulmonary vein ligation as described above (ligation of right pulmonary veins was carried out in one animal of this group). These dogs subsequently received intravenous injections (jugular vein) of fragmented autologous blood clot approximating 15 ml. in amount. The clots were given as a single intravenous dose in each case. The interval between ligature of pulmonary veins and clot administration varied from three hours to five days. Animals were then sacrificed and autopsied after post-injection periods ranging from four hours to eight days. Two animals were found dead in their cages, one and eight days respectively following clot administration. All of the above animals displayed numerous pulmonary infarcts. These were conspicuous in lungs with previously ligated pulmonary veins, but two animals also demonstrated prominent infarcts in the contralateral lung. Figures 1 and 2 illustrate the post mortem lung specimen of a dog given intravenous autologous blood clots several days subsequent to left pulmonary vein ligation. That pulmonary infarction was considerably more prominent in lungs with previously ligated pulmonary veins is of interest in view of the fact that the ligated lung in all probability received considerably less blood flow than the contralateral intact lung. Indeed, the fact that an appreciable portion of the total pulmonary blood flow (with potentially entrained emboli) coursed through the untreated (nonligated) lung was considered an undesirable feature of this model, and it was accordingly abandoned.

Bronchial Artery Ablation And Contralateral Pulmonary Artery Ligation

This approach, a two stage procedure, was utilized in a series of ten dogs. The initial step involved the ablation of the bronchial arterial supply to the right lung according to a method described by Ellis[6]. The method involved the appropriate injection of small quantities of vinyl acetate into the main right posterior bronchial artery. It was anticipated that this maneuver would transform the pulmonary arteries of the right lung into definitive end arteries without an appreciable collateral (bronchial arterial) supply. The secondary stage of the combined procedure (carried out approximately one to two weeks later) involved ligation of the left pulmonary artery, a procedure which diverted all pulmonary blood flow to the right lung. Under these circumstances the entire lesser circulation obligatorily coursed through an arterial bed which had been transformed into a definitive end artery circulation. Vulnerability to infarction by entrained thromboembolic particles was thus greatly enhanced.

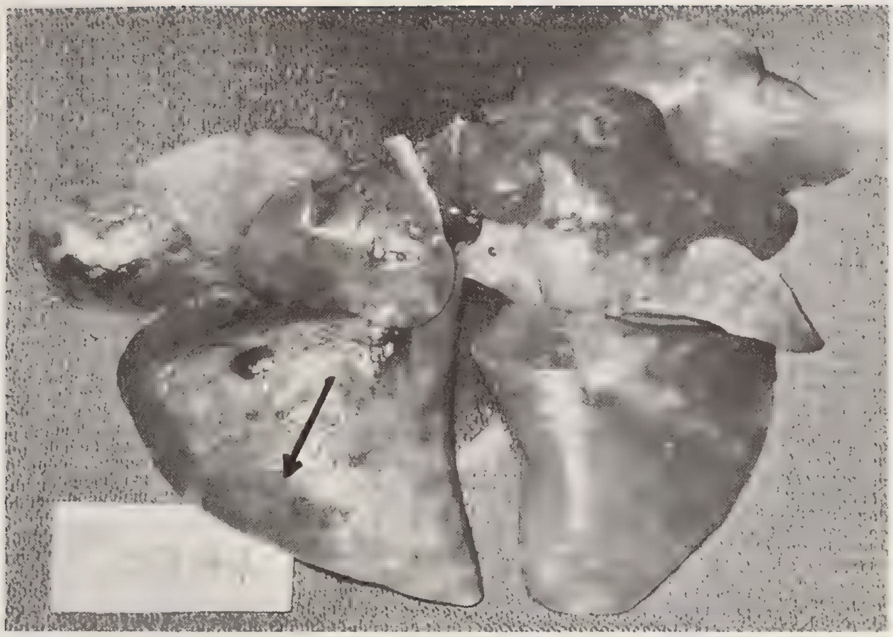

FIGURE 1. POSTMORTEM LUNG SPECIMEN FROM A DOG GIVEN 15 ML. OF FRAGMENTED AUTOLOGOUS BLOOD CLOT 5 DAYS FOLLOWING LIGATURE OF ALL LEFT PULMONARY VEINS. THE ANIMAL WAS SACRIFICED 4 DAYS AFTER THE CLOT INJECTION. THE LEFT LUNG DISPLAYS A LARGE (ARROW) AND SEVERAL SMALLER INFARCTS. CONGESTION AND PATCHY ATELECTASIS IS EVIDENT IN THE RIGHT LUNG.

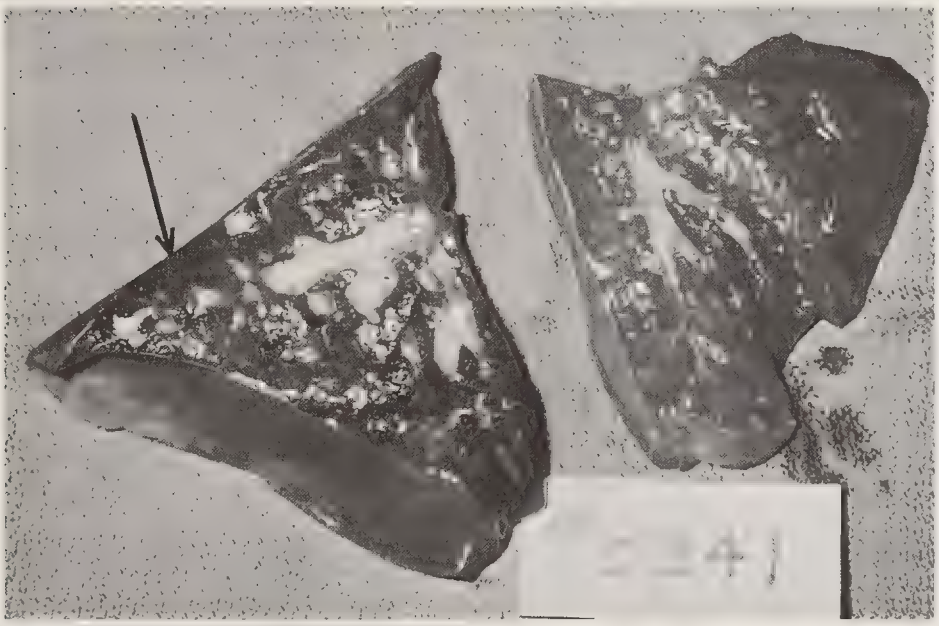

FIGURE 2. CUT SURFACE (LOWER LOBES) OF LUNG SPECIMEN SHOWN IN FIGURE 1. THE LARGE LEFT LOWER LOBE INFARCT DEPICTED IN FIGURE 1 IS AGAIN SEEN (ARROW). OTHER SMALLER AND IRREGULAR REGIONS OF INFARCTION ARE ALSO APPARENT IN THE LEFT LOWER LOBE.

Experimental Approach and Results

The initial seven animals in this series were utilized to perfect the necessary operative and injection techniques, as well as to establish the optimal time interval between the primary (injection) and secondary (left pulmonary artery ligation) stages of the combined procedure. It was found that vinyl acetate injections approximating 0.2 ml. usually resulted in satisfactory filling and ablation of the bronchial arterial supply to the right upper and lower pulmonary lobes in dogs weighing between 30 and 40 pounds. Significantly larger doses resulted in necrotizing and ulcerating mucosal lesions in the terminal trachea and main stem bronchi of both upper and lower right pulmonary lobes. A purulent, confluent focal pneumonitis of the right lung also accompanied these lesions. Figure 3 represents an example of such pathology. These complications were eliminated in later dogs, however, by the appropriate reduction of the vinyl acetate dose as given above. The final three dogs were prepared utilizing the dose adjusted vinyl acetate-ligation technique. A number of days (11-17) later these animals received 20 ml. of particulate autologous blood clot via the right jugular vein. Clot particles were carefully counted prior to injection. Two of three animals so injected demonstrated pulmonary infarcts, and in one dog it was also possible to identify emboli within the pulmonary arterial tree (Figures 4 and 5). In no animal, however, was it possible to identify infarcts equal in number to that of the injected emboli. Two possibilities existed to account for the quantitative disparity between the number of infarcts observed and the number of emboli introduced: (1) Not every embolus produced a recognizable infarct, or (2) several embolic particles became entrained in a single pulmonary vessel to produce a single infarct. Both situations would result in a disparity between the number of injected emboli and infarcts observed. The experimental findings suggest, however, that a lung modified by this particular technique is significantly more susceptible to infarction than the intact lung. On the other hand the variability of the bronchial circulation in the dog, especially with respect to anastomotic connections with other mediastinal vessels, gives rise to the possibility that the described plastic injection technique may at times fail to effect the desired complete ablation of the collateral blood supply to the right lung. Because of the difficulties cited above, further utilization of this procedure was deferred.

Renal Embolus Test System

The limitations of the pulmonary embolus test systems described above prompted the initiation of a series of experiments wherein the renal vascular bed and parenchyma were utilized as biologic indicators of embolic events. This approach involved ligation of the abdominal aorta of the dog approximately 1-1.5 cm. below the origin of the renal artery (but above the origin of the caudal mesenteric artery) together with the insertion of a ring of test material immediately above the origin of the renal vessels (but below the origin of the superior mesenteric artery). The vascular anatomy of the dog provides ample space for the insertion of such a test ring (8-10 mm. long) in animals of moderately large size. Under such circumstances all blood flowing through the test ring must course through the kidneys with the exception of a very minor fraction which may find egress from the aorta via a few minute posterior aortic branches. The kidney is well known to represent an organ which is highly susceptible to infarction in consequence of arterial embolization. Moreover, because of their relatively small size, they may be examined with great precision and in great detail at necropsy. Past experience in this laboratory has given the impression that this organ exceeds perhaps all others with respect to infarct susceptibility. It is fully realized that in a general way prosthetic devices implanted into the aorta are less prone to the development of surface thrombosis than implants into the inferior vena cava, due presumably in part to the higher flow velocities in the aorta. In this regard it is to be noted, however, that aortic ligation as described above serves to obligatorily reduce aortic blood flow velocity immediately above the level of the renal arteries (the site of test material implantation), because of concomitant aortic runoff from the more superiorly situated great arterial trunks. This circumstance would tend to create conditions which enhance thrombosis. In general, the method can be expected to represent a considerably more severe test situation with respect to thrombosis than a prosthesis implanted into the intact (unligated) aorta.

Experimental Approach and Results

Efforts to date have involved three series of experiments. An initial group of 12 dogs were subjected to aortic ligation alone as described above in an attempt first to ascertain whether or not they could withstand such a procedure, and secondly to establish the fact that spontaneous thrombosis and infarction did not occur in the kidneys in consequence of the operative intervention. The majority of animals in this series survived the procedure with no observable complications. A few animals, however, domonstrated ischemic lesions of the large bowel or pelvic biscera. Weakness of the hind extremities was an additional complication in some animals, but was generally compatible with survival. The large majority of dogs demonstrated neither renal nor other lesions grossly. In two dogs (early members of the series), however, microscopic examination of the kidneys revealed small ischemic lesions. The character of these lesions suggested that a number of minute embolic particles had somehow become entrained in the renal arterial circulation at the time of aortic ligation. An attempt was accordingly made to circumvent this complication by shifting the site of aortic ligation (initially 2-8 mm. beneath the takeoff of the renal arteries) to a point approximately 1 cm. caudal to this location (1.5 cm. below the origin of the left renal artery). No major aortic branches are bypassed by such a shift in aortic ligation site. Animals subjected to aortic

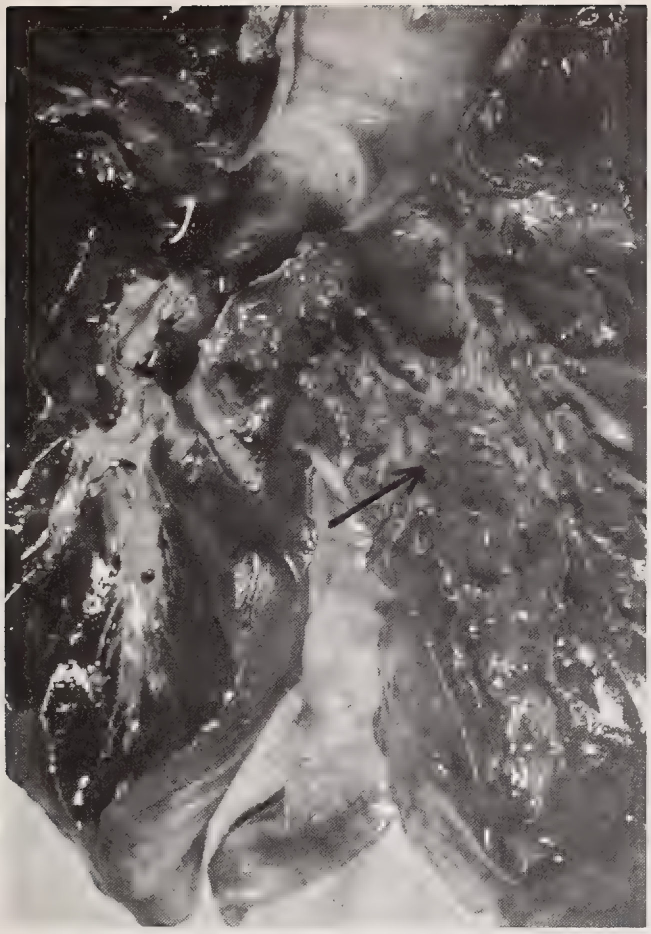

FIGURE 3. NECTORIZING AND ULCERATING MUCOSAL LESIONS (ARROW) OF THE RIGHT MAIN STEM AND LOBAR BRONCHI TOGETHER WITH SECONDARY CONFLUENT FOCAL PNEUMONIA. THESE LESIONS FOLLOWED THE INJECTION OF 2.0 ML. VINYL ACETATE INTO THE RIGHT POSTERIOR BRONCHIAL ARTERY OF A 40 LB. DOG.

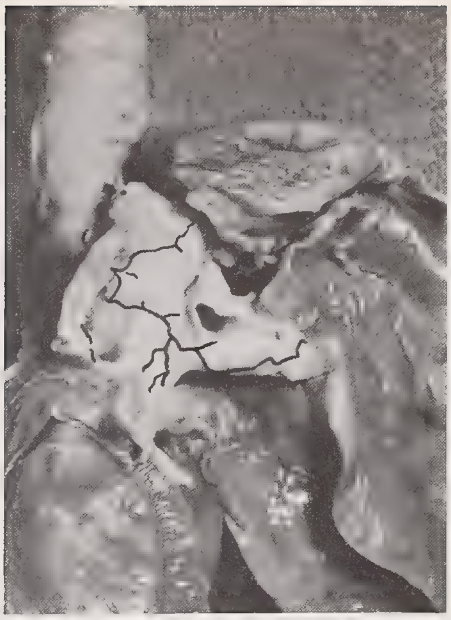

FIGURE 4. INJECTED BRONCHIAL ARTERIES (BLACK) TO RIGHT UPPER AND LOWER LOBES. VINYL ACETATE (0.2 ML.) HAD BEEN INJECTED 4 WEEKS PREVIOUSLY INTO THE RIGHT POSTERIOR BRONCHIAL ARTERY. VESSELS CONTAINING PLASTIC HAVE BEEN RETOUCHED FOR EMPHASIS.

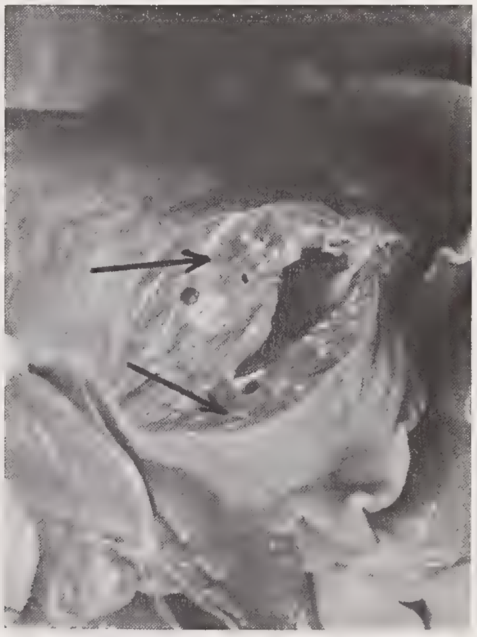

FIGURE 5. PORTION OF CUT SURFACE OF LUNG SHOWN IN FIGURE 4. COMPLETE EMBOLIC OCCULSION OF A PULMONARY ARTERY IS FOUND NEAR REGIONS BY EARLY INFARCTION (ARROW). THIS ANIMAL HAD PREVIOUSLY BEEN SUBJECTED TO THE COMBINED PROCEDURE OF RIGHT BRONCHIAL ARTERY ABLATION AND LEFT PULMONARY ARTERY LIGATION AS DESCRIBED IN THE TEST. 20 ML. FRAGMENTED AUTOLOGOUS BLOOD CLOT WERE THEN GIVEN INTRAVENOUSLY ON THE 17TH POSTOPERATIVE DAY. THE DOG WAS SACRIFICED ONE DAY LATER.

ligation in this more caudal location have generally survived with no observable renal complications. The experimental finds to date thus suggest that aortic ligation as described above may be carried out with long term survival, and without the subsequent occurrence of spontaneous thrombosis or renal infarction in the large majority of animals.

A second group of five dogs was subjected to the combined procedure of aortic ligation together with the subsequent injection of particles of autologous blood clot into the aorta immediately above the origin of the renal arteries. The animals were then sacrified one to three days later. Four out of five animals so treated showed numerous renal infarcts of various sizes. Figure 6 is a representative example of clot material used in this experimental group while Figures 7-9 represent a display of post-mortem findings encountered in one animal of this group.

The actual implantation of a mock aortic test ring coupled with the procedure of aortic ligation has been accomplished on a chronic basis in a single animal. The test ring consisted of a 1 cm. long, 7 mm. I.D. tubular segment of polyvinyl chloride, the surface of which had previously been coated with graphite-benzalkonium-heparin. The ring was inserted and positioned through a ventral longitudinal aortic incision created immediately below the point of subsequent aortic ligation. The ring was then secured in position by means of two sutures placed around the outer surface of the surrounding aortic wall. The animal was sacrificed seven days later. Necropsy findings included complete thrombotic occlusion of the test ring and subjacent aortic lumen to the point of aortic ligature. The kidneys displayed an infarct pattern consistent with multiple embolic episodes superceded by sudden massive and complete ischemia (Figures 10-11).

The composite studies described above suggest that the renal embolus test system may represent a feasible approach to the problem of detecting both prosthesis-induced thrombosis and embolism. Additional studies, especially those involving the implantation of aortic test rings, will be required, however, to more conclusively establish the validity and reliability of this test system.

TRAUMA-INDUCED REGRESSIVE LEUKOCYTE ALTERATIONS

The vulnerability of red blood cells to surface and perfusion-induced injury is now reasonably well established. On the other hand, it has generally been assumed that leukocytes are relatively resistant to trauma of this nature. Past experience in this laboratory, however, has suggested that leukocytes are in fact quite susceptible to injury upon exposure to foreign surfaces and perfusion systems. Thus, a considerable decrease in leukocyte phagocytic capability resulted when blood was exposed to plastic tubing. Even greater changes occurred after extended *in vitro* circulation with a blood pump[7]. The experiments described here represent further attempts to characterize the manifestations of surface and perfusion-induced injury. To create the degree of trauma necessary to elicit manifestations of injury in leukocytes, a blood exposure system consisting basically of a sterile closed loop of polyvinyl chloride tubing coupled to a roller pump was utilized. Pumping action served first to increase surface encounter. It, of course, additionally represented a source of purely mechanical trauma. The priming volume of the system consisted of approximately 50 ml. of anticoagulated (standard ACD solution) blood drawn under sterile conditions from adult mongrel dogs. A number of 16 hour *in vitro* perfusions (as further described in succeeding sections below) were carried out at room temperature (22-25°C.) to assess the effects of blood exposure to such a system upon leukocytes specifically. The perfusion system employed of course represents a marked departure from definitive *in vivo* circumstances. On the other hand the complicating effects of the reticuloendothelial system and hematologic compensatory mechanisms are absent and cannot, therefore, obscure perfusion-induced injury phenomena by the removal of injured cells and replacement with fresh normal cells.

Leukocyte Morphologic Aberrations

Control blood samples for these studies consisted of an unpumped aliquot of the same blood which was used to prime the perfusion circuit. The standard Wright's staining technique was used to examine both pumped and control blood samples. Distinct morphological alterations were encountered in some leukocytes from samples of pumped blood. These changes included: marked raggedness of overall cell contour, partial loss of cytoplasm and cellular shrinkage, changes in cytoplasmic granulation, nuclear distortion, homogenization of nuclear chromatin and occasional nuclear hyaline like change. A leukocyte from a sample of pumped blood is illustrated in Figure 12.

Outright Destruction of Leukocytes

Studies with the above test system sometimes demonstrated slight but distinct decreases in the total white cell count of pumped samples indicating that a certain small fraction of leukocytes present were destroyed in outright fashion.

Alteration In Leukocyte Differential Counts

Consistent relative decreases of mononuclear elements were encountered in differential counts of traumatized blood when compared to matched control samples. This finding suggests that the mononuclear blood corpuscles may be somewhat more susceptible to trauma than the granulocytic forms. It must be realized, however, that such changes in the leukocyte differential count may also have their basis in the differing cell life span of granulocytes and nongranulocytic leukocytes.

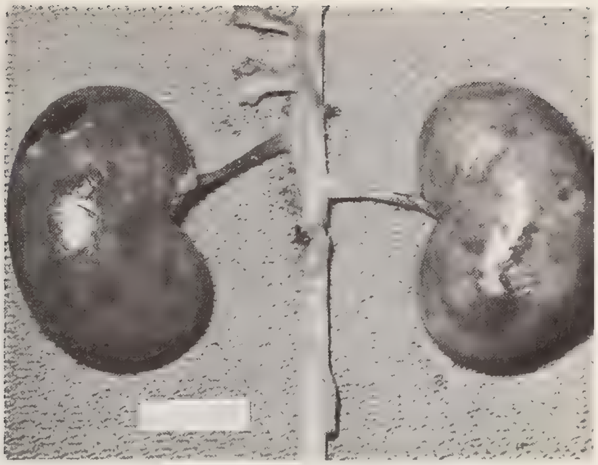

FIGURE 7. MULTIPLE BILATERAL RENAL INFARCTS (IRREGULAR DARK AREAS) SEEN AT NECROPSY IN A DOG SUBJECTED TO AORTIC LIGATION 14 DAYS PRIOR TO THE INTRA-AORTIC INJECTION OF PARTICULATE AUTOLOGOUS CLOT. THE ANIMAL WAS SACRIFICED 4 DAYS AFTER THE CLOT INJECTION. THE AORTIC LIGATURE HAS BEEN LEFT IN POSITION.

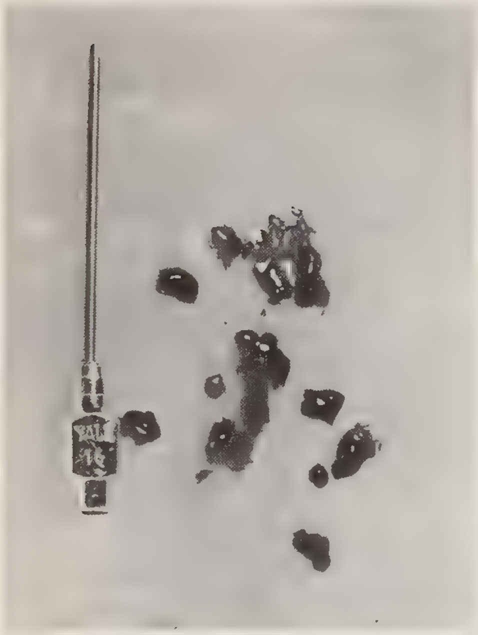

FIGURE 6. PARTICULATE AUTOLOGOUS BLOOD CLOT USED FOR INTRA-AORTIC INJECTION IN A DOG PREVIOUSLY SUBJECTED TO INFRA-RENAL AORTIC LIGATION.

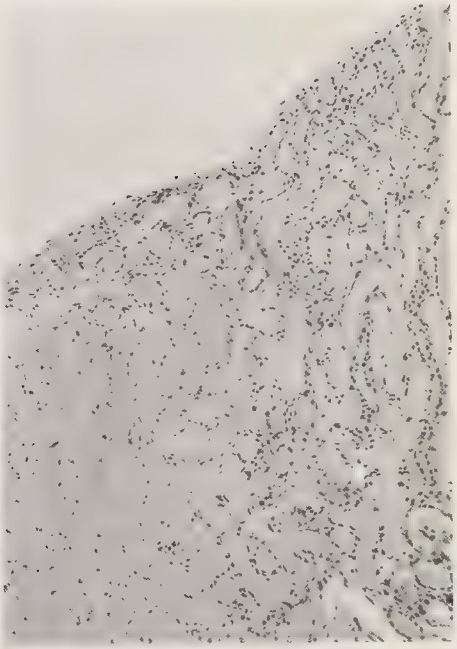

FIGURE 9. PHOTOMICROGRAPH OF INFARCTED RENAL TISSUE FROM A KIDNEY SHOWN IN FIGURE 8. COMPLETE COAGULATION NECROSIS (PALE ZONE) HAS OCCURRED ON THE LEFT. THE REGION TO THE RIGHT DISPLAYS LESS SEVERE ISCHEMIC DEGENERATIVE CHANGE.

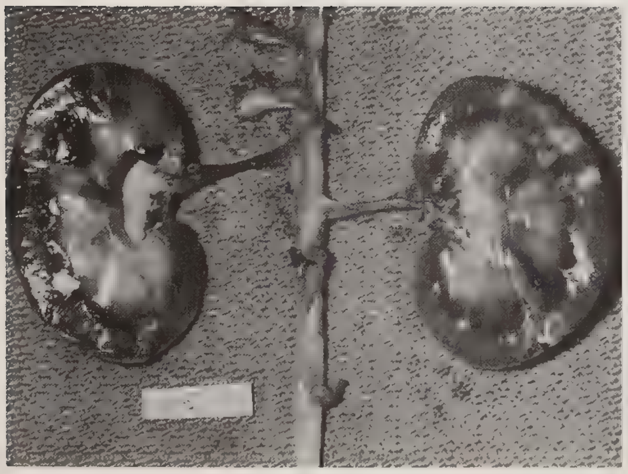

FIGURE 8. SPECIMEN SHOWING THE CUT SURFACE OF KIDNEYS DEPICTED IN FIGURE 7. BOTH HEMORRHAGIC INFARCTS (DARK ZONES) AND BLAND INFARCTS (PALE CORTICAL REGIONS) ARE PRESENT.

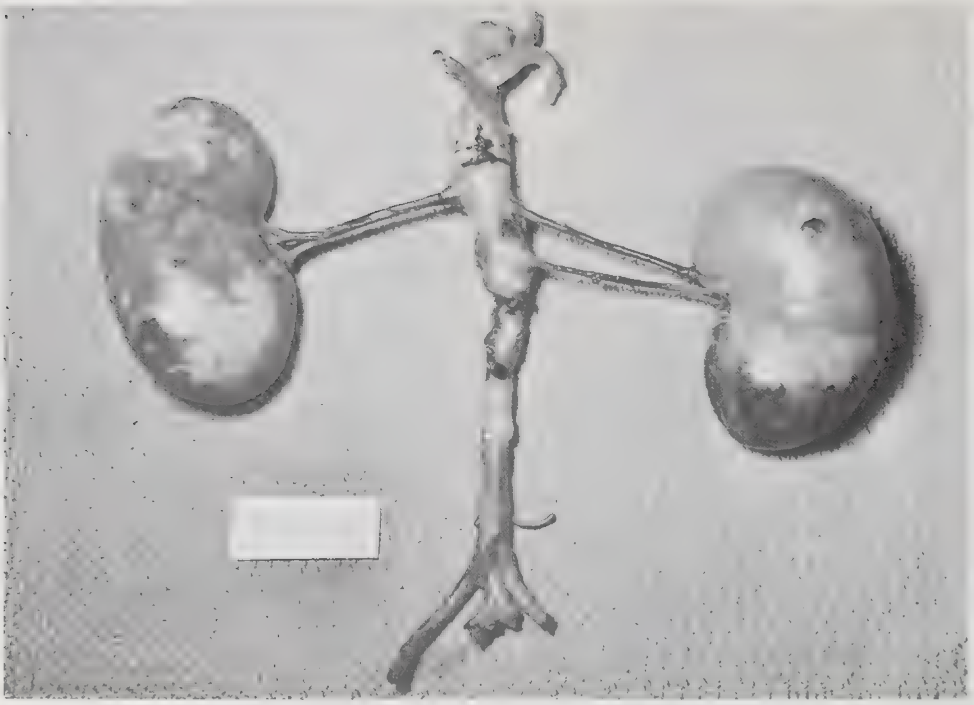

FIGURE 10. RENAL EMBOLUS TEST SYSTEM(AORTA UNOPENED). TWO SILK SUTURES ABOVE THE LEVEL OF THE RENAL ARTERIES SURROUND THE AORTA AT THE MOCK TEST RING POSITION. BOTH KIDNEYS DISPLAY INFARCTS OF VARYING SIZE.

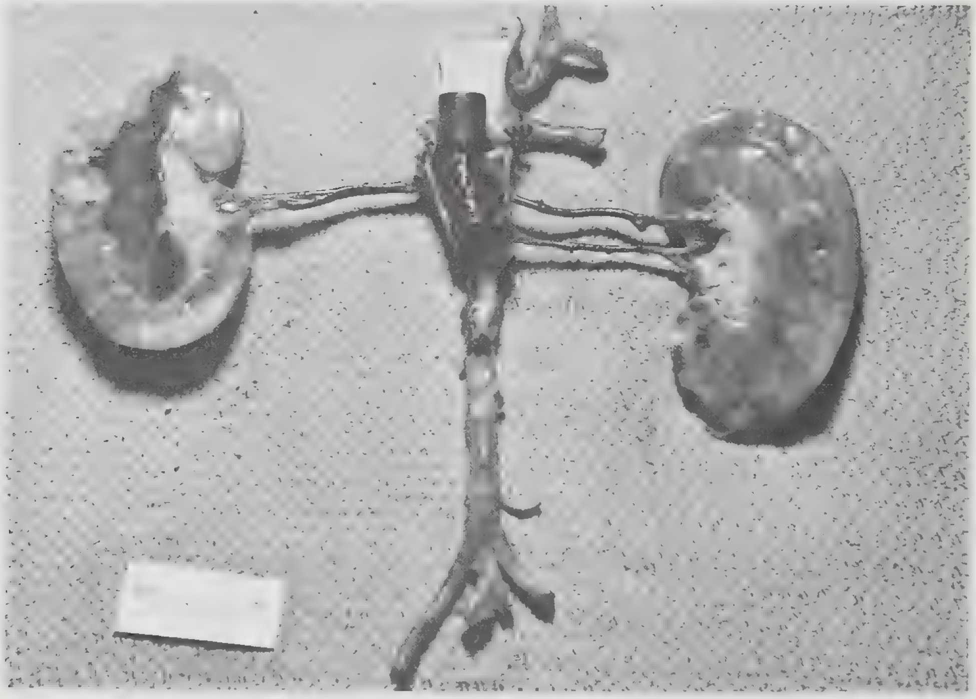

FIGURE 11. SPECIMEN OF FIGURE 10 WITH AORTA OPENED TO SHOW IMPLANTED MOCK TEST RING. A MASSIVE THROMBUS COMPLETE OCCLUDES THE LUMEN OF BOTH TEST RING AND SUBJACENT AORTA. THE CUT SURFACE OF THE KIDNEYS DISPLAYS A COMPOSITE OF SMALL AND MASSIVELY LARGE INFARCTS.

Leukocyte Oxygen Utilization

Control blood samples for these studies consisted both of aliquots freshly drawn from the donor animal (15 perfusions) at the time of termination of the perfusion, and of unpumped aliquots (3 perfusions) of the same blood which was used to prime the perfusion circuit. The latter controls were placed in very slowly rotating (1 rpm) segments of plastic tubing identical to that used for the pump circuit. A combined oximetric-Warburg technique was used for the measurement of leukocyte oxygen consumption. The method permitted correction for oxygen consumed by blood erythrocytes and platelets. Distinct decreases in leukocyte oxygen utilization were encountered in the large majority of samples of pumped blood when contrasted to controls. Leukocytes in the majority of pumped samples demonstrated decreases in oxygen utilization in excess of 60% in those experiments where controls consisted of blood samples drawn freshly from the donor animal at the end of perfusion. Lesser but yet distinct differences in leukocyte oxygen utilization were demonstrated between pumped and unpumped samples in those perfusions wherein control samples consisted of unpumped blood contained within the slowly rotating segments of plastic tubing. It is worthy of note that in these perfusions no apparent correlation appeared to exist between the observed decreases in leukocyte oxygen utilization and outright erythrocyte destruction in pumped samples as indicated by the final level of free plasma hemoglobin. The findings clearly demonstrate, however, that a distinct metabolic deficit (as evidenced by decreased oxygen utilization) may ensue in leukocytes which are traumatized by exposure to the system described above. This modality of leukocyte injury may be of considerable significance, since such definitive leukocytic functions as phagocytosis and cellular migration are dependent upon energy-liberating, oxygen-consuming intracellular processes.

REFERENCES

1. Jacobs, L., Klopp, E., and Gott, V. Studies on the fibrinolytic removal of thrombus from prosthetic swords. Trans. Amer. Soc. Artif. Int. Organs, 14:63, 1968.
2. Allison, P., Dunnill, M., and Marshall, R. Pulmonary embolism. Thorax, 15:273, 1960.
3. Karsner, H. Studies in infarction: II. Experimental bland infarction of the lung. J. Med. Res., 27:205, 1912.
4. Wyatt, J., Burke, D., and Hanlon, C. Morphologic study of canine lungs after ligation of the pulmonary veins. Am. J. Path., 29:291, 1953.
5. Hurwitz, A., Calabresi, M., Cooke, R., and Liebow, A. An experimental study of the venous collateral circulation of the lung. J. Thoracic Surg., 28:241, 1954.
6. Ellis, F., Grindlay, J., and Edwards, J. The bronchial arteris. I. Experimental occlusion. Surgery, 30:810, 1951.
7. Kusserow, B., and Larrow, R. Studies of leukocyte response to prolonged blood pumping. Effects upon phagocytic capability and total white cell count. Trans. Amer. Soc. Artif. Int. Organs, 14:261, 1968.

DISCUSSION

DR. BLACKSHEAR: I have a question for Dr. Kusserow which he could just answer by nodding his head. Was this an occlusive roller pump that you traumatized the platelets with? I have been requested to blow the whistle.

DR. KUSSEROW: Yes, the pump was totally occlusive.

DR. SAWYER: How long does it take to do that experiment? The important one, the one with the kidney?

DR. KUSSEROW: The usual procedure is as follows: The tube is first inserted immediately above the renal vessels, the aorta is ligated, incision closed, and the dog is returned to his cage. The sequence of events now depends on the nature of the tube surface. If one does a very careful job of GBH coating of the poly(vinyl chloride) plastic tube, and then sacrifices 5 days later, one may see a small amount or almost no thrombus on the ring itself. A few small renal infarcts may be present. If, however, one intentionally mars the ring a little so that the GBH coating is compromised, then one will obtain a very massive clot in perhaps three or four or even two days.

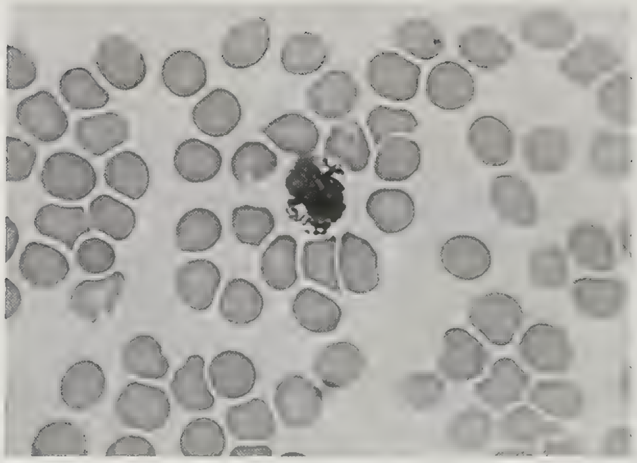

FIGURE 12. STAINED SMEAR FROM A SAMPLE OF PUMPED BLOOD. THE EOSINOPHIL PRESENT DEMONSTRATES NUCLEAR DISTORTION, CONFLUENCE OF LOBES AND HOMOGENIZATION OF CHROMATIN. CELL BOUNDARIES ARE RAGGED AND INDISTINCT. WRIGHT'S STAIN.

CHAPTER 22

NEW APPROACHES IN THE SELECTION OF MATERIALS COMPATIBLE WITH BLOOD

P.N. Sawyer and S. Srinivasan*

SUNY, Downstate Med. Ctr., Brooklyn, N.Y.

Thrombosis occurs at a solid (blood vessel wall or prosthetic material)- electrolyte (blood) interface. Therefore, it should depend on the electrochemical characteristics across the interface. Studies on a number of materials show that (i) with conducting materials, all those which establish negative rest potentials in blood**(NHE) tend to be antithrombogenic while those registering positive potentials are always thrombogenic; (ii) with insulator materials the homogenously negatively charged surfaces tend to be non-thrombogenic: (iii) conducting materials, even if they are normally thrombogenic at their spontaneous potentials (such as in the case of copper), when cathodically polarized to negative potentials are non-thrombogenic. The capacity across a metal-solution interface depends on the nature and extent of adsorption of chemical species on the metal. An inflection point was observed in the capacity-potential relation on a clean gold electrode immersed in blood at the critical thrombogenic potential (+100mv/NHE), indicating blood component adsorption above this potential. Powders of various insulator materials were mixed with blood to determine their blood destructive and antithrombotic characteristics. These studies show that chemically treated (sulfonated, carboxylated) insulator materials cause minimum destruction of blood components and prolong blood clotting times. In a bio-chemical approach to the study of the thrombosis problem, the extent of release of adenosine nucleotides from platelets exposed to powders of several metals was found to be considerably greater with the more noble metals (i.e., thrombogenic) than with the corrodible ones (i.e., antithrombogenic). The accumulated experience from these and related experiments clearly indicate the antithrombogenic characteristics of homogeneously negatively charged clean surfaces and the thrombogenic characteristics of both positively charged and unevenly charged surfaces.

**NHE - Normal Hydrogen Electrode

AN OUTLINE OF THE METHODS USED IN THE TESTING AND EVALUATION OF MATERIALS COMPATIBLE WITH BLOOD

Since thrombosis is a reaction which occurs at a solid (blood vessel wall or prosthetic material) - electrolyte (blood) interface, one will intuitively expect that the reaction occurs via an electrochemical mechanism. Several studies conducted in our laboratories over the past eighteen years support this view.[1-4] Before discussing the methods used for the testing and evaluation of materials for their compatibility with blood, it is worthwhile summarizing the evidence for an electrochemical mechanism from our past work:

(i) Under normal conditions, the blood vessel wall and blood cells have a negative surface charge density.

(ii) Injury, or atherosclerosis, makes the blood vessel wall less negatively charged and quite often even positively charged.

(iii) A decrease in pH increases the surface charge density of the blood vessel wall and blood cells. At a pH of approximately 4.5, the blood vessel wall and blood cells have a zero surface charge and below this pH, their surfaces are positively charged.

(iv) Antithrombogenic drugs increase the negative charge density of the blood vessel wall and of blood cells while thrombogenic drugs have the opposite effect and quite often even cause a reversal in sign of the surface charge of both the blood vessel wall and blood cells.

(v) With conducting prosthetic materials, all those which maintain a negative potential in blood vs the potential of the normal hydrogen electrode (NHE) tend to be antithrombogenic when clean, while those which register positive potentials (NHE) are invariably thrombogenic.

(vi) With insulator materials, the homogeneously negatively charged ones tend to be non-thrombogenic.

With this background information, several types of experiments were designed to test and evaluate materials for their blood compatibility. The methods used in this study are summarized in Table 1.

---

*Recipient of Career Scientist Award from the Health Research Council, City of New York (Contract No. I 542).

TABLE 1

METHODS FOR THE EVALUATION OF MATERIALS IN RESPECT TO THEIR COMPATIBILITY WITH BLOOD

IN VITRO STUDIES	IN VIVO STUDIES
1. Electrokinetic (surface charge) characteristics of insulator materials (i) Streaming potentials (ii) Electroosmosis	1. Long term stability. Implantation of (i) Tubes in canine thoracic aorta or thoracic inferior vena cava (ii) Heart valves in tricuspid annuli of calves
2. Electrochemical mechanism of thrombosis on conducting materials (i) Measurements of stable rest potentials in saline and in blood (ii) Electrode kinetic parameters using blood and its separated components (a) current - potential measurements (b) reaction orders (c) heats of activation (iii) Electrosorption data using blood and its separated components (a) capacitance measurements (b) ellipsometric measurements	2. Streaming potentials in blood on insulator materials
3. Determination of blood destruction and antithrombotic characteristics by use of material in powder form (i) Blood cell counts (ii) pH changes (iii) Clotting times (iv) Fibrinogen-fibrin conversions	3. Detection of critical thrombosis potentials on conducting materials by capacitance measurements as a function of potential
4. Biochemical studies on mechanism of thrombosis (i) Release of adenine nucleotides from platelets in presence of materials (ii) Extent of platelet destruction by materials by measurement of G-6-P and protein levels	4. Measurements of potentials of implanted conducting materials (tubes, valves) as a function of time
5. Ultrastructure of thrombus deposits formed on materials in dogs or calves (i) Electron microscopy (ii) Histology (iii) Ultraviolet microscopy-spectorscopy	

An important aspect of the investigation is the elucidation of the detailed electrochemical mechanism of the thrombosis reaction. Such a knowledge is of immense importance in the scientific, rather than empirical, selection of prosthetic materials. The most basic questions in the elucidation of the mechanism of an electrochemical reaction are:

(i) What is the role of adsorption of reactants, intermediates or products? As is well known, adsorption of species from solution is a potential dependent phenomenon.

(ii) Is charge transfer involved in the overall reaction? If this be the case, there are several well known methods in electrode kinetics (viz, determination of Tafel parameters, reaction orders, stoichiometric numbers, heats of activation, etc.) which may be used to determine the mechanism of the reaction.

(iii) Is electrophoretic deposition of colloidal particles (viz, blood elements) involved in the overall reaction?

From the work until the present time, one can eliminate the third mechanism i.e., electrophoretic deposition. There is sufficient evidence that both electrosorption and electron transfer are involved in the thrombosis reaction. This scheme appears quite plausible on conductive materials but one may wonder how one can hypothesize such a mechanism on insulator materials. In the latter case, it is very probable that the entities which initially adsorb on the surface possess some eletronic conducting properties and thereafter the electrochemical mechanism follows.

Several of the other experiments presented in Table 1 are not electrochemical. They are, however, very important in the selection and evaluation of materials for their compatibility with blood. Further, they will be useful in correlating the direct blood compatible characteristics with the electrochemical ones.

It is not possible to present the findings of all aspects of the work covered during the first year, in this paper. They are covered in great detail in the Annual Report on the Contract for the first year.[5] Two types of experiments which were developed during the year are described in some detail in the following sections. In the final section, an analysis is made of the materials which appear most promising from our work carried out until the present time.

EFFECT OF MATERIALS ON THE PLATELET RELEASE REACTION

Introduction.

The experimental work done so far shows that the blood platelet's surface reactions are very important in the development of the hemostatic plug and thrombus formation on blood vessel wall.[6,7] All metazoan cells, so far examined, possess a net negative charge on their surfaces. Sawyer and his associates have demonstrated that electrical charge on the blood vessel wall plays an important role in maintaining blood in a free flowing liquid state.[1-4] A change in the net electrical charge of either vascular endothelial cells or platelets probably plays an important role in the initial step in intravascular thrombosis. With the exception of visible platelet deposition on foreign surfaces in the Petschek apparatus,[8] "viscous metamorphosis" of platelets and platelet aggregation appear to constitute the first visible evidence of intravascular thrombus formation in flowing blood. During these interreactions, a large proportion of the adenine nucleotides and the other platelet constituents appear to be released from platelets into the surrounding media.

Numerous agents - thrombin, immune complexes, collagen, latex particles, epinephrin and serotonin - cause platelets to aggregate.[9] Each of the mentioned compounds induce energy changes within the platelets and cause release of adenine nucleotides into the surrounding medium. An attempt to explain the phenomenon of this release suggests that any agent which alters platelet surface charge will instigate membrane permeability changes which lead to release of adenine nucleotides and aggregation of platelets.

In the present work, determinations were made of the extents of release of adenine nucleotides in the presence of some metals. Metals and other materials are being evaluated and tested in respect to their antithrombogenic characteristics in our laboratories as well as several others. Correlations have been made between the electrochemical interfacial characteristics of the materials in blood or other electrolytes having nearly the same ionic composition as blood and the usefulness of the materials for prosthetic devices. In the case of metals, the metals high in the electromotive series (e.g. aluminum, magnesium, zinc, cadmium) tend to be antithrombogenic while the noble metals are invariably thrombogenic.[1-4]

For the present study, three metals were selected - one corrodible (Al) and two noble ones (Au and Pt).

In addition to adenine nucleotides, glucose-6-phosphate levels were also determined to ascertain whether platelet destruction occurs in the presence of the foreign materials.

Experimental.

Experiments were carried out with suspensions of washed platelets from rat's blood. The separation and washing of platelets were carried out according to the technique of Ireland.[10] Two incubations were carried out simultaneously. One contained the powder of the test metal. The other with no foreign material served as a control. Following the incubation procedure, suspensions of control and experimental samples were separated into supernatant and platelet button fractions by centrifugation. The platelet button was then resuspended in the incubation medium. Both fractions were then deproteinized with perchloric acid and centrifuged to remove all traces of protein. The subsequent supernatant solution was neutralized with potassium hydroxide. The neutralized extracts of supernatant and platelet button fractions were then stored at 20°C prior to quantitative determination of adenine nucleotides and glucose-6-phosphate.

Adenine nucleotides (ATP, ADP, AMP) and glucose-6-phosphate (G6P) levels were determined in both platelet-free supernatant extracts and in platelet button extracts utilizing specific enzyme reactions.

Results.

In Figure 1, are shown the percentages of the three adenine nucleotides and G6P in the supernatant fractions of washed platelets after exposure to the three metals. Corresponding results of control experiments are also shown. The results may be summarized as follows:

ATP: The percentage quantities of the ATP in the supernatant fractions of all samples are quite small.

ADP: With Pt, release is fairly large. With Au, it is less and with aluminum much less. The control sample like the test sample containing aluminum, shows very little ADP release.

AMP: With Pt, the amount of AMP in supernatant fractions is the highest (70%). Au shows similar values (60%). With aluminum, it is still less similar to the control.

G6P: With Pt (71%), Au (52%), Al and control (20%).

Discussion and Conclusions.

1. There is a loss in the total amounts of ATP after exposure of platelets to the metals Pt and Au. Correspondingly, there is a marked increase in the total quantities of AMP and G6P in these cases. These results suggest that there is a conversion of the ATP in the presence of glucose to AMP and G6P.
2. There is a significant ADP release from platelets in the presence of Pt, less with Au, and much less with Al.
3. G6P, an intracellular compound, was measured in an attempt to determine if there was gross cell damage. That G6P in the button remained constant would indicate absence of damage resulting in leakage. However, the increase in the supernatant suggests that there was considerable leakage of cell contents. Thus, the question of cell damage has not been resolved. It is an interesting possibility that G6P is released in the process of "platelet release". Electron microscopic studies of the platelets, exposed to the metals, could yield information on possible destruction.
4. In previous work from our laboratories, it was shown that aluminum is non-thrombogenic while platinum and gold are thrombogenic.[1-4] The present experiment gives a further correlation between the thrombogenic character of a metal (viz by release of ADP, like the chemical compounds which do the same and cause platelets to aggregate) and its position in the electromotive series.

DETECTION OF THROMBOSIS ON CONDUCTING SURFACES BY CAPACITANCE MEASUREMENTS

Introduction.

The capacitance method had been used extensively for the determination of adsorption of entities such as atomic hydrogen, oxygen, oxides, hydrocarbons, alcohols, aldehydes and acids on electrodes from solutions.[11,12] Frumkin[12] proposed an empirical relation between the measured double layer capacity (C) and degree of coverage (θ) of adsorbed material on the electrode

$$C=C_0\ (1-\theta)+C_a \qquad (1)$$

where C_0 and C_a are the capacities when $\theta=0$ and $\theta=1$ respectively.

Since the capacitance at an electrode-solution interface is affected by adsorption of species on electrodes and an adsorption step of proteins or blood coagulation factors is involved during thrombosis at the critical potential,[1-4] determination of the capacity at a conducting material-blood interface should probably lead to the detection of thrombus deposition on a conducting material. The critical potential for thrombus deposition on metals is about 0-100mv/NHE.[1-4] Thus it was decided to study the capacity-potential (C-V) relation on a gold electrode in blood, both *in vitro* and *in vivo*, to check if there was any unusual behavior in the C-V plot at the critical potential. Gold was selected for this study because it is possible to work on this metal over a long potential range (over a volt) in which its surface is free of adsorbed species such as oxygen or oxides.

Experimental.

Electrical circuitry. The capacitance measurements were made using a capacitance meter developed recently by Gileadi and Tshernikovski.[13] The block diagram of the electrical set-up for the measurement of double layer capacities on electrodes is shown in Figure 2. A pair of test electrodes, auxiliary electrode and reference electrode are necessary.

Cell for in vitro studies. The cell used for the *in vitro* studies is shown in Figure 3.

Electrode arrangement for in vivo studies. The gold electrodes were inserted through side branches of carotid or femoral arteries, just as in the case of the experiments carried out to determine the critical thrombogenic potential on metals.[3]

Measuring techniques. In the *in vitro* studies, capacity-potential relations were performed on gold electrodes (clean and thrombus covered) in saline +ACD (control) and in blood. For the measurement of capacity, the gold electrodes were maintained at the same d.c.potential and a small a.c. triangular wage was superimposed between the two electrodes. The amplitude of the resulting square wave, which is proportional to the capacitance was measured. Further, the measurements were made in two ways - either leaving the gold electrode at a constant potential and measuring the capacity after a fixed time (1-3 mins.) starting at the lowest potential and increasing the potential in steps of 100 mv, or measurement of capacity while varying the potential linearly with time.

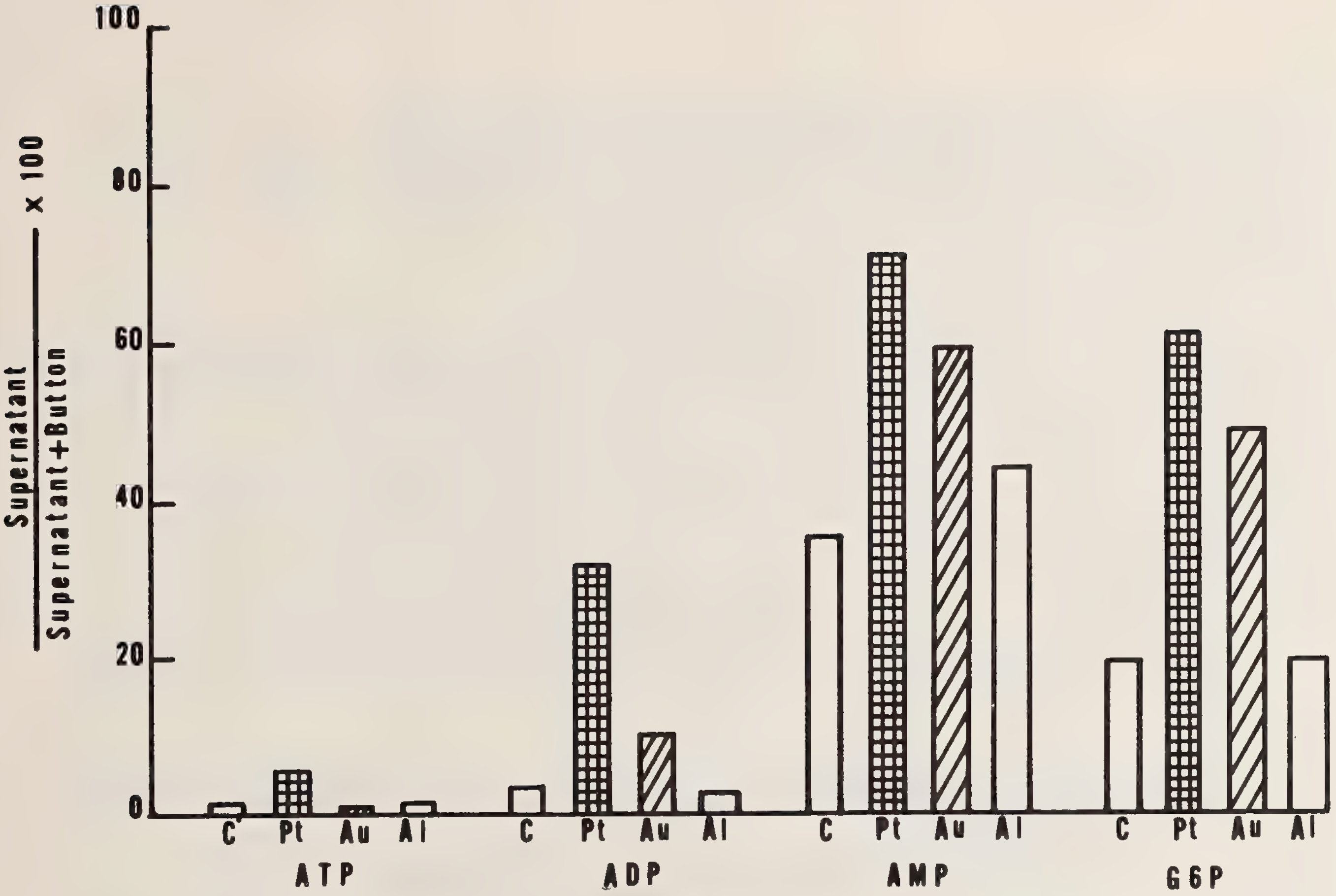

FIGURE 1. PERCENTAGE OF ADENINE NUCLEOTIDES AND GLUCOSE-6-PHOSPHATE IN SUPERNATANT SOLUTION AFTER CENTRIFUGATION OF SUSPENSION OF PLATELETS, EXPOSED TO SOME METAL POWDERS.

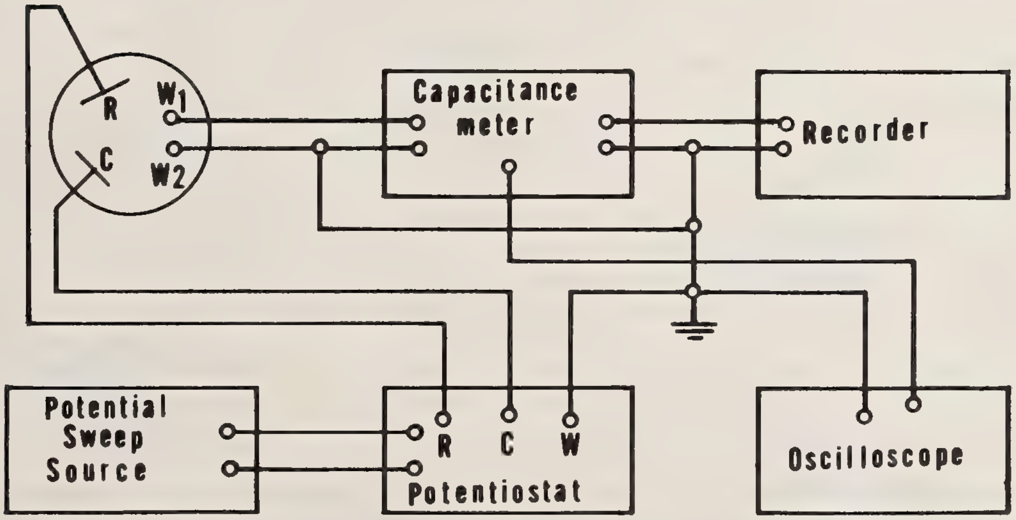

FIGURE 2. BLOCK DIAGRAM OF ELECTRICAL CIRCUIT FOR MEASUREMENTS OF CAPACITY AT ELECTRODE-ELECTROLYTE (E.G. SALINE, BLOOD) INTERFACE.

Results.

The results of the capacity-potential relations on a gold electrode (clean and thrombus covered) in saline +ACD are shown in Figure 4. Figure 5 shows the capacity potential relation on a gold electrode in blood *in vitro*; for comparison the C-V relation on a clean gold electrode in saline is also found in Figure 5. Figure 6, shows the capacity-potential relation on a gold electrode in blood *in vivo*.

Discussion.

There are several interesting features of the results:

(i) the relation on clean gold in saline shows a continuous increase of capacity with potential;

(ii) on the thrombus covered electrode in saline, the C-V relation passes through a maximum at -100 mv vs Ag/AgCl (+100mv vs NHE). The capacities are lower on the thrombus covered electrode than on the clean electrode throughout the potential range due to adsorption of several components of blood on the electrode;

(iii) the C-V relations on gold electrodes in blood are similar in the *in vitro* and *in vivo* experiments showing an inflection point around -200 to -100 mv vs Ag/AgCl (0 to + 100mv/NHE). The potentials at the inflection points coincide with the maximum of the C-V relation for the clot covered gold electrode in saline;

(iv) at potentials cathodic to the inflexion points, the capacities are higher and there is a fairly steady decrease of capacity with potential whereas at potentials anodic to the inflexion points, the capacities are lower and practically constant;

(v) the potential at the inflexion point is coincident with the critical potential for thrombus deposition on metal electrodes[3] and hence one may use this method for the detection of thrombus formation on conducting surfaces.

Future work.

The capacitance-potential relations will be made on other conducting materials in blood. In addition, the effect of antithrombogenic drugs on the capacity-potential relations will be examined.

AN ANALYSIS OF THE MORE PROMISING MATERIALS AT THE PRESENT TIME

Materials investigated on contract during first year.

The materials which have been either partly or completely tested during the first year are listed in Table 2.

TABLE 2

MATERIALS, PARTLY (P) OR COMPLETELY (C), TESTED IN RESPECT TO THEIR COMPATIBILITY WITH BLOOD

Metals	Alloys	Semiconductors	Insulators
Magnesium (C)	Stainless steel 304 (C)	Carbon (P)	Glass (pyrex, corex, soda) (P)
Aluminum (C)	Stainless steel 309 (C)	Bioelectric polyurethane (P)	Teflon (untreated, electrically treated, chemically treated-surface containing sulfonate, hydroxyl or carboxyl groups) (C)
Zinc (P)	Stellite (P)		
Nickel (P)	N 155 (P)		
Cobalt (P)	Inconel (P)		
Titanium (P)	Hastalloy (P)		
Copper (C)			Untreated and chemically treated Dacron (P)
Platinum (C)			Ioplex (anionic, cationic, neutral) (P)
Gold (C)			Carboxy methyl cellulose (P)

The materials are classified under metals, alloys, semiconductors and insulators. This classification is useful because several of the methods for the testing of the materials depends on the electronic conductivity of the materials. Metals and alloys have about the same electronic conductivity but a distinction between them yields information on the influence of alloying on the usefulness of the materials.

The methods used for the testing and evaluation of materials are presented in Table 1. Due to lack of time, all the materials listed in Table 2 have not been subjected to all of the experiments given in Table 1.

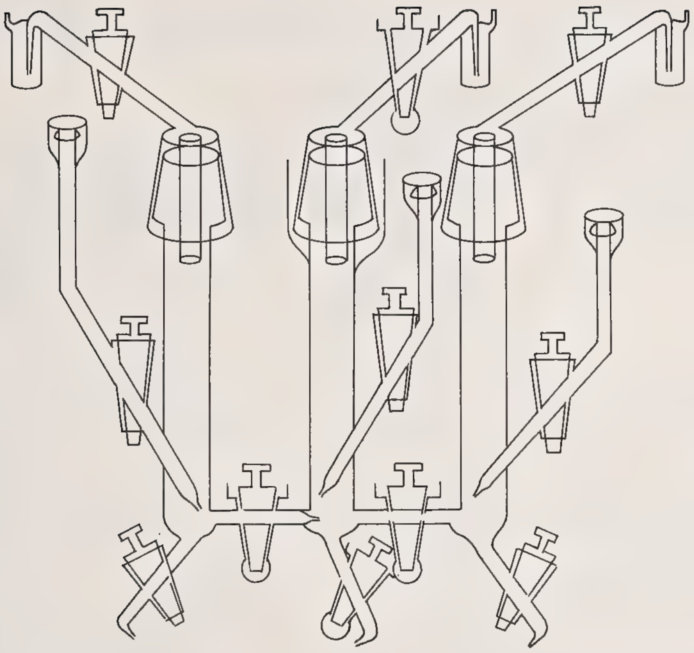

FIGURE 3. CELL FOR MEASUREMENT OF CAPACITY OF METAL ELECTRODES IN SALINE OR IN BLOOD. CENTER COMPARTMENT IS FOR PAIR OF TEST ELECTRODES; LEFT HAND SIDE COMPARTMENT IS FOR REFERENCE ELECTRODE; RIGHT HAND SIDE COMPARTMENT IS FOR COUNTER ELECTRODE.

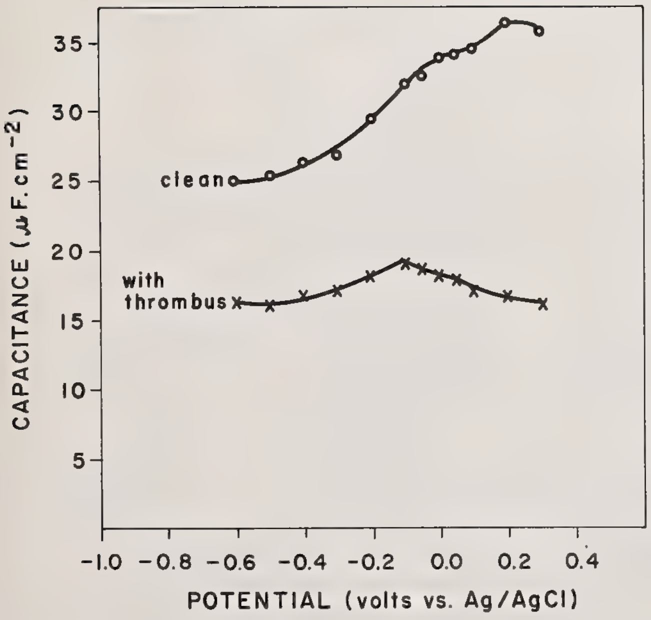

FIGURE 4. CAPACITY-POTENTIAL RELATION ON A CLEAN AND ON A THROMBUS-COVERED GOLD ELECTRODE IN SALINE SOLUTION CONTAINING ACD.

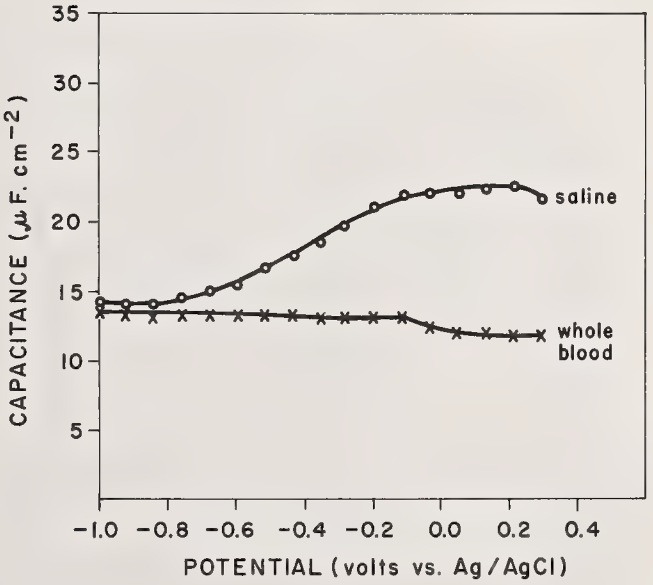

FIGURE 5. CAPACITY-POTENTIAL RELATION ON A GOLD ELECTRODE IN CITRATED BLOOD IN VITRO. CURVE IN SALINE IS SHOWN FOR COMPARISON.

The more promising materials, investigated during first year, and evidence for their usefulness.

Of the materials mentioned in Table 2, only a few show promise (Table 3).

TABLE 3

THE CURRENT POSITION OF THE MORE PROMISING MATERIALS TESTED AND EVALUATED

Material	Source of Material	Evidence for Usefulness of Material				Present Problems with Materials	Degree of Usefulness
		Potential (V) in blood vs. NHE or Zeta potential (ζ) in Krebs/1000 mv	Blood Destruction	ADP Release	Tube and Valve Implantation		
Aluminum	several	$V \approx -700$	Minimal	Minimal	No thrombus deposition	Corrosion	B
Titanium	Smeloff Cutter (Valve) and T.C.A.	$V \approx 100$	No data	No data	No thrombus deposition	None	B-A
Stellite	Starr Edwards	$V \approx 100$	Minimal	No data	No thrombus deposition	Pannus formation	B
Carbon	Carbone Corporation	$V \approx 400$	Minimal	Minimal	Junctional thrombus in tube	Overgrowth of Neo-intima	B
Sulfonated Teflon	American Cyanamid Corporation	$\zeta \approx -25$	Minimal	No data	Good	-	A
Carboxylated Teflon	American Cyanamid Corporation	$\zeta \approx -15$	Minimal	No data	Junctional thrombus formation in some	Thrombus formation in some	C

This Table shows: (i) the source providing the material, (ii) the evidence in which usefulness is judged, (iii) the present problems with the use of the material and, (iv) the degree of usefulness. The grading system for the degree of usefulness is as follows: A - Very good; B - Good; and C - Fair.

Materials being currently tested and evaluated.

At the time of writing of this article, extensive testing is underway of the materials provided by several companies. The nature of the materials, the companies providing them and the experiments being carried out are found in Table 4. *In vivo* testing of materials as tubes capable of being implanted in the vascular tree have been carried out with materials from four groups. (American Cyanamid, Battelle, Amicon and Monsanto Research.) These materials were initially tested *in vitro* to determine their general physical, chemical and electrochemical characteristics and then implanted either as tubes in the thoracic inferior vena cava (TIVC) for two hours, and/or two weeks (if they proved to be antithrombogenic in two hours). The two-hour and two-week tests have proven to be very good and we think that the TIVC is a very good vessel for a critical test. In this *in vivo* evaluation in the vena cava we have taken a slightly different path from that of Dr. Gott. A longer tube 3 -4cm long with uniform diameter, because of exposure of blood to a layer surface area should provide ample information concerning its antithrombogenic character in the short periods it is implanted.

Some materials have recently been received from Union Carbide, Melpar, Polysciences and the Goodyear Research Corporation all of which are now undergoing rather extensive testing. Three groups have had sufficiently complete testing that the results can be reported. These include those from Battelle, Monsanto Research and Amicon. As shown in Tables 5 and 6, the materials provided by Battelle appear quite promising. Both positive and negatively charged surfaces-negative heparinized and positive polyquarternary ammonium coated-were sent to us by Battelle. The characteristic surface charge characteristics of these materials are indicated in the last column under zeta potentials which are the most important parameter in Table 5. Table 6 shows in general that the untreated silicone rubbers are nearly as good as the heparinized surfaces provided us by the Battelle group. The quarternary ammonium coatings were positive and produced rapid thrombosis at inflow sites.

TABLE 4

EXPERIMENTAL WORK BEING CARRIED OUT ON THE RECENTLY OBTAINED MATERIALS

Source of Material	Material	Experiments being carried out with material				
		Streaming Potential	Blood Destruction	Implantation as: Tube	Valve	Other
American Cyanamid Company	Chemically and electrically treated insulators	X	X	X	X	
Amicon Corporation	Anionic, cationic and neutral ioplexes	X	X	X		Electroosmosis
Battelle Memorial Institute	Positively (quarternary ammonium salt) and negatively charged (heparinized) insulators	X	X	X		
Goodyear Research Corporation	Bioelectric polyurethane		X		X	Measurement of potential in blood
Gulf General Atomic Inc.	Carbon, Si doped or chemically treated		X			Measurement of potential in blood
Melpar Inc.	Chemically treated carboxy methyl cellulose		X	X		Electroosmosis
Monsanto Research Corporation	Heparinized insulators	X	X	X		
Polysciences Inc.	Chemically treated membranes		X	X		Electroosmosis
Thermo Electron Corporation	Electrets	X		X		
Union Carbide Corporation	Polyelectrolytes		X	X		Electroosmosis

TABLE 5

RESULTS OF STREAMING POTENTIALS VS PRESSURE MEASUREMENTS AND CALCULATED VALUES OF ZETA POTENTIALS ON SOME UNTREATED AND CHEMICALLY TREATED FLEXIBLE SILICONE RUBBER TUBES

Battelle Code No.	Surface Active Group	Concentration of Krebs Solution	Dimensions		Slope dE/dP mv/cm, Hg	Zeta Potential mv
			ID,mm	Length,cm		
	Untreated	K/1000	10	3	$\frac{60}{40}$	-3.2
	Heparinized	K/1000	10	3	$\frac{65}{40}$	-3.4
	Quaternary Ammonium Salts	K/1000	10	3	$\frac{-90}{40}$	+4.8
	Quaternary Ammonium Salts	K/1	10	3	$\frac{-.3}{40}$	+15.9
	Heparinized	K/1	10	3	$\frac{+.3}{40}$	-15.9
	Untreated	K/1	10	3	$\frac{+.4}{40}$	-21.2

TABLE 6

RESULTS OF IMPLANTATION OF FLEXIBLE SILICONE RUBBER TUBES IN CANINE THORACIC INFERIOR VENA CAVA

Tube Code No. SUNY	Battelle	Surface Active Group	Chronic/acute	Period of Implantation	Condition of Tube	Remarks
P-34-69 4.25.69		Untreated	Chronic	14 Days	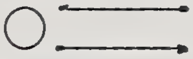	Sacrificed
P-35-69 4.25.69		Untreated	Chronic	11 Days	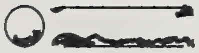	Junctional Thrombus
P-36-69 4.25.69		Quaternary Ammonium Salt	Chronic	14 Days	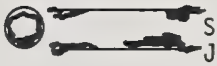	Sacrificed Junctional Thrombus
P-47-69 5.1.69		Quaternary Ammonium Salt	Chronic	6 Days	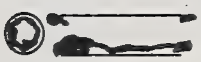	Junctional Thrombus 30% Occlusion
P-46-69 5.1.69		Heparinized	Chronic	14 Days	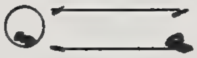	Sacrificed Junctional Thrombus
P-46-69 4.28.69		Untreated	Acute	5 Hours	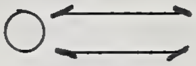	Clean
P-41-69 4.29.69		Quaternary Ammonium Salt	Acute	3 Hours 20 Min.	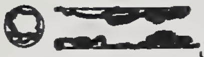	Junctional Thrombus
P-42-69 4.29.69		Heparinized	Acute	5 Hours	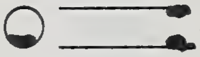	Junctional Thrombus
P-45-69		Quaternary Ammonium	Acute	3 Hours 50 Min.	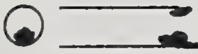	Junctional Thrombus

Right ← Hepatic
atrium blood flow

Table 7 illustrates the electrokinetic characteristics of the various neutral cationic and anionic charged ioplexes provided by the Amicon Corp.

TABLE 7

ZETA POTENTIALS OF SOME MATERIALS IN KREBS/1 SOLUTION
AT A pH OF 7.2 - 7.4, AS DETERMINED BY ELECTROOSMOSIS MEASUREMENTS

Material and Code No.	Company providing materials	No. of Expts.	Zeta Potential mv Krebs	Remarks
Neutral 45% film	Amicon	3	+4.88 ± 0	The pores of the Neutral film membranes are rather large. Thus giving the solution a free passage either way I →A or A →I. This makes the direction of flow rather erratic - sometimes + orientation sometimes - orientation. Unless these pore sizes can be modified some, a definite result is impossible.
Neutral 59% film	"	3	+2.93 ± 0.7	
Neutral 67% film	"	3	+3.91 ± 0	
0.5 Cationic film	Amicon	3	+15.64 ± 0	
ioplex 103 .0.27 Cationic 81% film	"	3	+ 8.14 ± .43	
0.5 Anionic 50% film	Amicon	3	-7.82 ± 0	
0.8 Anionic 52% film	"	3	-8.79 ± 0	
0.5 Anionic 63% film	"	3	-6.84 ± 0	
0.8 Anionic 70% film	"	3	-14.66 ± 0	
0.5 Anionic 79% film	"	3	-14.66 ± 0	
1.3 Anionic 76% film	"	3	-17.58 ± 0	
ioplex 103 0.15 Anionic 37% film	"	3	+6.84 ± 0.8	
ioplex 103 0.7 Anionic film	"	3	-9.77 ± 0	

They have provided us with a large number of ioplexes with varying surface charge. The surfaces of the ioplex membranes (Table 8) have frequently proven mechanically unstable, whether positively or negatively charged at implantation. Most of these surfaces have displayed some evidence of thrombus deposition very shortly after implantation and in almost all instances after two or three hours. There has been relatively little consistency in the surfaces and we are unable to explain this. It is very difficult to come to any significant conclusions concerning these surfaces tested in vivo.

Table 9 contains streaming potential measurements for a number of materials with 3 and 7% heparin coatings from the Monsanto Research Corporation. The surfaces are all negatively charged. Those with the higher heparin concentration have a more negative zeta potential. Several epoxy tubes were sent to us with either 3 or 7% coatings as well as one or two control epoxies (Table 10). The control epoxy tubes seemed to do relatively well. It is noted that most of the epoxy tubes fractured or disintergrated leading to hemorrhage and junctional thrombi formation. In instances where this occurred it was difficult to interpret the results of these materials. In the acute animal, neither the 3 or 7% coatings kept the tubes completely free from junctional thrombus formation or of some small amount of mural thrombus formation. The control tube in this instance appears to have done almost as well as either 3 or 7% heparin during an acute five hour implantation. The major problem with these epoxy samples are their mechanical instability.

The materials which we have received from several other corporations mentioned in Table 4 have been received so recently that it has not been possible for us to complete the evaluation of the materials.

The information in general tends to confirm the general hypothesis that negatively charged surfaces are more resistant to thrombus formation than positively charged surfaces.[1-4] It seems to be true for non-conductive materials such as many of the polymers tested. However, the results of electrochemical testing techniques here have been considerably more sophisticated than in the case of the more easily evaluated metal surfaces. It has been our experience, with materials from several of the companies, that as they have repeatedly produced surfaces for us the uniformity of the surfaces has tended to improve and the results of in vivo testing have correspondingly been more uniform and more satisfactory.

TABLE 8

RESULTS OF IMPLANTATION OF IOPLEX TUBES IN CANINE THORACIC INFERIOR VENA CAVA

Tube Code No.		Chronic/acute	Period of Implantation	Condition of Tube	Remarks
SUNY	Amicon				
P-80-68 10.2.68	Anionic 0.5	Chronic	13 Days	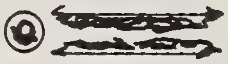	80% occlusion. Inner ioplex capsule separated causing mechanical occlusion, leaking and thrombosis
P-81-68 10.4.68	Anionic 0.5	Chronic	5 Days	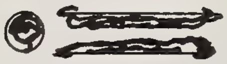	80% occlusion. Inner ioplex capsule separated causing mechanical occlusion, leaking and thrombosis
P-101-68 11.26.68	Anionic 0.5	Chronic	21 Days	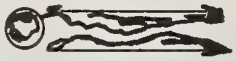	90% occlusion. Inner ioplex capsule separated causing mechanical occlusion, leaking and thrombosis
P-102-68 11.26.68	Anionic 0.5	Chronic	46 Days	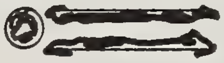	Sacrificed-80% occlusion ascites
P-25-69 4.22.69	Control	Chronic	14 Days	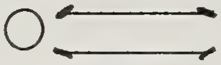	Sacrificed
P-26-69 4.22.69	Cationic	Chronic	14 Days	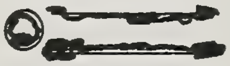	60% occlusion Junctional Thrombus Sacrificed
P-43-69 4.29.69	Anionic 0.5	Acute	5 Hours	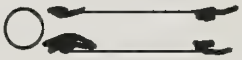	Sacrificed Junctional Thrombus attached to vessel wall
P-44 4.29.69	Cationic	Acute	5 Hours	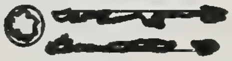	Sacrificed Junctional Thrombus attached to tube

Right ← Hepatic
atrium blood flow

TABLE 9

RESULTS OF STREAMING POTENTIALS VS PRESSURE MEASUREMENTS AND CALCULATED VALUES OF ZETA POTENTIALS ON SOME FLEXIBLE HEPARINIZED EPOXY TUBES IN KREBS/1000 SOLUTION

Monsanto Code No.	Percent Heparin	Concentration of Krebs Solution	Dimensions ID,mm	Dimensions Length,cm	Slope dE/dP mv/cm, Hg	Zeta Potential mv
	3	K/1000	10	3.0	$\frac{175}{40}$	-9.3
	7	K/1000	10	3.0	$\frac{110}{40}$	-5.8
	3	K/1	10	3	$\frac{+.3}{40}$	-15.9
	7	K/1	10	3	$\frac{+.5}{40}$	-26.5

TABLE 10

RESULTS OF IMPLANTATION OF FLEXIBLE EPOXY TUBES IN CANINE THORACIC INFERIOR VENA CAVA

Tube Code No. SUNY	Tube Code No. Monsanto	Percent Heparin on Surface	Chronic/acute	Period of Implantation	Condition of Tube	Remarks
P-27-69 4.22.69	NBP 92126 69-03-27-02	Control	Chronic	14 Days	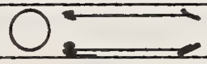	Sacrificed
P-28-69 4.22.69	NBP 92127 69-03-27-03	3	Chronic	18 Hours	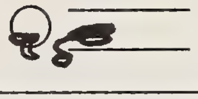	Proximal defect in tube-broken Haemothorax led to death. Mechanically unstable
P-30-69 4.24.69	" "	3	Chronic	2 Days	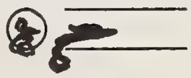	Proximal defect in tube-broken Haemothorax led to death. Mechanically unstable
P-31-69 4.24.69	NBP 92128 69-03-27-04	7	Chronic	4 Days	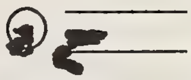	Proximal defect in tube-broken Haemothorax led to death. Mechanically unstable
P-32-69 4.24.69	" "	7	Chronic	12 Hours	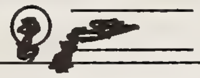	Proximal defect of tube Haemothorax
P-33-69 4.24.69	" "	7	Chronic	18 Hours	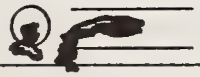	Proximal defect of tube Haemothorax
	Sacrificed after 5 Hours					
P-37-69 4.28.69	NBP 92126 69-03-27-02	Control	Acute	5 Hours	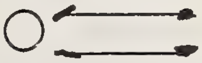	Junctional Thrombus
P-38-69 4.28.69	NBP 92127 69-03-27-03	3	Acute	5 Hours	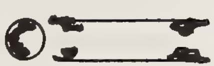	10% occlusion Junctional Thrombus
P-39-69 4.28.69	NBP 92128 69-03-27-04	7	Acute	5 Hours	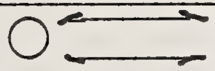	Clean

Right ← Hepatic
atrium blood flow

ACKNOWLEDGEMENTS

The authors wish to thank Dr. T.C. Detwiler, Dr. J.G. Stempack and Dr. L. Vroman for providing the facilities of their laboratories to carry out the biochemical, electron microscopic and ellipsometric investigations respectively.

Significant contributions to the work described in this paper and in the Annual Report for 1968 on the contract PH 43-68-75 were made by Drs. R. Zivkovic, E. Gileadi, M.E. Lee, R. Rubin, B. Stanczewski, A. Parmeggiani and Messrs. M. Ranganathan, C.B. Burrowes, T.R. Lucas, R. Morrison, T.E. Kasper, J.L. Cohen, N.A. Chase, L. Rubin, A.I. Garfinkel, E.J. Ginchansky, M.J. Touger, H. Pollack and S. Gottlieb.

REFERENCES

1. Sawyer P.N. (ed), Biophysical Mechanisms in Vascular Homeostasis and Intravascular Thrombosis, Appleton Century Crofts, New York, 1965.
2. Sawyer P.N. and Srinivasan S., Metallic and plastic prosthetic devices as vascular wall substitutes: biophysical criteria and methods of evaluation, J. Biomed. Mat. Res., 1:83, 1967.
3. Sawyer P.N. and Srinivasan S., Studies on the biophysics of intravascular thrombosis, Am. J. Surg., 114:42, 1967.
4. Sawyer P.N. and Srinivasan S., Thrombosis: a surface chemical phenomenon, submitted for publication to Acta Surgica Scandinavica.
5. New Approaches in the Selection of Materials Compatible With Blood, Annual Report on Contract (Principal Investigator: P.N. Sawyer) No. PH 43-68-75 with Artificial Heart Program, National Heart Institute, National Institutes of Health, Bethesda, Maryland for 1968.
6. Mustard J.F., Glynn M.F., Nishizawa E.E. and Packham M.A., Platelet surface interaction: relationship to thrombosis and hemostasis, Fed. Proc., 26:106, 1967.
7. Hughes J., The pathophysiology of hemostasis, Thromb. et. Diath. Haemorr., 8:41, 1962.
8. Petschek H., Adamis D. and Kantrowitz A.R., Stagnation flow thrombus formation, Trans. Amer. Soc. Artif. Int. Organs, 14,256, 1968.
9. Zucker M.B., A.D.P. and collagen induced platelet aggregation _in vivo_ and _in vitro_. Thromb. et. Diath. Haemorr., 26 (Suppl): 175, 1967.
10. Ireland D.M., Effect of thrombin on the radioactive nucleotides of human washed platelets, Biochem. J., 105:857, 1967.
11. Piersma B.J. and Gileadi E., The mechanisms of electrochemical oxidation of organic fuels, Chapter 2 in J.O'M. Bockris and B.E. Conway (eds), _Modern Aspects of Electrochemistry_, Vol. 4, Plenum Press, New York, 1966.
12. Frumkin A.N. and Damaskin B.B., Adsorption of organic compounds at electrodes, Chapter 3 in J.O'M. Bockris and B.E. Conway (eds), _Modern Aspects of Electrochemistry_, Vol. 3, Butterworths, Washington, 1964.
13. Gileadi E. and Tshernikovski N., New techniques for double layer capacitance measurements at solid metal electrodes, To be published.
14. Gileadi E., Srinivasan S. and Sawyer P.N., Electrochemical methods for the detection of thrombus formation on conducting surfaces. J. Electroanal. Interf. Electrochem, 21:P 6, 1969.

DISCUSSION

MR. SALYER: I have one question for Dr. Sawyer. It has to do with the fact that so many of our samples broke, and I wanted to remark that apparently his test is a little rougher mechanically as well because Dr. Gott was able to handle those same samples without them breaking. However, the DETA cured samples are flexible and much stronger. I assure you that the next samples you get will be more suitable.

DR. SAWYER: Thank you. I think some of the problems with those test samples is that the tubes are longer and they flex everytime the heart beats on the atrium. You note that they all flex at the atrial side,not at the hepatic impulse side.

MR. SALYER: Do you want them to be made a little stiffer?

DR. SAWYER: Well, they could be a bit more elastic but still not too compressible so that my vascular fellow can tie them in, or he can try to tie them more strongly. Why don't you try them stronger first.

MR. SALYER: Yes, we will try to do that.

DR. BLACK: I have a question for Dr. Sawyer also. In the work you reported on measuring electrode capacitance in whole blood. How were you able to distinguish between protein adsorption on the surface and just the attraction of the blood elements?

DR. SAWYER: Anything which coats that electrode will change its capacitance. What Dr. Srinivasan and coworkers are trying to do is something very sophisticated in a very simple way. They are trying to determine when the first layers deposit on the surface. It is a most sophisticated way to examine adsorption. The minute the first layer deposits on that electrode, there will be a change in the capacitance.

DR. BLACK: Maybe what I should ask is "What indeed did you find was the first layer that was attracted?"

DR. SAWYER: I don't think Dr. Srinivasan really knows because what he now has to do is develop electrodes which are suitable for electron microscopy. He has to develop a gold coated foil to use as his electrode and then he can actually fix that and look at it through the electron microscope.

DR. BLACK: I would like to mention some work that has been going on in our laboratories at the University of Pennsylvania. We have been doing the same experiment, Dr. Svare has been conducting these. He has been looking at simple amino acids on pure metal surfaces in physiological saline in the absence of all the proteins and blood fractions and he finds that some of them in particular are adsorbed on copper at an extremely low concentration, at microgram levels. There is a major change in the capacitance of the surface long before adsorption occurs. In fact, he gets a very radical capacitance change on the order of a factor of two at one thousandth of a monolayer of the adsorbate.

DR. SAWYER: That's good. At what potential does this take place?

DR. BLACK: I think on copper at pH 7, it takes place at about 100-200 mv. It is very similar to the potentials which you mention. Of course, this is on a different metal.

DR. SAWYER: It doesn't really matter. It's not metal really, it is the potential that matters.

DR. BLACK: Well, unfortunately we think it is metal, because we do not see the same thing on chromium.

DR. SRINIVASAN: Yes, it is metal and it will depend on the potential of zero change of the metal in this medium. As far as chromium is concerned I do not know where the potential of zero change is in neutral medium.

DR. MARSHALL: I have a question to ask of Dr. Sawyer. I would like to know if he sterilized the Ioplex materials, and if so, how?

DR. SAWYER: No, we did not sterilize them, because we didn't know how to. We figured, if we sterilized them we would ruin them, and we assumed that you sent them to us at least clean. I figured it would be better if we tested them clean than not at all.

DR. MARSHALL: You can sterilize them by hydrochloric acid wash. I'll send you the procedures, but essentially it is immersed for one hour in 30% HCl, rinsed and then soaked in NaOH for one hour and washed till neutral.

DR. SAWYER: I'll bet if we continue to put them in as we get them from you, just the way we have gotten them, we'll get better results than if we sterilize them in 30% HCl. There is no evidence of infection around these by the way.

DR. HASTINGS: This is a question for both Dr. Sawyer and Dr. Kusserow: I just wondered what they think the lungs would look like if they had been prepared by Dr. Kusserow's technique, following Dr. Sawyer's inferior vena caval implants?

DR. SAWYER: I thought that the technique was perfectly gorgeous, Frank.

DR. LEONARD: I would like to ask Dr. Sawyer a question. You indicated, I think, Dr. Sawyer that there was a reason for the difference in the thrombogenic or non-thrombogenic character between carboxylated Teflon and sulfonated Teflon.

DR. SAWYER: No, I am rather satisfied with both of those surfaces, too. The last batches were pretty homogeneous and the carboxylated and sulfonated surfaces were tested both in vitro and in vivo. That's all I can report to you.

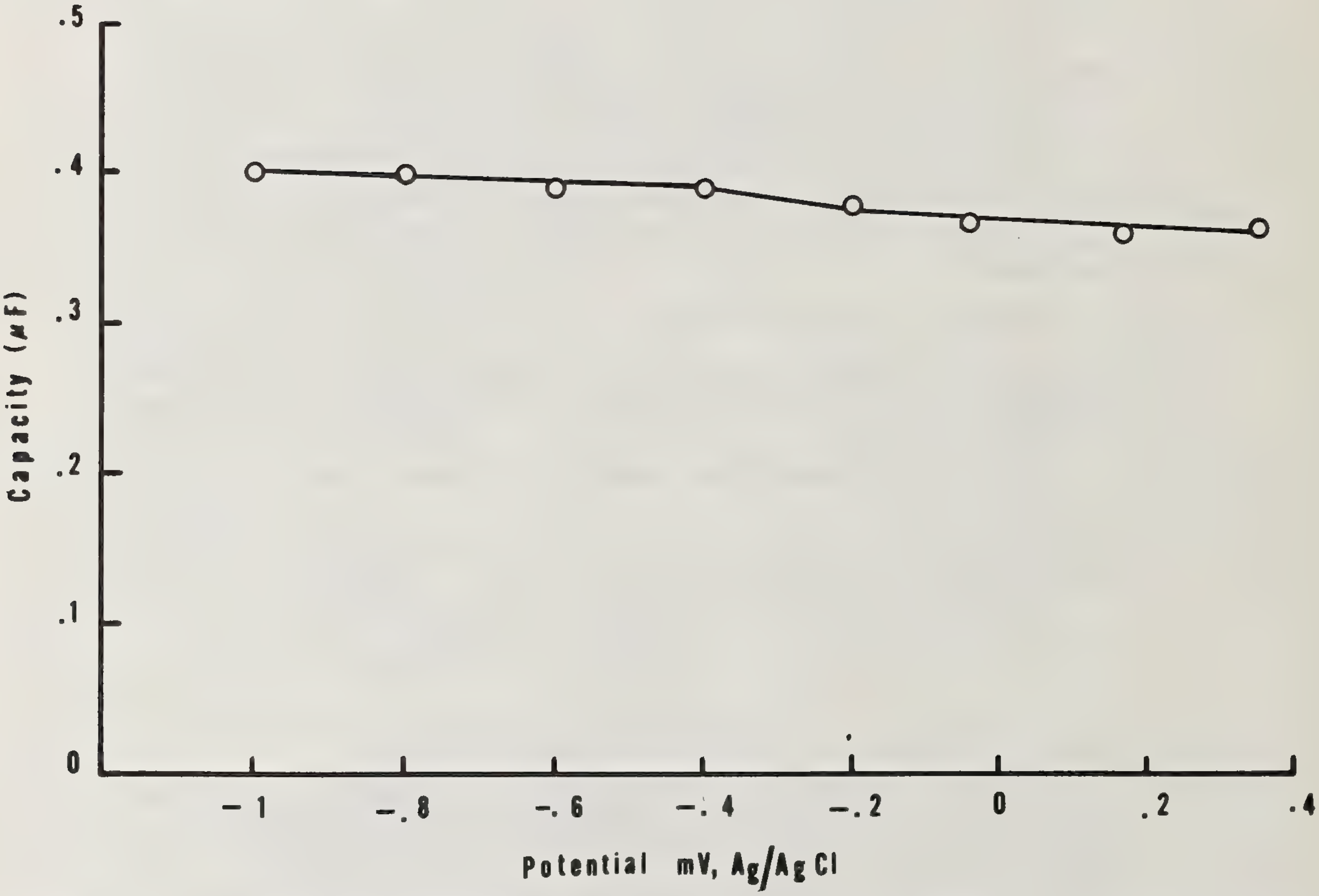

FIGURE 6. IN VIVO CAPACITY-POTENTIAL RELATION ON A GOLD ELECTRODE INSERTED INTO A CANINE CAROTID ARTERY.

CHAPTER 23

IMMUNOGENIC EFFECTS OF MATERIALS ON PLASMA PROTEINS

I.J. Stern, A.A. Kapsalis, and B.L. Neil

Travenol Laboratories, Inc.

Morton Grove, Illinois

A possible characteristic of materials which may have long term toxic potential is the promotion of immunigenicity in adsorbed autologous plasma proteins. Bases for this study lie in observations of others that proteins are adsorbed generally by materials (R.D. Falb, et al., NHI Contract PH-43-64-496, report of 30 March 1967), may be subtly denatured by adsorption [D.K. Chattoraj and H. Bull, J. Am. Chem. Soc. 81, 5128 (1959)], and may acquire greatly enhanced immunogenicity as a result of adsorption [S. Kochwa, et al., J. Immunol. 99, 981 (1967)]. Implants of materials promoting immunogenicity in autologous proteins would present constant antigenic stimuli to the recipient which might predispose towards autoimmune phenomena [H.M. Pretty, et al., Blood 32, 205 (1968)] or neoplastic plasma cell transformations (J.H. Vaughan in "Immunological Diseases", Little, Brown and Co., pp.723-4). Tests for immunogenicity are performed with materials samples of smooth surface and high surface-area-to-volume rations. Ideally, materials with 0.5 m^2 surface area are sealed in polyvinyl chloride bags and agitated gently at 37°C for 24 hrs. in the absence of gas interfaces, with about 20 ml of heparinized rabbit plasma isolated without contact with glass or air. A sample of the exposed plasma is retained for analysis and later use as antigen, and the remainder is injected into the original donor rabbit in an attempt to stimulate an immune response. The formation of antibodies is determined by interfacial ring, gel diffusion, passive hemagglutination, and passive cutaneous anaphylaxis techniques. Initial results indicated that immunogenicity was not induced by contact with blood processing equipment. Repeated freezing and thawing produced little or no denaturation discernible by cellulose acetate or immunoelectrophoresis, but the plasma was rendered immunogenic. Plasma treated with alkali was immunogenic as well as grossly denatured by the above electrophoretic criteria. Results obtained with several material test samples will be discussed.

INTRODUCTION

One possible consequence of exposure to foreign surfaces is the subtle denaturation and subsequent promotion of immunogenicity in autologous plasma proteins so that they become antigenic for the host. The basis for this hypothesis lies in observations in several laboratories that foreign surfaces immersed in plasma acquire at least a monomolecular layer coating of protein which is partially denatured[1,2]. The process of adsorption, at least to polystyrene, has been demonstrated to increase greatly the antigenic activity of heterologous antigens[3,4]. Whether autologous plasma proteins which have been adsorbed and subsequently desorbed may be rendered antigenic, and whether this induction of antigenicity varies with different material surfaces is the principle goal of this research.

Immunogenic effects of materials intended for long term implantation may be related to subtle, chronic toxic effects. If autologous protein were adsorbed, denatured, and released from an implanted material, there would be present in the host a constant antigenic stimulus. Adsorption, denaturation, and desorption could be envisioned as occurring possibly at the material surface or at the surface of a protein monolayer, which Lyman and his co-workers[5] have described as irreversibly adsorbed in vitro. It seems improbable, however, that in vivo there would not be at least some desorption and replacement of the monolayer. Although small quantities of denatured autologous proteins undoubtedly are removed by naturally-occurring scavenger mechanisms, in atopic[6] or immunologically deficient[7] patients, or in debilitated patients desensitization may not occur. Some extreme reactions to plastic implants in lower animals, such as the induction of plasma cell tumors in mice[8] and the formation of neoplasms in rats[9] are reminiscent of diseases in man thought to be related to constant antigenic stimuli. Moreover, it is conceivable that foreign material implants might be involved in autoimmune phenomena by modifying host antigens just enough to render them antigenic, while they still retain cross-reactivity with native antigen[10]. It is important to note again, that while increased antigenicity due to adsorption to plastic has been described for heterologous proteins, that is, human IgG antigen in rabbits, the induction of antigenicity by foreign surface contact in autologous proteins, that is, of rabbit protein for the same donor rabbit, has not been described.

IMMUNOGENIC TEST PROCEDURE

In the test developed here, about 60 ml. of blood are removed from 2-2.5 kg. rabbits with polypropylene syringes containing about 1,000 units of heparin. The blood is inserted beneath the mineral oil layers in polycarbonate tubes, and after centrifugation the plasma is withdrawn directly through polyvinyl tubing into polyvinyl chloride blood transfer bags (surface area 198 cm^2, Figure 1). Material samples are sealed into the bag previously, and sterilized by steam when water is present, or by ethylene oxide in dry samples. Ioplex resin samples were sterilized with formaldehyde which was subsequently removed by washing with isotonic saline. The ethylene oxide sterilized samples were heated at 55°C under vacuum for 2 hours to remove residual gas. Shown here are an unsealed bag, and a bag sealed with carbon-coated zirconium oxide granules inside. Tests with spore strips in similar bags confirmed the efficiency of our sterilization procedures. Other samples sealed in the bags with about 20 ml of water added to simulate the conditions during testing are shown in Figure 2. All of the residual air bubbles may be removed by careful manipulation and gentle suction at the inlet tube.

The general plan of the test (Figure 3) was to expose plasma of a donor animal to a large surface area of material for 24 hours at 37°C in the absence of gas interfaces. Part of the exposed plasma was frozen for later use as antigen, and the remainder was lyophilized and injected back into the original donor rabbit in an attempt to induce antibody formation. Five animals were used for each variable or for each test sample.

The detection systems used here were chosen to pick up the major classes of antibody types. Gel diffusion detected precipitating antibodies and was the least sensitive of the tests used. Passive hemagglutination of formaldehyde-sensitized sheep erythrocytes detected precipitating and agglutinating antibodies. Finally, passive cutaneous anaphylaxis (PCA) in the guinea pig detected some precipitating and agglutinating antibodies as well as the tissue-sensitizing class. All samples were tested for sterility by plating on blood agar after exposure.

To obviate effects of the processing equipment and container surfaces, extensive control experiments were performed to determine the antigenicity of isolated plasma. As shown in Table 1 plasma which was simply removed from a rabbit and re-infused intravenously either all at once or in several weekly injections gave no reactions. Lyophilization followed by 5 weekly injections in Freund's adjuvant plus an intravenous injection adsorbed to calcium alginate also gave no reaction. Rather disturbing to us at this stage was the finding that deliberate denaturation of plasma by repeated freezing and thawing or alkaline treatment also gave no reaction, at least with the simple autologous system shown here. On the possibility that "incomplete" antibodies were present, Coombs' serum was included in the passive hemagglutination test. Although some technical difficulties were encountered in this system, 3 of 4 surviving rabbits developed antibodies to their own alkali-denatured plasma, but none were detected as a result of processing, lyophilization, or freeze-thaw denaturation.

TABLE 1

EFFECTS OF PROCESSING EQUIPMENT AND CONTAINER SURFACES ON THE AUTO-IMMUNOGENICITY OF RABBIT PLASMA
1. AUTOLOGOUS ANTIGEN

	Positives/Total No. in Group			
		Passive Hemagglutination		
Treatment	Gel Diffusion	Direct	+ Coombs' Reagent	PCA[f]
None[a]	0/5	0/5	0/5	0/5
Lyophilization[b]	0/5	0/5	0/5	0/5
Freeze-thaw[c]	1/4	0/4	0/4	0/4
Alkali[d]	0/4	0/4	3/4	0/4
Shaking[e]	0/5	0/5	---	0/5

[a] No treatment: Multiple reinjection of native plasma

[b] Lyophilization: Plasma lyophilized and injected at 5 weekly intervals in Freund's adjuvant and once adsorbed to Ca-alginate

[c] Freeze-thaw: After 5 cycles of freezing and thawing, plasma was lyophilized and injected as in b above

[d] Alkali: Plasma was brought to pH 10 with NaOH, neutralized, lyophilized, and injected as in b above

[e] Shaking: Plasma was shaken 24 hrs. without an air interface in PVC bags at 37°C, lyophilized, and injected as in b above

[f] PCA: Passive Cutaneous Anaphylaxis.

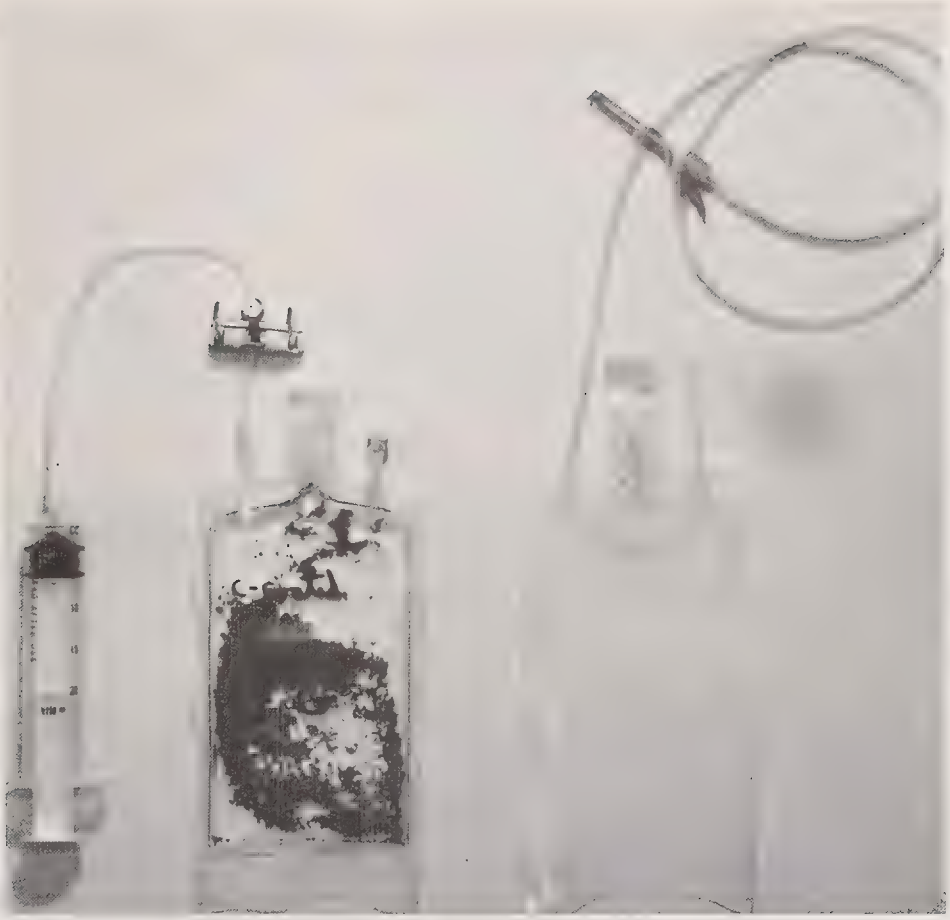

FIGURE 1. POLYVINYL CHLORIDE BLOOD TRANSFER BAGS. ON RIGHT - UNSEALED; AT LEFT - BAG SEALED WITH 5 GM OF C-COATED ZrO_2 GRANULES INSIDE IN 20 ML OF ISOTONIC SALINE.

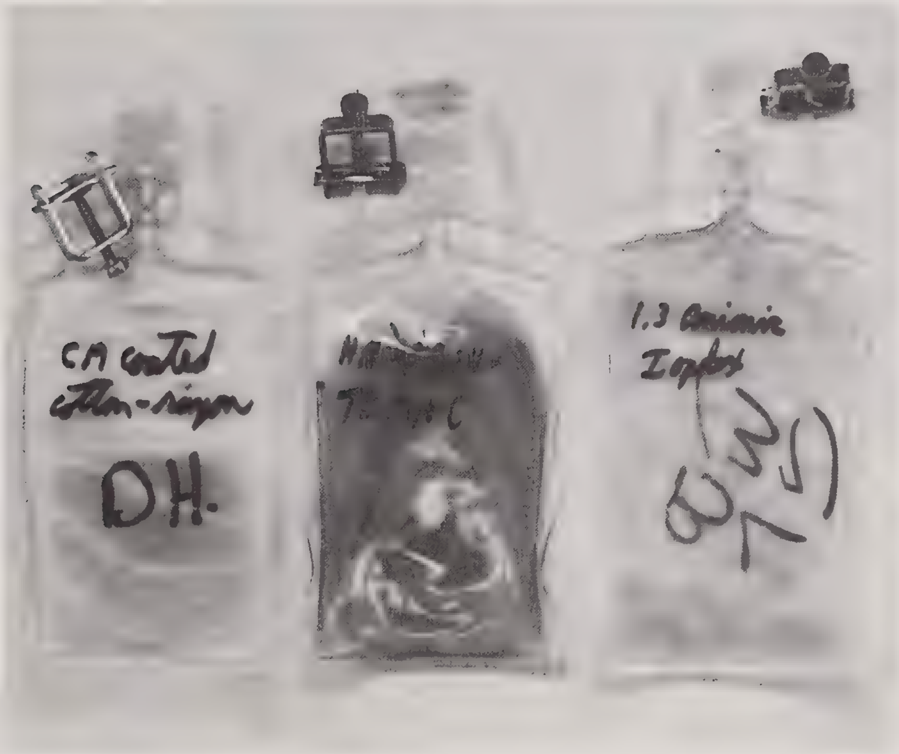

FIGURE 2. LEFT TO RIGHT- CARBOXYMETHYL CELLULOSE-COATED COTTON RAYON MATRIX, HEPARINIZED TDMAC-COATED MONOFILAMENT, AND IOPLEX RESIN SAMPLES IN ABOUT 20 ML OF ISOTONIC SALINE.

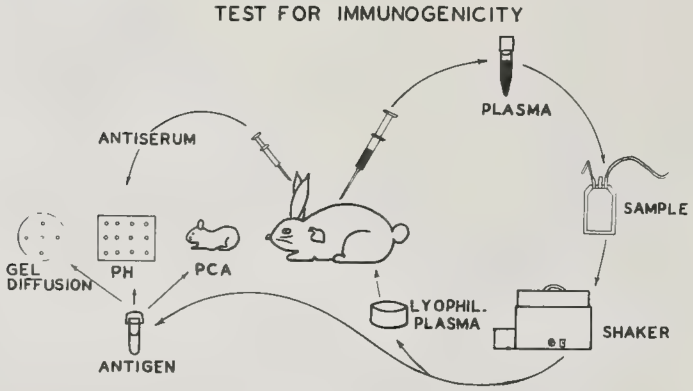

FIGURE 3. SCHEMATIC REPRESENTATION OF THE IMMUNOGENIC TEST PROCEDURE.

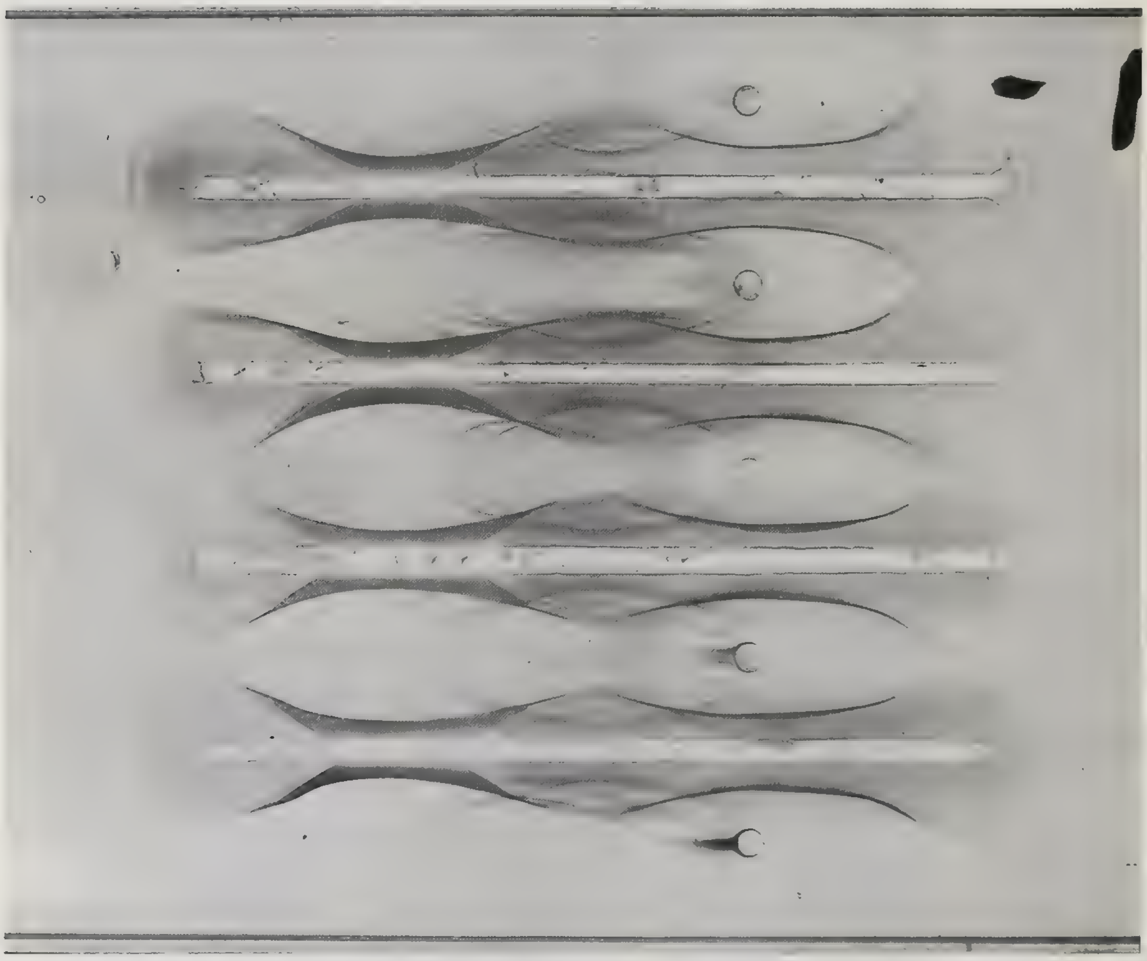

FIGURE 4. IMMUNOELECTROPHORETIC PATTERNS OF NORMAL RABBIT PLASMA (TOP WELL, CENTER WELL), LYOPHILIZED PLASMA (SECOND WELL), AND FREEZE THAW-DENATURED PLASMA (FOURTH AND FIFTH WELLS). PLASMA IN THE BOTTON (FIFTH) WELL WAS LYOPHILIZED.

Attempts to demonstrate antibodies to autologous, denatured antigens were not, of course, unique to our laboratory. A number of years ago Milgrom and Witebsky[11] demonstrated in rabbits the antigenic activity of slightly denatured autologous gamma globulin. Although McCluskey and his co-workers[12] claimed that deliberate (freeze-thaw or alkali) denaturation was required before antibodies to autologous gamma globulin would be formed, Williams and Kunkel[13] demonstrated antibody formation to autologous gamma globulin isolated under the mildest of conditions. A common finding for all of these workers was the low reactivity of the antisera against the autologous antigen, but very high reactivity against human gamma globulin. Apparently the rabbit gamma globulin molecule may be denatured in such a way as to reveal antigenic sites similar to those of human gamma globulin. Testing suspected antisera with human gamma globulin as antigen, then, was a sensitive method for detecting antibody formation in rabbits in response to injected, partially denatured autologous plasma.

This test with human gamma globulin (Cohn Fraction II) was applied to our control antisera with the results shown in Table 2. While even deliberately denatured samples were negative, in the gel diffusion test antisera for the shaken samples gave detectable precipitin lines. In passive hemagglutination only the deliberately denatured plasmas were positive, with respectable titers. PCA showed only the lyophilized plasma to be non-reactive.

TABLE 2

EFFECTS OF PROCESSING EQUIPMENT AND CONTAINER
SURFACES ON THE AUTO-IMMUNOGENICITY OF RABBIT PLASMA
2. HETEROLOGOUS ANTIGEN - HUMAN γ-GLOBULIN

	Positives/Total No. in Group			
	Gel Diffusion[a]		Passive	
Treatment	Low Antigen	High Antigen	Hemagglutination	PCA[d]
None	0/5	0/5	0/4	---
Lyophilization	0/5	0/5	0/4	0/5[c]
Freeze-Thaw	0/4	0/4	4/4[b]	4/4
Alkali	0/4	0/4	4/4[b]	3/3
Shaking	1/5	2/5	0/5	2/5

[a] Low Antigen = 1 mg/ml
High Antigen = 20 mg/ml
[b] Titer^{-1} = 512
[c] Same results whether simple injection or injection in Freund's adjuvant.
Highest antiserum dilution = 10^{-1}
[d] Passive Cutaneous Anaphylaxis

The important conclusion to be drawn from this experiment was that shaking plasma overnight in a polyvinyl chloride blood transfer bag apparently produced some denaturation which led to the formation of antibodies against human gamma globulin. If we may extrapolate from the observations of Milgrom, Witebsky and Kunkel described above, it appeared that the rabbit gamma globulin was affected by shaking. Although this aspect of testing was positive in the most important control experiment, we thought it might be possible to adjust our detection methods so as to detect major immunogenic effects in the background of minor changes caused by containers and processing. A final important note to be emphasized here was that with native autologous antigen alone except for the weakly positive reaction observed with gel diffusion essentially no antibody could be detected by any method.

During these experiments cellulose acetate electrophoresis and immunoelectrophoresis were used as alternative methods to examine denaturation. With the control samples cellulose acetate electrophoresis revealed denaturation only after alkali treatment. Immunoelectrophoresis, although qualitative, was much more sensitive, and in Figure 4 were shown comparisons of normal rabbit serum (center well) lyophilized plasma (upper 2 wells), and freeze-thaw denatured plasma (lower 2 wells). No meaningful differences were detectable here. After alkaline denaturation, however, (Figure 5, upper 2 wells) changes in mobility and optimal precipitation zone were prominent. Plasma samples exposed to nylon monofilament or to carbon-coated ZrO_2 (lower 2 wells) were identical to normal rabbit serum (center well).

Some photomicrographs of materials samples are shown in Figure 6. The carbon-coated zirconium oxide, although it was extensively tumble polished had a lightly pitted surface. Surface area determined by gas adsorption at Gulf General Atomic Laboratories was 6000 cm^2 for the 5 gm. sample used here. Because the surface area available to proteins was probably less than that available to gas molecules, the surface area was calculated roughly by assuming a mean particle diameter of 0.7 mm, with a result of 1075 cm^2 of surface per 5 gm. sample. A particle of the Ioplex resin sample was shown here to portray its irregular nature. No surface areas were calculated, but particle sizes were generally about 2 mm across. Likewise with carboxymethyl cellulose-coated cotton rayon matrix, no surface areas were calculated. The gross sample dimensions were 6 x 6 cm, but the fibrillar nature of the matrix made a large surface available. Other samples, such as nylon monofilament or heparinized TDMAC-coated monofilament had surface areas of 783 and 5000 cm^2 respectively.

Exposure of rabbit plasmas to the various materials samples gave the results shown in Table 3. Here, as in the previous tables, the highest number of positive animals are shown, each having been bled at 3, 5, and 7 weeks after the last antigen injection. Since we were trying to establish whether any response at all could be detected, the earliest samples, that is plasma exposed to nylon monofilament or autoclaved carbon-coated ZrO_2 were injected in the same rigorous injection schedule as the shaken control - 5 intramuscular injections of 10 mg each in Freund's adjuvant spaced at weekly intervals, plus 1 intravenous injection of antigen adsorbed to calcium alginate. Plasmas from the remaining samples were reconstituted in water to original concentration and 2 ml were given intravenously at 2 one-week intervals followed by a single intravenous injection of calcium alginate-adsorbed antigen.

TABLE 3

IMMUNOGENICITY OF RABBIT PLASMA AFTER EXPOSURE TO LARGE SURFACE AREAS OF FOREIGN MATERIALS

		Gel Diffusion		Hemagglutination		PCA	
Material	Source	Autol.	H γ-G	Autol.	H γ-G	Autol.	H γ-G
Nylon Monofilament[a]	Commercial	0/5	0/5	4/5[d]	0/5	4/5	3/5
Carbon-coated ZrO_2[b]	Gulf General Atomic						
Autoclaved		0/4	2/4	3/4	0/4	3/4	2/4
Vacuum outgassed 900°C		0/5	5/5	1/5	4/5	1/5	4/5
CMC-coated cotton-rayon matrix	Melpar, Inc.	0/4	1/4	2/4	0/4	1/4	0/4
Uncoated cotton-rayon matrix		0/3	0/3	2/3[e]	2/3	0/3	1/3
Anionic Ioplex, 0.50	Amicon Corporation	0/4	0/4	2/4[e]	4/4	1/4	3/4
Cationic Ioplex, 0.75		0/5	0/5	4/5	0/5	1/3	5/5
Anionic Ioplex, 1.3		0/4	0/4	2/4[e]	1/4	0/4	1/4
Heparinized TDMAC[c] monofilament	Battelle Memorial Institute	0/5	0/5	3/4	1/5	0/4	0/5

[a] Surface area about 783 cm^2 per sample

[b] Surface area by nitrogen adsorption = 6000 cm^2

Surface area assuming spheres of mean diameter 0.7 mm, 3500 particles per gram, 1075 cm^2

[c] Surface area about 5000 cm^2 per sample

[d] $Titer^{-1}$ = 8 for 4 animals. With Coombs' reagent added, $titer^{-1}$ = 256

[e] $Titer^{-1}$ below 16; $titers^{-1}$ of 2 not considered positive.

In the gel-diffusion test, no precipitin lines could be detected in any sample with autologous antigen. Human gamma globulin, however, at high concentrations gave precipitin lines with ZrO_2 - treated samples, but because of positive reactions with this antigen shown earlier in the controls, these lines were of doubtful significance.

In the hemagglutination test frequent positive results were obtained among the various samples, but the results varied with the time of bleeding. For example, with nylon monofilament the 5-week bleeding results were as shown; for the 7-week sampling only 1 animal was positive. The addition of Coombs' reagent intensified the hemagglutination reaction for ZrO_2, and reciprocal titers of 256 were obtained in 2 animals. With autoclaved ZrO_2 only 2 of 4 animals were positive on the first 2 bleedings. On the 3rd bleeding, however, 3 of 4 were positive. Vacuum-outgassed heated ZrO_2 seemed less reactive, with only 1 of 5 animals positive on the first 2 bleedings; none were positive on the last bleeding. Similar results were obtained for carboxymethyl cellulose and its backing, and for the Ioplex gels. Plasmas exposed to heparinized TDMAC-coated monofilament elicited positive reactions only on the second bleeding. Because of the consistently negative results with native controls, the above positive reactions were considered significant.

The hemagglutination results with human gamma globulin antigen were considered of doubtful significance here, even though the shaken control was negative. Hopefully, further experiments on shaken plasma alone will clarify the meaning of cross reactivity with human gamma globulin.

The detection of autologous antigen-antibody combination by passive cutaneous anaphylaxis (PCA) reflected only partially the results of passive hemagglutination. Agreement was found in the deliberately-denatured controls which were negative with both PCA and hemagglutination, and with samples exposed to nylon monofilament and autoclaved, carbon-coated ZrO_2, which were positive.

Several samples, however, registered positive in passive hemagglutination and negative in PCA - the carboxymethyl cellulose support matrix, the 1.3 anionic Ioplex, and the heparinized TDMAC-coated monofilament were examples. In our hands, passive hemagglutination was more sensitive than PCA.

With human gamma globulin as antigen in the PCA test almost every sample was positive on at least 1 bleeding. As before, the positive control experiments rendered these data of doubtful significance. Whether antisera to heterologous antigens may have any significance in disease of immunologic etiology is unknown.

DISCUSSION

The most important conclusion to be drawn from the results just presented was that contact of plasma with large surfaces of foreign materials may denature autologous proteins in a subtle way, so that they become immunogenic for the host. Anti-gamma globulin antibodies after open heart surgery have been demonstrated by Pretty and co-workers[14] who suggested as possible causes mechanical trauma during extracorporeal circulation or contact with prosthetic valve materials.

Although precipitating antibody could not be detected, significant reactions were observed with the more sensitive passive hemagglutination and PCA techniques using autologous whole plasma antigen. Milgrom and Witebsky[11] described their inability to detect antibody with whole serum as antigen, although they and several others mentioned earlier[12,13] were able to demonstrate immunogenic activity in very modestly denatured, isolated autologous rabbit gamma globulin. The marked reactivity towards human gamma globulin after injecting rabbit antigen observed by the above workers was interpreted to mean that denaturation exposed antigenic determinants in common with both species.

It is tempting to presume that exposure to foreign material surfaces denatured other than gamma globulin protein and that this was partly the cause of the lack of agreement between the autologous and heterologous antibody detection system.

Because of the qualitative nature of the procedure described here, no comparison or judgements of materials are yet possible. The apparent lack of precipitating activity in antisera to contact denatured plasma made it more difficult to determine which serum proteins were denatured because immunoletrophoretic analysis was not possible. Whether different materials denature different proteins is another question as yet unanswered. An initial unsuccessful attempt to determine grossly whether the gamma globulin fraction was denatured by surface contact with nylon will be repeated. The testing of plasma fractions isolated by gel chromotography or density gradient centrifugation should permit determining by hemagglutination or PCA reactions which fractions were antigenic. Hopefully, additional experiments relating the effects of time, temperature, surface area, and agitation rate will permit meaningful comparisons of various materials, so that known characteristics may be correlated with immunogenicity and the ideal non-immunogenic surface defined. In the future more sensitive, quantitative physical methods may permit the detection of subtle molecular changes produced by various materials, but at present such changes apparently may be detected best by immunologic means.

REFERENCES

1. D.K. Chattoraj and H. Bull. Electrophoresis of Adsorbed Protein. J. Am. Chem. Soc. 81, 5128-33 (1959).
2. R.D. Falb, G.A. Grode, M.T. Takahashi, and R.I. Leininger. NHI Contract PH 43-64-496, Development of Blood-Compatible Polymeric Materials. Battelle Memorial Institute, 30 March, 1967.
3. S.D. Litwin and J.M. Singer. The Adjuvant Action of Latex Particulate Carriers. J. Immunol. 95, 1147-52 (1965).
4. S. Kochwa, M. Brownell, R.E. Rosenfield, and L.R. Wasserman. Adsorption of Proteins by Polystyrene Particles. I. Molecular Unfolding and Acquired Immunogenicity of IgG. J. Immunol. 99, 981-86 (1967).
5. D.J. Lyman, J.L. Brash, S.W. Chaikin, K.G. Klein, and M. Carini. The Effect of Chemical Structure and Surface Properties of Synthetic Polymers on the Coagulation of Blood. II. Protein and Platelet Interactions with Polymer Surfaces. Trans. Am. Soc. Artif. Int. Organs 14, 250-55 (1968).
6. W.B. Sherman in "Immunological Diseases," M. Samter and H.L. Alexander, eds. Little, Brown, and Company, Boston, 1965. pp.503-05.
7. J.H. Vaugham, Second Editor's Comment, ibid. p. 734.
8. R.M. Merwin and G.H. Algire. Induction of Plasma-cell Neoplasms and Fibrosarcomas in BALB/c Mice carrying Diffusion Chambers. Proc. Soc. Exp. Biol. Med. 101, 437-39 (1959).
9. B.S. Oppenheimer, E.I. Oppenheimer, I.Danishevsky, A.P. Stout, and F.R. Eirich. Further Studies of Polymers and Carcinogenic Agents in Animals. Cancer Res. 15, 333-40 (1955).
10. R.S. Weiser, Q.N. Myrvik, and N. Pearsall, "Fundamentals of Immunology." Lea and Febiger, Philadelphia, 1969. p. 281.
11. F. Milgrom, E. Witebsky. Studies on the Rheumatoid and Related Serum Factors. I. Autoimmunization of Rabbits with Gamma Globulin. J. Am. Med. Assn. 176, 56-63 (1960).

12. R.T. McCluskey, F. Miller, and B. Benacerraf. Sensitization to Denatured Autologous Gamma Globulin. J. Exp. Med. 115, 253-74 (1962).
13. R.C. Williams, Jr., and H.G. Kunkel. Antibodies to Rabbit γ-Globulin after Immunizing with Various Preparations of Autologous γ-Globulin. Proc. Soc. Exp. Biol. Med. 112, 554-61 (1963).
14. H.M. Pretty, H.H. Fudenberg, H.A. Perkins, and F. Gerbode. Anti-Gamma Globulin Antibodies after Open Heart Surgery. Blood 32, 205-16 (1968).

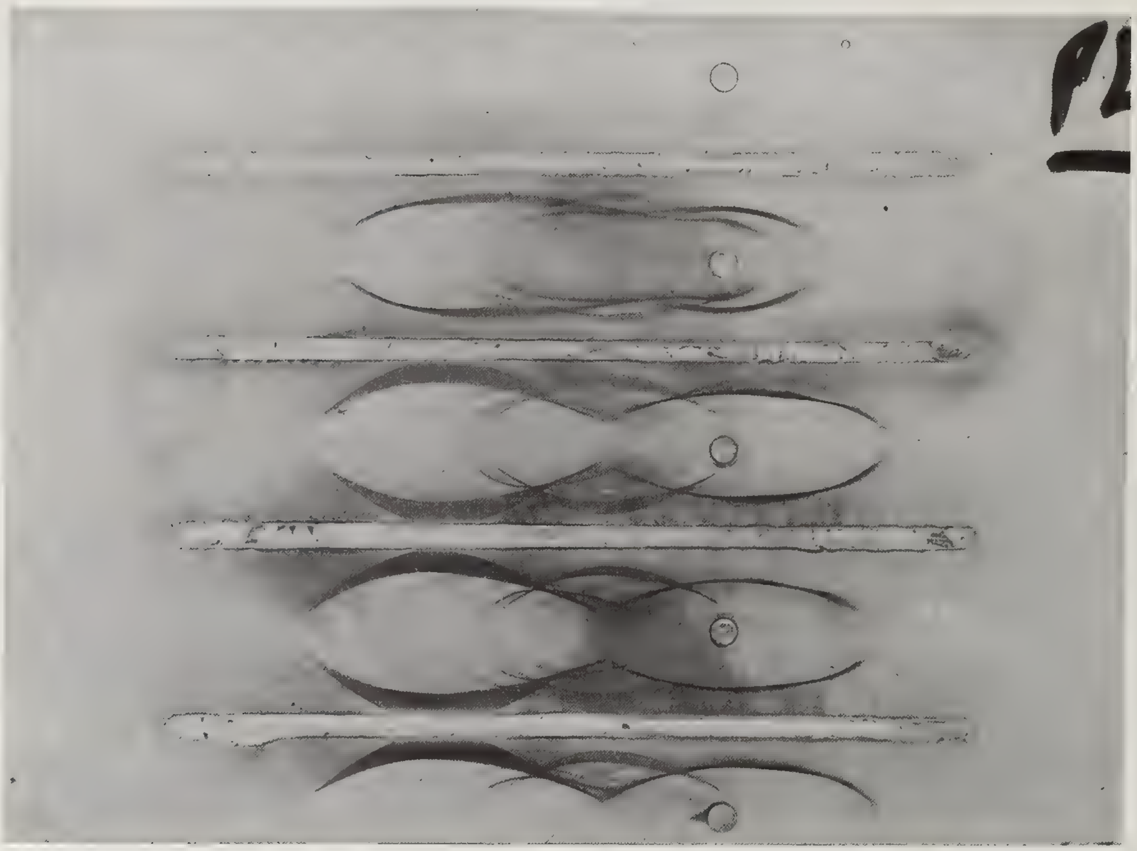

FIGURE 5. IMMUNOELECTROPHORESIS OF ALKALI-DENATURED PLASMA (TOP 2 WELLS) AND PLASMAS EXPOSED TO NYLON MONOFILAMENT AND C-COATED ZrO_2 GRANULES (BOTTOM 2 WELLS). CENTER WELL CONTAINED NORMAL RABBIT SERUM.

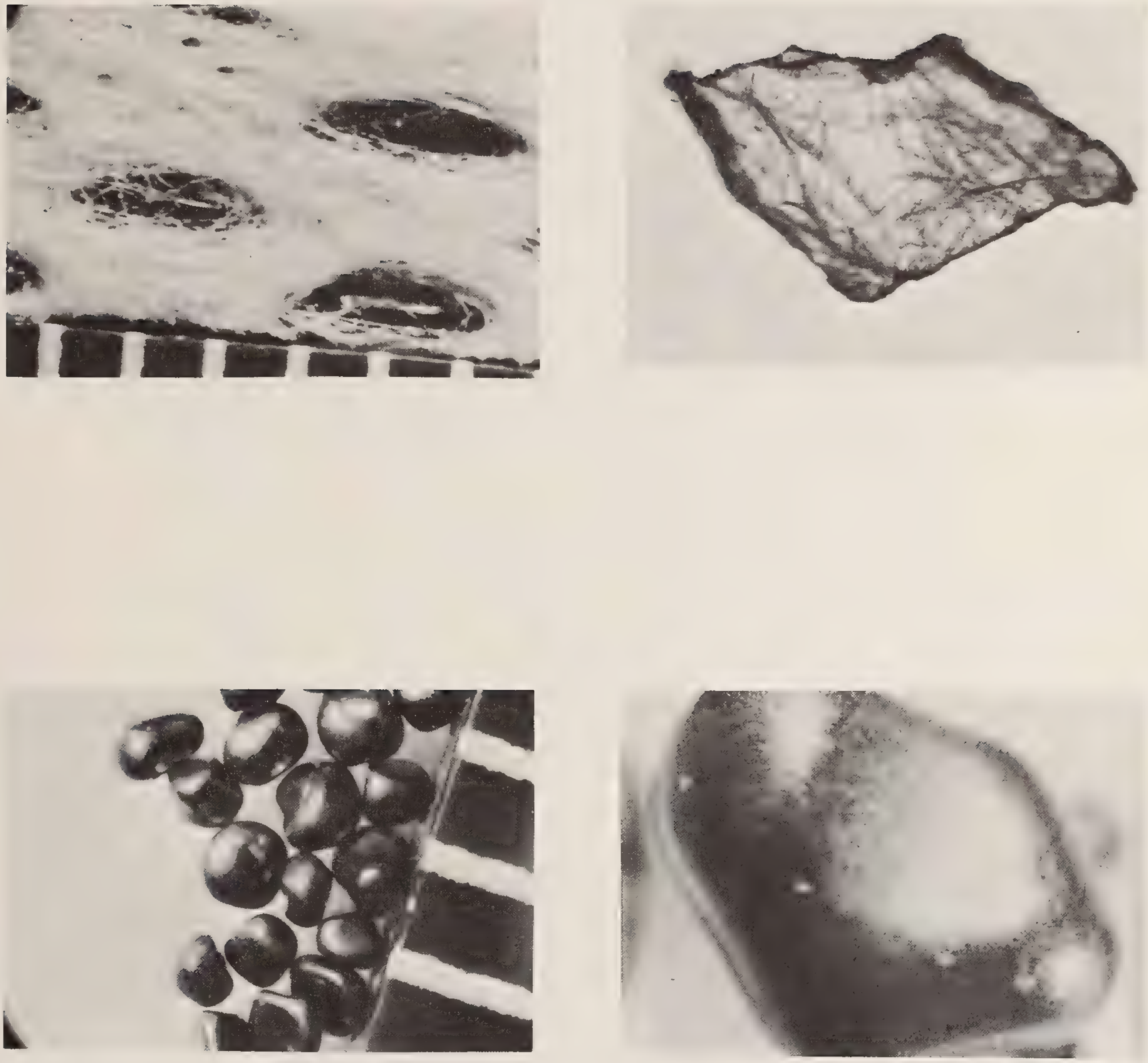

FIGURE 6. PHOTOMICROGRAPHS OF CARBOXYMETHYL CELLULOSE-COATED COTTON RAYON MATRIX (UPPER LEFT), PARTICLE OF IOPLEX GEL (UPPER RIGHT), AND C-COATED ZrO_2 GRANULES (LOWER). THE WHITE LINES (LOWER LEFT), ARE 1 MM. APART. THE FINELY PITTED SURFACE OF ONE GRANULE IS SHOWN AT LOWER RIGHT.

SECTION III

BLOOD FLOW THROUGH BLOOD PUMPS AND VALVES

Chairmen: Allen K. Ream, M.D.
Charles E. Branch

INTRODUCTION

Major problems in the development of circulatory assist devices and valves have been clotting and the destruction of the formed elements of the blood. While these phenomena are due in part to the prosthetic materials used, a major problem needing further investigation is the flow of blood, through and adjacent to such devices. Factors that may be involved include turbulence, shear, and rapid changes in pressure caused by the pump. The purpose of this contractual program is to develop basic theorems and fundamental data pertaining to flow at such sites as prosthetic valves, points of connection, and pumping sites in order to define the design limits for devices in contact with flowing blood. In this regard it is important to look at the microscopic flow patterns as well as the more obvious gross patterns.

CHAPTER 24

THROMBUS FORMATION ON ARTIFICIAL SURFACES

H.E. Petschek and P.N. Madras

Avco Everett Research Laboratory, Everett, Mass.

A number of chambers have been developed which allow the observation of thrombus formation on artifical surfaces while varying the rate of blood flow. Using this chamber, a sequence of reactions in thrombus formation has been observed on polyurethane and on a wide variety of other materials supplied for evaluation.

Platelets are always the first formed element to attach to a surface, but do not necessarily lead to thrombus formation. In all regions where thrombi form, leukocytes also become attached to the surface. In an area occupied by leukocytes, platelets draw together but do not necessarily form aggregates. In contrast to platelets, however, the tendency for leukocytes to stick to the surface appears to be both flow and chemistry dependent and may represent an important link between blood flow and thrombus formation.

In all observations on different materials, the above sequence could be determined in thrombus formation. However, significant differences in the rate at which these events occurred were found. These differences permit a comparison of materials regarding their tendency for platelets to adhere, for leukocytes to adhere and for thrombus formation.

It appears at present that those surfaces which show least tendency for leukocytes to adhere may be the most non-thrombogenic.

INTRODUCTION

While the chemistry of blood platelets and individual clotting factors has been studied and described in great detail, the relevance of any of these individual factors to hemostasis or thrombus formation is poorly understood. This gap in our knowledge is in part due to the fact that relatively little work has been done on the problem of thrombus formation in flowing blood. Work which has been done in this area has concentrated on thrombus morphology in moving blood as opposed to clot morphology in stagnant blood. The emphasis was on the gross and microscopic appearance of the clot or thrombus, and not on the role which was played by the movement of the blood. This experiment was designed to observe thrombus formation on clear artificial surfaces, in which blood flow is known precisely so that shear rates at the surface and diffusion of platelets and proteins to the surface were well controlled. In addition, this experiment enables one to compare a variety of materials with regard to their thrombogenicity under reproducible flow conditions. It is this latter aspect of the work which will be emphasized in this paper because, at present, our knowledge of the importance and role of blood flow in itself is rather incomplete.

The experiment[1] consists of leading fresh blood from a dog's carotid artery through a chamber (Figure 1) to a 25 mm diameter microscope cover slip which is rigidly held in place by the construction of the chamber. This chamber is then fixed to the stage of a microscope which, by using dark field illumination, enables one to observe what is happening beneath the cover slip. The carotid artery of the dog is led through a hollow stainless steel tube which may be fixed to the chamber in such a way that the central portion of the blood stream is led to the center of the cover slip from which it diverges in a radially symmetric pattern to a collecting gutter shown at the edge of the cover slip. By varying the diameter of the inlet hole and the gap between the cover slip and the bottom of the chamber, and by varying the withdrawal rate from the flow regulator, different blood velocities are obtainable. As was discussed in the first reference, such stagnation flows have been explored in considerable detail in the aerodynamic literature. The blood velocity and surface shear vary directly with distances from the stagnation point.

Mongrel dogs weighing about 15 ± 5 kg are used in the experiment. They are anesthetized with nembutal and the carotid artery exposed. Standard Lee-White clotting times are done on these animals and show a range of about 6 to 12 minutes.

Five chambers have been designed for use in this experiment. These chambers have different geometries so that the flow varies considerably from chamber to chamber. The flow parameter[1] varies from about one reciprocal second to about fifty reciprocal seconds.

Descriptions of thrombus formation on glass have been discussed previously.[1,2] Briefly, platelets cover the surface in a monolayer rapidly after about one minute of flow in which nothing visible has happened. They are followed from three to ten minutes later on glass by the appearance of wedge-shaped thrombi with the apex of the wedge pointing toward the stagnation point and the thrombus growing rapidly downstream away from the stagnation point and slowly upstream toward it. The fact that the thrombi form as wedges indicates that glass is a nonhomogeneous surface, with regions that are more thrombogenic than other regions acting as the initiators of thrombus formation. The thrombi, once initiated, go on to form with a geometry not unexpected from the type of flow situation which exists.

However, if the surface were absolutely homogeneous, one would expect that thrombus would start to form at virtually the same time at any given distance from the stagnation point because, at a given radius, the transport of necessary materials to the surface coupled with the tendency for the thrombus to be sheared off the surface is identical. This is indeed what happens with uniformly highly thrombogenic surfaces as will be shown later.

COMPARISON OF THROMBUS FORMATION ON ARTIFICAL SURFACES

In this section the growth of thrombi on polyurethane will be described. This is done because polyurethane is the most easily used relatively nonthrombogenic foreign material in the flow experiment being easily layered on to glass cover slips. Thus we have used polyurethane as a standard on which to observe the growth of thrombi and from which to compare thrombogenicity of other materials.

Following the description of thrombus formation on polyurethane, a comparison of polyurethane and other materials supplied for evaluation by various contractors of the Artificial Heart Program Office will be described.

Thrombus Formation on Polyurethane.

The sequence described in this section has been studied on polyurethane, but seems applicable with only minor differences to any foreign surface upon which thrombus forms. It appears that platelets and leukocytes are most essential to thrombosis on foreign surfaces, so our observations regarding these blood elements is discussed in a qualitative manner. Their possible interaction is also discussed in this section. Following this section is a brief introduction to the quantitative techniques which will be applied to these observations in the remainder of the contract year.

Platelet Phenomena. Observation using reflected light and an oil immersion lens (100X objective) enables one to see only blood elements which touch, or are stuck to, the surface.[1]

Platelets start to arrive at the surface as soon as the flow starts, but it requires 20 to 60 seconds before they stick. After about four minutes, a monolayer covering the surface may be seen under oil immersion. In many runs, no thrombus forms for the next three hours, and in these cases no visible change takes place in the platelets attached to the surface. If a cover slip is removed from the chamber at any time after the monolayer forms, up to three hours, and if no thrombus has formed on this cover slip, it will exhibit reproducible platelet morphology (Figure 2). After the cover slip has dried, it has a "ground glass" homogeneous appearance, except in the support region (Figure 3). With Wright stain and magnification, this homogeneous appearance is seen to consist of individual platelets which do not interact with each other (Figure 2). The remarkable observation is the fact that no changes visible by light microscopy occur after platelet deposition in those runs in which no thrombus forms.

White Cell Phenomena. In many runs, white cells form a circle around the stagnation point. In this circle, the platelets form small clusters in the vicinity of white cells and bare areas of surface appear between platelets which do not attract further blood elements (Figure 4). However, in the white cell circle, individual platelets in clusters can still be detected by light microscopy, except in the infrequent case in which a true platelet aggregate may be found.

The same two elements, leukocytes and platelets, show a similar, but more pronounced, interaction when a thrombus forms on the surface. In the thrombus region, the platelets migrate together, forming platelet aggregates, and lose their identity by light microscopy. Leukocytes which also have lost their cellular definition, such as their cytoplasmic membrane and nuclear detail (Figure 5), are also trapped in these aggregates.

The white cell circle becomes inportant when added to the following three observations. First, that platelets within the white cell circle undergo characteristic changes in morphology. They lose the independent appearance noted in Figure 2 and form aggregates. In only one run, done with Dow Corning material RB 1512, which is fairly thrombogenic, did an actual thrombus form in this region (Figure 15) but whenever a white cell circle forms the changes in platelets are similar to changes occurring in the thrombi (Figure 5).

The second observation is that all thrombi which form on artificial surfaces have leukocytes in them. As suggested earlier, such thrombi may be attributed to surface inhomogeneities on relatively nonthrombogenic surfaces. However, these irregularities attract leukocytes in addition to forming thrombi. No white blood cells are seen on surfaces in which platelet deposition but no thrombosis occurs.

Third, that on the surface outside the white cell circle and away from any thrombi, platelets are able to form a monolayer and appear independent of each other. This appearance may be retained for periods up to the limit of our runs, or three hours. The morphology of the platelet monolayer does not change from the time of its formation at a few minutes until thrombi form, and these thrombi are always preceded and accompanied by leukocyte deposition. In Figure 3, the bulk of the surface is covered by a platelet monolayer away from the wedge-shaped thrombus.

The coincidence of platelet changes and the presence of leukocytes lead to the postulate that leukocytes are relevant factors in the formation of thrombi on foreign surfaces. Since the

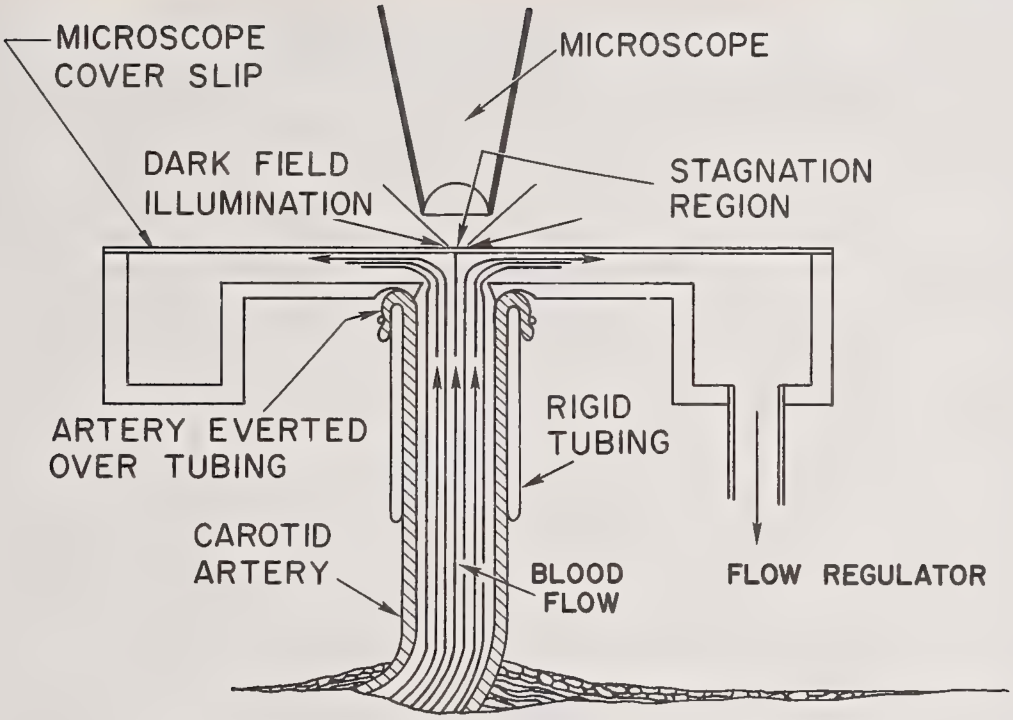

FIGURE 1. SCHEMATIC DIAGRAM OF THE FLOW CHAMBER. THROMBUS FORMATION ON THE UNDERSIDE OF THE COVERSLIP IS OBSERVED IN THE NEIGHBORHOOD OF THE STAGNATION POINT. NOTE THAT STREAMLINES REACHING THIS AREA COME FROM THE CENTER OF THE ARTERY AND HAVE NOT CONTACTED THE WALLS OF THE HOLE IN THE BOTTOM OF THE CHAMBER. THE FLOW REGULATOR PROVIDES A STEADY FLOW AT A LOW WITHDRAWAL RATE. STAGNATION FLOW PARAMETER CAN BE VARIED USING CHAMBERS WITH DIFFERENT HOLE DIAMETERS AND DIFFERENT SPACING BETWEEN THE TOP AND BOTTOM OF THE CHAMBER.

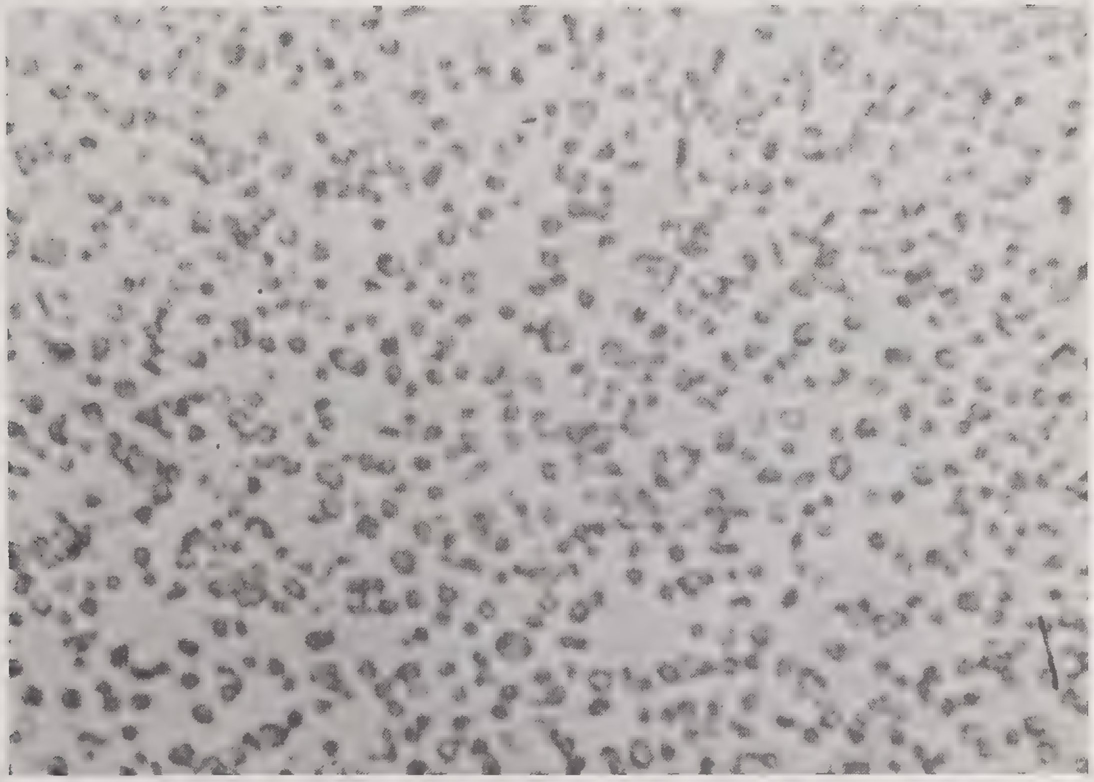

FIGURE 2. PLATELETS ON SURFACE AFTER 3-HOUR RUN SHOWING NO INTERACTION

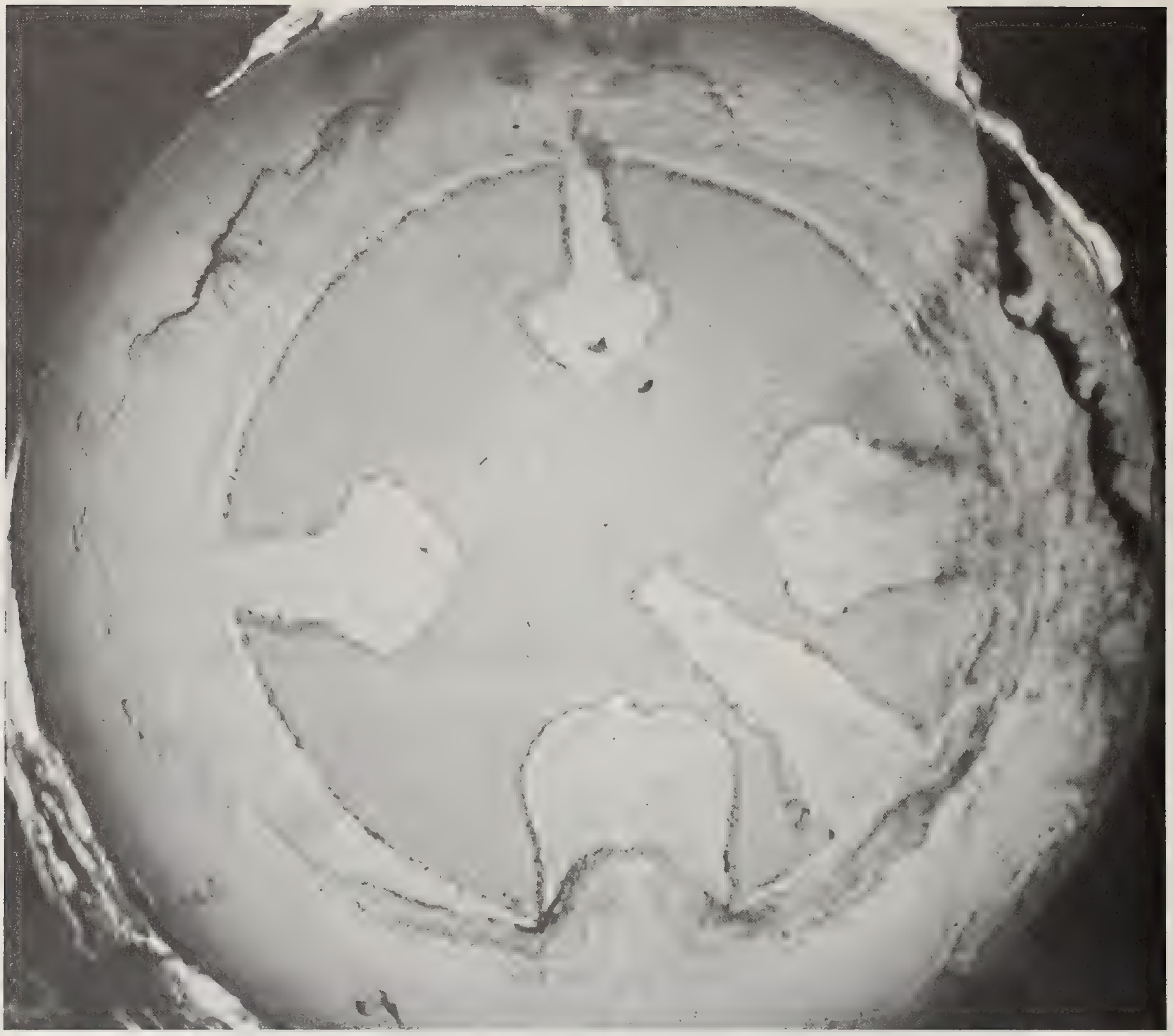

FIGURE 3. POLYURETHANE COVERSLIP REMOVED AFTER THREE HOURS. NOTE THE LARGE SOLITARY THROMBUS AND FROSTED APPEARANCE REPRESENTING DISCREET, NONRELATIVE PLATELETS.

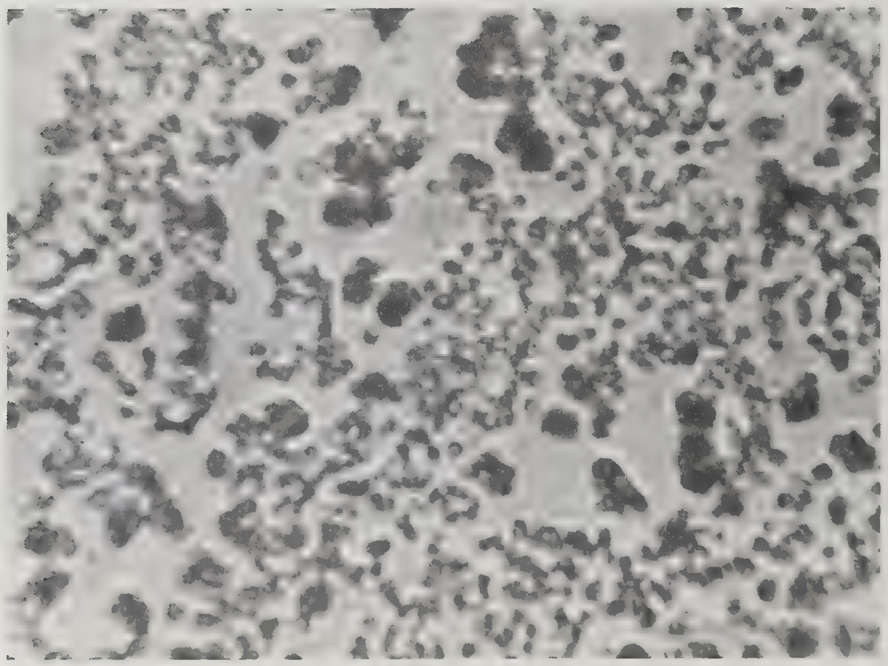

FIGURE 4. STAINED COVERSLIP SHOWING PLATELET MORPHOLOGY IN LEUKOCYTE CIRCLE.

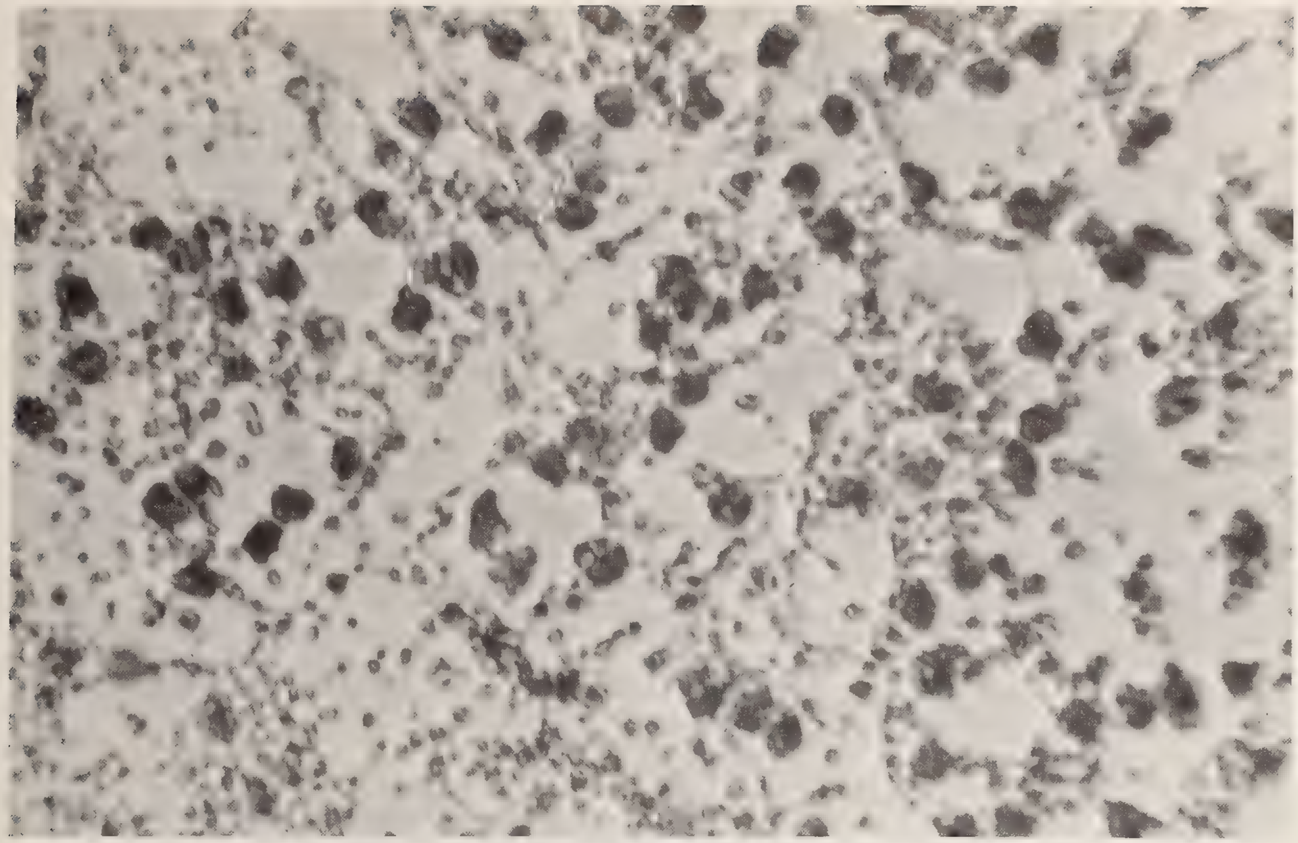

FIGURE 5. STAINED COVERSLIP SHOWING PLATELET MORPHOLOGY IN REGION NEAR THROMBUS.

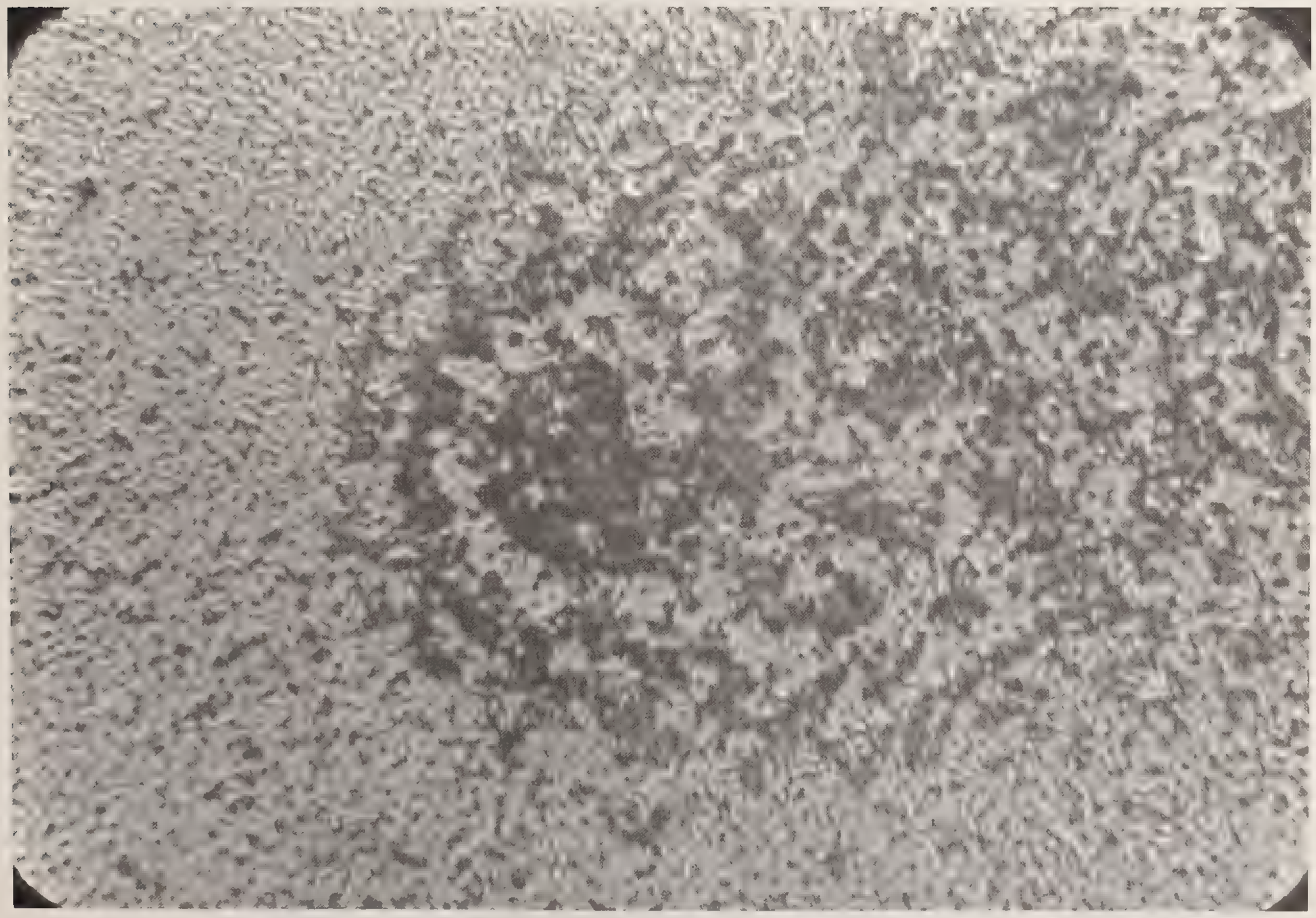

FIGURE 6. LEADING EDGE OF THROMBUS. HERE THE GROSS DISTORTION OF PLATELET MORPHOLOGY SURROUNDING THE THROMBUS CAN BE SEEN (WRIGHT STAIN).

leukocyte appearance and not platelet appearance is flow dependent, the leukocytes may be the agents through which flow is related to thrombus formation.

It should be stressed that the above view is unorthodox, and that leukocytes do not seem to play a role in thrombus formation in vivo. Furthermore, the amount of data on hand to support the above theory is insufficient. Thus, the authors present the leukocytes in this unique role because they feel that work is necessary to explore this phenomenon in more depth.

Independently of whether the attached leukocytes lead to platelet aggregation or whether the platelet aggregation leads to leukocyte attachment, the appearance of platelet aggregates within this very slow flow region suggests an incipient thrombus. For example,it is reasonable to hypothesize that still slower flows than have been used may lead to the formation of a definite thrombus. Further work in this direction will be pursued during the remainder of the contract period. However, since the present results suggest that the white cell circle may correspond to a different mechanism of thrombus formation than the one leading to the wedge-shaped thrombi discussed in the next section, this may be an important area for further study.

Thrombus Formation. The thrombi form as wedges exactly as described on glass in a previous contract report.[1] These wedges grow rapidly downstream in the wake of the original thrombus (Figures 3 and 6) and more slowly upstream toward the stagnation point. They may also grow by increasing their wedge angle and thus encompassing greater segments of the cover slip. These thrombi grow three-dimensionally down into the flow as well as along the surface. It is not possible, however, to observe quantitatively their growth into the bulk of the flow.

During the flow, these thrombi can be seen to consist of many platelet aggregates surrounded by white cells (Figure 6). In these aggregates, the platelets are completely indistinguishable by light microscopy. The white cells in these aggregates have no well defined cytoplasmic membrane, and their nuclear detail is also somewhat obscured. Around these aggregates are regions where flow continues in a highly distorted manner.

Quantitative Results.

Protein Layer. During a short period of time at the beginning of each run, blood flow near the surface can be seen; however, no surface interaction phenomena are visible in the microscope. After this period, platelets begin to settle on the surface. During this time interval, a protein layer is presumably deposited on the surface and modified such that it becomes attractive to platelets. Figures 7 and 8 show measurements of the time required before the first platelet attaches to the surface. Figure 7 suggests that there is no significant difference between the conditioning time of the surface protein layer on glass and polyurethane and that the conditioning time is independent of flow parameter over a wide range. In an attempt to reduce the scatter in the data, a more standardized technique of surface preparation was developed. Furthermore, the experimental technique was modified to permit observation from the first instant of blood flow. This data appears to confirm the observation that the protein layer conditioning time is independent of flow. This in turn suggests that the changes in the surface conditions required to attract platelets occur as surface reactions rather than being influenced by the rate at which the flow brings new proteins to the surface.

Platelet Attachment Rate. Measurements have also been made of the rate at which platelets settle on the surface following this conditioning time. Assuming that the platelet arrival rate is simply proportional to the area of the surface which is not already occupied by platelets, one derives the following formula:

$$\frac{N_f - N}{N_f} = e^{-Kt} \qquad (1)$$

where N_f is the final surface density of platelets; N is the surface density at a time, t, after initiation of platelet settling; and K is the reciprocal of the characteristic time in which the surface becomes fully covered with platelets.

Figure 9 shows an example of the history of the platelet density on the surface in one case with $(N_f - N)/N_f$ plotted on semi-log paper versus time. Since these curves typically fall on a straight line they are in agreement with Equation (1) and measurement of the slop of this line provides a measure of the rate of attachment.

In Figure 10 this rate is plotted as a function of the flow parameter, A. For comparison, the rate at which platelets would reach the surface simply by being on a streamline which approaches within 1.5 microns of the surface is shown. Also, the rate of arrival which would be expected for ordinary Brownian diffusion of platelets with a diffusion coefficient of 10^{-9}cm^2/sec is shown. It can be seen that both of these mechanisms are grossly insufficient to account for the observed arrival rate and a more rapid mechanism for platelet diffusion is required.

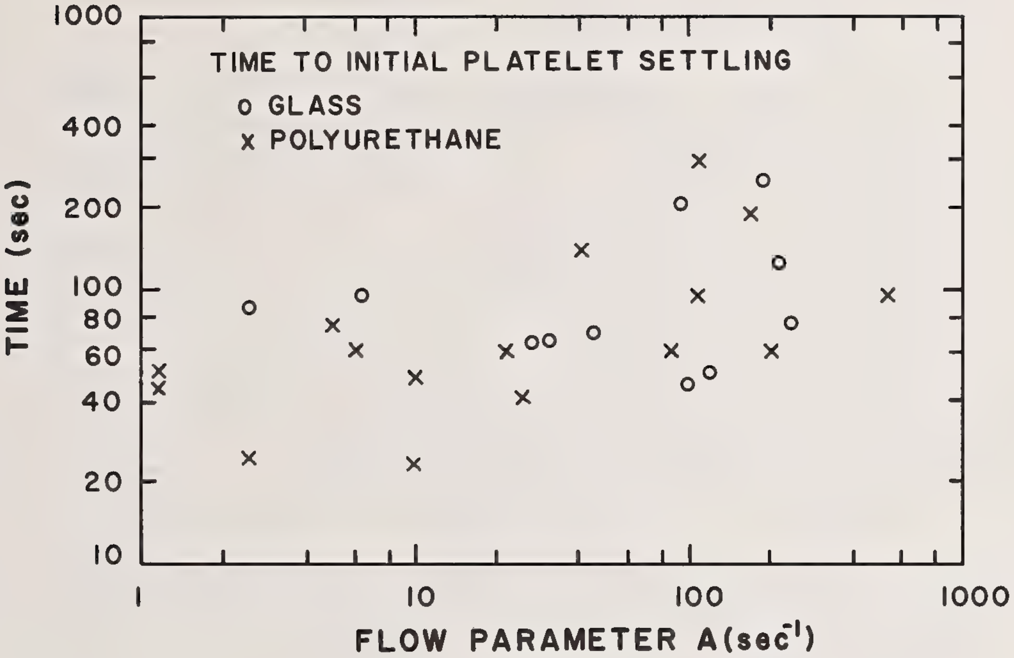

FIGURE 7. TIME TO INITIAL PLATELET SETTLING VS FLOW PARAMETER A FOR BOTH GLASS AND POLYURETHANE IS SHOWN. NOTE THAT NO SIGNIFICANT DIFFERENCE IS SEEN BETWEEN THESE TWO VERY DIFFERENT MATERIALS, BUT THAT THE SCATTER IN RESULTS FOR BOTH MATERIALS IS VERY LARGE.

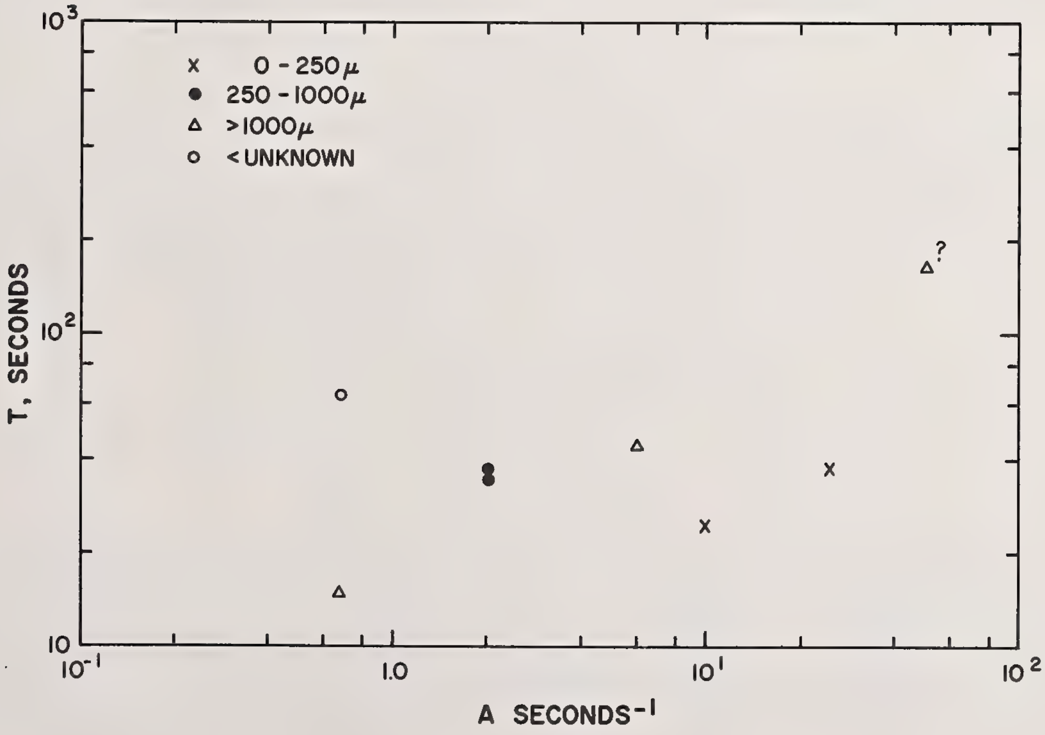

FIGURE 8. TIME TO INITIAL PLATELET SETTLING VS A FOR POLYURETHANE PREPARED BY A UNIFORM TECHNIQUE WITH DIFFERENT POINTS REPRESENTING DIFFERENT RADII FROM THE STAGNATION POINT. THIS GRAPH SHOWS NO A DEPENDENCE AND NO RADIUS DEPENDENCE. HENCE, THE CONCLUSION THAT PLATELET DEPOSITION IS NOT RELATED TO FLOW CONDITIONS AT A SURFACE.

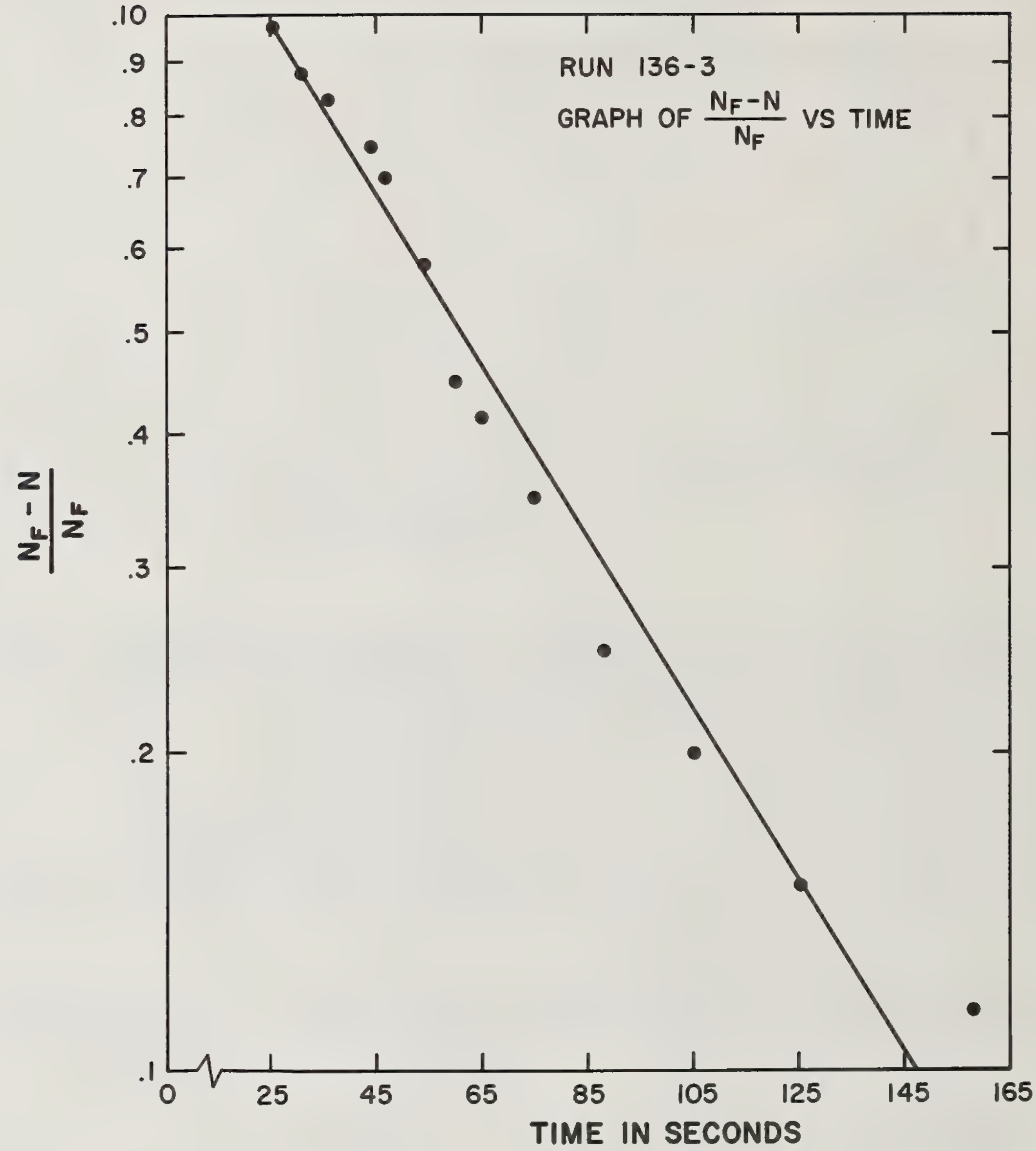

FIGURE 9. $(N_f - N)/N_f$ VS TIME. SEE EXPLANATION IN TEXT.

In Figure 11 the same data is replotted as a function of $A^{3/2}\ r^{2/3}$ It has been suggested that diffusion in the presence of a shear flow might be enhanced by red cell tumbling according to the law $D = 10^{-8}\ \partial u/\partial y\ cm^2/sec$ where $\partial u/\partial y$ is the shear. Using this assumption, the rate of arrival of platelets at the surface is given[1] by the solid line in Figure 11. While this theoretical estimate comes closer to the experimental observations, it also does not correctly account for the dependence on flow and radius.

Although the above data shows clearly that platelet diffusion is significantly enhanced by red cell tumbling, the mechanism is not at present understood quantitatively. During the remainder of the present contract period, we anticipate that more data will be collected which may lead to some clarification of both the diffusion mechanism and the probability of attachment of platelets.

Although the platelet attachment rate contains several phenomena of fundamental interest, it is not at present clear that this rate is directly related to thrombus formation. Two of the materials which we have evaluated form platelet monolayers very slowly. Yet both of these materials did eventually give rise to thrombi during a run. On the other hand, another material which we have tested did form a monolayer of platelets very quickly but showed no thrombus formation over the subsequent 2- to 3-hour experiments. Examples of the first material types which attract platelets slowly are the material developed by Shell, coded LR 10850-88, and material TC-3 produced by Thermo Electron Corporation. The thrombus seen on Shell's material, however, was definitely relatable to a dirt spot on the material, while the thrombus seen on the Thermo Electron material may have been due to contamination during shipment. However, thrombi did form and adhere to these materials even though they attracted platelets very slowly.

White Cell Phenomena and Platelet Aggregation. Observation of the flow during a run reveals that the leukocytes move more slowly than the flow next to the surface. In the slow flow chambers, a small fraction of the leukocytes become adherent to the surface in the region around the stagnation point, forming a circle in which many white blood cells are adherent to the surface.

The diameter of this circle is strongly flow dependent, decreasing rapidly with increased flow rate. In Figure 12 the diameter is plotted as a function of the flow parameter, A. The arrow at the left indicates an apparent diameter larger than the available field of observation. The arrow at the right indicates the absence of a white cell circle. Extrapolating the observed diameters to this value of A would suggest a diameter comparable to that of an individual cell, thus explaining the absence of the white cell circle at this and higher values of A.

It may be shown[1] that a radius which corresponds to constant shear varies as $A^{-3/2}$. A line with this slope is plotted at a magnitude which best fits our data. This slope is seen to be in agreement with the data indicating that the white cell circle is indeed limited by a constant value of shear which is approximately equal to 0.6 sec^{-1}. It is interesting to note that this value corresponds roughly to the value of shear at which the non-Newtonian viscosity of blood becomes significant.

RESULTS OF MATERIAL EVALUATION

Using the flow chambers, a test has been developed which allows one to compare the formation of thrombi on artificial surfaces without the necessity of observing events continuously. While continuous observation is preferable, it would limit the applicability of the test to only those materials having suitable optical properties. Thus, runs of fixed duration are performed, often with no observation possible during the run, and the cover slips are then removed for staining with Wright stain.

Each evaluation consists of a single dog experiment in which five runs are planned.

Run	Chamber	A(sec^{-1})	Duration (min)
1	5	25	2
2	1	2.5	2
3	3	10	10
4	4	1.0	120
5	2	10	120

Performing the runs as listed above enables one to obtain a number of significant facts concerning the material under study.

To study platelet settling, two runs are performed in chambers having widely varying values of A. In some cases, as with Shell BM 4 and BM 1, the chamber having the higher A value led to greater platelet coverage at 2 minutes. However, Dow Corning material RB 1522 had the opposite effect. This result implies that platelets may be sticking quickly but weakly to the Dow material, and are thus blown off by the higher shears in Chamber 5. In contrast, the chemical reaction which causes platelet adhesion to the Shell materials seems to proceed more slowly, but perhaps this bond, once formed, is stronger.

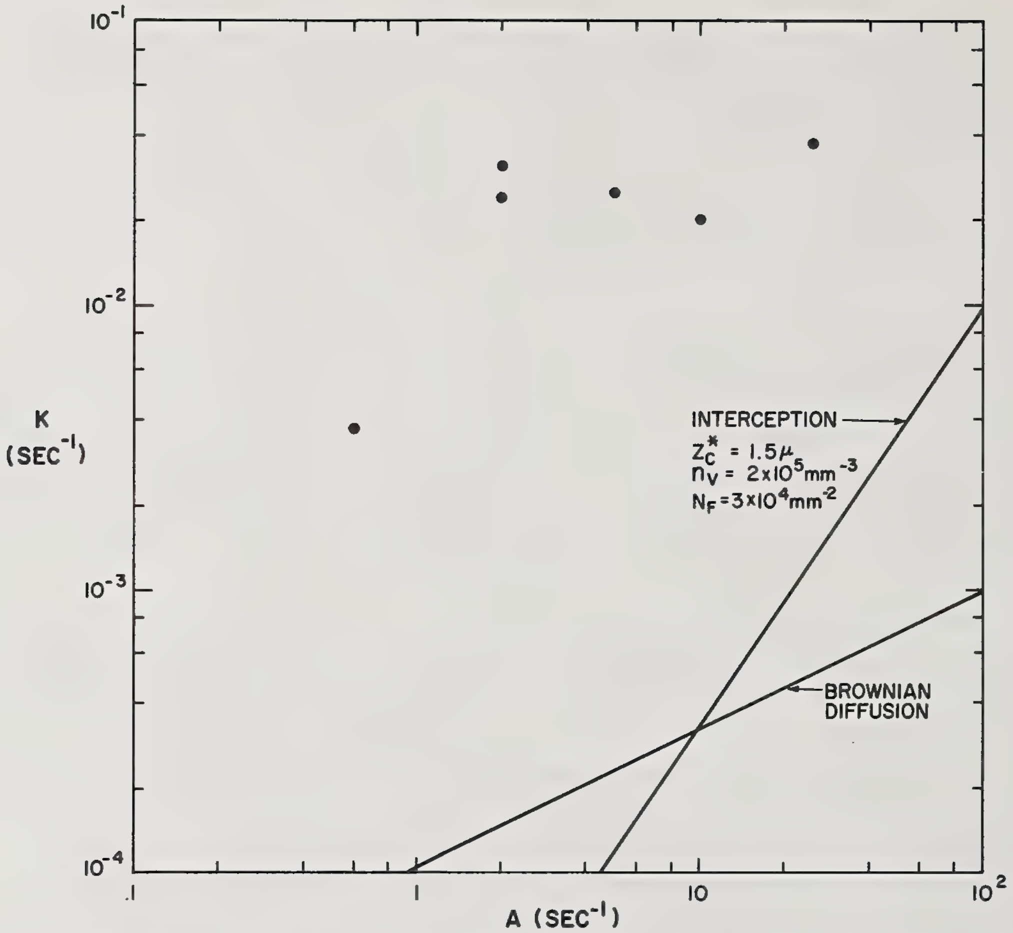

FIGURE 10. THE CONSTANT, K, DESCRIBING PLATELET ARRIVAL RATE IS PLOTTED AGAINST THE FLOW PARAMETER, A, OF THE CHAMBER. IT IS SEEN THAT K IS RELATIVELY CONSTANT AND INDEPENDENT OF A, THE DATA IS COMPARED TO PLATELET ARRIVAL RATES BASED ON BROWNIAN DIFFUSION AND ON TRANSPORTATION OF PLATELETS TO THE SURFACE BY THE FLOW INDEPEDENT OF DIFFUSION (LINE LABELED "INTERCEPTION"). ALL THE DATA IS FAR IN EXCESS OF EITHER OF THESE TWO MECHANISMS.

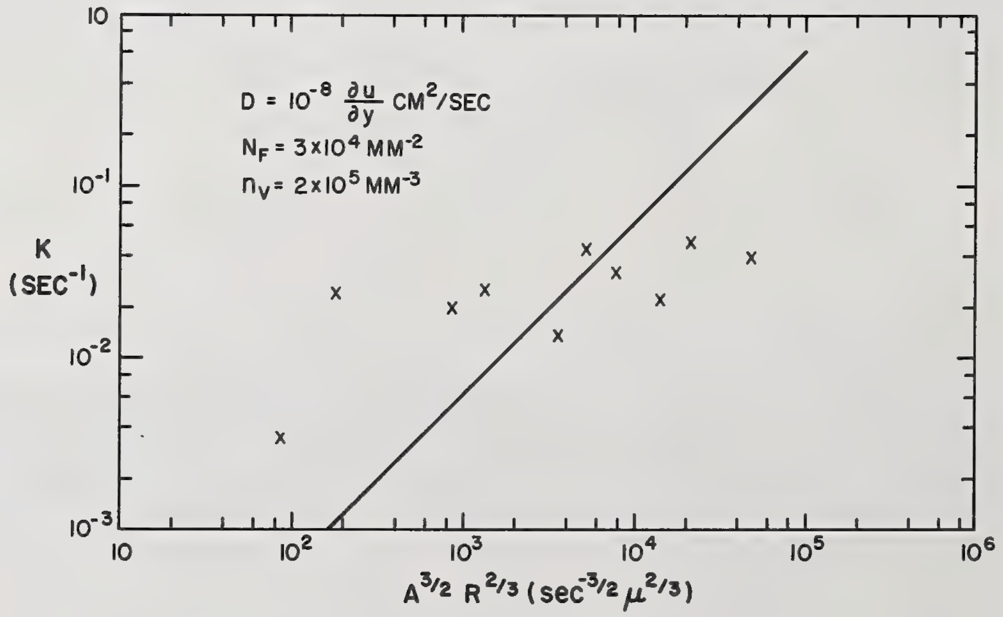

FIGURE 11. SEE TEXT FOR EXPLANATION.

One intermediate duration run is performed. This time, from experience, is set at 10 minutes which is sufficient to allow some thrombi to form or some platelet aggregation which can be detected on staining the cover slip.

The next run is a long duration run done with Chamber 4. This is the lowest flow chamber and might hence be the one most prone to form extensive thrombi. If possible, the formation of thrombi in this run is observed. Should this not be feasible the run would probably be stopped after two hours if nothing happened to disturb the overall withdrawal rate of blood before that time.

If Chamber 4 develops thrombi before the two-hour limit, the run is discontinued and a chamber having a flow parameter ten times as great is substituted for Chamber 4. The run is then repeated looking for the same events as described in the preceding paragraphs for Chamber 4.

Certain small variations from the above protocol occurred. These were in runs in which the material proved to be highly thrombogenic, thus causing the experimenter to feel that better results could be obtained by varying the protocol slightly. These variations do not affect the conclusions.

It is instructive to compare three cover slips of relatively nonthrombogenic, mildly thrombogenic and highly thrombogenic materials. These are respectively polyurethane (B.F. Goodrich Estane 5740 x 140), Dow Corning RB 1512, and Amicon, neutral ioplex. The polyurethane, Figure 13, shows a single thrombus which presumably formed on a surface irregularity, and a "frosted" appearance on the remainder of the cover slip, where no platelet aggregation could be seen, even after three hours exposure to blood. The Dow Corning RB 1512 material showed a thrombus at the stagnation point as well as numerous small thrombi elsewhere on the surface (Figure 14). Finally, neutral ioplex, which is highly thrombogenic became uniformly coated with thrombus which formed first at a large distance from the stagnation point and grew concentrically inwards. The thrombus shown in Figure 15 is more dense at a large radius and tapers to be relatively clear near the stagnation point.

The overall results obtained from applying this protocol to the materials is presented in Tables 1 to 5. The legend which precedes these tables should be consulted to aid in the interpretation of the column headings.

CONCLUSIONS

As a rapid but somewhat crude summary of the results in Tables 1 to 5, in Table 6 all the materials are rated on a scale of one to five regarding their effect on platelets, attraction for leukocytes, and thrombogenicity. The larger numbers show the greatest effect. The most thrombogenic material, Amicon's Cationic Ioplex, is rated five in all categories except for effect on platelets which was impossible to observe. Shell material BM-1 is given the value of one in all categories as it was the most nonthrombogenic.

TABLE 6

Material	Platelets	Leukocytes	Thrombi
Shell			
BM-1	1	1	1
BM-4	2	2	2
BM-15	?	?	2[a]
LR10850-88	2	3	3
Dow Corning			
RB 1622	5	4	4
RB 1519	5	4	4
Amicon Ioplex			
Cationic	?	5	5
Neutral	?	4	4
Anionic	?	3	2
Thermo Electron			
TC-3	3	3	4
No. 1	2	2	2
Avcothane			
Heated	2	2	1
Unheated	2	2	1

[a] Based on Run 4, Chamber 4, where some thrombus was seen in small ripples on the surface; not sufficient to cause flow separation.

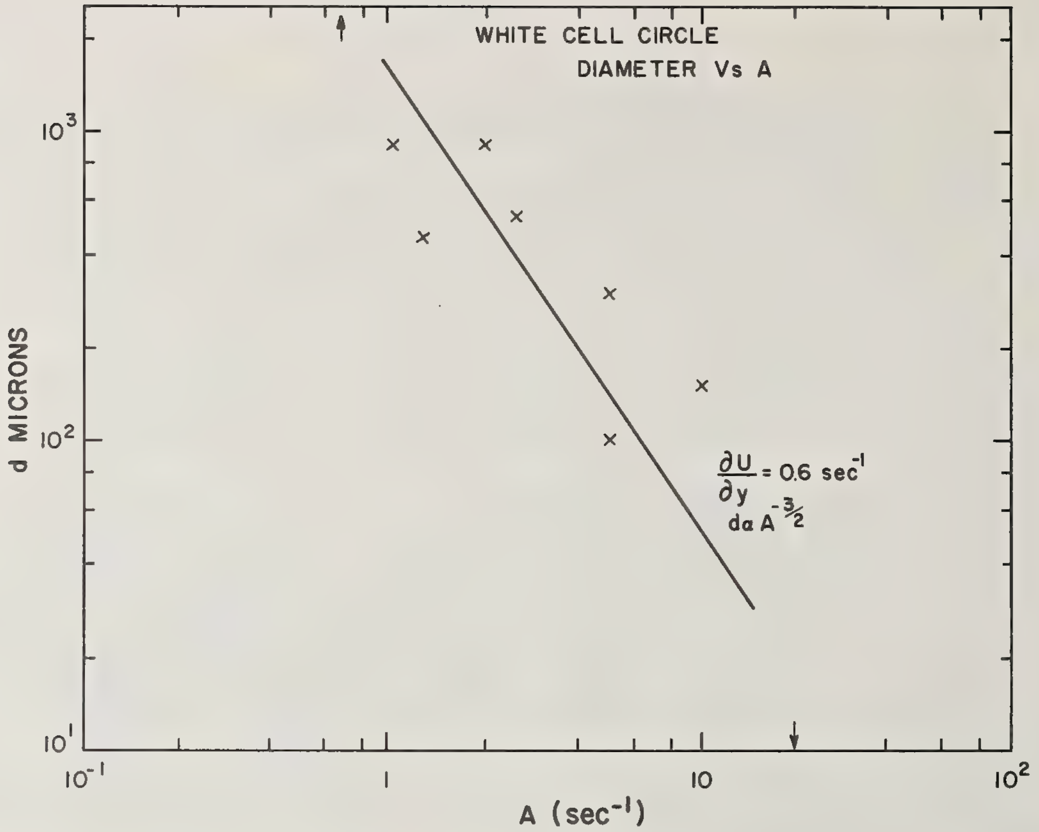

FIGURE 12. DIAMETER OF WHITE CELL CIRCLE VS A. THE SOLID LINE IS DESCRIBED BY d $A^{-3/2}$ WHICH IS A LINE OF CONSTANT SHEAR. THIS SHEAR IS 0.6 SEC^{-1}.

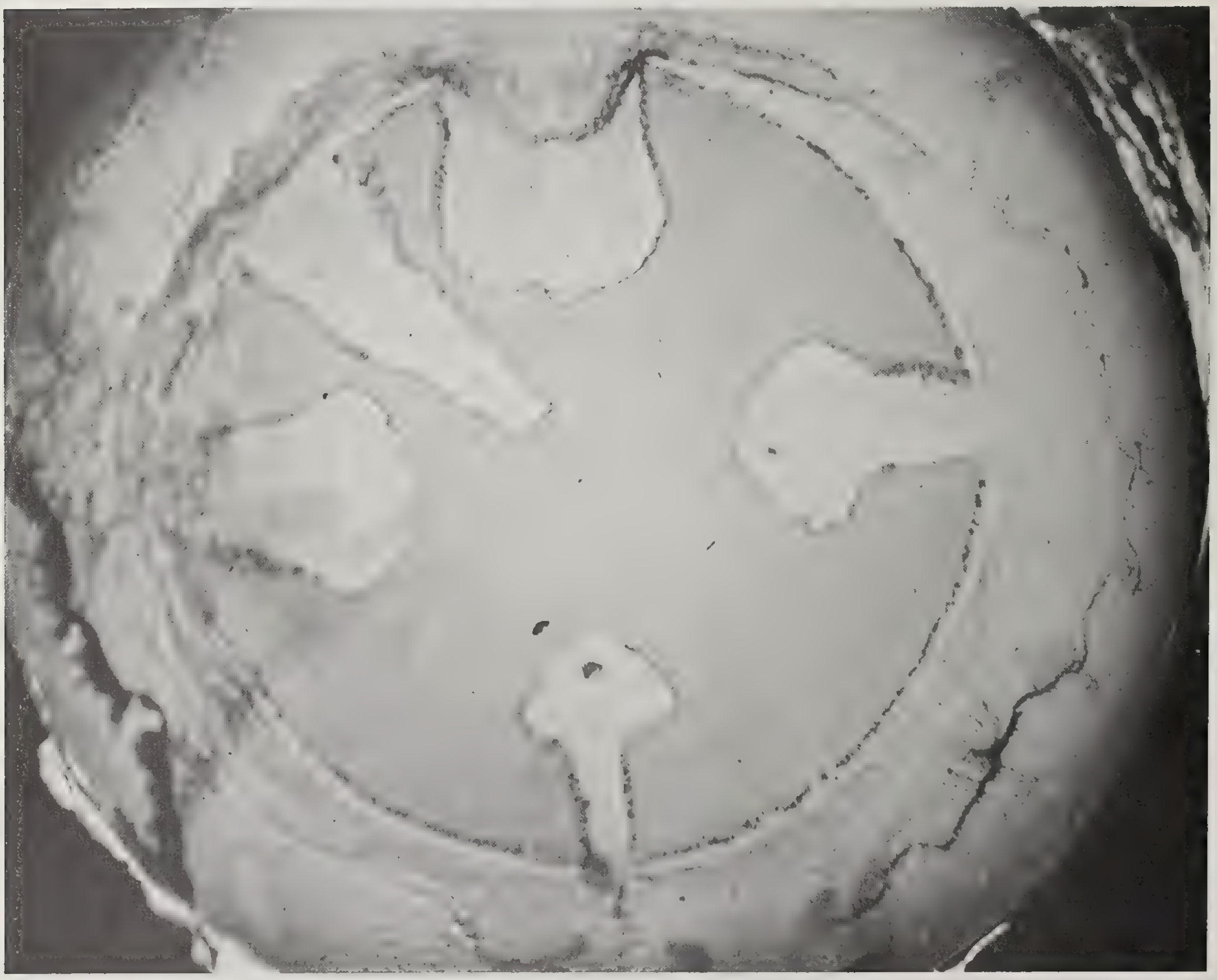

FIGURE 13. POLYURETHANE COVER SLIP SHOWING SINGLE THROMBUS AFTER A 3-HOUR RUN.

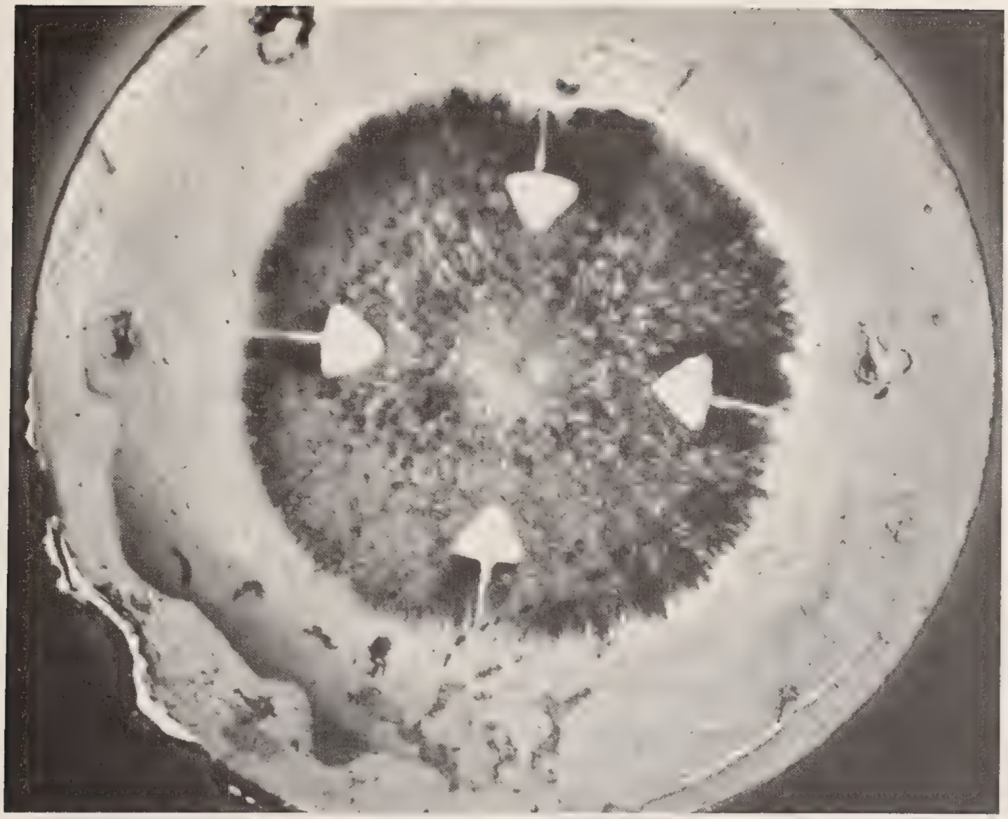

FIGURE 14. COVERSLIP FROM DOW CORNING MATERIAL RB 1512 REMOVED AFTER A 10-MINUTE RUN. NOTE MANY SMALL THROMBI POINTING TO THE STAGNATION POINT AND SOLITARY THROMBUS ON THE STAGNATION POINT.

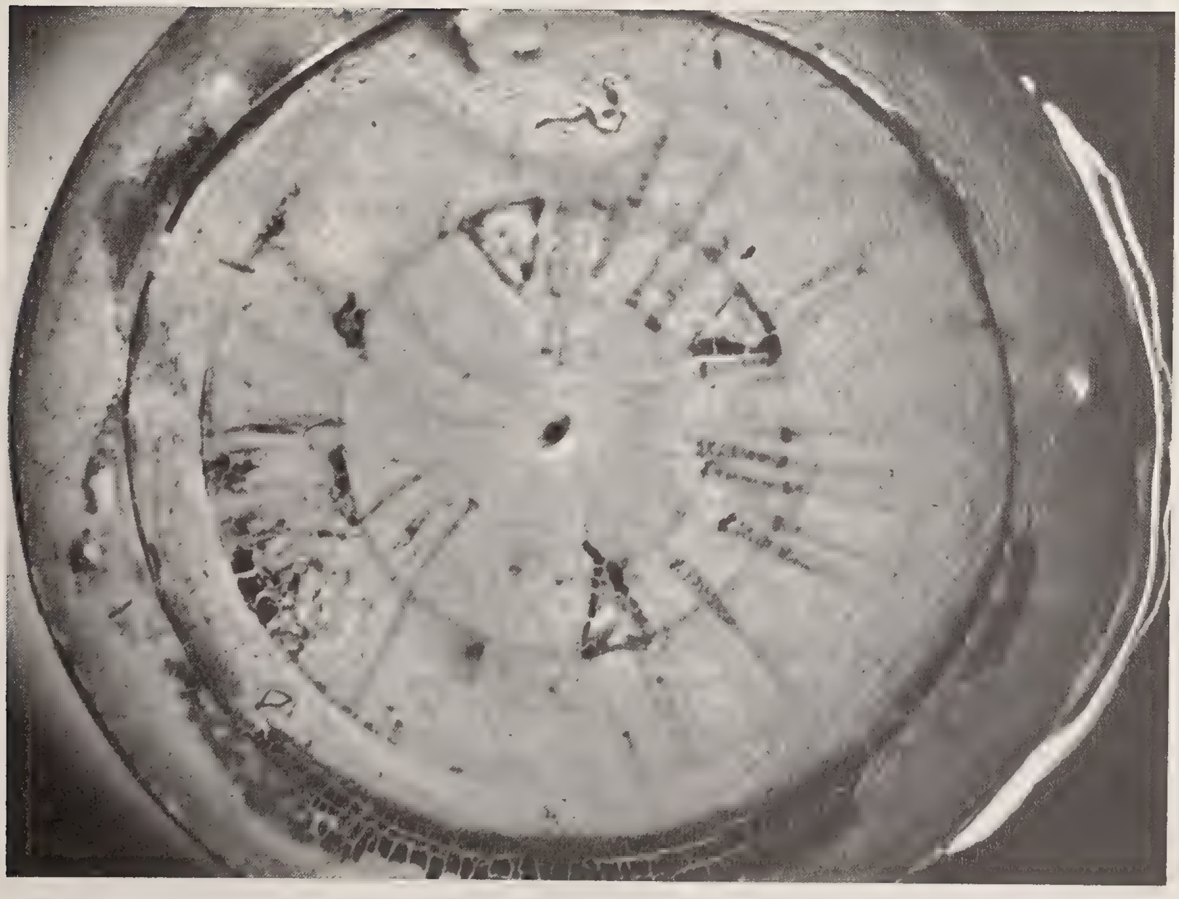

FIGURE 15. COVER SLIP REMOVED FROM AMICON, NEUTRAL IOPLEX AT 9-1/2 MINUTES.

DISCUSSION

DR. BLACKSHEAR: In the circle in which you observe leukocytes sticking did you have a chance to observe whether or not the red cells were aggregated in clumps larger than the leukocytes?

MR. PETSCHEK: The leukocytes within the circle appear to stick more or less individually. The stained cover slip doesn't have any red cells on it, and the flow itself doesn't seem to show any pronounced rouleaux formation although this is within the significantly non-Newtonian viscosity region.

DR. LUDWIN: Do you have any comments you can make regarding protein adsorption with regard to pattern or thickness on the surfaces of these materials?

MR. PETSCHEK: There is this phenomenon; the platelets do not attach until the blood has flowed for 30 to 50 seconds on polyurethane. This indicates that there is some time involved in the formation of a protein layer. That is the extent of information on the protein layer, that I have.

DR. LEONARD: There is indication that platelet adhesion is inhibited on glass in the presence of citrate. Have you examined your polymer films under these conditions; could you tell me whether perhaps there is the same underlying mechanism of platelet adhesion?

MR. PETSCHEK: Are you suggesting systemic citration of the animal? We are dealing with blood that is coming directly from the carotid artery.

DR. LEONARD: I understand that. Once you get citrate into this region, then there is a question as to whether platelet adhesions would occur, under these conditions.

MR. PETSCHEK: I haven't done anything of that nature.

DR. LEONARD: What I am trying to get at here is what is the nature of the forces that hold the platelet to the polymer surface?

MR. PETSCHEK: Well, we haven't worked with citrated blood. The only experiment we have done in which there is a chemical change in the blood, is that we have done a few experiments with heparinized dogs. These do not show differences in adhesion of the platelets.

DR. LEONARD: Heparin presumably doesn't inhibit the adhesion of platelets on glass. But citrate does. And it would be of interest to try it in the presence of citrate.

MR. PETSCHEK: Possibly. I think that that would be done more practically using a beaker of citrated blood. We have tried to avoid changes in the natural blood configuration.

DR. REAM: One final question.

DR. ROTH: Have you attempted to correlate the results of the tests rating the various coatings with the results of Dr. Galt.

MR. PETSCHEK: Not in detail. No. Grossly there is some agreement. Within the Amicon Ioplex group of materials for example, there is a definite correlation with other results that the anionic is markedly better than the neutral and cationic. But, we haven't tried a detailed correlation.

DR. REAM: Thank you very much Mr. Petschek.

REFERENCES

1. Petschek, H.E., Adamis, D. and Kantrowitz, Arthur, "An Experimental Preparation for the Study of Thrombosis on Artifical Surfaces Under Controlled Flow Conditions," Annual Report, Contract PH43-67-1120, February 1969; also, Avco Everett Research Laboratory, Research Report 314, September 1968.
2. Petschek, H., Adamis, D. and Kantrowitz, A.R., "Stagnation Flow Thrombus Formation," Vol. XIV Trans. Amer. Soc. Artif. Int. Organs, 1968, Contract PH43-67-1120.

LEGEND FOR TABLES 1 TO 5

Column Heading	Interpretation
Material	The material being evaluated identified by supplier and supplier's code number, except for Thermo Electron No. 1 which is the first sample sent to us by Thermo Electron Corporation.
Duration	Time of run in minutes.
% Monolayer	This is a subjective impression of the number of platelets compared to the total which would complete the surface monolayer.
Degree of Aggregation - Indicated by 0 to 4+	0 - No interaction between platelets which are on the surface. 1+- Platelets have grouped together leaving some surface regions blank. Each platelet has retained its identity by light microscopy. 2+- Platelets have lost individual identity in some clumps, thus probably indicating the start of true platelet aggregation. 3+- Approximately half the platelets have aggregated. 4+- Complete platelet aggregation - usually accompanied by or preceding extensive thrombus formation in the chamber.
White Blood Cells	0 - No leukocytes on surface 1+- Sparse white cells - seen only in leukocyte circle or around starting support thrombi. 2+- Large white cell circle or uniform covering of surface with diffuse white cells. 3+- More dense covering than 2+. 4+- Tightly packed leukocytes - usually occurring in a region from which a thrombus has been removed.
Thrombi	Number indicates how many thrombi were found on a surface and the percentage of surface covered. When a thrombus formed on a surface and was pulled off in dismantling the chamber, the region of surface originally covered by the thrombus has a characteristic appearance somewhat independent of the surface from which the thrombus was removed. This appearance, which is indicated by capital F (for thrombus footprint) consists of many white cells, often closely packed together in a hexagonal mosaic pattern, and almost total lack of platelets. The density of leukocytes remaining in the footprint is the most variable parameter between different materials and seems directly related to the tendency of the thrombus to adhere to the surface. Thus, a notation 4F in the "thrombi" column indicates that the majority of surface was covered by thrombi which were removed from the cover slip before staining.

TABLE 1

CHAMBER NO. 1

A = 2.5 sec^{-1}

			Stained Cover Slip				
Material	Duration Min.	Observation During Run	% Mono-layer	Degree of Aggregation	White Blood Cells	Thrombi	Comments
Shell							
BM-1	2	No changes	10	0	0	0	
BM-4	2	"	20	0	0	0	
BM-15	2	"	--	-	-	-	Material shrivelled-No observation possible
LR10850-88	5	Leukocyte circle formed	100	0 (except in WBC circle)	circle with some platelet aggregates	0	
Dow Corning							
RB 1622	2	Impossible because of surface opacity	100	1+	-	0	Platelet aggregation starting only on supports.
RB 1519	2		100	1+	-	0	
Amicon Ioplex							
Cationic	2	No changes seen	-	-	-	-	Material shrivelled-No observation possible
Neutral	-	----	-	-	-	-	
Anionic	43	1st thrombus 23 min grew rapidly Leukocytes covered surface by 10 min	-	-	-	-	Material shrivelled-No observation possible
Thermo Electron							
TC-3	2	No changes	10	1	1	0	
No. 1	2	"	1.0	0	0	0	
Avcothane							
Heated	2	Too opaque	100	0	0	0	
Unheated	2	"	100	0	0	0	

TABLE 2

CHAMBER NO. 2

$A = 10\ \text{sec}^{-1}$

			Stained Cover Slip				
Material	Duration Min.	Observation During Run	% Mono-layer	Degree of Aggregation	White Blood Cells	Thrombi	Comments
Shell							
BM-1	83	WBC circle Support thrombi only	100	0	1+	0	
BM-4	45	Support thrombi	100	2+	2+	0	Support thrombi larger than BM-1
BM-15	40	Material detached No gross thrombi	---	-	-	-	Material detached
LR10850-88	61 1/2	17 1/2 min to 1st thrombus 31 min to 2nd thrombus	75	0	1+	2	Platelet aggregation only in vicinity of thrombi
Dow Corning							
RB 1622	34	Extensive thrombi on cover slips	100	4+	4+	4F	
RB 1519	55		100	4+	4+	4F	
Amicon Ioplex							
Cationic	8 3/4	Covered with thrombus at 6 minutes					Material shrivelled-No observation possible
Neutral	18 1/3	Thrombi started at 3 3/4 minutes and grew rapidly but not as fast as Cationic Ioplex					
Anionic	-	-----					
Thermo Electron							
TC-3	60	Thrombus	100	2+	2+	1F	
No. 1	-	-----	---	-	-	-	
Avcothane							
Heated	65	-----	100	0	Few around stagnation point	-	
Unheated	60	-----	100	0	Circle	-	Some platelet clumping in WBC circle only

TABLE 3

CHAMBER NO. 3

$A = 10\ \text{sec}^{-1}$

			Stained Cover Slip				
Material	Duration Min.	Observation During Run	% Mono-layer	Degree of Aggregation	White Blood Cells	Thrombi	Comments
Shell							
BM-1	10	3-4 WBC near S.P.	100	0	0	0	Support thrombi very small
BM-4	10	No changes	100	2+	2+	0	
BM-15	10	No changes	---	-	-	-	Shrivelled on drying
LR10850-88	10	No changes	---	-	-	-	Shrivelled on drying
Dow Corning							
RB 1622	10	Opacity too great for observation	100	4+	4+	Multiple small thrombi	
RB 1519	10						
Amicon Ioplex							
Cationic	10	1st thrombus 2 1/2 covered by 8 min					Material shrivelled-No observation possible
Neutral	9 1/2	Entirely covered by 9 1/2 min					
Anionic	4	None on surface					
Thermo Electron							
TC-3	10	Thrombi	100	4+	4+	4+	Concentric thrombus formation
No. 1	10	No thrombi	100	0	70μ circle	0	Some platelet aggregation in WBC circle
Avcothane							
Heated	10	-----	100	0	0	0	
Unheated	10	-----	100	0	0	0	

TABLE 4

CHAMBER NO. 4

$A = 1\ \text{sec}^{-1}$

			Stained Cover Slip				
Material	Duration Min.	Observation During Run	% Mono-layer	Degree of Aggregation	White Blood Cells	Thrombi	Comments
Shell							
BM-1	90	Only support thrombi	100	0	0	Supports	
BM-4	40	Stagnation region Thrombus forced run stoppage	100	2+	2+	1	
BM-15	65	Thrombus in folds of swollen material	---	-	-	-	Shrivelled
LR10850-88	31-1/2	1st thrombus 12-1/2 min; 2nd thrombus 14 min	75	-	-	2	Leukocytes, platelets and aggregates seen only in region of thrombi
Dow Corning							
RB 1622	32-1/2	Opacity too great for observation	---	-	-	F	Cover slip completely thrombosed
RB 1519	60		---	-	-	F	When thrombi removed, leukocytes found adherent to surface
Amicon Ioplex							
Cationic	13	Thrombus started at 8-1/2 min and complete at 9-1/2 min	---	-	-	-	Shrivelled on drying
Neutral	27	By 10 min the entire viewing region was covered with thrombus	---	-	-	-	
Anionic	8	None	100	0	1+	-	Some leukocytes near stagnation point
Thermo Electron							
TC-3	73	-----	---	-	-	4+	Single large thrombus adherent to material
No. 1	60	-----	100	1+	1200μ circle 2+ elsewhere	3	Single main thrombus in stagnation point region with small other thrombi nearby
Avcothane							
Heated	179	-----	100	0	circle	0	Some platelet clumping in WBC circle
Unheated	41-1/2	-----	100	0	circle	0	Some platelet clumping in WBC circle

TABLE 5

CHAMBER NO. 5

$A = 25\ sec^{-1}$

			Stained Cover Slip				
Material	Duration Min	Observation During Run	% Mono-layer	Degree of Aggregation	White Blood Cells	Thrombi	Comments
Shell							
BM-1	2	No changes	60	0	0	0	
BM-4	2	"	50	1+	0	0	
BM-15	2	"	--	-	-	-	Material shrivelled-No observation possible
LR10850-88	2	"	variable	0	0	0	Sparse to almost complete monolayer
Dow Corning							
RB 1622	2	"	50	0	0	0	
RB 1519	2	"	100	0	0	0	
Amicon Ioplex							
Cationic	10	1st thrombus 3-3/4 min. Covered at 6 min.	--	-	-	-	Material shrivelled-No observation possible
Neutral	2	No changes	--	-	-	-	
Anionic	56	"	100	0	0	0	
Thermo Electron							
TC-3	2	"	75	1+	0	0	
No. 1	2	"	--	-	-	-	Broken cover slip
Avcothane							
Heated	2-1/2	-----	100	0	0	0	
Unheated	2	-----	100	0	0	0	

CHAPTER 25

BEHAVIOR OF BLOOD CELLS NEAR WALLS

P. L. Blackshear, Jr., K. H. Keller, R. J. Goldstein,
F. D. Dorman, M. Rosenberg

University of Minnesota
Minneapolis, Minnesota

Several groups at the University of Minnesota are studying the flow of blood near walls. Each focuses on a region limited by the technique. These regions overlap. Starting nearest the wall, the studies are: "Distance 0-1000 Å. Resolution 1Å." Ellipsometric studies of deposits on chrome-plated slides following exposure to cells show that red cells stick to surfaces not first exposed to protein and leave behind a 30Å thick deposit of material. Cells did not stick to surfaces that have been first exposed to plasma until lysolecithin was added. "(D) 0-1000 Å, (R) 10Å." The surface contact microscope shows that red cells in plasma rarely settle closer than 0.1μ from the wall and that there is evidence of microscopic reversibility of cell motion near walls. "(D) 0-1000μ , (R) 2 μ." The 3-D microscope shows red cells in ghost suspensions display velocity vectors with marked lateral components. "(D) 0-1000 μ, (R) 1-10 μ" The uptake of radioactivity of a plasma-free suspension of red cells in a radioactive cholesterol-coated tube increases sharply at wall shear rates of ≈ 1000 sec^{-1}. No such jump occurs when cells are absent. "(D) 0-1cm, (R) 0.01cm." The Laser-Doppler technique is used to measure velocity components of pigmented cells in ghost suspensions. These research efforts combine to give the means for studying the relevant particle behavior in flowing blood in those regions where wall induced lysis and mass transport near walls are important.

INTRODUCTION

A group made up of faculty and graduate students at the University of Minnesota representing several Engineering and Biological fields have been exploring ways of measuring cell motion in flowing blood both remote from and near foreign surfaces, the nature and stability of wall deposits and some mechanical and compositional aspects of the adhesion of cells to foreign surfaces. The motivation for this work lies in the desire to understand the influence wall encounter has upon thrombus formation (immediate and delayed) red cell lysis (immediate and delayed) white cell destruction or mobilization and to better understand the magnitude and nature of particle behavior throughout the flow on diffusional processes in blood.

There is ample evidence to show that there is interaction between these processes and that events at the wall are further influenced by the nature of the protein deposit which in turn depends upon the nature of the underlying surface and the flow past the surface.

For example: Gott and his associates show that surface composition, geometry and flow interact in a complex way to influence thrombus formation. The influence of surface coatings on hemolysis has long been known. More recently Steward and Sturridge, our group and many others have demonstrated an influence on surface composition, geometry and adjacent blood flow on hemolysis. Lyman and, independently, Petschek have shown in interplay between white cell adhesion, wall composition and local blood flow.

Many authors have published on the influence of surface composition on wall deposits. Ponder and, independently, Rosenberg and Watters of our group have shown that cell wall adhesivity depends upon the nature of the wall deposit. Falb and Leininger have evidenced that hemolysis influences the clotting times in vitro involving whole blood. Brain has shown how fibrin strands can cut and alter red blood cells in vitro as well as in vivo. Lyman has shown evidence that white cells sticking to foreign proteins on foreign walls influence platelet deposition and by inference red cell stickiness. Petschek has shown some evidence of interaction between white cell, foreign wall, flow, thrombus formation and occasionally red cell adhesion.

Our group has shown that there is an influence of particle rotation and migration on diffusional processes of particles and solutes in the presence of velocity gradients.

Goldsmith and Mason have shown that in dilute suspensions particle deformability and size determine the speed with which a deformable particle moves to the center of a tube. Takano et al show that in concentrated suspensions of oil droplets in water there is a residual effect in that the larger droplets take an equilibrium position at the center of a tube (in steady or pulsatile flow) forcing smaller particles near the wall. Farhaeus had earlier made similar observations on flowing blood showing that the large white cells assume a position near the tube center unless aggregated red blood cells displace them. Weed has recently demonstrated that a reduction in cell ATP causes a marked decrease in deformability of the red blood cells. Thus stored, abused, sequestered, or perhaps aged cells would be forced by the flow to the outer periphery of tube flow, perhaps exacerbating the effect of wall encounter. There is the possibility that skimming layer thickness depends upon the population of stiff cells in addition to hematocrit and flow.

In our previous years' work we have shown an interplay between flow and wall-cell adhesion that leads to lysis. Thus, in all three regions near a wall of interest in artificial internal organ design:

a. 0 - 100 A, the region where chemical and electrostatic forces operate,
b. 0 - 10,000A, the skimming layer where fluid dynamic forces tend to keep particles away from the wall, and
c. 0 - 100μ to 1 cm, where red cell motion induced by the shear dominates the diffusion of smaller particles,

there is an intimate interplay between particle motion and biochemical factors. It is our feeling that engineers familiar with particles and flow working with biologists familiar with blood chemistry, meeting and arguing frequently can contribute to a better understanding of these phenomena; ours is such a group. The activities and results of the current year's work by this group are summarized in the following figures.

PARTICLE BEHAVIOR IN GHOST SUSPENSIONS

A method for studying particle behavior in concentrated particle suspensions pioneered by Mason, later adapted to blood by Goldsmith, has been employed by us to examine instantaneous particle velocity vector distribution in simulated blood. Two lines of attack are being pursued (strobed 3-D microscopy and laser scattering) and will be discussed. The extent to which the results model whole blood depends upon the properties of red blood cell ghosts which in turn depend upon the method of ghost production.

The procedure for ghost preparation is shown below in Table 1. This procedure is unique and, therefore, the properties of the ghosts may be in several respects unique.

TABLE 1

GHOST CELL PRODUCTION

(1) Remove plasma and white cells by refrigerated centrifuge (Servall LV-2), at 4080 g for 10 minutes.
(2) Wash separated erythrocytes with 4 parts Normazal (Commercial Saline) or 0.9% Saline at 4080 g for 10 minutes.
(3) Resuspend cells in 4 parts 310 im. Osm 0.155 M NaH_2PO_4 and 0.103 M Na_2HPO_4 with pH 7.4.
(4) Weigh the ice made of distilled water at a rate of 7 gm ice/cc of solution and pour washed cells on this ice, let them set until the ice melts. This results in hemolysis.
(5) Spin down ghosts and wash them twice with 4 parts 310 im. Osm KCl-NaCl solution (Aqueous solution of 0.135 MKCl and 0.027 M KCl and 0.027 MNaCl) with pH 6, at 13200 g for 30 min.
(6) Separate ghosts from washing solution and resuspend them in 310 im Osm Phosphate Solution. Add 5% of 0.2 M ATP.

Morphological Assay.

Figure 1 shows a Coulter Counter size distribution of the original dog cells and of the ghosts resulting from the application of the above procedure. The volume distribution change from cells to ghosts is less than the variations in cells taken from different dogs.

The shape and projected diameters of cells and ghosts in serum are sufficiently alike to suggest that surface areas are (within normal tolerance) the same.

Rheological Assay.

Tests have been run over a range of shear rates and hematocrits with ghosts suspended in plasma and serum. These results are summarized in the next two figures.

Figures 2a and 2b show the influence of shear rate on the viscosity of cells and ghosts respectively in plasma at different hematocrits. The strong dependence on shear rates for both at low shear rates suggests (according to Merrill and others) that rouleaux formations are similar for the two populations. Microscopic inspection confirms that the stationary ghosts in plasma form rouleaux. In obtaining this data no attempt was made to alter the scum that forms at the plasma-air interface in the Brookfield viscometer. This obviously influences the low shear rate data for plasma so that the magnitude of the effect of rouleaux cannot be accurately determined.

Figures 3a and 3b show the influence of shear rate on the viscosity of cells and ghosts in serum. The fact that concentrations of ghosts effect the viscosity in the way shown at high shear rates suggests that the viscosity of the intracellular fluid is not appreciably different from that of the serum. The fact that as shear rates are lowered the viscosity of ghost suspensions increases at high hematocrits (while micrographs of ghosts in serum at rest show no rouleaux) suggests that the ghost membrane resists distortion much the same as the red blood cell does.

Thus from a rheological point of view the chief differences between ghost and red blood cell behavior are due to the lower intracellular viscosity in ghosts. As a consequence, over normal hematocrit ranges, the viscosity of ghost suspensions is only weakly dependent upon hematocrit.

Goldsmith's results show that in dilute suspensions the important factors in determining the speed with which a particle is accelerated away from a wall in flow is particle size and particle deformability. If the skimming layer thickness and cell concentration distributions at normal hematocrits are similarly influenced, then, in these respects, the ghosts are excellent models of red cells.

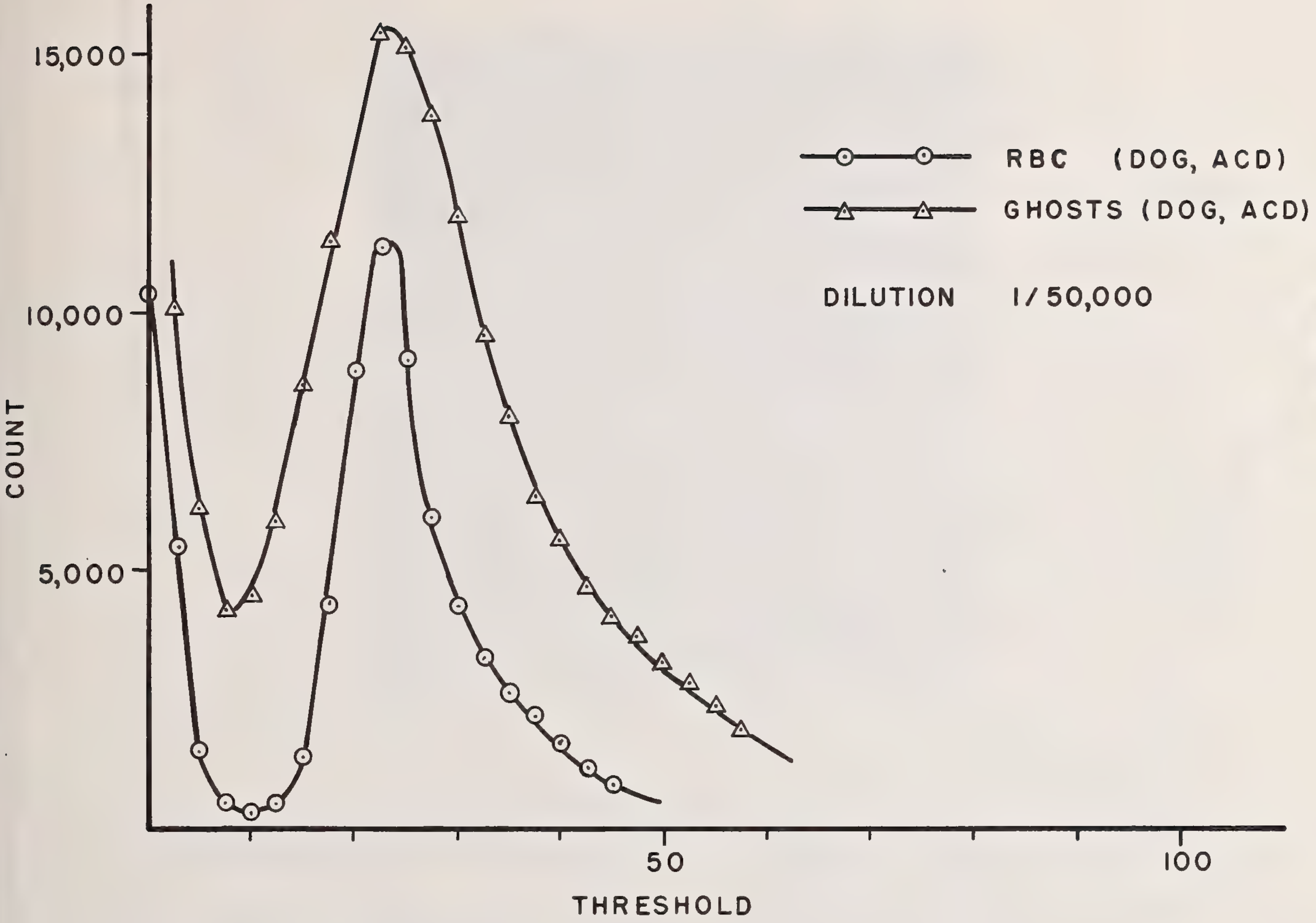

FIGURE 1. COULTER COUNTER SIZE DISTRIBUTION OF ORIGINAL DOG CELLS AND OF GHOST DOG CELLS.

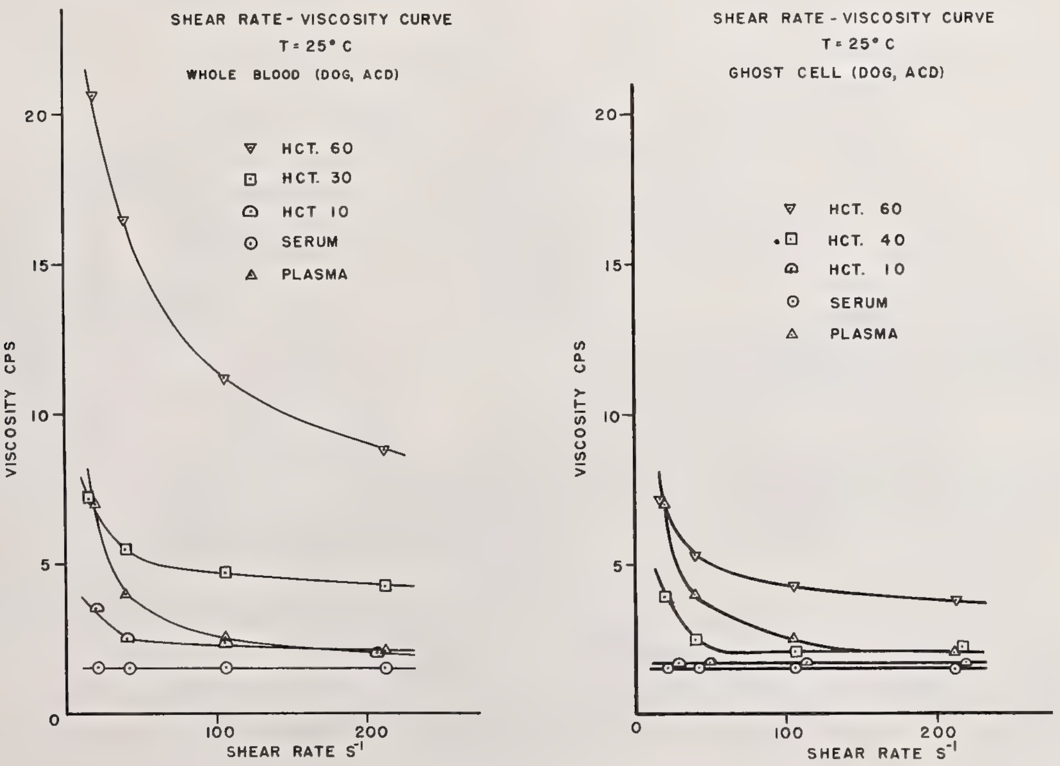

FIGURES 2a AND 2b. INFLUENCE OF SHEAR RATE ON THE VISCOSITY OF CELLS AND GHOSTS RESPECTIVELY.

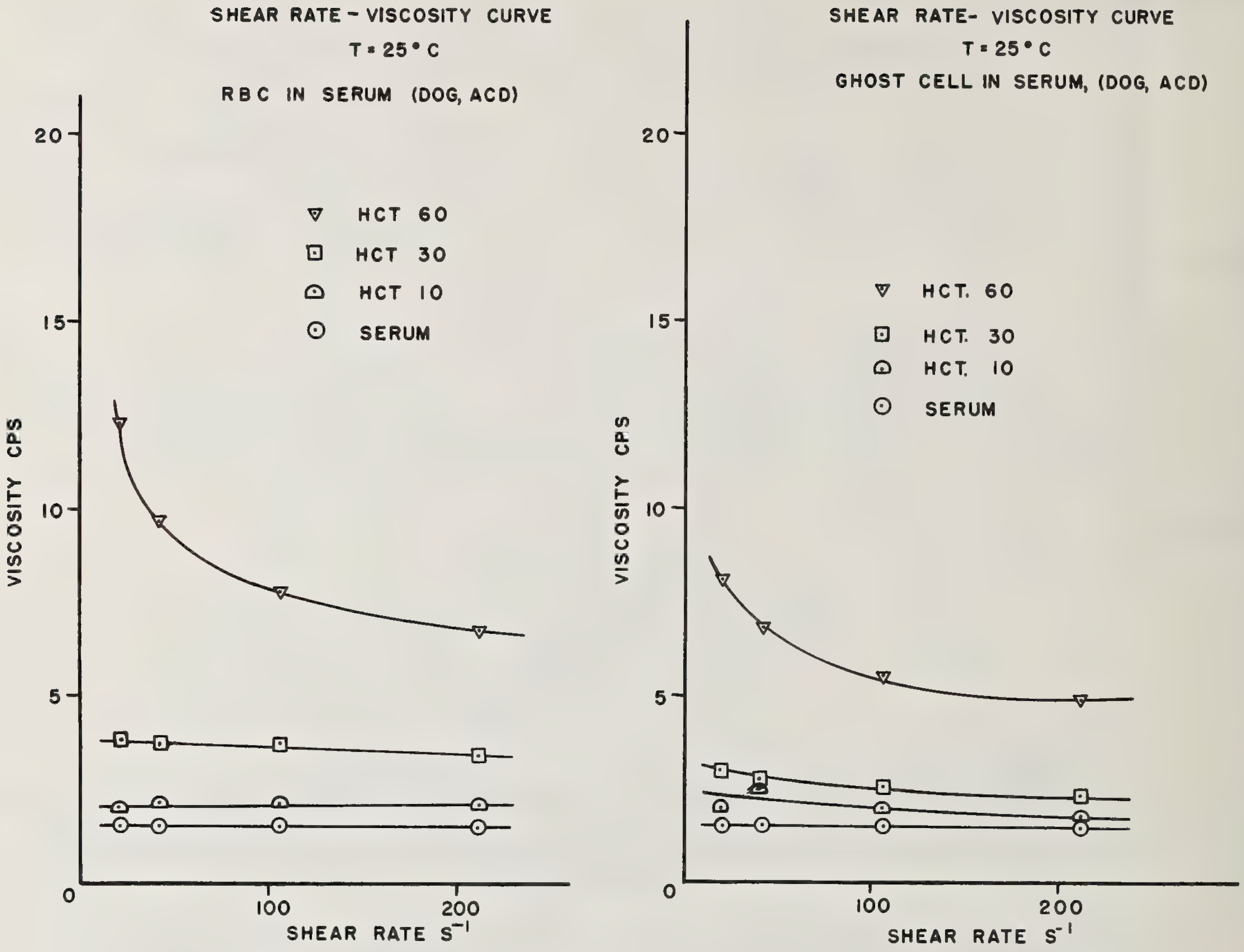

FIGURES 3a AND 3b. INFLUENCE OF SHEAR RATE ON THE VISCOSITY OF CELLS AND GHOSTS IN SERUM.

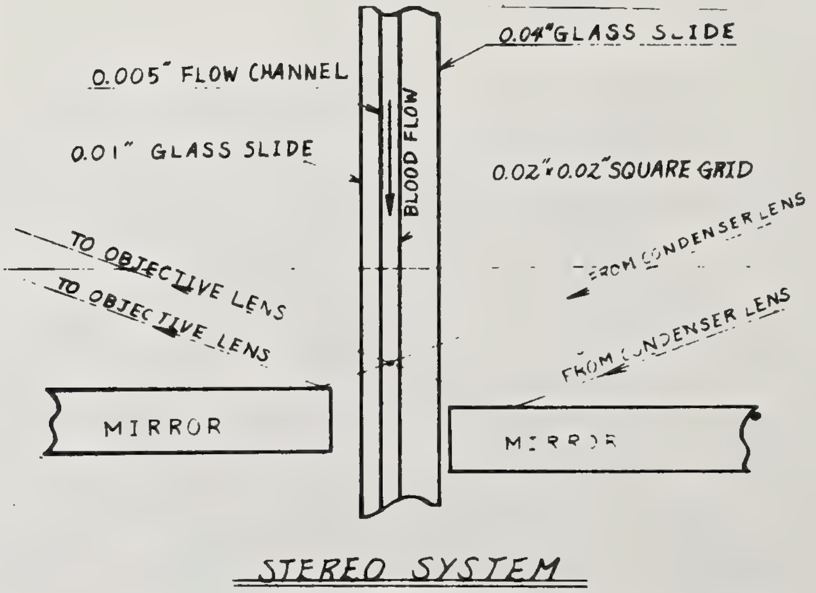

FIGURE 4. STROBED 3-D PHOTOGRAPHY APPARATUS.

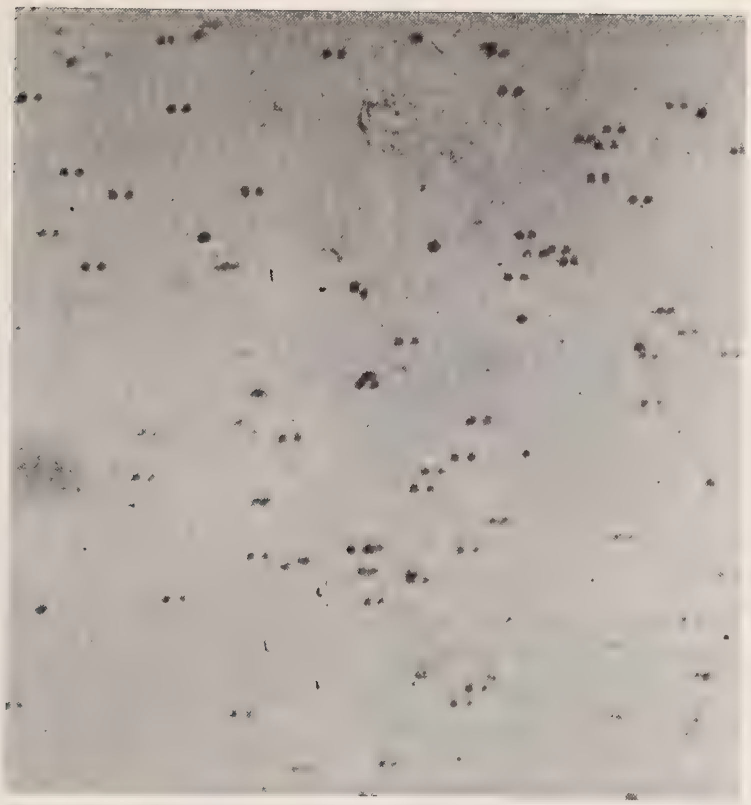

FIGURE 5. APPEARANCE OF PARTICLES WHEN ILLUMINATED TWICE IN RAPID SUCCESSION.

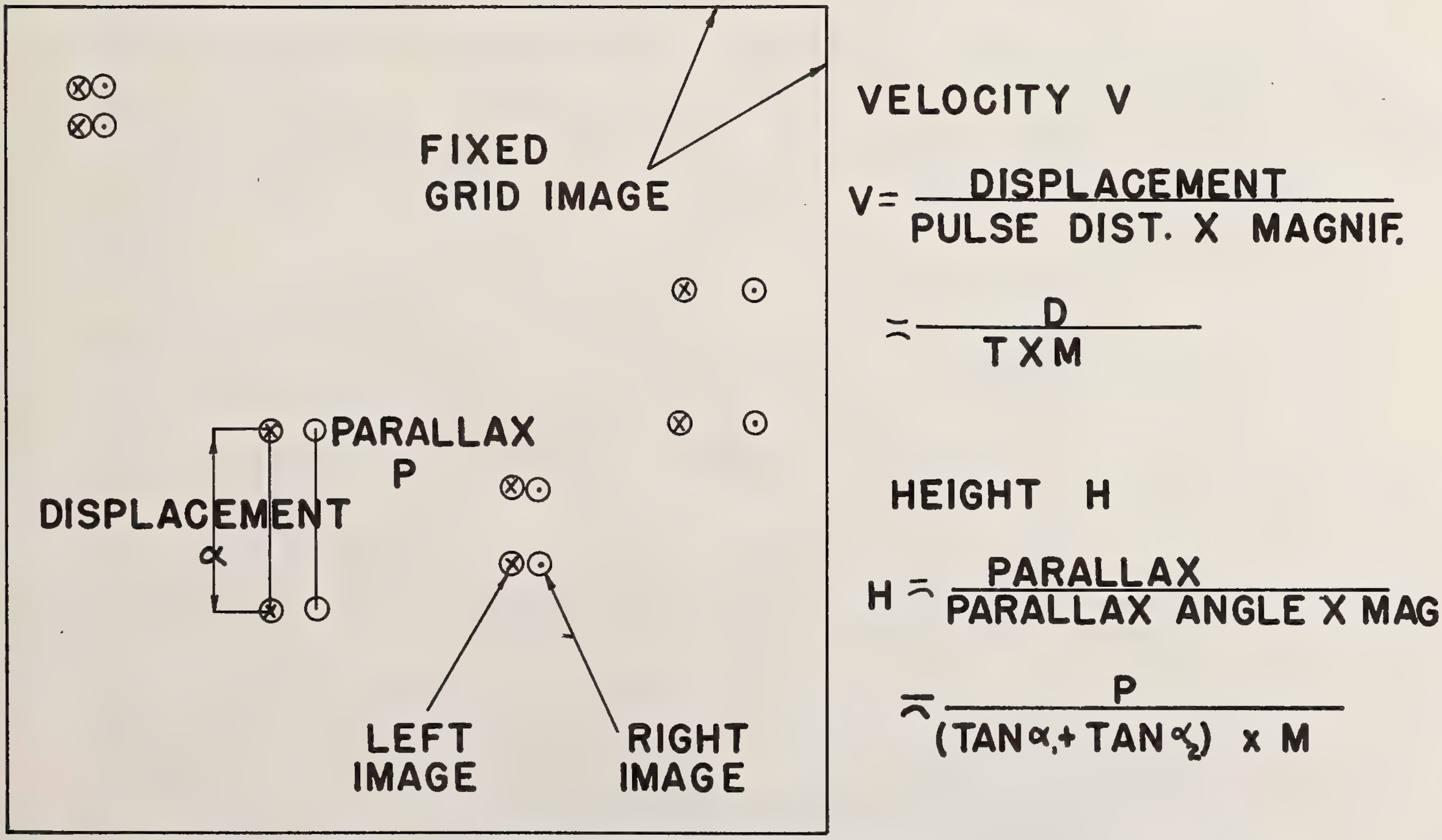
FIXED
GRID IMAGE
PARALLAX
P
DISPLACEMENT
α
LEFT
IMAGE
RIGHT
IMAGE
VELOCITY V
V = DISPLACEMENT / PULSE DIST. X MAGNIF.
≃ D / T X M
HEIGHT H
H ≃ PARALLAX / PARALLAX ANGLE X MAG
≃ P / (TAN α₁ + TAN α₂) x M

FIGURE 6. SIMPLIFIED MAPPING PROCEDURES.

Optical Properties

Measurements on light absorbed in red cell and ghost suspensions are employed to infer the capabilities of the laser scattering technique and will be summarized later.

STROBED 3-D PHOTOGRAPHY

The Apparatus.

The method developed by us for obtaining 3-D photographs of pigmented cells in ghost suspensions was described at last year's contractors' meeting. The next several figures review the method. Figure 4 shows the details of the test section showing how two sets of images with a 8-1/2^o included angle are obtained. Figure 5 shows how the images of particles appear when illuminated twice in appropriately rapid succession on the stereo pair and Figure 6 shows how these appear superimposed. Here each pigmented cell appears as four images. This contains enough data to obtain all three velocity and position vectors for each cell.

Results and Discussion.

The nomenclature to be used in the next several figures is illustrated in Figure 7. Here $\bar{v}_x$ is mean particle velocity in the direction of flow and v_x' is the local perturbation about the mean. Because the y dimension of the test section is so much greater than the z dimension, we focus our attention on data obtained near the center of the y coordinate where $\frac{\partial \bar{v}_x}{\partial y} \approx 0$.
The system then can be considered in this region to be two-dimensional with respect to the mean flow. The velocity profile for $\bar{v}_x + v_x'$ is shown in Figure 8.

Cell Population Distributions.

A plot of the $\frac{\partial \bar{v}_x}{\partial z}$ vs z is also shown in Figure 9. Local values of effective viscosity can be inferred from $\mu = \tau_{wall} \frac{z}{b} \left(\frac{\partial \bar{v}_x}{\partial z}\right)^{-1}$. Within the limits of our resolution $\frac{\partial \bar{v}_x}{\partial z} \propto z$; the effective μ appears to be constant. No inference can be drawn from this regarding ghost population distribution in view of the weak dependence of μ upon hematocrit at these velocity gradients as shown in Figures 4a and 4b.

On the other hand the population distribution of pigmented cells can be obtained by number count from the data photographs. These counts are shown in Figure 9. Here can be seen a suggestion that a population maximum occurs near the tube center.

There is no reason to expect the red blood cell should distort more readily hence migrate more readily with applied stress than the ghosts do. Thus, there is reason to believe there is a variation in the ghost population distribution across the channel, having a maximum concentration at the center of the channel. By inference, blood in tube flow may have similar concentration distributions.

Velocity Fluctuations.

Values of the vector component $\bar{v}_x + v_x'$, v_y' and v_z' are shown in Figure 10. Values of $\sqrt{v_i^2}$ for these components are shown in Figure 11. Particularly noteworthy are the following:

a. The perturbation velocities are anisotropic. The variation of these RMS values ($\bar{v}_x'$) across the duct is different.

$\bar{v}_x'$ does not tend to zero at the walls whereas both $\bar{v}_y'$ and $\bar{v}_z'$ do. $\bar{v}_x'$ has a distinct depression at the center of the duct whereas in the others the depression is not so distinct. Note that $\bar{v}_z'$ is non vanishing where $\frac{\partial \bar{v}_x}{\partial z}$ does vanish and that $\bar{v}_y'$ is substantial despite the fact that $\frac{\partial \bar{v}_x}{\partial y} = 0$.

Perhaps of most immediate practical importance is the region of diminishing amplitude in v_z' near the wall. In these runs this region is approximately 15μ perhaps 3 - 5 times the mean skimming layer thickness predicted for this hematocrit. Thus, the full enhancement effect of red cell movement in mass transfer processes will become operative where concentration boundary layers are thicker than 15μ.

Of additional interest is the inference that can be drawn from this data relative to the importance of turbulent flow. Recall that in fully developed turbulent pipe flow there is a region near the wall where the velocity profile is nearly laminar. This is depicted in Figure 12. We may calculate the conditions under which the boundary of the laminar sublayer equals 15μ. These calculations are shown in Figure 13. We see that for mean flow velocities on the order of 1000 cm/sec or greater, the influence of turbulence should be felt in the region $z \leq 15\mu$.

There is a significant body of data accumulated in our laboratory and elsewhere showing that in tube flow and in the Fleisch hemoresistometer, hemolysis jumps in the neighborhood of 600 cm/sec. In our jet tests, Figure 14, we show that without walls red blood cells can withstand turbulent velocities of 2000 cm/sec. Thus, it would seem likely that lysis involving turbulent flow of blood near walls occurs because of wall encounter and not due to in-bulk forces.

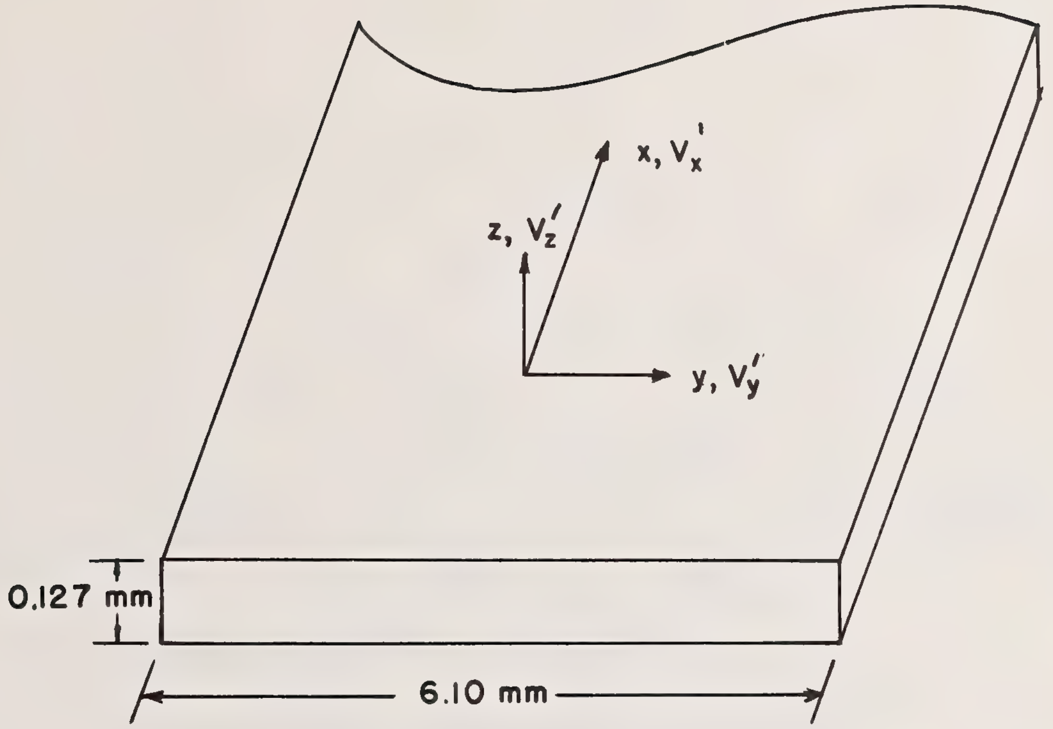

FIGURE 7. NOMENCLATURE USED IN THE NEXT SEVERAL FIGURES.

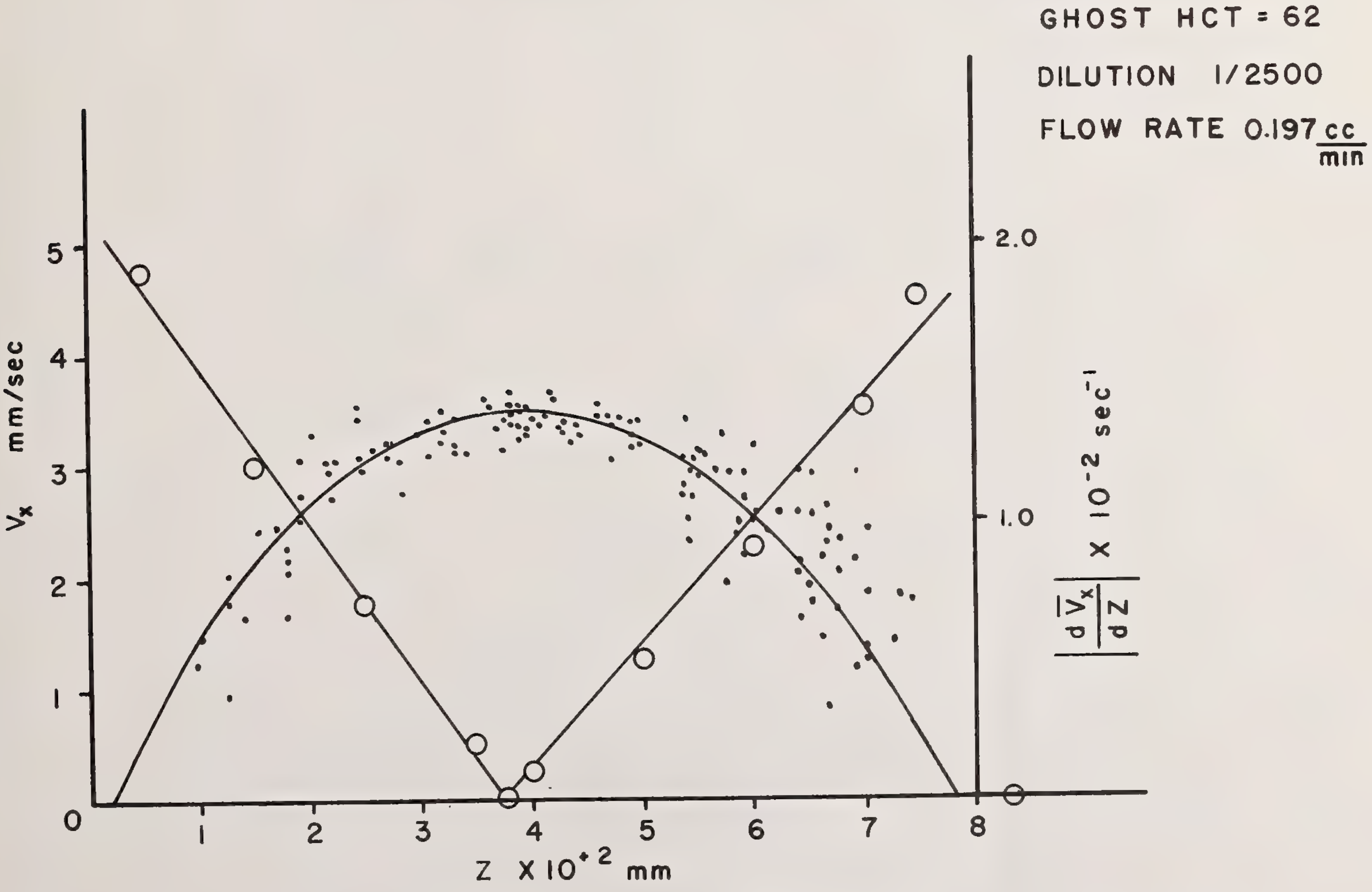

FIGURE 8. VELOCITY DISTRIBUTION OF RED BLOOD CELLS.

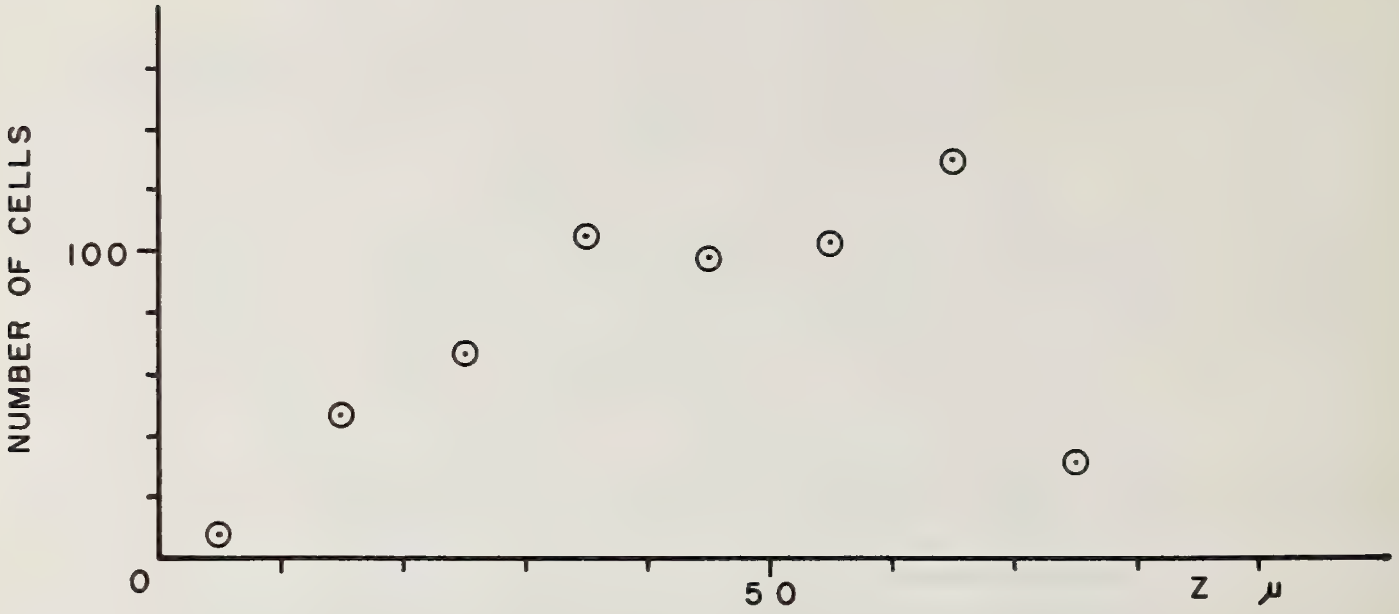

FIGURE 9. CELL DENSITY DISTRIBUTION.

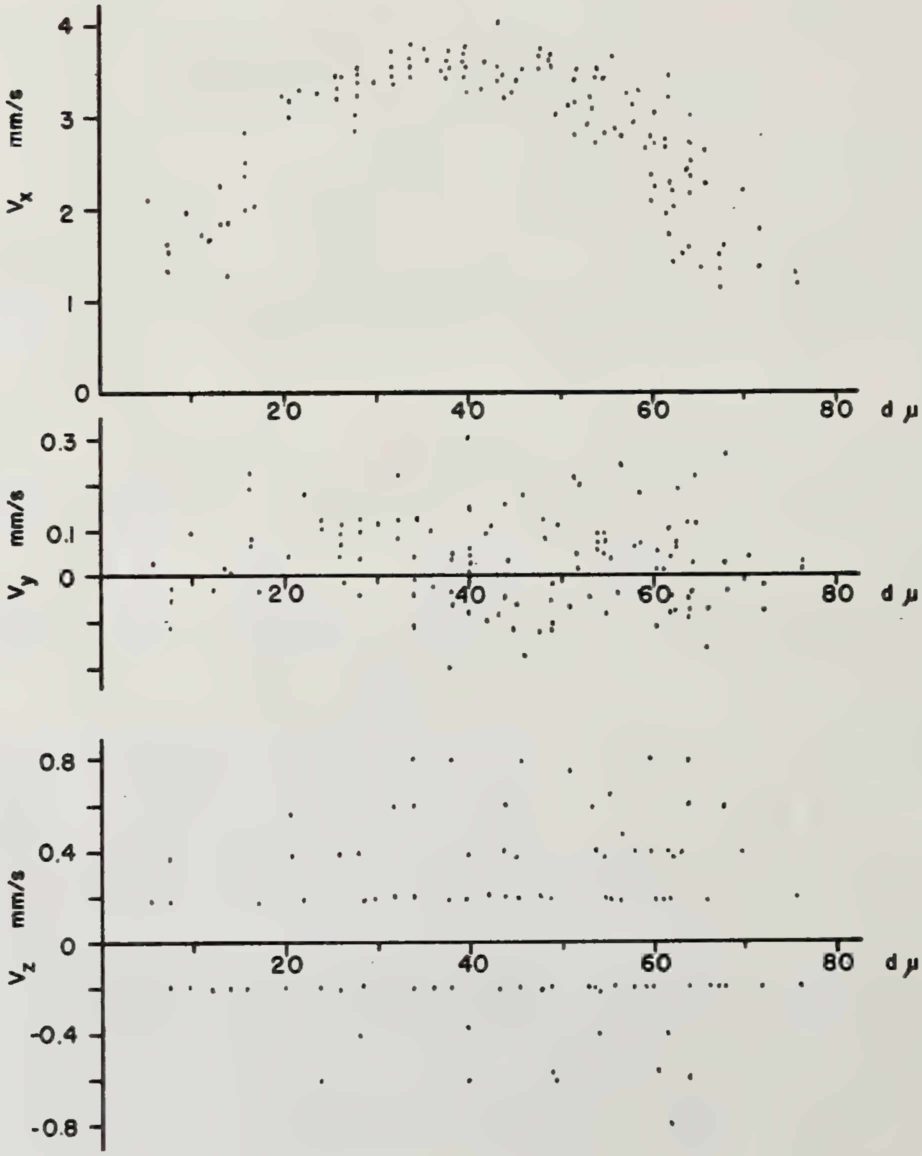

FIGURE 10. SEE TEXT FOR EXPLANATION.

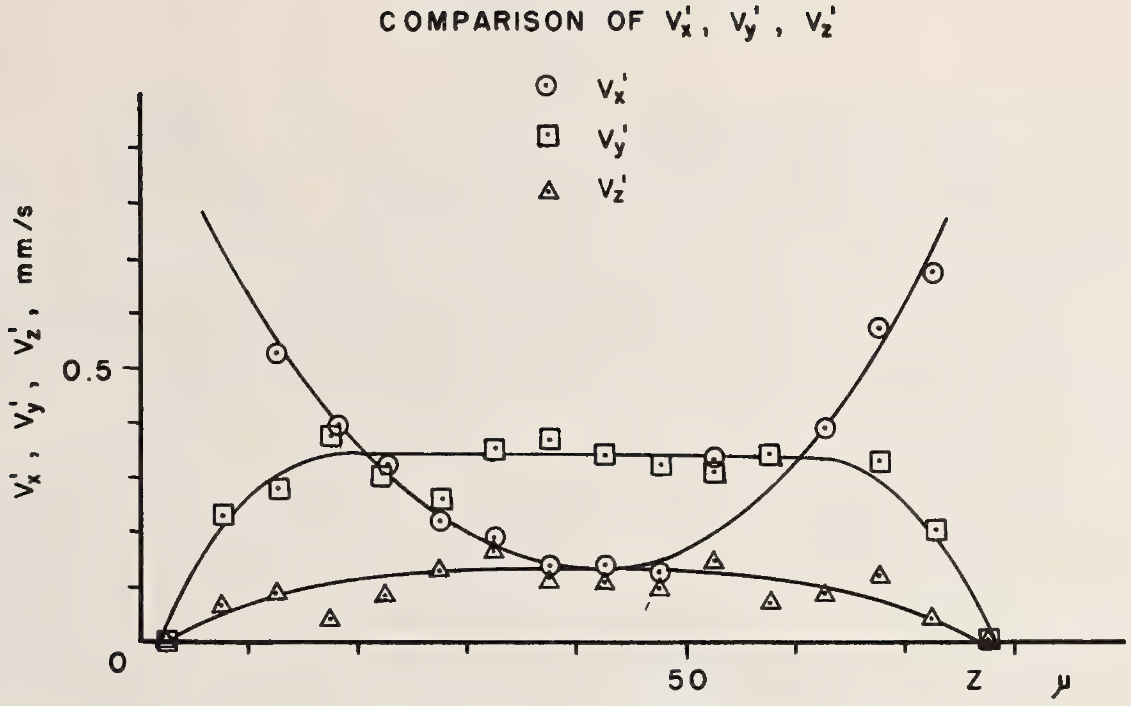

FIGURE 11. SEE TEXT FOR EXPLANATION.

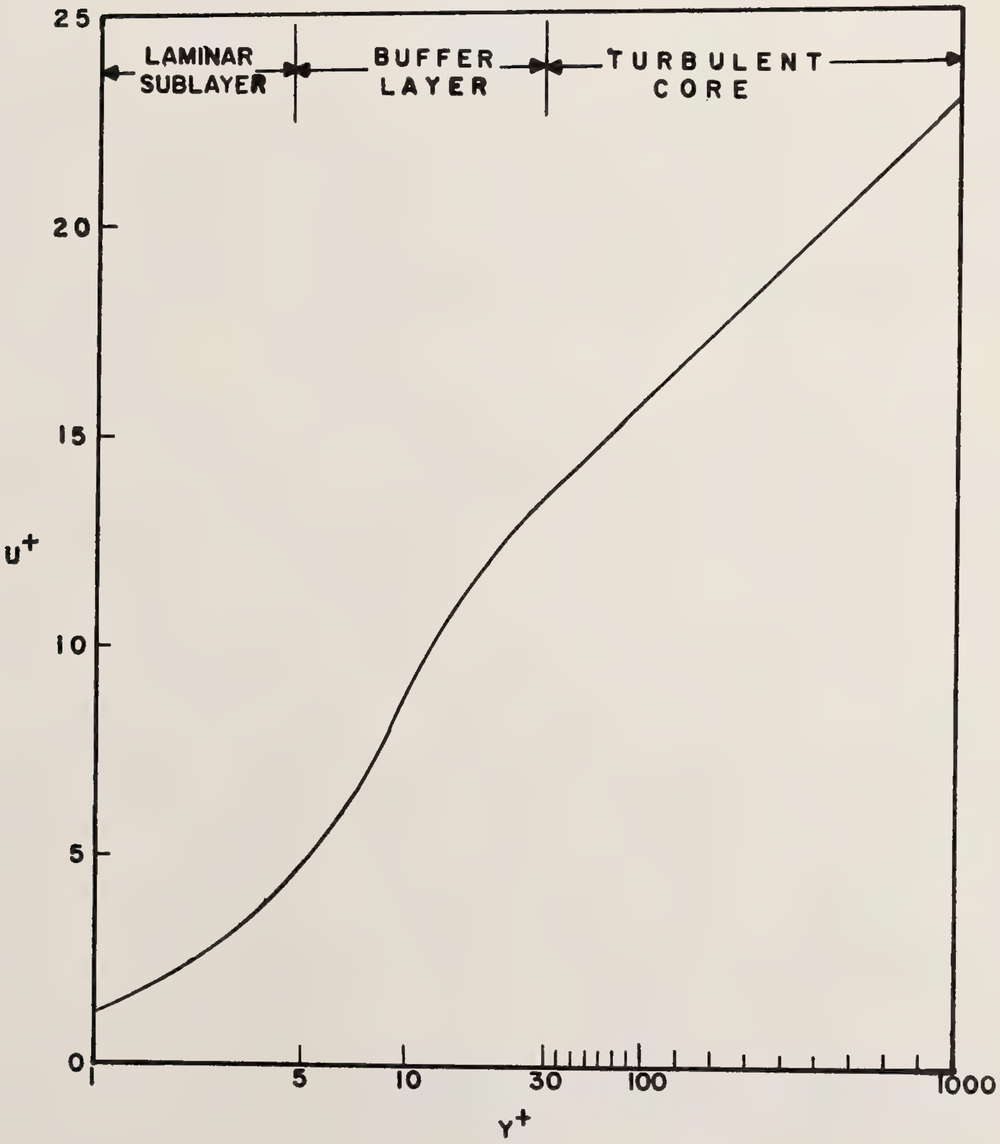

FIGURE 12. TURBULENT PIPE FLOW.

Laminar Sub layer boundary is for $y^+ = \frac{y}{\nu}\sqrt{\frac{\tau_w}{\rho}} = 5$

we ask for the conditions where $y = 15\mu$

$$y = 15 \cdot 10^{-4}\,\text{cm} = \frac{y^+ \nu_w}{(\tau_w/\rho)^{1/2}}$$

$$\text{But} \quad \frac{\tau_w}{\rho} = \frac{f\,Um^2}{8}$$

$$f \approx 0.02$$

$$y^+ = 5$$

$$0.01 \leq \nu_w \leq 0.02 \;\text{cm}^2/\text{sec}$$

$$15 \cdot 10^{-4} = \frac{5\,\nu_w\,20}{Um}$$

or

$$650 \leq Um \leq 1300\,\text{cm/sec}$$

FIGURE 13. CALCULATIONS FOR TURBULENT PIPE FLOW.

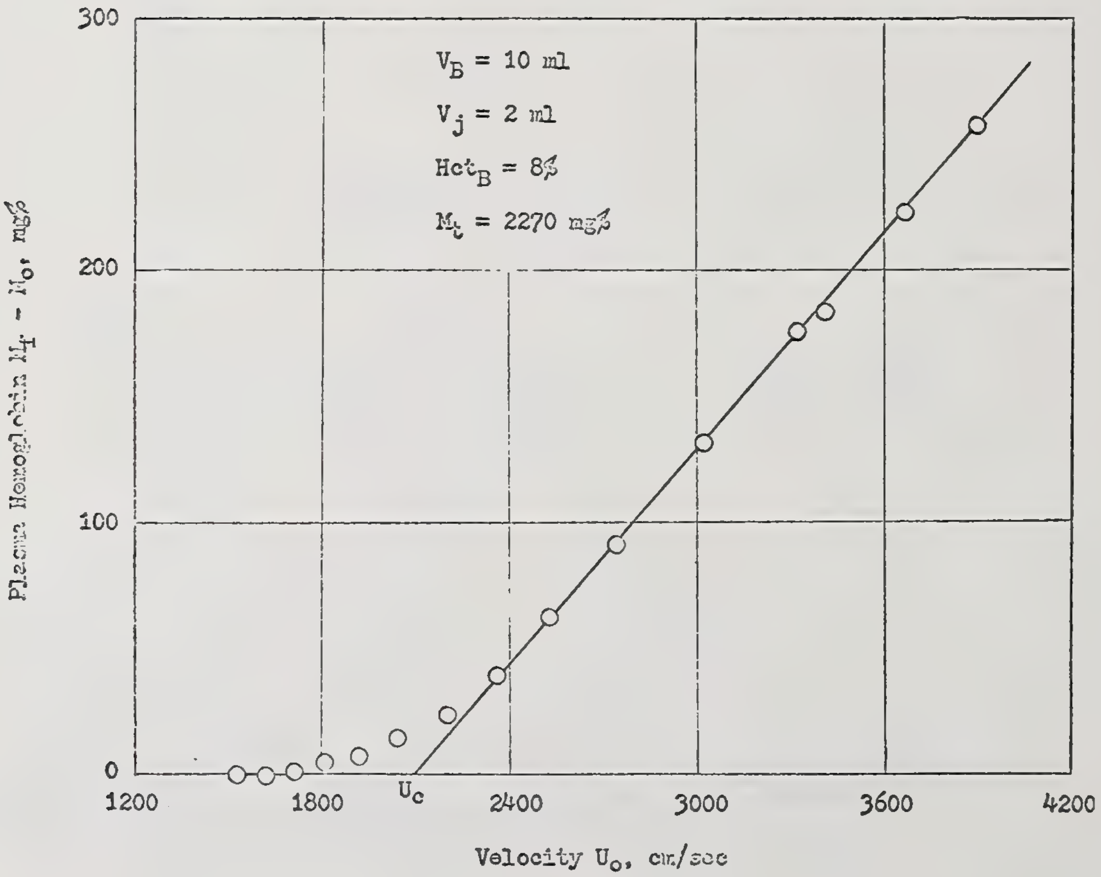

FIGURE 14. REPRESENTATIVE DATA FOR HUMAN BLOOD.

Correlation Parameters.

Efforts to obtain correlations between v_z' and v_y' as well as between v_z' at two positions have resulted in the following tentative conclusions. The only correlations observed over dimensions which are large compared to red blood cell diameters are those of v_y' as a function of y. These displayed a scale of approximately 2.5 mm.

Assuming the scale of the other components is of the order of the single red blood cell, the diffusion of species associated with the moving cell should be $D \times 10^{-8} \frac{\partial \bar{v}_x}{\partial z}$ which is approximately the value derived from Collingham's model experiments and from Goldsmith's particle movement in blood. The particle-induced diffusion near the center of the flow chamber is obviously not related to local velocity gradients; it is thus (similar to turbulent transport processes) a function of the entire flow. We infer then that the domain of influence of one particle in motion must extend well beyond one cell diameter.

Just as v_x', v_y', v_z' are not the same, the diffusion produced by these perturbations are not the same. Thus, the estimate of order of magnitude of particle motion-induced diffusion given last year before this group (Figure 15) should be interpreted as follows. When the velocity gradient reaches the value indicated anywhere in a cross section the effect of particle motion on diffusion will be somewhere in the flow on the order of magnitude shown. The actual effect will be anisotropic, will not be uniquely related to the local velocity gradient, but depends on the entire profile in an as yet undetermined manner.

In reviewing the utility of the 3-D photographic technique it seems ideally suited for measuring velocity and position vectors of randomly distributed particles over a relatively large field of view. It is thus a promising tool for assessing the position and motion of platelets and white blood cells as well as concentration distributions and movement of the red blood cells.

LASER-DOPPLER VELOCITY MEASUREMENTS

The Laser-Doppler system for the measurement of fluid velocity has been described by Goldstein and Kreid in a previous report. Figure 16a is a schematic or the optical system employed.

The design of the Laser-Doppler system required information concerning the light scattering properties of red cells and ghosts. A system was assembled and measurements were made of scattered intensity vs. observation angle as shown in Figure 16b. As a check on the reliability of the apparatus similiar data was taken employing one half micron polystyrene spheres as shown in Figure 16c. A program was written to calculate the Mie theory scattering prediction and agreement was good for the poly styrene spheres. The Mie theory prediction for the red blood cells does not correlate well with the data since red blood cells are non-spherical, absorbing and electrically conducting in violation of the assumptions of the Mie theory. The data agrees in order of magnitude but the predicted oscillations in amplitude are not observed.

ATTENUATED TOTAL REFLECTION MICROSCOPY (ATR)

ATR has been used to observe cell wall encounter (i.e., cells brought to within 1000Å). The apparatus is shown in Figure 17. Some observations are summarized below:

a. The leading meniscus introducing cells in a dry flow chamber;
   i) Causes an increase in hematocrit behind the meniscus
   ii) Forces the cells closer to wall behind meniscus
   iii) Leaves debris stuck to wall
b. Increasing hematocrit increases wall encounter
c. Increasing the flow velocity changes the character of the wall encounter in saline suspension.
   i) At low velocities (wall shear rates <1 sec^{-1}) cells come close to wall but never stop moving.
   ii) As velocity increases cells appear to pause momentarily at the wall and then move on.
   iii) Further increases in velocity (up to wall shear rates of 300 sec^{-1}) increases the frequency of cells approaching wall, pausing, then moving on.
d. Some observations of microscopic reversibility have been made. At a low wall shear rate (≈1 sec^{-1}) encounters have been observed to be reversible and repeatable. For example, upon stopping the flow and reversing it a cell that had just careened into and out of the field of view could be forced to follow its path over and over again. This suggests that some cells near the wall behave as though they are non-deformable at some low shear rates.
e. In time the surface becomes more and more cluttered with debris which ATR illuminates. However, for each such stationary spot that forms hundreds of cells have appeared in the same position and passed on.

Hemolysis studies in tube flow were conducted in the apparatus shown in Figure 18. Injecting blood of varying hematocrit through a stainless steel 23 gage hypodermic needle at shear rates up to 300,000 sec^{-1} (where hemolysis is due to terminal jet lysis) gave results shown in Figure 19. Note that:

a. At low hematocrit (<30%) hemolysis was extremely small until shear rates as high as 10^5 sec^{-1}. This corresponds to a wall shear stress of up to 10,000 dynes/cm^2.
b. As hematocrits increased beyond 40, hemolysis became appreciable at wall shear rates of $10^4 sec^{-1}$ and increased with increasing shear rate.

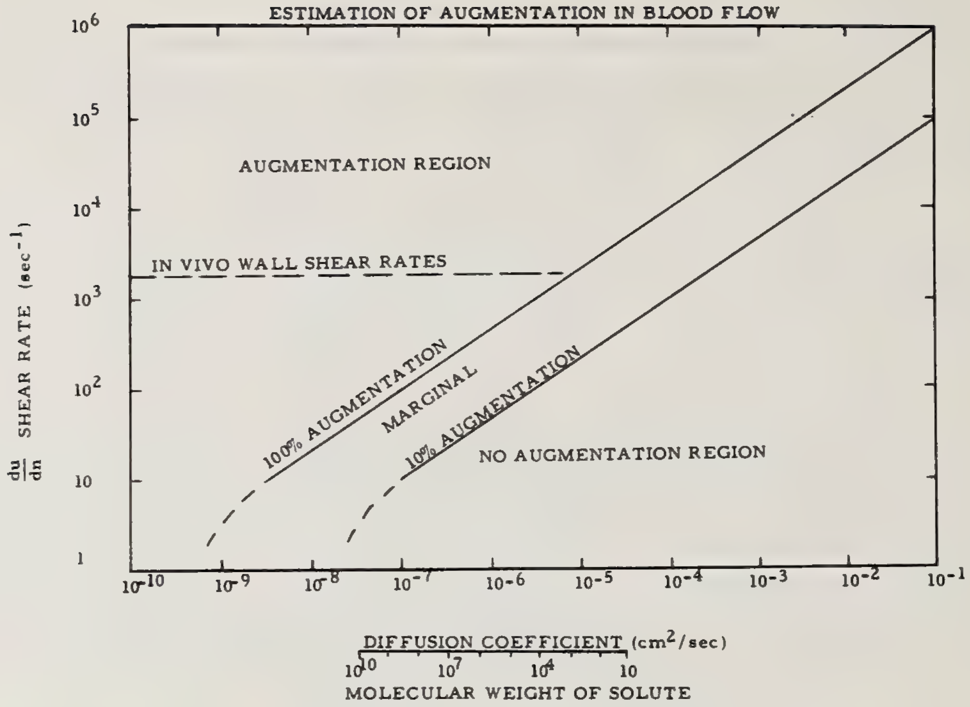

FIGURE 15. FLOW RELATED AUGMENTATION OF DIFFUSION IN BLOOD. SOLUTE WITH DIFFUSION COEFFICIENT ON ABSCISSA SHOULD BE AUGMENTED AS SHOWN. EXAMPLE: A SOLUTE WHOSE MOLECULES D IN BLOOD IS 10^{-6}cm^2/sec DIFFUSES AT A RATE 2.10^{-6} WHEN THE LOCAL $\frac{du}{dy}$ IS 3.10^2 sec^{-1}.

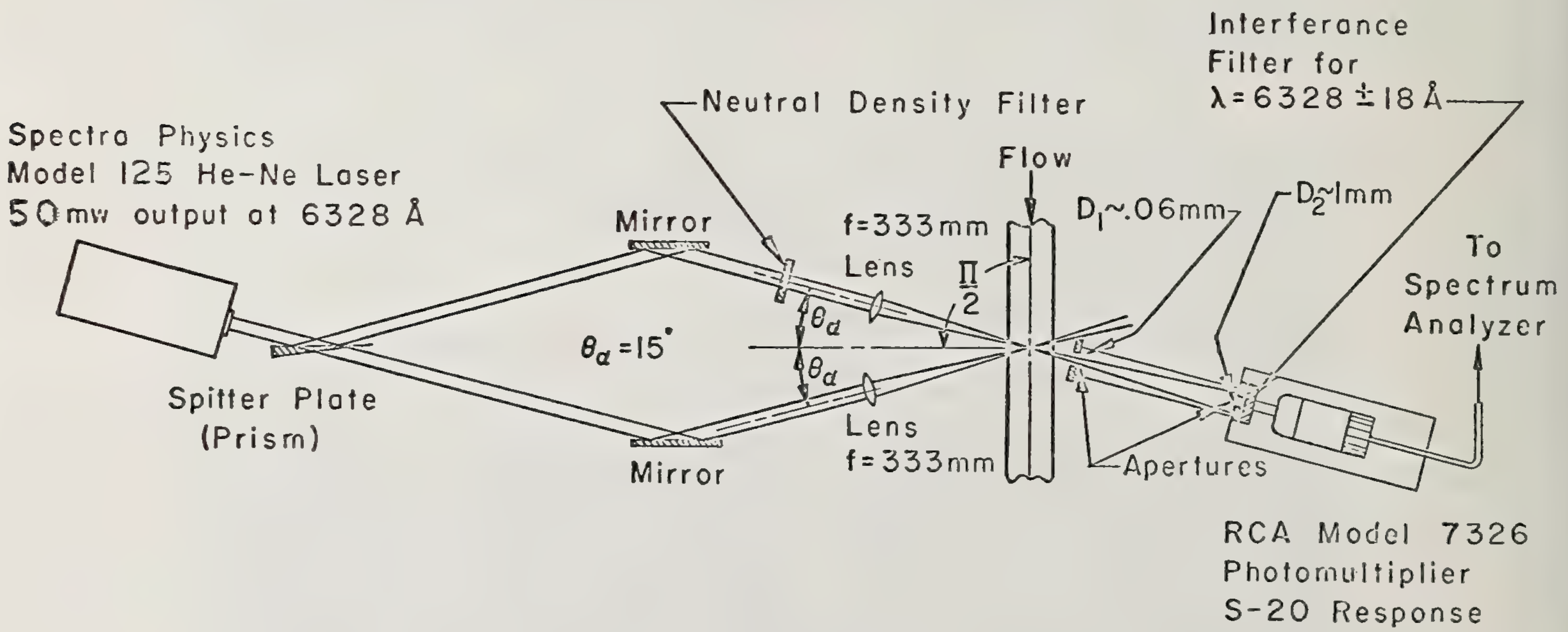

FIGURE 16a. SCHEMATIC OF THE OPTICAL SYSTEM.

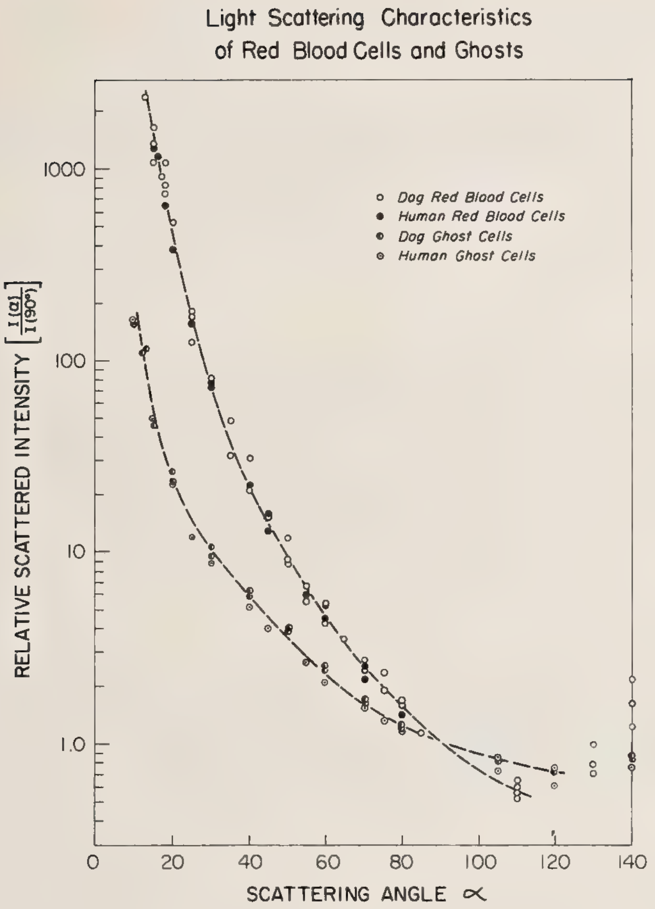
Light Scattering Characteristics of Red Blood Cells and Ghosts

FIGURE 16b.

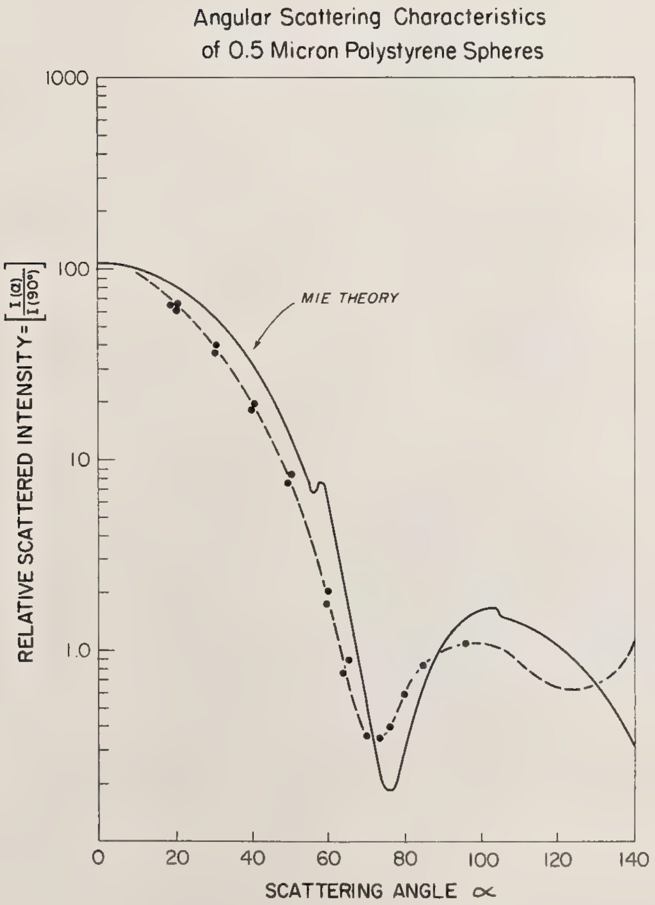
Angular Scattering Characteristics of 0.5 Micron Polystyrene Spheres

FIGURE 16c.

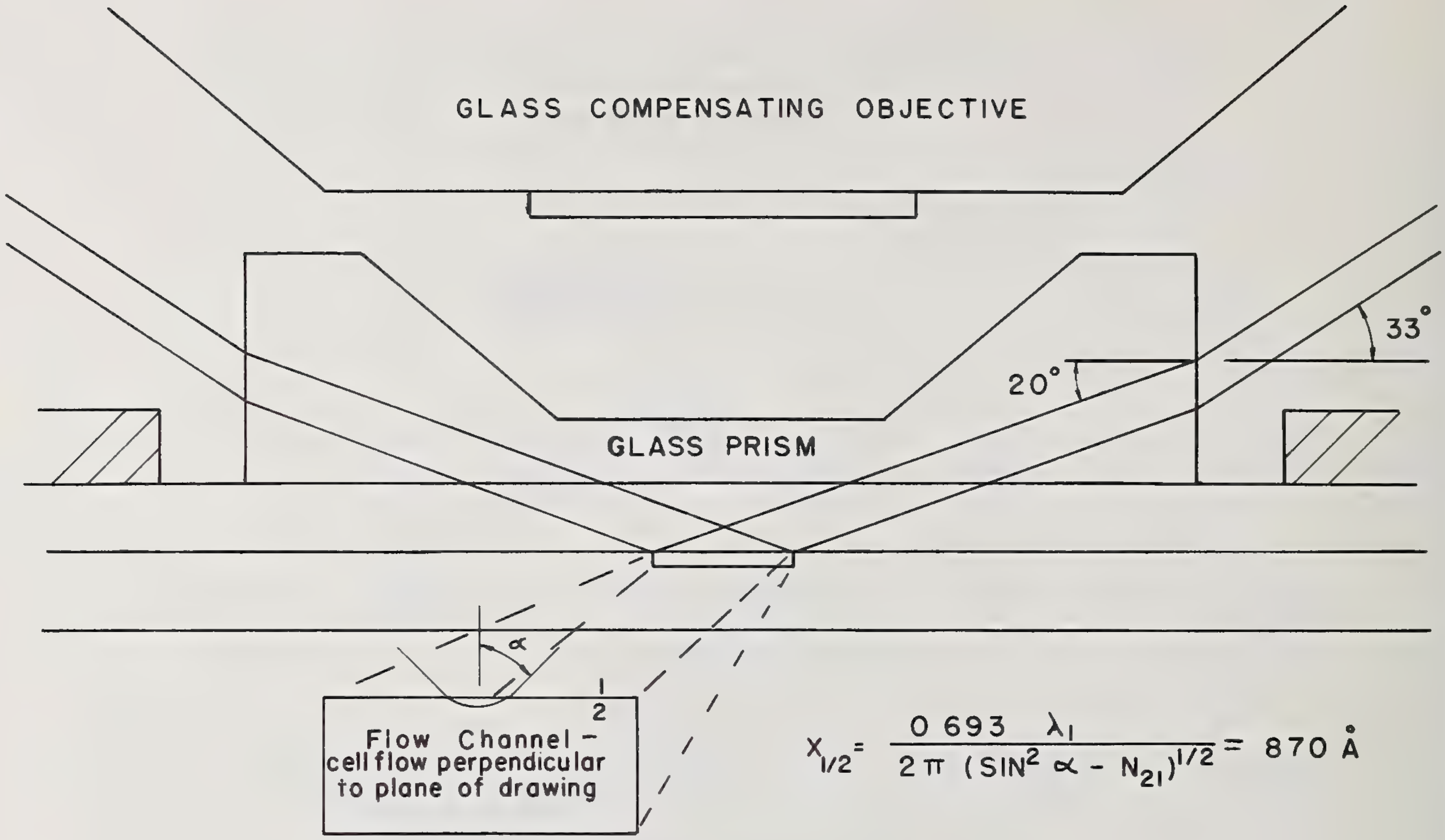
GLASS COMPENSATING OBJECTIVE
33°
20°
GLASS PRISM
α
1
2
Flow Channel - cell flow perpendicular to plane of drawing
$X_{1/2} = \frac{0\ 693\ \lambda_1}{2\pi\ (\sin^2 \alpha - N_{21})^{1/2}} = 870\ \text{Å}$

FIGURE 17. ATTENUATED TOTAL REFLECTION MICROSCOPY.

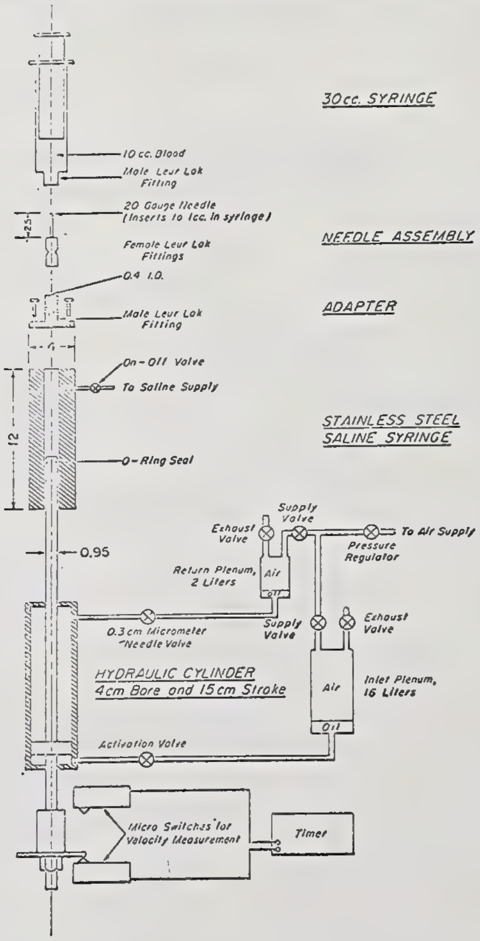

FIGURE 18. APPARATUS FOR HEMOLYSIS STUDIES IN TUBE FLOW.

c. At a hematocrit between 75 and 80 there is a dramatic increase in hemolysis at wall shear rates $<10^4 \sec^{-1}$ with up to 50% of the cells lysed at shear stresses <40,000 dynes/cm^2.
   We infer that:
   - i) This very high degree of lysis is not due to wall encounter but to phenomena taking place in the bulk.
   - ii) Since greater bulk shear stresses can be tolerated at lower hematocrits we attribute this lysis to cell-cell plus shear stress interaction.
   - iii) The fusing of cells within the tube and subsequent lysis in the turbulent jet at the tube exit is being explored as a possible explanation.

In addition post alimentary lipemia causes no dramatic increase (over fasting blood) in RBC lysis at hematocrit <40.

Cholesterol Exchange

Results from experiments where washed cells in saline flow through a long tube coated with radioactive cholesterol are shown in Figure 20. From this data we infer that:

a. Some cells which strike the wall remain there at shear rates $<10^3 \sec^{-1}$.
b. At wall shear rates $>10^3 \sec^{-1}$ struck cells appear to be removed from the wall.
c. At shear rates $>10^3$ cells which strike the wall do not appear to stick.
d. The dependence of uptake of cholesterol on hematocrit and flow velocity is still poorly understood. There is, however, a dramatic increase in uptake when cells are introduced into the flowing saline suspending phase.
e. It is clear that the cholesterol is bound to the cells; virtually none is found in the suspending media.

WALL DEPOSITS

Wall deposits have been examined ellipsometrically, by means of stains, by surface contact angle measurements and by a vibrating crystal resonance technique. In this work there is evidence that wall deposits can be altered by high shear stress near walls and will depend on the surface properties of the wall. In the limit of gentle agitation the findings listed below apply for deposits on chromium plated glass:

a. Washed cells stick to clean surfaces and leave a 30Å deposit when removed.
b. Plasma on a clean surface leaves a 30 Å deposit.
c. RBC's settling on a plasma protein deposit do not stick and do not leave an additional deposit.
d. RBC's to which sublethal amounts of lysolecithin have been added do stick to the plasma protein deposit and leave an additional 20Å deposit when removed.

ELECTRON MICROGRAPHS OF CELL FRAGMENTS

Electron micrographs have been taken of representative cells and fragments following a variety of tests. These tests include: cells treated with lysolecithin and a study of: fragments resulting from high shear stress lysis. Some of the results include:

a. In no case was the appearance of the unit membrane in a fragment different from the intact cell.
b. Cells treated with lysolecithin undergo fragmentation.
c. Cell fragments become smaller as shear stress causing the lysis becomes greater.

As can be seen in the above, there is at every level intimate interplay between fluid mechanical and biochemical factors that dictate the way the components of flowing blood interact with foreign surfaces.

Although it is too early to predict blood behavior in the variety of flow configurations, blood states, and component materials anticipated in artificial organ design, some semiquantitative inferences can be drawn for simple tube flow. Figure 21 is designed to show certain domains of fully developed flow of blood in a tube and some things germain to hemolysis that can be said about these domains.

Here we see a map of mean velocity vs. diameter. The map is divided first into a turbulent and laminar regime by a line Re $\frac{Ud}{\nu}$ = 2000. In the laminar regime there is a region where wall shear rates exceed 100,000 $\sec^{-1}$ where we have observed in bulk lysis at high hematocrits, due to some phenomena associated with cell-cell encounter. For shear rates below about 1000 $\sec^{-1}$ cells which hit the wall apparently stick and agglutination (and possibly cell alteration) ensues. This value is undoubtedly dependent upon wall material. In between these two regimes is a region marked "safe" laminar region. How safe this region is depends upon cell and wall roughness, upon hematocrit and probably on how deformable cells are. If the cells are healthy, the walls smooth (roughness <1μ) and the hematocrit normal it should be possible to flow cells through within this region with no lysis.

The turbulent region is also divided into several subregions: Above the velocity = 2000 cm/sec in bulk shear stresses should lyse the cells. Above the velocity = 600 cm/sec line, turbulence should invade the micro turbulent boundary layer and cause an increased interaction with the wall.

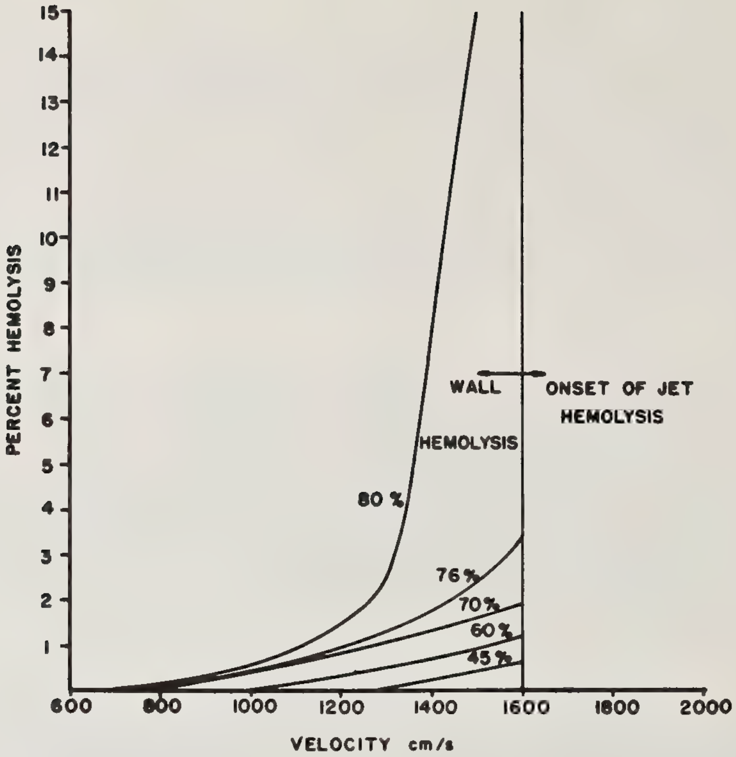

FIGURE 19. DOG'S BLOOD AT DIFFERENT HEMATOCRIT INJECTED INTO SALINE THROUGH A 23 G NEEDLE.

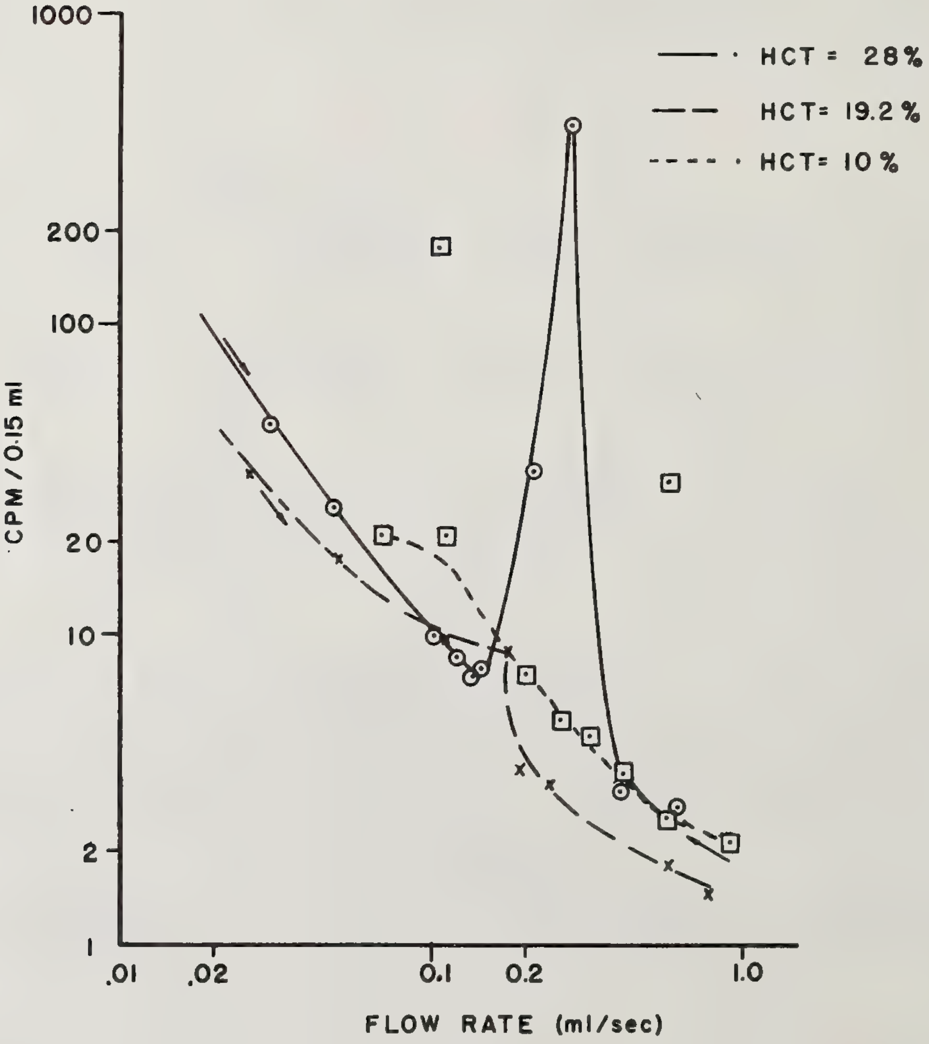

FIGURE 20. RADIOACTIVE CHOLESTEROL EXCHANGE EXPERIMENT.

Between the velocity = 600 cm/sec and the transition line there should be a regime in which the turbulent flow is as safe as in the "safe" laminar regime with the same reservations.

These remarks hold for red cell lysis. It is not clear at present if these regimes are also safe for white cells and/or platelets.

The present series of experiments should make it possible to establish firmly the existence of "safe" regimes and to map similar safe zones for other flow configurations. This information will make it possible for artificial organ designers to recognize the restraint required, and more important to recognize the sometimes unexpected latitude available.

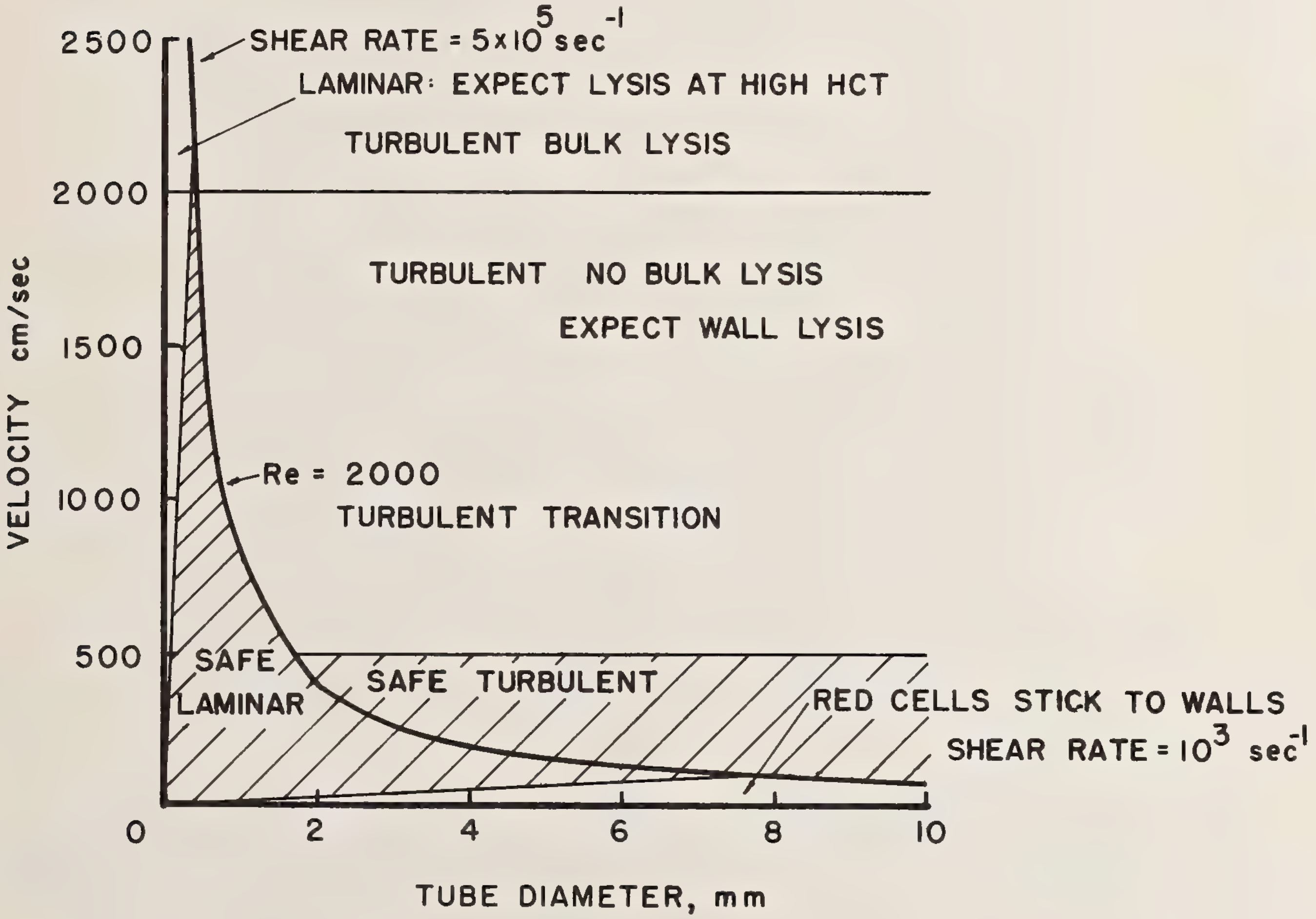

FIGURE 21. DOMAINS OF FULLY DEVELOPED FLOW OF BLOOD IN A TUBE.

CHAPTER 26

STUDIES OF BLOOD FLOW IN AND ADJACENT TO BLOOD PUMPS

S. M. Scala, N. R. Kuchar, M. P. Sherman
General Electric Company, Philadelphia, Pa.

and

L. U. Lilleleht
University of Virginia, Charlottesville, Va.

The objective of this study is the investigation of the hydrodynamic aspects of hemolysis and clotting in and adjacent to artificial blood pumps and other blood processing devices. The study is focused on the determination of the permissible ranges of the various flow parameters such that they may be held within desired physiological limits while minimizing hemolysis and thrombus formation. The equations of motion in which blood is treated as a non-Newtonian fluid consisting of a mixture of red cells, rouleaux and plasma are presented. The boundary conditions utilized allow for finite length, variable cross sectional area and blood vessel distensibility. Numerical results are presented for the streamline patterns and the pressure and velocity distributions for a number of geometries of physiological interest. A phenomenological model for blood based on experimental data expressing the rheological properties in terms of hematocrit and fibrinogen concentration has also been derived and solutions of the non-Newtonian equations of motion, giving details of the velocity profiles and pressure and shear stress distributions have been found for steady and unsteady flows in circular tubes. A new model is presented for the self-collisions of erythrocytes and red cell collisions with surfaces. The model includes the electrical double layer, London-van der Waals forces and the low Reynolds number hydrodynamic forces. The model has a small potential well at about 100 Å from the cell wall corresponding to rouleaux formation, and a potential barrier at about 15 Å which prevents agglutination except for those energetic collisions which overcome the repulsive forces and lead to hemolysis. *In vitro* experiments with "pseudo-blood" were conducted in distensible tubing for a range of geometries including uniform tubing, constrictions (stenoses) and bifurcations. Comparisons between the theory and the experiments are made.

INTRODUCTION

Among the many problems associated with the design of effective artificial hearts are those which are related, totally or partially, to the blood flow through the device. These include mechanical hemolysis, which can be caused by excessive red cell collisions induced by turbulence or high shear stresses in the flowing blood, and thrombus formation, which may be promoted in regions of long residence time due either to slow blood motion or trapped vortices.

The blood flow research being carried out at the General Electric Company is aimed at determining ways to prevent these hemodynamic problems in artificial hearts. The study is being carried out using an integrated program of theoretical and *in vitro* experimental research. This paper describes the progress achieved during the present contractual period.

In order to understand these hemodynamic phenomena so that one may design devices which effectively prevent them, it is necessary first to relate the macroscopic flow patterns which can occur in blood pumping devices to the geometry of the passages, the flow rate, and pulsation frequency. Then, the dynamics of the physical processes which occur on a cellular level, such as cell collisions must be investigated and related to the macroscopic flow dynamics.

In the theoretical studies carried out during the previous contract period, the investigation of the macroscopic time-dependent blood motion and its laminar stability was based on the use of the time-dependent Navier-Stokes equations derived for the flow of homogeneous Newtonian fluids. This kind of modeling was utilized to develop new understanding and information about unsteady blood flow through rigid ducts in the complex geometries of interest for blood pumping devices.

However, it is recognized that the flow of blood through the vessels or artificial devices is strongly dependent on the rheological properties of the blood, which is to say the flow is ultimately dependent on the composition and structure, at the molecular and cellular levels, of the blood. Whole blood is a multicomponent fluid, being a heavy suspension of cellular particles in a watery solution, the plasma. As might be expected, since whole blood is very complex rheologically, there are many unusual and anomalous flow phenomena associated with it, some of which are important in the hemolysis process. Hence, in order to utilize a more realistic model for the blood rheology in the studies, the analysis of the macroscopic blood flow patterns is now being extended to include multicomponent effects in which plasma, red cells, and rouleaux are the three major constituents of the blood.

Moreover, the effects of wall elasticity have also been introduced into the model. Also, a phenomenological non-Newtonian model for blood is being developed and utilized to study the rheological effects on flow patterns, pressure drops and the laminar-turbulent transition process.

During the previous contract period, work on the theoretical model of the collisions between red blood cells, and red blood cells and walls, (with emphasis on violent collisions leading to mechanical hemolysis) was begun. A potential energy curve for the collisions between cells, and cells and walls, was obtained by considering the molecular forces in the cells, walls, and plasma dielectric as well as the hydrodynamic forces on the cells. Only one orientation was considered, namely, collisions parallel to the axis of symmetry. In the present contract period, this work is being continued and extended to include the hydrodynamic forces acting over the entire range of intercellular separation and to include collisions at arbitrary orientations and possible effects of cell deformation. The results of the collision analysis for arbitrary orientation can be integrated, knowing the relative frequency of each type of collision, to give hemolysis rate as a function of shear rate. Since theoretical studies necessarily forecast useful and meaningful experimental work, and should be guided by experimental data, it is important that certain experiments be carried out in conjunction with the theory. During the previous study period, meaningful in vitro experiments complementing the analytical studies focussed on the study of the macroscopic flow patterns in constrictions and bifurcations and the transition from laminar to turbulent flow using a Bentonite solution as the fluid.

These experimental investigations are now being extended to include the study of blood flow patterns and distributions of cellular elements in and near constrictions, orifices, valves and bifurcations, using a specially developed particulate suspension, "pseudo-blood". The boundary between laminar and turbulent regimes is also being investigated with this special suspension.

The end product of these theoretical and experimental studies is the further development of comprehensive analytical and semi-empirical methods for predicting the presence of high shear stresses, turbulence and trapped vortices which can lead to excessive red cell collisions, red cell deformation, hemolysis and clotting. With these types of predictors, it should be possible to correlate the macroscopic flow dynamics with the associated microscopic consequences and hence to define the ranges of design variables such as flow rate, pulsation frequency, and geometrical parameters which can be used in the design of artificial hearts without introducing excessive hemolysis and thrombus formation.

MACROSCOPIC BLOOD FLOW PATTERNS

Our first objective is to determine the functional relationship between the blood flow pattern, the blood vessel geometry, the blood vessel distensibility and the entrance and exit conditions of the flow regions of interest, for time-dependent flow over a complete heart cycle.

Last year a theoretical model was developed for the flow of blood in large blood vessels which was based on the following physical assumptions.

1. In a large blood vessel, blood behaves as a Newtonian fluid whose motion is governed by the Navier-Stokes equations.
2. The blood vessel wall is rigid.
3. Blood is a fluid having a large but finite speed of sound and hence is actually a compressible fluid.
4. Beyond the flow region of specific interest, the blood vessel has a constant cross section and is of infinite extent.

Then, utilizing the complete time-dependent Navier-Stokes equations, numerical calculations of the resulting flow patterns were carried out for flow in blood vessels of circular cross section, having minor and major constrictions (stenoses). In our calculations, the streamline patterns and the corresponding velocity distributions within the geometrical regions treated were found to be reasonable from a physiological point of view. However, it was found that the pressure calculated at the entrance of a large blood vessel, necessary to accelerate the blood from rest to the maximum value normally measured in the aorta, was much larger than the physiologically observed pressure in the left ventricle.

Consequently, in order to eliminate this abnormally high calculated entrance pressure, and in fact bring it into the range of the ventricular pressure we know should exist, we were led to the consideration of two alternatives.

One alternative would be to specify physiologically correct data for both velocity and pressure at both the inlet and the outlet stations of the specific flow region of interest, and of course, we would then have to modify our mathematical model so as to accept these boundary conditions as prescribed quantities, rather than calculated quantities. This would dictate that we use the conventional approach where one specifies the physiologically correct pressure levels by first assuming that blood is an incompressible fluid, (that is, the speed of sound in blood would have to be assumed infinite). This approach also avoids the question of the coupling of the blood flow in the specific region of interest to the remainder of the circulatory system. However, this would also tend to preclude the determination of the effect on the pressure level of other physiological phenomena, such as a blood vessel distensibility and downstream area changes, which would not be desirable.

Another approach is to retain the capability of calculating the pressure distribution, but to investigate the separate and combined effects of each of the previously mentioned physical assumptions. That is, since in our earliest calculations we did not observe the correct pressure levels in the blood vessel, and since the blood does not necessarily behave as a Newtonian fluid, and since the blood vessels are distensible rather than being rigid, and since the cross-sectional area of the flow passages is not constant with distance, we concluded that a better model was required.

During the present contract period, we have replaced the second and fourth aforementioned assumptions by the following:

2. The blood vessel wall is viscoelastic.
4. The flow beyond the region under study must be characterized by realistic boundary conditions at the exit of the flow passage being studied.

In a given computation, we generally confine our attention to a specific region of interest; that is, the domain of the computation is only a small portion of the entire circulatory system. Consequently, boundary conditions must be provided for the region under investigation which represent the presence of the remainder of the system in which the flow is not being computed explicitly. To see how this thought fits into the mathematical model, let us treat the following simplified case.

Consider an infinite rigid tube of constant cross-sectional area. Suppose at some downstream point we can ignore radial gradients, in which case our equations reduce to a one-dimensional system in which the two independent variables are t (time) and y (axial distance). In this case, one of the characteristics of the system of equations is defined by,

$$\frac{dt}{dy} = \frac{-1}{C - V_y}$$

where C is the speed of sound and V_y is the axial velocity. If we let Z be the corresponding characteristic variable, then the corresponding characteristic equation has the form,

$$\frac{\partial Z}{\partial t} = (C-V_y)\frac{\partial Z}{\partial y} \qquad (1)$$

Suppose for the moment we consider (1) as a single equation in Z. Since in our problem V_y is small compared to C, the mathematical characteristics of this equation are almost straight lines, with only a small amount of curvature.

On each of the characteristic lines, Z is constant or Z maintains the value with which it was tagged at t = 0. If our region of computation is $0 \leq y \leq y_1$ then in the region R (swept out by mathematical characteristics) the value of Z is determined solely by initial conditions, without additional boundary conditions. Suppose that a solution is desired at some point outside this region, say $t = t^*$ and $y = 0$. Then, this value of Z is determined by the value of Z at $t = 0$, $y \approx Ct^*$. If we are to stay in region $0 \leq y \leq y_1$, we must then impose a boundary condition at $y = y_1$, $t = t^{**} = t^* - y_1/C$.

Consequently, the boundary condition at $y = y_1$ should be determined by what the formulator of the problem assumes about the downstream behavior. This is a very crucial part of the formulation of the problem and needs to be strongly emphasized. As indicated by the physics of the problem, there is a strong upstream influence produced by the downstream system of blood vessels, and therefore one is not surprised to see this same fact reflected in the mathematical model. It should also be noted that there is a great deal of freedom in this choice of the boundary conditions, and it is important that any such choice be related to a physical assumption about the downstream behavior. In effect, one can consider the influence of the downstream system as manifesting itself in the form of an "admittance" at the exit station of the region of computation. If we assume a stationary fluid at t = 0, then Z = 0 at t = 0. Consequently, Z = 0 in the region R. Suppose now that beyond $y = y_1$ we want to assume an infinite rigid tube of constant diameter, in which the flow will have negligible radial gradients. Then, this is quite simply imposed as a boundary condition at $y = y_1$, namely

$$\frac{\partial Z}{\partial t} = 0 \text{ at } y = y_1 \qquad (2)$$

In terms of the variables ρ and V_y this becomes,

$$\frac{\partial \rho}{\partial t} = \frac{\rho}{C}\frac{\partial V_y}{\partial t} \qquad (3)$$

Making use of the equation of state,

$$(P - P_o) = \frac{C^2}{g}(\rho - \rho_o)$$

P = Pressure (atmospheres)
C = Speed of sound (ft./sec.) = 4820
g = gravitational acceleration constant
ρ = density (lb./ft.^{3}), ρ_o = 62.5

equation (3) can be put in the following form

$$\Delta P = P - P_o = 4.43\,\Delta V_y \qquad (4)$$

Equation (4) is the precise boundary condition that we first imposed at $y = y_1$, and we believe that this represents an infinite rigid tube of constant diameter beyond $y = y_1$, (in accordance with the original assumptions 2 and 4).

As an example, consider the problem in which the tube is filled with a stationary fluid at t = 0. Let the fluid be accelerated to some final steady-state velocity by either injecting fluid at y = 0, or by applying a pressure at y = 0. In the body a maximum value for this final velocity would be approximately 1.5 ft./sec. The driving pressure needed to achieve this is then given by equation (4).

$$\Delta P = 6.64 \text{ atmospheres} \tag{5}$$

If a negligible pressure drop exists over the region $0 \le y \le y_1$, then of course this final pressure will be achieved throughout this region. In our numerical solutions of the governing partial differential equations this is indeed the result we obtained. One notes that this value is about 30 times greater than the pressure rise actually observed in body measurements. This result demonstrates conclusively that when the effects of the finite speed of sound of blood are included in the model then the assumption of an infinite rigid tube beyond the region of computation is completely unrealistic.

We first note that in the body the blood vessels bifurcate in such a way that the total cross-sectional area downstream of the branching point is larger than the upstream cross-sectional area. To obtain some insight into the effect of increasing area, we consider that position $y = y_1$ is upstream of the bifurcation and that $y = y_2$ is downstream of the bifurcation. For simplicity, we first assume that beyond $y = y_2$ we again have an infinite rigid tube of constant cross-sectional area. Consequently, our previous discussion can be applied, thereby concluding that at $y = y_2$, the boundary condition is again given by equation (3). The question is how to specify a boundary condition at $y = y_1$ which would simulate the proper condition at $y = y_2$.

Consider, as before, the problem in which the final steady velocity is specified at $y = 0$, say $V_y = V_0 = V_1$. Then the final steady velocity V_2, which will be obtained at $y = y_2$, is easily obtained from the conservation of mass equation,

$$[\rho V_y \pi R^2]_{y=0} = [\rho V_y \pi R^2]_{y=y_1} = [\rho V_y \pi R^2]_{y=y_2} \tag{6}$$

In this equation ρ can be considered constant, thereby obtaining,

$$V_2 = V_1 \left(\frac{R_1}{R_2}\right)^2 \tag{7}$$

The corresponding pressure at $y = y_2$ is then calculated from equation (4). If we again assume that the pressure drop is negligible between y_0 and y_2, we have the following conclusion:

> Let ΔP_1 be the driving pressure required when fluid in a rigid infinite tube of constant diameter is accelerated from rest to a final velocity, $V_y = V_1$. Let ΔP_2 be the driving pressure required when fluid in an infinite rigid tube containing a bifurcation (area increase), is accelerated from rest to the same final velocity (that is $V_2 = V_1$ at $y = 0$). Then,

$$\frac{\Delta P_2}{\Delta P_1} = \left(\frac{R_1}{R_2}\right)^2 \tag{8}$$

This result is quite easily incorporated into the boundary condition at $y = y_1$ by modifying equations (3) and (4) as follows:

$$\frac{\partial \rho}{\partial t} = \left(\frac{R_1}{R_2}\right)^2 \frac{\rho}{C} \frac{\partial V_y}{\partial_y} \tag{9}$$

$$\Delta P = 4.43 \left(\frac{R_1}{R_2}\right) \Delta V_y \tag{10}$$

An actual calculation was then performed with the full axially-symmetric partial differential equations for flow through a tube containing an area increase (in the region $0 \le y \le y_2$). The final driving pressure obtained was indeed the one given by equation (8). It is clear that if one is designing a system of rigid tubes to transport blood, then a downstream area increase will decrease the required pumping pressure as given in equation (10).

Within the body, the downstream area variation is not the only factor which contributes to the determination of the pumping pressure. Another mechanism which we believe to be essential to the development of a realistic theory of hemodynamic phenomena is the distensibility of the blood vessels. In our formulation, the overall mathematical model utilizes a coordinate system which permits motion of the walls and consequently it is necessary only to specify the manner in which the wall moves.

Our first attempt to provide for the effects of wall motion was to use an equation of the form:

$$\Delta R = c \, \Delta P \tag{11}$$

where c is an appropriate constant.

This simple equation, which states that as the pressure rises, the blood vessel instantaneously dilates, immediately led to computational instabilities. In fact, oscillations built up so quickly (after only two or three computational time steps) that the resulting behavior probably should not be thought of as instability in the usual sense. Several difficulties in the use of equation (11) are immediately discernible. One of these is that the inlet radius is not fixed (presumably at the inlet to the aorta, distension is not nearly as great as further downstream). The other difficulty is that equation (11) seems to put no maximum on ΔR (which is not compatible with the fact that the more the wall expands, the more difficult it should become to expand further). We attempted to alleviate these areas of possible difficulty by modifying equation (11) in the following manner:

$$\frac{dR}{dP} = c\,\frac{f_1(y)}{f_2(P)} \tag{12}$$

where

$$f_1(y) = \frac{y^2}{a + y^2} \tag{13}$$

$$f_2(P) = 1 + b(P - P_o)^2 \tag{14}$$

a, b are constants.

The function $f_1(y)$ serves to anchor the entrance point $y = 0$, while the function $f_2(P)$ represents the physiologically observed result that the force required to further distend a blood vessel becomes larger as it undergoes distension. Since $f_1(0) = 0$, $dR = 0$ at $y = 0$, hence the inlet radius is fixed. For large values of y, $f_1(y) \rightarrow 1$, i.e., the equation is effectively unchanged here. The constant a simply adjusts the length of the transition region; f_2 acts to reduce $\frac{dR}{dP}$ for large P. These changes were then incorporated into the digital computer program. Although the oscillations were damped somewhat, reasonable answers could still not be obtained.

At this point it was decided to uncouple the wall motion from the flow by specifying the wall motion "a priori" in an attempt to isolate the difficulty. We employed the following equation:

$$R(t,y) = R_o(y) + \frac{ay}{b^2 + y^2} \tag{15}$$

where $R_o(y)$ gives the geometry at $t = 0$, and the parameters a and b varied with time. Note that equation (15) keeps R fixed at $y = 0$, but the remainder of the wall undergoes a "wave" motion. Equation (15) and appropriate modifications to the boundary conditions were incorporated into the program. The resulting calculations were found to be well behaved without any sign of instability. It was then concluded that the instabilities were a result of the manner in which equation (12) coupled the flow to the wall motion.

At this point a careful investigation was made with respect to the actual boundary conditions that were being used at the wall. After considerable analysis of the characteristic variables, a very interesting fact emerged, namely that the boundary conditions required by the governing partial differential equations (as opposed to the arbitrarily imposed boundary condition, equation (12) related $\frac{\partial R}{\partial t}$ to dP. Note that this is inconsistent with equation (12) which relates $\frac{\partial R}{\partial t}$ to $\frac{\partial P}{\partial t}$. It was then found that data of the appropriate form does exist. The following correlation is given for the thoracic aorta of a dog (Peterson, Jansen and Powell, Circ. Res., Vol 8, 1960, p. 622)

$$P - P_o = \frac{d_1}{R_o}(R - R_o) + \frac{d_2}{R_o}\frac{\partial R}{\partial t} \tag{16}$$

We assume that equation (16) actually gives the normal component of the wall motion. After allowing for variable cross-section, and after inserting the functions f_1 and f_2, which appear in equation (12) equation (16) takes the following form:

$$\frac{\partial R}{\partial t} = \sqrt{\frac{1 + \frac{\partial R}{\partial y}^{2}}{K_1}}\left\{\frac{c_1 R_o(P - P_o)\, f_1(y)}{f_2(P - P_o)} - (R - R_o)\right\} \tag{17}$$

Using the data of Peterson et al,

$R_o C_o = 4.38 \times 10^4$, ft./lb m
$K_1 = 3.55 \times 10^{-2}$, sec.

where R_o was taken to be .02 ft.

Equation (17) was incorporated into the program. No computational instabilities were observed, however, since we utilized the expression for $f_1(y)$ given in equation (13), no distension of the blood vessel was calculated during the first small fraction of a second. The reason for this was that the aforementioned expression for $f_1(y)$ provided for tethering at the inlet to the blood vessel and not at any point downstream. Consequently, the effect of the passage of a pressure wave through the blood was to initiate both axial and radial motion in the blood in such a way as to promote distension of the blood vessel all along its length. Thus, the region of distension was unconfined (i.e.,unspecified) and hence the amount of distension produced by the passage of the finite pressure wave was in fact negligibly small.

It immediately became clear that in order to calculate the motion of blood into a blood vessel, it is not only necessary to consider the degree of tethering at the inlet of the region under investigation, but also the degree of tethering beyond the inlet.

In the human body, the degree of tethering is not a constant, but rather is related, for example, to the compliance of the local surrounding tissue and to the number of bifurcations in the vicinity of the point in question.

In order to incorporate an outlet tethering constraint into the model, the following functional form was derived for $f_1(y)$

$$f_1(y) = \frac{y^2}{a_1 + y^2} \left[\frac{L - y^2}{(L - a_2)^2 + (L - y)^2} \right] \tag{18}$$

Preliminary computations have now been made with equations (14), (17) and (18).

The effect of wall elasticity on the streamline patterns is illustrated in Figure 1, where comparisons are given for flow through a blood vessel, having either a rigid wall, or an elastic wall. This figure is based on our preliminary computations.

When the blood vessel is rigid, then one obtains the streamline patterns shown in Figure 1.A. When the walls are elastic, then the result is that the streamlines are initially directed toward the wall as filling of the blood vessel begins. This streamline pattern is shown in Figure 1.B. At a later point in time when the pressure in the vessel exceeds the driving pressure, the inlet valve closes and the discharge part of the cycle shown in Figure 1.C proceeds. These initial calculations also indicate that the required pumping pressure required to accelerate the blood from rest is considerably less than that calculated for a completely rigid tube.

BLOOD FLOW STABILITY

Whole blood is a multicomponent fluid, being a suspension of cellular elements in a saline solution, the plasma. Because of this, blood is generally non-Newtonian; that is, as it flows, its apparent viscosity is dependent upon the shear rate or velocity gradient. Furthermore, the rheological properties of blood depend upon such factors as hematocrit and the concentrations of plasma proteins, particularly fibrinogen.

The objective of much of our work is to determine the effects of blood's unique rheological properties on the pressure drops (i.e., pumping requirements), velocity distributions, shear stress distributions, and laminar-turbulent transition characteristics associated with typical flows in blood pumps and mass transfer devices such as artificial kidneys and blood oxygenators. This information will aid in the design of blood-handling devices having acceptable hemolytic and thrombogenic characteristics.

Another part of our work had been concerned with evaluating the effects of non-Newtonian blood rheology using a phenomenological model based on the examination of experimental data published in the literature.

Nearly 100 papers on blood rheology have been examined. Broadly speaking, a salient characteristic of this literature is the inconsistency of its data. This is due primarily to the fact that until very recently some of the important factors in blood rheology were not recognized and hence were not controlled or investigated in the experiments. Also, biomedical investigators often failed to make full use of the science of rheology when designing the experimental procedures.

Nevertheless, several points emerged from these papers. Briefly, they are:

1. The apparent viscosity of blood decreased with increasing shear rate, up to shear rates of about 100 $\sec^{-1}$. and is relatively constant thereafter.
2. The apparent viscosity of blood increases with increasing hematocrit.
3. Whole blood has a small yield stress, which vanishes if the fibrinogen is removed.

In recent years a reasonably consistent qualitative theory for the rheological behavior of blood has emerged which explains rather well the data taken under controlled conditions. In brief, this theory ascribes the rheological behavior of blood to the reversible aggregation of red cells into rouleaux at zero and low shear rates, while increasing the shear rate results in the gradual breakup of these aggregations into smaller and smaller units, thus decreasing the resistance to flow. The forces causing aggregation are intermolecular in nature and depend partly on the composition of the plasma.

Based on the experimental data, a phenomenological model for blood rheology has been formulated. It is assumed that a suitable approximation for the stress tensor $\bar{\bar{\tau}}$ is

$$\bar{\bar{\tau}} = -p\bar{\bar{I}} + n\,(\bar{\bar{\Delta}})\;\bar{\bar{\Delta}}$$

where p is the pressure, $\bar{\bar{I}}$ the unit tensor, $\bar{\bar{\Delta}}$ the deformation tensor, and n a scalar function of $\bar{\bar{\Delta}}$. The particular form of n chosen is

$$\left[n = \left\{ m \left| \sqrt{\frac{1}{2}(\bar{\bar{\Delta}} : \bar{\bar{\Delta}})} \right|^{n-1} + \frac{1}{2}\,\frac{\tau_o}{\left| \sqrt{\frac{1}{2}(\bar{\bar{\Delta}} : \bar{\bar{\Delta}})} \right|} \right\} \quad \text{for } (\bar{\bar{\tau}} : \bar{\bar{\tau}}) > 2\tau_o^2 \right]$$

and,

$$\bar{\bar{\Delta}} = 0 \text{ for } (\bar{\bar{\tau}}:\bar{\bar{\tau}}) < 2\tau_o^2 \qquad (19)$$

This describes a fluid having a "power law" viscosity coefficient and a non-zero initial yield stress.

The parameters m, n, and τ_o are taken to be empirical functions of hematocrit H and fibrinogen concentration C_f. These functions have been evaluated using data which is felt to be valid (that is, data taken from experiments which used viscometers which permit a single shear rate to exist throughout the fluid at each operating point, eliminated free-surface effects in the blood, and recognized the importance of factors such as hematocrit and plasma protein concentrations; these data are largely due to Merrill's and Burton's groups). Preliminary relationships are

$$\begin{aligned} m &= (.0105)e^{.054H} \\ n &= 1 - (.0045)H \\ \tau_o &= (3 \times 10^{-5})\, C_f^2\, (H-5) \end{aligned} \qquad (20)$$

In order to gain an understanding of the effects of the blood's non-Newtonian rheological properties on the flow in blood pumps and other blood handling devices, a typical kind of flow is being investigated. This is the flow of an incompressible fluid which moves in a straight, rigid, circular tube. The flow is assumed to be pulsatile, axisymmetric and fully developed, so that the blood velocity is directed axially and is a function of the radial coordinate and time only. In this case, the governing equations of motion can be derived in the following form which includes the conservation of mass and momentum.

Continuity Equation (Mass Conservation)

$$\frac{\partial u}{\partial x} + \frac{\partial v}{\partial r} + \frac{v}{r} = 0$$

Momentum Conservation

$$\rho\frac{\partial u}{\partial t} = -\frac{\partial P}{\partial x} + \frac{\partial \tau}{\partial r} + \frac{\tau}{r}$$

$$0 = \frac{\partial P}{\partial r}$$

Phenomenological Equation

$$\tau = \left\{ m\left|\frac{\partial u}{\partial r}\right|^{n-1} + \frac{\tau_o}{\left|\frac{\partial u}{\partial r}\right|} \right\} \frac{\partial u}{\partial r}$$

τ = shear stress $\quad \frac{\partial u}{\partial r}$ = velocity gradient

τ_o = yield stress $\quad$ m = consistency index

n = pseudoplastic index

Once one has selected H and C_f, the values of m, n and τ_o are obtained from equations (20) and are utilized in the phenomenological equation for τ, the shear stress above. The pressure gradient is specified to be a pulsatile function of time, with a steady part added to give a net forward blood flow over a pulse cycle:

$$\frac{\partial p}{\partial x} = f_o + f_1 \cos(\omega t). \qquad (21)$$

This type of flow is particularly useful in determining the effects of the non-Newtonian rheology of blood, because several Newtonian flows which are presently used in describing blood flow are special cases of this formulation. For instance, if $f_1 = 0$, $\tau_o = 0$, and $n = .1$, the above equations describe a Poiseuille flow, while for $f_o = 0$, $\tau_o = 0$, and $n = 1$, they describe the Newtonian oscillatory flow used by Womersley and many other investigators for blood flow. Thus, the results for non-Newtonian cases can easily be compared with known (Newtonian) solutions and the rheological effects determined.

Several analytical solutions to the above equations have been obtained for limiting cases of interest. These are for the cases:

1. $n = 1$, $f_1 = 0$, $\tau_o = 0$
2. $n \neq 1$, $f_1 = 0$, $\tau_o = 0$
3. $n = 1$, $f_1 = 0$, $\tau_o \neq 0$
4. $n \neq 1$, $f_1 = 0$, $\tau_o \neq 0$
5. $n = 1$, $f_1 \neq 0$ $\tau_o = 0$

The solutions obtained will be useful for comparison with the most general solution, that for n, f, and τ_o all different from zero.

At present, the solution for general values of the parameters is being sought using a finite-difference numerical technique. The problem is treated as an initial-value problem, with the flow taken to be zero until time t = 0, when the pressure gradient is applied. Then the time history of the velocity field is followed. The finite-difference equations will be solved using a digital computer.

The solution will be obtained for ranges of hematocrits and fibrinogen concentrations of physiological interest. Once the velocity profiles are known, their laminar-turbulent stability boundary will be investigated using the unsteady flow stability theory developed during the previous contractual period.

RED CELL COLLISION DYNAMICS

The theoretical prediction of hemolysis rates caused by the mechanical trauma of violent red cell collisions, found in flows with high shear rates in and adjacent to blood pumps, is also being investigated by modeling the erythrocyte collision process.

Most of the effort during the first year was directed toward the understanding of the electrical forces between erythrocytes. Some results are shown in Figure 2. Because of the deformability of the erythrocytes and the high contact pressures generated in close approach, the regions of the two cells in close proximity can be assumed to be parallel flat plates. The electrical force per unit area, a function of two as yet unknown parameters, the red cell surface potential and effective dielectric constant, is represented for varying intercellular gaps. The theory includes the "electrical double layer" forces and the London-Van der Waals forces. The electrical double layer forces depend on the surface potential. The important result is that electrical forces are negligible for distances greater than about 2 x 10^{-2} microns, (200A). Hence, the motion of red cells is dominated by hydrodynamic forces except during the brief time of very close approach in cell-cell and cell-wall collisions. The weak attractive force at about a hundred Angstroms leads to rouleaux formation. The strong repulsive barrier of about 10 to 20 Angstroms prevents the agglutination of cells. We hypothesize that mechanical hemolysis occurs when the repulsive barrier is overcome in violent collisions. Most of our present effort is directed to determining the hydrodynamic forces on the erythrocytes.

The motion of red cells through the surrounding plasma and the collision of red cells with one another or with walls occurs in the "low Reynolds number," "creeping flow" or "Stokes flow" hydrodynamic regime. The Reynolds number, Re, is defined

$$Re = \frac{\rho V L}{\mu} \tag{22}$$

where ρ is the characteristic (plasma) density, μ the characteristic (plasma) viscosity, L the characteristic length (erythrocyte diameter) and V the characteristic speed (relative collision speed). The Reynolds number is very small for the red cell collision problem. The low Reynolds number approximation is obtained if the equations of motion are nondimensionalized and the terms proportional to the Reynolds number are neglected. These are the nonlinear inertial terms and the nonsteady term. The neglect of the nonlinear term permits the use of the powerful techniques of linear analysis (superposition, transform techniques, separation of variables, etc.) on the remaining linear equations. The neglect of the nonsteady term is less important. The remaining equation is "quasi-steady", i.e., at each instant a steady state equation is valid. The nonsteady term could be retained, the added term being handled with a Laplace transform. However, this term is usually negligible when the nonlinear inertial term is negligible. The resulting equations are:

$$\begin{aligned} \mu \nabla^2 \vec{V} &= \nabla p \\ \nabla \cdot \vec{V} &= 0 \end{aligned} \tag{23}$$

where $\vec{V}$ is the velocity vector, p is the pressure and ∇ is the usual vector differential operator.

Even with the simplifications of the low Reynolds number approximation, it is a formidable task to theoretically model the flow in a dense suspension such as the red cells form in blood. Certain limiting cases have been considered in the literature. When the gap between the cells is very small, less than about 10^{-1} or 10^{-2} micron, we can use the lubrication or thin-film approximation. Lubrication theory applies when two parallel or nearly parallel surfaces have a gap between them very much smaller than the length of the surfaces. The flow becomes insensitive to the flow conditions beyond the edge and we get some generalization to Poiseuille flow.

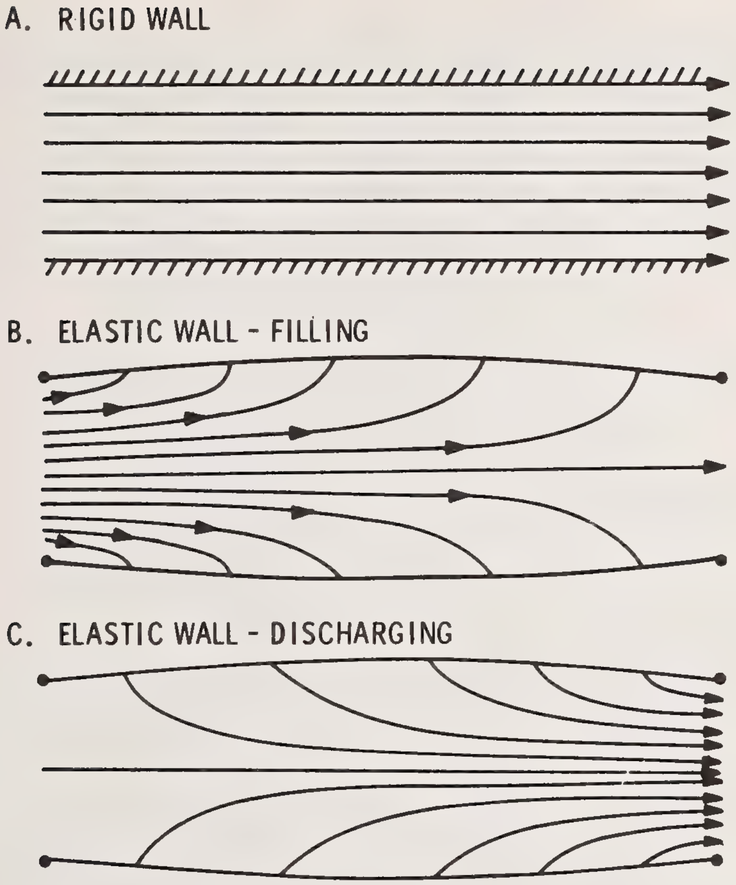

FIGURE 1. BLOOD FLOW PATTERNS.

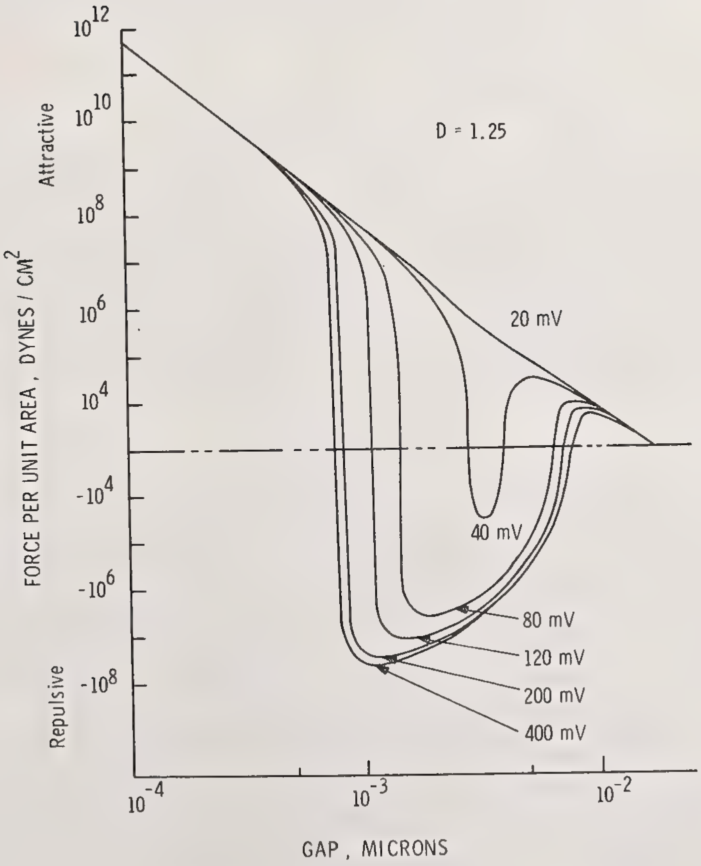

FIGURE 2. NET ELECTRICAL FORCE BETWEEN TWO PARALLEL FLAT PLATES IN BLOOD PLASMA.

In the limit where the erythrocyte is far from any other body, the force on it is readily computed using existing theory. In the practical case of interest where the intercellular distance is compared to a diameter, no existing solutions exist. We have been studying this case. In particular we are considering coaxial collisions first, because of their relative simplicity. Coaxial collisions will not be frequent in blood because of the very high resistance to close approach in this position. However, because the hydrodynamics are linear, we can break up the forces in a complex collision (with rotary, axial, and other linear relative motions) into those created by each complication and add the parts to get the resultant.

For coaxial collisions of two flat disks, we can use the axisymmetric stream function form of equations (23)

$$E^2(E^2\psi) = 0 \tag{24}$$

where $E^2$is a linear operator similar but not identical to the Laplacian:

$$E^2 = \frac{\partial^2}{\partial r^2} - \frac{1}{r}\frac{\partial}{\partial r} + \frac{\partial^2}{\partial z^2} \tag{25}$$

and the stream function ψ is defined by

$$\begin{aligned} V_r &= \frac{1}{r}\frac{\partial\psi}{\partial z} \\ V_z &= \frac{1}{r}\frac{\partial\psi}{\partial r} \end{aligned} \tag{26}$$

For the coaxially colliding disks a distance h apart, the boundary conditions are;

$$\begin{aligned} r &= 0: && \psi = 0,\ V_r = 0 \\ z &= 0: && \psi = 0,\ V_z = 0,\ \frac{\partial V_r}{\partial z} = 0 \\ z\to &= \infty: && \psi = 0;\ V_r = 0,\ V_z = 0 \\ r\to &\ \ \infty: && \psi = 0;\ V_r = 0,\ V_z = 0 \\ z &= \frac{h}{2}\ (o \le r \le 1): && V_r = 0,\ V_z = -V \end{aligned}$$

A schematic of the streamlines is shown in Figure 3. This shows the fluid being forced out from between the disks and flowing around them.

The appropriate transform for equation (24) is the J_1 Hankel transformation.

$$\Phi(z,\lambda) = \int_0^\infty rJ_1(\lambda r)\,[\psi/r]\,dr$$

$$[\psi(z,r)/r] = \int_0^\infty \lambda J_1\,(\lambda r)\Phi\,d\lambda \tag{28}$$

SinceΦ and Φ/z are continuous at $z = h/2$, we can solve for $C(\lambda)$ and $D(\lambda)$ in terms of $A(\lambda)$ and $B(\lambda)$. Inverting the Hankel transforms, we are led to two sets of dual integral equations for the two unknown eigenfunctions $A(\lambda)$ and $B(\lambda)$. One equation comes from the continuity of the second axial derivative of the stream function for $z = h/2$ and $r > 0$, while another comes from the continuity of the third derivative in the same position. The two equations valid for $z = h/2$ and $1 > r > 0$ involve the value of the stream function and of its axial derivative. Note that the usual second order partial differential equation with split boundary values leads to one set of dual integral equations while our fourth order equation leads to two sets. We solve the equations using a technique developed by Tranter using the properties of the Weber-Schafheitlin discontinuous integrals. Some numerical results appear in Figure 4.

EXPERIMENTAL STUDIES

Another part of our work concerns the experimental aspects of particle-fluid suspension flow. A mixture of synthetic flexible-walled micro-capsules and water, hereafter referred to as pseudo-blood, is being used to mimic the flow behavior of real blood. The main objective of this work is to investigate the effect of suspended flexible particles on the laminar velocity profiles and on the transition to turbulence. Steady as well as pulsatile flows in rigid and specially designed distensible-walled tubing, with constrictions and bifurcations, are being used. Furthermore, attempts will also be made to detect regions of high shear and trapped vortices near constrictions and bifurcations. These experimental results are then to be compared with the theoretical computations previously described.

The difficulties associated with visual investigations of detailed blood flow patterns in vessels other than capillaries, as well as the instability and unavailability of whole blood, have prompted the development of pseudo-blood suspensions. Successful pseudo-blood suspensions are to exhibit, at room temperatures and at particle concentrations equivalent to the normal hematocrit, the same rheological properties as whole blood at body temperatures. Furthermore, the pseudo-blood suspension should cost less and be less opaque that the real blood in order to facilitate flow visualization in reasonably-sized experimental equipment.

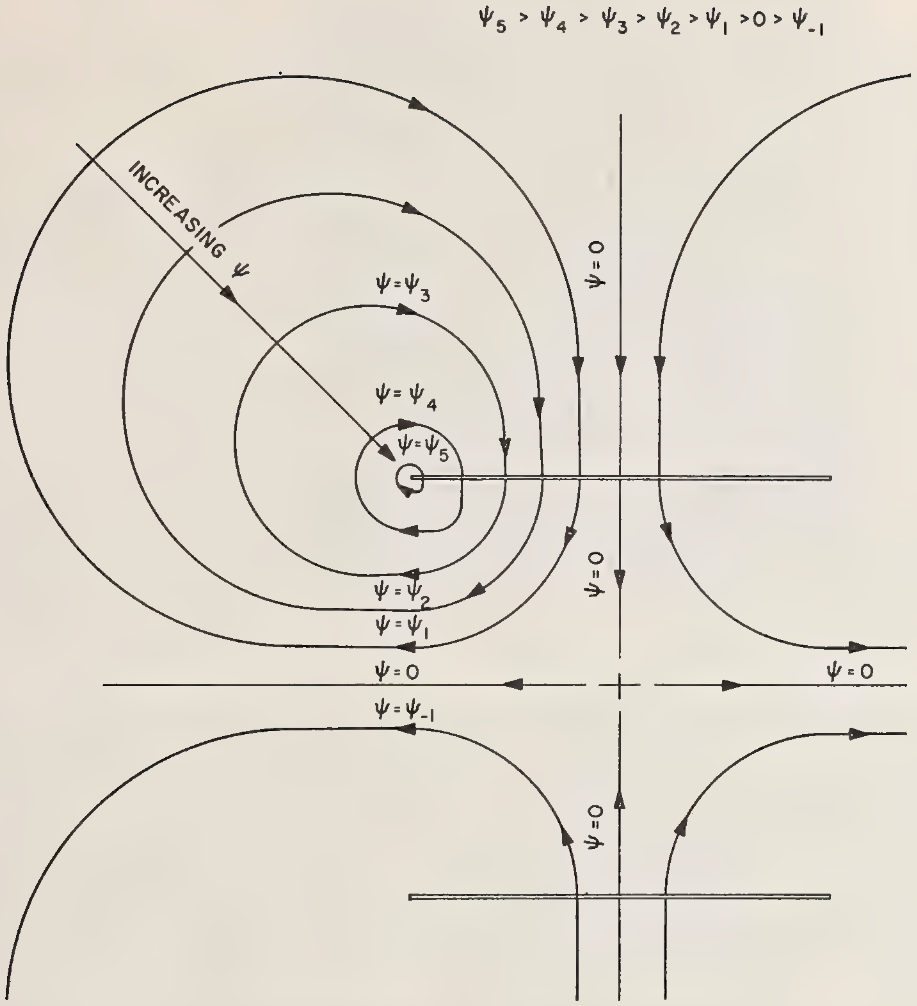

FIGURE 3. SCHEMATIC DIAGRAM OF FLOW STREAMLINES AROUND TWO COLLIDING DISKS.

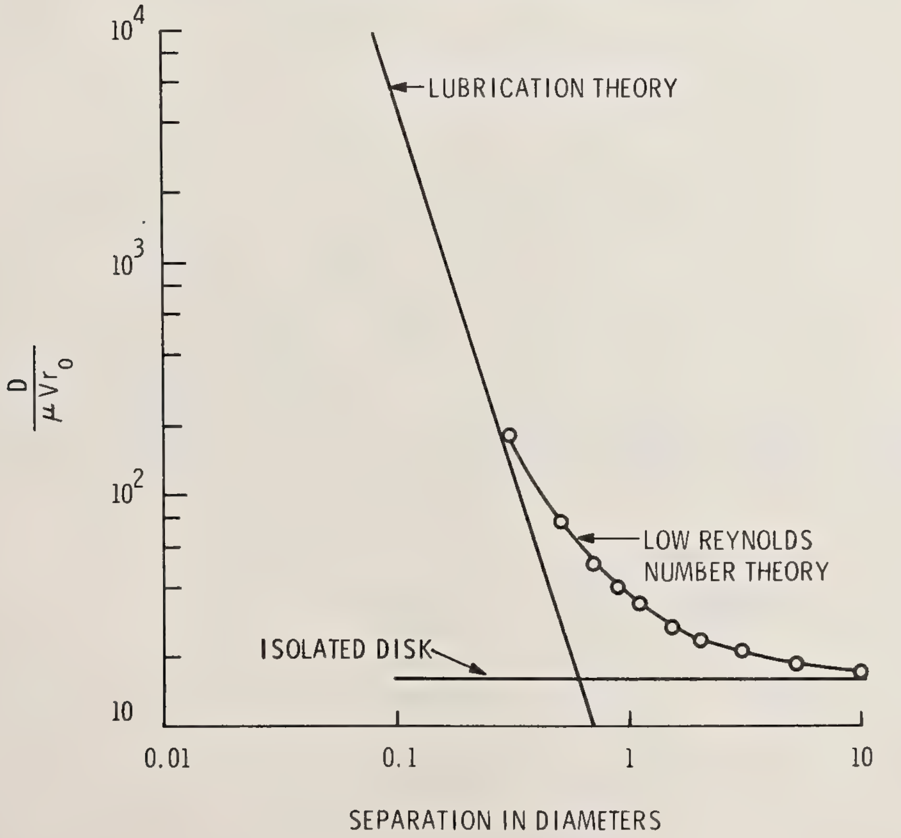

FIGURE 4. HYDRODYNAMIC MODEL FOR RED CELL COLLISION DYNAMICS.

The suspension used to date in this investigation consists of castor oil droplets encapsulated by flexible gelatin walls using a simple coacervation technique. The microcapsules are suspended in water of an aqueous solution of carboxy-methyl-cellulose (CMC). The latter is used to raise the viscosity of the continuous suspending phase to match that of blood plasma.

The average diameter of the microcapsules can be varied from approximately 10 to 1000 microns. Throughout the production steps, the capsules are generally spherical in shape. However, after the removal of the coacervating salt during the capsule washing procedure, the larger particles have a tendency to collapse. This appears to be the result of water penetrating and extending the gelatinous wall material. The capsules can be returned to their original spherical shape by increasing the salt concentration in the suspending phase. Thus, the salt content of the pseudo-plasma could be used to regulate the shape of the microcapsules if this should prove to be desirable. Some typical microcapsules are shown in Figure 5.

The flexibility and integrity of the microcapsules has been further demonstrated by forcing them through small capillaries. Breakage of the elongated particles became significant only after a critical length to diameter ratio of approximately 10 is exceeded.

The apparent viscosity of the pseudo-blood is affected primarily by the particle concentration and the viscosity of the suspending phase. Figure 6 compares the viscosities of typical pseudo-blood suspensions at room temperature with those of whole blood at 37C and at various hematocrit levels. Although there is some question about the accuracy of the volume concentration determination for the pseudo-blood suspensions, the data does indicate that suspensions can be produced with viscosity equivalent to that of blood at approximately the same particle concentration. Efforts are currently being made to improve the accuracy of the particle volume per cent determinations. The effects of the particle size, size distribution, and shape on the suspension viscosity are yet to be determined.

Another of the main objectives in developing pseudo-blood suspensions was to produce a synthetic mixture which is sufficiently transparent to permit visual tracking of suitably tagged particles in vessels of approximately arterial size. This is possible with the currently available pseudo-blood at microcapsule concentrations up to approximately 10% by volume. A better matching of the refractive indices of the encapsulated phase and the suspending phase is necessary to improve the transparency of the suspension at higher particle concentrations. This problem is currently being attacked from two directions: (i) organic materials with refractive indices lower than that of caster oil are encapsulated, and (ii) the microcapsules are suspended in sucrose solutions. The addition of sucrose to the suspending phase increases its viscosity as well as the refractive index. This may, therefore, eliminate the need for CMC in the pseudo-plasma. However, the sucrose concentrations needed for refractive index and viscosity matching are not identical and a compromise will have to be worked out.

The experimental work on the laminar-turbulent transition of pseudo-blood suspensions has been confined to some preliminary runs in straight rigid tubing as the result of some delays in obtaining suitable hot-film anemometer probes. The preliminary data indicate that hot-film anemometer probes mounted flush with the vessel wall are capable of detecting transition to turbulence in the bulk of the fluid. Figure 7 shows typical anemometer output signals at successively high bulk velocities for water and an aqueous 6% by volume suspension of microcapsules respectively. First signs of flow instability appeared at a Reynolds number of approximately 1850 with the microcapsule suspension as compared with a critical water Reynolds number of 2050 in the same equipment.

Use of a conical hot-film probe protruding into the flow field has been ruled out by the excessive disturbances in the anemometer output signal, even at rather low velocities. This is believed to be the result of the separation of flow past the protruding probe and/or the collisions of individual microcapsules or clusters with the sensing element. In Figure 8, the output signals for Reynolds numbers from approximately 1800 to 2300 are shown, covering a range of conditions for laminar, transitional and turbulent flow. The relatively smooth signal shown as the bottom trace is for laminar flow and the blips for disturbances are associated with the arrival of a microcapsule at the probe. Note that these blips continue to appear as the Reynolds number is increased. The difficulties with the protruding hot-film probes indicate that the currently available probes of this type are not suitable for the detection of trapped vortices in the wake of obstructions and in bifurcations. These experiments will have to be conducted using flow visualization techniques and high-speed photography.

Determination of laminar velocity profiles in suspension flow are awaiting the development of more transparent pseudo-blood fluids. Although these experiments could currently be made with dilute suspensions of microcapsules, the measurements are believed to be of more significance if made at particle concentrations equivalent or as close as possible to the whole blood hemotocrit levels.

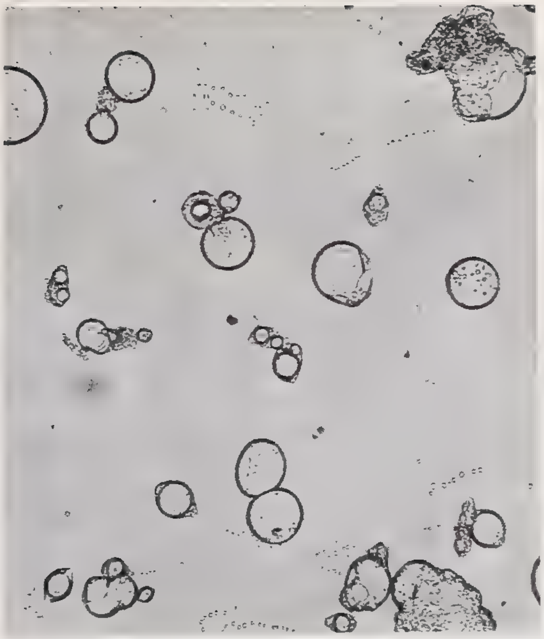

FIGURE 5. PHOTOGRAPH OF MICROCAPSULES IN SUSPENSION.

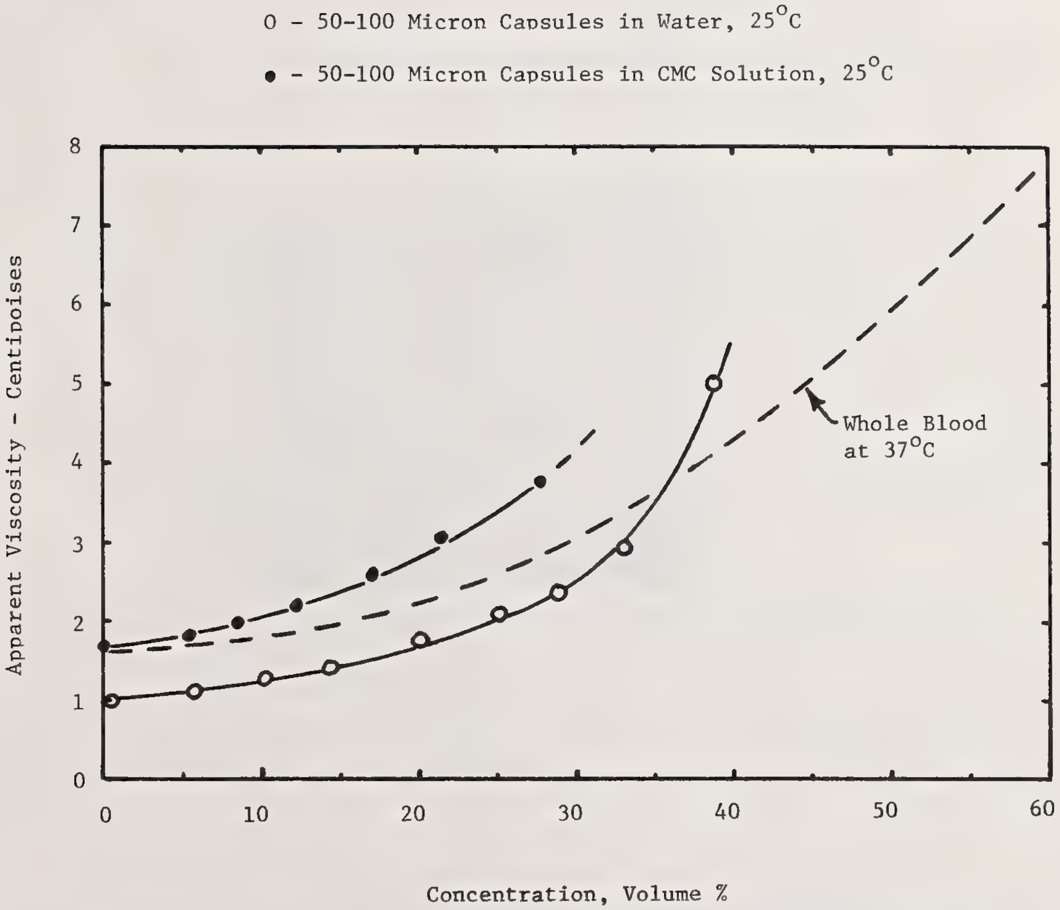

FIGURE 6. EFFECT OF CAPSULE CONCENTRATION ON SUSPENSION VISCOSITY.

FIGURE 7. 6% CAPSULES, SURFACE PROBE TRANSITION AT RE≅1850.

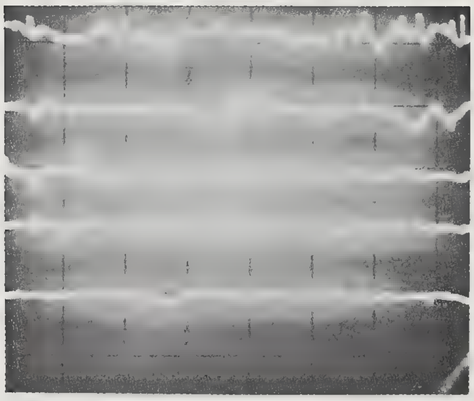

FIGURE 8. 10% CAPSULES, CONICAL PROBE TRANSITION AT RE≅1900.

DISCUSSION

DR. ROTH: Since the work apparently involved a tremendous amount of computer time, I wonder why you haven't considered elastic wave propagation in the conduit wall itself, both radial modes and axial modes. I would think these elastic waves would be quite important since you apparently have considered the sonic velocity in the fluid itself.

DR. SCALA: What we're trying to do is add one complication at a time. If we were to try to put all of the governing equations on the computer, in one fell swoop, which is within our capability, we would be working in the dark. Now, if we start out with a rigid wall and we investigate the effects of geometry, such as introducing a constriction, or a bifurcation, then we can sort out the effects of geometry. If we then go from a Newtonian model to a non-Newtonian model and do the flow calculations for precisely the same geometry, in other words, keeping everything else fixed, we can then ascertain the effects of a non-Newtonian rheological model. As a next step, we allow for the distensibility of the wall, in which we uncouple the governing partial differential equations for the wall itself, and have the moving wall appear only as a boundary condition on the flow equations. We can then calculate the primary effect of a distensible wall, which in the case of the aorta is to allow the aorta to fill partially before blood proceeds downstream. In other words, we feel that our calculations show that in the first small fraction of a second, the first motion of the fluid is to act to fill the aorta, and then as the aortic valve closes, more of the blood will proceed downstream. So, what you suggest is something which is within our capability; we could try to do that, but we would not then be able to sort out the separate effects, as readily as with the procedure we are now using.

DR. ROTH: Well, but you did include tethering which I take to mean a rigid hoop placed downstream at some appropriate point. This condition seems far less important and less realistic than the traveling waves along the conduit itself.

DR. SCALA: Well, I think that before one looks at the mathematical details of the coupling between the partial differential equations for the blood vessel itself, with the partial differential equations for the fluid, one must first obtain as much information as possible about the fluid motion, particularly when one is interested in such complex geometries as stenosis and bifurcation. For example, one way to avoid the question of the viscoelastic behavior of the wall, is to treat the case of a rigid wall, because one can conceive of devices in which one insists that the wall material be rigid. I'm not recommending that one use rigid walls you understand; what I am saying is that we're trying to learn what the relationship is between the rheological properties of the blood, the viscoelastic properties of the blood vessel through which the blood is flowing, and the flow patterns which result. The use of the tethering constraint delimits the region which undergoes distension.

DR. LAIRD: I think it is physically inconsistent to talk about what happens in the first fraction of a second as a distributed phenomenon along the whole length of the distensible tube. It is correct to talk about the Windkessel, but that concept is only valid when the elastic inertial wave has had time to propagate to and fro along the tube. The other question I had was, what is the physical interpretation of the rather complicated wall boundary condition that you used; the one with the partial differentials. I didn't follow the physical argument.

DR. SCALA: Are you referring to the third equation, for R/ t?

DR. LAIRD: Yes.

DR. SCALA: I'll come back to that. The first statement that you made was that it didn't appear to be physically meaningful to talk about the first fraction of a second. Well, since we are going to consider the effect of an entire heart cycle on a local region, and are solving a time dependent problem, we can certainly stop the computer at any point and ask, "What do we have thus far"? All I'm saying is that since we are calculating an entire cycle, and are calculating the flow field variables as a function of time and space, unlike the Windkessel model which is a "lumped" model, not a distributed representation, we are solving a time dependent problem, and are certainly in a position to look at what we have computed as we proceed. Now, with regard to the third equation, which we utilized as a boundary condition for the wall motion; it is a viscoelastic representation, which can be shown to satisfy physiological data. This equation is a mathematical representation of the fact that the radius changes with time in a way that is proportional to the pressure rise. It is also dependent on the nonlinear variation of the radius with static pressure, based on the data for that particular blood vessel, and on the tethering constraint. In other words, many of the experimental data on the relationship between distention and pressure are obtained post mortem by taking a particular blood vessel and filling it with a static fluid at various pressures measuring the resulting radius. Hence, many of these data are obtained under static conditions. Now, there are other data which have been obtained under dynamic conditions, and we would like to see more of this kind of data, which shows that there is a viscoelastic lag in the system and that the radius does not change instantaneously with pressure, and this is what our third equation represents.

DR. LIGHTFOOT: I would like you to comment briefly, if you would, on the comparison between your work and the work by Womersley, who found a simple compliance expression to work quite well for his description of pulsatile flow.

DR. SCALA: Womersley was able to get some rather elegant results because of the nature of the assumptions that he made in his original governing flow equations. In his work, Womersley generally assumes that the nonlinear terms may be neglected in the equations for the motion of the blood. Moreover, he generally treats the case of an infinitely long straight tube. This enables him to obtain an elegant closed form result, or in any case, simpler numerical results. But then, his procedure may be dead-ended, because it does not allow one the latitude of studying other effects in a logical sequence within the framework of those assumptions. That is, we're trying to construct a model in which one can investigate separate effects by adding a particular complication to those which were already included. We could compare our work directly with Wormersley, if we were to try to put in the same physical boundary conditions that he did. But we would expect our results to be different from his since we retain the nonlinear terms.

DR. REAM: Thank you, Dr. Scala.

SECTION IV

CARDIAC CONTROL PARAMETERS

Chairmen: Allen K. Ream, M.D.
Charles E. Branch

INTRODUCTION

The circulatory assist devices to be developed under the Artificial Heart Program should be sufficiently responsive to the needs of the body for moderate ambulatory activities by the patient. It is recognized that the intact heart meets the needs of the body by responding to a myriad of local and remote mechanical, neural, biochemical and other stimuli. It is unrealistic to expect that these control systems can be described completely, let alone reproduced precisely along with their necessary sensing transducers. Nevertheless, the patient with the ventricular assist device must respond adequately to many of the factors facing the normal person in everyday life; indeed the automatic control systems of his device must never permit catastrophic inadequacy of regulation. Accordingly the program is supporting studies which will lead to the development of practical control systems of circulatory assist devices.

CHAPTER 27

CARDIAC CONTROL: HEART RATE OPEN LOOP RESPONSE

E. Dong, H. Glaze, E. Stinson, C. Weaver

Stanford University Medical Center
Stanford, California

Last year we reported that cardiac autotransplantation results in the absence of sinus arrhythmia, increased blood and plasma volume, decreased diuresis to acute volume load, absence of infusion tachycardia, and diminished cardiac output response to infusion. That these alterations existed in a preparation which conforms to "Starling's Law" suggested that rate and frequency would be important although not absolutely necessary for optimal control of an artificial heart.

These studies are the first in which we document the open loop response of heart rate and peripheral resistance to alterations of ventricular rate and filling. Method: during cardiac autotransplantation the heart is removed and sutured by transection of atrium. Thus, a rim of atrium (containing the sino-atrial node) is still responsive to the central nervous system. The ventricle and attached atria are now termed "donor heart". Under anesthesia the animal was studied by driving the donor atria with a voltage controlled pacemaker in sine and square wave configurations and in a stopbeat mode. A bipolar intracavitary (atrial) lead, respiration, ECG, and arterial pressure were recorded. Mathematical work for the development of the transfer function between blood pressure and heart rate has not been completed but the initial data support the assumptions made. Opening the loop at the atrial level is important for studying the control of the cardiovascular system. The remnant atrial rate (now called the P'-P' interval) can be measured so that the system response is identified: (arterial pressure, baroceptors, central nervous system, motor nerve and pacemaker tissue).

Results: Static -	RR	800	700	600	500	400	300
	P'-P'	320	338	343	380	383	453
	AP	125	130	130	132	130	143

Stop-beat - P'-P' control 450 milliseconds, on the 5th beat the P'-P' is 420 and it reaches its minimum (300 milliseconds) 30 beats post "R arrest".

INTRODUCTION

The development of a good controller for an artificial heart requires understanding quantitatively the variable behavior of the normal cardiac pump and the variable impedance that the vascular system loads on the heart. The basic mechanical determinants of cardiac output include the input load or Starling mechanism, the heart period, and the output load or input peripheral impedance. Presently, the relative roles of heart rate and the peripheral impedance loading the heart are not clearly delineated. Furthermore, the overall neural control of each of these parameters is not well characterized.

The intent of this study is to document and to develop mathematical models for arterial blood pressure control of heart period and for arterial blood pressure control of peripheral impedance. The central thrust of this work is in using the cardiac-autotransplanted dog (autograft) as a biological tool for eliciting these control laws. The heart of this biological model may be viewed as an autonomous, free-running pump without direct central nervous control, but having Frank-Starling type characteristics. The remainder of the autograft's cardiovascular system is completely intact. With this preparation, the donor heart rate can be electronic pacemaker controlled with synchronous atrioventricular contraction. Also, the autograft's basal heart rate is low, generally below 70 BPM; this allows pacemaker control of the heart rate over a wide range.

Last year we reported that cardiac autotransplantation results in the absence of sinus arrhythmia, increased blood and plasma volume, decreased diuresis to acute volume load, absence of infusion tachycardia, and diminished cardiac output response to infusion. These abnormalities did not preclude long-term autograft survival, but it seemed reasonable to expect that control of heart rate and arterial pressure waveform would improve system performance.

This paper (1) briefly reviews the classical concepts in the homeostasis of arterial blood pressure, (2) considers the closed-loop multipath feedback mechanisms which we want to characterize, (3) describes the autograft as a biological tool for studying these control mechanisms on an open-loop basis, (4) describes our present experimental protocol and measurement techniques, and (5) concludes with several figures of dynamic data recorded from an autograft in studying the arterial blood pressure control of heart period.

Figure 1 shows a conceptual schematic of the reflexes involved in the homeostasis of arterial blood pressure.

The broad lines indicate neural links and the single lines represent mechanical events.

The representation for peripheral impedance with flow as input and pressure as output is only conceptual; in reality both flow and pressure are the input variables to peripheral impedance.

Generally when arterial pressure increases, the baroreceptor nervous activity increases. The resulting afferent neural impulses impinge upon the vasomotor center and are processed. The vasomotor center output neural impulses sent over motor pathways cause (1) a decrease in the magnitude of peripheral impedance, (2) a decrease in the force of contraction, and (3) an increase in heart period. These alterations tend to restore arterial pressure to its original state. The respiratory center is included, because of the strong connection between respiration and heart period.

To understand closed-loop behavior, the following open-loop responses need clarification: arterial pressure-to-input peripheral impedance, arterial pressure-to-heart period, arterial pressure-to-force of contraction, and respiration-to-heart period.

The main problem in characterizing these input-output responses is that the input variable cannot be freely changed over a wide range. The input variable is constrained by neural and/or mechanical feedback in the closed-loop or normal dog. By eliminating neural control of the heart pump, one of the major control loops is opened.

Figure 2 is a conceptual schematic for the control of arterial blood pressure in the autograft. The ventricle and attached atria are now termed donor heart. As described, the donor atrium can be pacemaker excited. During cardiac autotransplantation the heart is removed and sutured by transection of the atrium. Thus, a rim of atrium containing the sino-atrial (SA) node is still responsive to the central nervous system. The SA node initiates the depolarization of the host atrium and the brief electromagnetic field generated specifies the firing rate of the SA node. A bipolar intracavitary or extracavitary atrial lead is used to measure this small field and the resulting signal spikes are called P-waves.

Altering arterial pressure in a prescribed manner is desirable for investigating the open-loop arterial pressure-to-host heart rate response. It is reported that the baroreceptors are responsive to the actual waveshape of arterial pressure. At normal operating levels the three main features of the pressure waveform detected by the baroreceptors are its mean level, positive rate of change, and the pulse period, or the R-R interval of the limb ECG. Voltage-controlled pacing of the donor heart modulates the arterial pressure's period according to any desired voltage function. Mean pressure can be changed by using chemical vasoconstrictors and vasodialators, or by altering blood volume, or by inflating a balloon in the thoracic aorta of a hypovolemic dog. The positive derivative of the pressure pulse is determined in part by the force of heart contraction and the peripheral impedance; hence pulse derivative is not directly controllable. However, the autograft model does provide us with substantial control over two characteristics of the natural arterial waveform.

In studying the arterial blood pressure-to-input peripheral impedance response, blood pressure changes can be achieved by altering ventricular rate and heart filling. The dotted line from arterial pressure to the respiratory center indicates that in much of our experimental data there is a strong correlation between respiratory rhythmic activity and blood pressure changes. In order to maintain blood gas composition near the autograft's control state, artificial respiration was not used during these experiments.

In the following figures attention is given to (1) the respiration-to-heart period response with arterial pressure fixed and (2) arterial pressure-to-heart period response with respiratory activity viewed as biological noise.

The first two data figures (Figures 3 and 4) are the open-loop respiration-to-host heart period responses. Heart period is the reciprocal of heart rate. These data were recorded when the arterial blood pressure was at steady-state. The top line spike train specifies the R-onset times of the limb ECG. Here, the donor heart is paced at a period of 500 milliseconds which is a rate of 120 BPM. The voltage waveform at the top is proportional to thoracic circumference and is our measure of respiration. The lower function is host heart period or P-P interval. The vertical lines of this function specify where the P-onset times occurred. The discrete amplitudes equal the times between two successive P-wave onsets. The scale is for heart period only and is in tenths of seconds. For example, the number 14 means 1.4 seconds; 1.4 seconds corresponds to an instantaneous heart rate of 43 BPM.

Notice that the heart period shortens following inspiration in a regular manner. The large P-P intervals attained implies that the motor neural activity caused by blood pressure is high. That respiratory activity is strongly coupled to host heart period is shown by the 2-to-1 changes in instantaneous heart period.

These open-loop data demonstrate that at least two of the explanations generally proposed[1] to account for the respiratory-heart period response are not dominant causes. The first explanation is that the transient change in intra-arterial blood pressure occurring with respiration affects the heart rate reflexly. As stated, our data was taken with a non-changing intra-arterial pressure waveform. Hence, any heart rate changes cannot be evoked by arterial pressure. The second explanation is that the increase in inflowing venous blood during inspiration accelerates the heart reflexly via stretch receptors in the atria and ventricles. This cannot be the cause since the autograft's donor heart is denervated.

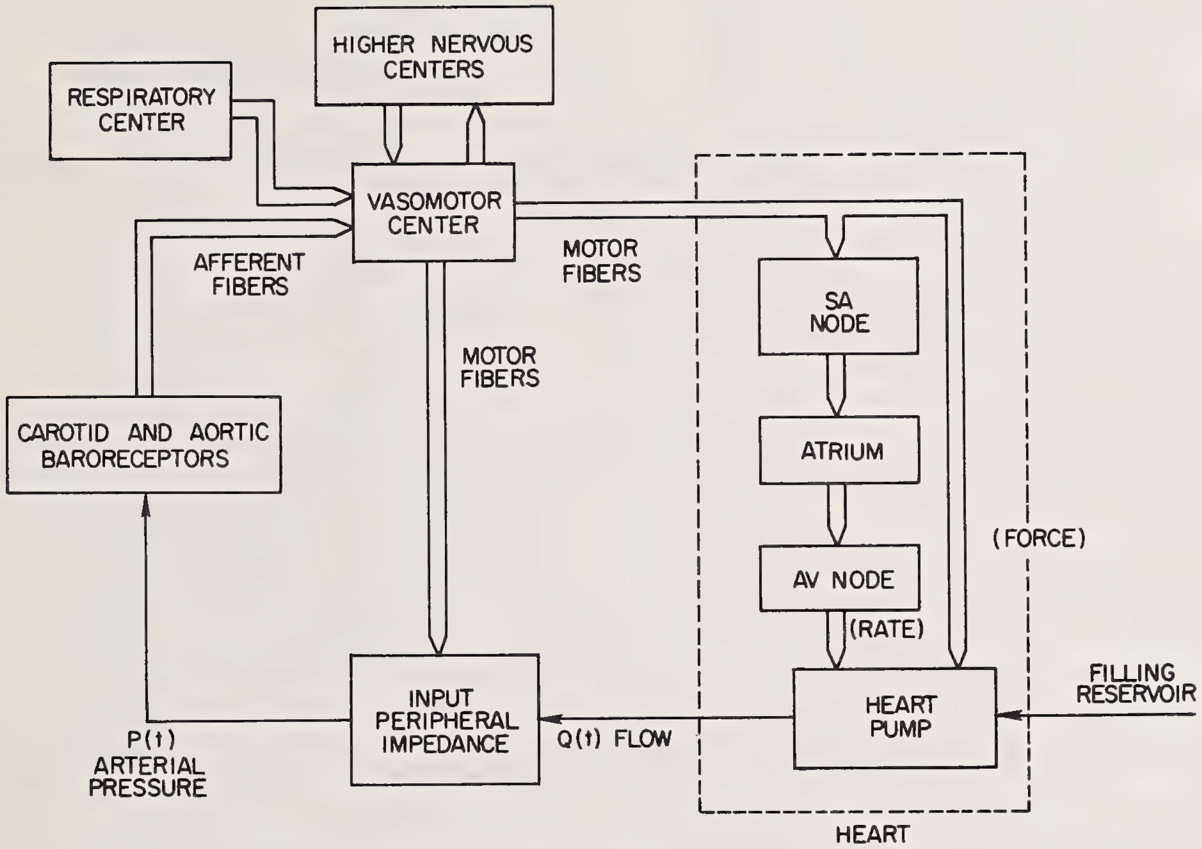

FIGURE 1. CONCEPTUAL SCHEMATIC OF THE REFLEXES INVOLVED IN THE HOMEOSTASIS OF ARTERIAL BLOOD PRESSURE.

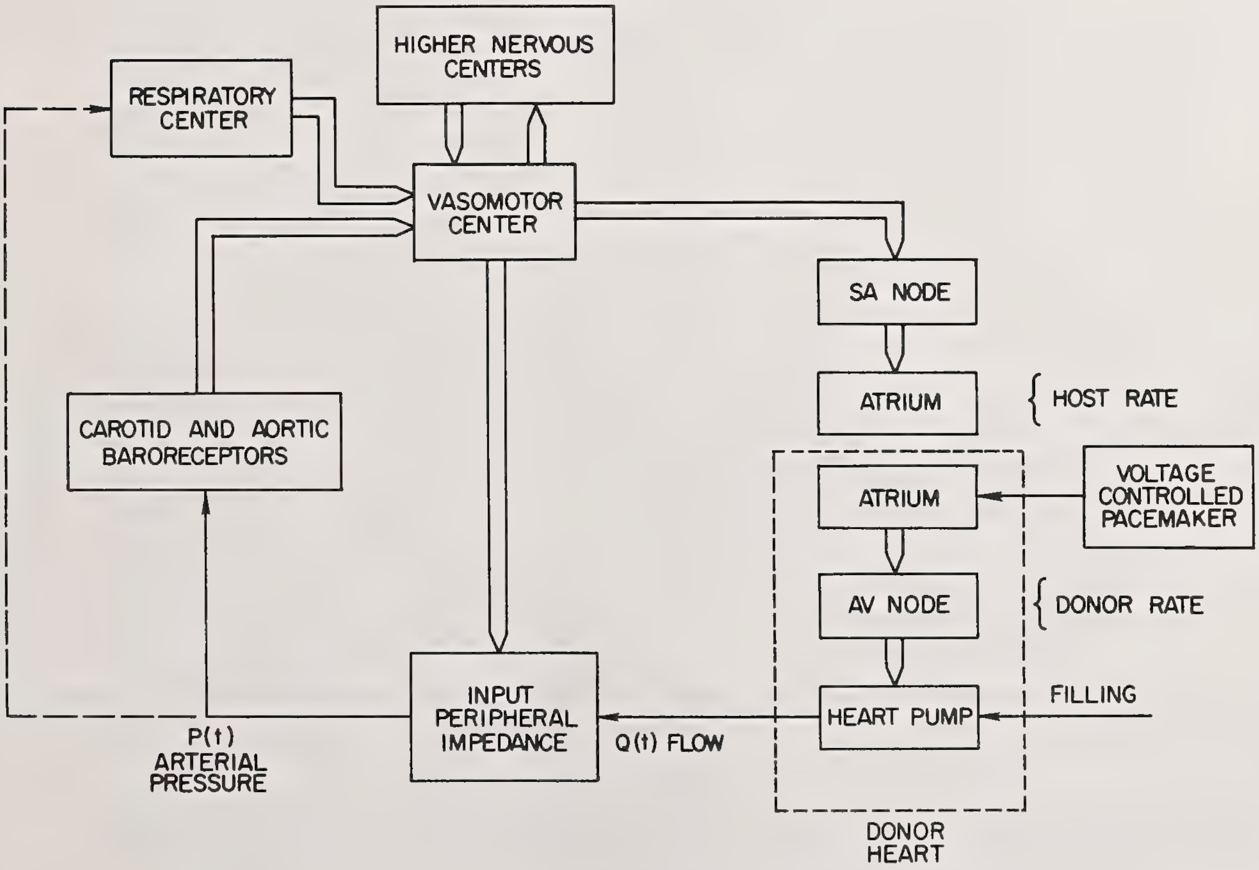

FIGURE 2. CONCEPTUAL SCHEMATIC FOR THE CONTROL OF ARTERIAL BLOOD PRESSURE IN THE AUTOGRAFT.

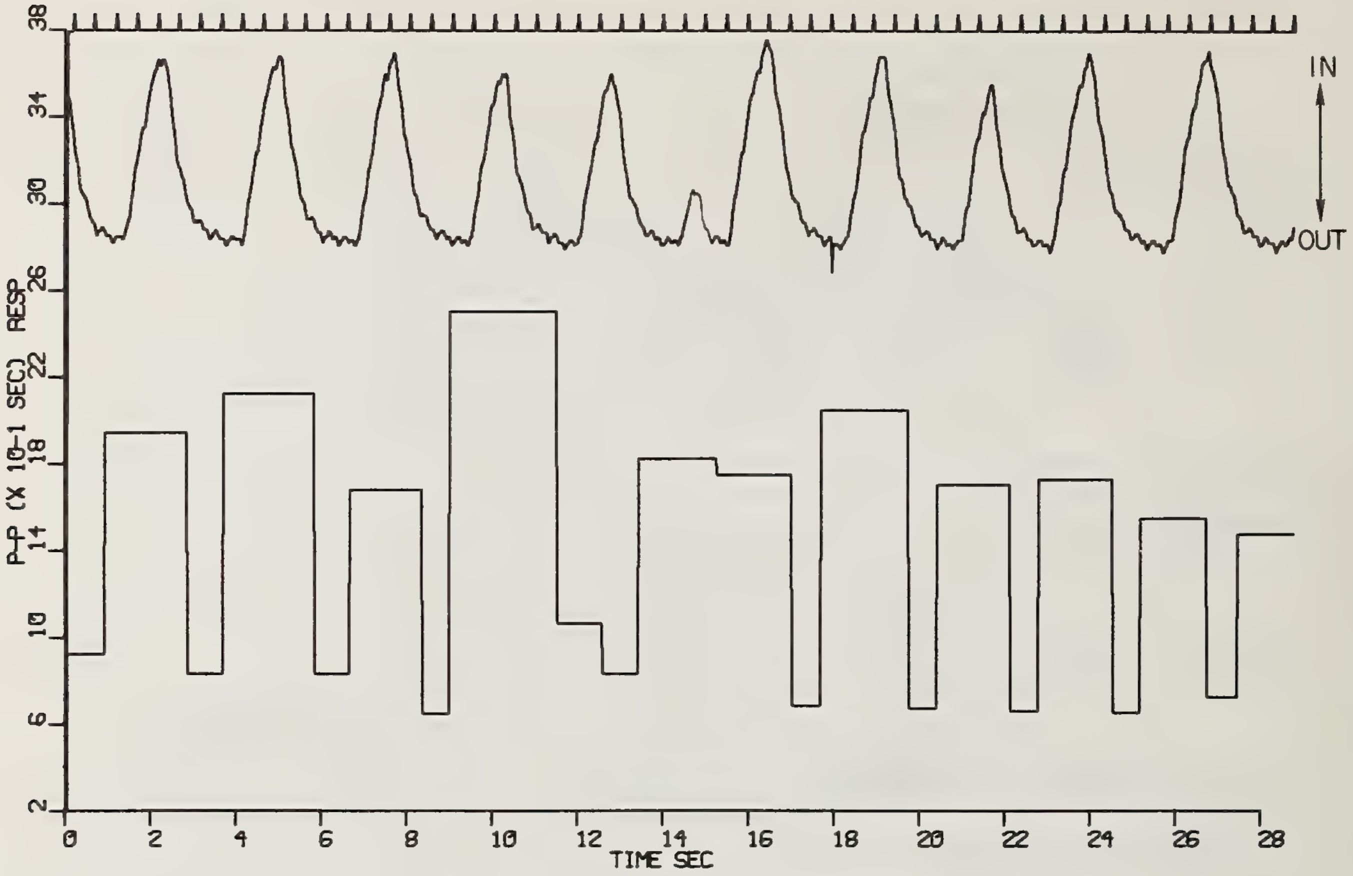

FIGURE 3. OPEN-LOOP RESPIRATION-TO-HOST HEART PERIOD RESPONSES.

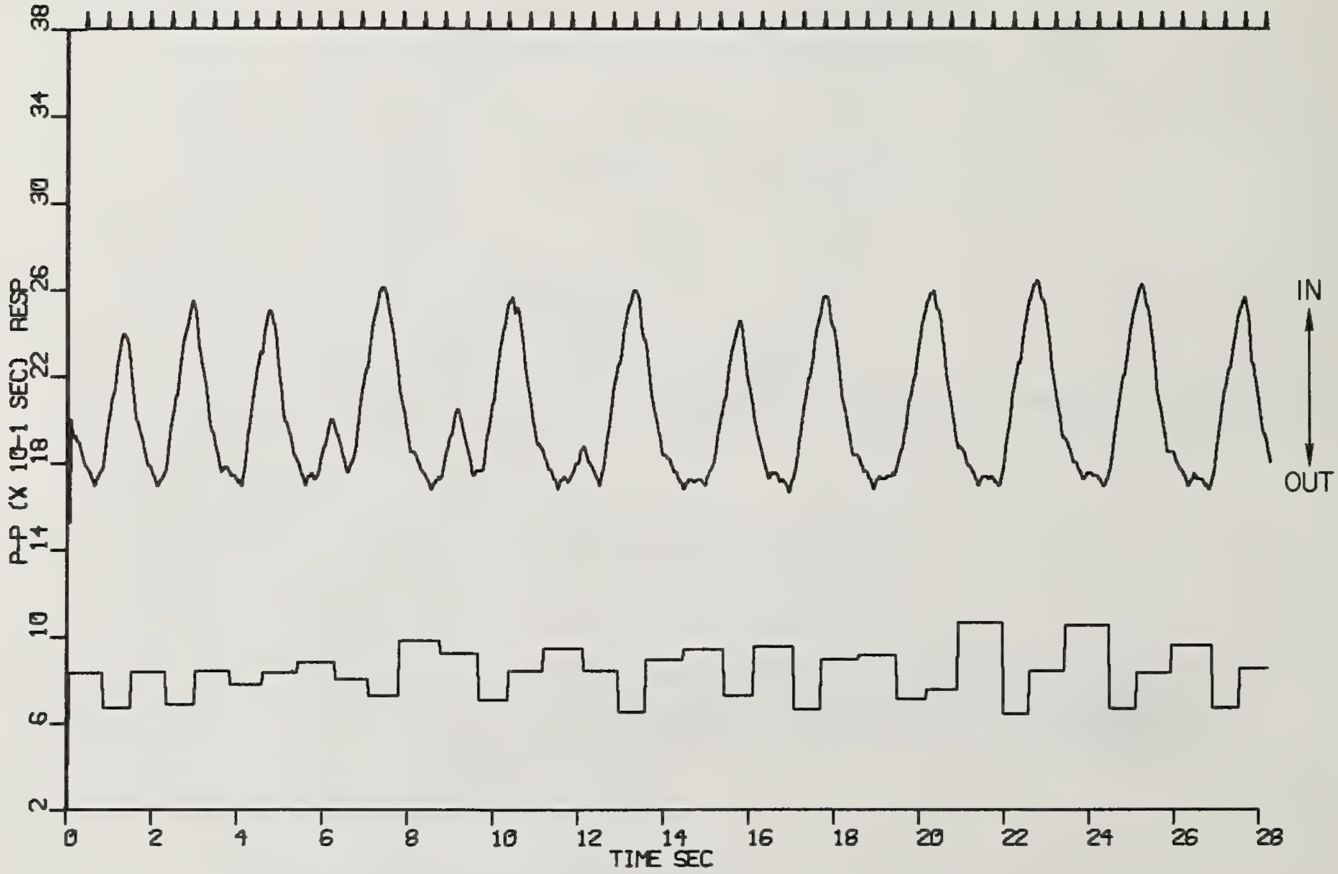

FIGURE 4. OPEN-LOOP RESPIRATION-TO-HOST HEART PERIOD RESPONSES.

Figure 4 shows another open-loop respiratory-to-host heart period response. Again arterial blood pressure is at steady-state. Notice that at this resulting low heart period, respiration does not modulate P-P interval by the same percentage as it did in the previous slide. This behavior supports the theory that the lungs are a source of impulses which exert a suppressing influence upon the cardio-inhibitory center, especially during inspiration.

We expect the autograft and normal dog's respiratory-to-heart period responses will differ substantially. The normal dog's carotid sinus and aortic reflex are a form of negative feedback. This feedback mechanism will, therefore, diminish the magnitude and alter the dynamics of the pure or open-loop respiratory-to-heart period response.

Figure 5 and the next four figures (Figures 6, 7, 8, 9) are autograft data obtained from measurements in studying the arterial blood pressure-to-host heart period response. Donor heart period or R-R interval is the time between the R-onset times of successive limb ECG spikes. (For practical reasons, all R-R intervals exceeding 1000 milliseconds are clamped to 1000 milliseconds). Host heart period or P-P interval is the time between successive P-wave spikes. The interval data were computed on an IBM 360/50 computer. The waveform labeled respiration is a voltage proportional to thoracic circumference. Arterial blood pressure is presented as recorded with a Whittaker strain-gauge pressure transducer.

As in the previous figures, visually the rapid fluctuations in P-P interval are well correlated with respiration. Since the P-P interval maxima occur when respirator activity is small, we suggest viewing the upper envelope of these P-P interval data as the best estimate of noiseless P-P interval data.

This ensemble of dynamic events occurred when the pacemaker was first set at approximately 500 milliseconds and then turned off. The donor heart stops beating. As pressure decreases, P-P interval decreases as expected. About 10 seconds after pacemaker shut-off, the donor heart begins to beat on its own at a period of approximately 800 milliseconds. Following 30 seconds of normal beating the heart slows again, due to instability of the donor nodal rhythm. In both cases of decreasing pressure, the P-P interval saturates at about 300 milliseconds; this corresponds to a heart rate of 200 BPM. However, the P-P interval time courses in approaching saturation differ. Where the decreasing pressure is pulsatile, saturation does not obtain as rapidly as for the non-pulsatile pressure case. This is true even though the P-P interval is initially higher in the non-pulsatile case.

For both time segments just prior to the two cases of decreasing pressure, arterial blood pressure has a mean of 92 mm Hg and a mean positive derivative of 250 mm Hg/sec. The first time segment has a R-R interval of nearly 500 milliseconds and a P-P interval exceeding 1100 milliseconds. The second segment has a R-R interval of about 800 milliseconds and a P-P interval below 900 milliseconds. The 200 milliseconds difference in P-P interval data can be attributed to the difference in the R-R interval data since the other main pressure characteristics (mean and mean positive derivative) are essentially the same for both time segments.

In Figure 6, using a voltage controlled pacemaker, the donor heart period is modulated about a center period of 600 milliseconds according to a triangular voltage. The R-R interval deviation is approximately 200 milliseconds or 35 percent. The modulating period is about 95 seconds and only one period is shown. Mean arterial blood pressure increases from 83 to 93, and then decreases to 83 mm Hg. These actual changes in mean arterial pressure are relatively small because input peripheral resistance changes rapidly enough to compensate for mean pressure changes. Arterial pressure mean positive derivative does not change significantly over the entire time record. Hence the upward trend of P-P interval is caused mainly by increasing mean pressure and decreasing R-R interval. P-P interval then decreases because R-R interval increases and mean pressure decreases.

Triangular modulation of R-R interval about a center period of 500 milliseconds is shown in Figure 7; the modulation deviation is 200 milliseconds. The modulating period is 95 seconds. Mean arterial pressure increases from 88 to 97, and then decreases to 88 mm Hg. Positive derivative of the pressure pulse does not change significantly for the entire record. Hence, both decreasing R-R interval and an increasing mean pressure cause the P-P interval data to increase. Respiration activity is high throughout the record. Respiration can decrease P-P interval significantly, as shown at the far left where P-P interval decreases to 400 milliseconds.

In Figure 8, the R-R interval is triangularly modulated about a center period of 600 milliseconds. The percent modulation is 35 and the modulating period is 20 seconds. Beat mean arterial pressure varies periodically between 75 and 98 mm Hg. Input peripheral resistance does not change rapidly enough to compensate for these pressure changes, as it did in the previous slides. Again respiratory rhythm is fast; the dog is panting here. The mean positive derivative of arterial pressure decreases with decreasing R-R interval. Even so, as R-R interval decreases, mean pressure increases; thus causing P-P interval to increase. P-P interval varies periodically from approximately 700 to 1000 milliseconds with the same periodicity, but slightly delayed from the R-R interval waveform.

Figure 9 shows the same ensemble as in the previous figure except the R-R interval modulating period is now 10 seconds instead of 20 seconds. The P-P interval oscillates at the same basic frequency. However, now the delay between the R-R interval minima and the P-P interval maxima is more conspicuous. This transport delay is approximately 250 milliseconds.

The beat mean arterial pressure fluctuates between 85 and 100 mm Hg. As R-R interval decreases, mean pressure increases and conversely. The mean positive derivative of arterial pressure decreases with decreasing R-R interval. Hence, the mean pressure and R-R interval changes are more dominant in determining P-P interval than is the mean positive derivative.

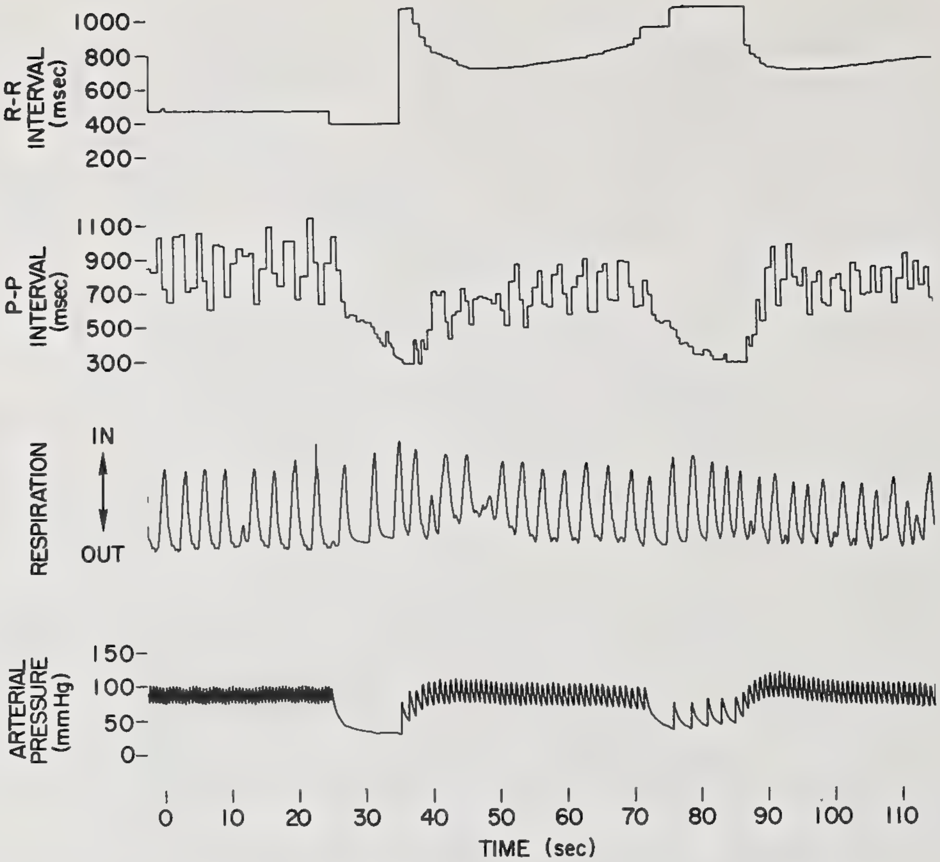

FIGURE 5. AUTOGRAFT DATA IN STUDYING THE ARTERIAL BLOOD PRESSURE-TO-HOST HEART PERIOD RESPONSE.

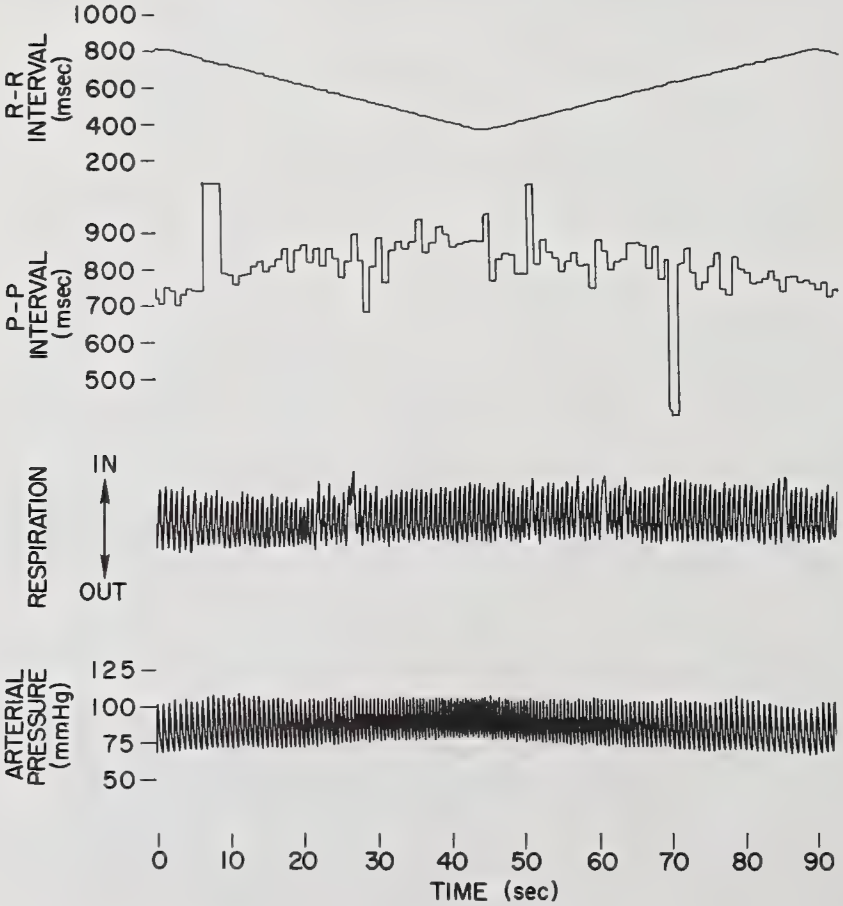

FIGURE 6. AUTOGRAFT DATA MEASURED IN STUDYING THE ARTERIAL BLOOD PRESSURE-TO-HOST HEART PERIOD RESPONSE.

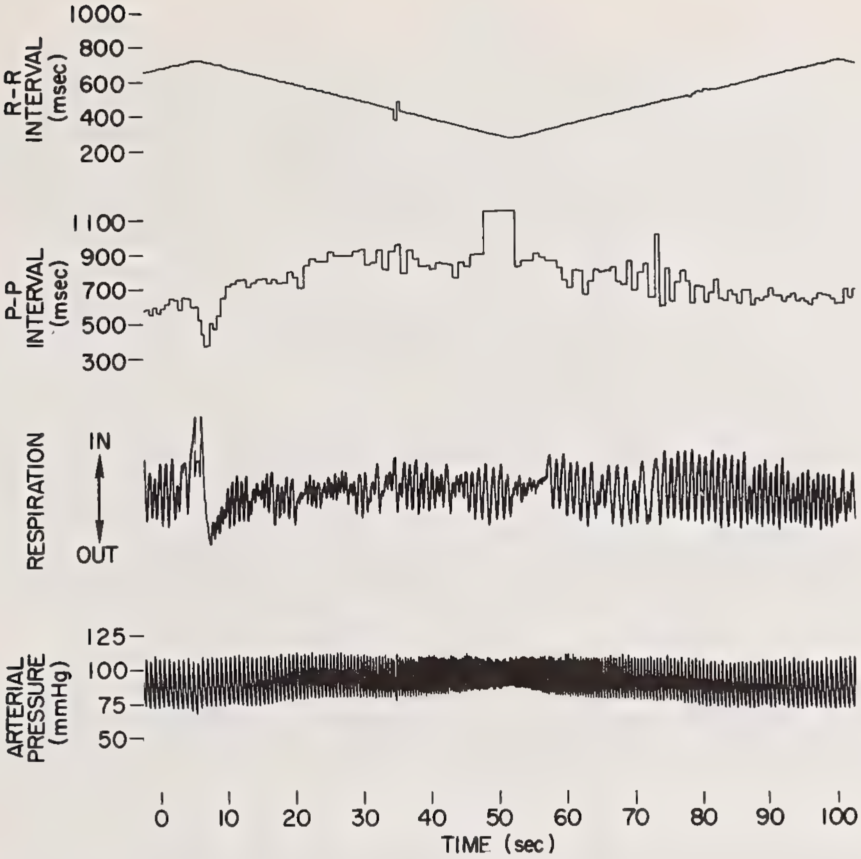

FIGURE 7. AUTOGRAFT DATA MEASURED IN STUDYING THE ARTERIAL BLOOD PRESSURE TO HOST HEART PERIOD RESPONSE.

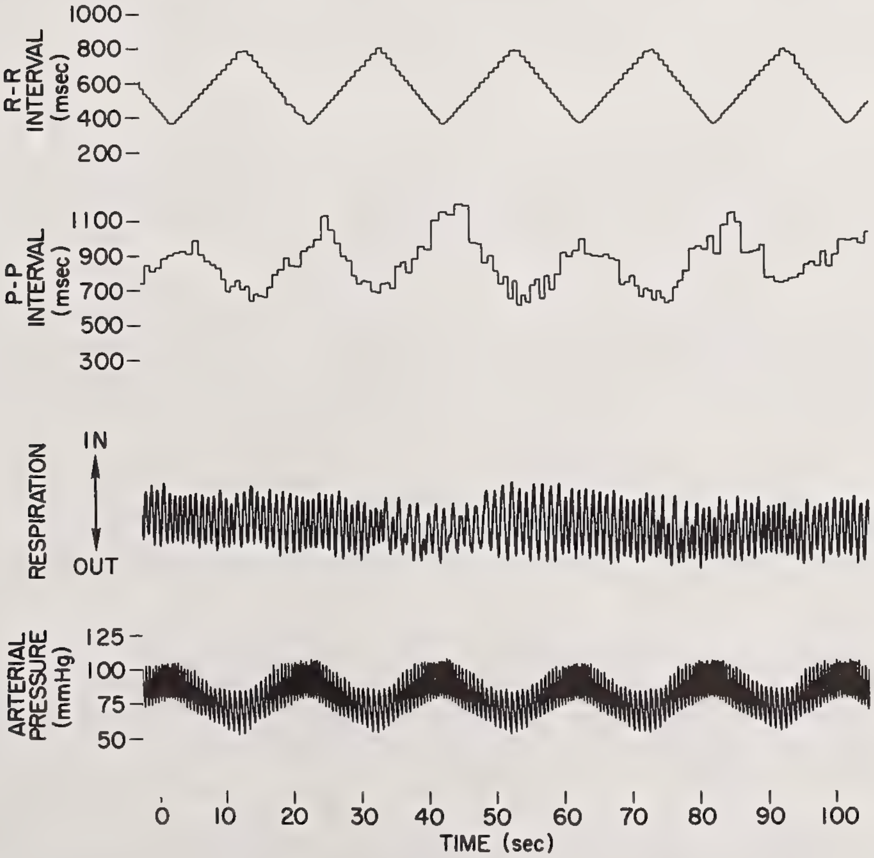

FIGURE 8. AUTOGRAFT DATA MEASURED IN STUDYING THE ARTERIAL BLOOD PRESSURE-TO-HOST HEART PERIOD RESPONSE.

CONCLUSION

The autograft was introduced as a biological analog of a dog equipped with an uncontrolled artificial heart. Previous experiments indicated that circulatory function would improve if the autonomous transplanted heart was controlled. We suggest controlled pacing of the donor heart for this improvement. In order to determine a heart period control law which is based on heart input and output mechanical events, two major feedback responses are being studied: (1) overall open-loop arterial blood pressure control of host heart period, and (2) overall closed-loop arterial blood pressure control of input peripheral impedance.

In the autograft preparation, the heart-rate control loop is opened at the atrial level, distal to the SA node. Controlled electronic pacing of the donor heart then provides a means of varying arterial pressure for eliciting the responses described. Unlike nearly all experimental preparations used for studying the homeostasis of blood pressure, the autograft's sino-aortic baroreceptors remain intact and undamaged.

The studies discussed today were the first in which we document the open-loop response of heart period to arterial pressure and respiration. Although the exact functional homeostatic reasons for the respiratory-heart period response are unknown, three statements can be made: (1) that the open-loop respiratory-heart period response exists, (2) that the percent heart period variation increases with increases in vagal tone, and (3) that several of the classical explanations accounting for this response in the normal dog cannot be valid.

Since the arterial pressure-to-heart period response is altered by respiration, it is vital to understand the nature of these alterations. We demonstrated that the host heart period is responsive to arterial pressure according to reflex laws already established.

REFERENCE

1. McCrady, J.D., et al.: Neural origin of the respiratory - heart rate response. Am. J. Physiol., 211(2):323-328, 1966.

DISCUSSION

DR. REAM: I have a brief question for you. In view of your introduction, one might term your paper heart rate with neural open loop response. I wonder if you can tell me briefly the significance of the control modes that remain.

DR. DONG: Well, last year we described some abnormalities in the autograft. There is an absence of sinus arrhythmia, an increased blood and plasma volume, decreased diuresis to acute volume load. These abnormalities did not preclude long-term autograft survival. We have autografts at Stanford that survived for over two years. Since the pressure waveform is different in an autograft, we expect the peripheral impedances differ, as well.

DR. WILLMAN: This is extending the question just asked. To ask if perhaps exercise is not the most common physiological phenomenon which influences peripheral resistance, and therefore also alters impedance, to which there is a response by the blood pressure mechanism. Has it not been demonstrated that the auto transplanted heart, in response to exercise, does increase cardiac output and indeed increases the cardiac rate? Therefore, the question arises: Is this response perhaps not due to a neuro-hormonal loop? Then, does this preparation actually represent a completely open loop or is it only an attenuated loop? Another question I might ask in relation to that last figure, which very nicely demonstrated a response of blood pressure to rate, at that time, even at a heart rate of 140 the systolic blood pressure was only 100. The question is, was the preparation, at that point, modified?

DR. DONG: I appreciate Dr. Willman's work on auto transplant response to exercise. These preparations are not pure biological analogs of the artificial heart. They do respond to neuro-hormonal influences. But as he has demonstrated and we have demonstrated as well, the degree of circulatory response to exercise in the auto transplant is diminished. The questions arising then, are, is this diminution due to a lack of central nervous system control, and if we can find some arterial pressure parameters and close the loop with a heart rate control might we be able to completely correct the abnormality? The second question, about a particular experiment, is whether or not the pressure was low. Throughout all the experiments we are able to separate particular data out of the long continuous experiment. The data shown in the figure were selected because they do show these changes. We are now doing the experiments on unrestrained animals. We have found approximately the same thing at different levels of arterial pressure. One of the nice aspects of this particular preparation is that we can change mean arterial pressure by bleeding the dog or over-transfusing or giving some other drugs such as vasoconstrictors so that we can change the parameters involved. We selected that particular figure because it did show the response that we wanted to show.

MR. PURDY: The dominant control mechanisms for heart output are both left and right atrial pressures, and you were measuring, as one of your dominant input variables, the arterial pressure. Is there a reason for that or had you planned to include atrial pressure as well as part of your input data.

DR. DONG: The dominant input parameter to heart rate control is arterial pressure. We think the dominant input parameter to cardiac output is left and right atrial pressure.

MR. PURDY: Would not your experiment be an ideal technique for actually examining the complete control capability of an artificial heart?

DR.DONG: Well, we think so, and we will be working on it during the coming year.

DR. TOPAZ: My only problem with understanding this control system is trying to show that these controls work without knowing what the cardiac output is. Is there any data on what the cardiac output was when you were changing the rate?

DR. DONG: In the initial experiments that we demonstrated here the cardiac output was not measured. In the last month and a half we have been able to put flow transducers on the aorta and maintain them for several weeks. We have not yet analyzed that data.

DR. NORMANN: I just wonder if you would care to comment on the transfer function centrally, since you do use pressure as the input. Have you quantitated your data enough to describe them in a similar manner as Dr. Kezdi and his group have done; such as the frequency response of the circulatory centers?

DR. DONG: We have not. That is what we are trying to develop at the present time as Mr. Glaze mentioned. These are the very first data coming off our biological model. We spent the first six months of the last fiscal year developing the biological preparation that you see. It has required development of the flow system, pressure system measurements of heart rate, intra-atrial heart rate, and computer methods of separating the pacemaker spike from the intra-atrial activity. We are going to come up with what we think will be the transfer functions and transformations involved. We haven't gotten that mathematical work done yet. We have simply accumulated the physiologic data.

DR. REAM: Thank you Dr. Dong and Mr. Glaze.

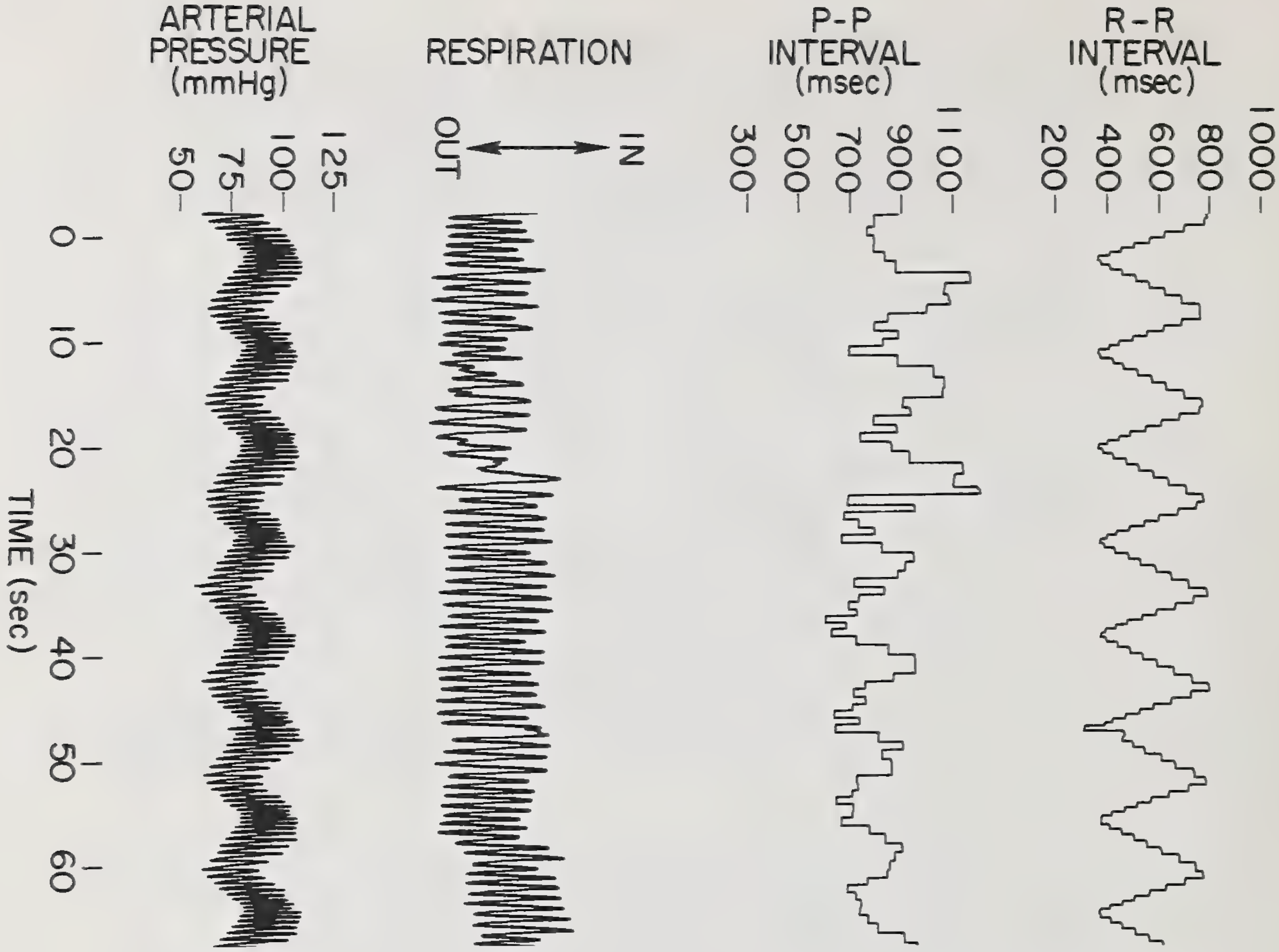

FIGURE 9. AUTOGRAFT DATA MEASURED IN STUDYING THE ARTERIAL BLOOD PRESSURE-TO-HOST HEART PERIOD RESPONSE.

SECTION V

OXYGENATOR DEVELOPMENT

Chairmen: Allen K. Ream, M.D.
Charles E. Branch

INTRODUCTION

As part of the goal of developing ventricular assist devices the Artificial Heart Program is considering the use of a blood oxygenator as part of a system for long-term perfusion to assist the failing heart. An important limitation to use of the presently available blood oxygenators is the harm they cause to blood due to denaturation of proteins and lipoproteins and destruction of cellular and non-cellular elements. There is evidence that the presence of a direct blood/gas interface is a major problem in the long-term use of these oxygenators. Other investigators have approached the problem by attempting to design oxygenators without a blood/gas interface; these include both membrane and liquid interface devices. However, most of these oxygenators have limitations due to poor gas transport, poor hemodynamics, high cost, and difficult assembly. The poor gas transport, due primarily to poor and varying blood flow patterns, results in the necessity for a large surface area and high priming volume. The problems of high cost and difficult assembly limit the use of these oxygenators on a large scale. An additional problem with these oxygenators is that the efficiency tends to decrease when scaling up from a small test cell to a high capacity unit. This is due to poor blood manifolding, shunting, and varying flow resistance in the individual oxygenating subunits. Studies aimed at the design, fabrication, and testing of more effective blood oxygenators for clinical use are in progress.

CHAPTER 28

BLOOD OXYGENATOR WITH PREFORMED, MEMBRANE-LINED, CAPILLARY CHANNELS

P. Dantowitz & A. Borsanyi

Monsanto Research Corporation, Everett, Mass.

Arterialization of blood in parallel capillaries about 200μ effective diameter requires a thin membrane barrier (<60μ) if full advantage is to be taken from this geometry for both oxygen and CO_2 transfer. This presentation deals with the design, construction and evaluation of a membrane oxygenator which will utilize thin film (5-10μ) coated capillary channels. The basic functional element of the device consists of two 23.1 x 11.6 cm substrate sheets, one of which is flat and the other preformed with 580 parallel grooves 11.6 cm long and about 200μ x 200μ cross section. When pressed together the two sheets delineate a flat layer of parallel capillaries with rated blood flow of 60 ml/min and pressure drops of 80 mmHg. The substrate material is a highly porous, hydrophobic mix rolled onto a stainless steel screen support. Elements can be stacked to form larger capacity units. In the first year of the program feasibility was demonstrated by in vivo testing in which oxygen uptake was close to the original goal of 80 $ml/min/m^2$. In the second year we made improvements in the geometry of the blood side to reduce shunts and maldistribution. Progress was also made in applying the thin coating of silicone rubber to the grooved and flat substrates. Dog perfusions have been carried out for up to 6 hours. Occasionally red cell aggregation has caused a sharp rise in the head of pressure necessary to maintain the rated flow. This phenomenon, which is fully reversible upon washing the oxygenator with saline, is not completely understood. Gas exchange data from in vivo testing show considerable scatter, only a portion of which can be explained. Data will be discussed in detail in the presentation.

INTRODUCTION

This report is written at the end of the second year of development effort on our version of an improved membrane oxygenator. The major goal has been to minimize the blood contacting surface required for both oxygen uptake and carbon dioxide elimination. It has long been recognized that blood film geometry is the most important factor governing oxygen uptake. Our early studies convinced us that a capillary configuration of the smallest practical size would be advantageous and so we selected an equivalent diameter of 200μ. An arbitrary blood shear limit of 100 $dynes/cm^2$ was imposed to avoid excessive trauma, which dictated 50,000 capillaries for an oxygenator with a five liter per minute blood flow. The capillary length (11.5 cm.) was selected to raise the saturation from 60% to 90%, based upon an estimate of oxygen uptake rate of 80 $ml/min\text{-}M^2$.

OXYGENATOR CONSTRUCTION

Figure 1 shows conceptually how the capillaries are made. We start with a thin sheet of a microporous matrix made of Teflon-bound carbon backed by a fine mesh stainless steel screen. One sheet is grooved to form three sides of a square cross-section capillary and an ungrooved sheet of the same material forms the fourth side. For ease of fabrication the profile of the grooved sheet is actually trapezoidal as shown in Figure 2. A thin film (∿0.5 mil) of silicone rubber is cast in situ on both the grooved and ungrooved sheets to prevent direct contact between blood and gas.

Although the film covers over 95% of the area flaws do exist but blood does not leak through the hydrophobic pores. To emphasize this point it is noted that acute in vivo experiments were successfully carried out without any film at all. It is this tolerance to flaws which allows us to use a film thin enough to obtain carbon dioxide removal in excess of 100 $ml/min\text{-}M^2$. Most membrane oxygenators are operated with blood pressure higher than oxygen pressure to avoid bubbling in the event of a leak. Our oxygenator is always operated in this fashion because any reversal in pressures is certain to result in oxygen bubbles entering the blood stream through the flaws in the film.

The main feature of the oxygenator construction is the smooth transition from the blood manifolds to the many hundreds of capillaries. The basic building block of the oxygenator is the module which is made as follows. The 10" x 10" microporous matrix is folded in half, as shown in Figure 3, and the edges are sealed to form an open-ended envelope with the screen on the inside. Rubber spacers are placed inside the envelope to provide structural support and to guide oxygen flow along the matrix surface. Figure 4 shows a partial end view of the envelope with the oxygen spacers in place. Here the smooth transition from manifold to capillaries is clearly visible. Oxygen flows into the paper and blood flows from left to right. To complete the module, curved, die-cut rubber gaskets are cemented to the top and bottom of each envelope forming the individual elements of the blood inlet and outlet manifolds. Half of the modules are made starting with a grooved matrix; the other half with an ungrooved matrix. A pair of modules, one grooved and the other ungrooved, delineate 600 blood capillaries with a rated capacity of 60 ml/min.

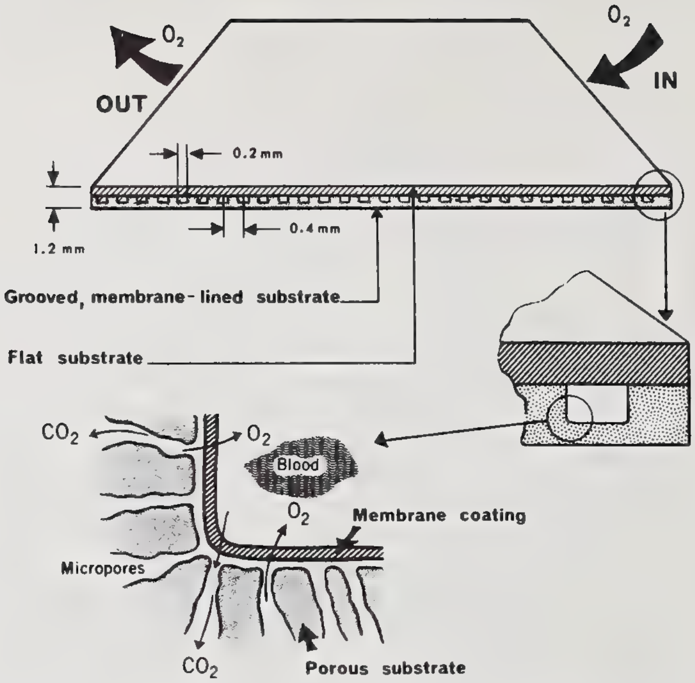

FIGURE 1. SCHEMATIC REPRESENTATION OF MEMBRANE-LINED, CAPILLARY OXYGENATOR.

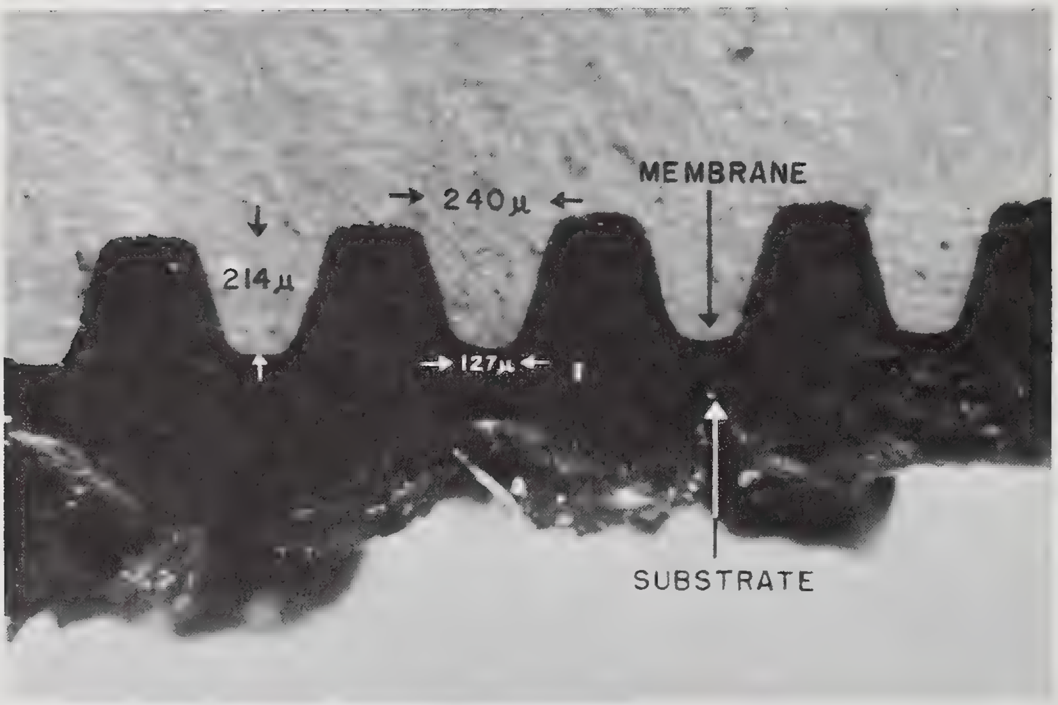

FIGURE 2. MICROPHOTOGRAPH OF A CARBON-TEFLON SUBSTRATE SHEET GROOVED THROUGH FEEDING BETWEEN APPROPRIATE ROLLERS, AND LINED WITH A SILICONE RUBBER FILM USING THE FLOAT-COATING TECHNIQUE.

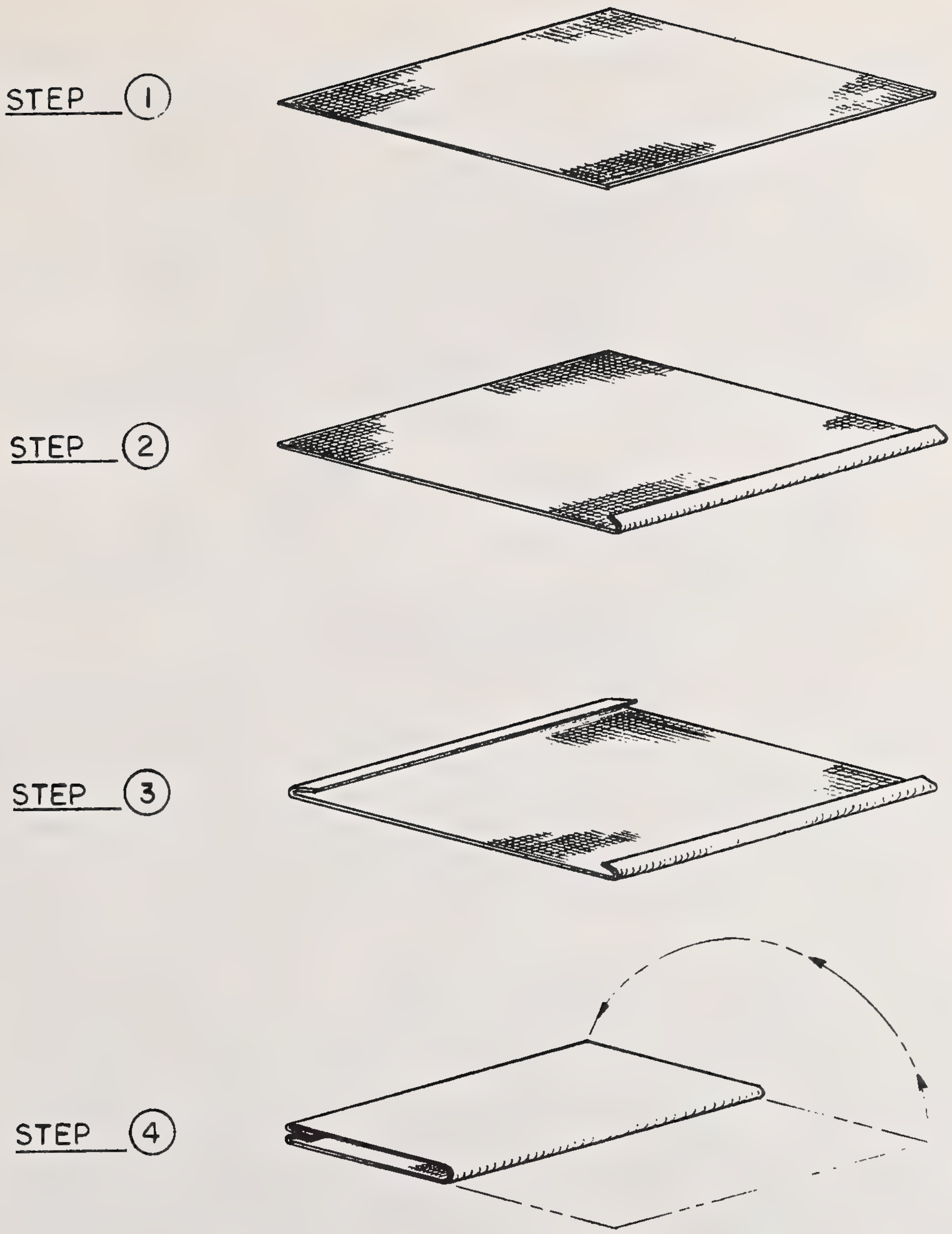

FIGURE 3. SUBSTRATE FOLDING PROCESS.

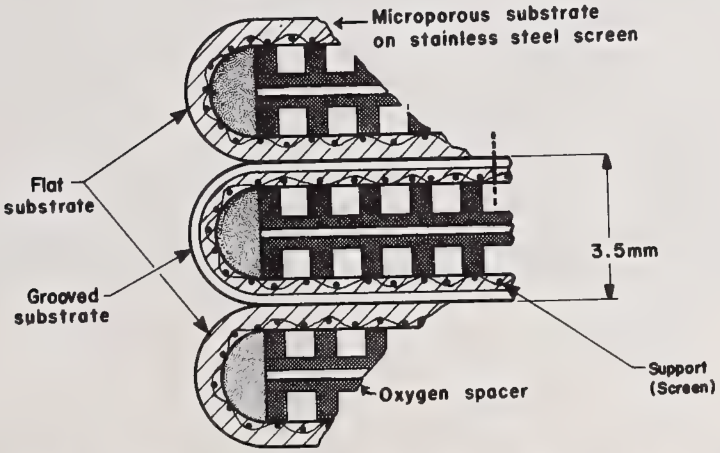

FIGURE 4. FOLDED ENVELOPE DESIGN SHOWING HOW THE MEMBRANE-LINED SUBSTRATE (FLAT OR GROOVED) IS WRAPPED AROUND THE OXYGEN SPACERS.

An oxygenator with a rated capacity of any multiple of 60 ml/min may be constructed by alternately stacking grooved and ungrooved modules on top of one another (Figure 5). First an ungrooved module is placed on a Plexiglas endplate which contains blood inlet and outlet connections. The subsequent modules alternate between grooved and ungrooved. The stack ends with an ungrooved module which is specially fitted with a flat plastic bag inside the envelope. The bag is pressurized during operation to keep the grooved modules pressed tightly against the ungrooved. The blood pressure would otherwise force the modules apart to flow in a sheet rather than in the capillaries. A second Plexiglas endplate completes the assembly, which is then clamped together with a set of tie bolts. The blood inlet and outlet manifolds are formed by the superposition of the rubber gaskets. The construction of the oxygen spacers allows the manifold gaskets and the adjoining edges of the modules to be compressed to provide a blood seal. An oxygen distribution manifold is built on one side of the machine and the excess gas escapes to the atmosphere on the other side.

The unit shown in Figure 6 contains five flat and four grooved modules, forming eight layers of capillaries. It has a rated blood flow of 480 ml/min, an estimated gas exchange surface area of 0.41 M^2, and a priming volume of 150 ml, 20 ml of which are in the capillaries and 65 ml in each of the manifolds.

DEVELOPMENT TESTING

A series of ten oxygenators with a single layer of capillaries (rated flow 60 ml/min) was tested in the fall of 1968, and in February of this year a series of five oxygenators with two layers of capillaries (rated flow 120 ml/min) was tested.

Except for pressure drop testing with water, these machines were evaluated in vivo according to the attached test procedure.

Design improvements were introduced in the course of both series of tests so that the results have little statistical validity; however, one observation is worthy of note. In testing some of these small units in vivo, a rapid and large increase in blood pressure drop was experienced at the beginning of the test. In most instances the blood pressure drop was so high that the test was aborted. Subsequent flushing with saline invariably restored the normal pressure drop characteristic (with saline), making it unlikely that clotting was the cause of the difficulty. A second oxygenator on the same animal often behaved normally and to further confuse matters the same oxygenator sometimes behaved normally on a different animal. The best guess we can make at this time is that the capillaries are occluded by an agglomeration of red cells, associated possibly with a high sedimentation rate observed with some of the dogs. Despite this difficulty, and as a result of generally encouraging data, a series of 5 machines with 8 layers of functional capillaries was fabricated. The in vivo testing of these machines was done at Brown University under the direction of Dr. P. M. Galletti. He also authored the following section on results and the attached section on testing procedure.

RESULTS

Oxygen Transfer

Under conditions of decreasing input oxygen saturation (Figure 7), the output saturation remains in the neighborhood of 100 per cent until input saturation drops below 70 per cent. If one arbitrarily selects an output saturation of 95 per cent as the minimal goal, then the 8 element unit is able to handle its rated flow of 450 ml/min as long as input saturation is above 62 per cent. The oxygen uptake under such conditions amounts to 67 ml/min/m^2. Higher oxygen transfer rates can be obtained when the incoming blood is more markedly desaturated, but the output saturation no longer reaches 95 per cent.

Under conditions of constant inlet saturation and blood hemoglobin content (Figure 8) oxygen transfer increases linearly up to the rated flow or somewhat beyond, then reaches a plateau of about 85 ml/min/m^2. There again the output oxygenation remains above 95 per cent up to a blood flow of 1125 ml/min/m^2 of gas exchange area.

The data obtained with 5 units of the ML-8 series are pooled in Table 1 and Figure 9. At the rated flow, the oxygen uptake varies between 50 and 70 ml $O_2/m^2/min$, depending upon the input conditions. Higher oxygen uptakes are possible at higher blood flow rates and for lower inlet oxygen saturation. It appears unlikely that the oxygen transfer rate could exceed 100 ml/min/m^2.

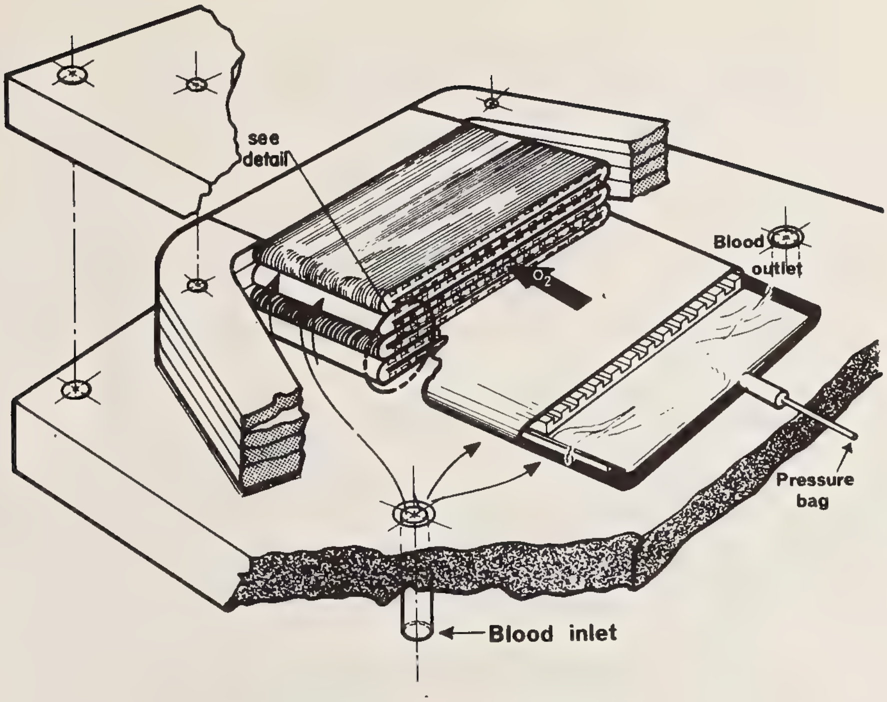

FIGURE 5. EXPLODED VIEW OF AN ASSEMBLED OXYGENATOR UNIT, INDICATING THE RELATIONSHIP OF BLOOD FLOW TO GAS FLOW, AND THE LOCATION OF THE PRESSURE BAG. THE ELEMENTS IN THE CIRCLE AT THE EDGE OF THE EXCHANGER ARE DETAILED IN FIGURE 4.

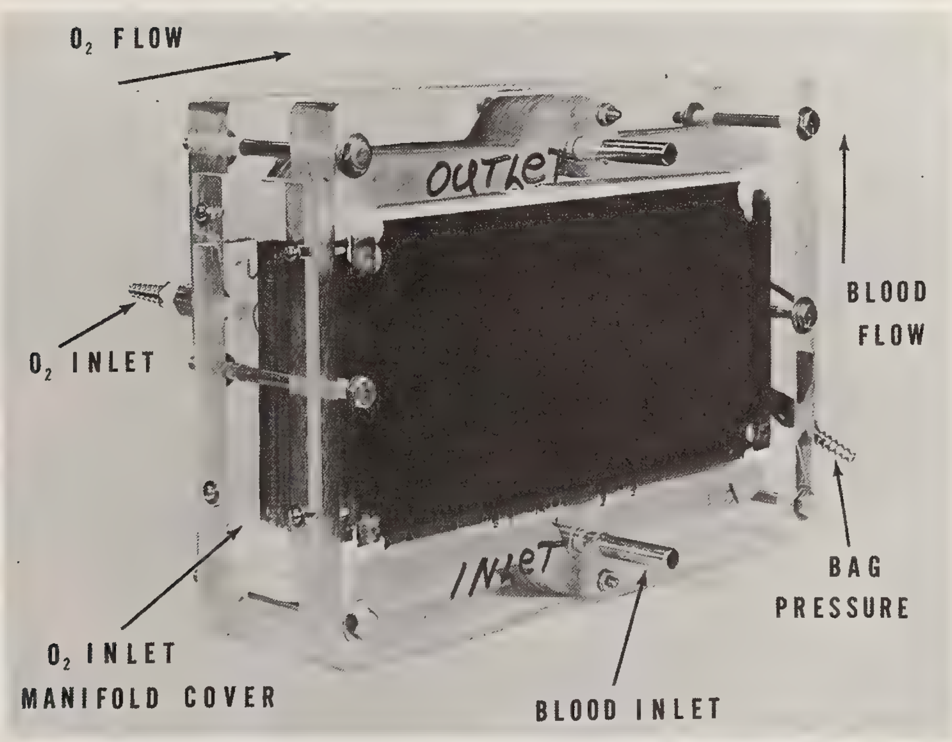

FIGURE 6. PHOTOGRAPH OF 8 ELEMENT OXYGENATOR UNIT.

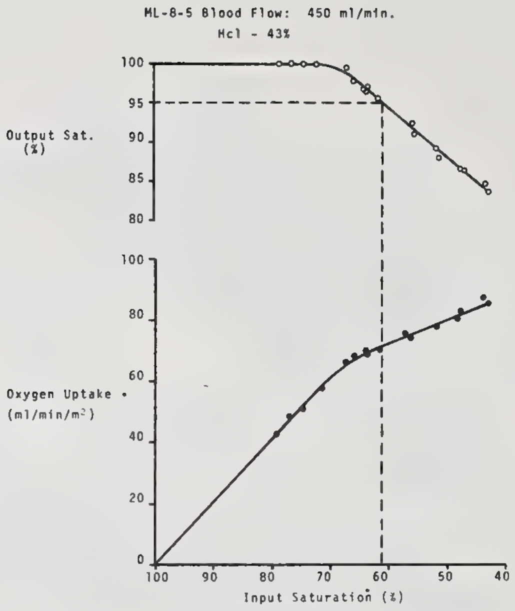

FIGURE 7. PLOT OF BLOOD OXYGEN SATURATION AT THE OUTLET OF THE OXYGENATOR (IN%) AND OXYGEN TRANSFER RATE (IN ML/MIN/M^2 OF EXCHANGE AREA) VERSUS BLOOD OXYGEN SATURATION AT THE INLET (IN%). BLOOD CARRYING CAPACITY FOR OXYGEN, BLOOD FLOW AND OXYGEN FLOW WERE KEPT CONSTANT THROUGHOUT THIS EXPERIMENT.

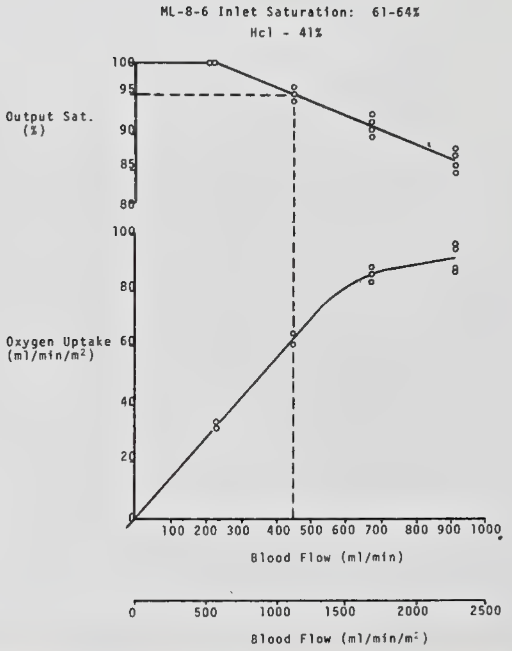

FIGURE 8. PLOT OF BLOOD OXYGEN SATURATION AT THE OUTLET OF THE OXYGENATOR (IN%) AND OXYGEN TRANSFER RATE (IN ML/MIN/M^2 OF EXCHANGE AREA) VERSUS BLOOD FLOW RATE THROUGH THE OXYGENATOR (UPPER SCALE IN ABSOLUTE VALUES, ML/MIN; LOWER SCALE RELATED TO EXCHANGE AREA, ML/MIN/M^2). BLOOD OXYGEN SATURATION AT THE INLET AND GAS CARRYING CAPACITY WERE KEPT CONSTANT THROUGHOUT THIS EXPERIMENT.

TABLE 1

OXYGEN AND CARBON DIOXIDE TRANSFER IN MEMBRANE-LINE CAPILLARY LUNG

		Blood Flow Rate			
		230 ml/min	450 ml/min	670 ml/min	920 ml/min
O_2 transfer*	Input satur. 75 ± 2%	27.0 ± 3.1	47.8 ± 3.8	73.8 ± 6.8	-----
	Input satur. 65 ± 2%	32.7 ± 1.0	63.7 ± 4.5	80.7 ± 4.2	92.2 ± 6.1
	Input satur. 55 ± 2%	43.9 ± 0.2	71.2 ± 4.7	------	-----
CO_2 transfer*	All input conditions	50.7 ± 18.9	81.0 ± 35.4	101.6 ± 48.3	-----

*mean ± standard deviation

CO_2 Transfer

Carbon dioxide exchange rates are more difficult to measure because of the uncertainty involved in the various nomogram readings. Nevertheless the unit displayed a remarkable ability to eliminate CO_2. Most of the readings were obtained with inlet pCO_2 between 35 and 45 mm Hg. At the rated flow the pCO_2 drops across the membrane lung varied between 8 and 14 mm Hg, and the pH rose by 0.02 to 0.05 units. The calculated CO_2 removal is usually in excess of the oxygen uptake, pointing to an average respiratory exchange ratio of 1.3.

DISCUSSION

Generally the results are good and compare favorably to our original performance goals. The ability to reach 100% output saturation at low blood flows or high inlet saturation is particularly gratifying because shunting was a persistent problem until the latter stages of development. The high carbon dioxide removal rate clearly demonstrates the effectiveness of the thin film of silicone rubber. Despite these positive aspects of the results further discussion is warranted.

All of the machines tested had a blood pressure drop almost twice as high as that expected based upon both experience on smaller machines and pressure drop tests with water. We note in passing that the pressure drop results with water agree well with theoretical predictions, verifying the capillary geometry.

In view of the occasional occlusion experienced with the small units, the possibility of the same phenomenon causing the high pressure drop cannot be excluded. The possibility that some of the capillaries were occluded is supported by the fact that in some cases a substantial increase in pressure drop (at constant blood flow) was observed during the test. On the other hand, water tests conducted just prior to the *in vivo* testing showed a large increase in pressure drop over that found in similar tests conducted a week or so earlier. The latter tests were conducted using a different test set up and different instrumentation which may in part explain the discrepancy. It is unlikely that testing differences account for the entire difference in pressure drop, suggesting that the capillary geometry had changed, due perhaps to local yielding of the microporous matrix. In any event, further study should be conducted to explain the unexpected high pressure drop and if possible it should be corrected.

SUMMARY

The use in a blood oxygenator of a thin, supported silicone rubber membrane has exhibited higher CO_2 elimination rates than previously reported on other membrane oxygenators. Although some practical difficulties have yet to be overcome, the design concept holds the promise of continuing increase in oxygen uptake by improvement of blood film geometry and in CO_2 removal by even thinner silicone rubber films.

ATTACHMENT

Test Procedure

A standard circuit for partial heart-lung bypass (veno-arterial pumping with oxygenation) was used for the evaluation reported here. Conditioned dogs with a hematocrit of about 45%, and initially anesthetized with α-chloralose, served as a source of venous blood. Small doses of pentobarbital, and the addition of a dead space to the tracheal tube permitted the control of the oxygen saturation and the CO_2 content of the incoming blood. The extracorporeal circuit, made of Silastic® tubing 3/16" I. D., includes a closed venous reservoir (a 150 ml reinforced Silastic® bag), two 360° roller pumps, a flat plate heat exchanger (set for a blood temperature of 37°C) and the oxygenator unit located about 40 cm below heart level. The use of two pumps in the testing circuit permits the unit under scrutiny to be separated hemodynamically from the vascular system, and the evaluation of the effect is blood recirculation if needed (none in this case). Blood flow through the unit is measured by pump calibration. The head of pressure at the oxygenator inlet, and the differential pressure between inlet and outlet are monitored continuously as is the arterial pressure of the donor animal. The oxygenator is fed with dry oxygen at a flow of 5 L/min. The blood flow is started at half the rated flow of the unit, under a shim pressure of 8 PSI and kept there until stabilization of the differential pressure recording indicates complete mixing between the donor animal's blood and the heparinized saline used to prime the circuit (350 to 400 ml). Paired inlet and outlet samples can then be obtained for the determination of gas transfer under various experimental conditions of flow and blood gas concentration. The hematocrit ratio is kept close to 40% by an intravenous saline drip, and heparin is added every hour (2 mg/kg), following an initial dose of 4 mg/kg. The duration of an evaluation procedure is about 6 hours.

Blood Gas Determinations

Every pair of inlet and outlet samples is analyzed in duplicate for hematocrit (microhematocrit centrifuge), oxygen saturation (American Optical oxymeter, recalibrated for dog blood using a spectrophotometric technique), pH (Radiometer microelectrode), pCO_2 and pO_2 (Instrument Laboratories). Oxygen capacity of dog's blood is taken as Hct x 0.324 x 1.34. CO_2 contents are read from the Singer-Hastings monogram on the basis of directly measured parameters. The precision of oxygen transfer rates measured under such conditions is ± 5%. The precision of measurements for carbon dioxide transfer rate is in the order of ± 25%, unless very wide (and quite unphysiological) differences between input and output conditions are achieved.

DISCUSSION

DR. L. J. ARP: I am wondering, in the surviving animals, did you see any cases of pneumonia and, if so, how do you account for this?

DR. DANTOWITZ: Almost all of the animals survived the experiments, and they were sacrificed at the end of the experiment. I do not believe there were any cases of pneumonia.

DR. WEISSMAN: How big was the pressure drop you were talking about in your 450 cc/minute unit?

DR. DANTOWITZ: In general, it was close to 200 mm of Hg, perhaps a little less, e.g., 180.

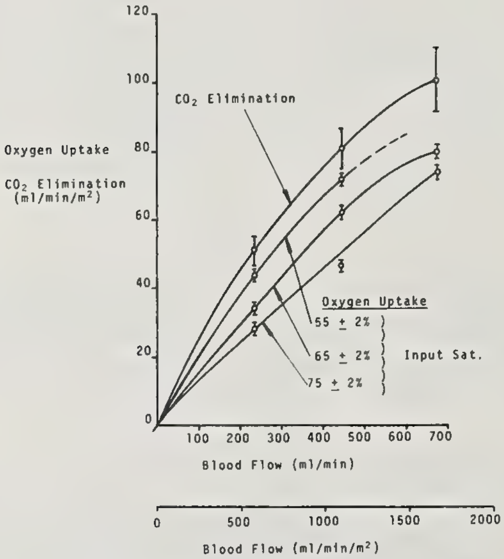

FIGURE 9. PLOT OF OXYGEN AND CARBON DIOXIDE TRANSFER RATES VERSUS BLOOD FLOW THROUGH THE OXYGENATOR. POOLED DATA FROM 5 EVALUATION PROCEDURES, SELECTING MEASUREMENTS MADE AT THREE DIFFERENT BLOOD OXYGEN SATURATIONS AT THE INLET OF THE ARTIFICIAL LUNG (55, 65 AND 75%). CORRESPONDING CO_2 TRANSFER RATES FROM THE SAME EXPERIMENTS. DATA POINTS INDICATION MEAN ONE S.E.M.

CHAPTER 29

DEVELOPMENT OF A CAPILLARY MEMBRANE BLOOD OXYGENATOR

R.P. deFilippi, F.C. Tompkins, J.H. Porter, G.W. Harris

Abcor, Incorporated, Cambridge, Mass.

Both experimental and theoretical work has been carried out in parallel during the current contract year. *In vitro* and *in vivo* evaluation of small oxygenators containing 100 silicone rubber capillaries was continued to establish a firm basis for scale-up to larger sizes. Oxygen exchange rates were in the range of 40 to 100 cc/min-m^2 depending on blood flow rate. In larger capillary bundles having a blood flow capacity of about 500 cc/min, the exchange rate was lower (30-50 cc/min-m^2), and the reason for this decrease with scale-up is presently being sought. *In vivo* hemolysis rates are quite low (HI≈0.16g hemoglobin/100 ℓ blood flow) compared to bubble and disc oxygenators (HI≥1.8), and platelet removal is minimal. A bundle of ten helically coiled capillaries was tested *in vitro* to evaluate the effect of secondary flow. Oxygen transfer rates were increased to as high as 120 cc/min-m^2. The latest literature data on oxygen and carbon dioxide transport in whole blood has been assimilated and incorporated into our existing computer program for predicting theoretical performance. Further *in vitro* and *in vivo* tests on 500 cc/min oxygenators is in progress in preparation for the design and construction of oxygenators of sizes up to those large enough for total bypass.

INTRODUCTION AND BACKGROUND

The need for a short-term extracorporeal blood oxygenator is well known. Two potential applications exist: a) total substitution for the lung function during open heart surgery, and b) partial assists for periods of acute reversible lung failure, as encountered in hyaline membrane disease, for example. The basic requirements for a blood oxygenator are:

1) High oxygen and carbon dioxide transmission rates are required for a high efficiency unit of minimum surface area.
2) Low priming volume is desirable for reduction of donor blood requirements.
3) Hydraulic resistance to blood flow must be minimized to reduce or eliminate the need for extracorporeal pumping.
4) Blood flow should be laminar, since turbulent flow is damaging to formed elements of the blood.
5) In a membrane oxygenator, oxygenating gas flow must be so distributed as to minimize gas side resistance to mass transfer and stagnation or channeling effects.

A design which satisfies the above requirements is a capillary membrane oxygenator, the capillaries being constructed of a gas-permeable membrane. The small diameter blood conduits give high blood phase mass transfer efficiency and low priming volume per unit of membrane surface area. Blood trauma is minimized by elimination of blood/gas interfaces, and the capillary concept allows completely laminar flow in low shear fields. By using a large number of capillaries in parallel, a low pressure drop is achieved.

During the first year's program, blood oxygenators containing three capillaries were studied *in vitro* to determine the effect of capillary diameter and wall thickness. These results were then used as the basis for scaling-up to 100-capillary bundles. Extensive evaluation of this size bundle was carried out both *in vitro* and *in vivo*. Effects of gas side configuration and non-thrombogenic surface treatments on mass transfer were investigated. Operating experience showed that efficient, low volume units could be built based on the capillary concept. Initial data indicated that carbon dioxide transfer might be the limiting factor in oxygenator design.

A mathematical model of the capillary bundle oxygenator was derived, based on the well known Graetz correlation for heat transfer in a tube. This correlation was modified to account for both mass transfer resistance in the blood phase and diffusional resistance in the membrane, but a negligible gas-phase resistance was assumed. The Graetz correlation suggests that data be plotted in terms of two characteristic dimensionless system parameters, the Sherwood number and the Graetz number. The Sherwood number is the ratio of the convective mass transfer rate to the diffusional mass transfer rate in the liquid, and the Graetz number represents the ratio of characteristic times for diffusion and convection and is proportional to flow rate. The advantage of such a correlation is that, by using these dimensionless groups, all data for small and large capillary bundles may be plotted on the same curve. This gives an excellent guide for scaling-up to full-scale bundles, which has been the primary objective of the present year's work. It also gives a basis for comparison between the theoretical and measured oxygen transfer rates.

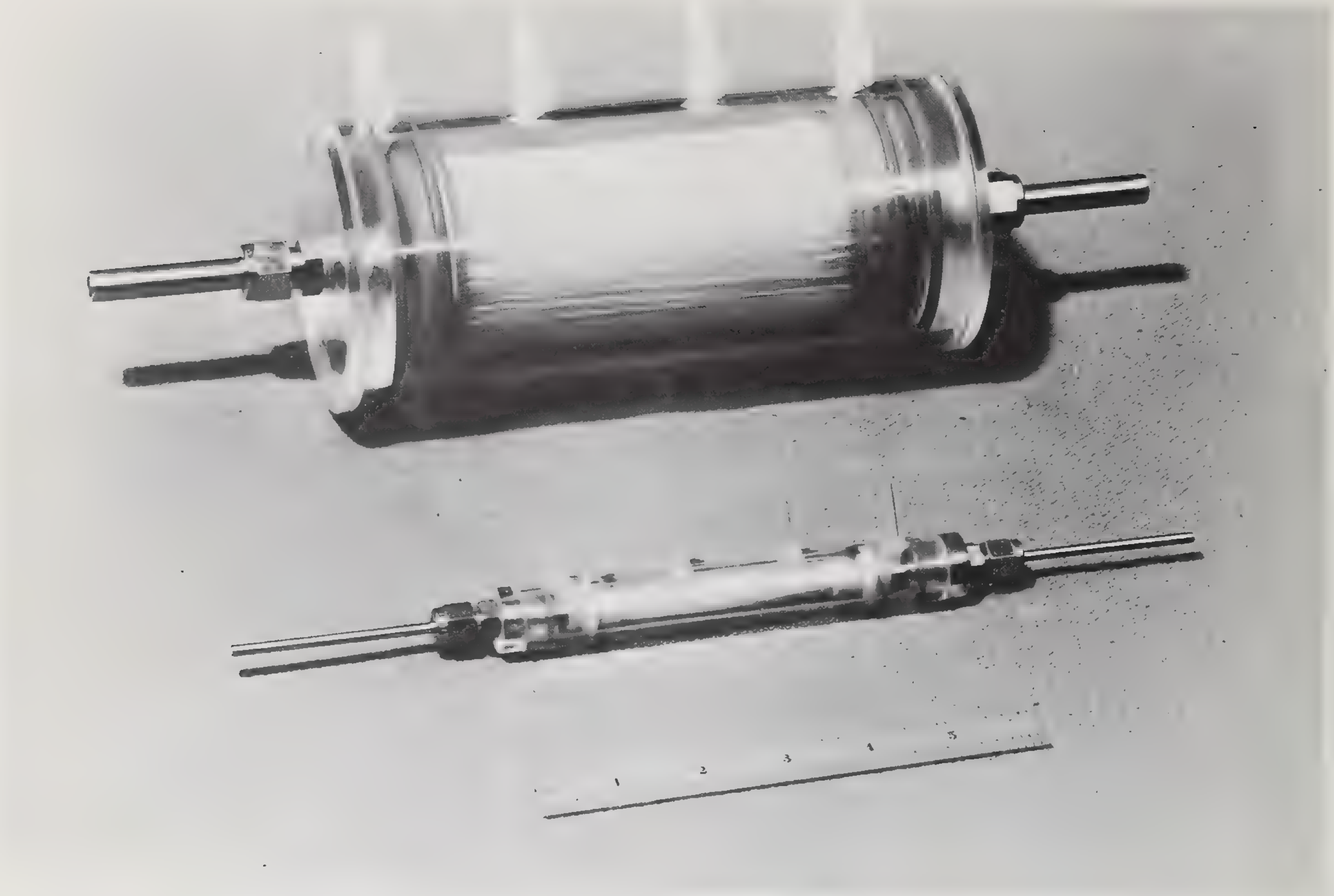

FIGURE 1. 10 CC/MIN AND 500 CC/MIN CAPILLARY MEMBRANE BLOOD OXYGENATOR.

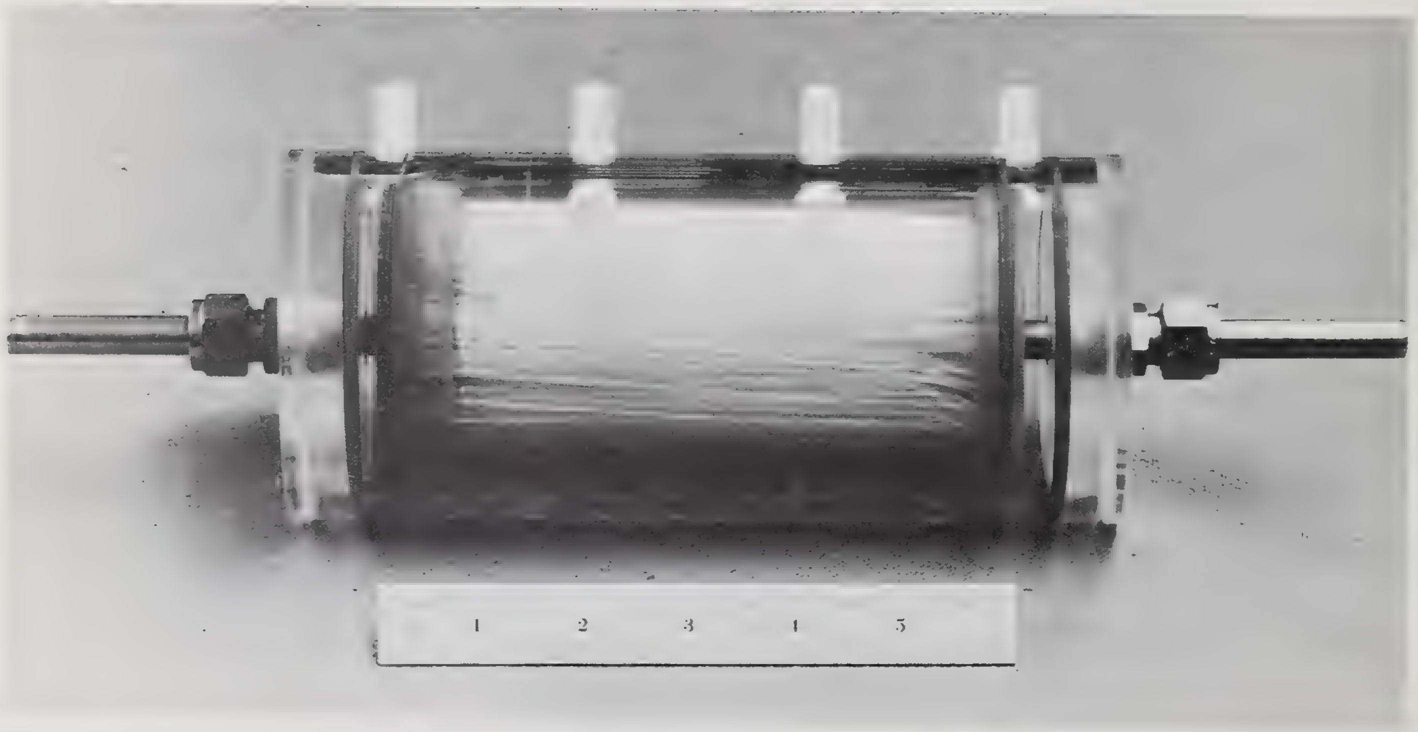

FIGURE 2. 500 CC/MIN CAPILLARY MEMBRANE BLOOD OXYGENATOR.

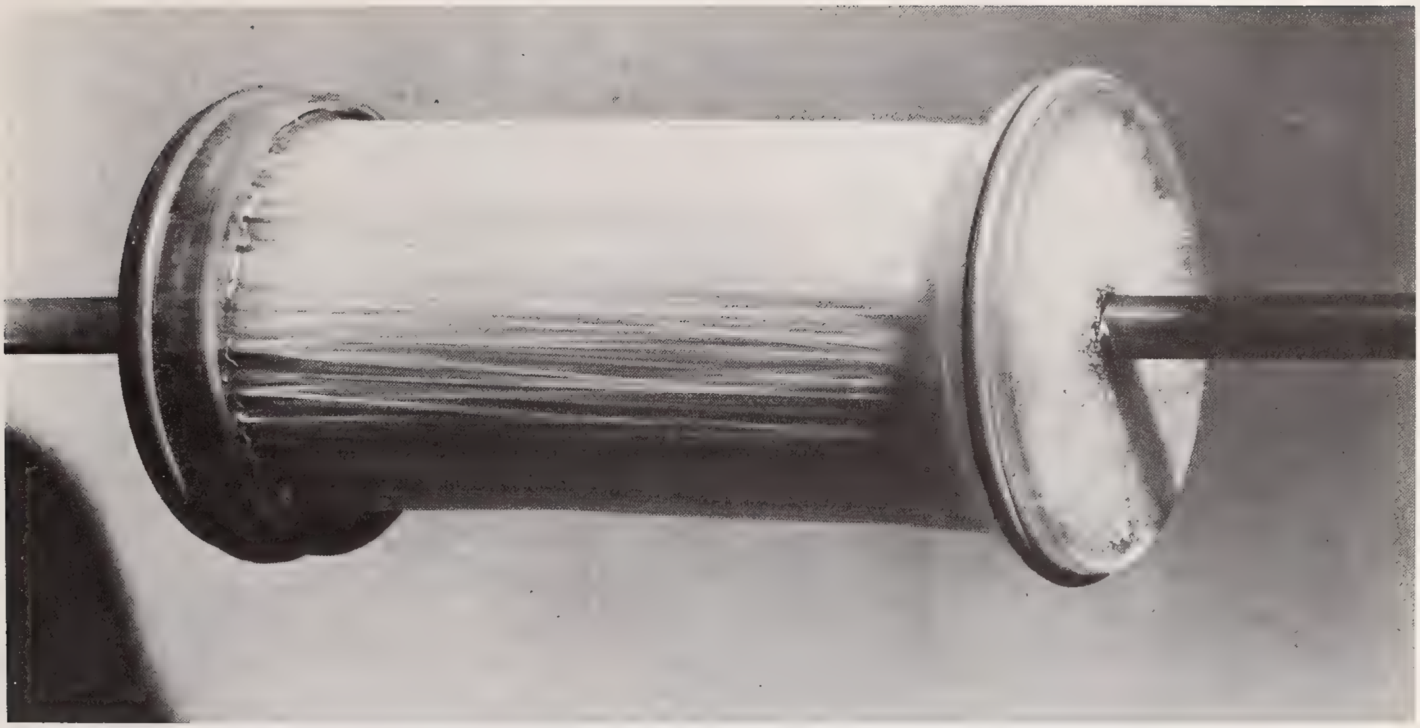

FIGURE 3. CLOSE-UP VIEW OF CAPILLARY BUNDLE FOR 500 CC/MIN OXYGENATOR.

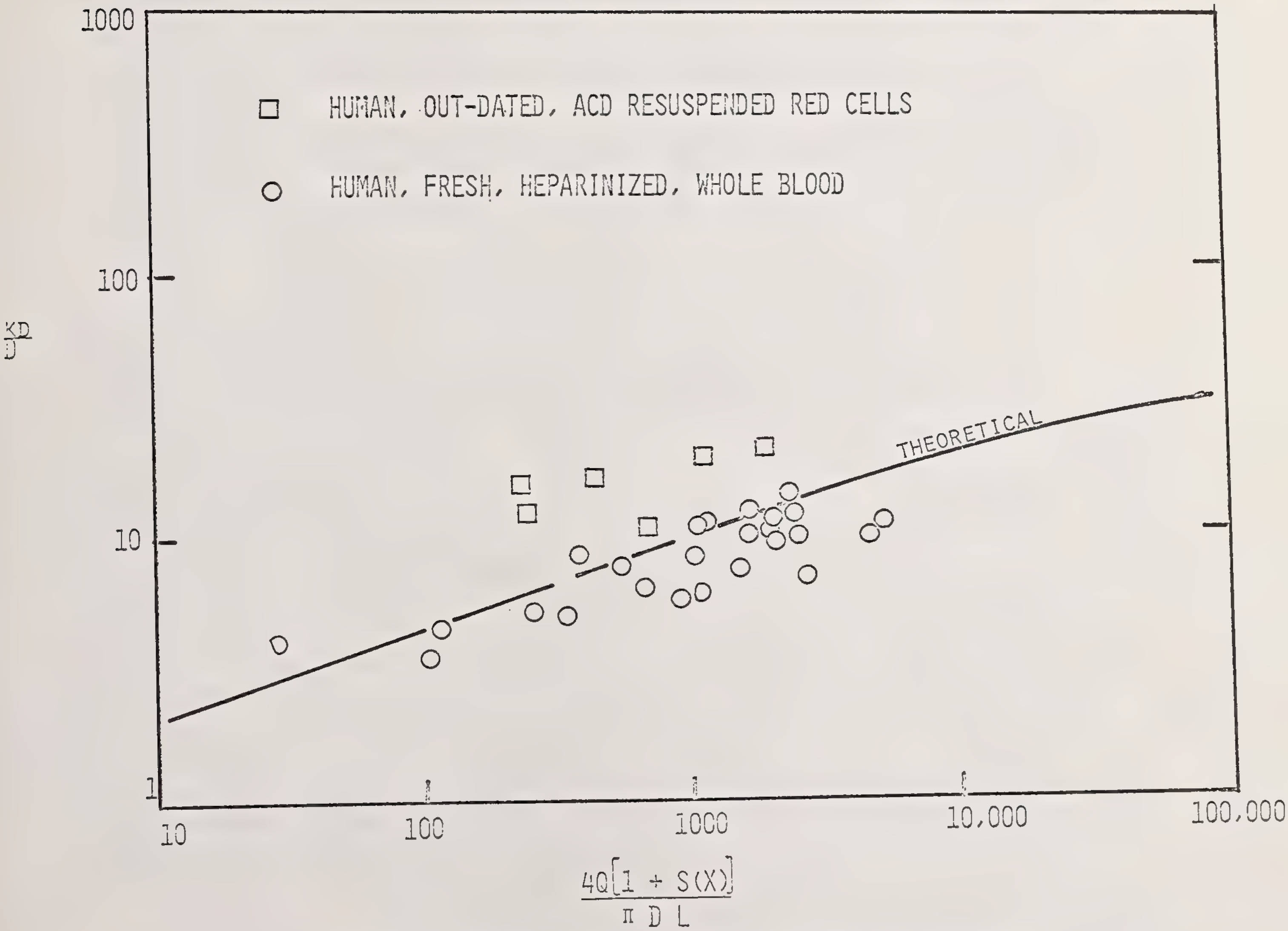

FIGURE 4. IN VITRO OXYGEN TRANSFER IN 100-CAPILLARY OXYGENATORS.

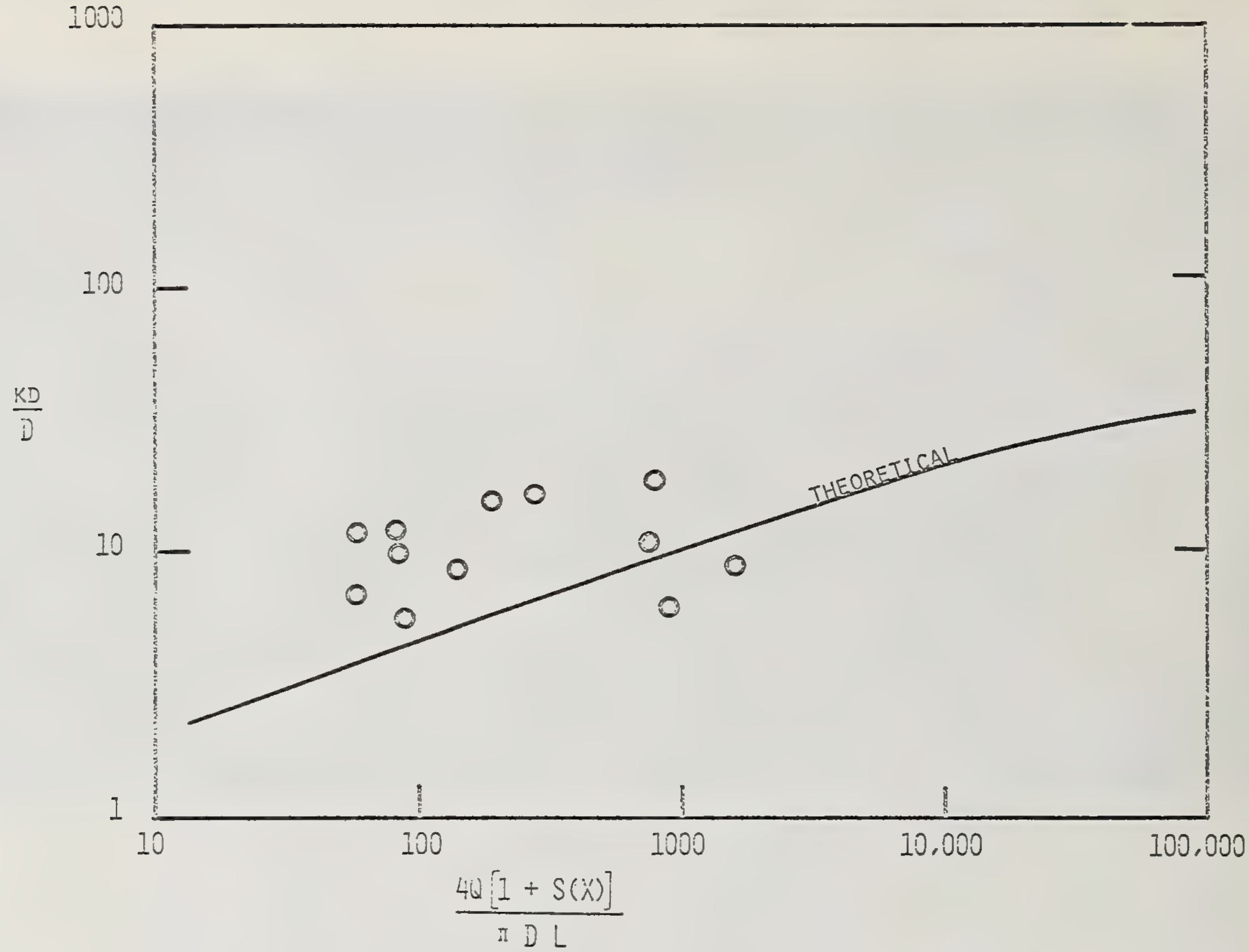

FIGURE 5. IN VITRO OXYGEN TRANSFER IN 100-CAPILLARY OXGENATORS.

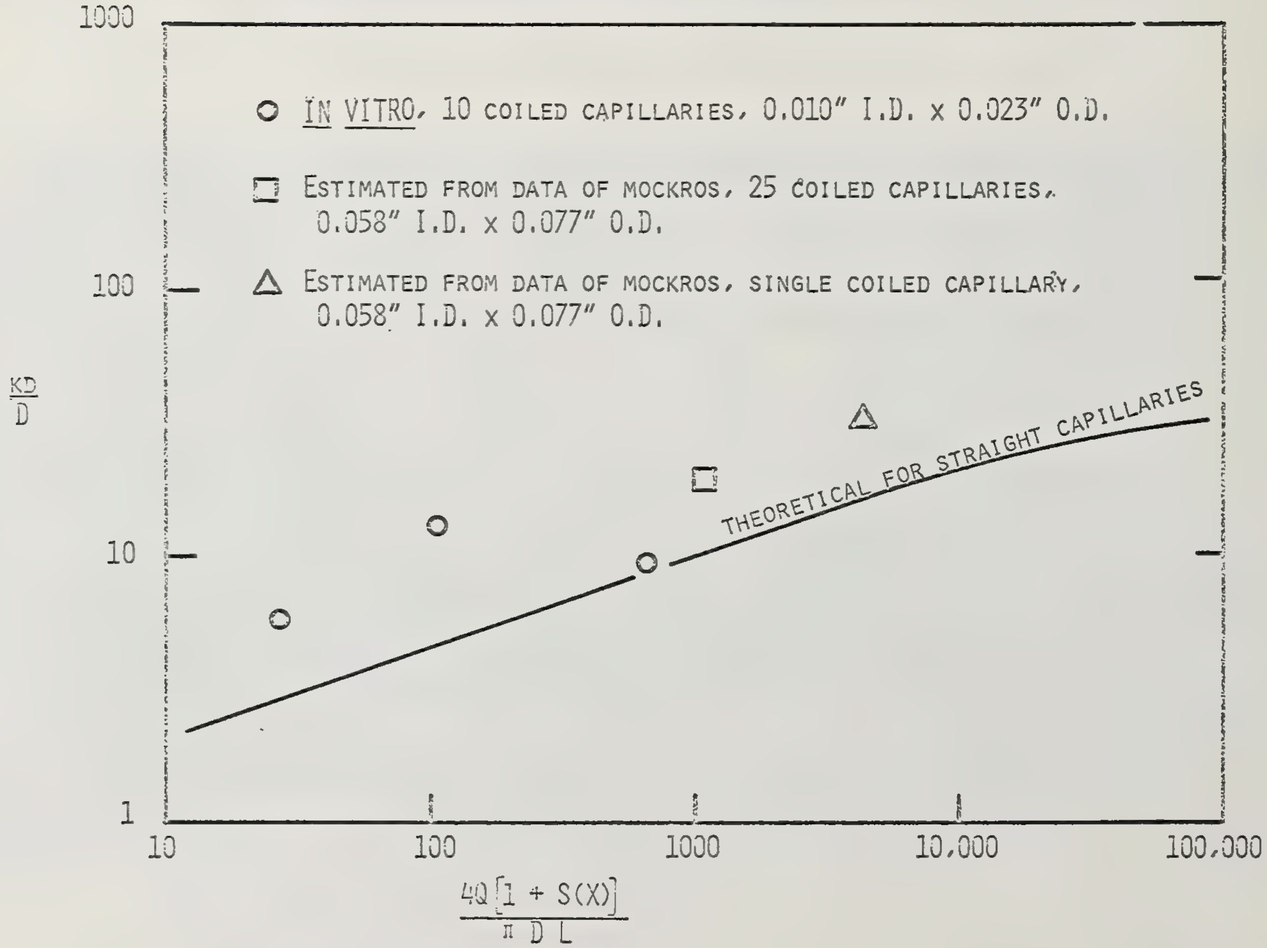

FIGURE 6. EFFECT OF SECONDARY FLOW ON OXYGEN TRANSFER IN COILED CAPILLARIES.

TABLE 1

CHARACTERISTICS OF INTERMEDIATE-SCALE BLOOD OXYGENATOR

Blood Flow	300-500 cc/min
Oxygen Partial Pressure	50 mm Hg in
	100 mm Hg out
Priming Volume Including Headers	130 cc
Carbon Dioxide Partial Pressure	50 mm Hg in
	40 mm Hg out
Hydraulic Pressure Drop	80 mm Hg
Number of Capillaries	4,600
Active Length	10 cm
Capillary Dimensions	280 μ I.D. x 625 μ O.D.

The additional design constraints are the hydraulic resistance equation for laminar flow in parallel capillaries and the carbon dioxide material balance equation with the requirement that the pCO$_2$ must be reduced from 50 mm Hg to 40 mm Hg.

Figure 7 shows mass transfer data obtained *in vitro* with a 500 cc/min oxygenator. The data fall on a line whose slope agrees quite well with the theoretical prediction, but whose vertical position is somewhat below the theoretical line, as was the case with the smaller bundles. It is apparent that the mass transfer efficiency per unit area decreases somewhat as the number of capillaries is increased.

These 500 cc/min oxygenators were then tested *in vivo* on dogs, and the results are shown here also. One can see that the mass transfer rates are still quite close to those predicted by theory; however, in this case there is considerably more scatter in the data. In particular, one of the bundles seems to give higher mass transfer rates than the other one. Some clotting and leakage occurred in this bundle, however, and there may have been an error in the estimate of the effective surface area used in the calculations. It is probable that the lower points best represent the actual oxygen transfer rate.

These bundles were run in a veno-arterial mode with a roller pump providing blood flow through the unit. Hemolysis rates were measured in the second bundle and gave an increase in plasma hemoglobin of about 3 mg %/hr, approximately 2 mg %/hr of this being caused by the roller pump itself. From these rates, one can calculate a hemolysis index, defined as $V(dC/dt)/Q$. The oxygenator has a hemolysis index of approximately 0.2 (g plasma hemoglobin formed/100 ℓ blood flow) which is considerably lower than the hemolysis indices of one to two g/100 ℓ that one measures in bubble and disc oxygenators. It is also encouraging to note that the platelet count did not decrease during the six-hour run. Quite recently, a 24-hour animal test was successfully completed. Data are summarized in Table 2. Analysis is not completed, however it is evident that constant transfer rates were achieved over this run.

TABLE 2

SUMMARY OF 24-HOUR *IN VIVO* TEST

Elapsed Time Hours	Blood Flow, cc/min	pO$_2$, mm Hg		pCO$_2$, mm Hg		Hematocrit, Volume Per Cent	Platelet Count, No. Per mm^3	White Cell Count No. Per mm^3
		V	A	V	A			
0	---	-	-	-	-	-	304,000	8,500
1	300	40	94	28	23	44	259,000	1,400
2	400	53	128	31	27	45	209,000	4,400
3	400	53	91	29	25	44	201,000	5,500
9	400	-	-	29	24	45	315,000	16,100
13	400	-	-	24	23	44	265,000	14,200
17	400	-	-	30	21	42	---	---
22	400	46	118	-	-	40	---	---
23.5	300	39	85	38	37	40	164,000	14,000
24	400	43	74	43	37	-	---	---

AN OXYGENATOR FOR TOTAL BYPASS

Based on the *in vitro* and *in vivo* data obtained from the 100-capillary bundles and on the larger 500 cc/min bundles, a 5 liter/min capillary bundle has been designed. The characteristics of this oxygenator are shown in Table 3.*

*NOTE: As of this writing, no data are available on this oxygenator.

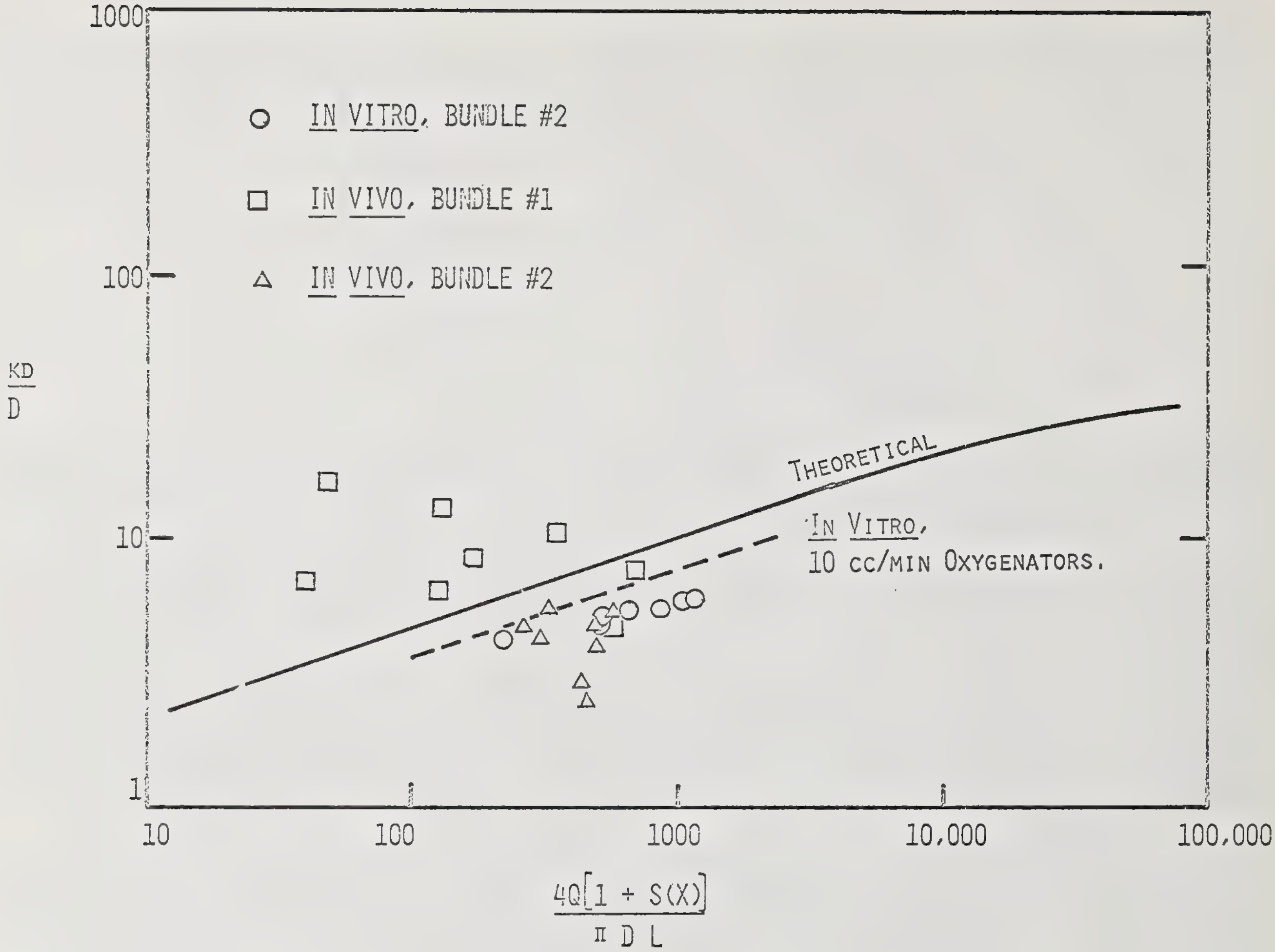

FIGURE 7. OXYGEN TRANSFER IN 500 CC/MIN OXYGENATORS.

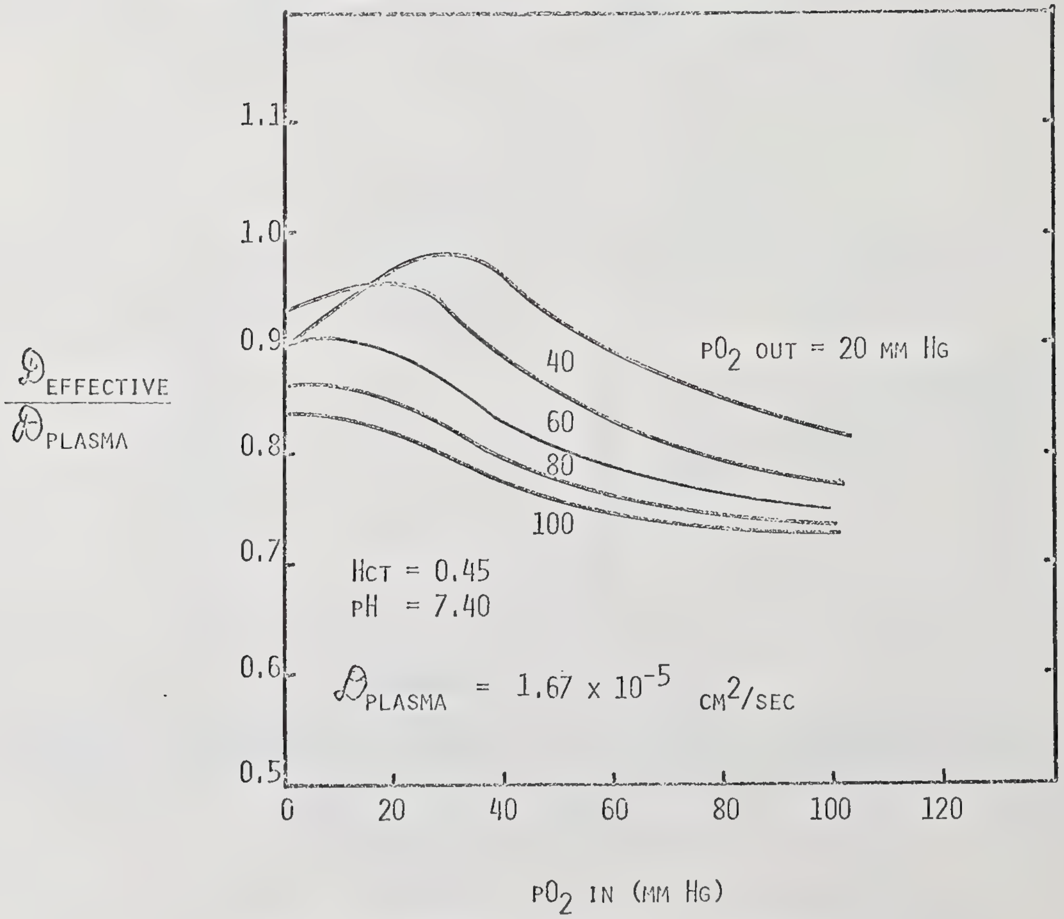

FIGURE 8. EFFECTIVE OXYGEN DIFFUSIVITY IN WHOLE BLOOD.

The first figure shows a 100-capillary bundle and a 4,600-capillary bundle which has the capacity for approximately 500 cc/min of blood flow. A 5 liter/min blood oxygenator for total bypass would contain approximately ten times as many capillaries as the larger bundle shown here. The capillaries are made of silicone rubber and have an inside diameter of 280 μ ± 13 and an outside diameter of 625 μ ± 25. Figures 2 and 3 show other views.

MASS TRANSFER IN 100-CAPILLARY BUNDLES

I would now like to discuss some of the interesting findings of the early part of this second year's work. The first *in vitro* data had been obtained using a synthetic blood made by resuspending outdated ACD packed red cells in isotonic saline. It was decided that some of these measurements should be repeated at the 100-capillary level using fresh whole heparinized human blood to more closely simulate the clinical situation. Figure 4 shows a comparison of data obtained using fresh heparinized blood and ACD blood. These data are presented in terms of the Graetz plot mentioned earlier. The Sherwood number is plotted on the ordinate, this being the mass transfer coefficient times the capillary diameter divided by the oxygen diffusivity. On the abcissa is plotted the Graetz number which is four times the flow rate per tube times the quantity one plus the chord slope of the oxyhemoglobin saturation curve, this quantity divided by pi times the diameter of the capillaries times the length of the capillaries. Points lying higher on the graph represent higher oxygen transfer rates. Points lying farther to the right represend data taken at higher flow rates. The solid line shown on the graph represents the computer solution to the mathematical model derived for oxygen diffusion through silicone rubber capillaries into whole blood. It is obvious from this figure that mass transfer into ACD blood appears to be more rapid then into fresh heparinized blood. Data by Darling and Roughton suggest that the high transfer rates to ACD blood are only apparent. They found that in buffered hemoglobin solutions containing known amounts of methemoglobin (a product formed from hemoglobin during the natural aging process in stored blood), the hemoglobin oxygen saturation curve was shifted toward higher saturations at lower PO_2 values. The presence of methemoglobin is not accounted for in the analysis, and may be significant in outdated red cells (at least three weeks old), causing higher apparent efficiencies to be calculated when the normal saturation curve is used. Because outdated ACD red cells were used, it is possible that a certain amount of hemoglobin had changed to methemoglobin and caused the high apparent transfer rates.

The recent data obtained with whole blood lend support for the theoretical prediction, although the measured transfer rates are somewhat lower than the predicted ones.

Figure 5 shows similar data taken *in vivo* with 100-capillary oxygenators using dogs. The *in vivo* oxygen transfer rates are higher than those measured with the fresh heparinized blood *in vitro*. There are no apparent reasons for this difference. However, it should be remembered that the oxygen saturation curve used for calculating Sherwood numbers *in vivo* is based on human blood, whereas, the *in vivo* measurements were made on dog blood. Any difference in oxygen saturation characteristics between these two bloods would cause an apparent difference in oxygen transfer rates. It is encouraging to note that the mass transfer data most typical of clinical situations, namely, that taken on fresh whole heparinized human blood, agree fairly closely with the theoretical prediction.

SECONDARY FLOW EFFECTS

The major resistance to mass transport in most membrane oxygenators lies in the blood phase, rather than in the membrane. In a capillary membrane oxygenator this mass transfer rate can be increased by inducing secondary flow inside the tubes. This causes a rapid turnover of the highly oxygenated laminar boundary layer into the bulk of the blood. One way of inducing this kind of secondary mixing process is to coil each tube into a helix with a ratio of helix diameter to tube diameter of about ten, a theoretically optimum value (2, 3). This was done in an Abcor bundle containing ten capillaries, and oxygen transfer was measured *in vitro*. The results are shown in Figure 6. They indicate that transfer rates two or three times as large as those observed in straight tubes can be obtained. These data agree with Sherwood numbers estimated from data published previously by Mockros using helical coils.

Unfortunately, it would be difficult and expensive to fabricate a compact oxygenator containing many coiled capillaries with small helical diameters. Thus, in spite of improved transfer rates, this approach does not appear promising.

MASS TRANSFER IN 500 CC/MIN OXYGENATORS

Table 1 lists the dimensional characteristics of the 500 cc/min oxygenator. It was designed based on carbon dioxide transfer being limiting and using a carbon dioxide transfer rate of 80 cc/min/m^2, which is typical of the rates obtained in the small bundles.

TABLE 3

DESIGN FOR 5 ℓ/MIN CAPILLARY BLOOD OXYGENATOR

REQUIREMENTS	
Blood Flow - 5 ℓ/Min	
Oxygen Partial Pressure	50 mm Hg in 90 mm Hg out
CO_2 Partial Pressure	50 mm Hg in 40 mm Hg out
CHARACTERISTICS	
Number of Capillaries	43,000
Active Length	10 cm
Priming Volume in Capillaries	450 cc
Priming Volume in Headers	750 cc
Hydraulic Pressure Drop	80 mm Hg

DIFFUSIVITY OF OXYGEN IN WHOLE HUMAN BLOOD

One of the most important parameters needed for the Graetz correlation is the diffusivity of oxygen in blood. We have derived a theory which predicts this diffusivity over a wide range of pO_2, hematocrit, pH, and temperature. Theory combines the work of Buckles[8] and Keller[4], and the data of others[5-7,9]. Oxygen is transported by ordinary diffusion through plasma both inside and outside the red cell. In addition, oxygen is transported from one side of the red cell to the other in the form of oxyhemoglobin. The hemoglobin-oxyhemoglobin equilibrium has been found to be rapid compared to oxygen diffusion across the cell wall or oxyhemoglobin diffusion through the cell.

The result of calculations for typical physiological conditions are shown in Figure 11.

SUMMARY

In summary, capillary membrane oxygenators have been completely characterized with respect to oxygen transfer up through the 500 cc/min size both *in vitro* and *in vivo*. In general, the oxygenation rate is slightly lower than that predicted by an analogy of the Graetz correlation. No problems have been encountered in scaling up to this level. These data have been used for the last ten-fold scale-up to a 5 ℓ/min oxygenator for total bypass. Data on this oxygenator will be obtained by the end of the second contract period. Also, more complete CO_2 transfer data will be obtained.

REFERENCES

1. Darling and Roughton, *Amer. J. Physiol.*, *137*, 56 (1942)
2. Eisman, M.M., and Mockros, L.F., *21st Ann. Conf. of Eng. in Med. and Biology*, Vol. 10, p. 12.3 (1968)
3. Weissman, M.H., and Mockros, L.F., submitted to *J. Eng. Mech. Div., Proc. ASCE*.
4. Keller, K.H., and Friedlander, R.K., *J. Gen. Physiol.*, *49*, 663 (1966).
5. Adams, L.R., and Fatt, I., *Respiration Physiology*, *2*, 293 (1967)
6. Moll, W., *Respiration Physiology*, *1*, 357 (1966)
7. American Physiological Society, *Handbook of Physiology*, *I*, #III, Williams and Wilkins, 1964, p. 767
8. Buckles, R.G. "An Analysis of Gas Exchange in a Membrane Oxygenator," Ph.D. Thesis, Chem. Eng., M.I.T. (1966)
9. LaForce, R.C., and Fatt, I., *Tr. Faraday Soc.*, *58*, 1451 (1962)

DISCUSSION

DR. REAM: We have a short time available for questions.

DR. EBERHART: In the abstract it was mentioned that on the larger scale device, the oxygen exchange rate was lower, and the reason for the decrease with scale up is presently being sought. Could you comment on that please?

DR. TIMMINS: The oxygen exchange rate on the larger device ranged from numbers in the neighborhood of 30-35 up to about 50-55. Based on our in vitro and in vivo work with the smaller scale devices and our theoretical work, we have reason to believe that we should be able to get somewhat higher exchange rates than this, perhaps in the range of 80.

DR. EBERHART: Is this due to circulating the oxygen around the tubes?

DR. TIMMINS: It could be due to that, and we are looking specifically at the question of whether, in the larger device, there are occluded tubes where the surface is not available for exchange and very shortly we will be able to report on these studies.

DR. BIXLER: Dr. Timmins, we were struck by the relative insensitivity of your apparent Sherwood numbers to changes in Graetz number. I realize it should be only a cube root dependence and the scatter of the experimental data tends to wash this out, but it did seem that your Sherwood numbers were staying approximately constant in both your early in vitro and particularly in your in vivo results. I do not have an explanation for this behavior, but perhaps you could amplify on one point: Did you change the Graetz number in any way other than by changing blood flow rate? Have you looked at shorter tubes or different diameter tubes?

DR. TIMMINS: We have looked at some small variations in length and we have looked at a substantial variation in diameter, ranging from the smallest diameter tested of about 5 mils, which was a material other than silicone rubber, up to a 50-60 mil diameter, and over that range, the data did correlate quite well with the Graetz plot. On the figure which I showed for the intermediate scale results, there was a dashed line which represented the best fit to all of the data that we obtained with the small scale devices. It did have the same slope that one would expect from the theoretical curve.

DR. LAIRD: Could you tell me what the helix radius/tube radius ratio was in the experiments in which you attempted to enhance transport with secondary flow?

DR. TIMMINS: Yes, the ratio of helix radius to tube radius for these experiments was 10. The data of Mokros was for about 10, I think it was actually 12, but it was right in that range. Above that ratio, the enhancement effect drops off substantially and below that it improves.

DR. PETROVICK: Did you conduct any flow pattern or profile measurements at the input of the header and relate these to clotting or turbulence-related clotting?

DR. TIMMINS: We have done dye-injection tests to work out the flow patterns, both in the headers and also down the bundle of tubes. We have seen no substantial areas of turbulence or high vorticity, and so we don't really feel this to be a major problem. We are looking at the introduction of the blood into the header tangentially as well as head on; we have had good luck with this in another device that we have been working on.

DR. REAM: Thank you, Dr. Timmins.

CHAPTER 30

HOLLOW FIBERS FOR USE IN MEMBRANE OXYGENATORS

B. J. Lipps, W. E. Skiens, E. A. McLain
and P. D. Oja

Dow Chemical Company, Walnut Creek, California

The object of this study was to produce and evaluate hollow fiber capillaries prepared from a variety of synthetic polymer materials for potential use as membrane oxygenators in artificial heart devices. Commercially available gas-permeable capillaries are unsuitable for inclusion in an operable membrane oxygenator because of their: 1) low percent open cross-section area, 2) large internal diameter, and 3) prohibitive cost. The gas permeabilities and predicted ease of hollow fiber spinning of the selected materials were initially evaluated in flat membrane form. The polymers studied include polycisisoprene, poly-4-methylpentent-1, polybutadiene, poly (propylene co-ethylene), poly (butadiene co-styrene) polyisobutylene, poly (ethylene co-octene) and an experimental silicone rubber. The most promising of those materials were selected for conversion into hollow fiber form. Hollow fibers ranging in size from 30 to 300μ I.D. with 40-65 percent open cross-sectional area have been successfully prepared from: 1) poly-4-methylpentene-1, 2) modified poly-4-methylpentene-1 and 3) the experimental silicone rubber. Gas permeability measurements indicate that these fibers have respectively 1/20, 1/4, and 2/3 the oxygen and carbon dioxide permeability of Silastic membranes. Good *in vitro* blood compatibility has been reported for the modified poly 4-methylpentene-1.

The object of this study was to produce and evaluate hollow fiber capillaries prepared from a variety of synthetic polymer materials for potential use as membrane oxygenators in artificial hearts. Commercially available gas permeable capillaries are unsuitable for inclusion in an operable membrane oxygenator because of their: (1) low percent open cross-sectional area, (2) large internal diameter, and (3) prohibitive cost. Hollow fiber materials studied included polycisisoprene, poly-4-methylpentene-1, polybutadiene, poly(propylene-co-ethylene), poly(butadiene-co-styrene), polyisobutylene, poly(ethylene-co-pentene), and an experimental silicone rubber.

The program has been divided into the following sections:

1. Material Acquisition and Construction of Permeability Measuring Apparatus
2. Membrane Preparation and Initial Permeability Evaluation
3. Development of More Permeable Poly-4-Methylpentene-1 Membranes
4. Hollow Fiber Spinning and Permeability Evaluation
5. Preliminary Evaluation by NHI of Hollow Fibers and Membranes

GAS PERMEABILITY MEASURING APPARATUS

A modified Dow Gas Permeation Cell and the ancillary equipment were constructed for the measurement of flat membrane permeabilities. Gas permeabilities were measured according to the basic method outlined in ASTM Designation D-1434 (1962 Revision). The gas transmission rate with this cell was determined from measurements of pressure change and subsequent calculation of the volume of gas transmitted through the membrane from a chamber of gas at a specified temperature and essentially constant pressure (driving force).

The pressure change was measured and recorded with a Statham Transducer and Van Lab Recorder. The membrane permeability was calculated (utilizing a computer program) by means of a least squares slope of the logarithm of the relative driving force versus time plot. Silastic membrane gas permeabilities measured with this system have agreed well with literature values.

Hollow fiber loop cells were substituted for the modified Dow Cell to measure the gas permeability of hollow fibers. The open ends of a loop of hollow fiber were potted with an epoxy resin and the cured resin cut with a sharp knife to provide a tube sheet. The fiber loop and tube sheet were then inserted in a copper tube to provide a test cell. This loop cell easily withstood pressures far in excess of the 15 psi driving force applied during the permeability test. All permeability measurements were made at 37°C.

MEMBRANE PREPARATION - INITIAL SCREENING OF PROMISING MATERIALS

Eight membrane materials were selected for initial membrane screening studies as potential gas permeable hollow fibers primarily because of their reported oxygen permeability relative to silicone rubber (1). Each material appeared to be capable of being spun into hollow fibers but with varying degree of spinning equipment modification. A summary of the materials which were screened and the membrane preparation data is listed in Table 1. The results of these screening studies are presented in Table 2.

TABLE 1

MEMBRANE MATERIAL AND PREPARATION DATA

Material	Supplier	Trade Name	Melt Press[a] Temp. °C.	Remarks
Poly(dimethylsiloxane) (Medical Grade Silastic)	Dow Corning	Silastic Rubber	---	Well-known material
Silicone rubber (1965-X 30738)	Dow Corning	Experimental Material	135	Possibly low level of amines
(1968-X 30738)	Dow Corning		150	
Polybutadiene	Goodyear Tire & Rubber Company	Budene 501	230	
Poly(butadiene-co-styrene) (80-85% butadiene)	Shell Oil Co.	Shell S 7705	210	
(75.5-77.5% butadiene)	Goodrich-Gulf Chemical, Inc.	Ameripol 1502	230	
Polycisisoprene	Goodyear Tire & Rubber Company	Natsyn 400 Natsyn 410	230 230	
Poly-4-methylpentene-1	I.C.I.	TPX	260	Additional information on blood compatibility in the text
Poly(ethylene-co-propylene)	Enjay Chemical Company	Vistalon 404 Vistalon 4504 Vistalon 4608 Vistalon 3708	230 230 230 230	
Poly(ethylene-cooctene-1) (6.5% octene)	The Dow Chemical Company	Experimental Resin	210	
Polyisobutylene	Enjay Chemical Company	Vistinex L 80 Vistinex L 140	230 230	

a) All membranes were cooled at 150°C./minute

TABLE 2

SUMMARY OF MEMBRANE PERMEABILITY MEASUREMENTS WITH UNMODIFIED MATERIALS

Material	Permeability $\left(\frac{\text{cc (STP) cm}}{\text{cm}^2\text{ sec. cm Hg}} \times 10^9\right)$		Permeability Relative to Silastic		Predicted Ease of Hollow Fiber Spinning
	Oxygen	Carbon Dioxide	Oxygen	Carbon Dioxide	
Poly(dimethylsiloxane) (Medical Grade Silastic)	64	253	1	1	—
Experimental Silicone Rubber (1965-X 30738)	25	119	.39	.47	+
Experimental Silicone Rubber (1968-X 30738)	36	155	.55	.61	+
polybutadiene	14	79	.22	.31	- -
poly (butadiene-costyrene) (80-85% butadiene)	4.4	25	.070	.10	-
poly (butadiene-costyrene) (75.5-77.5% butadiene)	3.4	18	.053	.071	-
polycisisoprene	5.7	23.5	.089	.093	- -
poly-4-methylpentene-1 (TPX)	3.6	9.4	.055	.037	+ +
poly (ethylene-copropylene)					
Vistalon 404	4.4	16	.069	.063	-
Vistalon 4505	4.2	16	.068	.063	-
Vistalon 4608	3.4	13	.053	.051	-
Vistalon 3708	3.0	12	.047	.047	-
poly (ethylene-co-octene-1) (6.5% octene)	.6	1.9	.009	.008	+ +
polyisobutylene	.4	1.1	.006	.004	- -

The measured gas permeabilities of the unmodified, heat-molded materials are listed and compared to Dow Corning Silastic Medical-Grade Silicone Rubber. Each listed value represents an average of measurements with at least two different membranes with a maximum variation between samples of 20% of the average. These measurements substantiate for the most part the values reported by Salame.[1]

The predicted ease of hollow fiber spinning was attributed to each material as a result of the experience gained during heat molding of the membranes for permeability studies. This predicted ease of spinning is also presented in Table 2. A three plus (+++) rating was accorded the cellulose esters with which a great deal of spinning experience has been gained. A three negative (- - -) rating represents a definitely non-spinnable polymer without significant modification of the spinning system.

These screening studies indicated that poly-4-methylpentene-1, TPX®,* has the highest gas permeability of the two materials judged most easily spun into hollow fibers. The gas permeability of TPX® was found to be about 1/18 to 1/24 that of Silastic. Thus, TPX® was judged to have marginal gas permeability for inclusion into an acceptable size hollow fiber oxygenator. In contrast, the experimental silicone rubber had a gas permeability of about 55 to 60 percent that of Silastic. Studies indicated that this material was definitely spinnable but with somewhat more development effort than required for TPX.®

Both of these materials should be reasonably compatible with blood and were felt to be the most promising hollow fiber materials for the blood oxygenator, expecially if the TPX® permeability could be enhanced without jeopardizing its blood compatibility. TPX® has received FDA approval for use in contact with food and is being used in medical syringes which intimately contact blood.[2]

DEVELOPMENT OF MORE PERMEABLE TPX® MEMBRANES

The gas permeability of TPX® has been increased, as evidenced by membrane and hollow fiber measurements, by over 1000 percent through the inclusion of aqueous insoluble additives into the polymer matrix. The presence of these additives tends to reduce crystallinity and possibly provide diffusional paths of significantly higher transport rate through the swollen structure of the polymer. Amoco Indopol Polybutenes** and Dow Corning 200 Fluids have been studied as additives. These oils are known to be non-toxic, non-irritating, and find many applications in contact with food products. Silicone oil, 200 Fluid®, is the additive of choice because of its high inherent gas permeability. Thus, the object was to include as much silicone oil into the TPX® structure as is consistent with acceptable strength. Two techniques to accomplish this have been studied:

a. Hot melt blending of silicone oil and TPX® prior to membrane formation. It appears that at least one part of silicone oil can be blended with one part of TPX® by weight while retaining acceptable physical properties. The quantity of silicone oil which can be successfully incorporated into the structure decreases with increasing silicone oil molecular weight.

Extraction studies with saline solutions indicate no detectable leaching of the silicone oil from TPX® -silicone oil membranes. Similar in vitro extraction studies with human blood and one M^2 hollow fiber devices are underway. Blood compatibility studies conducted by a separate NHI contractor showed that the TPX® -silicone oil blend was more compatible with blood than either the TPX® alone or the TPX® -polybutene blend. These studies showed that the TPX® -silicone oil blend compares well in blood compatibility with some of the more promising materials yet tested.

b. Hot melt blending of polybutene oil with TPX® followed by a postfabrication exchange of the polybutene oil for silicone oil. This substitution may be accomplished either by extraction of the polybutene oil with xylene followed by replacement of xylene with silicone oil or direct leaching and replacement of the polybutene with silicone oil. With this approach, higher molecular weight silicone oil, such as Dow Corning 360 Medical Fluid-20 centistoke, can be incorporated into the TPX® structure.

The preferred TPX® -silicone oil blend appears to be about a one part TPX® to one part silicone oil of 10 centistoke viscosity. The oxygen and carbon dioxide permeabilities for this blend, as measured on membranes, are about 0.25 and 0.20 that of Silastic. However, hollow fibers produced from this blend had oxygen and carbon dioxide permeabilities of about 0.50 that of Silastic. The cause of this difference in measured gas permeabilities is under investigation and is thought to reflect differences in blending and melt cooling rates between the membrane and fiber forming systems. These increased gas permeabilities represent an improvement of from 500 to 1000 percent over the unmodified TPX® polymer. The tensile strength and tensile yield stress of this blend were found to be about 0.17 that of unmodified TPX®. The data from which these conclusions are drawn are presented in Tables 3 and 4. Table 3 presents the measured gas permeabilities for TPX® -silicone oil blends and for TPX® -L10-silicone oil blends in membrane form. Table 4 presents the results of stress-strain measurements on membranes of different TPX® blends.

* ICI America, Inc. - TPX® methylpentene polymer.

** Amoco Indopol L10 is the preferred polybutene.

TABLE 3

MEMBRANE GAS PERMEABILITIES

TPX-Silicone Oil Blends

Material & Blend Ratio (By Weight)	Melt Press. Temp. ^0C	Gas Permeability $\left(\frac{cc(stp)\cdot cm}{cm^2\ sec\cdot cm\ Hg} \times 10^9\right)$ O_2	CO_2
TPX	260	3.6	9.4
TPX:Silicone Oil (2 centistoke)(1:1)	190	19.5	39.5
TPX:Silicone Oil (2 centistoke)(1:4)	180	20.5	55.3
TPX:Silicone Oil (10 centistoke)(1:1)	230	15.4	36.0

TPX-Indopol L10 - Silicone Oil Blends

Material & Blend Ratio (By Weight)	Melt Press. Temp. ^0C	O_2	CO_2
TPX:L10:Silicone Oil (20 centistoke) (1:.75:.25)	210	12.1	37.6
TPX:L10:Silicone Oil (20 centistoke) (1:.5:.5)	190	15.6	47.6
TPX:L10:Silicone Oil (5 centistoke) (1:1.5:.5)	190	15.4	37.2
TPX:L10-Silicone Oil (5 centistoke) (1:1:1)	180	16.3	45.4
TPX:L10:Silicone Oil (5 centistoke) (1:.5:1.5)	210	17.9	49.0

TABLE 4

RESULTS OF STRESS-STRAIN MEASUREMENTS ON MEMBRANES[a]

Material & Blend (by Weight)	Tensile Strength (psi)	Tensile Yield Stress (psi)	Ultimate Elongation (%)
TPX	2958	3304	3.00
TPX:L10 (1:1)	658	597	8.75
TPX:L10 (1:2)	471	399	9.75
TPX:L10 (1:3)	256	253	7.25
TPX:Silicone Oil of 10 centistoke (1:1)	639	580	6.50
TPX:L10:Silicone Oil of 20 centistoke (1:0.5:0.5)	513	501	8.00
Experimental Silicone Rubber 1968-X30738	1402	No Yield Point	554.75

a) Average of Ten Measurements

Although the second technique studied to increase TPX® permeability, post exchange of L10 for silicone oil, introduces a fiber treatment step, this approach has the advantages of: (1) possible increased permeability over the resin blending approach and (2) the final fiber need only contain TPX® and higher molecular weight medical grade silicone oil. This additional fiber treatment step is automatable and should present no long-term operational difficulty. The preferred blend with this approach, as determined from membrane studies, is a TPX® - L10 blend of one part TPX® to two parts L10 with a post exchange of the L10 for 20 centistoke silicone oil. The post exchange of L10 produces a membrane about twice as permeable as the TPX® - L10 blend. The oxygen and carbon dioxide permeabilities for this post exchanged membrane is about 0.34 and 0.26 that of Silastic. These membranes have tensile strength and tensile yield stresses of about 0.10 that of TPX®. Measured gas permeabilities for the TPX® - L10 blends and the post exchanged membranes are presented in Table 5.

TABLE 5

MEMBRANE GAS PERMEABILITIES

TPX-Indopol L10 Blends

Material & Blend Ratio (By Weight)	Melt Press. Temp. °C	Gas Permeability $\left(\frac{cc(stp)\cdot cm}{cm^2\ sec\cdot cm\ Hg}\times 10^9\right)$	
		O_2	CO_2
TPX	260	3.6	9.4
TPX:L10 (1:.5)	230	7.8	22.2
TPX:L10 (1:1)	200	9.6	26.8
TPX:L10 (1:2)	190	11.0	33.0
TPX:L10 (1:3)	180	12.5	39.2
TPX-Indopol L10 Blends Exchanged with Silicone Oil			
TPX:Indopol-L10 (1:1). L10 Exchanged for Silicone Oil- 20 centistoke	190-200	14.6	43.5
TPX:Indopol-L10 (1:2) L10 Exchanged for Silicone Oil - 20 centistoke	180	22.3	66.3
TPX:Indopol L10 (1:3) L10 Exchanged for Silicone Oil - 20 centistoke	170-180	23.6	65.0
TPX:Indopol-L10 (1:1) L10 Exchanged for Silicone Oil - 10 centistoke	190-200	13.0	29.4
TPX:Indopol-L10 (1:1) L10 Exchanged for Silicone Oil - 5 centistoke	190-200	16.2	40.3

These two approaches to increased gas permeability have been extended to other poly α-olefins for comparison with TPX®. Brief studies of modified polyisobutylene and polyethylene membranes showed them to be appreciably less permeable than comparably extended TPX®. This indicates that the polymer structures, even in these highly swollen membranes, still greatly influence the gas permeability.

HOLLOW FIBER SPINNING AND PERMEABILITY EVALUATION

Hollow fibers have been successfully spun with the following materials: 1) TPX®, 2) TPX®: L10 (1:1)*, 3) TPX®: L10:Silicone Oil (5 csk)(1:0.5:0.5), 4) TPX®: Silicone Oil (10 csk)(1:1) & (1:1.5) and 5) experimental silicone rubber.

A listing of the fibers spun to date and their measured gas permeabilities are presented in Table 6. Table 6 also contains a comparison between the measured hollow fiber permeabilities and those measured for comparable membranes. With the three different TPX® blends good agreement exists between the hollow fiber and membrane permeabilities with the exception of the TPX®-silicone oil blend. The cause of this discrepancy is under investigation, as noted earlier. Except for the unmodified TPX® the fiber gas permeabilities are slightly higher than those measured with membranes. This increased permeability possibly results from the faster cooling rate with the hollow fibers, which favors decreased crystallinity.

The gas permeability of TPX® hollow fibers decreases with decreasing fiber size. Since the method of producing the different sized fibers is simply to draw the molten polymer at different rates, one immediately suspects that fiber orientation is increased with the smaller fibers causing a decrease in fiber permeability.

Table 7 lists a comparison of stress-strain measurements for hollow fibers and membranes. The fibers show about the same ultimate strength relative to TPX® as did the membranes.

Six samples of hollow fibers have been supplied to NHI for evaluation. Two 150 gram samples of 30μ I.D. and 45μ I.D. TPX® hollow fibers were supplied for evaluations. A few grams of 60μ I.D. TPX®-L10-silicone oil (1:0.5: 0.5) hollow fibers and three small samples of the experimental silicone rubber hollow fibers have been supplied for evaluation.

Samples of TPX® hollow fiber weaves have been prepared to study the influence of fiber twisting and filler spacing with 45μ I.D. fibers. These weave samples are presently under evaluation.

* Parts by weight

TABLE 6

COMPARISON OF HOLLOW FIBER AND MEMBRANE GAS PERMEABILITY

Material & Blend (by weight)	Hollow Fiber					Membrane		
	Spin Temp., ^{0}C	Ave. I.D., μ	Average Wall Thickness μ	Permeability $\left(\frac{\text{cc (STP) cm}}{\text{cm}^2\cdot\text{sec. cm Hg}} \times 10^9\right)$ O_2	CO_2	Melt Press. Temp. ^{0}C	Permeability $\left(\frac{\text{cc (STP) cm}}{\text{cm}^2\cdot\text{sec. cm Hg}} \times 10^9\right)$ O_2	CO_2
TPX	280	200	20	3.2	9.2	260	3.6	9.4
TPX	280	45	9	2.8	7.9	"	"	"
TPX	280	30	7.5	2.3	5.2	"	"	"
TPX:L10 (1:1)	230	300	50	11.5	29.2	190-200	9.4	26.8
TPX:L10:silicone oil (5 centistoke) (1:0.5:0.5)	235	400	62	22.1	60	200-210[a]	15.6	47.0
"	235	120	28	18.2	52.1	" "	"	"
"	235	60	20	16.5	49.0	" "	"	"
TPX: Silicone Oil (10 cstk.) (1:1)	230	190	40	40	130	200-210	15	36
Experimental	250	310	40	44	214	165-177[b]	36	155
Silicone Rubber: Silicone oil(20 cstk.)(9/1)	250	225	28	55	211	" "	"	"
	250	127	20	49	188	" "	"	"

a) Silicone Oil (20 centistoke)

b) Experimental Silicone Rubber only.

TABLE 7

COMPARISON OF STRESS-STRAIN MEASUREMENTS

Fiber and Membrane Material (Ratio of Plasticizer) Fiber Size	Ultimate Strength, % TPX Hollow Fibers	Membrane
TPX	100	100
TPX/Silicone Oil (10 cstk.) (1:1) 130 μI.D.	20	18
TPX/Silicone Oil (10 cstk.) (1:1.5) 130 μI.D.	8	-
TPX/Indopol L10 (1:1) 300 μI.D.	17	22
TPX/Indopol L10 (1:1.5) 200 μI.D.	6	-
TPX/Indopol L10 (1:2) 320 μI.D.	4	16
TPX/Indopol L10 (1:3)	-	8
TPX:L10:Silicone Oil of 20 cstk. (1:0.5:.05)	11	17

SUMMARY

The gas permeabilities and predicted ease of hollow fiber spinning of the selected materials were initially evaluated in flat membrane form. The polymers studied include polycisisoprene, poly-4-methylpentene-1, polybutadiene, poly(propylene co-ethylene), poly (butadiene co-styrene) polyisobutylene, poly(ethylene co-octene) and an experimental silicone rubber. The most promising of those materials were selected for conversion into hollow fiber form. Hollow fibers ranging in size from 30 to 300μ I.D. with 40-65 percent open cross-sectional area have been successfully prepared from : (1) poly-4-methylpentene-1, (2) modified poly-4-methylpentene-1 and (3) the experimental silicone rubber. Gas permeability measurements indicate that these fibers have respectively, 1/20, 1/4, and 2/3 the oxygen and carbon dioxide permeability of Silastic membranes. Good in vitro blood compatibility has been reported for the modified poly 4-methylpentene-1.

REFERENCES

1. Salame, M., "A Correlation Between the Structure and Oxygen Permeability of High Polymers". ACS Polymer Preprints, 8.
2. Modern Plastics, May 1967.

DISCUSSION

DR. deFILIPPI: I noticed in the data which you showed, comparing the permeability of hollow fibers against membrane for the extended TPS, i.e., the TPX extended with silicone oil, that while the O_2 permeability goes up by about a factor of three, the CO_2 permeability appears to stay the same if I read that chart right. Do you have any explanation for this?

DR. LIPPS: I don't believe that is so. The ratio between the O_2 and the CO_2 permeability appeared to remain constant. This is usually a good indication that you do not have pinhole leaks and we follow this very closely. The values were 40 and 130. Therefore, the actual ratio between the O_2 and CO_2 remained constant at about 3.

DR. BIXLER: Historically, microcrystalline polymers have been difficult to extend with oils or to externally plasticize, particularly with respect to long-term syneresis of oil, stress cracking, and problems of this nature. Now you reported to us that you have seen no silicone oil extraction in 24 hours of circulation. Was this through fibers by the way?

DR. LIPPS: Yes, this was through the fibers.

DR. BIXLER: I would caution you to look at long-term syneresis effects, i.e., slow exudation of the silicone oil, in your microcrystalline TPX polymers due to slow recrystallization. I would expect this to be most pronounced in your fibers since they appear to be lower in crystallinity than your flat sheets due to more rapid quenching from the melt.

DR. LIPPS: Yes, we have kept our eye on this, and we have observed samples for over six months now and have not noticed this phenomenon.

DR. BRUCK: I was wondering whether you have given any thought to studying copolymers in order to reduce the crystallinity of your system instead of using external plasticizers.

DR. LIPPS: We have. However, we have not found an acceptable system to date, and we have no data. An initial attempt to use copolymers was studied in the poly (ethylene co-octene) material.

CHAPTER 31

A HOLLOW FILAMENT FABRIC BLOOD OXYGENATOR

T. L. Williams, L. H. Bosher, T. Nakamura

Medical College of Virginia, Richmond, Va.

During the first contract year, we constructed and evaluated two models of the hollow filament fabric blood oxygenator. These demonstrated the expected mechanical and flow properties and the ability to oxygenate up to 1500 cc of canine blood per minute. Their capacity was severely limited by the low gas permeability of the only available hollow filaments (medium density polyethylene). Since then emphasis has been on obtaining more permeable hollow filaments. The criterion of relative permeability has been the ability to transmit CO_2 from within the filaments to the surroundings at a pCO_2 in the range 710 to 810 mmHg. This criterion was chosen because the venting of CO_2 is the really critical characteristic of any membrane oxygenator. An apparatus for measuring the permeation of CO_2 under those conditions has been developed. Hollow filaments from two types of polymers having much higher permeability than polyethylene were obtained. The first type, a methyl pentene, appears to have a permeability about six to eight times as great as polyethylene. Twelve samples based on this polymer, varying in inside diameter from 25 to 100 microns have been evaluated, and an optimum inside diameter of 60 μ selected. Such filaments are now being woven to fabric for evaluation in the oxygenators. The single sample of filaments made from a silicone copolymer appears to be about 25 times as permeable as the polyethylene. Work on improved spinning is underway. Further studies on cleaning and sterilizing procedures, and on blood trauma in the oxygenator are encouraging. An arteriovenous shunt with the small polyethylene oxygenator interposed was operated at flow rates of 1000-1400 cc per minute on dogs for four hours. Flow rate and pressure gradient were stable, plasma-hemoglobin remained very low (not over 5 mg%), other parameters showed no remarkable changes, saline washings of the oxygenator before each procedure were negative, blood cultures were sterile, the dogs survived.

INTRODUCTION

The objective of this study has been to design, construct and evaluate a membrane blood oxygenator which would have a large membrane area in a small overall volume, and would be free from many of the mechanical difficulties inherent in designs shown in the literature. The basic idea was to use as membranes the walls of capillary tubes through which oxygen would flow while blood would flow around and between them. This idea, of course, is not new, but other designs have used capillaries of 300 micra inside diameter and many feet long, while the present design would use many more capillaries with an inside diameter of some 50 micra and only a few inches long. To arrange the capillaries in a proper spacing, and hold them in position, they would be woven into a fabric, and many layers of such fabric would be stacked together to form the active element. These ideas are shown in the sketch in Figure 1. Note that the fabric is cut into squares, and the border of each square impregnated to seal the edges and to provide a gasket between layers. The present design is shown in Figure 2. When filled to its full capacity of 200 fabric sheets its height is 12 cm, its diameter is 20 cm, its calculated membrane area is 8.0 M^2 and its priming volume 350 cc.

The basic requirement of the project from the beginning was a source of permeable hollow filaments suitable for weaving and compatible with blood. The first experiments were done with fabric made from solid nylon monofilaments, to check on the mechanical design and hydrodynamic properties, and to detect any obvious blood damage. A supply of fabric woven from hollow polyethylene filaments was then obtained and was used in most evaluations of the two model oxygenators which were constructed. It was realized that the permeability of polyethylene is quite low compared with that of silicone rubber or even of Teflon, but it was sufficiently high to detect substantial oxygenation.

EXPERIMENTAL

The most pertinent data on performance are shown in Table 1. The first three experiments were done in vitro, with canine blood circulating through a laboratory oxygenator ventilated with 93% nitrogen, 7% CO_2, to "deoxygenate" the blood, add CO_2 and deliver "venous" blood to the hollow filament oxygenator. Blood samples were taken simultaneously proximal and distal to the fabric oxygenator for measurement of per cent saturation and blood gases. Oxygen transmission was calculated from the change in per cent saturation and the known whole blood hemoglobin. It is apparent that the oxygen transmission depends on the saturation of the incoming blood. In the first two runs, disc oxygenators were used for "deoxygenation," and were insufficient. In the third, a Bentley

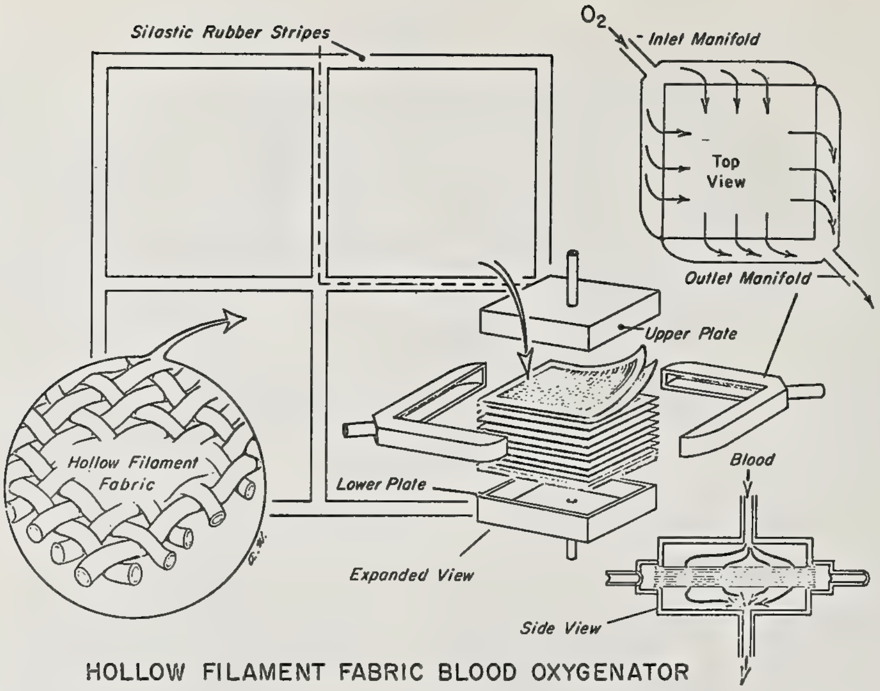

FIGURE 1. HOLLOW FILAMENT FABRIC BLOOD OXYGENATOR.

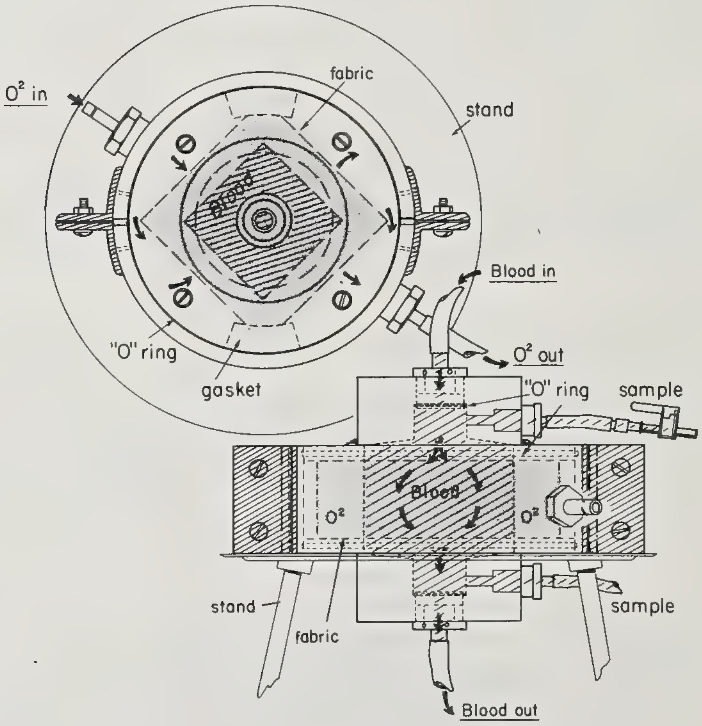

FIGURE 2. PRESENT BLOOD OXYGENATOR DESIGN.

TABLE 1

CIRCULATION EXPERIMENTS - SELECTED DATA

Model B Oxygenator - 100 Fabric Layers - 4.0 M^2 Area

Date	Blood Flow	% O_2 Saturation		ΔO_2	pCO_2 mmHg	
	cc/min	Proximal	Distal	cc/min	Proximal	Distal
(1) 7/1	500	78	95.5	20	35	33
(2) 7/3	500	72	96	30.5	39	35
(3) 7/8	815	63	85.5	31.8	40	43
		Partial By-Pass on 22 Kilo Dog				
(4) 7/10	630	62	93	33.5	37	39
7/10	750	63.5	89	33.0	37	37
		200 Fabric Layers-8.0 M^2-Partial By-Pass-25 Kilo Dog				
(5)	1,500	65.0	92.4	66		

bubbler was used, and was adequate. This run probably represents the true capacity of the oxygenator at this blood flow rate.

Experiment number 4, an in vivo partial by-pass shows about the same capacity for this oxygenator. In experiment number 5, the total capacity of the oxygenator, 200 layers of fabric, was used. As expected, we were able to double the blood flow rate and the oxygen transmission. The data is consistent and seems to represent the true permeation capacity of this particular polyethylene. It should be noted, however, that data on the ventilation of CO_2 are variable, and not really satisfactory in any case.

To approach the goal of oxygenating 4-5 liters of blood per minute, it was necessary to find a hollow filament material at least five times as permeable as this polyethylene, and preferably ten or more times as permeable. This search has been in progress for a number of months. Fortunately, several corporations have become interested in hollow fibers for a number of uses. They have supplied altogether sixteen samples representing various sizes and wall thicknesses from three types of polymers. The most prevalent type is a polymer of methyl pentene known as TPX. The second is a copolymer of methyl silicone with other materials, and the third is an experimental silicone rubber. All have shown promise - as well as problems. In every case except one, the samples received consisted of only a few ounces or less; not enough to weave into fabric for actual trial in the oxygenator. A simple apparatus has been devised for measuring the relative permeability of these samples and the rates of gas flow through them. Since the search was for large differences, refinements were not required. Furthermore, the samples were not always uniform in size or shape so that rigorous mathematical treatment of the data did not appear to be justified.

The apparatus consists essentially of a gas buret, using mercury, to provide a known supply of gas at any desired pressure from 25 to 150 mmHg, a second gas buret using Nujol or silicone oil to receive the exit gas at atmospheric pressure, and manometers for pressure measurement. The test sample is a strand of 20 to 130 individual filaments, depending on their size. The two ends of the strand are potted in glass tubes using paraffin or a silicone composition and leaving the open tips of the filaments exposed. Total strand length is 8 inches and the exposed length in the center where permeation is possible is 3.5 inches. The latter figure corresponds with the exposed length of filaments in the oxygenator.

The sample strand is suspended between the two burets. It may be suspended in air or any other gas. It may also be suspended in a circulating buffer solution containing an indicator whose color changes as CO_2 is absorbed. This color change is observed as the buffer passes through the cuvet of a Spectronic 20 photometer.

The rate of permeation of CO_2 from inside the tubes to the surroundings was selected as the criterion of relative permeability. This choice was partly because venting of CO_2 is the critical property of a membrane oxygenator and partly because CO_2 is easy to detect. It was also reasoned that the permeation of CO_2 through the different fibers from the inside out would be in the same order and similar proportions to the permeation from blood outside to the inside of the filaments. This may not always be true as is shown below.

To compare the permeation through filaments of varying sizes, advantage is taken of the relationship that if the fraction of the total cross section which is hollow is held constant, the volume of gas permeating through a unit length in unit time is independent of fiber diameter. Since this fraction of hollow space varied only between 40% and 50% (with one notable exception), the relative permeation was first expressed in cc per minute per filament. A correction for variation in the fraction of hollow space can be applied if closer comparison is desired and if a reliable figure for this fraction is available.

The rate of flow of gas through the filaments at practicable pressures is also of primary importance in the ventilating of CO_2 from blood. The pCO_2 in venous blood is only 45 mmHg. If CO_2 is allowed to accumulate in the flowing gas the ΔpCO_2 between the blood and the flowing gas, and consequently the rate of ventilation, may be seriously reduced. This means that with more permeable polymers, the rate of flowing gas must be increased proportionately to take full advantage of the inherent permeability. Fortunately, the rate of gas flow at a given pressure drop is proportional to the fourth power of the inside diameter. A relatively small increase in fiber diameter will result in a large increase in gas flow. This is doubly fortunate since, as of today, the most permeable polymers appear to be the most difficult to spin to small sizes.

In a typical experiment with the above described apparatus the procedure is: (1) Check the sample for gas leaks at 100 mmHg internal pressure with air; (2) measure the flow of air and of CO_2 through the sample at 50 mm and 100 mmHg inlet pressure (i.e., the rate of loss from the input buret and the rate of collection in the output buret) with the sample suspended in air; (3) immerse sample in circulating buffer and observe loss of CO_2 from the input buret and the change in per cent transmission on the spectrometer vs. time. Measurements of the rate of gas output are also made at intervals. All gas volume measurements were reduced to RTP.

In step (2), with samples of low or moderate permeability there was usually a small difference between the measured input and output of CO_2 which might represent permeation to the atmosphere. However, this was variable and not considered as reliable as the spectronic data. In step (3), the semilog plots of per cent transmission vs. time gave good straight lines between 20% and 100% transmission. The slope of these lines (compared with calibration curves) gave a direct measure of the CO_2 absorbed in the buffer per minute.

In the case of certain large filaments the flow of gas at pressure drops of 50 or 100 mmHg was too large to measure conveniently. In such cases a capillary bleed was used on the exit end of the test sample. Most of the pressure drop then occurred across the bleed, the partial pressure of CO_2 was nearly constant throughout the sample, and a low but steady flow maintained.

As mentioned above, the permeation can be estimated by volume changes or by the spectrometer readings. For samples of low permeability the difference was small. For highly permeable samples this is definitely not the case. For instance with a sample of experimental silicone rubber immersed in the buffer and with an internal partial pressure of CO_2 of about 800 mmHg, the rate of absorption of CO_2 was 1.35 cc per minute (Table 2).

TABLE 2

PERMEATION THROUGH SILICONE RUBBER

Sample - 20 filaments, 3.5 in. exposed length
Internal partial pressure CO_2 - 785 mmHg

Suspended in	Permeation	
	by Spectrometer	by Volumes
Buffer	1.35 cc/min	
Air		2.5 cc/min
CO_2 (760 mmHg)		0.25 cc/min

The same sample suspended in air at the same partial pressure showed a loss of 2.50 cc/min. When the same sample was suspended in a flask of CO_2 at atmospheric pressure the gas loss was reduced to 0.25 cc per minute. This series of experiments has been repeated several times with the same result. Changing the rate of circulation of the buffer made no difference in absorption by the buffer. It seems certain that under our conditions the buffer is unable to absorb the CO_2 as rapidly as it penetrates this highly permeable polymer in air. We conclude that this is a solid to liquid boundary problem which occurs at this high partial pressure difference and permeation rate. It may, or may not occur at the blood to polymer interface with a low partial pressure difference, in a working oxygenator. We accept the high figure as describing the true permeability of these filaments.

Table 3 shows a tabulation of the relative permeation measured on the several items tested.

TABLE 3

RELATIVE PERMEABILITY OF HOLLOW FILAMENTS TO CO_2

	Permeation per strand cc/min	Filaments per strand	Permeation per filament cc/min	Relative Order
Polyethylene	0.058	100	0.00058	1.0
Poly(methylpentene)				
Dow Chemical	0.500	100	0.00500	8.6
Source #2	0.430	100	0.00430	7.4
Silicone Copolymer				
General Electric	0.534	20	0.027	46.0
Experimental Silicone Rubber				
Dow Chemical	2.51[a]	20	0.125[a]	216.[a]
			0.085[a]	145[a]

[a] The very high observed permeation for this item is due in part to its thin wall and high hollow fraction - 62.7%. Calculation converting to a hollow fraction of 50% gives the lower figures shown.

The figures are averages from a large number of tests, and are at best approximate. However, they do show the great improvement which could be made if any of the three could be made available in a size and form suitable for weaving. Work on improved spinning methods for all three is continuing and we are quite hopeful.

In fact, we hoped to have a poly(methylpentene) fabric stack evaluated in time for reporting at this meeting, but ran into textile problems. We thought they had been overcome, and not until we had the fabric in the oxygenator did we discover that a small percentage of the filaments had developed longitudinal cracks and were leaking.

Such textile problems should be expected, and they can not be attacked until sufficient quantities are available for actual operation on textile machinery. The two types of polymers comprised of silicones are both quite elastic. They should have no brittleness problems. And much has been learned in the last few years about the weaving of elastic yarns. With two or three pounds of either of these yarns we should be able to construct an oxygenator whose limitations would not be in gas transport, but in fluid flow through the oxygenator. Suitable compromises between filament size and permeability should be easily reached by experiment.

In the course of these studies we have confirmed the theoretical predictions based on round tubes. For instance, two samples made of the same polymer, one with inside diameter 40.6 μ, outside diameter 57.9 μ and hollow fraction of 49.1% and the other with inside diameter 62.4 μ, outside diameter 90.8 μ and hollow fraction 47.3%, have practically the same permeation per filament, 0.42 and 0.40 cc per minute respectively. We have also confirmed that with our far from perfect hollow tubes, the gas flow at a given pressure drop is closely related to the fourth power of the average inside diameter.

In addition to the studies described above, the search for evidence of blood damage due to mechanical effects has been continued. In a series of seven experiments an arteriovenous fistula was created in the dog between the femoral artery and vein with the small fabric oxygenator interposed in the line. Oxygen was not passed through the tubes. Pressure gradient across the oxygenator, screen filtration pressure, plasma hemoglobin, platelet count, platelet adhesiveness, hematocrit and white blood cell count were measured within 5 minutes after establishing the arteriovenous fistula and 4 hours later. Blood cultures were taken at the beginning and end of the experiment.

Three milligrams of heparin per kilogram were administered to each animal prior to cannulation and 1/6 of the dose was given every 30 minutes until conclusion of the experiment. An electromagnetic flow meter was positioned in the Tygon line distal to the fabric oxygenator. In the last 4 experiments flow rates in excess of 1,000 cc/min. were achieved.

At flow rates between 1,000 and 1,500 cc the maximum pressure gradient across the oxygenator did not exceed 40 mmHg. In no instance did the pressure gradient increase during the four-hour experiment. The average gradient was 31 mmHg at the beginning and 21 mmHg at the end of the run, whereas flow rates averaged 674 cc/min. at the beginning and 799 cc at the end.

The hematocrit and white blood cell count remained constant. The plasma hemoglobin increased little or not at all (average of 5 mg% early; 9 mg% late). Indeed, in none of the experiments in which negative cultures were obtained at the end of the experiment was there any increase in plasma hemoglobin.

No statistically important changes were noted in platelet counts, the average initial and final values being 207,000 and 203,000. In no case was a truly significant decrease noted. Platelet adhesiveness averaged 58% and 63% initially and finally. In only one instance was a significant decrease noted (90% to 69%). Screen filtration pressure (by the method of Swank) in six experiments averaged 138 mmHg initially and 182 mmHg finally. But in four of the six experiments there was actually a decrease in the screen filtration pressure.

In four of the first six experiments positive blood cultures developed by the end of the experiments. More rigorous cleaning and sterilizing methods led to consistently negative cultures in the last three experiments.

DISCUSSION

These experiments represent a continuation of earlier investigations undertaken to evaluate the effect of the fabric oxygenator on blood. The arteriovenous fistula allows testing *in vivo* of the oxygenator without a mechanical pump.

The results of these experiments indicate minimal trauma to the cellular elements of the blood during acute experiments lasting 4 hours. The polymer employed in this fabric oxygenator was polyethylene and the results do not necessarily apply to other polymers. However, it is suggested that the geometry of the oxygenator is acceptable in terms of blood trauma. The stability of platelet counts and pressure gradients was especially impressive. When tubes are available of polymers more permeable to carbon dioxide and oxygen the effect of the fabric oxygenator on blood will be tested in longer experiments and during post-perfusion survival.

DISCUSSION

DR. COVAL: Dr. Williams, I wonder whether you have any evidence to support your hypothesis that oxygen transport is limited by the filament material and not by the geometry of your apparatus.

DR. WILLIAMS: We have tried to measure the problems which exist on the blood side. When we change our speed of operation (our speed of flow), instead of getting as many people do a considerable change in the oxygen transport, we find that there is very little change at all. We suspect that that is due to the fact that the passage of any element of blood through this stack of fabric is a very tortuous one. Individual threads woven into the fabric are not in even register, and two layers adjacent to each other couldn't possibly be in register over much of an area, so that the blood is going back and forth in two directions. It is tumbling as it passes through, and we think this must give the necessary turbulence, or whatever is required to eliminate a large part of this boundary effect. We have no proof; that's the way we can explain it to ourselves.

DR. COVAL: Perhaps you could calculate the amount of oxygen you could expect to be transported through the walls of your filament and compare it with what you obtained.

DR. WILLIAMS: That is difficult when you're dealing with such a tangled mass of fibers. The fibers are not really uniform you know, and they are not always round. They are frequently flattened in weaving and we have not been able to satisfy ourselves, that we could calculate what should happen in such a mass of fibers. I would like very much to be helped in that regard.

DR. COVAL: Your present upper limit of oxygen saturation is about 90. Does this low level not concern your prospects of scaling up?

DR. WILLIAMS: On many occasions, we have been higher than that. I think the highest figure was 94. We have a very difficult time with the dog, now, getting any saturations higher than 95 on our particular oximeter with which they were measured. I suspected that our oximeter may read a different figure for human blood than for canine blood, but 95 is about the best we have been able to get.

MR. MATHEWSON: In your experiments of blood damage, I notice that there is no drop or no change in pressure drop over the four hour experiment. Do you inspect the equipment after the experiment to see whether there is any sign of blood thrombus?

DR. WILLIAMS: Of course, that is what we were looking for in the measurement of that pressure gradient: some alteration in the blood, some deposition in the critical passages, and we would expect that if anything like that happens, there would be an increase. Actually, we have noticed many times that if we take blood which has been standing, in a blood bag overnight for instance, from a dog that was bled the night before, that the gradient will be higher initially for a given flow, and then will go down. We think that aggregation of cells must have taken place during the night, and it frequently happens that the pressure gradient goes down. We have never had the pressure increase during a run that finished as a sterile preparation.

MR. MATHEWSON: Did you ever inspect the fabric after the experiment?

DR. WILLIAMS: Yes, we do not have very much fabric. Consequently, we attempt to use the same lot in a number of experiments, so we have to have a cleaning procedure to remove anything which is in there and to get it thoroughly sterile and free from pyrogens again. I do not think that you would want me to explain the entire procedure here. However, it takes quite a bit of washing with alkaline and finally with acid solutions, and then again with distilled water in order to get the oxygenator into shape. I think that something is deposited. I think there is a little debris going around in every animal's blood, and that there are some things which are tangled and which have to be removed by chemical means. This is what we are trying to do. We can report, though, that we have made quite a number of experiments in which, after sterilization, we have washed out the oxygenator, including the fabric and all, quite thoroughly with sterile saline. We find that it gives a sterile culture, and also that it is free of pyrogens, so we feel safe in using it again.

DR. SCALA: A moment ago, in answer to a question, you mentioned the word turbulence; I would like to make a comment here. You had used the word turbulence in reference to the tortuous passage for the motion of the blood between the non-aligned layers of capillaries. I think a better term to use would be enhanced mixing, rather than turbulence, because the flow is probably laminar at the low Reynolds numbers which are present in your blood oxygenator. I think that the increase in efficiency is due to better mixing, not to turbulence, because I immediately think of turbulence as a deleterious effect which promotes hemolysis. Would you please comment on that?

DR. WILLIAMS: I really do not know how to judge what goes on within that fabric stack. We have pumped water through it and dropped a stream of colored liquid on top and tried to follow its passage, but as soon as it has buried itself four or five layers in the pack, then we cannot see it anymore. Just what is happening, I do not know, but I do know that if you take only three layers of fabric after one of these experiments, and try to look through it with a microscope, or look through it with light behind, we find very few things that look like clean passages. The filaments are overlapping; and so just which way, and at which time, and in which direction the blood goes, we do not know, but we know it must be going in a tortuous path.

DR. SCALA: It is a standard laboratory technique to generate turbulence by inserting a grid into a flowing stream; it could be done in any fluid, gas or liquid. My only point was that perhaps the flow velocities are low enough, so that while you are getting a tortuous path which enhances the efficiency of the mass transport processes, nevertheless, the flow is not turbulent in the standard sense.

DR. WILLIAMS: I'd be perfectly willing to accept that, ir. I know that there are people who have worked with oxygenators with a tube wound in a helical pattern so that there would be some centrifugal effect to throw cellular elements against the walls as it goes round and round. I am sure we have got a great deal of that going on inside of our fabric stack.

CHAPTER 32

DEVELOPMENT OF CAPILLARY NETWORK MEMBRANE OXYGENATORS

R. L. Hauser, D. H. Thompson

Hauser Research and Engineering Co., Boulder, Colo.

and

J. A. Jacoby

Denver, Colorado

A unique geometry was studied in this contract, consisting of an interconnecting capillary network. The capillaries were made of porous nickel coated with silicone rubber, or of just silicone rubber. The network was manifolded for oxygen flow within capillaries. Oxygenator elements were made with 2.5 square meter diffusional area within 0.7 liter priming volume. Blood flow pressure drop was low and mixing was excellent. As of this writing, reliable leak-free elements have not yet been made with sufficient diffusion for complete blood oxygenation. Continuing research is expected to provide an efficient, economical membrane oxygenator.

INTRODUCTION

The objective of this study has been to develop a membrane oxygenator with high diffusional surface area per unit of priming volume. Basis for the study is a unique material with an interconnecting network of capillaries. Elements are manifolded for gas flow within the network and blood flow between the capillaries. Such an oxygenator could possibly provide a membrane surface area of about 2.5 square meters within a priming volume of 1 liter.

CONCEPT

A unique material geometry was conceived as the basis for this oxygenator. Its closest parallel in prior developments is the woven hollow fabric oxygenator of Dr. Williams at the Medical College of Virginia.

The basic geometry is that of a reticulated urethane foam, Scottfoam (trademark, Scott Paper Company), which is very commonly used in clothing, upholstery and packaging. The foam is produced in a number of pore sizes, ranging from 10 to 100 pores per inch, Figure 1. Surface area is dependent upon the pore size, as noted in Table 1.

TABLE 1
SCOTTFOAM CHARACTERISTICS

Porosity, ppi	Surface Area	
(pores per inch)	in^2/in^3	cm^2/cm^3
10	12	4.7
20	26.6	10.5
30	42.5	16.7
45	69	27.2
60	95	37.4
80	135	53.1
100	173	68.1

This foam can be plated chemically, using silver, copper or nickel salts with proper activation and reducing agents. Upon the very thin metallic surface, electroplating can be accomplished to increase thickness and build a stiff tube around each urethane filament. When the metallic plating is thin, it can be permeable to gas transmission. Nickel electroplate is porous if thickness doesn't exceed .002 inch. The urethane foam is easily removed from within the metal by heating it to decomposition temperature. A few holes are broken in the structure to permit the gaseous products of pyrolysis to escape. A slight carbonaceous residue is left within the capillaries. Oxygen flow is directed within the capillaries, and blood flows in the approximately 95 percent void space between capillaries. This phase separation is accomplished by sealing a void surface and by opening many of the capillary terminations. This geometry provides high surface area per unit volume, excellent blood mixing by random flow within the network, and low blood-phase diffusional resistance because of this good mixing.

DESIGN AND FABRICATION

Three different designs of oxygenators have been prepared on this contract. In time sequence, they have been a cylindrical oxygenator, a stack of "melba toast" elements, and an all silicone network.

Cylindrical Design

The initial design was based upon slip-fitting gaskets to seal between oxygenator elements and the housing. A cylindrical unit was designed, as shown in Figure 2. Each element of capillary network was prepared with cylindrical seals at the gas-blood interfaces and with flat seals between elements to maintain gas transfer, Figure 3. The seals and manifold were cast of Silastic 382, and capillaries were exposed by grinding and electrochemical etching, Figure 4. This design was effective for preparation of components and evaluation of concepts, but it was difficult to obtain efficient manifold seals.

The cylindrical oxygenator was made with an acrylic sleeve, aluminum end caps, Silastic gaskets and a stainless center post and tubing connectors. An oxygenator with six elements and a 1-liter priming volume is shown in Figure 5.

The six-element oxygenator was set up for a blood flow test with pump and manometer. A water-glycerol solution with 5 centipoise viscosity was pumped through the unit with flow rates varied from 1 to 5 liters/minute. Pressure drops through the system were measured. Similar tests were made without the elements in the unit, to measure the pressure drop of the blood line. Results are shown in Table 2:

TABLE 2
SIMULATED BLOOD FLOW PRESSURE DROP

Flow Rate (liters/minute)	P (foam) mm Hg	P (blood line) mm Hg	P (total) mm Hg
1	1.3	6.4	7.7
2	2.6	12.8	15.4
3	3.9	19.2	23.1
4	5.2	25.6	30.8
5	6.5	32.0	38.5
6	7.8	38.4	46.2

These tests indicate that blood flow resistance is not a significant concern in the oxygenator with 10 ppi capillary network. An extrapolation from Scott data on flow properties through foam provides an estimate of 26 mm Hg pressure drop for blood at 5 liters/minute for a 45 ppi network having 2.5 square meters of membrane surface area. This pressure drop is in the same magnitude as that normally experienced for human blood circulation through the lungs.

The first two cylindrical oxygenators delivered for blood oxygenation tests were opening-night flops. The first unit leaked at the manifold seal against the central spindle, and oxygen flows of 3 and 6 liters/minute made it into a bubble oxygenator. The second unit was tested with a pressure gauge on the oxygen supply, and operation appeared to be satisfactory at 0.5 psi with flow only 0.5 liter/minute of oxygen. When flow was increased to 1 liter/minute, bubbles appeared, indicating a new leak in the unit.

The third test was made with elements pre-tested for oxygen flow to 4 liters/minute (20 mm Hg), and then proof tested to show no leakage at 40 mm Hg. Poor oxygen pressure regulation damaged this unit at 3 psi. The fourth unit was tested with better control and gave the results shown in Table 3.

Slight blood leakage from manifold into the capillary network decreased the area efficiency of this unit approximately 50 percent. Small, slow bubbles were also observed during the oxygenation tests. Oxygen transfer was approximately 20 cc/minute.

Troubles with the manifold seals prompted a revised design, similar in many respects to that of Dr. Williams at Virginia.

"Melba Toast" Elements

Sheets of Scottfoam 1/8" thick were electroplated with nickel as the basic unit of this design. Window frame seals were obtained by edge casting or by silk-screen techniques using Silastic 382. Elements were made of 45 ppi and 80 ppi Scottfoam, as shown in Figure 6. A stack of elements with oxygen and blood manifolds is illustrated in Figure 7, and is shown schematically in Figure 8.

First experiment with elements of this design were a failure, due to lack of oxygen flow through the capillary network. To date, all of the "Melba Toast" elements have either leaked air bubbles at low pressure or networks have had very limited oxygen flow.

All-Silicone Network

Because the nickel network has less than 10 percent porosity, efficiency of the metal network is limited. For this reason, elements have been made of copper-plated foam with Silastic 2000 to .002" thickness. These foams were then stacked as shown in Figure 9 and frames were cast of Silastic 382.

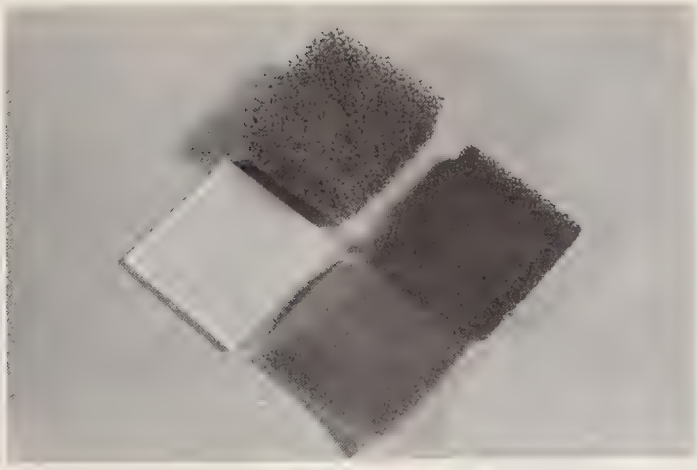

FIGURE 1. SCOTTFOAM SAMPLES. CLOCKWISE FROM TOP 10 PPI, 1" THICK; 20 PPI, 1/2" THICK; 45 PPI, 1/8" THICK; 80 PPI, 1/8" THICK.

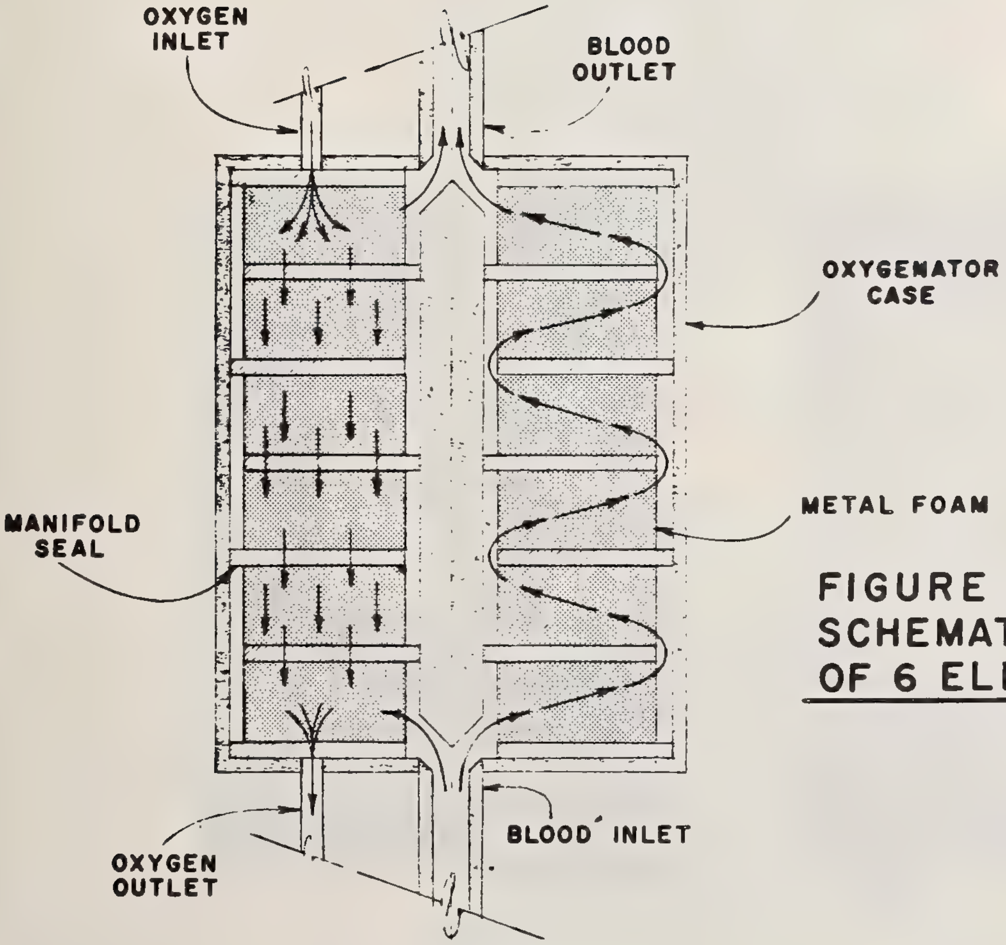

FIGURE 2
SCHEMATIC CROSS-SECTION OF 6 ELEMENT OXYGENATOR

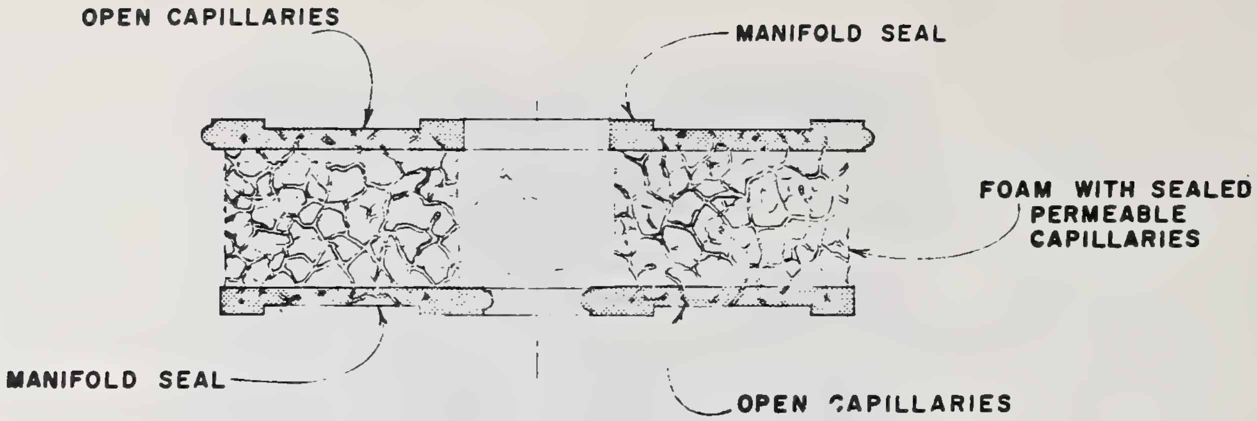

FIGURE 3 - CROSS SECTION OF MANIFOLD SEAL AND CAPILLARY NETWORK

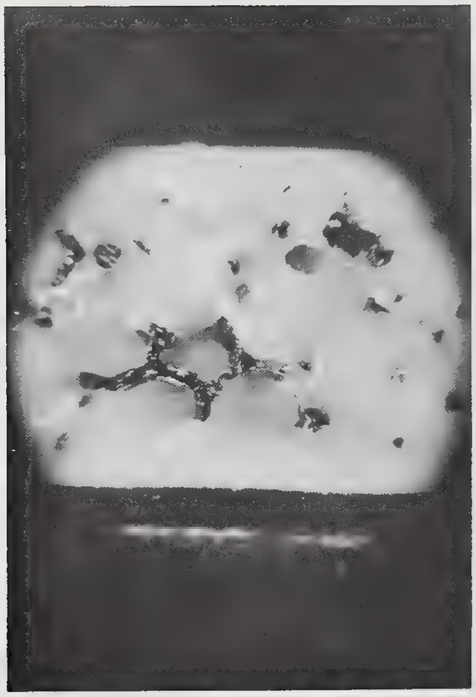

FIGURE 4. PHOTOMICROGRAPH OF CAPILLARY NETWORK AT OXYGEN MANIFOLD SEAL. SCALE APPROXIMATELY 20 X.

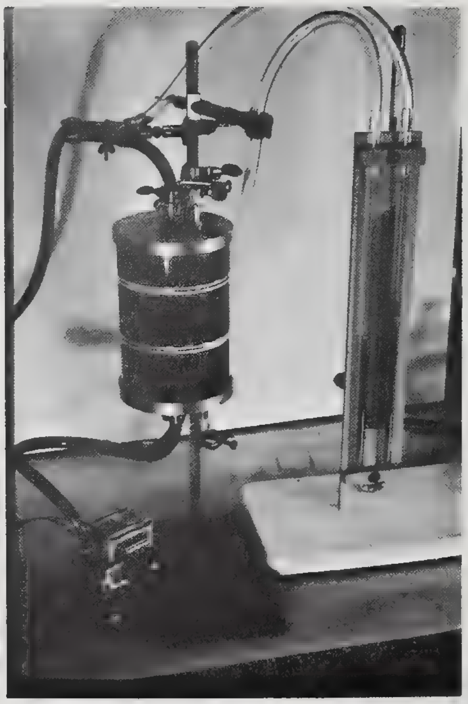

FIGURE 5. CYLINDRICAL OXYGENATOR ASSEMBLED FOR BLOOD FLOW TEST.

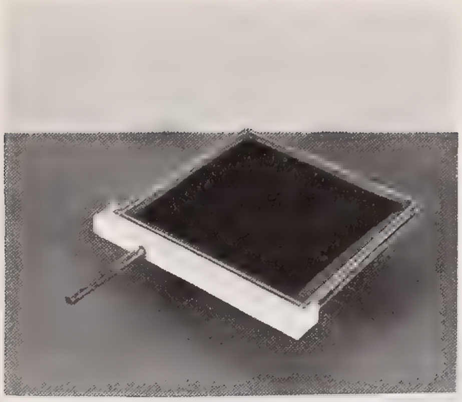

FIGURE 6. TWO "MELBA TOAST" ELEMENTS WITH OXYGEN MANIFOLD IN PLACE.

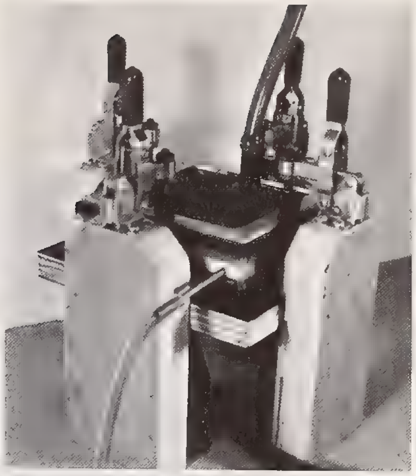

FIGURE 7. "MELBA TOAST" ELEMENTS IN CLAMPED BLOOD MANIFOLDS.

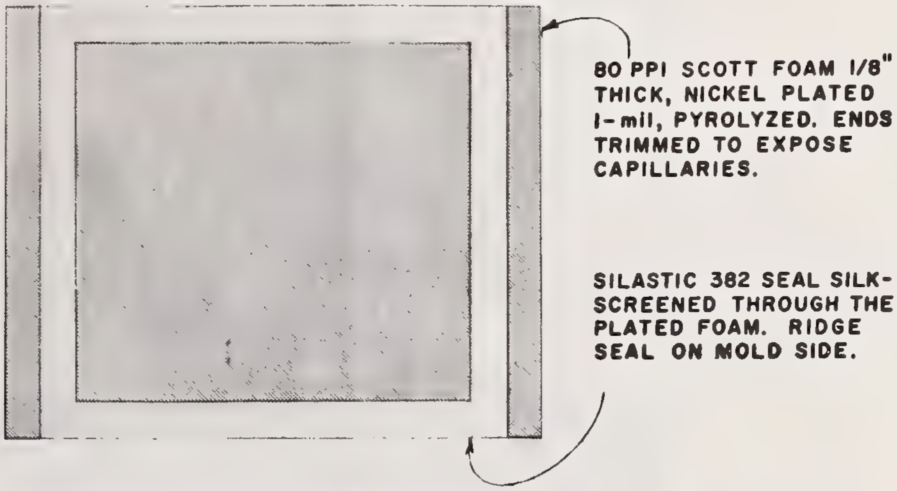
80 PPI SCOTT FOAM 1/8" THICK, NICKEL PLATED 1-mil, PYROLYZED. ENDS TRIMMED TO EXPOSE CAPILLARIES.
SILASTIC 382 SEAL SILK-SCREENED THROUGH THE PLATED FOAM. RIDGE SEAL ON MOLD SIDE.

INDIVIDUAL ELEMENT

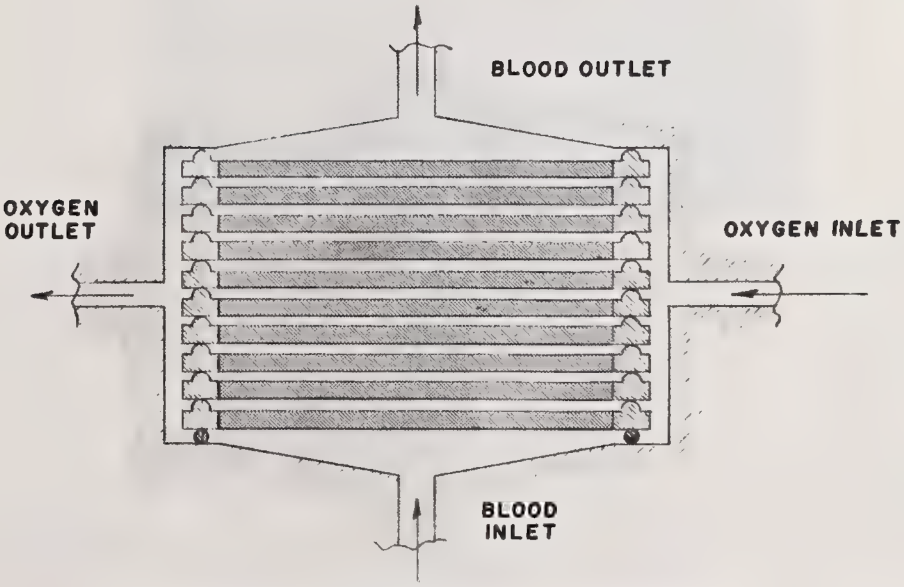

SECTION THROUGH STACKED OXYGENATOR

FIGURE 8 - MELBA TOAST OXYGENATOR

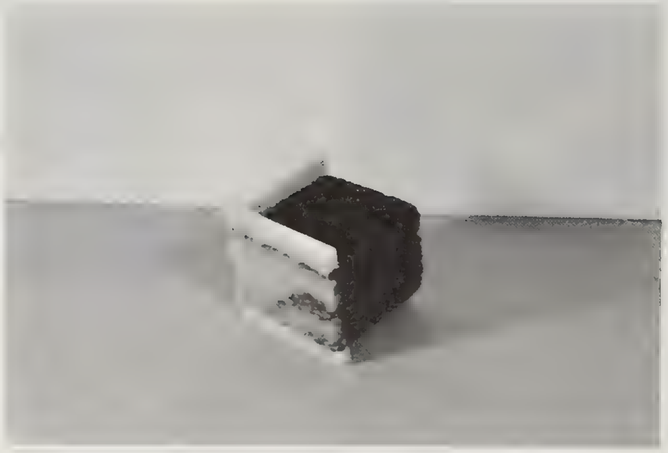

FIGURE 9. ALL-SILICONE OXYGENATOR WITH SEALS CAST ONTO TWO OF THE FOUR SIDES.

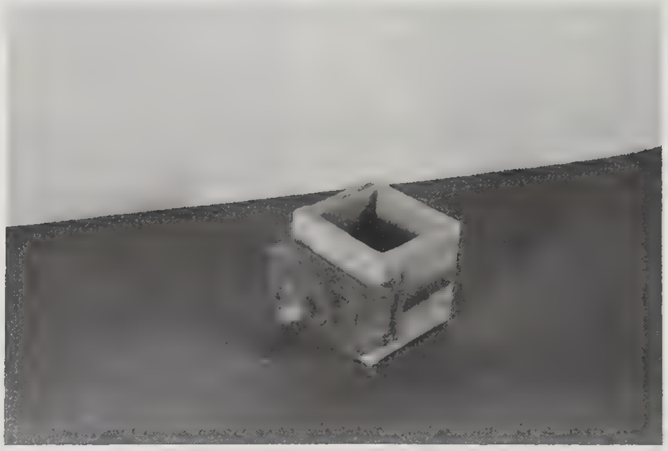

FIGURE 10. ALL-SILICONE OXYGENATOR WITH ALL FOUR SIDES CAST AND WITH OXYGEN MANIFOLD IN PLACE. BLOOD MANIFOLDS NOT YET ASSEMBLED.

TABLE 3
PERFORMANCE OF OXYGENATOR NO. 4

Preparation: 2 elements, 10 ppi, cylindrical
surface area 1450 sq. cm.
leak tested to .85 psi, O_2 flow of 3 l/min. @ 0.5 psi

Tests: $25^{o}C$, Blood, 4 units A^{+} outdated, 12,000 units heparin
Flows -- liters/minute

Time	Blood Flow	O_2 Flow	O_2 Pressure	N_2 Flow	Oximeter		pH	
					A	V	A	V
9:04	1	2	1.5	3	39.5	39		
9:22	1	3	1.5	2	42	38		
9:41	1	4	1.8	1	40	38		
9:59	2	4	1.8	1	34	34		
10:16	3	4	1.8	1	20	20		
10:38	1	5	2.6	1	34	26		
10:58	2	5	2.4	1	29	26		
11:17	1	6	3.1	1	48	36	6.80	6.84
11:43	1	6	3.1	1	52	46		

The copper was then exposed by light grinding, and "Dutch Mordant," a copper etchant, was introduced into the network. This left a silicone network with 100 percent area efficiency.

Ends of the oxygenator were made of silicone rubber, and tubes were assembled for blood flow. Oxygen entry was accomplished with a small box attached to one side, Figure 10.

The all-silicone oxygenator has not yet been tested for *in vitro* performance. This unit has 6 cubic inches of foam with 0.10 square meter surface area. It could be capable of 36 cc/minute oxygen transfer with no blood phase resistance.

DISCUSSION

MR. SALKIN: I was wondering whether you have a consistent pressure drop from one manifold to the next.

MR. HAUSER: Are you referring to the blood pressure drop or the oxygen pressure drop?

MR. SALKIN: The oxygen.

MR. HAUSER: Just about every unit we have made so far has been somewhat different from the other. So that we don't have a good measure of consistent characteristics.

DR. JACOBEY: The development of a membrane oxygenator can be divided into three steps, the development and fabrication of geometric configuration, physico-chemical evaluation of efficiency of mass transfer, and physiological testing. Although the first stage has been prolonged in our efforts, the second stage seems promising. The most efficient membrane currently available is being used in a geometry that provides both large surface area per unit volume and substantial mixing although the Reynold's number falls within what would be described as that of laminar flow. Tests to be carried out include *in vitro* transfer of oxygen and carbon dioxide and *in vivo* total bypass studies for 4 hours and partial bypass studies plasma hemoglobin, platelets, fibrinogen and protein electrophoresis will be evaluated. In the future we visualize incorporation of this device in a compressible chamber to produce a compact disposable pump oxygenator and further potential may be possible utilization of this geometry and material as an implantable artificial lung.

CHAPTER 33

DEVELOPMENT OF A LIQUID-LIQUID BLOOD OXYGENATOR

R.P. deFilippi, R.M. Anderson,
J.H. Porter and G.W. Harris
Abcor, Incorporated, Cambridge, Massachusetts

and

Yukihiko Nosé
Cleveland Clinic, Cleveland, Ohio

An experimental blood oxygenator has been tested wherein a falling fluorocarbon (FC-43®) film inside a vertical Teflon® tube contacts a rising column of blood. Oxygen and carbon dioxide transfer occurs across the moving interface between two immiscible liquids, thus eliminating the need for membranes or blood-gas contacting. The liquid-liquid contacting device is operable over a wide range of blood and fluorocarbon flow rates without the formation of fluorocarbon emboli. No detectable blood components are removed and no foreign substances are introduced. *In vivo* hemolysis rates with the falling fluorocarbon film are an order of magnitude less than with disc or bubble oxygenators. Intravenous injections of fluorocarbon slugs have shown that there is no apparent chemical toxicity and that the fluorocarbon can be removed from the body at rates up to 0.2 cc/kg body weight/day, apparently by exhalation. Because of the high interfacial velocities in the counter-current liquid-liquid contactor, high mass transfer rates are possible. Oxygen and carbon dioxide flux rates of 30-80 cc/min-m^2 and 40-150 cc/min-m^2, respectively, have been measured *in vitro* and *in vivo*. Based on these measurements, several different devices based on multiple cylinders or parallel plates have been designed having blood flow capacities of five liters per minute.

INTRODUCTION

Extracorporeal blood oxygenators have been in clinical use for many years, but there is still considerable need for improvement of these devices. Attention has been focused recently on devices which avoid direct blood/gas contact by transferring gases through a semi-permeable membrane. The blood/membrane interface has been found to be less traumatic. However, blood hemolysis rates are still high enough to limit the use of membrane blood oxygenators to several hours duration.

The research to be discussed here deals with a completely new concept in blood/gas exchange. The key feature is the fact that blood is brought into gentle contact with an immiscible liquid for interfacial mass transfer of dissolved gases, so that blood/gas and blood/solid interfaces are not required. The essential features of the liquid-liquid blood oxygenator are shown in Figure 1. A carrier liquid containing a high level of dissolved oxygen is introduced into a reservoir from which it flows over the lip of a vertical column. If the surface properties of the solid wall are similar to those of the carrier liquid, the latter will form a thin, uniform film which flows down the column wall. The carrier liquid exits at the column base through an outflow line which is used to maintain the appropriate level of the carrier/blood interface near the column base. The blood is introduced through a central feedline above this carrier level, so that it flows into the column without droplet formation. Blood flows upward in the core of the column, countercurrent to the carrier liquid film. Gas transport occurs across the interface between the thin film of flurocarbon and the upward flowing column of blood.

There are several advantages of a liquid-liquid exchanger of this type for use in blood oxygenation.

1) Overall gas transport can be higher because of the absence of the membrane resistance.
2) It appears that the liquid-liquid interface of the annular configuration shown causes less blood hemolysis then a blood/membrane interface.
3) Transport rates at the liquid-liquid interface will be constant over a long period, whereas blood components might tend to accumulate at membrane surfaces over extended periods, thus reducing oxygenator performance.

There have been two main objectives of this first year's program.

1) To determine the oxygen and carbon dioxide transport characteristics and the hydrodynamic behavior of the liquid-liquid exchanger.
2) To determine the long-term physiological effects of blood/carrier liquid contact.

Experiments designed to accomplish the first objective have been carried out at Abcor in Cambridge, while experiments on physiological effects have been done at the Artificial Organs Laboratory of the Cleveland Clinic, under the direction of Dr. Yukihiko Nosé.

MASS TRANSFER EXPERIMENTS IN VITRO

An experimental liquid-liquid oxygenator incorporating a single vertical tube was used in the first experiment (Figure 2). A perfluorocarbon liquid was chosen as the carrier liquid because of its high solubility for oxygen and its immiscibility with blood. The specific liquid used was FC-43®, consisting primarily of a completely fluoridated tributyl amine. Teflon® was chosen as the material for the vertical cylindrical tube because it was found to be preferentially and completely wetted by the fluorocarbon. A translucent thin-walled Teflon column was supported by a thicker plexiglass tube to allow for partial transparency during operation. Fresh, whole heparinized human blood was chosen for the *in vitro* tests because it most closely represented the clinical situation. Most of the mass transfer measurements were carried out in a tube having an inside diameter of 11 mm, but 8 mm and 4 mm tubes were also studied.

In vitro mass transfer data are presented in Table 1. They represent runs wherein column length, column diameter, blood flow rate and fluorocarbon flow rate were varied. One can see that oxygen transfer rates ranged from 30 to 70 cc/min/m^2, but in some cases flux rates greater than 100 cc/min/m^2 were obtained. The oxygenator operation was quite stable with no evidence of foaming, fluorocarbon embolus formation, or rivulet flow.

TABLE 1

IN VITRO GAS TRANSFER DATA

Blood Flow cc/min	Fluorocarbon Flow cc/min	Column Length cm	Column Diameter cm	Gas Transfer Rate cc/min-m^2
20	55	36	1.1	51
20	103			57
30	55			34
30	103			51
30	172			53
20	55	53	1.1	24
20	103			38
20	172			33
22	80	36	0.8	60
22	142			77

A simple and fairly accurate method of correlating these data is shown in Figure 3. This is based on the well-known Graetz correlation for heat transfer in a tube of constant wall temperature. In the case of the liquid-liquid oxygenator, the blood is visualized as flowing in laminar flow inside a tube whose wall is the interface between the blood and the fluorocarbon. The oxygen concentration in the fluorocarbon film is assumed to be constant and all the resistance to mass transfer is assumed to be in the blood phase. The Graetz correlation suggests that the mass transfer be expressed in terms of the Sherwood number, which is a ratio of convective mass transfer to diffusional mass transfer. Sherwood number, as plotted on the ordinate here, is simply the mass transfer coefficient times the diameter of the blood column divided by the diffusivity of oxygen in the blood phase. The Graetz correlation suggests that the blood flow rate be expressed in terms of the Graetz number which is shown on the abscissa as the mean velocity of the blood phase relative to the interface, times the square of the diameter of the blood column, divided by the diffusivity in the blood phase times the length of the blood column, and multiplied by a factor which accounts for not only the physical dissolution of oxygen in blood plasma, but also the reaction of oxygen with hemoglobin to form oxyhemoglobin. The data shown here were taken on a column that is 53 cm long and 1.1 cm inside diameter, giving an estimated blood column diameter of 0.78 cm.

It is obvious from the data in this figure that most of the mass transfer rates measured are slightly higher than those predicted by the theory. This could be due to the fact that most of the data are taken in the transition region between laminar flow and turbulent flow, whereas, the theory assumes laminar flow throughout. It is certainly possible that, to the extent that turbulence is occurring in the blood column, the mass transfer rate would be slightly higher.

IN VIVO MASS TRANSFER STUDIES

A similar single vertical tube liquid-liquid oxygenator was tested on several dogs, using a roller pump to pump blood from the femoral vein through the oxygenator to the femoral artery. The effect of blood flow rate from 10 to 50 cc/min and fluorocarbon flow rate from 55 to 172 cc/min was studied. Each experiment lasted about four hours and the data are summarized in Table 2. The average oxygen transfer rate is 52.5 cc/min/m^2 as compared to 38.5 cc/min/m^2 for a similar run *in vitro*. Carbon dioxide transfer was almost twice as rapid as oxygen transfer, and

---

FC-43® - 3M Company
Teflon® - E. I. duPont deNemours & Company

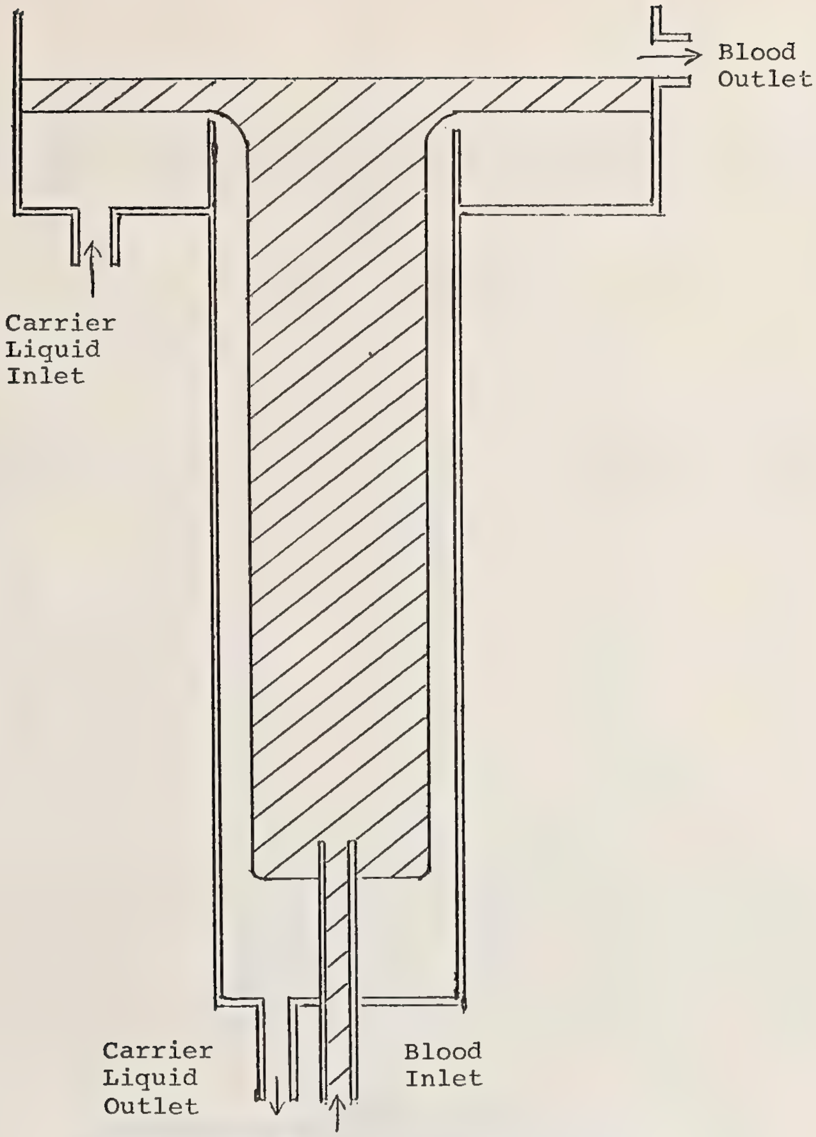

FIGURE 1. SKETCH OF LIQUID-LIQUID CONTACTING DEVICE.

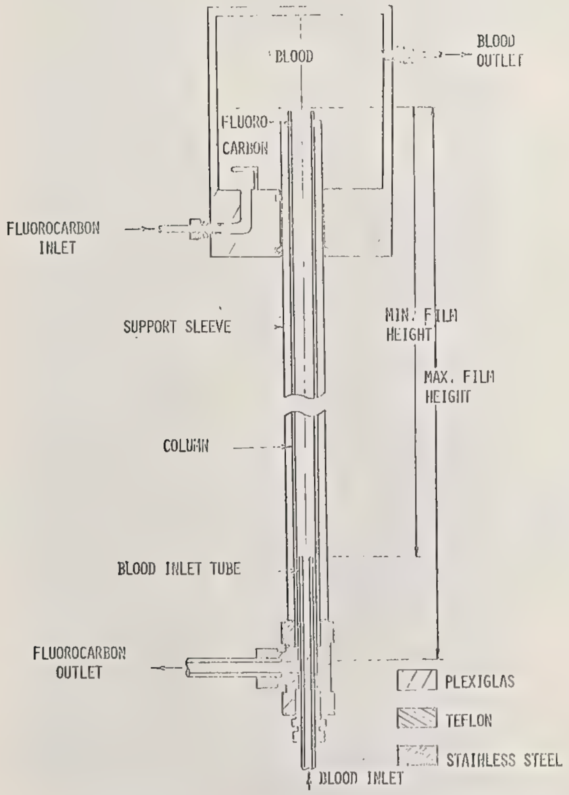

FIGURE 2. EXPERIMENTAL LIQUID-LIQUID BLOOD OXYGENATOR.

the oxygenator appears to be oxygen transfer limited over the physiological range, rather than carbon dioxide transfer limited, as is usually the case with membrane oxygenators.

TABLE 2

IN VIVO GAS TRANSFER DATA

Column Length: 36 cm

Column Diameter: 1.1 cm

Blood Flow cc/min.	Fluorocarbon Flow cc/min.	pO_2, mm Hg		pCO_2, mm Hg		Gas Transfer Rate cc/min-m^2
		V	A	V	A	
15	55	47	54	44	42	22
20	55	41	54	46	43	33
25	55	34	38	50	47	28
15	103	59	79	43	35	36
20	103	52	61	43	39	62
25	103	55	70	47	40	86
35	103	54	64	48	42	61
15	172	47	73	41	35	68
20	172	39	60	41	36	110
25	172	39	52	41	35	100

These data can be used to design a full-scale liquid-liquid oxygenator having a blood flow capacity of 5 liter/min. The characteristics of such an oxygenator are shown in Table 3. It is seen that the major disadvantage of such an oxygenator would be the large priming volume required. This can be considerably reduced by going to smaller vertical tubes or to any other geometry which would allow a smaller blood channel dimension. We have demonstrated operability in vertical cylinders as small as 4 mm inside diameter using fresh, heparinized blood. No mass transfer measurments have been made yet in the 4 mm tube, but assuming that the Graetz correlation holds, one would calculate a priming volume less than 2 liters for a device incorporating tubes of this size.

TABLE 3

DESIGN OF 5 ℓ/MIN LIQUID-LIQUID OXYGENATORS

Tube Diameter cm	Tube Length cm	Oxygen Flux Rate cc/min-m^2	Number of Tubes	Priming Volume cc
1.1	36	50	400	13,700
0.8	36	69	400	7,200
0.4	36	137	400	1,800

PARALLEL PLATE OXYGENATOR

To eliminate some of the difficulties involved in a multiple tube oxygenator, Abcor has designed and tested a parallel plate cross-flow oxygenator such as the one shown in Figure 4. Fluorocarbon is introduced under pressure into the top reservoir and flows through slits onto parallel plates. It is collected in a reservoir at the bottom and is removed through the bottom exit line. Blood enters through the side of the parallel plate device and flows very slowly across between falling films of fluorocarbon to exit at the other side of the device. Because of the high velocity of the fluorocarbon film relative to that of the blood, the main circulation pattern is one of downward blood flow along with fluorocarbon flow near the interfaces on either side of each blood channel, with recirculation of blood back-up through the center of each channel. A parallel plate device having a transfer area of roughly 0.2m^2 has been proved easily operable over a wide range of blood and fluorocarbon flow rates. Plate spacings as small as 4 mm has been proven operable. This device is much easier to control than the vertical cylinder oxygenator and shows promise of being quite easily scaled-up simply by increasing the number of parallel plates.

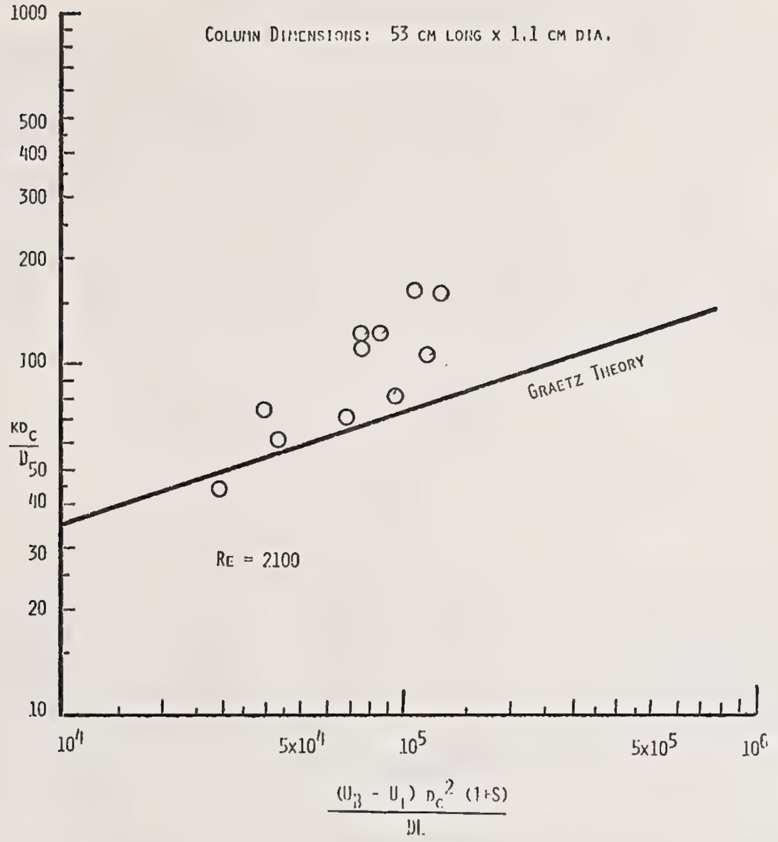

FIGURE 3. MASS TRANSFER IN THE LIQUID-LIQUID BLOOD OXYGENATOR.

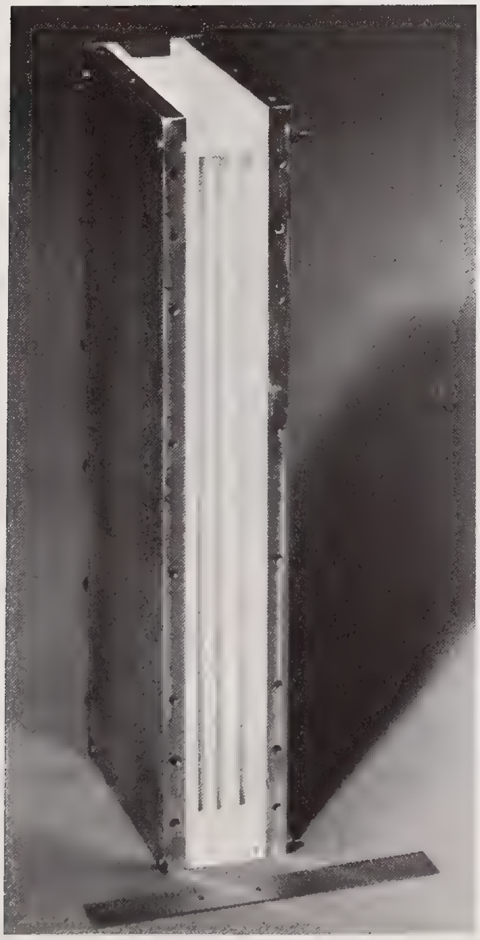

FIGURE 4. PARALLEL PLATE CROSS-FLOW OXYGENATOR.

IN VITRO EFFECTS OF FLUOROCARBON ON BLOOD

The purpose of these experiments was to determine the effect on various blood parameters of contacting blood with fluorocarbon. Fresh, heparinized, human blood or ACD human blood was placed in a Teflon container with an equal amount of FC-43. Care was taken to completely eliminate any blood/gas interface. The container was then rotated axially at 50 rpm for several hours while being held at 37°C. After specific periods of contact time the blood and fluorocarbon were sampled, and a series of analyses were made. These analyses included: plasma hemoglobin, cell volume, red cell and white cell counts, cell morphology, platelet count, plasma fibrinogen, and electrophoresis studies for albumin, alpha-1, alpha-2, beta, phi, gamma, and total protein, alpha-lipoprotein, and beta-lipoprotein. To ascertain the effects of Teflon a series of blanks was run with blood alone under the same experimental conditions. The results of these *in vitro* contacting studies are shown in Table 4. No differences were found between the fluorocarbon-contacted samples and the control samples. It is encouraging that FC-43 does not remove any of the proteins monitored during these *in vitro* tests.

TABLE 4

TWENTY-FOUR HOUR FC-43 - BLOOD CONTACTING STUDIES

	0 Hrs. Control	24 Hrs. Control	24 Hrs.
Hematocrit	46	44	43
White Cell Count (per mm^3)	4,000	3,500	3,750
Platelet Count (per mm^3)	175,000	55,000	60,000
Fibrinogen (mg%)	380	360	360
Plasma Hemoglobin (mg%)	4.6	10.8	9.8
RBC Morphology	Normal[a]	Normal[a]	Normal[a]

[a] Many RBC's crenated, but otherwise normal

IN VIVO HEMOLYSIS STUDIES

The small vertical tube oxygenator was tested on four dogs to measure the extent of hemolysis. In these tests, the oxygenator was connected from femoral artery to femoral vein, thus eliminating the need for a pump. In two cases the oxygenator was operated as usual with a flowing fluorocarbon film, and in the other two cases there was no fluorocarbon flow, so that the blood contacted the Teflon wall instead. Measurements of plasma hemoglobin as a function of time are shown in Figure 5. It is seen that the rate of plasma hemoglobin increase is much greater without the fluorocarbon film. This indicates that the liquid-liquid interface is much less traumatic than the liquid-solid interface. The data from the liquid-liquid case give a hemolysis index of 0.12 g/100 ℓ, which is even lower then the 0.2 g/100 ℓ hemolysis index that Abcor has measured in a capillary membrane oxygenator.

TOXICITY STUDIES

During the operation of the liquid-liquid oxygenator with fluorocarbon, it is conceivable that an accidental upset would cause some fluorocarbon to be introduced into the body. To determine the effect of such a dosage of fluorocarbon, several types of injection studies have been made. In the first series of studies, slugs of fluorocarbon were injected intravenously into dogs. All the fluorocarbon samples were preheated to 37°C and saturated with oxygen before injection. The results of the intravenous slug injections are shown in Table 5. The first two dogs died after 0.1 ml of FX-80/kg. Autopsies showed extensive hemorrhages and severe pulmonary edema. Ten dogs received intravenous injections of FC-43. If the individual dose was 0.8 ml/kg, the dosage proved fatal after 1.6 ml/kg total. If the dose was lowered to 0.4 ml/kg, it was tolerable for from four to eight injections, and two dogs survived for much longer periods of time. The last dog is still alive.

TABLE 5

FC-43 INTRAVENOUS INJECTION STUDY

Dog No.	Dose of Inject.	Freq. of Inject.	No. of Inject.	Total Dose (ml)	Survival Time (Days)
727-K	0.4 ml/kg/inj.	3 Times/Week	4	16	7
608-K			7	28	13
695-K			46	184	98
693-K			50	200	110
624-K		5 Times/Week	8	32	12
716-K			5	20	5
723-K	0.8 ml/kg/inj.	3 Times/Week	1	8	2
745-K			2	16	3
665-K		5 Times/Week	2	16	2
714-K			2	16	2

A large amount of data was obtained on these dogs and it is summarized in Table 6. Particularly notable are the increase in white blood cell count and LDH level and a gradual decrease in cell volume and hemoglobin. Autopsies always revealed partially hemorrhagic and congested lungs and distended right ventricles. Red and white thrombus formation was observed in the pulmonary artery and right ventricle. The liver, spleen, and kidney were macroscopically normal. Microscopic examinations showed varying degrees of pulmonary edema accompanied by severe acute polymorpho nuclear infiltrate. In the longer survivor, pathologic findings showed chronic lipoid pneumonia with focal granulomatous reaction.

TABLE 6

LONG RANGE SHIFTING OF BODY VARIABLES DURING INTRAVENOUS INJECTIONS

	Long Range Changes Observed
Total Bilirubin	No Change
Alkaline Phosphatase	No Change
Blood Urea Nitrogen	No Change
Uric Acid	No Change
Glucose	No Change
Albumin	No Change, or Slightly Less
Total Protein	No Change
Calcium Ions	No Change
Cholesterol	No Change
Lee-White Clotting Time	No Change
Inorganic Phosphorus	No Change
SGOT	Slight Increase
LDH	Increase
White Blood Cells	Increase
Red Blood Cells	Decrease
Hemoglobin	Decrease
Cell Volume	Decrease

The next set of injections more typically represent what might be caused by accidental liquid-liquid oxygenator upset. Intraaortic injections of slugs of FC-43 were given and always immediately resulted in a grand mal type seizure, followed by coma and death.

In addition to slug injections, emulsions of FC-43 were prepared by mixing 20% by volume of FC-43 with a 5% dextrose solution, and with the addition of either Pluronic F-68® or dog albumin as a surfactant. In these emulsions, 99% of the fluorocarbon particles had diameters less then 2 microns.

Pluronic F-68® - Wyandotte Chemical Corporation

The dogs receiving intraaortic injections of emulsions also experienced a grand mal type seizure, but they recovered within 20 minutes. In most cases the dogs were anesthetized before injections to avoid this reaction. The survival of dogs receiving slug injections is shown in Table 7. SMA-12 and hematological findings showed no remarkable changes. Autopsy findings showed that macroscopically the heart, liver, and spleen had no pathological changes. Microscopic examination of the lungs showed focal intra-alveolar hemorrhages, passive congestion, and focal histocytic pneumonities with desquamation of alveolar lining cells. In the liver there was marked passive congestion and, in the kidney acute, tubular degeneration with focal acute tubular necrosis.

TABLE 7

INTRAAORTIC INJECTION STUDY

Dog No.	Slug or Injection	No. of Injections	Total Dose (ml/kg)	Survival Time	Cause of Death
751-K	Slug	1	.4	Less than 20 hours	Brain Damage
749-K	Emulsion	4	1.6	13 days	Sacrificed - Prolonged Coma
780-K	Emulsion	12	4.8	26 days	Cardiac Tamponade

	Before Injection	3 hours After Injection	6 hours After Injection
Chol. (mg%)	210	215	215
Ca^{++} (mg%)	10.8	10.9	10.7
Inor. Phos. (mg%)	6.2	5.5	7.2
Total Bili. (mg%)	0.1	0.1	0.2
Alb. (gm%)	2.2	2.1	2.0
T.P. (gm%)	5.9	6.5	6.2
Uric Acid (mg%)	0.7	0.7	1.0
B.U.N. (mg%)	11	11	12
Glu. (mg%)	100	110	125
LDH (W.U.)	125	105	100
Alk. Phos. (K.-A.U.)	8	9	9
SGOT (K.U.)	30	50	45
WBC	7,500	29,000	3,200
RBC	6,000,000	8,000,000	9,000,000
CV (%)	42	56	57
Hb (gm%)	14.5	19.7	19.6
Platelets	300,000	180,000	210,000

These injection studies show that, in spite of the fact that fluorocarbon is quite inert when contacted with blood _in vitro_, it is rather toxic when injected intravascularly. The direct chemical toxicity of FC-43 on body metabolism is probably quite small as evidenced by the fact that many body chemical factors as seen in this study showed minimal changes over extended periods of time. The toxicity seems to be more mechanical in nature. The fluorocarbon droplets obstruct the capillaries, especially in the lung, and they also seem to have an immediate effect on brain function. Enhancement of intravascular blood clotting also seems to be a result of FC-43 injections. Whether this clotting is caused by a chemical change or a simple mechanical obstruction, is still not clear. It is certainly clear, however, that, in order to have a practical liquid-liquid oxygenator, a very effective fluorocarbon exclusion device is essential to avoid any unexpected intravascular introduction of flourocarbon.

SUMMARY

Tests of the physical performance of the liquid-liquid oxygen exchanger _in vitro_ and _in vivo_ have shown oxygen exchange rates in the range of 30-70 cc/min-m^2, accompanied by sufficient CO_2 transfer. Gas exchange was measured using a 1.1 cm-diameter Teflon column, with a fluorocarbon liquid film flowing down the wall, and blood flowing up the central core. Use of parallel columns of this diameter would result in an excessive priming volume for the oxygenator. Thus, tests have been initiated using a 4 mm-diameter column, and a crossflow parallel-plate device, both of which would reduce priming volume substantially. Both test devices have been operated successfully, although gas exchange characteristics have not yet been evaluated.

Extensive work has been performed on the physiological effects of blood-fluorocarbon contact. _In vivo_ tests showed that hemolysis was lower in the liquid-liquid exchanger than in a membrane oxygenator. In vitro contacting studies indicated that neither plasma proteins nor formed elements in the blood were damaged or extracted by fluorocarbon. In toxicity evaluations with dogs, daily intravenous dosages as high as 0.4 ml/kg administered as single slugs, were tolerated by some animals for several months. Similar intraaortic injections resulted in coma and death, while intraaortic injections of fluorocarbon/dextrose solution emulsions were tolerable.

In general, good gas exchange, low hemolysis rates, and apparent lack of chemical toxicity of fluorocarbon liquid point to the potential success of the liquid-liquid device as an oxygenator.

DISCUSSION

DR. JACOBEY: You mentioned briefly in your introduction that you had considered surface tensions. I wonder what the difference in surface tension between your fluorocarbon and blood was. It seems to me this would be an important phenomenon both as regards gas transfer and in terms of adequate dispersion of the blood. Wouldn't it be possible to get a surface tension difference that would be less than your fairly large difference in specific gravity to allow reaccumulation of the blood on the top and still have better dispersion?

DR. deFILLIPPI: First, the surface forces we do find come into play when we go to very small diameter columns. You can calculate a force balance on the attempt to introduce a blood droplet into a column of fluorocarbon, and those forces do indeed balance the buoyancy due to the density differences. I cannot remember a good number for the surface tension of blood. The surface tension of these fluorocarbons is on the order of about 15 dynes per square centimeter, which is quite low.

DR. BLACKSHEAR: When Murray Rosenberg studied cell culture or any sort of culture with an aqueous phase in contact with a fluorocarbon phase, anytime he has proteins in the aqueous phase he forms a monolayer, sometimes a multiple layer on the interface. The thing that concerns me is that you have to flow the fluorocarbon through this system. Presumably, you flow the interface, too, and it seems for every square centimeter of interface you flow through the system you must scavenge at least the monolayer of the plasma protein. I was not clear in your blood damage test if the damage test included the effects of the flowing interface or whether this was exposure to an agitated but constant interface. I wonder if you could clarify that please?

DR. deFILLIPPI: To respond to the latter first, the samples were contained in a cylinder which was rotated where presumably there was indeed turnover of the interface while that was going on.

DR. BLACKSHEAR: But there was not a free flow from a reservoir to a reservoir in this test. It was just an agitated constant volume of blood?

DR. deFILLIPPI: There was constant volume of fluorocarbon; that is correct. Now, in our experimental tests, and I would say also I would visualize in the operation of this device, the inventory of fluorocarbon would remain constant. What we do experimentally is to cycle it through an oxygenating system. So it is not necessary, it seems to me, to feed and bleed fluorocarbon into the system and thus remove proteins from the system in this way.

I am not familiar with the data that you cite. I would expect, however, that you would get an equilibrium buildup of protein in the bulk of the fluorocarbon. You would then get the equilibrium surface concentration associated with that, and I would expect that that might limit the amount of protein extraction that occurs. Experimentally, thus far, based on the in vitro tests that we have run, this appears to be the case.

DR. KUSSEROW: I wonder if you would be kind enough to describe in somewhat more detail the method used to detect possible entrained globules of fluorocarbon. Secondly, I wonder if during the in vivo experiments with the oxygenator there was any autopsy study of the tissues. I presume you carried out a vein-to-artery type of perfusion. Were the tissues specifically examined to see whether or not there might have been small emboli and resultant infarction? Thirdly, I was interested in your data relating to blood trauma. I interpret these as indicating that the system with the fluorocarbon present is considerably less traumatic than the system in which blood was exposed directly to bare Teflon. Do you further imply from these data that there is no, or very minimal, blood damage in the absolute sense? I was somewhat concerned by the drop in platelets and the lesser drop in the white cells.

DR. de FILLIPPI: To answer briefly the first question (and I would like to ask Dr. Nose to respond to questions on cells and tissue damage), the blood samples were taken from the line returning to the animal and these samples were simply examined under a microscope to look for emboli. In other situations, we deliberately emulsified fluorocarbon in blood and we had a good idea of the size of emboli that can be expected for the amount of shear that might be produced in the oxygenator. In order to produce very small emboli, we have had to use relatively high shear in standard viscometers. Perhaps, Dr. Nose, you would care to comment on that also.

DR. NOSE: Yes, Dr. Kusserow, this is Yuki Nose of Cleveland Clinic answering your question. If we inject the fluorocarbon slug in dogs intravenously, we always get pulmonary lesions. They are intra-alveolar hemorrhage and pulmonary edema, and this was especially prominent in dogs that died within a short period of time. For instance, if we inject FC 43 slugs up to 0.8 ml/Kg body weight, then the animal usually dies in 24 to 48 hours. If the dose is less (0.4 ml/Kg three times per week), the dogs can survive more than several days and have the findings of more likely chemical pneumonitis. Two dogs survived more than three months, receiving more than 200 ml of FC 43. One of the dogs survived about 96 days. It is very interesting to see the lungs where the deposition of lipids has taken place; in other words, it may be called lipoid pneumonia. I realize that dogs who received large doses of fluorocarbon developed a gradual decrease of the hematocrit and blood red cell count, so maybe this has something to do with it. Pathologically, there might be four possibilities: one is a mechanical obstruction of the capillaries in the lung by the fluorocarbon. Second, the obstruction of capillaries by fluorocarbon gas; and maybe the third is the enhanced intravascular clotting tendency which is introduced by intravascular FC 43. In quite a large number of the dogs, we have seen a mass of red and white thrombus in the right atrium, right ventricle, and also in the pulmonary arteries. Also, clotting time studies indicated that there is a temporary shortening of the blood clotting times. Maybe intravascular clotting is induced originally by the fluorocarbon, or maybe secondary due to decreased flow. Fourthly, there are the direct chemical effects of fluorocarbon which I am not certain of at this time. In conclusion, I am not sure which possible causes play the main roles, but there is a vast difference in the toxicity tolerance doses; one dog may tolerate up to 300 ml of fluorocarbon, and another can tolerate only 10-20 ml. So maybe the explanation is that not one, but several factors are involved. Does that answer your question?

DR. KUSSEROW: Yes, I hasten to add that I was most intrigued by this very ingenious approach on the one hand, and yet I do want to endorse your concern over the possiblity of embolization of this material, especially into the arterial tree where even very minute emboli can be lethal, especially if emboli should happen to be carried into the upper branches of the aortic tree.

DR. NOSE: Maybe I should add something more. We used a fluorocarbon experimental oxygenator on four dogs by means of an arterio-venous shunt. One dog died instantaneously with massive introduction of fluorocarbon and three survived. We checked all the SMA 12 and routine hematological studies. They were normal, except for a rather short clotting time. We sacrified one dog one week following a five-hour perfusion. Surprisingly, we found that his lungs also had local intra-alveolar hemorrhages and also slight pulmonary edema. So maybe judging from these findings, this dog might also have gotten some fluorocarbon intravascularly. Regarding the intra-aortic injection, usually 0.1 ml/Kg body weight FC 43 slug injection is fatal. If we use an emulsion, dogs can tolerate 1 ml/Kg emulsified FC 43 for about 10 injections. Every time injection is made, the animal shows convulsion, incontinence, etc., which last for half an hour. So, I would like to stress the necessity of an embolus exclusion device for this type of oxygenator.

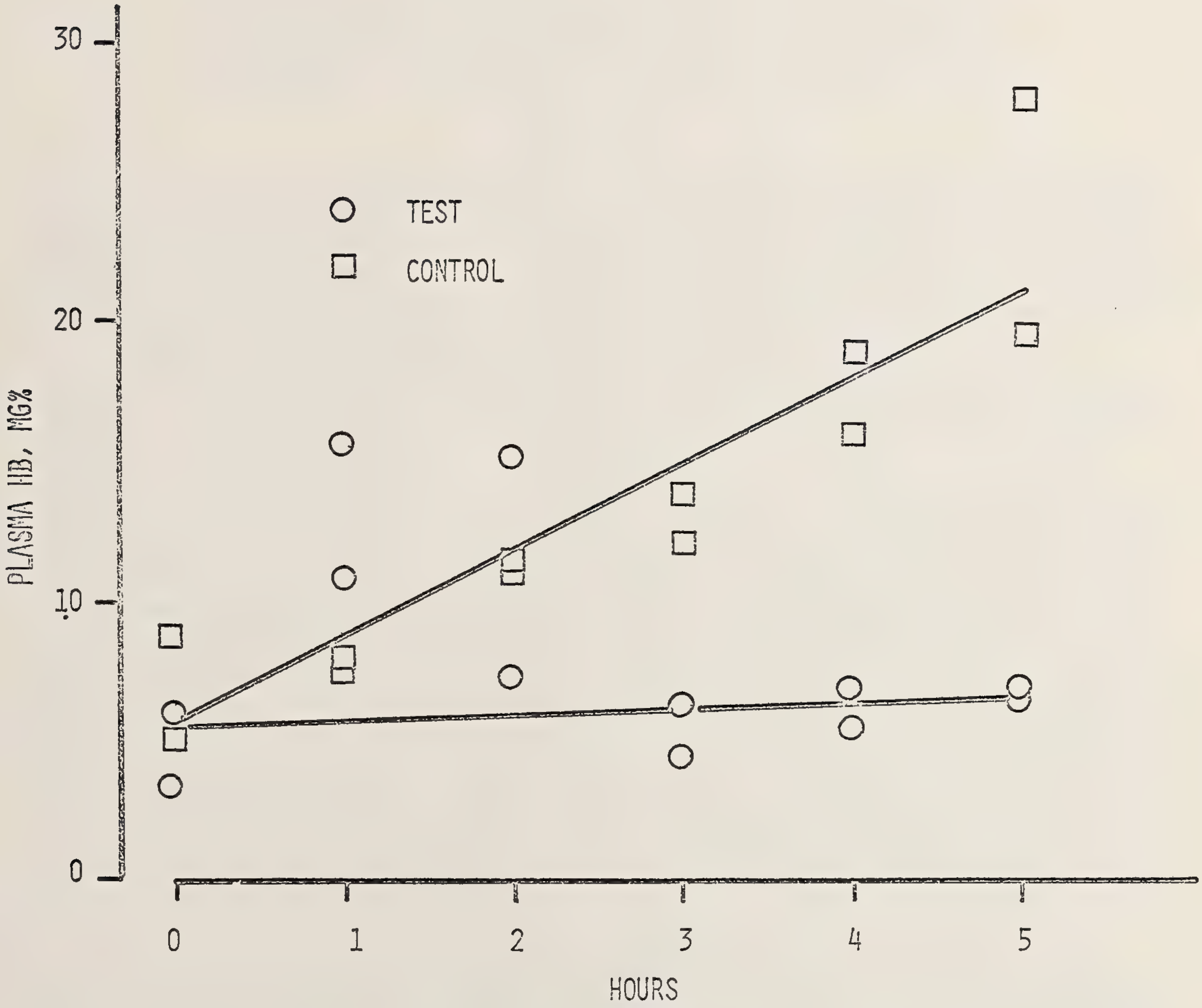

FIGURE 5. HEMOLYSIS STUDIES WITH LIQUID-LIQUID OXYGENATOR (FC-43).

CHAPTER 34

DEVELOPMENT OF A COUETTE OXYGENATOR

K. H. Keller

University of Minnesota, Minneapolis, Minn.

The purpose of this project is to develop a membrane oxygenator in which the blood flow field induces rotation of the red blood cells, thus promoting plasma mixing and reducing the resistance of the plasma to oxygen transport. A concentric cylinder device has been built and tested which induces a Couette flow field and a blood shear rate of up to 2000/sec. In the initial design using a G.E. XD polymer membrane, a blood throughput rate of 850 cc/min, and a blood layer thickness of 1 mm, uptake rates were about 25 ml(STP)/(sq.m.)(min) without rotation and 160 ml(STP)/(sq.m.)(min) with rotation (shear rate of 1500 inverse sec), representing an improvement of a factor of 6 due to flow-induce red blood cells rotation. A modified design with reduced dead space and improved bearing and seal construction is presently being tested.

DESIGN CRITERIA

In the normal resting condition, about six liters of blood per minute pass through the lungs, absorbing oxygen at a rate of approximately 250 mℓ (STP)/min and desorbing CO$_2$ at a slightly lower rate. The oxygen concentration in the entering blood is about 40 mm Hg and it must absorb enough gas to leave at about 95 mm Hg in order to provide a sufficient driving force for oxygen to be transferred into the tissues as the blood circulates around the body. The carbon dioxide concentration of blood entering the lungs is 46 mm Hg and it is reduced by CO$_2$ desorption to 40 mm Hg in the pulmonary venous blood. This latter figure is of particular importance since various circulatory control functions appear to use it as an input signal.

These very fundamental considerations provide the basis for establishing the functional requirements of any gas exchange device intended to substitute for the lungs. They may be summarized as follows:

1. The device must be capable of processing blood at the relatively high rate of five to six liters per minute.
2. It must have a minimal priming volume since the availability of blood is quite limited.
3. The blood leaving the exchanger must have well-controlled, essentially fixed levels of gas concentration.

In addition to these functional requirements, however, a further constraint and one that is frequently limiting, is that the device must satisfy these exchange requirements while causing no more than minimal damage to the blood. Blood damage of various sorts appears to occur in all extracorporeal flow circuits primarily, though not exclusively, from thrombosis and hemolysis. While the factors contributing to such damage are not completely understood, particularly in the case of hemolysis, it seems clear that interactions with foreign surfaces play a primary role.[1] Therefore, a reasonable goal in the design of an artificial organ is to minimize contact between the blood and foreign surfaces. A further obvious goal is to insure that any surfaces in contact with blood are made of materials that are minimally damaging. Since gas-blood interfaces are notoriously poor in this respect, most current design efforts are directed toward the development of membrane oxygenators. These efforts fall into two categories: the development of new membrane materials and the development of improved blood flow dynamics. Our own work has centered in the second of these areas.

The consequence of these functional requirements can be seen immediately by noting that steady state conservation of mass implies that the average time that an element of blood spends in the gas exchange device, τ_{res}, is given by:

$$\tau_{res} = \frac{V^*}{Q} \qquad (1)$$

where V is the active exchange volume (priming volume exclusive of dead space) and Q is the volumetric throughput. Since Q is 6 liters/minute, if we aim for a priming volume of less than 500 mℓ, the gas exchange process must be completed in less than 5 seconds, or, in more general terms, to minimize the priming volume for a given throughput rate, we must minimize the gas exchange time.

The full implications of this can be seen by considering the qualitative picture of gas exchange shown in Figures 1a and 1b. In Figure 1a, a system is shown in which blood flows at a relatively high rate through the oxygenator element. As a result, the boundary layer remains relatively small, the resistance to transport through the blood is low, and the rate of uptake consequently high. However, the average outlet concentration of oxygen in the blood is low and thus the third criterion is not met. By slowing the flow rate in the same unit, the situation depicted in Figure 1b would result. Since the blood remains in the unit longer, the boundary layers join by the time it exits and the blood is fully saturated. However, the average boundary layer thickness is much greater and

---

* Nomenclature is explained in section immediately preceding references.

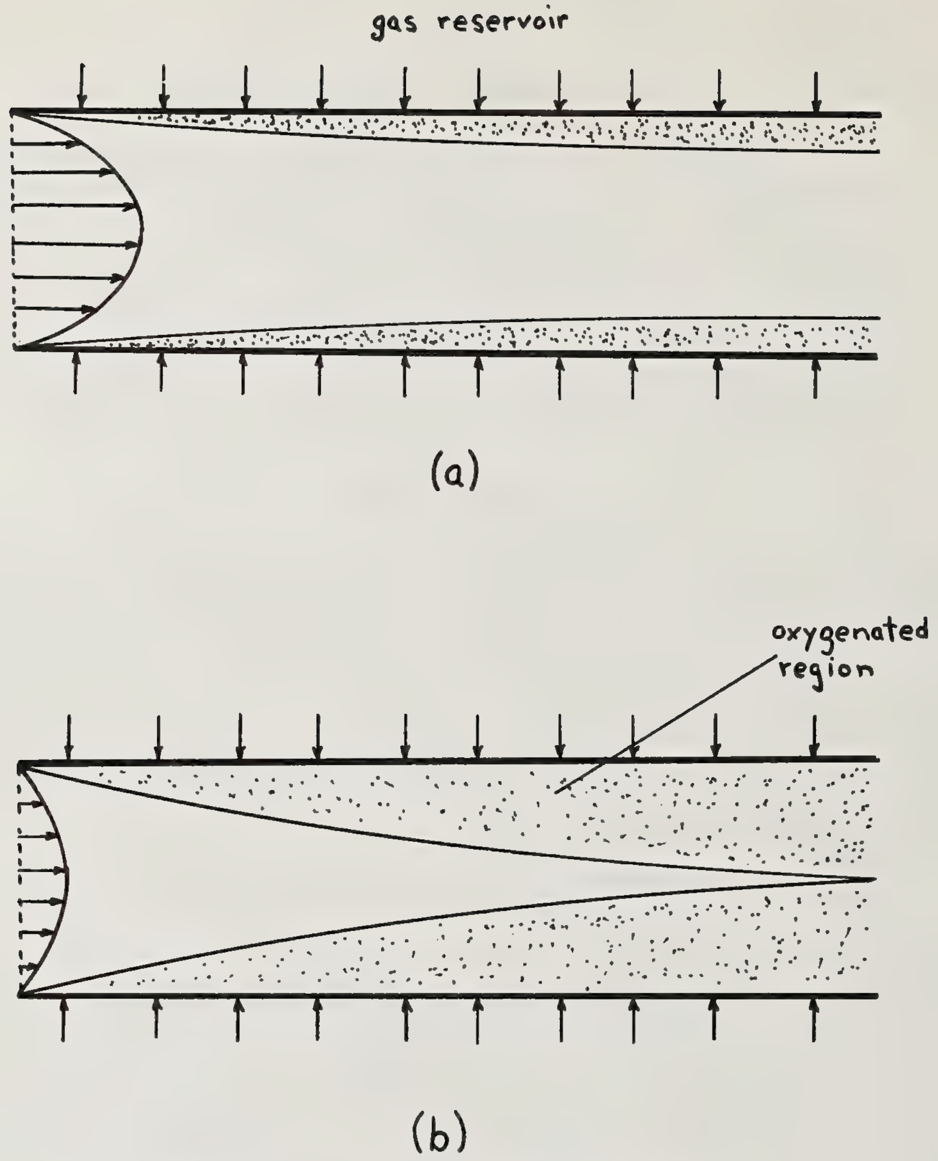

FIGURE 1. QUALITATIVE PICTURE OF GAS EXCHANGE.

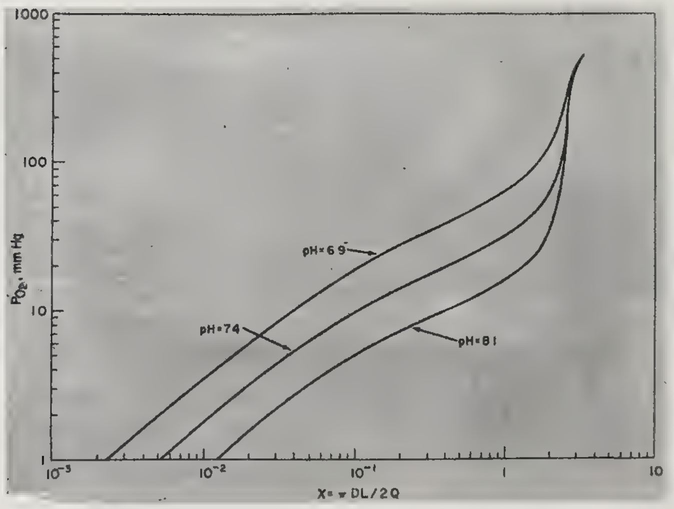

FIGURE 2. CALCULATIONS OF BUCKLES.

thus the rate of uptake is considerably decreased. The problem, then, is to design a unit constrained to oxygenate essentially to completion, but one which allows that process to occur in an acceptably short period of time.

Analytically, the problem of quantifying the above observations by an appropriate solution to the species conservation equation is hopelessly complex. A variety of simplifications have been proposed and attempted[4,5,6] the most important of which are that blood can be modeled as homogeneous and that the reversible reactions occurring are sufficiently rapid that the chemical species are near equilibrium at all times. Under those circumstances, the solution for the rate at which the amount of gas in the system changes can be expressed in the dimensionless form:

$$\frac{d\overline{\theta}_i}{d\xi} = f_{V*}\left(\Phi_i, \frac{1}{\gamma_i}\right) \tag{2}$$

where

$$\overline{\theta}_i = \frac{\overline{p}_i - (p_i)_{\xi=0}}{(p_i)_g - (p_i)_{\xi=0}} \tag{3}$$

and

$$\xi = \frac{x}{L} \tag{4}$$

Note that criterion (3) is equivalent to the requirement that $(\overline{\theta}_i)_{\xi=1}$ must reach a certain minimum value, or that the integral of Eq. (2) must reach that value.

The group γ_i is given by:

$$\gamma_i \equiv \frac{D_i \alpha_i}{(D_i)_m (\alpha_i)_m} \frac{\delta}{b} \tag{5}$$

and is the relative resistance of membrane and blood-to-gas transport. Its value is zero in a completely blood transport-limited situation, in which case Eq. (2) is independent of γ_i ; it is infinite in a membrane-limited situation, in which case Eq. (2) depends only on the membrane properties.

Φ_i is a modified Graetz number given by:

$$\Phi_i \equiv \frac{(D_i)_{eff}}{b^2} \frac{L}{\overline{v}} \tag{6}$$

where the quantities $(D_i)_{eff}$ are, respectively, for oxygen and carbon dioxide:

$$(D_{O_2})_{eff} = \frac{D_{O_2}}{1 + \frac{dc_{HbO_2}}{d\,C_{O_2}}} \tag{7}$$

$$(D_{CO_2})_{eff} = = \frac{D_{CO_2}\left(1 + \frac{D_{HCO_3}}{D\,CO_2} \frac{K}{C_{H^+}}\right)}{1 + \frac{K}{C_{H^+}}} \approx D_{CO_2} \tag{8}$$

and K is the equilibrium constant for the reaction:

$$CO_2 + H_2O \rightleftarrows HCO_3^- + H^+ \tag{9}$$

Φ_i can be interpreted as the ratio of the blood residence time $(V/Q = L/\overline{v})$ and a diffusional relaxation time $(b^2/(D_i)_{eff})$. $\frac{d\overline{\theta}_i}{d\xi}$ varies monotonically with Φ_i and $\frac{1}{\gamma_i}$ so that we seek to minimize γ_i and maximize Φ_i in order to reach the required level of $\overline{\theta}_i$ in the shortest possible time.

By calculating γ_i for the membrane materials presently available, it can be shown that blood film resistance for oxygen transport is limiting while membrane and blood have comparable resistances for CO_2 transport. Therefore, our immediate concern has been with the oxygenation problem where we expect the uptake rate to be a function of Φ_{O_2} primarily.

We note from Eq. (7) that $(D_{O_2})_{eff}$ is always smaller than D_{O_2} since the slope of the hemoglobin oxygenation curve appears in the denominator. Therefore, the rather paradoxical circumstance arises that the effect of the chemical reaction is to slow the response time of the blood. This is illustrated quite well in the calculations of Buckles[4] shown in Figure 2 where the rate of change of average oxygen concentration varies widely depending upon the local slope of the oxygenation curve. Because of the large capacitance of blood for oxygen, however, one should not infer a lowered rate of uptake associated with the increased response time.

As Eq. (8) shows, this effect does not appear in $(D_{CO_2})_{eff}$ so that the response time for CO_2 desorption is much shorter than that for O_2 uptake. This provides an additional justification for neglecting the CO_2 desorption problem in this particular study.

In summary, there are three approaches to maximizing the value of the left side of Eq. (2) for a blood-limited-transport situation: we can modify the velocity field to magnify the functional dependence of $d\bar{\theta}_i/d\xi$ on Φ_i ; we can increase Φ_i by decreasing b ; we can increase $(D_i)_{eff}$ to increase Φ_i . Until now, with some notable exceptions[7], major efforts have been directed at decreasing b . The question that arises is what effect the decrease of b has on blood damage in oxygenators. This question has been difficult to answer because there have been few models of the damage process available. One of the directions our design work has taken has been the evolution of a mathematical model for the damage process.

Since progress in the development of anti-thromobogenic surfaces has been encouraging, the problem of hemolytic blood damage may ultimately prove to be the limiting factor in long-term extracorporeal circulation. At present, the most feasible approach to this problem has been to minimize interfacial contacts between red blood cells and the surfaces of the oxygenator. To determine how best to accomplish this, we are presently examining a two-zone model of blood flow (skimming layer and core) with damage at the wall occurring in a first-order process. Preliminary results indicate that in many important cases, decreasing the channel spacing will increase the amount of hemolytic blood damage. While this work is incomplete, it suggests the importance of seeking to minimize priming volume by maximizing $(D_{O_2})_{eff}$.

A variety of phenomena are reflected in the value of $(D_{O_2})_{eff}$, including the fact that diffusion occurs through a heterogeneous medium, that secondary flow phenomena may superimpose on the basic flow field, that local flow phenomena may augment plasma mixing, and that chemical reaction is occurring. The first and last of these effects are relatively independent of oxygenator design, but the others are not. Early efforts to increase $(D_{O_2})_{eff}$ have been made either by the simple expedient of putting disturbances in the flow[8,9] or by the more sophisticated technique of inducing secondary flows[7,10]. Our efforts have been aimed at attempting to utilize a secondary flow phenomenon arising from the shear flow of a particulate suspension.

PARTICLE ROTATION INDUCED DIFFUSION

It has long been known that when a single particle is subjected to a fluid shear field, as shown in Figure 3, it rotates at a rate that will depend upon the shear rate and the shape of the particle. If the particle is spherical the rotation occurs at a steady angular rate $\omega = \frac{1}{2} (\frac{dv}{dy})$. If the particle is not spherical it tends to remain in a position aligned with the flow for relatively long periods of time and with its long axis normal to the flow for shorter periods. An excellent review of the hydrodynamics of dilute particle suspensions is presented by Goldsmith and Mason[11].

Since the fluid is viscous, as the particle rotates it drags with it a surrounding region of fluid, in effect stirring the region and giving rise to an eddy diffusion phenomenon. The order of magnitude of this effect can be estimated from an analysis similar to the Prandtl mixing length development[12]. In a previous report we showed that, as a first estimate, the diffusion coefficient associated with the particle rotation is given by:

$$D_p \approx \frac{\delta^2}{8} \left(\frac{dv}{dy}\right) . \qquad (10)$$

Under circumstances where D_p is large compared with the Brownian motion diffusion coefficient, particle-induced rotation can clearly have an important effect. Since δ is approximately 8μ , for D_p to be ten times the Brownian motion D_{O_2} (which has a value of 1.01×10^{-5} cm^2/sec at 25°C in stagnant blood[13], $\frac{dv}{dy}$ must be at least 1250 sec^{-1}. The increase in the overall value of D_{O_2} that results from particle rotation is much more difficult to assess. In concentrated blood suspensions, interactions among the blood cells decrease the rate of rotation of the cells so that Eq. (18) will certainly be in error. On the other hand, the increased cell concentration tends to increase the influence of particle rotation on the overall effective diffusion coefficient. While work is continuing on analyzing the effect mathematically, it has seemed more appropriate to test its importance experimentally and, in particular, its usefulness in augmenting gas transport in the plasma.

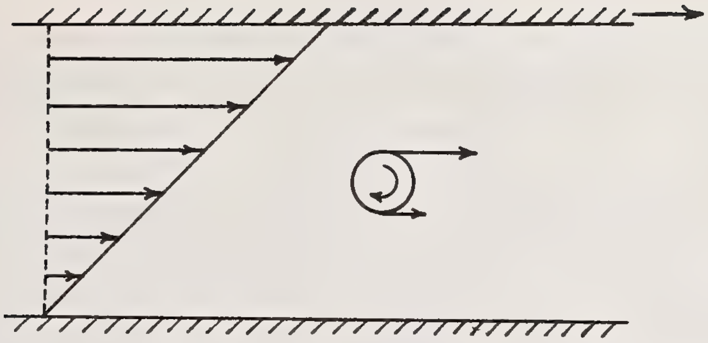

FIGURE 3. SINGLE PARTICLES SUBJECTED TO A FLUID SHEAR FIELD.

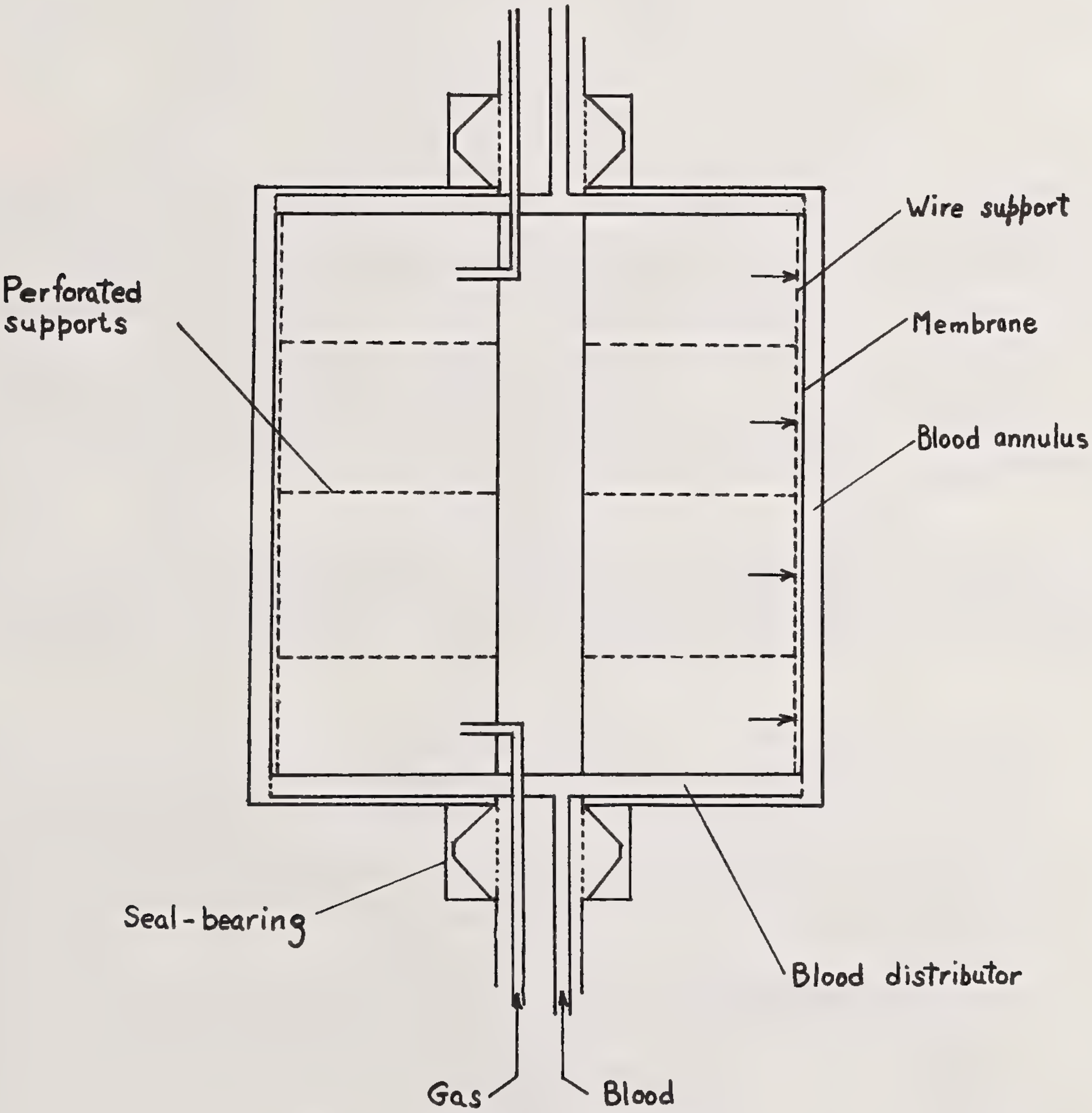

FIGURE 4. DIAGRAM OF FIRST MODEL OF THE COUETTE OXYGENATOR.

DESIGN DESCRIPTION

Since D_p will be proportional to the local value of the velocity gradient, parabolic flow fields, which always contain regions of low shear, appeared to us to be intrinsically inefficient for bringing about particle-induced transport augmentation. Moreover, such flow fields are brought about by pressure drops over the channel length and they introduce a coupling between the rate of blood flow through the system and the local shear rate. This interaction reduces the flexibility of design (in terms of the rotation phenomenon) and leads ultimately to systems with very high pressure drop and relatively narrow channels.

To avoid these problems, we decided to utilize a Couette flow field, a flow brought about by the relative movement of two parallel surfaces. This has the advantage of exhibiting a shear rate which is both independent of position and easily adjustable by changing the relative velocity of the two surfaces. From a design point of view, a cylindrical Couette field is particularly simple and was therefore selected. The cylindrical Couette field has no net throughput, so we superimposed on it an axial flow through the gap. This introduced a slight parabolic profile in the axial direction, that is, in the direction normal to the Couette velocity field. The net flow is slightly helical.

A diagram of the first model of the Couette oxygenator is shown in Figure 4. The inner cylinder is made up of a series of support plates around which are wrapped a stainless steel wire mesh screen and a highly gas-permeable polymer film. The outer cylinder is constructed of Lucite and has an outside diameter of one foot and a height of one foot. The annular gap between the gas-permeable membrane and the inner surface of the outer cylinder is 1 mm.

The membrane used was a .001" copolymer film containing silicone rubber identified by G.E. as XD polymer. Transport in the gas phase both in bulk and through the wire mesh screen was assumed to be very efficient compared with transport through the membrane and in the blood.

In operation, oxygen and blood enter the unit through the bottom, the gas passing to the inner region of the inner cylinder and the blood being distributed in the annular region. Both gas and blood also pass out through the top. The inner cylinder is stationary; the outer one is capable of being rotated by a motor drive at varying rates up to 120 RPM inducing shear rates up to 2000 sec^{-1} in the blood. A recirculating system, shown in Figure 5, provides for closed circuit operation for testing. Deoxygenation is accomplished by a DeWall oxygenator through which nitrogen is bubbled in place of oxygen. No temperature control was provided for so that oxygenation occurs at room temperature.

In the initial experiments, provision was made for measuring oxygen concentration either upstream or downstream of the oxygenator using an oxygen electrode mounted in a Beckman temperature-controlled cuvette. The degree of hemoglobin saturation was determined using oxygenation curves in the literature[15]. A standard rotameter was used to measure blood flow rate and a stroboscope to determine the cylinder rotation rate.

RESULTS AND DISCUSSION

Runs on this first model were made with washed human red blood cells resuspended in Ringer's solution at a hematocrit of 40%. Data on uptake rates were first obtained with the outer cylinder stationary. Rotation of the cylinder was then begun and additional uptake data recorded. Finally, the cylinder rotation was stopped and data again taken on uptake rates. The results are shown in Table 1.

TABLE 1

RESULTS OF OXYGENATOR EXPERIMENTS USING HUMAN RED BLOOD CELL SUSPENSIONS AT $25^0 \pm 1^0C$

Relative time change	$(pO_2)_{in}$ mm Hg	$(pO_2)_{out}$ mm Hg	$\Delta(\%HbO_2)$	uptake rate $m\ell O_2(STP)/m^2min$
Begin run, cylinder stationary. Pump flow 0.7 liters/min.				
0 min	14	20		
30 min	10	12.5	11%	49.2
Start cylinder rotation at 85 ± 5 RPM. Pump flow unchanged.				
35 min	10	40		
60 min	13	77	37.4%	167.5
Stop cylinder rotation. Pump flow unchanged.				
65 min	15	46		
90 min	12	15	9%	40.4

It can be seen that uptake rates increased by a factor of approximately 4 when the cylinder rotation was such that the shear rate in the blood was approximately 1350 sec^{-1}. The maximum rate of uptake was about half of the theoretical value for the membrane.

Since the outside cylinder was the one rotating, Taylor vortices should not have been present. However, the possibility existed of other flow perturbations resulting from flat spots on the membrane support structure. To check on the degree of augmentation that might have resulted from such perturbations rather than from red blood cell rotation, a similar set of runs was performed using water in place of blood. These results are shown in Table 2.

TABLE 2

RESULTS OF OXYGENATOR EXPERIMENTS USING WATER AT 25°±1°C

Relative time	$(pO_2)_{in}$	$(pO_2)_{out}$	Uptake rate
Begin run, cylinder stationary, pump rate 0.7 liters/min.			
0	56 mm	182 mm	$10.0\ \frac{ml\ O_2}{min\ m^2}$
60	44 mm	156 mm	
Begin cylinder rotation at 93±8 RPM. Flow rate unchanged.			
75	54 mm	243 mm	$27.5\ \frac{ml\ O_2}{min\ m^2}$
160	52 mm	360 mm	
Stop cylinder rotation. Pump flow unchanged.			
220	45 mm	171 mm	$11.4\ \frac{ml\ O_2}{min\ m^2}$
260	37 mm	165 mm	

Note that augmentation under these circumstances did occur, but only by a factor of about 2 1/2. Two effects make quantitative comparisons between the two sets of data difficult. The driving force variation in the water runs was not insignificant, the log mean value varying by 15-20% between rotational and non-rotational runs. This would tend to yield erroneously low values of uptake on the rotational experiments. On the other hand, the support structure flat spots which we believe are responsible for the augmentation in the water runs would have created local lower shear regions which would decrease cell-rotation induced augmentation. Fortunately, these two effects lead to errors of opposite sign and therefore tend to cancel each other.

The appearance of flow perturbations in the water runs is not, in itself, disturbing since the resulting augmentation does increase oxygen uptake rates. However, it makes it difficult to assess the true importance of the particle-induced augmentation phenomenon itself. Moreover, we have postulated that the introduction of secondary flow phenomena to augment transport is most useful if it does not simultaneously increase the rate of contact of red blood cells with the wall and thereby increase the hemolysis rate. Gross secondary flow phenomena are likely to have this effect, but the local agitation brought about by red blood cell rotation is less likely to have this result. Therefore, we were particularly interested in redesigning the device to reduce the gross secondary flow effect in order to study the particle-rotation effect more closely.

REVISED DESIGN

The current design is shown in Figure 6. The basic structure of the new unit is made of stainless steel and the unit has been reduced in size; the new diameter is approximately 6" and the active height approximately 8". The inner cylinder is a steel cylinder perforated with 3/8" diameter holes. A stainless steel screen is wrapped around the perforated cylinder and the XD polymer membrane around that. A compression ring at top and bottom seals the membrane on its edges; heat sealing augmented by a silicone-base tape is used on the membrane's end.

The problem of maintaining an adequate seal-bearing has been reduced by half since the bottom seal has been eliminated; all flow lines penetrate the unit at the top. The priming volume of the oxygenator itself is about 40 cc and the membrane transfer area is 52 in^2. The gap thickness is .024" or approximately 0.6 mm.

In the testing circuit, two additional changes have been made. A Sarns roller pump has replaced the rather unwieldy finger-pump previously used and an oximeter has been added to the instrumentation to provide a direct reading of percent saturation of hemoglobin.

RESULTS AND DISCUSSION OF REVISED DESIGN

The results for water runs with the new design are shown in Table 3. The flow perturbation induced diffusion augmentation has been substantially reduced. In all runs it was less than 25% of the unsheared value. The actual uptake rates of oxygen are somewhat higher than those in the runs on the first design, but this is not inconsistent with the fact that the much smaller active exchange volume (about 40 mℓ compared with about 250 mℓ on the earlier design) resulted in a shorter residence time and consequent decreased boundary layer thickness.

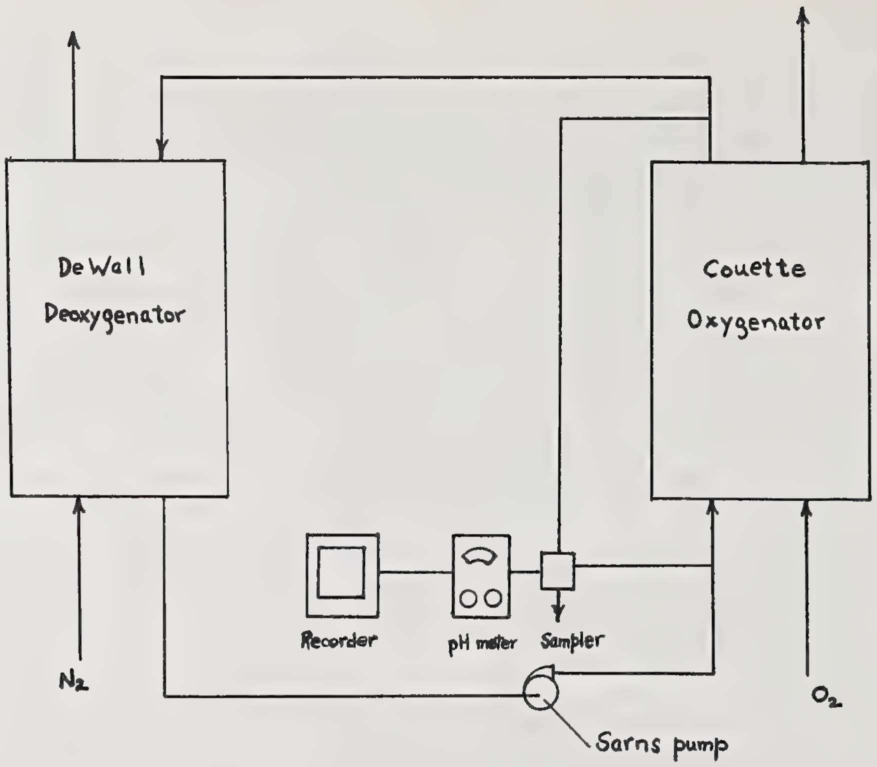

FIGURE 5. RECIRCULATING SYSTEM.

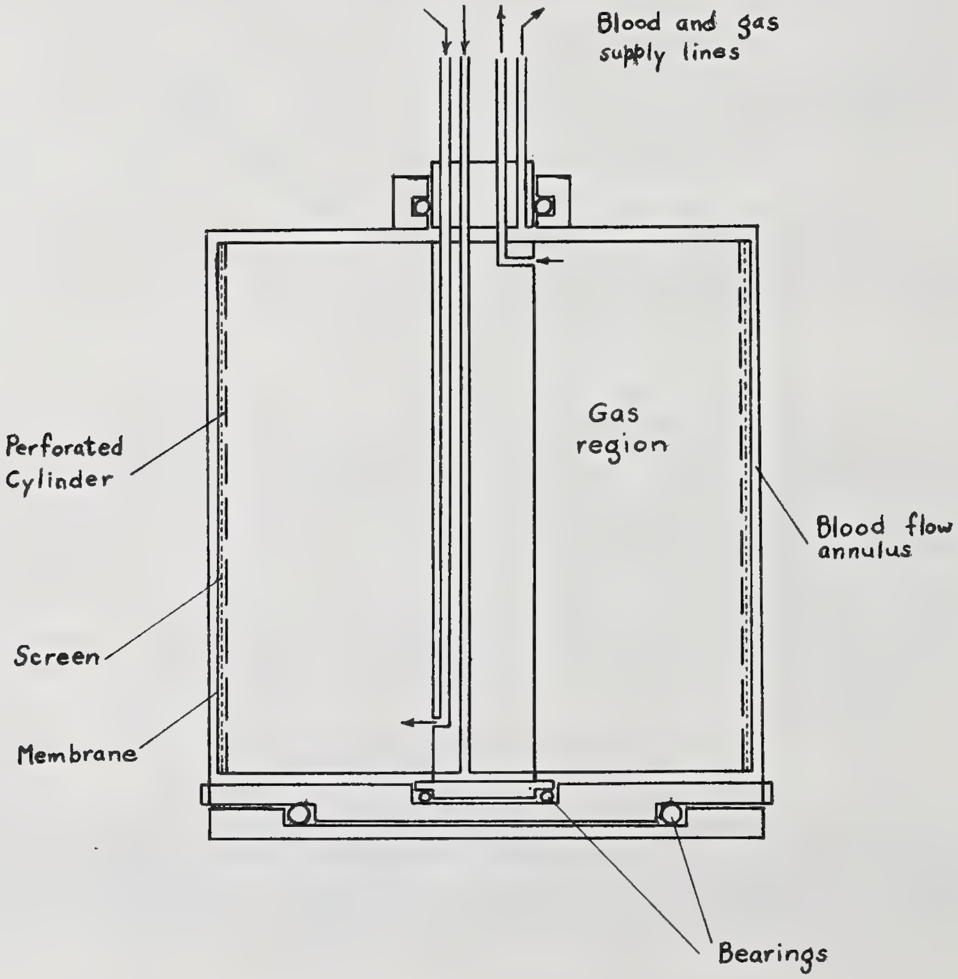

FIGURE 6. CURRENT COUETTE OXYGENATOR DESIGN.

TABLE 3

RESULTS OF WATER EXPERIMENTS WITH 2ND OXYGENATOR AT 22^{0}C

Flow rate	RPM	$(pO_2)_{in}$ mm Hg	$(pO_2)_{out}$ mm Hg	uptake rate $mlO_2(STP)/m^2min$
325 cm^3/min	0	31	120	32
"	30	33	132	35.6
"	46	30	127	34.9
"	107	29	137	38.8
136 cm^3/min	0	60	245	30.2
"	60	67	290	37.1

Selected data for the blood runs are shown in Table 4. The data indicate that augmentation by red blood cell rotation does occur. The conversion factor from RPM to shear rate is 13.2 sec^{-1}/RPM so that runs at 30, 60, and 120 RPM correspond to 396, 792, and 1584 sec^{-1} respectively. Uptake rates are approximately doubled although there is some evidence that the increase is not linear. As expected, the uptake rate at lower throughput rate is less than that at the higher throughput.

TABLE 4

RESULTS OF BLOOD EXPERIMENTS WITH 2ND OXYGENATOR

Flow rate	RPM	(pO_2)in mm Hg	(pO_2)out mm Hg	$\Delta(\%HbO_2)$	uptake rate $mlO_2(STP)/m^2min$
140 cm^3/min	0	19	20	3%	23.7
"	60	19	21.5	6%	47.5
"	120	20	22.5	5.5%	43.5
72 cm^3/min	0	21		2%	8.6
"	121	21	25	5.5%	23.6
"	180	21		7%	30.2
140 cm^3/min	0	37	43	2%	15.8
"	60	37	47	3.3%*	26.4
"	115	37	49.5	4.16%*	32.9

We are still encountering significant difficulty with leakage from the blood space to the gas space and in assuring accurate readings of the percent saturation of inlet and outlet blood. Efforts are now underway to correct these difficulties. Further modification of the collar sealing the membrane at the top is being undertaken and all sampling lines are now constructed of glass to avoid leakage of oxygen in between the system and the measuring cuvette. In addition, in future runs, the blood will be buffered to a lower pH to flatten the oxygenation curve, thus decreasing the sensitivity of the results to small errors in measuring percent saturation or pO_2.

BLOOD DAMAGE

One of the important questions which must be asked about this oxygenator is to what extent the blood is damaged during its oxygenation. The present experimental apparatus does not provide a feasible method for evaluating such damage. The DeWall deoxygenator, which is a bubbling device, is known to be intrinsically traumatic to blood and it would not be possible to separate its damaging effects from those of the Couette unit. When the Couette design progresses to an acceptable point, a recirculating system containing only the Couette oxygenator will be tested to establish its effect on hemolysis.

From a more theoretical point of view, the question of relative damage in the present oxygenator and in designs not utilizing secondary flows depends upon the effect of the secondary flows on the movement of red blood cells to and from the walls of the device. If the effective diffusion coefficient of red blood cells increases more than the effective diffusion of oxygen does, then relative damage (the cells damaged per unit of blood oxygenated) will increase. If the opposite is true, damage will be less. With particle-induced rotation, the answer to this question will depend upon whether particle rotation increases more or less than particle translation in the shear field. In concentrated cell suspensions such as blood, it would appear that rotation* will, in fact, increase more than translation, but this has yet to be shown.

* For purposes of diffusion augmentation, an oscillating movement of the cells without complete rotation is all that is required for an effective rotational augmentation.

CONCLUSIONS

1. Particle-rotation induced transport augmentation appears to be effective in promoting gas transport through plasma.
2. A Couette flow field design permits oxygenation of blood in layers about ten times as thick as those employed in membrane oxygenators without significant secondary flows. Moreover, the transport rates achievable are of the order of the permeability of existing membrane materials.
3. Hemolytic damage during oxygenation must be investigated to determine the effect of the secondary flows on the rate of collision of red blood cells with walls.

ACKNOWLEDGEMENTS

This work was supported by the National Heart Institute under NHI Contract No. Ph-43-67-1419, which is gratefully acknowledged.

The experimental work in this project has been performed by Mr. Michael Overcash who has made extensive contributions to the overall effort.

NOMENCLATURE

b = Half-spacing between parallel plates, cm.
C_i = Concentration of the i^{th} species, gmoles/cm^3.
D_i = Brownian motion diffusion coefficient, of species i cm^2/sec.
D_{O_2} = Apparent diffusion coefficient of O_2 in a dynamic heterogeneous syspension, cm^2/sec.
$(D_{O_2})_{eff}$ = Apparent diffusion coefficient of O_2 in a heterogeneous suspension in which a chemical reaction occurs which is not accounted for explicitly, cm^2/sec.
D_p = Apparent diffusivity induced by particle rotation, cm^2/sec.
L = Length of an oxygenation channel, cm.
Q = Total blood flow rate through oxygenator, cm^3/sec.
$\bar{v}$ = Average velocity in a channel, cm/sec.
V = Total blood priming volume, cm^3.
α_i = Solubility of the i^{th} species, $m\ell$(STP)/$m\ell$.
γ_i = Ratio of membrane resistance to blood resistance defined by Eq. (5).
δ = Diameter of a red blood cell, cm.
ν_i = Stoichiometric coefficient of i^{th} species.
ξ = Dimensionless distance along oxygenator x/L.
Φ_i = Modified Graetz number given by Eq. (6).

SUBSCRIPTS

g = Parameter associated with the gas phase.
m = Parameter associated with the membrane phase.
o = Value at the blood inlet.

REFERENCES

1. Bernstein, E. F., Blackshear, P. L. and Keller, K. H., Am. J. Surgery, 114, 126 (1967).
2. Hershey, D. and Hesselberth, J., A.I.Ch.E. National Meeting, New York (1967).
3. Spinak, R. B., Transport of Carbon Dioxide in Erythrocytes, Master's Essay. University of Minnesota, 1969.
4. Buckles, R. B., Merrill, E. W. and Gilliland, E. R., A.I.Ch.E. Journal, 14, 703 (1968).
5. de Fillippi, R. P. et al, Trans. Am. Soc. Art. Int. Organs, 14, 236 (1968).
6. Spaeth, E. E. and Friedlander, S. K., Biophysical J., 7, 827 (1967).
7. Weissman, M. H. and Mockros, L. F., J. Eng. Mech. Div., A.S.C.E., 94: Em 3, June 1968.
8. Bluemle, L. W. et al, Trans. Am. Soc. Art. Int. Organs, 6, 38 (1960).
9. Landé, A. J. et al, Trans. Am. Soc. Art. Int. Organs, 14, 227 (1968).
10. Drinker, P. A. et al, Augmentation of Membrane Gas Transfer by Induced Secondary Flows, Surgery (in press).
11. Goldsmith, H. L. and Mason, S. G., in Rheology, Theory and Applications, F. R. Eirich, Ed., Vol. IV (1968).
12. Bird, L. B., Stewart, W. E., and Lightfoot, E. N., Transport Phenomena, p. 629, Wiley (1960).
13. Stein, T. R., Augmented Diffusion of Oxygen, Ph.D. Thesis, University of Minnesota, 1968.
14. Pierce, E. C. II and Dibelius, N. R., Trans. Am. Soc. Art. Int. Organs, 14, 220 (1968).
15. Severinghaus, John W., in Handbook of Physiology, Section 3, Vol. II, Edited by Fenn, W. O. and Rahn, H., pp. 1475-1487 (1965).

DISCUSSION

DR. KUSSEROW: Dr. Keller, do you feel that the centrifugal force which acts on the red cells in your Couette system is at all a significant factor in compromising the efficiency of oxygenation in the device?

DR. KELLER: Well, if there is a centrifugal force, it will tend to decrease the efficiency because the membrane is on the inner cylinder. I don't believe it is a significant force, but the only reason I have for saying so is that there is such a very small density difference between the cells and the suspending medium for the kind of centrifugal force we are putting on them; the first unit had a diameter of twelve inches, the second one eight inches; we are only rotating at rates of about 150 RPM's, so we are not getting any kind of significant force on them during the time that they remain in the oxygenator which varies from approximately 10 to 30 seconds. So I don't think that is a problem at the moment. We intend to experiment using the outer membrane as the transferring one. Perhaps I will then have reason to change my mind.

CHAPTER 35

DESIGN AND FABRICATION OF BLOOD OXYGENATOR FOR CIRCULATORY ASSIST DEVICES

E.C. Peirce

Emory University School of Medicine, Atlanta, Georgia

and

W.F. Mathewson, Jr.

General Electric Company, Schenectady, New York

The evaluation of General Electric silicone copolymer, with regard to gas exchange capability and blood trauma studies, continued. Both oxygen and carbon dioxide transfer have been studied as a function of membrane support technique, membrane thickness, blood film thichness and flow rate, and shim pressure in the Peirce oxygenator. To further evaluate the usefulness of this membrane material, it has been compared with Teflon and the disc oxygenator in paired *in vitro* experiments to distinguish the difference in blood trauma. Comparable circuits were primed with 500 ml fresh heparinized blood simultaneously drawn from the same dog. One used a six-inch Esmond oxygenator with 13 convoluted discs run at either 75 or 100 rpm. Another used a Peirce lung with $0.5M^2$ of Teflon or copolymer membrane. Six-hour tests were run at 500 ml/minute flow and 37^oC. Each experiment represented 360 circulations of the entire blood volume. Supplied gas was 3% CO_2 in air. Blood held at 37^oC or 25^oC was used for control. Tests included: Plasma hemoglobin (PHb), cell counts, O_2 saturation, glucose, lactic dehydrogenase (LDH), viscosity, prothrombin time (PT), partial thromboplastin time (PTT), euglobulin clot lysis (ECL), fibrinogen, pH, pCO_2, and culture. Trauma could not be assessed by cell counts, changes in viscosity, PT, PTT, ECL, or fibrinogen. LDH values correlated with time but only in individual experiments. PHb levels provided a satisfactory measure of trauma. Copolymer membranes with intrinsic point support caused little more trauma than the circuit alone, while the inclusion of polyvinyl coated fiber glass screen between the copolymer membrane resulted in severe trauma. The disc, run at 75 rpm, was comparable to the Teflon membrane lung but was much more traumatic at 100 rpm.

INTRODUCTION

Over the past year, the purpose of this program has been to prepare screen supported and point (cone) supported copolymers (polycarbonate/silicone rubber) membrane envelopes and to evaluate those envelopes in the Peirce lung configuration for gas exchange capabilities and blood damage characteristics. The best of these envelope configurations was then to be produced in sufficient quantities for more extensive blood damage tests and for long-term (24 hours) dog perfusions.

The following relates the results of those program tasks, and in addition provides sufficient analysis to yield the basis for future work.

GAS EXCHANGE

During the course of this two-year program many combinations of membrane and membrane support have been evaluated for gas exchange and blood damage characteristics in the Peirce artificial lung. However, the combination of copolymer (polycarbonate/silicone rubber) with cone support, as shown in Figures 1 and 2, gave the best overall gas exchange and blood damage performance. Therefore, the gas exchange discussion will focus on the copolymer, cone support systems.

The experimental results for that system are summarized in Figure 3 through Figure 6. The oxygen transfer was calculated from the AV difference and the blood flow rate. The blood channel height was calculated from blood holdup measurements. From inspection of Figures 5 and 6, it can be concluded that oxygen transfer can be correlated best with blood channel height. This correlation is shown in Figure 7. Maximum transfer occurs at minimum channel height which is achieved at low blood flows and high shim pressures. It is obvious then that membrane distension remains as the major problem in achieving good gas exchange at high blood flow rates. The relative significance of distension, blood film and membrane resistance, with regard to oxygen transfer and oxygen/carbon dioxide balance, can be seen from the following analysis.

The oxygen transfer through the membrane is given by:

$$N_{O_2} = k_m A(P_g - P_i) \qquad (1)$$

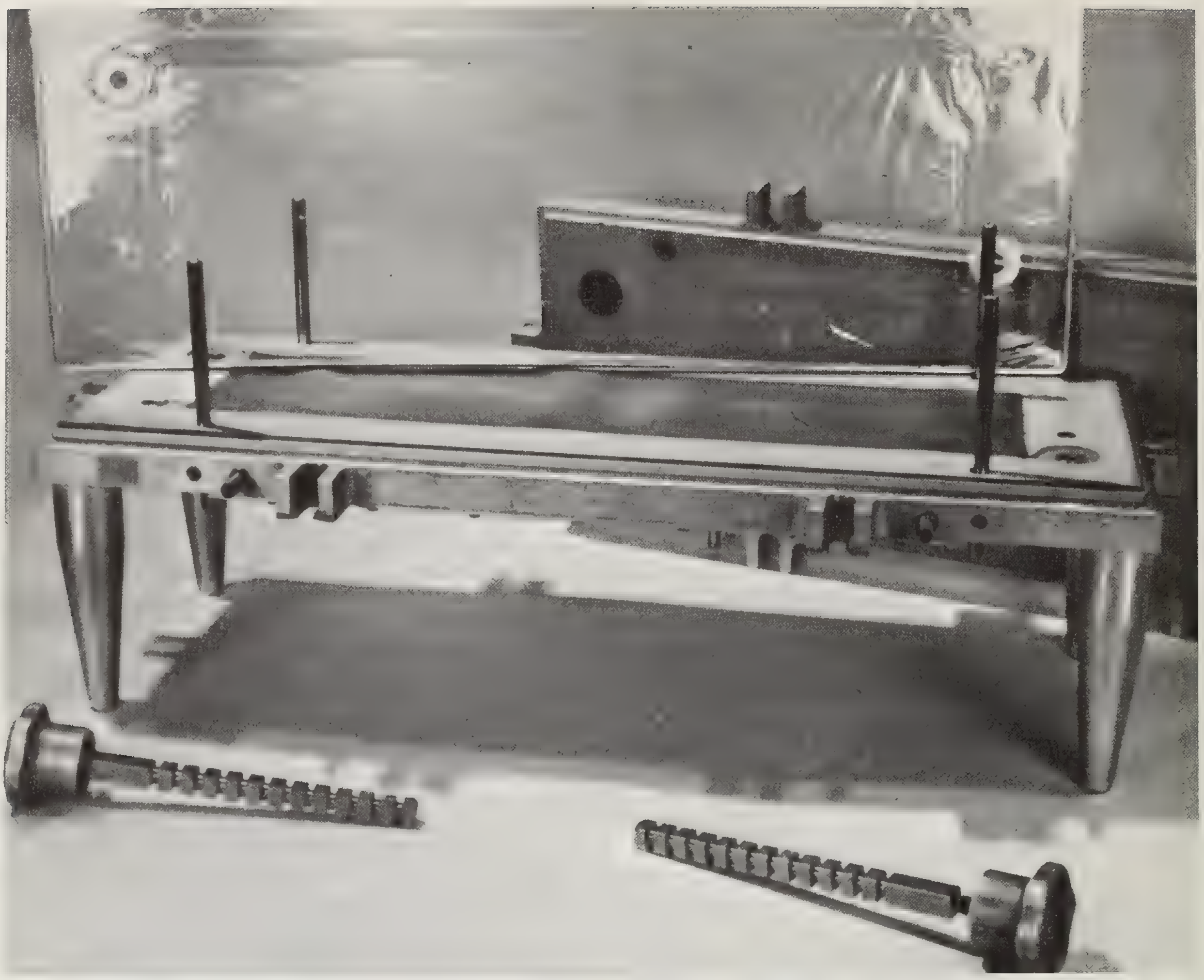

FIGURE 1. PEIRCE LUNG WITH COPOLYMER MEMBRANE ENVELOPE.

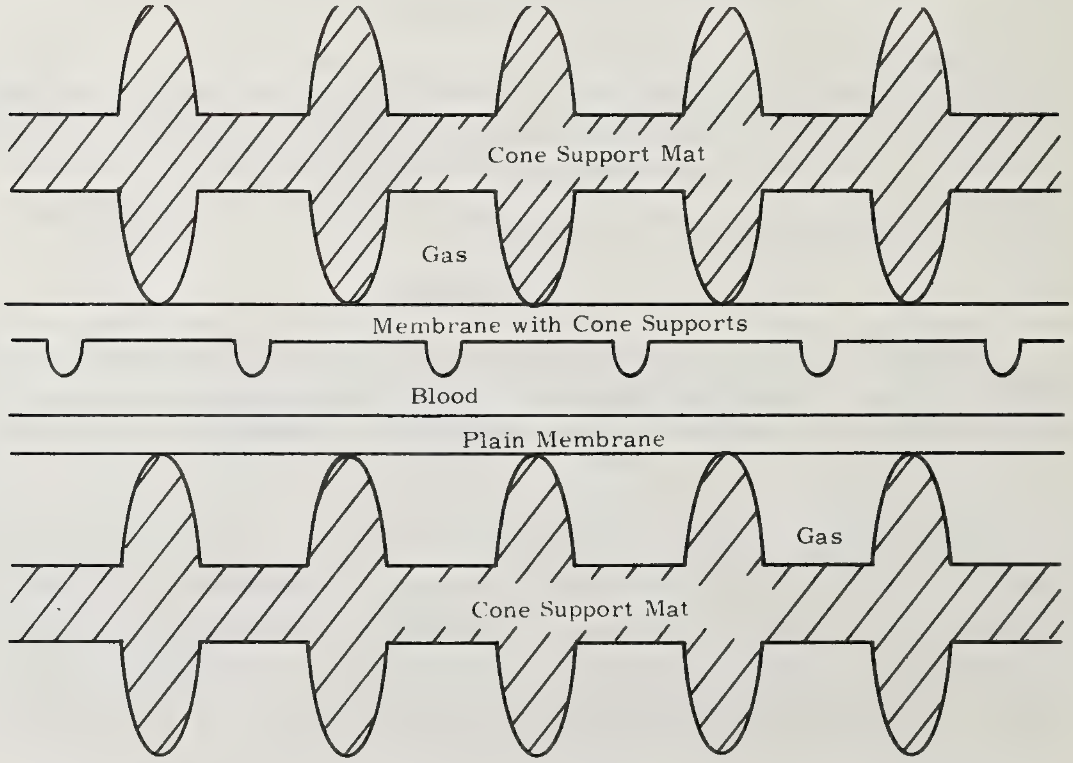

FIGURE 2. SCHEMATIC SECTION OF MEM 213 CONE MEMBRANE ENVELOPE WITH CONE SUPPORT MAT.

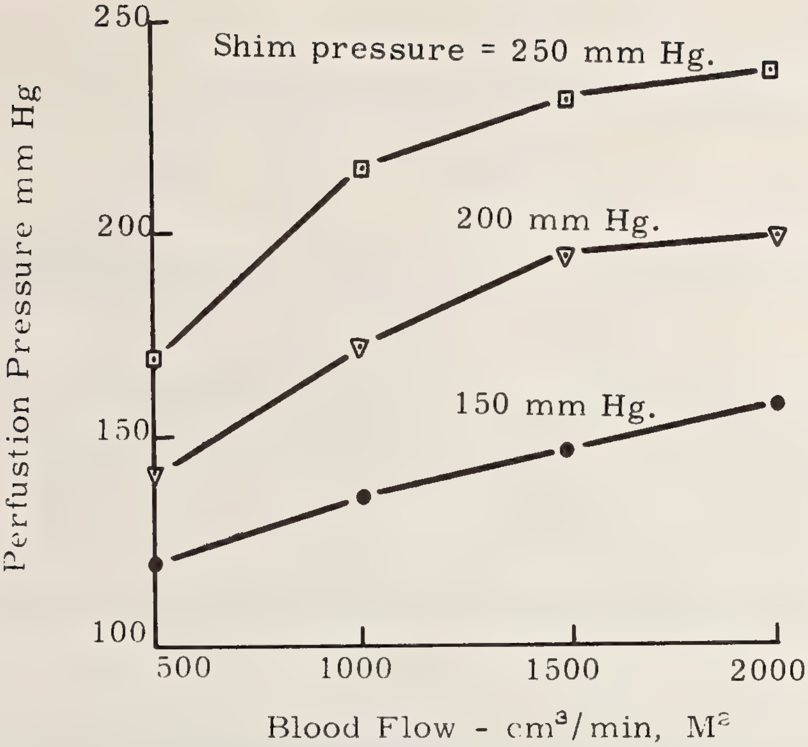

FIGURE 3. PERFUSION PRESSURE VERSUS BLOOD AT VARIOUS SHIM PRESSURES.

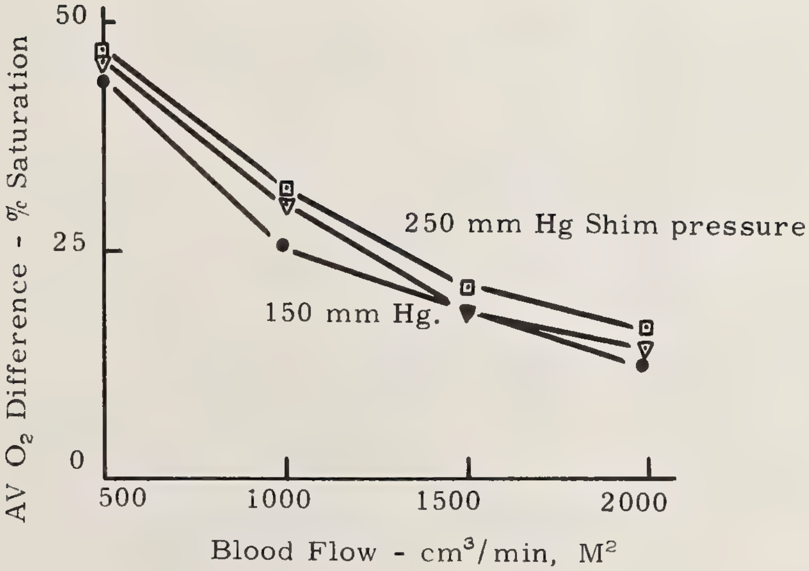

FIGURE 4. BLOOD SATURATION INCREASE VERSUS BLOOD FLOW AT VARIOUS SHIM PRESSURES.

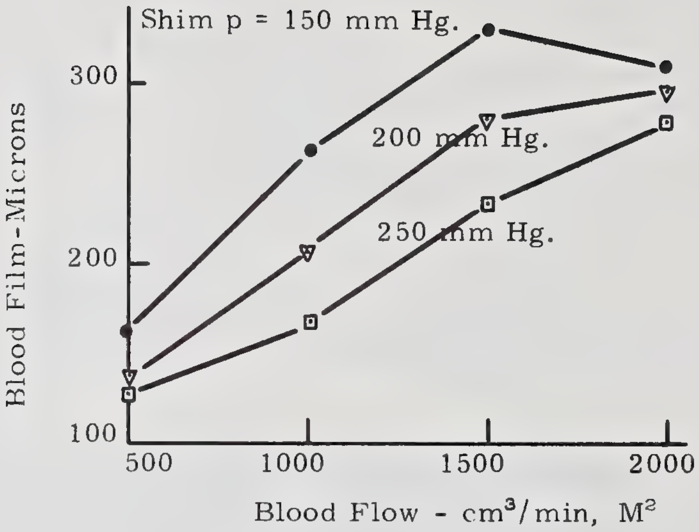

FIGURE 5. AVERAGE BLOOD CHANNEL HEIGHT VERSUS BLOOD FLOW AT VARIOUS SHIM PRESSURES.

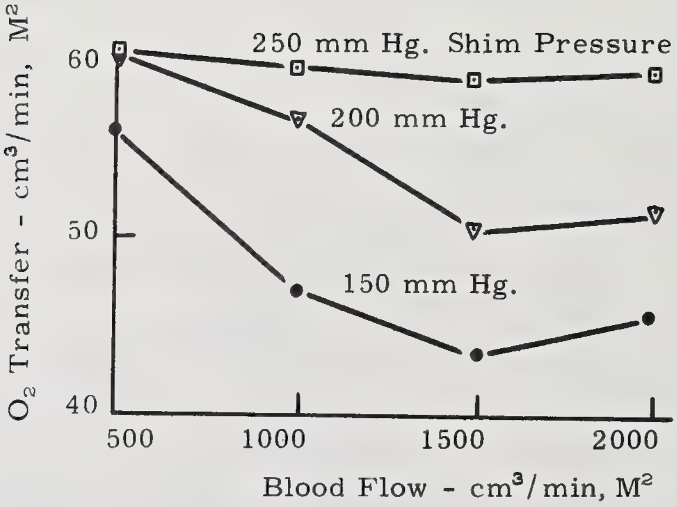

FIGURE 6. OXYGEN TRANSFER VERSUS BLOOD FLOW AT VARIOUS SHIM PRESSURES.

where N_{O_2} is the transfer in cm^3/sec., A is the area in cm^2, P_g is the partial pressure of oxygen in the gas phase in atm., P_i is the partial pressure of oxygen at the membrane/blood film interface, and k_m is the membrane transfer coefficient in cm^2/sec., atm.

The membrane mass transfer coefficient, k_m is a constant for any combination of material, gas, and thickness. Its value is determined by:

$$k_m = \frac{P_r}{t_m} \tag{2}$$

where P_r is the membrane permeability in cm^2/sec., atm., and t_m is the membrane thickness in cm.

The oxygen transport through the blood is given by:

$$N_{O_2} = k_b A\alpha(P_i - P_d) \tag{3}$$

where k_b is the blood mass transfer coefficient in cm/sec., α is the solubility constant of oxygen in plasma in cm^3 (STP)/cm^3, atm., and P_d is the partial pressure of oxygen that would be in equilibrium with the bulk of the blood.

Since P_i is difficult to measure experimentally, it is useful to define an overall mass transfer coefficient to eliminate P_i:

$$N_{O_2} = K_{og}A(P_g - P_d) \tag{4}$$

Equations (1), (3), and (4) can be combined to relate mass transfer coefficients:

$$\frac{1}{K_{og}} = \frac{1}{k_m} + \frac{1}{\alpha k_b} \tag{5}$$

From Figure 7, and the results of previous experiments, one might expect the following relationship to be valid for any given planar design.

$$k_b = \frac{C_t D}{t_b} \tag{6}$$

where C_t is a constant, D is the diffusion coefficient in cm^2/sec. and t_b is the blood channel height in cm.

Equations (5) and (6) can be combined to yield:

$$\frac{1}{K_{og}} = \frac{1}{k_m} + \frac{t_b}{\alpha C_t D} \tag{7}$$

Assuming $(P_g - P_d)$ is approximately constant at 0.92 atm., K_{og} can be calculated from the experimental data.[9] A plot of $1/K_{og}$ versus t_b should result in a straight line with a slope of $1/\alpha C_t D$ and an intercept of $1/k_m$. (Assuming an average membrane thickness of 1.5 mils results in a predicted intercept of 0.31×10^4 atm., sec./cm.). This along with the experimental results are shown in Figure 8. From the slope calculation, and assuming $\alpha = 0.0256$ and a diffusion coefficient, D, in the range of 1×10^{-5} cm^2/sec. C_t falls in the range of 10 to 15. That is the average mass transfer blood film thickness is 1/10 to 1/15 that of the blood channel height.

For diffusion without chemical reaction in a planar configuration, one would expect C_t to have a value of 4. Since oxygen transfer is achieved with diffusion with a rapid chemical reaction, values of C_t in the range of from 4 to something up to 20 might be expected. The exact value will depend on the specific flow geometry of a given planar design.

It should be noticed from Figure 8 and also from Figure 7 that oxygen transfer and the blood film coefficient, k_b, are generally lower than expected in the region of low blood channel heights. The reasons for this appears to be occlusion of a portion of the active area of the membrane when one tries to achieve these channel heights by applying excessive shim pressures. However, the remainder of the gas exchange analysis will demonstrate that this present design limitation is of little consequence if one is to achieve good oxygen/carbon dioxide balance in membrane oxygenators with the presently available practical membrane materials.

The relative transfer of carbon dioxide and oxygen as a function of blood resistance can be estimated by combining equations (4) and (5) to yield:

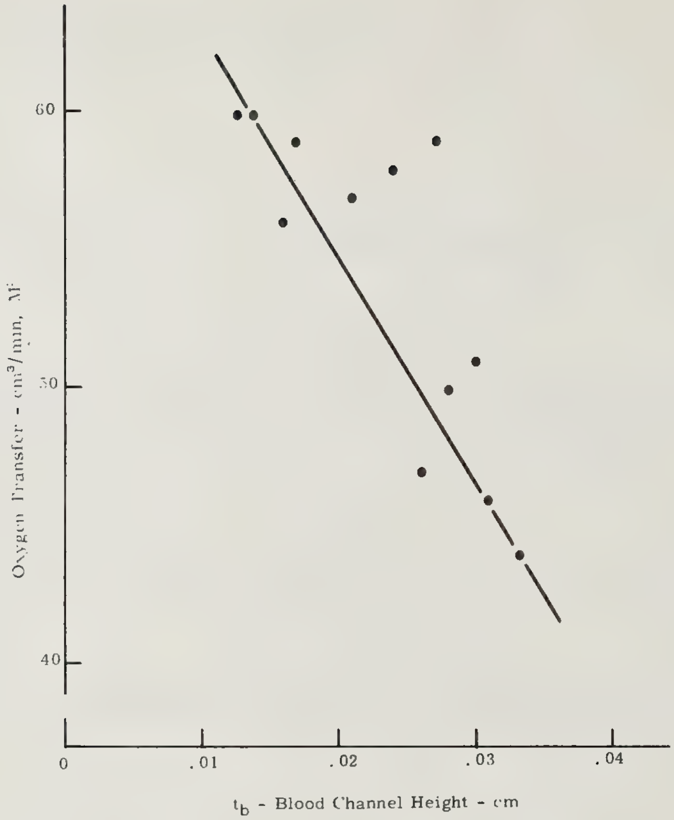

FIGURE 7. OXYGEN TRANSFER VERSUS AVERAGE BLOOD CHANNEL HEIGHT.

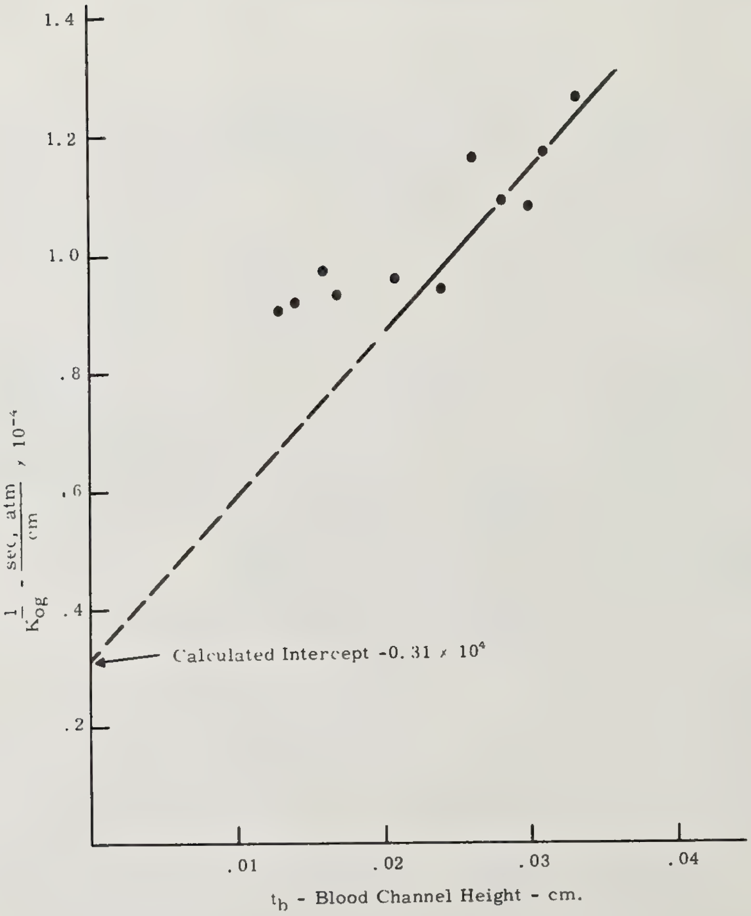

FIGURE 8. OVERALL OXYGEN TRANSFER RESISTANCE VERSUS AVERAGE BLOOD CHANNEL HEIGHT.

$$\frac{N_{CO_2}}{N_{O_2}} = \frac{(P_g-P_d)_{CO_2}}{(P_g-P_d)_{O_2}} \times \left[\frac{\dfrac{1}{k_{m\ O_2}} \quad \dfrac{1}{\alpha_{O_2}\ k_{b\ O_2}}}{\dfrac{1}{k_{m\ CO_2}} + \dfrac{1}{\alpha_{CO_2}\ C_k\ k_{b\ O_2}}} \right] \tag{8}$$

where $C_k = \frac{k_{b\ CO_2}}{k_{b\ O_2}}$

The fixed values for this analysis are:

$(P_g-P_d)_{CO_2} \simeq 0.053$ atm.

$(P_g-P_d)_{O_2} \simeq 0.92.$ atm

$\alpha_{O_2} = 0.0256$ cm^{3}O$_2$ STP/cm^3, atm.

$\alpha_{CO_2} = 0.46$ cm^3 CO$_2$ STP/cm^3, atm.

Since k_b CO$_2$ and k_bO$_2$ are mass transfer coefficients for diffusion with rapid chemical reaction, the ratio, C_k, will not only be dependent on the diffusion coefficient for these gases, but also will be dependent on the blood's specific capacity to hold the gas reaction products. This capacity is greater for the carbon dioxide products than the oxygen products. When these factors are analyzed as first approximation one would conclude that the value of C_k should lie between 1 and 2.

Given the above inputs, one can proceed to analyze the expected CO$_2$/O$_2$ transfer balance as a function of membrane characteristics and the oxygen/blood mass transfer coefficient. From the analysis summarized by Figure 8 one can conclude that design values of k_bO$_2$ should lie between 10^{-3} and 10^{-1}cm/sec. as minimum and maximum. Thus this is the range covered in Figure 9. The results are shown in Figure 9 for 0.0005 inch Teflon and for 0.001 inch polycarbonate/silicone copolymer. The analysis for dimethyl silicone rubber were also completed, however, the values fall close to those for the copolymer except that the curve is shifted slightly to the right in the case of the rubber.

This theoretical analysis is confirmed, at least in part, by the actual results of the gas exchange experiments as shown by the averaged value of all experiments with the copolymer, cone support membrane envelope. The most significant conclusion of the analysis is that with 0.001 inch copolymer or silicone rubber membrane there is little one can do, over what has been demonstrated to date, to improve the gas exchange efficiency of the system while maintaining good CO$_2$/O$_2$ balance. However, there are obvious advances to be made by developing techniques to fabricate practical devices with membrane thickness even less than 0.001 inch. For then reasonable CO$_2$ exchange can be maintained at the higher oxygen fluxes associated with lower blood mass transfer resistance.

BLOOD TRAUMA

This is the second step in proper evaluation of a gas exchange device and is a complex problem because it involves measurement of changes in the principle constituents of blood.

1. Red blood cells: both immediate hemolysis and occult red cell damage.
2. White blood cells: destruction, morphologic change and functional alterations.
3. Platelets: agglutination, destruction and morphologic alteration.
4. Coagulation factors: this includes platelets, proteins, and other substances.
5. Plasma proteins: this includes changes in the physical and biologic properties of the proteins, separation of lipid from lipo-proteins, and immunogenic changes.
6. Plasma lipids: this includes a study of chylomicrons, lipid derived from lipoproteins, and changes in neutral fat derivatives.

Because of variations in the fragility of blood taken at different times and from different individuals, discrimination in trauma studies is considerably enhanced by running paired experiments, one of which serves as a control.

Because the effects of trauma to blood are moderated by having an animal in the circuit, critical tests for trauma are best carried out under *in vitro* conditions.

Two parallel circuits each included gas exchange device, heat exchanger, ventricle pump, and flow probe.

1. Peirce membrane lung with 0.5 M^2 membrane.
    - a. Teflon 0.5 mils
    - b. Copolymer, 1 mil or thicker, with intrinsic cone point distribution pattern.
    - c. Copolymer envelopes, nominally 1 mil, with polyvinyl or RTV silicone coated fiber glass screen inserts.
2. Six-inch polycarbonate disc oxygenator with thirteen 5-1/8 inch convoluted discs.

Each circuit was run with 500 ml of whole fresh blood, a single donor being used for both circuits. Sufficient additional blood was obtained for an unperfused control at 37°C and often, additionally, at 25°C.

Circuits were run at 500 ml/min. The membrane lung was shimmed to 150 mmHg. The disc was driven at 75 or 100 rpm. Temperature was maintained near 37^{o}C. Gas supplied was 3% CO_2 in air at about 1 liter per minute. Appropriate amounts of heparin, neomycin, and glucose were added to circuits and controls at intervals. Sterilization was by ethylene oxide or soaking in neomycin sulfate 1:1000 (flow probes only).

The following determinations were made on blood from each control sample and each circuit:

1. Every 2 hours (regularly): plasma hemoglobin (PHb).
2. Every 2 hours (in some experiments): plasma lactic dehydrogenase (LDH), blood lactate, plasma pH, pH at 40 mm Hg pCO_2 (pH_E), packed cell volume (PCV), and red cell count (RBC).
3. Zero control and 6 hours (regularly): viscosity (cone plate), glucose, white blood count (WBC), platelet count, partial thromboplastin time (PTT), prothrombin time (PT), euglobulin clot lysis (EGL), fibrinogen, routine culture, O_2 saturation, pH, pH_E, and PCV.
4. Zero control and 6 hours (in 4 experiments): osmotic fragility studies were made on the 37^{o}C control sample and on blood from each circuit.

In six paired experiments, 3 at 25^{o}C and 3 at 37^{o}C, the oxygenators were excluded to permit evaluation of the circuits alone. The remaining paired experiments were divided as follows:

	Total	Analyzed
Copolymer (1 mil) in envelopes with 3 mil cone points on one side (copolymer-cone)	17	11
Teflon	10	5
Copolymer in envelopes with methyl silicone or polyvinyl covered fiber glass inserts (copolymer-screen)	12	12

In addition to obtaining values for the mean and standard error of the mean for data from each category of oxygenator, the hemolysis values, WBC, and platelet damage data were analyzed by paired t-test. In the case of the PHb, the corresponding control value was subtracted from the experimental disc and membrane value before their comparison. The results are as follows:

Bacteriology. Positive cultures and high associated hemolysis necessitated discarding one complete experiment and two disc tests.

Acid-base changes. O_2 saturation and pCO_2 remained within reasonable limits in all experiments. There was a progressive rise in non-carbonic acids (NCA) which was considerably greater for perfused blood than for non-perfused controls. Approximately 50% of the NCA increase was accounted for by lactate.

Blood cell damage. Significant decreases in the number of white blood cells were seen in the disc and in the copolymer screen experiments. Significant decreases in platelet counts occurred in the copolymer-cone, disc, and copolymer screen experiments.

Coagulation factors. No changes of sufficient magnitude to occasion clinical aberrations of coagulation or clot lysis were observed.

Plasma hemoglobin. Each type of membrane differed significantly from the other two in the degree of measured hemolysis. The copolymer-cone envelopes showed significantly less hemolysis than the disc, the Teflon membrane, and the copolymer-screen combinations ($p<0.001$). The Teflon and copolymer-screen were less satisfactory than the disc on the basis of hemolysis. They differed significantly from each other only after 6 hours. These results are summarized in Figure 10.

Lactic dehydrogenase. The plasma hemoglobin level correlated well with the LDH level in individual experiments but pooled data showed no significant correlation.

Miscellaneous. Significant differences in plasma glucose, blood viscosity, and osmotic fragility were not observed between groups.

In summary, the use of paired trauma tests proved to be a useful and discriminating experimental model in terms of immediate red cell damage. Damage to white cells and platelets in general correlated well with red cell hemolysis but were not as discriminating. Gross plasma protein damage was not demonstrated on the basis of measurements of viscosity, fibrinogen, and other clotting factors. Larger increases in NCA in perfused blood compared to non-perfused control samples suggested the possibility of occult red cell damage but was inconclusive because the precise cause of this phenomenon is not known.

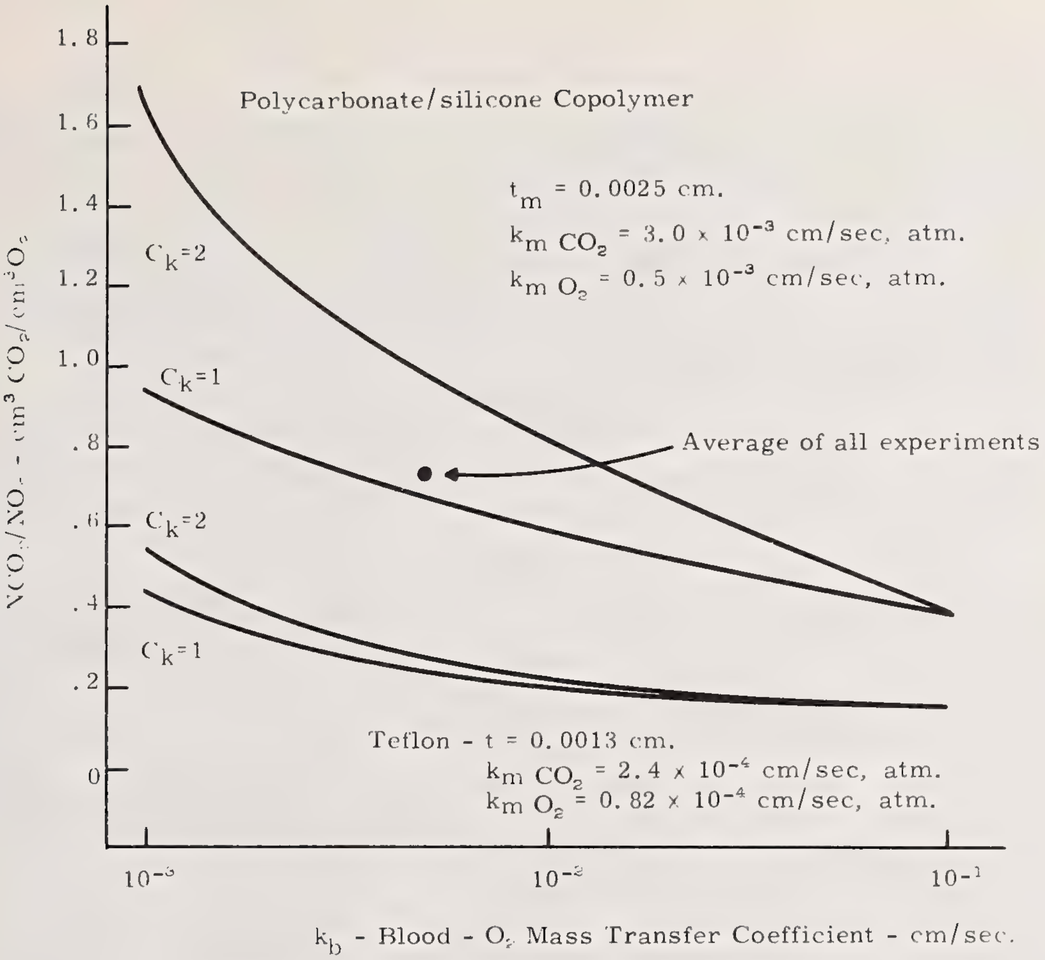

FIGURE 9. CARBON DIOXIDE/OXYGEN TRANSFER BALANCE VERSUS OXYGEN/BLOOD MASS TRANSFER COEFFICIENT.

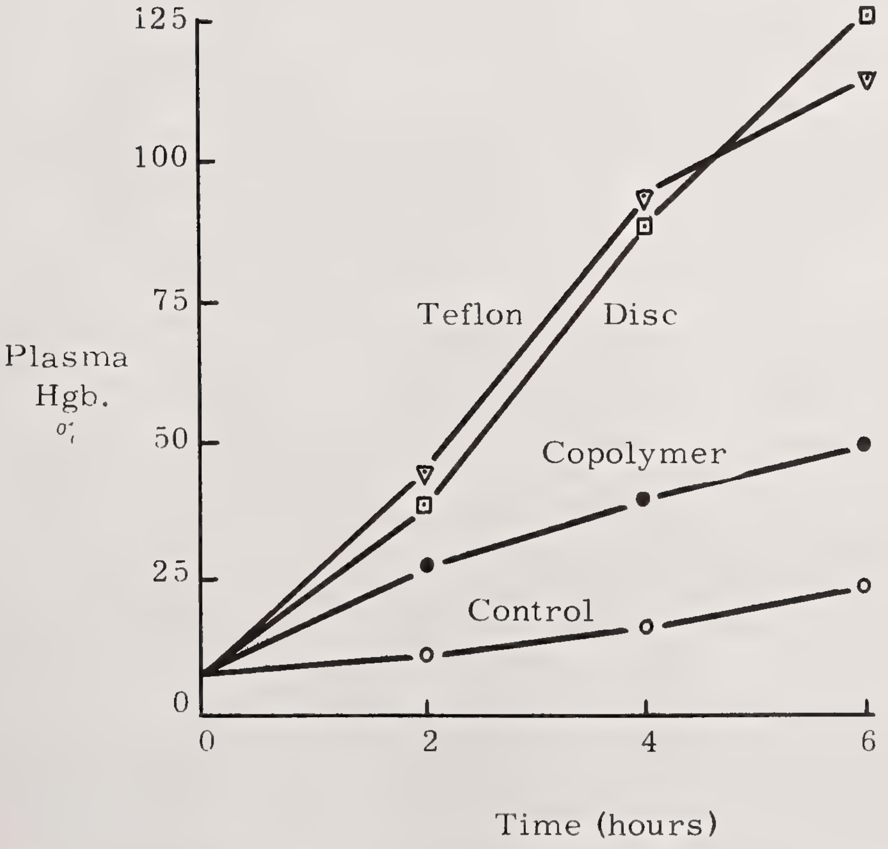

FIGURE 10. PLASMA HEMOGLOBIN LEVELS VERSUS PERFUSION TIME FOR VARIOUS PERFUSION SYSTEMS.

The chosen in vitro test is a fairly rigorous test for gross red cell damage. The experiment permitted a single passage of the entire blood volume once per minute, or 360 passages in the 6-hour experiment. On the basis of the results, the following preliminary conclusions seem indicated:

1. The rate of cumulative in vitro hemolysis decreases with time when copolymer-cone membranes or Teflon are employed. The estimated cumulative rate of hemolysis of 0.15 mg/min for the copolymer-cones at blood flow rates of $1L/M^2$/min is only a little greater than the level thought to be tolerable for prolonged periods. For partial bypass, therefore, this type of membrane would be expected to perform satisfactorily for long term bypass.
2. Copolymer-screens were found to be excessively hemolytic under the test conditions employed. Use of this membrane-screen configuration, therefore, appears to be potentially dangerous.
3. To provide a full evaluation of blood trauma, additional tests are needed, especially careful evaluation of protein denaturation, and occult red cell damage.

ANIMAL EXPERIMENTS

This is the third step in the pre-clinical evaluation of a lung device. A number of options are available including arterio-venous, veno-venous, and veno-arterial bypass. Each of these has special hemodynamic characteristics and different implications in terms of produced trauma.

Two general experimental protocols were chosen:

1. Twenty-four hour partial bypass in lightly anesthetized dogs. This procedure was selected for the following limited objectives:
    a. Evaluation of blood trauma in perfusions of sufficient length to be of clinical value.
    b. An opportunity to compare the function of various sizes of lungs used in a variety of ways:
        (1) Arterio-venous perfusion without a pump.
        (2) Veno-venous perfusion with a single pump.
        (3) Veno-arterial perfusion with two pumps.

To date, only (1) and (2) have carried out.
    c. To permit development of a protocol comparable to one that might be used in human assisted circulation.

2. Five-hour perfusions in unanesthetized chronically instrumented animals had the following major objectives:
    a. To obtain data on blood trauma.
    b. To study the hemodynamic effects of arterio-venous perfusion in conscious animals.

For the twenty-four hour perfusion experiment, the animals were anesthetized with morphine-chloralose and supplemented as needed to maintain light anesthesia. For arterio-venous perfusion the lung consisted of either 0.5 or 1.0 M^2 of copolymer-cone membrane envelopes. Temperature was maintained at a normal level by utilizing the lung water jackets. The circuit included a flow probe and a bubble trap. The femoral artery and femoral vein on one side were utilized and arterial and venous pressure monitoring catheters were inserted through the vascular cannulas. In addition, the ECG, heart rate, respiratory rate, respiratory velocity, extracorporeal flow, esophageal temperature, dog weight, and shim pressure were recorded. Blood was analyzed for hematocrit, oxygen saturation, acid-base change, viscosity, osmolality, plasma hemoglobin, glucose, sodium and potassium, lactic dehydrogenase, coagulation factors, blood lactate, and formed elements. Blood culture was taken on completion. Urine flow and osmolality were measured. In addition, paired plasma and urine creatinine values were obtained at intervals to measure glomerular filtration rate.

Animals were given suitable doses of neomycin sulfate, heparin, intravenous fluids, and blood. On completion heparin was neutralized with Polybrene. RISA blood volume measurements were made in some animals and in others radiochromium red cell survival studies were carried out. The RISA animals were sacrificed at one week while the radiochromium animals were kept for three weeks.

In the veno-venous perfusion experiments, a ventricle pump and a reservoir were added to the circuit. Blood was taken from the right atrium via a right external jugular cannula and was returned via a femoral vein. Central venous pressure was monitored by way of a catheter inserted through the return cannula. A femoral artery was catheterized for aortic pressure.

Five-hour perfusions in unanesthetized animals were carried out using 1.0 M^2 lungs with either copolymer-cone or copolymer-screen envelopes. Animals were sedated with chlorpromazine and morphine sulfate. Some were perfused at normal body temperature and others were cooled to approximately 30°C. Animals were previously instrumented with an ascending aortic electromagnetic flow probe and a left ventricular pressure transducer. Female animals were used and an episiotomy was performed to permit ready catheterization of the urinary bladder. Animals were trained to lie on the operating table for periods of five to six hours without anesthesia. Cut-downs were carried out under local anesthesia, blood being taken from the right atrium via the external jugular vein and returned by way of a femoral artery. Circuits contained two roller pumps, a heat exchanger, a flow probe, a bubble trap, and a reservoir. Hemodynamic measurements included left ventricular pressure, left ventricular end-diastolic pressure, left ventricular dp/dt, aortic flow, stroke volume, and external cardiac work. Laboratory data roughly similar to that collected in the twenty-four hour perfusions were obtained though no blood volume or red cell survival studies were made.

The twenty-four hour perfusions have resulted in long-term survivors in all instances. Blood flow approximated 500 ml/M^2/min in each experiment. In the arterio-venous perfusions this necessitated lowering the shim pressure to approximately 60 mm Hg. The principal problem has been bleeding from the cut-downs which has necessitated relatively large volume blood replacement. Dogs have appeared to be in excellent condition throughout the procedures with the exception of two who had rather severe homologous blood reactions at the beginning. In both of these, hemodynamic and acid-base deterioration, occasioned by the reactions, was corrected during the remainder of the perfusion without special treatment. In no instance was an antacid required. All animals showed prompt reversal of anticoagulation with a single calculated dose of Polybrene. In most of the perfusions there was a progressive reduction in the platelet count but it generally did not fall below 50% of the control. The white blood count generally fell initially but exceeded the control at 24 hours. Glomerular filtration rate was usually well maintained. In more than half, the plasma hemoglobin level reached a peak at 12 hours or earlier and then fell progressively. The 24-hour plasma hemoglobin level ranged from 9.4 to 100 mg% (50.5 ± 13.5) (uncorrected for control values of 3.3 to 9.8 mg%). Some adherent solid material, suggesting fibrin or platelet deposits, was found in manifolds and on surfaces after 24 hours.

Nine five-hour veno-arterial perfusions were carried out using a 1.0 M^2 lung. The flow rate through the lung was maintained slightly above 1L/M^2/min throughout the perfusion. On the average, platelet levels were moderately diminished on completion and white cell levels were moderately increased. Heparin anticoagulation was promptly reversed as in the twenty-four hour perfusions. Plasma hemoglobin levels ranged from 34 to 177 mg% (79.4 ± 13.8) (uncorrected for control values). In one instance, where the plasma hemoglobin level was 105 mg%, the circuit plasma hemoglobin was 930 mg% prior to the start of perfusion. In an experiment where plasma hemoglobin was 177 mg%, copolymer screens were used and the animal had a severe empyema. It was a clinical impression that the animals perfused using a lung with copolymer-cones were more alert during the perfusion than the animals perfused with lungs utilizing copolymer-screens. In one instance an animal experienced cardiac arrest and a period of hypoxia exceeding 12 minutes prior to the start of perfusion (possibly on the basis of pulmonary air embolus). This animal was resuscitated by the perfusion which proceeded relatively normally. In three instances animals had rupture of the ascending aorta as a result of erosion by the electromagnetic flow probe. One animal went into deep shock soon after heparinization and prior to the start of perfusion. In all experiments, it was possible to continue the perfusion by aspirating shed blood from the chest and returning it to the perfusion circuit. In each case of aortic rupture, the complication clearly antedated the perfusion and became clinically apparent only after heparinization.

In summary, experiments so far carried out indicate that the copolymer-cone lung may be used in a variety of perfusion configurations and that the degree of blood trauma is acceptable for experimental long-term perfusion. The need for improvement in blood manifolding and the shape of the cone fields is apparent.

Twenty-four hour arterio-venous and veno-venous perfusion have been carried out in a manner that might be clinically acceptable. Blood trauma has not been great; there has been no mortality, and morbidity appears to be acceptably small. These data, taken together with the results of *in vitro* trauma studies, indicate the desirability of utilizing the lung clinically, expecially in experimental situations where adequate therapy is not available for pulmonary insufficiency.

A series of five-hour veno-arterial perfusions in conscious chronically instrumented animals demonstrates the efficacy of the copolymer lung for emergency cardiovascular support.

DISCUSSION

DR. BLACKSHEAR: I could not understand the data on oxygen transfer versus flow. The effect of the oxygen transfer versus flow seemed to decrease the amount of oxygen transported. I am not referring to the amount transported per gram.

DR. PEIRCE: Well, in this one configuration, if one increases the velocity of flow, one increases the thickness of the blood film and also presumably decreases the uniformity of the blood distribution within the unit, unless one simultaneously increases the shim pressure and that is what causes that particular relation.

DR. BLACKSHEAR: The increases in the thickness of the film would seem to me to have the opposite effect. It should have lowered the saturation and therefore caused a higher transport of oxygen, so it is conceivable that it is all due to the non-uniformity effect? Or does the membrane press against the fingers that back up the structure at high pressures, and thus cut down on the capacity?

DR. PEIRCE: No, I think it is simply that one gets poorer gas exchange into a thick film than into a thin film, and this more than offsets the effect produced by an increased flow. However, I couldn't analyze it more than that.

DR. LUDWIN: The abstract says that the supplied gas was 3% CO_2 in air. I would ask what were your reasons for using air, and, secondly, whether you could compare this with the results that you might expect with oxygen?

DR. PEIRCE: Well, the air was used only in the in vitro blood trauma experiments, and the 3% CO_2 in air was used to maintain the CO_2 and pO_2 within reasonable limits during the six hours of exposure of the blood. Of course, in all of the experiments that were done with animals, only 100% humidified oxygen was used in the gas phases.

CHAPTER 36

PROGRESS IN THE TESTING AND DEVELOPMENT OF PRACTICAL FLAT PLATE MEMBRANE OXYGENATORS FOR CARDIO-PULMONARY ASSIST

A. J. Landé, R. N. Tiedeman, V. A. Subramanian,
S. J. Fillmore, C. W. Lillehei

Cornell University Medical College
New York, New York

In order to test our disposable membrane oxygenators, we inserted vena caval and arterial catheters through the external jugular and carotid of anesthetized dogs. While still anesthetized, the dogs were subjected to partial veno-arterial bypass and breathed with 8%O_2, 92%N_2. Although some useful information on oxygenation and CO_2 removal was obtained, this was an unstable preparation and the dogs soon died. Partial perfusions of awake dogs that had had catheters inserted 24 hours previously under anesthesia were then undertaken. Perfusions of 10 dogs for 24 hours yielded 5 long-term survivors. Perfusions of 5 dogs for 48 hours yielded 2 long-term survivors. Mortality could be traced to technical mishaps and pneumonia. Although a variety of parameters were studied, morbidity was limited to a temporary reduction in platelets. A decrease in hemoglobin was noted; however, plasma hemoglobin only reached the range of 50 mgm.% and no priming or replacement blood was required.

INTRODUCTION

Development of membrane blood oxygenators has been an integral part of the development of open heart surgery. Kolff noted that his artificial kidneys yielded red blood and he made a coil device with polyethylene membrane for this purpose. In the 1950's Clowes performed over 150 open heart operations with membrane oxygenators (Figure 1) and in the ensuing year's other equally distinguished investigators have made additional contributions. The theoretical superiority of membrane blood oxygenators over bubble and filming, types which allow direct contact between blood and gas, is generally conceded, and the work of Lee and his associates in protein denaturation has defined perhaps the most important difference between membrane and direct gas interface devices. We have utilized one of their techniques in our laboratory to demonstrate the difference in protein denaturation between membrane and bubble oxygenators. Figure 2 illustrates data from experiments in which aliquots of plasma were either pumped through a bubble oxygenator or a membrane oxygenator for prolonged periods of time during which specimens were taken periodically and examined in a spectrophotometer after having been centrifuged at low speed to remove the coarse flocculent precipitants. A distinct hazy appearance soon became evident in test tubes of bubble-oxygenated plasma compared with the membrane-oxygenated plasma which retained a clarity which was almost indistinguishable from control aliquots. This optical density is thought to be related to protein denaturation which consists of the disruption of lipoproteins and release of lipid and protein parts. Other advantages of membrane oxygenators which we were able to confirm in our studies will be detailed later. All these point to the conclusion that oxygenation of blood with membrane devices is far more physiologic than with the devices which are in general use today.

Perhaps the sole reason why membrane oxygenators have not actually dominated has been their lack of practicality. The Clowes device required painstaking dismantling, cleaning, assembly, testing and sterilization between uses. Some devices which have actually become available in disposable form are too small for adult clinical use or have had to sacrifice some of the potential advantages of membrane oxygenators, such as fixed small blood volume. The principal objective of this work has been the design and construction of prototype membrane oxygenators by techniques that would be amenable to mass production. Then further development of such devices might become truly practical and economically feasible. We now plan to turn our attention toward developing and demonstrating the potential uses to which these devices may be put. Aside from obvious employ in open heart surgery where far more complicated and prolonged procedures may be contemplated than were feasible in the past, we are particularly interested in using these devices for assist to the failing cardiopulmonary system. Extracorporeal bypass including a membrane oxygenator is particularly well suited for this purpose since it results in the flow of pressurized oxygenated blood and may be applied via peripheral arteries and veins without resort to major surgical manipulations.

Our basic membrane oxygenating device has been described in detail elsewhere. It will suffice here to describe the general principles of design which were utilized. Short thin parallel blood flow paths are desirable for gas transfer and minimum priming volume. The flat plate configuration was chosen because of simplicity of manifolding and the applicability of available membranes. Methods of manufacture were utilized which are suitable for mass production. We recognize that a number of excellent membrane oxygenators have been designed and built in years past but thought that a contribution might be made in making such devices available for general use. Hence thermoplastic molding technology and a modular design which required few kinds of parts, which in turn could be assembled by machine, were utilized. A self-contained free standing device was arrived

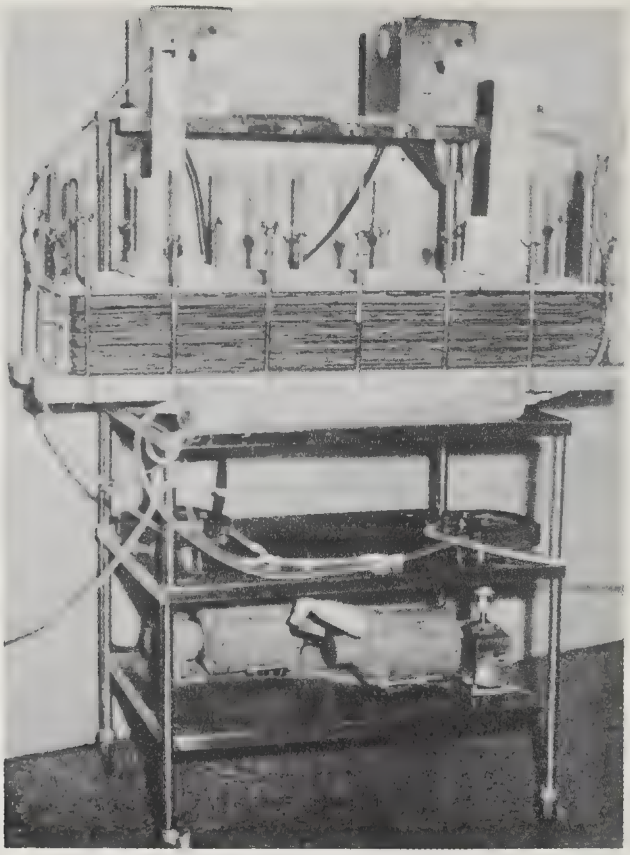

FIGURE 1. MEMBRANE OXYGENATOR.

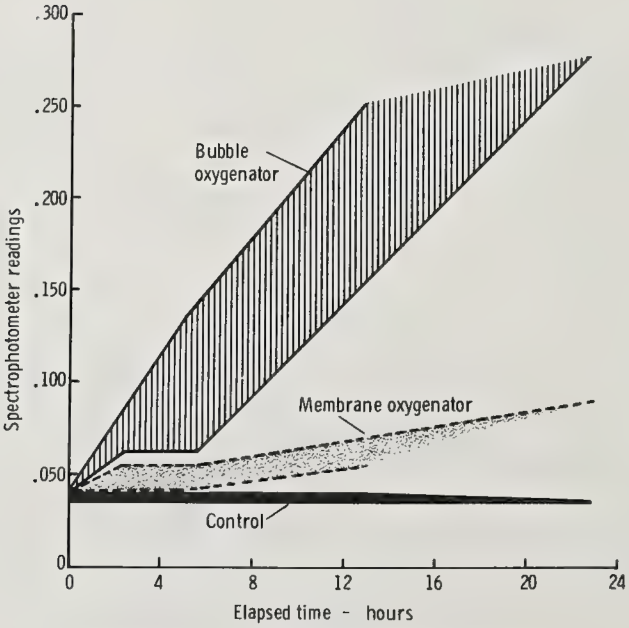

FIGURE 2. PLASMA DENATURATION STUDY.

at (Figure 3). This could be assembled, tested and sterilized in the factory for single use and subsequent disposal. Such devices have been tested *in vitro* and *in vivo* in animals. Recently a number of clinical experiences have added to our knowledge of their capabilities. A number of conclusions have been drawn concerning features of design and construction which should be incorporated in a production model. We believe that even shorter, more precise, firmly supported flow paths should be provided for blood and that this could be achieved by further innovations in design. We recognize more than ever that matters of practicality of construction are of the very first importance and that if we do not give them such consideration, these devices will remain no more than occasional research tools.

IN VIVO TESTING IN A PATHOLOGIC PREPARATION

Introduction.

In our early *in vivo* experiments we attempted to duplicate and study the hypoxia which has been noted to occur in patients suffering from cardiogenic shock secondary to myocardial infarction. The rationale for these experiments was that if the hypoxia could be corrected, then perhaps the afflicted heart would muster sufficient energy to survive long enough to recover. We desired also to study gas transfer through our devices under conditions which were optimal.

Experimental Method.

Eight 20-25 Kg. dogs were anesthetized with "suritol," after which endotracheal tubes were inserted and their cuffs inflated. The animals were attached to a respirator and ventilated with room air while blood vessels were being exposed for cannulation. Sampling catheters were inserted antigrade into the pulmonary artery and retrograde into the left ventricle under fluoroscopic control. Large bore catheters were then installed in veins in the groin and neck to which the pump oxygenator could be connected. A simple circuit was used which consisted of a venous reservoir feeding a roller pump which in turn forced blood through a 1 M^2 of membrane oxygenator and back into the animal via a bubble trap. The animals were placed on bypass at various rates of blood flow. The respirator was next connected to a source of 8% oxygen, 92% nitrogen mixture and the system was allowed to equilibrate before sampling was begun from the blood flow lines and sampling catheters. Venous and arterialized pO_2, pCO_2 and pH were determined at various blood flow rates using an IL blood gas analyzer. Hemoglobin and plasma hemoglobin levels were also determined at intervals. The animals were sacrificed before regaining consciousness. Volumes of oxygen transferred into blood were calculated.

Results.

Up to 75 cc. of oxygen per minute could be introduced into blood through a 1 M^2 of membrane device (Figure 4). The pCO_2 was reduced an average of 9 mm Hg partial pressure between oxygenator inflow and outflow (Figure 5) and increases in pH of 0.01-0.03 units were also measured. During veno-venous perfusion significant increases in pO_2 could be detected at the pulmonary artery level when the machine was turned on. Plasma hemoglobins rose no higher than 75 mg % over four hours in any of the dogs.

Discussion.

These animals which had been anesthetized, instrumented, and subjected to an 8% oxygen atmosphere constituted a pathological preparation which was of limited but definite value. The data indicating that oxygen transfer through 1 M^2 of membrane may be as high as 75 cc./min. at 1500 cc blood flow are impressive but must clearly be read in light of the peculiar circumstances of the experiment. The veno-venous route is uniquely suited for obtaining a high rate of oxygen transfer. This is because there is no requirement that the output from the oxygenator achieve arterial oxygen saturation levels and therefore there is no limit to the rate at which blood may be flowed through the oxygenator. Thus at 1500 cc flow per M^2 of membrane much oxygen may be transferred into unsaturated blood but only low % saturation levels may be achieved. These dogs which were being ventilated with 8% O_2 were especially unsaturated and thus their blood was especially avid for O_2. Since there is no limit to the flow rate at which veno-venous bypass might be performed, this route may well have merit. It will be of even greater interest to note in Figure 3 that at 500 cc blood flow only approximately 35-40 cc of oxygen could be transferred through 1 M^2 of membrane per minute. However at this flow rate nearly 100% oxygenation could be achieved. These rates of oxygen transfer are still greater than will be reported further on. This is again because of the extreme desaturation of this venous blood. The average ΔpCO_2 of 9 in these experiments was generally adequate to bring distinctly elevated pCO_2's down to high normal levels. Thus these experiments provided us with an evaluation of our oxygenator design. This experiment was deficient, however, in that it provided little information concerning other parameters which are of even greater importance, such as blood damage and animal morbidity and mortality. These animals after being subjected to anesthesia, instrumentation and hypoxia were unstable and several died before and during perfusion. The 1 M^2 of membrane oxygenators were insufficient in size to replace the whole oxygen deficit, especially since oxygen introduced into the venous blood might actually be removed in its ensuing passage through lungs which were being ventilated with 8% oxygen. It was of interest that plasma hemoglobins remained below 75 mg % over several hours of perfusion in all of these animals. Acidosis after a

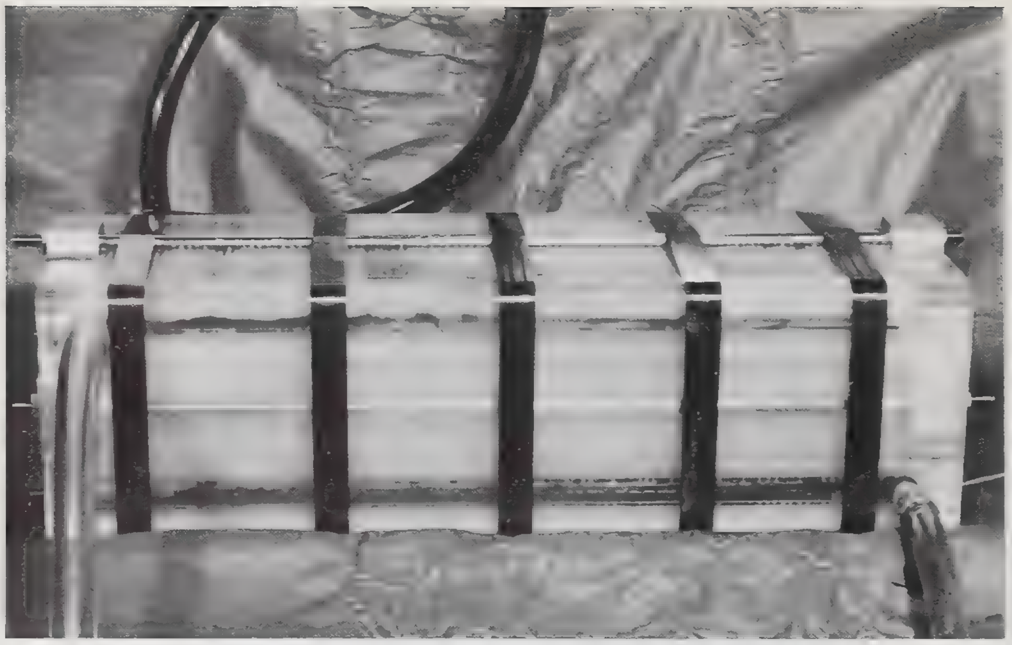

FIGURE 3. SELF CONTAINED FREE STANDING MEMBRANE OXYGENATOR.

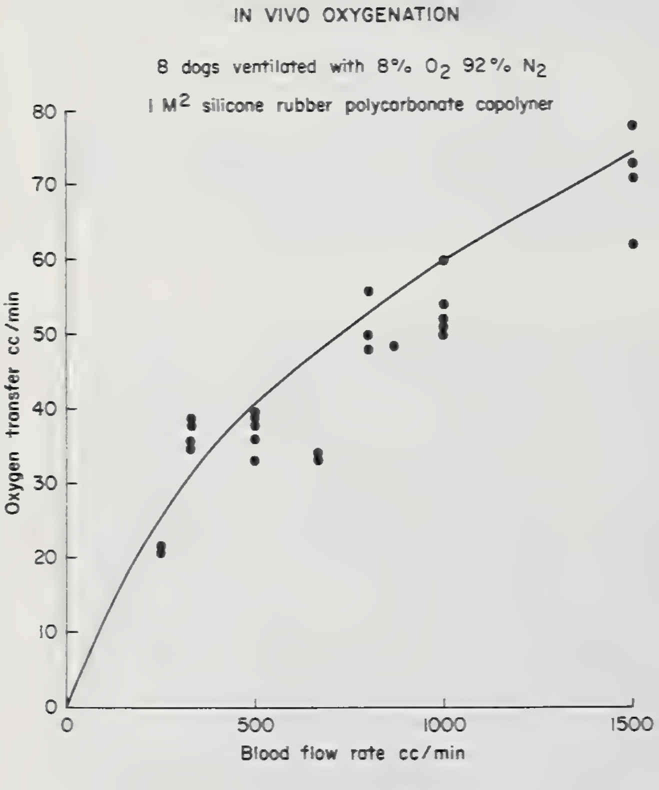

FIGURE 4. IN VIVO OXYGENATION.

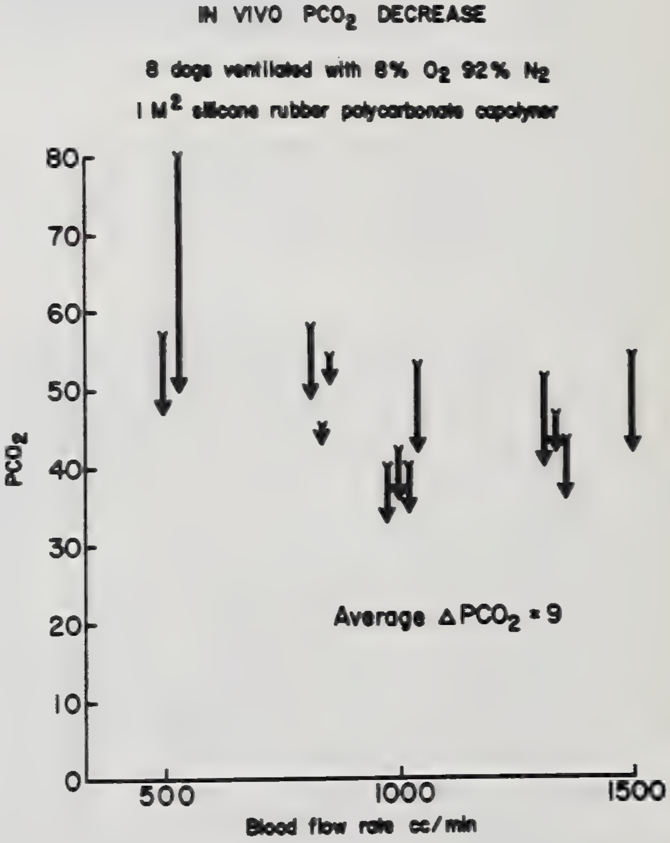

FIGURE 5. IN VIVO pCO_2 DECREASE.

short time in most of these experiments made meaningful hematologic and chemical data difficult to obtain. Finally the experiments gave no information about animal survival upon being subjected to assist with the membrane oxygenator. This series of experiments then was of interest primarily as an initial in vivo evaluation of the gas transport capability of the membrane oxygenator. The veno-venous route is of interest since it allows an inordinately large amount of gas to be transferred. It is a route of perfusion which may be of clinical value in selected situations.

TWENTY-FOUR HOUR VENOUS-ARTERIAL PERFUSIONS

Introduction.

The purpose of this surgical experiment was to assess survival and hematologic factors in prolonged partial heart-lung bypass with membrane oxygenators.

Methods.

Ten 15-25 Kg. dogs were anesthetized with pentobarbital and had the largest catheters the vessels would accept placed in the right atrium via the right external jugular vein and in the left carotid artery. These arterial and venous catheters were looped about the animals' necks and connected to form wide-open arterio-venous fistulae. No heparin was given at that time. Twenty-four hours later when the effect of anesthesia had worn off and the animals were behaving completely normally, the catheters were inspected and declotted if necessary. Only then were the animals placed on bypass, in a fully awake and unmedicated state (Figure 6). A 1 M^2 of membrane oxygenator was utilized in 9 cases. In one case a 3 M^2 of membrane device was used. A collapsible reservoir devised from a blood collection bag received the venous blood from the animal by gravity drainage. Any accumulation of air in the reservoir could be withdrawn through a vent, leaving no direct blood-gas interface in the entire system. The venous reservoir was suspended from the scale pan of a roller pump console which also held the oxygenator (Figure 7). Since the rate of rotation of the primary driving pump was controlled by the weight of the elements on the pan and since these included the collapsible bag which was the only significantly expansile element in the entire system, the extracorporeal volume was maintained automatically. An adjustable clamp on the venous return limited the flow rate. The primary roller pump drew blood from the venous reservoir and drove it through the oxygenator and on into the arterial system of the dog. A pressure sensitive monitor and automatic cut-off, attached directly after the primary pump, prevented excess pressure. No bubble trap or blood filter was utilized. No blood heat exchanger was required. To prevent heat loss, the oxygen was heated. In addition, conventional infra-red lamps were directed at the oxygenator and tubing. A secondary pump was utilized to recirculate blood through the oxygenator. The recirculation pump was kept turning at all times, even while perfusion was interrupted, so that hot spots would not develop from the form of heating that was employed. The oxygen was humidified to limit water vapor loss across the membrane and to ensure that any small amount of blood which leaked across the membrane would be carried out rather than drying and caking on the membrane. Halfway through the series, a conventional hospital humidifier equipped with a 40 mm Hg pressure limiting device was adopted. This ensured that high oxygen pressures could not arise and force oxygen bubbles across the membrane into the blood. For these experiments the extracorporeal circuits were cleaned with an aqueous zephiran solution and rinsed with copious amounts of tap water. Then they were flushed with sterile saline and finally primed with approximately 1500 ml of "Normosol" balanced electrolyte solution. More recently the oxygenators have been gas sterilized. They and the sterile tubing are merely connected and flushed with sterile saline to remove the sodium bicarbonate powder which is used to keep the membranes from sticking. Thirty mg of heparin were added to the prime which was allowed to circulate for a few minutes. The temperature of the system was regulated to 37°C. The dog was given 3 mg/Kg of heparin intravenously after which the catheters were connected to the heart-lung machine. The venous reservoir which contained approximately 700 ml of priming solution accounted for a substantial part of the total prime. Bypass was commenced by small increments over 10 minutes. This was done in order to make the onset of hemodilution as benign as possible for awake animals. The primary pump was set at 500 ml/min. with the 1 M^2 oxygenators and 1500 ml/min. with the 3 M^2 oxygenator. The secondary pumps were set at 1000 ml/min. and 3000 ml/min. respectively. Heparin and fluids were administered at a rate of 3 mg/Kg/hour of heparin and 100 ml/hour in the earlier experiments and 50 ml/hour of fluids in the later experiments. A constant infusion pump simplified control of these flow rates. This amount of heparin was ample and has been decreased in subsequent experiments. The animals were allowed to move about their cages but were watched by an attendant to prevent excessive twisting and kinking of the blood tubing. Food and water were allowed ad lib and intake and output were noted. The recirculation pump was occasionally turned to four times the constant rate to insure that all blood channels were open and oxygenating. This resulted in a small increase in the maximum pressure of the system from approximately 180 mm Hg to 200 mm Hg. Samples were taken periodically for a variety of studies. The hematin method was used for plasma hemoglobin determination.

When animals died they were autopsied and the microscopic and gross pathology examined. No animals were sacrificed since this was primarily a study of survival. At the end of the 24-hour periods of partial bypass, the blood remaining in the devices was transferred to intravenous fluid bottles from which it was reinfused into the animals. A luerlock side vent in the connector between the arterial and venous catheters served as a handy site for reinfusion of this blood. Following this the catheters were removed from the arteries and veins which were then ligated. Subsequent to

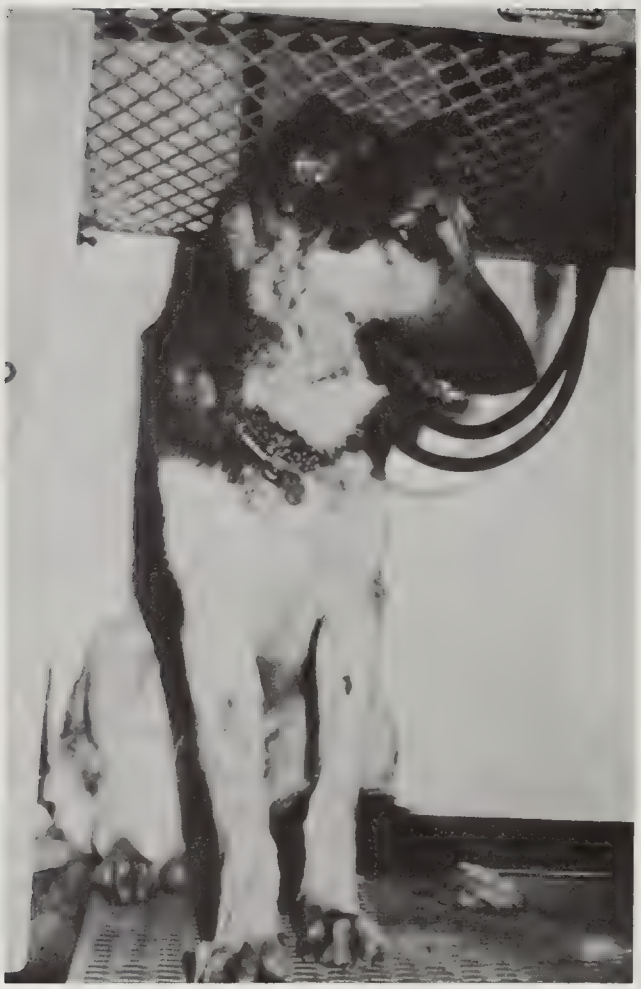

FIGURE 6. ANIMAL PLACED ON BYPASS IN FULLY AWAKE AND UNMEDICATED STATE.

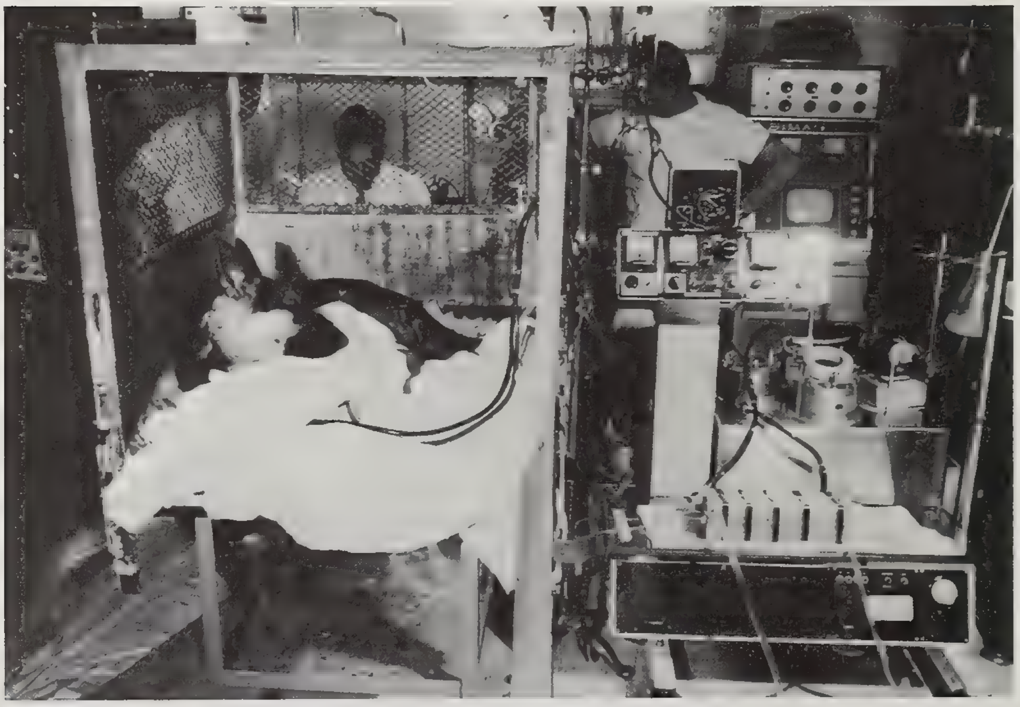

FIGURE 7. VENOUS RESERVOIR SUSPENDED FROM SCALE PAN WHICH ALSO HOLDS THE OXYGENATOR.

this series of experiments one animal was lost during the reinfusion period and we suspect this was related to the added burden of the large open arterio-venous fistula. Therefore, the arterial side of the fistula is now clamped during reinfusion. Following this the animals were allowed to walk upstairs to their cages. Blood sampling was continued during subsequent days and weeks.

Results.

Five of these ten 24-hour dogs survived the entire procedure and remained as long-term survivors (Table 1).

TABLE 1

24-HOUR VENO-ARTERIAL PARTIAL BYPASS 10 DOGS

5 Long-Term Survivors
5 Deaths
  3 Technical Mishaps
  2 Pneumonias

Two of the dogs that died did so acutely during the run, as a result of massive O_2 emboli before the oxygen pressure limiting device was added to the system. O_2 embolus has not been a problem since. An additional death occurred during a run in a dog that had been used previously for two other unrelated experiments. Examination of this dog's lungs demonstrated acute hemorrhagic pneumonia. Two dogs died 6 and 10 hours following perfusion. One of these had pneumonia and the other death was at least in part due to a technical mistake which had resulted in the infusion of a considerable quantity of tap water into the animal's circulation. At 500 ml partial bypass with a 1 M^2 of membrane oxygenator, nearly 100% oxygenation was always obtained (Table 2).

TABLE 2

24-HOUR VENO-ARTERIAL PARTIAL BYPASS 10 DOGS

(Typical Results)

Blood Flow	500 cc/min
Recirculation Rate	1000 cc/min
V-A $\Delta\%\ O_2$	25%
O_2 Transfer	25 cc/M^2
V-A $\Delta\ pCO_2$	5 mm Hg
pH	No Change
Hct	40 → 30%
Hgb.	12 → 9 Gm.
Pl. Hgb.	20 → 80 mg %
Platelets	250,000 → 20,000
WBC	No Change
Burr cells	Some
Acanthocytes	Some
SGOT	15 → 25
SGPT	15 → 20
BUN	No Change
Creatinine	No Change

An average increase in percent of oxygenation through the oxygenator was 25%. The amount of oxygen actually transferred through a 1 M^2 device at 500 ml basic flow and 1000 ml recirculation averaged 25 cc. This is not as high as in the earlier series of experiments, however it should be noted that those had been derived from dogs whose venous O_2% saturations were lower and whose extracorporeal blood flow rates per membrane area were much higher, giving higher O_2 partial pressure gradients across the membranes. The average decrease in pCO_2 was 5 mm of Hg. This was approximately one half of what we achieved earlier where venous pCO_2's remained within normal limits. The pH also remained normal in these animals. An average hematocrit decrease of 10% occurred between pre-operative and 24 hours post-operative, when body fluids had stabilized. Hemoglobin decreased an average of 3 gm during the same period of time. Plasma hemoglobin increased on the average to no more than 80 mg % during 24 hours. Hemoglobinuria was never noted. No blood was given these animals in the prime or before, during, or after the runs. No animal died with a low hemoglobin or hematocrit or high plasma hemoglobin. A radical change did occur in platelets, on the average from 250,000 at the beginning down to 20,000 at the end of the run. However, platelets returned rapidly to half the pre-operative value within 5-6 hours of the perfusion, indicating that the bone marrow had not been suppressed. Some burr cells and acanthocytes were seen when blood smears were examined. No changes in SGPT or SGOT were seen. BUN and creatinine remained unchanged. It should be noted that in the one animal which was perfused at approximately 1500 ml/min. basic flow, 3000 ml/min. recirculation for 24 hours, no greater changes were seen in any of these studies. It appears that increasing the flow from approximately 1/4 total bypass to 3/4 total bypass did not make a significant difference in any of these parameters including plasma hemoglobin.

Discussion.

As much was learned from our failures as from our successes in this series of experiments. A number of technical mishaps were perhaps inevitable when we were dealing with awake animals that were free to move about in their cages and capable of twisting arterial and venous lines, etc. In adapting conventional blood pumps for use in prolonged perfusions a number of lessons had to be learned and some of these were unfortunately at the expense of the experimental animals. The relative lack of measurable blood parameter changes and the long-term survival of 5 of 10 animals with a minimum of apparent morbidity encouraged us to embark on a series of longer procedures.

48-HOUR VENOUS-ARTERIAL PERFUSIONS

A series of 5 dogs were perfused for a period of 48 hours using methods and procedures identical to those prescribed for the 24-hour dogs in the preceding section. Results as regards hematologic and chemical parameters were essentially the same. No priming or transfusion blood was given at any given time in this series of experiments, as before. The first dog of this series made it through the 48-hour run apparently unaffected but unfortunately escaped his handlers during the process of removing the arterial cannula and bled to death before he could be brought under control. The second dog survived unaffected and remains living and well up to this day. The third 48-hour dog, although appearing relatively well at the end of the run, expired some 2 hours later and unfortunately no autopsy was performed. As mentioned before this A. V. fistula was still wide open at the time of death and high output cardiac failure may have contributed. Hypokalemia as low as 2.8 was also noted in the subsequent analyses of serial blood samples from this experiment and may well have played a role in his demise. A fourth attempt at a 48-hour run was interrupted after 36 hours because of demands on the pump team dictated by patient needs. That animal appeared unwell when the experiment was terminated and he died some 6 hours later. At autopsy one lung lobe showed red heparinization consistent with pneumonia. Subsequent analysis of serum samples from this experiment also showed low potassium levels. A fifth dog survived the 48-hour perfusion unaffected and he also remains living and well to this day. Thus 2 of 5 forty-eight hour perfusions were highly successful and the deaths which followed the other perfusions were not necessarily attributable to the oxygenator itself.

ARTERIO-VENOUS PERFUSION OF PUPPIES

We are greatly indebted to an excellent senior medical student at Cornell, David L. Schenkar, for an interesting series of studies directed at exploring a possible therapy for infants afflicted with respiratory distress syndrome. His study was undertaken to solve some of the problems which have been related with studies of this form of therapy and to demonstrate that pumpless arterio-venous partial bypass is a safe procedure in infant beagle puppies.

Methods.

Eleven conditioned infant beagle puppies weighing 3 to 4.5 Kg were studied to determine control white cell counts, platelet counts, total and plasma hemoglobin and total proteins. They were anesthetized eight hours prior to the perfusion with fast acting barbiturates and under sterile conditions, an arterio-venous fistula was created from the common carotid artery to the jugular vein with 8-12 French catheters. Intramuscular procaine penicillin was given. Puppies were allowed to awaken and food was withheld until the experiment the next morning, when control studies were again done.

The perfusion system was assembled under sterile conditions. Special sharp-interface connectors linked the puppy, via 3/16 in. Tygon tubing, to the one meter-square membrane oxygenator, Pemco low-volume heat exchanger and Sweden single-pass bubble trap. Recirculation, when used, was maintained by a conventional Sarns roller pump at variable flows. This practically isovolemic system was pre-primed and adjusted to puppy mean arterial pressure with less than 200 cm^3 of either dextran, normosol, autologous or homologous whole blood after which time no blood was added to the system. Priming temperature and pH were adjusted to 37°C and 7.4 respectively. Perfusion rate was initiated and controlled by partial release of the adjustably clamped arterial catheter and the animal allowed to move about freely in his cage, eat or sleep during the experiment. During the perfusion heparin was infused in dose equivalent to 2 mgm/Kg /3 hrs. and the weight of the puppy and oxygenator was observed.

Continuous monitoring of EKG, left ventricular end-diastolic pressures, central venous pressure, arterial, venous and oxygenator pH, pO_2 and temperature, total flow, oxygenator gas flow, respiratory rate, pulse and blood pressure was done. Studies also included control and experimental serum sodium and potassium concentration, plasma glucose and hemoglobin, hematocrit, white cell and platelet counts, urine analysis for protein, sugar, acetone, and hemoglobin, peripheral blood sugar, reticulocyte counts and serum protein, BUN, SGOT, and SGPT. Reticulocytosis and hematocrit were followed for at least three weeks post-perfusion and random animals were sacrificed for gross and microscopic pathological examination within two hours post-perfusion.

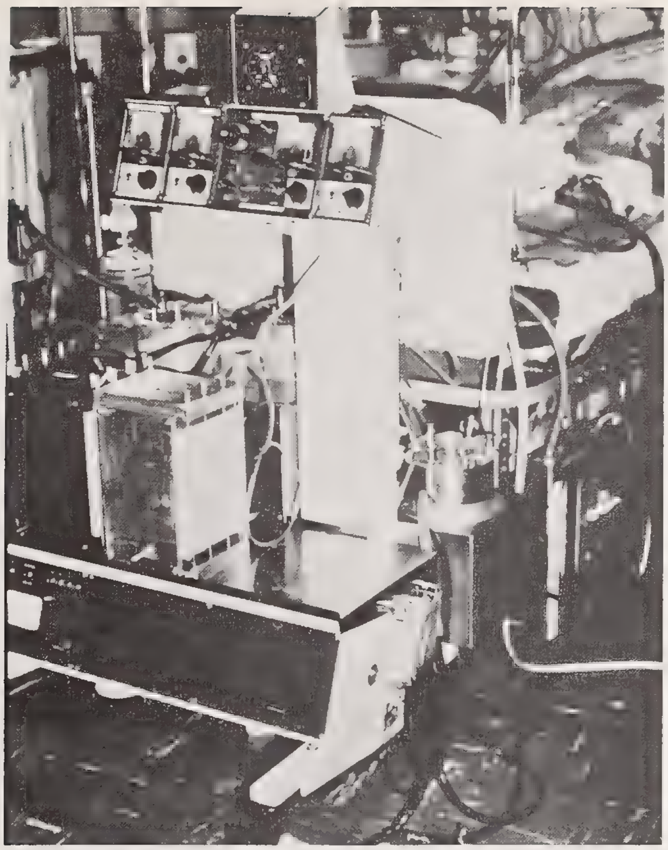

FIGURE 8. 3 M^2 OXYGENATOR.

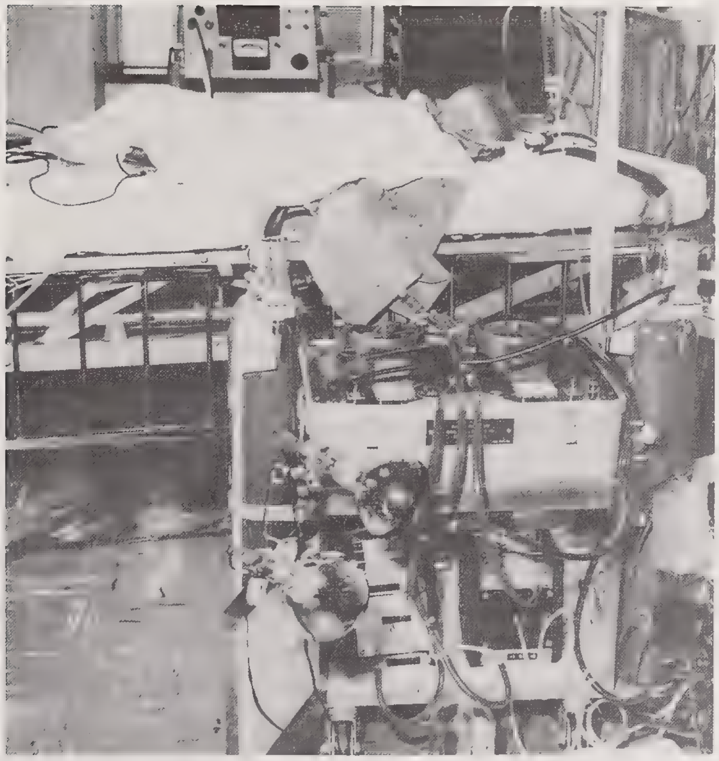

FIGURE 9. 1 M^2 OXYGENATOR.

All animals (8) survived 8-24-hour perfusions except the initial three, which were lost to technical errors. During the entire perfusion, the puppy ate, walked or slept although most of the animals were somewhat lethargic due to at least eight hours of open arterio-venous shunting before the experiment. Rectal thermistor temperature stabilized at 37°C and was exactly controlled by heat-exchanger water temperature which never rose above 42°C and other vital signs remained near control values. Puppy peripheral arterial pO_2 remained at about 75-85 mm Hg while blood return to the venous system from the oxygenator was as high as pO_2 450 depending on the O_2 flow. At flow rates of 125 to 175 cm^3/min. the $\Delta\, pCO_2$ across the oxygenator was about 10 mm Hg (puppy arterial pCO_2 25 mm Hg to oxygenator pCO_2 15 mm Hg). The pCO_2 was easily controlled by addition of CO_2 to the gas flow. Pre and post oxygenator pH were about 7.5-7.4 respectively.

During perfusion there was no elevation of SGOT, SGPT or BUN and total protein decreased as much as 1 gm %. Hematologic studies showed hematocrit decrease of less than four points during the 24-hour experiments even though brisk intravenous infusion ran continually. WBC's were variable and platelet counts decreased precipitously only to rise within 24 hours to control levels. Peripheral blood smears showed only a few burr cells, and reticulocyte count increased until the fourteenth post-perfusion day, during which time hematocrit correction began. Plasma hemoglobin rose to as much as 100 mgm % in one experiment but was cleared within 5 hours after perfusion ended. Urinalysis during the experiment showed no protein or hemoglobin.

EKG remained unchanged during the tests and left ventricular end-diastolic pressure did not rise.

Four randomly selected animals were sacrificed for gross and microscopic examination of heart, brain, liver, lung, kidney and muscle which showed a few scattered pulmonary fibrin thrombi in only two. Three animals were lost to the initial experiments: two to cannulation accidents and sepsis and one to spontaneous hematoma of the mesentery followed by shock. The remaining four animals are 1-1/2 to 2-1/2 month long-term survivors at this writing.

Discussion.

The results achieved by this talented medical student illustrate that perfusion via this potentially very useful arterio-venous route need not be harmful even to very small puppies. The studies likewise again demonstrate the relative absence of hematologic and chemical aberrations related to such perfusions. The type of rigidly supported blood flow path device used would be of especial importance for premature infants because of its capacity to maintain a constant extracorporeal blood volume. This would ensure a constant blood volume in a very small infant which could otherwise be thrown into shock or failure by fluctuations in volume as would be possible in devices which have less well supported membranes. Modular construction of these devices makes it possible to tailor oxygenator size to fit the patient.

CLINICAL EXPERIENCES

Introduction.

After extensive animal laboratory testing including that related above, we have undertaken nine veno-arterial perfusions in moribund patients. This was for prolongation of life and in the constant hope that salvage might be achieved. Due to these experiences, we have gained considerable new knowledge regarding the application of membrane oxygenators to patients in assist situations. More important still, perhaps, has been the recognition of some of the actual problems which must be faced and some glimpses of possible solutions.

Methods.

The same techniques and equipment were utilized as had been used in the 24-and 48-hour dog and puppy experiments. Adaptations were made where required to fit the specific clinical situation. We have settled on 2, 3 M^2 oxygenators (Figure 8) as apparently ample for even total bypass of adults and one or more 1 M^2 units for pediatric work (Figure 9). A standard roller pump console with 2 pump heads, one for veno-arterial pumping and the other for the recycling of the blood through the oxygenator have been used. Recycling does seem to us a worthwhile adjunct, useful for providing some movement of blood through the oxygenator when it is temporarily not receiving blood from the patient and also as a definite aid in promoting additional oxygen transfer through the membranes when the amount of membrane available is marginal. We think this additional oxygenating capacity is highly comforting and the price which has to be paid in terms of damage to blood is so inconsequential as to not be detectable. The pump set-up was essentially the same as for the 24- and 48-hour experiments. No heat exchanger nor bubble trap were used. The time from first indication that the treatment will be needed until the perfusion of the patient has commenced has been cut to as little as one-half hour when the circuit has been prepared in advance. The sterile circuit is flushed with saline followed with a prime of bank blood. A full 1000-1500 cc blood prime has been used in most patients because, as will be noted below, in their poor condition a large blood space develops which must be filled with colloid. Cannulation of the femoral artery and vein is carried out simultaneously with pump preparation. We have settled upon proximal and distal directed catheters placed through adjacent sites in both arteries and veins so that the leg involved may also be perfused. Warming blankets supplement the heat added by the heated oxygen and the infrared lamps directed at the oxygenators themselves. These heat sources are more than adequate for maintaining body temperature during assist but it is inadequate for the rapid temperature changes which are needed for heart surgery. For cardiac surgery we have placed a blood heat exchanger in the venous line before the reservoir. This site of insertion prevents air embolus due to the addition of a heat exchanger in mid-run. Blood samples for gases are taken from the arterial and venous lines to the oxygenator. Direct arterial catheters for sampling the patient are inserted whenever possible. The same catheter is also important for pressure movements. The rate of perfusion is directed by the rate of venous return. In most of these moribund patients, we found ourselves performing essentially total bypass at rates varying between 2000 and 4000 cc per minute in adults and 500-1000 cc in infants. Heparinization is carried out at a rate of 3 mg per kilo at the beginning of the procedure and additional heparin has been added only to convert transfused blood. Lee-White clotting times are followed from time to time to be certain that clotting is not imminent. In general no additional heparin is required even in extended perfusions.

Results.

Oxygenation and CO_2 removal have been more than adequate since we decided to use 6 square meters of membrane in adult perfusions. This is indicated both by blood gases which show pO_2 well over 100 mm Hg on the arterial side, and CO_2 removal which is commensurate. pH has also remained normal and in some cases has been alkaline without addition of buffers. Hemolysis as indicated by plasma hemoglobin accumulations has been minimal in these clinical perfusions. We have seldom seen plasma hemoglobin concentrations rise over 100-150 mg % even where total bypass was carried out for extended periods of time. On one occasion a patient was placed on a bubble oxygenator for one hour before being attached to the membrane. Plasma hemoglobin rose to over 1000 mgm % in one hour on the bubble oxygenator and gradually came down to less than 80 mgm % in the ensuing 16 hours on the membrane. Only on one occasion were the plasma hemoglobin levels greatly increased on the membrane oxygenator. It is believed that this was due to the position in which the oxygenators were placed. The support plates were horizontal unlike all the other runs where the membrane support plates were vertical. It is thought that since blood circulates so slowly through the multiple short (3 cm) flow paths (average time of approximately 6 seconds to traverse 3 cm) that there would be time for a significant number of cells to settle by gravity out of the laminar flow and contact the membrane. Perhaps with vertical positioning of the plates such contact does not occur. Our criterion of refractory cardiac arrest insured that, without the membrane, life would have been measured in minutes. The fact that perfusions could be carried out for an average of 15 hours and as long as 38 hours while electrocardiographic signals continued demonstrates the effectiveness of the membrane device for restoring and maintaining the viability of at least some internal organs. In general however the arterial pressures obtained on the oxygenator in these central nervous system damaged patients have been unsatisfactory, apparently due to peripheral vascular collapse. Only 50-60 mm Hg pressure was obtained even at extremely high rates of extracorporeal flow. Pressor drugs have met with little success in helping this situation. Our most recent patient however has encouraged us to believe that given more favorable criteria of patient selection, some of these physiologic problems will be solved. Our most recent patient was a 2 year old who had had a Mustard procedure performed for complete transposition of the great vessels. Despite correction of the anatomical defect, he continued to have poor vital signs including pressures which were detectable between 40 and 50 mm of Hg systolic. He was also quite cyanotic from low cardiac output. He was, on the other hand, still reactive when placed on the membrane oxygenator for the purpose of keeping him alive so that preparations might be made to re-explore him. When placed on the oxygenator at a flow of approximately 50 cc per kg per minute which was all he would return, he immediately became quite pink and warm in his extremities and awakened. Most astonishing, both before and after his re-exploration, systolic pressures could be elevated from 40 mm Hg to 200 mm Hg merely by turning on the machine. This is the first situation we have encountered where we were truly assisting a weakened heart in the presence of a semi-intact central nervous system. This child remained on the membrane pump oxygenator through his second operation and was successfully taken off bypass several hours later. The connecting cannulae and the oxygenator remained attached to him, ready to be turned on in case of further need. He then suffered an additional cardiac arrest and was left with fixed dilated pupils. Thereafter it was impossible to obtain satisfactory arterial pressures with the assist.

Discussion.

Thus it appears that while more extensive means of assist will probably be required for patients who have been damaged to the point where they are unable to maintain a peripheral resistance, there are indications that patients who are merely in shock refractory to conventional pharmacologic forms of treatment will respond readily with high arterial pulse pressures when subjected to partial assist with the membrane oxygenator.

CONCLUSIONS

In *in vivo* and *in vitro* testing of flat plate membrane oxygenators in our laboratory certain conclusions have been reached. As short as 3 cm blood flow paths have been achieved in some of our designs ensuring minimal resistance through the devices. Rigid membrane support mechanisms allow relatively exact control to be exercised over the blood film thickness minimizing differential flow patterns. Our earlier devices utilized Bluemle cone supports, which posed difficulties in preparing the mold and in the actual molding process. Boring of some 14,000 small holes in our original mold was a time-consuming and demanding process. Furthermore each hole must be filled separately with plastic and each contains a small air bubble at its tip making the filling quite difficult. In our most recent designs, we have utilized extremely fine ridges of plastic to support the membranes. These should not be confused with the coarse ridges which may be found in some other blood oxygenating and dialyzing devices. In fact the ridges we are now working with are spaced about half as far apart as the closely spaced cones. The grooves which form such ridges are relatively easy to machine with great uniformity and plastic molding of ridges is far more precise than of cones since the plastic tends to roll down the mold cavity and fill grooves with much greater accuracy at much lower molding pressures. The pedestals which we included in our prototype mold to hold the constant relationship between neighboring support plates were quite successful. Occasional wide ridges would also serve quite satisfactorily. Extreme importance must be given to scaling up these devices to a more practical size. Our prototype device consisted of support plates and frame plates and a total number of 200 parts were required for each one square meter unit. Six square meters of membrane required some 1200 parts, which is obviously not practical. For this reason, larger plates are desirable and this need not result in longer flow paths. In fact we have reduced the flow path from 5 cm to 3 cm in such designs. By modifying the manifolding system we have eliminated the need for frame plates, thus further halving the number of parts required. Thus in some of our newest designs only some 100 parts compared to 1200 parts are required to support 6 M^2 of membrane. Since the larger parts cost very little more than the smaller ones and are no more difficult to assemble, a considerable saving can be achieved. More and better membranes are becoming available and as they do so they will be easily incorporated in these flat plate devices. Our in vivo perfusions indicate that these devices of themselves are not harmful. They indicate that we must explore a variety of methods of using these membrane oxygenators in order to benefit the broadest possible spectrum of patients. This is because, under clinical conditions, it will be impossible to be very selective about which patients to treat with assist devices and when. While some proposed assist devices could be used only with a narrowly defined group of patients at a specific time in their clinical course, we foresee that we will actually be faced with patients ranging from those requiring little more than pharmacologic agents on through balloon assist and oxygenation assist and finally transiently passing through periods when they will need total bypass. We therefore plan to develop systems of assist which could automatically deal with these circumstances. Our failure to achieve adequate systolic pressures while perfusing moribund patients with constant flow would seem to indicate that we should develop systems for infusing blood in pulsatile fashion, preferably during diastole. This may be done utilizing our oxygenators themselves as pumps (Figure 10). By intermittently increasing and decreasing the pressure on the oxygen side of the membranes and including one-way blood valves in the system, this can indeed be done quite efficiently. While the membranes are being pulled apart by decreased O_2 pressure, blood enters between them and when the pressure on the oxygen side is increased the blood is pushed out through the outflow check valve. This is actually a very efficient pumping mechanism which needs to be studied further for its effect on blood and on the whole animal. A very important finding for this purpose is that this pumping action can be achieved using negative pressure alone (Figure 11), thus eliminating the possibility of forcing oxygen bubbles across the membrane into the blood. In this mode of operation, the membrane is drawn in and among the closely spaced membrane supports till the negative pressure is released, and then the elastic recoil of the membrane forces the blood out of the device at more than adequate pressures. One could accomplish diastolic augmentation by these means. An alternative method which interests us greatly is that of combining intra-aortic balloon pumping with membrane pump oxygenation. Recognizing that infusion of blood through narrow catheters is a difficult way to achieve a high pulse pressure without excessive trauma to blood, we hope to use a balloon pump simultaneously. The balloon pump alone is useful in a narrow, well defined group of patients who have some cardiac output and good lungs and a fairly regular heartbeat. On the other hand without all of these criteria the method falls down. We propose to combine the positive pumping and oxygenating action of the membrane oxygenator with diastolic augmentation of the balloon pump and perhaps more importantly with its collapsing function during systole. The heart would then find a lower pressure against which to disgorge its load of oxygenated blood from the lungs. Then it might be possible to convert some total bypass procedures to partial assist procedures by allowing the patient's heart and lungs to assume at least part of their natural functions.

We will also be exploring other uses of these versatile membrane blood oxygenating devices. Their use in heart surgery and in the support of cardiac and pulmonary transplantation is planned. Some far more difficult and time consuming cardiac surgical procedures might be attempted with the support of such devices. Their use in pediatrics, and in assist to diseased lungs are large fields worth exploring. Acute episodes such as pulmonary embolus and aspiration of gastric contents both might be supported for several days with favorable results. Organ preservation for transplantation is another area where membrane oxygenation might well find extensive use. Also basic scientific or investigative uses might be mentioned. For instance we have been cooperating with Dr. Charles McSherry of Cornell in an investigation of the "Vietnam lung" in which both membrane oxygenators and hyperbaric chambers are used in delimiting the causes of this oxygen toxicity disease. We see uses even further afield, as for instance in an artificial gill for a diver which would allow him to ascend from great depths without fear of the "bends" and allowing him to return to shipboard without need of a decompression chamber. There are then multiple areas of development that might take advantage of the development of practical devices for membrane oxygenation. We foresee that our laboratories will be kept busy with these possibilities for several years to come.

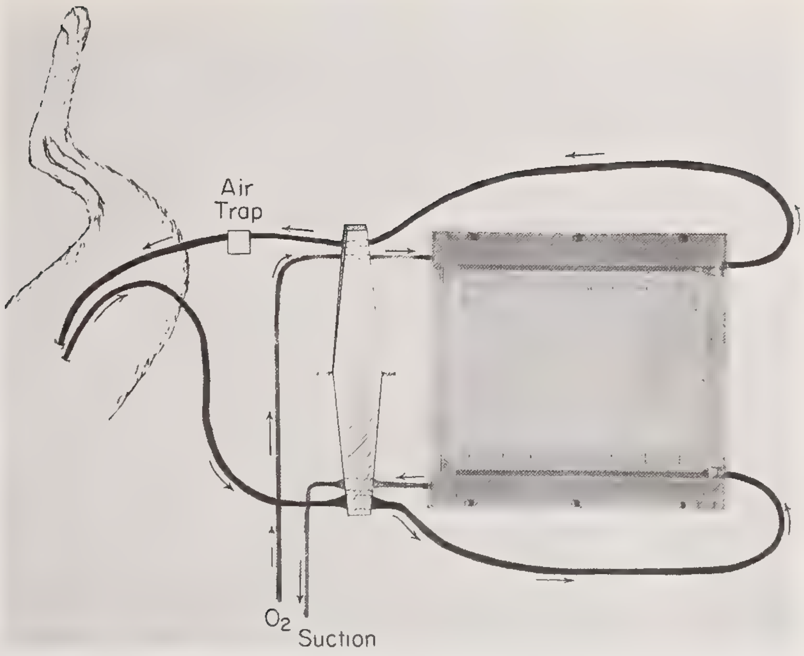

FIGURE 10. PUMPLESS VALVELESS MEMBRANE PUMP-OXYGENATOR.

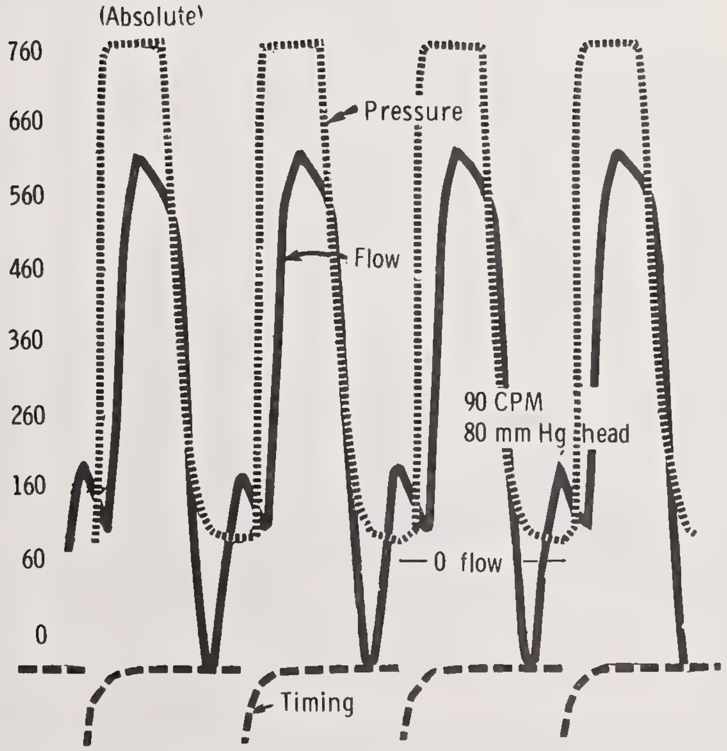

FIGURE 11. PUMPING ACTION USING NEGATIVE PRESSURE ALONE.

REFERENCES

1. Landé, A. J., Carlson, R. G., Perschau, R. A., Lange, R. P.,Sonstegard, L. J., Lillehei, C. W. A new membrane oxygenator-dialyzer. Surg. Clin. of N. Am., 1967, 47:1461-1470.
2. Landé, A. J., Parker, B., Subramanian, V., Carlson, R. G., Lillehei, C. W. Methods for increasing the efficiency of a new dialyzer-membrane oxygenator. Trans. Amer. Soc. Artif. Int. Organs, 1968, 14:227-230.
3. Lande, A. J., Fillmore, S., Subramanian, V., Solomon, H., Edwards, A., Killip, T., Lillehei, C. W. In vivo evaluation of a practical membrane oxygenator. Circulation, 1968, 38:121 (No. 4, supplement, No. VI).
4. Landé, A. J., Fillmore, S. J., Subramanian, V., Tiedemann, R. N., Carlson, R. G., Bloch, J. A., Lillehei, C. W. 24-hour venous-arterial perfusions of awake dogs with a simple membrane oxygenator. Trans. Amer. Soc. Artif. Int. Organs, 1969, 15.

DISCUSSION

DR. EBERHARDT: Dr. Lande, what was your cannulation system on your clinical partial bypasses?

DR. LANDE: In all of these cases we have gone into the femoral artery and vein. In case we start doing simultaneous pumping with the balloon, we will have to amend that and go into the upper extremity because otherwise we might get a paradoxical effect. Every time we pulsed the balloon we might get a decrease in pressure. I think that there are vessels in the upper extremity that would do just as well.

DR. EBERHARDT: And you obtained 3-1/2 liters a minute through the bypass circuit?

DR. LANDE: With six square meters, yes, and this seemed to be quite adequate. The venous blood returned at a higher pO_2, indicating that we were more than meeting the patient's requirements.

DR. HOLDEFER: Dr. Lande, would you summarize the mortality in the eight clinical veno-arterial perfusions?

DR. LANDE: 100%. The last patient was weaned off the pump but arrested two hours later , got widely dilated pupils, and could not be brought around thereafter.

DR. HOLDEFER: Did you monitor atrial pressure during these perfusions, and what were the values?

DR. LANDE: We did not monitor atrial pressure, but we monitored central venous pressure, and we tried to keep these at values more or less normal for patients in a heart surgery intensive care unit. Normal pressures for these patients are around 16-20 cm of water. We would like to have venous pressures a little higher than normal because that could increase our venous return. Interestingly enough, however, no great drop of venous pressure occurred when we started taking blood from the central venous system into the oxygenator. I had expected that this would decrease the central venous pressure, but it doesn't. As far as the mortality, I think I explained that most of these patients were really moribund and beyond return when we started.

CHAPTER 37

DEVELOPMENTS TO IMPROVE THE BRAMSON MEMBRANE OXYGENATOR

R. C. Eberhart, M. L. Coval

Institute of Medical Sciences
San Francisco, California

We report biochemical and engineering investigations of the Bramson oxygenator. Photometric and photographic techniques were developed which allowed us to map O_2 saturation and blood streamlines throughout the individual gas exchange cell. A numerical technique, based on Hele-Shaw flow, was also developed to calculate the local velocity vector. Local oxygen flux, pO_2 drop across the blood layer and local oxygen mass transfer coefficients were calculated from these data. A mass transfer correlation parameter was modified to resolve variations of pH, temperature, hemoglobin and inlet saturation between experiments. Simple modifications of the Bramson machine, based on these analyses, have increased the oxygen exchange efficiency by 40%, with 60% increase in blood pressure drop. In clinical blood samples obtained during heart lung bypass, consistent changes have been observed in the plasma protein pattern obtained with the procedure of analytical acrylamide gel electrophoresis. The technique was modified to allow routine separation of more than 40 human plasma proteins. A quantitation procedure was developed to measure the protein content of individual bands in the gel. The concentrations of several proteins were found to change as a function of the length of the bypass. Some of these proteins were identified as haptoglobins. Other studies of blood trauma included erythrocyte osmotic fragility and screen filtration pressure.

INTRODUCTION

Our contract called for investigations to improve an existing, clinically proved membrane oxygenator, the Bramson oxygenator. We shall deal here with two topics: engineering studies of the gas exchange performance and biochemical investigations of the response of blood to extracorporeal circulation.

I. ENGINEERING STUDIES

The engineering work was constrained to the Bramson geometry; Figure 1 depicts the blood flow in thin circular sheets defined by layers of plastic screen and adjacent silicone rubber membranes. The central blood inlet and four outlets cause the blood streamlines to form a cloverleaf pattern. The screens maintain the spacing of the membranes, and also induce a mild stirring action which improves the gas exchange. Fifteen cells, identical to that shown in the figure, arranged in parallel, are capable of adequately oxygenating up to 5 liters per minute blood flow. The system is oxygen-limited, and we therefore devoted our attention to methods of improving the oxygen transfer efficiency. This would be effected by varying the relative thickness of the screens, thereby controlling the blood flow. The complexity of the blood flow through the screens prevented a theoretical analysis, and our approach was therefore primarily experimental.

Methods. We built a one cell oxygenator consistent with the Bramson design, with transparent end plates to allow us to see the blood flow, (Figure 2). We constructed a scanning bichromatic photometer; this device measured the depth averaged oxygen saturation fraction at points throughout the cell. The measurements were relatively insensitive to blood flow rate, blood thickness and the presence of screens and semi-transparent membranes. Figure 3 presents the oximetric calibration curve obtained for one screen design. The standard deviation at any point did not exceed 2% saturation. The nonlinear form of this curve is due to the scattering sources in the light path.

Our in vitro experimental technique called for progressive deoxygenation of fresh human blood, discarded from heart-lung bypass in the day's surgery. We de-oxygenated in the same chamber to be used for oxygenation. We attempted to regulate the blood to a standard inlet condition: 50% oxygen saturation, pH 7.3, temperature 37, pCO_2 50 mm. Hg., hemoglobin concentration 12 gm. %. The blood was then re-oxygenated by one pass through the oxygenator; all gas exchange measurements were obtained in the 5 to 10 minutes available during this transient experiment.

We obtained 2 dimensional maps of blood streamlines by inserting small catheters into the blood layer, injecting dyes and photographing the results.

Results. We constructed composite maps for each screen design, showing the local blood thickness, lines of constant oxygen saturation and blood streamlines. Stream tubes carry equal flows in these pictures.

The results for the existing Bramson design in Figure 4, indicate the major part of the blood flow is restricted to the shorter paths between inlet and outlet. The dips in isosaturation lines near the inlet are due to a large jet of blood issuing from the inlet port. Note that this could not be discerned by our streamline mapping technique. Far from the inlet the isosaturation lines are inflected towards the outlet port: one can show that the oxygen flux into the blood decreases rapidly as the isosaturation and streamlines approach congruence. The humped isosaturation lines close to the outlet are caused by a weld of the plastic screens which creates a barrier to the flow.

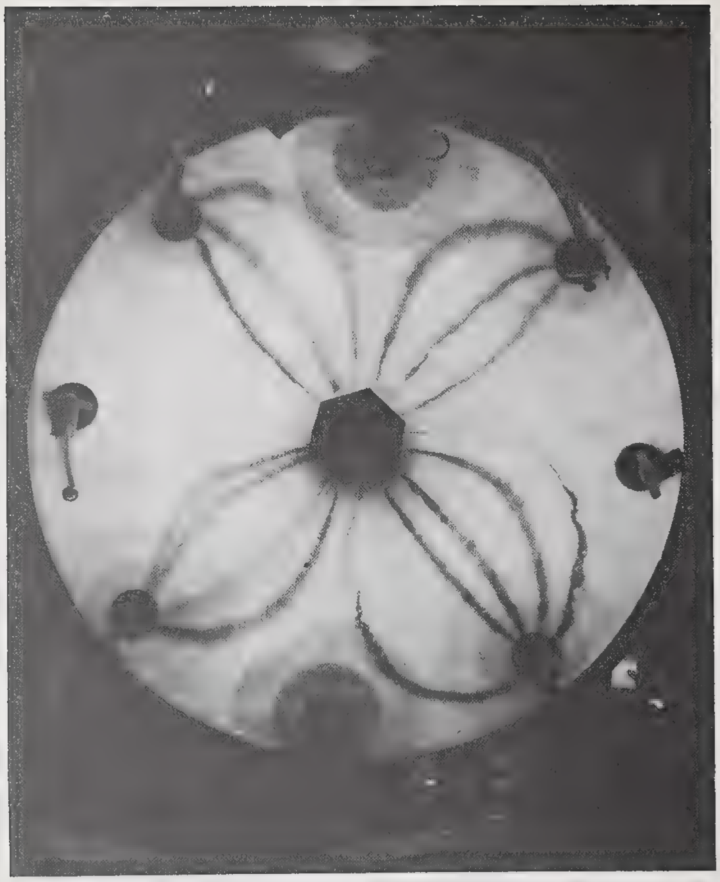

FIGURE 1. STREAMLINES IN THE GAS TRANSFER CELL. CLINICAL MODEL.

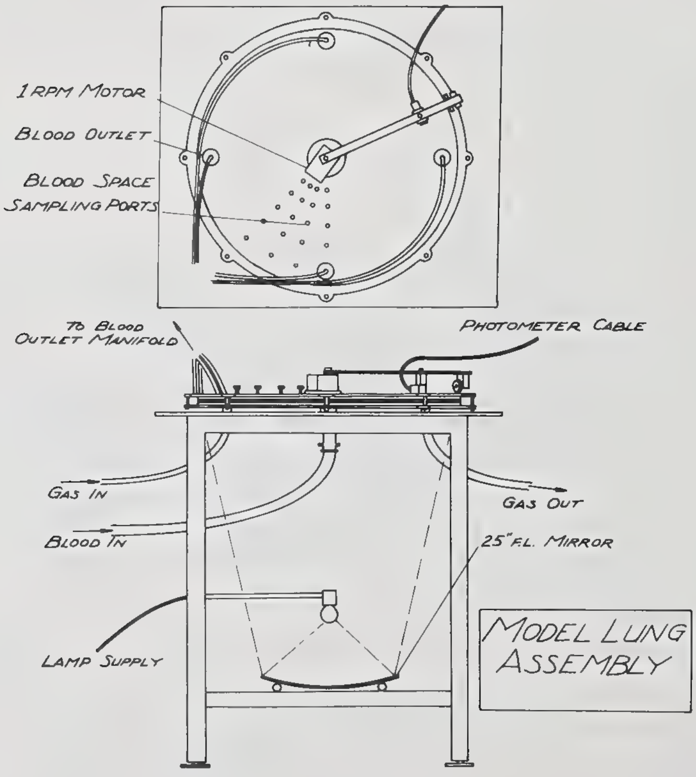

FIGURE 2. ONE CELL OXYGENATOR

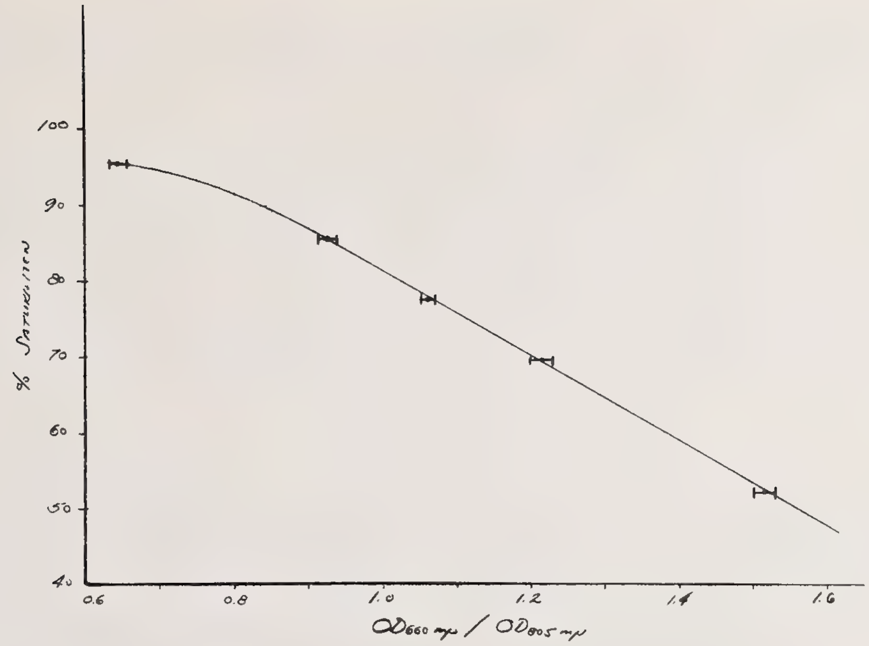

FIGURE 3. O_2 SATURATION CALIBRATION OF MARK VII SCREEN. CURVE BASED ON 70 GRID POINTS.

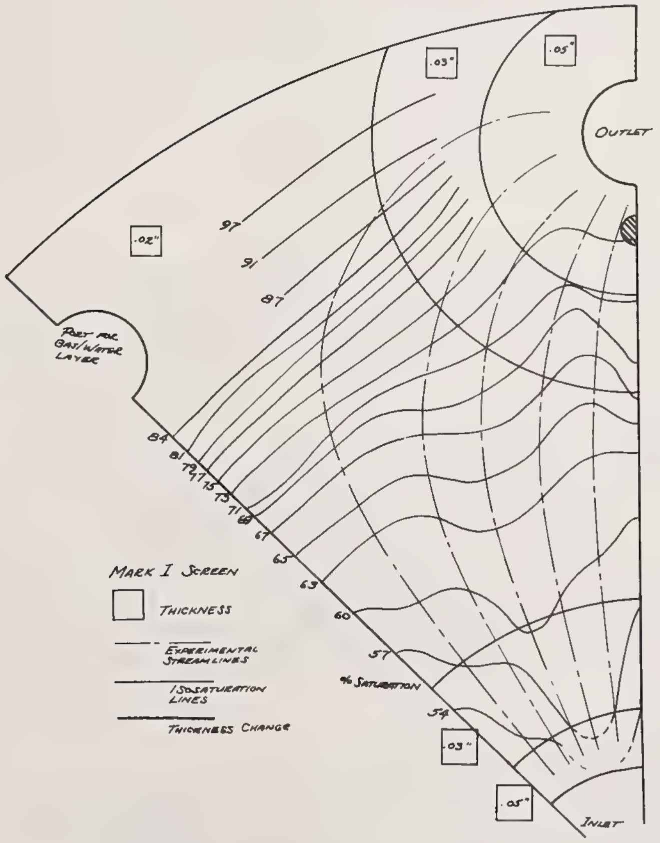

FIGURE 4. SATURATION AND STREAMLINE MAPS FOR THE CLINICAL OXYGENATOR. BLOOD FLOW 300 ML/MIN.

Figure 5 shows the resolution possible with the scanning photometer. The inlet ports were clogged with burned material in this experiment, constructing the orifices and increasing the penetration of blood jets into the cell. The visualizations of these jets align with known orifice positions. Incidentally, these effects cannot be seen by eye. The behavior in the rest of the cell follows that of the last slide.

Figure 6 presents the results of our best design to date. We effect a compromise between increased oxygenation efficiency and increased blood pressure drop. We have diverted much of the blood flow to the peripheral region by inserting a relatively thin layer at the shorter inlet-outlet paths. The blood flow in the periphery is much higher, as seen by the shift of streamlines upward from the results of Figure 4. The isosaturation lines support the diversion of the flow by the sharp drops, coinciding with the transition to the thin layer. One sees vestiges of inlet jets in this relatively slow flow experiment.

Analysis. For the case of two dimensional blood flow in artificial lungs, one can simplify the governing fluid flow equations. One deletes the inertial terms from the Navier-Stokes equations, provided the reduced Reynolds Number,

$$Re_t' = Re_t \left(\frac{2t}{x}\right)^2 << 1$$

t : half thickness
x : path length

We have carried out such simplifications and have been able to create a digital code to solve for the local blood velocity vector in the presence of arbitrary changes in the blood layer thickness. Good agreement between experiment and theory exists for simple screen designs. Poorer agreement exists for the more complex screens of our improved design, shown in Figure 7. Errors are started in the highly sensitive inlet region, and are amplified in the .010 layer. These errors are caused in part by our assumption of clear channel flow. We are inserting a drag term in the simplified equations to account both for the streamline offset and the low pressure drop down the channel. Discrepancy is also produced by our inability to match the uniform flow boundary condition, important in this case.

With a simple mass balance one may proceed to calculate the local oxygen flux. Returning to Figure 6 we see local flux values enclosed in circles. There is a rapid decline in oxygen flux with distance from the inlet; there is also some inverse relationship with blood layer thickness. For purposes of illustration we also show pO_2 at the membrane-blood interface. This calculation proceeds from the fact that oxygen diffusion through the thin membrane must be normal to the plane of the blood layer. Note that the major pO_2 drop must occur within the blood layer; this holds true for all but the largest flux in this experiment. Therefore, despite the mixing effects of the blood screens, the largest resistance to oxygen exchange occurs in the blood layer of the Bramson oxygenator.

We introduce the collect of three experiments in Figure 8. ht/Φ, the Sherwood number, is plotted versus $\frac{x}{t}[Re_t\ Sc]^{-1}$. The abcissa can be redefined as $[\text{Lewis} \cdot \text{Graetz}]^{-1}$ but the desired form indicates the dependence on path length x, half thickness, t, and Schmidt Number Sc, in addition to Reynolds Number, h, a local oxygen transfer coefficient, is defined as

$$h = \frac{g}{\underset{\text{wall}}{pO_2} - \underset{\text{bulk}}{pO_2}}$$

g : local specific O_2 flux

These data, for two separate designs, different blood flow rates and almost identical blood inlet conditions, demonstrate the sensitivity of oxygenation efficiency to the development of a concentration boundary layer. They do not account for varying blood conditions. Despite the mixing induced by the blood screens there is a four-fold decrease in efficiency between the inlet and fully developed boundary layer regions. 85% of the surface area of the Bramson oxygenator obtains at $\frac{x}{t}[Re_t\ Sc]^{-1}$ greater than 0.1. The remaining 15% of the surface is up to four times as efficient. Design in another geometry is clearly suggested by these results. The solid line is a least squared fit to a third order power function. The scatter of data beyond $\frac{x}{t}(Re_t\ Sc)^{-1} = .1$ is caused by variations in screen thickness. The trend of the data in the absence of screen thickness change is to a constant Sherwood Number. For this condition we find a fully developed concentration profile after 100 thicknesses.

We have prepared an iterative calculation scheme, based on the computer solution for blood velocity vector and the dimensionless oxygen efficiency. This will allow us to obtain, entirely by numerical analysis, the oxygen exchange in channel flow geometries in the presence of blood screens. A simple example of this scheme for a short path oxygenator, 6 cm. long, 0.5 mm. thick, in rectangular geometry, gives a net specific oxygen flux of 90 ml/M^2-min at a blood flow of 16 L/M^2-min, (6 cm/sec).

The General Oxygenator Transfer Function.

There has been controversy about the effects of blood conditions on reported values of specific oxygen flux. The following plot, Figure 9, has been useful to us in resolving the effects of pH, inlet saturation, etc., on the mean oxygen exchange rate. We multiply the inlet/outlet, or A-V difference, $G/1.34\ C_{Hb}$ by the group $\left[\frac{dpO_2}{dS} Z\right]^{1/2}$. The slope of the dissociation curve is taken at the average of inlet and outlet saturations, at pH 7.4, 37°C. Z is the product of pH and temperature corrections to the dissociation curve, as reported by Severinghaus.

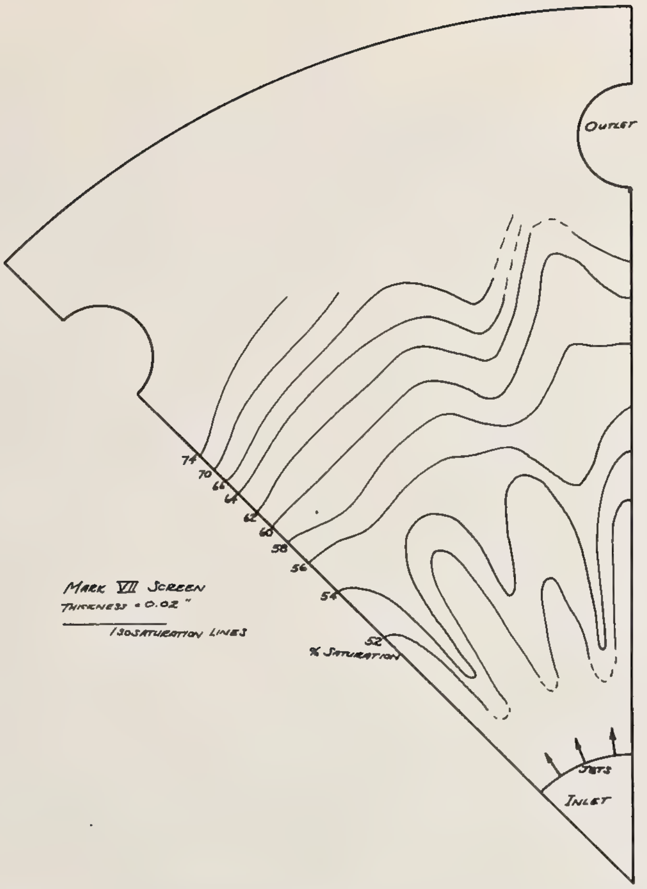

FIGURE 5. SATURATION MAP. INLET ORIFICES CONSTRICTED. NOTE EFFECTS ON SATURATION OF INLET JETS.

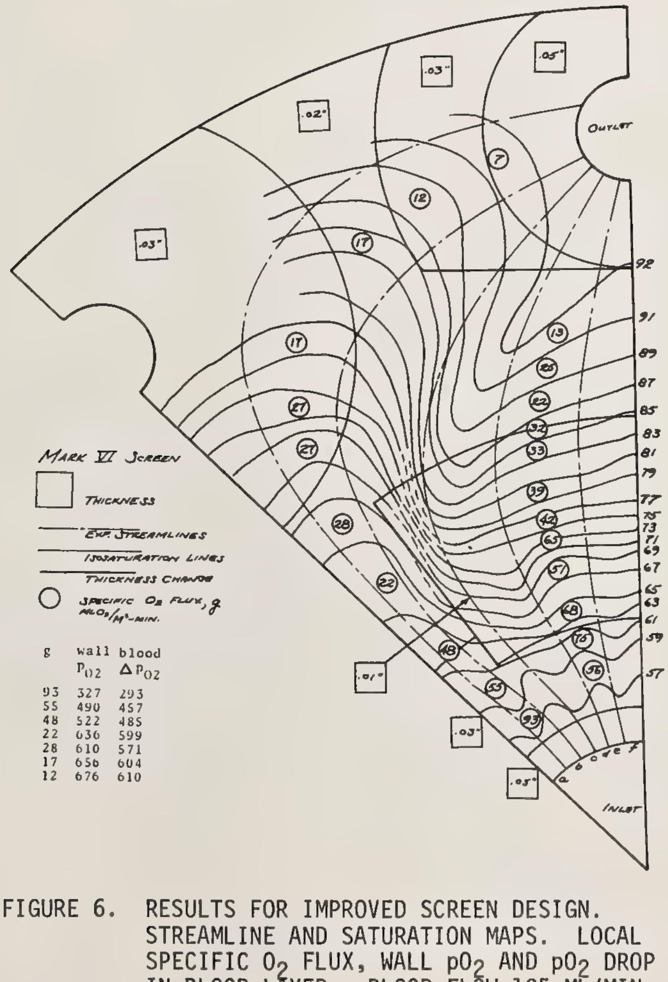

g	wall P_{O2}	blood ΔP_{O2}
93	327	293
55	490	457
48	522	485
22	636	599
28	610	571
17	656	604
12	676	610

FIGURE 6. RESULTS FOR IMPROVED SCREEN DESIGN. STREAMLINE AND SATURATION MAPS. LOCAL SPECIFIC O_2 FLUX, WALL pO_2 AND pO_2 DROP IN BLOOD LAYER. BLOOD FLOW 195 ML/MIN FOR WHOLE CELL.

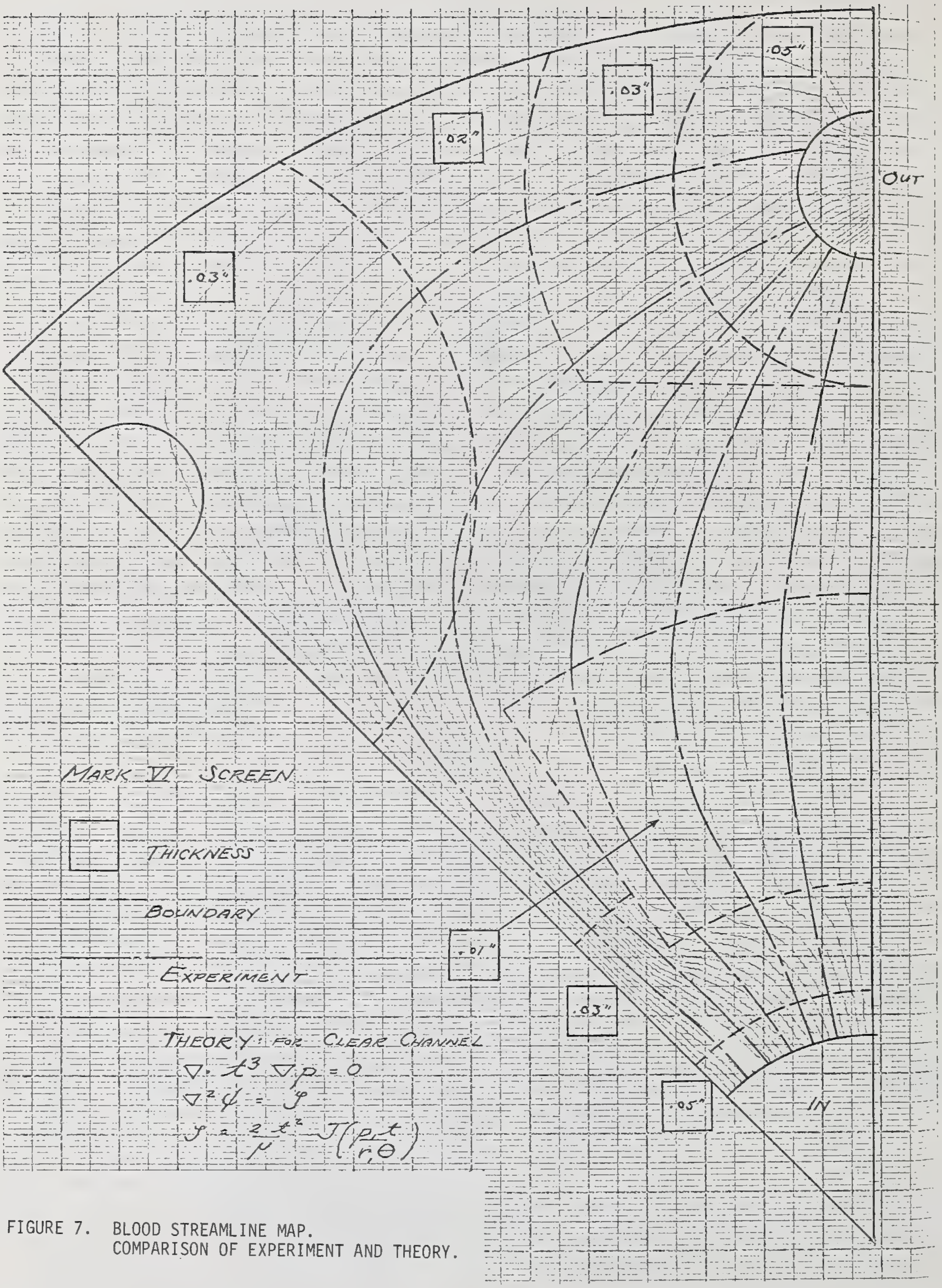
.05"
.03"
.02"
OUT
.03"
MARK VI SCREEN
THICKNESS
BOUNDARY
EXPERIMENT
THEORY: FOR CLEAR CHANNEL
$\nabla \cdot t^3 \nabla p = 0$
$\nabla^2 \psi = \varphi$
$\varphi = \frac{2 t^2}{\mu} J\left(\frac{p, t}{r, \theta}\right)$
.01"
.03"
.05"
IN

FIGURE 7. BLOOD STREAMLINE MAP.
COMPARISON OF EXPERIMENT AND THEORY.

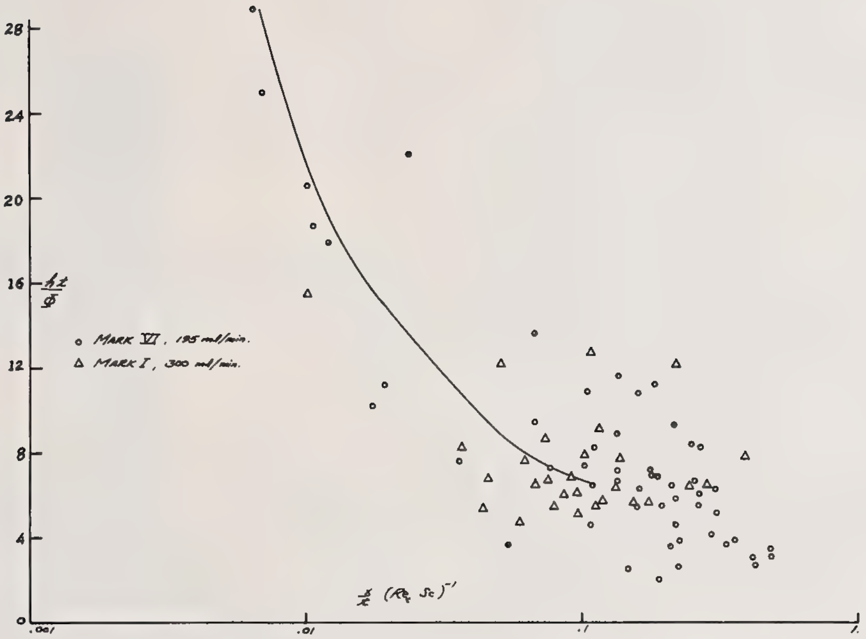

FIGURE 8. DIMENSIONLESS CORRELATION OF OXYGEN TRANSFER DATA:
g: O_2 TRANSFER COEFFICIENT. ML/CM^2 SEC MM Hg
t: CHANNEL HALF THICKNESS. CM
Φ: BLOOD O_2 PERMEABILITY. ML/CM SEC MM Hg
Re_t: HALF THICKNESS REYNOLDS NUMBER
Sc: SCHMIDT NUMBER

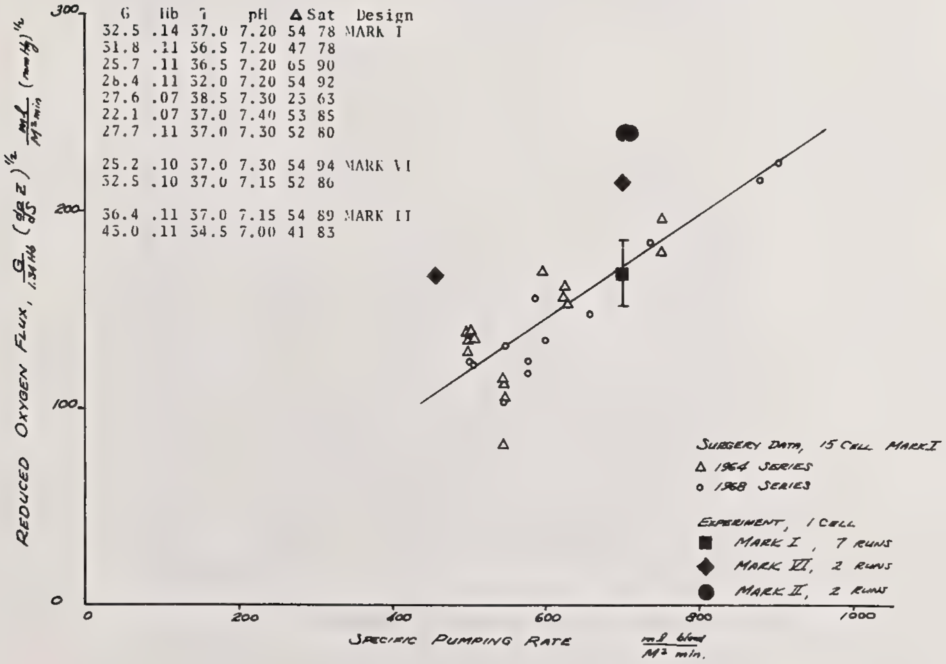

G	Hb	T	pH	Δ	Sat	Design
32.5	.14	37.0	7.20	54	78	MARK I
31.8	.11	36.5	7.20	47	78	
25.7	.11	36.5	7.20	65	90	
26.4	.11	32.0	7.20	54	92	
27.6	.07	38.5	7.30	23	63	
22.1	.07	37.0	7.40	53	85	
27.7	.11	37.0	7.30	52	80	
25.2	.10	37.0	7.30	54	94	MARK VI
32.5	.10	37.0	7.15	52	86	
36.4	.11	37.0	7.15	54	89	MARK II
43.0	.11	34.5	7.00	41	83	

FIGURE 9. OXYGENATOR TRANSFER FUNCTION.

The dots are 15 cell Bramson oxygenator performance on 10 patients in surgery over a wide range of temperature, inlet saturation and hemoglobin concentration. The square symbol is the mean of 7 one cell experiments, in vitro, over the indicated range of blood parameters. Note one cell performance is not degraded by 15 cell clinical operation. The diamonds and circles present in vitro performance of two improved blood screen designs in the circular Bramson geometry. Flux increases of 27% and 42% are achieved in the two improved designs: associated blood pressure drops are increased 60% and 170%, respectively. This plot resolves the performance decrease at high specific blood flow of the conventional A-V difference plot. It appears likely that the correlation will accurately show the advantages of various oxygenator designs.

Summary.

In summary, we have developed experimental methods of local oxygen saturation and blood velocity analysis which should apply to all channel flow membrane oxygenators. We also have a computer code for local 2 dimensional velocity analysis, including arbitrary changes in blood thickness. We have presented dimensionless oxygen exchange efficiency correlations which have allowed us to design and build improved oxygenators. Finally, we have been able to resolve a wide range in blood inlet conditions with a general oxygenator transfer function.

II. BIOCHEMICAL ANALYSIS

The work of our laboratory has focused on the development of methods to determine the amount of damage inflicted on blood by artificial devices, especially by heart-lung machines. This trauma to the blood limits the usefulness of most current heart-lung machines for prolonged perfusion.

This problem has been recognized for at least ten years, but progress toward solving it has been minimal. Some of the evidence accumulated suggests that denaturation of plasma protein is involved, and thus about a year ago we began a broad survey of plasma proteins with a technique called analytical acrylamide disc gel electrophoresis. This separation technique allows one to see about 20 human plasma proteins of the two-hundred known human plasma proteins. By modifying the technique to include one stacking layer and five separating layers of increasing gel concentration, we were able to double the number of proteins that can be seen in the tiny cylinders of acrylamide gel. We have been able to distinquish routinely 40 to 50 protein bands after staining with amido black.

In blood samples obtained during the clinical use of heart-lung machines we have seen consistent changes in the appearance and concentration of several human plasma proteins. In brief, after the electrophoretic separation, the gels are stained for proteins, so that the different bands are visible. We have also developed a method of measuring the dye concentration in individual bands.

Human plasma has a characteristic pattern which varies from person to person, and may be as individual as a fingerprint. It also shows typical changes in response to various diseases.

In Figure 10, the resolution obtained with the standard technique can be compared with the results of our modification of this procedure. The proteins which can be seen include albumin, ceruloplasmin, transferrin, α-, β-, and γ-globulins, and lipoproteins.

In Figure 11, by means of specific staining procedures, ceruloplasmin and transferrin have been identified.

In Figure 12 the reproducibility within a single run of the method is seen.

Figure 13 shows a typical picture of changes which develop in human plasma samples during total bypass with a disc oxygenator. A number of proteins are seen to increase, and one decreases. A number of differences in the intensity of staining of individual bands can be seen. The fifth gel was stained for haptoglobins with a benzidine stain, and it is evident that some of the bands which have reacted with this stain are identical in location to some of those bands whose concentration is changing.

In Figure 14, a duplicate set of the gels in Figure 13 were stained for haptoglobins, and it is evident that there is a general increase in the concentration of these bands. We have attempted to determine whether this was perhaps related to the slight increase of hemoglobin from hemolysis, but have not observed similar changes in the presence of an excess of hemoglobin. The relevance of this increase in haptoglobin concentration is the object of our current investigations.

In order to quantitate the changes which are visible in gel electrophoresis, we have been led to develop the following procedure: individual dyed bands are cut as single discs from the gel. The dye is then quantitatively extracted in dimethyl sulfoxide. In Table 1, separate dyed bands of protein were extracted at 50° or 100°, and both the increase in absorbance and the stability of the color were observed. After ninety minutes, the absorbance of the dye (amido black) has reached a constant level in the dimethyl sulfoxide and remains constant, within the limits of experimental error, for at least 19 hours. The extraction involves placing the disc of gel in 0.8 ml. of the solvent, in capped tubes, at a temperature between 50° and 100°, for about two hours. The absorbance is measured at the absorption maximum, 625 millimicrons. It is necessary to treat all gels in an identical manner, particularly during the destaining and slicing steps.

After electrophoretic separation of 5, 10 and 20 microliters of plasma, the eluted absorbance of three bands of dyed protein was determined, and the absorbance or concentration of each is proportional to the original sample volume (Figure 15).

In Figure 16, the protein concentration of a number of bands has been followed in plasma samples obtained from a clinical case. The protein concentration of this group of bands did not vary significantly during the operation. The last blood specimen was obtained sixty minutes after the perfusion had ended. Some of the determinations were done in duplicate and the repeatibility of the technique is indicated by the degree of scatter.

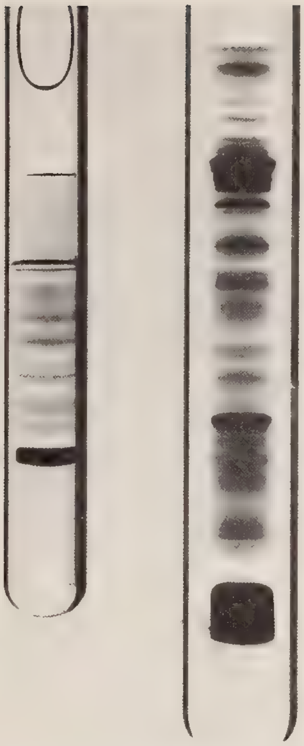

FIGURE 10. COMPARISON OF HUMAN PLASMA PROTEIN SEPARATION BY THE CONVENTIONAL TECHNIQUE, AND RIGHT, OUR TECHNIQUE.

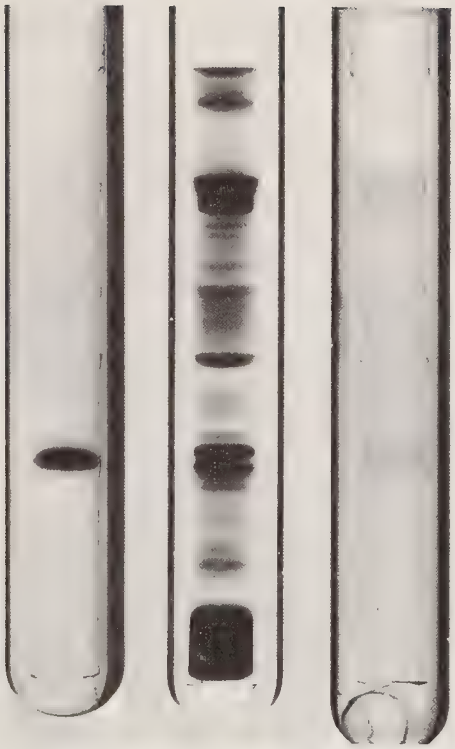

FIGURE 11. IDENTIFICATION OF CERULOPLASMIN ON THE LEFT, AND TRANSFERRIN, RIGHT.

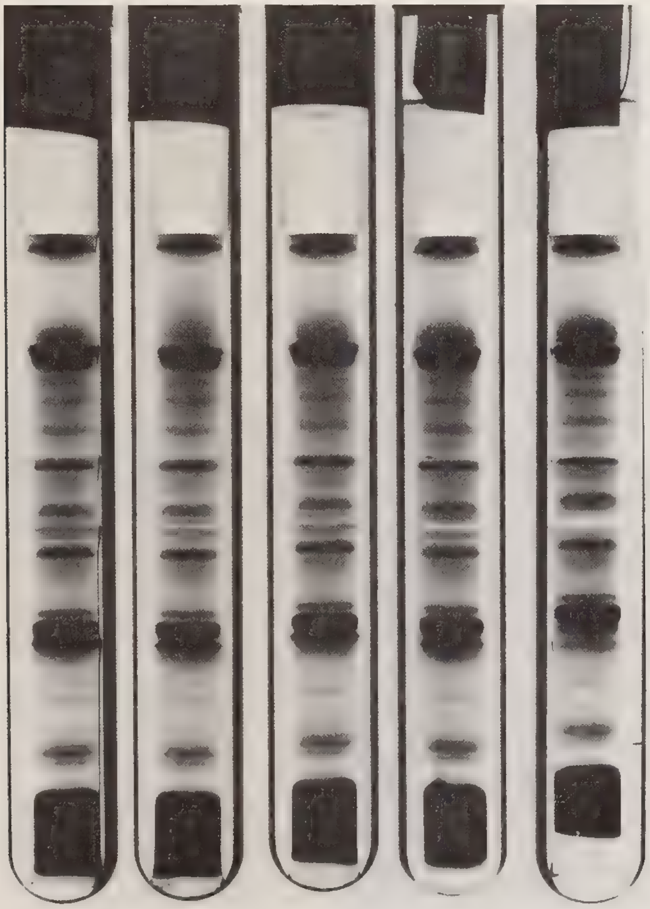

FIGURE 12. REPRODUCIBILITY OF THE METHOD WITHIN A SINGLE RUN.

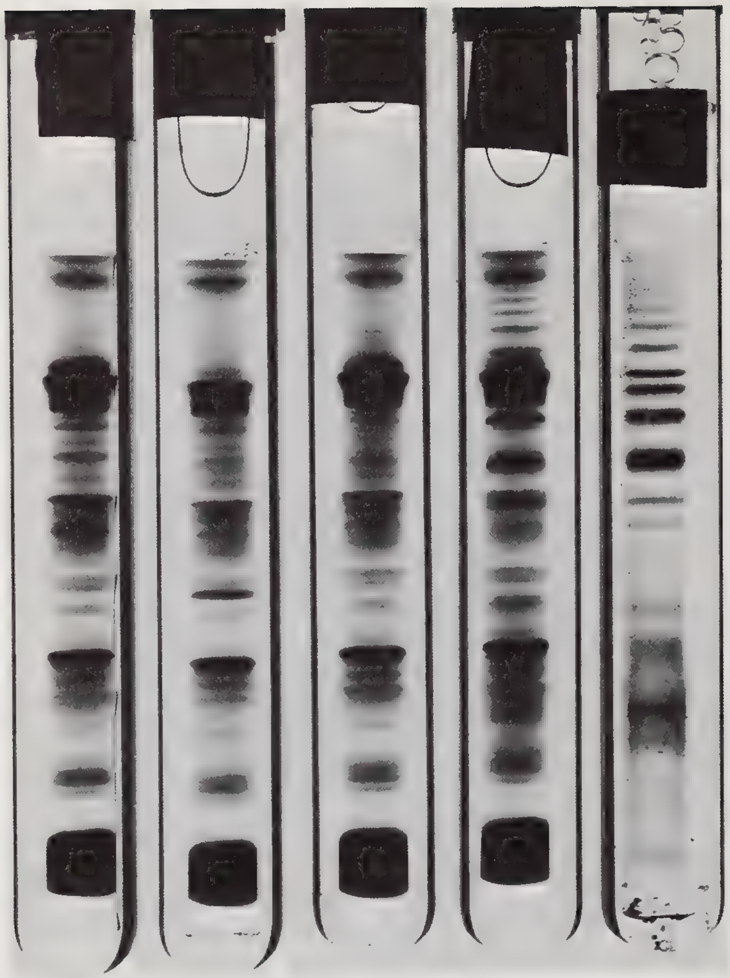

FIGURE 13. THE PLASMA SAMPLES IN THE FIRST 4 GELS WERE OBTAINED AT 10, 30, 60, and 127 MINUTES AFTER PERFUSION WAS BEGUN IN A CLINICAL CASE WITH A DISC OXYGENATOR. THE FIRST 4 GELS WERE TREATED WITH A GENERAL PROTEIN STAIN AND THE 5th GEL, A DUPLICATE OF THE 4th, WAS STAINED FOR HAPTOGLOBINS WITH A BENZIDINE STAIN. IT IS EVIDENT THAT SEVERAL OF THE BANDS WHICH INCREASE MARKEDLY ARE HAPTOGLOBINS.

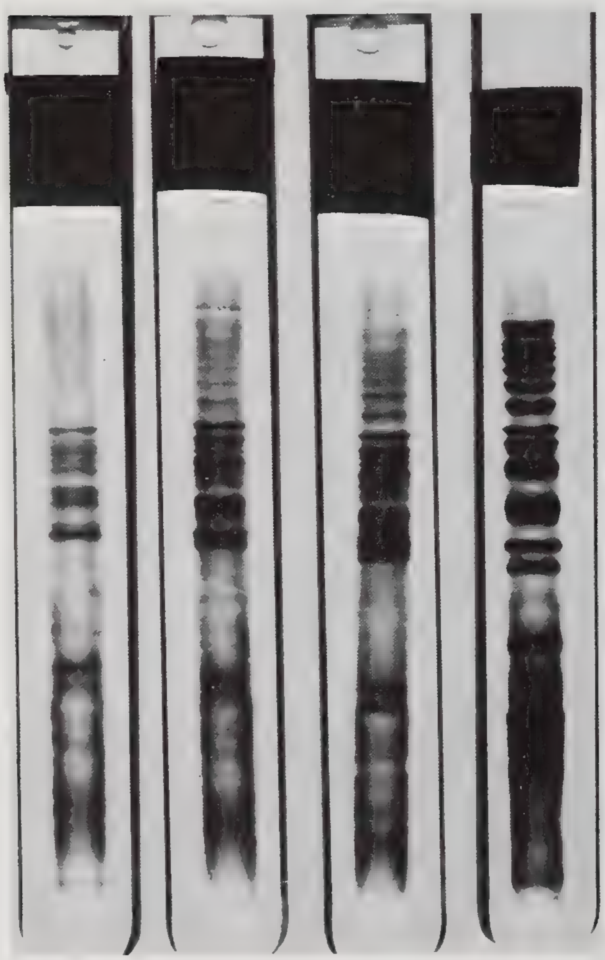

FIGURE 14. A DUPLICATE SET OF THE GELS IN FIGURE 13 WERE STAINED FOR HAPTOGLOBINS. IT IS EVIDENT THAT THERE IS A GENERAL INCREASE IN THE CONCENTRATION OF THESE BANDS.

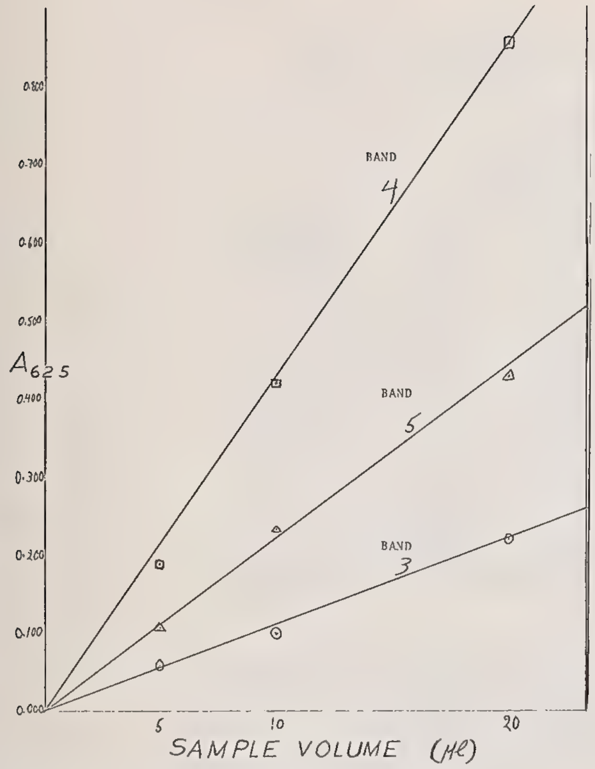

FIGURE 15. ELUTED ABSORBANCE OF THREE BANDS OF DYED PROTEIN.

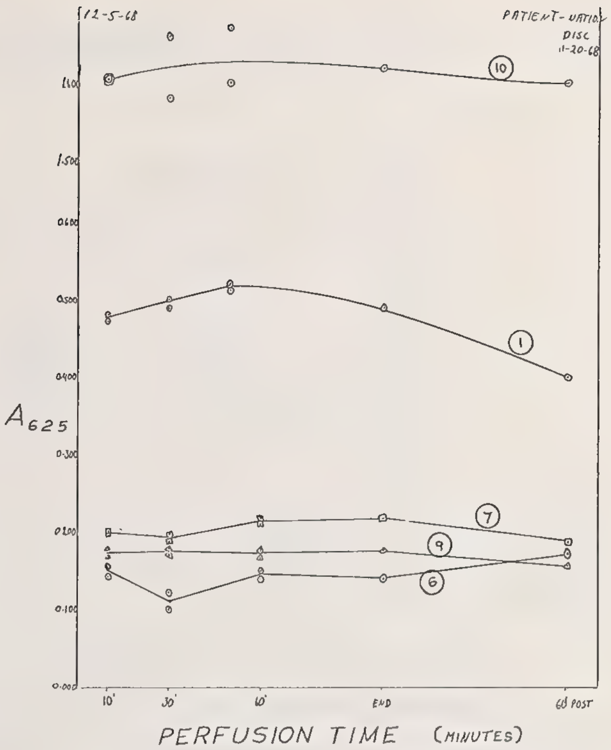

FIGURE 16. PROTEIN CONCENTRATION OF BANDS IN PLASMA SAMPLES OBTAINED FROM A CLINICAL CASE.

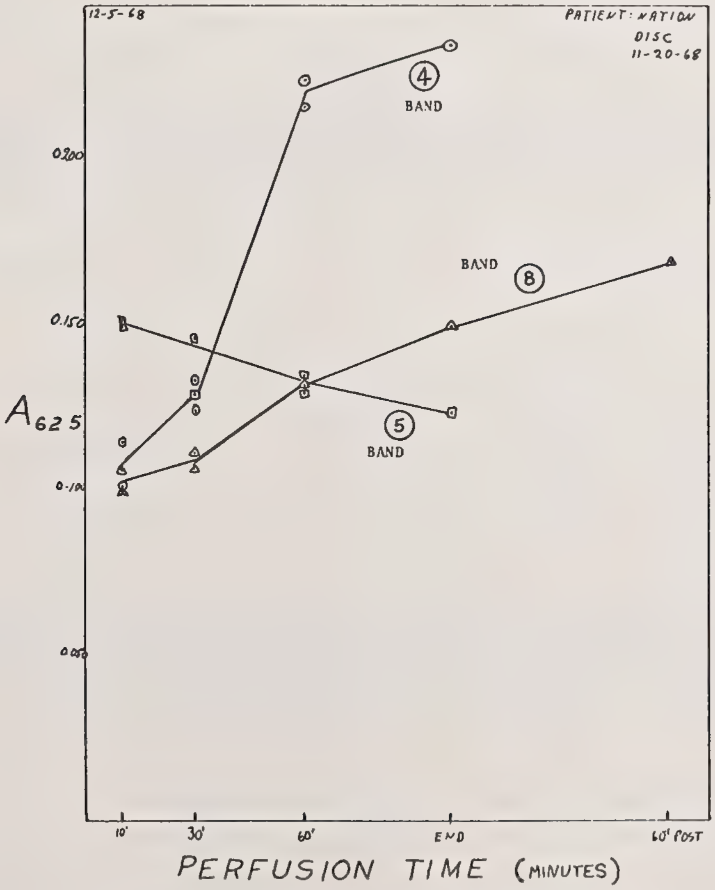

FIGURE 17. PROTEIN CONCENTRATION OF BANDS IN PLASMA SAMPLES OBTAINED FROM A CLINICAL CASE.

TABLE 1

RATE OF EXTRACTION AND STABILITY OF AMIDO BLACK IN DIMETHYL SULFOXIDE

Tube No.	Temperature	Absorbance (625 millimicrons) Time (minutes) 30	60	90	120	19 hours
1	100	0.819	0.880	0.875	0.872	0.871
2	100	0.889	0.910	0.895	0.896	0.890
3	100	0.695	0.726	0.722	0.732	0.742
4	51.5	0.874	1.080	1.112	1.117	1.126
5	51.5	0.565	0.625	0.625	0.625	0.635
6	51.5	0.788	0.840	0.831	0.830	0.825
DSMO vs H_2O	100	-0.002	-0.002	-0.003	-0.002	-0.002

Two albumin bands (from separate gels) were cut out and divided into approximately three equal pieces, each then placed individually in 3.5 ml. of dimethyl sulfoxide (tubes 1-6). Tubes 1-3 were kept at 100° C, 4-6 at 51.5° C. Absorbance measurements were made at the indicated intervals at 625 millimicron, the absorption maximum.

In Figure 17, there are some bands from the same run whose concentration did change significantly during the operation. Band No. 4 is one of the haptoglobins.

These methods have been developed to the stage where they can be used to follow the concentration of a considerable number of proteins in human plasma. They are now being used in our continuing investigations on the trauma dealt to blood by heart-lung machines and other artificial devices. The complete details of the procedure are available and will be published elsewhere.

ACKNOWLEDGEMENT

The determination, the dedication, the brains and hard work of Mrs. Cynthia Osborne and Mrs. Phyllis Friedman were essential to this work.

DISCUSSION

DR. FALB: I would like to congratulate you on your very nice piece of work with proteins. I wonder if you could elaborate on your concentrations of buffer and acrylamide in the separating gels. Or is that too complicated?

DR. COVAL: I think it is too complicated to go into right now. There are too many details.

DR. FALB: How many bands did you slice the gels into?

DR. COVAL: I think in the experiment you saw, we had ten.

DR. FALB: The reason is that you could not get a good densitometer to read the band; is that correct?

DR. COVAL: I do not think there are any sufficiently sensitive densitometers.

DR. STERN: Two questions: Were you able to see the appearance of new proteins in the circulating plasma, or was this a conversion of native protein into another band? Secondly, I noticed you had results of density in proportion to the sample amount, or was this proportional to protein concentration?

DR. COVAL: I do not think at the moment that we can identify the source of proteins which increase in concentration. We did present a year ago some data where we observed that many of the same bands appeared in plasma which had been denatured *in vitro*.

DR. STERN: It was not clear as to whether the straight line relationship that you had shown was due to actual protein concentration in the gel itself or just to different quantities of extracted gel. For it to be reliable you would have to demonstrate that the extracted dye was proportional to protein concentration in each band.

DR. COVAL: We had one figure which was intended to show that. We used the same plasma and we just varied the volume of the proteins. I think the amounts of separate proteins can be assumed to vary as the volume of plasma does. In our routine tests on plasma obtained during clinical use of oxygenators, we measure the protein concentration in each sample and set the volume accordingly, so that all of the gels contain the same amount of protein, the same total amount.

DR. deFILLIPI: What is the basis for the correlation shown which utilizes (oxygen exchange rate)x(slope of oxygen saturation curve)yz as a parameter?

DR. EBERHART: You cannot develop it from theory. It is strictly a manipulation of the data usually obtained from surgery. We had observed that, depending on the oxygen saturation of the venous blood, there would be changes in the efficiency of the device. We sought to account for this dependence and have been successful, at least for this short series of patients.

DR. LONG: There are some changes that occur in the plasma protein in patients who have suffered various forms of trauma, surgical and burn trauma, for example. Have you done any controls on the changes in the plasma proteins in your patients undergoing cardiopulmonary bypass versus patients with comparable degrees of injury but without exposure to a heart-lung machine?

DR. COVAL: We have not done such controls and we need to. Nevertheless, the doubts which have plagued me concerning the significance of our observations are now at peace. There are many other types of trauma in such operations. However, the changes we have seen are related primarily to the use of the oxygenator, rather than to other variables such as cardiac suction which we had found not to be a factor during the duration of the anesthetic. In summary, based on the limited control studies we have done, the only correlation is with time on the oxygenator.

CHAPTER 38

THE TIDAL-FLOW OXYGENATOR - PRINCIPLES, CONSTRUCTION AND PRELIMINARY EVALUATION

E. F. Leonard, R. M. Koffsky, H. R. Krumholz

Artificial Organs Research Laboratory
Columbia University, N. Y.

A membrane oxygenator based on the tidal-flow concept has been designed, constructed, and tested. This concept was developed earlier as a hemodialyzer[1] The tidal-flow oxygenator in addition to its gas exchange capability is able to accept blood at venous pressure and deliver it at arterial pressure levels with no auxiliary or serial blood pump in the system. The basic construction of the exchange device of the system includes a continuous strip of membrane (presently silicone base material folded transversely to a convenient size, supported by frames die-cut from a suitable material (i.e., latex, silicone rubber). The frames are sandwiched between two end plates, enclosing a defined volume and completing a unit. The membrane divides the enclosed volume into blood and gas spaces. These spaces reciprocate in size from zero to the completely enclosed volume as the incoming and egressing flows cause the membrane to move over its excursion of one frame thickness. Six such units are packaged into one cartridge with two sets of three units operating serially and in complementary fashion. A mechanical system has been constructed to control cartridge function. This operator controls flow and has a rudimentary CO_2 bleed control as well. Initial tests with sodium sulfite in place of blood indicate oxygen uptake rates of 100 ml/min at an oxygen pressure of 15 psig and a "blood" flow rate of 540 ml/min through a membrane area of 0.95 M^2.

INTRODUCTION

The tidal-flow oxygenator is intended to be a membrane gas exchanger capable of handling flows up to the normal human cardiac output and satisfying basal gas exchange requirements. In this paper the tidal flow principle is explained; technical ramifications of the principle which are important to oxygenator design are considered; and the present status of the development effort is summarized. An appendix summarizes the use of sodium sulfite solutions as an oxygen absorbent for preliminary testing of oxygenators.

TIDAL FLOW PRINCIPLE

The principal working component of the tidal flow oxygenator is a moving membrane which serves both as a surface across which gas exchange occurs and as a pumping diaphragm. Useful tidal flow configurations exhibit large ratios of transport surface area to filling volume, a requirement imposed on all homeostatic artificial organs. To achieve a high area to volume ratio, the membrane across which transport occurs is folded between frames so as to present a large working area in a small volume, as shown in Figure 1. Flow is achieved by alternately filling and emptying the spaces formed by the membrane folds as shown in Figure 2. Clearly a tidal flow unit must have a cyclic flow pattern. Typically the areas desired, the volumes permitted, and the flowrates imposed result in cycles which range in length from 12 to 50 seconds (i.e., 6 to 25 seconds for filling and a like interval for emptying). Since a cyclic flow of this periodicity is of no biological value, tidal flow units are arranged in parallel; one unit is always filling while its counterpart is emptying and *vice versa*. An idealized flow pattern is shown in Figure 3. A further (and final) complication of the basic design arises from the experimental observation that tidal flow units show better gas exchange with shorter operating cycles. Shorter cycles can be obtained while area, volume, and throughput are maintained at desired levels by using several smaller units arranged in series. Figure 4 is a schematic view of a "multiplex" gas exchanger cartridge consisting of 6 units: two parallel, oppositely acting trains of 3 units each. Each unit alternately fills and empties acting oppositely to its serial and parallel neighbors.

TECHNICAL RAMIFICATIONS

The design equations for a tidal flow exchanger are simple. If n is the number of frames of area a and thickness t in each unit, if the cartridge has m stages (corresponding to 2 m units), and if the total flowrate is Q one can compute the following quantities:

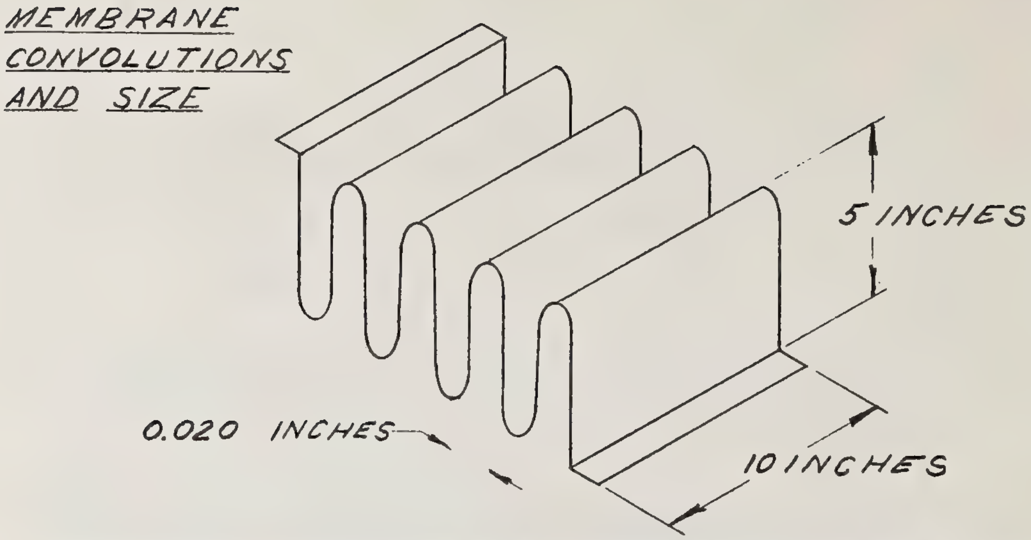

FIGURE 1. FOLDING OF MEMBRANE BETWEEN FRAMES SO AS TO PRESENT LARGE WORKING AREA IN A SMALL VOLUME.

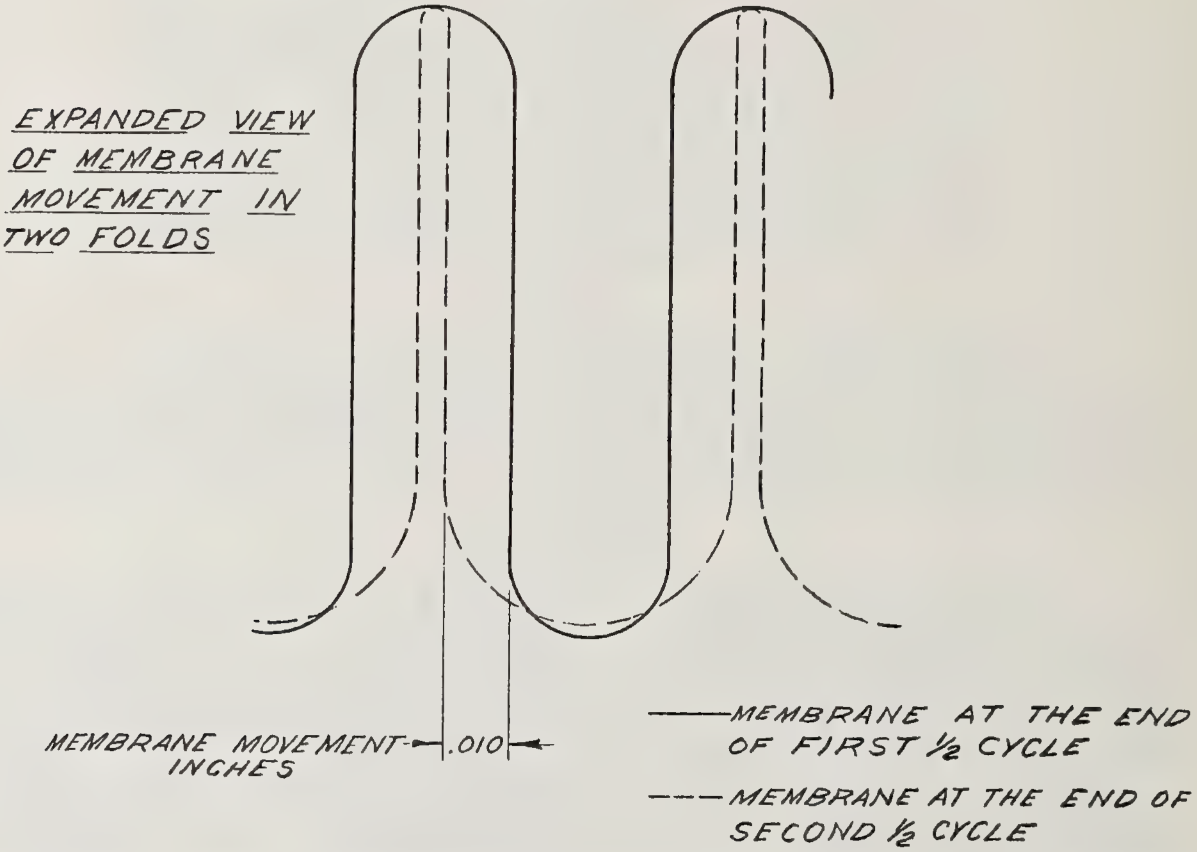
EXPANDED VIEW OF MEMBRANE MOVEMENT IN TWO FOLDS
MEMBRANE MOVEMENT INCHES
.010
——MEMBRANE AT THE END OF FIRST ½ CYCLE
---MEMBRANE AT THE END OF SECOND ½ CYCLE

FIGURE 2. FLOW ACHIEVED BY ALTERNATELY FILLING AND EMPTYING THE SPACES FORMED BY THE MEMBRANE FOLDS.

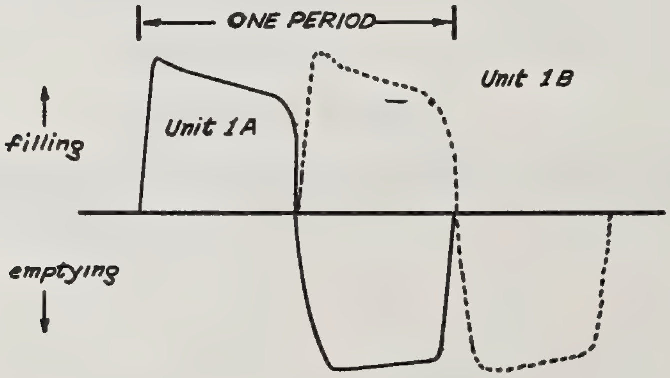

FIGURE 3. IDEALIZED FLOW PATTERN.

transport area:

$$A = 2a\ m\ n$$

operating volume:

$$V = a\ m\ n\ t\ (\underline{\text{not}}\ 2a\ m\ n\ t)$$

total cycle length:

$$T = 2a\ m\ n\ t/Q = 2V/Q$$

membrane velocity:

$$v = Q/(a\ n)$$

As opposed to most reciprocating pumps, the "piston" (membrane) velocity of the tidal flow exchanger is very low, about 0.02 cm/sec for a 2 M^2 3-stage cartridge pumping 4 l/min. Presumably this low velocity results in unusually gentle pumping action.

For a normal 2 M^2, 3-stage exchanger using frames each of which presents a useful area of 178 cm^2 each unit will contain n = 18 frames, will have an operating volume of 750 cc and a cycle length of 22 sec. when the cartridge is processing 4 L/min. of blood. In addition to these design parameters, details of frame configuration are important. Frames must be designed to permit nearly complete emptying in each cycle and reasonably uniform blood distribution over the membrane area. The frame material must be soft enough to function as a gasket but rigid enough to facilitate assembly and provide dimensional control. At present frames are constructed of gum rubber. A further advantage of the tidal flow configuration is the ease with which simple frames (adequate at least for development up to final stages) can be readily hand- or machine-cut from sheets of an appropriate elastomer.

Control of flow and gas exchange in multistage tidal flow systems is essential to their effective performance. Operating gas pressures may be determined by either flow or transport considerations (Figure 5). Flow considerations control in the filling of stage 1: gas pressure must be enough less than venous pressure at the cannulation site to overcome pressure losses in the venous cannula and permit timely filling. Transfer to stage 2 requires a pressure difference between stages 1 and 2 but permits the absolute level of the two pressures to be as high as may be desired to facilitate oxygen transport. Similarly only the pressure difference must be controlled to effect transfer from stage 2 to stage 3. Gas space pressure during the emptying half-cycle for stage 3 must be fixed appropriately above the arterial pressure against which the oxygenator discharges. These pressure relationships are shown in Figure 5. It is important to note that, in a 3-stage unit, blood can be in contact with hyperbaric gas for two-thirds of its residence time and that pressure differences, not pressure levels, are responsible for controlling flow.

A control device has been constructed to supply required gas pressures and to operate tubing occluders which direct blood flow through successive stages. Figure 6 is a photograph of a gas-exchange cartridge mounted on the control unit. A timing motor operates switches which actuate pneumatically -driven tubing occluders; the same motor drives four pistons which create the movements of gas which are used to control flow between stages 1 and 2 and stages 3 and 4. (Four piston-cylinder assemblies are required for the four units involved two others have also been mounted on the unit shown in Figure 6 to support an alternative scheme for stage 1 filling.) A vacuum pump is presently used to create the slightly hypobaric pressures needed to fill stage 1.

During the blood-emptying half of its operating cycle the gas side of each unit is pressurized from a common, high-pressure oxygen manifold; during this time the gas volumes of the cylinders associated with the units in stages 2 and 3 are driven toward their minimum, some of the gas being bled to atompshere to dissipate carbon dioxide while the balance enters the units. At the end of this half-cycle, the units in stages 2 and 3 are isolated from the manifold and the volume of the cylinder increased, causing the unit to fill with blood at a controlled rate.

STATUS OF DEVELOPMENT EFFORT

Tidal-flow gas exchangers and an associated control device have been constructed and tested in vitro. No rates of exchange with blood have yet been observed, but design levels of oxygen transfer have been demonstrated using an oxygen-absorbing solution in place of blood. Figure 7 shows transfer rates for a 0.95 M^2 cartridge as a function of flowrate at three different manifold pressure levels.

Present studies are directed toward optimizing fluid dynamical performance by modification of cartridge design, examination of the effects of membrane stiffness, and minor redesign of the control device (for example: installing time delays on occluder opening lines to eliminate regurgitation). Following completion of these studies brief in vivo tests will be performed to corroborate oxygen transport rates obtained with absorbent, to obtain carbon dioxide transport rates, and to assess possible coagulation problems.

APPENDIX

Blood is not in all respects or at all times, an ideal fluid to use in testing blood gas exchangers. It is clearly the fluid of choice in demonstrating the ultimate utility of a device. However it is difficult accurately to measure oxygen uptake in and carbon dioxide release from blood, to deoxygenate blood in in vitro circuits, and to maintain constancy of its properties during long experiments. This last problem in particularly acute when devices are being tested which have been only partially devlcped.

When one desires to measure the ability of a device to take up oxygen, solutions of sodium sulfite may be used in place of blood. When properly catalyzed this solution rapidly and

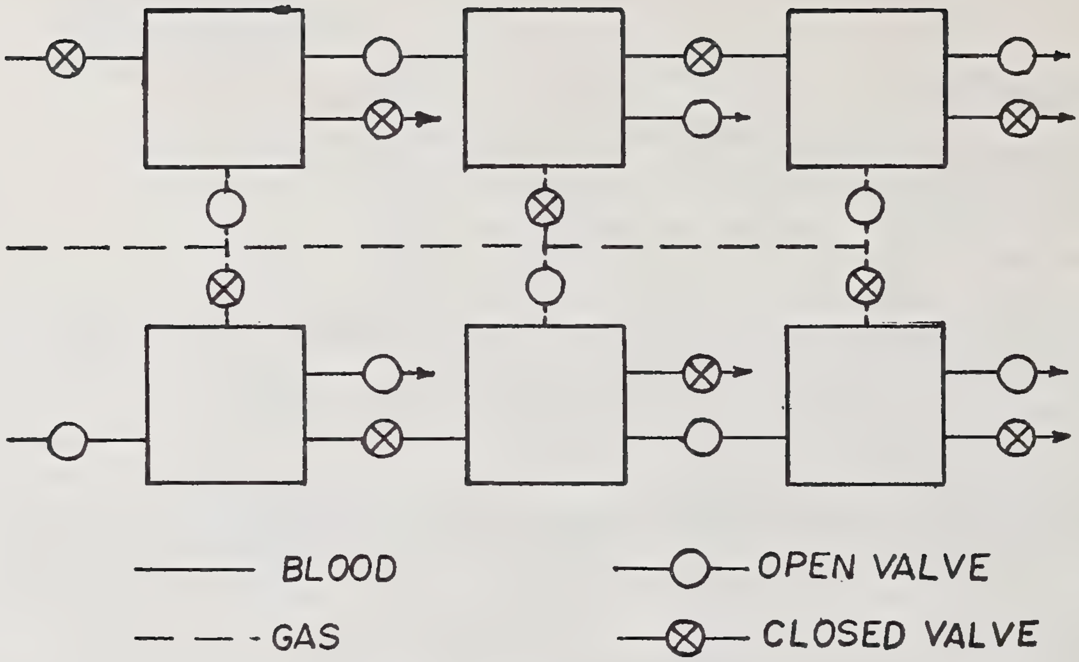

FIGURE 4. MULTIPLEX FLOW PATTERN.

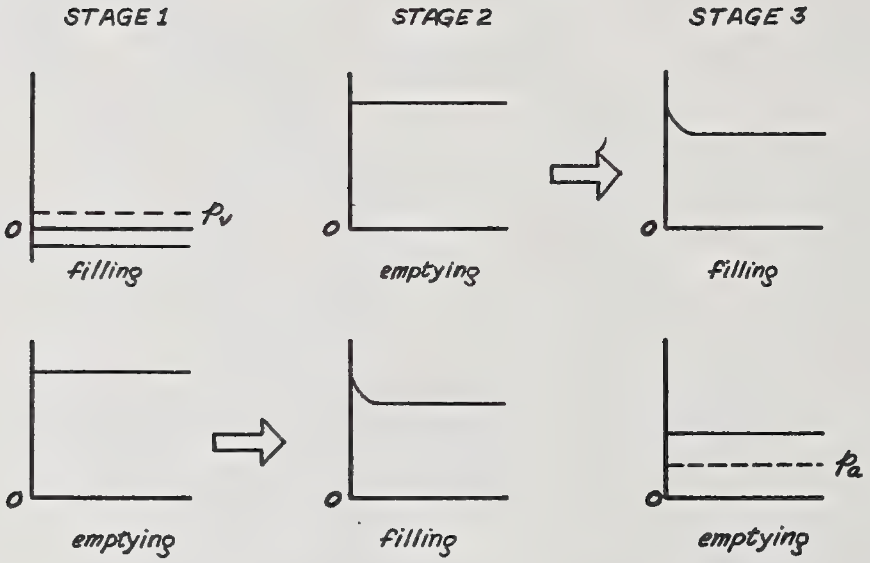

FIGURE 5. OPERATING GAS PRESSURES DETERMINED BY EITHER FLOW OR TRANSPORT CONSIDERATIONS.

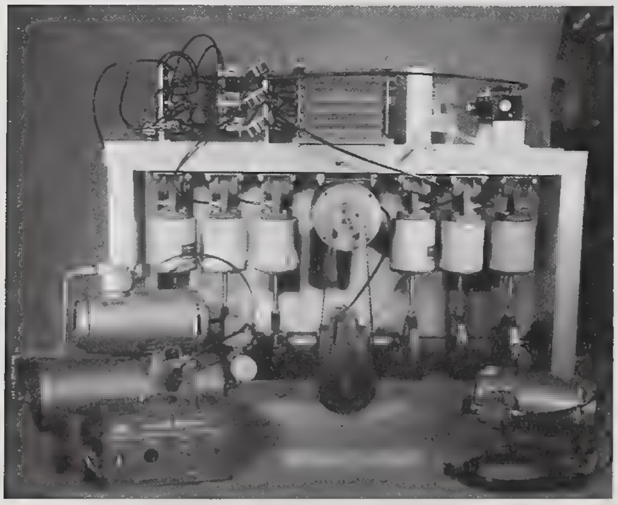

FIGURE 6. TIDAL FLOW OXYGENATOR (PROTOTYPE).

irreversibly takes up oxygen. Because the reaction is not reversible and the chemicals inexpensive, the solution is discarded after a single pass through the system. The reaction is given by the equation

$$SO_3^{=} + 1/2O_2 \xrightarrow{Cu} SO_4^{=}$$

The test solution is made up of 15.7 gm anhydrous sodium sulfite and 0.125 gm copper sulfate pentahydrate per liter, yielding a solution which is 0.125 molar with respect to sulfite. Oxygen uptake is determined by the difference in sulfite content of influent and effluent solution, samples of each having been quenched in an identical quantity of iodine solution[*] more than sufficient to allow the following reaction to go to completion:

$$H_2O + SO_3^{=} + I_2 \rightarrow SO_4^{=} + 2I^- + 2H^+$$

By determining the difference in excess iodine between the two samples, the oxygen uptake can be calculated. This determination is made by titrating the quenched sample solutions with sodium thiosulfate solution (.02 molar; 4.96 g of sodium thiosulfate pentahydrate per liter of solution) in the presence of starch indicator to determine the amount of unreacted iodine. This is a common titration considered in many textbooks of analytical chemistry.[2]

Each mole of iodine consumed by the sample implies that one-half mole of oxygen was taken up by that sample.[≠]

REFERENCES

1. Leonard, E. F., Robert M. Koffsky, J. E. Casterline & R. F. Cascone., A New Tidal-Flow Dialyzer: In Vivo, In Vitro, and Mathematical Assessment. Vol. XIII, Trans. Amer. Soc. Artif. Int. Organs, 208. 1967.
2. Pierce, W. C., and E. L. Haenisch, "Quantitative Analysis" 3rd ed. Wiley, New York (1948).

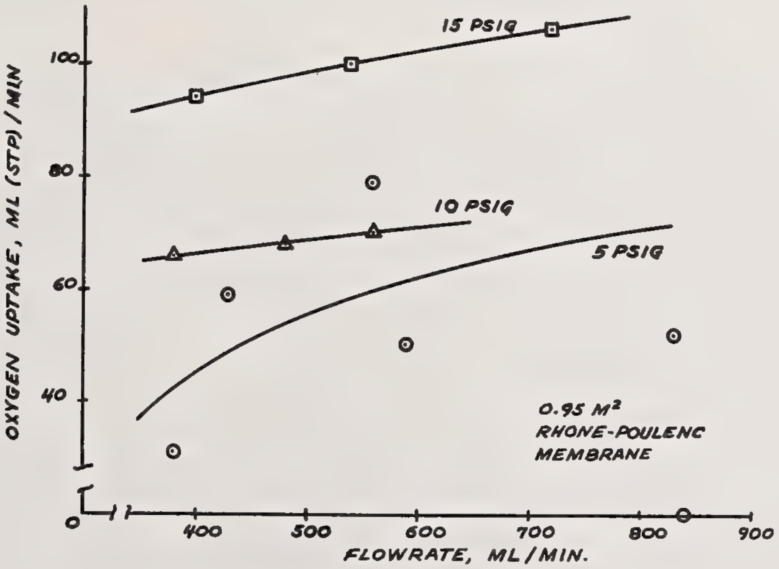

FIGURE 7.

---

[*] 3.97 g resublimed iodine and 10.0 g potassium iodide per liter of solution.

[≠] Sample calculation: titration of influent sample after iodine addition, 42.7 ml; titration of effluent sample after iodine addition 31.2 ml; size of sulfite samples from exchanger 10.0 ml; flowrate through exchanger, 1700 ml/min.

(42.7 - 31.2) x .02 molar $S_2O_3^{=}$ = 0.25(10 ^{3}) moles $S_2O_3^{=}$ consumed = 0.125(10 ^{3}) moles I_2 consumed = 0.0625(10^{-3}) moles O_2 taken up. 0.0625 x 10^{-3} x 1.7$(10)^3$/10 = 0.0106 moles O_2 taken up per minute or about 230 ml (STP) O_2 per minute.

Note that of the several solutions only the thiosulfate concentration enters into the calculation whence its concentration should be known accurately while other concentrations need only be approximated. It is important that sample volumes be accurate and that iodine quench volumes be identical.

DISCUSSION

CAPT. CALKINS: Have you considered using fluidic control for your oxygenator?

DR. LEONARD: If you ask the question: "Have you considered?," I can answer: "Yes, we have considered," but if you mean, "Have we done anything?," then the answer is "no." While we are aware of this possibility, and find it very attractive, we do not have in our own shop the technology or the know-how to implement it. I think it is a very logical thing to do in the future; and we would anticipate that fluid controls would provide improved simplicity, reliability, and even the opportunity to operate the system completely without any electrical parts. This would be desirable, for example, when it was being used in transport.

CAPT. CALKINS: For your reference, back in 1964 some investigators at Harry Diamond Laboratories considered this idea for a different application from what you are dealing with. These experiments are described in a document which is available through the Clearinghouse (Mon, George: "Design and Development of a Membrane Oxygenator", Clearinghouse Report No. AD 450728). It shows a system in which you can use a bistable unit. I do not know if it would directly fit your application, but it would probably give you a lead as to how you can adapt it.

DR. KELLER: Have you tried to determine how you would scale the sulfite data to the reversible oxygen reaction, either in terms of the concentration of the sulfite or the difference between the reversible or irreversible reactions? I am wondering whether or not you have done anything which would give you some idea of the rate of uptake as affected by having substituted the sulfite reaction for the reversible reaction, and what difference there may be in the concentrations. Are these concentrations about the same as those of hemoglobin?

DR. LEONARD: The quick and appropriate answer to that question is that the sulfite concentration (as one would not expect from theory) does not affect the rate at which the reaction proceeds. This is a finding in our hands and those of others who, as you know, have attempted to use this technique in developing fermentation equipment. It is possible, although it was not the case in the experiments which I have reported, to adjust the sulfite concentrations so that the oxygen capacity of the sulfite is identical to the capacity of blood. One should specify what is meant by 'capacity.' The irreversible capacity of the sulfite can be made equal to the reversible capacity of blood which still does not mean that we have exactly the same situation. A Master's Thesis carried out at Columbia University (George Greene, Chemical Engineering, 1969) forms the basis of our understanding of the relation between blood and sulfite oxygen uptake. The flow conditions used there were not those in the tidal-flow oxygenator. They were very high Reynolds number flows. Under those conditions we found that the transport rate to the sulfite was less than the transport rate to blood and we ultimately concluded (in nice agreement with the "Minnesota hypothesis") that the agitation of the boundary layer by red cells in high shear fields accelerated the transport in blood over that which would have been observed if cellular material had not been present. That would indicate that under those conditions - an important proviso - the sulfite was, if anything, a conservative technique. Because we have very good rates of oxygen transport to sulfite in the tidal-flow system, some conservation in the sulfite system is desirable. Still, I am not at all sure we will be able to completely confirm these when we run blood through the system.

CHAPTER 39

SPIRAL COIL BLOOD OXYGENATOR

K. Abel

Litton Industries
Minneapolis, Minnesota

An oxygenator of the Kolobow spiral coil configuration capable of providing adequate respiratory gas exchange for blood flows up to 5 liters per minute is under development. Highly specialized membrane design is required for the configuration in order to achieve maximum gas exchange with minimum oxygenator size. A cooperative task of membrane development and testing between Litton-Rhone Polenc (Paris) and Litton-Fuji Polymer (Tokyo) has been completed. This part of the program has resulted in the establishment of high volume sources of suitable high quality membrane for use in both spiral coil and conventional membrane oxygenators. The incorporation of these membranes into the spiral coil oxygenator and testing of the oxygenator is now in progress.

INTRODUCTION

During the year, this group has been working on a program of fabrication and testing of a Kolobow spiral coil oxygenator with up to 5 liter/min blood flow capacity.

Continuing studies on the application of membrane oxygenators in extended-term extracorporeal circulatory assist has added substantial evidence to the desirability of this class of oxygenator over previous classes featuring direct blood-gas interfaces. The most recent and most significant reported work is that of Kolobow, et al.[1] Kolobow has reported 50 ml/kg/min for more than 100 hours with minimal blood destruction or evidence of morbidity. In a subsequent personal communication, he has indicated successful bypass for longer than one week with equally good results.

The high efficiency of the Kolobow oxygenator is due to specific design and operational features which have been described adequately in several of Dr. Kolobow's publications.[2] The specific features include:

1) Surface configuration of the membrane.
2) Oscillation of the oxygen pressure between -100 to 0 mm Hg (atmospheric pressure).
3) Thin, uniform blood film layer.

The specific advantages of the design not related directly to oxygenation efficiency include:

1) All blood contacting surfaces can be disposed of after a single use.
2) The blood volume is fixed and largely independent of perfusion pressure.
3) The unit exhibits a low perfusion pressure.
4) Oxygenated blood leaving the membrane lung can be pulsatile independently of the blood pump.
5) All surfaces in contact with the blood are of non-toxic plastic materials known to have low thrombogenic characteristics and known to produce minimal protein denaturation.
6) It has a compact shape requiring a minimum of special handling or fixtures for effective use.

The key factors in achieving the specific advantages noted above are: (1) the spiral coiling (which maintains uniformity of blood film layer and blood volume without complex or bulky pressure pads or plates); (2) the thin screen-like space within the membrane envelope (exposed only to oxygen); and (3) the open knit fabric support within the silicone rubber membrane.

The rubber thickness of the membrane is not a key factor in oxygenation efficiency; increasing the membrane thickness from 0.002 inch to as much as 0.008 inch decreases the oxygen transfer rate by less than 10 percent. The limiting factor for oxygen transfer is the blood boundary layer resistance. This resistance is decreased as a result of the thin blood layer and the pulsatile oxygen gas flow which produces a "stirring" action at the membrane surface. Carbon dioxide elimination, however, does depend on the membrane thickness. Nevertheless, with membranes thinner than 0.005 inch, the overall design is also satisfactory with regard to carbon dioxide exchange.

Of all these factors, we have found the membrane specification to be the major hindrance in our goal to achieve a reliable, reasonable cost membrane oxygenator. A significant number of membrane samples (more than two dozen) from seven commercial firms have been examined for applicability in this oxygenator design. Of these seven firms, three have demonstrated the ability to manufacture membranes suitable for the design. The first firm* developed the membrane in conjunction with advisory support from Dr. Kolobow over approximately a four-year period. Their full output is reserved for their own commercial program. The second firm** has developed the manufacturing capability during a six-month period in conjunction with advisory support from Litton and indirectly from Dr. Kolobow. The manufacturing techniques are somewhat different between the two firms, but the resulting membrane is highly similar. The third firm* has modified a previously developed dip-coating technique to produce a membrane which shows considerable promise and is of the highest quality.

---

* Dow Corning Corp., Medical Products Division, Midland, Michigan.

** Rhone-Polenc, Paris, France, as represented through their subsidiary Rhodia, Inc., New York, N.Y.

Table 1 lists most of the samples we have tested to date.

TABLE 1

SAMPLES TESTED

Manufacturer	Sample	Cost[a]	Suitability for Spiral Coil Unit
Dow Corning	Nylon knit reinforced	Not available for sale	Highly suitable
Rhone-Polenc	RP 11		Marginal
	RP 12		Not suitable
	RP 13	$ 200	Not suitable
	RP 112		Not suitable
	RP 114		Suitable
	RP 115		Suitable
Fuji Polymer	Square weave #1		Not suitable
	Square weave #2		Not suitable
	S-81		Marginal
	S-98	$ 90	Marginal
	S-99		Not suitable
	S-100		Not suitable
	Special		Suitable (with reservations)
Waters	Standard oxygenator membrane	$ 60	Not suitable
GE	Single-backed	$1125	Not suitable
	Double-backed	$1250	Not suitable
	Unbacked	$1000	Not suitable
	Copolymer	$ 500	Not suitable
Ferro/Cordo	Fiberglass Dacron Weave	$ 40	Not suitable
Esco	"Silescol"	Not available for sale	Not suitable

[a]Cost is membrane only, 5 sq meter per oxygenator.

In Table 2 are listed the companies who have supplied these samples and their addresses.

TABLE 2

SUPPLIERS OF MEMBRANES

Rhodia, Inc.
600 Madison Avenue
New York, New York 10022
Attn: S. Andreani

Waters Co.
P. O. Box 529
Rochester, Minnesota
Attn: P. Nelson

General Electric Co.
1 River Road
Schenectady, New York 12305
Attn: J. Kesglow

Fuji Polymer Industries, Ltd.
No. 6-7, 1-Chrome, Kamimeguro
Meguro-ku, Tokyo
Attn: M. Horikawa

Ferro Corp., Cordo Division
3512 - 20 Helms Avenue
Culver City, California 90230
Attn: H. Reffe

Dow Corning Corp.
Medical Products Division
Midland, Michigan 48640
Attn: I. Hutchinson

Esco Rubber, Ltd.
Walsingham House, 35, Seething Lane
London, England
Attn: W. Shupak

---

*Fuji Polymer, Tokyo, Japan

REFERENCES

1. T. Kolobow, W. Zapol, J.E. Pierce, "High survival and minimal blood damage in lambs exposed to long-term (4-5 days) veno-venous pumping with a polyurethane chamber roller pump, with and without a membrane oxygenator", presented at ASAIO Meeting, Atlantic City, New Jersey (1969).
2. Specifically: T. Kolobow and R.L. Bowman, TASAIO 9:238-243 (1963); and T. Kolobow, W. Zapol and J. Marcus in "Organ Perfusion and Preservation", ed. by J.C. Norman, Appleton-Century-Crofts, New York (1968).

EDITOR'S NOTE: The following is a discussion of a blood oxygenator system, using nonthrombogenic coatings. It was presented by Dr. Akio Wakabayashi, University of California, Irvine, at the conclusion of this series of presentations by the Artificial Heart Program contractors.

DISCUSSION

DR. WAKABAYASHI: Although the concept of extracorporeal circulation was promulgated more than 150 years ago, the artificial oxygenation of blood was not achieved until 1937 when Dr. Gibbon successfully applied heparin to the circuit. Thirty-two years later, we succeeded in oxygenating blood without heparin. Today I would like to report briefly our studies to you. The first slide shows a photograph of the entire system: the venous cannula, venous return tubings, a Kay-Cross disc oxygenator, a roller pump, a Brunswick heat exchanger, and an arterial cannula. (Slide) The entire system is totally coated with our nonthrombogenic film coating, polyurethane-polyvinylgraphite film, which I described in detail previously. A short bridge between the venous and arterial lines serves to maintain circulation to prevent clotting and to maintain blood temperature while the heart-lung bypass is not in use. The second slide shows a close-up view of the coated discs. (Slide) The third slide is a close-up view of the mounted oxygenator. (Slide) As you can see, the top of the Pyrex glass cylinder is not coated, so that we can see through it while the blood is flowing. The fourth slide shows a close-up view of the coated Brunswick heat exchanger. (Slide) The last slide is a close-up view of the coated tubing set. (Slide)

We have done thirteen animal experiments without heparin. The system was primed with stored ACD blood, Ringer's lactate, or five percent dextrose in water.

Duration of total cardiopulmonary bypass was two hours in ten dogs, three hours in one, two and a half in one, and four hours in one. Two animals were excluded from the survival experiment because of non-related causes. Nine out of eleven dogs survived. During bypass, Lee-White clotting time remained within normal limits, usually six or seven minutes. Hematocrit was stable, and blood loss was minimal. Upon completion of bypass, clot formation was carefully inspected. We found clots always on the inner tube of the heat exchanger at the sites of entrance and exit. Also, a small amount of clots was often noticed on one or two discs near the entrance and exit. The other parts were free from clotting. Calcium gluconate was routinely given to the patient, 500 mg. per 500 ml. of ACD blood. Acidosis was common but not severe. Sodium bicarbonate was used in some cases but not routinely. Since our purpose was to investigate the feasibility and effects of heparinless total cardiopulmonary bypass, we tried not to use any drugs.

We feel that an oxygenator housing should be re-designed to minimize turbulence, and a heat exchanger should be changed so that over-heating can be avoided.

The present study indicates that a total cardiopulmonary bypass without heparin is possible by means of our nonthrombogenic coating. We are hopeful that this may permit open heart surgery with minimal operative and postoperative bleeding, and more importantly, may be used to assist a cardiogenic shock patient for a prolonged time.

DR. BLACKSHEAR: How did you get away with not using heparin?

DR. WAKABAYASHI: We have so many complications of operative and postoperative bleeding, and the reason for this is that we completely heparinize the patient. Heparinization is easy but after we finish open heart surgery sometimes we have difficulty in neutralizing heparin by use of protamine sulfate. This is the reason why we try to avoid the use of heparin so that we have very little amount of blood loss during and after surgery. The total blood loss after 2 hours of total cardiopulmonary bypass in this series was always less than 100 cc which is very little compared to heparinized bypass. We tried to establish heparinless heart-lung bypass so that we can do open heart surgery with minimal blood loss. Eventually we might develop a nonthrombogenic membrane oxygenator. We used polyurethane-polyvinyl-graphite coatings which I described yesterday.

DR. HOLDEFER: I am not suggesting that you did not examine these animals postoperatively for signs of central nervous system dysfunction, but Dr. Ivan Brown several years ago, in the study of deep hypothermia, pointed out that many times dogs have significant loss of cerebral tissue without exhibiting clinical signs of central nervous system dysfunction. In your autopsy examination, did you examine the brain microscopically?

DR. WAKABAYASHI: We did not use microscopic studies. Also, we did not open the skull but we feel, of course, that we should examine the brain. And also, before we try to apply this technique to human patients we will, of course, have to re-design the oxygenator and heat exchanger. Also, we must have a very efficient filter system. Then we can apply this unit to clinical open-heart surgery.

SECTION VI

CIRCULATORY ASSIST DEVICES

Chairmen: Frank W. Hastings, M.D.
Lowell T. Harmison, Ph.D.
Anthony M. Bruno, M.D.
William P. Sears, M.D.

INTRODUCTION

The development of therapeutic circulatory assist devices which could return the cardiac patient to a useful position in society is a major goal of the Artificial Heart Program. This requires the development of a variety of devices and related techniques which will effectively provide the therapy required by the patient, depending upon his type of heart disease and existing clinical condition. The Artificial Heart Program is interested in the development and evaluation of three classes of devices - emergency support, temporary short-term support, and permanently implantable devices. Work on several of these is currently being supported.

CHAPTER 40

EVALUATION OF THE ANSTADT VENTRICULAR ASSIST DEVICE IN ACUTE AND CHRONIC STUDIES

E. Tragus, H. Wallace, J. Marchesini, M. Bendon, P. Jennings,
W. Zerby, R. Thorn, and W. Blakemore

University of Pennsylvania, Philadelphia, Pennsylvania

Evaluation of the Anstadt mechanical ventricular assist module was performed with chronic and acute studies. Chronic implantation experiments evaluated assistor cup design and materials. Silastic and polyurethane were used. Initially, the original design cup was implanted in dogs that were not assisted and allowed to survive. Failure to survive for more than 48 hours led to design modifications consisting of changes in housing form, position of sidearms, intratubal pressure, presence or absence of the atrioventricular flange and its corrugation, fibrillation and defibrillation and type of incision. Conclusions are that a Silastic-coated glass housing with a Silastic liner, electrode implanted into liner, corrugated flange, right angle sidearms and left thoracotomy permitted longest survival. One animal survived for two weeks and at that time was fibrillated and assisted without thoracotomy for three hours, maintaining good urine output and blood pressure. In acute studies animals were assisted for 1, 3, 6, and 9 hours. No significant differences were observed between Silastic-lined or polyurethane-lined cups, nor the presence or absence of flange corrugation, with regard to hemodynamic and enzyme measurements. An additional group was assisted for four hours and renal function was measured.. Renal plasma flow, tubular function and glomerular filtration rate were adequate during this time. In another group of animals, assist was synchronized with the EKG and compared to non-synchronous assist. Synchronization produced better cardiac output, blood pressure, and flow of thoracic duct lymph. Synchronized assist also permitted a reduction in the sustained negative pressure necessary to hold the cup on the heart.

INTRODUCTION

Acute and chronic studies were performed in animals with the Anstadt device to evaluate its possible use as a clinical means of mechanical ventricular massage. Chronic studies were designed to assess the effects on the heart and other vital organs of chronic implantation of the assistor cup. This means of assistance could be of potential value in patients who develop a myocardial infarction complicated by concomitant failure or irritability or in those patients who develop a cardiac arrest. The acute study was performed to evaluate the early physiological effects of assistor cup placement upon the heart.

GENERAL DESCRIPTION OF THE MARK IVa SYNCHRONIZED PROGRAMMER (SMEC, INC.)

The Mark IVa Synchronized Programmer provides for mechanical ventricular assistance and electrical stimulation of the heart. The programmer utilizes state-of-the-art circuitry for maximum reliability and versatility. The synchronizer section features maximum reliability in QRS recognition despite neuromuscular impulses and electrical interference. Delay modules and minimum and maximum assistance rate circuits are provided to add to its versatility.

This programmer is ideally suited for any other circulatory assist system (i.e., the intra-aortic balloon) and related applications in peripheral circulation and resuscitation.

A particular ECG lead combination may be selected by a seven position switch and is connected into the high input impedance preamplifier. This circuit features extremely fast overload recovery time. Thereby the electrocardiogram and synchronization is restored almost immediately after defibrillation with the ECG leads connected to the patient.

All filtering circuits are active filters providing for sharp low and high frequency cutoff (60 db per decade). Low frequency cutoff points at 2, 5, 10 or 15 cycles (3 db down) eliminate interference from neuromuscular impulses and electrolytic potential variations due to electrode movement. High frequency filters at 35, 65, 130 or 260 Hz (60 db per decade) eliminate electrical noise interference. A 60 cycle line filter having an extremely narrow rejection band eliminates line frequency interference between the two "hot" lines of the electrocardiogram. In the pass band, the synchronizer has extremely flat amplitude characteristics.

The automatic gain control (AGC) provides for the constant adjustment of the synchronizer gain as variations in the input amplitude of the ECG occur. It varies this gain over a 250% amplitude range with selectable sampling rates. A meter is provided for readout of an acceptable gain within the AGC operating range.

Bipolar trigger circuits provide a trigger pulse at either 65 or 40% (normal and high sensitivity) of the maximum permissible signal amplitude as determined by the overload light of the automatic gain control circuit.

The maximum rate module limits the instantaneous rate of any synchronized assistance. It therefore provides for the rejection of extra systolic pulses or of assisting only part of the stimulus input pulses. Whenever a pulse is rejected in the range of 30 to 250 pulses per minute, a maximum indicator is automatically lighted.

The minimum rate circuit provides for the minimum assisted rate during synchronized or unsynchronized circulatory support. In the synchronized mode it will automatically introduce assistance should the input stimulus signal fail. Its 10 to 300 pulses per minute range provides for the greatest flexibility in cardiac support or resuscitation.

The first delay module will delay any trigger signal from 6 to 250 mSec (when on), thereby the assistance may be delayed for a particular mode of operation.

The second delay module (off, or 6 to 250 mSec delay range) provides for a difference in timing between mechanical assistance and stimulation. Thereby electrical stimulation or pacemaking may precede mechanical assistance or vice versa. An indicator light is provided to show when either the stimulation or the mechanical ventricular assistance is delayed.

The stimulator provides a completely floating (not common to any other terminal in the programmer) pulsed direct current signal for cardiac stimulation. This stimulation pulse has a duration of 15 mSec and is adjustable between 0 and 5 volts output. A polarity reversing switch makes lead reversing unnecessary. A blanking signal from the stimulator is sent to the synchronizer to prevent triggering on the stimulation pulse. Thereby the leads used for ECG detection may simultaneously be used for cardiac stimulation. Because the stimulator blanking pulse will produce blanking of the input signal, it should be kept off when not in use.

The systole duration module provides for one phase of the mechanical assistance. It is adjustable from 0.1 to 3 seconds. It is important to keep the systole duration less than the reciprocal of the rate of assistance for proper operation of the programmer. The systole duration module drives the solenoids with a non-linear current pulse. In this manner the solenoids are initially driven with a large current for rapid activation and held with a small current for rapid disengagement.

The frequency meter may be used to detect the rate of incoming stimuli (input position) or the rate of assistance (out position).

The percent systolic meter gives an indication of the percentage of systolic duration. Thereby constance systolic to diastolic ratios can readily be maintained.

Modifications to the Synchronized Programmer.

The synchronized programmer for MVA was modified to incorporate a "blood channel" which results in assistance only being provided when blood pressure would fall below a pre-selected minimum. This circuit connects to any mean or pulsatile arterial pressure output from an auxiliary preamplifier. Once the circuit results in MVA being provided when the blood pressure falls below a set minimum, then assistance is provided until a mean level of blood pressure 40% higher than this "cut in" level has been achieved.

GENERAL DESCRIPTION OF CUP DEVELOPMENT

The level of development of the old style of MVA cup consisted of a rigid glass shell with a Silastic (Dow Corning Trademark for medical silicone rubber) diaphragm cemented to the glass shell. This cup provided adequate short-term total circulatory support, but was hampered by the following disadvantages:

Mechanical

1) The glass shell was a rigid obstructive shell hindering the positioning and movement of the heart.
2) Glass shell is fragile.
3) Hose connections restricted positioning of the cup.
4) Liner was likely to break.
5) Pulsatile hoses too large in diameter.
6) The liner did not move with ventricles in unassisted implants.

Materials

1) Glass is relatively incompatible with body tissue. (This was minimized by the use of only Pyrex glass in contrast to glass with lead or other impurities.)

Redesign of Hose Connections to Cup.

The conventional hose connections pointing in a direction from the orifice to the apex of the cup were unsuitable for chronic implants as the hoses would restrict the movement of the cup and ventricles in a vertical or apex/aortic axis of the heart. When the hoses were brought out of the cup at an angle perpendicular to this axis the movement was much more readily permitted.

Helium Adaptor.

Conventionally 1/2" O.D. and 3/8" I.D. pulsatile pressure hoses are used on dog cups for MVA with air. When helium is used as a pneumatic fluid instead of air, the much lighter helium (helium has an atomic weight of 4 compared to air's 80% nitrogen atomic weight of 14) permits 14/4 reduction in the area of the I.D. of the pulsatile pressure hose. This in turn permits a reduction of the helium tube internal diameter to 60% of the air pulsatile tubes. As a result the following tubes were used with a helium to air interface located 18" from the MVA cup:

1) Pulsatile pressure line 1/8" I.D., 1/4" O.D.
2) Sustained negative line 1/16" I.D., 1/8" O.D.

A drawing of the helium adaptor is shown in Figure 1.

Polyurethane Lining.

Following is a list of the pertinent data of Silastic and polyurethane:

1) Dow Corning Silastic #372 Medical-Grade Silicone Rubber Sheeting (as used in the previous cup liners)

Tensile strength	350 psi
Durometer Hardness, Shore A	40
Color	cloudy clear

2) B. F. Goodrich Type 5707F1 Estane (Polyurethane)

Tensile strength	8000 psi
Durometer Hardness, Shore A	95
Color	clear

From this data calculations for a 65 mm cup with a 100 mm of mercury positive pressure are shown in Figure 2. These indicate that a 50 mil Silastic liner would be necessary compared to a 2 mil polyurethane liner. This thin polyurethane liner has hardly any interference on the free movement on the ventricles as shown in Figure 3. Thereby, the ventricles are permitted to move much more readily with the diaphragm in an unassisted implant. The method for the polyurethane liner fabrication used the following technique after several modifications. A mixture of one part type 5707 Estane (polyurethane) was mixed with nine parts tetrahydrofurane. Glass molds were dipped into this solution and allowed one hour drying time between dips. After about six dips and a 24-hour curing time an excellent 4 mil liner could be pulled from the glass mold.

Since the polyurethane does not stretch, the liner has to be made adequately large so that it can provide the necessary systole. If the liner is too large, too much of a compression of the ventricles may occur with a resulting effect of the ventricles being pushed out of the cup.

Cementing of Liner to Glass Cup.

The hard polyurethane liner readily pulled away from the orifice and apex cement surfaces bonding the liner to the glass shell using the glass cup and the Silastic adhesives (G. E. RTV-108 and 118). In Table 1 the pertinent data of available silicone adhesives are listed. It was discovered that not only is a high tensile strength necessary, but even more important is a high resistance to tearing, or a high tear strength. As such, the apex bonding was done with Dow Corning RTV-3145 adhesive and the orifice bonding was done by pulling the liner over the outer edge of the cup and cementing it on the outside of the cup with RTV-118. A summary of accelerated life tests for empty cups and 200 mm of pulsatile positive pressure is shown in Table 2.

TABLE 1

SILICON RUBBERS

Adhesive Use
Air Cured

GENERAL ELECTRIC, Manufacturer

NUMBER	HARDNESS	PSi	TEAR	COLOR	SHRINKAGE	% PERM. ELONGATION
RTV-108	30	350	45	transparent	1.0%	400
RTV-112	30	300	25	white	1.0%	350
RTV-118	27	520	33	transparent	0.3%	350
RTV-511	45	350	25	white	0.2% to 0.6%	180
RTV-102	30	350	45	white	1.0%	400
RTV-830	50	800	100	beige	-	250

DOW CORNING, Manufacturer

NUMBER	HARDNESS	PSi	TEAR	COLOR	SHRINKAGE	% PERM. ELONGATION
RTV-3140	25	300	20	clear	not listed	450
RTV-3145	33	800	125	gray	not listed	675

New Cup Design.

A newly developed molded cup design is shown in Figure 4. This cup uses Dow Corning type 186 silicone rubber in its shell. This and other silicone rubbers are summarized in Table 3.

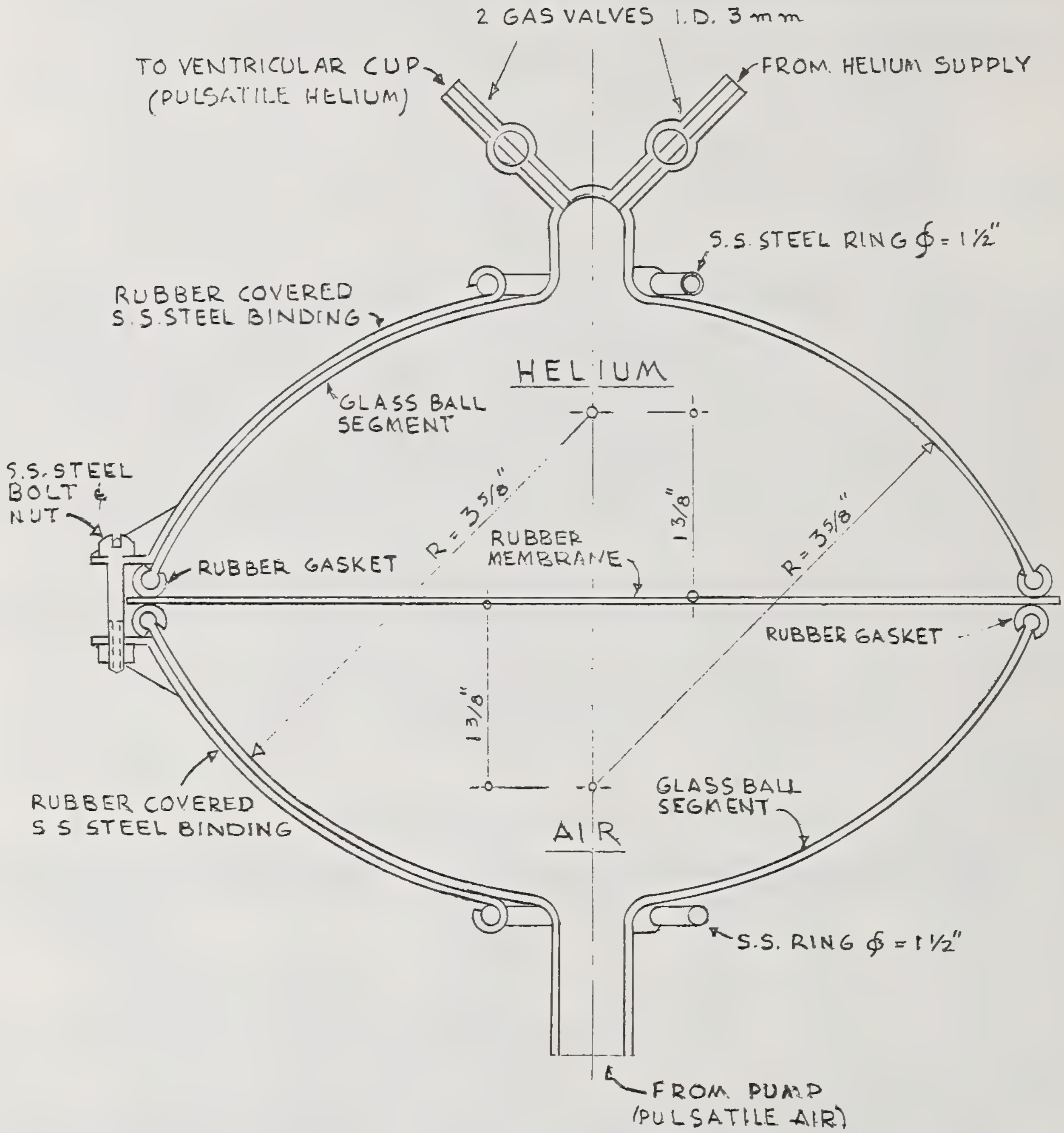

FIGURE 1. HELIUM ADAPTOR.

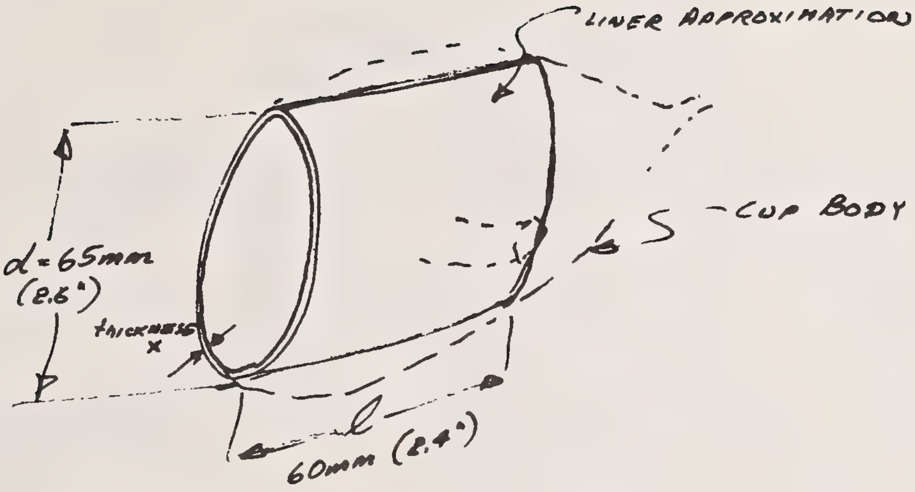

100 mm Hg PRESSURE = 1.9 lb/in²

Let tension/end = PRESSURE ON LINER CYLINDER

$= \text{AREA} \times \text{PRESSURE}$

$= (2.4)\left(\frac{\pi d^2}{4}\right)(100\text{mm Hg})$

$= 2.4\left(\frac{\pi 2.6^2}{4}\right)(1.9)$

$= 24.4 \text{ lb}$

tensile stress (FOR TEARING) $= \frac{\text{tension on end}}{\text{area of end}} = \frac{24.4\text{ lb}}{\pi d x}$

$x = \text{thickness} = \frac{24.4}{\pi(2.6)(8\times10^3)}$ (POLYURETHANE)

$x = 0.4$ mil (POLYURETHANE)

$x = 10$ mil (SILASTIC)

(A 5x SAFETY FACTOR ALLOWED FOR UNEVEN STRESS AT ENDS AND FOR REASONABLE FLEX LIFE)

FIGURE 2. CALCULATION OF CUP LINER TENSILE STRESS.

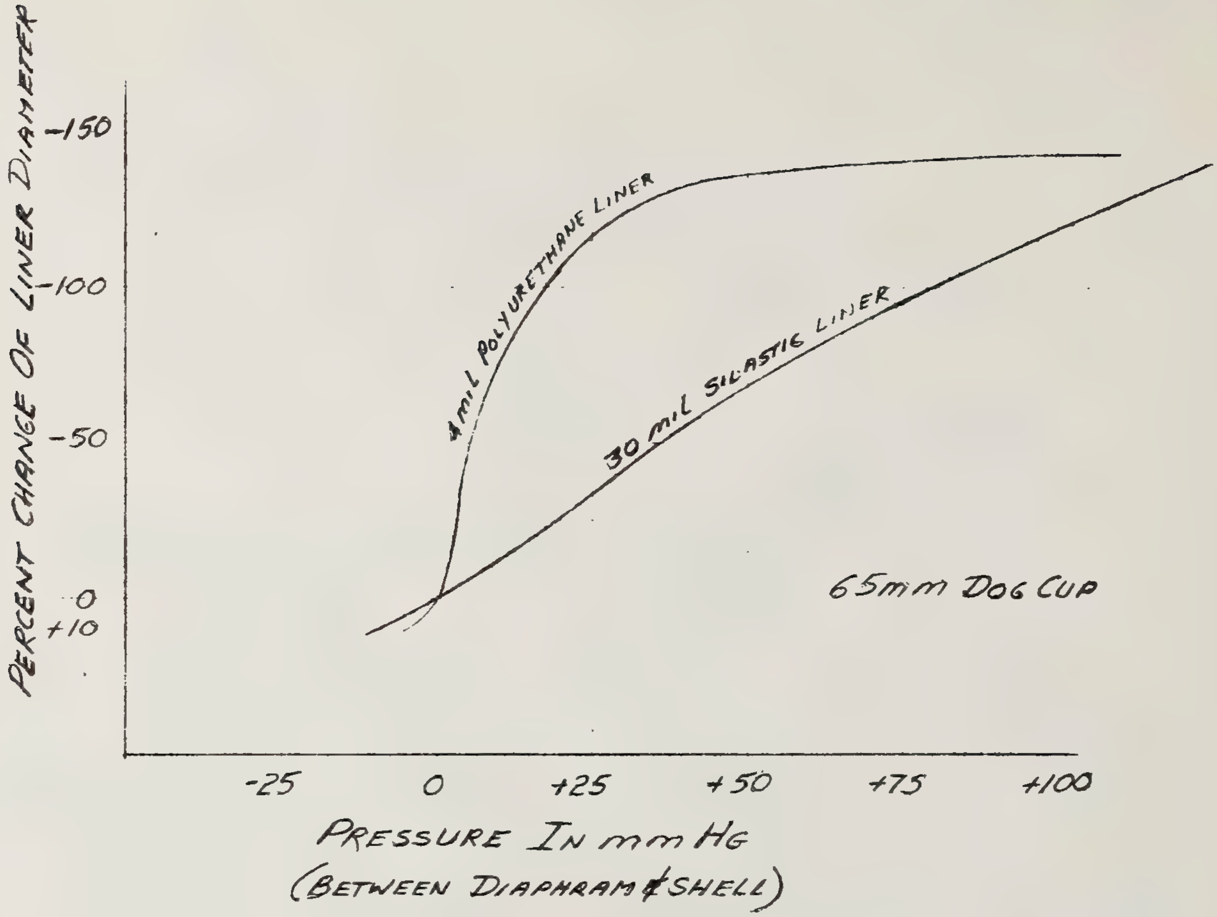

FIGURE 3. COMPARISON OF PULSATILE PRESSURES TO INFLATE EMPTY SILASTIC AND POLYURETHANE LINERS.

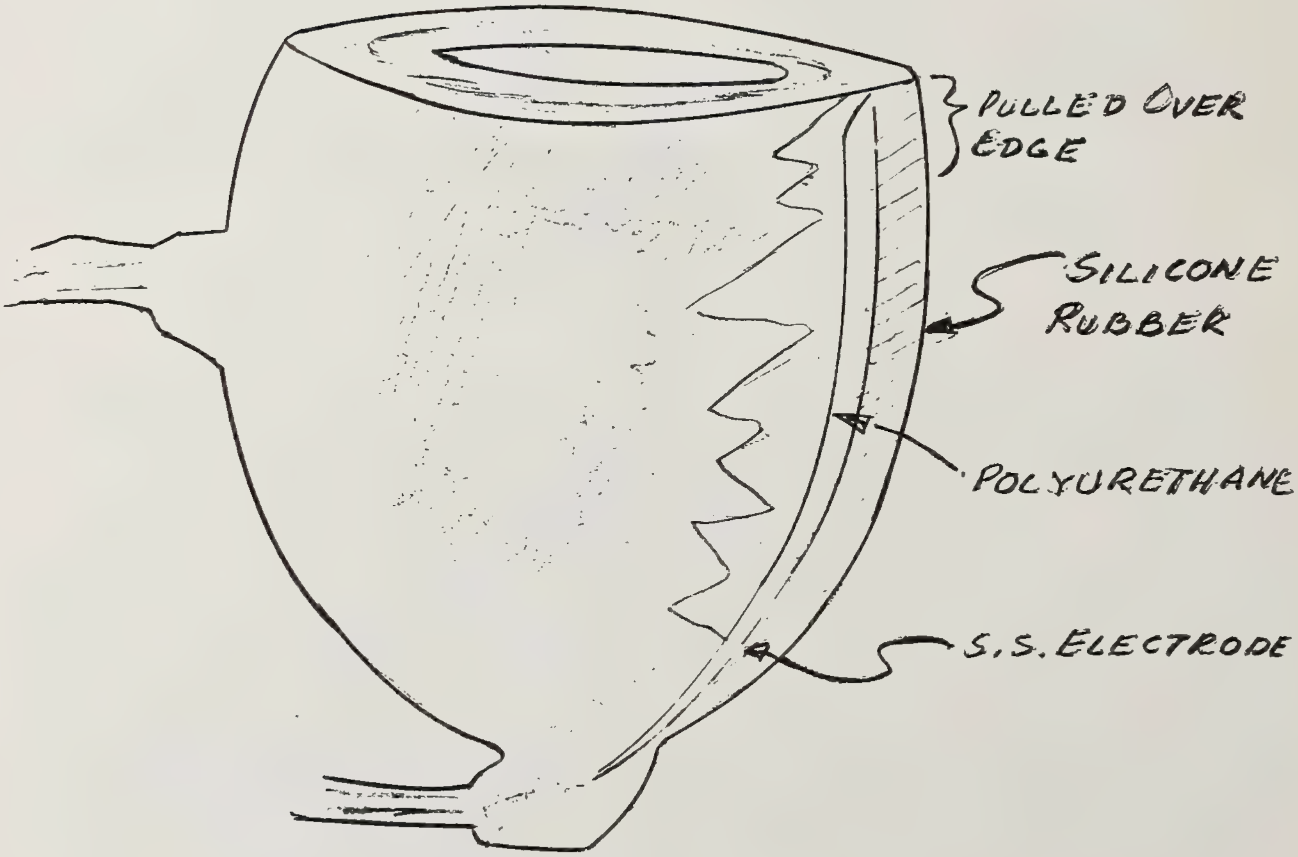

FIGURE 4. NEW SILICONE RUBBER/POLYURETHANE CUP W/SS ELECTRODE.

TABLE 2

ACCELERATED LIFE TESTS FOR EMPTY CUPS

(200 mm pulsatile positive pressure)

Cup	Conventional	Conventional	Conventional	Conventional	Electrode	Electrode
Liner	Silastic (0.030)	Polyurethane	Polyurethane	Polyurethane	Polyurethane	Polyurethane
Adhesive	GE/RTV118	GE/RTV118 (Top) GE/RTV108 (Apex)	GE/RTV118 (Top) GE/RTV108 (Apex)	GE/RTV118 (Top) Dow 3145 (Apex)	GE/RTV118 (Top) GE/RTV108 (Apex)	GE/RTV118 (Top) Dow 3145 (Apex)
Construction	Conventional	Conventional	Liner Pulled Over Orifice Edge and Cemented on Outside	→		
Minutes Until Failure (Typical)	5	30	80	250	8	250
Cause of Failure	Liner Torn	Liner Separated from Glass at Orifice	Liner Separated from Glass at Apex	→		

TABLE 3

SILICONE RUBBERS

For use in making cupshell or potting (molding) compound
Catalyst Cured

DOW CORNING, Manufacturer

NUMBER	HARDNESS	PSi	TEAR	COLOR	SHRINKAGE	% PERM. ELONGATION
Resin #184	40	900	15	clear	none	100
#182	40	900	15	clear	0.1%	100
#186	30	800	100	clear	none	480
#187	30	800	100	black	none	480

GENERAL ELECTRIC, Manufacturer

NUMBER	HARDNESS	PSi	TEAR	COLOR	SHRINKAGE	% PERM. ELONGATION
RTV-615	35	925	25	clear	0.2%	150
RTV-11	45	350	180	white	0.2% to 0.6%	180
RTV-41	50	500	200	white	0.2% to 0.6%	200
RTV-602	15	-	-	clear	0.2%	2
RTV-630A	70	850	90	blue	<.2%	300

The cup has the following advantages:

1) A semi-flexible shell which may more readily be inserted through a smaller surgical opening.
2) The shell is clear.
3) It uses a nonbreakable polyurethane liner.
4) A stainless steel electrode securely clamps the liner at the apex of the cup.
5) The silicone rubber shell is lighter and more compatible than glass.
6) The cup is unbreakable.

CHRONIC ANIMAL STUDIES

Preparation.

Adult mongrel dogs weighing 35 to 50 pounds were anesthetized with sodium pentobarbital. A median sternotomy or left thoracotomy was performed. Appropriate peripheral vessels were catheterized for measurement of arterial blood pressure and central venous pressure. A limb lead electrocardiogram was attached, modalities were recorded on an Offner recorder. In this group of chronic studies ventricular massage was not instituted in the animals. Various designed assistor cups were placed onto the heart and the animals were observed for three hours. The cups were then left on the heart, the chest was closed, and they were returned to their cages.

Group I. Three dogs had implantation of cups of the original design. This consisted of a glass housing with an internal Silastic diaphragm which fits over the ventricle leaving the atria free. The diaphragm is attached to the housing by a bonding agent over the apex and also over the base of the housing. This creates a chamber between the diaphragm and the housing which communicates with the sidearm of the housing. Tubing is attached to the sidearm for alternating positive and negative air pressure and to a small inlet at the apex for negative pressure to hold the cup on the heart. A small rim, the flange, at the base of the cup also aids in maintaining the cup on the heart. Neither physiological nor biochemical monitoring was carried out in this group of animals.

Results: All three animals died, one in one hour, one at twenty-four hours and one at forty-eight hours. The dog that expired at one hour died of ventricular fibrillation. Post mortem examination in the other two animals demonstrated an indentation in the atrioventricular groove which was the anatomical location of encirclement by the flange.

Conclusion: The thick rigid Silastic tubing which was attached to the sidearm was noticed to have created a lever system with the intercostal space through which they were brought out when placed subcutaneously. Angulation of the cup upon the base of the heart was theorized as to the cause of death in these animals. These observations lead to the study of Group II.

Group II. Three dogs had the same type of assistor cup implanted. However, a median sternotomy incision was used. This incision was used as a means of avoiding the lever system which was incriminated as the cause of death in the Group I animals.

Results: There was an increase in the central venous pressure and a decrease in the blood pressure during three hours of observation in all three animals. The chest was closed and animals placed in their quarters. Two animals died within twenty-four hours and one animal died in seventy-two hours. Autopsy revealed a minimal amount of pleural effusion as well as compression and indentation of the atrioventricular groove.

Conclusions: These findings necessitated changes in cup design if long term survival with cup implantation was to be achieved. These findings then lead to Group III and Group IV.

Group III. Three animals had the original cup design implanted without tubing, two animals of these three had cups with the regular flange and one animal had a cup with a flange which was one-half of the diameter of the original flange.

Group IV. Three dogs had the original cup design implanted without tubing. The flange was also removed from these cups.

Results: Group III. One animal died in five days, one animal in four weeks and the animal with one-half diameter flange was sacrificed at thirty weeks. Autopsy of the first two animals demonstrated dilation of the atria and compression of the atrioventricular groove. A fibrin envelope was found to encase the heart in the first two animals. There was a minimal amount of pleural effusion present and dense adhesions were found which were attached to the surrounding structures. The dog which was sacrificed at thirty weeks had minimum fibrosis and tissue reaction. There was no pleural fluid or ascites. There was no atrial dilation.

Results: Group IV. One animal died in four days because of intrathoracic bleeding. The other two animals survived and were deliberately sacrificed after six weeks and five months. The animal sacrificed at six weeks demonstrated a very intense fibrous envelope over the entire heart with evidence of liver congestion, splenic congestion, ascites and edema of the bowel. The animal sacrificed at five months showed that the cup had slipped and was only partially on the heart. That is, the apex of the heart was within the cup and this was quite small while the remainder of the heart was dilated and edematous. The entire heart was also encased by a thick fibrous coat with numerous adhesions to the surrounding structures. Four thousand cc of ascitic fluid was present as well as splenic and hepatic engorgement and edema of the bowel. Measurements obtained during intervals prior to sacrifice demonstrated elevated central venous pressures and decreased blood pressures.

Conclusion: Cup design even without tubing attached to the sidearms or flange allowed for an increase in survival from days to weeks. However, congestive heart failure was still present. These observations lead to a new cup design.

Group V. A thinner and more oval glass housing was created. The negative pressure outlet at the apex of the cup was moved up along side of the sidearm which was used for alternating positive and negative air pressure for massage. A platinum electrode was embossed into the apex of the cup to enable easy fibrillation and defibrillation with the closed chest and the wire leading from it was coated in Silastic. The flange at the base of the cup was corrugated over .5 cm perpendicular to the edge of the cup. No change was made in the thickness of the Silastic liner at this time.

Results: Three animals had implantations of this new cup. One died in twenty-four hours, one in ten days. Autopsy again demonstrated pleural effusion, dilated atria, visceral and hepatic congestion and a fibrous envelope over the heart. The third dog was taken to the operating room fifteen days postoperatively. The subcutaneous tubing for sustained negative pressure and for alternating positive and negative pressure, as well as the lead to the electrode were exposed. Without opening the chest ventricular fibrillation was accomplished via the exposed lead and mechanical ventricular, assistance was instituted via the tubing. This was continued for three hours. Prior to the onset of mechanical ventricular massage the mean arterial pressure was 160 mm Hg. After one hour of massage it fell to 86 mm Hg, at two hours it was 66 mm Hg, and at the end of three hours it had returned up to a level of 100 mm Hg. Central venous pressure, which was elevated before ventricular fibrillation was instituted, was a control value of 6 mm Hg. It progressively rose reaching a peak of 16 mm Hg at the end of three hours of massage. Defibrillation was attempted but could not be accomplished and the animal was sacrificed (Figure 5). Autopsy findings once again demonstrated a fibrin envelope over the entire heart, pleural effusion of a minimal amount, and a marked fibrous reaction and adhesions to the surrounding structures. In addition, heart worms were present in the right side of the heart.

Conclusion: New cup design did result in an improvement in animal survival. However, further evaluation is necessary.

Group VI. Three animals had the newly designed cup implanted. These cups, however, had a polyurethane liner rather than a Silastic liner.

Results: Two animals died in twenty-four hours, one animal died in fourteen days. The findings on autopsy were the same as those described previously. Measurement of SGOT, SGPT, CPK, and LDH for five days after implantation showed a return to control values of all except LDH (Figures 6, 7, 8, 9).

Conclusion: Polyurethane was of no aid in preventing complications of chronic cup implantation in this small group.

ACUTE ANIMAL STUDIES

Group I. Eight dogs were utilized. Blood pressure, central venous presure, and electrocardiograms were monitored in the manner described previously. Periodic blood samples were obtained for SGOT, SGPT, LDH, and CPK. Median sternotomies or thoracotomies were performed and assistor cups were implanted upon the heart following electrical fibrillation. Two animals had mechanical ventricular massage for one hour, two for three hours, two for six hours and two for nine hours. The original cup with a non-corrugated flange was used and the animals were sacrificed immediately after completion of the assist. Representative specimens were obtained for microscopic examination of the heart, lungs, liver and kidneys.

Results: Mean arterial blood pressure for the entire group was 134 mm Hg during control and 111 mm Hg after nine hours of massage. Central venous pressure during control was 3.5 mm Hg and at nine hours of massage was 12 mm Hg (Figure 10). No correlation could be found between the duration of mechanical ventricular assistance and the analysis of LDH (Figure 11) or SGPT (Figure 12). SGOT and CPK demonstrated a progressive rise as duration of massage continued (Figures 13 and 14).

Group IA. Two additional dogs had mechanical ventricular massage for six hours using the original cup and a corrugated flange.

Group IB. Two additional dogs using the new cup design with polyurethane liner, corrugated flange and helium gas instead of air as the pumping vehicle had mechanical massage for six hours. SGOT, SGPT, CPK, and LDH showed a progressive rise as duration of massage continued (Figure 15).

Observations during the short term studies consistently demonstrated that the flexibility of the Silastic liner was limited and that the amount of air pressure needed to reach the control preassist blood pressure was 30 to 50 mm Hg higher. After a search polyurethane was selected to be tested as the cup liner because it was more flexible and stronger than Silastic and could adapt itself to the configuration of the heart more readily. Simultaneously various gases were examined which could be used to replace the air system. Helium was chosen because it was lighter than air and there was less friction. This combination of helium gas as the pumping medium and the polyurethane liner made it possible to mechanically massage the heart at a significantly reduced positive air pressure of assistance and to achieve a blood pressure equal to that obtained using air as the medium for pumping when a Silastic liner was used. Also, it was found that the sustained negative pressure, which was necessary when a Silastic liner was used to keep the cup on the heart, was virtually eliminated when helium and polyurethane were used. An additional observation of the polyurethane helium system is that if the atria dilated during massage and the CVP became elevated as was seen routinely when a Silastic liner and air were used, this atrial dilatation and elevation of pressure could be reduced by increasing the duration of systolic ejection from 45 to 60 per cent (Figure 16).

Group II. Three dogs. Difficulty encountered during fibrillation and defibrillation with the assistor cups on the heart resulted in the development of a platinum electrode being incorporated into the cup liner. Fibrillation can now be accomplished with the electrode and a lead which runs from it to the subcutaneous tissues and defibrillation can be accomplished by passing a pacemaker wire into the right ventricle via the jugular vein. By attaching a current to these two wire leads the heart can then be defibrillated.

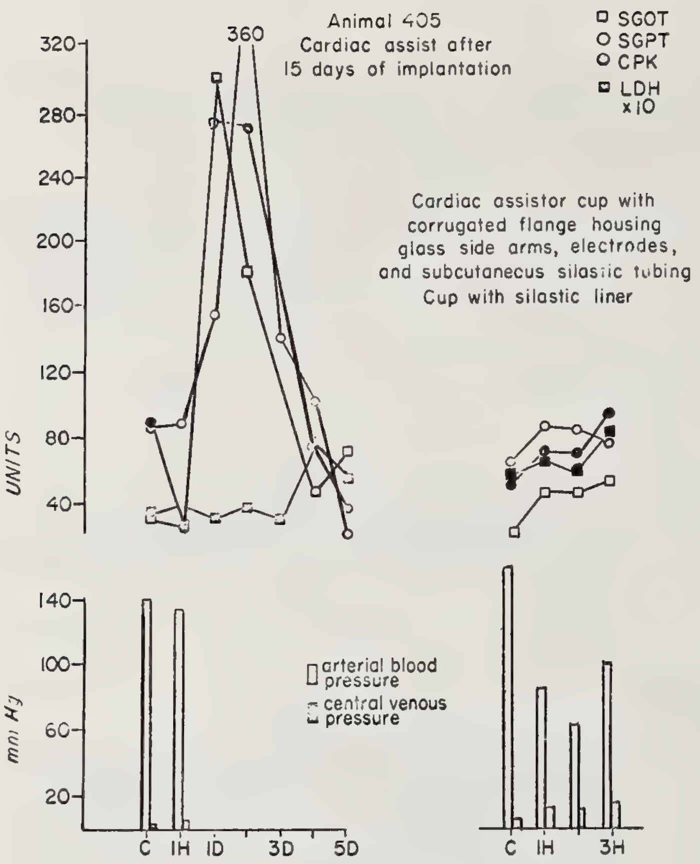

FIGURE 5.

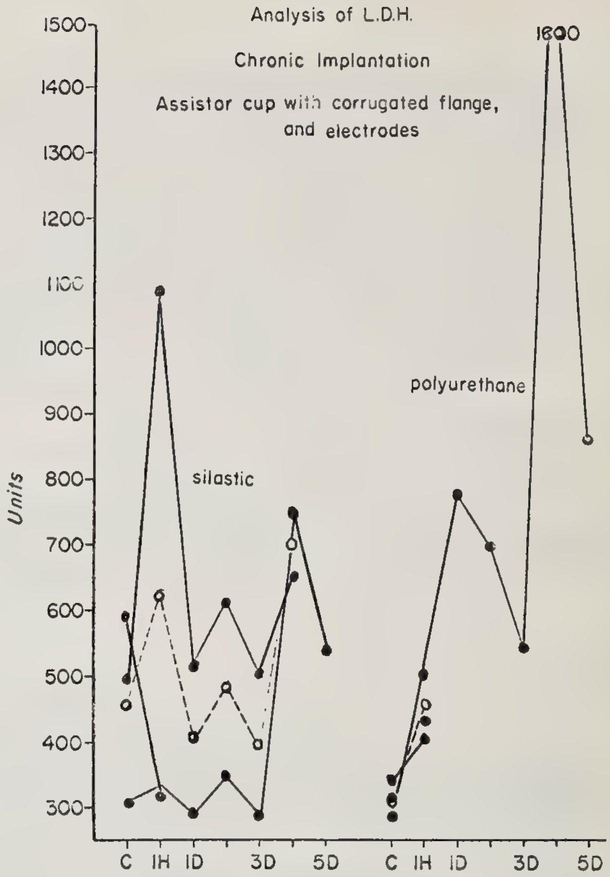

FIGURE 6.

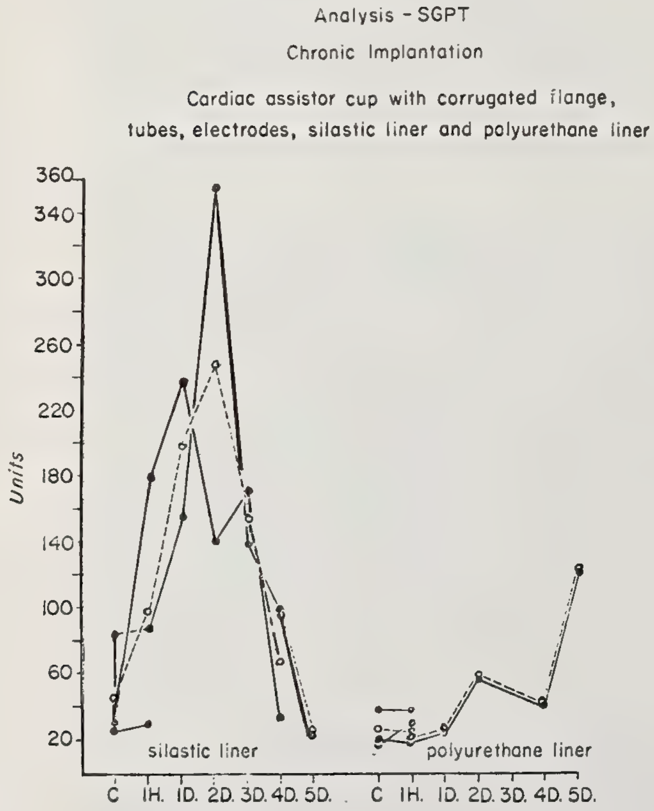

FIGURE 7.

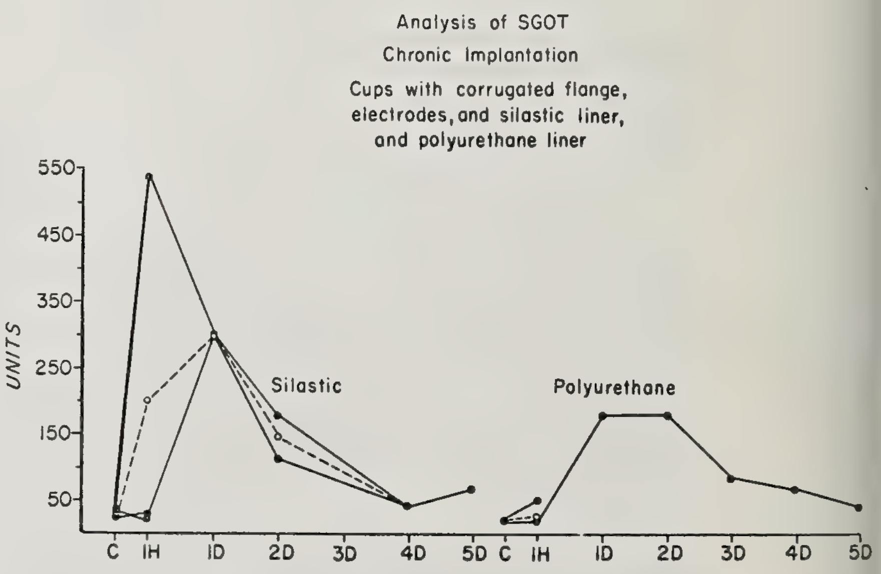

FIGURE 8.

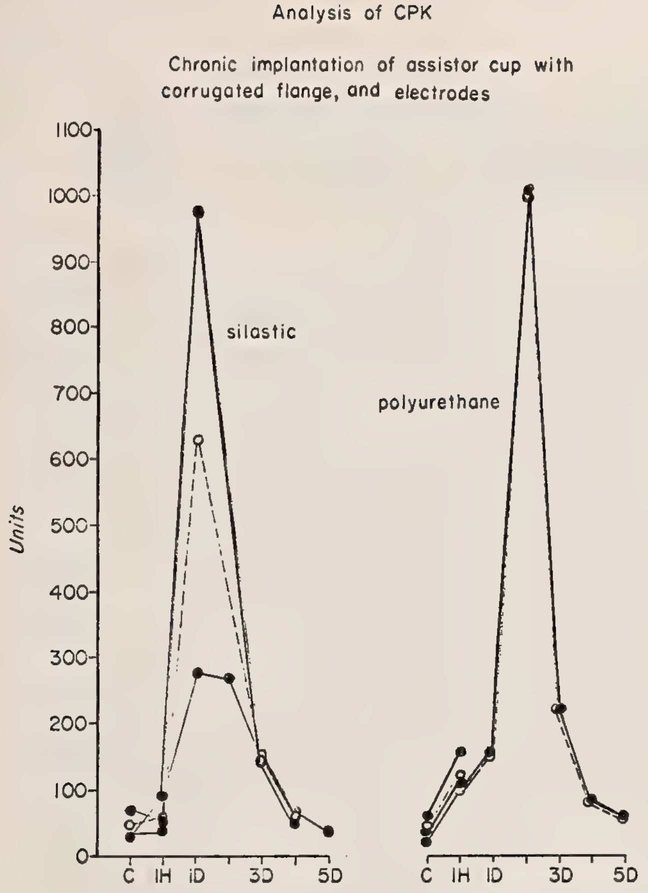

FIGURE 9.

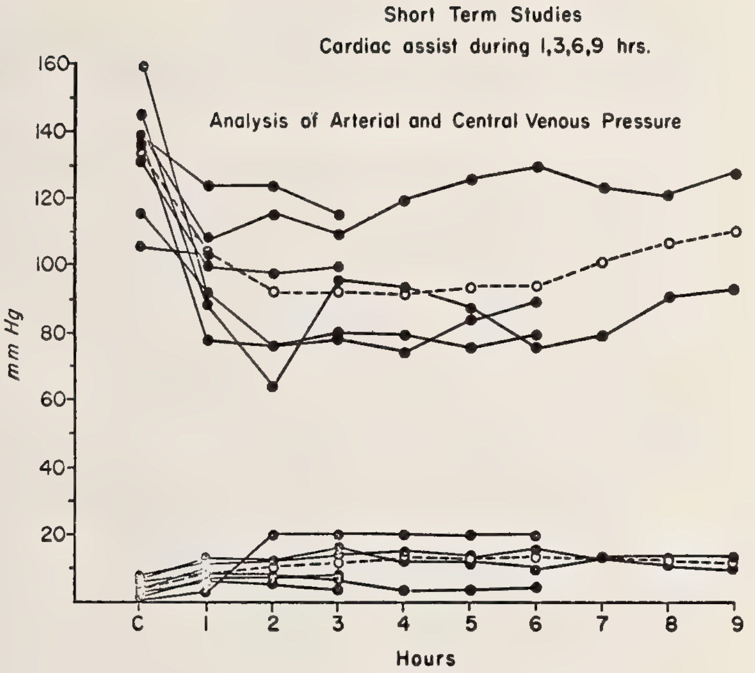

FIGURE 10.

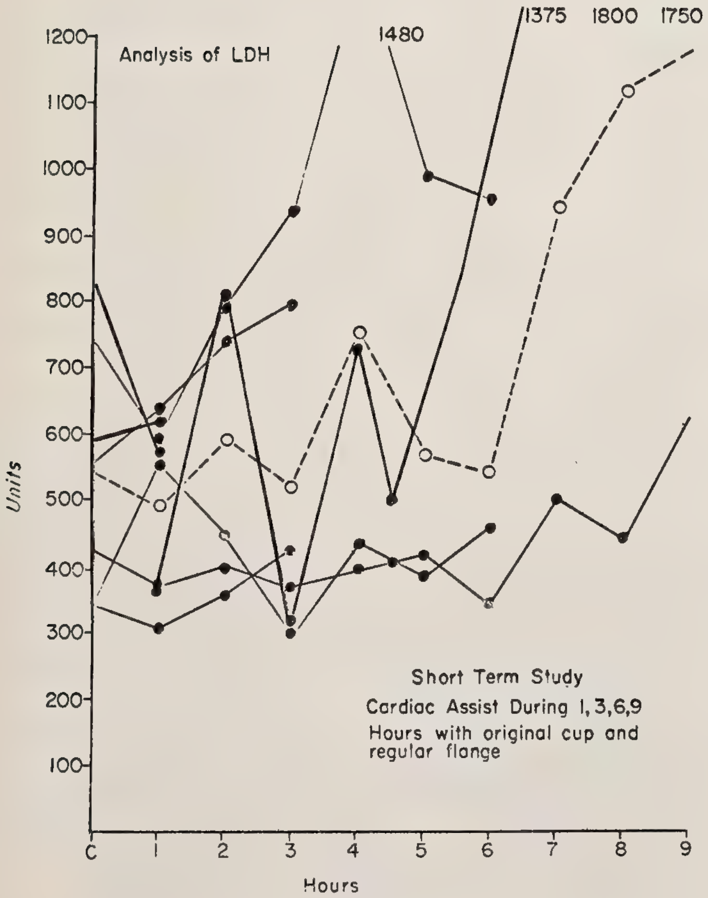

FIGURE 11.

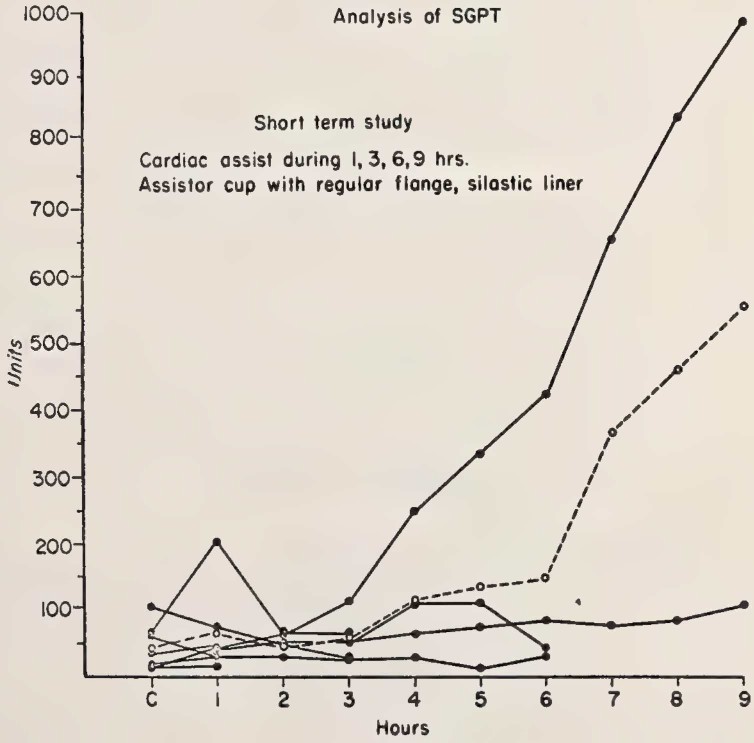

FIGURE 12.

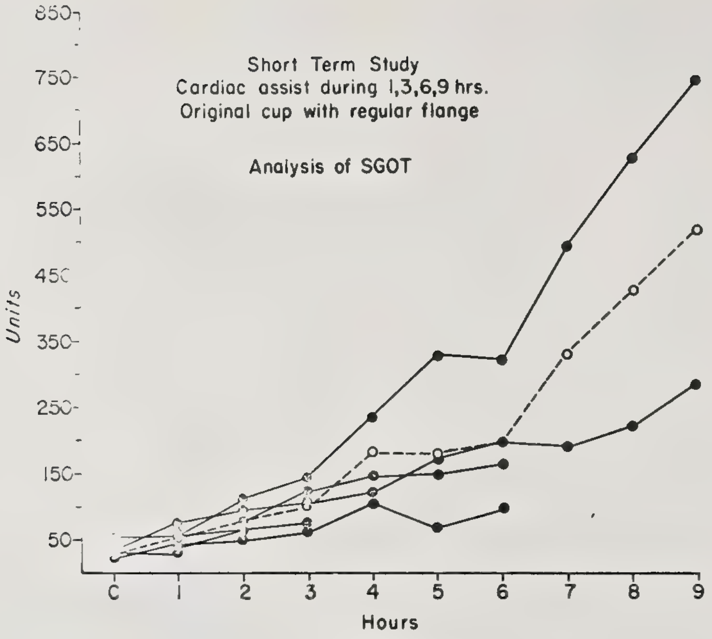

FIGURE 13.

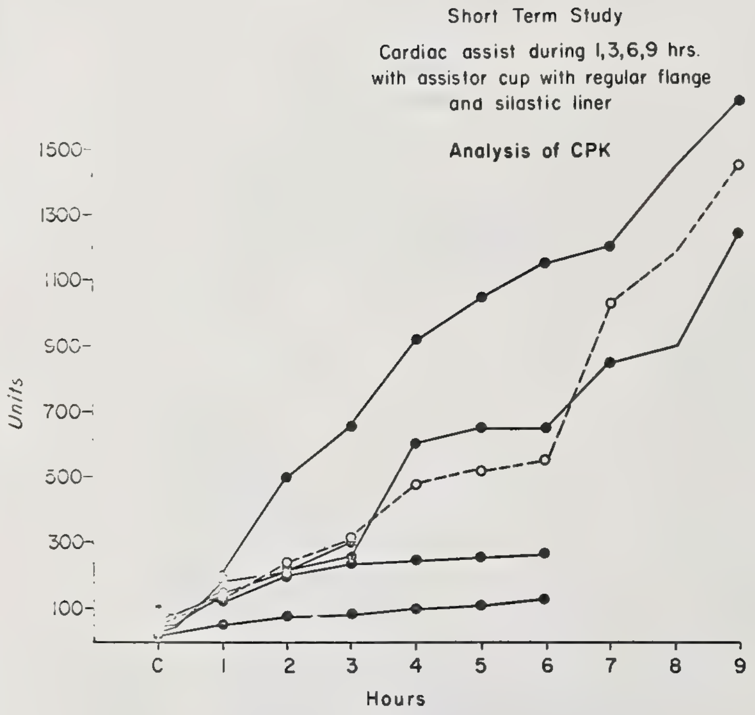

FIGURE 14.

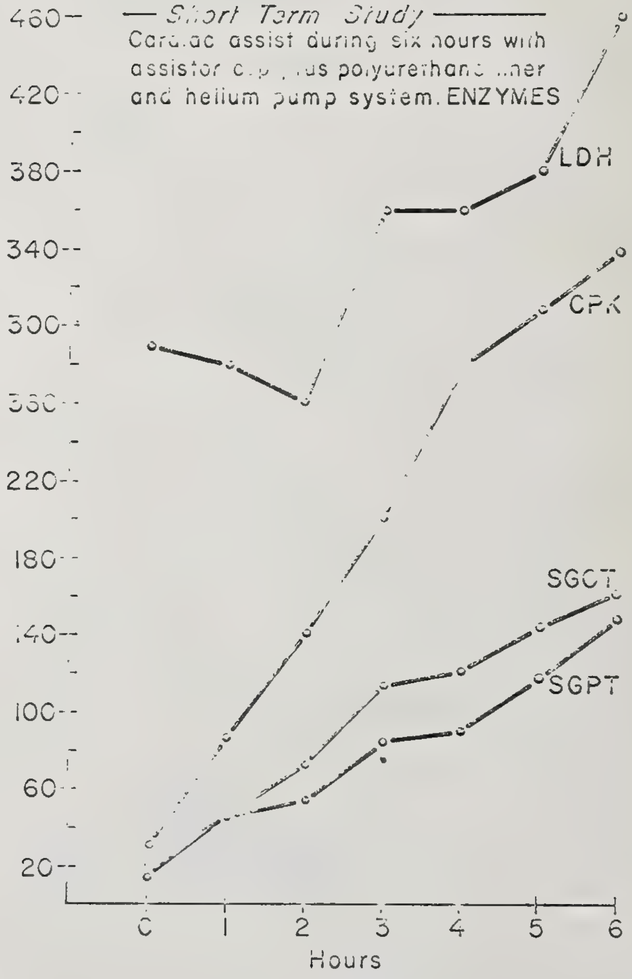

FIGURE 15.

Group III. Thirteen dogs. Thirteen dogs had mechanical ventricular massage for four hours. Renal function was evaluated as to the efficacy of mechanical cardiac massage for in vivo preservation of potential renal allografts. The data obtained was presented at the meeting of the American Society of Artificial Organs in Atlantic City, N. J.

Group IV. Pulse wave form evaluation. Six dogs were utilized for this portion of the study. The dogs were anesthetized and the left femoral artery had a catheter inserted retrograde to the aortic arch for measurement of blood pressure and pulse wave configuration. The left femoral vein had two catheters inserted retrograde, one to the right atrium and one to the pulmonary artery for measurement of pressure. Mechanical ventilation was then instituted and a left thoracotomy and pericardiotomy were performed. The aorta had a Carolina instrument square wave flow probe attached for measurement of cardiac output less coronary flow. The cup used had a Silastic liner with a corrugated flange and the driving force was compressed air. Application of the cup caused a reduction in mean arterial blood pressure from a control value of 98 mm Hg to 82 mm Hg when assist was begun. The air hose dampening pressures were 25% systolic and 25% diastolic.

Dampening. With the use of compressed air as a driving medium and no reduction in the velocity of the air, a square wave pulse is generated. By attaching a constriction to the systolic and diastolic air lines this pulse can be modulated to form a bell-shaped curve rather than a square wave curve. The lever system producing this air hose constriction can reduce the circumference of the tubing from 100% or no dampening to 0% at which time there is no air flow.

Previous work has demonstrated that the most physiological appearing pulse wave, as seen in the arterial blood pressure tracing, was obtained when dampening was 25% systolic and 25% diastolic.

Previous work has also demonstrated that without dampening the air pressure is so forceful that the heart is ejected from the cup. This portion of the study was carried out to evaluate the configuration of the arterial pulse wave, and to correlate its modification with the cardiac output, pulmonary artery pressure, central venous pressure and blood pressure.

Application of the cup caused a reduction in mean arterial blood pressure from a control value of 98 mm Hg to 82 mm Hg when assist was begun and dampening was 25% systolic and 25% diastolic. Pulmonary artery pressure increased from a control value of 17.5 mm Hg with a systolic of 29 and diastolic of 0 to 22 mm Hg with a systolic of 53 and a diastolic of 5.3. Right atrial pressure increased from a control value of 2.5 mm Hg to 8 mm Hg. Cardiac output fell from a control value of 1020 ml/min. to 745 ml/min. at one hour of assist. The systolic per cent dampening was then maintained constant at 25 and the diastolic per cent dampening was increased from 25 to 50 to 100 per cent, respectively. Blood pressure at 25 systolic and 25 diastolic per cent dampening was a mean of 76 mm Hg with a central venous pressure of 7, a pulmonary artery pressure of 19, and a cardiac output of 695 ml/min. Increasing the diastolic per cent of dampening to 50 per cent caused a reduction in blood pressure to 69 mm Hg, an increase in central venous pressure to 9, an increase in pulmonary artery pressure to 29, and an increase in cardiac output to 755 ml/min. Increasing diastolic dampening to 75 per cent elicited a blood pressure of 71 mm Hg, a central venous pressure of 8 and a pulmonary artery pressure of 2 mm Hg and a cardiac output of 635 ml/min. Increasing the dampening to 100 per cent diastolic demonstrated a blood pressure of 68, a CVP of 9, a PAP of 20 mm Hg and a cardiac output of 635 ml/min.

Systolic dampening was then increased to 50 per cent and maintained at 50 per cent, and diastolic dampening was evaluated at 25, 50, 75 and 100 per cent, respectively. With a 50 per cent systolic and 25 per cent diastolic dampening, a blood pressure of 68 mm Hg was obtained, central venous pressure of 7 and a mean pulmonary artery pressure of 28.5 mm Hg. However, the systolic, diastolic ratio of the pulmonary artery pressure at this level was 71/-1. The cardiac output was 700 ml/min. With a systolic ratio of 50 per cent and a diastolic ratio of 50 per cent, the mean arterial blood pressure was 65.5 mm Hg, central venous pressure was 6.3, the pulmonary artery pressure was 37 with a systolic of 83 and a diastolic of 5.6 and the cardiac output was 645 ml/min. Increasing the diastolic to 75 per cent resulted in blood pressure of 63 mm Hg, a central venous pressure of 6.5, a pulmonary artery pressure of 36 with a systolic-diastolic ratio of 80 to 3 and the cardiac output fell to 607 ml/min. Increasing the diastolic to 100 per cent and maintaining the systolic at 50 per cent did not demonstrate any difference in the pressure measurements or in cardiac output from previous 75 per cent dampening.

The systolic per cent of dampening was increased to 75 per cent and maintained at this value and the diastolic was evaluated at 25 per cent, 50 per cent, 75 per cent and 100 per cent. Mean arterial blood pressure when systolic dampening was 75 per cent and diastolic 25 per cent, was 67 mm Hg. Central venous pressure was 7 mm Hg and the pulmonary artery pressure was 40 mm Hg mean with a systolic of 90 and a diastolic of 3. Cardiac output was 650 ml/min. Increasing the diastolic to 50 per cent brought a reduction in blood pressure to 57.5 mm Hg, no change in central venous pressure, an increase in the pulmonary artery pressure to 46 mean and 109 systolic and 2 diastolic, and no change in cardiac output. Increasing the diastolic per cent to 75 and 100 per cent demonstrated no changes in mean arterial blood pressure, central venous pressure, and pulmonary artery pressure. However, cardiac output was reduced to 612 ml/min. and 619 ml/min., respectively (Figure 17).

Conclusions: The pulse wave characteristics can be seen in Figure 17 . A pulse wave configuration similar to the control can be obtained only when the systolic dampening is at 25 per cent. Increasing the diastolic dampening percentages while maintaining a 25 per cent systolic dampening did not modify the pulse wave configuration nor adversely affect the cardiac output or pressures.

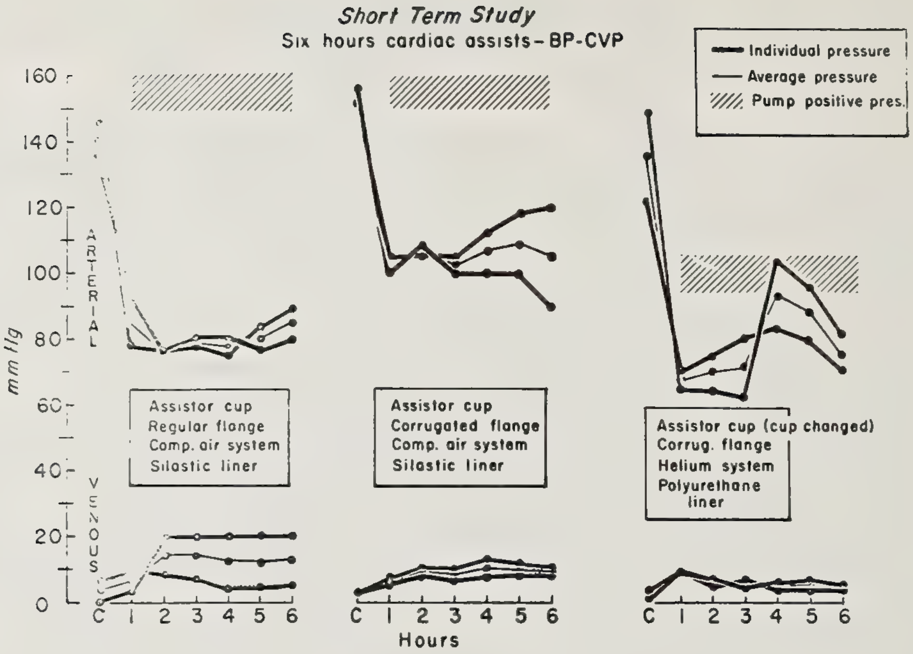

FIGURE 16.

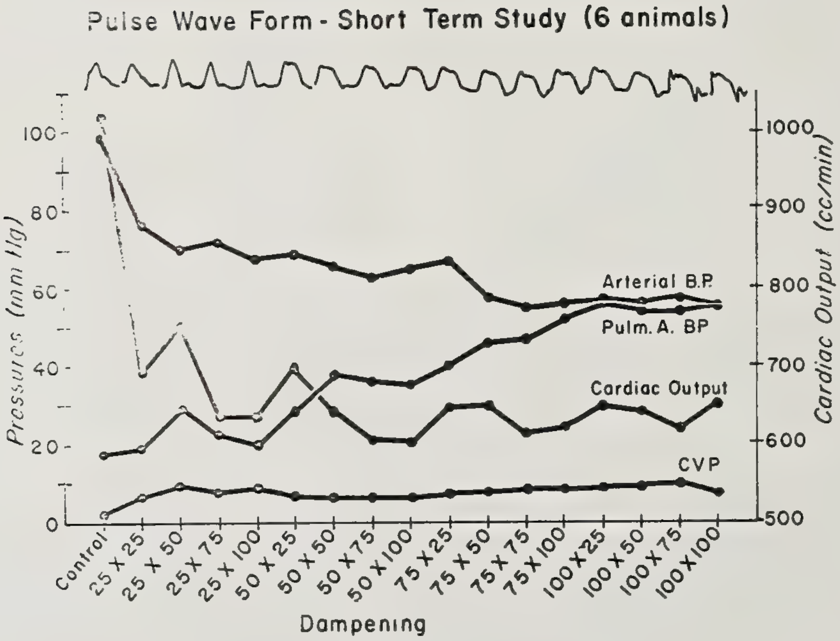

FIGURE 17.

Large increases in pulmonary systolic artery pressure as high as 120 mm Hg are uniform findings when dampening of the systolic air line is increased above 25 per cent. This occurs because the air pressure is so forceful that the volume of blood in the right ventricle is ejected with a high velocity.

PATHOLOGY

Microscopic examination of representative sections of the heart, lung, liver and kidneys were evaluated. Definitive work and documentation of the effect of both chronic implantation and acute assist on these organs has not been fully realized. This report is preliminary and pertains only to eight of the animals. Inference as to myocardial reaction to cup implantation can be made which should be confirmed upon completion of the study.

Representative sections of the apex of the heart, the left ventricle including the septum and anterior descending artery, and the atrioventricular groove at the origin of the left circumflex artery were examined. To minimize prejudice in reporting, the pathologist was not informed as to which part of the protocol the specimens were obtained. A qualitative and quantitative attempt to grade myocardial reaction both as to degree of trauma and tissue response was carried out. Ten parameters of reaction were evaluated in five different grades of response (Table 4).

TABLE 4

KEY TO MYOCARDIAL REACTION

	0	±	+	++	+++
1. Edema	none	nonartifact widening of interstitium	-	-	large protein containing spaces
2. Congestion	none	few RBC's in vessels	subepicardial vascular congestion not in myocardium	vessels distended with RBC's also in myocardium	RBC's in vessels & interstitium
3. Muscle degeneration	none	rare hyperpigmented or atrophic fibres	groups of hyperpigmented fibres	dark vacuolated nuclei; loss of nuclei	necrosis
4. Fibrin deposition	none	few subepicardial strands	thin epicardial layer	thick epicardial layer	large mass of layered fibrin
5. Polymorphs	0-1	2-5 phpf[a]	small groups in subepicardial region	many in subepicardial region	numerous in all fields
6. Lymphocytes	0-1	2-5 phpf[a]	"	"	"
7. Plasma cells	0-1	2-5 phpf[a]	"	"	"
8. Giant cells	none	equivocal giant cells	rare	"	"
9. Fat necrosis	none	occasional necrotic cell	small foci of necrosis	subepicardial & myocardial	diffuse
10. Fibrosis	none	epicardial only	subepicardial fat	"	diffuse

a) phpf: per high power microscopic field

The most constant adverse reaction was that of fibrin deposition and fibrosis limited to the epicardium and subepicardial region. As six of the eight animals' hearts were those which had chronic implantation and not assist, one may infer at this time that the reaction was due to implantation of a foreign material and restriction of cardiac motion (Tables 5, 6, 7).

TABLE 5

APEX MYOCARDIAL REACTION

		0	±	+	++	+++
1.	Edema	X X X X	X X X X			
2.	Congestion		X X	X	X X X	X X
3.	Muscle degeneration	X	X X	X X	X X X	
4.	Fibrin deposition		X	X X X X	X	X X
5.	Polymorphs	X X	X X X	X X X		
6.	Lymphocytes	X X X X X	X X X			
7.	Plasma cells	X X X X X X	X	X		
8.	Giant cells	X X X X X X X X				
9.	Fat necrosis	X X X X X X X X				
10.	Fibrosis	X X X X	X	X	X X	

TABLE 6

ATRIO-VENTRICULAR GROOVE MYOCARDIAL REACTION

		0	±	+	++	+++
1.	Edema	X X X X X	X X X			
2.	Congestion		X X X		X X X X	X
3.	Muscle degeneration		X X X X X	X X X		
4.	Fibrin deposition		X	X X X X X		X X
5.	Polymorphs	X	X X	X	X X X X	
6.	Lymphocytes	X X	X X X X X	X		
7.	Plasma cells	X X X X	X X X X			
8.	Giant cells	X X X X X X X X				
9.	Fat necrosis	X X X X	X	X X X		
10.	Fibrosis	X X	X X	X X X X		

TABLE 7

LEFT VENTRICLE MYOCARDIAL REACTION

		0	±	+	++	+++
1.	Edema	X X X X	X X X X			
2.	Congestion		X X	X	X X X X	X
3.	Muscle degeneration	X	X X	X X X X X		
4.	Fibrin deposition		X X	X X X	X	X X
5.	Polymorphs	X	X X X X	X	X X	
6.	Lymphocytes	X X X	X X X X X			
7.	Plasma cells	X X X X X X X		X		
8.	Giant cells	X X X X X X X X				
9.	Fat necrosis	X X X X X X	X	X		
10.	Fibrosis	X X X X	X	X X X		

DISCUSSION

DR. HASTINGS: Any discussion?

DR. ROTH: I noticed that most workers are using gas of one kind or another to drive these diaphragms. I have always wondered why liquids were not used. The compressibility of the liquid driving medium is approximately that of the load liquid, you could reduce the flow volume of the driving liquid and, also, you could more readily shape the driving impulse and thereby attain great fidelity of diaphragm motion.

DR. TRAGUS: I don't know why we did not use liquid. We used helium, but I appreciate your suggestion. I have no answer for it.

DR. KLINE: I am very happy to see that you are getting around to going back to an elastic outer shell which is comparable to my original device covered by U.S. Patent in my name and reported in my Doctoral Thesis in 1962, A Biomedically Engineered Myocardial Prosthetic System. I think you will find that it is more adaptable and advantageous over the rigid outer shell you had been using before for MVA.

DR. ROGERS: Basically, where were the pressures taken of the driving air or hydrogen? Were they taken at the energy generating unit or were they taken in the space between the elastic liner and the cup?

DR. TRAGUS: They were taken at the airline itself, right before it was attached to the cup.

DR. ROGERS: Then they were not inside the cup?

DR. TRAGUS: No, they were not inside the cup.

DR. ROGERS: The final small passage would affect the pressures considerably. There will be a considerable difference between these values and the actual cup itself, I think, which will account in part for the differences in driving pressure.

DR. KENNEDY: This presentation contained interesting information. I would like to ask a few questions relevant to closed chest defibrillation of your animals in which mechanical ventricular assist cups had been placed previously. As I understand it, closed chest defibrillation was not effective; I wonder if this does not mean that the cup acts either as an insulator or as a semiconductor. Secondly, could you describe in somewhat greater detail just how closed chest defibrillation was carried out with a pacing catheter.

DR. TRAGUS: Yes. The cup did act as an insulator. We found that in open chest experiments, when we tried to defibrillate the animals to get the cup on, it was quite difficult. We could only achieve it in one out of twenty or thirty attempts. Our engineer, the co-designer of this unit, hit upon the idea of fitting an electrode into the base of the cup. By this means it was quite easy to defibrillate the animal. In the animal that I demonstrated to you, in which we could not defibrillate, we then went on and studied as to why we could not defibrillate, and we hit upon the idea of putting an electrode through the vein to the right ventricle so we could have opposing plates. By using the defibrillator we could hook it up to the electrode leads from the cup which was around the apex to the pacemaker wire, which was the most available that we had, hook it up to those two and defibrillate the animal. This was in open-chest experiments; we have not done this in any closed chest experiments.

UNIDENTIFIED DISCUSSANT: I would lik you to explain what was meant by the 25% air flow systolic and 25% diastolic, twenty-five percent of what? And must they not add up to 100%?

DR. TRAGUS: I am sorry if I did not make that clear. By the 25% air flow systolic and 25% diastolic, I mean that the air hose carrying the positive pressure can be reduced in its diameter and therefore in its volume from 100% to 0% or no air flow. A 25% constriction is 1/4 of its total diameter, while 75% is 3/4 and it is just a term to denote the percent reduction of the air flow that goes through the air tubing, whether it is 25% of the total air flow or 50%.

DR. HASTINGS: One more question.

DR. SATINSKY: If I understood you correctly, you stated that you get better pressures when you increase systolic ejection from 45% to 60%.

DR. TRAGUS: Duration of systolic ejection time?

DR. SATINSKY: Yes, now in the long run, at the expense of diastolic filling, wouldn't this have a deleterious physiological effect?

DR. TRAGUS: We have not carried these animals past 9 hours, but Dr. Ansted is here. He has kept animals alive, I think, on continuous pumping for approximately three to four days, and perhaps he could answer that.

DR. HASTINGS: I think we better go on to the next paper.

CHAPTER 41

NEW MODIFICATIONS FOR MECHANICAL VENTRICULAR ASSISTANCE (MVA)

D. Skinner, Mary Dutka, R.N., A. Raciti,
P. Schiff, G. Anstadt

The Johns Hopkins University School of Medicine
Baltimore, Maryland

The purpose of this contract was to evaluate Silastic-coated rigid assister cups for chronic implantation, fabricate and evaluate flexible assisters, develop synchronization for MVA, and study the effects of synchronized MVA in dogs. When implanted around the heart, inactivated rigid assister cups coated with Silastic caused decreased cardiac action and compression of the base of the heart. The longest survivor with an implanted cup lived 10 days. Coronary artery flow during MVA given to the fibrillating heart by rigid cups was studied by cineangiography, flow meters, and radioisotope washout. Flows comparable to control levels were demonstrated. Flexible assisters were fabricated to the investigator's specifications by the Dow Corning Corporation. Using flexible cups to assist the fibrillating heart, hemodynamics and metabolism during 3-5 hours of assistance were comparable or better than results achieved using rigid cups. Cardiac damage was significantly less, and flexible cups were better tolerated during chronic implantation. An electronic programmer to synchronize MVA to the QRS was developed and proved to be extremely accurate in following arrhythmias. The delay time between the QRS until pressure was applied to empty the ventricles averaged 40 msec, so that mechanical systole occurred before the myocardium contracted actively. Hemodynamics and metabolism during synchronized MVA were well maintained. Measurement of heart work by oxygen consumption and coronary flow during synchronized MVA demonstrated that both were decreased, so that there was not a net increase in coronary flow relative to heart work as seen when MVA was given to the fibrillating heart. The potential value of synchronized ventricular assistance employing flexible cups will be assessed and problems will be discussed.

INTRODUCTION

Direct mechanical ventricular assistance (MVA) employing the device invented by Anstadt can provide total circulatory support to the fibrillating or arrested heart for periods in excess of 24 hours followed by long-term survival. Following the initial description of this system by Anstadt, Schiff, and Baue [1], MVA was subjected to experimental evaluation of its physiologic effects and applications by Skinner, Camp and Anstadt at the USAF School of Aerospace Medicine during 1966 and 1967. [2,3,4] These experiments demonstrated that hemodynamics, metabolism, and hematologic parameters were well maintained while the circulation was provided entirely by this mechanical means. Applications investigated included cardiac resuscitation, reducing the mortality from acute myocardial infarction, preserving cadaver organs in vivo for subsequent transplantation, maintaining the circulation during cooling to achieve profound hypothermia and prolonged circulatory arrest without extra-corporeal circulation, and studying mechanical control of the heart action and its effects on peripheral circulatory responses. Pathology of the hearts assisted by this means was evaluated.[5] Other work with MVA has been described by Anstadt and Britz,[6] Anstadt and Baue,[7] Tragus et al,[8] Attai, Veith and co-workers, [9,10] and Hoffer, Almond et al.[11] Human applications have been reported from three institutions.[9,12,13]

Further studies with this method have been conducted at The Johns Hopkins University School of Medicine during 1968 and 1969 with support from a grant by the National Heart Institute to study applications of ventricular assistance given to the fibrillating heart, and a contract awarded by the Artificial Heart Program to make and evaluate improvements and modifications in the apparatus. The objectives of the contract, which are the subject of this report, were to develop, fabricate, and evaluate a programmer for synchronization of the MVA to the beating heart, to design, fabricate, and evaluate three types of flexible assister cups, to modify rigid cups for chronic implantation in dogs, and to study the effects of synchronized assistance in dogs with and without coronary artery ligation.

Assistance is given by a cup lined with a Silastic diaphragm bonded at the apex and rim. The ventricles are held in the cup by suction. To effect systole and diastole, alternating positive and negative air pressures are delivered through the side arm opening into the space between the cup and diaphragm. All experiments previously performed with this device were done with the fibrillating heart. The atria remain outside the device when it is properly applied. Mean atrial pressures are generally less than 15 mm Hg. Waves greater than 30 are uncommon. Left ventricular and aortic peak systolic pressures range from 90 to 130 mm Hg. Left ventricular early diastolic pressures are frequently negative, and end diastolic pressures are less than 15 mm Hg.

EVALUATION OF CORONARY ARTERY FLOW DURING MVA GIVEN TO THE FIBRILLATING HEART

The effects of ventricular assistance given to the fibrillating heart were studied by cineangiographic right and left heart injections of radiopaque material. With the heart fibrillating, mitral valve action was demonstrated to be competent. Several cineangiographic sequences demonstrated that ventricular emptying of both right and left ventricles was quite adequate with this device assisting the fibrillating heart. The filling of the right and left coronary arteries was seen following left ventricular injections. Aortic root injections demonstrated competency of the aortic valve and excellent filling of both coronary arteries. Selective coronary arterial injections demonstrated adequate filling of the distal vessels. The coronary arteries filled during diastole and emptied during systole.

The effects of ventricular assistance on coronary flow were studied by other techniques. An electromagnetic flowmeter probe was placed on the left anterior descending coronary artery in five dogs, and coronary flow was measured with the heart beating normally and during ventricular fibrillation and assistance. During assistance flow increased markedly in diastole and decreased in systole. Mean coronary flow in all five dogs equalled or exceeded the baseline levels. If an assister cup was employed which was too small for the heart, coronary arteries were compressed and coronary flow was reduced. For optimal hemodynamics and coronary flow, it was important to use a proper sized assister cup which could easily be judged by visual comparison of heart and assister sizes.

Myocardial blood flow was measured by ^{133}Xe washout from the mycardium to compare tissue perfusion before and during assistance. When injected into a coronary artery, an inert gas such as ^{133}Xe diffuses rapidly throughout tissue. The rate of washout or disappearance is inversely proportional to the flow per gram of tissue. In five dogs, the rate of disappearance of ^{133}Xe following injection of 10^4 to 10^5 counts per minute dissolved in less than 0.5 cc of saline was determined by a RIDL scintillation counter placed over the heart. The half time of isotope washout was averaged from four or five baseline determinations and compared to half time values from four to seven determinations made while MVA was given to the fibrillating heart. In the five dogs, values during ventricular assistance averaged from 53 to 85% of baseline myocardial perfusion levels.

CHRONIC IMPLANTATION OF RIGID ASSISTERS

Standard assister cups previously developed, consisting of an outer glass shell and an inner Silastic diaphragm, were prepared for chronic implantation by coating the outside of the assisters with Silastic to reduce tissue irritation. This was done by the Dow Corning Corporation. Following application to the heart in an inactive phase, no difficulty was encountered in maintaining cup position on the heart for prolonged periods. When the assister was applied initially, blood pressure fell sharply, and gradually returned to baseline levels. Cardiac output measured by an electromagnetic flow probe on the pulmonary artery dropped to an average of 56% of baseline levels immediately following cup implantation in five dogs Cardiac output recovered to an average of 87% of baseline levels when the thoracotomy was closed. The dogs died 3, 18, 18, and 24 hours, and 10 days after cup implantation. At autopsy, there was a groove on the base of each heart at the point where the assister rim had impinged. There were no cardiac ruptures. In the animal which survived for 10 days, the groove was particularly deep over the right atrium near the A-V groove. The tip of the intermediate lobe and both diaphragmatic lobes showed evidence of pressure necrosis. The right lower lobe was congested and hemorrhagic. There were 1200 cc. of purulent sanguinous fluid in both pleural cavities. In this dog, pressure from the rigid cup on the adjacent lungs caused necrosis and death of the animal. This study suggested that approximately one week would be the upper limits of time during which it might be feasible to leave a rigid assister cup in place.

Disadvantages apparent from the use of rigid cups included the large size of thoracotomy opening required to insert and remove the device, the potential hazard of breakage, the possibility of coronary artery compression at the rigid cup rim, pressure necrosis of adjacent structures following prolonged implantation, and the previously described necrosis of the right ventricular outflow tract at the point where the assister rim crossed the right ventricle. Each of these drawbacks might be obviated by the development and use of flexible assister cups.

DESIGN, FABRICATION, AND EVALUATION OF FLEXIBLE ASSISTERS

In collaboration with the Dow Corning Corporation, flexible assisters were fabricated. These consisted of a Dacron reinforced Silastic outer shell, and a Silastic inner diaphragm installed in one of three different ways. In the early experiments with this device, it seemed necessary to use rigid cups to maintain suction on the heart during rapid pressure changes. However, maintaining suction and cup shape were not problems with the flexible cups. Using the flexible device to assist the fibrillating heart in nine dogs, mean blood pressure was 81 mmHg, and mean cardiac outputs were 82% of levels measured during normal heart action. Following three to five hours of assistance, mean arterial pH was 7.39 compared to 7.55 during the control period. P_{O_2}, P_{CO_2}, and excess lactate production did not change significantly. Each of these results was comparable or better than results of similar studies using rigid cups. In six dogs, survival was observed following five hours of ventricular fibrillation and flexible cup assistance. Each heart was successfully defibrillated, and five dogs survived until sacrificed one to two weeks later. At autopsy, cardiac damage was significantly less than usually observed with rigid cups. Necrosis at the level of the cup rim was notably absent. These new flexible assisters appeared as effective as the rigid cups and offered significant advantages.

Body tolerance to chronic implantation of flexible assisters was assessed in nine dogs. As with the rigid cups, blood pressure dropped acutely when the flexible assister was applied in an inactive mode to the beating heart, but recovery appeared more rapid. In two animals, blood pressure after implantation of the cup and thoracotomy closure was better than baseline levels. The acute drop in cardiac output to 55 to 70% of control levels immediately following the cup implantation was less marked than that observed with the rigid cups. Following thoracotomy closure, cardiac outputs increased to at least 80% of the baseline values and returned to levels of normal heart action in two dogs. Arrhythmias were not noted unlike the situation when rigid cups were applied. Three of the nine dogs died approximately one day after flexible assister implantation, but the other six lived from nine days to more than a month, and two are still living, yielding a much better survival than had been observed with the rigid cups. At autopsy in dogs which died, fluid, ranging between 75 to 2000 cc, was found in the chest cavity and some evidence of damage to adjacent lung was apparent. In each dog, satisfactory cup position was found at autopsy and by serial X-ray examinations. In only three of the animals was there a significant groove around the base of the heart where the assister had impinged, and in only one of these animals was there evidence of coronary artery compression. There was no gross evidence of myocardial infarction in this dog. Flexible cups clearly appeared to be better tolerated during chronic implantation.

Based upon four year's experience with cup evaluation, criteria for an ideal assister can be suggested. Flexible assister cups are preferable to those with rigid outer shells. The depth should be 10% greater than the diameter at the orifice. Design of the cup orifice should allow good suction and contact with the heart without compromise of the coronary arteries. The outer shell of the cup should be able to stand a pressure of at least 300 mmHg without breaking, and a negative 150 mmHg with the heart inside the cup without the shell buckling. The diaphragm should be bonded to the cup at the rim and over a distance from the apex up to 20% of the cup depth. The apex is left open for a 1/4 inch diameter suction line. Bonding of the diaphragm to the outer shell has not always been adequate in the current Silastic cups. Strength of bonding should be sufficient so that the pressure range from +300 to -150 mmHg will be resisted without separation of the diaphragm from the cup. The inner diaphragm surface must be smooth and compatible with the epicardium to reduce irritation and pericarditis. The outer structure of the shell should be compatible for implantation within the chest for at least one to two weeks without causing undue inflammatory reaction. Materials employed should be able to withstand autoclaving. The cup should allow conductivity of the electrocardiogram to the rest of the body or else provide a conductive mechanism within its wall to permit EKG monitoring. The substance used for the diaphragm should have a high flex life so that breakage will not occur at the point of bonding. This has been a major problem with Silastic diaphragms. Ideally, these diaphragms should withstand 30 days of continuous pumping without diaphragm or bonding breakdown. Although a slight elasticity in the diaphragm is desirable, this should not permit the walls of the diaphragm to approximate when the cup is pumped at 200 mmHg. Ideally, the outer shell and cup diaphragm should be transparent so that the heart condition can be seen through the device. The currently employed Silastic devices meet most but not all of these criteria. The major drawback has been a low flex life with resulting high breakage rates during use. It is hoped that better materials or fabriaction for these devices will be identified and made available for testing during the next contract year.

SYNCHRONIZATION FOR MECHANICAL VENTRICULAR ASSISTANCE

Until the current year, nearly all experiments with MVA were conducted during intentional ventricular fibrillation. Preliminary experiments during the past three years indicated that it might be desirable to synchronize MVA to the beating heart. A programmer was developed for this purpose. Based on the findings of others that the major portion of ventricular energy expenditure occurred during the rise in the ventricular pressure curve,[14] it was postulated that to decrease heart work, assistance should be provided before the myocardium contracted. To prevent interference with diastolic filling or coronary flow, assistance should be given in the interval between the electrocardiographic QRS signal and the normal rise in left ventricular pressure, a time of approximately 70 mSec. Criteria for extreme accuracy in QRS detection during rapid ventricular multifocal arrhythmias, and a total system response time of less than 70 mSec were established.

Reliable QRS detection was obtained by selecting the largest amplitude QRS frequency component, a value between 15 and 30 Hz, and separating this from neuromuscular and other low frequency baseline changes, 60 Hz line, and high frequency noise interference by the use of variable three section active filters with an exceptionally flat frequency response. Other preamplifier and synchronizer characteristics included a total system common mode rejection ratio of 2,000,000:1, and an overload recovery time after defibrillation of less than one second. An automatic gain control for changes of QRS amplitude over a 250% range, selectable maximum and minimum rate control to allow assistance on alternate input triggering or to pulse automatically at low heart rates, two delay modules to make the programmer adaptable to other assist systems, a pacemaker stimulator, rate meter, and percent systole meter were all incorporated into the final programmer.[15]

When synchronized at full bandwidth to a normal electrocardiogram, solenoid valve activation occurred approximately 10 mSec after initiation of the QRS complex. The total delay of the system from initiation of the QRS until pressure was delivered to the ventricles varied between 40 and 60 mSec in 12 dogs. Recordings of EKG, solenoid activation signal, and left ventricular pressure rise demonstrated that the time from QRS initiation to the upswing of left ventricular pressure occurred from 10 to 35 mSec faster during synchronized MVA than during normal heart action. To determine accuracy of the frequency selection synchronizer, the device was tested against a ventricular arrhythmia occurring in a patient with a severe myocardial infarction. During four and one-half hours of monitoring, the overall accuracy of the programmer was greater than 99%. Accuracy was tested in dogs in which acute myocardial infarctions were caused by circumflex coronary artery division. The number of QRS complexes not detected within the minimal and maximal rate settings of the programmer was less than 1% of the total beats. At heart rates of greater than 200, it was found beneficial to set the maximum rate limiting switch setting at a lower value and to assist only alternate beats. This proved desirable hemodynamically to permit sufficient ventricular filling time at the faster pulse rates.

To assess the physiologic effects of synchronized ventricular assistance, studies of coronary flow, myocardial work and the effectiveness of synchronized ventricular assistance in treating myocardial infarction were evaluated. To measure coronary flow and heart work, a GBH-coated catheter was sutured into the coronary sinus so that all coronary sinus flow was diverted through an extracardiac shunt into the right atrium. This permitted direct measurement of coronary sinus flow and sampling of blood for oxygen content, lactate, pyruvate, and SGOT levels. When compared to simultaneously obtained aortic blood samples, myocardial oxygen consumption and excess lactate production could be measured. Blood oxygen content was measured directly by a polarographic technique standardized against VanSlyke determinations. Comparison of the averages of 18 coronary sinus flow determinations made in each of 8 dogs during 30 minutes before application of synchronized MVA to the average of 18 coronary sinus flow measurements made during two hours of synchronized assistance demonstrated that coronary sinus flow decreased significantly in each dog. Averages of three aortic-coronary sinus oxygen content differences before and during assistance showed an increase in five, no change in one, and a decrease in two. Myocardial oxygen consumption decreased in all eight dogs during synchronized assistance. The ratio of coronary sinus flow to oxygen consumption did not change significantly overall. Excess lactate levels during and after two hours of synchronized assistance showed no evidence of anaerobic metabolism.

These results differ from observations made previously employing the same experimental technique to measure coronary sinus flow and oxygen consumption during assistance given to the fibrillating heart with or without coronary artery division. In 18 of 20 dogs, the ratio of coronary sinus flow to oxygen consumption increased during assistance given to the fibrillating heart.

Coronary flow during assistance synchronized to the beating heart was studied in four dogs by the electromagnetic flowmeter or Xenon washout techniques. During synchronized MVA, flows in the anterior descending coronary artery showed no change or an increase over control levels, similar to results obtained when coronary flow was studied by this technique during MVA given to the fibrillating heart. Xenon washout from the myocardium was diminished during synchronized MVA compared to baseline levels, results again comparable to those seen in the earlier experiments studying perfusion of the fibrillating heart given ventricular assistance.

The canine model previously employed to study the effects of circulatory assistance upon survival following myocardial infarction was used to evaluate MVA synchronized to the beating heart. Following left circumflex coronary artery division at its origin, the mortality of dogs given standard supportive treatment, oxygen, sympathomimetic amines, and defibrillation when necessary, has resulted in a 33% 24-hour survival rates in each of three experiments conducted more than a year apart.[16] Using this data as control values, survival following LCCA division was evaluated when the infarcted heart was given five hours of synchronous MVA commencing 30 minutes after infarction. In all other respects, assisted animals were treated like those in the control groups. Twelve of thirteen dogs which received synchronized MVA survived more than 24 hours after LCCA division. Nine survived more than 48 hours, and eight became long-term survivors which were eventually sacrificed one to three weeks later. Infarction was verified by electrocardiograms and by autopsy in each dog. Eight of the thirteen dogs develops ventricular fibrillation shortly after LCCA division. Six of these animals became long-term survivors after five hours of synchronized MVA. These results demonstrated significantly increased long-term survival when MVA was given synchronized to the heart beat and were comparable to results previously reported demonstrating significantly increased survival when ventricular fibrillation was induced and complete circulatory support was given by ventricular assistance.[3]

We had previously attributed this increase in survival when MVA was given to the fibrillating heart to the reduction in myocardial work while coronary flow was maintained at control levels. However, the experiments conducted with synchronized MVA did not demonstrate the relative increase in coronary flow compared to heart work which was seen with the fibrillating assisted heart, and yet survival following infarction was equally improved when MVA was given to either the beating or fibrillating heart.

DISCUSSION AND SUMMARY

Mechanical ventricular assistance offers several advantages as a temporary method for partial or complete circulatory support. These include ease and rapidity of application which is necessary for emergency cardiac resuscitation, simplicity of concept and control, and absence of vascular cannulations or blood-to-foreign surface interfaces. Canine survival following 72 hours of ventricular fibrillation and MVA has recently been accomplished by Anstadt. The upper time limit of this approach to mechanical circulation is probably about one week. Disadvantages include the need for open thoractomy, but this is not a serious objection in the types of patients for whom clinical applications have been investigated. Other disadvantages such as the size of thoracotomy wound, damage to the heart and adjacent structures, and need to maintain the heart in ventricular fibrillation, have largely been overcome by the development of flexible assister cups and synchronization during the past year's contract work. Several equipment modifications and evaluations are still desirable, and form the subject of next year's contract. These include the need for better materials in the assister so that flexion breakage will be reduced, development of a hand pump to aid in transportation of assisted patients, further investigation of the relative merits of synchronously assisting the beating heart or assisting the intentionally fibrillated heart, and investigation of the type and importance of pulse pressure wave shaping which can be obtained.

The basic equipment and physiologic rationale for MVA seem well worked out and evaluated. Research applications have been demonstrated in several areas, as a method to study hypothermia, control of the circulation, myocardial infarction, and organ preservation and function. The time has come when only clinical trials can tell what the ultimate value of this approach will be in humans. To our knowledge, there have been 16 clinical applications of this device at four institutions to the present time. In nearly every instance, MVA was employed as a final desperate attempt to restore life or organ function when all other resuscitative maneuvers had failed, and evidence of patient viability was absent or diminished. Cardiac outputs of up to 5.5 liters per minute have been obtained, and blood pressures have been adequately restored. Although only one patient has been able to maintain circulation after discontinuance of the device, there has been good evidence of improved organ function and overall patient status in these last ditch resuscitation attempts. EEG activity was improved in one patient in whom this was measured. Fibrillation has returned to the flaccid heart on several occasions, urine output has been restored, and severe acidosis has been corrected. The experimental and initial clinical experiences fully support further clinical trials of MVA in carefully selected patients in whom there is some hope for successful maintenance of life, and in whom no better established form of treatment is now available.

REFERENCES

1. Anstadt, G.L., Schiff, P., and Baue, A.E. Prolonged circulatory support by direct mechanical ventricular assistance. Trans. Amer. Soc. Artif. Int. Organs 12:72, 1966.
2. Skinner, D.B., Anstadt, G.L., and Camp, T.F., Jr. Applications of mechanical ventricular assistance. Ann. Surg. 166:500-512, 1967.
3. Skinner, D.B., Anstadt, G.L., and Camp, T.F., Jr. Acute circulatory support by mechanical ventricular assistance following myocardial infarction. J. Thorac. Cardiov. Surg. 54:785-794, 1967.
4. Skinner, D.B., Anstadt, G.L., and Camp, T.F., Jr. Mechanical ventricular assistance: applications of a method for total cardiac support. Bull. Soc. Internatl. Chir. (accepted for publication).
5. Coogan, P.S., Casey, H.W., Anstadt, G.L., and Skinner, D.B. Acute and long-term effects of direct mechanical ventricular assistance in the dog. Arch. Path. 87:423-431, 1969.
6. Anstadt, G.L. and Britz, W.E., Jr. Continued studies in prolonged circulatory support by direct mechanical ventricular assistance. Trans. Amer. Soc. Artif. Int. Organs 14:297, 1968.
7. Anstadt, G.L. and Baue, A.E. Mechanical ventricular assistance for prolonged support of the heart. Surg. Forum 17:148, 1966.
8. Tragus, E.T., Moore, J.R., Baue, A.E. and Blakemore, W.S. Mechanical cardiac massage for *in vivo* preservation of renal allografts. Trans. Amer. Soc. Artif. Int. Organs Vol. 15, 1969 (in press).
9. Attai, L.A., Veith, F.J., Furman, S., Denize, A., Boley, S.J., Robinson, G. and Gliedman, M.L. Intracorporeal cadaver organ preservation by mechanical ventricular assistance. Surg. Forum 19:202, 1968.
10. Veith, F.J., Attai, L., Koerner, S., Gliedman, M.L. Functional evaluation of lungs transplanted after varying ischemic intervals and after preservation by mechanical ventricular assistance. Presented at Society of Thoracic Surgeons, January, 1969. To be published in Ann. Thorac. Surg.
11. Hoffer, R.E., Almond, C.H., Elefson, E.E., Anido, H., MacKenzie, J.W. Mechanical ventricular assistance for circulatory support in acute coronary artery occlusion in the pig: the Anstadt cup. Dis. Chest 53:502-506, 1968.
12. Skinner, D.B., Schechter, E., Hood, R.H., Jr., Camp, T.F., Jr. and Anstadt, G.L. Mechanical ventricular assistance in human beings. Ann. Thorac. Surg. 5:131-140, 1968.
13. Baue, A.E., Tragus, E.T., Anstadt, G.L. and Blakemore, W.S. Mechanical ventricular assistance in man. Circulation 37:Suppl. 2:33-36, 1968.

14. Sarnoff, S.J. et al. Hemodynamic determinants of oxygen consumption of the heart with special reference to the time tension index. Amer. J. Physiol. 192:148, 1958.
15. Schiff, P., Skinner, D.B., Dutka, M. and Anstadt, G.L. Synchronization of direct mechanical ventricular assistance to the electrocardiogram. Trans. Amer. Soc. Artif. Int. Organs Vol. 15, 1969.
16. Skinner, D.B., Davis, W.G., Jr., Camp, T.F., Jr. Left circumflex coronary artery division in dogs given supportive treatment. Ann. Thorac. Surg. 7:242, 1969.

DISCUSSION

DR. RASSMAN: I would like to ask, when you obliterate the constriction on the pulmonary outflow tract with this new device, why don't you get pulmonary edema? As you know, we tried to obliterate the pulmonary constriction and we induced pulmonary edema in each case. Secondly, we also implanted a similar device in six animals over long periods of time. Of the six, two animals died of infection, and four lasted for a period of up to two months. In our opinion, such cups can be tolerated for longer periods of time. We had the opportunity to treat one additional patient in the past three weeks. The patient who was on a heart-lung machine and had a low blood pressure was put on the assist device. We were able to maintain the circulation very nicely. Thank you.

DR. SKINNER: With the flexible cup design we are now using, the reduction in right ventricular outflow tracts compression is relative, because we still see a gradient on pullback pressure tracings through the outflow tract. The flexible rim does not seem to be digging in as severely and we are not seeing the necrosis which we saw with rigid assistors. We agree that the flexible cups will be tolerated better by the body and our longest flexible implant in the inactive mode has now been more than three weeks, and some of these animals are still living.

DR. JACOBEY: I wondered if you considered the possibility in your findings that the striking decrease in coronary sinus flow might be due to partial occlusion of the coronary sinus by the assist device. This might be clarified by your A-V differences across the heart in this situation. Did you get those values? Secondly, you did not say anything about pathological studies of the coronary vessels themselves, and I wondered whether you have seen arteritis or occlusion secondary to your treatment. I gather that you haven't found any myocardial necrosis in the long-term implants?

DR. SKINNER: The A-V differences across the coronary sinus have been generally decreased or unchanged. They inversely parallel the ratios of the flow to myocardial oxygen consumption. We do not think the coronary sinus has been obstructed, because we have a large cannula holding it open, and the cannula is held in place by a suture placed around it. In previous work, which I did not review today, we assisted the fibrillating heart with a similar cannula in the coronary sinus, and did not see this reduction in coronary sinus flow. Flow remained essentially unchanged with assistance to the fibrillating heart which is why there was a difference in the ratio of flow to oxygen consumption between the two preparations, one with the fibrillating heart and one with assistance synchronized to the beating heart. Oxygen consumption decreased in both. We have been disturbed about how to measure coronary blood flow most meaningfully and that is why we have used five different ways of trying to assess coronary flow: angiography, flow meter, isotope washout, coronary sinus flow, and microspheres. We have not reported the data yet, but we have used distribution of radioactive microspheres injected into the left atrium as a way of measuring coronary flow, and this also shows that coronary flow is maintained at about control levels after the heart is fibrillated and assisted. You asked about pathology. In the 24-hour studies, we have seen small areas of myocardial necrosis, but no more extensive than those seen in the six hour studies which were reported by Drs. Coogan, Casey, Anstadt and us in the April issue of Archives of Pathology. So, we think going to longer times has not significantly increased the amount of cardiac damage, and we think we are seeing less necrosis in the myocardium with the new flexible assistor. We have not seen coronary thrombosis or arteritis, either acutely or in dogs that have been allowed to survive more than a year after assistance, and then been sacrificed and subjected to pathological studies.

DR. JACOBEY: Have you done pathological studies of hearts treated for more than 48 hours?

DR. SKINNER: No.

DR. LUDWIN: Could you comment on the pulse rate and also on the partitioning of each cycle between systole and diastole?

DR. SKINNER: The normal dog under barbituate anesthesia has a rapid spontaneous pulse rate so we run assisted animals with fibrillating heart at a pulse rate of about 110 to 120. We found, unlike the previous report, that a systolic duration of 35-40% gives us better hemodynamics, and we think that allowing adequate time for ventricular filling is important.

DR. BOLOOKI: Mr. Chairman, may I show four slides, please? I just wanted to mention some of the problems we may get into when we begin clinical trials on this type of device. We have not used your type of device, but just the simple bubble oxygenator with a portable pump on patients who have been referred to us by medical colleagues. The first slide shows the results obtained in the Jackson Memorial Hospital coronary care unit during 1967 and 1968 (Slide). As you notice, from the slide, there are 32 deaths per year. Of these, 11 patients had acute myocardial rupture, and I do not think we can get to them rapidly enough, at least not with our present facilities and speed. However, there were 21 patients, whom we might be able to help. We have been called to see four patients since last December 1968, three of them were already in ventricular fibrillation, and they were given cardiac massage; one of them, open chest cardiac massage. All these patients were immediately placed on the portable pump oxygenator and because they could not be defibrillated, they were taken to the operating room and placed on total cardiopulmonary bypass.

Immediately an attempt was made to assess their coronary circulation. This was done by on-table coronary angiography, which is shown in the next slide. (Slide) You notice in the slide that in the left and right coronary arteries of this particular patient, there is practically a total block on both sides at one cm from takeoff. The next slide shows the situation encountered in another patient. (Slide) In this woman, you notice that the left coronary artery fills up only for a distance of about one cm, and there is no filling of the right coronary artery at all. These x-rays are taken by direct hand injection of 25-50 cc of 50% Hypaque. Another method that we use to assess the coronary circulation or its collateral circulation is by injection of 5 cc of methylene blue into the root of the aorta. (Slide) As you can see, the area of infarct can be delineated very well, but in regards to overall circulation to the heart, there is not very much circulation. What could be done for such a heart with counterpulsation or with any other type of device we really do not know. In some of the patients we tried to resect the infarcted area. The heart was practically like jelly and did not take any sutures. On cutting through the left ventricle there was no bleeding at all, which obviously shows that the heart did not have any effective circulation. In wonder if we should spend time using an assist device to pump this type of patient for two or three or four hours, while we do not know the state of coronary circulation. Thank you.

DR. SKINNER: Thank you Dr. Bolooki for pointing out the clinical problems that will be encountered. We feel that it is important to have a method available that can be quickly applied and that will gain immediate control over the patient's circulation, when the patient is dying from acute myocardial infarction. This will permit time for the kind of studies that you have referred to so that these can be done in some sort of organized and controlled manner without chaos and while attempts to treat the patient are initiated. Whether the ultimate treatment for these patients will be infarctectomy, acute coronary artery surgery, heart replacement by transplantation, a totally replaceable mechanical heart or another method is still not clear, but I think that the type of temporary assist methods we are talking about will give us a way of keeping the patient alive while he is being evaluated, and prepared for definitive treatment.

CHAPTER 42

COMBINED PERIPHERAL AND THORACIC MODALITIES OF SYNCHRONOUS EXTERNAL PRESSURE ASSIST

W. Birtwell, F. Giron and H. Soroff
Tufts-New England Medical Center Hospitals
Boston, Massachusetts

External pressure actuators have been produced for the hindquarters and thorax of the dog to provide pressure pulses with a peak value from 50-200 mm. Hg. synchronous with cardiac activity. Hydraulic operation results in minimal system delay (30-50 milliseconds) and sharp pressure pulses. In normal animals the diastolic peak pressure in the root of the aorta has been raised by 30-60 mm Hg and the systolic pressure reduced by 20-40 mm Hg. Retrograde flow pulses from 6-10 cc. have been recorded in the descending aorta with similar increases in the antegrade flow. The thoracic venous pressure remains at control level while the venous bed in the actuated portion of the body reflects the applied external pressure. In 10 animals with experimentally produced acute left heart failure by serial ligation of branches of the left coronary arteries, external assist reduced the end-diastolic pressure in the left ventricle from 20 mm Hg to 3 mm Hg and decreased peak ventricular pressure by 25-40 mm Hg. Initial experiments in normal dogs with the thoracic unit functioning every other heart beat indicated that the driving pressure in the aorta was increased by 25 mm Hg and the peak flow in the carotid artery was increased by 100% with an intrathoracic pulse pressure of 40 mm Hg. In these experiments, the diaphragm coupling between the thorax and abdomen has been greater than the coupling which was experienced with the peripheral modality.

INTRODUCTION

External pressure assist produces counterpulsation pressure effects in the arterial system and assists the circulation by regional application of pulsating external pressure synchronous and properly phased with cardiac action. The peripheral modality is phased so that the pressure in the root of the aorta is increased during cardiac diastole by a retrograde flow pulse from the peripheral arterial system produced by the application of a positive pressure pulse to the hindquarters of the dog. The thoracic modality is phased so that the intrathoracic pressure is positive during cardiac systole increasing the driving pressure in the descending aorta at no energy cost to the left ventricle. The effectiveness of the system is determined by the magnitude of the differential pressure which is created between the pressurized regions and the extent to which the arterio-venous driving pressure is phasically increased.

Under contract #PH-43-68-1438 equipment has been developed to facilitate the study of the effectiveness of the combined peripheral and thoracic modalities using the dog as the experimental animal. Physiologic studies have been performed using normal animals and coronary occlusion preparations.

TECHNICAL DEVELOPMENTS

For several years we have studied the problems relating to the creation of a cyclic pressure pulsation on a portion of the body. Form fitting pneumatic systems, pneumatic systems with liquid coupling, and hydraulic systems have been utilized. The approach which has been followed in this development has proved to be a satisfactory solution practical for clinical application. This system can accommodate a wide variation in the size and shape of the body. The water used for liquid coupling is sealed in a leak proof non-distensible seal. The pressure coupling provided by the system reduces damping to a level which makes possible rapid cyclic pressure pulses with peak values in excess of 200 mm Hg peak at a rate of 200 pulses per minute or more. The design of the seal minimizes the motion of the body which is caused by the unbalanced force created by the pressure. The noise level of the equipment can be reduced to an acceptable value.

The Peripheral Actuator and Seal

Figure 1 is a photograph of the actuator which has been produced to accommodate the hindquarters of the dog. The seal which has been produced to our design by the Jobst Institute is a double walled tube 10" in diameter and 34" long. The material is neoprene impregnated tightly woven nylon cloth produced to Jobst specifications. Two longitudinal seams secure the inner and outer walls to each other for the entire length of the seal forming two compartments. Filling hoses are incorporated in each compartment. The construction of the seams is such that the seals provide long service without leaks and withstand pressure far in excess of the peak pressure which is required.

The seal is housed in a rigid aluminum split cylindrical housing. The two half sections are hinged and driven by a hydraulic cylinder. The bore (1" diameter) and stroke (1") of the hydraulic

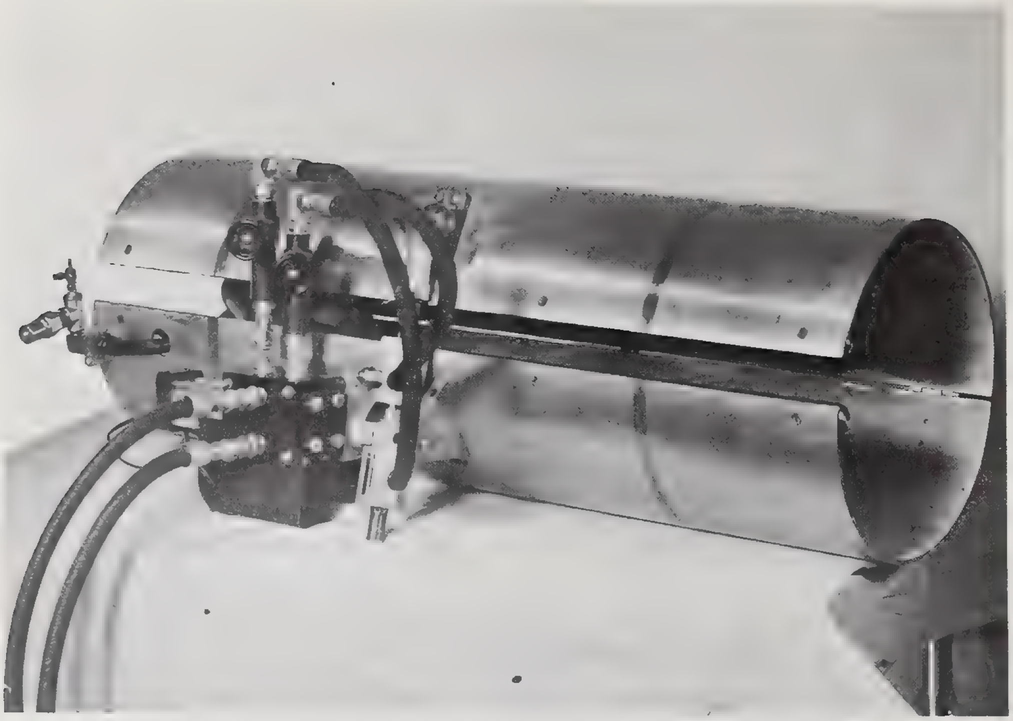

FIGURE 1. THE PERIPHERAL ACTUATOR HOUSING AND SEAL.

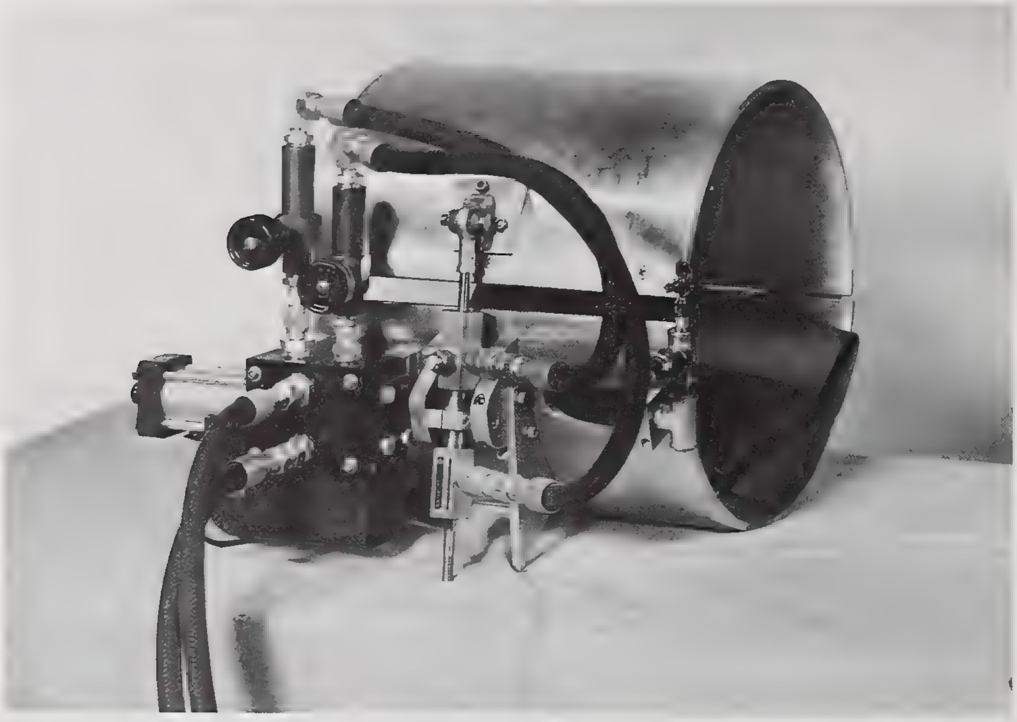

FIGURE 2. THE THORACIC ACTUATOR HOUSING AND SEAL.

cylinder were selected to provide the proper pressure conversion ratio and volume displacement. The split cylindrical housing converts the high pressure (200-2000 PSI) low volume displacement pulse from the hydraulic power supply to a low pressure (0-200 mm Hg) high volume pulse in the seal.

A 4-way solenoid valve mounted on the housing energizes the hydraulic cylinder in both directions. Flow control valves are provided to control the velocity of the cylinder motion.

In operation, the seal and actuator housing are slipped onto the hindquarters of the dog. The proximal end of the housing is located about 2" below the diaphragm. The seal is filled with water through the filling hoses to an ambient pressure of 15-20 mm Hg. The hydraulic hoses from the solenoid valve are connected by means of self-sealing quick disconnects to the hydraulic power supply. The solenoid valve is triggered by a synchronous electronic control (produced under contract PH-43-67-1117) triggered by the ECG. The peak pressure produced in the seal and on the body of the animal is determined by the adjustment of the hydraulic pressure. In the peripheral system, the ratio of the hydraulic supply pressure to seal pressure is 340/1.

Figure 2 is a photograph of the actuator housing and seal which has been produced to pressurize the thorax. This device is 12" in diameter and 12" long. The design and function of this actuator is identical to the peripheral system.

Figure 3 is a photograph of the high pressure hydraulic power supply and the synchronous breathing system. A gear pump rated at 1 gallon/minute at 3000 PSI is driven by a 2 HP, 3/60/220 V 1800 RPM induction motor. The pump is mounted on a 1" gallon supply tank of oil. Pressure relief and adjustment valves, an accumulator with pressure adjustment system, pressure gauges and quick disconnects are included to provide a complete hydraulic power supply with two adjustable pressure outlets.

Figure 4 is a schematic diagram showing the hydraulic connections and controls for one actuating system. The internal pressure relief valve is set at 2000 PSI. The accumulator pressure can be adjusted from 0-2000 PSI by means of a nitrogen pressure system. The pressure regulating valve is adjustable from 0-2000 PSI. Flexible high pressure oil lines from the solenoid valve are attached to the power supply by means of self-sealing quick disconnects. The flow regulating valves are provided to control the speed of the hydraulic cylinder in both directions. The system is operated in a pressure limited mode causing the cylinder to stop when the pressure in the seal balances the pressure in the cylinder.

Figure 5 illustrates the response of the system in an in vitro study using a rigid body to replace the animal. The bottom curve is the electrical duration signal in the synchronous electronic control. The pulse period is 650 milliseconds with a systole duration of 325 milliseconds. The top recording shows the pressure produced in the seal. The initial rise in seal pressure occurs about 30 milliseconds after the start of the electrical duration signal. This delay is a measure of the operation time of the solenoid valve. The center recording is taken from a pressure sensing balloon placed on the surface of the stimulated body. The initial rise in pressure at this point occurs 50 milliseconds after the start of electrical systole. A similar delay is seen at the end of systole duration causing the duration of the pressure signals to be very nearly equal to the electrical duration.

Table 1 shows the pressure characteristics of the system at various pulse ratio and system pressures.

TABLE 1

CHARACTERISTICS OF SYSTEM

Pulse Rate	System Pressure P.S.I.	Systole Duration m. sec.	System Delay m. sec.	Tank $\frac{dp}{dt}$ mm Hg/sec	Time to Peak Pressure m. sec.	Balloon Catheter $\frac{dp}{dt}$ mm Hg/ sec.
60	600	480	30	4,000	100	2,000
60	1,000	480	30	6,000	60	5,000
60	1,500	480	30	10,000	80	15,000
90	600	360	20	3,000	110	2,000
90	1,000	360	30	5,000	70	5,000
90	1,500	360	30	12,000	60	8,000
120	600	290	30	4,000	90	2,000
120	1,000	240	30	7,500	60	5,000
120	1,500	240	30	11,000	50	8,000
150	600	100	30	3,000	80	2,000
150	1,000	100	30	7,500	70	5,000
150	1,500	100	30	14,000	70	8,000
180	600	100	30	5,000	80	1,500
180	1,000	100	30	9,000	70	3,500
180	1,500	100	30	10,000	70	6,000

The system delay is constant at 30 milliseconds. The rate of change of pressure varies with system pressure from 3000-14000 mm Hg/sec. On the surface of the body the range of dp/dt is from 2000-8000 mm Hg/sec.

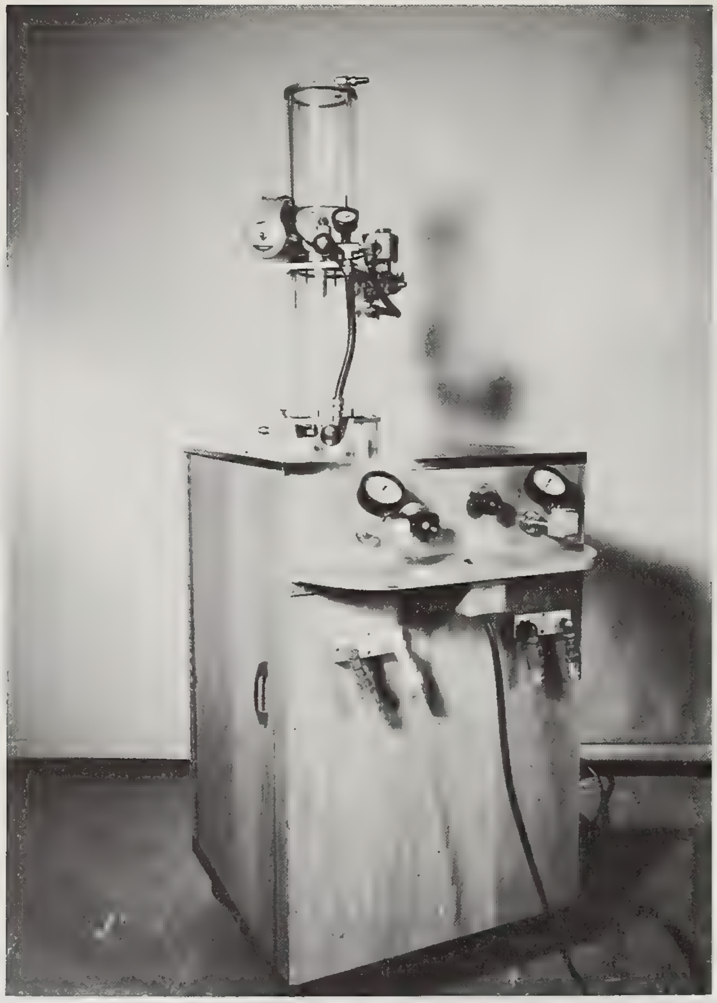

FIGURE 3. THE HYDRAULIC POWER SUPPLY.

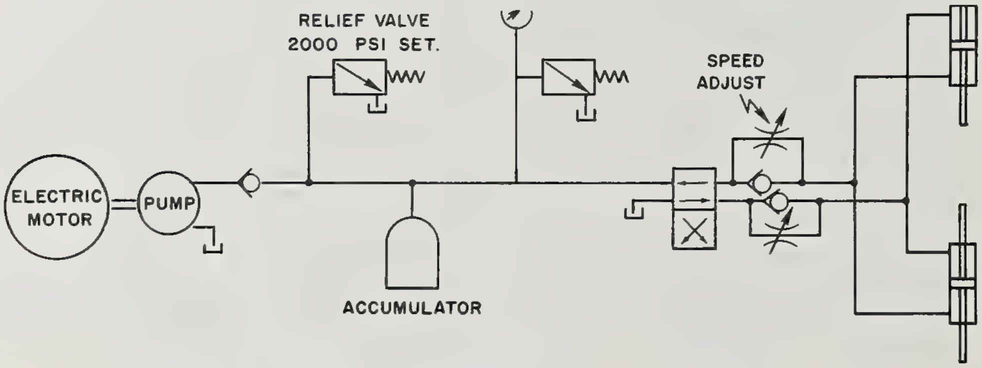

FIGURE 4. SCHEMATIC DIAGRAM OF HYDRAULIC CIRCUITRY.

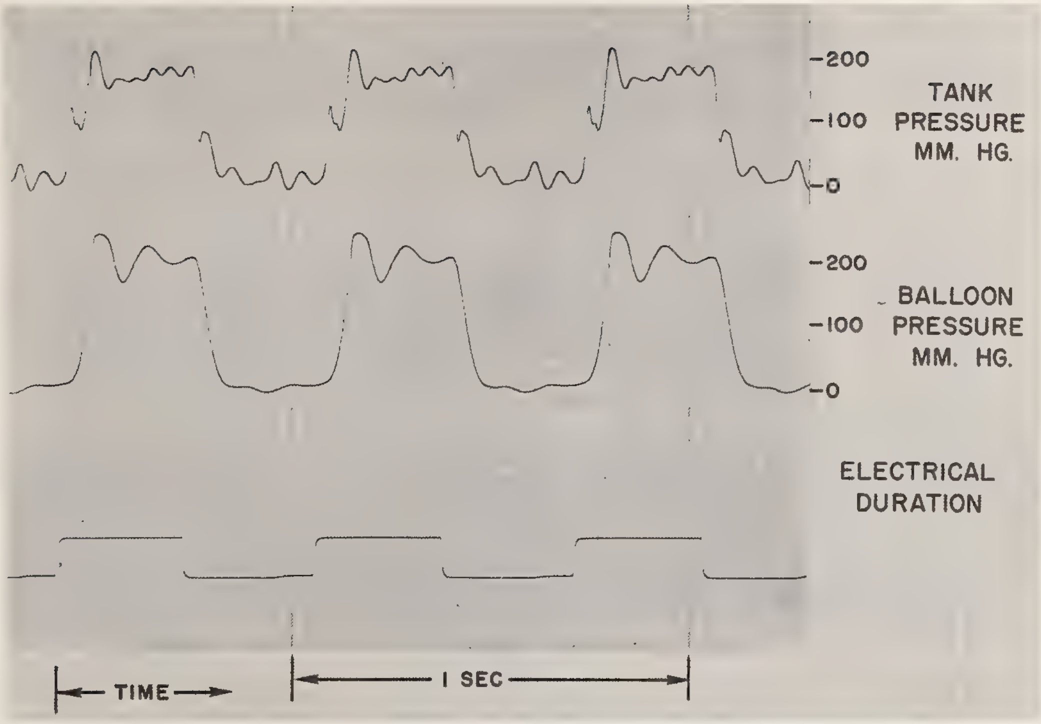

FIGURE 5. IN VITRO STUDY OF PERIPHERAL ACTUATOR.

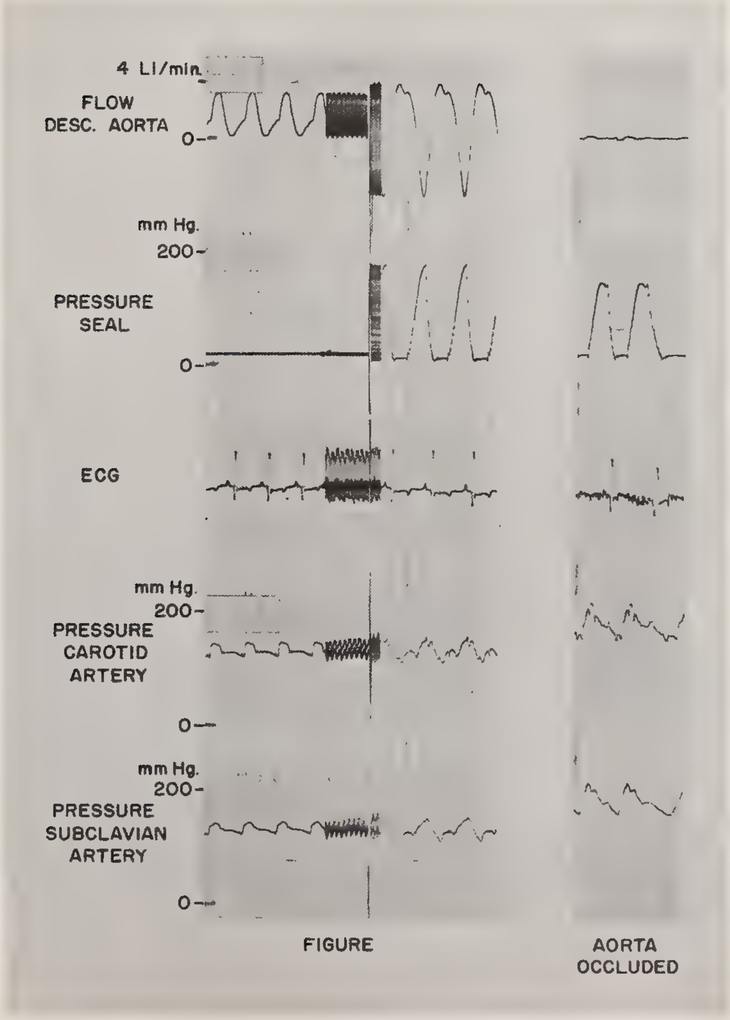

FIGURE 6. IN VIVO TEST CURVES OF PERIPHERAL MODALITY.

The operating characteristics of the system are modified by several damping effects introduced by the hindquarters of the dog. The shape of the inner seal must conform to the body of the animal. This introduces a shape instability and reduces the effective tethering of the inner and outer walls of the seal. At the foot end of the system, the unsupported area of the seal is large. Motion of tissue and the body also increases the damping effect. Despite these damping factors, this system provides sharp pressure pulses at pulse rates in excess of 200 beats/minute.

Physiologic Studies with the Peripheral System.

Under this Contract, 72 acute and 12 chronic studies have been performed using the dog as the experimental animal. These experiments served the following purposes:

1. Test and evaluation of the equipment which has been produced and determination of the optimal mode of operation.
2. Studies of the steady state hemodynamic status in the actuated portion of the vascular bed.
3. Studies of the hemodynamic response of the assisted portion of the vascular bed.
4. Determination of appropriate animal preparations for the future studies of coronary occlusion and left heart failure.

Since the system which has been produced for the peripheral modality is an improved version of a prototype which had been studied for more than two years, little difficulty was encountered in the initial studies. From the outset, excellent hemodynamic results were obtained, motion of the animal was minimal, and the equipment was proved to be dependable and responsive with substantial reserve capacity.

Figure 6 most clearly describes the basic hemodynamic function of this type of circulatory assist. At the left control values of flow in the descending aorta, seal pressure, ECG, and pressure in the carotid artery and subclavian artery are shown from top to bottom. The flow in the descending aorta is unidirectional with a variation from 200 cc/min to 3400 cc/min during the cardiac cycle. The pressure measured at the carotid artery is almost identical to the pressure in the subclavian artery.

The center set of recordings shows the effects of the peripheral modality of external assist on these variables. The peak forward flow in the descending aorta increases and a retrograde flow pulse is seen during the positive pressure pulse in the seal. The peak retrograde flow is coincident with the peak positive pressure in the seal. Inspection of the carotid and subclavian pressure pulses shows them to be substantially the same with a peak diastolic pressure of 150 mm Hg (an increase of 25 mm Hg) and a peak systolic pressure of 125 mm Hg (a decrease of 20 mm Hg). It is significant that although the catheters were approximately at right angles to each other, no measurable difference is seen in the pressure pulse. This indicates that motion artifacts in the pressure measuring system are negligible. Further evidence of this is shown by the series of recordings at the right. A snare was used to occlude the aorta proximal to the electromagnetic flow probe. The flow ceases and the pressure curves show the elimination of the diastolic pulse. The elevated aortic pressure during this period is the result of the increased peripheral resistance.

The forward and retrograde aspects of flow in the descending aorta were integrated and plotted in Figure 7 as a function of peak seal pressure. The forward flow increases from 7.6 cc/pulse to 15.6 cc/pulse while the retrograde flow increases from zero to 7.7 cc/stroke as the seal pressure is increased to 150 mm Hg. The net flow perfusing the hindquarters remains remarkably constant indicating that the pulsating external pressure does not compromise the circulation in the actuated portion of the body. This graph also indicates that the pressure and flow effects of the assist saturate at seal pressures in excess of arterial pressure when the ambient pressure in the seal is held constant.

Figure 8 illustrates the steady state pressure and flow conditions in the venous bed during external assist. When the pressure cathether in the inferior cava is advanced into the legs, the pressure pulse is almost identical to the seal pressure in both magnitude and phase. As the catheter is withdrawn into the abdomen the pressure reflects the lower pressure produced by the system in the abdomen as a result of damping. As the catheter is withdrawn from the system, the pressure drops abruptly to normal venous pressure. Since the flow pulse in the inferior cava is normal, these data indicate that the venous bed is quickly pumped to low volume by the venous pumping effect of the pulsating external pressure. This is consistent with the relatively constant perfusion flow to the hindquarters previously documented. The venous pulse pressure in the system maintains the driving pressure approximately constant.

Figure 9 shows a pressure survey of the arterial system during external pressure assist. The wedged pressure in the femoral artery is similar to the seal pressure. As the catheter is withdrawn, the pressure produced by the external pressure pulse is superimposed on the arterial pressure. The pressure pulse attenuates in the abdominal aorta and changes its phase relationship with the antegrade pulse. In the thoracic aorta the counterpulsated pressure waveform is seen.

The effects of the peripheral modality of external assist in a coronary occulsion preparation are seen in Figure 10. In this preparation, all branches of the left circumflex and anterior descending coronary arteries are serially tied. In many animals the end diastolic pressure in the left ventricule rises to 10-20 mm Hg. During the control periods, the end diastolic pressure in the left ventricle is 20 mm Hg. During external assist, the end diastolic pressure returns to normal and the peak systolic pressure is reduced by 25 mm Hg. The peak diastolic pressure in the aortic arch is increased to 165 mm Hg.

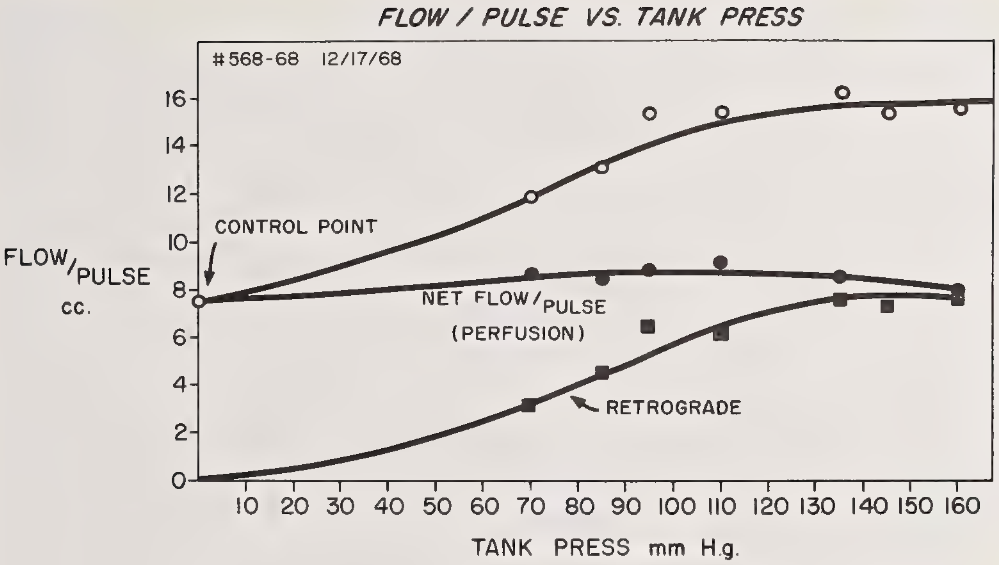

FIGURE 7. ANTEGRADE AND RETROGRADE FLOW VS SEAL PRESSURE.

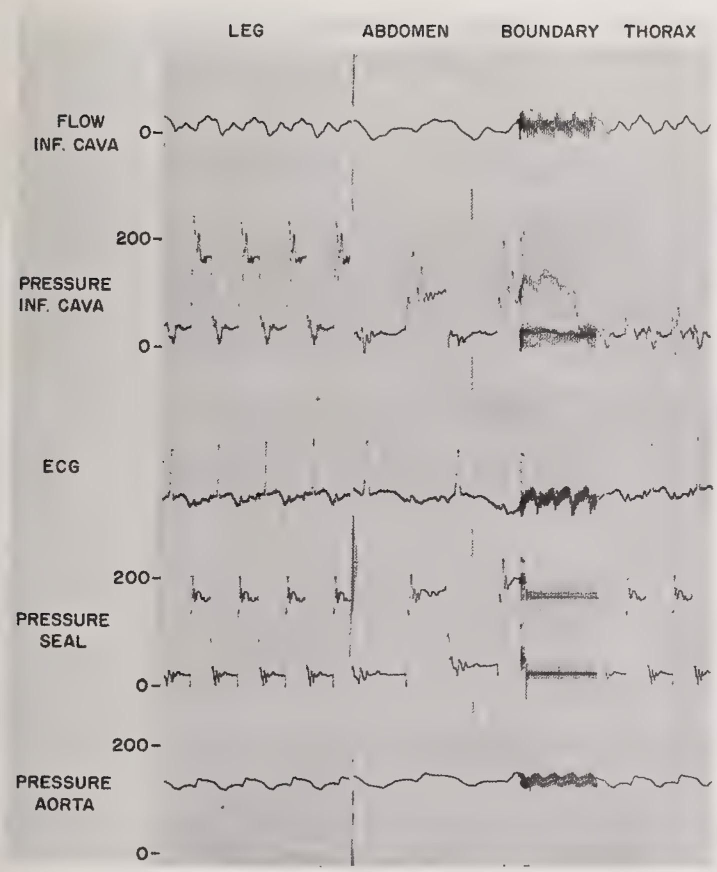

PRESSURE SURVEY OF INFERIOR VENA CAVA

FIGURE 8. SURVEY OF VENOUS BED IN PERIPHERAL SYSTEM.

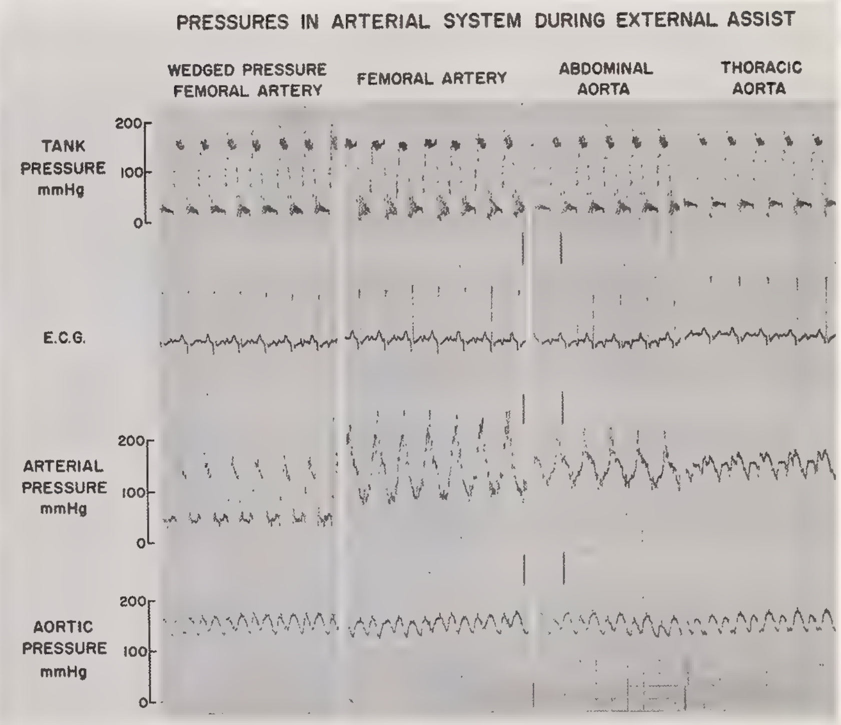

FIGURE 9. SURVEY OF ARTERIAL BED IN PERIPHERAL.

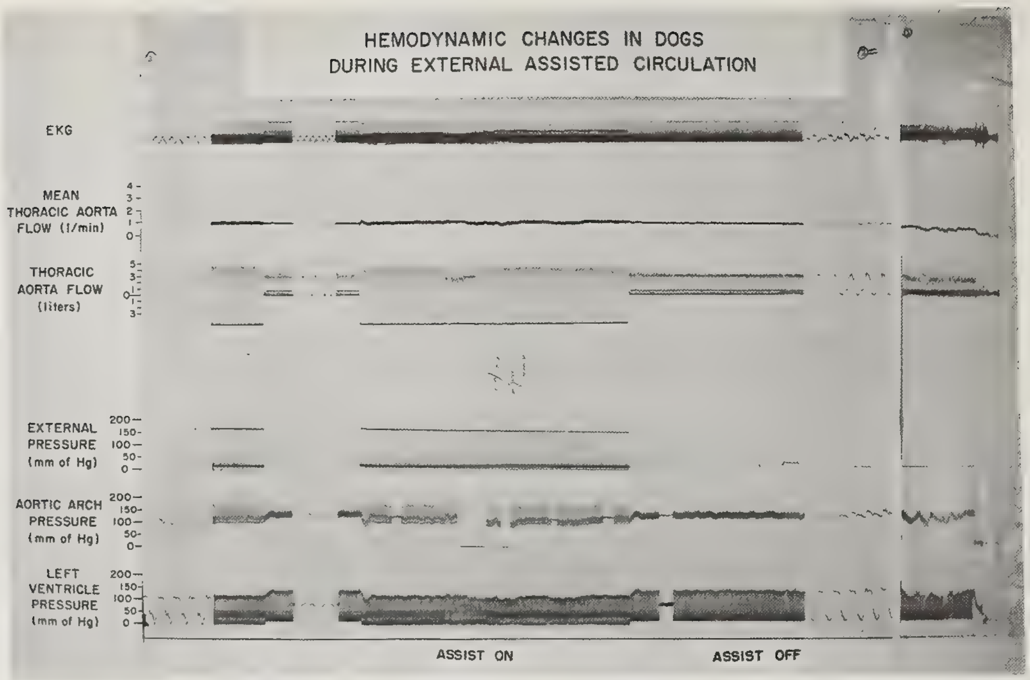

FIGURE 10. EFFECTS OF EXTERNAL ASSIST ON END DIASTOLIC LV PRESSURE.

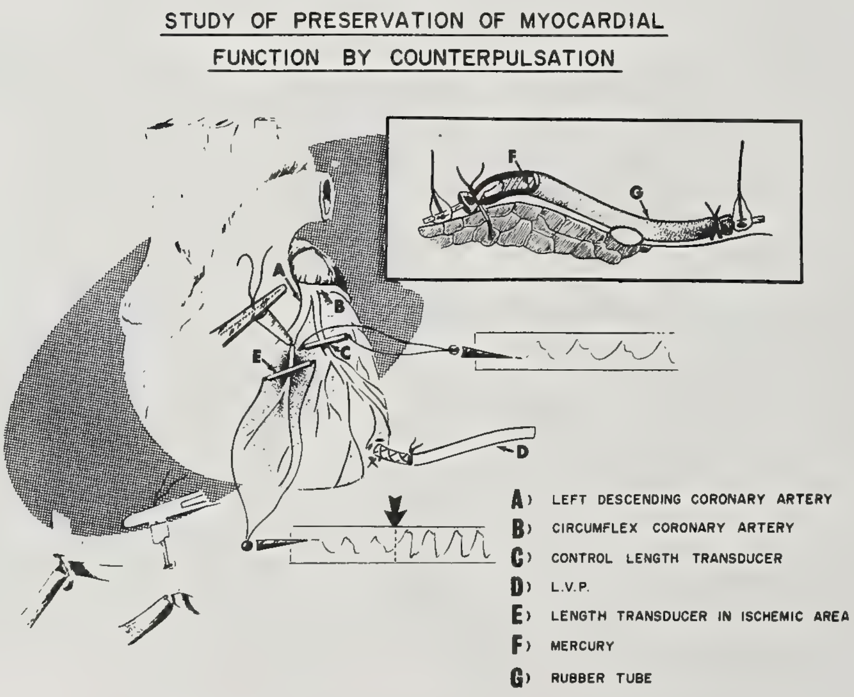
STUDY OF PRESERVATION OF MYOCARDIAL
FUNCTION BY COUNTERPULSATION
A
B
C
D
E
F
G
A) LEFT DESCENDING CORONARY ARTERY
B) CIRCUMFLEX CORONARY ARTERY
C) CONTROL LENGTH TRANSDUCER
D) L.V.P.
E) LENGTH TRANSDUCER IN ISCHEMIC AREA
F) MERCURY
G) RUBBER TUBE

FIGURE 11. DIAGRAM OF STRAIN GAUGES ON LEFT VENTRICLE.

The average hemodynamic results in five experiments are tabulated in Table 2.

TABLE 2

HEMODYNAMIC CHANGES IN DOGS DURING EXTERNAL CIRCULATORY ASSIST

		Before Ligation	After Ligation	During Assistance
[a] Aortic Pressure (mm Hg)	Systolic	138	127	99
	Diastolic	106	95	124
[a] Left Ventricular Pressure (mm Hg)	Systolic	140	130	100
	Diastolic	1	9.8	0.60
[a] Mean Aortic Flow (cc/min)		1,420	1,200	860
[b] Cardiac Output (cc/min)		1,450	1,100	1,400

[a] Average from 5 observations

[b] Average from 2 observations

The control values of the measured variables are shown at the left. After the ligation procedure, the aortic pressure and the mean flow in the descending aorta fell as indicated. The end diastolic pressure in the left ventricle increased to an average of 9.8 mm Hg. At the right the effects of external assist are shown. The aortic systolic pressure was reduced to 99 mm Hg. and the diastolic pressure was increased to 124 mm Hg. The end diastolic pressure in the left ventricle was reduced to normal. The reduced mean flow in the descending aorta reflects the retrograde flow provided by the external assist and does not represent a reduction in cardiac output.

The effects of the counterpulsated waveform on flow to an ischemic area of the myocardium are shown in the following figures. In this preparation shown in Figure 11 mercury-in-rubber strain gauges are sutured to the myocardium; one in an area which will be made ischemic by tying a branch of the anterior descending artery and the other at a position not affected by the tie. The branch artery is tied for a 45-minute period which in 9 control animals (Figure 12) resulted in almost total loss of function (18% return) when the tie is removed. In 9 animals which were counterpulsated during the 45-minute period of occulsion the muscle recovered 80% of its control function as illustrated in Figure 13. Counterpulsation for one hour before the occlusion also resulted in 60% recovery of function. This preparation provides a sensitive indication of the effects of the assist on the perfusion to an occluded area of myocardium.

The Thoracic Modality of External Assist.

The original experiments which we performed in 1965 to study right heart assist by synchronous breathing provided counterpulsation effects in the pulmonary vascular bed to reduce right ventricular pressure. Figure 14 shows the synchronous pulsations in intrathoracic pressure and the effects of phasing on the right ventricular pressure. All pressures are measured with respect to atmospheric pressure. Therefore, the intrathoracic pressure must be subtracted from the right ventricular pressure to determine the actual transmural pressure of the ventricle.

The thoracic modality now under investigation assists the left ventricle by providing a positive intrathoracic pressure during cardiac systole. In the preliminary experiments which were conducted to evaluate the effectiveness of the equipment, diaphragm motion damped the positive pressure pulses which were created in the thorax. Restriction of the abdomen by a non-distensible vest reduced the damping effect of the diaphragm and made possible intrathoracic pressure pulses with peak values from 15-40 mm Hg at an elevated mean pressure.

Figure 15 describes the effects on flow in the carotid artery, aortic pressure and intrathoracic pressure. At the left, the control values are shown. The center set of recordings documents intrathoracic pressure pulsations with a peak value of 45 mm Hg synchronous and in phase with every heart beat. The peak flow in the carotid artery increased by 25% with no change in mean flow. The transmural pressure in the left ventricle (aortic systolic pressure-intrathoracic pressure) was reduced. The recordings at the right show the effects with positive intrathoracic pressure pulses produced with every other beat. The peak carotid flow with the assisted beat is increased by 100% and the aortic peak systolic pressure is increased by 25 mm Hg while the transmural pressure of the left ventricle is reduced. These results support the concept of the thoracic modality and illustrate the possible limitation which coupling through the diaphragm may impose.

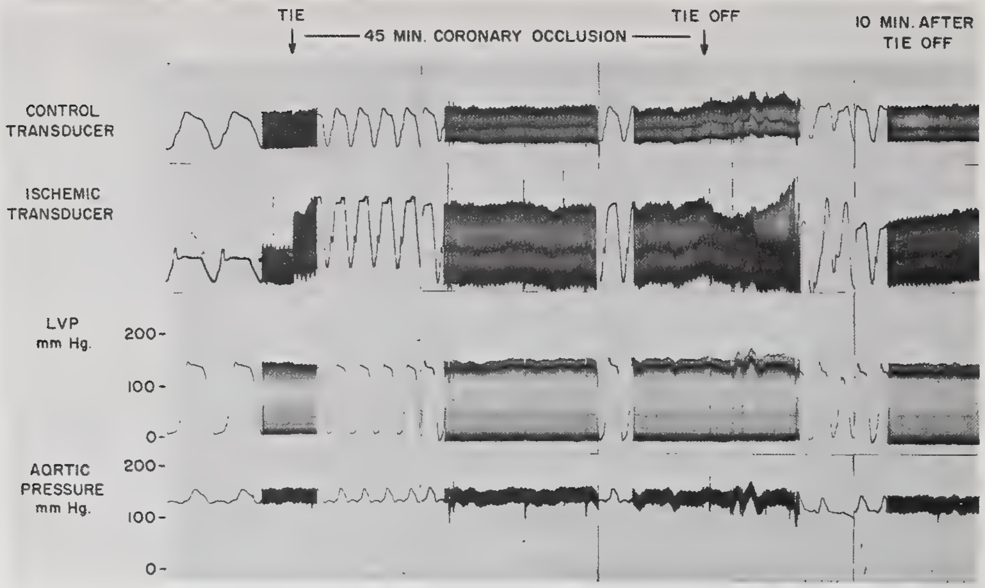

FIGURE 12. CONTROL STUDY OF 45 MINUTE OCCLUSION.

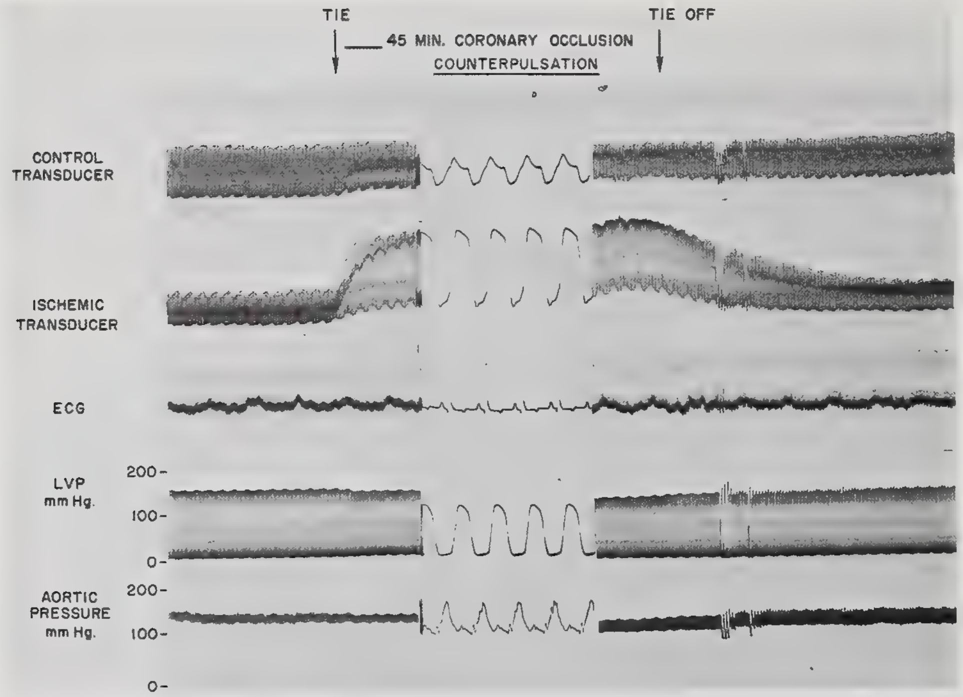

FIGURE 13. THE PLASMA SAMPLES IN THE FIRST
4 GELS WERE OBTAINED IN L)

DISCUSSION

DR. GREENFIELD: We have been concerned in the past with the use of unphysiologic pressure in the lung. I was wondering whether or not the lungs were examined, and whether or not they showed any damaging effects from the excessively high intrathoracic pressure?

MR. BIRTWELL: We have not seen any such effects, although I cannot say that complete pathologic studies have been made. I think the important thing to note here is that although the intrathoracic pressure may be high, this does not necessarily indicate any high transmural pressure across the capillaries of the lung. The capillary pressure is increased too. In other words, we have a situation here similar to that which one might find in a hyperbaric chamber, in which the patient may be at three atmospheres but this in no way affects the cardiovascular system.

DR. ROSENSWEIG: I would like to commend the authors on what I think is probably the most exciting contribution to this field since Dr. Harken and Birtwell initially proposed counterpulsation in 1958. I would like to ask two questions. Firstly, have you monitored your right atrial or pulmonary artery pressures in these experiments to see whether there is any rise that might be hazardous or which might precipitate pulmonary edema in these animals. Secondly, in your clinical applications have you been able to achieve the diastolic augmentation effect that you have demonstrated here in animals?

MR. BIRTWELL: I will try to answer your first question. As you might suspect, making physiologic measurements under these circumstances is rather difficult and one has to be very careful about motion effects on pressure sensing catheters and equally careful about the effects of the pulsating pressure on, for instance, electromagnetic flowmeter probes, whose function is dependent on a rather good contact between the probe and the artery. We have used several systems, including catheter assist transducers and so forth, and I must admit that even today we are not happy with our measurements. Nevertheless, the indications are as we showed. The figure, I think, to which you are referring was a figure that was done a long time ago when we were investigating synchronous breathing; and our preoccupation now is not with the effects on the right ventricle, but rather the effects on the left ventricle. We are trying to increase the driving pressure so that we can more effectively assist a patient who is in profound shock. Does that answer your first question?

DR. ROSENSWEIG: No, I was really thinking in terms of enhancement of venous return, whether this might precipate failure.

MR. BIRTWELL: You are probably referring to the last slide. In that slide, we showed every other slow pulse in the carotid artery to be increased. But rather, we intended to show that there was no increase in mean flow. One would suspect then that this means that every other pulse was increased and every other one decreased. We have also seen this in the descending aorta. We have tried another approach to substantiate the fact that the normal probes, the extravascular probes, were giving a good indication. You are absolutely right. Many of these effects may be caused by pulsating changes in the venous return. And we cannot say, at this time, the extent to which this occurs. It is interesting, however, that the increased flow comes with the increased aortic pressure pulse. And in order to guess what we are seeing would imply that the venous return is to be restricted during that beat so that the filling pressure for the next beat is less, causing a smaller flow in every other unassisted beat. I cannot really answer your question. I can answer your second question with regard to our ability to provide diastolic augmentation in the face of shock under clinical circumstances. The answer is that we can. In the patients we have done so far, who have been in profound shock, we have almost invariably elevated the diastolic pressure to above systole. We have seen increases in mean pressure, and we have seen evidences of increase in cardiac output. I never attempted to measure it under the circumstances.

DR. KENNEDY: I, too, would like to commend Mr. Birtwell and his associates for what, in theory, should be a widely applicable method of assisted circulation. Would it be possible for you to clarify for the audience the figure in which vena caval pressures were recorded along the margin and in which high transients, presumably from inferior vena cava, were recorded as high as 160 mm Hg? In theory, this might not be very good for hepatic function.

MR. BIRTWELL: Because of the valving in the venous bed, we have always suspected that very quickly after a pulse or two, the venous bed is pumped essentially dry. We wanted to document this by measuring the pressure in the various portions of the vena cava. As you can see in the slide, the flow in the inferior vena cava is not remarkably pulsatile (Slide). As we were creating very high pressure pulses, which were represented as an impedance drop in the inferior cava, quite obviously we had tremendous slow pulses. Therefore, the pressure in the inferior cava, as reflected in the leg, represents a collapsed vessel which is functioning very much like the waterfall effect in many of the other portions of the vascular bed when the extramural pressure is of the same order of magnitude as the intramural pressure. Therefore, the increase in the venous pressure is essentially the same in that part of the system as the increase in the arterial pressure. This causes no increase in the driving pressure and the flow through the assisted portion of the body remains essentially constant. Now, as we withdraw the catheter from that position in the limb to the abdomen, we see the pressure decreasing, and one might interpret that as an impedance pressure drop in the inferior cava. However, when you look at the flow pulse, you can see that this is not true. We have also measured the pressure in the abdomen, the extravascular pressure, and found that to be decreased in a similar fashion. So that the pressure pulse simply gives you an indication of the pressure in the belly of the animal. Now the most important thing is to look at the boundary. If this pressure drop from the assisted portion to the unassisted portion were an impedance drop, it could not drop from better than 100 mm Hg to normal values in a matter of moving the catheter an inch. Therefore, it is reasonably obvious that the venous vascular bed in the system is operating in a collapsed state and that we can obtain pressures in it of the same order of magnitude as the system pressures because the venous bed is acting like a tambour and this in no way causes a large pressure pulse in the assisted portion of the venous bed.

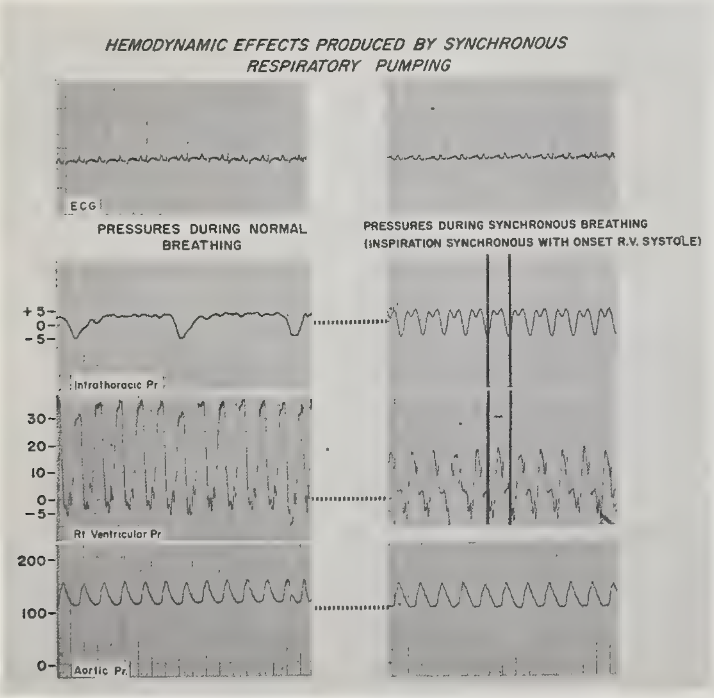

FIGURE 14.

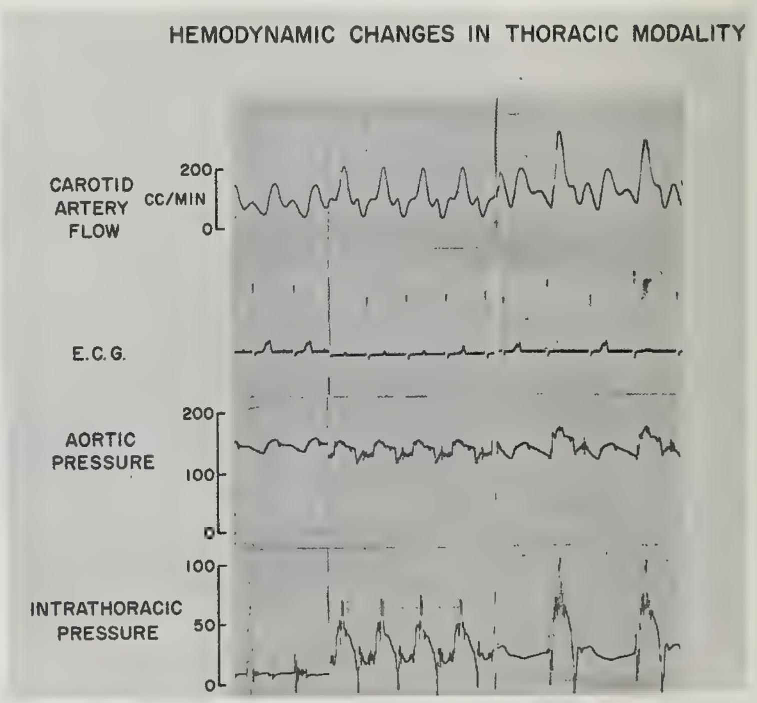

FIGURE 15.

CHAPTER 43

SEQUENCED EXTERNAL PULSATION IN THE THERAPY OF CARDIOGENIC SHOCK

L. Cohen, D. Porterfield, J. Mitchell, and C. Mullins

University of Texas
Southwestern Medical School
at Dallas
Dallas, Texas
and
Hamilton Standard Division of United Aircraft Corporation
Farmington, Connecticut

Cardiogenic shock is the cause of death in over 100,000 individuals each year. A variety of ventricular assist devices has been used in the therapy of cardiogenic shock but cannulation of one or more major vessels is usually necessary. Although external pulsation is not a new concept, the sequenced application of external pressure is anticipated to provide increased diastolic augmentation due to increased diastolic return of blood to the central circulation. A series of bladder cuffs placed on the arms and legs is inflated and deflated rapidly by a pneumatic pressure system utilizing solenoid valves phased with the electrocardiographic signal. The cuff bladders are inflated during early diastole in a sequential manner starting distally on each extremity. Arterial blood from the extremities is returned to the central circulation causing an augmentation to central aortic pressure and possibly in coronary arterial filling. At the onset of each ventricular systole the cuffs are rapidly deflated so that resistance in the periphery is lessened, thereby decreasing the after load against which the left ventricle must pump. The animal phase of the program utilizes baboons (sp. Papio papio) as the anatomy of these primates resembles that of man. During right and left heart catheterization, intracardiac pressure, cardiac output, coronary flow and cineangiographic ventricular volumes are measured in a controlled state and with Sequenced Pulsation. In 4 baboon experiments to date, Sequenced Pulsation has led to diastolic augmentation in 2 animals. The next laboratory phase of the program will be with animals in cardiogenic shock. Upon completion of the animal phase, the assist device will be applied to human subjects during catheterization, then to patients in cardiogenic shock.

INTRODUCTION

The 100,000 annual deaths in the United States which can be attributed to the 60 to 80 percent mortality rate in cardiogenic shock patients clearly indicate a requirement for more effective therapy than is now available for application.

For the past year, Hamilton Standard and our sub-contractor, Southwestern Medical School, have been engaged in a program designed to evaluate a cardiac assist technique known as Sequenced Pulsation which may well help to fill this need. Initial goals set for the first year of the program were:

1. The design and fabrication of an electro-mechanical system for application of sequenced pulsation to baboon and human subjects, and;
2. Physiological evaluation of the technique with
   a. Normal baboons
   b. Baboons in cardiogenic shock, and subject to prior NHI approval:
   c. Human volunteers undergoing routine cardiac catheterization.

During the past eleven months a complete sequenced pulsation system with facilities for application to baboons and humans has been designed, developed and fabricated. Over the past four months at Southwestern Medical School a total of eleven (11) experiments have been performed with baboons as test subjects. No human evaluation has been attempted to date.

Among the most promising new techniques for supporting the failing circulatory system are those which employ the principle of synchronous counterpulsation. Each of these techniques involves the reduction of systolic pressure and the increase of diastolic pressure in the aorta in order to decrease the work of the left ventricle while maintaining or increasing mean pressure and coronary perfusion.

Arterio-arterial counterpulsation removes blood from the arterial tree during cardiac systole and returns it during diastole.

Veno-arterial counterpulsation removes both venous and arterial blood during systole and returns it to the arterial tree during diastole.

Aortic balloon counterpulsation does not remove blood from the body but manipulates pressure in the aorta by controlled inflation and deflation of an intra-aortic balloon. In each of these methods, minor surgery is required for placement of catheters and the blood is brought into contact with the foreign material which constitute the pumping mechanism.

In an attempt to provide the benefits of counterpulsation without requiring surgery or exposure of blood to any foreign materials, several investigators have investigated various methods of applying synchronous external pressures to the limbs in order to manipulate circulatory pressures and obtain counterpulsation.

The Sequenced Pulsation technique for external counterpulsation provides two significant features which have not been previously investigated:

1. Each limb is divided into several zones, the pressure pulse applied to each zone being individually controlled as to timing and amplitude. This makes possible a programmed limb "milking" action which is expected to result in maximum blood volume manipulation by the pumping device.
2. The torso, head, and airway are subjected to a controlled constant positive pressure. This should permit control of central venous pressure and augments flow of arterial blood to the limbs during cardiac systole. (It is important at this point to understand that while increased torso and airway pressure increases aortic pressure referenced to the atmosphere, it should have no effect upon the pressure differential across the ventricles and thus no direct effect upon cardiac work.) By application of constant positive pressure to the torso and airway we should achieve an effect equivalent to application of negative pressures to the limbs during cardiac systole.

ENGINEERING ASPECTS

In order to evaluate the sequenced pulsation technique, it has been necessary to design and build a system which includes the following provisions:

1. A suit device for application of individual pressures to nine limb zones and a head and torso chamber for use with baboon and human subjects.
2. A pneumatic source for providing power to the suit device.
3. A control system to provide:
    a. Individual zone pressure pulse sequence timing controls based upon the subject's EKG signal.
    b. Individual zone pressure pulse amplitude and duration control.
    c. Head and torso chamber pressure and air flow rate control.

Through the course of the sequenced pulsation program, we have considered the electro-mechanical system to be a research tool and not as an end item for general clinical use. Consequently, the design has emphasized flexibility, versatility, functional performance and minimum development costs.

Sequenced Pulsation System.

The block diagram in Figure 1 shows the physical components which comprise the system. The sequenced pulsation suit is the key item with its head and torso chamber and multiple limb cuffs. The baboon suit is shown here with five arm zones and four leg zones. (The human suit configuration is slightly different, having four arm and five leg zones because of the difference in limb length.) Each limb zone is individually pressurized so that pressures can be applied in any desired sequence. The normal pumping sequence, of course, involves pressurizing from the distal to proximal zones. Air flows to the suit are provided by the pneumatic console which, in turn, is controlled by the electronic control module. Air for the head and torso pressurization is provided by a system contained in the pneumatic console. Pressure and vacuum pumps which provide the motive force for inflation and deflation of the limb cuffs are the remaining system components.

The suit is composed of a head and torso chamber with a zipper closure which permits rapid access to the head and thorax. A plastic faceplate permits observation of the subject during operation of the system. Limb penetration seals consist of doubled folds of sheet rubber which automatically inflate when torso pressure is applied. The chamber itself is fabricated from flexible laminated nylon-latex material. It is designed for a working pressure of 100 mm Hg.

The limb cuffs are designed around standard blood pressure cuff bladders. The cuffs themselves are fabricated of nylon material with adjustable fasteners for maximum flexibility in application. The cuffs were conservatively designed for a working pressure of 200 mm Hg and have been successfully operated at 500 mm Hg in the course of the physiological evaluation program. Two complete suits have been designed and fabricated; one sized for a 55 pound baboon and one for a 160 pound human male.

Sequenced Pulsation Electronic Control. The basic element of any counterpulsation system is the device which permits precise timing control of the applied pumping action. Figure 2 shows a block diagram of the electronic module which provides this control function for the Sequenced Pulsation System. This controller utilizes the electrocardiogram (EKG) signal as a basic timing reference and provides individually controlled solenoid valve driving signals for each of the nine limb zones. The EKG signal is amplified and fed to the EKG trigger circuit which generates a pulse upon detection of the steepest negative slope in the EKG signal. In practically all normal and abnormal EKG signals this trigger pulse will occur at a point in the RS interval of the QRS complex.

The trigger circuit output pulse is fed to a period analog generator which generates and stores for one cycle an output voltage analog of the duration of each cardiac cycle. Each trigger pulse also fires a ramp generator which provides an output which at any instant is an analog of the time elapsed since the initiation of the current cardiac cycle. A voltage divider on the output of the period analog generator permits adjustment of that signal to any desired fraction of the cardiac period analog.

SEQUENCED PULSATION SYSTEM

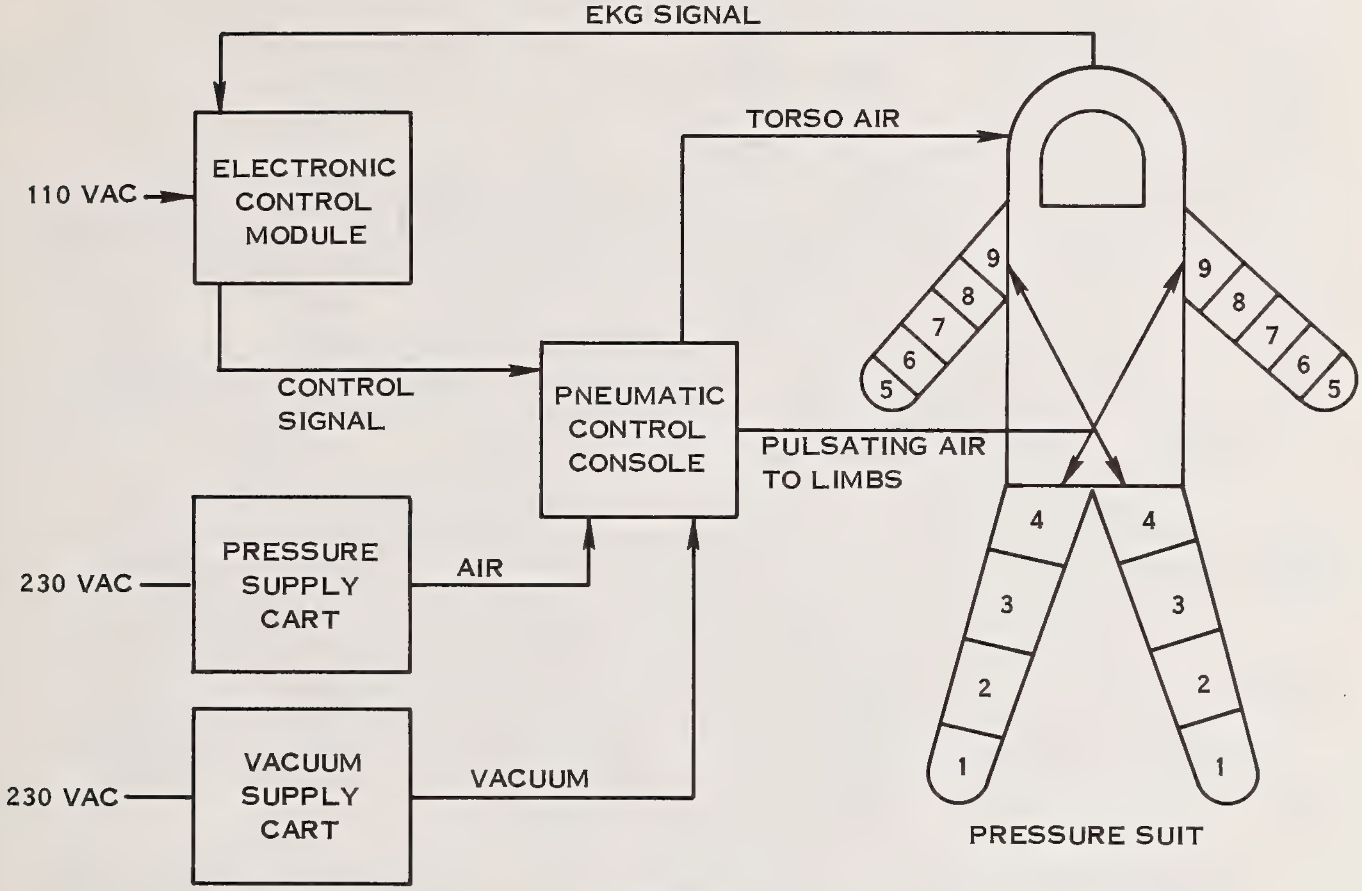

FIGURE 1

SEQUENCED PULSATION ELECTRONIC CONTROL (SINGLE CHANNEL SHOWN)

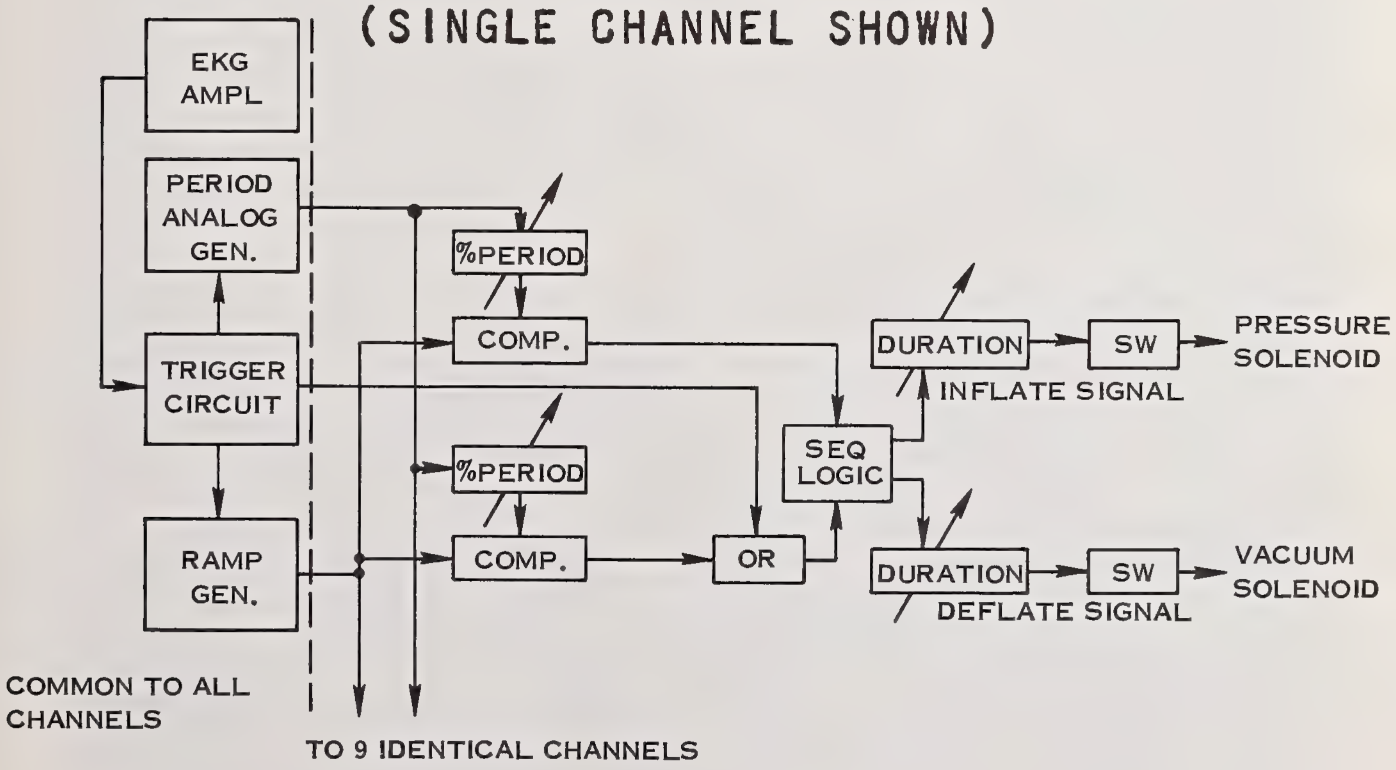

FIGURE 2

A comparator circuit produces an output pulse when the ramp generator signal is equal to the output of the period analog generator voltage divider. Thus the comparator circuit can be made to fire after the elapse of any desired fraction of the cardiac cycle. One such comparator circuit is provided for each zone inflation control solenoid and one for each zone deflation control solenoid. This permits the inflation and deflation time of each limb zone to be independently controlled. At the output of each comparator circuit is a pulse duration control circuit which determines the length of time which each solenoid valve remains open during each cycle. This feature permits accurate control of zone pressure in the range of 50-500 mm Hg while using relatively high (1,500 mm Hg) operating pressures to achieve rapid filling of the pressure cuffs. The outputs of the pulse duration controls actuate reed relay circuits to drive the solenoid valves in the pneumatic controller. The controller provides four adjustments for each limb zone: Inflate delay, Inflate end pressure, Deflate delay, Deflate end pressure. A pressure monitoring circuit not shown in this figure is provided for displaying and recording zone sequence and pressure pulse form in any suit during sequenced pulsation.

Sequenced Pulsation Pneumatic Control. Figure 3 shows the basic components of the pneumatic control console. Pressure and vacuum lines from the carts supply the pressure and vacuum manifolds which in turn supply the solenoid valves for each zone. A regulator valve provides control of the manifold pressure which in turn affects zone filling time. The deflate solenoids are normally open and the inflate solenoids are normally closed so that limb pressures are automatically removed in case of a power failure.

A vane type air pump located in the pneumatic console provides filtered air to the torso chamber at adjustable flow rates up to 6.5 cubic feet per minute as required for respiration and removal of metabolic heat. Torso air temperature and flow rate are displayed on the controller panel.

Figure 4 shows the essential components of the system: The baboon suit is shown with its head and torso section and limb zones assembled. The pneumatic control console forms the base of this assembly and the electronic controller with its four individual control knobs for each zone in the upper unit. Not shown are two portable units containing the pressure and vacuum pumps.

The equipment described above was installed at Southwestern Medical School at Dallas in February of this year eight months after receipt of contract. Since that time Dr. Lawrence Cohen and his associates have carried out a physiological evaluation program which is discussed below.

PHYSIOLOGICAL EVALUATION

The primary goals of a cardiac assist device are twofold. Since myocardial oxygen requirements are closely related to the tension developed by the myocardium in systole, a cardiac assist device should diminish the external work of the heart by reducing the afterload of the left ventricle. Secondly, since approximately 70% of the coronary flow occurs during diastole, the assist device should augment central aortic diastolic pressure, thereby augmenting filling of the coronary arteries.

In 1961, Clauss, Birtwell, Harken, et al[1] reported on a counterpulsation device which involved cannulation of the femoral arteries. By synchronization with the electrocardiogram, the pump aspirated blood from the femoral arteries during cardiac systole and returned blood to the central circulation during diastole. Soroff, et al[2], using synchronized counterpulsation in dogs, noted that the mean systolic pressure was lowered by approximately 40 mm Hg, and the tension time index by 39%. Coronary blood flow rose by an average of 50%, and the average reduction in myocardial oxygen consumption was 22%. Jacobey, et al[3,4], in a canine preparation in which cardiogenic shock was caused by injection of microspheres into the coronary circulation, demonstrated an improvement in survival from 30% to 70% in animals counterpulsed for two hours.

Arterial to arterial counterpulsation involves a surgical procedure in order to isolate the femoral arteries. The need for sterile technique generally necessitates that the procedure be carried out in an operating room. The critically ill patient often must be moved to the sterile hospital area, thereby experiencing a delay before counterpulsation can be initiated. In addition, since the counterpulsator is an extracorporeal pump, anticoagulants must be utilized in order to prevent fibrin and clot from forming in the device. Hemolysis of red blood cell elements is a frequent concomitant of prolonged patient assist. Anesthesia may be necessary during the surgical procedure. For these reasons, it would be desirable if a totally external cardiac assist device could be developed.

Dennis[5], Osborne[6], Soroff[7] and their respective co-workers have investigated external sleeves, pressure suits, and chambers utilized for counterpulsation. Although favorable hemodynamic results have been achieved in animals, these external assist devices have not yet had sufficient clinical use to judge their efficacy.

One of the potential limitations of an external pressure cardiac assist device is the possibility of large proximal vessels in the extremities undergoing compression before smaller, more distal vessels. Return of blood to the central circulation during diastole might thereby be inhibited. The concept of sequential pulsation directs itself toward avoiding proximal occlusion of extremity vessels. A series of bladder cuffs placed on the arms and legs are inflated and deflated rapidly through a pneumatic pressure system utilizing solenoid valves phased with the electrocardiographic signal. The bladder cuffs are inflated at beginning diastole in a sequential manner, starting

SEQUENCED PULSATION PNEUMATIC CONTROL

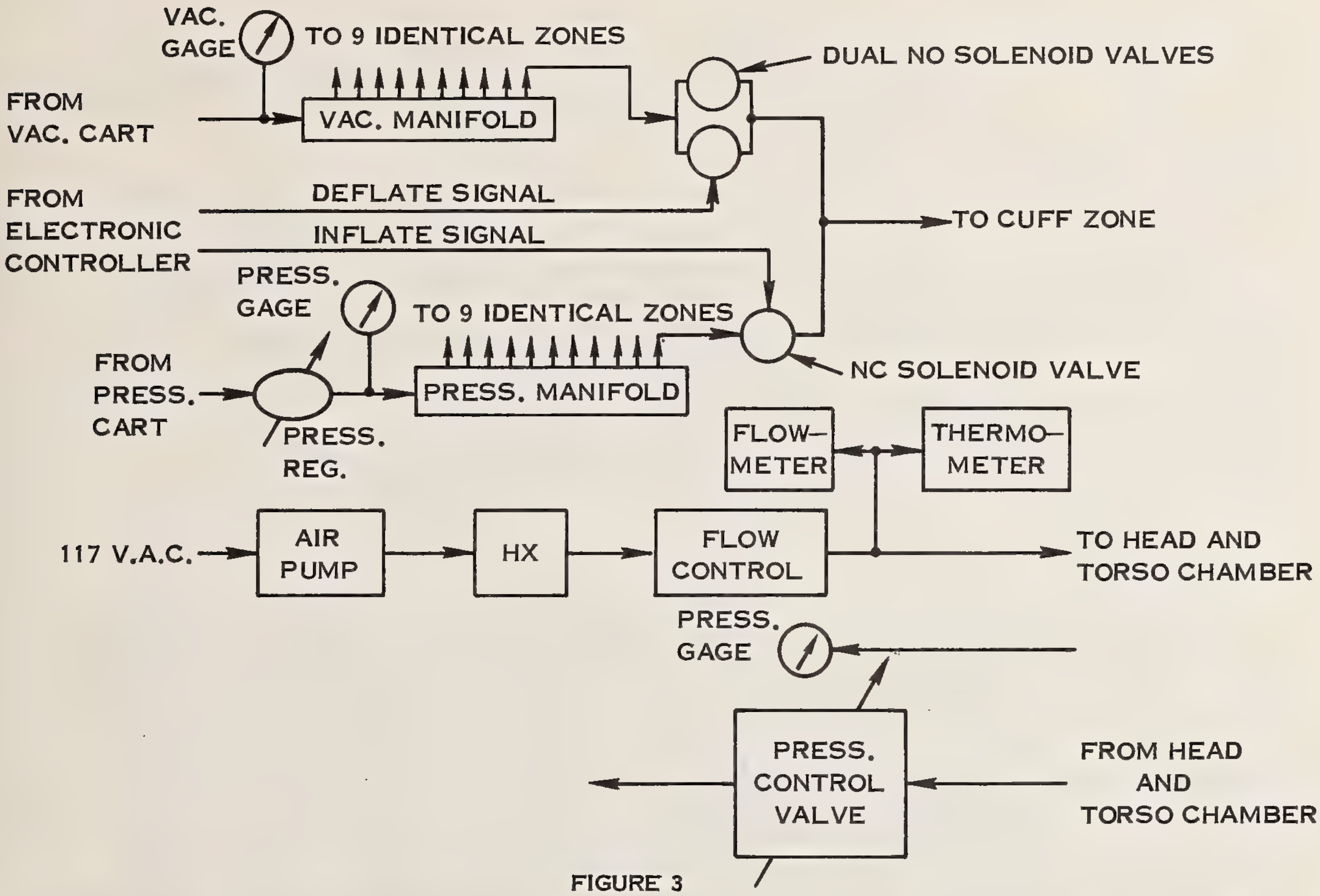

FIGURE 3

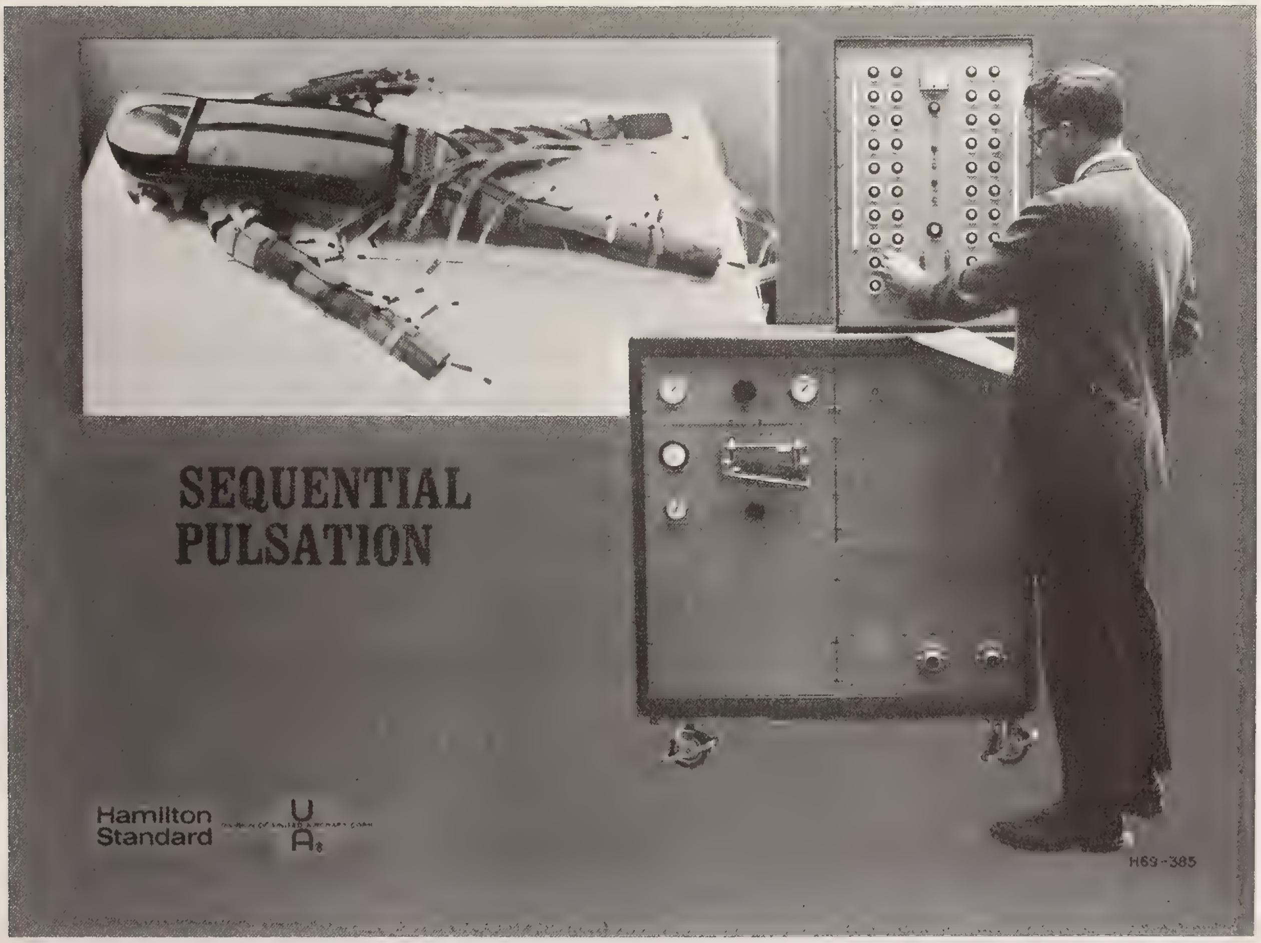

FIGURE 4

distally on each extremity. At the onset of ventricular systole, the cuffs are rapidly deflated, so that resistance in the periphery is lessened, thereby decreasing the afterload against which the left ventricle must pump. The central torso is exposed to constant pressure of between one and two pounds per square inch.

Experimental Results.

The animal phase of the program utilizes baboons (sp. Papio papio) as the anatomy of these primates resembles the anatomy of man.

Figure 5. In six of eleven experiments, it was possible to obtain physiologic measurements. Cardiac output rose between 5% and 50%, with an average rise of 25% during sequenced pulsation.

Two examples of the change in arterial pressure wave form are seen in the next Figures, and are representative of six of the ten experiments performed. (Figures 6 and 7) The control state appears on the left, and the arterial wave form during sequenced pulsation appears on the right. In each instance, (Figure 8), the area under the systolic part of the curve fell between 7% and 60%, with an average fall of 34%. There was an augmentation in the diastolic area of the arterial pressure pulse ranging from 5% to 70%, with an average of 26%.

Figure 9. The ratio of diastolic area of arterial pressure pulse to systolic area of the arterial pressure pulse was compared at control, and with sequenced pulsation. The diastolic to systolic area ratio averaged 0.47 at control, and rose to 0.97 during sequenced pulsation.

SUMMARY

In summary, during the last year a flexible sequenced pulsation system has been designed and fabricated. Using this equipment, cardiac output and diastolic augmentation data have been obtained in normal baboon experiments. These data indicate that the technique does produce increased cardiac output and diastolic pressure augmentation. As a result of this year's activity and evaluation, we recommend that the present system be modified to make it more convenient for clinical use. The human suit should be redesigned for ease of application to catheterized human subjects and fabricated in two sizes to increase the number of potential recipients. The physical size and the noise generated by the pneumatic power supply units should be reduced so that the system will be more acceptable in a hospital patient area rather than being confined to the laboratory.

The physiological evaluation program should include extended testing of animals with myocardial infarctions and in cardiogenic shock. Sequenced pulsation should be evaluated on human volunteers undergoing routine cardiac catheterization and lastly on patients in cardiogenic shock. The end product should be a conclusion as to the merits of sequenced pulsation as a cardiac assist technique for relief of cardiogenic shock in humans.

REFERENCES

1. Clauss, R. H., Birtwell, W. C., Albertal, G., Lunzer, S., Taylor, W. J., Fosberg, A. F., and Harken, D. E.: Assisted Circulation I: The arterial counterpulsator. J. Thoracic Cardiovasc. Surg., 41:447, 1961.
2. Soroff, H. S., Levine, H. J., Sachs, B. F., Birtwell, W. C., and Deterling, R. A. Jr.: Assisted Circulation II: Effects of counterpulsation on left ventricular oxygen consumption and hemodynamics. Circulation, 27:722-31, 1963.
3. Jacobey, J. A., Taylor, W. J., Smith, G. T., Gorlin, R., and Harken, D. E.: A New Therapeutic Approach to Acute Coronary Occlusion, I. Production of standardized coronary occlusion with microspheres. Am. J. Cardiol., 9:60, 1962.
4. Jacobey, J. A., Taylor, W. J., Smith, G. T., Gorlin, R., and Harken, D. E.: A New Therapeutic Approach to Acute Coronary Occlusion, II. Opening dormant coronary collateral channels by counterpulsation. Am. J. Cardiol., II:218, 1963.
5. Dennis, C., et al: Studies on External Counterpulsation as Potential Measure for Acute Left Heart Failure. Tr. Am. Soc. Artif. Int. Organs, 9:186, 1963.
6. Osborn, J. J., Main, F. B., and Gerbode, F. L.: Circulatory Support by Leg or Airway Pulses in Experimental Mitral Insufficiency. Circulation, 28:781, 1963.
7. Soroff, H. S., Birtwell, W. C., Giron, F., Collins, J. A., and Deterling, R. A. Jr.: Support of Systemic Circulation and Left Ventricular Assist by Synchronous Pulsation of Extramural Pressure. S. Forium, 16:148, 1965.

DISCUSSION

DR. SOROFF: I believe that the addition of this concept of sequenced pulsation is a very interesting one and potentially a useful one. However, it is quite apparent that the amount of equipment required is extremely complicated. Since the whole concept is based on the hypothesis that the large vessels, being compressed, may trap blood in the smaller vessels, I wonder what evidence we have for this. In other words, have you assisted animals or will you assist animals with sequenced pulsation versus the pulsation applied simultaneously?

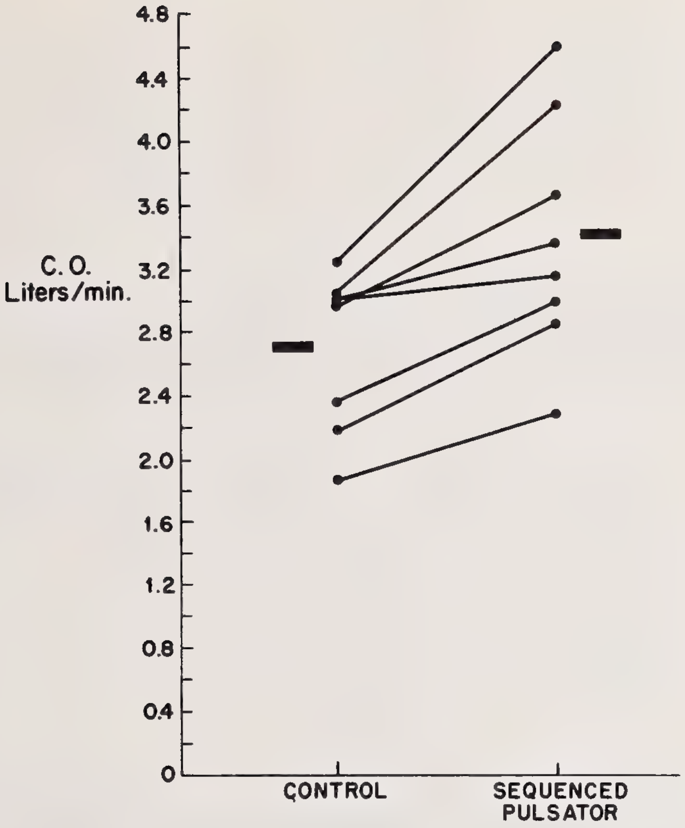

FIGURE 5. CARDIAC OUTPUT DURING SEQUENCED PULSATION.

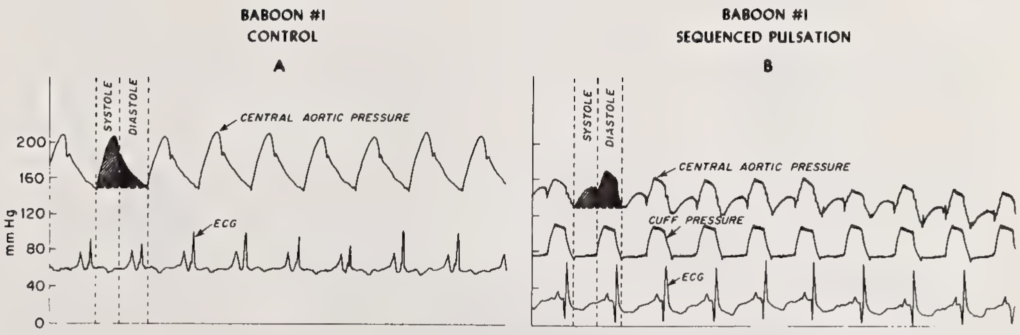

FIGURE 6. CHANGE IN ARTERIAL PRESSURE WAVE FORM.

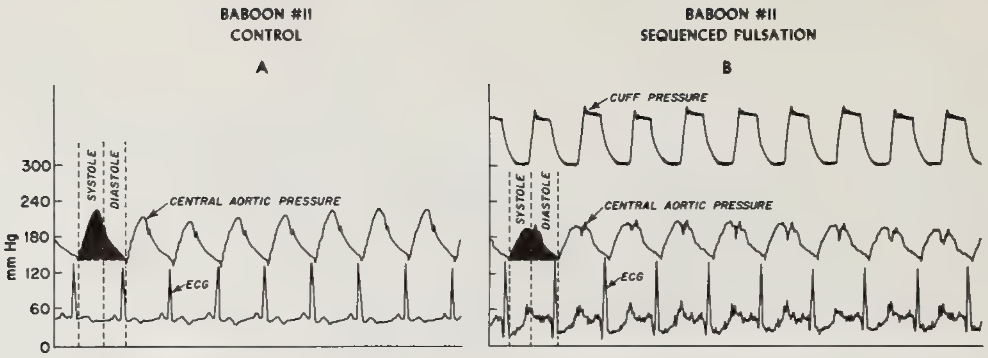

FIGURE 7. CHANGE IN ARTERIAL PRESSURE WAVE FORM.

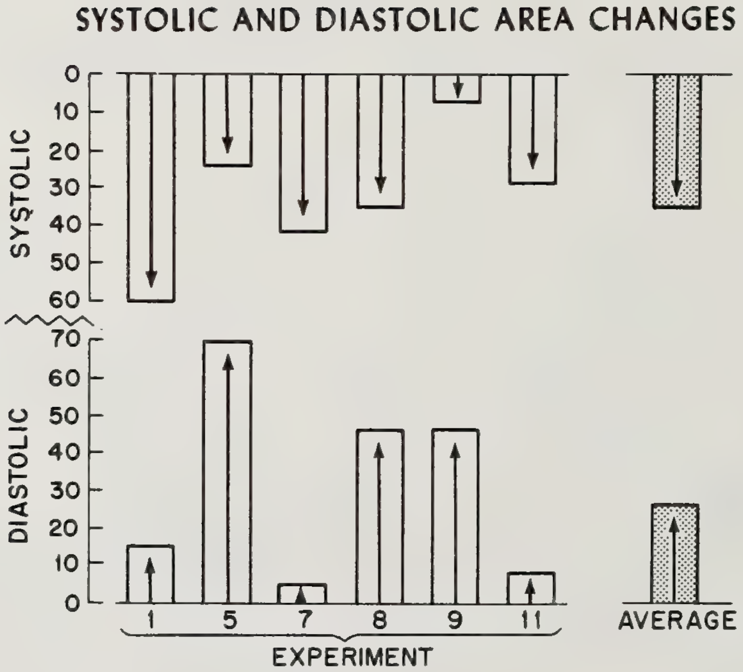

FIGURE 8.

DR. COHEN: That is a very good question and the point is very well taken. The considerations at this time are solely theoretical. Yet, in the next phase of the program, we anticipate using intravascular flow meters and testing pulsation in both the sequenced and simultaneous mode. Because of the flexibility of the sequenced pulsator, regardless of its timing potential, we will be able to apply sequenced or alternatively simultaneous pressures to the extremities. That aspect of this theoretical consideration will be looked at.

DR. FEOLA: In evaluating the performance of the assist device, it seems a good deal depends upon the physiological state of the experimental animal, i.e., whether the animal is a normal animal or in experimental cardiogenic shock. I just wonder whether you can compare the diastolic aortic augmentation, and the reduction of peak systolic pressures in normal animals, to animals at shock levels. In other words, were you able to demonstrate any salutory effects in animals in cardiogenic shock.

DR. COHEN: I would like to emphasize that the data which were presented this morning were those of the first phase of the program. We have had this device for evaluation for only a four-month period and we felt obliged to try to work out some of the physiology in normal animals prior to placing our animals in cardiogenic shock. We have just this past week started on the second phase of the animal experimentation, which involves putting the animals into cardiogenic shock. We are about to start to collect data to see if there is any difference in the animals in shock as opposed to the animal whose cardiovascular system is intact. I am certain that information will be forthcoming and it carries a very high priority in our program.

MAJ. ANSTADT: It is encouraging to see that more emphasis is being put on what I would like to term indirect methods of circulatory support. In this regard, with the present emphasis on methods of circulatory assistance, it would be helpful, I think, to divide all methods of circulatory support into two broad classes, namely direct and indirect methods. The direct methods are those which actually require direct contact with the blood for their application. On the other hand, indirect methods have a more conservative approach in that they attempt to support the circulation without contacting the blood. I think undue attention has been given to the direct methods of circulatory support in relation to indirect methods. In the light of the present knowledge, formidable unsolved problems confront us in the area of direct contact of blood with any artificial device or surface. Basically, we do not know yet how to touch blood. Indirect methods do not solve these basic problems, but instead avoid them. In this respect, indirect methods of circulatory assistance are more conservative and worthy of much more attention than they are being given today.

DR. COHEN: Major Anstadt, I appreciate your comments. You have certainly been one of the pioneers in the area of cardiac assist devices, and we appreciate your comments concerning the indirect method.

DR. DODGE: I think this is a very interesting approach to the problem, but I have trouble deciding whether the results that you observed were due to diastolic augmentation of the arterial pressure, or whether, in fact, you were enhancing venous return. I really did not see any data that would allow me to decide. I think this is of critical importance to the problem. Dr. Rackley, in our group, has been doing augmentation of filling by infusing dextrin and the results today look as though when its filling gets above a pressure somewhere around 20 or 22 mm Hg, you really do not gain much beyond that. It seems to me that this is a critical decision with respect to how one goes about this, and really what is the true effect of this system of pulsation.

DR. COHEN: The point is well taken, Dr. Dodge. If one looks at the cardiac output data, it might well be that the cardiac output was augmented by increased venous filling. The cardiac output was augmented by 24%, but augmentation of venous return or decrease in ventricular afterload could explain that finding. If one looks at the pressure tracings demonstrating diastolic augmentation, that can only be explained by an effect upon the arterial side of the circulation and could not be explained by an augmented venous return.

DR. BRUCK: I wonder how soon after instituting counterpulsation, your physiologic data was obtained, and whether you observed a change with increased duration of augmentation?

DR. COHEN: The pressure data indicate that diastolic augmentation occurs almost simultaneously with turning on the counterpulsator. Immediately with the very first beat we see some degree of diastolic augmentation which reaches a maximum for that particular animal in about four beats. In terms of the cardiac output determinations, we generally turn on the pulsator for about a minute and at that point take a measurement of cardiac output. We have not, in rapid succession, measured cardiac output because of the time limitations necessary for a cardiac output determination. When we do use a flowmeter in the arterial system, I think we will get some idea of how rapidly the changes in cardiac output come about.

DR. BRUCK: I am more concerned with how rapidly the animals may deteriorate afterward.

DR. COHEN: Again, when we turn the sequenced pulsator off, the wave form changes immediately. In terms of cardiac output data, we have not looked at the second-to-second changes attendant upon turning the sequenced pulsator off. Our flowmeter data will address themselves to how rapidly the hemodynamic changes revert to a control state after the sequenced pulsator is turned off. The flowmeter is a very important part of our second phase. I hope that I have answered your question.

DR. BRUCK: I meant that, during continuous counterpulsation, did you lose some of the initial results that you obtained as the duration of augmentation continued?

DR. COHEN: We have used the counterpulsator continuously for periods of up to one half hour, and the diastolic augmentation has not diminished at all. Once the animal does achieve a certain level of diastolic augmentation, this level appears to be maintained for as long as the device is utilized.

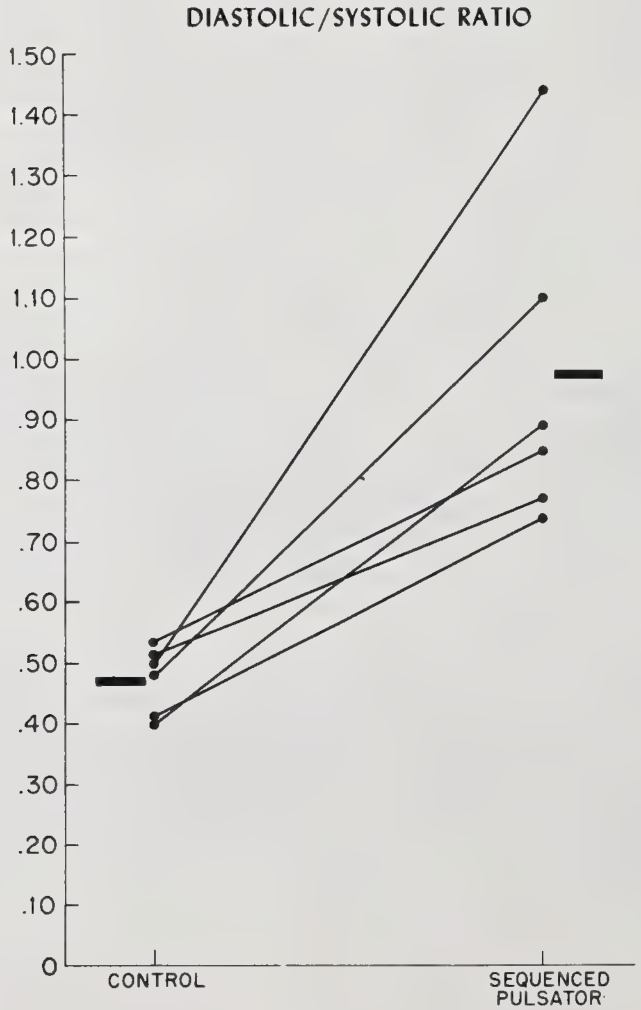

FIGURE 9.

CHAPTER 44

FLUID MECHANICS OF INTRA-AORTIC BALLOON COUNTER PULSATION

A. Shapiro, M. Jaffrin, C. Clark, V. Sreedhara Murthy
T. McMahan

Fluid Mechanics Laboratory
Department of Mechanical Engineering
Massachusetts Institute of Technology
Cambridge, Massachusetts

The technique of intra-aortic balloon pumping, which consists of counterpulsing a balloon positioned in the descending aorta, has been studied both theoretically and by means of an experiment in which the cardiovascular system is modelled by a lumped hydraulic circuit. An attempt has been made to explain the local fluid mechanics around different types of intra-aortic balloons. A general theory for counterpulsation devices has been developed for the arterial system represented as a network of tapered elastic tubes. An analytical model of the arterial system was developed, based on the reported physiological measurements of input impedance, and on approximate physical dimensions available for man and for dogs. Experimental observations and theoretical understanding of the operational modes of the balloon have led to criteria for design of constrained balloons. Also presented is a comparison between the analytical results, which consider the balloon as a loss-free volume source, and measurements made with the experimental model.

INTRODUCTION

Left ventricular assistance by intra-aortic balloon pumping requires the insertion into the aorta of a long narrow balloon mounted at the end of a catheter (Figure 1). A gas supply (pressure and suction) connected to the external end of the catheter is triggered by means of EKG signals so that the balloon operates in counter pulsation to the left ventricle. Removal of gas from the balloon during heart systole reduces the pressure against which the left ventricle must pump, whereas the introduction of gas at high pressure into the balloon during diastole serves to pump the blood through the arterial system.

The main effect of balloon pumping is to reduce both the peak and the mean systolic pressures in the aorta and left ventricle, thereby reducing the effort and mechanical work required by the ventricle in ejecting its stroke volume and the myocardial oxygen requirement. Another favorable feature is the possibility of producing a selective redistribution of blood flow: for example, increased flow through coronary arteries.

The primary objectives of the present study are the understanding and evaluation of various generic types of intra-aortic balloons, with specific reference to the mechanics of the balloon and to the local fluid mechanics, in order to provide a rational basis for the design, improvement, and optimum operation of such balloons. Among the parameters which must be optimized are the ratio of balloon to heart stroke volumes, the phase and duration of inflation and deflation, the location, geometry, and construction of the balloon. A systematic optimization of a heart assist device by means of animal experiments would be time-consuming and costly. We wish to demonstrate the feasibility of simple, theoretical and laboratory models which possess the essential features of the human arterial tree and allow experiments or calculations to be performed quickly and economically. In the electrical analogs of the human circulatory system proposed by various authors, there has been no attempt to include assist devices.

First, a theoretical representation of the arterial tree, the "tapered elastic tube model" which complies with the available physiological data and allows a logical interpolation of the missing ones, is developed to provide the basis for a general theory of counterpulsation in the arterial system. This theory is valid not only for an intra-aortic balloon but also for other arterio-arterial types of assist devices. Only a crude model of the balloon (pressure node-volume source) is set up at this stage. Secondly, a hydraulic experiment is built, (1) to test the validity of the simple theoretical model of the balloon, and (2) to permit an experimental investigation of the detailed fluid mechanics around the balloon. These experimental results will eventually lead to any necessary refinement of the model for the balloon, and to design of constrained balloons which can overcome the defects of a limp balloon.

The philosophy which underlies the present work is that for the full and effective development of the intra-aortic balloon pump, which is a complex system, it is necessary to carry out both theoretical and experimental investigations of the various components into which the system may be divided, and to establish a fundamental understanding of the balloon operation. Hence the present program of research is designed to provide a basic engineering understanding of the mechanics and fluid mechanics of aortic balloon operation. This should provide a rational basis for the evaluation of systems currently in use, for the design of balloons of various types, and for the selection of suitable cycles of operation for new systems. The particular aspects of the program of developing the intra-aortic balloon technique on which we are engaged should provide sound guidelines for more effective and economical techniques of building and testing laboratory prototypes, for testing of prototypes in animals, and for the interpretation of the results of such tests.

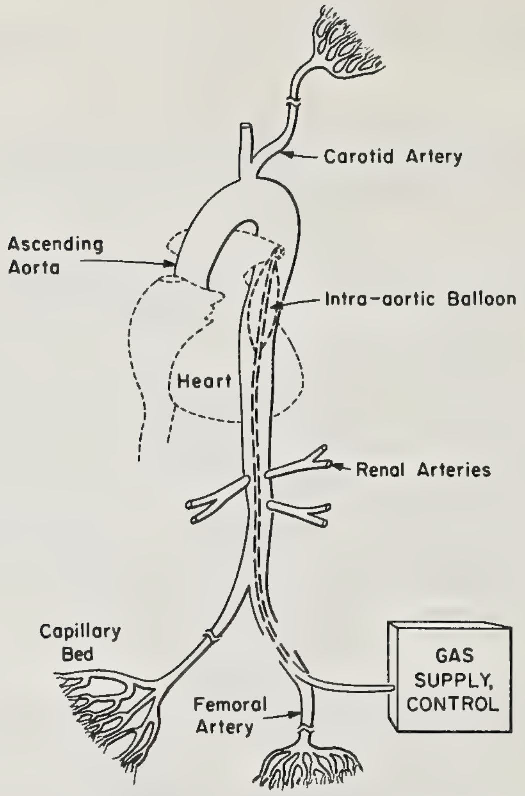

FIGURE 1. INTRA-AORTIC BALLOON PUMPING.

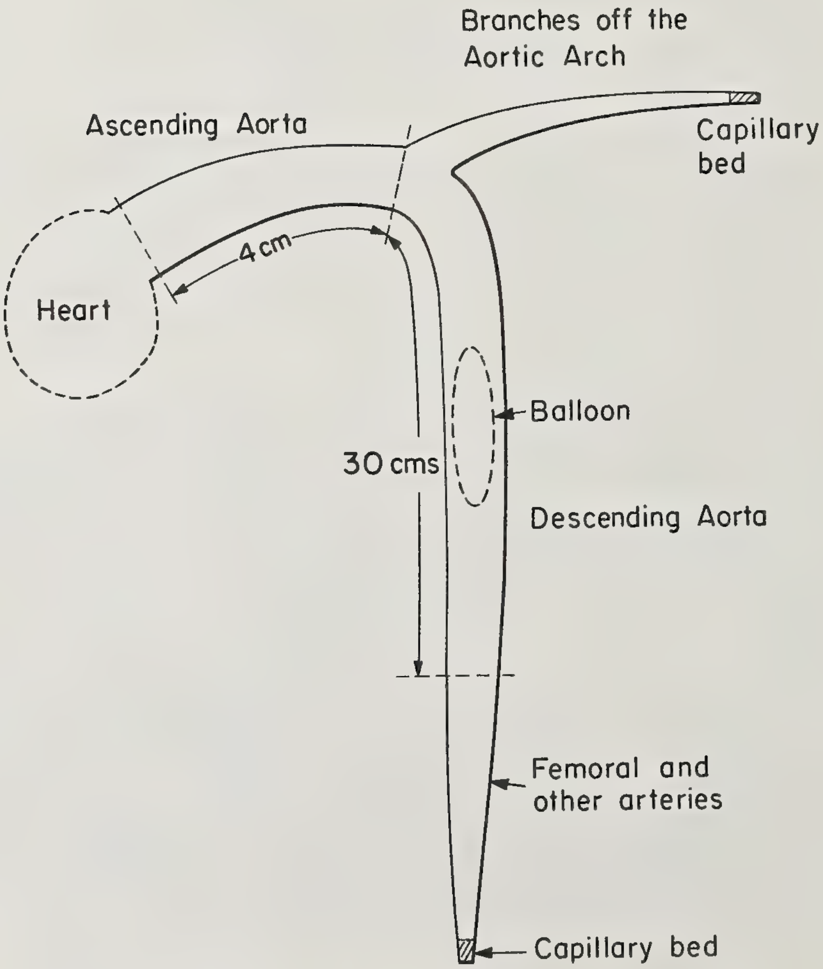

FIGURE 2. TAPERED TUBE MODEL OF THE ARTERIAL SYSTEM.

THE TAPERED ELASTIC TUBE MODEL

A general representation of the arterial tree is required for theoretically evaluating the effect of any counterpulsator in the cardiovascular system. A crude model, which has been adopted by many investigators so far, is the simple "Wind Kessel" model comprised of one lumped capacitance (corresponding to the total capacitance of the arterial system) and one lumped linear resistance (accounting for the resistance of the capillary bed). The Wind Kessel model is, however, not adequate for predicting the effect of the balloon on the arterial system, as well as the behavior of the balloon itself, since the local fluid motions near the balloon and the consequent bubble blowing phenomenon are heavily dependent on the distribution of various impedances in the arterial tree. As an example, in the extreme case where all the compliance of the system is lumped at one end of the balloon, the limp mode of inflation would consist of only one bubble at the end closest to the lumped compliance. For a given pressure of the gas introduced into the balloon, the balloon stroke volume for this one-bubble mode of inflation is considerably less than that for a double-bubble inflation, such as occurs if the compliance were divided between the two ends of the balloon. Thus, the Wind Kessel model, which not only lumps the total capacitance and resistance into single elements, but also neglects all the inertia of the fluid, is inadequate for evaluating any counterpulsator. With this in mind, a new representation of the arterial tree by a cascade of tapered elastic tubes has been developed.

The proposed arterial model, as depicted in Figure 2, consists of a network of tapered elastic tubes arranged so as to best represent the aorta in which the counterpulsating device would be located, with the rest of the arterial system lumped into tapered compliant tubes terminating in pure resistances. The ascending and the descending portions of the aorta are each represented as a tapered elastic tube. The branches off the aortic arch together with their capillary beds, and the major arteries at the end of the abdominal aorta along with their capillary beds, are each lumped into one tapered elastic tube terminating in a characteristic impedance, which in addition to being equal to the resistance of the corresponding capillary bed is also equal to the pure resistance at the end of the tube. This choice clearly implies that there are no perceptible reflections from the capillary beds of an arterial tree. The taper factor Ω defined as $\Omega = c \frac{d}{dx} (\ln Z_0)$, where c is the wave speed and Z_0 is the characteristic impedance ($Z_0 = \sqrt{L/C}$, where L is the inertance and C the capacitance per unit length of the tube), is assumed constant throughout the model. The numerical values of the parameters and dimensions in the model are established from the reported arterial input impedance measurements of some investigators, and from the average values of the wave speed in different portions of the vascular bed. It is assumed that 20% of the flow passes into the branch upstream of the balloon. The relations between the pressures and flow rates at different locations along the aorta are obtained by solving the dynamical equations for tapered tubes. This provides transfer functions relating the input to the output impedance for each region of the arterial model, upstream and downstream of the balloon. With the knowledge of the local fluid mechanics of the counterpulsating device, the effect of the counterpulsator on, say, the pressure in the proximal aorta may be calculated from this theory.

The simplest model of the balloon, at least in so far as it is an element of the total arterial system, is that it be treated as a loss-free volume source. That is, as a first approximation, the balloon is taken as a pressure-node in the arterial system. This model may, subsequently, require modification on the basis of studies of the detailed fluid mechanics around the balloon. The heart is considered to be a positive flow source, since the true behavior is not known.

For the loss-free source model, the relationship between pressures and flows at different locations in the aorta may be supplemented by two more equations connecting the pressures and flows at the two ends of the balloon. Since the balloon has been shrunk to a point, the pressure there must be equal to the balloon pressure, p_b, and the difference between the flow rates at the two ends of the balloon must be given by the balloon flow input, q_b (rate of increase of volume of gas inside the balloon).

These observations together with the relations between the pressures and flow rates in the rest of the arterial system give two equations between the four quantities p_h, q_h, p_b, and q_b, and hence, in principle, given any two of the four, the other two may immediately be calculated(p_h and q_h are respectively the pressure and flow rate at the heart).

Purely to illustrate how the theory may be used to predict the effect of balloon operation, an example of the effectiveness of the balloon (represented as a loss-free volume source) is given by Figure 3. For this case, the heart flow was assumed unaltered and was represented by the Fourier components up to the third harmonic. Then the requirement was imposed that the pressure at the heart be constant, and the question was asked as to how the balloon volume should vary in order to achieve this end. Figure 3 also shows the pressure at the location of the balloon. A peak systolic efficiency defined as the percentage decrease in the peak systolic pressure, may immediately be calculated as

$$\eta_{\text{peak systolic}} = \frac{|p_h|_{\text{max, unassisted}} - |p_h|_{\text{max, assisted}}}{|p_h|_{\text{max, unassisted}}}$$

$$= 14.2\% \qquad \text{(from Figure 3)}$$

In this case, the balloon stroke volume is about 55% of the heart stroke volume.

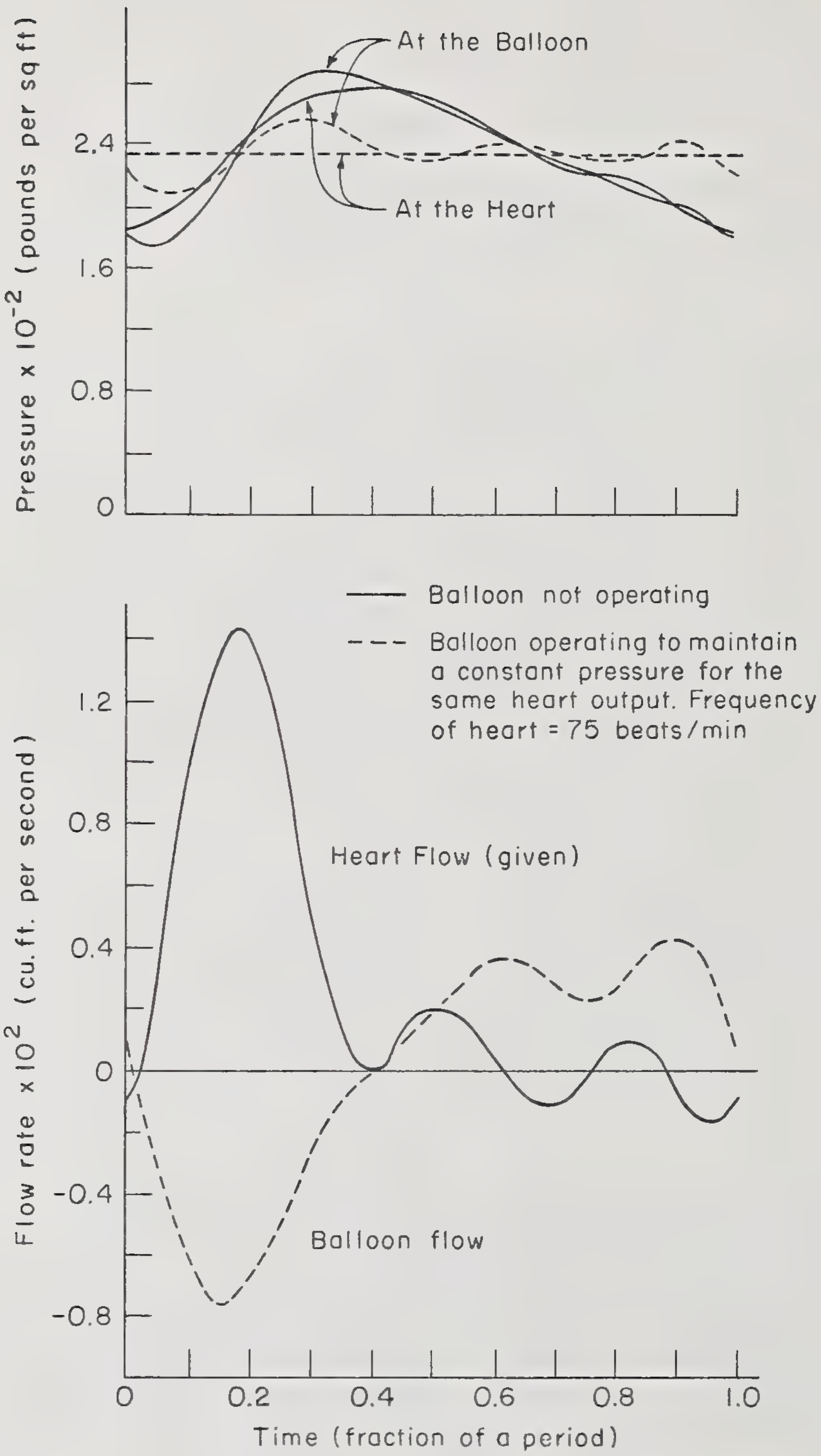

FIGURE 3. REQUIREMENTS OF BALLOON BASED ON LOSS-FREE VOLUME SOURCE MODEL OF BALLOON FOR A GIVEN HEART OUTPUT.

EXPERIMENT

The necessity for a fluid mechanical model derives not from the hope of presenting a superior representation of the arterial system but from the lack of an adequate mathematical model of the intra-aortic balloon itself. The pressure-mode model of the balloon is not consistent with even the most elementary fluid model of the balloon as a volume-displacing device due to the bubble blowing phenomenon. In fact, no consistent mathematical description of the fluid mechanics in the vicinity of the balloon is yet available. Instead of trying to model the experiment closely after the human circulatory system at an expense in complexity and in instrumentation capability, a geometrically simple experiment is designed to present the same flow impedance as that of the human system as seen from the heart and from the balloon looking both upstream and downstream. Schematics of the hydraulic model and its electrical equivalent are displayed in Figure 4. The test-section, representing a section of the descending thoracic aorta, is a straight rigid transparent tube of uniform bore. A side branch upstream of the test section but downstream of the pressure port p_h, measuring source or left ventricular pressure, represents the branches off the aorta upstream of the balloon. For convenience of instrumentation and observation, the inside diameter of the model aorta was made twice the approximate mean inside diameter of the human aorta. This geometrical scaling of the experiment requires appropriate changes in the dynamic parameters of the experiment, as will be explained later.

The heart is simulated by a flow source consisting of a steady flow pump working in parallel with a piston-in-cylinder which provides a sinusoidal reciprocating flow. It is thus idealized in two respects: it represents the true cardiac flow-time curve by only the zeroth and first harmonics; and it assumes the left ventricle to be a flow source with infinite output impedance, i.e., with flow rate independent of the output pressure, which is an idealization roughly true for healthy hearts but not so true for the failing heart. The flow source is not given a finite internal shunt impedance principally because this impedance is not known, but experiments may be done simulating such a finite impedance by lumping it with the impedance of the representative upstream branch. Water is used in the experiment. Whereas the Reynolds number similarity is not perfect, this is not significant because viscous effects are important only in the resistances which are adjusted separately. The distensibility of the arterial system is represented by three lumped capacitance elements. Each is a closed vertical tube in which a predetermined volume of air trapped above the liquid surface acts as a linear spring for small displacements. One of these air springs lies downstream of the balloon in the model aorta, one upstream, and one in the branch circuit. Peripheral resistances are also modeled by lumped components, these being porous tubes at the ends of both the main and the branch circuits through which the flow passes into atmospheric-pressure sumps which simulate the venous system. A return line connects the two sumps to the low-pressure side of the flow source.

The three porous discs (Figure 4) in the circuit were primarily intended to have very low resistances compared to the tubes and to serve only as flow-meters for determining the flows at those locations. They also turned out to be useful extra variables in the process of matching the impedance of the lumped circuit experimental model with the impedance of the arterial system which has distributed capacitance, represented by both the physiological measurements and the tapered elastic tube calculations presented earlier.

The balloon itself is mounted on a rigid 1/2" (outside diameter) catheter which extends straight through the test section. It is inflated via a large-volume constant-pressure reservoir when a cam actuated microswitch on the reciprocating flow pump opens a solenoid valve attached to the catheter. The balloon and catheter exhaust to the atmosphere when another cam-driven microswitch opens the exhaust valve at the end of the catheter. The duration and phase of both cams driving the microswitches are adjustable.

a. Impedance Comparison.

Figure 5 shows several comparisons of the input impedance at various harmonics of the fundamental heart frequency, as seen (a) looking from the heart downstream, (b) looking from the balloon upstream, and (c) looking from the balloon downstream. Both modulus and phase are shown. In the curves representing the tapered transmission line model, the balloon mid-point is assumed to be 6" from the heart. Also plotted in Figure 5 are the flow impedances actually measured in man[5] and dogs[6]. O'Rourke's dog measurements[6] have been scaled to the size of man. The assumptions here are that although the dog's and man's anatomy are different, their input impedance curves must be essentially similar when plotted vs. frequency on a dimensionless scale.

It is not possible to find a set of values for the elements of a lumped circuit which present an impedance exactly equivalent to that of a distributed parameter circuit over a range of frequencies. It may be possible, however, to find a set which approximately matches the two circuits over a limited frequency range. The curve in Figure 5, representing the lumped parameter model, was computed on the basis of the circuit shown in Figure 4. This represents the outcome of approximately thirty trials for the impedance computations, each trial taking different values for the R's and C's, but leaving the L's fixed, since these are dependent on the geometry of the model and more difficult to change. A trial-and-error process, while lengthy and difficult, is apparently the only practical procedure for this matching operation since the requirement of matching over the range of at least the first three frequencies over-determines the specification for the lumped values.

b. Modelling Laws for Changing the Scale of the Lumped Parameter Model.

Having specified, by the above procedure, values for the impedance elements of a lumped parameter circuit to represent the arterial system, the task is now to determine, how these values must be changed to maintain dynamic similarity when all physical lengths in the fluid circuit are multiplied by a constant factor (geometric similarity).

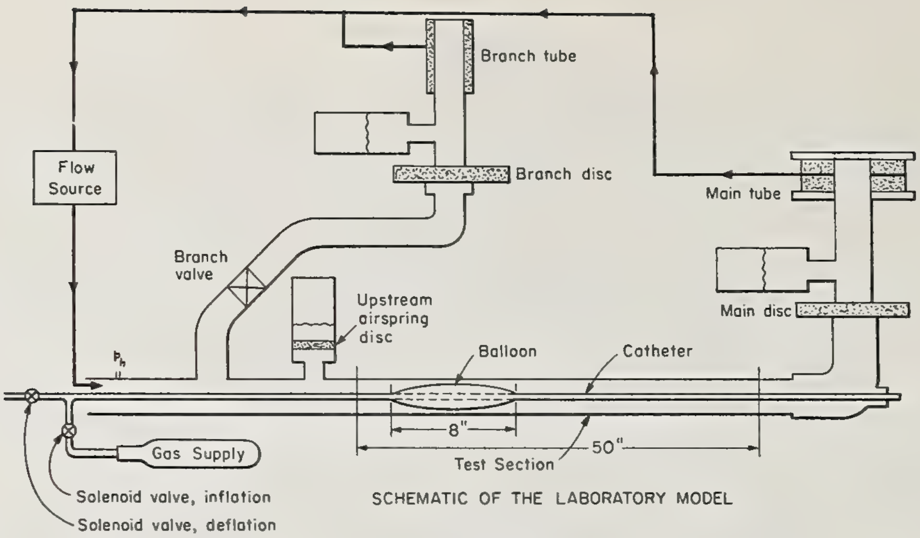

SCHEMATIC OF THE LABORATORY MODEL

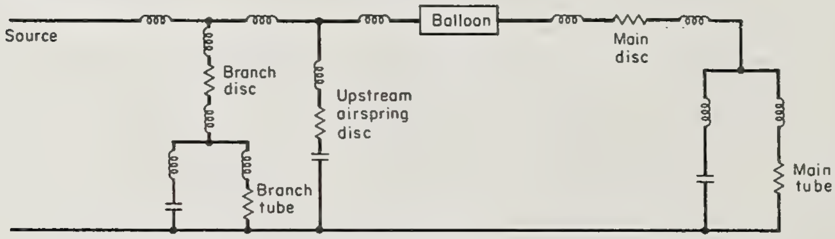

EQUIVALENT ELECTRICAL CIRCUIT

FIGURE 4.

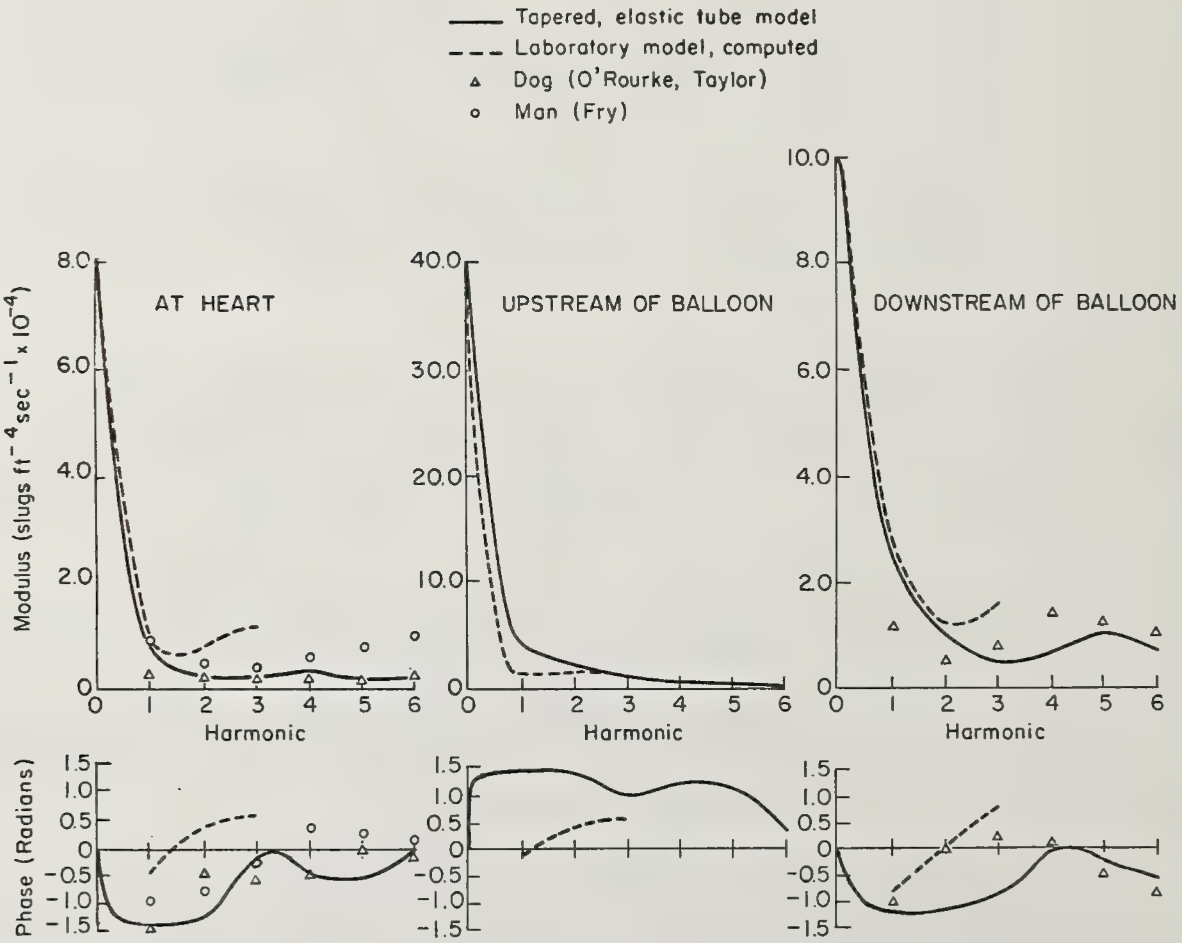

First Harmonic = 7.86 Radians/Second

FIGURE 5. IMPEDANCE COMPARISON.

The pressure, or any other dependent variable measured anywhere in the system, may be expressed as a function of nine parameters:

$$p = p(\ell, f, q, \theta, \rho, C, R, L, g)$$

where:

ℓ = any of the several lengths, such as aortic radius, balloon length
f = any of the several frequencies, such as fundamental heart frequency
q = any of the several volume flow rates, such as cardiac output
C = any of the capacitances, such as branch air spring capacitance
R = any of the resistances, such as main tube resistance
L = any of the inertances, such as test section inertance
θ = table angle with respect to the horizontal
ρ = density
g = acceleration due to gravity

From these nine parameters, the following six independent dimensionless groups may be formed:

$$\frac{g}{f^2\ell}, \quad \frac{q}{f\ell^3}, \quad \theta, \ LCf^2, \quad \frac{R}{fL}, \quad \frac{\rho}{L\ell} \quad .$$

Dynamic similarity requires these groups to be invariant under a change of scale. We multiply all lengths by 2, leaving the density and the acceleration due to gravity unchanged. Thus, between the model and the prototype, the changes to be incorporated are:

$$\frac{\ell_{model}}{\ell_{proto}} = 2 \quad \text{(chosen)}, \qquad \frac{L_{model}}{L_{proto}} = \frac{1}{2} \quad \text{(same density)},$$

$$\frac{f_{model}}{f_{proto}} = \frac{1}{\sqrt{2}} \quad \text{(same gravitational acceleration)}$$

The modelling laws for other variables immediately follow.

$$\frac{q_{model}}{q_{proto}} = 4\sqrt{2}, \quad \frac{C_{model}}{C_{proto}} = 4, \quad \frac{R_{model}}{R_{proto}} = \frac{1}{2\sqrt{2}}$$

$$\theta_{model} = \theta_{proto}$$

The dimensionless group associated with the dependent variable, pressure p, is $p\ell^4/\rho q^2$ and therefore all pressures follow the law

$$p_{model}/p_{proto} = 2.$$

c. Instrumentation.

Pressure transducers measure the pressure differential across each of the three porous discs and two porous tubes, and thus can be calibrated to read flow through each of these elements when the values of the porous resistances are known. It is also possible to measure the gauge pressures at the position corresponding to the aortic valve, in the catheter, and at each of four stations along the wall of the test section where the balloon is located. The motions of the balloon may be filmed by a high-speed motion picure camera which views the balloon through the transparent test section. A potentiometer, driven by a rack and pinion mechanism actuated by the reciprocating flow pump, is included as one arm of a Wheatstone bridge circuit, thus obtaining a voltage signal representing the position of the reciprocating flow pump piston. This piston position voltage is arranged to be interrupted during the time when either the intake or exhaust valve of the balloon is open, so that balloon cycle information is available in the same signal. Two large copper ring electrodes make up the test section wall ahead of and behind the balloon, and five smaller rings interrupt the wall at regular intervals in the vicinity of the balloon. A constant electric current is caused to flow through the circulating liquid from the upstream to the downstream current electrodes. It is now possible to record the voltage across any pair of intermediate electrodes and have a measure of the local cross-sectional area of the annulus bounded by the test-section wall and the balloon.

d. A Preliminary Experiment Testing the Linear Impedance Element Assumption.

The flow forced through the model is given by

$$q_h(t) = \bar{q}_h + q_{h0} \cos \omega t \quad .$$

The pumps were set to provide zero net flow over the second half of the period corresponding to diastole. The steady component of flow $(\overline{q}_h)$ was adjusted to represent the cardiac output of a failing heart (half the normal output). A limp balloon, 8 inches long, made of Tygon with a wall thickness of approximately 0.01 inch was mounted on the catheter. Its stroke volume was about 1.9 times that of the flow source. It is recognized that this value is much larger than can be attained in a human subject, but it was chosen for preliminary experiments in order to give prominence to the effect and behavior of the balloon. The cams controlling the balloon cycle were set to provide balloon inflation and deflation starting at flow phases π and 0, respectively, as shown in Figure 6. The deflation valve remains open approximately half the cycle, the inflation valve a shorter time. "Heart pressure", flow across the main and branch discs and the main tube, piston position and balloon cycle, intracatheter balloon pressure, and pressures immediately upstream and downstream of the balloon were recorded against time. These measurements were performed for three frequencies, taking two conditions of the experiment for each frequency: branch valve open and branch valve closed. In some of the experiments, motion pictures were taken at a framing speed of 1000 frames/sec.

Gauge pressure measured at the pressure port corresponding to the heart is shown in Figure 6 versus time. The left half of the figure is shaded below the pressure curve obtained when the balloon was not operating: the right half of the figure is shaded beneath the balloon-operating pressure curve. The combined flow from the reciprocating and steady-flow pumps is represented schematically below. It is apparent that the balloon reduces the mean systolic pressure and increases the mean diastolic pressure, as it was designed to do. An unforeseen consequence of the balloon operation is the sharp pressure rise following collapse of the balloon midway through the deflation period. This "stopping shock" is interpreted as a result of the abrupt termination of the radially-inward directed liquid motions around the balloon when the balloon reaches zero displacement volume. The motion pictures show the expected "bubble blowing" phenomenon, the ends of the balloon inflating before the center and apparently nearly occluding the test section. A comparison was made of gauge pressure measured just ahead of and just behind of the balloon. This is presented in Figure 7, where both pressures have been traced from the oscillograph record using the piston/microswitch signal (just below) as a time reference. A preliminary conclusion is that there is very little measurable difference between the pressures at any time, and therefore the loss-free source or pressure-node model of the balloon may indeed be justified.

An important first use of the pressure and flow data measured in the experiment when the balloon was not operating is the calculation of input impedance from the heart measured at the three frequencies of operation. This is found by measuring the pressure amplitude and phase at the heart station and dividing that amplitude by the flow amplitude of the reciprocating flow pump. The experimental impedance results are compared with values computed on the basis of the circuit shown in Figure 4 for three frequencies and two cases, branch valve open and closed. The comparison shown in Figure 8 includes analytic points computed on the basis of two different sets of resistance values, a "high resistance" and a "low resistance" set corresponding to the possible extremes in linearized resistance. All of the porous elements are slightly nonlinear, and in addition to this, there was some experimental scatter in the resistance calibrations. The "low" and "high" resistance sets correspond to the extremes of this possible variance in resistance. The comparison is seen to be quite reasonable. A tentative conclusion is that the flows and pressures in our experimental set-up are reasonably well predicted by a linear-element mathematical model of the apparatus.

THE MECHANICALLY-CONSTRAINED BALLOON

The limp balloon used in this experiment cannot support a pressure difference until inflation is complete. Non-uniform inflation such as bubble blowing can occur, which may decrease the efficiency of the balloon as a heart assist device.

One technique for overcoming this disadvantage of simple limp balloons is to incorporate beams parallel to the catheter which force the balloon to take a specific shape while inflating (Figure 9). These beams are pinned to the catheter at one end and to a sliding joint at the other end. Thus, the balloon has two stages of inflation. In the first stage each fold inflates like an individual limp balloon, with bubbles at the ends separated by the still undeflected beams. In the second stage, as the gas pressure inside increases, the balloon skin begins to support tensile stress and the beams bend radially outward. The beams continue to bend until the balloon becomes approximately cylindrical in its mid section. Therefore, the constrained balloon cannot occlude the aorta until the maximum stroke volume has been attained and does not create pockets of high pressure fluid trapped between the ends, since the beams insure longitudinal passages for the fluid to escape. Another advantage is that the beams could be fitted with strain gauges giving a signal proportional to the balloon volume.

CONCLUSION

Most of the efforts so far have been directed to insure that the laboratory model describes adequately the physiological situation. At the present time, therefore, a working system, which will yield many results economically and rapidly, has been set up. Two problems of fluid mechanical origin and of great importance to balloon operation have been recognized. They are the bubble blowing phenomenon caused by non-uniform inflation of the balloon and the high pressures generated by the stopping wave during deflation. We are trying at present to overcome these problems. We expect in the near future to be able (1) to predict the effect of intra-aortic balloons for different physiological states of health, age and exercise, (2) to optimize the performance of intra-aortic balloons.

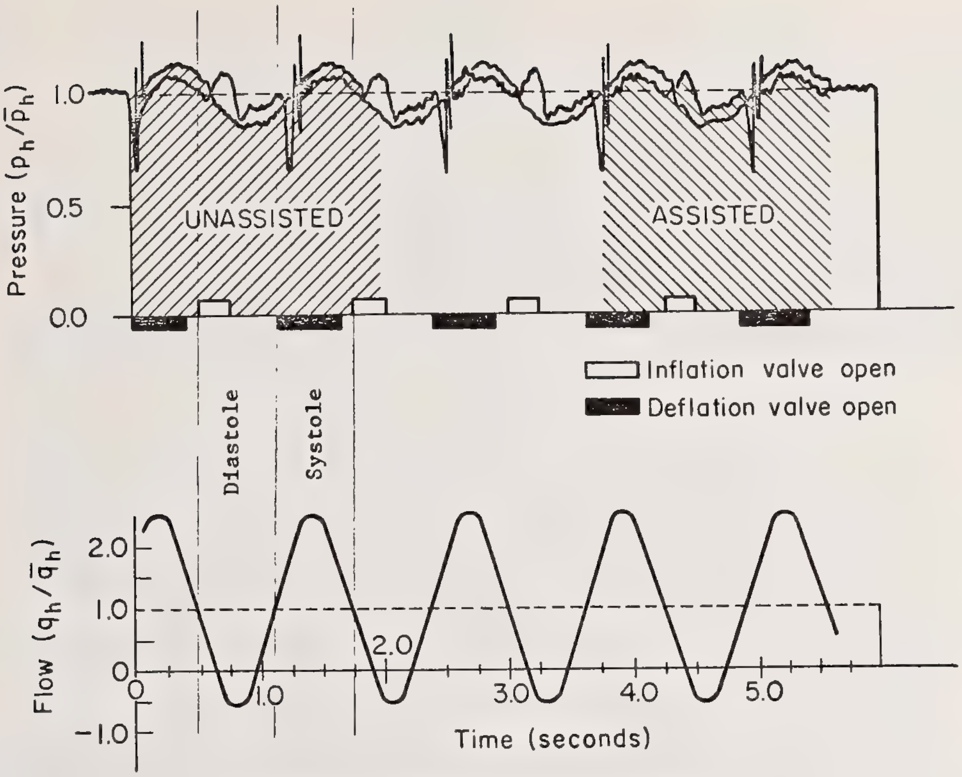

FIGURE 6. PRESSURE AND FLOW AT HEART.

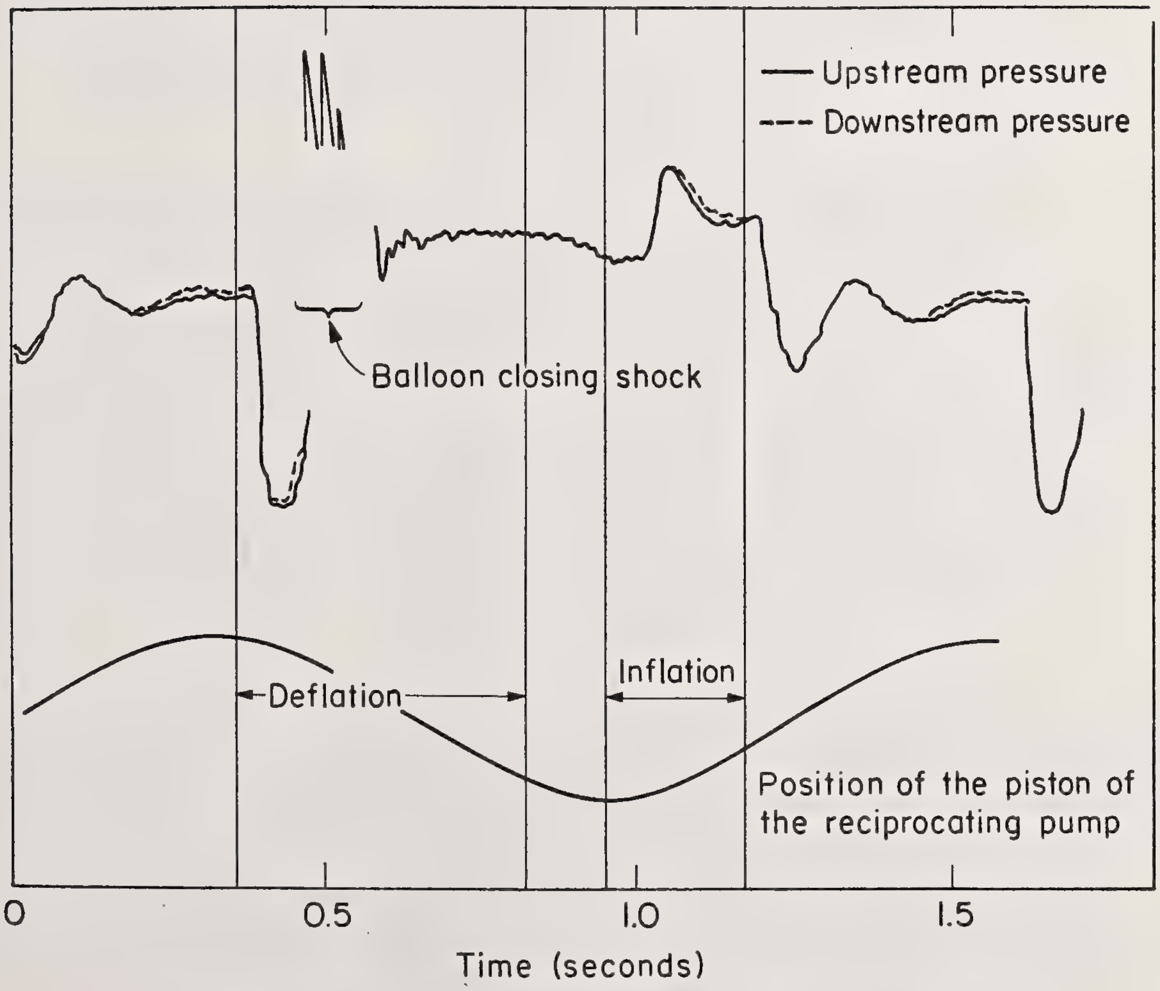

FIGURE 7. PRESSURE AT THE UPSTREAM AND DOWNSTREAM ENDS OF THE BALLOON.

REFERENCES

1. Shapiro, A.H., Jaffrin, M.Y., Clark, C., McMahon, T.A., Chiu, W.S., "Annual Technical Progress Report on the Development of an Intra-Aortic Balloon Pump", July, 1968.
2. Shapiro, A.H., Jaffrin, M.Y., Clark, C., Murthy, V.S., McMahon, T.A., "Preliminary Version of the Annual Technical Progress Report on "Engineering Development of Intra-Aortic Balloon Pump", May 1969. Contract No. PH-43-67-1114.
3. Noordergroff, A., Jager, G.N., Westerhog, N., Circulatory Analog Computers, North Holland Publishing Co., Amsterdam, 1963.
4. Laird, J.D., Madras, P.N., Jones, R.T., Kantrowitz, A.R., Kothari, M.L., Buckley, M.J., and Austen, W.G., "Theoretical and Experimental Analysis of the Intra-Aortic Balloon Pump", Trans. Amer. Soc. Artif. Int. Organs, XIV, 338-343, 1968.
5. Attinger, E.O., Pulsatile Blood Flow, McGraw Hill, New York, 1964.
6. O'Rourke, M.F., and Taylor, M.G., "Input Impedance of the Systematic Circulation", Circulation Research, 20, 365-379, April, 1967.

DISCUSSION

DR. ROTH: I would like to repeat a question I asked an earlier speaker. Why is gas filling of a balloon used here instead of a liquid?

DR. JAFFRIN: In order to inflate and deflate a balloon rapidly, it would require very high pressures due to the high inertia of the liquid and this would probably be dangerous to use in a patient.

DR. ROTH: This depends how you shape the wave form of the liquid, and since the impedance match between the material outside the balloon and inside the balloon would be essentially one, I think you could have much better control.

DR. JAFFRIN: It is true that with liquid you would have better control of the shape of the balloon, but as I said, it would require very high pressures because the inertia of a liquid would be much higher than the inertia of gas and I understand that users of the balloon employ light gases like helium.

DR. HASTINGS: One more question.

UNIDENTIFIED DISCUSSANT: I would like to know the thickness of the membrane.

DR. MURPHY: It is 20/1000 of an inch.

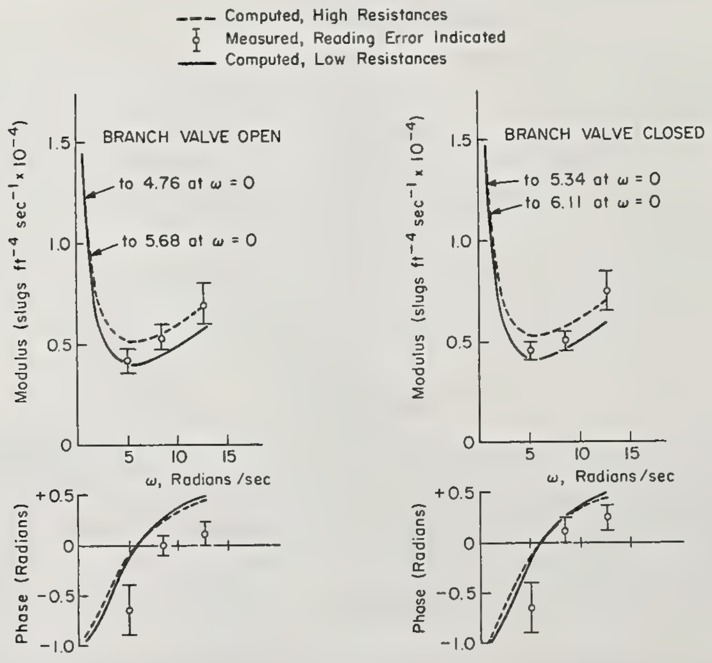

FIGURE 8. INPUT IMPEDANCE AT THE HEART, FOR THE LABORATORY MODEL.

CHAPTER 45

DEVELOPMENT OF AN INTRA-AORTIC BALLOON ASSIST DEVICE

J. M. Evans and G. E. McGinnis
Westinghouse Electric Corporation
Pittsburgh, Pennsylvania
and
B. G. Brown, W. D. Gundle, D. L. Trump, M. D. Ramos, and V. L. Gott
Johns Hopkins University
Baltimore, Maryland

During the past year we have continued physiological evaluation of the intra-aortic balloon, made improvements in the total system, and provided assistance to the Artificial Heart Program. Studies of renal function, chronic implantation, coronary collateral flow, and the effects of a triple balloon were conducted. Ten chronic experiments were done to determine the effect of diastolic augmentation on renal artery pressure and blood flow, urinary output, creatinine clearance, and sodium and potassium excretion. In all cases, augmentation with the balloon positioned in the thoracic aorta did not alter the above indices of renal function. Chronic implantation studies showed that balloons prepared with a variation of the TDMAC process yield excellent results for up to four days. Experiments in the mechanisms of coronary collateral flow indicate that retrograde flow collected from the cannulated distal coronary artery occurs essentially during diastole, and is proportional to the diastolic trans-collateral pressure difference. This result indicates that systolic contraction may mechanically occlude these collateral channels. Based on the results of the coronary collateral flow studies, a triple balloon has been designed which will selectively increase aortic root mean diastolic pressure without compromising the rest of the circulation. With reference to system improvements, the minimum time to failure of balloons subjected to cyclic testing has been increased by 30%. Development of the assist device has included improved gas porting in the actuator, redesigned and improved ECG amplifier and 60 Hz filter, improved automatic gain control circuit, and simplified trigger setup. Two assist device consoles, plus intra-aortic balloons, have been provided for independent evaluation.

INTRODUCTION

During the past year, the cooperative program of Westinghouse and Johns Hopkins has been continued with the objective of the development of a simple, safe, and highly reliable intra-aortic balloon assist device suitable for clinical evaluation. The accomplishment of this objective involved investigation of three major areas: physiologic evaluation, device improvement, and interaction with the physiologic evaluation teams under contract to the National Heart Institute. Studies of the physiologic effects of intra-aortic balloon diastolic augmentation involved investigation of the effects of balloon position on renal function, the evaluation of improved balloon designs, the elucidation of the mechanisms of intercoronary collateral flow, and evaluation of the efficacy of non-thrombogenic balloon coatings. Under device improvement, extensive life testing of balloons was performed to provide data for reliability estimation, a prototype was constructed to evaluate improvements in circuit design among which were improved ECG amplifiers and simpler triggering controls, and incorporation of additional safety features including an excessive balloon pressure alarm and a low gas supply warning. In the area of providing assistance to the programs of the National Heart Institute and its supporting contractors, we have fabricated balloons for physiologic effects testing, provided assistance and guidance to the physiological effects testors and balloon fabricators, and developed specifications for and begun construction on the first 10 of 40 assist devices.

PHYSIOLOGIC EVALUATION

Renal Function.

A series of six 8-hour renal function studies was carried out in two chronic canine preparations that were undergoing balloon diastolic augmentation. The dogs were trained and fully awake throughout the procedure. Aortic root and renal artery pressure and renal artery flow were measured by means of chronic indwelling catheters and flow probes. The bladder was exteriorized so that each ureter could be cannulated for urine collection. Urine output, creatine clearance, Na^+ and K^+ excretion were determined during an 8-hour period during which balloon augmentation was applied first in the thoracic aorta and then in the abdominal aorta. Initial results show that all the above indices of renal function are unaffected with balloon diastolic augmentation in the thoracic aorta. In the abdominal aorta, the balloon produces very high pulsations in renal artery flow and pressure. In response to this, one dog experienced a 30% decrease in urinary output, but the other indices were unaffected. In the second dog, all indices increased 10%.

Coronary Collateral Studies.

Studies by Gundel have demonstrated that coronary collateral flow is acutely enhanced by approximately 40% during diastolic augmentation. Collateral flow was estimated by the retrograde flow technique (Figure 1), in which the ligated coronary vessel was cannulated distally. Backflow from the ischemic zone was collected and weighed. In these studies, mean aortic root pressure was maintained constant with a reservoir. Under these circumstances, a change in collateral flow would be due to changes in the waveform, through its effects on ventricular dynamics. Enhanced collateral flow was not seen to remain elevated after discontinuing balloon diastolic augmentation following two hours of pumping. This cast some doubt on the popular notion that arterio-arterial pumping "blows open" the collateral bed.

Recent studies to further clarify the dynamics of collateral flow have taken the following direction: Using a blood reservoir and varying amounts of balloon diastolic augmentation, it is possible to vary aortic diastolic pressure while maintaining a constant systolic pressure. Conversely, diastolic pressure can be held constant, while systolic pressure varies. Collateral flow is unaffected by changes in systolic pressure, and is linearly related to the diastolic trans-collateral pressure differential. This is illustrated in Figure 2 and is more graphically shown in Figure 3. These findings may be interpreted in the following way: 1) There is little or no collateral flow occurring during systolic ejection. That is, myocardial contraction and intra-ventricular pressure sufficiently collapse the collaterals so as to prevent passage of blood. 2) Collateral flow, per heartbeat, is well correlated with the simple expression:

$$Q = \frac{A_oP_d - PCP_d}{R_d}$$

where A_oP_d is the mean aortic diastolic pressure and PCP_d is the mean diastolic peripheral coronary pressure. R_d is the diastolic collateral bed resistance. R_d is related to the number and caliber of the collateral vessels, and to the amount of myocardial stretch prevailing (LVEDP). These findings have been observed in five of five experiments; and it is strongly expected that this mechanism will stand the test of further experiments and statistical evaluation.

Triple Balloon.

Based on the observation that aortic root mean diastolic pressure is the mechanical determinant of coronary collateral flow, a balloon was designed to selectively increase aortic root mean diastolic pressure. This is called the triple balloon. It represents a refinement of the double balloon catheter discussed last year at this time. The basic double balloon has an added small cuff balloon which is positioned just proximal to the brachiocephalic trunk when the catheter is approximately located. The cuff balloon is expanded and collapsed through a small, separate catheter. Its expansion at aortic valve closure completely obstructs the ascending aorta, thus forming a closed chamber above the aortic valve. Subsequent expansion of the main ascending aortic balloon, in conjunction with the decending aortic balloon, causes high diastolic pressures in the ascending aorta. In order to achieve this effect, the cuff balloon should begin its expansion 30 msec or more before the main balloons. Studies of triple balloons were conducted in nine dogs. The following are exemplary responses. Figure 4 shows that the triple balloon can increase mean aortic root pressure and left circumflex coronary flow by 15-20% without significantly reducing carotid artery flow. "Double balloon" means that the independent cuff balloon is held in the collapsed condition. Figure 5 is another example of hemodynamic alterations caused by this catheter. In this one, the triple balloon elevates mean aortic root diastolic pressure, but flow in the brachiocephalic trunk diminished by 25%. Figure 6 is an example of the effectiveness of the triple balloon in the situation of acute coronary occlusion. From the moment of ligation of the left anterior descending coronary artery, the left ventricle begins to fail, as evidenced by the decline in peak ventricular systolic pressure, here represented as X's connected by a dot-dash line. This ventricular weakening continues even when the "double balloon" is activated, however, with the onset of the "triple balloon" (occlusive cuff is activated), the ventricle beings to recover its contractile power. Concomitant with the increase in ventricular function is a striking increase in aortic root mean pressure, left circumflex coronary flow, and retrograde flow, as collected from the distally cannulated left anterior decending artery which is permitted to bleed externally during collection. Again, during this experiment, the most constant correlate of retrograde flow was mean aortic root diastolic pressure, and not mean aortic root pressure. When the triple balloon is operative, there is an initial decrease in the mean carotid artery pressure, however, with ventricular recovery, the carotid mean eventually is increased.

Chronic Implantation.

Studies this year are a continuation of last year's chronic implantation studies. In order to facilitate circulatory assistance during instances when total systemic anticoagulation is undesirable, a flexible thromboresistant surface, polyurethane-TDMAC-heparin, has been given preliminary evaluation using intra-aortic balloon catheters chronically implanted in the canine aortic bloodstream via a laparotomy and terminal aortotomy.

In general, treated balloons - both pumped and unpumped - performed better in terms of thromboresistance than untreated control balloons in the same circumstances. However, even with the most satisfactory group of surface-treated balloons, there was significant thromboembolism in several cases.

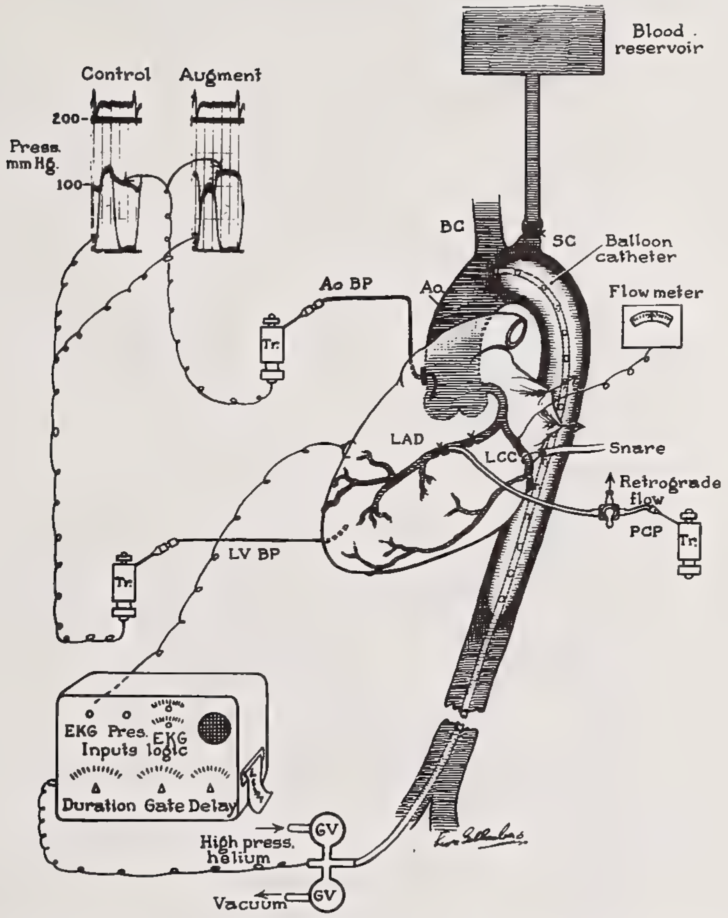

FIGURE 1. RETROGRADE TECHNIQUE FOR MEASUREMENT OF CORONARY COLLATERAL FLOW.

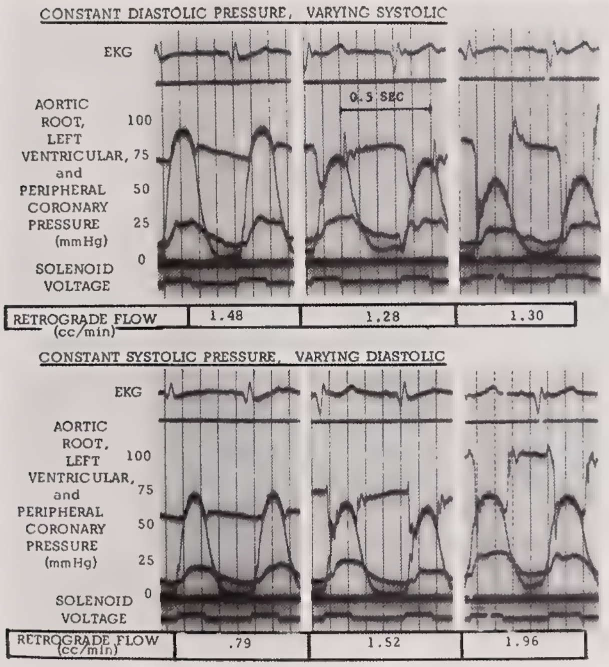

FIGURE 2. THE CONTRIBUTION OF THE TWO PHASES OF THE CARDIAC CYCLE TO LEFT ANTERIOR DESCENDING RETROGRADE FLOW. IN THE TOP SERIES, RETROGRADE FLOW IS RELATIVELY UNCHANGED AS DIASTOLIC PRESSURE IS HELD CONSTANT AND SYSTOLIC PRESSURE IS VARIED. CONVERSELY, WHEN SYSTOLIC PRESSURE IS HELD CONSTANT AND DIASTOLIC PRESSURE IS VARIED, THE RETROGRADE FLOW INCREASES STRIKINGLY WITH INCREASED DIASTOLIC PRESSURE. FURTHER ANALYSIS OF THIS STUDY SUGGESTS THAT COLLATERAL RESISTANCE IS VERY HIGH DURING SYSTOLE. THEREFORE, LITTLE OR NO COLLATERAL FLOW OCCURS DURING SYSTOLE.

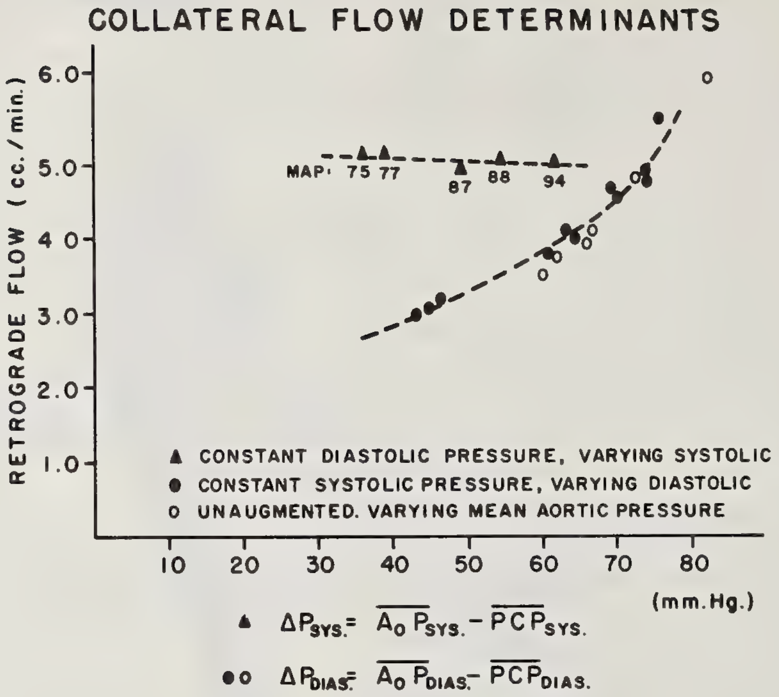

FIGURE 3.

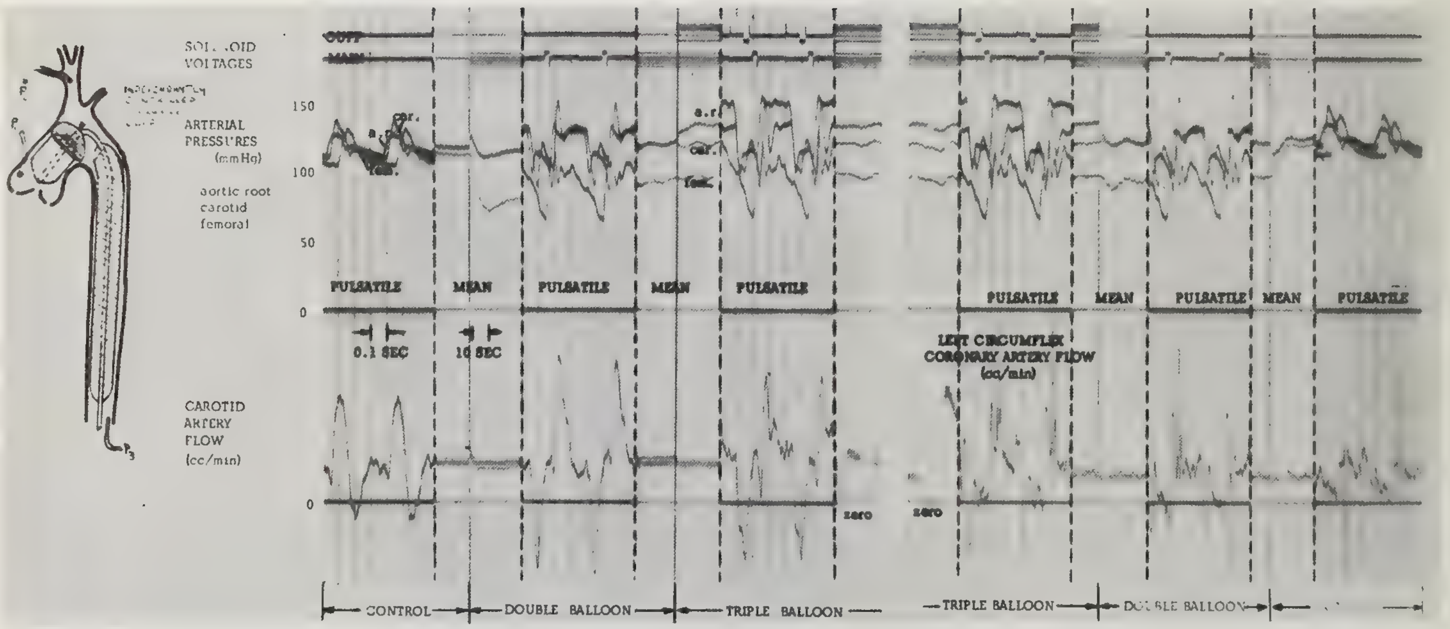

FIGURE 4. EFFECTS OF THE TRIPLE BALLOON ON CORONARY FLOW.

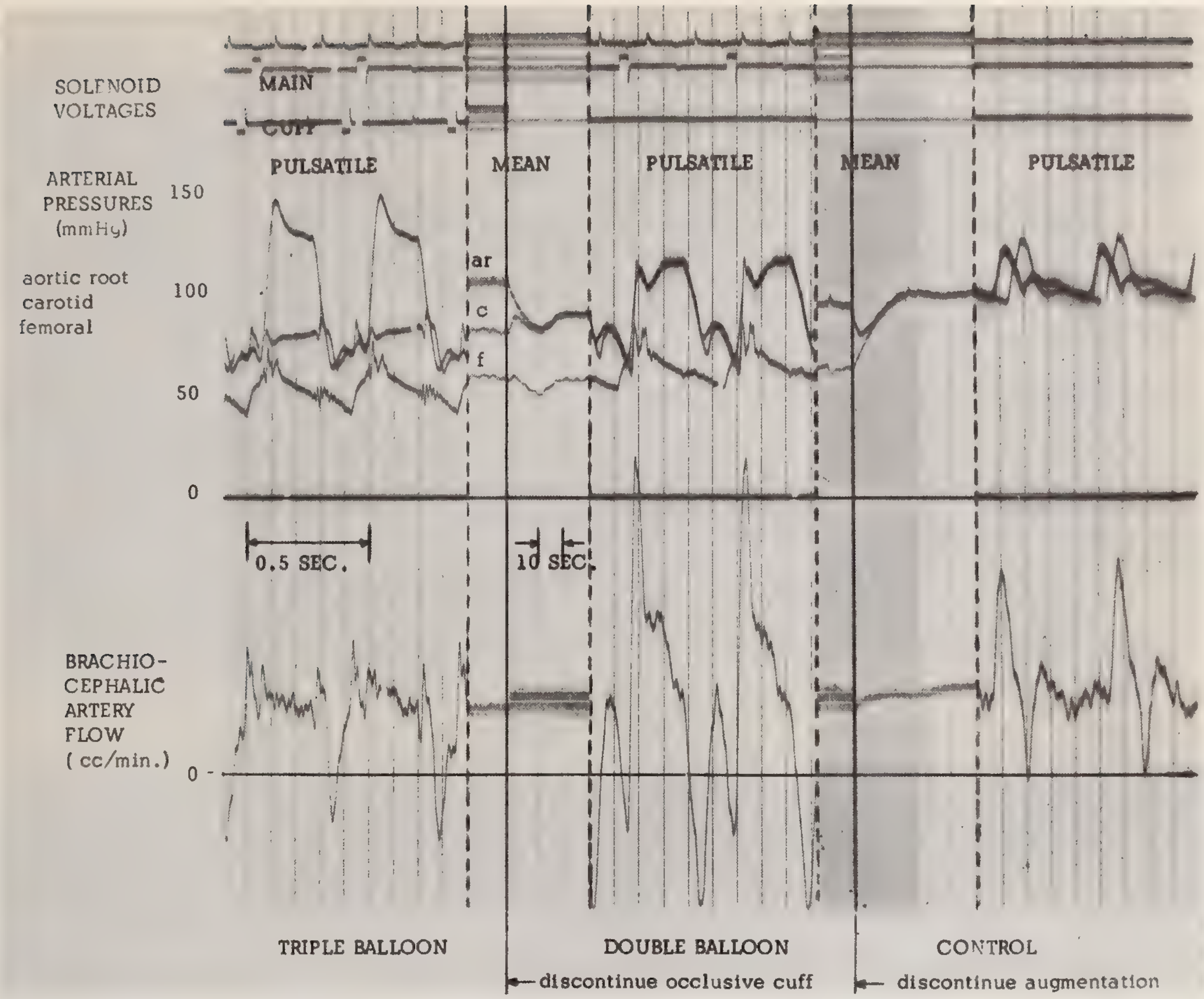

FIGURE 5. COMPARISON OF THE HEMODYNAMIC EFFECTS OF TRIPLE AND DOUBLE BALLOON DESIGNS.

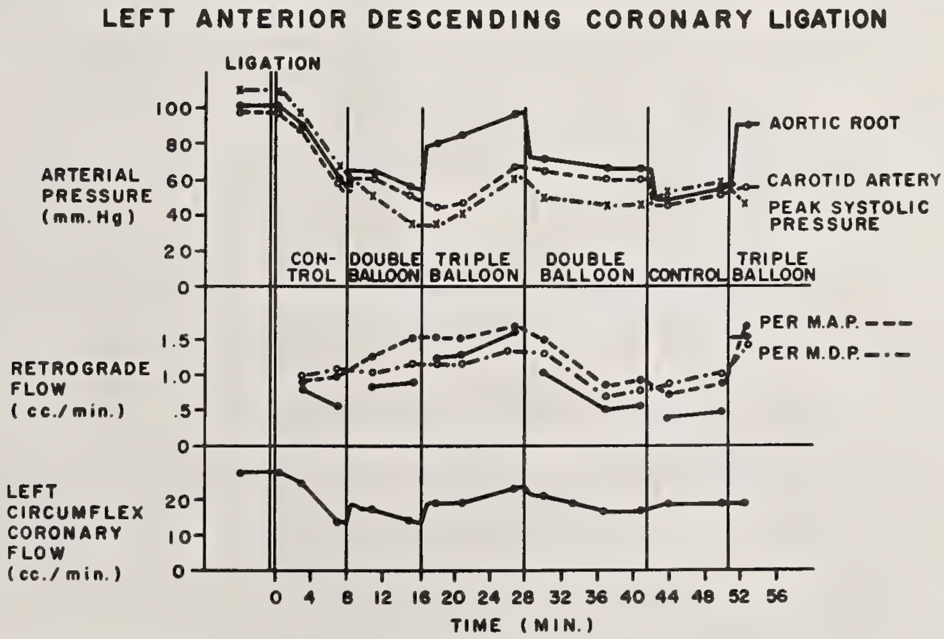

FIGURE 6. COMPARISON OF EFFECTS OF DOUBLE AND TRIPLE BALLOONS AFTER LIGATION OF THE LEFT ANTERIOR DESCENDING CORONARY ARTERY.

We must conclude that while the TDMAC balloon treatment is significantly better than no treatment, the performance in dogs does not merit implants in unheparinized humans.

DEVICE IMPROVEMENT

A great number of improvements and refinements were made in the engineering design of the components of the assist device and in the area of operational procedures. Balloon fabrication procedures were modified to achieve better quality control and greater reliability. Splitting of the film during the curing stage was observed when the difference between dewpoint and ambient temperature was less than 16^0. By preconditioning the Jello mandrel (Figure 7) to eliminate free surface moisture and fabricating the balloons in a controlled humidity, this problem was circumvented.

Cyclic life testing of balloons has been continued and the failures occurring in this program were correlated with evidence of foreign particle inclusion and microscopic bubbles in the film. More carefully controlled dipping techniques reduced the incidence of bubbles in the film and switching the fabrication of the balloons to a clean room minimized inclusion of dust particles in the film. Life testing was carried out by cycling balloons in a heated saline bath for periods up to 112 days (Figure 8). The results of these tests are shown in Table 1.

TABLE 1

CYCLIC TESTS OF BALLOONS FABRICATED FROM POLYURETHANE

Series Number	Balloon Number	Dia. at Start (in.)[a]	Dia. at Day Indicated	Thickness (in.)[b]	Days to Failure	Days to Termination	Failure Mode	Comments
89	1	0.63		0.0051	39		Pinhole at bubble site	
	2	0.62		0.0059		112		
	3	0.58		0.0051		112		
	4	0.61		0.0052		80		Balloons were terminated to make room for others.
	5	0.60		0.0062		80		
	6	0.60		0.0065		80		
	7	0.62		0.0060		80		
	8	0.62		0.0053		80		
106	10	0.78	0.78 11th	0.0055		52	Test terminated	
	11	0.78	0.78 11th	0.0054	52		Operator error (burst)	
	12	0.78	0.78 11th	0.0055	52		Operator error	
	13	0.78	0.78 11th	0.0054		52	Terminated	
	14	0.78	0.78 11th	0.0056	52		Operator error	
	15	0.78	0.78 11th	0.0054		52	Terminated	
106A	1	0.73	0.80 24th	0.0050		65	Terminated	
	2	0.78	0.80 24th	0.0060	50		Pinhole	
	3	0.80	0.82 24th	0.0060		45	Burst	
	4	0.73	0.78 24th	0.0050		45	Burst	Burst due to failure of solenoid on 45th day.
	5	0.78	0.78 24th	0.0060		45	Burst	
	7	0.78	0.79 24th	0.0060		45	Burst	
	8	0.78	0.80 24th	0.0060		45	Burst	

a Average of 4 measurements at 1 psi.
b Average of 8 measurements.
Series 89, 106 - Mix #43
Series 106A - Mix #47

Test Conditions:
Cycle rate - 70/min
Inflation pressure - 200 mmHg
Imersion in 110^0 saline bath during test

Statistical analysis of this data indicates that the probability of a balloon lasting for a period of 14 days under the conditions of test is 0.94 with a confidence limit of 0.90. The polyurethane balloon material was also subjected to exposure to subcutaneous fluids, saline and plasma for periods of 14 days and no significant changes in its mechanical strength were found.

The polyethylene catheters which were initially used for dog experimentation were found to be subject to kinking when used with calfs. Subsequently, catheters were constructed of extruded high density polyurethane which does not soften at body temperatures, is highly resistant to kinking and will return to its original shape after being kinked (Figure 9).

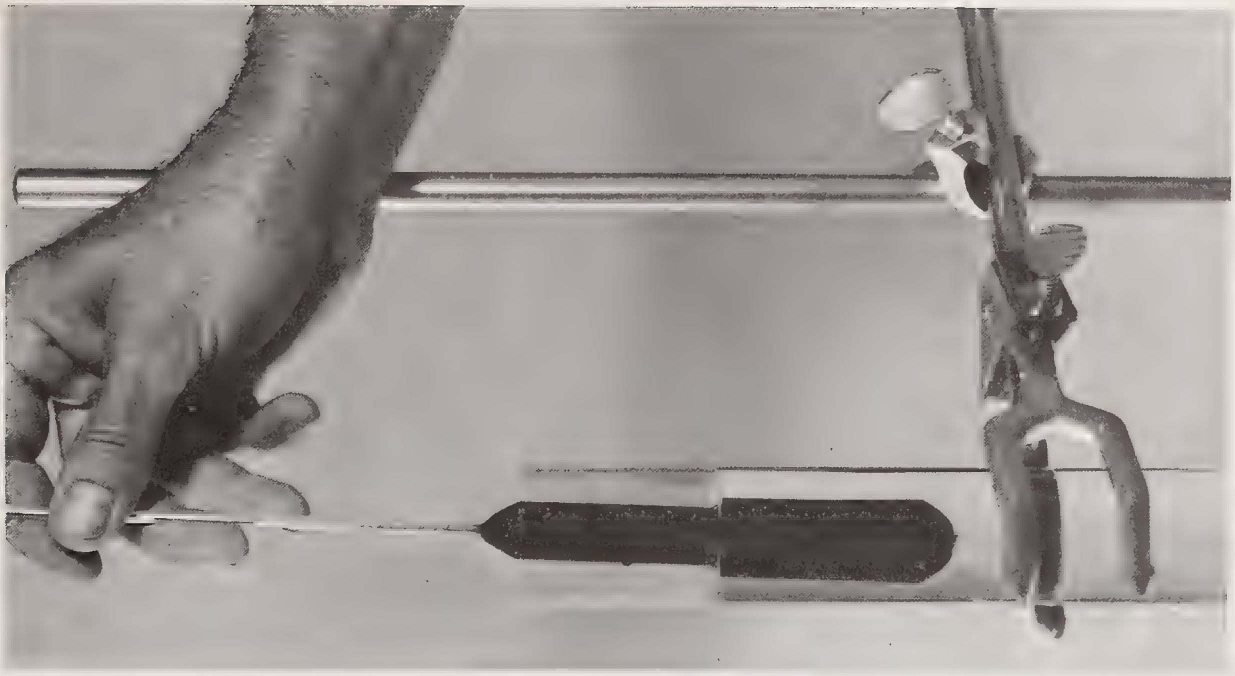

FIGURE 7. CONSTRUCTION OF POLYURETHANE BALLOON BY DIPPING OVER JELLO MANDREL.

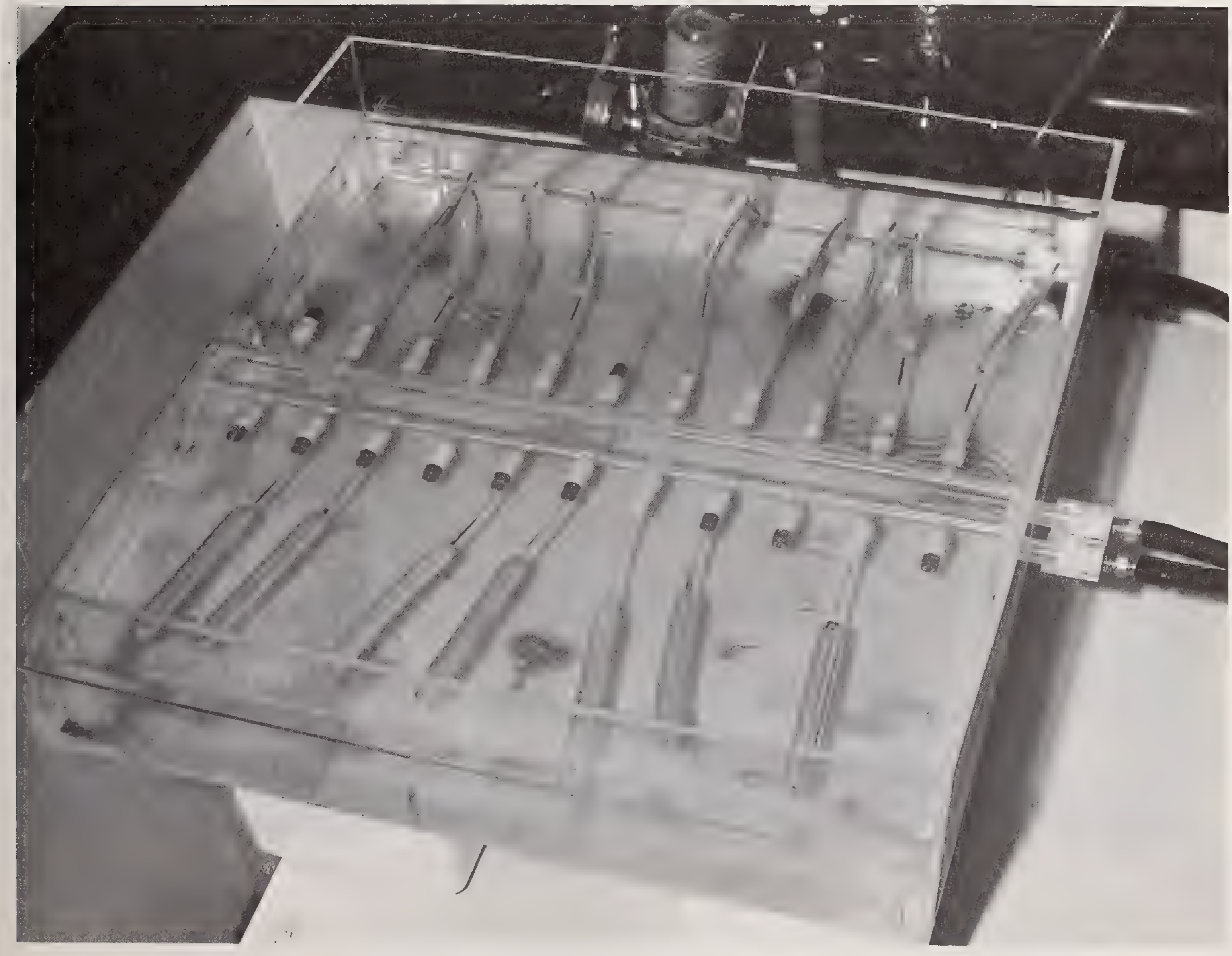

FIGURE 8. CYCLIC LIFE TESTING OF BALLOONS.

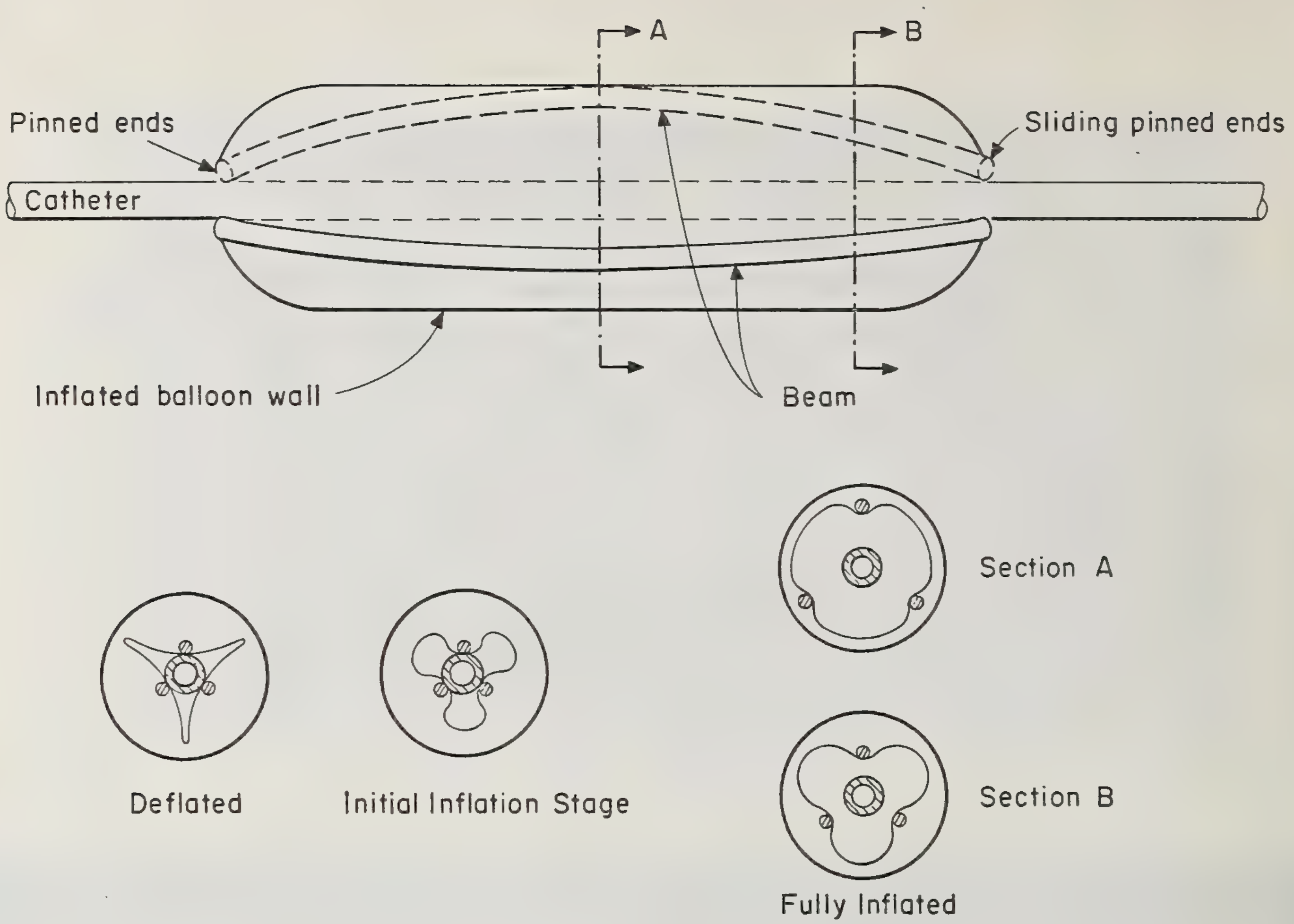

FIGURE 9. CONSTRAINED BALLOON WITH LONGITUDINAL BEAMS.

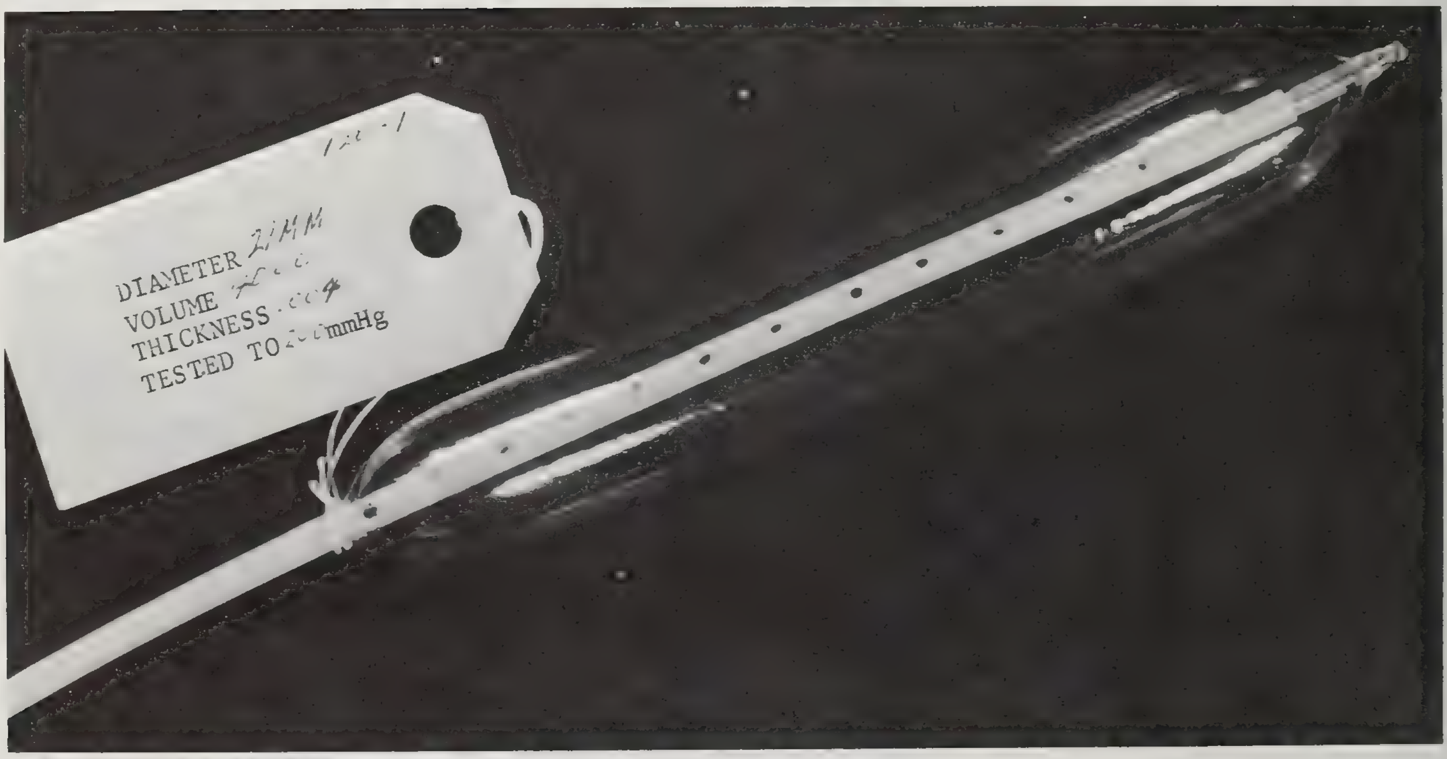

FIGURE 10. PHOTOGRAPH OF BALLOON CONSTRUCTED ON POLYURETHANE CATHETER.

Extensive modifications were made on the control circuitry which were designed to improve its function and reliability and to simplify setup and operational procedures. Evaluation of the prototypes (Figure 10) constructed last year revealed that low ECG signal input levels led to occasional missed beats. The automatic gain control circuitry was redesigned so that the system would respond to signals as low as 0.25 mv peak and the response of this circuit was increased so that it could follow changes in waveform amplitude more reliably.

Excessive delays were noted between occurrence of a QRS complex and balloon collapse. These delays were traced to phase distortion of the waveform in the input amplifier and 60 cycle filter. The band width of the amplifier was extended and the common mode rejection improved so that the system could be operated without the filter. The final design includes an optional 60 cycle filter of the parallel T design which introduces minimum phase delay.

Early control circuitry allowed the balloon to remain inflated if the circuitry missed a QRS complex. Additional timing circuits were added which imposed a limit on the inflation time and allowed operation of the device in a combined predictive immediate collapse mode.

In the area of simplifying setup and operational procedures, we have added circuits to simplify the initial setup and calibration of system pressure. We have simplified triggering setup by establishing a set of fixed parameters to enable rapid change from one waveform type to another, all circuits which control balloon inflation and deflation are timed from the occurrence of a QRS complex which enables alteration of one point in the cycle without affecting the others, and we have revised the timing circuit so that calibrated linear controls now appear on the front panel. In addition to the above modifications, we have supplemented the spurious triggering, low pressure, and loss of triggering alarms with alarms which indicate low tank pressure, excessive balloon pressure, and a sonic indication of an alarm condition.

Modification made to the pneumatic and balloon actuation system include incorporation of a compact oilless vacuum pump in the system, a simpler and more compact actuator design, improved sound conditioning of the solenoid valve, and reduction of the noise level during operation to approximately 40 db. A recirculating system which would reduce the gas requirements for operation was designed and evaluated.

PROVISION OF ASSISTANCE TO THE PROGRAMS OF THE NATIONAL HEART INSTITUTE

We have provided assistance to the National Heart Institute, its programs, and its supporting contractors in many areas and they, in turn, have been most generous in supplying us with information, advice, and constructive criticism which has been invaluable to the progress of our program. In all, we supplied over 100 balloons to various investigators for physiologic evaluation. We provided two prototype control systems to the physiologic effects groups under Dr. Kennedy in Cleveland and Dr. Galysh in Chicago. We provided assistance in the initial orientation of these groups with the prototype and maintained communication throughout the program.

We have advised Western Gear in California of the many problems associated with the production of clinical quality balloons using our technique and are delighted to find that they are now producing excellent quality balloons.

Finally, we have developed specifications for a compact assist device incorporating display, control, and pneumatic functions in one unit which has been designed to simplify setup and operational procedures and will deliver the first 10 of 40 units to the National Heart Institute by the end of July 1969. Figure 11 shows the control panel of the device. The top panel incorporates an oscilloscope for display purposes, the middle panel contains controls for balloon inflation and deflation and alarm indications, and the lower panel houses the vacuum supply and pressure regulation. Controls which are normally used only during calibration and setup are recessed behind the three panels on the right-hand side of the console.

CONCLUSIONS

We find that the last year has been a challenging but satisfying one in that we are close to the realization of extensive scientific evaluation of the concept of balloon diastolic augmentation utilizing safe, simple, and reliable equipment. We have especially enjoyed the interaction with other members of the scientific and medical community which this program has afforded us. The evaluation of the prototype consoles during the past year by the physiologic effects testers in Chicago and Cleveland has been especially helpful in our attaining our objectives. Finally, we look forward to assisting the National Heart Institute in the attainment of its present and future objectives.

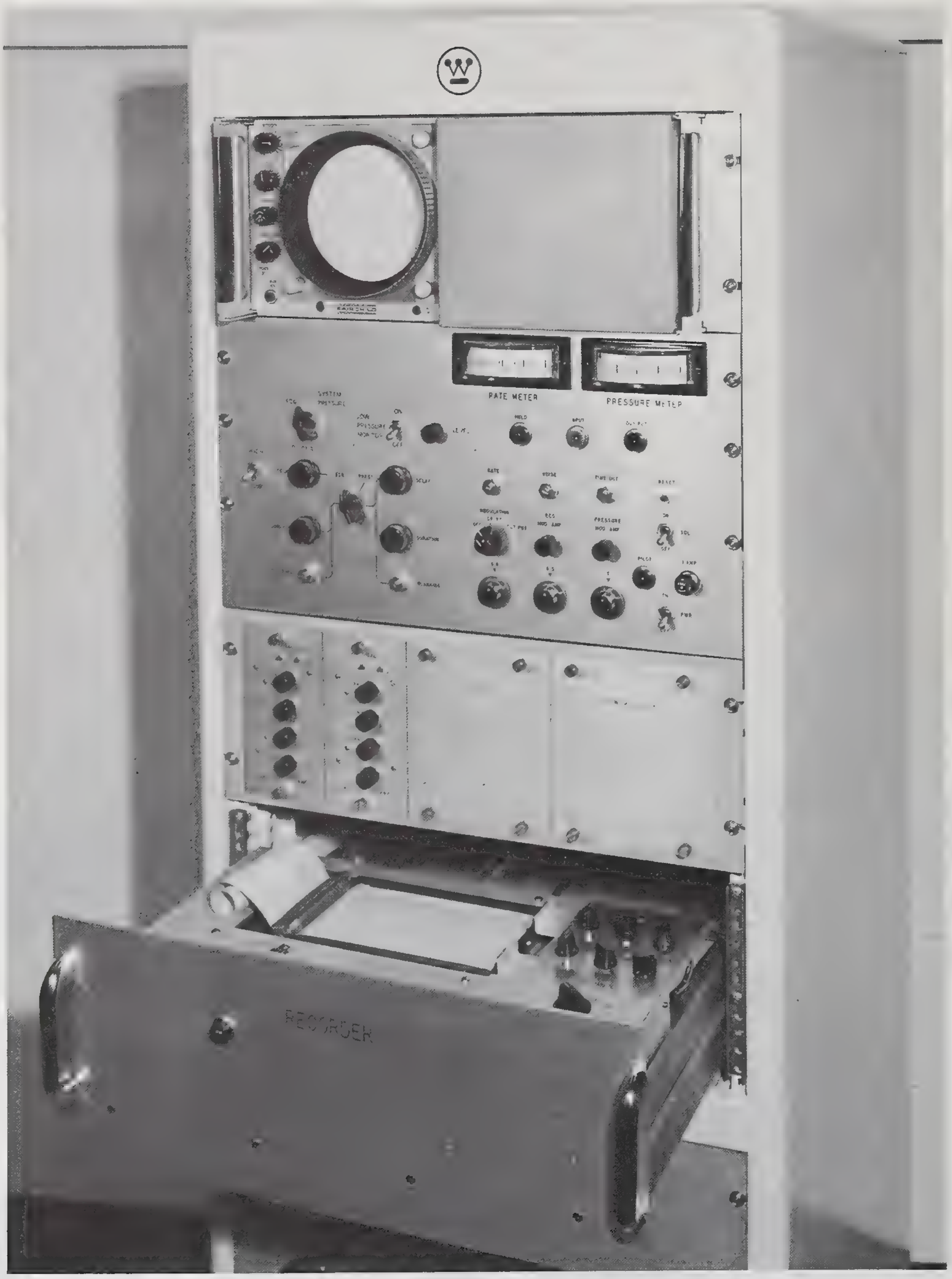

FIGURE 11. PROTOTYPE ASSIST DEVICE.

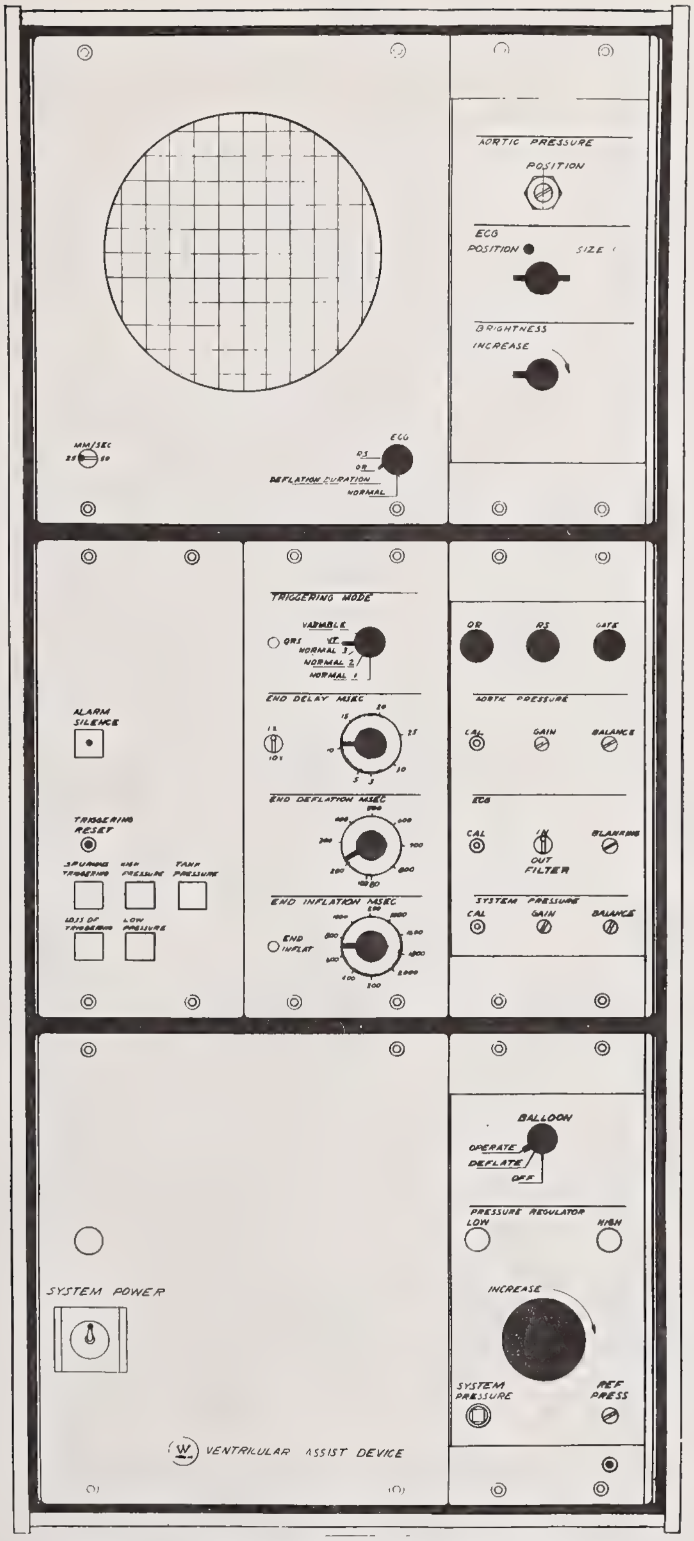

FIGURE 12. FRONT PANEL OF NEW ASSIST DEVICE.

DISCUSSION

DR. KANTROWITZ: Dr. Hastings, I wonder if I might make a few comments. First, I have enjoyed both of the papers on balloon pumping, although I must admit I did not understand the first paper. I hope that they will be able to reduce the arithmetic by next year so that surgeons can understand it. Our program at Maimonides Hospital in Brooklyn has been entirely supported by the National Heart Institute grants program and we have been interested in phase shift balloon pumping for some three or four years. I thought it might be of some interest to this group to report our clinical use of the device. Our balloon is a rather simple design. It contains only one chamber of about 33 cc. It is activated by helium and synchronized to the electrocardiogram with rather sophisticated, I think, electronic circuitry. Rather than limiting the number of gas ports in the balloon, we have used a metal braid which permits literally thousands of ports. We don't think that there is any problem regarding the effectiveness of pumping which results from the sequential inflation of different sections of the balloon, provided the balloon is not occlusive. We do agree that there can be a problem when the balloon is totally occlusive. In patients, we have been able to recognize this situation and correct it in one of two ways. One, we can increase the arterial pressure of the patient usually by giving just a little bit of Levophed and expanding the aorta. Then the characteristics of the arterial pressure curves become very obvious and we can thus reduce or release a totally obstructing balloon. A second method which we have used is to take the balloon out and replace it with a second balloon of a smaller diameter. At any rate, we have used this balloon pump now in the past two years in about 30 patients. These patients are all patients in deep cardiogenic shock who have been treated by the medical men in our hospital, and they have come to the conclusion that none of these patients could be retrieved. Roughly, this group of 30 patients can be divided into three sub-groups. One group, which we call a delayed shock group, consists of patients who developed their cardiogenic shock more than 36 hours after the appearance of their myocardial infarction. In this group, we have not been able to retrieve any, i.e., all of these patients have died. We have been able to bring the remaining two thirds of the patients out of cardiogenic shock, although three of them have died on the assist device. Nine of the patients have gone on to become long-term survivors, in that they have gone home. The remaining patients were short-term survivors, living for a period of one day to about one week. We do think that this is a modality which offers great hope in the treatment of cardiogenic shock. I might mention that the device is now commercially available for investigative use. Thank you very much.

DR. KUHN: I would like to support Dr. Evans' remarks concerning the so-called third balloon, but I also want to ask him a question about it. First of all, in support of this, I can cite some of our own evidence which would indicate that central aortic counterpulsation alone, either by balloon or by blood counterpulsation, when there is profound hypotension, in experimental acute myocardial infarction, has not been associated in our hands with significant cardiac metabolic improvement or in hemodynamic improvement. However, when the coronary flow is increased by a non-phased balloon in the abdominal aorta, much more striking hemodynamic and cardiac metabolic improvement have been obtained, including reversal of left ventricular excess lactate production. We have interpreted this as being due to increased coronary flow in an ischemic situation, not obtainable in sufficient degree by counterpulsation alone in the central aorta. When you mentioned the third balloon in your device, I didn't hear any detail as to how this was phased or whether it was phased. I wonder if you could give us some detail on that.

DR. EVANS: The phasing of the triple ballon is that an occlusive cuff is inflated in the first portion of diastole before the main balloon is inflated. The occlusive cuff seals off the ascending aorta and a small balloon between the occlusive cuff and the heart is then inflated along with the main balloon which is in the descending thoracic aorta.

DR. KUHN: That is deflated in systole?

DR. EVANS: It is deflated during the systolic period.

DR. FEOLA: Do you have any survival data showing that animals in cardiogenic shock treated with a triple or double balloon survive longer than animals treated with a single balloon or animals not treated with a balloon at all?

DR. BROWN: There have not been extensive survival studies with the triple balloon. In the few dogs that we studied increased ventricular function appeared to parallel the increase in collateral flow. We think the fact that one can elevate aortic root diastolic pressure with the triple balloon is the basic attribute, and that survival should parallel increased collateral flow. Since increased myocardial survival should be the primary goal of LV assist, we think the triple balloon will be effective.

DR. FEOLA: The basic question is whether patients in coronary shock are better treated with vasopressors or vasodilators, i.e., by an increase or a decrease in total peripheral resistance. It seems to me that a triple balloon or double balloon will produce an increase in total peripheral resistance. True, this will increase the coronary flow, but it will also increase the pressure component of left ventricular work. Experimental data, particularly those from the laboratory of Dr. Lilleleht, prove that when this happens, survival of dogs in cardiogenic shock is literally curtailed, while an increase in survival follows the increase in the volume component of left ventricular work.

DR. SCOTT: I am wondering if the retrograde flow after ligation had a determination of the oxygen content, in order to see to what extent this represented improved perfusion of the capillary bed.

DR. BROWN: We did not measure the oxygen content of the retrograde flow, but it has been evaluated by Donald Gregg in his laboratory. He finds that, in all cases, retrograde flow is at the same saturation as arterial oxygen saturation. It represents flow coming from an arterial source, somewhere, presumably it is on its way to the capillary bed, but it is at arterial oxygen saturation, i.e., arterial blood.

DR. SCOTT: I do not think that this necessarily eliminated a venous shunt to an artery-to-artery connection.

DR. BROWN: The collateral network represents an artery-to-artery connection; it is going from, in our case, the left circumflex to the left anterior descending artery. It cannot be a venous A-V shunt because we are not in a venous line when we collect retrograde flow. So it is an A-A connection and that is what an arterial collateral flow presumably is, arterial to arterial.

DR. SCOTT: I don't believe I want to continue this further. The point I am really making is that the volume of retrograde flow following section of the artery distal to the point of ligation may be an overestimation of the arterial flow to the infarcted area under these circumstances.

DR. BROWN: Again, pertinent information comes out of Dr. Gregg's laboratory. He and Dr. Kattus did an extensive study using an isotopic determination to measure collateral flow, and found that retrograde flow was almost identical to this isotopic determination when the myocardial isotope content was taken into account. Donald Gregg estimates that retrograde flow is within 85% of the actual collateral flow.

UNIDENTIFIED DISCUSSANT: We have done some studies with the coronary circulation and phasic pressure. When you elevate diastolic pressure, maintaining systolic pressure at a constant level, you change the mean aortic pressure, which changes the system considerably. What you actually want to do is to elevate diastolic pressure and maintain the mean pressure at a constant; therefore, you would have to drop the systolic pressure. Under those circumstances, when this is done just to the coronary circulation isolated from the cardiovascular system, the coronary flow does not change.

DR. SATINSKY: You stated that maintaining systolic balloon pressure and increasing diastolic pressure is salutory for the coronary circulation. I assume the reverse is true for renal circulation. What would be the desideratum?

DR. BROWN: The effect on the renal circulation does not depend on whether the pulse is during cardiac systole or diastole. In the heart, I guess higher pressure is required in systole than in diastole since the heart has a higher resistance in systole, at least in the collaterals than in the coronaries. However, counterpulsation in the renal bed does influence its function.

DR. SATINSKY: The question is that since it has been shown more recently that pulsatile flow is significant, if you elevate balloon diastole to favor coronary flow, wouldn't that be at the expense of renal or other systemic flow?

DR. BROWN: We have studied that problem with balloon pumping, and the flow to the branches of the aorta did not change. The mean flow did not change; it merely became much more pulsatile. If the balloon acts as an obstructive device in the aorta during diastole, then the diastolic pressure is reduced or mean pressure is reduced in the kidney bed. If the balloon is not obstructive then the diastolic pulsation will be apparent throughout the arterial system and pressure will be elevated in diastole both above and below the balloon.

MR. WILLIAMS: During the life testing, could you tell us at what rate the balloons were cycled? What were the positive and negative pressures used to exercise the balloons?

DR. EVANS: The balloons are exercised at approximately seventy cycles per minute. The positive pressure was 200 mm of Hg and it lasted for approximately two thirds of the cycle. The negative pressure was house vacuum and that is a variable in our testing setup, probably in the range of 15 to 16" of Hg.

MR. WILLIAMS: At what pressure was the water bath?

DR. EVANS: That was at atmospheric.

MR. WILLIAMS: And for how long a period per day was testing accomplished?

DR. EVANS: Twenty-four hours.

DR. ROSENSWEIG: In reference to Dr. Satinsky's question, in other forms of counterpulsation in the ischemic heart preparations, we have demonstrated enhancement of renal femoral and carotid flow in addition to coronary flow during the periods of counterpulsation. I would like to make one point in terms of the augmentation of the coronary flow by the triple balloon. I think there is no question that you get greater diastolic augmentation and enhancement of coronary flow, but I think in the ischemic heart preparation, there may be a critical level of augmentation that is required and I wonder whether the increased complexity of the triple balloon is necessary to produce enhancement of flow to the minimal required level.

DR. EVANS: I do not think we know the answer to your question, as yet.

CHAPTER 46

LEFT HEART ASSIST DEVICES

T. Akutsu, H. Takagi, H. Takano and C. Farish

University of Mississippi Medical Center
Jackson, Mississippi

Both series-type and bypass-type air-driven left heart assist devices have been constructed. The V-shaped implantable series-type device has an air-driven outlet valve. The volume of two sizes of this device is 65 and 95 ml respectively. The bypass-type device has 6 chambers arranged in a hexagonal shape and functions in a peristaltic fashion. The 6 pumping chambers are formed by a one-piece tube divided into 6 sections with 6 rigid outer housings. The device fills as it pumps. The control system for the series-type device has a rate compensation circuit which can automatically change the systole-diastole ratio with changes in pulse rate. The control system for the bypass-type device allows pumping once every 2nd to 8th trigger, and can adjust the number of functioning chambers from 6 to 3. Twenty-eight acute experiments with the series-type device were performed in calves. Extracorporeal circulation was used during implantation. With Model 1 (65 cc), the decrease in LV systolic pressure area was 25 to 30%. With Model 2 and the calf normotensive, the decrease was 52.4% with the valve off and 61.5% when on. With the calf hypotensive (80/50 mm Hg) at a cardiac output of 3.5 l/min., the decrease was 76.3% with the valve off and 82.5% when on. Two acute experiments using the bypass-type device were done in calves. When the pulse rate was 120 in 1:1 trigger using all chambers, alternate peak LV output decreased about 80%, with an average decrease of LV systolic pressure area of 11.6%. Using 2:1 trigger, every other LV output decreased about 90%. Decrease of LV work load varied from 38.5 to 49%. In 3:1 trigger, the average area of 3 consecutive LV pressure curves was almost the same as control. When the number of chambers used was decreased to two and one in 2:1 trigger, aortic peak flows decreased markedly during pumping, and those in between showed 40 to 25% increase. Decrease in LV work load ranged from 25 to 15%.

PUMPING DEVICE

Series-type device.

A human adult-sized device has been constructed. The essential design of the device is the same as that for dogs; the device is pneumatically driven and has an outlet valve which is also driven by compressed air. In designing an original cast the following points were kept in mind: 1) the device should be suitable for use both in human-sized animals and in human adults without changing its shape and size and 2) the volume should be greater than 50 ml. Unfortunately, however, the contours of the chest cavity of human adult-sized animals, such as the sheep and the calf are quite different from those of the human. In order to test a device of 60 ml. capacity which fits snugly in the left upper chest cavity of a 150 lb. adult, we have to use a calf weighing about 180 lbs. which has a narrow chest in the right-to-left direction. Our design has been changed from U-shaped device for dogs to a V-shaped device (Figure 1). The first model has the volume of 65 ml., and the second 95 ml. **Increase in the volume was achieved by modification of the air-driven outlet** valve. The new valve has been designed to be shorter and wider than the original. Therefore, more room has been saved for increase of the capacity of the pumping chamber without changing the overall length.

The construction, materials, and fabrication techniques for the new human adult-size device are essentially the same as those for the device designed for dogs.

Peristaltic pump device. Principle of the pump.

Thrombus formation in prosthetic blood pumps, especially around the valve, still remains a prime problem to be solved. Our bypass-type heart assist device does not have conventional type valves. The device consists of six chambers which work in a peristaltic fashion being driven by compressed air. Therefore, each chamber works as a valve as the peristaltic movement proceeds (Figure 2). This device has two outstanding features: 1) It is in reality an avalvular pump in which the successive pumping of six pumping chambers simulates valve action. Our current work with pneumatically activated flow valves indicated that they do not contribute to clot formation like other types of valves. 2) This device fills as it pumps. This means that at the end of one pumping cycle the unit is already filled to capacity and does not require additional time to fill before beginning its next pumping cycle. Also, when pumping during diastole of the natural heart, the unit will be pumping and simultaneously filling when there is most readily available blood in the left

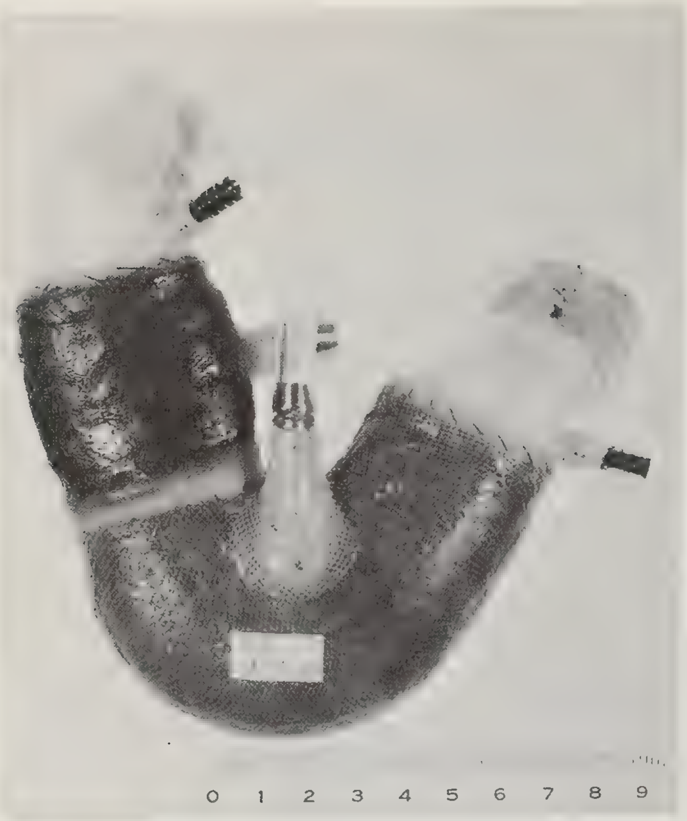

FIGURE 1. PICTURE OF A V-SHAPED SERIES-TYPE HEART ASSIST DEVICE (MODEL 1). RIGHT SIDE CUFF WILL BE CONNECTED TO THE ASCENDING AORTA BY END-TO-END ANASTOMOSIS, AND LEFT SIDE CUFF TO THE DESCENDING AORTA BY END-TO-END ANASTOMOSIS. DARKER SQUARE PART BELOW THE LEFT SIDE CUFF IS THE AIR-DRIVEN OUTLET VALVE.

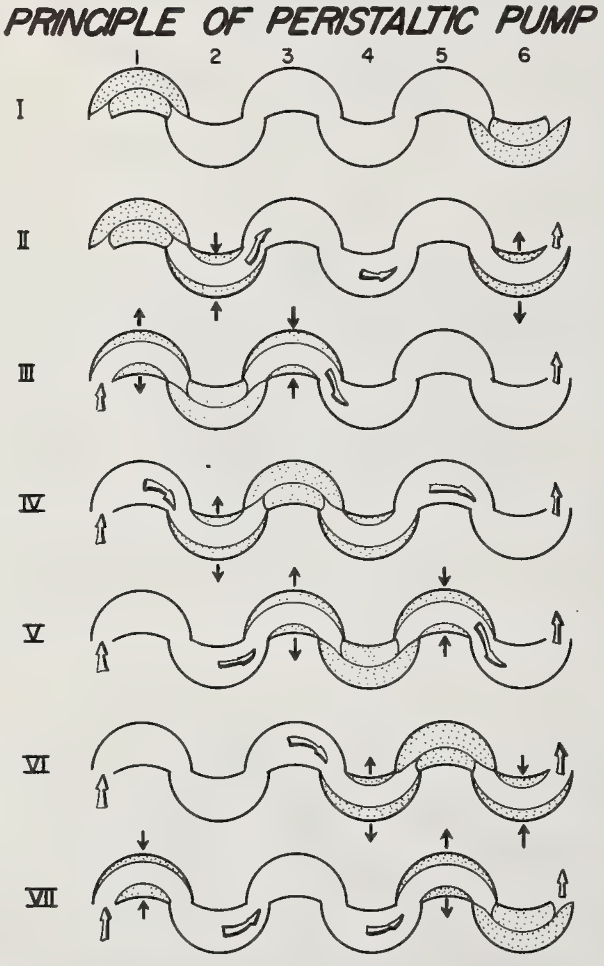

FIGURE 2. PRINCIPLE OF THE 6-CHAMBERED PERISTALTIC BY-PASS TYPE LEFT HEART ASSIST DEVICE.

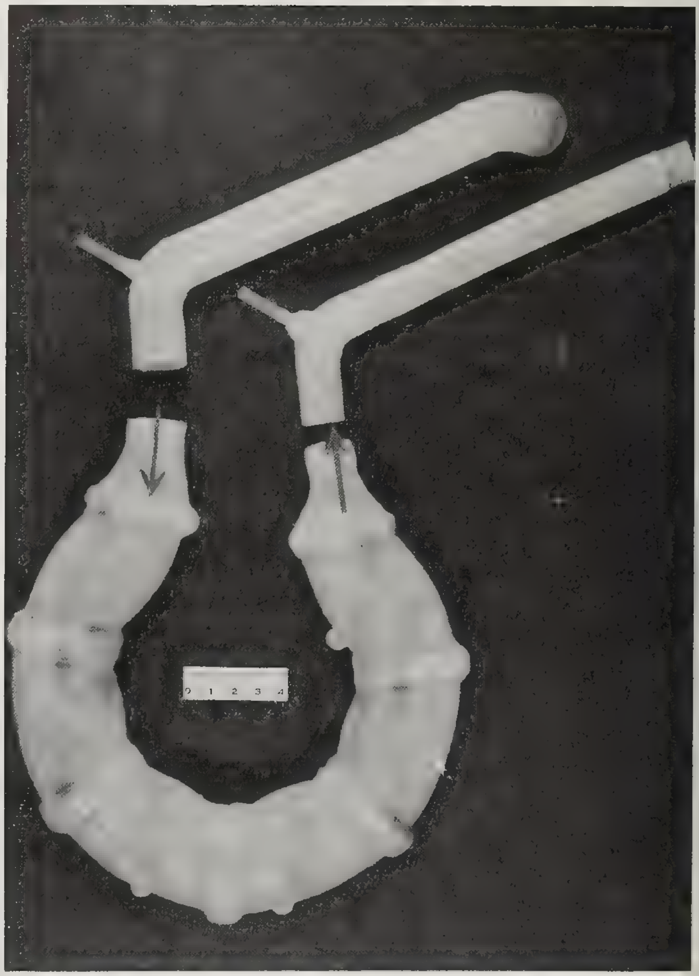

FIGURE 3. PICTURE OF THE 6-CHAMBERED AIR-DRIVEN PERISTALTIC PUMP.

atrium in the beginning of diastole. This eliminates one of the major disadvantages of the sac or diaphram type of bypass pumps; i.e., the lack of sufficient blood to fill them. This is especially true of these two types of pumps when they are employed at high heart rates.

Peristaltic pump device.

The six chambers have been arranged in a hexagonal shape on the same plane (Figure 3). The middle four chambers are exactly the same shape, and the two at either end of the pump are mirror images of each other. In order to achieve quick closure and opening of the chamber and not to prevent irregular and incomplete closure as seen in a round tube, the cross-section was made in the shape of a 60° ellipse. Since the cross-sectional area is the same all the way, the inside of the pump is essentially a hexagonal single tube, having no pocket, recess or groove. The outside of the tube was divided into six sections with six rigid housings. The tube which constitutes six pumping chambers as well as six valve chambers was made of Silastic. The six housings made of fiberglass-resin were completely covered with Silastic. A connector also made of Silastic was attached to each inlet and outlet of the pump. A short piece of Dacron graft was attached at the tip of the connector.

CONTROL AND DRIVING SYSTEM

System for series-type device.

The original unit consists of a cardioscope displaying the ECG, selectable frequency cut-off controls, adjustable trigger circuits, and adjustable delay, injection (systolic time), filling (diastolic time), dropout and internal triggering time circuits. The trigger controls are normally adjusted so that the unit triggers on the R-wave of the ECG, and is delayed for the necessary interval in order for injection to occur after the T-wave. Our unit can be triggered at any point from the P- to S-wave of the ECG. The cardioscope is intensity modulated during the injection period. At the end of the injection time, filling starts automatically and continues for a preselected time.

If the unit fails to receive an ECG trigger for a selected dropout time, it automatically gates on audio and visual alarms and switches to the internal trigger. Two successive ECG triggers turn the alarms off and return the unit to normal operation automatically.

The unit has a rather unique circuit, automatic rate compensation system. The circuit has been designed in order to change the delay duration automatically as the heart rate changes. If the heart rate increases, the delay duration becomes shorter. The purpose of this automatic rate compensation is to maintain the ejection period of the pump immediately following the -T- wave of the animal's heart.

The major changes in the design of the new system are as follows: 1) It has completely transistorized ECG preamplifiers and **trigger amplifiers.** 2) It has transistorized horizontal and vertical deflection circuits. 3) It has three built-in function generator curves. 4) It has a completely redesigned power supply utilizing an AC to DC converter to allow emergency stand-by operation on no voltage batteries. 5) It has incorporated into it a high trigger detector in order to lock the unit open and sound alarms in the event of a loss of an ECG lead which would cause the unit to start triggering on 60 cycles. 6) Individual circuits have been incorporated into each individual printed circuit board.

System for peristaltic pump.

Figure 4 shows the system for the peristaltic pump in a pretriggered or hold condition, the first and 6th chambers are closed (Figure 5). An external trigger pulse causes the device to enter the transient state. At this stage chamber 2 is closing as chamber 6 is opening. The pulse which triggers the transient state simultaneously activates a time base generator with a time period long enough to allow chamber 2 to close completely and chamber 6 to expand and fill. At the end of this time period the base generator puts out a pulse triggering the next transient state, during which chamber 3 closes as chamber 1 opens. This trigger pulse also activates a second time base generator set for an interval sufficiently long to allow chamber 3 to close and 1 to open completely. Then, the time base generator triggers the next transient state. It can be seen that while one chamber is completely closed, the chamber adjacent to it on the output side is closing and the one adjacent to it on the input side is opening. This peristaltic pumping action continues through the entire phase. At the end of the phase the device returns to the pretriggered or hold condition, and remains in this condition until another external trigger pulse is received.

This pulse could come from a control circuit such as the one we are presently using, and could coincide with the end of the delay time so that the assist device pumps during the diastole of the natural heart. If desired, this trigger pulse could coincide instead with the beginning of the delay period so that the device would pump simultaneously with the natural ventricle. Or, if desired, the control circuit could be allowed to drop out, and the device run on the internal trigger generator. This would allow pumping of the device asynchronously with the natural heart's action at a rate selected by the operator. Provision was also made in the peristaltic pump control unit for continuous pumping. We feel that as the natural heart recovers from surgery, injury or disease, that necessitated the use of the ventricular support device, the work load could be returned to it gradually, rather than putting the entire work load on it suddenly, when the support device is removed. To facilitate this we have incorporated, between the trigger output of the control circuit and the peristaltic pump control, a trigger count-down device that allowed us to pump on every second, third, fourth, fifth trigger, etc. An additional means for decreasing the work load of the support pump and thus increasing the load on the natural ventricles will be discussed below.

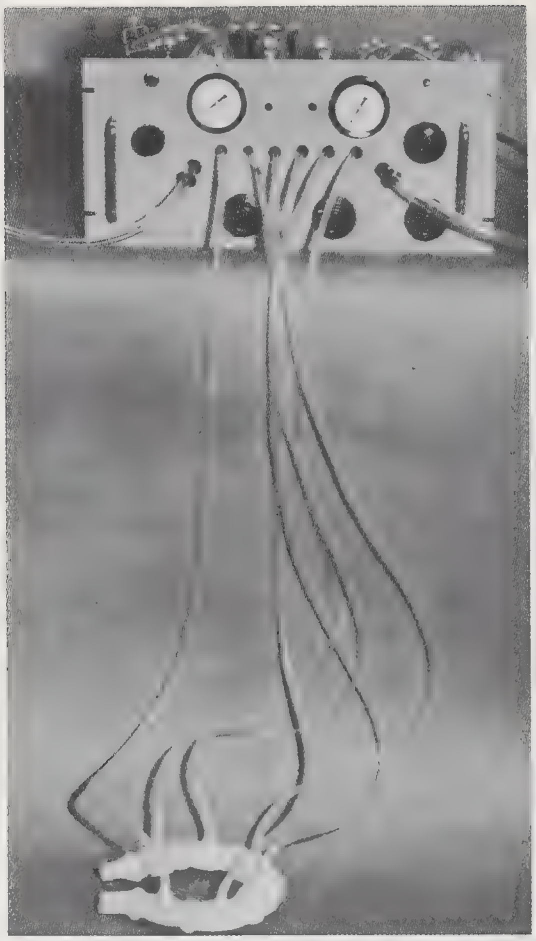

FIGURE 4. PICTURE OF THE CONTROL AND DRIVING UNIT CONNECTED TO THE PERISTALTIC PUMPING DEVICE.

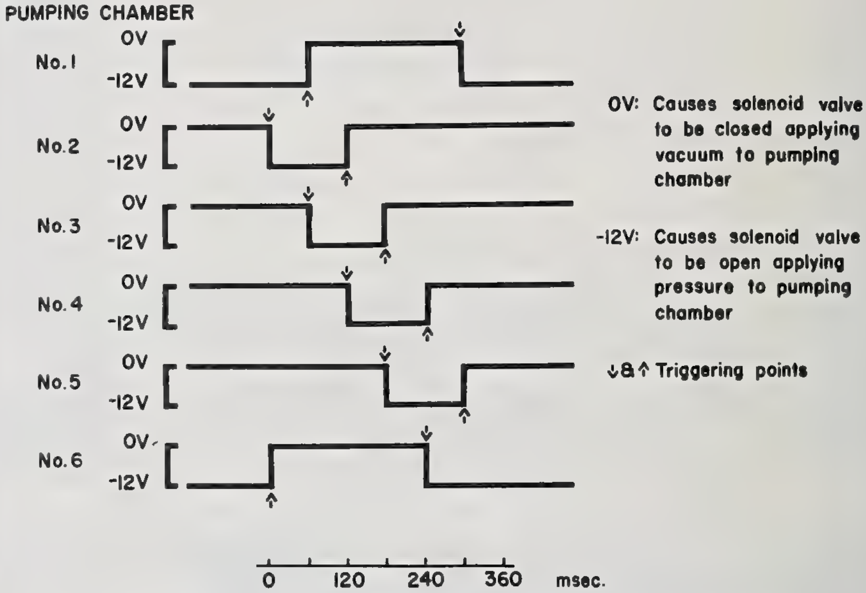

FIGURE 5. DIAGRAM OF THE SEQUENTIAL ELECTRICAL CONTROL OF THE 6-CHAMBERED PERISTALTIC PUMP.

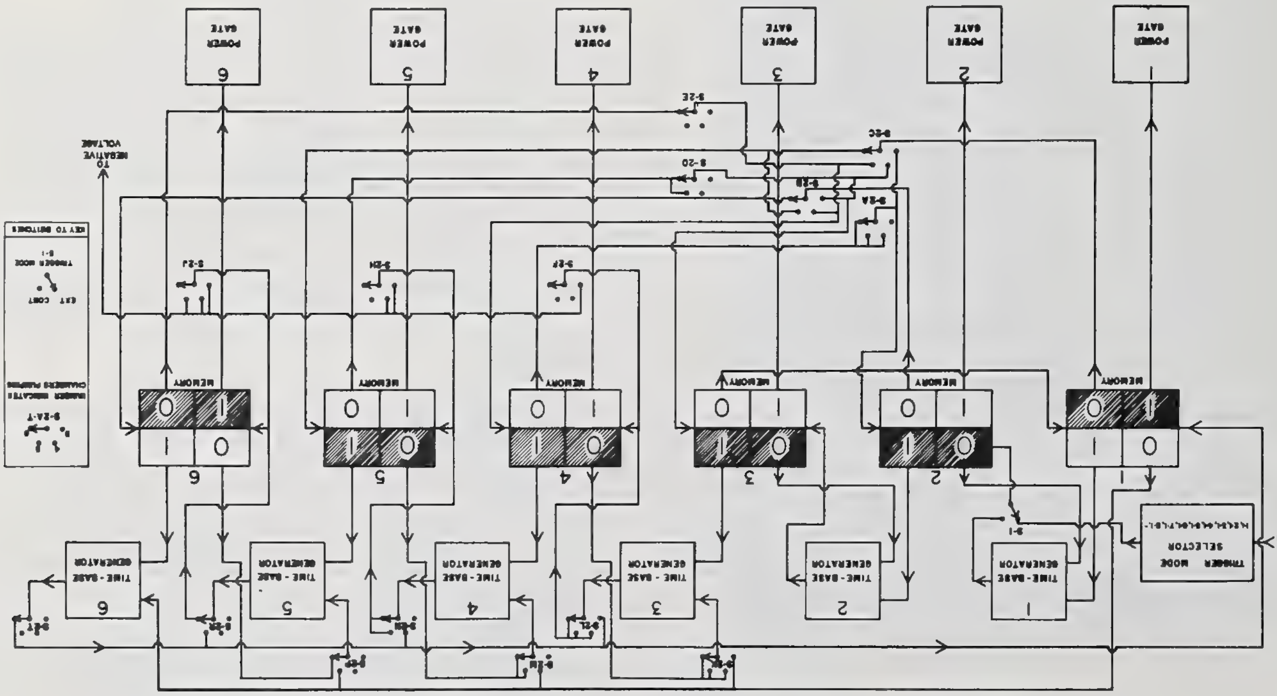

FIGURE 6. BLOCK DIAGRAM OF THE CONTROL UNIT FOR THE PERISTALTIC PUMP.

The control system consists of six bistable memory circuits, six solenoid power gates and six time base generators (Figure 6). However, only five of the time base generators will be needed when the trigger pulses originate externally and the device is operated at maximum stroke volume. Correspondingly fewer time base generators will be needed when the stroke volume is reduced, as this will be accomplished by using only five, four, or even three, of the pumping chambers. The switching circuit made this possible. When some of the pumping chambers are not in use they become straight tubes. Thus, we have achieved a stepwise increment or decrement of stroke volume. This is the second means of gradually increasing the work load on the natural ventricle as it recovers.

BENCH-TOP TESTS

Tests of bypass-type pump.

Pumping characteristics of the device have been determined by bench-top tests using a test circulatory system. Left atrial pressure was fixed at around 10 cm H_2O, and mean arterial pressure at around 90 mm Hg. Time of pumping all 6 chambers was constant, 360 msec until the pulse rate up to 200. Therefore, one cycle at PR of 60 in 1:1 trigger was the same as that at PR of 120 in 2:1 trigger. Changes in length of cycle at PR over 200 was due to the shortening in the opening time of chambers No. 1 and No. 6. The total closing time from No. 2 chamber through No. 5 chamber stayed constant. The system would not function properly when the pulse rate was faster than 200. There was some regurgitation when No. 1 chamber closed. Cardiac outputs did not change in proportion to the trigger. The higher the pulse rate, the larger the decrease. For instance, at PR 60, cardiac outputs in 2:1 trigger decreased to 55 to 62% of those in 1:1 trigger, and at PR 120 decreased to 30 to 43%. Maximum cardiac output obtained was 5 l/min. with air pressure, 300 mm Hg, vacuum - 10 mm Hg, PR 164, using all chambers. In the first control system maximum time of one cycle available for each chamber is approximately 120 msec. The diameter of the air tubes used was 5 mm which was the same as that used in the series-type heart assist devices with the capacities of 65 and 95 ml. Air pressure required to achieve sufficient compression of each chamber was much higher than expected. The wall suction available in the laboratory was not strong enough to expand the chambers within a limited time.

Bench-top tests for series-type pump.

These tests have been performed using the mock circulatory system and the timer designed for dog-sized devices. The left chamber of the total artificial heart designed for 150 lb. sheep was used as a pump which corresponds to the natural left ventricle. This combination made it possible to test two different types of pumps simultaneously. By using a 10 liter capacity Fisher-Porter flowmeter, the pump was regulated so that the flow was around 5 liters per minute.

DEVICE FACILITATING CONTINUOUS PUMPING WITHOUT ATTENDANCE

The necessity for constant observation has been an obstacle to the achievement of long-term continuous artificial pumping in experimental animals without difficulties with either electrical or pneumatic connections, or both. In some laboratories where night shift personnel are not available, the period of artificial pumping has been limited to 8 to 10 hours a day. Our device to circumvent this consists of three components: 1) a percutaneous lead, 2) a universal coupling, and 3) a pulley system (Figure 7).

The percutaneous lead consists of a Silastic body through which pass two stainless steel pipes for the pumping chamber and the valve chamber pressure lines. A piece of Dacron velour is glued around the Silastic to encourage tissue ingrowth. Since the Silastic lead is both flexible and compressible, it buffers the twisting action of the air tubes and thus promotes wound healing. The construction of the universal coupling is essentially the same as that designed for use on dogs except that the pipes through the device are larger since the air line diameter is larger for calves. The pulley system was designed for more safety and better efficiency of the whole device. It consists of one double wheel unit, and another freely rotating wheel which is fixed on the edge of the animal cage. The upper wheel of the double wheel unit slides on a bar across the top of the cage. The universal coupling and the balancing weight are hung on each end of a rope which is spun between the lower wheel and the wheel fixed on the cage. The coupling moves smoothly up and down as the animal stands or lies down.

ANIMAL EXPERIMENTS

Patency experiments with dog-sized series-type devices.

These experiments were continued to investigate thrombus formation in the inlet side of the device. Thirty-three experiments were done. In the first group a stainless steel ring was used at the connecting end of the inlet cuff, and in the second group a Dacron graft was used.

In the first group of nine dogs, the ring was completely covered with Silastic, and a piece of Dacron velour was attached on the outside for tissue ingrowth. It was found that connection of the inlet cuff with a ring was technically more difficult than when a Dacron cuff was used. Six were lost from technical failures; one by tear of the aorta, and from brain damage due to prolonged aortic occlusion, one from bleeding, and three from the ring slipping out. One dog died from bleeding, on the outlet side on the 8th postoperative day. Two died from thrombo-emboli on the 7th and

14th postoperative days (Figure 8). The results of these and of earlier similar experiments indicate that thrombus formation is greater in the ring type connection than in any other type of construction, eventually causing thrombo-emboli no matter how smooth the edge is made.

In the second group, numbers of dogs which died by various causes unrelated to thrombi were five from technical failures, one from atelectasis 13 days postoperatively, two from unknown causes 10 to 12 days postoperatively, one from infection (9th day postoperatively), four from bleeding (6th, 7th, 8th, 11th days postoperatively), and one by pyelonephritis (72nd day postoperatively). Eight dogs which died from thrombo-emboli survived from four to 36 days. Late death by bleeding was due to insufficient fusion between the Dacron graft and the aorta. This was caused by overcoating the graft with Silastic-xylene solution. In the eight dogs which died from thrombo-emboli there were no visible thrombi or very few found at the Silastic-Dacron junction. Figure 9 shows a specimen recovered from a dog which was sacrificed on 542nd postoperative day. One dog remains alive for 270 days (May 20, 1969).

Studies of regional myocardial blood flow.

One of the main functions of the heart assist device is to augment the coronary flow by counterpulsation. There are numerous reports describing a net increase in the coronary flow during counterpulsation. However, there is no report available concerning the effect of counterpulsation on the blood flow in the area distal to the occluded coronary artery. This series of experiments was designed to elucidate the effect of counterpulsation on the regional coronary blood flow with the use of Rb^{86} clearance.

After injection of Rb^{86} dogs were sacrificed, and the heart was taken out. Measurements were done with myocardial specimens taken from the following parts of the heart: Three portions each from the right atrial side and the septal side of the right ventricular wall (RV), upper and lower portions from the anterior and posterior sides both in the septum (S) and the left ventricular wall (LV).

In five control dogs the left anterior descending branch was ligated immediately after the bifurcation from the circumflex branch. In two of five control dogs the ligature was placed proximal to the septal branch. In seven dogs a series-type assist device was employed after ligation of the coronary artery at the same place as in the control group. In two of them, the septal branch was also ligated.

In the control group a slight increase was noted in the endocardial side of RV. Compensatory increase was noted both in S and LV particularly in the LV side of S and in the endocardial side of LV except in the anterior lower portions of both S and LV where the flow decreased almost to 20% (Figure 10). When the septal branch was not ligated, the decrease in the anterior lower portion of S was slight. By pumping with an assist device after ligation of the coronary artery a marked increase, larger on the endocardial side, was noted in RV (Figure 11). Increases in S and LV were also considerable, except in the anterior lower portions. The anterior lower portion in LV did not show any improvement except in one dog. We cannot give an explanation for this. In the anterior lower portion in S, even when the septal branch was ligated, the flow increased 50% although the value was still on 30% of the normal average.

Development of a new technique for implantation of new human-sized series-type devices in calves and acute hemodynamic studies.

Thirty-three experiments were performed. In order to obtain as much working room as possible around the ascending aorta, both the brachio-cephalic artery and the aortic arch were dissected and occluded temporarily during anastomosis of the inlet cuff of the device to the proximal end of the bisected ascending aorta. Therefore, two arterial cannulas had to be inserted each via the right femoral and the right carotid arteries. Venous blood was drawn from one cannula inserted into the inferior vena cava through the right atrial appendage and from another cannula inserted into the superior vena cava through the right jugular vein. Extracorporeal circulation was done using three roller pumps and a bubble oxygenator.

In the first two experiments the calves used weighed 180 lbs. The device was inserted without difficulty and pumping continued for three hours. After these experiments two changes had to be made: 1) The direction of the outlet cuff and 2) the size of both cuffs from 25 mm to 22 mm. Vent drainage from the left ventricle was done and coronary perfusion was performed during anastomosis of the inlet cuff to the ascending aorta.

The stroke volume of calves used was larger than the capacity of the Model 1. The decrease in left ventricular pressures was small, and was larger when the outlet valve was off than when it was on, which was expected. When the heart was still in failure after the extracorporeal circulation was stopped, the decrease in the systolic area of the left ventricular pressure was around 30%.

In the last eight experiments, Model 2 which had the volume of 95 ml. was implanted. When the calf was in good condition having a high blood pressure of 130/80 mmHg, decreases in the area of the systolic portion in the left ventricular pressure curves were 52.4% with the valve off, and 61.5% when on. When the calf was in poor condition with the blood pressure of 80/55 mmHg and the cardiac output of 3.5 l/min., they were 76.3% when the valve was off, and 82.5% when on. (Figure 12). The systole-diastole ratio in calves we used was 1.5 to 2.25 which was much larger than that in human beings or dogs. Therefore, the basic delay time at the pulse rate of 75 was set at 340 msec when the unit was triggered by the R-wave. The time from the triggering point (A) to the start of the expansion of the pumping chamber (B), and the time from B to the minimum point of the ascending aortic pressure (C) before the left ventricular contraction were 30-40 msec, and 20 msec respectively.

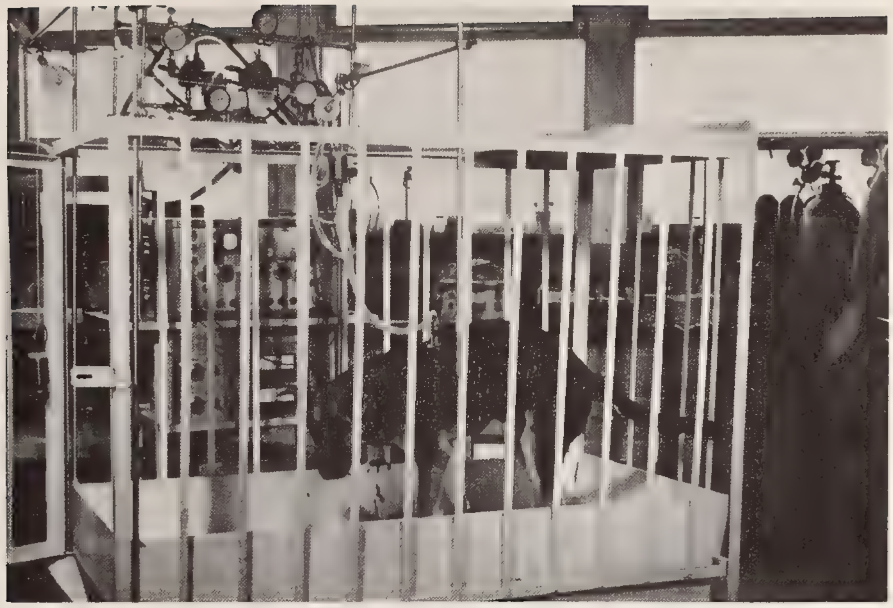

FIGURE 7. PICTURE OF THE DEVICE WHICH FACILITATES CONTINUOUS PUMPING ALLOWING THE DOG FREE MOVEMENT. THE DEVICE CONSISTS OF THREE COMPONENTS: 1) PERCUTANEOUS LEAD WHICH IS SEEN FIXED ON THE BACK OF THE DOG, AND 2) UNIVERSAL COUPLING SHOWN JUST BELOW THE UPPER EDGE OF THE FRAME AND 3) PULLEY SYSTEM ATTACHED TO THE FRAME OF THE CAGE.

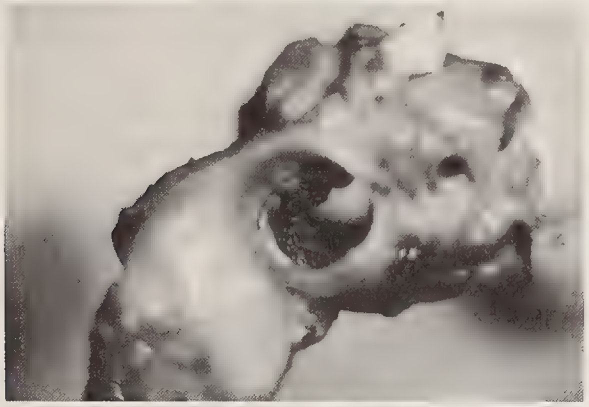

FIGURE 8. SPECIMEN RECOVERED FROM A DOG WHICH DIED BY THROMBOSIS ON THE 14th POSTOPERATIVE DAY. NOTICE THICK THROMBI FORMED ALL AROUND INSIDE THE RING.

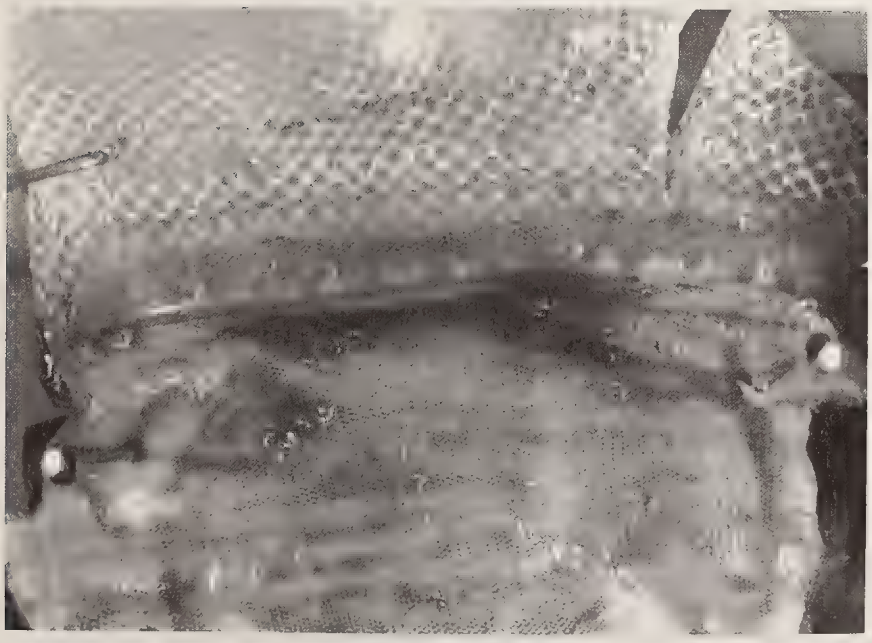

FIGURE 9. SPECIMEN RECOVERED FROM A DOG WHICH WAS SACRIFICED 542 DAYS AFTER IMPLANTATION. NOTICE A SMALL AMOUNT OF THROMBI COMPLETELY COVERED WITH SMOOTH PSEUDO-INTIMA AT THE SILASTIC-DACRON JUNCTION.

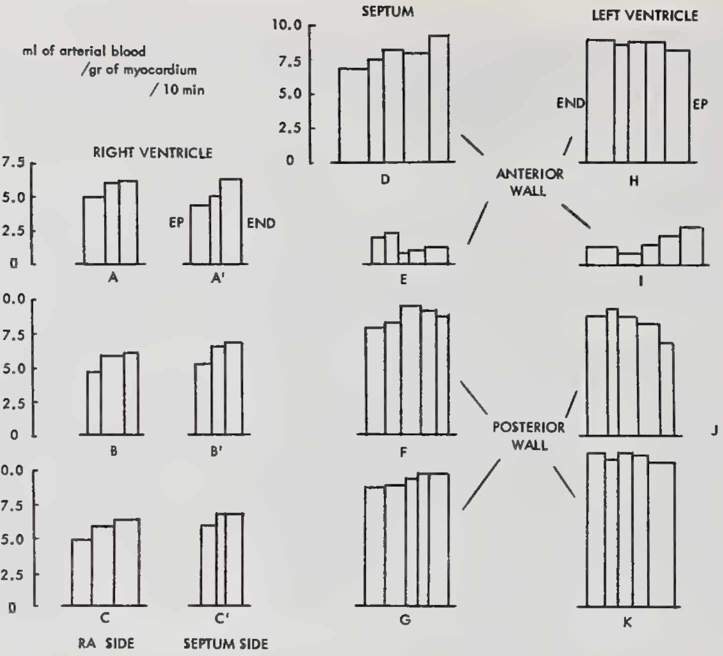

FIGURE 10. REGIONAL MYOCARDIAL BLOOD FLOWS FOLLOWING OCCLUSION OF THE LEFT ANTERIOR DESCENDING BRANCH EP = EPICARDIAL SIDE. END = ENDOCARDIAL SIDE. RA = RIGHT ATRIUM.

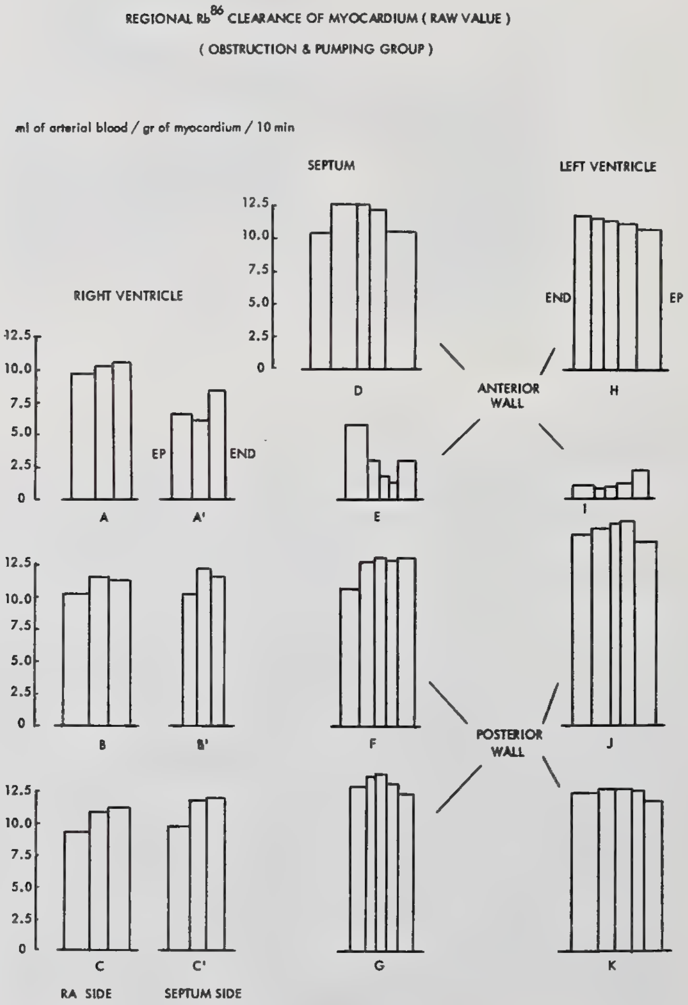

FIGURE 11. REGIONAL MYOCARDIAL BLOOD FLOWS DURING COUNTERPULSATION WITH A SERIES-TYPE LEFT HEART ASSIST DEVICE FOLLOWING OCCLUSION OF THE LEFT ANTERIOR DESCENDING BRANCH.

However, C never reached 0. This means the pumping chamber was not quite ready when the left ventricle started to contract. This problem may be **solved** either by improving the exhaust line or by triggering on the P-wave. However, as previously mentioned, the duration of diastole in calves is so short that the time from the end of the T-wave to the P-wave is about 100 msec at normal pulse rates, which is not long enough to completely empty the large pumping chamber. If this problem is solved, complete atrialization of the left ventricle should be possible with Model 2 device.

Acute animal experiments with peristaltic bypass-type device.

Five acute experiments were done in calves which weighed from 74 to 80 kg. Anesthesia was induced with Surital and maintained with Fluothane. After the chest was opened through the left fourth intercostal space, the outlet connector end was first connected to the descending aorta by end-to-side anastomosis. On completion of anastomosis of the inlet side connector to the left atrium, the device and connectors were filled with heparinized normal saline. The ECG was taken by the chest lead. During pumping the device was placed on the left chest wall. The following parameters were measured; bypass flow, flows in the ascending aorta and pulmonary artery, and pressures in the left atrium and left ventricle. Air pressure used was 450 mm Hg. Vacuum used varied according to the pulse rate. As described in the bench-top tests, wall suction was not strong enough when the pulse rate was high especially in the Model 2 (larger model). This hindered us to obtain larger cardiac output at pulse rates higher than 100.

When triggers were changed from 1:1 to 5:1, ventricular pressure curves showed a regular gradual increase with the lowest pressure curve at the triggered pulse (Figure 13). The area of the systolic portion of left ventricular pressure curves as compared with the control were 0% in 1:1 trigger, 1.6% and 18.3% in 2:1, 33.6%, 49.3% and 82.2% in 3:1, 32.2%, 57.9%, 83.6%, and 95.4% in 4:1, and 36.8%, 44.1%, 80.9%, 93.4% and 80.9% in 5:1. Their changes according to the number of chambers used in 1:1 trigger were 0% when four chambers were used, 37.3% when three chambers were used, 86.7% when two chambers were used, and 110.7% when one chamber was used (Figure 14). Thus, when all four chambers were used in 1:1 trigger, complete atrialization of the left ventricle was achieved. Gradual changes in the bypass flow was possible by changing either triggering or number of chambers used.

SUMMARY

Two models of a new human adult-sized series-type heart assist device have deen designed and constructed. The volumes of each model are 65 and 95 ml. They can be implanted in calves weighing around 180 lbs. and also in adult patients without changing the volume and shape. A new control and driving system has been designed. We are supposed to construct six such units, one for our own use and five under subcontract. A prototype device facilitating a continuous pumping without attendance has been constructed. Thirty-three patency experiments were done with series-type devices in dogs with an emphasis on the inlet side construction. Large thrombi apparently always form around the connecting line when a ring was provided at the end of the inlet cuff. With modification in design and improvement in construction technique no visible thrombus or very few were found at the Silastic-Dacron junction. When the graft is carefully connected with a few crimps eliminated at the junction and with a proper use of Silastic glue, death by thrombo-emboli would be avoided.

Regional myocardial blood flow studies following ligation of the left anterior descending branch were performed and the effect of pumping with series-type assist devices was investigated in dogs. A new implantation technique for adult-sized series-type devices has been established in calves using a pump-oxygenator, and some acute experiments have been performed for hemodynamic studies. Using a device of Model 2, left ventricular work load has been considerably reduced. A peristaltic bypass-type heart assist device has been designed for human adults and large animals such as calves. In calf experiments complete atrialization of the left ventricle has been achieved. Further increase of maximum cardiac output should be possible by applying stronger suction, by preventing regurgitation, and by increasing the time duration of one cycle. The first control unit functioned satisfactorily. Stepwise changes of the pumping volume have been achieved either by changing triggering or by changing the number of chambers used.

DISCUSSION

DR. JAFFRIN: I wonder what makes you choose this type of pump rather than the ordinary type of a roller pump. Do you expect that the rate of hemolysis will be lower with your pump, because I understand that it operates with complete occlusion over a larger section of the tube, and the rate of hemolysis may be large.

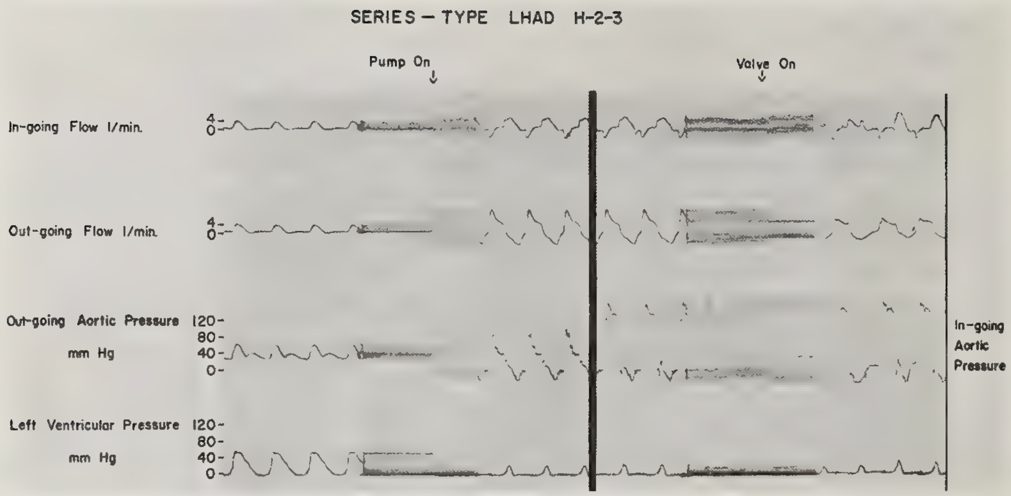

FIGURE 12. OBSERVED HEMODYNAMIC CHANGES BY PUMPING WITH A SERIES-TYPE LEFT HEART ASSIST DEVICE. NOTICE A MARKED DECREASE IN LEFT VENTRICULAR PRESSURES DURING ARTIFICIAL PUMPING.

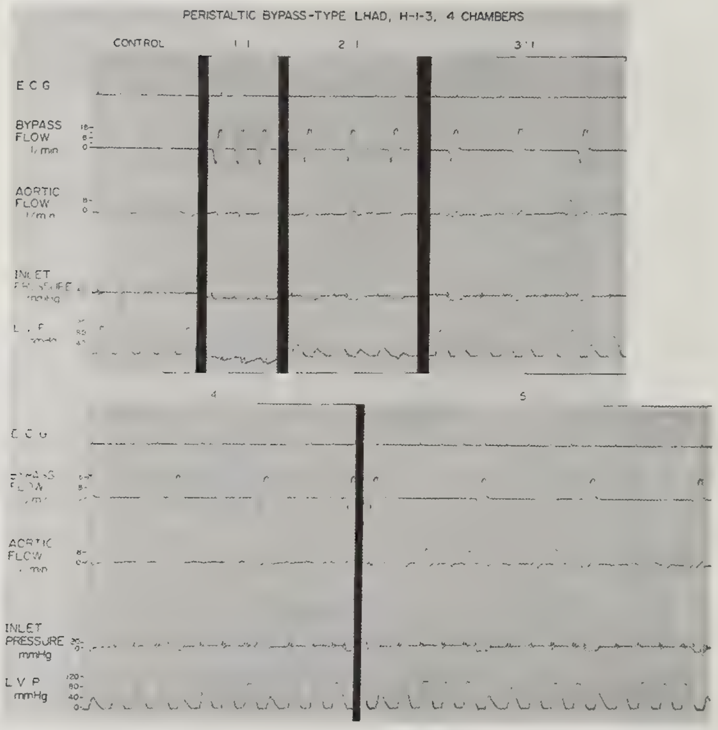

FIGURE 13. HEMODYNAMIC EFFECTS OF CHANGES IN TRIGGERS DURING PUMPING WITH THE PERISTALTIC BYPASS-TYPE DEVICE. NOTICE COMPLETE ATRIALIZATION OF THE LEFT VENTRICLE IN TRIGGER 1:1, AND STEPWISE REGULAR CHANGES IN LEFT VENTRICULAR PRESSURES ACCORDING TO CHANGES IN TRIGGERS.

DR. AKUTSU: We did not do any chronic experiments yet, so I do not know what kind of hemolysis you will have. The series type was used in one dog last year for a period of 16 days. One week afterwards, the plasma free hemoglobin was 36 mgs %.

DR. ATSUMI: We have been developing a portable driving mechanism for the artificial heart, utilizing a fluid amplifier system. You can see the system of an artificial heart around the sheep. We tried to drive an artificial heart with this system. The projection slide shows a diagram of the system (Slide). What do you think about the possibility of a portable driving mechanism for left heart bypass?

DR. AKUTSU: I didn't get the question.

DR. HASTINGS: I think the word is "portable."

DR. AKUTSU: Well, I think you have to provide some means for the patient to move around. Maybe the control system could be placed under the wheelchair. Of course, it is good to have that type of device.

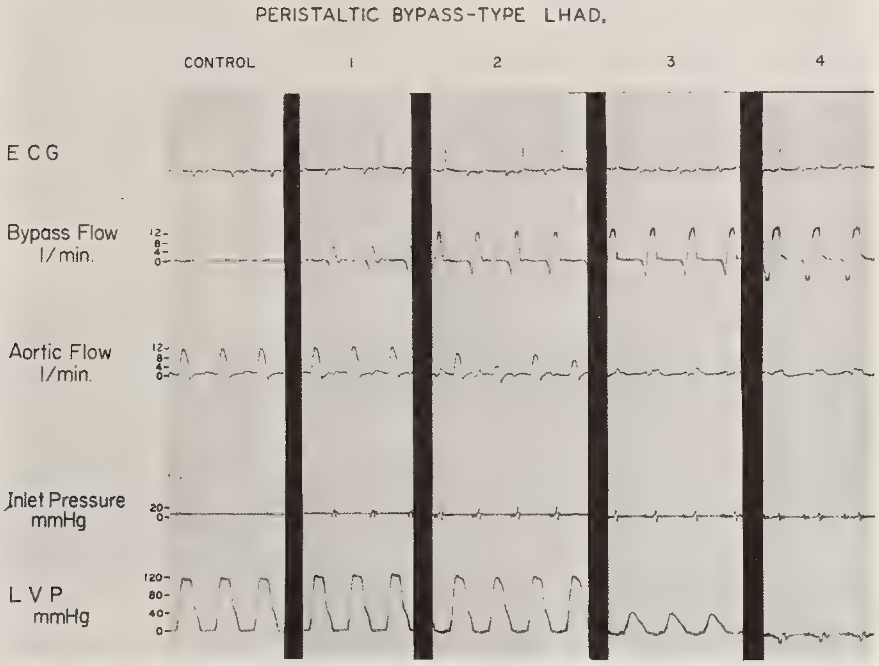

FIGURE 14. HEMODYNAMIC EFFECTS OF THE PERISTALTIC BYPASS-TYPE DEVICE BY CHANGING NUMBER OF CHAMBERS USED. TRIGGER USED WAS 1:1. NOTICE COMPLETELY FLAT LEFT VENTRICULAR PRESSURES AND ALMOST NO CARDIAC OUTPUT FROM THE LEFT VENTRICLE WHEN ALL FOUR CHAMBERS WERE USED.

CHAPTER 47

THE IN-SERIES SUBCUTANEOUS EXTERIORIZED PUMPING VENTRICLE WITH POSITIVE ACTING VALVE

F. Giron, W. Birtwell, H. Soroff

Tufts-New England Medical Center Hospitals
Boston, Massachusetts

A pneumatically operated, tubular, prosthetic ventricle designed for subcutaneous implantation has been produced. The molded silicone rubber ventricle, lined with Dacron velour, has been implanted in 12 dogs to study the long-term physiologic effects of non-actuated prostheses. Two animals survived for one month, and 4 for one week or more without the use of anti-coagulants. The linings which formed on the velour surface were of irregular thickness, often ridged in areas of curvature, and rough. The poor survival rate experienced in this series and the activity and excitability of the healthy survivors lead to the choice of the calf as the experimental animal for chronic studies of the effects of continuous actuation of the prosthesis. Of the first 6 calves in which the prosthesis was implanted for patency studies without actuation, 1 survived for more than 3 months, 3 survived for 3 weeks to 1 month, and 2 died 3 days after the procedure as a result of technical errors. Pulmonary infection was the cause of death in all animals except the 3-month survivor which succumbed to an uncontrollable infection at the site of the prosthesis. The use of anti-coagulants has resulted in the development of smooth, thin, glistening linings well adherent to the Dacron velour. In acute studies, 3 models of distal valve operation have been studied: passive-open to provide counterpulsation, pressure-loaded to provide a controllable differential between the proximal and distal pressure, and active-pressure operation for normal valving. The pressure loaded mode permits the elevation of coronary perfusion pressure to a selected level above the distal aortic pressure. The hemodynamic effects of the in-series pumping ventricle have been documented previously in acute studies. Initial experience with the calves indicates the feasibility of chronic studies using continuous pneumatic actuation.

INTRODUCTION

At the completion of the initial contract year, we had produced an "in-series" prosthetic left ventricle along the lines described in our original publication of 1965. The prosthesis, manufactured by the Brunswick Manufacturing Company Incorporated of Quincy, Massachusetts, was made of silicone rubber with inner and outer linings of Dacron velour. It consisted of three parts (Figure 1) connected by specially designed connectors made of nylon. It was felt that this type of construction would provide the necessary flexibility to allow the orientation of the prosthesis to be varied in order to conform for the differences in size and anatomical characteristics of each dog. Fifteen of these prostheses, along with three synchronous power supplies and an actuator were produced (Figure 2).

The present extension of the contract called for improvements in the connecting pieces of the prothesis, the development of equipment to facilitate chronic actuation of the prosthesis and three series of in vitro, acute and chronic studies to determine the hemodynamic characteristics of the device. Each one of these tasks has been performed. But, since chronic actuation of a prosthesis installed in a normal animal was the primary goal of this contract, the work schedule proposed originally, was modified as experience dictated in order to more readily accomplish this goal.

The final details of the construction of the connecting pieces are shown in Figure 1. A tubular projection, covered with Dacron velour provides a male connector which fits into a counterbore in the connector located in the other element. The resulting junction presents no shoulder on the internal surface of the lumen. Externally, the junction is secured by the plastic ring as shown. This design results in a rigid connection of more bulk than the rest of the prosthesis and as will be indicated has produced pressure necrosis in the skin of three animals.

In vitro studies of the prosthesis were carried out in a system which provided a continuous pulseless flow for the measurement of resistance and a sine wave modulation for the measurement of impedance. The resistance drop across the prosthesis was shown to be 1 mm Hg at a flow of 8 liters per minute. At lower flow rates, the resistance drop was less than 1 mm Hg and hence difficult to measure accurately. When the flow was modulated by a sine wave hydraulic generator, the essentially sinusoidal pressure ripple was 90^{0} out of phase with the modulated flow, indicating that the impedance was substantially inertial. At a DC flow rate of 8 liters per minute and a modulation of plus or minus 39.5 cc per second, the ripple pressure drop across the prosthesis was 4.2 mm Hg peak.

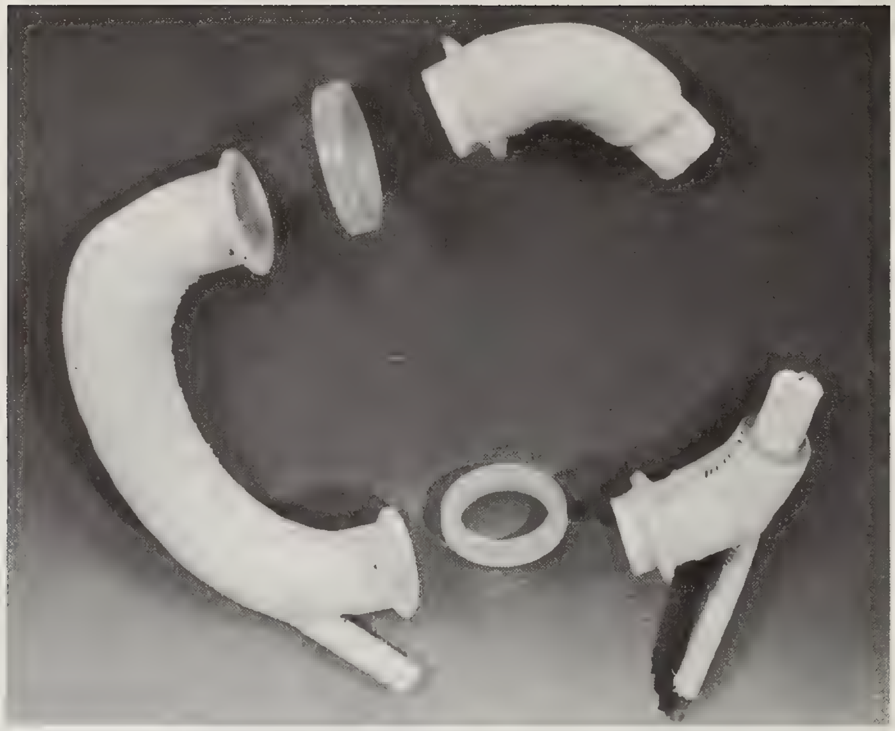

FIGURE 1. PROSTHESIS USED IN THE DOG.

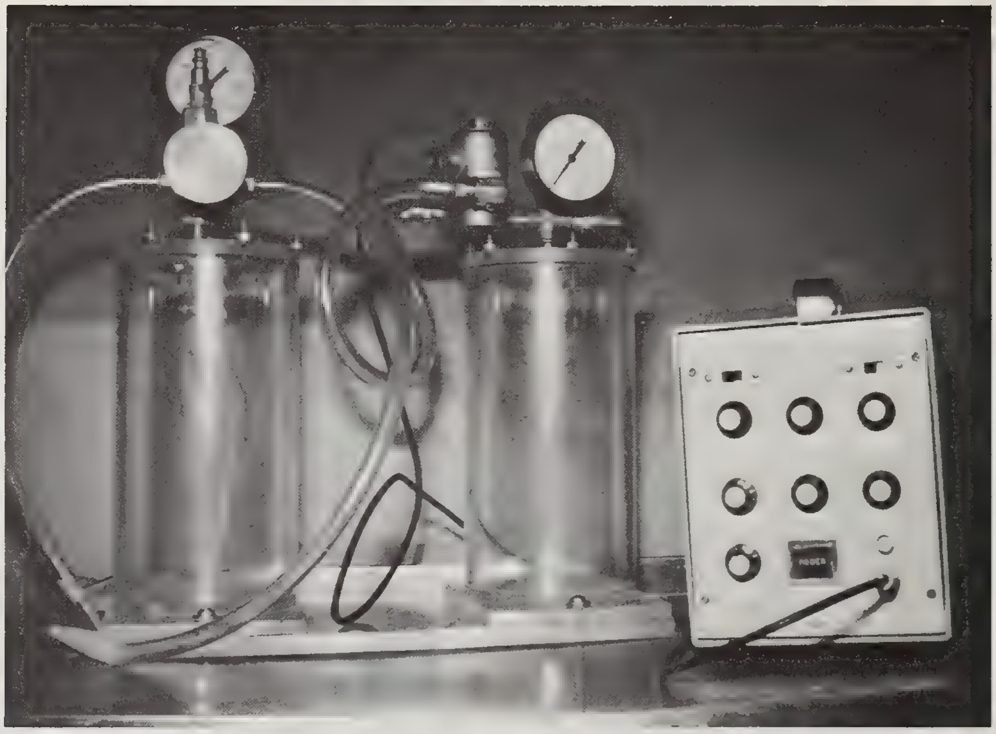

FIGURE 2. ELECTRONIC POWER SUPPLY.

Acute studies of the hemodynamic characteristics of the prosthesis were performed in five dogs and reported in last year's annual report. In summary, it was shown that the pressure gradient across the prosthesis, measured from left ventricle to the descending aorta averaged 20 mm Hg and was mainly related to the right angle anastomosis. Activation of the prosthesis, provided with a valve resulted in a 70% reduction of the left ventricular pressure (Figure 3).

CHRONIC EXPERIMENTS

Our greatest efforts during this contract were concentrated on the solution of problems related to chronic survivals. In this regard, we will present the approaches and results in the dog, our early experience using the calf as the experimental animal, and finally our present approach to the problem.

Four types of operative procedures were used in the dog as presented schematically in Figure 4. In Type I a double thoracotomy was made on the left side of the chest in the 4th and 7th intercostal spaces. The proximal and distal anastomoses were made end-to-side to the ascending aorta and descending aorta at the level of the 4th and 7th rib respectively. The aorta was occluded distal the proximal anastomosis. The prosthesis was exteriorized and brought out of the chest through openings made by removing a small portion of the fifth and seventh ribs. The skin and platysma muscle were separated from the underlying tissues between the two incisions in order to provide space for the location of the prosthesis in a subcutaneous position.

In Type II a double thoracotomy was made in the left side. The proximal anastomosis was made end-to-side at the site of the amputated brachiocephalic artery. The distal end of the brachiocephalic artery was anastomosed to the subclavian artery. The procedure was completed as in Type I.

In Type III the proximal anastomosis was made at the level of the ascending aorta via a thoracotomy performed at the level of the right 4th interspace. The prosthesis was placed from right to left side across the chest in a subcutaneous position and anastomosed to the descending aorta through another thoracotomy on the left 8th intercostal space.

In Type IV a thoracotomy was performed in the left side at the level of the 5th interspace. The proximal anastomosis was performed at the level of the amputated subclavian artery. The prosthesis was exteriorized through the apex of the chest, brought back in a subcutaneous position, re-entering the thorax through the same thoracotomy to be anastomosed to the descending aorta. The aorta was ligated between the two anastomoses.

Anesthesia

Initially, the dogs were anesthetized with sodium pentobarbital, 30 mgm/Kg given intravenously. A cuffed endotracheal tube was inserted and attached to the Harvard respirator. The animals were ventilated at a fixed volume with the expiratory phase exhausting to the atmospheric pressure. With this technique the pCO_2 values fell to 20 mm Hg or below, and the pO_2 values which had been in the range of 100-200 mm Hg at the onset fell to 50-60 mm Hg during the procedure. The pH gradually fell to the range of 7.1 to 7.2 indicating a profound metabolic acidosis despite the respiratory alkalosis. In an attempt to improve the pulmonary gas exchange during anesthesia, the exhaust of the Harvard respiratory was connected to an underwater seal which prevented the complete collapse of the lungs during the expiratory phase. With this modification, the values of the blood gases were maintained in a more physiologic range.

In a series of four dogs, after induction of the anesthesia with pentothal and succinyl choline, the dogs were maintained with fluothane, oxygen and succinyl choline using an Emerson respirator. This type of anesthesia did not materially improve the results obtained with the Harvard respirator.

The diversion of blood through the prosthesis was accompanied by hypotension requiring transfusion. Between 200 to 500 cc of blood were used during the procedure in the early experiments. In the late experiments, the blood loss was maintained and replaced with Dextran. It was felt that one of the causes contributing to the pulmonary congestion observed in the animals at post-mortem examination could be related to homologous transfusion and for this reason transfusion of blood was avoided. Fluid replacement was kept to a minimum during the procedure for fear of overloading the circulatory system. Between 500 to 1,000 cc of lactated Ringer's was infused during the intraoperative period.

Postoperative management

After the completion of the operation, the animals were taken to an intensive care unit and the following measures were carried out:

In the first experiments, the dogs were allowed to be on their right side. Unsuccessful attempts were made to change the position of the dogs so that they would lie on their left operated side, leaving the intact left hemithorax unobstructed. In the last experiments, the dogs were ambulated on the day of surgery, and a thick foam rubber pad was placed in the cage to allow the dog to lie on his operated side, leaving the unoperated side unobstructed. Respiration, pulse, and temperature were recorded at hourly intervals. 600,000 μ of penicillin and 0.5 gm of streptomycin were given twice daily. In the last dogs a valved thoracotomy tube was left in place at the time of surgery which allowed for continuous drainage of air and blood, and for early ambulation of the animal. The tube was removed after three days.

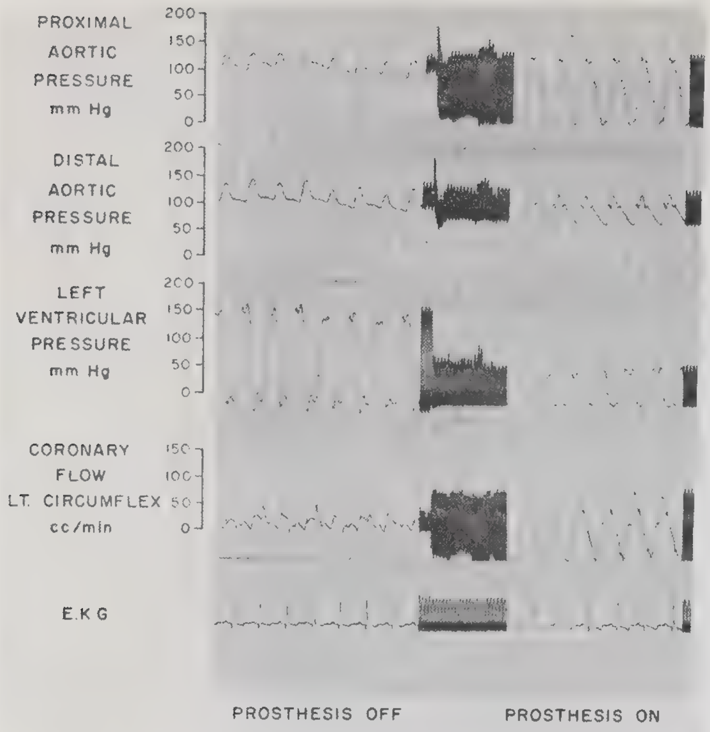

FIGURE 3. HEMODYNAMIC CHANGES OBTAINED IN THE DOG IN ACUTE EXPERIMENTS.

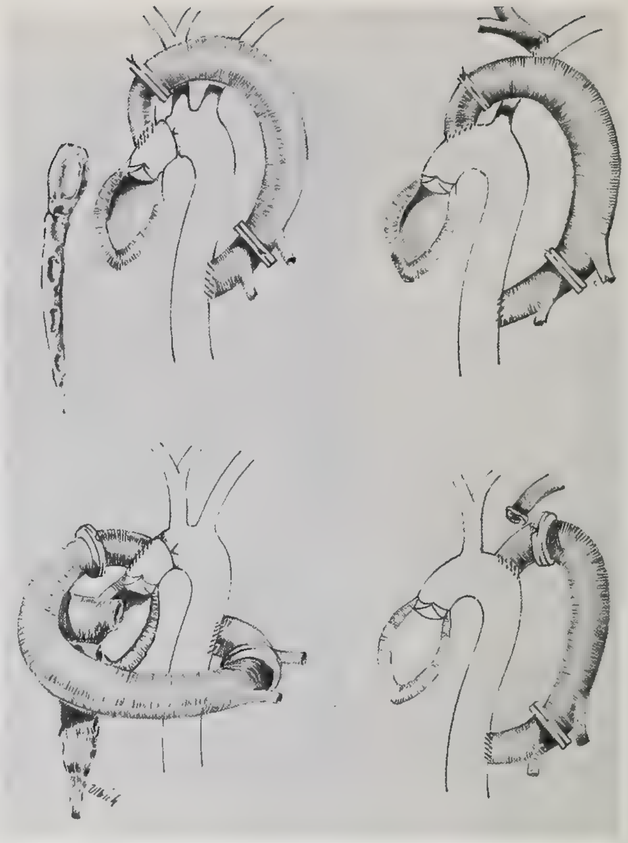

FIGURE 4. SCHEMATIC REPRESENTATION OF THE TYPE OF OPERATIONS USED IN THE DOG.

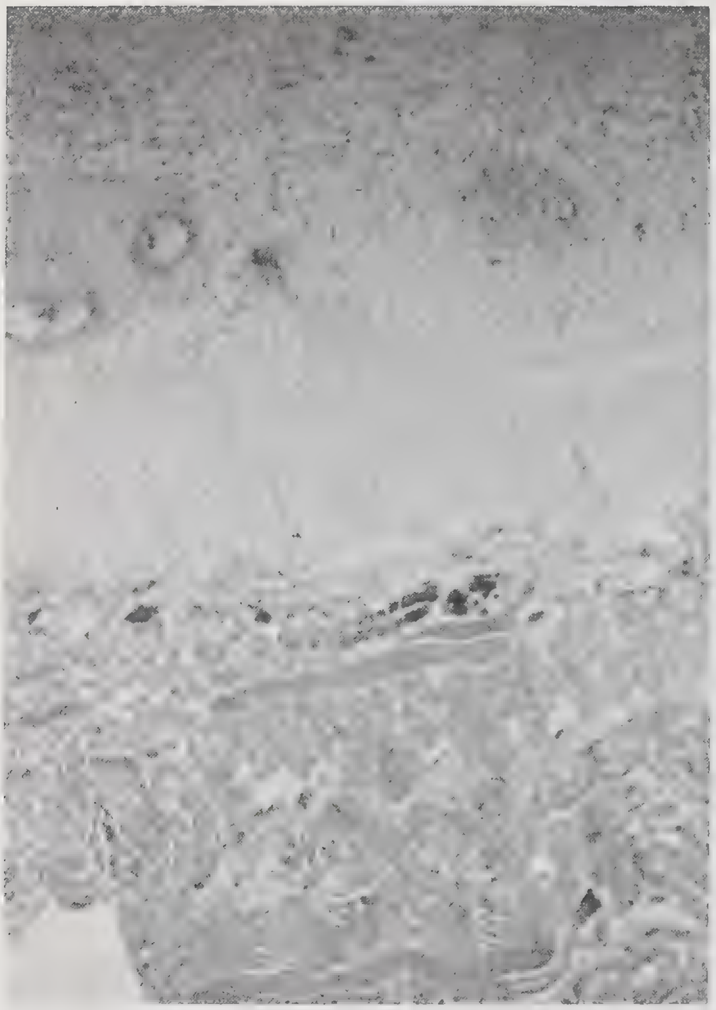

FIGURE 5. MICROPHOTOGRAPH OF PROSTHESIS AFTER ONE MONTH IN THE DOG.

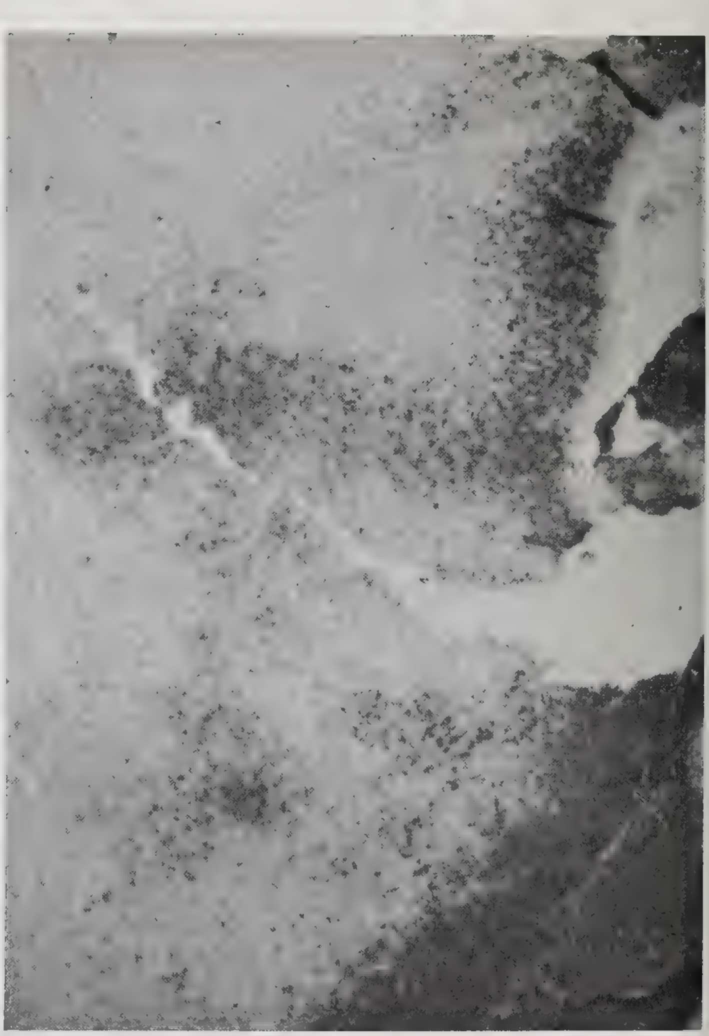

FIGURE 6. MICROPHOTOGRAPH OF INNER LINING.

Survival.

The results of this series of experiments are tabulated in Table 1.

TABLE 1

POSTOPERATIVE SURVIVAL

Type of Operation	# of Dogs	Survival	Postmortem
I	5	Average: 19 hours Range: 7-36 hours	Pulmonary Congestion Heart Failure
II	2	1 Day 2 Days	Undetermined Hypertension during procedure
III	1	20 hours	Hemorrhage proximal anastomosis
IV	12	Average: 11 days Range: 6 hours-36 days	Multiple causes
IVa	2	13 Days 12 hours	Bleeding through the velour

The longest survival time for the animals that were submitted to operation Type I was three days. At postmortem examination, pulmonary congestion was a common finding. To rule out the possibility of left heart failure produced by constriction at the level of the anastomosis in the ascending aorta, the operations Type II, III and IV were designed in order to improve the proximal anastomosis. Also, the left atrial pressure was monitored in two animals, and it remained within normal limits until the time of death.

For reasons that are difficult to identify the dogs submitted to procedure IV appeared to tolerate the operation better and survived for longer periods of time. Out of 12 dogs, two survived for one month and four for one week or more. They died or were sacrificed because of infection or bleeding. Two of the early deaths were attributed to thrombosis of the prosthesis.

Patency studies

In the dogs that survived for three days or less, there was no evidence of incorporation of the prosthesis by the surrounding tissues . The device in this early stage appeared surrounded by hemorrhagic fluid. An inner lining of laminated fibrin, 1 to 2 mm thick, covered the inside of the prosthesis. A study of the prostheses that were available for examination in the one month survivals revealed the following findings: The prostheses appeared well incorporated with dense connective tissue penetrating the outer velour as shown in Figure 5.

The most significant findings were encountered in the inner lining (Figure 6). In three prostheses studied, the inner lining was of irregular thickness and consistency. The surface appeared smooth and firm in some areas, rough and granular in others. It appeared that there was deposition of fibrin in the areas of curvature, producing a lining with a thickness of up to 5 to 6 mm. The thickness was greater in the area of the distal connector, where the prosthesis is narrower, resulting in a very narrow path for the blood flow. In one of the prostheses, the distal end was totally obliterated by well-organized fibrin.

In the pumping portion of the prosthesis, the thicker lining appeared in the area of the lesser curvature of the prosthesis. At the same time, ridges of fibrin were observed (Figure 7). In the pre-sacrifice x-ray examination, the prosthesis was found to be almost obliterated in the 35 day survivor. In the other animal, increased thickness in the distal portion of the prosthesis was visualized.

The potential of this kind of lining as a source of emboli was documented in one of the animals in which a kidney infarction was found (Figure 8).

In summary, the lining developed in the prosthesis appeared to have undesirable thickness, poor adhesion to the velour and an irregular surface. The excessive thickness of the lining is a finding consistent with the experience of other workers with whom we have discussed this problem and is probably related to the lack of porosity of the prosthesis. The use of Heparin has been suggested as a solution to this problem but we have not anticoagulated the dogs. On the other hand, the poor adhesion was traceable to the use of excessive moulding pressure which was exerted during construction of the prosthesis and which caused the silicone rubber coating to penetrate the velour.

To further elucidate this point, a Dacron velour graft was constructed, of approximately the same shape as the prosthesis, but without the silicone backing. The graft was implanted in two dogs. One animal died in 24 hours and the other died seven days after the operation due to bleeding through the graft. Nonetheless, the latter graft showed a thin, uniform, smooth inner lining, in contrast to the thick undesirable lining found in the nonporous prothesis.

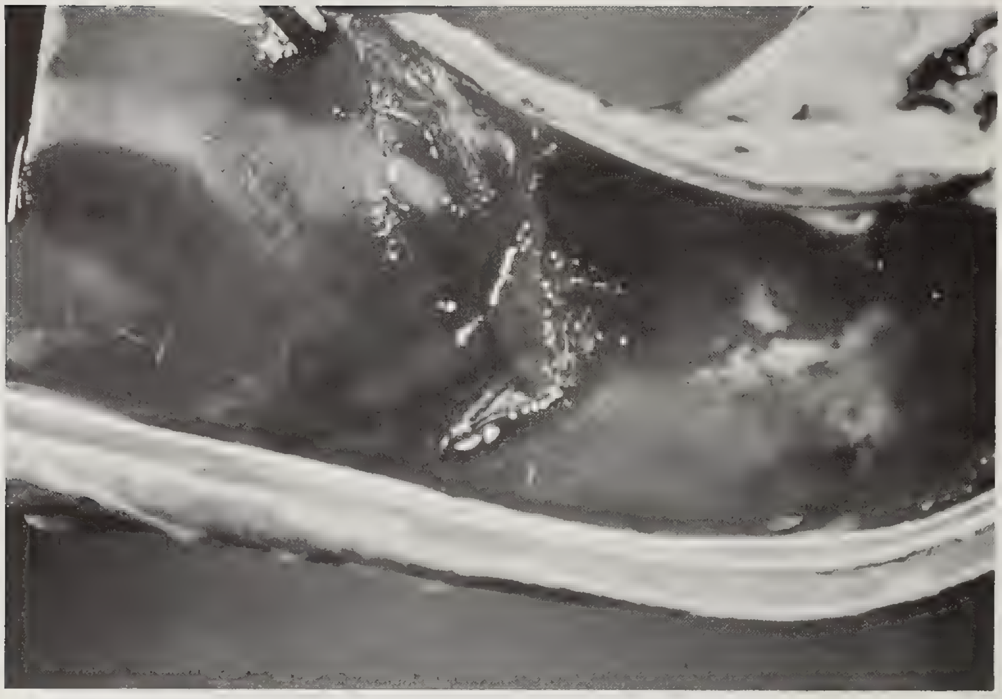

FIGURE 7. PHOTOGRAPH OF PROSTHESIS SHOWING RIDGES OF FIBRIN.

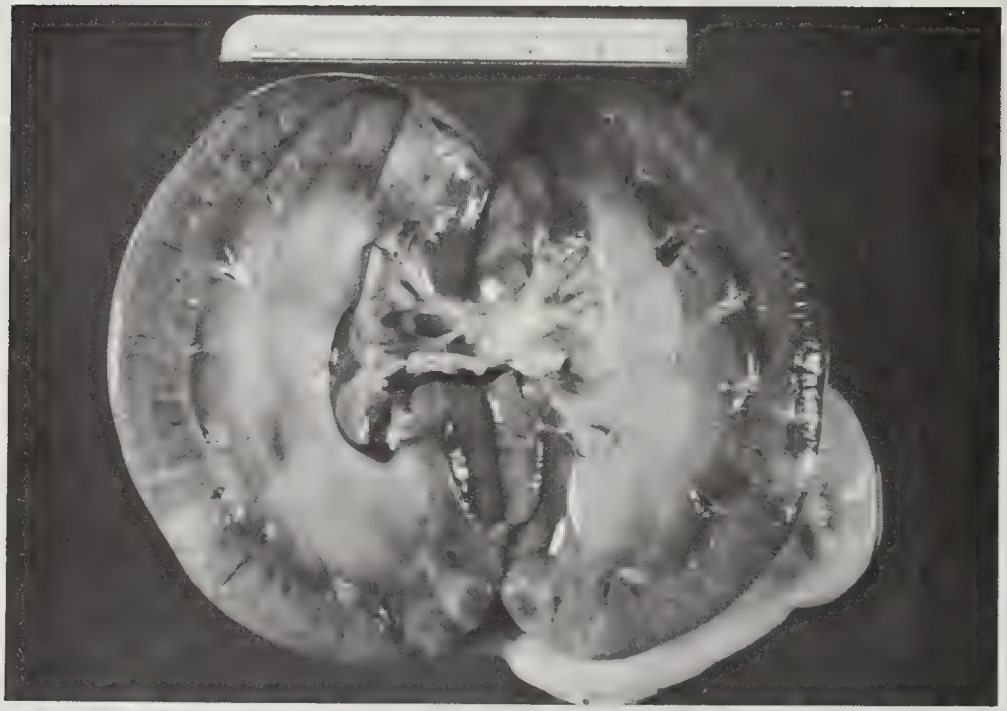

FIGURE 8. AREA OF INFARCTION IN THE RIGHT KIDNEY.

Chronic Actuation

Experience with the surviving dogs clearly indicated that the activity and excitability of the healthy survivor would make continuous actuation of the prosthesis difficult. We were forced to extensively review the technique which we had planned to use during the period of preparation of the prosthesis. Others have also experienced this problem and have found the calf to be docile and generally inactive. In view of the problem outlined above, it was decided to use the calf as a more suitable animal for chronic studies.

CALF EXPERIMENTS

Six chronic studies and one acute experiment were performed in this series. In the six initial experiments, the dog prosthesis was modified for use in the calf in the following manner:

The proximal and distal connectors were cut at a level where the diameter of the lumen was 20 mm. At this level a 20 mm Dacron graft of 10 cm length was sutured. The prosthesis, thus modified, was installed using two different operative approaches. The calves were anesthetized with Pentothal, Fluotane and oxygen. Flaxedil, 1 mgm/kilo was used as relaxant and the ventilation was assisted using the Harvard respirator at a tidal volume of 700 cc. In two calves the operation was performed in the following manner (Figure 9).

The chest was entered at the level of the 5th interspace. The proximal anastomosis was performed end-to-side in the aortic arch, distal to the brachiocephalic artery. The distal anastomosis, also end-to-side, was placed one inch distal to the proximal anastomosis and the aorta was occluded between the two using an umbilical tape ligature. The prosthesis was exteriorized subcutaneously by removing a small segment of the 3rd anteriorly for the proximal connecting graft and a posterior segment of the 7th rib for the distal connecting graft.

In four calves the operation was modified in the following way (Figure 10).

The chest cavity was entered and a 20 mm Dacron graft was anastomosed end-to-side to the brachiocephalic trunk, which is approximately 20 mm in diameter, and descending aorta respectively. At this point the aorta was clamped and divided distal to the brachiocephalic artery while the 20 mm Dacron graft served as a bypass for the distal perfusion of the animal. The prosthesis was then connected in-series, end-to-end to the divided aorta. Once the installation of the prosthesis was completed a ligature was placed at the origin of the brachiocephalic artery. The end result of this arrangement was to have the prosthesis located "in-series" with the left ventricle with no arterial branches, (except the coronaries), between the heart and the prosthesis. The brachiocephalic artery is perfused by the Dacron graft, where the flow is reversed when the ligature is placed at the origin of the brachiocephalic artery. The reason for this complicated procedure lies in the impossibility of performing an anastomosis in the ascending aorta of the calf due to the short length of the vessel.

Postoperatively the animals were maintained on chest suction and antibiotics. During the first three days Heparin 50 mg every 4 hours were given. Afterwards the animals were treated with coumadin at a dosage appropriate to maintain the prothrombin time between 20 to 20 seconds for a four-week period.

The results are summarized in Table 2.

TABLE 2

POSTOPERATIVE SURVIVAL

Type of Operation	# of Calves	Survival	Postmortem
I	2	3 months 20 days	Skin necrosis infection and thrombosis of the prosthesis
II	4	3 days 3 days 28 days 23 days	Pulmonary edema resulting from excessive airway pressures Pneumonia

Although the first two calves survived for three months and 20 days respectively, the grafts were grossly infected and thrombosed. The next four animals died of pulmonary complications. However, they survived for periods from 3 to 23 days, allowing assessment of the characteristics of the lining. The inner lining was thin, glistening and adherent to the velour (Figure 11).

An evaluation of the experience in the first six animals indicated that the prosthesis which was designed for the dog did not have a sufficient capacity to accommodate the cardiac output of the calf. This judgement was made on the basis of our experience in two of these calves in which we found that the hemodynamic effects produced by the actuation of the prostheses were minimal.

The prosthesis was then modified in the last two calves based upon the data obtained from the following acute experiment. A bellofram type of pump with a controllable stroke volume was installed in the circulation instead of the active portion of the prosthesis utilizing the Type II operation. Figure 12 shows the hemodynamic results obtained using a stroke volume of 60 cc.

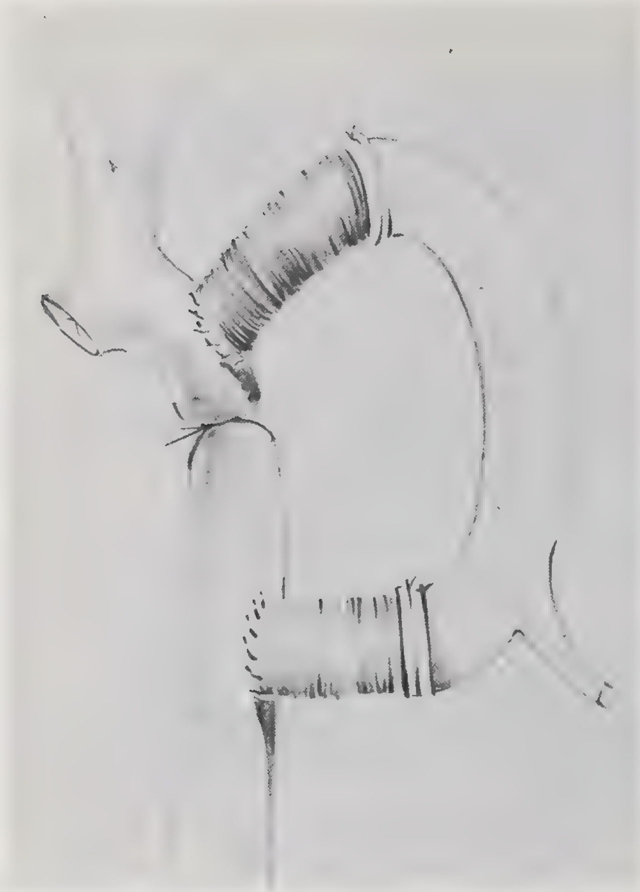

FIGURE 9. OPERATION TYPE I USED IN THE CALF.

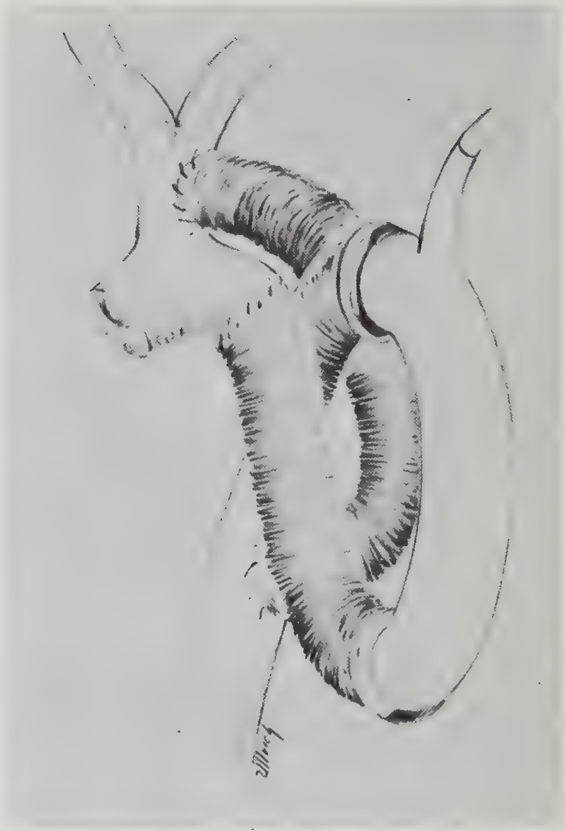

FIGURE 10. OPERATION TYPE II USED IN THE CALF.

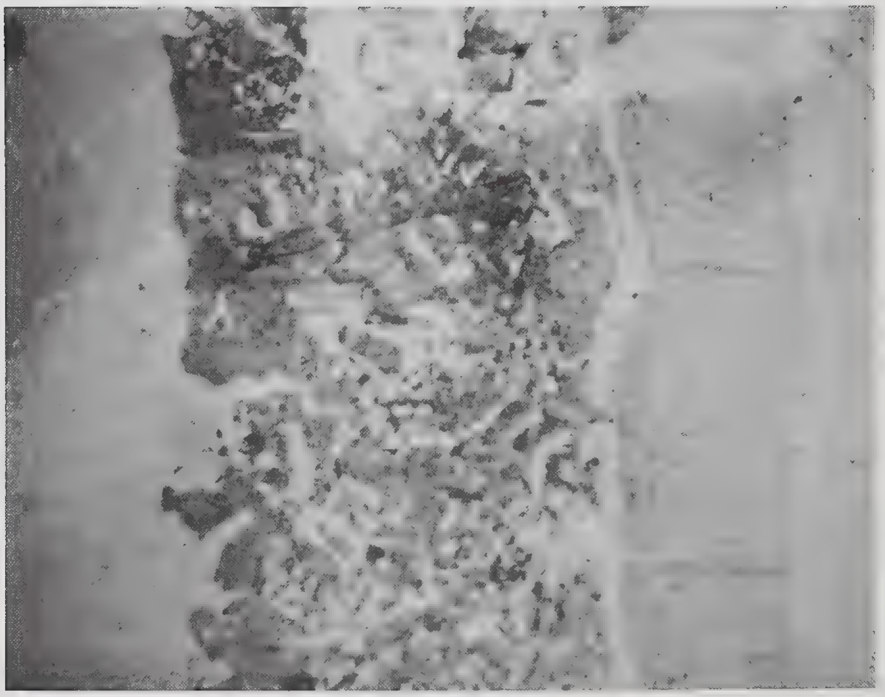

FIGURE 11. MICROPHOTOGRAPH OF INNER LINING OBTAINED IN THE CALF.

These modes of operation of the distal valve were calculated. The flow distal to the prosthesis, the EKG, the aortic pressure proximal and distal to the prosthesis and the left ventricular pressure were measured. The control values are seen on the left. Next the changes which are produced by counterpulsation with the discharge valve open are shown. The flow distal to the prosthesis regurgitates into the prosthesis during the suction phase of the pump. Left ventricular pressure is reduced to 110 mm Hg and the aortic diastolic pressure is increased to 160 mm Hg. The next series of curves was produced by applying a fixed pressure compressing the discharge valve. The regurgitant flow is reduced or eliminated, the proximal aortic diastolic pressure is increased to 220 mm Hg peak. The distal aortic pressure remains essentially constant and left ventricular pressure is reduced to 90 mm Hg peak. The series of recordings at the right show the effects which are produced when the discharge valve is actively closed during the suction phase of the pump and opened during pump systole. With this mode of operation, the proximal aortic pressure peak during pump systole is reduced and regurgitant flow is eliminated.

Based upon these data the model of the prosthesis which is under current investigation is shown on Figure 13. The potential stroke volume of the prosthesis is 120 cc. The prosthesis is made using silicone rubber laminated to a fabric surface of velour using RTV silicone adhesive. Two calves have been studied. One is alive at three weeks and is being used for patency studies, and an attempt was made to actuate the other calf. Unfortunately, the animal died of air embolism due to a defect in the prosthesis.

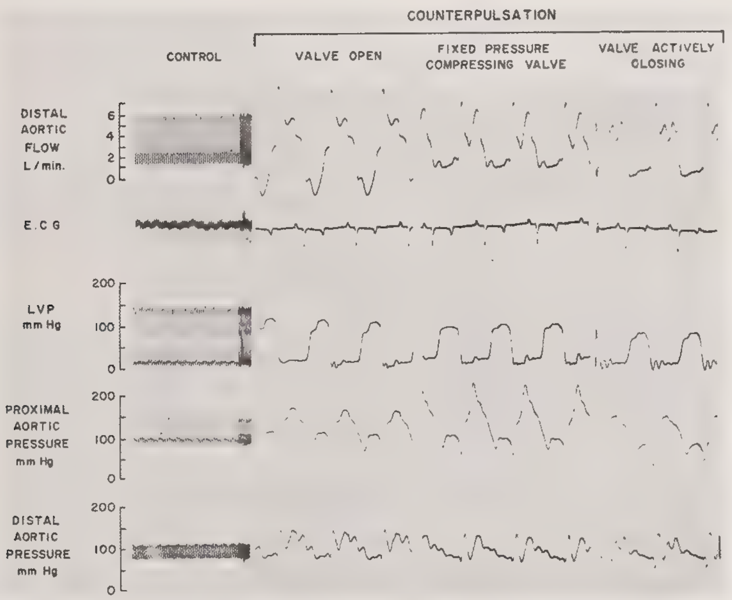

FIGURE 12. HEMODYNAMIC EFFECTS OBTAINED IN THE CALF.

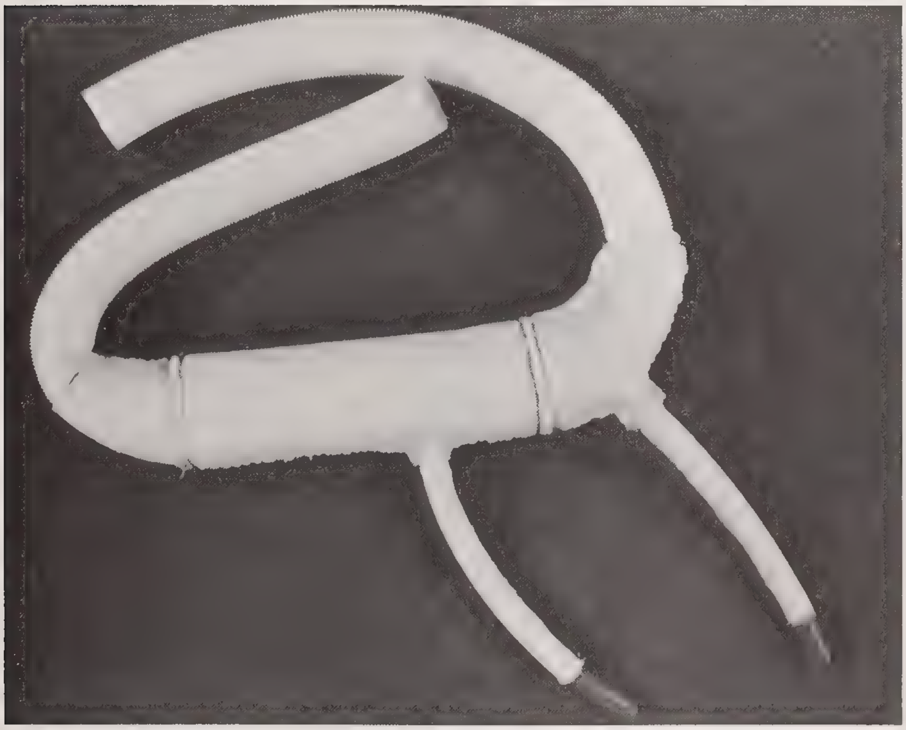

FIGURE 13. PROSTHESIS DESIGNED FOR USE IN THE CALF.

CHAPTER 48

DEVELOPMENT AND INITIAL PHYSIOLOGICAL EVALUATION OF THE CO-PULSATION TECHNIQUE FOR CIRCULATORY ASSIST

B. Hochman
Hamilton Standard, Farmington, Connecticut

T. Sato
Yale University, New Haven, Connecticut

W. Sugg
Southwestern Medical School, Dallas, Texas

An electrohydraulic servo system and blood pump was constructed to evaluate the efficacy of a circulatory assist technique which amplifies the systolic pressure pulse. Preliminary *in vivo* data have been obtained with the co-pulsation system. The hemodynamic changes induced by co-pulsation were as follows: (1) pressure ratio of mean descending aortic pressure to mean ascending aortic pressure increased up to 2.6:1; (2) left ventricular systolic pressure and tension-time-index decreased by approximately 30 percent and 40 percent respectively; (3) left ventricular stroke volume increased by approximately 10 percent; (4) left ventricular external work decreased by approximately 30 percent; (5) left ventricular end-diastolic pressure decreased slightly (3-4 mm Hg); (6) left ventricular ejection fraction slightly increased (about 5 percent), and left ventricular end-systolic volume decreased by approximately 10 percent. Co-pulsation has proved effective in decreasing left ventricular work as measured and defined by these parameters.

INTRODUCTION

The technique of co-pulsation and its initial development have been discussed in detail previously, and this paper very briefly describes what co-pulsation is, and the mechanism for achieving it. This is followed by a report on the major technical problems and progress occurring during this past year's testing and development. This is followed by a section reporting the *in-vivo* evaluations by Dr. T. Sato of Yale University.

CO-PULSATION DEVELOPMENT

Co-pulsation is a method of amplifying the pressure waveforms in the aorta during *systole*. This is accomplished by means of a blood pump in series with the aorta, and an associated driving servo mechanism, and timing and control system. The co-pulsation system is a research tool which will permit the evaluation of this mode of assist. If such assist proves beneficial it may provide a basis for design of cardiac assist devices and artificial hearts.

Co-Pulsation Original Configuration

Figure 1 shows the co-pulsation original configuration. The co-pulsation system provides the left ventricle with an expanding low pressure receiver during systole, thereby reducing the work load of the ventricle. At the same time, that is, coincident with systole it adds energy to the blood by amplifying the wave form presented by the left ventricle. By a combination of lowering of the inlet pressure and raising of the outlet pressure it establishes and maintains a set ratio between blood pump input and output pressures. Three co-pulsation servo systems were constructed, one for continued development at H.S.D., one for physiological evaluation by Dr. T. Sato at Yale, and one for evaluation by Dr. W. L. Sugg at Southwestern Medical School. As initially constructed, the co-pulsation systems had faults that manifested themselves as poor system response, resonances, and instabilities. This prevented true co-pulsation operation since a ratio could not be maintained over the course of a systolic waveform. However, the left ventricle would see an expanding low pressure receiver and energy would be added to the aorta during systole, therefore physiological evaluation was begun. The results of this evaluation will be discussed shortly by Dr. Sato.

Coincident with the preliminary physiological evaluation, development of the H.S.D. co-pulsation system continued. The resonance phenomena were observed *in vitro* in the range of 15 to 30 cps and took the form of a 3 x to 10 x increase in either input or output pressure of the blood pump in response to the actuator piston input stroke. The causes of these resonances were identified as hydraulic coupling inertia in conjunction with the compliance of air in the actuator and a soft seal.

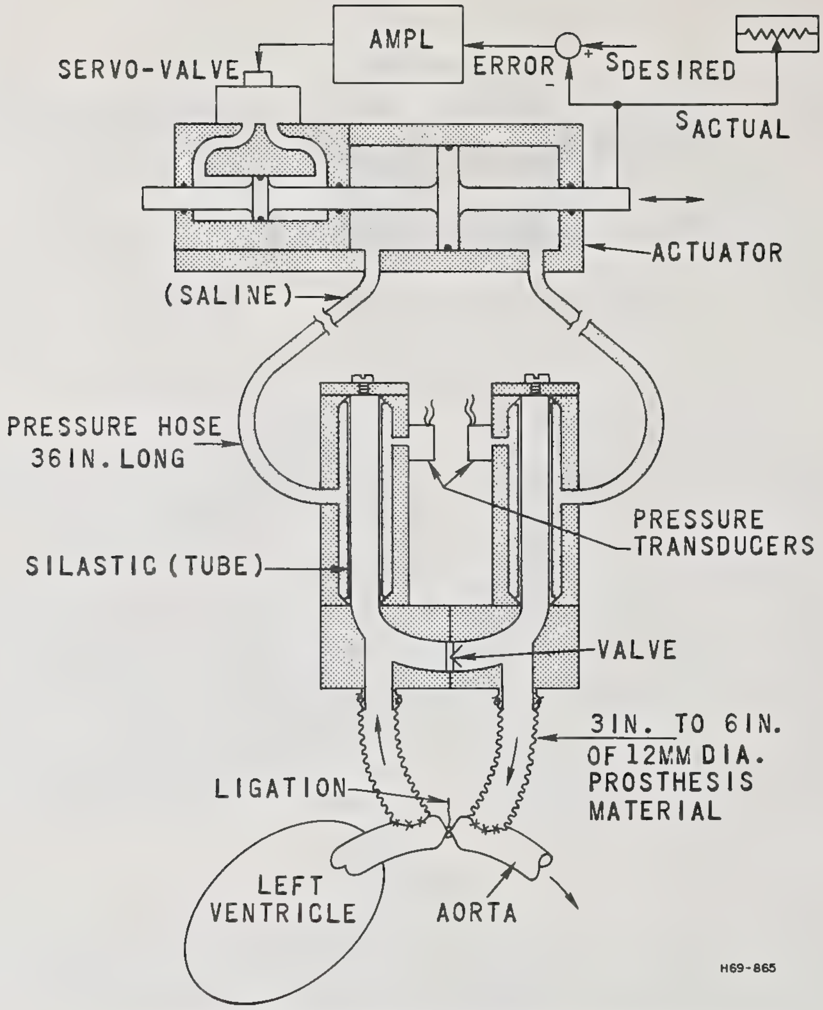

FIGURE 1. CO-PULSATION HYDRAULIC COUPLING SYSTEM INITIAL ARRANGEMENT.

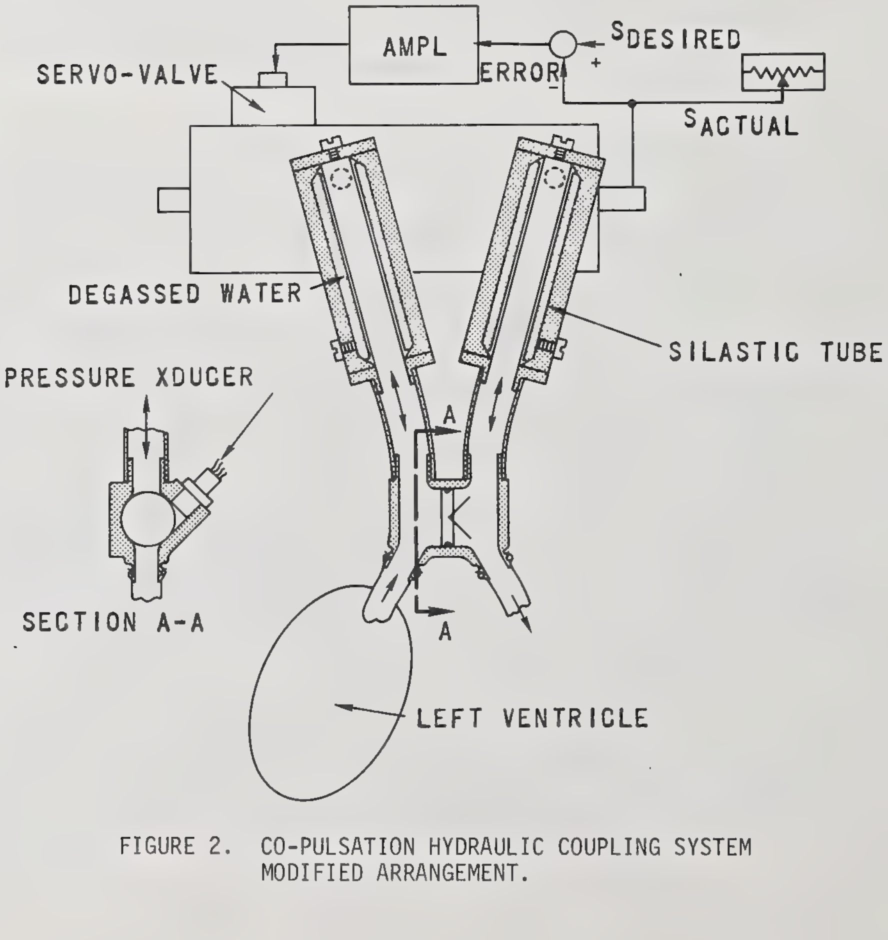

FIGURE 2. CO-PULSATION HYDRAULIC COUPLING SYSTEM MODIFIED ARRANGEMENT.

Co-Pulsation Hydraulic Coupling System Modified Configuration.

The system was modified as shown in Figure 2 by close coupling of the blood pump to the actuator and by hardening of the seals. This pushed the resonances out beyond 30 cps as shown in Figure 3.

Investigation of the electrohydraulic servo actuator indicated a rough motion and a first order lag at about 15 cps. The poor response was caused by the inability of the system to overcome hysteresis within the servo valve and actuator. The system levels were "normal" but, a servo actuator rod seal designed to leak to the return line reduced the pressure sensitivity of the system and prevented it from overcoming the hysteresis. A carbon film position feedback potentiometer was a significant contributor to the rough response, (i.e., numerous small discrete steps of motion). The actuator performance was improved by the following: Optimization of the driving amplifier in terms of gain and phase, modification of the actuator seals, substitution of a low friction, infinite resolution linear variable differential transformer for the potentiometer, and raising the hydraulic pressure from 1,000 psig to 1,500 psig. Test of the modifications indicated a response flat to 30 cps with less than 55^{0} phase lag.

Development of the electronic compensation to match the pressure ratio loop characteristics to the in vivo impedances, required in vivo determinations of the canine left ventricular impedance and aortic impedance. These measurements were made in conjunction with Dr. W. Sugg and Mr. G. Templeton of Southwestern Medical School. By varying the frequency of a pressure source generator and observing the pressure perturbations in the aorta and left ventricle during systole and diastole it has been possible to obtain measurements of Z_{LV}. These measurements were utilized to design electronic compensation for the pressure ratio control loop, On in vitro tests, this compensation provided stable closed performance at unit gain to 10 HZ. An improved system has been delivered to Yale for continued evaluation.

PHYSIOLOGICAL EVALUATION

Materials and Methods.

Twenty-nine normal mongrel dogs weighing approximately 20 Kg. were used for the development of surgical technique, to familiarize the research staff with the operation of the pumping device as well as its control in in vivo performance, and for the physiological measurements. The hemodynamic data presented here consisted of 17 co-pulsations performed in 9 dogs in which data to evaluate were obtained.

Surgical Procedures. Anesthesia was induced and maintained with pentobarbital sodium, 30 mg. per kilogram bodyweight. Respiration was kept constant with a mechanical respirator and a cuffed endotracheal tube. The left chest was entered through the fourth intercostal space. In the first several experiments, the inflow pump and outflow pump were connected to the ascending and the descending aorta respectively with Dacron graft by end-to-side anastomosis, and then the ascending aorta was ligated between the proximal anastomosis and the brachio-cephalic trunk (Figure 4). In the later experiments, however, in which hemodynamic study was performed, the descending aorta was transsectioned distal to the left subclavian artery and the inflow and the outflow side of the pump were connected end-to-end to the proximal and the distal ends of the transsectioned aorta respectively with Dacron graft which has a bypassing graft between the inflow graft and the outflow graft. During the pumping procedure this bypassing graft was occluded. The brachio-cephalic trunk was ligated and the cerebral circulation was maintained through the branch graft extended from the outflow graft of the pump, the left subclavian artery was cannulated for ascending aortic pressure measurement, and ligated distally, thus all blood flow was made to pass through the pump during pumping procedure. Heparin, 2 mg. per kilogram of bodyweight, was injected before connection of the pump to the aorta.

Physiological Measurements. The catheters[*] for measuring blood pressures were placed in the left ventricle through the apex, ascending aorta via the left subclavian artery, and descending aorta via the femoral artery. Pressures were measured with Statham P23Db strain gauge transducers and recorded on Electronics for Medicine Model DR-8 recorder. Cardiac output and coronary blood flow were measured with two electromagnetic flow meters[+] through flow transducers[#] affixed to the ascending aorta and the left circumflex branch of the coronary artery respectively and recorded on the same recorder as pressures. After all measurements were finished, calibrations of blood flow were performed by injecting the determined volume of blood into the involved vessels. The mean values of blood flow and pressure were determined by electrical integration. Tension-time index (TTI) was determined by planimetrical integration of the area under the systolic portion of the left ventricular pressure curve. The rate of rise of left ventricular pressure during isovolumic contraction period (dP/dt) was calculated from the slope of left ventricular pressure curve. The stroke work of the left ventricle was calculated by multiplying the left ventricular mean ejection pressure minus left ventricular end-diastolic pressure, by the stroke volume. Hemodynamic measurements were performed before, during and after co-pulsation following establishment of hemodynamic equilibrium.

---

[*] Cardiac catheter, 8 Fr., U. S. Catheter and Instrument Corporation.

[+] RC1000 Electromagnetic flow meter, Micron Instruments.

[#] Micron MC series transducer, lumen diameter 16mm. (for the aorta) and 2.5mm (for the coronary artery)

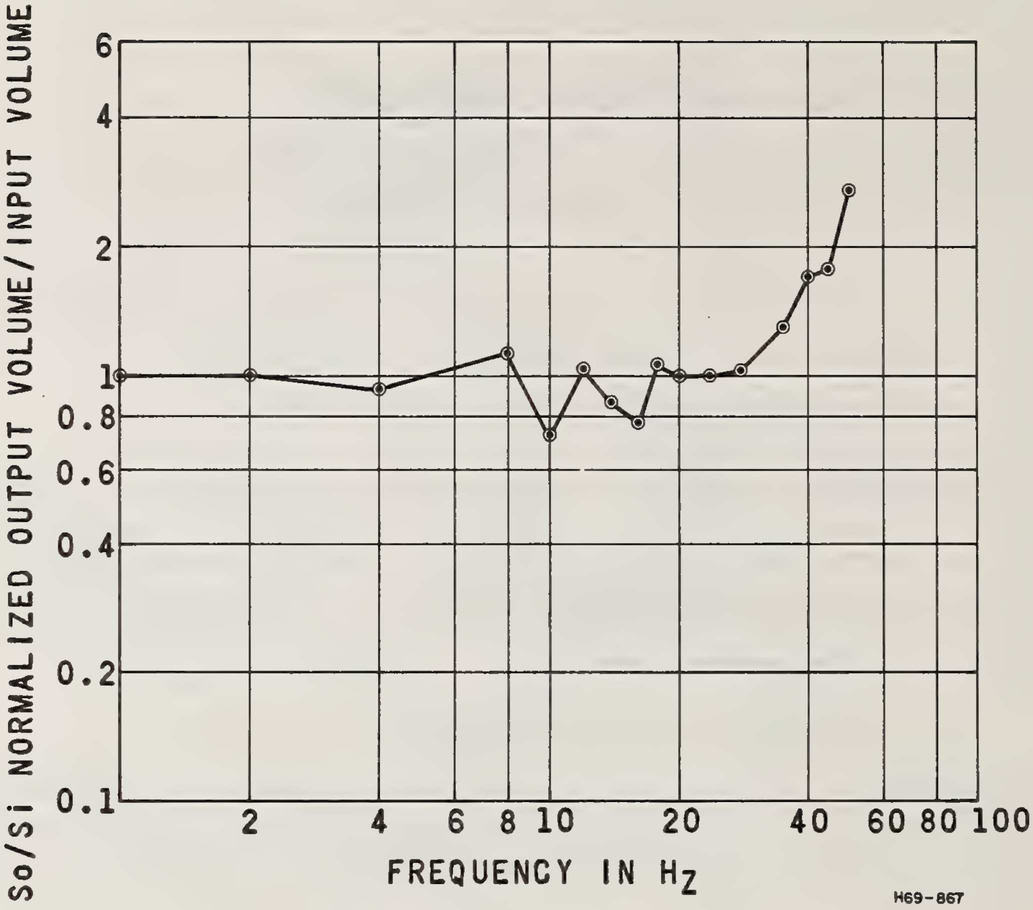

FIGURE 3. HYDRAULIC COUPLING RESPONSE EVALUATION.

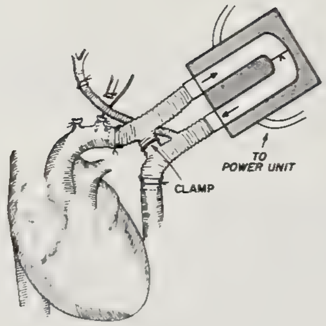

FIGURE 4. CO-PULSATION PUMP SURGICAL LOCATION.

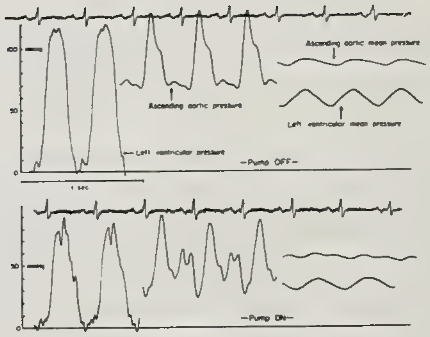

FIGURE 5. CHANGES IN HEMODYNAMIC PARAMETERS.

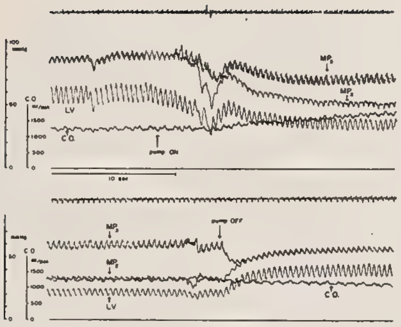

FIGURE 6. CHANGES IN HEMODYNAMIC PARAMETERS.

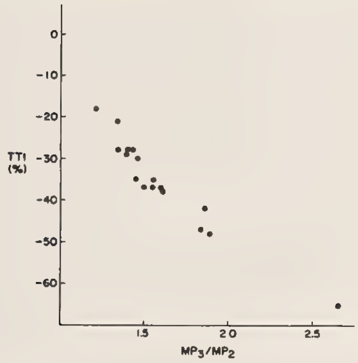

FIGURE 7. CHANGES IN TTI AND THE PRESSURE RATIO.

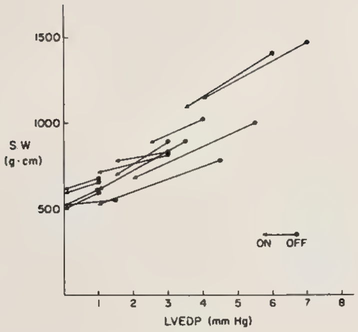

FIGURE 8. CHANGES IN CARDIAC FUNCTION.

Results

The mean control left ventricular peak pressure of 99 mm.Hg. decreased to 75 mm. Hg when the co-pulsation was on, and TTI decreased by an average of 33%. Heart rate decreased slightly by co-pulsation. Left ventricular end-diastolic pressure decreased by an average of 2.5 mm. Hg and left ventricular work per minute decreased by an average of 23%. The rate of rise of left ventricular pressure during isovolumic contraction period decreased by 22%. The mean control ascending aortic pressure of 74 mm. Hg decreased to 50 mm. Hg. The mean descending aortic pressure increased in some experiments but decreased in other experiments and, thus, no statistically significant change could be found. The pressure ratio of descending aortic pressure to ascending aortic pressure (MP_3/MP_2) was increased by an average of 52% by co-pulsation. Cardiac output increased by 19%. Coronary flow, however, decreased by 19%. These hemodynamic data obtained in 9 co-pulsations performed in 9 dogs are summarized in Table 1, and actual pattern change and transient process of change in the hemodynamic parameters are shown in Figures 5 and 6.

TABLE 1

HEMODYNAMIC CHANGES INDUCED BY CO-PULSATION

		CONTROL	PUMP ON	RELATIVE CHANGE
H.R.	(per min.)	123 ± 28	118 ± 26	- 3.4 ± 2.3%
LVSP	(mm.Hg)	99 ± 24	75 ± 21	- 24 ± 7 %
LVEDP	(mm.Hg)	3.9 ± 1.7	1.3 ± 1.2	- 2.6 ± 0.8 mm.Hg*
TTI	(mm.Hg·sec.)	2820 ± 520	1940 ± 620	- 33 ± 9 %
dP/dt	(mm.Hg/sec.)	1470 ± 420	1160 ± 380	- 22 ± 7 %
MP_2	(mm.Hg)	74 ± 21	50 ± 20	- 34 ± 11 %
MP_3	(mm.Hg)	72 ± 22	71 ± 23	- 2 ± 11 %
MP_3/MP_2		0.96 ± 0.05	1.46 ± 0.23	+ 52 ± 21 %
C.O.	(ml./min.)	1060 ± 200	1260 ± 280	+ 19 ± 9 %
C.F.	(ml./min.)	49 ± 11	45 ± 12	- 19 ± 5 %
LVW	(Kg.·M.)	1.18 ± 0.42	0.87 ± 0.26	- 23 ± 12 %

*Change in absolute value.
The figures represent Mean ± Standard Deviation
Though the change in MP_3 is not statistically significant, changes in other hemodynamic parameters are all statistically significant ($P<0.01$).
H.R.: Heart rate, LVSP: Left ventricular systolic pressure, LVEDP: Left ventricular end-diastolic pressure, TTI: Tension-time-index per minute, MP_2: Ascending aortic mean pressure, MP_3: Descending aortic mean pressure, C.O.: Cardiac output, C.F.: Coronary flow, LVW: Left ventricular work.

The relationship between the relative change in TTI and the pressure ratio (MP_3/MP_2) is presented in Figure 7 using the data obtained in 17 co-pulsations performed repeatedly in 9 dogs. A statistically significant correlation was found between these hemodynamic parameters. The changes in cardiac function as expressed in the frame of reference of stroke work and ventricular end-diastolic pressure are shown in the Figure 8. A definite trend of change in cardiac function by co-pulsation could be recognized.

Coronary Flow. Coronary flow was decreased by co-pulsation as far as the data obtained to date (by measuring the blood flow of the left circumflex branch of the coronary artery) are concerned. There are various factors affecting the coronary flow[2] and the most important factors are the perfusion pressure (aortic pressure) and the resistance of the coronary vessels[3]. In our experiments the major cause for decreasing coronary flow is oscillation of the system which results in "noisy" waveform of the aortic pressure providing the coronary vascular bed with inadequate perfusion pressure. Technical improvements to eliminate oscillations are being instituted. On the other hand, a myocardial oxygen consumption study is underway to establish whether or not the decrease in myocardial oxygen consumption is greater than the decrease in coronary flow, because coronary flow should be discussed in relation to myocardial oxygen requirement and the reduction of the left ventricular work load is of prime importance.

SUMMARY

The new concept for ventricular assist, co-pulsation, has been proposed and a physiological evaluation of this newly designed pumping device has been performed from the hemodynamic aspect. Co-pulsation has proved effective in decreasing the left ventricular work load. In this preliminary study coronary flow decreased. The system awaits further technical improvements with respect to system stability. Coronary flow remains to be evaluated in relation to myocardial oxygen requirement using improved co-pulsation system.

REFERENCES

1. Sarnoff, S.J., Braunwald, E., Welsh, G.H., Jr., Case, R.B., Stainby, W.N., and Macruz, R. Hemodynamic Determinants of Oxygen Consumption of the Heart With Special Reference to the Tension-Time-Index. Amer. J. Physiol., 192 (1):148, 1958.
2. Katz, A.M., Katz, L.N., and Williams, F.L. Regulation of Coronary Flow. Amer. J. Physiol., 180:392, 1955.
3. Gregg, D.E., and Sabiston, D.C., Jr. Current Research and Problems of the Coronary Circulation. Circulation, 13:916, 1956.

DISCUSSION

DR. JARON: First of all I would like to congratulate the authors on this new concept which is interesting and intriguing. However, I would also like to bring up a couple of points. In general, when one uses an in-series assist device one relies on a functioning left ventricle. It may be only partially functioning but the left ventricle has to continue to put out some amount of blood. In order to design a system which keeps the ventricle viable there are certain boundary conditions which have to be met and I think the copulsation technique has not met one or more of these boundary conditions, as evidenced by the data presented here. These conditions are either increased perfusion of the coronary circulation or a considerable reduction in oxygen concumption of the ventricle, which can also keep the myocardial muscle viable. Neither of these conditions is met by copulsation.

DR. SATO: We have not completed the studies of myocardial oxygen consumption, so at present one cannot say whether it reduces myocardial oxygen consumption or not. The basic idea of the copulsation is an increase of the diastolic pressure in the ascending aorta and the reduction of the left ventricular systolic pressure.

DR. JARON: One of the principal effects of copulsation is the reduction of diastolic pressure, and therefore, coronary perfusion is going to be lowered.

DR. SATO: Preliminary investigations indicated that diastolic pressure was reduced by oscillations in the system, but we expect the improved system to provide slightly increased diastolic pressure as shown in the preliminary test of the improved system. More experimental use of the improved copulsator is required for definitive conclusions.

DR. SOROFF: I still fail to understand how the coronaries would be perfused. It seems to me that the major effect is to decrease the systolic pressure and increase the distal diastolic pressure. Can you explain again, how the coronaries will receive increased perfusion.

MR. HOCHMAN: During the piston return stroke of the actuator and ventricle, blood flows from the proximal ventricle through the pump valve. The pressure drop through the valve necessitates that the pressure in the proximal pump ventricle be greater than that in the distal ventricle. Consequently, ascending aortic pressure before the pump is slightly higher than the pressure in the aorta distal to the pump, thereby providing a greater potential for coronary perfusion.

CHAPTER 49

DEVELOPMENT AND EVALUATION OF A LEFT VENTRICULAR-AORTIC ASSIST DEVICE

W. Bernhard, C. LaFarge

Surgical Research Laboratory, Childrens Hospital
Boston, Massachusetts

S. Kitrilakis, T. Robinson
Thermo Electron Corporation, Waltham, Massachusetts

A totally implanted assist device capable of complete functional replacement of the left ventricle is being developed and evaluated in animal experiments. Improved blood interface configuration, hydrodynamic characteristics and valve function, decreased pressure drops, and increased life and reliability have been incorporated in the series of pump models designed, developed, fabricated, and tested to date. Thirty studies of 7 to 120 days duration have been performed in healthy calves, with 1500-3000 ml/min. assisted circulation provided continuously by the blood pump. In some experiments, the flocked Dacron pump matrix was seeded with bovine fetal fibroblasts to accelerate pseudoendothelial development. In 20 animals, sacrificed after 30 to 120 days by bypass, histologic study of the lining revealed masses of viable fibroblasts and collagen attached to the Dacron matrix. Identification of fetal cells was accomplished with liquid scintillation using C^{14}-thymidine. Blood trauma was minimal and consisted of 15% hematocrit reduction, temporary (14 day) increase in incubated osmotic fragility, and a 24 hour increase in mechanical fragility. Erythrocyte survival (D.F.P.^{32}) was reduced approximately ten percent (24 day half-life). Red cell mass (Cr^{51}) was also less, with a reciprocal rise in plasma volume. Plasma hemoglobin, haptoglobins, reticulocyte count, platelets, and intracellular cations were unchanged. Reduction of left ventricular pressure to atmospheric levels has been demonstrated in acute studies in calves. The maintenance of the normal hemodynamic state during acute left ventricular failure (induced in chronic pump implantations) has also been demonstrated.

INTRODUCTION

Prolonged periods of assisted circulation have been accomplished in calves utilizing a pneumatically-actuated, double-valved pump interposed between the left ventricular apex and the descending thoracic aorta.[1] The device functions by accepting blood from the left ventricle during systole and ejecting it into the aorta during diastole. With an effective stroke volume of 60 milliliters, pump action lowers left ventricular peak pressure and causes a reduction in stroke work in myocardial energy comsumption.[2]

The internal pump lining consists of flocked Dacron fibrils embedded in a polyurethane substrate. The resultant matrix encourages deposition of a uniform fibrin layer within the pumping chamber and on the valve housings and struts. Organization of this protein layer differs considerably from that observed in a Dacron vascular prosthesis, because the impermeable nature of the pump precludes connective tissue ingrowth. For this reason, cellular elements necessary for development of a pseudoendothelium must be derived from blood circulating through the device, and nourishment of the entire lining is dependent upon diffusion of nutrient materials.

Previous investigations have demonstrated that a fibrin-cellular lining developed in multicentric fashion on both the static and flexing pump surfaces.[3] However, this process invariably proceeds at a slow and unpredictable pace. In an effort to accelerate development of the interface, the Dacron surfaces of the most recent pump (Model VI) were seeded with bovine fetal fibroblasts previously grown in tissue culture. These allogeneic cells were selected because of their rapid reproduction *in vitro*, and the hope that their primitive nature would not evoke a major immunologic response from the recipient animals.

This report contains an evaluation of the use of fetal fibroblasts in the formation of a fibrocellular blood-material interface, and includes an appraisal of the hematologic effects of prolonged assisted circulation upon the protein and cellular elements of blood. In addition, the evolution of the current device from an engineering standpoint is recorded, along with a series of physiologic observations made during cardiac catheterization in chronic pump animals.

MATERIALS AND METHODS

Engineering Description.

The development of an assist device capable of long-term function in animals continued with the design, fabrication, and testing of blood pumps and other devices shown in Table 1.

TABLE 1.

LEFT VENTRICULAR-AORTIC ASSIST DEVICE DEVELOPMENT

June 1968 through April 1969

Component or Device	Number Fabricated	Purpose	Results
1. Assist Device Model V & Va	4	To achieve extended chronic survival for studies of blood interface development and effects of pump on blood and organs.	Up to 76 days duration of continuous chronic pumping.
2. Assist Device Model VI	2	Improved hydrodynamic characteristics, reduced valve pressure drops, more reliable assembly procedure.	Bladder tear occurred after 8 days of pumping in first chronic implant.
3. Assist Device Model VIa	7	Revised bladder shape and thickness to reduce stresses and increase life and reliability.	Up to 40 days chronic pumping.
4. Assist Device Models VIb-VIi:	15	Revised inflow and outflow valves in attempt to reduce thick fibrin deposition.	
Model VIb	1	Unflocked polished inflow valve seat and guide pins.	12 days chronic pumping.
Model VIc	1	Unflocked polished inflow and outflow valve guide pins.	51 days chronic pumping.
Model VId	1	Same as VIc but use of Hughson wash primer begun, giving improved adhesion of polyurethane to stainless steel.	23 days chronic pumping.
Model VIe	2	Larger diameter inflow valve disc, polished inflow and outflow valve guide pins.	Up to 30 days of chronic pumping.
Model VIf	3	Same as VId but with stainless steel valve seats as well as guide pins unflocked and polished.	Up to 41 days of chronic pumping.
Model VIg	3	.010 inch long Dacron flock fibers on all pump surfaces except valve discs.	Up to 98 days of chronic pumping.
Model VIh	2	.010 inch long Dacron flock fibers but with polished valve seats and guide pins.	Up to 96 days of chronic pumping (continuing).
Model VIj	4	.010 inch long Dacron flock fibers but with Teflon valve discs and Teflon covered disc guides.	Up to 40 days of chronic pumping (continuing).

Improvements in hydrodynamic characteristics were achieved in pump Model VI, including reduced pump filling and ejection pressure drops, reduced flow separation, and improved surface washing. Extensive use of hydrodynamic models, such as those shown in Figure 1 was made in the development. Flocking techniques were modified to improve flock uniformity and adhesion of the polyurethane flock cement to stainless steel pump components.

A major part of the development effort with pump Model VI was devoted to achieving improved uniformity and decreased thickness of the fibrin deposits which form around the struts of the inflow and outflow valves. A variety of valve configurations was designed, fabricated, and evaluated in calves for this purpose. Two lengths of Dacron fibrils were also investigated. The .020" long fibers used initially have been replaced by .010" long fibers in pump Model VI, as shown in Figure 2.

Assist Pump Implantation.

In a selected series of 28 calves, partial left ventricular bypass was undertaken for periods of 30 to 120 days. Although pump implantation was routinely accomplished without cardiopulmonary bypass, systemic heparinization was instituted prior to connection of the device to the circulation. Postoperatively, anticoagulation was maintained with heparin (125 units per kilogram every four hrs.) for a period of 14 to 30 days, followed by the administration of oral sodium warfarin (5.0 milligrams/24 hrs.). Prothrombin times, obtained twice weekly, were maintained at 2.5 times the control value.

The pump was actuated pneumatically by a control system which was either triggered from the R-wave of the electrocardiogram or operated at a fixed rate.[4,5] In these experiments, 7 animals were pumped synchronously, and 21 calves underwent asynchronous assisted circulation. Flows were maintained between 1500 and 3000 milliliters per minute, and pump rates ranged from 30 to 60 beats per minute.

Physiologic Observations.

Methods and procedures for the evaluation (both acute and chronic) of calves have been described previously.[6] During acute studies, the animal was anesthetized with pentobarbitol and halothane, and catheters were placed in various cardiac chambers and vessels for blood sampling and pressure measurements. In certain instances, electromagnetic flow probes were used to evaluate pulmonary artery flow (cardiac output), aortic and assist pump blood flows. During chronic studies, electromagnetic flow probes were left in place for monitoring during the awake state and for evaluation of the response of the animal (and the assist device) to an exercise load.[7]

Since the last annual report, attention has been directed to two areas: cardiac catherization of calves with chronically-implanted, continuously pumping assist devices, and biplane, angiographic analysis of left ventricular function.

For these latter purposes, calves were anesthetized, and respiration was supported with a positive pressure ventilator. Catheters were introduced into the right carotid artery and positioned in the left ventricle and aorta. Two left ventricular catheters were used for an injection of Renovist and simultaneous monitoring of left ventricular pressure during the biplane angiogram. The third catheter was positioned in the aorta, both for monitoring and for coronary artery infusion. In addition, the myocardial electrocardiogram, pump stroke volume, biplane changer exposure signal, and the timing signal from the Cordis II dye injection are continuously monitored by a seven-channel Sanborn tape recorder. All recordings were obtained with an eight-channel Sanborn photographic recorder.

After the initial catheterization, baseline measurements were made, followed by a biplane angiogram performed in a non-pumping state. Similar angiograms were obtained in control and sham animals. A period of stabilization ensued, with optimization of pumping, following which a biplane angiogram was made during pumping to permit evaluation of the effect of assist device operation upon ventricular function. After further physiologic data were obtained, catheters were removed and the animal was returned to the laboratory to continue chronic pumping studies.[1]

Data thus obtained were reduced, and measurements were made of stable ventricular complexes (recorded during the biplane angiogram) for calculation of dP/dt and hoop stress. The anterior-posterior and lateral frames of the biplane angiogram (numbered to correspond with the Elema-Scholander signal recording) were then measured for area by planimeter and for major axes. The data were processed serially through three programs in the Harvard 940 Computer Center, which yielded the desired left ventricular function data: end-diastolic and end-systolic volumes, stroke volume ejection fraction, ventricular mass, semi-minor axis, radius of curvature, stroke work and power, stress, and a maximal rate of change of pressure (circumferential radius and strain).[8] For indexed values, all data were normalized by the square root of weight, $\sqrt{(Kg)}$, the most accurate method for animal and man.

A recent study has been undertaken for induction of acute left ventricular failure by infusion of carbon dioxide gas (in measured quantities) into the left coronary artery. Preliminary evaluation has been made to assess the effects of the assist device on ventricular pressures, volumes, and function during such a state. A protocol similar to that described above was used.

Hematologic Investigations.

The following laboratory determinations were performed in each calf from one to three times per week: erythrocyte morphology studies on peripheral blood smears; plasma hemoglobin concentration;[9] reticulocyte count (using methylene blue stain); serum haptoglobin determination;[10] serum iron;[11] fibrinogen levels;[12] platelet counts; blood urea nitrogen;[13] serum bilirubin levels;[14] serum proteins;[15] [16] prothrombin time;[17] sodium and potassium (I.L. flame photometer); chlorides (Buchler-Cutlove Chloridometer); hematocrit; erythrocyte mechanical fragility;[18] incubated osmotic fragility;[19] red blood cell survival (D.F. ^{32}P isotope technique);[20] red cell volume (^{51}Cr Sodium Chromate); and plasma volume determinations (^{125}I labelled R.I.H.S.A.).[22]

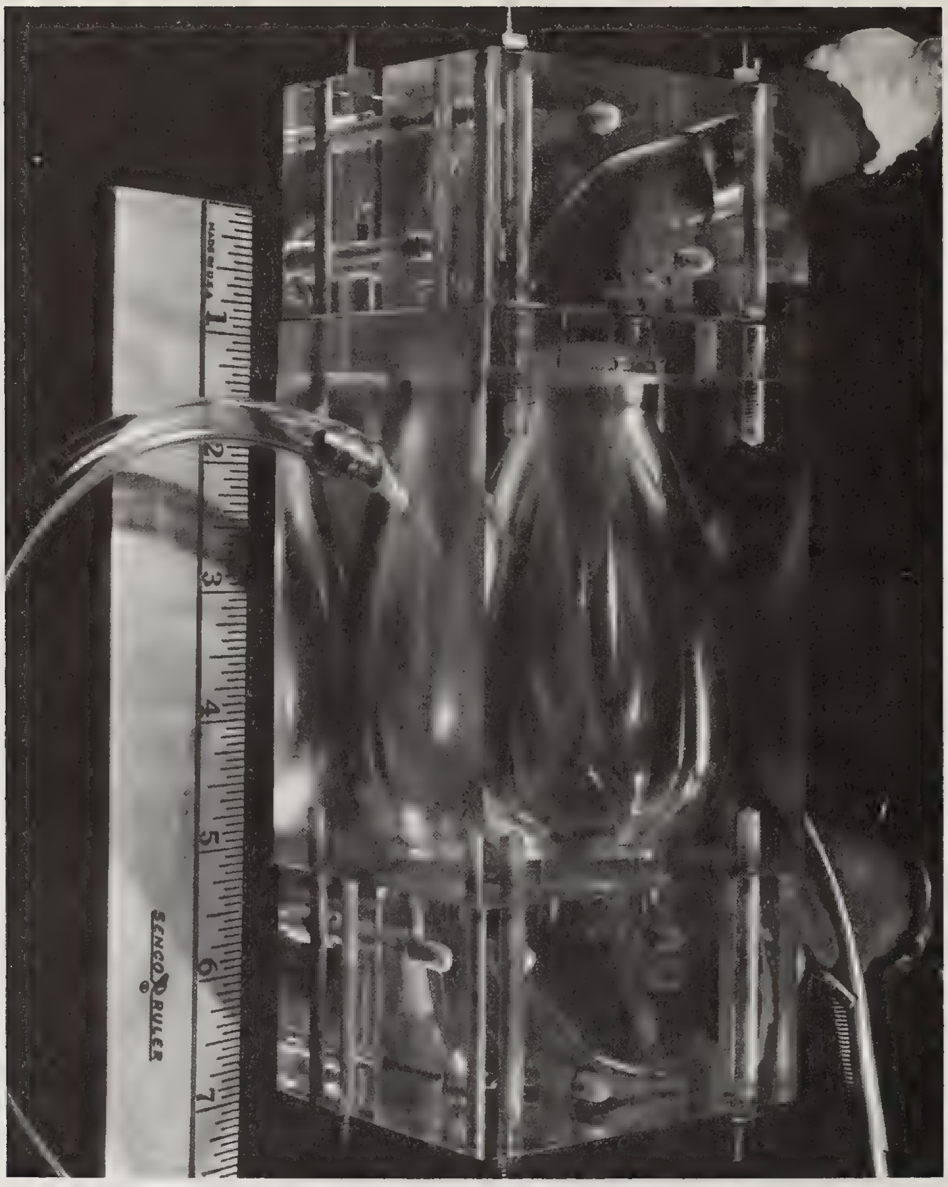

FIGURE 1. A TRANSPARENT PROTOTYPE OF ASSIST DEVICE MODEL VII FOR HYDRODYNAMIC TESTING.

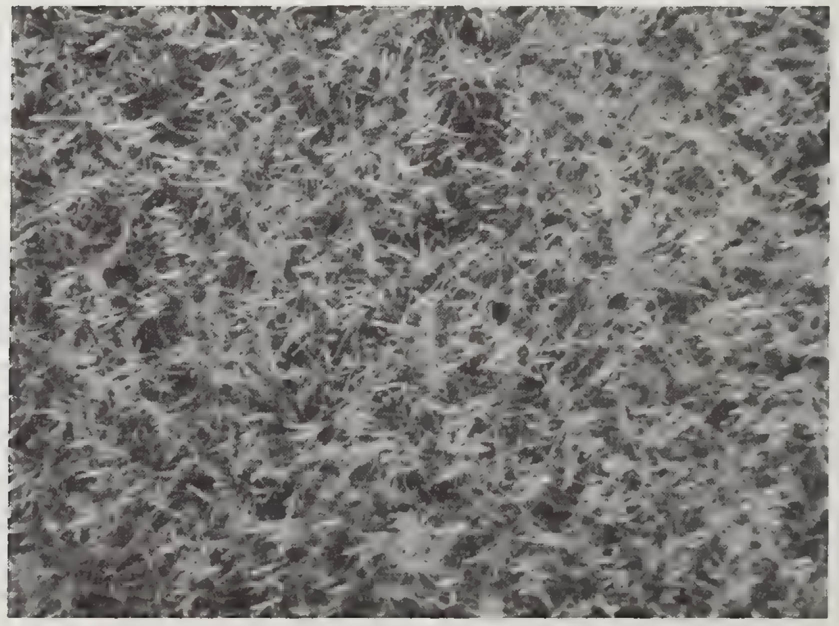

FIGURE 2. A MAGNIFIED VIEW OF THE PUMPING CHAMBER FLOCKED INTERFACE. THE DACRON FIBERS ARE 10 MILS LONG AND 1 MIL IN DIAMETER.

Cell Culture Technique.

The method utilized for the culture of bovine fetal fibroblasts has been reported recently.[22] Fetuses of 2.0 to 4.0 months gestation were employed as the source for skeletal muscle and connective tissue (Figure 3). The muscle segments were cleansed in Hank's Balanced Salt Solution and minced into sections approximately 1.0 gram in weight. Trypsinizing of these sections in a trypsin-EDTA solution was continued until an aliquot of the supernate from each flask contained an average of 5 x 10^5 cells per milliliter. The suspension was decanted into conical tubes containing calf serum to inactivate the trypsin. After centrifugation at 2000 revolutions per minute, the supernate was discarded, and the cell pellet resuspended in nutrient medium 199 (enriched with calf serum and buffered to a pH of 7.30). The suspension was divided into polypropylene petri dishes, each dish containing a concentration of 1 x 10^5 cells per milliliter. Incubation in desiccators at 37° followed (Figure 4).

Rapid cell division was noted in 12 hours, resulting in a doubling of the fibroblast population every 24 to 48 hours. When a uniform monolayer developed, the cells were separated from the plastic surface and divided.

In subculture, the medium was replaced with Hank's Balanced Salt Solution (without calcium ions), to raise the pH of the monolayer from 7.30 to 8.0. Loosening of the monolayer was then effected with a trypsin-EDTA solution. This solution was decanted and medium containing calf serum was added to the residual film to inactivate the trypsin and prevent cell lysis. The harvested cells were divided and replated with additional medium and then incubated, Figure 5.

Application of Fetal Cells to Prosthetic Pump Surfaces.

Thirty million pooled cells (prepared as for subculture) were collected in a sterile tube and decanted into the pump. The device was then sealed for 60 minutes at room temperature. After this interval, the fluid media were collected, and a cell count was performed to indicate the number of retained fibroblasts at the moment of connection to the circulation.

During surgical implantation of the pump, fibroblasts were allowed to remain on the interface (exposed to air) for periods of 5 to 15 minutes, while the vascular connections were accomplished. Previous observations indicated that fibroblasts in contact with a moist Dacron surface remained viable for periods of 30 minutes with no evidence of damage.

Gross and Microscopic Pathology.

Complete autopsies were performed on all animals sacrificed during the period of investigation. In addition, a comparative evaluation of the pump lining was performed in six calves receiving fibroblast-seeded devices and in 22 control animals.

RESULTS

Engineering Data.

An axial cross-section of assist pump Model VI is shown in Figure 6. The blood flowing from the left ventricle is passed through the inflow tube and inflow valve to the pump chamber or bladder. Here, blood is ejected from the pump through the outflow valve, tube, and Dacron graft to the thoracic aorta. Air pressure, supplied by an external control system through a percutaneous connector to the space between the rigid aluminum housing and the polyurethane pumping chamber, is used to eject the blood which fills the bladder. The internal surfaces of the pump are coated with Dacron fibrils embedded in a polyurethane adhesive.

The assembled assist device is presented in Figure 7. The Dacron velour covering permits fixation to the left hemi-diaphragm. The percutaneous connector consists of an air-line and three myocardial, electrocardiographic leads.

A summary of weight and volume characteristics of assist pump Model VIa is shown in Table 2.

TABLE 2

CHARACTERISTICS OF ASSIST PUMP MODEL VIa

Overall weight, dry	261 grams
Overall external volume	255 ml
Maximum internal volume	128 ml
Inlet tube volume	19 ml
Outlet tube volume	18 ml
Maximum pumping chamber volume	91 ml
Maximum stroke volume	76 ml
Maximum recommended stroke volume(a)	60 ml

(a)This stroke volume provides 1mm or greater separation between chamber walls in the end ejection position. Touching walls are undesirable because of possible damage to blood and the autologous lining.

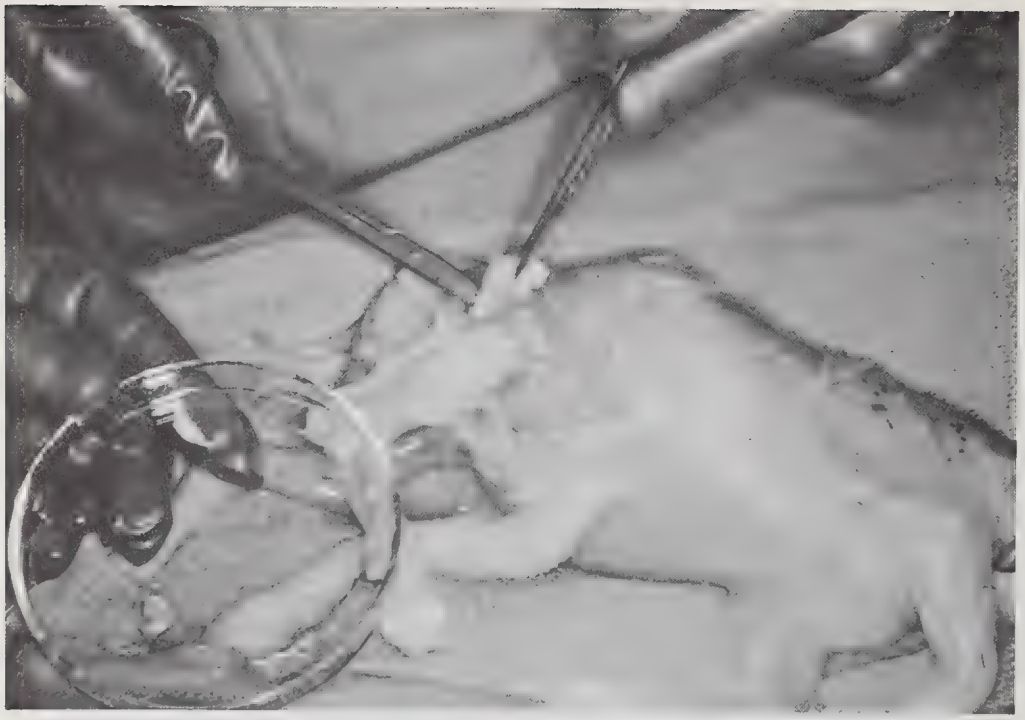

FIGURE 3. CALF FETUS (3.0 MONTHS GESTATION) DURING REMOVAL OF CONNECTIVE TISSUE PRIOR TO CELL CULTURE.

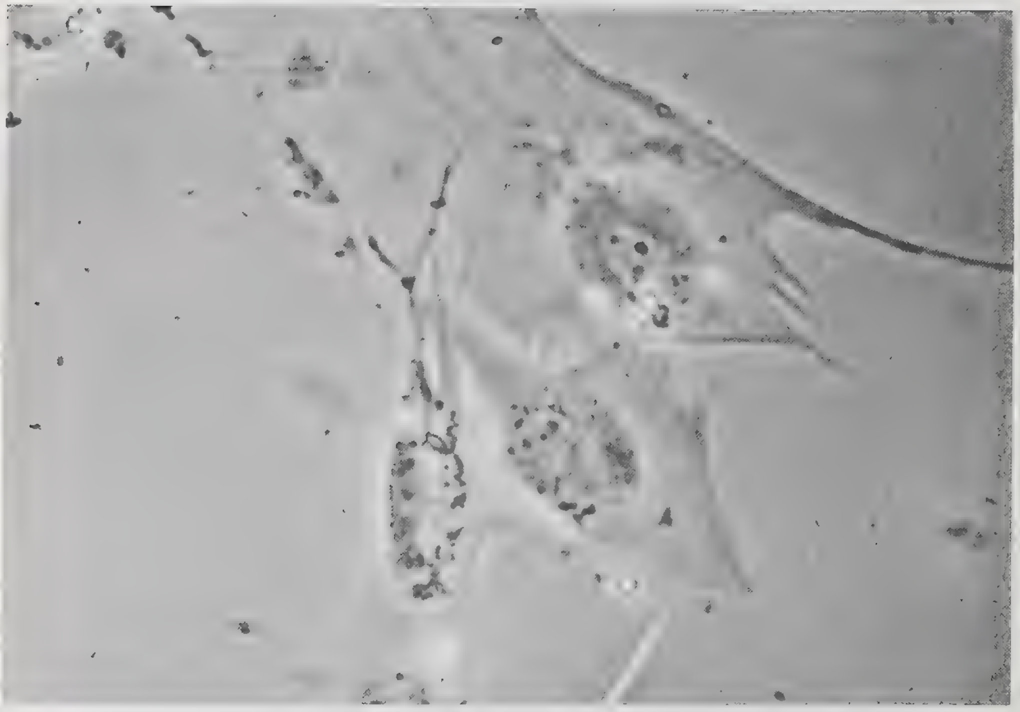

FIGURE 4. CALF FETUS FIBROBLASTS DURING INCUBATION, 8 HOURS AFTER DISPERSION OF CELLS FROM FETUS. CELLS ARE BEGINNING TO FORM A MONOLAYER.

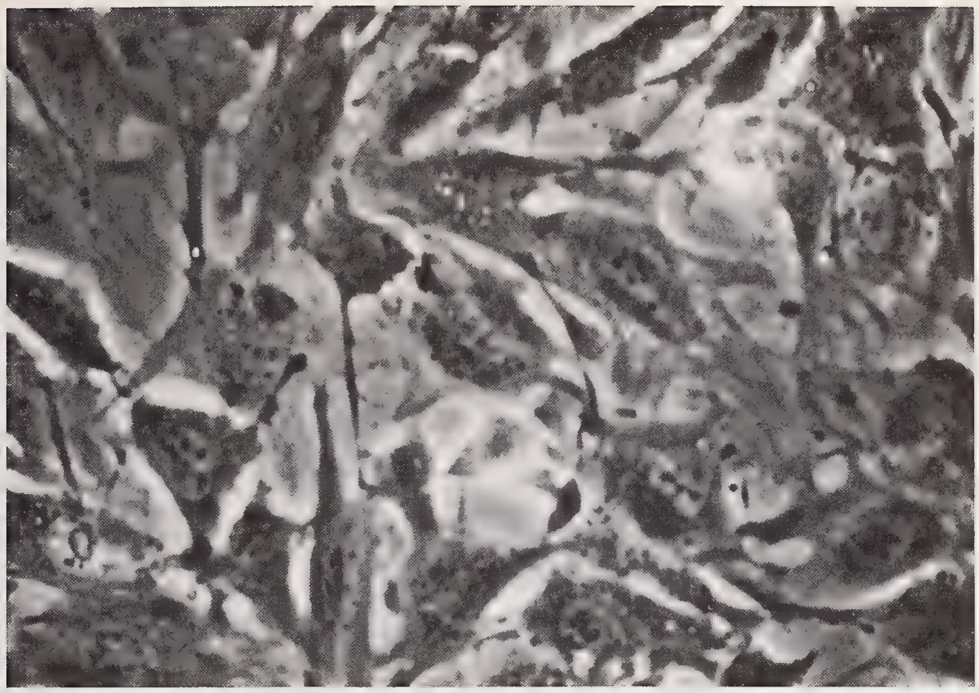

FIGURE 5. FETAL FIBROBLASTS AFTER 24 HOURS OF INCUBATION. CELLS ARE READY FOR TRANSFER TO A PUMP OR CAN BE DIVIDED AND MAINTAINED IN CULTURE. CELLS CAN BE KEPT GROWING FOR 7-8 WEEKS.

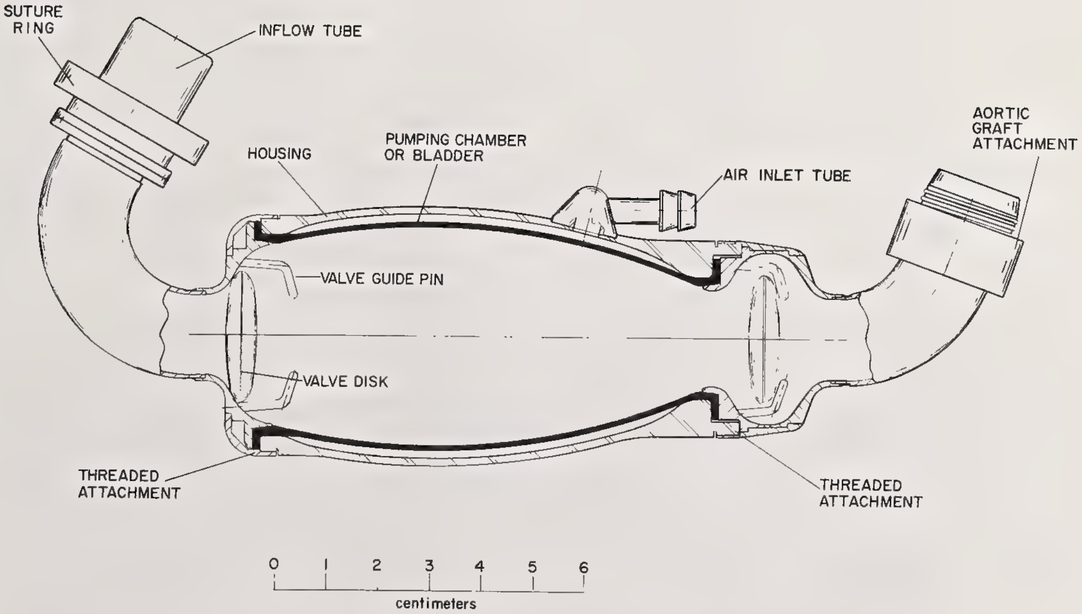

FIGURE 6. SCHEMATIC DIAGRAM OF ASSIST DEVICE MODEL VI.

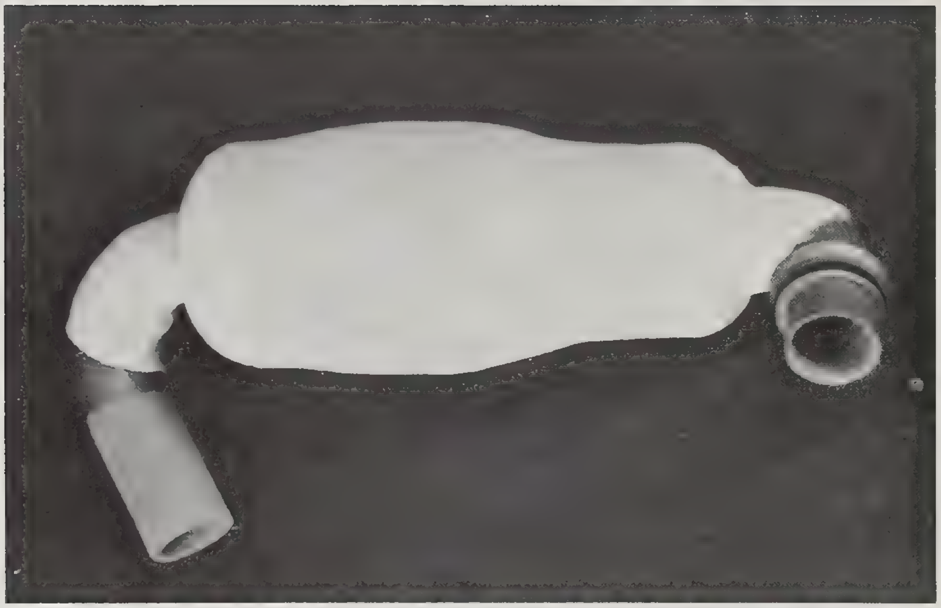

FIGURE 7. PHOTOGRAPH OF THE DOUBLE-VALVED, PNEUMATICALLY-ENERGIZED ASSIST PUMP MODEL VI UTILIZED IN THESE EXPERIMENTS. DACRON CLOTH ON THE OUTER SHELL OF THE PUMP PERMITS SUTURE FIXATION TO THE LEFT DIAPHRAGM.

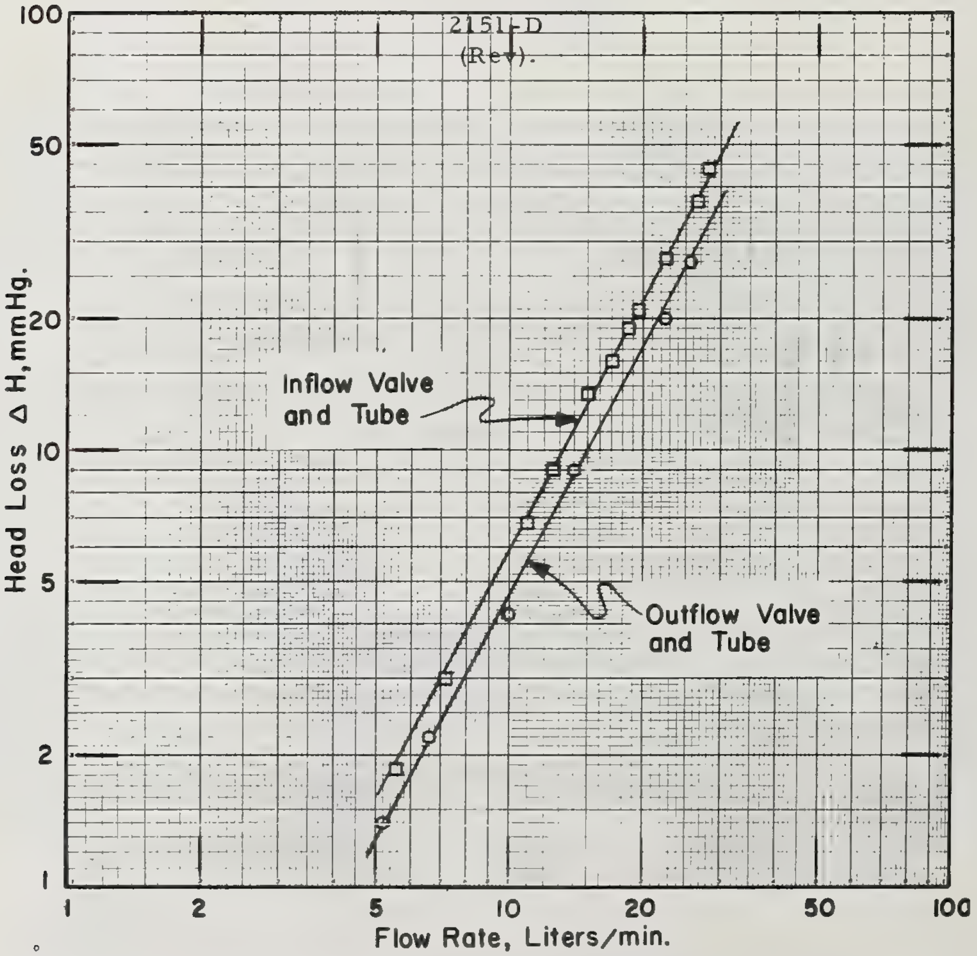

FIGURE 8. STEADY FLOW EXPERIMENTAL DETERMINATION OF HEAD LOSS THROUGH INFLOW VALVE AND INFLOW TUBE, AND THROUGH OUTFLOW VALVE AND OUTFLOW TUBE, TECO ASSIST PUMP MODEL VIa. WATER AT 68° F.

A maximum stroke volume of 60 ml was recommended to prevent touching of pumping chamber walls and attendant damage to blood and the autologous lining.

Steady flow tests of frictional or stagnation pressure drops through the inflow tube and valve and the outflow tube and valve have been performed. The results are included in Figure 8. At a mean flow rate of 6 liters per minute, peak flow approximated 20 liters per minute, necessitating a filling pressure differential of 22 mm Hg and an ejection pressure differential of 17 mm Hg. The compliance or pressure differential versus volume of the pumping chamber has been measured statically and is included in Figure 9. The partially-filled bladder was seen to provide five to 10 mm Hg of filling pressure.

Assist Model VII is presently being designed, developed, fabricated, and evaluated in vitro and in vivo. The objectives of this device are to provide a stroke volume of 100 ml and to reduce filling and ejection pressure differentials. An axial cross-section drawing of this pump is shown in Figure 10. The device is similar in design to Model VI, except for the horn shapes of the inflow and outflow tubes, the larger valve discs and pumping chamber, and the stainless steel housing adapted to pneumatic or hydraulic actuation. A photograph of the assembled assist device is shown in Figure 11. A summary of the characteristics of this assist device is given in Table 3.

TABLE 3

WEIGHT AND VOLUME CHARACTERISTICS OF TECO ASSIST PUMP MODEL VII FOR CHRONIC IMPLANTATION AND PNEUMATIC ACTUATION

Overall weight, dry	490 grams
Overall external volume	450 ml
Maximum internal volume	212 ml
Inlet tube volume	30 ml
Outlet tube volume	22 ml
Maximum pumping chamber volume	160 ml
Maximum stroke volume	140 ml
Maximum recommended stroke volume[(a)]	100 ml

[(a)] This stroke volume provides 1 mm or greater separation between chamber walls in the end ejection position. Touching walls are undesirable because of possible damage to blood and the autologous lining.

Partial Left Ventricular Bypass.

Twenty-eight animals underwent continuous assisted circulation for periods of 30 to 120 days.

TABLE 4

DURATION OF PARTIAL LEFT-VENTRICULAR BY-PASS IN 20 CALVES

(Flows of 1500-3000 ml/minute)

Days of pumping	30-49	50-69	70-89	90-120
Number of calves	10	6	4	8

Nine of this group, including six with devices containing bovine fetal fibroblasts, were sacrificed to permit evaluation of the blood-material interface.

Pumping was terminated in six calves (after 60 and 100 days), because of empyemas which developed around the pneumatic tube leading to the external control system. In four other animals, detachment of the Dacron pump matrix occurred due to separation of the polyurethane adhesive from the underlying silastic rubber. This resulted in an immediate obstruction of the pump lumen, followed by clot formation. The separation was caused by a lack of polymeric linking between the polyurethane adhesive and silastic elastomer, and was subsequently eliminated by switching to a polyurethane elastomer for pump chamber fabrication.

The remaining four animals were sacrificed because of gradual obstruction of the disc valves by clot. Thrombus accumulated at the base of the valve struts and gradually compromised the lumen. Five animals remain alive and well, 34, 62, 72, and 86 days postoperatively.

Physiologic Data.

Acute physiologic studies and cardiac catheterizations in chronic pump animals have confirmed previous observations on the effects of a left ventricular-aortic assist device: cardiac output was adequately maintained or increased , as was aortic pressure, and left ventricular pressure was reduced, to an extent determined by the percent of cardiac output captured by the pump (pressure can be reduced to zero when the pump captures the entire stroke volume). At the same

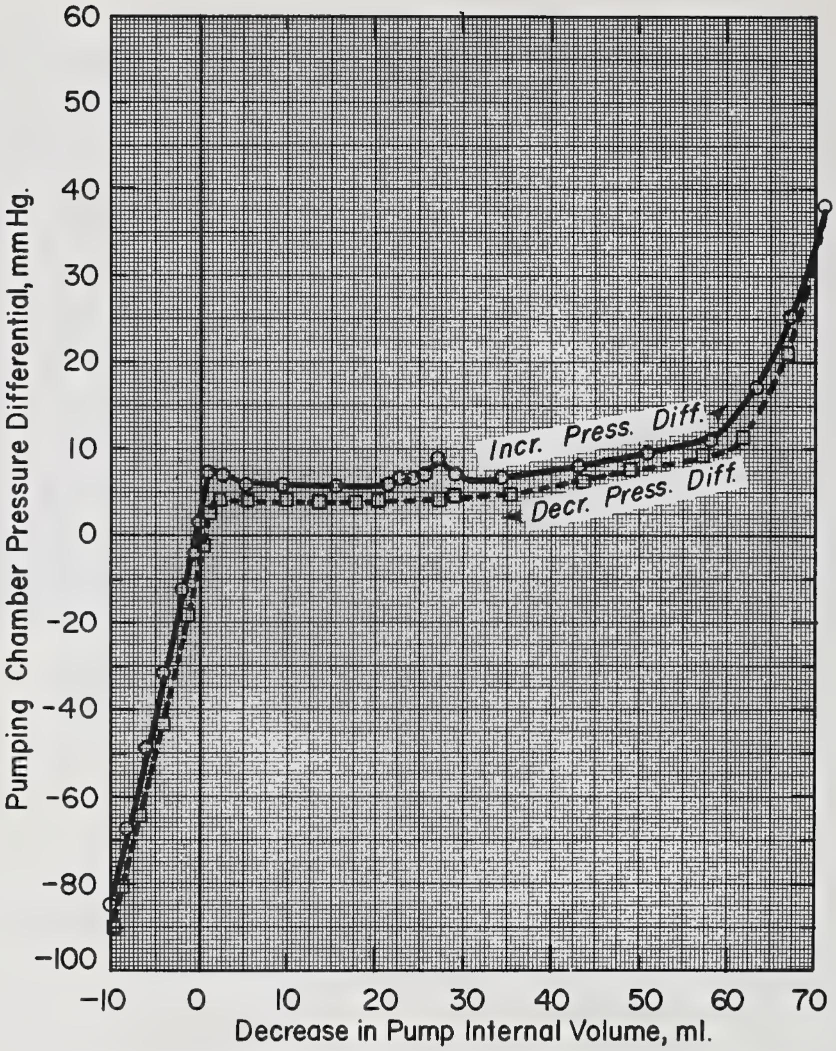

FIGURE 9. PUMPING CHAMBER COMPLIANCE TEST RESULTS PUMP MODEL VIa.

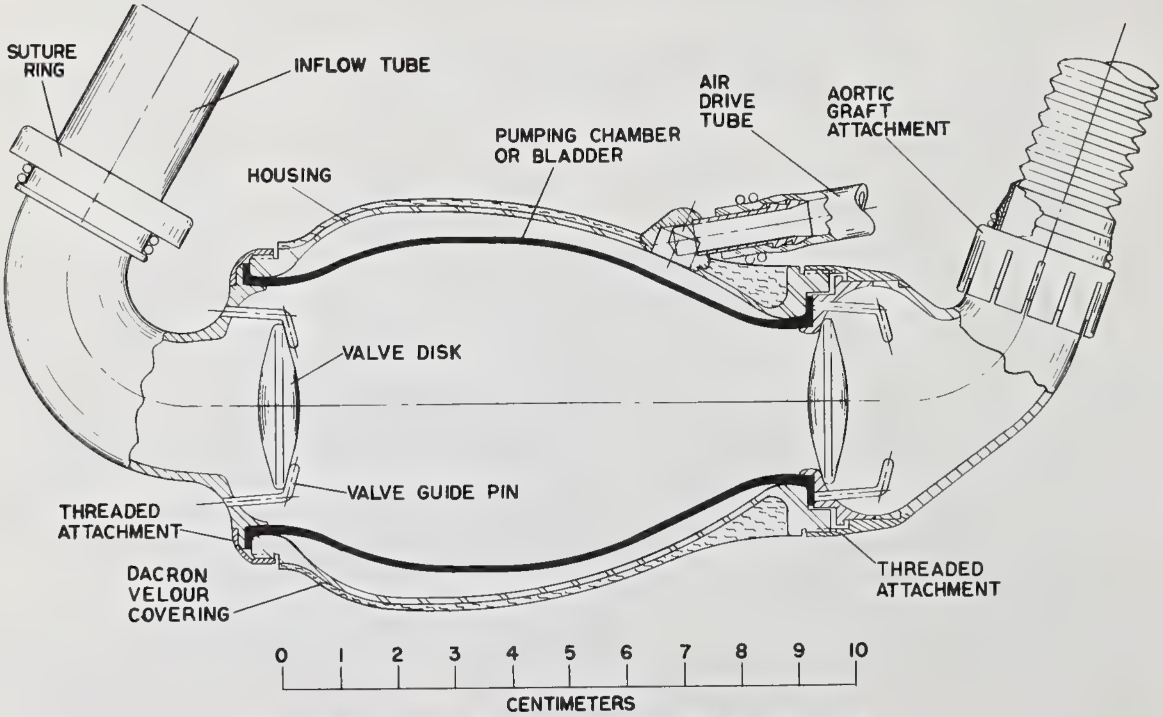

FIGURE 10. AXIAL CLOSS-SECTION VIEW OF PUMP MODEL VII.

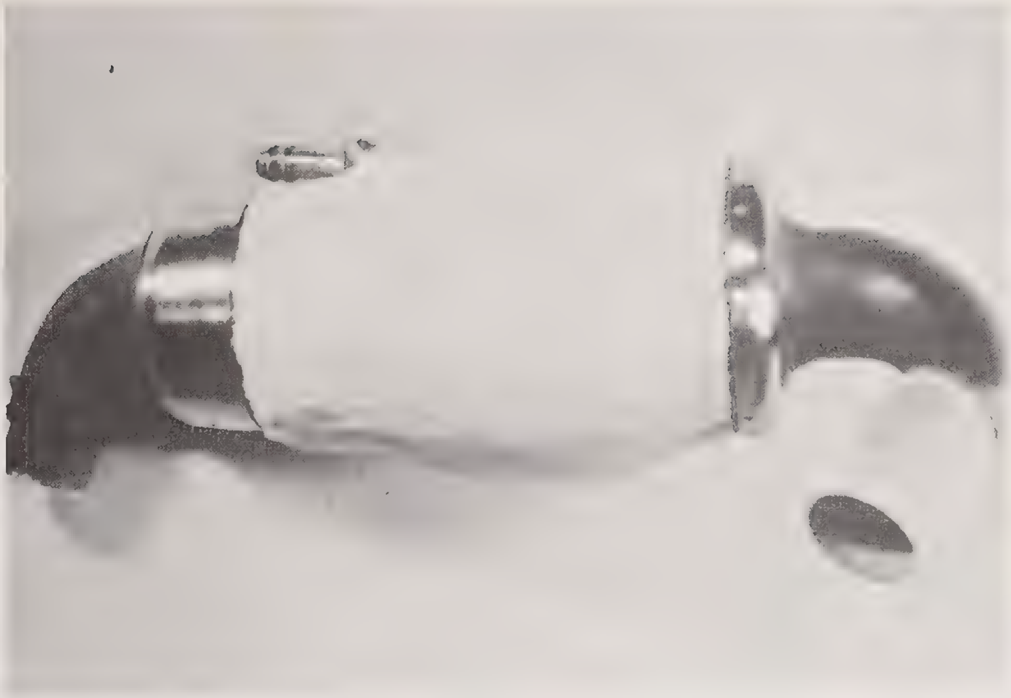

FIGURE 11. PHOTOGRAPH OF PUMP MODEL VII.

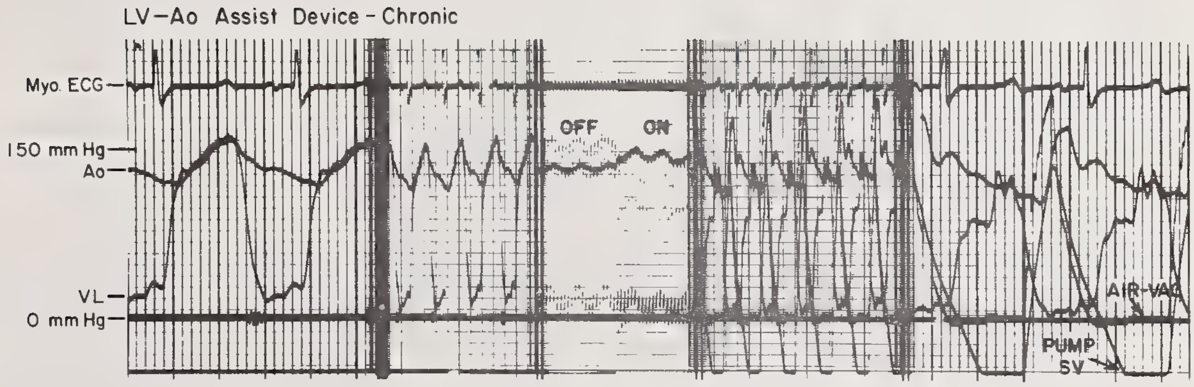

PUMP STATUS	PRESSURES (mm Hg)		RATES (per min)		PUMP OUTPUT (L/min)	PUMP SV (ml)
	LV	Ao	HEART	PUMP		
OFF	160/24	158/118 (138)	98	—	—	—
ON	122/16	170/105 (150)	95	95	(5.7)	(60)

Calf # 95 p̄-op 14 days

FIGURE 12. THE EFFECTS OF LV-AO ASSIST DEVICE ON AO AND LV PRESSURES DURING COUNTERPULSATION, MEASURED AT CARDIAC CATHETERIZATION.

time, left artrial pressure was reduced, as was left ventricular end-diastolic pressure. An example of the normal functioning of the device, when it captured less than the total cardiac output (but with a respectable pump output) is shown in Figure 12. On the left is the control state, in the center is the activation sequence of the pump, and on the right is the effect on the pressures. The latter consisted of a decrease in left ventricular pressure, accompanied by a slight increase in aortic pressure.

An example of a study in which the total cardiac output was captured by the pump is illustrated in Figure 13. Again on the left, the control state is illustrated; the pump is activated in the center of the panel, and the right side demonstrates a reduction of left ventricular pressure to approximately zero mm Hg. Concomitantly, aortic pressure increased and heart rate slowed, possibly due to neural feedback mechanisms.

To date, biplane angiographic analysis has been carried out in six calves: two controls, one sham-operated animal, two animals with pumps implanted (but not pumping), and two animals in which the pumping was of routine and maximum effectiveness. Using this biplane angiographic information to calculate the various parameters of left ventricular function, it was possible to demonstrate that a normally-functioning left ventricular assist device tends to reduce end-diastolic and end-systolic volumes towards normal. In addition, there is some improvement in the ejection fraction, and sometimes a slight increase in cardiac output. Maximal rates of change in pressure decreased, pari passu, with energy requirements. In the animal where left ventricular pressure was dropped to zero mm Hg, the same general effect was seen. An even more marked reduction of maximum dP/dt occurred with a decrease in stroke work, power, and end-diastolic and end-systolic volumes.

In preliminary experiments, involving the induction of acute, transient (reversible) left ventricular failure (by infusion of carbon dioxide selectively), the assist device proved capable of maintaining hemodynamic stability. For example, a typical progression in data from the control state to acute failure is shown in Figure 14. In a less dramatic example of failure induced by the CO_2 method, the effect of the assist device is illustrated in Figure 15. Left ventricular end-diastolic pressure is lowered (as is the peak systolic)while aortic perfusion pressure is slightly improved. These effects were also illustrated in Figure 12, where left ventricular failure occurred spontaneously. In both examples, the pressures are not lowered dramatically, since the left ventricular stroke volume exceeded that of the pump. Left ventricular peak pressure fell, with a concommitant rise in left ventricular end-diastolic and atrial pressures. A consistent fall in aortic pressure also developed, as well as a small increase in heart rate. Ventricular assistance further reduced the left ventricular peak pressure, returned the end-diastolic pressure toward normal, and produced a rise in systemic pressure (to control levels). Long-term heart failure experiments have not yet been possible, but it is anticipated that the same phenomena (as illustrated in Figure 15) should apply to that state as well as to the acute state. The dependent factor is the ability of the pump to continue to accept a significant amount of cardiac output, synchronized or unsynchronized.

Hematologic Investigations.

Studies of erythrocyte morphology revealed the presence of marked anisocytosis. The red cells were predominantly microcytic with no nucleated red cells noted. Reticulocytes never exceeded 1.0 percent, and serum haptoglobins remained in the normal range (1.0 to 10.0 milligrams percent). Plasma hemoglobins did not exceed 12 milligrams percent, and serum iron, fibrinogen, platelets, BUN, Bilirubin, total proteins, and serum electrolytes were unchanged from control values.

Examination of the sodium and potassium transport in calf erythrocytes was undertaken in an effort to detect evidence of cell membrane damage produced by chronic bypass. However, our investigations indicated an absence of the transmembrane pump found in the human red cell. Instead, calves were noted to have intracellular sodium and potassium values close to the plasma concentrations of these cations. Accordingly, no meaningful changes in the control or post-pumping specimens were noted in Table 5.

TABLE 5

SODIUM AND POTASSIUM TRANSPORT IN CALF ERYTHROCYTES

	Intracellular Na^+ mEq/L.	Intracellular K^+ mEq/L.	Plasma Na^+ mEq/L.	Plasma K^+ mEq/L.
Control (Unoperated) calves (8)[a]	86.2	16.6	132.2	4.40
Calves with pump implant (12)[a]	83.1	18.8	138.1	4.0
Human control (20) values (15)[a]	10	95	140	3.5

(a) Mean values

Serial hematocrit determinations in 28 chronic experiments were compared with similar data previously obtained in eight animals (shams) undergoing a left thoracotomy alone. These data indicated a slight reduction in hematocrit after pump implantation, with a gradual return toward the control level. Mechanical fragility evaluation indicated a temporary increase in red cell fragility for 24 to 48 hours. After this period, the plasma hemoglobin levels in the traumatized samples dropped to the normal range. Incubated osmotic fragilities were slightly increased for 7 to 14 days after pump implantation. However, these determinations also returned to the normal range within 30 days. Erythrocyte survival time was investigated using D.F. ^{32}P., since our previous experience revealed that a ^{51}Cr label did not attach strongly to the bovine hemoglobin molecule. However, the ^{51}Cr isotope was sufficient to permit red cell volume measurements, and ^{125}I labeled RIHSA could be used successfully for plasma volume determinations. In both unoperated (control) calves and those with pump implants, whole blood volume was measured first, followed by red cell half-life determination. This order proved to be essential, since ^{32}P interferes with the counting of ^{51}Cr and ^{125}I.

Red cell survival and whole blood volume measurements in six unoperated animals and 12 pump calves are presented in Tables 6 and 7.

TABLE 6.

WHOLE BLOOD VOLUME AND RED CELL SURVIVAL IN SIX CONTROL CALVES

Calf Number	Red Cell 1/2 Time (Days)	Red Cell Vol. RCV/kg ml / ml/kg	Plasma Vol. PV/kg ml / ml/kg	Whole Blood Vol. WBV/kg ml / ml/kg
70	18	1352 15.3	4528 51.1	5880 66.4
72	19	1311 19.2	3874 56.7	5185 75.9
71	26	1152 14.4	4173 52.4	5325 66.8
86	12	1990 29.8	3686 55.2	5676 85.0
87	14	1717 26.1	3008 45.7	4724 71.8
31	15	1409 20.4	3413 49.5	4822 69.9
Average (ml/kg)	17.4	20.9	53.6	72.6
Standard Deviation	4.5	6.0	5.1	7.0

A small drop in red cell survival occurred in the pump animals (16.8 days) as compared to the controls (17.4 days). Red cell volume, indexed to body weight, was also decreased (17.7 ml/per Kg in the pump calves and 20.9 ml/Kg in the controls), but blood volume indices were almost identical (17.6 ml/Kg in the controls and 72.3 ml/Kg in the pump calves). A small increase in plasma volume in the latter group compensated for the change in red cell mass noted, resulting in whole blood volumes almost equal to the controls.

Evolution of the Blood-Pump Interface.

In 22 animals receiving unseeded pumps (controls), the autologous lining within the device consisted of fibrin plus a number of small regions containing proliferating fibroblasts and collagen. In some instances, these pseudoendothelial islands were surrounded by hyalinized fibrin completely devoid of cells. The thickness of the interface varied from 250 microns to 3.0 millimeters, with the largest accumulations of the unorganized fibrin noted along the flexion creases of the pump chamber and at the base of the valve struts. In contrast, the permeable Dacron graft segment was always completely endothelialized. This latter process developed by extension of the intima from the aortic anastomosis and by direct fibroblastic invasion of the interstices of the graft.

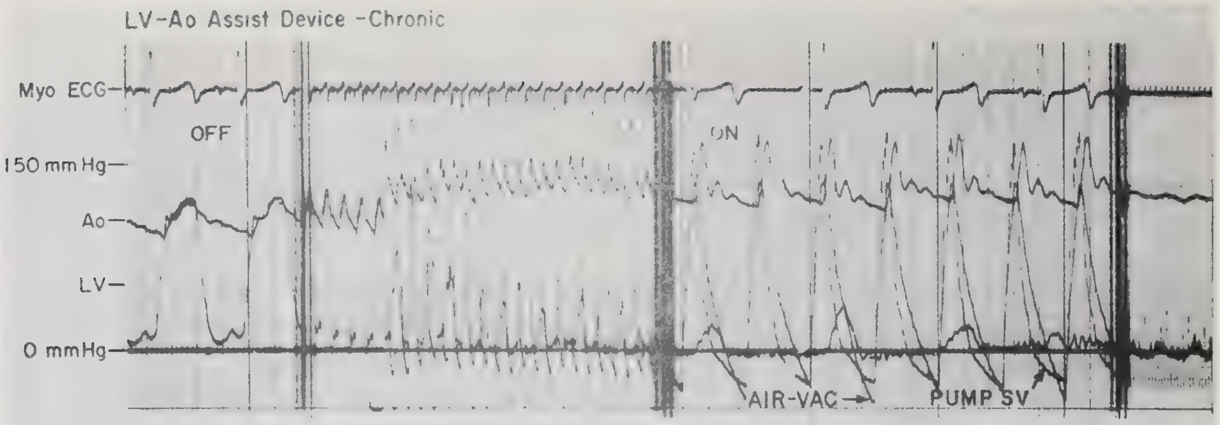

PUMP STATUS	PRESSURES (mm Hg)		RATES (per min)		CO (L/min)	PUMP SV (ml)
	LV	Ao	HEART	PUMP		
OFF	122/12	118/93(110)	88	—	—	—
ON	0 to 35/0	160/118(126)	70	119	6.0*	50*

Calf #95 $\bar{p}$-op 14 days

*Approximate

FIGURE 13. LEFT VENTRICULAR-AORTIC ASSIST DEVICE OFF AND ON WITH VENTRICULAR PRESSURE REDUCED TO 0 MM Hg.

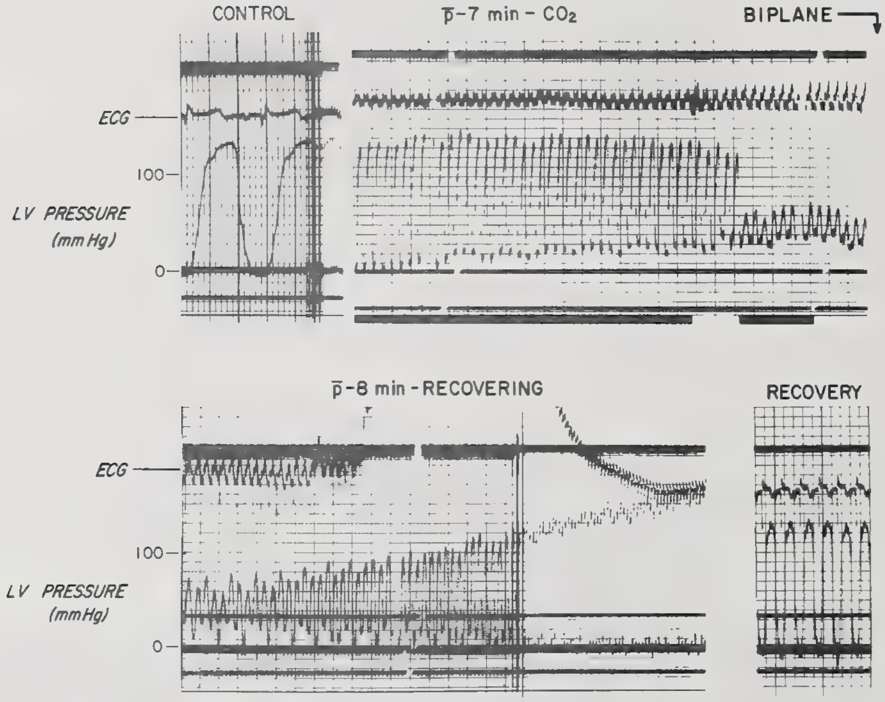

CALF # 50 (Cell)

FIGURE 14. ACUTE LEFT VENTRICULAR FAILURE INDUCED BY CO_2 INFUSION INTO A CORONARY ARTERY. CONTROL LV PRESSURE 120/0-4; PRE-BIPLANE DECREASE TO 48/30 (7 MINUTES); OVERSHOOT DURING RECOVERY TO 170/0-8(8-1/2 MINUTES); AND RETURN TO CONTROL BY 12 MINUTES (128/0 MM Hg). NOTE ISCHEMIC PATTERN IN ECG AND REVERSION, BY 12 MINUTES, TO NEAR NORMAL.

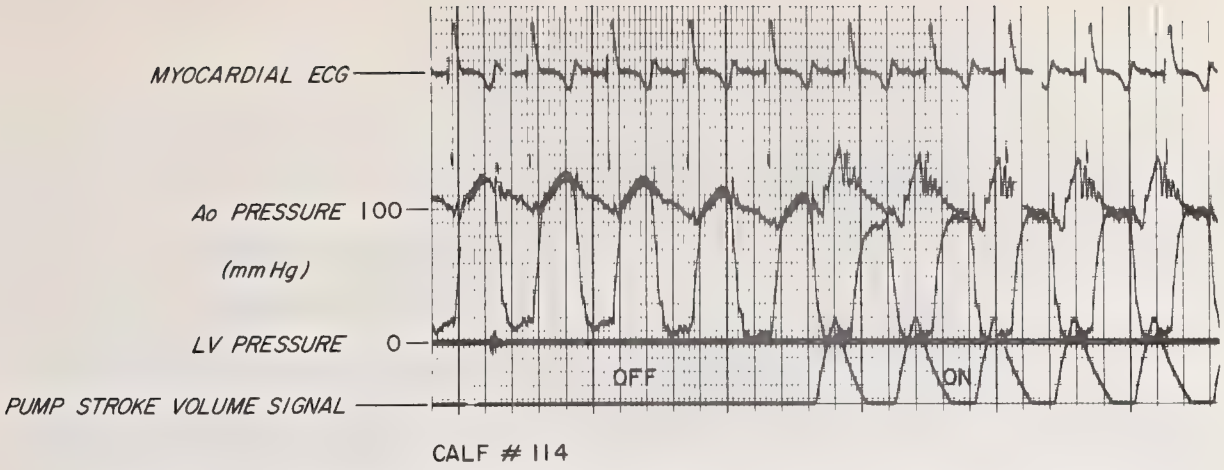

FIGURE 15. THE EFFECT OF LEFT VENTRICULAR-AORTIC ASSIST DEVICE ON ACUTE LV FAILURE INDUCED BY CO_2 INFUSION INTO A CORONARY ARTERY, NOTE REDUCTION IN LV END-DIASTOLIC (18 MM Hg TO 10 MM Hg) AND PEAK SYSTOLIC PRESSURES AND INCREASED AORTIC PRESSURE DURING ACTIVE PUMPING.

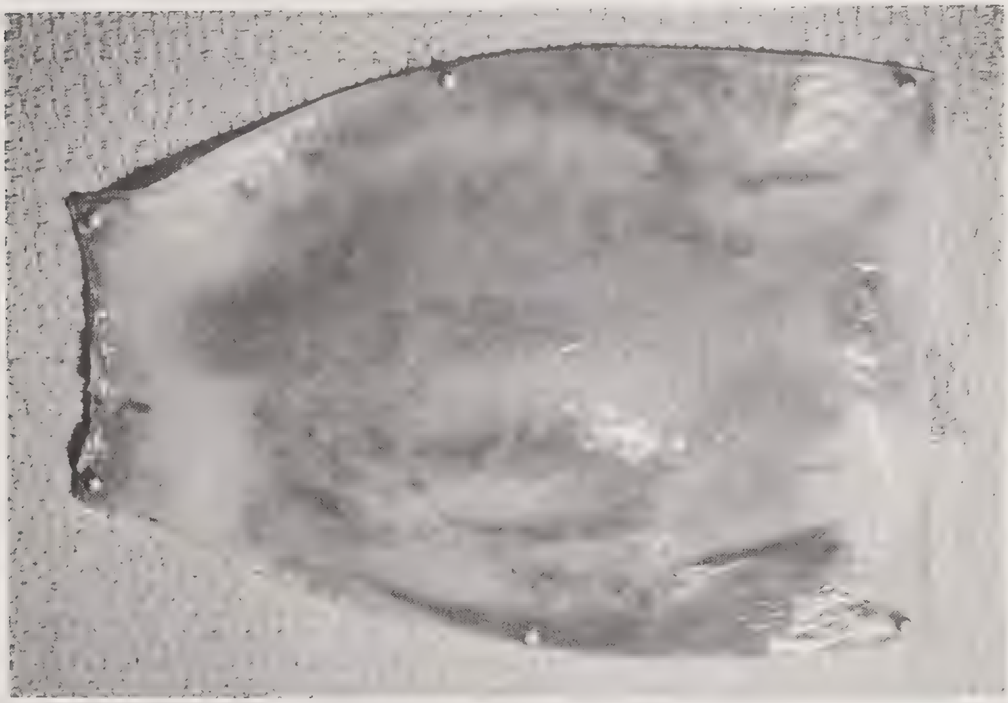

FIGURE 16. PUMP BLADDER (CHAMBER) REMOVED AFTER 30 DAYS OF CHRONIC LEFT HEART BYPASS SHOWING SMOOTH LAYER OF FIBROBLASTS AND COLLAGEN COVERING THE SURFACE.

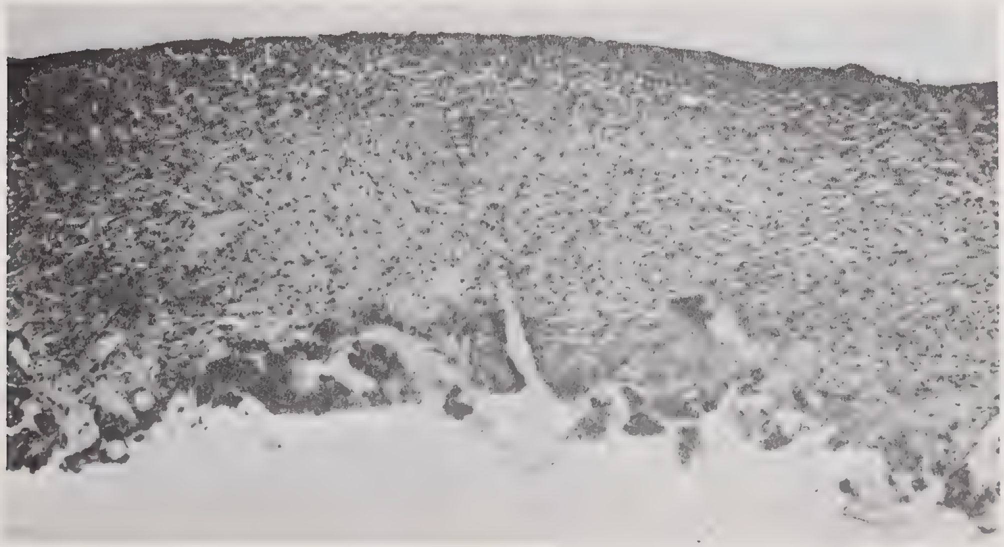

FIGURE 17. FETAL FIBROBLASTS (90 POWER) LAYERED AT SURFACE OF PUMP CHAMBER. COLLAGEN FIBERS (PRODUCED BY THE FIBROBLASTS) CAN BE SEEN BELOW THE SURFACE LAYER OF CELLS; DACRON FIBRILS ARE PRESENT AT THE BASE.

TABLE 7.

WHOLE BLOOD VOLUME AND RED CELL SURVIVAL IN 11 CALVES WITH ASSIST PUMPS

Calf Number	Red Cell 1/2 Time (days)	Red Cell Vol. RCV/kg ml/ml/kg	Plasma Vol. PV/kg ml/ml/kg	Whole Blood Vol. WBV/kg ml/ml/kg
77	16	1840 20.9	5239 59.5	7079 80.4
80	24	1465 17.4	5038 59.2	6503 77.1
96	10	1443 18.1	4192 52.7	5635 70.9
97	15	1010 11.6	3525 40.5	4535 52.1
95	12	874 11.5	4399 57.7	5273 69.2
104	20	1504 20.1	4691 62.7	6194 82.8
108	14	1205 15.8	3233 42.4	4437 58.2
110	11	894 10.9	5016 61.2	5910 72.1
111	34	1707 21.0	5129 63.3	6836 84.4
112	14	1646 21.1	4804 61.6	6449 82.7
114	14	2098 26.2	3156 39.5	5254 65.7
Average (ml/kg) Standard Deviation	16.8 7.0	17.7 4.9	54.6 9.3	72.3 10.6

The appearance of the pump lining was considerably improved in the six animals with assist devices containing bovine fetal fibroblasts. In specimens examined after 30 to 60 days of continuous assisted circulation, broad sheets of fibroblasts and considerable quantities of collagen were noted Figure 16. Layers of spindle-shaped cells were frequently present at the surface of the interface, and the cellularity often continued down to the Dacron fibrils at the base of the pump chamber wall. These cells, and the surrounding collagenous fibers, firmly fixed the fibrocellular lining to both the flexing and stationary surfaces of the pump (Figure 17.)

DISCUSSION

The ability to carry out mechanical circulatory support in 28 calves for period of 30 to 120 days indicates the potential merit of our left ventricular-aortic assist pump. In addition, serial hematologic studies, undertaken to detect the presence of major cellular or protein damage produced by prolonged periods of pumping, disclosed very few abnormalities. Erythrocyte half-life determinations were found to be slightly reduced from controls, as were red cell mass measurements performed simultaneously. However, no change in total blood volume occurred, since a small, compensatory increment in plasma volume developed in each animal within the first two weeks following pump implantation.

Gross hemolysis was never observed, and there were only transient increases in mechanical red cell fragility and incubated osmotic fragility. Platelets remained in the normal range, as did serum protein values, fibrinogen, serum electrolytes, blood urea nitrogen, and total serum bilirubin. It is apparent, therefore, that blood trauma is not an important limiting factor in prolonged assisted circulation at flow rates up to 3.0 liters per minute.

From a physiologic standpoint, it is clear that the assist device is capable of maintaining a satisfactory cardiac output up to a maximum of eight liters per minute. With the proposed increase in stroke volume from 60 ml to 100 ml, the capability of pump Model VII should be increased to the point where consistent reductions in left ventricular pressure and work will be seen. It is clear that reduction of pressure in the atrium and ventricle is largely, if not entirely, dependent upon the full stroke volume.

The investigations involving biplane angiographic evaluation of left ventricular function (in the normal animal and in the animal with acute left ventricular failure) have indicated that the function of the left ventricle is improved in several significant ways. First, a reduction in end-diastolic and end-systolic volumes is the basis upon which the respective pressures are reduced, while maintaining a normal stroke volume and ejection fraction. This mechanism serves to protect the Frank-Starling mechanism of heterometric autoregulation of ventricular output, by filling volume and pressure. Second, any reduction in heart rate which accrues(Figure 12, is beneficial, since heart rate is expensive in terms of myocardial energetics. Third, in this same vein, the beneficial changes in tension, stress, and maximum dP/dt all tend to operate in the same direction that of lowering the cost of cardiac output. While a satisfactory animal model of chronic left ventricular failure (particularly myocardial fibrosis) is not yet available, the acute studies (with carbon dioxide) suggest that the left ventricular-aortic assist device responds, in the failure state, as one would predict from the data obtained in healthier animals. Hemodynamically, then, the conclusion to be drawn from these studies is inescapable: The prime requirement of a left ventricular assist device, like that of the heart, is to accept and pump forward an adequate stroke volume.

A desire to accelerate the development of pseudoendothelium on the flocked Dacron surface of our assist pump prompted us to seed the device with bovine fetal fibroblasts grown in tissue culture. Transfer of cells to prosthetic surfaces was accomplished easily, and after connection of the pump to the circulation, the existence of stationary fluid at the boundary layer prevented a washout of cells by the high velocity blood flow.

Examination of cell-seeded pump linings, at the time of animal sacrifice, presented a striking contrast with the control. Broad sheets of fibroblasts were present throughout each section of the pump chamber, with layers of spindle-shaped cells aligned at the surface. There was an abundance of collagen present, and only scattered areas of hyalinized fibrin. The entire surface was thinner than the control specimens and extremely adherent to the underlying Dacron matrix. The results of these efforts to improve the blood-material interface has been encouraging.

The primitive allogenic fetal cells employed in these experiments proliferated rapidly, and did not evoke an immunologic response from genetically dissimilar recipient calves. Both fibroblasts and fibrocytes were observed in the microscopic section of the linings, which suggests that the fetal cells either matured in vivo or were gradually replaced by mature fibrocytes from the host. In either case, the result was a stable, cellular interface.

The fact that fetal cells could be grown with considerable ease in the laboratory further suggests that they may be of importance in other areas of cardiovascular research. At present, investigations are underway to improve methods of cell application to prosthetic pump surfaces.

SUMMARY

1. Assisted circulation has been carried out in a selected series of 28 calves at flow rates of 1500-3000 milliliters per minute for periods of 30 to 120 days.
2. A variety of hematologic studies were performed, including red cell survival determinations and measurements of red cell mass. These revealed only minor evidence of blood trauma produced by chronic pumping.
3. Since development of a clot-free blood interface is the limiting factor in longer periods of bypass, an effort was made to accelerate the formation of pseudoendothelium on the flocked Dacron matrix of our assist device. The experiments involve preliminary seeding of the lining with bovine fetal fibroblasts previously grown in tissue culture. Microscopic comparison of assist pumps containing fetal cells with other unseeded devices revealed a greater degree of cellularity and organization of the fibrin layer in the seeded pump.

REFERENCES

1. Bernhard, W. F., LaFarge, C. G., Robinson, T. C., Yun, I., Shirahige, K., and Kitrilakis, S. An improved blood interface for left ventricular bypass. Ann. of Surg., 168: 750-764, 1968.
2. Filler, R. M., Bernhard, W. F., Bankole, M., LaFarge, C. G., and Robinson, T.: An implantable left ventricular-aortic assist device. Journal of Thoracic and Cardiovascular Surgery, 54: 795-802, 1967.
3. Bernhard, W. F., LaFarge, C. G., Jockin, H., Kitrilakis, S., and Robinson, T.: Chronic left ventricular bypass with an implantable ventricular-aortic assist pump. Circulation (In press) 1969
4. LaFarge, C. G., Bernhard, W. F., Robinson, T. C., Kitrilakis, S., Yun, I., and Shirahige, K.: Physiological consequences of acutely and chronically implanted direct left ventricular-aortic assist devices. A.S.A.I.O Transactions XIV: 316-322, 1968.

5. LaFarge, C. G., Hausain, M., Ono, K., Robinson, T. C., and Bernhard, W. F.: Biplane angiographic evaluation of chronically implanted left ventricular-aortic assist devices. Transactions XV, (in press), 1969.
6. Phys. Evaluation of blood pumps in animals, 1st annual report, NHI.
7. LaFarge, C. G., Robinson, T. C., Kitrilakis, S. S., Bernhard, W. F.,: Physiologic Response to Exercise During Chronic Assisted Circulation, Circulation, 38: VI-121, 1967.
8. LaFarge, C. G., Husain, M., Ono, K., Robinson, T. C., Bernhard, W. F.,: Biplane angiographic evaluation of chronically implanted left ventricular - aortic assist devices, Trans. Amer. Soc. Artif. Int. Organs, Vol 15 (In press), 1969.
9. Crosby, W. S. and Furth, F. W.: Determination of plasma hemoglobin in whole blood. Blood 11: 380, 1956.
10. Tarukoski, P. H.: Quantitative spectrophotometric determination of haptoglobin. Scandinavian J. of Clin. Lab. Invest. Vol. 18 pp. 80-86, 1966.
11. Young, D. S. and Hicks, J. M: Method for the automatic determination of serum iron, Journal of clinical pathology. Vol. 18, pp. 98, 1965.
12. Rattenoff, O. D. and Menzie, C.: A new method for measurement of fibrogen in small samples of plasma. Journal of Laboratory and Clinical Medicine, 37: 316, 1951.
13. Marsh, W. H., Fingerhut, B., and Miller, H.: Automated and manual direct methods for the determination of blood urea. Clinical Chemistry, 11: 624, 1965.
14. Malloy, W. T., and Evelyn, K. A.: D-termination of bilirubin with photoelectric calorimeter. Journal of Biological chemistry. 119: 481, 1937.
15. Kirk, P. L.: Kjedahl method for total nitrogen. Anal. Chem. 22: 354-358, February, 1950.
16. Kingsley, G. R.: A rapid method for separation of serum albumin and globulin. Journal of Biological Chemistry. 133:731-735, May, 1940.
17. Quick, A. J.: The prothrombin and hemophilia in obstructive jaundice. Journal of Biochemical Chemistry, 109: LXXIII, 1935.
18. Fleisch, A.: Mechanical fragility determinations, Schweiz, Med. Wschr., 90: 186, 1960.
19. Dacie, J. W.: Osmotic fragility after incubation. The Hemolytic Anemia. Number 1: 40, 1954.
20. Mizuno, Perman, V., Bates, F. W., Schultze, M. O. : Life span of thrombocytes and erythrocytes in normal and thrombocytopenic calves, Blood, 14: 708, 1959.
21. Button, L. N., Gibson, J. G., Walter, C. W.: Simultaneous determination of the volume of red cells and plasma for survival studies of stored blood. Transfusion, 5: 143, March-April, 1965.
22. Bernhard, W. F., Hasain, M., George, J. B., and Curtis, G. W.,: Fetal fibroblasts as a substratum for pseudoendothelial development on prosthetic surfaces. Surgery (In press) 1969.

DISCUSSION

DR. C. W. HALL: I want to congratulate the authors on a beutiful presentation. I would make one suggestion. We have recently described a technique whereby skeletal muscle can be taken at the time of the operation, macerated in a Waring blender and made into a tissue brie which can then be seeded onto the surface of any type of thromboadherent surface, and this will give you the identical result without involving some of the drawbacks of tissue culture.

DR. JARON: If one uses such a pump and compels all the blood to flow through the pump, then I am a little bit confused as to the difference between this pump and the pump which utilizes the aorta and, therefore, maybe incorporates the aortic valve in its design. Also, the data showed increases in cardiac output; however, if I'm not mistaken, the data did not show how this cardiac output is distributed to the different organs and to the coronary circulation. I am also wondering whether the authors have any data regarding the oxygen consumption of the myocardial muscle.

DR. LaFARGE: I can't tell you about the distribution of the total cardiac output amongst the various organs, since this would require a host of flowmeters: individual organ flows varying as they do, from moment to moment. In those that we have measured, for example, the coronary artery blood flow, which you especially pointed out, and carotid flow, during the time when the output and the pressure are increased by the activation of the device, these flows do respond as you would expect. There is a slight absolute increase in coronary flow as well as a relative increase in coronary flow with respect to the reduction in left ventricular pressure, which, as you would anticipate, leads to a decrease in myocardial oxygen consumption. I can't yet separate out the various influences on myocardial oxygen consumption (peak ventricular pressure, wall tension and stress, dP/dt, heart rate, and coronary perfusion pressure) in this kind of setting; I don't think anyone is wise enough to do that.

DR. JARON: Your data showed that the tension in the wall remains the same.

DR. LaFARGE: The data in the first figure that I showed (calf No. 87) only illustrated that the rate of change of strain remained unchanged. I haven't the time to show you the more complicated data from the other calves including the one in which the pressure was reduced to zero. However, tension responds as you would expect it to: it falls in proportion to the decrease in pressure and the radius of curvature. In the animal experiment which I showed (calf No. 87), the pressure was reduced by roughly 50% but no significant reduction in tension was calculated from the biplane data.

DR. JARON: My first question was in regard to the difference between this device and the device which will be connected to the aorta, utilizing the aortic valve.

DR. LaFARGE: There is no device to my knowledge which accepts blood from the aorta and is capable of reducing ventricular peak pressure to zero, of maintaining coronary perfusion pressure, and at the same time of being able to pump levels of 5 to 7 liters per minute, which we can do even now with the 60 milliliter model of the left ventricular-aortic device.

DR. JARON: But in principle, it seems to me that the same device could be connected to the aorta and achieve the same results with one less hole in the ventricle.

DR. LaFARGE: The basic hemodynamic difference between the left ventricular aortic device and an aortic-aortic pump concerns the perfusion pressure seen by the coronary and possibly the carotid arteries. The former device will maintain near-normal mean and pulsatile perfusion pressures to all organs, since the aortic valve remains closed when the pump assumes all the work of the left ventricle. The aortic-to-aortic pump must accept blood through the aortic valve, and consequently the coronary arteries see the same level of pressure during systole as does the left ventricle. If peak left ventricular pressure is reduced to levels near zero, then coronary perfusion pressure is similarly reduced to zero. During diastole, coronary perfusion pressure is then elevated to aortic pressure levels or higher, depending upon pump design and actuation.

DR. KUSSEROW: I do want to compliment the team from Boston City, Boston-Children's, on their very spendid progress and on a truly beutiful presentation. I do have a few questions, however; first, what level of anticoagulation have you been using in your long-term animal studies?

DR. BERNHARD: We begin with heparin for the first day or two. We start coumadin at about the third or fourth day and the animals receive 5 milligrams of coumadin each day (maintainance dose). We do prothrombin times twice a week, maintaining them at about 2-1/2 times those of the controls.

DR. KUSSEROW: With this level of anticoagulation, have you noted any problems with regard to hemorrhage, spontaneous hemorrhage?

DR. BERNHARD: No, we have not had any problems with the calves at all. However, deep intramuscular injections are avoided in the calves.

DR. KUSSEROW: Secondly, have you noted any evidence of infarction in the peripheral organs, especially in the long-term surviving animals, first with regard to particles of flock that may have possibly come loose and, secondly, bona fide thromboembolic particles?

DR. BERNHARD: In terms of the flock, we really have pretty good attachment of the flock this year, better than last year; and we have not had any problems with washout as we presented last year. In terms of thromboembolic complications, we haven't seen any. What we have seen is a build-up of thrombus around the valves, and we have had to sacrifice animals (four out of twenty-eight in the group discussed) because of lack of pump function due to obstructed valves. Where we have good valve function, as in the ones that I showed you, I am sure all of those animals would have gone another 100 days, except for a fairly massive empyema due to the percutaneous leads which necessitated sacrifice, and consequently we haven't seen peripheral thromboemboli. We could expect to see it because there has been thrombus around valves in four instances, but we haven't observed it.

DR. KUSSEROW: Fine, just one or two more questions. Have you noted any thickening of your pseudoendothelium over the expanse of the pump bladder itself? This conceivably might be a problem with regard to flexibility and proper excursion of the pumping bladder.

DR. BERNHARD: In the control bladder at 100 days that I showed, there definitely was thickening of the interface. However, with the fetal cell work, it has remained much thinner up to 105 days; I would say the maximum thickness has been a millimeter. The maximum thickness on the control bladder was 2 or 3 millimeters in several areas. What will happen when we finally get to 200 days, I don't know but I think with some good furtune during this next year we should be able to push on further.

DR. KUSSEROW: Then, just a final question; this subject area came up yesterday. I was most intrigued by your choice of fetal cells as liners for the pump bladder, and this choice is interesting to me because it is made in the face of the now established biological phenomenon of rejection of cells from another individual. It is, in fact, an allograft and I just wonder, despite the very nice linings that you have shown us today, and which are truly remarkable, whether or not, in your long-term animals again, there has been evidence of any kind of cellular necrosis, presumably on the basis of immune rejection, and secondly, whether you had any opportunity to test for the emergence of anti-fetal tissue cell antibodies.

DR. BERNHARD: These are allogenic cells, but this is an avascular surface and so, if one were to see an immunologic reaction, it would obviously be completely different from the ones that were usually associated with connections to the vascular system. Whether or not the fibrocytes that we see in the interface (they are definitely two kinds of cells) are mature cells of fetal origin or allografts, or whether these cells are replaced gradually by the body and the mature fibrocytes are actually host cells, we don't know, but on the other hand, we don't really care as long as the interface appears quite stable. So it may be that there is no rejection here, but rather replacement, as there is in a cornea, for instance; but, on the other hand, we have no evidence for this so far. Again, we are out at 100 days, and we should have seen something during this interval of time if we were going to have a rejection phenomenon. In terms of looking for antibodies, we haven't done this. It has been suggested to us and we are going to do it.

DR. KUSSEROW: When are you going to put this excellent device on the market?

DR. LaFARGE: No answer.

DR. RASSMAN: I would like to add my congratulations with the other discussants. A number of years ago, Dr. Lillehei's laboratory reported that left heart bypass would have, as an effect on the right side of the heart, a relative increase in external work of the right side. In the one clinical trial that we've had, about 6 or 9 months ago, the worst of our realizations came true. A patient with mock left heart failure went into right heart failure while undergoing left heart bypass. I'd like to ask whether this system parallels the left heart bypass and what the effects may be on the right side?

DR. LaFARGE: I believe that was Dr. Lillehei's report to the ASAIO about 2 or 3 years ago. In perhaps 15% of all studies where we see a total increase in total output of the combined assist device and left ventricle, we do see an increase in right ventricular work, but in none of them has there been a significant increase. I would not expect an animal under such circumstances to go into right heart failure, unless one were to invoke a complicating pulmonary perfusion problem.

DR. RASSMAN: Have you had any opportunity to produce bi-ventricular disease and study this point?

DR. LaFARGE: Yes, we will have this opportunity; we are investigating several different techniques which create either unilateral failure or bilateral failure. We are also in the process now of working on a bilateral assist device combination for use in total heart failure.

MR. PURDY: Your results are certainly extremely encouraging. I have two questions. One is to Dr. Robinson. What is the hydraulic efficiency of your device, before and after the endothelialization of the wall surface? In other words, what kind of hydraulic pumping efficiency are you getting, the output power of the blood divided by the input power to your hydraulic pumping system?

DR. ROBINSON: The overall pumping efficiency has been measured only in vitro and not in vivo; we don't expect much differential because the effect of autologous lining on bladder compliance is not very much and the decrease of the area of the inflow and outflow tubes and valves has not been much. The hydraulic efficiency depends upon pumping rate and flow rate from the device, but in pump Model VI it varies from about 85% down to about 60% over the usual range of operation. We expect it to be higher in pump Model VII, which is designed partly for the purpose of improving overall efficiency of operation.

MR. PURDY: My second question is: What was the basis for your selection of a disc rather than a ball? Would not a ball have a lower drag coefficient in your flow stream?

DR. ROBINSON: We designed disc valves to have pressure drops which were tolerable in terms of left ventricular pressure drop and pump efficiency. We are presently achieving pressure drops and flow profiles in the inflow tube and valve which appear to be satisfactory. A primary reason for the selection of a disc valve was to provide more axial length of the bladder or pumping chamber and thereby to increase the effective stroke volume of the device.

DR. BUCHANAN: I was confused about your distinction between control and experimental animals with regard to red cell survival. Fifteen to seventeen days doesn't really sound like very long red cell survival. Are these control animals that have a pump in? What do you get on normal calves that don't have anything in them?

DR. BERNHARD: The control data are on normal calves; sixteen to nineteen days is our normal red cell half life in calves using DFP^{32} as the isotope.

DR. GIANNOTTI: I understand that the left ventricular pressure was approximately 20 millimeters pumping against that inlet loss on the valve rather than the zero that you are striving for. The question is, at what point do you think there would be a basic physiological difference made if that level were boosted by another 20 millimeters? Do you think an additional 20 millimeters in that left ventricular output would make a basic change?

DR. LaFARGE: No answer.

CHAPTER 50

TOTAL HEART REPLACEMENT DEVICE AND ITS CONTROL AND DRIVING SYSTEM

T. Akutsu, H. Takagi, H. Takano, C. Farish

University of Mississippi Medical Center
Jackson, Mississippi

A pair of air-driven total prosthetic hearts for use in sheep have been designed and constructed to be implanted inside the pericardial sac. Each side of the heart has been made of a single piece of Silastic including two valves. The outlet valve is bicuspid with an S-shaped closure line. One such valve functioned in a test circulatory system 24 hours a day for six months. The inlet valve, an oval mono-membrane type, has a large cross-sectional area and is built completely inside the ventricle. An automatic control and driving system presently under construction will regulate the cardiac output through a servo-control mechanism using atrial pressures as reference. The systole-diastole ratio will also be controlled. Thirteen experiments were performed in sheep weighing about 67 kg. The control and driving machine used was a simple manual system which has two main dials indicating the duration of systole and diastole in milliseconds. The pulse rate and systole-diastole ratio was easily determined from a nomogram. Average time of extracorporeal circulation was 69 min. Average time required for connection of artificial hearts was 41 min. Two sheep were lost by irreparable tear of each aorta and pulmonary artery. Severe hypoxia due to improper extracorporeal circulation killed two others. Four sheep which were pumped from one to three hours died from bleeding at the atrial edges. Three died from air emboli resulting from insufficient removal of residual air in one and from suction of air through the left atrial monitoring tubing in two. They were pumped each for 7, 12, and 8 hours. One sheep died after 8 hours of pumping from thrombo-emboli originating from side monitoring tubes that had improper antithrombogenic treatment. Two major causes of death, bleeding and air-emboli, have been eliminated each by application of double pursestring sutures and by low pressure-vacuum gauges.

TOTAL HEART REPLACEMENT DEVICE

Our total heart replacement device has been designed to be implanted inside the pericardial sac of sheep which weigh around 150 pounds. The natural heart has a large reserve capacity and can increase its cardiac output greatly by increasing the stroke volume, but the stroke volume of the prosthetic heart is limited to the volume of the filled ventricle. Any further increase in cardiac output can be obtained only by increasing the pulse rate, because the artificial ventricular wall cannot stretch. Therefore, the new total heart does have as large a capacity as possible and still fit within the pericardial sac. (Figure 1).

Since thrombi occur mostly around the valves in any type of artificial heart, considerable effort was directed toward improvement of the valve design in the new heart. Each side of the heart was constructed in one piece and includes two valves. The outlet valve is the bicuspid type and its closure line is S-shaped (Figure 2). Since the total length of the bicuspid leaflets' S-shaped edges is the same as the circumference of the 55^{o} elliptic orifice, the valve opens fully without resistance. One such valve functioned in the observation chamber in our test circulatory system 24 hours a day for six months.

The inlet valve, which is an oval mono-membrane valve, has a large cross sectional area for better inflow and has been built completely inside the ventricle (Figure 3). The orifice opening into the ventricle was greatly enlarged without increasing the heart size by positioning it obliquely and by making it elliptical in shape. During diastole a slight movement of the large, thin, convex membrane which closely parallels the ventricular wall, yields a large opening. During systole the pressure produced in the ventricle pushes the membrane against the ventricular wall, which itself acts like one leaflet of a bicuspid valve. Satisfactory function of this valve has been demonstrated in the test circulation.

The left ventricle is round and thick, and the right is flat and concave fitting the left ventricular contour when they are combined. Both ventricular walls were provided with several thick ridges along the direction of flow for reinforcement and also to increase resilience. Without these ridges, particularly in the left ventricle, "incarceration" took place during systole. In order to prevent this, the left ventricular wall was fixed to the housing along both sides of the inlet valve. With this construction the ventricular contraction became regular and distortion of the inlet valve leaflet during systole was eliminated.

All parts which come in contact with blood were made of Silastic. From the original master cast of each side of the heart made of plaster of paris, a RTV Silastic 589 mold was made. Polyethylene melted in a container over the fire was poured into the mold to make the same cast as the original plaster of paris cast. After layering Silastic sheet on the polyethylene cast, it was hung upside down and the layered Silastic cured in an autoclave. While curing, the polyethylene was melted out. The heart, thoroughly cleaned in distilled water, was then inserted into the outer housing. The housing of the ventricle was made of fiberglass-resin and completely covered with this Silastic sheet outside and with Silastic coating inside so that the ventricle could be fixed to it, both with Silastic glue and by additional continuous sutures along the edges. Rings embedded in Silastic for connection at four places--two atria, aorta, and pulmonary artery--were made of stainless steel. The final procedure of the fabrication was complete recoating of both the inside and the outside of the heart with Silastic solution to prevent exposure of any Dacron mesh and to cover any pinholes or other minor defects.

The leakage of blood or air through the atrial suture line was a serious problem when continuous sutures were used. When the heart parts were made separately, the technique of securing it with continuous sutures was established in dogs, since only the combined atria were fixed in place first. After we started using the model in which each side of the heart was made all in one piece, technical difficulties caused a bleeding problem in sheep. Later, a rapid and secure mode of atrial connection was achieved by providing a metal ring embedded at the end of each atrium to be fixed by a purse-string suture. This technique has reduced the time required for complete connection of the total prosthetic heart from an average of 60 minutes to an average of 43 minutes.

CONTROL AND DRIVING SYSTEM

The control system presently in use has two main dials with digital figures, indicating the duration of systole and diastole in milliseconds (Figure 4). The pulse rate and ratio of systolic to diastolic intervals can be easily determined from a nomogram (Figure 5). In the present system, however, changes in pumping conditions must be made manually. By insertion of a compliance reservoir in the air pressure line between the three-way solenoid valve and the heart pump, the sharp rise and fall in ventricular pressure curves have been eliminated and round-shaped curves grossly similar to the natural ventricular pressure curves have been obtained.

Since we believe that it is still too early to simplify and miniaturize the control and driving system, our new system has been designed so that it would duplicate the action and response of the natural heart as nearly as possible. The new system consists basically of a segmented line function generator whose output is fed into a multiplier. The other input to this multiplier is the sum of a bias voltage and a voltage corresponding to the mean atrial pressure which is derived from a pressure transducer and an averaging filter. The output of the multiplier is fed into a servo amplifier which in turn drives a servo motor and positions a servo valve allowing a corresponding pressure to be fed into the pumping chamber. This chamber pressure is sensed by a pressure transducer, whose output is fed back to the input of the servo amplifier to provide a conventional closed loop servo system.

The atrial pressure sensing system becomes active only during diastole. We do not use the mean atrial pressure as a reference pressure. There are two reasons: (1) When a circuit is made so that the mean atrial pressure is used as a reference pressure, such a circuit would have a certain amount of lag or delay time. The undesirability of this feature is debatable, but we would like to see the system respond faster to a given change in atrial pressure. This would reduce the likelihood of inhibition of venous return by back pressure when the system should respond to an increased venous return as, for example, during sympathetic stimulation. (2) In contradistinction to the action of the natural heart, which actually causes an atrial suction effect during ventricular contraction, the prosthetic heart has, in our experience, produced back pressure in the atria during ventricular contraction. This effect has occurred to various degrees with all valves we have tested in the total replacement device. With certain types of valves, this is apparently caused by regurgitation, with others it appears to be caused by a distortion of the valve, reflecting a back pressure into the atrium. In any case, this back pressure increases the mean atrial pressure and causes an increase in the pressure during ventricular contraction. The subsequent increase in ventricular pressure could cause a further increase in atrial back pressure. This, then is a positive feedback system that could, under certain conditions, cause numerous detrimental effects on the operation of the control circuit. The very least detrimental effect that could be expected is the limitation of the gain at which the system could be operated. In our system selective gating techniques have been used to achieve control as follows: The atrial pressure sensing system will be active only during diastole. At the end of the preceding systole, an appropriate gating circuit removes the chamber pressure measuring system from the input to the servo amplifier. At the same time, the atrial pressure measuring system is switched into the input of the servo amplifier. The polarity of this signal is such that a positive pressure in the atrium causes the servo system to apply a vacuum to the ventricular pumping chamber. This then will be a closed loop servo system whose objective is to keep the atrial pressure at the selected reference level. We have planned to use zero and +4 mmHg as the reference points for the right and left atrium respectively. The amount of vacuum necessary to keep the atrial pressures at their reference levels will be a function of the amount of blood

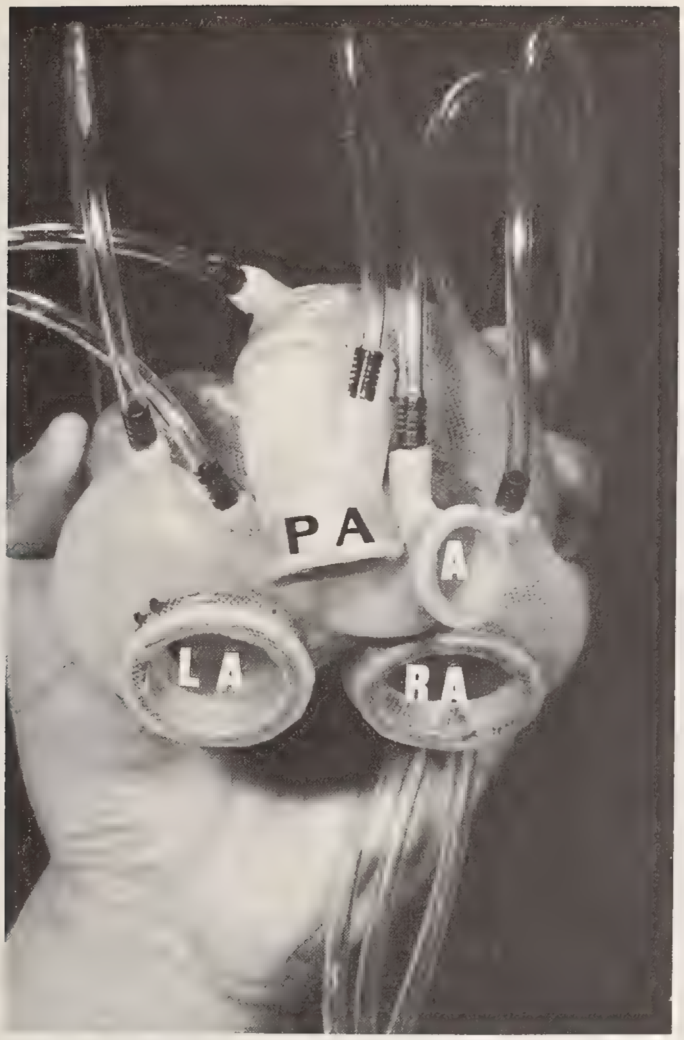

FIGURE 1. TOTAL ARTIFICIAL HEART DESIGNED FOR 150 LBS. SHEEP. RA: RIGHT ATRIUM. PA: PULMONARY ARTERY. LA: LEFT ATRIUM. A: AORTA. SIX SIDE TUBINGS ARE ATTACHED TO EACH CHAMBER AND VESSEL. THEY ARE USED TO REMOVE AIR BEFORE PUMPING STARTS AND TO MONITOR PRESSURES DURING PUMPING. AIR LINES FOR DRIVING ARE NOT SEEN.

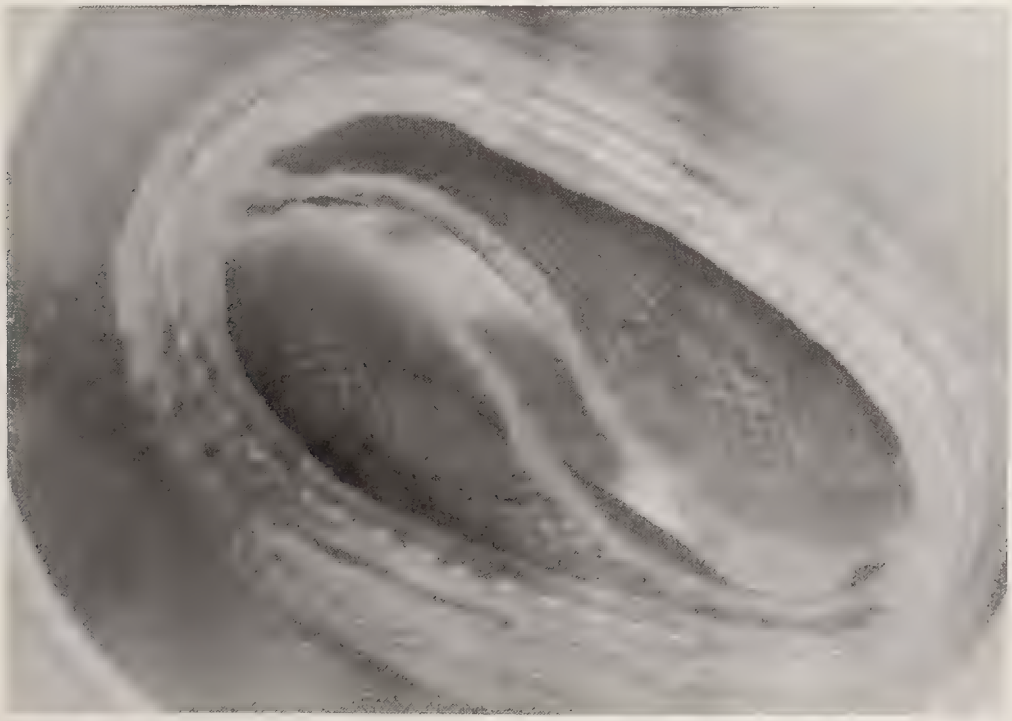

FIGURE 2. S-SHAPED BICUSPID OUTLET VALVE FOR TOTAL ARTIFICIAL HEART.

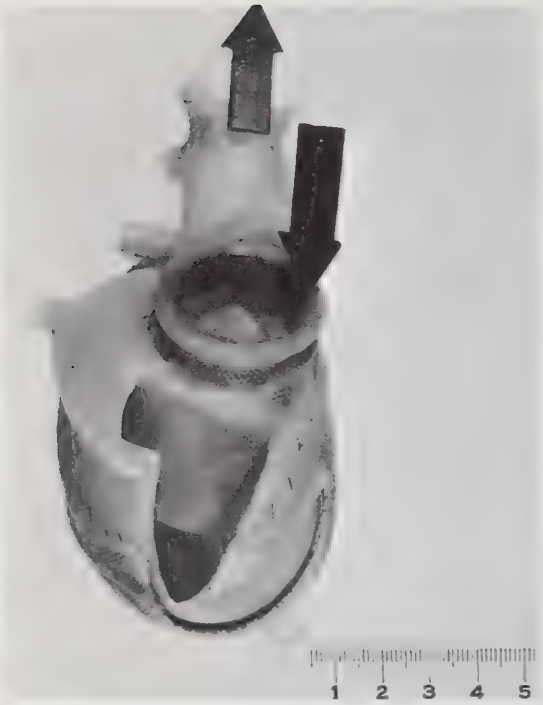

FIGURE 3. LEFT SIDE OF THE HEART. DARK ARROW SHOWS THE ENTRANCE TO THE LEFT ATRIUM THROUGH A RING. A LARGE MEMBRANE BELOW THE RING WHICH IS HALF WAY IN THE ATRIUM AND HALF WAY IN THE VENTRICLE IS THE BUILT-IN MONO-MEMBRANE INLET VALVE.

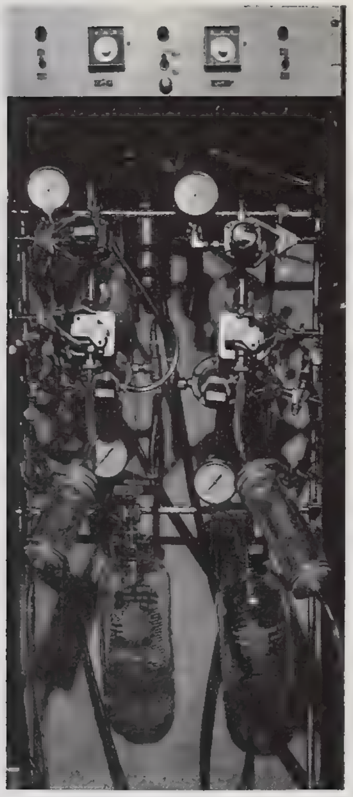

FIGURE 4. MANUAL CONTROL AND DRIVING SYSTEM. EACH SIDE HAS A PRESSURE GUAGE AND A VACUUM GUAGE CALIBRATED IN MM Hg. TWO PRESSURE REGULATORS ARE LOCATED IN THE CIRCUIT IMMEDIATELY AFTER EACH CONNECTION TO THE COMPRESSED AIR SOURCE. PRESSURE RESERVOIRS ARE INSERTED AFTER THE SOLENOID VALVE ELIMINATE SHARP PRESSURE CHANGES IN THE LINE. THE TIMER HAS TWO DIALS, ONE FOR SYSTOLE AND THE OTHER FOR DIASTOLE, BOTH CALIBRATED IN MILLISECONDS.

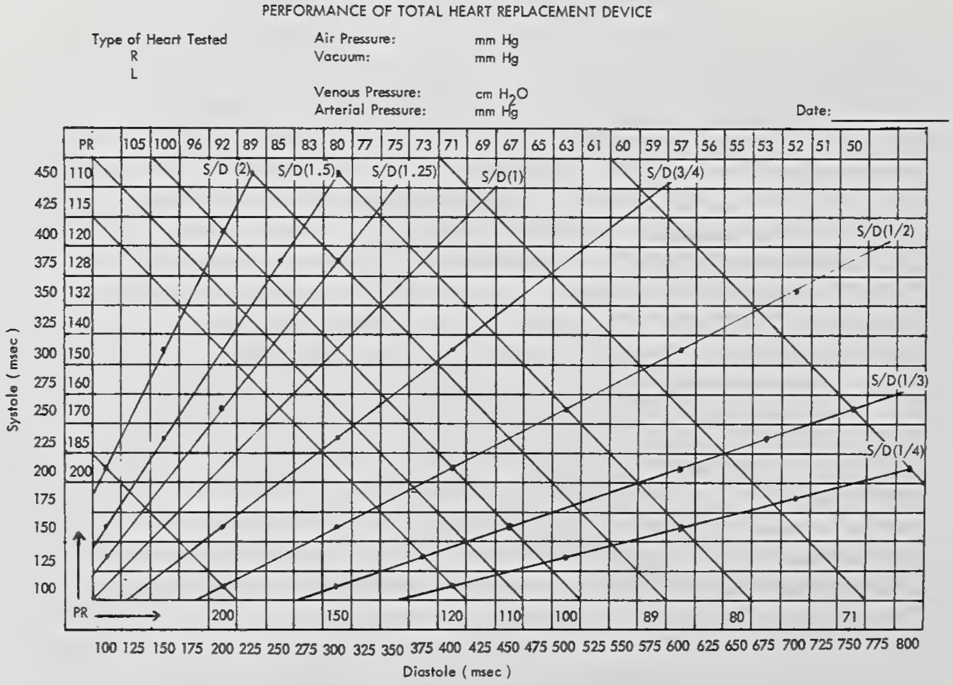

FIGURE 5. NOMOGRAM SHOWING RELATIONS AMONG PULSE RATE, DURATION OF SYSTOLE AND DIASTOLE, AND SYSTOLE-DIASTOLE RATIO. DURATIONS OF SYSTOLE AND DIASTOLE ARE SHOWN WITH INCREMENT OF 25 MSEC.

returning to the respective atrium. Therefore, the voltage driving the torque motor for positioning the proportional pneumatic valve will be a function of this same blood flow. This voltage will give us an indication of the blood flow into each pumping chamber at any given moment. If we integrate this signal during diastole, we will have an indication of the total blood flow into the chamber during this period.

We will "hold" this integral voltage in order to control the strength of the next ventricular contraction. This voltage will be switched to one of the inputs of a multiplier, during the period of the next systole. The other input will be a contoured wave form to simulate normal ventricular pulse pressure. During the systolic period, the chamber pressure measuring system will be switched into the input of the servo amplifier. This voltage will be opposite in polarity to the other input, which is the multiplied contoured wave form, and will be a feed back signal to null the servo system.

We use the signal controlling the right heart servo motor during diastole to control also the pumping rate of the artificial heart. This means that venous return will control the pumping rate of both pumping chambers. In order to receive the optimal beneficial effect of an increased pumping rate, it is necessary to control the ratio of systole to diastole (S/D ratio).

This will be accomplished automatically in our wave form generator. Both the rate control and the S/D ratio control will be accomplished automatically on a beat-by-beat basis. The initial condition and the slope of the S/D ratio change will be adjustable by the operator. This will allow for changes in position of the animal. In the natural heart, the S/D ratio has been demonstrated to change with variations in heart rate and in the animal's position. Therefore, this adaptability is desirable in artificial hearts.

We have planned to have several other features incorporated into the system: (1) a beat-by-beat readout of the pumping rate. (2) A readout of the systolic and diastolic time periods. (3) A display and recorder output of the minute volume of blood being pumped by both sides of the artificial heart. This will be accomplished by multiplying the integral of the diastolic filling control by the heart rate. We need this for both chambers in order to study the capacitance changes of the pulmonary and systemic systems on a beat-by-beat basis. (4) Direct control of the pumping rate by triggering the system on the "P" wave taken from the atrial remnant.

ANIMAL EXPERIMENTS

Prior to animal experiments, performance tests of the total artificial heart were done in the test circulatory system in relation to air pressure, vacuum, venous pressure, arterial pressure, pulse rate, systole-diastole ratio, and cardiac output.

Pairs of series No. 1 through No. 8 of Model No. 1 were implanted in 17 sheep which weighed from 54.5 to 81.8 kg. All sheep were not fed for two days before experiments.

Anesthesia.

Anesthesia was induced by intravenous injection of 2.5% Surital and maintained with 0.3 to 0.5% of Fluothane. When the sheep moved or tried to breathe on his own, Anectine was given rather than increasing the amount of Fluothane.

Implantation Surgery.

The chest was opened through the left 5th intercostal space. In order to obtain a sufficient room in the area of the short ascending aorta, the branchio-cephalic artery and the aortic arch were dissected free to be occluded during implantation. This procedure required two arterial cannulations, one from the left femoral artery and the other from the left carotid artery. The left jugular vein was used for cannulation of the superior vena cava. The inferior vena cava cannula was inserted through the right atrial appendage. Recently, it has been found possible to dissect both venae cavae inside the pericardial sac, eliminating the necessity of opening the right chest cavity. This apparently helped keep the right lung well inflated. Extracorporeal circulation was done with two roller pumps and a bubble oxygenator.

After occlusion of all blood flow into and out of the heart, the heart was removed, starting first with dissection of the aorta and the pulmonary artery as close to the ventricle as possible, then the ventricles. In preparing the atrial edges for connection, two points were important in order to facilitate secure and easy connection of the atria: (1) the interatrial septum should be split sufficiently starting from the middle of the non-coronary aortic valve cusp to give a sufficient length of the atrial edge on both sides, and, (2) the coronary sinus should be sufficiently freed close to the sinus opening and cut between the two ligatures. After this, connection of the prosthetic heart was done in the following order: right atrium, left atrium, aorta and pulmonary artery. Even when the connection was made by tying of a purse-string suture placed around the atrial edge over the ring embedded in the artificial atrium, bleeding was a problem. It has been found that it was from small vessels arising from the bottom of the atrium and opening into the fat in the atrio-ventricular groove. This problem has been solved by applying double purse-string sutures.

After completion of connection, residual air was removed by replacement with saline through a side tube attached to each chamber. Removal of air from the right side first was easy, since the right ventricular side tube came to the highest point to accumulate air when the heart was fixed. Air in the left side was then removed. After removal of air, the side tubes were used as pressure monitoring tubes. Immediately after extracorporeal circulation ceased, the prosthetic heart started pumping. During the first 20 beats, only the descending aorta was opened, and the brachio-cephalic artery was kept closed to prevent the brain from getting air which might have been left in the left ventricle. The presently available manually-operated control and driving system was used. As soon as the chest was closed, the sheep was put on the floor in a normal sitting position, supported by several wide canvas bands attached with springs to a specially designed frame. Thus, the sheep was supported about 10 to 15 cm above the floor to prevent compression of the various tubes and to keep the sheep comfortable.

Both atrial pressures were continuously monitored. Usually right ventricular output and pressures of any two chambers were continuously recorded. The reason that the right ventricular output was measured rather than the left, was because there was always room to put an electromagnetic flow probe around the natural pulmonary artery. Oxygen saturation rate and pH of arterial blood were checked periodically.

Results.

Time of extracorporeal circulation varied from 53 to 90 minutes. Time required for connection of the total artificial heart ranged from 29 to 51 minutes. In 8 sheep,time of artificial heart pumping was less than 5 hours. It was 7 hours in one, 8 hours in two, 12 hours in two, 14 hours in one, and 18 hours in one. The first preliminary experiment was performed to see fitting of the new model and to investigate surgical techniques. It was terminated after 3 hour pumping. In the last sheep the chest was too small for the artificial heart used, and was not able to close. The experiment was terminated after two-hour pumping.

Causes of death of 15 sheep were: tear of pulmonary artery and aorta due to mismatch in size in two sheep, pneumothorax due to breakage of the housing in one, improper extracorporeal circulation in two, thrombo-emboli originated from side tubes in two, uncontrollable bleeding from the atrial edge in four, and air emboli in four. Air emboli occurred by insufficient air removal from the left ventricle in one, air suction from the atrial pressure monitoring line in two, and breakage of the left ventricle in one. (Table 1).

TABLE 1

CAUSES OF DEATH

Causes of Death	No. of Death	Time of Pumping
Air Emboli:		
Residual air in artificial heart	1	7 hrs.
Atrial pressure monitoring line	2	12 hrs., 8 hr.
Breakage of Left Ventricle	1	12 hrs.
Bleeding	4	1 hr., 1 hr., 3 hr., 2 hr.
Thrombo-emboli: From Side Tubes	2	8 hrs., 18 hrs.
Pneumothorax: Breakage of Housing	1	14 hrs.
Tear:		
Pulmonary artery	1	0 hr.
Aorta	1	0 hr.
Inadequate Extracorporeal Circulation:		
Blood Loss	1	3 hrs.
Hypoxia	1	3 hrs.
Sacrificed	2	3 hrs., 2 hrs.
TOTAL	17	

Shortly after the sheep was placed on the floor in a normal sitting position, pressures always became very stable requiring almost no adjustment of the driving machine. Oxygen saturation rate in arterial blood always decreased temporarily lower than 80% immediately after the extracorporeal circulation was stopped and the artificial heart started pumping. Following gradual recovery, it became perfectly normal as soon as the sheep was placed on the floor (Figure 6). All five sheep survived longer than 8 hours completely recovered from anesthesia. The one which survived 18 hours was able to stand firmly, drank water, and behaved normally (Figure 7).

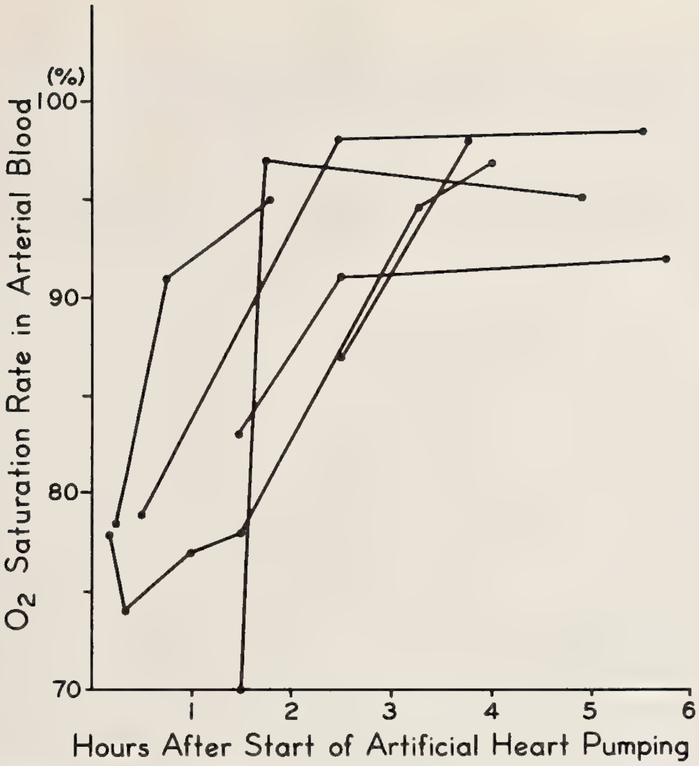

FIGURE 6. OXYGEN SATURATION RATE IN ARTERIAL BLOOD AFTER ARTIFICIAL HEART HAS STARTED PUMPING. NOTE THE INITIAL LOW OXYGEN SATURATION RATE WHICH ALWAYS TAKES PLACE IMMEDIATELY AFTER ARTIFICIAL HEART STARTS PUMPING, AND THE FOLLOWING RAPID IMPROVEMENT AS SOON AS THE SHEEP IS PUT ON THE FLOOR IN HIS NORMAL SITTING POSITION.

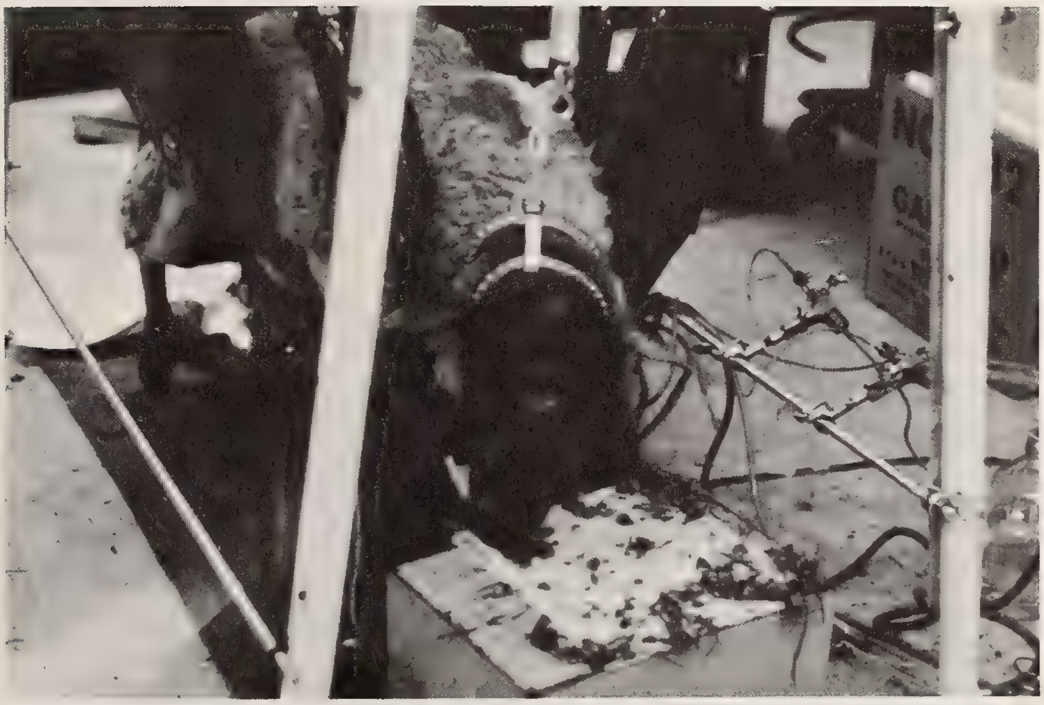

FIGURE 7. A SHEEP WHICH SURVIVED FOR 18 HOURS. EVENTUAL DEATH WAS CAUSED BY THROMBOEMBOLI ORIGINATED FROM ALL POLYVINYL CHLORIDE SIDE TUBES. THE INSIDE OF THE ARTIFICIAL HEART WAS FREE OF THROMBI. PICTURE WAS TAKEN AFTER 10-HOUR PUMPING. HE COMPLETELY RECOVERED FROM ANESTHESIA, WAS ABLE TO STAND FIRMLY, DRANK WATER, AND BEHAVED NORMALLY.

SUMMARY

Our new total heart replacement device, driven by a simple manually-operated control and driving system, has been proved to give sufficient cardiac output to maintain the life of sheep weighing around 150 lbs.

Among three major causes of death, bleeding from the atrial edge and air emboli have been eliminated each by application of double purse-string sutures and by utilization of low pressure-vacuum gauges. Clot formation in side tubes still remain unsolved.

Overall surgical techniques have been established. It is obvious that the result has been improving judging from longer survivals in recent experiments.

DISCUSSION

DR. NOSE: I would like to offer my congratulations on the wonderful work that Dr. Akutsu did. I would like to ask two questions. One is cardiac output and atrial pressure relationships of Dr. Akutsu's heart. For instance, if atrial pressure is increased from 0 to 5 cm water, how much does the cardiac output increase? I hear that in your data you have a high incidence of air emboli. Maybe this cardiac output and atrial pressure relationship (so called Starling's regulation) is not so steep. Maybe this is why, if atrial pressure is lower than it should be, then by accident air is introduced into the artificial heart because of poor venous pressure sensitivity. Number two is: You showed that in the initial stage of heart pumping you have low oxygen saturation, and you mentioned that at that time the systole to diastole pumping ratio was 1:4. According to our experience, we always have poorer pulmonary function if this ratio is less than 25% in one heart beat. Maybe that poor oxygenation in your animals might have some relation to this short duration of systole. I would like to ask, why you use 1/4 systole ratio at the early stage of pumping.

DR. AKUTSU: For the first question, I do not think air emboli are responsible because of the relation between the carotid and left atrial pressures. As was shown in the slide, in two cases, air emboli did work their way from the left atrial pressure monitoring system by mistake. We have since changed to a closed system, using a pressure gauge, so that we do not have that trouble anymore. For the second question, the reason why we are using a ratio of 1:4 in the beginning while the chest is being closed, is because of the fact that we have the height of the total heart at about 10 cm. We have to think about the height of systolic pressure and, therefore, cannot use high suction. We have to use a longer diastole, and it does not look like an effect on the oxygenation by the sheep's own lung. Recently, we have found another way to improve the oxygenation during the closing of the chest. In the chronic animal that we did last week, the oxygenation saturation was about 94%, while the animal was still on the table and the chest was being closed.

DR. KWAN-GETT: I would like to congratulate Dr. Akutsu on his fine work. I think 55 hours survival is the longest reported as yet. Incidentally, you did not say whether you used a calf or a sheep. I would like to make several comments about inflow valves. We too in our total replacement experiments have found that the larger diameter inflow valves have lower resistance and make the heart easier to control. However, we have found that prosthetic valves in clinical use are quite adequate, except at the junction between different types of material, for instance, a Silastic to titanium junction. These junctions usually act as a site for clot formation. In the case of Dr. Akutsu's heart, I think it has a flap type valve made of the same material as the blood sac. A comment on the systole to diastole ratio: In our own experiments, we have found that when we change the ratio, it generally has very little or no physiological effect, although, as Dr. Akutsu said, you may have to change some of your driving parameters. A comment on the blood oxygenation: We found in sheep that the level of the left atrial pressure was extremely important, especially when on pump oxygenator bypass. I am wondering whether or not Dr. Akutsu had a left atrial vent in position at all times, until he started his prosthetic device. We found that if we adequately vented until the instant we started up the prosthetic device, that our arterial oxygenation would stay well above 90% at all times. One final question, I would like to know some details of the cause of death in the 55 hour's survival. In most of our experiments, which have gone up to 50 hours, we see a terminal picture which looks to me like an irreversible shock, showing a gradual fall in blood pressure, a decrease in peripheral resistance, pooling of blood and a widening of the pulse pressure. I would like a comment on your levels of hemolysis please.

DR. AKUTSU: Left atrial pressure usually is maintained at levels around 5 cm water at all times. One half to one hour before the animal died it was behaving quite normally. Until that time, the cardiac output was maintained at around 4.5 liters and arterial pressure was about 120 and coronary artery pressure was 45. The animal looked very good, suddenly its respiration stopped and there was no sense to continue pumping. We, therefore, terminated the experiment. The cause of death was due to thromboemboli originating from the side tubes. At autopsy the device was completely free of thrombi internally.

SECTION VII

PHYSIOLOGIC EFFECTS OF CIRCULATORY ASSIST DEVICES IN ANIMALS

Chairmen: William P. Sears, M.D.
Lowell T. Harmison, Ph.D.

INTRODUCTION

Studies on the physiological effects of circulatory assist devices in animals and on the performance characteristics of such devices are required before they can be considered for use in humans. Groups that are developing circulatory assist devices under the Artificial Heart Program are, of course, making such studies of their own devices. In addition, the Artificial Heart Program is having such studies made by other groups to ensure the depth and bredth of evaluation required for circulatory assist device development. In order to avoid even the appearance of non-objectivity or competitive bias in circulatory assist device development, groups with circulatory assist device development programs of their own are not considered eligible for contracts in this area.

CHAPTER 51

CONTINUING EVALUATION OF THE BAYLOR LEFT VENTRICULAR BYPASS DEVICE

E.F. Bernstein, M.A. Shea, and D.A. Spyker

University of Minnesota
Minneapolis, Minnesota

The Statham-Baylor Left Ventricular Bypass Device (BLVB) was initially evaluated *in vitro* to determine its performance characteristics, most efficient operating parameters, and hemolysis rates. Acute hemodynamic studies in normal calves revealed minimal pressure and flow changes, with the BLVB generally replacing 5 to 25% of the control cardiac output, but never exceeding 2.5 L/min. Variations in pump control parameters produced similar responses to those seen in the previous *in vitro* studies. BLVB implantation in calves for up to 12 days of continuous pumping demonstrated problems with pump and connector thrombosis, pump diaphragm leaks, development of a moderate anemia, transient leukocytosis, increasing plasma volume, transient tissue enzyme elevations, and frequent pulmonary complications. Extensions of these studies include the development of a reproducible model of acute mitral insufficiency. Measurements of left ventricular function, including LV dp/dt, aortic flow acceleration, LV stroke work, and LV power, are rapidly and strikingly decreased. Following BLVB insertion, pumping of 2-3 L/min is possible since left atrial pressure is high. Left ventricular function changes little, however, and calf survival is prolonged only briefly. In a parallel effort, an optimal BLVB pump controller has been designed, following hybrid computer simulation of a cardiovascular system and pump. Predicted measurements of benefit are comparable to measured experimental values. A sensitivity analysis based on the reduction of flow work resulted in defining optimum delay and duration settings for extensive ranges of heart rate and peripheral resistance.

PART I

EVALUATION OF THE BAYLOR VENTRICULAR BYPASS DEVICE

INTRODUCTION

The Baylor Left Ventricular Bypass Device (BLVB) was designed as a paracorporeal pneumatically driven pump assist device for left ventricular bypass.[1] A previous report from this laboratory documented the operational and performance characteristics of the drive and control console, a schedule of pump operating parameters and performance under varied conditions, the acute hemodynamic response of normal calves to insertion of the BLVB, and the response to variation of pump controls in both acute anesthetized and chronic unanesthetized calves.[2] In addition, experience with chronic implantation of the device in 19 normal calves was reported, with observations concerning causes of pump failure, causes of animal death, and detailed hematologic and chemical observations.[3]

During the past year, emphasis in this continuing evaluation of the BLVB has shifted to measurements of benefits rather than tolerance, and to efforts at developing appropriate control systems.

The present report details our continuing studies with the BLVB in the following areas:

1. The development of an experimental cardiac failure model (acute mitral insufficiency).
2. The hemodynamic response of calves with induced acute mitral insufficiency to cardiac assistance with the BLVB.
3. The determination of optimal BLVB pump controls.

DEVELOPMENT OF A TEST MODEL OF CARDIAC FAILURE

Previous experimental evaluations of the BLVB device have been performed in normal animals. These were designed to test the animal's tolerance to prolonged pumping of a large fraction of his cardiac output. However, such experiments do not permit an evaluation of the potential benefit of the device in pathologic situations. Therefore, a consistent model of cardiocirculatory failure was sought, and the hemodynamic alterations accompanying this model documented, as a baseline for therapeutic testing of the BLVB.

An ideal experimental cardiac failure model is not yet available. Varying definitions of cardiac failure further complicate the problem of such model design. Some of the criteria of failure which have been offered include (1) an inadequate cardiac output, (2) inadequate emptying of cardiac chambers, (3) increased ventricular end diastolic pressure or decreased compliance, (4) inadequate tissue oxygenation, and (5) dilatation of the cardiac chambers.[4] Efforts to mimic human congestive heart failure, or myocardial infarction and shock, have included the following approaches:

1. Coronary artery obstruction, by ligation of the left anterior descending, left circumflex, multiple small coronary artery branches or coronary microsphere injection.[5-9]
2. Creation of a large arteriovenous fistula (produces high output failure - a poor test model for the flow assist device under evaluation).[10,11]
3. Cardiotoxic drugs - angiotensin, l-norepinephrine, pentobarbital, and endocardial iodine.[12-15]
4. Variations of intravascular volume - either hypo or hyper-volemia.[16,17]
5. Outflow obstruction - pulmonary artery or aortic constriction. [18,19]
6. Acute valvar insufficiency - by disruption of the tricuspid or mitral valves. [16,20-22]

After careful review of the pertinent literature, and a number of unrewarding efforts at producing predictable cardiac failure by several of the above approaches, an experimental approach involving the creation of acute mitral insufficiency was developed. The advantages of this method include (1) simple surgical technique, (2) uniform development of severe circulatory failure, (3) evidence of failure by progressive elevation of left ventricular end diastolic pressure, and (4) immediate and significant elevation of left atrial pressure, which would favor the filling of the BLVB device.

The approach involves the passage of a perforated cylindrical device through a purse-string suture in the left atrial appendage and through the mitral valve, to create a common left atrioventricular cavity. The degree of mitral insufficiency can be graded by varying (1) the diameter of the device and (2) the number and size of the perforations in the hollow cylinder (Figure 1).

METHODS AND MATERIALS

Thirty-five calves weighing between 50 and 100 kilograms were fasted for sixteen hours preceding the experiment. The animals were lightly anesthetized with intravenous sodium thiamylal. Following endotracheal intubation, 0.25% Halothane anesthesia was administered through a Fluotec device with a positive pressure respirator. Controlled ventilation by the Method of Donawick[23] (high pressure of 30-33 cm of water and large tidal volume) was used to prevent atelectasis and maintain adequate oxygenation during thoracotomy, through the fifth intercostal space. Pressure catheters were inserted directly into the descending thoracic aorta, through the azygos system into the right atrium, by direct puncture into the pulmonary artery, and into the left atrium and left ventricle through a purse-string suture in the left atrial appendage. Flow probes were placed around the ascending thoracic aorta immediately above the aortic valve and around the left main coronary artery at its origin. Two purse-string sutures were placed around the base of the left atrium, and the failure device was inserted through the left atrial appendage to lie within the opened mitral valve. The purse strings were secured for hemostasis. An obturator was constructed for each device to facilitate atrial insertion (Figure 2). It was removed following device placement through the mitral valve.

Pressures were measured with Statham Model SP37 Blood Pressure Transducers and were recorded on a Beckman Biomedical Dynograph 504D Recorder. Cardiac output and left coronary artery flows were determined with Biotronex BL610 pulsed-logic flow meter. Left ventricular functions were computed by Biotronex BL620 and BL622 modules. Left ventricular pressure-time-product (PTP) was determined with a compensating polar planimeter.[24] The time interval from the onset of left ventricular contraction to mdP/dt (t_c-mdP/dt), the ratio of mdP/dt to the simultaneously developed left ventricular pressure (mdP/dt/IP), and the time interval from the onset of ascending aortic flow to maximum dQ/dt were measured from appropriate tracings.[25]

During the developmental stages, nine different models of mitral insufficiency devices were fabricated (Figure 1).

Model 8 was used in the last 15 experiments and appeared to be most satisfactory. Model 9, which has a smaller outer diameter, was developed for use in small calves, or for more chronic circulatory failure and was not used in any of these experiments. As depicted in Figures 1 and 2 multiple perforations in the devices permitted the free regurgitation blood into the left atrium during systole.

RESULTS - ACUTE MITRAL INSUFFICIENCY

A summary of our experience with the induction of acute mitral insufficiency in 35 calves is detailed in Table 1. Of these, 9 experiments were considered technical failures of the insertion procedure, and in 4 others either the device or the animal was considered unsuitable for the experiment. Data from 14 experiments with the successful induction of acute mitral insufficiency yields a mean survival time of 2.3 hours following insertion. No animal survived more than 4 hours.

The hemodynamic alterations in a "typical" animal with acute mitral insufficiency are illustrated in Figures 3 through 8. Right atrial and pulmonary artery pressures did not change appreciably during the course of the experiments. Immediately following insertion of the failure device, left atrial pressure rapidly increased, and paralleled left ventricular pressure (Figure 3). Both left ventricular and aortic pressures rapidly decreased to approximately 30% of control values (Figures 4 and 5).. Immediately after device insertion, cardiac output decreased to approximately 50% of control and then slowly continued to decline (Figure 6). In contrast, left coronary artery flow increased strikingly shortly after device insertion (Figure 7) and then gradually declined.

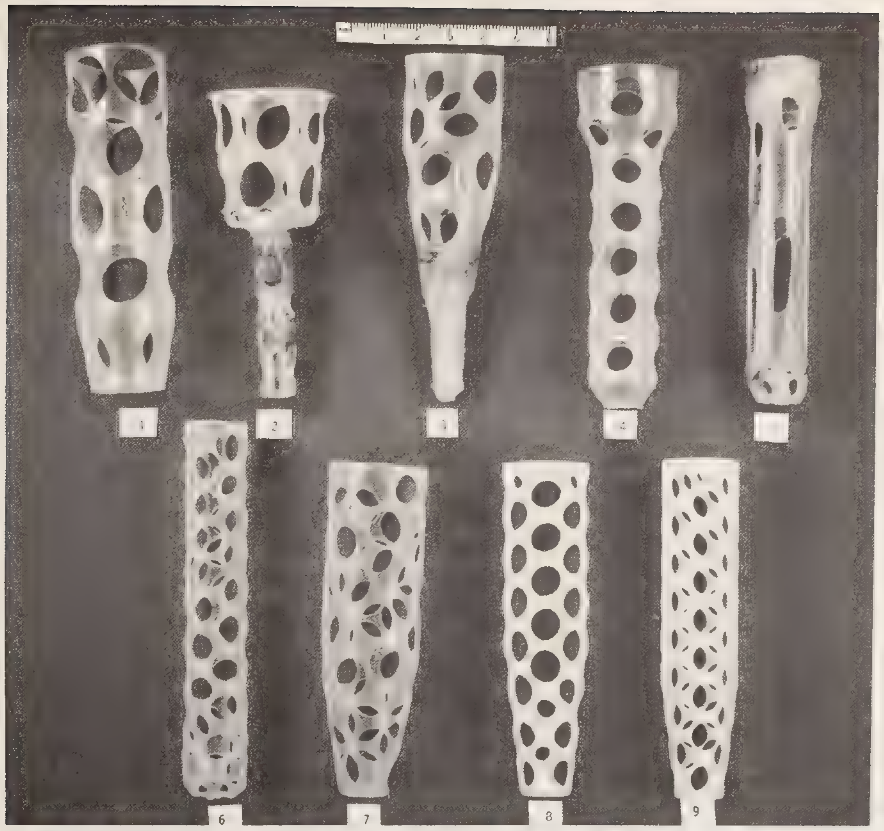

FIGURE 1. THE PERFORATED CYLINDERS DEVELOPED FOR THE PRODUCTION OF ACUTE MITRAL INSUFFICIENCY, BY PASSAGE THROUGH THE MITRAL VALVE OF THE CALF.

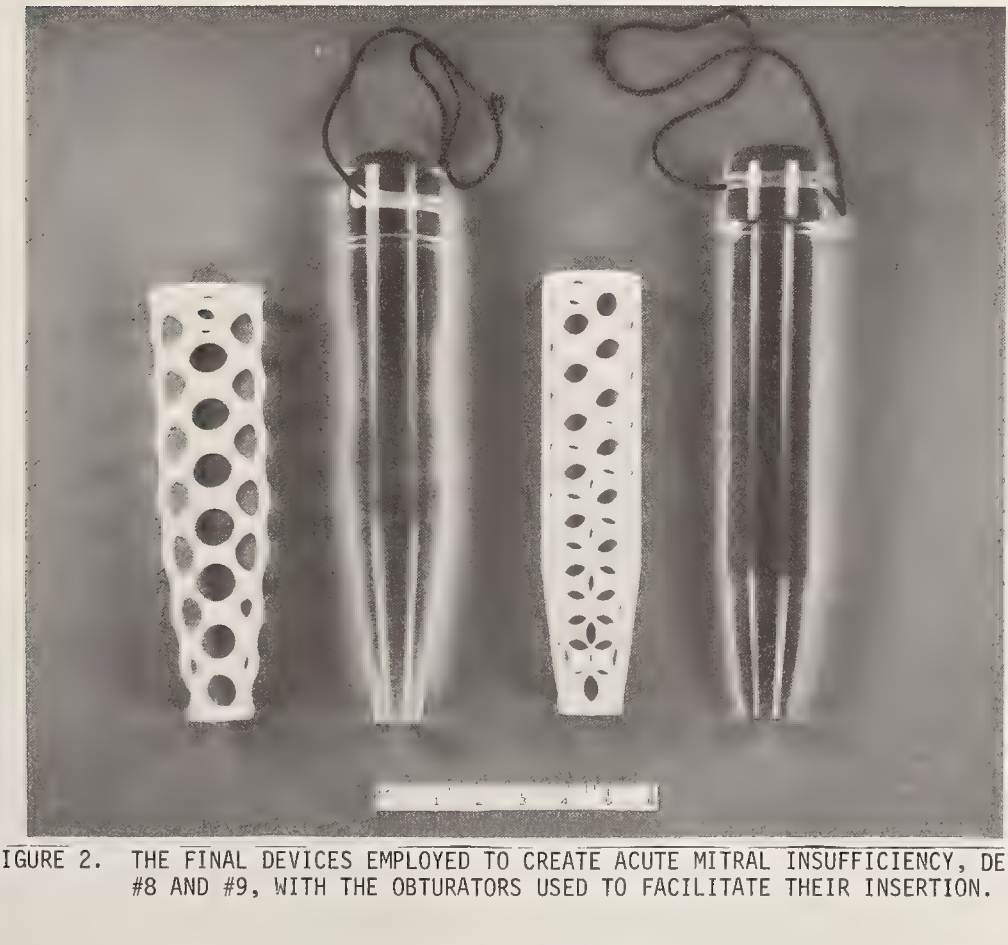

FIGURE 2. THE FINAL DEVICES EMPLOYED TO CREATE ACUTE MITRAL INSUFFICIENCY, DEVICES #8 AND #9, WITH THE OBTURATORS USED TO FACILITATE THEIR INSERTION.

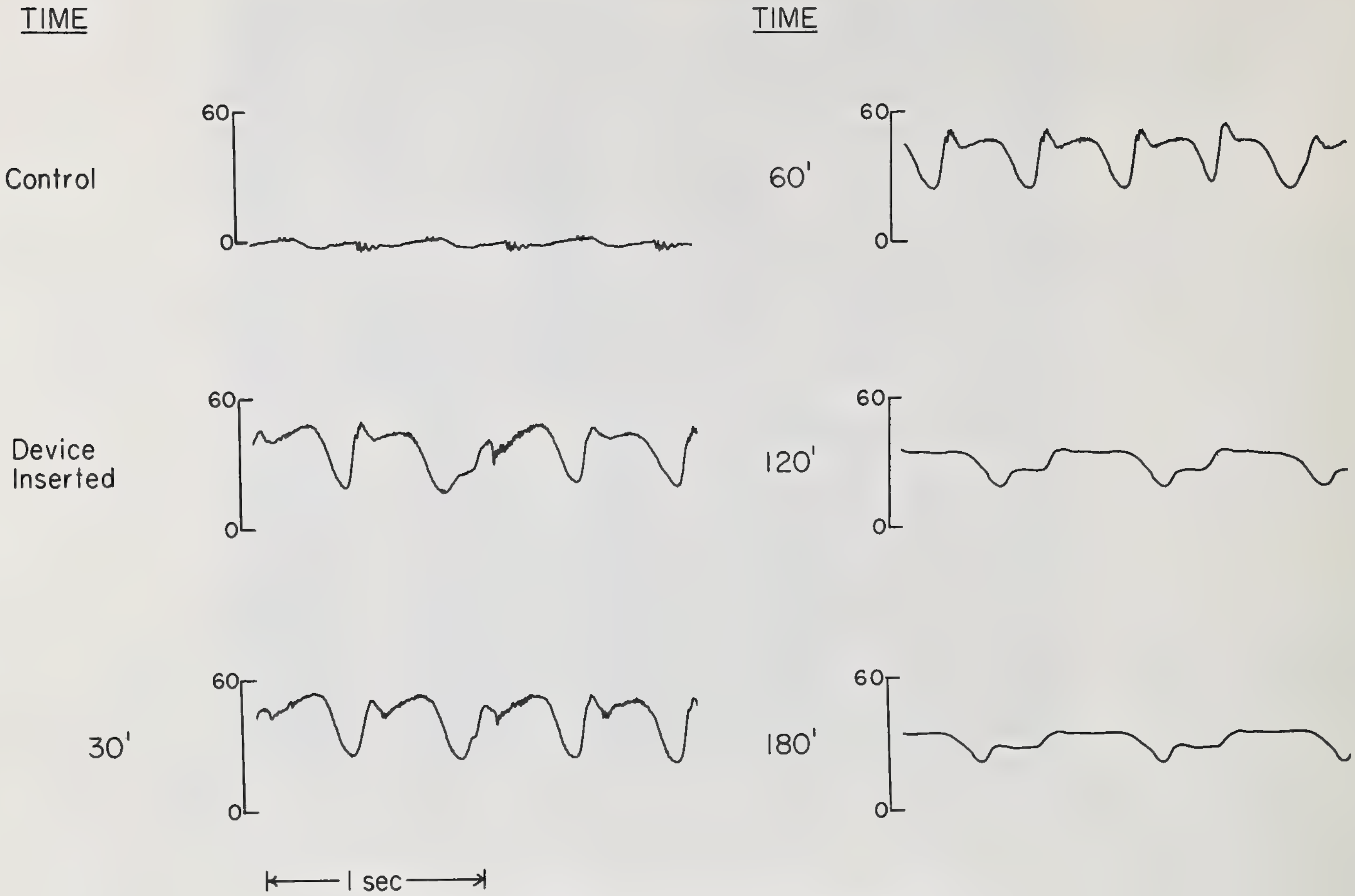
Left Atrial Pressure (mmHg)

FIGURE 3. HEMODYNAMICS OF ACUTE MITRAL INSUFFICIENCY.

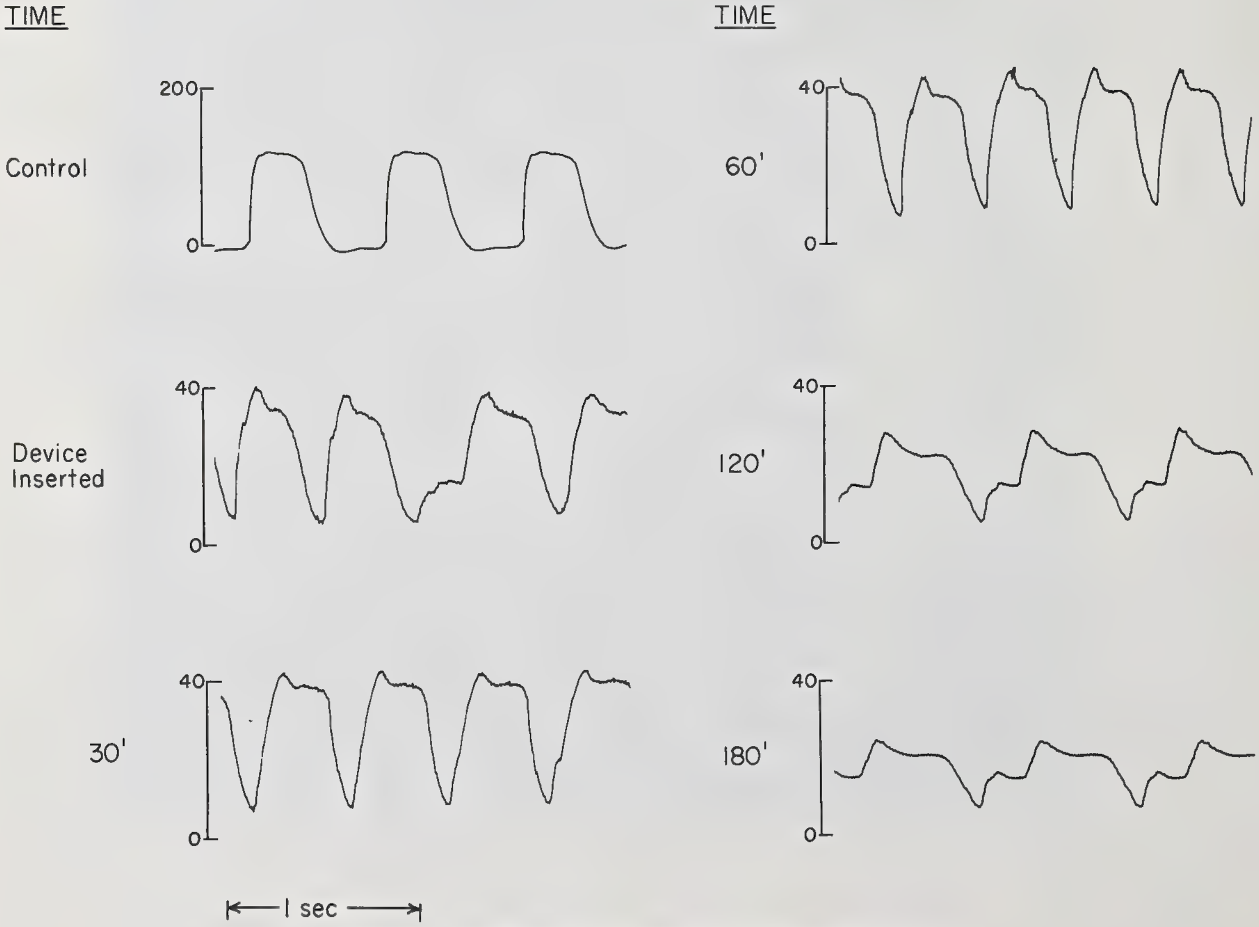
Left Ventricular Pressure (mmHg)

FIGURE 4. HEMODYNAMICS OF ACUTE MITRAL INSUFFICIENCY.

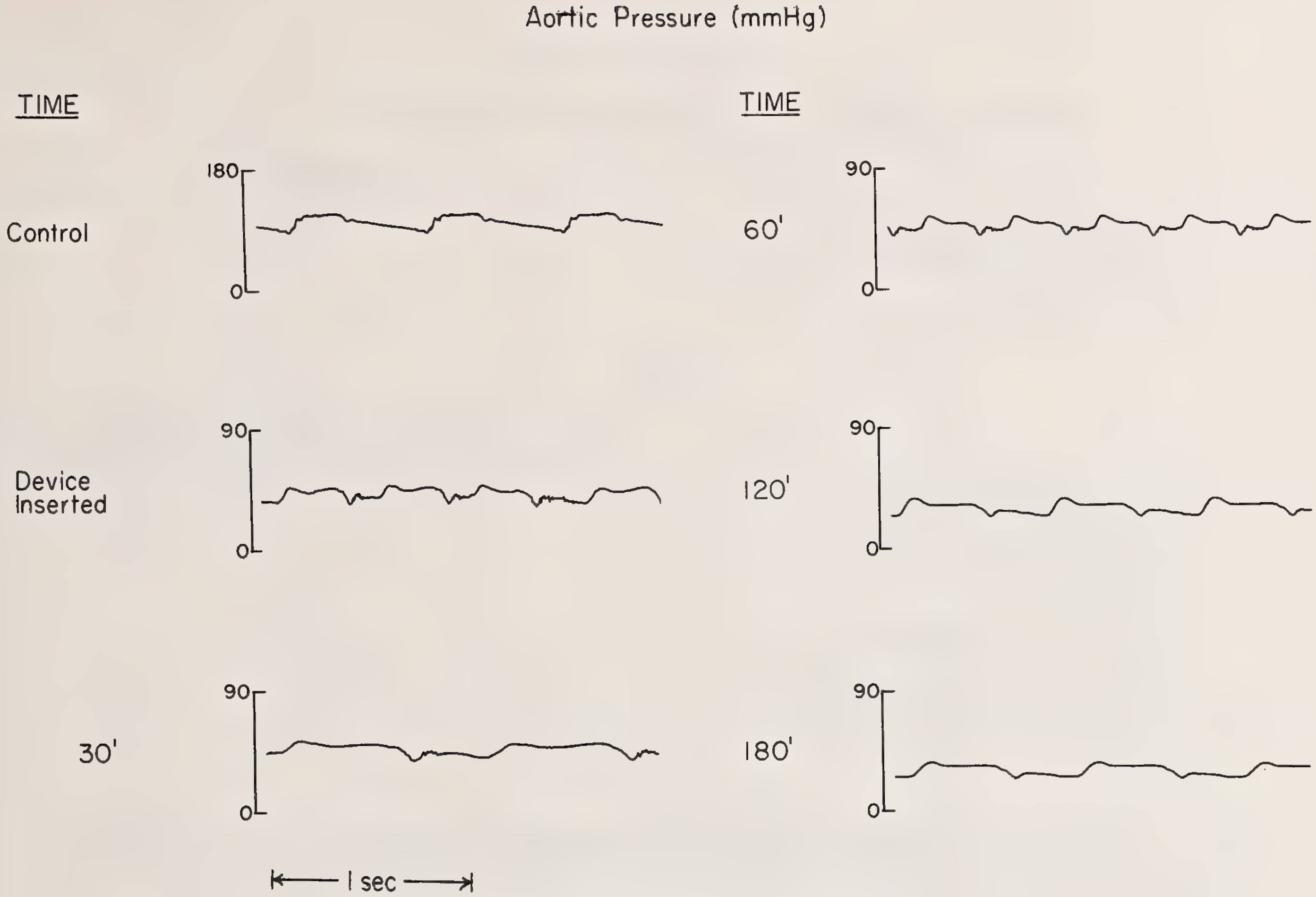

FIGURE 5. HEMODYNAMICS OF ACUTE MITRAL INSUFFICIENCY.

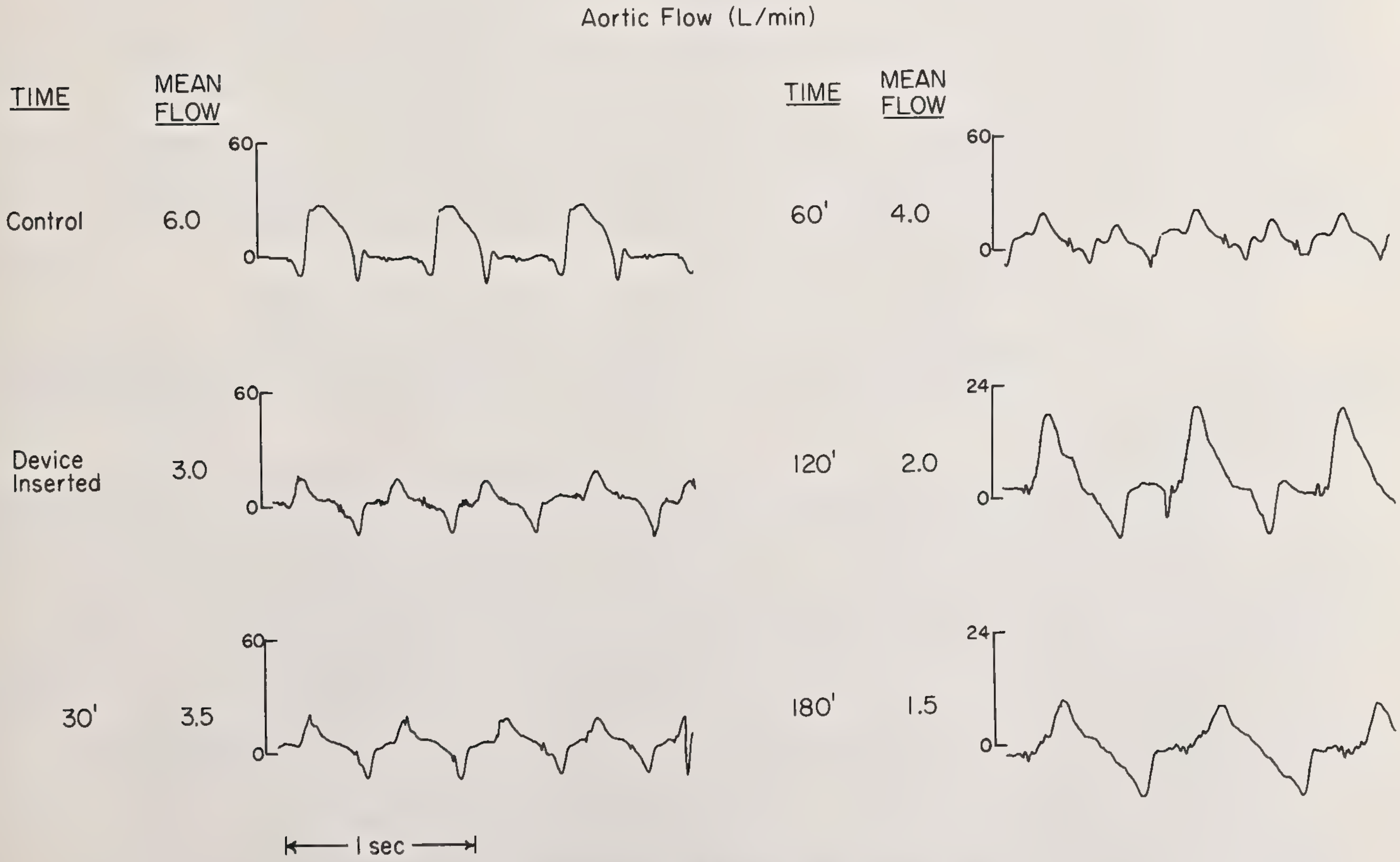

FIGURE 6. HEMODYNAMICS OF ACUTE MITRAL INSUFFICIENCY.

TABLE 1

SUMMARY OF EXPERIENCE WITH ACUTE MITRAL INSUFFICIENCY IN CALVES

	No. of Calves
Total experience	35
All MI devices pump insertion not attempted	18
MI device + BLVB insertion	17
Technical failures	9
Device or animal unsuitable	4

RESULTS

	No. of Calves	Mean Survival after MI Device Insertion (hrs.)
Technically successful MI device insertion	14	2.3 (0.5 - 4.0)(a)
Technically successful MI device (all devices) insertion and BLVB pumping	8	5.1 (1.75 - 10.25)
Final MI device, implantation only	1	3.7 (--)
Final MI device, BLVB successfully inserted, and pumping begun	4	5.7 (1.75 - 10.25)

(a) Range

Tracings of analog computed left ventricular function parameters demonstrate rapid and persistent declines in maximum rate of change of left ventricular pressure, ascending aortic flow acceleration, power and stroke work (Figure 8).

Data documenting the development of left ventricular failure and declining left ventricular function in the entire experimental group of animals are presented in Figures 9 and 10. Mean LVEDP rapidly increased from 8.0 to 15.4 mm Hg, and then continued to increase in the surviving animals. Cardiac output fell to 50% of control values immediately following insertion of the failure device (Figure 9), declining from a mean of 7.9 to 3.5 liters/min. A gradual decrease continued over the following hours of observation. Mean left coronary artery flow increased from 179 to 312 ml/min immediately following device insertion. Coronary flow then gradually declined, but remained well above control values for the first 2 hours of the failure period. Subsequently, coronary flow decreased rapidly, in association with general deterioration of cardiac function.

An example of left ventricular function data is demonstrated in Figure 10. The maximum rate of rise of left ventricular pressure and maximum ascending aortic flow acceleration abruptly declined to approximately 50% of control values, followed by a continued parallel decrease in both functions. Left ventricular stroke work and power also declined abruptly to approximately 20% of control values immediately following device insertion.

HEMODYNAMIC RESPONSE OF ANIMALS WITH ACUTE MITRAL INSUFFICIENCY TO BLVB PUMPING

In 17 calves, following successful insertion of the mitral insufficiency device, the Baylor Left Ventricular Bypass Device was then inserted in the left atrial-aortic position. In 8 of these experiments, the pump was successfully inserted prior to the death of the animal and pumping begun with the chest left open.

The average survival time of these 8 animals was 5.1 hours. The mean survival time of the 4 animals subjected to mitral insufficiency device No. 8 and BLVB pumping, was 5.7 hours.

The course of a typical experiment with acute mitral insufficiency and BLVB pumping is depicted in Figures 11 through 16. An abrupt rise in left atrial pressure followed the onset of acute mitral insufficiency (Figure 11). Left ventricular pressure abruptly decreased (Figure 12), as did aortic pressure (Figure 13). The initial decline in cardiac output (Figure 14) was comparable to that seen in animals subjected to acute mitral insufficiency without cardiac support. The increase in coronary flow was not as marked following the initiation of BLVB pumping (Figure 15). In addition, the decline of left ventricular function (Figure 16) was not quite as marked.

A comparison of mean left ventricular end diastolic pressure in the animals with acute mitral insufficiency and those in which pumping was initiated is depicted in Figure 17. In contrast to the rapid and sustained increase in LVEDP following initiation of mitral insufficiency, with BLVB pumping there was a progressive decrease in LVEDP, which returned to normal values and remained at these levels during the lifetime of the surviving animals.

Cardiac output, which was measured as ascending aortic flow, fell to 50% of control values following insertion of the mitral insufficiency device (Figure 18). With the onset of BLVB pumping there was a transient increase in ascending aortic flow. However, within 60 minutes of the

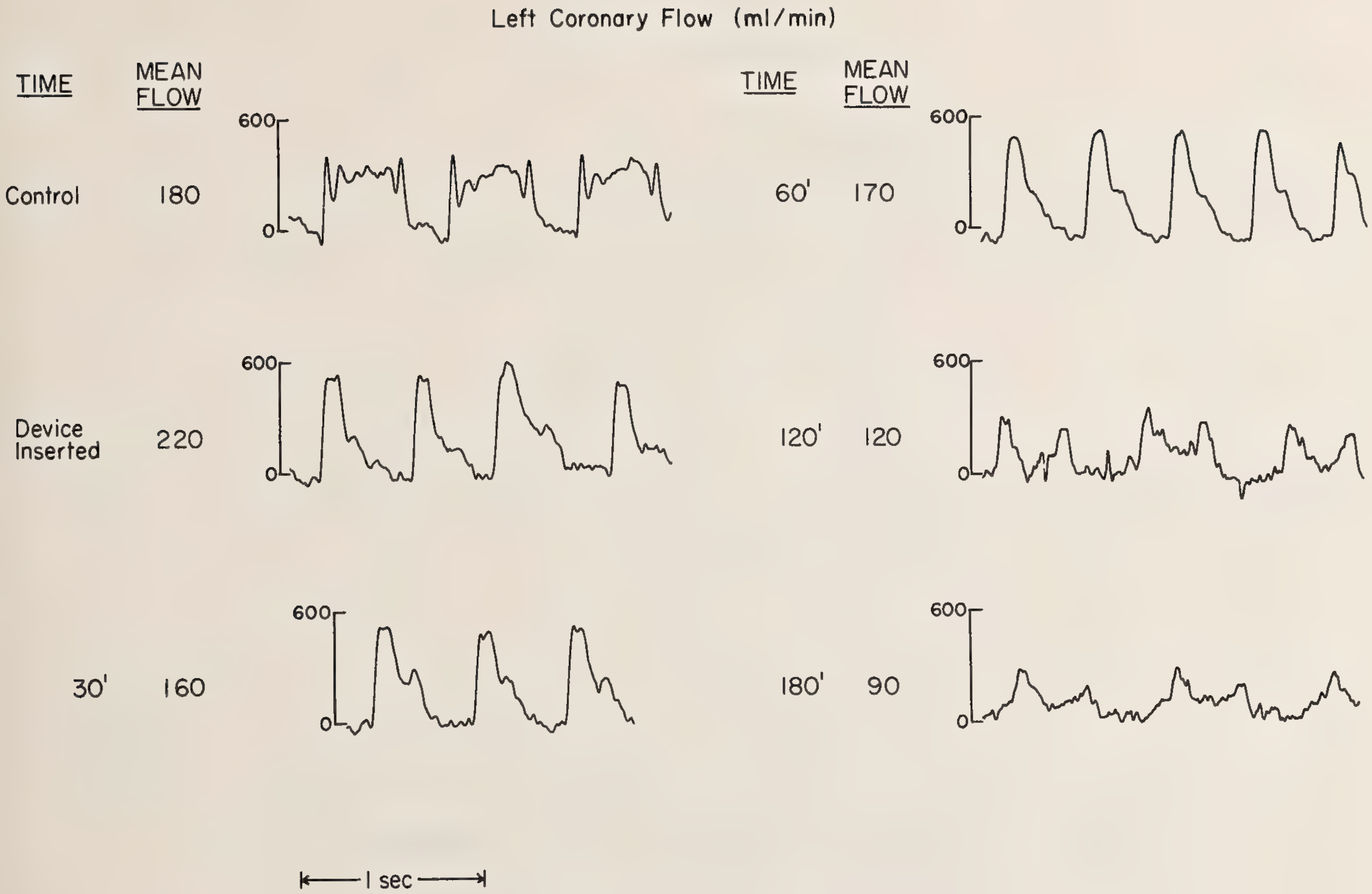

FIGURE 7. HEMODYNAMICS OF ACUTE MITRAL INSUFFICIENCY.

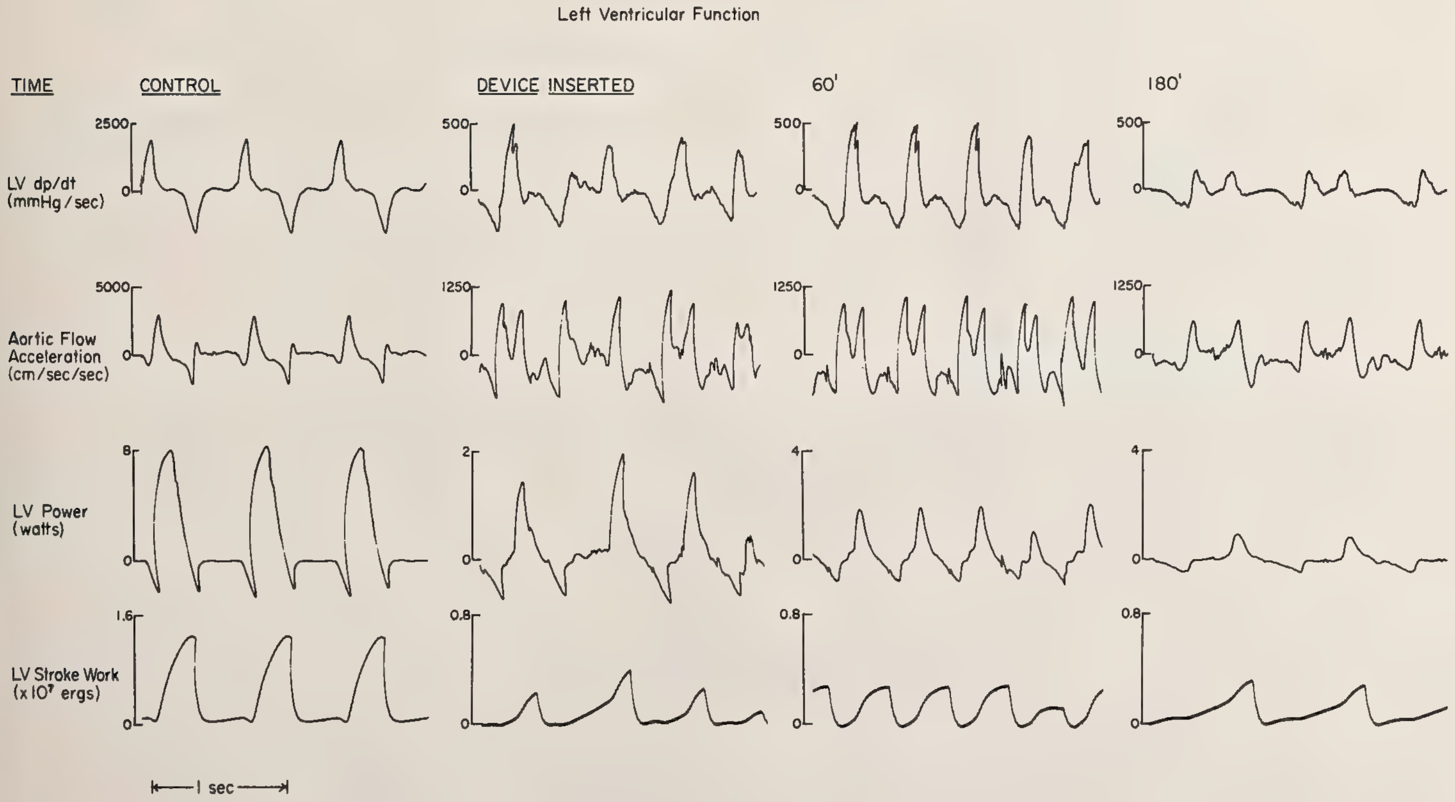

FIGURE 8. HEMODYNAMICS OF ACUTE MITRAL INSUFFICIENCY.

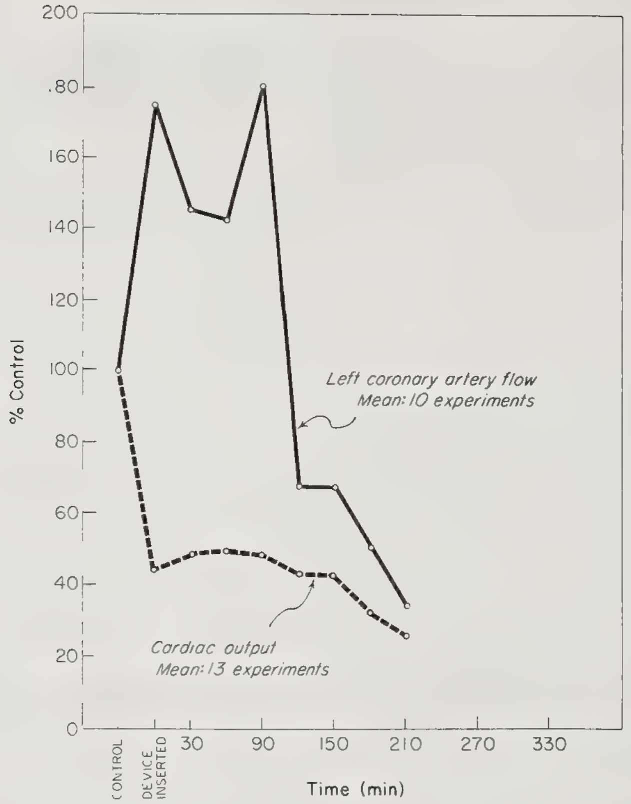

FIGURE 9. EFFECT OF ACUTE MITRAL INSUFFICIENCY ON CARDIAC OUTPUT AND LEFT CORONARY ARTERY FLOW.

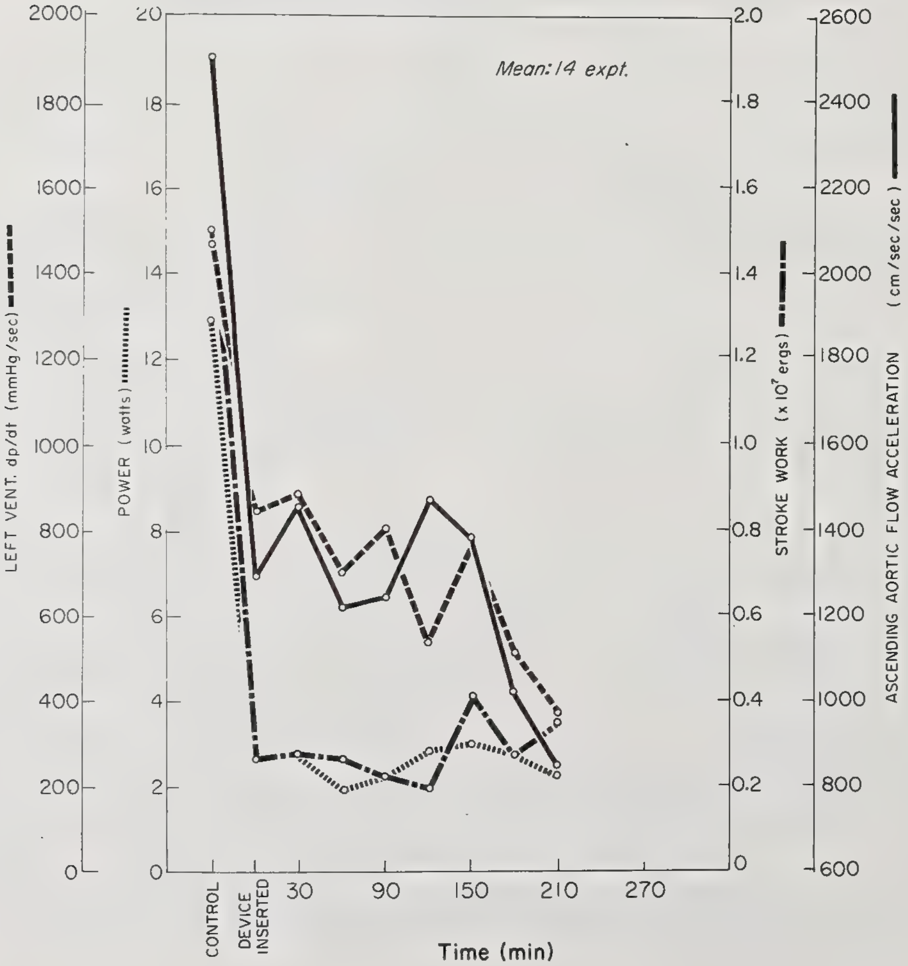

FIGURE 10. EFFECT OF ACUTE MITRAL INSUFFICIENCY ON LEFT VENTRICULAR FUNCTION.

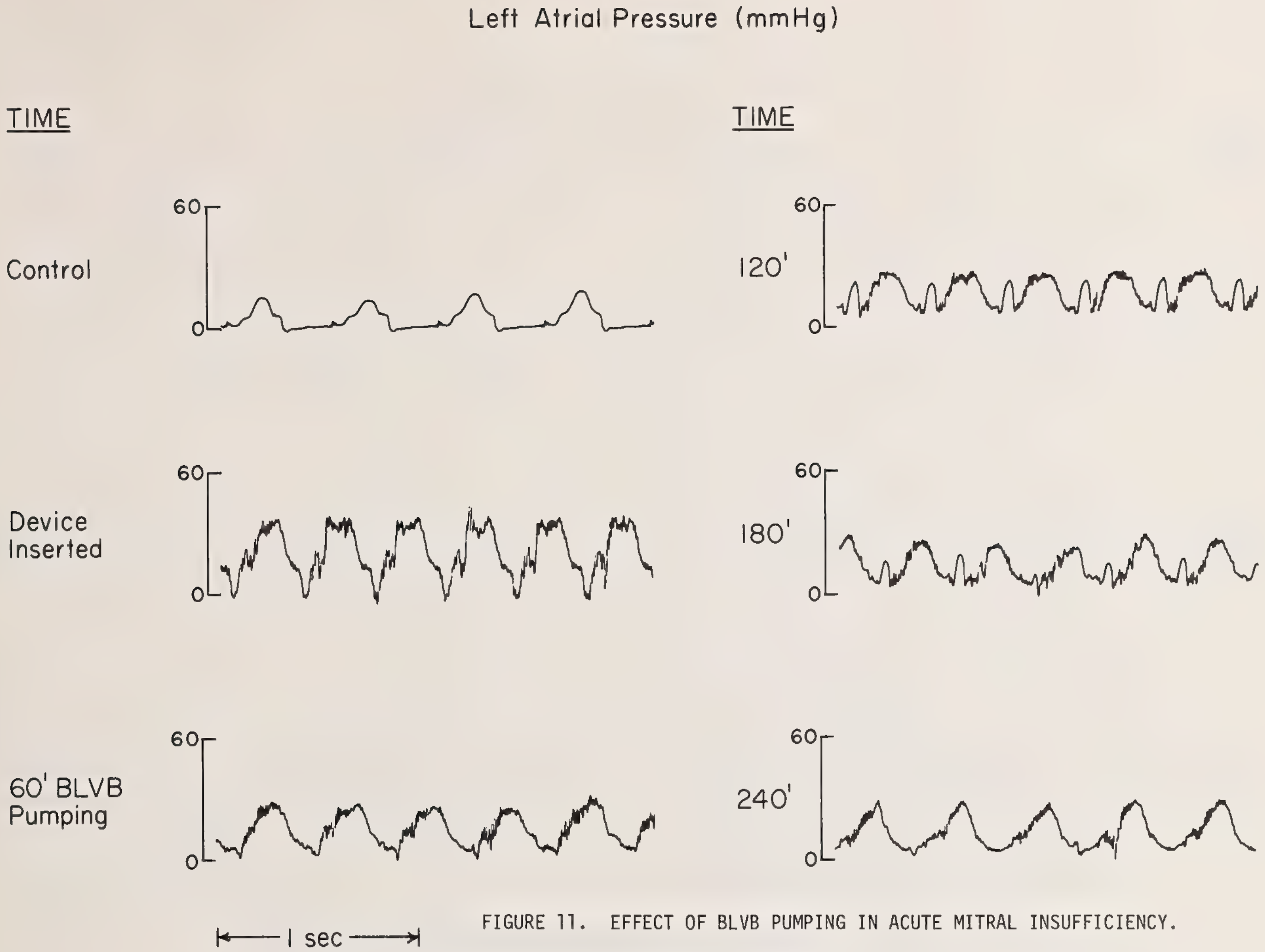

FIGURE 11. EFFECT OF BLVB PUMPING IN ACUTE MITRAL INSUFFICIENCY.

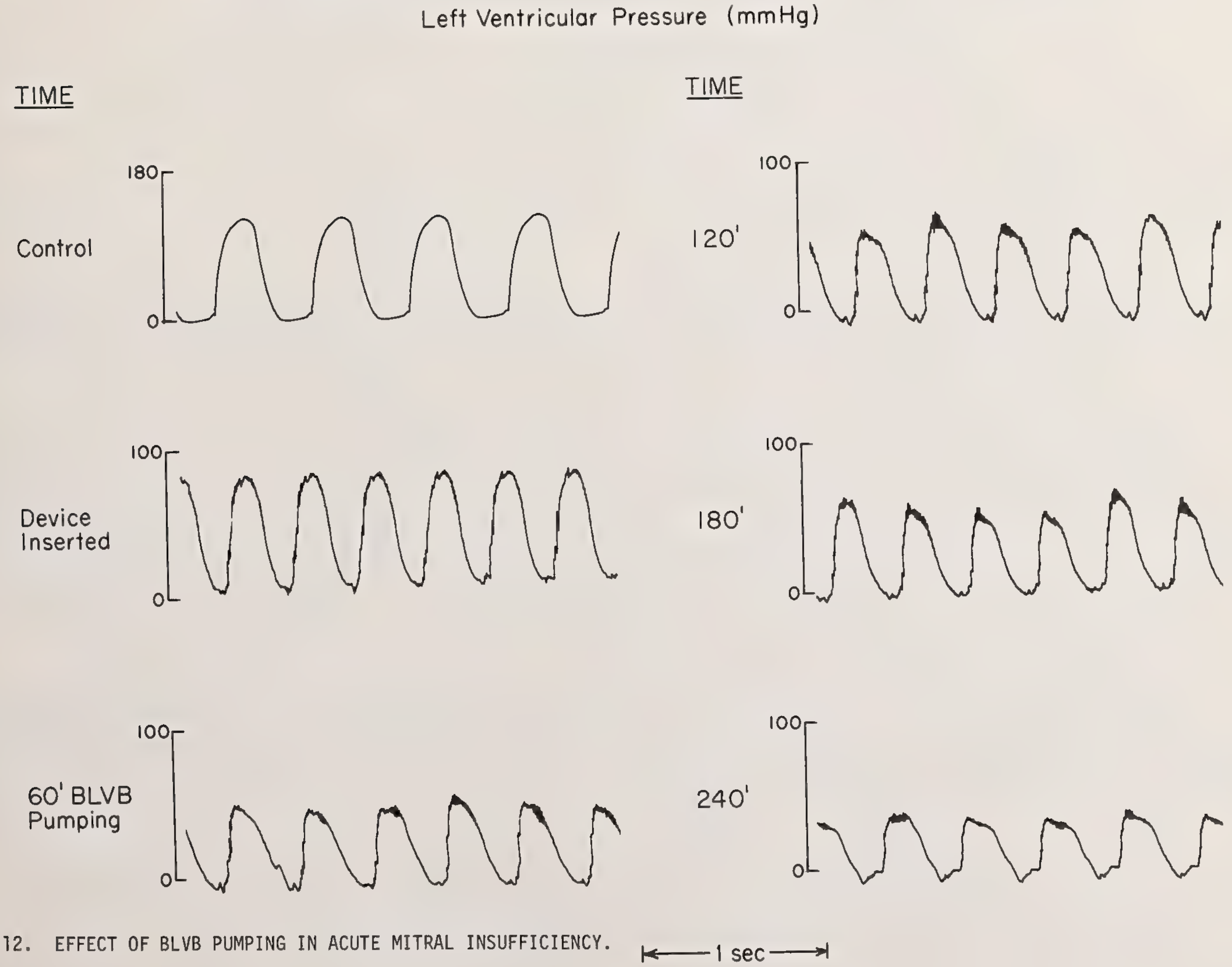

FIGURE 12. EFFECT OF BLVB PUMPING IN ACUTE MITRAL INSUFFICIENCY.

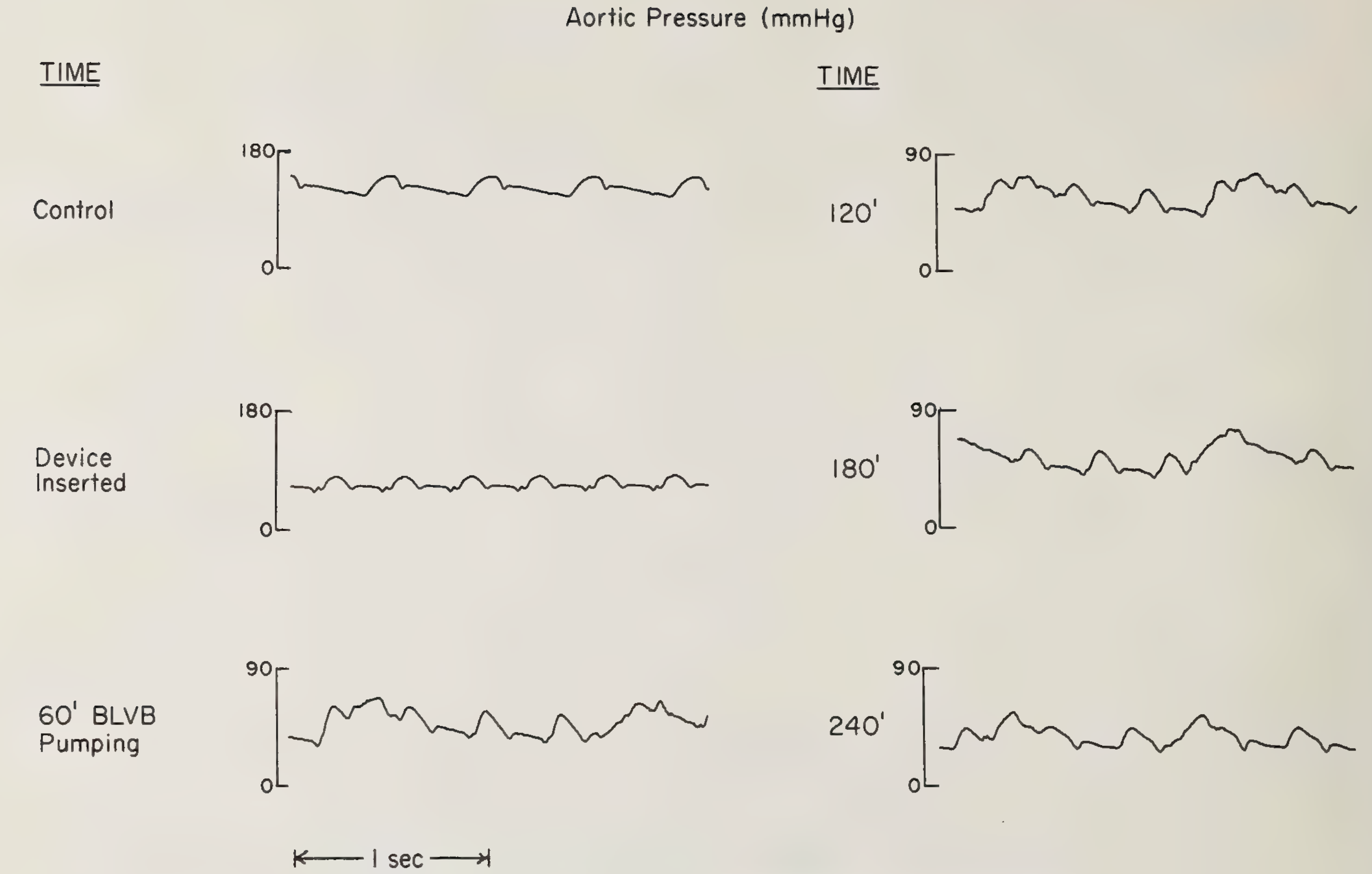

FIGURE 13. EFFECT OF BLVB PUMPING IN ACUTE MITRAL INSUFFICIENCY.

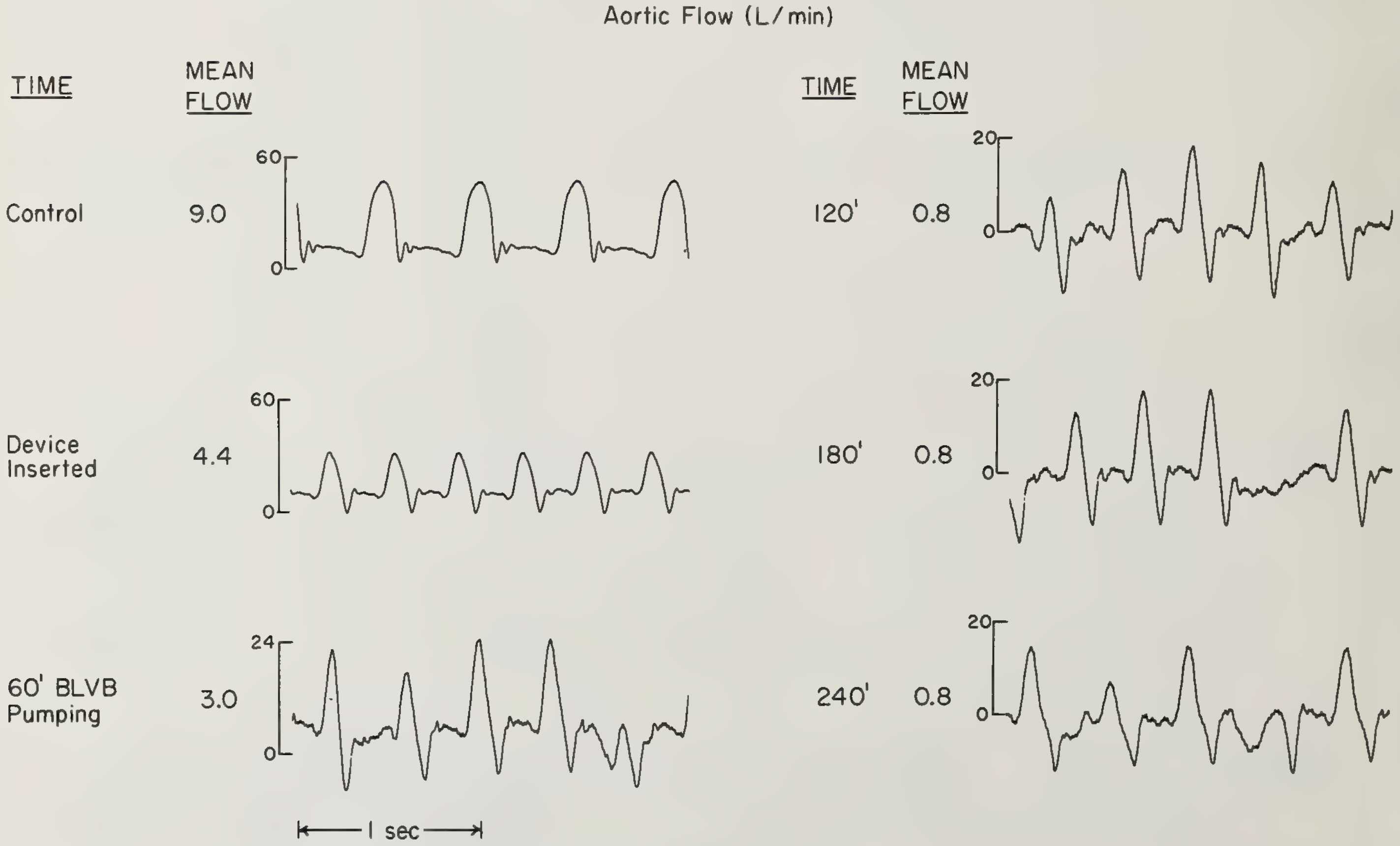

FIGURE 14. EFFECT OF BLVB PUMPING IN ACUTE MITRAL INSUFFICIENCY.

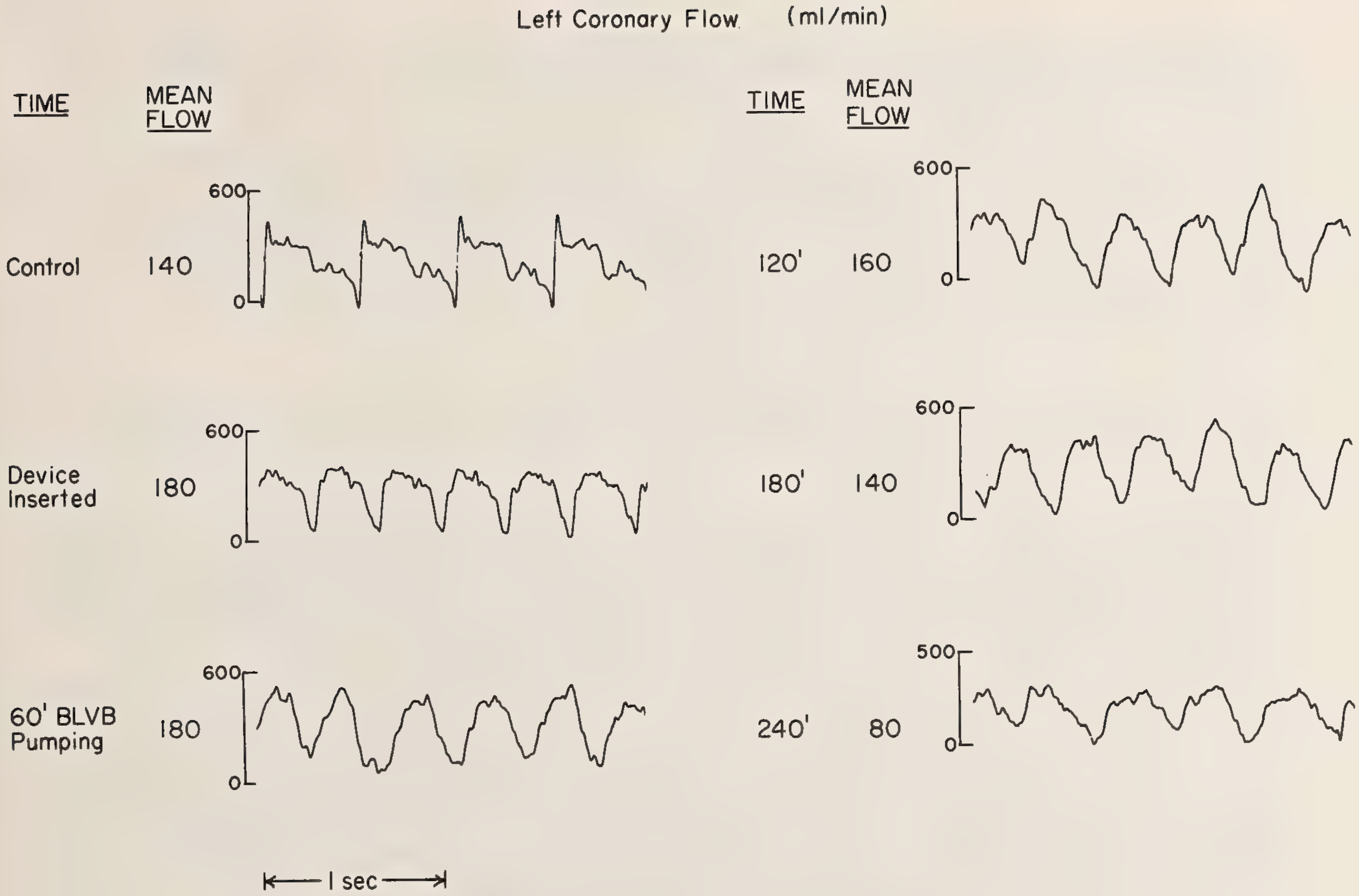

FIGURE 15. EFFECT OF BLVB PUMPING IN ACUTE MITRAL INSUFFICIENCY.

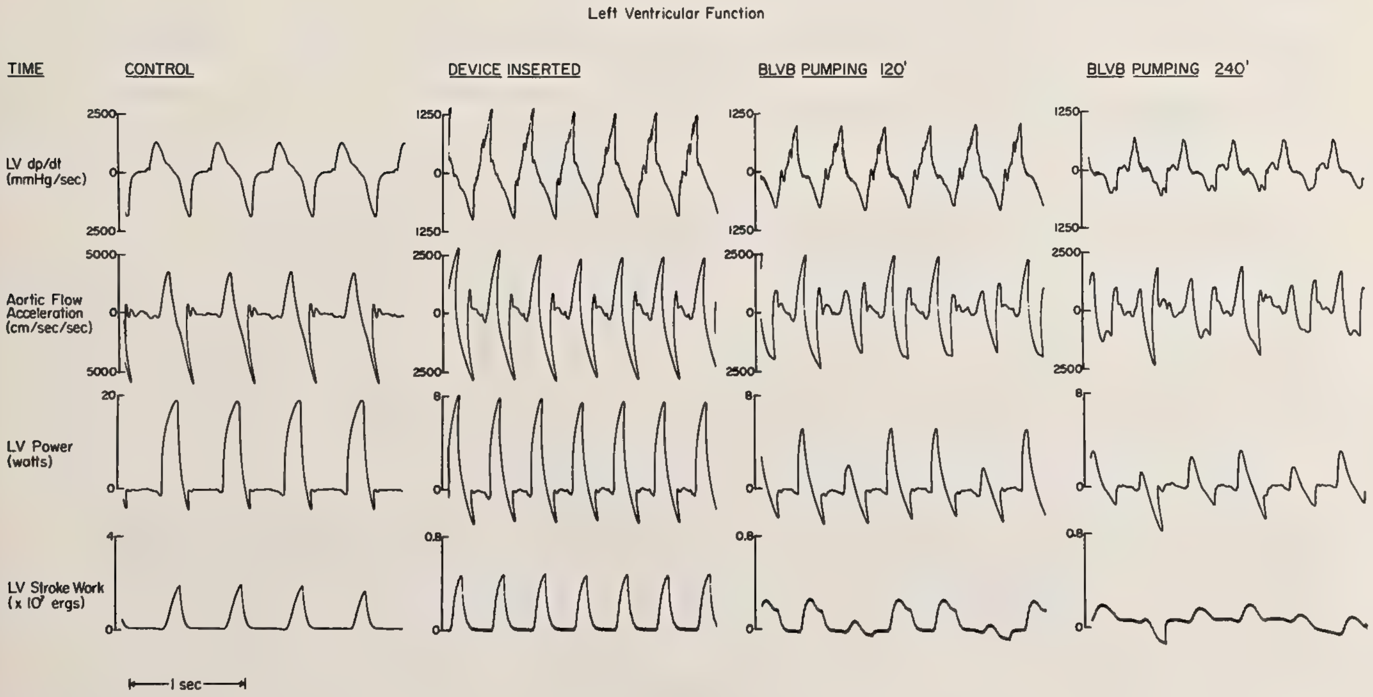

FIGURE 16. EFFECT OF BLVB PUMPING IN ACUTE MITRAL INSUFFICIENCY.

onset of pumping cardiac output fell to less than 40% of control values, where it remained throughout the continuing experimental course. BLVB pump output ranged from 1.5 to 2.9 liters/min, and, when added to ascending aortic flow, increased total aortic inflow to 47-62% of control cardiac output.

The increase in left coronary flow was not as marked or as prolonged as in the pure mitral insufficiency animals, once the BLVB was inserted. Whereas the unsupported animals sustained a marked decline in coronary flow approximately 90 minutes after the onset of mitral insufficiency, in the BLVB supported animals coronary flow was maintained at control levels or higher until their death (Figure 18). Mean left ventricular function data is presented in Figure 19 and does not significantly differ from the measurements presented in animals with mitral insufficiency without cardiac assistance.

DISCUSSION

The appropriateness of the cardiocirculatory failure model adopted and the therapeutic effects of BLVB pumping must be judged on the basis of measurements of left ventricular contractility and work.

The three commonly accepted criteria of cardiac failure which appear to be met by this model include an increase in heart rate, an increase in left ventricular end diastolic pressure, and a decrease in cardiac output.[4] The sharp decline in each of the measured indices of left ventricular contractility and work also testifies to the massive nature of the insult to left ventricular function provided by the acute mitral insufficiency device employed. Observations of these mean functions following the insertion of the BLVB device and the initiation of pumping did not demonstrate significant changes in the indices of contractility and work to suggest evidence of significant benefit from pumping, when compared with the unsupported animals.

Three factors do appear to demonstrate beneficial effects associated with employment of the BLVB device. These include (1) prolongation of survival time, (2) continued normal or elevated coronary artery flow and (3) the return of left ventricular end diastolic pressure to normal levels.

The increase in mean survival time from 2.3 to 5.1 hours with BLVB pumping must be evaluated in the light of the experimental conditions of continuous anesthesia and prolonged thoracotomy, both of which may have serious and additive deleterious effects. The support offered by BLVB pumping resulted in increasing total aortic inflow, in comparison to the non-supported animals, and in a modest increase in mean aortic pressure. This may well explain the sustained coronary artery flows in the range of normal control in the BLVB supported animals.

The changes in LVEDP do appear to be significant, since a definite decrease was observed in 6 of the 8 animals in which such data was available after the onset of BLVB pumping - the LVEDP in the other two animals remaining unchanged.

The alterations of coronary artery flow observed following insertion of the mitral insufficiency device are of considerable interest. Gregg suggests that the primary determinants of coronary artery flow include aortic blood pressure, reflex vasomotor nervous control of the coronary arteries, and myocardial oxygen demand.[29]

The most likely explanation for the profound initial increase in coronary flow which follows the insertion of the mitral insufficiency device is myocardial cellular anoxia. A sharp decline in cardiac output and aortic blood pressure occur simultaneously.

Eckenhoff has demonstrated that maximal coronary artery dilatation occurs when the arterial oxygen saturation falls to 50% of normal.[30]

In Kennedy's experiments, an increase in coronary sinus oxygen content was noted in animals in which left ventricular failure was induced by l-norepinephrine and multiple coronary ligations. Large coronary arteriovenous shunts were demonstrated with glass beads, suggesting that coronary vascular resistance also decreased significantly.[17]

The marked decline in cardiac output following the development of acute mitral insufficiency must be attributed to the regurgitation of a large fraction of left ventricular blood into the left atrium. Other possible explanations include obstruction of pulmonary venous inflow by the failure device, and inadequacy of the left ventricle to completely empty during systole because of the presence of the device in the ventricular cavity. The subsequent continuing decrease in cardiac output, however, must be attributed to progressive deterioration of cardiac function. Flow support by the BLVB at 2 to 3 liters/min failed to significantly alter the eventual outcome of any of these experiments, although life was prolonged an average of 2 to 3 hours.

The use of various contractility and work indices tend to confirm the severity of myocardial damage produced by the acute mitral insufficiency preparation. BLVB pumping does appear to have significant effects in reducing maximum aortic acceleration, and tends to decrease left ventricular power and work, while increasing the left ventricular pressure-time-product. Whether this is of significant benefit to the left ventricle can only be a matter of conjecture at this time. However, the prolongation of life associated with pumping appears to be significant, and does suggest the importance of the continued improvement in coronary flow and decreased LVEDP which result from pumping.

SUMMARY

The development of a model of cardiocirculatory failure in calves based on the initiation of acute mitral insufficiency is presented. Animals with acute mitral insufficiency and BLVB pumping demonstrate (1) prolongation of survival time, (2) continued normal or elevated coronary artery

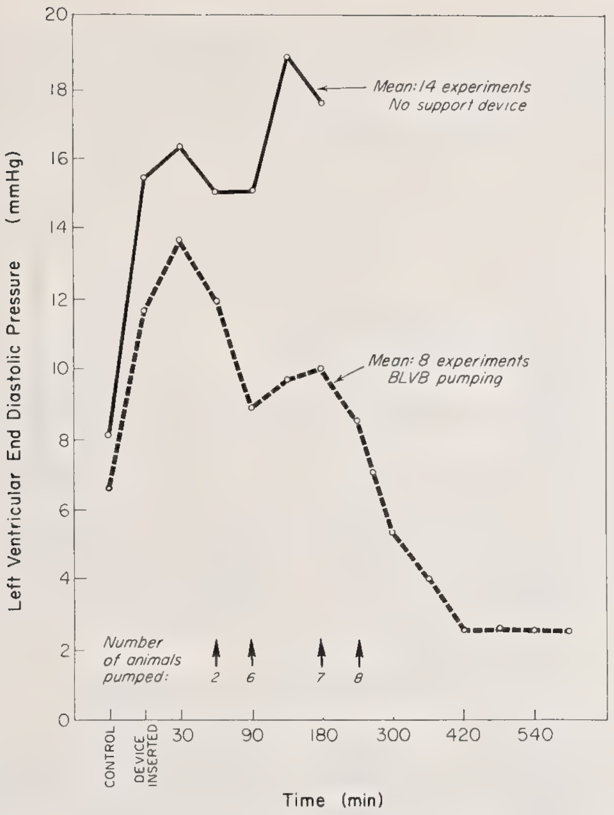

FIGURE 17. LVEDP FOLLOWING ACUTE MITRAL INSUFFICIENCY ± BLVB PUMPING.

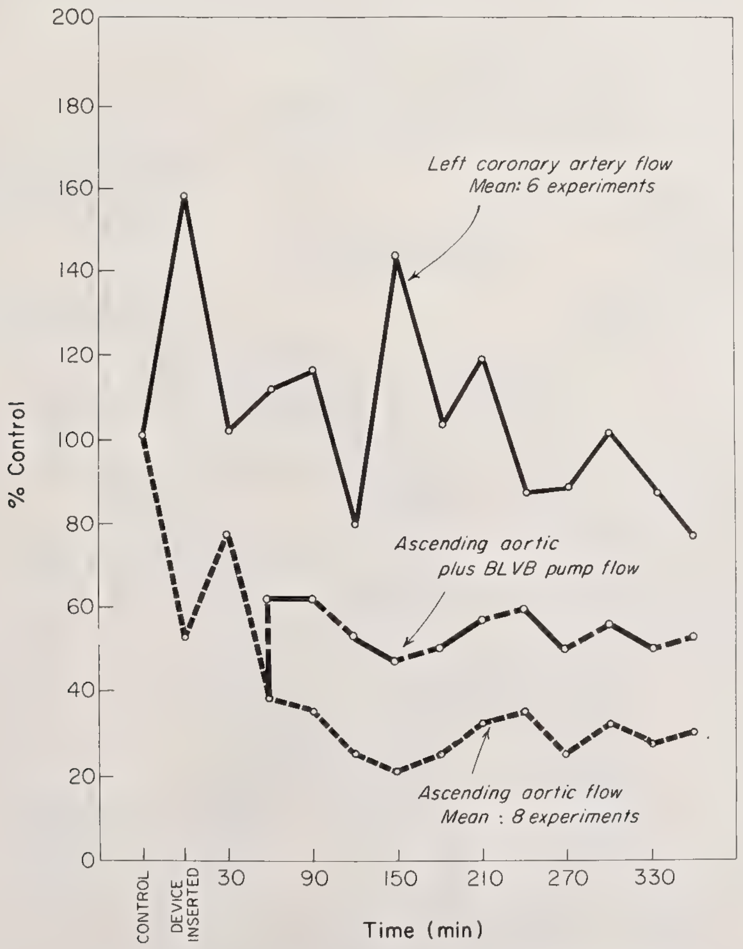

FIGURE 18. EFFECT OF ACUTE MITRAL INSUFFICIENCY AND BLVB PUMPING ON ASCENDING AORTIC AND LEFT CORONARY ARTERY FLOW.

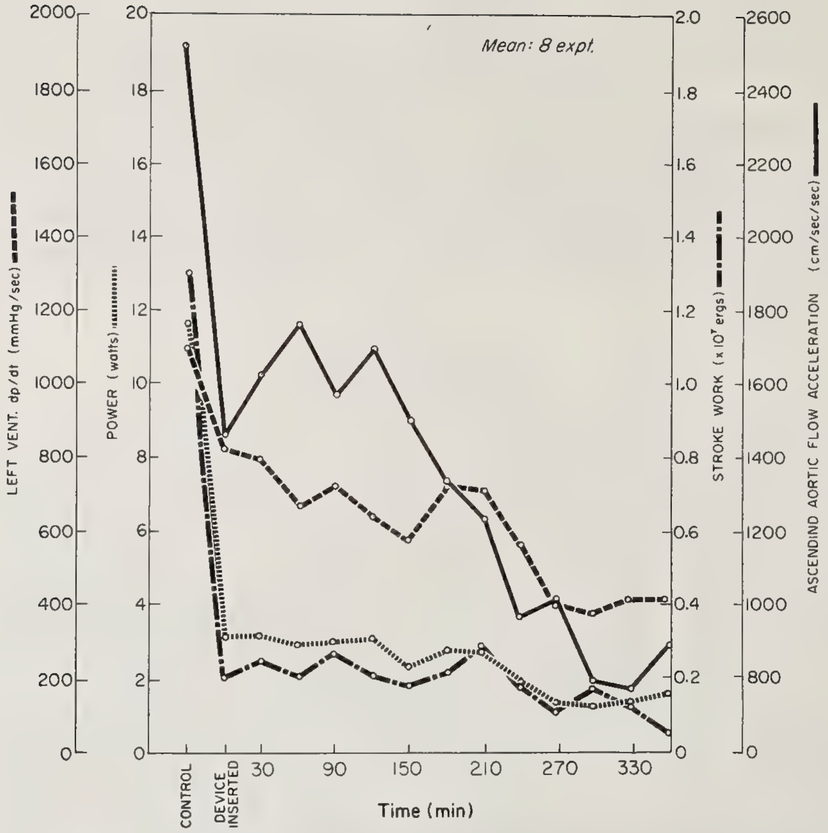

FIGURE 19. EFFECT OF ACUTE MITRAL INSUFFICIENCY ON LEFT VENTRICULAR FUNCTION WITH BLVB PUMPING.

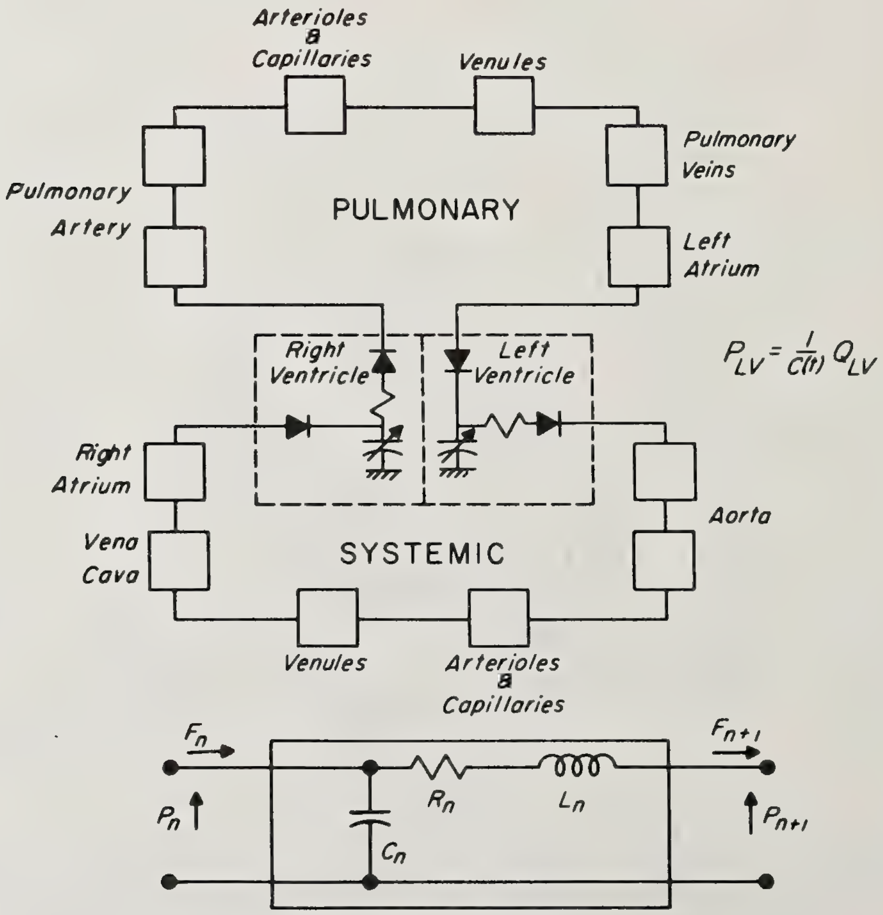

FIGURE 20. CARDIOVASCULAR MODEL.

flow and (3) the return of left ventricular end diastolic pressure to normal levels, when contrasted with animals with cardiocirculatory failure alone. BLVB pumping reduced maximum aortic flow acceleration, and decreased left ventricular power and work, while increasing the left ventricular pressure-time-product. An evaluation of synchronous and nonsynchronous pumping revealed no consistent or significant alterations in left ventricular contractility or work as a result of synchronous pumping.

PART II

DESIGN OF AN OPTIMAL PUMP CONTROLLER

INTRODUCTION

The objective of this section of the present investigation is an analysis of the effects of pumping with the Baylor Left Ventricular Bypass Device on left ventricular function, and the selection of optimal controller settings for such a device through the use of a hybrid computer model.

Using a hybrid computer, a model of the cardiovascular system was developed and evaluated, and a model of the Baylor Left Ventricular Bypass Device and Statham controller was developed. Pump control was then formulated as an optimal control problem, in which the cost functional was related to combined heart and pump stroke volume, the time-tension index and flow work. Heart rate and peripheral systemic resistance were arbitrarily chosen as independent variables, and optimum (minimum flow work) delay and stroke duration settings were found for ranges of those variables.

EXPERIMENTAL

The cardiovascular model is depicted in Figure 20, and typical wave forms from it are shown in Figure 21. Figure 22 shows the relationship between systole and diastole.

This model did not include any of the physiological control loops on heart rate or contractile force since these were to be among the independent variables for this investigation.

The acceptability of the cardiovascular model was based on reasonable pressure and flows throughout the model, as well as the analysis of cardiac output, flow work and peak dP/dt* as a function of contractile force, peripheral systemic resistance, blood volume and diastolic compliance. Table 2 and Figure 23 show the printout and recordings for one such run. The definition of pump delay and duration are depicted in Figure 24.

TABLE 2

PRINTOUT FOR VARIATION OF CONTRACTILE FORCE

Heart Rate = 73.8 per minute
Systole = 358. milliseconds
Diastole = 455. milliseconds

Stroke Volume
Heart = 75.140 milliliters
Pump = .040 milliliters

Cardiac Output = 5.5451 liters per minute
Pump output = .0029 liters per minute
Combined output = 5.5480 liters per minute

Time tension index = 5.0310 Normalized = .9068
Flow work = 3.9080 Normalized = .7044

Capillary Resistance	Blood Volume	Diastolic Compliance	Peak DP/DT	Stroke Volume	T.T.I.	Flow Work
1201.	4.635	.400	4.679	75.030	5.023	3.897
1201.	4.536	.400	2.546	59.950	4.334	2.503
1202.	4.635	.401	3.599	70.280	4.828	3.426
1201.	4.634	.400	4.393	73.790	4.972	3.773
1201.	4.636	.400	5.215	76.840	5.106	4.093
1201.	4.638	.400	6.048	78.840	5.211	4.317
1201.	4.637	.400	6.895	80.060	5.286	4.459
1201.	4.638	.400	7.858	81.180	5.363	4.610
1201.	4.638	.400	8.939	82.310	5.435	4.767
1201.	4.639	.400	10.172	83.580	5.511	4.940
1202.	4.628	.401	2.704	63.340	4.591	2.801

---

*dP/dt is the time derivative of left ventricular pressure; the peak occurs during isovolumetric contraction.

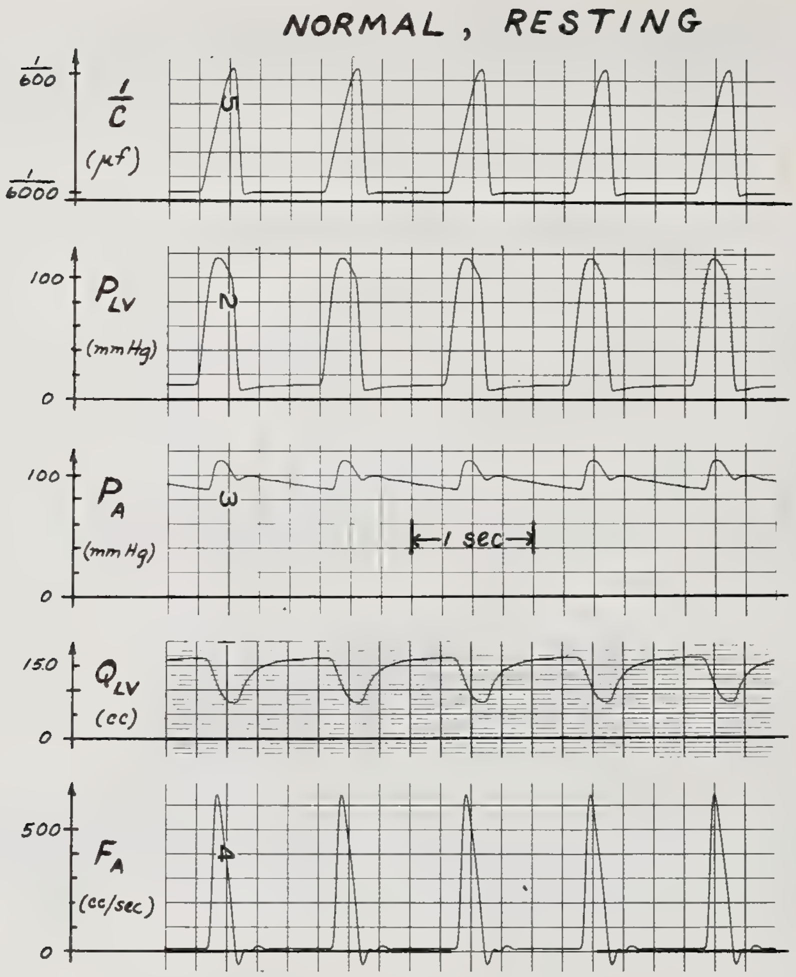

FIGURE 21. WAVEFORMS FROM CARDIOVASCULAR MODEL.

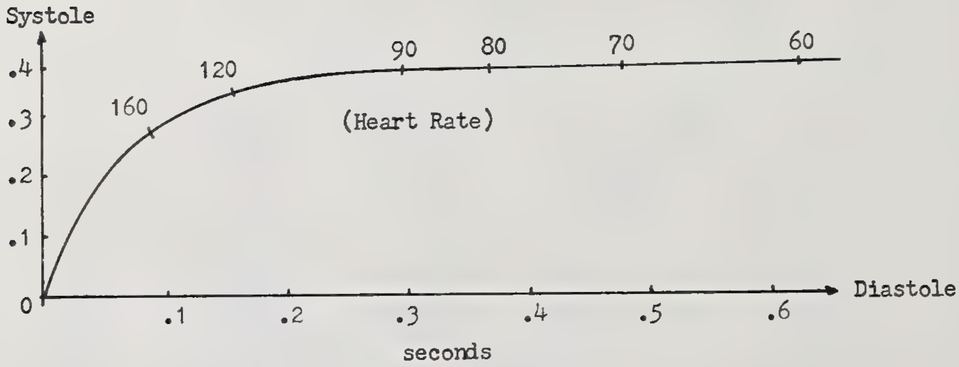

FIGURE 22. RELATIONSHIP BETWEEN SYSTOLE AND DIASTOLE.

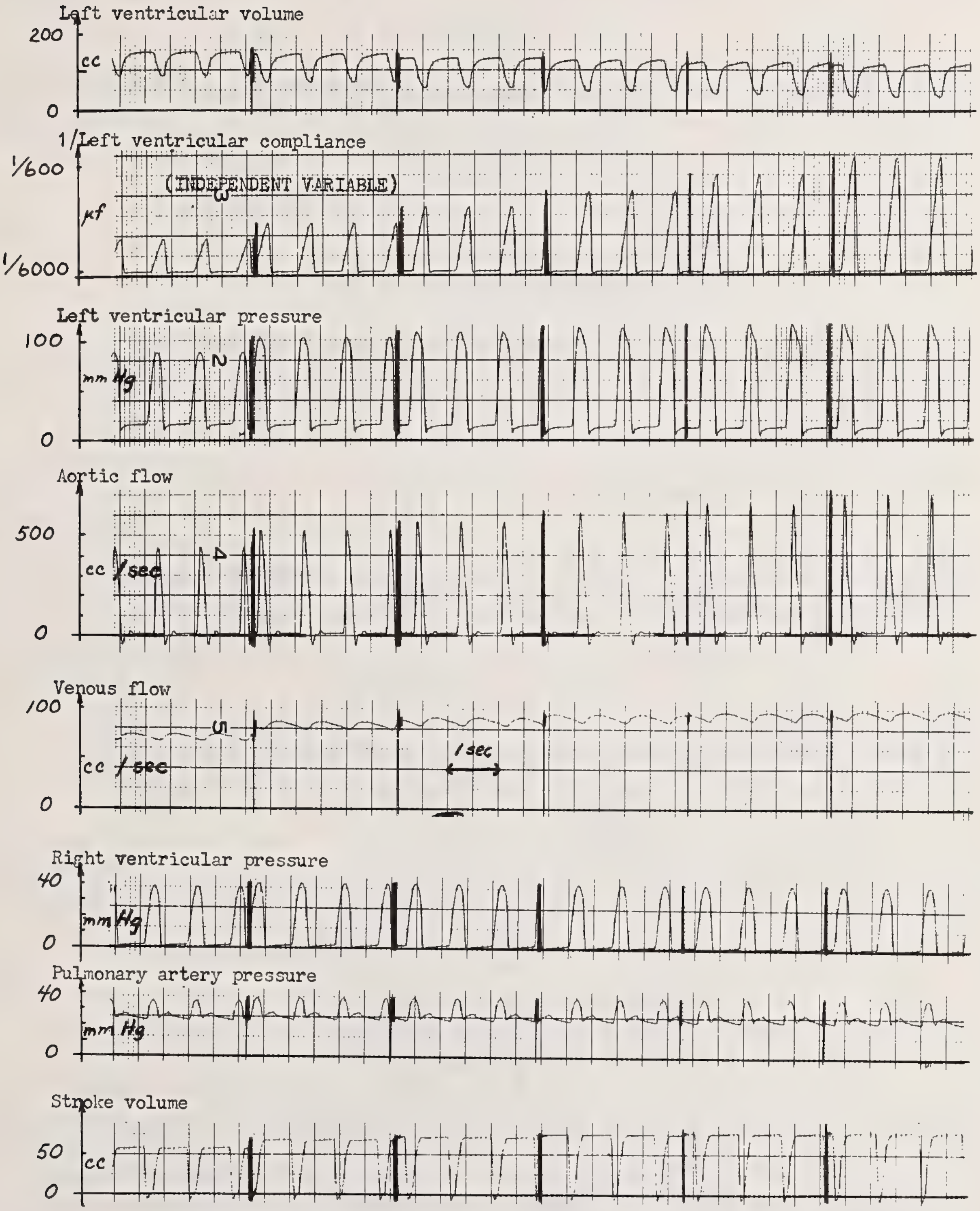

FIGURE 23. RECORDING FOR VARIATION OF CONTRACTILE FORCE.

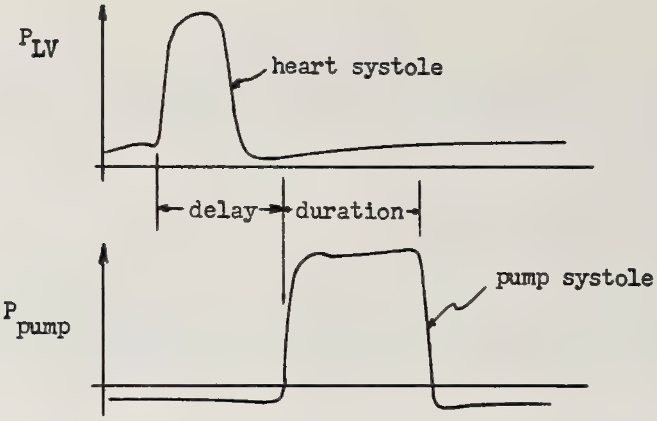

FIGURE 24. DEFINITION OF PUMP DELAY AND DURATION.

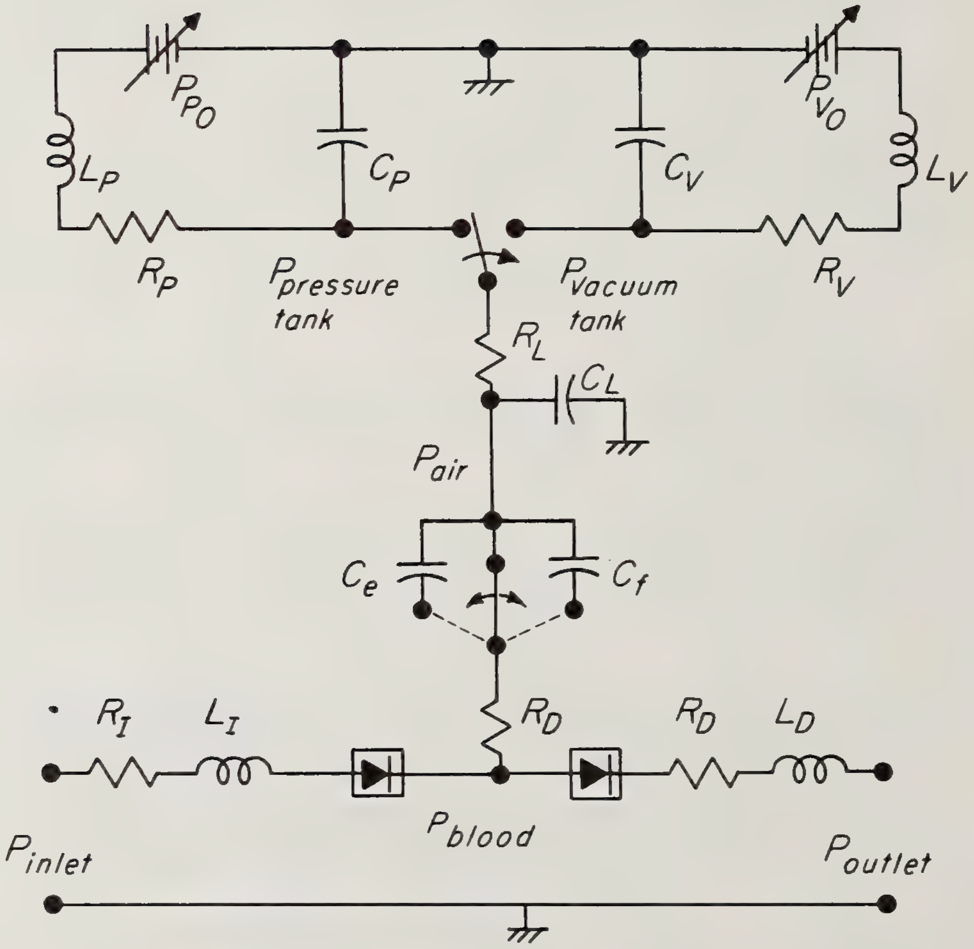

FIGURE 25. PUMP AND CONTROLLER MODEL.

Figure 25 is the fluid mechanical analog of the pump and controller which was used for this investigation. The stroke volume as a function of duration for the model is given in Figure 26 and compared with actual in vitro pumping of calf blood. Recording of pressures and flows for a 500 millisecond stroke duration is given in Figure 27.

Sensitivity Analysis.

In the following analysis of left atrium-to-aorta (LA-A) and left ventricle-to-aorta (LV-A) bypass pumping, as well as optimum parameter selection, synchronous operation was assumed. The pump model was triggered from the cardiovascular model and pumped one stroke for each heart beat.

The mechanical work done by the left ventricle was defined as

$$\text{Flow Work} = \int_0^T (P_{LV} \cdot F_A)dt$$

where

P_{LV} - left ventricular pressure

F_A - flow through the aortic valve

T - period = 60/Heart rate

It is believed that the actual mechanical work accounts for a small fraction of the myocardial energy expenditure.[10] A simple indicator of this "non-flow work" is the

$$\text{Time Tension Index} = \int_0^T P_{LV}dt$$

The following four figures (Figures 28 through 31) present the effect of varying the duration and delay on the stroke volumes, time tension index and flow work for each configuration.

Left Atrium→Aorta.

Heart stroke volume and flow work have a minimum at a duration of about 500 milliseconds while the TTI is largely unchanged. From Figure 29 it is clear that cardiac function is quite insensitive to delay. This also suggests that asynchronous pumping would be equally acceptable.

Left Ventricle→Aorta.

The TTI is also relatively insensitive to delay and duration, but heart stroke volume and flow work exhibit clear minima in both parameters.

Qualitative conclusions from this analysis suggest that:

1. Neither of the two configurations significantly changes the non-flow energy expenditure.
2. Due to improved filling pressure the LV-A assist is able to carry more of the mechanical work load.
3. The LA-A assist is quite insensitive to delay and would possibly be more effective pumping asynchronously since its rate could then be adjusted to maximize output.

Optimal Pump Control.

The formulation of the pump control as an optimal control problem required the definition of criteria of benefit (or cost functional with the other sign), that is a precise mathematical statement of the desired end. The cost functional selected was:

$$\text{Cost} = -\text{Benefit} = K_1(\text{C.S.V.}) + K_2(\text{T.T.I.}) + K_3(\text{F.W.})$$

where

Cost - scaler functional to be minimized

C.S.V. - combined stroke volume = Heart S.V. + Pump S.V.

K_1, K_2, K_3 - relative weightings $K_1 \leq 0$, K_2, $K_3 \geq 0$

The question of optimal switching times can then be posed as follows:

Given: A particular set of cardiovascular parameters (heart rate, contractile force, etc.), controller pressure and vacuum and cost functional weightings (K_1, K_2, K_3).

Find: The delay and duration which minimize the cost (maximize benefit).

A simple gradient search was chosen to answer this question. Heart rate and peripheral systemic resistance were arbitrarily chosen as independent variables as well as various values of K_1, K_2, K_3. Since a suggested application of these results was the operation of a feedback controller, the optimum duration of a feedback controller, the optimum duration is displayed vs. the mean left atrial pressure (instead of peripheral resistance which could not be measured directly in an animal). The particular case represented in Figure 32 is for $K_1 = K_2 = 0$, $K_3 = 1$, i.é., cost = flow work.

To operate a controller, the heart rate and mean atrial pressure would be measured and the optimum delay and duration (from table look up or functional representation) returned by the computer to set the controller for the next heart beat.

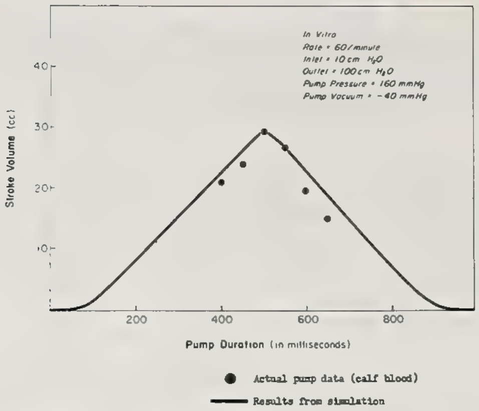

FIGURE 26. PUMP STROKE VOLUME VS DURATION.

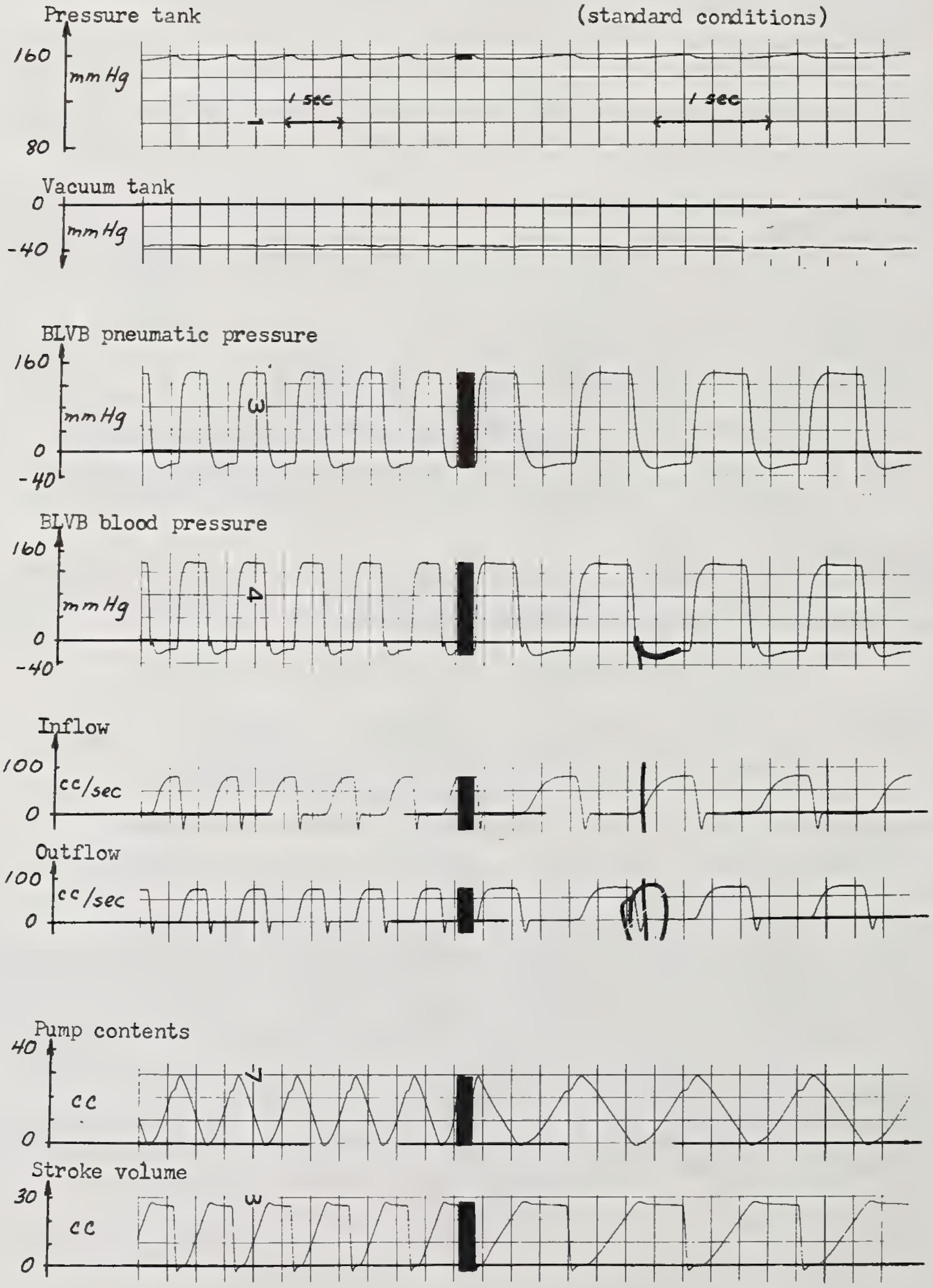

FIGURE 27. RECORDING OF IN VITRO PUMP MODEL.

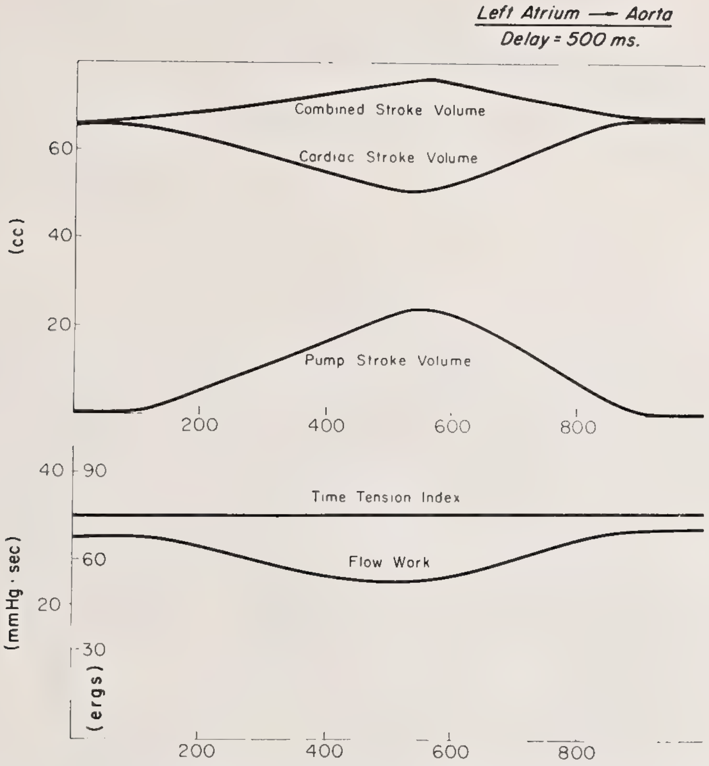

FIGURE 28. EFFECT OF VARYING THE DURATION AND DELAY ON THE STROKE VOLUMES, TIME TENSION INDEX AND FLOW WORK.

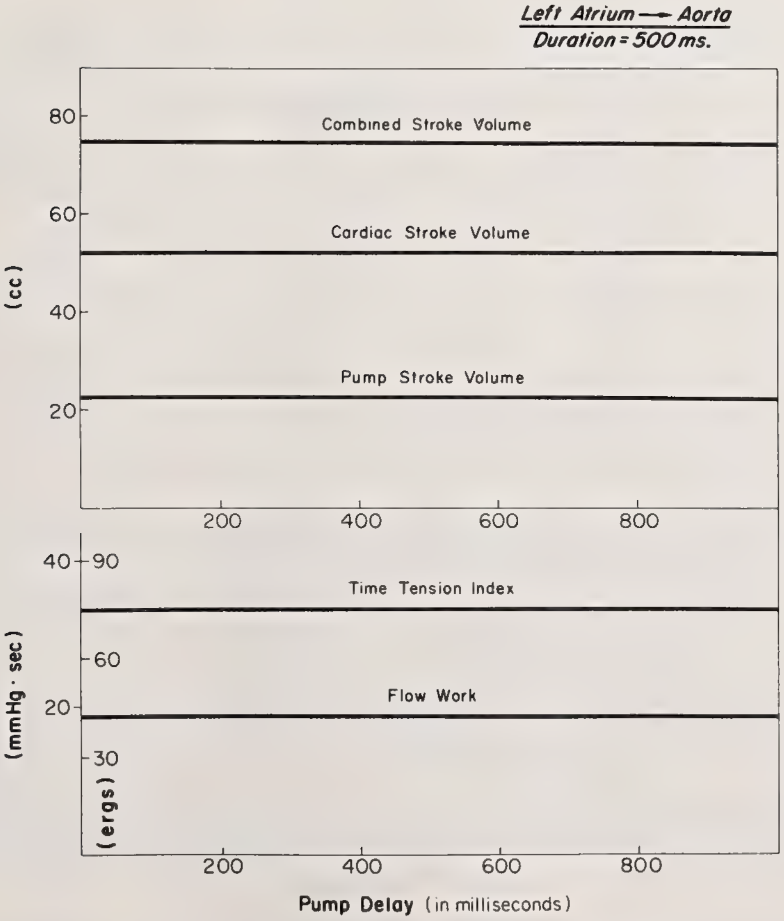

FIGURE 29. EFFECT OF VARYING THE DURATION AND DELAY ON THE STROKE VOLUMES, TIME TENSION INDEX AND FLOW.

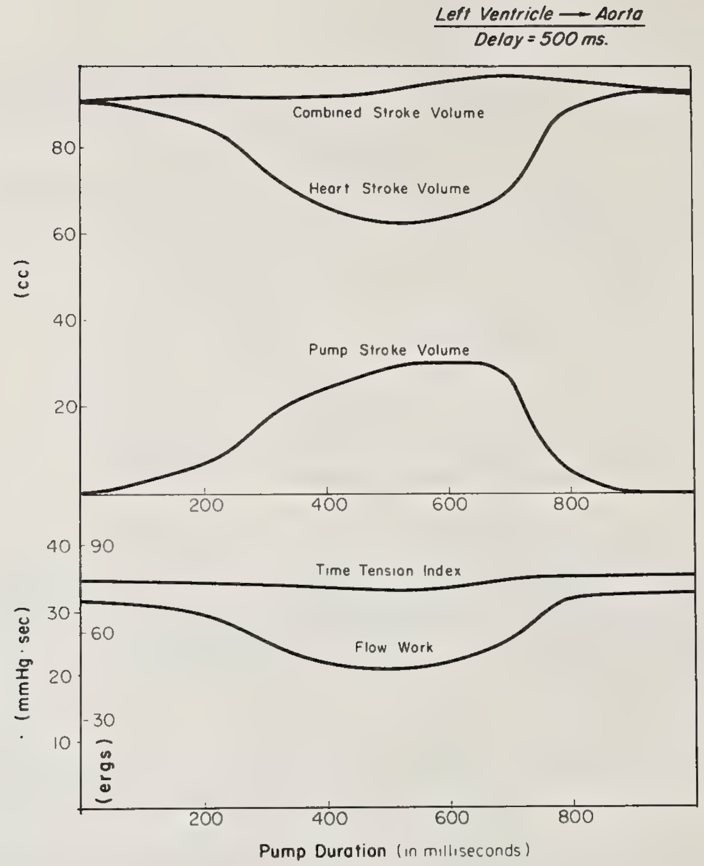

FIGURE 30. EFFECT OF VARYING THE DURATION AND DELAY ON THE STROKE VOLUMES, TIME TENSION INDEX AND FLOW WORK.

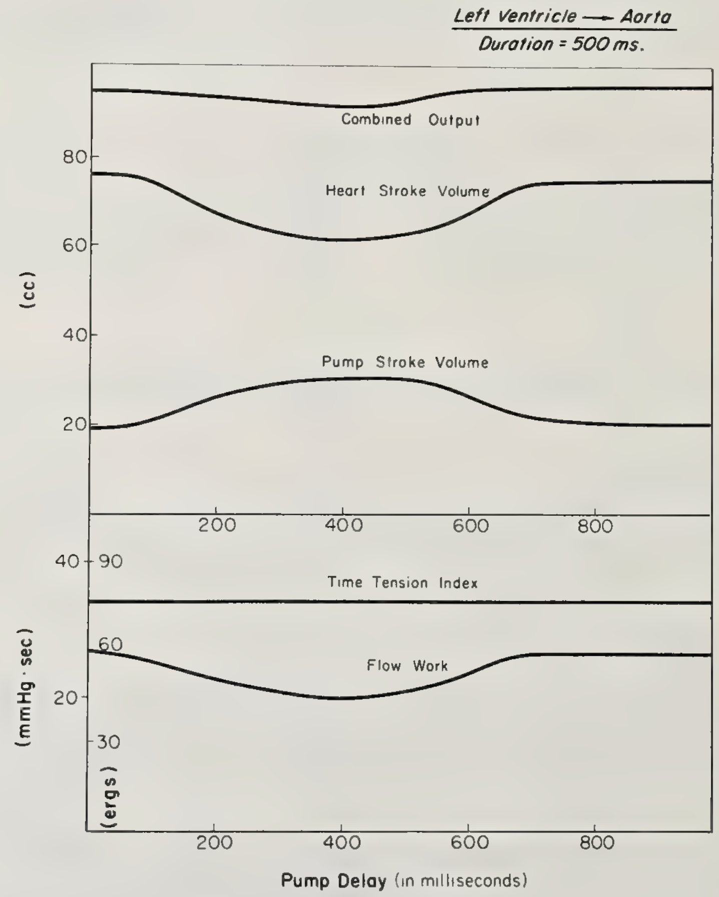

FIGURE 31. EFFECT OF VARYING THE DURATION AND DELAY ON THE STROKE VOLUMES, TIME TENSION INDEX AND FLOW WORK.

Summary.

A hybrid computer cardiovascular model was evaluated, and a comparable model of the BLVB device and Statham controller was developed and accepted on the basis of in vitro operation. Although the simplifications and assumptions were rather severe, the results are still reasonable and helpful.

The sensitivity of cardiac output, combined output, time tension index and flow work to the control parameters (delay and duration) for both left atrium-to-aorta and left ventricle-to-aorta configurations were evaluated.

Optimum delay and duration were then found for ranges of heart rate and peripheral resistance for various cost functional weightings.

REFERENCES

1. DeBakey, M. E., Liotta, D., and Hall, C.W.: Left Heart Bypass Using an Implantable Blood Pump. In Conference on Mechanical Devices to Assist the Failing Heart. Washington, D.C.: National Academy of Sciences-National Research Council, 1960.
2. Shea, M.A. and Bernstein, E.F.: Evaluation of the Functional Capability of the Baylor Left Ventricular Bypass Device. Trans. Amer. Soc. Artif. Int. Organs, XV:1969.
3. Bernstein, E.F. and Shea, M.A.: Evaluation of the Baylor Left Ventricular Bypass Device. Conference on the Artificial Heart Program of the National Heart Institute, June, 1968.
4. Werko, L.: Current Status, Unsolved Problems, and Future Directions on Congestive Heart Failure Research. Amer. Heart Journal 70:402, 1965.
5. Bloch, J.H., Pierce, C.H., Manax, W.G., Lyons, G.W., and Lillehei, R.C.: Experimental Cardiogenic Shock. Arch. Surg., 91:77, 1965.
6. Ellis, P.R., Lee, C., Wong, S.H., DelRosario, V.C., Hyland, J.W. and Prator, G.: Assisted Circulation in Treatment of Experimental Heart Failure. Arch. Surg., 90:879, 1965.
7. Small, M.L.: A Standardized Experimental Preparation of Cardiogenic Shock. Surgery, 60:1051 1966.
8. Joison, J., Kumar, R., Hodd, W.B., Jr. and Norman, J.C.: An Implantable System for Producing Left Ventricular Failure for Circulatory Assist Device Evaluation. Trans. Amer. Soc. Artif. Int. Organs, XV:1969.
9. Glass, B.A., Carter, R.L. and Albert, H.M.: Experimental Myocardial Infarction: Effect on Cardiac Output and Response of the Heart After Surgical Excision. The Amer. Surgeon, 33:912, 1967.
10. Taylor, R.R., Covell, J.W. and Ross, J., Jr.,: Left Ventricular Function in Experimental Aorto-Caval Fistula with Circulatory Congestive and Fluid Retention. J. Clin. Invest. 47:1333, 1968.
11. Friedberg, C.K., Lasser, R.P., Allen, D.F., Furst, S.E. and Gabor, G.E.: Production of Chronic Elevation of Left Ventricular End Diastolic Pressure in Dogs: Hemodynamic & Renal Studies. Circulation Research, XV:1, 1964.
12. Ross, J., Jr., Covell, J. W. and Sonnenblick, E.H.: The Mechanics of Left Ventricular Contraction In Acute Experimental Cardiac Failure. J. Clin. Invest., 40:299, 1967.
13. Kelly, D.T.: Electrical Pacing of the Heart with Observations on the Single and Paired Electrical Stimuli During Acute Reversible Experimental Heart Failure in the Anaesthetized Dog. S.A. Medical Journal, 42:432, 1968.
14. Chapple, J. C., and Connolly, J.E.: Efficacy of Left Heart Bypass in the Treatment of Acute Heart Failure. Surgery Forum, 15:262, 1964.
15. Wennemark, J.R., Pokornowski, R.F. and Gilbert, R.P.: Experimental Chronic Right Ventricular Failure Produced by Endocardial Application of Dilute Iodine Solution. Soc. Exper. Biol. Med. Proceedings 122:967, 1966.
16. Chaptal, P.A., Akutsu, T. and Kantrowitz, A.: Hemodynamic Effects of a Mechanical Auxiliary Ventricle Following Induced Heart Failure in Dogs. J. Thorar. & Cardiov. Surg. 52:377, 1966.
17. Kennedy, J.H., Haiderer, O., Reid, J.D. and Bailas, N.: Experimental Heart Failure. Arch. Surg. 93:759, 1966.
18. Spann, J.F., Bussino, R.A., Sonnenblick, E.H.: Production of Right Ventricular Hypertrophy with and Without Congestive Heart Failure, in the Cat. Soc. Exper. Biol. Med. Proc., 125:522, 1967.
19. Kenner, H.M. and Wood, E.H.: Intrapericardial, Intrapleural, and Intracardiac Pressures During Acute Heart Failure in Dogs Studied Without Thoracotomy, Circ. Research, XIX:1071, 1966.
20. Aldinger, E.E. and Brown, J.A.: Cardiac Decompensation in Dogs Subjected to Chronic Congestive Heart Failure. Jap. Heart J., 8:507, 1967.
21. Tatooles, C.J., and Braunwald, N.S.: Sustained Paired Electrical Stimulation of the Heart: Hemodynamic Effects in the Presence of Experimentally Produced Heart Failure. Surgery, 59:102, 1966.
22. Chidsey, C.A., Kaiser, G.A., Sonnenblick, E.H., Spann, J.F. and Braunwald, E.: Cardiac Norepinephrine Stores in Experimental Heart Failure in the Dog. J. Clin. Invest., 43:2386, 1964.
23. Donawick, W.J., Nara, Y. and Baue, A.E.: Techniques for Successful Cardiopulmonary Bypass in the Calf. J. Clin Res. 9:79, 1969.
24. Goldenbert, A.L., Brown, L. and Dennis, C.: Relative Evaluation of Left Heart Bypass Whether Pulsatile or Pulseless, with Counterpulsation as Technique for Myocardial Augmentation. Suppl. I to Circ., XXXV and XXXVI:188, 1967.

25. Snider, M.T., and Galletti, P.M.: Left Ventricular Adaptation to Partial Heart-Lung Bypass and Arterio-Venous Pumping, Trans. Amer. Soc. Artif. Int. Organs, XIV:311, 1968.
26. Noble, M.I.M., Trenchard, D. and Guz, A.: Left Ventricular Ejection in Conscious Dogs: I. Measurement and Significance of the Maximum Acceleration of Blood from the Left Ventricle. Circ. Res., XIX:139, 1966.
27. Rushmer, R.F.: Initial Ventricular Impulse. A Potential Key to Cardiac Evaluation. Circ., XXIX:268, 1964.
28. Reis, R.L., Enright, L.P., Hannah, H., III and Morrow, A.G.: The Effects of Epicardiectomy on the Performance of the Acutely Ischemic Left Ventricle. J. Thor. & Cardiov. Surg., 56:647, 1968.
29. Gregg, D.E.: Coronary Circulation in Health and Disease. Lea and Febiger, Philadelphia, Pa. 1950.
30. Echenhoff, J.E., Hafkenschell, C.M., Landmesser, C.M. and Harmel, M.: The Coronary Circulation in the Dog. Am. J. Physiol., 148:582, 1947.
31. Liotta, D., Crawford, E.S., Cooley, D.A., DeBakey, M.E., de Urquia, M. and Feldman, L.: Prolonged Left Ventricular Bypass by Means of a Intrathoracic Pump Implanted in the Left Chest. Trans. Amer. Soc. Artif. Int. Organs, VIII: 90, 1962.
32. Sarnoff, S.J., Braunwald, E., Welch, G.H., Case, R.B., Stainby, W.N. and Macruz, R: Hemodynamic Determinants of Oxygen Consumption of the Heart With Special Reference to the Tension-Time Index. Am. J. Physiol. 192:148, 1958.
33. Katz, L.: Analysis of the Several Factors Regulating the Performance of the Heart. Physiol. Rev. 35:91, 1955.
34. Levin. H.J. and Wagman, R.S.: Energetics of the Human Heart. Amer. J. Cardiol., 9:372, 1962,
35. Dennis, C., Hall, D.P., Moreno, J.R. and Senning, A.: Reduction of the Oxygen Utilization of the Heart by Left Heart Bypass. Circ. Res., X:298, 1962.
36. Nose, Y. et al, "Experimental Use of an Electronically Controlled Prosthesis as an Auxiliary Left Ventricle", Trans. Amer. Soc. Artif. Int. Organs, IX:269, 1963.
37. Laird, J.D. et al, "Theoretical and experimental analysis of the intra-aortic balloon pump", Trans. ASAIO, Vol. 14, 1968, pp. 338-343.
38. Rudinger, G. , "Review of current mathematical methods for the analysis of blood flow," Biomedical fluid MECHANICS Symposium. New York: ASME 1966, pp. 1-33.
39. Womersley, J.R., "An elastic tube theory of pulse transmission and oscillatory flow in mammalian arteries," Wright Air Dev., Rpt. WADC-TR 56-614, 1957.
40. Jager, et al, "Oscillatory flow impedance in electrical analog of Arterial System," Circulation Research, Vol. 16, 1965, pp. 121-132.
41. McLeod, J.,"PHYSBE, a physiological simulation benchmark experiment," Simulation, Vol. 7, No. 6 Dec. 1966, pp. 324-329
42. Beneken, J.E.W., "Electronic analog computer model of the human blood circulation," in Pulsatile Blood Flow, McGraw-Hill, 1963, pp. 423-432.
43. Nabbefeld, N.C., "Hybrid computer modeling of cardiovascular dye-dilution experiments," MS Thesis, University of Wisconsin, 1968.
44. Rushmer, R.F., Cardiovascular Dynamics, Saunders, 1961, p. 50.
45. Galletti, P.M., "Dynamics of artifically supported circulation," in Engineering in the Practice of Medicine, W & W 1967, pp. 249-266.
46. Velichenko, V.V. "Optimal control for equations with discontinuous right-hand sides," Automatica i Telemekhanika, Vol. 27, No.7, 1966, pp. 20-30.
47. Spyker, D.A., "Gradient techniques of flight path optimization," MS Thesis, Purdue University, 1966.

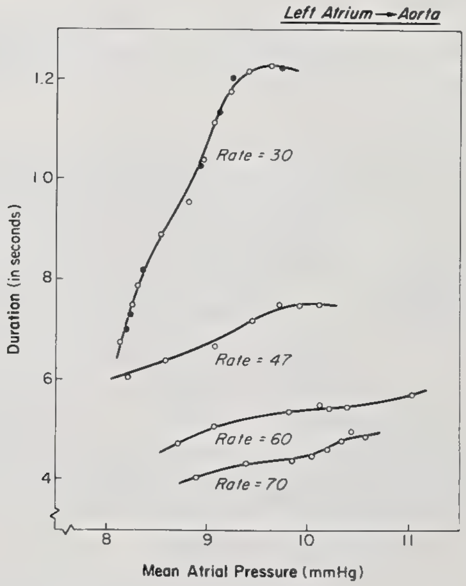

FIGURE 32. OPTIMUM DURATION VS ATRIAL PRESSURE (MINIMIZING FLOW WORK).

DISCUSSION

DR. HALL: I think one of the most perplexing problems, in trying to evaluate the various devices is the very fact that we do not have an adequate animal test model for heart failure. I want to congratulate the authors on the beautiful technique which they have evolved. I do want to ask one question of Dr. Bernstein; Do you think that if the bypass pump had a greater volume, you could obtain prolonged survivals?

Dr. BERNSTEIN: I could not predict the duration of survival, but we certainly felt that the rather limited capability of the pump in terms of volume flow restricted its potential benefits to the animal. As I indicated in the talk, the average pump flow rate was in the range of 2 liters per minute. These calves have a normal cardiac output of almost 8 liters per minute, so that the best this pump could do is in the range of 25% of normal output. And here, too, we imposed a very severe test for any support device. I am not sure that any device would be able to permit prolonged survival, but I certainly would agree with the suggestion that you are making, that a major factor was the limitation of pump flow.

DR. KWAN-GETT: My question touches a little on what Dr. Hall asked. I would like to ask Dr. Bernstein and other investigators who make assist devices, how do we know how much assistance we should give? You have an assist device that can take 25% of total flow. Some left heart bypasses can take 100% of total flow and so the natural heart may have no output. However, I do not think we have had any indication of how much assistance we should give. Should we keep the left atrial pressure normal so that we do not get pulmonary edema? Should we share the load or should we keep the blood pressure normal? Another question is: How long should we assist?

DR. BERNSTEIN: I can only sympathize with the question that you have asked; I think the answers obviously are not available. The question you asked is also one reason that Dr. Spyker began investigating the use of optimum control theory for the possible control of such a device. We obviously need good criteria of benefit and do not have them as yet.

DR. LaFARGE: My presentation will follow this paper, and it gives me an opportunity to comment on Dr. Bernstein's time rather than my own. In answer to Dr. Hall's question, the answer is certainly yes. I certainly agree with Dr. Bernstein that the amount of failure that you can relieve is dependent upon the volume capability of the pump. In other words, as long as the animal cooperates by only having 2 liters per minute of failure, then, he will be helped, and his failure will be reversed. As long as the failure was greater than the ability of the pump to relieve that fraction of the output, then the pump failed to reverse the failure. This was certainly true in the case under discussion.

CHAPTER 52

A PHYSIOLOGIC EVALUATION OF THE BAYLOR LEFT VENTRICULAR BYPASS

C. G. LaFarge & W. F. Bernhard
Surgical Research Laboratory
Children's Hospital, Boston
and
T. C. Robinson
Thermo Electron Corp.
Waltham, Massachusetts

An engineering and physiological evaluation of the Baylor left atrium-to-aorta assist device has been completed. Circulatory analog studies have been performed to analyze the hydrodynamic, mechanical, and electronic functions of the blood pump and its control system. The hemodynamic, hematologic, and pathologic effects of pump function in healthy calves has been studied in short- and long-term experiments. A total of 9 animal experiments have demonstrated that the device is capable of assisting the systemic circulation by a maximum of 2.5 liters/minute for periods up to 45 days, with an average of 20 days. Blood trauma was significant early in each study, but the hematocrit increased, and osmotic and mechanical fragilities decreased during the experiments. Effective pump function was terminated in these experiments by the development of a thick non-uniform fibrin layer on all the Dacron velour surfaces of the pump, preventing adequate pump filling and proper valve and diaphragm action.

INTRODUCTION

The Baylor Left Ventricular Bypass (BLVB) is a mechanical assist device designed to aid the patient in left ventricular failure by partial unloading of the left ventricle. This is accomplished by removing blood directly from the left atrium and returning it, in ventricular diastole, to the descending thoracic aorta, thus bypassing the left ventricle partially.

The study reported here was concerned with the evaluation of the BLVB in several phases: in an analog of the circulatory system, in short-term studies of hemodynamic effects in animals, and in long-term studies (3 to 44 days) of the hemodynamics and of the effect of continuous blood-pumping on hematologic and on other organ functions.

A two-fold purpose was served by this study; data were generated concerning the performance of the BLVB itself, and indirectly these data have contributed materially to an understanding of the behavior of cardiac-assist devices in general and of the criteria by which they should be designed, developed, and used.

MATERIALS AND METHODS

The Assist Device.

The assist device under consideration is illustrated in Figure 1. The pump has a clear Lexan shell in two parts which are held together by a threaded-steel ring: the lower half has an inlet and outlet tube, each of which houses a valve with a Silastic ball, with a Statham electromagnetic flow probe on the inflow side. Special Dacron-covered Silastic , steel spring-reinforced grafts are attached to each of these arms. The inflow graft is sutured to the left atrium, and the outflow graft is sutured to the descending thoracic aorta. In the interior of the lower half of the pump, a continuous lining of Dacron velour is cemented in place. A Silastic diaphragm covered internally with Dacron velour occupies the upper half of the pump shell, which in turn is attached by the air-drive line to the electropneumatic control unit. During the compression of the bladder, blood is delivered through the outflow line to the aorta, and during the vacuum phase, the pump is filled via the inflow line from the left atrium.

The control unit is simple to operate, is reliable, and provides the following: a control for unsynchronized or synchronized pumping from every heart beat to every 16 beats; an air pressure control and gauge for the pumping phase; a vacuum control and gauge for the filling phase; a calibrated control for regulating the duration of the ejection phase; threshold and delay controls for sensing of the R-wave of the electrocardiogram and for timing the activation of the pump at any selected interval in the cardiac cycle; a signal generator for triggering the assist device automatically should the ECG signal become unavailable; and manual controls for filling or emptying the pump during its implantation into an animal.

The monitoring unit contains the electronics for the electromagnetic flowmeter, an ECG amplifier, a cardiotachometer, and an uncalibrated oscilloscope for visual display of ECG, pressure and flow signals.

In Vitro Studies.

Since it is difficult, if not impossible, to control and measure all the parameters to be evaluated in an animal experiment, a circulation analog provides an opportunity to look individually at the effects of changing "cardiac" parameters as well as to evaluate the effect of individual variations in the control parameters and to determine the optimum control settings. For this purpose, the BLVB was attached to an analog circulation, as illustrated in Figure 2. A modified Hydrospace mock loop was used. Basically, it consists of Harry Diamond Laboratory analog left and right ventricles, left and right atria, and analog vascular systems including resistance and compliance networks for the pulmonary and systemic circuits. It is regulated by a control system using arterial pressure feedback circuits. Electromagnetic flowmeters were used to measure flow from the "left ventricle" as well as from the "pulmonary artery", the latter measuring the analog of total cardiac output. Assist device inflow was monitored by the Statham meter on the BLVB. Sanborn 267 B pressure transducers were used to measure aortic, left ventricular, left atrial, internal BLVB, and air drive pressures. These monitored parameters were recorded on a 4-channel Sanborn direct-writing system.

In addition to the studies of control and analog circulation relationships, assessment was made of the "on and off" effects of the pump in the normal analog state, in left ventricular failure, and during various "arrhythmias". These latter two states were of particular interest, since they are difficult to evaluate in the living animal. From these studies, it was possible to predict with considerable accuracy the behavior of the BLVB in subsequent animal experiments, as will be illustrated.

Functional Analysis.

The circulation analog was further modified, as in Figure 3, to permit detailed evaluation and characterization of BLVB function in the form of parametric relationships between control system parameters and BLVB output. Lumped parameter resistance and compliance elements were used everywhere except for the simulated aorta, where a distributed parameter element was provided along with a lumped compliance. Mean aortic flow was measured directly by means of a stop watch and graduate. An engineering analysis of the control and monitoring units was also performed in order to characterize their performance. The design and operation of each major component of these units were analyzed. From this analysis, adequacy and range of performance, and reliability were determined.

Surgical Implantation

Calves were used for this study except for one experiment with a miniature pig. Prior to surgery, the animal was anesthesized with intravenous pentobarbital sodium (25 mg/kg), and maintained by Halothane. Additional muscular relaxation was maintained by the use of Flaxedil, 1.0 ml, repeated as necessary. Respirations were controlled with a Bennet positive-pressure ventilator. The calves ranged in weight from 80 to 100 kg.

A left postero-lateral thoracotomy was made and the chest was entered through the left fifth intercostal space. The left lung was retracted medially and the descending aorta exposed at a point exactly opposite the base of the left atrium. The pleura over the aorta was incised for a distance of 4 cms and a partially-occluding vascular clamp was placed on the aorta to permit suturing of the arterial limb of the pump. The Dacron graft of the arterial limb was trimmed so that approximately 1.0 cm of the graft was left for the anastomosis with 4-0 Tevdek sutures. After completion of this suture line, a clamp was placed across the arterial tube and the vascular clamp removed, thereby achieving hemostasis at the suture line. When this was accomplished, the vascular clamp was again applied and all clots were evacuated from the lumen of the outflow tube.

The lung was next retracted laterally and the pericardium opened above and parallel to the left phrenic nerve. A vascular clamp was placed on the left atrial wall for a distance of approximately 4 cms. An incision was made and the atrial limb of the inflow graft was sutured in position. This anastomosis was carried out in such a manner as to leave approximately 5 mms of the atrial tube projecting into the lumen of the left atrium. A running 4-0 Tevdek suture was utilized for the first layer of the anastomosis, followed by a second running suture of 5-0 arterial silk. The final step in the prescribed procedure was the application of a single coat of Eastman-910 adhesive to seal the anastomosis further.

The clamp was removed from the posterior wall of the left atrium and blood aspirated up into the tube. All bleeding points were stopped with sutures of 5-0 arterial silk. The vascular clamp was then reapplied and all blood aspirated from the atrial tube. At this point in the procedure, the animal was anticoagulated, using 1.5 mg/kg of heparin.

The BLVB was then connected to the atrial and arterial grafts and all air was evacuated from the pump, using carbon dioxide gas at a flow of 6 L/min. Approximately 2 minutes were allowed for this procedure, following which the pneumatic driveline was connected to the dome of the pump and the bladder was compressed. After the removal of the arterial clamp, allowing blood to enter the arterial tube, the atrial clamp was removed to permit blood to enter the pump from that chamber. Active pumping then began. A #30-French catheter was then placed in the left pleural space for drainage, the fifth and sixth ribs were approximated and the chest closed in routine fashion.

The calves used in acute studies were continued on heparin throughout, and the first two chronic implantations (Figure 4) were heparinized during the first 24 hours. All subsequent animals received heparin only during the surgical implantation procedure.

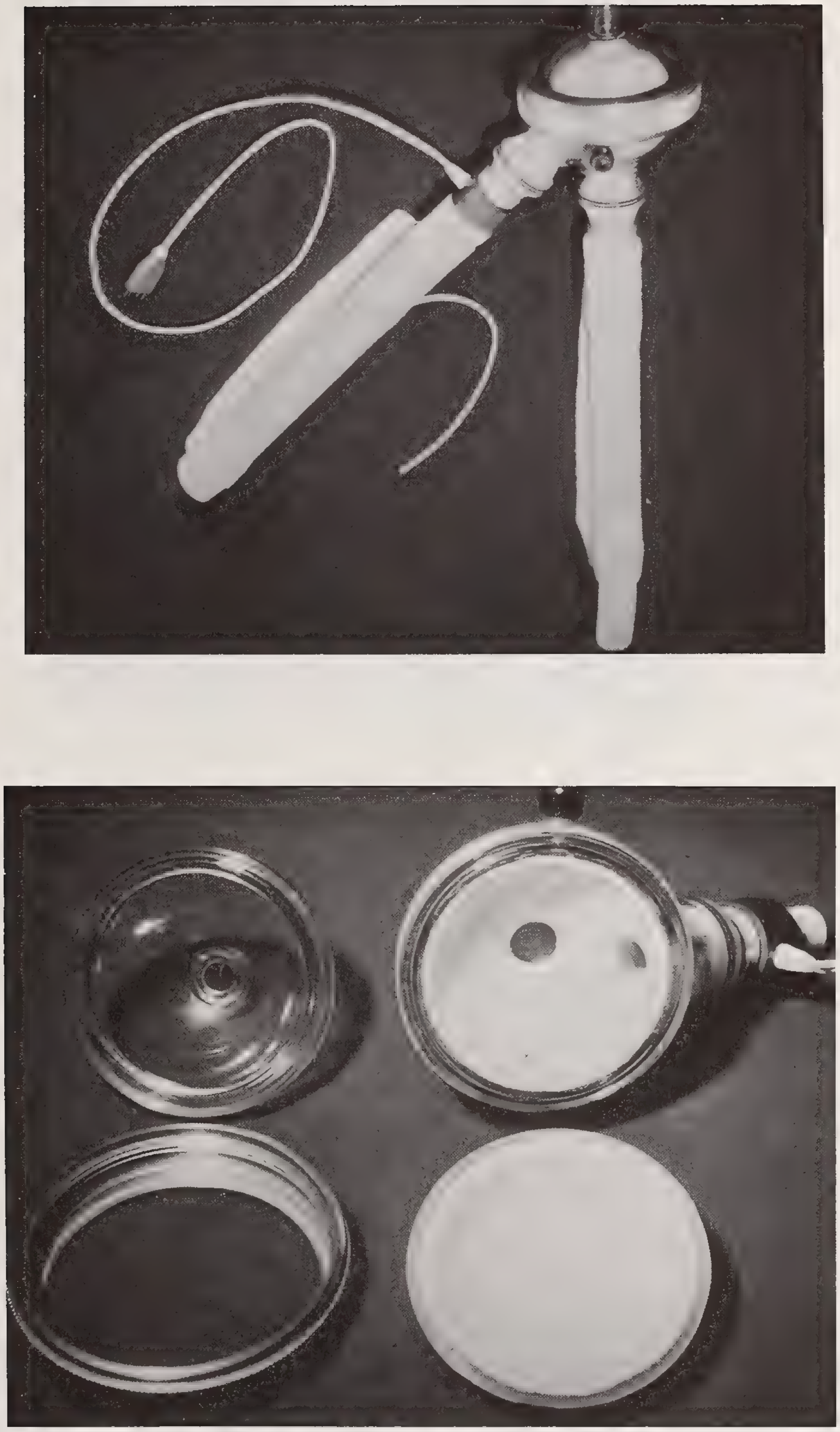

FIGURE 1. A AND B. BAYLOR LEFT VENTRICULAR BYPASS.

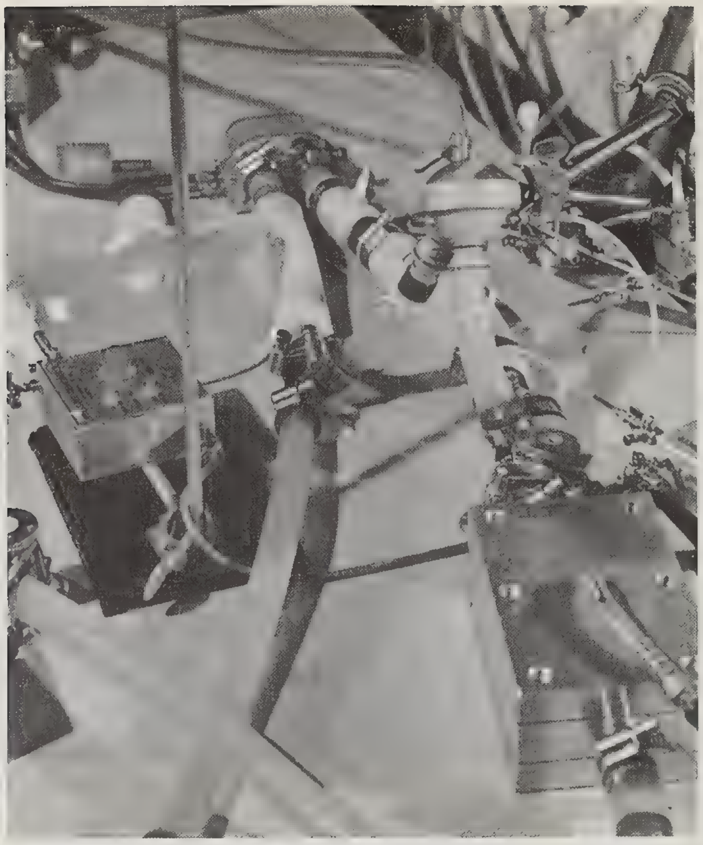

FIGURE 2. BLVB ATTACHED TO AN ANALOG CIRCULATION.

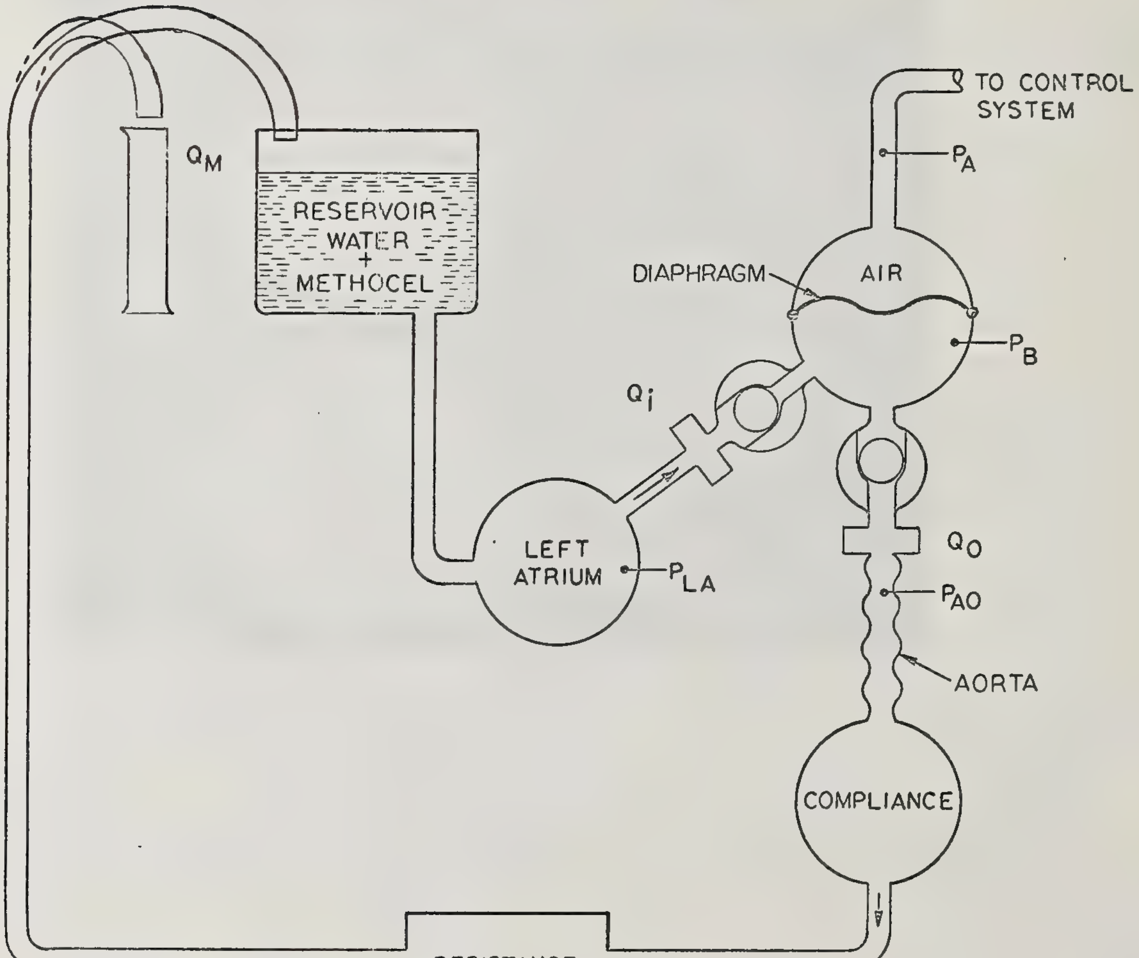

FIGURE 3. MODIFIED CIRCULATION.

Acute In Vivo Studies.

For the purpose of evaluating the hemodynamic effects of the pump on flows and pressures during variations in control parameters, pumps were implanted in three animals for periods of 3 to 6 hours: one of these animals was a miniature pig, the other two were calves. For this phase of the study, the monitoring equipment consisted of an 8-channel Sanborn direct-writing recorder and oscilloscope. Inputs were derived from 4 or 5 pressure transducers, an ECG, and two or three other signal sources. Among the latter were the Colsen densitometer (dye dilution cardiac output), the Carolina Medical Instruments' square-wave electromagnetic flowmeter, the Statham air-drive pressure and stroke volume signals, and thermistor temperature probes. In all animal studies, venous and arterial catheters were inserted into the right atrium, ventricle, or pulmonary artery for blood sampling and measurements of pressure, as well as for injection of indocyanine dye for cardiac output curves. Arterial catheters were placed in the left ventricle, left atrium and aorta. Another connection was made to the pumping chamber of the BLVB.

Chronic In Vivo Studies.

Implantation of the BLVB was carried out in six animals for extended periods of time (3 to 44 days) with continuous pumping. Nine pumps or pumping diaphragms were used in this phase of the evaluation. Periodic assessment was made of flows and pressures, phonocardiograms, and ECGs, with the animal awake and resting. In addition to these hemodynamic parameters, a wide variety of hemotologic and other organ function data were obtained. They included hematocrit, red and white blood cell counts, hemoglobin, mean corpuscular hemoglobin content and concentration, reticulocytes, platelets, mechanical and osmotic fragilities, plasma hemoglobin, osmolarity, serum sodium, potassium, and chloride, blood urea nitrogen, lactic acid dehydrogenase, serum glutamic oxaloacetic transaminase, bilirubin, fibrinogen, prothrombin and partial thromboplastin times, and thromboelastogram.

Of the nine experiments performed, one was terminated because of acute separation of the pump from its graft, two because of separation of the Dacron velour from the Silastic bladder, one because of clotting secondary to an electrical failure, and the other five because of clotting of the BLVB and its grafts. In each of these latter five instances, the experiment was terminated when the maximum pump output fell below 0.5 L/min. The animal was sacrificed, a detailed post-mortem examination done, and sections sent for microscopic analysis of organs. The pump itself was disassembled, photographed, and preserved.

RESULTS

Circulation Analog Dynamics.

The performance of the BLVB in the circulation analog is illustrated in Figure 5. Pulmonary flow, representing total cardiac output, is denoted by the letter P, systemic flow by the letter S. The difference between them represents the output of the BLVB. On the left of the figure the pump is off; on the right; it is on. Total cardiac output (P) is essentially unchanged whether or not the pump is actuated. Systemic flow, initially equal to pulmonic flow, is reduced by 1.2 L/min, which represents the output of the BLVB. There is essentially no change in either atrial or arterial pressures, and the left ventricular peak pressure is reduced by 25 to 35 mmHg. These findings are quite typical of those seen in acute animal experiments.

"Left ventricular failure" was induced by the simple device of decreasing ventricular drive pressure from 16 to 10 psi, as illustrated in Figure 6. Concomitantly, the BLVB was turned off. Analogously, the cardiac output fell, and left atrial pressure rose from 2 to 10 mmHg. Aortic pressure also fell slightly. When the BLVB was reactivated, as illustrated in Figure 7, the left atrial pressure immediately fell from 9 to 1 mmHg, while aortic pressure remained substantially unchanged. Cardiac output, on the other hand, rose from 2.2 to 3.3 L/min. It is also important to remember that during this recording, the right ventricular output remained unchanged. The significance of this will be discussed below.

During experiments in which "arrhythmias" were induced, similiar observations were made. In the case of total cessation of cardiac function (as in fibrillation or standstill), illustrated in Figure 8, the expected events took place: cardiac output dropped and left atrial pressure fell to levels below zero (minus 1 mmHg), while right atrial pressure rose from one to 8 mmHg. In this example, the "pulmonary capillary resistance" was held at zero units, and the pulmonary arterial pressure of 8 mmHg was sufficient to provide adequate filling of the BLVB and maintenance of a cardiac output of 2.8 L/min. In a subsequent experiment, the pulmonary resistance was gradually increased until the pulmonary artery pressure reached 16 mmHg, with only a slight decrease in total flow. At higher resistances, pulmonary flow gradually ceased, and, consequently, the BLVB became non-functional. This phenomenon was also seen in an animal experiment, to be discussed below.

Functional Analysis.

Control system function does not directly determine the stroke volume of the assist device. The control parameters which can be selected are filling vacuum ejection or air-drive pressure, and ejection duration and rate. Delay and heart rate-to-pump rate ratio can be selected for pump synchronization with the electrocardiogram. The stroke volume, one of the essential parameters of pump function, is indirectly determined by two sets of conditions: by filling time and filling pressure or vacuum, and separately by emptying time or ejection duration and ejection pressure. Reliable pump

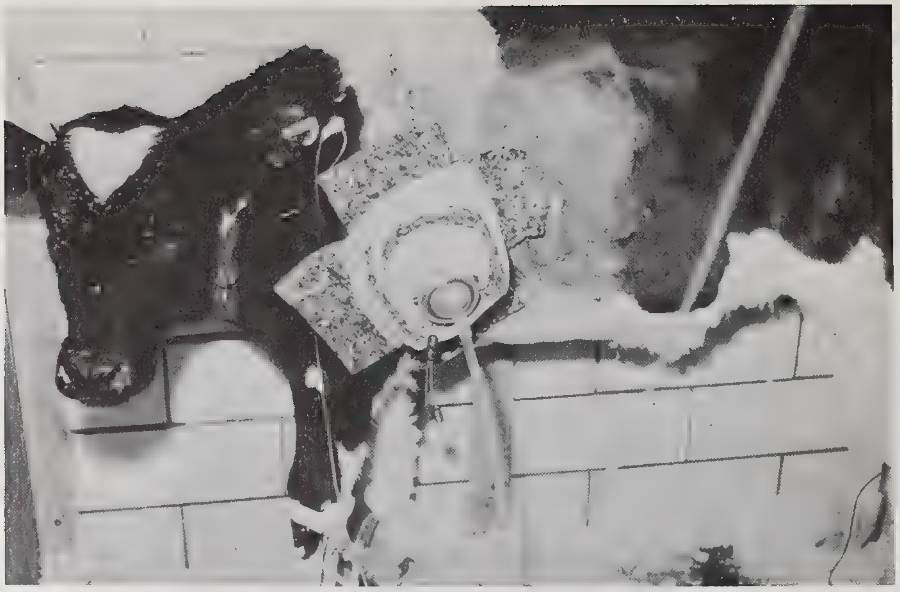

FIGURE 4. CHRONIC IMPLANTATION IN CALF.

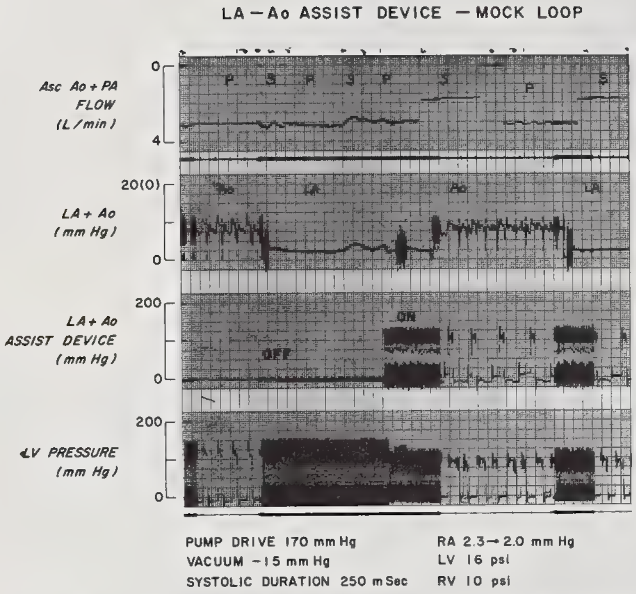

FIGURE 5. PERFORMANCE OF BLVB IN THE CIRCULATION ANALOG.

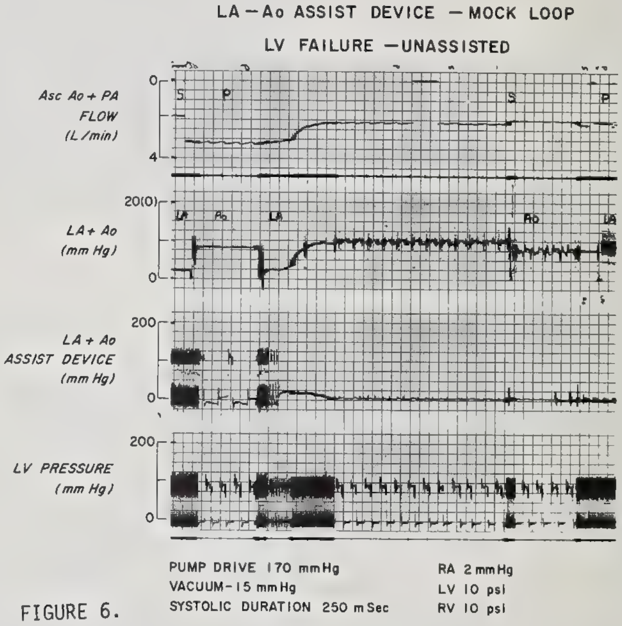

FIGURE 6.

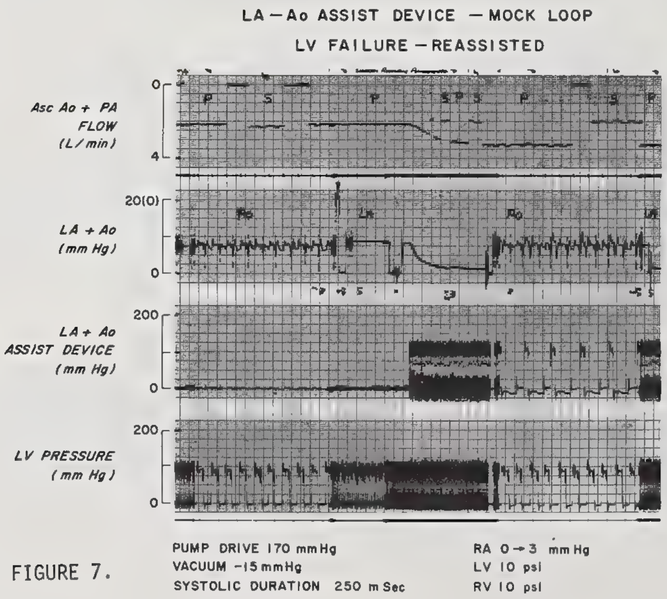

FIGURE 7.

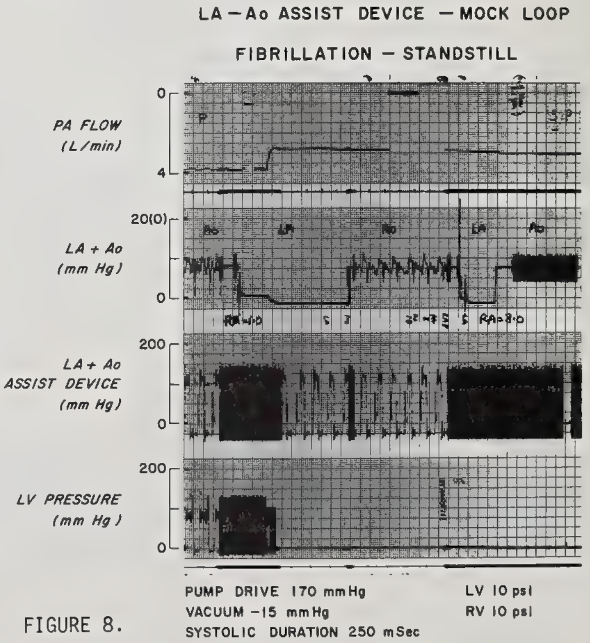

FIGURE 8.

function at approximately constant volume has been possible on the mock loop and in healthy animals for small changes in synchronized pumping rate, provided that the pump was permitted to fill completely and that ejection pressure and duration were chosen to prevent complete diaphragm collapse. This, the most stable mode of operation, results from filling the pump completely during each pump cycle and was used in all animal and mock loop studies.

The impedance presented by blood flow through the pump is largely resistive, except at very short ejection or filling durations when inertial effects become significant. The resistances to flow through the inflow tube and valve, and through the outflow tube and valve, are shown in Figure 9 with pressure drops proportional to the square of the steady flow rate.

In Figure 10, pump diaphragm compliance is shown to be small, less than 10 mmHg from completely filled (at 0 pumping chamber pressure differential) to an end-ejection volume of about 40 ml.

The pump stroke volume varies approximately linearly with duration for the primarily resistive flow impedance at any fixed pressure differential. Stroke volume has been determined as a function of duration and the range of pressure differentials for both the ejection and filling phases, thus characterizing pump and control system performance.

Figure 11 shows a typical plot of stroke volume versus ejection durations selected on the control system. A maximum stroke volume is reached; with longer durations the stroke volume is decreased due to inflow valve leakage from the pump to the left atrium.

Figure 12 shows a family of such measured constant pressure curves which characterize pump ejection. The pressure differential for each curve is the air-drive pressure measured on the control system gauge minus the mean aortic pressure set at 90 mmHg. Neither these pressures nor their difference varied more than a few mmHg during ejection. It is seen that a maximum ejection stroke volume of 46 to 50 ml can be obtained at ejection durations of 200 to 500 milliseconds, requiring air-drive pressures of 130 to 220 mmHg. Vacuum was adjusted in all cases to the minimum level required to completely fill the pump.

Figure 13 shows a typical plot of stroke volume versus measured filling duration at a fixed filling pressure differential.

A family of measured constant pressure curves which characterize pump filling is given in Figure 14. The filling pressure differential is left atrial mean pressure minus control system filling pressure read from the vacuum gauge; this differential changes negligibly during pump filling. It is seen that a maximum pump stroke volume of 46 to 50 ml is achieved at 350 to 800 ms filling durations, requiring 20 to 80 mmHg vacuum.

The important components of the gas or pneumatic drive unit and our experience with their function for approximately 140 days of total operation are given in Table 1.

TABLE 1

CHARACTERISTICS OF STATHAM CONTROL SYSTEM COMPONENTS: DRIVE UNIT

Component	Function	Remarks
Compressor and Vacuum Pumps, Reservoirs, and Servoregulators for Pressure Selection	To provide high and low pressure source and sink to empty and fill pump	Pressure and vacuum regulation ± 5% Good readibility and selectability of levels No cross-coupling below 2000 ml/min pump flow rate, or levels of vacuum ± 20 mmHg No failures
Solenoid Valve and Electronic Drive	To switch between high and low pressure reservoirs	Approximately 8 ms response time; less than 10% of duration rise time at usual chronic pumping conditions No failures
Rate and Duration Controls	Select pumping rate and pump ejection duration	Calibration within 5% or 10 ms/min duration error Good readibility and selectability Rate control on side panel somewhat inconvenient No failures
Redundant System	Back-up for electronic control circuitry and switching solenoid	Occasional unexplained switching to redundant system No failures

In brief, this unit has been reliable and performed as intended by the designers. No failures have occurred. Calibrations have been sufficiently accurate in acute and chronic studies; the range of pressure, vacuum, rate, and ejection duration is adequate; the ease of selection and readability of these parameters is good; the operation of the unit is predictable and quiet. Cross-coupling between

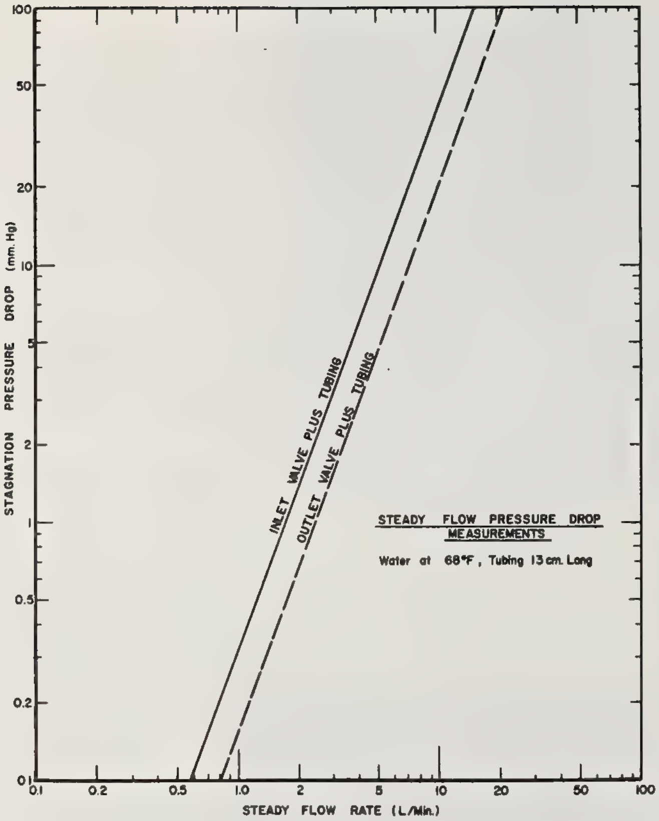

FIGURE 9.

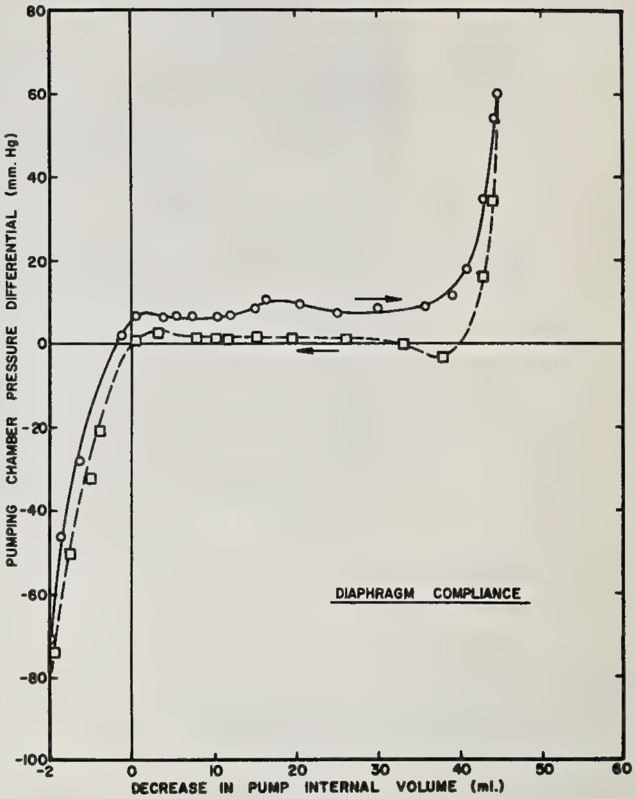

FIGURE 10.

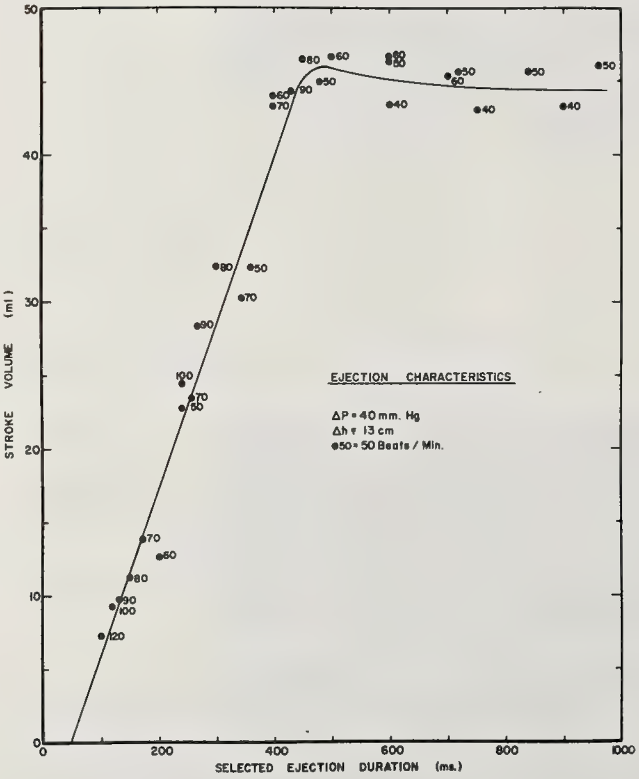

FIGURE 11.

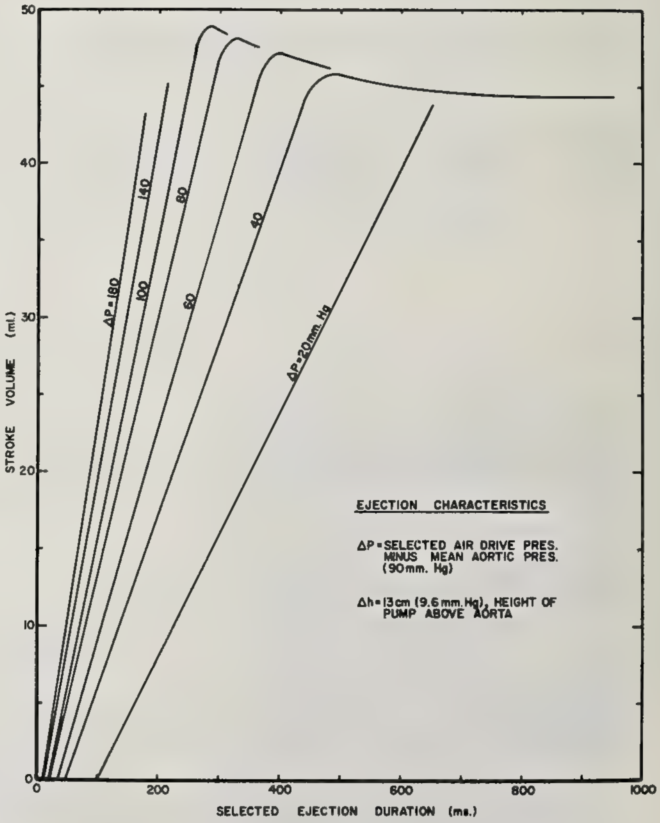

FIGURE 12.

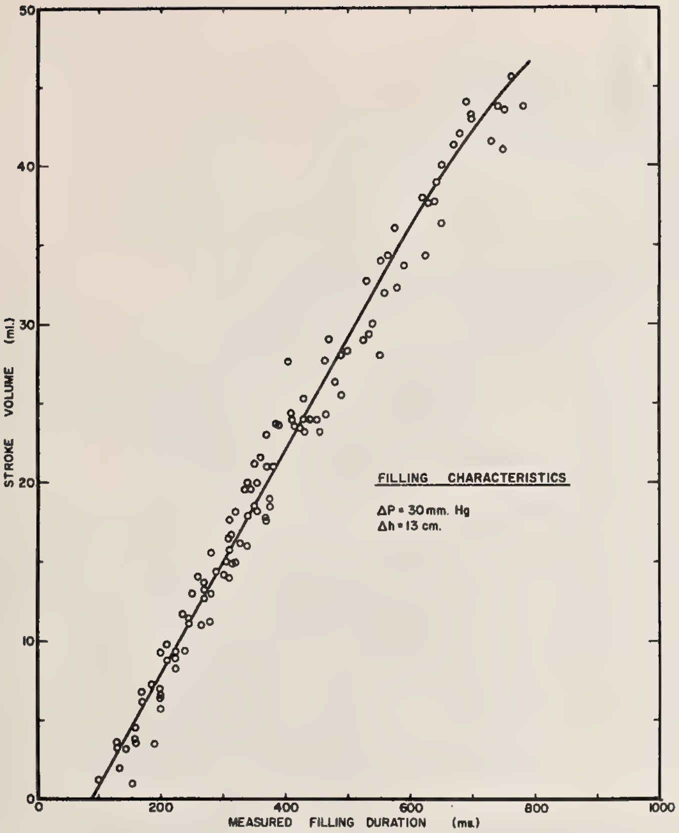

FIGURE 13.

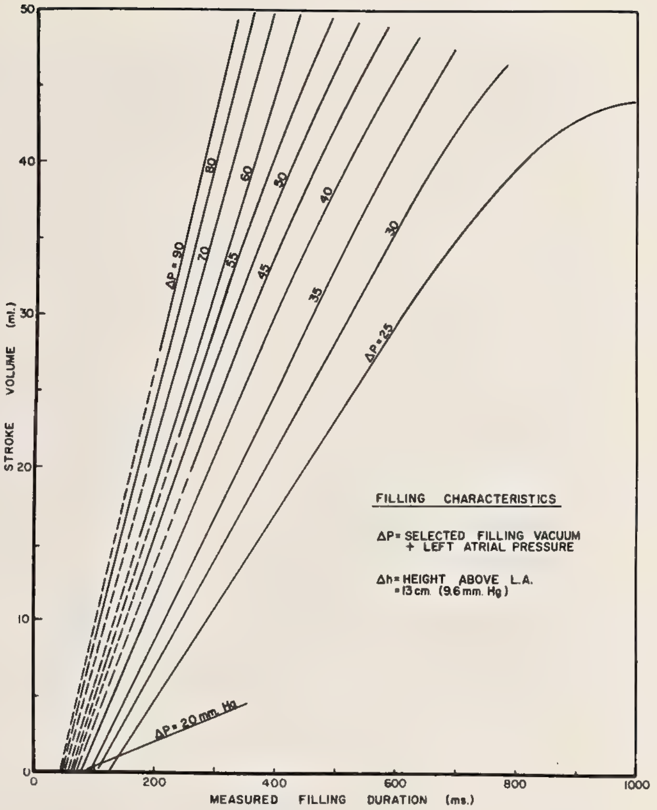

FIGURE 14.

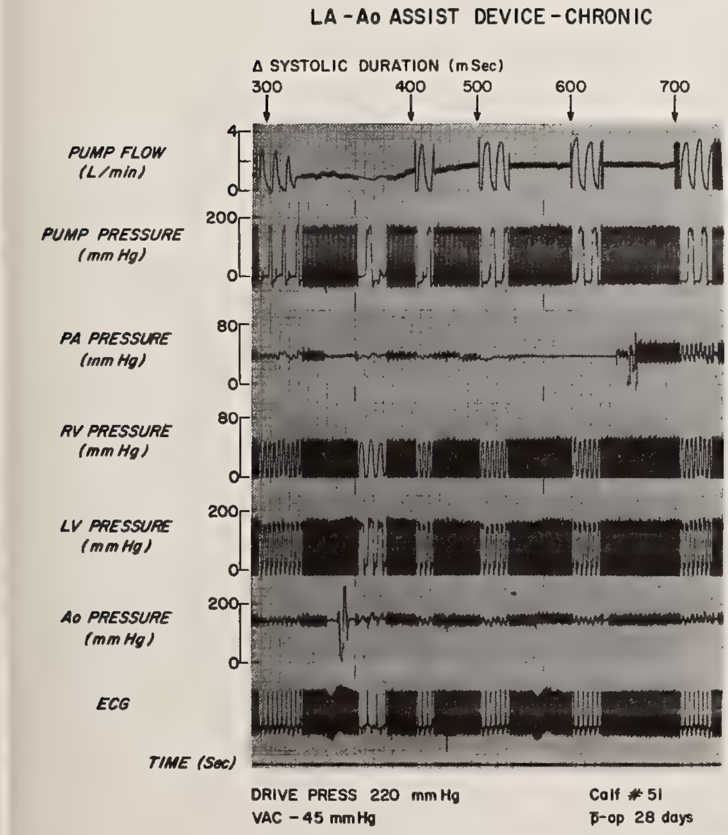

FIGURE 15.

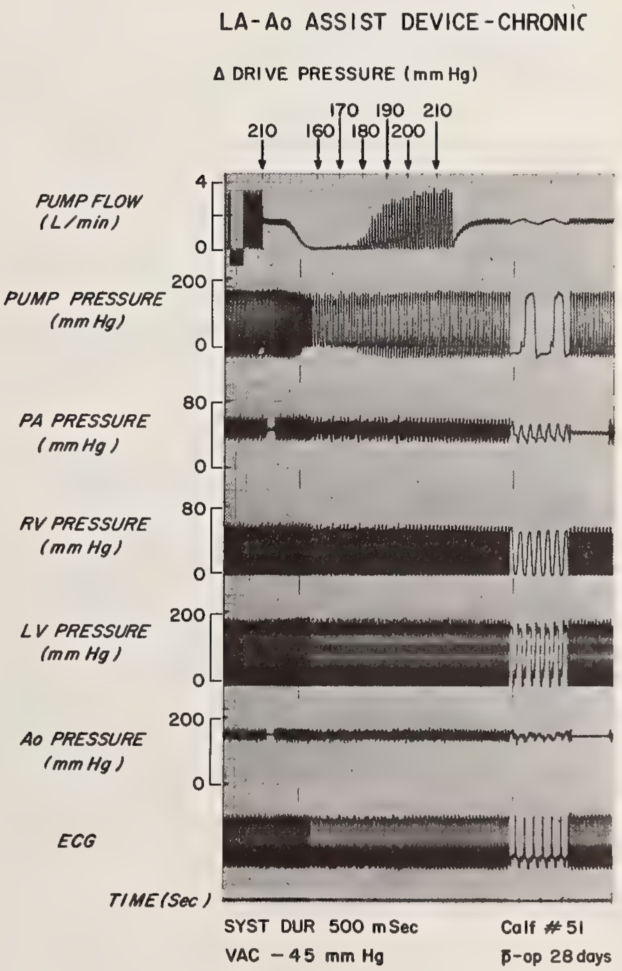

FIGURE 16.

pressure and vacuum supplies occurs only at the extreme settings such as high vacuum and high pressure at large pump flow rates. These extremes have not been reached in acute or chronic animal experiments.

Table 2 summarizes some problems which have been encountered with the major components of the monitor unit.

TABLE 2

CHARACTERISTICS OF STATHAM CONTROL SYSTEM COMPONENTS: MONITOR UNIT

Component	Function	Remarks
Electrical Power Supplies	To supply power to all control system components	1 failure of main power supply 1 failure of oscilloscope power supply
Oscilloscope	To monitor control system variables and other selected inputs	No calibrations; qualitative monitoring only No failures
ECG Amplifier, R-wave Detector, Cardiotachometer	To monitor ECG, trigger drive unit synchronously, and read heart rate	1 repair at Statham 1 replacement at TECO Complicated R-wave detection and Triggering controls
Electromagnetic Flowmeter and Amplifier	To monitor input flow to assist pump	1 repair at Statham 1 replacement at TECO Ground loop problem prevented simultaneous flow monitoring and ECG triggering was repaired but use of other instrumentation can make this problem recur.

The most serious problems were associated with the ECG and flow amplifiers. Failures of these components occurred and a ground loop problem prevented simultaneous pump inflow monitoring and ECG triggering of the assist device when other instrumentation was used. These problems did not seriously affect the safe operation of the assist device.

Acute In Vivo Studies.

In acute animal experiments, evaluation was made initially of the effects on pump performance of altering the important control parameters (systolic duration, drive pressure, filling vacuum, and activation frequency). These are illustrated in Figures 15 through 18.

Figure 15 illustrates the effect of increasing the duration of pumping at constant heart and pump rates. The only substantial change is an increase in total flow pumped by the BLVB, with the optimum for these conditions occurring at a systolic duration of 500 msec duration.

The effect of a change in the air-drive pressure is illustrated in Figure 16. Optimum air-drive pressure in this animal is just above 200 mm Hg, with an output at that level of 1.6 L/min. Note also that during the time when the pump was not active (160 mm Hg drive pressure), the vacuum effect was also not seen in the pump pressure recording. No other substantial change in pressure is seen.

A change in filling vacuum, illustrated in Figure 17, produces the expected result; a cessation of pump filling in this instance at levels below -20 mm Hg, with no other substantial change. Optimum filling pressure (vacuum) at this point lies below -40 mm Hg.

The predictable effect of increasing the heart-to-pump rate ratio is illustrated in Figure 18. A minimum flow of 800 ml per minute is pumped by the BLVB when operating every seventh cardiac cycle. Gradually increasing the frequency of activation, the optimum pump output of 1.7 L/min is achieved with an activation of every third cardiac cycle. This is not usually the case with a "fresh" pump, where the optimum ratio is 2:1. This animal, however, was 28 days post-operative, and the pumping diaphragm had become relatively non-compliant.

Table 3 summarizes pump operation and gives the maximum output conditions. The pumping rate is determined by the sum of the ejection and filling durations.

TABLE 3

BLVB CHARACTERISTICS

Max. Stroke Volume	46-50 ml
Min. Ejection Duration . .	200 ms
Min. Filling Duration. . .	350 ms
Max. Pumping Rate.	100 bpm
Max. Mean Flow Rate. . . .	4.8 L/min

Other considerations determine the maximum pumping rate and output for animal experiments. Large negative left atrial pressures during pump filling cannot be tolerated (cavitation hemolysis inflow tube occlusion by atrial wall) and necessitate moderate levels of vacuum and filling duration. Very short ejection durations at full stroke volume may result in significantly increased blood damage (Waring Blender syndrome). Pump stroke volume was not permitted to reach the maximum because the diaphragm touching the walls of the pump may abrade the autologous lining and increase blood damage. Thus pump output during in vivo studies has been maintained below 2.7 L/min, below 45 ml stroke volume and below 60 beats/min.

As discussed earlier in relation to the circulation analog, studies of flow and pressure were made in the acute animal experiments. An example is illustrated by Figure 19. The optimum settings for this pump were found, and the activation ratio was best at 2:1, or every other cardiac cycle. Total cardiac output was 3.6 L/min, with 1.5 L/min ejected into the aorta directly by the left ventricle, and 2.1 L/min bypassed through the pump. Comparing the two periods of inactivation with the periods of activation, there is reflected in left ventricular peak pressure a reduction of 11% on the alternate beat prior to which atrial volume was accepted by the pump. No significant change is noted in aortic, left atrial or right ventricular pressures.

The extent to which the left ventricular peak pressure may be decreased by pumping is dependent upon the ability of the BLVB to accept a large portion of the cardiac output. In Figure 20, drawn from the acute experiment with the miniature pig, the total cardiac output was 2.2 L/min, of which the pump, ejecting essentially every other beat, accepted from zero to 80% of the total stroke volume, depending upon the timing of pump filling. Thus, left ventricular pressure (I) is reduced by 50% (90 mm Hg control to 45 mm Hg) every other cycle during which the pump accepts this large proportion of the left ventricular stroke volume (15 ml pump, 20 ml pig).

On the left-hand side of the illustration, the left ventricular pressure recording reflects the characteristics of the effect of varying the delay, the time between the "R"-wave of the ECG and the onset of pump ejection. Optimum pumping begins with isometric ventricular diastole and ends with isometric ventricular systole.

Two examples of the effects of serious arrhythmias are shown in Figures 21 and 22. Twelve minutes after the activation of the pump during its implantation, a previously-repaired air leak in the inflow graft leg of the pump reopened, and allowed air to enter the system. This was corrected immediately, but air entered the coronary arteries, and the ventricles began to fibrillate. The curious feature of the fibrillation, illustrated in Figures 21 and 22, is that the atria continued to contract. This is reflected in the artifact in the left atrial and ventricular pressure tracings.

The left-hand panel of Figure 21, recorded after 3 hours of continuous pumping during fibrillation, illustrates the acute cardiac failure that ensues when pumping is discontinued. Left atrial pressure rises from 4 to 20 mm Hg. Cardiac output drops to zero, aortic pressure drops to very low levels, while left-ventricular and pulmonary-arterial pressures increase slightly due to the continued activity of the atria. The cardiac failure thus induced is relieved by reactivation of the BLVB. The cardiac output (maintained by the device) is 2.2 L/min, as illustrated in the right panel of this illustration.

The direct contribution of the atria to the filling of the BLVB is illustrated in Figure 21. With the ventricles fibrillating and the atria contracting, atrial fibrillation was electrically induced in the center of the illustration. Left atrial pressure fell rapidly to -20 mm Hg, and pulmonary artery pressure began to fall, as did aortic pressure, reflecting decreased efficiency of the pump. With spontaneous return of the left atrium to sinus rhythm, the situation is corrected. This figure emphasizes the well-known fact that, in the absence of right heart function and in the presence of normal or elevated pulmonary vascular resistance, the return of blood to the left side of the heart will not be adequate for filling of a left ventricular assist device.

Once again, the implications of the circulation analog study in terms of ventricular failure and fibrillation were borne out in the animal experiments.

Chronic In Vivo Studies.

During the six chronic animal experiments (3 to 44 days), a number of studies were conducted to evaluate control parameters and the function of the BLVB. One study, conducted 28 days postoperatively, was illustrated in Figures 17 through 20. Another example, taken from the same animal, is illustrated in Figure 23. It is included here because it represents the pattern seen in all of the experiments: as the interior of the BLVB and its grafts accumulate clot, there is progressive obstruction of flow and a gradual diminution in bladder compliance. Initial flows in this experiment were 2.3 L/min, falling to 1.6 L/min after 28 days of pumping, and, as in Figure 23, to 1.2 L/min after 40 days. Also illustrated are the loud ejection and filling murmurs which were recorded, representing the obstruction of blood flow by the presence of thrombus. Four days later, the flow was recorded at 0.5 L/min, and the experiment was discontinued. In Figure 23, the pump is operating asynchronously. At comparable rates, no difference was noted in the output of the pump or the effect on left-ventricular or aortic pressures during synchronous versus asynchronous pumping, either acutely or chronically, in any experiment.

LA-Ao ASSIST DEVICE-CHRONIC

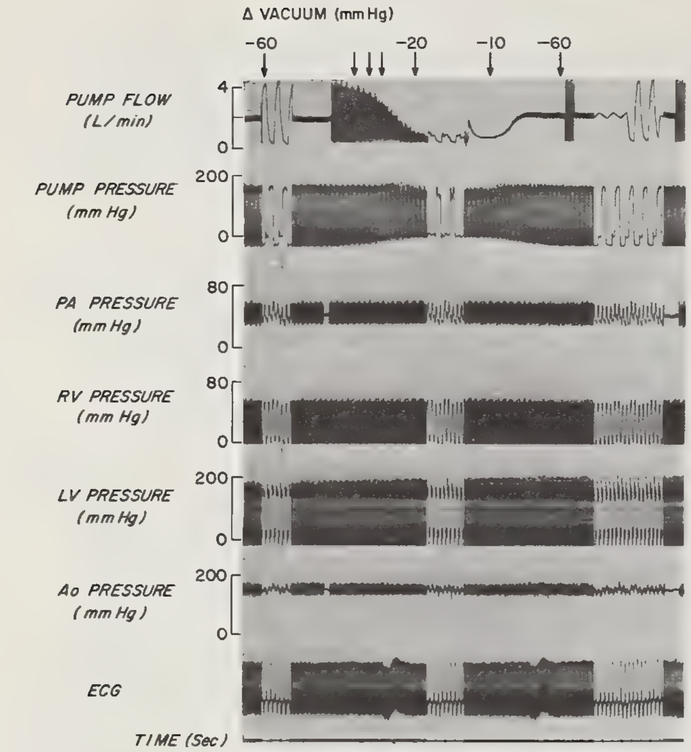

SYST DUR 500 mSec
DRIVE PRESS 220 mmHg

Calf # 51
p̄-op 28 days

FIGURE 17.

LA-Ao ASSIST DEVICE-CHRONIC

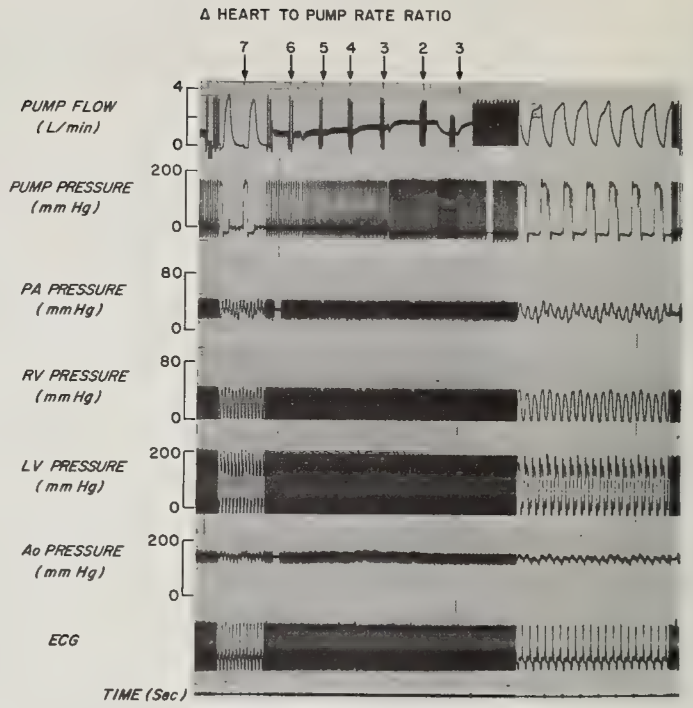

SYST DUR 500 mSec HR-150/min
DRIVE PRESS 220 mm Hg RR-30/min
VAC-45 mm Hg

Calf #51
p̄-op 28 days

FIGURE 18.

LA-Ao ASSIST DEVICE-ACUTE

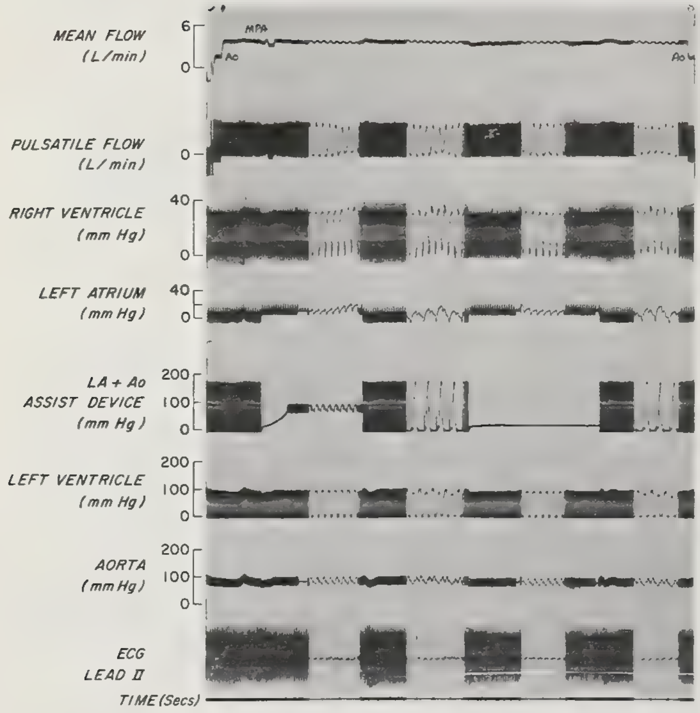

PUMP DRIVE 205 mm Hg
VACUUM -40 mm Hg
SYSTOLIC DURATION 150 m Sec

FIGURE 19.

LEFT ATRIUM TO AORTA IN-PARALLEL ASSIST DEVICE

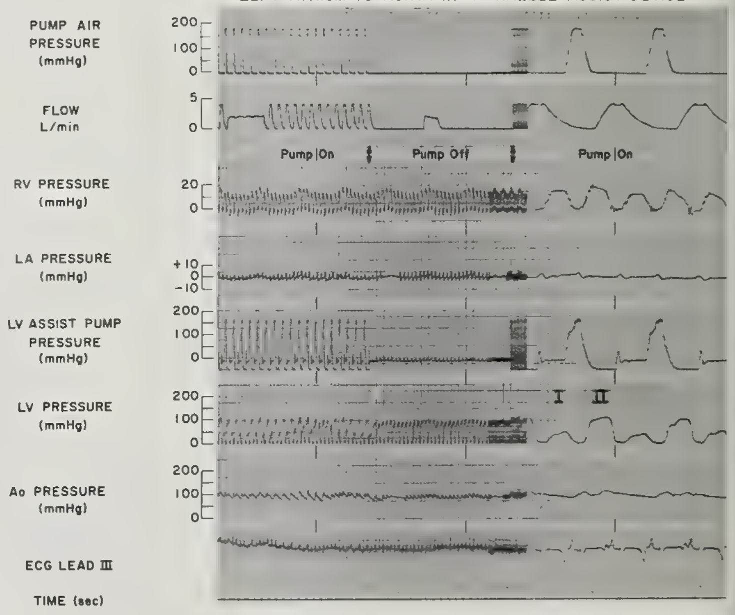

Systolic Duration......200m Sec
Delay................Random
Pump Stroke Volume ... 39ml

Pump Air Pressure....270mmHg
Pump Filling Vacuum...-50mmHg

FIGURE 20.

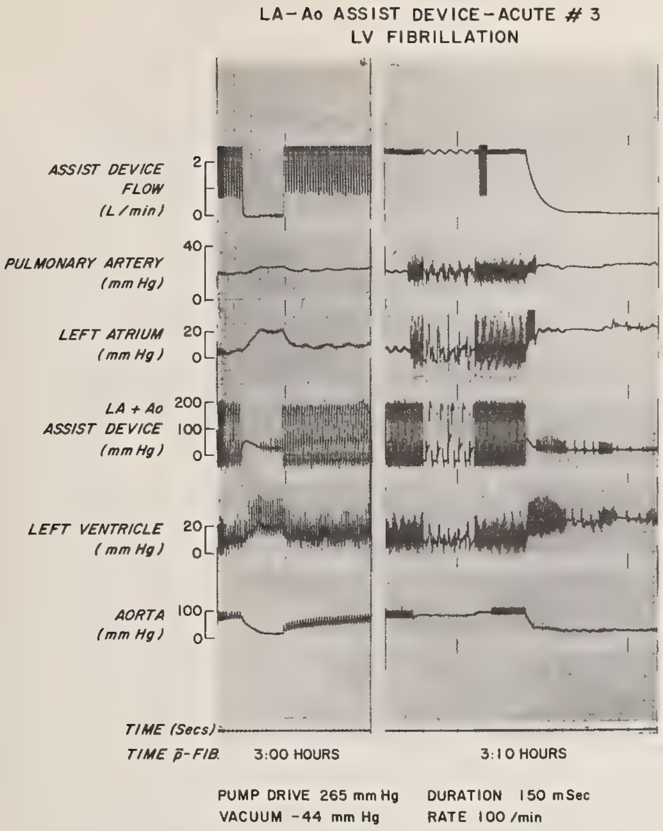

FIGURE 21.

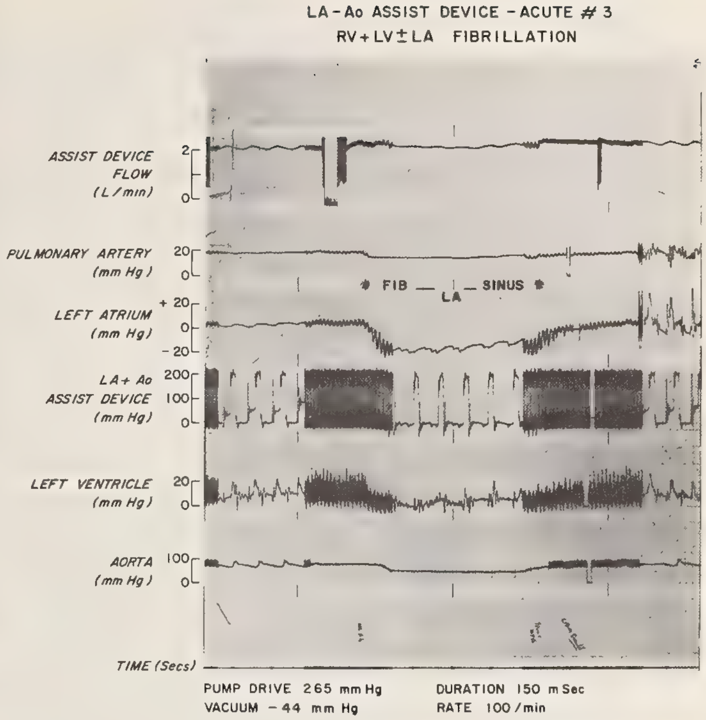

FIGURE 22.

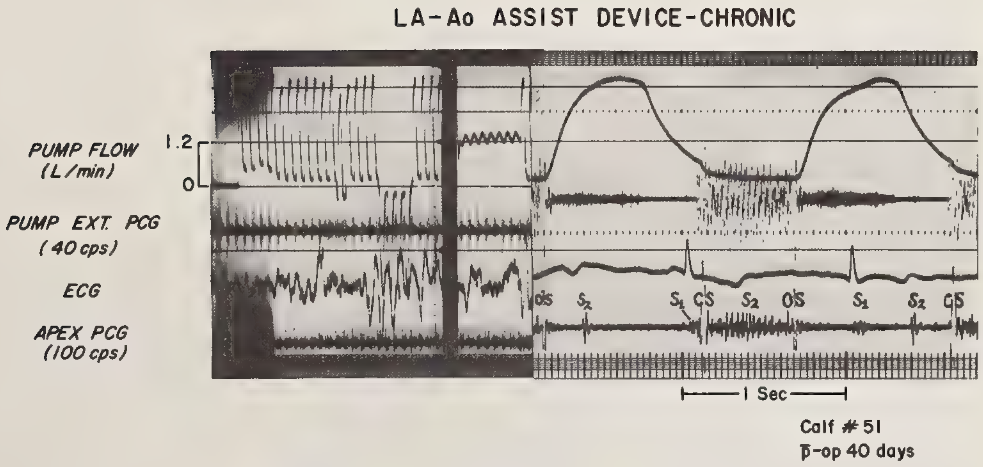

FIGURE 23.

Hematologic and Organ Function Data.

Of all of the quantities measured (see Methods), only four remain abnormal after the immediate post-operative period, especially when compared with similar data taken in sham-operated animals: hematocrit, incubated osmotic fragility, mechanical fragility, and red blood cell survival time. Other quantities, such as SGOT, may remain abnormal for the first two weeks after surgery, but return to normal levels after that point.

The hematocrit remains somewhat low and the red blood cell survival time continues to be somewhat shortened up to the maximum pumping time of 44 days observed in this study. The red blood cell fragilities also remain somewhat abnormal, but tend to return toward normal levels after 3 weeks.

Post-Mortem Studies.

The principal pathological problem encountered was the formation of layers of thrombus within the Baylor Left Ventricular Bypass Pump during chronic studies. All of these studies were performed without anticoagulation (Table 4).

TABLE 4

LA-AO ASSIST DEVICE

Calf #	Time Pumping	Heparin*	Comment
5-A1	6 hours	Yes	Acute, unsynchronized
69-A2**	6 hours	Yes	Acute, synchronized (pig)
47-A3	3 hours	Yes	Acute, inflow air leak Ventricular fibrillation
48-C1	3 days	24 hours	Rapid clotting: pump, valves, grafts; sacrificed.
49-C2	4.5 days	24 hours	Inflow graft clot; separation of pump and outflow; sacrificed.
51-C3	44 days	***	Acute study (28 days) Total pump clotting; sacrificed.
67-C4	9 days	***	Inflow graft clot; sacrificed.
70-C5A	8 days	***	Velour-Silastic separation. Pump replaced.
70-C5B	11 days	***	Power failure; sacrificed.
100-C6A	11 days	***	Velour-Silastic separation. Diaphragm replaced.
100-C6B	8 days	***	Clotted pump: Diaphragm replaced.
100-C6C	8 days	***	Entire pump clotted. Sacrificed.

* 1.25 mg/kg
** Miniature pig
*** Implantation only

No other major abnormalities were found by post-mortem examination, and the organs of the animals were normal except for occasional small thromboemboli. Six chronic studies were performed, and three bladders were changed during the experiments. Considering this total as nine experiments, six of these were terminated because of clotting and obstruction to blood flow in either the pump (5) or the inflow grafts (1), or both (1).

The second bladder in chronic animal #5 and the second and third bladders in chronic animal #6 were clotted, as were those in animals 1, 3, and 4 (Table 4). The clot took the form of a web encircling the orifice of the inflow graft (2 experiments), a long adherent thrombus in the inflow (6) and outflow (1) grafts, and of moderate (5) or marked (1) deposition of layers of fibrous thrombus within the pumping chamber. The clots in the grafts were long, adherent to the walls, and obstructive to blood flow. Obstructive clot was also present in the ball valve housings. The body of the pump itself contained layers of clot laid down in a way which was apparently influenced by the blood flow patterns. An example of such a pump is illustrated in Figure 24.

Three pump bladders were replaced during the studies for two reasons: separation of the Dacron velour from the Silastic bladder (2 instances), and clotting of the diaphragm of the bladder (1 instance). In Calves Nos. 5 and 6, both being pumped at a drive pressure of 180 mm Hg, a vacuum of -40 mm Hg, and a systolic duration of 400 msec, separation of the Dacron velour from the Silastic diaphragm began to occur on the fifth and ninth days, respectively. This was noted in the form of a bleb of plasma which appeared between the two surfaces and which grew gradually in size until it occupied at least half of the total surface area, at which point the animal was taken to the operating room and anesthesized. In animal No. 5, the entire pump was replaced. In animal No. 6, just the flexible diaphragm was exchanged, a procedure which proved extremely simple. When this second diaphragm became less flexible on the nineteenth day of pumping, it was also replaced, and a third one continued to be activated until the twenty-seventh day, at which point no level of pressure or vacuum would generate a flow of greater than 300 ml/min.

Two experiments ended traumatically: animal No. 2, after 4-1/2 days of pumping, suddenly experienced separation of the outflow graft from the outflow leg of the pump. Exsanguination and death resulted immediately. In the second instance, animal No. 5, after successful replacement of his pump, was pursuing an uneventful course when, 11 days after his second operation (19 days of pumping), he chewed through the electrical power cord to the control unit, thereby voluntarily discontinuing pumping. Fifteen minutes later, when discovered, his pump was hopelessly clotted, and the experiment was discontinued. Table 2 summarizes all of the animals studied and their outcome.

DISCUSSION

Three important criteria should be met by a left ventricular assist device in advance of its use in clinical left ventricular failure: it should be safe to use, it should perform the job for which it was intended, and it should place no extra burden upon either the patient or the surgeon.

The safety to the patient and the reliability of the device are of prime importance. In the studies reported, it was evident that both of these requirements were less than adequately fulfilled; in all of the studies, with BLVB activated at optimal settings for maximum flow rates, the grafts, the valve housings, and the pumping chamber all accumulated layers of a shaggy, fibrinous material, some of which was subsequently released in the form of small thromboemboli. Similarly, in two instances, inadequacy in the adhesion of the Dacron velour to the Silastic bladder led to their separation, with consequent diminution in functioning stroke volume and subsequent clotting. The separation did not, of itself, create a hazard, but rather expressed itself in the secondary manner described.

The other hazards which were encountered included the air leak in the inflow graft line, due to a faulty manufacturing process, and the sudden separation of the pump from the outflow graft (calf No. 2). The first is a question of materials and fabrication reliability. The second is a question of design: the recommended procedure was the fixation of the graft limb to the pump by heavy plastic tapes. In spite of this prescribed procedure, this coupling loosened with time, and would present a material hazard to the patient. The problem was solved, in our laboratory by employing heavy silk buttress sutures to reinforce the attachments of all subsequent pumps to their grafts.

For the purpose of clarifying the relationship between control parameters and hemodynamic function of the BLVB, a hypothetical example is illustrated in Figure 25. The "optimum" relationship between systolic and diastolic duration and the pump's inactive period in any given cardiac cycle (assuming synchronous operation) is shown for a systolic duration of 300 msec, a vacuum of -40 mm Hg, an air-drive pressure of 180 mm Hg, and a heart rate of 60 beats per minute. Normal pump ejection is followed by complete filling and a brief inactive period before the onset of the succeeding cycle. This inactivity compensates for small variations in heart rate (see line 10, where a shorter cardiac cycle is illustrated).

The systolic duration control determines the length of time used for ejection of stroke volume. In the first example (line 2), a slight increase over optimum systolic duration leads to a prolongation of pump systole, but adequate filling of the pump will still occur although the cushion of the inactive period is now lost. A further increase in systolic duration (line 3) will not permit adequate time for filling of the pump, and with each succeeding beat the flexible bladder will be progressively depressed until no further pump filling or ejection occurs. Conversely, a decrease in systolic duration will decrease the amount of flow through the pump while not substantially interfering with adequacy of subsequent pump filling, and a decrease in effective pump stroke volume results.

Diastolic filling duration is controlled by the vacuum. Any decrease in vacuum produces a decrease in filling rate and a prolongation of pump diastole, as shown in line 5. Diastole is prolonged, but does not interfere with the subsequent cycle. Any further decrease in vacuum prolongs diastolic filling beyond the onset of the subsequent pump cycle and precisely the same phenomenon occurs as with marked increase in systolic duration: the pump is progressively depressed to its maximum point and ejection and filling cease. In contrast, an increased vacuum with decreased diastolic filling duration is analogous to a decrease in systolic duration (line 7).

Air-drive pressure, in the presence of an unchanging ejection duration, is responsible for the determination of stroke volume and the pressure at which blood is delivered to the aorta. When this pressure is increased, systolic emptying is more complete and, thus, the pump requires a greater time to fill. In the example in line 8, the required filling time again encroaches upon the subsequent cycle, resulting in a gradual emptying of the pump. A decrease in drive pressure will have the same effect as a decrease in systolic or diastolic durations: a decrease in effective stroke volume.

With the other three parameters unchanged, a small increase in heart rate will have an effect analogous to that seen with a small increase in systolic or diastolic duration; the pump maintains its stroke output and fills adequately, as illustrated in line 10. A further increase in heart rate (line 11) again produces an effect analogous to that seen with markedly increased diastolic or systolic duration. A decrease in heart rate (line 12) has an effect analogous to a decrease in systolic or diastolic duration: pump ejection and filling are adequate, but a wasteful inactive period ensues before onset of the subsequent contraction.

Keeping these relationships in mind, the discussion of BLVB function in vivo which follows may be clarified.

The maintenance of an adequate cardiac output, in the state of irreversible left ventricular failure, becomes the joint responsibility of the assist device and what remains of left ventricular function. The results of the animal studies provide the conclusion that the maximum flow rate of which the pump is capable, at optimum settings, is 2.5 L/min. In practical terms, the flow rate does not usually exceed 2.1 to 2.2 L/min. To the extent, then, that the degree of left ventricular failure present in the patient involves a circulating volume up to 2.2 L/min, the BLVB will certainly be adequate in accepting that share of the responsibility for maintaining cardiac output. This was illustrated above in Figures 7, 8, and 21. When this degree of failure is exceeded, the BLVB will not be able to correct the failure state, and a physiological decline will be inevitable.

There is relatively little effect on aortic pressure (perfusion pressure) by pumping synchronously or asynchronously. This parameter is regulated by the central and peripheral nervous system networks, and will continue to be autoregulatory just as long as cardiac output is maintained, from whatever source, and tissues are adequately perfused.

Although the necessity for reducing the left-ventricular peak pressure to low levels is not as yet known, it is theoretically desirable. The BLVB produces little effect in animals with cardiac outputs in excess of 3 L/min, since it is limited to a minute volume of 2.5 liters. When cardiac output exceeds this latter figure, left-ventricular pressure is only slightly reduced (Figures 19 and 20); when the cardiac output is as low as 2.2 L/min (Figure 20), the device can perform much better in this regard.

Maximum rate of pump activation is also limited: it is not possible to fill the pump to maximum effective stroke volumes at an activation rate exceeding 60 beats per minute.

A stable animal model of chronic left ventricular failure is not yet available for use in evaluating such a device. It should perform, however, as illustrated in the circulation analog (Figures 6 and 7) and in the acute animal experiment (Figure 21).

The behavior of any left ventricular assist device in the face of serious cardiac arrhythmias has been demonstrated here, as elsewhere. Two considerations are important: the presence of right heart function and the level of pulmonary vascular resistance. The former has been demonstrated previously, and was also shown in the circulation analog experiment (Figure 8). The effect of the absence of right ventricular function was also demonstrated in the acute animal experiment (Figure 21). The effect of the BLVB on total cardiac failure, produced analogously, was that as long as pulmonary vascular resistance remained at extremely low levels, blood could continue to return to the right side of the heart, and the BLVB could fill adequately. In the presence of normal or elevated resistance levels, this "passive return" ceased, and the pump rapidly lost its effectiveness, as illustrated in the right-hand panel of Figure 20.

The third and final criterion, that of surgical simplicity, appears to have been met adequately by this device. The relatively simple left thoracotomy does not necessarily present an undue burden to the patient. The pump does, however, require 2 grafts (inflow and outflow) which extend through the skin and are fixed to the rib cage. These lines are a potential source of infection, although it is doubtful that the BLVB would remain in situ for a sufficiently long period of time for serious complications in this respect. On the other hand, it has proved simple to change either the pump or the flexible diaphragm, since both parts are external to the chest.

The use of Eastman 910 adhesive did not prove satisfactory when used on pump parts in contact with tissue: severe local tissue necrosis resulted.

Finally, it is worth commenting that the control unit (which houses the pressure-vacuum and timing controls), has proved to be a reliable unit: it was easy to adjust, unambiguous in its settings, and functioned well throughout the course of the experiments.

DISCUSSION

DR. HALL: I want to congratulate the authors on this work. I would like to ask one question. In the case where the clot continued to build up, were you obtaining full excursion of the diaphragm of the pump? I ask this because we have experienced the same thing and usually this occurred because the animal had temporarily occluded one of the tubes, or the power unit had gone off for a short period of time, or the pump rate had been decreased to the point that a stagnant area arose inside the pump for a very short period of time - long enough to allow clots to continue to build up.

DR. LaFARGE: Your point is well taken. As Dr. Bernhard indicated in our earlier presentation, we have technicians working 24 hours a day. They watch the animals very carefully and try to make adjustments so that the diaphragm flexes to its largest volume capability without hitting the far wall. This decreased the time required for clots to build up. Effectively, during the first two weeks anyway, the level of pumping could be maintained around 2 liters, 1.7 to 2 liters, per minute, by continuing to do this. We kept the rate at about 40 beats a minute and usually closer to 50 in order to try to avoid the stagnant period as much as possible. The animals were watched very closely with the exception of the one which exsanguinated during the Harvard Medical Faculty meeting when everybody was out of the building.

DR. HASTINGS: One final question.

UNIDENTIFIED DISCUSSANT: I note, Dr. LaFarge, that the presence of thrombi within the pump is a very common finding. Did you resort to any type of anticoagulation during the perfusion period? It was not quite clear.

DR. LaFARGE: This was a source of hot debate early in the program, to be or not to be, to coagulate or not to coagulate. In our two initial experiments with animals, we continued heparinization for 24 hours and then stopped because at that point Dr. Bernstein and I were advised by Dr. Hall that the pump was designed to be used without anticoagulation except at the time of implantation. With the exception of the initial two studies, therefore, all the rest of the animals were anticoagulated only during the implantation procedure.

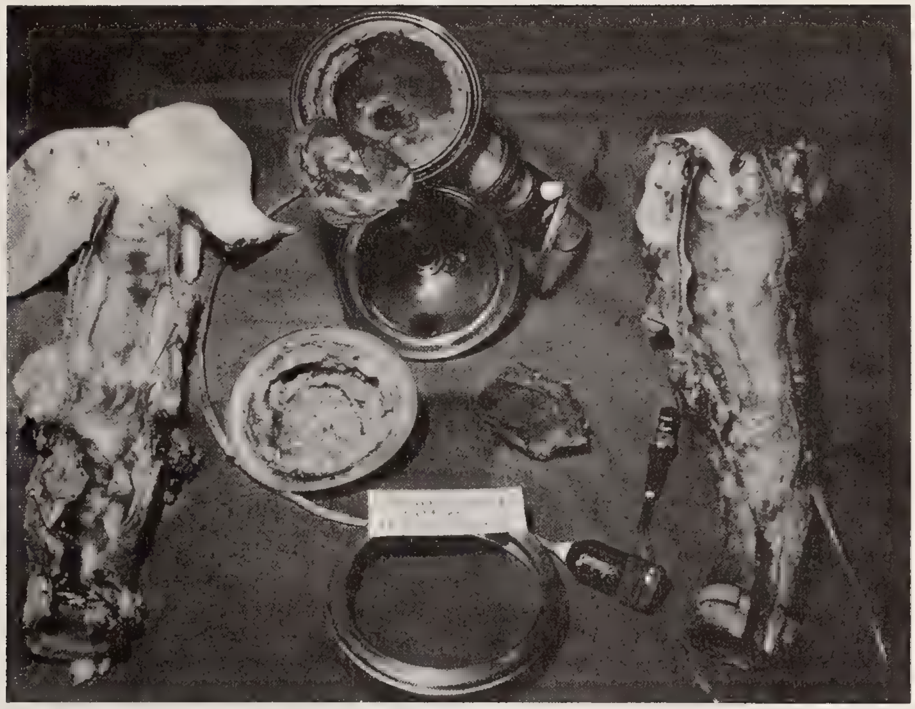

FIGURE 24.

RELATIONSHIPS BETWEEN PUMP FUNCTION PARAMETERS

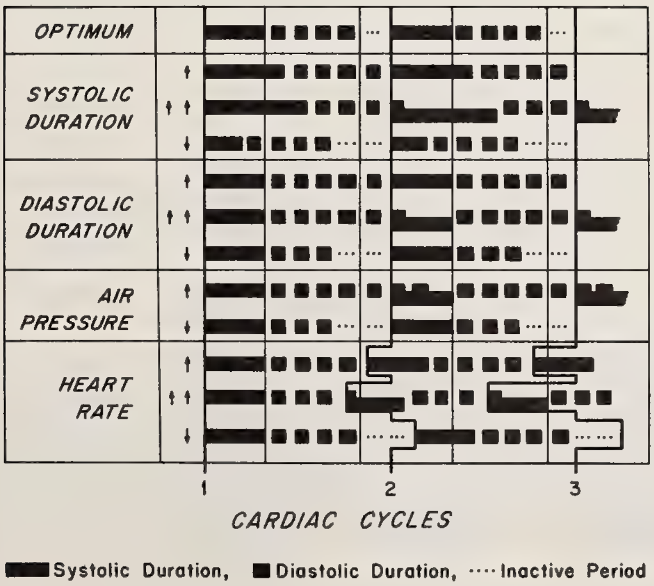

FIGURE 25.

CHAPTER 53

ASSISTED CIRCULATION: EXPERIMENTAL INTRA-AORTIC BALLOON PUMPING

M. Feola, N. A. Normann, O. Haiderer, J. H. Kennedy

Cleveland Metropolitan General Hospital
Case Western Reserve University
Cleveland, Ohio

I. Hemodynamic Observations in Experimental Acute Left Ventricular Failure: An acute left ventricular failure (LVF) preparation was developed in 60 dogs pretreated with reserpine, by ligation of coronary artery branches and by propranolol-chlorpromazine infusion. In 15 dogs with LVF_1, characterized by 15-25% reduced cardiac output and mean aortic pressure, IABP reestablished normal hemodynamics. In 15 dogs with LVF_2, characterized by further reduction in previous parameters, plus elevated left ventricular end diastolic and mean left atrial pressures and central venous blood desaturation, IABP improved all parameters within three hours. In these two groups of dogs, IABP decreased tension-time-index and minute work; increased stroke volume, mean aortic pressure, coronary flow, myocardial contractility (dp/dt) and oxygen utilization. In 12 LVF_3 dogs characterized by above 40% decreased cardiac output, mean aortic pressure, coronary and systemic flows, IABP had insignificant hemodynamic effects, compared to a group of eight untreated dogs, and did not prevent progression of failure or prolong survival.

II. Aortic Baroreceptor Output: In anesthetized dogs, the nerve impulses were recorded from the left vagus nerve and by analog-computational techniques separated from activity in other fiber groups. The results demonstrate that balloon "pumping" increases and drastically alters the output pattern in aortic baroreceptor nerve fibers. Operation of the balloon reduces the baroreceptor output ("BRO") during systole, a reduction which, however, is outweighted by the increase caused during diastole. Thus, total "BRO" (integrated over 10 second periods - "N_{10}") increased. The temporal relationship between heart action and "pump" timing appears as a more critical parameter than the direct interpretation of the pressure tracings would indicate.

I. INTRA-AORTIC BALLOON PUMPING (IABP) AT DIFFERENT LEVELS OF EXPERIMENTAL ACUTE LEFT VENTRICULAR FAILURE

INTRODUCTION

Pumping devices, based upon the principle of Counterpulsation, have been in experimental development and evaluation since 1957 (Casten).

Intra-aortic balloon pumping (IABP), introduced in 1962 (Moulopoulos, Topaz and Kolff), would have the advantages of not requiring thoracotomy, major vascular surgery, or extracorporeal circulation, and being of relatively rapid applicability, easy synchronization and actuation. As to the effectiveness of hemodynamic performance, evaluation of the experimental data presently available is limited by the great variance of experimental models, and of the criteria for definition and quantification of acute heart failure and "coronary shock."

The present study had the following objectives:

1. Development of an experimental model, bearing the closest possible resemblance to the clinical situation;
2. Establishment of criteria for the classification of acute left ventricular failure in stages or levels;
3. Study of the effects of IABP in a group of normal animals, to have a baseline point of reference;
4. Study of the effects of IABP at different levels of failure;
5. Establishment of indications and limitations of the method;
6. Improvement of the device and potentiation of its effects.

MATERIALS AND METHODS

I. IABP in Normal Dogs.

Ten normal mongrel dogs, of 15 kg average weight, were used. Anesthesia was induced with Sodium Pentobarbital (25 mg/kg), and maintained with additional doses as required. Ventilation was assisted with a Bird Respirator using 100% oxygen, via an endotracheal tube.

A tubular balloon (Westinghouse model), 0.005 mm in thickness, 12-16 mm in diameter, 15-22 cc in volume, varying with the size of the animal, was inserted through the left femoral or common iliac artery, the tip reaching the origin of the left carotid artery. The balloon was inflated with helium (150-200 mm Hg) and deflated with a vacuum pump. EKG synchronization and pumping were actuated by means of a Westinghouse console and solenoid pump.

The chest was opened with a median sternotomy. (Figure 1)

Catheters, for pressure measurement and blood sampling, were inserted into: ascending aorta through the left carotid artery; the left ventricle through the apex; the left atrium through a segmental left pulmonary vein; the superior vena cava through the left jugular vein; the abdominal aorta, distal to the balloon, through the right femoral artery. Electromagnetic flow transducers were inserted around the root of the aorta, the right carotid and left renal arteries. A siliconized tube was anchored at the ostium of the coronary sinus and connected by a Y-tubing to a large-bore Bardic catheter, inserted through the right jugular vein into the right atrium. A three-way stopcock, at the end of the Y-connection, allowed measurement of coronary sinus flow by gravity drainage and sampling. Preliminary experiments with this continuous shunting arrangement indicated that flow was not impeded. Two small catheters were inserted into the ureters, for measurement of urinary output.

LVP, mean left atrial pressure (MLAP), aortic pressures proximal and distal to the balloon were monitored continuously with Statham pressure transducers. Flow at the root of the aorta (AoF), renal (ReF) and carotid (CaF) flows were monitored, using calibrated flow transducers and biotronix electromagnetic flow meters. Flow zero was taken as the late diastolic value of the pulsatile wave form.

An EKG was derived from transthoracic needle electrodes. All these parameters were recorded continuously with an Electronics for Medicine recorder, both on paper and on tape. CVP was monitored with a water manometer. Blood samples were taken from the arterial, central venous and coronary sinus lines, for determination of pH, pO_2, pCO_2, Hct., O_2 vol. %, lactate and pyruvate. Euvolemia was maintained by the administration of Ringer's Lactate, four times the amount of calculated blood loss, plus 5% dextrose/W, 20 drops per minute. Heart rate (HR) was derived from the EKG. CO was calculated from the flow at the root of the aorta. Tension-Time-Index per minute (TTI/min.) was derived, according to Sarnoff's method, as the product of the mean aortic systolic pressure x systolic ejection x heart rate. Left ventricular minute work (LVMW) was calculated from a modification of Gorlin's formula, which uses 3/4 of peak LVP in place of the mean aortic pressure:

$$\begin{array}{l}\text{LVMW}\\ \text{(kg-m/min.)}\end{array} = \frac{(Q \times 1.055)\ (\text{LVP} \times 0.75 \times 13.6)}{1000}$$

Q = cardiac output L/min.
1.055 = specific gravity of blood
LVP x 0.75 = 3/4 of systolic LVP
13.6 = specific gravity of Hg

Total peripheral resistance (TPR) was calculated as:

$$\begin{array}{l}\text{TPR}\\ \text{(Units: mm Hg/L min.)}\end{array} = \frac{\text{AoP} - \text{CVP (in mm Hg)}}{\text{CO (L/min.)}}$$

Coronary sinus flow (CSF) was recorded as cc/100 gm LV/min. Left ventricular oxygen consumption (MVO_2) was calculated as the arterio-coronary sinus O_2 difference in vol. % x CSF. Left ventricular efficiency was calculated with the formula:

$$\text{LV Eff.} = \frac{\text{LVMW (in kg-m/min.)}}{MVO_2 \times 2.06 \ \text{(the energy equivalent in kg-m of 1 cc of } O_2)}$$

"Excess Lactate" of the left ventricle was calculated by the method of Huckabee:

$$XL - (L_v - L_a) - (P_v - P_a) \times (L_a - P_a),$$

Where XL = excess lactate
v = coronary sinus
a = aorta
L = mM lactate
P = mM pyruvate.

Left ventricular weight was calculated from the body weight, after the method of Herrmann.

Heart rate, LVP, MAoP, TT/min., LVMW, MVO_2, LV Eff., TPR, CO, CaF, ReF, CSF were recorded after the preparation was stabilized. IABP was then carried out for one hour. Recording of the same parameters was obtained at the onset of pumping, and at 15, 30, 45, 60 minutes. These first ten experiments revealed the first limiting factor of IABP: the occurrence of tachyarrhythmias and dysrhythmias. Abnormal QRS complexes, either broader than 50 msecs, or of a voltage lower than 1/3 of 1 millivolt, would produce failure of the device to trigger properly, leaving the balloon often inflated for several beats. Shifting heart rates, particularly tachycardia, above 160 beats/min., would render proper phasing more difficult to obtain. In order to assess the performance of IABP in optimal conditions, it was decided to use a constant infusion, for the duration of the experiment, of Propranalol, in a dose small enough not to produce significant myocardial depression, and yet adequate to maintain a normal, slow rhythm, averaging 130 beats/min. In order to balance the beta-adrenergic blocking effect of Propranalol, Chlorpromazine was added for its alpha-adrenergic blocking effect. The optimal dose of both substances was found to be 0.012 mg/kg/min.

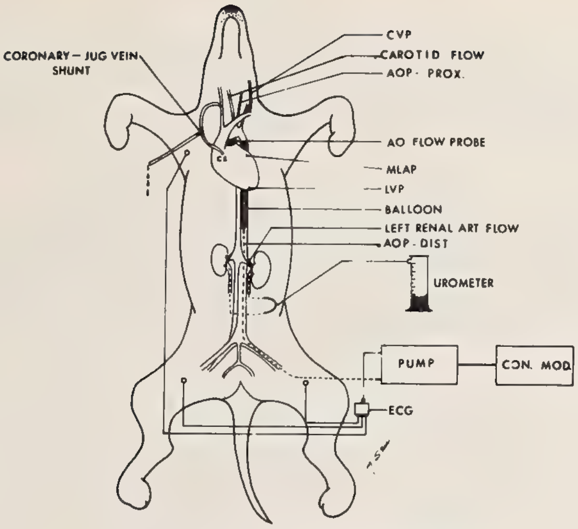

FIGURE 1. MEDIAN STERNOTOMY.

EXPERIMENTAL ACUTE LEFT VENTRICULAR FAILURE
(LVF1)

I. PRE-TREATMENT WITH RESERPINE. (0.1mg / Kg / day x 3 days)
II. CONSTANT INFUSION OF PROPRANOLOL CHLORPROMAZINE. (0.012 mg / Kg / min)
III. LIGATION OF ADR-LEFT CORONARY ARTERY-LOWER THIRD. PLUS LIGATION OF COLLATERAL EPICARDIAL VESSELS.

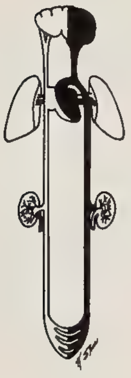

1. EKG ISCHEMIC CHANGES.
2. 10-25% DECREASE IN CARDIAC OUTPUT.
3. 10-25% DECREASE IN MEAN AORTIC PRESSURE.
4. 10-25% DECREASE IN CORONARY SINUS FLOW.
5. 10-25% DECREASE IN SYSTEMIC FLOWS AORTIC, CAROTID, RENAL
6. 0-10% INCREASE IN T.P.R.

FIGURE 2.

EXPERIMENTAL ACUTE LEFT VENTRICULAR FAILURE
(LVF2)

I. PRE-TREATMENT WITH RESERPINE (0.1 mg / Kg / day x 3 days)
II. CONSTANT INFUSION OF PROPRANOLOL-CHLORPROMAZINE (0.012 mg / Kg / min)
III. LIGATION OF ADR-LEFT CORONARY ARTERY, MIDDLE THIRD PLUS LIGATION OF COLLATERAL EPICARDIAL VESSELS.

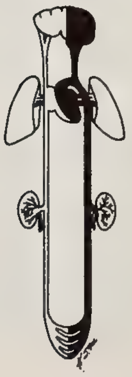

1. EKG ISCHEMIC CHANGES.
2. 25-40% REDUCTION IN CARDIAC OUTPUT.
3. 25-40% REDUCTION IN MEAN AORTIC PRESSURE.
4. 25-40% REDUCTION IN CORONARY SINUS FLOW.
5. 25-40% REDUCTION IN SYSTEMIC FLOWS
6. ELEVATION OF LVEDP.
7. ELEVATION OF MEAN LEFT ATRIAL PRESSURE.
8. INCREASE IN TOTAL PERIPHERAL RESISTANCE.
9. INCREASE IN CENTRAL VENOUS BLOOD DESATURATON.

FIGURE 3.

EXPERIMENTAL CORONARY SHOCK
(LVF3)

I. PRE-TREATMENT WITH RESERPINE (0.1 mg/Kg/day x 3 days)
II. CONSTANT INFUSION OF PROPRANOLOL CHLORPROMAZINE (0.012 mg/Kg/min.)
III. LIGATION OF ADR. LEFT CORONARY ARTERY UPPER THIRD PLUS LIGATION OF COLLATERAL EPICARDIAL VESSELS

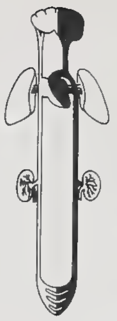

1 EKG ISCHEMIC CHANGES
2 >40% DECREASE IN CARDIAC OUTPUT.
3. >40% DECREASE IN MEAN AORTIC PRESSURE.
4. >40% DECREASE IN CORONARY SINUS FLOW
5. >40% DECREASE IN SYSTEMIC FLOWS (AORTIC CAROTID. RENAL)
6. INCREASE IN TPR
7. OLIGURIA (>50% REDUCTION IN U.O.)
8 METABOLIC ACIDOSIS
9 DECREASE IN ARTERIAL PO_2
LACTIC ACIDEMIA.
10 EXCESS LACTATE IN CORONARY SINUS BLOOD.
11. ELEVATION IN LVEDP & MLAP

FIGURE 4.

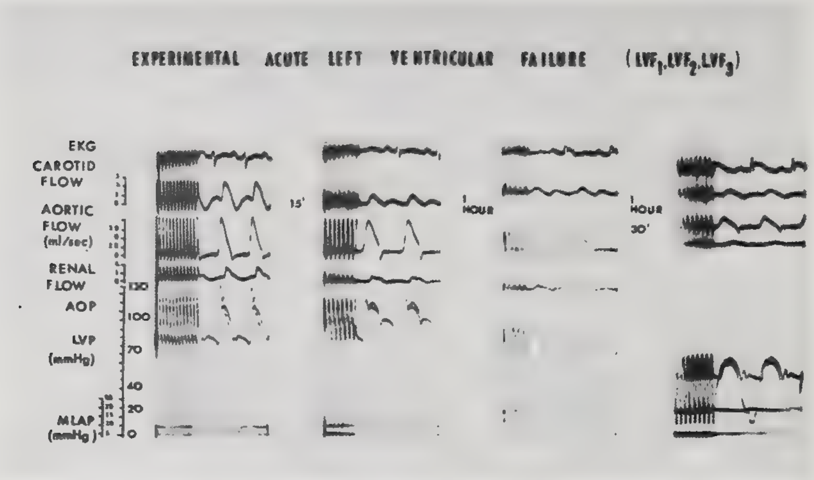

FIGURE 5.

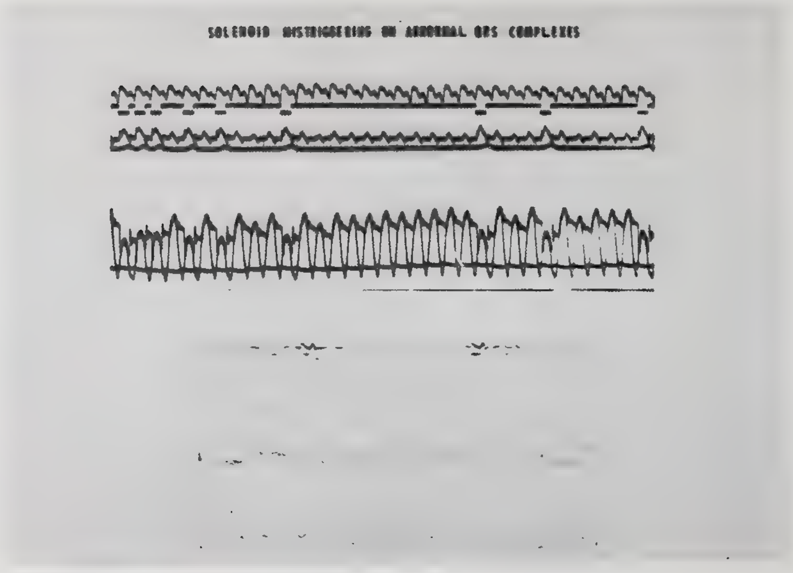

FIGURE 6.

Ten dogs, so prepared, were used for a second group of "normal experiments." IABP was carried out for one hour. Recording of the same hemodynamic and metabolic parameters was carried out in the same fashion. It is this second group of animals that represents our "baseline point of reference."

II. IABP at Different Levels of Experimental Acute Left Ventricular Failure (LVF).

A standardized model of experimental myocardial infarction-acute left ventricular failure was reproduced in 65 dogs. Normal mongrel dogs, of 15 kg average weight, were pretreated with Reserpine, orally, 0.1 mg/kg/day x3 days, for the purpose of depleting the myocardium of catecholamines, and decreasing myocardial irritability. After all cannulations, as in previous experiment, and baseline recording of hemodynamic and metabolic parameters, the constant infusion of Propranalol and Chlorpromazine in equal doses of 0.012 mg/kg/min. was started via a Harvard injector. After one hour, the anterior descending ramus of the left coronary artery was ligated at its upper, or middle, or lower third. Collateral vessels were ligated over a 30 min. period, to the point of complete ischemia (as evidenced by I.V. Fluorescein and examination under ultraviolet lamp) of a small (approximately 1/3), a medium (1/2), or a large (2/3) area of the left ventricle.

Preventing the development of acute ventricular fibrillation, severe dysrrhythmias by pharmacologic means, coronary ligation to the point of complete ischemia had the effect of producing an adynamic left ventricle, with consequent acute "pump failure." The size of the ischemic area determined the severity of failure. The preparation was stable, with no spontaneous fluctuations toward recovery and with minimal incidence of ventricular fibrillation.

LVF_1 was reproduced in 15 dogs by ligation of the anterior descending ramus of the left coronary artery in the lower third supplemented by ligation of collateral epicardial vessels, to the point of complete ischemia of a small area (1/3) of the left ventricle, characterized by: 1) 15-25% decrease of cardiac output; 2) 15-25% decrease of mean central aortic pressure; 3) 15-25% decrease of coronary sinus flow; 4) 15-25% decrease of systemic flows (aortic, carotid and renal); 5) Increase in TPR (Figure 2). After 1/2 hour, allowed for the stabilization of the preparation, IABP was carried out for two hours. Hemodynamic and metabolic sampling were taken before, at the onset of pumping, and at 30, 60, 90, 120 minutes.

LVF_2 was reproduced in 15 dogs by ligation of the anterior descending ramus of the left coronary artery in the middle third, supplemented by ligation of collaterals, to the point of complete ischemia of a medium-size area (1/2) of the left ventricle, characterized by: 1) 25-40% reduction in CO, MAP, CSF, Systemic flows; 2) Elevation of left ventricular end diastolic pressure (LVEDP) and mean left atrial pressure (MLAP) above 12 mm Hg; 3) Increase in TPR; 4) Increase in central venous blood desaturation (Figure 3). After 1/2 hour, allowed for the stabilization of the preparation, IABP was carried out for 1-3 hours. Hemodynamic and metabolic sampling were taken before, at the onset of pumping, and at 30, 60, 90, 120, 150, and 180 minutes.

LVF_3 (Coronary Shock): Reproduced in 20 dogs, by ligation of the anterior descending ramus of the left coronary artery, in the upper third, supplemented by ligation of collaterals, to the point of complete ischemia of a large area (2/3) of the left ventricle, characterized by: 1) 40% or greater reduction in CO, MAoP, CSF, Systemic flows; 2) Increase in TPR; 3) Oliguria (greater than 75% reduction in UO);4) Lactic acidemia; 5) Drop in arterial pH and pO_2; 6) Appearance of excess lactate in coronary sinus blood; 7) Increase in LVEDP and MLAP (Figure 4). Eight dogs were left untreated and used as control. Their survival time averaged 90 minutes; all dogs were dead within two hours. IABP was carried out in 12 dogs. Hemodynamic and metabolic sampling were taken before, at the onset of pumping, and at 30, 60, 90, 120 minutes (Figure 5).

RESULTS

A. Mechanical Performance of Westinghouse Device.

EKG Discrimination. The present Westinghouse console (the one evaluated by us) works on a preset range of QRS complexes, configuration and amplitude. Failure of triggering on abnormal QRS complexes leaves the balloon inflated for several beats (Figure 6). Resetting of the console is done manually, by way of three separate screws (controls labeled: QR, RS, Gate). While transient arrhythmias disappear before any resetting can be carried out, severe dysrhythmias, represented by rapid sequence of low voltage, widened, upward and downward deflection QRS complexes, make any resetting impossible. In these cases, the balloon remains inflated, or it works in an erratic fashion, with unpredictable, probably deleterious hemodynamic consequences. Shifting heart rates also require manual resetting. Ventricular fibrillation produces, as expected, failure of triggering.

Fail-Safe Features. Rupture of the balloon occurred in one animal, with acute helium embolism and immediate death.

Ease of Operation. The present system requires a person that is very familiar with its electronic and pneumatic controls.

Balloon Size and Pressure. The relationship size of the balloon - diameter of the aorta is a critical one: the balloon is to be large enough to produce definite diastolic augmentation, small enough not to be "occlusive." This relationship is a dynamic one: at the stage of "shock," as the central aortic volume and pressure are reduced, and the aortic diameter is reduced, a proper sized balloon becomes "occlusive." We have seen by Aortograms that, in this situation, the balloon expends its energy more in the expansion-retraction of the aortic wall than in the propulsion of blood.

Balloon inflation-deflation pressure is another important factor. At the stage of "shock," diastolic augmentation can be obtained, within certain limits, by increasing balloon inflation pressure. But deflation, with this mode of pumping, has a sucking effect upon the aortic branches, as evidenced by reversal of flow in the carotid and renal arteries (Figure 7).

Position of the Balloon. The best position is with the tip immediately distal to the left carotid artery. Hemodynamic performance is less effective with a more distal position, while a more proximal position causes carotid backflow with deflation of the balloon.

B. Hemodynamic Performance.

IABP in Normal Dogs. The results of 1 hour pumping in a group of 10 normal dogs confirm Galletti's theory that the introduction of a pump into a circulatory system becomes a perturbation or intrusion into its control mechanisms. They also confirm that the control mechanisms "reset", to return the disturbed hemodynamics toward normal (Figures 8, 9, 10, Tables 1 through 5).

TABLE 1

HEMODYNAMIC-CARDIAC METABOLIC EFFECTS OF IABP IN NORMAL DOGS[a]

	# Dogs	Baseline	IABP	15 min	30 min	45 min	60 min
HEART RATE (beats/min)	10	130[b] (10)	120 (5)	120 (5)	120 (5)	110 (5)	120 (5)
LVP (mm Hg)	"	130 (10)	110 (5)	112 (5)	112 (5)	130 (5)	130 (5)
MAP (mm Hg)	"	124 (4)	128 (4)	114 (4)	114 (4)	128 (4)	134 (4)
CO (Cardiac Output minus Coronary Flow) (ml/kg/min)	"	99 (3)	120 (5)	106 (5)	106 (5)	94 (2)	99 (3)
CSF (ml/100 gm LV/min)	"	52 (4)	48 (2)	46 (2)	46 (2)	48 (2)	52 (2)
CaF (ml/kg/min)	5	14 (2)	16 (2)	15 (2)	15 (2)	12 (2)	14 (2)
ReF (ml/kg/min)	"	9.3 (2)	11 (3)	10 (3)	10 (3)	9.3 (2)	9.3 (2)
TTI/min (mm Hg/seconds)	10	1230 (130)	810 (90)	920 (90)	920 (90)	1050 (120)	1140 (120)
TPR (units: mm Hg/L min)	"	40.60 (8)	34.71 (5)	34.67 (4)	34.67 (4)	44.32 (9)	43.95 (8)
LVMW (kg/m/min)	10	2.083 (0.33)	2.130 (0.33)	1.927 (0.16)	1.927 (0.16)	1.971 (0.22)	2.083 (0.33)
MVO$_2$ (ml/100 gm LV/min)	10	6.75 (5)	6.54 (4)	6.43 (4)	6.43 (4)	6.44 (4)	6.65 (5)
LVME (%)	10	37% (3)	41% (3)	39% (3)	39% (3)	39% (3)	38% (3)
dp/dt LVP (mm Hg/sec)	10	1200 (5)	1300 (5)	1300 (5)	1300 (5)	1280 (5)	1280 (5)

[a] Mean weight = 15 kg (±3); dogs treated with Propranalol-Chlorpromazine 0.012 mg/kg/min; after anesthesia (Pentobarbital 25 mgm/kg) and thoracotomy.

[b] Mean values, with standard error in parenthesis.

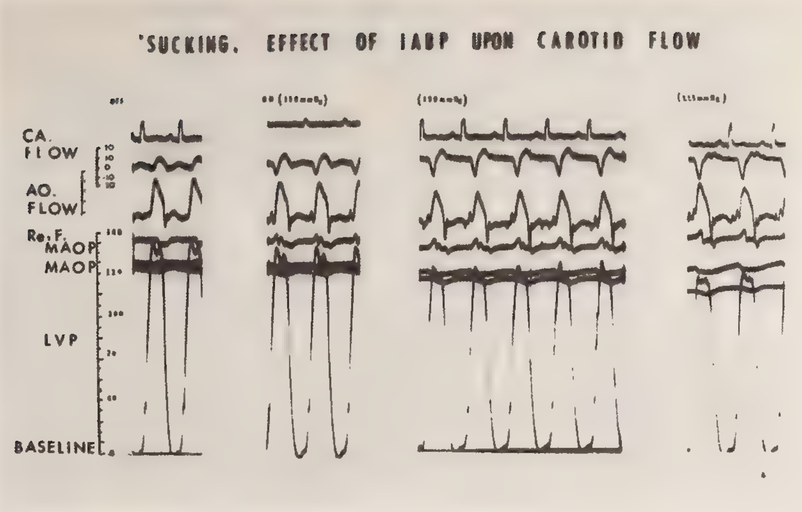

FIGURE 7.

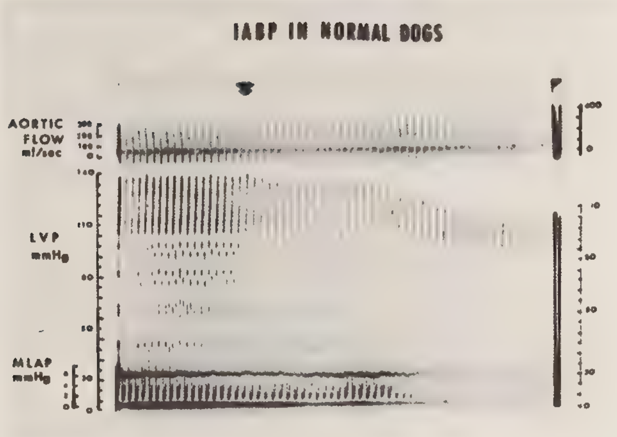

FIGURE 8.

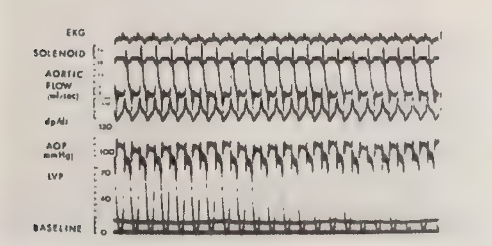

FIGURE 9.

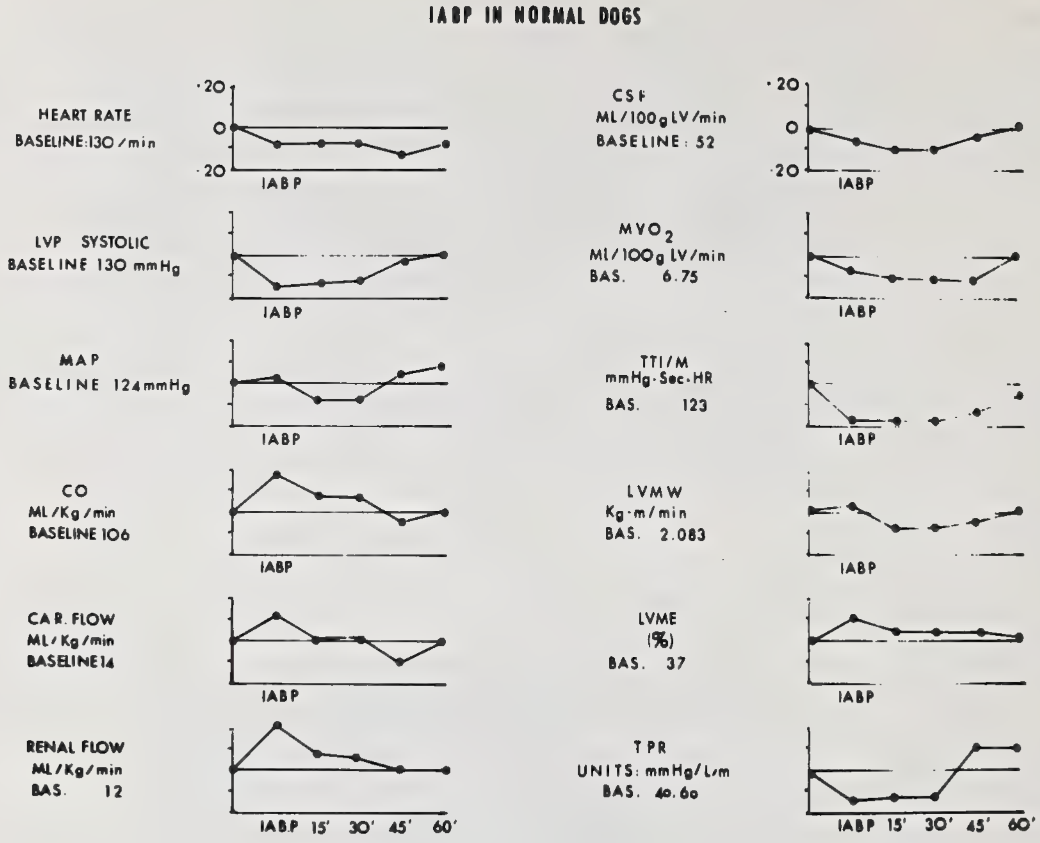

FIGURE 10.

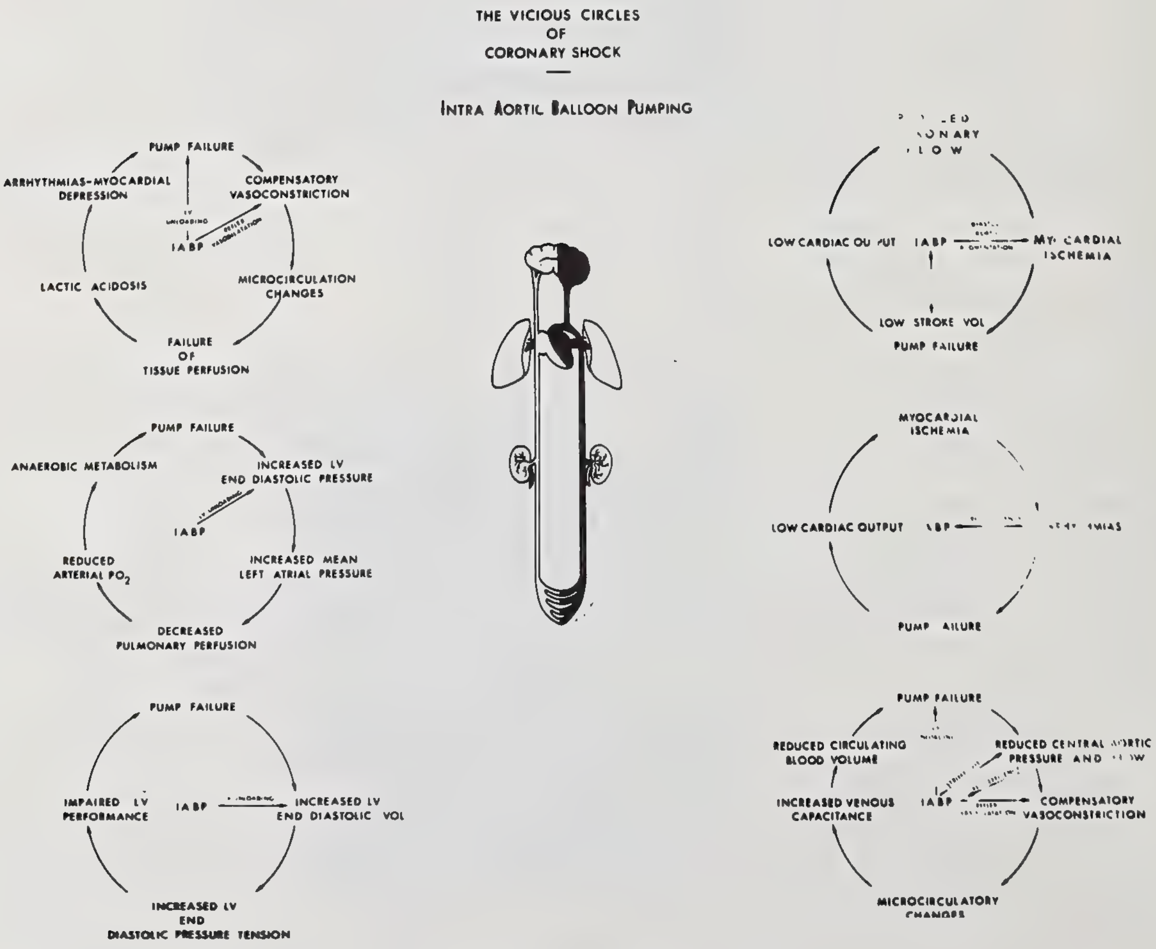
THE VICIOUS CIRCLES OF CORONARY SHOCK
Intra Aortic Balloon Pumping
PUMP FAILURE
COMPENSATORY VASOCONSTRICTION
MICROCIRCULATION CHANGES
FAILURE OF TISSUE PERFUSION
LACTIC ACIDOSIS
ARRHYTHMIAS-MYOCARDIAL DEPRESSION
IABP
LV UNLOADING
REFLEX VASODILATATION
PUMP FAILURE
INCREASED LV END DIASTOLIC PRESSURE
INCREASED MEAN LEFT ATRIAL PRESSURE
DECREASED PULMONARY PERFUSION
REDUCED ARTERIAL PO2
ANAEROBIC METABOLISM
IABP
LV UNLOADING
PUMP FAILURE
INCREASED LV END DIASTOLIC VOL
INCREASED LV END DIASTOLIC PRESSURE TENSION
IMPAIRED LV PERFORMANCE
IABP
LV UNLOADING
CORONARY FLOW
MYOCARDIAL ISCHEMIA
LOW STROKE VOL
PUMP FAILURE
LOW CARDIAC OUTPUT
IABP
MYOCARDIAL ISCHEMIA
ARRHYTHMIAS
PUMP FAILURE
LOW CARDIAC OUTPUT
IABP
PUMP FAILURE
REDUCED CENTRAL AORTIC PRESSURE AND FLOW
COMPENSATORY VASOCONSTRICTION
MICROCIRCULATORY CHANGES
INCREASED VENOUS CAPACITANCE
REDUCED CIRCULATING BLOOD VOLUME
IABP
REFLEX VASODILATATION

FIGURE 11.

TABLE 2

PEAK SYSTOLIC

LVP

(10 NORMAL DOGS)

	Baseline	IABP	15 min	30 min	45 min	60 min
1	135	112	114	114	132	134
2	126	110	112	112	120	124
3	124	108	110	110	126	124
4	140	115	117	117	135	135
5	130	110	112	112	130	130
6	120	105	107	107	125	125
7	138	115	116	116	134	136
8	125	108	110	110	128	125
9	136	114	114	116	132	134
10	122	106	108	108	126	122

TABLE 3

CARDIAC OUTPUT MINUS CORONARY FLOW

(ml/kg/min)

NORMAL DOGS

Baseline	IABP	15 min	30 min	45 min	60 min
99	120	106	106	94	99
102	124	110	110	96	100
100	120	108	108	96	100
98	115	110	110	96	98
98	120	110	110	96	100
101	122	110	102	96	100
102	125	111	111	96	102
102	124	109	109	95	100
96	115	102	102	96	96
96	116	104	104	96	96

TABLE 4

AORTIC PRESSURES: PEAK SYSTOLIC/END DIASTOLIC

(mm Hg)

NORMAL DOGS

	Baseline	IABP	15 min	30 min	45 min	60 min
1	135/94	112/72	114/76	114/76	132/80	136/86
2	126/90	110/76	112/76	114/78	120/78	124/82
3	124/85	108/74	110/76	110/76	126/78	124/78
4	140/90	115/65	117/72	118/74	135/78	135/80
5	130/90	110/72	112/72	112/74	130/80	130/82
6	120/88	105/65	107/68	108/68	125/74	125/74
7	138/90	115/76	116/76	118/76	134/80	136/82
8	125/80	108/64	110/64	110/66	128/72	125/72
9	136/90	114/66	114/68	116/68	132/74	134/84
10	122/82	106/60	108/60	108/64	126/84	122/82

TABLE 5

PEAK DIASTOLIC AORTIC PRESSURE

(mm Hg)

NORMAL DOGS

	Baseline	IABP
1	110	134
2	110	130
3	95	124
4	100	130
5	100	132
6	100	134
7	100	134
8	98	128
9	100	126
10	90	120
	mean = Baseline 100	mean = IABP 129
		% increase 29%

The effects of IABP are of two orders: a direct mechanical effect (decrease of LV afterload; diastolic aortic augmentation) and a reflex vasomotor effect (slowing of heart rate; peripheral vasodilatation). The two-step decrease in peak LVP is an expression of this dual phenomenon. TTI/MIN decreases in virtue of both: decrease in systolic mean aortic pressure, and shortening of ejection time.

LVMW was calculated with a modified Gorlin's formula, which takes into consideration not the aortic pressure, which is altered by the pumping effect, but the isovolumetric phase of LV systole. The immediate slight increase must be due to the great increase in stroke volume; the subsequent decrease reflects the decrease in LVP.

MVO$_2$ Oxygen utilization decreases with pumping, while left ventricular mechanical efficiency (LVME) increases.

MAoP after a transient elevation due to the mechanical effect of pumping, decreases, paralleling the decrease in total peripheral resistance.

C.O. increases in virtue of a significant increase in stroke volume. As the ejection time is shortened, increase in stroke volume appears to be due to an increase in myocardial contractility. This is evidenced by an increase in dp/dt of LVP.

Coronary Flow. Measurement of coronary sinus flow (CSF) was found to be the most satisfactory method of measuring coronary flow. CSF decreased with pumping, reverting to control values at the end of 1 hour. This decrease in flow was associated with a decrease in oxygen consumption and paralleled the decrease in left ventricular minute work and tension-time index.

This curve lends support to the theory of autoregulation of coronary flow.

IABP at Different Levels of Left Ventricular Failure. The primary circulatory changes in acute left ventricular failure are: 1) decrease in cardiac output; 2) compensatory increase in total peripheral resistance; 3) elevation of left ventricular end-diastolic pressure and mean left atrial pressure, with diminution of pulmonary perfusion and hypoxia. These phenomena set into motion a series of vicious circles, which lead to failure of tissue perfusion, anaerobic metabolism and shock (Weil and Shubin, 1968 - Dietzman et al., 1969) (Figure 11). IABP tends to break these circles, by increasing stroke volume, decreasing total peripheral resistance, reducing LVEDP ("unloading of the left ventricle") and improving coronary flow (Laird et al., 1968 - Brown et al., 1966 - Kantrowitz et al., 1968).

IABP is however subject to the following limitations: 1) As any other method of arterio-arterial pumping, it is limited in its performance by the fact that only a minor part of the total circulating blood volume is contained in the aorta; this volume is further reduced in acute heart failure by a shift of blood from the systemic to the pulmonary circulation (Burton, 1966). 2) The progressive decrease in central aortic diameter, from the progressive decrease in pressure and flow, creates an "occlusive effect" of the balloon (Moulopoulos et al., 1962). 3) The progressive decrease in stroke volume reaches a critical point, when sudden deflation of the balloon has a "sucking effect" upon the carotid and renal arteries, with production of backward flow.

Performance of IABP was evaluated in terms of:

1. Improvement of cardiac output;
2. Unloading of the left ventricle (change in TTI);
3. Maintenance of mean aortic pressure;
4. Reduction of total peripheral resistance;
5. Improvement of coronary flow;
6. Left ventricular minute work;
7. Left ventricular mechanical efficiency.

Figures 12-17 and Tables 6-20 demonstrate the varying degree of change of the parameters studied at the three levels of failure.

TABLE 6

HEMODYNAMIC-CARDIAC METABOLIC EFFECTS OF IABP IN DOGS IN LVF_1

	# Dogs	Baseline	LVF_1	IABP	30 min	60 min	90 min	120 min
HEART RATE	15	120[a]	120	110	110	100	100	110
(beats/min)		(10)	(5)	(5)	(2)	(2)	(2)	(2)
LVP	"	120	104	100	104	104	106	110
(mm Hg)		(10)	(4)	(4)	(5)	(5)	(5)	(5)
MAP	"	94	80	85	84	85	90	90
(mm Hg)		(3)	(2)	(3)	(2)	(2)	(3)	(3)
CO	"	106	83	99	93	106	106	106
(ml/kg/min)		(6)	(3)	(4)	(3)	(3)	(3)	(3)
CSF	"	42	34	36	38	40	42	40
(ml/100gm LV/min)		(2)	(2)	(3)	(2)	(3)	(3)	(3)
CaF	"	15	12	15	15	18	18	18
(ml/kg/min)		(3)	(3)	(2)	(3)	(3)	(3)	(3)
ReF	"	10	8	11	10	10	10	10
(ml/kg/min)		(3)	(2)	(3)	(3)	(3)	(3)	(3)
TTI/min	"	2256	2004	1870	1680	1683	1782	1620
(mm Hg/seconds)		(120)	(70)	(70)	(62)	(62)	(75)	(50)
TPR	"	56.25	60.80	54.36	57.14	50.62	53.75	53.75
(units: mm Hg/L min)		(4)	(4)	(3)	(4)	(3)	(3)	(3)
LVMW	"	2.066	1.397	1.602	1.565	1.789	1.812	1.803
(kg/m/min)		(0.066)	(0.33)	(0.16)	(0.20)	(0.32)	(0.32)	(0.42)
MVO_2	"	6.43	6.34	5.87	5.90	5.92	5.68	5.60
(ml/100gm LV/min)		(10)	(5)	(5)	(5)	(5)	(5)	(5)
LVME	"	41	28	41	41	45	52	50
(%)		(3)	(3)	(3)	(3)	(4)	(4)	(3)

a Mean values, with standard error in parenthesis.

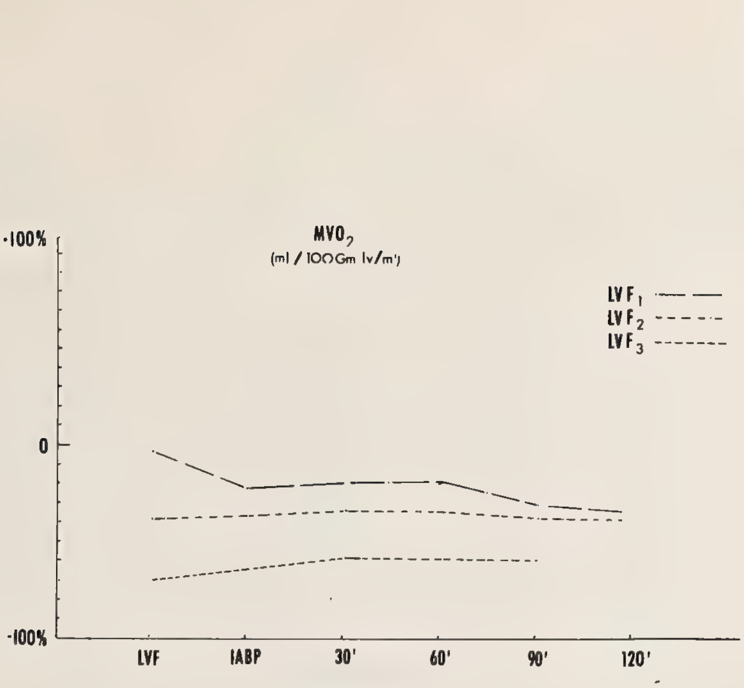

FIGURE 12.

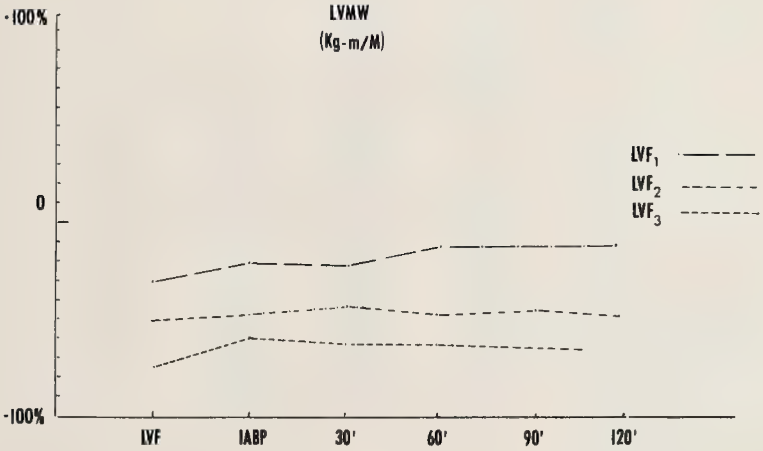

FIGURE 13.

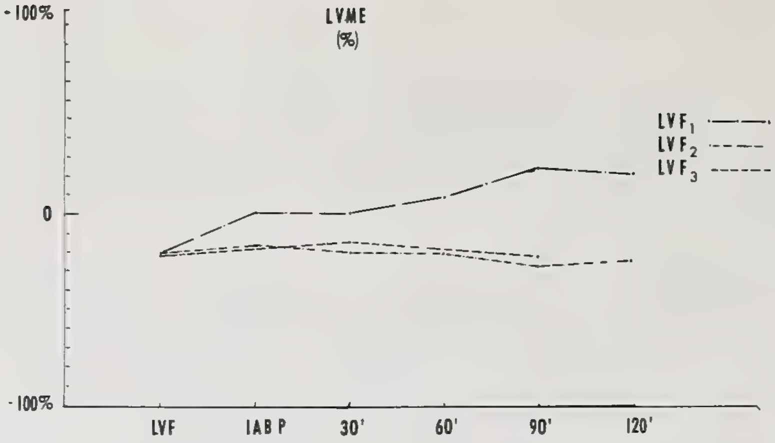

FIGURE 14.

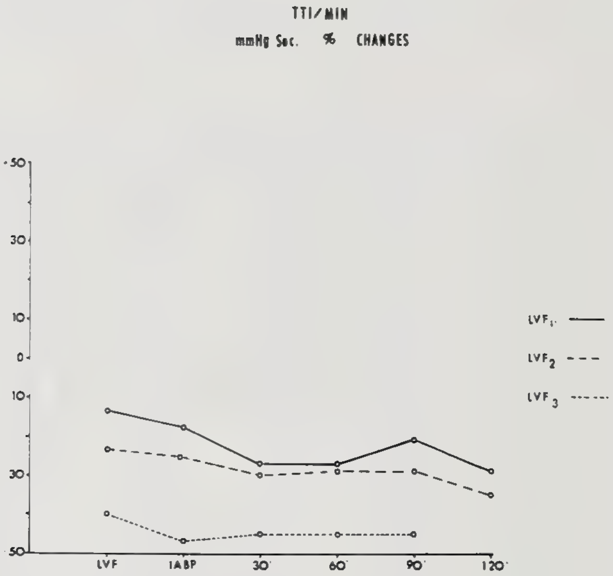

FIGURE 15.

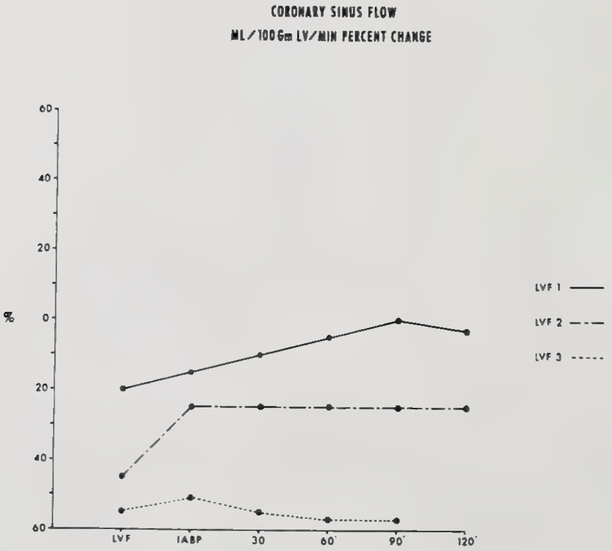

FIGURE 16.

TABLE 7

PEAK SYSTOLIC

LVP

(15 DOGS IN LVF_1)

	Baseline	LVF_1	IABP	30 min	60 min	90 min	120 min
1	128	110	100	106	110	116	124
2	130	108	104	109	109	111	115
3	110	100	96	98	98	102	106
4	130	106	104	104	104	106	120
5	120	108	98	100	100	110	120
6	124	104	96	100	98	110	120
7	120	104	100	104	104	106	110
8	124	108	104	110	114	120	124
9	128	108	100	110	110	120	126
10	126	108	100	110	116	126	126
11	110	100	96	99	99	101	105
12	112	100	96	98	98	100	112
13	114	100	100	100	110	114	114
14	120	104	96	100	112	120	120
15	120	104	96	100	100	100	116

TABLE 8

CARDIAC OUTPUT MINUS CORONARY FLOW

(ml/kg/min)

LVF_1

	Baseline	LVF_1	IABP	30 min	60 min	90 min	120 min
1	110	84	100	94	108	108	108
2	105	83	99	93	105	105	105
3	100	82	98	92	105	103	103
4	100	80	95	90	103	103	103
5	103	82	101	94	108	108	103
6	102	80	96	94	104	104	105
7	102	82	97	92	105	105	103
8	106	83	99	93	106	106	106
9	104	84	100	94	107	107	104
10	112	86	103	96	108	108	109
11	112	86	102	96	109	109	109
12	100	80	95	90	103	103	103
13	102	81	96	91	104	104	104
14	106	84	100	96	103	103	106
15	110	86	100	96	104	104	109

TABLE 9

AORTIC PRESSURES: PEAK SYSTOLIC/END DIASTOLIC

AoP LVF_1

Baseline	LVF_1	IABP	30 min	60 min	90 min	120 min
128/86	110/80	100/64	106/64	110/72	116/74	124/80
130/90	108/78	104/70	108/70	108/72	110/74	115/75
110/74	100/74	96/66	98/66	98/66	102/70	106/70
130/90	106/88	104/82	104/84	104/84	106/88	120/90
120/85	108/76	98/62	100/62	100/64	110/70	120/76
124/90	104/70	96/64	100/64	98/64	110/72	120/80
120/90	104/66	100/62	104/70	104/70	106/72	110/75
124/84	108/64	104/56	110/60	114/64	120/74	124/80
128/88	108/68	100/54	110/58	110/58	120/70	126/75
126/80	108/60	100/52	110/56	116/60	126/60	126/64
110/75	100/68	96/58	99/64	98/66	100/68	105/68
112/78	100/65	96/56	98/56	98/60	100/60	112/68
114/75	100/70	100/66	100/66	110/70	114/72	114/75
120/80	104/70	96/60	100/62	112/62	120/70	120/70
120/80	104/72	96/62	100/65	100/65	100/72	116/72

TABLE 10

PEAK DIASTOLIC AORTIC PRESSURE

(mm Hg)

LVF_1

	Baseline	IABP
1	90	110
2	96	120
3	82	110
4	95	115
5	90	110
6	96	120
7	95	112
8	90	110
9	94	120
10	88	115
11	80	100
12	84	102
13	80	100
14	90	110
15	90	110

mean Baseline	mean IABP
89	111

% increase
+24.7

TABLE 11

HEMODYNAMIC-CARDIAC METABOLIC EFFECTS OF IABP IN DOGS IN LVF_2

	# Dogs	Baseline	LVF_2	IABP	30 min	60 min	90 min	120 min
HEART RATE (beats/min)	15	110[a] (5)	100 (5)	100 (5)	90 (5)	90 (5)	90 (5)	80 (5)
LVP (mm Hg)	"	140 (10)	98 (4)	90 (4)	94 (4)	86 (2)	86 (2)	84 (2)
LVEDP (mm Hg)	"	2.5 (1)	12.5 (2)	12.5 (2)	7.5 (1)	7.5 (1)	2.5 (.5)	2.5 (.5)
MLAP (mm Hg)	"	2.5 (1)	15 (2)	15 (2)	10 (1)	10 (1)	5 (.5)	2.5 (.5)
MAP (mm Hg)	"	104 (4)	74 (2)	84 (2)	82 (2)	84 (1)	86 (2)	86 (2)
CO (ml/kg/min)	"	110 (5)	77 (3)	87 (3)	90 (3)	90 (3)	94 (2)	94 (2)
CSF (ml/100gm LV/min)	"	53 (3)	35 (2)	39 (2)	38 (2)	40 (2)	40 (2)	39 (2)
CaF (ml/kg/min)	"	20 (4)	14 (2)	16 (3)	16 (3)	18 (3)	18 (3)	18 (3)
ReF (ml/kg/min)	15 (3)	16 (3)	11 (3)	13 (3)	14 (3)	14 (3)	14 (3)	14 (3)
TTI/min (mm Hg/sec)	"	2508 (120)	1500 (80)	1100 (70)	800 (70)	890 (70)	845 (70)	640 (70)
TPR (units: mm Hg/L min)	"	61.21 (4)	71.47 (4)	62.06 (4)	58.51 (4)	60.00 (4)	58.86 (4)	58.86 (4)
MVO_2 (ml/100gm LV/min)	"	8.13 (10)	6.52 (5)	6.57 (5)	--	6.64 (5)	--	6.57 (5)
LVMW (kg/m/min)	"	2.484 (.40)	1.208 (.10)	1.253 (.10)	1.355 (.20)	1.238 (.20)	1.293 (.20)	1.272 (.20)
LVME (%)	"	29 (3)	23 (3)	24 (3)	--	21 (3)	--	22 (3)
Central Venous Blood Desaturation	"	15% (5)	29% (8)	--	--	26% (8)	--	17% (5)
dp/dt LVP (mm Hg/sec)	"	1200 (4)	900 (2)	940 (2)	1200 (3)	1200 (3)	1210 (3)	1210 (3)

[a] Mean values, with standard error in parenthesis.

TABLE 12

PEAK SYSTOLIC LVP

(15 DOGS IN LVF_2)

	Baseline	LVF_2	IABP	30 min	60 min	90 min	120 min
1	130	94	86	90	84	84	82
2	140	100	90	92	88	86	86
3	130	98	96	94	86	86	86
4	144	102	96	94	90	86	88
5	146	100	96	96	88	88	90
6	130	100	94	94	88	88	90
7	145	100	90	92	92	94	96
8	140	98	90	94	86	84	84
9	142	98	96	92	94	86	84
10	145	100	92	94	88	86	86
11	140	102	94	96	90	90	86
12	136	100	90	92	94	90	86
13	132	94	88	90	84	82	82
14	138	96	88	86	86	84	84
15	150	102	94	98	88	88	86

TABLE 13

CARDIAC OUTPUT MINUS CORONARY FLOW (ml/kg/min)

LVF_2

	Baseline	LVF_2	IABP	30 min	60 min	90 min	120 min
1	112	78	88	92	92	95	95
2	112	78	86	88	94	94	95
3	115	80	87	87	87	94	96
4	115	80	90	93	93	96	96
5	114	80	86	87	88	92	94
6	112	78	88	92	92	95	95
7	112	76	86	87	87	92	94
8	110	77	87	90	90	94	94
9	112	78	90	90	90	94	94
10	108	74	86	90	90	92	94
11	110	78	86	90	90	94	94
12	105	74	84	87	87	92	92
13	110	76	85	88	88	94	94
14	106	78	88	88	88	92	92
15	106	78	85	88	88	95	95

TABLE 14

AORTIC PRESSURES: PEAK SYSTOLIC/END DIASTOLIC
(mm Hg)
AoP LVF_2

Baseline	LVF_2	IABP	30 min	60 min	90 min	120 min
130/85	94/75	86/65	90/65	84/68	84/70	82/70
140/90	100/80	90/72	92/74	88/72	86/70	86/70
130/90	98/75	96/70	94/68	86/65	86/65	86/65
144/110	104/80	94/62	96/70	90/64	86/64	88/64
146/100	100/74	96/70	96/66	88/60	88/60	90/65
130/80	100/72	94/62	94/62	88/60	88/60	90/64
145/100	100/80	90/65	92/65	92/65	94/70	96/72
140/100	98/80	90/65	94/65	86/60	84/60	84/65
142/100	98/80	96/68	92/62	94/66	86/65	84/65
145/92	100/84	92/75	94/75	88/65	86/65	86/65
140/80	102/72	94/62	96/65	90/60	90/60	86/60
136/80	100/72	90/60	92/64	94/64	90/65	86/62
132/85	94/78	88/70	90/70	84/60	82/60	82/65
138/80	96/72	88/62	86/60	86/60	84/60	84/60
150/110	102/90	94/80	98/84	88/75	88/75	86/80

TABLE 15

PEAK DIASTOLIC AORTIC PRESSURE
(mm Hg)
LVF_2

	LVF_2	IABP	
1	82	94	
2	90	100	
3	84	94	
4	90	100	Mean LVF_2 86
5	80	94	
6	80	94	Mean IABP 104
7	90	100	
8	90	130	Increase %
9	90	110	17.4
10	90	110	
11	84	94	
12	82	96	
13	82	100	
14	88	100	
15	94	104	

TABLE 16

HEMODYNAMIC-CARDIAC METABOLIC EFFECTS OF IABP IN DOGS IN LVF_3

	# Dogs	Baseline	LVF_3	IABP	30 min	60 min	90 min	120 min
HEART RATE	12	120[a]	100	100	100	100	100	--
(beats/min)		(5)	(5)	(5)	(5)	(5)	(5)	
LVP	"	130	74	72	74	76	74	--
(mm Hg)		(10)	(2)	(2)	(2)	(2)	(2)	
LVEDP	"	2.5	15	15	12	15	15	--
(mm Hg)		(1)	(5)	(5)	(5)	(5)	(5)	
MLAP	"	2.5	15	15	15	15	15	--
(mm Hg)		(1)	(5)	(5)	(5)	(5)	(5)	
MAP	"	110	62	66	64	64	64	--
(mm Hg)		(5)	(3)	(4)	(3)	(3)	(3)	
CO	"	96	42	68	56	53	53	--
(ml/kg/min)		(5)	(3)	(3)	(3)	(3)	(3)	
CSF	"	70	33	35	32	30	30	--
(ml/100gm LV/min)		(5)	(2)	(2)	(2)	(2)	(2)	
CaF	"	18	8	5.3	5.3	5.3	5.3	--
(ml/kg/min)		(2)	(2)	(2)	(2)	(2)	(2)	
ReF	"	10	4	4	4	4	4	--
(ml/kg/min)		(3)	(1)	(1)	(1)	(1)	(1)	
TTI/min	"	2640	1610	1390	1500	1560	1560	--
(mm Hg/sec)		(150)	(75)	(62)	(75)	(75)	(75)	
TPR	"	73.79	91.90	61.76	71.76	76.25	76.25	--
(units: mm Hg/L min)		(5)	(8)	(5)	(5)	(5)	(5)	
MVO_2	"	8.55	5.38	--	5.82	--	5.80	--
(ml/100gm LV/min)		(10)	(3)		(3)		(3)	
LVMW	"	2.027	0.510	0.789	0.675	0.654	0.636	--
(kg/m/min)		(.60)	(.10)	(.10)	(.10)	(.10)	(.10)	
LVME	"	21	17	--	18	--	17	--
(%)		(4)	(3)		(3)		(3)	
Arterial	"	7.40	7.27	--	7.28	--	7.15	--
pH		(.3)	(.3)		(.3)		(.1)	
Central Venous	"	15	48	--	49	--	51	--
Desaturation		(3)	(3)		(3)		(3)	
Excess Lactate	"	-1.60	+0.19	--	+0.35	--	+0.78	--
		(.03)	(.02)		(.02)		(.02)	

[a] Mean values, with standard error in parenthesis.

TABLE 17

PEAK SYSTOLIC LVP

(12 DOGS IN LVF_3)

	Baseline	LVF_3	IABP	30 min	60 min	90 min	120 min
1	120	72	70	72	74	72	--
2	134	78	74	74	76	75	--
3	128	74	70	72	74	72	--
4	136	75	70	72	74	74	--
5	130	74	70	70	74	72	--
6	130	74	72	74	76	74	--
7	128	72	72	70	74	74	--
8	138	76	70	72	76	74	--
9	140	76	72	70	74	72	--
10	122	72	72	74	74	74	--
11	124	74	72	72	76	76	--
12	140	76	74	76	78	76	--

TABLE 18

CARDIAC OUTPUT MINUS CORONARY FLOW (ml/kg/min)

LVF_3

	Baseline	LVF_3	IABP	30 min	60 min	90 min	120 min
1	95	42	66	55	55	55	--
2	100	44	70	58	56	56	--
3	101	45	72	59	55	55	--
4	94	40	66	54	50	50	--
5	94	42	68	58	56	56	--
6	96	42	68	56	53	53	--
7	100	44	70	58	56	56	--
8	100	45	71	59	56	56	--
9	101	44	70	59	55	55	--
10	92	40	65	54	51	51	--
11	91	39	65	53	50	50	--
12	93	44	70	58	56	56	--

TABLE 19

AORTIC PRESSURES: PEAK SYSTOLIC/END DIASTOLIC (mm Hg)

AoP LVF_3

Baseline	LVF_3	IABP	30 min	60 min	90 min
120/78	72/50	70/46	72/50	74/54	72/54
134/90	78/66	74/64	74/66	76/66	75/60
128/80	74/50	70/50	72/48	74/50	72/50
136/90	75/60	70/55	72/55	74/55	74/60
130/80	74/54	70/46	70/46	74/50	72/50
130/80	74/55	72/50	74/52	76/54	74/54
128/78	72/50	72/50	70/50	74/52	74/50
138/100	76/54	70/48	72/50	76/50	74/50
140/90	76/70	72/60	70/60	74/62	72/64
122/84	72/62	72/60	74/64	74/62	74/62
124/80	74/56	72/50	72/50	76/52	76/52
140/90	76/58	74/50	76/50	78/50	76/54

TABLE 20

PEAK DIASTOLIC AORTIC PRESSURE (mm Hg)

LVF_3

	LVF_3	IABP
1	54	64
2	70	90
3	60	70
4	66	80
5	58	70
6	60	70
7	60	75
8	60	70
9	74	90
10	70	80
11	66	80
12	64	80
	mean LVF_3 63.5	mean IABP 76.5
		% increase 20%

Changes were the most definite at the stage LVF_1, when mechanical efficiency was increased 60%.

In LVF_2, the main effect of IABP appeared to be the unloading of the left ventricle, as evidenced by a return to normal of the elevated LVEDP and MLAP, with a sustained systolic LVP. "Unloading" produced an increase in myocardial contractility, as evidenced by an increase in dp/dt of LVP and stroke volume. Coronary flow was little improved; this curve paralleled that of MAoP, demonstrating a pressure dependent relationship.

In LVF_3, the hemodynamic effects of IABP were insignificant. Lack of improvement in tissue perfusion was evidenced by progressive deterioration of urinary output, central venous blood desaturation, arterial pH, coronary excess lactate. Survival was not improved.

The "occlusive effect" of the balloon at the stage of shock was best demonstrated by cine-aortogram.

Indications and Limitations of IABP.

This study suggests that if IABP is to be used as a method of assisted circulation, it must be used before the occurrence of shock.

Attempts at Improvement and Potentiation.

Anti-arrhythmic agents. The use of Reserpine, Propranalol and Chlorpromazine, in appropriate doses, makes synchronization of the device easier, performance more effective.

Inotropic agents (Glucagon). Glucagon injected at a dose of 0.7 mg/kg/min, after one hour of pumping at the stage of LVF_3, produced remarkable hemodynamic improvement in a group of nine dogs. Stroke volume, coronary and systemic flows, mean aortic pressure were increased, while LVEDP and MLAP reverted to normal in seven out of nine animals. LVMW and MVO_2 increased, however, to 36% and survival was shortened.

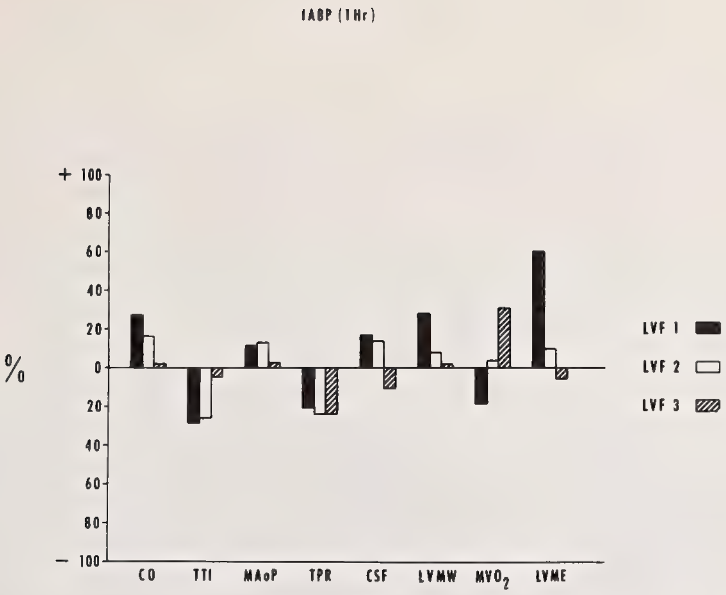

FIGURE 17.

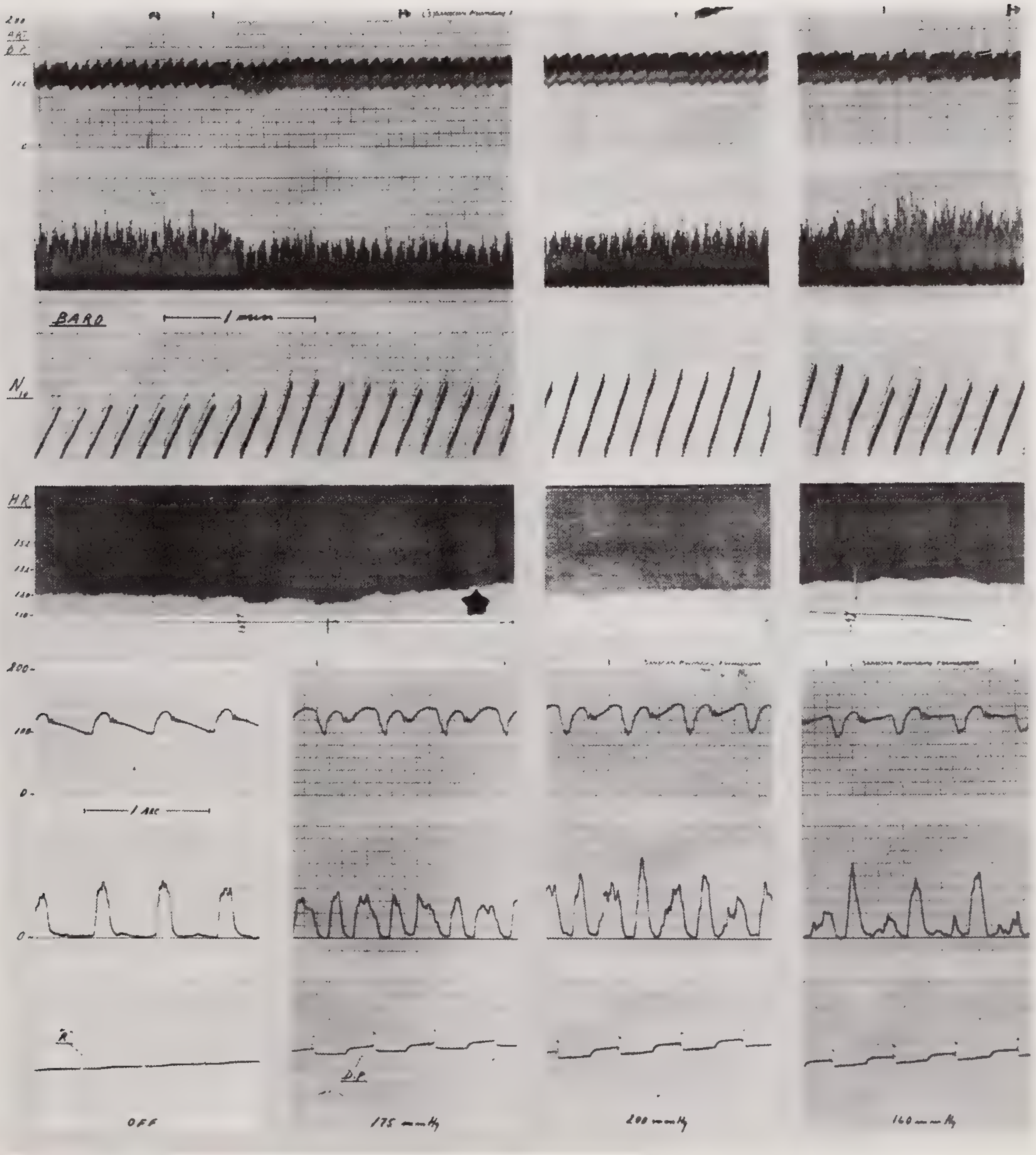

I. A. BALLOON ASSISTANCE

FIGURE 18. SEE TEXT FOR EXPLANATION.

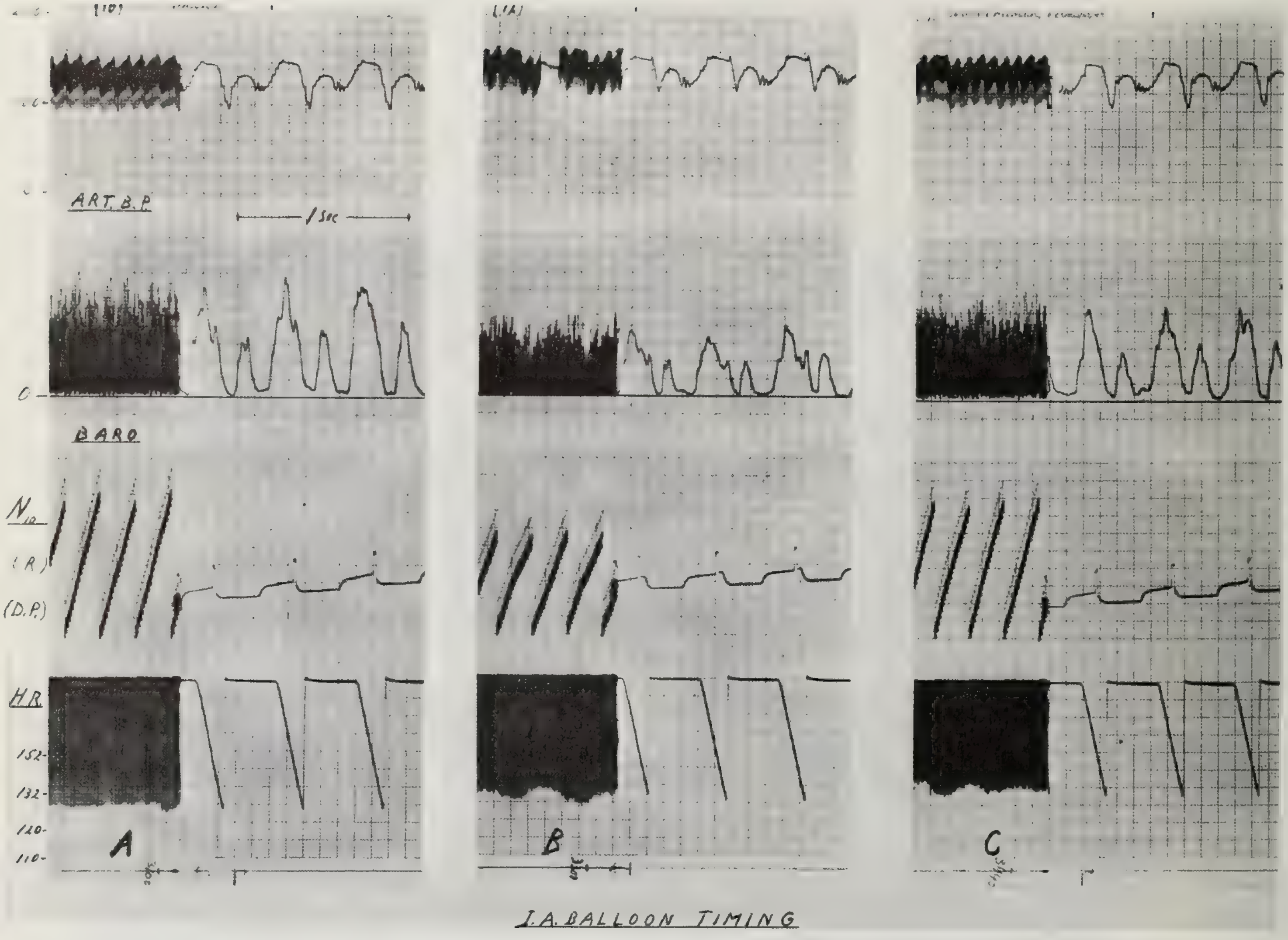

FIGURE 19. SEE TEXT FOR EXPLANATION.

Plasma volume expansion (Low molecular dextran). Infusion of 500 cc of low molecular dextran after one hour of pumping increased stroke volume, coronary and systemic flows, with no improvement in LVEDP and MLAP, and with increase in LVMW and MVO_2.

A "see-sawing" method of aortic counterpulsation. Thinking of counterpulsation as a method of left ventricular assistance, one is reminded of the paired, coordinated action that goes into see-sawing.

The "occlusive" effect and the "sucking" effect of IABP at the stage of experimental coronary shock indicate a lack of coordination between the primary and the auxiliary pump.

It is possible that an automated pumping system, with a volume and pressure variable balloon, activated by an instantaneously monitored stroke volume, could carry to the stage of LVF_3 the beneficial effects noticed in stages LVF_1 and LVF_2.

SUMMARY

1. An experimental model for canine acute myocardial infarction-left ventricular failure has been presented.
2. The criteria have been presented for the definition and classification of acute LVF in three stages.
3. The effects of IABP have been described, in the normal and in animals at different stages of failure.
4. The presented data indicate that IABP is an effective method of left ventricular assistance, before the occurrence of "shock."
5. At the stage of experimental coronary shock, IABP is limited in its performance by the drop in central aortic pressure and volume, and the drop in stroke volume.
6. The "occlusive" and the "sucking" effects of IABP have been described as limiting factors in its performance.
7. A "see-sawing" method has been proposed, of coordinated stroke volume-aortic counterpulse.

II. INTRA-AORTIC BALLOON ASSISTANCE AND AORTIC BARORECEPTOR OUTPUT

The operation of an auxiliary pump for assisting the heart will of necessity modify or determine pressure-flow characteristics in the arterial tree. Pressure contours in aorta and carotid arteries are of particular interest, not only because of their direct hemodynamic relevance, but also because of their effects on baroreceptors located in the walls of these vessels. From the baroroceptors originates feedback information which, via neural pathways, reaches the central nervous system and thus contributes to neuro-humoral control of cardiac and vascular functions.

As part of an investigation into the involvement of the autonomic nervous system in circulatory control, we have examined how the operation of an intra-aortic balloon changes the pattern of impulses originating in baroreceptors, strategically located in the aortic arch. In the dog, the group of nerve fibers conducting these impulses, joins the vagus nerve within the chest and remains part of this nerve throughout most of its course in the neck. Electrodes were placed on the left cervical vagus, and from the impulses thus recorded those of baroreceptor origin were selectively isolated by the employment of analog-computational methods.

Representative data are reproduced in Figure 18: Paper speed in the upper half of the figure was 1 mm/sec. and in the lower half 50 mm/sec. In each half, the traces represent (from top to bottom) proximal aortic pressure; envelope of baroreceptor output ("BRO"); baroreceptor output integrated over ten seconds ("N_{10}" = height of heavy bar); and finally, in the upper half, in the bottom trace, the border indicates beat-beat heart rate. Superimposed on the N_{10} bar are a brief square wave substitute for the ECG R-wave and the drive pressure - the latter obtained from a transducer in the console. In the first panel to the left the balloon is passive; the neurogram displays the characteristic BRO during systole. Start of balloon operation is indicated on the N_{10} trace: the total BRO increase reached the maximum level after 15-20 seconds. Interestingly, heart rate showed only a transient slowing which was followed by an increase to above control level. In the high-speed tracing, the following features stand out: BRO caused by cardiac ejection during systole and by balloon inflation during diastole is clearly delineated; the cardiac contribution was reduced from that during the control period; the diastolic BRO was 50-100% greater (by area) than that occurring during systole. In the next panel (third from left) an increase of inflation pressure from 175 to 200 mm Hg caused a further increase in BRO. The last panel depicts the consequences of reducing the inflation (drive) pressure to 160 mm Hg. A reduction of diastolic BRO would be expected; the reason for the systolic increase, however, cannot be deduced from any changes in static pressure, pulse pressure, or pressure derivative.

In Figure 19 are reproduced data which illustrate the effects caused by a change of timing. Using drive pressure as an indicator, deflation of the balloon is seen in panel "A" to occur just about synchronously with the R-wave. An increased deflation delay of about 35 msec (panel "B") led to a rather surprising reduction of both systolic, diastolic, and total BRO. Again, blood pressure contours do not readily explain the changes observed in the neurogram. In the last panel ("C") is seen how BRO returned to previous levels as the deflation delay was reset to the shorter duration.

In summary, with respect to intra-aortic balloon assistance, the following points may be made at this time:

1. The aortic baroreceptor neurogram may be changed drastically and reflect in a sensitive manner mode of balloon operation.
2. Total BRO is increased.
3. Aortic baroreceptor output appears as a more sensitive indicator of proximal aortic hemodynamics than the intra-aortic pressure (recorded with arterial catheter and extracorporeal transducer).
4. The data do not permit any conclusions as to systemic consequences; those aspects constitute the objective of our next series of experiments.

REFERENCES

1. Birtwell, W. C., Soroff, H. S., Wall, M., Bisberg, A., Levine, H. J., and Deterling, R. A., Assisted circulation: I. An improved method for counterpulsation. TASAIO 8:35, 1962.
2. Brown, B. G., Goldfarb, D., Topaz, S., and Gott, V. L., Diastolic augmentation by intra-aortic balloon: Circulatory hemodynamics and treatment of severe acute left ventricular failure in dogs. J. Thorac. Cardiov. Surg. 53:789, 1967.
3. Casten, G. G., Murphy, W. P., and Alley, J. C., Augmentation of diastolic arterial pressure by mechanical means: effect on coronary sinus flow. Circulation 16:866, 1957.
4. Clauss, R. H., Birtwell, W. C., Albertal, G., Lunzer, S., Taylor, W., Fosberg, A. M., and Harken, D. E., Assisted circulation: I. Arterial counterpulsator. J. Thorac. Cardiov. Surg. 41:447, 1961.
5. Cronin, R. F. P., and Calatayud, J. B. Hemodynamic effects of synchronous arterio-arterial pumping after experimental myocardial infarction. Am. J. Cardiol. 768, June 1963.
6. Dietzman, R. H., Bloch, J. H., Feemster, J. A., Idezuki, Y., and Lillehei, R. C.: Mechanisms in the production of shock, Surgery 62:645, 1967.
7. Ellis, P. R., Lee, C., Wong, S. H., Del Rosario, V. C., Hyland, J. W., and Prator, G., Assisted circulation in treatment of experimental heart failure. Arch. Surg. 90:879, 1965.
8. Goldfarb, D., Knikerbocker, G. G., Jude, J. R., and Bahnson, H. T.: Treatment of circulatory failure with a new system for selective diastolic augmentation. Surgery 56:547, 1964.
9. Hahnloser, P. B., Gallo, E., and Schenk, W. J., The hemodynamics of counterpulsation. J. Thorac. Cardiov. Surg. 51:366, 1966.
10. Kantrowitz, A., Tjønneland, S., Krakauer, J., Buhner, A. N., Phillips, S. J., Yahr, W. Z., Shapiro, M., Freed, P. S., Jaron, D., Sherman, J. L. Jr., Clinical experience with cardiac assistance by means of intra-aortic phase shift balloon pumping. TASAIO, 14:344, 1968.
11. Laird, J. D., Jones, R. T., Austen, W. G., and Buckley, M. J., Observations on the dynamics of an intra-aortic balloon pump. In Digest of the seventh International Conference on Medical and Biological Engineering, Copenhagen, 1967, p. 29-4.
12. Lefemine, A. A., Low, H. B., Cohen, M. L., Lunzer, S., and Harken, D. E. Assisted Circulation: III. The effects of synchronized arterio-arterial counterpulsation on myocardial O_2 consumption and coronary flow. Am. Heart J. 64:789, 1962.
13. Moulopoulos, S. D., Topaz, S., and Kolff, W. J.: Diastolic balloon pumping (with carbon dioxide) in the aorta: mechanical assistance to the failing circulation. Am. Heart J. 63:669, 1962.
14. Schilt, W., Freed, P. S., Khalil, G., and Kantrowitz, A., Temporary non-surgical intra-arterial cardiac assistance. TASAIO, 13:322, 1967.
15. Shea, T. M., Watson, R. M., Piotrowski, F., Dermksean, G., and Case, R. B., Anaerobic myocardial metabolism. Amer. J. Physiol. 203:463, 1962.
16. Weil, M. H., and Shubin, H. Shock following acute myocardial infarction: Current understanding of hemodynamic mechanisms. Progress in Cardiovasc. Dis. 11:1, 1968.
17. Watkins, D. H., and Duchesne, E. R.: Postsystolic myocardial augmentation: Physiological considerations and techniques. J. Appl. Physiol. 17:61, 1962.
18. Willman, V. L., Cooper, T., Riberi, A., and Hanlon, C. R., Cardiac assistance by diastolic augmentation. Hemodynamic evaluation on dogs with complete heart block.

DISCUSSION

DR. JACOBEY: I want to congratulate the authors on their very interesting study of intraaortic balloon counterpulsation. I think their conclusions, as transferred to the human regarding the treatment of shock, point up the very interesting question that so far today has not been alluded to, and that is the relative efficiency of counterpulsation by means of the intraaortic balloon. By way of this, I would just like to mention our last four clinical cases in severe cardiogenic shock. These patients were treated by a similar modality using cannular counterpulsation. This is shown in my first slide. The cannula was inserted via the left subclavian artery and placed at a position 3 cm from the aortic valve. In this way, the pressure changes are produced where they are needed; at the aortic valve and the coronary arteries. Of these last four patients we had three survivors, two of whom died at about one month. Both of these had severe myocardial fibrosis from previous infarctions. The third one is doing well now at six months (Slide). As you can see in the slide, the cannula is put in from the left subclavian artery and its position at the tip is approximately 3 cm from the aortic valve. The small extension beyond that is a pressure catheter which measures the pressures at the aortic valve. The next slide shows an actual tracing, taken in a patient (Slide). This slide demonstrates fairly readily the types of changes that can be produced with this method of counterpulsation. On the left you have counterpulsation going on; and you can see that the systolic pressure is 100, and the diastolic 126. During the middle phases of the slide you can see this is without counterpulsation and the systolic has risen 34 mm of mercury and diastolic has fallen to 82 or approximately 44 mm of mercury. The next slide shows another patient and, again, the same type of changes are produced with this method (Slide). I think this brings up the question of what the efficiency of the intraaortic balloon is. However, in addition to that, I would like to ask the authors if they would comment on what their experience has been with potential complications. This subject has not been brought up today. How many balloon ruptures did you experience? What kind of aortic damage do you get? You talked about aortic flap with a balloon. Was there any actual damage or rupture? Where were your pressure monitors placed when you measured aortic pressures? Were they in the area of the balloon, or around the aortic valve?

DR. KENNEDY: How much time do we have to answer that question?

DR. SEARS: Approximately one minute.

DR. KENNEDY: Time does not really permit my sharing with you all the data from our group this year. Dr. Katubig, of the Department of Pathology at Cleveland Metropolitan General Hospital, carried out intraaortic balloon pumping in 20 cadavers with pacing mode at 160 mm Hg drive pressure. The cadavers were all atherosclerotic and ranged in age from 38 to 89 years. There were no ruptures of the aorta nor of the balloon. On the other hand, Dr. Feola had one balloon rupture in 60 dog experiments. Microscopically, there was abrasion of the endothelial cells from the surface as has also been reported by B. G. Brown from Westinghouse Laboratories. There was intense staining, presumably by hemoglobin, of the intimal surface. In three of twenty cadavers, the balloon could not be inserted because of severe aortoiliac atherosclerosis. In four additional subjects, when the balloon was inserted, there was stripping of the intima and free atheromatous debris was found in the aorta.

CHAPTER 54

PHYSIOLOGIC EFFECTS AND ENGINEERING EVALUATION OF INTRA-AORTIC BALLOONS AND CONTROL CONSOLES

F. T. Galysh, A. S. Patel and C. Y. Lin

Travenol Laboratories, Inc.
Morton Grove, Illinois

Westinghouse balloons and control console, Western Gear balloons, and the Avco Model 5 console were evaluated. Observed balloon defects were: balloon pinholes, catheter wall breakdown and subsequent kinking, and slip joint dislodgement. Catheter kinking was found in the mock circulatory system (MCS) to be mechanistically associated with longitudinal balloon-catheter movements. Inflation-deflation characteristics of the ends vs. the central portion of single segment balloons were studied in the MCS using an electrical technique. ECG triggering evaluation studies were performed on the Avco and Westinghouse controllers over a variety of clinical arrhythmias. Pressure triggering circuits of both consoles could not discriminate the animal's pulse pressure from the aortic pressure rise elicited by balloon inflation. Surgical installation of ~22 mm diameter, 40-50 ml, 14 Fr catheter balloons in calves (C) and ~15 mm, ~25 ml, 14 Fr catheter balloons in dogs (D) was a simple procedure, but was attended with thrombosis of the femoral artery insertion site and circulatory insufficiency (weakness) of the extremity in calves. Hemodynamic studies were carried out in the MCS and in calves and dogs with normal cardiac status. Mean diastolic pressure ($\overline{P}_d$) in the aortic root was ↑ (increased) 48% in D and 12% in C; aortic root mean pressure was ↑ 13% in D and unchanged in C; abdominal aortic $\overline{P}$ was ↓ 19% in D and 11% in C; $\overline{P}_{LV}$ was ↓ 8% in D and 7% in C; cardiac output as pulmonary artery blood flow (Q_{PA}) was ↓ 4% in D and 2% in C; $Q_{cor.art.}$ was unchanged in dogs and ↓ 4% in calves; $Q_{renal\ art.}$ was ↓ 19% in D and 8% in C. Differences in responses of $\overline{P}_d$ between these species are attributable to lower aortic compliance in dogs and pigs as compared to calves and sheep. Renal clearances (GFR and ERPF) in calves were not altered by one week of continuous pumping. Four techniques to achieve the clinical counterpart of chronic cardiac failure in calves and dogs failed.

INTRODUCTION

This report summarizes work performed during the period from July 1, 1968 through mid-May, 1969. The objective of our efforts was to perform engineering and physiologic effects evaluations of single segment intra-aortic balloons supplied by Westinghouse and Western Gear Corporation as well as Westinghouse and Mark II, Model 5 Avco control consoles. Figure 1 shows a Westinghouse balloon and its control console. At the top of the console is the monitoring oscilloscope to help adjust electronic control knobs on the next two sections so that proper synchronism of the balloon pumping is obtained with the use of the skin ECG. The small portable transparent unit is called a pneumatic actuator, the pneumatic control knobs being in the lowest section.

The balloon, of course, is to be deflated during ventricular systole and inflated during diastole by gas flows through the catheter, which contains holes in that section which is within the balloon.

ENGINEERING EVALUATION OF CONSOLES

Extensive *in vivo* and *in vitro* studies provided the following findings:

The consoles were found to be reasonably reliable. In the Westinghouse console we had experienced several malfunctions such as loose control knobs of amplifier, inadequate balance capacity for the system pressure transducer, inoperative aortic pressure measurement facility, loose electrical contacts of the power supply module and solenoid clogging due to hair being sucked through the balloon port. Most of these were corrected by Westinghouse Corporation and the rest prevented by appropriate precautions.

Table 1 summarizes evaluations related to the design aspects of the Westinghouse console. The lumen size of the solenoid to balloon connector was smaller than the inner diameter of the balloon catheter, thus providing a major resistance to gas flow. This may be important, especially for deflation of the balloon. Subsequently Westinghouse Corporation increased the lumen size of all connectors of the solenoid ports to a considerably larger size.

On several occasions, an implanted balloon ruptured and the blood which rushed into the pneumatic ports of the console made it non-functional until time consuming cleaning was done. Even though these incidents mainly reflect the unreliability of the balloons, they also indicate the necessity of including a blood safety trap between the balloon and console. Also a spare balloon and actuating system may be required in clinical use.

TABLE 1

DESIGN ASPECTS - WESTINGHOUSE CONSOLE

1. Lumen size of solenoid port connector.
2. Actuator failure following balloon rupture.
3. Insufficiency of balloon deflation response time.
4. Anticipation mode of triggering.
5. Termination of balloon inflation duration.
6. Vacuum pump.

For the 50 ml. balloons used in calves we observed indirect evidence that in the time between the recognition of the "R" wave and ventricular contraction, deflation of the balloon was insufficient as seen in Figure 2 as the initial ventricular pressure peak. This deduction was confirmed by the absence of this peak when either the balloon was turned off or when the anticipation mode of triggering was used. This peak, thus,is the indication of higher impedance seen by the ventricle because of insufficient balloon deflation.

In the anticipation mode of triggering the deflation of the balloon could be initiated just prior to an oncoming systole by using the previous beat's "R" wave. This mode could not be used unless R-wave to R-wave duration remains almost constant, a most unlikely condition in clinical patients. If R-wave to R-wave duration varies and such a mode of triggering is used, then balloon inflation during ventricular systole may occur. The termination of the inflation duration cannot be independently selected as in the Avco console. Only the next "R" wave will initiate deflation. Consequently, if the oncoming "R" wave fails to be recognized, the balloon will remain inflated during the next ventricular systole, an undesirable logic.

The vacuum pump provided in the Westinghouse console is noisy as contrasted with that in the Avco console. Many of the design aspects of the console appear now to be improved as reported earlier in these proceedings by Dr. Evans.

And now a brief discussion of the comparative triggering capacities of the two consoles follows.

Table 2 shows a variety of human clinical arrhythmias available as Series 110 to 129 tape cartridges from Physiological Training Company which were used to evaluate triggering capacity.

TABLE 2

COMPARATIVE EVALUATION OF ECG TRIGGERING CAPACITY

Type of ECG	Westinghouse Console	Avco Console
Sinus Rhythm, Sinus Bradycardia, Sinus Tachycardia, Sinus Arrhythmia	S[a]	S
Premature Atrial & Ventricular Contractions	S	S
Atrial Tachycardia with or without Block	I.M.[b]	S
Atrial Flutter	S	S
Atrial Fibrillation	I.M.	S
Nodal Rhythm	I.M.	S
Nodal Tachycardia	S	S
1st, 2nd, and 3rd Degree AV Block	S	S
Ventricular Tachycardia	I.M.	I.M.
Bundle Branch Block	S	S
Ventricular Fibrillation	No QRS complexes & hence meaningless triggering	
ECG Artifacts (Poor Electrode Contact, Patient Movement, AC Interference)	I.M.	I.M.
Paroxysmal Atrial Tachycardia with or without Block	S	S
Nodal Premature Contractions	I.M.	I.M.

[a] S - Satisfactory Triggering

[b] I.M. - Isolated Mistriggering

PROCEDURAL DIFFERENCE IN READJUSTMENT FOR ECG TRIGGERING

Westinghouse console requires time consuming readjustment. This is due to quantitative nature of readjustment which requires the operator to confirm amount of correction selected by him by observing several beats.

Avco console readjustment is simple, quick discrete selection of next of the three positions of the gain switch.

On the whole, both consoles have fairly good capacity to handle these variations of the ECG. But the Westinghouse console required more frequent triggering adjustment in comparison with the Avco console. The procedural differences for adjustment of both consoles must also be stressed in terms of difficulty of adjustment as well as time required for same. For the Avco console a three position gain switch required switching to the next gain position, a simple quick discrete procedure. For

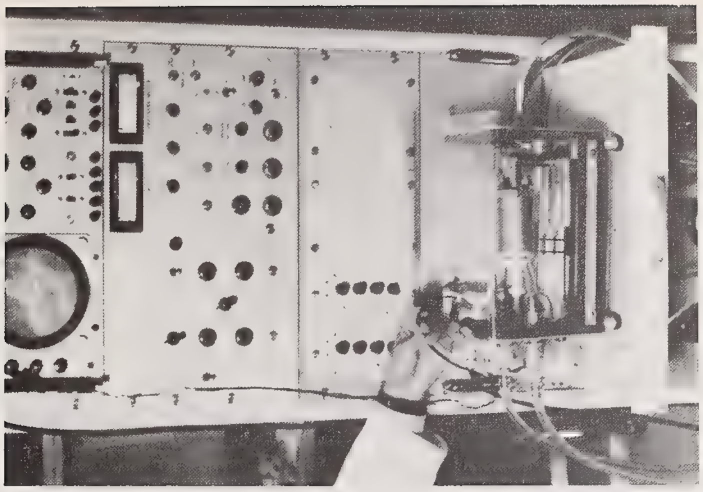

FIGURE 1. WESTINGHOUSE BALLOON AND ITS CONTROL CONSOLE.

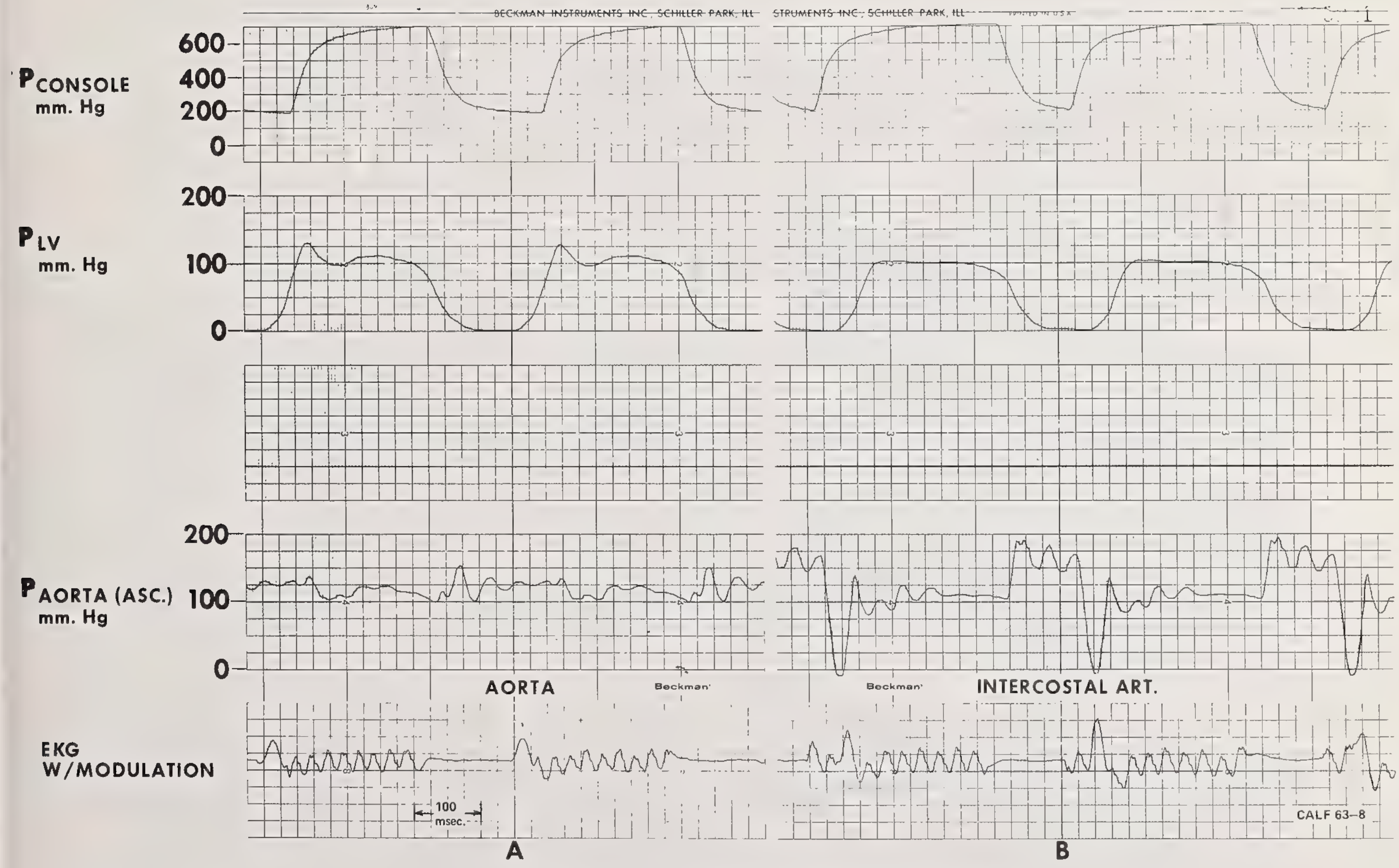

FIGURE 2. INSUFFICIENT BALLOON DEFLATION.

the Westinghouse console, on the other hand, triggering adjustment was difficult and time consuming as it required quantitative adjustment of one or more of three controls, namely: QR slope, RS slope, and pulse width T, and the operator had to observe several beats to confirm the amount of adjustment selected by him.

Both the consoles have a triggering mode using the aortic pressure pulse. Its evaluation in animal studies revealed that whenever a sufficiently large aortic pressure pulse existed, the triggering was satisfactory. But when the aortic pressure pulse was low, the detection circuit failed to distinguish between the aortic pressure pulse and the pressure pulse due to balloon inflation and mistriggering resulted.

Figure 3 shows the Mock Circulation System (MCS) which was used for intra-aortic balloon *in vitro* studies. A Harry Diamond laboratory ventricle, which uses a fluidic amplifier, served as the heart for this simplified systemic circulation system. A suitable aorta (24 mm. in diameter) specially fabricated such that the balloon could be inserted and lateral pressures along its length could be measured, was used. A brachiocephalic trunk analog with appropriate resistance was added to the aorta in order to achieve through it about 30% of the total cardiac output, thus simulating flow to the anterior portion of the body. The aorta was connected to the peripheral systemic load resistance, the output of which returned to the heart via a venous capacitance bag. The level of the venous reservoir determined the filling pressure of the heart. The pressure in the aorta was measured by a pressure transducer via a catheter and could be adjusted to the desired value by a simple feedback system which pneumatically controlled the systemic load resistance. The feedback controller controlled pressure of the air on the rubber diaphragm in the resistance box, which in turn controlled its cross-sectional area and hence the value of the resistance. The ECG for proper synchronism of the assist device was obtained as a pulse from a battery at the instant the fluidic amplifier was triggered by a solenoid controlled by a stimulator such that systole of the heart began.

The flows were measured by electromagnetic flow probes and the pressures at various locations were measured by Statham pressure transducers.

For normal cardiac circulation simulation, a 37 ml., 15 mm. diameter non-occlusive balloon pumping response is shown in Figure 4. The ventricular pressure was reduced from 150 to 115 mm. of Hg. The cardiac output was reduced from 2.86 to 2.44 liters/minute. The brachiocephalic flow was reduced from 0.95 to 0.82 liters/minute. The mean pressures in the ascending aorta (P_1), along the length of balloon (P_2, P_3) and the descending aorta (P_4) were reduced by about 15 mm. of Hg. due to pumping by this non-occlusive balloon. Figure 5 shows the response due to a 58 ml. occlusive balloon 24 mm. in diameter. The ventricular pressure was reduced from 150 to 105 mm. of Hg. The cardiac output was reduced from 2.8 to 2.5 liters/minute, while the brachiocephalic flow was increased from 0.95 to 1.15 liters/minute. It should be noted that unlike its non-occlusive counterpart, the occlusive balloon raised the mean aortic pressure (P_1) in the ascending aorta and along the length of the balloon (P_2, P_3) by about 25 mm. of Hg, but the occlusive balloon also decreased the pressure (P_4) in the descending aorta by about 20 mm. of Hg. Not only in the MCS, but also in experiments on calves and dogs we observed such effects.

Under failing cardiac status simulation, the details of which are given in our six month report, and which was far from pathologic failure in animals, both types of balloon acted as an effective pump, raising the cardiac output and pulse pressure considerably.

In order to study the nature of inflation-deflation characteristics of the balloon a specially fabricated aorta shown in Figure 6 was used. Eleven silver rings (5 mm. in width, 22 mm. in diameter) were fixed in sequence at a distance of 25 mm. apart to the inside wall of this analog made from silicone rubber. The balloon was placed within the segment of the aorta containing these rings and circulation of saline was established in the MCS. A constant current was designed to pass through the column of saline between the two end rings while the balloon was inflated and deflated at a cardiac rate of 75 beats/minute. The voltage signal between a pair of rings was, thus, inversely proportional to the average cross-sectional area of the saline column surrounding the balloon between that pair. The time course of each balloon inflation-deflation cycle was thus represented as an example shown in Figure 7 by the signals obtained between pairs of rings along the length of the balloon.

The technique showed that the ends of the balloon represented by signals S_1, and S_4, inflated earlier than the middle portion, a phenomenon also reported by others in last year's annual meeting as "bubble blowing."

BALLOON DEFECTS

The next several figures show a variety of defects observed in intra-aortic balloons supplied by Westinghouse and Western Gear, detected either in the course of our pre-experimental checks or animal experiments. Figure 8 depicts a balloon typical of those with crazed, rough surfaces with contained inclusions. Early balloon catheters (Figure 9) were incompletely covered with polyurethane balloon material with junctional polyethylene-polyurethane areas serving as a nidus for clot formation. Aneurysmal swellings (Figure 10) occurred in two balloons following inflation to pressures less than 200 mm. Hg; these balloons were rejected from animal evaluation studies. Slipjoint displacement out of the end of the balloon (Figure 11) and out of the catheter (Figure 12) also occurred in animal experiments.

Of more serious consequences were lateral balloon wall pinholing and leaks (Figure 13) at points of balloon wall stress from repeated creasing at the base of the balloon, the so-called umbrella effect. This occurred in six animals pumped from 28 minutes to 15 hours with balloons having

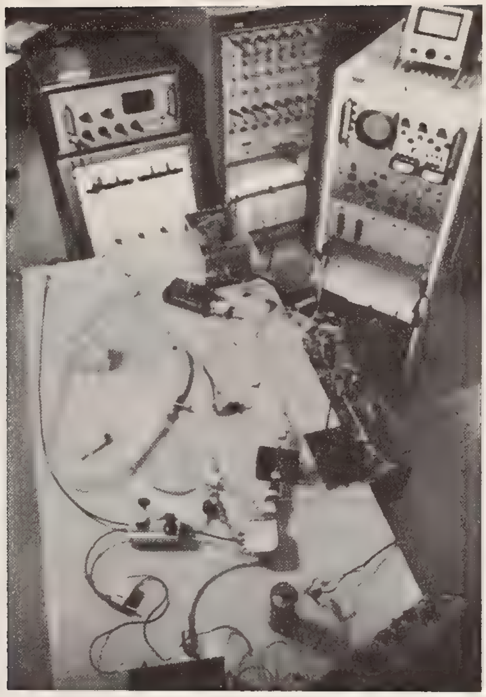

FIGURE 3. MOCK CIRCULATION SYSTEM.

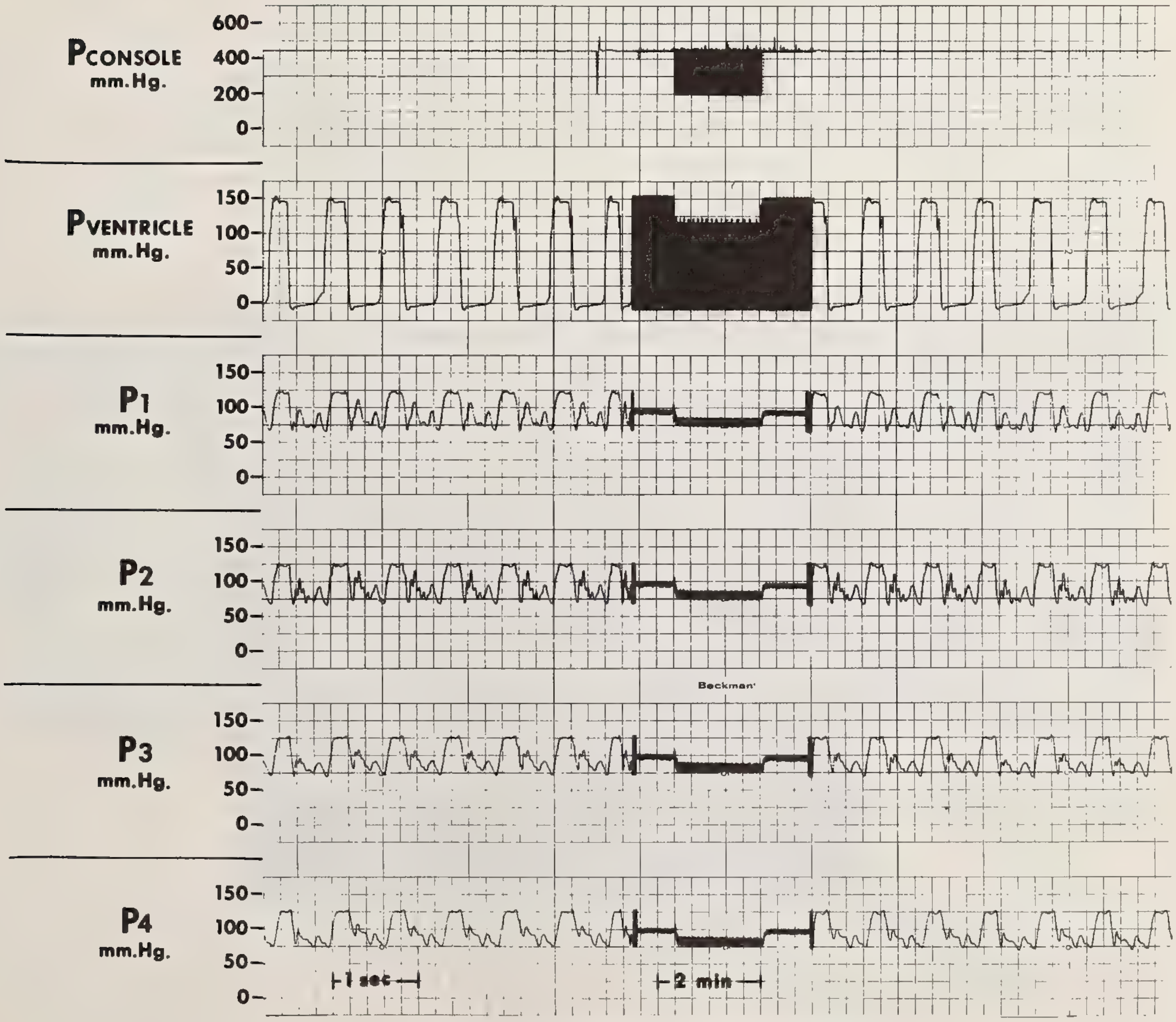

FIGURE 4. NON-OCCLUSIVE BALLOON PUMPING.

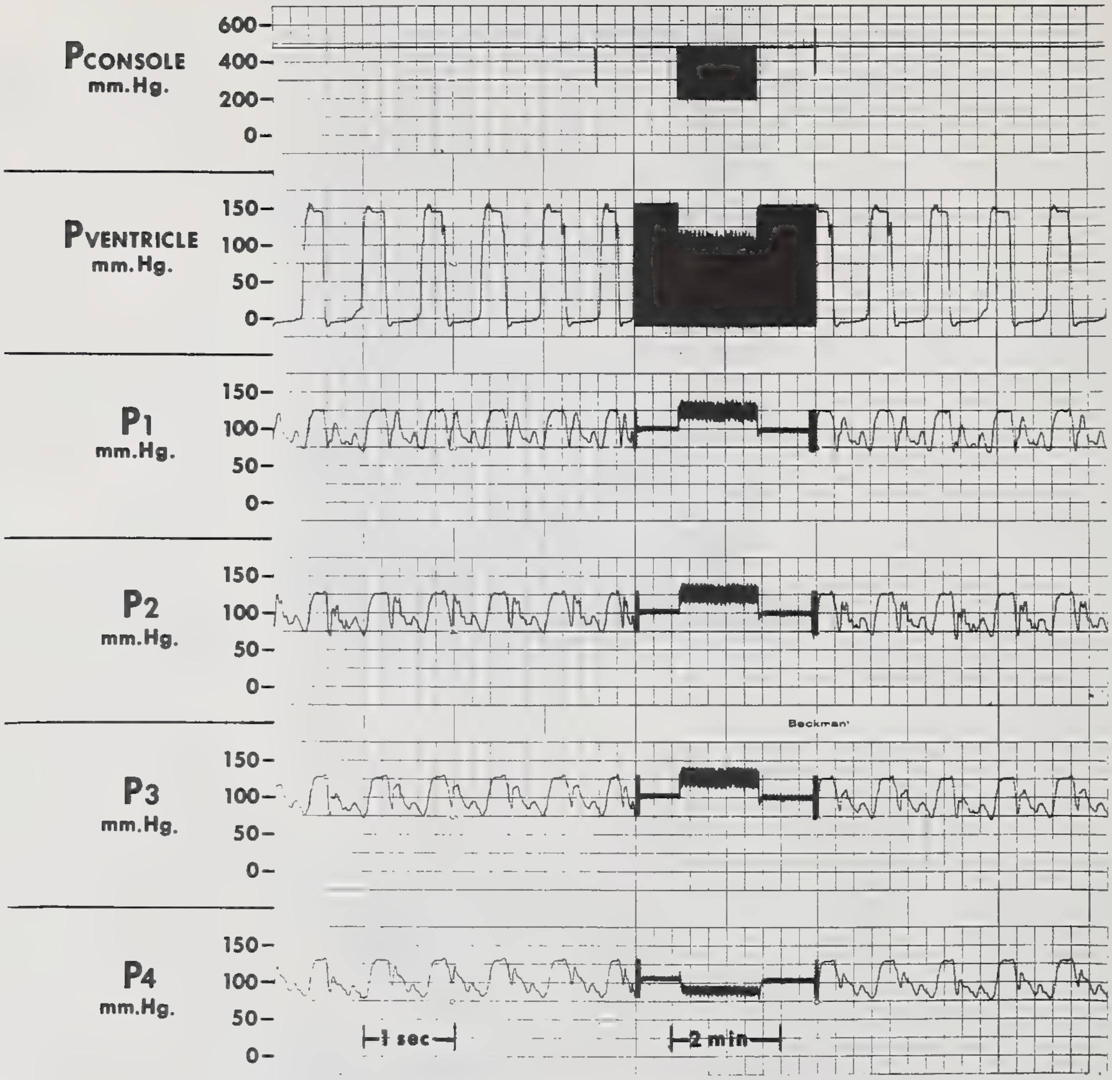

FIGURE 5. OCCLUSIVE BALLOON PUMPING.

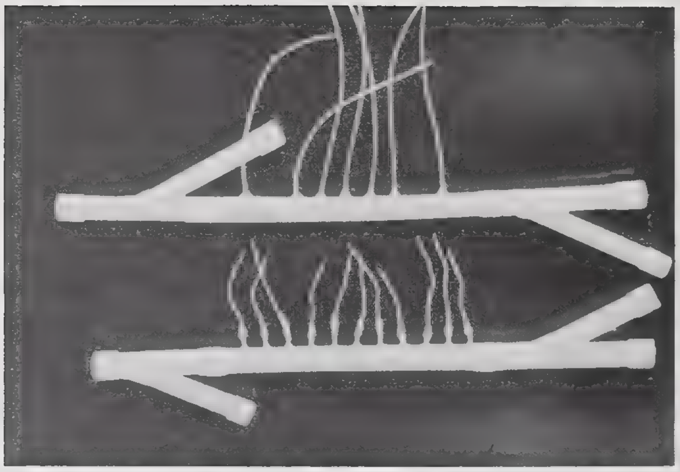

FIGURE 6. SPECIALLY FABRICATED AORTA USED TO STUDY INFLATION-DEFLATION CHARACTERISTICS OF THE BALLOON.

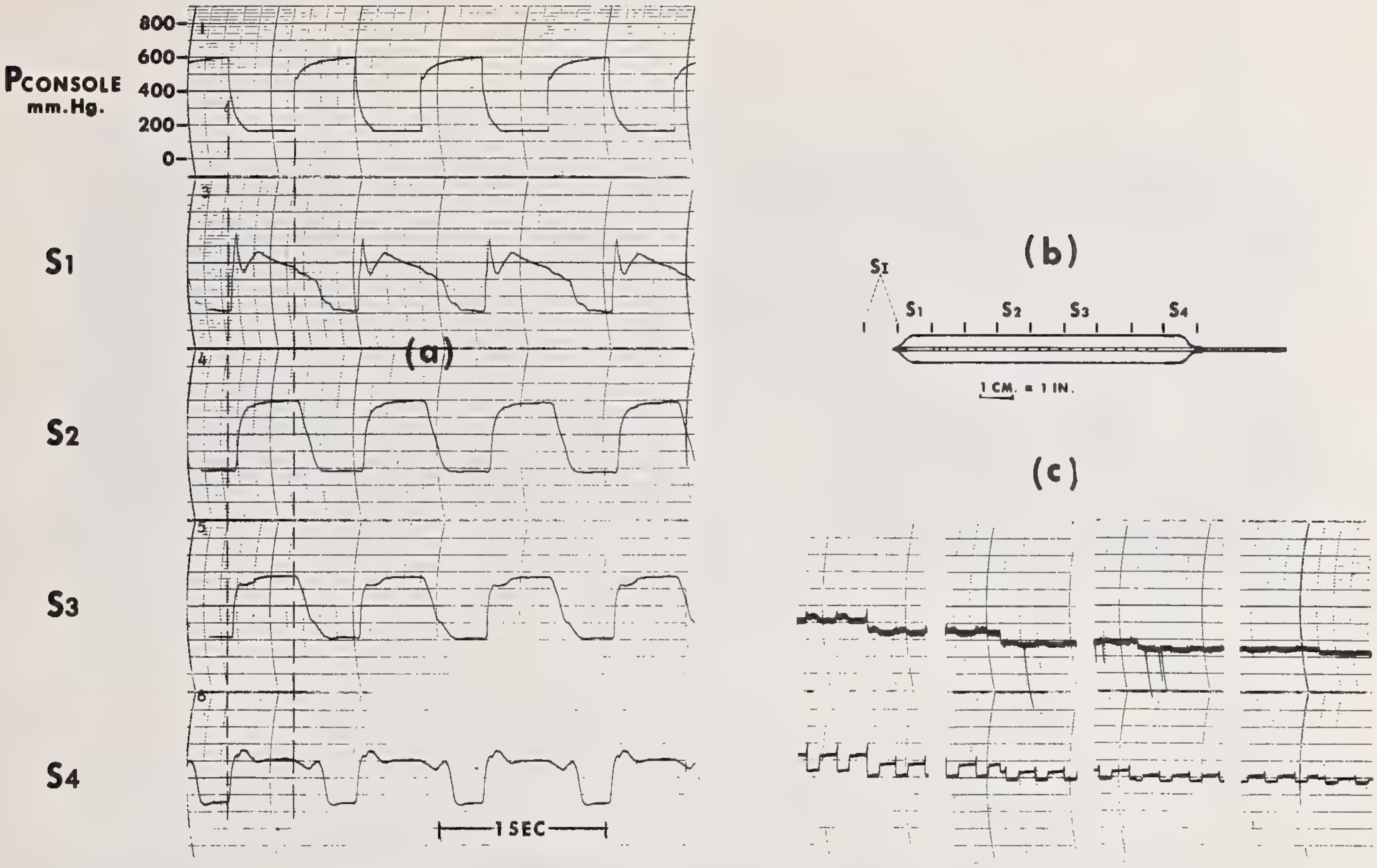

FIGURE 7. TIME COURSE OF BALLOON INFLATION-DEFLATION CYCLE.

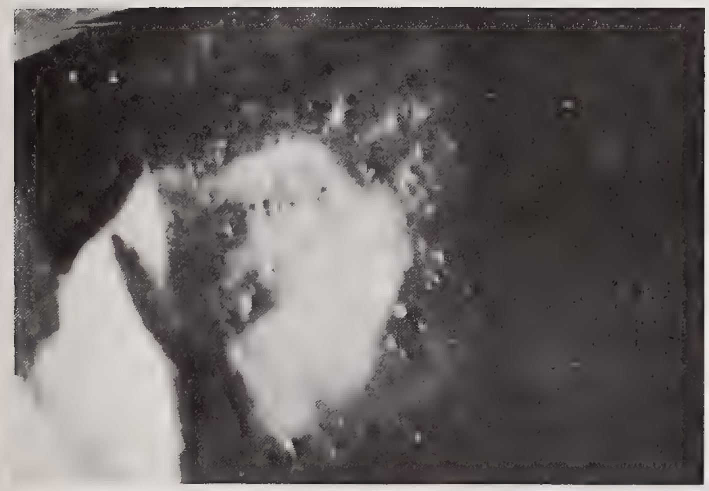

FIGURE 8. BALLOON WITH CRAZED, ROUGH SURFACE.

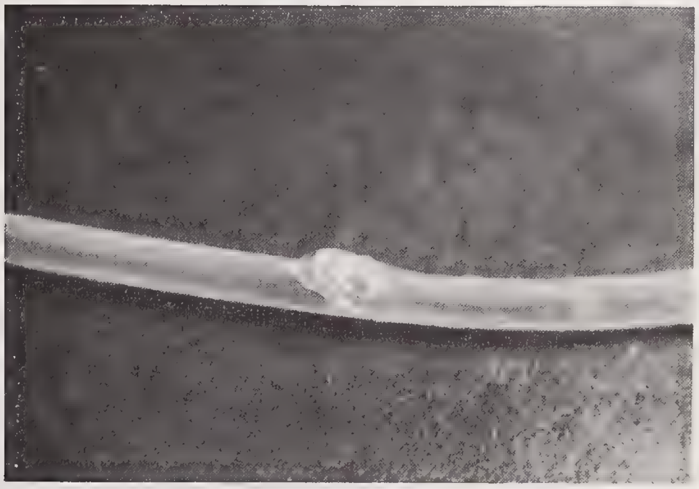

FIGURE 9. EARLY BALLOON CATHETER WITH INCOMPLETE COVERING WITH POLYURETHANE AND JUNCTIONAL POLYETHYLENE-POLYURETHANE AREAS SERVING AS A NIDUS FOR CLOT FORMATION.

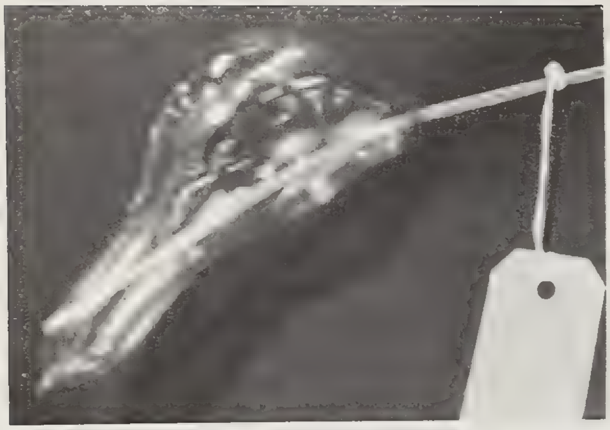

FIGURE 10. ANEURYSMAL SWELLING IN BALLOON FOLLOWING INFLATION.

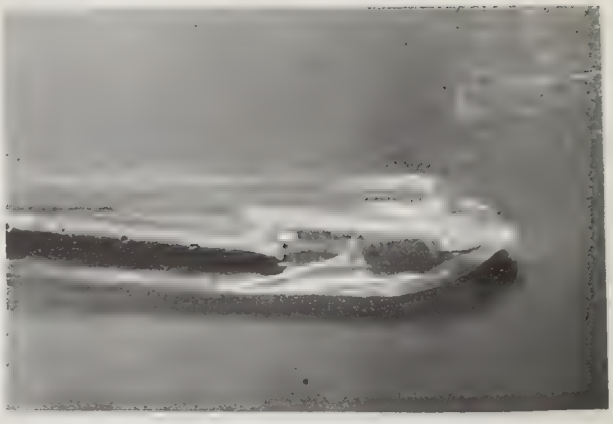

FIGURE 11. SLIPJOINT DISPLACEMENT OUT OF THE END OF THE BALLOON

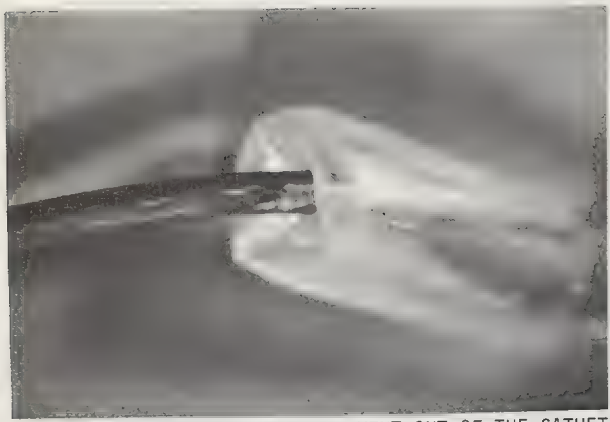

FIGURE 12. SLIPJOINT DISPLACEMENT OUT OF THE CATHETER.

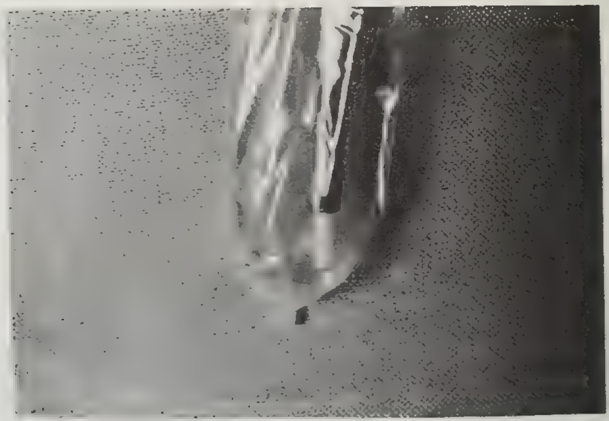

FIGURE 13. LATERAL BALLOON WALL PINHOLING AND LEAKS.

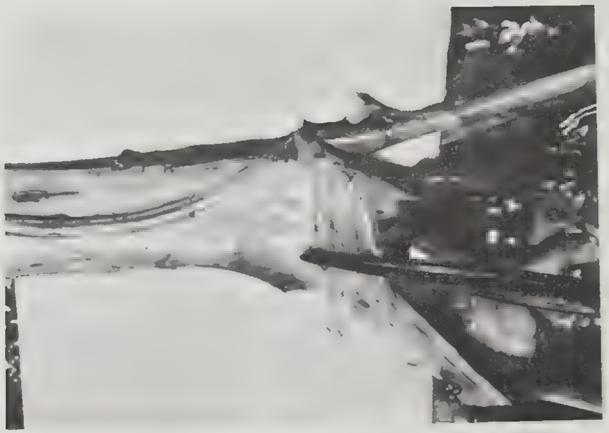

FIGURE 14. CATHETER WALL BREAKDOWN WITH KINKING.

a wall thickness under 5 mils and caused death in two animals with gas embolization of the coronary arteries. Catheter wall breakdown with kinking (Figure 14) occurred in seven animal experiments with serious consequences (Figure 15). This figure shows that when such occlusive kinking occurred, the balloon remained inflated, and obstructed the aorta, resulting in persisting hind limb paralysis in these calves, thus requiring termination of these experiments. Catheter kinking was found in the mock circulatory system to be mechanistically associated with longitudinal balloon-catheter movements with similar indications at necropsy of calves. Inasmuch as balloon catheter kinking has not, to the best of our knowledge, been reported in dog experiments, there may be danger in extrapolating findings relating to safety from this species to man, which in turn argues for use of a species more closely approximating the size of the clinical patient.

Factors contributing to these various defects have been in part identified in our laboratories and the problems resolved to variable degrees by the balloon fabricators.

SURGICAL INSTALLATION

Surgical installation of the balloons via the femoral artery presented no special problems except in a miniature pig with its small peripheral arteries. Thrombosis was uniformly observed around the portion of the 14 Fr catheters within the iliac and femoral arteries of calves. Long standing arterial insufficiency to the lower extremity and extension of thrombus to the contralateral iliac artery, observed in our animal experiments in spite of heparinization, represent a potential danger when extrapolated to the clinical patient. Insertion of the balloon via a Dacron graft sutured end-to-side on the exposed femoral artery may reduce occlusion of same as suggested by Kantrowitz.

ACUTE HEMODYNAMIC STUDIES

Figure 16 illustrates methods used and the hemodynamic responses recorded on Beckman and Grass oscillographs. Left ventricular pressure was measured with a Whittaker Model 1017 transducer inserted either via the left atrium or a left ventricular apex stab wound. Ascending aortic and left main coronary artery blood flows were measured with Carolina Medical Electronics square wave electromagnetic flow transducers and meters. Aortic root and abdominal aortic pressures were measured via catheters by Statham P23 transducers. These measured data were also recorded on a Precision Instruments FM tape recorder. The taped data were subsequently analyzed with a Simulator 240 analog computer as shown in the right panel. The computed data consist of beat-by-beat integrated ventricular pressure, dP_{LV}/dt, integrated stroke power to obtain stroke work, integrated diastolic blood flow in the left main coronary artery and the pressure in the aortic root. The last two integrations are done only during diastole during which the balloon inflates as a pump.

Figure 17 depicts hemodynamic responses in a 70 Kg. calf to pumping with an occlusive 40 ml. balloon of 22 mm. diameter. Although respiratory oscillations render interpretation a little difficult, the central panel shows that the left ventricular peak pressure was reduced about 15 mm. Hg, mean blood flow in the aortic root and left main coronary artery were essentially unchanged, aortic root mean pressure was unchanged, while, as in MCS studies, the abdominal aortic pressure was reduced 20 or 25 mm. Hg. The integral of left ventricular pressure was reduced by ~15%, dP_{LV}/dt was slightly reduced and stroke work was reduced by ~25%. During diastole, the integral of left main coronary artery flow was increased by ~30%, although mean flow was unchanged. The integrated aortic root diastolic pressure was also increased about 18% in this calf with no change in mean aortic root pressure.

Figure 18 depicts in the center panel a hypotensive response evoked by an overdose of sodium pentobarbital. In this condition, an occlusive balloon acted as a pump to slightly increase ascending aortic mean flow as well as aortic root mean pressure, while coronary mean flow and abdominal aortic pressure remained unchanged. The computed integrals of diastolic coronary flow and aortic root pressure were increased about 50% in this condition.

Non-occlusive balloons produced qualitatively similar results except that abdominal aortic and aortic root pressures were slightly reduced in calves. The computed variables mentioned above were also changed in a qualitatively similar fashion by the non-occlusive balloon.

To date, a total of 32 calves, 6 dogs and 1 pig, all with normal cardiac status have been pumped in acute hemodynamic studies. Table 3 summarizes acute hemodynamic studies carried out in 21 calves and 4 dogs.

TABLE 3

HEMODYNAMIC STUDIES

Parameter	Change In Dog	Change In Calf
Mean Diastolic pressure in the aortic root	+48%	+9.6%
Mean pressure in the aortic root	+13%	Unchanged
Mean pressure in abdominal aorta	-18.8%	-9.6%
Peak pressure in left ventricle	-10%	-7.3%
Pulmonary artery blood flow	Unchanged	Unchanged
Coronary blood flow (left main)	Unchanged	Unchanged
Renal blood flow	-18.0%	-8.0%

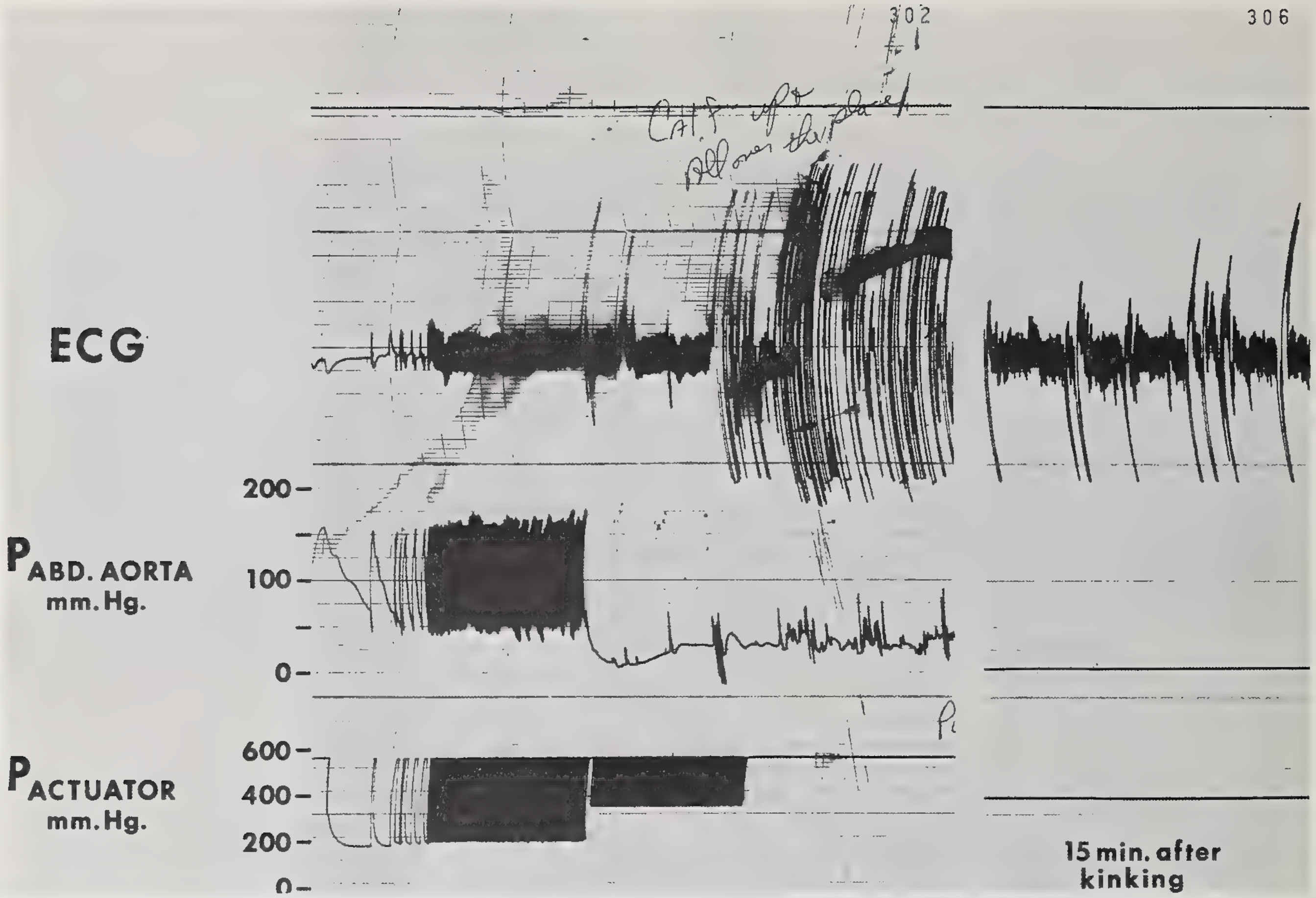

FIGURE 15. CATHETER WALL BREAKDOWN WITH KINKING OCCURRING IN ANIMAL EXPERIMENTS WITH SERIOUS CONSEQUENCES.

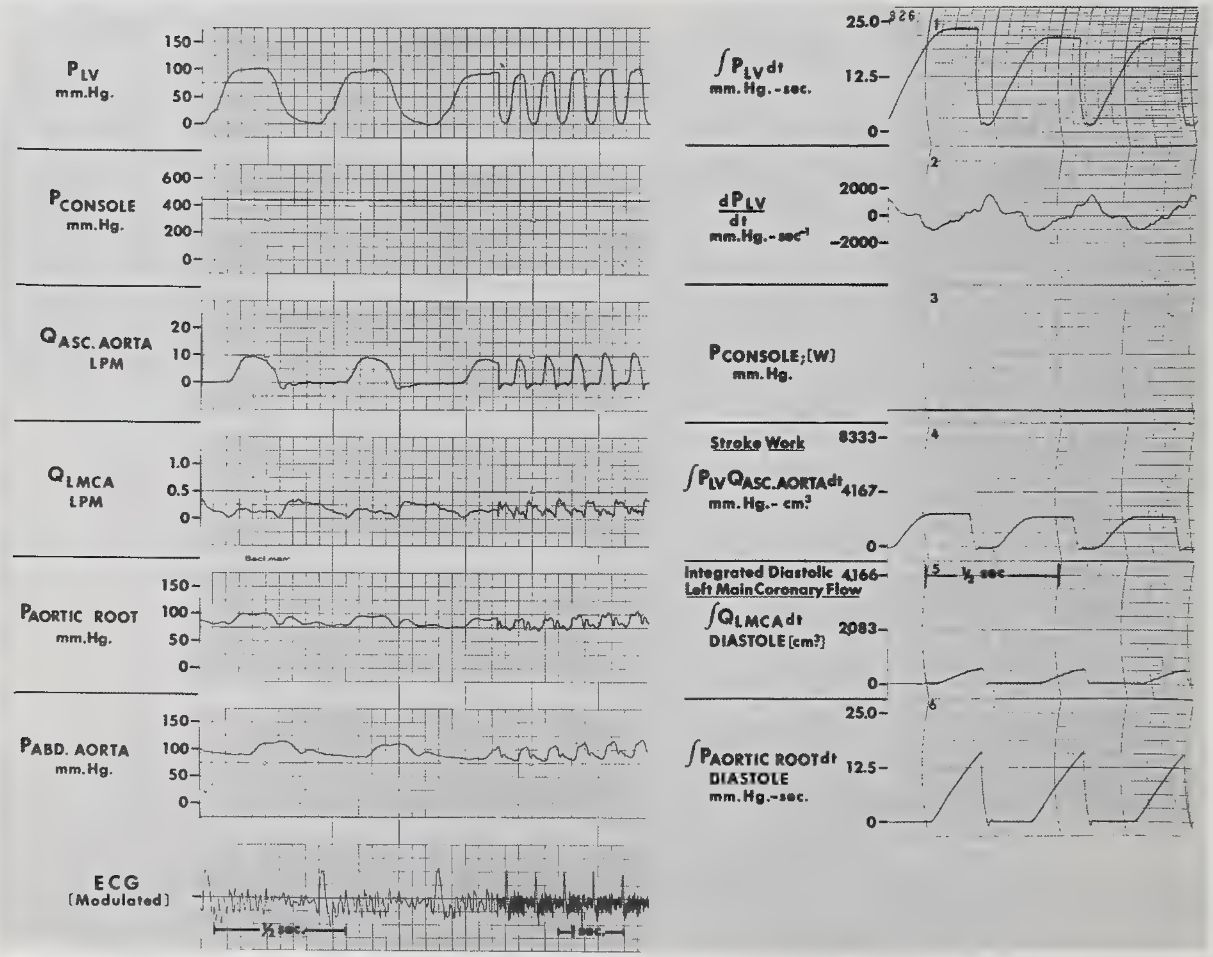

FIGURE 16. METHODS USED AND THE HEMODYNAMIC RESPONSES RECORDED ON BECKMAN AND GLASS OSCILLOGRAPHS.

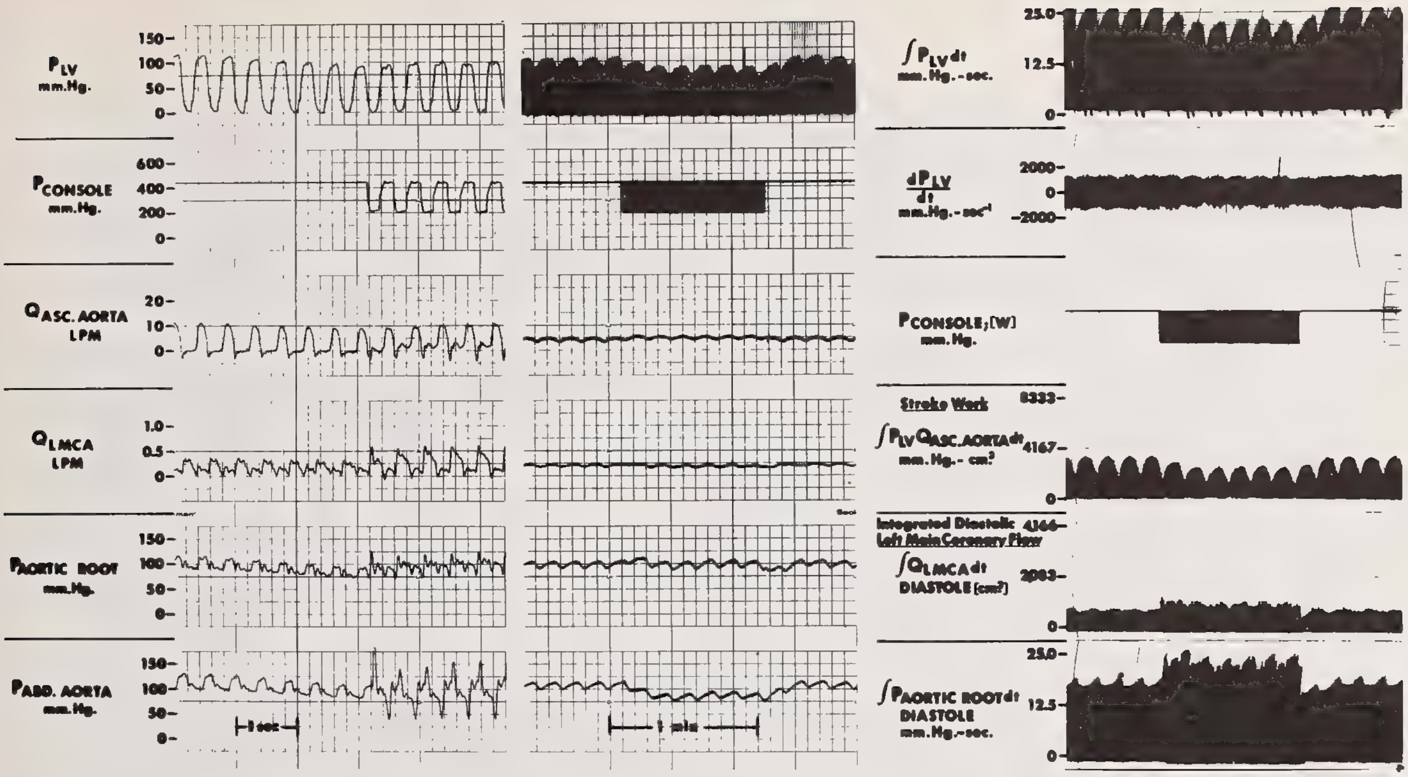

FIGURE 17. HEMODYNAMIC RESPONSES IN CALF TO PUMPING WITH OCCLUSIVE BALLOON.

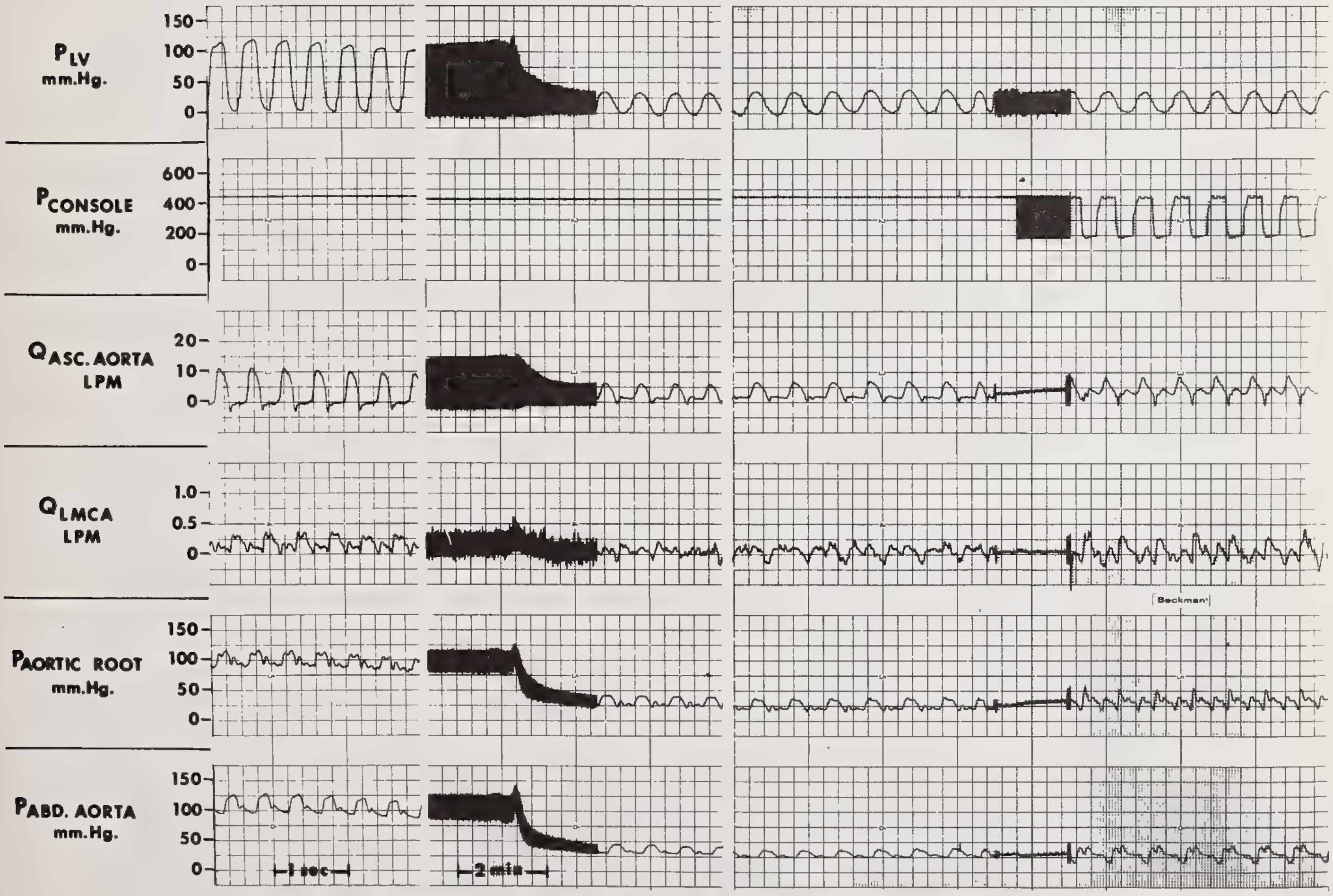

FIGURE 18. HEMODYNAMIC RESPONSES TO AN OVERDOSE OF SODIUM PENTOBARBITAL.

The magnitudes of responses differ quite markedly between calves and dogs as shown. Diastolic pressure augmentation was much greater in the dog. Abdominal aortic mean pressure, mean peak left ventricular pressure and renal artery blood flow were reduced as shown during intra-aortic balloon pumping. Coronary flow, cardiac output and heart rate were not appreciably changed.

The mean diastolic pressure in the aortic root of calves could be almost doubled (Figure 19) upon transient occlusion of the brachiocephalic trunk. This finding, along with the fact that only minimal diastolic augmentation was obtained in calves suggested that vascular capacitance and resistance may indeed be important determinants of the extent of diastolic augmentation which can be attained during balloon pumping.

Figure 20 illustrates aortic pressure-volume (compliance) diagrams as a mean of three experiments in each species. Aortae, from the aortic valve to the iliac arteries (and including the great vessels off the arch), were infused with autologous blood at a constant rate of 150 ml./min. while recording intraluminal pressure on a recorder. All aortae were freshly excised and maintained at 37°C. V_o represents the initial volume contained in the aorta at atmospheric pressure.

It is apparent that the compliance of the aorta of the calf is greater than that of the dog. At the indicated operating point of 50 mm. Hg, 20 and 40 ml. volume displacements evoke pressure changes in the dog 5 to 6 times as great as those in calves. At a 100 mm. Hg operating point, these displacements are associated with 4- to 5-fold greater pressure changes in dogs as compared with those in calves.

STUDIES IN CHRONICALLY PUMPED CALVES

Studies were carried out in five healthy unanesthetized calves pumped with intra-aortic balloons continuously 24 hours/day for periods ranging from 3 to 7-1/2 days. These studies were intended:

(1) To assess reliability of the balloons and the two consoles submitted for evaluation.
(2) To assess renal function in terms of glomerular filtration rate and effective renal plasma flow.
(3) To assess hematologic and blood biochemical responses to prolonged pumping.
(4) To assess organ and tissue changes (especially of the aorta) to chronic pumping.

Balloon rupture was observed after 74 hours and on the fourth day of pumping in each of two animals, which in one case resulted in blood entering the pneumatic system of the Avco console. Balloon catheter wall breakdown in a Westinghouse balloon with a thin-walled polyethylene catheter was observed as a consequence of torsion on that portion immediately under the skin which resulted in pumping of helium gas in large quantities into subcutaneous and retroperitoneal spaces. The Westinghouse catheter problems appear to have been eliminated with submission of new balloons bearing sturdy 85 Shore D Spiretex polyurethane catheters. Twice, Western Gear balloon catheters broke down at the sleeve holding the Luer metal fitting to the catheter thus allowing sero-sanguinous fluid to enter the pneumatic conduit.

The Avco console performed well during chronic pumping of four animals except for an instance of oscilloscope failure which was traced to a coronal arcing short in the high voltage circuit. The vacuum pump of the Westinghouse console overheated, failed to maintain vacuum, and had to be substituted for periodically with another pump. Additionally, the solenoid in the Westinghouse actuator began to stick after four days of continuous pumping and required relubrication.

Because distinct reduction in abdominal aortic mean pressure and renal blood flow was observed in acute studies, renal clearance studies were initiated. A single i.v. injection, double radioisotope technique as described by Blaufox and Merrill was utilized to study glomerular filtration rate, effective renal plasma flow and filtration fraction in these chronically pumped calves. The next three figures (Figure 21-23) revealed that there was no consistent or striking decrease in G.F.R., renal plasma flow (except in Calf 58-8 in which the depicted increase in plasma flow was correlated with a persistent hypertension evolving only in this calf after 48 hours of continuous pumping), or in the filtration fraction. On the basis of these data, there is no evidence that glomerular or tubular function was overtly modified in these calves.

COAGULATION, HEMATOLOGIC AND BIOCHEMICAL PARAMETERS

The next series of tables (Tables 4-9) depict observed changes in a host of coagulation, hematologic and biochemical parameters in these chronically pumped calves.

Table 4 shows that:

(1) The one-stage prothrombin time was elevated somewhat in these animals which were kept heparinized to a Lee-White time of 20 to 30 minutes.
(2) Fibrinogen was elevated perhaps as a response to continuous heparinization.
(3) Platelet count was depressed but never was less than 104,000/mm^3 in any of the five calves.

Table 5 summarizes the RBC variables in these calves.

(1) The highest plasma hemoglobin value observed was 14 mg.% after 48 hours of pumping.
(2) The depression of total hemoglobin, hematocrit and RBC counts paralleled each other. These findings which were not accompanied by changes in plasma hemoglobin, corpuscular volume or hemoglobin concentration, may reflect sequestration of blood in the periphery and decrease in circulating blood volume, already suggested to occur following counterpulsation by Sugg and co-workers in 1968.
(3) Osmotic fragility of RBCs was not altered.

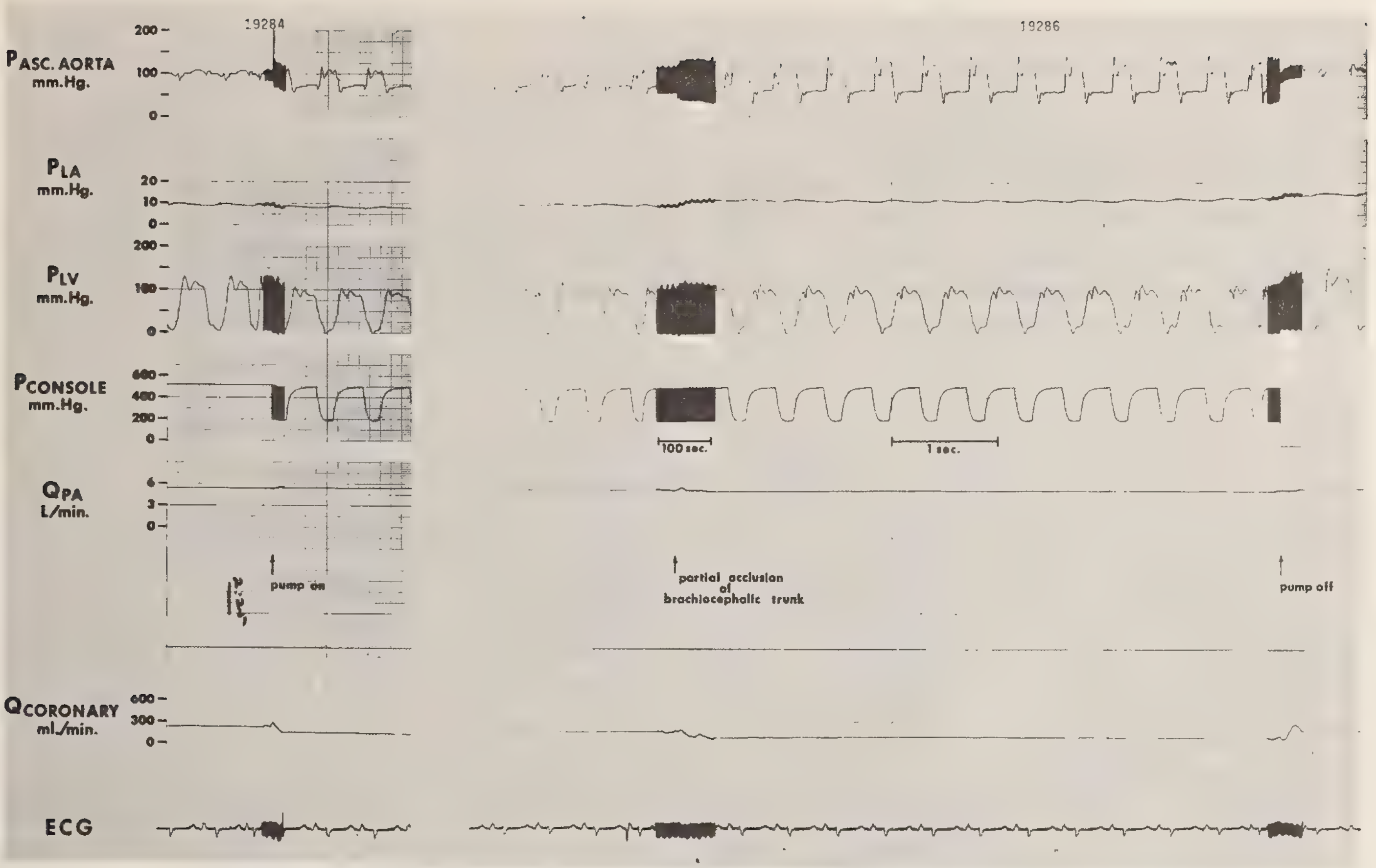

FIGURE 19. HEMODYNAMIC RESPONSES TO TRANSIENT OCCLUSION OF THE BRACHIOCEPHALIC TRUNK.

SPECIES	Pressure Change mm.Hg.									
	Hypotensive Condition (50 mm. Hg.)					Normotensive Condition (100 mm. Hg.)				
	DOG	PIG	GREY HOUND	SHEEP	CALF	DOG	PIG	GREY HOUND	SHEEP	CALF
20 ml. volume displacement	78	60	40	22	14	70	47	30	22	16
40 ml. volume displacement	152	108	70	46	25	160	110	58	60	32

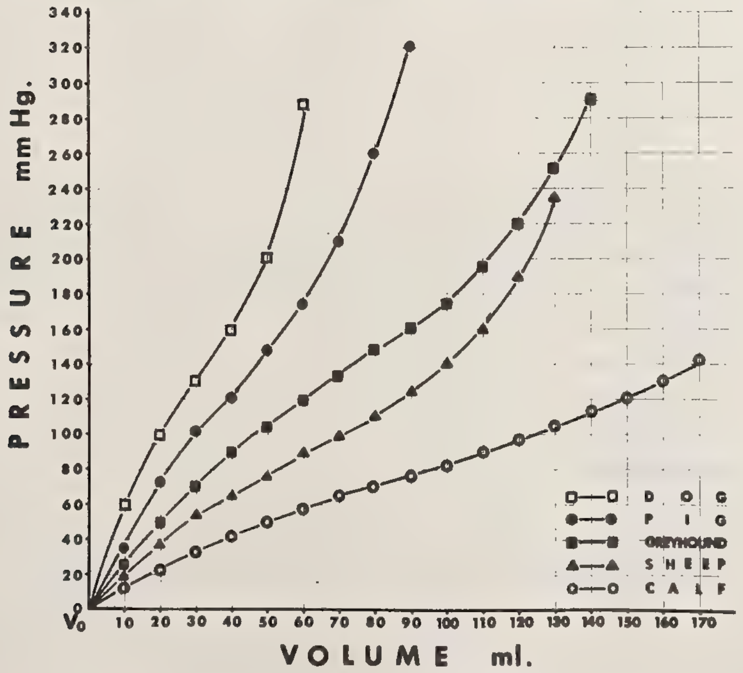

FIGURE 20. AORTIC PRESSURE-VOLUME (COMPLIANCE) DIAGRAMS FOR FIVE SPECIES.

TABLE 4

COAGULATION VARIABLES, AS MEAN % CHANGE FROM CONTROL

Variable	Control			Days Pumped			
		1	2	3	4	5	6
1-Stage PT, sec	17.2	+106[a]	+39	+16	+81	+31	+25
Fibrinogen, mg. %	386	+39	+77[b]	+134[c]	+126	+136[a]	+49
Platelet Count, X 10^3	504	-35[b]	-46[c]	-54[b]	-30	-33	-20[a]

a P = <0.05
b P = <0.01
c P = <0.001

TABLE 5

HEMATOLOGIC VARIABLES, AS MEAN % CHANGE FROM CONTROL

Variable	Control			Days Pumped			
		1	2	3	4	5	6
Plasma Hb, mg. %	12.3	-77	-46	-72	-94	+13	+16
Total Hb, Gm. %	12.0	-12[a]	-20[a]	-21	-15	-21[a]	-19
Hct., %	37	-12[b]	-19[a]	-23	-18[a]	-20	-18[a]
RBC Count, X 10^6	9.86	-12[a]	-17	-23	-18	-23	-13
Mean Corpusc. Vol., μ^3	37.7	0	-3	-2	+1	+4	-5
Mean Corpusc. Hb, μμg.	12.1	+1	-5	0	+2	+6	-6
Mean Corpusc. Hb, Conc., %	32.2	+2	-2	+1	+1	-2	-1
RBC Fragility, % NaCl							
Start	0.69	-1	+4	+3	+6[c]	-1	-1
Complete	0.37	-3	+3	+3	+7	+4	+4
Mean	0.51	+2	+2	+2	+4	+1	+1

a P = <0.05
b P = <0.01
c P = <0.001

TABLE 6

HEMATOLOGIC VARIABLES, AS MEAN % CHANGE FROM CONTROL

Variable	Control			Days Pumped			
		1	2	3	4	5	6
WBC Count, X 10^3	7.8	+29	+56[b]	+22	-6	-20	-3
Diff. Count, %							
Polymorphs	36.8	+78[b]	+51[b]	+48[b]	+15	-10	-8
Lymphocytes	60	-46[a]	-27	-28[a]	-9	+4	+11
Monocytes	0.6	-100	-42	+167	+84	0	+167
Eosinophils	2.6	-38	0	-38	-38	0	-96

a P = <0.05
b P = <0.01

Table 6 shows some elevation of the white blood cell count in response to surgical stress with prompt return to control levels. Table 7 depicts increased levels of the transaminase enzymes with return to normal levels a few days postsurgically. Total LDH values were also elevated somewhat. Ornithine carbamyl transferase, OCT, a liver specific enzyme did not elevate to pathologic levels, thus along with other parameters, confirming the integrity of liver function during chronic pumping.

TABLE 7

SERUM ENZYME VARIABLES, AS MEAN % CHANGE FROM CONTROL

Variable	Control			Days Pumped			
		1	2	3	4	5	6
SGOT, Hyland Units	87	+340	+490[a]	+510[a]	+506	+186	+107
SGPT, Hyland Units	14.3	+124	+173[a]	+157	+192	+105	+82[a]
SGOT/SGPT	6.28	+59	+107	+113	+14	+56	+17
OCT, Sigma Units	118	-19	+12	+57	+39	-58	+76
Total LDH mU/ml.	624	+82[a]	+117	+85	+48	+85	+38

a P = <0.05

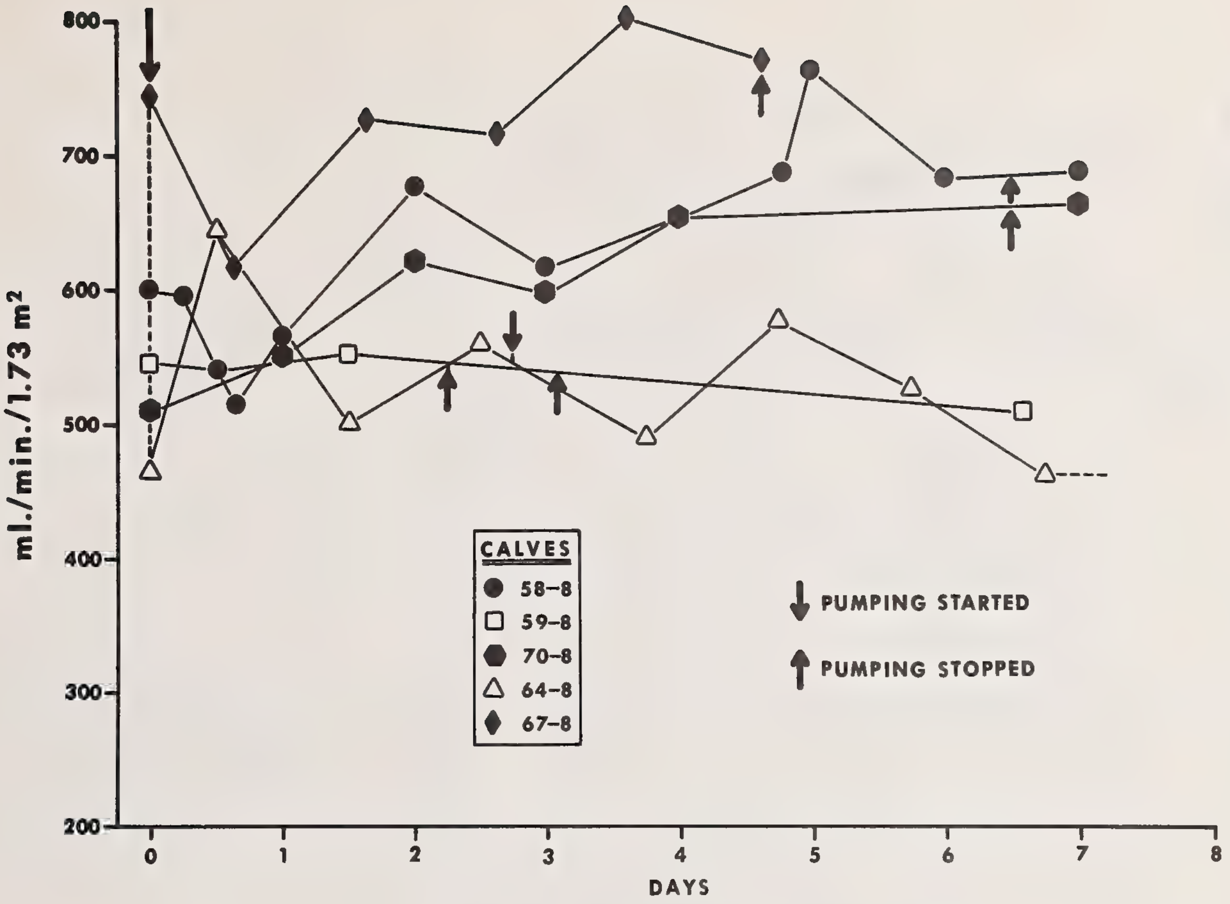

FIGURE 21. GFR IN CHRONICALLY PUMPED CALF.

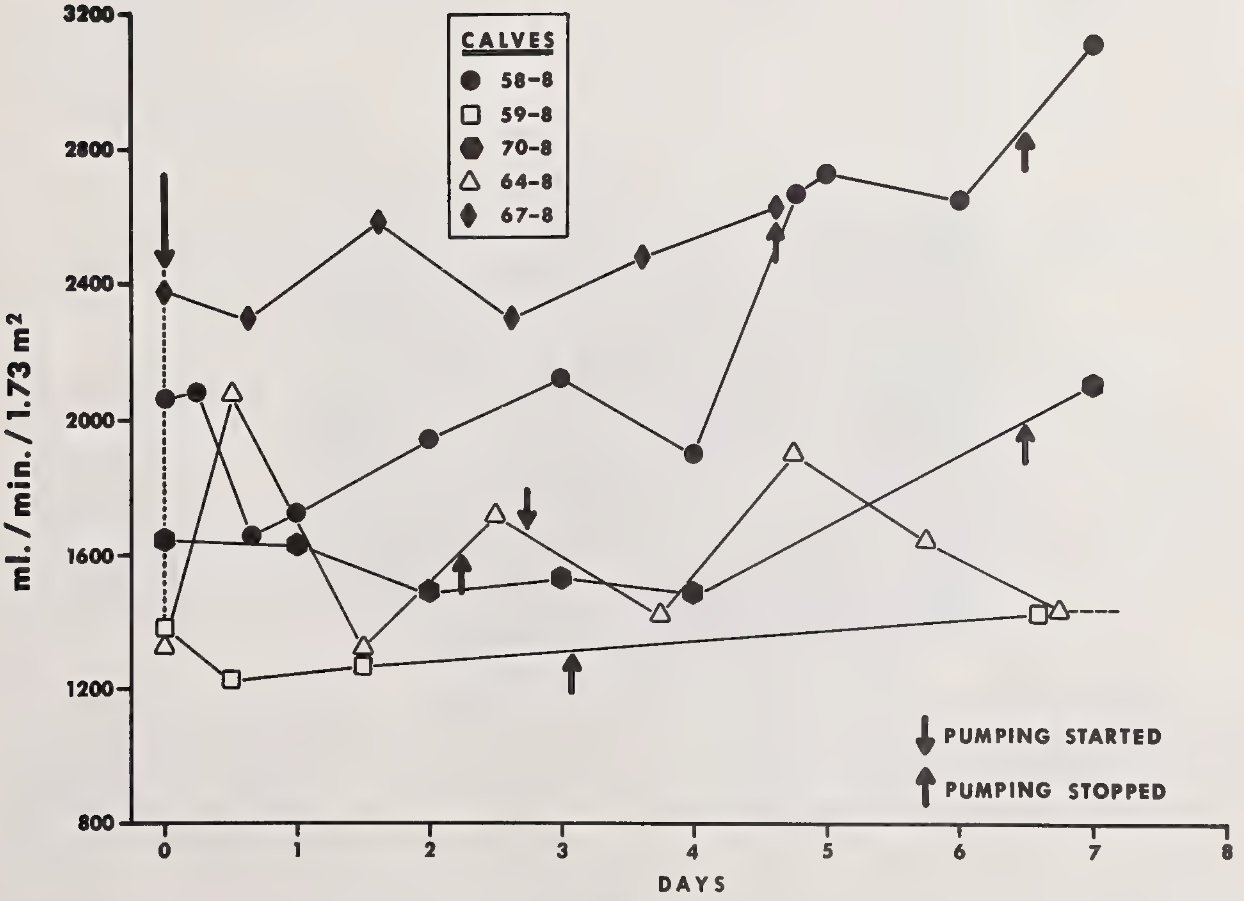

FIGURE 22. ERPD IN CHRONICALLY PUMPED CALF.

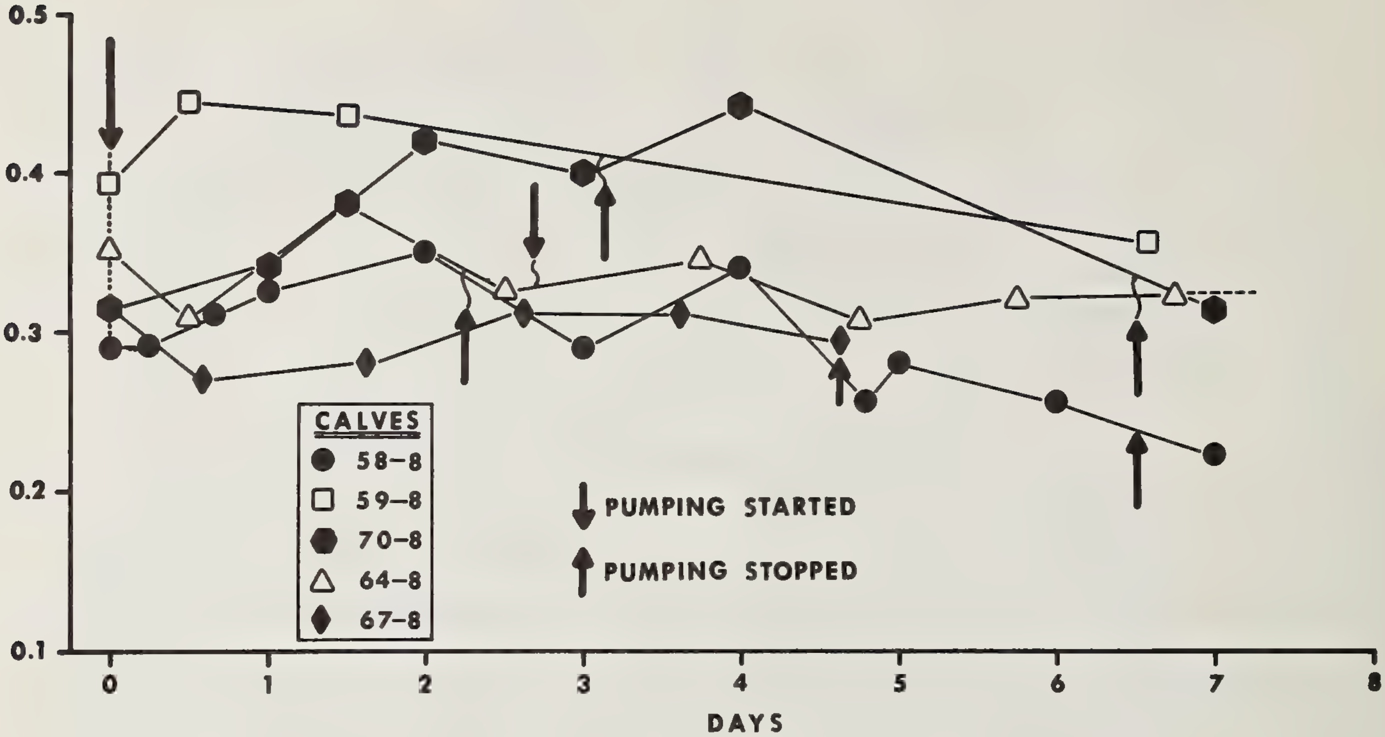

FIGURE 23. FF IN CHRONICALLY PUMPED CALF.

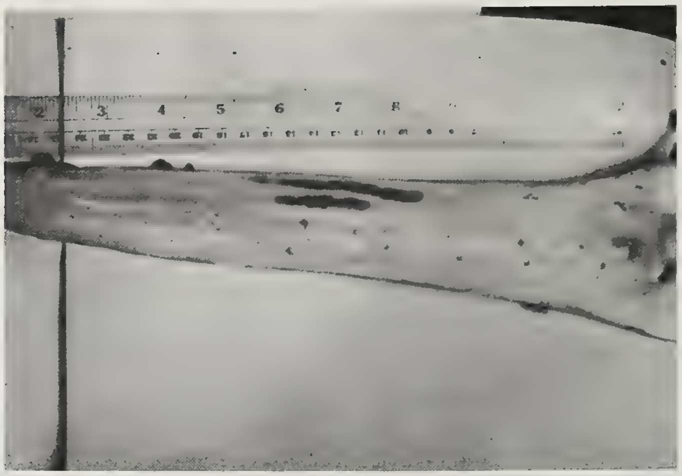

FIGURE 24. LOCAL PATHOLOGIC CHANGES IN THE THORACIC AORTA ATTRIBUTABLE TO THE BALLOON.

TABLE 8

SERUM ELECTROLYTE VARIABLES, AS MEAN % CHANGE FROM CONTROL

Variable	Control	Days Pumped					
		1	2	3	4	5	6
Na^+, mEq./l.	150	-2	0	-1	+1	-3	-4
K^+, mEq./l.	4.96	-4	-10	-1	+12	+1	+3
Ca^{++}, mEq./l.	5.72	-5	0	+7	-7	-10	-3
Mg^{++}, mEq./l.	2.42	+2	-20[a]	-8	-21	-23	-21
Cl^-, mEq./l.	98.9	+4	+4	+6	-7	+1	+2

a P = <0.05

TABLE 9

MISCELLANEOUS BIOCHEMICAL VARIABLES, AS MEAN % CHANGE FROM CONTROL

Variable	Control	Days Pumped					
		1	2	3	4	5	6
BUN, mg. %	13.8	+5	-20	+22	-22	+22	-7
Glucose, mg. %	95	+24	+5	0	-10	+16	-5
Inorg. Phosph., mg. %	8.4	-14[a]	-7	-7	-6	-28	-17
Uric Acid, mg. %	1.3	-35[a]	-49[a]	-50[a]	-46	-69	-23
Total Protein, Gm. %	6.88	-9	-2	-5	-12	-3	+1
Total Bilirubin, mg. %	0.2	+31	+17	+75	0	+50	0
Alk. Phosph., mU/ml.	173	-21[a]	-26	-49[a]	-65	-51	-30
Serum Lactate, mg. %	9.2	-17	+38	-56[a]	-32	-32	-28
Serum Pyruvate, mg. %	0.84	-4	+38	-37	-10	-21	-7
Lactate/Pyruvate	10.9	-13	-8	-28	-30	-12	-5

a P = <0.05

Table 8 illustrates that serum electrolytes were not altered in these calves.

The final table in the series (Table 9) shows that there were no physiologically or pathologically significant changes in blood urea nitrogen, glucose, inorganic phosphorus, uric acid, total protein, bilirubin, serum lactate and pyruvate, while alkaline phosphatase seemed to be reduced.

In summary, chronic pumping with intra-aortic balloons in calves is not associated with any alarming hematologic alterations. Our data suggest redistribution of blood to peripheral reservoirs, which can be confirmed only by further study.

NECROPSY STUDIES

Necropsies were performed on 15 calves receiving Westinghouse intra-aortic balloons and 12 calves with Western Gear balloons. Twenty-four of the calves were pumped for less than 12 hours and the remaining three calves were pumped from three to six and one-half days. Balloon end inflation pressure never exceeded 200 mm. Hg.

Local pathologic changes in the thoracic aorta attributable to the balloon were occasionally seen grossly, and in almost every calf microscopically. The worst case in terms of gross findings is shown in Figure 24.

The most common microscopic finding in the thoracic aorta adjacent to the balloon was the loss of the endothelial lining of the aorta, characterized by absence of the endothelial nuclei. The severity of this loss did not appear to be related to the duration of pumping. With long durations (3 to 6-1/2 days) of pumping with occlusive balloons, chronic inflammatory cell infiltration of the intima was seen, along with granular changes in the internal elastica. Intimal hemorrhage and fibrin deposition was a common finding in many of the pumped animals. Besides the deendothelialization noted above, the intima was eroded and edematous and the internal elastica was fragmented. The media showed occasional hemorrhage and edema.

HEART FAILURE ANIMAL MODEL STUDIES

We have attempted to achieve a stable cardiac failure model in a total of twenty calves utilizing three techniques: (1) selective staged coronary artery ligation; (2) chemical infarction with direct intramyocardial injection of formalin; and (3) ventriculotomy and resuturing. Although distinct left ventricular infarction was present in chronic survivors, no definitive hemodynamic evidence of left heart failure, except for moderate increases in left ventricular end diastolic and left atrial pressures, was observed.

CONCLUSION

The many unresolved questions regarding the use of intra-aortic balloons as counterpulsation devices, some mentioned above, suggest that further studies are required. These studies should include those of:

(1) Stability and integrity of balloons during long-term pumping.
(2) Characterization and comparisons of human aortic compliance, especially in graded arteriosclerotic conditions which should elucidate optimal animal models for balloon studies.
(3) Hemodynamic responses in heart failure models.
(4) Additional comparative hemodynamic and pathologic effects of occlusive versus non-occlusive balloons.
(5) Postinfarction ECG triggering problems
(6) Balloon deflation-inflation dynamics.

DISCUSSION

DR. JARON: First of all, I would like to compliment the authors on a very comprehensive study. There is one thing, however, that bothers me, and it is the same thing that bothered me with regard to the last paper we heard. It was already alluded to that the size of the aorta is a very important factor in the effectiveness of the balloon. Now, in preliminary work that we carried out at Maimonides, we also found that the effectiveness of the balloon is very much dependent upon the timing. As a matter of fact, it is very critically dependent on the correct timing of the balloon in relationship to the cardiac cycle. Now, in order to be able to evaluate the hemodynamic effectiveness of the intraaortic balloon, I had a feeling that one has to control very carefully both the size of the balloon in relationship to the size of the aorta and the correct timing of the balloon in relation to the cardiac cycle. Otherwise, it is very difficult to get any kind of valid conclusion with regard to the hemodynamic testing of the balloon. As a matter of fact, I suspect that in Stage 3 of the failure presented in the last paper, one of the reasons why the balloon was not effective was because the size of the balloon was too large compared to the size of the aorta.

DR. GALYSH: We used both occlusive and non-occlusive balloons. At the aortic root in the calf, the aorta was about 25 mm ID and down to about 16 mm at the level of the diaphragm. We used both 15 mm diameter and 22 mm diameter balloons. I think with regard to the timing, we try to adjust timing so that we will be deflating adequately in such a manner that the ventricle would not be seeing an increased impedance. Further, we adjusted the duration of inflation to maximize the aortic root pressure increase during diastole. We also found that the equilibrated end inflation pressure in the balloon was an important factor, that 100 - 150 mm Hg was much less effective than our standardized inflation pressure of 200 mm Hg.

DR. JARON: My remark was not directed towards this presentation in particular. In general, when we are embarking on the testing of balloons, I think it is very important to control our experiments.

MR. FREED: I would like to join Dr. Jaron in complimenting both groups for a substantial amount of good work and I just would like to add for the benefit of those that may not be aware of it that there are other groups in the country, Maimonides being one of them, that do use balloons that do not leak, do not tear, and do not kink.

EDITOR'S NOTE: The Travenol balloons were tested according to National Heart Institute request and specifications to establish the minimum thickness at which they would be safe. The balloons that ruptured were extremely thin.

DR. LAIRD: I do want to second the remark of Dr. Jaron about the importance of the size of the balloons, compared with that of the aorta. All the evidence that you showed in which there is a drop in mean abdominal aortic pressure is, as we illustrated in our 1968 ASAIO paper, a very easily detectable symptom of what has been referred to earlier as the bubble blowing phenomenon. Referring to the remarks earlier by Dr. Jacobey, it is not really fair to contrast to the remark Dr. Jacobey made before raising the question of the efficiency of the balloon vs. other techniques. It is not really fair to place a balloon in a situation where its efficiency is by definition compromised. The other point that I would like to make is that I would differ with Dr. Patel's suggestion, that the thing to do with these consoles is to put a trap in the lines so that the blood from a ruptured balloon does not get into the console. The object of clinical application of the balloon pumping is not to protect the console. It takes impeccable, really stringent, quality control standards, in the process of making these balloons to insure that rupture does not happen. We have never had a balloon break or rupture in a case where it has passed quality control standards, and we have pumped a lot of balloons under very severe conditions.

DR. PATEL: I agree with Dr. Laird. I think the balloon should be one which should not rupture.

DR. LAIRD: The other thing I want to say is that although I understand that you were not operating the AVCO console in this particular mode, the AVCO console does have an isolating piston in it which moves between stops. This makes it possible to operate the balloon in a manner so that it inflates very rapidly and yet does not end up under transmural wall tension. This has a profound effect on the fatigue life and reliability characteristics of the balloon, and you wouldn't have had quite so many problems if you operated it that way. It is possible for example to inflate a full 30 cc of a balloon in 50 - 70 milliseconds with that console, and still end up with no pressure differential inside the balloon at the end of the inflation.

DR. JACOBEY: I, too, would like to congratulate you on a well formulated study. I wonder about these balloons. They have talked about their quality control. What about the size? In counterpulsation with a cannula, we always take a great deal of pain to assure the proper size cannula because it makes a great deal of difference in the efficiency that we get. Are there different sizes for obviously different size aortas in large people, small people, men, women, etc? I wondered what your plans are for that. Secondly, as far as arrhythmias are concerned, I found a very nice answer to it in this regard, in paired pacing. We have taken patients who have various sorts of arrhythmias and have paced them with very good success and have had results that have been as good as any we have had in patients.

DR. LAIRD: In our preparations for the clinical trials in pumping, we do at the moment have two sizes of balloons available. We are not sufficiently sophisticated to be able to discriminate in fine detail as to the precise size of the aorta, but we have a girl size and a boy size.

UNIDENTIFIED DISCUSSANT: Isn't that going to be a problem for you? Not being able to simulate sufficiently the proper size?

DR. LAIRD: So far, clinically, it has not been a problem because we have taken the approach of being very conservative in the selection of the outer diameter of the balloon compared with the minimum of all the data we could collect out of the literature, as well as that which we collected ourselves on the diameter of the aorta. The biggest balloon is 16 mm in diameter at its biggest point, is long, and has tapered ends.

CHAPTER 55

DEVELOPMENT OF FABRICATION TECHNOLOGY FOR CIRCULATORY ASSIST DEVICES

J. Sprung

Western Gear Corporation
South Gate, California

The activities of Western Gear Research Center have been directed toward two objectives. The first is the development of techniques to produce pre-production quantities of an intra-aortic balloon/catheter emergency assist-type device. The balloon/catheters are produced by the repetitive dipping of a water-soluble gelatin mandrel into a solvent solution of thermoplastic polyurethane material, drying between coats, and after building up a five mil film, removing the soluble gelatin mandrel by dissolving in hot water gently pumped in and out through the inflation holes in the catheter. Basic technique was developed by Westinghouse. Several sample balloon/catheters have been submitted to Travenol Laboratories for *in vivo* evaluation. Results to date from seven (7) units indicate that at least six (6) days of continuous operation have been recorded when used with the Avco controller-actuator console. Major problem areas include fabrication of the balloons from a polyurethane solution that is extremely sensitive to environmental conditions, excessive flexing of the balloon film due to variations in the slip-joint design of the shrinkage compensator, kinking of the catheter and excessive softening of the catheter at body temperature. Since present fabrication methods have resulted in a high percentage of rejects, an improved mandrel material, more stable film material and an improved production technique are indicated. The second objective is the fabrication of prototype devices such as blood pump components for left heart assist devices. This activity has just been initiated and only preliminary design approaches have been investigated.

INTRODUCTION

The development activities of the Western Gear Research Center have been directed by the Artificial Heart Program toward two objectives. The first is the development and improvement of fabrication techniques to produce pre-production quantities, that is, more than twenty units of the same design, of emergency assist type, intra-aortic balloon/catheter devices. The second objective is the fabrication of prototypes in quantities of less than ten (sometimes hopefully even one) of devices designated by the Project Officer. The balloon/catheter development is a continuation of a program initiated by the Westinghouse Research Group to produce inflatable devices which can be evaluated *in vitro* and *in vivo*.

These devices, components and materials of construction have been modified as required by the Project Officer, and have undergone several evolutionary design changes. The physical and mechanical characteristics of the fabricated devices have been evaluated to insure their efficacy, safety and reliability. They have been tested *in vitro* under simulated test conditions and samples have been submitted to Travenol Laboratories for *in vivo* evaluation.

I. DEVELOPMENT AND IMPROVEMENT OF FABRICATION TECHNOLOGY FOR CIRCULATORY ASSIST DEVICES

A balloon/catheter can be defined as an inflatable device consisting of a spindle-shaped balloon formed around the distal, perforated end of a long catheter tube. The initial design had a spherical radius on both ends. The intermediate designs had a conical distal end which became more sharply tapered. The current design has a conical configuration on both ends and is approaching the shape of an elongated football. (Figure 1) The fabrication process starts with the preparation of the tube sub-assembly. This consists of a temporary stiffening rod, a catheter tip slip-joint that is required as a shrinkage compensator and the catheter tube itself. This tube is 3/16" O.D. x 36" long. It is No. 5400-USC1-USA-14 supplied by U. S. Catheter, Inc., of Glen Falls, N. J., and has a "Luer-Lok" on one end. The other end is temporarily corked with a polyethylene plug and the entire tube is dipped in polyurethane solution up to the Luer fitting. The coated tube is allowed to dry and a second coat of polyurethane is applied. After this second coat has dried, the polyethylene plug is removed and the desired number of holes are drilled through the tube within the length to be enclosed by the balloon. The hand fabricated catheter tips are assembled with an estimated gap to provide about 3/8 to ½ inch for anticipated longitudinal shrinkage. The temporary stiffener rod is inserted into the tube down to the catheter tip.

METHODS

Two methods of mandrel preparation have been employed: water soluble gelatin and, more recently, a water soluble, inorganic salt product.

Gelatin Mold Assembly.

The preparation of the gelatin mold assembly consists of glass tubing, the upper catheter indexing plug and the lower tip locater plug. The catheter tube sub-assembly is inserted into the mold and is ready for the pouring of the soluble gelatin mandrel. The prepared gelatin is poured slowly into the mold (Figure 2) and the upper indexing plug is positioned. The mold is then refrigerated two to 12 hours. The Westinghouse No. 43 polyurethane solution is prepared in a controlled environment room by mixing B.F. Goodrich "Estane" polyurethane, tetrahydrofurane, 1,4 dioxane and 2 methoxyethyl acetate. These materials are mixed slowly for 12 hours and are then filtered. Moisture content is analyzed and the solution viscosity is checked prior to dipping. The molds are removed from the refrigerator and the plugs are removed from the glass tubing. The mold is dipped into warm water and the tube is slipped off the gelatin. The gelatin mandrel is allowed to dry and then the ends are shaped by hand molds (Figure 3). The film bonding areas of the mandrel are carefully cleaned by wiping with warm water. The mandrels are suspended on a rack for one hour to condition the surface. The dipping environment room must be controlled for temperature, relative humidity and ventilation drafts. The urethane solution is somewhat toxic and prolonged exposure to solution fumes must be avoided. The solution is poured into a graduate of sufficient height to permit complete immersion plus two inches excess.

A flow-coating technique has been used to try to compensate for the flowing down of solution from the upper part of the mandrel during the dipping procedure. This is done by holding the mandrel horizontally over a drip pan and pouring the solution over the upper quarter of the mandrel and about one inch onto the catheter tube. This flow-coat is allowed to dry prior to proceeding.

The gelatin mandrel is now ready for balloon fabrication. The catheter is held vertically and the mandrel is slowly lowered into the solution until the solution covers the gelatin mandrel and about two inches up onto the catheter tube (Figure 4). The motion is immediately reversed and the mandrel is slowly lifted out of the solution and the catheter is suspended for ten minutes for drying before the next dipping cycle. The coating operation is repeated eight to ten times until a 3.5 mil to 4.0 mil film thickness has been formed. After the last coat has been formed, the assembly is allowed to cure in a dust-free environment for 12 hours.

The uniformity of balloon catheter devices produced by this method depends entirely upon operator technique. Reliable duplication of end configuration, diameter and volume is problematical.

Rigid Mold Assembly.

With the recent requirement to produce devices to close, specific tolerances, and since the flexible gelatin mandrel method produces devices that are only relatively uniform, a new rigid mandrel material is currently being investigated. This inorganic salt product is commercially available as "Rigidax-W.S." and is supplied by Argueso Co., Inc., Mamaroneck, N.Y.

The preparation of the Rigidax mandrel begins with the design of an aluminum mandrel pattern. This pattern is made larger than the finished balloon by the amount of estimated shrinkage of the balloon. Final size of the pattern is developed by trial silicone rubber molds (Figure 5). After the diametrical shrinkage has been established, the longitudinal shrinkage can be calculated and the final pattern size is determined. The pattern is used to make a two-piece silicone rubber mold that has a longitudinal parting line. This mold incorporates both end configurations, a precise locater for the molded catheter tip slip-joint and a locating groove section for centering the catheter tube. When the final design for production has been determined, this rubber mold will be replaced with a highly polished, aluminum mold. The catheter tube slip-joints are now uniformly cast in an aluminum, laboratory type of mold, using Uralane No. 8158-A polyurethane from Furance Plastics Co. (Figure 6).

The catheter tube is prepared by inserting the distal end into an accurately engineered drill jig and is drilled to a uniform pattern. The Rigidax material is prepared by melting the pellets, which are the size of grains of rice, in a beaker while stirring continuously. An electrically heated dispensing unit equipped with a 30 RPM gear motor and wiping-type agitator is recommended by the supplier of Rigidax. The catheter sub-assembly is prepared by inserting a molded catheter slip-joint into the end of the drilled catheter tube allowing the revised estimated gap for shrinkage. The stiffener rod is inserted from the Luer-Lok end and extends all the way through to the slip-joint. This sub-assembly is positioned in the bottom half of the mold with the catheter tip slip-joint indexed in the distal end of the mold cavity and the catheter tube nested in the groove provided for it.

The melted Rigidax is poured into the mold cavity until level with the parting line surface (Figure 7). The upper half of the mold is positioned, clamped and the mold is immediately rotated around the longitudinal axis. After 15 minutes, this produces a hollow shell of rigid, water soluble material around the encapsulated catheter tube and slip-joint. The mold is opened, the Rigidax mandrel is removed and the parting line is cleaned. The surface of the mandrel is not as smooth as gelatin so a thin coating of polyvinyl alcohol is sprayed over the mandrel. After one hour, the polyvinyl alcohol is very carefully cleaned off the polyurethane tip and tube surfaces. The mandrel is now ready to dip.

A ten-station mechanical dipping machine has been designed and built. This has been installed inside a temporary conditioned environment room and is operated from outside by remote control. The mandrels are attached to the moveable section of the machine in the raised position. The polyurethane solution is poured into graduates located under each mandrel assembly. By remote control, the moveable section lowers the mandrels into the solution, reverses immediately and raises the mandrels into the drying position (Figure 8). Control of speed and direction is still being handled by the Research

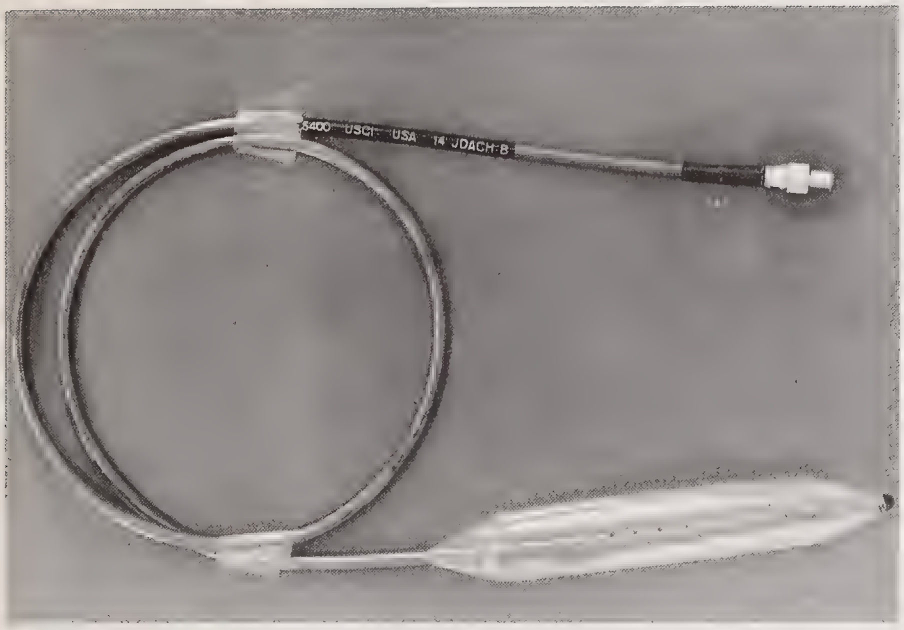

FIGURE 1. INTRA-AORTIC BALLOON/CATHETER EMERGENCY ASSIST-TYPE DEVICE.

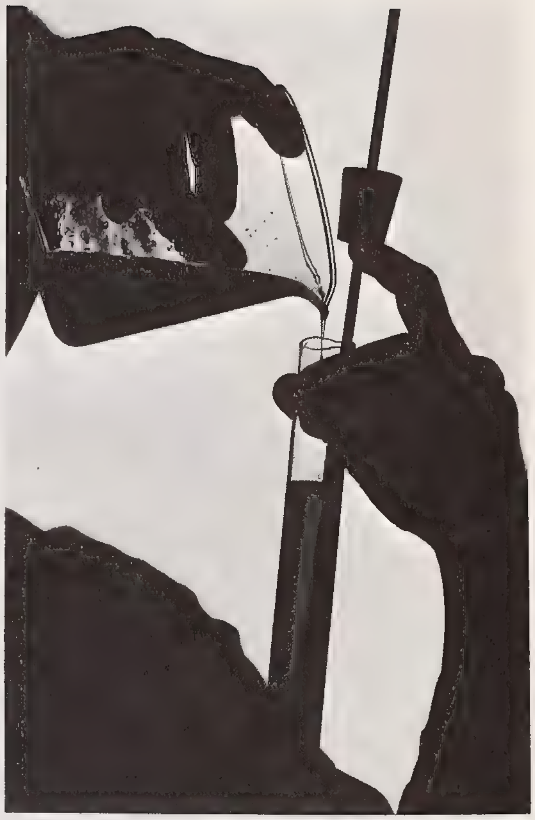

FIGURE 2. POURING OF GELATIN INTO MOLD.

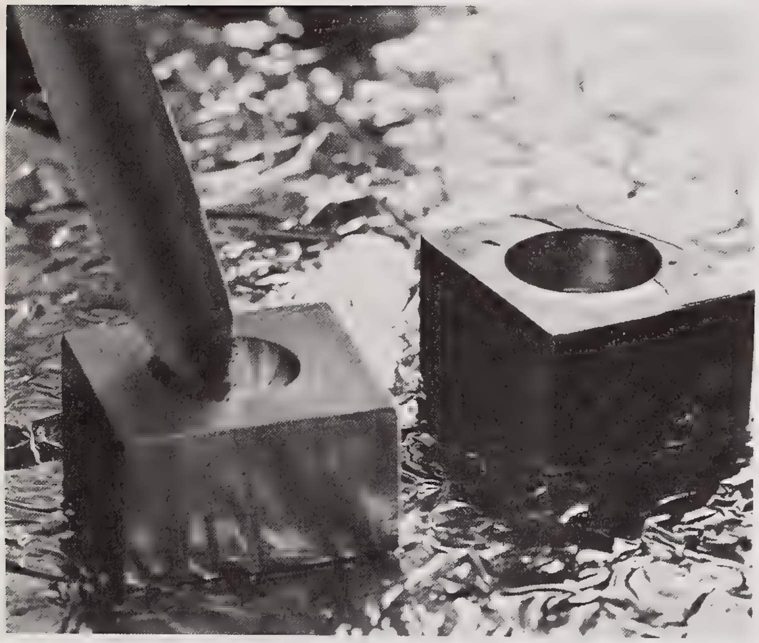

FIGURE 3. GELATIN MANDREL IS ALLOWED TO DRY AND THEN THE ENDS ARE SHAPED BY HAND MOLDS.

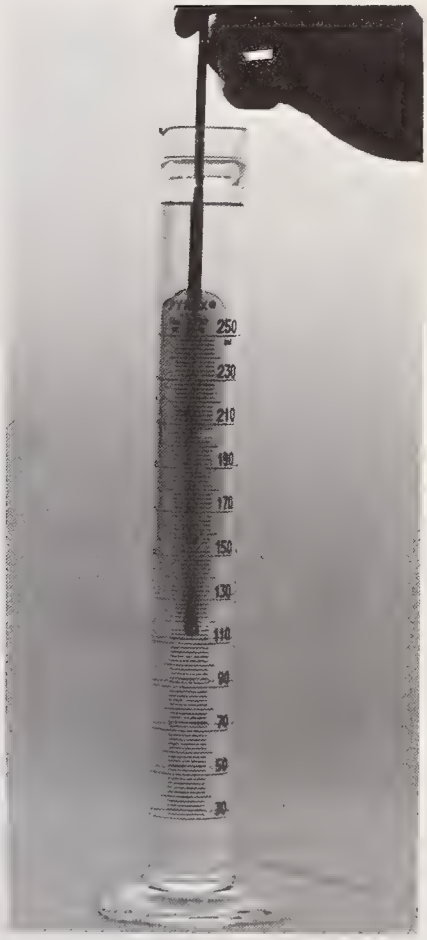

FIGURE 4. THE CATHETER IS HELD VERTICALLY AND THE MANDREL IS SLOWLY LOWERED INTO THE SOLUTION.

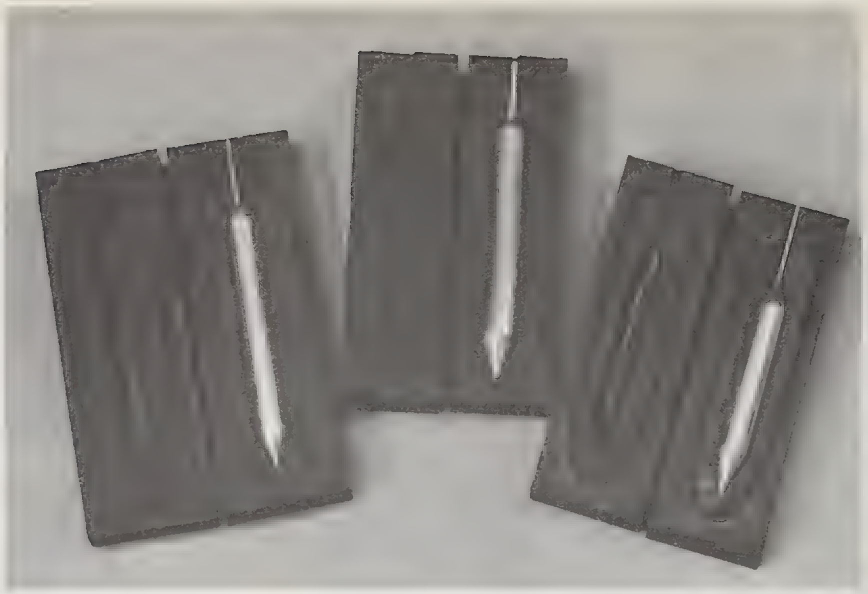

FIGURE 5. TRIAL SILICONE RUBBER MOLDS.

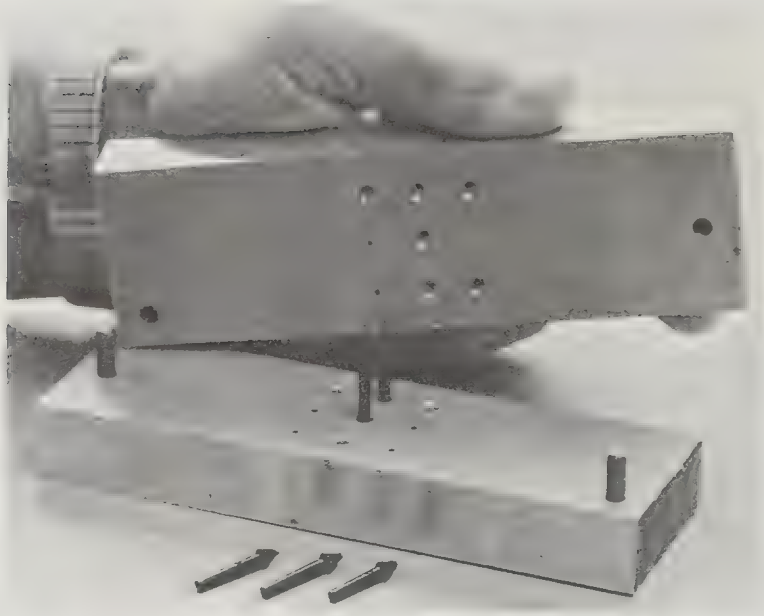

FIGURE 6. CATHETER SLIP-JOINTS ARE UNIFORMLY CAST IN ALUMINUM.

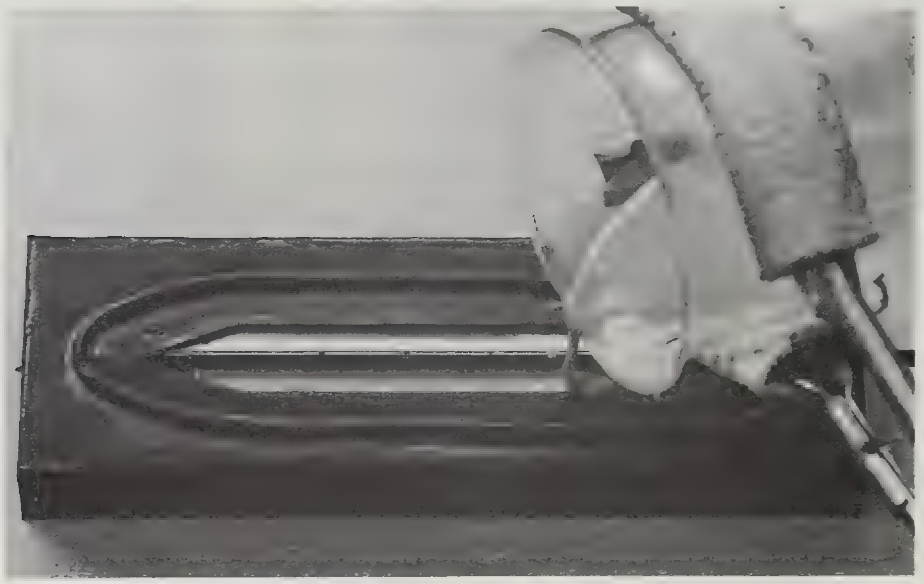

FIGURE 7. MELTED RIGIDAX IS POURED INTO THE MOLD CAVITY.

Engineer; however, this can be automated after we have obtained sufficient data on dipping and withdrawal rates to insure uniform film thickness. The dipping cycle is repeated as required until a 3.5 mil to 4.0 mil film thickness has been formed. After the last dip, the mandrel is left in the raised position and allowed to dry for at least 12 hours. It is then placed in the oven and heated for one hour at 135°F.

Further Preparative Techniques.

After the curing period, the excess material is removed from the tip and reshaped by dipping into polyurethane solution.

The stiffener rod is removed from the catheter tube and a small diameter polyethylene tube is inserted through the catheter tube down to the balloon. Lukewarm water at low pressure is circulated for several hours. This process is continued until the mandrel material has been completely removed through the ventilating holes in the catheter tube (Figure 9).

The final drying is done by circulating anhydrous nitrogen through the balloon to remove residual moisture, and the device is ready for inspection.

Quality Control.

Quality control consists of:

1. Visual inspection for gross defects: dirt, pin-holes, tip protrusion, surface irregularities, etc.
2. Preliminary film thickness measurement by measuring deflated balloon with an Ames spring-loaded film thickness gauge. Probe size is .25" diameter, double wall measurement is taken and averaged (Figure 10).
3. Leak test consists of inflating the balloon with air at 200 mmHg pressure and submerging in water. (Companion test to No. 4). Observe for visible bubbles. A second leak test determines rate. The change in pressure and volume at 180 mmHg initial pressure is noted over a one-hour period (Figure 11).
4. Balloon diameter is checked by inflating with air to 200 mmHg pressure. This pressure is held for 15 seconds while the GO and NO-GO gauges are applied to the balloon. Optical methods will be developed to avoid touching the film to measure the diameter.
5. Balloon displacement is measured by immersing the balloon vertically into water at 73°F and read gross volume of deflated and then the inflated balloon. Net displacement is recorded.
6. Working pressure test: Balloon is re-inflated to 200 mmHg with fixed amount of air and is allowed to remain for 60 seconds. If pressure remains constant or does not change more than 5% in 60 seconds, the part is acceptable.
7. Fatigue resistance: Balloon is immersed horizontally in a sealed container with back pressure of approximately 150 mmHg applied. By alternately inflating the balloon with 10 psig air and deflating, the balloon is cycled once per second. If displacement volume per cycle increases more than about 10%, the part has failed (Figure 12).
8. Ultimate failure: Balloon is inflated at rate of 1 psi per minute to failure as defined by formation of aneurism. Record pressure at failure.
9. Solvent Retention: Condition device 24 hours at ambient, then dry balloon catheter with dry nitrogen to constant weight. Record accurate weight, condition at 100°F for 4 hours, record weight change.
10. Hydrolytic Resistance: Prepare 3 tensile specimens; condition 24 hours at ambient followed by immersion in normal saline solution of 100°F, 24 hours, determine 300% and ultimate tensile values per ASTM D-412-66.

We think that comment is necessary on test methods 3, 4, 5 and 6 above. These test pressures were established to conform with the requirements of the Project Officer. The stress level in the balloon film under test varies directly with the diameter of the balloon. At the minimum film thickness of 0.0035 inch, the stress in the 22 mm diameter balloon is 478 psi, whereas on the 16 mm diameter balloon, the stress is only 348 psi. These two points are illustrated on the load-deflection curve of the graph (Figure 13). Note that the higher point is approaching the knee of the curve. The shape of the curve indicates that balloon distension is occurring (volume is increasing) beyond that which would exist in *in vivo* testing or service in the presence of diastolic (back) pressure. Since the balloon material can be expected to exhibit some creep under stress, the slow rates of pressurization and hold periods are likely to be additive in exaggerating volume. It is suggested that these tests on the larger size balloons be conducted at internal pressures representative of net pressures in service, to avoid providing misleading measurements.

RESULTS

Results of Testing of Balloon/Catheters Fabricated by Gelatin Mandrel Method.

Results obtained from the gelatin mandrel method of fabrication have been recorded for a total of 130 devices.

Results from Travenol's *in vivo* testing have been received for three of the seven submitted balloon/catheters. Over 12 hours of satisfactory performance were reportedly experienced with the first device, with no significant problems in either catheter or balloon. Separation of the balloon film from the end of the small polyethylene tubing used in the slip-joint was experienced, but was repaired. Softening of the catheter was noted, but did not appear to constitute a major problem since

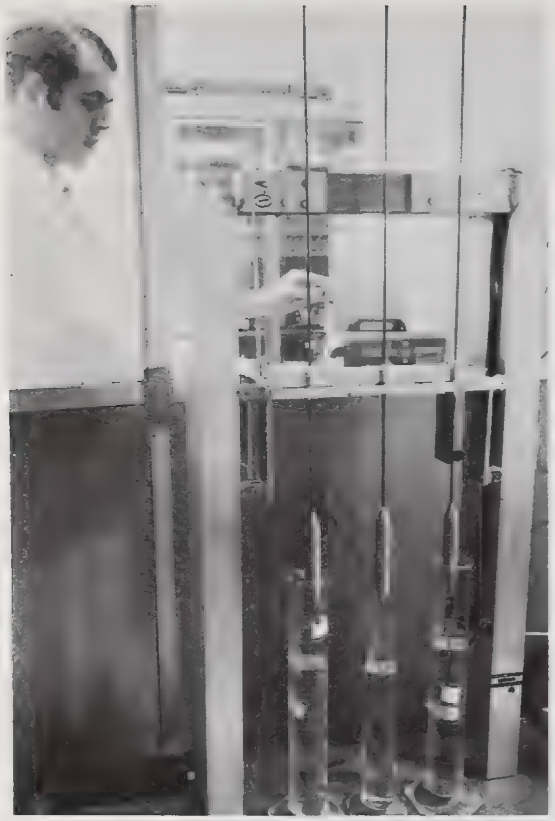

FIGURE 8. BY REMOTE CONTROL THE MOVABLE SECTION LOWERS THE MANDRELS INTO THE SOLUTION, REVERSES IMMEDIATELY AND RAISES THE MANDRELS INTO THE DRYING POSITION.

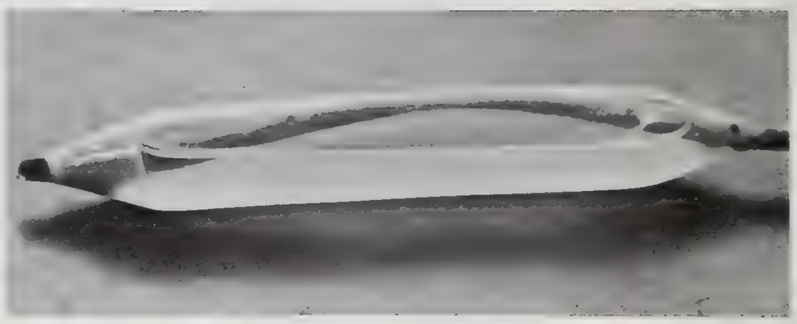

FIGURE 9. REMOVAL OF THE MANDREL MATERIAL BY LUKEWARM WATER AT LOW PRESSURE.

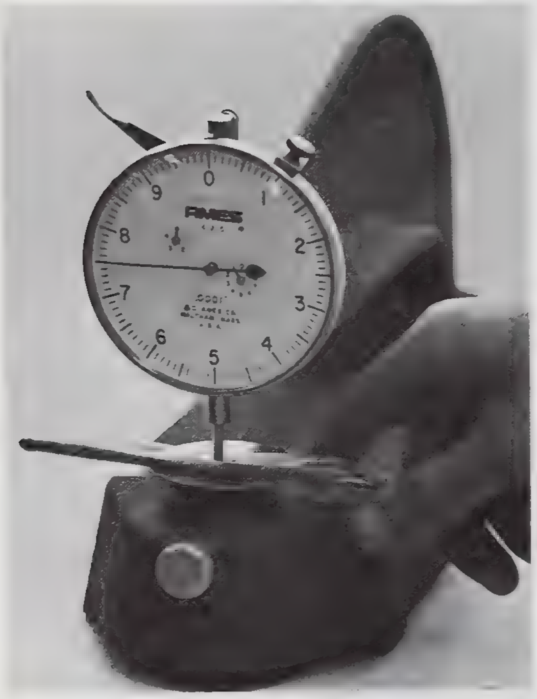

FIGURE 10. PRELIMINARY FILM THICKNESS MEASUREMENT.

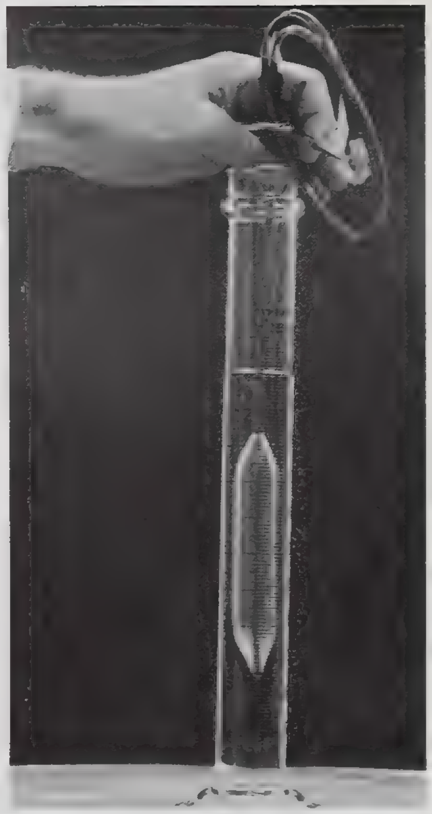

FIGURE 11. LEAK TEST.

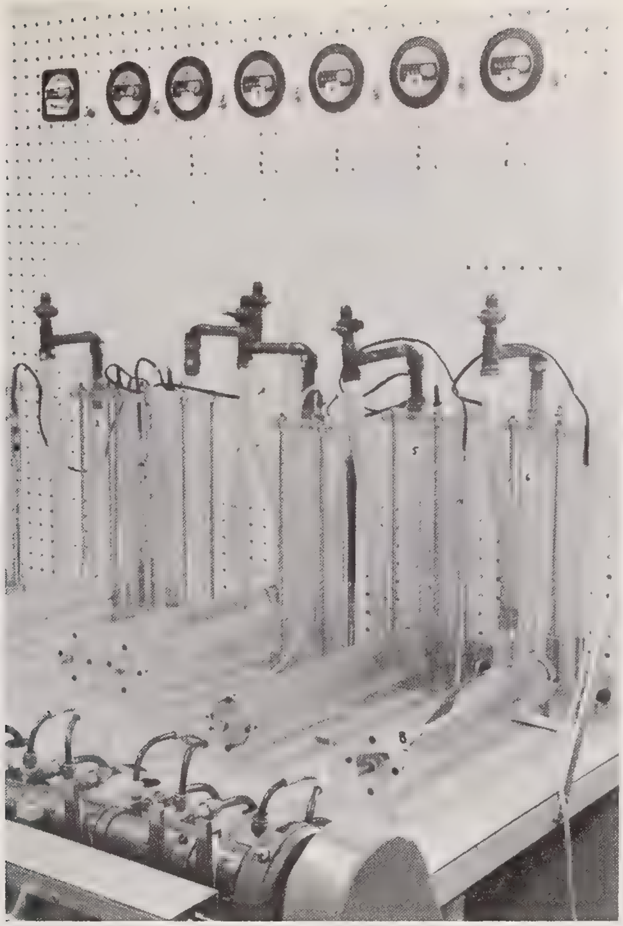

FIGURE 12. FATIGUE RESISTANCE MEASUREMENT.

REPRESENTATIVE LOAD-DEFLECTION
RELATION IN BALLOON FILM

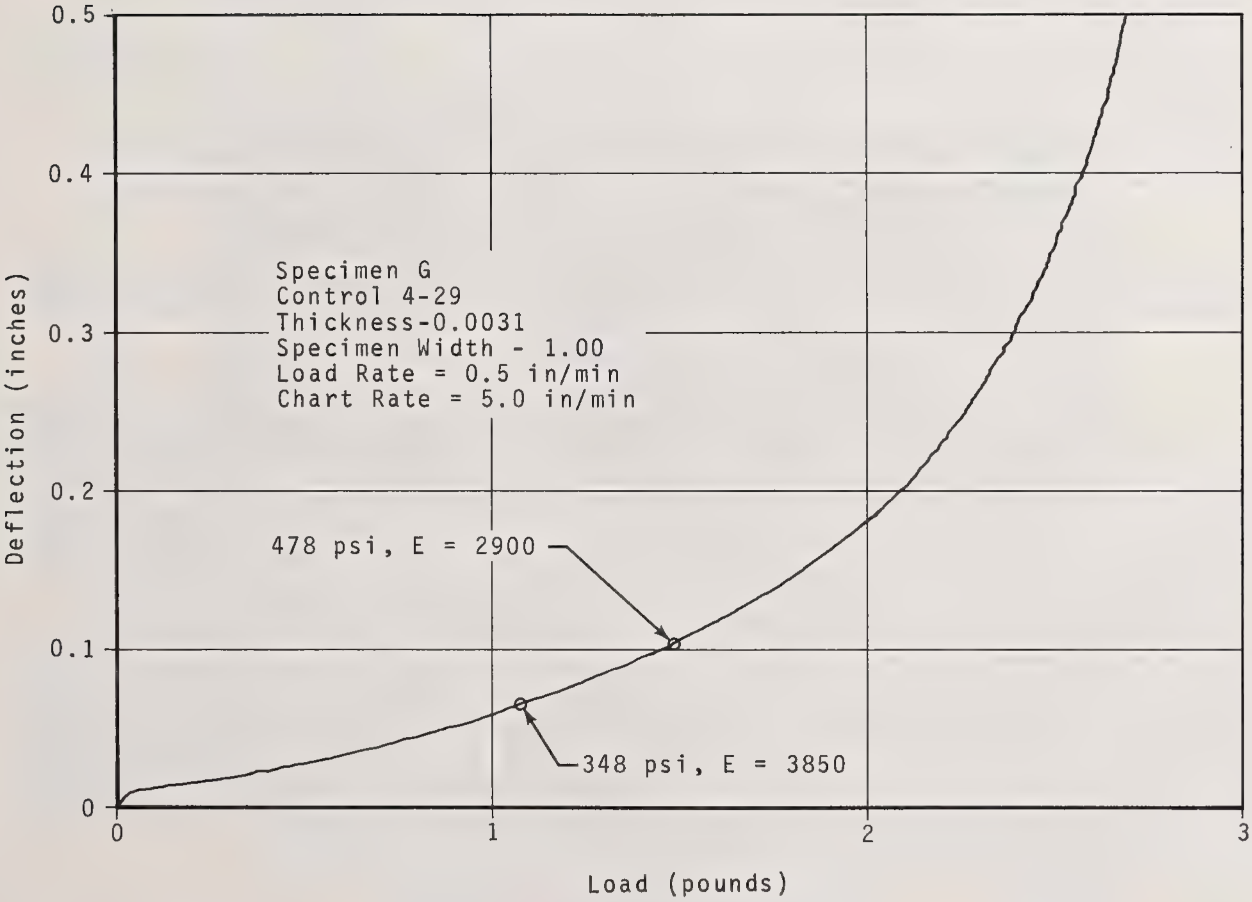

FIGURE 13

this device was evaluated successfully in two test animals. Six additional devices were then submitted for evaluation, with several units having a redesigned slip-joint configuration to prevent separation of the balloon film from the catheter previously experienced. Three major problem areas were defined from the in vivo testing of two of these units: The first was that too loose a fit between components of the slip-joint used to compensate for balloon film shrinkage appeared to cause repetitive umbrella-like folding and unfolding of the balloon during inflation and deflation resulting in the formation of creases which ultimately split. A more severe problem experienced during in vivo use of these two devices was kinking of the catheter. The third problem experienced during testing of the fabricated devices was excessive softening of the catheter making relocation difficult, if not impossible. This softening might also have contributed to the kinking of the catheter, although Travenol Laboratories theorized that the cause of the kinking might be in the operational mode of the controller-actuator.

A tentative fabrication procedure was established for producing pre-production quantities of balloon/catheters. A ten percent rejection level was experienced with this procedure. An analysis of the time required for the major phases of the fabrication and inspection indicated that an improved mandrel material and production technique is required. Preliminary quality control parameters and acceptance criteria were developed. A tester was constructed to assess life expectancy of the devices under repetitive inflation and deflation cycling action.

Results of Testing of Balloon/Catheters Fabricated by Rigid Mold Method.

Results obtained from the Rigidax mandrels are just being compiled; however, initial indications show a marked improvement in uniformity of film thickness, diameter and volume.

Specifically, there have been improvements on:

1. A consistently improved uniformity of film appearance. A clear uniform slightly frosty effect due to inside pebbly surface of sprayed PVA.
2. A consistent, as dipped, volume, diameter and length. The variation of volume, etc., at 200 mmHg is a function of film thickness which is not due to association with Rigidax.
3. Relative ease of dipping. Humidity control does not require critical, difficult limits. To date, solutions have not caused visual rejection associated with the solution per se.
4. More uniform thickness. Due to more uniform shape, i.e., extraneous run-off minimized.

CONCLUSIONS

1. Gelatin mandrels permit immediate variations in end configuration for design change investigation.
2. Gelatin mandrels are dimensionally unstable for fabrication within the specific tolerances recently adopted.
3. The polyurethane dipping solution is only relatively stable and we have found it more difficult to control on gelatin mandrels than on Rigidax mandrels.
4. The longitudinal shrinkage of the film after removal of the mandrel and the expansion under prolonged internal pressure require additional investigation.
5. The Rigidax mandrel material appears to offer a method for standardization of mandrel size and end configuration.
6. The machine dipping technique produces more uniform film formation than hand dipping.
7. Environment controls of the dipping area with provisions for proper ventilation protection for operators are required.

II. FABRICATION OF PROTOTYPE DEVICES

In addition to the activities on balloon/catheter fabrication, Western Gear Research has investigated the fabrication of prototype devices, such as blood pump components for left heart assist devices.

METHODS

We have received a model of Dr. Akutsu's series-type device and have prepared several combination molds for casting expendable mandrels for the housing sections of the device (Figure 14). These housing sections are for the valve chamber and the pump bladder section. Since these mandrels are expendable, we have molded them hollow of a low melt polyethylene wax material. The molds themselves are two-piece with irregular mating parting lines and are of laminated construction with a silicone rubber inner surface supported for strength with a rigid plaster outer shell. The method of fabrication of these molds is more involved than the molds for the balloon/catheter mandrels.

The model is coated with a release agent and then completely covered with a quarter-inch layer of clay. This encapsulated model is then half-embedded in clay. A plaster reinforcing outer shell is cast over the upper half of the model. When this is hard, the assembly is inverted and the clay is removed from the upper half of the mold. A tongue and groove register pattern is modeled into the clay remaining in the lower section. A layer of silicone rubber is carefully applied to assure a uniform coating over the model and the register pattern. A plaster reinforcing outer shell is cast over the silicone rubber. The assembly is again inverted, the upper reinforcing shell is removed and the clay is carefully scraped out of the shell. The model is coated with a thin layer of silicone rubber and the upper shell is replaced over the model (Figure 15). The assembly is clamped and ro-

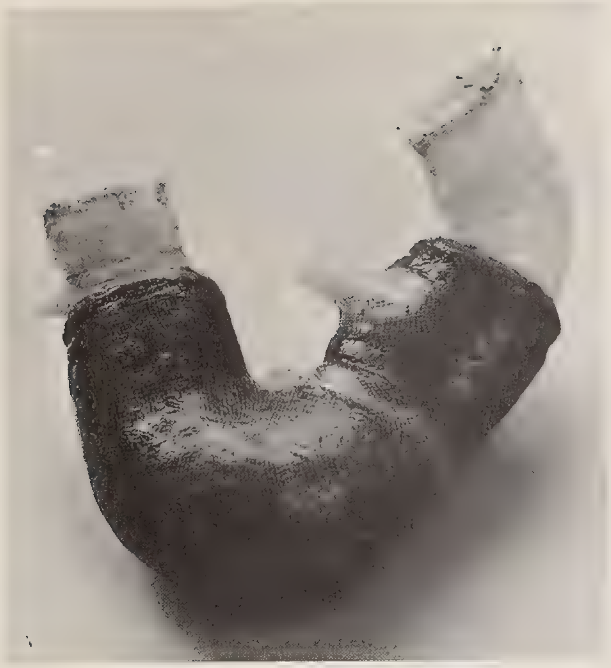

FIGURE 14. EXPENDABLE MANDREL.

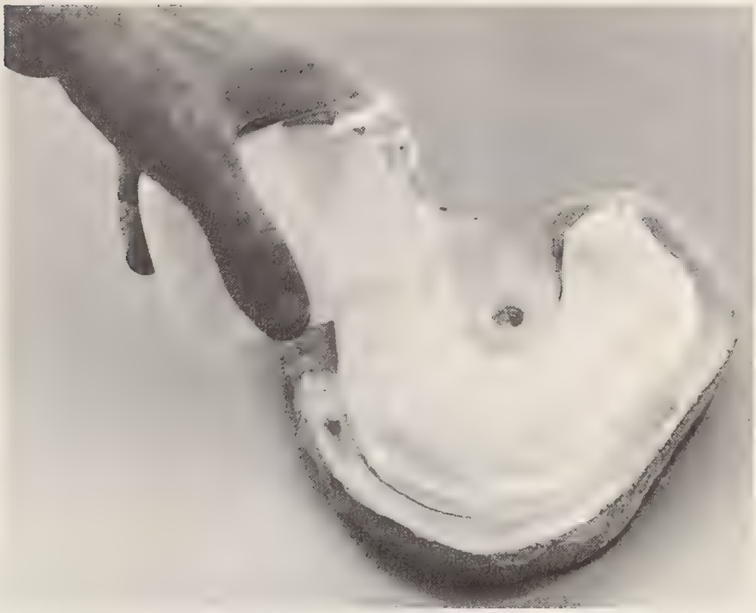

FIGURE 15. THE MODEL IS COATED WITH A THIN LAYER OF SILICONE RUBBER AND THE UPPER SHELL IS REPLACED OVER THE MODEL.

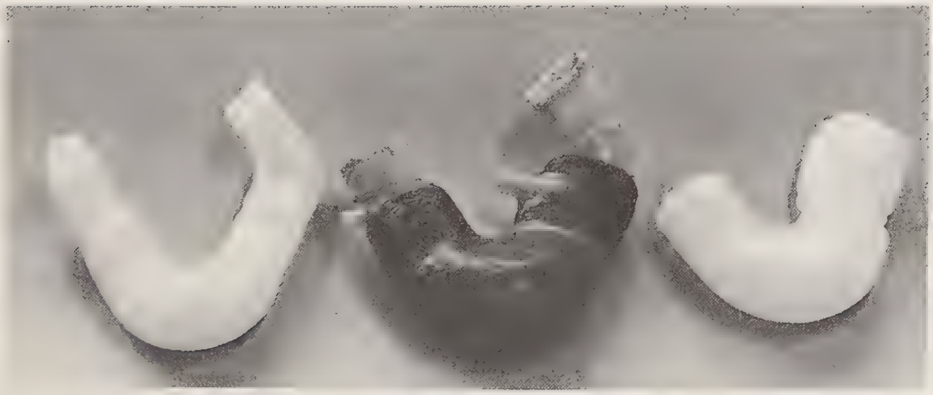

FIGURE 16. SEE TEXT FOR EXPLANATION.

tated so that a sprue section provided at the parting line can now be used to complete the filling of the silicone rubber cavity. When the mold has dried completely, the model is removed. The mold is reclamped and the sprue section is used to pour a low melt polyethylene wax into the mold cavity. The finished part becomes an expendable mandrel around which an epoxy part will subsequently be formed (Figure 16).

Samples of these expendable mandrels have been submitted to Dr. Akutsu for approval. Since this activity has just been initiated, and has been of low level priority, our investigation has been principally in evaluating fabrication techniques. As requested by the Contract Office, we will expand our efforts.

DISCUSSION

DR. BYCK: We have observed that balloons fabricated from melt extruded polyurethane may represent an improvement over solution cast balloons from the point of view of reproducible durability. In general, one obtains urethane films which have consistently fewer inhomogeneities which may be acting as rupture points. I was wondering if you have any plans to investigate extrusion or blow molding or any other form of melt fabrication?

MR. SPRUNG: We have been following a plan approved by the project officer. Blow molding would give us a mold parting line that would not be permitted.

DR. BRUNO: I'll make this brief, the hour is late. You are to be complimented on a work of art and indeed a labor of love, but I'd like to leave you with a humorous note. In 1958, I was in Rome with Professor Valdoni and we were faced with the problem of coronary angiography. We took a Charles Dotteer catheter, modified it, and added what the Romans called American parachutes to it (which could only be bought at the PX during the war). We used this balloon catheter; it worked very effectively. I don't recall any failures in the balloon catheter, but let me say, you have come a long way since then.

MR. SPRUNG: Thank you, Dr. Bruno. Before I leave, I would like to give my card to all these experts who know how to make balloon catheters and I would like to enter into co-experiments, so before you leave will you please tap me on the shoulder; I have a large number of cards.

MR. CULP: In the fabrication of your balloons, have you done anything to evaluate the exterior surface characteristics of the balloon?

MR. SPRUNG: The exterior surface of the balloon begins with the smooth aluminum mandrel and we reproduce this with our silicone rubber mold. Ultimately, this silicone rubber mold should be replaced with a hollow, smooth aluminum mold which will give us the final surface of the balloon. We cover the mandrel as you saw with poly(vinyl alcohol) and examine this very closely because the smoothness of the poly(vinyl alcohol) surface is reflected in the final film surface formation.

MR. CULP: Thank you. In the spraying of the poly(vinyl alcohol), do you measure the surface roughness of the sprayed coating?

MR. SPRUNG: No, we haven't measured the roughness. We observe the light reflection from the surface.

CHAPTER 56

A NEW ANIMAL MODEL MYOCARDIAL INFARCTION

W. Elzinga, W. Kaufman, D. Upright and D. Powell

Hittman Associates, Inc.
Columbia, Maryland

Coronary thrombosis was precipitated in dogs by magnetically removing blood-borne microscopic iron particles (approximately four micron mean diameter) at a designated site on the coronary artery. Four groups of animals were studied: an acute feasibility group (two dogs), a control group consisting of sham-operated, iron particle-injected animals (particle controls-four dogs) and magnet implanted, non-particle injected animals (magnet controls-four dogs), a dose-response group (12 dogs), and a progressive infarction study group (nine dogs). In the control group, the iron particles increased the white blood cell count (WBC) shortly after injection. No tissue necrosis was found in any organs reviewed. The implanted perivascular magnet causes a local inflammatory response. Doses of 0.2 gm/Kg, 0.1 gm/Kg, and 0.025 gm/Kg (injected by vein five days postsurgery) precipitate iron-positive thrombi beneath the magnet. The average vessel occlusion for each dose level was 60 percent (13 dogs), 38 percent (four dogs), and three percent (four dogs), respectively. Serial electrocardiogram (EKG) and enzyme (LDH, SGOT, and CPK) data postinfarction confirm myocardial infarction. In the progressive study, dogs autopsied three hours, 12 hours, and 24 hours post-particle injection (PPI) did not have thrombi in the anterior descending artery; however, many small branches distal to the magnet were occluded with iron-positive fibrin thrombi. In those dogs autopsied 3, 8, 11, 14, and 21 days PPI, large,organizing, iron-positive thrombi were present in the anterior descending artery. Soon after particle injection (three hours), the enzymes LDH, SGOT, and CPK were sharply elevated and peaked between 8 and 12 hours PPI.

INTRODUCTION

To determine the usefulness of a circulatory assist device, it is necessary to test it in experimental animals. Although certain useful information can be derived from tests performed in the normal healthy animal, the real test comes from the experimentation in the cardiac impaired animal.

We have developed a new technique for the preparation of an animal model which we believe will be useful in the testing of assist devices.

- The technique allows the investigator to precipitate a coronary thrombosis at almost any site within the major coronary vessels.
- Gradual or stepwise narrowing of the vessel appears to be possible.
- The animal can be completely unrestrained during the development of the occlusion.
- The technique appears to be applicable to more than one animal species.

An animal model that mimics human disease has always been an important substitute in those cases where human experimentation is impractical or impossible. This model mimics human myocardial infarction in amany respects in that:

(1) A roughening of intima (collection of iron powder by the magnet) precipitates the formation of a thrombosis.
(2) The vessel is damaged at the site of the thrombus attachment.
(3) Serum enzymes (LDH, SGOT, and CPK) are elevated.
(4) **Electrocardiogram (ECG)** recording during myocardial ischemia, injury, and infarction are similar to those of humans.
(5) Cardiac arrhythmias are present during the attack, or early stages of occlusion.
(6) Secondary vessels distal to the site of the thrombus are commonly occluded.

Our procedure involves the implantation of a specially constructed magnet on the anterior descending branch of the left coronary artery of the dog. Any other appropriate site could also be used. After a surgery recovery period, microscopic iron particles (four microns mean diameter) are injected into a cephalic vein. The blood-borne microscopic particles are partially removed from the circulation at the site of the magnet and precipitate the formation of a coronary thrombosis.

METHODS

The perivascular magnets* were machined from Alnico V cylindrical bars. The finished magnets were essentially cylindrical with a machined air-gap and are best defined by referring to Figure 1. The magnets were magnetized after they were machined. Each magnet weighed 0.681 gram. Prior to implantation they were sterilized in Germicide** and thoroughly rinsed in sterile saline.

The carbonyl iron powder*** was essentially pure iron in the form of microscopic particles with a mean diameter of approximately four microns (90 percent of the particles were under seven microns and 70 percent were under five microns). The injection solution consisted of previously autoclaved iron particles suspended in normal saline at a concentration of one gram of iron powder per 10 cc of saline.

All of the animals used in the study weighed approximately 11 kilograms and were pure-bred beagles. To place the magnet on the coronary vessel a thoracotomy was required. The anterior descending branch of the left coronary artery was isolated for a distance of seven millimeters at the bifurcation. The magnet was placed over the artery and sutures were placed under the vessel and tied over the top of the magnet.

RESULTS AND DISCUSSION

This preliminary program was designed to test the feasibility of the magnet and microscopic particle technique for inducing myocardial infarction. The feasibility research effort was divided into four smaller studies:

1. Feasibility Study of Microscopic Particle Technique.

In acute open chest studies a magnet was placed on the anterior descending left coronary artery and coronary pressure was monitored distal to the magnet by cannulating a very small branch of this artery. Iron particles (0.1 gm/Kg of body weight) were then injected into the left ventricle. Figure 2 shows the results of this study, a sudden significant reduction of distal coronary pressure.

2. Study of the Pathological Effects of the Magnet and the Iron Particles.

The favorable results from this study led us to believe that the technique was feasible. Therefore, we decided to perform tests on a group of animals to study the pathological effects of injecting iron into the circulatory system of dogs. Furthermore, four additional dogs each had a magnet implanted on the anterior descending coronary artery; no particles were injected and these animals served as a magnet control group. These two control groups were monitored periodically (ECG, hematology). Both groups were autopsied at the termination of the experiment.

a. In the so-called "particle control" animals a sham operation was performed. A magnet was positioned on the coronary vessel and then removed. After the animals recovered from the sham surgery they received 0.2 gm/Kg of iron by venipuncture (cephalic vein).

The effects of the injected iron on serum enzymes and blood components are shown in Figures 3 and 4 and Table 1. Serial ECG data (leads I, II, aVL) from all the dogs revealed that the particles do not alter the electrical activity of the heart. The particles consistently elevated the white blood cell count (WBC) (mainly neutrophils).

After the 21 day period, the animals were sacrificed and microscopic slides were prepared of various organs. No histological evidence of tissue necrosis was found in the following organs: lymph nodes, lungs, liver, spleen, pancreas, kidneys, urinary bladder, stomach, large and small intentines, testicles, brain, adrenals, and bone marrow. The heart was sliced transversely from the base to the apex approximately every five to six millimeters. The myocardium and internal structures of the heart were normal. Large amounts of iron were found in the spleen, liver, and lungs. Smaller amounts of iron were dispersed in the lymph nodes (tonsil, cervical, popliteal, pulmonary, and mesenteric) and kidneys. Therefore, we found no structural evidence that these particles harm the animal, at least until 21 days after particle injection. The animals appeared normal in behavior.

b. In the so-called "magnet control" animals a magnet was implanted but no particles were injected.

The presence of the perivascular magnet in the dogs had little effect on serum enzymes and blood components (Table 2). The magnet was found to elicit a local inflammatory response, observed at autopsy, in the adjacent tissues. Consistently elevated T waves were noticed in the magnet control group after magnet implantation.

The results of the two control studies suggested that the animals could live indefinitely with either the magnet or the particles. However, more extensive testing is required to substantiate this. After determining that the particles and the magnet do not cause serious damage to the animals, the third phase, a dose response study, was initiated.

---

*Permag Corp., Jamaica, New York

**Bard-Parker Co., Rutherford, New Jersey

***General Aniline and Film Corp., Linden, New Jersey

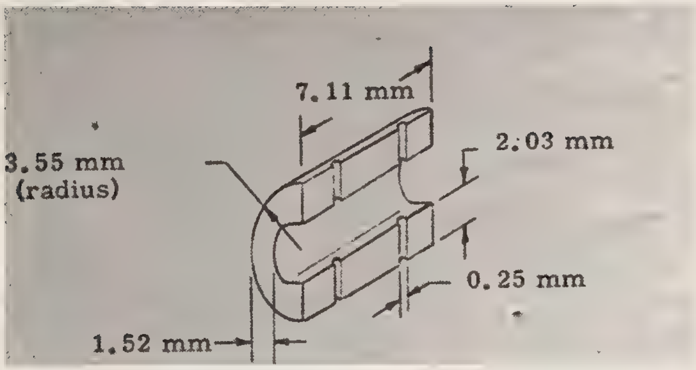

FIGURE 1. DIAGRAM OF MAGNET USED FOR IMPLANTATION ON CORONARY VESSEL.

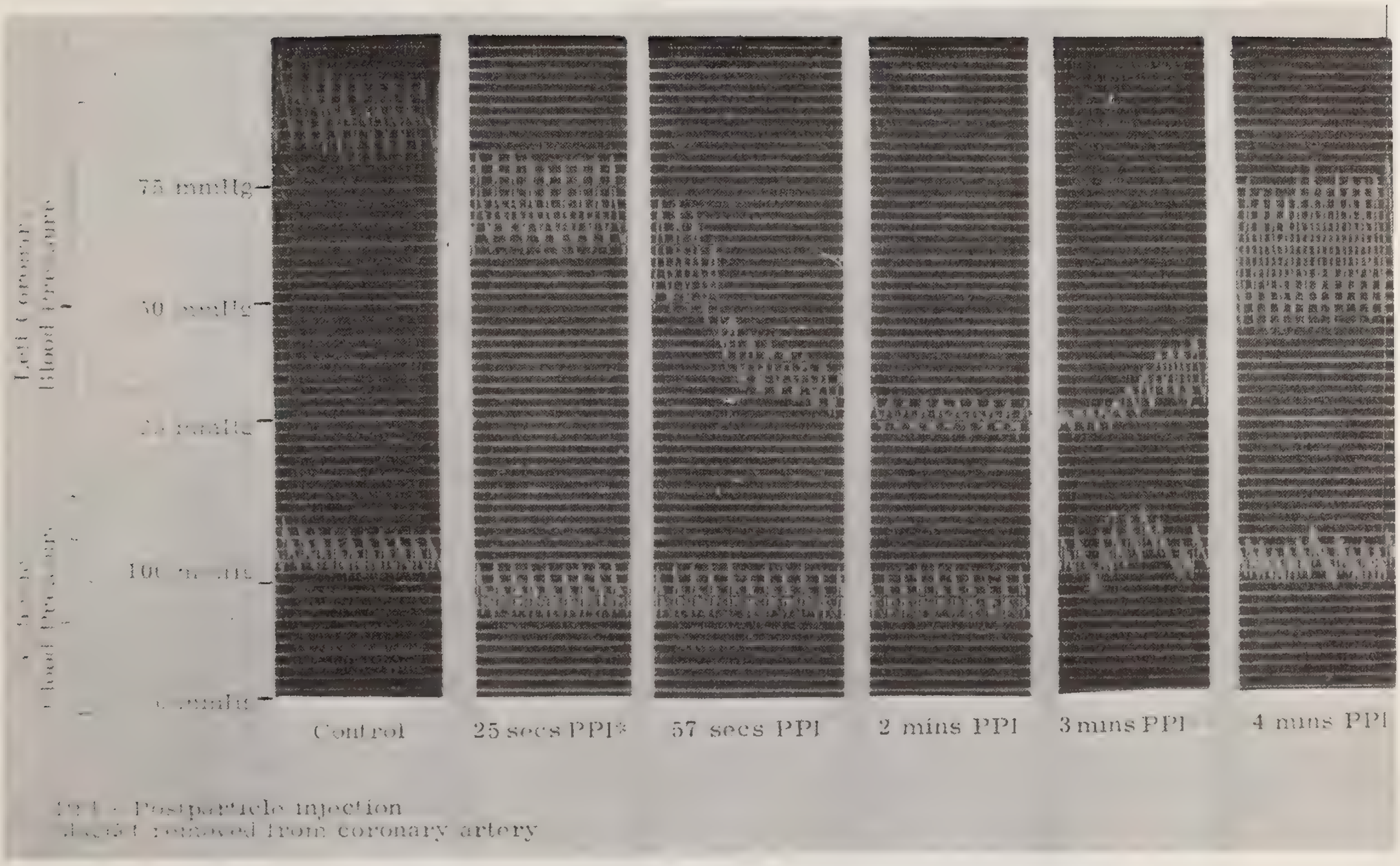

FIGURE 2. CHANGES IN SYSTEMIC BLOOD PRESSURE AND ANTERIOR DESCENDING LEFT CORONARY ARTERY BLOOD PRESSURE DISTAL TO THE PERIVASCULAR MAGNET BEFORE AND AFTER PARTICLE INJECTION (PAPER SPEED 25 MM/SEC)

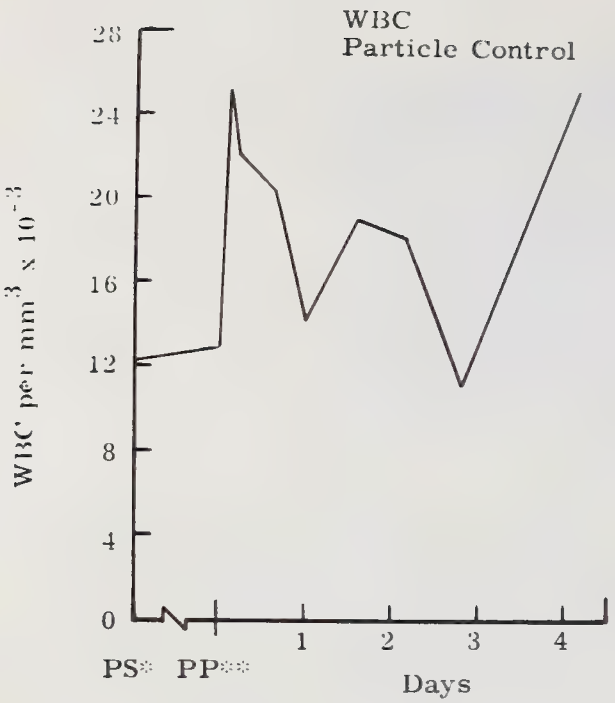

FIGURE 3. CHANGES IN WBC IN RESPONSE TO IRON INJECTIONS (FOUR DOGS).

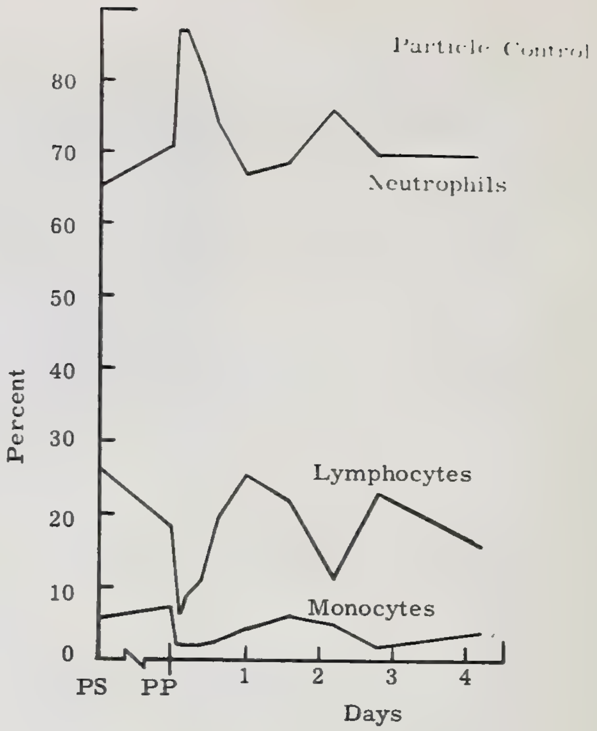

FIGURE 4. CHANGES IN NEUTROPHILS, LYMPHOCYTES AND MONOCYTES IN RESPONSE TO IRON INJECTIONS (FOUR DOGS).

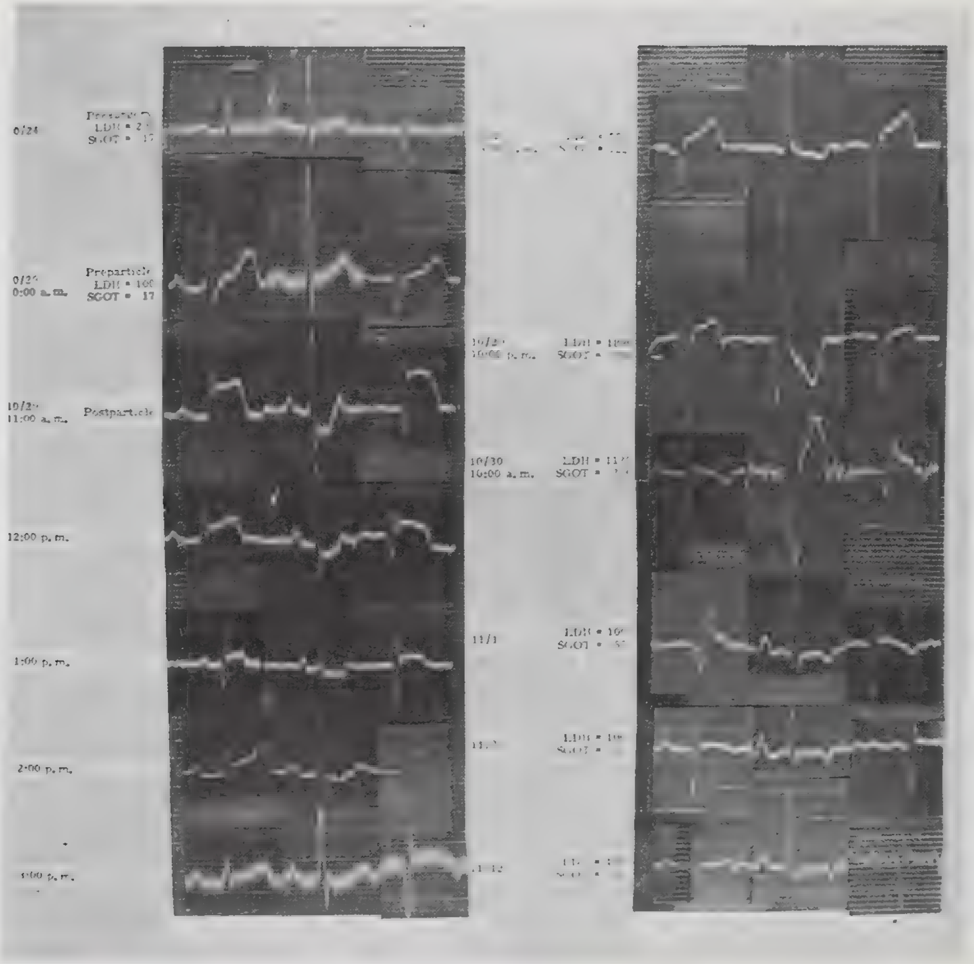

FIGURE 5. SERIAL ECG AND ENZYME DATA FROM PARTICLE INJECTED (0.2 GM/KG) DOG.

TABLE 1

SUMMARY DATA SHEET FOR SHAM OPERATED PARTICLE CONTROL STUDY

			Days After Iron Particle Injection								
	Presurg. Aver. n	Prepart. Aver. n	1(am) Aver. n	1(pm) Aver. n	2 Aver. n	3 Aver. n	5 Aver. n	8 Aver. n	11 Aver. n	14 Aver. n	21 Aver. n
HCT(%)	48.5[a] 4	49.2 3	48.7 2	49.5 4	46.8 4	46.8 4	43.8 3	47.5 4	45.8 2	49.5 1	47.5 1
HGB(gm%)	15.1 4	13.9 4	15.2 3	15.2 4	14.5 4	14.3 4	14.3 3	14.5 4	14.4 2	15.4 1	14.4 1
RBC(10^6mm^3)	6.73 4	6.67 4	6.81 3	6.77 4	6.58 4	6.35 4	6.52 3	6.61 4	6.43 2	6.98 1	6.02 1
WBC(mm^3)	12,150 4	12,725 4	24,800 3	21,980 4	21,225 4	20,200 4	14,200 3	19,100 4	18,300 2	11,300 1	25,000 1
Seg. Neuts(%)	61.8 4	71 4	86.5 4	87.2 4	81.3 4	74 4	67 4	68 4	76 3	70 1	70 1
Lympho.(%)	25.7 4	18.3 4	6.3 4	7.8 4	11 4	19 4	25 4	22 4	15.3 3	23 1	16 1
Mono.(%)	5.5 4	6.7 4	2.3 4	1.5 4	1.8 4	2 4	3.8 4	5.5 4	4.7 3	2 1	4 1
LDH(units)	488 4	663 4	558 4	440 4	958 4	478 4	713 3	675 4	643 3	280 1	490 1
SGOT(units)	16 4	28 4	52 4	32 4	34 4	16 4	18 3	27 4	26 3	39 1	14 1

[a]Average value for n dogs
n = number of dogs

TABLE 2

SUMMARY DATA SHEET FOR MAGNET CONTROL STUDY

		Days After Magnet Implantation							
	Presurg. Aver. n	4 Aver. n	5 Aver n	6 Aver. n	8 Aver. n	11 Aver. n	14 Aver. n	16 Aver. n	23 Aver. n
HCT(%)	44.5[a] 4	43.7 3	46.8 4	48.4 4	45.1 4	46.9 4	45.3 4	43.0 3	42.2 3
HGB(gm%)	13.5 4	13.9 3	14.6 4	15.1 4	13.9 4	15.0 4	13.8 4	13.5 3	13.5 3
RBC(10^6mm^3)	6.17 4	6.08 3	6.75 4	6.79 4	6.25 4	6.53 4	6.55 4	4.38 3	5.84 3
WBC(mm^3)	18,000 4	11,800 3	13,200 4	17,300 4	21,600 4	14,700 4	12,000 4	12,600 3	10,500 3
Seg. Neuts(%)	61 4	62 4	73 4	65 4	74 4	68 4	63 4	55 4	68 4
Lympho.(%)	31 4	32 4	22 4	27 4	14 4	22 4	25 4	30 4	25 4
Mono.(%)	5.5 4	4 4	3 4	4 4	8 4	6 4	9 4	10 4	2 4
LDH (units)	730 4	365 4	438 4	438 4	718 4	375 4	438 4	408 4	230 4
SGOT (units)	30 3	21 4	19 4	19 4	31 4	13 4	22 4	18 4	35 4

[a]Average value for n dogs
n = number of dogs

3. Dose Response Study.

In the dose response study (Table 3), three dose levels of iron were investigated: 0.2, 0.1, and 0.025 gm/Kg of body weight. Identical magnets were again implanted at the same site as in the magnet control study. When the animals recovered from surgery, the suspension of iron was injected into the cephalic vein. Electrocardiograms and blood data were periodically monitored postparticle injection. These dogs were again autopsied at the termination of the experiment.

TABLE 3

SUMMARY SHEET FOR ALL DOSE LEVELS

Dose Level	No. of Dogs	Enzyme Activity	EKG	Vessel Thrombosis		Heart Pathology
0.2	4	Elevated (all dogs)	Severe arrhythmias (all dogs); ST elevation; Q waves	Primary 67%	77%	Small subacute apex and subendocardial
				Primary 100%		Large acute (magnet to apex)
				Primary 67%		Large subacute (magnet to apex)
				Primary 75%		Massive transmural (magnet to apex)
0.1	4	Normal (all but one dog)	Severe arrhythmias (all dogs); prominent T waves	Primary 67%	36%	Small apex
				Primary 33%		Small apex
				Primary 12%		Normal
				Primary 33%		Small right ventricle
0.025	4	Normal (all dogs)	Severe arrhythmias (all but one dog)	Primary 12%	3%	Minute focal
				None		Normal
				None		Minute focal
				None		Normal

At the 0.2 gm/Kg level, changes in the ECG and serum enzymes indicated that myocardial damage had occurred (Figure 5). Hematological data, with the exception of the serum enzymes, appeared normal in this group. Myocardial infarction was histologically verified in all dogs at this dose level (Figures 6 and 7). Sections of the coronary vessel beneath the magnet revealed the presence of coronary thrombosis in all dogs (Figures 8, 9, and 10). Furthermore, many secondary thrombi were found in branches of the anterior artery distal to the magnet. Both primary and secondary thrombi were iron positive with Perls' Prussian Blue and Owens' iron stains. Microincineration of a section of the thrombosed vessel revealed the presence of a significant amount of iron. The iron was found lightly dispersed throughout the thrombi with focal accumulations near the vessel walls.

At the 0.1 gm/Kg dose level, occurrence of arrhythmias in the serial ECG data was suggestive of myocardial impairment. The serum enzymes LDH and SGOT were, however, within normal limits. Myocardial infarction was verified histologically and was confined mainly in the apex of the heart. Iron-positive thrombi (primary and secondary) were present in all dogs at this dosage. The degree of vessel occlusion was considerably less when the 0.1 gm/Kg group was compared to the 0.2 gm/Kg dogs.

The 0.025 gm/Kg dose group did not exhibit signs suggestive of heart damage. Only one dog had a small primary thrombosis beneath the magnet.

4. Progressive Infarction Study.

The final investigation in this series was a study of the progression of the iron precipitated coronary thrombosis. Magnets were again implanted on the left anterior artery of nine dogs and 0.2 gm/Kg of iron was injected into the cephalic vein after a five day recovery period. The animals were sacrificed according to the following schedule: 0.5, 1, 2, 3, 5, 11, 14, and 21 days postparticle injection. A complete autopsy was performed on each dog. Special emphasis was placed on the pathology of the coronary arteries and the myocardium.

The hematological and enzymatic results of the study are shown in Figures 11, 12, and 13. The progression of the iron precipitated coronary thrombosis is described in Table 4. Iron containing thrombi, as determined by staining, were present in all stages of the study, from four hours up to 21 days postparticle injection. In those dogs autopsied shortly after particle injection (4, 12, and 24 hours), only secondary thrombi were found in branches of the anterior descending artery distal to the magnet. In those dogs sacrificed in the later stages of the study (8, 11, 14, and 21 days), both primary thrombi, i.e., thrombi beneath the magnet, and secondary thrombi were present.

Histological examinations of the coronary thrombi in the early stages of the study (4, 12, 24, and 72 hours) showed that they were composed primarily of fibrin, inflammatory cells, and many iron particles. In the later stages of the study (5 to 21 days), the thrombi contained iron and fibrin but were lined with endothelium and classified as organized thrombi. Sections of the coronary vessel beneath the magnet, submitted to microincineration, revealed that a large quantity of iron was in the thrombosis.

Severe arrhythmias were evident in all but one dog soon after particle injection. Figure 14 shows that 77 percent of the arrhythmias started within six hours postparticle injection. In general,

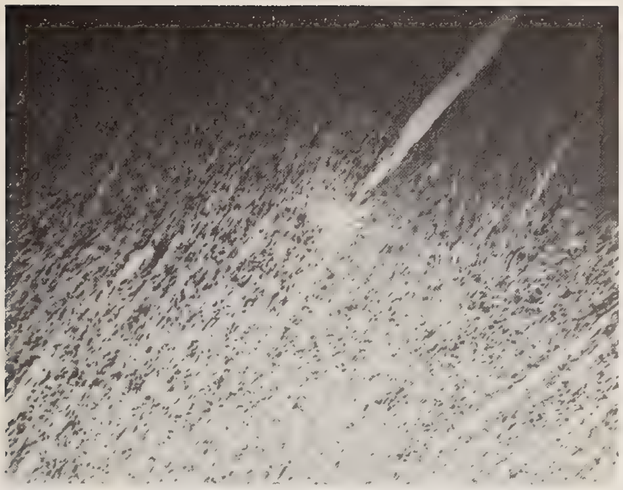

FIGURE 6. EIGHT-DAY INFARCT SHOWING EDGE OF LIQUEFACTION NECROSIS, LOWER HALF. MARKED INFILTRATION OF LEUKOCYTES AND FIBROBLASTS ARE EVIDENT (100x).

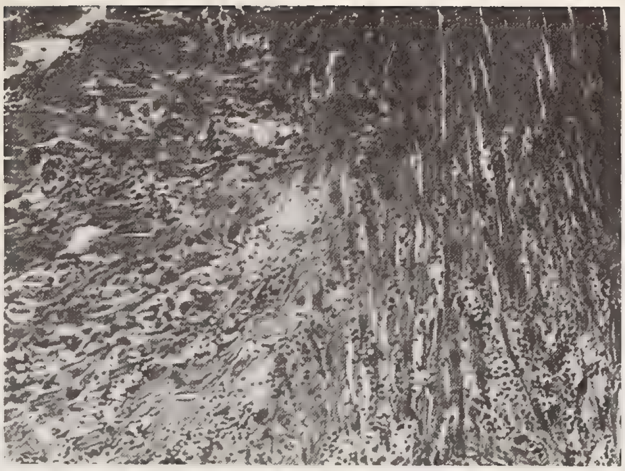

FIGURE 7. FIVE-DAY INFARCT SHOWING MARKED INFILTRATION OF LEUKOCYTES AND RED BLOOD CELLS (100x).

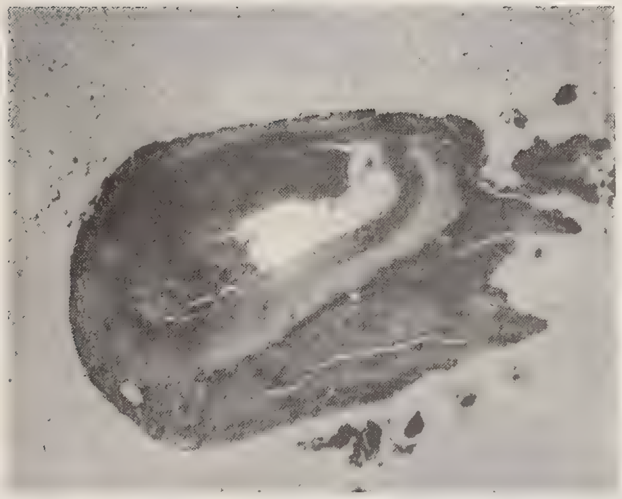

FIGURE 8. PHOTOMICROGRAPH OF IRON PRECIPITATED CORONARY THROMBOSIS WITHIN VESSEL BENEATH MAGNET (25x).

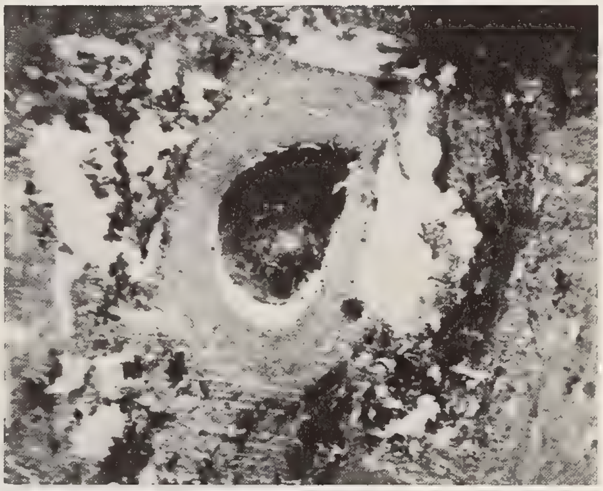

FIGURE 9. PHOTOMICROGRAPH OF IRON PRECIPITATED CORONARY THROMBOSIS WITHIN THE VESSEL BENEATH THE MAGNET SHOWING TOTAL OCCLUSION OF THE VESSEL (35x).

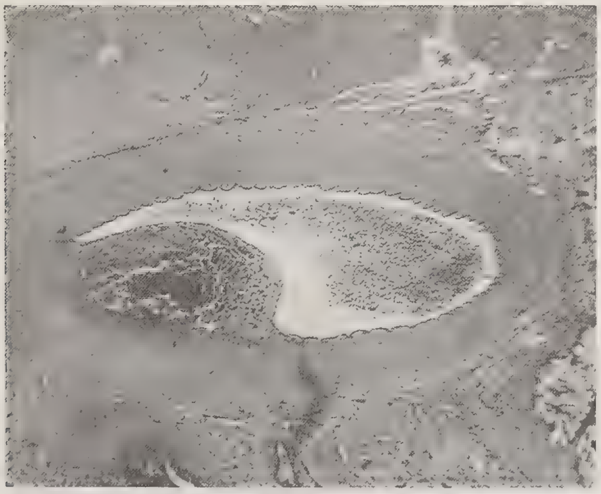

FIGURE 10. PHOTOMICROGRAPH OF IRON PRECIPITATED CORONARY THROMBOSIS WITHIN A BRANCH OF THE ANTERIOR DESCENDING ARTERY DISTAL TO THE MAGNET (35x).

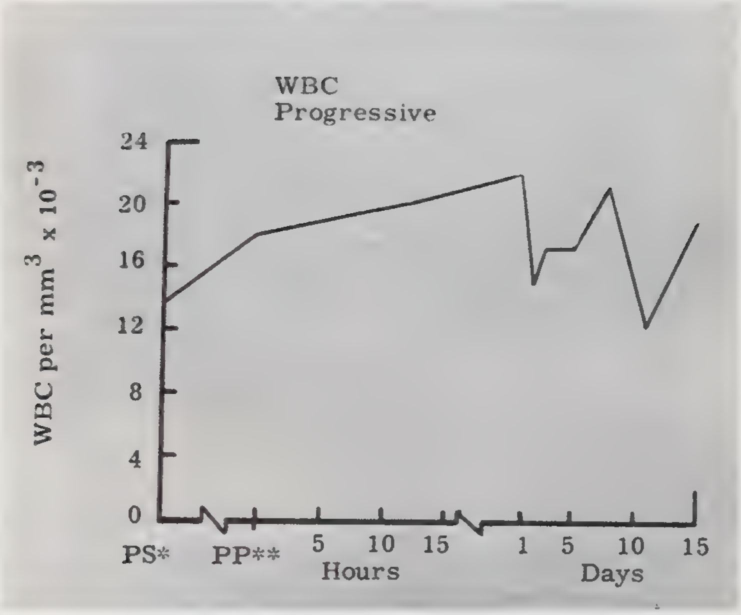

FIGURE 11. CHANGES IN WBC IN RESPONSE TO IRON INJECTIONS (NINE DOGS).

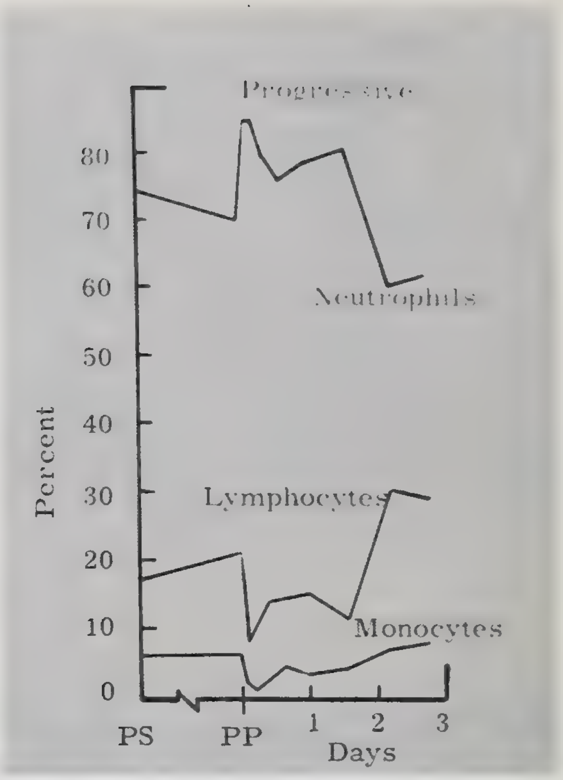

FIGURE 12. CHANGES IN NEUTROPHILS, LYMPHOCYTES, AND MONOCYTES IN RESPONSE TO IRON INJECTIONS (NINE DOGS).

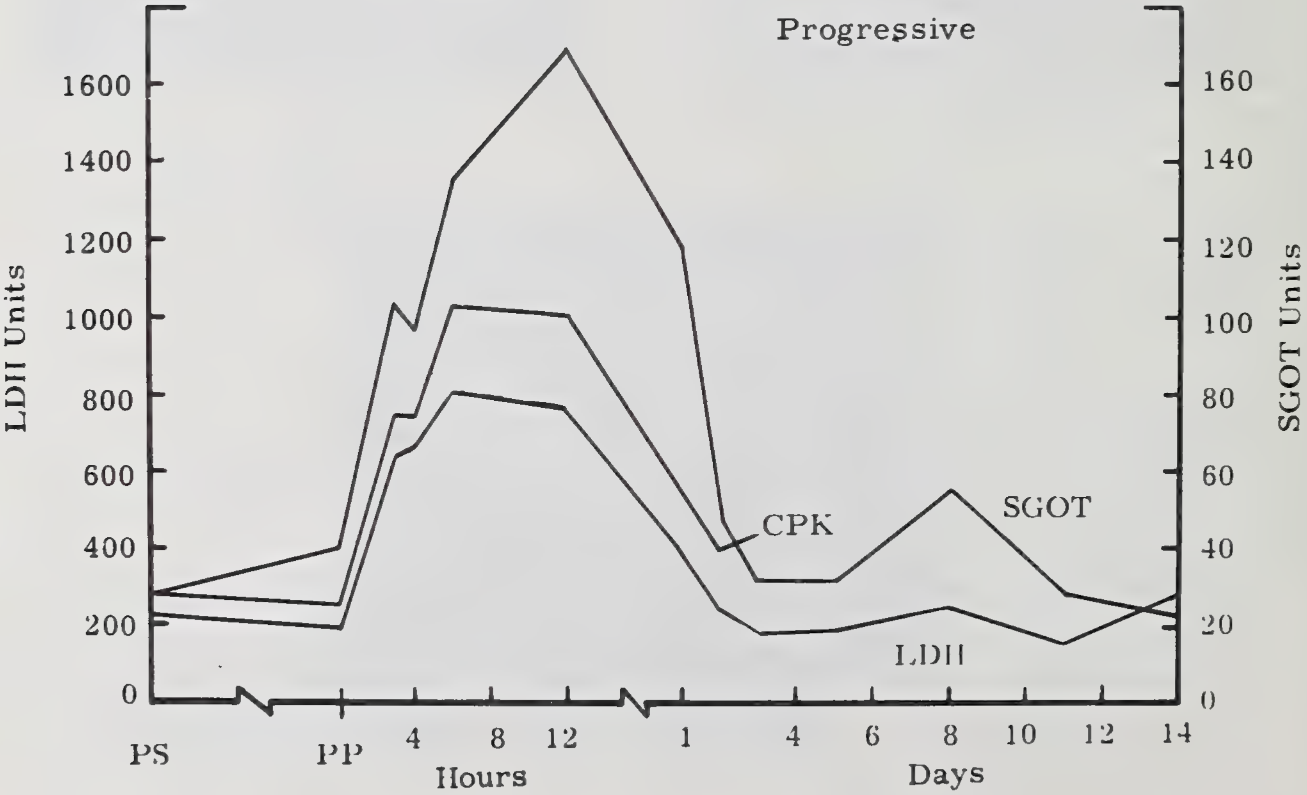

FIGURE 13. CHANGES IN LDH, SGOT, AND CPK POSTPARTICLE INJECTION (NINE DOGS).

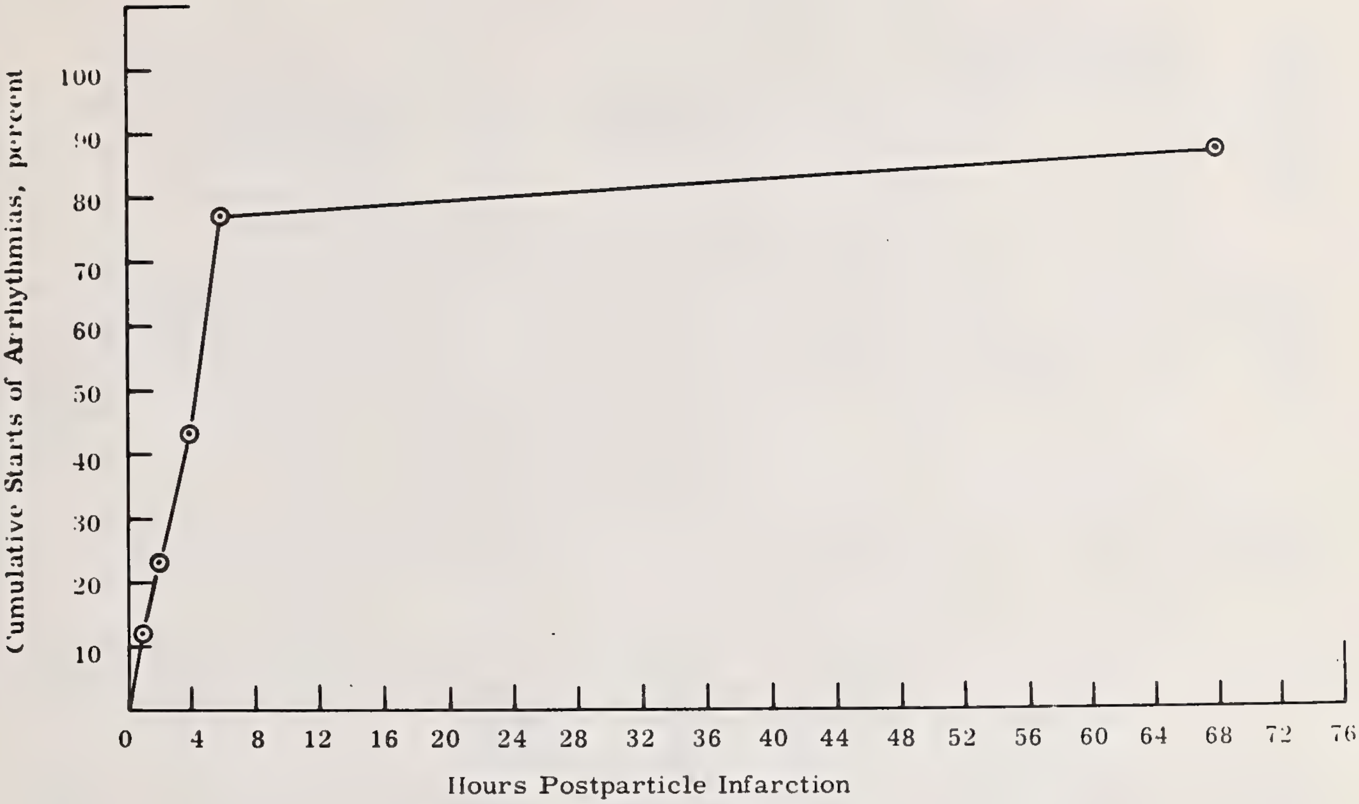

FIGURE 14. CUMULATIVE STARTS OF ARRHYTHMIAS IN NINE DOGS RECEIVING 0.2 GM/KG IRON.

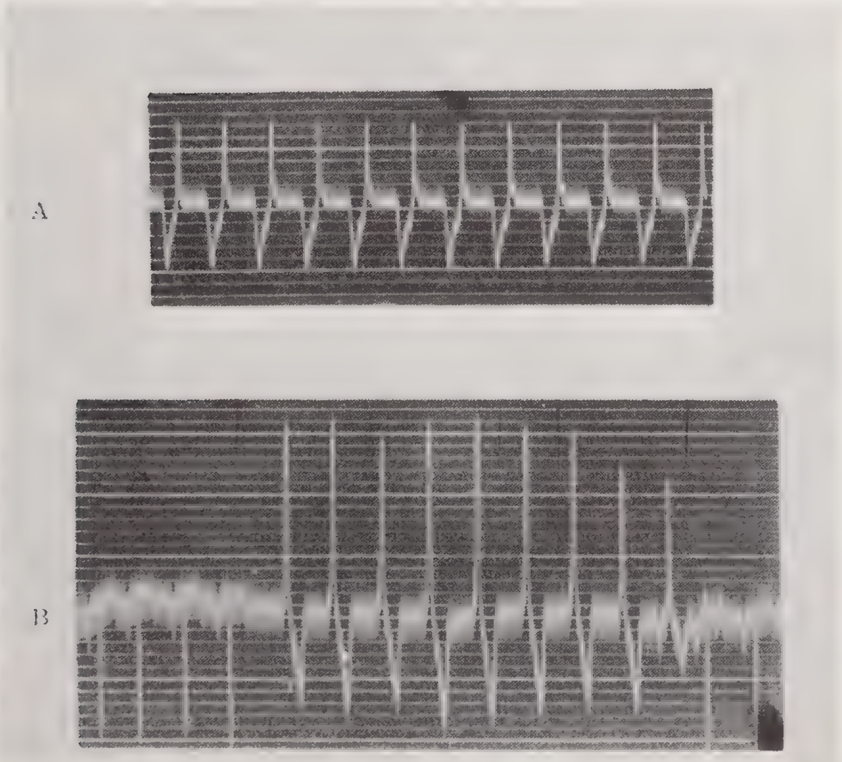

FIGURE 15. CHARACTERISTIC ARRHYTHMIAS OCCURRING SOON AFTER PARTICLE INJECTION; (A) LEAD I, BURST OF VENTRICULAR TACHYCARDIA; (B) LEAD aVI, PAROXYSMAL VENTRICULAR TACHYCARDIA AND PERIODIC INVERTED P WAVES.

TABLE 4

SUMMARY OF PROGRESSIVE INFARCTION STUDY

Dog No.	Enzyme Activity	Duration of Arrhythmias	EKG Data		Vessel Thrombosis	Heart Pathology
			Preparticle	Post Particle		
OTNIA #3 (12 hr.)	Elevated	6 hrs.	Elevated T wave; inverted T	Prominent T waves; severe arrhythmias	Fibrin; secondary; vessel normal	Necrosis around magnet only (subacute).
BJVHIA (24 hr.)	Elevated	8 hrs.	Inverted T; arrhythmias third day	Severe arrhythmias; prominent T waves	Fibrin; secondary; vessel normal	Necrosis around magnet only (subacute).
FTLIA #5 (2 day)	Elevated	2 hrs.	Elevated ST; inverted T	Gross ST elevation; severe arrhythmias	Fibrin; secondary; vessel normal	Necrosis adjacent to magnet; expired four hours PPI.
ZGNRA #3 (3 day)	Elevated	24^{+}hrs.	Elevated ST; inverted T	Gross ST elevation; inverted T wave; tachycardia; arrhythmias	Fibrin; primary 100%; secondary; vessel damaged	Necrosis adjacent to magnet; acute infarction in septum.
LAAMA #3 (3 day)	Elevated	0 hrs.	Elevated ST; inverted T	Prominent T waves	Organizing; secondary; vessel normal	Necrosis adjacent to magnet; normal.
LAUCI #3 (8 day)	Elevated	71 hrs.	Elevated ST; inverted T	Prominent T waves; pronounced ST elevation; severe arrhythmias	Organizing; primary 50%; secondary; vessel damaged	Necrosis adjacent to magnet; massive, transmural, and subacute from magnet to apex.
KHNIA #4 (11 day)	Elevated	18 hrs.	Elevated ST; elevated T	Ventricular tachycardia; severe arrhythmias	Organizing; primary 67%; secondary; vessel normal	Necrosis adjacent to magnet; moderate subacute apex; multiple focal acute from magnet to apex.
LAAMA #2	Elevated	68 hrs.	Inverted T	Elevated ST; tachycardia; severe arrhythmias	Organizing; primary 33%; secondary; vessel normal	Necrosis adjacent to magnet; several focal subacute left ventricular wall.
LAUCI #1	Elevated	42 hrs.	Elevated T waves; inverted T waves	Grossly elevated ST segments; severe arrhythmias	Organizing; primary 60%; secondary; vessel damaged	Subacute, massive, transmural from magnet to apex.

the arrhythmias lasted for a considerable duration after particle injection (in one case for 71 hours). In most cases, the arrhythmia was ventricular in origin, ventricular tachycardia being present in most dogs. In one dog, however, sinus tachycardia was evident. Inverted P waves were periodically observed in some of the tracings demonstrating that atrial depolarization was from the atrioventricular node to the sinoatrial node. A sample ECG tracing is shown in Figure 15.

At the request of the Artificial Heart Program Office, we are extending the application of this technique to other animal species. We are currently testing procedures for inducing myocardial infarction complicated with congestive haart failure in the Holstein calf. The procedure is to first induce a generalized infarction in the heart by using very small plastic microspheres. Several days after this, an additional infarction is caused by the iron and magnet technique. It is our hope that, depending upon the amount of iron injected, various levels of congestive failure can be accomplished.

DISCUSSION

DR. KRALIOS: I would like to congratulate you for your original work and would like to ask you two questions: What do you think are the advantages of your method as opposed to the accepted methods of coronary ligation? You have to open the chest and, as opposed to the injection of microspheres through a transarterial coronary catheter, you have uncontrolled secondary distal thrombosis. The second question: Do you think that the increase of the white blood cells usually resulted from the infarction itself or was it a general reaction of the reticuloendothelial system to the injection of the iron particles?

DR. ELZINGA: To answer the first question, as you know, it would require too much time. However, as you notice, the mortality of this particular technique was very low when compared to the direct ligation technique. I think that the model that best mimics human coronary occlusion and myocardial infarction is probably a better model. In regard to the next question, the white blood cells do rise during myocardial infarction; however, in the sham operated animals, which were iron particle injected (venipuncture), the white blood cells did rise and there was no evidence of myocardial infarction.

DR. FEOLA: Two questions: 1. What was the incidence of ventricular fibrillation immediately upon infarction; and 2. Do you have hemodynamic measurements to relate the extent of the infarcted area to the severity of failure? Are the particular changes definitive or transient?

DR. ELZINGA: This was only an initial feasibility study. We did not measure hemodynamic parameters. We are presently doing this in the calf.

DR. HARRIS: This is a very elegant way of producing myocardial infarction in the dog, but I would like to question whether or not it does have any advantages over thoracotomy and ligation? There, for sure, you know exactly where you are placing your obstruction and as for losing animals in ventricular fibrillation, if you will follow the two stage method that is in the literature and has been there for almost 20 years, you can avoid most of the ventricular fibrillations that come early. Also, your own evidence seems to indicate that you are not getting a particularly gradual occlusion since you have your arrhythmias developing within six hours. Now, in the two stage ligation technique, there is no arrhythmia of any consequence for four to seven hours, when they begin to develop, reaching maximal frequency at 10 to 15 hours. So, the time of onset would suggest that you are occluding fairly quickly with the magnet and that you are going to extra trouble to do the same thing, not quite as precisely as you would do it with ligatures.

DR. ELZINGA: This may be true. We believe that over a period of time you can slowly inject iron into the animal and slowly increase the coronary thrombosis and eventually occlude the vessel. As for the occurrence of the early arrhythmias, we believe that during the formation of the primary thrombosis, emboli are being formed which in turn occlude secondary vessels.

DR. NORMANN: Maybe I missed this, but did you examine the interaction between your iron particles and components of blood, and related to that, have you found signs of emboli in brain, kidney and so forth?

DR. ELZINGA: Of course, it is very difficult to determine whether or not emboli were present in organs other than the heart, but to the best of our knowledge, from extensive pathological examination of all the organs listed, we did not see vessel occlusion in other organs than the lungs.

DR. RICE: How strong was your magnetic field?

DR. ELZINGA: I am not prepared to answer that question right now. This, of course, depends upon the size of the magnet. In these particular studies, the magnetic field was the same for each magnet.

CHAPTER 57

A STUDY OF THE OVINE THORAX AND ASSOCIATED STRUCTURES

W. D. Anderson

University of Minnesota
Minneapolis, Minnesota

The objective of this study has been to describe and illustrate the gross morphology of the thoracic wall and intrathoracic anatomy of sheep and relate these findings to comparable structures in man. The thorax of adult mature sheep of mixed breeds was illustrated while directly viewing the dissected cadavers. Plastic cast preparations were made of the arterial and venous systems using Tensol cement (manufactured by the Imperial Chemical Industries, Ltd., Great Britain). When directional terminology for the quadruped differed from that of man, the human term has been included in parenthesis. The shape of the ovine bony thorax and the character of the endothoracic fascia differed from that of man while the pleural cavities were similar. The ventral (anterior) mediastinum and _in situ_ position of the lungs, pericardial sac, its attachments and pericardial sinuses resembled that in man. The surfaces of the ovine heart were similar to the human; however, the distribution of the coronary arteries corresponds to one of the common variations seen in man. Pulmonary, aortic and atrioventricular valves of sheep and man were similar morphologically in number and position of valvules and cusps. In 50 ovine aortic arches studied, the aorta was characterized as giving origin to a single branch, the brachiocephalic trunk. The bronchoesophageal artery arose from the aorta at the level of the hilus of each lung and coursed to the esophagus and lung. The terminations of vegal and sympathetic fibers have been traced and photographed with the use of the Zeiss operating microscope. The azygos venous system in sheep was found to be poorly developed while the hemiazygos vein on the left was the predominant venous drainage of the thoracic wall.

REVIEW OF LITERATURE

Strangeways (1904), Chauveau (1910), Ellenberger and Baum (1891 and 1943), Sisson and Grossman (1954), Seiferle (1956), Habel (1964 and May (1964) have contributed most to the scant anatomical knowledge available today concerning the gross and subgross anatomy of the ovine thorax. On the other hand, the exhaustive anatomic descriptions of the human thorax by Grant (1958 and 1962), Gardner, Gray and O'Rahilly (1960), Anson (1963), Pernkopf (1963) and Hollinshead (1967), have contributed to the thorough knowledge of this region of the body in man.

Dimensions of the ovine bony thorax, heart and great vessels appear unavailable in the literature. Likewise, data concerning plastic cast preparations of the arterial system do not seem abundant. The Latin nomenclature for the pectoral musculature as adopted by the World Association of Veterinary Anatomists (1963) and used by Habel (1964) is the most current nomenclature for muscles forming the thoracic wall of the sheep. In this study an attempt has been made to use current nomenclature for all structures of the thorax; however, for easier interpretation by those unaccustomed to Latin terminology, the anglicized form of the most current nomenclature will often be used.

MATERIALS AND METHODS

Fifteen adult, cull sheep of mixed breeds, principally of female sex and weighing between 124-206 lbs. were used in this study. For that portion of the study dealing with the bony thorax, the thoracic skeleton was prepared by immersion in hot running water for five hours. At the end of this period the skeleton was cleaned and dried in preparation for study and illustration. Gross and subgross dissection were carried out in other cadavers after formalin-fixation and latex injection of the arterial system. Plastic cast preparations were made of the arterial and venous systems using Tensol cement* (Figure 1). After hardening, all tissues were digested using concentrated hydrochloric acid. This leaves an accurate representation of the macro- and microcirculation.

RESULTS AND DISCUSSION

Bony Thorax.

In all ovine specimens 13 pairs of ribs were present. There were eight sternal or true ribs and five asternal or false ribs. The sternum of the sheep was composed of six fused sternebrae and divided into _manubrium sterni_, _body_ and _xiphoid process_ (Figure 2). Ribs one through eight articulated with the fovea of the sternum and ribs nine through thirteen articulated by costal cartilages with the preceding cartilage.

---

* Tensol cement, manufactured by Imperial Chemical Industries, Ltd., Great Britain.

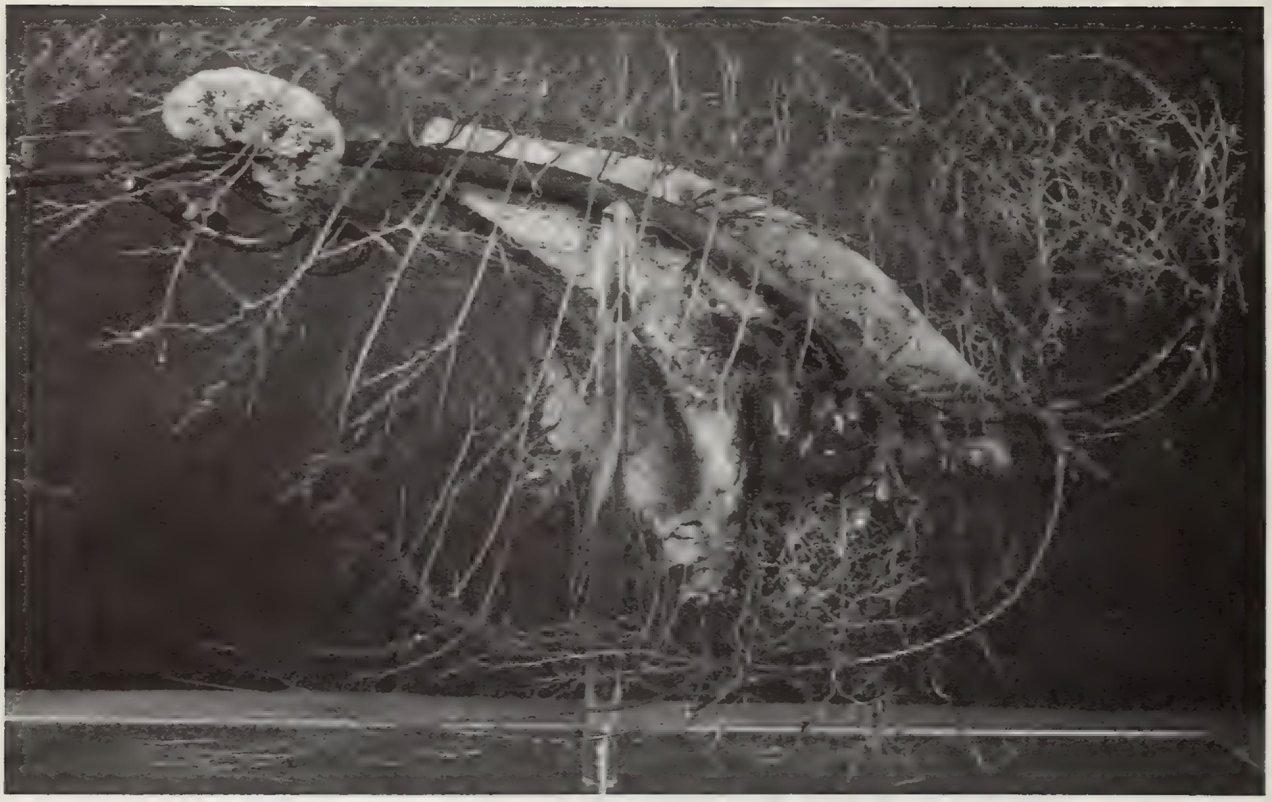

FIGURE 1. PLASTIC CAST PREPARATION.

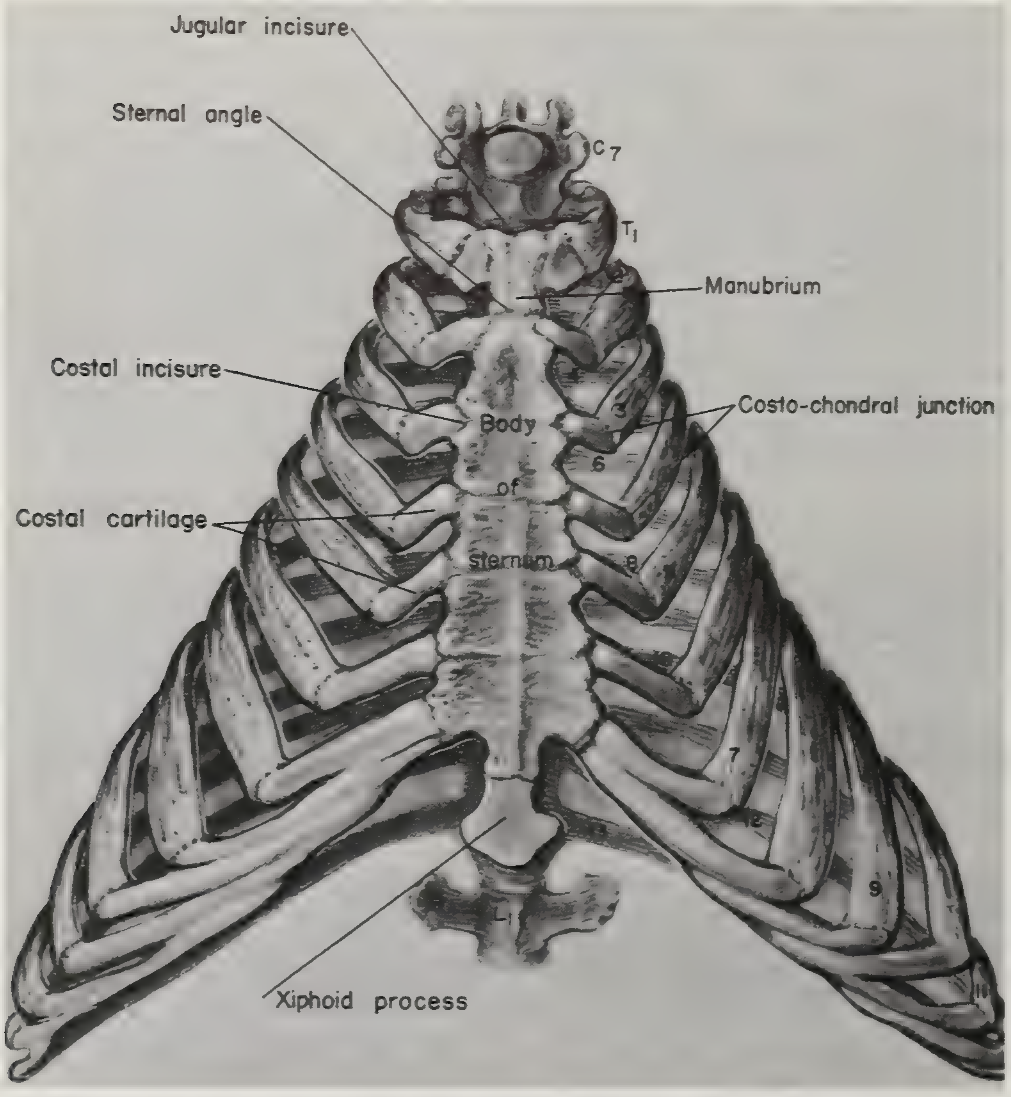

FIGURE 2. VENTRAL (ANTERIOR) VIEW OF SKELETON OF OVINE THORAX.

The ovine thoracic cage was laterally compressed and formed a truncated cone (Figure 2). The body of the sternum was a flattened structure extending approximately 16 cm. from manubrium to xiphoid process. At its cranial end the body was deviated upward at approximately a 10 - 14^0 angle and the manubrium (which is 5.0 cm. long) continued the upward deflection an additional few degrees toward the seventh cervical vertebra. The ventrodorsal (anteroposterior) diameter of the cranial thoracic aperature was thus further reduced by the upward curvature of the manubrium so that the mean diameter of the thoracic inlet was 5.0 cm.

Bony Thorax. Comparable features, sheep and man.

Differences in bony thorax noted were: (a) shape in general, (b) dimension of the cranial (superior) thoracic aperature, (c) number of ribs present and ribs articulating with the sternocostal and costovertebral joints.

The cranial thoracic aperature, or thoracic inlet as it is commonly called, of sheep differed from that in man. The greatest diameter of the thoracic inlet in man is the transverse one (Figure 3); while in sheep it was the ventrodorsal (anteroposterior) diameter. The boundaries of the thoracic inlet are similar in both: namely the first thoracic vertebra dorsally (posteriorly), the first pair of ribs laterally and the manubrium sterni ventrally (anteriorly).

The ribs which form the lateral walls of the thorax follow an obliquely downward angle of approximately 20^0 in man. In the sheep, ribs one through six were directed cranially; while ribs six, seven and eight were nearly vertically oriented and the remaining five ribs were directed caudally (Figures 4, 5).

The Ventral and Lateral Walls of the Ovine Thorax.

Both Latin and English nomenclature appear in the literature to describe the pectoral muscles in the sheep. Although both will be used in this text, in accordance with the custom in this country today, the Anglicized term will be used wherever possible.

Pectoral muscles.

For purposes of simplification the sheep had two pectoral muscles like man; however each was divided into two heads. Thus there was a superficial pectoral muscle of sheep homologous to the pectoralis major of man and a deep pectoral homologous to the pectoralis minor (Figure 6). The thoracic musculature in the sheep as in man was covered by skin, superficial fascia and structures contained within the fascia. When the skin over the thorax, axilla and brachium was reflected, the cephalic vein was seen to course upward from the medial surface of the carpus to the cranial surface of the elbow joint. The vein then crossed the distal portion of the brachiocephalicus muscle, ran parallel to the descending pectoral and dipped medial to the sternocephalicus muscle to join the external jugular vein near the thoracic inlet.

Deep pectoral muscles.

The ascending pectoral was a thick, deep lying muscle which originated from the caudal (inferior) 12 cm. of the sternum and from the deep fascia lateral to the xiphoid process. Its muscle fibers passed upward and forward to insert on the medial surface of the proximal brachium (Figure 7). The cleidoscapular head of the deep pectoral was either absent or minimally developed in all specimens studied.

Deeper muscles and associated structures of thorax.

After reflection of the ovine pectoral muscles the serratus ventralis m. (serratus anterior m. in man) was seen to attach at the costochondral junctions of ribs two through six, and dorsally on ribs seven and eight (Figure 7). The fibers coursed upward and forward to insert on the medial surface of the scapula. The long thoracic nerve coursed caudally across the surface of the serratus ventralis approximately 12 cm. dorsal to the costochondral junctions of ribs two through six. The lateral cutaneous branches of intercostal nerves could be seen to emerge dorsal to the ventral edge of the serratus ventralis.

The external and internal intercostal muscles, relatively thick in the sheep, bridged the gap between ribs. (Figure 8).

The Ventral (Anterior) Mediastinum and In Situ Position of the Thoracic Viscera.

The ovine heart within its pericardial sac extended from the second intercostal space to the level of the sixth rib (Figure 9). Its apex was directed slightly to the right of the median plane and the pericardial sac was anchored to the sternum by poorly developed fibrous bands, the sternopericardial ligament. The sternocostal surface of the heart was partially covered by the right and left apical lobes and right middle lobe of the lung. In the young it was also partially covered by the thoracic portion of the thymus. The fibrous pericardium was coated by a layer of pleura and was crossed near the base of the heart by the right and left phrenic nerves. Cranial (superior) to the heart the mediastinum enclosed considerable amounts of adipose tissue as well as the thoracic portion of the thymus which will vary in size according to age.

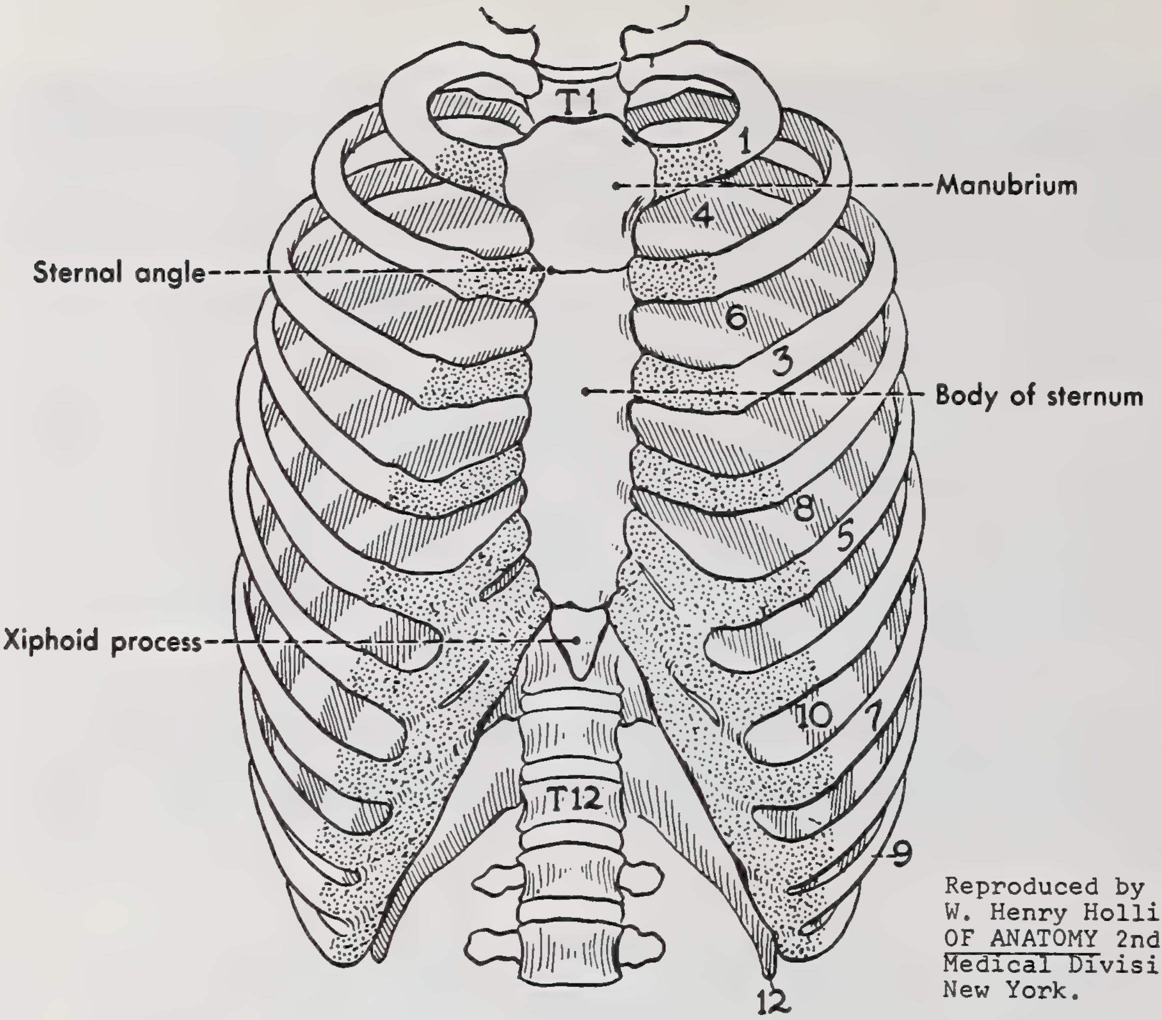

Reproduced by permission from:
W. Henry Hollinshead, A TEXTBOOK OF ANATOMY 2nd ed., 1967. Hoeber Medical Division, Harper and Row, New York.

FIGURE 3. ANTERIOR VIEW OF THE SKELETON OF THE THORAX.

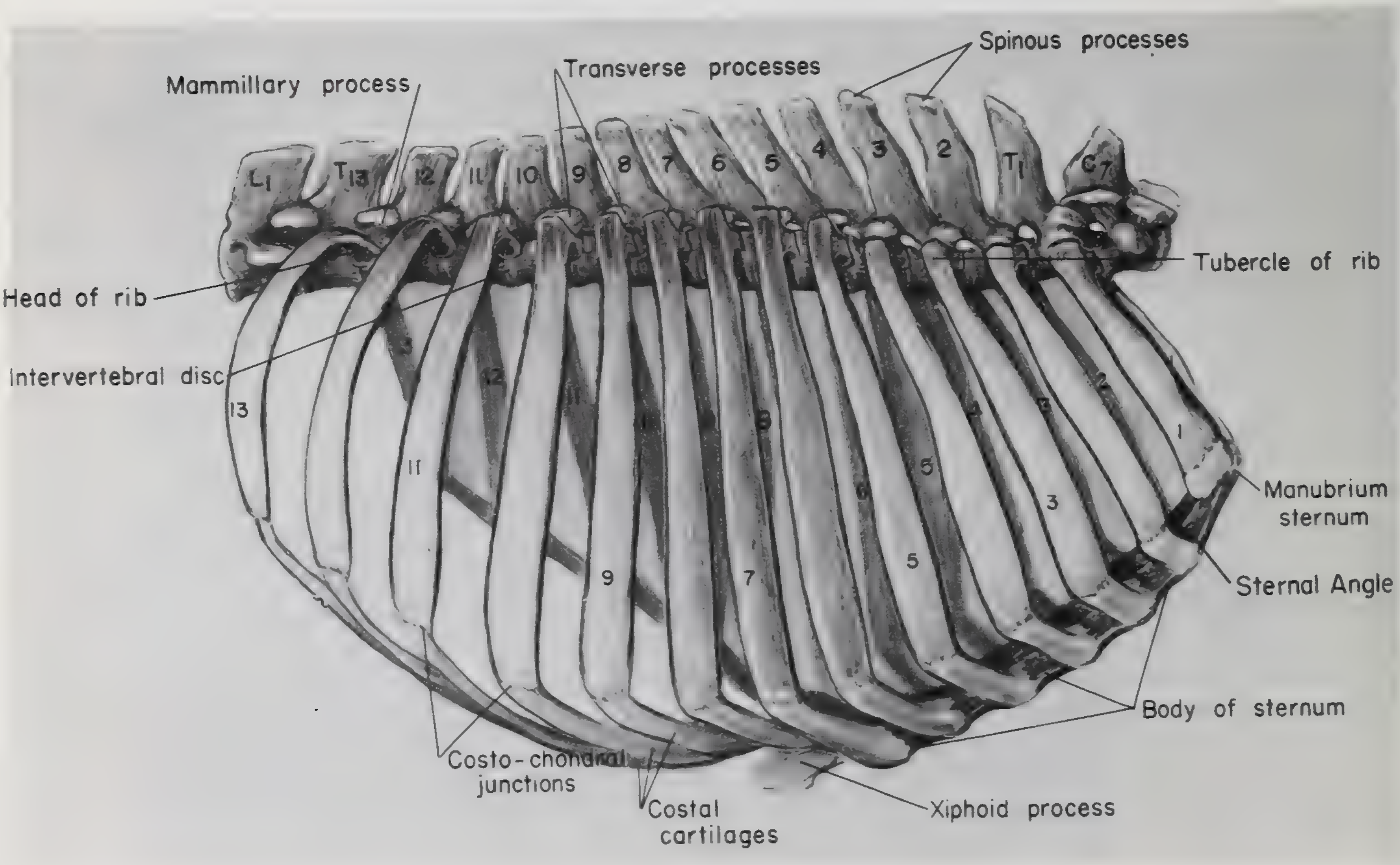

FIGURE 4. RIGHT LATERAL VIEW OF OVINE BONY THORAX.

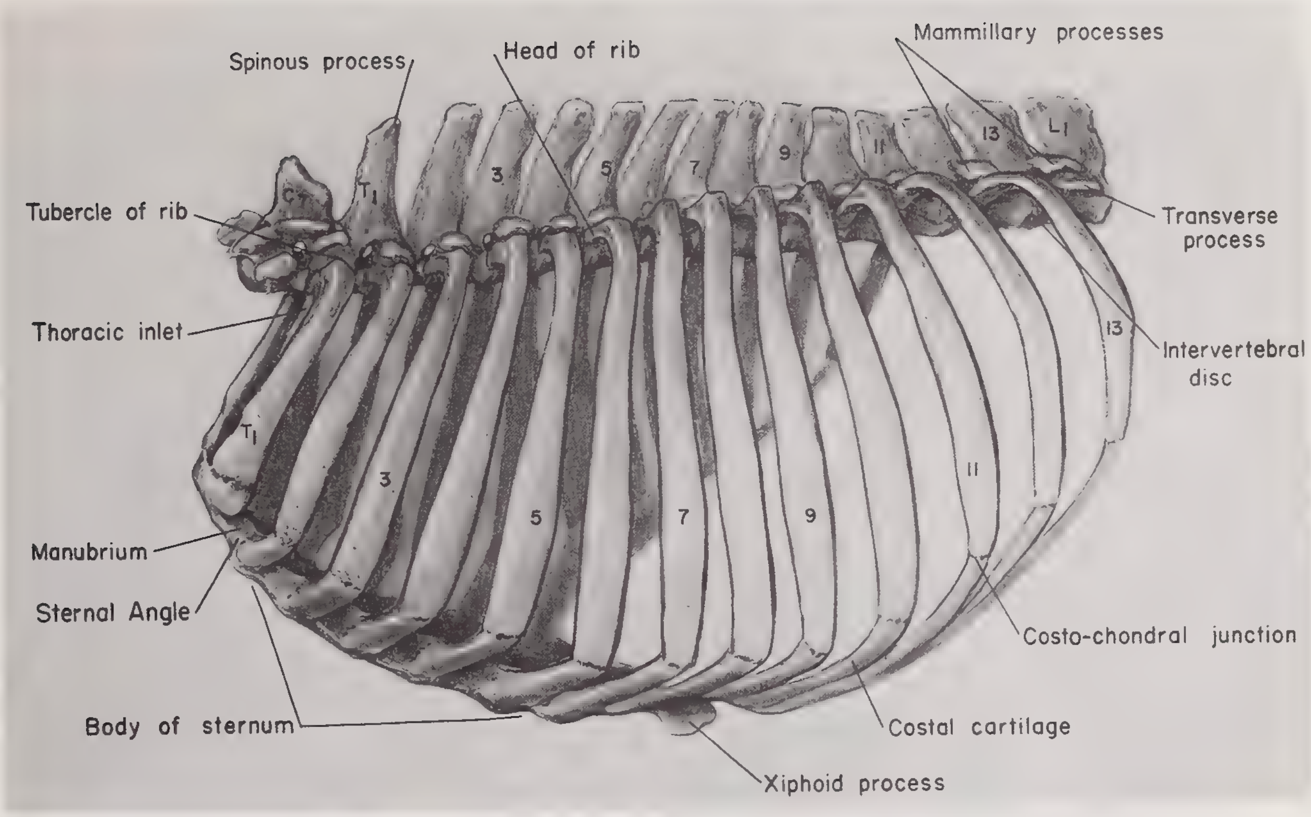

FIGURE 5. LEFT LATERAL VIEW OF OVINE BONY THORAX.

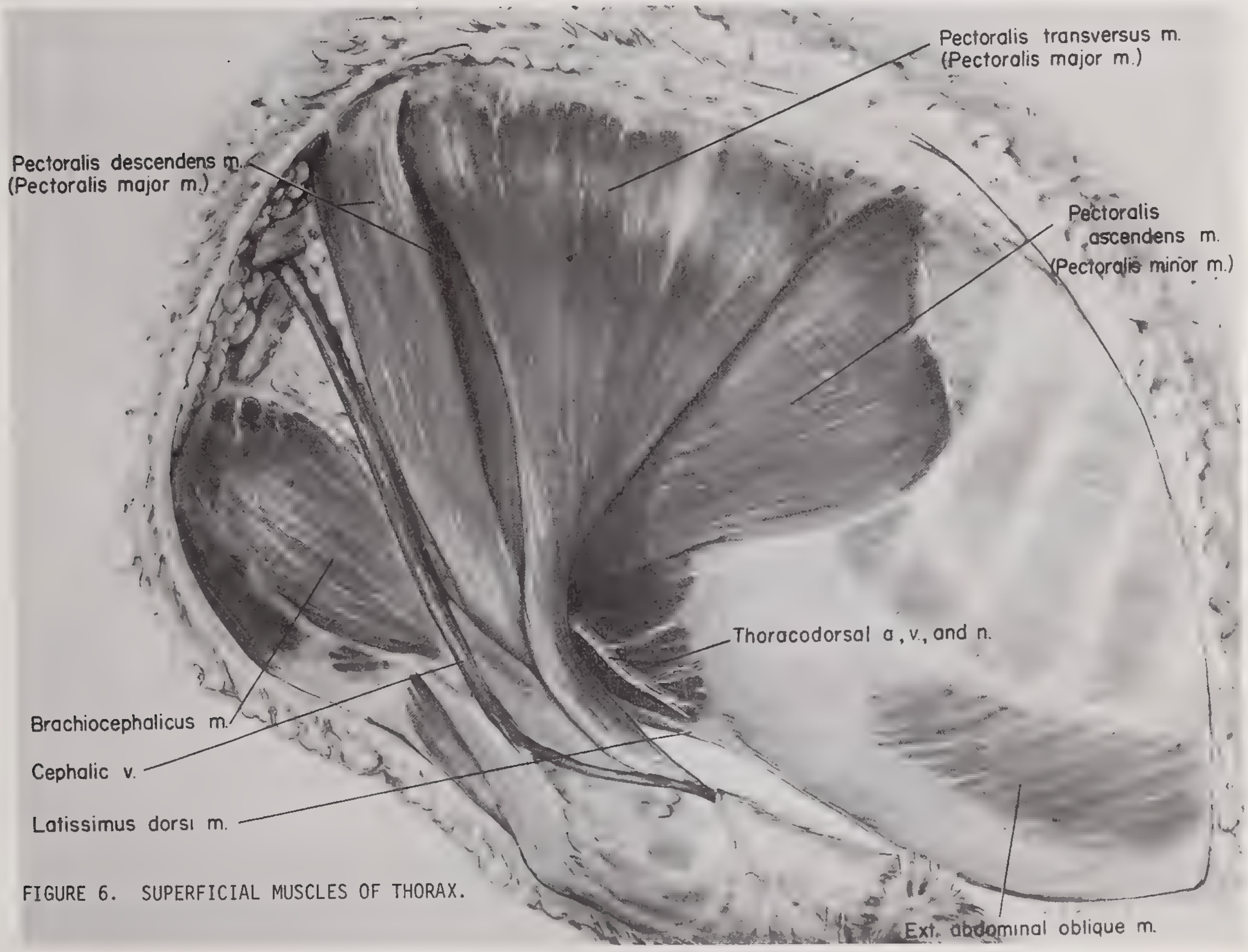

FIGURE 6. SUPERFICIAL MUSCLES OF THORAX.

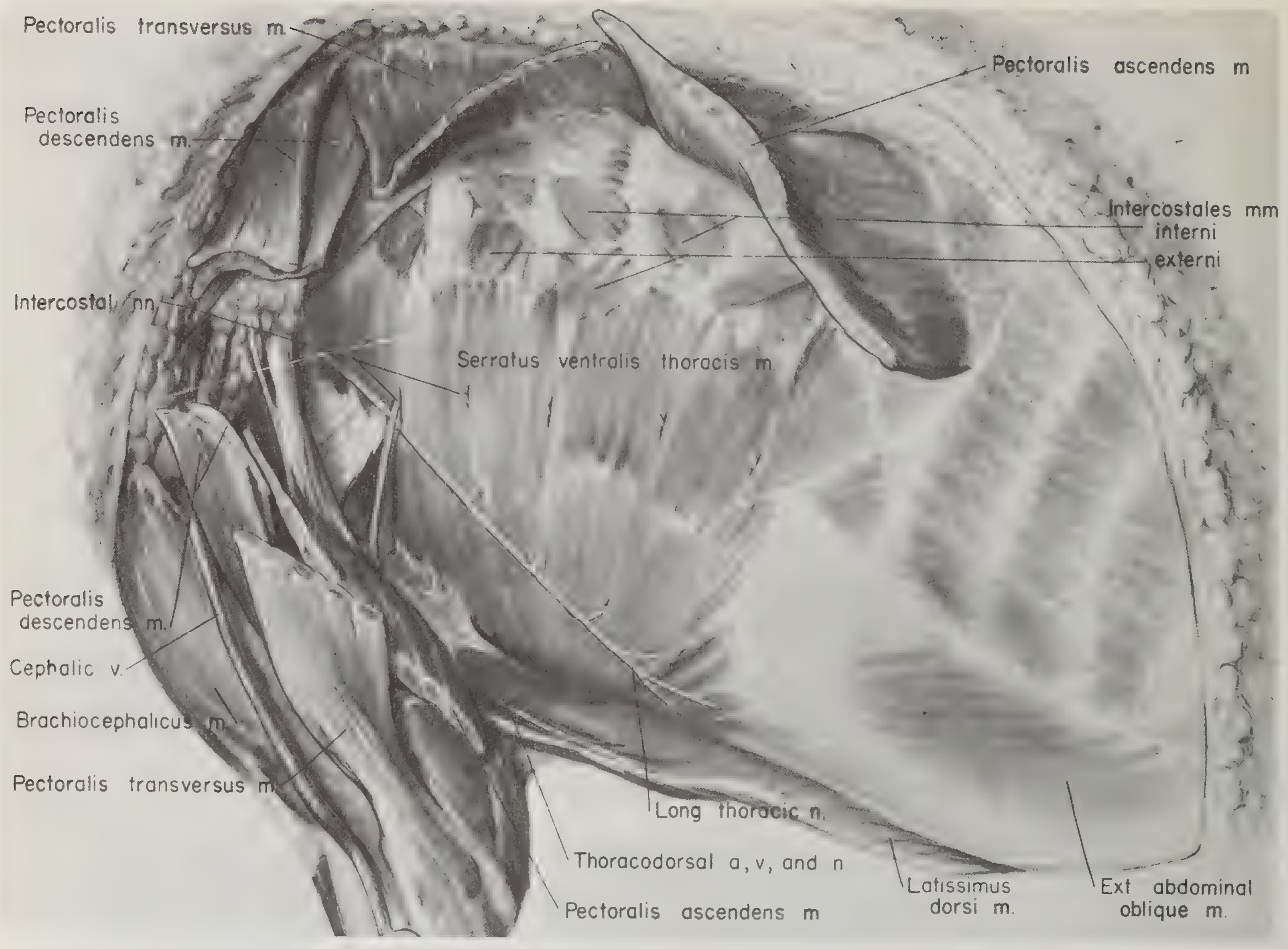

FIGURE 7. RIGHT LATERAL WALL OF OVINE THORAX.

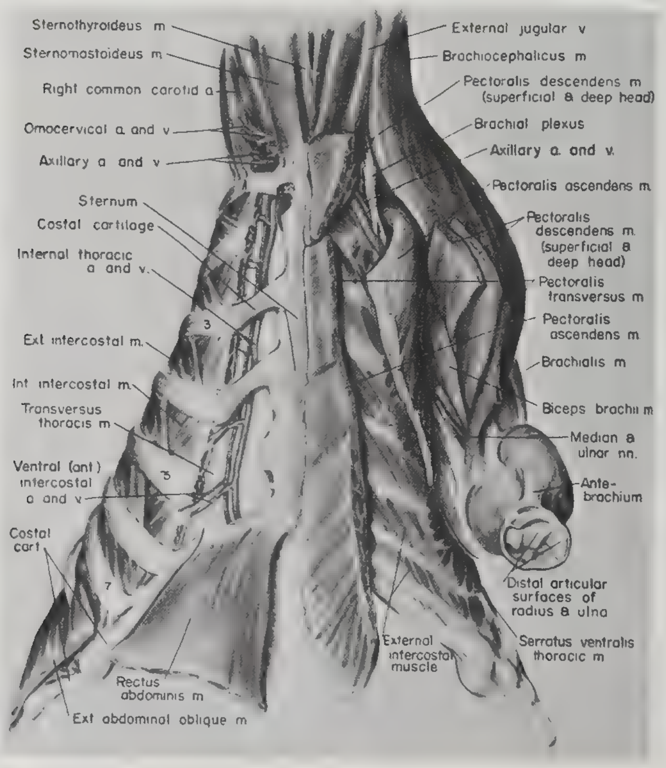

FIGURE 8. VENTRAL (ANTERIOR) WALL OF THE OVINE THORAX.

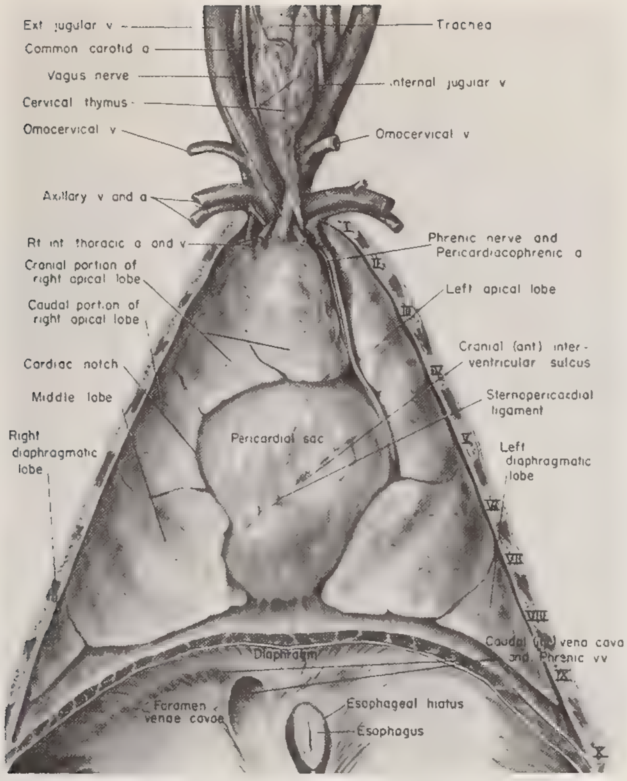

FIGURE 9. VENTRAL (ANTERIOR) MEDIASTINUM & IN SITU THORACIC VISCERA.

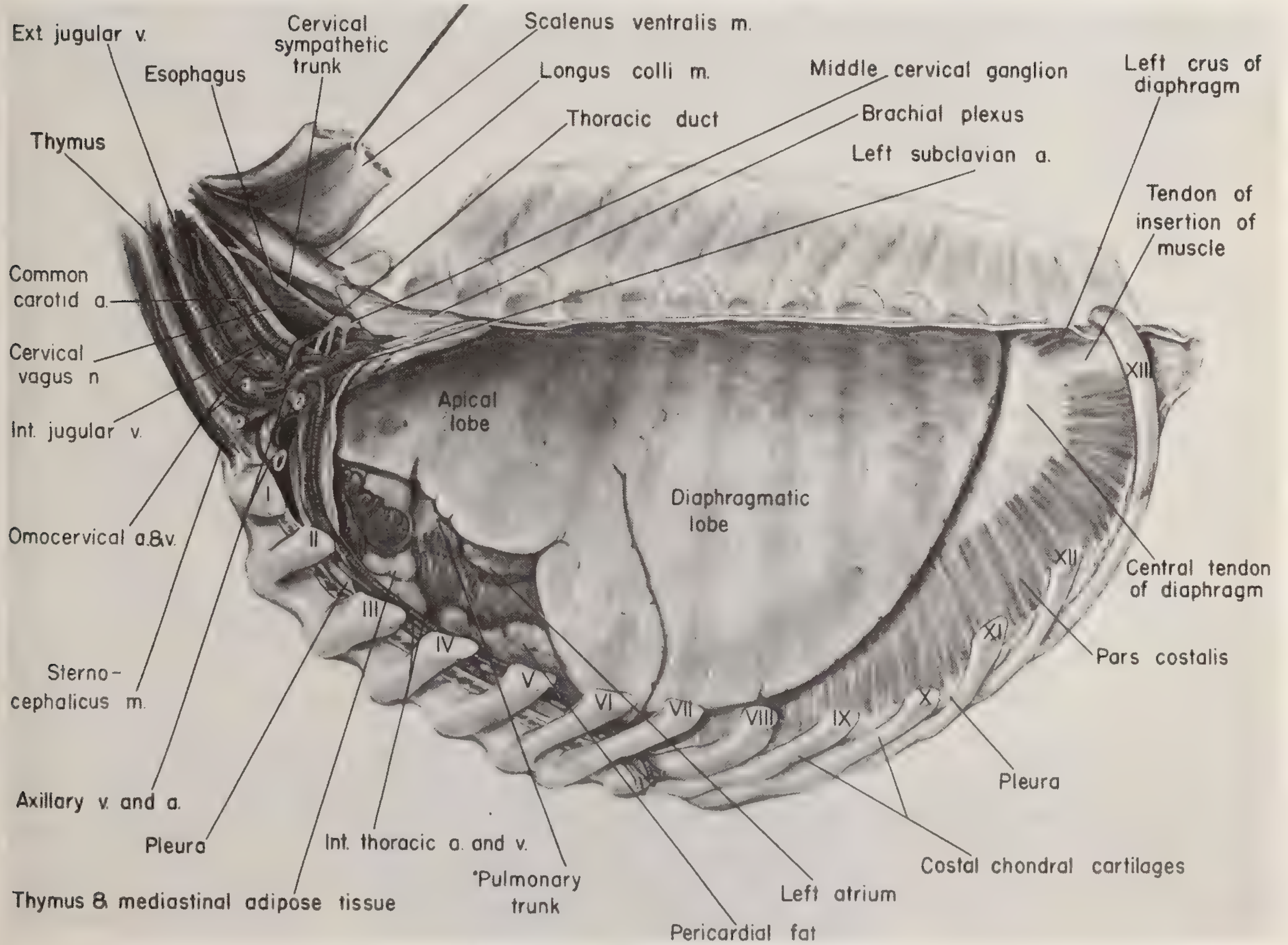

FIGURE 10. THORACIC VISCERA IN SITU.

The heart was positioned slightly obliquely in the thorax with its base dorsal (posterior) and its apex just above the sternum at the level of the sixth costal cartilages. The mean distance from the base to apex in five hearts was 12.9 cm.; while the circumference taken at the coronary groove was 29 cm. The mean weight of 54 ovine hearts was 222.9 gms.

Lungs.

When the two pleural cavities were opened, the lungs and pleural sacs overlapped all but a central triangular portion of the pericardial sac. The right lung, larger than the left, had apical, middle (formerly cardiac lobe) diaphragmatic and accessory or intermediate lobes. The apical lobe, well developed on the right, had a deep fissure which separated it into cranial and caudal portions. The mediastinal surface of the caudal portion of the right apical lobe and the right middle lobe formed a cardiac impression as well as an impression for the cranial vena cava. The cardiac notch, formed principally by the apical lobe but to some extent by the middle lobe, on the right, and by the cranial and caudal portions of the left apical lobe, left exposed the the sternocostal surface of the heart. (Figures 10, 11).

The left lung, unlike the right, had only two lobes, namely apical and diaphragmatic. The left apical lobe, smaller than the right, had cranial and caudal portions and was separated from the diaphragmatic lobe by a deep fissure lined with pulmonary pleura. There was a remarkable similarity in the sternocostal surfaces of man and that of the sheep (Figure 12).

Heart, Great Vessels and Associated Autonomic Nerves.

Pericardium. When the pericardial cavity was opened, the visceral layer of serous pericardium was seen to be reflected around the pulmonary trunk and ascending aorta thus enclosing both vessels. This square shaped area of the pericardial cavity behind the vessels was the *transverse pericardial sinus* (Figure 13). The blind, semilunar-shaped sinus, poorly developed in the sheep, below the transverse sinus was the *oblique pericardial sinus*. The cranial boundary of the oblique sinus was formed by the caudal (inferior) vena cava on the right and the pulmonary veins on the left. The sinuses resemble those of man (Figure 14).

Heart-External anatomy. Cardiac Vessels: The two coronary arteries are named the same for quadrupeds as in man; namely, *left* and *right* coronary arteries (Figure 15). Their origins from the left and right aortic sinuses within the ascending aorta are likewise homologous to primates. The *left coronary artery* which supplied most of the sheep heart emerges from behind the left side of the pulmonary trunk and bifurcated into a descending branch, the *cranial (anterior) interventricular artery* and a *circumflex* branch. The cranial interventricular artery descended in its sulcus with the great cardiac vein to the apex of the heart where it entered into a weak anastomosis with the *dorsal (posterior) interventricular artery*. The circumflex branch coursed to the left around the heart below the great cardiac vein and gave origin to the left marginal and caudal (posterior) ventricular arteries and terminated on the caudal surface of the heart as the caudal (posterior) interventricular artery (Figure 15). This termination of the left coronary artery corresponded to an uncommon pattern in man. The most common pattern in man is for the right coronary to supply the majority of the posterior surface of the heart rather than the left as is the case in the sheep (Figure 16).

The *right coronary artery*, smaller than the left, arose from the ascending aorta within the right aortic sinus and emerged from deep to the pulmonary trunk to course to the right in the coronary sulcus at the base of the right ventricle. It gave origin to tiny descending myocardial branches, a larger *right margin artery* on the acute surface of the heart and terminated on the caudal (posterior) surface as tiny twigs which descend toward the apex.

The majority of the cardiac veins paralleled the coronary arteries. The largest was the great cardiac vein which ascended in the cranial (anterior) interventricular sulcus on the right side of the cranial interventricular artery (Figure 15). Near the origin of the circumflex branch of the left coronary artery, the great cardiac vein turned sharply to the left and passed around the heart in the coronary sulcus. As is the case in man, the tiny oblique vein of the left atrium marked the change in name from great cardiac vein to *coronary sinus*. The coronary sinus in the sheep received the relatively large left azygos (hemiazygos) vein before emptying into the right atrium.

Heart-Internal anatomy. The internal anatomy of the ovine heart was similar to the well understood internal structure of the human heart. All normally present ostia found in the heart of man may be found in the ovine heart. The internal architecture of the atria and ventricles appeared quite similar to that of man and the similarity in the right and left antrioventricular valves and two semilunar valves is worthy of mention (Figures 17, 18).

Innervation. Two sets of nerves reach the ovine heart, one from the sympathetic trunk and one from the vagi.

Vagus nerves: The vagus nerve entered the thorax on the lateral surface of the esophagus, crossed beneath the subclavian artery and continued caudally parallel to the brachiocephalic trunk where it gave off a cradiac branch (Figures 19, 20). As the cardiac branch entered the pericardial sac, it coursed between the pulmonary and aortic trunks and at the region of the ligamentum arteriosum, sent a branch which recurred around the aortic arch and ascended on the medial surface of the

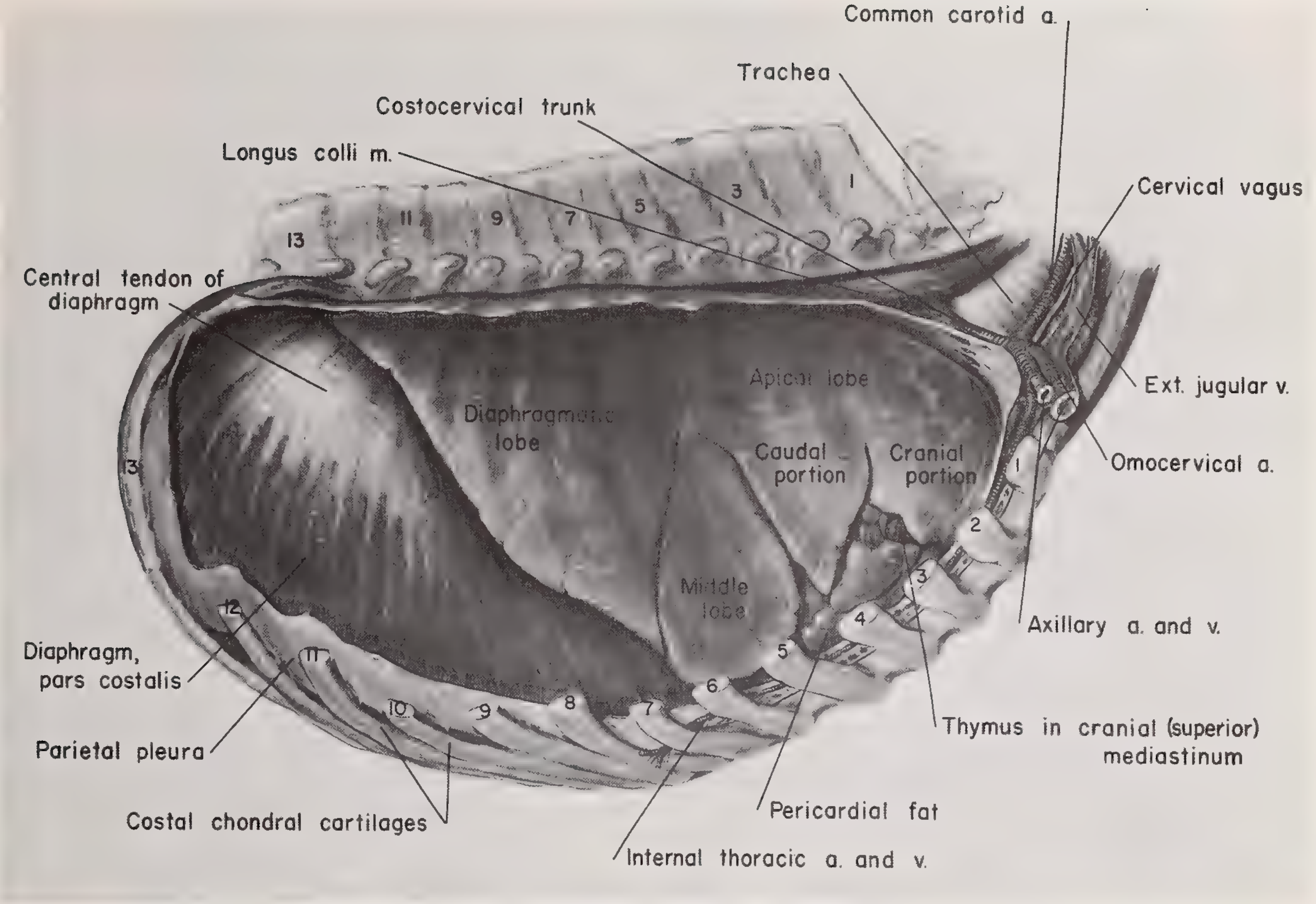

FIGURE 11. RIGHT SURFACE OF THORACIC VISCERA IN SITU.

Reproduced by permission from:
W. Henry Hollinshead, A TEXTBOOK
OF ANATOMY 2nd ed., 1967. Hoeber
Medical Division, Harper and Row,
New York.

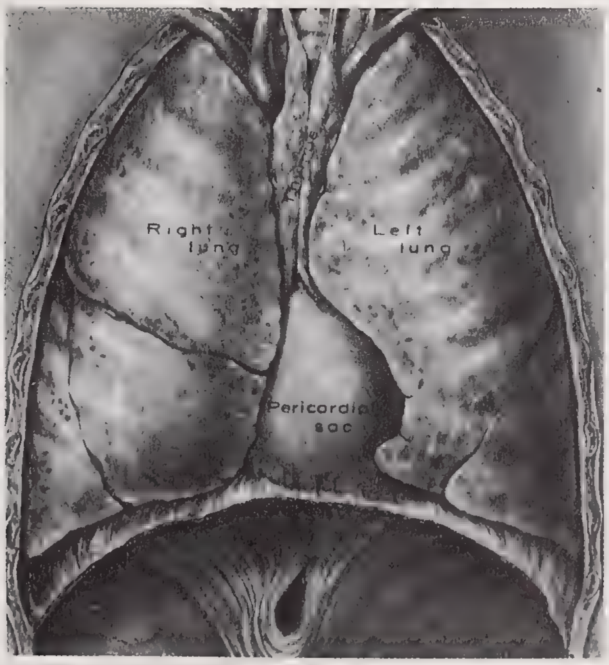

FIGURE 12. THE PERICARDIAL SAC IN SITU, OVERLAPPED BY THE LUNGS AND THE THYMUS.

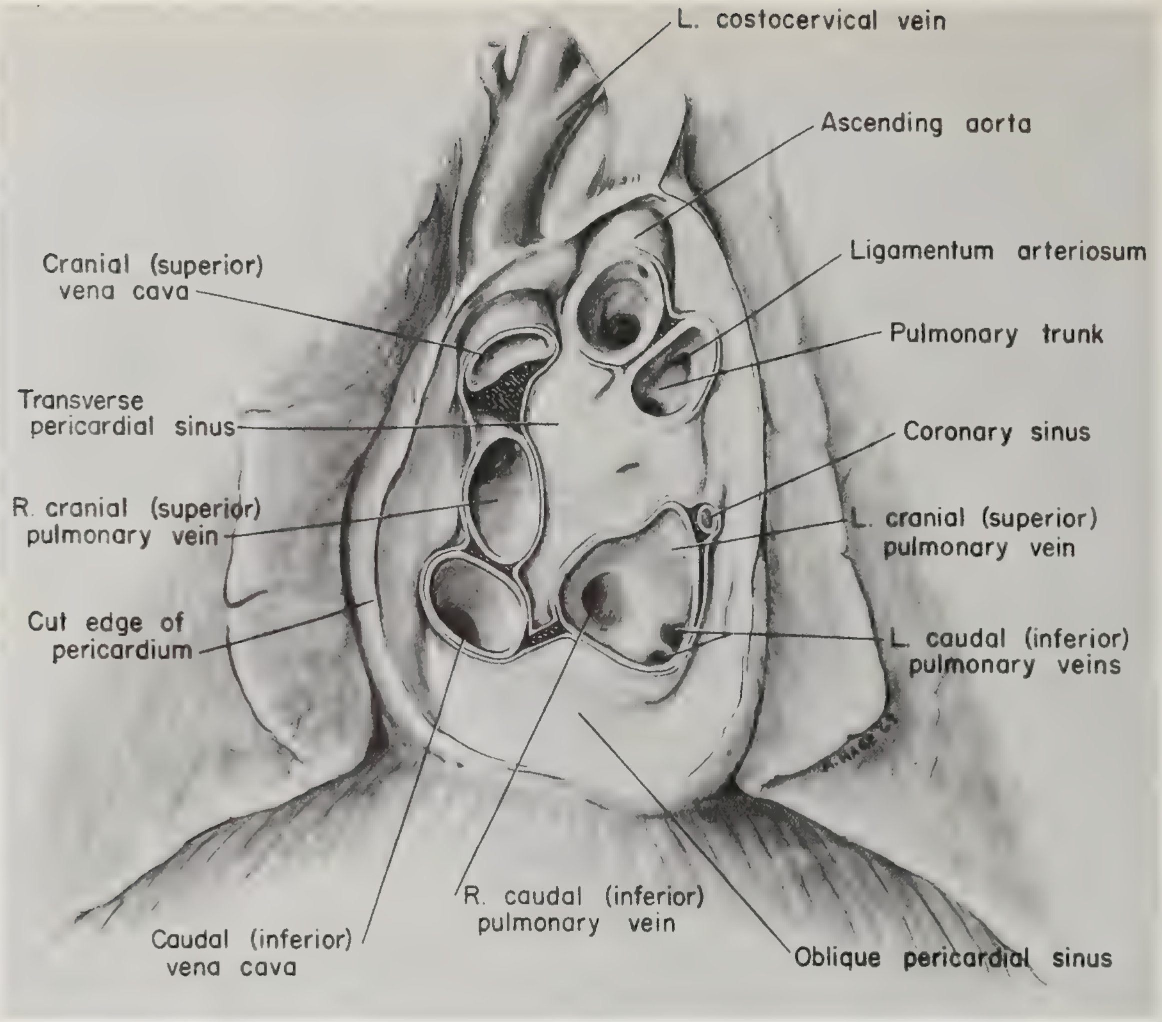
L. costocervical vein
Ascending aorta
Cranial (superior) vena cava
Ligamentum arteriosum
Pulmonary trunk
Transverse pericardial sinus
Coronary sinus
R. cranial (superior) pulmonary vein
L. cranial (superior) pulmonary vein
Cut edge of pericardium
L. caudal (inferior) pulmonary veins
R. caudal (inferior) pulmonary vein
Caudal (inferior) vena cava
Oblique pericardial sinus

FIGURE 13. ATTACHMENTS OF BASE OF HEART TO DORSAL (POSTERIOR) WALL OF PERICARDIAL SAC AND PERICARDIAL SINUSES.

Reproduced by permission from:
W. Henry Hollinshead, A TEXTBOOK OF ANATOMY 2nd ed., 1967. Hoeber Medical Division, Harper and Row, New York.

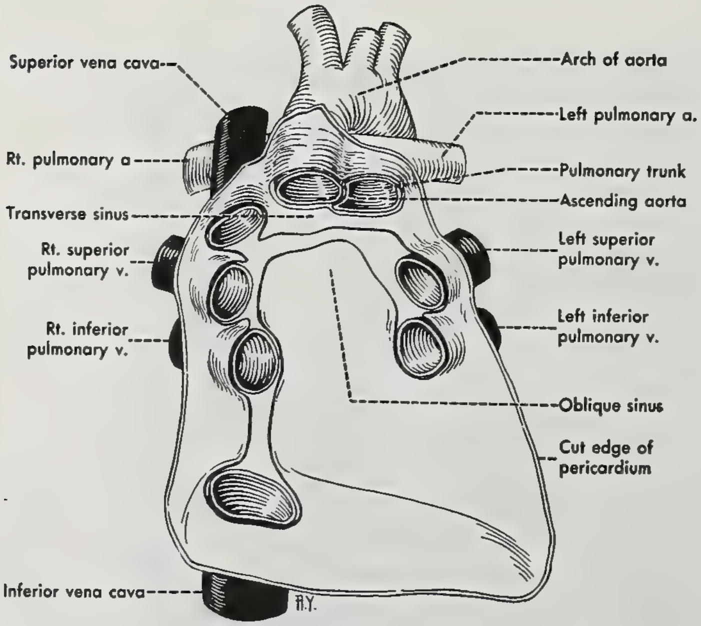

FIGURE 14. THE ATTACHMENT OF THE BASE OF THE HEART OF THE POSTERIOR WALL OF THE PERICARDIAL SAC, AND THE PERICARDIAL SINUSES.

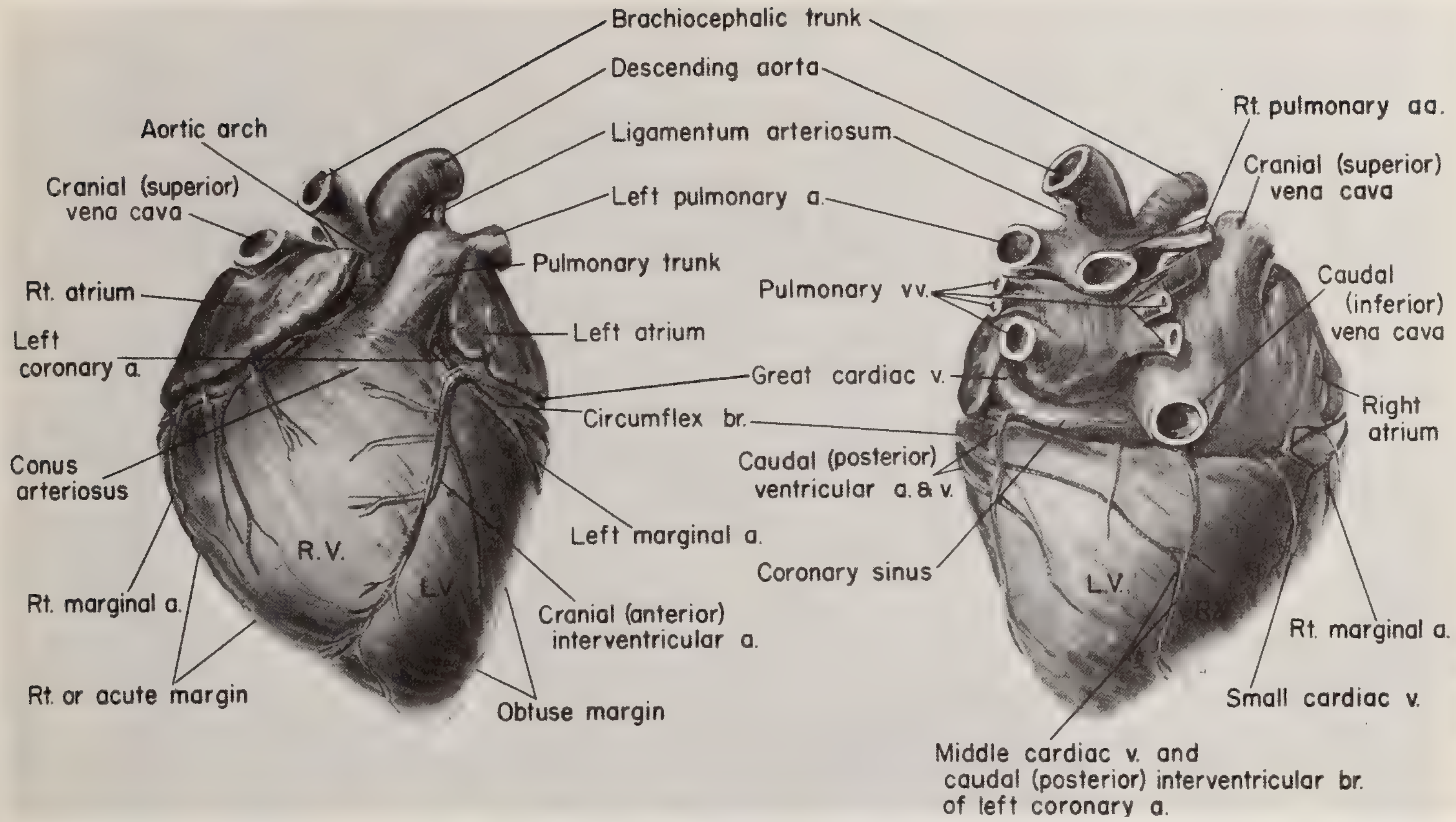

FIGURE 15. A. STERNOCOSTAL SURFACE OF OVINE HEART SHOWING CORONARY ARTERIES AND GREAT CARDIAC VEIN.

FIGURE 15. B. CAUDAL (POSTERIOR) SURFACE OF OVINE HEART DEMONSTRATING TERMINATIONS OF CORONARY ARTERIES & CORONARY SINUS.

Reproduced by permission from:
W. Henry Hollinshead, A TEXTBOOK OF ANATOMY 2nd ed., 1967. Hoeber Medical Division, Harper and Row, New York.

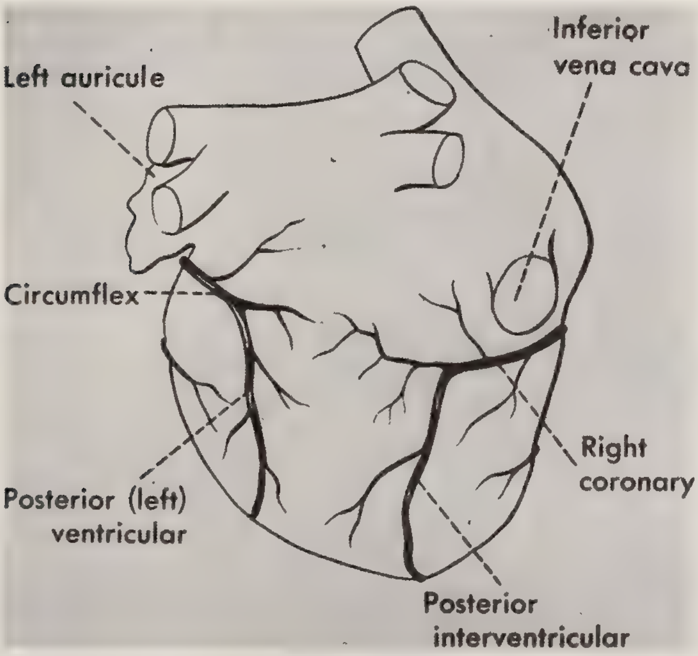

FIGURE 16. CORONARY ARTERIES IN MAN.

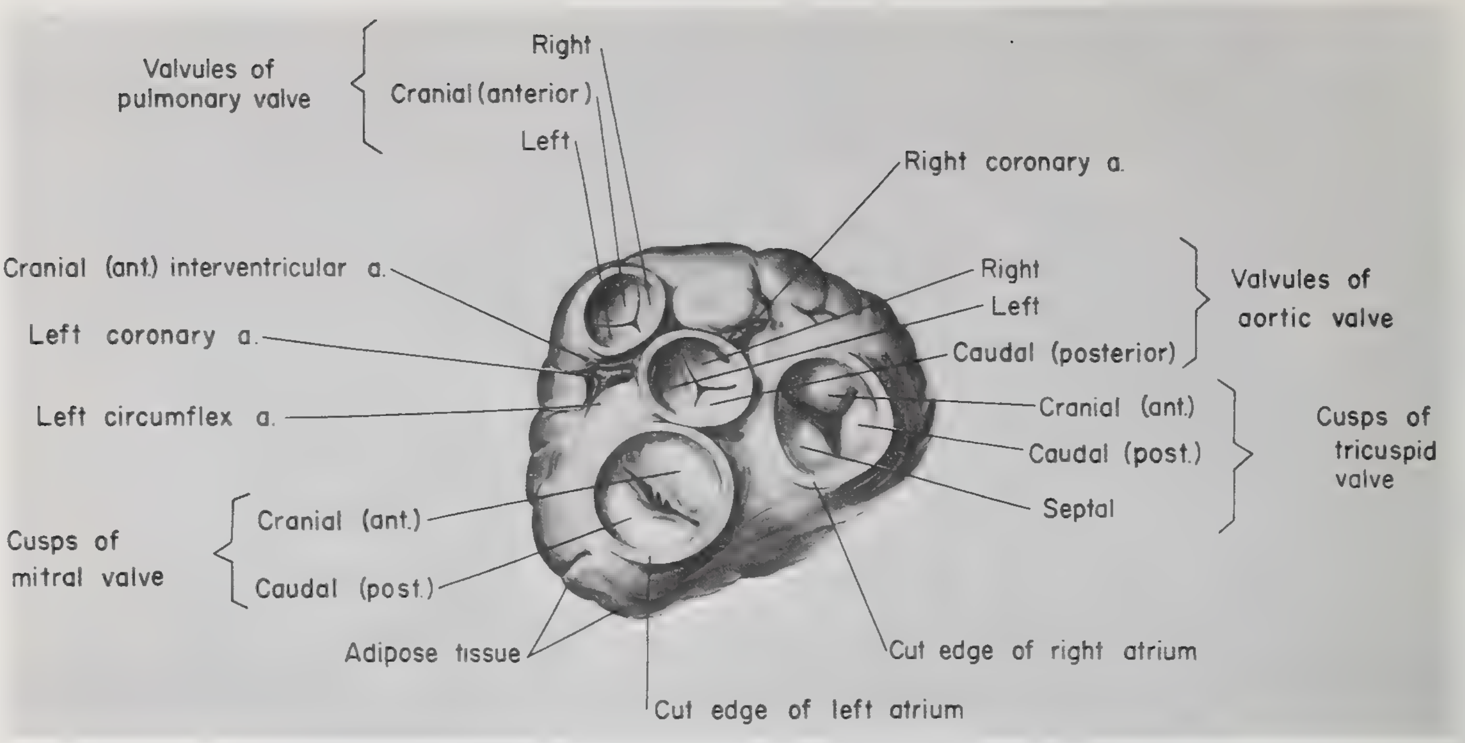

FIGURE 17. DORSAL (SUPERIOR) VIEW OF SEMILUNAR AND ATRIOVENTRICULAR VALVES OF OVINE HEART.

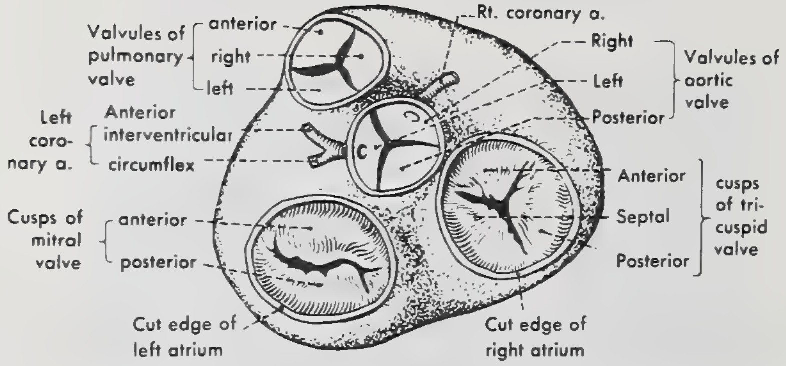

FIGURE 18. DIAGRAM OF THE VALVES OF THE HUMAN HEART, IN A VIEW FROM ABOVE, WITH BOTH ATRIA CUT AWAY AND THE AORTA AND THE PULMONARY TRUNK CUT A LITTLE ABOVE THE LEVELS OF THEIR VALVES.

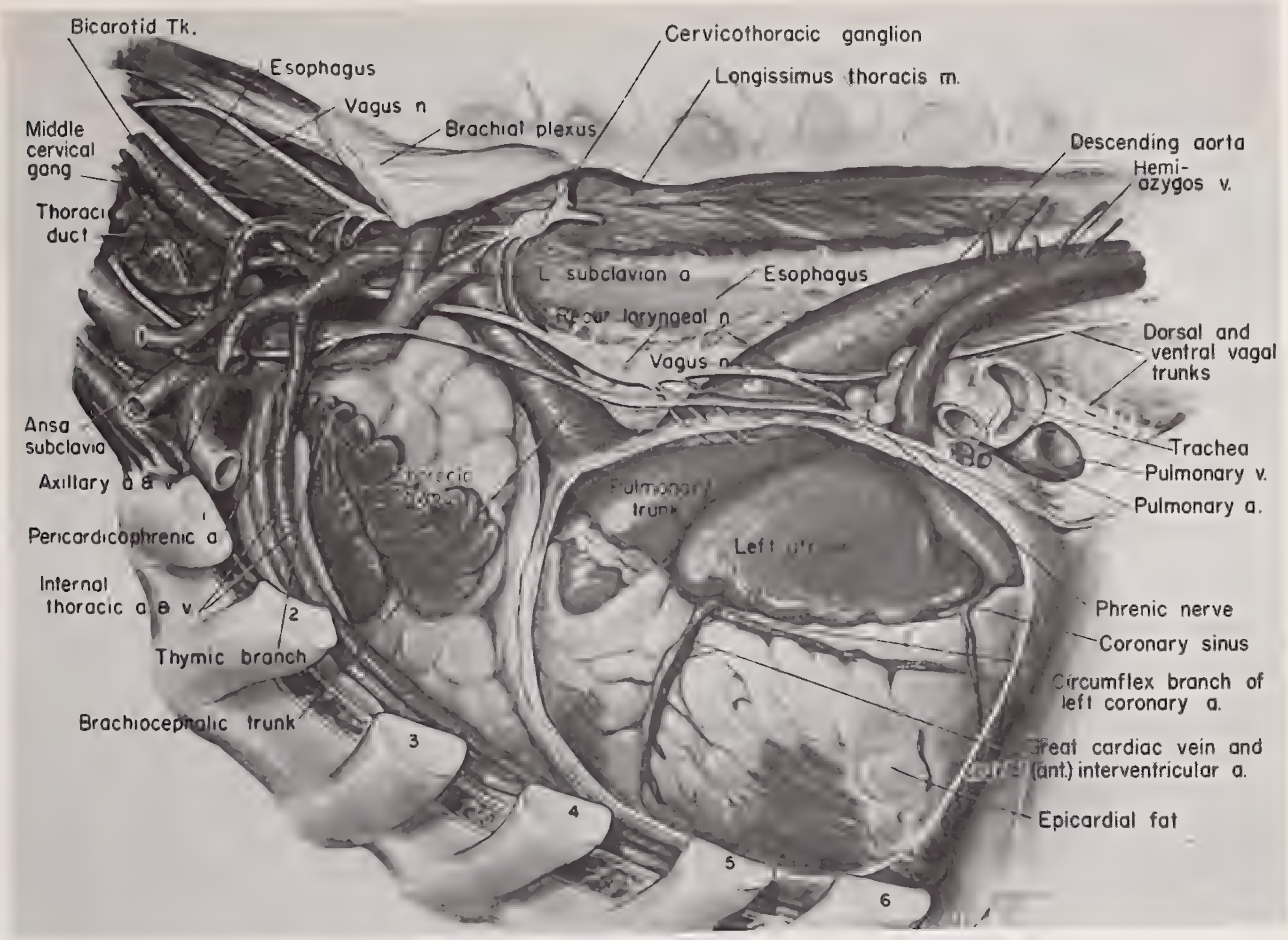

FIGURE 19. LEFT SURFACE OF HEART, GREAT VESSELS AND ASSOCIATED STRUCTURES.

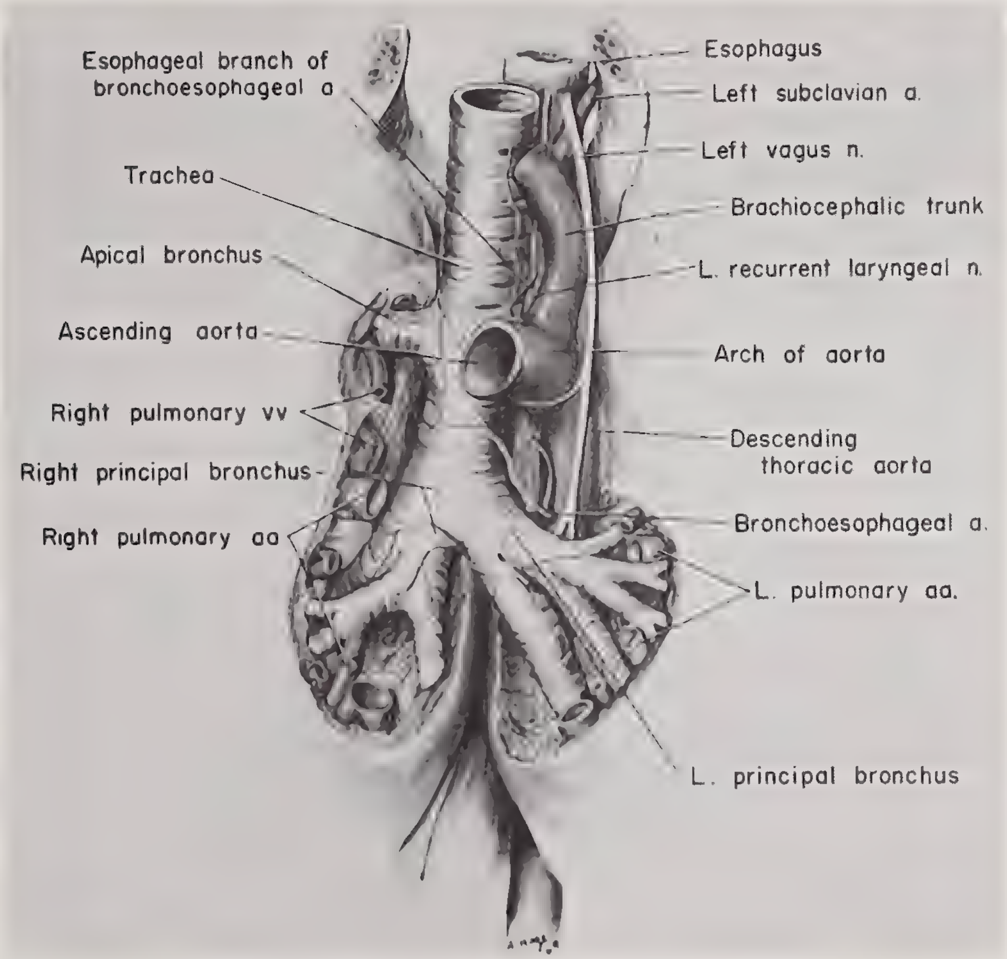

FIGURE 20. TRACHEA, BRONCHI AND ASSOCIATED STRUCTURES.

brachiocephalic trunk. This branch was the recurrent laryngeal nerve. As the recurrent laryngeal nerve continued cranially it passed beneath the subclavian artery and entered the carotid sheath in the caudal cervical region. The vagus, after it gave off the recurrent laryngeal nerve, continued along the ventrolateral surface of the descending thoracic aorta and reached the hilus of the lung. Small cardiac branches were given off at this point and penetrated the heart proper. Also, near the hilus of the lung at the esophageal plexus, each vagus bifurcated into a dorsal (posterior) and ventral (anterior) branch. The anatomy of this region resembles that of man (Figures 21, 22 & 23).

Sympathetic nerves: The sympathetic innervation of the thorax consisted of a complex system of small fibers with a multitude of variations possible for each specimen observed. A general pattern will be described, keeping in mind the possible variations. A chain of sympathetic ganglia ran parallel beneath and on either side of the vertebral column the entire length of the thorax with approximately one ganglion per vertebra.

The first thoracic ganglion and caudal cervical ganglion were fused into a large ganglion called cervicothoracic ganglion or stellate ganglion (Figure 24). Many small but distinct fibers arose from the cervicothoracic ganglion and coursed toward the pericardial sac and great vessels. These were sympathetic cardiac nerves. Near or on the surface of great vessels the sympathetic cardiac nerves united with the vagal trunk or passed in a craniomedial direction and looped around the subclavian artery. Other small branches passed directly from the cervicothoracic ganglion to the lateral surface of the trachea and coursed beneath the costocervical trunk. These branches united to form a small ganglion on the lateral surface of the trachea termed middle cervical ganglion. At approximately the fifth to sixth cervical vertebra the fibers from this ganglion continued cranially within the common epineurium of the vagal trunk. This constituted the vagosympathetic trunk as seen in the sheep.

Great Vessels. Ascending aorta: The ovine ascending aorta was approximately 2.4 cm. in diameter, 5.0 - 6.5 cm. in circumference and 2 1/2 cm. long (Figure 25). After it gave origin to the right and left coronary arteries, it ascended cranially (superiorly) and dorsally (posteriorly) in the middle mediastinum between the pulmonary trunk and the right atrium. It was invested with fibrous pericardium and shared a serous reflection with the pulmonary trunk. The origin of the aorta is somewhat dilated for at its origin was located three bulgings in its wall, the sinuses of the aorta. Each of the sinuses was named for the cusp of the aortic valve, namely cranial (anterior), right and left.

Arch of the aorta: The ascending aorta continued into the arch of the aorta and passed upward and slightly to the left. The aortic arch was approximately 6 cm. in circumference in the adult sheep. It was characterized by a single large branch, the brachiocephalic trunk and occasionally a small twig originated from the left surface of the arch at the level of the brachiocephalic trunk. This small artery descended to ramify over a portion of the right atrium. In 54 aortic arches examined the only large major branch of the aortic arch was the brachiocephalic trunk.

Descending thoracic aorta: After the origin of the brachiocephalic trunk from the aortic arch, the descending aorta rose to a position between the lungs and coursed caudally (inferiorly) approximately 6-9 cm. before giving off any major branches.

The bronchoesophageal artery (human, bronchial and esophageal branches) approximately 2-3 mm. in diameter, arose from the aorta at the level of the hilus of each lung (Figure 26). The artery immediately trifurcated and sent a long (12 cm.) branch caudally along the esophagus and a shorter branch (7 cm. long) cranially to the base of the pericardial sac and also small twigs to the esophagus. The middle branch (4-5 cm. long x 2 mm. diameter) curved toward the hili of the lungs where it divided into a right and left bronchial artery. In plastic cast preparation the bronchial arteries could be demonstrated coursing with the pulmonary artery and vein, above the bronchi and followed the vessels deep into the substance of the lung.

Azygos Venous System. Left azygos (hemiazygos) vein: Small ascending lumbar veins coursed high in the sublumbar region and united with the small subcostal vein to form the left axygos (hemiazygos) vein (Figures 27, 28). The vein continued cranially (superiorily) invested in endothoracic fascia. Deep to the parietal pleura and at each intercostal space it was joined by dorsal (posterior) intercostal veins until it reached the level of the fifth to sixth thoracic vertebra. At this level which is also cranial (superior) to the hilus of the lung, the vein turned ventrally (anteriorily) to enter the coronary sinus. As the left azygos ascended the dorsal (posterior) thoracic wall, its position was left of the descending thoracic aorta.

Right azygos vein: The right azygos vein (azygos in man) arose by small dorsal intercostal tributaries at the fifth and sixth thoracic vertebra and continued cranially receiving a dorsal intercostal vein at each intercostal space including the first intercostal (Figure 29). After receiving the first dorsal intercostal vein it turned sharply downward and coursed cranial to the apical branches and to the right of the trachea and right vagus nerve and emptied into the cranial vena cava at the level of the second thoracic vertebra.

Femoral triangle: The femoral triangle of the sheep was deeply located as it was covered by the sartorius muscle (Figure 30). The triangle contained from cranial to caudal, the saphenous nerve, femoral artery and vein. The saphenous artery arose from the femoral at the distal portion of the triangle and coursed downward superficially on the medial side of the thigh. The pulse may be taken from the saphenous artery as it courses from the triangle to the tarsus. The principal

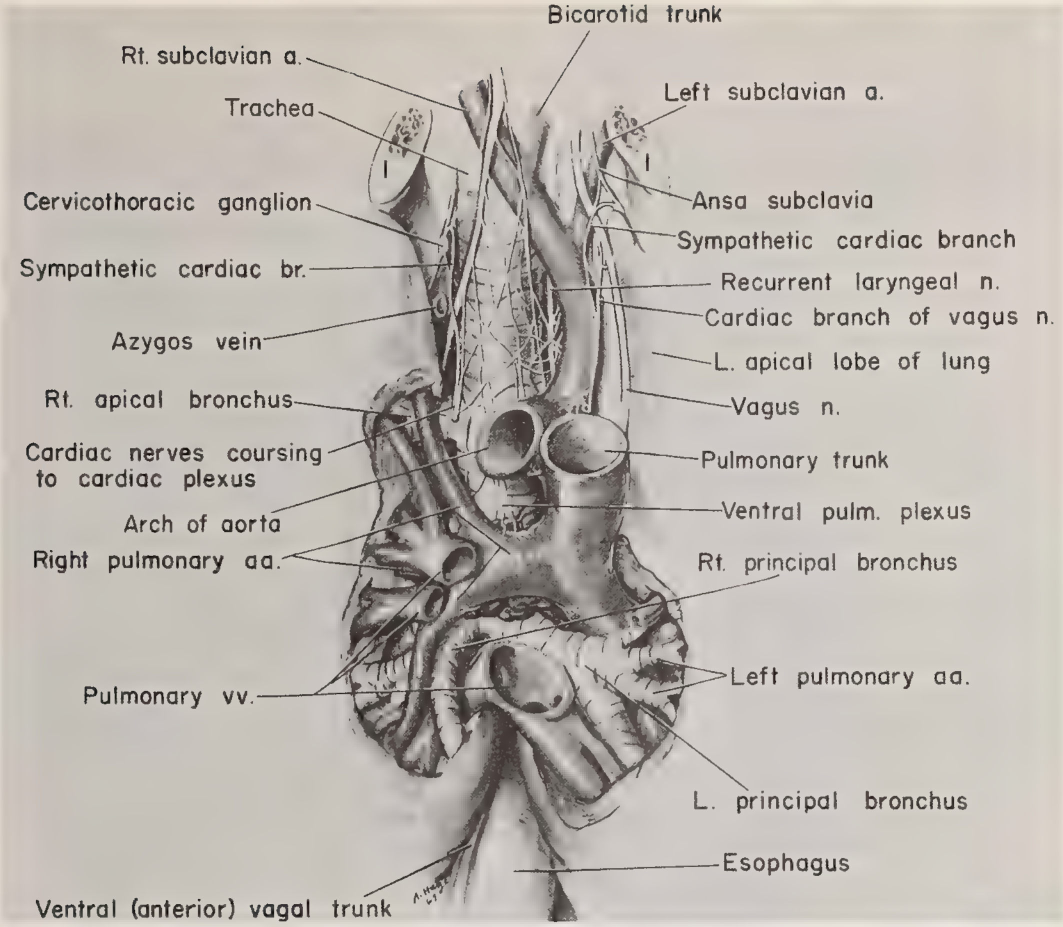

FIGURE 21. PULMONARY ARTERIES AND VEINS.

Reproduced by permission from:
J.C.B. Grant, AN ATLAS OF ANATOMY
5th ed., 1962. The Williams and
Wilkins Co., Baltimore.

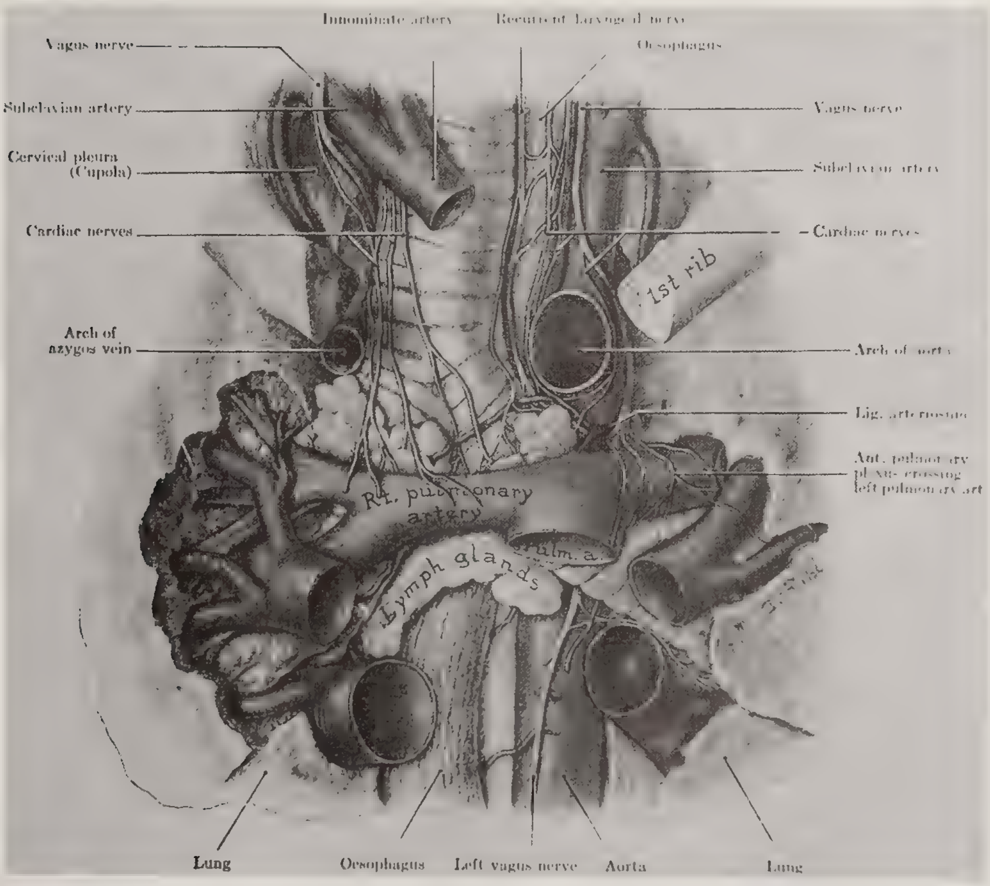

FIGURE 22. THE PULMONARY ARTERIES: SUPERIOR MEDIASTINUM.

Reproduced by permission from:
J.C.B. Grant, AN ATLAS OF ANATOMY
5th ed., 1962. The Williams and
Wilkins Co., Baltimore.

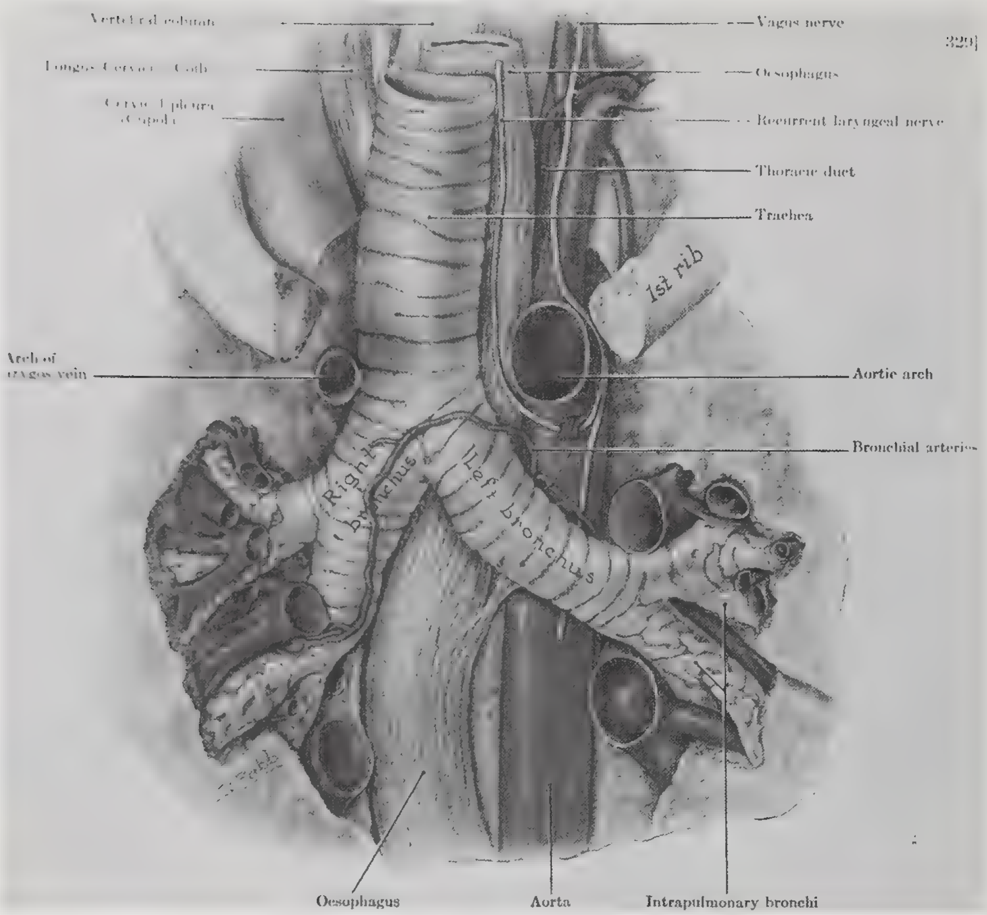

FIGURE 23. THE BRONCHI: SUPERIOR MEDIASTINUM.

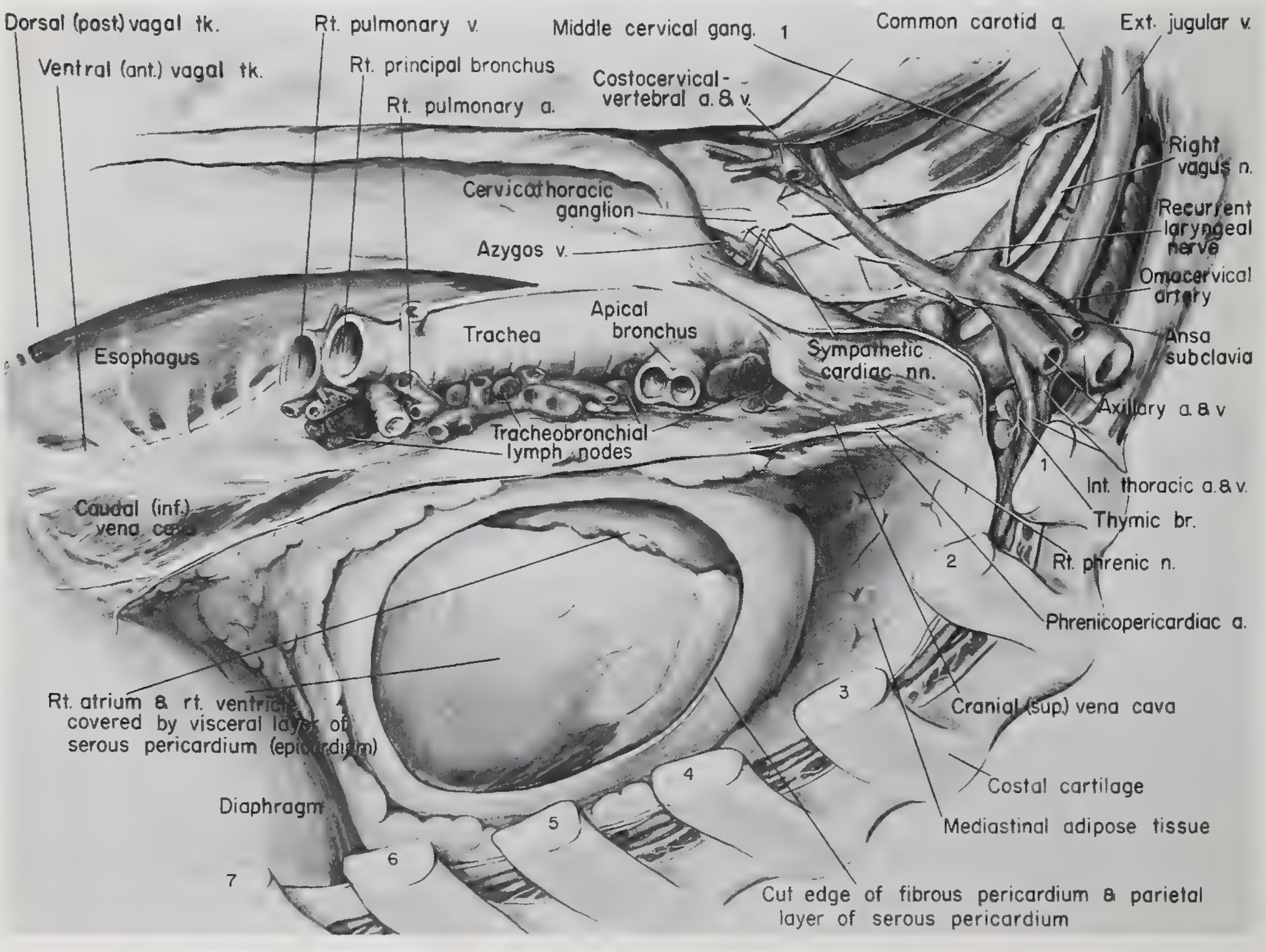

FIGURE 24. RIGHT SURFACE OF HEART, GREAT VESSELS AND ASSOCIATED THORACIC STRUCTURES.

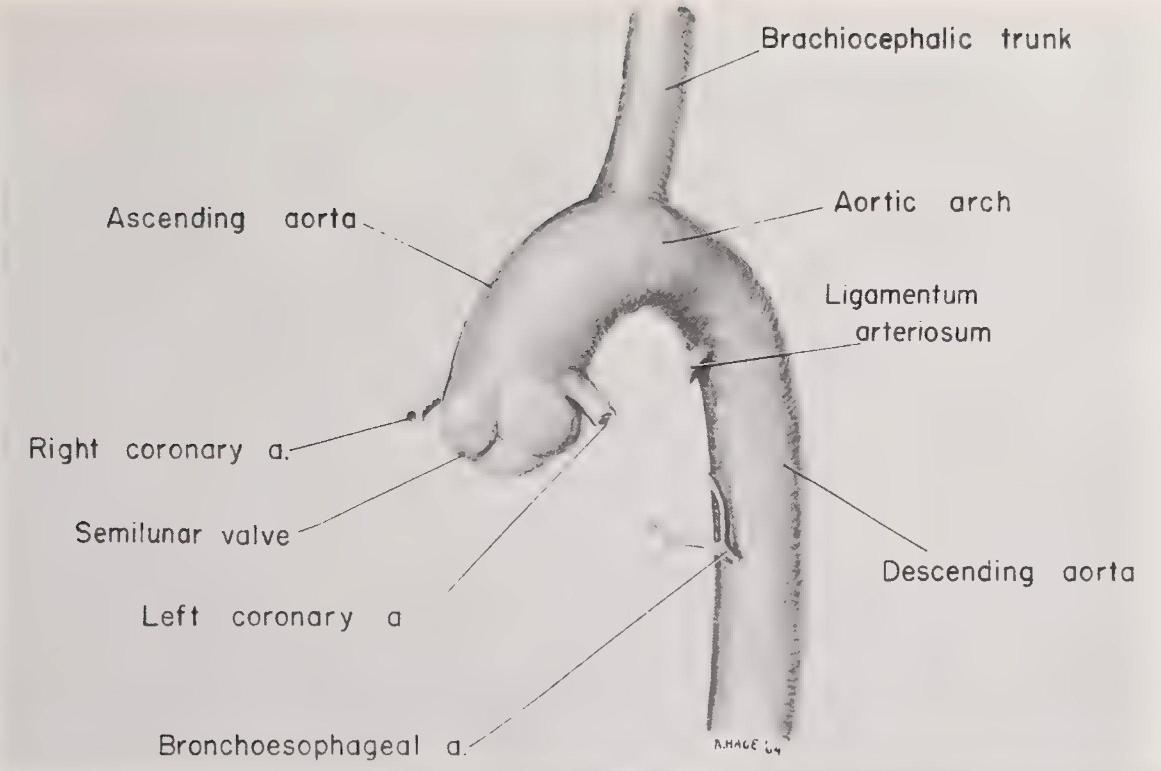

FIGURE 25. OVINE AORTIC ARCH.

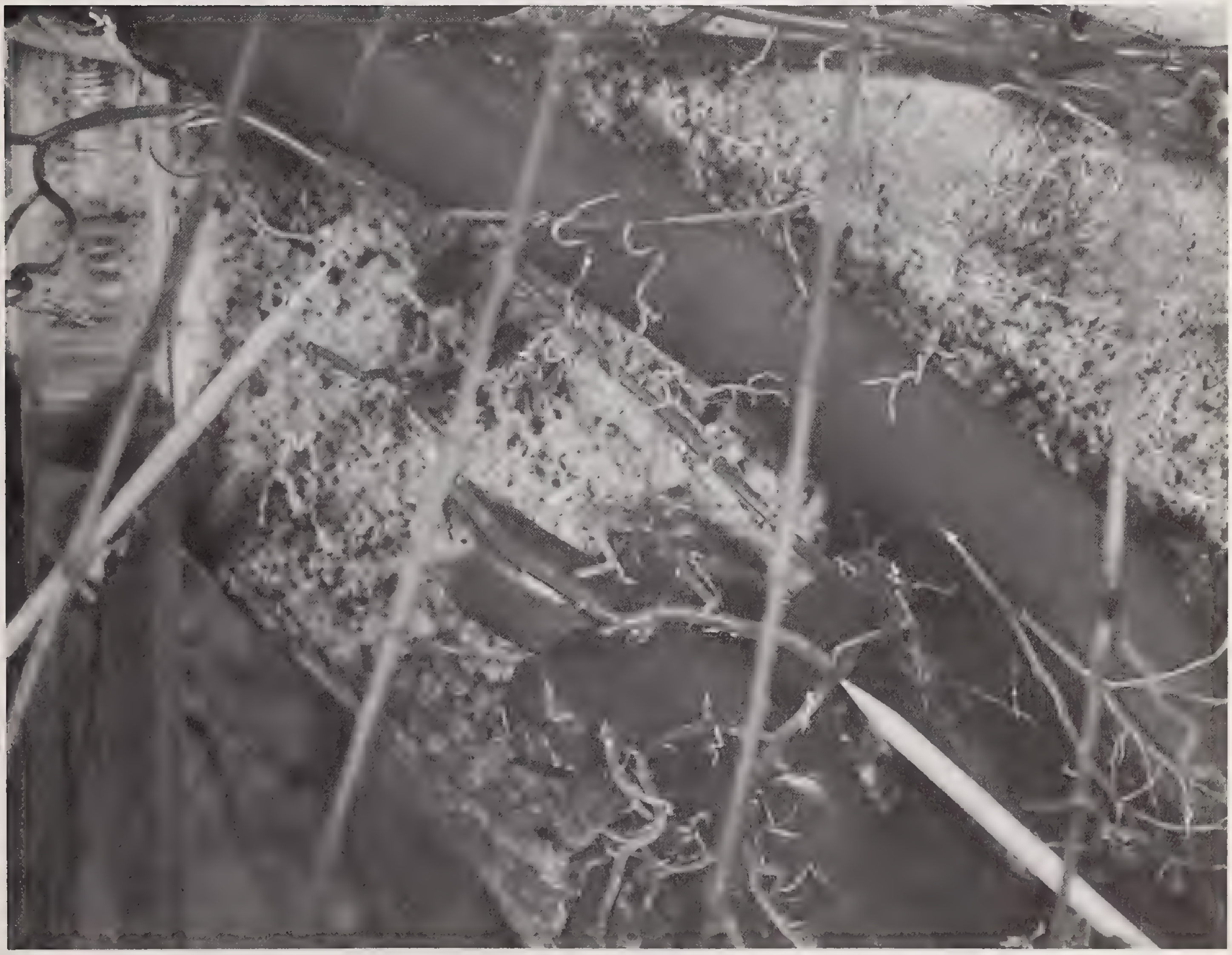

FIGURE 26. BRONCHOESOPHAGEAL ARTERY.

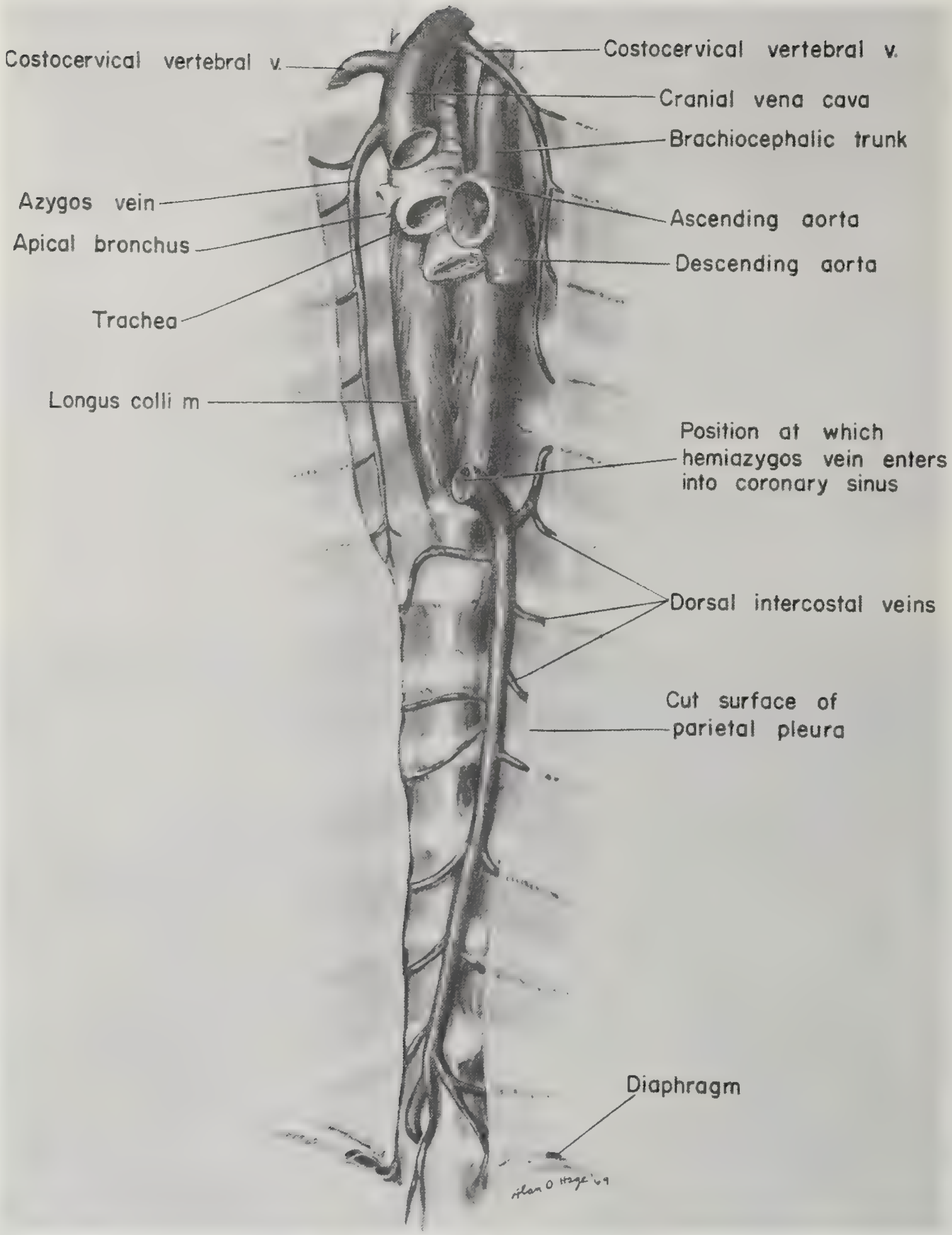

FIGURE 27. AZYGOS SYSTEM OF VEINS.

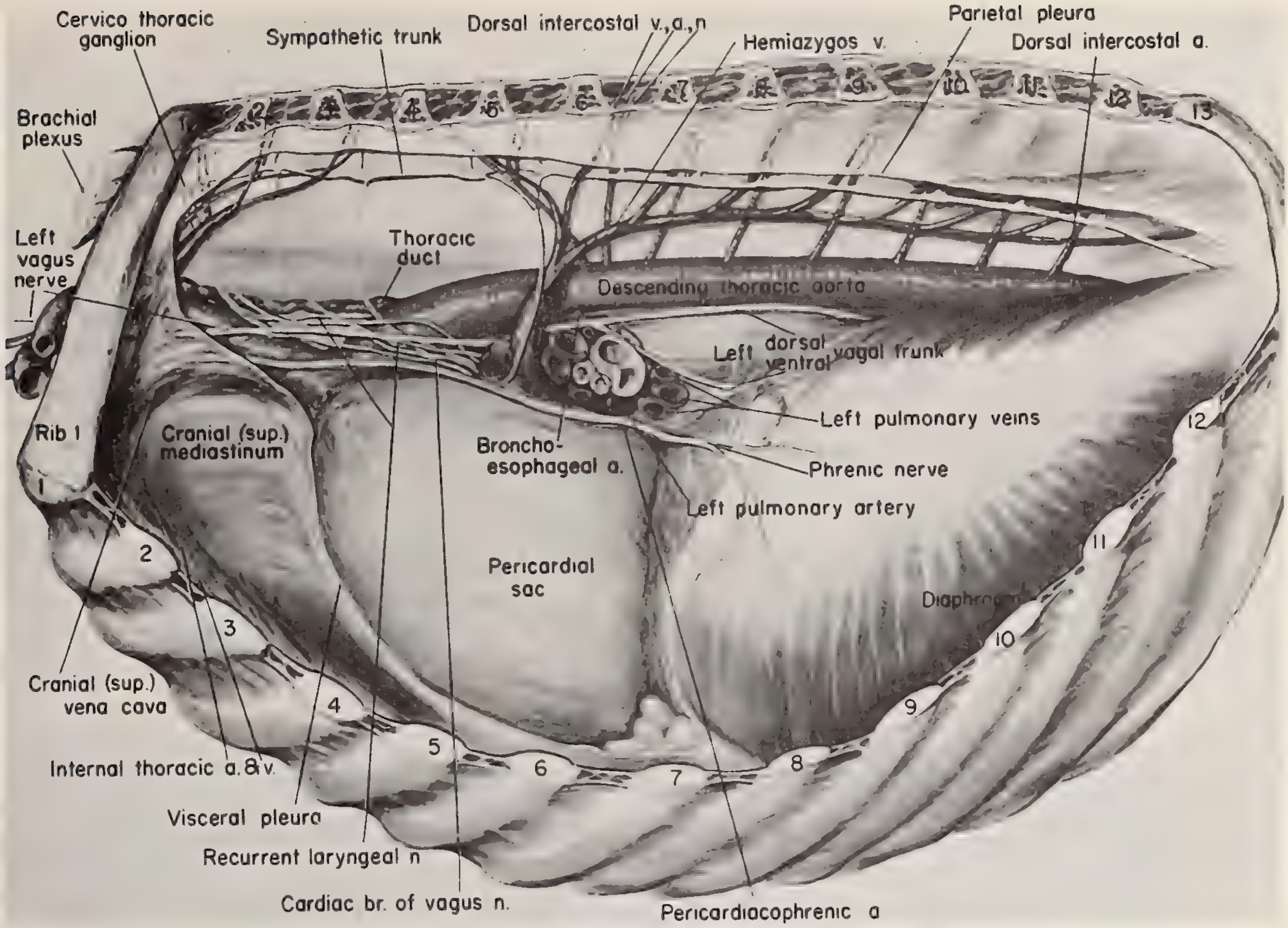

FIGURE 28. LEFT MEDIASTINUM ILLUSTRATING THE AXYGOS VENOUS SYSTEM.

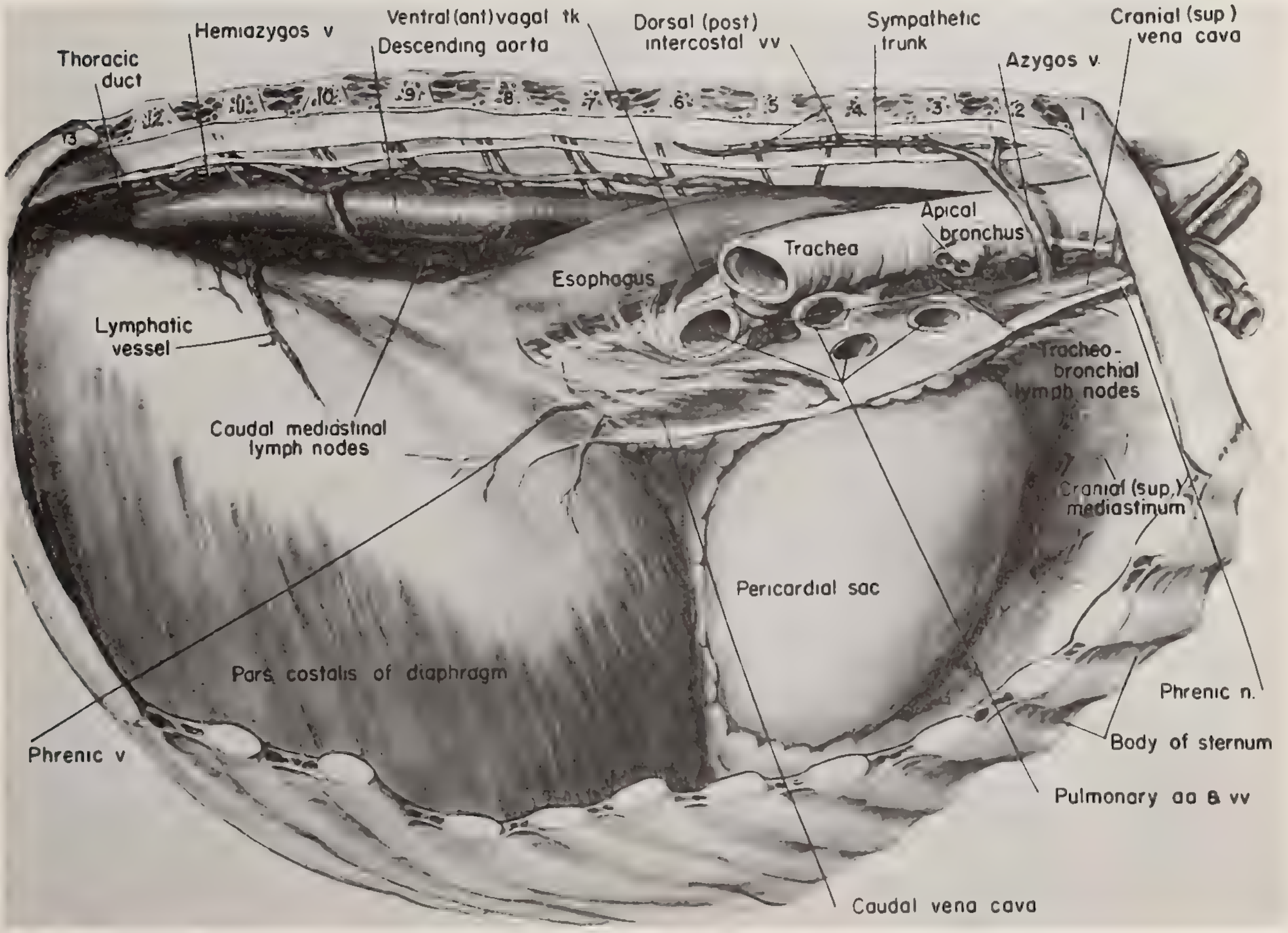

FIGURE 29. RIGHT MEDIASTINUM ILLUSTRATING THE AZYGOS VENOUS SYSTEM.

differences between the ovine femoral triangle and that of man are: (1) the sartorius muscle covers the triangle in the sheep while in man the sartorius muscle forms the lateral border of the femoral triangle, (2) the saphenous nerve rather than the femoral nerve occupies the triangle with the vessels in the sheep.

SUMMARY

The objective of this study has been to describe and illustrate the gross morphology of the thoracic wall and intrathoracic anatomy of the sheep and relate these findings to comparable structures in man. When directional terminology for the quadruped differed from that of man, the human term has been included in parenthesis. The shape of the ovine bony thorax and the character of the endothoracic fascia differed from that of man while the pleural cavities were similar. The ventral (anterior) mediastinum and in situ position of the lungs, pericardial sac, its attachments and pericardial sinuses resembled that in man. The surfaces of the ovine heart were similar to human; however the distribution of coronary arteries corresponded to one of the common variations seen in man. Pulmonary, aortic and atrioventricular valves of sheep and man were similar morphologically in number and position of valvules and cusps. In 54 ovine aortic arches studied the aorta was characterized as giving origin to a single major branch, the brachiocephalic trunk. The bronchoesophageal artery arose from the aorta at the level of the hilus of the lung and coursed to the esophagus and both lungs. The azygos venous system in sheep was found to be poorly developed on the right; while the hemiazygos (left azygos) vein was the predominant venous drainage of the thoracic wall on the left side.

REFERENCES

1. Anson, B. J., 1963. Atlas of Anatomy (ed. 3). Philadelphia: W. B. Saunders.
2. Chauveau, A., 1910. The Comparative Anatomy of the Domesticated Animals. (ed. 2) New York: D. Appleton and Co.
3. Ellenberger, W. and H. Baum, 1891. Systematische and Topographische Anatomie des Hundes. Berlin: Paul Parey.
4. Ellenberger, W. and H. Baum, 1943. Handbuch der Vergleichenden Anatomie der Haustiere (ed. 18).
5. Gardner, E., D. J. Gray, and R. O'Rahilly, 1960. Anatomy. Philadelphia: W. B. Saunders.
6. Grant, J. C. B., 1958. A Method of Anatomy (ed. 6). Baltimore: Williams and Wilkens.
7. Habel, R. E., 1964. Guide to the Dissection of Domestic Ruminants. Ann Arbor: Edwards Bros.
8. Hollinshead, W. H., 1967. Textbook of Anatomy. New York: Paul B. Hoeber.
9. Hollinshead, W. H., 1968. Anatomy for Surgeons (Vol. 1). New York: Paul B. Hoeber.
10. Hollinshead, W. H., 1968. Personal Communication.
11. Grant, J. C. B., 1962. An Atlas of Anatomy. (ed. 5). Baltimore: The Williams and Wilkens Co.
12. May, N. D. 1964. Anatomy of the Sheep. (ed. 2). Queensland: University of Queensland Press.
13. Nomina Anatomica Veterinaria, 1968. American Veterinary Medical Association. Berlin: Paul Parey.
14. Nomina Anatomica, 1967. Amsterdam: Excerpta Medica Foundation.
15. Pernkopf, E., 1963. Atlas of Topographical and Applied Human Anatomy. (Vol. 1 and Vol. 2). Philadelphia: W. B. Saunders.
16. Sisson, S., and J. D. Grossman, 1954. The Anatomy of the Domestic Animals. (ed. 4) Philadelphia: W. B. Saunders.
17. Seiferle, E., 1956. Grundsätzliches Zu Bau und Benennung der Haussauger - Lunge. Okajimas Folia Anat. Jap. L8: 71-81.
18. Vaughn, I., 1904. Strangeways Veterinary Anatomy (ed. 4) New York: William and Jenkins.

DISCUSSION

DR. KRALIOS: I would like to ask Dr. Anderson some questions: We noticed in four out of twelve sheep that a large anastomotic branch existed between the anterior descending, or the so-called anterior intraventricular branch, and the posterior descending branch. Is there any anastomosis between the coronary sinus and the hemiazygous vein? And also, I would like to know how large is usually the common wall between the atria because this is very important for the total replacement techniques. And now a question from Dr. Kwan-Gett, what are the dimensions of the epiglottis in sheep?

DR. ANDERSON: Well, I am aware from other studies that there is collateral circulation between the anterior and posterior intraventricular arteries or anterior descending and posterior descending branches. We have not demonstrated this collateral circulation very well in any of the calves. However, in the sheep that we have perfused, there is certainly collateral circulation from the anterior surface. Now, your second question was that you are concerned about the termination of the hemiazygous vein. Is that correct? The hemiazygous vein, which is the principal venous drainage of the thorax, commonly does empty into the coronary sinus. If one wants to locate the esophageal artery or the bronchial artery, one dissects medial to the hemiazygous vein. It is a very fine landmark.

DR. GALYSH: Dr. Anderson, have you had an opportunity to study the morphology of the wall of the aortic root? We have had numerous instances of aortic wall rupture in attempting to suture grafts of in-series assist devices on the aortic root wall.

DR. ANDERSON: Well, all I can tell you is that we have not studied the wall of the aorta that thoroughly, but we have made some observations. The wall of the aorta is probably thickest at the level of the hilus of the lungs. It is approximately 1/3 as thick at the distal portion of the descending thoracic aorta where it enters the hiatus. So, it may be worthwhile to be very cautious in the distal third of the ovine descending aorta, because it is very, very thin at this point.

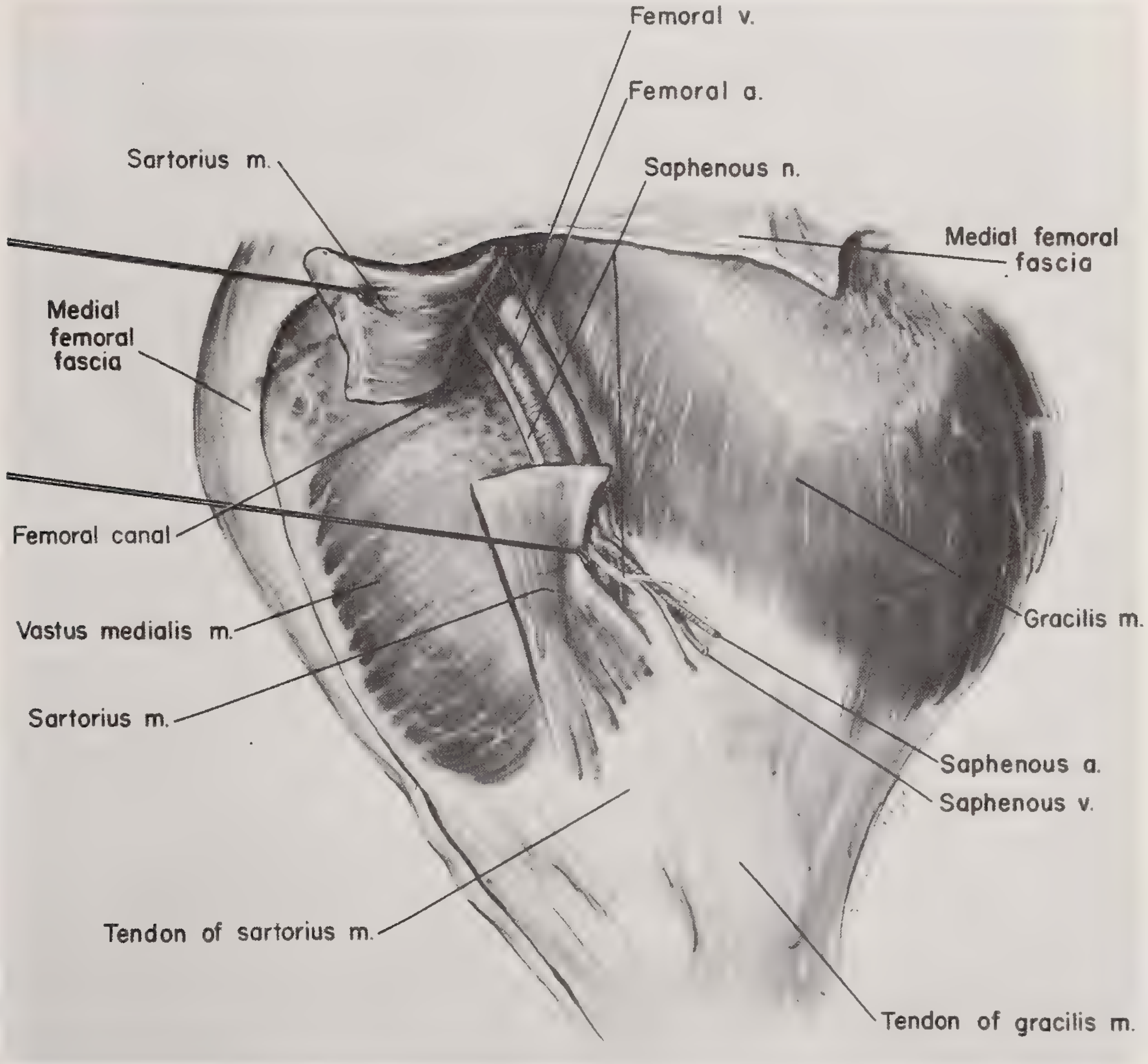

FIGURE 30. MEDICAL SURFACE OF PELVIC LIMB, FEMORAL TRIANGLE AND COMPONENTS.

SECTION VIII

INSTRUMENTATION APPLICABLE TO ARTIFICIAL HEART DEVELOPMENT AND USE

Chairmen: Allen K. Ream, M.D.
Charles E. Branch

INTRODUCTION

In the near future, a complete spectrum of assist devices (emergency, temporary, and permanent) and total heart replacements is envisioned, all requiring accurate experimental and clinical study. The development, selection, control and utilization of these devices require considerable sophistication in instrumentation technology, in many cases of a degree not currently available. This instrumentation is necessary in a broad range of areas: 1) A device must be developed with the aid of reliable and accurate pressure transducers, flowmeters, electrocardiograph-sensing apparatus, etc. 2) It must be tested, both by the developer and in other laboratories, in experimental animals under continuous operation for days, weeks, months or years (depending on its anticipated clinical use), using similar instrumentation. 3) Patients with heart disease must be identified and characterized; complete and accurate information must be obtained describing their cardiac, hemodynamic, metabolic, and general medical status using appropriate sensors and diagnostic techniques. 4) Using the data obtained from such a group of patients, those likely to require assist or replacement mechanical therapy must be identified and treatment begun. 5) Such treatment and its effect on the patient must be closely monitored and the data obtained properly and efficiently stored and analyzed. 6) During the course of such treatment instrumentation must be available to provide data needed for the decision to modify, alter, or stop mechanical assistance. 7) Permanently implanted assist and total heart replacement devices and their control systems must contain highly accurate and reliable transducers that are as small and efficient as possible since the total unit (assist or replacement device, energy source, control system) must be compact enough not to interfere with adjacent organ function.

CHAPTER 58

DEVELOPMENT OF A CONTINUOUS BLOOD pO_2 MEASURING SYSTEM

P. Reichner, Y. Tamari and G.E. McGinnis

Westinghouse Electric
Pittsburgh, Pennsylvania

The objective of this program is to develop a continuous, in-vivo, blood pO_2 measuring system. Continuous in vivo and in vitro analysis of blood pO_2 and pCO_2 is important for the monitoring and control of artificial heart devices and for the evaluation and control of blood oxygenators. The oxygen measuring device now under development uses solid electrolyte oxygen sensors with a circulating carrier gas in a null-balance system. The carrier gas composition is automatically adjusted to equilibrate the partial pressure of oxygen across the sensing membrane. This results in a measuring system with high accuracy that is essentially independent of the mass transfer characteristics of the membrane/blood interface, disposability for all elements that contact the body, freedom from calibration requirements, and no electrical potential within the patient. The oxygen in an N_2/O_2 gas mixture has been readily measured with the null-balance system to within 1 mmHg of a direct sample measurement. Membrane transfer of gases other than oxygen was found to cause significant errors in the O_2 measurement. These secondary gas transfer errors were eliminated by using a slightly more complex dual-null system which allows oxygen measurement of an $N_2/O_2/CO_2$ gas mixture with a deviation of less than 1 mmHg from the direct sample measurement. Feasibility has also been shown for the objective of developing a miniature catheter-tip device.

INTRODUCTION

The pO_2 of venous blood is an important measure of cardiac function. Of itself, pO_2 is a reflection of cardiac output; in conjunction with a suitable continuous oxygen consumption monitor, cardiac output can be measured continuously using the Fick relation. Because of this inherent relationship between blood pO_2 and circulatory system function, venous and/or arterial pO_2 are key parameters for monitoring the efficiency of ventricular assist devices. In addition, accurate pO_2 measurement is essential in the development and application of blood oxygenators.

The objective of this program is to develop a continuous, in vivo blood pO_2 measuring system. The oxygen measuring device now under development uses solid electrolyte oxygen sensors with a circulating carrier gas in a null-balance system. The carrier gas composition is automatically adjusted to equilibrate the partial pressure of oxygen across the sensing membrane. This results in a measuring system with high accuracy that is essentially independent of the mass transfer characteristics of the membrane/blood interface. In addition, the technique permits disposability for all elements that contact the body, freedom from calibration requirements, and no electrical potential within the patient. I will present a very brief review of the state-of-the-art techniques for pO_2 measurement, a description of the null-balance technique, and a summary of accomplishments during the present contract period.

The direct sensing of blood pO_2 is most commonly accomplished with a polarographic (Clark) electrode that is dependent upon the rate of oxygen transfer across a semipermeable membrane. In this sensor the current output, and thus the indicated pO_2, is a function of variables which are difficult to control in in vivo situations. The stability and accuracy of Clark electrodes are generally poor. The problem areas inherent to the Clark electrode include calibration, temperature, sensitivity, flow sensitivity, and deposition of blood elements on the membrane.

Calibration is usually done in vitro with a known gas. Since in vivo permeability of the membrane is but one part of the total resistance to O_2 flow (the other being the liquid-membrane interface layer), there is an offset that is a function of the relative permeabilities of the membrane and the liquid layer. Further problems are introduced by the need to ensure that the temperature is the same for the calibration conditions as it will be during measurements. Frequent recalibration is required.

Since the membrane permeability is temperature sensitive, it is necessary to maintain temperature constant during measurements. When doing in vivo work this can be a problem in pathological cases or in the case of hypothermic surgery.

It is very difficult to ensure constant blood velocity profiles in the in vivo situation. Changes in such profiles affect the readings due to changes in effective blood film permeability.

Probably the most significant effect on indicated blood pO_2 during continuous monitoring is caused by the deposition of blood elements on the membrane. This reduces the effective area of both the membrane and the surrounding blood layer and also changes the effective permeability of the latter.

In addition to the direct-reading polarographic electrode, oximetry may be used as an indirect method of evaluating pO_2. This method is based on the difference in the blood's reflection of light at two wavelengths. A system is available which employs a fiber optic bundle catheter for measuring *in vivo* O_2 saturation. The conversion from O_2 saturation to pO_2 requires knowledge of several other variable factors and the use of nonlinear curves that depend on temperature, pH (or pCO_2), and the pathology of the subject's hemoglobin. Since all of these are variable, both from patient to patient and variable in time for a given patient (especially during physiological stress), it is doubtful that this approach would yield accurate measurements of pO_2. Also the shape of the hemoglobin saturation curve would preclude measurements of arterial blood. Here an error of ±1% in the O_2 saturation could result in an error of ±10% in pO_2.

The mass spectrometer with a membrane-tipped hollow catheter has been investigated for blood gas measurements, but the high vacuum requirements, the complex and costly apparatus, and the critical nature of the membrane are severe limitations. The accuracy of this technique is also sensitive to membrane permeability variations.

THE NULL BALANCE SYSTEM

Consideration of the above problems leads to the conclusion that a measurement of blood pO_2 that is contingent upon the mass transfer characteristics of a membrane-blood film combination (*in vivo* or *in vitro*) will always be subject to the errors discussed. The development of a stable and accurate blood gas sensor requires, therefore, the minimization (or elimination) of this dependence. A null balance system accomplishes this and is made possible by employing the highly accurate and stable solid-electrolyte oxygen analyzer developed by Westinghouse.

The null balance system shown in Figure 1 measures the blood pO_2 in the following manner. A reference gas of adjustable oxygen concentration is pumped past a semipermeable membrane inserted in the blood stream. The gas then passes through one side of an oxygen cell where it is compared to the reference gas stream which comes directly from the reference gas mixing chamber. The output of this null sensor is the voltage

$$P_1P_2\, e_n = K \ln \frac{p_2}{p_1}$$

where p and p are the partial oxygen pressures on either side of the cell and K is a cell constant. This voltage will be zero when either of the following conditions occurs:

1) No transfer of gases across the membrane (true null); or
2) Transfer across the membrane of a gas mixture having a volume fraction of oxygen equal to that of the reference gas.

To eliminate condition 2, which is not a true null, the two reference gas streams (from the membrane and the mixing chamber) are scrubbed of CO_2 and H_2O and are passed through a second null cell (Figure 2). The scrubbing eliminates the changes in oxygen volume fraction caused by transfer of CO_2 and H_2O across the membrane and, if there is no significant membrane transfer of N_2, then the second cell voltage will be zero when there is no net transfer of oxygen across the membrane.

Since the membrane permeability to nitrogen is relatively low and the blood nitrogen pressure is fairly well known and constant, transfer of nitrogen is small and a null of the second cell precludes condition 2 for the first cell. Therefore, a null of both cells is a true null. The reference gas pO_2 at this condition is equal to that of the blood and may be measured by a third oxygen analyzer (readout sensor).

A servosystem controller uses the null cell output voltages to adjust the reference gas composition to automatically reach and maintain the null condition. Periodically, at an adjustable time interval, the null control system samples the null cell voltage. The system then makes a corrective gas composition adjustment by driving a valve at constant speed for a controlled time interval that increases with increased error (null) signal magnitude. The direction of valve rotation is controlled by relays and is based on the polarity of the null cell signal.

The key to the null system is its ability to determine accurately when two gases have the same pO_2. Figure 3 shows the predicted null resolution for the system with a 0.005" thick silicone rubber membrane and about a 0.004" thick blood film.

Consider an operating point where we are measuring a pO_2 of 100 mmHg with a null resolution of ±1 mmHg initially and changes in the film occur due to prolonged contact with blood. If we were using a membrane of 1 cm^2 area and due to exposure to blood the membrane/film permeability decreased so that the membrane transport of O_2 was affected by a factor of two (i.e., a 50% decrease), the change in null sensitivity would be only ±1 mmHg. The new null sensitivity would be ±2 mmHg. Compare this to a Clark electrode initially reading a pO_2 of 100 mmHg ±1 mmHg which is subject to the same conditions as above. Here, a 50% decrease in O_2 flow is a 50% decrease in current, and this is a 50% error (50 mmHg) in reading pO_2. This error is reduced somewhat in the Clark electrode by the use of membranes with lower initial permeability. Thus with the null balance system, only the error band is affected by changes in permeability while with an electrode the reading itself changes. This insensitivity to membrane characteristics makes possible external calibration and disposable catheter/membrane assemblies.

Prototype units of the oxygen analyzer that is used as the basis of the system have shown an accuracy capability consistently within ±0.25%. Figure 4 shows the variability in four units, each of which was used to measure known gases at five different O_2 concentrations. Table 1 lists the actual test data ranges for this plot.

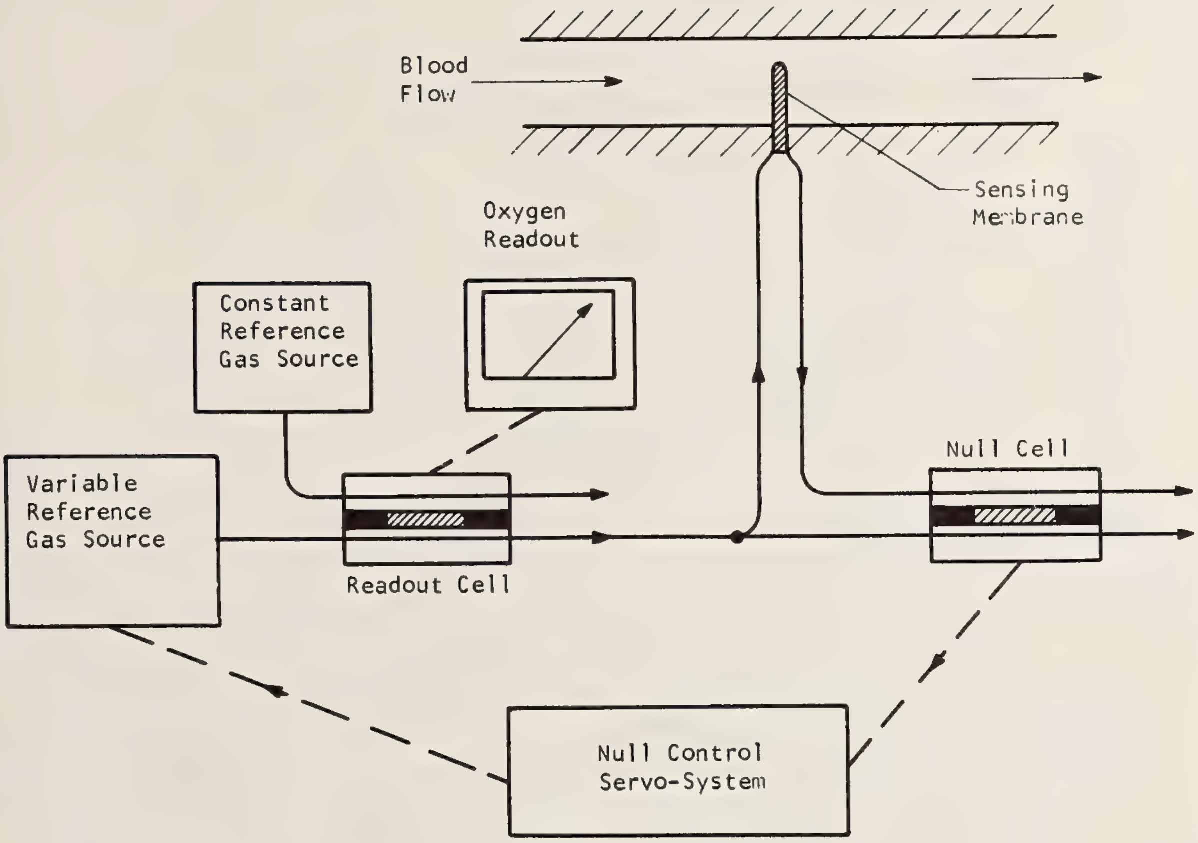

FIGURE 1. NULL BALANCE PRINCIPLE.

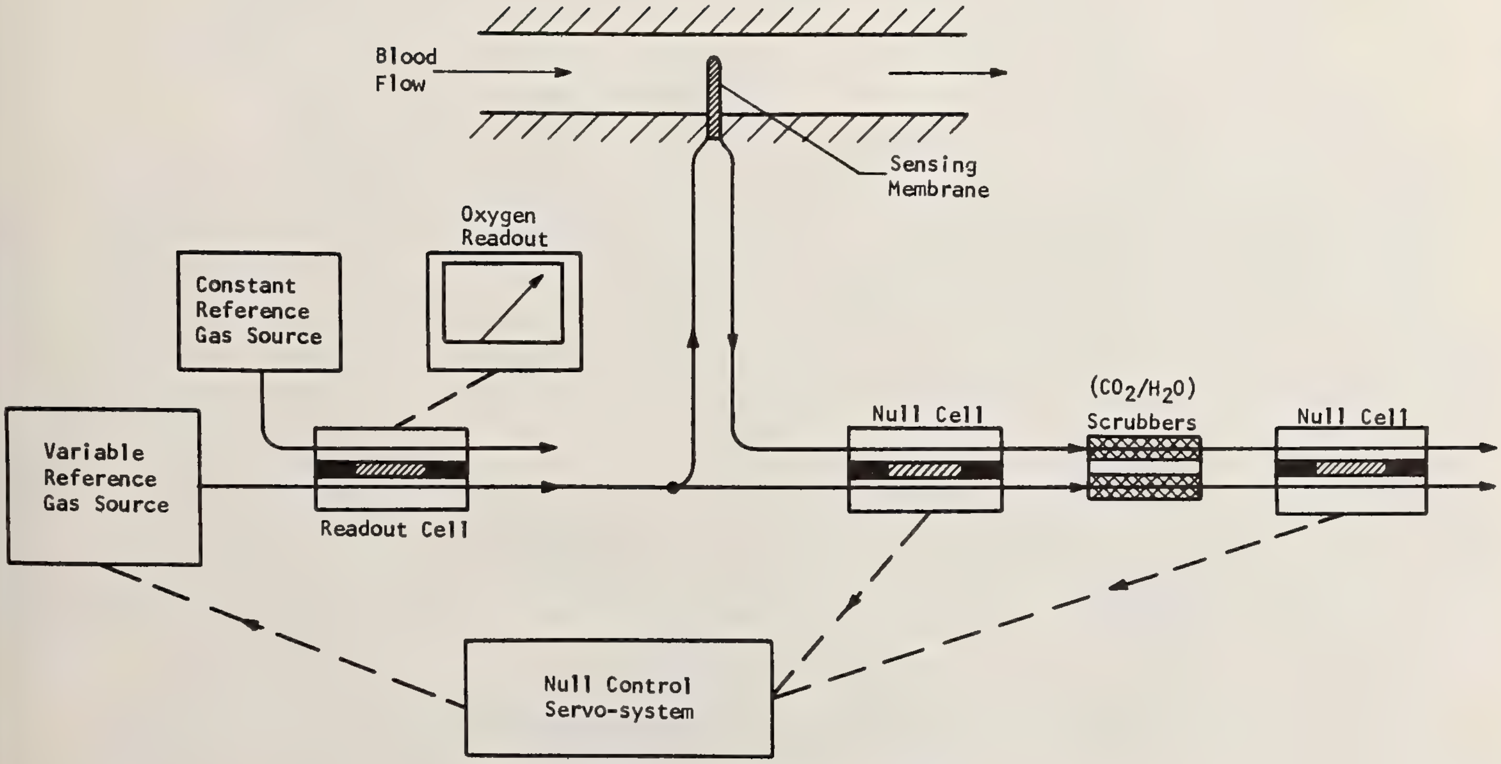

FIGURE 2. NULL BALANCE SYSTEM.

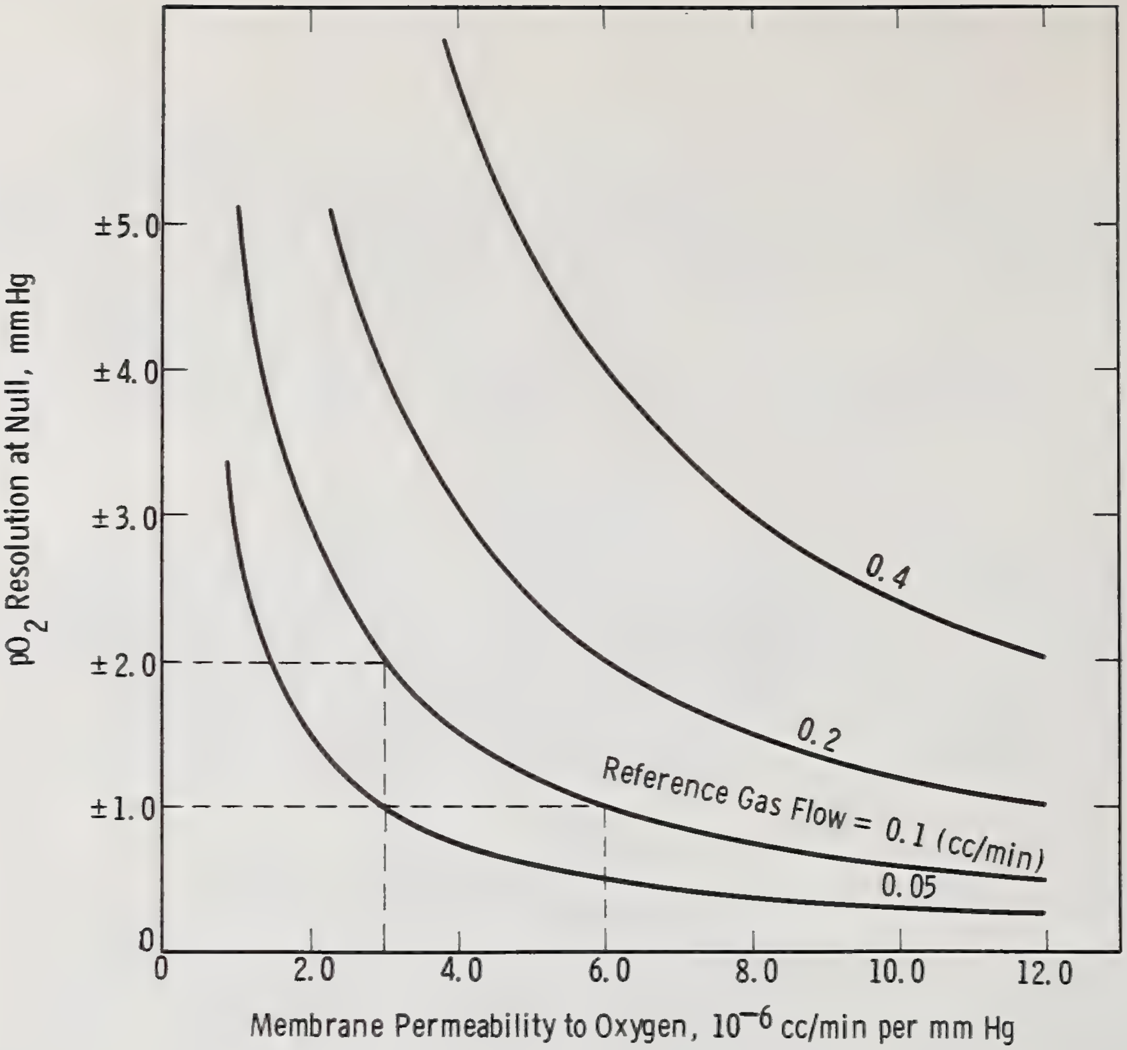

FIGURE 3. NULL SYSTEM RESOLUTION.

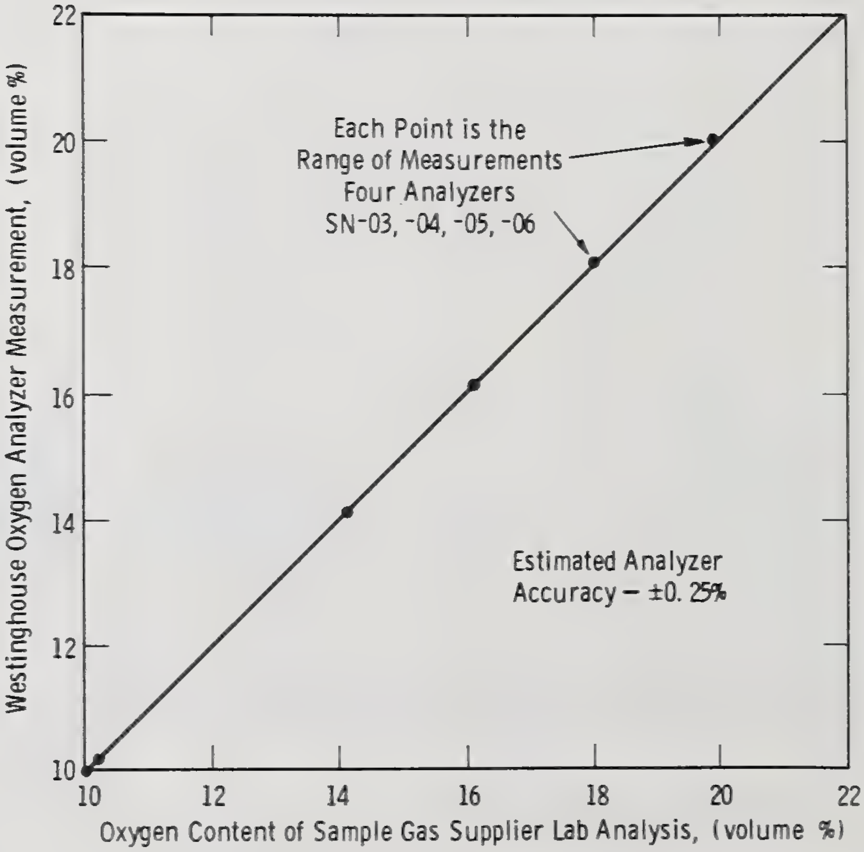

FIGURE 4. CALIBRATION EVALUATION OF WESTINGHOUSE MEDICAL OXYGEN ANALYZER.

TABLE 1

DATA FROM FOUR OXYGEN ANALYZER PROTOTYPES USED TO MEASURE KNOWN GASES AT DIFFERENT O_2 CONCENTRATIONS (SEE FIGURE 4)

Oxygen content, laboratory analysis	Oxygen analyzer measurement (range)
10.2%	10.19 to 10.24%
14.1%	14.03 to 14.10%
16.1%	16.11 to 16.13%
18.0%	18.03 to 18.06%
19.9%	19.97 to 20.01%

ACCOMPLISHMENTS

The resolution capability of the Model 209 Oxygen Analyzer was found to be about 10 μV. This is equivalent to a reference gas oxygen concentration difference, across the null cell, of about 0.002% (i.e., 5.000 to 5.002% O_2) to 0.006% (i.e., 15.000% to 15.006% O_2). At a reference gas flow rate of 0.1 cc/min, this resolution permits the detection of oxygen flow across the membrane greater than 2 to 6 x 10^{-6} cc/min. Therefore a small membrane area, about 1 cm^2, can be used for the catheter. (This is based on 1 mmHg ΔpO_2 across the membrane as an acceptable limit.)

The low flow rate of 0.1 cc/min necessitates a very low plumbing volume if a reasonable system response time is to be achieved. (A volume of only 1 cc would result in a response delay of about 10 minutes.) Problems of slow response and poor stability were found in the first designs of low-volume null sensors. These designs included a dual-bore tubular electrolyte (Figure 5) and a modification of the Westinghouse Model 209 Analyzer in which a tubular filler was added to reduce cell volume.

Preliminary designs of the catheter were of two basic types. Both contain about 1 cm^2 of membrane area. A co-axial tube arrangement is shown in Figure 6 in which the membrane is a 0.060" diameter, 1" (effective) length of silicone rubber tubing. The reference gas enters the central tube and then flows through a woven fiber sleeve that supports the membrane and returns through the annulus between the two co-axial tubes.

The second type was a parallel-tube design with a simple 0.012" x 0.025" diameter x 4" long silicone rubber tube which joins the ends of two parallel inlet and exit tubes and serves as the membrane. The parallel tube design has the advantages that the tubing is commercially available, the area can easily be changed, and it is simple to fabricate for bench testing. The larger diameter tubing is not available in thin wall sizes. Therefore, the parallel tube configuration was selected for initial prototype evaluation, although for clinical applications the co-axial tube design is expected to be less thrombogenic and therefore more desirable. A prototype of the parallel tube catheter was made and the membrane is shown in Figure 7.

Initial membrane bench tests were run with a scaled-up system (about 250 times the proposed catheter flow and about 180 times the membrane area). A membrane test fixture was constructed to hold a silicone rubber sheet and to provide the flow of a reference and sample gas along each surface of the membrane. It consists of two plates which are clamped over the membrane and two 6" diameter backup screens that allow the flow of gas along each face of the membrane. The gas stream (reference to sample) enters the screen passageway from a slot in the plate at one end of the membrane and travels along the screen to a similar exit slot at the other end of the membrane. The permeability of the sheet material was found to be about 50% greater than analytically predicted based on data in the literature. It is estimated, however, that the blood film reduces the effective permeability to about one fourth of the value for the rubber alone. A rough evaluation of response time was determined for diffusion flow through the 0.005" thick silicone rubber sheet. For both nitrogen and CO_2 the observed response time (63%) was about 10 seconds, but this value is about the same as that required to clear the volume of the test rig and therefore should only be considered as the upper limit for membrane response time.

In later tests with blood, a capillary tube type oxygenator under development by Abcor Corporation was used as the sensing membrane.

An analysis of the null balance pO_2 measuring system has shown that the diffusion of other gases through the membrane can cause a significant error in the pO_2 readout. This error is due to the change in volume fraction of oxygen caused by the addition or removal of other gases.

Figure 8 shows the calculated oxygen reading error (ΔpO_2) at unscrubbed null that is caused by the flow of either N_2 or CO_2 across the membrane. These curves are approximate and do not include secondary interactions of the different gas pressures.

In an attempt to eliminate the effects of CO_2 and water vapor transfer, these components were removed from the reference gas by scrubbers at the null cell inlet lines. It was expected that the modified system would produce no error if the reference gas had a nitrogen pressure equal to that of the blood. However, an error was observed experimentally that was attributed to partial pressure changes along the membrane.

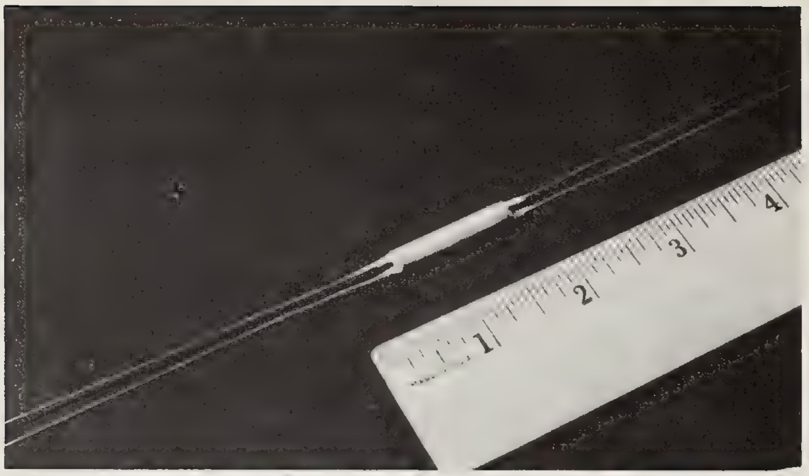

FIGURE 5. DUAL-BORE OXYGEN CELL.

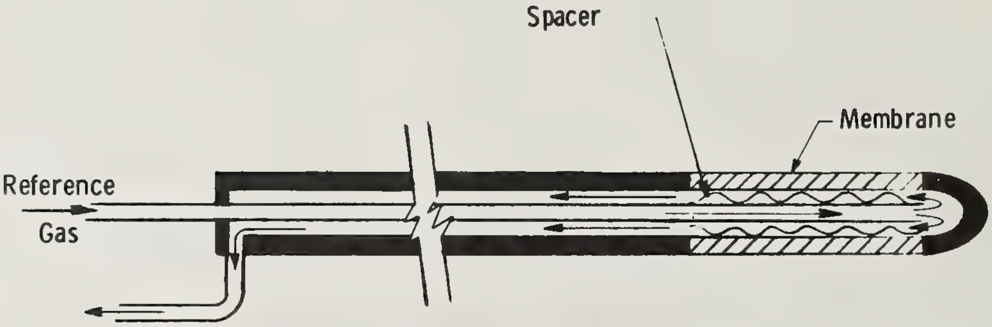

FIGURE 6. CO-AXIAL TUBE CATHETER DESIGN.

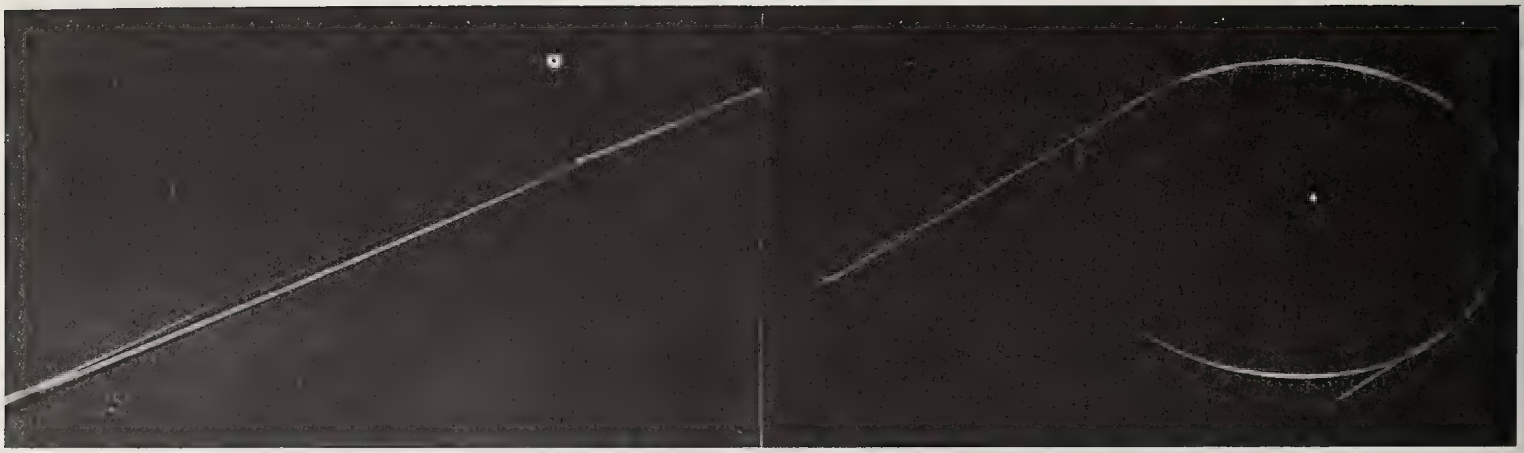

FIGURE 7. MEMBRANE/CATHETER.

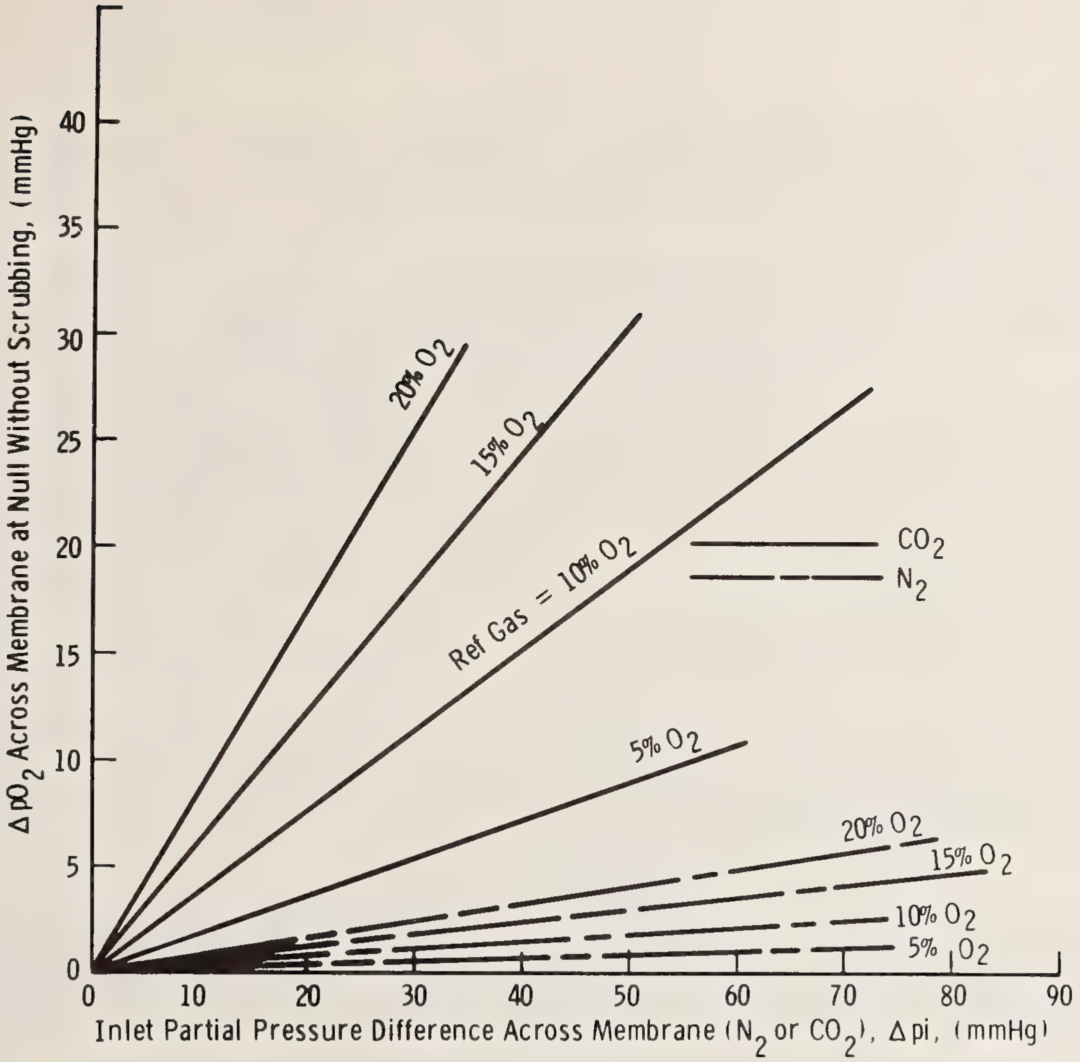

FIGURE 8. ERROR IN O_2 READOUT DUE TO N_2 AND CO_2 MEMBRANE TRANSFER.

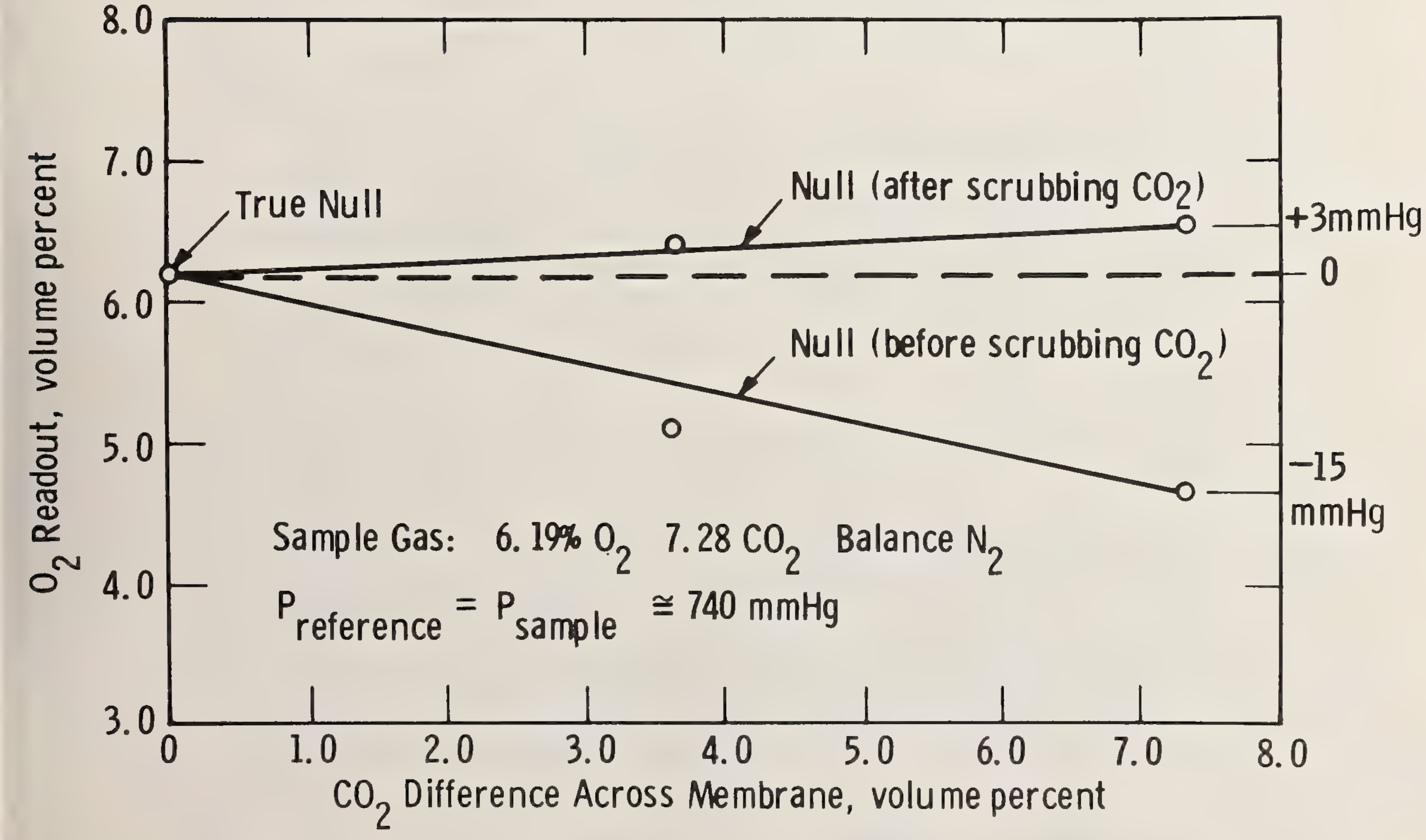

FIGURE 9. ERROR IN pO_2 READOUT DUE TO A pCO_2 DIFFERENCE ACROSS THE MEMBRANE.

Figure 9 presents the measured error in pO_2 readout caused by a pCO_2 difference between the sample and the reference gas. The deviation of the midpoints shown in Figure 4 is believed to be due to an error in the assumed CO_2 concentration in the reference gas. The CO_2 concentration at midpoint was approximated by maintaining a constant total flow rate and reducing the CO_2 flow to half of its measured value at true null.

A second null cell was added to guide the addition of CO_2 to the reference gas mixture. This second cell compared the oxygen contents before scrubbing at the membrane inlet and exit. With the first (scrubbed) null cell maintaining the zero for net oxygen flow, CO_2 was added to zero the second null cell so that membrane inlet and exit O_2 pressure were equal to each other and to the blood gas sample.

Tests were conducted to determine the error in pO_2 readout due to an established difference in total gas pressure across the membrane. The reference gas, outside of the silicone tubing of the Abcor oxygenator, was maintained at 60 mmHg above the total blood gas, which was at atmospheric pressure. When null was reached the pO_2 readout was about 6 mmHg above that of the sample gas.

A bubble-type oxygenator was used to maintain the blood pO_2, pCO_2, and pN_2 at the desired levels and to enable the indirect measurement of these partial pressures. Humidified gas was bubbled through the blood, thus equilibrating the blood gas composition. The bubble oxygenator was also used as the blood reservoir from which a small amount of blood passed through the membrane and then was pumped back to the oxygenator.

The readout display is composed of two null balance meters and an oxygen readout meter. The oxygen readout meter is capable of reading from 5% to 21% O_2. Output provisions are also available for direct recording of the null cell and oxygen readout cell voltages.

Measurements of pO_2 have been made using samples of both saline and blood, with oxygen in the range of 6% to 15% with carbon dioxide in the range of O_2 to 7%. With equal total gas pressures (reference and blood) the measurements have generally been within about 1 mmHg of the correct reading. Techniques are being studied to reduce the 6 mm error caused by total pressure inequality such as would occur in venous blood measurements.

CONCLUSIONS

The null balance technique of blood pO_2 measurement has been demonstrated to be feasible and accurate in bench tests with gases and saline, and in-vitro tests with blood. Preliminary prototype versions of the catheter, reference gas control system, and readout system have been fabricated. No significant problems are predicted, but further in-vitro and in-vivo tests are required to define and develop response time, long-term accuracy and stability, and reliability.

DISCUSSION

DR. FRIEDMAN: You just mentioned response time. What is the present response time for this system?

MR. REICHNER: We don't feel that the response time we have on the bench test setup is representative of that for the final system. We have just developed the control system and response time presently on the magnitude of change. For the changes that we normally run, from 21% oxygen to something on the order of 10% oxygen, it would be on the order of a half an hour with the control system. We can get it much faster if we manually adjust the composition or if we predict the composition for the first manual setting and then use the control system. If you are interested in fast response, we can change the system to give a fast response with a time lag due to transport. That delay in transport is going to be on the order of a minute.

DR. FRIEDMAN: Well, the question is this: If you are going to use this as a monitor, isn't it necessary to determine very quickly any change that occurs?

MR. REICHNER: We can alarm very quickly on rapid change, I mean on the order of half a minute to a minute.

DR. CAIRNS: What is the total volume of the active part of the system now, including detectors?

MR. REICHNER: We don't have the final detectors developed yet, but as I just said, if you take the volume of the catheter, transport time as now defined is on the order of half a minute and we would predict that the total system would be on the order of a minute. Does that answer your question?

CHAPTER 59

INSTRUMENTATION FOR ANALYSIS OF BLOOD LACTATE AND PYRUVATE

D. Williams and A. Doig

Monsanto Company
Everett, Massachusetts

Electrochemical monitoring of the LDH (cytochrome b_2) reaction of lactate with $K_3Fe(CN)_6$ is being investigated for the measurement of blood lactate. A thin enzyme layer is maintained between a platinum electrode and a dialysis membrane. Lactate diffusion into this layer produces pyruvate and $Fe(CN)_6^{-4}$ A potential is maintained at the platinum electrode such that $Fe(CN)_6^{-4}$ is oxidized back to $Fe(CN)_6^{-3}$. The resulting current is thus a measure of lactate. Whole blood can be used, but must be diluted with a buffer - $K_3Fe(CN)_6$ solution. Oxygen does not interfere in this method. However a background current in plasma and blood must be measured and subtracted. This can be accomplished electronically using a second similar electrode system, but without enzyme. A similar approach is being attempted with a $Fe(CN)_6^{-3}$ acceptor, pyruvate dehydrogenase, for the measurement of pyruvate in blood.

INTRODUCTION

Most analyses of organic blood components are presently performed by spectrophotometric methods. Recently many of these methods have utilized enzyme catalyzed reactions because of the specificity of such reactions. Electrochemical monitoring of these reactions may have definite advantages. For example, wide concentration ranges are measureable without dilution simply by scale switching and the test sample need not be optically clear. Most optical methods require precipitation of high molecular weight proteins, and they use a dilute filtrate for further analysis. The present methods can conceivably use undiluted whole blood.

At the beginning of the present contract no decision was made on the type of electrochemical measurement (for example, potentiometric or amperometric), or on the enzyme reactions which would be used. However, only the present, most successful approach will be described here.

ELECTRODE CONSTRUCTION AND ELECTRICAL CIRCUITS

A test system was required which would allow us to use a minimum quantity of enzyme and also set up a diffusion flux which would be repeatable. For this purpose a modified voltammetric membrane electrode[1] was developed prior to the start of the contract. A similar construction was used by Updike and Hicks[2] and the electrochemical methods for measuring $O_2$and CO_2 in blood use a basically similar electrode construction.

The electrode is composed of the following elements:

Electrochemical sensor (platinum electrode), enzyme reaction layer and diffusion and dialysis layer. (This final function can be supplied by the enzyme reaction layer held in a polymer membrane).

This electrode construction measures the enzyme substrate concentration as follows:

1. The necessary solution components are in nonvarying concentrations within the bulk of the solution. This may be assured by stirring, if necessary.
2. The reactant materials diffuse through the dialysis layer in proportion to their bulk concentrations. Certain unwanted components, such as oxygen combined with hemoglobin, are excluded. This dialysis layer also keeps the enzyme from diffusing into the bulk of the solution.
3. When reactant materials reach the enzyme reaction layer, reaction occurs and products form.
4. The electrochemical sensor measures the steady state concentration of the electrochemically active product.

A schematic diagram of the electrode is shown in Figure 1a. A 0.006 inch, 100-mesh nylon screen is used as the spacer for the enzyme layer. By decreasing the diffusion and reaction layer thickness, the response time of the device can be decreased. In other contract work (Contract PH-86-68-135) glucose oxidase has been incorporated into a polyvinylalcohol film. The response time of this system, using a stirred solution, was ~30 seconds.

Finally, the method requires a differential measurement against a similar electrode, without enzyme. We find the operational amplifier circuit of Figure 1b to be most convenient. The reference voltage of this system is set by a large auxiliary electrode, using the enzyme acceptor reduction (ferricyanide to ferrocyanide).

In the present study an operational amplifier system of the type described by DeFord[3] was used. When two electrodes were used, each signal was read versus ground to obtain the maximum information.

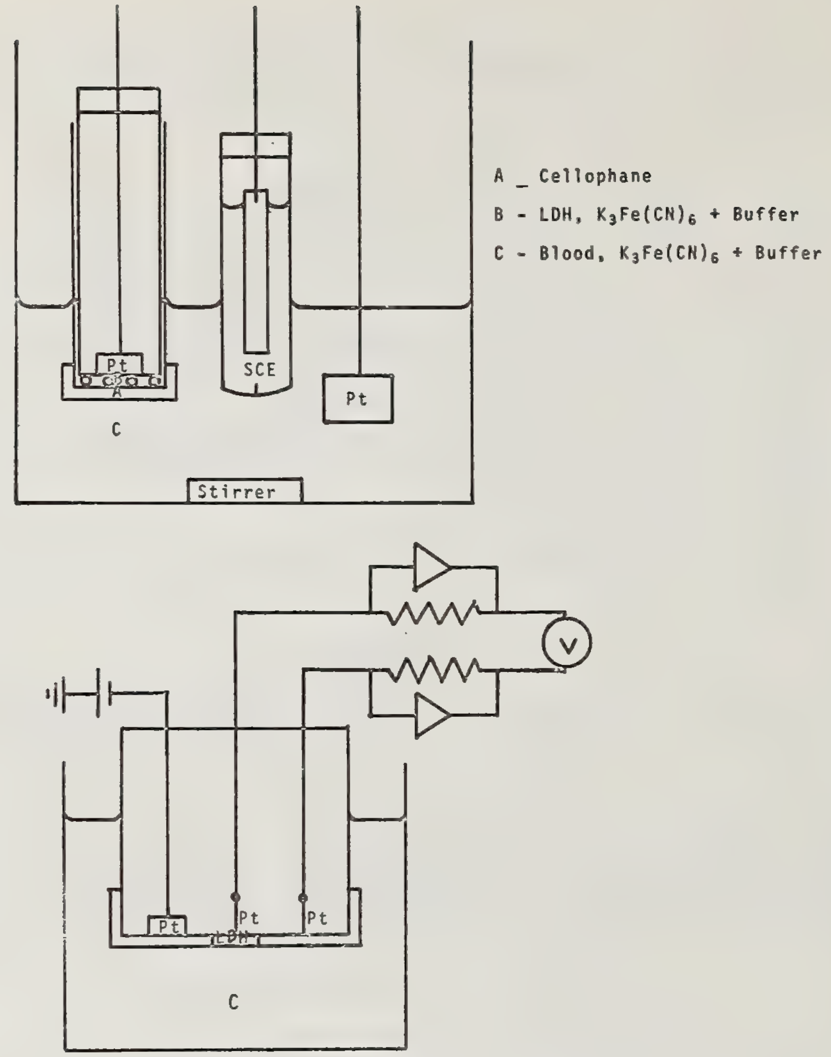

FIGURE 1. MEMBRANE ELECTRODE CELL DESIGN
A. TYPE USED. B. INSTRUMENT CONCEPT.

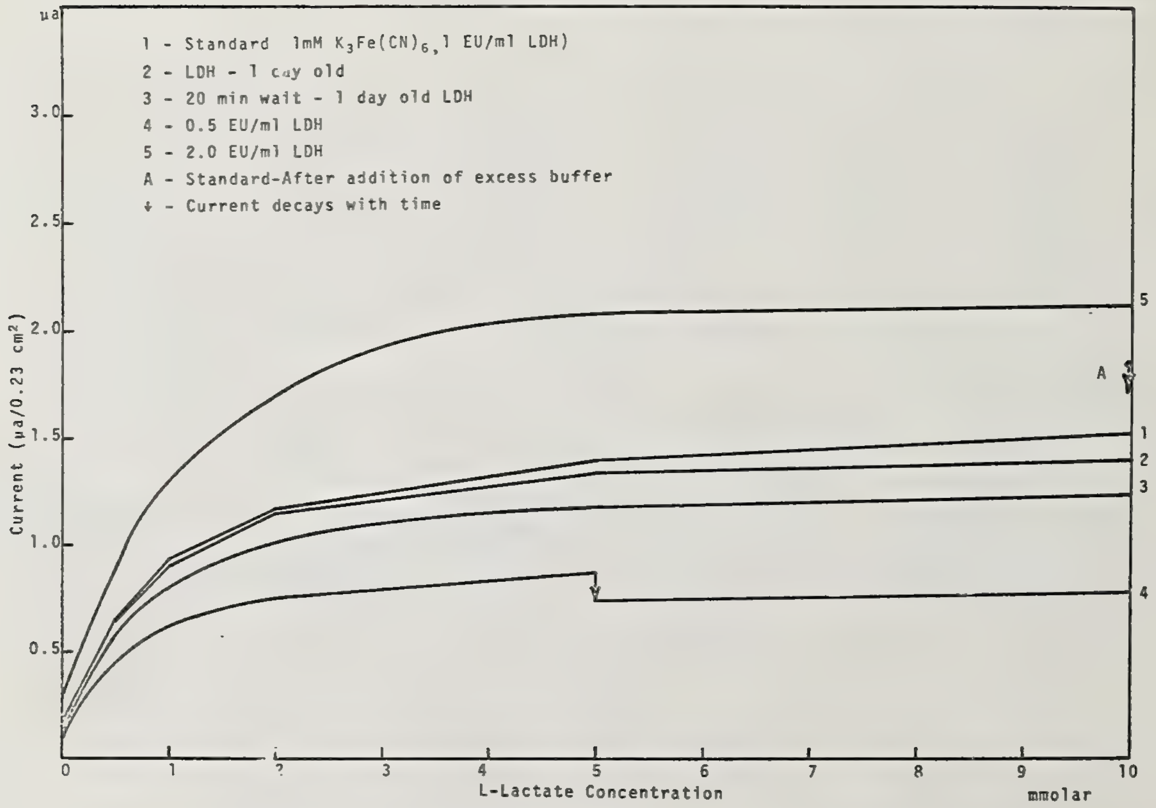

FIGURE 2. LACTATE ADDITION TO THE LDH (YEAST)- $K_3Fe(CN)_6$ SYSTEM.

LACTATE

Early work showed that the enzyme, lactate (cytochrome b_2) dehydrogenase from yeast, could be used with ferricyanide as the basis for a measurement of lactic acid. In most of the experimental work we used a modified voltammetric membrane electrode construction. Enzyme was contained in a thin layer (0.006 in.) adjacent to the electrode, and the reaction of lactate and ferricyanide in this layer was measured by the current generated by ferrocyanide electro-oxidation. The equations are:

$$\text{lactate}^{-1} + 2\,\text{Fe(CN)}_6^{-3} \xrightarrow{\text{LDH (yeast)}} \text{pyruvate}^{-1} + 2\text{H}^+ + 2\,\text{Fe(CN)}_6^{-4}$$

$$2\,\text{Fe(CN)}_6^{-4} \xrightarrow{\text{Pt}} 2\,\text{Fe(CN)}_6^{-3} + 2\,\text{e (at E = 0.4v vs SCE)}$$

Using this construction with a single layer of PUDO cellophane, an approximately steady state current was achieved within 10 minutes. This slow response time was found to be due primarily to slow diffusion through the enzyme reaction layer. It was not a function of enzyme reaction kinetics, since addition of ferrocyanide caused the same slow response as did addition of sodium lactate.

The quantity of enzyme in these tests was approximately 2 EU (EU = μ moles Fe(CN)_6^{-3} change/min). However, only 1% of this enzyme was in the electrode reaction layer. Hence only 0.02 EU would be required for the measurement at a 0.23 cm^2 area. The 2 EU quantity corresponds to 55 mg of product or 12.6 mg protein (LDH - Sigma Chemical Co., Type IV).

Tests with the lactate-LDH (yeast)-$K_3Fe(CN)_6$ system showed that deaeration of the system was not necessary. This would be expected since oxygen is not an acceptor for the enzyme, $K_4Fe(CN)_6$ is not air-oxidized under these conditions, and oxygen is not electrochemically reduced at this potential (+0.4 volts vs SCE).

Comparison of the current to that obtained with hydroquinone addition indicated that the percent conversion using this quantity of enzyme was greater than 25%.

Data showing the effect of increased lactate concentration on current are shown in Figure 2. Replotting these data as a Lineweaver-Burk plot (Figure 3) shows a linearity characteristic of an enzyme rate limitation. The best kinetic data are presumably at 0.5 EU/ml which yields values of I_m = 0.88 μa and K_m = 0.80 millimolar (lactate). Using the Faraday constant and the spectophotometric enzyme assay data, the enzyme kinetic limitation at high lactate concentration may again be shown. Thus, unless a large percent conversion is achieved, linearity will be lost at high lactate concentrations due to enzyme saturation.

Other problems which were encountered were the requirement of excess buffer as well as $K_3Fe(CN)_6$. This buffer was required in plasma and blood because the aerated dialyzed blood had a low buffer capacity and acid is generated in the reaction. This effect is primarily seen in a change of enzyme kinetics which decrease at the low pH generated at high lactate concentrations.

Data obtained using the dual electrode system are shown in Figure 4. A 10 mM $K_3Fe(CN)_6$ concentration was used to assure sufficient Fe(CN)_6^{-3} for reaction at the cathode without significant polarization. Approximately 1 millimolar L-lactate is a normal blood value.

Data obtained using plasma and whole blood with buffered $K_3Fe(CN)_6$ solution are shown in Figures 5 and 6. Both use a 20/1 dilution. The plasma data use a single measuring electrode, with and without enzyme, and 2 mM $K_3Fe(CN)_6$. The blood data use the dual electrode system and 10 mM. $K_3Fe(CN)_6$.

Presumably the high lactate level is due to the source of blood. The blood was collected from a slaughtered cow. The plasma was obtained within 4 hours after collection of the blood and glycolysis was inhibited by addition of 2 mg (NaF)/ml (blood). However, no real effort was made to obtain a representative lactate sample level.

Auxiliary techniques and developments on this contract include lactate analysis in blood by a separate method, and assay of LDH (yeast) by a pH-stat method.

The stability of LDH (yeast) has been evaluated in buffered-EDTA solution. A half-life of about 24 hours was observed for the enzyme at 20°C.

The lactate level of bovine blood as collected for the data of Figures 5 and 6, gave a value of 37 mg% lactate. The method used was based on a kit supplied by Sigma Chemical Company. The method uses the LDH (mammalian) catalyzed reaction of lactate to pyruvate. The lactate level is measured as a function of the concentration of the coenzyme, NADH, which is measured at 340 mμ. Aliquots of perchloric acid deproteinized blood were used. Standard samples showed excellent linearity of absorption with increasing lactate concentration.

PYRUVATE

The lactate measurement was emphasized at the start of the present contract because of the commercial availability of lactate dehydrogenase enzymes. The reversibility of this LDH reaction was attempted for use in the measurement of pyruvate. This was unsuccessful due to the electrochemical inactivity of NAD$^+$ and the nonreversibility of the diaphorase system.

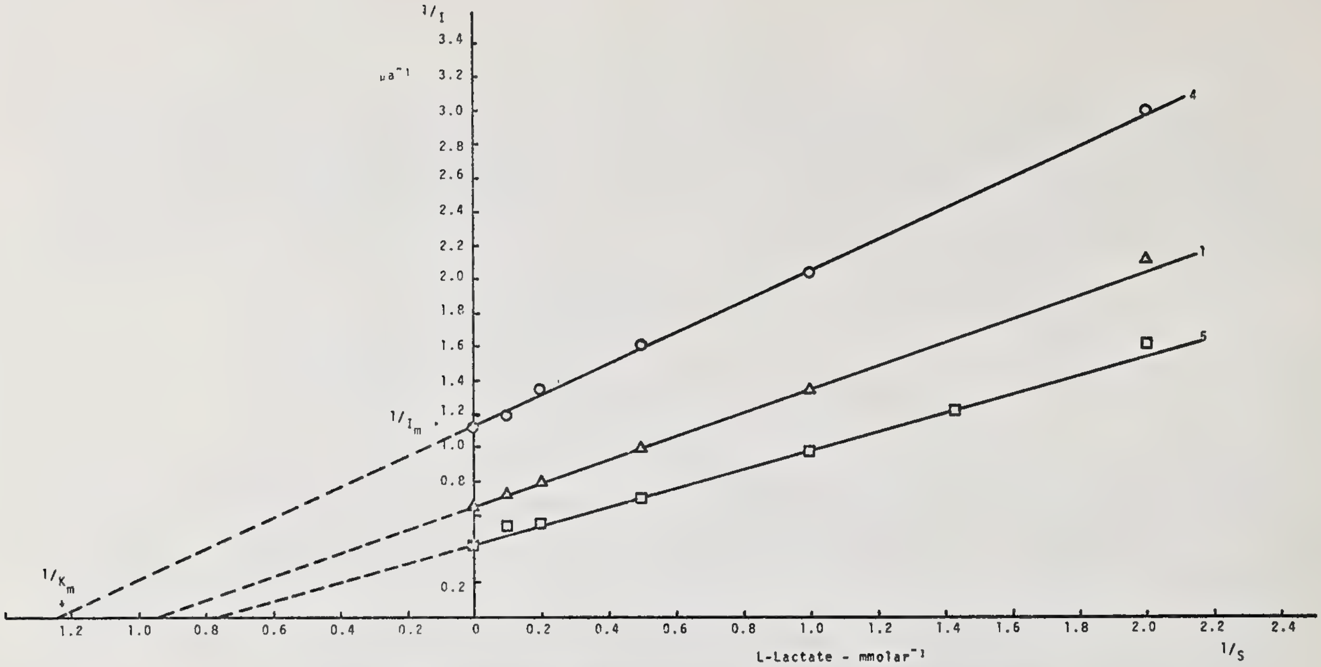

FIGURE 3. LINEWEAVER-BURK PLOT OF FIGURE 2 REACTION DATA.

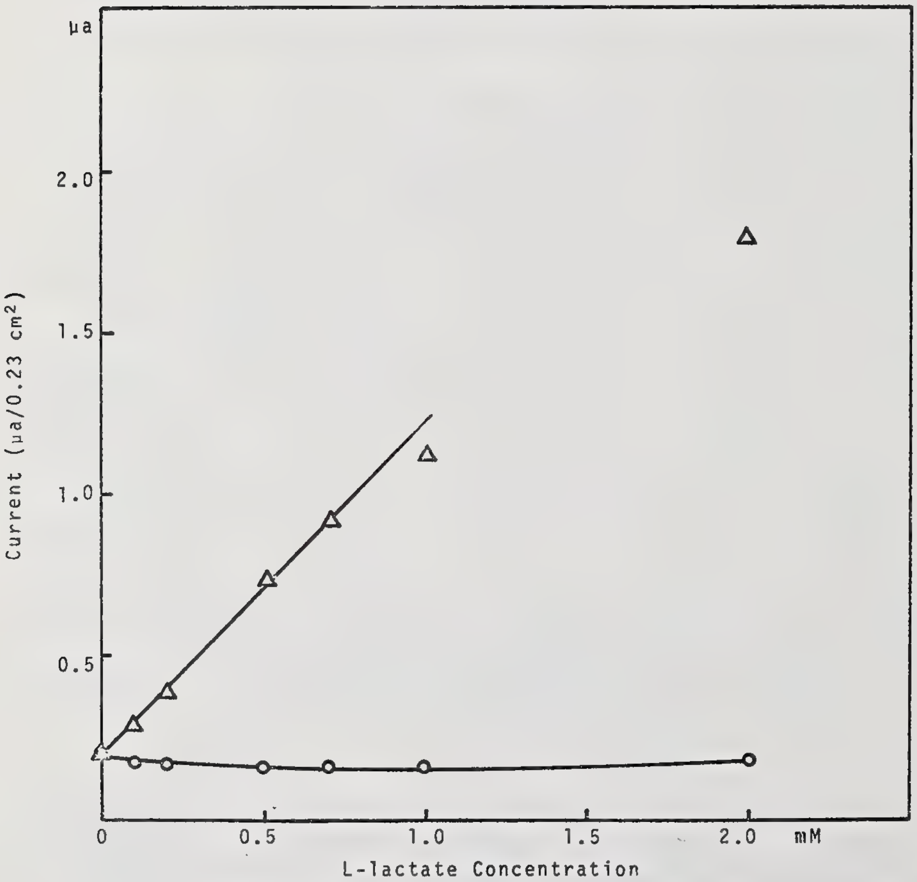

LDH layer - ~100 mg LDH
(2/5 vial) in 1 ml
Buffer, EDTA, 10 mM
$K_3Fe(CN)_6$

Test Solution - 100 ml
Buffer, 10 mM $K_3Fe(CN)_6$

FIGURE 4. DATA FROM DUAL ELECTRODE SYSTEM MEASURING LACTATE IN BUFFER.

We are presently involved in the isolation of pyruvate dehydrogenase (1.2.2.2) from E. coli B. cells. The enzyme, which was first isolated by Williams and Hager[4], oxidizes pyruvate to acetate and CO_2.

The presence of this enzyme can be measured spectrophotometrically by virtue of its ability to reduce potassium ferricyanide. Since pyruvate dehydrogenase has the capacity to transfer electrons like lactate dehydrogenase (yeast), it should be amenable to the electrochemical measurement of blood pyruvate.

REFERENCES

1. Bowers, R. C., Wilson, A. M., J. Am. Chem. Soc., 80, 2968 (1958).
2. Hicks, G. P., Updike, S. J., Analytical Chemistry, 38, 726 (1966).
3. DeFord, D. D., "Symposium on Electroanalytical Techniques, 133rd Am. Chem. Soc. Meeting," April 1958.
4. Williams, F. R., Hager, L. P., J. Biol. Chem., 236, PC 36 (1961).

DISCUSSION

DR. HARRIS: This appears to be a very promising method in your hands and concerns a problem which is a difficult and sticky one for those of us who are trying to measure lactate and pyruvate repeatedly in pathologic/physiologic experiments. How soon and how practical do you think it will be for some of the rest of us to use your method? Is it something that has to be done in your laboratory, or will it be available in a reasonable time for other laboratories?

MR. WILLIAMS: I really can't say how soon it will be available. Certainly, the electronics is something which would not be available in a clinical laboratory at present. You would have to develop it. Also, we do not have data which I would feel comfortable with in a clinical laboratory. The technique might be feasible but you would have some work to prove it as a clinical method. Therefore, I cannot tell you when it would be available to you.

DR. HARRIS: In a laboratory that does have some electronic and scientific capability to do their own development, will it be a tremendous job to set this up and to, let us say, supplement, test and carry on what you've already done?

MR. WILLIAMS: No, I don't believe it would be. Certainly, the electronic components are all readily available, and not extremely expensive. The problem is putting them together with the output assembly of an oxygen electrode. You might be able to use it by reversing leads and changing the potential.

DR. MUIR: Have you tried any membrane systems other than cellophane because I wouldn't expect equilibration of the system to be reached in the five minute diffusion period that you mentioned before proceeding with your test?

MR. WILLIAMS: The steady state diffusion is reached quite rapidly and in other experiments, in which we have used enzymes in a membrane, we have reached 90% of the final current value in about 30 seconds. Thus, it is similar to the oxygen electrode response time problem in that you do get a high current at the beginning, but you can set up a steady state. Fick's law will give you steady state approximation, and it would require about a minute.

DR. MUIR: Fick is not unfamiliar to me, but do you have any problems of deposition of plasma proteins on the membrane surface reducing the rate of lactate diffusion into your system?

MR. WILLIAMS: Excuse me, I didn't understand that question or hear it.

DR. MUIR: Do you have any problems with plasma proteins depositing on the surface affecting the rate? Can you minimize this with stirring?

MR. WILLIAMS: We have used stirring and, of course, on the platinum some of the high molecular protein does adsorb. However, you do have the problem on the membrane of possible deposition, as you do on oxygen electrodes.

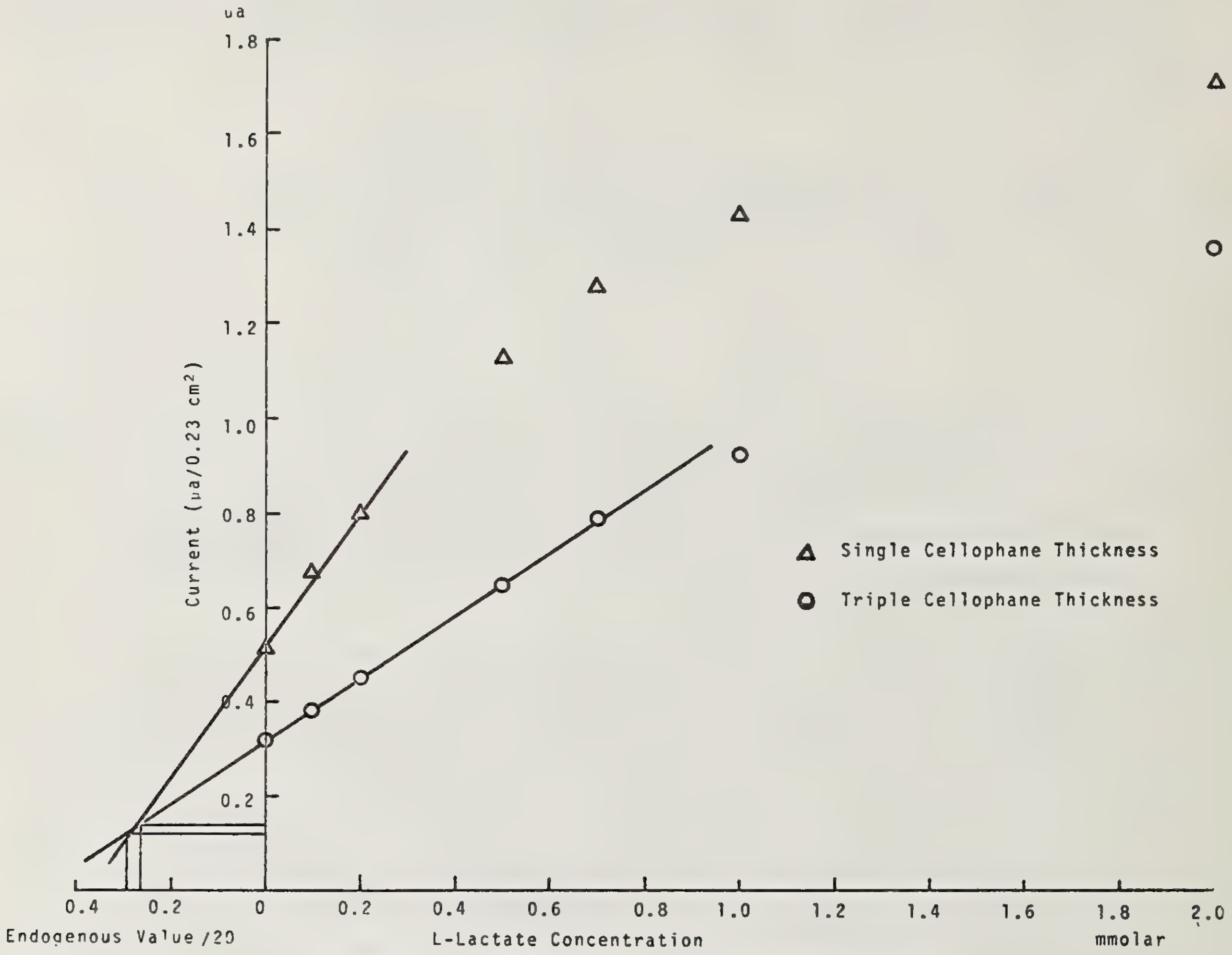

FIGURE 5. MEASUREMENT OF LACTATE IN BOVINE PLASMA.

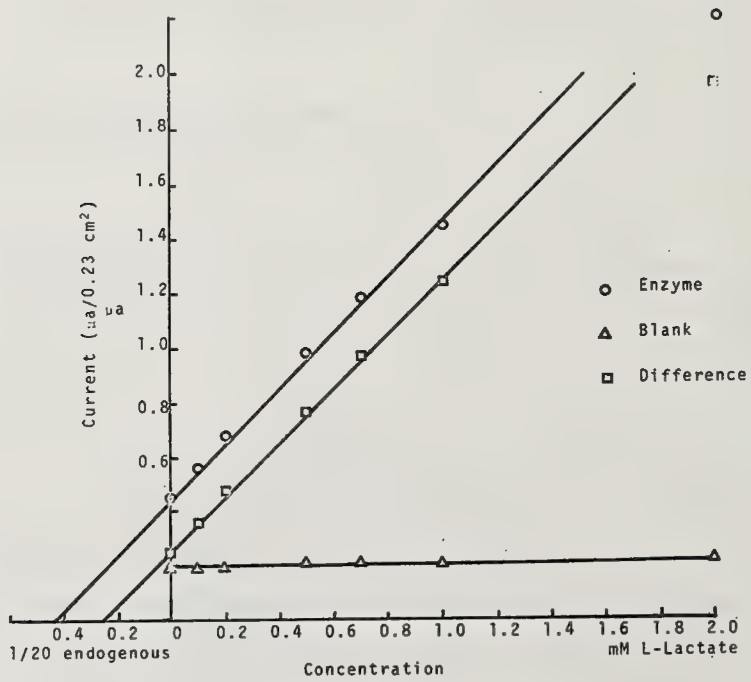

FIGURE 6. BOVINE WHOLE BLOOD LACTATE MEASUREMENT DILUTED 20/1 WITH BUFFERED 10 mM $K_3Fe(CN)_6$.

CHAPTER 60

CHRONICALLY IMPLANTABLE PRESSURE TRANSDUCERS

P. R. Perino

Statham Instruments, Inc.
Oxnard, California

This contract was for the development of chronically implantable differential pressure transducers with blood interface capability and utilizing a thoracic cavity pressure reference. The basic configuration of the transducer is a flat cylinder of 0.25" height. The pressure sensitive diaphragms are at the ends of the cylinder with the electrical cable connection between the two diaphragms. Diameters of 0.5", 0.375" and 0.25" with ranges of 40 to 350 mm Hg were investigated. Standard gage factor (2) thin film strain gages were used in preference to high gage factor semiconductor gages in order to optimize accuracy and stability. The transducer does not require a pressure reference external to the body and performs independent of ambient pressure variations. The inside of the transducer is hermetically sealed from the body fluid by welding all metal interfaces and ceramic fusing the electrical feedthrus. This design concept represents the ideal chronically implanted transducer where base line accuracy is required.

INTRODUCTION

For a strain gage pressure transducer, the simplest possible mechanical configuration is that of the diaphragm type as shown in Figure 1. Pressure is applied to the sensing diaphragm which deflects as a function of the pressure. The strain gages are attached to the back side of the diaphragm and respond to the pressure induced strain. An alternate configuration for a pressure transducer is the beam-diaphragm type shown in Figure 2. In this design concept, the strain gages are applied to the bending beam. The pressure is exerted against the force collecting diaphragm which is mechanically linked to the beam. For small size transducers, the relative characteristics of these two basic approaches are as follows:

DIAPHRAGM TYPE

1. Simplest possible mechanical construction.
2. Low range limitations due to membrane stresses developed as the diaphragm deflects to produce the stress level required by the strain gages.
3. Very difficult to provide hermetic seal by welding. The diaphragm is typically glued in place.
4. Not readily adaptable to a true differential type transducer by the addition of a second diaphragm.

BEAM-DIAPHRAGM TYPE

1. More complex to assemble.
2. Low pressure ranges obtainable because less force is required to drive the simple bending beam. The diaphragm can be designed to eliminate membrane tension.
3. Adaptable to all welded hermetic seal construction.
4. Adaptable to true differential type transducer by the addition of a second diaphragm.

All pressure transducers are basically of the differential type since the sensing element (strain gages) respond to the differential pressure across the diaphragm. The final transducer configuration may respond to absolute, gage, or differential pressure dependent on the final mechanical configuration. These principles are shown conceptionally in Figures 3, 4, and 5 respectively. In each case the pressure to be measured is assumed to be applied to the front side of the sensing diaphragm only.

The gage pressure construction represents the simplest possible type. In this design the reference (internal) side of the diaphragm is vented to the immediate vicinity of the transducer, it thus measures the difference between the pressure applied to the diaphragm and the pressure in the vicinity of the transducer body. The absolute pressure transducer is a variation of the gage pressure transducer whereby the internal reference side of the sensing diaphragm is evacuated and sealed at zero psia. This transducer is insensitive to the ambient pressure condition in the immediate vicinity of the transducer body. It measures the pressure applied to the diaphragm relative to the zero psia reference. A sealed gage pressure transducer represents a hybrid between the true gage and true absolute types. It is sealed with a one atmosphere internal reference pressure and is insensitive to variations of ambient pressure in the immediate vicinity of the transducer body. It is, however, subject to error due to the change in reference pressure as a function of temperature.

The differential pressure transducer exists in two basic configurations. As shown in Figure 5A (internal reference type), it is simply an extension of the gage pressure type construction. By incorporating a reference tube, the reference pressure can be obtained at a remote location rather

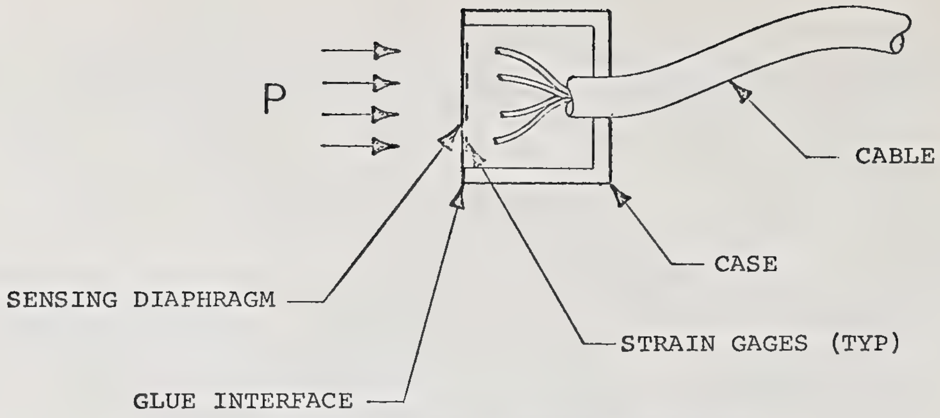

FIGURE 1. DIAPHRAGM PRESSURE TRANSDUCER.

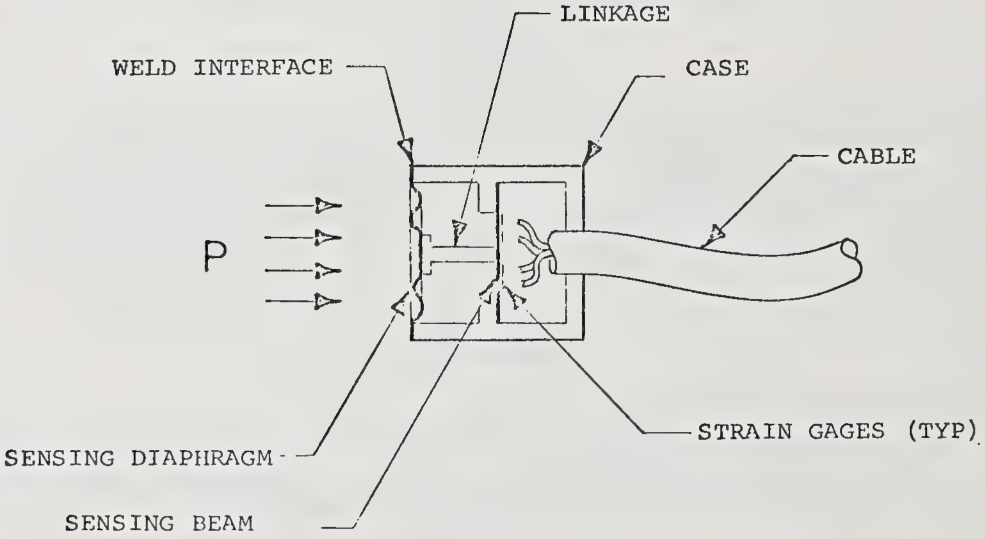

FIGURE 2. BEAM DIAPHRAGM PRESSURE TRANSDUCER.

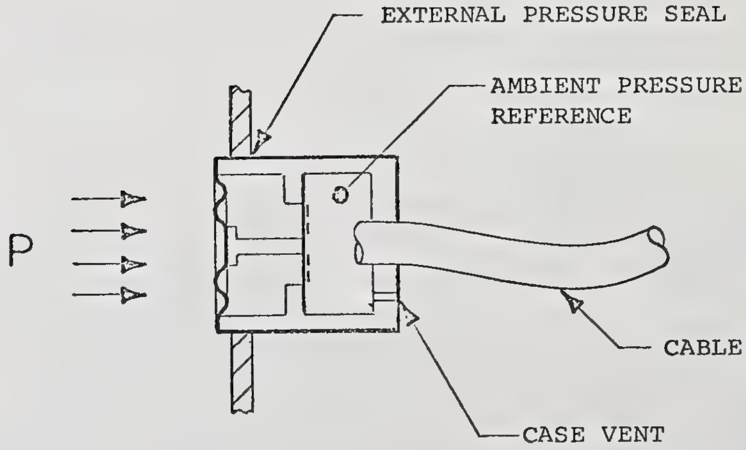

FIGURE 3. GAUGE PRESSURE TRANSDUCER.

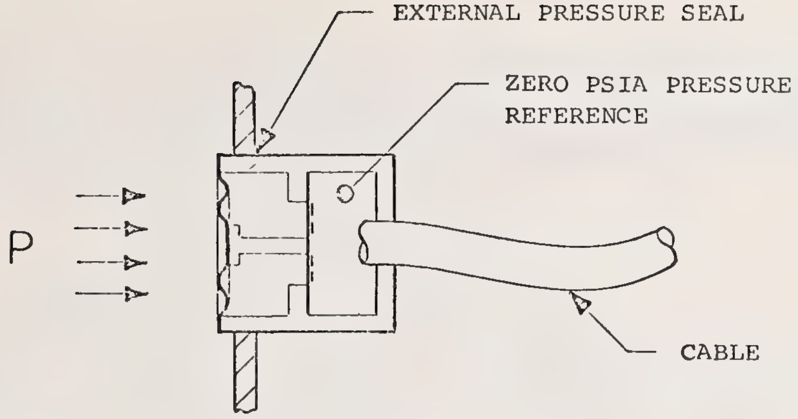

FIGURE 4. ABSOLUTE PRESSURE TRANSDUCER.

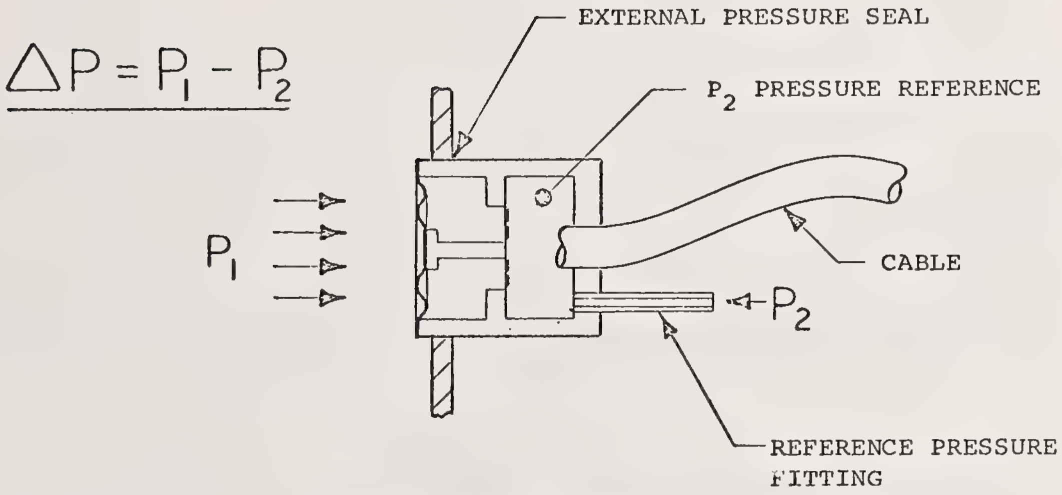

FIGURE 5. A. INTERNAL REFERENCE DIFFERENTIAL PRESSURE TRANSDUCER.

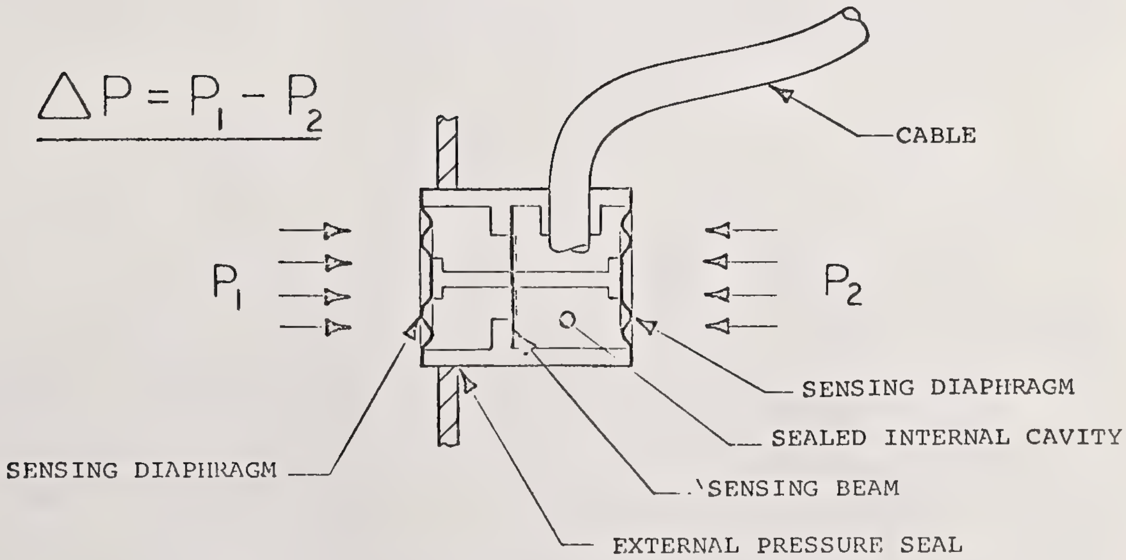

FIGURE 5. B. SEALED DIFFERENTIAL PRESSURE TRANSDUCER.

than in the immediate vicinity of the transducer body as in the gage pressure case. Otherwise these are identical construction transducers. The true differential pressure transducer construction of Figure 5B utilizes two sensing diaphragms. The inside of the transducer is completely sealed and is insensitive to the ambient pressure condition existing in the vicinity of the transducer body. A comparison of the relative characteristics of these basic types of transducers is given in Table 1 below:

TABLE 1

COMPARISON BETWEEN TRANSDUCERS

PARAMETER	GAGE	SEALED GAGE	ABSOLUTE	DIFFERENTIAL	
				INTERNAL REF.	SEALED
Response to pressure in vicinity of transducer body	Yes	No	No	Yes	No
Temperature error due to sealed reference pressure	No	Yes, Increases as range decreases	No	No	No
Lowest possible range (mm Hg)	<760 [a]	<760 [a]	760	<760 [a]	<760 [a]
Susceptible to permeation of body fluids in vicinity of transducer body	Yes	No [b]	No [b]	Yes	No [b]

[a] Lowest range is determined by mechanical design configuration.

[b] If hermetically sealed at all interfaces. When glued or potted construction is used, susceptibility to permeation exists.

TECHNICAL WORK TO DATE

A detailed study of the characteristics summarized in the Introduction Section was made. Small size strain gage pressure transducers of 0.250 to .065 inch diameter existed as commercial items. These transducers are typically assembled by adhesive interface connections which are susceptible to permeation during chronic implantation. Additionally, they are designed as gage transducers and required external venting for proper operation. If sealed at one atmosphere to eliminate the venting requirement, increased measurement error due to temperature effects are encountered. If used to measure differential pressure with an internal reference, body fluid is exposed to the strain gages and electrical circuits. Protection of these critical circuits and components by encapsulation without deteriorating the transducer performance is very difficult. At best this approach is suitable for acute implantation since permeation of the encapsulation will occur with time. Additionally, the hazard of patient damage due to electrical leakage current exists. It has been established that a leakage current as low as 10 microamperes produces fibrillation.

Therefore, it was concluded that the best design concept to meet the requirements of this contract was a true sealed differential type transducer using two diaphragms coupled to a sensing beam. This design permits low pressure ranges and can be hermetically sealed for chronic implantation. Performance is independent of ambient pressure variations and electrical current leakage due to body fluid permeation into the transducer is eliminated. However, the transducer is more complex to assemble and requires the development of appropriate techniques and tooling.

Semiconductor strain gages provide a signal output of 25 to 50 times greater than thin film metallic strain gages, thereby permitting an apparent equivalent reduction in full scale pressure range. However, when the performance of semiconductor strain gage transducer is interpreted in terms of long term stability and temperature variations, this apparent low range advantage is negated. The final criterion of importance then becomes the absolute error in mm Hg, not the rated pressure range. With these factors analyzed, the thin film strain gage was selected from an accuracy consideration.

The final transducer concept is shown in Figure 6. It is a true differential pressure transducer utilizing two diaphragms mechanically coupled to a sensing beam. Thin film strain gages of the metallic type with a gage factor of 2.0 are vacuum deposited on the sensing beam. This transducer is hermetically sealed and is designed for reference to thoracic pressure. It is, therefore, suitable for chronic implantation and is independent of ambient pressure variations.

At the start of this contract in the proposal, a range of 520 mm Hg for the 0.5 inch diameter transducer was indicated as the lowest range available using existing techniques for the double diaphragm type. This transducer utilized diaphragm and beam material with dimensions which represent the minimum currently in use. In order to produce the smaller size and lower range transducers, a prototype transducer was designed using substantially thinner material and new assembly techniques. Transducers were designed for 0.5, 0.375, and 0.25 inch diameters. A theoretical performance analysis for the three diameter transducers is given in Table 2.

TABLE 2

PERFORMANCE ANALYSES OF TRANSDUCERS

PARAMETER	UNITS	DIAPHRAGM ACTIVE DIA. 0.25	0.375	0.5
N.L. and Hys., Best Fit	% FS	.5	.25	.15
Non-repeatability	% FS	.15	.1	.1
Thermal Effects ±10^{0}F	% FS	.1	.1	.075
Stability, 1 year	% FS	.25	.25	.15
Total Error, RSS	% FS	±0.6	±0.4	±0.25
Minimum FS	mm Hg	350	125	60
Minimum Error	mm Hg	±2.1	±0.5	±0.15
Natural Frequency	Hz	2900	1800	1450

Techniques and tooling required to fabricate and assemble the differential pressure transducers have been developed. First generation prototype 0.5 inch diameter transducers produced a full scale range of 200 mm Hg. Additional 0.5 inch prototype transducers which will produce a lower range, as well as 0.375 and 0.25 inch diameter prototype transducers are in process.

In vitro and in vivo studies were conducted as part of the blood interface investigation. The basic concept for the blood interface is to separate the actual transducer sensing diaphragm from the blood system by a membrane, with the small intervening cavity filled with lymph. It was anticipated that this technique would permit the long term measurement of pressure without deterioration due to fibrin formation. Static and dynamic in vitro tests were made on silastic velour, pericardium, and urethane flocked dacron. The error associated with this interface technique was less than 1%. In vivo tests have been performed in a dog using preclotted dacron velour and silicon based dacron velour membranes. The results indicate that this technique produced suitable static and dynamic data for the eight (8) hour length of the experiment.

SUMMARY

Basically the work in the contract was directed at extending the lower range limit and reducing the size of differential pressure transducers while retaining existing accuracies. Only true hermetically sealed transducer assembly techniques coupled with high accuracy thin film strain gages were used in view of the long term implantation requirement.

Prototype transducers have been fabricated which lower the previously available range in the 0.5 inch diameter size from 520 mm Hg to 200 mm Hg; an improvement factor of 2.6. Design calculations indicate a possible improvement factor of approximately 9, providing a range of 60 mm Hg, is possible. Additionally, ranges of 125 mm for a 0.375 inch diameter and 350 for a 0.25 inch diameter are possible.

In vivo and in vitro tests have been conducted relative to the blood interface investigation. The results using a separating membrane and lymph filled cavity indicate that this concept is feasible.

DISCUSSION

DR. PATEL: Have you measured the frequency response of this transducer and, if so, what is it?

DR. PERINO: We have the theoretical value. We have not run actual sinusoidal pressure calibrations, but we do have the natural frequency at this point. The transducer alone varies from about 1,500 cycles for the half-inch diameter to 3,000 cycles for the quarter inch diameter. But, keep in mind that this is the natural frequency of the transducer in air. In any liquid system, the dynamics of the system dictate the frequency response of the measurements. The response of the transducer is sufficiently high so that you're now into the dynamics of the fluid system.

MR. REICHNER: Maybe I missed this during your presentation but could you clarify the application and also the objective as far as time of implant life for the intended application?

DR. PERINO: The contract was for a general purpose chronically implantable pressure transducer, so there was no specific application in mind other than to measure blood pressure in the body. The length of time is in the order of years, as opposed to short durations.

MR. REICHNER: You have not run any tests longer than 8 hours then, with the objective in terms of years? What I had in mind was the effect of depositions on the silicone rubber.

DR. PERINO: The work we did in terms of the blood interface was just a very small portion of the contract, and 8 hours is the maximum that we have run. The bulk of the contract was to develop the pressure transducer itself, independent of the blood interface.

MR. PURDY: One of the techniques of controlling an artificial heart is to measure the left and right atrial pressure, and these pressures are much lower than the pressures which you are measuring or which you are designing for. Could your transducer be used to measure pressures down in the ten to five millimeter range?

DR. PERINO: Well, measurement of pressures at lower range can be done with the same transducer with an increased error. At this point in time, we do not have a transducer which can have a constant accuracy as a percentage of a measurement that low. Additional development work would make this feasible, but at this point in time, it does not exist. You could, of course, measure it but your error factor becomes an increasing percentage of the measurement.

MR. PURDY: What would you estimate your error to be?

DR. PERINO: In the quarter inch design, we projected an error term of plus minus two millimeters of mercury. With the limited testing we have on prototype transducers, this is in the 6 mm of Hg class. The larger size, which is in the order of half an inch, is, of course, much better.

DR. TSIEN: My question is: How do you calibrate your system when you state that your transducer was accurate within certain limits. Do you calibrate dynamically or statically and with what standard instrument?

DR. PERINO: The transducer has been calibrated statically to a high degree of accuracy with a mercury manometer. We have done dynamic calibration at frequencies corresponding to the heart rate. These are not intended to be of the same degree of accuracy, but just to indicate ability to follow dynamic data. Static calibration via mercury manometers are very precise.

DR. TSIEN: This is all in vitro work, not in vivo?

DR. PERINO: This is in vitro, that's correct.

DR. TSIEN: No in vivo calibration was made?

DR. PERINO: The only calibration in vivo was a comparison calibration during the 8 hour test that I referred to. A catheter type transducer was installed outside of the body and comparison calibration was run, but there was no actual in vivo calibration. The intent here was to develop a transducer of sufficient accuracy and stability that would not require this type of in vivo calibration.

DR. TSIEN: Also, can you describe how you would mount this transducer inside the body? Is there a mounting problem?

DR. PERINO: The mounting problem was not looked at in this transducer during the course of this contract other than from the very generalized viewpoint that it must be mounted. Therefore, we merely put a thread on the outside body of the transducer. That was really beyond the scope of the project at this stage in time.

DR. TSIEN: In other words, you expect to have some interface material between the body and the transducer? Is that right?

DR. PERINO: That is correct.

DR. KONIGSBERG: You mentioned the stability of the thin film strain gauges. Can you tell us what the stability of the transducer was, let us say the quarter inch one, in millimeters of mercury in vitro and over how long a period?

DR. PERINO: Well, the stability of these designs has not been tested in that we are working here only with prototype transducers. The stability of thin film strain gauges in other transducers, not the ones in this contract, but other transducers that we have built by the thousands, is in the order of a tenth of a percent of full scale per year. Now, in millimeters of mercury, it's a function of what is full scale. If we're talking about a one hundred millimeter full scale, that is a tenth of a millimeter per year, but the transducers developed on this contract have not specifically been tested for long-term stability. They should have the same type of stability, however.

DR. REICH: Many of the problems you consider appear theoretical. We described a unit at the Houston meetings last fall which we developed with our colleagues at the Franklin Institute in Philadelphia, and we have been very pleased with its performance. The dimensions are somewhat smaller than yours. The sensing diaphragm is a semiconductor gauge, the smallest size 1.5 millimeters in diameter. The housing is titanium. The sensing surface of the transducer is apposed with a mica membrane fused onto a cup which seals the transducer diaphragm. The frequency response of this unit exceeds the requirements for the biologic work. We have had this implanted, facing the arterial circulation in prosthetic arterial grafts, for several weeks. The unit is temperature compensated, the temperature compensation being housed right in the pod, for plus or minus 5° C temperature ranges, and the accuracy full scale is better than 1%, with this particular instrument.

DR. PERINO: The only comment I have there is that unless it is designed as a true differential of the type I've shown up here, the double diaphragm type, it will be sensitive to atmospheric pressure variations and there is a large error associated with this.

MR. SPRUNG: What is the material of your sensing diaphragm?

DR. PERINO: The material that we worked with during this contract was type 347 stainless steel.

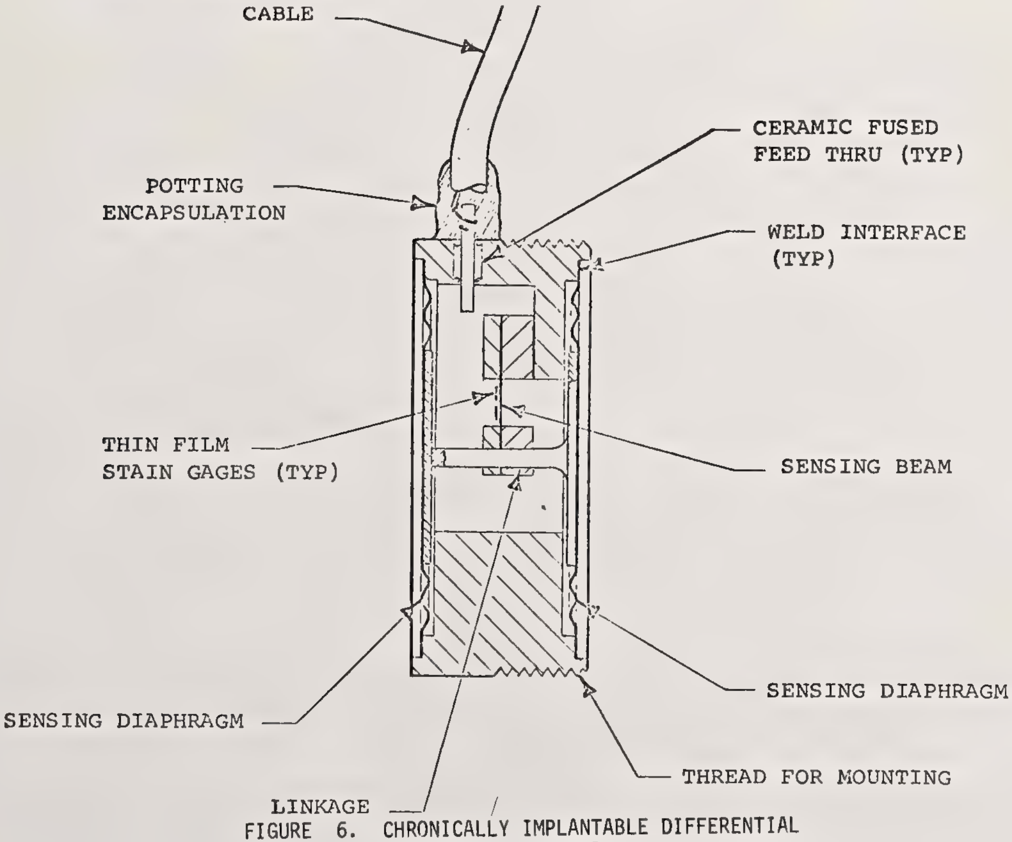

FIGURE 6. CHRONICALLY IMPLANTABLE DIFFERENTIAL PRESSURE TRANSDUCER.

CHAPTER 61

MINIATURE PRESSURE TRANSDUCERS

T. Corbin, M. Kienitz, T. Finnegan and F. Sutter
Corbin-Farnsworth, Smith Kline Instruments
Palo Alto, California

This program has been directed to the development of manufacturing ultra miniature capacitance transducers having a high frequency response, for intravascular pressure measurements. The transducers were first developed by NASA, Ames Research Labs, who built them in small quantities for test in dogs. Our program has had two principal goals: 1) to produce catheter-tip mounted transducers in sizeable quantities and with high yield, and 2) to design and test prototype implantable transducers. Under the first phase of the program, 50 catheter tip mounted transducers will be produced and delivered. The transducer sensing diaphragm is located at the end of a 40" long triaxial cable having a central airway. The cable outside diameter is only .043", allowing it to be inserted through a #17 needle. When in place, the transducer measures changes in blood pressure by measuring the tiny deflections of the diaphragm at the end of the cable. Capacity changes on the order of .02PF are measured. The central airway in the cable allows the transducer to be referenced at atmospheric pressure even when in place. Techniques for manufacturing transducers with high yield have been developed, as well as the techniques for building the .043 triaxial cable, triaxial connector with airway, and the assembling of them into working units. These catheters can be reused several times. In phase two of the program, a pair of implantable pressure sensors are being developed to be mounted in a single implantable package. One transducer is mounted in the blood stream at the measurement point; the other measures pressure of body fluids outside the cardiovascular system, such as in the interpleural space. The electronics for measuring the differential change in capacitance between the two transducers is a hybrid integrated circuit mounted in a hermetically sealed can. The implantable transducers are made of titanium, while the catheter mounted transducers are nickel steel.

CATHETER-TIP TRANSDUCER

Design Concept.

The concept employed in the design of the transducer is to use a very thin metal diaphragm separated by an air gap from a fixed plate, and to measure the pressure by the resulting change in capacitance produced by the deflection of the diaphragm. The diaphragm is extremely thin and is tightly stretched so that the device has good high frequency characteristics.

This transducer is situated at the end of a forty-eight inch long cable, which has a central airway connecting into the capacitor air gap, so that all pressure measurements are referenced to atmospheric pressure. The airway connection also allows a calibration pressure to be applied externally, while the catheter is in position.

Since the capacitance change caused by the diaphragm motion is extremely small, on the order of 10^{-13} farads for 300 mm. Hg pressure, and the transducer is at the end of a long cable, special techniques have to be used to make sure that changes in cable capacitance do not negate the readings. This is achieved by making the cable triaxial, and using the inner shield of this double shielded cable as a guard. If this inner shield can be driven by the same voltage as exists on the center conductor, then the capacitance to ground of the center conductor will be effectively zero, and the transducer capacitance will appear directly at the input terminals of the measuring amplifier. This requires special electronic techniques to achieve this result; these are described in the section on Electrical Design.

The outside diameter of the catheter cable is 0.043 inches, allowing it to be inserted into an artery through a #17 needle. The cable and transducers are made by semi-automated techniques, allowing for eventual quantity production. The catheter is connected to the electronic equipment by a special triaxial connector, which maintains the central airway, and at the same time protects the patient from any possible electrostatic shock hazard.

Mechanical Design.

There are three main aspects of the mechanical system: a) the transducer, b) the cable, c) the connector. These three areas have presented their own special problems of design and fabrication, which have been further compounded by the difficulties of mating the cell to the cable and the cable to the connector in such a way that a rugged construction was obtained.

Transducer Cell. The design of the transducer cell is illustrated in Figure 1. The hollow center stem (used for the airway) is fabricated from Kovar tubing into the shape of a nail-head. This is bonded to an outer Kovar sleeve by fusing with glass. After facing, the flat-head of the center stem forms the fixed plate of the capacitor, and the air gap is obtained by counterboring 0.0002 inches.

The diaphragm is fabricated from 46% nickel-iron foil 0.0001 inches thick. This is stretched, cleaned, and rim welded to the outer Kovar sleeve by overlapping spot welds. This operation is done in a jig to ensure that each spot is accurately positioned and of uniform size. Various other ways of achieving this rim weld were tried, but were unsuccessful.

This essentially completes the manufacture of the cell, except for a small cross cut on the center stem, used for attaching the center conductor of the cable.

The choice of materials used in the manufacture of the cell was dictated by several factors: The Kovar shell and stem were chosen for their property of producing a true hermetic seal with glass; 46% nickel-iron was chosen for the diaphragm because it is easily welded to Kovar, has a satisfactory modulus of elasticity and is available in foil without pin holes. The whole assembly forms a cell which has a temperature expansion characteristic such that the air gap which controls the capacitance remains sensibly constant.

Cable Design. Since it is imperative that the capacitance between the center conductor and the inner shield be tightly controlled, the initial cables were made by starting with a very small diameter coaxial cable as a base. Coaxial cable having an external diameter of 0.0008 inches was commercially available from Uniform Tubes. This was inserted in a Kynar sleeve with sufficient gap to form the airway, and the outside double wrapped with aluminum foil 0.0005 inches thick by 0.125 inches wide. This was held in place with a final covering of Kynar shrink tubing. After several of these cables had been made, it was discovered that the center conductor, which is 0.002 inches in diameter, was extremely brittle. Consequently, when the connection was made to the center stem of the transducer, the center wire would break, usually after final assembly was complete. This discovery required a re-design of the cable construction.

The present technique is to start with a 0.003 inch diameter copper magnet wire. This is inserted into Teflon tubing, and the outside is double wrapped with aluminum foil, using a specially designed wrapping fixture. Kynar tubing is then shrunk on and the outside double wrapped again with aluminum foil. A final covering of Kynar shrunk on completes the cable. This technique produces controlled cable fairly easily in quantity. Connections are made at each end to the shields by wrapping in a length of nickel-iron diaphragm foil for the last 2.0 inches of the cable.

Connector Design. The connector is ultra small like the cable. It is fabricated from brass shells, gold plated and sealed with epoxy. The design is such that the outer or ground shell makes contact first, so that the patient is protected from electrostatic shock.

The shells are all recessed so that it is impossible to accidentally touch any of them.

The cable end of the connector is provided with a strain relief, so that any cable tension does not rupture the center conductor.

Electrical Design.

The static capacitance of the transducer is on the order of 0.2 pf, with a full scale change of 0.1 pf. This small capacitance is several orders of magnitude smaller than the cable capacitances. For this to be measured accurately, the inner shield of the cable is used as a guard and is driven at the same potential as the inner conductor. This will effectively isolate the inner conductor from ground, so that the cable capacitance, and any variation in it, are cancelled. The first approach tried to achieve this result was to use a capacitance bridge.

Capacitance Bridge Approach. A block diagram of this approach is presented in Figure 2. The measuring circuit is a capacitance bridge, which measures the differential change in capacitance when pressure is applied to the diaphragm. In order to drive the inner or guard shield at the same potential as the center conductor, an amplifier with a gain of exactly one is required. It is to be noted that the circuit included by the amplifier is essentially a positive feedback system, wherein the input and output of the amplifier are connected by the capacitance between the inner conductor and inner shield. This is approximately 200 pf. It becomes obvious that as the gain of this amplifier approaches one, the circuit will tend to oscillate. We were unable to obtain a gain greater than 0.99 without instability occurring. This effectively cancels the 200 pf down to 2 pf. Thus, the other capacitances in the measuring bridge are also 2 pf, but this is still an order of magnitude higher than the capacitance of the transducer.

The accuracy and stability of the circuit depend on the gain of the amplifier remaining constant at 0.99, and the stray capacitances in the amplifier being carefully controlled.

With these limitations, this circuit has been successfully used with catheter transducers made on an experimental basis by the Ames Research Facility of NASA. Measurements of the temperature stability of the transducer were made in the lab and blood pressure measurements were taken using a dog. However, the device requires careful handling because of the inability to cancel the shield capacitance to less than 2 pf. It is felt that this circuit is not feasible as a manufacturing process; hence an alternate method is presently under consideration.

Transformer Bridge Approach. This alternate system is shown in Figure 3. The system uses a specially constructed transformer with a bifilar wound primary. The secondary winding is closely coupled to the primary and there is a double electrostatic shield between the primary and secondary

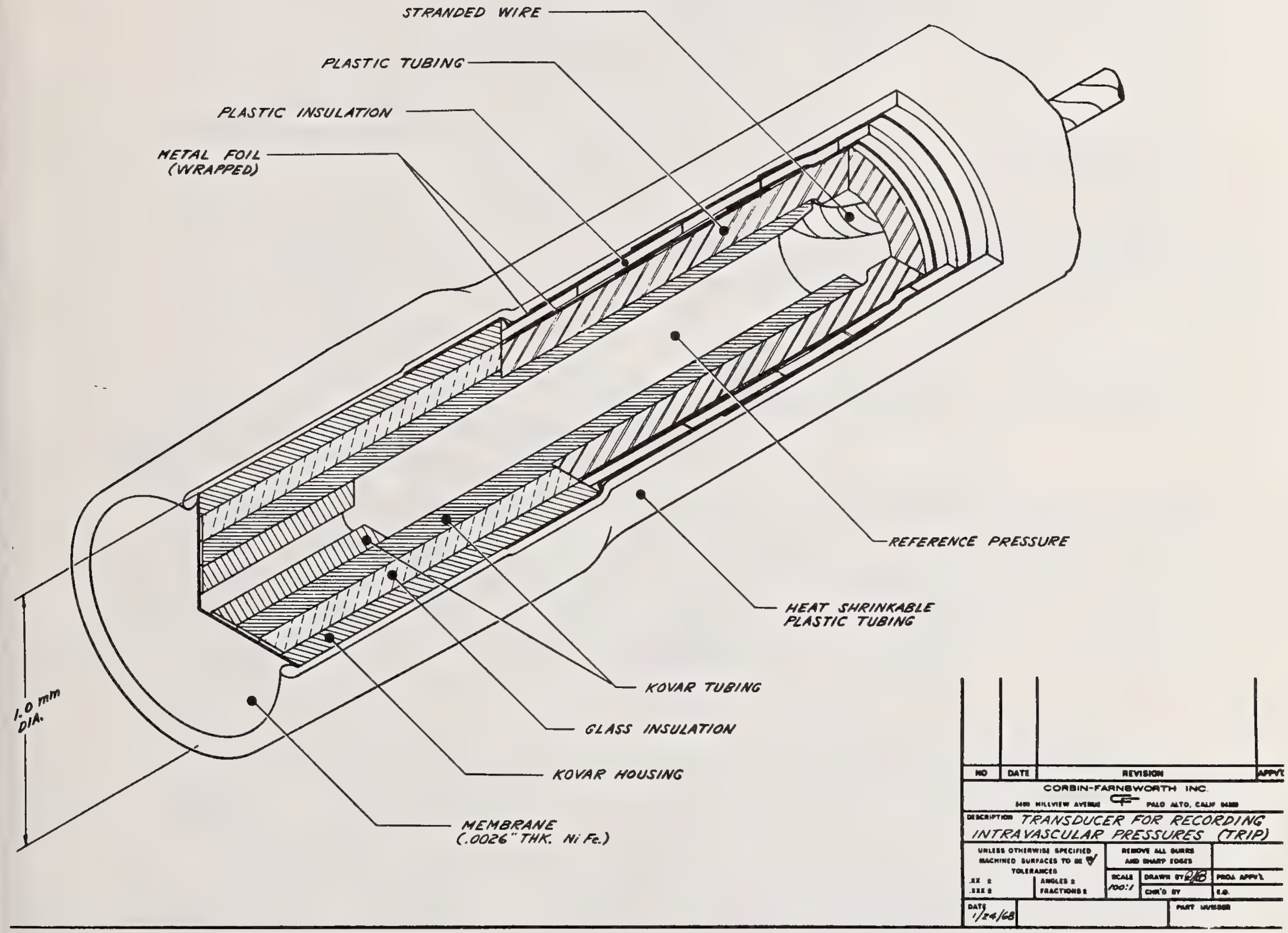
STRANDED WIRE
PLASTIC TUBING
PLASTIC INSULATION
METAL FOIL (WRAPPED)
REFERENCE PRESSURE
HEAT SHRINKABLE PLASTIC TUBING
KOVAR TUBING
GLASS INSULATION
KOVAR HOUSING
MEMBRANE (.0026" THK. Ni Fe.)
1.0 mm DIA.
NO
DATE
REVISION
APPV'D
CORBIN-FARNSWORTH INC.
HILLVIEW AVENUE
PALO ALTO, CALIF
DESCRIPTION TRANSDUCER FOR RECORDING INTRAVASCULAR PRESSURES (TRIP)
UNLESS OTHERWISE SPECIFIED MACHINED SURFACES TO BE
TOLERANCES
.XX ±
.XXX ±
ANGLES ±
FRACTIONS ±
REMOVE ALL BURRS AND SHARP EDGES
SCALE 100:1
DRAWN BY
CHK'D BY
PROJ APPV'L
E.O.
DATE 1/24/68
PART NUMBER

FIGURE 1a

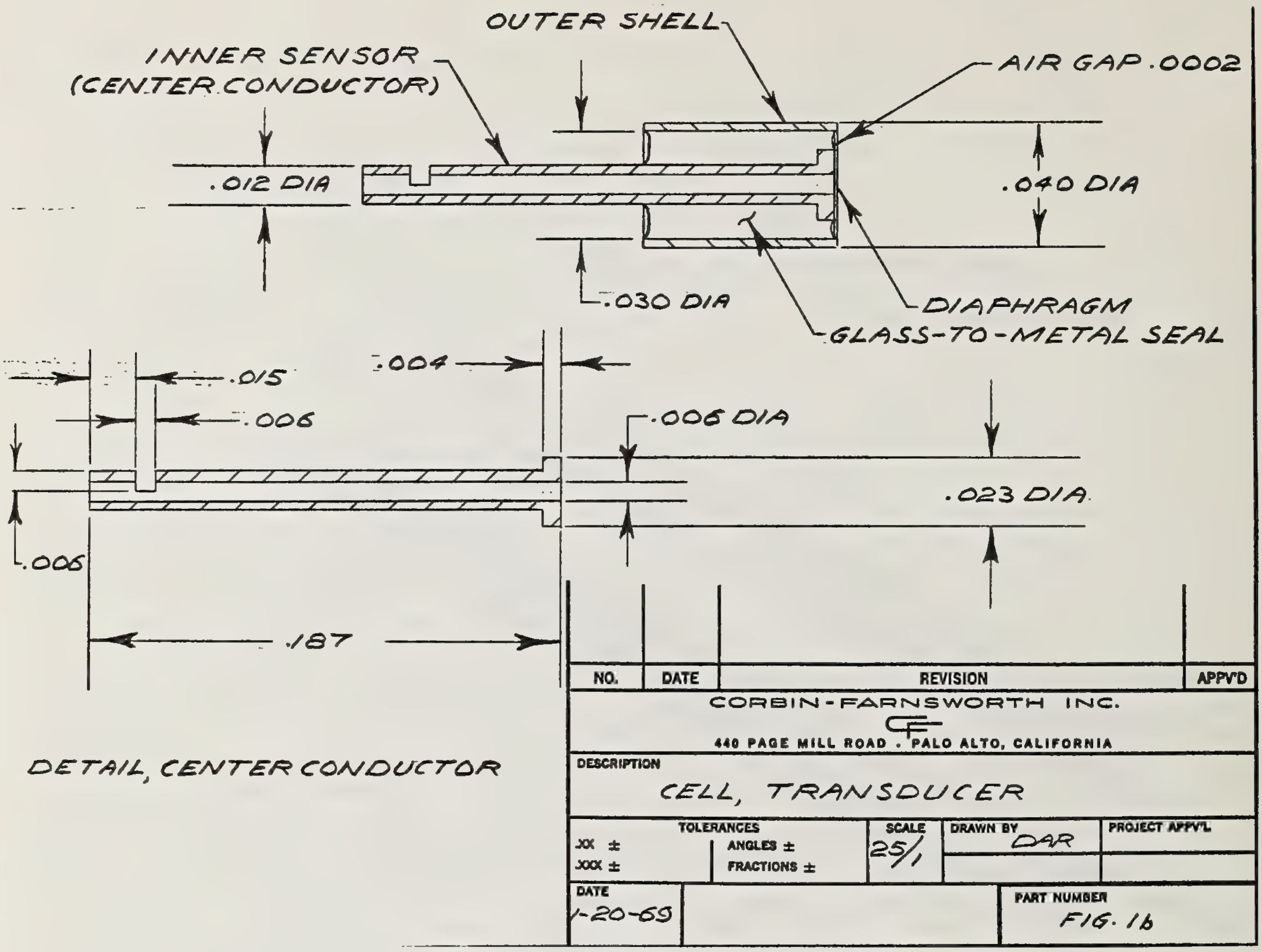

FIGURE 1b

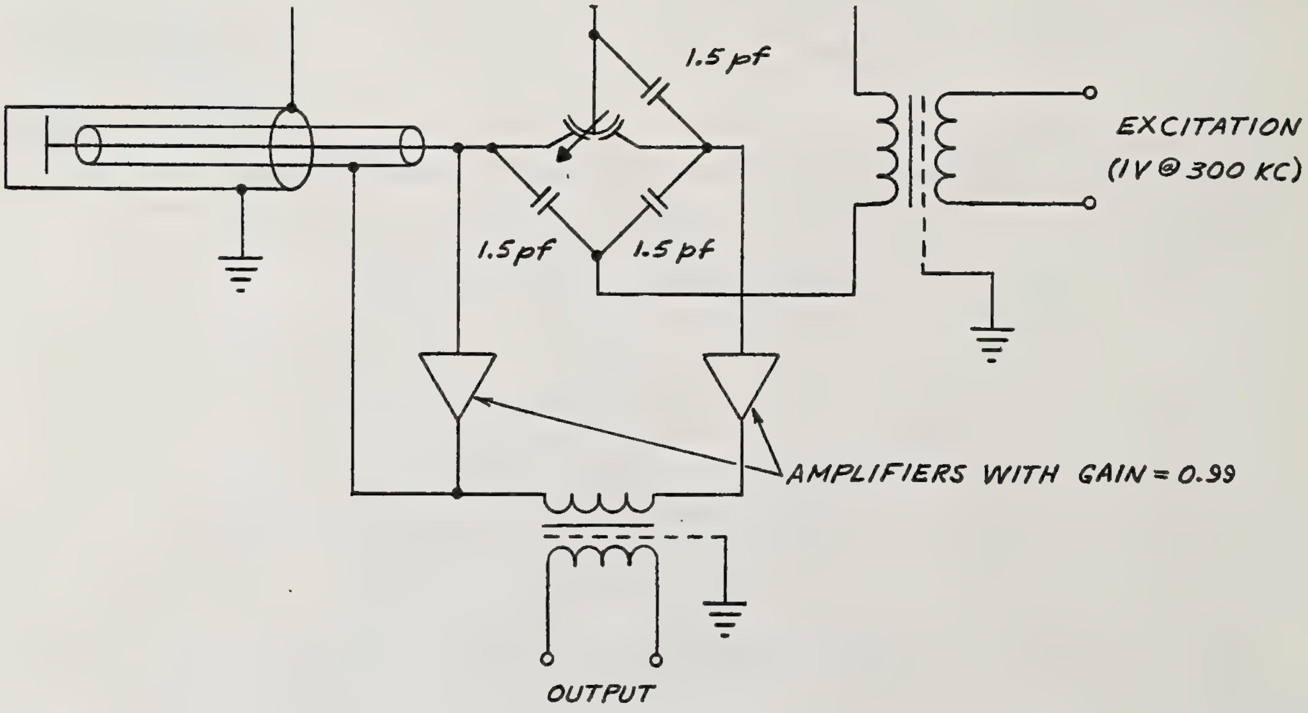

FIGURE 2. CAPACITANCE BRIDGE.

windings. The transducer capacitance is in series with one leg of the primary winding; the other leg having a corresponding fixed capacitance. The primary connections are arranged so that with zero pressure on the diaphragm, the currents in each leg are equal and opposite, so that zero flux is produced in the core. There will be no output in the secondary winding. When the diaphragm capacitance changes, a small differential flux is produced in the core which will produce a corresponding output at the secondary.

The inner shield of the cable is driven by the same voltage that is used to excite the transformer bridge. If the voltage across the primary winding approaches zero, then the potential difference between the inner shield and center conductor will also approach zero. This condition can be made to exist if the secondary winding of the transformer is coupled into a current amplifier. The transformer thereby becomes a current transformer and a step down turns ratio will provide a current gain.

One of the two electrostatic shields is also driven directly from the oscillator; the other shield being connected to ground. This shielding arrangement insures that the measuring circuit can be electrostatically isolated from ground, so that any stray capacitance will not effect the measurement. Practically, the transformer is wound using a Ferroxcube core. The primary is a conventional bifilar winding of 60 turns. The primary inductance was chosen to resonate with the shield capacitance. The first shield is a piece of the copper foil insulated with Mylar tape. The secondary winding is made from a piece of coax having a diameter of 0.013 inches, made by Uniform Tubes. This winding has 6 turns. The coax construction enables the secondary to be perfectly isolated from the primary system, so that unwanted output generated by common mode coupling is minimized.

This circuit has been successfully built and tried, although further work needs to be done to determine the optimum parameters.

An added complication is the fact that the cable has resistance losses associated with it. In order to obtain a good null at zero pressure, a second catheter cable is required on the opposite primary winding, so that the primary system is identical in each leg.

Initial work with this circuit shows that pressure differences on the order of 1 mm of Hg are detectable.

Auxiliary Circuits. The discussion so far has described the measuring circuits only. The final instrument will also include detection circuits designed to select either the systolic or diastolic pressure and to display the reading on a digital readout.

The peak tracking circuits use a sample-and-hold system with a sample interval of 2½ seconds. The system operates in a push-pull manner, so that a new pressure will be sampled during the hold interval. This allows an immediate update of the information at the end of the hold interval.

The digital display converts using a linear ramp and comparator system. Integrated circuit counters count the number of clock pulses generated during the interval between the ramp starting and comparison occurring. Both positive and negative values are displayed.

System Performance.

The temperature stability and linearity of a catheter transducer have measured using experimental devices produced by NASA. These results show that the temperature coefficient of the catheter is 0.1%/F° measured over a temperature range from 70 to 120 F, and a pressure range of 100 to 300 mm of Hg. The linearity is 1%. This is achieved by using linearizing circuits in the electronics to offset the natural non-linear relationship between the diaphragm pressure and the capacitance.

Both the temperature coefficient and linearity of the catheter-tip transducer were measured by applying reverse pressure to the diaphragm via the airway, which is normally vented to the atmosphere. This feature allows the catheter to be calibrated while in position if necessary, using a small displacement pump and a pressure gauge. The design of the displacement pump is such that no more than 2 cc. of air is injected if the diaphragm were to rupture during calibration.

IMPLANTABLE TRANSDUCER

Design Concept.

The implantable transducer will use the same principles as the catheter-tip transducer except that the diameter of the cell will be increased to 0.189 inches. Changes in the atmospheric pressure, or body reference pressure, will be sensed by a similar transducer suitably positioned. This will be covered with a ceramic filter which will allow slow changes of pressure to be sensed, but will prevent tissue growth from fouling the diaphragm. The differential capacitance between the two transducers will then be used to indicate the pressure.

Since the implantable transducer diameter is considerably larger than the catheter transducer, the capacitance of the diaphragm is correspondingly larger. This, plus the fact that there is no cable with which to contend, allows the capacitance to be measured directly. The electronics to measure the capacitance are fairly simple, and can be housed on a hybrid integrated circuit chip 5/8 inch square. The total transducer volume will be about 1 cubic centimeter. A drawing of the proposed device is shown in Figures 4 and 5.

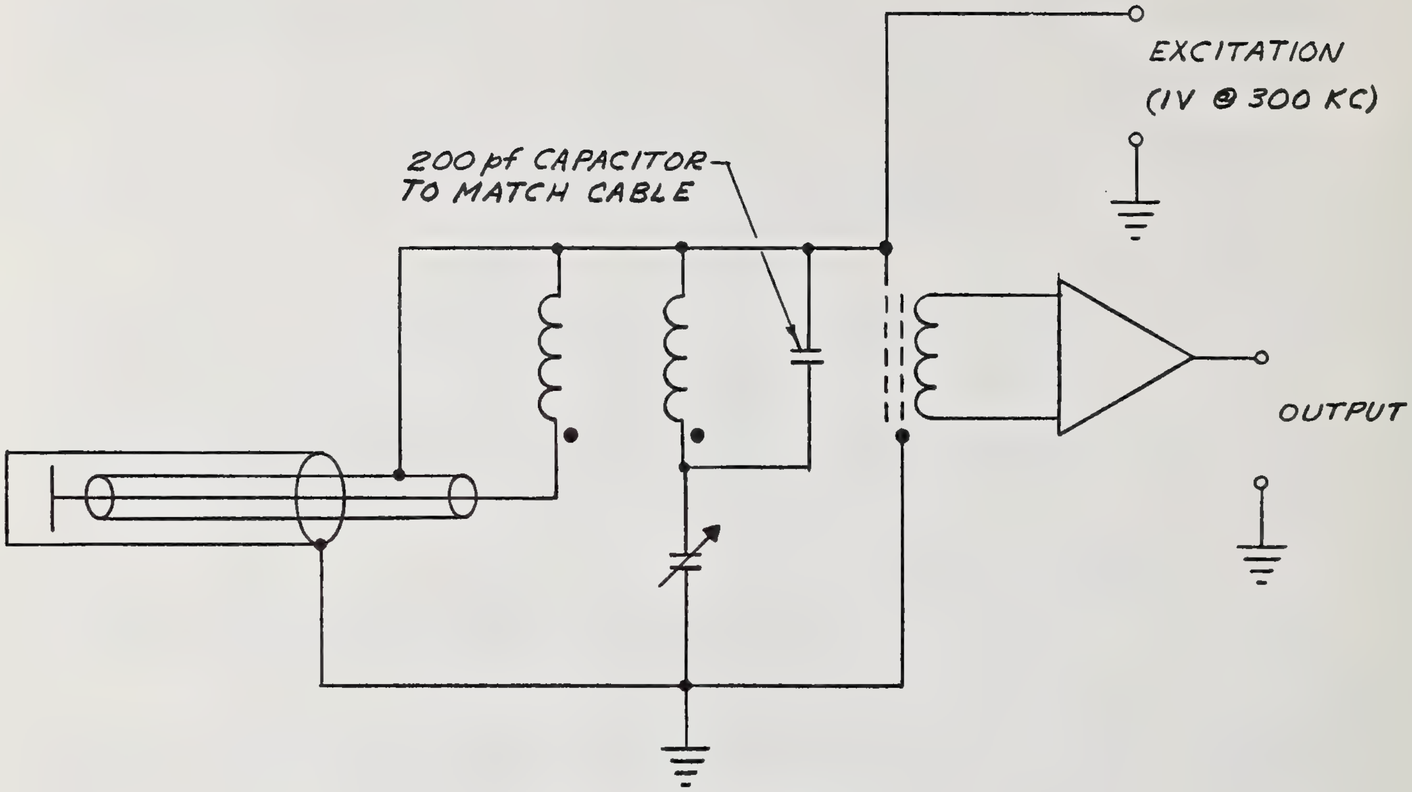

FIGURE 3. TRANSFORMER BRIDGE.

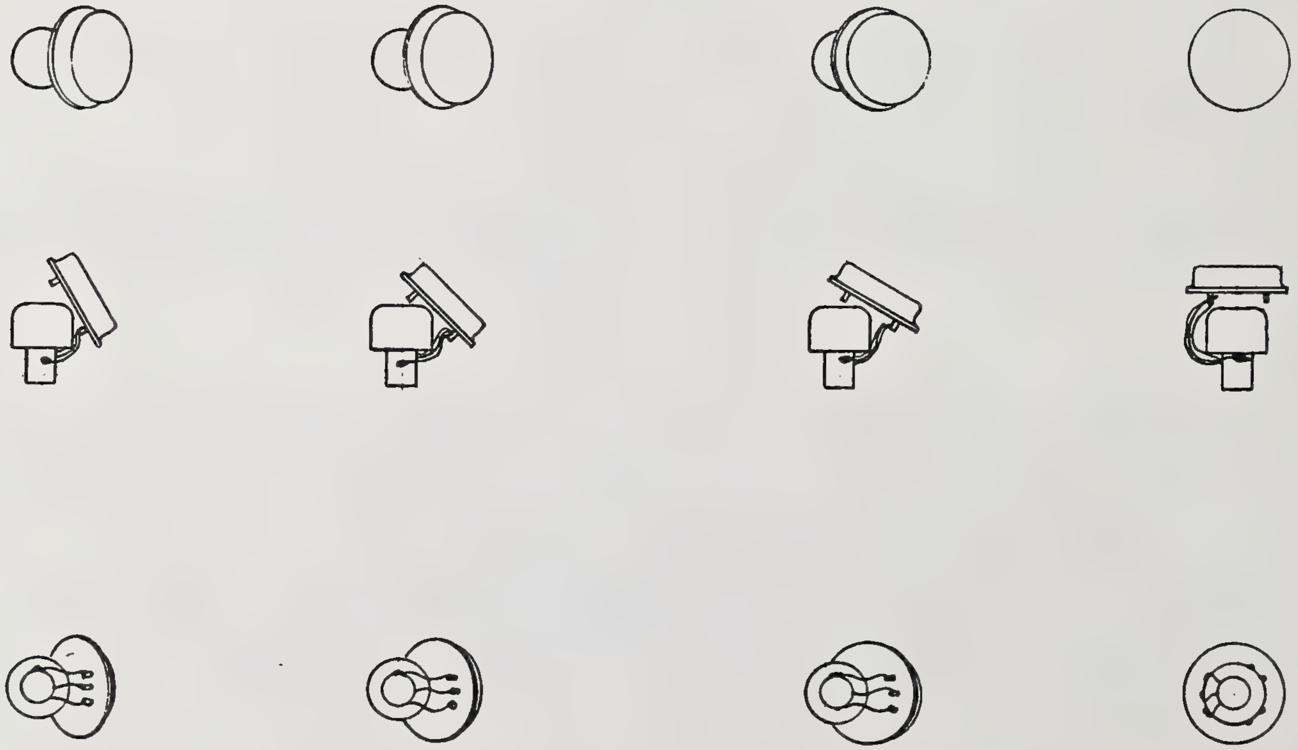

FIGURE 4. CELL & ELECTRONICS - IMPLANTABLE TRANSDUCER.

Mechanical Design.

At the present time it is proposed to fabricate the transducer from titanium, since this material appears to offer the best compromise between tissue compatibility on the one hand and structural requirements and availability on the other; although stainless steel type 316 L, Vitallium (cobalt-chromium) and other exotic alloys are also under investigation.

The material chosen has to be available commercially as a foil, with areas free of pin holes, and be weldable. It also has to be capable of forming a seal with glass.

The proposed cell assembly technique is shown in Figure 5. The center stem is Kovar tubing 0.012 OD x 0.003 wall, with a Kovar disc 0.125 inch diameter welded onto the end. This is sealed with glass to a titanium shell, one end of which is flared and faced. The transducer end is faced and counter-bored 0.002 inches, and the 0.0005 inch titanium foil diaphragm is spot-welded onto the shell. This process is repeated for the atmospheric pressure sensor. Connections are made to the center stems and the two transducers welded together. The ceramic filter is sealed in place with epoxy as are the connecting leads where they are brought through the transducer wall.

The electronics package is a separate assembly and is a welded titanium can housing a hybrid integrated circuit. After connections are made, it is fixed to the transducer with silastic rubber.

Electrical Design.

The capacitance change due to full scale deflection is on the order of 10 pf. This is measured in a simple capacitance bridge using a square wave excitation source at 1 M Hz. The power requirements are 5 V at 10 MA. The circuit is directly suitable for fabrication as a hybrid integrated circuit, and can be built on a chip 5/8 inch square.

DISCUSSION

DR. PERINO: The diaphragm material you mentioned was in the nickel iron class?

DR. CORBIN: That's right.

DR. PERINO: What is the history or knowledge on compatibility with blood?

DR. CORBIN: Well, the compatibility studies that were run by NASA, as I understand it, turned out quite well. This is why they chose the material. In addition, the catheters that they have been using now for a year and a half have been accepted quite well.

DR. PERINO: And what was the diameter of the catheter. I couldn't tell?

DR. CORBIN: It was one millimeter.

DR. REICH: Do you expect any problem with scarring on the pleural surface of the differential transducer?

DR. CORBIN: I don't think we're that far along yet. We are pretty much at the paper stage.

DR. TOPHAM: You stated some pretty strong characteristics for your transducer at the beginning of your talk. I wondered what experimental work or what justification you have for these characteristics of high linearity and low drift. There was nothing in the paper to justify this and I was wondering what you had done.

DR. CORBIN: Well, the linearity is primarily in the electronics. The characteristic motion of the diaphragm with pressure is not necessarily linear.

DR. TOPHAM. Have you used this device *in vivo* or where we could see some data that was collected from this transducer?

DR. CORBIN: A lot of this work was done by NASA. We have repeated it.

DR. TOPHAM: Is there a place that we could see the reference?

DR. CORBIN: Yes, at the Ames Laboratory.

DR. TOPHAM: Any publications?

DR. CORBIN: There have only been about 2 or 3 publications that I am familiar with, mostly by Dr. Sandler of Ames.

DR. HARRIS: In you abstract, a statement is made that these catheters can be re-used several times. I would like to have a definition of several, please, and also some idea of what they might cost?

DR. CORBIN: Our design goal is to exceed 100 times. The units that have been in use in Stanford I know have exceeded that at this point. The price is still unknown in our minds, but we expect it to be fairly reasonable, less than $500.00.

DR. ROTH: Nickel-iron alloys are very magnetostrictive generally and also ferromagnetic to a high degree. Are you concerned or rather, I should say I'm concerned with the presence of magnetic fields and their effect on transducer output. With all the electronic devices that we attach to subjects these days, nearby power lines and so on will induce deflections of the diaphragm.

DR. CORBIN: Well, I think you have a good point, and we are not totally satisfied with nickel iron as the only solution to the diaphragm problem. It is one that has been used by NASA, and we are trying to duplicate their work. We are also working with titanium and with stainless steel.

DR. REICHNER: There has been some concern lately over the introduction of electrical potentials within the body and the potential safety hazards. Could you comment on how your design is influenced by that?

DR. CORBIN: I am glad you brought that point up. The schematics that I showed were incorrect in that respect. The outer shell is shown connected to ground which is something that we would not do. Concerning the catheter and the associated electronics, if you notice the design of the connector itself, it is such that nobody can touch the live members at the end of the catheter accidentally. The current will be limited to two micro amps with two failures, available at the end of the membrane.

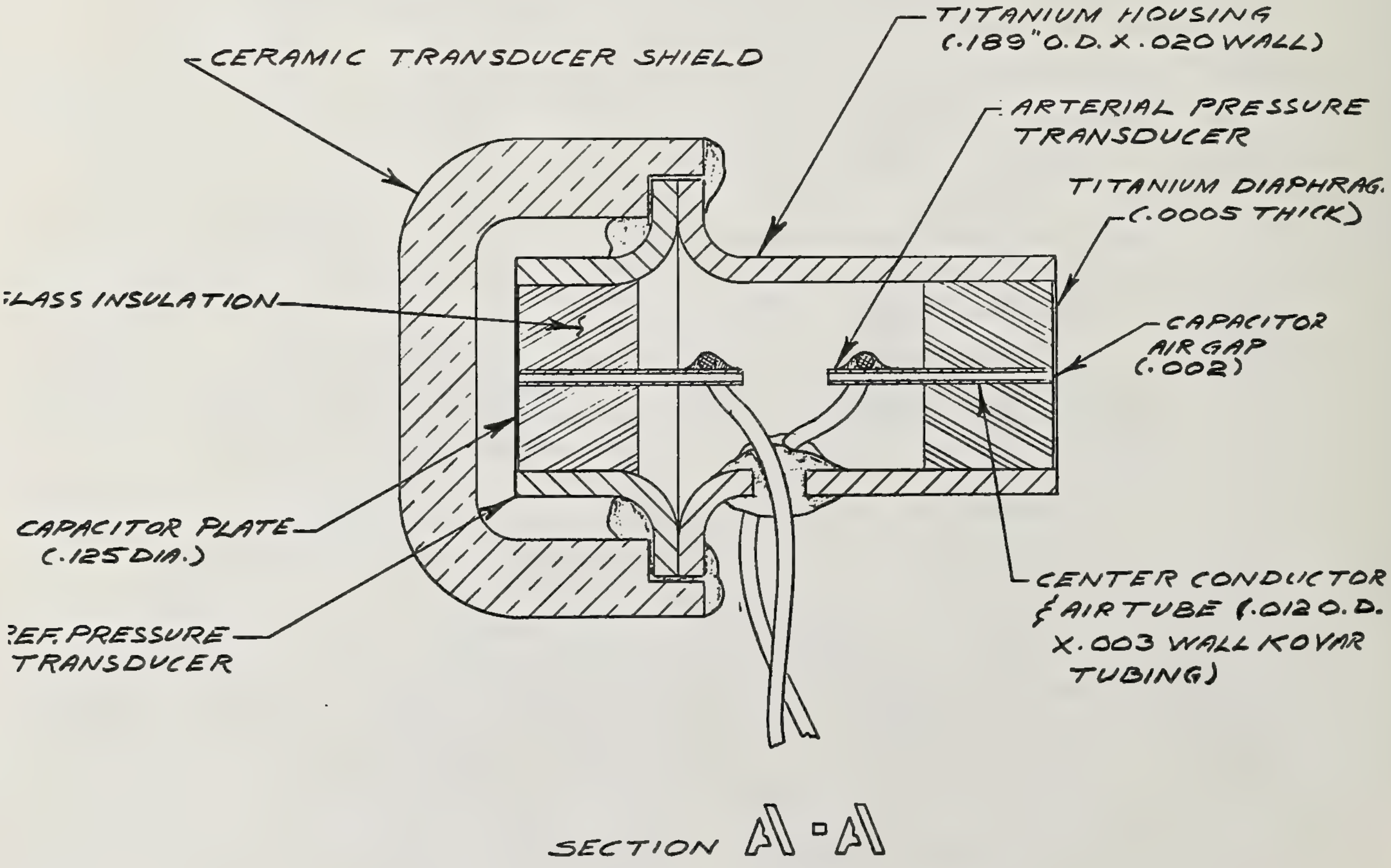
TITANIUM HOUSING (.189" O.D. X .020 WALL)
CERAMIC TRANSDUCER SHIELD
ARTERIAL PRESSURE TRANSDUCER
TITANIUM DIAPHRAG. (.0005 THICK)
LASS INSULATION
CAPACITOR AIR GAP (.002)
CAPACITOR PLATE (.125 DIA.)
CENTER CONDUCTOR & AIR TUBE (.012 O.D. X .003 WALL KOVAR TUBING)
EF. PRESSURE TRANSDUCER
SECTION A-A

FIGURE 5. CELL ASSEMBLY - IMPLANTABLE TRANSDUCER.

CHAPTER 62

IMPROVED DIAGNOSTIC ACCURACY IN ACUTE MYOCARDIAL INFARCTION WITH MULTI-CHANNEL ELECTROCARDIOGRAPHIC DATA ACQUISITION AND ANALYSIS

J. Cyprus
Texas Instruments
Houston, Texas

C. Blomqvist, A. Dowdy, S. Lightfoot and R. Putnam
Southwestern Medical School
Dallas, Texas

A study designed to correlate electrocardiographic, serum enzyme, and pathology data in cases of known or suspected myocardial infarction has begun. For each patient, the following measurements are made during the course of observation and treatment: (1) repeated simultaneous collection of 30 channels of electrocardiographic data from thoracic surface leads for a period of 10 seconds, and (2) repeated serum enzyme analysis. In those patients who succumb and are autopsied, detailed pathological examinations are performed. The electrocardiographic data is analyzed as follows: A suitable portion of the signal, spanning one cardiac cycle, is selected. The interval is then subdivided into ten time frames for further analysis. The data is subjected to a transformation which extracts a set of statistically independent ECG signals having maximal energy over each time frame. The number and energy distribution of these signals is being examined for correlation with the serum enzyme data and (when available) with pathology data. In addition, the ensemble of derived signals is being correlated with the original data to try to construct the geometry of conduction and hence to construct a map of viable and non-viable myocardium.

INTRODUCTION

Acute or healed myocardial infarction is recognized clinically in approximately 60 percent of all cases, there being little overall difference between standard electrocardiographic and vectercardiographic techniques.[1] Diagnostic tools which can provide an assessment of the extent of damage to the patient's heart with greater accuracy are desirable adjuncts to the development of both assist and replacement devices.

During the past several months, a computerized data acquisition and analysis system which is designed to collect and subsequently process 30 simultaneous channels of electrocardiographic data from a patient has been developed. This system is about to be placed into operation at the University of Texas Southwestern Medical School at Dallas as part of a study designed to improve diagnostic accuracy in acute myocardial infarction. This paper will describe the clinical protocol which will be followed, the equipment which has been developed, and the analytic approach which will be taken with the data gathered. An evaluation of the validity of this analysis must, of course await the execution of the clinical phase of the work, and will be reported at a later time.

CLINICAL PROTOCOL

Currently approximately 300 patients per year are admitted to the medical wards at Parkland Hospital and discharged with a diagnosis of acute myocardial infarction. Approximately 150 additional patients are admitted with a tentative diagnosis of acute myocardial infarction. The number of autopsies per year demonstrating acute myocardial infarction is about 45. This study will thus include the following four groups of individuals:

1. Acute myocardial infarction documented at autopsy.
2. Acute myocardial infarction documented by history and clinical and laboratory data.
3. Initial diagnosis of acute myocardial infarction disproved by clinical and laboratory data or at autopsy.
4. Control group.

For each patient, the following measurements will be made during the course of observation and treatment: (1) repeated simultaneous collection of 30 channels of electrocardiographic data from thoracic surface leads and (2) repeated serum enzyme analysis. In those patients who succumb and are autopsied, detailed pathological examination will be performed.

When a patient is admitted to this study, a reel of digital magnetic tape is assigned to his data. ECG data will be recorded three times during the first day of the patient's availability to the study, twice during the second day and once thereafter on the third and successive days, until his discharge. An initial file containing the patient's name, hospital file number, and the date of admission is placed onto the tape. Each time that ECG data is taken from that patient, the computer searches down the tape for the end of the previously recorded data, establishes a new file, and begins recording data there for 10 seconds. One reel of tape can easily hold 30 successive ten-second recordings for later analysis, which is more than adequate for the data associated with a single patient.

In conjunction with the gathering of the ECG data, routinely collected physiological data (WBC, blood sugar, temperature, etc.) will be used in the clinical evaluation of the patient. Particular emphasis will be placed, however, upon the results of carefully controlled serum enzyme measurements. Twice during the first day, and once thereafter, blood will be drawn from each patient. At various times during the patient's clinical course, the following enzymes will be assayed: creatine phosphokinase (CPK), serum glutamic oxalacetic transaminase (SGOT), lactic dehydrogenase (LDH) alpha hydroxybutyrate dehydrogenase (Alpha HBD), and in cases with an established diagnosis, LDH isozyme. This data will serve as a basis for inferring the presence and progress of acute MI, especially in the absence of post mortem corroboration.

The following data will be gathered from those patients who succumb to the myocardial infarct and are autopsied:

1. Heart weight. Presence or absence of dilation. Thickness of ventricular walls.
2. Status of the coronary arteries (dissection).
3. Presence of myocardial lesions. The heart will be studied with coronal sections of 4-5mm thickness, starting at the apex, and proceeding toward the base. Gross lesions will be measured in length, width, and breadth. Lesions will also be examined microscopically to confirm the gross appearance and to determine the age of the lesion.

EQUIPMENT

A block diagram of the computer system is shown in Figure 1. During data acquisition, the ECG signals go through an electrode harness, into the amplifier system, through the multiplexer and analog to digital converter, into the computer and onto digital magnetic tape. Thus, the first time the data reaches magnetic tape, it is in digital form. As soon as 10 seconds of data have been taken, the tape is spaced back to the beginning of the file just recorded. The data is then read back into the computer, and is sent through the digital to analog converter onto the cathode ray oscilloscope for visual confirmation of good quality by the medical technician. The technician can either accept the data by disconnecting from the patient, or request a fresh recording by moving one switch on the computer.

During data analysis, the reel of tape containing the desired patient's data is mounted onto the tape transport. The file to be analyzed is read from tape through the computer onto the drum. It is then read from the drum through the computer, through the digital to analog converter and onto the cathode ray oscilloscope as was done during acquisition. It is possible during analysis, however, to request that only one portion of the data (e.g., the time span associated with one cardiac cycle, the QRS interval, etc.) be displayed to a larger scale for closer examination. The data selected for reduction is then analyzed, and the results are presented on the cathode ray oscilloscope or on the typewriter as appropriate.

When the patient is first admitted, he is measured to establish the exact harness size and electrode placement. The electrodes are disposable, but they are left on the belts of the harness and re-used by applying additional electrode paste each time that data is taken again on that patient. The harness with three electrodes applied is shown in Figure 2. Silver-silver chloride electrodes were chosen for this study.

When actually gathering data, the harness contains 32 electrodes. One of these is defined to be the ground electrode, and one of them serves as the minus (-) input to every differential amplifier in the system. Each of the remaining 30 electrodes serves as the plus (+) input to its corresponding differential amplifier. In this manner, 30 bipolar ECG leads are created, all having the minus electrode in common. Figure 3 shows the harness on a subject, again with only 3 electrodes in place.

Because a conventional low frequency ECG amplifier produces an undesirable long time-constant exponential recovery signal when excited by an abrupt input transient, this system has been constructed using direct coupled (d-c) amplifiers. The frequency response of the amplifiers is from d-c to 300 Hz. The amplifiers chosen have an input impedance in excess of 1,000 megohms and a common mode rejection ratio in excess of 110 dB. They have been arranged to provide a fixed gain of 500. During the initial phases of checkout of the amplifier system, it was discovered that the electrodes tended to display different d-c potentials, some as much as 20 millivolts. This was, of course, sufficient to block the amplifiers. We have observed, however, that passage of a current of approximately 15 microamperes through each electrode, with the ground electrode used as a return for all the others, causes all the electrode half-cell potentials to approach each other to within 5 millivolts. Consequently, just before connecting the patient cable into the amplifier system, it is first plugged into a small chassis box containing a flashlight battery and 29 100-kilohm resistors wired in series with each electrode.

The multiplexer and analog to digital converter form a combined unit which is capable of converting 32 channels of data from the amplifiers. The dynamic analog range is a little over 8 volts centered about zero. The converter can operate at a speed of 1 msec for the set of 32 conversions, or at 31.25 microseconds each. It generates a digital representation of the input voltage of 14 bits plus sign. Of these 15 bits, the low order 12 bits are generally significant for the ECG data; the high order 3 bits provide the extra dynamic range needed to accommodate the d-c offsets from

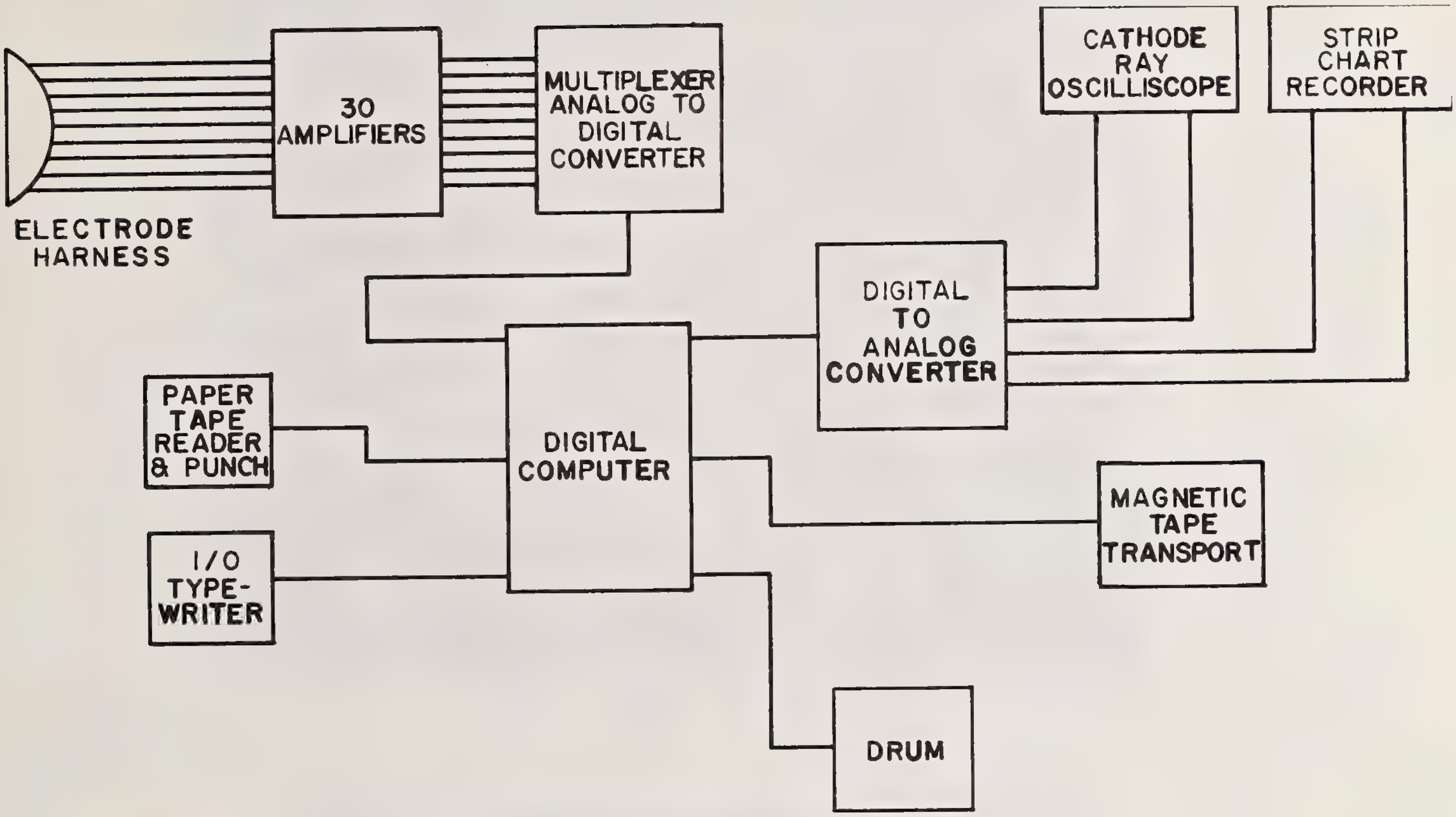

FIGURE 1. SYSTEM BLOCK DIAGRAM.

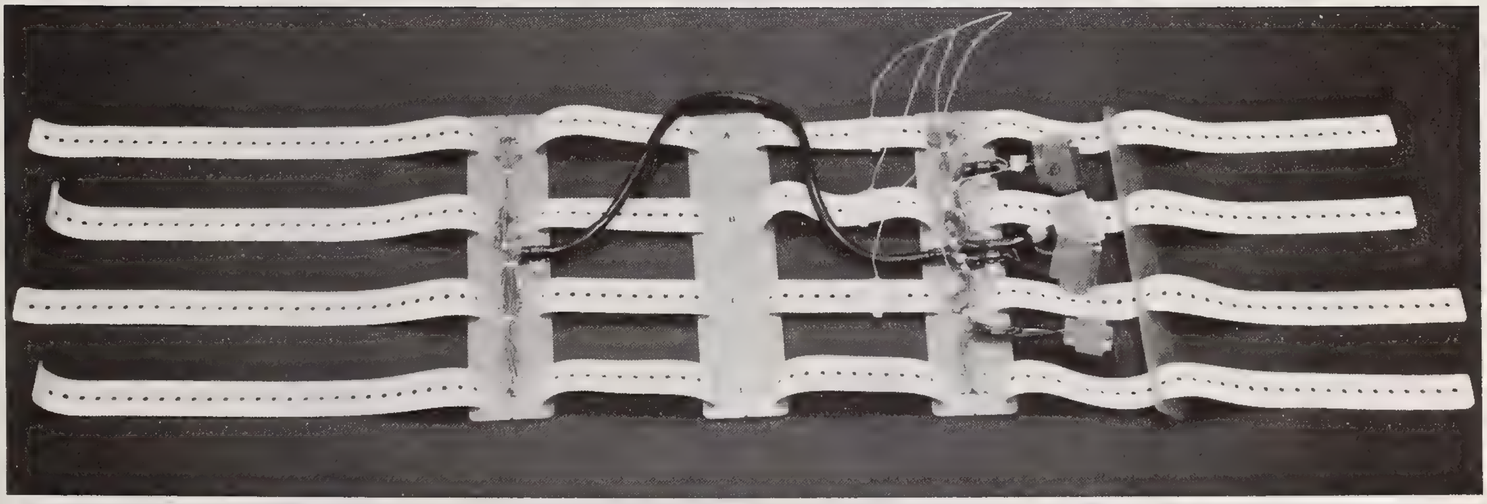

FIGURE 2. ELECTRODE HARNESS.

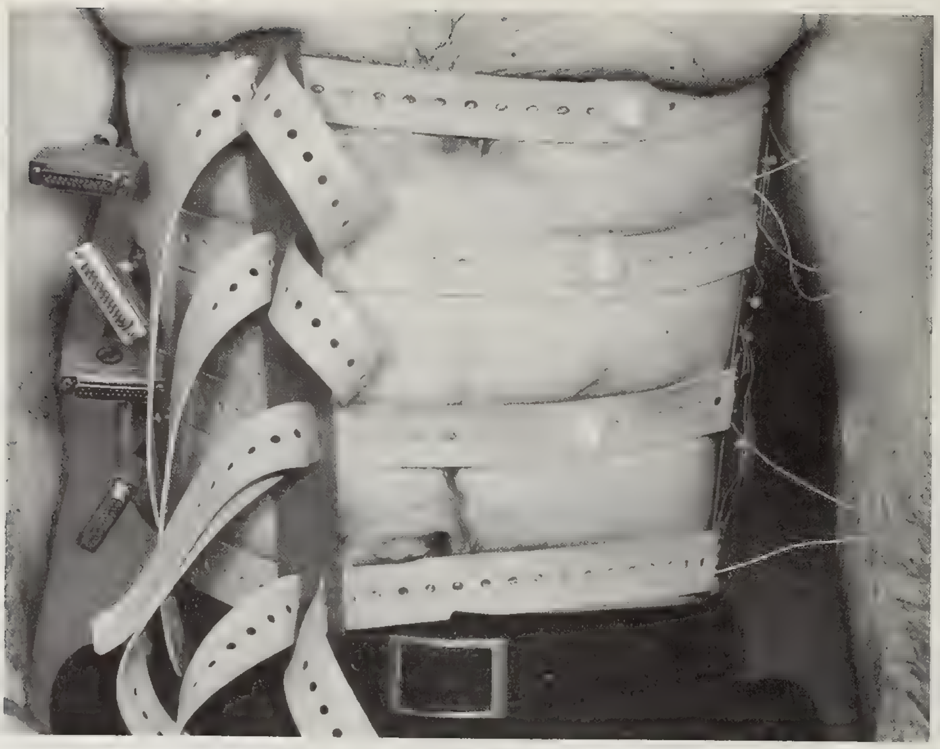

FIGURE 3. ELECTRODE HARNESS ON A PATIENT.

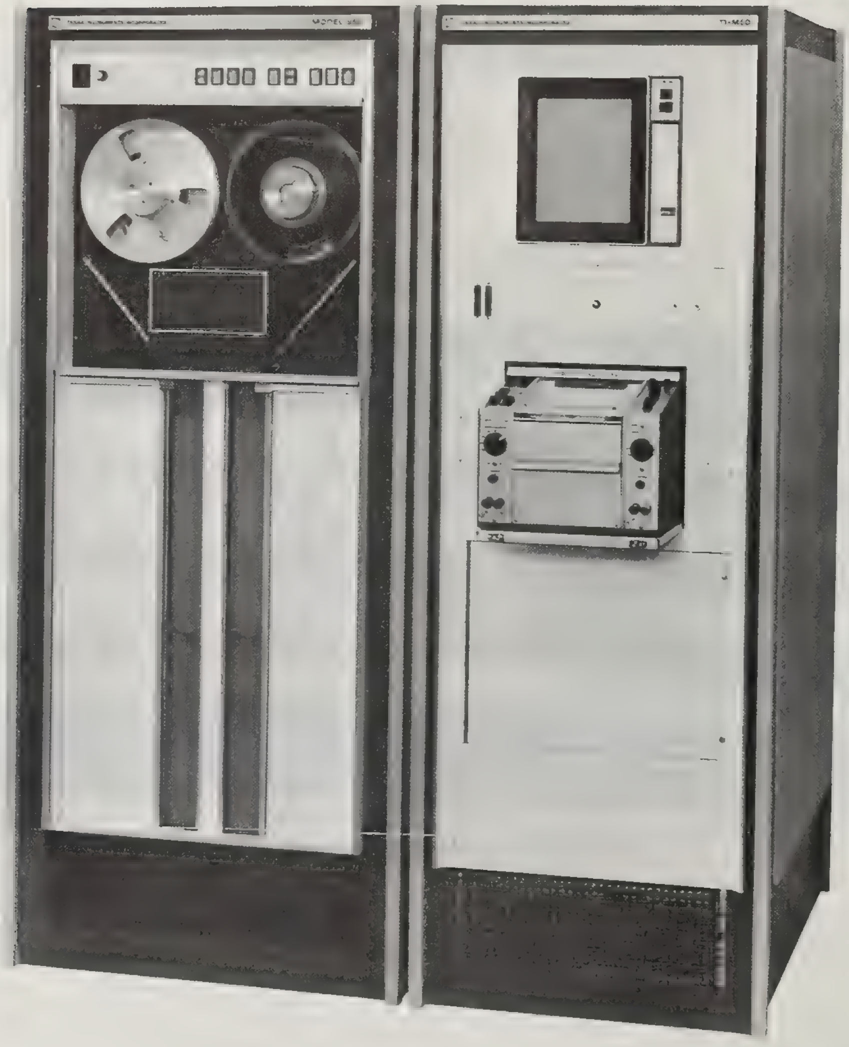

FIGURE 4. TAPE TRANSPORT AND AMPLIFIER CABINET.

the electrodes. The average (d-c) value of each lead is always subtracted from each data value before any display or processing is performed.

The digital computer is a small general purpose machine with a 1.5 microsecond CPU memory cycle and a 1.0 microsecond input/output memory cycle. It has a full instruction set, including double-length arithmetic, to facilitate the execution of the mathematical manipulations upon the ECG data. The core memory contains 4,096 words of storage.

The magnetic tape transport is a single-capstan computer grade office machine. Data is recorded in compatible nine-track format. The patient's ECG data is collected by the computer in a cyclic buffer in memory 2,048 words long, representing 64 samples for each of 32 data channels. The data is recorded continuously in records of 2,048 words each on tape concurrent with the data acquisition. The file associated with the ten seconds of data is made up of about 150 such records. Figure 4 shows a picture of the tape transport and the amplifier cabinet.

The digital to analog converter contains five channels, each of which has ten bits of conversion plus sign, for a total of 11 bits. One channel feeds the X-input to the memory oscilloscope; another feeds the Y-input. Two additional channels are used to feed a two-pen strip chart recorder. The fifth channel is used in a test mode to confirm that the amplifiers and analog to digital converter are working properly.

The magnetic drum has a capacity of over 390,000 words. It is organized into 192 tracks, each of which contains 2,048 words. During operation, the various programs which are to be executed are stored on the low order tracks of the drum. A system executive enables one to call for the various programs as required, such as the assembler, the data gathering program, the editing program, etc. In addition, the remainder of the drum is used during analysis to store a ten-second data file, various correlation coefficients, reduced traces, and other intermediate results.

The paper tape reader, paper tape punch, and I/O typewriter are conventional computer peripherals, and do not require further description.

Figure 5 shows the format in which a complete 10-second recording is presented. At the time that the photograph was made, only six of the 30 ECG amplifiers were in operation. In forming this display, the channels of data were individually scanned to compute their corresponding average values, which, as mentioned above, were then subtracted off. No attempt was made to correct for base-line shift, for our experience to date has indicated that with the electrodes and d-c coupled amplifiers being used, none is necessary.

ANALYTIC APPROACH

The construction of the equipment just described has been directed toward one goal: the acquisition of high quality simultaneous multi-channel ECG data in order to subject it to detailed analysis leading to an inference of the size and position of an infarct. The main analytic tool which will be applied to the ECG data is a multi-channel filter which will transform the 30 leads acquired from the surface electrodes into a reduced set of statistically independent leads, each of which has the property of maximal signal energy during some portion of the cardiac cycle.

The file containing the ECG data to be analyzed will be read in from the patient's reel of magnetic tape. The data will also be displayed on the face of the cathode ray oscilloscope. The investigator will then select the portions of the tracing which he wishes to analyze by typing time designations in through the keyboard of the typewriter. The times of demarcation of the signal will initially be obtained from manual measurement, and may be obtained at a later time through the application of prior data reduction in the computer center at Southwestern Medical School.

The portion of data selected for analysis will then be displayed on the screen of the cathode ray oscilloscope as confirmation that the desired interval has been selected. The data selected will then be transformed as shown in Figure 6.

The portion of signal selected is T samples long, and consists of 30 channels of redundant data. This data can be considered to be a matrix of dimension 30 X T. The covariance matrix (of dimension 30 X 30) will be computed for this data matrix. An iterative procedure will then be initiated to extract the largest eigenvalue and its corresponding eigenvector from the covariance matrix. This process will be continued until successive eigenvalues are not substantially decreasing.[2]

The eigenvectors so extracted are then used to form a multi-channel filter matrix of dimension P X 30, which is then applied to the original data to form a reduced set of leads having the following properties:

1. These reduced leads are linear combinations of the original 30 leads.
2. The reduced leads are statistically independent; i.e., their covariance matrix is diagonal.
3. The energy contained in each computed lead is proportional to its corresponding eigenvalue.
4. This set of reduced leads should be invariant with respect to reasonable variations in lead placement. Furthermore, it is derived without any a priori assumptions of the internal geometric and electrical structure of the subject.

The eigenvalues extracted from this process will be presented to the investigator, along with a plot of the reduced equivalent leads, versus time, during the interval selected. Our present working hypothesis is that the number and distribution of these eigenvalues for a particular interval of the cardiac cycle correspond to the number of degrees of freedom in the depolarization activity within the myocardium. In particular, we are expecting to find that when only viable myocardium is involved, there will be between one and four reduced leads produced by the process outlined

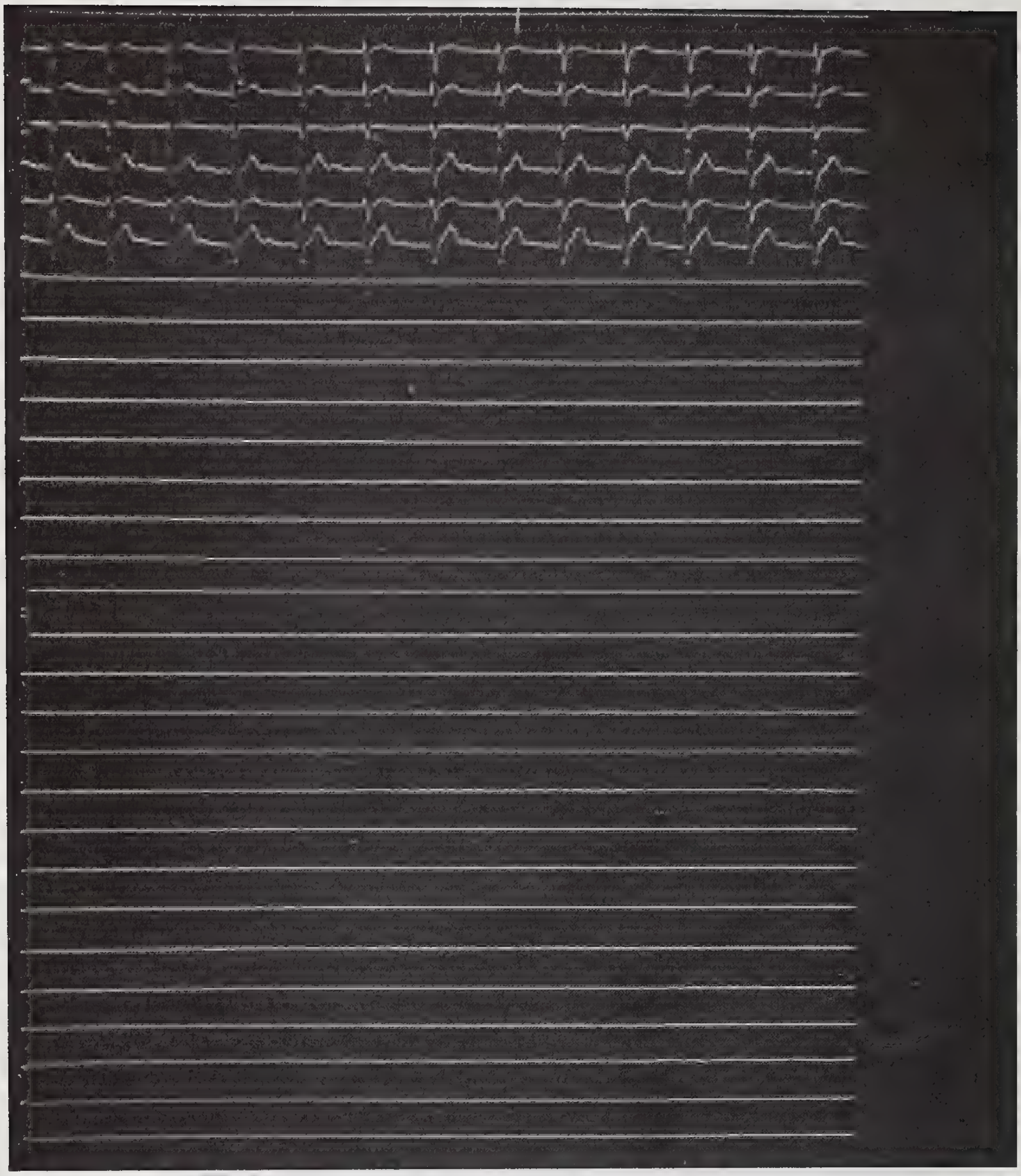

FIGURE 5. FORMAT IN WHICH A COMPLETE 10-SECOND RECORDING IS PRESENTED.

above, one or two of which will contain most of the signal energy; while infarcted tissue will cause the depolarization activity to split into alternate paths, and consequently will cause a larger number of reduced leads to be produced, along with a relatively uniform energy distribution.[3]

In addition, continuing with the hypothesis that this above process in fact produces components which are representative of the myocardial discharge, we shall attempt to estimate an equivalent geometric orientation of each of the reduced leads in an effort to reconstruct a three-dimensional model of the depolarization and repolarization activity.

Pairwise differences among the original 30 leads will be formed, thus producing 435 bipolar leads. These will in turn be cross-correlated with the reduced leads. The pair of leads whose difference produces the largest zero-lag cross-correlation with each reduced lead will be presented to the investigator as an indication of the inferred direction for that reduced lead.

SUMMARY

If this process is successful, it represents a solution to the inverse problem in electrocardiography based upon correlative statistical communication treatment of the signal, rather than a formulation of the field theory description of the subject. Execution of the clinical phase of this activity during the next several months as we attempt to infer the size and position of an infarction electrocardiographically will provide a basis for evaluation of the validity of this approach.

REFERENCES

1. Simonson, E. et al: Diagnostic Accuracy of the Vectorcardiogram and Electrocardiogram. A cooperative Study. American Journal of Cardiology. 17:829-878, 1966.
2. Kendall, M. G.: A Course in Multivariate Analysis. Hafner, New York City, 1957.
3. Pipberger, H. V.: Use of Computers in Interpretation of Electrocardiograms. Circulation Research 11:555-561, 1962.

DISCUSSION

DR. KAUFMAN: Do you have any noise interference from the lead contact?

DR. CYPRUS: The major problem with the lead contacts is not properly described as noise. There is one problem which I failed to mention but which is described in my presentation in the paper. We have gone to great pains to maintain direct coupling in the electrocardiographic system. Our motivation was to attempt to avoid the long period transients associated with low frequency a-c coupled amplifiers. We have observed that there is a substantial d-c offset from one electrode to another when placed upon the skin. It appears that we have succeeded in overcoming it and we are in the process of evaluating whether or not our technique does, in fact, overcome the d-c offset. But as far as noise, or 60 cycle pick-up, or even muscle artifact, I would say that they are really properly described by saying that they are negligible. The only problems we have really had with the electrodes is the d-c offset, because of having tried to maintain the d-c coupled system, and occasional tendency for an electrode to fail to make contact.

DR. HERROLD: What is the frequency response of your recording amplifier?

DR. CYPRUS: The amplifier itself is coupled from d-c up to approximately 300 Hz. We roll it off at approximately 300 Hz. The sampling rate of the converter can be as fast as 1 millisecond, but by virtue of the fact that we are attempting to run continuous data onto IBM compatible tape in gapped format with 2048 word records, the actual sampling rate turns out to be about 700 times per second instead of 1000.

DR. HERROLD: Thank you. Is the value judgement for a decision on an abnormality being made on the eigen value for the energy level?

DR. CYPRUS: The analysis has not as yet been implemented. The algorithin which we shall follow is that we shall extract the largest eigen-value, and we will continue extracting eigen values until we find one that is less than 1% of the size of the largest one. At this point, we shall terminate the process. The eigen value itself is proportional to the energy contained in the corresponding component.

DR. HERROLD: Yes, that is just the point that was bothering me. There has been quite a lot of research in this field, for instance by Langner in Philadelphia. This research seems to indicate that some valuable indications of an abnormality are sometimes contained in the very low energy high frequency components of the electrocardiogram.

DR. CYPRUS: Yes. For the time being, however, we shall terminate at one percent arbitrarily.

DR. HERROLD: Thank you.

DR. CYWINSKI: May I ask you, what was the reason for choosing 30 leads? The systems I am familiar with are utilizing 54 or 72 leads, or even more (like the IBM, Dr. Taccardi, and Dr. Rijlant systems).

DR. CYPRUS: The observation that I will make is that one tends to use equipment which is suitable for the problem, and which more or less is readily available. In particular we have utilized a multiplexer and analog digital converter which is available, using 32 channels. Other workers have used 50 channels and 127 channels and various other numbers of channels. In other words, what would one like? One would like one microsecond sampling with 1000 channels. And then, what will one accept as still being reasonable? One then compromises, I think, to what is available, without trying to push some instrumentation frontier unless it is necessary to do so. Thirty degrees of freedom, based upon published work appears to be too many. Yet 30 channels provide enough redundancy to make a statistical data extraction process take on some validity. So thirty was chosen as an engineering compromise as being reasonable, that at which we could maintain approximately 1 millisecond sampling, and that which was available to us.

DR. HERROLD: I noticed that you have apparently developed a new lead configuration. Now, most of the pattern recognition that has been done used the standard 12 leads with a Wilson Central terminal. Are you planning to establish a completely new baseline for detection of abnormalities? Or have you worked out a mathematical matrix to relate your lead configuration to what has been in current practice since 1903?

DR. CYPRUS: Aside from the fact that the standard leads are typically taken with the electrodes physically placed on the limbs, there are leads in the harness which are electrically fairly close to being equivalent to a limb lead. Specifically, the top belt has two leads that come fairly close to the location of the arms and the bottom belt has one lead which could in fact be taken as being approximately the same as left leg lead. So that if one wished to reconstruct the equivalent to leads I, II and III, or for that matter aVR, aVL, and aVF, forming the difference between two of the electrode signals that we are taking, will produce a standard three-lead system (I, II and III), and a straightforward linear combination of the three would produce the others. With respect to V_1, V_2, V_3, V_4, V_5, and V_6, and the Wilson Central terminal, the harness which we have would enable us to extract V_2, V_4, and V_6, but no V_1, V_3, and V_5, because we don't have quite that close a spacing across the thorax.

DR. HERROLD: Yes, I didn't notice when you reported that. Actually I think you have the capability to record $V_{7, 8, 9, 10, 11, \text{ and } 12}$.

DR. CYPRUS: Yes we do, again except for the spacing in our harness, omitting some of these. Our mathematical approach, however, is not based upon trying to correlate between conventional ECG observations that have been done before. But rather, and this is the key to the mathematical approach that we are taking, we are attempting to extract energy related signals from ECG data. We are going on the working hypothesis that the lead configuration that has been put on here or any other lead configuration, unless it is very poorly conditioned geometrically, would essentially result in the same output from the mathematical analysis that we are about to get into. In other words, we are predicting our mathematical approach here on the hypothesis that we have succeeded in extracting material which is representative of actual myocardial depolarization energy, independent of the placement of the lead. Of course, this is something which will be evaluated very critically during the next couple of months.

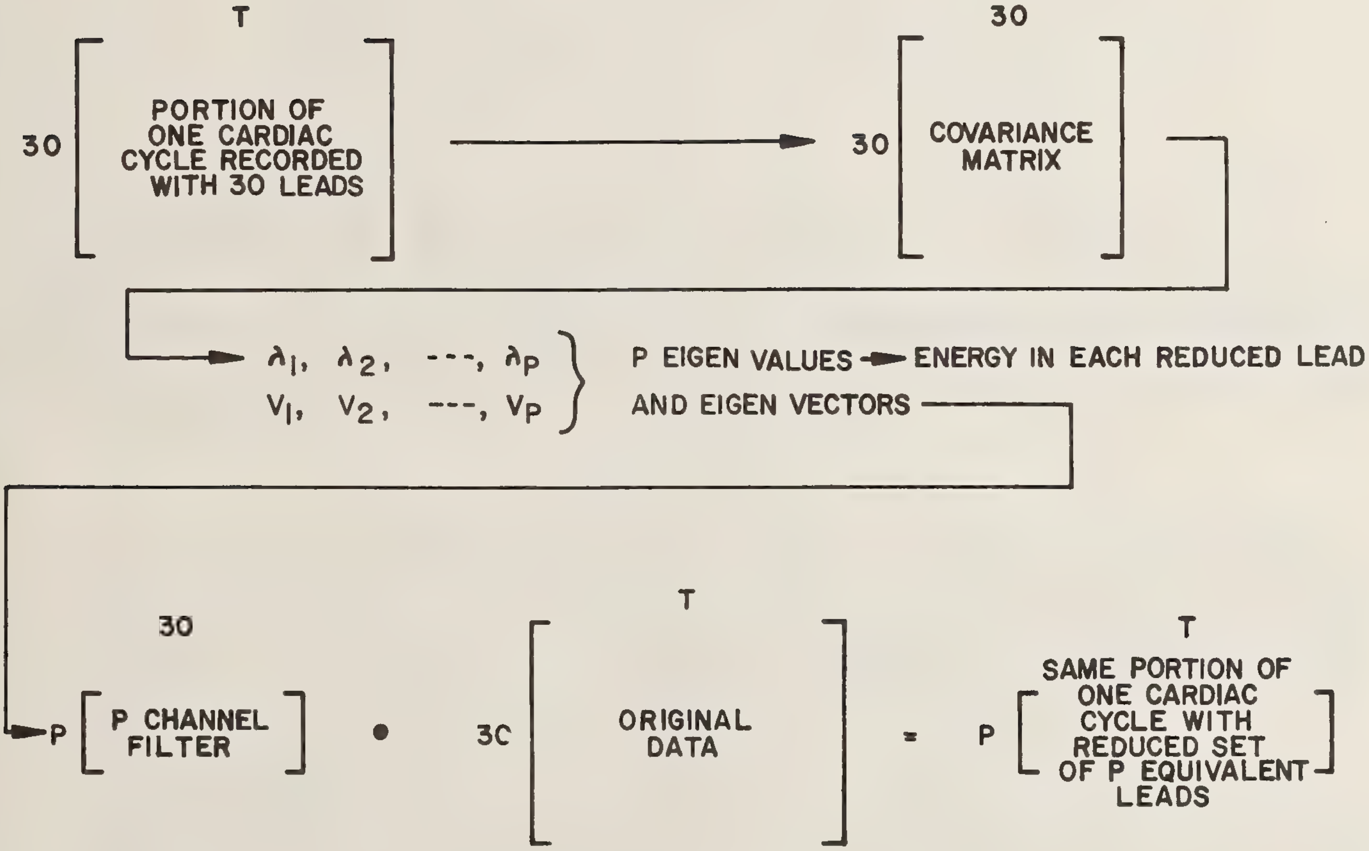
T
30
PORTION OF ONE CARDIAC CYCLE RECORDED WITH 30 LEADS
30
30
COVARIANCE MATRIX
λ1, λ2, ---, λP
V1, V2, ---, VP
P EIGEN VALUES
ENERGY IN EACH REDUCED LEAD
AND EIGEN VECTORS
30
P
P CHANNEL FILTER
T
3C
ORIGINAL DATA
=
T
P
SAME PORTION OF ONE CARDIAC CYCLE WITH REDUCED SET OF P EQUIVALENT LEADS

FIGURE 6. TRANSFORMED DATA.

CHAPTER 63

IMPLANTABLE IMPERMEABLE ENCAPSULANTS FOR ARTIFICIAL ORGANS

C. Enger and F. Rhinelander

Case Western Reserve University
Cleveland, Ohio
and
Cleveland Metropolitan General Hospital
Cleveland, Ohio

This project aims to develop a membrane impermeable to bodily fluids, for use as an encapsulant of implantable devices. Sheets of unvulcanized Silastic have been impregnated with various waxes -- beeswax, spermaceti and carnauba to date. The resulting membranes are being tested for ion permeability and water-vapor transmission; samples have been implanted into rabbits to test tissue compatibility. Ultraviolet microscopy studies, to determine the evenness of wax penetration, are to be carried out. The ion-permeability tests and the tissue compatibility tests are as yet incomplete. The water-vapor transmission tests indicate that 60-mil Silastic impregnated with spermaceti is superior to beeswax and carnauba-impregnated membranes, and to a control membrane of unimpregnated Silastic. Waxes additional to those mentioned above are being sought for impregnation into Silastic membranes.

INTRODUCTION

Medical grade silicone rubber (Silastic) has received wide acceptance over the past decade and has become the most widely implanted synthetic material in man. Its use as an encapsulant for electronic implants has been hampered by apparent ion migration as body electrolytes begin to penetrate[1].

Before embarking on the current project the principal author had devised a method to block permeation by impregnating Silastic with wax or oil. Continued studies, supported by this contract, have shown a major decrease in water vapor transmission and apparent ion permeation after impregnation. Compatibility studies have shown adequate acceptance of certain waxes by mammalian tissues. A new impermeable and flexible interface has thus been developed for isolation of artificial organs within living systems.

METHODS AND MATERIALS

Early attempts to impregnate Silastic with beeswax, by producing swelling of the cured material in xylene or ether, resulted in uneven penetration and incomplete permeation. This method was discarded in favor of a new technique which has shown superior results. Sixty-mil sheet stock of uncured Dow Corning Silastic is submerged in wax which has previously been heated to a fluid state at 150° C., the temperature at which Silastic is usually cured. The material is allowed to remain in wax at this temperature for 30 minutes. Upon removal and after cooling, an opaque and slightly swollen membrane, as contrasted to normal Silastic, is obtained (Figure 1). All of the experiments reported in this paper were carried out with Dow Corning Type 372 Silastic.

Tissue Compatibility.

Small samples of various types of beeswax and of spermaceti were implanted under aseptic conditions into the subcutaneous tissues of rabbits for a period of three weeks. The samples and surrounding tissues were then removed for routine histologic examination. All materials caused some degree of local cellular reaction of the chronic type, from very mild to moderate. The results are shown in Table 1, where the waxes are listed in the order of their decreasing tissue reactivity. Spermaceti is observed to show the best tissue acceptance.

TABLE 1

TISSUE REACTIVITY TO WAXES AFTER THREE WEEKS OF IMPLANTATION INTO RABBITS

Spermaceti	Very Mild
Beeswax, with Natural Propolis	Mild to Moderate
Beeswax (USP)	Moderate
Beeswax, Collected Directly from the Bee (Sucrose Diet)	Considerable to Severe

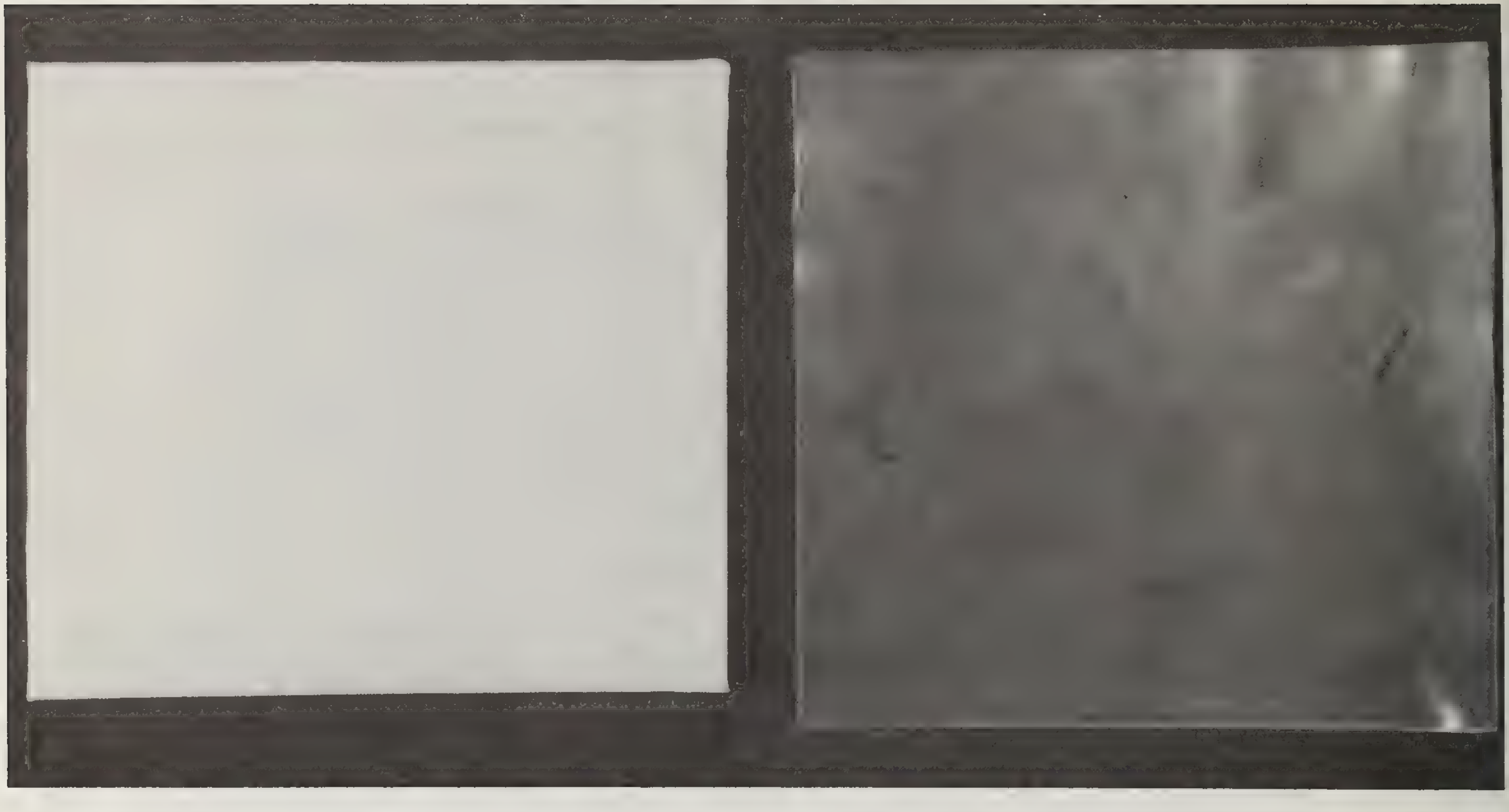

FIGURE 1. PHOTOGRAPHS OF SHEET OF UNTREATED SILASTIC (LEFT) AND SIMILAR SHEET OF SILASTIC IMPREGNATED WITH SPERMACETI (RIGHT).

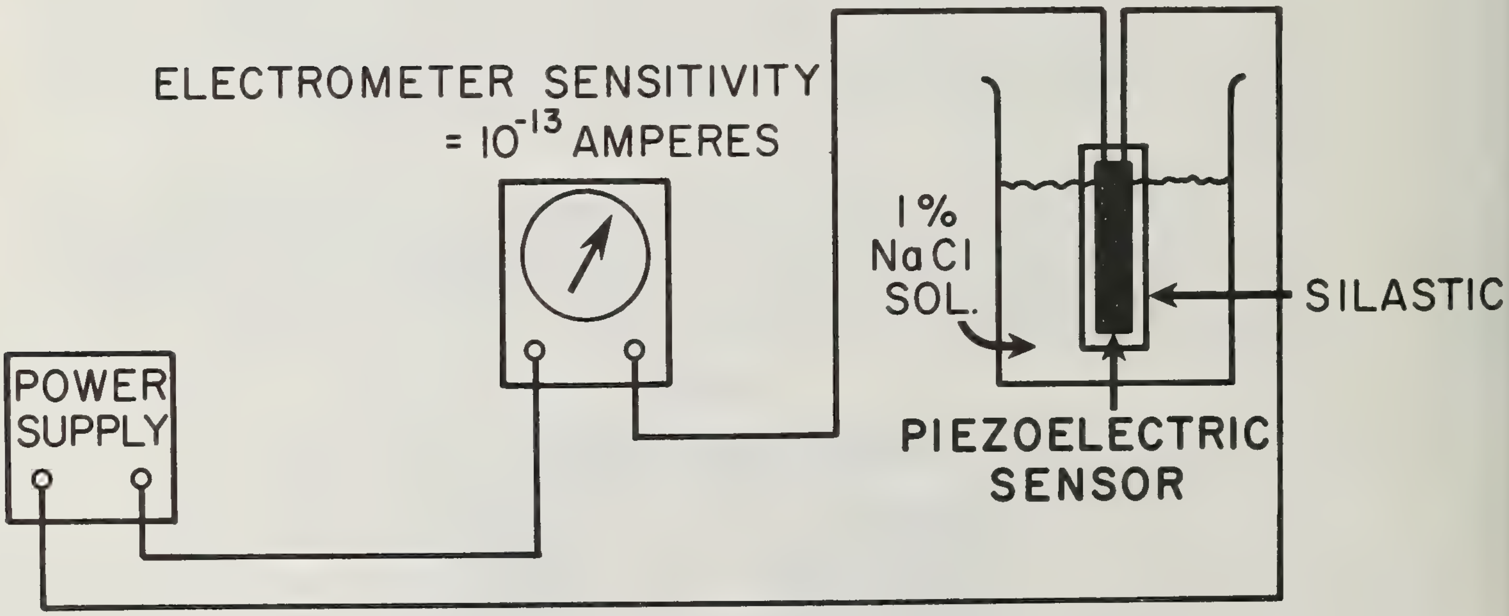

FIGURE 2. DIAGRAM OF TEST-RIG USED FOR COMPARING PERMEABILITY OF UNTREATED AND IMPREGNATED SILASTIC MEMBRANES.

Mechanical Properties.

Some changes in the mechanical properties of Silastic are observed after impregnation with wax. The initial mechanical tests have been conducted for us by Dow Corning, with the results shown in Table 2. Since the intended use is encapsulation, these small changes are not considered a problem.

TABLE 2

MECHANICAL CHARACTERISTICS OF UNTREATED AND WAX-IMPREGNATED SILASTIC MEMBRANES

Silastic Type 372 60mil Thick	Tensile (p.s.i.)[a]	Durometer	Elongation[a]
Control Unimpregnated	1,519	45	648
Carnauba Wax Impregnated	1,374	47	652
Beeswax Impregnated	1,294	43	620
Spermaceti Impregnated	1,170	46	597

[a] average of 3 specimens

Water Vapor Transmission.

Membranes impregnated with various naturally occurring waxes are being subjected to water vapor transmission tests, which are also being conducted for us by Dow Corning. The results for two waxes are shown in Table 3.

TABLE 3

WATER VAPOR TRANSMISSION OF UNTREATED AND WAX-IMPREGNATED SILASTIC MEMBRANES

Silastic Type 372 60mil Thick	
Control Unimpregnated	20.6^{-6}[a]
Carnauba Wax Impregnated	18.4^{-6}
Beeswax Impregnated	10.6^{-6}
Spermaceti Impregnated	4^{-6}

[a] cm^3 of gas/hr/cm^2 of membrane

You will observe that spermaceti impregnation produces a striking reduction in water vapor transmission as compared with unimpregnated controls, whereas carnauba wax impregnation produces only a slight reduction.

Permeability to Water and Ions.

Silicone rubber is known to transmit water vapor but theoretically it should not be permeable to electrolytes[2]. However, in early experiments on implantation of piezoelectric ceramics encapsulated with a pure Silastic membrane[1], we had observed a rapid decrease in electrical activity of the piezoelectric ceramic. Therefore, it appeared that ions, in addition to water, had migrated to the surface of the sensor. Experiments to test this were set up.

Piezoelectric ceramics[3], having an extremely high electrical resistance, are very readily inactivated by contact with any electrically conductive medium. Initially, we constructed an ion-permeability test-rig containing two compartments separated by the membrane to be evaluated. NaCl solutions of markedly different concentrations were placed in the two compartments, and an electric current was passed through the cell via an electrode in each compartment -- in an attempt to produce ion migration through the membrane. This test-rig, despite use of different concentrations of NaCl and of various electrical potential levels, proved to be too insensitive for our purposes -- possibly due to ambient electron leakage through the test-cell.

We then decided to eliminate the test-cell and use a piezoelectric ceramic sensor, protected by a Silastic pouch which was suspended in a beaker containing an NaCl solution. The sensor was a Bimorph (PZT-5H, Clevite Corp.) of 500 megohms DC resistance, measuring 6 cm x 0.5 cm, with an electrical lead from each surface to a power supply (9 VDC) and an electrometer of 10^{-13}-ampere resolution, as shown diagramatically in Figure 2. Any change in the electrical resistance of the Bimorph is detectable by this means.

The first membranes studied in this apparatus were 20-mil-thick unimpregnated Silastic in the form of pouches into which the sensor was inserted. The sensor was generally in direct contact with the inner surface of the membrane, but in occasional small areas, air intervened. The results are shown as electrical resistance curves in Figure 3. A rapid decrease in the resistance of the sensor is observed, from 500 to 0.04 megohms, equilibrium being reached after 22 minutes. Six unimpregnated membranes were tested with only slight variation.

A similar experiment was set up with pouches consisting of 20-mil Silastic impregnated with spermaceti. The results are also shown in Figure 3. The resistance of the sensor remained essentially unchanged over a period of 48 hours. Three such membranes were tested with consistent results.

Similar tests were run with a thin zone of inert non-polar fluid (3M Fluorochemical FC-75) interposed between the sensor and the inner surface of the pouch. The results are shown in Figure 4. When the pouch was composed of an unimpregnated Silastic membrane, there was a drop in resistance from 500 to 0.9 megohms. When a spermaceti-impregnated membrane formed the pouch, no appreciable drop in resistance took place -- the result being the same as when air, rather than non-polar fluid, occupied any space which was present between the sensor and the inside of the pouch. In three additional experiments, the spermaceti-impregnated membrane was allowed to remain in the test-rig for three days, and no appreciable change in resistance of the sensor was observed.

USP beeswax was used for impregnation of the Silastic membrane comprising the pouch in a few experiments, but it was less effective than spermaceti in maintaining high electrical resistance in the sensor.

DISCUSSION

The decrease in resistance of the sensor, when the pouch was composed of pure Silastic, indicates that ions must have reached its surface in an electrolyte solution. There are two possibilities: (1) water containing ions permeated the unimpregnated Silastic; or (2) inactive ions had been present on the outer surface of the sensor or on the inner surface of the pouch, and water alone then permeated the Silastic to activate these ions. Our experiments so far have not been able to differentiate between these possible events. However, regardless of which event occurs, impregnation of the Silastic membrane with spermaceti almost completely eliminates it.

This type of experiment does not give quantitative values for ion permeation, such as we had hoped to obtain with the test-rig in which the membranes were interposed between solutions of different ionic strength. However, it does permit us to compare different types of Silastic impregnation, where resistance to permeation of water alone, or of water containing electrolytes, is concerned.

Spermaceti[4], which has shown its superiority in all the parameters which we have tested so far, is a white crystalline wax obtained from the head case of the sperm whale, a member of the cetacean family (Figure 5). It has been used in the preparation of pharmaceuticals and cosmetics[5, 6] and has for many years been approved by the Food and Drug Administration for internal and external use in the human body. It has a melting point of 43.5^0 C. and maintains excellent electrical characteristics. The dielectric constant of spermaceti is 3.7 as contrasted to Silastic which is rated at 2.8. The effective alternating current conductivity of spermaceti is 17^{-12}ohms per cm^4. (These electrical constants were all measured after six months immersion in 3.5% NaCl solution[4]). The most important single advantage for in vivo applications of wax-impregnated Silastic is its electrical stability after long exposure to electrolytes.

We have shown that impregnation by two naturally occurring waxes can greatly enhance the effectiveness of Silastic as a barrier to the passage of water and electrolytes. Additional waxes and oils, especially others of cetacean origin, are to be tested in this connection. There is some evidence that a lower melting point is a factor of superiority.

The nature of the bond between Silastic and lipids remains to be determined, as does the permanence of this bond. For our purposes, these parameters can only be evaluated by in vivo experiments.

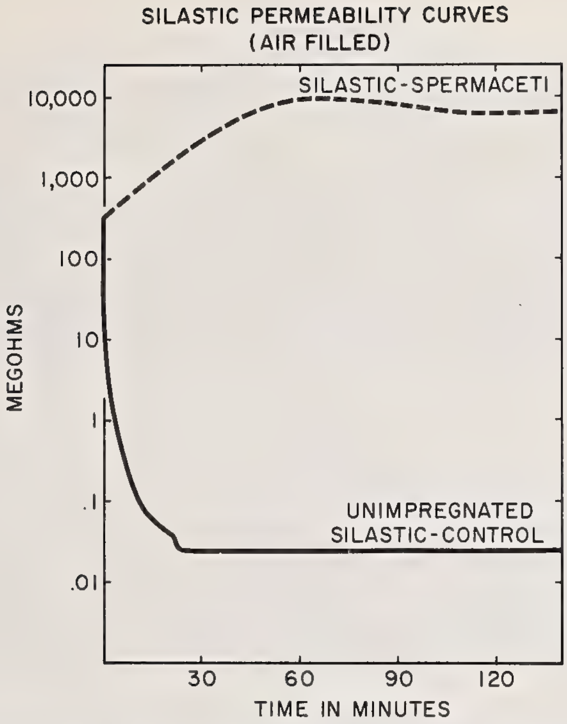

FIGURE 3. ELECTRICAL RESISTANCE CURVES COMPARING PERMEABILITY OF UNTREATED AND SPERMACETI-IMPREGNATED SILASTIC MEMBRANES IN DIRECT CONTACT WITH THE PIEZOELECTRIC SENSOR.

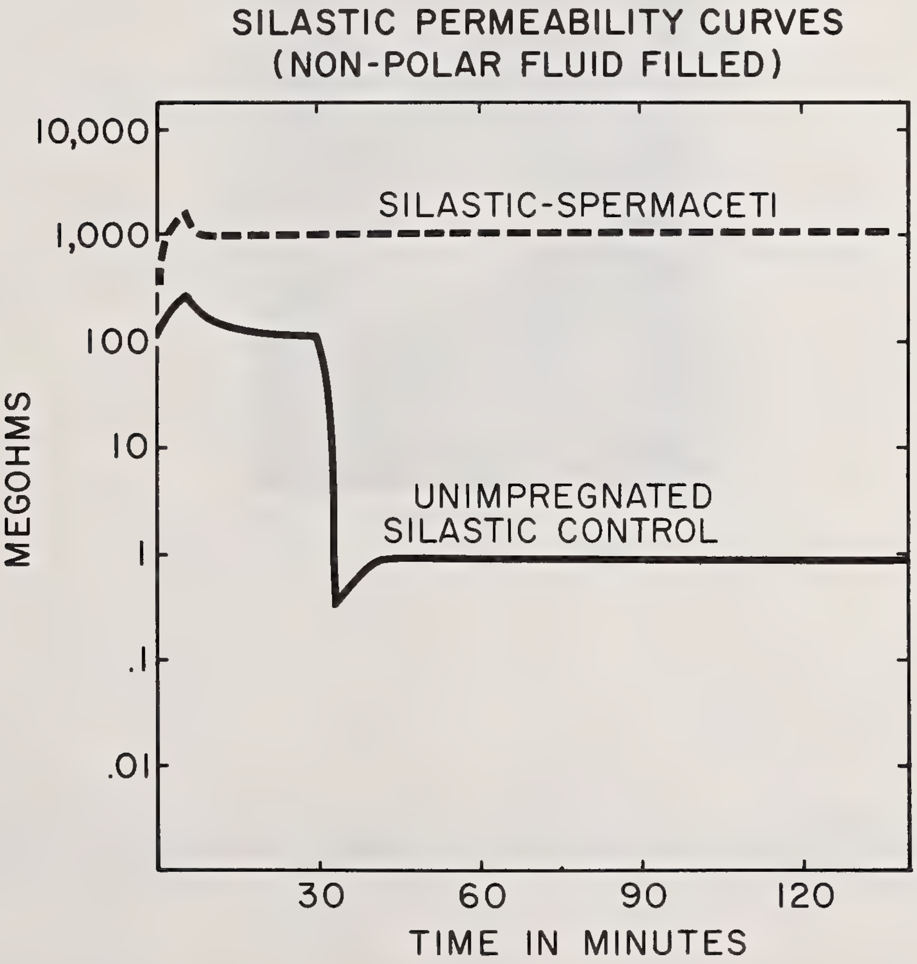

FIGURE 4. ELECTRICAL RESISTANCE CURVES COMPARING PERMEABILITY OF UNTREATED AND SPERMACETI-IMPREGNATED SILASTIC MEMBRANES SEPARATED FROM THE PIEZOELECTRIC SENSOR BY A THIN ZONE OF INERT NON-POLAR FLUID.

SUMMARY

Our studies have sought to develop a flexible impermeable encapsulant. Medical grade silicone rubber (Silastic), which is a widely used implantable material, is well known to be permeable to water. By use of a sensor of extremely high electrical resistance we demonstrated that Silastic was apparently permeable also to electrolytes.

We have subsequently shown that this apparent permeability to electrolytes can be greatly reduced by impregnation of the Silastic with certain naturally occurring waxes. Since our interest lies in the encapsulation of devices for implantation into bodily tissues, we have confined our investigation to waxes which are well tolerated by such tissues.

Of the waxes so far studied, in short-term experiments, spermaceti has revealed the best overall properties as an impregnant for Silastic.* Other waxes, and also oils, remain to be evaluated for possible superiority to spermaceti. Furthermore, permanence of the impregnation of Silastic by waxes and oils must be tested in long-term animal experiments.

REFERENCES

1. Enger, C. C. : A Piezoelectrically Powered Three-Gram Cardiac Pacemaker, Internat. Conf. on Engineering in Med. Biol., 7:79, 1967.
2. Braley, S., Dow Corning Corp.: Personal Communication.
3. Cady, W.: Piezoelectricity, Dover Pub., Vol. I & II, 1962.
4. Bennett, H.: Industrial Waxes, Chem. Pub. Co., Vol. I & II, 1963.
5. Gay, L. N.: The Nonantigenic Property of Beeswax, J. Allergy, 16: 195, 1954.
6. Bryson, J. D. & Code, C. F.: Prolonged Anticoagulant Action of Heparin in a Beeswax Mixture, Proc. Staff Meetings Mayo Clinic, 19: 100, 1944.

FIGURE 5. U.S.P. GRADE SPERMACETI OBTAINED FROM THE HEAD CASE OF THE SPERM WHALE.

---

* The process of impregnating silicone rubber with waxes and oils and the use of same is proprietary to Carl C. Enger and is presently being submitted to the United States Patent Office.

DISCUSSION

DR. NORMANN: As you mentioned Mr. Enger these encapsulants have been developed with flexibility, and I wondered what happened to the permeability factors under dynamic conditions. Do you have any data on that?

MR. ENGER: Yes. We have used similar materials to encapsulate piezoelectric pacemakers that I have been developing for some years. They require a slight movement of a piezoelectric ceramic element. This device encapsulated with a similar material has been placed in the pericardial cavity of a dog for six months. We are using a piezoelectric ceramic element which has an impedance of 500 - 1000 megohms and have seen very little reduction in the output of the generator. This degradation is at the very onset of the experiment and as we monitor the animal month after month we have not been able to detect any further change.

MR. REICHNER: You mentioned ion permeability. I am interested in the permeability to oxygen and other gases. Could you comment on that?

MR. ENGER: We have not been too interested in showing the permeability of the material to gases. There is a large amount of literature available, as you know, regarding the permeability of silastic to gases. I do know it is greatly reduced, but I don't know how much.

MR. KONIGSBERG: You mentioned that spermacite is brittle. Can I assume that it tends to be plastic at body temperature?

MR. ENGER: It loses a lot of its crystallinity at body temperature. One important matter that we have to remember is when we include it in silastic its atomic makeup is completely altered. We do not know whether all components of the wax are combining with the silastic. I know I can use spermaceti that has not been refined and has some coloration that is inherent in the unrefined material. This color does not go into the membrane which suggests there is some selective absorption of the material. We, of course, do not obtain a brittle membrane. The silastic is as flexible after we impregnate it as it is normally.

DR. JOHNSSON-HEGYELI: Did the permeability curves that you showed represent values at 37° C?

MR. ENGER: The permeability curves that you saw were all taken at room temperature which was approximately 72°F, and humidity controlled because you can imagine that a sensor of 1000 megohms is inclined to be affected greatly by moisture. Initial tests were run at elevated temperatures but no noticeable change in permeation could be detected. All final permeability tests were run at ambient room temperature for the sake of convenience.

CHAPTER 64

ENCAPSULATION PROCEDURE TO ISOLATE COMPONENTS FROM BODY FLUIDS

C. Nichols

Hydrospace Research Corporation
Rockville, Maryland

The technical objective of this program is to prepare and evaluate encapsulating materials that achieve reduced permeability by introducing high concentrations and/or selective distributions of impermeable inclusions to the base encapsulation. Reduced permeability is achieved by effectively increasing the diffusion path for body fluids. A mathematical model of the diffusion process has been developed that includes the effects of spherical and flake-type impermeable inclusions in the base material. The model indicated that hundredfold reductions of permeability should be theoretically possible for spherical inclusions and thousandfold reductions for flake-type inclusions. The present mathematical model does not include other mechanisms of permeation. Tests were conducted using Dow Corning RTB-382 as the base material and glass microspheres as the inclusion material. A volume fraction 0.70 inclusion was selected as a representative sample and permeation tests were conducted. Test results indicated that significant improvement in permeability reductions were obtained (1.6 fold compared to the theoretical sixfold improvement). The test results indicated what mechanisms of fluid transport are present. It is postulated that another mechanism involves "short channeling" of the diffusing material in the immediate vicinity of the interface between impermeable inclusions and the base material. Surface treatment of the spherical inclusions to reduce "short channeling" will be required to approach the theoretical improvement possible.

INTRODUCTION AND SUMMARY

The program was designed to provide the fabrication and testing of impermeable-inclusion-loaded, medically-acceptable encapsulation materials. The goals of the program are to develop encapsulation materials and techniques that will effectively isolate implanted components from body fluids, while retaining other necessary properties.

The technical approach is to load a standard, medically-acceptable, encapsulation material with impermeable inclusions which will partially block the diffusive path within the base material. In this way a less permeable coating material is formed while mechanical properties and surface characteristics are retained.

Seventeen separate aggregate formulations were prepared from basic filler and encapsulating materials selected from strength, toughness, permeability and biological acceptability considerations. The most promising were determined to be glass bubble microspheres uniformly distributed at concentrations up to 70 per cent by volume in medical-grade RTV elastomer; samples of which were further subjected to standard strength, toughness, permeability and absorption tests. Test results are reported and discussed.

The results of the permeability tests and their interpretation using predictive models, developed for diffusive penetration of the samples, indicate that significant potentials exist (up to 1000-fold improvements) for the inclusion-loading technique. The present results, however, display only marginal improvements. Recommendations are given for progressing beyond the present limitations.

RESULTS OF THE CURRENT PROGRAM

Reductions have been measured in the rate of water permeation, through the developed encapsulation formulations, to within approximately 60 per cent of the rate of permeation measured for samples consisting of only the pure base material. This level corresponds to an improvement of the effective fluid-transport resistance of the coating of 65 per cent over the fluid-transport resistance of the base material itself.

The materials formulation which produced this particularly significant result consisted of 60 per cent by volume 3M (Company) glass bubble microspheres (5-8 microns), Type B-22A, included in Dow Corning RTV 382 Medical Grade Elastomer cured with Dow Corning Catalyst M. Verification of this result was obtained through measurements involving five other samples with microsphere concentration levels ranging from 9 to 46 per cent by volume. The six samples involved in the corresponding data analysis and interpretation remained after two samples were discarded, from the original total of eight, because of their demonstration of anomalous fluid-transport rates.

Prediction is made from the statistical results, that the most likely improvement level that would be measured is 55 per cent if another sample 60 per cent microspheres by volume were to be prepared and tested. Furthermore, the statistical treatment establishes with a 95 per cent confidence level that the corresponding measured improvement level, for a new sample 60 per cent microspheres by volume, would fall within the range 22 to 85 per cent.

The strength and toughness characteristics measured for the 60 per cent by volume sample indicated no significantly adverse weakening effect due to the microsphere inclusions.

UNDERSTANDING OF THE PROBLEM

The understanding has been obtained, through the current program work, of the specific important mechanisms that are involved in permeation through a material containing impermeable inclusions; the potentials for obtaining improvements; the effects which specific levels of improvement concerning the individual mechanisms are expected to have upon the overall fluid-transport performance of the formulated encapsulating material; the limitations of the predictions and projections of the present mathematical models; and the problems that might be encountered in further development work.

A mathematical model has been developed, and satisfactorily verified by data, to relate the important parameters to the corresponding anticipated result. Two mechanisms have been identified as significantly controlling the steady fluid-transport rate through the developed encapsulating materials. The mechanisms are verified by the agreement of the data and the corresponding mathematical model developed upon this basis.

One mechanism, which provided the initial basis for the program, involves the transfer of material by diffusion through the bulk of the pure base material---a process which can be retarded by the presence of impermeable inclusions within the base material, provided the diffusivity of the base material does not significantly increase. The other mechanism involves short-channeling of the diffusing material in the immediate vicinity of the interface between the impermeable inclusions and the base material. Short-channeling is equivalent to an increase in the effective diffusivity in the vicinity of the interface; a phenomenon which may be attributed to the possible presence of a gas gap, a possible alteration in the electronic and physical structure of the base material due to bonding stresses, or both effects.

The effective diffusivity near the interface was found, from an analysis utilizing the mathematical model and the measured overall diffusion rates, to be constant to within a 95 per cent confidence limit of ±29 per cent. The mathematical model developed is verified to the extent that the computed effective diffusivity of the sphere-base material interface region is invariant since no efforts were made to provide various degrees of effective bonding at the interface.

A significantly high potential has been determined to exist for increasing the fluid-transport resistance of materials by using impermeable inclusion materials. Using the theory and corresponding mathematical model discussed above, a function has been developed to determine the maximum reduction in permeation rates that is possible using volume-loaded impermeable inclusion materials, provided there is no short-channeling at the sphere-base material interface. Improvement levels have been computed corresponding to selected levels of the volumetric loading of impermeable particles. Computed in addition are values of the theoretical upper limits (no short-channeling) of improvement levels corresponding to selected levels of area coverage when thin, oriented sheet and flake-type impermeable inclusions are considered. One-hundredfold (10,000 per cent) improvements in the fluid-transport resistance of the base material are projected for 93.5 per cent volumetric loading of spheres, 88.5 per cent area coverage of layer-oriented thin flakes, and 99.7 per cent coverage of layered sheets containing lattice spaced hole. A one-hundredfold increase in the fluid-transport resistance is equivalent to (a) a one-hundredfold increase in the time required for a coating material to permeate (leak) a given amount of fluid, and (b) a one-hundredfold decrease in the amount of fluid that will permeate through a coating material in a given period of time.

Using the mathematical model, the effect upon overall fluid-transport resistance has been determined of increasing the effective fluid-transport resistance near the sphere-base material interface and correspondingly adjusting the volumetric loading of spherical inclusions. Computations based on the results obtained in the present program project, for a 94.5 per cent volume loading level, a four-fold improvement in the fluid-transport resistance---provided the interface resistance remains constant. However, if the interface resistance were to be doubled, a fourfold increase would be projected for the 76 per cent loading level and a corresponding 16.5-fold improvement is projected for the 94.5 per cent loading level. A one-hundredfold improvement level is projected for the 94.5 per cent loading level provided the resistance of the interface material can be increased by a factor of 10 over the levels determined for the formulation methods of the present program.

There are several important limitations to the present theory and its corresponding mathematical models---all of which are attributable to two basic factors:

(1) Extensive time and effort is required in order to obtain exact solutions to the differential equations involved, or to obtain solutions by numerical or analog methods.

(2) The limited number of sample measurements which were incorporated in the analysis.

It necessarily follows as a result of the first factor that simplifying, but conservative, assumptions need be made, when resources are limited, in order to facilitate the construction of a workable, approximately accurate, mathematical model. To the extent that the model is approximate, rather than exact, the favorable evaluation of potentials is handicapped by the inherent conservatism and, more importantly, inaccuracies may arise in the verification of the theory by experiment. In addition, some important parametric influences may be overlooked by relying solely upon the simplified model. As far as the sphere diameter and other linear parameters are concerned, exact solutions to the differential equations involved are nondimensional in form as is the case for the simplified solutions obtained.

When a relatively large number of sample measurements are involved in an experiment, it will usually be found, through statistical analysis, that the range of values within which a subsequently determined measurement may be expected to lie (with a high level of confidence) will be relatively small compared to a corresponding range determined by the same experiment involving a smaller number of sample measurements. Since a limited number of sample measurements were incorporated in the analysis of the present program, the corresponding 95 per cent confidence band concerning projections based on the model and data is relatively broad. Figure 1 displays graphically both the theoretical and the measured effect of the concentration level of inclusion material on the permeation time (Figure 1).

A further limitation to applying the theory relates to the possible inaccuracies of its predictions and projections due to the simplifying assumption in the model development that the impermeable spheres are distributed on a uniformly spaced cubic lattice. In practice, however, the distribution appears to be relatively uniform, but random rather than ordered. Errors arising due to this assumption are probably relatively small, especially in cases where the volumetric loading of spheres is at a relatively low level. However, at higher loading levels some small error is probably involved. In fact, upper limits exist, in some cases, in the volumetric loading percentages then can be obtained. For spheres of a uniform size distributed on a uniform cubic lattice the maximum loading possible is 52.4 per cent; if distributed in the highest-density lattice configurations possible (close-packed hexagonal or face-centered cubic lattices) the maximum loading possible is 74.2 per cent. However, even higher loading densities, approaching 100 per cent, are possible when spheres of a variety of sizes are used together, even when only random spatial distributions are obtained.

Problems that are anticipated should further development be undertaken include the following general items:

(1) Maintaining satisfactory strength and toughness properties at higher levels of volumetric loadings.
(2) Developing a satisfactory surface bond that will increase the effective fluid-transport resistance of the sphere-base material interface by closing the possible "gas gap."
(3) Overcoming the possibility that short-channeling is due to an increase in the diffusivity of the base material itself, induced near the interface by molecular distortions produced by electrical force imbalances related to the interference in material continuity due to the sphere or, by other forces that may be involved at the interface.
(4) Maintaining a satisfactorily high level of quality control in coating material preparation.

DISCUSSION

DR. MOACANIN: You pointed out correctly that the maximum loading level would depend upon the size distribution of the microspheres. I would like to add, however, that the loading level would also depend on the surface characteristic of the microspheres. If you plan to use additives in order to affect gas permeation along the particle-matrix interface you are likely to also affect the maximum loading level.

We have done considerable work with fillers in our laboratory. We were able to show that for a given size or size distribution, the loading level for certain systems could be varied between 40 and 60% by using surface active additives.

DR. LEE: I was going to ask if you were using any chemical treatment of the surface, but Dr. Moacanin pre-empted my question. I would like to state that commercially we can get 80% by weight loading volumes and we do use surface treatment, because we can get higher loading volume with dry fillers. But the question I wanted to ask you is, why are you using spheres rather than flakes? It would seem to me that you are trying to make the maximum path length for water and ions, and flakes pack much better and give you rather significantly longer path lengths and spheres.

DR. NICHOLS: It turns out from the mathematical approach which we used, which incorporates some simplifying assumptions, that the theoretical limit for area coverage using flakes is greater. However, it is not many orders of magnitude greater. There is also a possibility of encountering the **distortion** in diffusivity near the interface, even when using flake type inclusions.

DR. LEE: It is difficult to get all the flakes to lie down the way you want them.

DR. NICHOLS: Yes, that would be a problem.

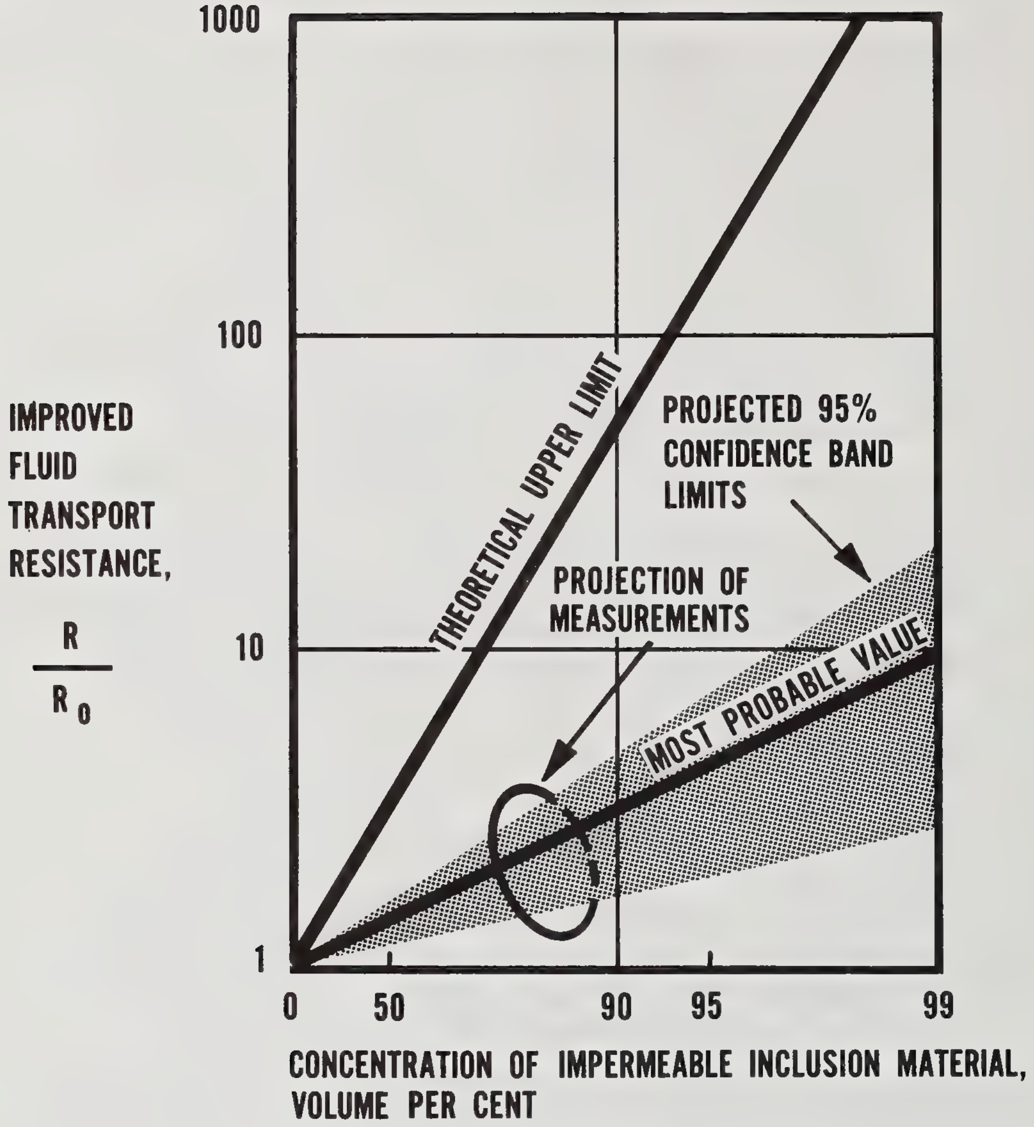

EFFECT OF CONCENTRATION OF SPHERICAL PARTICLES ON THE FLUID TRANSPORT RESISTANCE

FIGURE 1.

CHAPTER 65

DEVELOPMENT OF IMPROVED ENCAPSULATION MATERIALS FOR IMPLANTATION

H. Lee, A. Cupples, K. Neville, G. Culp and R. J. Schubert

Epoxylite Corporation
South ElMonte, Calif.

This program is intended to: (a) develop encapsulating resins suitable for long-term implantation in the body to serve as insulants for high impedance circuits used in artificial heart power sources and control devices, (b) develop methods for mounting artificial adnexa within the body, and (c) provide fast-response encapsulation and mounting fixture fabrication services. Epoxy-resin encapsulation systems have been developed with low water vapor permeability, low water absorption, and improved electrical properties. Concurrent with the encapsulation development, impermeable films of vacuum-deposited parylene have been investigated for use in sandwich constructions for some encapsulation applications. Results indicate the best systems so far developed preserve stable electrical properties in _in vitro_ testing in moist and fluid environments and are superior to those systems presently employed for pacemaker encapsulation. Three types of polyurethanes, segmented, polyester-based, and unsaturated, have been characterized for use as flexible, tissue-compatible overcoats for encapsulated artificial adnexa and for potential use in the fabrication of flexible stress-relief cones to prevent lead breakage on electrical units. Biodegradation studies in dogs have been initiated to confirm the suitability of the encapsulation materials and the polyurethane overcoats for use in biological environments. Scanning electron microscopy was used to determine histology and degree of surface attack on the implanted polymers. With regard to internal prosthopexy, an arrangement which distributes the weight of heavy artificial adnexa partly on bone and partly on soft tissue appears required. No directly applicable literature was found in a detailed _Index Medicus_ search. From 200 articles reviewed in detail, however, location adjacent to a section of stabilized rib cage is recommended, with weight being distributed to soft tissue by means of fabric tabs and to bone through the rib stabilization device. These devices are now being evaluated in cooperation with other contractors.

INTRODUCTION

In this part of our research for NHI, we have been concerned with developing plastic systems suitable for long-time implantation in the body -- both to protect artificial heart components as well as components of present-day pacemakers. We have also been instructed to develop a custom encapsulation service employing these systems for NHI contractors desiring to use it.

We have begun by developing encapsulation systems to permanently isolate electrical and mechanical systems from body fluids. The impermanency of paints and varnishes is well known. Perhaps less well known is the performance of thicker coatings -- encapsulation systems -- in severe environments. The present technology, for example, has not achieved an encapsulated electric motor that is suited for long-term operation under water. The problems involved with protecting printed circuits from high humidities, within allowable design parameters, are substantial. More generally, obtaining long-term junctions resistant to fluid leaks is not a simple or straightforward process.

For a variety of reasons, standard commercial encapsulation formulations -- nearly all based on the epoxy resins as the best available materials -- are not directly applicable to the present research. For one thing, water resistance of these formulations has been sacrificed to achieve other desirable properties including handling convenience, thermal shock resistance, etc. For another, curing requirements are often more open than with the delicate medical electronic components. In total, then, while using earlier experience as a starting point, we essentially began research afresh, selecting our starting materials on the basis of considerations which have been more or less well documented in the literature.

We have succeeded in producing systems which can be handled and cured within limitations imposed by medical applications and which appear suited for indefinite service inside the body -- at least so far as retention of electrical and physical properties are concerned. They are available through our encapsulation service.

As part of this research, and to clarify our own thinking as to the ultimate requirements we would have to satisfy, we reviewed the recent medical literature for clues as to how some of the heavier components anticipated in the implantable heart program might be permanently mounted. In this area, internal prosthopexy, we did not encounter more than cautionary notes indicating the problem is one of substantial magnitude. We _can_ conclude from the literature -- and this is something we all know -- that all artificial heart components and adnexa should be as small and as lightweight as possible.

DISCUSSION

Phase 1. Chemical Isolation Of Implanted Medical Prostheses.

The epoxy resins were selected as the most promising class of resins for use in developing encapsulation systems of low water sorption and low water vapor permeability.

Several characteristics of an epoxy-resin, curing-agent combination enables one to predict the approximate values for these parameters.

One of these characteristics is the oxygen/carbon (O/C) ratio for the resin. A lower O/C ratio implies enhanced hydrophobicity, since oxygen is the principal hydrophilic atom and carbon the principal hydrophobic atom. The influence of O/C ratio is demonstrated in Figure 1, where water sorption data are presented for epoxies with O/C ratios ranging from 0.15 to 0.28. These systems were all cured with the same amine and it can be seen that the relationship between O/C ratios and water pickup generally holds. Literally hundreds of epoxy resins are available to select from in order to obtain the O/C ratio which is as low as possible, consistent with handling requirements and reactivity considerations. Some are shown in Figure 2.

Another characteristic is the presence or absence of atoms along the resin chain more hydrophobic than carbon. Fluorine is particularly useful in imparting hydrophobicity. Some fluorinated epoxies similar to those chosen for testing under this program are shown in Figure 3.

While water sorption and water vapor permeability may be lowered by lowering the O/C ratio of the resin or using resins with hydrophobic substituents, it is also possible to decrease these values by the addition of nonreactive, low-molecular-weight diluents which serve to "plug up" intermolecular spaces. If chlorinated hydrophobic molecules are used, results are enhanced even further.

Based on such considerations, and taking into account the other application requirements, we selected resin systems suitable for initial screening.

We now come to the selection of the curing agent.

Of the curing agents available, diamines as a class offer the advantage of low cure temperatures, and, in the cured product, good resistance to degradation in a basic medium in the presence of enzymes, and elicit only moderate tissue response and relatively thin fibrous capsules when implanted in the body. Examination of the nitrogen to carbon ratio allows ball-park prediction of water resistance of resins cured with these amines, the lower N/C ratio giving the lower water pickup. Figure 4 illustrates this effect for the standard commercial resin cured with a series of alicyclic diamines. As can be seen, higher N/C ratios should be avoided to obtain low water pickup.

Of the diamines, long chain materials such as dodecane-1,12-diamine exhibit the greatest decrease in water sorption. However, because the distance between crosslinking points is great, it can be expected that such amines will prove to be unacceptably high in terms of water vapor permeability. Most other normally used classes of curing agents (especially the anhydrides) require cure temperatures of 200°F or over, making them unsuited for encapsulation of heat sensitive components.

Characterization of Cured Formulations. We tested a variety of formulations, with suitable controls, in terms of electrical properties, strength properties, water sorption, tissue reaction, and resistance to biodegradation.

Figure 5 illustrates dielectric loss factors for some of the systems. In this one, best electricals were obtained with the control resin (diglycidyl ether of bisphenol A), triethylene tetramine, and a chlorinated biphenyl diluent. The values for the low O/C resin (diglycidyl ether of tetramethyl bisphenol A) with the dicycloaliphatic amine (4,4'-diaminodicyclohexylmethane) were flat, indicating that the environment did not affect performance appreciably after 144 hours.

Figure 6 illustrates water pickup with time. As can be seen, the chlorinated material (Curve 5), which started with lowest dielectric loss, is suspect because of the water pickup, whereas system 4, which started with a relatively high loss and remained flat, exhibits the lowest water pickup, and appears to be preferred. The performance of Curve 1 is somewhat anomalous, showing nearly the lowest moisture sorption and yet the highest dielectric loss from Figure 5.

Results to date confirm, in a general way, the theory behind the present research, and confirm the superiority of even system 5, on the two figures, in comparison with system 2, (diglycidyl ether of bisphenol A cured with a resin adduct of diethanolamine) which can be taken as representative of the better commercial encapsulating systems suitable for use within the limitations of this program.

Microtensile bars of all systems were subcutaneously implanted in dogs and are being excised at three month intervals. In this manner, the effect of biodegradation on tensile strength over a one year period will be obtained.

Flexible Overcoating Systems. We know, from the literature, the desirable properties of silicone rubber for human implant applications. Less well known are the disadvantages, which include compatibility problems with other plastics, physical weakness, etc. Therefore, to increase our plastics armamentarium, as it were, we chose four polyurethane formulations for evaluation as potential overcoating systems, hoping that these would offer fewer disadvantages than the silicones, while offering equivalent tissue responses.

The two spandex polyurethanes, when subjected to the accelerated aging in the boiling water, showed rapid deterioration of electrical properties. Within 24 hours they were beyond the range of our equipment, a DK analyzer. Water sorption values for these materials were respectable at 2.10 and 1.30% for filled and clear spandex respectively. Water vapor permeability testing using an osmotic pressure system with ^{18}O enriched water showed them to be the most permeable of the systems tested (Table 1). Despite this relatively poor showing, the spandex materials have proven to be acceptable

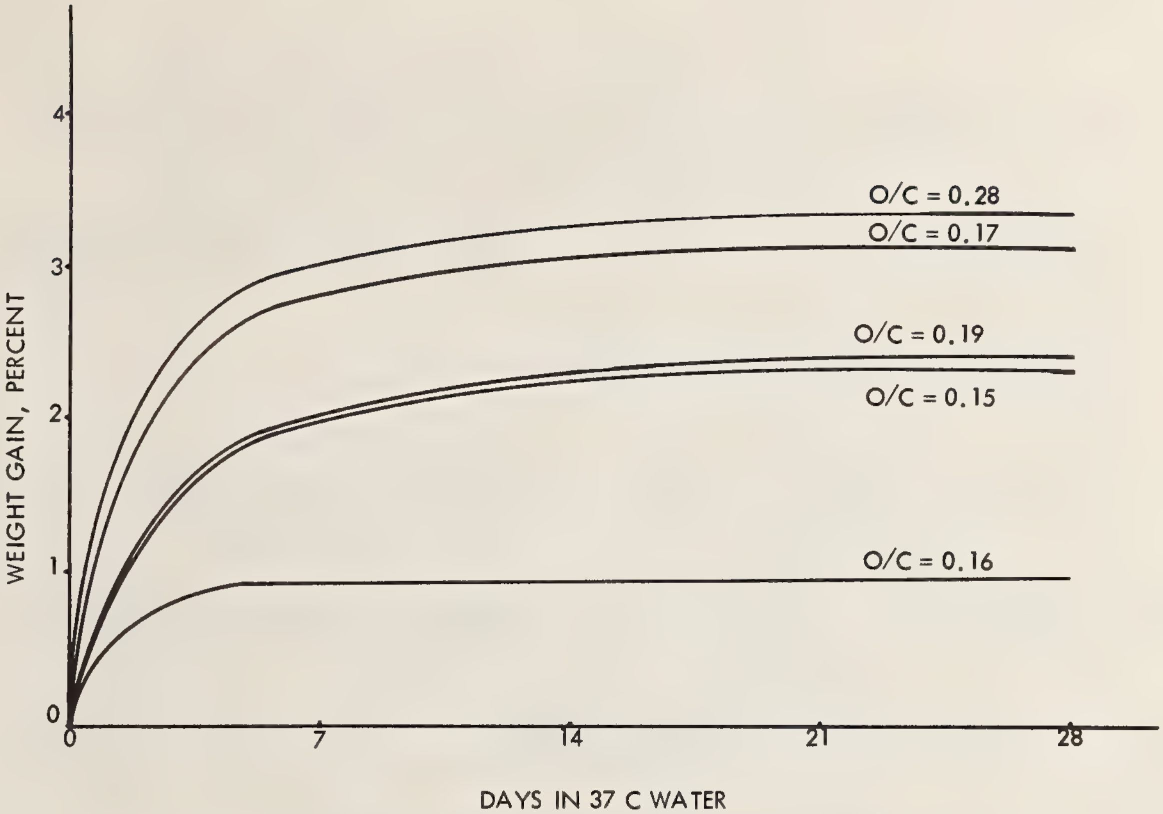

FIGURE 1. WATER SORPTION OF SEVERAL AROMATIC EPOXY RESINS OF VARYING O/C RATIOS. (ALL CURED WITH AN ALICYCLIC DIAMINE).

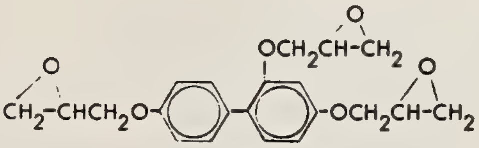

TRIGLYCIDYL ETHER OF TRIHYDROXYBIPHENYL, A TRIFUNCTIONAL AROMATIC EPOXY. O/C=0.28

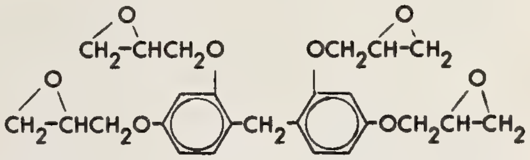

TETRAGLYCIDYL ETHER OF BISRESORCINOL F, A TETRAFUNCTIONAL AROMATIC EPOXY. O/C=0.32

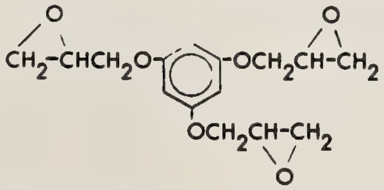

TRIGLYCIDYL ETHER OF PHLOROGLUCINOL, A TRIFUNCTIONAL MONONUCLEAR AROMATIC EPOXY. O/C=0.40.

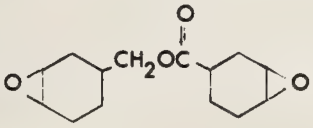

EPOXYCYCLOHEXYLMETHYLEPOXYCYCLOHEXANE CARBOXYLATE, AN ALIPHATIC EPOXY. O/C=0.31

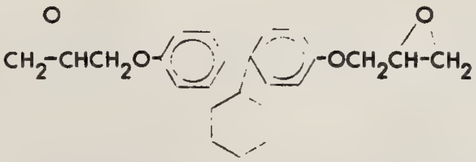

DIGLYCIDYL ETHER OF BISPHENOL C, A POLY-NUCLEAR AROMATIC-ALIPHATIC EPOXY.
O C 0.17

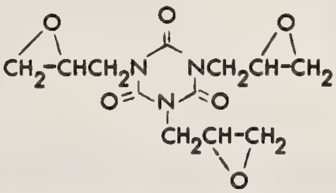

1,3,5-TRIGLYCIDYL ISOCYANURATE, A TRIAZINE-BASED EPOXY. O/C=0.50.

FIGURE 2. EXAMPLES OF AROMATIC AND ALIPHATIC, DI- AND TETRAFUNCTIONAL EPOXIES.

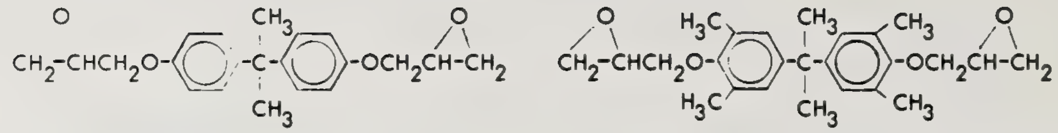

DIGLYCIDYL ETHER OF BISPHENOL A. O/C= 0.19.

DIGLYCIDYL ETHER OF TETRAMETHYL BISPHENOL A. O/C=0.16.

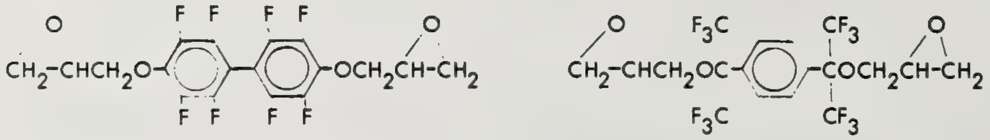

DIGLYCIDYL ETHER OF OCTAFLUOROBIPHENYL. O/C=0.22.

1,4-BIS[1'-(2,3-EPOXYPROPOXY)-1-TRIFLUOROMETHYL-2,2,2-TRIFLUORETHYL] BENZENE. O/C=0.22.

FIGURE 3. EXAMPLES OF METHYLATED AND FLUORINATED EPOXY RESINS COMPARED TO THE DIGLYCIDYL ETHER OF BISPHENOL A.

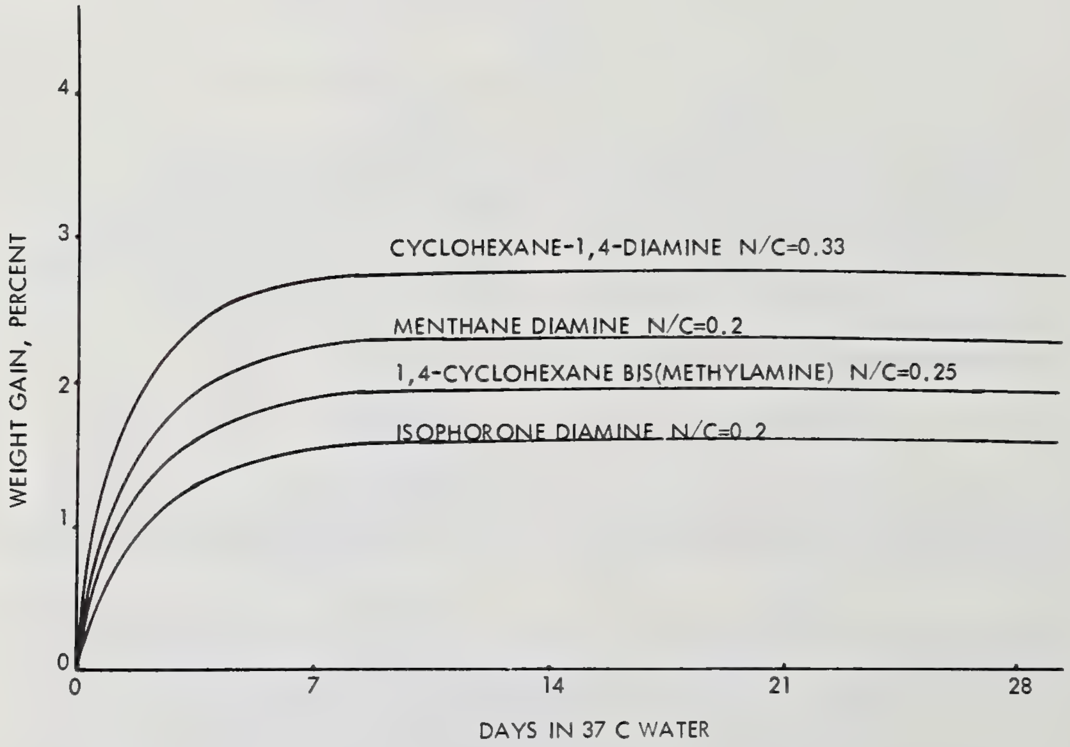

FIGURE 4. -WATER SORPTION OF MONONUCLEAR ALICYCLIC DIAMINES CURED WITH DGEBA.

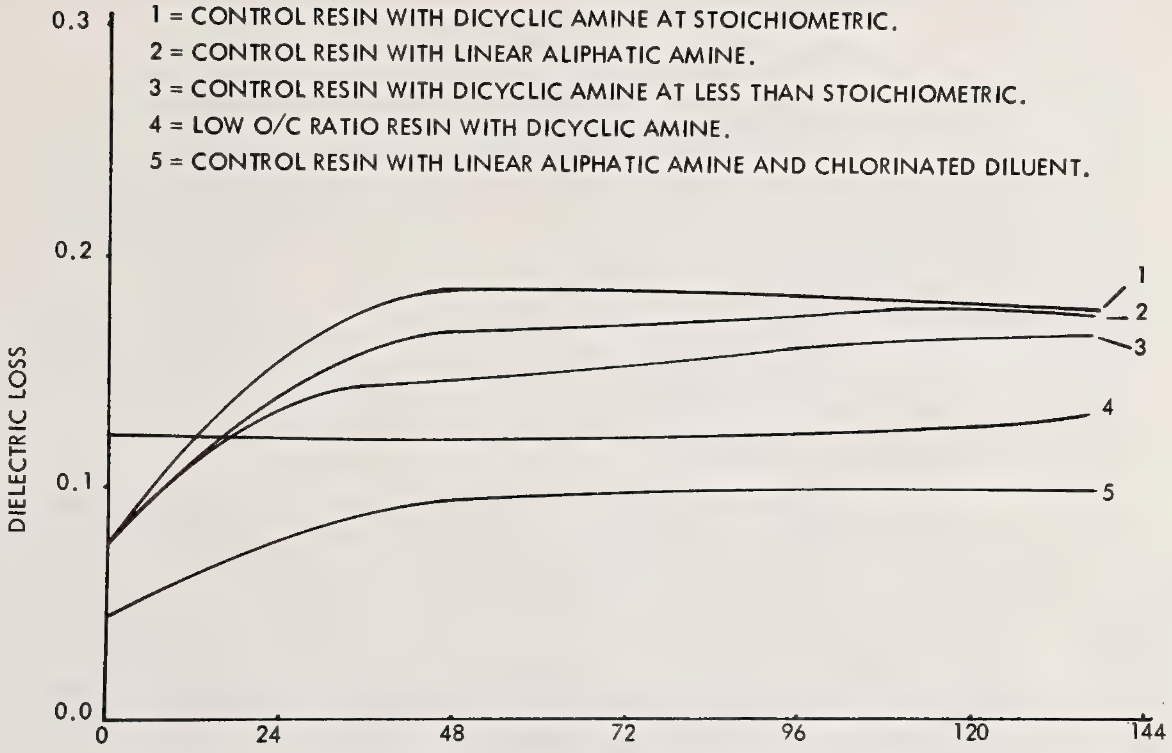

FIGURE 5. DIELECTRIC LOSS OF UNCOATED EPOXY ENCAPSULATION MATERIALS UPON ACCELERATED AGING IN 100 C WATER.

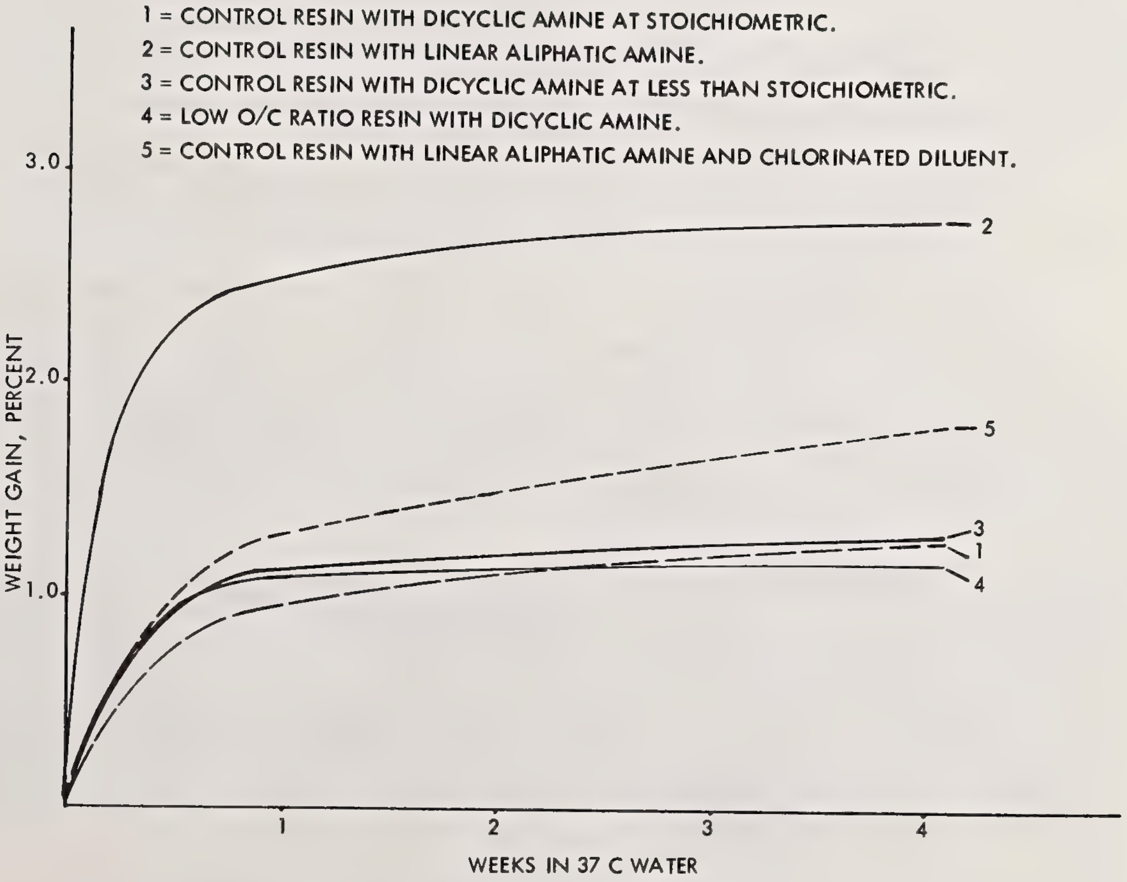

FIGURE 6. WATER SORPTION OF EPOXY ENCAPSULATION MATERIALS.

to the biological environment and therefore their evaluation is continuing since we do not plan to rely on them either as primary dielectric barriers or primary mechanical support members.

TABLE 1

RELATIVE PERMEABILITIES OF ENCAPSULATION COATINGS USING AN ^{18}O ISOTOPE ENRICHED WATER TECHNIQUE

Material	Relative Permeability (Change in ^{18}O Content, %)†
Clear, Segmented Polyurethane	0.209
Unsaturated Polyurethane	0.060
Polyester-Based Polyurethane	0.013
Chlorinated Parylene	0.001*
10% Dextrose Solution - Control	0.202

†All films tested for one week period.
*Corrected to 0.009" film thickness from actual 0.001" film thickness. Actual value = 0.008%. All other films are 0.009".

The third overcoating system is a flexible, unsaturated polyurethane of exceptional hydrolysis resistance. A curve of tensile strength vs. days in 100 C water for this material is shown in Figure 7. Unlike the two spandex polyurethanes which are solvent systems, this material is 100% solids and has potential use not only as an overcoating material, but also as a replacement for silicone rubber in the fabrication of stress relief cones on leads at their point of entrance into a prosthesis.

Retention of electrical properties for this material is good. After 144 hours in boiling water the dielectric loss factor changes from 0.102 to 0.283, which is only slightly worse than commercial epoxy systems. Despite its flexible nature and long polymer chains, water sorption is only 0.93%. This low value is due to the hydrophobic characteristics of the carbon-to-carbon backbone. Water vapor permeability is better than for the spardexes.

The last material to be tested, a polyester-based polyurethane, although giving lowest water vapor permeability values, deteriorated in electrical properties beyond the range of the DK analyzer within 24 hours.

The unsaturated polyurethane then, in terms of long range properties, is the most suitable material.

Parylene Coatings. In order to increase versatility of our encapsulation services, it would be desirable to have at our disposal some method for using one of the more impermeable films available to industry. A survey indicated that, as a class, the parylenes seemed to have the greatest potential for our uses.

Parylenes, aromatic, linear polymers, are theoretically suited to the encapsulation of medical prostheses because:

1. They are vacuum deposited on a part in less than 1 mil films at room temperature, thus being useful in the encapsulation of heat sensitive components and contributing virtually no weight.
2. As shown in Figure 8, the chlorinated versions are extremely impermeable to water vapor even in one mil films.
3. Being vacuum deposited, they cover sharp radii of curvature evenly without receding and causing uncoated areas.
4. The chemical nature of the polymers should prove them to be resistant to biodegradation by the body.

The materials, however, are rigid and in thin films, fragile. Their use by us is primarily intended to be in the fabrication of sandwich-constructed encapsulation coatings. Here (Figure 9) the linear chlorinated polymer is applied between two layers of epoxy with possibly another coating of the polymer followed by another coating of epoxy and finally a polyurethane overcoat. Such a construction would be extremely impermeable to body fluids.

Phase II. Encapsulation Service.

Several thixotropic versions of the low permeability formulations are offered in our custom encapsulation service for producing thick coatings and for wet lay up procedures such as are needed for the attachment of Dacron or nylon velour mounting tabs to the prostheses. Such mounting tabs, of course, are affixed over the initial epoxy/parylene coating.

A typical mock up version of an artificial heart system is shown before encapsulation in Figure 10. The same components, after encapsulation in a thixotropic low permeability epoxy but before attachment of nylon velour mounting tabs is shown in Figure 11 with its nylon "glove" in place.

Another encapsulated mock up artificial heart component is shown in Figure 12. This simulated battery pack was first encapsulated in epoxy and then received a layer of hydrolysis resistant polyurethane in which velour was imbedded.

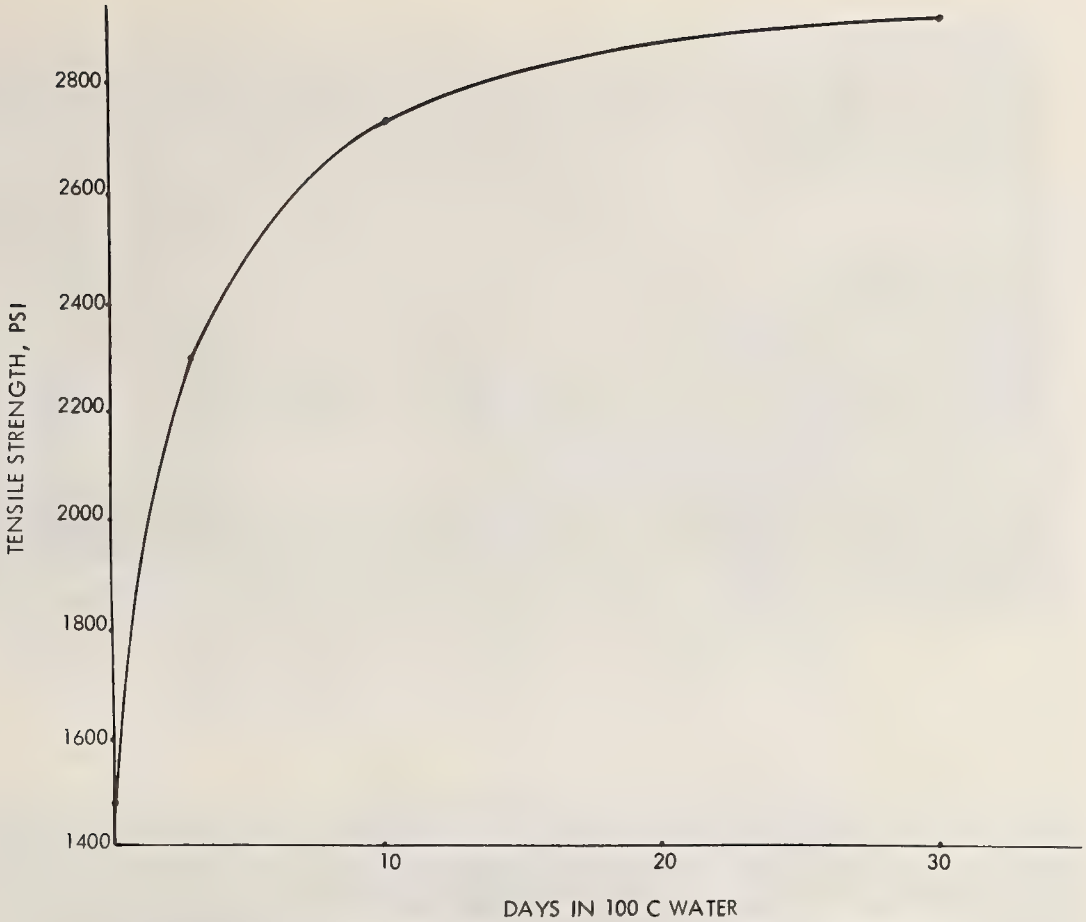

FIGURE 7. HYDROLYSIS RESISTANCE IN UNSATURATED POLYURETHANE #762.

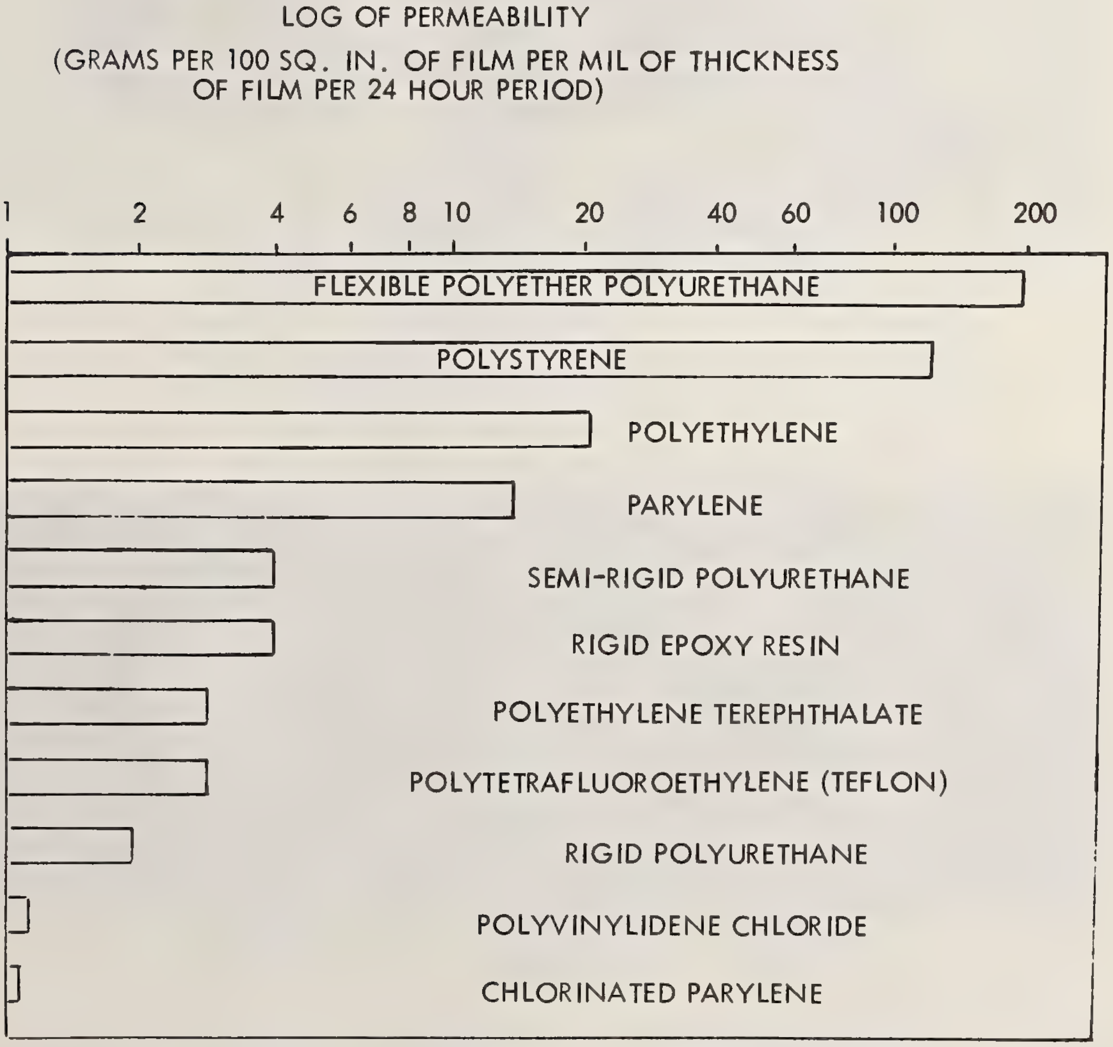

FIGURE 8. MOISTURE VAPOR TRANSMISSION OF LOW PERMEABILITY, UNFILLED POLYMERS.

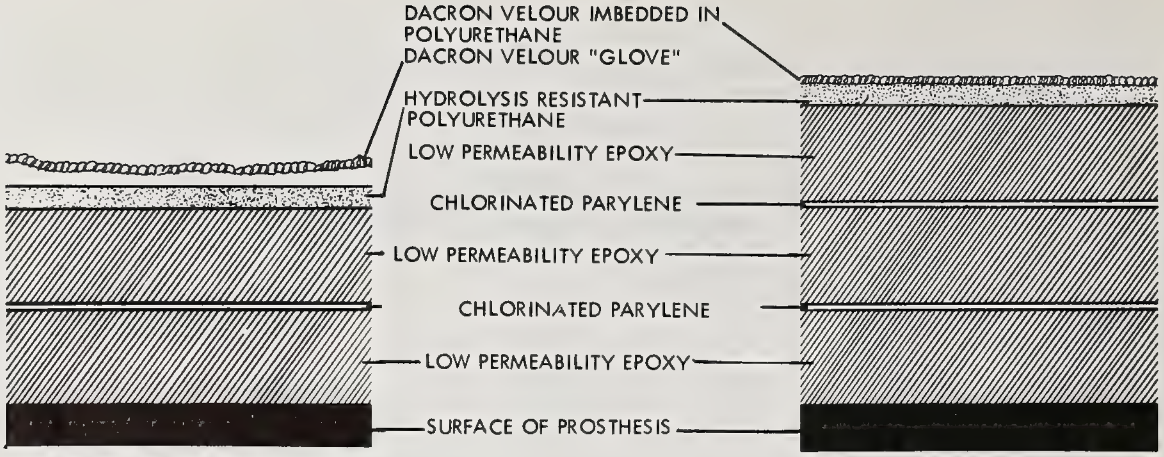

FIGURE 9. TWO POSSIBLE SANDWICH CONSTRUCTION METHODS OF ENCAPSULATING MEDICAL PROSTHESES USING A LOW PERMEABILITY EPOXY, CHLORINATED PARYLENE, A HYDROLYSIS RESISTANT POLYURETHANE, AND DACRON VELOUR.

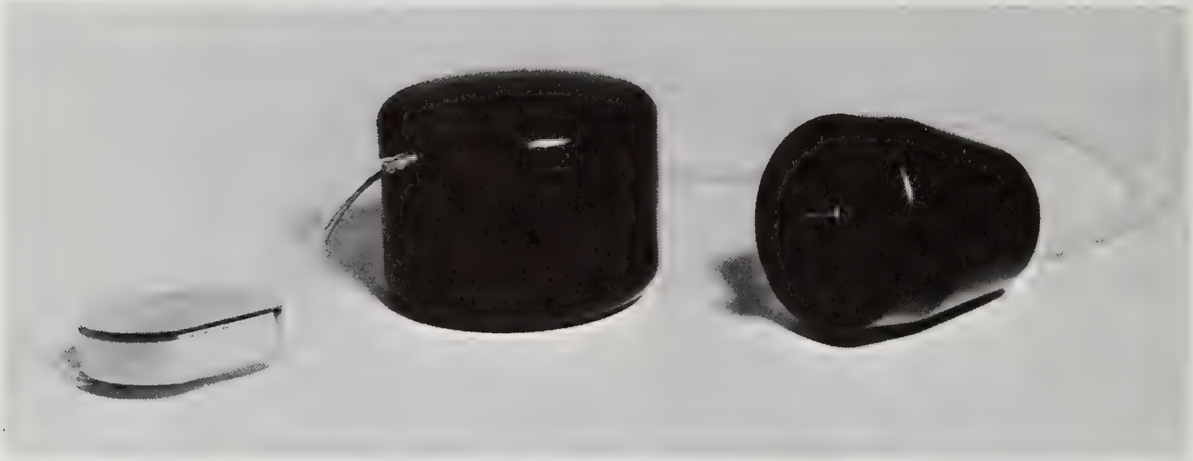

FIGURE 10. ARTIFICIAL HEART BEFORE ENCAPSULATION.

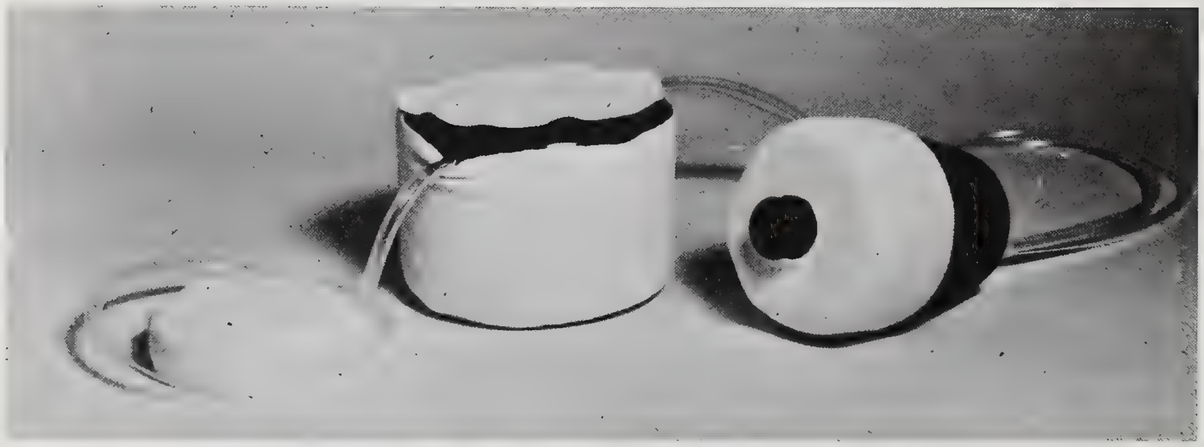

FIGURE 11. ARTIFICIAL HEART AFTER ENCAPSULATION.

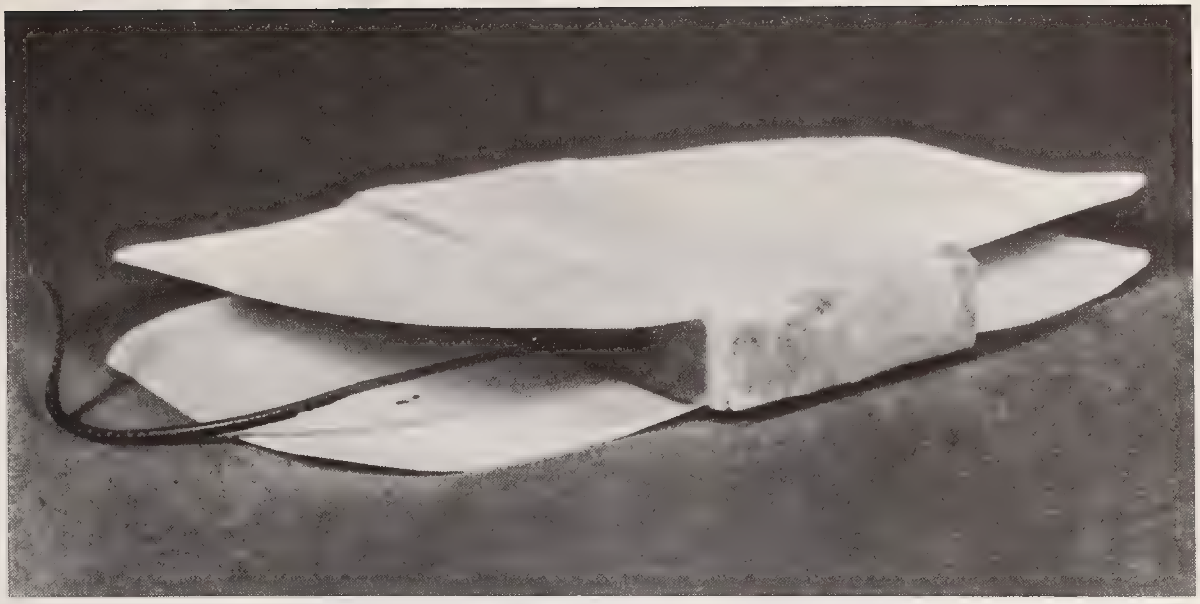

FIGURE 12. ENCAPSULATED BATTERY PACK.

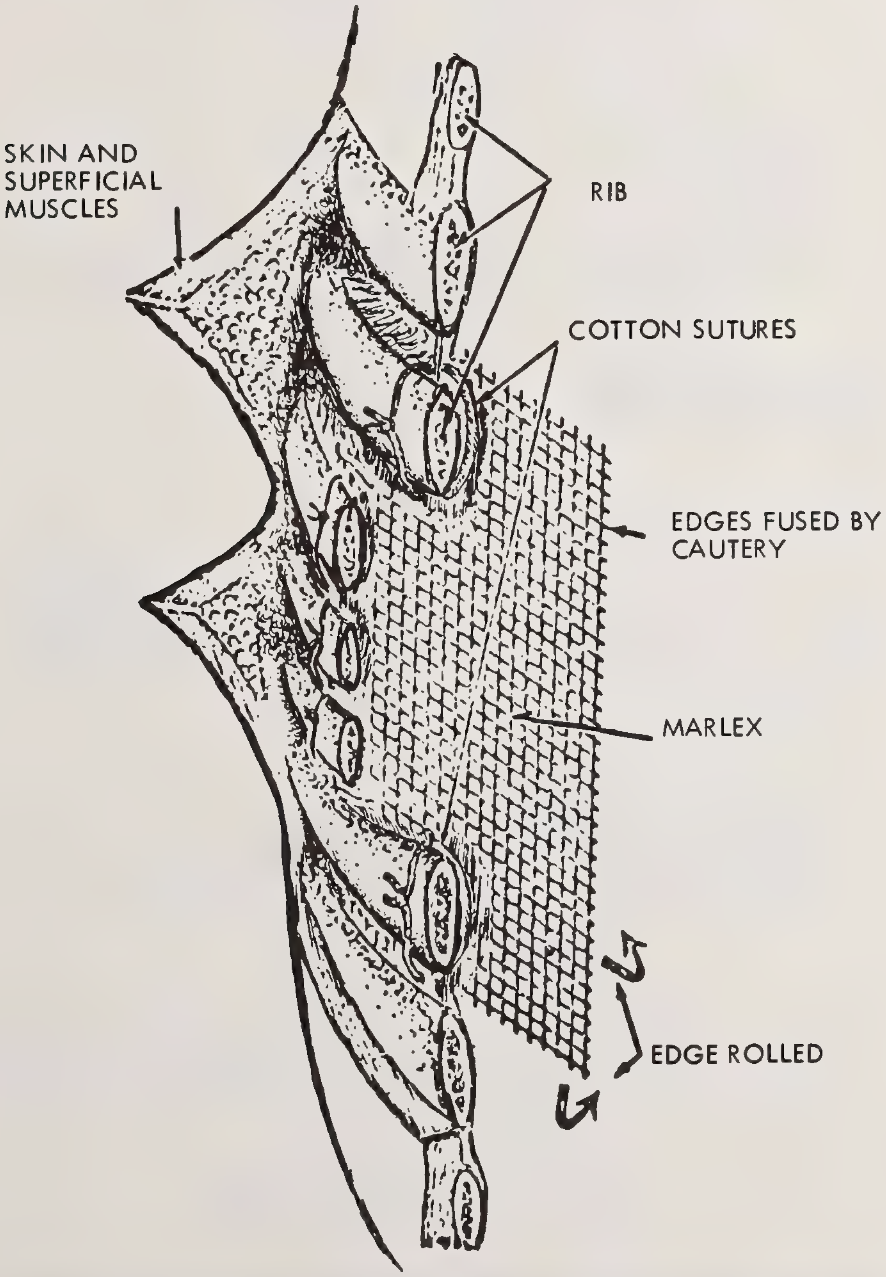

FIGURE 13. TECHNIQUE FOR INTRAPLEURAL FIXATION WITH POLYPROPYLENE MESH (REPRODUCED FROM ANN. SURG. 151:469-479, 1960).

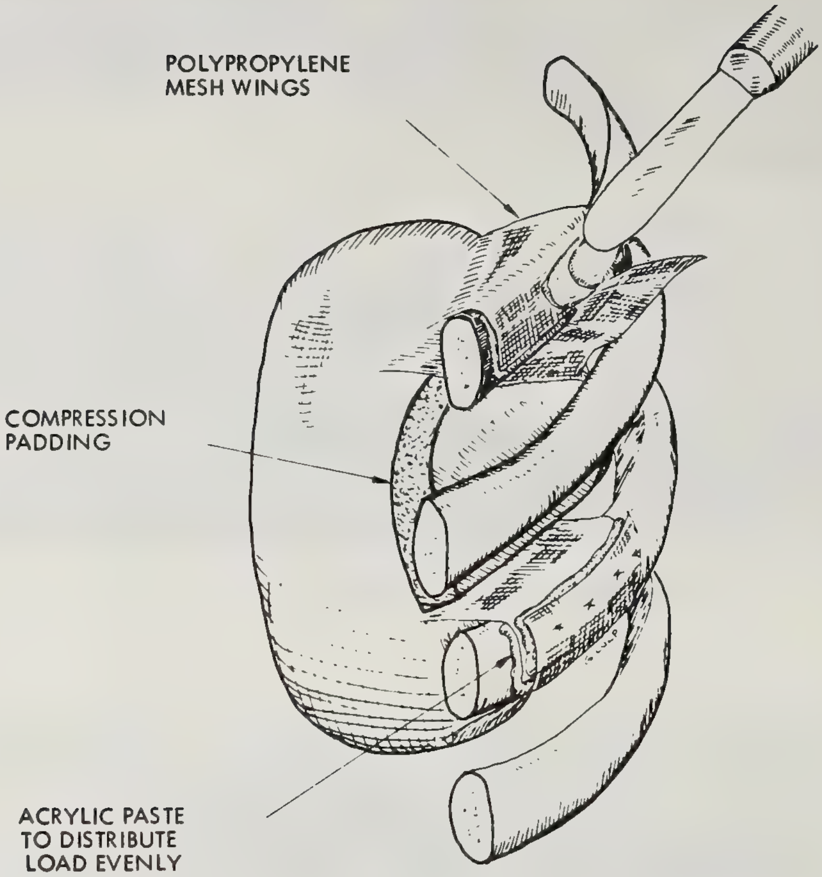

FIGURE 14. METHOD FOR ATTACHING ADNEXA WITH POLYPROPYLENE MESH AND ACRYLIC CURE-IN-PLACE PLASTIC. SOFT TISSUE SUPPORT MAY BE OBTAINED WITH ADDED DACRON MESH.

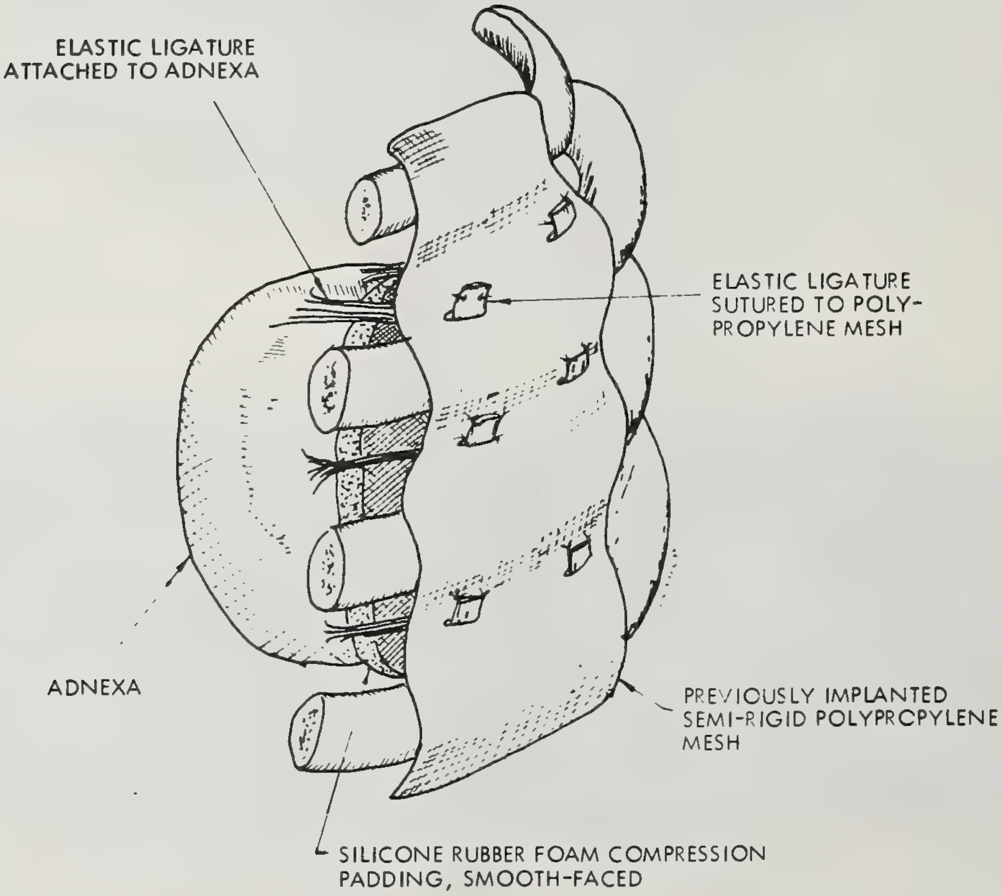

FIGURE 15. METHOD OF FORCE DISTRIBUTION TO SEMI-RIGID MESH AND THENCE TO RIBS AND INTERCOSTAL MUSCLES. INTERCOSTAL MUSCLES NOT SHOWN FOR CLARITY.

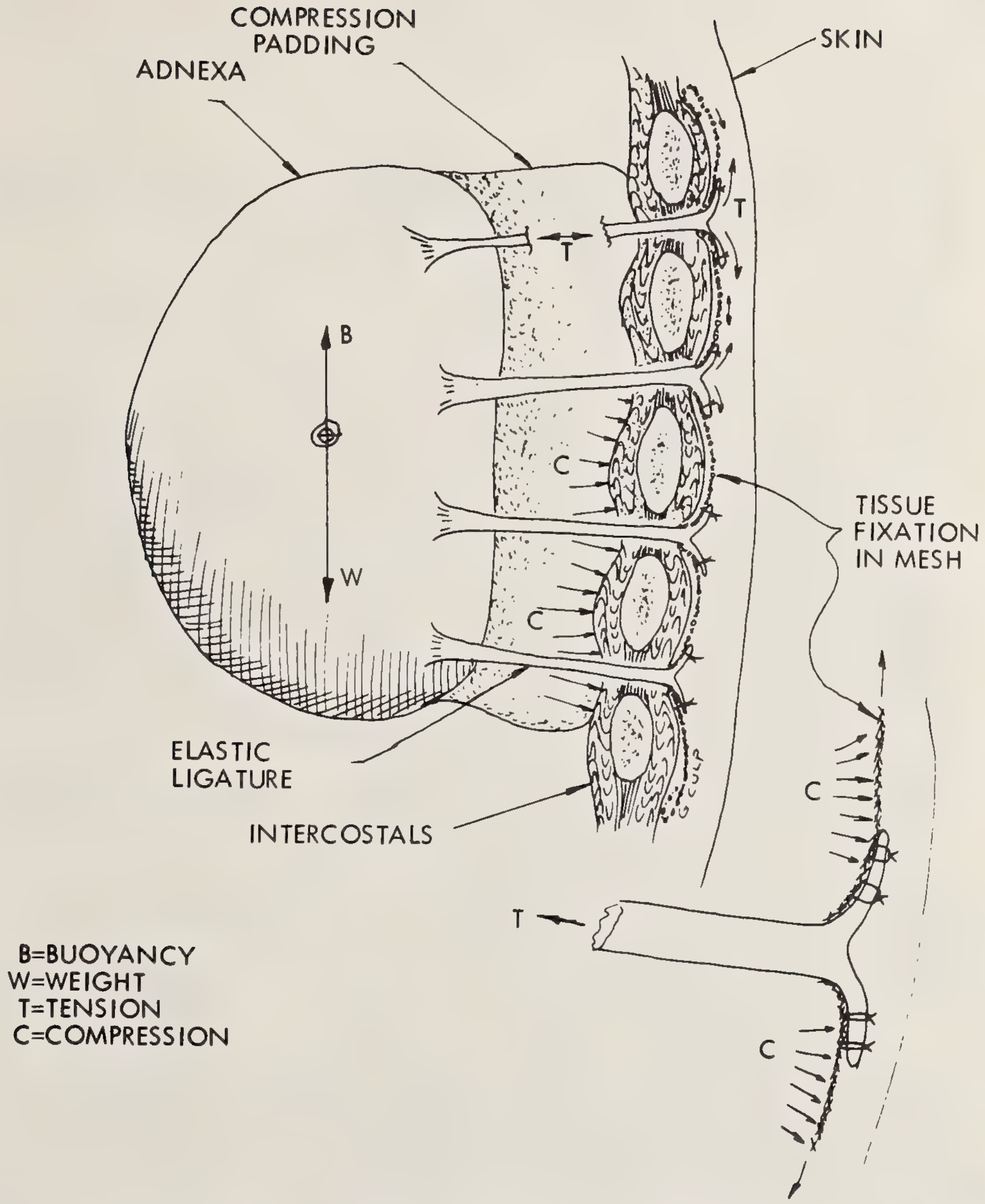

FIGURE 16. SCHEMATIC DRAWING SHOWING THE TRANSFER OF SUPPORT FORCES FROM THE ADNEXA TO THE ELASTIC LIGATURES THEN TO THE POLYPROPYLENE MESH, AND THEN FINALLY TO THE RIBS WITH THE EXTERNAL INTERCOSTALS ACTING AS A BUFFER.

Phase III. Mechanical Isolation.

The third aspect of this program involved a survey of medical literature in reference to the problem of long-term mechanical isolation and suspension of prostheses in the body. An item by item search of Index Medicus for 1964-1968 was conducted, with some 200 articles of greater or less relevance to the question being compiled. Simultaneously, a Medlars Search was instituted which ultimately produced approximately 90 articles, nearly all of which were without even peripheral value. This indicates that hard experimental data are missing, and that no totally firm conclusions are available at this time. However, from the literature, it is possible to present a general description of the problem areas and suggest that techniques applicable in unrelated surgical specialties might be modified to offer solutions.

Five problem areas were evident to us as being more or less critical for long-term satisfactory performance.

1. The literature on vascular prostheses suggests that late failures at anastomosis sites may be anticipated unless these sites are adequately reinforced in some manner. The solid-prosthesis, natural-vessel junction appears inherently weaker than the mesh-prosthesis, natural-vessel junction currently present with Dacron and nylon arterial prostheses and which itself is subject to late complications.
2. Although the literature, in particular relating to plastic surgical applications for tissue augmentation, is replete with the responses of soft tissue to relatively small plastic implants, it is silent with regard to tissue reactions to densities and configurations anticipated with some of the larger implanted artificial adnexa. Considerable evidence, both from the literature and our own research with percutaneous access devices, indicates that excellent tissue fixation can be achieved with fenestrated skirts or open-weave meshes. However, how well these will support relatively heavy objects remains to be determined.
3. When mounting to bone, it is generally recognized that static pressures in excess of capillary pressures will create erosion, and even at lesser pressure and under dynamic conditions, remodeling will occur. This would suggest that attachment techniques common with orthopedic surgeons should be avoided, since pins and screws tend to concentrate pressures over very small areas. Pressures should be more broadly applied, and this objective might be accomplished through the use of conforming pads or cure-in-place molding compounds.
4. On the assumption that the artificial adnexa will employ mesh tabs for tissue fixation, it is necessary to optimize materials for long term stability and strength retention in terms of imposed loads and resistance to body fluids. The literature suggests that polypropylene mesh might prove sufficiently strong in light weaves and provide the required stability. It appears preferable to less rigid meshes and to materials such as nylon, which has been shown to lose strength on implantation. The polypropylene, also, is reported to permit healing in an infected field.
5. Finally, methods should be investigated to provide surfaces which do not unduly provoke adhesions or soft tissue erosion when implants are to be located in the thoracic or abdominal cavity. It may be that special overcoats rich in heparin may be required to achieve this objective, or coverings of host tissue may be indicated.

It appears likely that the solution to problems of internal prosthopexy will require close collaboration between the engineers designing the artificial heart components and those dealing with mounting procedures.

If satisfactory adnexa of suitable weights and sizes can be designed, the most satisfactory mounting arrangement, while recognizing inherent disadvantages, would appear to involve sections of stabilized ribs. This location requires smaller and lighter weight components than are presently available.

Rib stabilization with mesh has been employed in clinical procedures; one arrangement is indicated in Figure 13. It would seem possible,then, to modify the concept for the mounting of heavier adnexa, as shown in Figures 14 through 16. In these figures, we have selected an intrathoracic location, which would probably create severe pulmonary and other complications, but which is presently necessitated by the dimensions of the available implants.

Optimally, we feel that only the artificial ventricles should be located in the chest cavity, and these should be tailored in size, weight, and density to resemble as nearly as possible the organ being replaced. The pump, controller, and batteries should be located elsewhere, and to minimize lead problems, as close to the ventricles as possible without unduly compromising the lungs.

DISCUSSION

MR. PURDY: There are two approaches for placing an artificial heart in the thoracic cavity. One is to bolt it to the sternum and the other is to use the pericardial sac as the support mechanism. In your recommendation, you suggested that some sort of a fabric be utilized which had been grown into the tissue. Will you comment on these other methods of attachment, please?

MR. CULP: We have not considered either of these methods at the present time. We have been given weight and sizes of the devices as well as the fact that there is a lack of biological material to act as an interface between the device and the lungs.

MR. PURDY: If it is in the pericardial sac, it would not contact the lung.

MR. CULP: That is true, but right now it is very difficult to say whether the pericardial sac could survive being put over the device.

MR. PURDY: To the first speaker I would also comment that two other approaches for creating a non-permeable material would be through the utilization of metals. In your technique, a non-permeable plastic is used, but instead nickel can be placed at very low temperatures on matrix as a barrier. The other approach would be to utilize aluminum. In other words, have you considered the use of a metallic barrier rather than an organic barrier, in your sandwich to confine the flow of fluid?

MR. CULP: We haven't worked with metals as yet.

DR. BYCK: I would like to compliment Dr. Lee and his associates on what appears to be an attractive approach to an impermeable encapsulant. I think I agree that polymer laminate materials represent a more promising approach than polymer mixtures or polymer composites. Needless to say, I was very interested in their use of Union Carbide's Parylene C, as you might expect. I might point out, as a practical measure of permeability, that we have succeeded in encapsulating reactive metal anhydrides, which are highly reactive to water, in such a way that these can be immersed in water without reaction and can be left exposed to moist atmospheres literally for periods of years without changes. I would, however, like to correct some small misconceptions which might be drawn from this paper regarding the Parylenes. Parylene C is one of several commercially available Parylenes, but is only one of perhaps one hundred experimental Parylenes which we have investigated which range in mechanical properties from very stiff materials to extensible materials. And I would also like to point out that while adhesion of Parylenes to surfaces is an experimental problem, we have always found that one can devise surface treatments which will permit rather excellent adhesion of Parylene polymers to virtually any surface desired.

MR. ROGERS: With reference to your support of the object, you said there is little information in the literature. We can add a little information from the point of view of sealing the space required for an energy source in the abdomen. It was done in the calf. We had an implanted object, the size of a football, and it was covered with ordinary Silastic out of a tube. It took about twenty tubes to cover it. They were put into the abdomen, and the calves were put out to pasture. We had seven of them, and the longest survival was almost a year. There was no percutaneous lead on them. We lost them for reasons unrelated to the device or the coating. Ultimately they made them of masonite. This absorbed water, and eventually stretched the coating, causing difficulty. But they were in no manner fastened, yet they stayed where they were, and remained so well encapsulated in an artificial film, that it was very difficult to remove them. We thought we would anchor them but we never did. I agree with your point of view on the pericardium. I think that ultimately if the ventricle is to be successful, it has to be such that it can be retained within the pericardium and this does present a problem.

MR. CULP: The specific gravity of your implanted device was that of water, was it not?

MR. ROGERS: Yes. We used an average density of just about that of the contents of the abdomen. It was just a little bit lower than water.

MR. CULP: In our case we have to work with devices that have a higher specific gravity. Adjusting specific gravity downward gives excessively large volumes.

SECTION IX

PERCUTANEOUS LEADS

Chairmen: Allen K. Ream, M.D.
Charles E. Branch

INTRODUCTION

At this stage of development, circulatory assist devices require tubes and/or wires passing through the skin. While with present techniques such percutaneous connections can be made reasonably safe for short periods while the patient is under close medical supervision, these techniques have not been proven suitable for long-term intrathoracic implants. The purpose of this contractual program is to devise and test in animals a long-term percutaneous lead system, for ultimate use in ambulatory humans, that can transmit electrical or fluid energy into the thoracic cavity for energizing circulatory assist devices. Problems to be solved include the attachment of a stable material to tissue which is continuously undergoing anabolic and catabolic change, the lack of antimicrobial resistance in avascular scar tissue, the good culture media for micro-organisms produced by desquamating tissues, the propensity of micro-organisms to develop resistance to antimicrobial agents, and the movements of tubes transmitting pulsatile fluid energy.

CHAPTER 66

DEVELOPMENT OF SATISFACTORY LONG-TERM PERCUTANEOUS LEADS

H. Lee, D. Ocumpaugh, G. Culp, A. Cupples

Epoxylite Corporation
South El Monte, Calif.

The lead which has been developed features a central percutaneous, cylindrical conduit which has an exterior flange and a subcutaneous fenestrated skirt. The central conduit passes the cannulae or electrical wires needed for artificial heart or assist device operation. The flange prevents overgrowth of the conduit, while the skirt provides immobilization when connective tissue invades the fenestrations. Animal experiments, including 88 leads in 23 dogs, 2 leads in 2 monkeys, and 10 leads in 4 pigs, were performed using 12 different materials of construction and 28 variations of configuration. Satisfactory lead performance is characterized by absence of serous weeping despite induced trauma by the free-ranging animal, continuous exposure to ubiquitous vivarium organisms, and externally applied broths of virulent bacteria. The apparently necessary histological precursor to satisfactory performance is epithelial encapsulation of all subcutaneous surfaces. The absence of epithelial encapsulation has, without exception, been associated with edema of adjacent tissue, with chronic serous or seropurulent weeping at the emergence site, and in some instances, peripheral exposure of the subcutaneous skirt. Subcutaneous implantation revealed no tissue toxicity due to any materials used in the leads: no lead construction materials, *per se* could be implicted in unsatisfactory performance. Minor variations of the configuration of the leads have not had statistically significant effects on lead performance. Docile animals, i.e., those that appear to ignore the emergence sites, have a higher incidence of satisfactory lead performance. We therefore conclude that animal-induced trauma, preventing the epithelial encapsulation in the first few weeks postoperative, is one cause of unsatisfactory performance.

INTRODUCTION

We set forth as the definition of a satisfactory long-term percutaneous lead a device that allows permanent access to inner body spaces, while at the same time, (a) not allowing the leakage of body fluids, (b) not allowing the ingress of virulent organisms, and (c) not losing its usefulness with time, while enduring the same trauma as the normal intact skin. This definition is somewhat more rigorous than that used by other investigators, since the retention of the device, or the level of the infection or foreign body reaction at the emergence site remaining clinically manageable, is all too often deemed sufficient for it to be considered successful. Our definition required that the device be treated in every way as the normal skin, which precluded the use of topical or systemic antibiotics or other special care.

The need for a device of this kind is illustrated by Figure 1, which shows an experimental, totally implanted cardiac system compared with the simplification possible in the implantation surgery and the postoperative maintenance of a system using a percutaneous lead.

The natural occurrence of percutaneous leads is infrequent. Figure 2 shows how a fairly good seal is formed when the oral epithelium turns downward and attaches to the tooth by means of the stratum cementum. The deer antler (Figure 3) is also a true percutaneous lead because it is a skeletal extension. Figure 4 shows a section through the antler skin comparable to the tooth insofar as the epithelium is turned downward and sealed by slight adhesion to the antler proper. The skin of the dog fish shark (*Squalus acanthias*) is covered with numerous placoid scales (Figure 5) which protrude from the skin. Here the down turning of the epithelium is not as prominent, but the flanged subcutaneous portion of the scale is important to the mechanical strength retention of the scale. A similar epithelium phenomenon is reported at the cut edge with the plastic artificial cornea.

Design of Percutaneous Leads.

To maximize the probability of success we emulated nature as closely as practicable in designing percutaneous leads. Figure 6 shows the optimized lead, which consists of a rigid plastic central conduit to pass the cannula or electrical cable, this attached to a semi-rigid, fenestrated skirt. The central conduit has a small flange at the top which, when the lead is in position in the skin, is in contact with the skin surface.

In nature epithelium is always observed to be attached to the percutaneous member by ingrowth or adhesion. Initially attempts were made to promote adhesion to the plastic central conduit by treating the surfaces in numerous ways, but no adhesion occurred. The configuration of the lead was then altered to enhance the downgrowth of the epithelium by moving the fenestrations of the skirt closer to the conduit.

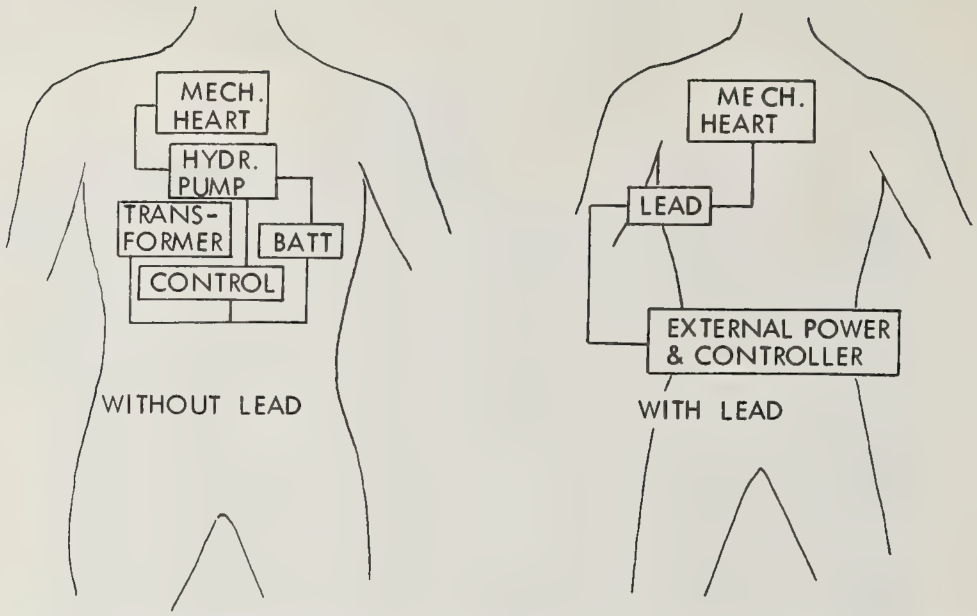

FIGURE 1. BLOCK DIAGRAM SHOWING SIMPLIFICATION OF AN EXPERIMENTAL COMPLETELY IMPLANTED CARDIAC ASSIST DEVICE USING A PERCUTANEOUS LEAD.

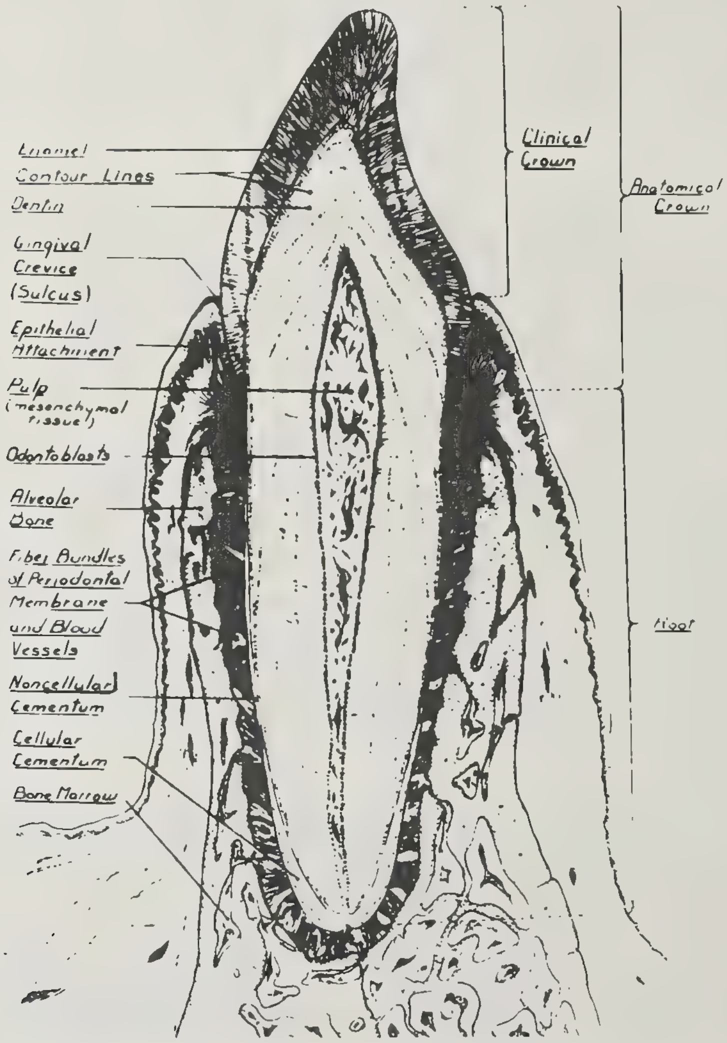

FIGURE 2. DIAGRAM OF A SAGITTAL SECTION OF A LOWER CENTRAL INCISOR TOOTH AND ATTACHMENTS.

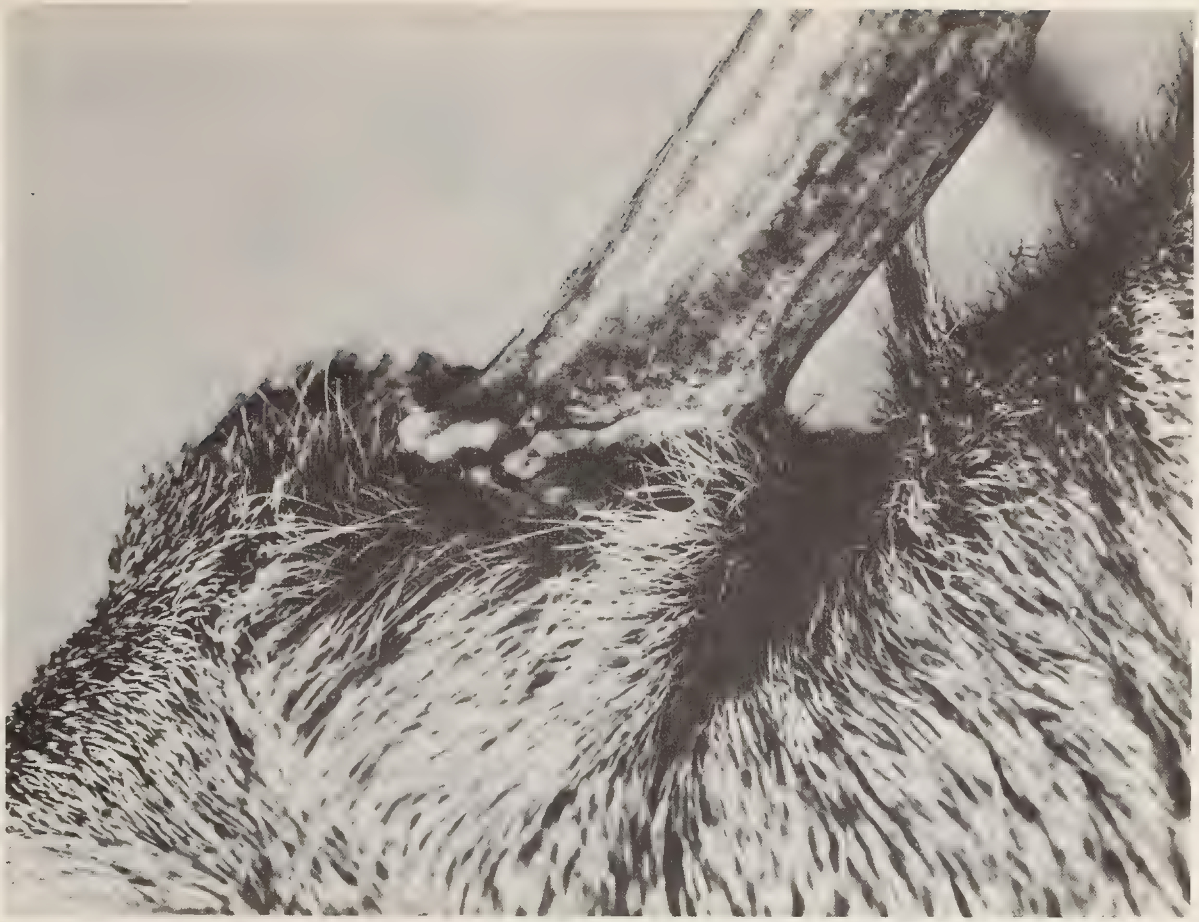

FIGURE 3. CLOSE UP VIEW OF DEER ANTLER SHOWING EXTERNAL FLANGE ABOVE EPITHELIAL ATTACHMENT POINT.

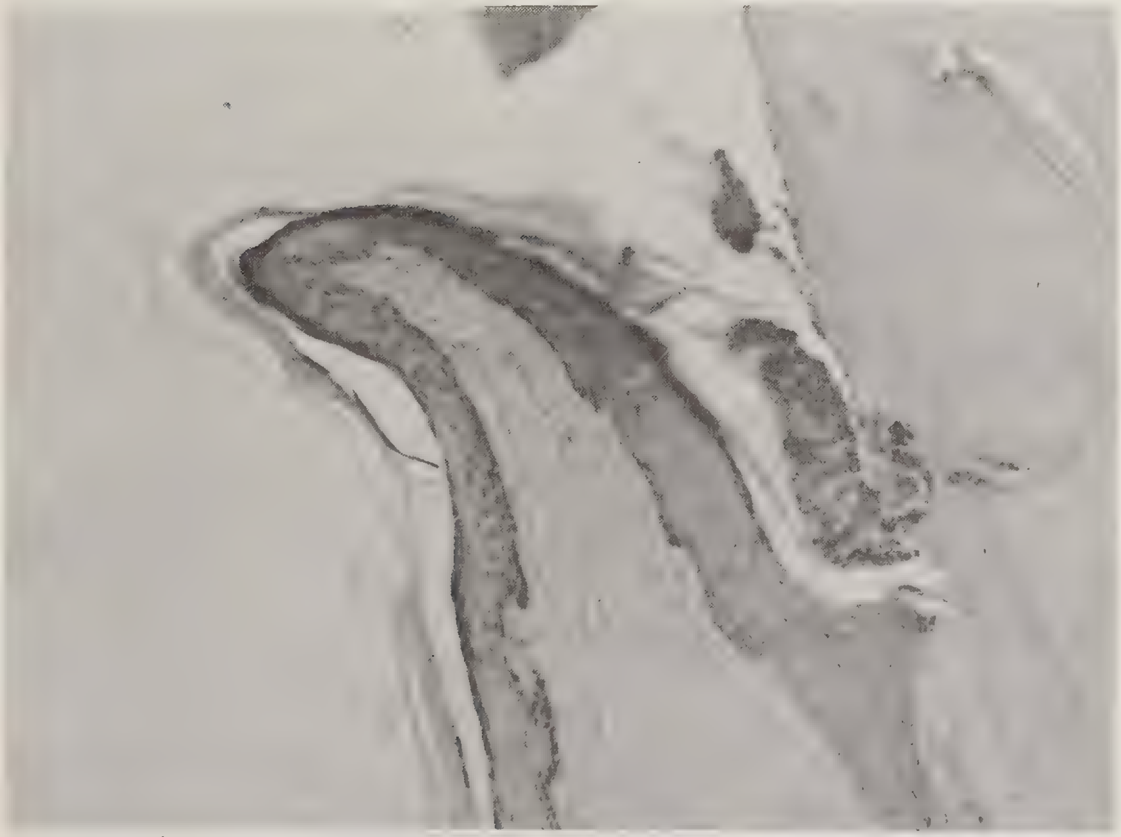

FIGURE 4. HEMATOXYLIN AND EOSIN HISTOLOGY SLIDE OF EPITHELIUM AT ATTACHMENT POINT TO DEER ANTLER.

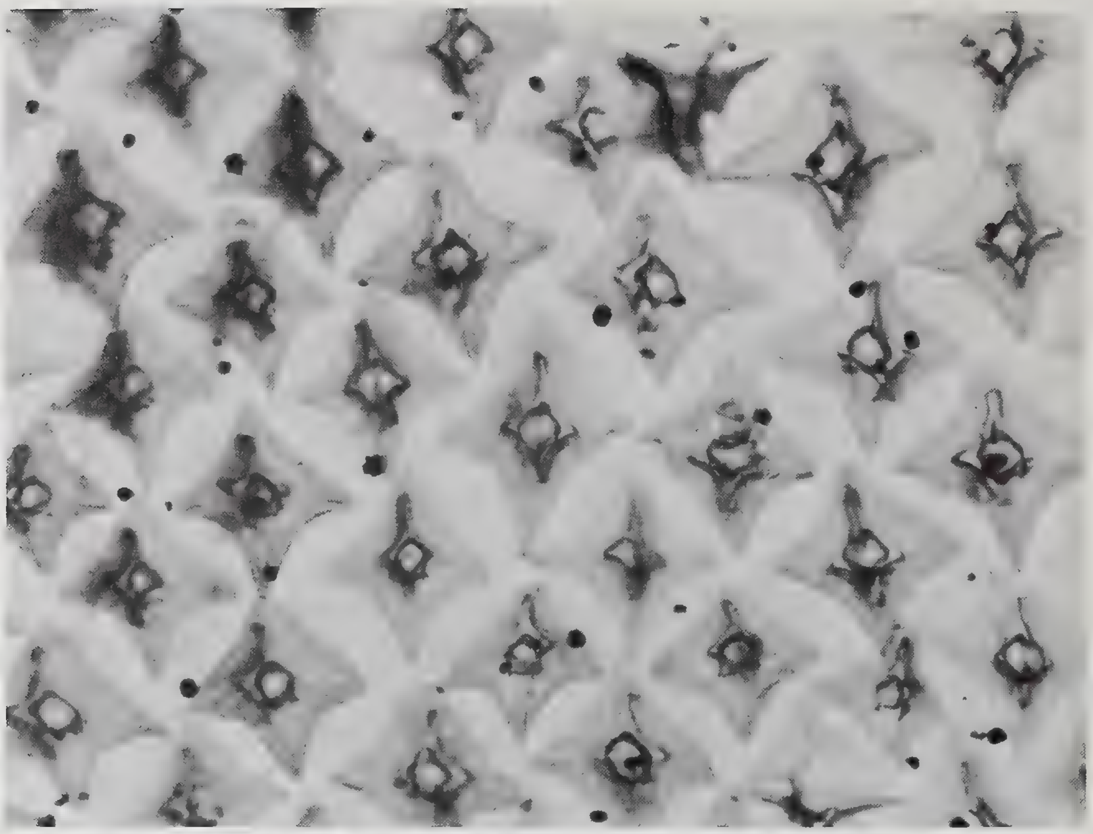

FIGURE 5. THIS IS A PLAN VIEW OF SHARK SKIN SHOWING PLACOID SCALES. ORIGINAL MAGNIFICATION 40x.

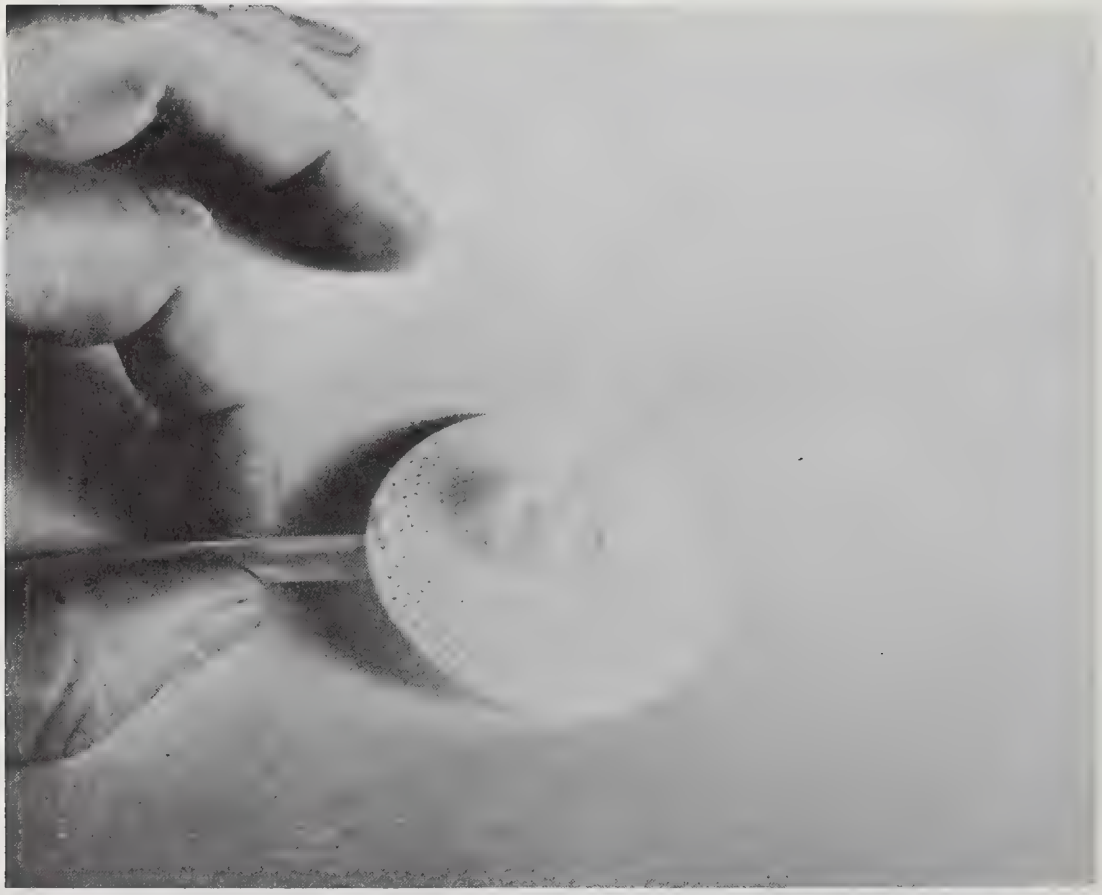

FIGURE 6. PERCUTANEOUS LEAD OF TYPE PROVEN MOST SUCCESSFUL UNDER THIS PROGRAM.

The conduit need only be large enough in diameter to pass the desired cannula size or electrical cable and still have sufficient wall thickness for structural strength. The height of the conduit, as measured from the upper surface of the skirt to the underside of the outer flange, is made slightly greater than the thickness of the skin. The skirt thickness is adjusted to give the proper flexibility and tensile strength, the exact values being functions of the physical properties of the particular material used. Typically, a Teflon skirt is one mm thick. The diameter of the skirt need only be large enough to prevent excessive motion of the skin adjacent to the conduit and to distribute stress over a larger area of intact skin. The fenestrations of the skirt were varied from 1/2 to 3 mm dia. early in the study to determine what effect this had on the degree of lead immobilization achieved by invading connective tissue. It appeared that a fenestration diameter equal to the skirt thickness gave the best results.

FABRICATION

Most leads were machined from cast billets. Particular care was taken in the machining to avoid lubricants of any kind that could later cause tissue reaction. Leads with Teflon skirts were assembled to rigid plastic conduits by casting the conduits around and through an inner row of fenestrations, since it is not practical to form a reliable adhesive bond to Teflon. It was paramount in the design of the skirts that the fenestrations be equally spaced, and that the per cent open area was held constant throughout the skirt. This was accomplished by the use of a special machine that positioned the skirt along an involute spiral, according to a prearranged computer program, during the fenestrating operation.

MATERIALS

Conduits for the leads were made of several formulations of rigid epoxy, rigid polyurethane, polypropylene, and Teflon. Skirts were made from flexible polyurethane, polypropylene, Teflon, and vitreous carbon fabric, and the untreated materials from which the conduits were made.

MATERIALS TESTING

It is important that the materials used do not lose strength after long-term implantation, as that they do not cause adverse tissue reaction. It could not be expected that the percutaneous leads would yield data on the effects of the plastics on the tissues, because of surgical trauma and the exposure of the subcutaneous tissues to the ambient ubiquitous organisms immediately after implantation. In addition, the shape of the leads does not lend itself well to the testing of physical properties. To circumvent these problems, tensile specimens were made according to ASTM Standard D1708-59T, except that all specimen dimensions were reduced to half value. These were implanted subcutaneously in the skin at the same level as were the skirts of the leads. At intervals of approximately six months, skin pathces containing some of the tensile specimens were excised, the tissue being given routine sectioning and staining, and the tensile specimens being pulled on a universal testing machine. Changes of hardness were noted using the indentation method per ASTM D1706-61 on the end tabs of the tensile specimens.

Because of the small dimensions of the tensile specimens, considerable variance of the tensile strength test results is expected. Because of the long-term nature of this testing, not enough specimens have been excised at this time to yield statistically significant results.

PREPARATION FOR IMPLANTATION

All leads were thoroughly washed and then extracted in a Soxhlet for three days. Contact with foreign protein was strictly avoided after extraction. Sterilization was by live steam at 250 F for 20 minutes USP. Effectiveness of sterilization was routinely verified using spore strips and autoclave tape.

IMPLANTATION

Naturally, rigorous sterile technique was employed in the implantation of the percutaneous leads. The leads were inserted by first making a lateral incision with length equal to the diameter of the lead skirt. Next, a pocket was formed in the fascia by blunt dissection. Then a hole was made in the center of the skin superior to the pocket that was just large enough to accommodate the neck of the conduit. An extremely sharp trephine was used to minimize the trauma at the cut edge. The lead was then inserted edgewise into the pocket and the conduit coaxed through the trephined hole. Tension in the skin was kept at a minimum. In most of the implantations a purse string suture was used near the cut edge around the conduit. The lateral incisions were closed with stainless steel sutures. Postoperative care consisted simply of vitamin supplements and mild oral antibiotics for four days.

This implantation protocol proved to be the least traumatic of all others tried. Eighty-eight percutaneous leads were implanted in 23 free-ranging mongrel dogs, 16 leads in Rhesus monkeys that were immobilized in executor chairs for three weeks, and 10 leads in four free-ranging pigs.

RESULTS

Mechanical Immobilization.

Within three weeks connective tissue invaded the fenestrations in the skirts of the leads (Figure 7). To measure the force required to extract the lead, a test animal was anesthetized and strapped to the testing machine (Figure 8). The protruding flange of the conduit was held in a clamp and the machine set to measure and record the force. In the case of the 2 in. dia. skirt with a 0.030 in. thickness and some 600 fenestrations, the extraction force recorded was 52 lbs. Since the dog only weighed 48 lbs., it is quite apparent why it was necessary to strap it down to the testing machine!

The mechanical collapse occurred by the umbrellation of the skirt (Figure 9). This placed all the tissue in the fenestrations in shear. Taking into account the area of the fenestrations, the 52 lbs. ultimate strength was equivalent to approximately 75 psi.

Effectiveness of Seal.

The effectiveness of the bacterial seal of the skin around the conduit was tested by swabbing with a broth of known virulent bacteria (Figure 10). Both well-sealed and weeping leads remained unchanged after the swabbing, and further tests were considered inconclusive.

Pressure testing of the seal was done by injecting dye subcutaneously near the conduit (Figure 11). In most cases the dye was forced through the skin at 2 to 10 times the normal body pressure and did not penetrate the junction of the skin and the conduit of the lead.

Appearance of the Leads.

A well-sealed lead (Figure 12) remains perfectly dry after healing. There is no scab or crusty residue after the drying of serous weepage. The skin near the conduit appears the same as the rest of the skin, and the lack of edema is conspicuous.

A poorly sealed lead (Figure 13) shows evidence of chronic or periodic serous weeping, edema, and in some cases, exteriorization of the edge of the skirt. In purulent leads, the appearance is that of a clinical infection or of a foreign body reaction, although it is not possible to tell which comes first, or to conclusively distinguish one from the other.

"Clinically Manageable" Lead.

As mentioned earlier, some investigators maintain that a clinically manageable lead, i.e., one that can be kept from extruding by the use of topical and systemic antibiotics, is satisfactory. However, this is not acceptable to our definition of a long-term lead, because the purulent and even the subclinically septic lead will most probably cause late complications due to sinus tract infectious migration.

The "clinically manageable" lead will appear dry for the first two to three months, with perhaps a small scab on one side of the conduit, and with perhaps some palpable edema. This lead must be regarded as highly suspicious, and in accordance with our long-term definition of satisfactory performance, is completely unacceptable (Figure 14).

A Clear-Cut Case.

There were no statistically significant differences in the performance of leads made of the several, demonstrably inert, materials. The incidence of satisfactory lead performance was considerably higher in the animals that paid little attention to, or ignored altogether, the leads. It appears evident from our data that the amount of self-induced trauma is largely responsible for the subsequent performance of the leads.

It is rare in medicine that a complex problem is resolvable in clear-cut terms. Figure 15 shows a composite photomicrograph of the epithelium adjacent to the conduit. Satisfactory leads, by our definition, have had most of the interior surfaces covered by downgrowing epithelium. Highly traumatized leads have not had this occur, and perform badly throughout their lives, either becoming "clinically manageable" or losing their function completely.

The downgrowth of epithelium performs two vital functions. First, it isolates the subcutaneous tissues from the plastic. Second, its natural bacteriostatic agents prevent bacteria from entering the inner spaces. The geometry of the lead is extremely important in that it determines the shape of the downgrowing epithelium and determines the travel distance of the bacteria to the interior spaces.

The clear-cut nature of the results was tested. If it was trauma that prevented the downgrowth of the epithelium, then an immobilized animal would yield 100 per cent satisfactory leads. It was impractical to immobilize dogs, so leads were implanted in Rhesus monkeys which were kept in executor chairs for three weeks postoperatively. These monkeys were then given complete freedom without intervention, or antibiotics, and the leads now, after two months, receive the same treatment as the normal intact epithelium, and have remained to this date 100 per cent satisfactory.

The importance of the clear-cut result of the epithelial downgrowth is best shown by histology.

Histology.

In successful leads, the epithelium grows down in the sulcus between the conduit and connective tissue, then over the skirt and down through the skirt fenestrations (Figure 15). In the process, it becomes keratinized. Eventually, the epithelium completely encapsulates the lead. This

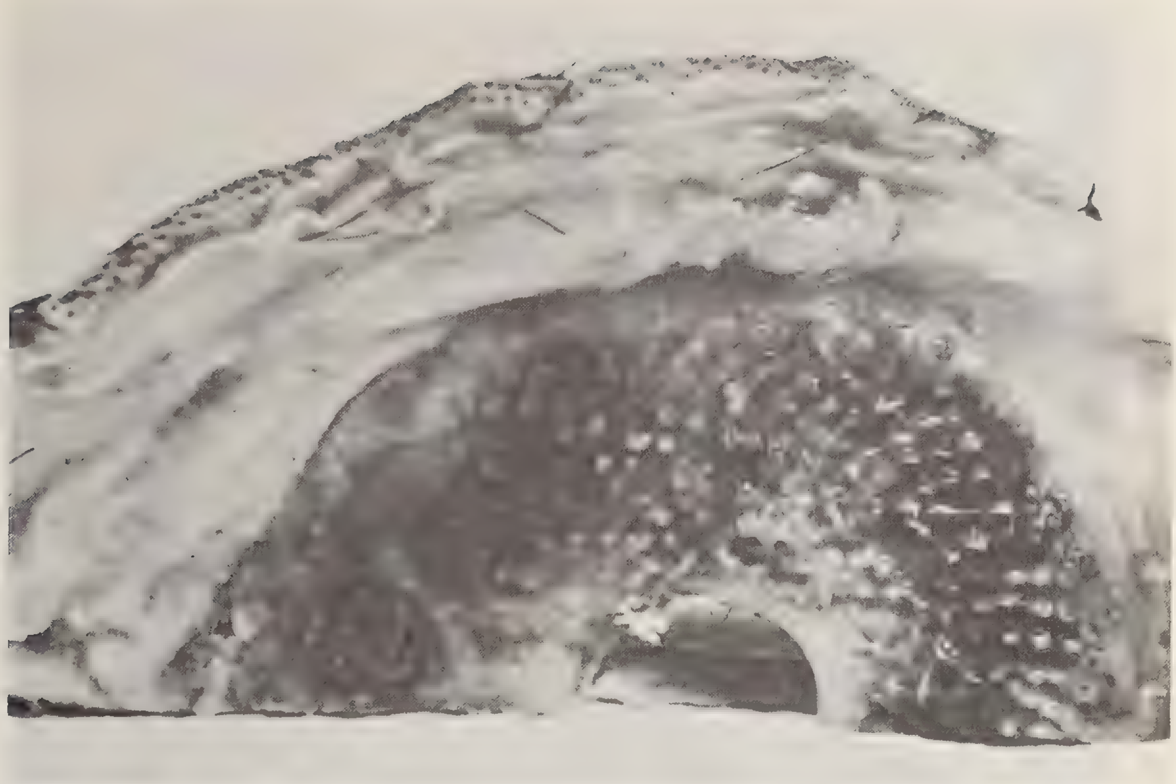

FIGURE 7. TISSUE FROM ABOVE LEAD B-7-3, DOG #206, SHOWING FINGERS OF SCAR TISSUE WHICH HAD BEEN GROWING IN FENESTRATIONS.

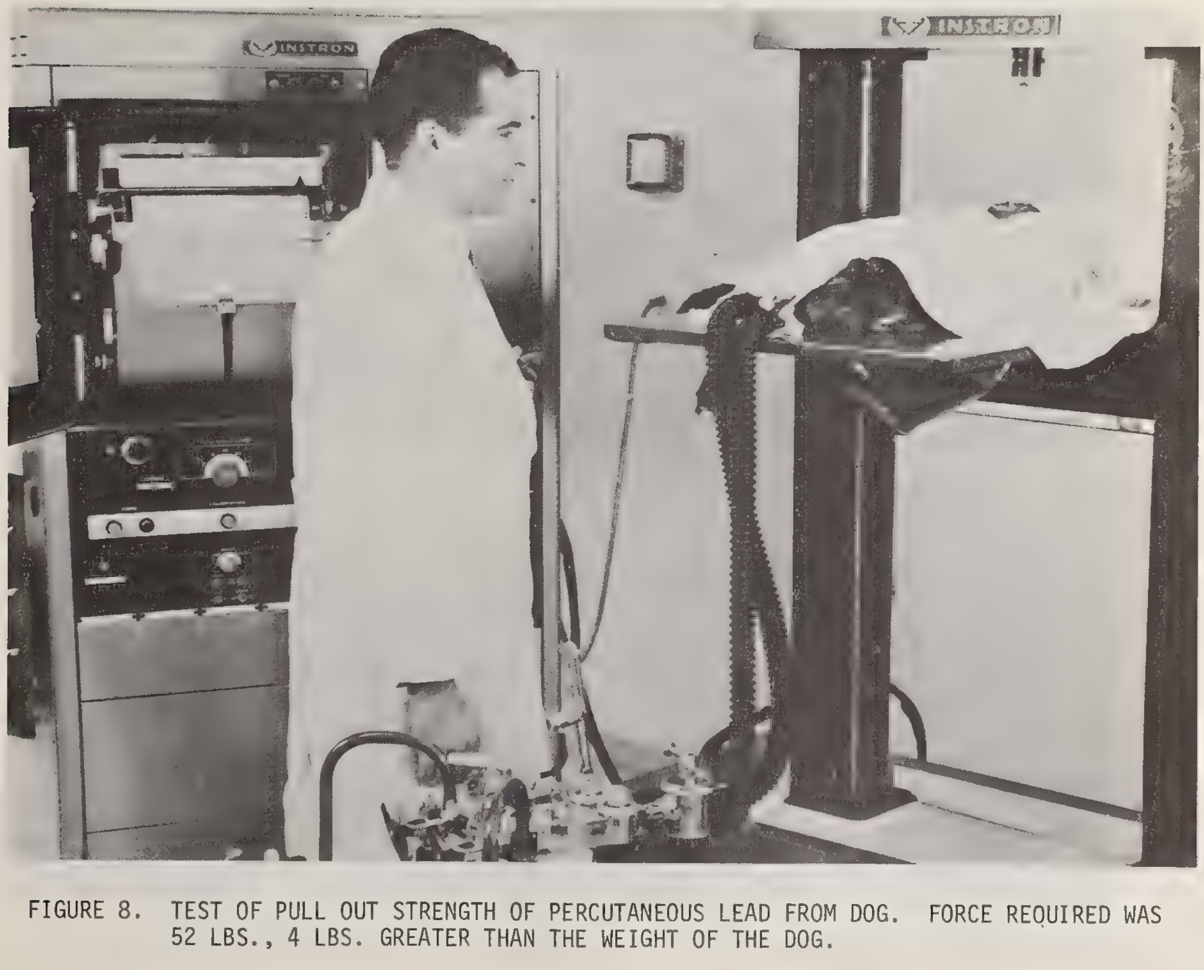

FIGURE 8. TEST OF PULL OUT STRENGTH OF PERCUTANEOUS LEAD FROM DOG. FORCE REQUIRED WAS 52 LBS., 4 LBS. GREATER THAN THE WEIGHT OF THE DOG.

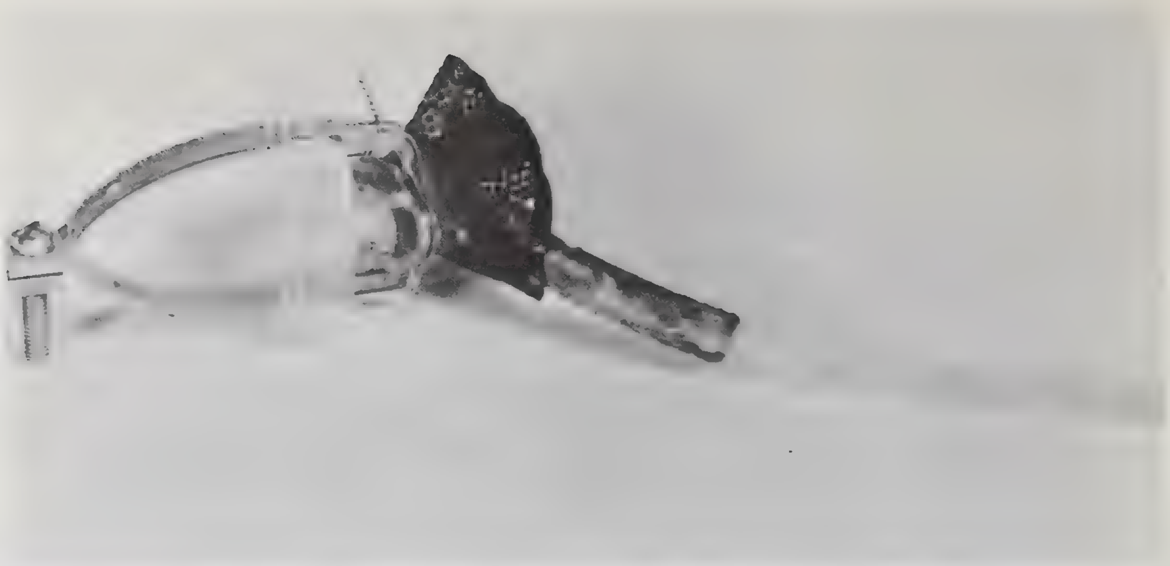

FIGURE 9. PERCUTANEOUS LEAD AFTER BEING PULLED FROM DOG SHOWING FAILURE MODE OF SKIRT.

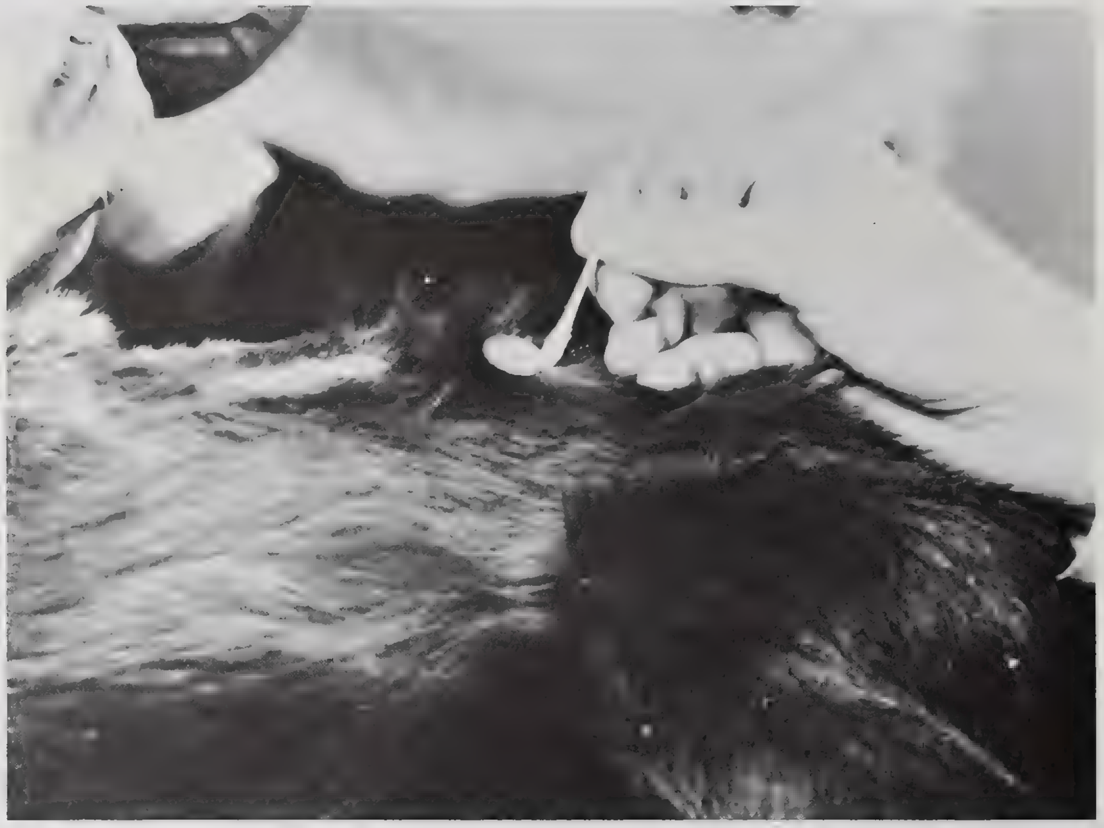

FIGURE 10. PERCUTANEOUS LEADS HAVE SUCCESSFULLY WITHSTOOD CHALLENGES OF PATHOGENIC BACTERIA.

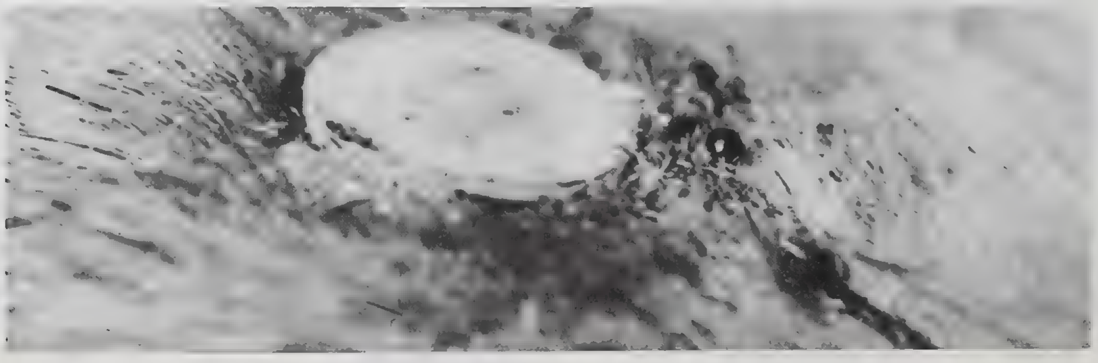

FIGURE 11. DYE BREAKS THROUGH SKIN OVER SKIRT BEFORE PENETRATING TO CENTRAL CONDUIT IN SOME CASES.

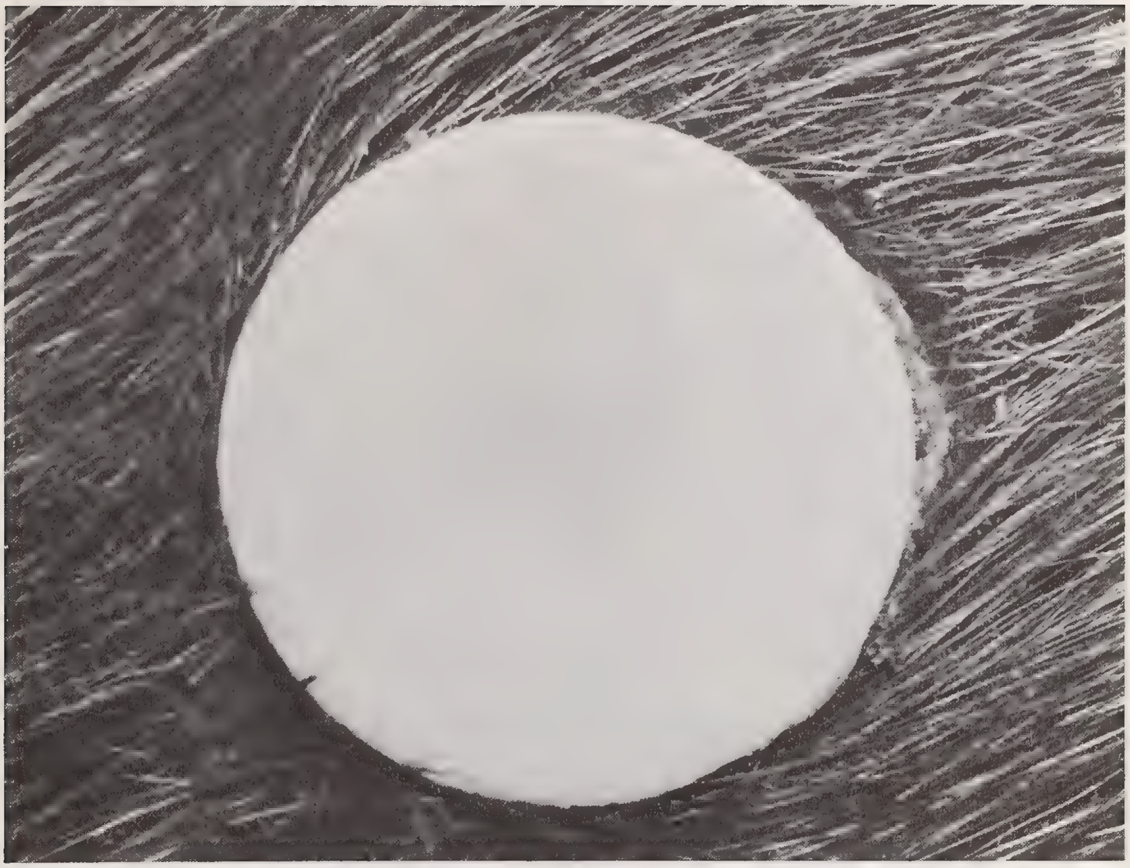

FIGURE 12. AN EXAMPLE OF A LEAD WHICH HAS REMAINED PERFECTLY DRY UP TO THE PRESENT. THIS PHOTOGRAPH WAS TAKEN 82 DAYS AFTER SURGICAL IMPLANTATION.

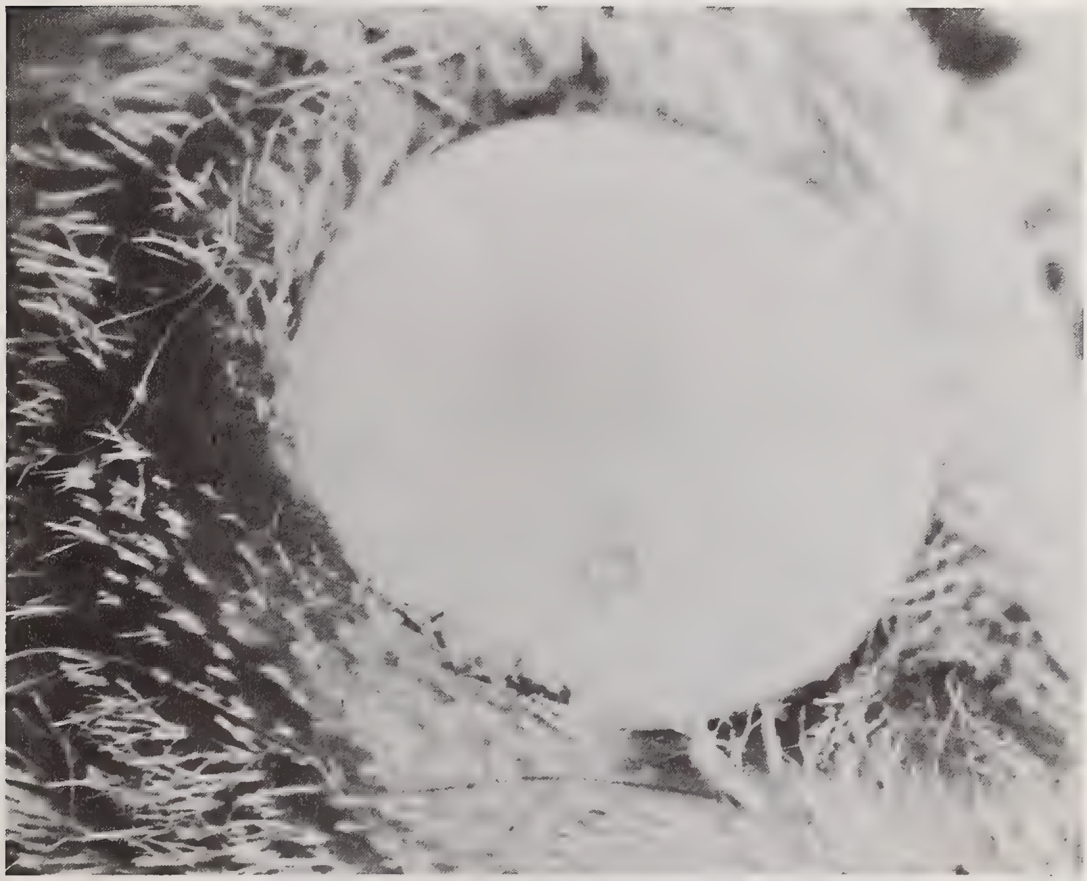

FIGURE 13. NOTE EDEMATOUS SKIN OVER SKIRT. THE LEFT CIRCUMFERENCE OF THE SKIRT LIFTS THROUGH SEVERED SKIN. SKIN RING IS NOURISHED THROUGH PEDICLE ON THE RIGHT.

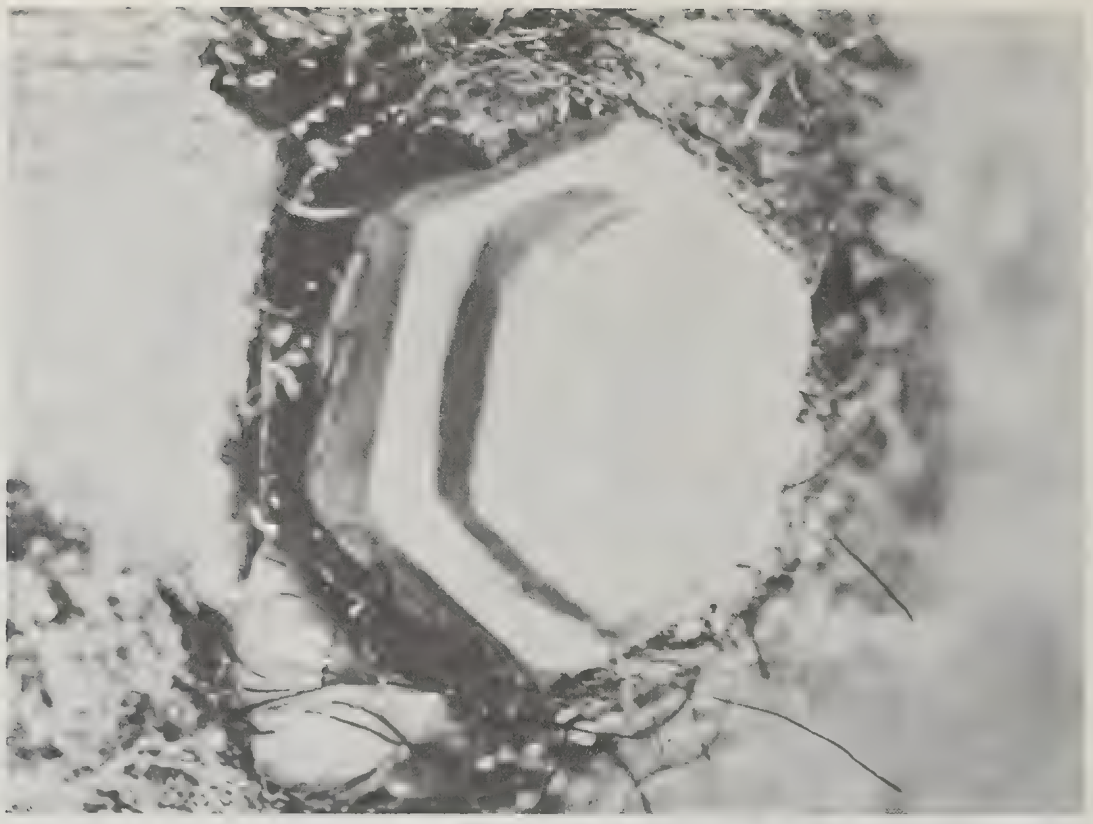

FIGURE 14. A "CLINICALLY MANAGEABLE" LEAD. THERE IS A SEROPURULENT EXUDATE AROUND THE SKIN CONDUIT JUNCTION. NOTE ALSO SWELLING IN THE SKIN AREA.

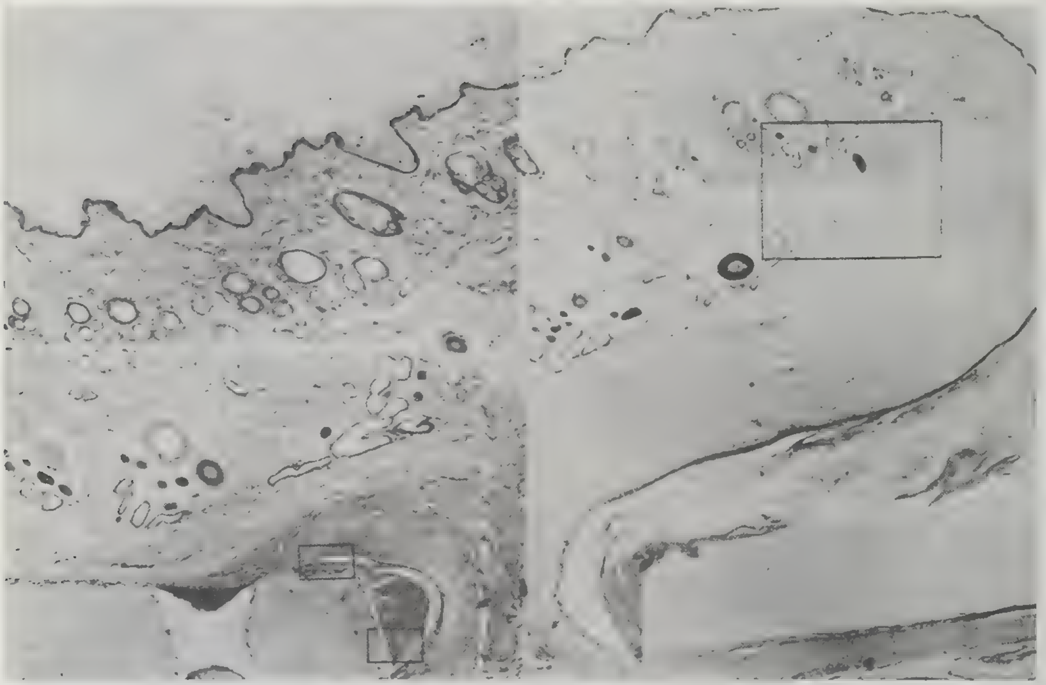

FIGURE 15. THIS IS A COMPOSITE MICROPHOTOGRAPH OF A SUCCESSFUL 280-DAY LEAD. EPITHELIUM HAS GROWN DOWN TO THE SKIRT AND THROUGH SKIRT FENESTRATIONS. UPPER BRACKET INDICATES INTERFACE BETWEEN SKIN DERMIS AND NEW CONNECTIVE TISSUE GROWTH. LOWER BRACKETS INDICATE KERATIN. HEMATOXYLIN AND EOSIN. ORIGINAL MAGNIFICATION 40x.

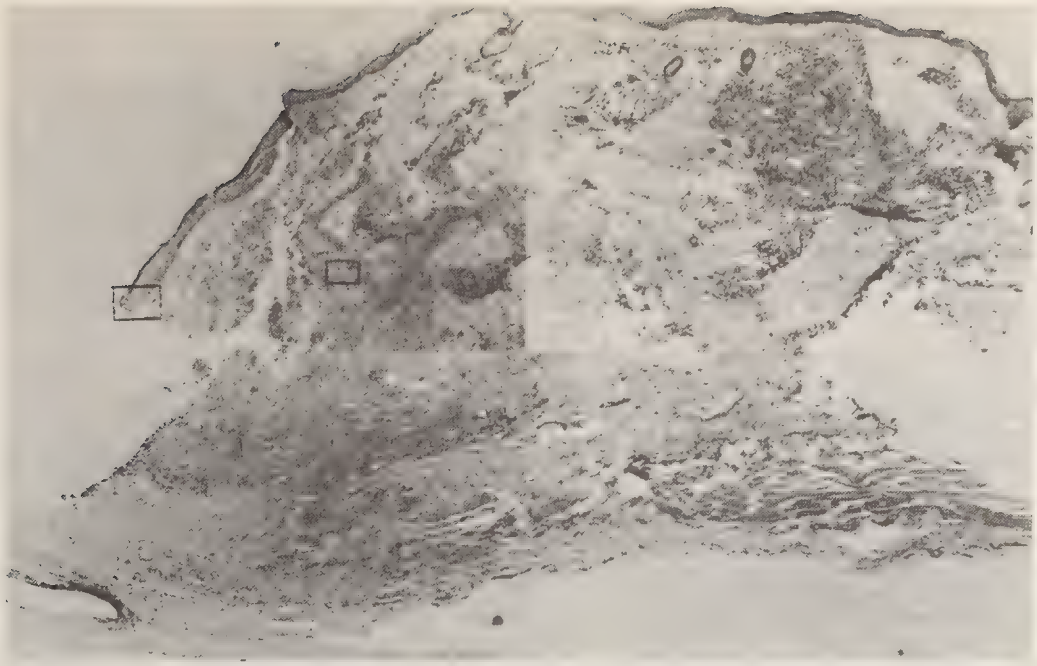

FIGURE 16. THIS IS A COMPOSITE MICROPHOTOGRAPH OF A PERCUTANEOUS LEAD WHICH APPEARED DRY FOR ITS ENTIRE 36-DAY HISTORY. PRESENCE OF MASSIVE GRANULATION TISSUE (RIGHT BRACKET) INDICATES LEAD WAS A FAILURE. THIS INFLAMMATORY TISSUE APPARENTLY IMPEDED EPITHELIAL DOWNGROWTH ALONG THE CONDUIT (LEFT BRACKET). HEMATOXYLIN AND EOSIN. ORIGINAL MAGNIFICATION 40x.

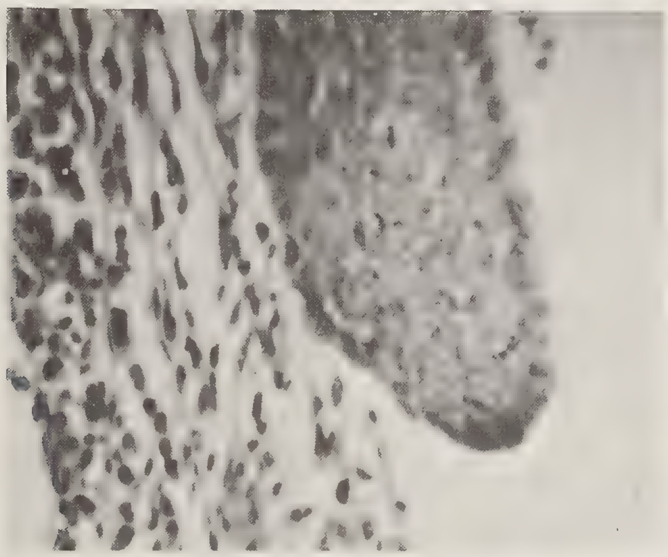

FIGURE 17. MICROPHOTOGRAPH SHOWING PERSISTENCE OF GRANULATION TISSUE IN UNSUCCESSFUL LEAD.

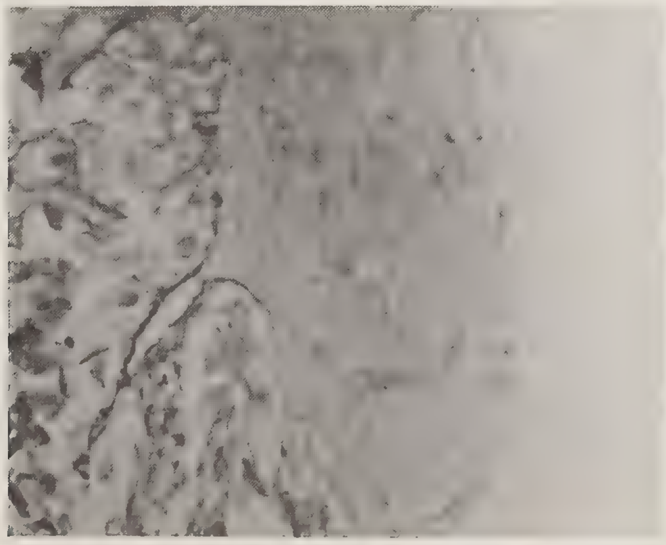

FIGURE 18. MICROPHOTOGRAPH SHOWING NEWLY FORMED EPITHELIUM GROWING IN THE SPACE BETWEEN THE PERCUTANEOUS LEAD AND CONNECTIVE TISSUE OF THE HOST.

keratinized epithelial barrier not only serves as an effective bacterial and fluid seal, but also diminishes the possibility of a long-term foreign body reaction between host tissue and implant.

It has been found that a specific progression of events occurs in the downgrading epithelium and subjacent connective tissue. The significant end result is that both the newly formed epithelium and connective tissue assume the appearance and staining characteristics of normal, healthy skin. This does not take place when there is an infection present. The following is a description of events which precedes a return to "normalcy".

1. The epithelium advances only when the granulation tissue disappears. In an unsuccessful lead, granulation tissue persists and appears to inhibit epithelial proliferation (Figures 16-17).
2. Newly formed epithelium growing in the space between the percutaneous lead and connective tissue of the host lacks several features of normal skin epithelium. It lacks a basement membrane, keratohyalin granules, keratin, and melanin (Figure 18).
3. Hypertrophy or increase in epithelial thickness occurs. Pyknosis (shrunken nuclei) is evident. In the underlying stroma, a reticular fiber network is synthesized by proliferating fibroblasts, replacing granulation tissue (Figure 19).
4. Glycogen granules appear in most epithelial cells, excluding the basal cell layer. Glycoproteins, intensely PAS-positive, appear in the connective tissue matrix. Mature collagen fibers are formed and are compressed into dense lamina (Figure 20).
5. Keratohyalin granules appear in superficial epithelial strata and keratinization begins. Hypertrophy is still evident. The epithelium is at least three times as thick as normal skin epithelium (Figures 21-22). Acid mucopolysaccharides, as well as glycoproteins, are laid down in the connective tissue ground substance. Collagen fibers are arranged in parallel rows, in contrast to normal dermal connective tissue (Figures 21-22).
6. Glycogen granules disappear from the epithelium. A basement membrane is formed (Figure 23). Evidences of cellular degeneration, such as pyknosis, are no longer apparent.
7. Excessive keratinization develops. The epithelium returns to a normal thickness of several cell layers. Moreover, collagen bundles assume the loose, feathery appearance and staining characteristic of skin dermis. However, hair follicles and other adnexa remain absent in the connective tissue beneath the downgrowing epithelium (Figures 24-25).
8. Neutrophils invade and digest some of the keratin. This is significant, as excessive keratin formation might cause extrusion of the implant (Figures 26-27).
9. Melanin granules, a feature of normal skin epithelium, gradually appear (Figure 28).

Finally then, the newly formed epithelium and subjacent connective tissue take on the typical character of healthy skin epithelium, save for loss of adnexa. The epithelium encapsulating the lead has a true basement membrane, keratohyalin granules, keratin, and melanin granules. There are no signs of cellular degeneration, particularly pyknosis. The underlying connective tissue has the morphologic and staining features of normal skin dermis.

As we have already said, these events do not take place when infection and concomitant inflammatory tissue are present near the downgrowing epithelium. The epithelial cells are pyknotic, and both keratin and keratohyalin granules are absent. The basement membrane appears imperfectly formed, and the underlying connective tissue has none of the characteristics of healthy skin dermis.

SUMMARY

Satisfactory performance of a percutaneous lead is associated with epithelial downgrowth. Failure is associated with absence of downgrowth. Many "clinically manageable" leads are truly failures because they require continuous treatment, i.e., cleaning of the wound and ritual application of antibiotics. Leads requiring such care are associated with little or no epithelial downgrowth.

It is postulated that epithelial proliferation between host tissue and the implant effectively isolates the lead from the surrounding tissue. Thus, this keratinized epithelial barrier diminishes the possibility of long-term foreign body reactions. Finally, as histological data have shown, the new epithelium and connective tissue surrounding the percutaneous device assumes the character of healthy skin. Two prominent points are therefore indicated: first, the process of epithelial downgrowth and encapsulation is not a pathological process; secondly, and more striking, the skin-like barrier is capable of providing as effective a bacterial and fluid seal as normal skin. This observation, more than any other, explains the need for epithelial downgrowth in a long-term percutaneous device which requires no post-operative care.

DISCUSSION

DR. REAM: I have one question for you. I wonder whether you would expect the normal process of desquamation, with this lining, to cause long term difficulty with the stability of the lead?

DR. OCUMPAUGH: You mean one of the leads might be extruded?

DR. REAM: Or would you have such problems with infection or accumulation of foreign matter as might cause degeneration of the tissue around the lead?

DR. OCUMPAUGH: There are no signs of infection, no inflammatory cells, no plasma cells seen approximately 2-1/2 to 3 weeks after the implant heals in an immobilized animal. And in all our monkeys, which are immobilized, we don't see any other signs of infection or inflammation. However, as far as the epithelial stability around the lead we don't know as yet. We feel that the anchoring flange will inhibit this type of response, but we don't know. This we'll have to wait for at least another year I would say.

DR. ROGERS: About 2-1/2 or 3 years ago, we started some implants in cows of a device quite similar to this. We implanted the device with the tube, so that the skin was closed, and then the tube was withdrawn after 30 days through the skin. Using this procedure in four animals, we withdrew a 5/16" diameter tube through the skin. It was placed quite near the backbone so that the calf couldn't rub against the fence, and the calves were put out to pasture without any attention. The shortest survival time was about 6 months and the budget caused us to sacrifice our longest survivor, just under three years when he weighed around 800 lbs. The leads stayed in very well, without any attention whatsoever. There was a small area of infection, usually around the tube, which remained. The only real difficulty we had was when rain water got in them; the flies could get around the tube and this maintained a small infected area, but the leads did last very nicely.

DR. CULP: Thank you very much. We noticed in leads which were chronically infected, that there was always a small, very dry scab between the emerging column or conduit and the host tissue. But on histologic examination we found it was always chronically infected. Apparently leukocytes and other inflammatory cells, keep migrating through the epithelium or near the epithelium and get into the interface there and dry. And that's an indication of a lead failure, in a sense, because chronic infection is an undesirable condition.

DR. ROGERS: I was wondering whether any care was given to the leads where they came through as far as you were concerned, the animal care, that is cleaning and washing?

DR. CULP: No, that was the point of the whole project, to obtain a percutaneous lead that required no care at all, including ritual application of antibiotics or washing beyond 4 days after the operation, but this only was achieved if we immobilized the animal until the lead healed.

DR. LUDWIN: Two questions. What was the material that you used and was this material selected as a result of previous preliminary experiments?

DR. CULP: It was selected as a result of a survey of the literature and Teflon, polyurethane and graphite were the materials used, three types of materials in three different types of leads. Do you have anything to add Dr. Lee?

DR. LEE: We also surveyed a number of rigid materials for the conduit as opposed to those used in the skirt. We used some rigid epoxies and rigid polyurethanes because of their convenience in fabricating, and various adhesives, but we started with generally recognized biologically inert materials.

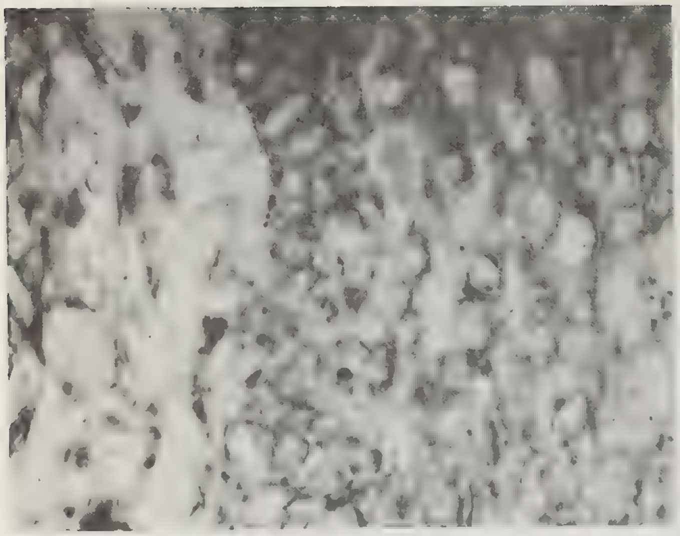

FIGURE 19. MICROPHOTOGRAPH SHOWING HYPERTROPHY OF EPITHELIUM.

FIGURE 20. MICROPHOTOGRAPH SHOWING GLYCOPROTEINS IN THE CONNECTIVE TISSUE MATRIX.

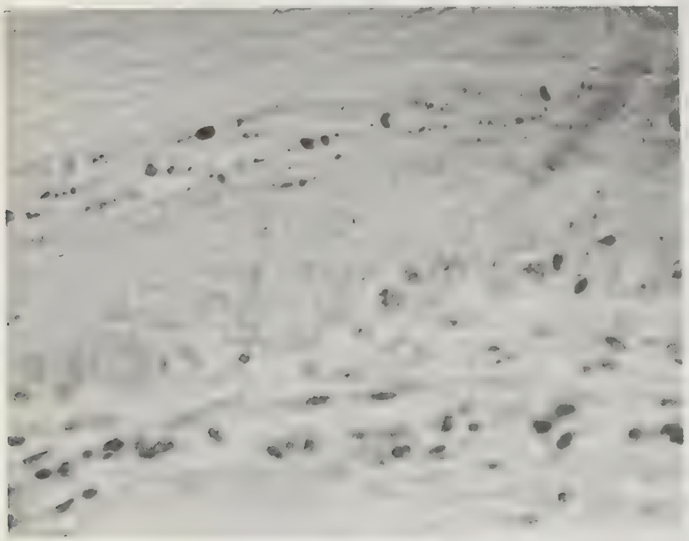

FIGURE 21. MICROPHOTOGRAPH SHOWING HYPERTROPHY OF EPITHELIUM.

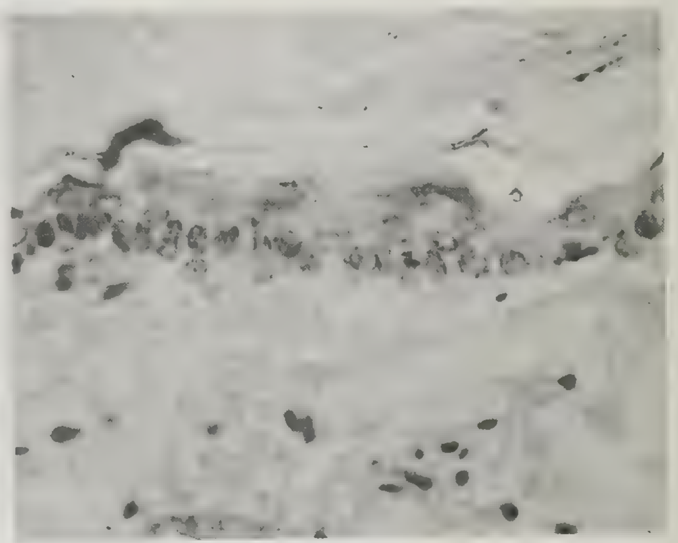

FIGURE 22. MICROPHOTOGRAPH SHOWING BEGINNING OF KERATINIZATION.

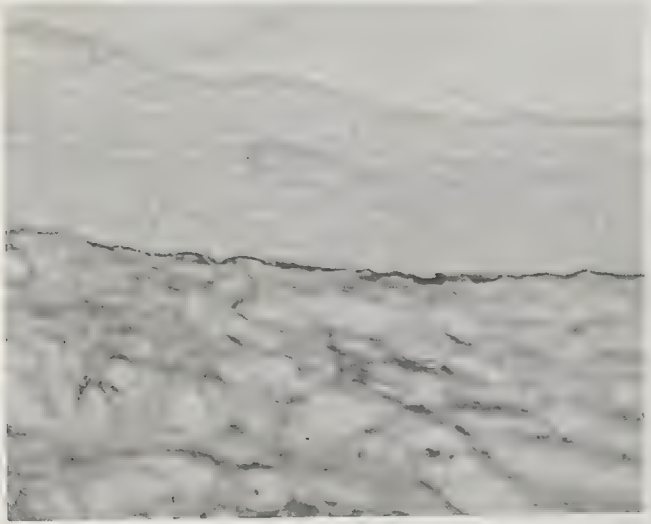

FIGURE 23. MICROPHOTOGRAPH SHOWING THE PRESENCE OF A BASEMENT MEMBRANE.

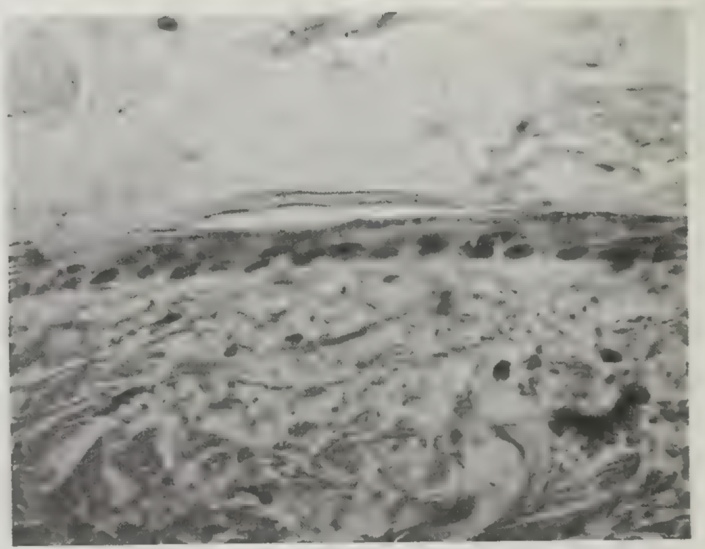

FIGURE 24. MICROPHOTOGRAPH SHOWING EXCESSIVE KERATINIZATION.

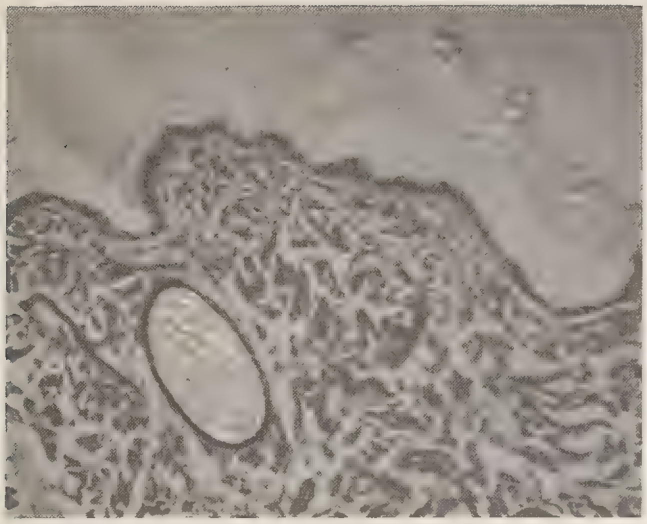

FIGURE 25. MICROPHOTOGRAPH SHOWING ABSENCE OF HAIR FOLLICLES AND OTHER ADNEXA IN NEWLY FORMED EPITHELIUM.

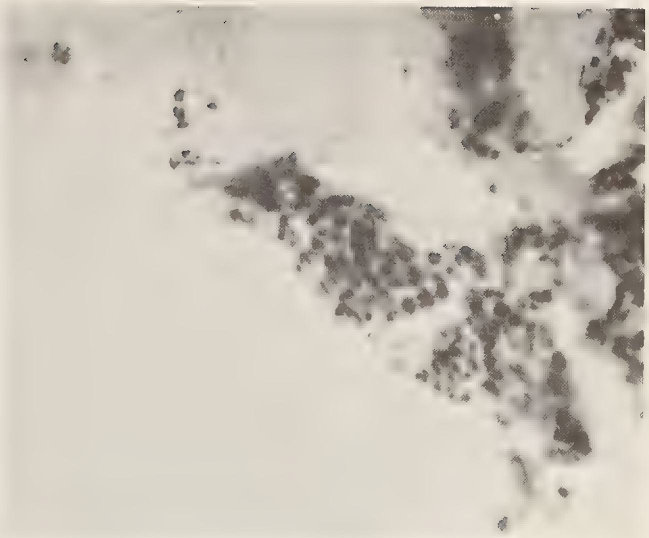

FIGURE 26. MICROPHOTOGRAPH SHOWING NEUTROPHILS INVADING AND DIGESTING SOME OF THE KERATIN.

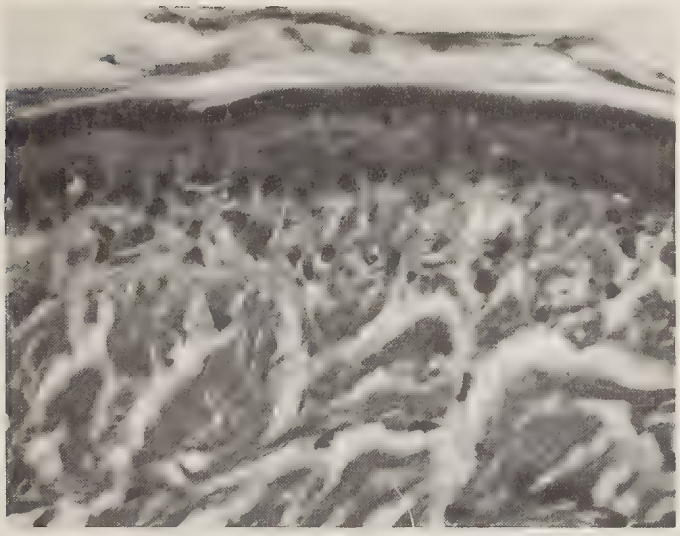

FIGURE 27. MICROPHOTOGRAPH SHOWING DIGESTION OF THE KERATIN.

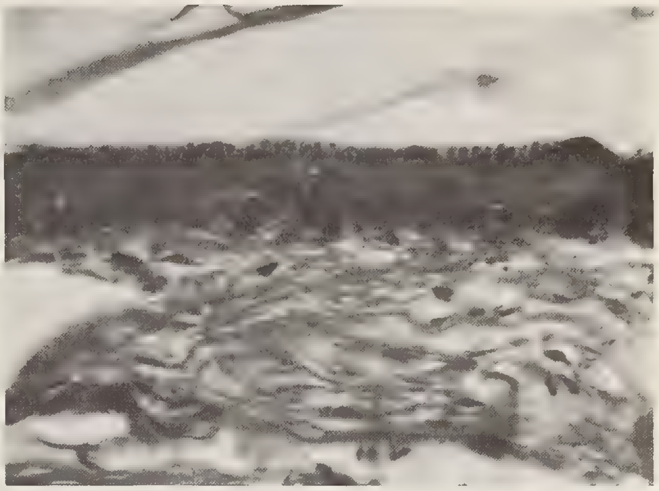

FIGURE 28. MICROPHOTOGRAPH SHOWING THE APPEARANCE OF MELANIN GRANULES IN THE NEWLY FORMED EPITHELIUM.

CHAPTER 67

BIOLOGICALLY COMPATIBLE POLYELECTROLYTE COMPLEX HYDROGELS FOR USE AS TISSUE/LEAD ADHESIVES FOR LONG-TERM PERCUTANEOUS LEADS

E. Friedman, L. Nelsen and H. Bixler

Amicon Corporation
Lexington, Massachusetts

Bacterial infection along the tract of a percutaneous lead can be reduced or avoided if the adhesive binding the lead to the tissue has the following properties: bacterial impermeation and inertia, good bonding to tissue and lead, adequate tensile and elastic properties, suitable cure times (0.1-24 hrs), and body compatibility and stability. The utility of polyelectrolyte complexes as such adhesives is under investigation. Preformed complexes of this type have demonstrated good body compatibility and adequate strength. Adhesion is brought about by the free radical in situ polymerization of one ionic monomer in the presence of the counterpolyion. The major problems thus far encountered are rapid gelation times, inadequate strength, and toxicity of one of the better adhesive systems. The adhesive systems studied contained sodium polystyrene sulfonate (NaPSS), polysodium acrylate (NaPAA) or styrene/maleic acid copolymer (SMA) as the polyanion in conjunction with 2-hydroxy-3-methacrylyloxypropyl trimethylammonium chloride (Q-1) as the cationic monomer. The (in vitro) tensile strengths of the hydrogels thus prepared are: NaPSS/Q-1, 111 psi with 25% elongation; SMA/Q-1, 20 psi, NaPAA/Q-1, 110-265 psi. Cure times were controlled by precooling the reactants. Current research is centering on extensive evaluation of the compatibility of these systems in vivo and on testing of the tensile strength and bacteria permeability of the gel systems.

INTRODUCTION

The large research and development effort concerned with the long-term implantation of circulatory assist devices in ambulatory humans is expected to lead to the realization of usable systems within the next few years. Under the present concept the power and control units for these devices must be located outside of the body. This requires that the percutaneous leads connecting the implanted device with the power and control units be inert to the body and resistant to infection at the lead tissue junction, and that this inertness and resistance be maintained for periods of time up to five years. The most important single problem concerning percutaneous leads has been found to be persistent infection at the skin/lead junction. It is towards this problem that the present program has been directed with the specific objective of developing an adhesive to seal off the tissue/lead junction and prevent the penetration of infection.

An adhesive that seals the percutaneous lead to the skin must have the following properties:

1. Impenetrability and inertness to bacteria.
2. Good bonding to tissue and lead.
3. Long-term body compatibility and stability.
4. Adequate tensile and elastic properties.
5. Suitable cure times (0.1-24 hours).

The first three requirements are easily defined; adequate tensile and elastic properties perhaps need further definition. The adhesive will be present as a relatively thin layer between the lead and the skin. The adhesive's modulus should be low enough to retain flexibility and prevent brittle failure and, in fact, should be lower than the modulus of skin. This would also allow the adhesive to retain its integrity during pulsation of the lead even if it had a somewhat lower tensile strength than the skin. Obviously certain tradeoffs are available here.

The adhesive's curing times must be long enough to allow for convenient application and short enough to allow for minimal setting difficulties. Twenty-four hours is a reasonable maximum. As is the case with tissue/tissue adhesives, cure times of the order of 10-20 min. are desirable, although in the tissue/lead case they are not mandatory since an adhesive that satisfies the other requirements is still useful even if it takes a day or so to fully cure.

This program has been concerned with the development of in situ formed polyelectrolyte complex hydrogels as tissue/lead adhesives. Several of these complexes (e.g., in the form of Diaflo® UM membranes) have been shown to be impermeable to bacteria and viruses[1], and they have also been found to be useful in a variety of biomedical areas such as contact lenses, dialysis membranes, antithrombogenic materials for blood-contacting prosthetic devices, etc.[2] The complexes are formed either by the association of two oppositely charged polyelectrolytes or by the polymerization of an electrolyte monomer in the presence of a polyelectrolyte of opposite charge. This is shown schematically in Figures 1 and 2. This process results in a gel which is insoluble in, but not impermeable to, water and low molecular weight body solutes.

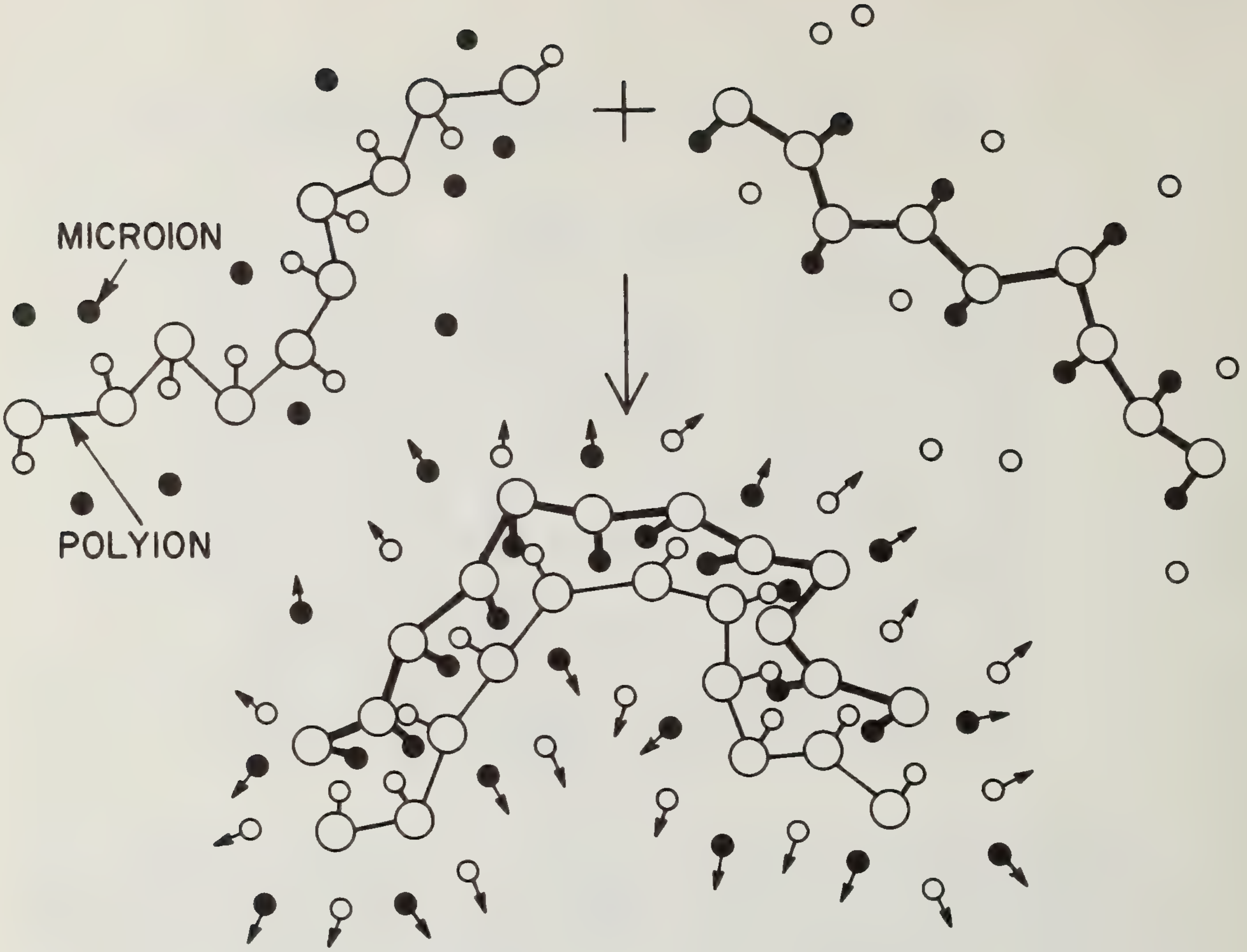

FIGURE 1. STOICHIOMETRIC REACTION.

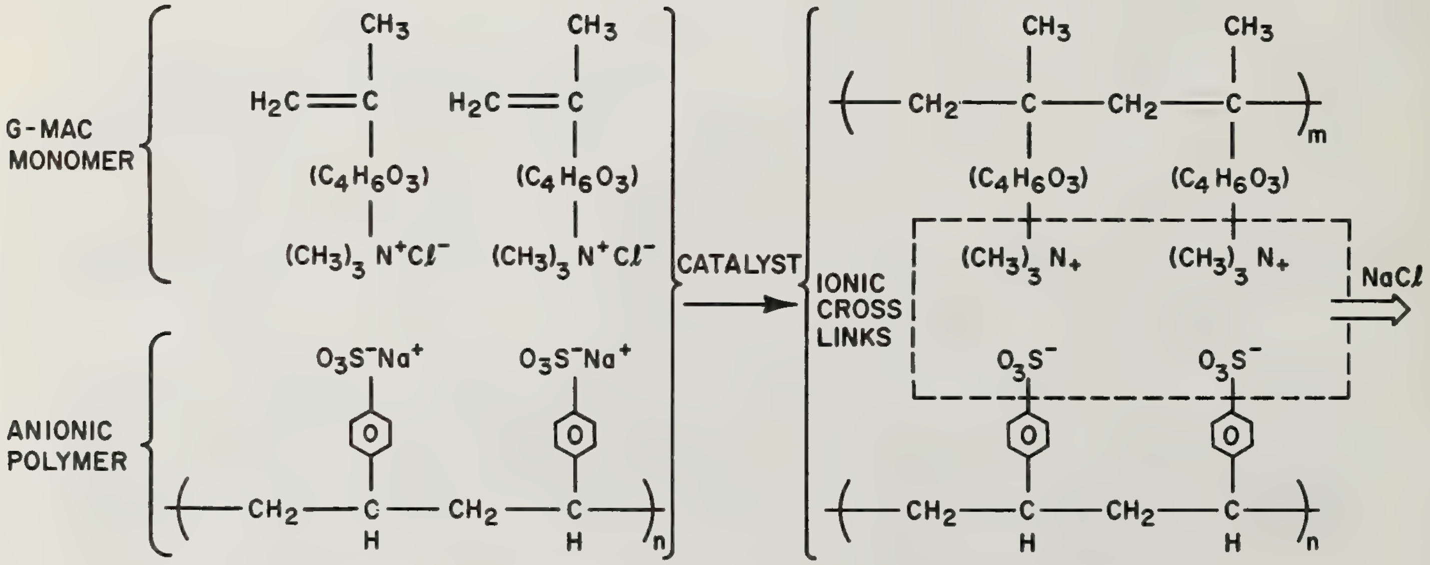

FIGURE 2. POLYMERIZATION OF G-MAC CATIONIC MONOMER IN THE PRESENCE OF ANIONIC POLYMER TO FORM A POLYELECTROLYTE COMPLEX.

EXPERIMENTAL

Polyelectrolyte Complexes Studied.

The constituents of the complexes considered under this program are shown in Table 1. The general method for preparing the adhesives has been described previously.[3]

TABLE 1

THE HYDROGEL POLYELECTROLYTE COMPLEXES WERE FORMED FROM:

Polyanions	
1. Sodium polystyrene sulfonate	(NaPSS)
2. Polysodium acrylate	(NaPAA)
3. Sodium salt of copolystyrene maleic acid	(SMA)
4. Sodium carboxymethyl cellulose	(NaCMC)

COMPLEXED WITH:

Polycations	
1. Polyvinylbenzyl trimethyl ammonium chloride	(P-VBTAC)
2. Poly-3-methacrylyloxy-2-hydroxypropyl trimethyl ammonium chloride	(Poly-Q-1)

A series of screening tests were performed in order to choose the most promising candidates. These procedures included *in vitro* adhesion as well as gel quality determinations. In general, it was found that good gels were not obtained when monomeric anions were used with polycations, and no good gels were obtained with NaCMC. Also, the gels made using Q-1 as the monomer were in all cases stronger than those using VBTAC. The results of the screening test left the systems shown in Table 2 to be considered for more detailed analysis and *in vivo* tests.

TABLE 2

ADHESIVE SYSTEMS STUDIED IN VIVO

1. NaPSS + Q-1 + redox initiator
2. SMA + Q-1 + redox initiator
3. NaPAA + Q-1 + redox initiator + aluminum subacetate
4. NaPAA + Poly-Q-1 + aluminum subacetate

The redox initiator used was ammonium persulfate plus sodium metabisulfite. Aluminum ions were found to be necessary for obtaining good water resistant gels with the sodium polyacrylate systems. They were added as the sparingly soluble subacetate salt since rapid addition of a supply of Al^{+++} ions caused instant local gelation and nonuniformity.

The weight ratios of the electrolyte monomers and polymers were set to give a stoichiometric equivalence between negative and positive groups. An exception to this was the NaPAA/Q-1 system where the addition of a stoichiometric amount of the Q-1 monomer caused salting out of the NaPAA, and an excess of the polyanion was used instead.

Gel Strengths.

The gels prepared from the systems listed in Table 2 all exhibited high elongation. A tensile test curve for a NaPSS/Q-1 gel is shown in Figure 3 and the data for four samples are shown in Table 3. The water content was 40-55 percent.

TABLE 3

INSTRON TENSILE TESTS ON NaPSS/Q-1 GELS

Strain Rate = 0.5 in/min, Sample Length = 0.75 in.

Sample	Thickness (in)	Width (in)	Breaking Strength (lb)	Tensile Strength (psi)
1	0.030	0.249	0.57	76
2	0.044	0.246	1.18	109
3	0.039	0.286	1.46	130
4	0.041	0.223	1.16	127

Average tensile strength = 111 psi

A gel sample prepared from two polyions (NaPAA/Poly-Q-1) rather than from the same monomer polymerized in the presence of the polycounterion exhibited greater tensile strength and lower, more controllable water contents than did the gels described above. The data for four samples are shown in Table 4. The water content was 75-78 percent. The variation in the data was due to lack of uniformity of the gel. The NaPAA/Q-1 gels prepared from the monomeric Q-1 were extremely weak - probably due to the high ratio of acrylate to Q-1 groups which could prevent long Q-1 chains from being formed. This high ratio, as mentioned above, is necessitated by the salting out problem. The SMA/Q-1 system was also very weak, probably due to the low molecular weight of the SMA (~50,000). It has also been found that when low molecular weight NaPSS (~40,000) was used, weak gels resulted.

TABLE 4

INSTRON TENSILE TESTS ON NaPAA/POLY-Q-1 GELS

Strain Rate = 2.0 in/min, Sample Length = 0.75 in.

Sample	Thickness (in)	Width (in)	Breaking Strength (lb)	Tensile Strength (psi)
1	0.026	0.261	0.76	112
2	0.024	0.259	1.38	223
3	0.028	0.235	0.76	115
4	0.024	0.258	1.64	265

Average tensile strength = 179 psi

The NaPSS normally used has a molecular weight of 4 million. Thus, it was concluded that the molecular weight of polyanions strongly affected the final gel strength.

In Vivo Experiments.

Animal experiments using dogs and rats were conducted with these materials in order to determine:

1. The basic compatibility of these polyelectrolyte complex adhesive systems with living tissue.
2. The bonding strengths of the adhesive systems to living tissue.
3. Any microscopic breakdown of the adhesive systems when exposed to the body environment.

The *in vivo* experiments were conducted at Children's Hospital Medical Center, Boston, under the direction of Dr. Robert Filler. Three sets of animal experiments were performed:

1. Adhesive and compatibility studies in dogs.
2. Long-term gel stability studied in the trunk musculature of dogs.
3. Adhesive tests in and under the skin of rats.

Adhesive and Compatibility Studies in Dogs. Adhesion of NaPSS/Q-1 and the NaPAA/Poly-Q-1 systems was investigated by implanting these adhesives in the trunk musculature of mongrel dogs. For these experiments, potassium persulfate and thiourea were used as the redox initiator in the NaPSS/Q-1 system, and $AlCl_3$ as well as aluminum subacetate was used as the gelling agent in the NaPAA/Poly-Q-1 system. The skin and fascia were sutured over the implant and then reopened a week later. In both cases adhesion was good and new tissue had grown into the adhesive. The NaPAA/Poly-Q-1 system appeared to be compatible with the body, but severe inflammation and necrosis had developed around the area of the NaPSS/Q-1 implants.

To investigate the cause of the incompatibility, solutions of NaPSS, Q-1, potassium persulfate, thiourea and sodium metabisulfate were injected under a dog's skin, and a preformed NaPSS/Q-1 gel was implanted. Only the injection of the NaPSS solution resulted in a toxic reaction. Various purification procedures applied to the NaPSS were not successful in reducing its toxicity.

NaPAA/Q-1 and SMA/Q-1 adhesives did not cause any toxic reactions.

Adhesion tests on dog's skin were also performed using the NaPAA/Poly-Q-1 and SMA/Q-1 systems. Aluminum chloride, aluminum isopropoxide or aluminum sulfate treated with stearic acid were added as gelling agents for the NaPAA/Poly-Q-1. The procedure was as follows: an incision was made in the skin, the adhesive applied and the incision held closed for 15 minutes. After 15 minutes an attempt was made to open the incision. In no case was the adhesion sufficiently strong to prevent the incision from opening.

Long Term Gel Stability Studies. In order to determine the long term physiological effects of the complex gels as well as the stability of the gels in the body milieu, preformed NaPSS/Q-1 and SMA/Q-1 gels were implanted in the trunk musculature of dogs. The gels were prepared by mixing the polymer first with the Q-1 and then with ammonium persulfate, and then soaking the material in a 10 percent solution of sodium metabisulfite. Control samples were maintained in 0.15 M NaCl buffered with phosphate to pH 7.5 at 37°C. Somewhat surprisingly, the gels softened in the control buffer solution while the NaPSS/Q-1 gel removed from the animal after one week was considerably harder and tougher than the initially implanted gel! In addition, the NaPSS/Q-1 gel caused severe toxic reactions.

Apparently the soaking in the sodium metabisulfite solution had extracted some of the Q-1 monomer before it could be polymerized, and thus: (1) prevented a water resistant gel from forming, and (2) the gel *in vivo* probably resulted from the transfer of divalent crosslinking ions by the body to the gel. The implication of this and the tissue ingrowth (discussed above) is that the adhesive should become stronger with time.

In order to investigate the toxicity and adhesive problems further using larger numbers of animals, rats were substituted for dogs in the subsequent experiments.

Adhesive Studies in Rats. The adhesives were applied to the rats as follows: The rat's abdomen was shaved, the incision was made through the skin only, the adhesive was applied and the skin was sutured or clamped. The incisions were opened after 1 day, 7 days and 35 days. The results are shown in Table 5.

TABLE 5

ADHESIVE IMPLANTS IN RATS

System	Days After Implant	Strength (psi)[a]	Remarks
SMA/Q-1	.02	23.2	Rat died 30 min. after surgery.
	1	2.6	
	7	28, 5.3	
NaPAA/Q-1	1	10	
	7	9.2	Holding together in places - may be healing.
	35		One incision open, one healed over.
NaPSS/Q-1	1	17	
	7	18	
	35		Skin healed over, hard pocket under incision.
NaPAA/Poly-Q-1	1		No adhesion.
	7	8.8	Abnormal tissue.
	35		Wounds open and necrotic.

[a] Rat skin tensile strength = 358 psi

Ether was found to be more suitable than nembutal as an anesthetic due to ease of application, control of sleep and quickness of recovery. The clamps which were used on the last 5 rats (due to the speed with which they could be applied) made it very difficult to study the adhesion since they injured the skin and were removed only with great difficulty (thus tearing at the incision area). Although the data from these tests are somewhat inconclusive because of these surgical difficulties and another series of tests is now underway using the NaPSS/Q-1 and NaPAA/Poly-Q-1 adhesives, it was observed that the rats did not react as strongly to the NaPSS/Q-1 as did the dogs. It was also found that the NaPSS/Q-1 adhesive had a pH of 8. At this pH, NaPSS/Q-1 forms a very weak gel. The strength and toxicity of the NaPSS/Q-1 system as a function of pH is presently being investigated. There also appears to be a strong reaction against the NaPAA/Poly-Q-1 system.

CONCLUSIONS

A series of polyelectrolyte complex hydrogels have been studied for potential use as adhesives for long-term percutaneous leads. Of the materials studied, two showed sufficient gel strengths to encourage further study: the NaPSS/Q-1 system initiated with ammonium persulfate and sodium metabisulfite (tensile strength = 111 psi) and the NaPAA/Poly-Q-1 system gelled with aluminum subacetate (tensile strength = 179 psi). Both materials had low modulus and thus high strain energies. Neither system demonstrated good adhesive properties and both elicited toxic reactions. The toxic reactions are apparently due to the toxicity of the one component (e.g., NaPSS) rather than any inherent toxicity due to the complex or the polymerization reaction. This has been demonstrated in work at Amicon on other programs that shows the implantation of preformed polyelectrolyte gels does not elicit toxic reactions. Work at Epoxylite has also shown that leads coated with preformed polyelectrolyte gels do not elicit toxic reactions.

REFERENCES

1. J. S. Rhim, L. B. Williams, Jr., R. J. Huebner and H. C. Turner; Fed. Proc., Item 2917 (1968).
2. L. L. Markley, H. J. Bixler and R. A. Cross; J. Biomed. Mater. Res., 2, 145 (1968).
3. J. H. Glaser, "Biologically Compatible, Synthetic Polyelectrolyte Complex Resins for Use as Tissue/Lead Adhesives for Long-Term Percutaneous Leads," NHI Contract PH43-67-1107, December 2, 1968.

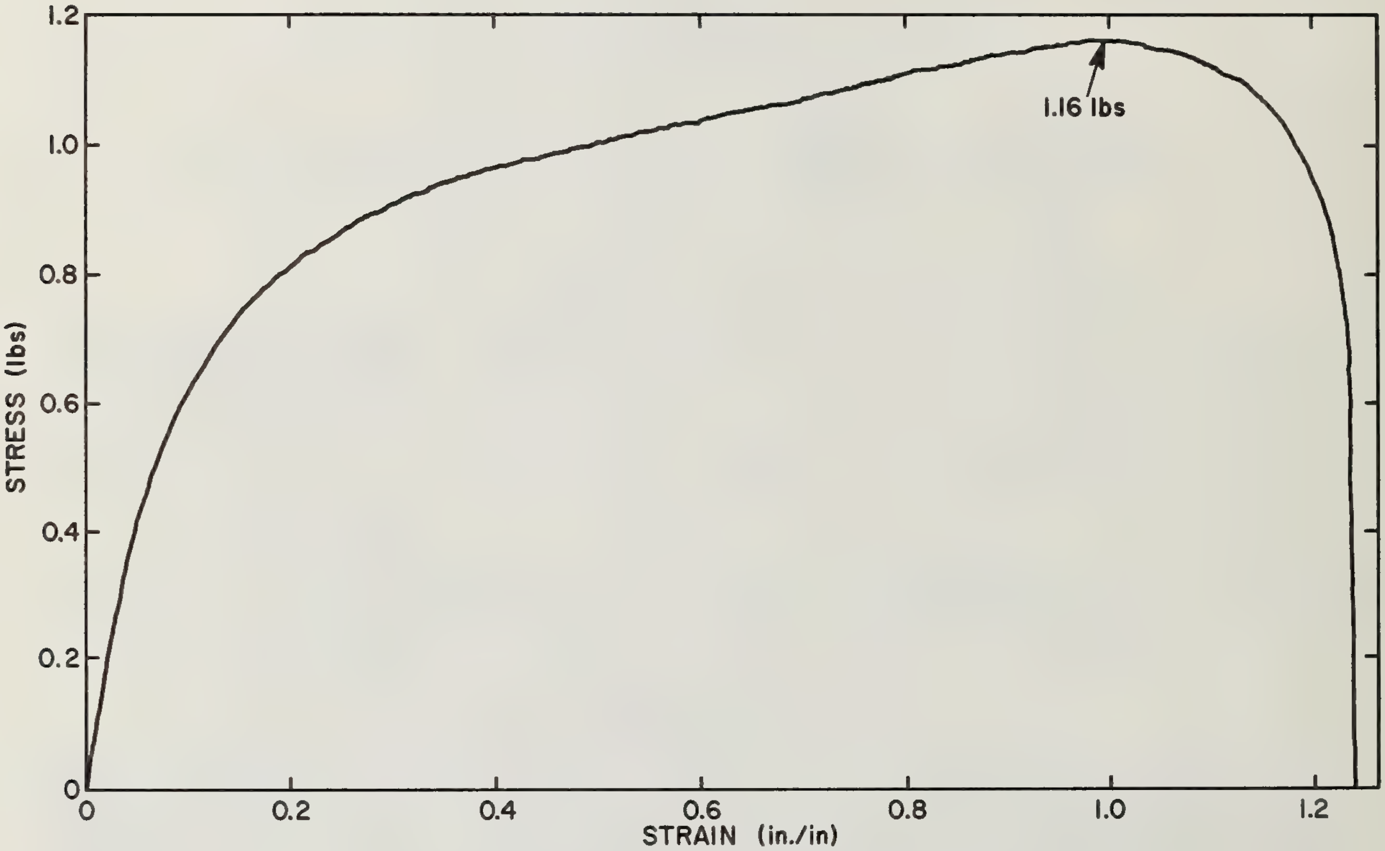

FIGURE 3. INSTRON TEST CURVE FOR NaPSS/Q-1 GEL.

SECTION X

BIOLOGICAL FUEL CELLS

Chairmen: Roger S. Powell
Lowell T. Harmison, Ph.D.

INTRODUCTION

In the development of artificial heart systems it appears highly desirable that the device ultimately be entirely implantable within the host. One source of power for such a fully implanted system that appears very attractive when considered functionally would be a biological fuel cell that would operate on chemical species normally found within the body. In its most attractive form, such a cell would extract its fuel and oxidizer and reject its waste products to the normal metabolic stream, modified if necessary by diet. The cell would consist of a prosthetic device permanently implanted into some location of the body by surgical procedures. Its effect upon normal body functions must be sufficiently moderate so that the body could adjust to the change in metabolism without long-term harmful effects. Current contract investigations have ranged from the development of specific electrocatalysts for oxygen reduction and blood carbohydrate oxidation (particularly glucose) through studies of reaction mechanisms and kinetics to development and testing of complete biological fuel cells.

CHAPTER 68

FEASIBILITY STUDIES - IMPLANTABLE BIOLOGICAL FUEL CELL

J. Batzold and M. Beltzer

Government Research Laboratory
Esso Research and Engineering Co.
Linden, New Jersey

In theory implantable biological fuel cells are attractive power sources for artificial heart devices. In practice, several difficult problems must be solved to provide a viable system. These problems stem from the attempt to operate the fuel cell in vivo, with a body fluid electrolyte, blood plasma, near normal body temperature. Blood plasma is seriously deficient in a critical property of any fuel cell electrolyte, the ability to resist pH changes caused by the production and consumption of hydrogen ions during anodic and cathodic electrochemical reactions respectively. This problem is further complicated by the low reactant concentrations present in blood plasma. Experimental measurements of the magnitude of these mass transfer limitations suggest that conventional fuel cells show little promise for this application and novel concepts are needed. A second problem, the electrochemical oxidation of glucose, has also been studied and two promising electrocatalysts based on platinum and ruthenium have been found. Two approaches to the solution of the major problem of mass transfer have shown promise. One approach involves the rapid flow of electrolyte through a porous electrode, whereby the diffusion layer thickness can be minimized. As a consequence, the limitations of pH changes and low glucose concentration are dramatically reduced, and acceptable performance for an anode operating on glucose in electrolytes similar to blood plasma appears to be within reach. Parasitic power requirements must be evaluated in this approach. A second approach involves the development of a solid state mediator cell, whereby the anodic and cathodic reactions are mediated through an impervious thin film of redox polymer. This system would eliminate the need for a body fluid electrolyte and thus avoid the electrolyte buffer limitations entirely. Experimental evidence for the operability of such a system has been obtained. Acceptable reaction mediation rates must now be demonstrated.

INTRODUCTION

An implantable biological fuel cell is one of the promising approaches to a power supply for an artificial heart. However, successful development will require the solution of a number of technical and engineering problems associated with the necessity of in vivo operation. The most immediate of these problems are currently being attacked at the Esso Research and Engineering Company under a contract from the Artificial Heart Program of the National Institutes of Health. In this presentation, the fundamental problems of fuel cell operation in blood plasma will be discussed, and the results to date of two promising approaches toward a solution of these problems will be described.

Serious difficulties arise in the use of body fluids such as blood plasma as electrolytes for fuel cell reactions. In aqueous media, the electrochemical oxidation reaction (anodic reaction) produces hydrogen ion, and the electrochemical reduction reaction (cathodic reaction) consumes this ion. Also, the potential of the respective electrode reactions are sensitive to the local hydrogen ion concentration at the electrode. As a result, if the electrolyte is in the neutral pH range and is a poor buffer, the production and consumption of hydrogen ion at the respective electrodes will cause large local changes in pH and a severe loss in potential. This is exactly the situation that pertains in the case of blood plasma. A schematic diagram illustrating the nature of this problem is shown in Figure 1.

The potential of a fuel cell reaction is also sensitive to the local concentration of the fuel. For example, let us consider the electrochemical oxidation of a soluble material at a fuel cell electrode. In a stagnant system the consumption of fuel at the electrode will set up a diffusion gradient, and as the current density (rate of reaction) is increased, a limit will be reached where the reaction rate is completely controlled by the rate of arrival of fuel molecules. The magnitude of this limit for a specific electrode configuration is directly proportional to the bulk concentration of fuel. The concentration of fuel, for example glucose, in blood plasma is quite low, i.e., about 0.01 Molar, at least an order of magnitude lower than that usually considered necessary for acceptable fuel cell performance.

Since both the pH and the glucose concentration limitations are basically mass transport problems, they are affected by any property of the electrolyte that influences mass transport. In the case of plasma, the higher viscosity of the medium compared to convential aqueous electrolytes will be a factor.

FEASIBILITY STUDY

As a first step in the feasibility study, the magnitude of the problem at the anode of a fuel cell caused by the electrolyte limitations of blood plasma was evaluated. The electrochemical oxidation of glucose served as the test reaction and two catalysts were used: platinum black and a proproprietary Esso noble metal catalyst having higher intrinsic activity for simple oxygenated hydrocarbon oxidation.

The buffer system studied consisted of potassium mono and di-hydrogen phosphate in equal molar amounts, over a concentration range from 1.5 Molar to 0.01 Molar, the latter approximating the buffer capacity of blood plasma. In actual fact, the main buffering system in blood plasma is bicarbonate-carbonate. However, in the absence of specific ion effects on electrode performance, which is the case here, the buffering capacity and not the particular buffer components is the major variable. The performance of conventional flag-type electrodes was measured with and without stirring to assess the magnitude of the buffer limitation. These conditions approximate those found during conventional fuel cell operation. The solutions contained 0.5 Molar glucose to avoid fuel concentration polarization problems and all tests were carried out at 37°C.

Over the current density range studied, no difference in performance was seen for buffer concentrations down to 0.5 Molar. At 0.01 Molar, approximately the buffer capacity of blood plasma, a large increase in polarization was noted which was reduced to some extent by stirring. This indicates that under conventional fuel cell conditions, the fuel cell anode would be severely limited by the poor buffering capacity of the plasma. Also, the effect was not sensitive to catalysis, a predictable result of a purely physical limitation.

Similar experiments were done using decreasing glucose concentrations at higher buffer concentration to evaluate the magnitude of fuel mass transport limitations. Here again, severe polarizations were encountered with limiting currents below 2 ma/cm^2 at the lowest fuel concentration. These data show that serious problems exist not only due to poor buffer capacity of blood plasma, but also due to low fuel concentration.

Theoretically, these effects will be additive. Data was obtained on electrode performance as both buffer capacity and glucose concentration were lowered toward physiological concentrations. These data are shown in Figure 2 and show the large effect on electrode performance in changing from adequate buffer and fuel concentrations to values close to the physiological ones. Clearly, even at current densities below 1 ma/cm^2, more than an order of magnitude lower than that required for a practical system, the anode is badly polarized. The increased viscosity of the blood plasma compared to that of conventional aqueous electrolytes used here would, of course, increase the severity of this problem.

It is important to realize that:

(1) the limitations predicted from theory and shown experimentally in this work apply not only to the anode, but also to the cathode;

(2) because of the nature of the buffering action of blood plasma, the pH limitation at the cathode will be even more severe than at the anode; and

(3) these effects are completely independent of catalysis factors, and therefore efforts to improve the catalytic activity of either anode or cathode catalysts without potential solutions to the mass transport problems is unrealistic.

POTENTIAL SOLUTIONS TO THE MASS TRANSPORT PROBLEMS

Two promising approaches toward solutions of these problems have been investigated and are listed in Table 1.

TABLE 1

TWO POTENTIAL SOLUTIONS TO THE MASS TRANSPORT PROBLEMS
1. Physical Approach Decrease stagnant layer thickness by flowing electrolyte through electrode.
2. Chemical Approach Mediate reactions at each electrode through a redox barrier to allow substitution of a better electrolyte.

One is a direct attack on the problem by reducing the diffusion gradient at the electrode surface, and the second is an indirect approach which could lead to a sealed fuel cell using a conventional acidic or basic electrolyte. The results obtained in these approaches will be discussed in turn.

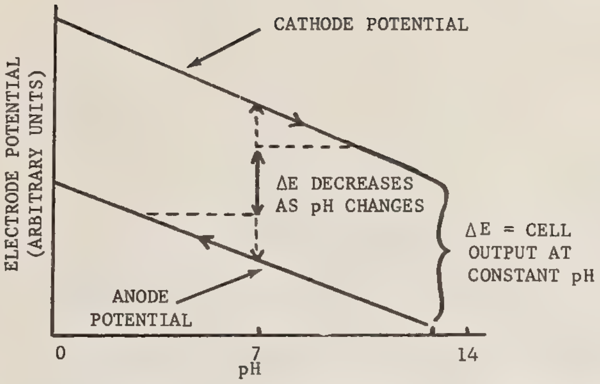

FIGURE 1. THE NATURE OF THE pH EFFECT OF ELECTRODE POTENTIAL.

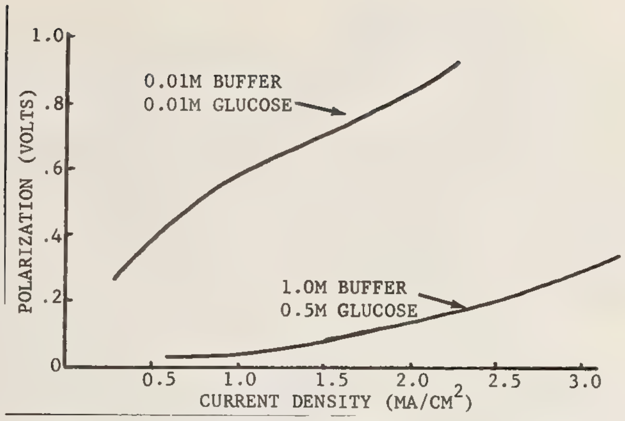

FIGURE 2. COMBINED EFFECT OF BUFFER AND GLUCOSE LIMITATIONS CAUSES SEVERE DEBIT.

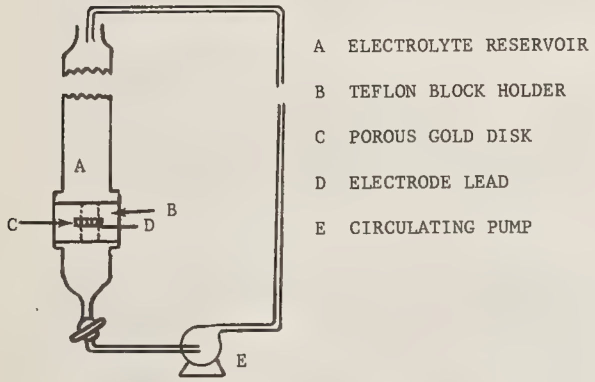

FIGURE 3. FLOW-THROUGH APPARATUS.

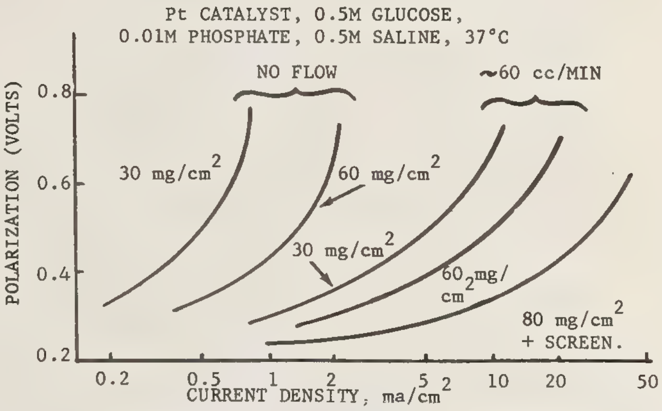

FIGURE 4. INCREASED PERFORMANCE POSSIBLE THROUGH ELECTRODE CHANGES.

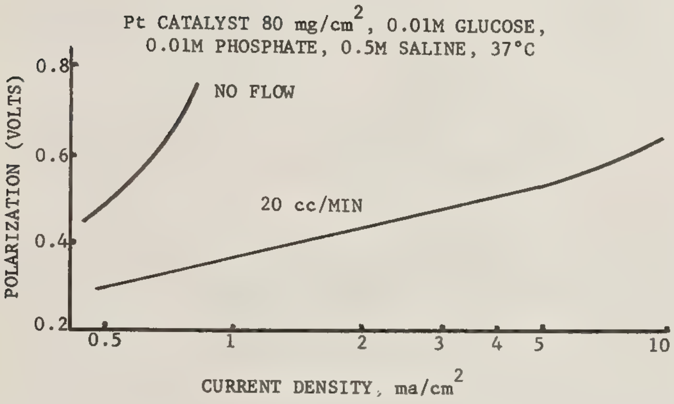

FIGURE 5. REASONABLE PERFORMANCE AT PHYSIOLOGICAL CONDITIONS.

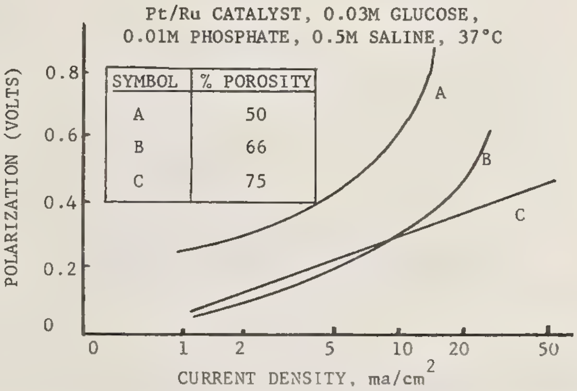

FIGURE 6. CONTROLLED POROSITY ELECTRODES GIVE HIGH PERFORMANCE.

A. Physical Approach.

The direct approach takes advantage of the large reduction in diffusion layers produced by flowing the electrolyte through a porous electrode, giving large relative motion between the electrode surface and the electrolyte. A diagram of the apparatus used is shown in Figure 4. It consists of a large cylindrical glass reservoir fitted with a nitrogen sparge, an auxiliary electrode, a thermometer and a Luggin capillary for measurement of electrode potential. Electrolyte temperature is controllable with an externally wrapped heating tape. Below the reservoir is mounted a Teflon electrode holder. In the initial evaluations, this contained a porous gold disk on which could be supported a layer of loose catalyst powder. Electrical connection was made by a ring of tantalum sheet, in contact with the gold disk, having an external tab. Later in the work, self-supporting porous electrodes were used. Below the electrode holder, an electrolyte collector was mounted, which led to a pump for recirculation of the electrolyte to the upper reservoir.

The utility of this device was demonstrated using platinum black catalyst, and electrolytes at varying buffer concentration. Performance curves were obtained for glucose oxidation using stagnant and flowing electrolyte. Electrolyte flow gave substantial increases in performance due to reduction of the diffusion layer thickness. Quantitatively, the improvement amounted to about an order of magnitude. In these experiments high glucose concentrations were used to eliminate concentration polarization from low fuel concentration. However, similar experiments at differing glucose concentrations showed a marked advantage for the flowing system at low glucose concentrations also.

Theoretically, the performance ought to be sensitive to electrode loading and electrode design. This proved to be the case. When more catalyst was used, the performance increased, the increase being about linear with catalyst loading. During these experiments, some channeling in the catalyst bed was observed, which would decrease the efficiency of the system. The addition of a gold-coated tantalum screen, pressed gently into the top of the bed for stabilization, gave a marked increase in performance. These data are shown in Figure 4.

This phase of the study ended with an evaluation of the performance of the improved electrode at both low glucose concentration and low buffer concentration. As shown by the data plotted in Figure 5, from a situation where the maximum current density was below 1 ma/cm^2, the use of electrolyte flow allowed at least 10 ma/cm^2 to be obtained. Thus, the use of this technique shows promise in minimizing the effects of mass transfer limitations, and efforts to improve on the catalytic aspects of the glucose reaction combined with further improvements in electrode structure were justified.

As a result of past programs, a number of catalysts had been developed having much higher intrinsic activity than platinum for the oxidation of simple oxygenated materials such as methanol. Accordingly, these catalysts were screened for glucose oxidation. Briefly, the findings of this study showed that, while a direct correlation did not exist between the activities for methanol and glucose, several catalysts exhibited much higher activities than platinum for glucose oxidation.

Using these more active catalysts, efforts were made to improve the performance capability of the flowing electrolyte system. The approach taken here was the preparation of structurally sound Teflon-bonded electrodes of controlled porosity. The latter was accomplished by incorporating a leachable component, for example calcium carbonate, whose removal introduces porosity into the structure. The porosity can be varied by changing the amount and the size of the incorporated material. This technique has given very promising results as shown in Figure 6. Glucose oxidation has been demonstrated at reasonable potentials out to very satisfactory current densities. As shown in Figure 7, even at physiological concentrations of glucose, the electrodes are operable out to 20 ma/cm^2 at 0.45 volts polarized, compared to less than 1 ma/cm^2 for a conventional electrode system (Figure 2). Further research in this area is expected to lead to even better performances. Also, this technique is directly applicable to a cathode where similar but more severe limitations exist.

Up to this point, only initial rather than long-term activities have been discussed. Since adequate electrode life is a prime requirement for an implanted cell, an assessment has been made of this property with the more active catalysts. These studies have shown that a problem exists in this area. Life tests have been operated at constant current for extended periods of time and show a gradual decline in performance. If the current is interrupted, partial restoration of performance is obtained as shown by the data plotted in Figure 8.

The most likely cause of this effect is the buildup in the electrolyte of an intermediate which is difficult to oxidize. This conclusion is strengthened by the observation that (1) addition of more glucose at the end of a life test gave no change in the rate of potential decay, i.e., the loss in performance was not due to lack of reactant and (2) the electrode itself could be easily regenerated at the end of the test showing that the loss in activity was not due to permanent loss in catalytic activity.

Some preliminary toxicity tests on mice have shown that the oxidation products are not toxic. Thus the electrode life problem might be alleviated in a real system by normal metabolism of the oxidized products, a kind of in situ purification process.

From the results obtained to date, the feasibility of overcoming the physical limitations of blood plasma by a flow-through electrolyte system seems promising. However, many problems remain to be solved, including the development of a satisfactory cathode and the engineering of a fuel cell system which meets the requirements of the Artificial Heart Program. Thus, significant progress has been made in the program so far and further research to develop a flowing electrolyte fuel cell should prove fruitful.

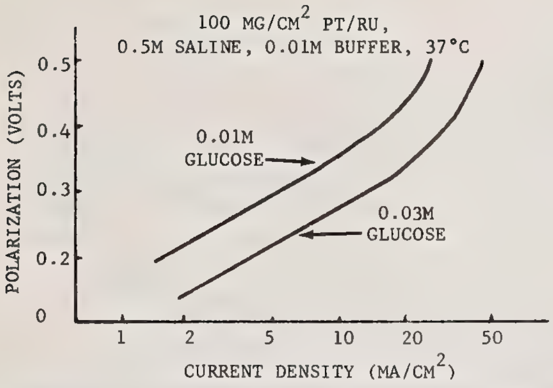

FIGURE 7. ELECTRODES ARE OPERABLE NEAR PHYSIOLOGICAL CONDITIONS.

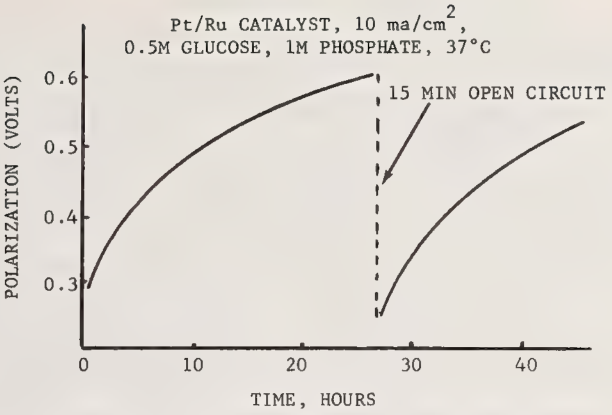

FIGURE 8. ELECTRODE LIFE IS A DEFINITE PROBLEM.

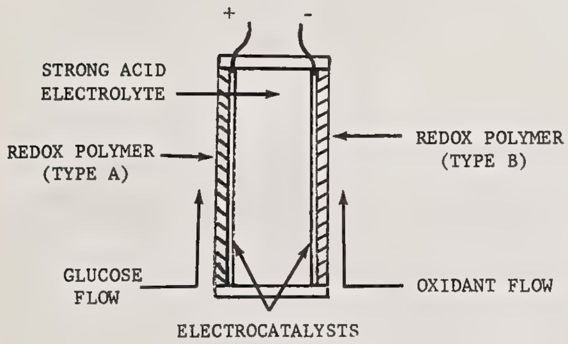

FIGURE 9. MEDIATOR CELL SCHEMATIC.

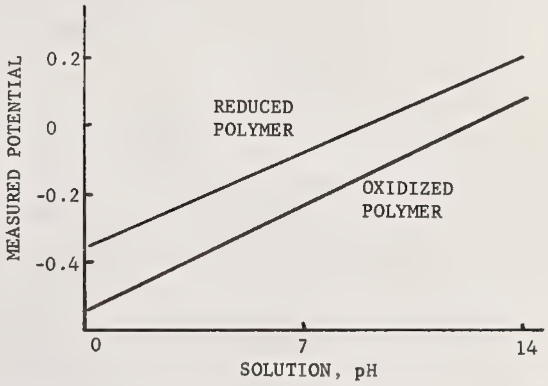

FIGURE 10. POLYMER ELECTRODE POTENTIAL SHOWS RATIONAL CHANGE WITH pH.

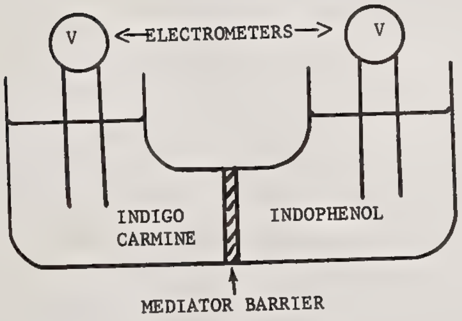

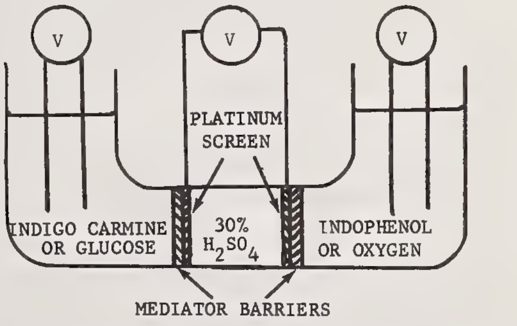

FIGURE 12. PRINCIPLE OF MEDIATOR FUEL CELL ESTABLISHED.

FIGURE 11. REACTION BETWEEN TWO REDOX DYE SYSTEMS CAN BE MEDIATED.

B. Chemical Approach.

The second approach toward the development of an implantable power source has a completely different direction. It is a solid state mediator system that in principle at least would eliminate any body fluid as the electrolyte of the cell. The principle of this device is best explained by an example.

Consider the properties of a non-porous film prepared by polymerization of a redox system such as hydroquinone/quinone. Such a film might be produced by polymerization of vinyl hydroquinone. Contact of the film on one side by an oxidizing agent would result in oxidation of the surface hydroquinone to quinone. These surface molecules could then react with underlying molecules such that an oxidation wave would pass through the membrane to the opposite side. If a layer of porous catalyst was present on the membrane face in contact with an electrolyte, electrochemical reduction could be effected. A similar situation can be postulated starting with an oxidized membrane and a reducing agent. This principle can then be applied to a fuel cell as shown in the schematic in Figure 9. Here we assume a hermetically sealed system, containing a strong acid electrolyte. The operation of the cell can be simply explained. At the left, glucose reacts with the redox membrane, giving the reduced form, the reaction proceeding until the reduction wave reaches the internal surface. Then, the electrochemical oxidation step occurs, producing hydrogen ions and electrons. The opposite reaction occurs at the right-hand side, with the oxidized form of the membrane being reduced, consuming electrons and hydrogen ions. Since the product of the anodic reaction (hydrogen ion) is consumed stoichiometrically in the cathodic reaction, the electrolyte is invariant. Also, since a strong acid or strong base can be used, no buffer limitation is present as is the case with plasma.

Demonstration of the applicability of this system has been a major goal in the work. The key component is quite obviously the membrane. Work was started with an experimental redox resin, Amberlite XE-239, from Rohm and Haas, which contains quaternary ammonium groups on a tertiary butyl hydroquinone skeleton. It was developed for removing oxygen from aqueous solutions and thus is designed with a large fixed porosity. Although the latter property is not desirable from the standpoint of rapid redox transfer, the ready availability of this material allowed work on the principle itself to begin.

Initially, the demonstration of the electrochemical activity of the resin was attempted. Electrodes were fabricated with both oxidized and reduced polymer and a conductive binder, and their potentials measured as a function of pH. As shown by Figure 10, at any given pH, the potential of the reduced and oxidized forms differ and each shows a pH dependence over the whole pH range examined. Although the response to pH differs somewhat from that of the monomer, the data shown here prove that the polymeric resin is capable of impressing a meaningful and stable potential at an electrode, and that the potentials, qualitatively at least, are in accord with electrochemical principles.

In the next set of experiments it was shown that the resin could undergo chemical oxidation and reduction cycles reversibly up to at least 10 cycles. The measured chemical redox capacity determined here was 0.55 ± 0.01 milliequivalents/gm. Batteries were then constructed using oxidized polymer as cathode and reduced polymer as anode. Although these were discharged successfully, only ~2% of the demonstrated chemical redox capacity could be used electrochemically even at very low current drains. This was no doubt caused by the poor ohmic contact between the polymer and the conductive binder and should be easily improvable with better electrode construction. The important point demonstrated here is that if the polymers can act as electrodes in a battery, they also could act as electrodes in a fuel cell where the oxidation and reduction of the polymer could be maintained chemically.

These results encouraged the preparation of impermeable barriers containing the resin. A relatively crude but effective approach was chosen consisting of suspending the resin in a molten polyethylene, pressing the suspension between smooth glass plates and recovering the film after solidification. Films made in this manner were about 40 mils thick. Films were tested by interposition between two chambers containing different redox dyes, one in the reduced form and one in the oxidized form. By following the potential of the individual solutions, it was shown that reaction between the two redox dye systems occurred, although they were separated by the impervious barrier. This experiment is outlined in Figure 11. Only one explanation is possible here: the reaction between the two dye systems was mediated by the barrier. Thus, the redox membrane principle has been demonstrated.

Using the experimental setup shown in Figure 12, the overall mechanism necessary for a solid state mediator fuel cell was then tested. A central compartment, filled with 30% sulfuric acid, was separated from two external compartments by two redox membranes having platinum mesh electrodes pressed into their inboard faces. The outer compartments were filled with the same two dye solutions tested originally. With time, a potential close to the theoretical 0.5 volt difference in potential of the two dye systems built up between the platinum mesh electrodes. Furthermore, the two electrodes could be discharged, although only at low current density. This demonstrates the concept of mediating a chemical reaction and extracting the energy electrochemically.

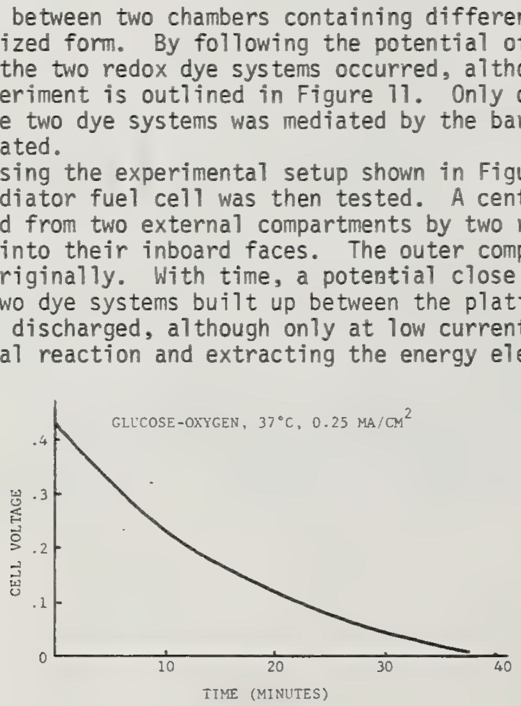

FIGURE 13. DISCHARGE CURVE, MEDIATOR FUEL CELL.

Recent work with this same apparatus has shown the development of electrical potential between the two platinum electrodes when the external chambers contain glucose solution and aerated solution respectively. In this case again, a potential greater than 0.4 volts built up between the two electrodes, and discharge of this potential at a current density of 0.25 ma/cm^2 was successfully demonstrated as shown in Figure 13. The voltage in this case dropped to zero since the mediation rate through the non-engineered redox barriers was limiting. Marked improvement in this property can be achieved by preparing actual redox membranes. Thus the principle of the mediator fuel cell has been conclusively demonstrated.

CONCLUSIONS

From the work done so far, several conclusions can be drawn:

(1) Blood plasma is such a poor electrolyte that fuel cells of conventional construction show little promise. Thus, development of electrocatalysts, while necessary, is not sufficient to ensure a practical system.

(2) Two approaches have shown promise in overcoming the problem: the flow-through principle and the mediator fuel cell.

(3) Many problems remain to be overcome. The more immediate are cathode and systems development for the flow-through approach and the demonstration of adequate mediation rates for the mediator fuel cell.

(4) No technical problem has yet been uncovered that appears insoluble. Thus further progress can be expected through additional research.

DISCUSSION

DR. BEAN: Have you done any analytical work to determine what products other than gluconic acid are produced in this cell?

DR. BATZOLD: We have recently been trying some flat plate chromatography, but we don't have any results that we are prepared to discuss yet. We are interested in the products of course, not only from the standpoint of the electrode poisoning phenomenon, but also from the possibility of toxicity. One thing we have done is to take some of the used electrolytes containing these products and tried some toxicity tests on mice and it turns out that the mice cannot tell the difference between the flush and the oxidized electrolyte. We did kill some mice because we injected too much potassium, but not because of the oxidized products.

DR. GINER: I have two questions. One is in the performance curve. How did you get them. How many millivolts per minute or how long were the points?

DR. BATZOLD: Basically, we normally take points about a half a milliamp square centimeter, one, two, five, ten, twenty, etc., and these points are taken for about ten minutes of operation.

DR. GINER: Do you hold at 10 minutes at this point?

DR. BATZOLD: Yes.

DR. GINER: My second question is: What is the specific conductivity of the ion membrane? Because that will be one of the factors that leads to your performance characteristics.

DR. BATZOLD: I think that is a question for my colleague.

DR. BELTZER: The question is not really one of conductivity. In fact, you don't want to conduct. The rate of interaction between the nearest neighbors on the polymer between the reduced form and the oxidized form is not really conduction. Essentially, its hydrogen transfer. In a sense it is almost like an organic equivalent of a palladium membrane.

DR. GINER: If so, I don't understand the concept.

DR. BELTZER: Basically, if you have a quinone grouping on a polymer, and the external quinone group sees a reducing agent and is reduced to the hydroquinone, it is possible that it can interact with the quinone underneath to form a semiquinone group. Not a quinhydrone but rather a semiquinone which can be stabilized because it is on the polymer. Then an additional molecule of reducing agent comes along and converts the external semiquinone to a hydroquinone and you can get interation throughout the polymer matrix, and thereby transmit chemical energy across the lattice.

If you look at the reaction of a quinone and hydroquinone to form a semiquinone this is equivalent to hydrogen transfer. It is the atoms rather than the ions or electrons that are transferred. The problem really is how fast does this interaction occur, and this is hard to say. For one thing, we have a suspension of this polymer in polyethylene, which results in a large fraction of dead space, and in addition the barriers as we make them presently are quite thick. We know that the mediation rate through this membrane is not rapid enough to maintain a steady state potential at a given current density. What the ultimate rate will be is difficult to answer. What we would like to do is to have an impermeable barrier made solely of the redox polymer.

DR. GINER: You would call that specific conductivity rate?

DR. BELTZER: Yes, there are polymers which are conductive. Recently, there was a polymer made by the oxidation of aniline through which current densities as high as an amp per square centimeter were passed. Now this conduction, it is not what we want, is indicative of the fact that you can get high rates of transfer and hence interaction across impermeable barriers.

DR. WROBLOVA: I just wanted to ask what was the potential scale on your graphs. Was the potential measured versus reversible hydrogen potential?

DR. BATZOLD: It was polarization vs. glucose theoretical which is similar to hydrogen.

DR. WROBLOVA: Thank you. Now, you also observed on certain of your polarization curves two Tafel sections with two different slopes at least in one case.

DR. BATZOLD: Well, we defined what looked like Tafel lines at low currencies, but they are actually very steep slopes, something on the order of I think 2/10 of a volt. I don't think these are true Tafel lines. Generally, it is just a bend at the end.

DR. WROBLOVA: We have worked under potentiostatic conditions defining steady state as $< 1\%$ of change in current over 30 min. long sections of Tafel lines with a slope of $\frac{2\,RT}{F}$ are then observed. I would also like to note that depending on the potential region the current decreases or increases in time. Do you observe an improvement of the electrode?

DR. BATZOLD: As far as the improvement of the electrode is concerned, what we have noticed, I guess you could call it that, is more a cyclic behavior where the electrode will polarize to a certain level and then suddenly improve quite rapidly. In fact, it may improve as much as a tenth of a volt, then slowly decay again, improve again, and eventually die. We have seen this before. Formaldehyde will do this on a platinum electrode quite nicely. It does not sound like the same sort of thing that you have found. I have never observed any long-term improvements.

DR. WROBLOVA: There is another point. The apparent reaction order is ~ 0.25, and thus the decrease of performance with decreasing concentration is not very large.

DR. BATZOLD: Well, we have not worked at all with constant potential devices.

CHAPTER 69

OXYGEN REDUCTION ON GOLD-PALLADIUM ALLOYS IN NEUTRAL MEDIA

J. Fishman and J. Henry

Leesona Moos Laboratories
Great Neck, N. Y.

The need to find active electrocatalysts for the selective reduction of oxygen in human body fluids motivated the study of Au-Pd alloys, to relate catalytic selectivity to the electronic configuration within the alloy series.

In the pH range 6.8-7.6, at 37°C, Pt, Pd, Au and Au-Pd alloys, in bulk and metal black form, displayed reproducible prime and steady state cathode activities. Prime activity and its rate of transition to the substantially lower steady state activity depend on the open circuit potential, which, in turn, depends on the prior polarization history, i.e., potential, degree of approach to the steady state and time on open circuit.

The open circuit potential tends spontaneously but slowly to the stable rest potential. Potentiostatically forced return to the stable value is associated with transient anodic currents.

It is thought that the described polarization phenomena could reflect the adsorption and removal of hydrogen peroxide from the catalyst surface.

Maximum activity for O_2 reduction at the steady state was found at about 35% and 65% (atomic) Au content for alloy blacks and at 30%, 40% and 75% for bulk alloys. Alloy blacks exceed Pt black activity by a factor of about 2-3. In the combined presence of 0.1 M NaCl, 1mg/ml dextrose, 0.25 mg/ml lactic acid and 0.3 mg/ml urea, the cathode activity of 35% and 65% Au-Pd blacks is suppressed by about 20% and 30% respectively, while that of Pt black by 70%.

Thus, some Au-Pd alloys are not only more active than Pt black for oxygen reduction in neutral media, but they are also more selective for this process.

INTRODUCTION

The work reported in this paper is concerned with the study and development of electrocatalysts for the oxygen cathode component of an implantable biological fuel cell. To be suitable for use in such a fuel cell, oxygen reduction catalysts must satisfy two primary conditions:

a) They must possess substantial activity in near neutral electrolyte media (pH 7.2-7.4) at 37°C, and
b) They must be selective for oxygen reduction in the presence of the various components of body fluids.

The achievement of the described catalyst characteristics involves the resolution of several known problems which are briefly discussed in the following paragraphs.

The oxygen electro-reduction process has been studied very extensively in recent years[1] and very efficient oxygen electrode structures have been devised that can support 4 amperes per cm^2 with about 250 mV polarization. These successful developments are, however, restricted to strong acid and alkaline electrolytes. The neutral and near-neutral region is a relatively unexplored territory as far as the oxygen reduction process is concerned. The previous work on the NIH implantable fuel cell project performed by Monsanto Research Corp.[2] and a recent paper by Hamman[3] suggested that in near-neutral media the rate of oxygen reduction on Pt and other noble metal catalysts will be a small fraction of that noted in acid and alkaline systems at the same electrode potential.

The achievement of electrocatalytic selectivity also presents serious obstacles. The commonly used oxygen reduction catalysts such as Pt, Pd, Rh, etc. tend to adsorb organic materials such as those found in body fluids and also to promote their electro-oxidation. Adsorption of organics poisons the catalyst for oxygen reduction by blocking active sites, while electro-oxidation of the organics will substract from or nullify entirely the current due to the simultaneously progressing oxygen reduction process. This problem of mixed electrode reactions will be discussed more fully in a later part of this paper.

Extensive research in electrocatalysis conducted at LML brought to light the remarkable spectrum of electrocatalytic properties possessed by the gold-palladium alloy series.[4,5] It was proposed that a study of the functioning of these alloy catalysts under the conditions of the implantable fuel cell holds promise for a substantial progress in achieving activity and selectivity for the oxygen reduction process. The alloys in the series are homogeneous, face centered cubic structures where the lattice constant changes in a nearly linear fashion from 3.88Å for Pd to 4.07Å for Au. The electronic configuration, however, changes significantly as Au is added to Pd. Palladium possesses approximately 0.55 - 0.60 d-band vacancies which are filled by alloying with gold. Most of the observed changes in the bulk properties of the alloys within the series are thought to be linked to the changes in electronic configuration. Significant transitions in the bulk properties of the alloys are found to occur in the 35 and 60 atomic percent Au composition regions. A listing of these properties will be found in several of the references appended to this paper.[4-6,10-19]

It is not surprising, therefore, that several studies of the catalytic properties of Au-Pd alloys reveal that these, indeed, undergo a transition in the same alloy composition regions where occur the bulk property transitions. Couper and Eley[6] studied the parahydrogen conversion on Au-Pd alloys and found that the activation energy for the process is 3,5kcal/mole on palladium-rich alloys and increases abruptly between 60 and 70 percent Au to the value of 8.5kcal found for gold-rich alloys. G. C. Bond[7], on reviewing this work, pointed out that the catalytic activity passes through a maximum at about 30 percent Au.

Gray et al[8] report that hydrogen chemisorbs on Au-Pd alloys immersed in H_2SO_4 only when the gold content in the alloy is below 60%. A sharp decline was observed in the change of the catalytic activity for the electrolytic hydrogen-evolution reaction in sulphuric acid on further increases in gold content beyond about 38% Au[9]. Dickens et al[10] studied the rate of recombination of hydrogen atoms and of oxygen atoms on Au-Pd alloys. They found an apparent activity maximum for hydrogen recombination in the 30% Au region. Although these authors state that there is no evidence of a correlation between alloy composition and its activity for oxygen atoms recombination, a closer examination of the reported results indicates that also in this case maximum activity may reside in the 30% Au composition region.

The experimental results obtained at Leesona Moos Laboratories bear special relevance to the objectives of the NIH program.[4,5] It was found that in strong alkaline electrolytes (30% KOH) smooth surface Au-Pd catalysts exhibit an activity maximum for oxygen reduction in the 35% (atomic) Au composition region, while alloy blacks show an activity maximum in the 50% Au composition region. It is significant that these activities exceed those of any other known catalyst under the same conditions. In acid media Au-Pd alloys exhibit a sharp maximum in activity for hydrogen oxidation at between 30% to 40% Au content and lose virtually all of this activity at gold contents in excess of 70%. The 30% to 40% Au composition region is also characterized by a remarkable resistance to poisoning by CO admixed to the hydrogen stream. In other words these alloys are selective for H_2 oxidation in the presence of CO. In principle, therefore, the Au-Pd series comprises highly active and also selective catalysts.

The task of exploring the usefulness of these catalysts in implantable fuel cells was divided into two general areas of investigation. In the first area the object was to determine catalyst activity as a function of alloy composition and to attempt to characterize the oxygen reduction mechanism in neutral electrolytes at 37°C. In the second area, the object was to study catalytic selectivity of Au-Pd alloys for oxygen reduction in neutral media in the presence of organic materials found in human blood.

EXPERIMENTAL

All alloys were prepared in the form of metal blacks by reducing with hydrazine an aqueous solution of the mixed metal chlorides. Subsequent investigations have shown that reduction with formaldehyde provided samples with greater activity. The alloy nature of the metal black product and its composition were verified by x-ray examination. The surface area of the metal black powder was determined by the BET method. The metal blacks were bonded with Teflon powder and mounted on a Pt screen. Each electrode contained 100 mg of catalyst powder per cm^2 of the Pt screen. All metal black electrodes were subjected to heat treatment at 300°C prior to testing, in order to "cure" the Teflon bond and to volatalize from the catalyst surface the absorbed chlorine containing compounds.

Oxygen saturated 1M phosphate buffers in the pH range 6.8 to 7.6 and at 37°C served as test electrolytes. Selectivity tests were performed by adding blood components to the electrolyte and studying the effect that these additives have on the oxygen reduction current. The effect of individual additives and of a mixture of additives was compared.

The experimental cell is shown schematically in Figure 1. Electrodes were polarized potentiodynamically and potentiostatically, and all potentials were measured with reference to a hydrogen electrode in the same system. Test electrodes were 2 cm^2 in geometric surface area.

RESULTS AND DISCUSSION

Oxygen Reduction.

The oxygen reduction process in neutral electrolytes on Pt, Pd, and Au-Pd is characterized by a reproducible phenomenon of two levels of activity. The initial activity, termed here the "prime" activity, of a potentiostatically polarized electrode changes with time to the considerably lower "stable state" activity. An example of this behavior is shown in Figures 2 and 3.

The current density supported by an electrode at the stable state at a given potential is completely reproducible. When an electrode operating at the stable state is placed on open circuit, its immediate rest potential is considerably below the original rest potential. The immediate rest potential, however, reverts slowly (in some cases over a period of 1-6 hours) to the original rest potential. The transition from the immediate to the original rest potential is associated with the regeneration of activity to the prime state. The above patterns of behavior are shown schematically in Figure 4. It is seen that the open circuit potential determines prime activity at a given polarization potential, while the polarization potential alone determines the final stable state activity.

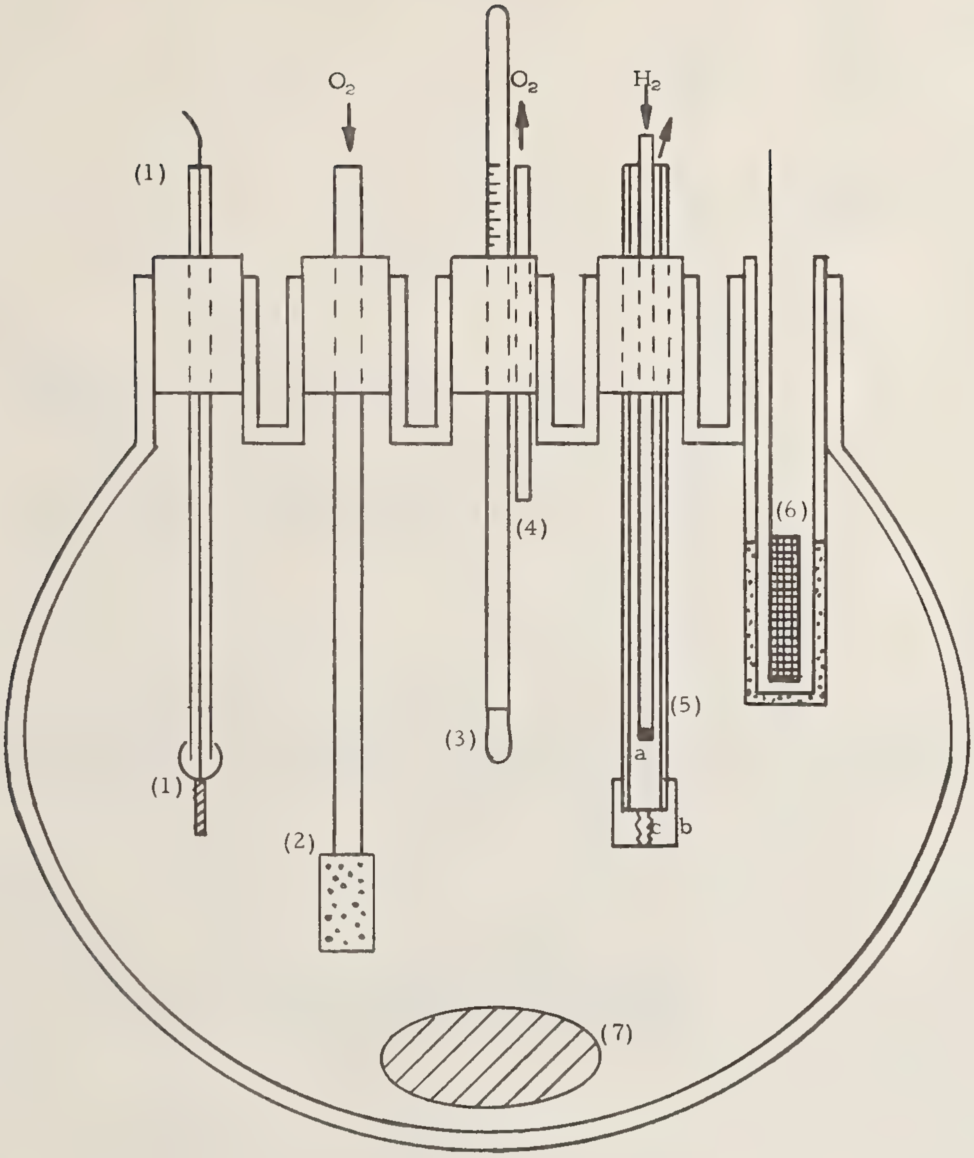

(1) Study electrode
(2) Gas disperser
(3) Thermometer
(4) Gas vent

(5) Reference electrode
a) Pt black electrode
b) Rubber sleeve
c) Asbestos wick
(6) Counter electrode .
(7) Magnetic stirring bar.

FIGURE 1. TEST CELL.

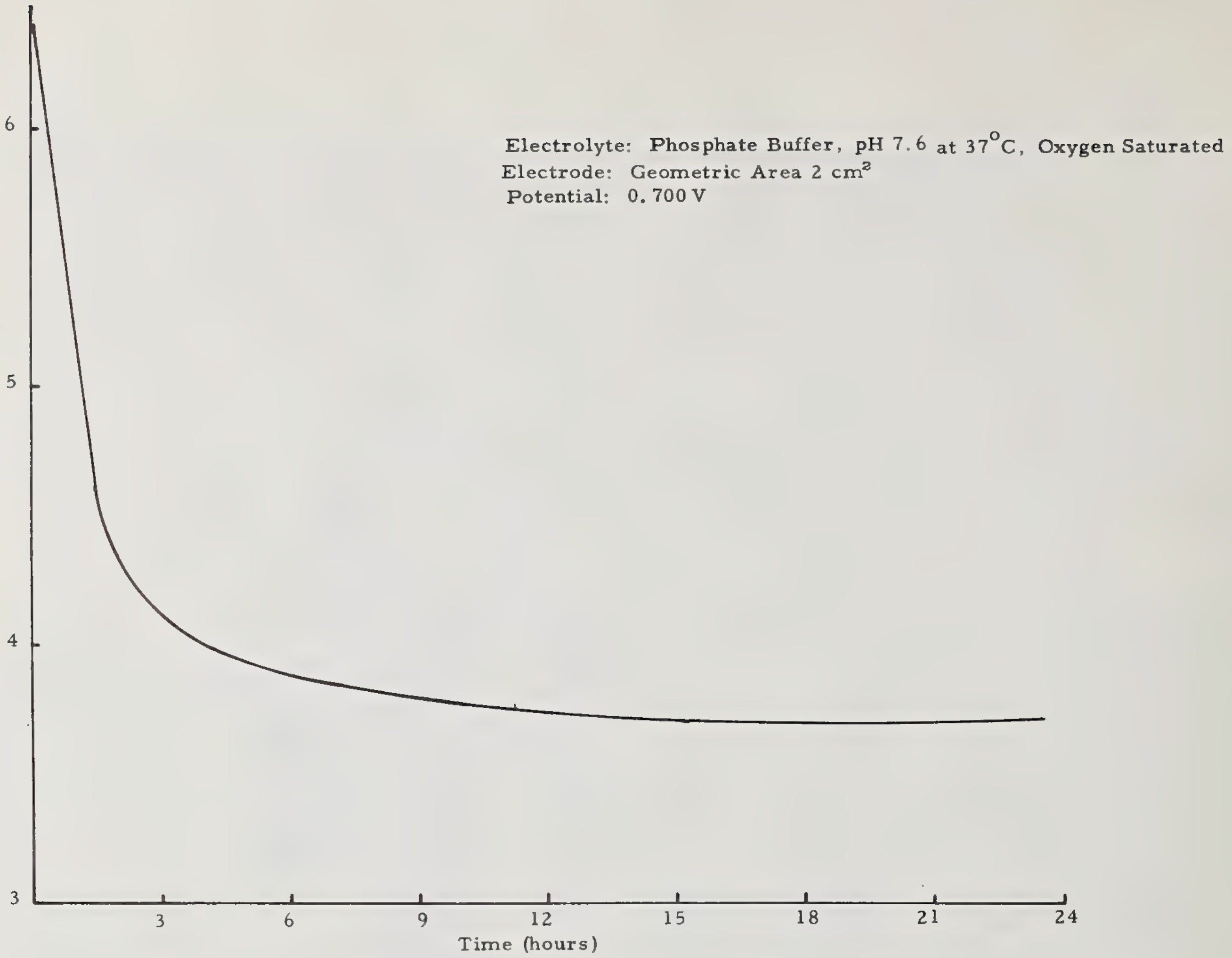

FIGURE 2. ACTIVITY TRANSITION OF 65% Au-35% Pd (ATOMIC) ALLOY BLACK CATHODE AT CONSTANT POTENTIAL.

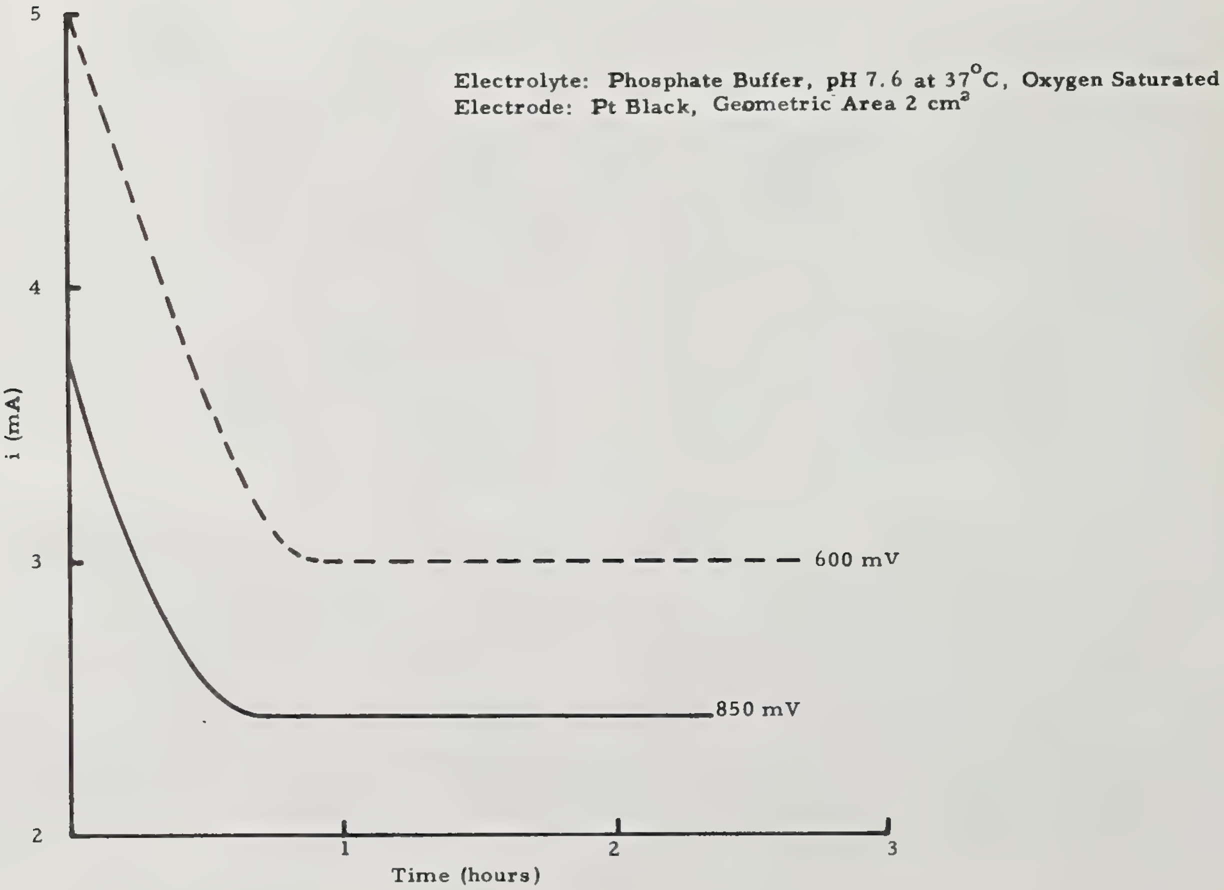

FIGURE 3. ACTIVITY TRANSITION OF A Pt BLACK CATHODE AT CONSTANT POTENTIAL.

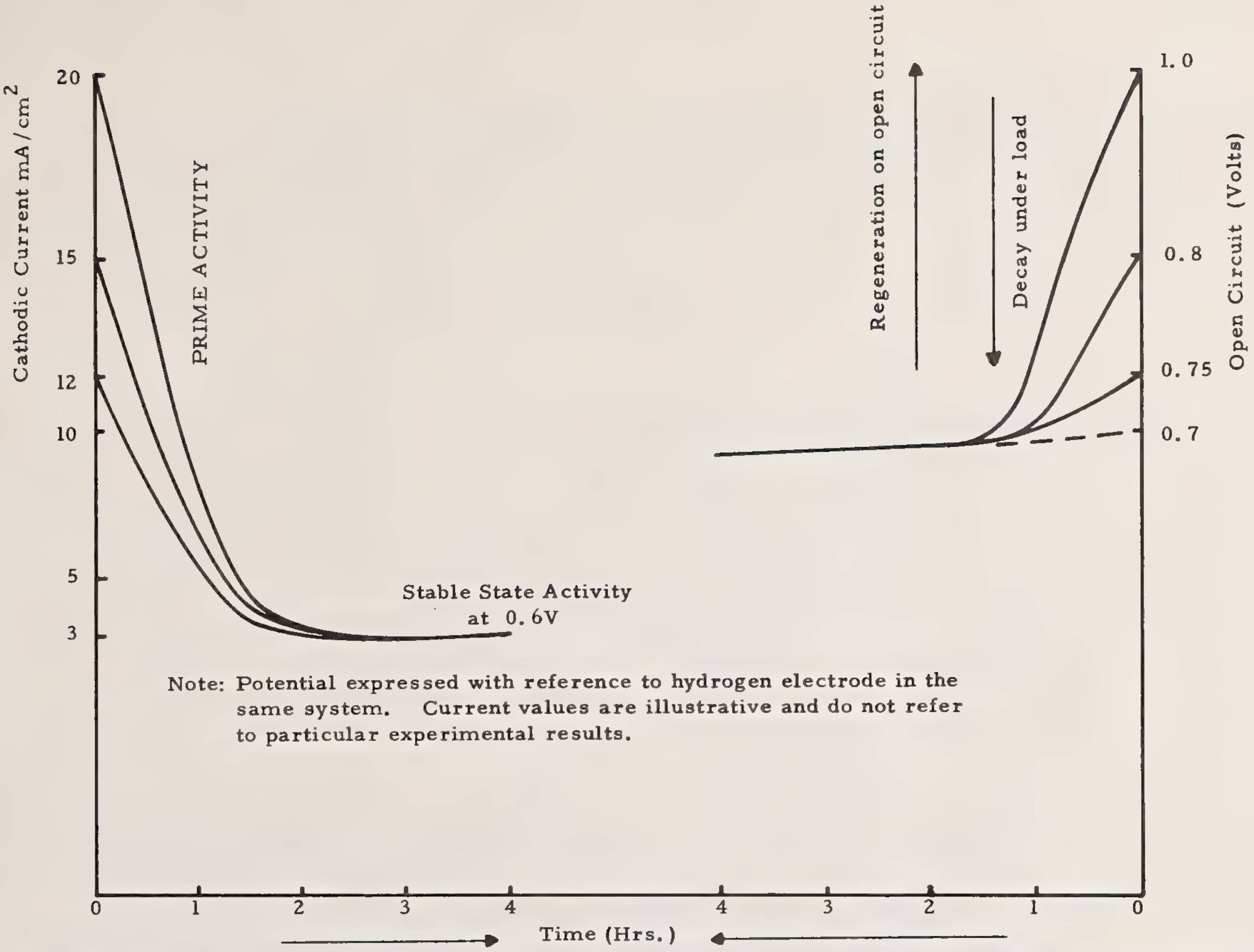

Note: Potential expressed with reference to hydrogen electrode in the same system. Current values are illustrative and do not refer to particular experimental results.

FIGURE 4. SCHEMATIC REPRESENTATION OF THE RELATION BETWEEN OPEN CIRCUIT POTENTIAL AND OXYGEN ELECTRODE ACTIVITY.

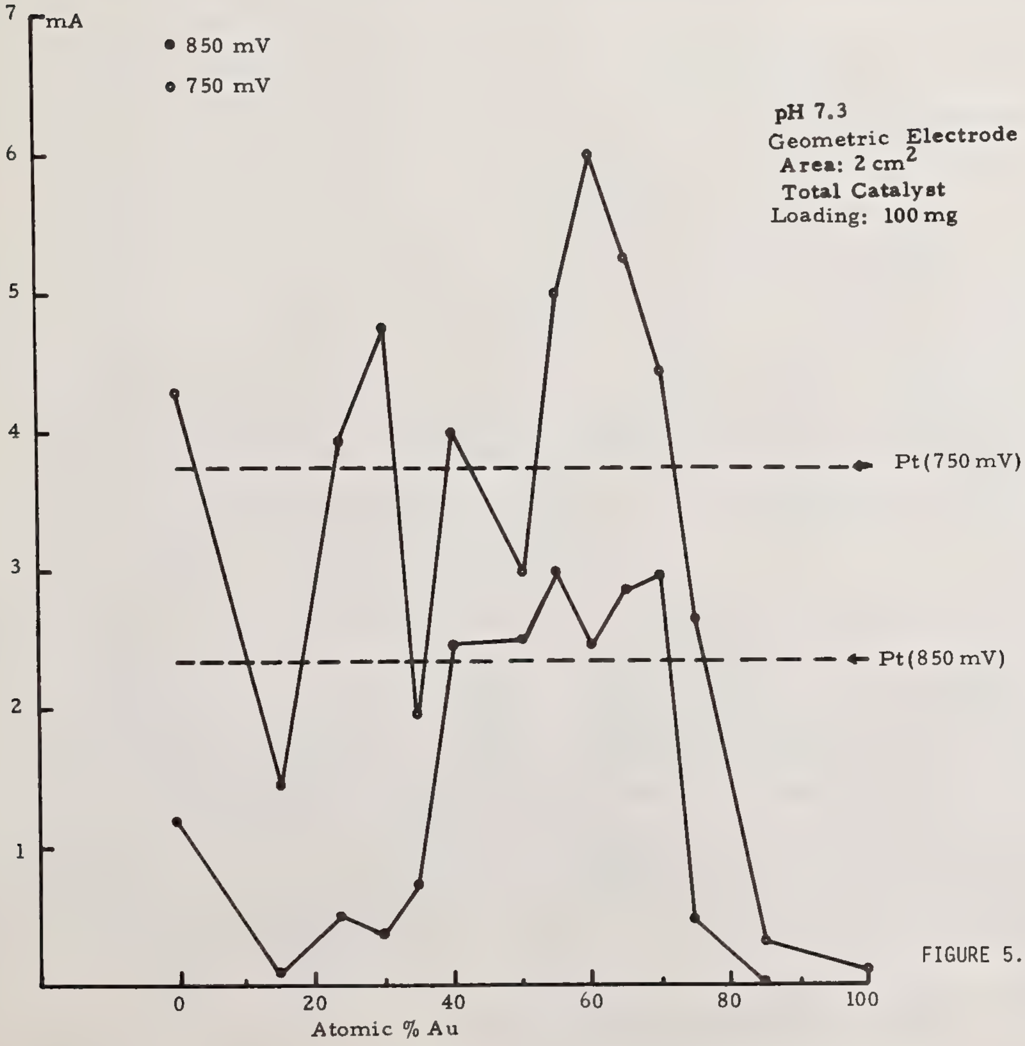

FIGURE 5. STEADY STATE ACTIVITY OF Au-Pd ALLOY BLACK O_2 CATHODES IN pH 7.3 BUFFER.

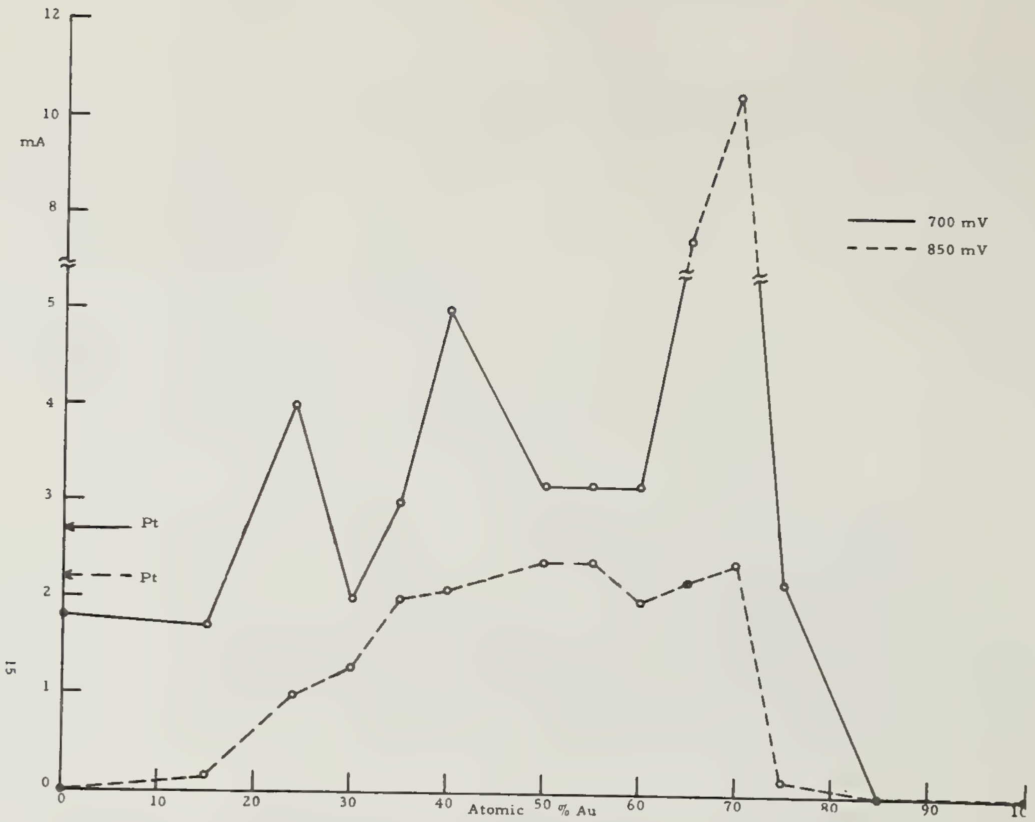

FIGURE 6. STEADY STATE ACTIVITY OF Au-Pd ALLOY BLACK O_2 CATHODES IN pH 7.0 BUFFER.

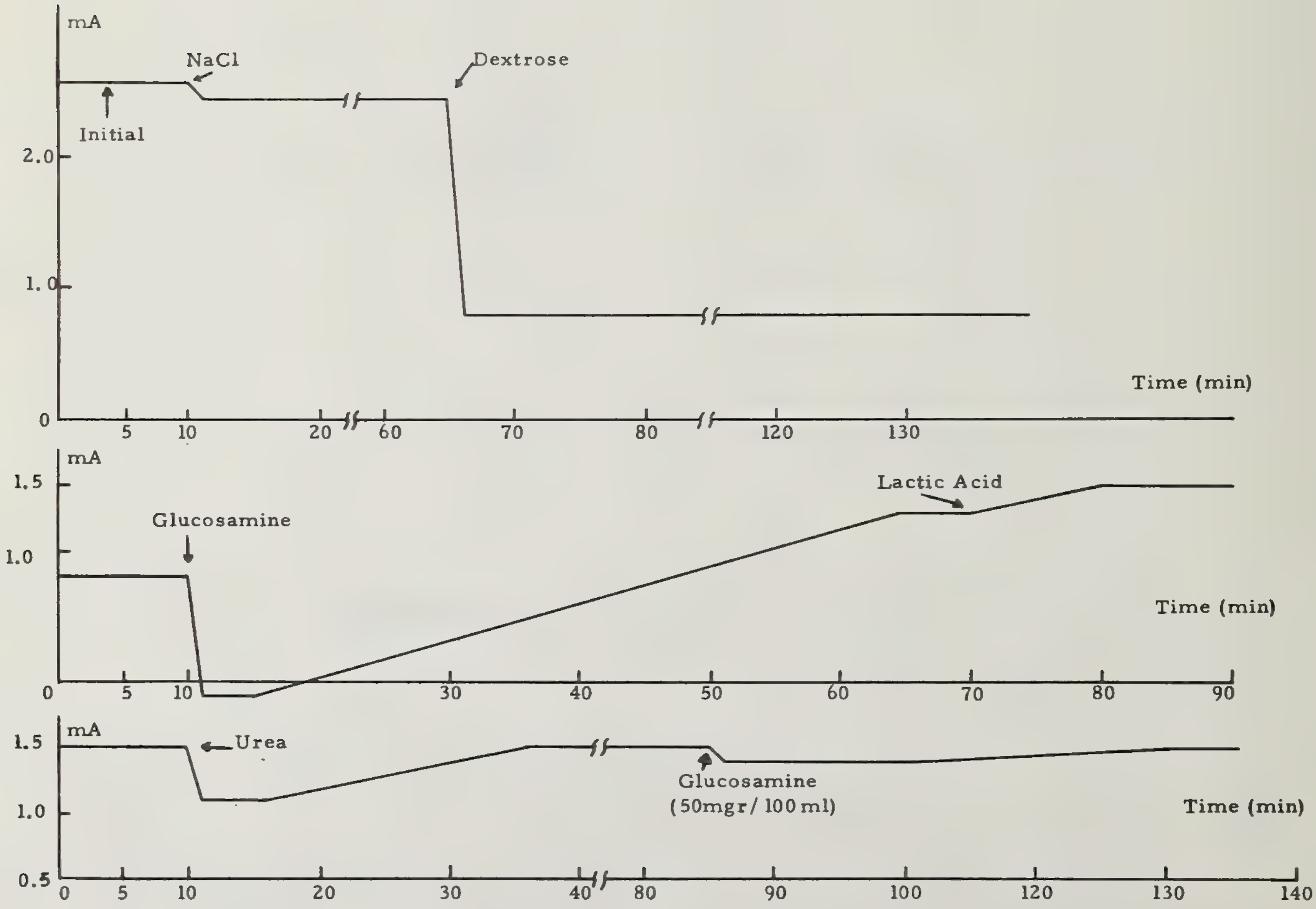

FIGURE 7. INFLUENCE OF ADDITIVES ON Pt BLACK O_2 CATHODES IN pH 7.4 BUFFER AT 0.800 V CONSTANT POTENTIAL.

The decay of prime activity under current load is associated with the decay in the immediate open circuit potential. (The phenomena described here also occur with smooth Pt cathodes, but not with Pt black cathodes, in strong acid electrolytes[11]). A hypothesis has been formulated to explain the described polarization patterns.

The most generally accepted sequence of reaction steps in the oxygen reduction process is shown below.[1]

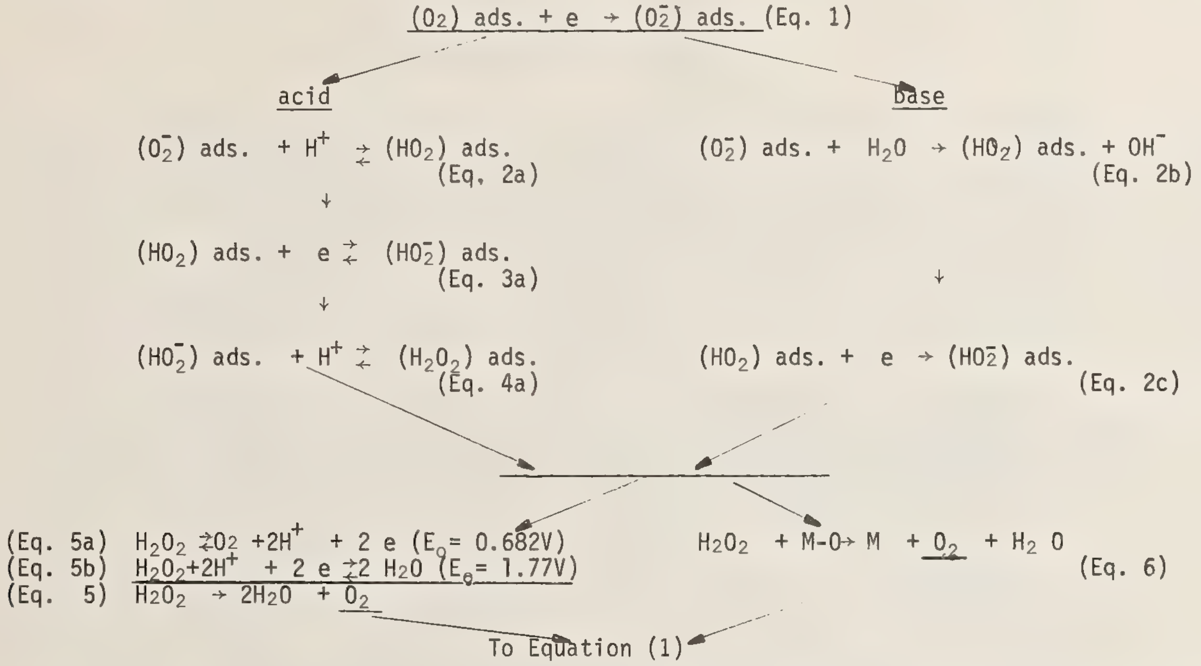

(O_2) ads. + e $\rightarrow$ (O_2^-) ads. (Eq. 1)

(O_2^-) ads. + H^+ $\rightleftarrows$ (HO_2) ads. (Eq. 2a)

(HO_2) ads. + e $\rightleftarrows$ (HO_2^-) ads. (Eq. 3a)

(HO_2^-) ads. + H^+ $\rightleftarrows$ (H_2O_2) ads. (Eq. 4a)

(O_2^-) ads. + H_2O $\rightarrow$ (HO_2) ads. + OH^- (Eq. 2b)

(HO_2) ads. + e $\rightarrow$ (HO_2^-) ads. (Eq. 2c)

(Eq. 5a) $H_2O_2 \rightleftarrows O_2 + 2H^+ + 2e$ ($E_0 = 0.682V$)
(Eq. 5b) $H_2O_2 + 2H^+ + 2e \rightleftarrows 2H_2O$ ($E_0 = 1.77V$)
(Eq. 5) $H_2O_2 \rightarrow 2H_2O + O_2$

$H_2O_2 + M\text{-}O \rightarrow M + O_2 + H_2O$ (Eq. 6)

Let it be assumed that the electrochemically formed hydrogen peroxide (Eq. 3a) or peroxide radicle (Eq. 2a) is neither readily desorbed nor readily decomposed, nor reacted in neutral and near neutral electrolytes (Eq. 5).

In other words, the active sites on the metal catalysts will be progressively blocked by adsorbed peroxide (radicle or ion), with an attendant decline in activity for oxygen reduction. A steady state will eventually be reached on the electrode where the rate of oxygen reduction is linked to the rate of peroxide removal from the electrode surface.

It is implied here that the hydrogen peroxide electrochemically formed at the electrode is differently bonded to the metal surface that is peroxide which is adsorbed from solution. This hypothesis is largely consistent with the observed phenomena. It accounts for the transition from prime to stable state activity. It also accounts for the open circuit potentials which would be governed by Eq. 5a where the surface coverage with peroxide determines peroxide activity. As the peroxide is slowly removed from the surface by desorption or decomposition, the electrode potential becomes gradually more positive. Since, as postulated, the open circuit potential is related to the degree of coverage of the electrode surface with peroxide, it will then also be related to electrode activity.

The "stable state" therefore, in terms of the hypothesis translates into "steady state" where the rate of oxygen reduction is linked to the rate of peroxide removal from the surface. If the hypothesis postulated here is substantiated in further studies, the development of an improved oxygen reduction electrocatalyst for near neutral and neutral electrolytes should involve, in one phase, a search for specific peroxide decomposing materials which can be incorporated in the studied metal catalysts to stabilize the prime activity of that catalyst.

An alternate hypothesis has also been formulated, which considers the possible role of surface oxides in the oxygen reduction process and the effect of formation and reduction of these surface oxides on catalyst activity. This latter hypothesis is, however, less favored since it requires the admission of more complex assumption.

In order to eliminate time effects, activity comparisons within the alloy series were made using the steady state activity values. Figures 5 and 6 show these comparisons at pH 7.3 and at pH 7.0 respectively. The values obtained with Pt black are also included. At pH 7.0 a marked activity maximum occurs in the composition range 60% to 75% (atomic) Au. At pH 7.3, activity maximum occurs in the composition range 50% to 70% (atomic) Au. (Previous studies[4] place the activity maximum at 50% Au in tests conducted in 5 N KOH. It would appear therefore that an increase in pH shifts the activity maximum towards compositions with lower gold content). In both media, activity becomes negligible when gold content exceeds 80% atomic. In both media, the activity of the best alloys exceeds considerably the activity of Pt black.

It appears, therefore, that in the near neutral media of interest (pH 7.2-7.4), Au-Pd alloys with gold content between 50% and 70% atomic, are the most active oxygen reduction catalysts uncovered so far. The activity of these catalysts can be further greatly enhanced if means are designed to stabilize the prime activity state.

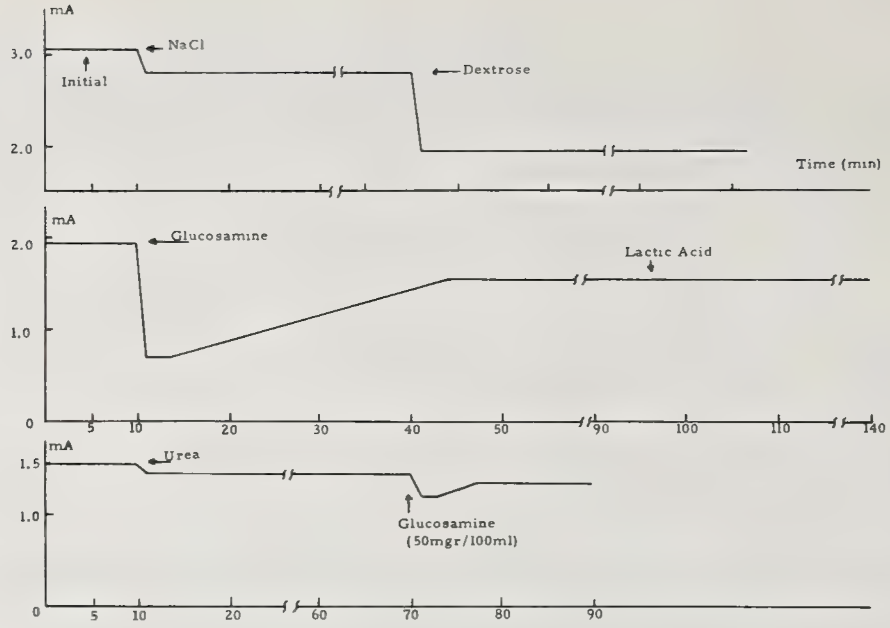

FIGURE 8. INFLUENCE OF ADDITIVES OF 65% Au-35% Pd ALLOY BLACK O_2 CATHODES IN pH 7.4 BUFFER AT 0.800 V CONSTANT POTENTIAL.

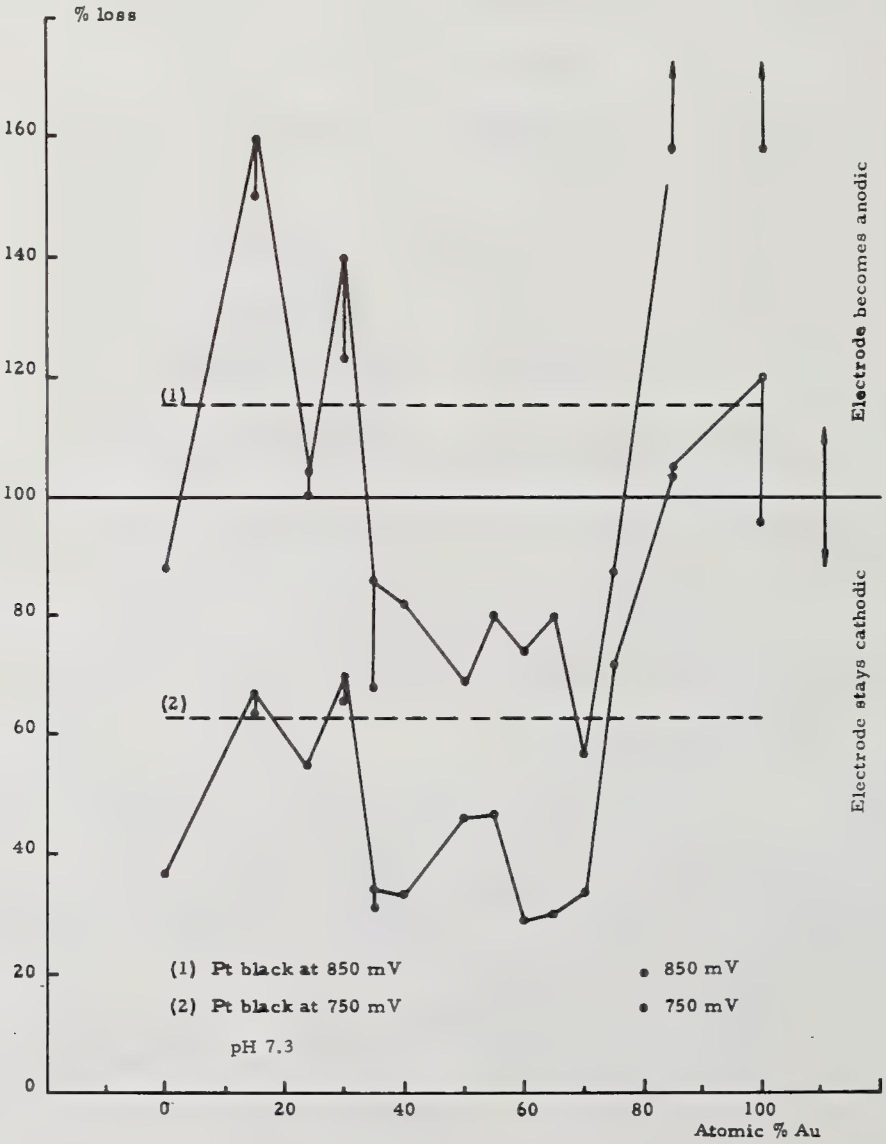

FIGURE 9. SEE EXPLANATION IN TEXT.

Electrocatalytic Selectivity.

Electrocatalytic selectivity of Au-Pd alloys was examined by noting the effect of blood components on the functioning of a potentiostatically controlled Au-Pd oxygen cathode. The experiments were performed in pH 7.4 and 7.3, 1M phosphate buffer. The following blood components were added either in succession or mixed:

Na Cl	0.1 M
Dextrose	1 g/1
Glucosamine	1 g/1
Lactic Acid	0.25 g/1
Urea	0.30 g/1

In order to eliminate time effects from the observations, all electrodes were permitted to achieve the steady state level of functioning as oxygen cathodes prior to introducing the additives into the system. Figures 7 and 8 illustrate the effect of successive additions of blood components to a Pt black system and to a 65% Au-Pd system respectively. Sodium chloride appears to have a relatively small current suppressing effect. Dextrose has a significantly greater effect on the Pt cathode than on the Au-Pd cathode. Glucosamine suppresses significantly the activity of both systems. The recovery of each system with time after the addition of glucosamine is believed to be due to the depletion of the substance by homogeneous oxidation in the oxygen saturated system. The Pt system, unexpectedly, recovers to a better activity than that prior to glucosamine addition. Also, unexpectedly, addition of lactic acid improved Pt cathode activity while it has no effect on the Au-Pd electrode. Urea has a relatively small effect on either electrode.

To characterize the systems under conditions more representative of those in a blood stream, the effect of adding a mixture of all the additives was determined. Figure 9 shows the results in pH 7.3 buffer. It should be noted that the influence of additives is expressed in percent loss of activity with respect to the initial (before introduction of additives) steady state readings. Readings were recorded after 10 minutes and after 60 minutes. Whenever two values for a given alloy composition are shown in Figure 9, the top value refers to the 10 minute reading.

It appears that the functioning of Au-Pd alloy cathodes with gold content between about 40 and 70 atomic percent is least affected by the combined additives. At 0.75 V, the active alloys lose, on the average, 30% of the cathodic current, while Pt black loses over 60% of the current under the same conditions. As shown in Figure 5, the above alloy composition range also comprises the most active electrocatalysts for O_2 reduction.

Alloys with gold content outside the above described range, which have been shown to be poor oxygen electrocatalysts (Figures 5 and 6), are strongly affected by the oxidizable additives. The current supported by these electrodes actually shifts from the cathodic to the anodic region when the additive mixture is introduced (Figure 9). In other words, these catalysts are substantially selective for the anodic process in the presence of oxygen, in contrast to the catalysts described in the previous paragraph, which are substantially selective for the cathodic process in the presence of oxidizable substances. To illuminate the recorded experimental results, it is useful to consider the nature of mixed electrode reactions.

Figure 10 describes graphically the behavior of an electrode on which a cathodic and an anodic reaction take place simultaneously. The condition that at open circuit the anodic and cathodic currents balance each other (zero net current) leads to the establishment of a mixed electrode rest potential Em. The resultant polarization curve is constructed by the algebraic summation of the contributing currents at various potentials. Figure 11 (a) and (b) describes two characteristically different cases. Figure 11 (a) corresponds better to an electrode acting as a cathode than as an anode in a mixed system. The mixed rest potential and the resultant net cathodic current polarization curve are both biased towards relatively positive potential values. The opposite situation is found in Figure 11 (b) which corresponds to an electrode acting better as an anode than as a cathode in a mixed system. Figure 11(a) may be considered as representing the behavior of Au-Pd alloys with gold content between about 40 and 70 atomic percent while Figure 11(b) as representing the behavior of the other alloys in the series.

The resultant polarization curves of Figures 10 and 11 represent idealized cases where it is assumed that there is no particular interaction between the reacting species. With real systems, however, the possibility is likely that the reaction kinetics of one process will influence the kinetics of the concurrent processes on the same electrode by competition of the reacting species for the available active sites on the electrode surface, or by some reaction between the adsorbed species. In order to assess how mixed reactions proceed on the studied Au-Pd alloys, separate steady state polarization curves were determined for:

- oxygen reduction in the absence of additives,
- dextrose oxidation in an argon purged system,
- oxygen reduction in the presence of dextrose.

The results are shown in Figures 12 and 13. The oxygen reduction curves show the expected features. The dextrose oxidation curves show a maximum which is much more pronounced in the case of the 55% Au alloy than in the case of the 85% alloy.

As a very simplified explanation of the dextrose curve, we consider that at potentials negative to the maximum region the process is one of dehydrogenation followed by the oxidation of the

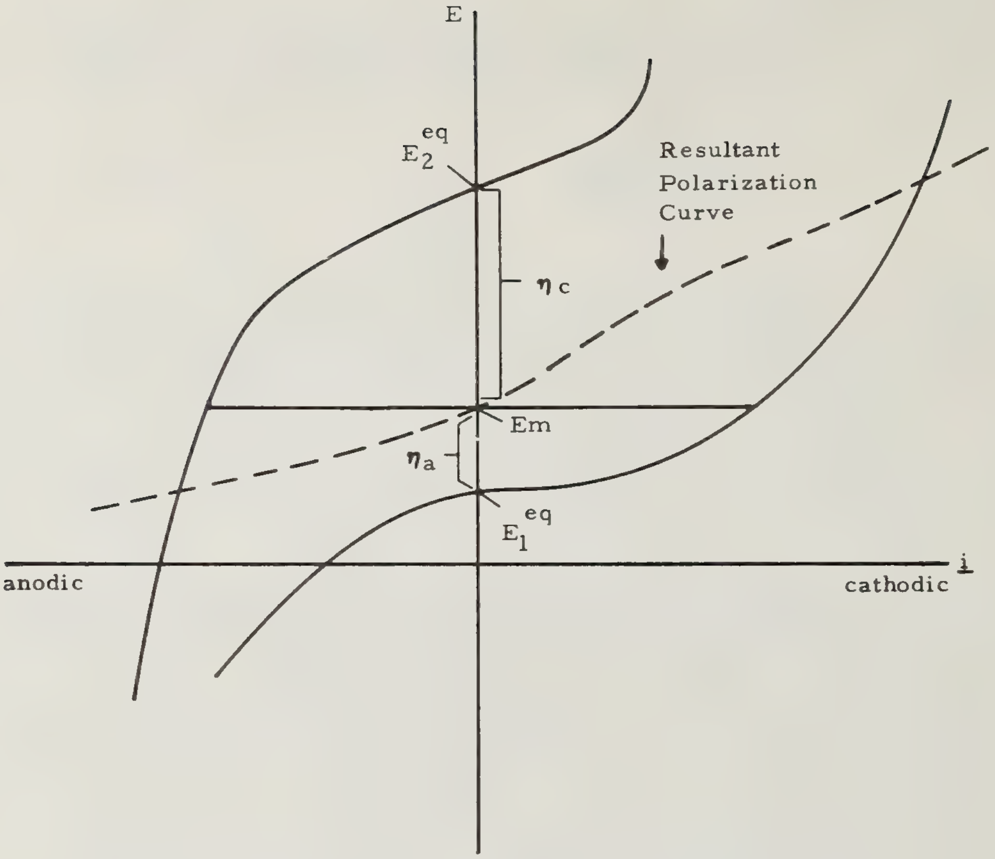

FIGURE 10. GRAPHIC DETERMINATION OF A MIXED POTENTIAL GENERATED AT A MIXED ELECTRODE BY THE COUPLING OF TWO ELECTRODE PROCESSES. (Reference: D. Gray and A. Cahill)

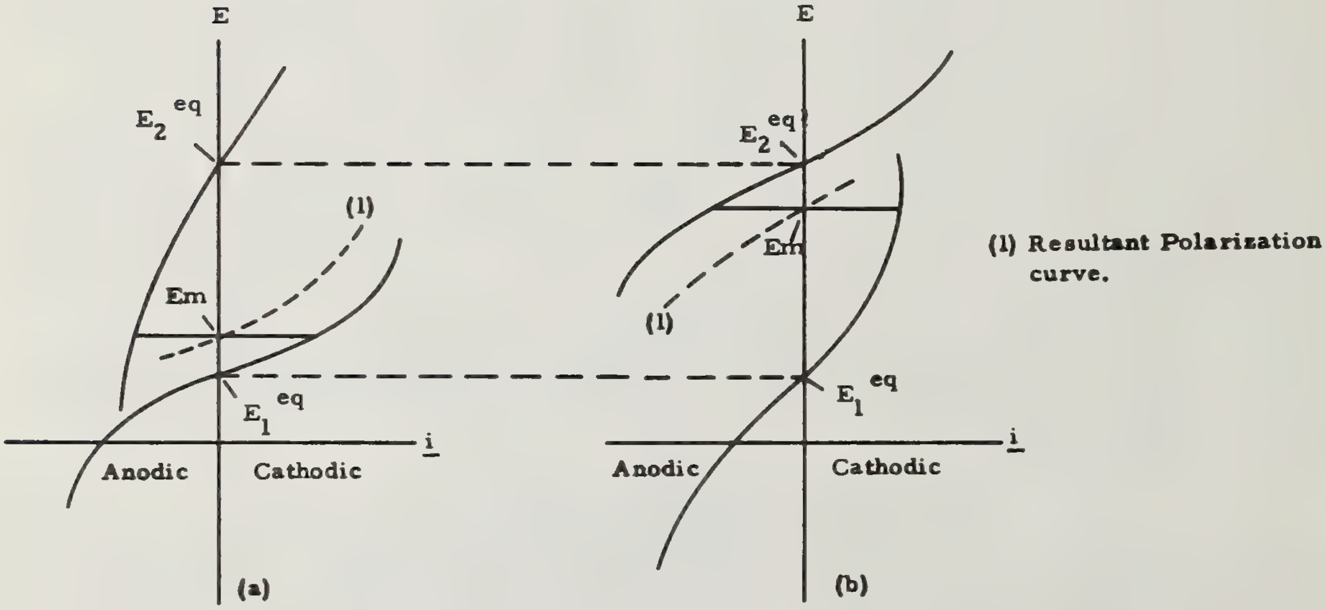

FIGURE 11. DEPENDENCE OF THE MIXED POTENTIAL ON THE RELATIVE POSITIONS OF THE PARTIAL CURRENT-VOLTAGE CURVES. (Reference 20)

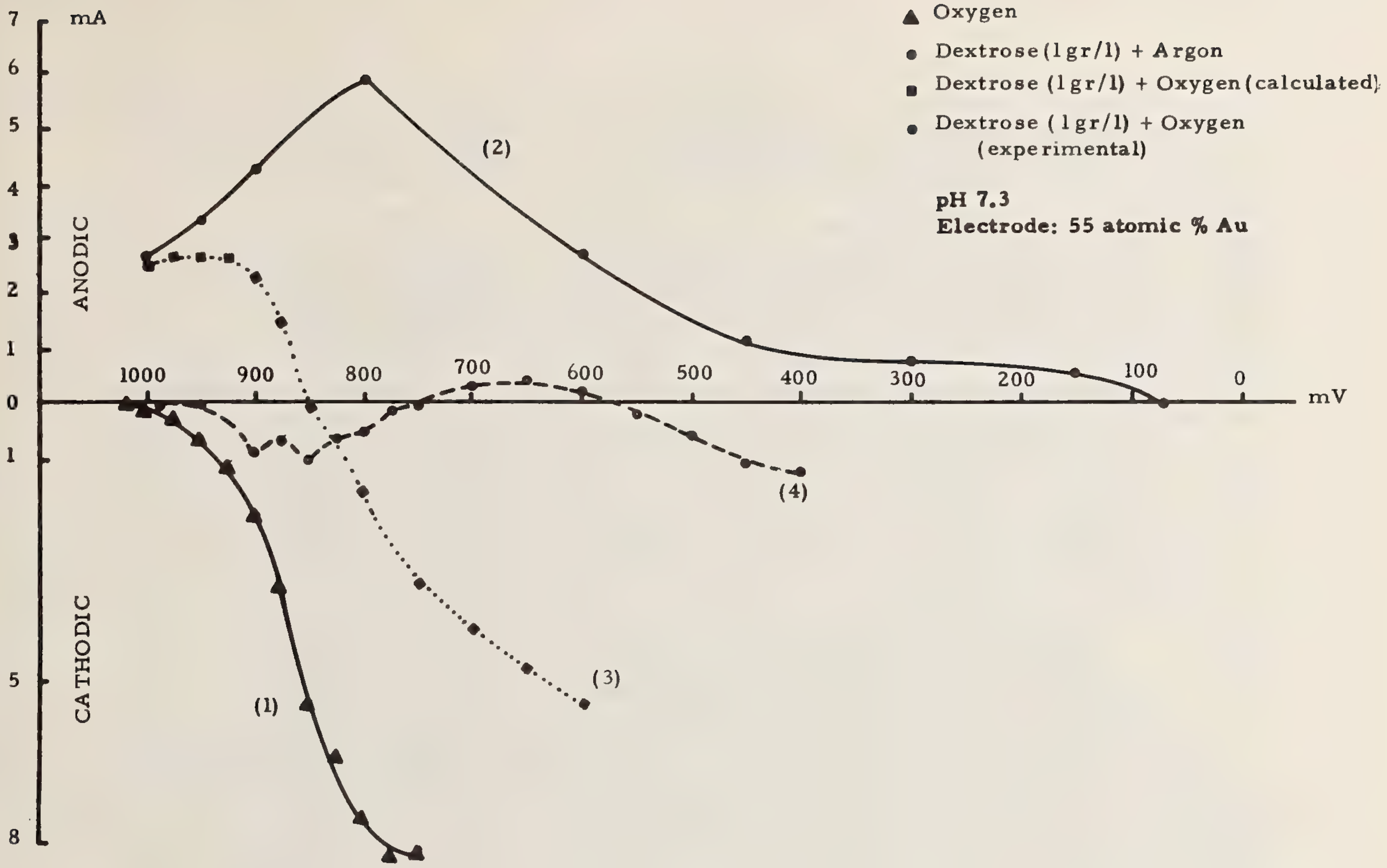

FIGURE 12. SINGLE AND MIXED POLARIZATION CURVES FOR DEXTROSE AND OXYGEN ON ALLOY BLACK ELECTRODE.

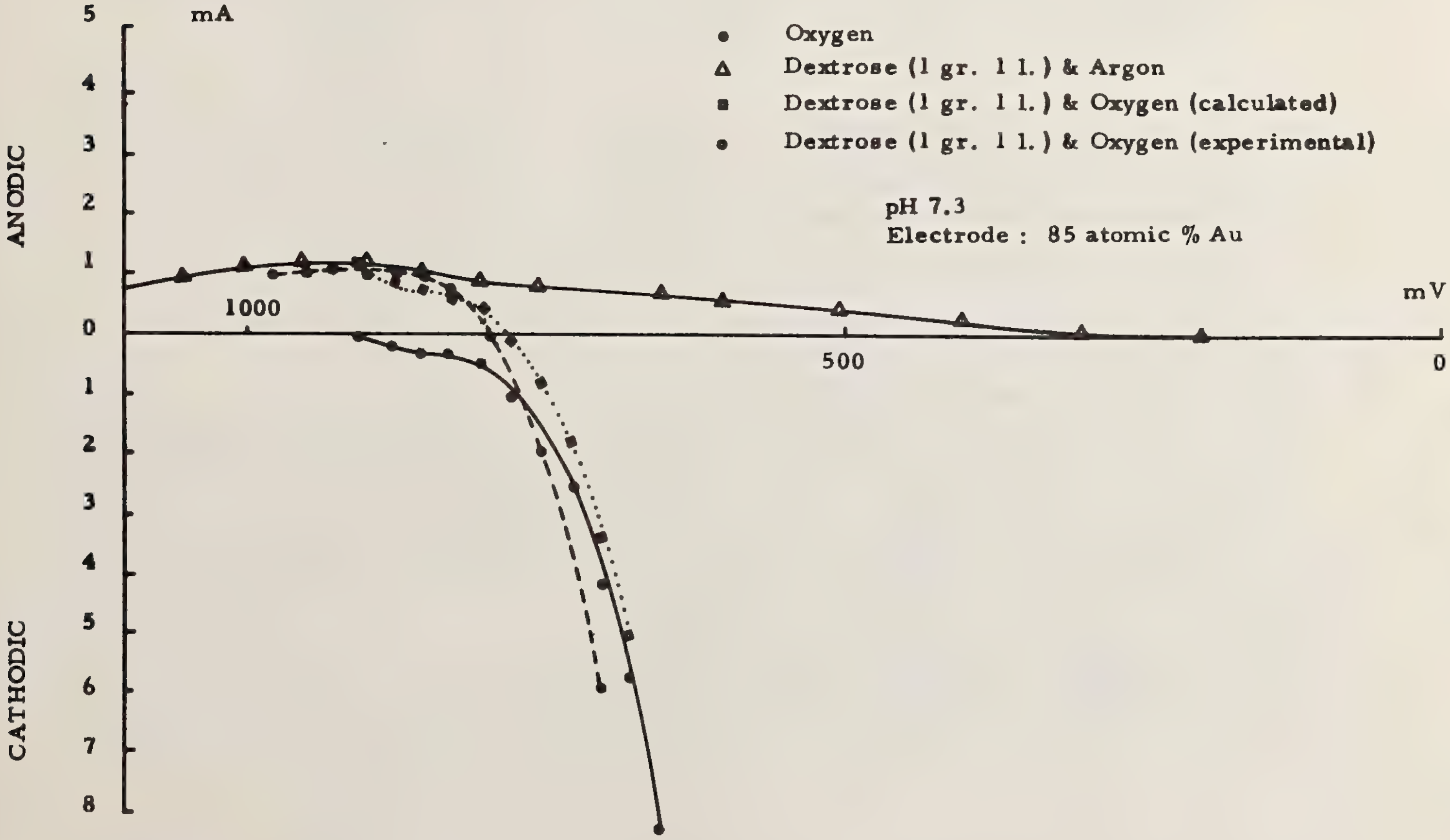

FIGURE 13. SINGLE AND MIXED POLARIZATION CURVES FOR DEXTROSE AND OXYGEN ON ALLOY BLACK ELECTRODE.

dissociated hydrogen. As the electrode is polarized to more positive potentials, the surface oxide which tends to form on the electrode is utilized to oxidize the carbon chain, giving rise to much higher anodic currents. Further increase in potential tends to increase electrode coverage with surface oxide, which in turn obstructs dextrose adsorption and causes the observed decline in anodic current.

The cathodic polarization curve in the presence of the mixed reactants was calculated and compared with the experimentally determined curve. In the case of the 55% Au alloy, the experimental curve is quite different from the calculated curve. The anodic and cathodic processes thus do seem to influence each other quite substantially in this case. The bias of this interaction is of interest in the context of this study program, since in the presence of both reactants the catalyst (55% Au-Pd) appears to be decidedly selective for oxygen reduction in the high potential region. In the case of the 85% Au alloy, however, the experimental curve obtained for a mixture of reactants is close to the calculated curve, suggesting that little interaction occurs between the anodic and cathodic processes. The results obtained in this case seem to correspond to the theoretical situation shown in Figure 11(b).

As indicated earlier, the Au-Pd system appears to comprise both anodic process selective and cathodic process selective alloys (Figure 9). A rather crudely arranged experiment was performed to prove the feasibility of deriving electric power from a mixed system in neutral media, by employing two oppositely selective alloys. A one molar, pH 7.3, phosphate buffer containing 1gr/1 of dissolved dextrose was saturated with oxygen. Two Au-Pd electrodes (alloy blacks) were introduced into the electrolyte. Distance between electrodes was about 0.5 cm, total geometric area of each electrode was 2 cm^2, while the total catalyst loading per electrode was 100 mg. The gold content of one alloy electrode was 55% and of the other 85%. The results are presented in Figure 14 (a) and (b). As expected from the results obtained previously the 55% Au electrode acts as the cathode and the 85% as the anode. Figure 14 (b) shows the stability of the cell (expressed as a power-time curve) over a period of 90 minutes. The 55% - 85% combination of electrodes was chosen as a result of a number of tests in which electrodes of various compositions were paired. In the limited series of tests performed, the 55% - 85% combination appeared to be the best match for the dextrose-O_2 cell.

The same electrodes were tested in an electrolyte containing the usual blood constituents (dextrose, glucosamine, lactic acid, urea, NaCl) and O_2. The results appear less good than for the dextrose-O_2 system. Matching of the electrode compositions was not attempted. It is believed that proper selection of electrodes would probably improve greatly the behavior of the cell, since it was noted that small changes in electrode composition result in important variations in fuel cell characteristics. The third curve in Figure 14(a) represents the E-i characteristics of a blood constituents - air fuel cell. Here again matching of alloy compositions was not attempted. Separate experiments have shown that the replacement of O_2 by air often seems to have a significantly enhancing effect on the anodic and/or cathodic behavior of each electrode and should be studied in detail.

Although Au-Pd electrocatalytic selectivity and activity in strong acids and bases has been demonstrated in earlier Leesona Moos Laboratories work, this is the first time that both anodic and cathodic selectivity has been shown to operate in systems of interest in the NIH program. The feasibility of drawing electric power directly from body fluids has thus been experimentally demonstrated.

REFERENCES

1. J. P. Hoare, The Electrochemistry of Oxygen (A Monograph), Interscience Publishers, New York, 1968.
2. First Annual Summary Report on Implantable Fuel Cells For An Artificial Heart, February 1968. National Heart Institute Contract PH 43-66-976, Monsanto Research Corp., Boston, Mass.
3. K. H. Hamann, Ber.d. Bunsengesellschaft, 71, 6, 612 (1967).
4. J. H. Fishman, Proceedings of the Second International Conference on Fuel Cells, (p244-247). SERAI, Brussels. (1967).
5. J. H. Fishman, and M. Yarish, Electrochem. Acta, 12, 579 (1967).
6. A. Couper, and D. D. Eley, Disc. Faraday Soc. 8, 172 (1950).
7. G. C. Bond, Catalysis by Metals, Academic Press, New York (1962).
8. T. J. Cray, R. B Rozelle and M. L. Soeder, Nature, London 181 (1964).
9. S. Schuldiner and J. P. Hoare, J. Phys. Chem. 61, 705 (1957).
10. P. G. Dickens, J. W. Linnett and W. Palczewska, J. Catalysis, 4, 140 (1965).
11. J. H. Fishman (Forten) and R. Roethlein, Paper #6, Theoretical Division, Electrochemical Soc. Meeting, Washington, D. C. 1964. Extensive treatment of the subject matter is contained in Leesona Moos Laboratories Internal Report SR 62-1-7237, "The Reduction of Oxygen on Platinum Cathodes in Acid Electrolytes" by J. H. Fishman (Forten) and R. Roethlein, (1963).
12. A. Maeland and T. B. Flanagan, Can. J. Phys. 42, 2364 (1964).
13. M. Hansen, Constitution of Binary Alloys, McGraw Hill, New York (1958).
14. H. J. Logie, J. Jackson, J. C. Anderson, and F. R. N. Nabarro, Acta Metall. 9, 707 (1961).
15. E. Vogt, Ann. Phys. 14, 1 (1932).
16. W. Koester, and T. Halpern, Z. Metallk. 52, 821 (1961).
17. V. Devi, C. N. Rao and K. K. Rao, Acta Metall. 13,44 (1965).
18. W. D. Copeland, and M. E. Nicholson, Acta Metall. 12, 321 (1964).
19. A. Nagasawa, Y. Matsuo and J. Kakinoki, J. Phys. Soc. (Japan) 20, 1881, (1965).
20. D. Gray and A. Cahill, J. Electrochem. Soc. 116, 443 (1969).

DISCUSSION

DR. BATZOLD: Could you clarify for me whether the data obtained in the last figure was obtained in 1M phosphate buffer with added body fluid, or actual body fluid?

DR. HENRY: This was 1M phosphate buffer at pH 7.3, plus the additives listed earlier in the concentrations mentioned. Oxygen or air were bubbled in the system.

DR. BATZOLD: Have you tried any experiments at very low buffer capacity, such as blood plasma?

DR. HENRY: No. This is not part of our program at the present stage.

DR. JAMES: Noble metals are excellent catalysts for heterogeneous reactions. I wondered if presumably dextrose and oxygen do not react together if they are dissolved in the same solution. Perhaps when these metals are present as well you get the heterogeneous catalysis of the reaction at the surface of the metals, so that you might have this reaction occur very rapidly under open circuit conditions. If so, would it have any effect on the body?

DR. HENRY: In one of the figures that we showed the case of the 55% alloy, the experimental curve does not correspond to the theoretically predicted curve. We do believe this may be due to some interaction between the two processes, that is oxygen reduction and hydrocarbon oxidation, in such a way that we get this unexpected behavior. We also believe that under open circuit conditions when no power is drawn from the system, there are some reactions occurring all the time, principally mixed reduction-oxidation reactions at each electrode.

DR. JAMES: If you throw a lump of platinum into the solution, the oxygen will presumably catalyze the reaction at the surface.

DR. HENRY: Yes, presumably.

DR. JAMES: This will have no effect on the body? You can leave these things in the body for a long time and have this heterogeneous catalyzed reaction going on? It won't affect anything?

DR. HENRY: We are always operating the unit under flowing conditions, so products of the reaction will be eliminated all the time. So nothing should harm the body.

DR. URBACH: I think your data confirm the fact that there is some interaction at the electrodes between the organic species and the oxygen. The fact that your mixed system shows an increased current over and above that of an oxygen alone indicates that the surface of your electrode has been reduced. It is well known that oxygen electrodes show better performance when the surface oxide is reduced. I think this supplies evidence that there has been a reaction going on.

DR. STONER: I have done some studies on various blood proteins in the isolated form as well as blood plasma in diluted and normal concentrations and studied the electrochemical behavior of these proteins at various anodes, using as anodes electron microscope grids with various metals deposited on them. I have found that the protein fibrinogen, which is present in the blood, actually forms a fiber on anode surfaces, i.e., if you pass an anode current. This fiber builds up slowly and eventually covers the electrode. This happens on copper, it happens on gold and on platinum. I was just wondering, if you immerse these anodes in the blood stream, will you also get these fibrinogen deposits which resemble fibrin, in addition to any other effects on formed elements.

DR. FISHMAN: What you are discussing now is actually a part of the engineering problem of how you prevent materials from approaching the electrode and depositing on it. We have at the present time no experience concerning this protein deposition problem. However, the use of selective membranes or films, isolating the electrodes from some blood component would eliminate the problem.

DR. STONER: I thought you said you had avoided these by your simple set up.

DR. FISHMAN: Yes. The set up was merely to demonstrate that one can immerse directly electrodes in a blood type fluid and derive power from it. This demonstrates that selectivity of the electrodes alone enables one to obtain electric power. Separation of the reactants is not necessary for the electrochemical reaction to proceed.

DR. TSIEN: The construction of your fuel cell seems to be quite simple, i.e. you simply stick two electrodes into the blood stream. I was wondering if there has been any consideration about the blood coagulation near the metal plate in the blood stream. Maybe in a matter of an hour, or perhaps a few minutes, your metal would be covered up with coagulated formed blood elements. Would the electrochemical action continue under those conditions?

DR. HENRY: Our tests were performed in phosphate buffers in which no coagulation problems were encountered, of course. If anything, the system improves with time under our working conditions. Over periods of approximately 8 hours the systems tested were stable or improved slightly. I should add at this point, that since these results were obtained, double or even more than double power densities have been achieved by better matching of the alloy composition.

DR. TSIEN: In other words you feel that there is no need for heparinization of your surface or anything like that?

DR. HENRY: We don't know. We are ready to give samples of our catalysts so that this question could be studied and answered properly.

DR. TSIEN: Do you not think that this is an oversimplification of the whole problem?

DR. FISHMAN: The problem is very, very complex. This is just one phase of it.

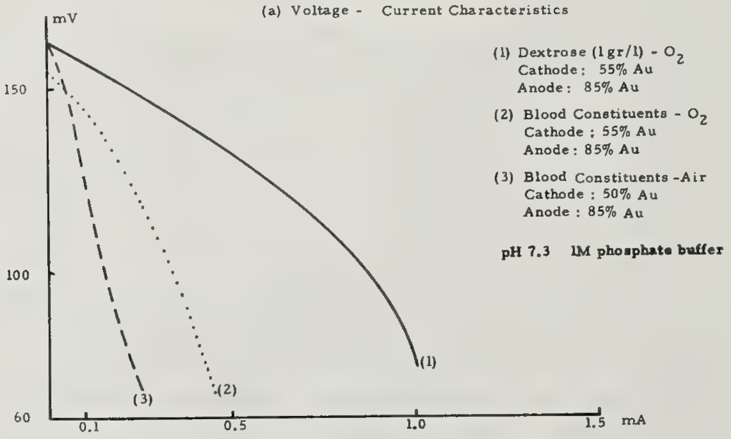
(a) Voltage - Current Characteristics

(b) Time behavior of cell (1) above

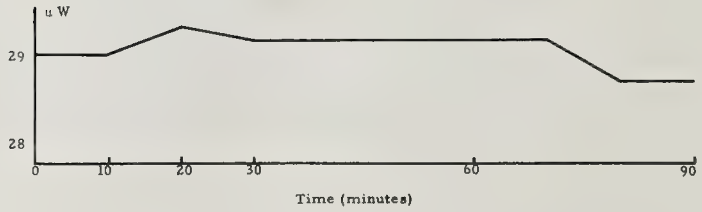

FIGURE 14. DIRECT FUEL CELL IN BODY FLUIDS.

CHAPTER 70

ANODIC OXIDATION OF GLUCOSE

J. Giner and P. Malachesky

Tyco Laboratories, Inc.
Waltham, Massachusetts

An implantable fuel cell is an ideal power source for artificial heart systems. With the objective of developing such a fuel cell working on oxygen and carbohydrates readily available in the blood, we have studied the mechanism of the anodic oxidation of glucose on smooth platinum electrodes in neutral solutions using transient electrochemical techniques. It has been found that glucose can be oxidized at potentials very close to the reversible hydrogen electrode to produce a chemisorbed product which can be irreversibly oxidized at higher potentials. This chemisorbed product has been tentatively identified as "reduced CO_2," an adsorbed species common to the oxidation of most organic fuels. It has been demonstrated that gluconic acid itself is oxidized at potentials where glucose is oxidized and therefore should not be the sole oxidation product. Determination of the rate of formation of the oxidation intermediate indicates that the electro-oxidation of glucose occurs via the open-chain or aldehyde form.

INTRODUCTION

The development of an implantable fuel cell to power artificial heart systems, based on blood carbohydrates and oxygen as reactants, is highly promising.[1] One of the hurdles that has to be overcome is the low performance of the blood carbohydrate anode (BCA). To improve this performance we have undertaken the task of elucidating the rate-determining steps and mechanism of fuel oxidation, in order to have a basis for more remedial development in the areas of electrocatalysts and/or electrode structure.

Specifically, we want to determine the nature of the limiting step in the over-all mechanism, the nature and effect of adsorbed intermediates, and the presence of dissolved intermediates. In addition to improving the performance of the glucose electrode, we aim to obtain engineering data which will allow the rational design of the most efficient total system.

It is well recognized that organic fuels such as methanol and propane can be oxidized in a fuel cell to CO_2.[2,3] It would be desirable for CO_2 (HCO_3^- at neutral pH) to be the final oxidation product of the BCA. This high faradaic capacity (i.e. 24 electrons/molecule) would necessarily insure a sufficient power output from the low concentration levels (ca. 10 mM) of the blood carbohydrates. For example, the conversion of glucose to gluconic acid, via a two-electron oxidation, yields 0.3 amp-hr per gram of fuel. Complete conversion of glucose to CO_2 would result in 3.6 amp-hr per gram of fuel.

In the following we describe some of the results obtained on the oxidation of glucose at smooth platinum electrodes under a variety of conditions.

EXPERIMENTAL

The electrochemical cell and techniques used here are those conventionally used in modern electrochemical kinetics. In addition, special care has been taken to achieve a reproducible platinum electrode surface and to use purified electrolyte solutions where necessary.

The following potential sequence, similar to the multipotential pulse electrode pretreatment developed by Gilman,[4] was used to achieve a well-defined Pt surface:

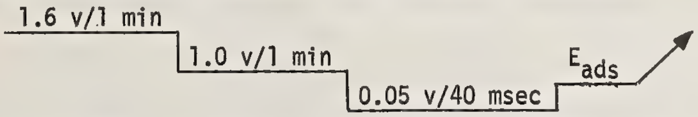

The step at +1.6 v vs. RHE is carried out with stirring by the purge gas; it serves to oxidize or desorb previously adsorbed contaminants. At the same time an oxygen film is formed on the surface.

The step at +1.0 v vs. RHE is first carried out for 30 seconds with stirring and then 30 seconds without stirring. The purposes of this step are to equilibrate the pH of the electrolyte near the electrode surface and to remove O_2. The oxygen film is retained during this step and prevents recontamination of the electrode surface.

In the step at +0.05 v vs. RHE the oxygen film is reduced and the electrode is now in an activated or "clean" state. The final potential step allows the adsorption or oxidation of glucose to occur. After a specified time at E_{ads}, a linear potential sweep (usually at 3.6 v/sec) is applied to the Pt electrode to analyze the adsorbed layer. At oxygen evolution, the potential sweep may be terminated or reversed to the initial starting potential of E_{ads}. During the linear potential sweep an I-E curve is recorded oscilloscopically and photographed.

While the multipotential pulse electrode pretreatment suffices for qualitative studies involving cyclic voltammetry, aqueous solutions of high purity must be employed, in addition, for more quantitative studies. The technique for solution purification which we have used involves the controlled potential adsorption of impurities on Teflon-bonded platinum fuel cell electrodes at low anodic potentials. Previous work in these laboratories has demonstrated the effectiveness of this approach.[5]

In order to establish standards of purity, it is necessary to have some means by which contamination may be monitored. We have used the cathodic galvanostatic charging method which assumes the deposition of a monolayer of atomic hydrogen before molecular hydrogen is evolved. The predominant face on polycrystalline platinum is the (100) plane which absorbs 1.3 x 10^{15} atoms/cm^2 or 210 μcoul/cm^2 in the deposition of a monolayer of H atoms. In the presence of adsorbable impurities these sites are "poisoned" and the charge required for the formation of hhe Pt-H monolayer (Q_H) decreases in proportion to the surface coverage.

We have purified a phosphate buffer solution (pH = 7.3) to a considerable extent by pre-electrolysis, using a high surface area Teflon-bonded platinum fuel cell electrode held at a potential of +0.25 v vs. RHE for a period of one week. Using the galvanostatic H-atom charging method, there was less than 5% coverage of the electrode with adsorbable impurities after adsorption times of up to five minutes.

QUALITATIVE CYCLIC VOLTAMMETRIC STUDIES

In order to obtain an over-all picture of the electrochemical oxidation of glucose at platinum electrodes, we devoted our initial effort to exploratory qualitative studies. By doing this we planned to acquire sufficient information to use in quantitative studies of oxidation mechanisms and electrocatalysts.

Using cyclic voltammetry on smooth platinum electrodes of well-defined surface character, we have investigated the influence of the following factors on the electro-oxidation of glucose:

(1) Nature of the buffer, i.e., bicarbonate vs. phosphate at pH = 7.3.
(2) Variations of pH in phosphate buffers (pH = 4.4 to pH = 8.8).
(3) Influence of specifically adsorbed anions such as chloride in both bicarbonate and phosphate buffers.
(4) Nature of reactant, i.e. glucose vs. gluconic acid.
(5) Effects of temperature.

Figure 1(a) shows a cyclic I-E curve on smooth platinum obtained at 4 v/sec in the buffer described above. The potential sequence described in the experimental section was used with E_{ads} +0.05 v vs. RHE. The time at E_{ads} was 5 seconds. We note that as we sweep from E_{ads} = +0.05 v vs. RHE to more anodic potentials, anodic current flows in the region of +0.05 - +0.40 v vs. RHE. This is due to the oxidation of the Pt-H monolayer formed at E_{ads} = +0.05 v vs. RHE. As E_{ads} is made more anodic, the magnitude of this current decreases since the formation of the Pt-H monolayer is potential dependent.

The region from +0.4 to +0.8 v vs. RHE is known as the "double-layer region." In the absence of any electroactive species, the current in this region is due only to the charging of the electrical double layer. At +0.8 v vs. RHE a monolayer of an Pt-oxygen or oxide film begins to form. Oxygen evolution occurs at +1.8 v vs. RHE.

On reversal of the sweep at +1.850 v vs. RHE, we can observe the reduction of the Pt-O monolayer in the region of +1.0 - +0.4 v vs. RHE. Formation of the Pt-H monolayer begins at +0.350 v vs. RHE.

In Figure 1(b), we have presented a cyclic I-E curve obtained at a smooth Pt electrode in a phosphate buffer containing 0.1M glucose at pH = 7.3 at 35°C. Three changes in the cyclic I-E curve are evident when compared to those to Figure 1(a).

First, the current in the region of Pt-H oxidation has increased. Secondly, a new anodic current peak is evident at +1.0 v vs. RHE. Finally, on sweep reversal, the reduction peak for Pt-O dissolution is followed and partially masked by a rather sharp oxidation peak in the region of +0.450 - +0.200 v vs. RHE.

We have ascribed the anodic current in the region of 0.0 to +0.6 v vs. RHE as primarily due to the oxidation of glucose. The new anodic current peak at +1.0 v vs. RHE was not observed in the phosphate buffer alone; therefore, it must be related to the oxidation of glucose or one of its oxidation products. The nature of this process will be discussed in more detail later. The presence of anodic current on the cathodic going portion of the cyclic sweep shows that oxidation of glucose takes place quite readily on an activated Pt surface formed by reduction of the Pt-O monolayer.

From these observations it appears that the rate of glucose oxidation to produce the intermediate is a maximum at +0.2 v vs. RHE and decreases at more anodic or cathodic potentials. This behavior is typical of the oxidation of most organic fuels. We will now consider the nature of the anodic process at +1.0 v vs. RHE.

Nature of Chemisorbed Intermediate.

It has been reported that the electro-oxidation of glucose at pH = 7.4 at platinized platinum electrodes gives rise to gluconic acid as the reaction product.[6] Therefore, we assumed that the oxidation process at +1.0 v vs. RHE in glucose oxidation was due to the oxidation of gluconic acid, the two-electron oxidation product of glucose. However, we discovered that gluconic acid behaved quite similarly on oxidation as glucose. An oxidation process occurs in the region of +0.05 - +0.40 v *vs.* RHE and the same oxidation peak at +1.0 v *vs.* RHE is present, as was the case in the oxidation of glucose. Therefore, it does not appear that this peak at +1.0 v *vs.* RHE in glucose oxidation is due to the oxidation of gluconic acid itself but is due to a common species arising from both gluconic acid and glucose on oxidation. Our further studies have identified this common species as "reduced CO_2."

"Reduced CO_2" is an adsorbed species first found by Giner on Pt electrodes in acidic solutions of CO_2.[7] He also reported the presence of this species on platinized platinum electrodes in the oxidation of partially oxygenated fuels such as methanol[8] and in the presence of saturated hydrocarbons.[9] We have demonstrated the similarity of the oxidation of "reduced CO_2" with the process found to occur in glucose oxidation at +1.0 v.

A pH = 7.35 phosphate buffer was saturated with CO_2 in the absence of glucose. After the appropriate electrode pretreatment, reductive adsorption of CO_2 was allowed to occur at various E_{ads}. A linear anodic sweep was applied to the Pt electrode and an I-E curve recorded. The oxidation peak at a +1.0 v in the CO_2-saturated system and that found in glucose oxidation were quite similar.

It does not appear that "reduced CO_2" formed by oxidation of glucose arises from the reductive adsorption of anodically evolved CO_2. Our experiments show that at potentials more anodic than +0.3 v *vs.* RHE "reduced CO_2" is not formed in the CO_2-containing buffer. Yet in the oxidation of glucose, we can see the oxidation process at +1.0 v which corresponds to oxidation of "reduced CO_2" at potentials greater than +0.3 v *vs.* RHE. This indicates that "reduced CO_2" is produced directly from glucose and not from anodically evolved CO_2, viz.

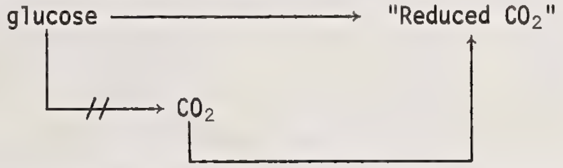

These results do not imply the complete oxidation of glucose to CO_2. Since gluconic acid also gives this same species, as reported previously, decarboxylation of the gluconic acid, as in the Ruff degradation, could yield CO_2 and an aldose of one less carbon.

A series of cyclic I-E curves were obtained at various temperatures. As expected, the currents increase markedly, indicating an increase in the rate of glucose oxidation with increasing temperature. Furthermore, a third anodic process at +1.3 v *vs.* RHE begins to manifest itself. This process is not observed in the oxidation of gluconic acid but only in the oxidation of glucose.

It was found that a buffer system at pH = 7.2 was easily achieved by saturating a 0.5M $NaHCO_3$ solution with CO_2. Although presence of CO_2 somewhat complicates the interpretation of data since the oxidation of "reduced CO_2" is evident in the base electrolyte alone, no essential differences are observed when the curves obtained are compared with those in the phosphate buffer, indicating that the effect of changing from a phosphate to a bicarbonate buffer system is negligible.

Effect of pH.

We have made a study of the effects of pH changes on glucose oxidation at smooth Pt in phosphate buffer systems in the absence of chloride from pH = 4.4 to pH = 8.8 at 35°C. It would appear that a pH of 7.3 is optional for glucose oxidation on Pt. A factor to be considered, however, is that of buffering capacity. At both extremes of pH studied here, buffering capacity is minimal. For the $H_2PO_4^-/HPO_4^=$ buffer used here, buffering action is a maximum at pH $\doteq$ 6.6. Some pH polarization effects, not found in the base electrolyte, are evident. The nature of these effects will be treated more explicitly in the future.

Effect of Chloride.

Specifically adsorbed anions such as chloride are known to affect the oxidation of organic fuels at platinum electrodes.[10] Inasmuch as chloride ion is a major ionic component of blood plasma, we have made a study of the effect of controlled addition of chloride ion (as NaCl) on glucose oxidation at +35°C in a phosphate buffer at pH = 7.3. A detailed study of the effect of chloride ion has also been made in the 0.5M $NaHCO_3/CO_2$ buffer system.

Two features of these I-E curves are of interest. First, on sweeping anodically, the oxidation peak at +1.0 v *vs.* RHE of "reduced CO_2" appears to be independent of chloride ion concentration. The magnitude of the current peak at +1.0 v *vs.* RHE after 10 seconds of adsorption at +0.2 v *vs.* RHE is somewhat decreased by added chloride. However, after 60 seconds of adsorption, even in 0.1M NaCl, the same amount of current due to oxidation of "reduced CO_2" is found in all cases. This would seem to indicate that the effect of Cl^- is kinetic in nature.

On reversal of the sweep, the usual sharp oxidation peak following oxide reduction shows a marked decline with increasing chloride ion concentration. Again we can conclude that the effect of chloride is to slow down the oxidation kinetics of glucose. It also appears to eliminate the high potential process at +1.2 v *vs.* RHE. The same results have been obtained in the HCO_3^-/CO_2 buffer system with added chloride.

Our qualitative results may be summarized as follows:

(1) The oxidation behavior of glucose and gluconic acid are quite similar. Both yield an adsorbed species akin to "reduced CO_2"; however, at potentials (>+1.2 v *vs.* RHE) a third oxidation step can be observed for glucose.

(2) The influence of the nature of the buffer system, i.e. bicarbonate *vs.* phosphate at pH = 7.3 is negligible.
(3) A pH of approximately 7.0 seems to be optimal for glucose oxidation. The effect of buffer capacity warrants investigation.
(4) Increases in temperature from 30° to 70°C enhance the rate of electro-oxidation of glucose.
(5) The effect of such specifically adsorbed anions as chloride appears to be kinetic in nature.

QUANTITATIVE STUDIES

In order to establish the role played by "reduced CO_2" in the oxidation of glucose we have made quantitative studies at smooth platinum electrodes in highly purified phosphate buffer solution. In particular we are interested in determining (a) the degree of electrode coverage and the nature of the chemisorbed product, (b) the kinetics of glucose oxidation and other soluble intermediates at low potentials (i.e. at potentials at which the poisoning intermediates are not further oxidized) and (c) the oxidation kinetics of the poisoning species.

Using a purified phosphate electrolyte at pH = 7.3 we have made measurements of surface coverage, θ_{org}, and Q_{ads} (the charge required to oxidize any adsorbed organic species) during the anodic oxidation of glucose. We have varied both the time and potential of adsorption in our studies. All measurements were made at 35°C. The glucose concentration was 8.2×10^{-2}M.

The experimental technique of measuring θ_{org} is essentially the same as described previously for monitoring solution purity. The decrease in the amount of charge required to deposit a monolayer of H-atoms on the Pt surface is measured with a cathodic galvanostatic pulse. The fraction of the surface occupied by the organic material, θ_{org}, is operationally defined as $1 - \theta_H$, where θ_H is the ratio of the cathodic H-atom charge under the given circumstances to the maximum value at the same temperature. The variation of θ_{org} with time and potential during the oxidation of glucose is shown in Figure 2.

From Figure 2 it can be seen that the initial rate of adsorption, i.e. $(d\theta_{org}/d\tau^{\frac{1}{2}})$, is a function of potential. $(d\theta_{org}/d\tau^{\frac{1}{2}})$ reaches a maximum at ca. +0.20 v *vs.* RHE. Changes in $(d\theta_{org}/d\tau^{\frac{1}{2}})$ have sometimes been attributed to variation in the mode of adsorption, i.e. the number of surface sites occupied per adsorbed molecule.

There are some distinct differences when the coverage data at 10 seconds and 300 seconds are compared. The data at 10 seconds reflect the initial rate of coverage, while the 300 second data are related to steady-state conditions. In Figure 3 it can be seen that the θ_{org} *vs.* E profile at 10 seconds is bell-shaped, typical of most organic fuels. However, at 300 seconds there is a broad potential region (+0.1 v - +0.4 v *vs.* RHE), where θ_{org} is relatively independent of potential.

If an anodic galvanostatic pulse is applied after adsorbing at constant potential, it is possible to measure the amount of charge necessary to oxidize the adsorbed organic species. It was determined that a current of 25 ma (66 ma/cm^2) was sufficient to prevent any appreciable quantity of glucose from adsorbing during the anodic current pulse. Thus, the measured values of Q_{ads} are due only to the oxidation of adsorbed species. Figure 4 depicts the variation of Q_{ads} with potential, with $(dQ_{ads}/d\tau^{\frac{1}{2}})$ being greatest in the region of +0.2 v *vs.* RHE. Figure 5 shows Q_{ads} *vs.* E profiles after adsorption times of 10 and 300 seconds. Again there is a distinct difference between the initial data and that obtained in the steady state.

For semi-infinite linear diffusion, with no retarding effect on adsorption because of blockage by adsorbed material, the accumulation of material on the electrode in quiescent solution is given by

$$Q_{ads} = 2n\ F \left(\frac{D}{\pi}\right)^{\frac{1}{2}} C\ \tau_{ads}^{\frac{1}{2}}$$

Here Q_{ads} is in coulombs per geometric cm^2, n is the number of electrons released in the oxidation of the adsorbate (for glucose, n = 24), and D and C are the diffusion coefficient and concentration (moles/cm^3) of glucose.

Using the data at +0.20 v *vs.* RHE the measured rate of accumulation of charge at the electrode is 264 μcoul/geom cm^2/sec$^{\frac{1}{2}}$. The calculated rate of accumulation of charge at the electrode using $C = 8.2 \times 10^{-5}$ moles/cm^2, $D = 6.2 \times 10^{-6}$ cm^2/sec and n = 24 is 530 m coul/geom cm^2/sec$^{\frac{1}{2}}$. This marked disparity of three orders of magnitude seems to indicate that the closed form of glucose is not the electro-active species. Using available literature data, the fraction of glucose present as the open or aldehyde form is 0.003% at equilibrium.[11] A recalculation of $(dQ_{ads}/d\tau^{\frac{1}{2}}_{ads})$, assuming that only 0.003% of the total glucose present can be oxidized, gives a value of 16 μcoul/geom cm^2/sec$^{\frac{1}{2}}$. This agreement to within an order of magnitude is encouraging, considering possible errors in the fraction of glucose present as the open-chain form. Based on a two electron oxidation to gluconic acid, with only the free aldehyde form electro-active the calculated value of $(dQ_{ads}/d\tau^{\frac{1}{2}}_{ads})$ is 1.3 μcoul/geom cm^2/sec$^{\frac{1}{2}}$. We have used plots of Q_{ads} *vs.* θ_{org} to characterize the adsorbed layer further.

By measuring the slope of a plot of Q_{ads} *vs.* θ_{org}, we can estimate the average oxidation state of the adsorbed material in the following manner. The fraction of H-atom sites occupied by the absorbate is θ_{org}, and when expressed in terms of the charge which would be involved in the oxidation of H-atoms if they were on θ_{org} sites, this corresponds to $\theta_{org} \times 210$ μcoul/cm^2. Since the oxidation of each

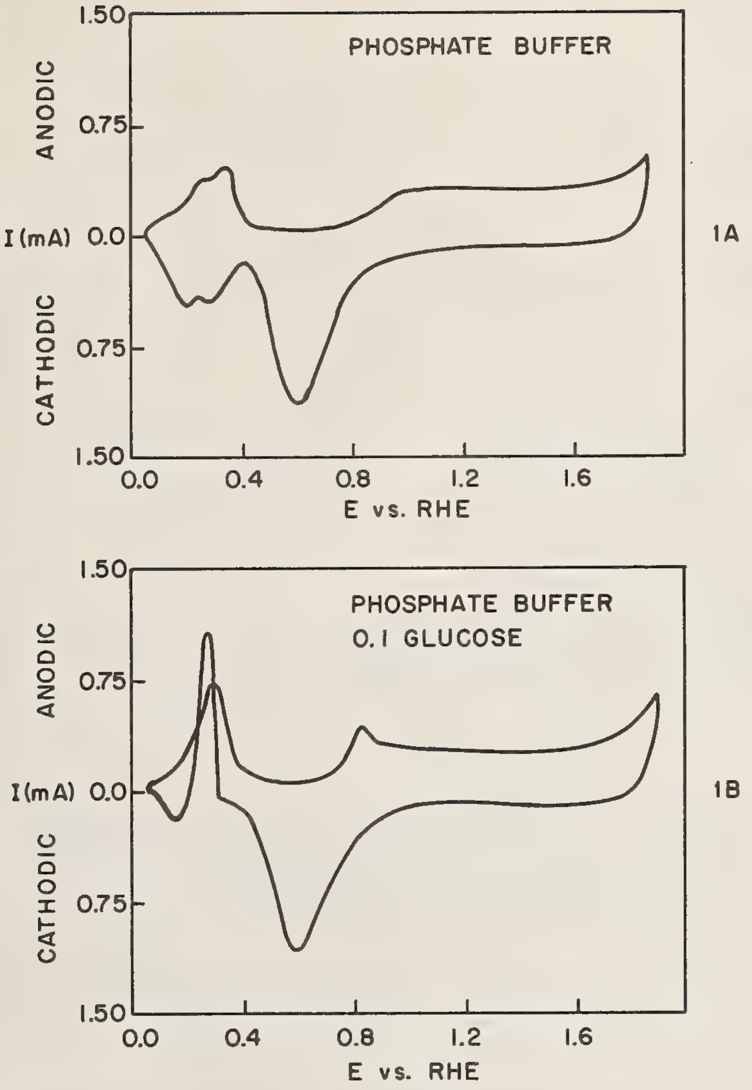

Fig. 1 Cyclic voltammetric sweeps on a Pt electrode in a pH = 7.3 phospate buffer with and without added glucose.

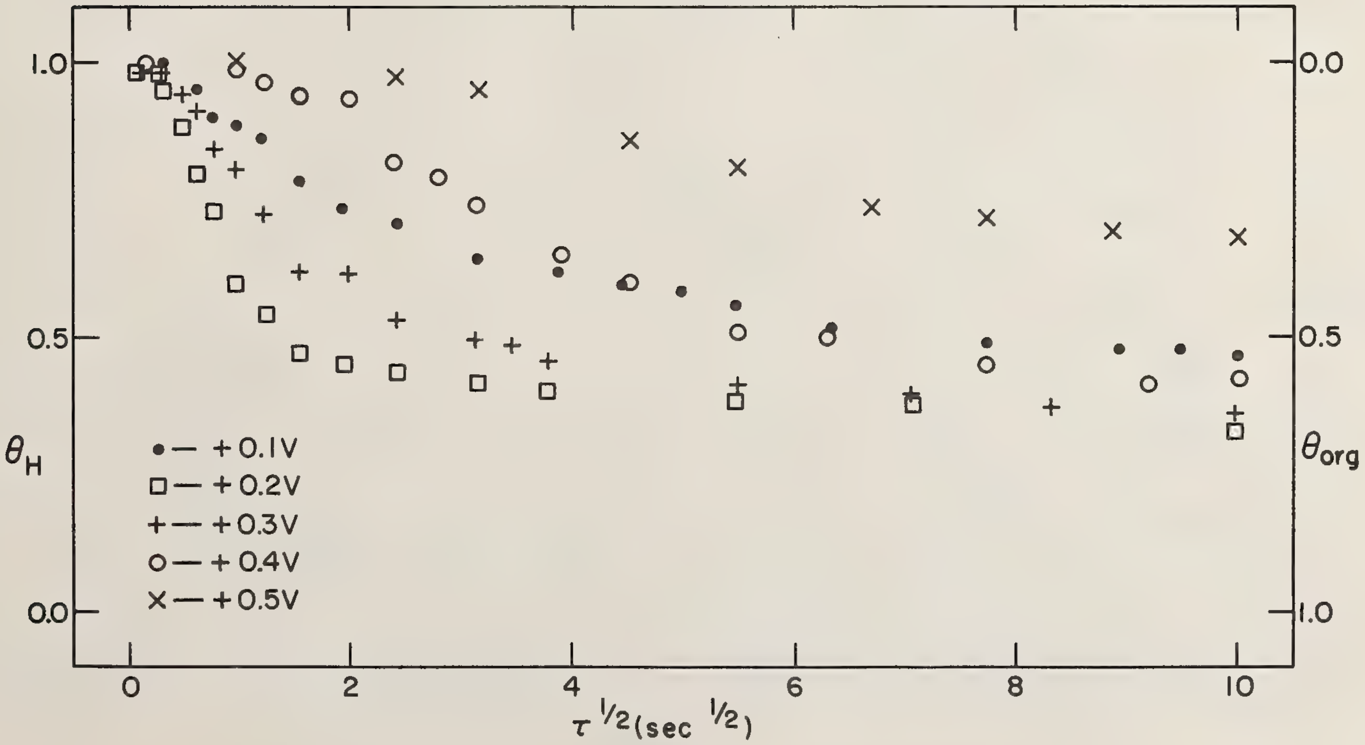

Fig. 2 Variation of θ_{org} with $\tau^{\frac{1}{2}}$ during glucose oxidation at pH = 7.3.

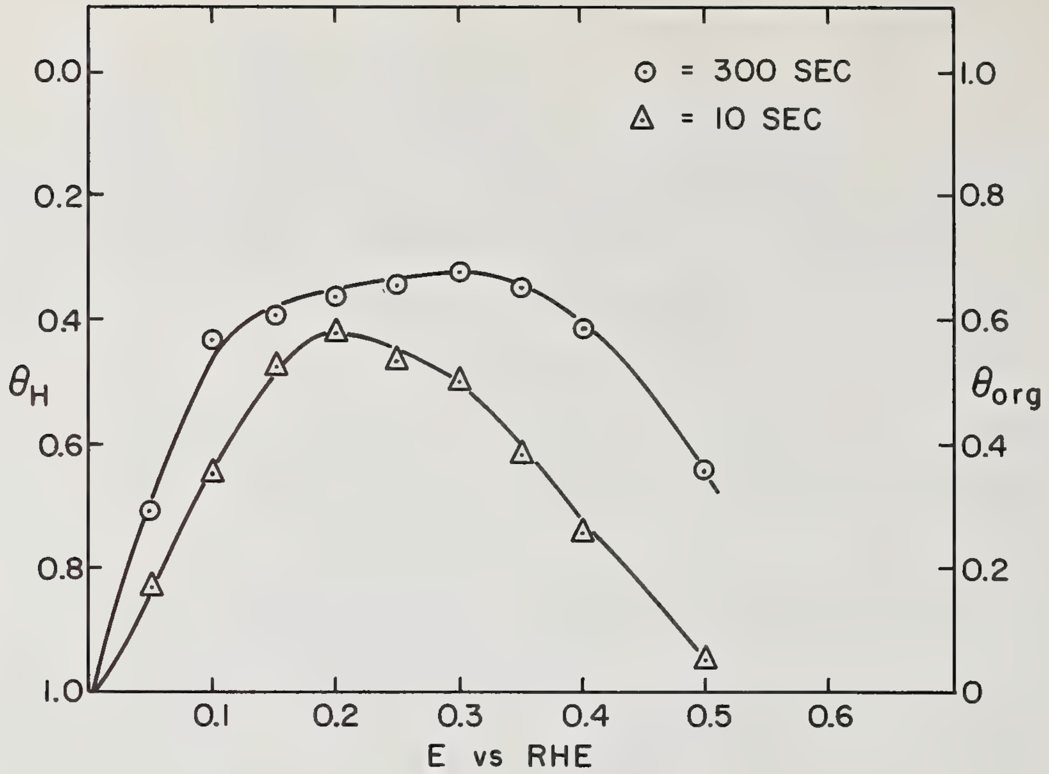

Fig. 3 Comparison of θ_{org} vs. E profiles for glucose oxidation after 10 seconds and 300 seconds.

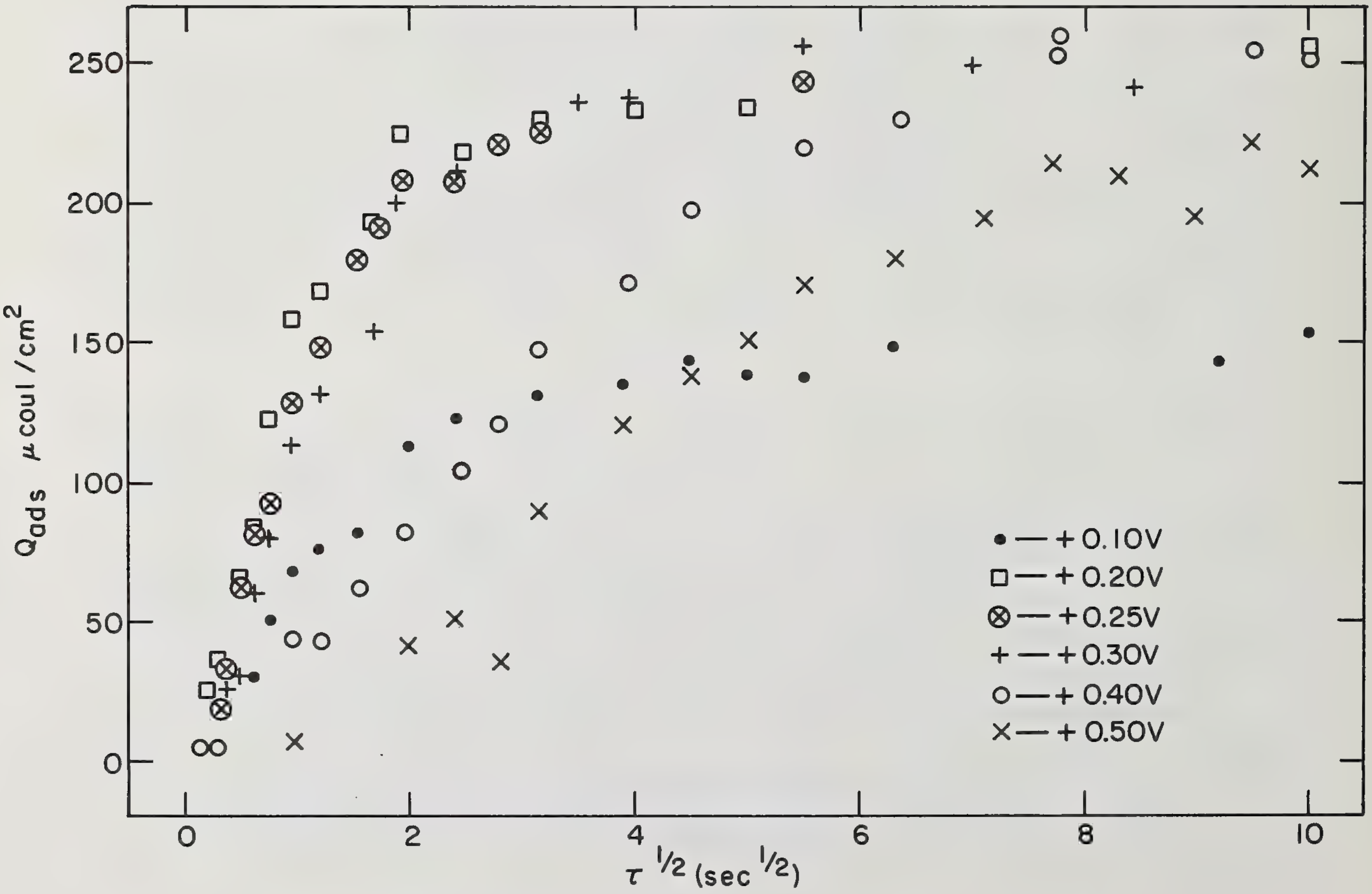

Fig. 4 Variation of Q_{ads} with $\tau^{\frac{1}{2}}$ during glucose oxidation at pH = 7.3

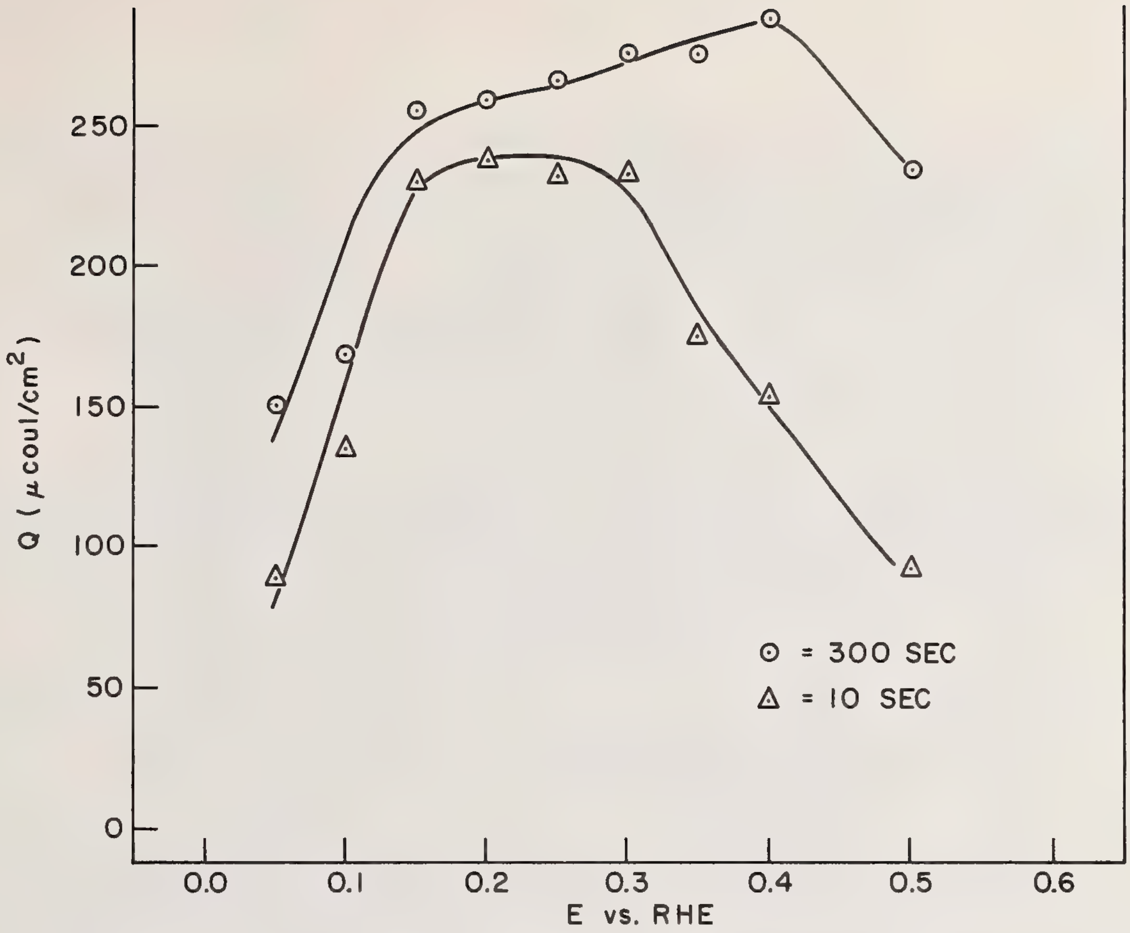

Fig. 5 Comparison of Q_{ads} vs. E profiles for glucose oxidation after 10 seconds and 300 seconds.

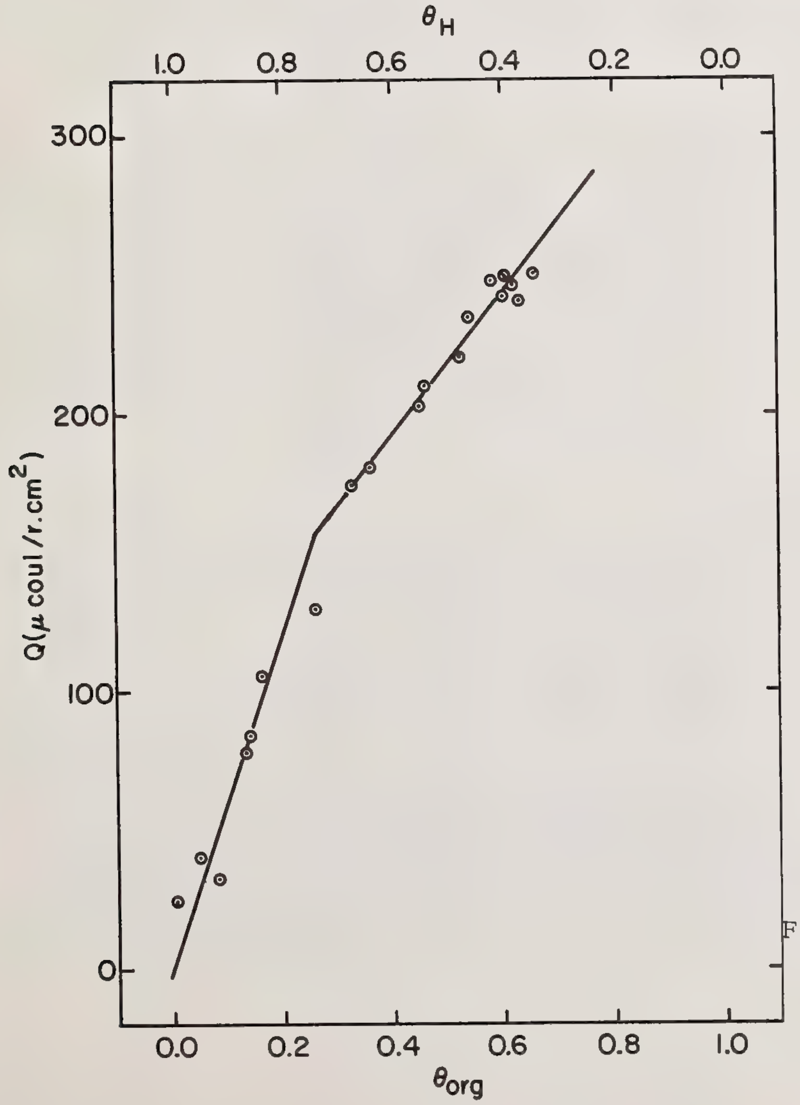

Fig. 6 Variation of Q_{ads} with θ_{org} during glucose oxidation at E_{ads} = +0. 3v vs. RHE.

H-atom involves a single electron, the slope of a plot of Q_{ads} vs. θ_{org} should be constant and should yield the average number of electrons, [e], involved in the ultimate, high potential oxidation of the absorbate per Pt surface atom which it covers. Any deviations from linearity in plots of Q_{ads} vs. θ_{org} can be taken as evidence for the presence of different adsorbed species or at least for different modes of bonding of the adsorbate.

Plots of Q_{ads} vs. θ_{org} for glucose oxidation do not appear to be linear. In Figure 6, which is a Q_{ads} vs. θ_{org} plot for E_{ads} = +0.3 v vs. RHE, there appear to be two distinct regions of linearity. At $\theta_{org} > 0.3$, [3] is 1.2 electrons/site. The value of 1.24 electrons/site at $\theta_{org} > 0.3$ is very close to that determined by other investigators for "reduced CO_2" of 1.2 - 1.4 electrons/site under different conditions (acidic solutions and higher temperatures).

SUMMARY

Detailed qualitative and quantitative studies have been made of the electro-oxidation of glucose on smooth platinum electrodes in neutral, buffered solution. Factors such as buffer nature, pH variations, temperature, nature of reactant, and the influence of specifically adsorbed anions have been investigated. We may summarize the results as follows:

(1) The oxidation behavior of glucose and gluconic acid are quite similar. Both yield an adsorbed species akin to "reduced CO_2"; however, at high potentials (> +1.2 v vs. RHE) a third oxidation step can be observed for glucose.
(2) The influence of the nature of the buffer system, i.e. bicarbonate vs. phosphate at pH = 7.3, is negligible.
(3) A pH of approximately 7.0 seems to be optimal for glucose oxidation. The effect of buffer capacity warrants investigation.
(4) Increases in temperature enhance the rate of electro-oxidation of glucose.
(5) The effect of specifically adsorbed anions such as chloride appears to be kinetic in nature.

We have demonstrated that gluconic acid itself can be oxidized at potentials where glucose is oxidized and therefore should not be the sole reaction product. Both glucose and gluconic acid give rise to a common absorbed species quite similar to the "reduced CO_2" found in the oxidation of other organic fuels such as methanol and propane. Furthermore, there is a high potential oxidation process which is only present in the oxidation of glucose and not gluconic acid. This indicates that there may be more than one pathway in the oxidation of glucose. Since gluconic acid has been found as a reaction product in glucose electro-oxidation,[6] one of these pathways may very well be the simple two-electron oxidation process. However, the presence of a "reduced CO_2" type of species and the further high potential oxidation process found only for glucose itself indicates the presence of another, more complex reaction pathway.

The presence of a "reduced CO_2" type of adsorbed intermediate in these qualitative studies does not, of itself, imply that complete conversion of glucose to CO_2 is possible. From evidence available there are two possible roles played by "reduced CO_2" in the oxidation of organic fuels. For methane and propane, the oxidation of "reduced CO_2" to CO_2 is the rate-determining step in the conversion of the organic fuel to CO_2.[12,13] However, the role of "reduced CO_2" in the oxidation of formic acid is different. It is formed as a side product and not as part of the predominant reaction pathway leading to CO_2 production.[14] Its role in the oxidation of formic acid is that of a poison to the main electrode reaction by blocking available surface sites from participating in the reaction. Experiments are now in progress which are designed to quantitatively establish the role of "reduced CO_2" in glucose oxidation.

We plan to extend our measurements to include high surface area platinized platinum electrodes, leading to the eventual development of efficient alloy electrocatalysts for the blood carbohydrate anode.

REFERENCES

1. Research Corporation 1st Annual Summary Report, "Implantable Fuel Cell for an Artificial Heart," Contract No. PH43-66-976, February 1968.
2. M. W. Breiter, J. Electroanal. Chem. 14, 407 (1967).
3. W. T. Grubb and C. J. Michalski, J. Electrochem. Soc. 111, 1015 (1964).
4. S. Gilman, J. Phys. Chem. 67, 78 (1963).
5. P. A. Malachesky, R. Jasinski, and B. Burrows, J. Electrochem. Soc. 114, 1104 (1967).
6. M. L. B. Rao and R. F. Drake, ibid. 116, 334 (1969).
7. J. Giner, Electrochemica Acta 8, 857 (1963).
8. J. Giner, ibid. 9, 63 (1964).
9. J. Giner, Paper presented at 15th C.I.T.C.E. Meeting, London, (1964).
10. B. I. Podlovchenko, O. A. Petry, and A. N. Frumkin, Dokl. Akad. Nauk SSSR, 153, 397 (1963).
11. J. M. Los, L. B. Simpson, and K. Wiesner, J. Am. Chem. Soc. 78, 156 (1956).
12. A. H. Taylor and S. B. Brummer, To be published.
13. S. B. Brummer and M. J. Turner, To be published.
14. S. B. Brummer, Paper presented at the Fall Electrochemical Society Meeting, Montreal, (October 1969), Abstract No. 331.

DISCUSSION

DR. CAIRNS: What was the temperature at which this work was done?

DR. MALACHESKY: All of this work was done at 35°C. We have made some qualitative measurements up as high as 70°C.

DR. CAIRNS: In the discussion of a couple of your plots, the Q versus time, and θ versus time, you were speaking about the rate of adsorption, but I think this simplified terminology may be a little bit misleading to some of us. This is really a net rate of adsorption, particularly at the higher potentials at which, I am sure you realize, there is electrochemical oxidation taking place simultaneously. Only at potentials in the range of say 0.2 to 0.3 volts does it become fairly accurate to speak of this as simply a rate of adsorption. Also, the relative amounts of the different species on the surface are much different at higher potentials, and therefore, it is not fair to compare these Q's as if they were measuring the same types of species and in the same relative amounts.

DR. MALACHESKY: Yes, that is very true. We know from the way that the plots of Q vs. θ behave that we have more than one adsorbed species, so it is not really correct to call these rates of adsorption.

DR. SRINIVASAN: Have you done any steady state work?

DR. MALACHESKY: No, we have not. We have made some preliminary measurements on platinized platinum electrodes at relatively short times. It appears that even after five minutes that you still can see current decay occurring under constant potential conditions.

DR. SRINIVASAN: The second question that I have concerns intermediates. Don't you think it is rather difficult to postulate a simple intermediate such as reduced CO_2 for the oxidation of a large number of organic compounds varying in molecular size and structure. From steady state work, the Tafel slope for the oxidation of a number of hydrocarbons is 2 RT/F, which would not be the case if the oxidation of reduced CO_2 is involved in the rate determining step.

DR. MALACHESKY: We have not really established what the role of "reduced CO_2" is in the oxidation of glucose. It appears that in the oxidation of methane on platinum in phosphoric acid the current which is available is actually limited by the oxidation of "reduced CO_2." In other words, the slow step in the overall conversion of methane to CO_2 is actually the oxidation of "reduced CO_2." But we have not established, as yet, what the role of "reduced CO_2" is in the actual reaction under discussion here.

DR. GINER: I wanted to add to what Dr. Malachesky said. Certainly so-called steady state measurements are very suspect because if you wait twenty minutes you get one Tafel slope; if you wait a half hour, you get another one. In studies with many of these reactions you have to be very careful in drawing conclusions from Tafel slopes. "Reduced CO_2" appears in the oxidation of methanol, formaldehyde, formic acid, and in all the aliphatic hydrocarbons. It doesn't appear when you oxidize ethylene on platinum, because ethylene is so strongly absorbed. It doesn't appear when you oxidize CO. So there are a couple of cases where "reduced CO_2" doesn't appear. In the other cases, as Dr. Brummer has shown at Tyco Laboratories, in addition to "reduced CO_2" you observe other intermediates. Also Dr. Malachesky has shown the presence of "reduced CO_2" in glucose oxidation, but it is very hard to say what the role of "reduced CO_2" is, but it is always there in the cases that I mentioned.

DR. STONER: I would like to address a question to Dr. Giner. I agree that the Tafel slope interpretation for the oxidation of such a large complex as glucose is complicated. But I wanted to ask two short questions. One is, I have done some studies on some fairly large hydrocarbons and their oxidation in various electrodes, and I have found that you get 100% oxidation to CO_2, plus or minus 1% or something like that. Now that 1% could, of course, completely cover the whole electrode. I think that is what you mean. You do not have a significant parallel reaction, but maybe you have a small amount of something which may block the electrode. If this is a small parallel side reaction, I could agree with you. However, in the oxidation of most of these saturated hydrocarbons we find a reaction order of unity; and if your rate determining step is 14 steps down (e.g., reduced CO_2) and it is a very small thing like a C-1 species, like you have often proposed, I do not understand how you could have a reaction order of one with respect to glucose. Can you explain that?

DR. GINER: We have not claimed that the oxidation of "reduced CO_2" is the rate determining step in glucose oxidation, nor have we mentioned a reaction order of one with respect to glucose. When you change the potential, for instance, in propane oxidation, the rate determining step changes. You find that at low potentials the oxidation of "reduced CO_2" is the rate determining step. However, at more anodic potentials, the adsorption of propane is the rate determining step at these potentials. So I don't say that the rate determining step is always the oxidation of "reduced CO_2." The "reduced CO_2" is almost always there, but its oxidation doesn't have to be the rate determining step.

DR. OSWIN: I would like to ask a simple question which is, do I take it from your presentation that you cannot say how many electrons are released by the oxidation of one molecule of glucose?

DR. MALACHESKY: Not at the present time -- we cannot be sure. It looks that from the measurements that you apparently may be just oxidizing the open-chain form, the aldehyde form. It does not appear that the actual bulk glucose concentration is actually electroactive.

DR. OSWIN: Your data seem to indicate that the number could be anything between 2 and 24 and it seems to me that from the point of view of engineering a device, it is absolutely vital to know the number of electrons accurately. Couldn't this be determined by a quantitative analysis and coulombic measurements? Isn't the number also likely to be potential dependent?

DR. MALACHESKY: Yes, those are measurements which we plan to make. We would like to know the oxidation products as a function of both time and potential. Platinized platinum electrodes with high surface areas are necessary in studies like these.

DR. GINER: May I add to this point that one of the very important findings here is that we are getting CO_2 from glucose. We don't know if we are oxidizing only one carbon to CO_2 or the whole glucose molecule to CO_2. I think that the situation is very similar to methanol where you can get CO_2 but you can also get formaldehyde and other products from the electrode reaction. This is the type of work that Dr. Malachesky mentioned that we are planning to do so that the engineers will be happy.

CHAPTER 71

SEARCH FOR A SPECIFIC CATALYST FOR ELECTROCHEMICAL OXYGEN REDUCTION IN NEUTRAL NaCl SOLUTION

A. Kozawa, V. Zilionis, R. Brodd and R. Powers

Union Carbide Corporation
Consumer Products Division
Palma Technical Center
Cleveland, Ohio

An implantable fuel cell which will drive an artificial heart requires a specific catalyst for oxygen reduction at the cathode. The specific catalyst applied on the cathode used in a blood stream should not catalyze a direct chemical reaction between molecular oxygen and glucose coexisting in the blood. In a search for such a catalyst, various carbons, graphites, metals, carbides, borides, blood components, and other catalytically active materials were tested in an isotonic saline solution (0.15M NaCl+0.1M phosphate buffer, pH 7.22), with and without 10 percent human blood added. These materials were first screened using linear sweep voltammetry techniques in quiescent solutions. More definitive measurements were carried out with a rotating disk electrode technique. It was found that ferric phthalocyanine deposited on graphite was the best catalyst among the materials tested. Ferric phthalocyanine was deposited on the electrode surface by dilution of sulfuric acid solution or by evaporation of a pyridine solution of phthalocyanine. The phthalocyanine catalyzed graphite (P.C.-Gr) electrode exhibited an open circuit voltage of +0.3 to +0.4 volt vs. S.C.E. in the O_2- saturated saline solution and the current capability as well as the current-potential curve taken at this electrode was approximately the same as that taken at a smooth platinum electrode. This P.C.-Gr electrode operated in whole blood and did not react with isotonic saline solutions containing glucose and gluconate. The importance of substrate material should be noted. It was found that ferric phthalocyanine was an excellent catalyst only when deposited on graphite and carbon. Ferric phthalocyanine deposited on Ti, Zr, and porous nickel electrodes was not active.

INTRODUCTION

An implantable fuel cell which will drive an artificial heart requires a specific catalyst for oxygen reduction at the cathode. The word "specific" means that the catalyst applied on the cathode used in a blood stream should not catalyze a direct chemical reaction between molecular oxygen and glucose which coexist in the blood. Without considering the details of the oxygen reduction reaction, the over-all process is given by the equation.

$$\begin{tikzcd} O_2 \arrow[r, "2e"] & H_2O_2 \arrow[r, "2e"] \arrow[l, bend right, "\text{surface decomposition}"'] \arrow[d] & OH^- \\ & \text{solution} & \end{tikzcd} \qquad (1)$$

The mechanism points out the importance of the intermediate H_2O_2 and its decomposition to OH^- or O_2 as well as the possible dissolution of H_2O_2. The catalyst must inhibit dissolution of H_2O_2 as well as speed the over-all process.

In a search for such a catalyst, various electrode materials such as graphites, carbides, borides, and metals were tested in an isotonic saline solution (0.15 M NaCl + 0.05 M phosphate buffer, pH 7.22) with and without the addition of human blood. In an early experiment, it was noted that human blood contains a catalyst which promotes the electrochemical reduction of oxygen on graphite and also on some metal electrodes. In order to identify the effective compound in blood, hemoglobin, catalase, hemin chloride and finally, by analogy, various metal phthalocyanines were tested. The purpose of this paper is to describe the results of these tests and some characteristics of ferric phthalocyanine on graphite, which is the best catalyst found so far in our studies of this system. In view of the limited time available here, detailed behavior of various metal, carbide, and boride electrodes will be presented elsewhere.

Many papers[1] have been published concerning electrochemical oxygen reduction in general. The investigations were carried out in concentrated KOH (7 to 9 M) and in H_2SO_4 and H_3PO_4 electrolytes because of an interest in fuel cell oxygen cathodes. Only a few papers have been published in which neutral salt electrolytes were used. Laitinen[2] studied oxygen reduction at a platinum electrode in buffer solutions of pH 3 to 12. Delahay[3] studied oxygen reduction in 0.2 N KCl solution (pH 6.9) at various metal electrodes. Oxygen reduction in NaAc-HAc (pH 7.0) solution at anodized and cathodized platinum electrodes and at a lithium-doped nickel oxide electrode was reported by Kozawa[4, 5]. All these studies indicate that the formation of H_2O_2 as an intermediate takes place in these salt solutions. This suggests that a catalyst which decomposes hydrogen peroxide should be a good catalyst for the cathode. However, the well-known platinized platinum electrode which decomposes H_2O_2 vigorously cannot be used for the present purpose since it is not a specific catalyst.

Phthalocyanines have been reported to be good catalysts for oxygen reduction[6, 7, 8] when used in strongly acid and strongly basic solutions. Jasinski[6,8] investigated cobalt phthalocyanine deposited on porous nickel in 35 percent KOH solution ($pH \cong 16$). A ferric phthalocyanine-carbon combination was investigated in 4.5 N H_2SO_4 ($pH \cong 0$) by Jahnke and Schönborn[7]. However, the performance of these materials has not been reported in neutral salt electrolytes.

EXPERIMENTAL

Chemicals and Blood.

Catalase, hemoglobin and hemin chloride were obtained from Calbiochem (Los Angeles) and stored in a refrigerator. Metal phthalocyanines and porphyrazines (Table 1) were obtained from Distillation Products Industries (Division of Eastman Kodak Company).

TABLE 1

PHTHALOCYANINES AND PORPHYRAZINES TESTED

1.	Phthalocyanine
2.	Chloroaluminum chlorophthalocyanine
3.	Diantimony phthalocyanine
4.	Cadmium octaphenylporphyrazine
5.	Fluorochromium phthalocyanine
6.	Copper octaphenylporphyrazine
7.	Copper phthalocyanine
8.	Polycopper phthalocyanine
9.	Ferric phthalocyanine
10.	Chlorogallium phthalocyanine
11.	Lead phthalocyanine
12.	Dilithium phthalocyanine
13.	Magnesium octaphenylporphyrazine
14.	Magnesium phthalocyanine
15.	Nickel phthalocyanine
16.	Chlororuthenium phthalocyanine
17.	Silver phthalocyanine
18.	Sodium phthalocyanine
19.	Tin 1, 1-phthalocyanine
20.	Uranyl phthalocyanine
21.	Vanadyl octaphenylporphyrazine
22.	Vanadyl phthalocyanine
23.	Zinc phthalocyanine

These compounds were used as received without purification. Figure 1 shows the general chemical structures[9] of three types of compounds, phthalocyanine, hemin, and porphyrazine. Human blood obtained from Parma Community Hospital was stored in a refrigerator and used within three days. The blood contained EDTA as an anticoagulant.

Solution.

An isotonic saline solution (0.15 M NaCl + 0.05 M phosphate buffer, pH 7.22) was prepared from reagent grade chemicals. It was used without further purification. Phosphate buffer was used because it is one of the major pH buffer systems in the blood[10].

Linear Sweep Voltammetry.

The isotonic saline solution was placed in a polarographic H-cell and a test electrode was placed in one arm. Current-potential (i-E) curves were taken in a quiescent nitrogen- or oxygen-saturated solution with a Controlled Potential and Derivative Voltameter (Model ORNL-1988A)[11]. Figure 2 shows the schematic setup. The electrode surface exposed to the solution was about 0.25 cm^2.

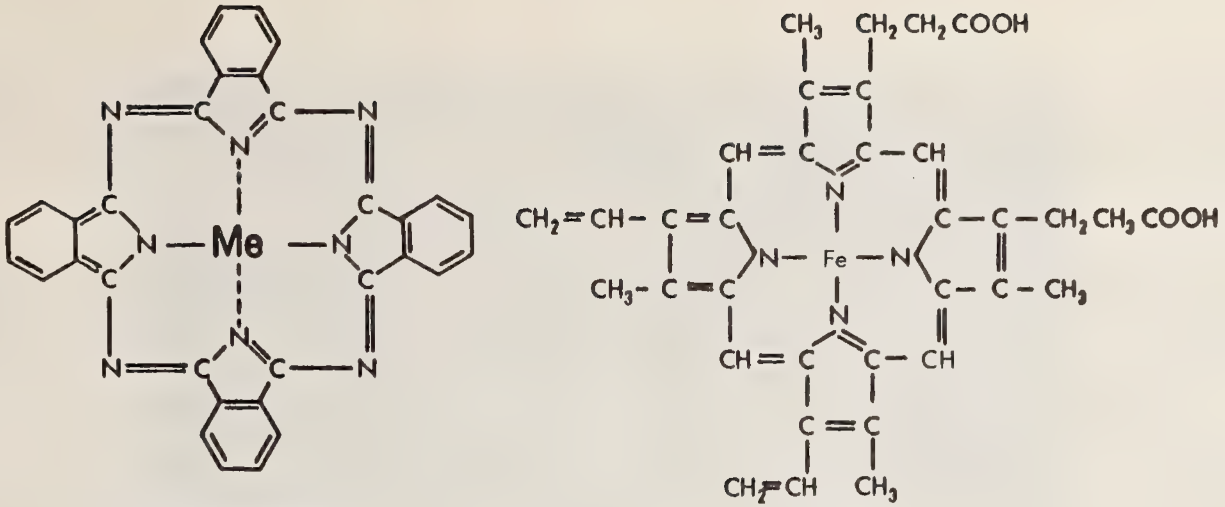

(a) PHTHALOCYANINE

(b) HEMIN

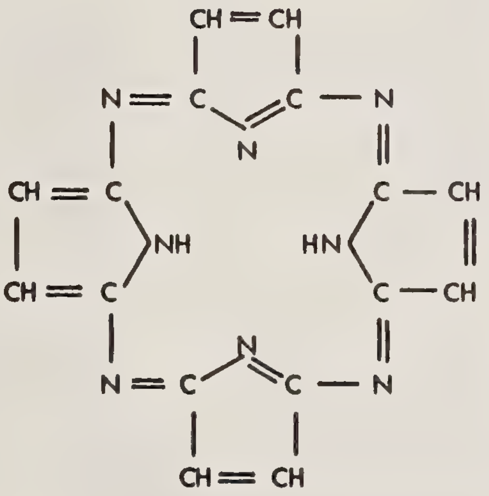

(c) TETRAAZOPORPHIN OR PORPHYRAZINE

FIGURE 1. MOLECULAR STRUCTURES OF PHTHALOCYANINES AND RELATED COMPOUNDS.(9)

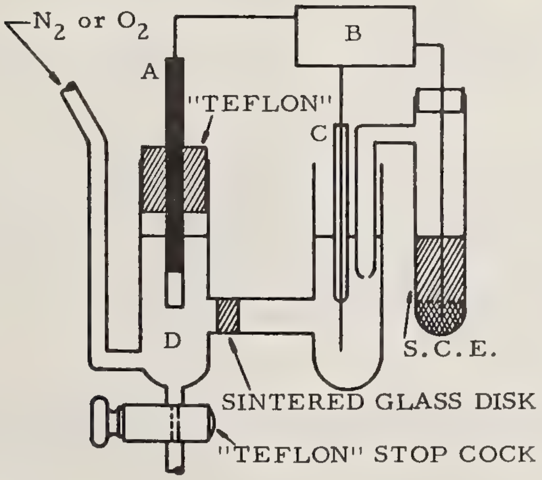

FIGURE 2. EXPERIMENTAL SETUP, STATIONARY ELECTRODE STUDIES.
- A. TEST ELECTRODE, PARAFFIN COATED EXCEPT THE EXPOSED PORTION OF ABOUT 0.25 CM^2.
- B. CONTROLLED POTENTIAL AND DERIVATIVE VOTAMMETER (MODEL ORNL-1988A).
- C. COUNTER ELECTRODE (Pt ELECTRODE).
- D. TEST SOLUTION (20.0 ML).

Paraffin was used to mask off the unused portion of the surface. The potential sweep rate was 0.25 volt per minute. Usually the i-E curve was first taken in a nitrogen-saturated solution, then twice consecutively in an oxygen-saturated solution, and finally in the solution to which blood or other material (catalase, hemin chloride, etc.) was added. All potential measurements were made using a saturated calomel reference electrode (S.C.E.).

Rotating Disc Electrode.

The rotating disc apparatus is shown in Figure 3. The structure of the graphite rotating disc electrode is shown in Figures 4 and 5. The area of the pyrolytic graphite rotating disc electrode was 0.268 cm^2 and that of the platinum electrode was 0.196 cm^2. The rotational speed was constant (120 rpm) throughout the experiments. The speed was monitored continuously by an electronic counter using a photocell. The voltage scanning rate was 0.1 volt per minute.

Before deposition of the catalyst, the pyrolytic graphite rotating disc electrode was polished using a microcloth on a mechanical wheel. If necessary, an alumina (0.3μ) suspension in water was used always ending with a wet polish on the plain microcloth. The electrode was press-fitted in a "Teflon" holder concentric to the rotating shaft. Electrical connection was established by a spring-loaded contact in the shaft. Epoxy resin was used to seal the imperfections between the "Teflon" and the electrode to prevent oxygen from diffusing into the test cell from the backside of the electrode. This also prevented solution from creeping up into the joint. After deposition of the catalyst, the electrode was washed with distilled water and mounted on the rotating disc apparatus.

The hydrodynamic equations for the rotating disc technique were solved by Levich[12]. The expression for the limiting current of a reaction controlled by mass transfer is given in Equation 2.

$$i_\ell = 0.62\ n\ F\ A\ C\ D^{2/3}\ \nu^{-1/6}\ \omega^{1/2} \qquad (2)$$

where i_ℓ = limiting current
n = number of electrons involved in the reaction
F = Faraday constant
A = area of disc
C = concentration of reactant in solution
D = diffusion coefficient
ν = kinematic viscosity
ω = angular frequency ($2\pi f$)

The equation takes into account that the effective surface concentration of the reactant can be varied by changes in rotation rate of the electrode. In this investigation, a constant rotation rate of 120 rpm was used. Therefore, the structure of the diffusion layer at the electrode surface was standardized for all electrodes. Comparisons of the activity of various electrode surfaces could be made without the added problems associated with diffusion.

RESULTS AND DISCUSSION

Effect of Blood.

Figure 6 shows the i-E curve at a stationary pyrolytic graphite electrode with and without blood addition to the saline solution. Two effects of blood addition were observed. First, at the foot of the i-E curve, the current is somewhat suppressed in the presence of blood, indicating the presence of some inhibitor in the blood at this potential region. Second, the current is considerably greater in the presence of blood over most of the potential range studied. Without blood, the i-E curve shows two steps which are similar to the polarogram of dissolved oxygen at a dropping mercury electrode; the first step being $O_2 \rightarrow H_2O_2$ and the second step being $O_2 \rightarrow H_2O$. A tentative explanation is that a substance or substances in the blood catalyze hydrogen peroxide decomposition at the electrode surface.

A number of i-E curves were taken at various metals (platinum, palladium, gold, silver, nickel, molybdenum, titanium, niobium, tantalum, zirconium), graphites, carbides, and borides. Among these electrode materials ZTA graphite[13] (high density graphite), platinum, palladium, gold, and silver showed fair to good activity for oxygen reduction. With the exception of platinum, the blood effect with these electrodes was quite similar to that of the pyrolytic graphite electrode shown in Figure 6. The current value for the platinum electrodes was considerably lower and the i-E curve shifted toward a more negative potential when 10 percent blood was added.

Effect of Catalase.

Figure 7 shows the effect of catalase. The effect of catalase on the i-E curve is essentially the same as that of the 10 percent blood addition, which was seen in Figure 6. This suggests that the blood effect may be due in part to the catalase present in the blood.

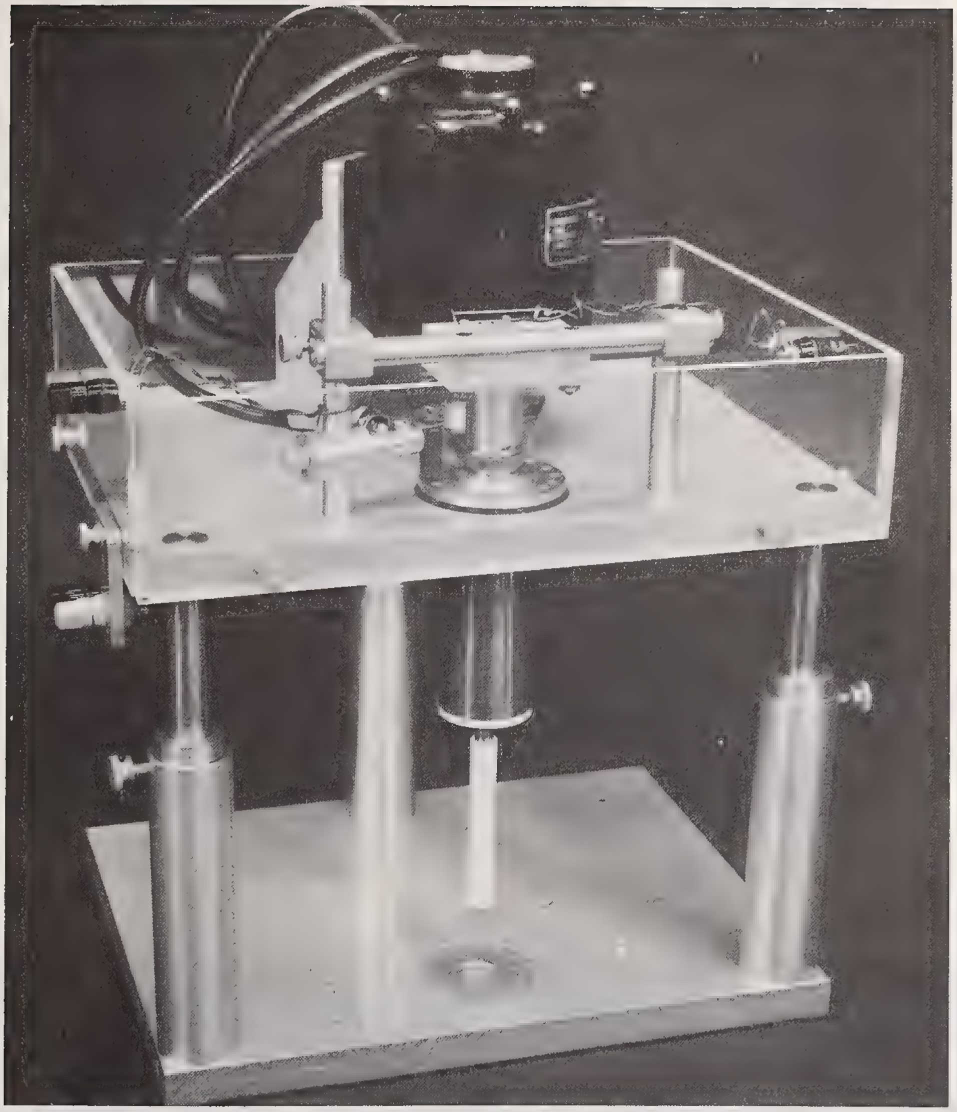

FIGURE 3. ROTATING DISC ELECTRODE APPARATUS.

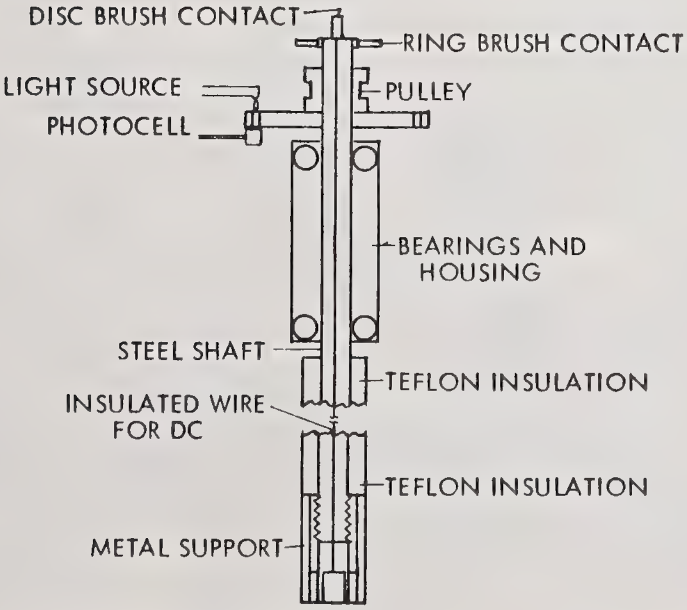

FIGURE 3A. SCHEMATIC OF ROTATING DISC APPARATUS.

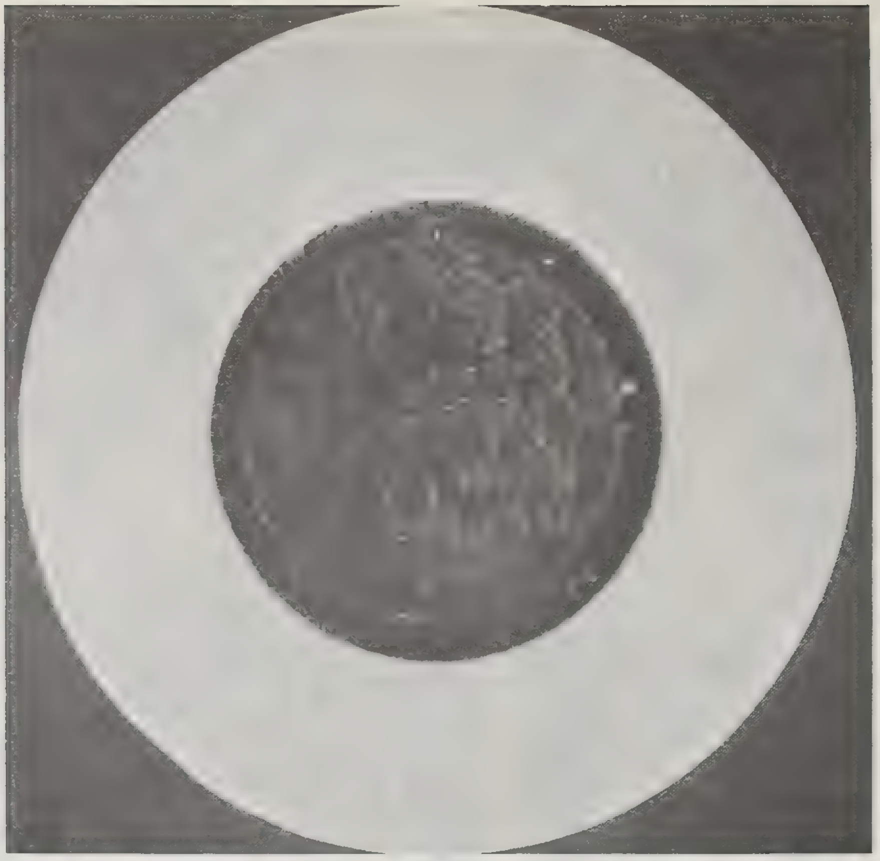

FIGURE 4. A PHOTOGRAPH OF THE SURFACE OF A ROTATING DISC ELECTRODE (0.268 CM^2).

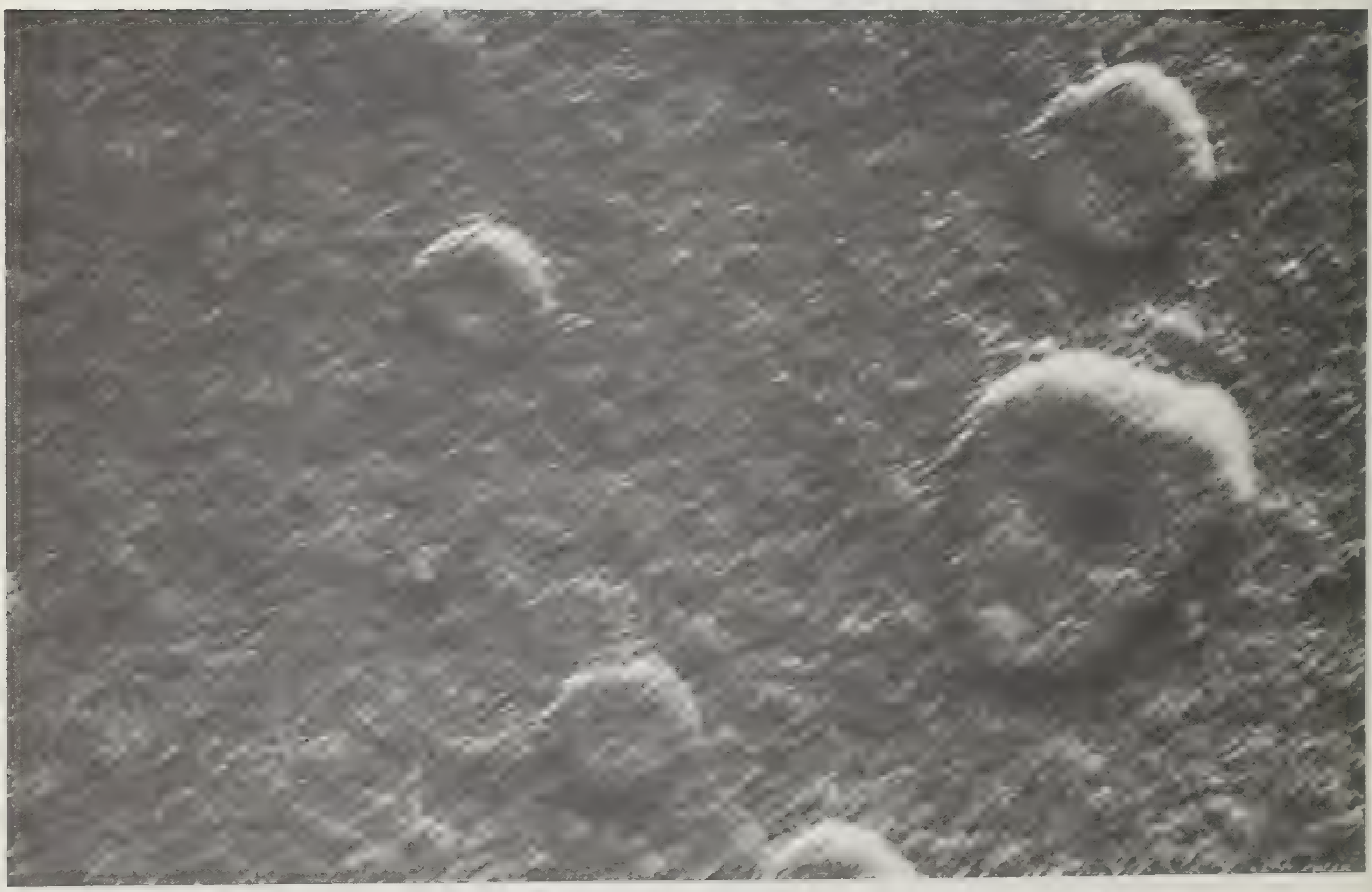

FIGURE 5. AN ELECTRON MICROSCOPE PHOTOGRAPH OF THE SURFACE OF PYROLYTIC GRAPHITE AT 40,000x MAGNIFICATION.

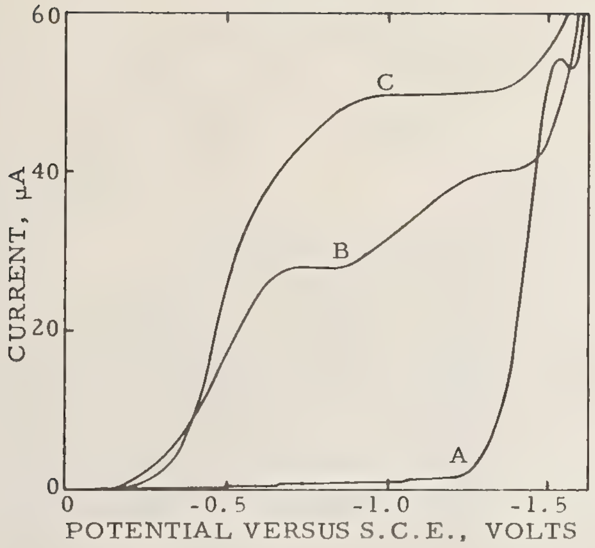

FIGURE 6. CURRENT-POTENTIAL CURVES BY LINEAR SWEEP VOLTAMMETRY IN 0.15 M NaCl (+ PHOSPHATE BUFFER, pH u.22) AT 24° C AT A PYROLYTIC GRAPHITE ELECTRODE (0.20 CM^2). CURVES ARE TAKEN IN A QUIESCENT SOLUTION.

A. N_2 - SATURATED SOLUTION.
B. O_2 - (1 ATM) SATURATED SOLUTION.
C. O_2 + 10% BLOOD (BY VOLUME).

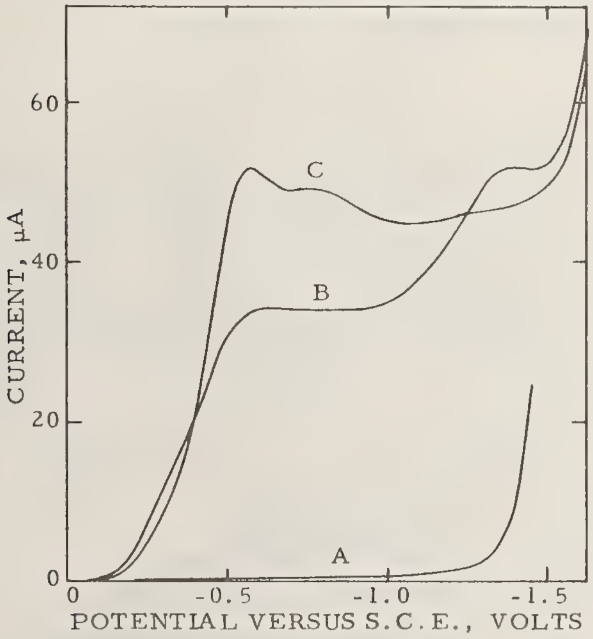

FIGURE 7. EFFECT OF CATALASE (BOVINE LIVER, A-GRADE). THE CURRENT-POTENTIAL CURVES WERE TAKEN AT A PYROLYTIC GRAPHITE ELECTRODE (0.245 CM^2) BY LINEAR SWEEP VOLTAMMETRY IN 0.15 M NaCl (+ PHOSPHATE BUFFER, pH 7.22) AT 23 ± 1° C. THE CURVES WERE TAKEN IN A QUIESCENT SOLUTION.

A. IN N_2 - SATURATED SOLUTION.
B. IN O_2 - SATURATED SOLUTION.
C. IN O_2 - SATURATED SOLUTION (20 ML) TO WHICH 0.5 ML CATALASE SOLUTION WAS ADDED.

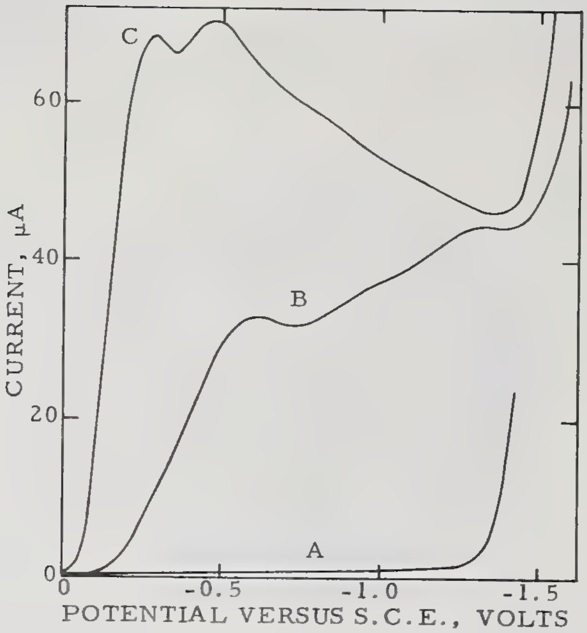

FIGURE 8. EFFECT OF HEMIN CHLORIDE. THE CURRENT-POTENTIAL CURVES WERE TAKEN AT A PYROLYTIC GRAPHITE ELECTRODE (0.260 CM^2) BY LINEAR SWEEP VOLTAMMETRY IN 0.15 M NaCl (+ PHOSPHATE BUFFER, pH 7.22) AT 23 ± 1° C. THE CURVES WERE TAKEN IN A QUIESCENT SOLUTION.

A. IN N_2 - SATURATED SOLUTION.
B. IN O_2 - SATURATED SOLUTION.
C. IN O_2 - SATURATED SOLUTION CONTAINING 10 MG HEMIN CHLORIDE,* THE CURVE WAS TAKEN AFTER BUBBLING O_2 FOR 30 MINUTES IN AN ATTEMPT TO DISSOLVE THE HEMIN CHLORIDE.

* added to 20 ML of the NaCl solution

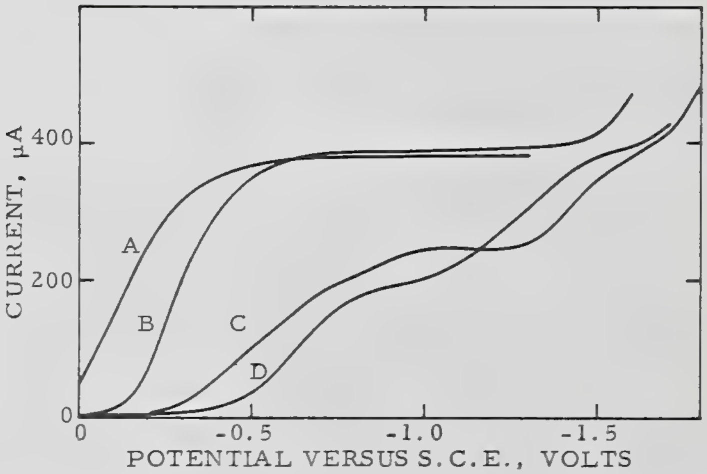

FIGURE 9. CURRENT-POTENTIAL CURVES TAKEN AT ROTATING DISC ELECTRODES IN OXYGEN-SATURATED 0.15 M NaCl (+ PHOSPHATE BUFFER, pH 7.22) AT 23° C. ROTATIONAL SPEED: 120 RPM, VOLTAGE SCANNING RATE: 0.1 VOLT/MINUTE, ELECTRODE AREA 0.268 CM^2.

A. FERRIC PHTHALOCYANINE DEPOSITED ON PYROLYTIC GRAPHITE.
B. POLYCOPPER PHTHALOCYANINE ON PYROLYTIC GRAPHITE.
C. SILVER PHTHALOCYANINE ON PYROLYTIC GRAPHITE.
D. UNCATALYZED PYROLYTIC GRAPHITE.

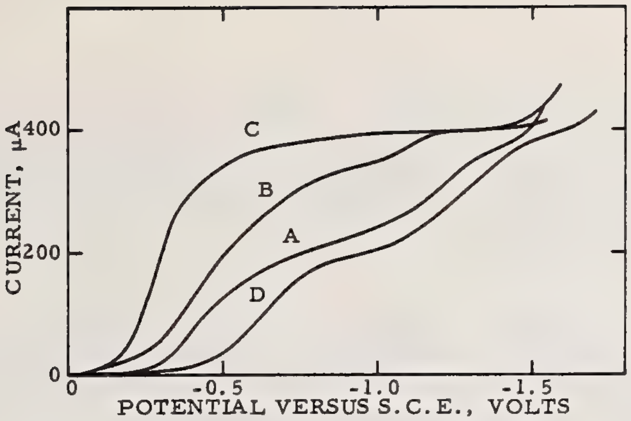

FIGURE 10. CURRENT-POTENTIAL CURVES TAKEN AT A PYROLYTIC GRAPHITE ROTATING DISC ELECTRODE IN OXYGEN-SATURATED 0.15 M NaCl (+ PHOSPHATE BUFFER, pH 7.22) AT 23° C. ROTATIONAL SPEED :120 RPM, VOLTAGE SCANNING RATE: 0.1 VOLT/MINUTE, ELECTRODE AREA 0.268 CM^2.
A. COPPER OCTAPHENYLPORPHYRAZINE DEPOSITED ON PYROLYTIC GRAPHITE.
B. COPPER PHTHALOCYANINE ON PYROLYTIC GRAPHITE.
C. POLYCOPPER PHTHALOCYANINE ON PYROLYTIC GRAPHITE.
D. UNCATALYZED PYROLYTIC GRAPHITE.

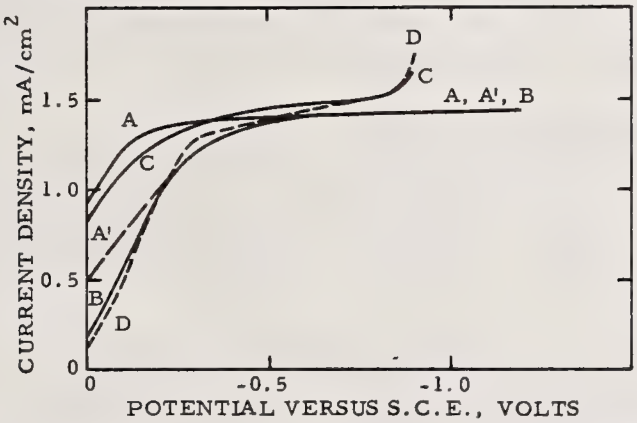

FIGURE 11. CURRENT-POTENTIAL CURVES AT ROTATING DISC PYROLYTIC GRAPHITE, ON WHICH FERRIC PHTHALOCYANINE WAS DEPOSITED, AND BRIGHT PLATINUM ELECTRODES IN OXYGEN-SATURATED 0.15 M NaCl (+ PHOSPHATE BUFFER, pH 7.22) AT 23° C. ROTATIONAL SPEED: 120 RPM, VOLTAGE SCANNING RATE: 0.1 VOLT/MINUTE.
CURVE A, A¹. FERRIC PHTHALOCYANINE-GRAPHITE ELECTRODES.
TWO DIFFERENT ELECTRODES WITH DIFFERENT ACTIVITY.
B. FERRIC PHTHALOCYANINE-GRAPHITE ELECTRODE. THE CURVE WAS TAKEN AFTER STANDING AT ZERO VOLT FOR 15 MINUTES.
C. BRIGHT PLATINUM ELECTRODES AFTER POLISHING.
D. BRIGHT PLATINUM ELECTRODES AFTER USE.

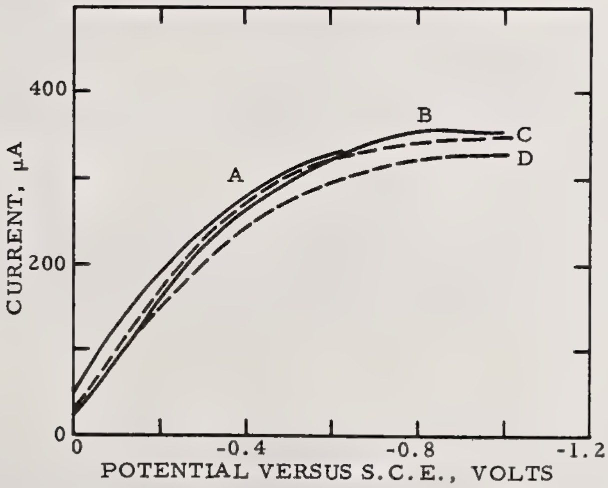

FIGURE 12. EFFECT OF GLUCOSE ON CURRENT-POTNETIAL CURVES FOR PYROLYTIC GRAPHITE WITH FERRIC PHTHALOCYANINE ELECTRODES. OXYGEN SATURATES SOLUTION AT 23° C, ROTATIONAL SPEED: 120 RPM, VOLTAGE SCANNING RATE: 0.1 VOLT/MINUTE.
CURVES 1 AND 2. SOLUTION IS 0.15 M NaCl + PHOSPHATE BUFFER.
3. ABOVE SOLUTION CONTAINING 100 MG GLUCOSE/100 ML.
5. ABOVE SOLUTION CONTAINING 200 MG GLUCOSE/100 ML.

Effect of Hemin Chloride.

The effect of hemin chloride is shown in Figure 8. Although hemin chloride dissolves slowly in the saline solution, stirring for 30 minutes brought sufficient hemin chloride into the solution to influence the i-E curve. As seen in Figure 8, the i-E curve shifts considerably toward a more positive potential and the current is much higher than in the control curve. It was confirmed that the reacting species here was not hemin chloride, since in the nitrogen-saturated hemin chloride solution, the i-E curve gave essentially zero current.

Effect of Phthalocyanines.

The i-E curves were taken at a catalyzed rotating disc electrode sweeping from zero volt versus S.C.E. toward a more negative potential. In most of the tests, the scanning was stopped at -1.0 volt in the first run, and in the second run with the same electrode, the potential was scanned to around -1.7 volts. The potential was limited to -1.0 in the first run because it was felt that excessive cathodization might completely alter the nature of the catalyst. However, since the i-E curves for the first and the second runs were approximately the same, the catalyst does not appear to be affected by the potential in saline solution.

Figure 9 shows i-E curves which illustrate good, fair, and poor activities. The best activity for oxygen reduction was observed with ferric phthalocyanine (curve a) which was comparable to the activity of a smooth platinum electrode. Fair activity was exhibited by polycopper phthalocyanine (curve b). Fluorochromium phthalocyanine, chloroaluminum phthalocyanine and copper phthalocyanine also gave fair activity in the test. Other metal phthalocyanines, such as silver, did not exhibit good activity for the oxygen reduction reaction at graphite electrodes.

Figure 10 compares phthalocyanine compounds having copper as a central metal, polycopper phthalocyanine, copper phthalocyanine, and copper octaphenyl porphyrazine. The results show that the polymerized copper phthalocyanine is more active than the unpolymerized one, and that copper phthalocyanine is more active than a copper porphyrazine.

Comparison of Ferric Phthalocyanine, Hemin and Platinum.

The use of hemin chloride as a catalyst has some disadvantages. Even though it has a tendency to be strongly adsorbed on the pyrolytic graphite surface, it is soluble in neutral salt solutions. Thus, hemin chloride must be continuously supplied to the electrode surface to prevent its eventual loss by dissolution in body fluids. Ferric phthalocyanine is a more active catalyst than the hemin chloride for the electroreduction of oxygen. Since ferric phthalocyanine is insoluble in neutral salt solutions, it will remain on the electrode surface and not lose activity by dissolution in body fluids.

Figure 11 compares the ferric phthalocyanine on graphite and bright platinum as catalysts for oxygen reduction in the isotonic saline solution. The rotating disc electrodes of smooth platinum and graphite with ferric phthalocyanine were assumed to be polished to the same surface roughness so that the curves in Figure 9 are a fair comparison of the catalytic activity of oxygen reduction on these electrodes. The current value at -0.5 to -0.8 volt at the ferric phthalocyanine-graphite electrode is roughly the same as that at the platinum electrode. This suggests that oxygen is being reduced directly to water by a four-electron transfer process ($O_2 + 4H^+ + 4e \rightarrow 4H_2O$) at the ferric phthalocyanine-graphite electrode in this potential range. It is interesting to note that the current-potential curve at the ferric phthalocyanine-graphite electrode has one step, rather than two steps which are observed at an uncatalyzed graphite electrode (curve d, Figure 9). Such a two-step curve indicates the possibility that oxygen is reduced in two steps, (1) $O_2 \rightarrow H_2O_2$, and (2) $O_2 \rightarrow H_2O$, at negative potentials. Because of these observations, hydrogen peroxide decomposition is considered an important characteristic of the oxygen electrode catalyst. The influence of the catalyst on the reaction mechanism is not clear. It is possible that the catalyst speeds the rate of decomposition of hydrogen peroxide either to oxygen, which is then reduced, or to OH^-, so that the peroxide decomposition step is not observed. It may also be possible that the catalyst changes the reaction mechanism so that peroxide is not produced as an intermediate.

It was also observed that the initial open circuit potential of the ferric phthalocyanine-graphite electrode in this saline solution (about +0.3~+0.4 volt versus S.C.E.) was higher than that of the platinum electrode (about +0.2 volt versus S.C.E.).

Effect of Glucose.

Figure 12 shows the effect of glucose at a rotating disc pyrolytic graphite electrode catalyzed with ferric phthalocyanine. Approximately 10^{-4}g/cm^2 of the catalyst was applied to the electrode.

The results indicate that the ferric phthalocyanine-graphite electrode is not sensitive to the presence of glucose. The ferric phthalocyanine catalyst does not appear to catalyze a direct chemical reaction between glucose and oxygen, since the oxygen reduction current is not appreciably influenced by the presence of glucose.

Effect of Substrate Material.

Besides graphite, other corrosion resistant substrate materials such as nickel, zirconium, and titanium were investigated as substrates for ferric phthalocyanine. It was found that ferric phthalocyanine deposited on titanium, zirconium, and nickel was not active for oxygen reduction in this saline solution.

CONCLUSION

In summary, the influence of blood additions to saline solution on the oxygen reduction reaction appears to be due primarily to catalase and hemin chloride. Both of these compounds exhibit characteristics of catalysts for the oxygen reduction reaction. Phthalocyanines, which have a similar structure to that of hemin chloride, were also found to be active catalysts for the oxygen reduction reaction in saline solution. Ferric phthalocyanine deposited on graphite appears to be a specific catalyst for oxygen reduction in saline solution.

ACKNOWLEDGMENT

The authors gratefully acknowledge the assistance of William L. Adams.

REFERENCES

1. See J. P. Hoare, "The Electrochemistry of Oxygen", Interscience Publishers (1968).
2. H. A. Laitinen and I. M. Kolthoff, J. Phys. Chem. 45, 1061 (1941).
3. P. Delahay, J. Electrochem. Soc. 97, 198, 205 (1950).
4. A. Kozawa, J. Electroanal. Chem. 8, 20 (1964).
5. A. Kozawa and E. B. Yeager, ONR Technical Report No. 1, Contract No. 1439 (09), Nov. 1, 1964.
6. R. Jasinski, U. S. Patent No. 3,410,727 (Nov. 12, 1968).
7. H. Jahnke and M. Schönborn, a paper "Electrocatalysis on Organic Semiconductors", presented at the 19th CITCE Meeting, Detroit, (September 26, 1968).
8. R. Jasinski, J. Electrochem. Soc. 112, 526 (1965).
9. F. H. Moser and A. L. Thomas, "Phthalocyanine Compounds", Reinhold Publishing Corp. (1963).
10. H. A. Harper, "Review of Physiological Chemistry", p. 167 (1965) Lange Medical Publication, Los Altos, California.
11. M. T. Kelly, H. C. Jones, and D. T. Fischer, Anal. Chem. 31, 1475 (1959).
12. V. Levich, Physiocochemical Hydrodynamics, Trans. Scripta Technica, Inc., Prentice Hall, Inc. (1967).
13. Advanced Material Information Bulletin No. 3 (Union Carbide Corporation, Carbon Products Division) May 1962.

DISCUSSION

DR. OSWIN: When comparing the platinum and graphite/phthalocyanin surfaces you polished your electrode surfaces to get a low surface roughness. Presumably this would give a surface roughness of 1.2-1.5 for Pt, but you would have to deposit phthalocyanin on the graphite after polishing and depending on the method of deposition used, this could increase the roughness factor up to 10X. The technique that you used for the deposition is important since it will determine the surface roughness factor. I wondered if you could say how you carried out the deposition?

MISS ZILIONIS: The phthalocyanin was deposited from ice cooled sulfuric acid solution, diluting it with water.

DR. KOZAWA: The rotational speed is only 120 rpm, so that the thickness of the diffusion layer is much greater than the surface roughness. Therefore, in the potential range, in which a diffusion limited current is observed, the surface roughness factor in comparing the two electrodes is insignificant. However, the surface roughness factor becomes important in comparing the current capability at the bottom of the S-shaped current-potential curve. We do not know the true surface area or the roughness factor of these electrodes at this stage of our work. The present work is a rough survey of a large number of compounds and electrode materials.

CHAPTER 72

ON THE DESIGN OF CATALYSTS FOR BIOLOGICAL FUEL CELLS

C. Bocciarelli

Pennsylvania Research Associates
Philadelphia, Pennsylvania

A new theory of metallic catalysis has been developed which is based on the electron density of a metal under the further requirement that the catalyst show nearly complete immunity to chemical attack. Catalysts designed on the basis of this theory have been produced and tested. These differ from previous practice as they are crystalline powders (mounted in Teflon), not blacks. As specific oxygen electrodes in neutral or alkaline solutions, they outperform existing catalysts such as platinum black by a very wide margin. For example, the gold-copper alloy catalyst at a potential range of 0.85 to 0.75 volt in 5N KOH yields current densities from 300 to 1000 ma/cm^2, whereas platinum black prepared and operated under identical conditions gives current densities from 100 to 300 ma/cm^2. Studies on the design of glucose electrodes have also been carried out.

INTRODUCTION

The search for a better fuel cell catalyst has been going on for several years substantially without success. A single company, for instance, has tested more than 2,000 materials in the hope of finding an improvement to Pt black. Such unsuccessful searches have made it apparent that unless a logical approach is substituted for random searches, the remarkable potential of the fuel cell may never be achieved.

The rate of reaction of a fuel cell is dependent on the catalyst. If, for instance, at the H_2 electrode of a H_2-O_2 fuel cell Pb were used as a catalytic metal instead of Pt, the performance of the cell would be essentially nil. Present catalysts are too costly, and even more important, too inefficient to optimize performance and reduce initial costs and sizes to acceptable levels. A subtler point is that unless an optimal design goal exists, no evaluation of the real potentials of fuel cells in specific applications can be reached. These goals would be completely different if improved catalysts permitted significant (say a factor of five) increase in current density and hence in power density at a given voltage.

As is well known, a catalyst is a material that in some rather mysterious way greatly accelerates a chemical reaction. In the particular case of fuel cells a number of conditions, as for instance the necessity of very high conductivity in the catalyst, limit the choice to metals. Consequently the properties of a metal have to be found that, if optimized, can best cause an electron to be adsorbed or emitted by an electrode. These conditions are required to burn a fuel, as for instance H_2 in the presence of O_2. It has been known for some time that at the surface of metals and in its immediate vicinity very high fields are present, corresponding to the height of the Fermi distribution in the metal and to the work function, the work function being the additional potential above the Fermi level which restrains the electrons from leaving the metal. The sum of the Fermi energy and the work function is generally called the electron affinity, W_A. The author found (Figure 1) that a simple relationship existed between W_A and E_F, the depth of the Fermi sea. On the basis of a simple theory, strictly speaking valid only for isotropic materials, the height of the Fermi sea can be expressed in terms of the electron density of the metal.

THEORETICAL INVESTIGATION

In a theoretical investigation, the author has shown that the values of W_A can be derived theoretically in a way that agrees completely with experimentally observed facts. The electron affinity turns out to be a function only of the bulk electron density, as is true also for the Fermi level.

It is a rather striking fact that all materials having high catalytic properties are materials showing high values of W_A.

Again on the basis of a rather simple hypothesis, a theory was developed that explained how high values of W_A are essential and differentiated between the requirements of an electron donor and an electron acceptor catalyst. This meant that it should be possible to develop a catalyst that may work very well as an O_2 but not at all as an H_2 catalyst.

Another requirement of a catalyst is its "nobility", that is its chemical inertness to attack by both very strong bases and very strong acids. This is not an a priori requirement for biological fuel cells that must work in very nearly neutral electrolytes. However, even in this case the desired long life and the general inaccessibility of a fuel cell imbedded in a human body make this requirement very valid.

All this narrows the choice to noble metals. It is not fortuitous that a high value of W_A and nobility go together. It is known that the materials most resistant to chemical attack are not pure metals but some intermetallics which are ordered stochiometric alloys; that of these, the

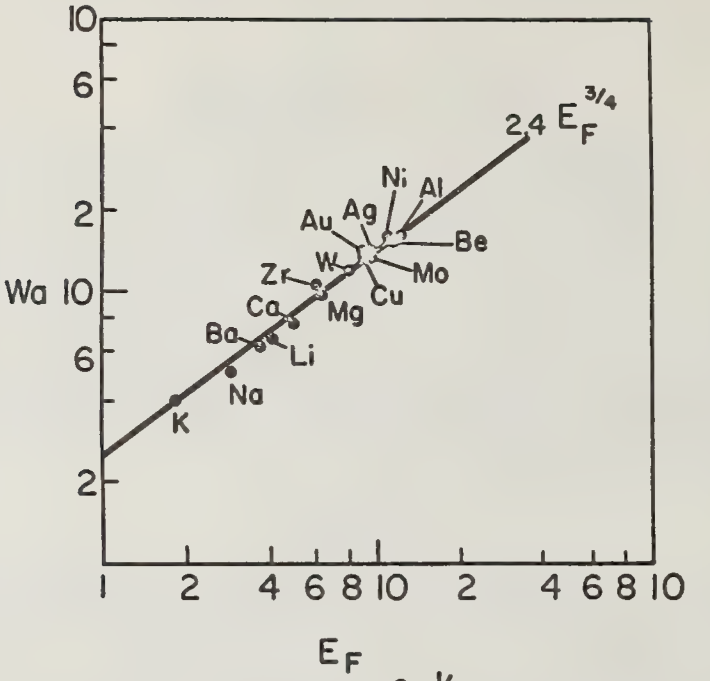

$$W_A = 3.48\,\hbar\left(\frac{ne^2}{m}\right)^{1/2} = 2.35\ E_F^{\ 3/4}$$

FIGURE 1. RELATIONSHIP BETWEEN W_A AND E_F.

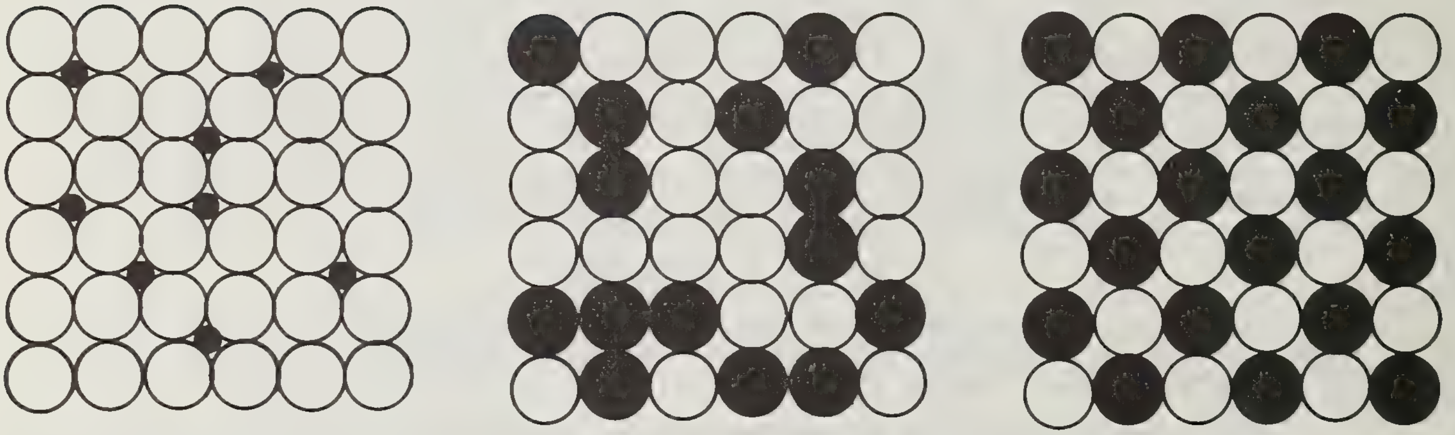

(a) Interstitial

(b) Substitutional (Random)

(c) Substitutional (Ordered)

FIGURE 2. ORDERED ALLOYS.

alloys of Au and Cu show not only spectacular resistance to chemical attack but also high initial electron density. Finally, it is known that this electron density can be increased by addition of multivalent impurities.

These ordered alloys are illustrated schematically in Figure 2 (A. H. Cottrell, Theoretical Structural Metallurgy. Edward Arnold and Company, London, 1951.), showing diagrammatically the differences among various possible alloys. The ordered lattices happen only in cases where the metals are soluble in each other to a great extent and then only in the immediate neighborhood of precise atomic ratios such as 50-50 or 25-75. When these occur the properties of the resulting alloys can differ markedly from the properties of their constituents. For instance, the AuCu alloys are enormously more resistant to chemical attack than either Au or Cu.

The theory also indicated that the higher density faces of single crystals would be of higher activity. This motivated us to obtain oriented single crystals as very fine powders, since increasing subdivision of the material should result in increased activity. The problem therefore is to obtain these materials in the form of very fine powders which consist of minute single crystals of alloys of AuCu to which trivalent impurities such as Al and Ga have been added.

METALLURGICAL WORK

We started by evaporating these materials on Single Crystal 100 faces of NaCl to a thickness of approximately 1,000 A^O. At these very small thicknesses, the components of the alloys will diffuse rapidly into each other until an equilibrium situation is reached, a process that by standard metallurgical methods may take weeks and months. These thin lamina can be floated off the salt, mounted on Ni meshes and tested for catalytic activity. Figure 3 shows the results of such a test compared to Pt bright. It will be noticed that all or nearly all of the new catalysts outperform Pt bright.

Of course these currents are lower than we would prefer for many fuel cell applications, but it is interesting to note (Figure 4) that the catalytic material improved with additional percentages of trivalent impurity as predicted by theory. It was also shown, and this was perhaps the most encouraging point reached in these preliminary investigations, that perforated lamina which could admit O_2 to one-cm^2 fuel cells performed surprisingly well. From these preliminary experiments one could assume that these catalysts would be indeed satisfactory, provided that they could be mounted somehow like the blacks in Teflon slurries. To do so, these catalysts would have to be finely subdivided powders. A rough order of magnitude calculation showed that these powders could not improve on Pt black unless it were possible to reduce them to about 1μ average size.

Initially, materials with high dopant content were used because at higher electron concentrations the crystal form changes from fcc to bcc; and while the fcc is malleable, the bcc is known to be brittle. In order to obtain the desired single crystals, we used a Bridgeman technique. This consists essentially in slowly freezing a cylindrical column of molten metal beginning at the lower end.

Extremely slow motions of the order of 3 mm/hr. are required, so that more than one working day was used to obtain a crystal. While we obtained coarsely polycrystalline material where few single crystals were of the order of 6-8 mm on a side, success with this approach was not obtained until we were ready to adopt the high temperature "hot shot" method to be described. Furthermore, this approach led to uncertitudes about the actual composition of the crystals. Nevertheless, these crystals gave very good results after grinding and incorporating in a Teflon electrode. Figures 5a and 5b show their performance as single crystals compared to Pt bright initially and after 18 hours. It shows an advantage over Pt by a factor of 7 or 8 initially, improving to at least 70 after 18 hours. These crystals, ground to a .5μ size and incorporated in Teflon electrodes, gave satisfactory results. Figure 6 shows results obtained with Al doped AuCu. This technique is of course, most effective with the higher impurity concentrations for which more brittle material is obtained. Other techniques, however, may be exploited when using lower impurity concentrations and hence more malleable materials.

It is known that malleable materials can be ground with suitable surfactants, provided that the initial charge consists of rather fine powder, say of the order of 100 μ. To get to this size, we made use of what is essentially a high temperature shot tower using a carbon crucible with a fine bottom opening of the order of 10 mils. Normally the surface tension keeps the diffused metal from pouring through the opening but, on applying a few pounds pressure of Argon, a fine spray could be obtained which solidifies while falling into perfect balls of the desired order of magnitude (See Figure 7). It can be shown that these spheres will be of uniform composition and be single crystals, a fact that is further attested to by the fine reticulation of equispaced normal lines that cover their surfaces. These tiny balls were ground to approximately .3μ size.

RESULTS

As expected, the new catalysts proved to be excellent electron acceptors, and hence excellent oxygen side catalysts, and relatively ineffective as fuel catalysts. Figure 8 shows the results obtained with three successive electrodes with AuCu plus 22 at % Ga. These results were obtained in actual cells, Pt black (American Cyanamid) electrodes being used as H_2 electrodes.

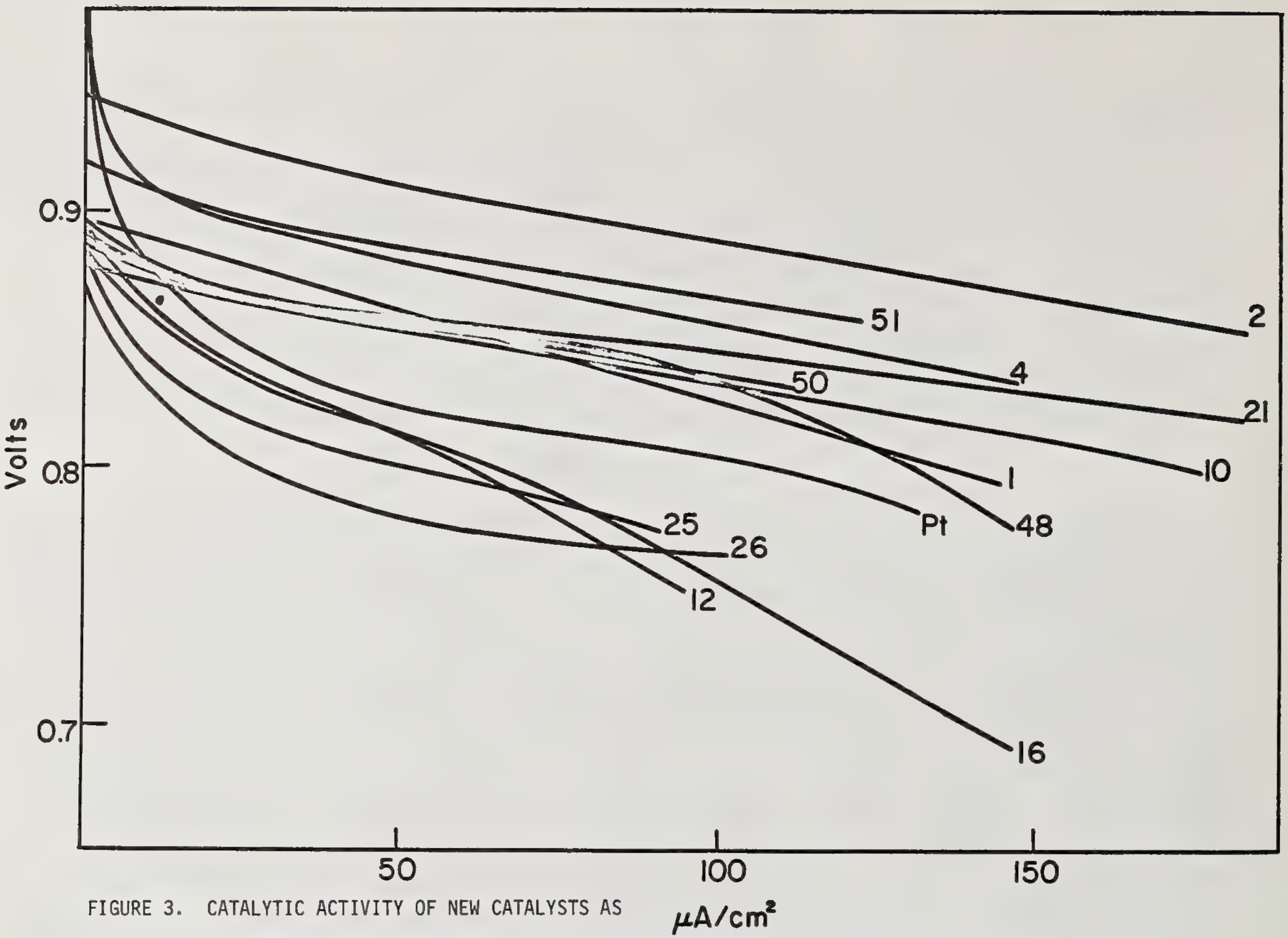

FIGURE 3. CATALYTIC ACTIVITY OF NEW CATALYSTS AS COMPARED WITH Pt BRIGHT.

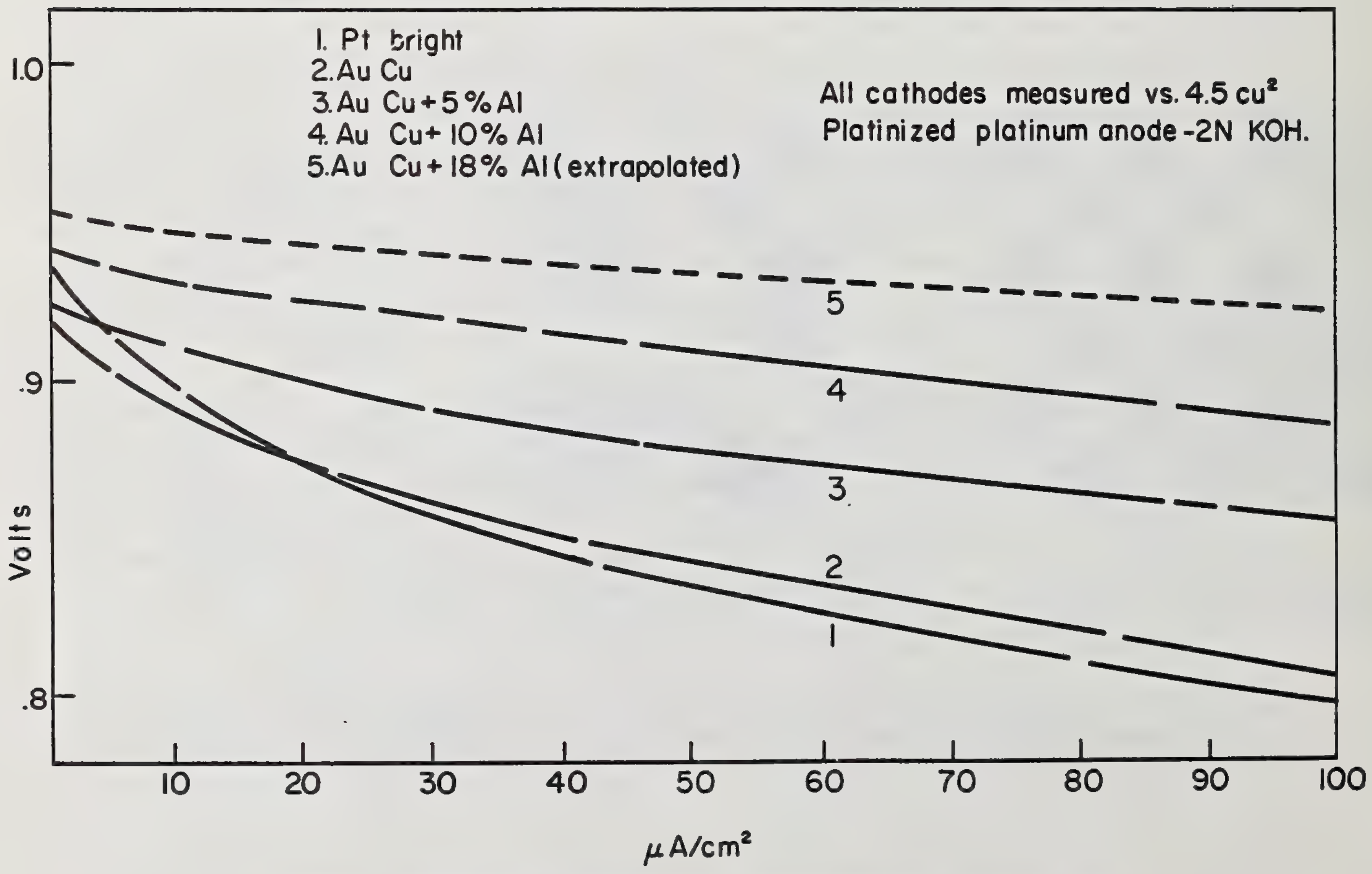

FIGURE 4. IMPROVEMENT OF CATALYTIC ACTIVITY WITH ADDITIONAL PERCENTAGES OF TRIVALENT IMPURITY.

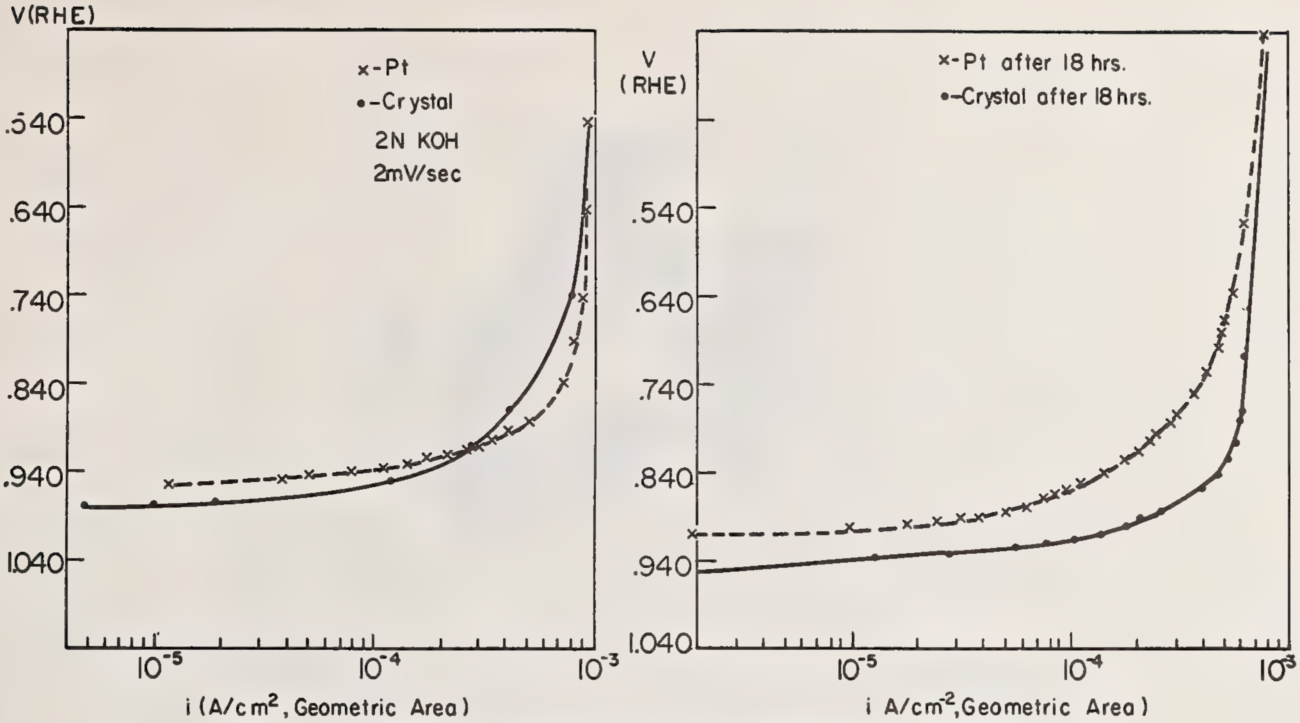

FIGURE 5. PERFORMANCE OF SINGLE CRYSTALS AS COMPARED WITH Pt BRIGHT INITIALLY AND AFTER 18 HOURS.

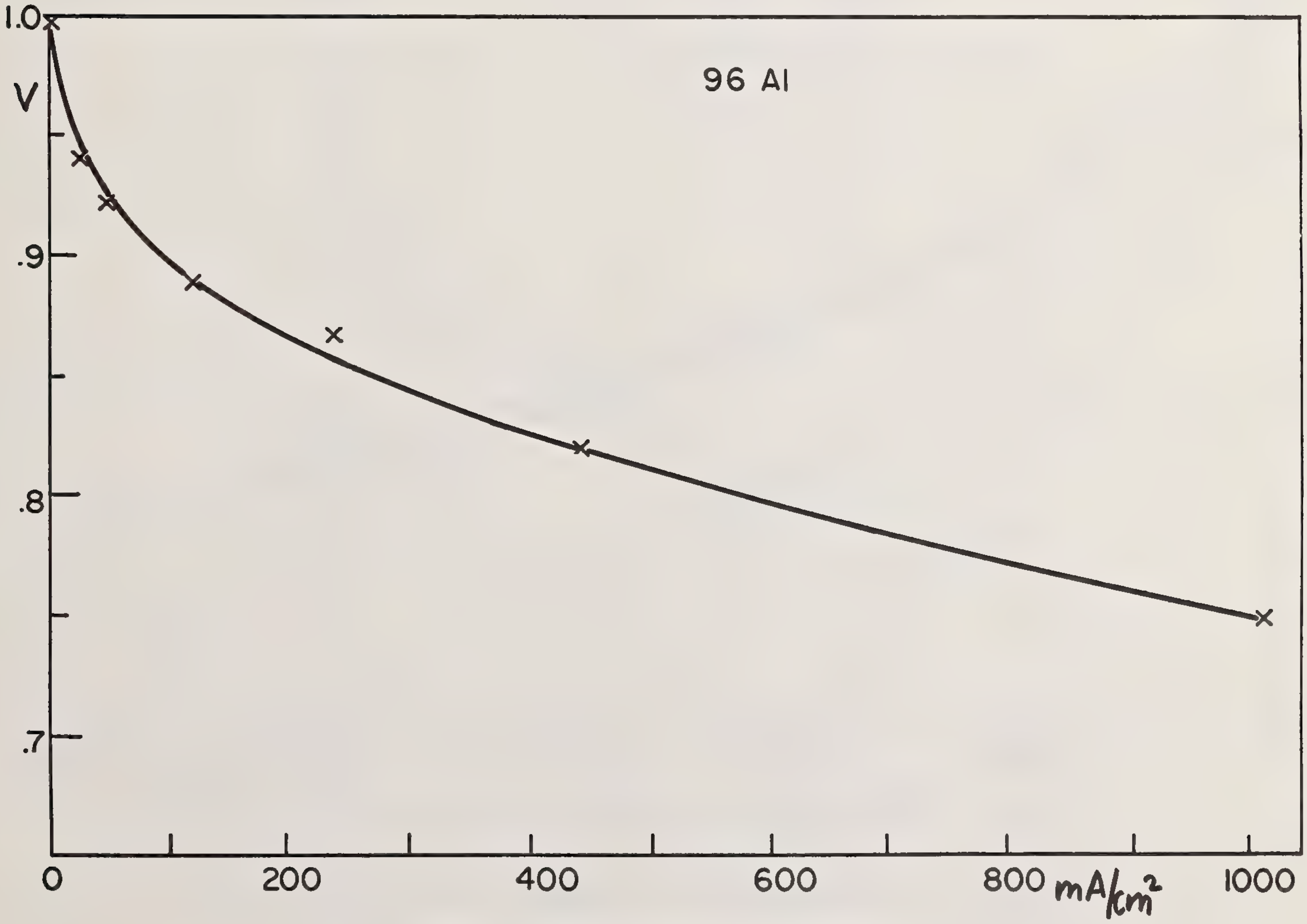

FIGURE 6. RESULTS OBTAINED WITH Al DOPED AuCu.

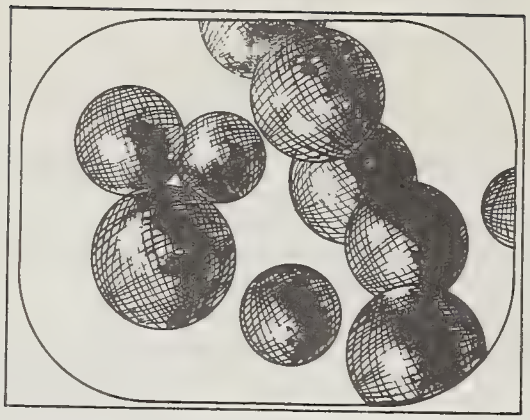

FIGURE 7. SPRAY SOLIDIFIED INTO BALLS OF THE DESIRED ORDER OF MAGNITUDE.

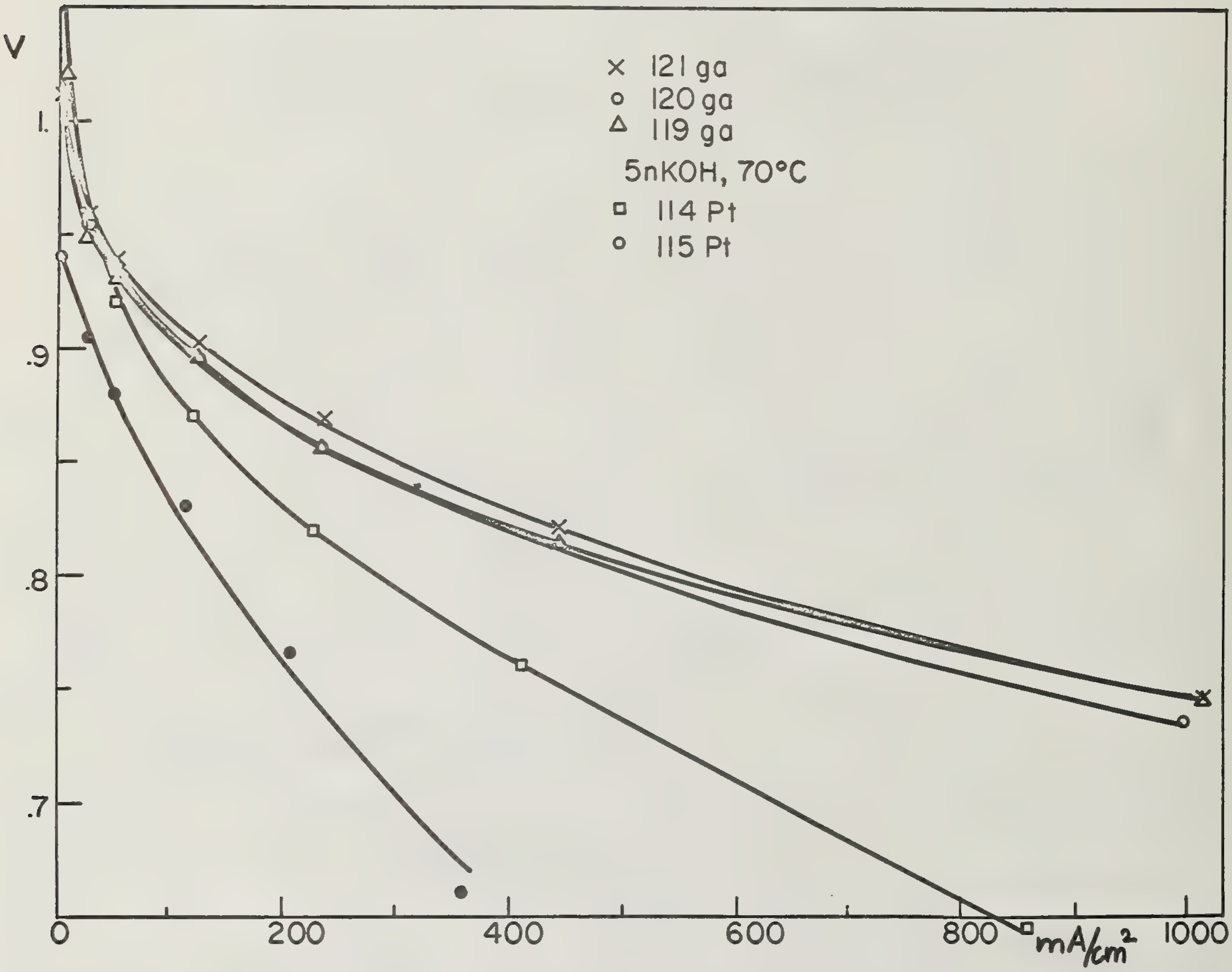

FIGURE 8. RESULTS OBTAINED WITH THREE SUCCESSIVE ELECTRODES WITH AuCu PLUS 22 AT % Ga.

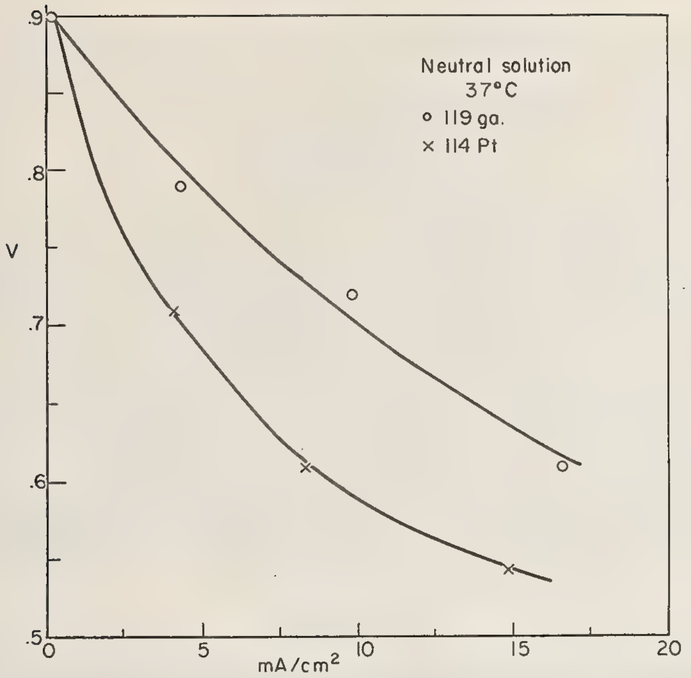

FIGURE 9. COMPARISON OF RESULTS OF #119 Ga AND #114 Pt.

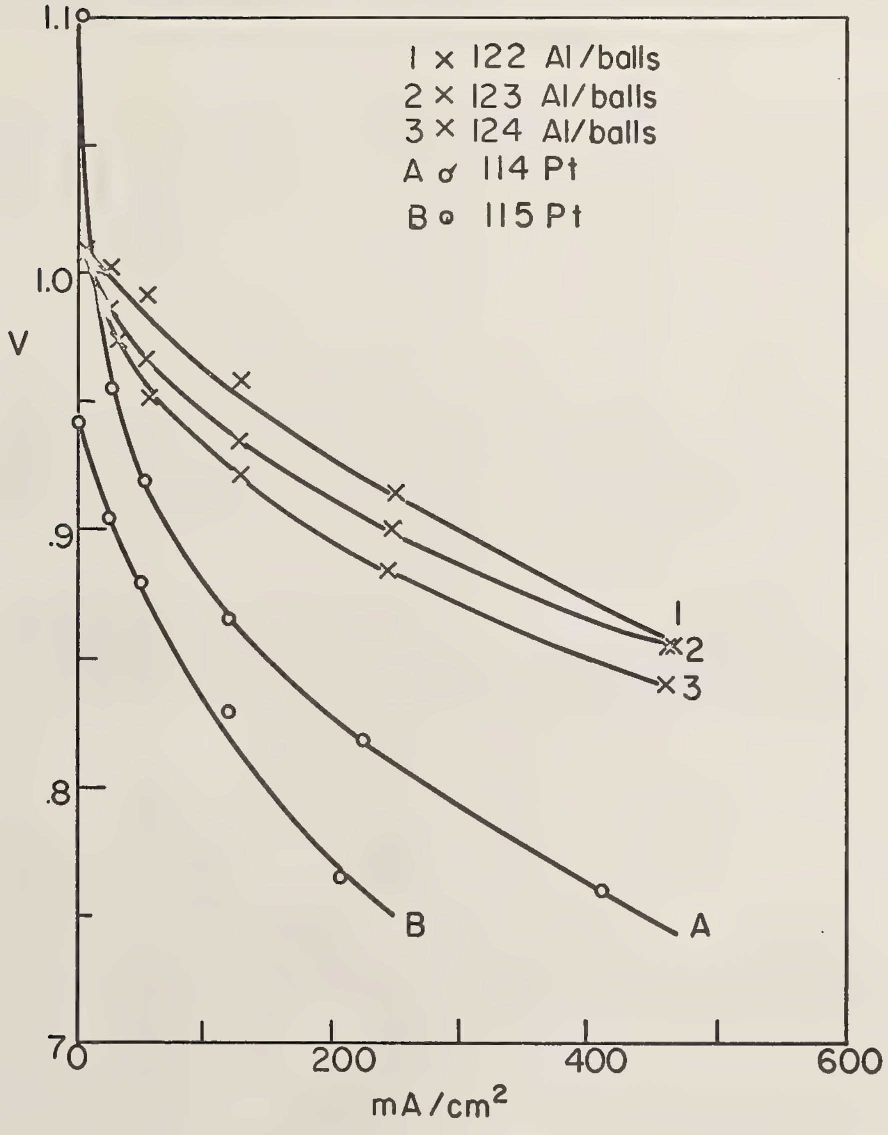

FIGURE 10. RESULTS WITH AuCu.

The spacing was 30 mils of fuel cell asbestos. The temperature was approximately 70°C, the electrolyte 5 N KOH. Note that the results for the three electrodes are nearly identical.

For comparison we also show the results obtained with Pt black similarly mounted. Not only are the results obtained with Pt black markedly inferior, but also they show a larger spread in performance, about 2 to 1. Even greater spreads are characteristic of blacks. This is important because a designer confronted with such characteristics knows that if he chooses a medium value as a design target, he more than doubles the cost of the electrodes.

The catalyst exceeds Pt by a factor of 2 to 3 through most of the useful range. Moreover, a further improvement in performance is expected. It should be possible to reduce the grain size, now about .5μ, to about .05μ. The resulting increase in current should be roughly proportional to the decrease in grain size. Figure 9 compares the results between our #119 Ga and #114 Pt shown on the preceding figure, but the electrolyte is now neutral (pH 7.39 at 35° C), and the temperature is body temperature (36 - 37° C). The currents therefore are very much reduced. Note that the horizontal scale extends only to 25 ma/cm^2 instead of 1 a/cm^2. However, the current ratios between the two curves remain about the same as before. Thus with further decreases in catalyst size more satisfactory current levels can be expected.

Finally in Figure 10 we show our most recent results obtained with AuCu, Al doped. The conditions are similar. These represent a considerable improvement on the curves shown in Figure 8. Compared to Pt the current advantage averages about a factor of 6. Power densities of about .25 watts at .7 V and .7 watts at .8 V are being obtained. Corresponding increases may be expected in neutral solutions.

CONCLUSIONS

It has been shown that advantages obtained in developing catalysts to work for O_2- H_2 fuel cells will extend to biological fuel cells when the requirement of near neutrality of the electrolyte is mandatory. All the preceding work refers exclusively to the oxygen electrodes. Since the final fuel to be burnt is not going to be H_2 but glucose, the limitations at the fuel electrode are also severe. Some progress has been made in understanding the requirements of a catalyst for a glucose electrode. New catalysts designed to improve its performance are being developed.

ACKNOWLEDGEMENT

This work was supported partly under NIH Contract PH43-68-1417 and partly under NASA Contract NAS7-574.

DISCUSSION

DR. STONER: I hate to argue with success; however, the concept of electrocatalysis is wrong from the view of gaining energy for electron transfer at one electrode since you must eventually put the electron back into the system at the other electrode. The best catalyst for a given electrode reaction will be one whose coverage or adsorption behavior is idealized; i.e., one which significantly adsorbs reactants and desorbs products. Perhaps you have achieved this is your copper-gold electrodes.

DR. BOCCIARELLI: I think I can anser some parts of your question, but not all of it. First of all, yes we do expect to develop hydrogen side electrodes also. Second, there may be some truth to what you say, but we have improved the electrocatalyst relative to standard hydrogen electrodes. All we did was on the oxygen side.

CHAPTER 73

IMPLANTABLE FUEL CELL FOR AN ARTIFICIAL HEART

R. Drake

Monsanto Research Corp.
Boston Lab.
Everett, Massachusetts

Research and analysis has required a substantial modification of the original neutral electrolyte cell concept that involved free solution exchange at flat, planar electrodes. Problems with mass transfer of reactants and products, electrode kinetics at neutral pH, and non-selective catalysts have led to the design and evaluation of an "acid" electrolyte cell (pH = 1.4) that requires phase separation of gaseous O_2 at the cathode and hydrogen from dextrose at the anode through a Pd foil. Prototype cells have been designed that have performed in vitro at 0.6 volt/cell at 50 $\mu a/cm^2$ with flat electrode structures. Design studies are underway to extend this performance by providing larger exchange surface areas in the electrode structures. An in vitro and in vivo evaluation of these prototype cells is planned as well as for a "second generation" prototype in which the results of a component optimization study are included.

INTRODUCTION

For the past three years, Monsanto Research Corporation has been determining the feasibility of, and defining and seeking solutions to the problems in developing, a completely implantable, trophically energized fuel cell power supply for an artificial heart. Initial analysis showed that to avoid a permanent epithelial penetration, blood carbohydrates and blood oxyhemoglobin-O_2 were the only feasible reactants.

PRELIMINARY MODEL SYSTEM

In order to define problems and organize the research effort, a model system was proposed very early in this work[1]. That concept (Figure 1) considered only a very simple unit cell composed of two juxtaposed, porous, hydrophilic electrodes covered with blood compatible, permeable membranes through which reactants and products freely diffused. The electrodes are separated by an electrolyte member in ionic equilibrium with blood (i.e., pH = 7.4). The model was used to calculate the dimensions of the physical, electrochemical and physiological parameters and constraints in the system allowing an assessment of the major problem areas requiring attention.

These are, in general, the electrokinetic and mass transfer limitations in utilizing the unique reactants in the blood stream at their relatively low prevailing concentrations and in the highly specialized environment in which the fuel cell must operate.

Research effort was directed toward developing and evaluating electrode structures and catalysts adapted for this application, determining the rate limitations at each electrode, and evaluating the limiting mechanisms.

The results of this research and further analysis indicated, in our opinion, that any module developed using the concept outlined previously had a low probability of successfully producing the required electrical power (5-20 watts) in a volume sufficiently small to be implantable (<100 in^3 est.). This judgment was based on the following facts:

1. Pt is the only O_2 reduction catalyst that really performs well in any fuel cell and it is very susceptible to "poisoning" by reducing agents in the blood (i.e., mixed potential reaction kinetics).
   For example, a Pt/Pt electrode in an aerated stirred phosphate buffer solution containing 0.5M dextrose acquires an open circuit potential at least -0.6v from R.O.E.[2]
2. The transport of oxygen from blood is highly mass transfer limited, the largest resistance existing in the molecular O_2 diffusion layer in the plasma. The exchange surface areas associated with a flat planar electrode geometry are not large enough to supply the oxygen requirements.
   It can be calculated that if the O_2 diffusion resistance is similar to that encountered in membrane oxygenators (as it should be since the plasma diffusion layer is the largest component of resistance and is common to both) the limiting current density to be expected is two orders of magnitude below that required in the model (i.e., 0.3 ma/cm^2 vs. 30 ma/cm^2 required).[2,3,4]
3. The reduction of gaseous O_2 in neutral electrolytes is severely limited by "pH polarization"--a build-up of product OH^- due to poor buffering kinetics.
   Figure 2 provides documentation for this statement. The data is for a porous gas diffusion electrode and shows that larger polarizations are encountered in neutral electrolytes. There is nearly 7 orders of magnitude difference in the rate constants for the reactions of hydroxyl ion with CO_2 and hydrogen ion respectively, indicating the reasons for the lack of buffering.[5]

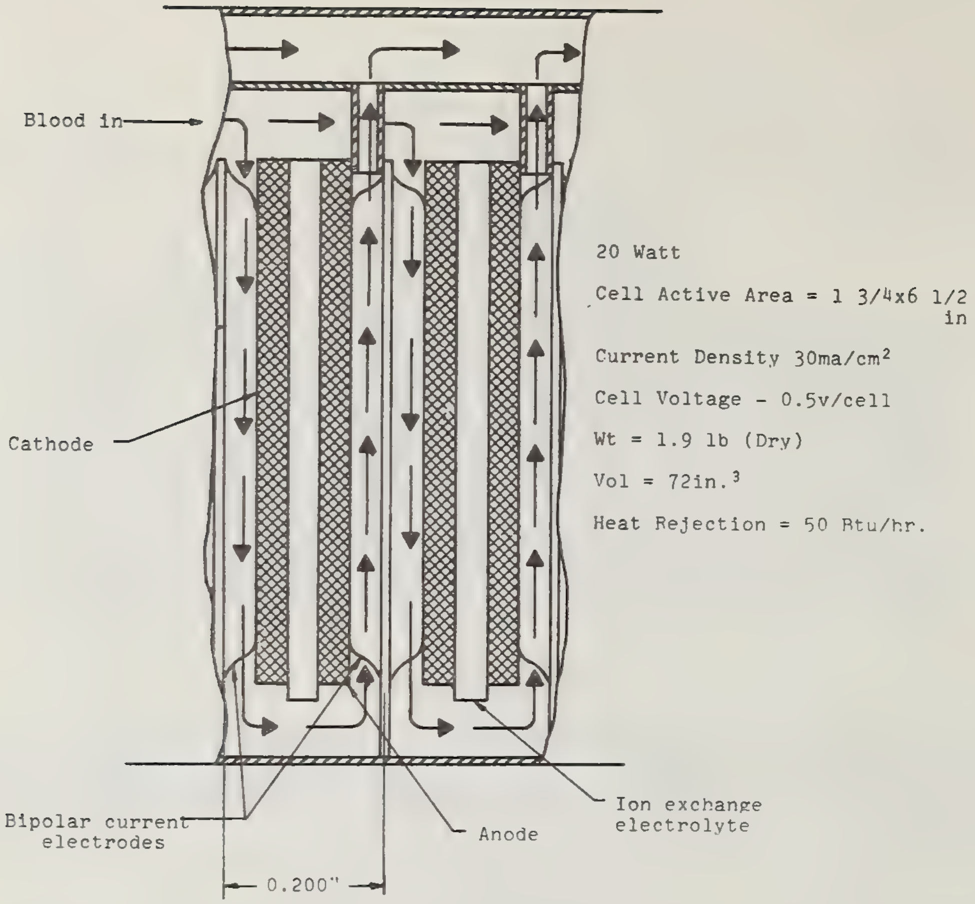

FIGURE 1. DESIGN CONCEPT FOR FUEL CELL POWER SUPPLY FOR AN ARTIFICIAL HEART.

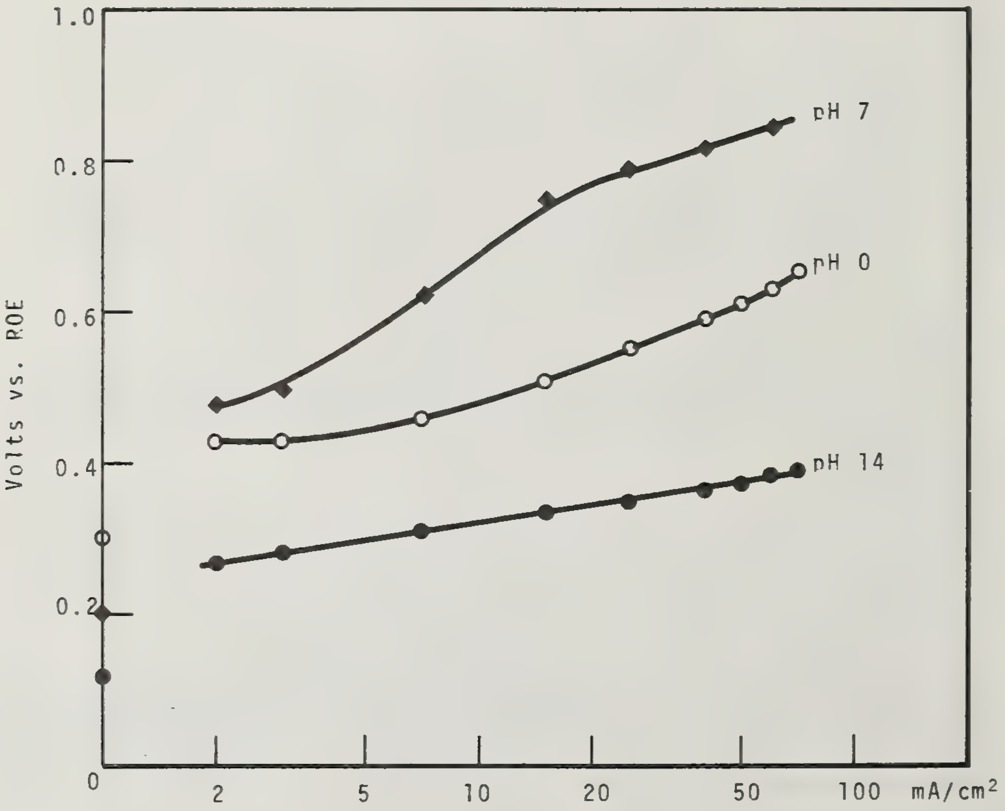

FIGURE 2. TAFEL PLOTS OF REDUCTION OF OXYGEN AT MRD-Pt ELECTRODES AS A FUNCTION OF pH.

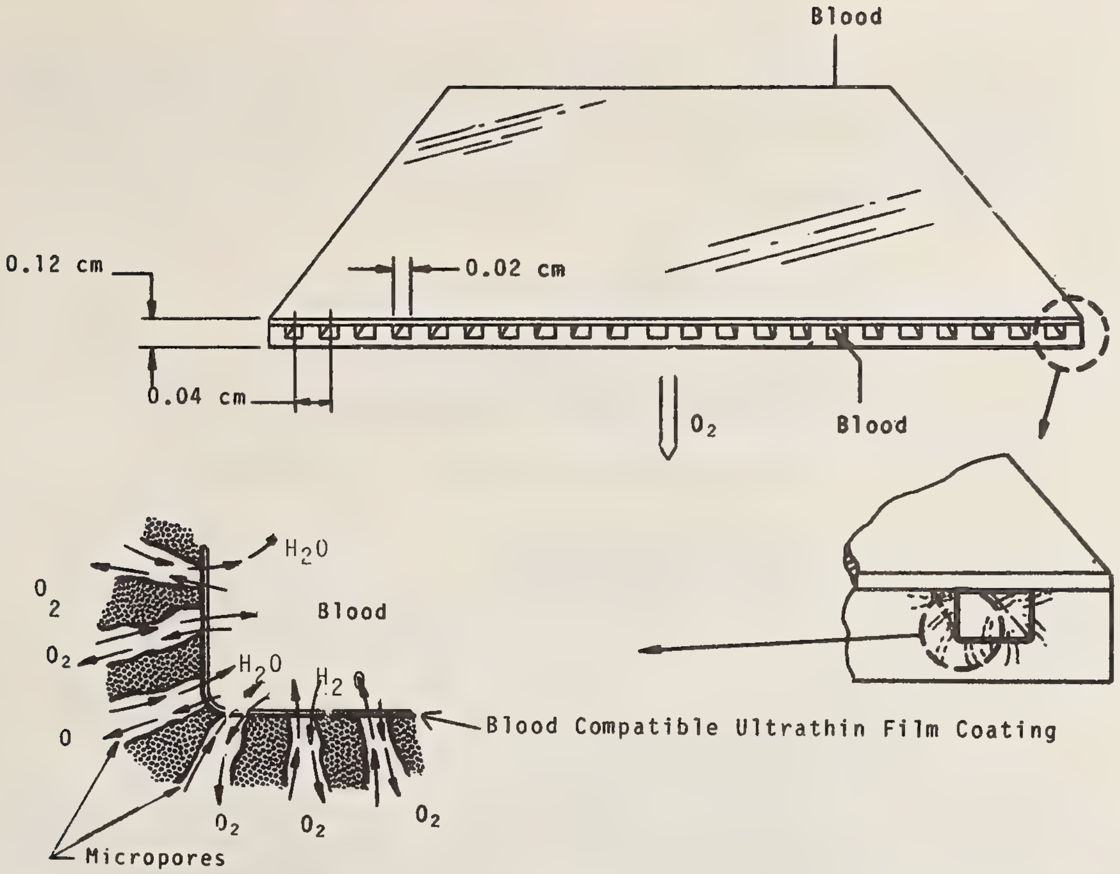

FIGURE 3. ULTRATHIN FILM COATED CAPILLARY MEMBRANE DEOXYGENATOR (CONCEPTUAL SKETCH).

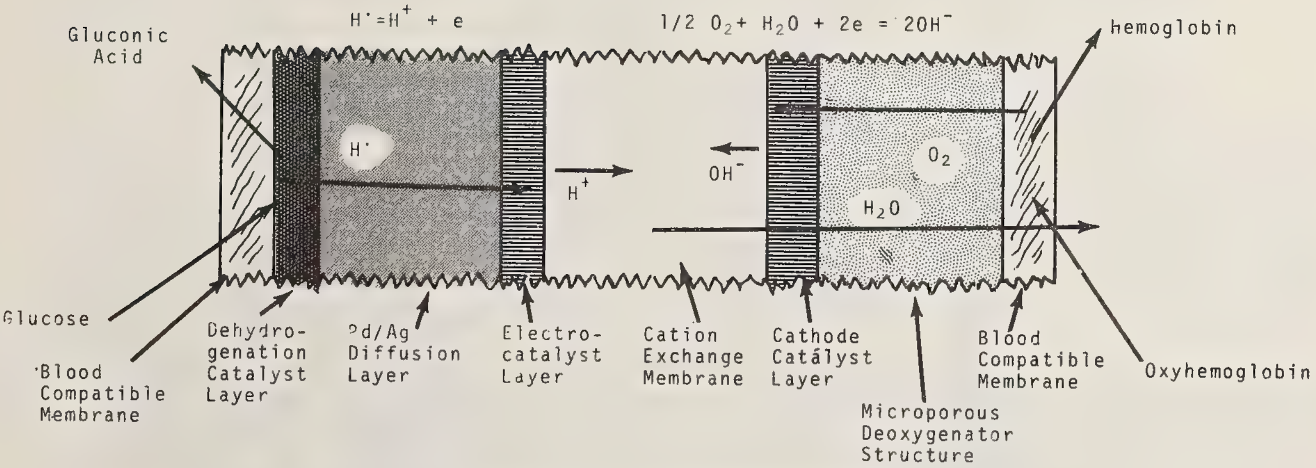

FIGURE 4. Pd DIFFUSION CELL SCHEMATIC.

4. The electro-oxidation of dextrose on the best electrodes is limited by mass transfer both of the dextrose itself (because of low prevailing concentration) and of the product gluconic acid that adsorbs strongly on the electrode in the potential region of interest.[6] Flat planar electrode geometry may not supply sufficient exchange area to alleviate these problems.
   For example, the maximum diffusion layer thickness can be calculated from:

$$\delta = \frac{D_L \Delta C}{\vec{N}_G}$$

where $\vec{N}_G = \frac{I}{nFA} = 15 \times 10^{-8}$ g-moles/cm^2-sec

for 30 ma/cm^2 and a 2e dextrose oxidation

D_L = dextrose diffusion coefficient in the diffusion layer

$\simeq 1 \times 10^{-5}$ cm^2/sec

ΔC = concentration gradient

$= 1 \times 10^{-5}$ moles/cm^3 maximum

$$\delta = \frac{10^{-5} \times 10^{-5}}{15 \times 10^{-8}} = 6.7 \times 10^{-4} \text{ cm}$$

This is very close to 10^{-3} cm, the usual limit assumed for vigorously stirred solutions.[7]

REDESIGN CONSIDERATIONS

Two approaches are possible in attacking these problems. One modification would provide a completely porous, flow-through cell in which the A.-V. pressure differential would be used to hydraulically "pump" blood or a blood dialysate through the cell. The resulting flow would certainly promote the necessary mass transfer processes (the improvement depending greatly on the degree of local convective mixing realized at the active surfaces). However, the problems associated with cathode poisoning by dextrose or other oxidizable constituents would be alleviated only to the extent that the concentration of these constituents could be reduced by passage through the anode first. The feasibility of this approach seems to us to rest on the discovery of much more selective electrode catalysts. Preliminary evaluation of the most promising new O_2 reduction catalysts developed in house and reported in the fuel cell literature (e.g., Au, Ag, Pd, Pt alloys, transition metal additions to noble metals, O_2 carrying chelates, tungsten bronzes, special carbons such as "blood char") was not promising.[2]

The other approach that we have emphasized attempts to solve these problems by:

1. Alleviating the mass transfer limitations through capillary flow electrode structures in which the exchange surface area/unit bulk volume ratio is high and convective mixing at the capillary walls is promoted by the hemodynamic shear developed by the flowing stream.
2. Phase separation of both reactants and complete solution isolation of the fuel cell electrolyte allowing the use of a lower pH electrolyte (e.g., a cation exchange membrane) in which the performance of Pt catalyzed O_2 reduction electrode is greatly improved.

Phase separation of gaseous O_2 from flowing blood is relatively easy to visualize as simply running an artificial lung in reverse. The specific capillaried structures have been demonstrated on a concurrent oxygenator contract and the operating principle is shown in Figure 3. As O_2 is reduced at the catalytic surface, an O_2 gas partial pressure gradient is established in the microporous substrate and this serves as the driving force to transport O_2 to the catalyst and, ultimately, to deoxygenate the blood flowing in the capillaries. As will be shown later, H_2O is the only product of the cell reaction and is removed via vapor phase counter diffusion in response to P_{H_2O} differences between the cell electrolyte and the flowing blood.

The question of whether specific deoxygenator structures can be produced that supply sufficient gaseous O_2 to support the cell reaction in bulk volumes small enough to be implanted has been explored.[2,4] In brief, the feasibility, given the current state-of-the-art in the relevant materials technology, may rest with the value of the total effective diffusivity of O_2 in blood including facilitated transport mechanisms. This value and its variation with physiological and physical parameters is not well characterized at present.

The phase separation at the anode involves a combination of a carbohydrate dehydrogenation catalyst and a solid Pd-Ag diffusion foil that transfers the abstracted hydrogen to a hydrogen oxidation catalytic layer on the other (electrolyte) side of the foil.

A schematic of the operating principles of the proposed cell is shown in Figure 4.

The composite anode is intended to be used with a hemodialysis membrane that screens out the cellular and high molecular weight elements but allows the diffusion of the carbohydrate fuel into the catalyst layer where the fuel undergoes a dehydrogenation reaction. For example, dextrose is converted to gluconic acid, that counter-diffuses back through the membrane, and an adsorbed hydrogen

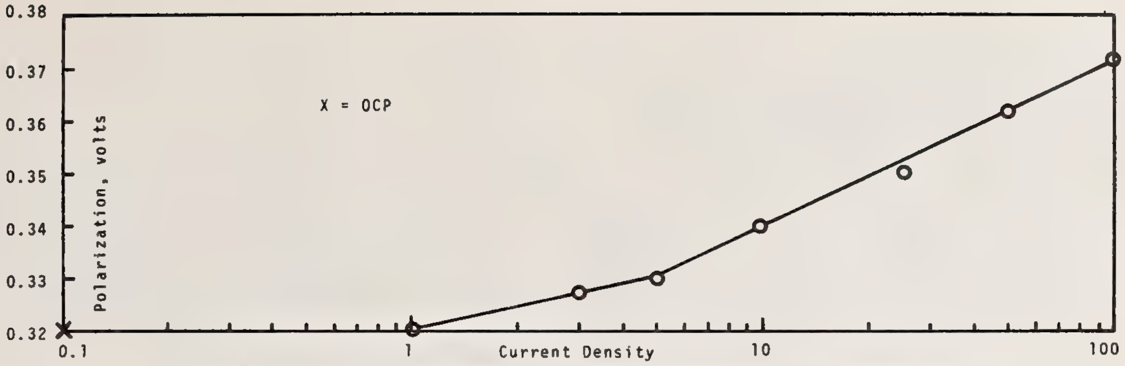

FIGURE 5. POLARIZATION CURVE - O_2 REDUCTION SOLUTION. STANDARD CELL.

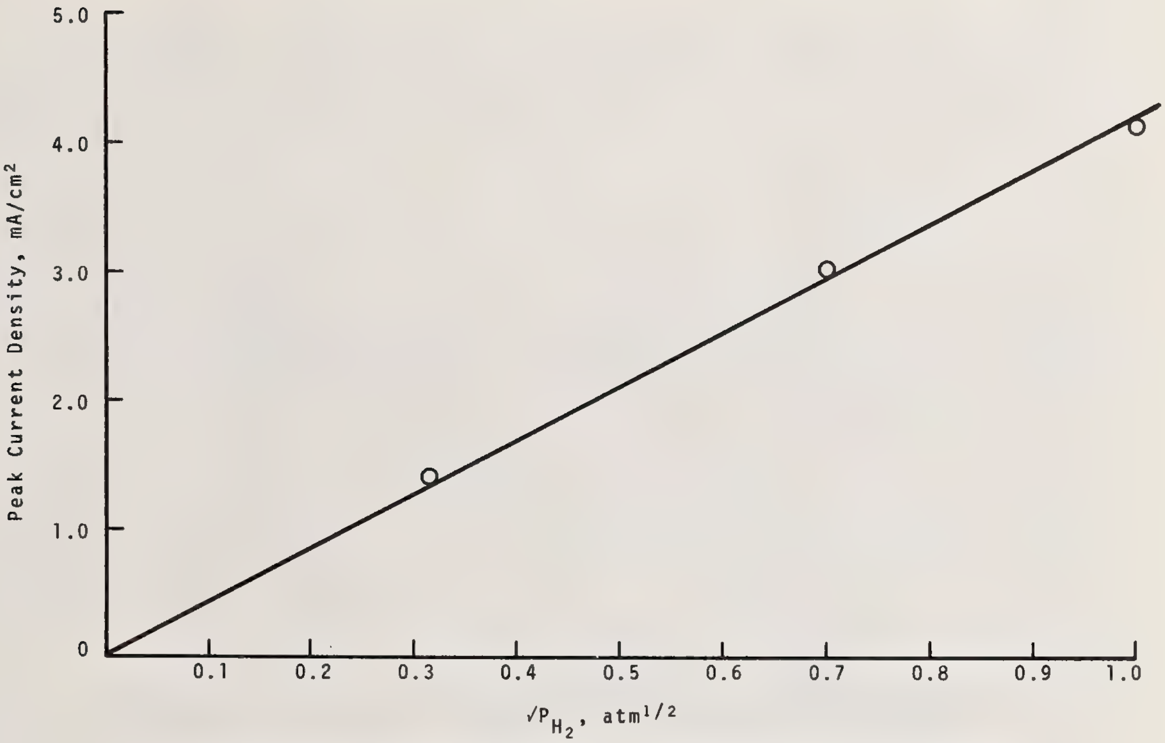

FIGURE 6. EFFECT OF PARTIAL PRESSURE OF HYDROGEN OR PEAK CURRENT DENSITY.

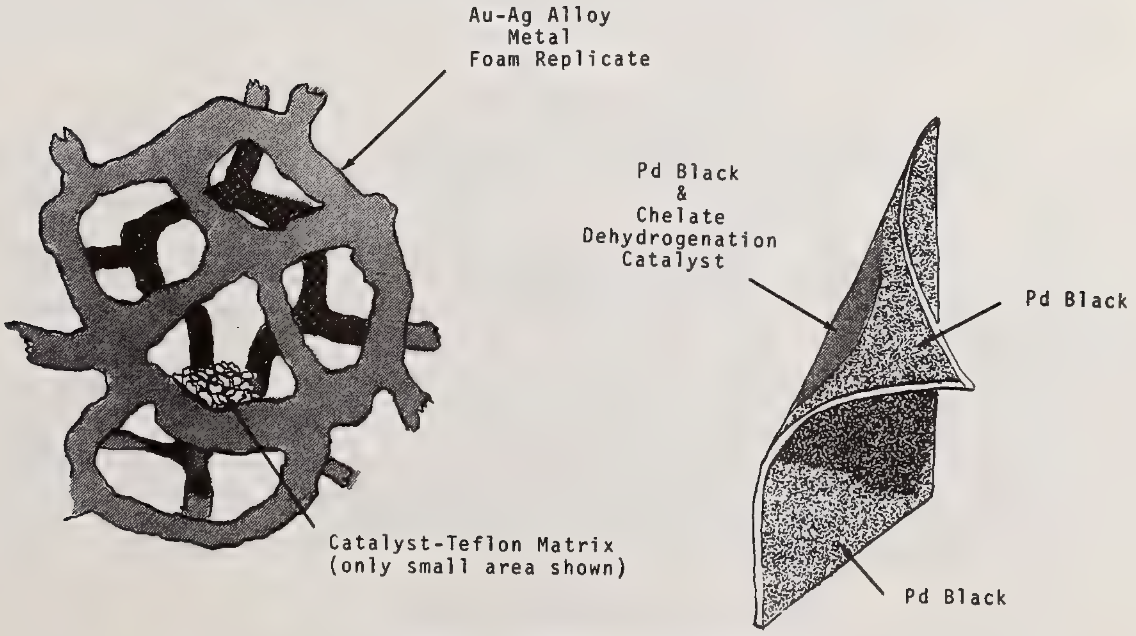
Au-Ag Alloy Metal Foam Replicate
Pd Black & Chelate Dehydrogenation Catalyst
Pd Black
Catalyst-Teflon Matrix (only small area shown)
Pd Black

FIGURE 7. COMPOSITE ANODE STRUCTURE.

species. The hydrogen is absorbed into the Pd/Ag foil where it is transported through the foil in response to a concentration gradient, to the catalytic surface on the interior side. There it undergoes electro-oxidation to form hydrogen ion.

The third necessary component of the cell is the electrolyte-separator. Because of the phase separation of reactants, a completely sealed cell is used and the electrolyte can be at a different pH than that of the physiological environments. Ideally, a caustic electrolyte would be best for the O_2 reduction reaction, however a caustic electrolyte would eventually be neutralized by contact with gaseous CO_2 in the deoxygenator. An acid electrolyte approximately isotonic with blood is preferred (e.g., 0.17N H_2SO_4, pH = 1.4). This is conveniently supplied by a strong acid ion exchange membrane. As H_2O is produced in the cell reaction, the solution is diluted, increasing the P_{H_2O} above the electrolyte, thus providing the driving force for removal of product H_2O from the cell via counter diffusion through the deoxygenator.

DEVELOPMENT AND EVALUATION OF NEW DESIGN

Experimental work was aimed at answering several critical questions central to the operation of this type of cell.

1. Can O_2 in solution be utilized by a porous gas diffusion electrode? An experiment was run using a standard hydrophobic porous gas diffusion electrode (a proprietary electrode developed by Monsanto Co. for N_2H_4/air fuel cells consisting of a Pt black catalyst supported on a sintered polytetrafluoroethylene-carbon substrate). The electrode was tested with a 4% O_2-5% CO_2 gas mixture bubbled into a buffered saline solution on the uncatalyzed side and an acid electrolyte on the catalyzed side. Figure 5 is a polarization curve for this electrode and clearly shows that dissolved O_2 in the solution can serve as the reactant source.
2. Will sufficient hydrogen diffuse through a Pd/Ag foil at 37°C to support an electro-oxidation reaction? Pd-25% Ag foils 0.001" thick were oxidized in air at high temperatures to activate the surface and then tested in a half-cell unit in which one side was exposed to gaseous H_2 mixtures (Ar diluant) and the other to an acid electrolyte. The data in Figure 6 show that not only will hydrogen diffuse at this temperature but the process follows Siebert's law, indicating mass transfer rather than surface reaction control.
3. Can dextrose be efficiently dehydrogenated under physiological conditions and can the abstracted hydrogen species be transferred into the Pd/Ag foil? Most time and effort was expended on this problem this past year. The approach used was to study coordination compounds with known interactions with aldehyde groups (e.g., metal phthalocyanines, Cu salicylaldehyde and acetylacetone chelates, organometallic noble metal hydrides and phosphines) that could also be firmly deposited on Pd foils. Although some success was obtained, particularly when charge transfer mediators or "promoters" such as 2-hydroxypyridine or chloranil were included, the results generally showed low or irreproducible activities. The surface properties of the foil and the methods of cleaning and deposition were found to be quite critical.
   Finally, the combination of a proprietary noble metal catalyst with a chelate was found to have distinct advantages on a concurrent program.
   The specific structures used are shown in Figure 7. The solid foil is palladized on both sides and a chelate catalyst deposited on one side. An Au/Ag alloy porous matrix containing a noble metal alloy catalyst is spot welded to the foil.
   The results of a slow voltage sweep test on this electrode are shown in Figure 8 and clearly indicate that the process of dehydrogenation, diffusion of the hydrogen through the foil and subsequent electro-oxidation can be linked together to effect the desired phase separation.

COMPLETE CELL TESTS

In order to evaluate the basic feasibility of the new design, a simple single cell unit was constructed and tested (Figure 9). As can be seen, no attempt was made to provide high exchange surface areas by incorporating capillary flow channels, the cell was intended only to demonstrate the basic processes.

This cell utilized a standard, planar, hydrophobic, porous gas diffusion fuel cell cathode and a planar Pd-Ag foil anode with an integral dehydrogenation catalyst layer and a commercially available strong acid ion exchange membrane. When tested in an air-saturated, buffered saline solution containing 0.01M dextrose, performance levels of 0.6 v/cell at 50 μa/cm² were realized for over three thousand hours.

A separate evaluation under contract of the complex anode operation was made by testing a similar cell in a special rig that allowed the cathode surface to be exposed to air, thus greatly reducing the cathode polarization. The data in Figure 10 were taken with an unstirred buffered saline solution, 0.01M in dextrose, in contact with the composite anode. The results indicate that the anode is performing its multiple functions satisfactorily and that the major limitation on performance exists at the cathode. Further experimentation suggested that this limitation was primarily mass transfer resistance in abstracting the dissolved molecular O_2 from the solution.

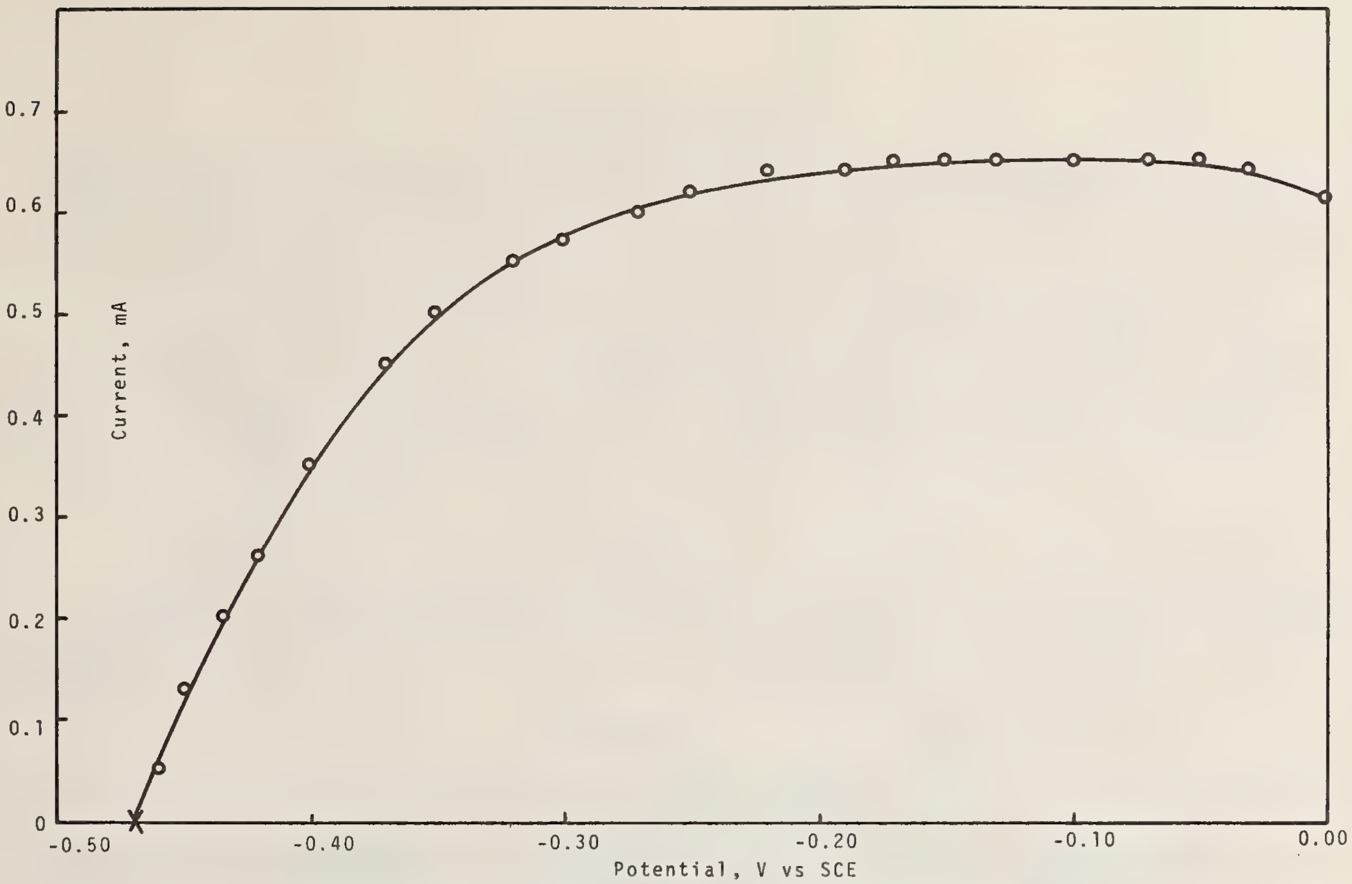

FIGURE 8. POTENTIOSTATIC SWEEP OF HIPORE (PROP. CAT)/(PdPc) Pd-Ag Foil-Acid Cell DEXTROSE CONS. = 0.5 M.

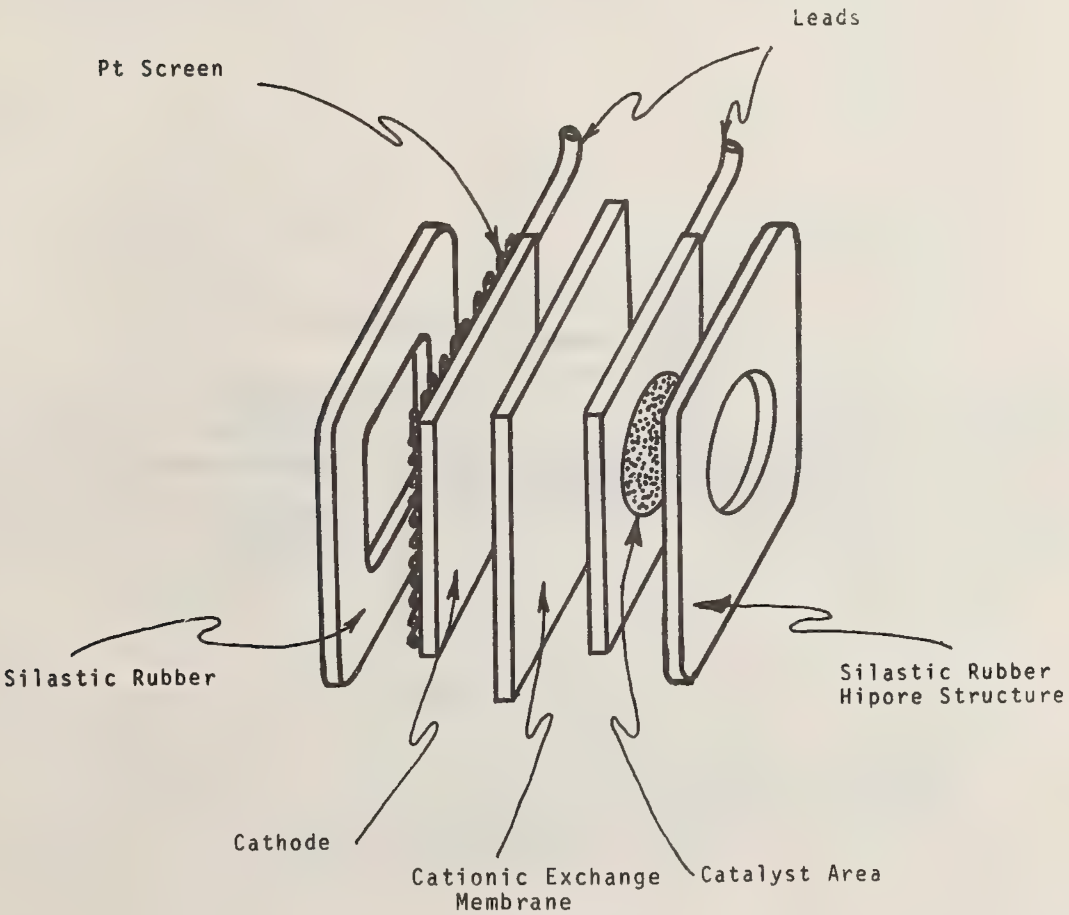

FIGURE 9. DIAGRAM OF ACID CELL.

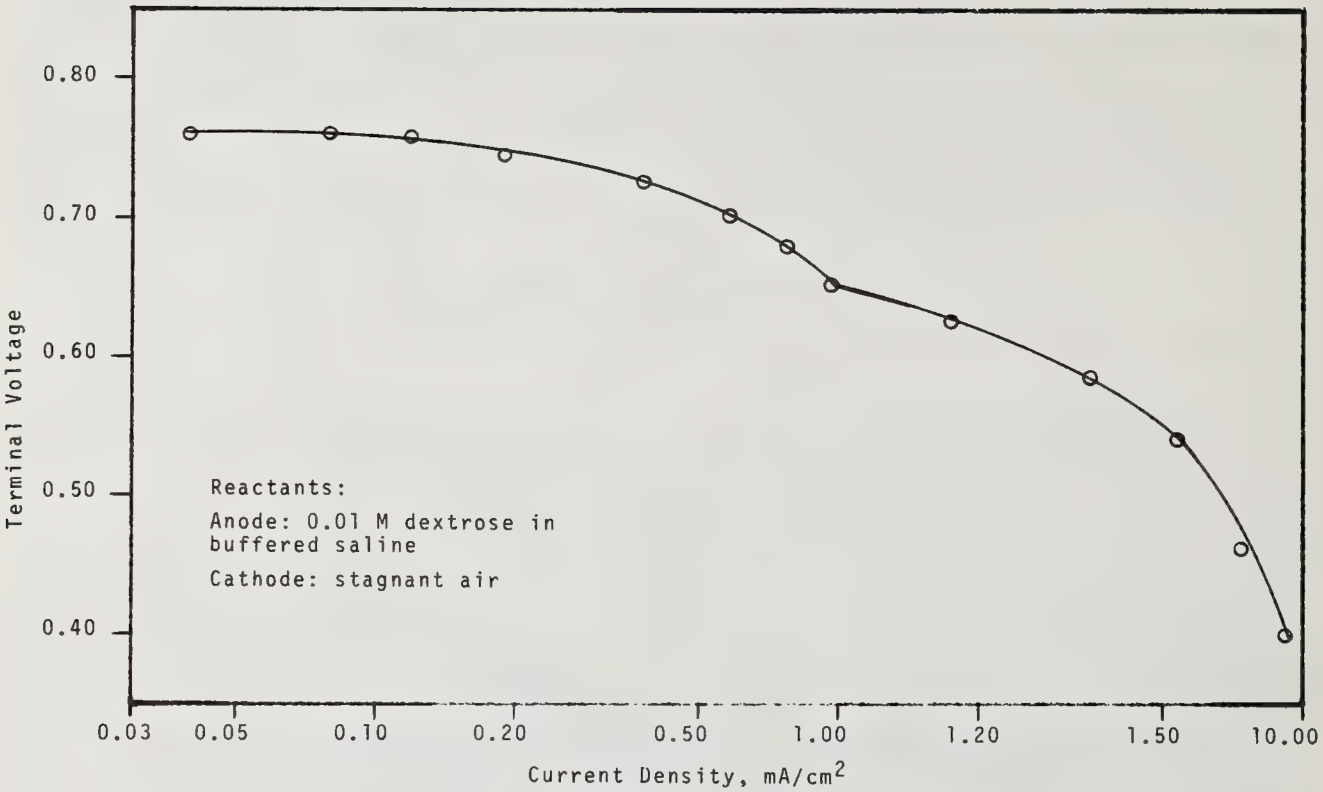

FIGURE 10. FULL CELL POLARIZATION CURVE.

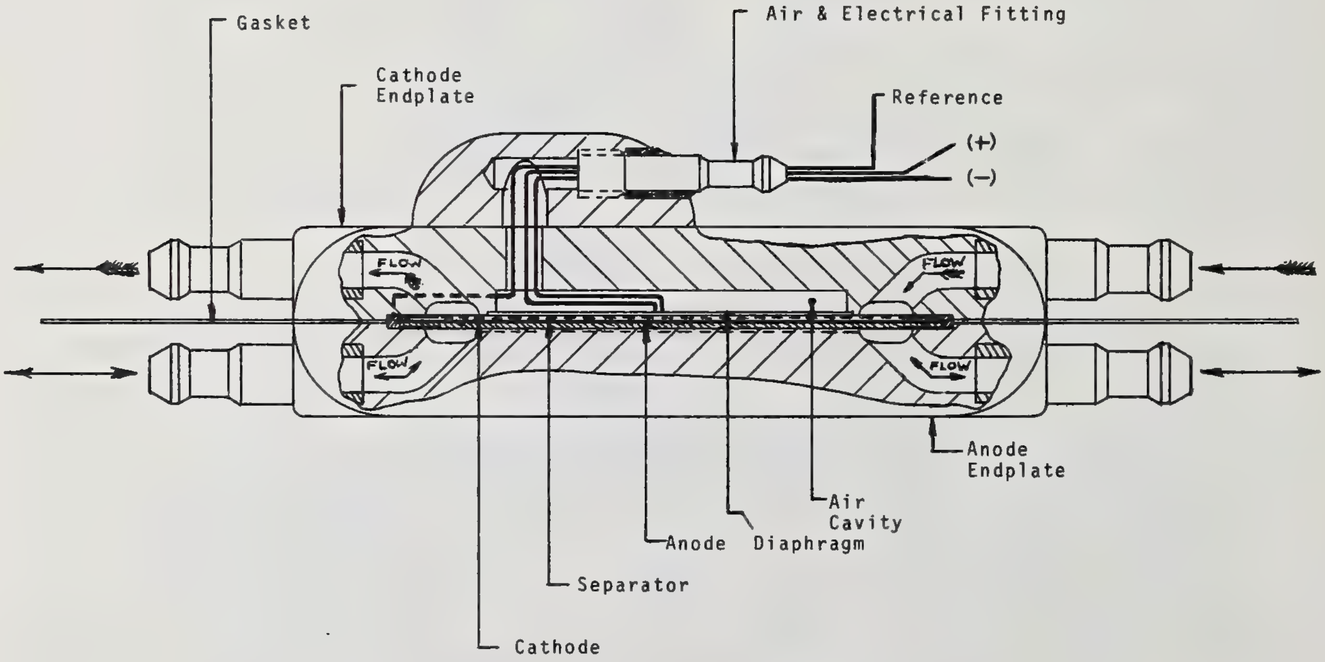

FIGURE 11. RESEARCH PROTOTYPE CELL.

PROTOTYPE IMPLANTABLE CELL

The results of this work were sufficiently promising to justify a proposed extension of the technology into a "first generation" paracorporeal and in vivo study aimed at demonstrating state-of-the-art performance with high surface area-capillaried electrode structures and acquiring a first look at problems inherent in actual operation in vivo on flowing blood. A single cell research prototype has been designed and a test program outlined (in concert with Dr. B. K. Kusserow, University of Vermont) to accomplish these objectives.

The cell design is shown in Figure 11. The deoxygenator capillary channels are formed by rolling grooves (8 mil x 8 mil) into the uncatalyzed side of the cathode prior to curing. The open side of the channels are sealed by an air pressurized silicone rubber diaphragm. Anode blood flow channels are machined into the endplates. The cell itself is compression edge sealed.

The planned test program includes in vitro tests with aerated buffered saline containing 0.01M dextrose, paracorporeal with dogs in a femoral artery to femoral vein shunt, and an intra-abdominal implantation study with a distal aorta to vena cava shunt.

ACKNOWLEDGMENTS

The author wishes to acknowledge the technical contributions to the program of S. Messinger, J. J. O'Connell, S. Matsuda, G. Arzoumanidis, M. Deibert, N. Masse, and D. Williams of the MRC Boston Laboratory Staff; C. Satterfield and C. Colton of MIT; and B. Kusserow of the University of Vermont. In addition, the support of Drs. Frank Hastings and Lowell Harmison of the Heart Institute is gratefully acknowledged.

REFERENCES

1. R.F. Drake, et al., First Annual Summary Report, "Implantable Fuel Cell for an Artificial Heart", 28 June 1966 to 28 June 1967, Contract No. PH43-66-976.
2. R.F. Drake, et al., Second Annual Summary Report, "Implantable Fuel Cell for an Artificial Heart", 28 June 1967 to 28 June 1968.
3. Dr. T. Kolobow, NIH, Washington, D.C., private communication, September 1966.
4. C.K. Colton and R.F. Drake; Analysis of In Vivo Deoxygenation of Human Blood: A Feasibility Study for an Implantable Biological Fuel Cell, Trans. ASAIO, in publication.
5. R.P. Bell, Quarterly Reviews, 169 (1959).
6. MLB Rao, R.F. Drake, Studies of Electrooxidation of Dextrose in Neutral Media, J. Electrochem. Soc., 116, 334 (1969).
7. S. Glasstone, An Introduction to Electrochemistry, D Van Nostrand,1942, pp. 448-452.

DISCUSSION

DR. MRAVA: Can you tell me if any of your planned in vivo testing will incorporate the capillary type deoxygenator?

DR. DRAKE: Yes it will.

DR. MRAVA: In its very next phase?

DR. DRAKE: In its next phase, yes.

DR. MARTINI: Can you tell me what you're hoping for in terms of watts of power output per square cm of cell area?

DR. DRAKE: In this particular unit?

DR. MARTINI: When it gets developed, yes.

DR. DRAKE: No, you're going to have to define that. I feel that this unit is simply a research prototype, not a finished unit.

DR. MARTINI: Well, in this last unit you described, what do you hope to get from that?

DR. DRAKE: This last unit which is the first research prototype; I guess it is really only fair to say, since it is the first attempt, that we will be satisfied with any power density that can be realized. The unit is designed to supply sufficient reactants to maintain a current density of 5 ma/cm^2. If we realize the same cell performance as in previous tests, the power density would be 2.5 milliwatts/cm? This assumes the mass transfer problems are completely solved, which is unlikely.

DR. OSWIN: I would just like to make a couple of comments on the mass transfer aspects which you have introduced into the new design. You stated that you plan to use forced convection to reduce the boundary layer thickness and thus increase the rate of mass transfer to the electrode but to do this you have introduced into the system two membranes which increase the thickness. The hydrodynamic conditions will not affect this extra barrier.

Secondly, it is very difficult to conceive of a membrane which will permit the perfusion of glucose to the palladium silver electrode without at the same time permitting the diffusion of oxygen. If both oxygen and glucose reach the electrode surface then you have the old problem of selectivity.

The last point I would like to make is: Have you calculated how much power you are going to need to pump the liquid through the capillaries at a rate sufficient to reduce boundary layer thickness significantly?

DR. DRAKE: The first question refers to the fact that we have developed capillary structures in order to solve some of the mass transfer problems but then added a couple of membranes which certainly increase the mass transfer problems. The membranes are there to completely isolate the electrolyte of the cell in order to operate at a lower pH because the oxygen reduction kinetics in neutral saline are so low. I assume by membranes you mean the palladium silver foil and the deoxygenator substrate material.

DR. OSWIN: The deoxygenator membrane and your hemodialysis membrane.

DR. DRAKE: Oh, the dialysis membrane. We will eventually need a completely blood compatible surface. I can state almost categorically that neither the oxygenator substrate nor the catalyst layers on the anode side are going to be permanently blood compatible surfaces. What I envision for these membranes eventually is something like a layer of tissue cultured endothelial cells that would be 15 to 30 microns thick but continuous over the blood contracting surfaces. A 15 micron layer certainly does have some mass transfer resistance but not like a 1 mil cellophane membrane. To answer your second question concerning the presence of oxygen and glucose at the palladium-silver foil simultaneously, both species certainly diffuse through the dialysis membrane. However, the concentration of dextrose is an order of magnitude above the concentration of dissolved molecular oxygen in blood plasma, i.e., 10^{-2} moles/l for dextrose and 10^{-3} moles/l for oxygen. If the diffusion coefficients are approximately the same the concentrations at the catalyst surface will be in the same ratio, and the dehydrogenation reaction should dominate.

DR. OSWIN: Well, the power is really the point. Have you calculated how much extra sort of power you are going to need? What sort of power are you going to need to get effective flow through the capillaries?

DR. DRAKE: The pressure drops through the capillaries are actually very small. We have done a study that was reported at the last ASAIO meeting by Clark Colton in which we developed a model system based on Buckle's work but aimed specifically at deoxygenation rather than oxygenation. We find that there are many problems but that the pressure drop through the capillary structures is quite modest. And, of course, the pumping power requirements are directly proportional to the pressure drop.

DR. GINER: I want to make a comment on the 2.5 milliwatts per cm^2. I think this is a conservative estimate, and that a complete module would produce good power. If, for example, you use 10 cells of about 10 x 10 cm. and these can be made very compact, you get about 2.5 watts, which is sufficient to supply the needs of a sleeping man. The 7 watts that are needed for an awake exercising man is within reach. I hope we can do very much better than that but I will say in essence it's not as bad as people working with bigger fuel cells may think.

DR. DRAKE: I do not want to be held to that 2.5 milliwatts per square cm. for these initial tests. I said at the time that if we got the same kind of cell performance that we did in vitro work with the mass transfer problem solved, it would be 2.5 milliwatts per square cm.

DR. GINER: I make this comment because I have heard many of my colleagues working on other types of fuel cells. for example, a 500 watt cell, that they are quite skeptical but they do not realize that we need only about 7 watts or something like that.

DR. DRAKE: 7 to 20 watts.

DR. GINER: You could take double the number of cells and can build them very, very close.

DR. DRAKE: The cells that we are presently working with are about 30-35 mils thick.

DR. MARTINI: This includes blood passages and everything?

DR. DRAKE: Not in the prototype, no. It does not. I'm talking about a single cell.

DR. MARTINI: What would be the center distance between one cell and the next one?

DR. DRAKE: We are talking about a single cell - we are not trying to build modules at this stage. I would not even guess on what the center to center cell dimension might be in a multi-cell module. We feel that a unit to be implantable has to be under 100 cu. inch in volume. The largest volume contribution in the type of cell we are considering is taken up by the deoxygenator structures themselves. We need a tremendous amount of surface area to get the required oxygen exchange. We feel that it is feasible to provide that surface area within bulk volumes under 100 cu. inch. It has not yet been done, but it is feasible.

DR. URBACH: You alluded to the pressure drop in your oxygen system. Now, the oxygen partial pressure in the blood is somewhat less than one fifth of an atmosphere, and you are going to have a fairly low pressure at the cathode. Therefore, there are possibilities for accumulations of all sorts of partial pressure, that is of other constituents. Have you considered these?

DR. DRAKE: Yes, the other partial pressures really are only nitrogen, carbon dioxide, and water. The acid electrolyte is carbon dioxide rejecting. This is why we did not use a caustic electrode, which would have performed better electrochemically, but which would have been neutralized eventually by contact with CO_2.

DR. URBACH: In practical fuel cell devices we find that very small fractions of impurities in oxygen accumulate. A poisoning or blanketing effect results from the impurities. This in turn ultimately leads to impairment in the function of the cathode, and you have to do something about this.

DR. DRAKE: The cathodes we are using are the cathodes that were developed by the Monsanto Company for their hydrazine air fuel cells. These have been operated for literally thousands of hours on impure air supplies with very little impairment of performance. I think one possible explanation is that there is so much platinum catalyst on these electrodes. I am not prepared to say what happens when these impurities have to be volatile in order to be eliminated from the interior of the cell. Any contaminant would have to be in the vapor state to reach the cathode catalyst surface anyway.

SECTION XI

EFFECTS OF ADDITIONAL ENDOGENOUS HEAT

Chairmen: Roger S. Powell
Lowell T. Harmison, Ph.D.

INTRODUCTION

An artificial heart system will necessarily consist of several sub-systems such as: the blood pump, an energy supply or storage system, a system to convert stored energy for input to the blood pump, and a control system. These systems may be based upon various physical principles and operating concepts but whatever these principles and concepts, the efficiencies of the various components will be less than 100% and therefore heat will be liberated in their operation. In addition, some of the operating concepts which are under consideration contain Carnot cycle heat engines and hence require a heat sink into which waste heat can be rejected. Heat from both sources will be released into the body, either accidentally or intentionally. Studies are currently underway to determine the physiologic effects of heat and to define the limits on temperature and total thermal energy that may be dissipated in the body.

CHAPTER 74

STUDIES ON THE EFFECTS OF ADDED ENDOGENOUS HEAT AND ON HEAT EXCHANGER DESIGNS

M. F. Gillis and P. C. Walkup

Battelle Memorial Institute
Pacific Northwest Laboratories
Richland, Washington

In order to define limits on tolerance of added endogenous heat from an internal source, using blood as a coolant, electrically energized heaters were surgically implanted in the descending thoracic aorta of miniature swine and power levels of 0 to 60 watts (0-4.7 watts/cm^2 flux, 0-1.1 watts/ kgm body weight) applied for periods up to and exceeding twelve months. High ambient temperatures (over 80-85^{O}F) or pyrexic states produce severe hyperthermia at the higher power levels, necessitating discontinuance of power to prevent death. Otherwise, no alteration of physiologic function has been observed. There are no gross or microscopic lesions unequivocally attributable to added endogenous heat, and hematologic/serum biochemical changes are minimal to absent in both heated and control (0 watt) animals. Gamma irradiation of implants (0.3 megaroentgens, cobalt-60) and nylon velour coating of percutaneous lead bundles has essentially eliminated problems of infection. A specially designed leather swine harness continues to be highly successful in extending percutaneous lead life and eliminating skin trauma. Extended area heaters having longitudinally finned lumens of carbon (antithrombogenic coating by Gulf Atomic Corporation) appear to be compatible with hemic and hemodynamic requirements as well as increasing heat transfer per unit length over straight tubular designs. Preliminary results with Dacron-flocked exchange surfaces *in vivo* indicate higher thermal resistances than previously predicted, creating serious concern regarding their applicability to artificial heart systems using heat cycle engines.

INTRODUCTION

In order to define the ability of a host animal to tolerate endogenous heat produced by an implanted source, using blood as a coolant, miniature swine were instrumented for long-term studies. In this third year of effort, major emphasis was placed on producing truly long-term preparations, allowing essentially uninterrupted continuance of added endogenous heat for periods in excess of 12 months.

Results of the first two years of study[1,2] indicated that miniature swine with implanted thoracic aorta heat exchangers could probably tolerate power inputs up to and including 60 watts (4.7 watts/cm^2 flux; 1.1 watts/kgm body weight) for extended periods without significant alteration of physiologic function, and the findings this fiscal year tend to confirm those predictions.

CONCLUSIONS

The following conclusions have been drawn from or further supported by the research of the past year:

Barring high ambient temperature, concurrent systemic infection causing fever, or occlusion of blood flow through the exchanger by thrombus formation at the junction of DeBakey prostnetic and aorta, Hanford Miniature Swine females weighing 53 to 80 kilograms can tolerate 60 watts added endogenous heat via a standard GBH heat exchanger placed in the thoracic (descending) aorta (4.7 watts/cm^2 flux, up to 1.1 watts/kgm body weight) for periods in excess of 12 months without gross alteration of physiologic function.

High ambient temperatures produce discomfort, increased respiratory rate and increased rectal temperature to an extent dependent on power level. Room temperatures in excess of 85^{O}F are generally intolerable for 60-watt animals, whereas 20-watt animals respond to increased ambient temperatures similar to 0-watt controls.

Added endogenous heat of 40 watts or more augments the febrile response of animals suffering from mild occult infection. Added endogenous heat at the rate of 60 watts so exaggerates the rise in body temperature associated with mild systemic infection that heater power usually must be temporarily discontinued to prevent severe hyperthermia. Hematologic and serum biochemical changes are minimal to absent in heated and control animals. Trends which do occur are slight and either occur in both heated and control animals or else are of questionable significance in light of statistical dispersion. Reticulocyte depression continues as an unexplained phenomenon in both control and heated animals.

Gamma irradiation of implants (cobalt-60 source) at the reduced exposure of 0.3 megaroentgens provides satisfactory sterilization of heaters and instrumentation for implantation in these studies, however, degradation of electrical leadwire and its insulation may still occur to a slight degree.

Nylon velour coating of percutaneous lead bundles and use of the specially designed leather swine harness[2,3] continues to prove highly successful in experimental preparations by extending percutaneous lead life, preventing lead track infection, and eliminating skin trauma. Multiple redundancy in percutaneous leads has reduced considerably the attrition rate due to percutaneous lead failure within the animal. This is barely satisfactory for our strict experimental purposes; it most definitely is not a satisfactory answer to the general and widely recognized problem of maintaining percutaneous lead integrity for long periods.

Extended area heaters having longitudinally finned lumens (carbon, antithrombogenic coating by Gulf Atomic Corporation) continue to appear to be compatible with hemic and hemodynamic requirements. Preliminary results with Dacron-flocked exchange surfaces indicate higher thermal resistances than previously predicted, creating serious concern as to the applicability of flock/tissue layer exchange surfaces to heat cycle engines.

DISCUSSION

Surgical Observations.

Thirteen implant operations were performed during the past year, all but four being standard GBH heaters interposed in the thoracic (descending) aorta following the procedures described in detail in annual reports for fiscal years 1967 and 1968.[1,2] No significant alterations in procedure were necessary; the Karajunction technique of Dacron prosthetic anastomosis and heater implantation continues to be highly successful, with surgical times seldom exceeding two hours (skin-to-skin) and surgical mortality zero.

Twelve of the above animals were subsequently put on experiment. In one case a special heater design was tried, consisting of a standard GBH heater around which had been bonded nylon velour fabric, fuzzy side out. This was to be a preliminary evaluation of a technique for providing mechanical support of implants having specific gravities much greater than one, the principle being to promote intimate bonding of the entire surface area of the implant with the surrounding fibrous scar tissue. Unfortunately the left lung became involved in the healing process, wrapping itself around the heater and attaching itself to the velour surface. The animal died three weeks later of acute pulmonary hemorrhage.

Ambient Temperature Effects.

As covered in previous reports, ambient temperature was observed to have a marked effect on respiratory rate and, at higher temperatures, on the ability of swine to tolerate their added heat load. Continued observations verify this phenomenon, a factor which may become of considerable practical importance in the adaptation of artificial heart power sources to human implantation. Some of the information gained during the past year on control and 60-watt animals is summarized in Figure 1.

Pyrogenic Hyperthermia Effects.

On several occasions we have observed heated miniature swine to exhibit fevers, apparently of infectious origin. Rectal temperatures rose to above 104°F and heater power was discontinued temporarily to prevent serious hyperthermia. An immediate lowering of rectal temperature was observed, though it remained high enough to suggest the continued presence of pyrogenic influences (above 102.5°F). In a few days this returned to normal, heater power was reinitiated without a subsequent rise to fever level, and the animal continued on experiment without incident.

This suggests that the added heat burden of a heat exchanger (or power source/energy converter) may become intolerable during mild fevers of pyrogenic origin. At least it can certainly be expected that the presence of the heat-producing implant will augment the effects of a hyperthermia of hypothalamic origin, regardless of the cause.

Subjective Observations on Ambient Temperatures and Fever.

It is possible to differentiate between hyperthermia due to added endogenous heat and febrile conditions arising from systemic infection. In the former, the animal attempts to compensate for the increased heat load: the skin is warm and respiration rate increases, even to the point of panting, while rectal temperature rises relatively little. In the latter, rectal temperature rises dramatically while respiratory rate continues to be similar to control animals in the same room; the skin may be quite cool to the touch, indicating an overall tendency to conserve rather than dissipate body heat.

Curious observations were made during a period of unusually cold weather when outside temperatures dipped to below or near zero degrees Fahrenheit and the cage rooms were frequently in the low sixties. Three 60-watt animals experienced fever and anorexia of unknown etiology during this time, and it became necessary to turn off heater power as rectal temperatures indicated approaching hyperthermia of serious proportions. In each case, recovery from the febrile condition (usually within 2 or 3 days) was accompanied by shivering, and the animal returned to 60-watt heating with apparent gratitude. Shivering ceased, the animal relaxed and slept. Control animals, on the other hand, are apparently as content at 60°F as at 75°F.

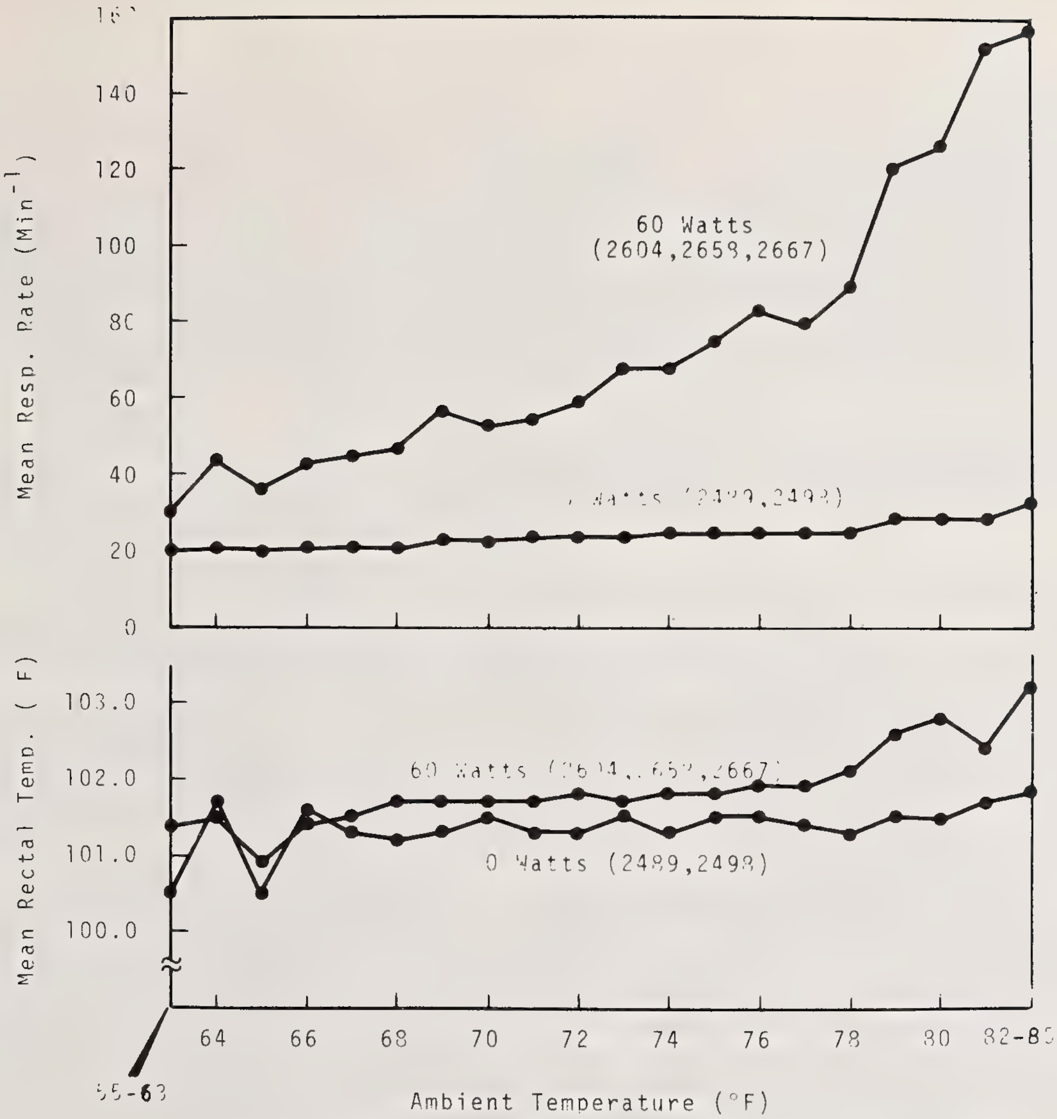

FIGURE 1. RESPIRATION RATE AND RECTAL TEMPERATURE VARIATION WITH AMBIENT TEMPERATURE FOR THREE 60-WATT AND TWO CONTROL (0-WATT) ANIMALS. MEANS PLOTTED ARE DERVIED FROM OVER 1000 DATA FOR 60 WATTS AND OVER 600 DATA FOR CONTROLS.

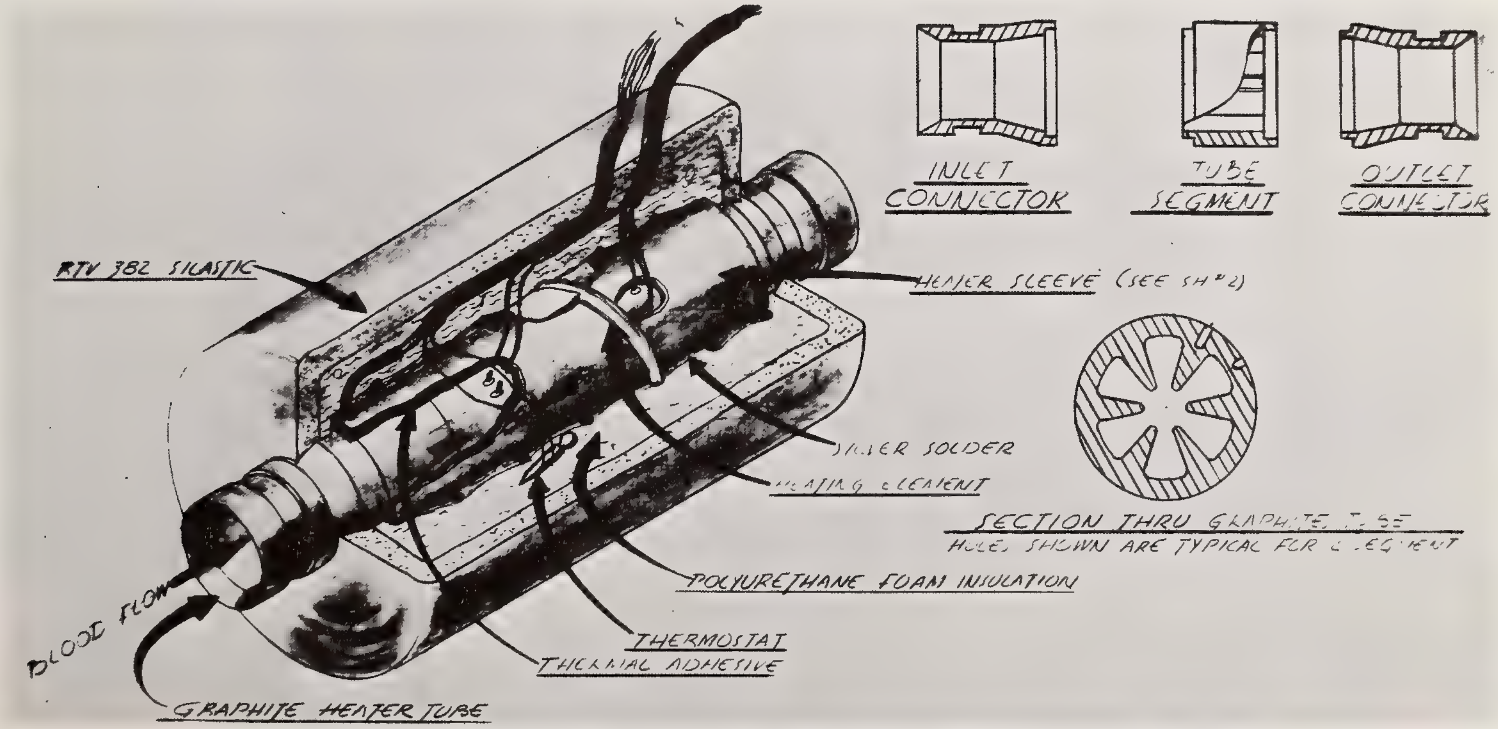

FIGURE 2. HEATER ASSEMBLY - EXTENDED AREA (INTERNALLY FINNED) HEAT EXCHANGER.

Hematologic Observations.

Changes in the hemogram of heated and control animals are generally slight to absent. Packed cell volume (PCV), hemoglobin, erythrocytes (RBC), eosinophils and immature forms experience only transient postsurgical changes. Basophils and monocytes show no significant change. Reticulocyte depression, reported previously, continues to be seen and has yet to be explained. It occurs in both control and heated animals, suggesting that the cause is either cage confinement or the presence of the foreign body implant, or both. A slight depression in total leukocytes is seen which has not been previously reported. This occurred only in heated animals, involving a loss of segmented neutrophils and, to a slightly lesser degree, lymphocytes. The data are not unequivocal at this point, and verification of such a trend must await collection of additional data on very long-term animals.

Serum Biochemical Observations.

Serum biochemical changes in long-term 60-watt animals are generally absent. Previously reported elevations (inconsistent) in gamma globulin are once again seen in all animals, including controls, but the means usually agree with presurgical values within standard deviation.

Necropsy Observations.

Gross Postmortem. Gross findings continue to be similar to those observed in the past. There have been no findings which can be specifically related to added endogenous heat, although isolated lesions have yet to be explained.

The skin of several caged swine have developed areas of hyperkeratosis which are whitish in appearance, raised, hairless, and flake when rubbed. They resemble a chronic mycosis, however a culture of one specimen for fungi was negative. It is possible that these lesions, most frequently found around the face and anterior dorsum of the back, are related to the lack of sunshine and air movement in the strict confines of the metabolism cage. They seldom appear until at least three months of such confinement and appear noninflammatory. Similar lesions are seen, albeit less frequently,on swine housed outdoors.

The lead exit wounds characteristically exhibit a ring of crusty exudate surrounding the lead bundle, under which is found moist but intact skin. In only one case was lead tract purulence present, in association with a large abscess near the shoulder which apparently arose from a contaminated suture in the vicinity. This tract stopped about 5 cm outside the thoracic cavity. The immediate vicinity of the heater is typically free of infection, comprised of a scar tissue capsule 2-5 mm in thickness enveloping the implanted device. The implant is held quite securely by this capsule, as well as by incorporation of the velour-covered lead bundle in bizarre bone reformation occurring at the split periosteum of the removed rib. Soft innocuous adhesions of the left lung over the scar tissue capsule and throughout about half the remainder of parietal pleura on that side are always found, a typical end result of prolonged intrathoracic surgery. A single exception was the case in which the diaphragmatic lobe of the lung had wrapped around and adhered to the velour surface of the heater. The animal died (three weeks postoperative) as a result of massive pulmonary hemmorhage in the vicinity.

All animals had ring-shaped thrombi at the anterior and posterior junctions of Dacron DeBakey prosthetic and aorta. These varied in size, the smallest occupying (when pulled away from the wall) about one-fourth the lumen of the vessel and the largest causing total occlusion of the vessel with subsequent heater destruction by self-heating. The GBH-coated heater lumens were typically clear of thrombus formation except for two or three small (less than 1 mm high) attached nodules. The Dacron-flocked lumen heater was one of those destroyed by self-heating following occlusion, so no examination of the lumen as to thrombogenicity or pseudointimal infiltration was possible.

The gross appearance of regional lymph nodes continued to be similar to that reported in the past, changes being restricted to slight enlargement with occasional edema. A single exception was found where the internal iliac nodes were obviously active as a result of a chronic purulent metritis. Gross kidney lesions consisting of whitish areas in the cortices were observed in two cases. A detailed description of their microscopic appearance is given in the next section. The animals had been on 60 watts for 6-1/2 months and 40 watts for 2-3/4 months, respectively. Conversely, necropsy examination of an animal which had been on 60 watts for one year revealed no gross lesions whatsoever.

Histopathology.

In general, the thyroid, brain, pituitary, lung (remote to implant), intestines, urinary bladder, pancreas, cardiac muscle, ovaries, spleen, adrenal glands, spinal cord (at level of thoracolumbar junction), uterus and bone marrow appear histologically normal.

Superficial and visceral lymph nodes (prescapular, prefemoral, superficial inguinal, internal iliac, mesenteric, hepatic) continue as in the past to show varying degrees of mild reactive hyperplasia of the lymphoid germinal follicles, similar to follicles undergoing antigenic stimulation.

Liver sections continue to show evidence of mild to moderate passive congestion of the sinusoids and central veins, with swollen hepatic parenchymal cells and bile retention. Such mild changes may be related to increased resistance to blood flow at the heater, however, enlarged parenchymal cells, reported in the past, may also be due to foreign body reaction.

Kidney lesions are ordinarily limited to slight hypercellularity of some glomeruli and occasional small infarctions with a variable degree of hypertrophy of the epithelial lining of the tubules, all relatively common findings in the past. Cases which had obvious gross lesions also had marked microscopic changes characterized by rather widespread interstitial fibrosis and glomerulitis (occasionally having progressed to complete destruction and sclerosis), with hypertrophy and hyperplasia of tubular epithelium, arteritis with occasional occlusion through proliferation of media, and areas of necrosis and/or infarction. Proteinaceous casts were commonly seen in these sections, with severe damage of the glomeruli in those regions.

Sections of aorta near the anastomosic site show the usual changes described in earlier reports, characterized by cellular infiltration (in response to the silk suture material) and chronic, fibrosing granulomatous reaction over the entire adventitial surface (in response to surgical isolation during the implant procedure). Tissue flaps submitted were verified to be organized or organizing thrombi.

Extended Area Heater- Engineering Analysis.

The results of an experiment in which an extended area (finned) heater was implanted in the thoracic aorta of a miniswine were reported in the last annual report. This heater remained patent for 24 postsurgical days, including eight hours of heating at powers of 40 to 60 watts just prior to necropsy. The heater was found to be completely free of clots and thrombi.

This year the heater was rebuilt and implanted in another miniswine. The assembly is shown in Figure 2. The heater lumen is constructed of POCO AXZ-5Q1 graphite and the heat transfer surface coated with a proprietary antithrombogenic coating by Gulf Atomic Corporation. The fin geometry was designed so that the same cross-sectional flow area was provided as with the standard tubular blood heaters (0.13 in^2) and the heat transfer area per unit length was about 2-1/4 times as great (3 in^2/in vs. 1.32 in^2/in). The total heat transfer area is about 3-1/4 times as great as in the standard heaters.

Thermistors were installed in the fins and in the wall midway between the fins at two locations, 1/4 and 2/3 of the total distance downstream from the leading edge. Data obtained from these thermistors are shown in Figures 3, 4, 5 and 6.

It will be noted that the fin temperatures exceed the wall temperatures, due to the higher thermal resistance between the thermistor location within the fin and in the heat transfer surface as compared to the situation in the relatively thin heater wall. It will also be noted that the upstream and downstream heater wall temperatures are practically the same. This suggests that little or no boundary layer formation exists, unlike the case of straight tubular heaters.

Heat transfer coefficients calculated from available data are summarized in the following table.

TABLE 1

CALCULATED HEAT TRANSFER COEFFICIENTS - EXTENDED AREA HEATER

Power, W	Heat Flux, Btu/hr ft^2	Mean Wall Temp., ^oF	h(Btu/hr-ft^2-^oF)
10	750	104	250
30	2250	108	322
50	3720	112	337
70	5250	115.5	362
90	6750	119	375
110	8250	123	377

The range of coefficients (250 to 377) is somewhat higher than reported for the 12" straight tubular (acute experiment) heater (mean value 200).

Dacron Flock Coated Heater - Engineering Analysis.

Two heaters with Dacron-flock lining were implanted and temperature data obtained at various heater power inputs. The temperature indicated by the two thermistors in each of the two heaters was recorded at each power level. The entire run was repeated the following day. Since the differences were small between thermistors in one heater, between average temperatures in the two heaters, and between average heater temperatures in the two runs, all data was grouped for each power level with the following results:

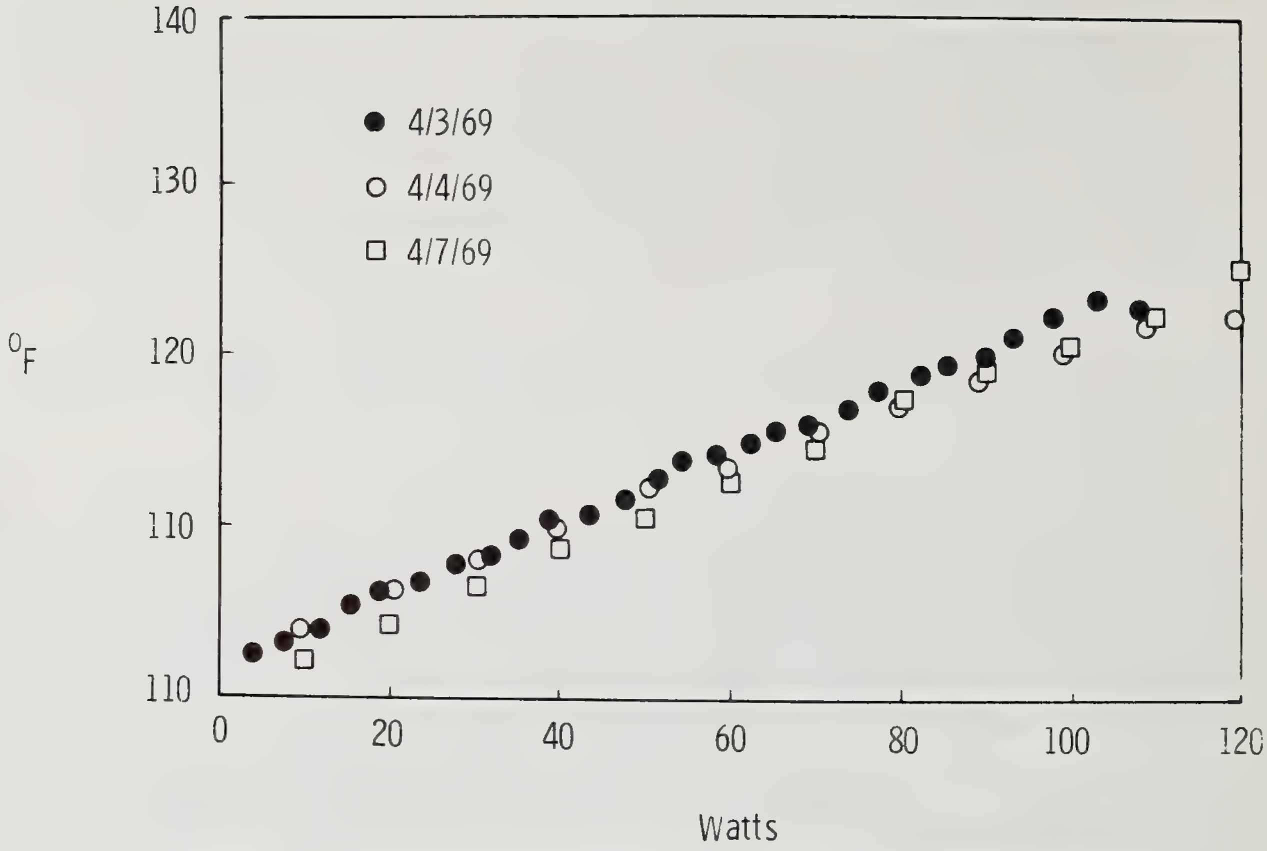

FIGURE 3. EXTENDED AREA HEAT EXCHANGER WALL TEMPERATURE VS POWER, UPSTREAM (0.535" FROM LEADING EDGE).

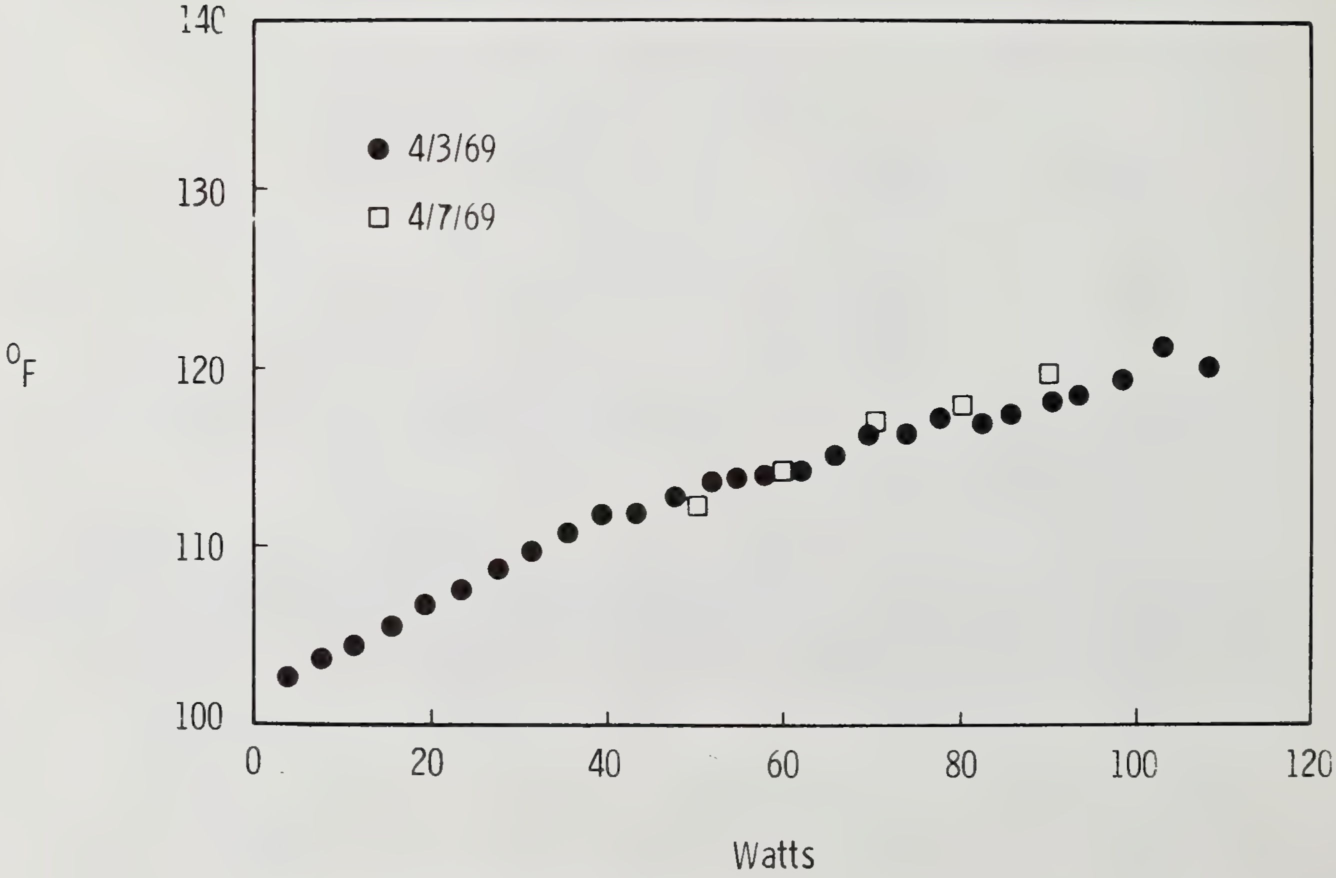

FIGURE 4. EXTENDED AREA HEAT EXCHANGER WALL TEMPERATURE VS POWER, DOWNSTREAM (1.46" FROM LEADING EDGE).

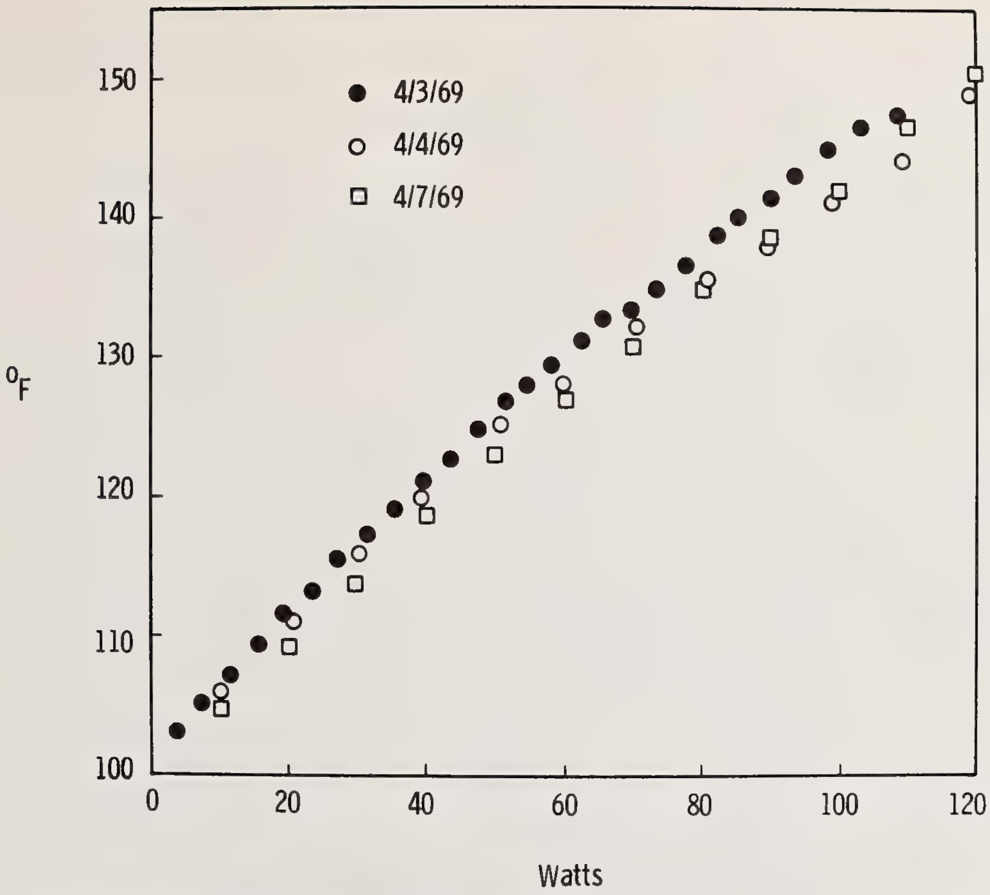

FIGURE 5. EXTENDED AREA HEAT EXCHANGER FIN TEMPERATURE VS POWER, UPSTREAM (0.535" FROM LEADING EDGE).

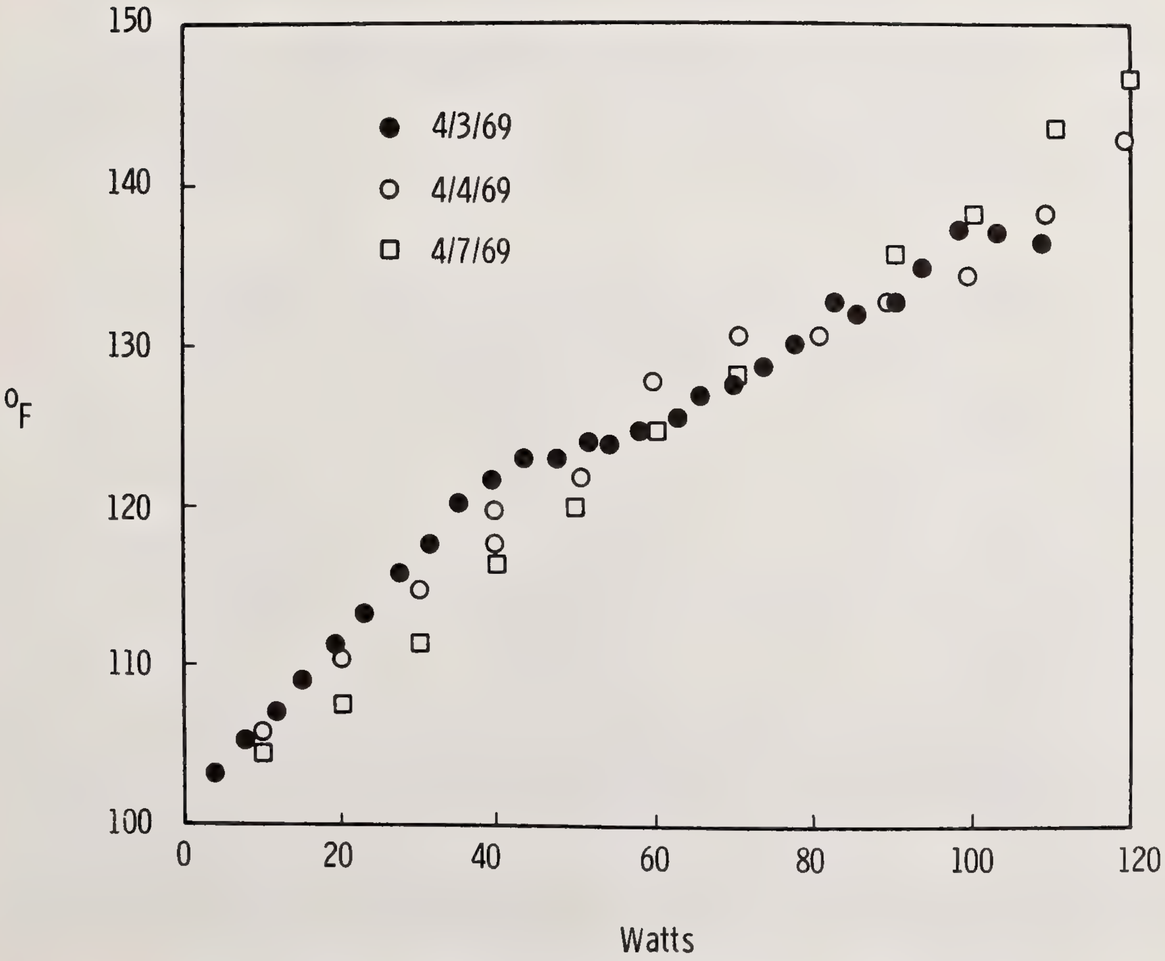

FIGURE 6. EXTENDED AREA HEAT EXCHANGER FIN TEMPERATURES VS POWER, DOWNSTREAM (1.46" FROM LEADING EDGE).

TABLE 2

DACRON FLOCK COATED HEATER TEMPERATURES

Watts	Watts/cm^2	Mean[a] Wall Temp. ($^\circ$F) ± Std. Dev.
0	0	100.9 ± 0.5
5.5	0.43	111.1 ± 0.9
10.5	0.82	119.3 ± 1.9
15.3	1.20	126.8 ± 2.6
20.5	1.61	135.7 ± 3.9
26.4	2.07	145.8 ± 5.2

[a] Mean of all four thermistors (two heaters) and both runs (n = 8).

This demonstrates, for example, that to keep the wall temperature below 120°F (at this stage of fibrin organization), one must not exceed a flux of about 0.8 watts/cm^2. Under such conditions, a 40-watt dissipation requires an exchange surface area of about 50 cm^2.

The data from Table 2 are plotted in Figure 7. For comparison purposes, corresponding wall temperatures are plotted for typical standard GBH-coated heaters (no flock). The difference in wall temperature between the two cases (Figure 8) is a measure of the thermal resistance of the flock-fibrin coat. From these data the thermal resistance per unit area of the flock-intimal layer is found to be a constant equal to 18°F/watt/cm^2.

The data obtained indicate that the use of the blood pump bladder, as a heat transfer interface, may be more problematical than is generally believed. In the Rankine cycle engine concept, for example, waste heat is to be dumped into the bloodstream via the blood pump hydraulic actuating fluid. This fluid also serves as the cooling medium engine for exhaust steam condensation. Variations in the condenser temperature could affect the system efficiency to the point where the engine could stall. For example, a modest increase in the thermal resistance across the heat transfer interface (the blood pump) would cause a corresponding increase in the hydraulic fluid-condenser cooling fluid temperature, an increased condenser temperature would reduce engine efficiency, and require the dumping of more waste heat. Increased heat load across the heat transfer interface would further increase the condenser temperature. Continuation of this diverging feedback process would eventually elevate the condenser temperature to the point where the engine would stall.

The Rankine engine-powered total heart prosthesis will have to dissipate 16 to 48 watts of waste heat, depending on the system load and the efficiency developed. If it is assumed that the blood pump will be the equivalent of a CHMC-TECO assist device, a total heat transfer area of about 114 cm^2 would be available for heat transfer. The calculated thermal resistance of the 0.030 inch thick polyurethane bladder (k - 0.121 Btu/hr-ft^2 - $^\circ$F-ft), and the estimated blood heat transfer film, were combined with the measured flock-fibrin layer thermal resistance to produce the results shown in the following table.

TABLE 3

ESTIMATED THERMAL RESISTANCE OF FLOCKED BLADDER EXCHANGE SURFACE

Assumed Heat Transfer Area - 114 cm^2

Heat Load	16 Watts	48 Watts
Bladder Thermal Resistance	0.179 F/watt	0.179 F/watt
Bladder Δt	2.86 F	8.58 F
Flock Thermal Resistance	0.168 F/watt	0.205 F/watt
Flock Δt	2.68 F	8.05 F
Blood Film Thermal Resistance	0.112 F/watt	0.112 F/watt
Blood Film Δt	1.79 F	5.37 F
Total Thermal Resistance	0.496 F/watt	0.496 F/watt
Total Δt From Outside of Bladder to Bulk Blood	7.33 F	22.0 F

The computed 2.7 to 8.1 F temperature rise across the flock layer thus can be significantly greater than the "nominal" 2 F previously estimated.[4] The estimated variation of 15 F in condenser temperature from minimum to maximum load is somewhat less than would be the actual case because the thermal resistance due to the film on the hydraulic fluid side of the condenser was not included. On the basis of Carnot thermal efficiency, this 15 F increase in condenser temperature would cause a decrease in cycle efficiency of 1%. While the power system may well have adequate capacitance and damping to handle transients of this magnitude without instability, its ability to handle condenser temperature changes of, say, two or three times this amount (causing efficiency decreases of two or three percent) may be questionable.

REFERENCES

1. Twelve-Month Technical Progress Report on a Study on the Effects of Additional Endogenous Heat Relating to the Artificial Heart (Contract PH-43-66-1130) to the National Heart Institute, Bethesda, Maryland; Clearinghouse for scientific and Technical Information, Springfield, Virginia -- PB-177328; Pacific Northwest Laboratory, Richland, Washington, August 10, 1967.
2. Second Twelve-Month Technical Progress Report on A Study on the Effects of Additional Endogenous Heat Relating to the Artificial Heart (Contract PH-43-66-1130) to the National Heart Institute, Bethesda, Maryland; Clearinghouse for Scientific and Technical Information, Springfield, Virginia; Pacific Northwest Laboratory, Richland, Washington, December 30, 1968.
3. Karagianes, M. T., "An Instrumentation Harness Assembly for Long-Term Use on Miniature Swine," Journal of Applied Physiology 25 (5): November, 1968 (641).
4. Huffman, F. N., and Doyle, E. F., "Design of an Implantable, Rankine-Cycle Circulatory Support System", ASME Winter Annual Meeting and Energy Systems Exposition, Paper 68-WA/ENER-10, New York, December 1-5, 1968.

DISCUSSION

MR. PURDY: What was the delta T from the wall surface to the blood? In one of your charts I noticed that you plotted temperature as a function of the thermal energy and the data indicated 30°F.

DR. GILLIS: You mean _in vivo_?

MR. PURDY: Yes, in the animal.

DR. GILLIS: We don't know. The thermistors are located in the wall and we really don't have any idea of what the temperature is right at the base of the flock layer.

MR. PURDY: What do you consider the primary design criteria for implantable heat exchangers? Is it blood temperature rise?

DR. GILLIS: We haven't reached any conclusion on this, yet, on a chronic basis of 18 months' continuous heating. It appears from our results so far that perhaps 130°F interface temperature may be tolerable.

MR. PURDY: What would this represent, a 30°F temperature gradient from heater wall to blood?

DR. GILLIS: Roughly.

MR. PURDY: The second question is with respect to flow through your device. Does this flow in swine correspond to that which you might expect through the human heart, or was it less? At 60 watts was the blood volume flow rate comparable to the volumetric flow rate say 7 liters/min. that you might expect in the human heart? I'm trying to get an idea of how you can relate your measurements to the actual requirement for a human heart?

DR. GILLIS: The thoracic aorta blood flow (from earlier measurements) will run from 2000 to 3500 ml/min. We are in the descending aorta, so it cannot equal cardiac output.

MR. PURDY: The third question. You were concerned about the drop across the flock material? Why were you concerned about that drop? Are you mainly concerned about the characteristics of the engine or are you concerned about some biomedical problem?

DR. GILLIS: I am concerned here about the effect of increased thermal resistance on engine efficiency. I didn't have time to mention the effect of heat on the autologous cellular layer itself. If the cellular layer is present, will it continue to exist at these elevated temperatures; or if it has not developed yet, will it develop in the presence of these elevated temperatures? These are questions which have to be answered in the future.

MR. PURDY: Thank you.

DR. HUFFMAN: After our planned paper, I do have a few slides that will bear on this and I think it is probably best to wait until then to comment.

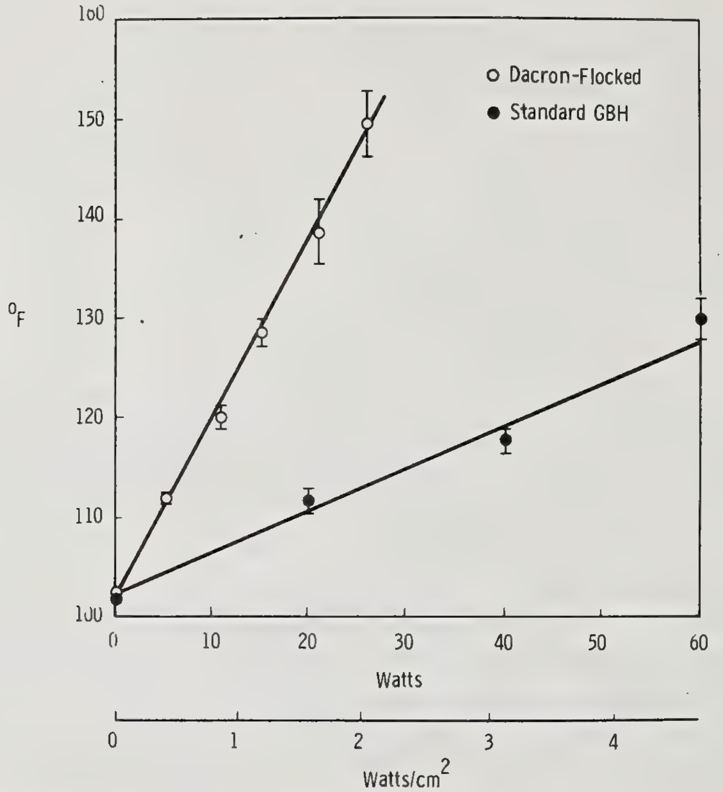

FIGURE 7. MIDLINE HEATER WALL TEMPERATURE VS POWER, DACRON-FLOCKED AND STANDARD GBH HEATERS.

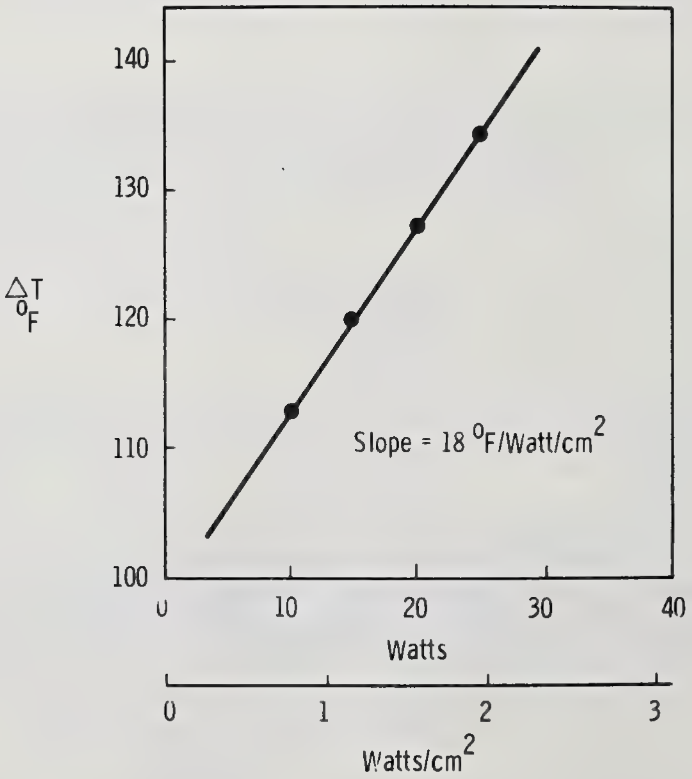

FIGURE 8. THERMAL RESISTANCE OF HEATER FIBRIN/FLOCK COATING.

CHAPTER 75

STUDIES OF THE EFFECTS OF ADDITIONAL ENDOGENOUS HEAT

R. Rawson

John B. Pierce Foundation Laboratory
New Haven, Connecticut

Three general areas of study have been investigated relative to the effects of additional endogenous heat: 1) effects on the thermoregulatory responses of dogs and sheep; 2) histological changes at the blood or tissue interface in dogs and sheep; and 3) effects on body temperature cycles in dogs. In short term experiments in which respiratory frequency, respiratory evaporative heat loss, and certain body temperatures were measured in dogs, it was confirmed that no significant thermoregulatory responses could be elicited in 25 kg dogs subjected to additional endogenous heat loads of 0.6-0.7 watts/kg in a neutral or warm environment. In 50-60 kg sheep, a 0.5-0.6 watts/kg heat input was immediately followed by a significant increase in panting in the absence of a rise in temperature of skin or brain thermoreceptors. This was interpreted as evidence of the operation of unknown deep body temperature receptors. Histological studies in sheep have confirmed previous findings of marked vascularization of fibrous encapsulation tissue around implanted prostheses which have a tissue interface temperature maintained at 43-45°C, and that potential heat exchange to adjacent tissue regresses with time if encapsulation continues in the absence of high temperature at the interface. In dogs, histological examination of ingrowth in the aortic heat exchanger lumen lined with flocked Dacron revealed some indication of an epithelioid movement along the blood-lumen interface.

OBJECTIVES

In our recent work at the Pierce Laboratories in New Haven, we have been looking at three aspects of the additional endogenous heat problem:

1) the effects on the thermoregulatory responses in dogs and sheep;
2) the histological changes at the blood or tissue interface in these two animal species; and
3) the effects on body temperature cycles in dogs.

EXPERIMENTAL

Effects of Endogenous Heat on Thermoregulatory Responses in Dogs and Sheep.

Two methods of introducing additional endogenous heat were employed. First, dogs were implanted at Boston Children's Hospital with the straight tube heat exchanger of Thermo Electron Corp. shown in the lateral radiograph in Figure 1.

The exchanger was anastomosed into the descending aorta by means of a Dacron graft material, and two pairs of flexible wire leads were exteriorized through a subcutaneous tunnel to a point between the scapulae. A Diaderm percutaneous lead button shown in Figure 2 was used to obtain a skin-prosthesis graft which was effective in sealing the lead entry from invasion by organisms for several months. The neck of the button was covered with Dacron felt and a layer of Dacron mesh to provide an effective matrix for ingrowth of vascularized cutaneous tissue. A Dacron skirt helped to immobilize the button when it became incorporated with ingrowing tissue. Figure 3 shows this prosthetic device in a dog four months after implantation.

The heat exchangers implanted in dogs lay distal to the vessels supplying blood to the head as illustrated in Figure 4 showing a fibrous tissue encapsulated exchanger still attached to the aortic arch which had been sectioned at the heart. One pair of wire leads supplied DC current to the heater coil around the tube exchanger; the second pair of leads permitted measurement of tube surface temperature at the discharge end with a calibrated thermistor. The tube was lined with a layer of flocked Dacron in contact with the bloodstream and the temperature measured was not that of the blood-Dacron interface, but was a monitor of tube temperature which was higher than the blood layer temperature when heat was introduced.

The second method of endogenous heating utilized the convective heat transfer capability of vascularized tissue instead of direct heat transfer at a blood interface. This method of course requires a much larger heat exchange area. This was accomplished by implanting in the abdominal cavity of sheep, four strip heaters measuring approximately 2 x 6 inches and 3/8 inch thick, making a total heat exchange surface area of 96 square inches. Two of these strip heaters are shown in Figure 5. The direct heat source was a flat, close wound coil of #34 gage copper wire. On top of this was wound a second coil of #36 copper wire which was heated by the inner coil, and whose resistance measurement permitted an estimate of its temperature to better than 0.1°C. The heater-sensor system was cast in a uniform layer of medical grade epoxy incorporating Dacron mesh skirts for suturing the implants to the abdominal wall. A pair of heaters was implanted on the right and left side as shown in Figure 6. Lead wires were again exteriorized dorsally through a Diaderm button.

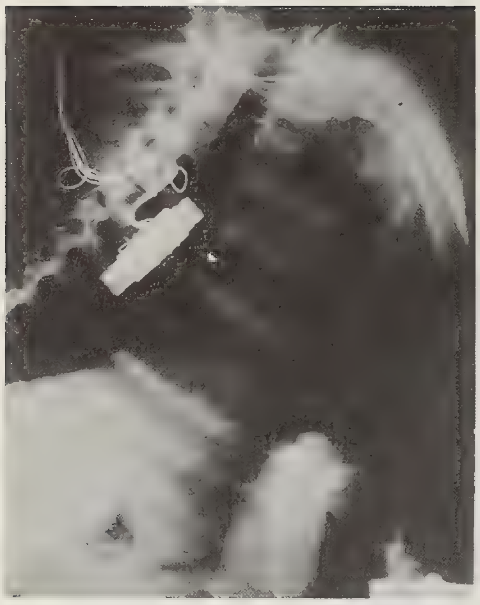

FIGURE 1. LATERAL RADIOGRAPH SHOWING STRAIGHT TUBE HEAT EXCHANGER IMPLANTED IN DOG.

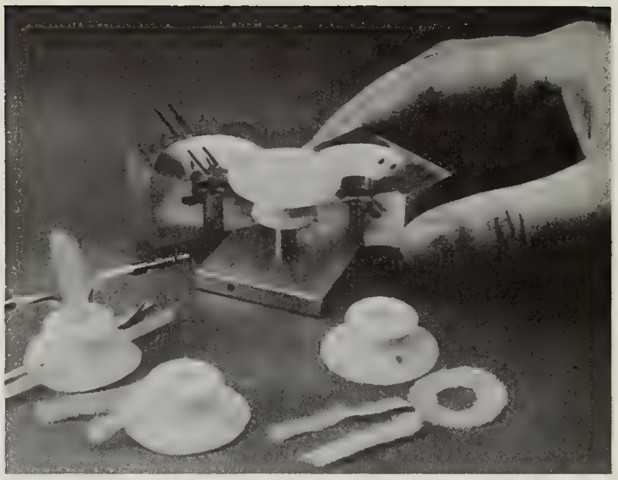

FIGURE 2. DIADERM PERCUTANEOUS LEAD BUTTON USED TO OBTAIN A SKIN-PROSTHESIS GRAFT.

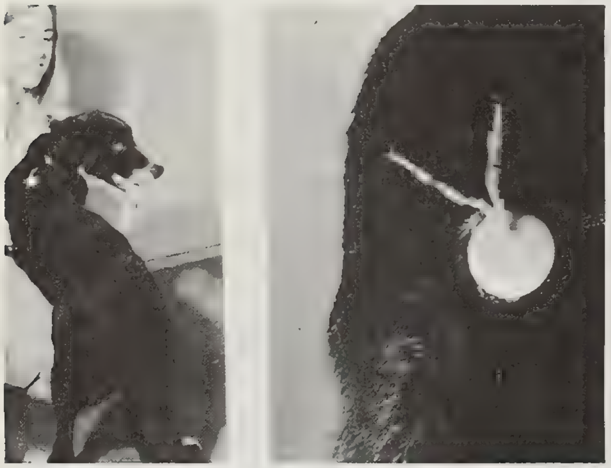

FIGURE 3. PROSTHETIC DEVICE IN A DOG FOUR MONTHS AFTER IMPLANTATION.

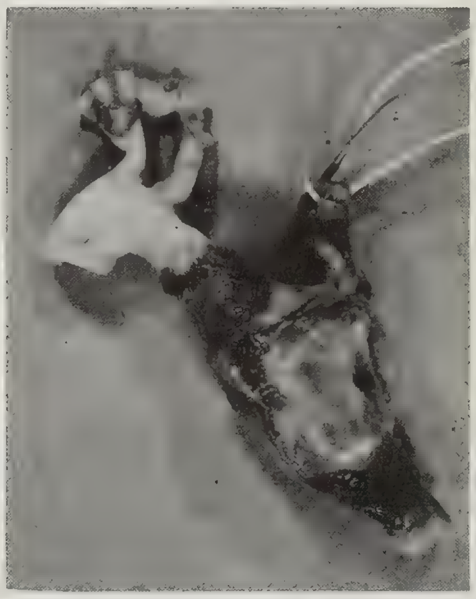

FIGURE 4. FIBROUS TISSUE ENCAPSULATED EXCHANGER STILL ATTACHED TO THE AORTIC ARCH WHICH HAD BEEN SECTIONED AT THE HEART.

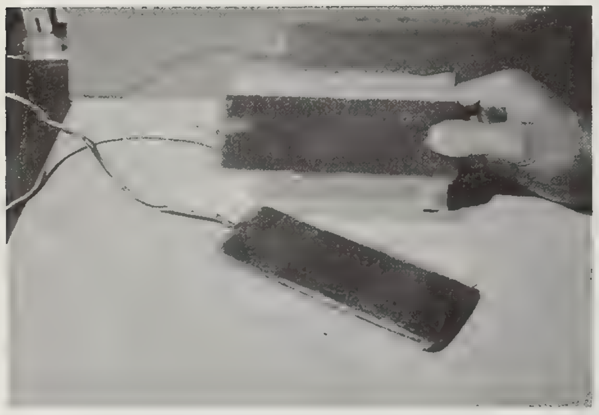

FIGURE 5. TWO STRIP HEATERS.

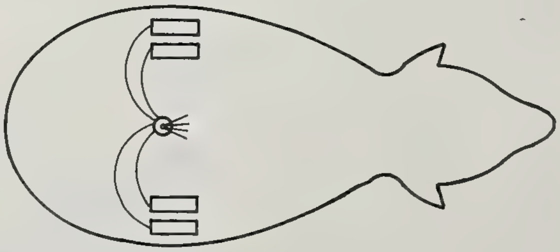

FIGURE 6. PAIR OF HEATERS ARE IMPLANTED ON THE RIGHT AND LEFT SIDE OF THE ANIMAL.

From calibration data of the heaters in a stirred water bath prior to implant, a heat transfer coefficient for each heater was determined, thus measurement of heat source temperature and power input permitted calculation of heater-tissue interface temperature *in vivo*. Dogs and sheep were trained to walk a treadmill in a climate chamber while wearing a breathing mask and other equipment associated with the measurement of physiological parameters in cold, neutral, and hot environments. Shown in Figure 7 is the instrumentation for measuring heart rate, respiratory frequency, respiratory evaporative heat loss and oxygen uptake along with temperatures of the skin, vagina, brain, and venous return from the head. All data were scanned each minute, and subsequently analyzed by an IBM 1130 Computer System.

Last year, we reported at this conference on data from eleven dogs prepared as just described and supplied to us for testing. It was found in our experiments that under an endogenous heat input load of 0.6 watt/Kg in a neutral environment, the dog was quite able to dissipate this additional endogenous heat by increasing its respiratory frequency and evaporating more water from the upper respiratory tract. The additional endogenous heat load amounted to 30% of the resting metabolic heat production. In man, an additional load of 25 watts would amount roughly to 30% of his resting metabolic heat. It was concluded from these findings that if the animal or man were in the average environmental conditions where normal heat loss mechanisms were permitted to operate, the additional heat load from a total heart implant with power source would not constitute significant thermal stress to generate hyperthermia. It was shown, however, that in a dog anesthetized with nembutal, 0.6 watt/Kg of additional endogenous heat produced marked hyperthermia due to the depression of the thermoregulatory mechanism of panting.

Effects of Endogenous Heat on Body Temperature Cycles in Dogs and Sheep.

During the recently concluded contract period, more studies were designed to further investigate these short term effects of additional heat loads in dogs subjected to environmental thermal stress. Only two dog preparations were available during this period however, and only one of these animals was trainable to the climate chamber regime. The second dog continued to show panic and destructive tendencies during a 2-week training period. Both animals demonstrated slow physical deterioration, with death from intrathoracic hemorrhage occurring 60 days after prosthesis implantation. One of these dogs was used to monitor deep body temperature continuously with and without heat input while confined to its pen. The second animal was tested in the climate chamber in short term experiments in an effort to establish a maximum environmental thermal stress tolerable to the dog while receiving additional endogenous heat. It was found that although this dog would cooperate in experiments conducted in an environmental temperature around 27°C, the animal would not tolerate experimentation on him at temperatures any higher for more than a few minutes. His vigorous and continuous efforts to tear off the breathing mask at these higher temperatures of course precluded the obtaining of meaningful data from the experiment. His intolerance was not an effect of additional endogenous heat.

In ten experiments conducted in environmental temperatures of 19-27°C, our earlier findings with respect to endogenous heat load tolerance were confirmed. The computer plot shown in Figure 8 is representative of the typical response obtained from the dog when 0.6 watt/Kg of heat was dissipated to the blood. The top curve is a profile of the temperature recorded from the thermistor at the discharge end of the exchanger, and indicates its temperature range when heat was introduced. This point in the heat exchanger rose 10.5°C with heat on, the blood temperature being about 39.4°. The blood temperature was slightly higher than the recorded rectal temperature, a relationship normally observed. The curve of metabolic heat production, second from the top, shows a rate of 3-4 watts/Kg at the beginning of the experiment, and its fluctuations were followed closely by those of the respiratory heat loss curve just below it, showing approximately 1-2 watts/Kg heat loss through evaporation or roughly 2/3 of the metabolic heat production. Rectal temperature shown at the bottom was relatively steady throughout the experiment, and is a fair indication of an unchanging body heat storage, and competent body temperature regulation largely through the avenue of respiratory heat loss.

In this experiment, at 25 minutes, the dog lay down and appeared to fall asleep. The heat production and evaporative loss rapidly declined. At this time 0.6 watt/Kg of endogenous heat was introduced for 15 minutes as indicated by the first black bar, and there appeared only small transients in heat loss of 0.3 watt/Kg. It is apparent that there was no tendency for the rectal temperature to undergo any significant change in this short period. The animal regulated well to this amount of additional endogenous heat as it did to normal endogenous heat when aroused and exercised at 1-mile per hour, to increase metabolic heat production to almost twice its resting level. In other experiments where endogenous heat was introduced simultaneously with exercise, there was likewise evidence that the dog was able to easily regulate his body temperature under these conditions.

This dog lived in a pen for a period of 18 days before he died, and a temperature closely representing that of the aortic blood was recorded every hour. The temperature monitoring was accomplished in the following manner: The thermistor incorporated into the discharge end of the heat exchanger at the time of its assembly provided a means of measuring the exchanger tube temperature. The temperature was recorded on a Leeds & Northrup Speedomax which was turned on for ten minutes every hour by a time switch. When the recorder turned on, the power to the heat exchanger turned off, thus a series of cooling curves was recorded as shown in the typical readout in Figure 9. The temperature recorded at the end of the ten minute cool-off period was taken as a close estimate of the blood temperature, and a fair estimate of the average deep body temperature. This method was

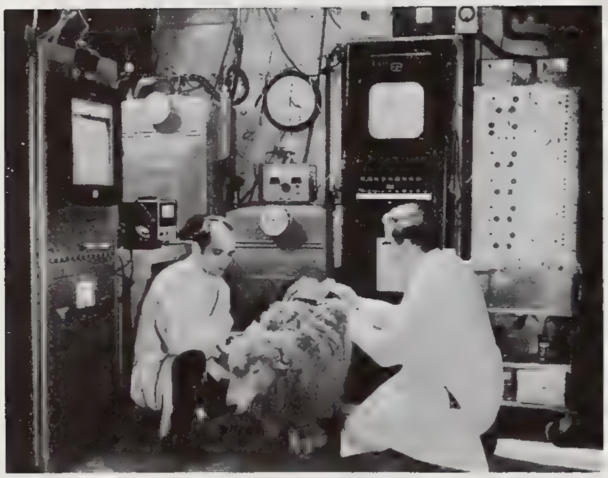

FIGURE 7. INSTRUMENTATION FOR MEASURING HEART RATE, RESPIRATORY FREQUENCY, RESPIRATORY EVAPORATIVE HEAT LOSS AND OXYGEN UPTAKE ALONG WITH TEMPERATURES OF THE SKIN, VAGINA, BRAIN, AND VENOUS RETURN FROM THE HEAD.

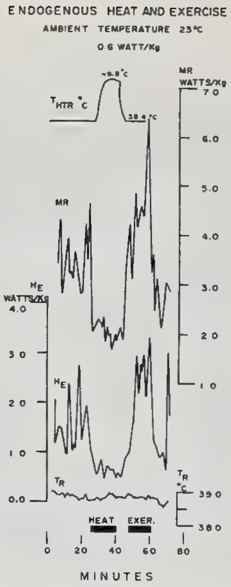

FIGURE 8. COMPUTER PLOT SHOWING TYPICAL RESPONSE OBTAINED FROM A DOG WHEN 0.6 WATT/KG OF HEAT IS DISSIPATED TO THE BLOOD.

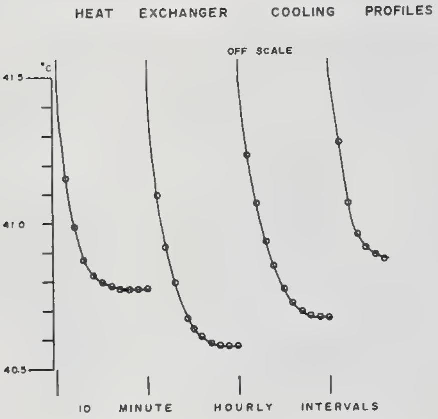

FIGURE 9. HEAT EXCHANGER COOLING PROFILES.

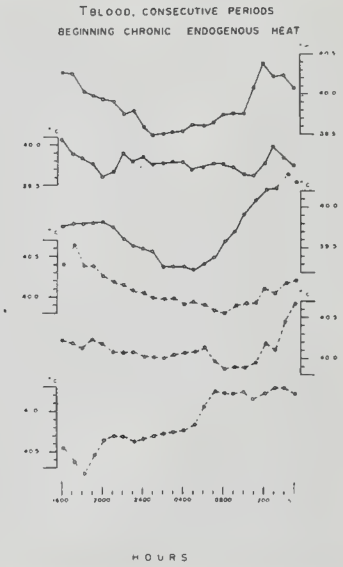

FIGURE 10. BLOOD TEMPERATURE CYCLES AT THE BEGINNING OF CHRONIC ENDOGENOUS HEAT.

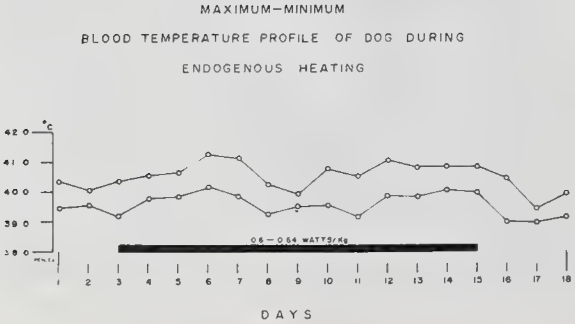

FIGURE 11. MAXIMUM-MINIMUM BLOOD TEMPERATURE PROFILE OF DOG DURING ENDOGENOUS HEATING.

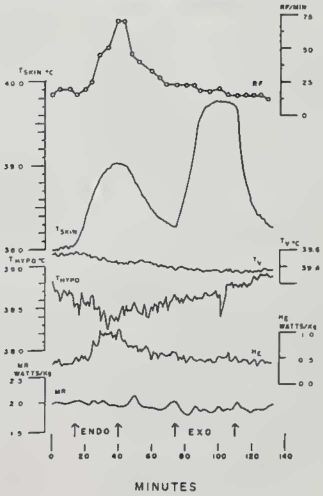

FIGURE 12. RESPONSE TO ENDOGENOUS HEATING IN A NEUTRAL ENVIRONMENT. SHEEP, 0.5 WATTS/Kg, T_a = 200° C.

preferred to temperature measurements from the rectum with its attendant difficulties of lead breakage. When the hourly temperature readings were plotted against time, 24-hour body temperature cycles were obtained as shown in Figure 10. The top three 24-hour cycles are without additional endogenous heat, then 0.6 watt/Kg of heat was introduced for the following days. When the maximum and minimum body temperatures were plotted for each of 18 days, a graph shown in Figure 11 was obtained.

At the initiation of endogenous heating at the end of the third cycle, the maximum and minimum temperatures underwent a transient rise and fall over the following 6-day period. The slow rise and decline appeared to repeat itself over the next 7 days. Since we do not have such consecutive recordings from this dog without endogenous heat, we cannot say that endogenous heat influenced this weekly rhythm, but it does show that over a heating period of 12 days, there was no maintained increase in deep body temperature, and the dog was able to regulate to this additional endogenous heat adequately, suggesting undisturbed thermoregulatory function over this time span. The other of the two dogs, the more destructive one, was also monitored in this way, and although consecutive periods of 3-4 days of recording could be obtained which showed essentially the same temperature values, no uninterrupted long-term heating record could be obtained because of power and monitoring lead breakage. It is believed that these temperature data may be safely extrapolated to hot environments for both dog and man. The additional input of 1/3 of the resting metabolic rate in man in thermal equilibrium with environments where radiant and evaporative heat losses are greatly reduced but not abolished, would result in no more stress than the heat generated by slowly moving the extremities.

In our studies on sheep with strip heaters in the abdominal cavity, the heat load tolerances in short term experiments parallel those of the dog experiments in neutral environments. In a hot environment of 38°C, a sheep with 3 inches of fleece, however, still equilibrated with his environment while receiving 0.6 watt/Kg of heat, but its vaginal temperature levelled off at about 0.5°C higher than without additional endogenous heat.

In addition to this confirming data, an important basic physiological finding was made in the sheep experiments. Figure 12 illustrates an experiment in which a 40 Kg ewe, implanted with four strip heaters and allowed to equilibrate in a 23°C environment was subjected to 0.5 watt/Kg of additional endogenous heat, to raise strip heater surface temperatures to 43°C. Five to seven minutes after the onset of heating, the respiration frequency and respiratory evaporative heat loss rapidly increased to a new level, and remained there until heating was discontinued. During the same time course, the temperature of the hypothalamus decreased and returned to its original level after heat was turned off. Skin temperature measured over the site of the heater implants rose approximately one degree, the skin thermocouples being heavily insulated to the environment with a 2-inch layer of urethane foam. The importance of this observation lies in its relationship to the currently held concept that the two major groups of thermal receptors having to do with body temperature regulation are those in the skin and the hypothalamus. Yet the hypothalamic temperature declined when heat was introduced into the abdomen. When the skin surface was heated over the locations of the implanted heaters, by means of 2 x 6 strip heaters strapped to the skin, until the skin temperature was raised to a level higher than when heated from the inside as shown in the graph, there were no thermoregulatory responses initiated. The most probable explanation of this phenomenon is that in these sheep preparations, deep body thermoreceptors capable of driving thermoregulatory responses, were being stimulated by warmed blood drained from muscle and visceral tissue in the region being heated. Recent investigations at Indiana University have uncovered rather conclusive evidence of the existence of thermally sensitive nerve endings in the femoral vein of the cat. It is quite likely that the large veins of the sheep, including the vena cava, also contain thermoreceptors, and that these were being stimulated to overdrive the thermoregulatory system to lose heat and thus drop the hypothalamic temperature. This possibility has obvious importance to a program of design and implantation in man of heat generating devices. In man, the thermoregulatory responses corresponding to panting in the sheep are skin vasodilation and sweating. At least cognizance of the possibility of stimulating deep body temperature receptors, even though it may not seriously impair body temperature regulation, is strongly suggested by these findings.

Histological Changes Due to Endogenous Heat.

In our previous Annual Reports, we have described an interesting difference observed between the histological structures of fibrous encapsulation tissue found around heated and unheated strip heaters in sheep. We have learned that the body is capable of adapting to what are ordinarily considered noxious or damaging temperatures by vascularization of the normally dense, avascular, fibrous tissue, thus increasing convective heat transfer to lower the surface temperature of the heater. This process has been noted to be most obvious at an original surface temperature of 45-46°C, and in about 3 weeks from the onset of heating, the surface temperature may have declined as much as two degrees.

We conducted another experiment to determine the effect of initiating heating after the fibrous capsule had formed in the absence of heat. Three months after implantation, it was found that a given power input to a heater raised its surface temperature 3-4 degrees higher than did the same power input a few days after implantation. This was ascribed to the insulation properties of an avascular fibrous capsule formed around the heater. Biopsy of the capsule through the abdominal wall provided a specimen shown in Figure 13. Van Gieson stain for elastic tissue showed no significant vascular channels in this 2 mm layer as evidenced by the absence of gray or black staining of vessel walls or capillary sphincters. Thirty days later a second biopsy shown in Figure 14 demonstrated the growth of a vascularized layer of tissue beneath the dense avascular layer to the right.

The gray or black stained vessels are prominent in this new layer, and consist of minute vessels 20-300 microns in diameter in the prepared figure.

After vascularization had occurred, it was found that the convective heat transfer had significantly increased over that observed after 3 months of avascular capsule formation, and was greater than that observed immediately after heater implantation. This finding has significance with regard to heat exchanger efficiency in man in that if a method of heat dissipation to tissue were to be employed, increased convective heat transfer would probably still obtain even after insulative encapsulation of an exchange surface had occurred.

SUMMARY

In summary, our major findings indicate that an additional heat load of up to 0.6 watt/Kg in dogs in neutral or slightly warm environments is easily dissipated in the conscious animal by increased respiratory heat loss. Unshorn sheep, in a 38°C environemnt, underwent a body temperature increase which levelled off at about 0.5°C higher than basal level. Also, in short term sheep experiments, it was clearly demonstrated that the respiratory mechanism could be overdriven to cool the cerebral circulation and decrease hypothalamic temperature - a phenomenon probably dependent upon unknown deep body thermoreceptors. Finally, good evidence has been obtained that the adaptive response of vascularization to high temperatures is still operative after an initial fibrous capsule has formed around the heat source.

DISCUSSION

DR. W.E. STEWART: I caution the use of sheep as an animal to compare to man as far as heat dissipation. First of all they have no sweat glands. Secondly, they get rid of most of their heat by way of their respiratory system so that I think we should be using dogs or calves. Dr. Ken Blaxter at the Rowett Research Institute, Scotland, over the last 20 years, has conducted extensive work on sheep in environmental control chambers in order to study the efficiency of their digestion and their means of getting rid of heat. With three inches of wool, there is almost no loss of heat by way of convection or conduction. In fact, the loss by radiation is very small when the amount of wool exceeds 1/4 of an inch. Third, sheep have a dynamically varying, exothermic forestomach bacterial fermentation digestive mechanism.

DR. RAWSON: Well, thank you very much for those comments, Sir. I don't think that we are trying to extrapolate from sheep to man in heat dissipation. We're simply saying that in sheep there appears to be deep temperature thermoreceptors which may possibly exist in all higher vertebrates. The sheep's major avenue of heat loss is not from his lungs, but it is from his upper respiratory tract namely, from his nasal passages where there is an excellent heat exchanger in operation as shown by Dr. Anderson's excellent acrylic injections of the sheep head displayed out in the hallway to the conference room. Incidentally, if you will look closely at the acrylic injection of the sheep head in the area which was the base of the brain, you will see an acrylic cask of a small plexus which is the plexus described by Baker and Hayword. This is an excellent heat exchange which cools cerebral circulation in the sheep. The venous return from the nasal passages where water is evaporated and blood is cooled passes through this plexus and cools the cerebral circulation. It seems to be some kind of a built-in mechanism for detecting the sheep's brain overall temperature, and this is probably the phenomenon responsible for the observation that I showed in the slide where the hypothalamic temperature dropped precipitously when the sheep started to pant.

DR. STEWART: It is known that when dogs run a flock of sheep a few hundred yards, the sheep will die of heat prostration. They just can't get rid of the excess heat, so you are going to see differences in the sheep showing that they markedly vary from man, dog, or other animals. When the sheep pants, very little air circulates via the nasal airways.

DR. RAWSON: Yes, I will agree 100% the sheep is quite different in his temperature regulation mechanisms than man, in fact, his regulation appears quite sloppy at times, and the temperature varies depending upon any number of unknown variables.

EDITORS NOTE: This work was also supported because of Dr. Stewart's point. Little data on tolerance of additional endogenous heat was available. It was felt that data from animals of human size, with rejection primarily dependent on respiratory mechanisms, might indicate the range of minimum safe thermal loads for man, even with some compromise in thermo regulatory mechanisms, as might occur after surgery or with multi-system disease.

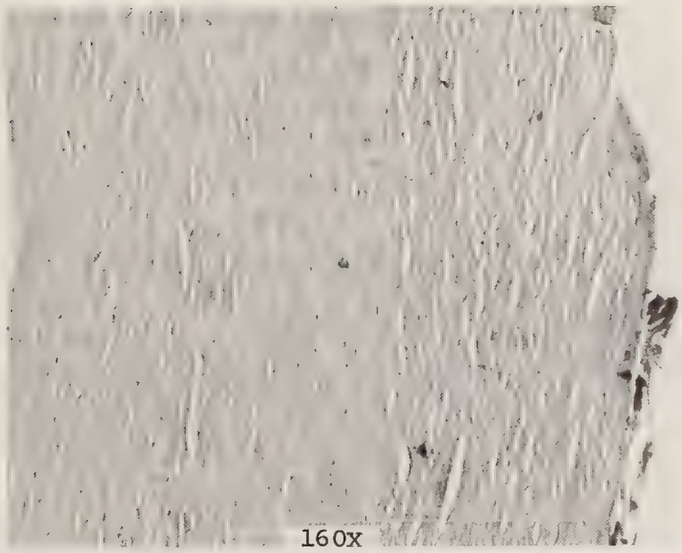

FIGURE 13. MICROPHOTOGRAPH SHOWING AVASCULAR FIBROUS CAPSULE FORMED AROUND THE HEATER. ORIGINAL MAGNIFICATION 160x.

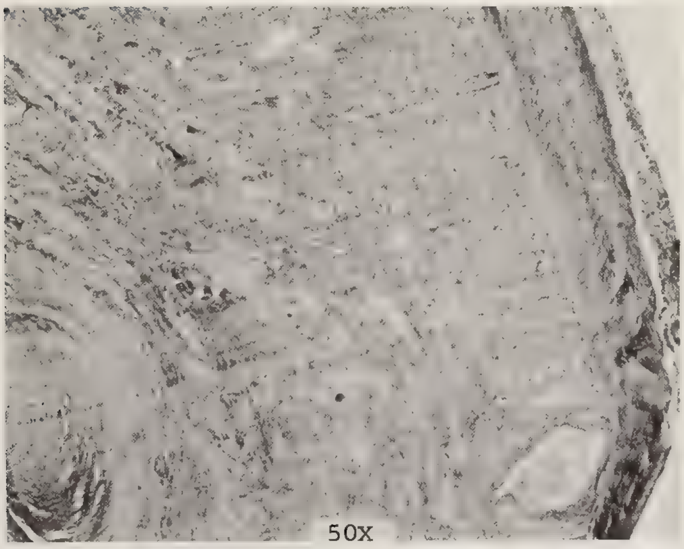

FIGURE 14. MICROPHOTOGRAPH OF BIOPSY TAKEN 30 DAYS LATER, DEMONSTRATING THE GROWTH OF A VASCULARIZED LAYER OF TISSUE BENEATH THE DENSE AVASCULAR LAYER TO THE RIGHT TISSUE.

CHAPTER 76

EFFECTS OF INTRACORPOREAL HEAT AND RADIATION ON DOGS

J. Norman, C. Pegg, G. Sandberg, R. Lee
Sears Surgical Research Laboratories
Boston, Mass.

F. Huffman
Thermo Electron Corporation
Waltham, Mass.

The body must be capable of dissipating the reject heat from the power source which drives the blood pump(s) of an implantable circulatory support system. If the energy source is a radioisotope, the body must also tolerate nuclear radiation exposure. The objective of these studies is to characterize the effects of additional heat and nuclear radiation on dogs by implanting blood-cooled heat exchanger in the thoracic cavity using Pu-238 (plutonium-238) capsules as well as RES (radiation equivalent sources) capsules which simulate the Pu-238 neutron and gamma radiation environment. Implantation entails excision of a segment of the descending thoracic aorta and replacement with a titanium tube heat exchanger. Within the observation periods (16 watt Pu-238, 18 mos.; 24 watt Pu-238, 10 mos.; RES , 10, 10, and 8 mos.) all radioisotope dogs are in apparent good condition except for chromosomal changes in their lymphocytes cultured *in vitro* after phytohemmaglutinin stimulation, similar to those found in patients after radiation therapy. Serial hematologic, endocrine, hepatic and renal function tests are within normal limits. These continuing studies indicate that the temperature regulation mechanisms of mongrel dogs adjust to dissipate additional endogenous heat loads up to 0.8 watt/kg (corresponding to a heat flux of 1 watt/cm^2 and a maximum blood temperature rise of 4^{0}C within the exchanger) and that the anticipated reject heat and dose rate levels from an implantable circulatory support system may be permissible.

INTRODUCTION

All totally implantable circulatory support systems reject heat from the power source driving the blood pump. The reject heat levels vary with the energy storage and conversion techniques used. Projected thermal conversion systems may require the body to dissipate up to 40 thermal watts. If the energy source is a radioisotope, the body must also tolerate chronic nuclear radiation exposure. The studies of the feasibility of using the circulating blood as a means of dissipating additional heat were undertaken four years ago as part of our cooperative artificial heart program. Before describing the present year's activities, we will first discuss the rationale of the program and summarize the previous work.

The objective of the studies on the effects of additional endogenous heat has been to characterize the effects of additional heat and nuclear radiation on dogs. The effects of additional heat alone were studied using electrical heat exchangers during the first year of the program. During the past 18 months, the combined effects of heat and radiation were investigated using Plutonium-238 (Pu-238) sources. Composite radioisotope sources (RES) roughly equivalent in neutron and photon radiation levels to those of Pu-238 were implanted in dogs in order to evaluate the effects of radiation alone.

Studies of the effects of additional endogenous heat have been approached by excising a segment of either the descending thoracic or the abdominal aorta and replacing it with a metal tube heat exchanger. The initial studies used titanium or 304 stainless steel blood tubes to which a resistance heater was brazed. The heater section was thermally insulated with Fiberfrax and encapsulated in layers of RTV (GE Silicone Rubber) and Silastic. The inside surfaces of the blood tubes were treated in a variety of ways including mechanical polishing, electropolishing, silicone coating, acid dipping ultrasonic cleaning and heparin bonding. Most of the exchangers were stainless steel and bonded with heparin after the graphite substrate was soaked in benzalkonium chloride. Before dying of infection, one animal survived 240 days while continually dissipating 14 watts. The other dogs died from a wide variety of causes, with no apparent correlation with thermal input. Infection originating at the exit point of the wire leads was a continuing problem and sometimes resulted in fatal peritonitis. Clotting associated with the blood tube claimed another large fraction of the animals. One of the few clear effects of the heat was the initial rise in body temperature from 1 to 3^{0}C above the baseline temperature. Body temperatures then declined and stabilized within 24 hours to temperatures usually less than 0.5^{0}C higher than the preheated value. Acute experiments showed that if the temperature of the heat exchanger exceeded 44^{0}C, there was a high probability of clotting. These data strongly suggest a correlation between clotting and infection associated with the percutaneous electrical leads.

A totally implantable circulatory support system fueled with a radioisotope would provide patients with a degree of freedom that cannot be realized with rechargeable systems. A radioisotope source permits tentative evaluations of the radiobiologic effects from using such an energy source.

EXPERIMENTAL

A discussion of the economic, radiation and design factors which determine the choice of a radioisotope fuel for powering an artificial heart is beyond the scope of this paper. However, Plutonium-238 (Pu-238), Thulium-171, Promethium-147 and Tritium are candidate fuels. Plutonium-238 was chosen as the radioisotope fuel for these studies because of its availability, relatively low radiation, reasonable power density, long half-life and established heat source technology.

In support of these studies, the Atomic Energy Commission supplied two Pu-238 heat and radiation sources fabricated by Mound Laboratory. Although the two Pu-238 sources have different thermal outputs (16 and 24 watts), the capsule dimensions are identical. A drawing of the Pu-238 capsule is shown in Figure 1. The plutonium metal (80 percent Pu-238) is contained inside a welded tantalum liner 0.030 in. thick. The tantalum liner is compatible with metallic plutonium up to temperatures of 400°C and includes a void volume (1.1 times the fuel volume) for helium gas buildup from alpha particle decay. The tantalum liner is hermetically sealed in a helium atmosphere within a thick-walled (approximately 0.100 in.), welded Haynes-25 outer container. The capsule is approximately 1.6 in. in diameter and 0.6 in. high. The 16-watt source contains 35 g of plutonium. The heat sources weigh approximately 170 g. All the Pu-238 implants have employed essentially the same heat exchanger design shown in Figure 2. The aluminum heat conductor is cast onto a 3/8-in. diameter titanium tube, 4 in. long. The inside of the blood tube is coated with graphite-benzalkonium-heparin. The heat exchanger is jacketed in Fiberfrax thermal insulation and encapsulated in Silastic. The assembly weighs about one pound after source loading and encapsulation.

The procedure for implanting the radioisotope heat exchanger is shown in Figure 3. At most, three intercostal arteries are divided for implantation. A segment of the descending aorta is removed and short lengths of Dacron tubing are sutured to the cut ends of the aorta. The heat exchanger is then secured to the graft segments and aortic flow reestablished. The Pu-238 capsule is then inserted into the heat exchanger.

Figure 4 shows the maximum rise in coolant temperature through the heat exchanger as a function of flow. The ordinate is the temperature difference between the wall of the heat exchanger tube and the incoming coolant plotted as a function of flow rate, parametric in coolants and pumping modes. Blood and saline were the coolants; both steady and pulsatile flows were studied. As expected, saline is a better coolant because of its higher thermal conductivity and lower viscosity. It is interesting that in the case of both blood and saline the pulsatile flow gives significantly better heat transfer than does steady flow. Since the cardiac output in a 40 kg dog is about 3500 ml/min., the maximum blood temperature rise for the 24-watt source is around 2-1/2°C. Of course, only a small fraction of the blood per pass is exposed to a temperature rise this high, since the bulk blood temperature increase is only a few tenths of a degree centigrade. The rectal temperatures in six animals over the first 24 hours following implantation of the 16-watt capsule are shown in Figure 5. Notice the drop in temperature due to exposed heat transfer areas during the procedure. These temperatures increased as shown and returned to normal ranges by the day following operation. Implantation of the higher power 24-watt source required the immediate use of cooling blankets to prevent heat stroke.

The implantation of a Pu-238 source immediately subjects the animal to the effects of both heat and radiation. In order to separate these factors, a composite source was built which simulates the radiation from the Pu-238 sources, yet generates negligible heat. The design of the radiation equivalent source is shown in Figure 6. The source dimensions are identical with those of the 16- and 24-watt Pu-238 sources. The Americium-241/Beryllium neutron source has an output intermediate between the 16- and the 24-watt Pu-238 sources. A Strontium-90 (Sr-90) bremsstrahlung source is used to simulate the gamma output of Pu-238. The total dose rate from the radiation equivalent source is comparable to that from the 24-watt Pu-238 source. These sources have been implanted in the chest cavities of three mongrel dogs. A summary of current radioisotope dogs is given in Table 1.

TABLE 1
SUMMARY OF CURRENT RADIOISOTOPE DOGS

Identification	Sex	Approx. Weight (Pounds)	Type of Source	Date of Implant	Months Since Implant
Plutina	Female	80	16-Watt Pu-238	26 Sept. 1967	20
Wolf	Male	70	24-Watt	7 May 1968	13
3403	Male	59	RES[a]	24 April 1968	13
3308	Female	56	RES[a]	24 April 1968	13
4172	Female	45	RES[a]	24 July 1968	11

[a] Neutron and photon dose rates from RES (radiation equivalent source) approximate those from 24 watt Pu-238 capsule.

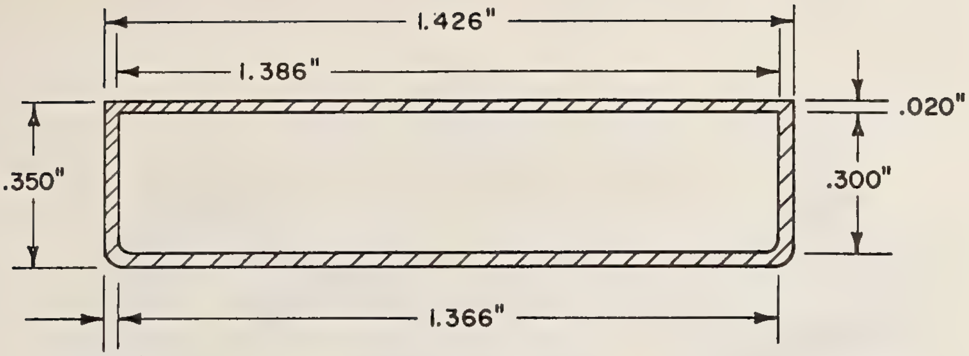

Tantalum Inner Liner

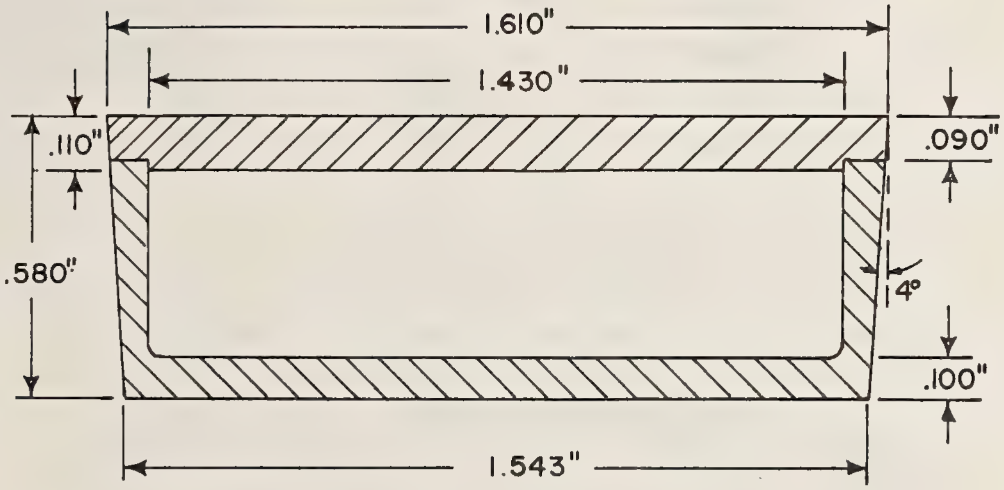

Haynes 25 Outer Capsule

FIGURE 1. PLUTONIUM-238 SOURCE DIMENSIONS.

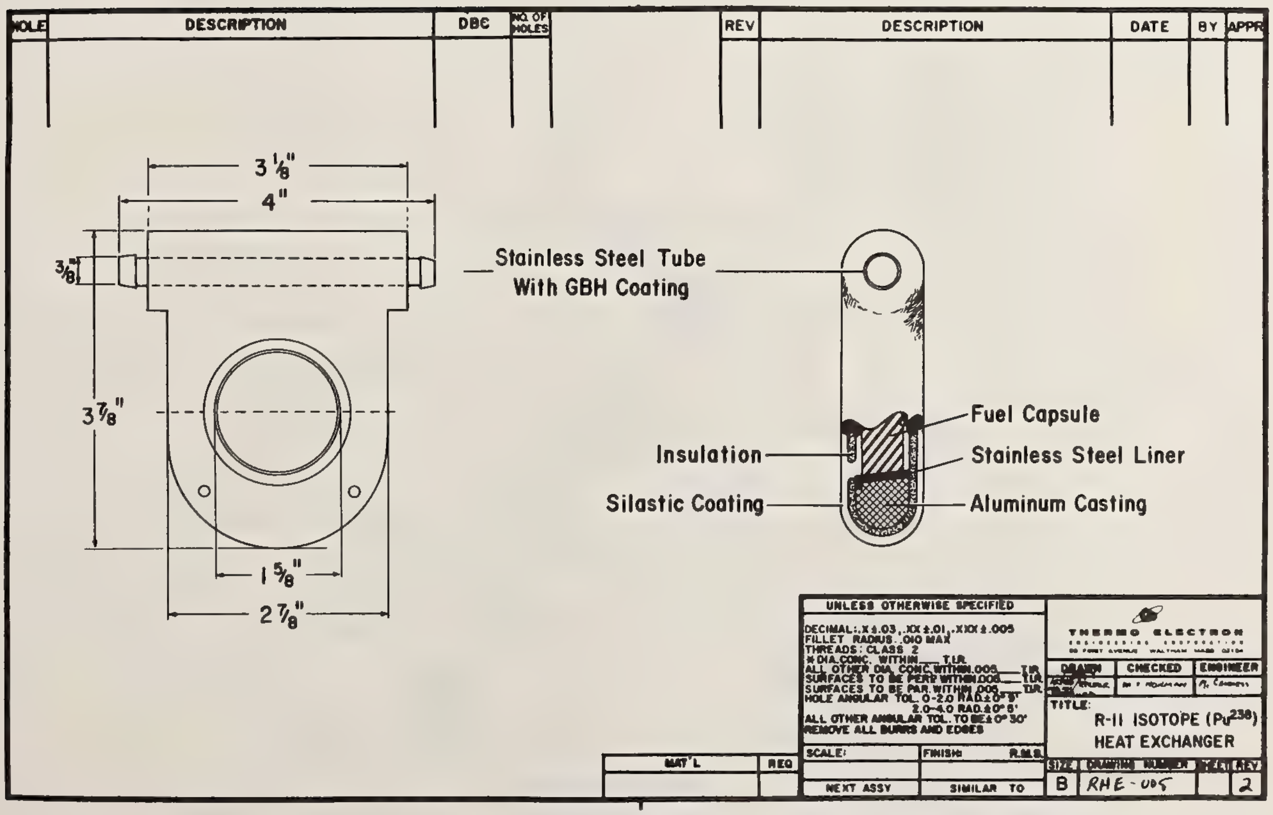

FIGURE 2. RADIOISOTOPE HEAT EXCHANGER DESIGN.

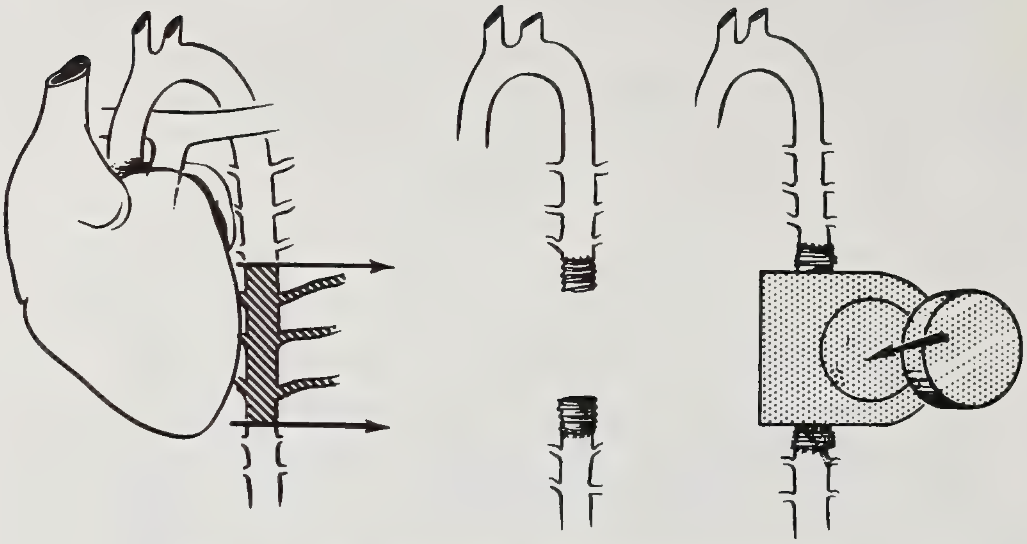

FIGURE 3. STEPS IN THORACIC IMPLANT OF Pu-238 CAPSULE.

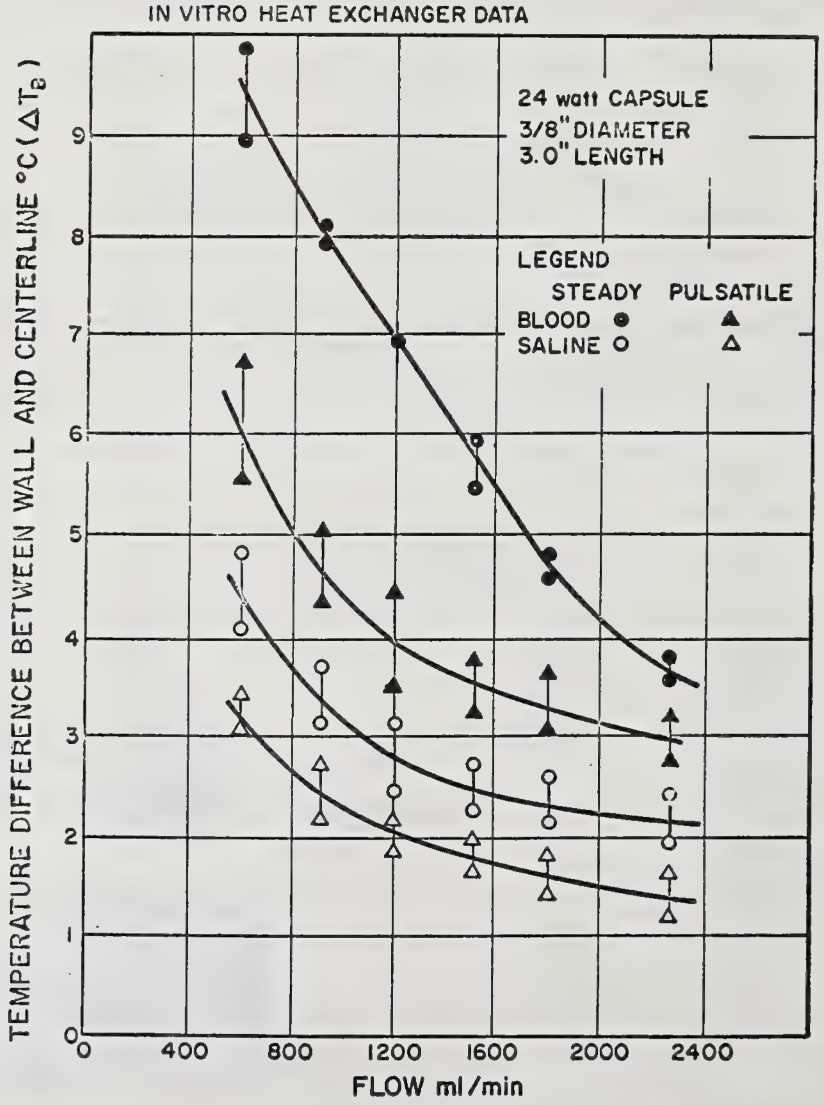

FIGURE 4. DIFFERENTIAL COOLANT TEMPERATURE AS A FUNCTION OF FLOW RATE.

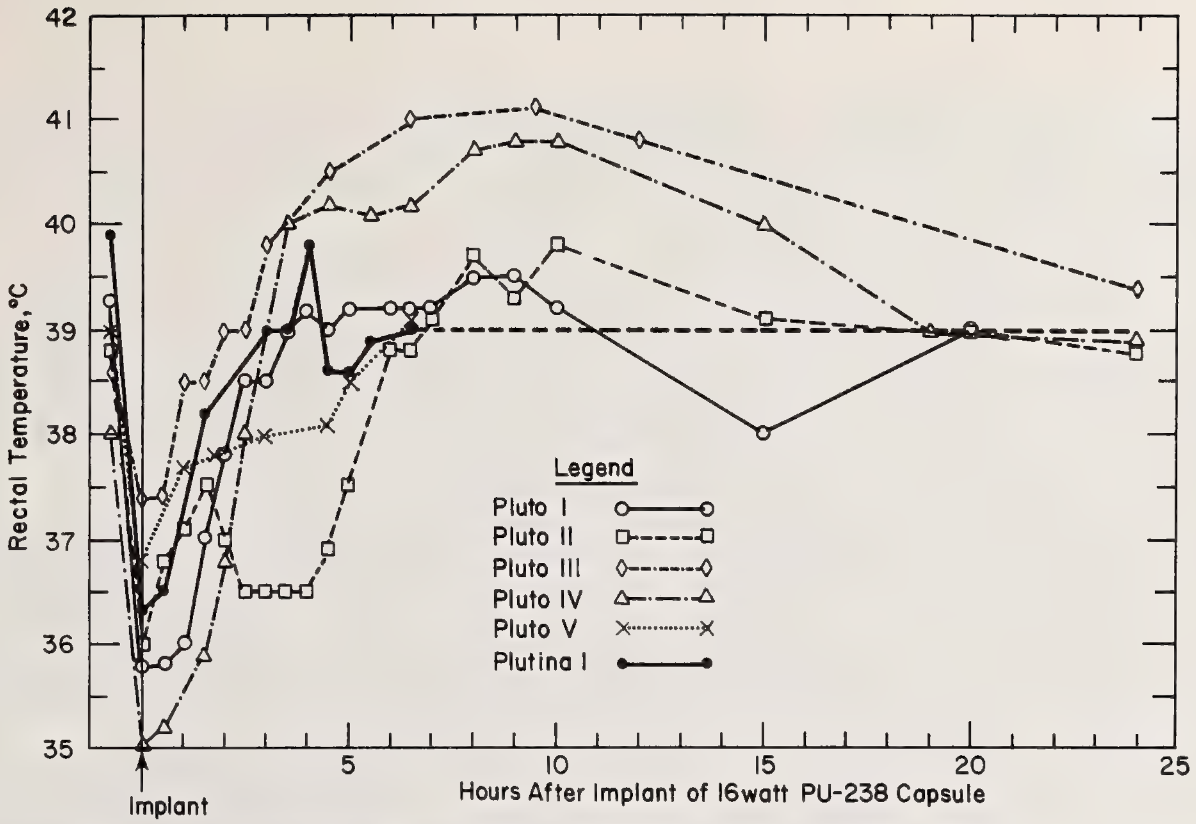

FIGURE 5. RECTAL TEMPERATURES FOR THE FIRST 24 HOURS AFTER IMPLANT; SIX DOGS 16-WATT CAPSULE.

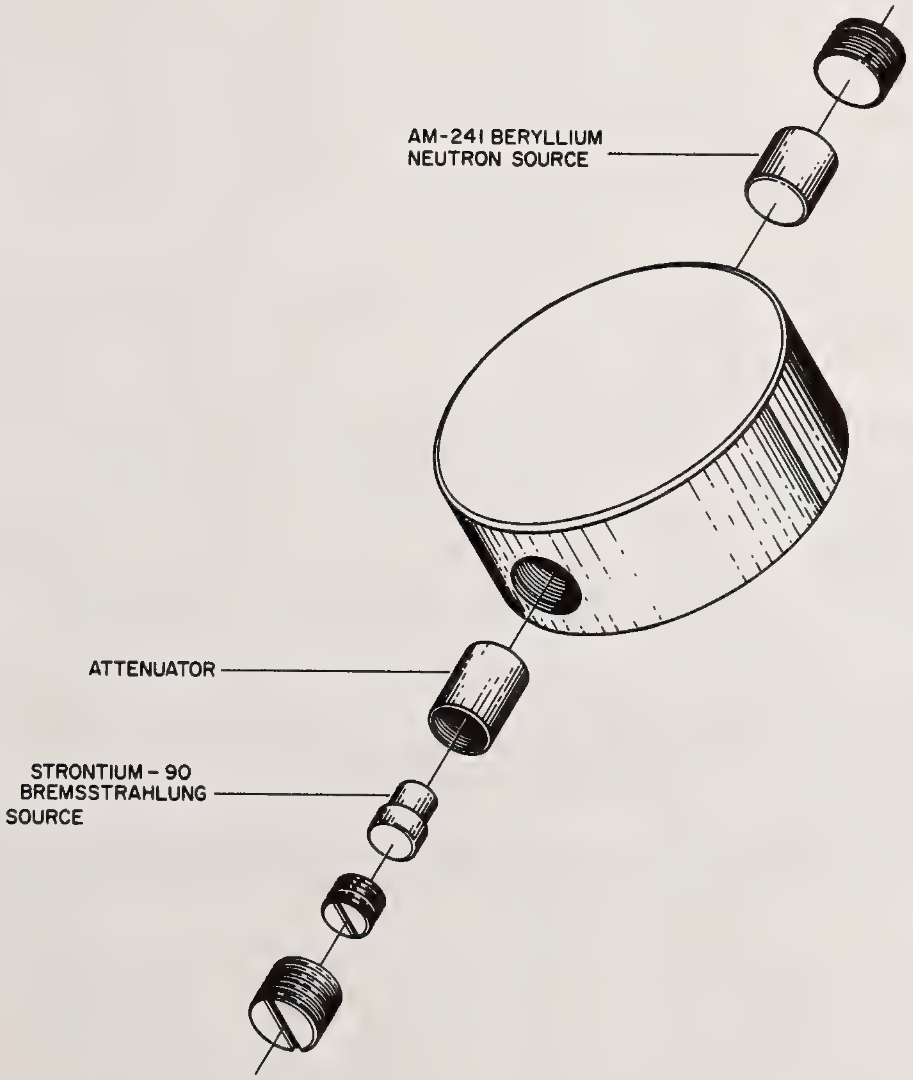
AM-241 BERYLLIUM NEUTRON SOURCE
ATTENUATOR
STRONTIUM - 90 BREMSSTRAHLUNG SOURCE

FIGURE 6. RADIATION EQUIVALENT SOURCE.

The most significant results of these studies are the long-term survivals in apparent good condition of all dogs implanted with radioisotope capsules (both Pu-238 and RES). An 85-pound female dog (Plutina) has had a 16-watt Pu-238 source implanted in series with her descending aorta for over 20 months. A 70-pound male dog with an implanted 24-watt Pu-238 source is in similar good condition after 13 months. Three animals with radiation equivalent sources are also in apparent good condition after periods up to 11 months.

Hematologic, hepatic, renal, and metabolic data have been recorded on all animals as a function of time since implantation. Hematologic and weight data of Plutina are given in Figure 7. The blood parameters all fall within normal canine limits. Normal blood urea nitrogen, uric acid and electrolyte levels, as shown in Figure 8, indicate unaltered renal function. Monitoring of hepatic function, as measured by bilirubin, enzyme and protein levels, is shown in Figure 9 and continues to be normal. Thyroid function remains normal. Serum calcium and phosphate levels remain within the normal range, indicating unimpaired parathyroid function. The physiologic data for dogs containing radioisotope sources show similar stable patterns. All of the dogs appear to be in good condition. No change in their behavior is evident.

These experiments are especially significant since the dose rates at the surface of the heat exchanger are many times higher than the maximum on the surface of the projected Pu-238 power source for driving blood pumps. In this case, more compact source geometry, distance, limited shielding and higher purity fuel can all be used to reduce the dose rate. The maximum dose rate at the surface of the 16-watt exchanger is about 600 mrem/hr, while the dose rate on the surface of the 24-watt heat exchanger is around 1000 mrem/hr. Figure 10 gives the gamma plus neutron dose rate as a function of distance from the source. The gamma and neutron dose rates are approximately equal at the capsule surface. The air values were measured by Mound Laboratory while the tissue dose rates were calculated and normalized to the air data. The dose rate falls sharply with distance from the source, primarily due to geometric attenuation rather than to absorption in the tissue.

An exploration of the effects of the implanted radioisotope sources on somatic cells has begun. These studies have revealed the only radiation effect yet found. Figure 11 shows a photomicrograph of a representative field of lymphocytes cultured _in vitro_ after phytohemagglutinin stimulation. The specimen was taken from Plutina eleven months after implantation of the 16-watt Pu-238 capsule. This figure shows no mitoses and virtually no lymphocytes along with debris. This result is to be compared to a representative field of a control animal in Figure 12 which shows 8 mitoses and many healthy lymphocytes. Although all radioisotope-bearing animals display this aberrant pattern, the peripheral white cell concentrations have been maintained within normal limits in all cases. This result is a typical reaction to exposure levels far less than those received by the dogs in this study. Thus far, the effect appears benign. The fact that the radiation exposure is non-uniform and protracted helps the animals tolerate the insult. Since the lymphocyte aberrations are present in both Pu-238 and RES animals, it is concluded that the effect is due to radiation rather than to heat.

Two of the radiation equivalent source dogs were mated and a litter of 9 pups were born eight months ago. The three surviving pups appear to be normal. Although this mortality rate is high, it is not clear that this is due to radiation.

CONCLUSIONS

Because of the limited number of experimental animals and restricted test periods, the conclusions drawn from these studies must be considered as tentative. However, on the basis of present experience, it appears highly probable that:

1. _Transient Thermal Input_
   Experimental animals adjust their temperature regulation mechanisms to dissipate up to 24 watts of additional endogenous heat without significant elevations in core temperature.
2. _Chronic Thermal Input_
   The additional endogenous heat is tolerated by dogs for periods up to 20 months and continuing.
3. _Heating Index_
   Additional endogenous heat loads of approximately 0.8 watt/kilogram may be dissipated without apparent ill effects for periods up to 13 months and continuing.
4. _Radiobiological Effects_
   No discernible radiation effects, other than anticipated lymphocyte abnormalities, have been identified.
5. _Intravascular Prosthesis Material_
   After a review of the patency of titanium and 304 stainless steel blood tubes used in these studies, titanium would appear to be the superior material for intravascular prostheses.

In summary, these studies are encouraging that the anticipated levels of reject heat and radiation produced by a totally implanted circulatory support system can be tolerated by human beings.

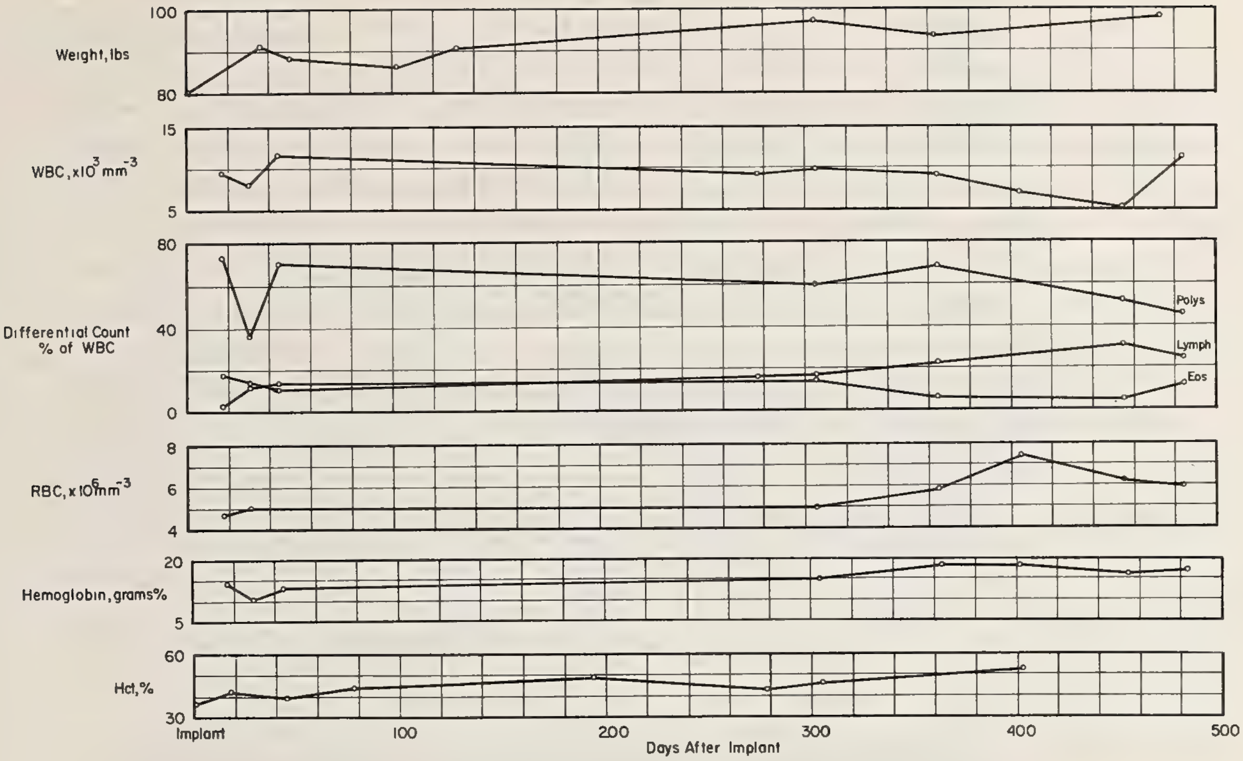

FIGURE 7. HEMATOLOGY AND WEIGHT DATA OF PLUTINA VERSUS TIME.

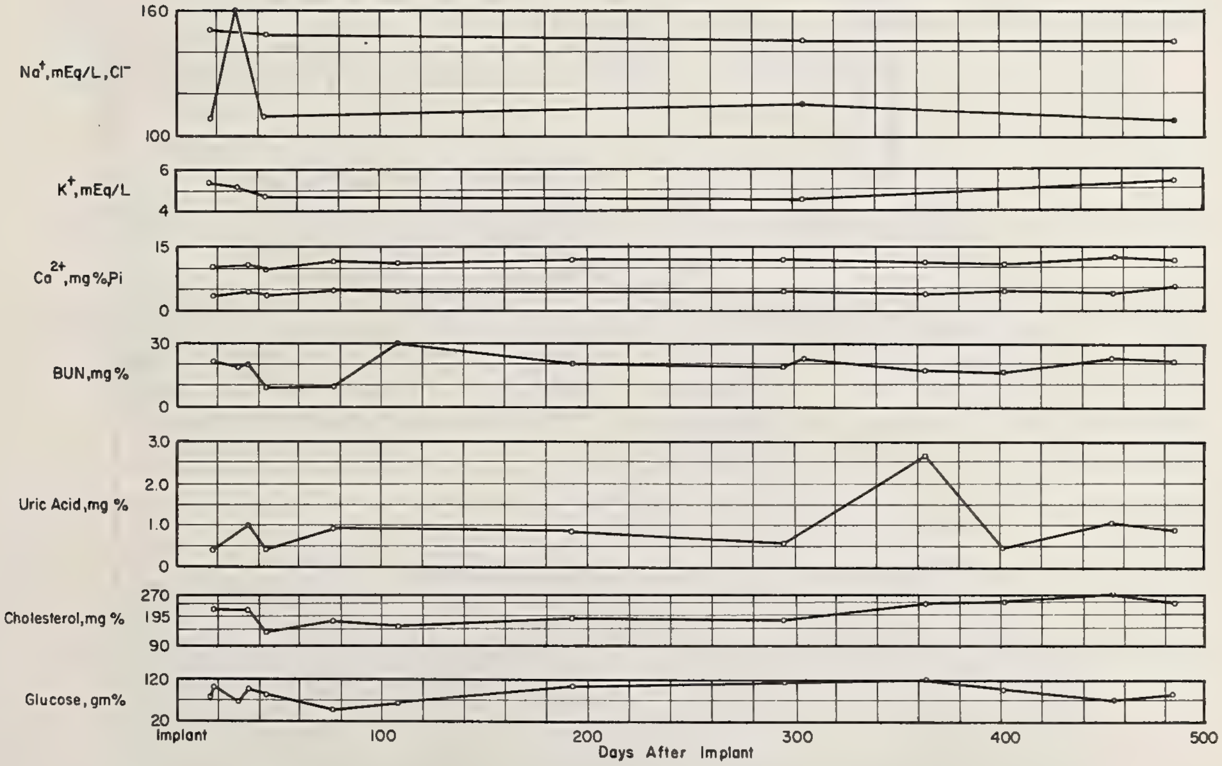

FIGURE 8. RENAL FUNCTION, CHOLESTEROL AND GLUCOSE DATA OF PLUTINA VERSUS TIME.

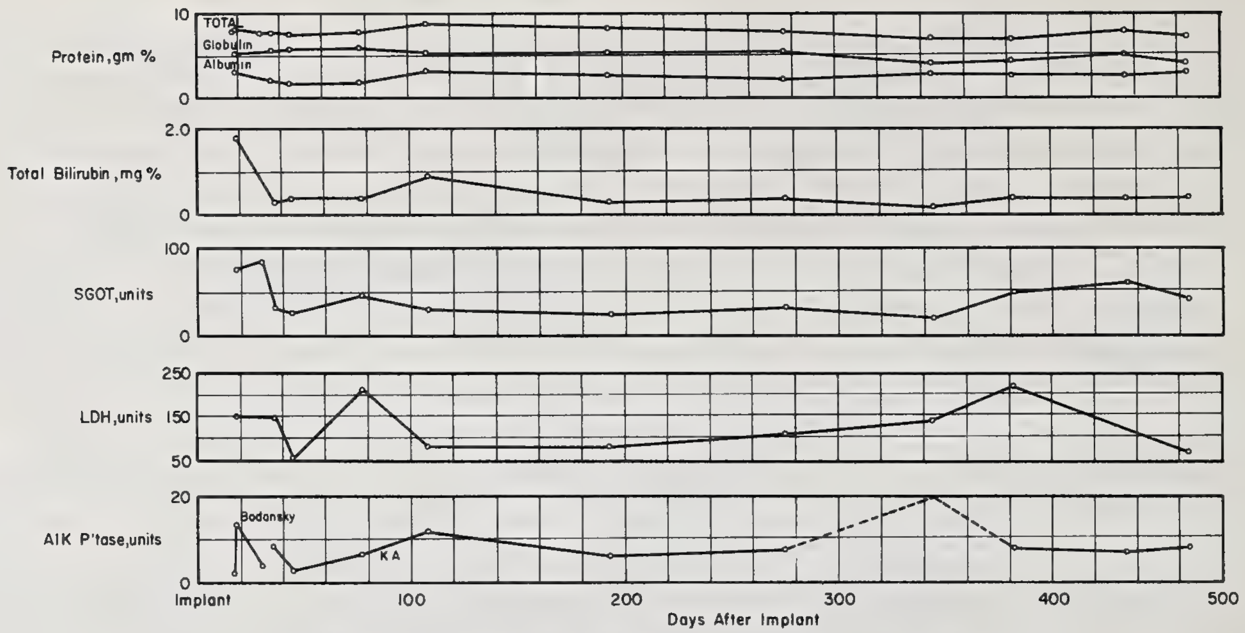

FIGURE 9. LIVER FUNCTION DATA OF PLUTINA VERSUS TIME.

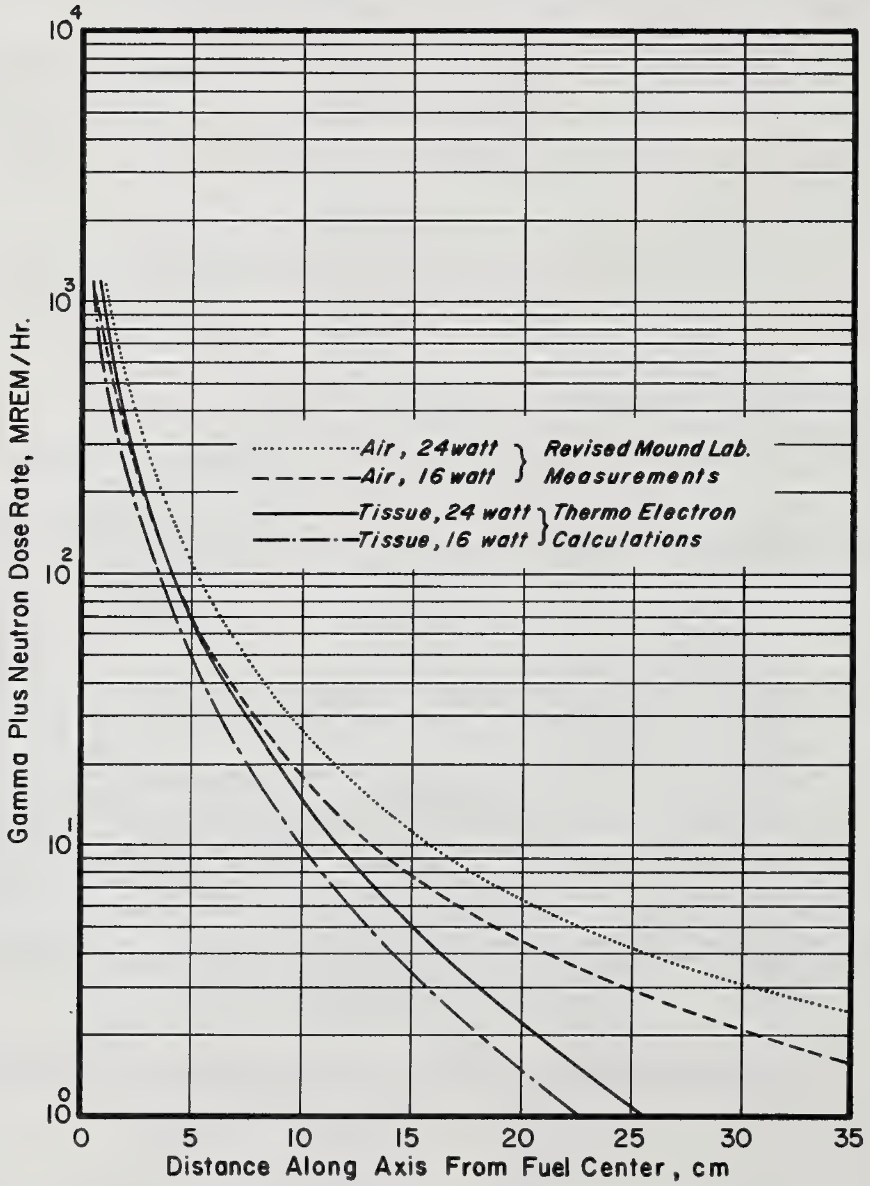

FIGURE 10. DOSE RATES FROM 16 AND 24 WATT PLUTONIUM-238 CAPSULES.

REFERENCES

Norman, J. C., LaFarge, G., Harvey, R., Robinson, T. and Bernhard, W. F.: Experimental Model for Inducing Acute and Chronic Hyperthermia; Developmental Methods and Preliminary Observations as Related to Power Requirements of Cardiac Prostheses. Transactions of the American Society for Artificial Internal Organs, 12: 282, 1966.

Bernhard, W. F., Norman, J. C., Harvey, R., LaFarge, G., Robinson, T. and van Someren, L.: An Investigation of Induced Chronic Hyperthermia and In Vivo Heat Dissipation. Journal of Thoracic and Cardiovascular Surgery, 52: 611, 1966.

Norman, J. C., LaFarge, C. G., Harvey, R., Robinson, T., van Someren, L. and Bernhard, W. F.: Heat Dissipation: A Common Denominator of Implantable Power Sources for Cardiac Prostheses. Surgical Forum, 17: 162, 1966.

LaFarge, C. G., Robinson, T., Bernhard, W. F., Harvey, R. J. and Norman, J. C.: Chronic Hyperthermia in Dogs: Responses to Pyrexia and Exercise. Circulation(SupplementIII)34: 152, 1966.

Harvey, R. J., Robinson, T. C., Bernhard, W. F., Norman, J. C., van Someren, L. and LaFarge, C. G.: Evaluation of the Rankine steam Cycle as a Power Source for a Portable Artificial Heart. Proceedings of Biomedical Engineering Symposium, Progress in Biomedical Engineering. Ed. L.J. Fogel and F. W. George, Spartan Books, Washington, pp. 259-269, 1967.

Norman, J. C., Covelli, V. H., McCandless, W. J. C. and Bernhard, W. F.: Feasibility of Implantable Pu-238 Power Sources for Circulatory Assist Devices. Circulation Supplement, 36: 200-201, 1967.

Norman, J. C., Harvey, R. J., Covelli, V. H., McCandless, W. J. C. and Bernhard, W. F.: Implantable Power Sources: Continuing Studies. Proceedings of 20th Annual Conf. on Engineering in Medicine and Biology, Boston, 9: 3.4, 1967.

Harvey, R. J., Robinson, T. C., McCandless, W., Bernhard, W. F., Bankole, M. A. and Norman, J. C.: Studies Related to Heat Transfer and Flow in an Aortic Prosthesis. Digest 7th International Conf. Med. & Biol. Engineering, Stockholm, p. 389, 1967.

Norman, J. C., Covelli, V. H., Bernhard, W. F. and Spira, J.: An Implantable Nuclear Fuel Capsule for an Artificial Heart. Amer. Soc. Artif. Intern. Organs, 14: 204-208, 1968.

Huffman, F. N., Covelli, V. H., Sandberg, G., Lee, R., Norman, J. C. and Spria, J.: Studies of Reject Heat and RAdiation from Implanted Radioisotope Sources. Winter Annual Meeting of Am. Soc. of Mech. Engineers, Engineering Systems Exposition, New York, 1968.

Norman, J. C., Covelli, V. H., Bernhard, W. F. and Spira, J.: Implantable Nuclear Fuel Capsules for Artificial Hearts: In Vivo Dosimetry. Surgical Forum, 19: 140-141, 1968.

Norman, J. C., Covelli, V. H., Bernhard, W. F. and Spira, J.: In Vivo Nuclear Power (16 & 25 Watt Pu-238) Sources for Artificial Hearts. Circulation Supplement No. VI, 38 (4): 49, 1968.

Pegg, C. A. S., Joison, J., Sandberg, G., Huffman, F. and Norman, J.: Intracorporeal Irradiation Without Heat: Studies of Nuclear Heat Sources. Clinical Research. 16 (4): 517, 1968.

Pegg, C., Sandberg, G., Lee, R., Huffman, F. and Norman, J.: Effects of Intracorporeal Sr 90-Am 241/Be Sources (RES) Simulating Radiation Fields from Pu-238-Fueled Artificial Hearts. Fed. Proc. (Abst.), 28 (2): 789, 1969.

DISCUSSION

DR. GILLIS: You mentioned that 150 degrees was the design limit for condenser temperature and on our particular heater, which, granted, had a rather thick fibrin flock coat, the 150 degree wall temperature point was reached at about 28 watts. This is what concerned us because of the possible future need for 40 watts or more heat dissipation.

DR. HUFFMAN: I'd like to ask you if any anticoagulant was given to the animal during the period in which the tissue was growing?

DR. GILLIS: We avoided this on purpose because we wanted a fibrin coat to lay down immediately after surgery.

DR. HUFFMAN: Even with an anticoagulant, one obtains a fibrin deposition. However, the thickness of the coating appears to be limited when the anticoagulant is given during the period in which the autologous lining is building. Also, as I noted previously, about 40 to 50% of the heat actually comes out on the surface of the components. It is hard to limit the surface loss to less than this. With a complete circulatory support system, there would be quite a bit more area exposed directly to the tissue than in this experiment. This increased area would tend to keep the condenser temperature down.

MR. PURDY: I'd like to congratulate both of you gentlemen on your presentation and the work you have done. It is very interesting and I think certainly a step forward towards the use of radioisotopes for heat sources for Rankine cycle systems. I have two questions: the first question concerns the thermal drop in the blood pump system. At approximately the 30 watt power level that you mentioned, what were the temperature drops from the surface to the blood?

DR. HUFFMAN: The temperature across the bladder is the difference between the rectal temperature (being typical of the blood temperature) and the temperature of the water in the drive line. This difference would be about an 18° F rise. The temperature drop down the drive column of water which couples the blood pump to the actuator was too small to measure. The drop was about 1° F. Now the other temperature rise depends on how good the heat transfer is from the condenser to the water column. We believe that this can be limited to something like 10° F.

MR. PURDY: What was the volumetric flow rate and what is the surface area of your heat exchanger surface?

DR. HUFFMAN: The surface area of the bladder is something like 100 sq. cm. I don't remember the volumetric flow rate.

MR. PURDY: With respect to your 16 and 24 watt implantable sources, you mentioned that the dose rate on the surface of the 16 watt was 800 millirem per hour and the 24 watt was 1000 millirem per hour. Could you tell me what the contributions were for gamma and neutrons and what biological conversion factors you used to convert from millirads to millirems for the neutron dose rate?

DR. HUFFMAN: The neutron and gamma components, in millirems per hour, were roughly equivalent on the surface. The RBE that was used was that of NBS Handbook 63.

MR. PURDY: Do you remember what it was in the tens, for example?

DR. HUFFMAN: It was close to ten.

DR. CLARKE: Did I understand you to say that there were no metaphase plates in the cells of the experimental animals, in all microscopic fields examined?

DR. NORMAN: No, that's not true at all. The examples we showed you were the most severe changes, actually about 50 fields are counted and three culture tubes are set up on controls as well as serial cultures on each of the radiation equivalent source animals as well as the 16 watt and 25 watt plutonium source animals. In some fields counted, you can see relatively normal lymphocyte mitoses and this, of course, has been described in our report. I think we've had something in the range of 50 illustrations through the past year on different myelocytic cultures. However, you can see metaphase plate arrest on the third day following the lymphocyte cultures. We can also show you relatively normal appearing microscopic fields. If you scan the entire microscopic slide, there is a differential between normal and experimental animals. The significance of these observations is an object of further study. As you know, patients who have had radiation in childhood may show this type of lymphocyte arrest in adulthood. There are probably three populations of lymphocytes: short lived, long lived and a third type with a half life of more than 20 years. This moves us into the area of immunology and the circulation of lymphocytes and opens up another new area of study of these specific animals. Often, in the radiation equivalent dogs, you see relatively normal leukocyte mitoses, which is included in the report.

DR. CLARKE: Have you done any karyotypic studies at all?

DR. NORMAN: Yes. The karyotypes aren't changed at all. In terms of karyotypes, we consider the lymphocyte chromosomal pattern as part of karyotyping. This involves other experiments, transplantation experiments, where we used the female xy and xx chromosome appearances to determine whether or not in these transplantation experiments we had a female or male donor. The karyotypes in the lymphocytes that are undergoing mitoses are relatively normal.

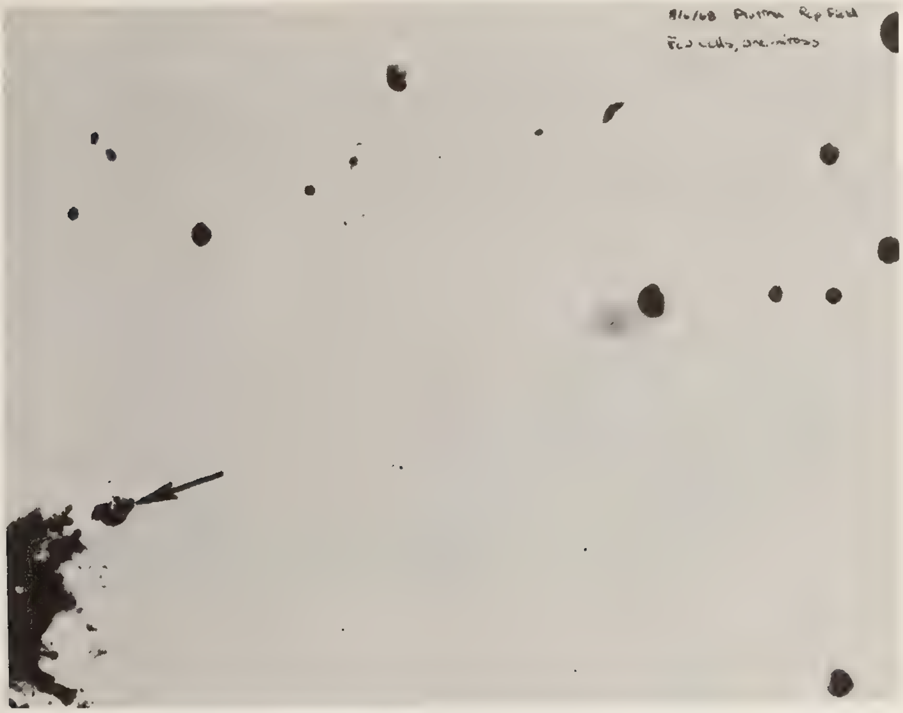

FIGURE 11. ANOTHER FIELD (ORIGINAL MAGNIFICATION 10x) OF LYMPHOCYTES CULTURED FROM PLUTINA (FEMALE), ELEVEN MONTHS AFTER 16 watt Pu^{238} FUEL CELL IMPLANTATION SHOWING A FEW LYMPHOCYTES AND ONE MITOSIS INDICATED BY THE ARROW (COMPARE WITH FIGURE 11).

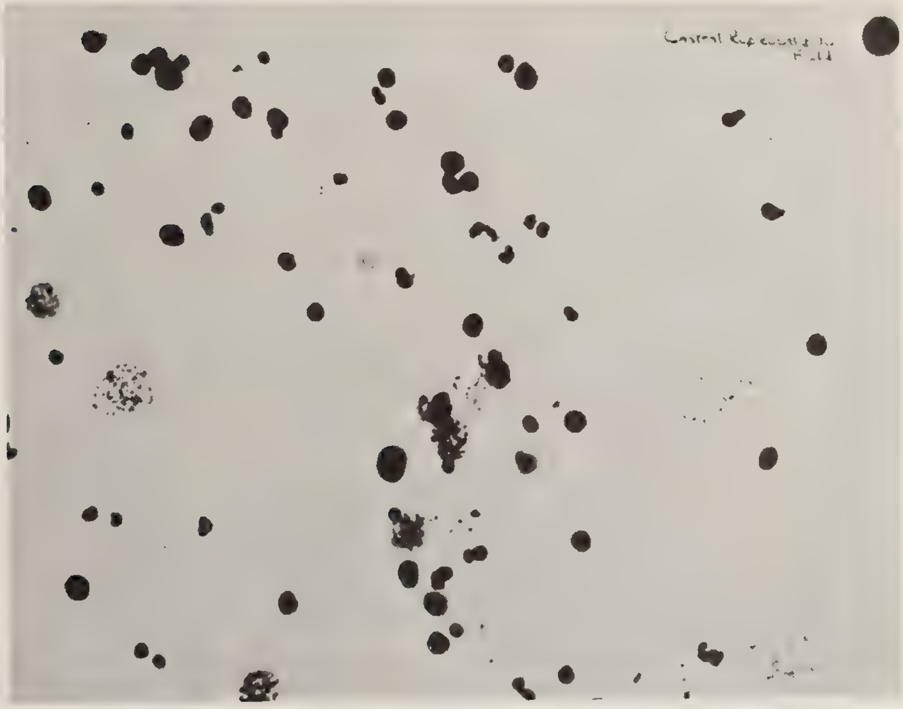

FIGURE 12. CONTROL REPRESENTATIVE FIELD (ORIGINAL MAGNIFICATION 100x) OF LYMPHOCYTE CULTURE OF NORMAL FEMALE DOG #4202 SHOWING EIGHT MITOSES, AND ROUND MODERATELY DARK STAINING HEALTHY LYMPHOCYTES.

SECTION XII

IMPLANTABLE ENERGY SYSTEMS

Chairmen: Roger S. Powell
Lowell T. Harmison

INTRODUCTION

The development of high performance, reliable and safe implantable energy systems is absolutely essential to the achievement of implantable cardiac assist and heart replacement devices. The stringent requirements of energy systems for biological applications are not significantly different in terms of complexity from energy system requirements for space applications, i.e., inertness to environmental effects, minimal volume and weight, response to required load demands, high efficiency, reliability, safety, etc. The systematic approach to providing energy to drive cardiac assist or replacement devices can be divided into (1) selection of a source of energy; (2) selection of the means of storing sufficient energy to provide patient mobility and rehabilitation; (3) selection of the means for conversion of the energy from the source to the final use form; (4) selection of the means of controllling the flow of energy to the blood pump; and (5) interfacing the energy system with the blood pump itself. As the degree of implantability increases, the requirements of the energy system and the associated problems become more difficult. Despite the increased complexity, the advantages of complete implantation (the elimination of problems of percutaneous leads, the minimization of patient psychological problems, and the increase in patient mobility and rehabilitation) make it a most desirable goal.

CHAPTER 77

A POWER TRANSFORMER FOR MECHANICAL HEARTS

A. Thumim, G. Reed, F. Lupo, G. Myers and L. Cortes

New York University
New York, New York

A power transformer which is capable of transmitting over 30 watts of power through intact skin has been constructed and tested in animals. Modified models of the transformer which have an efficiency of 80 to 90% can also be used at higher power levels to charge implanted power storage devices. With proper cooling of the primary, power in excess of 100 watts has been transferred. The device which works at audio frequency range of 3 to 30 k_c is double tuned and air gap variations between 8 to 15 mm and lateral motion of ±1 cm can be tolerated with little reduction in power transfer. The device consists of two circular "cup cores" 6 cm in diameter, weighing 300 g each; one is placed subcutaneously and one, externally. The internal unit is stabilized by a Teflon "skirt" sutured to the fascia, and by a molded cup on the external unit. The electronics consists of a multivibrator followed by a transistorized power switching stage. Acute and chronic tests in five dogs and three sheep indicate no deleterious effects. The measured temperature rise is less than 3°C inside the encapsulation and 1°C at a point 3 cm distal to the unit. The new feature is a method of permitting large variations in air gap, accomplished by tuning the transformer so that it becomes "double tuned," and then making the coupling coefficient greater than the critical value for the nominal skin thickness. Thus, as the air gap is increased, the coupling coefficient approaches the critical value and the power transferred increases slightly and then decreases. The study confirms that the power transformer can transmit adequate power for energizing an artificial heart and with some modification can be adapted to transmit higher levels of power for charging implanted storage devices. In accordance with expectations implanted units that have been removed after long-term implantation show good ingrowth of fibrous tissue through the Teflon skirt which fixed the unit firmly in its position.

INTRODUCTION

An implanted artificial heart requires approximately 30 w of power for its operation. The present state of the art of batteries of this capacity precludes their implantation for substantial periods of time. Development of biologically inert materials has not yet progressed to the point where it is feasible to power devices by wires passing through intact skin for long periods of time. As a result, the method which has proved to be most attractive is to couple electrical energy into the interior of the body by means of electromagnetic induction. It is also becoming evident that the trend will be toward systems that will include an implantable energy storage device and in this case it is desirable to be able to remove any external connections or unit from the patient between charging intervals. Schuder[1] has done the initial investigations and experiments in radio frequency power transmission through intact skin. He has shown conclusively that this approach is practical. Schuder has made most of his devices work at frequencies in the neighborhood of 455 KHz. He has also undertaken extensive experiments to determine any possible effects of tissue damage caused by the radiation at these frequencies, and in general has found such damage to be negligible. His approach has been to make a radio-frequency transformer with two "pancake" windings, one on the outside and one on the inside of the body. At the frequencies he uses, iron cores are not necessary.

The approach taken by the investigators in the work described in this paper was to follow the general philosophy used by Schuder, but to use low audio frequencies in the range 3,000 to 15,000 Hz. To get efficient coupling at these frequencies, iron cores (made from ferrite) are required. When such cores are used, a transformer with a relatively small size and weight results so that the total weight of the implanted portion of the transformer is approximately the same as that of a cardiac pacemaker, and is comparable to weights reported for higher frequency devices. Thus, no penalty seems to be present when this approach is used. On the other hand, certain advantages exist when low audio frequencies are employed, principally simplicity in the electronics. Power at the appropriate frequencies can be generated efficiently with simple electronics, using either a battery or line current as a basic power source. Eddy current losses in tissue are negligible at the frequencies employed. While the presence of a core means that core losses now must be included, the net efficiency of the transformer reported here (for 30 w of transmitted power) is up to 90 percent, which is about the same as has been reported for the radio-frequency devices. Evidently, most of the losses in both the high and low frequency devices are in the copper winding, and the lower frequencies reduce the copper loss sufficiently so that the sum of copper and core losses at both frequencies approximately equals the copper losses at the higher frequencies. An additional advantage, which would be realized if these devices were in common use, is that there is less possibility of radio-frequency interference from the electronics or from the transmitter. At frequencies of 455 KHz, and at power levels of 30 w, interference might be noticeable in radio and television receivers.

PHYSICAL DESCRIPTION OF THE DEVICE

Physically, each half of the transformer is a ferrite cup core, 6 cm in diameter and 2 cm thick. A typical unencapsulated unit is shown in Figure 1. The cores are fabricated from commercial ferrite cores, which are usually made in much larger sizes. Thus, it is necessary to reduce the size of the cores by machining them with diamond tools. The windings have roughly 200 turns, 22 gage copper wire insulated with double formvar enamel. The weight of each unit, when encapsulated, is 8 oz. The encapsulation consists of an initial impregnation with silicon rubber, followed by a thin coating of biologically-inert epoxy resin. The windings are made on an ordinary coil winder, and no special winding patterns are used. Because of the nature of the implants, it is not feasible to use paper for interwinding insulation. Therefore, it has been found that great care must be taken in winding the coils to avoid scraped insulation and the resulting shorted turns, which tremendously increase losses. In the primary coil of the transformer a bifilar winding is used. It consists of two one hundred turn windings of 22 gage wire in parallel. The secondary is a single winding of 220 turns. This configuration reduces the copper losses of the primary as well as the voltage across it (for a given load). External connections are made with lead wire of the type used in pacemakers, which is highly fatigue resistant. Both the primary and secondary are tuned, as is shown in Figure 2, by means of capacitors. Because the Q of the secondary is low the tuning of the capacitor in the secondary is not very critical. However, the initial proper tuning is important in the primary circuit. It has been found to be more convenient to choose first a frequency that will guarantee over-critical coupling for the airgap and load used, and then tune the device by means of decade capacitors in the primary and secondary. Once the device is tuned these decade capacitors can be replaced with commercially available capacitors of the proper values. The entire device can be fabricated from available components.

The voltage supplied by the basic audio frequency power source is between 30 to 100 v rms depending on the load impedance and power source. The voltages across the primary capacitor and primary winding at resonance are of the order of 200 v, but during tuning it may be several times higher so care must be taken to use adequate insulation. In the current model, which has a 200 turns bifilar primary and 220 single coil secondary, the load current is 0.75 amps and the load voltage is 36 v (on a 50 ohms load).

One of the major problems in transformers of this kind is the maintenance of proper coupling between the primary and secondary cores. This requires both proper physical alignment across the airgap and proper tuning for this airgap. The problem of physical alignment of the transformer is reduced by the particular tuning method used. Proper tuning of the primary and secondary units can materially increase the range of motion which the units can undergo and still maintain good coupling. Figure 3 is a plot of output voltage versus frequency for a double tuned transformer. Several curves are shown for different values of the coupling coefficient k. It can be seen that at resonant frequency maximum output will occur if the coupling coefficient is k_c. This is called the critical coupling. For a given transformer geometry, load, and frequency of operation critical coupling occurs at a particular airgap. If the airgap is reduced the transformer becomes overcoupled, k_3 and k_4 in Figure 3. If the airgap is increased, the transformer output drops, k_2 and k_1 in Figure 3. The tuning method employed makes the transformer over-coupled (k_3 in Figure 3) at the nominal airgap used. Now the transformer output will not drop immediately when it is misaligned, but will first increase as the coupling approaches critical coupling k_c and only then start dropping (to k_2). It is clear from the same figure that for the over-critical transformer proper power transfer will be maintained as the oscillator frequency is shifted about f_o such that the unit becomes less sensitive to the source frequency.

If the units are brought closer together so that the thickness of the airgap decreases below the nominal value, the power output will still decrease, but not very rapidly, because the decrease in the power transfer as a function of coupling coefficient is slow for over-coupled transformers. In any case, the most common problem would be increase in the airgap or lateral motion of the units. As a result of this tuning method, the airgap can change in size from 8 to 15 mm with a 10 percent drop in transmitted power. Lateral misalignment of 2 cm can be tolerated too with a drop of only 10 percent in transmitted power. When properly aligned, the oscillator's frequency can also be changed over a range of more than 3 KHz with a 10 percent drop in output power.

The electronic circuit currently employed (Figure 4) consists of an astable multivibrator which generates square waves of the required frequency. Its output is amplified by a single amplification stage which then drives through a transformer two power transistors. The output power amplifier stage is a push-pull switching stage. This permits direct driving of the tuned primary circuit (which has no D.C. path). The efficiency of this power unit is high because the power transistors are switched between saturation and their off positions.

A problem which has been observed in other devices of this type is migration of the implant. That is, because of various changes in the tissues, the implanted part moves with respect to the external part, resulting in reduced coupling and higher losses. To minimize this possibility, the external device is encapsulated in a shallow cup shown in Figure 5. Since the internal device causes a bulge in the skin, the projections on the external portions can engage the internal portion, and prevent lateral motion. Also a Teflon mesh has been attached to the implanted unit and is sutured to the tissue fixing the implant in its position.

ELECTRICAL CHARACTERISTICS

This section will discuss the electrical characteristics of the transcutaneous power transformer. Of prime importance are the losses in the device. Figure 6 shows both the core losses and the copper losses when the output power is 30 w and the airgap is 1 cm. These measurements were done with a transformer consisting of a 200 turns single coil primary and a 200 turns secondary at 3700 Hz. As may be seen, optimum power transfer occurs at a load resistance of 150 to 300 ohms, although the optimum is fairly broad. The capacitors and the frequency are adjusted for the airgap at critical coupling, as will be discussed later. For the optimum load resistance, the efficiency is approximately 90 percent. These measurements were made by what is known as the "three-voltmeter method." In this method, voltages across the generator, capacitor, and transformer primary are measured. The fact that the vector diagram must close, along with the known relationship between current and voltage in the capacitor, permit computing voltage, current, and phase angle. Two points in this curve have been checked and verified by placing the unit in a calorimeter. Similar measurements to Figure 6 have been repeated on a bifilar transformer at over critical coupling. The optimum load range is lower (50-150 ohms), and the losses are slightly lower mainly because of reduced copper losses.

The optimum value of load resistance may be changed by altering the number of turns in the transformer, the capacitors, and the frequency. The size of the core may also be changed, but this in general is complicated because of the difficulty in obtaining larger cores and in machining the hard ferrites. It is probably desirable to use a flatter core of a slightly larger diameter to achieve over critical coupling in the cases in which more than 30 watts have to be transmitted.

The effect of airgap variations is shown in Figure 7(a) for the critically tuned single coil primary transformer. In this experiment, the capacitors and the frequencies were adjusted for the 1 cm airgap. The airgap was then varied and the power transfer measured. In general, the frequency and capacitors may be adjusted so that the maximum value of power transmission occurs at the actual airgap. Figure 7(b) and 7(c) show the variation in power output versus airgap and lateral misalignments for a bifilar overcoupled transformer. It can be seen that for a transformer that was tuned to transmit 30 w at a nominal airgap of 1 cm the power increases as the airgap is increased and only after it reaches a peak at a distance at which the coupling is critical, it starts dropping. Figure 7(c) shows the output power versus lateral misalignment. Here too the power increases initially as the unit shifts out of position and after it reaches a peak it starts dropping. When the device is implanted in an animal, the parameters are adjusted for the skin thickness actually encountered. No additional adjustments should be necessary in general but since the input impedance of the device is approximately resistive at the optimum setting, periodic adjustments can be made in the case of a chronic implantation. In this way, it is possible to compensate for variations in skin thickness (due to accumulated fat, for example), by means of external measurements and adjustments.

Effects of frequency variation are shown in Figure 8(a) for the critically coupled transformer. In this case, all parameters are adjusted for the 1 cm airgap, and the frequency is then varied. In Figure 8(b) the same measurement is repeated for the over coupled transformer. It can be seen that now the power transfer is much less sensitive to frequency changes and the oscillator's frequency stability is not an important consideration.

ANALYSIS OF THE DEVICE

In conventional power transformers the coupling coefficient k is assumed to be unity, but in this case it is much smaller than unity and the analysis is different than that for regular power transformers. The analysis given here is for a critically coupled transformer but most results are indicative of what is expected of a slightly overcoupled transformer. Figure 2 shows the transformer circuit with both primary and secondary tuned to series resonance by means of capacitances C_1 and C_2, respectively. R_p is the winding resistance of the primary and R_s is the winding resistance of the secondary. The load resistance is R_L and the power source has a voltage V_g and a source resistance R_g. Let

$$R_1 = R_g + R_p$$

$$R_2 = R_s + R_L$$

then

$$Q_1 = \frac{W_o L_1}{R_1}$$

$$Q_2 = \frac{W_o L_2}{R_2}$$

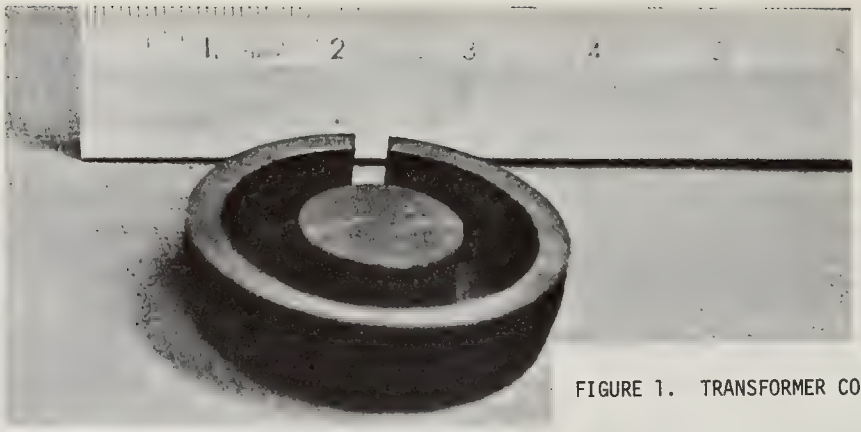

FIGURE 1. TRANSFORMER CORE.

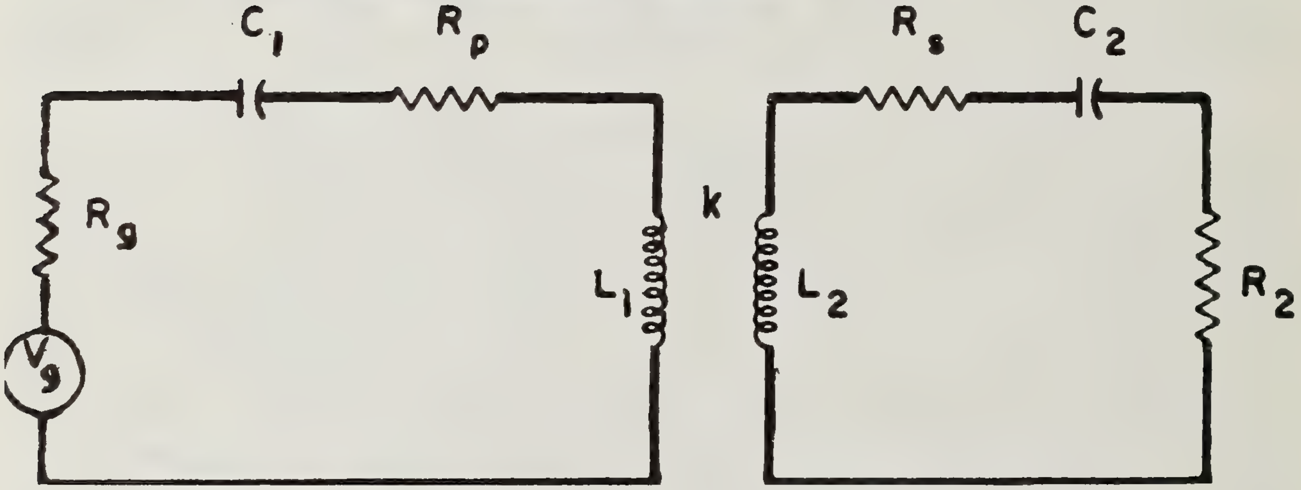

FIGURE 2. BOTH THE PRIMARY AND SECONDARY ARE TUNED BY MEANS OF CAPACITORS.

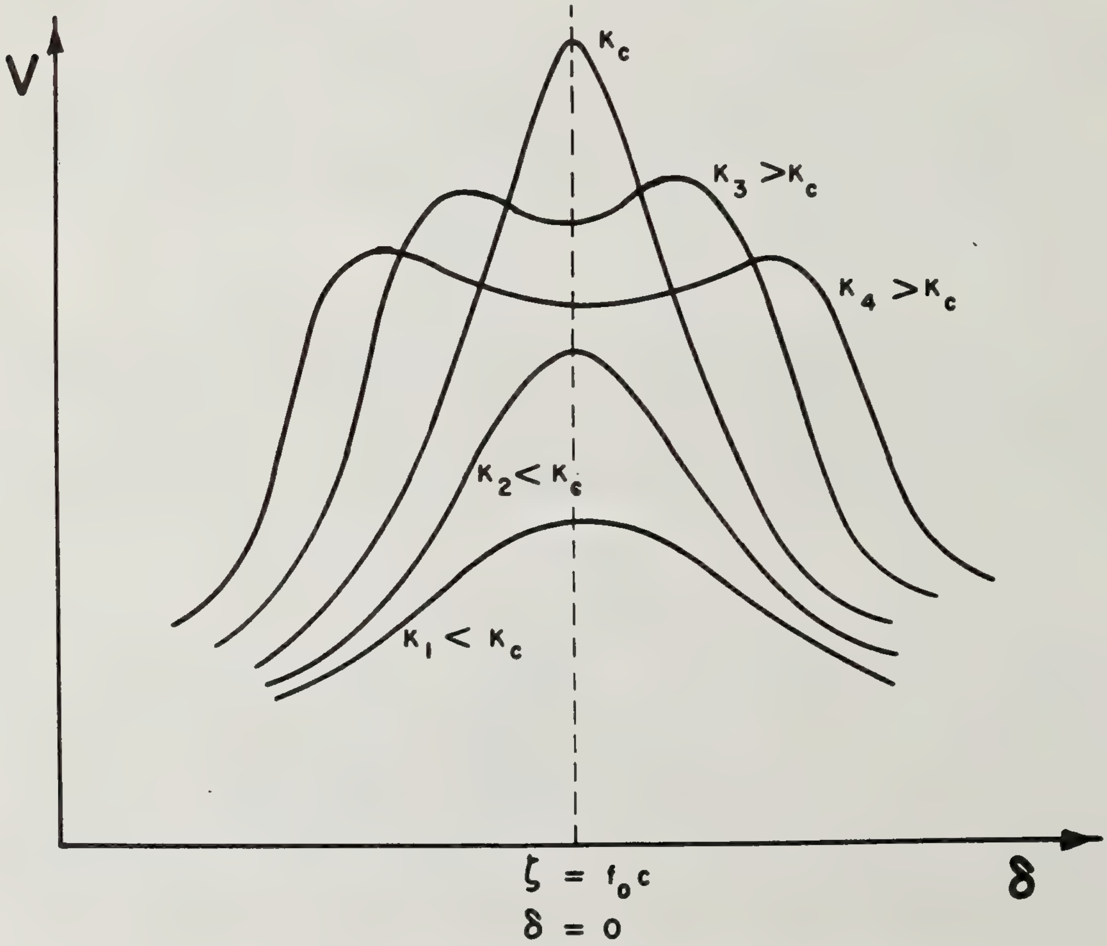

FIGURE 3. OUTPUT VOLTAGE VERSUS FREQUENCY, DOUBLE-TUNED TRANSFORMER.

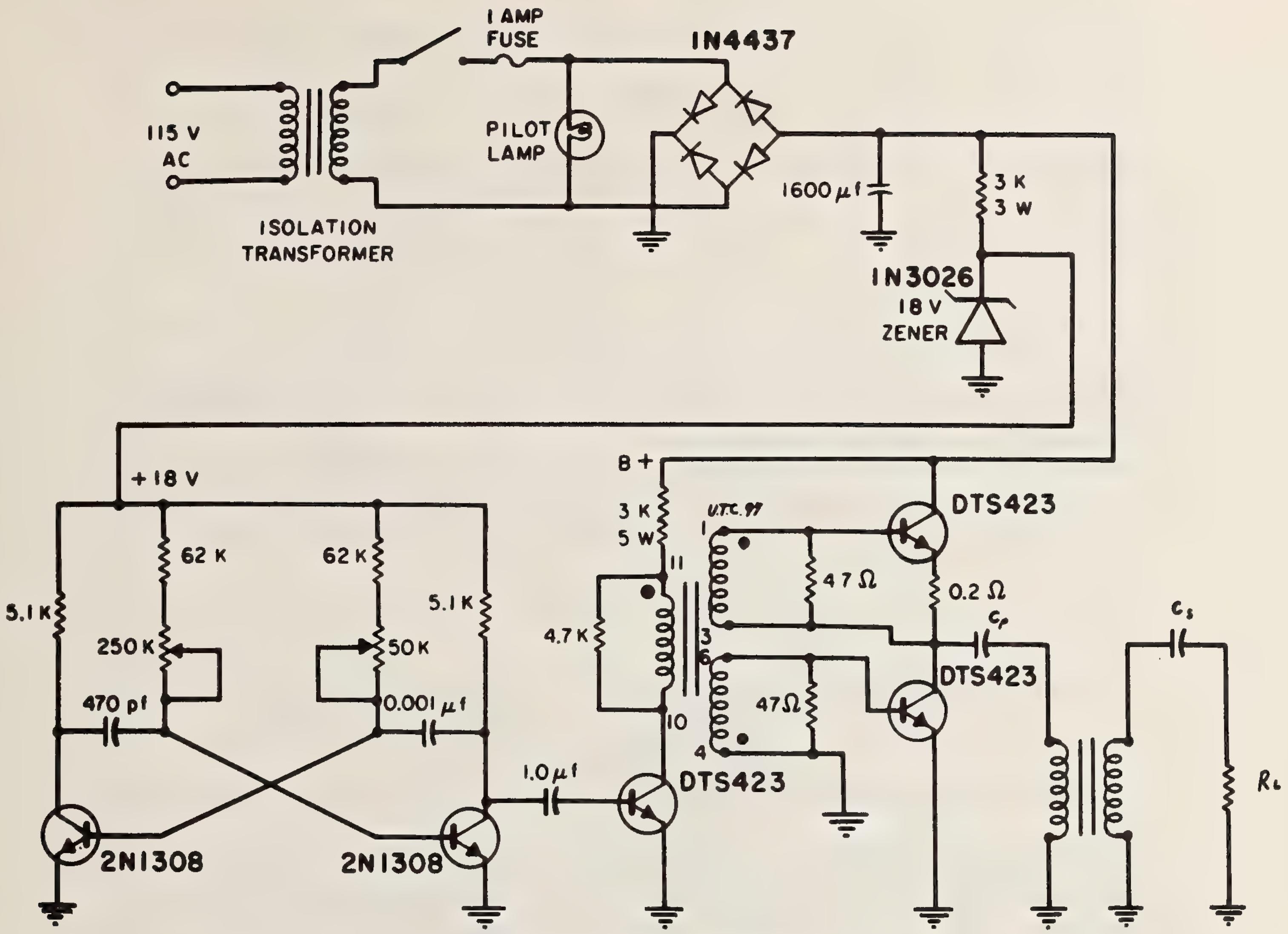

FIGURE 4. CIRCUIT DIAGRAM.

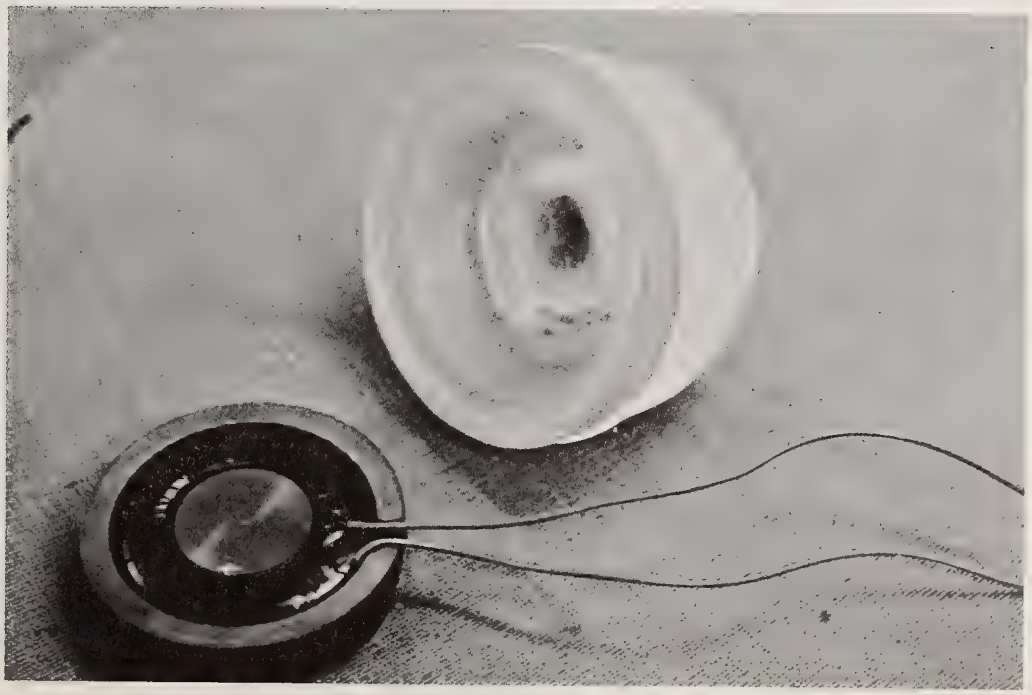

FIGURE 5. ENCAPSULATION AND CUP.

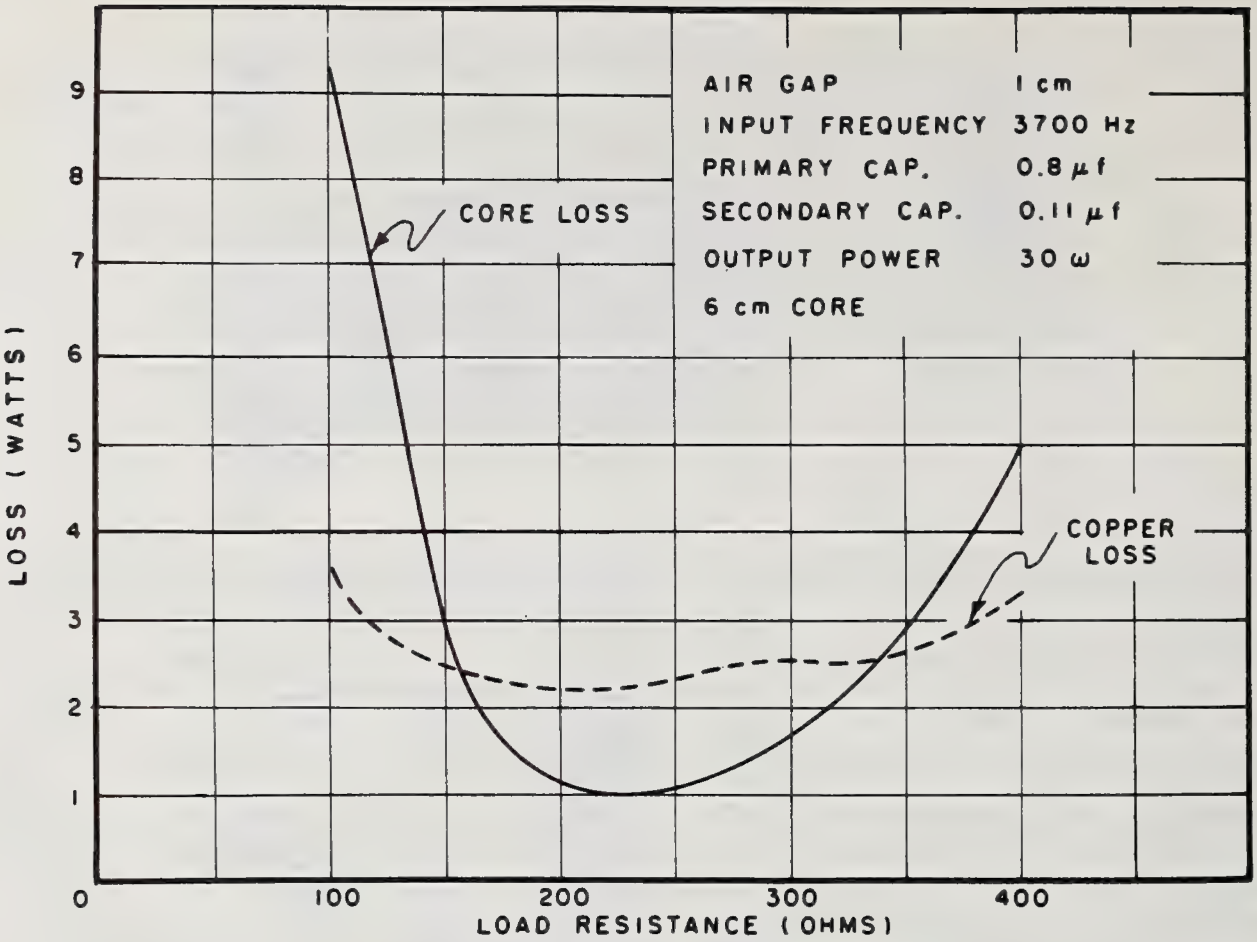

FIGURE 6. LOSSES VERSUS LOAD RESISTANCE.

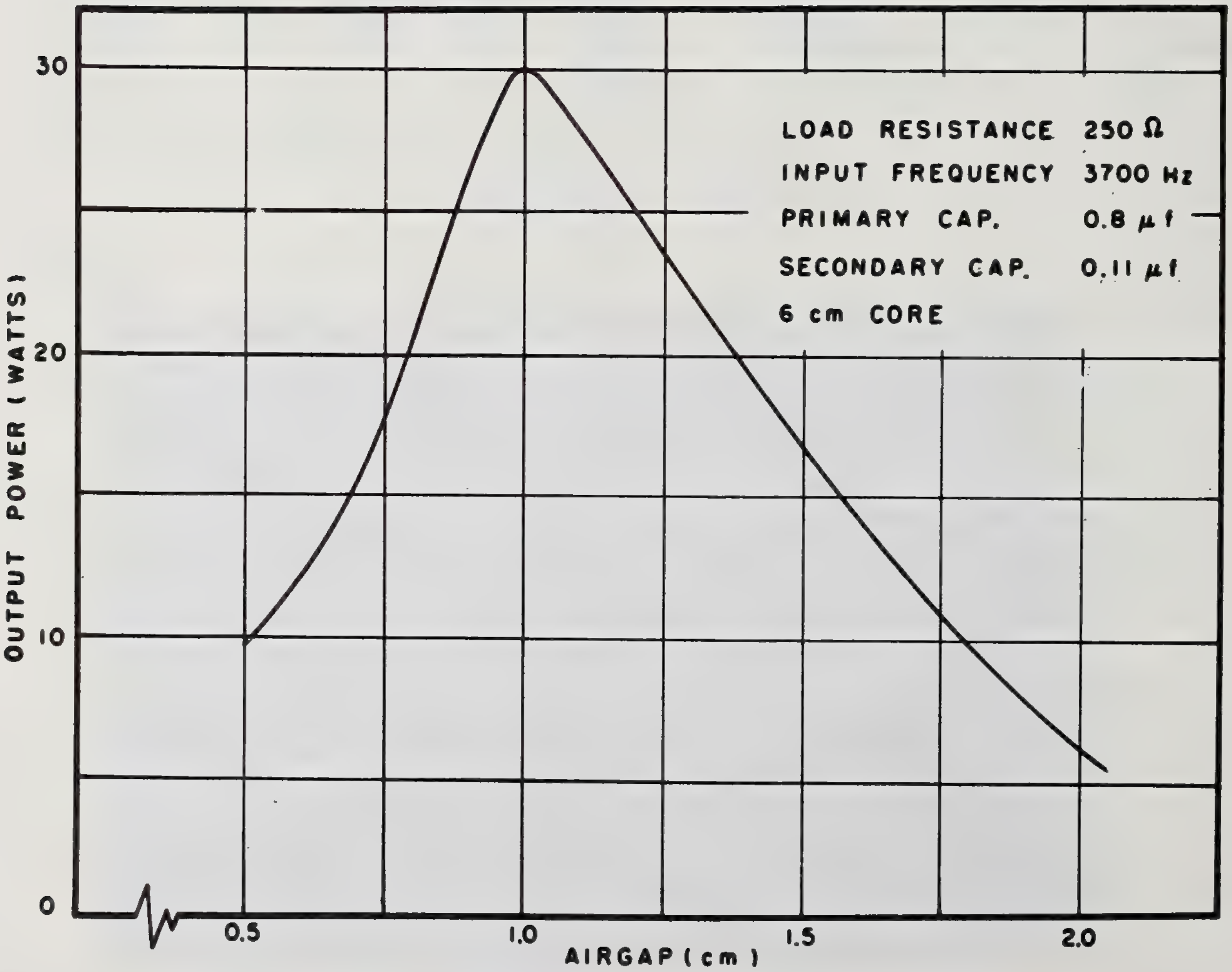

FIGURE 7. (a) POWER OUTPUT VERSUS AIRGAP, CRITICALLY TUNED.

it can then be shown that at the resonant frequency

$$\frac{I_2}{I_1} = -\frac{L_1}{L_2}\,\frac{k}{\frac{1}{Q_1Q_2} + k^2}$$

If $k = 1/\sqrt{Q_1Q_2}$ it is called the critical coupling coefficient k_c and with this coupling coefficient the current gain at resonance is maximized.

In our case k has a value that is determined by the core's geometry and by the separation between the primary and secondary.

$$Q_1 = \frac{W_oL_1}{R_1} = \frac{W_oL_1}{R_g + R_p} \quad \text{and} \quad Q_2 = \frac{W_oL_2}{R_2} = \frac{W_oL_2}{R_s + R_L}$$

It is desired to maximize Q_1 and Q_2 with a given R_L.

R_g is the source resistance and it is made as small as possible by the design of the power amplifier stage. R_p is the resistance of the primary and it is a function of L_1. It cannot be decreased without changing L_1 (for a given core), hence an optimum choice for L_1 has to be made. This sets the value for L_1/R_1.

R_L is the load resistance; this value will be specified by the user and it is assumed here to be a few hundred ohms. The same argument as for L_1 and R_p holds for L_2 and R_s. Here too an optimum value should be chosen which specifies L_2/R_2.

As has been stated before, k is given by the transformer's geometry. It is desired to make this the critical coupling k_c. C_1 and C_2 have to be chosen such that

$$W_o^2 = \frac{R_2R_1}{L_1L_2k^2}$$

under this condition

$$\frac{I_2}{I_1} = -\frac{L_1}{L_2}\,\frac{1}{2k^2}$$

The efficiency of the power transfer is

$$\eta = \frac{I_2^2R_L}{I_1^2(R_g + R_p) + I_2^2(R_s + R_L)}$$

If R_L is much larger than R_1 and R_s and I_1 is of the same order as I_2, η can be made high.

In this calculation, losses in the core material and in the tissue have not been included. As was shown in Figure 6, the core losses are less than one-half of the copper losses. Furthermore, the optimum load resistance for both losses occurs at the same value. Thus, this analysis may be used to indicate the correct operating points.

Saturation in the ferrite core must always be considered. The actual voltage applied to the transformer winding may be quite high (about 150 to 800 v depending on coil ratios and load impedance), since the generator voltage is multiplied by the Q of the primary circuit. Cores which have sufficiently wide cross-sectional area must be employed to avoid saturation. It can be shown that the power transfer capability of a transformer of this type is proportional to its volume, a direct result of saturation effects. If the flux density is kept sufficiently low to prevent saturation, as in the devices constructed, then the core losses are not important at the optimum points as may be seen in the figure.

IMPLANTATION TESTS

A point of major importance in a device such as this is the effect of tissue reaction. At the frequencies employed here the major tissue reaction will come from rejection of the plastic, and from heating. Plastic rejection has been tested by implanting a dummy unit in a dog for a period of nine months. To date, no rejection has occurred.

Temperature rise has been tested in acute experiments by implanting the devices in dogs, operating them with the proper parameters so that the losses are correct, and measuring temperature rises by implanted thermistors. The results of one such experiment are shown in Figure 9. In this case, two thermistors were used: one on the outside of the internal core (but inside the encapsulation); and one in the tissue, 3 cm away from the unit. The time constants are quite long, of the order of 1 hour. The curve shows that the temperature rise inside the encapsulation is 3°C while it is only 0.9°C 3 cm away. Tests from other investigators[2] have indicated that such a rise is acceptable. It is interesting to note that most of the losses in this device are in the external unit, not the internal implanted unit. This is because the coupling coefficient of the unit is 0.5 so the flux density in the implanted unit is one-half that of the external unit. The current in the primary required to couple the power through the airgap is proportionately greater than in the secondary. Thus both core and copper losses are greater in the primary. In spite of the fact that losses in the implanted unit are almost negligible, the fact that the external unit is in immediate contact with the skin causes noticeable temperature rises inside the body. For 30 watts

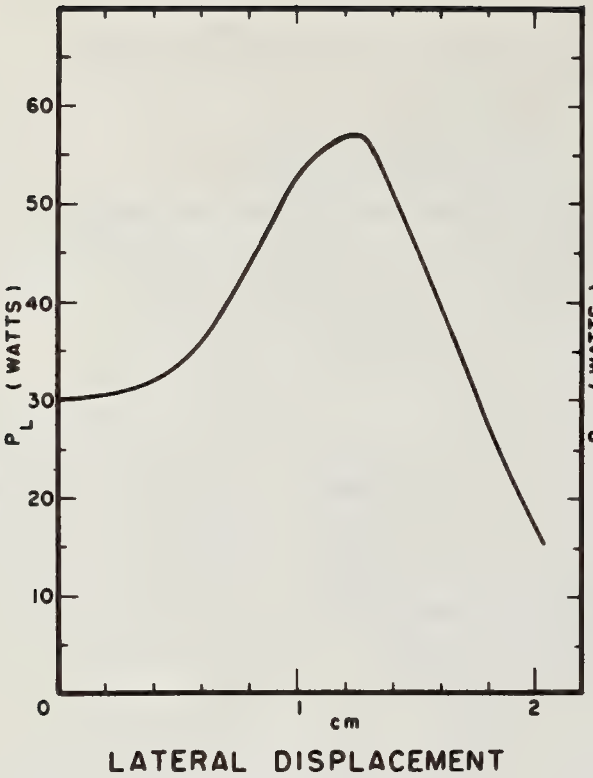

FIGURE 7. (c) POWER OUTPUT VERSUS LATERAL DISPLACEMENT, OVERTUNED.

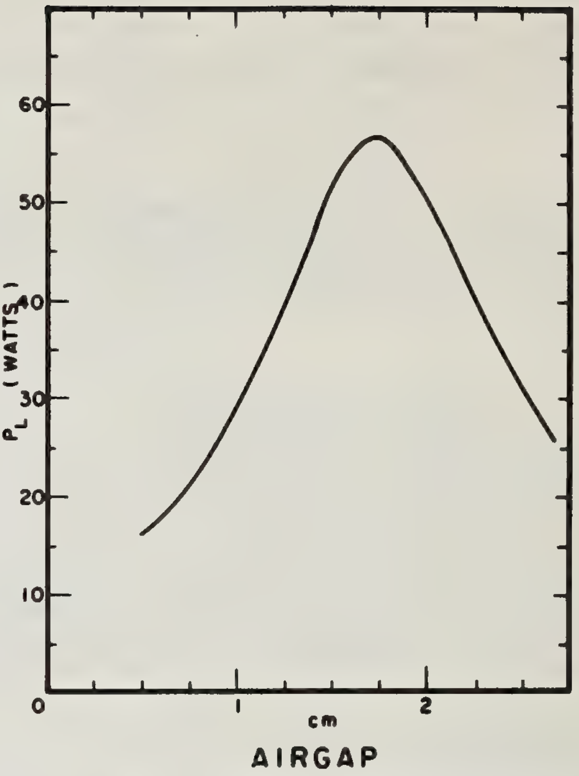

FIGURE 7. (b) POWER OUTPUT VERSUS AIRGAP, OVERTUNED.

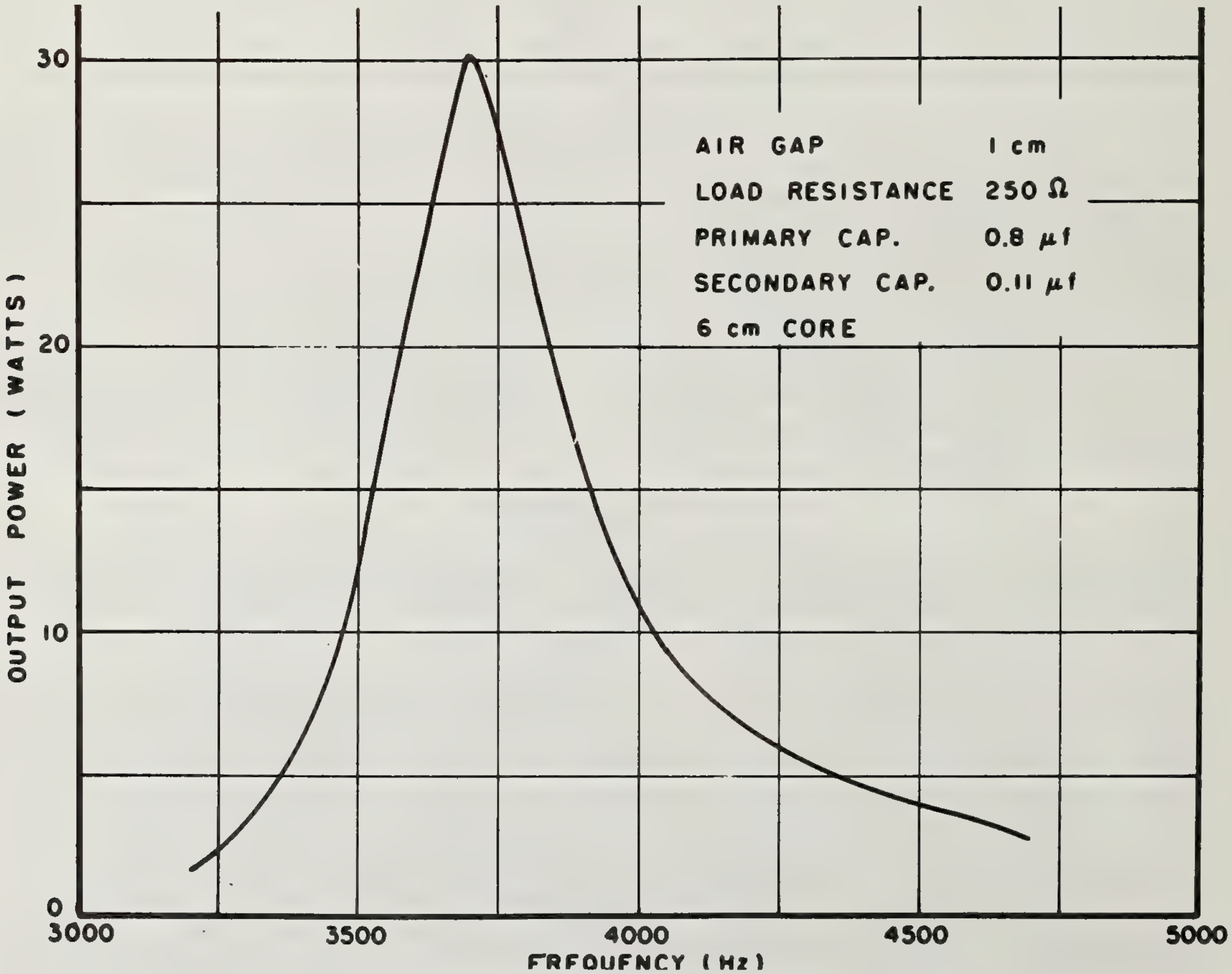

FIGURE 8. (a) POWER OUTPUT VERSUS FREQUENCY.

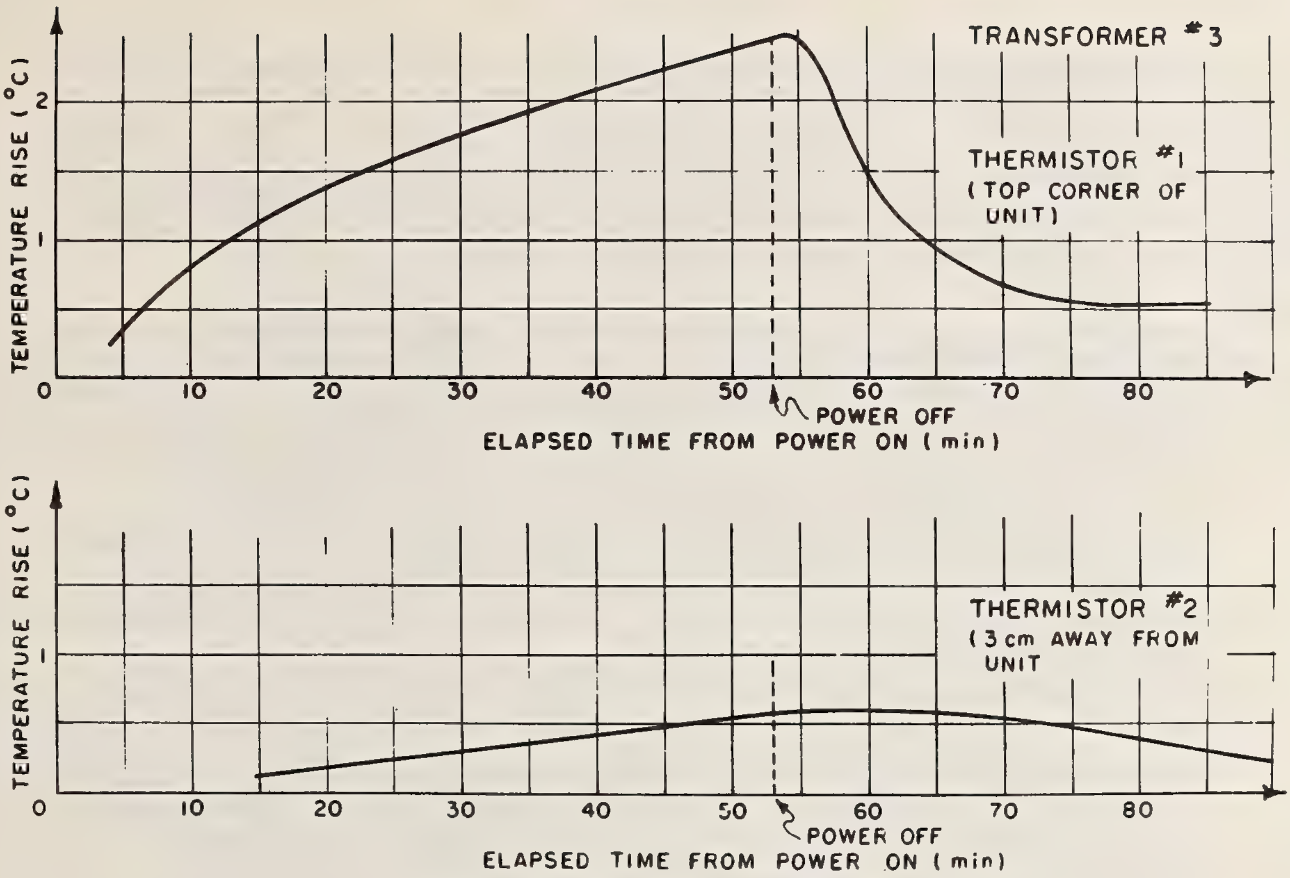

FIGURE 8. (b) POWER OUTPUT VERSUS FREQUENCY.

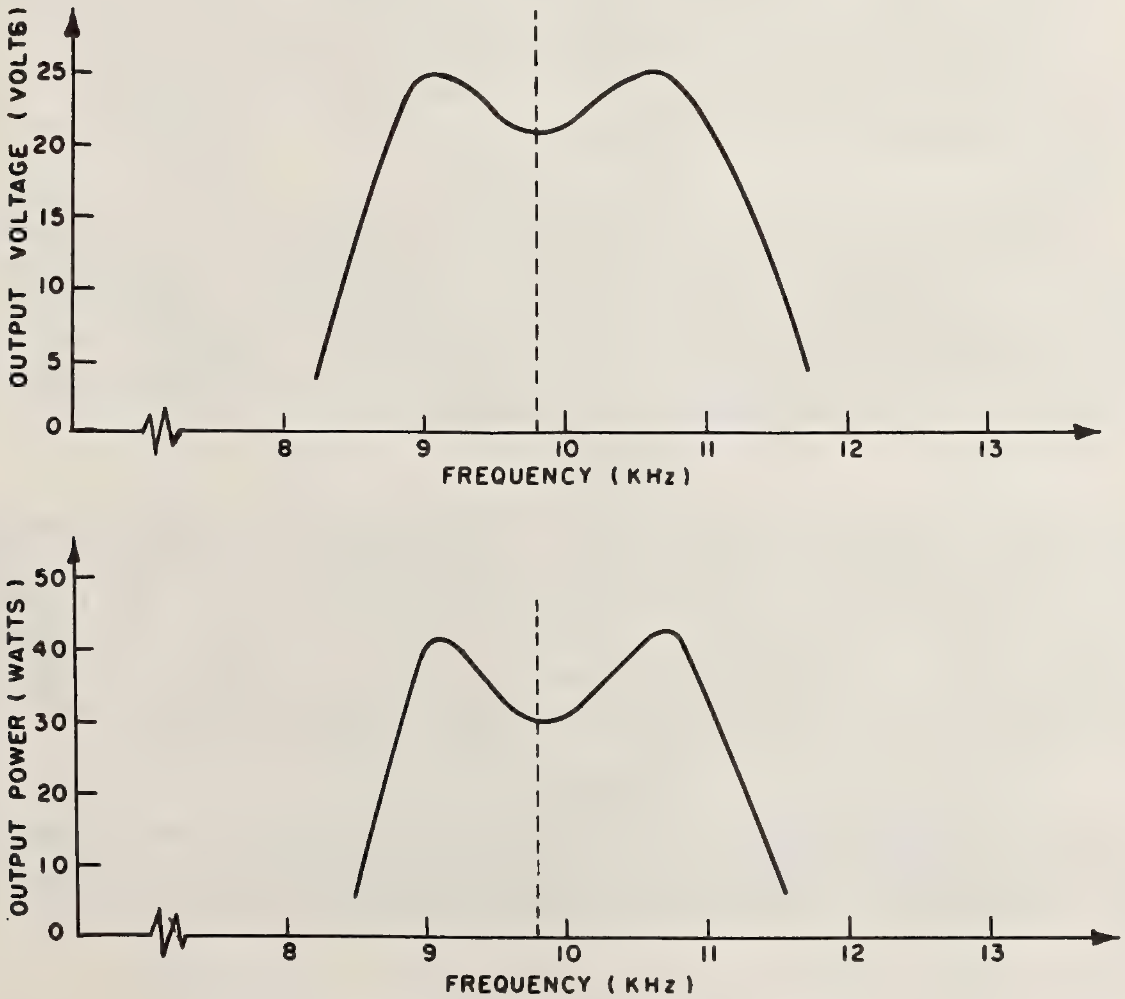

FIGURE 9. TEMPERATURE MEASUREMENT DURING TEST.

power transfer no external cooling of the primary is necessary but if the transformer is to be used at higher power levels (as may be desired when charging implanted energy storage devices) cooling of the primary is desirable. The initial acute _in vivo_ testing was performed in dogs. Only one chronic test was performed in a dog. This chronic implant was a dummy unit to test body reaction and no leads were attached to the unit. For chronic _in vivo_ testing the sheep was selected as the experimental animal. For a variety of reasons, this animal is superior to the dog in instances where leads must be taken from the animal to outside equipment. Because the sheep will stand relatively immobile in a pen, he lends himself to this sort of testing.

Methods.

Acute and chronic _in vivo_ testing was performed in three sheep, weighing between 70 and 80 lb. The experiments were all performed under general anesthesia employing sodium pentothal for induction, followed by endotracheal intubation and Halothane inhalation anesthesia. A total of seven implantations were performed in the sheep. The experience permits certain conclusions to be drawn:

1. Optimal site of implantation is on the lateral aspect of the thoracic cage midway between the arm and the costal margin. In this site, the external unit (primary coil) can be positioned and maintained with relative simplicity by a belt of webbed plastic.
2. The skin incision is best placed more caudally, over the abdominal wall and is carried down through platysma. In the areolar plane beneath the platysma, a pocket is created in the position described above. Hemostasis must be meticulous.
3. The secondary unit is placed into this pocket and the leads are passed through a long subcutaneous tunnel caudally and posteriorly to emerge from the skin through a separate stab wound well away from the transformer site.
4. Sterilization of the implanted unit may be by any of the usual methods. If gas sterilization is used, thorough airing of the unit is essential for implantation and probably requires a minimum of 24 hours. Autoclaving, and cold sterilization with Warfarin were also used. No significant differences were noted among these three techniques of sterilization. Minor amounts of fluid did collect in some of the subcutaneous pouches. One required aspiration, in the others, spontaneous resorption occurred. It was felt that the fluid accumulation was more likely a reaction to less than optimal mixing of the epoxy or to impurities in the Silastic coating. Medical grade Silastic was not available for the early implants.

In the first animal, necrosis of the skin over the units occurred. Implantation in this animal was in two areas on the same side. One unit was planted in the flank and the second unit was planted over the chest wall. Necrosis occurred over the first unit about four weeks after implantation, and two weeks after implantation of the second unit in the same animal as the first. It is postulated that the two incisions required and the extensive undermining of the skin performed, were duly responsible for depriving these elevated areas of skin of their blood supply, thereby permitting necrosis to occur. Subsequent implantations have not revealed necrosis. At no time has infection been a problem, although all animals have been maintained on antibiotics for the first five-postoperative days.

A dummy unit was implanted in the contralateral side of the sheep who suffered necrosis of the skin over two previous units. This sheep was well and no necrosis developed. It was killed by a dog after six months. On examination no infection or rejection were evident. Three more units were implanted in two other sheep. One was removed after 6 months of implantation and the other after 8 months. Power transfer was affected to these units intermittently. At the termination of the experiment the units were removed from the sheep. No infection or rejection was evident. In accordance with expectations these implanted units show good ingrowth of fibrous tissue through the Teflon skirt which fixed the unit firmly in its position. The units removed showed no deterioration and upon _in vitro_ testing performed as before original implantation.

CONCLUSIONS

The results of these investigations have shown that a transformer for transferring power into the body for an artificial heart is feasible at low audio frequencies. The implanted unit with its encapsulation is a flat disk 75 mm in diameter and approximately 25 mm high. Its weight is approximately 8 oz. With this unit at least 30 w of power can be transmitted through the skin at efficiencies of about 90 percent. By proper choice of parameters and tuning of the unit, power can be transmitted to a wide range of loads through an airgap of up to 15 mm. Power transfer can be maintained also when the unit is moved laterally up to 2 cm from its proper position. Long term implantation in sheep show no adverse reactions to the implanted units. Tissue ingrowth fixed the units firmly in position and proper power transfer was possible to these implanted units throughout.

REFERENCES

1. Schuder, J. C. and Stephenson, H. E., Jr., "Energy Transport and Conversion for a Permanently Implanted Artificial Heart," Trans. Am. Soc. Art. Organs, Vol. 9, 1963, p. 286.
2. Rawson, R. O., Hardy, J. D., and Vasco, K. A., "Visceral Tissue Vascularization: An Adaptive Response to High Temperature," Science, Vol. 158, 1967, p. 1203.

DISCUSSION

MR. WARNER: What was the temperature rise as measured in the tissue directly between the two units of the transformer when operating at the 100 watt level?

MR. THUMIN: I did not give that number because we did not conduct any continuous in vivo experiments at the 100 watt level. The curves were obtained at 30 watts and the temperature rise between the two units was roughly about 1.5 degrees. I did not show that in the slides. The reason that the temperature rise was slightly higher between the units than 3 cm distal is due to the fact that heating is caused both from the external and internal units. If a 100 watt device is used, some external cooling is needed which we did not supply. We only did short term experiments at the 100 watt level. The temperature in this case will be primarily a characteristic of the cooling of the primary coil because most of the heating in this place is due to the primary. By cooling one you could limit the temperature rise to about three degrees, which is acceptable.

DR. ROTH: You did not mention flux density in skin interface, but it is axial, and this will produce a constant compressive force between primary and secondary. Do you have figures on the flux density and the compressive force between units?

MR. THUMIN: We did not do exact measurements, but the flux density that we have is about 2000 gauss at maximum. The compression is rather minimal. We have more pressure due to the elastic belt than due to any type of electromagnetic forces.

DR. FRIEDMAN: What is the expected total weight of the external and internal units (in humans)?

MR. THUMIN: The internal unit is roughly 8 ounces and it goes up to about 9 ounces depending on the size of wire used. This, in turn, depends on the load impedance. The external unit is heavier depending on the size of the cup. The core itself is about the same weight of 8 ounces. The entire weight depends upon the size of the positioning cup used. For sheep, we use a larger cup and then the total weight was about 12 to 13 ounces. For use on humans, it could be made lighter. I would say that about 10 ounces would be a good weight.

DR. TOPAZ: How many times was the external device removed by the sheep in the eight months after it was implanted?

MR. THUMIN: The cup was knocked off quite often. I should say that we did not apply power continuously, but for a period of hours at a time, mainly because we did not have the personnel to sit there with the unit for a long period of time. It is true that the cup was knocked off by the sheep, but we feel that with a human being, this problem will not exist. It was mainly knocked off because the sheep was pressing it against the side of the cage. What we tried to do though is that in addition to the elastic webbing, we added a mesh. The mesh was pasted to the wool of the sheep with glue and this positions the unit very well. We find that this reduces the number of "removals."

DR. TOPAZ: I would like to point out that if this device was removed while it was delivering power to an artificial heart, the patient would not be able to put the unit back in place within a few seconds. The experience with kidney shunts is that people are not very careful with these external tubes.

MR. THUMIN: This is true, but as I said, we worked on the power transformer rather than on the strapping procedures which would again be different in the sheep than in human beings. Therefore, we did not put that much emphasis on the strapping technique. This would be something that other people would have to do in due course. In addition, let me point out that my feeling is that at least some type of internal storage device will be necessary. It seems a little bit hard to believe that a device which could break down (which is, after all, only a circuit) would be expected to power a heart device without any backup system. At least a few minutes or maybe a few hours of stored energy supply should be provided.

DR. KENNEDY: I have enjoyed this paper very much. Have the authors any data on the theoretical minimum mass for the internal component?

MR. THUMIN: As far as the mass is concerned, there are two factors we cannot avoid. One is the volume of the core material to be used. It is well known from the theory of transformer design that the power transmitted depends on the volume of the core. We feel we cannot reduce it by much. The second factor is the copper wiring. In order to reduce the copper losses, we have to use heavy copper wire in order to reduce the winding resistance. If the load impedance is kept high, it may be possible to get high efficiency with slightly thinner wire. But it seems to me that 8 ounces is about the minimum that could be attained. We were not able to do any better.

MR. TSIEN: Is the load resistance of the secondary circuit outside or inside of the skin? Will this 30 watt heating effect of the load resistance affect the performance of your transformer? Secondly, have you considered the skin irritation due to this device? Maybe the transformer causes itching which, in turn, makes the sheep wish to get rid of it. If so, the same thing might happen in humans.

MR. THUMIN: Let me answer the first question first. Maybe it was not clear, but we conducted the power out of the animal. The 30 watt power was not dissipated internally. The heating effect that was shown was heating due to losses in the secondary and primary only. The power was transmitted out through wires that needed to be led through the skin. There was no heating effect due to the load resistance. As far as the second question is concerned, again, in humans, one would probably have a completely different situation than with sheep and we did not feel that the sheep had shown any signs of trying to knock the unit down willfully. Usually it happens because it somehow rubs or leans against the cage or sits down. With some of the earlier units, when we did not know exactly the correct positioning for the unit, the leg motion sometimes would remove the unit when the sheep sat down. But we did not do any other work as far as the comfort factor to the sheep is concerned.

DR. BRUNO: I want to compliment you on a very interesting paper and ask if you have looked into the possibility of various types of coverings, that is, various types of skin grafts. Are you using a full thickness at this time? Have you considered any other types of skin grafts and have you considered covering, possibly with a synthetic fiber of sorts which would be incorporated into the skin and thereby reduce the resistance across the skin?

MR. THUMIN: As far as the first question is concerned, we tried different thicknesses and found that if we put the units as low as possible and if the tissue between the two units was as thick as possible, we got the best results because blood circulation was not hampered too much. The optimal site of implantation is in the abdominal wall, and the incision is carried down to the areolar plane beneath the platysma. As far as grafts are concerned, one of the reasons we conducted this study was that there is nothing that we knew about which would give good adherence to tissue. If we could get any type of plastic material that would allow us to have good interface with the skin for a long period of time, we could pass the wire in and out directly and then no transformer would be needed at all. We could not find anything to allow us to carry wires through the skin or any type of plastic tubing that could be inserted through the skin for a long period of time without infection. That is why we undertook this study.

CHAPTER 78

SKIN TRANSFORMER AND POWER CONDITIONING COMPONENTS

P. Newgard and G. Eilers

Stanford Research Institute
Menlo Park, Calif.

We have previously demonstrated acute tolerance of animals to transcutaneous power transfer of from 20 to 120 W by the intact-skin transformer technique. During this past year we have conducted prolonged experiments to establish the longevity of the implants and to explore the increase in heat dissipation capability of the implant with the expected increase in local vascularity. Heat flux at the coil tissue interface was increased from the two hundred-three hundred W/m^2 range used in acute experiments to nine hundred W/m^2 over a three-month interval without excessive tissue temperatures. With each incremental increase in heat dissipation, the local tissue temperature immediately increased. This was followed generally within a few days by a decrease to near normal temperature. This response continued with increases in heat dissipation up to the nine hundred W/m^2 level. An energy transmission system was designed employing the SRI skin transformer to supply power to a piezoelectric pump/storage battery combination. It was discovered that low-voltage rectifiers are especially difficult to drive efficiently from the skin transformer. Harmonic currents, which are required for rapid switching and high efficiency, cannot be obtained from the skin-transformer secondary, owing to the presence of leakage reactance. A hydraulic control and reservoir unit was designed and built to adapt to an existing blood pump for hydraulic actuation. The device presents a low hydraulic impedance for hydraulic fluid displaced during systole.

BACKGROUND

Last year we reported on short-term several hour experiments demonstrating the power-handling capabilities and design characteristics of an intact-skin transformer. We had demonstrated tolerance of animals to both the mechanical trauma and heat dissipation up to 300 W per square meter of implanted surface. We had arrived at a workable geometry that allowed the transmission of power from 20 to 120 W at frequencies from 60 to 20,000 Hz. It further appeared that there was an optimum frequency range around 400 Hz to 2,000 Hz.

We also reported that the problems still to be resolved included long-term retention of implanted coils and that we had not yet explored to what degree we may expect vascularity to increase in the tube pedicle flap--especially in response to severe heat loads.

LONG-TERM IMPLANT TESTS

It now appears that our difficulties with maintaining implants were due in large part to our using percutaneous leads to monitor internal temperatures and to route the power back out to a load. During this past year we have maintained six implants without percutaneous leads for an average of 9½ months and a maximum of 12 months. These coils have been constructed of aluminum windings with silicone-rubber covering 1-mm thick and have used a loose-fitting dacron-tricot fabric overlay to promote tissue ingrowth and provide mechanical support. During the past year, no incidents of infection or rejection have occurred.

Two coils have been maintained in two goats since October 1968 with continuous transmission of power to heat the coils, producing heat-flux levels from 200 W/m^2 to 940 W/m^2.

Heat flux was increased in four steps over a period of three months. Figure 1 shows the plotted temperature at the coil/tissue interface. There were several instances of a radical decrease in interface temperature after only one to four days. More typically, the accommodation required a week to a month. We believe it is significant, however, that dissipation of heat--even at the level of 940 W/m^2--is accomplished with interface temperatures at about the same level as the initial temperature prior to the experiment.

SKIN TUNNEL SURGICAL PROCEDURE

We have previously reported on the use of the tube pedicle flap surgical procedure to implant the secondary transformer coil. During the past year we have attempted a somewhat different surgical technique--the skin tunnel procedure. The skin-lined tunnel is constructed so that it traverses the aperture of the secondary coil. Figure 2 is a series of seven photographs showing implantation of the coil in a female human cadaver below the right breast. Figure 2(a) shows the coil, and Figure 2(b) shows two parallel incisions separated by a distance equal to the interior periphery of

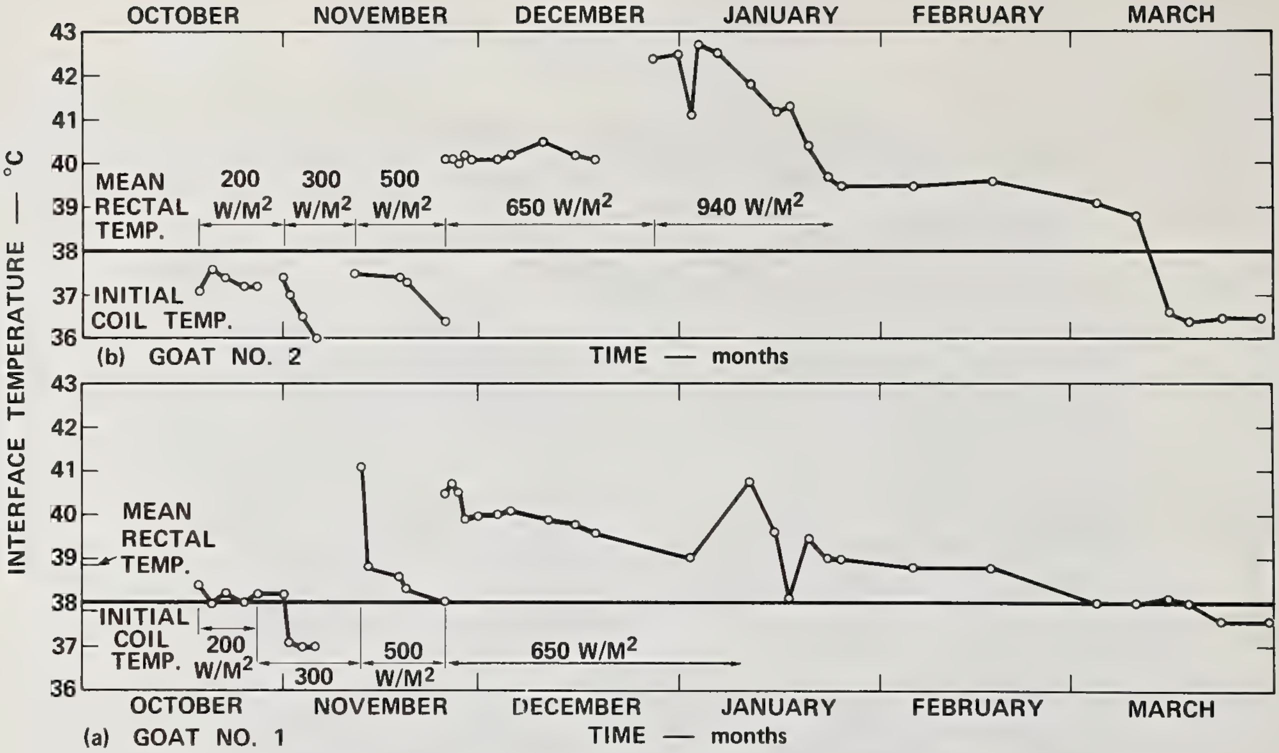

FIGURE 1. INTERFACE TEMPERATURE AS A FUNCTION OF TIME (OCTOBER THROUGH MARCH 1969).

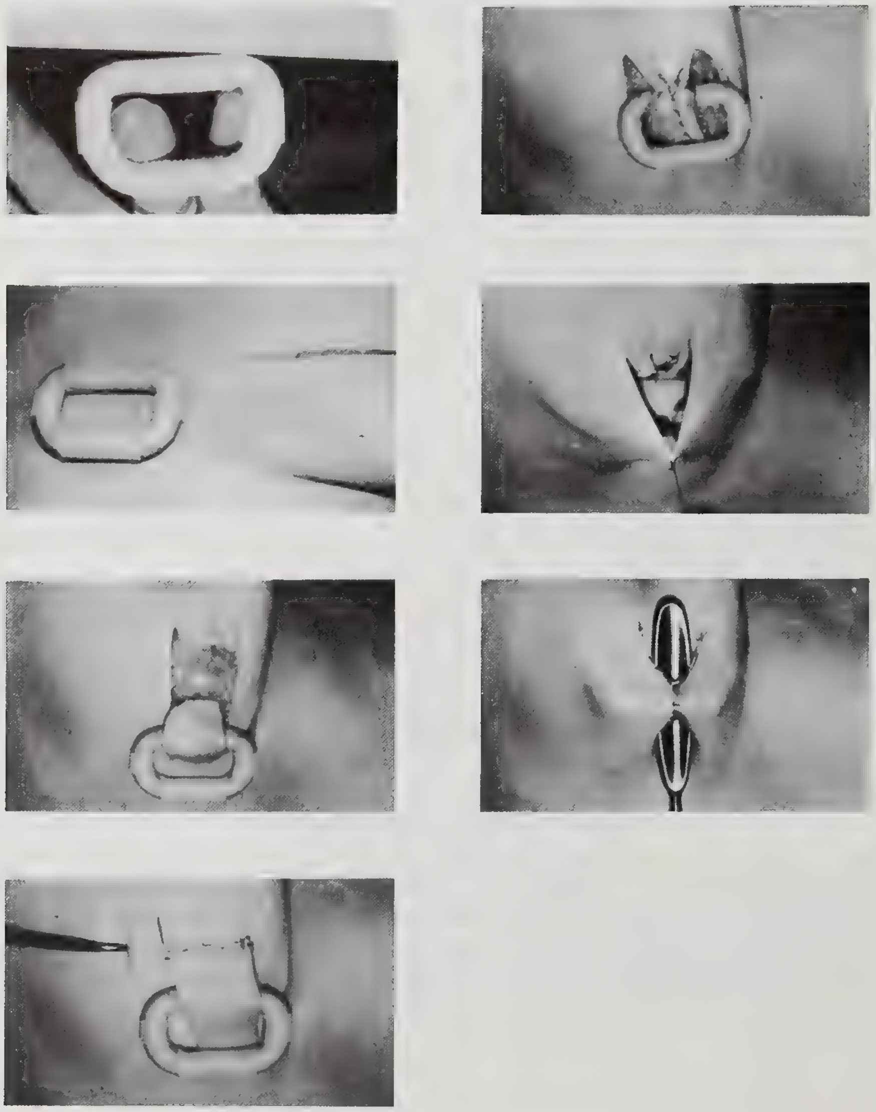

FIGURE 2. CONSTRUCTION OF THE SKIN TUNNEL.

the coil. In Figure 2(c), the two parallel incisions have been joined by a cross incision to form a pattern like the letter "H". The two small flaps thus formed are separated from the tissue substrate and then sutured together within the window of the coil. This is shown in Figure 2(d). The skin within the coil is then formed into a tube, as shown in Figure 2(e). Figure 2(f) shows the surrounding skin being pulled over the coil to complete the skin tunnel, as shown in Figure 2(g). Moderate tension has been noted when the wound edges are advanced over the coil.

The procedure was also performed on a calf cadaver--once in the iliac focca and twice in the inframammary area. A live calf experimental preparation failed to heal because the calf experienced extreme bloating and the suture line dehisced at one week.

At this time the technique appears to be feasible, but it is unproved by animal experiments.

COMPONENT DEVELOPMENT

The greatest portion of our efforts during the past year has been devoted to the development of power-transmission components for a heart-assist system specified by the Artificial Heart Program Office. The technique chosen for this work was a passively filled, bypass pump, shown in Figure 3. The electrical system that provides power for operation of the hydraulic pump is shown in Figure 4.

Our area of responsibility for electrical components included the development and delivery of the exterior ac/ac converter, the skin transformer, the ac/dc converter, the battery-charging controls, and the emergency-function switch to apply power from the batteries whenever the main power source is interrupted. In practice, it was also found expedient to use components of the emergency-function-switch circuit to control power delivery to the dc/ac inverter and piezoelectric motor in response to control signals derived from hydraulic flow sensors. This provided control of pump output in synchronism with the heart.

All of the electrical components shown in Figure 4 were constructed and operated under various simulated load conditions. Primary input power was obtained from the 110-V 60-Hz commercial line. In order to use a small, lightweight (120 gm) skin transformer, the input power was converted to 1200-Hz square waves before being applied to the transformer primary. This frequency was chosen as a compromise between the heavier transformer design that would result from lower-frequency inputs and the high leakage reactance that accompanies higher-frequency designs.

An internal three-cell NiCd storage battery was incorporated within the system to provide power to the Pz motor during periods when the primary power source was interrupted, either accidentally or intentionally. Because of the presence of the battery and the need for 120-Hz excitation to the PZ motor, a dc/ac inverter was needed. Although the NiCd battery could have been kept on line at all times, this was not done, because it was feared that this would cause the battery to be continually exercised--charged and discharged--as the load presented by the PZ motor changed throughout the heart cycle. Exercising the battery in such a manner is not recommended, as it tends to shorten the battery's life. To disconnect the battery from the inverter during periods when primary power was available, a solid-state switch was added that derived its control signal from the presence or absence of 1200-Hz ac at the secondary of the skin transformer.

The PZ motor, which was designed and built by Energy Research and Generation, Inc., was expected to require 440 V rms at about 20 W resistive load at its input terminals. It was considered advisable to present a nearly sinusoidal voltage to the input terminals to prevent further increases in the peak stresses experienced by its internal components. Because the PZ motor, owing to the nature of its construction, presents a substantial shunt capacitance across its input terminals, there is further incentive to keep the harmonic content of the drive signal low; large harmonic content--such as would be present in a square wave, for instance--would require that high peak currents flow at the input terminals--a situation that inevitably leads to reduced efficiency in the electrical driving components.

As a direct result of the shunt capacitance just mentioned, the power factor of the pump departs from unity. The factor computed on theoretical ground is 0.6 leading, which means that a total of about 33 VA must be supplied. During experimental work with the PZ pump, the power factor was measured and found to be considerably less than the above figure. This was explainable on the basis of observed modes of malfunction within the PZ pump, and there is no reason to expect that the 0.6 figure would not be attained if the motor were functioning properly.

In order to attain high efficiency in the dc/ac inverter, a switching-mode design was chosen, which, of course, produced at its output a square wave. Since the application of this square wave directly to the PZ input terminals would have been detrimental to the PZ motor operation and would have caused excessive peak currents to flow at each transition, a series-resonating inductance was added. For resonance, the inductor must store the same amount of electrical energy as the capacity of the PZ motor when the two are connected in series and driven at 120 Hz. The amount of energy stored in the capacitance on the average, is easily calculated. For 440 V rms applied to the input and 20 W resistive load producing a power factor of 0.6, the capacitance is found to be approximately 0.18 μF. The average energy stored in the capacitance is then about 1.8 J.

An inductor that is capable of storing 1.8 J on the average with 120-Hz excitation and that does not lose an appreciable portion of this energy each cycle to hysteresis effects turns out to be of considerable size in comparison to the other electrical components. The inductor we used for testing was probably far from optimum design for this application, but its size can be taken as a first approximation to what might ultimately be attained through careful design. It was about half the size of the PZ motor and weighed as much as the balance of the circuitry to be implanted, i.e., everything exclusive of the external ac/ac converter, the battery, and the skin transformer.

Two approaches that might be considered as alternatives to the series inductor are a linear amplifier driver and a high-frequency switching-mode design. The linear amplifier approach is inherently limited to roughly 80 percent efficiency because of dissipation in the active elements; this is a theoretical limitation and cannot be improved by choice of components or circuit design. The high-frequency switching-mode design, which was suggested to us by Dr. Hamlin of the General Electric Co., would employ a high-frequency variable-duty-cycle solid-state switch. Variation of the duty cycle in a sinusoidal fashion would produce the needed 120-Hz sine wave output, but with the efficiency of a switching-mode design. A small inductor placed in series with the switch would smooth out the high-frequency variations in output current, leaving only the 120-Hz component.

The first of the above alternatives was neither seriously considered nor implemented because of the premium on efficiency. The second, which is potentially capable of producing the 120-Hz sine wave at very high efficiencies, involves a large amount of circuit development, and the added complication may in the long run offset its advantages. For the present, however, it appears to be the only approach to higher efficiency dc/ac conversion that can meet the needs of the PZ motor.

Probably the most serious problem encountered in the circuit design was voltage drop across semiconductor junctions. With the dc voltage levels being determined by the 3-cell, 3.6-V NiCd battery, even the drop across a saturated switch can produce appreciable power loss. Because of this, active switches were used to rectify the output of the skin transformer in place of silicon or germanium diodes. The switches were driven into saturation during the appropriate portion of the cycle and were so arranged that they produced full wave rectification. A schematic of a typical arrangement is shown in Figure 5.

It should be noted in connection with the rectifier switches and the battery-disconnect switch that the power losses incurred in the saturated-switch configuration can appraoch those of the diode junction. Referring to Figure 6, the base drive current can be supplied via a transformer winding or directly from the supply line via a current-limiting resistor. In order to keep the collector-base drop below about 0.1 V, the base current must be at least one-tenth of the collector current for currently available power transistors. If this base current is supplied from a transformer winding, a current-limiting resistance may still have to be included to overcome changes in emitter-base voltage with temperature fluctuations or difference from one transistor to another. If, on the other hand, the base current is obtained from the dc supply directly through a resistive dropping element, the losses in the dropping element become appreciable, easily exceeding those incurred in a simple diode junction.

HYDRAULIC SYSTEM

As a further part of our work to supply components for the NHI heart-assist system mentioned above, we became responsible for the design and construction of the portion of the hydraulic system between the PZ hydraulic pump and the blood pump. Referring to Figure 3, our responsibilities included the hydraulic reservoir, the hydraulic valve, the control sensors, and packaging of these components to minimize hydraulic losses.

The assist technique chosen for this application is passive-filling, i.e., the ventricle provides the hydraulic energy to fill the blood pump. Then, at a later interval in the cardiac cycle, the hydraulic pump supplies power to expel blood from the blood pump into the arterial system. The degree of assistance afforded by this technique is directly related to the amount of blood that is diverted away from the aortic valve to the mechanical device. Thus, one important criterion for design of the hydraulic system is that its hydraulic input impedance be minimized in comparison with the input impedance of the normal physiological receiver. Our area of design was the reservoir and valve system to fit an existing blood pump; so we attempted to minimize hydraulic losses in this area to be compatible with the overall requirements for minimum input impedance.

Another portion of our work was to provide the sensors and the hydraulic and electrical controls to synchronize the assist device with the heart over a frequency range of 60 to 180 beats per minute. The approach used to minimize the hydraulic input impedance can best be explained by referring to the three dynamic components of hydraulic impedance. Total impedance is the instantaneous sum of capacitive, resistive, and inertial impedances. A low capacitance was attained by providing a distensible flaccid-bag reservoir in direct communication with the intrathoracic cavity. The pressure necessary to fill the reservoir was found to be a maximum of 17 mm Hg for a 50 ml stroke volume. Low resistive losses were attained by providing a flow path through the sleeve valve of Figure 5, approaching two square inches of open area. The resistive drop through the open valve was measured to be 1.0 mm Hg at a 30-l/min flow rate. A negligible inertial load was achieved by reducing the path length between the blood pump and the reservoir to about 0.1 inch. The reservoir is actually wrapped completely around the pump and separated from it only by the valve mechanism.

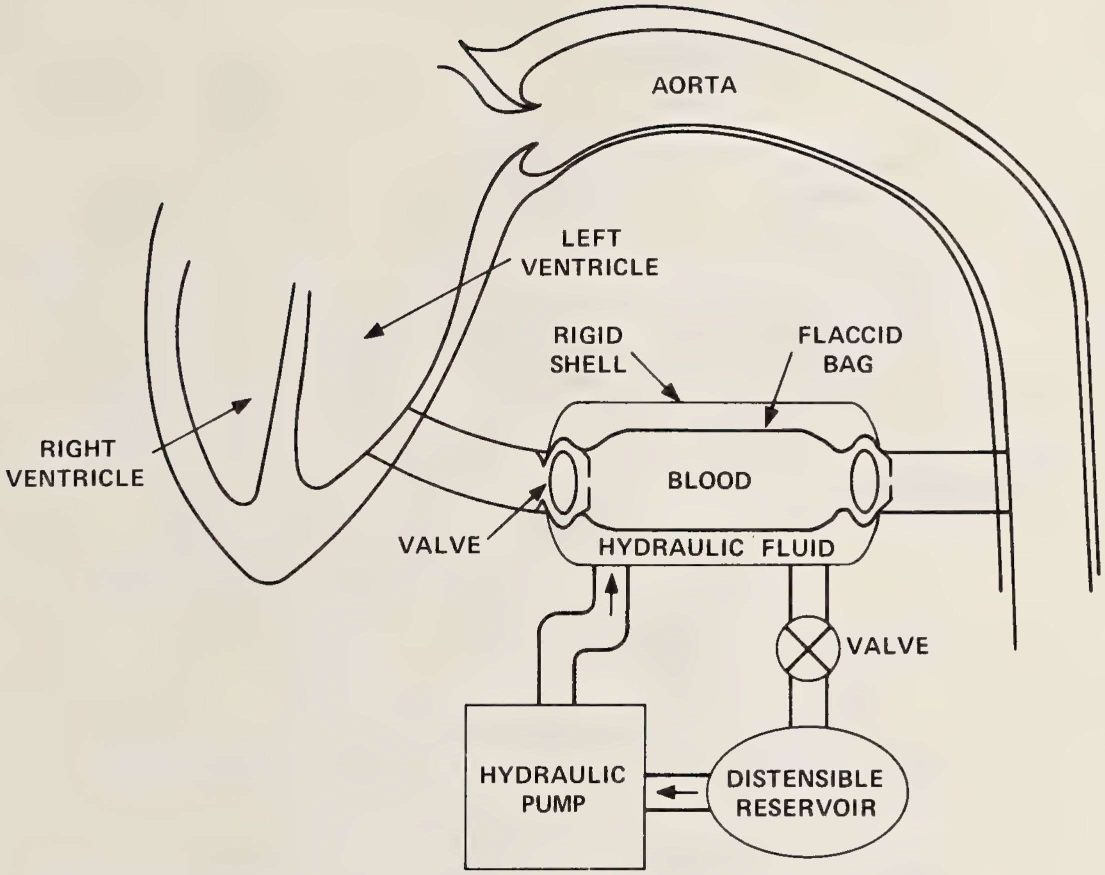

FIGURE 3. LEFT-VENTRICLE-TO-AORTA ASSIST CONFIGURATION.

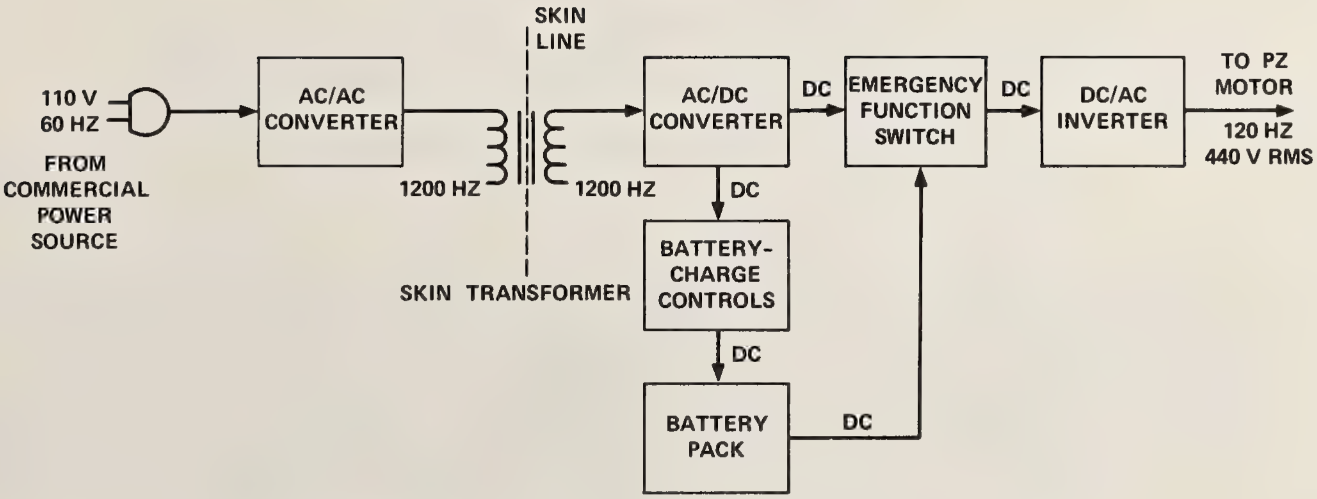

FIGURE 4. ELECTRICAL POWER SUPPLY FOR PIEZOELECTRIC PUMP.

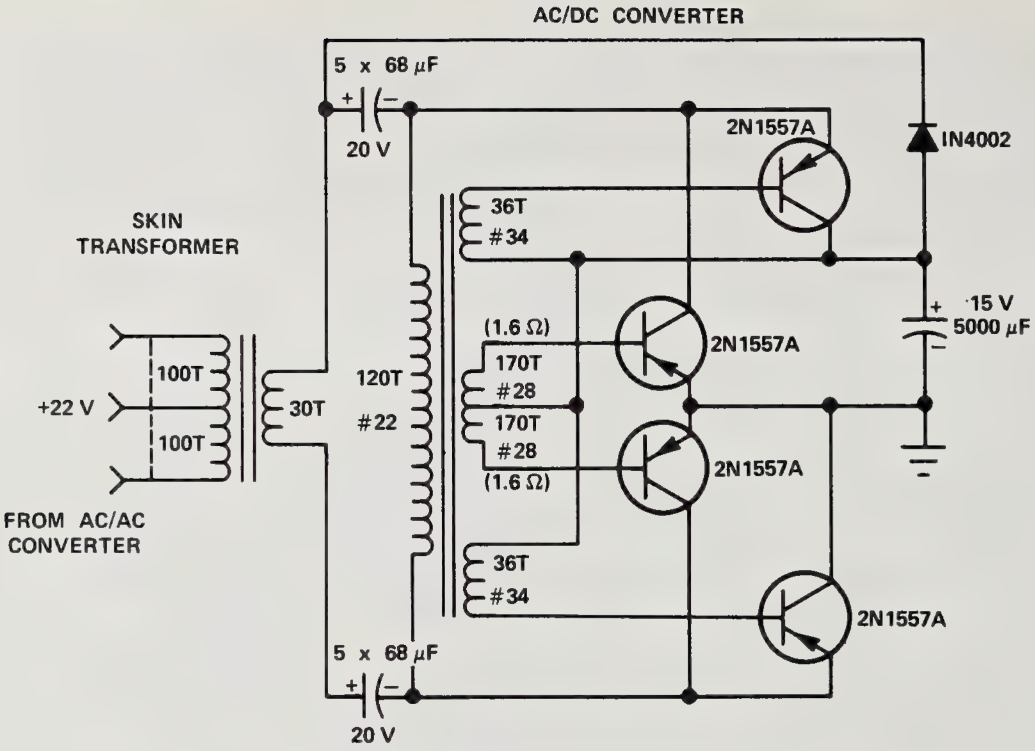

FIGURE 5. AC/DC CONVERTER, BATTERY CHARGER, AND SWITCH CONTROL.

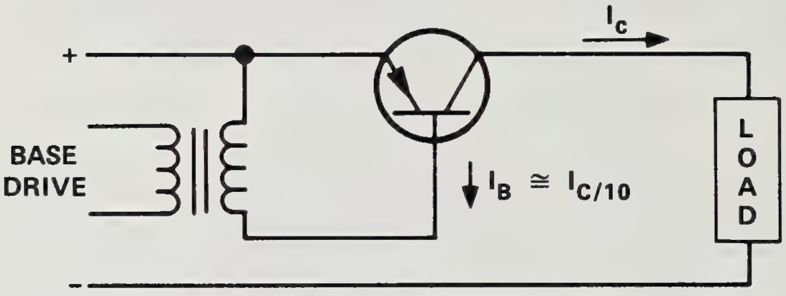

(a) TRANSFORMER WINDING

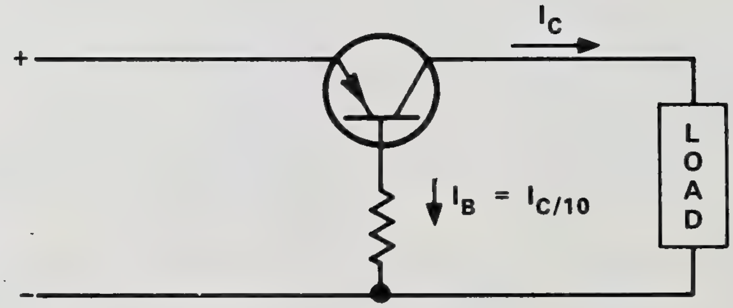

(b) FED FROM OPPOSITE SUPPLY TERMINAL

FIGURE 6. SATURATED SWITCH CIRCUIT.

Figure 7 shows a cross-sectional view through the combined blood pump, control valve, and reservoir unit. The device is depicted at a time just prior to physiological systole. The blood pump has been emptied of blood, the sleeve valve is spring-loaded in the open position with an array of 144 holes allowing flow from the interior of the rigid housing through the valve to the exterior reservoir volume. Hydraulic fluid has been transferred from the reservoir to the interior of the blood pump, thus exhausting the reservoir. In this condition, the device is ready to receive the systolic ejection from the left ventricle.

When heart ejection occurs, blood will enter the blood pump bladder, enlarging it, and forcing hydraulic fluid through the open sleeve valve into the exterior reservoir. A flow sensor (not shown in the figure) is actuated by the pressure drop across the sleeve-valve ports. When this sensor indicates the cessation of flow due to cardiac action, and a reservoir position sensor indicates that the reservoir is distended as shown by the dotted lines, then electrical power is applied to the energy converter to pump the hydraulic fluid from the reservoir volume into the interior of the blood pump. The ducting is so designed that flow in this hydraulic circuit must pass the lip of the sleeve valve. This creates a pressure drop across the end cap of the sleeve valve, which forces it to move against the spring to the closed position as long as the hydraulic pump operates. Pump operation is terminated by a pressure-actuated switch which senses that the exterior reservoir has collapsed, i.e., all available hydraulic fluid has been transferred from the reservoir to the blood pump. This insures that the blood pump is also exhausted of available blood.

Figure 8 shows photographs of the combined blood pump and hydraulic system. This unit has not yet been implanted for in vivo tests of the control system. Its critical components and functions have been individually tested, with the following results.

(1) Sleeve valve open--pressure drop at 30 l/min flow = 1.0 mmHg.
(2) Sleeve valve closed--leak flow at 150 mmHg = 1.6 l/min
(3) Sleeve valve actuation time--less than 30 ms.
(4) Flow sensor switching occurs at a flow rate of 15 l/min through the sleeve valve.
(5) Reservoir limit switch operates at a reservoir pressure of 1.5 mmHg below intrathoracic pressure.

There are several areas in which we anticipate possible problems as the hydraulic unit is applied in animal trials. For one, the switch logic may not function in response to the systolic flow level obtainable from a damaged heart muscle. This may lead to the inclusion of more logic circuitry or even to the alternative control mode of running the assist device open-loop (asynchronously with the heart). In this mode, the assist-pump operation would be based only on the degree of reservoir filling.

With the present design, the exterior reservoir is not as compliant as it should and could be. This should be resolved by molding in thinner sections and by modifying the geometry.

Perhaps the most basic problem we foresee is with the concept of passive filling during systole. To be effective, the assist device must compete with the normal physiological receiver for the blood flow. The flow will be divided inversely proportional to the hydraulic input impedance of the two potential receivers. Thus, it is interesting to compare each component of this critical characteristic. Table 1 illustrates the relative magnitude of these impedances in terms of the driving pressure necessary to cause a pulse of blood flow characteristic of a normal human adult systole.

TABLE 1

COMPARISON OF INPUT IMPEDANCES

Hydraulic Impedance Component	Geometrical Dependence	Typical Pressures (mm Hg)			
		Physiological Receiver	Mechanical Assist System		
		D = 1 inch L = 2 inches	D = 5/8 L = 3	D = 3/4 L = 3	D = 7/8 L =3
Capacitive	Independent	100	20	20	20
Resistive	$\times \frac{1}{D^4}$	5	33	16	8.5
Inertial	$\times L/D^2$	20	77	52	39

It is assumed that we can indeed reduce the capacitive load on the left ventricle from a mean pressure of 100 mmHg to some low value such as 20 mmHg. It is further assumed that the critical length of hydraulic ducting in the mechanical system will be about 3 inches. This is the path length from the left ventricle wall to the interior of the auxiliary blood pump. Table 1 illustrates the critical dependence of the resistive and inertial components of input impedance on duct diameter. The pressures tabulated represent the maximum instantaneous load on the left ventricle due to each component of impedance. It can be seen that the duct size must approach the 1-inch diameter of the physiological receiver to significantly reduce the load on the left ventricle if one requires passive filling of the assist device during physiological systole.

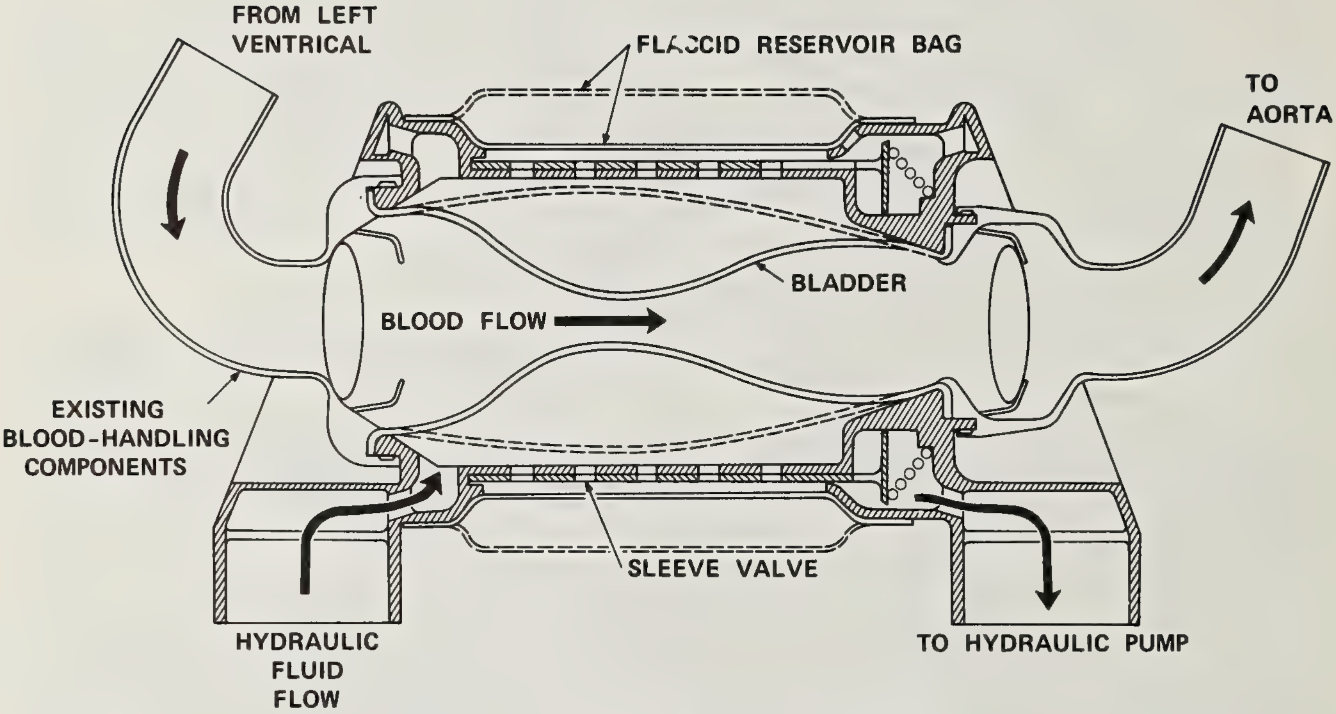

FIGURE 7. BLOOD PUMP AND HYDRAULIC UNIT.

If a portion of each stroke volume could be removed from the ventricle during diastole--prior to systole--then peak flow rate and peak accelerations would be reduced and the peak instantaneous pressures would be reduced. This appears to be a valid alternative and a possible way out of a difficult design problem. Another alternative--really an extension of the same philosophy--is to run the assist device asynchronously, allowing it to fill throughout one or more heart cycles until the blood pump is fully distended before the assist pump is actuated. This would produce the lowest left-ventricle pressure possible with a given duct geometry. However, there would be an occasional time during which the physiological heart contraction would coincide with assist-pump actuation. During this cycle, the heart would not be assisted, nor would it be additionally loaded to any appreciable degree.

Both the workability of these various control options and their effectiveness in achieving the desired result will best be decided during animal experiments. The present state of our analytical and modeling ability simply does not allow the determination of an optimum technique.

PLANS FOR THE COMING YEAR

We plan to continue the development of the intact-skin transformer technique, primarily by the practical--and sometimes painful--process of applying it to real system requirements. This will be augmented by continued animal experiments with surgical implantation techniques and long-term power transfer. We are presently constructing electrical power equipment to supply two dc electro-hydraulic energy converters. Our concept for hydraulic drive and control of the blood pump will be improved along the lines previously mentioned. We also have plans to convert to a fully hydraulic control concept, including all sensors and pump-control actuators. Beyond this, we plan to assist NHI in preparing early animal experiments that will further expose problem areas, and hopefully will determine the optimal control techniques for cardiac assistance.

DISCUSSION

DR. SATINSKY: In that diagram of your pump, I gather that the ejection force of the left ventricle is required to fill the bladder. What is the real use of this ejection force? Since the very nature of the assist means that the heart is in trouble, if it falls below a certain level, will cardiac output be sufficient? Secondly, since filling of the bladder is passive, what safeguard have you provided to prevent the ejection from the left ventricle to meet the total body resistance rather than being emptied, as it was, under conditions of other systems, and then having the secondary pump overcome the total body resistance. In other words, it would seem to me that, at least I got the impression, that a great load is put on the left ventricle and it is open to the resistance as reflected in the aorta before the pump may give its assist.

MR. NEWGARD: Well, I think I can answer the first question, but I am not sure what the second one is. Indeed, the load is critical. A hydraulic system must have very large openings and short lengths of ducts in order to significantly reduce the load and this is a severe problem. In a figure which time did not allow me to show, I have illustrated that passage diameter between a heart and the pump must approach a dimension like one inch before you can reduce pressures to 20-40 mm Hg, and this is a very difficult problem in the passive filling device. As I said, this has not been used in an animal or in a good overall test. We have measured this drop on the bench. It is significant, and I think that it is a great problem. It is a difficult hydraulic design problem.

MR. BLUMLE: You indicated that your sleeve valve design has the frequency response of about 30 cycles, yet apparently the hydroelectric energy hydraulic motor operates at a frequency of 120 cycles. I wonder if you might comment on how you intend to make the two systems together?

MR. NEWGARD: Yes, the sleeve valve does not operate with every pump stroke; it operates only for long duration cycles, one heart cycle time, not pump time.

MR. BLUMLE: Well, then how do you accumulate the output of the hydraulic electric motor?

MR. NEWGARD: The hydroelectric motor has its own high speed valving in the pump.

DR. LUDWIN: Can you make any projection or any estimate of the shape of the pulse pressure wave that will be generated as a result of the function of this unit?

MR. NEWGARD: Essentially, a square wave with rounding at the corners. The control mode envisioned here would be to turn the pump on at full rate of 18 liters per minute and then turn it off.

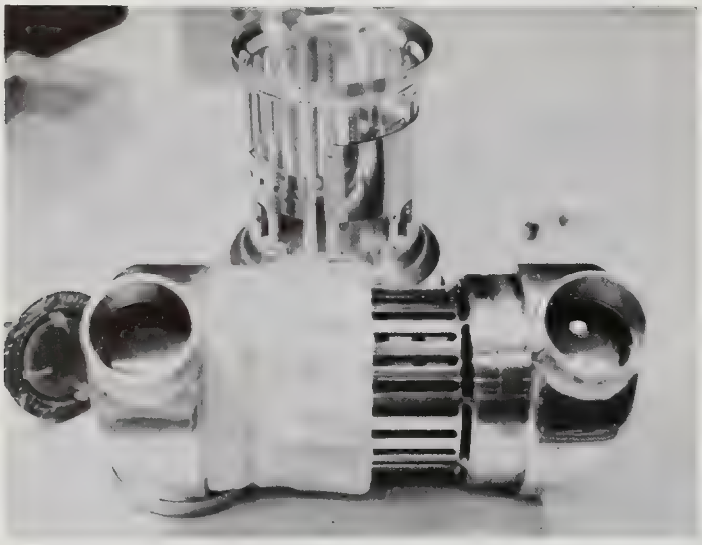

(a) PUMP ASSEMBLY

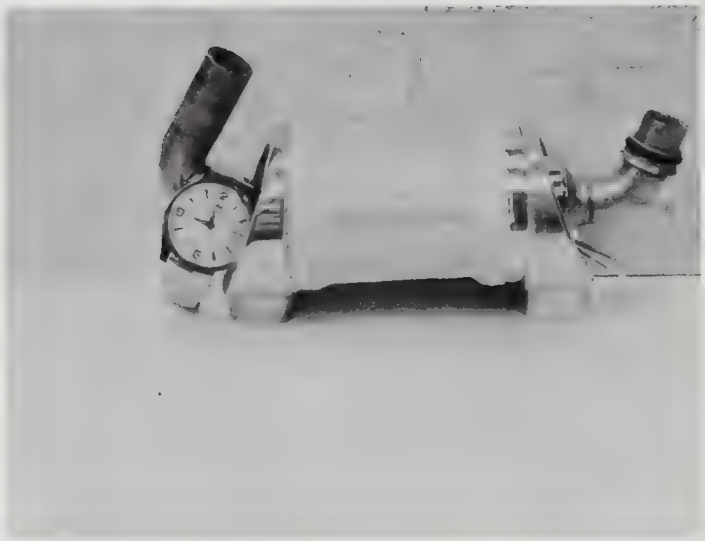

(b) COMPLETED PUMP

FIGURE 8. HYDRAULICALLY ACTUATED BLOOD PUMP.

CHAPTER 79

ENERGY TRANSMISSION THROUGH THE INTACT SKIN

L. Heimlich and F. Christiansen

Biomedical Systems Department
Hamilton Standard
Division of United Aircraft
Farmington, Connecticut

T. Sato
Yale University
New Haven, Connecticut

A system has been developed to transmit 40 watts of regulated electrical power across the intact human skin. The transmitted power may be utilized to supply energy to artificial heart assist devices.

Radio frequency transport of electrical power is accomplished by inductive coupling between external and internal coils. Transport via inductive coupling has been shown to be very efficient, provided the coils are not too small and the separation between the coils is not too great in relation to their diameter.

The system consists of an external power and regulation control unit, transmitting coil and implanted energy receiver unit. The control unit contains the fundamental RF source and power amplifier as well as the control signal conditioning circuitry. The implanted energy receiver unit, in addition to supplying power to an implanted load, contains power sensing and control circuitry that generates a control signal frequency proportional to the received power.

The 530 KHz RF signal is generated by a crystal-controlled oscillator. Class S amplification and solid state switching regulation are utilized for high efficiency. The demodulated control signal is used to control the switching regulator which, in turn, controls the RF power delivered to the load.

Demonstration of a closed loop for power regulation indicates possible solutions for power control over variable physiological conditions. In particular, the system has the capability to transmit power across the intact skin with the feedback control signal transmitted back via the same power transmission coils. Use of state-of-the-art technique and components has resulted in minimal size and weight units.

In vitro and *in vivo* evaluations of the system are being conducted at present. Large semi-restrained pigs are used for the *in vivo* tests.

INTRODUCTION

The Energy Transmission Through Intact Skin System (ETTIS) is designed to provide a means of transferring energy across intact skin for subsequent use by an artificial heart (Figure 1). The energy is transferred by means of inductive coupling between an extracorporeal transmitting coil and an implanted receiving coil. The unique aspect of this system is that the power transmitted is constant and relatively insensitive to movements between the coils (±1/2 inch at one inch axially and ±1-1/2 inch radially). The system power regulation is accomplished by using a voltage controlled oscillator to generate a 22 KHz control signal in the receiver and transmitting it to the extracorporeal coil which is tuned to approximately 530 KHz and 22 KHz.

The system described in this presentation was designed and built during the initial contract period (1967-1968). Throughout the present program it has not been necessary, nor required, to change the basic electronic design.

The objectives of the program include the following:

1. Long-term *in vivo* testing of implanted energy receiver subsystems.
2. *In vitro* testing of Energy Receiver Units (ERUs) in physiological saline.
3. Evaluation of the overall applicability of the system with respect to efficiency of power transmission, the degree and nature of tissue damage, compatibility with conditions of implantation and ability to permit adequate hygiene and reasonable patient activity, and
4. To provide RF energy transmission systems to operate with and directly connect to piezoelectric, electric motor and thermal implantable energy conversion systems with implantable energy storage.

In this report, a description of the system is briefly presented, followed by a discussion of the program's accomplishments over the past year.

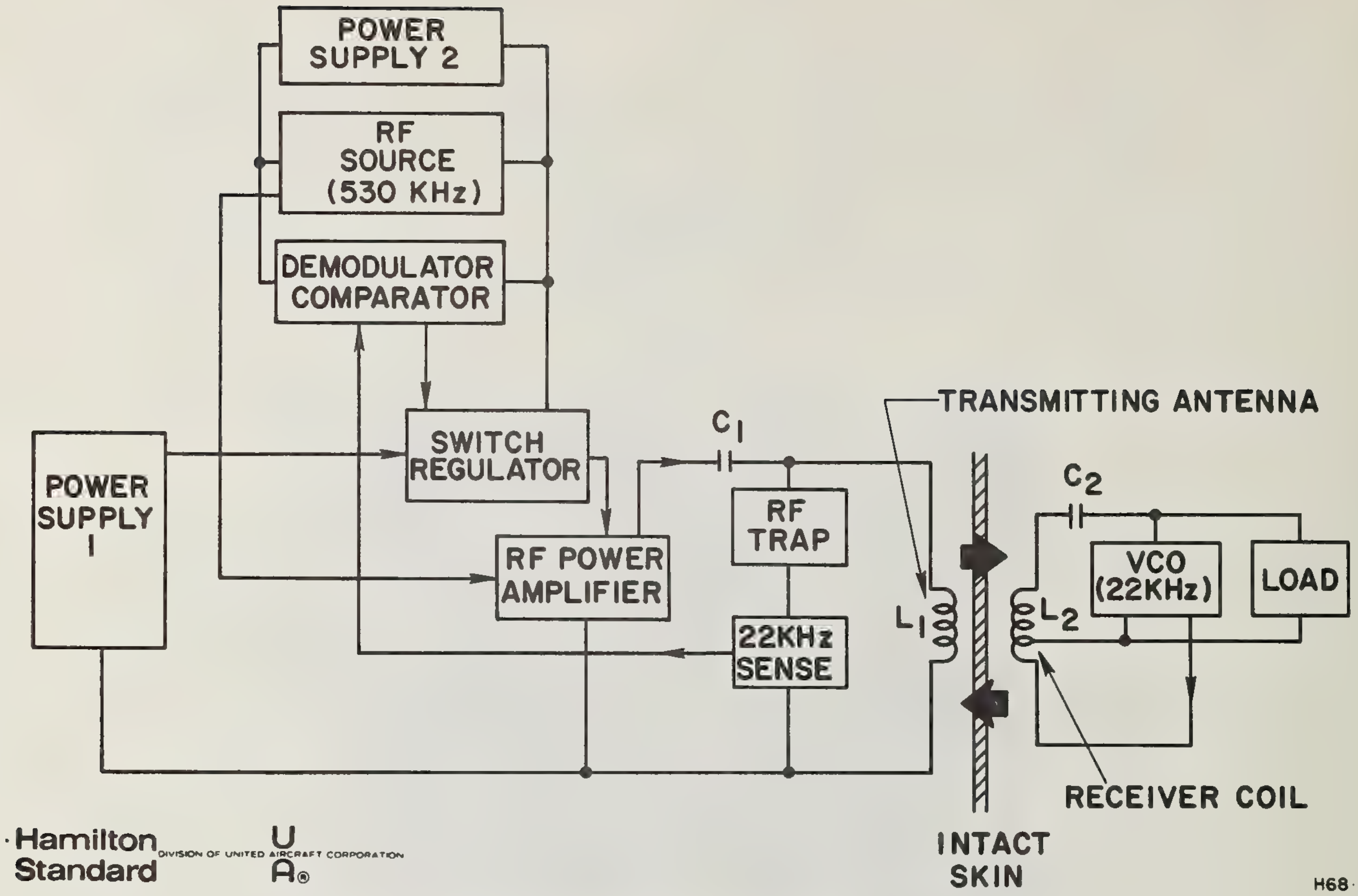

FIGURE 1. RF ENERGY TRANSMISSION THROUGH INTACT SKIN.

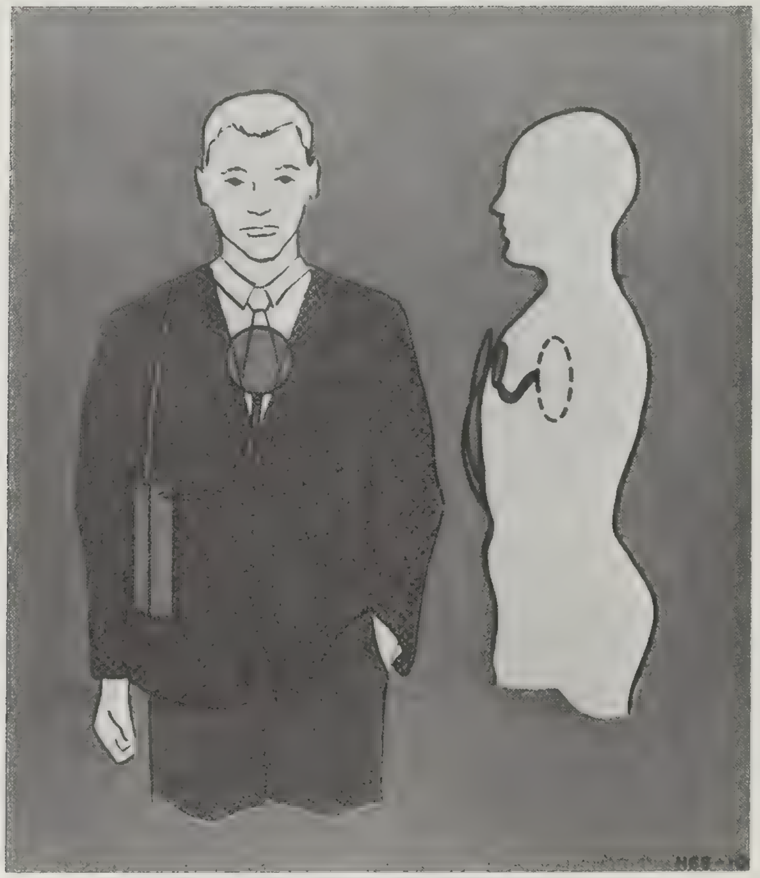

FIGURE 2. RF ENERGY TRANSMISSION SYSTEM.

EXPERIMENTAL

The Hamilton Standard system, designed to transmit approximately 40 watts of controlled electrical power across the intact skin, is shown in Figure 2. The power transport frequency of 530 KHz is generated by a crystal-controlled oscillator and applied to a Class S amplifier. A voltage-controlled oscillator, physically located within the implanted receiving unit, senses the induced voltage at 530 KHz and the fluctuations due to axial and radial displacements between the two coils. This intelligence is transmitted to the transmitting antenna coil which is tuned resonant at both the power transmission and voltage sensing frequencies, 530 KHz and 22 KHz respectively. Upon amplification and demodulation, the control signal is applied to a switching regulator power supply. This supply, amplitude modulates the Class S RF amplifier which is proportional to load voltage variations, thereby completing the control loop.

The physical appearance of the complete energy transmission system is shown in Figure 3. The Energy Control Unit is approximately 8" x 8" x 4" and weighs about ten lbs. Attached to the rear panel of the energy control unit is the energy transmission antenna. The large six-inch diameter coil is attached to the skin over the area of the smaller implanted Energy Receiver Unit. The Energy Receiver Unit which is approximately 3-1/2" in diameter and weighs 6 ounces is implanted in a subcutaneous pocket provided by simple surgical technique. The performance of the energy transmission system is measured by the effective regulated power transmsmission over a variable degree of coil alignment. The system has been designed to regulate within five percent of the total power delivered over a wide range of both radial and axial displacements of the primary coil relative to the secondary coil. Figures 4 & 5 indicate actual system performance measurements for radial and axial coil displacements respectively. On each figure the upper curve marked "unregulated" is a measure of open loop system response. The lower "regulated" curve is a measure of system closed loop response.

The range of actual system axial regulation extends from one-half inch separation at the low end to over one inch and three quarters at the upper end, as shown (Figure 5). Over the regulated range, the output power is 44.2 watts. Also shown on the curves is the overall system efficiency at the control limits. As expected, system regulation is within the five percent level considered acceptable. The basic energy transmission system has the capability of transmitting approximately 40 watts of electrical power into a 50 ohm resistive load. In the anticipated application of the ETTIS system to energy conversion systems, the actual load and power requirements must be matched. One method of accommodating the various loads and power factors would be to modify the basic system to perform the appropriate function. However, in the interest of economy and expediency, it was deemed more advantageous to design and build a matching system to interface the present transmission system with the energy conversion systems. In the case of the motor and thermal conversion techniques, the matching system consists of a relatively small passive network physically located between the energy receiver unit and the particular conversion load. Piezoelectric energy conversion system matching can be accomplished within the energy control unit.

The in vitro test was established for the purpose of observing the performance and reliability of the energy receiver unit, exclusive of the side effects of the in vivo environment. The test consisted of immersing the energy receiver unit in a heated normal saline bath for an extended period of time while transmitting power to an artificial load (Figure 6). The test assembly consisted of a plastic saline water bath container mounted directly above the transmission coil. The transmission coil, similar to the one used with the complete system, is recessed in the test rig bottom plate and covered with a thin plastic disk to protect it from excess water exposure. A receiver coil support stand is mounted above the test tank. The coil is immersed in the saline bath and the height adjusted for the desired power transmission. The connector and implantable lead assembly are attached to the energy receiver unit and brought out of the tank to an artificial load. The saline bath is heated to 98^{0}F by a simple aquarium heater. Power is delivered to the transmission coil from a standard 530 KHz broadcast transmitter. Eight separate test assemblies are run in parallel and are powered by the single 500-watt transmitter.

As of June 1, 1969 we have accumulated over 46,000 hours of testing. Three of the original eight units in the in vitro test have been successfully operating for over a year. The first three failures had the effect of corroding and destroying the polyurethane connector (Figure 7). In addition, one had a "burn hole" along the periphery (Figure 8). The cause of these failures is believed to be a breakdown of the urethane material due to insufficient insulation. A thin covering of encapsulant in the area where the "burn hole" appeared was believed to be the result of vigorous grinding while the units were being smoothed out. These observations and the fact that the units were in saline leads us to the conclusion that poor insulation, especially on the tips of the connectors, allowed low resistance paths for the current and caused the subsequent breakdown of the material. The first three failures were all related to the connector. It is felt that until a better connector can be developed it would be advantageous to eliminate the source of unreliability by bringing a cable directly from the ERU circuit out through the polyurethane encapsulant. Another improvement in the system would be to increase the thickness of the encapsulant to provide greater insulation and exert better quality control during encapsulation.

The fourth failure (Figure 9) appeared as a melting and charring of its top side (above the components) of the polyurethane. The unit was destroyed to the extent that immediate determination of the failure was not possible. The fifth failure was similar to the fourth, but not as extensive. The difficulties with the encapsulant have led us to investigate other materials and methods of encapsulation.

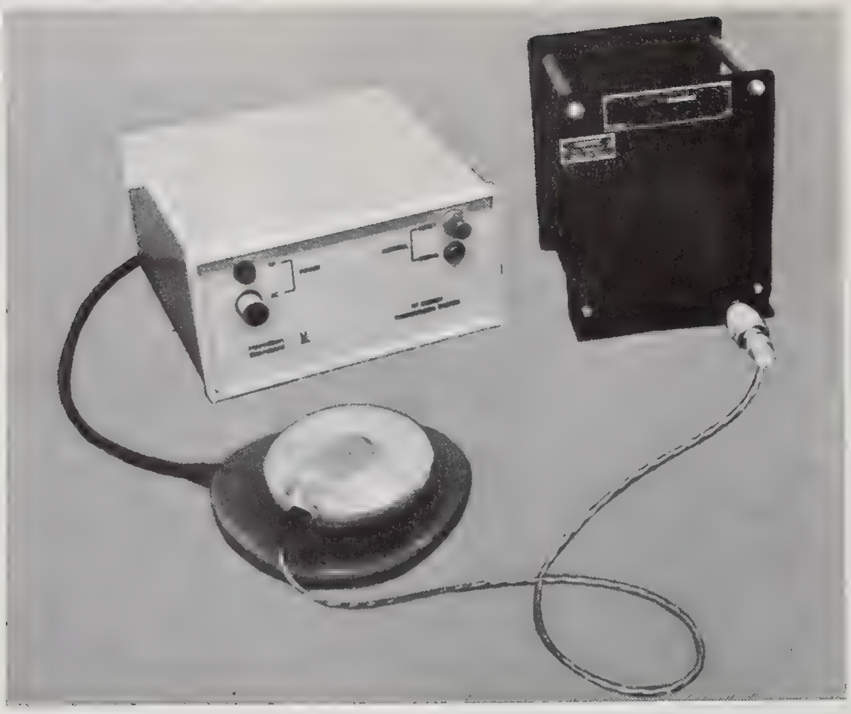

FIGURE 3. TRANSMISSION SYSTEM.

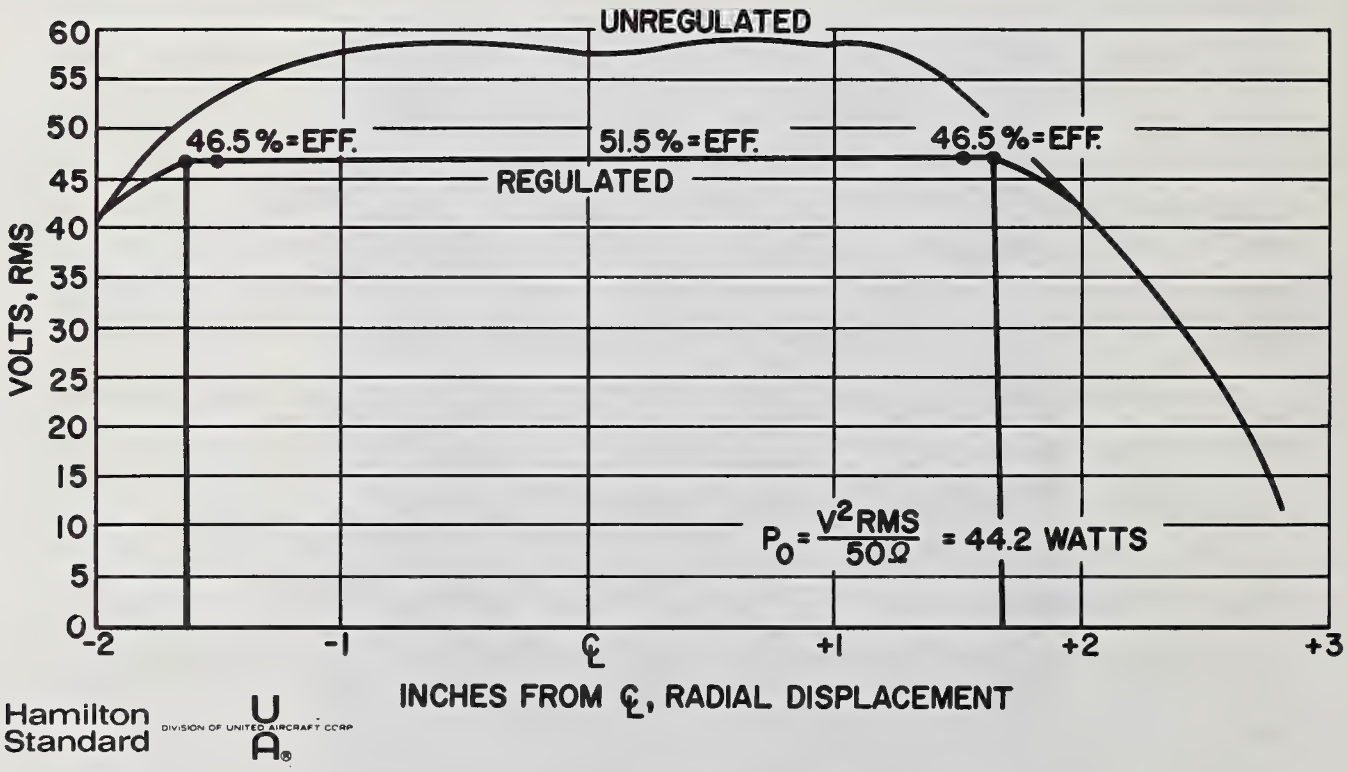

FIGURE 4. SYSTEM PERFORMANCE-RADIAL REGULATION.

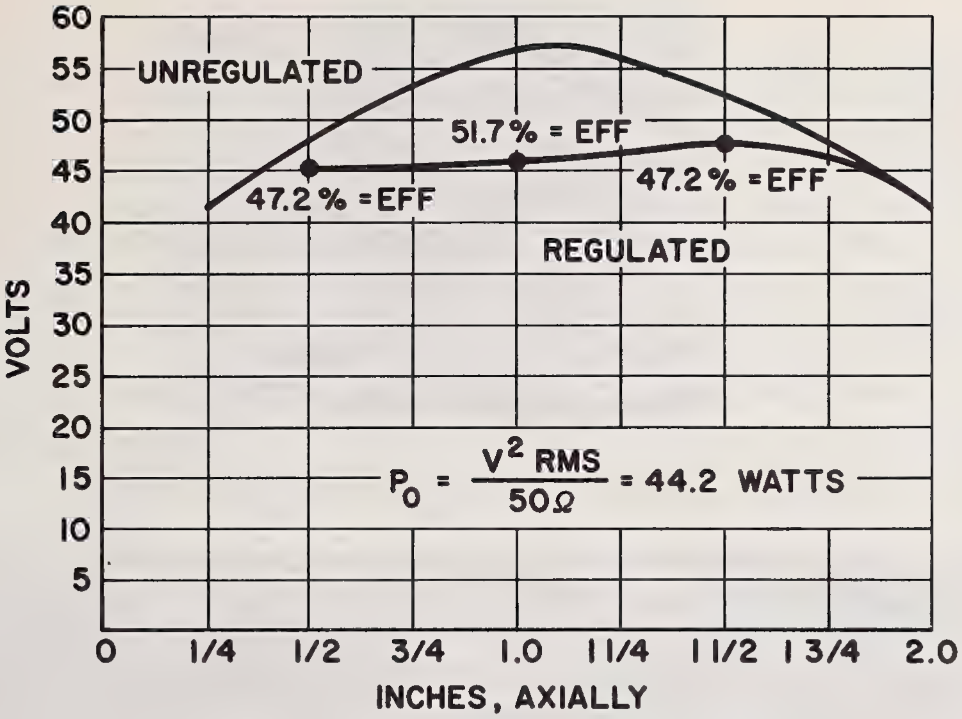

FIGURE 5. SYSTEM PERFORMANCE-AXIAL REGULATION.

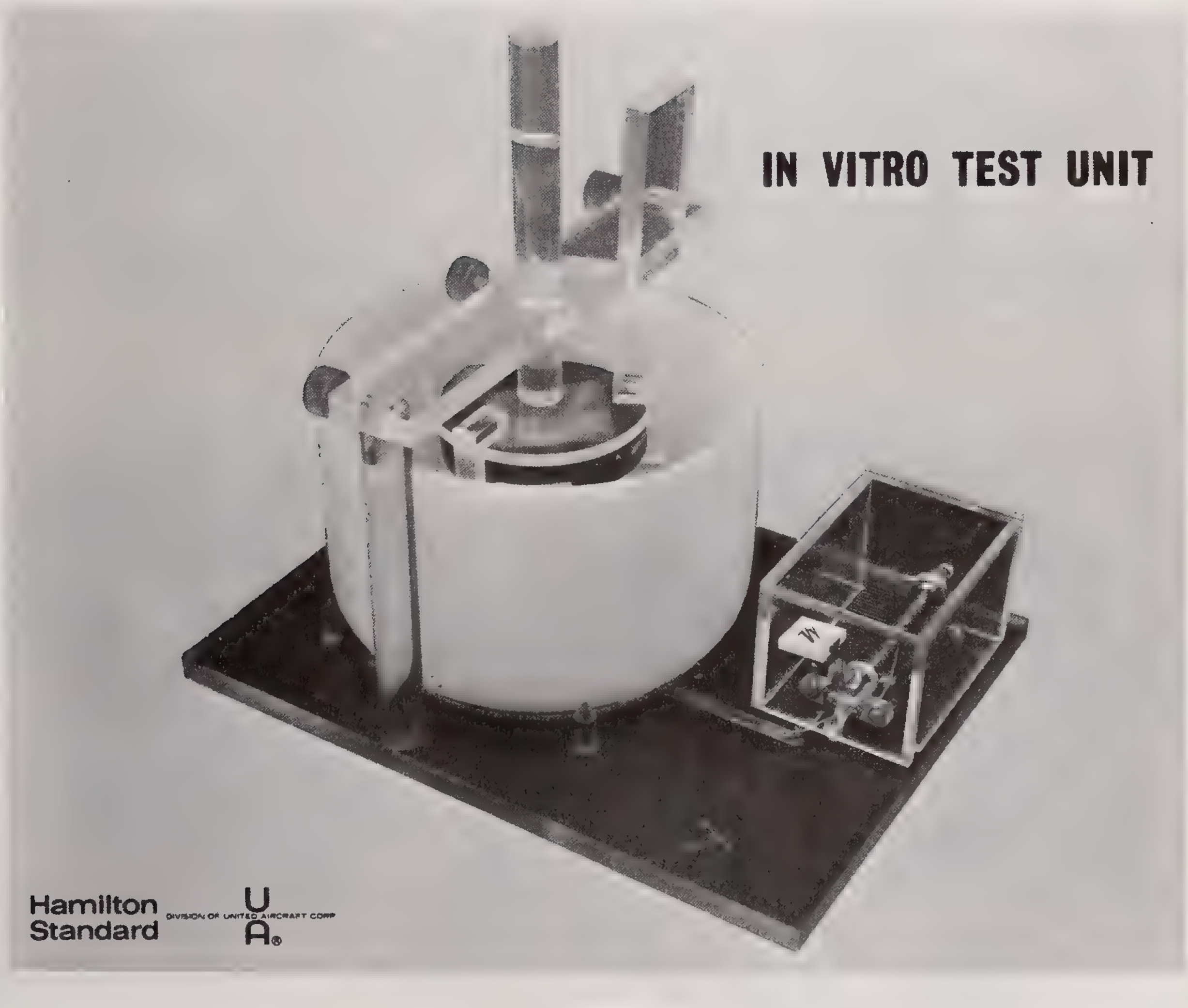

FIGURE 6.

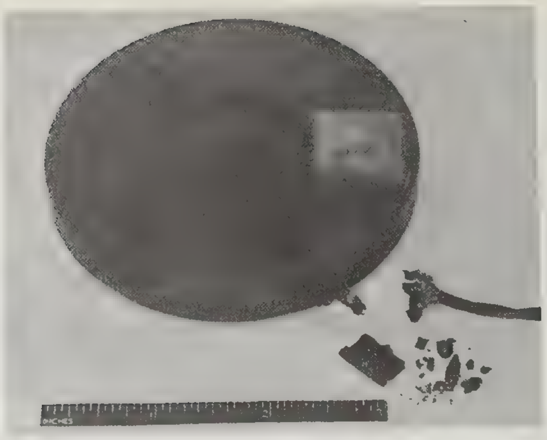

FIGURE 7. ENERGY RECEIVER UNIT IN VITRO CONNECTOR FAILURE.

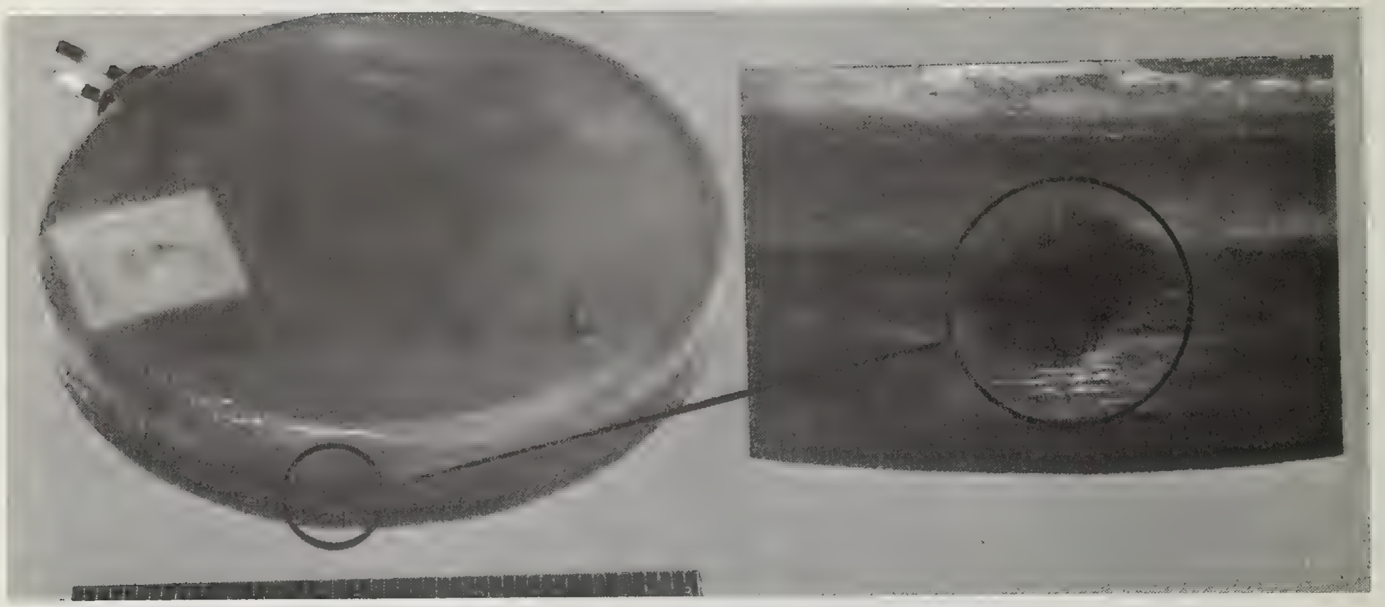

FIGURE 8. ENERGY RECEIVER UNIT IN VITRO ENCAPSULANT FAILURE.

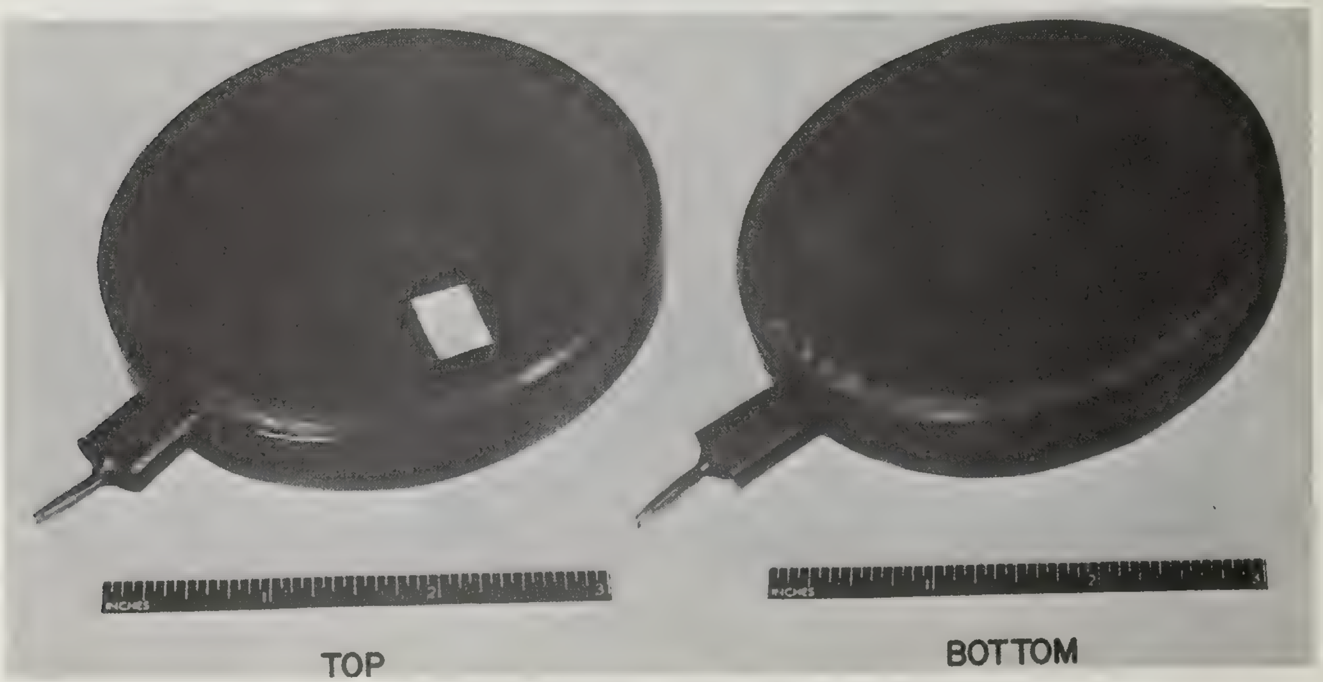

FIGURE 9. ENERGY RECEIVER UNIT NO. 14 AFTER 5600 HOURS OF OPERATION.

Yale Medical School, as part of their responsibility on this contract, conducted the in vivo evaluation of the units. Figure 10 represents the in vivo test configuration. The main problem in devising a test setup was the question of where to dissipate the 40 watts of energy transmitted across the skin. The solution to this was to bring a cable from the implanted receiving unit out through the skin (by a diadermal button) and connect it to a load box situated above the pig's stall. The control unit was also situated above the stall. The transmitting coil or antenna is connected to the control unit by means of extendable telephone cables. The first four receiving units and associated connectors were implanted in miniature swine with the diaderm buttons providing a means for bringing the cable out from the body implantations. In the fifth and sixth implantations, however, the diaderm button and the whole lead wire were totally implanted to avoid infection. Ninety-nine days after implantation the first receiver coil unit was removed because of an infection in the wound. This infection was caused by the continual scratching of the pig up against the cage. The second and third failures were discovered after an attempt was made to transmit across the skin. Using an ohmmeter it was discovered that there was an open circuit between the two leads projecting out of both pigs' backs. The implanted systems and units were removed. In the implanted portion, the lead wire revealed severe knotting, twisting and bunching of the copper fibers enclosed within the polyurethane lumen and the copper fibers were strained to the point of fracture. (This condition was more severe in the unit which had been implanted for 64 days.) The portion of the wire that was taped to the pig's back showed green corrosion.

An analysis of the lead failures indicated that corrosion was the primary cause of failure, and flexing was secondary. The ability of fluids to contaminate the copper cables was evident after a review of the test procedures. After the cable had been brought out from the diaderm button it was left either hanging or taped to the back of the pig. The end of the cable was open to its environment; there was no seal. The latter was easily dealt with. Stainless steel jackets were placed over the exposed copper wires. The problem of flexing presented greater difficulties. The solution was to increase the resistance to compression and twisting by enveloping the copper cable with an Elgiloy stress relieving coil. Figure 11 is a photograph of the completed strengthened cable. The Elgiloy spring is wrapped around the two cables and Silastic tubing is placed over the whole assembly. In addition to using Elgiloy, urethane was injected into any cavities or spaces which could possibly accumulate moisture and corrode the cable. After being implanted in pigs for up to 6 months there was no deterioration of any part of the cable which was treated. The end portions of the cable, which were not reworked were found to be fractured and corroded.

Subsequent failures of implants with strengthened cables after 4 and 6 months in animals resulted from the failure of the connectors. These units, which did not cause any gross tissue damage, had to be removed because of an open circuit on the female side of the connector. Our latest technique has been to directly weld the strengthened cable to the male pins of the ERUs. In the new units, presently under construction, the connector has been eliminated.

CONCLUSION

In May, 1969 a complete Energy Transmission System was delivered to the National Heart Institute, who arranged for its implantation in sheep. After almost 300 hours of transmission there is no indication of any major defects in the system or the animals. An investigation is also being conducted to determine whether polyurethane should be eliminated since it might be a source of failure. The control unit, as discussed above weighs about 10 lbs. and has a volume of 256 cubic inches. As need requires, it is felt that significant reduction in the unit's weight and size can be expected within the bounds of existing technology. In the months ahead it is planned to continue to transmit in vivo and to work with the energy conversion groups in order to achieve the objectives of the Artificial Heart Program.

DISCUSSION

DR. SATINSKY: While the effort is very laudible, it seems to me that the crux of the entire matter of utilizing the externally derived energy is its effect on the biological preparation, particularly as it relates to carcinogenesis. Is there any work in the in vivo studies that has been carried out in this regard? Because no matter what success you might have technically, the preparation might result in severe damage to the body tissues, and even the long range biochemical effects.

MR. HEIMLICH: I agree with you. The more significant work is in the in vivo area, but our problems with the cables and with the encapsulation of the materials prevented us from getting to that stage, and the little evaluation which was done through in vivo experiments was not enough to give us conclusive results. We plan to obtain these physiological data in the future.

MR. DOLAN: A small comment with regards to that last question. Some of this in vivo work has been done, starting in 1961. As a matter of fact it is still being carried on and the results are negative to date.

MR. HEIMLICH: There has been a considerable amount of work done by Dr. J. Schuder in the transmitting of energy across the intact skin. We plan to do some of this work ourselves in the future.

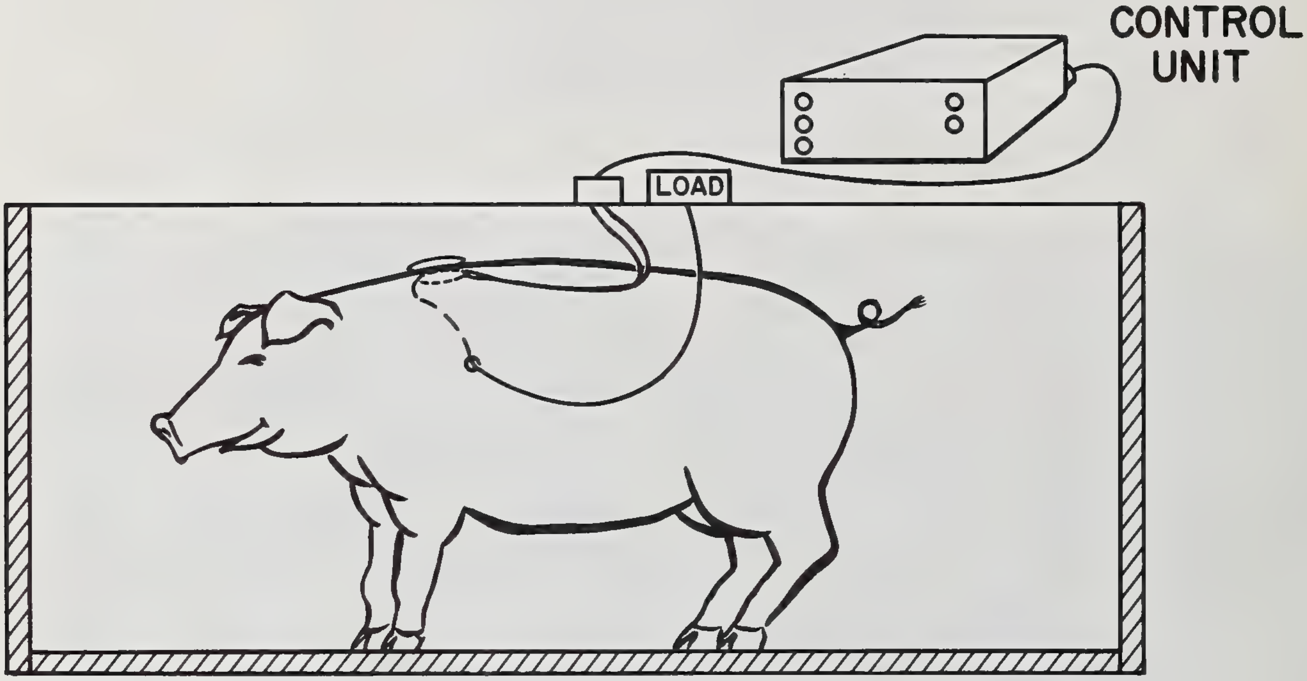

FIGURE 10. IN VIVO TESTING.

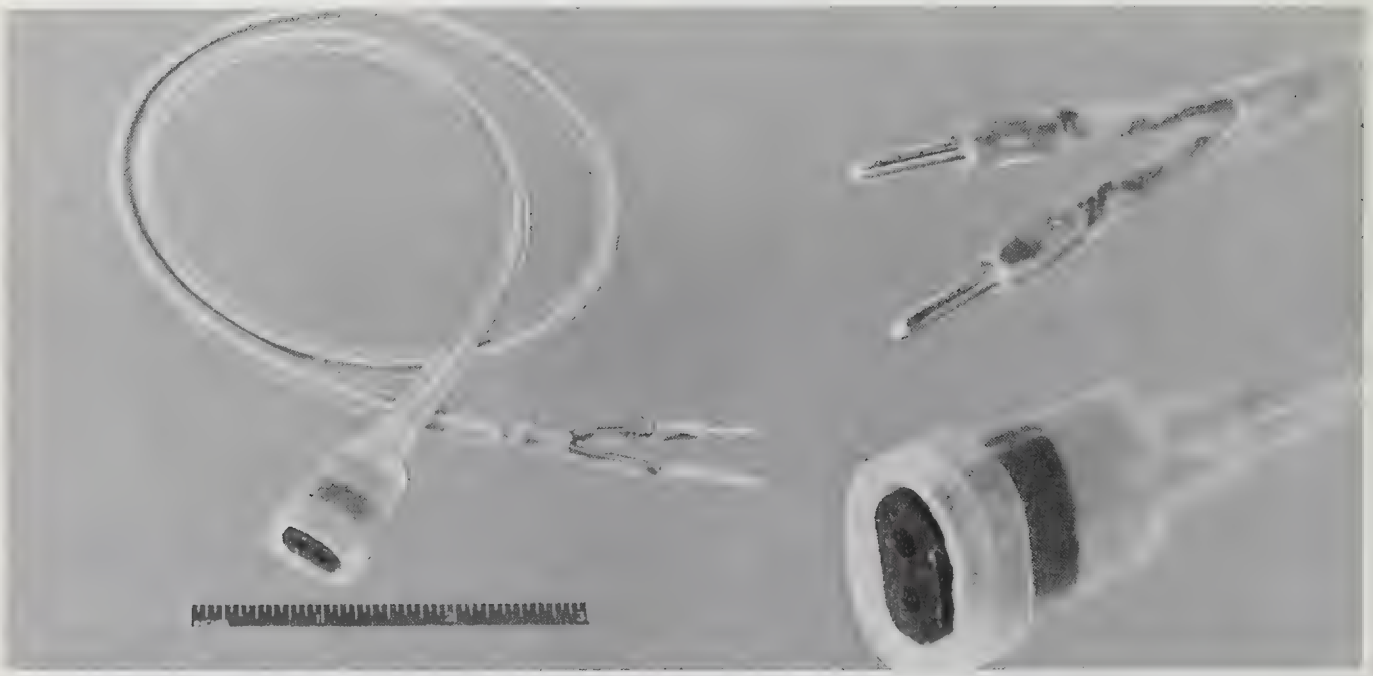

FIGURE 11. ENERGY RECEIVER UNIT CABLE WITH POLYURETHANE, ELGILOY AND SILASTIC.

CHAPTER 80

IMPLANTABLE ENERGY SYSTEM FOR A CARDIAC ASSIST DEVICE

J. Chambers

Statham Instruments
Oxnard, Calif.

The purpose of the program was to develop an energy system to power a circulatory assist device. The project includes integration of components and testing of the system. The basic energy converter is a small DC torque motor coupled to a ball and screw actuator to convert rotary motion to linear motion. The linear output is directly coupled to a bellows which uses hydraulic fluid to drive the blood pump. The energy converter allows passive filling of the blood pump; in addition, a bias towards filling of the blood pump may be provided if indicated. The system is developed to synchronize with the end of biologic systole and can provide varying blood output volumes. The primary control for this response is flow into the blood pump from the left ventricle. The energy converter is driven by a transcutaneous energy transmitter and may be driven temporarily by an implanted battery. Power conditioning components have been designed to drive the converter from either of these two energy sources.

INTRODUCTION

The current program has required Statham Instruments to develop an energy converter unit which employs an electric motor such as a torque motor coupled to a blood pump through a mechanical linkage such as a rolamite mechanism. The coupling medium between the energy converter and the blood pump is to be a fluid. Systems are to be delivered including associated electronic control and interface equipment required to adapt to a prototype drive system, to various blood pumps and to other components. Figure 1 is a schematic of the system as it has evolved to date. The blood pumps have been supplied by Thermo Electron Engineering Company and the initial transcutaneous transformer was supplied by New York University. The batteries have been supplied by General Electric Corporation. The system has five basic units. The Thermo Electron blood pump, the Energy Converter that actuates the blood pump, a power package that contains switching circuits, circuits for DC-DC conversion and circuits for rectifying the incoming AC signal. The final components considered for implantation are the secondary of the transcutaneous transformer and the battery pack.

EXPERIMENTAL

At the beginning of the program, the energy conversion unit shown in Figure 2 was proposed. This unit is made up of a rotary torque motor, a rolamite to linear translation mechanism and a metal bellows as a fluid pump. This drawing is schematic only and a number of functional designs based on this principle were developed during the first few months of the program. A typical example is shown in Figure 3. This particular figure uses a 4-roll rolamite approach in order to obtain stability in the rolamite drive system.

Continuing work with the rolamite concept demonstrated that this type of mechanism presented a number of special problems. The metal bands are extremely delicate and easily broken, and the mechanism must be extremely precise to avoid band creep around the rollers. Attempts to optimize the system always resulted in a relatively large and heavy torque motor that used less than 360° rotation for full stroke. Investigations of the possibility of the rolamite mechanism as a gear reducer also met with failure because of the tendency of the rolamite band to creep.

Because of the difficulties with the rolamite principle, the energy converter shown in Figure 4 was developed. This energy converter utilizes a small multiple-turn torque motor which rotates a ball screw. The nut of this ball screw is attached to the bellows and produces the translatory motion. This design resulted in an energy converter that had a weight less than the torque motor alone in the rolamite approach. The current torque motors utilize brushes and investigation is under way to replace these with brushless motors in future designs. Contact with manufacturers of these motors indicate that they have the ability to produce a motor with similar output characteristics to the one we are now using and within the same package size. To date these energy converters have demonstrated efficiencies in translating electric power to hydraulic power ranging from 11% to 18.5% depending upon stroke volume and required eject force. A variety of appraoches for the control of the energy converter and its synchronization with the biologic heart have been investigated. The initial thinking on the control method utilized the output from a pressure transducer located in the inflow of the blood pump just below the left ventricle.

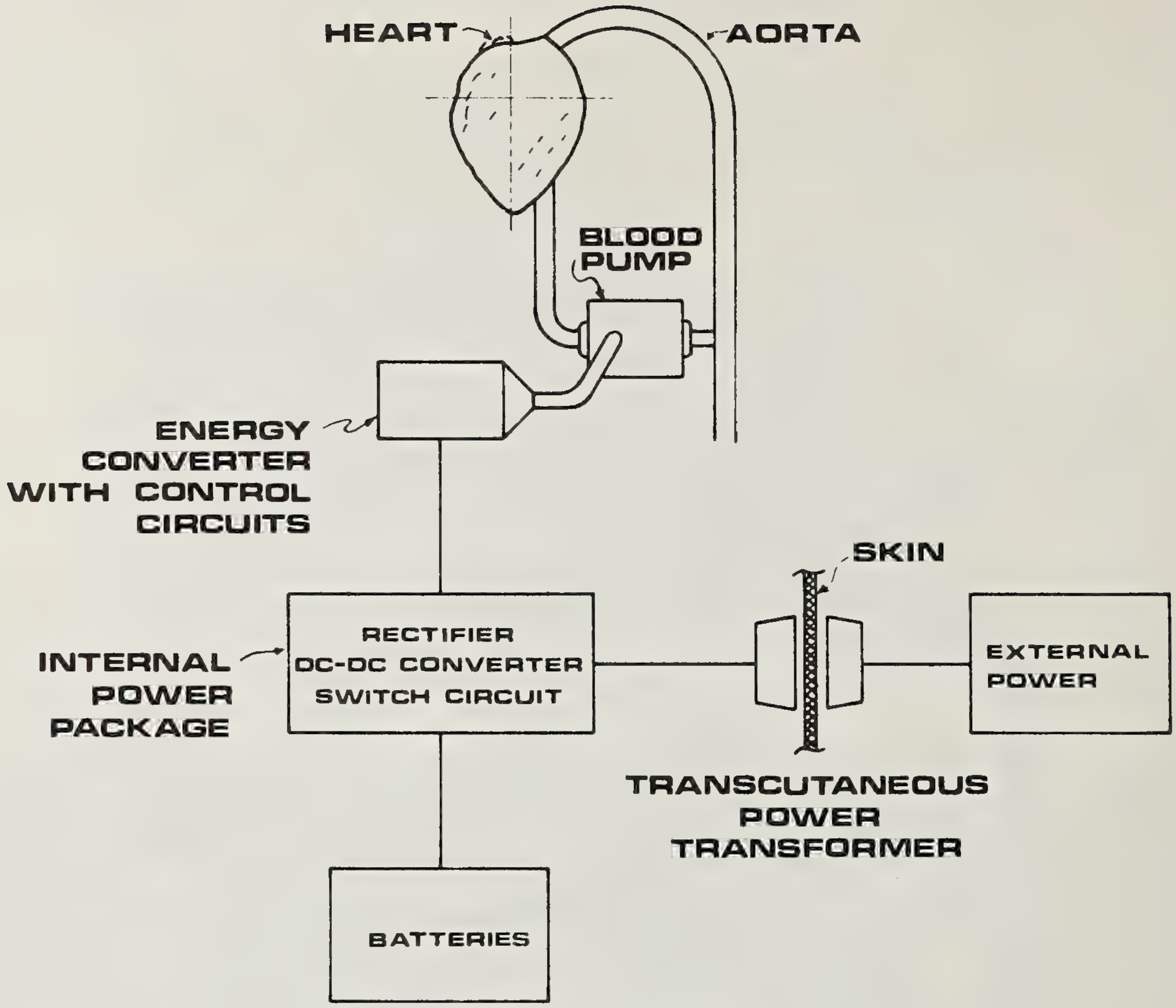

FIGURE 1. CARDIAC ASSIST SYSTEM.

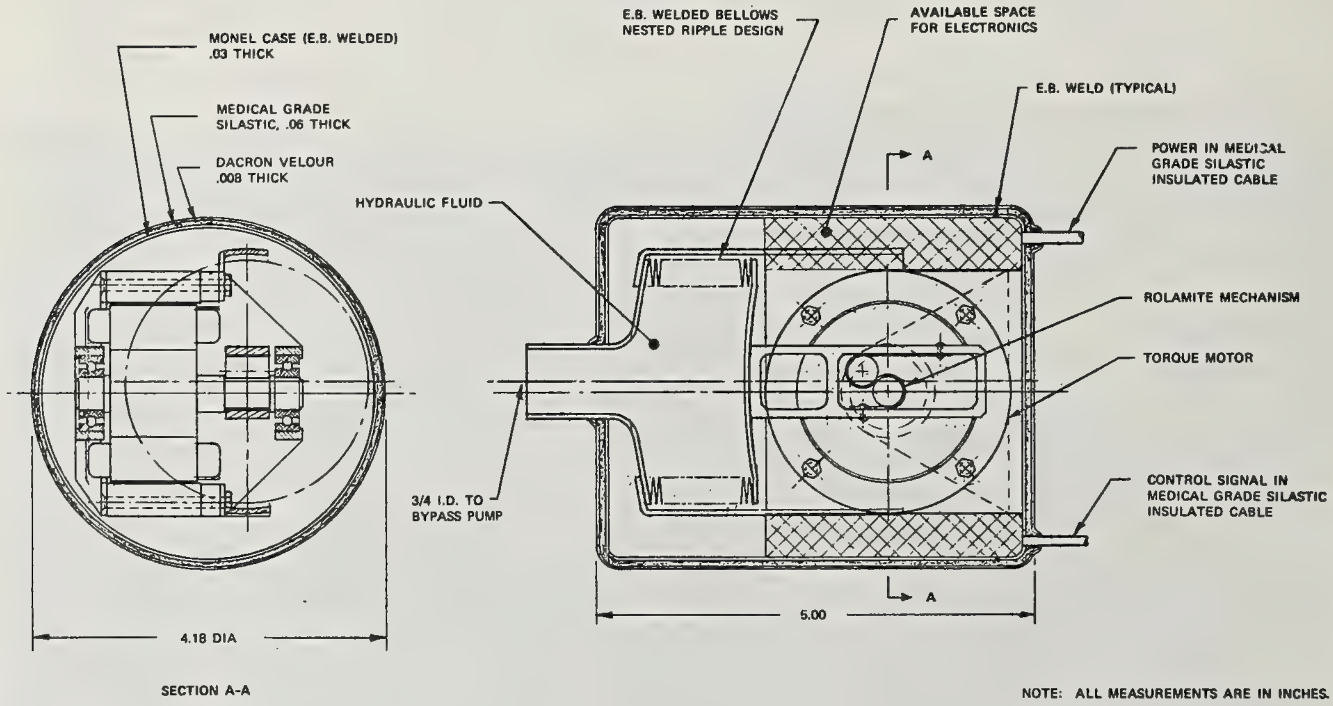
MONEL CASE (E.B. WELDED) .03 THICK
MEDICAL GRADE SILASTIC, .06 THICK
DACRON VELOUR .008 THICK
HYDRAULIC FLUID
E.B. WELDED BELLOWS NESTED RIPPLE DESIGN
AVAILABLE SPACE FOR ELECTRONICS
E.B. WELD (TYPICAL)
A
POWER IN MEDICAL GRADE SILASTIC INSULATED CABLE
ROLAMITE MECHANISM
TORQUE MOTOR
CONTROL SIGNAL IN MEDICAL GRADE SILASTIC INSULATED CABLE
3/4 I.D. TO BYPASS PUMP
A
5.00
4.18 DIA
SECTION A-A
NOTE: ALL MEASUREMENTS ARE IN INCHES.

FIGURE 2. HYDRAULIC PUMP AND TORQUE MOTOR - ROLAMITE DRIVE, TYPICAL NONOPTIMIZED DESIGN CONCEPT.

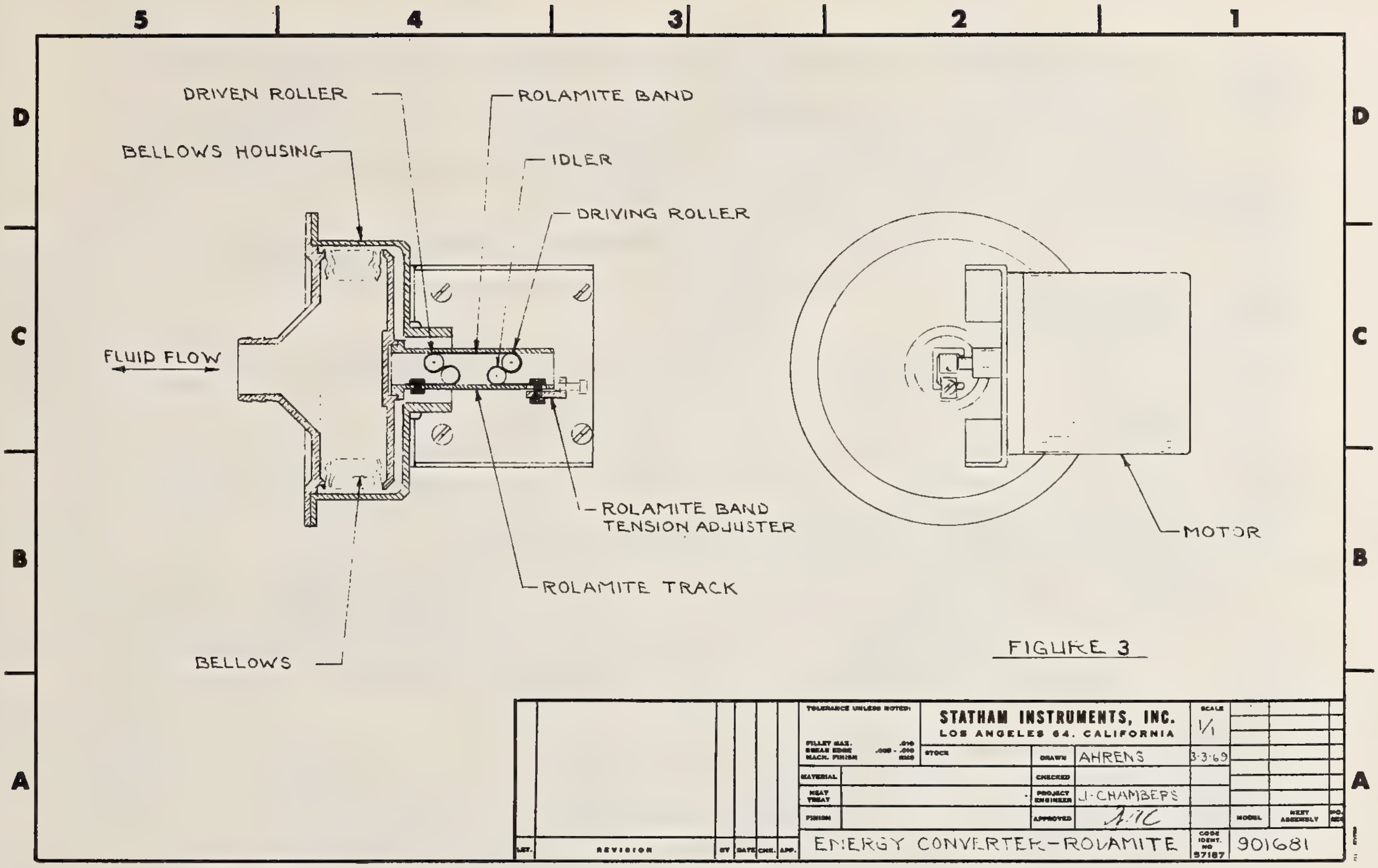

FIGURE 3.

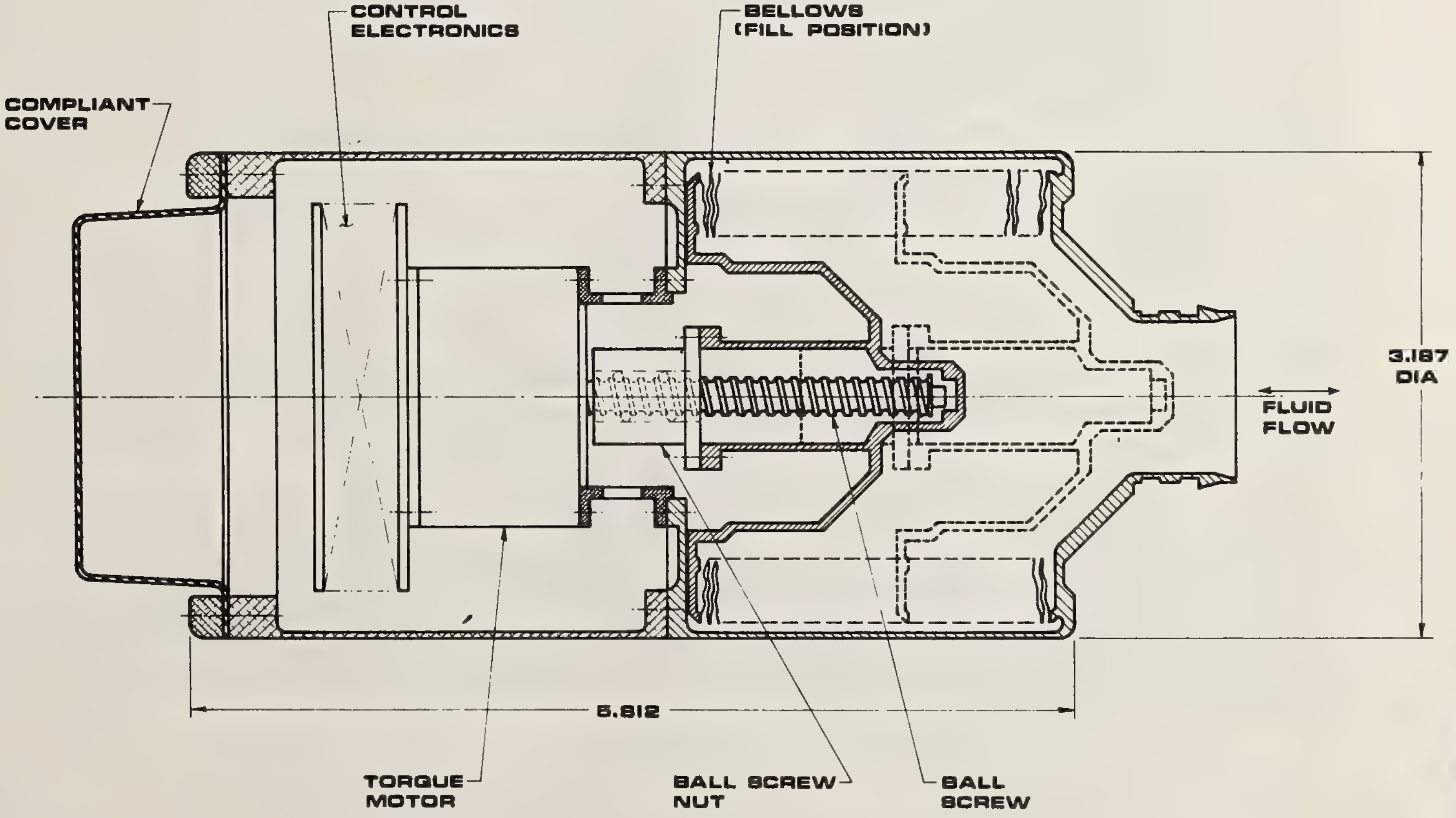

FIGURE 4. BALL SCREW ENERGY CONVERTER.

In the first control mode investigated, the filling of the blood pump would be initiated by a rise in ventricular pressure and the fill force applied to the energy converter would be pre-set. The eject from the energy converter would be triggered by a negative slope of ventricular pressure. The filling interval with this control approach would take place only during biologic systole.

In the second control approach, filling began immediately after mechanical systole and continued through biologic diastole and systole. The mechanical ejection would again be initiated by a negative or falling ventricular pressure. This control approach provided a longer filling interval and again, the filling force was pre-set electrically.

The third control mode is similar to the last mode except that the filling phase of the blood pump is servo controlled. In this approach, the system undertakes to maintain left ventricular pressure at or below a pre-set value. Ejection again takes place on the falling slope of left ventricular pressure.

The next mode that was investigated also utilized a servo controlled fill cycle for the mechanical system, but in this case ejection of the system took place only when the blood pump was full. In general, this system operated asynchronously and did not attempt to avoid eject during biologic systole.

A fifth system was also investigated that would utilize servo control fill, but would eject under either of two conditions. If the negative ventricular pressure was encountered before the blood pump was full, it would eject in a synchronized mode. If the blood pump completely filled before the end of the subsequent ventricular contraction, it would then eject immediately. This control approach is essentially a combination of the last two.

The above control modes and especially the last one, gave encouraging results but before they could be completely investigated, the control approach that we are now investigating was developed following a suggestion of Doctor Harmison of NHI. The system does not employ a pressure transducer, but rather, the spring characteristics of the bellows in the energy converter provide the filling force. Ejection takes place as a result of either cessation of the flow of the blood into the blood pump or if the blood pump should become completely filled. In this latter case, of course, even though more blood may be available, filling stops since the blood pump is full. Eject will then take place.

This system operates in either a synchronous or asynchronous mode. Mock loop tests have shown that the cessation of fluid flow following simulated left ventricular contraction will trigger the energy converter to eject. Under most conditions, therefore, the system synchronizes with the simulated biologic heart; but also has the capacity of operating at whatever rate is required in order to handle the total volume of blood presented to it. The mock loop that has been used during these studies is shown in Figure 5. The mock loop is shown with the Thermo Electron pump in place to simulate the relationship in a biologic system. The mock loop itself consists of a 50 cm^3 pneumatically powered pump that simulates the biologic heart. The flow from this pump travels through a simulated aorta into a pressure chamber with a compliant member. The fluid then flows through a clamp that simulates peripheral resistance through a flow meter and into a second chamber covered by a compliant member. This chamber is open to atmosphere and simulates the left atrium. Flow returns from this simulated atrium to the simulated heart. Three flow probes are also included in the mock loop. One of these for measuring total system flow is located in the inflow to the simulated biologic heart. The second flow probe is on the aorta and third flow probe is located on the outflow of the blood pump. Figure 6 shows representative curves taken during testing with the mock loop and demonstrates a reduction in ventricular pressure as a result of the action of the energy converter blood pump combination.

As mentioned earlier (Figure 1), implantable batteries are provided for emergency power in the event there is a failure from the external power system through the transcutaneous transformer. Our present systems employ three nickel cadmium batteries that develop 3.73 volts. These batteries operate into a DC-DC converter that boosts their voltage to the required 28 volts for the operation of the motor in the energy converter. The conversion efficiency is 70%. The batteries are packaged separately and a second package contains the DC-DC converter. The second package also contains a rectifier to convert the transcutaneous transformer voltage from AC to DC. A battery charging circuit is included and a switching circuit in this package senses the loss of external power and switches to internal battery operation. This same switching circuit switches the batteries off when external power is restored. The current batteries operating at body temperature have been able to give operation of six minutes. It is expected that improved batteries or the use of more cells together with improved efficiencies in converter circuits will increase this operating time.

The transcutaneous transformer we have used in this program is the same design developed by New York University, but we have modified the tuning circuits. Figure 7 is a schematic showing the difference in the circuit used by New York University and modifications we have made. With this modified circuit, we have been able to obtain 50 watts DC operating at 6.9 kilohertz through the transformer. Our measured efficiency is 68% between primary and secondary of the transformer. We made some investigations of other transcutaneous transformer designs utilizing U shape ferrite cores, and obtained some preliminary encouraging results. In one unit operating at 17 kilohertz, we obtained a power output of 34 watts with 60% efficiency. The weight of the subcutaneous unit without encapsulation was 33 grams.

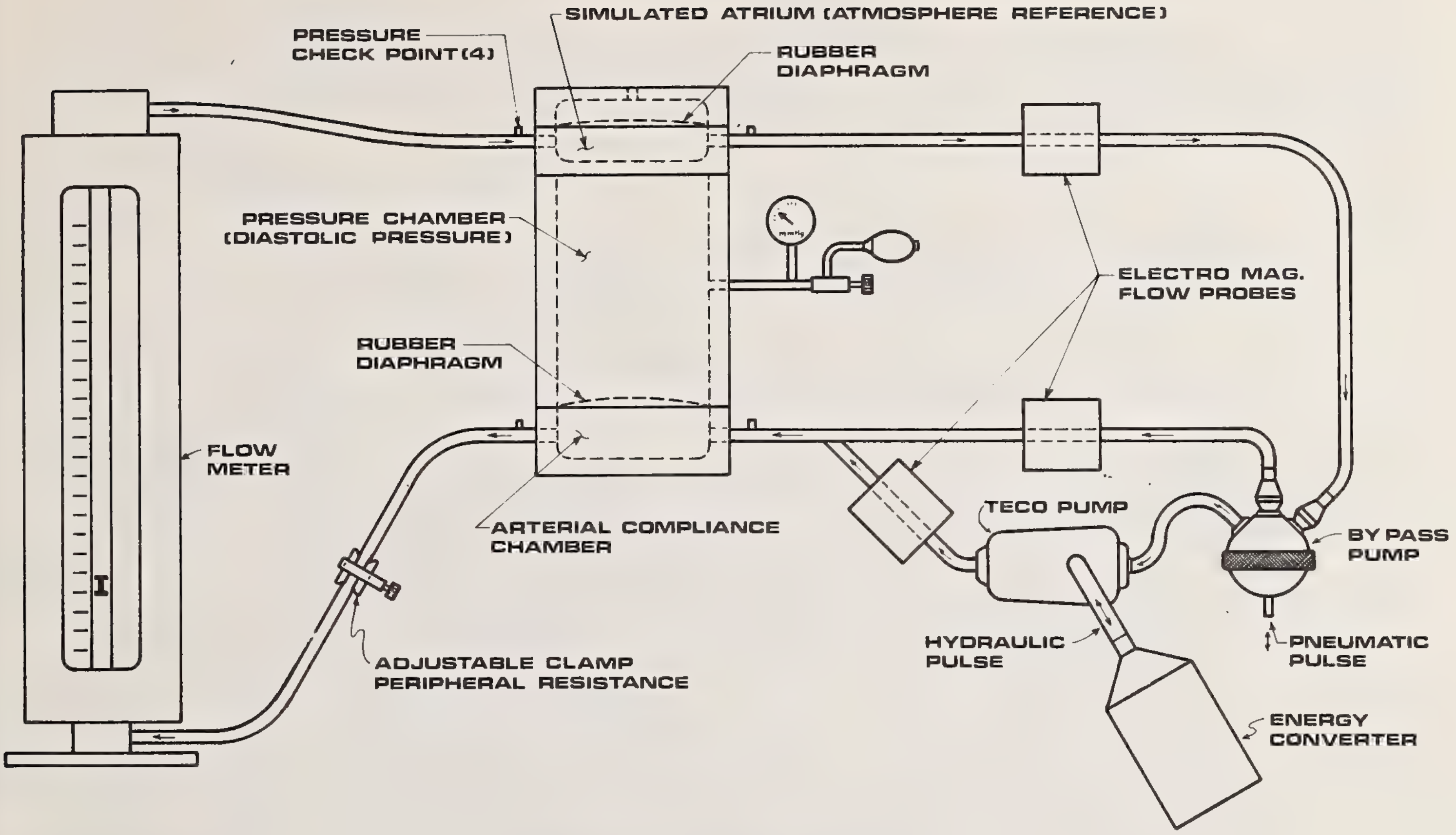

FIGURE 5. MOCK CIRCULATORY SYSTEM.

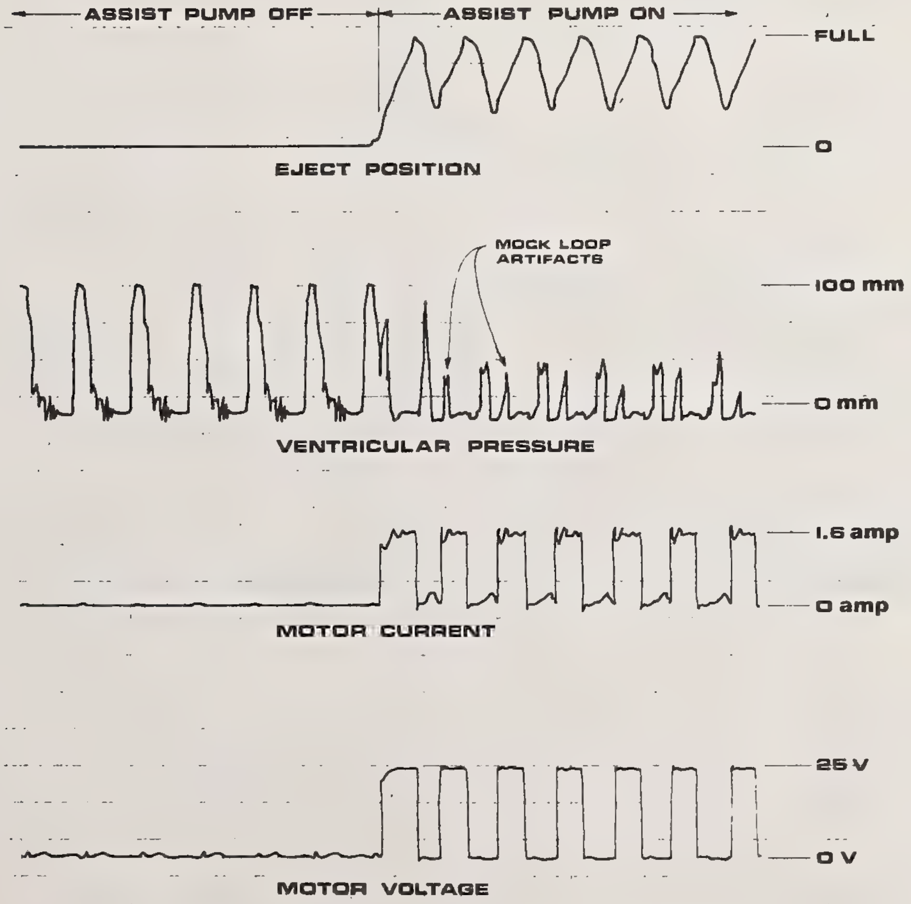

FIGURE 6. LVP PRESSURE REDUCTION IN MOCK LOOP.

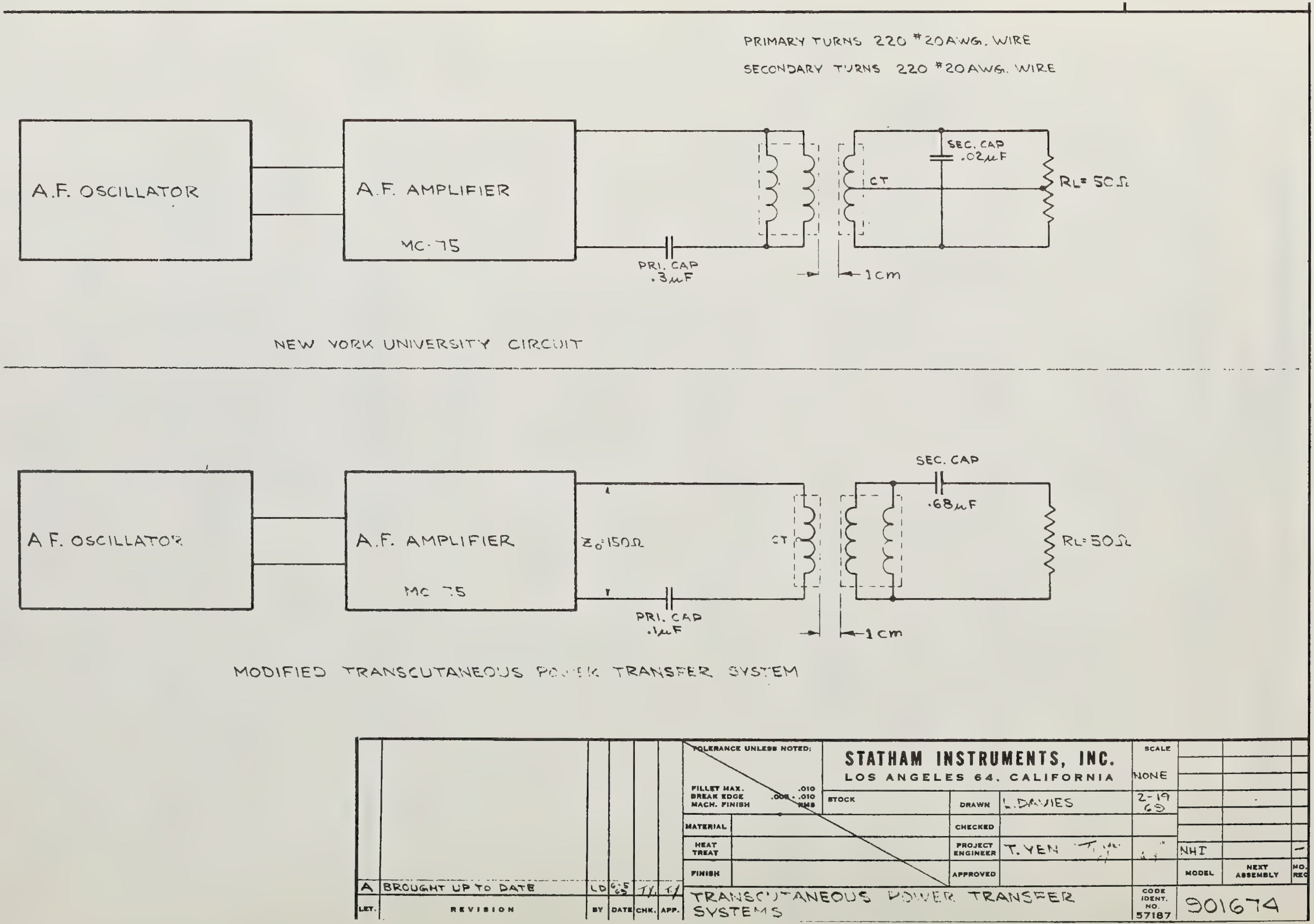
PRIMARY TURNS 220 #20AWG. WIRE
SECONDARY TURNS 220 #20AWG. WIRE
A.F. OSCILLATOR
A.F. AMPLIFIER
MC·75
PRI. CAP .3μF
CT
SEC. CAP .02μF
RL= 50Ω
1cm
NEW YORK UNIVERSITY CIRCUIT
A.F. OSCILLATOR
A.F. AMPLIFIER
MC 75
Z₀=150Ω
PRI. CAP .1μF
CT
SEC. CAP .68μF
RL=50Ω
1cm
MODIFIED TRANSCUTANEOUS POWER TRANSFER SYSTEM
TOLERANCE UNLESS NOTED:
FILLET MAX. .010
BREAK EDGE .005 - .010
MACH. FINISH RMS
MATERIAL
HEAT TREAT
FINISH
STATHAM INSTRUMENTS, INC.
LOS ANGELES 64, CALIFORNIA
STOCK
DRAWN L.DAVIES
CHECKED
PROJECT ENGINEER T. YEN
APPROVED
SCALE NONE
2-19 65
NHI
MODEL
NEXT ASSEMBLY
NO. REQ
A BROUGHT UP TO DATE LD 6-5 65 T.Y.
LET. REVISION BY DATE CHK. APP.
TRANSCUTANEOUS POWER TRANSFER SYSTEMS
CODE IDENT. NO. 57187
901674

FIGURE 7.

SUMMARY

In summary, a complete cardiac assist system has been assembled and tested. The system receives power through a transcutaneous transformer and is capable of emergency operation using implanted batteries. This system has demonstrated its ability to synchronize with the simulated biologic heart and has shown the ability to reduce left ventricular pressure in a mock loop system.

DISCUSSION

DR. CAIRNS: What is the total weight of the system that is implanted now or will be implanted and what do you think is practical to hope for in the next two to four years?

DR. CHAMBERS: The total system?

DR. CAIRNS: The total implanted portion or implantable portion of the system.

DR. CHAMBERS: That is a very difficult question to answer at this stage of development, because this involves encapsulation and so forth. I really don't have very good data on that. I really would rather not make a guess; it would be a total ball-park figure. We have not weighed the components in their final states. The energy converter itself weighs approximately 2 lbs. with its internal electronics, the power pack is relatively heavy, probably 5 to 6 lbs. at this point. The weight of the batteries is fairly well established, but I do not know what it is, and of course, the transformer was reported earlier.

MR. POWELL: Perhaps you could give an indication of the dimensions of the converter and the power pack?

DR. CHAMBERS: The energy converter dimensions were on the slide. This is one of several versions of the energy converter. Its outer diameter is approximately 3 inches and its overall length is in the neighborhood of 5 inches. The dimensions of the current power pack probably are 1-1/2 x 5 x 7 inches. The batteries run about 5 inches. It depends upon how you pack them, of course, but they are relatively thin, about 5/8 inches thick. About three of them end to end would be about 6 inches long and about 2-7/8 inches high.

DR. MARTINI: How much power must be supplied to the power transformer compared to the power supplied to the pump?

DR. CHAMBERS: Some of our data indicate that we have been putting in the neighborhood of 5 to 6 watts hydraulic power into the blood. This requires approximately 40 watts into the secondary of the transcutaneous transformer.

MR. GEBBEN: A pneumatic drive would reduce vibrations caused by inertia reaction forces that result from accelerating and decelerating the pumping fluid. Since the drive system operates between 0 and 120 mm Hg (gauge) pressure, the compressibility effects of gas will be approximately 20% of the total gas volume. In other words, the pneumatic drive would operate with relatively incompressible characteristic which would not increase the system size appreciably. Have you considered the use of a pneumatic drive system instead of the hydraulic system presented?

DR. CHAMBERS: No. The requirements of the program require hydraulic coupling and the hydraulic system would minimize the size of the energy converter. Surprisingly enough, we operate this into a mock loop, and there are rather small reactive forces and very small torsional forces. The energy converter is quite quiet. It doesn't make much noise at all.

CHAPTER 81

DEVELOPMENT OF AN ELECTROHYDRAULIC ENERGY SOURCE TO POWER AND CONTROL CIRCULATORY ASSIST DEVICES

N. Griffith and W. Burns

Indiana University Medical Center

Recently developed circulatory assist and total cardiac replacement blood pumps require hydraulic or pneumatic energy transfer mechanisms to pump blood. An implantable electrohydraulic energy source, consisting of a high-speed rotary pump, a brushless DC motor and the attending control system has been developed. This configuration, drawing power from implantable batteries or a transthoracic energy transmission system, delivers 10 watts of hydraulic power (3 psi at 7.6 gal/min) to the circulatory assist device. A 1:1 volumetric correspondence is maintained to ease control problems and minimize blood trauma. Operating at high speed (15,000 RPM) to achieve high efficiency and power output/volume indices, the motor and pump are coupled through either a 3:1 magnetic gear reducer or a 1:1 magnetic coupler. Since the pump-motor system is completely immersed this configuration isolates the motor interior and rotating parts from the corrosive, isotonic solution and permits flexibility in matching the pump and motor. Pumps with specific speeds of 2260 and 6350, which have marked differences in zero-flow power drain and pressure-flow characteristics, were fabricated to evaluate their pulsatile flow-generating capabilities and their effect on selecting the control logic. Hydrodynamic bearing designs for the pump and motor were considered in the interest of reliability. The electrohydraulic energy source is being integrated to a circulatory assist device for evaluation. Control logic for the system is based on monitoring the hydraulic fluid energy state in the blood pump, thus reflecting the output condition of the natural heart. Total system performance is reviewed and recommendations for continuing development are suggested.

INTRODUCTION

Implantable blood pumps, power conversion systems, energy sources, and blood-compatible materials are being developed to relieve the prevalent condition of the failing heart. As illustrated by this conference, extensive development efforts in this area bear witness to the profound importance of this problem in society today. Groups of workers, serving on integrated bio-medical engineering teams, have been concentrating on the formidable problems associated with control, packaging, blood-material compatibility, energy sources and the blood-pumping function itself. Partial success of circulatory assist devices and artificial hearts in the past several years would indicate that significant progress is being made.

Indiana University Medical Center personnel have been conducting research and development for a total cardiac replacement for over six years. The objective of these efforts has been to develop an implantable artificial heart capable of either prolonged or interim intrathoracic operation which would deliver the required pulsatile blood-flow to ensure satisfactory tissue perfusion. The displacement of blood by hydraulic or pneumatic pressure from a contained area which can fill in a variable displacement manner appears to be the preferred approach and is represented in many blood pumps today (Figure 1).

Following conceptual definition of the blood pump mechanism and primary control law, one of the first steps is the development of a miniature, efficient, controllable energy source to serve as the prime mover in effecting the blood pumping function. The electrohydraulic energy source (EHES), consisting of an electric motor and pump, was chosen for development early in artificial heart research, because it inherently possesses many characteristics necessary for good blood pumping and control. The EHES, functioning with a 1:1 blood-to-hydraulic fluid volumetric correspondence in a displaceable bladder configuration, offers many advantages. Hydraulic pumping subjects the blood constituents to normal physiological pressure and flow levels, so blood trauma and hemolysis are maintained at near normal levels. Evenly distributed hydraulic forces tend to reduce stress on the bladder materials which may experience millions of flexures, and hydraulic energy is transferred to the blood efficiently and reliably without transient high pressure gradients. Direct volumetric measurement of the non-compressible hydraulic fluid permits accurate monitoring and control of the total system.

Use of a small, immersible electric motor as the prime mover for the EHES opens the door for miniaturized control electronics and makes possible the use of complementary implantable batteries, biological fuel cells and transthoracic/electro-magnetic energy transmission systems. The electric motor and hydraulic pump may be compactly designed to permit integration within the blood pump mechanism. Thus, long hydraulic connections, introducing dynamic response problems are eliminated. The specific characteristics of the pump and motor may be selected to yield the appropriate control transfer function. Complete immersion of the EHES in hydraulic fluid, permits direct transfer of the 15 watt motor heat loss to the blood. If a fluid, isotonically similar to blood is used as the pumping medium, gradual molecular transfer through blood pump membranes should cause no foreign element problems, and bladder material design problems may be reduced.

Concomitant with the artificial heart development, we have undertaken the contractual development of an EHES to power and control various types of cardiac prostheses. The spectrum of these prostheses ranges from implantable, left-ventricular assists, which may relieve the heart's work load while healing, to intra-thoracic, total heart replacements. The objective of this effort then is to develop and test an implantable EHES system consisting of a brushless dc motor, mixed-flow, hydraulic pump and the required control system to power and control a variety of circulatory assist devices (CAD). In addition, we have recently undertaken the integration of the EHES and CAD in order to further test in vivo operation of the EHES.

The purpose of this paper then is to discuss the operation, development considerations, and resultant performance of this EHES. Development concepts for the integrated EHES-CAD system and anticipated performance will be presented.

CAD Operation.

The EHES is to power and control CADs similar to that depicted in Figure 1. This particular CAD is connected between the apex of the left ventricle and the ascending aorta. Developed by Thermo Electron Corp. in both hydraulic and pneumatic pumping configurations, the device relieves the work load required of the ailing left ventricle by effectively reducing the apparent hydraulic impedance during ventricular systole (CAD diastole). The energy source then applies pressure energy to the blood bladder during ventricular diastole (CAD systole) to effect the required instantaneous blood pressure and flow levels. As described in a later section, the EHES is being incorporated into a hydraulic valving and control logic system which will supply and accept hydraulic fluid directly to/from the CAD through large diameter, short tubing.

Pumping Requirements.

Specification of the overall, and individual EHES components (brushless dc motor, hydraulic pump, etc.), depend upon the establishment of the systems' intended function, control law, power and performance requirements, and the existing operational environment.

If the EHES, combined with the CAD, is to relieve the left ventricle (that portion of the heart pumping the high pressure, systemic vasculature) of its work load, to permit healing, then merely by definition, the EHES must be capable of generating, as a minimum, the pressure, flow and power level normally generated by the left ventricle.

The normal heart maintains a continuous flow of blood through the peripheral vasculature by pumping blood in a pulsatile manner. Clearly the instantaneous pressure flow and power levels defining the pulsatile blood flow waveform are considerably higher than the average or mean values. For the normal heart in average man (16 to 50 years of age), Figure 2 illustrates the approximate operational performance regions for pressure, flow, and power that the left ventricle delivers under resting to moderate-work conditions. The mean pressure power, and flow operating range is defined by Region A. Region C defines the instantaneous operating range assuming that a sinusoidal aortic flow waveform is generated. This is a simplifying assumption. However, it is doubtful that an EHES-CAD will be able to exactly duplicate the natural aortic waveform. Notice that 10 watts of instantaneous power, 155 mm Hg @29 l/min (the maximum power point on Region C) is required to achieve the mean power level of 3.8 watts for moderate work conditions.

ELECTROHYDRAULIC ENERGY SOURCE (EHES) DEVELOPMENT

In consideration of the above discussion, a cardiac replacement or assist device, operating under moderate work conditions, would require the EHES to deliver 10 watts of hydraulic power, 155 mm Hg @29 l/min. Confidence to pursue this development was based upon the success of previous brushless d-c motor and mixed-flow pump development with primary subcontractors, Micro-Pump and Sperry, Marine Systems Division.

The general configuration for the EHES consists of a high-speed electric motor, a "kinetic" hydraulic pump and a means for coupling the two components. Based on 1) the necessity for supplying the hydraulic equivalent of natural heart performance, 2) the implanted environment and anatomical space constraints and 3) the availability of a d-c electrical energy source, the following general development specification was established (Table 1).

System design was referenced to providing the pulsatile-flow capability of ten watts with an efficiency of 40% so that a maximum of only 15 to 20 watts need be dissipated. Other workers had been developing various types of implantable, electric energy sources and converters, so the availability of 24 volts d-c was assumed. Hydraulic power control over a wide range was to be a function of load demand, so the hydraulic load state was to be detectable in the motor input variables of current and/or commutation frequency. This condition requires that the speed-torque characteristics of the motor and pump be properly matched.

Since implantable operation was the objective, immersion of all components in isotonic fluid was specified. This criterion eases elastomeric bladder design but complicates the design and selection of metallic components. Immersible operation, of course, required that the motor interior either run "wet," or that special seals and/or indirect magnetic coupling be provided between the motor and pump assembly.

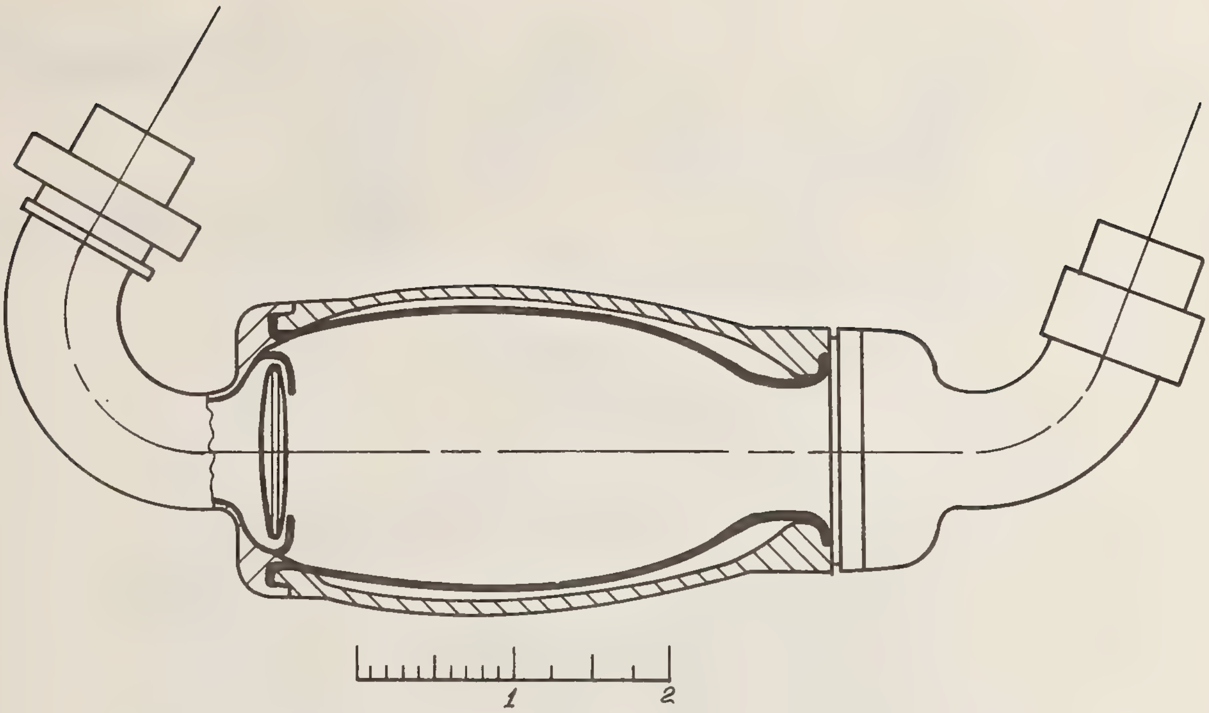

FIGURE 1. THERMO ELECTRON CORPORATION - CIRCULATORY ASSIST DEVICE.

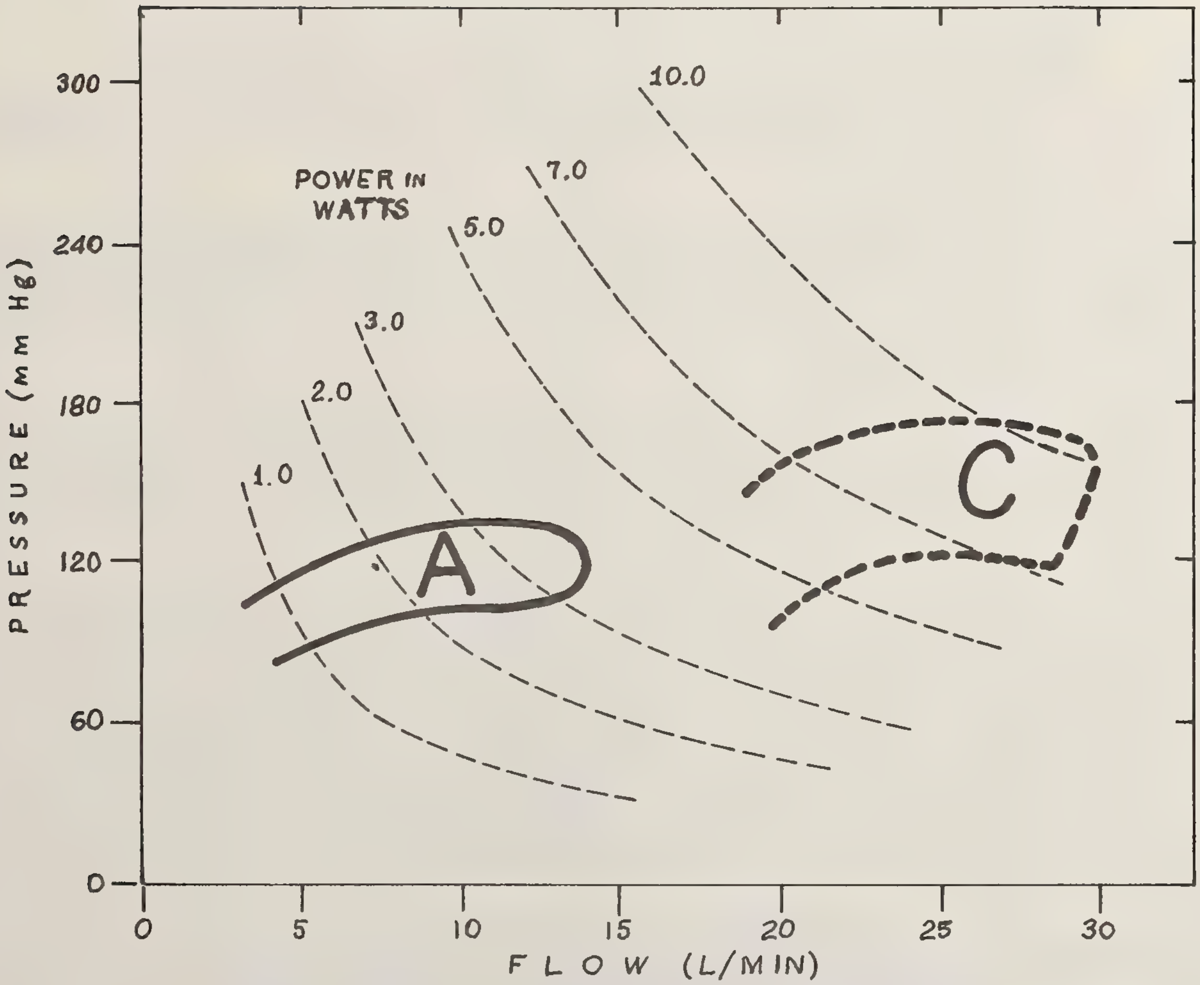

FIGURE 2. MEAN AND INSTANTANEOUS CARDIAC PERFORMANCE AVERAGE MAN, AGE 16 to 50 YEARS.

TABLE 1

EHES SPECIFICATIONS

Overall System Performance	
Power Output (hydraulic)	10 Watts
Pressure	3 psi (155 mm Hg)
Flow	7.6 Gal/min (29 l/min)
Efficiency	>40%
Power Input (electric)	25 Watts
Volts	24 V DC
Characteristic	
Pulsatile-Flow Capability	
Power state information available through electrical variables	
Power control over 40% to 120% range of system design point	
Reliability -- Maximum Possible, MTBF > 80,000 hrs.	
General Configuration	
Brushless dc motor	
Centrifugal-to-axial type hydraulic pump	
Size - smallest possible size consistent without compromising other criteria	
Operational Environment	
Immersible Operation	
Isotonic fluid (0.9% NaCl solution wt.)	
Temperature	37°C

Several motor-pump configurations were considered for development. Variations include:
1) Motor, 1:1 magnetic coupler, mixed-flow pump
2) Motor, shaft-coupled to mixed-flow pump
3) Motor, 3:1 magnetic gear-reducer, centrifugal pump
4) 2 motor-pump system

The EHES ultimately developed (Item 1) is depicted in Figure 3. It consists of 1) the brushless d-c motor, 2) 1:1 magnetic coupling providing motor interior sealing, and 3) a mixed-flow hydraulic pump. The centrifugal pump system was also developed.

Brushless D-C Motor Development.

The brushless d-c motor was selected for development, because it possesses the high performance characteristics of the conventional d-c motor while incorporating the long-life, high reliability features of "solid-state," electro-optical commutation. Operating at high speeds (15,000 rpm) these motors achieve good efficiency operation (65%) from low voltage d-c and characteristically have high, $\frac{\text{power output}}{\text{volume}}$ indices. Complete immersion of the motor interior in certain fluids is also possible with the brushless configuration.

Within its design operating range, these motors exhibit the standard, linear torque-speed and current-torque characteristics associated with conventional "brush" motors. These brushless motors are, however, torque-limited. The "field" in the motor is actually provided by the permanent magnet rotor, which has a relatively short magnetic length. Thus, if the current to the stator winding is not limited, particularly during startup, stall or transient acceleration, the current may generate an excessively high field which demagnetizes the rotor.

Motor Operation. The brushless d-c motor, Figure 4, consists of four major assemblies: a permanent magnet rotor, stator windings, a rotor position-sensing assembly (lamp, photo-sensors, shutter), and solid-state commutation circuitry (not shown). Functionally, the motor operates in the same manner as a conventional d-c motor in which the permanent magnet rotor establishes the field. With the Sperry motor, however, conventional, brush commutation is replaced by an electro-optical rotor sensing unit and a solid-state switching system. Current in each coil of the delta-wound armature is reversed cyclically by the switching network, thus establishing a magnetic field in the armature that is in space quadrature with the rotor field. Logic for the network is provided by semi-conductor photo-sensors which are alternately illuminated by a stationary light source. Attached to the permanent magnet rotor is a shutter which sequentially directs a light beam at the photo-sensor as the rotor turns. In turn, the photo sensors drive the switches causing stator current to flow in the direction that develops maximum torque.

Motor Design Considerations. Previous hydraulic pump development efforts indicated that pump efficiencies approaching 70% could be expected. Since the pump delivers ten watts of hydraulic power, the purpose of motor development crystallized easily. In addition to the Table 1 criteria, the

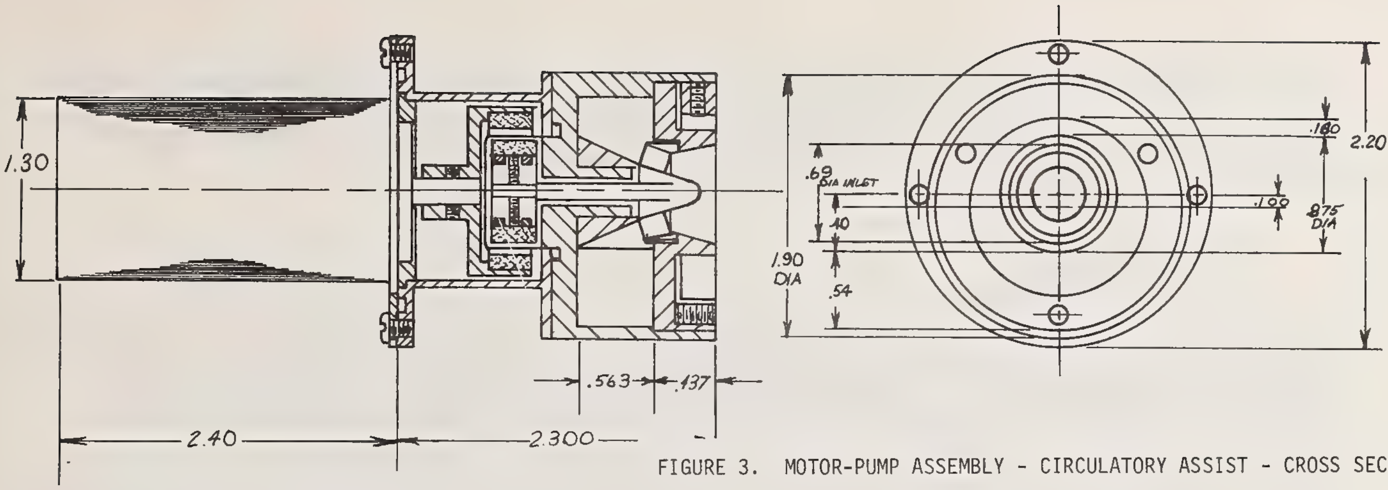

FIGURE 3. MOTOR-PUMP ASSEMBLY - CIRCULATORY ASSIST - CROSS SECTION.

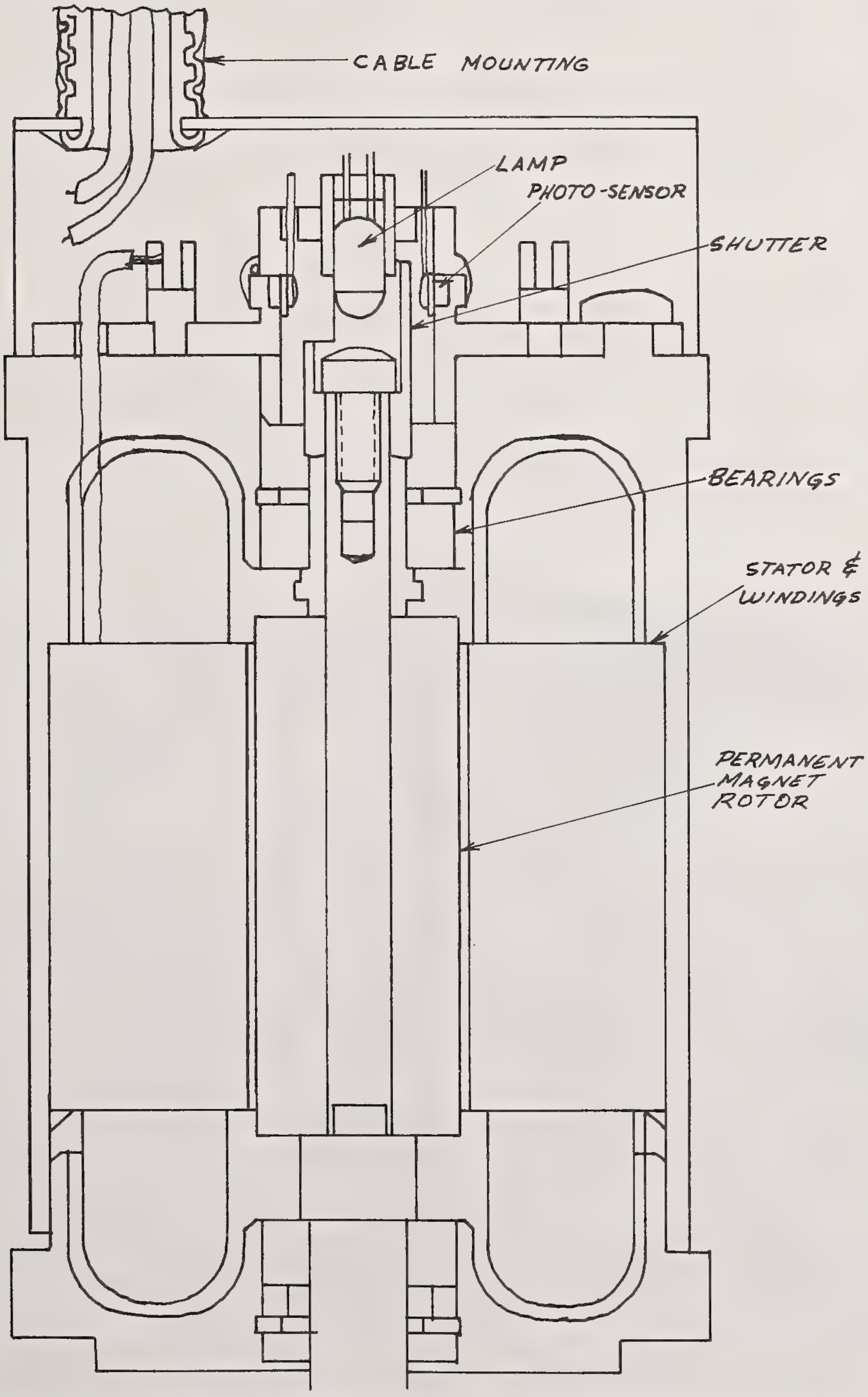

FIGURE 4. BRUSHLESS D-C MOTOR - CROSS SECTION.

motor was designed to deliver 14 watts of shaft output to the pump in a package amenable to implantable operation. With power output defined, three factors determined the motor configuration: 1) motor speed vs. volume/length ratio, 2) operation of the motor interior exposed or isolated from the isotonic fluid, 3) location of the commutation electronics.

The relation $\frac{Po}{N} \propto D^2L$ where,

Po = power output
N = motor speed
D = stator diameter
L = stator length

is used as a similarity criterion in motor design, because it relates the approximate motor performance to the physical configuration by dependently including the magnetic circuit variables, flux density and magnetomotive force. This relation discloses that minimum motor volume for a given power level is achieved by designing for highest speed operation. In addition, motor volume $\frac{(\pi D^2L)}{4}$, decreases with diameter while the length increases for a given Po/N figure. This in turn permits higher rotor speeds due to decreased centrifugal forces and viscous drag. Longer motor dimensions also permit more efficient utilization of wire, because the end turns comprise a smaller fraction of the stator length. The motor diameter, however, can only be decreased to the point of maintaining sufficiently low reluctance paths in the stator and providing adequate room for the coil windings. The permanent magnet, magnetomotive force is proportional to magnet length (rotor diameter in this case), so a minimum rotor diameter must also be maintained. Figure 5 illustrates the tradeoff between speed and stator stack length for stator diameters of 2.0 and 1.3 in., for each of two motors delivering 14 watts of output power. At 15,000 rpm with stator a stacklength of 1.05 in., nearly a 30% reduction in volume (also weight) is realized by the 1.3 in. dia. motor as compared with the 2.0 in. motor.

If the motor interior is flooded with fluid during operation, the necessity for sealing would be eliminated with considerable savings in system complexity and cost. However, viscous drag for the speeds of operation considered could decrease overall efficiency considerably. Viscous drag tests were run on a rotor-stator combination with similar dimensions to the motor actually developed. At 15,000 rpm, the viscous power loss was four watts -- 28% of the required output power. This loss could be reduced somewhat by operating with smaller air gaps. Although the Sperry motor can operate in fluid, operation in saline solution causes several problems. Leakage currents between the phototransistors, conducting through the solution could cause switches to turn on at inopportune times resulting in asynchronization or causing short-circuits in the switching circuitry. In addition, the high rotational speed of the lamp shutter could introduce damaging pressures on the incandescent lamp. This problem could be alleviated by inserting a glass header between the photo-sensor, lamp assembly and the fluid. This would be effective -- and expensive. Therefore, due to viscous losses, photo-sensor reliability problems and excessive development costs, the motor was developed for "dry" operation.

With the motor interior isolated, ball bearings could be used, but their presence introduced the spectre of a catastrophic failure. An investigation on bearing reliability data was initiated. Depending on the bearing fit and pre-load, similar bearings, under similar operating conditions to those defined above, effected 10% failure ranging from 60,000 to 20,000 hrs. with MTBF figures ranging from 90,000 to 20,000 hrs., respectively. Ball bearings were included in the design, however, development of hydrodynamic bearings was initiated for long-term considerations - 10 years. A self-contained, hydrodynamic bearing, with centrifugal action, lubrication and capillary action sealing features was designed. Development was discontinued due to funding considerations.

Motor Description. Table 2 defines the design specifications, and Figure 6 is a photograph of the motor components.

The external surfaces, motor casing and end cap are constructed of stainless steel to prevent corrosion. The motor interior is isolated from the fluid by the magnetic coupler, utilizing a non-magnetic membrane cup and O-ring seal applied to the casing flange. The rotor is shown with size 618 ball bearings which are lubricated with Andox "C" lubricant. The permanent magnet, polarized perpendicular to the axis is pressed onto the stainless steel shaft. The stator and coil windings, photo-sensor assembly, motor end cap and the commutation electronics wafer are also shown. The commutation electronics wafer, to be encapsulated in RTV 3120, is remotely located from the motor by a silicone rubber-covered cable. Stan-Rel circuit components have been used in the first prototype motor. However, to enhance reliability, Hi-Rel, i.e.,"burned-in," components will be used in the final module. Control of the motor is provided through a simple input voltage control circuit, which includes the current-limiting function. The current is limited to 1.6 a to prevent rotor demagnetization. Access points on the input control circuitry permit monitoring motor current or commutation frequency for power state or speed measurement, respectively. Pulse-width-modulation has been applied to the circuitry, effecting speed control from 100 rpm to 20,000 rpm.

Motor Performance. The performance characteristics for the first prototypes are depicted in Figure 7. Maximum power design point, 10 watts (1.25 oz.-in. @15,500 rpm) has been achieved. The linear characteristics, short of current-limiting, are exhibited. Design efficiency specifications were exceeded with a maximum efficiency at 21.5 volts of 68%.

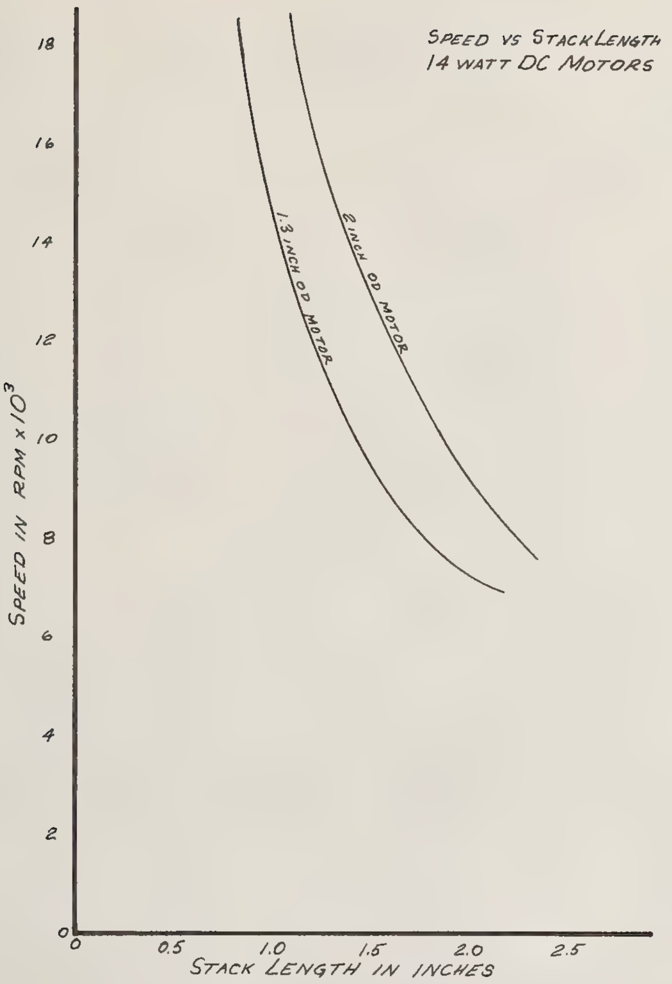

FIGURE 5. MOTOR VOLUME/SPEED RELATION, 14 WATT MOTORS.

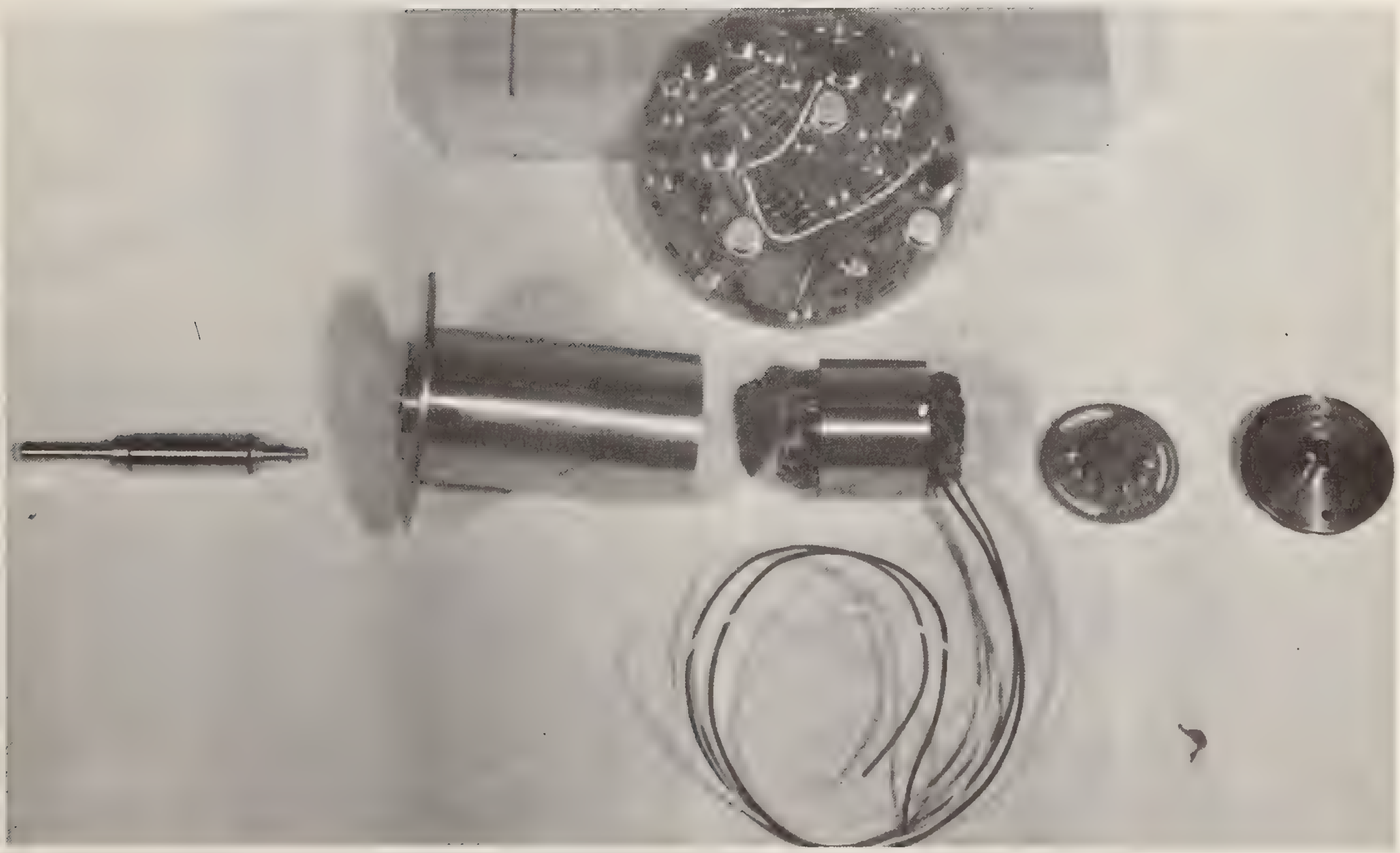

FIGURE 6. BRUSHLESS D-C MOTOR COMPONENTS.

TABLE 2

MOTOR SPECIFICATIONS

Performance	
Power Output (max)	14 watts
Speed	15,500 rpm
Torque	1.25 oz.-in.
Power Output (max efficiency)	9.7 watts
Speed	14,500 rpm
Torque	0.9 oz.-in.
Efficiency	>65%
Power Input (max)	23 watts
Voltage	24 v
Current	.95 a
Current Max	1.6 a
Power Input (max efficiency)	14.4 a
Voltage	21.5 v
Current	.67 a
Size	
Motor Diameter	1.3"
Motor Length	2.4"
Environment	
Isotonic Solution	.9% NaCl (wt)
Temp	≈37°C

With power supply ripple of 3 volts rms, the motor speed will track frequencies less than 200 Hz. Between 200 Hz and 10 KHz, the motor is insensitive to ripple. Above 10 KHz, the high-frequency components, shunted through by capacitive coupling, cause the electronic switches in the commutation circuits to come out of saturation. In this condition excessive current is drawn, and the motor slows.

Hydraulic Pump Development.

The pumps considered for development range in pump "type" from centrifugal to axial-flow pumps. These pumps designed in sizes sufficiently small for implantation, are easily capable of delivering the physiological pressures and flow required with efficiencies approaching 70%. Reliability of the overall EHES system is enhanced through the use of these pumps, because they can be ruggedly designed and should realize little wear. Short of gross fluid contamination or material failure, the pump is probably the most reliable component.

Pump Design Considerations. Hydraulic pump development was concerned with selecting the smallest, most reliable and efficient "pump type" that would provide the appropriate pressure-flow characteristic dependent upon selection of several possible motor operating speeds. Several motor-pump configurations were being considered for development to provide a broad range of system performance and size characteristics. Selection of the hydraulic pump for this application requires the consideration of the following primary parameters: (a) size, (b) pump speed, (c) load sensitivity, and (d) the pressure-flow characteristic. The relations between these characteristics at design point vary depending upon the pump type selected.

Note: Pump Design Criterion. A criterion of similarity often used in the design of centrifugal to axial flow pumps is the term "specific speed," where,

$$N_s = \frac{N\ (Q)^{1/2}}{H^{3/4}} = \frac{\text{pump speed (flow)}^{1/2}}{\text{(pressure head)}^{3/4}} = \frac{\text{rpm}\ \ \text{gpm}}{(\text{FT, } H_2O)^{3/4}}$$

Pump types can be related to each other performance-wise by specification of their specific speed. And, in turn, the relation between the above mentioned parameters, size, speed, etc., can be estimated.

Purely centrifugal pumps are characterized by low specific speeds, N_s = 1000 or less. Axial flow pump specific speeds are 10,000 or greater. Mixed-flow pumps are intermediate. Figure 8 correlates the pressure-flow characteristics and power input requirements for pumps with particular specific speeds.

Referring to Figure 8, the power input requirement, as a function of flow, can be determined for a particular specific speed. These curves are referenced to constant pump speed. Therefore, since power is proportional to the product of torque and speed, the input torque variation may be correlated to the pressure-flow characteristic.

Since the design operating point of 10 watts, 3 psi (6.93 ft, H_2O) @ 7.6 gal/min, has been determined, a linear relation between pump speed and specific speed remains,

$$N_s = \frac{N\ (Q)^{1/2}}{H^{3/4}} = \frac{N\ (7.6)^{1/2}}{\left(\frac{6.93}{17}\right)^{3/4}} = .5\ N(\text{rpm})$$

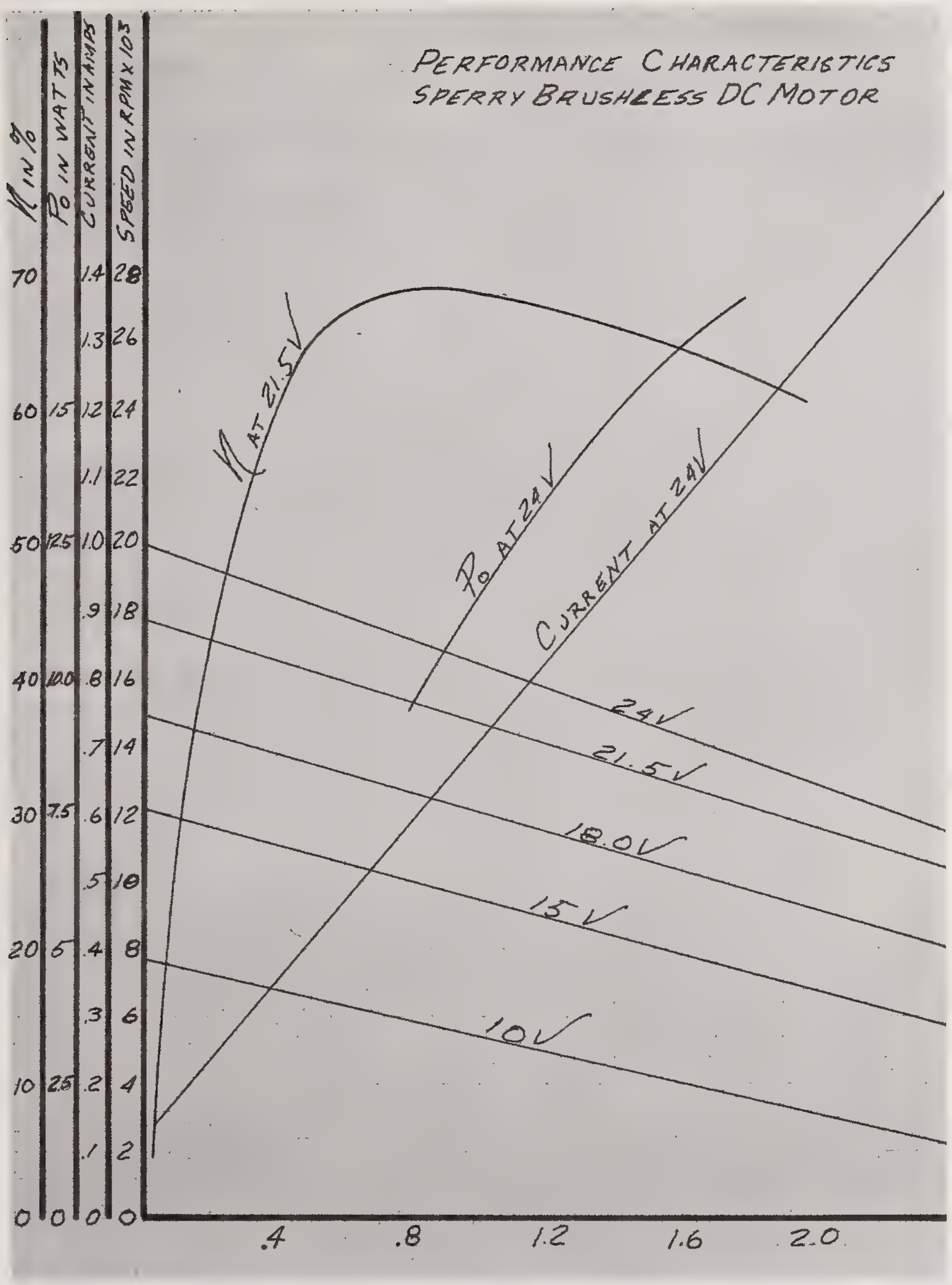

FIGURE 7. MOTOR PERFORMANCE CHARACTERISTICS.

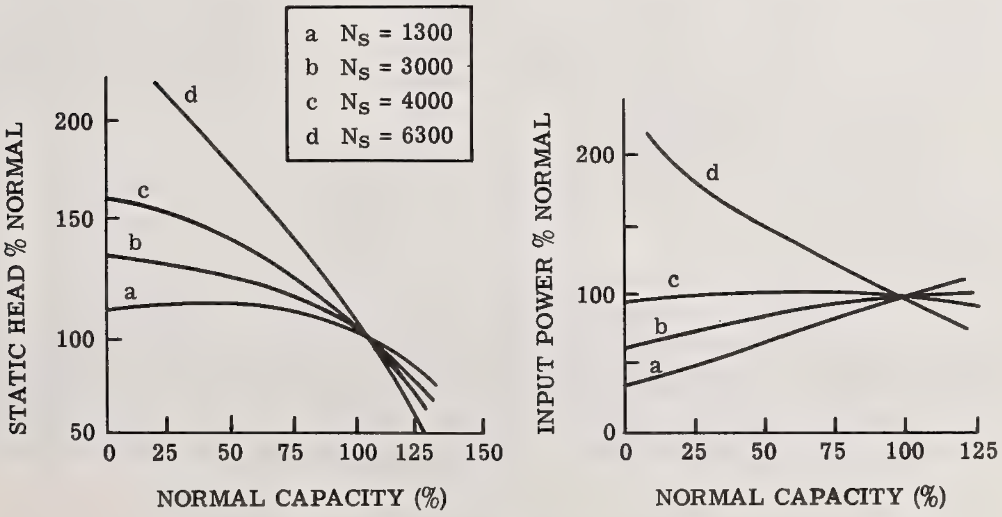

FIGURE 8. NORMALIZED PUMP SIMILARITY CHARACTERISTICS.

Selection of the appropriate pump characteristic required depends on the pump's 1) capability for generating pulsatile flow, 2) power dissipation at flow shutoff, and 3) reflection of the hydraulic load through the prime mover.

To realize pulsatile flow, the relatively flat pressure curve associated with the centrifuged pump, e.g., curve (a), Figure 8, would be preferable. That is, during ejection, the pressure, once developed, stays relatively constant as the flow passes through zero to peak values. Power drain at shutoff is clearly down for the low specific speed pumps. The pump must also reflect the hydraulic load to the motor through variation in torque and speed to permit determination of the hydraulic power state for control purposes. Pumps with low specific speeds (less than 3000, curve b), or high specific speeds (greater than 5000 by interpolation), reflect changes in flow by loading the motor with torque changes which effect a corresponding change in motor current. Pumps with low specific speeds would be preferable then, because they provide both the proper pressure-flow characteristic, minimum power drain at shutoff, and the power state information. A pump with a specific speed of around 6000 provides adequate control information, but its steep pressure-flow characteristic may be less desirable. To minimize power drain during pump shutoff, when the torque requirements are highest, would require control logic to reduce input power. For a given set of pressure-flow conditions, centrifugal pumps are larger in diameter, and run at slower speeds than corresponding mixed-flow pumps.

Pump Development. Two basic pump designs were considered, a centrifugal and high-speed, mixed-flow pump. The centrifugal pump was to be coupled to the motor by a 3:1 magnetic speed reducer which provides motor sealing and pump speed reduction. The mixed-flow pump was coupled to the motor by a 1:1 magnetic coupler.

With the 3:1 magnetic speed reducer, the motor operates at 15,000 rpm, driving the pump at 5,000 rpm. Thus the pump could be designed with a specific speed of around 2500, giving the desirable characteristics associated with the low, specific speed pump operation. Breadboard centrifugal pumps were fabricated and design performance characteristics were realized. This design was shelved, however, because the 3:1 magnetic gear reducer could not be designed to generate the required breakaway torque with the space available. The high-speed, mixed-flow pump, driven by the 1:1 magnetic coupler operation at motor speed of 15,000 rpm was designed to satisfy the following conditions:

Mixed-flow hydraulic pump.		
	Power Output (max)	10 watts
	Pressure	3 psig
	Flow (max)	7.6 gal/min
	Flow (max eff.)	6.0 gal/min
	Efficiency (max)	70% or greater
	Specific Speed	6,350
	Pump Speed	15,000
	Fluid	0.9% NaCl (wt)
	Temp	37°C
	Size	1.9 in. dia. x 1.3 in. long
Drive		1:1 Magnetic Coupler
	Input Speed	9,000-15,000 rpm
	Input Breakaway Torque	3 in.-oz. or greater
	Size	1.4 in. dia. x 1.0 in. long

Pump Construction. The pump and coupler cross-section and component layout are shown in Figures 3 and 9, respectively. The pump components are mounted in a cup-shaped housing, the volute chamber. The impeller and driven magnet assembly are shown mounted on the shaft which receives central bearing support from the cone-shaped figure forming the central surfaces of the volute chamber. The bearing is constructed of polytetrafluoroethylene material which has a very low coefficient of friction. Most of the pump parts, have been fabricated with a modified polyphenylene oxide plastic, Noryl. Noryl was selected for pump component fabrication because of its 1) corrosion resistance to isotonic fluid, 2) light weight (pump component weight, 4 oz.), 3) machinability and 4) dimensional stability. Machining the complex curvatures of the mixed-flow impeller and the volute chamber is accomplished by computer-programmed, numerically-controlled milling. The computer program includes the facility for impeller design reiteration.

The 1:1 magnetic coupler consists of 1) the outer housing which mounts and seals the pump and motor, 2) an inner, non-magnetic, fluid barrier, sealing cup interposed between 3) the driven magnet located on the motor shaft and 4) the driven magnet on the pump impeller shaft.

Hydraulic Pump Performance. Performance curves recently obtained for the first mixed-flow pump and magnetic coupler are shown in Figure 10. Pressure-flow curves for several different pump speeds illustrate the relatively steep P-Q curves associated with a 6350 specific speed pump. Design point pressures and flow have been clearly realized. Maximum efficiency of 55% at 14,000 rpm is below the design goal of 70%. Most of this loss is attributed to viscous drag in the coupler and bearings. Efforts to reduce the losses are continuing. Note that the torque versus flow characteristic has less slope than that predicted from the pump similarity curves (Figure 8). This difference may be related to viscous losses also. It must be realized that the pump similarity laws

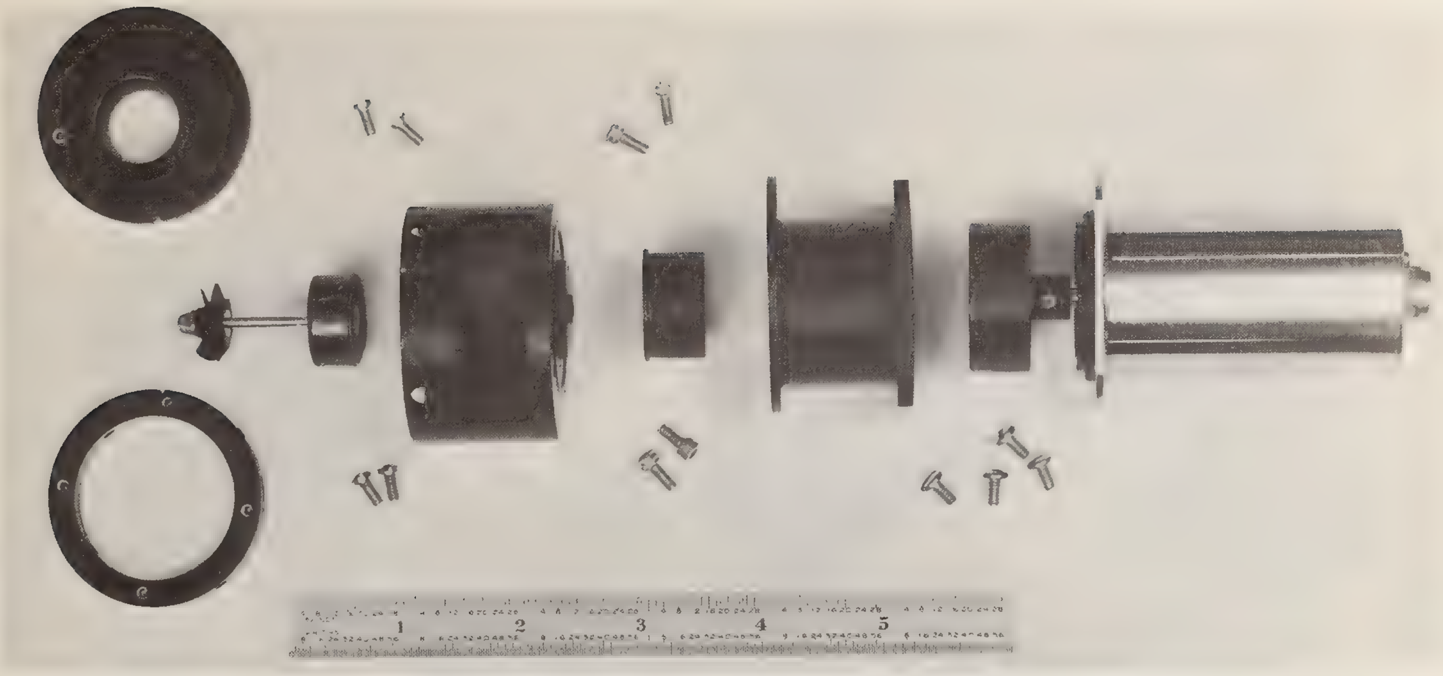

FIGURE 9. MIXED-FLOW, MAGNETIC COUPLER COMPONENTS.

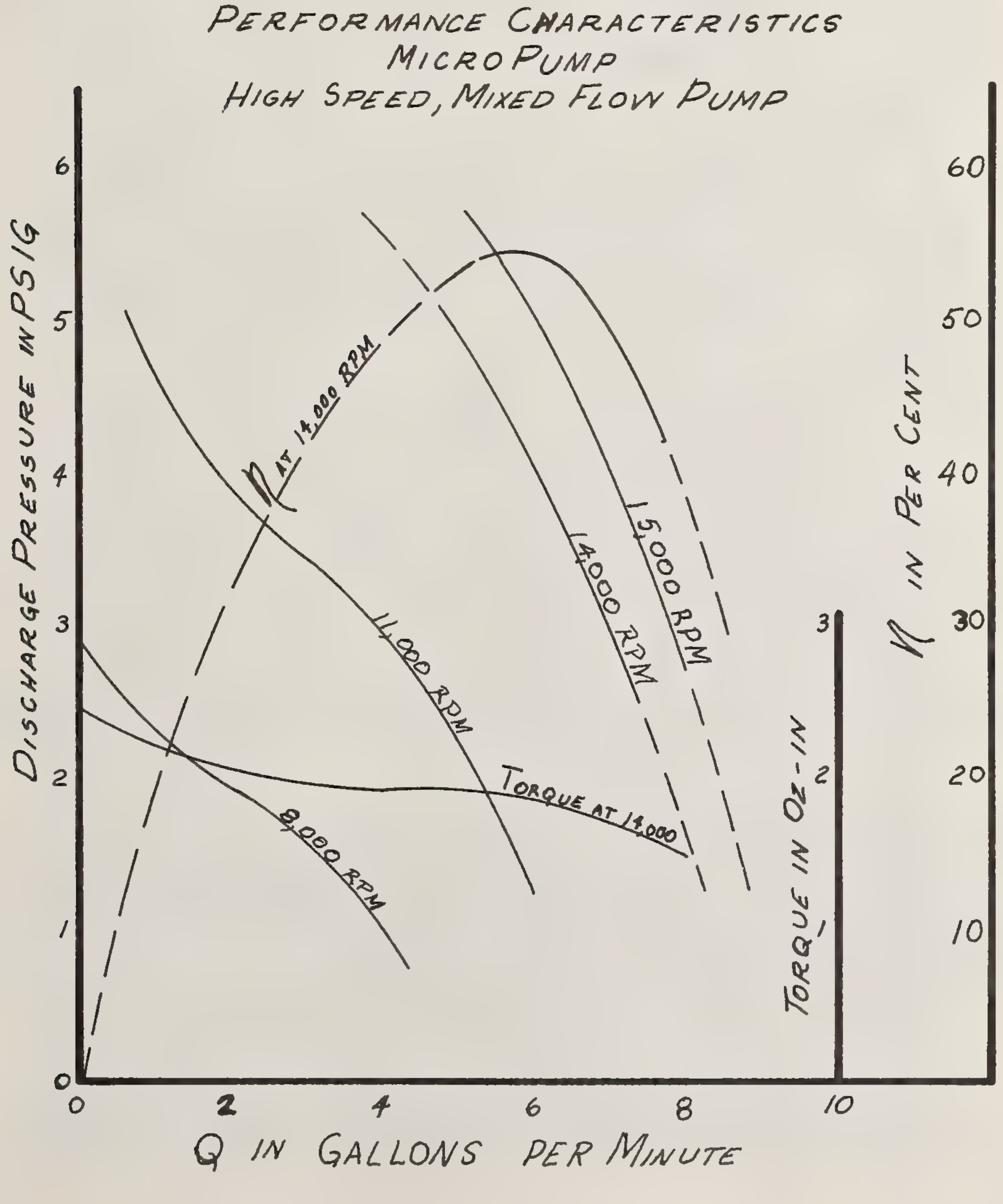

FIGURE 10. MIXED-FLOW PUMP CHARACTERISTICS.

are generally based on huge pumps. Consequently, they must be judiciously applied to miniature pump design.

EHES System Performance.

Figure 11 shows the integrated EHES system consisting of the brushless d-c motor, mixed-flow pump, magnetic coupler, and remotely located commutation electronics wafer. In the finished form, the wafer will be encapsulated, and there will be no connector on the cable. The connector and unpotted wafer condition is required at this point to permit testing and assembly of CAD valve components about the motor.

Figure 12 represents the combined motor-pump performance data. Operating with an input motor voltage of 24 volts, maximum design point of 3 psi and 7.6 gal/min was realized. Best efficiency of 40% occurs when operating at 22.7 volts.

Superposition of the P-Q map on to Figure 2 (Ref. 3 psi @7.6 gal/min; 155 mm Hg @29 l/min) provides complete coverage of Region C. Thus, subject to the hydraulic impedance limitations of a given blood pump and control system, the EHES as developed here should be capable of delivering pulsatile flow at instantaneous flow rates that would permit the dependent subject to perform moderate work efforts.

EHES-CAD SYSTEM INTEGRATION

Indiana University and Bendix Research Labs are presently involved in the integration of the EHES with a hydraulic power control package and electronic logic to drive a Circulatory Assist Device such as that developed by the Thermo Electron Corporation. The presence of the required input power to the EHES is assumed.

Fundamentally, the EHES must be hydraulically connected to the TECO-CAD so that, during cardiac diastole, the EHES serves as a hydraulic energy source for the CAD. During cardiac systole, the total EHES-CAD system must appear as a minimum impedance, hydraulic sink. Hydraulic control must be provided to switch the system between these two phases of operation, and control logic is required to determine when switching should occur.

A schematic of the integrated EHES-CAD system is shown in Figure 13. The primary control element, a two-position, three-way main valve controls fluid transfer between the hydraulic pump, reservoir, and the CAD. After filling of the blood pump (CAD diastole), the main valve switches to the position shown. This permits isotonic fluid to be pumped from the reservoir to the CAD causing ejection of blood (CAD systole) into the descending thoracic aorta. Upon completion of pumping, the main valve is switched to the opposite position (CAD diastole) in which the hydraulic pump output is blocked and fluid flows from the blood pump to the bellows reservoir. The main valve is actuated in one direction by a low-flow, solenoid-operated pilot valve utilizing hydraulic pump output pressure. A spring returns the valve in the opposite direction. The system is designed for continuous operation of the motor-hydraulic pump, but during CAD diastole, motor voltage can be reduced to minimize power consumption.

In this closed volume system, the bellows mechanism permits the reservoir volume to vary in direct correlation to the fluid and/or blood flow. The reservoir has a fixed minimum volume established by a mechanical stop and during each cycle empties the same minimum volume. This ensures that only a maximum, predetermined amount of hydraulic fluid can enter the blood pump. The volume is adjusted to prevent contact of the opposing blood bladder surfaces. This minimizes hemolysis of blood cells and eliminates possible damage to the newly-developed, autologous bladder lining.

A single sensing element, a velocity transducer attached to the bellows plate, provides the necessary signal for actuation of the valve-switching, control logic. The transducer generates a voltage proportional to the bellows plate velocity. Direct correlation, integration and differentiation of this signal, respectively, provides proportional information on the hydraulic fluid/blood flow rate, volume displacement and flow acceleration.

All components of the EHES system are immersed in the isotonic fluid and are surrounded by a fluid-filled, flexible, amorphous bag. Via the bag and the bellows, the system is referenced to intra-thoracic pressure and thus experiences the same pressure excursions as the natural heart. The bag permits the reservoir bellows-mechanism to be insensitive to mechanical displacement perturbations by any contiguous organs.

EHES-CAD System Testing and Evaluation.

Initial system testing will be conducted on a simplified, cardio-vascular simulator. The lumped-parameter, hydraulic impedance load has been fabricated for this purpose. A cardiac pulse source will consist of a periodically, interrupted pressure head to the CAD. This hydraulic head will be equal to the maximum pressure that the left ventricle is expected to generate (20 mm Hg). Failure of the EHES-CAD system to satisfy minimum ventricular pressure relief specifications will be evidenced by the generation of abnormally long CAD diastolic periods. CAD output performance will be determined by measurement and observation of fluid flow and pulse shapes.

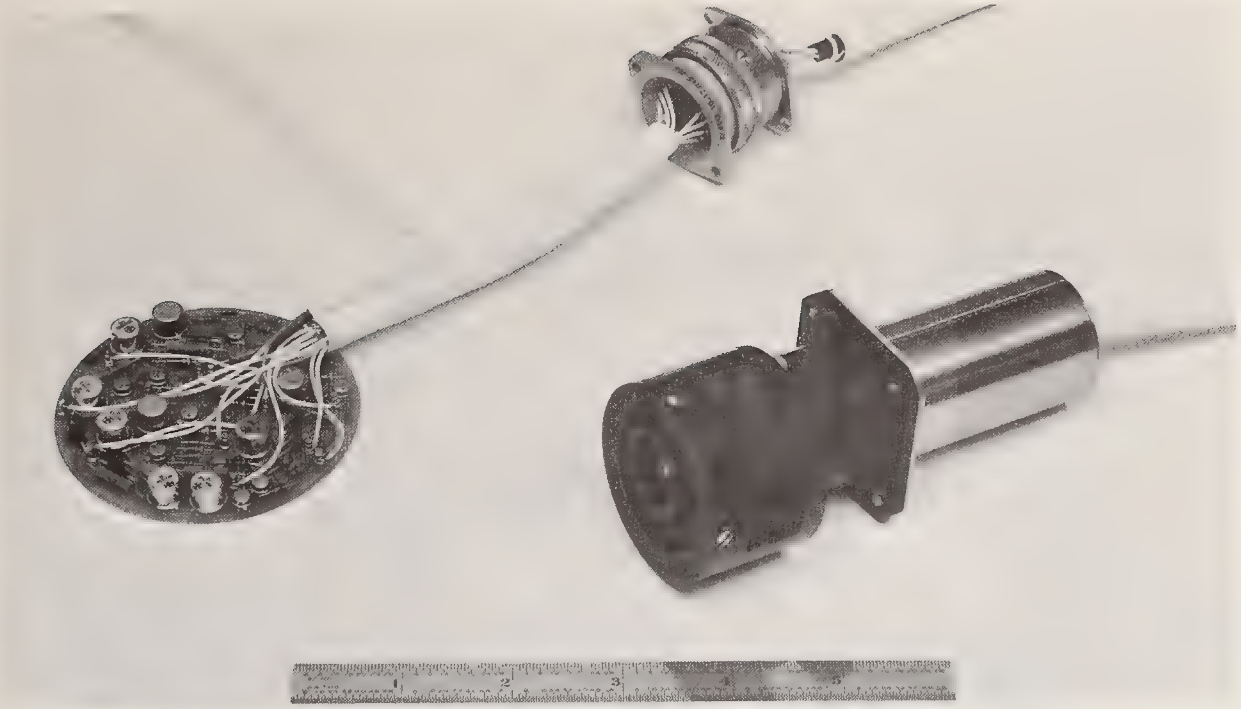

FIGURE 11. ELECTROHYDRAULIC ENERGY SOURCE ASSEMBLY.

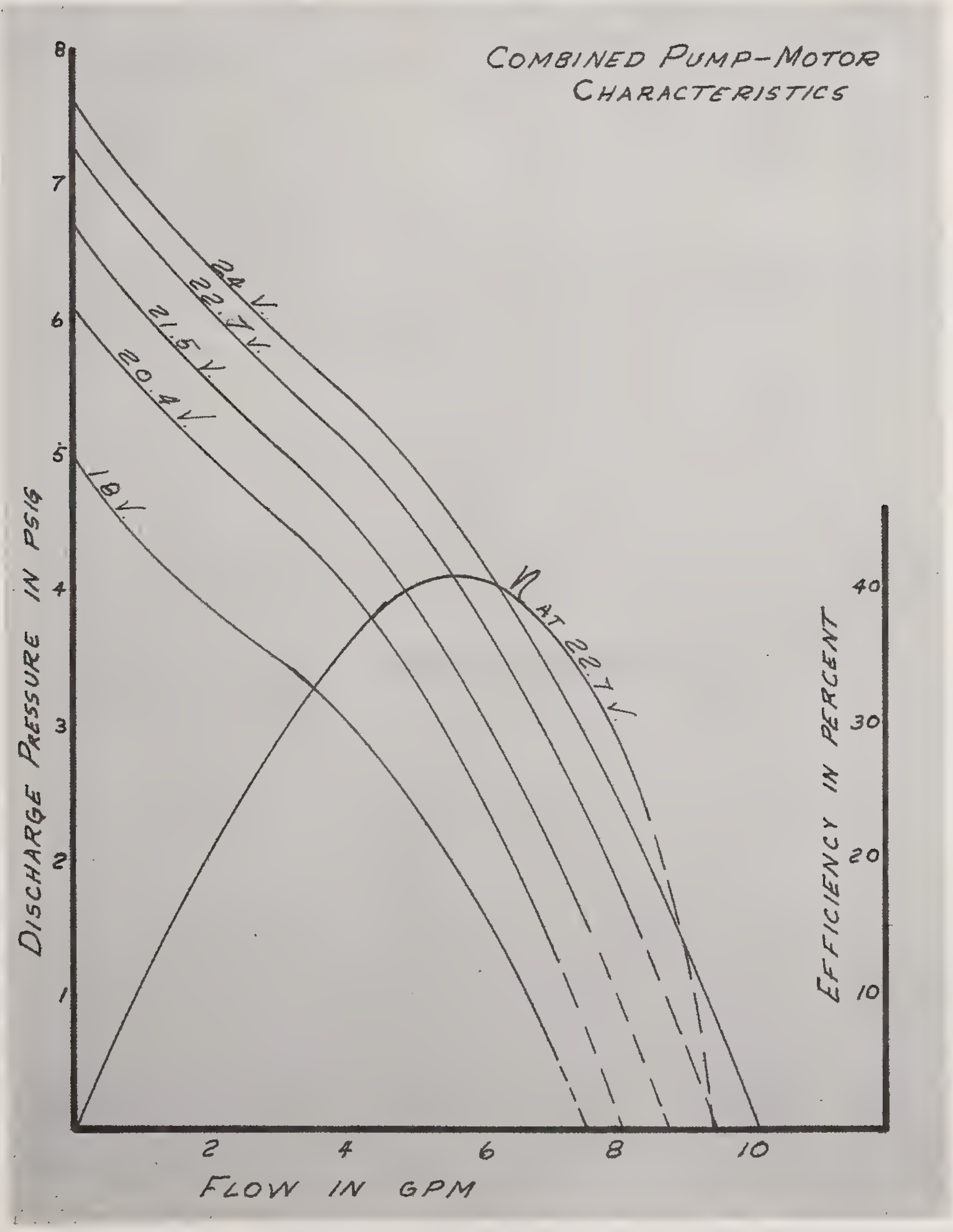

FIGURE 12. ELECTROHYDRAULIC ENERGY SOURCE CHARACTERISTICS.

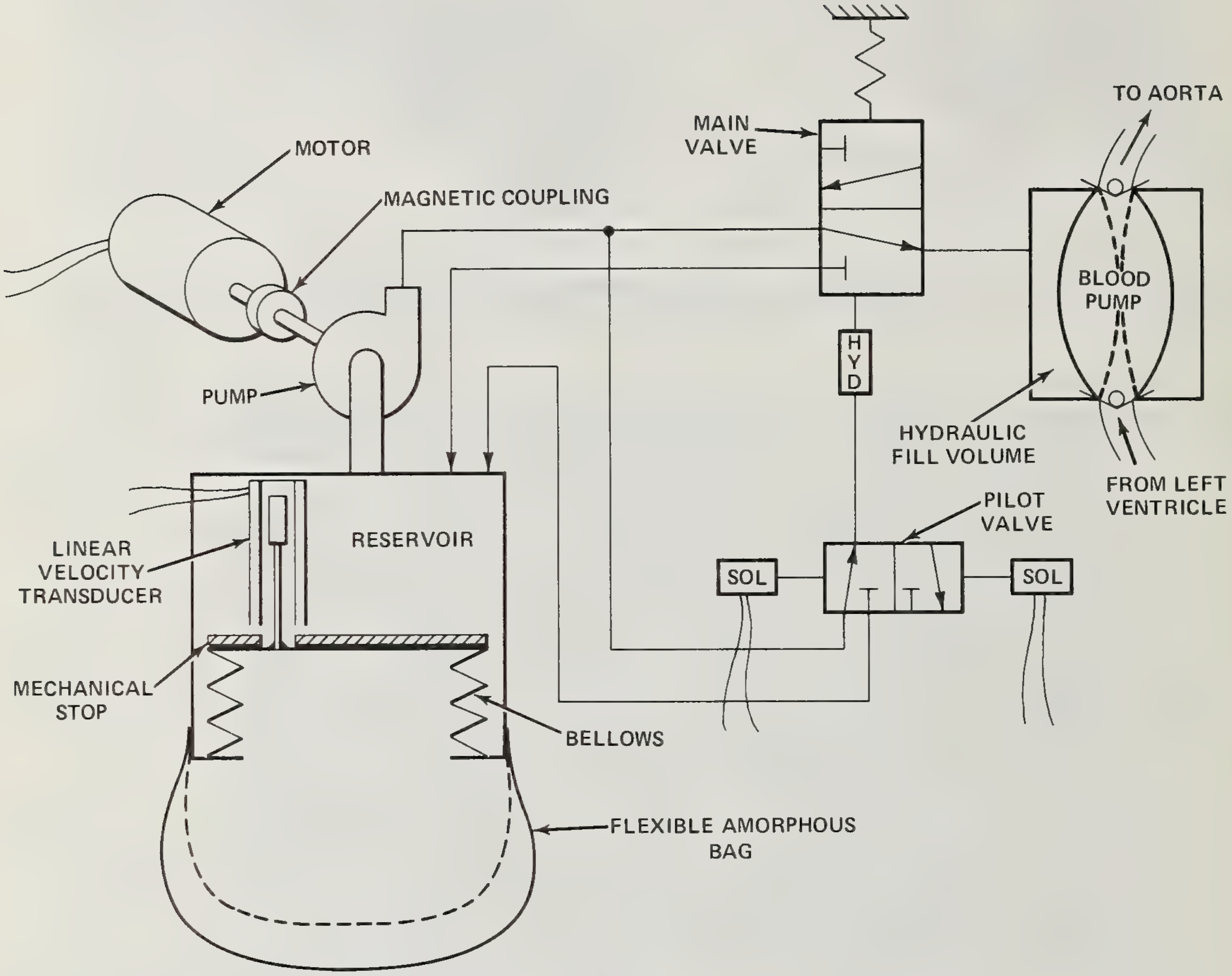

FIGURE 13. INTEGRATED EHES-CAD CONTROL: LOGIC SCHEMATIC.

ACKNOWLEDGEMENTS

The authors would like to acknowledge the following workers for the perceptive and valued contributions to this and allied development efforts.

Bendix Research Laboratories:
Mr. B. Teitelbaum
Mr. J. Kremidas
Mr. J. Madurski

Micro-Pump Corporation:
Mr. T. Martin
Mr. W. Conner

Sperry, Marine Systems Div.:
Mr. R. Rakes
Mr. R. Fischer

Indiana University:
Mr. S. Barbarich

DISCUSSION

DR. ROGERS: I congratulate you on your work. I have been interested in your progress since you started. In connection with the electric motor, I think some comparison can be made with another one. We have been working on motors similar to those that you are interested in , but at speeds about 4000 to 4500. This motor actually meets the same requirements that you have. We found relatively satisfactory performance using a directly submerged centrifugal pump which provides 7.5 PSI at 21 liters/min. with inputs of about 25 watts. The motor has been developed to run submerged, either sealed or flooded. The volume of the pump and motor was approximately 9 in^3. In the matter of the controls, the University of Pennsylvania has been working on automatic internal controls as has been reported at the 21st ACEMB in Houston last fall. At that time, a totally implantable artificial heart in an in vivo implantation in a 190 lb. calf demonstrated individual atrial feedback controls of ventricular output within 0-18 mm Hg. Pulse was controlled internally. The device responded to barometric pressure changes automatically. An external percutaneous lead supplied energy. We think it does present a standard of simplicity preferable to that of a complex system. The system that we are speaking of uses hydro-mechanical controls with a single work and control fluid. A mock system had functioned for 2-1/2 years in 1965. Component and system reliability have been supported by component testing.

DR. NG: What is the noise level of the motor and pump units. Are the frequency and amplitude of the noise tolerable for implantation?

DR. GRIFFITH: We have not run this pump and motor system in the final configuration yet; we have operated it in standard hydraulic test fixtures and as far as this steady state operation indicates, the noise level will not be any problem. Hydraulic valving could conceivably introduce noise.

MR. BENSON: There are a few points that I would like to question. The first question has to do with efficiency. Now if I run the numbers through my mind, as you presented them, I get something in the order of 40% efficiency. I question though, whether or not the efficiency can be obtained in driving just a left ventricular assist device when one looks at the cycling time involved. Now you are running a 12000 or 15,000 RPM motor at normal cardiac beats, say 70-100 beats/min. One is talking about a few hundred milliseconds for the pump to come up to speed to sustain this delivery and then to shut off. I am wondering just how you can maintain these efficiencies under this type of cycling operation, or are you dead-ending the pump?

DR. GRIFFITH: Well, obviously, that is steady state efficiency. There are two modes of operation available for this pump and motor unit. You can either shut the motor and pump off hydraulically at the output, or input, or you can turn the motor on and off electrically. We have just recently realized rise time data on the pump and motor indicating that the pressure buildup time constant is 20 milliseconds. If a person would operate the electric motor in an on-off condition, you would not be dissipating energy during the circulatory assist device diastole. The alternative is, that you could reduce power during diastole. At any rate, with the 20 millisecond time constant, the pump motor pumping during the 2/10 of a second cardiac pulse length interval, spends only about 25% in accelerating and decelerating. Obviously, it is not going to have 40% overall efficiency.

MR. BENSON: Thank you, the second question I have concerns the type of water you are using. It is natural tap water or is it deaerated?

DR. GRIFFITH: It is an isotonic solution, 0.9% NaCl by weight. Currently we are simply testing the system with water.

MR. BENSON: Have you noticed any cavitation problems in the pump when one operates the pump at the same equilibrium CO_2 concentration as that occurring in the blood? It is difficult to pump champagne, that's what I am getting at.

DR. BURNS: I really don't know what the exchange rate through the membranes will be to get CO_2 into the system, but if it is not cavitating tap water, it probably would not cavitate CO_2.

MR. PURDY: Do you think that a motor and gear train operating at 15,000 RPM will last for 10 years?

DR. BURNS: Reliability problems in the motor-pump system are focused primarily on the motor bearings, because high reliability solid-state components have been incorporated. Hydrodynamics bearings have progressed through preliminary design in the interest of achieving a 5-year MTBF.

MR. PURDY: Exactly what type of sensor is used as your control system input, a flow meter or a pressure transducer?

DR. BURNS: Sensing of the hydraulic fluid/blood flow state is done through the linear velocity transducer mechanically attached to the bellows. Since bellows displacement is proportional to stroke volume, blood volume, flow and acceleration are available.

MR. GEBBEN: Have you evaluated the gyroscopic effects that result from the angular momentum of the motor and the pump? What problems might the gyroscopic effects cause in relationship to patient discomfort and to the attachment of the equipment?

DR. BURNS: We have not evaluated the gyroscopic effect of the complete motor pump and rotating fluid system. The gyroscopic moment of the motor alone at 15,000 RPM is negligible.

DR. MRAVA: Can you estimate the total weight and volume of the total implantable portion of your drive system, including hydraulic control system?

DR. BURNS: The electrohydraulic power control package has an estimated weight of 2-3 pounds.

DR. ROTH: When you measured the 20 msec. start and stop times, what sort of mountings were required to prevent the unit from rolling off the bench? These torques will act to tear the unit away from tissue in *in vivo* situations.

DR. BURNS: Regardless of the 20 msec. time constants for motor-pump start-stop times, the motor can exert only a maximum of 2.2 oz-in of torque. Consequently, the mounting is designed accordingly. The hydraulic control valve, on the other hand, could conceivably cause the buildup of somewhat greater forces through abrupt deceleration.

CHAPTER 82

ELECTROMAGNETIC IMPLANTABLE ENERGY CONVERSION SYSTEMS

J. W. Christie, G. M. Benson

ERG, Inc.
Oakland, California

This paper presents the current status of a research and development program sponsored by the NHI to determine the performance of advanced electromagnetic energy converters that may be employed to power blood pumps in implantable artificial heart systems. Theoretical and experimental results are presented for electromagnetic machines which indicate that a high frequency parametric oscillator operating on the variable reluctance principle and directly coupled to a positive displacement double acting fluid pump offers promise in terms of reliability, efficiency, compactness and controllability over the complete operating range required. The basic design of this electromagnetic-hydraulic (EMH) converter is based on a 2-pole magnetic oscillator consisting of a core and coil assembly for each pole and a laminated iron disc armature. Under operation the armature is pulled toward one re-entrant magnet structure (pole) on one half-cycle and then pulled the opposite way by an identical magnet structure on the alternate half-cycle. By commutating the two field coils an efficient energy transfer between coil is achieved which increases the power factor at the terminals. The mechanical forces, efficiently produced by the alternating magnetic fields, are sufficient to directly drive a hydraulic plunger, which may be the armature. By this action electric power synchronously pumps an isotonic fluid at a rate and pressure sufficient to directly displace blood from a bladder-type blood pump. Performance trade-offs and operating characteristics of these converters are described for both valved and valveless (peristaltic) pumps. System integration approaches incorporating these non-rotating, bearingless, vibration-balanced, statically sealed converters are potentially promising systems.

INTRODUCTION

Under resting conditions, the biological heart of an adult delivers slightly over one watt of average pump power to the blood stream. During moderately heavy exercise, this figure increases to perhaps eight watts average. The normal biological heart weighs in the neighborhood of 300 grams, has an efficiency of between 5 and 25 percent, and a longevity which is typically some 70 years.

The problem of designing an artificial heart which even approaches the performance specification of the biological heart has proven to be a difficult one. One important portion of the problem revolves around the need for converting energy into mechanical form to actually drive the heart. If the energy is transported into the body in electrical form, then a suitable electrical to mechanical energy converter is needed. The present paper suggests one general approach to the problem of making the electrical-mechanical conversion. A companion paper suggests an alternate approach.

ARTIFICIAL HEART SYSTEM

A generalized system for an artificial heart is shown diagramatically in Figure 1 and consists of four subsystems: an energy source and storage subsystem, an energy conversion subsystem, a control subsystem, and a blood pump subsystem.

A more specific system, depicted in Figure 2, functions as follows. Electrical power is provided by the power source, such as a wall-socket or a battery, and is transferred to the ac/ac or dc/ac power conditioner which provides a high frequency* ac output. This output is then inductively coupled through the skin into the body where a portion of the power is fed to an ac/ac power conditioner and the remainder to an ac/dc converter. The power conditioner provides power at an appropriate frequency, voltage and wave-form to the control unit which supplies controlled power to the electromechanical energy converter. The ac/dc converter delivers dc power at an appropriate rate to the battery for recharging the battery. When the external power is disconnected, by removing the inductive coupling, the battery delivers dc power to the dc/ac inverter which in turn supplies ac power to the control unit. The control unit, in turn, delivers controlled power to the electromechanical energy converter. The control unit controls power to the energy converter through the use of sensors, such as a pressure transducer located in the proximal tube. The energy converter converts the electrical energy to fluid energy, which in turn is transferred through a valve galley and fluid switch to an assist device. The fluid is first pumped from the accumulator to the assist device where it deforms a bladder thereby displacing the blood, contained within the bladder, through a check valve into the descending thoracic aorta. At the completion of the blood delivery stroke, which occurs during diastole, the hydraulic switch is reversed and the fluid is transferred from the assist device into the accumulator, allowing blood to flow into the assist device during cardiac systole. This cycling process is repeated for each heart beat. As a result, the blood delivered to the aorta by the assist device is synchronized in phase-opposition with the normal cardiac systole and is of equal stroke-volume. The duration of delivery is adjustable by varying the fluid delivery rate produced by the pump (energy converter), but must be shorter than cardiac diastole. The assist device may be actively filled with blood by transferring the fluid from the assist device through the pump and into the accumulator during cardiac systole or the assist device may be passively filled by allowing the blood to displace the fluid from the assist device into the accumulator. In passive filling the heart must supply the energy to displace the fluid through the fluid loop during cardiac systole and results in a higher load on the left ventricle than does active filling. However, this load probably cannot be entirely eliminated owing to the possibility of creating a suction in the left ventricle during cardiac systole. Having described the operation of this system let us now consider the power requirements.

---

* The frequency probably should be at least 10 k Hz in order that the mechanical noise, produced by the inductive coupling, be inaudible (above 20 k Hz).

The average pump power delivered to the blood by the natural heart is about 7-8 watts during exercise and about 80 percent of this is delivered during less than 40 percent of the time. As a result, the peak pump power delivered to the blood by the heart is about 20 watts during exercise. If an assist device is to match this peak cardiac output then the device obviously must have the capacity of also delivering about 20 watts of power to the blood. However, if the delivery time of the assist device is extended to twice that of cardiac systole during exercise then only 10 watts need be delivered to the blood during the assist delivery period. In Figure 2 the assist device is assumed to match the natural cardiac output and therefore have a capacity of delivering up to 20 watts of pump power to the blood. The complete system, in turn, must have a sufficient power capacity to provide this peak pump power to the blood, even though, under this condition the duty cycle may be low (40 percent) and the operating time short (several minutes). Representative system parameters that are then required are shown in Figure 2. If the assist device has an overall efficiency of 80 percent at the 20 watt blood power output level then 25 watts of fluid power need be delivered to the assist device. If the overall efficiency of the energy converter/pump assembly is 70 percent, including flow losses in the fluid loop, and if the power factor of the energy converter is 0.8 then about 45 watts VA need be furnished to the energy converter by the control unit. If the control unit efficiency is 90 percent then 50 watts VA must be delivered to the input terminals of the control unit. At these conditions 50 watts VA would be required at a pulse rate of 3 per second with a pulse duration of about 100 m sec. The electrical frequency would typically be in the 120-400 Hz range throughout this pulse duration.

An artificial heart system for a total heart replacement would have similar requirements since the assist device would become the left ventricle and the blood pump for the right ventricle would probably replace the accumulator shown in Figure 2. If, in addition, power is to be furnished for atrium assist then the fluid circuitry and controls would become more complex but the peak power supplied should not change appreciably. Under these conditions the artificial right and left ventricles would operate in phase-opposition and deliver equal stroke-volumes.

The above parameters are based on optimistic component efficiencies not yet achieved in the laboratory and on the assumption that the integrated system is carefully balanced and precisely matched. Such demands on the electrical system, which supplies power to the control unit at an appropriate wave-form, voltage and frequency and balanced to prevent power back-flow through the static power conditioners, combined with the demands on the energy converter/fluid loop system describe the enormity of the systems engineering problem represented by a compact, implantable system that possesses the reliability and lifetime required by an artificial heart system.

ENERGY CONVERTER

This paper describes but one method of converting electrical power to fluid power for driving either an assist device or a total heart replacement. The method employs an electromagnetically driven positive displacement pump that operates at frequencies significantly above cardiac frequencies. The frequency transformation occurs in the blood pump, which acts as a fluid accumulator that is successively filled by many small discrete displacements occurring at high frequency. Figure 3 graphically describes this frequency transformation. The blood-displacement is plotted as a function of time for two operating frequencies of an assist device or a left ventricle blood pump. At 180 beats/min. the blood is displaced in about 1/10 sec. by fluid pumped into the assist device in 24 discrete pulses (assuming a 240 pulse per sec. delivery from the positive displacement pump). At a pulse rate of 70 beats/min. the blood is displaced in about 3/8 sec. by fluid pumped into the assist device in 88 discrete pulses (assuming a constant frequency of the displacement pump). In this figure the blood is assumed to refill the assist device without pump assist, i.e., passive filling and results in a smooth profile for the second-half of the blood displacement-time trace.

The primary reason for operating the converter at a frequency significantly higher than cardiac frequency is due to the fact that the energy output per cycle per unit volume of the converter is fixed, primarily by electrical efficiency limitations in practical systems. Presently available conductors and ferromagnetic materials, when operated at body temperature, impose losses

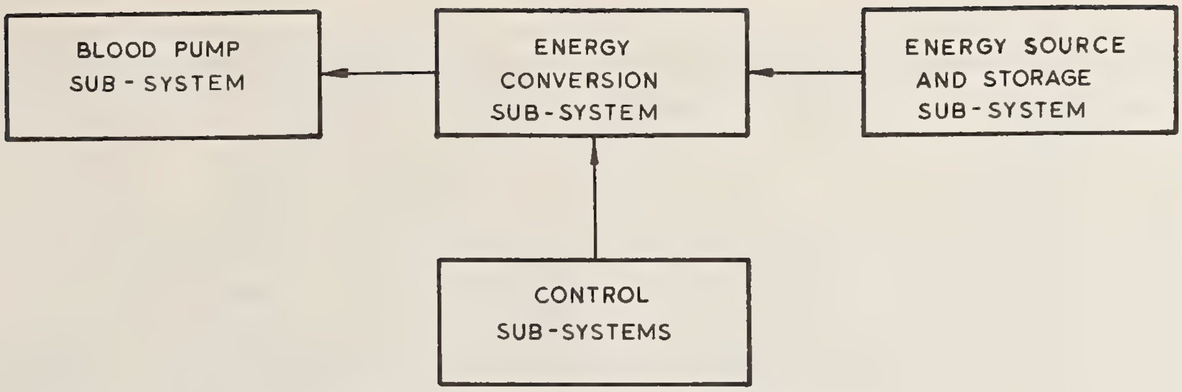
BLOOD PUMP SUB - SYSTEM
ENERGY CONVERSION SUB - SYSTEM
ENERGY SOURCE AND STORAGE SUB - SYSTEM
CONTROL SUB - SYSTEMS

FIGURE 1. AN ARTIFICIAL HEART PUMP SYSTEM.

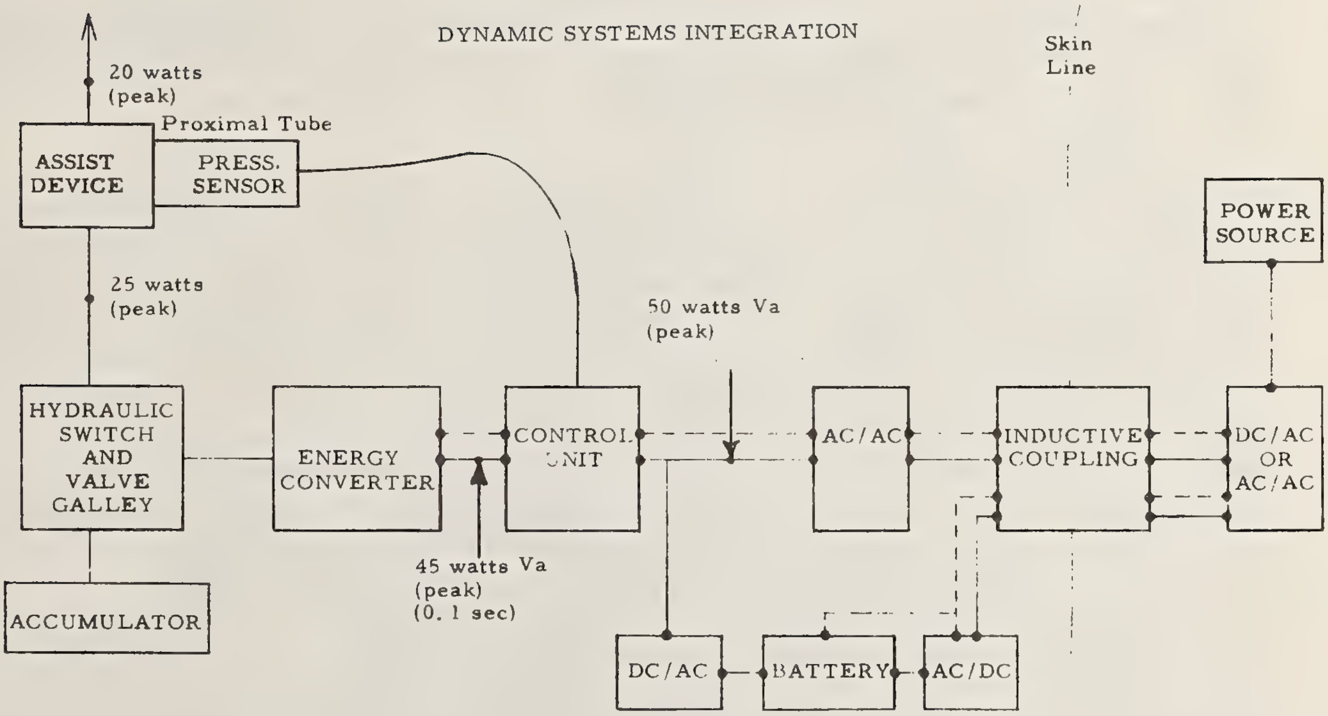

Blood displacement (max.): 100 cc
Systole (min) 0. 1 sec
Blood P (max.) 140 mmHg: 1.9×10^4 n/m^2
Peak power (blood output): ~20 watts
Blood pump efficiency: .8

FIGURE 2. DYNAMIC SYSTEMS INTEGRATION.

that markedly increase with energy density. In order to minimize these losses the energy density needs to be decreased which, in turn, results in an unwieldy and massive converter if operated at cardiac frequency. However, as the frequency is increased the hydraulic losses increase, primarily in the pump and set an upper limit on operating frequency. For a positive displacement reciprocating pump this frequency limitation presently appears to be in the 200 Hz range (400 pulses/sec. for a double acting pump).

The choice of a positive displacement pump is based upon its capability of matching the wide range of pressure-head and flow-rate required for driving an assist device or a total heart replacement at cardiac output. The flow-rate range is of the order of ten whereas the pressure-head range is approximately two. The flow-rate, pressure-head relationship is not a unique function but is dependent on operating conditions with higher heads required at higher flow-rates. The advantages of positive-displacement reciprocating pumps over rotary pumps, such as axial flow, mixed-flow and centrifugal flow pumps, lie in their flexibility in regard to flow-rate (capacity), pressure-head, and speed (frequency), their nearly uniform efficiency under a wide range of operating conditions, their markedly higher efficiencies in small capacities and their capability of matching the demands of the assist device, particularly the crucial demand of increasing head with higher flow-rate. Since no other pump is known to possess these characteristics together with that of rapid response and the ability to overdrive a stalled ventricle, only a high-frequency, positive-displacement, reciprocating pump was considered. One suitable driver for the positive displacement pump is an electromagnetic oscillator that directly drives the reciprocating pump. Alternate drivers include electrostatic oscillators and piezoelectric drivers. A companion paper describes piezoelectric drivers.

Considering several different electromagnetic oscillators, including linear induction motors, moving coil oscillators and solenoids, the only electromagnetic oscillator which possesses a sufficiently high force per unit of loss (copper and iron losses) and per unit of weight and volume is a variable gap, variable reluctance oscillator.

The variable reluctance oscillator may operate as a resonant system, when coupled to an appropriate mechanical reactance, and achieve reasonably high efficiencies. One such design has produced 50 watts shaft output with 68 watts input to an oscillator weighing 2 kgm and operating at a mechanical resonance of 60 Hz. Alternately the oscillator may operate non-resonantly and achieve faster response, smaller size and weight, greater flexibility and higher overall efficiency . Such a converter may be classified as a parametric oscillator.

One such design which we have worked on is a non-resonant variable reluctance (parametric) oscillator which is schematically shown in Figure 4 where the dimensions are given in inches. This unit is a two-pole, single-phase oscillator, having a separate coil and core for each pole, which operates as follows. Voltage is applied to one coil which produces a current and hence a magnetic field that pulls the laminated armature toward this pole thereby reducing the reluctance of the magnetic circuit by reducing the air-gap. This coil is then electrically connected to the opposite coil and the stored magnetic energy is transferred to this opposite pole, owing to the high reluctance of this opposite pole. Additional electrical power is then supplied to the opposite pole to make up for the mechanical work produced, and the losses due to coil, core, friction and windage. The magnetic field in this opposite pole pulls the armature toward that pole. This pull-pull oscillation is transferred by the centrally positioned drive stem to the pump piston, shown in Figure 4 without a pump housing. The electrical switching from one coil to the other is performed by a commutator operating at supply frequency. As a result, the mechanical frequency is equal to the supply frequency. Commutating in this manner decouples the circulating electric energy from the terminals, which reduces the I^2R losses, greatly improves the power factor to a level comparable to conventional electric motors operating at rated load, and minimizes the back-flow of electric power into the static inverter. In addition, a wide range of voltage wave-forms may be used, ranging from square-wave to sinusoidal.

As a result of this operation, the two-pole, variable gap, variable reluctance machine has no equivalent in rotary machines and presents unique operating features in terms of efficiency, pull-out force, response, and electrical terminal characteristics as a function of frequency and load.

Typical characteristics of the variable reluctance unit, shown in Figure 4, are presented in Figure 5. The force-displacement characteristic for a 1.5 mm stroke at a frequency of 60 Hz and a peak B field of about 6,000 Gauss are shown. The force was determined by measuring the hydraulic pressure in each blocked pump chamber. The difference in force shown for the upper and lower chambers is due to hydraulic asymmetry. The asymmetry in force developed by each pole is due to unmatched poles. The maximum stroke allowed by the pole gap is 2.5 mm. At a frequency of 200 Hz and a stroke of 1.5 mm the mechanical output corresponds to about 55 watts whereas with the 2.5 mm stroke the force-displacement corresponds to about 100 watts output.

The pump housing, which connects to the variable reluctance unit, is shown in Figure 6 and operates as follows. Fluid is drawn through the inlet manifold into the inlet reed valves and flows through the inlet diffusers into the pump chamber. On the delivery cycle the fluid is transferred from the pump chamber through the delivery reed valves and flows through the delivery diffusers into the outlet manifold. Owing to the double-acting pump operation, two delivery strokes occur for each pump cycle. The outlet manifold contains gas-loaded diaphragms (not shown) which act as hydraulic capacitors (bounce chambers) that match the hydraulic inductance of the oscillating flow and thereby provide a nearly uniform delivery rate. The large clearance between the pump piston and the pump cylinder heads reduces flow losses caused by high temporal flow velocities. The double convolution,

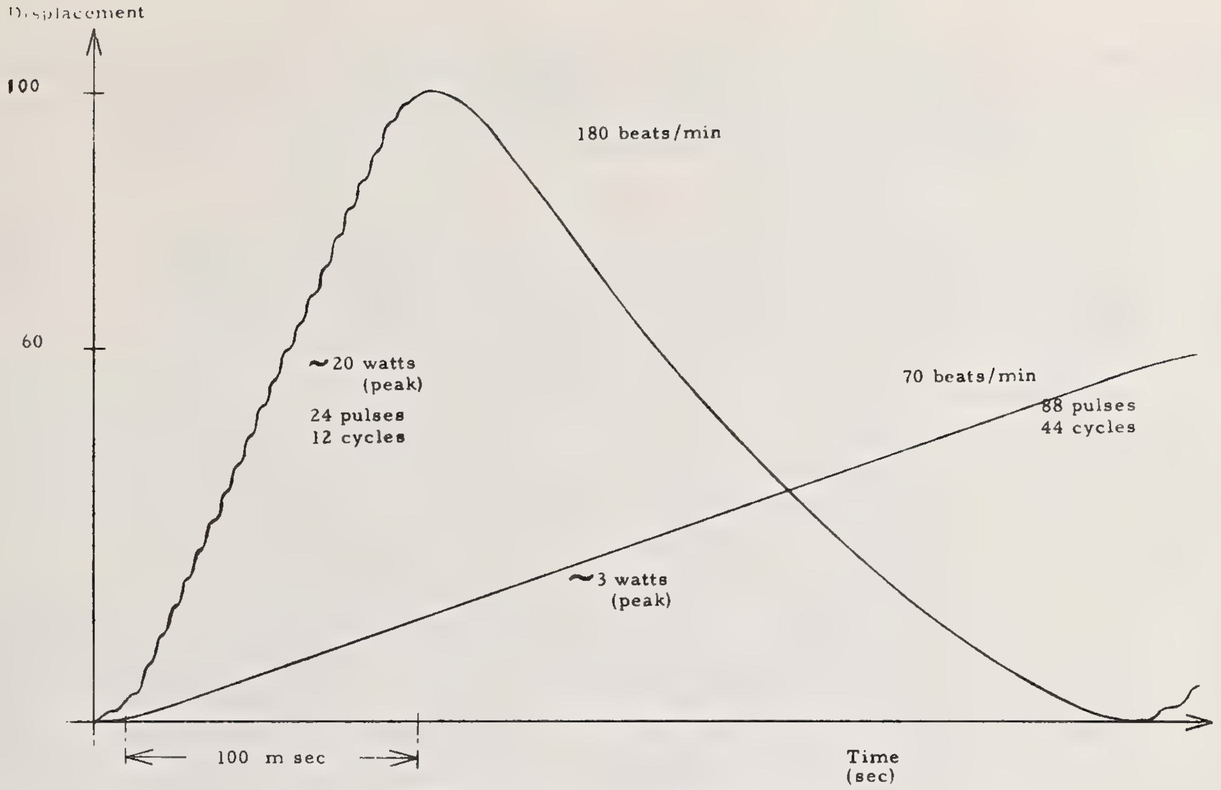

FIGURE 3. BLOOD DISPLACEMENT VS TIME.

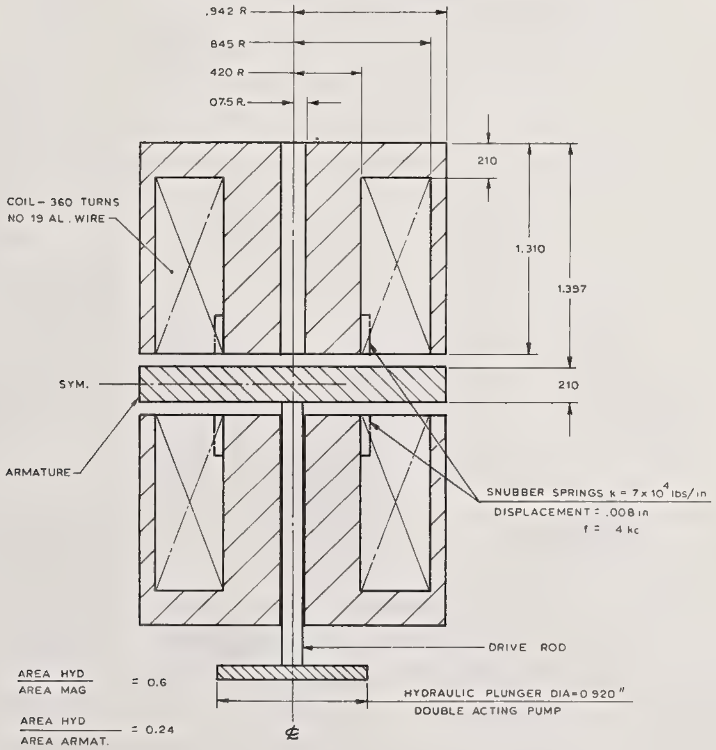
.942 R
845 R
420 R
07.5 R.
210
1.310
1.397
210
COIL – 360 TURNS NO 19 AL. WIRE
SYM.
ARMATURE
SNUBBER SPRINGS k = 7 x 10⁴ lbs/in
DISPLACEMENT = .008 in
f = 4 kc
DRIVE ROD
AREA HYD / AREA MAG = 0.6
AREA HYD / AREA ARMAT. = 0.24
HYDRAULIC PLUNGER DIA = 0.920"
DOUBLE ACTING PUMP
℄

DESIGN PARAMETERS - 40 Lpm, 200 cps

1. HYDRAULIC WORK RATE ≃ 55 WATTS (600mm Hg)
2. PEAK B FIELD ≃ 10 KILOGAUSS
3 ARMATURE-PLUNGER KINETIC ENERGY ≃ 24 JOULES, MASS = 76 Gr
4. UNIT WEIGHT ≃ 2 Lbs

DIMENSIONS ARE IN INCHES.

FIGURE 4. SECOND GENERATION VR UNIT.

metal bellows attached to the piston circumference provides a positive seal, a radial restraint, a low-friction seal and a spring action. The multi-convolution metal bellows attached to the piston crown seals the drive stem and the variable reluctance oscillator from the pump chamber.

Several attempts were made to have the armature act as a combination armature and pump piston but the flow losses, hydraulic damping and lack of design flexibility in matching the oscillator to the pump resulted in using a separate hydraulic module attached to one end of the oscillator, as shown in Figure 4.

The use of reed valves permits high discharge rates with minimum pressure drop, fast response and a smooth straight-through hydraulic flow. Dynamic analysis of reed valves shows that a reed valve will produce a flow area opening that is at least an order of magnitude greater than poppet valves or sleeve valves for the same work performed in opening the valves and for the same opening times. The reed valves are opened and closed by the fluid pressure differential generated across the valve by virtue of the flow rate through the valve. However, the primary disadvantage of reed valves is the high pressure-loss produced at the valve discharge section as a result of the sudden expansion in flow cross-section at this location. In order to reduce this loss a diffuser is required at the valve discharge section which gradually reduces the fluid velocity from that at the valve discharge section to that at the pump chamber or the delivery manifold. The gradual reduction in fluid velocity minimizes flow losses, limited only by wall-friction effects. The extent of the reduction in pressure losses achieved by the diffusers is shown in Figure 7 for a reed valve of 2.5 cm width, 6 mm height and 8 mm active length. The top curve represents the measured pressure drop caused by the valve and the valve cage. The next lower curve represents the pressure drop caused by just the reeds. Intersecting these two curves are curves representing the calculated pressure drops for three reed openings, where the pressure drops are caused by the sudden expansion in flow area from that at the reed valve delivery section to that of the 2.5 cm diameter-delivery manifold. The points of intersection of these curves agree with measured reed valve openings for the respective flow rates. The third lower curve represents the pressure drop caused by the sudden expansion to the cross-sectional area of the valve-cage. The experimental data indicate that the fluid senses the two separate expansions as one, indicating that the jet-streaming effect produced by the reed valve exit-orifice continues into the delivery manifold. The lowest curve represents the pressure drop produced by a gradual expansion in flow area provided by a diffuser. This pressure drop is attributed solely to friction between the wall and the fluid. The advantage of a diffuser is obvious.

A typical reed valve test module with exit diffusers and an entrance diffuser is shown in Figure 8. The entrance and exit cross-sections of the module are 2.6 cm diameter circular sections which permit installation on a closed-loop flow bench for performance evaluation of the valve. The flow direction is specified by the arrows located at the circular cross-sections of the module.

Figure 9 is a photograph of the variable reluctance oscillator (shown in Figure 4) attached to a breadboard hydraulic module (pump). The supporting fixtures provide flexibility in testing various VR oscillator designs and hydraulic module configurations. In this fixture both the gap and the stroke can be independently varied. The section between the pump and the oscillator provides space for instrumentation, such as displacement and force transducers. Tests performed on oscillators using this test bed have provided data which correlate with theory and give confidence to prototype design specifications. Efficiencies of approximately 60 percent have been measured on this test bed which permit extrapolations to higher efficiencies for better matched units.

A prototype VR oscillator and hydraulic module are shown in Figure 10 where the dimensions are given in cm for a unit that is designed to produce a flow-rate of 25-30 liters/min. against a pressure head of 4 psi, which corresponds to a hydraulic output of 12-15 watts. Continued improvements in design and operation should enable this unit to produce higher flow rates and output power levels.

The simplicity of design exhibited by this unit is noteworthy. The only moving component is the integral armature, drive stem and pump piston that are radially aligned by the double convolution bellows at the pump and the flexure rings (not detailed) at the armature. The pump piston contains a Frahm vibration balancer, which balances the reaction force produced by the oscillating armature, drive stem and pump piston. As a result of the simplicity of this design and the endurance test data taken on components, it is felt that a lifetime of ten years may be achieved for this unit.

The flexure rings which provide the radial restraint for the armature and the non-linear rebound spring force for the armature, drive stem and pump piston consist of flat rings composed of a rim and spokes mounted to a center support, as shown in Figure 11, where the ring is installed on an endurance tester and driven by a solenoid. More recent designs incorporate profiled spokes and a narrower rim with several rings mounted axially in series and alternately joined at the rim and the hub. Such a design permits tailoring of the force-displacement characteristics of the flexure ring assembly and a reduction in size and weight while still maintaining high endurance lifetimes.

The complete prototype VR converter and hydraulic module are sketched fully assembled in Figure 12 and form the VR-EMH package. Present data indicate that the overall length of this unit may be decreased from that shown, resulting in a packaged weight of about 300 gms, while maintaining a flow-rate capacity of 25-30 liters/min.

A bidirectional pump chamber is shown in Figure 13, in which two inlet valves and two delivery valves are illustrated. An external flow switch, which switches the flow from one inlet-outlet valve set to the other, is not shown. This design permits active filling of an assist device or the operation of a total heart replacement.

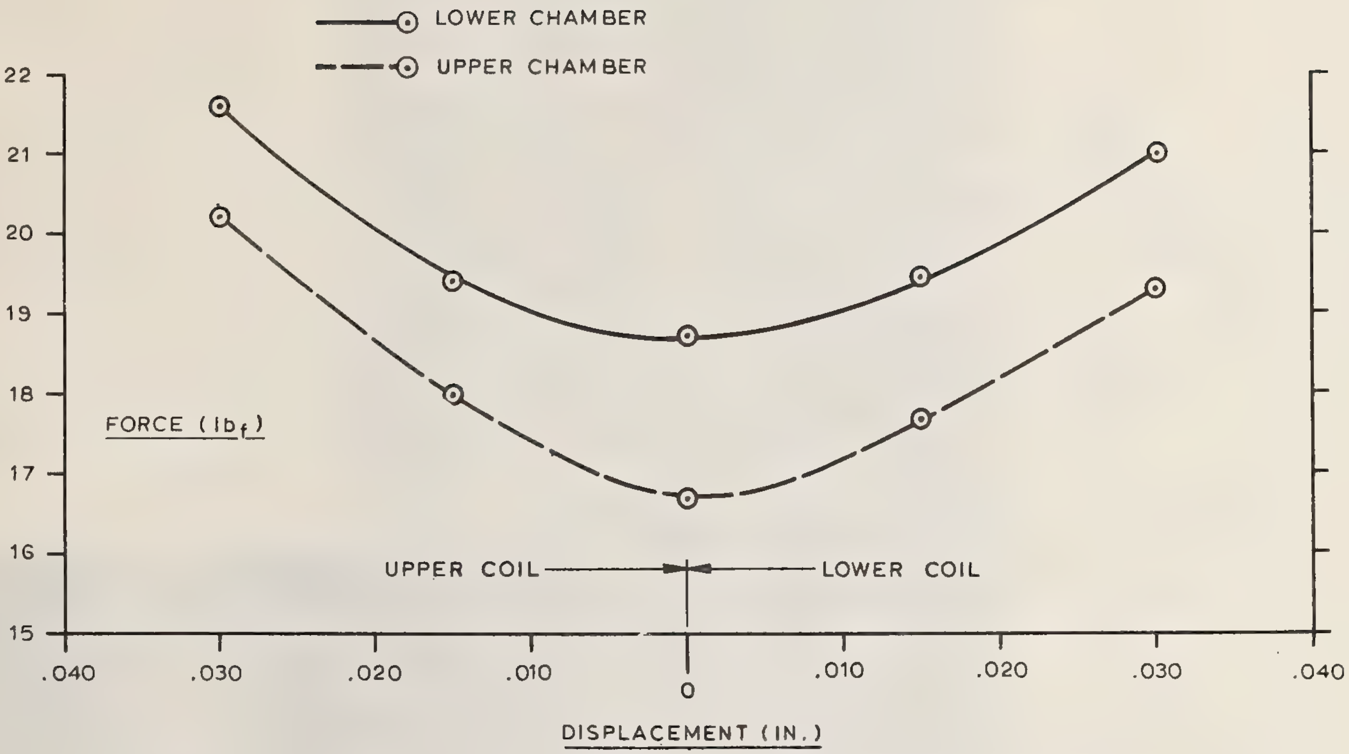

FIGURE 5. FORCE-DISPLACEMENT RESPONSE OF SECOND GENERATION VR MOTOR @60 Hz.

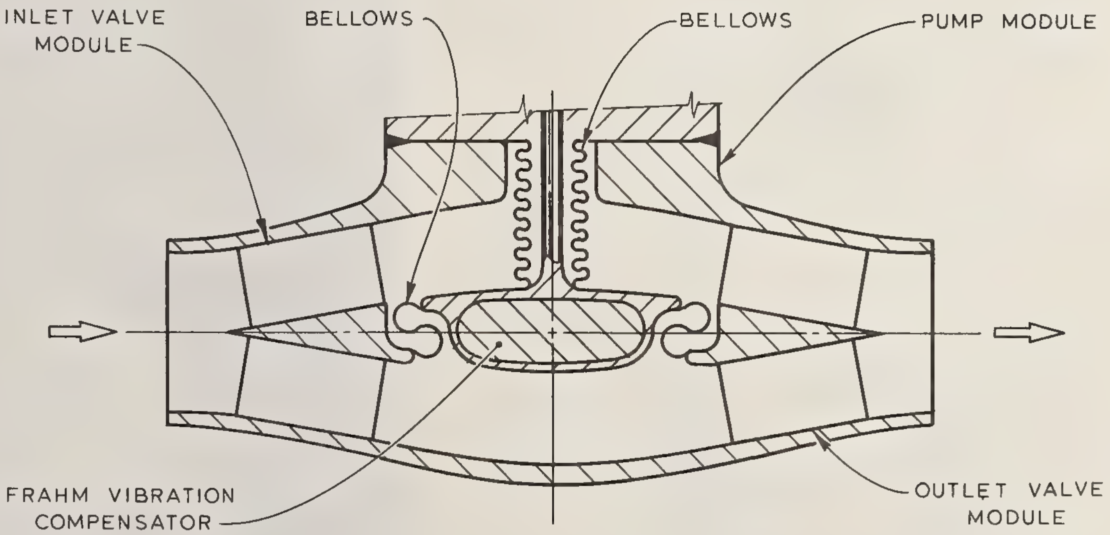

FIGURE 6. HYDRAULIC MODULE.

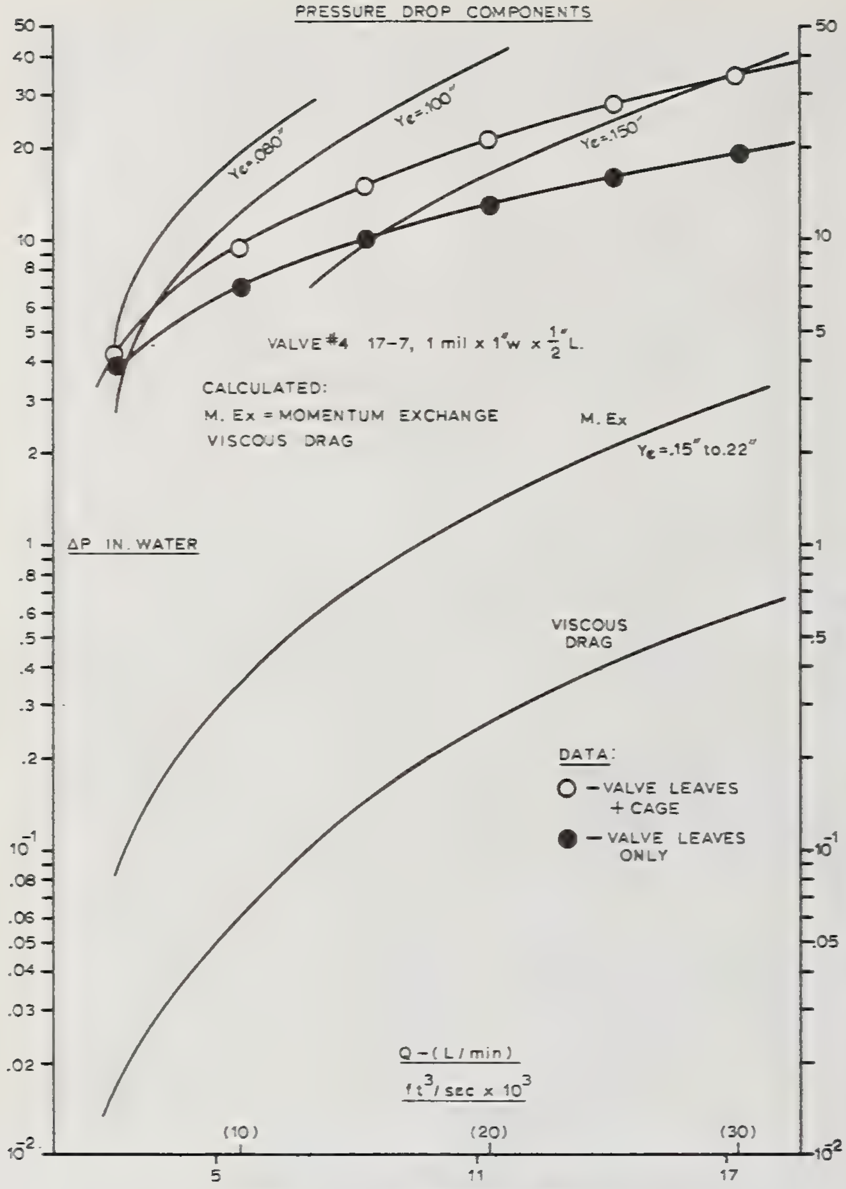

FIGURE 7. PRESSURE DROP COMPONENTS.

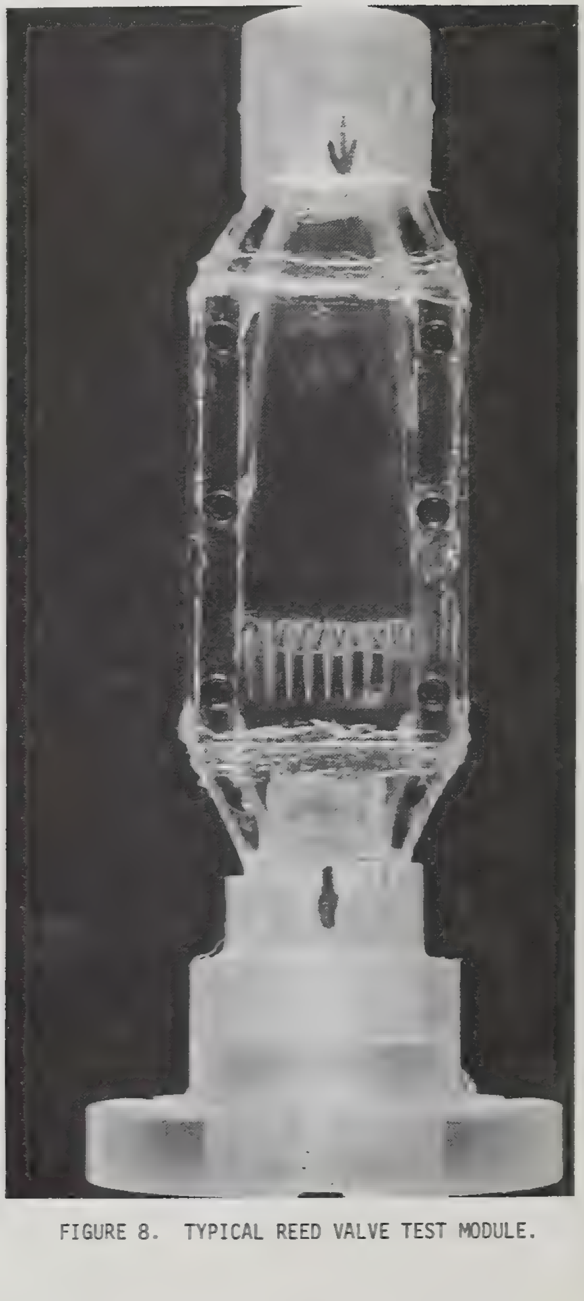

FIGURE 8. TYPICAL REED VALVE TEST MODULE.

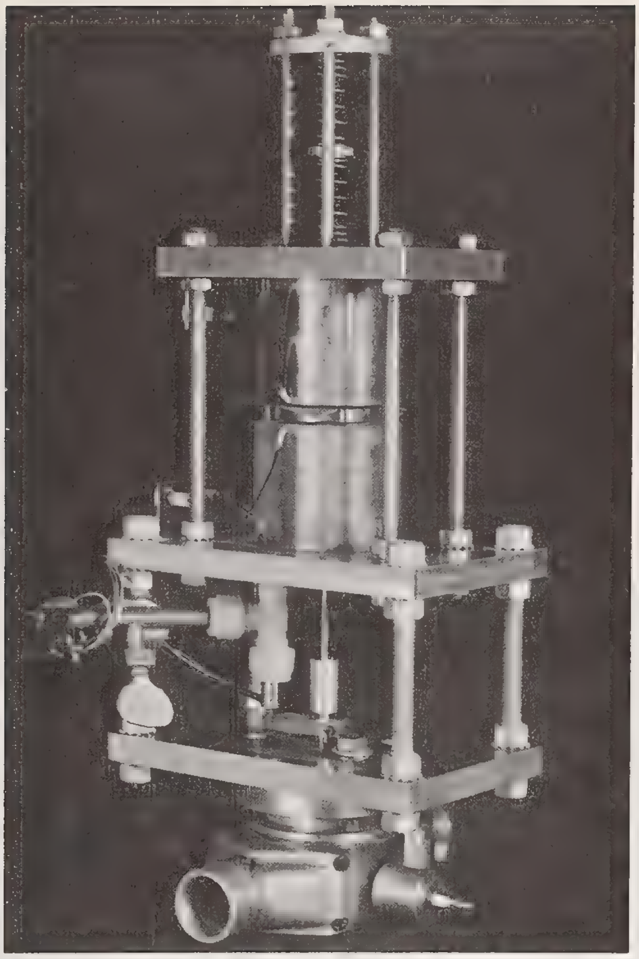

FIGURE 9. VARIABLE RELUCTANCE OSCILLATOR ATTACHED TO A BREADBOARD HYDRAULIC MODULE.

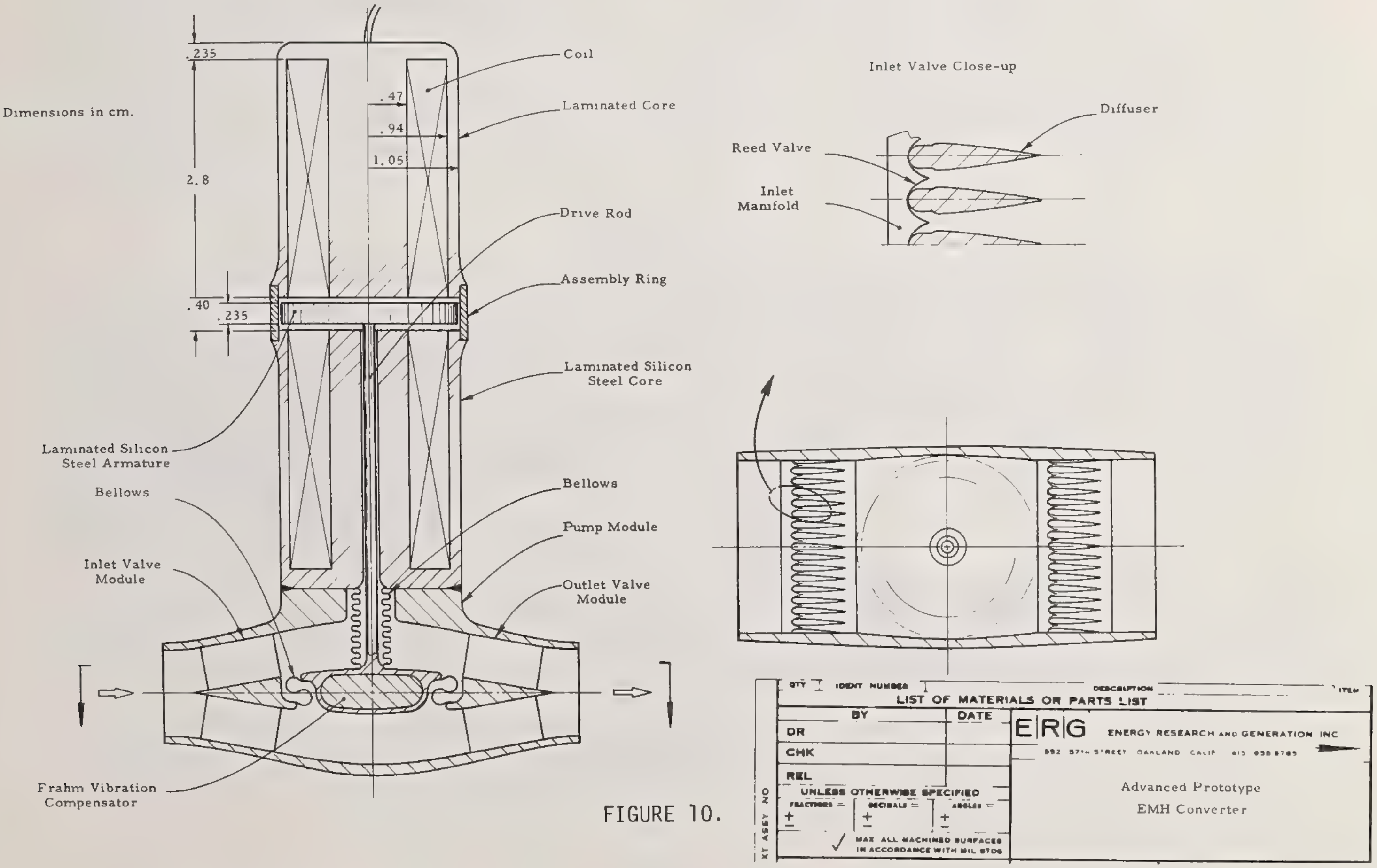

FIGURE 10.

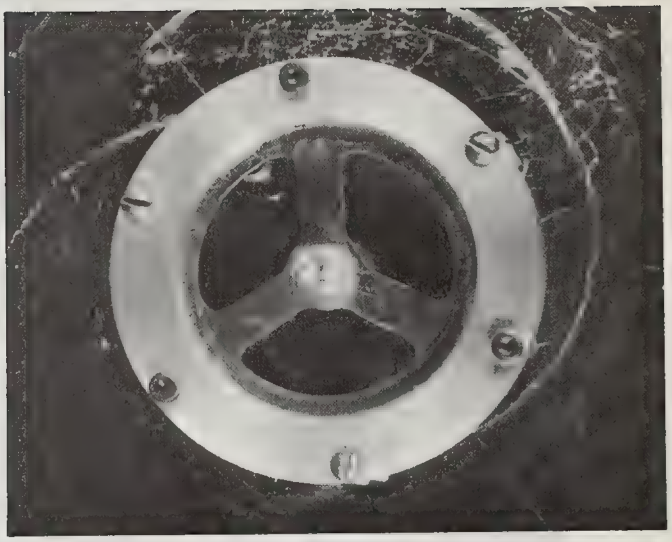

FIGURE 11. FLEXURE RING USED TO PROVIDE RADIAL RESTRAINT FOR THE ARMATURE.

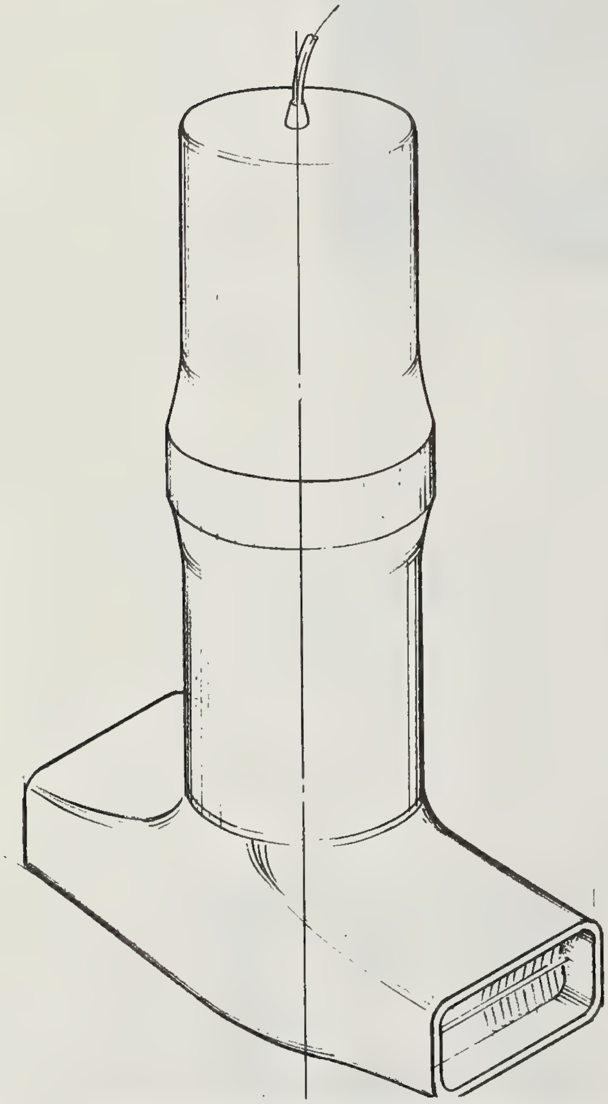

FIGURE 12. SCHEMATIC DRAWING OF ADVANCED PROTOTYPE VR-EMH CONVERTER.

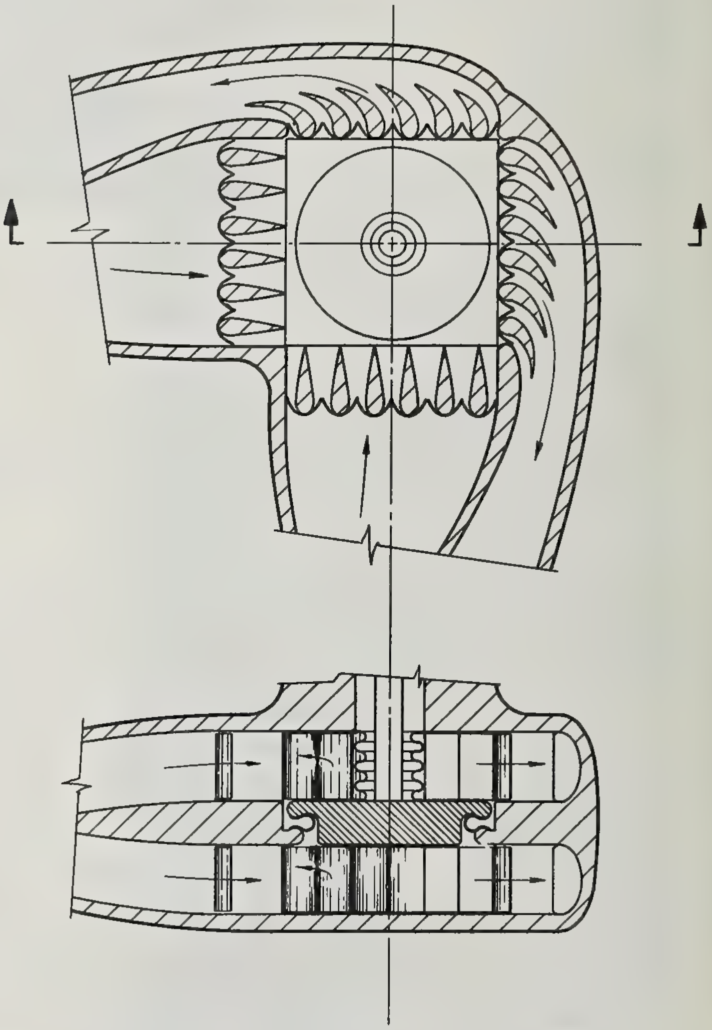

FIGURE 13. BIDIRECTIONAL PUMP CHAMBER.

PERISTALTIC PUMP

A valveless pump that is driven by a variable reluctance energy converter is shown in Figure 14 in the form of a high frequency peristaltic pump. The converter consists of six 2-pole variable reluctance oscillators with each oscillator pair driven by a separate phase of the three-phase power that is supplied to the unit and each pair driven in phase opposition so as to achieve an effective separate phase for each 2-pole unit. Each 2-pole unit sequentially pulls the metal belt, containing discrete laminated armatures, toward the respective energized pole, thereby generating a travelling wave action in the belt. This travelling wave displaces fluid contained between the belt and the pole pieces producing a steady outflow of fluid as a result of the double-acting pump operation. The frequency of the travelling wave is synchronous with the supply frequency and results in flow-rate control by variable frequency supplied to the unit. Commutation between pole pairs of each 2-pole unit is similar to that of the previously described single 2-pole oscillator. Bidirectional fluid flow is produced by switching the phases applied to the unit. The design details shown include sharp leading and trailing edges of the belt, provision for constant belt tension and effective fluid flow diffusers which minimize the pressure losses associated with sudden expansions of flow area.

CAVITATION

One problem in high speed pumps, such as high rotational speed rotary pumps and high frequency reciprocating pumps is cavitation caused by a sudden decrease in local pressure within the hydraulic circuit. For hydraulic fluids which contain appreciable quantities of dissolved gases, particularly CO_2, the cavitation is caused by gas evolution from the locally supersaturated liquid that is suddenly depressurized, the result being similar to gas bubble evolution from carbonated beverages that are suddenly depressurized. The extent of this problem is shown in Figure 15 which depicts the volume of CO_2 dissolved in water as a function of temperature. Since presently used bladders in assist devices are permeable to CO_2 gas then the concentration of gas dissolved in the isotonic fluid should equilibrate with that of the blood. Under these conditions the gas solubility is sufficient to produce pseudo-cavitation caused by gas evolution. The result of this pseudo-cavitation is to markedly decrease the through-put or volumetric capacity of the pump. Experiments have been performed which demonstrate that the flow from either high speed centrifugal pumps or reciprocating pumps can be completely arrested using carbonated water. Under these conditions no audible noise is generated - in marked contrast to the noise level generated when cavitation occurs in fully deaerated water. In order to overcome this problem a closed fluid loop was constructed which incorporates a deaeration section which maintains a fully deaerated fluid. For an implanted system a deaerated fluid probably may be maintained by using metal coatings on the fluid side of the bladder of the assist device and on all internal surfaces of the fluid loop. An alternate solution is to use a fluid having a low gas solubility. This requirement eliminates most fluids including fluorinated hydrocarbons (such as Freon* fluids). One fluid that was tested successfully was Dowtherm SR-1**; however, the viscosity of this fluid is about an order of magnitude higher than that of water at body temperature.

Several fluid additives were tested to determine their long term stability and activity in reducing dissolved gases or in reducing fluid friction. The only additive that indicated any promise is a friction reducing additive (polyethylene oxide: Polyox***). However, its lack of stability under high shear rates for extended time periods in a flow loop caused a gradual decay in its friction reducing properties to that of the base fluid (water).

GAS COMPRESSOR

The requirement for a completely gas sealed fluid loop for high speed liquid pumps provides an opportunity for investigating the use of gaseous working fluids to drive the assist device. The results of such a study, based primarily on Freon, indicate that the additional power consumption required for compressing the gas is more than off-set by the reduction in pressure losses experienced in the pump valves, fluid loop and assist device when compared with water as the working fluid. In addition, the use of gas bearings and simplified valving for reciprocating compressors offers additional advantages. Alternately several valveless compressor designs that are directly driven by high efficiency electromechanical converters are available. The reliability of these sealed units should be at least equivalent to that achieved by modern sealed household refrigerators, especially since no sliding or rotating components would be employed.

CONCLUSIONS

A 2-pole, variable gap, variable reluctance, vibration-free, oscillator that directly drives a matched-positive displacement, reciprocating, reed-valved pump offers a promising design for an electromechanical converter which is capable of delivering fluid power to a ventricular assist device or a total heart replacement. This design incorporates a bearingless, metal bellows-sealed unit having no rotating components or sliding surfaces. Modifications of this basic unit include valveless, peristaltic, bidirectional pumps and valved and valveless gas compressors. Ultimate sizes for 20-25 watt fluid output powers at 200 Hz appear to be less than 50 cc with weights of less than 400 gms. The advantages of simplicity, long-lifetime, reliability, compactness and high response rates during a cardiac cycle are balanced by electromechanical conversion efficiencies that are no higher than those of high-performance rotary electric motors when operated at rated load and are detracted by the somewhat higher commutation losses than occur in electronically commutated rotary motors.

---

* Trade Mark of E. I. duPont de Numours and Company, Inc., Wilmington, Del.

** Trade Mark of Dow Chemical Company, Midland, Michigan.

***Trade Mark of Union Carbide Company, New York, N.Y.

REFERENCE

1. "Development of a Miniature Reciprocating Cryogenic Refrigerator for Space Applications", AFFDL-TR-67-78, R. W. Breckenridge, Jr., Arthur D. Little, Inc., Cambridge, Mass.

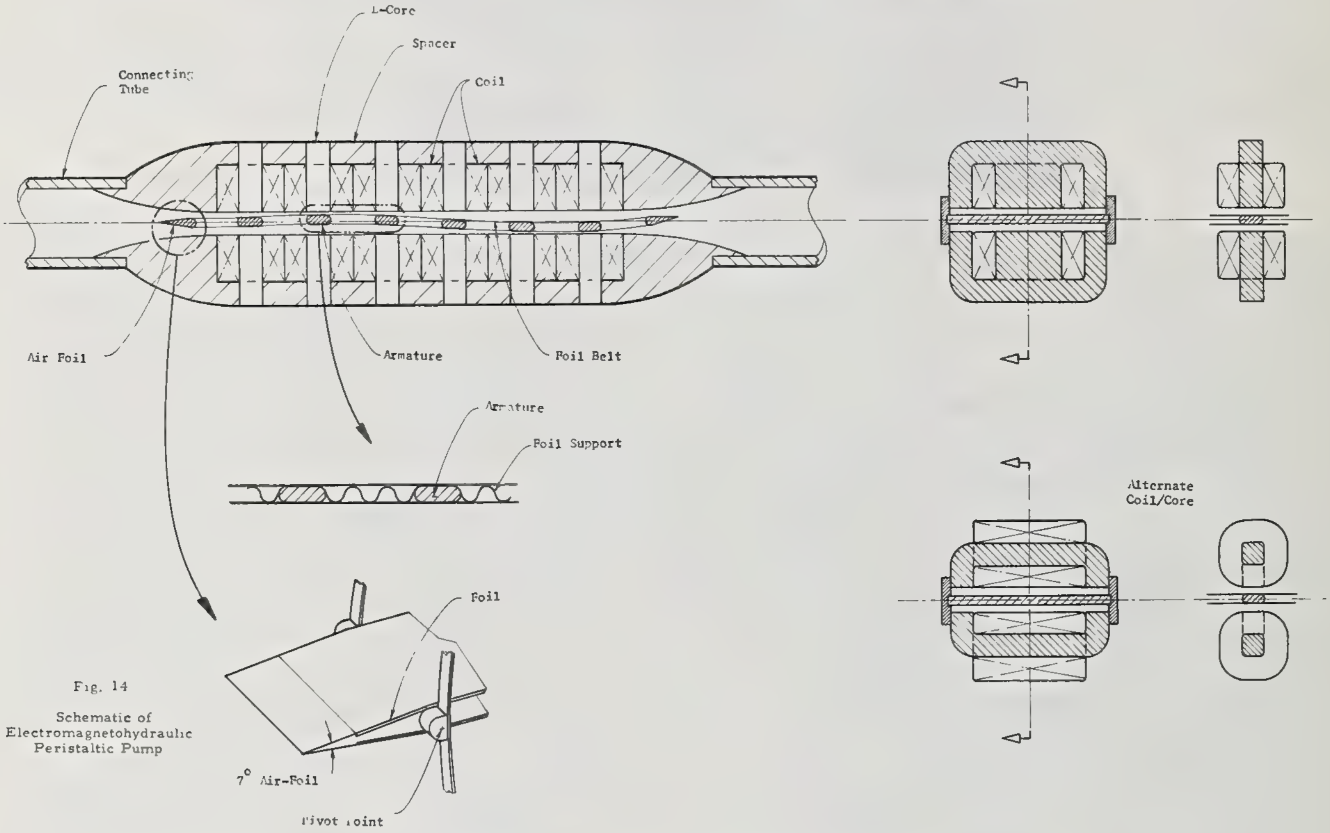

FIGURE 14. SCHEMATIC OF ELECTROMAGNETOHYDRAULIC PERISTALTIC PUMP.

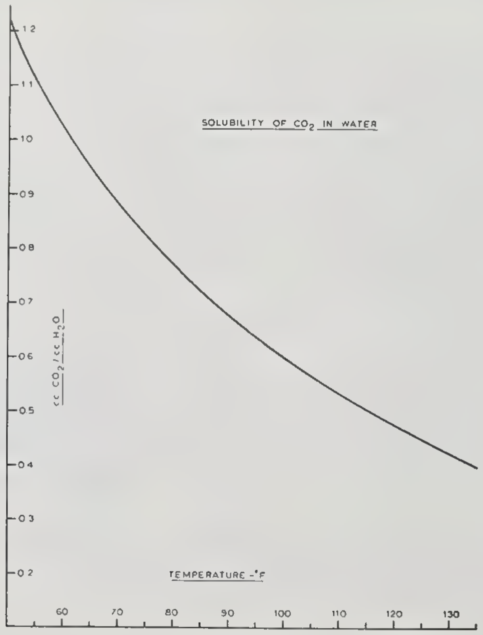

FIGURE 15

CHAPTER 83

DEVELOPMENT OF A PIEZOELECTRIC DRIVER FOR AN ARTIFICIAL LEFT VENTRICLE

P. Smiley, C. O'Neill, W. Olander, J. Creighton*

Physics International Co.
San Leandro, Calif.

A program of development work on a piezoelectric driver for an artificial left ventricle is described. The objective was to convert the high force, low-displacement output of a piezoelectric device into a low pressure, large displacement pulsatile hydraulic output that could be accurately and rapidly controlled and synchronized with the natural heart. Initial efforts were directed at the design of equipment to demonstrate feasibility. Later design work was aimed at reducing the size, weight, and power consumption of the piezoelectric driver and at the solution of problems in electrical insulation and reliability. Inadequate data on the performance of piezoelectric ceramic materials at high electric fields necessitated a program of piezoelectric properties measurement. Piezoelectric strain was measured at 180 volts/mil. Improvement of assembly techniques and insulation methods gave reliable operation up to 124 million operating cycles at 85 volts/mil. The energy available from a stack of piezoelectric disks (or the work done by a piezoelectric driver) increases as the square of the applied electric field. Several bench model experimental drivers were built and tested. The most successful was a hydraulically amplified model that produced a stroke volume of 58 cc against a discharge pressure of 130 mmHg with a systolic duration of 200 msec with check valves from a blood pump currently under development by another contractor. This is equivalent to an output of 7 liters/min at 120 strokes/min.

INTRODUCTION

Physics International Company has been working for several years on piezoelectric energy conversion systems for various industrial and commercial applications such as fuel injectors, fast response valves, and metering pumps. Under the Artificial Heart Program we are developing a piezoelectric driver for circulatory assist devices.

The advantages of applying piezoelectric technology to a circulatory assist device are primarily:

1. Instantaneous controllability with respect to amplitude and timing.
2. Mechanical simplicity giving reliability and endurance.
3. High energy-density and efficiency.

In the course of this program five experimental drivers were built and tested *in vitro*. The most recent model succeeded in reaching the output goals for the contract--an output within the range of human requirements. It produced output flow of several liters/minute when coupled with a simulated blood pump. To achieve this output, we had to solve a number of technical problems in the design and fabrication of piezoelectric energy converters, and conduct a materials program to measure properties of piezoelectric ceramics at high electric fields.

EXPERIMENTAL

This presentation begins by discussing the use of piezoelectric materials to convert electrical energy into hydraulic energy. This is followed by a discussion of the experimental drivers that we have built and tested.

The Use of Piezoelectric Materials to Convert Electrical Energy into Hydraulic Energy.

A piezoelectric material is a solid that will produce a precise change in dimensions in proportion to an applied voltage. Figure 1 shows the basic piezoelectric element--a thin ceramic disk with a conductive coating on both sides. If we apply a dc voltage, the thickness will increase as shown by the curve at the right. For PZT-5H, the strain is about 0.003 in./in. at 150 V/mil. We have measured strains up to 200 V/mil. Figure 2 shows the theoretical maximum work that can be done by a unit volume of piezoelectric material.

---

* Now at Lawrence Radiation Laboratory of the University of California at Livermore.

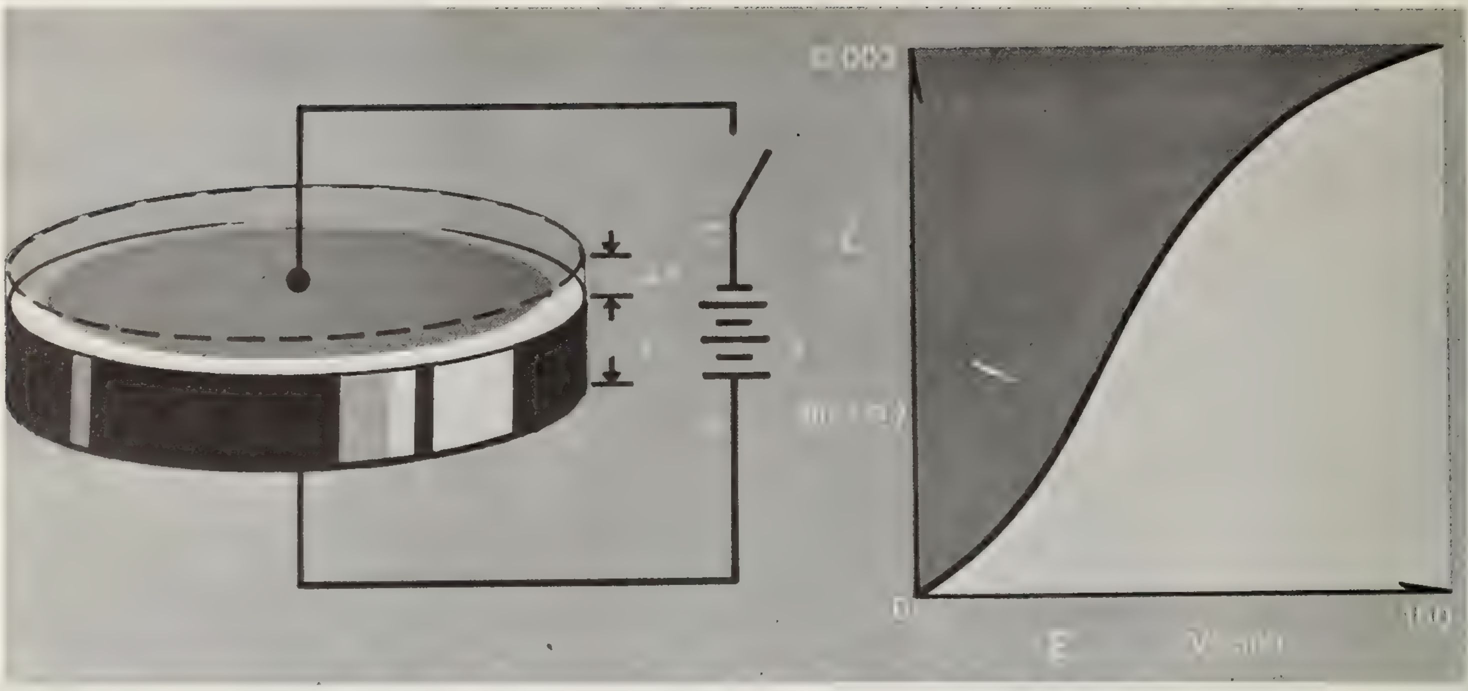

FIGURE 1. STRAIN OF A PIEZOELECTRIC DISK.

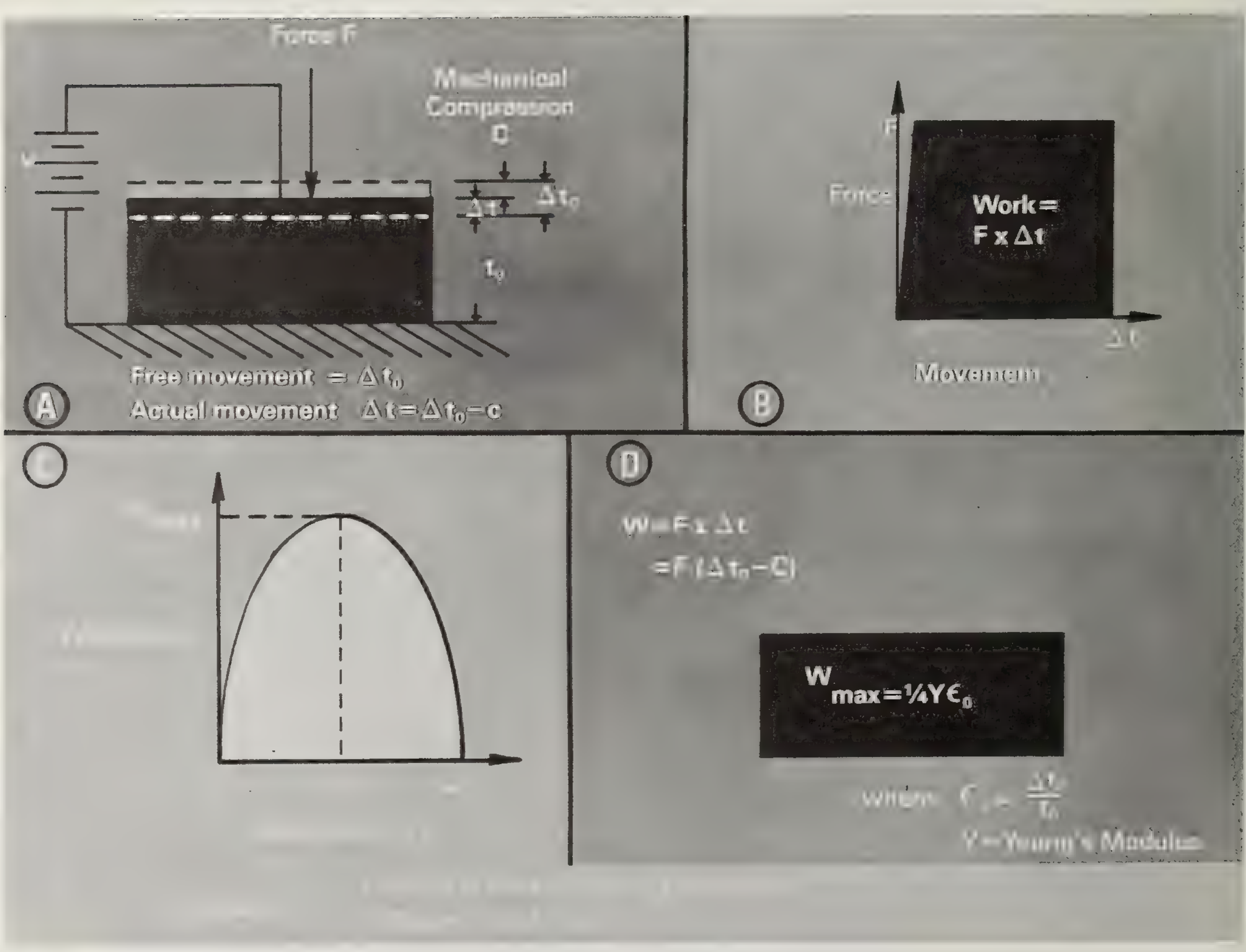

FIGURE 2. WORK DONE BY PIEZOELECTRIC MATERIAL PER STROKE.

If the disk exerts a force on some load, useful work will be done. The resultant movement is the difference between the free movement and the mechanical compression of the disk. We will assume that the applied force is constant as shown in panel B. Panel C shows that the maximum work is done when the optimum force is applied and the resultant movement is 1/2 the free movement. Then the maximum work available per stroke is given in panel D. This is for a pulsed dc mode and with a constant force. A material like PZT-5H is capable of producing 2.5 J/in.^{3}/stroke or 20 J/kg/stroke.

By using thin disks we can achieve high electric fields with low voltages, but the movement from a single disk is very small. To increase the movement, we stack several thin disks and connect them in parallel electrically. Now the movement is a few thousandths of an inch. The force that can be generated is several thousand pounds (Figure 3). We considered two alternatives that can be used to impedance match the stack to a load requiring much larger movement and a smaller force. One is a hydraulic amplifier in which a large piston drives a small plunger through a hydraulic fluid. The plunger motion can be 100 times as much as the stack. The force is reduced by the same factor.

Another is a mechanical amplifier where the motion is amplified by sagittal linkages. We started by building one model of each type from which we would select one type for further development.

Experimental Piezoelectric Drivers.

Figure 4 shows the basic piezoelectric energy converter with hydraulic amplification, a low-pressure diaphragm chamber, and a blood pump. The plunger movement is transferred to a diaphragm which forces fluid at low pressure into the blood pump housing to compress the bladder. Return springs pull the diaphragm back on the intake stroke, creating a slight negative pressure in the diaphragm chamber to assist filling. The system responds to a trigger signal such as the EKG "R" wave. A dc pulse is supplied to the stack, and the driver displaces the entire stroke volume in one stroke, timed with the natural heart. This mode maintains the minimum number of cycles (i.e., one for each stroke of the heart) and employs a minimum number of operating components to enhance endurance and reliability. The first model of the hydraulically amplified driver contained 12 PZT-5H disks, 1-1/2-in. diam.by 1/4-in. thick (Figure 5). The piston and plunger were sized to amplify the motion 100 times. The high-pressure chamber was sealed by a single O ring on the plunger. The return spring was a compression spring around the plunger. The diaphragm used is not shown. When we tested this driver with a dog-sized auxiliary ventricle, it delivered 1.0 liters/min with 37 mm Hg ventricular outlet pressure, i.e., 15 cc/pulse, 70 pulses/min. The major losses were due to friction on the plunger by the seal and the return spring.

The mechanically amplified driver, (Figure 6) contained 128 disks, 1.5-in. diam by 0.040-in. thick. We refer to this device as a radial diaphragm driver because a cylindrical diaphragm is pushed outward radially by sagittal links or straps connected to two plates, one at each end of the piezoelectric stack. When the stack expands, the straps, which are curved inward, straighten and push the diaphragm outward. When tested with commercial check valves, this model delivered 1.1 liters/min. at 70 mm Hg outlet pressure (35 cc/pulse at 31 pulses/min.).

After evaluating design problems with the mechanical and the hydraulic driver, we selected the hydraulic design for development. Figure 7 shows the next model. We reduced the friction on the plunger by a factor of three by a change in the seal design. The plunger and cylinder form the primary seal. A small amount of fluid leaks past the primary seal and is contained by a secondary seal and returns to the high-pressure chamber through a check valve during the intake stroke. The pressure on the secondary seal is limited to about 500 psi permitting a metal bellows to be used in future designs. The metal bellows will provide a positive seal without friction. Its compliance will not affect operation. The stack contained 14 disks, 1.5-in. diam.by 0.250-in. thick. This model delivered 2.8 liters/min at 75 mm Hg, outlet pressure (24 cc/pulse, 120 pulses/min). To double this output, we used two stacks and two low-pressure chambers in the next model (Figure 8). This was a more compact model.

As predicted, the stroke volume of this driver was twice that of the Mark III; however, the frequency response was lower because of the drive tubes and junction connecting the two low-pressure chambers. This driver delivered 4.0 liters/min against 80 mm Hg outlet pressure. The pressure in the diaphragm chambers was about 130 mm Hg (33.5 cc/pulse at 120/min). The maximum stroke volume was 60 cc. After evaluating this design for incorporation of metal bellow seals, we found that compactness would be sacrificed by using two bellows. So we chose the single chamber design for the next model.

Figure 9 shows the latest experimental model, the Mark III X and the test apparatus. The piezoelectric stack is contained in the steel cylinder; below that is the Plexiglas diaphragm chamber. The chamber is connected to the valve assembly to the left. The valves are from a prototype TECO blood pump. The fluid is pumped from the container on the right into the pressurized Plexiglas outlet chamber on the left. The gauge at the top measures pressure in the outlet chamber. This pressure is controlled by a self-bleeding regulator. Figure 10 shows output or stroke volume times frequency in liter/min as a function of outlet pressure. The pulse rate was 120/min. The numbers above the data points give the mean pressure in the diaphragm chamber. In this case we used check valves from a Harvard apparatus laboratory blood pump that had quite high resistance to flow. With a larger diaphragm the driver has delivered up to 8 liters/min.

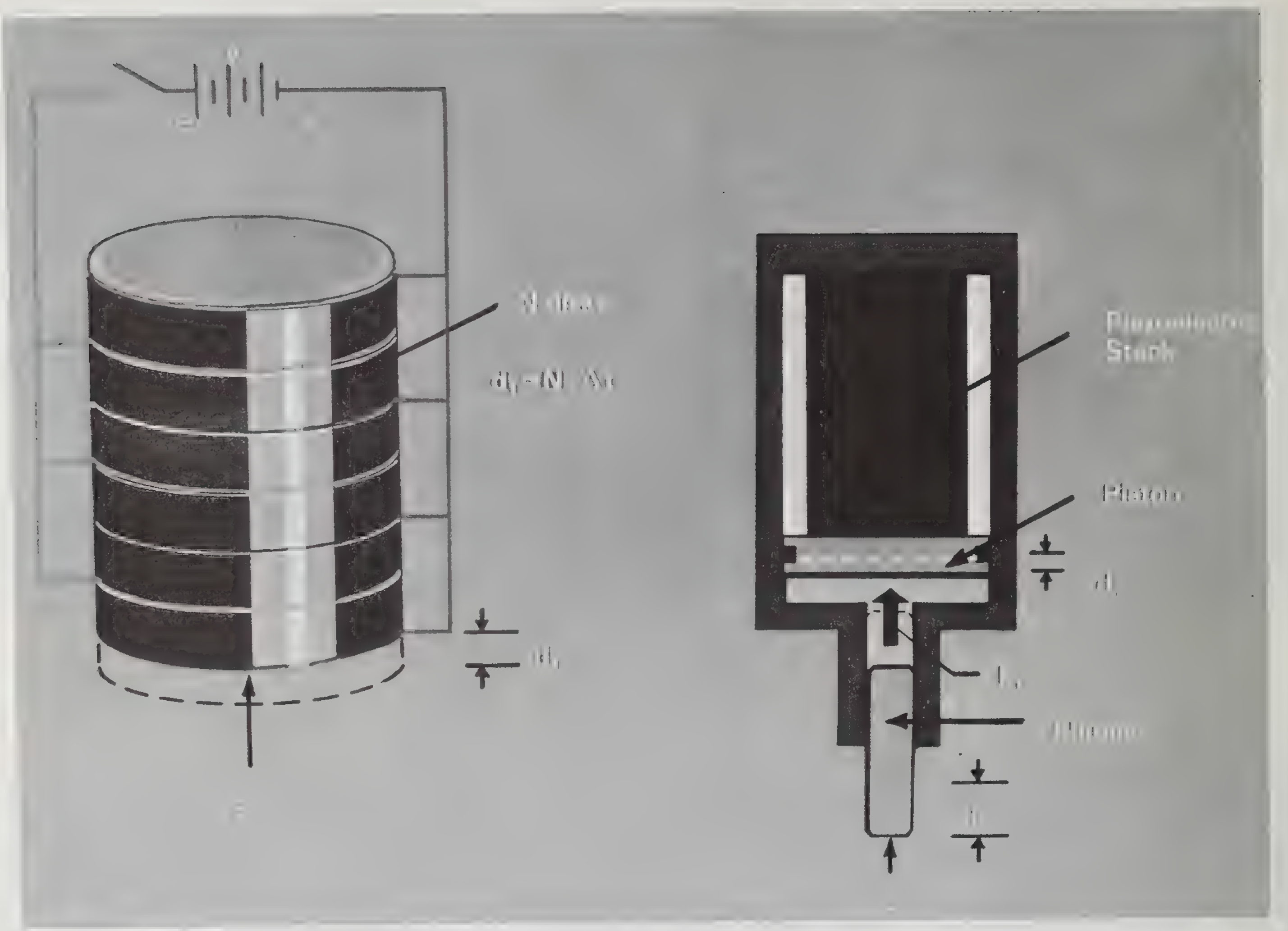

FIGURE 3. BASIC PIEZOELECTRIC ENERGY CONVERTER.

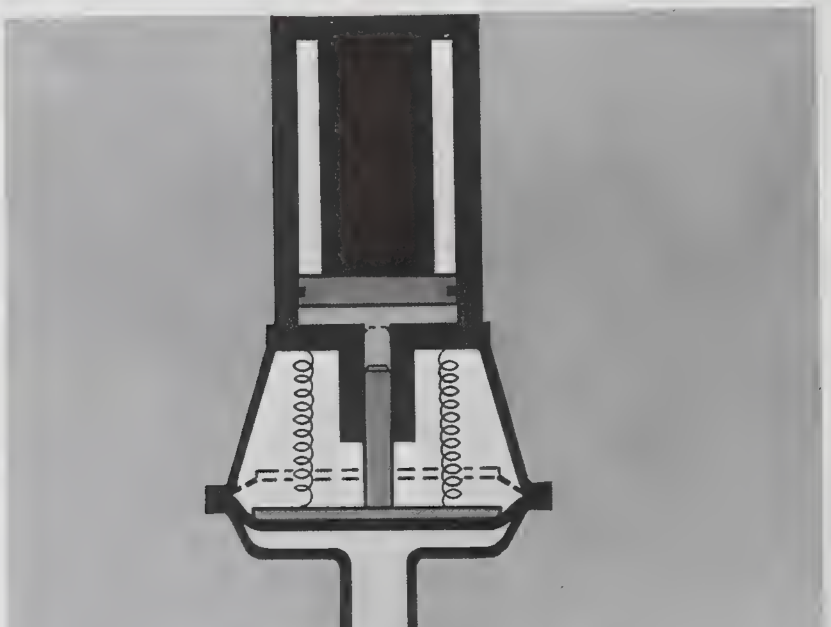

FIGURE 4. PIEZOELECTRIC DRIVER FOR AN AUXILLARY VENTRICLE.

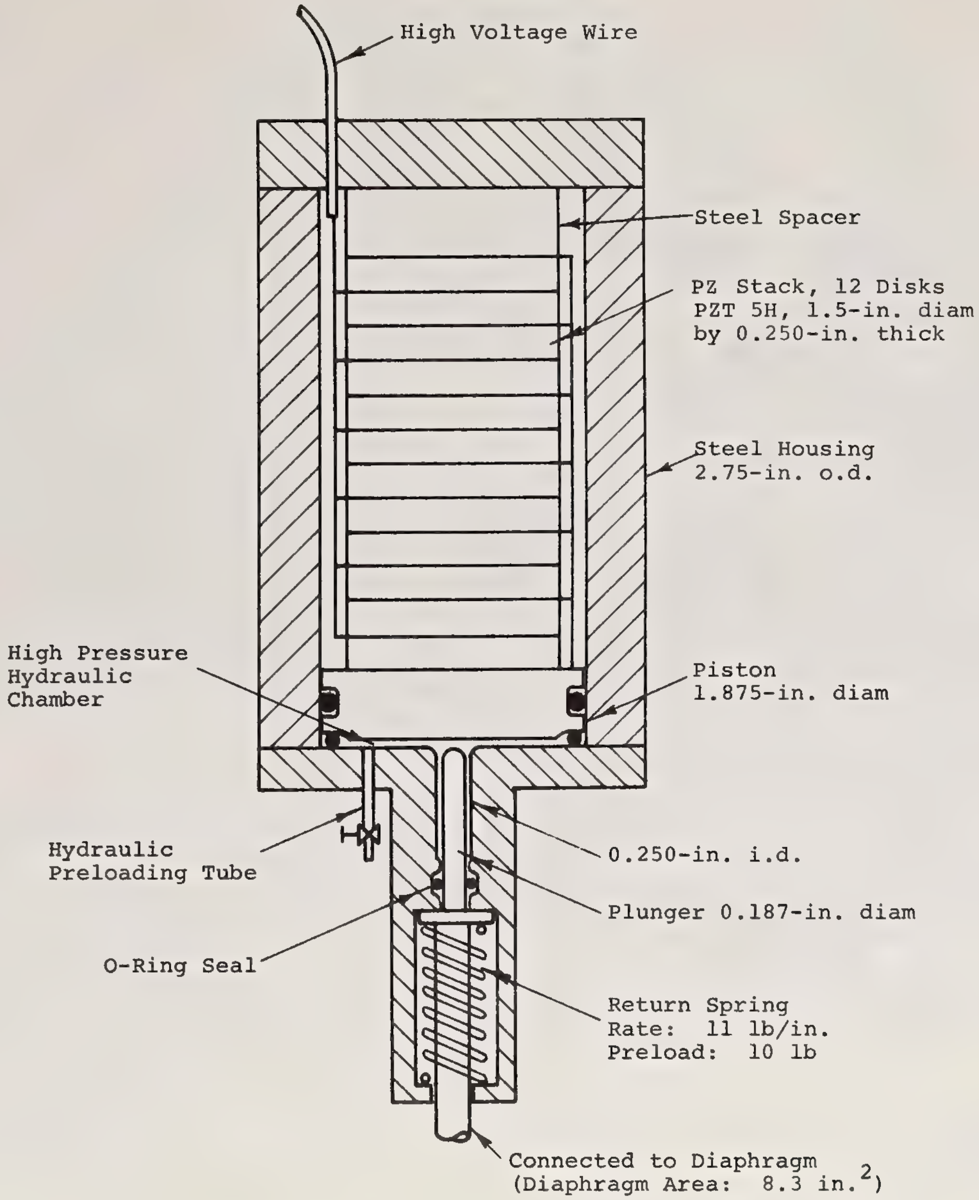

FIGURE 5. MARK I HYDRAULICALLY AMPLIFIED DRIVER.

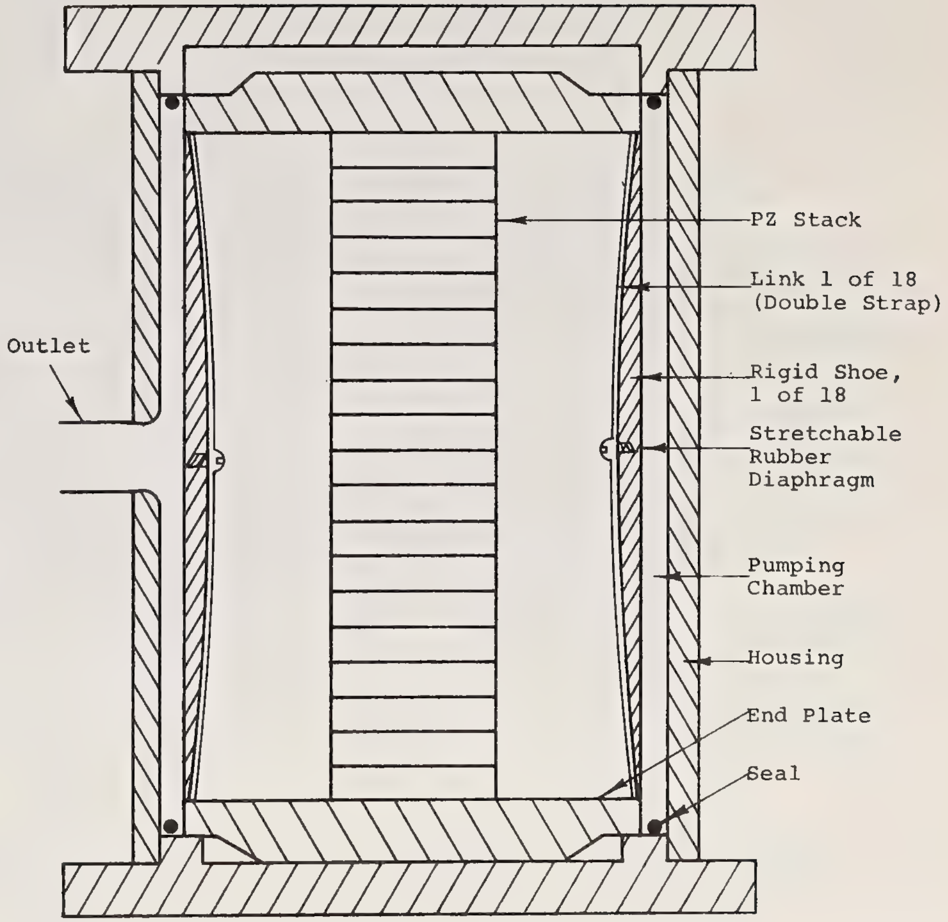

FIGURE 6. MARK II RADIAL DIAPHRAGM DRIVER WITH SHOES.

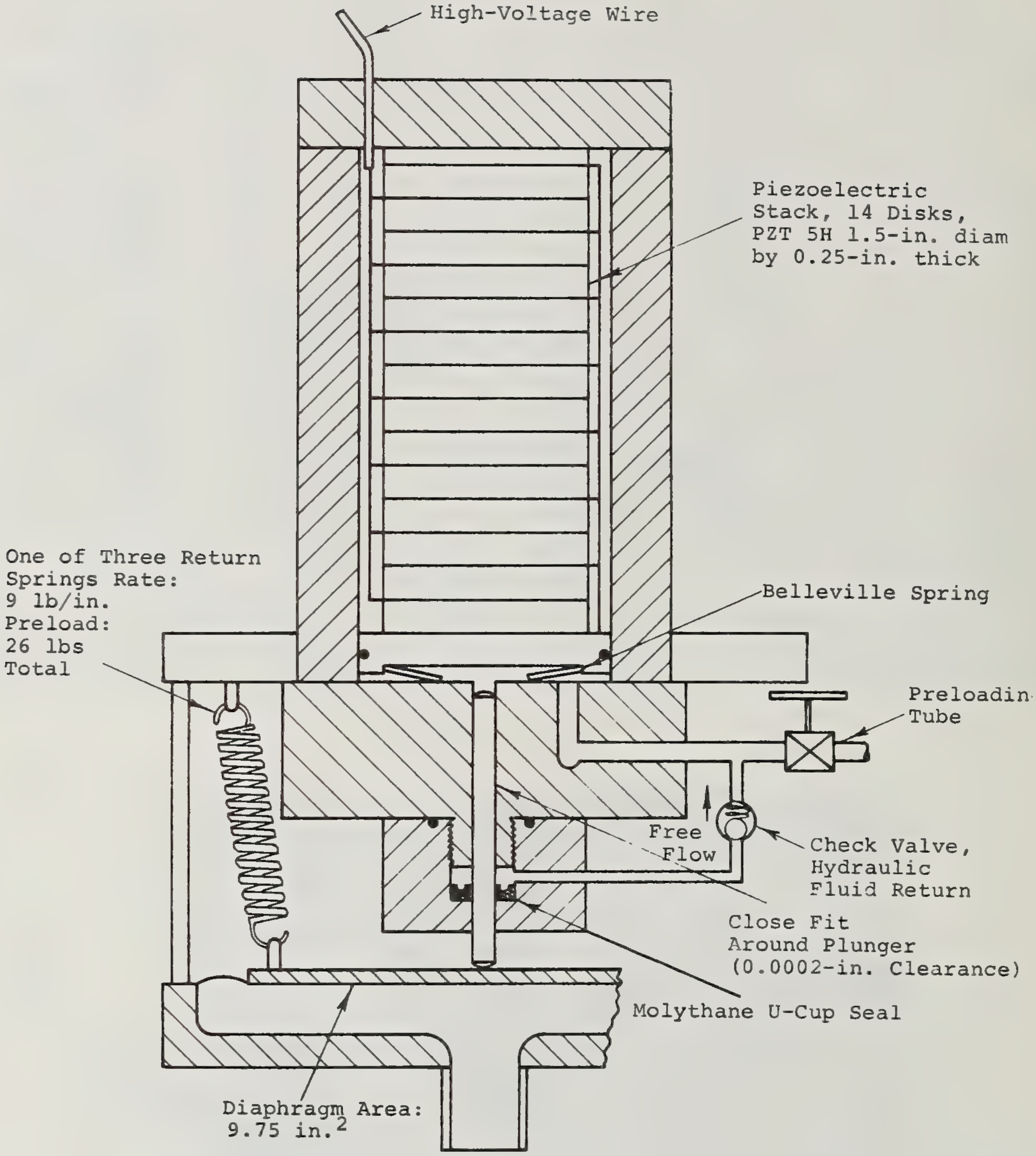
High-Voltage Wire
Piezoelectric Stack, 14 Disks, PZT 5H 1.5-in. diam by 0.25-in. thick
One of Three Return Springs Rate: 9 lb/in. Preload: 26 lbs Total
Belleville Spring
Preloadin Tube
Free Flow
Check Valve, Hydraulic Fluid Return
Close Fit Around Plunger (0.0002-in. Clearance)
Molythane U-Cup Seal
Diaphragm Area: 9.75 in.²

FIGURE 7. MARK III HYDRAULICALLY AMPLIFIED DRIVER.

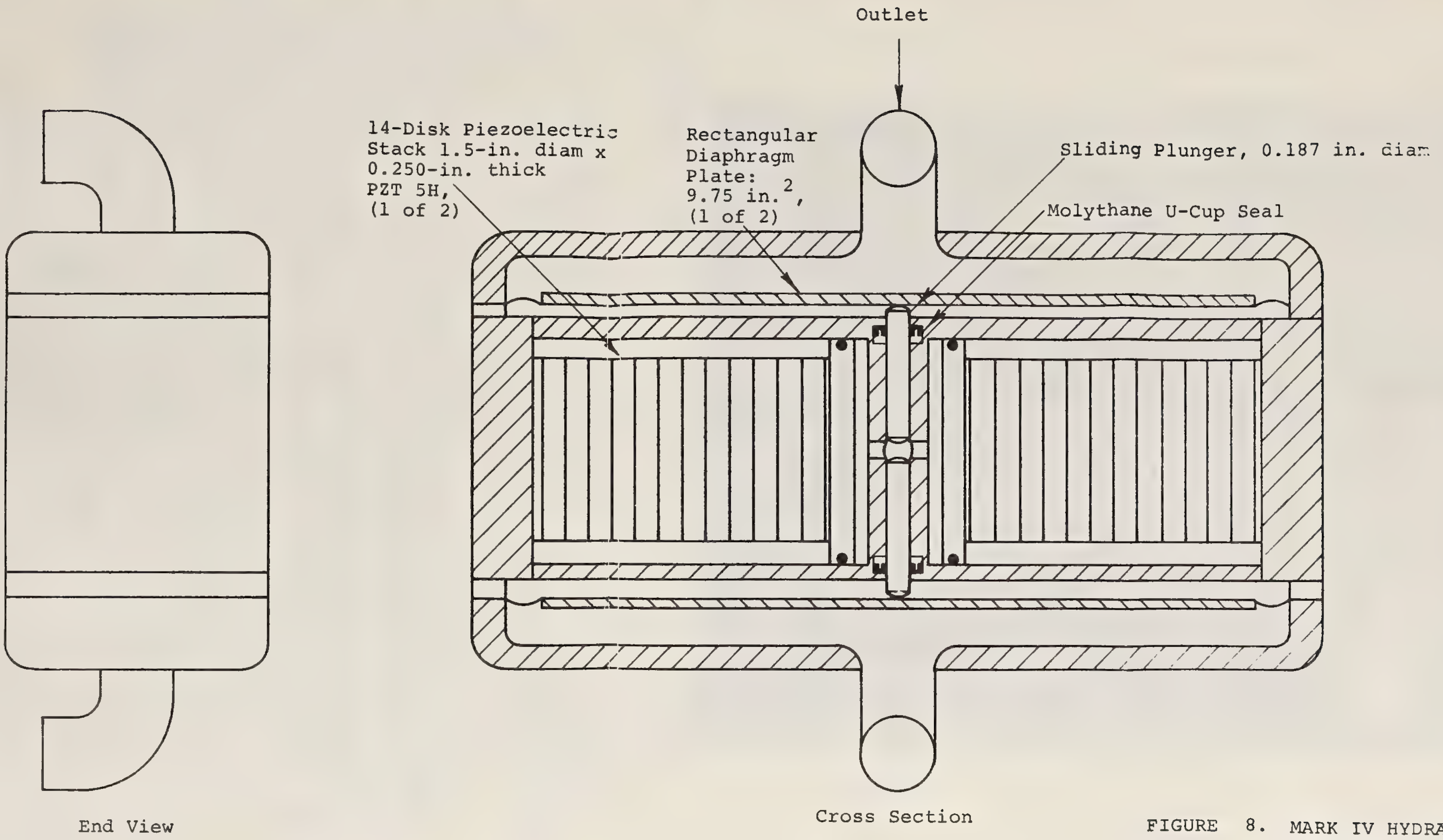

End View

Cross Section

FIGURE 8. MARK IV HYDRAULICALLY AMPLIFIED DUAL COMPONENT DRIVER

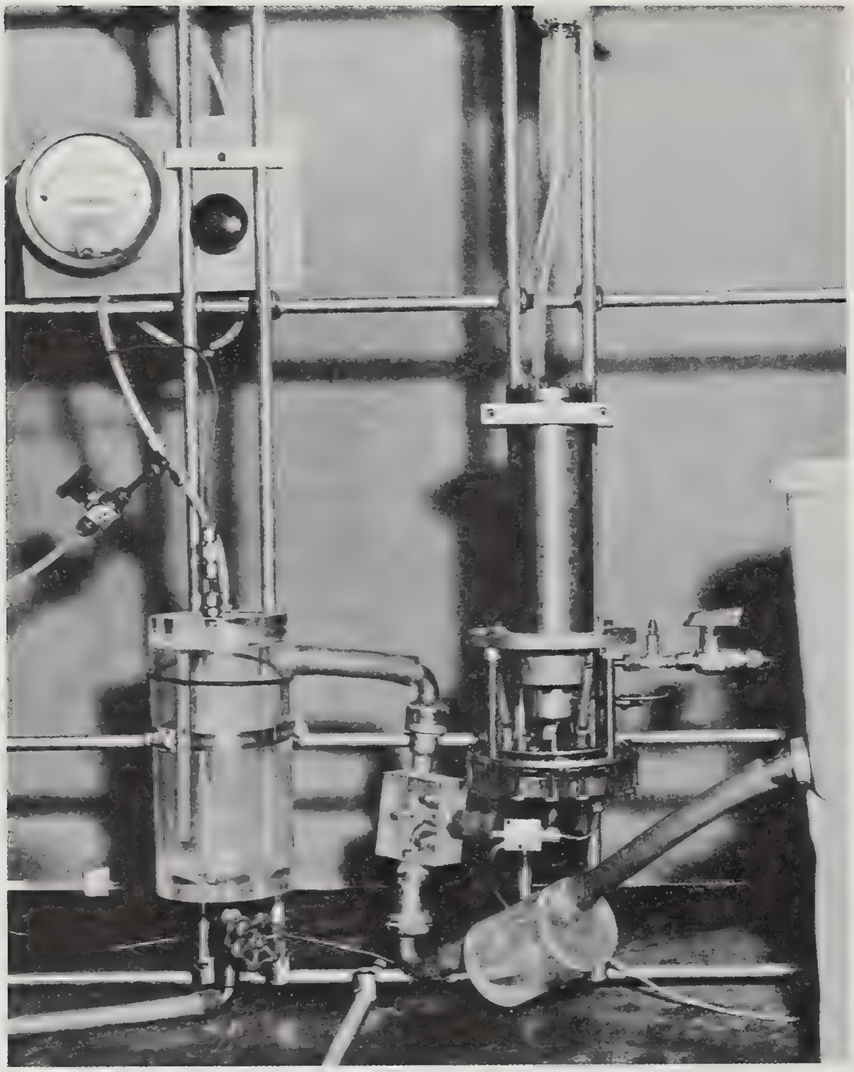

FIGURE 9. MARK III X HYDRAULICALLY AMPLIFIED DRIVER AND TEST APPARATUS.

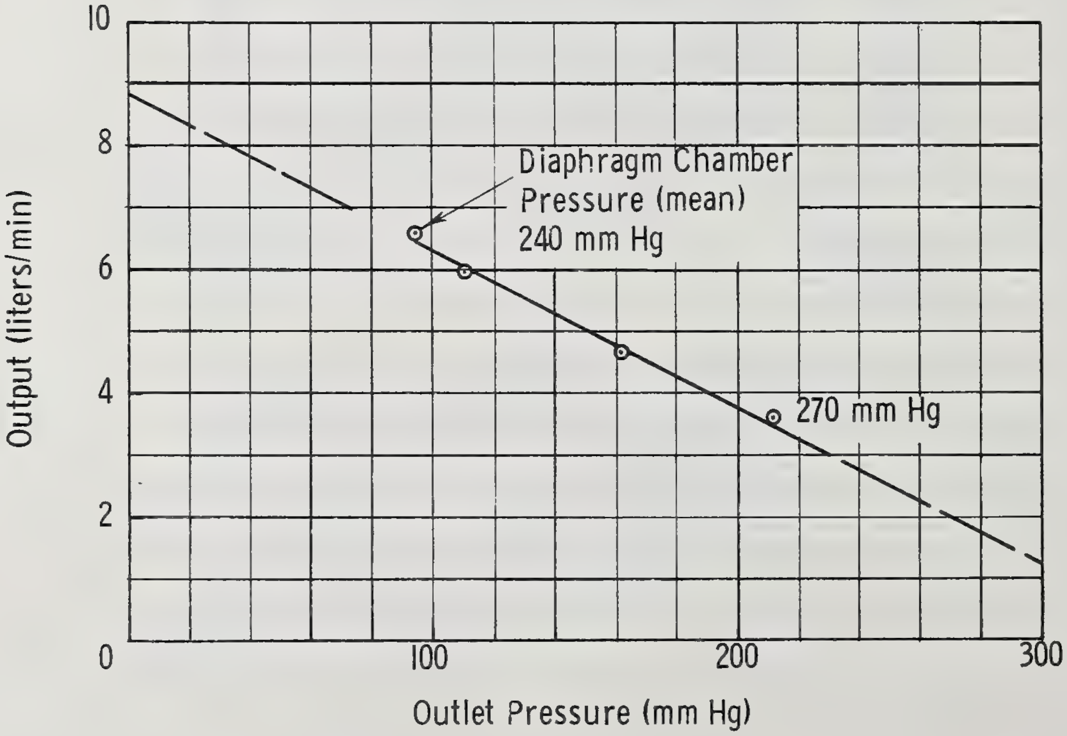

FIGURE 10. OUTPUT OF THE MARK III X DRIVER AT 120 STROKES/MIN.

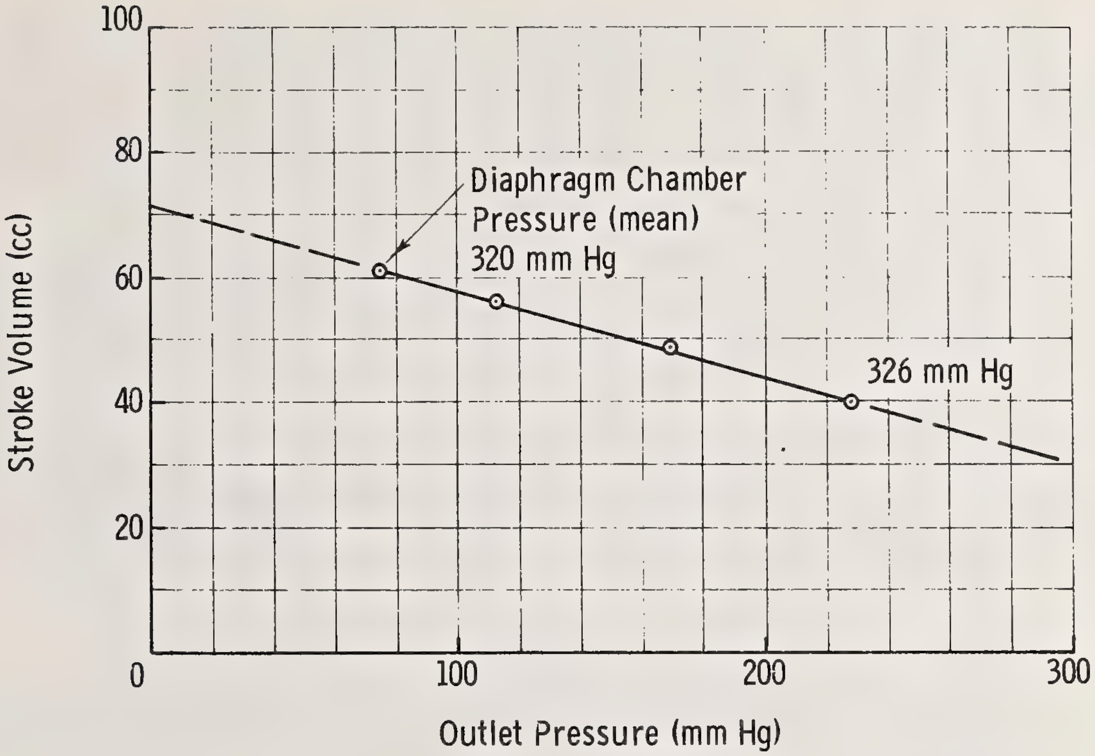

FIGURE 11. STROKE VOLUME OF THE MARK III X DRIVER: PULSE DURATION = 200 MSEC.

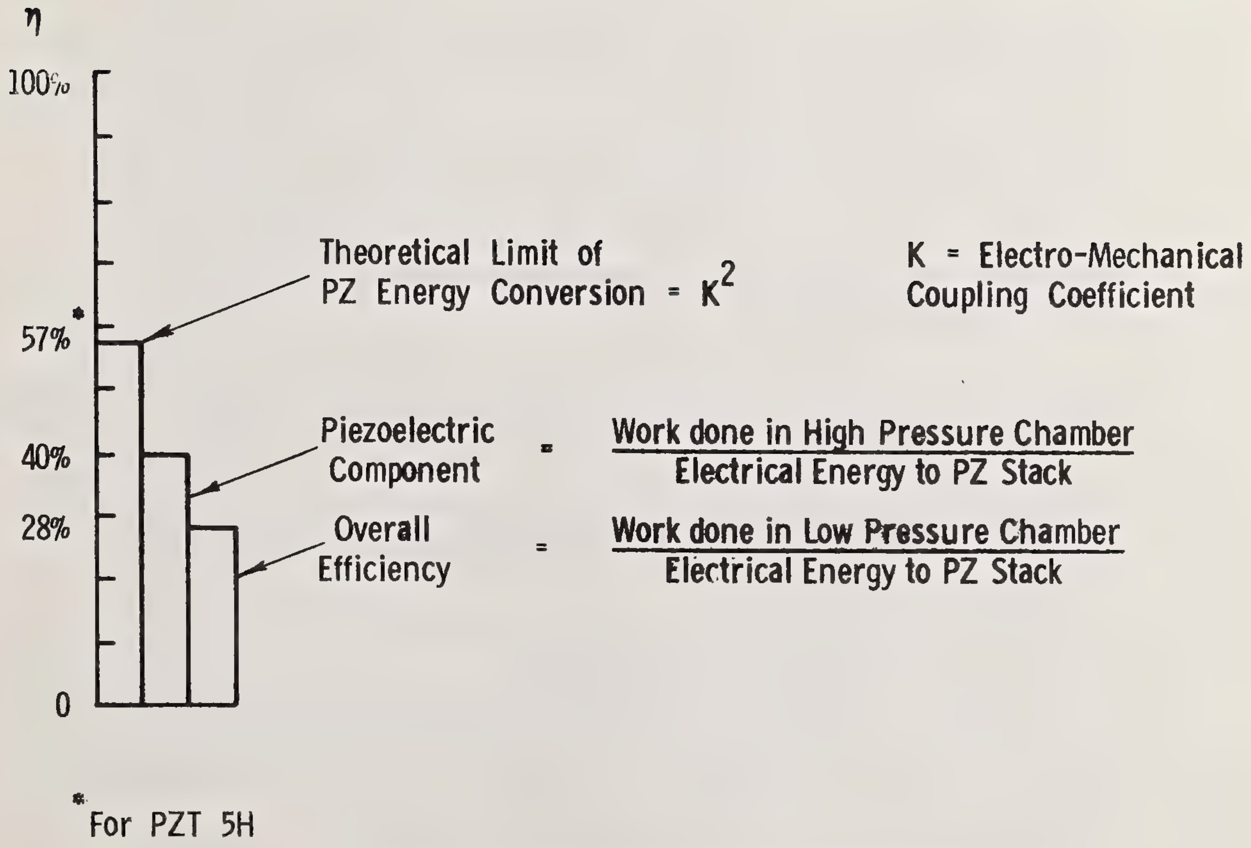

FIGURE 12. MEASURED PIEZOELECTRIC DRIVER EFFICIENCIES.

Stroke volume as a function of outlet pressure is plotted in Figure 11. The pulse duration was 200 msec. The data were taken in single pulses with adequate time between pulses for complete filling. Again, numbers over the data points indicate mean pressure in the diaphragm chamber. With a larger diaphragm, the stroke volume has been up to 77 cc with a 200-msec pulse duration, (60/220 mm Hg). We have determined some efficiencies of Mark III X by measuring the electrical charge supplied to the stack, and the pressure and displacement in the high- and low-pressure chambers. We will define the piezoelectric component efficiency as the work done in the high-pressure stage divided by the electrical energy supplied. The overall driver efficiency is the work done in the low-pressure chamber divided by the electrical energy supplied. It is assumed that no energy is recovered when the stack is discharged.

The measured piezoelectric component efficiency is 40% and the measured overall driver efficiency is 28%. Maximum efficiency is limited by the mechanical coupling coefficient in any piezoelectric device. For a material like PZT-5H this limit is 57% (Figure 12). Mark III X contains 12 in.^{3} of piezoelectric material--1500 g. Our laboratory measurements show that the amount of work done by Mark III X can theoretically be done by 1 in.^{3} or 125 g. The energy density is 2.3 J/in.^{3} per stroke or 18.5 J/kg with a field of 150 V/mil. This is calculated from strain measurements at that field.

We have tested piezoelectric stacks of 0.040-in. thick disks to 85 V/mil successfully. By using this electric field in a driver we believe that we can reduce the piezoelectric stack volume by more than a factor of two. We have started a company-financed program to develop improved piezoelectric materials for high strain application. With a moderate degree of success in this effort, we can expect another factor of three reduction. Then the driver would require only two cubic inches of material, 250 g (Figure 13).

SUMMARY

To summarize our accomplishments, this program has:

1. Developed a piezoelectric driver capable of producing an output flow of 8 liter/min.
2. Demonstrated that the driver can be controlled as to the quantity pumped and timing of pulses.
3. Tested a piezoelectric stack at 85 V/mil for the equivalent of 2-1/2 years of operation without degradation.
4. Made laboratory measurements to show that it is possible to reduce the size of the piezoelectric stack by a factor of ten from the present size.

DISCUSSION

DR. KENNEDY: I would like to compliment the authors on this interesting work, well presented, and to ask what measures for isolation of the piezoelectric material from the basically hostile body environment are projected for future implantation?

As is well-known to this audience, piezoelectric materials are high-impedance devices, and are therefore inactivated by minor amounts of moisture.

Our own project group has been interested in implantable piezoelectric power sources since 1964. The problem of encapsulation in a flexible medium impervious to body fluids has been so great, that our colleague, Dr. Glencoe, developed an end-loaded harmonic-mode piezoelectric generator in an effort to avoid this problem.

DR. SMILEY: The piezoelectric component will be entirely enclosed in a hard metal enclosure. The seal as I mentioned would be a metal bellows seal, and the high voltage wires and so forth would all be enclosed in a welded conduit so that there would be a complete metal seal all around.

DR. BENSON: Thank you for a very interesting movie on piezoelectric pumps that was certainly demonstrative in pumping red fluid. I have a couple of questions. One is, did you ever measure the power factor on a pump over several cycles?

DR. SMILEY: No we have not done that but we have plans to do so in the future (i.e., to integrate instantaneous power).

DR. BENSON: This is one of the problems in piezoelectric single pulse actuation. We have made similar measurements in the past and have obtained very low power factors, which implies a tremendous problem -- in coupling a static inverter to the piezoelectric stack. The second question is in terms of efficiency. We saw the value for K squared for PZT-5H and we all recall that the K factor is strongly dependent upon voltage fields. If you are talking in terms of a couple of volts per meter or thereabouts then the value of K presented is the correct number. If you go to higher fields K decreases. Now, I wonder if you have made a specific measurement of the efficiency of the system, rather than using a low field K value.

DR. SMILEY: We did make measurements of efficiency but as far as the coupling coefficient for high voltages, no. The coupling coefficient I reported was the one published for low fields.

DR. BENSON: Did you measure the efficiency, and what is the efficiency?

DR. SMILEY: It was 40%.

DR. BENSON: 40%. And this was electrical energy input to hydraulic energy output?

DR. SMILEY: Yes.

DR. BENSON: That is very high, indeed. The final question is what was the weight of the pump you have shown?

DR. SMILEY: The one that was shown, of course, is large. The piezoelectric stack weighed 1500 grams.

DR. BENSON: What was the weight of the whole unit, though?

DR. SMILEY: I don't know what the whole unit weighed. The projected weight of the piezoelectric component vs. the piezoelectric weight would be about 2 to 1. So if you have 250 grams of piezoelectric material you have 500 grams total.

DR. BENSON: Is this based on experimental data?

DR. SMILEY: Yes.

DR. TSIEN: I want to compliment you on the engineering achievement in this pumping operation, but I was wondering if any assessment has been made on the traumatic effect on the blood being pumped in this kind of a mode. We were very much interested to develop some sort of a blood pump to simulate the natural heart condition, and we were warned by the medical profession that any reciprocating action or drastic screening of the blood will cause short term traumatic and long term disastrous effects. I was wondering if this has been determined?

DR. SMILEY: Well, of course the fluid we are driving is intermediate fluid which would be displaced to a circulatory assist device like the TECO blood pump. The pulse wave shape, wave form, etc., can be controlled so that you get essentially desired physiological parameters.

DR. ROTH: With an efficiency of 40%, about 60% of the input energy is converted to heat. Your stack is insulated from the metal cartridge. What means do you have for ultimately getting rid of the heat that has developed in this pack?

DR. SMILEY: That heat would be dissipated in the resistor which would be mounted somewhere in contact with the intermediate fluid.

DR. ROTH: I am talking about the heat developed in the piezoelectric material.

DR. SMILEY: That heat is conducted through the metal.

DR. ROTH: How? It is separated from the metal, is it not?

DR. SMILEY: There is a liquid insulating fluid.

DR. ROTH: The cartridge is filled with liquid?

DR. SMILEY: Yes.

DR. SIPIN: What is the amplitude of voltage waveform applied to the piezoelectric stack?

DR. SMILEY: The amplitude of these particular stacks was 34 volts per mil or 8-1/2 K on a quarter inch thick disk. Thinner disks and hence lower voltages will be used in the future.

DR. SIPIN: How is the voltage wave obtained?

DR. SMILEY: The input was an electrically-mechanically switched pulse from a large capacitor charged by a variable DC power supply.

DR. SIPIN: How do you intend to obtain this waveform in a unit suitable for implantation?

DR. SMILEY: We have a scheme for an implantable power supply which charges the stack in small steps at high frequency, and discharges it through a resistor.

DR. BLUMLE: What was the insulating fluid used?

DR. SMILEY: At the present time we are using peanut oil.

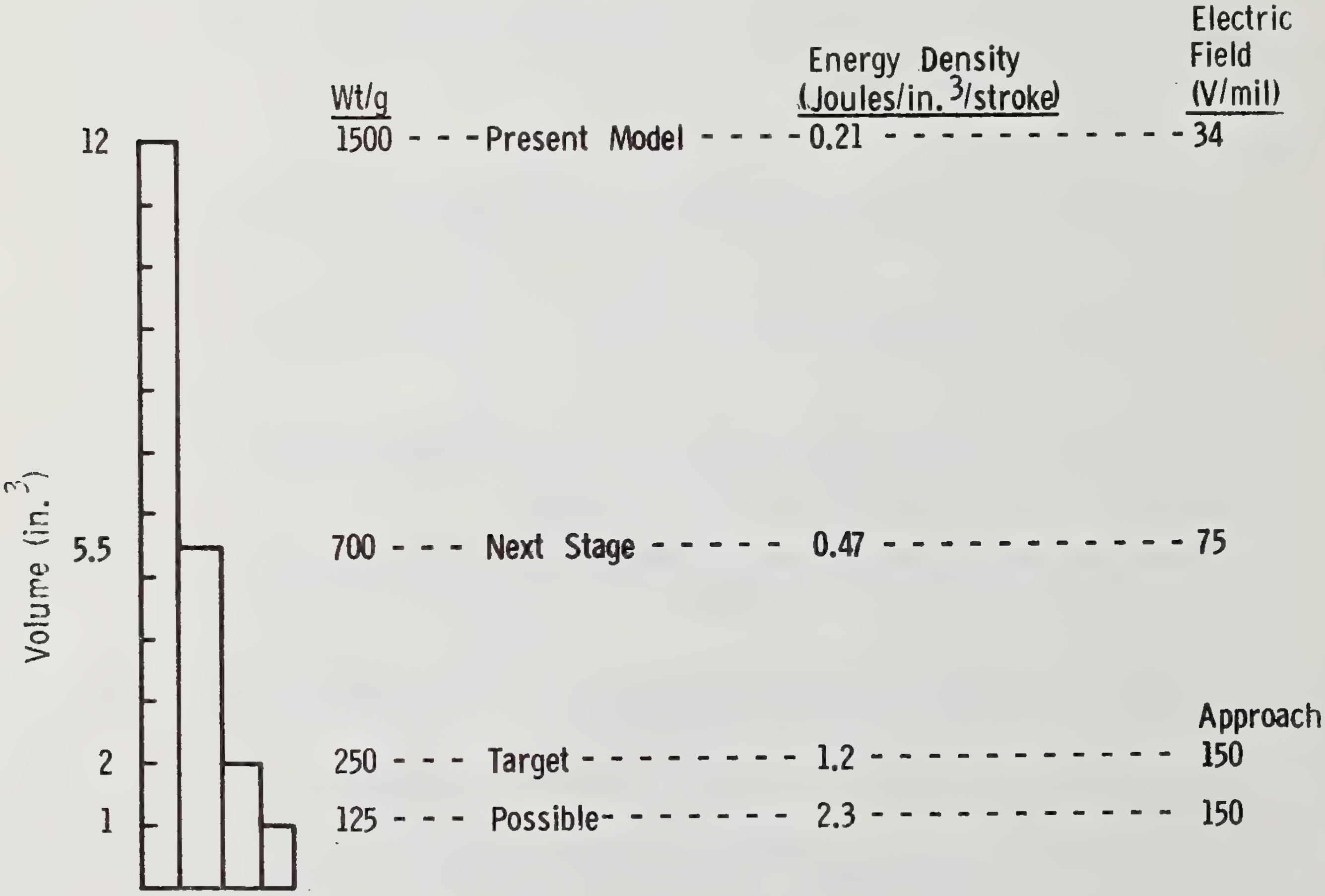

FIGURE 13. PIEZOELECTRIC MATERIAL REQUIRED FOR HEART ASSIST DRIVER.

CHAPTER 84

PIEZOELECTRIC IMPLANTABLE ENERGY CONVERTERS

G. Benson, J. Christie

ERG, Inc.
Oakland, Calif.

Results of work sponsored by NIH on piezoelectric (PZ) electromechanical energy converters are given. The operating principles and performance levels of PZ materials are reviewed and compared with more conventional electromechanical energy converters. This comparison suggests that efficiency, reliability and compactness can be maximized by exciting the PZ material at an ac voltage frequency determined by the mechanical resonant frequency of a mass loaded spring biased oscillator. A reduction in the oscillator mass is achieved by the use of a mechanical transformer which effectively couples the high-force, low-displacement output of the PZ material to the low-force, high displacement of the oscillator. This transformer employs differential area, mercury filled, metal bellows of advanced design which drive a double-acting positive displacement pump whose variable displacement output is determined by the ac voltage applied to the PZ module. Experimental results for preliminary designs are presented and compared with theory. Designs are described that operate at either cardiac frequency or at high frequency with mechanical frequency transformation. Endurance tests on advance PZ modules were conducted to over several billion cycles under high electric field and mechanical strain conditions without measurable degradation. Electromechanical conversion efficiencies for PZ modules were determined to be in the ninety percent range for practical operating conditions. Mechanical output energy densities of over 0.1 J per cycle per cc of PZ material were reproducibly obtained. Flow rates of over 40 liters/min. against a pressure head of 150 mm Hg were produced by the hydraulic pump at frequencies up to 200 Hz. As a result, resonant, high-frequency PZ driven double-acting, positive displacement pumps appear promising for hydraulically driving artificial blood pumps, provided that their complexity, when compared with other energy converters, can be justified.

INTRODUCTION

The rationale for investigating piezoelectric motors, for use as electromechanical energy converters in implantable artificial heart systems, is that it has proven difficult to achieve suitable performance characteristics from the more conventional electromagnetic mechanical converters, such as high-speed rotary electric motors, solenoids and torque motors, which have been under continuous development for several decades. While there is reason to believe that suitable electromagnetic mechanical converters may eventually be developed, the problems inherent in such a development, based upon the extensive work performed on these converters to date, strongly suggest the desirability of simultaneously pursuing other energy conversions methods. A recent study[1] on alternate electromechanical conversion methods indicates that the only other promising methods that are presently known are advanced electrostatic parametric converters, piezoelectric motors and electro-expansive dielectric converters, which all operate as electric field machines rather than magnetic field machines, as do conventional electromechanical converters. In both machines the electric or magnetic field generates a force which results in mechanical work output, provided movement occurs. The work output and energy density in both is limited by the electric or magnetic fields that can be maintained in the materials. The energy density is maximized by using materials having high permittivities or high permeabilities which concentrate the electric or magnetic fields, respectively. These materials exhibit saturation, i.e., are capable of concentrating only a limited quantity of electric or magnetic energy per unit volume or unit mass. As a result, an electromechanical converter can convert only a limited quantity of electrical to mechanical energy per cycle or stroke of operation. Therefore, in order to minimize size and weight, these converters have to operate at as high a frequency as possible, limited only by the mechanical components and the frequency dependent losses, which detract from overall converter efficiency. If the frequency is limited by the application, then, the higher the energy density that is converted per cycle, the lower the size and weight of the converter, other parameters being equal. Even though specific machine designs may enhance certain performance parameters, such as overall efficiency, size and weight, reliability and response times, the basic limitations imposed by dielectric and magnetic materials still exist and ultimately govern the machine characteristics.

Confining our discussion now to electric field machines, the operation of these is governed by the field response characteristics of the material. These characteristics may be represented by displacement charge-electric field curves, in which the area enclosed by a cycle represents energy density, similar to that expressed by temperature-entropy curves for thermodynamic cycles, in which the electro-responsive material is replaced by the working fluid.

Representative displacement charge-electric field (D-E) curves for several dielectric materials are shown in Figure 1. In Figure 1a, a linear piezoelectric material, such as quartz, is shown in which a positive field is applied and then removed. The area enclosed by the cycle, traced on these coordinates, represents the loss exhibited by the piezoelectric material for this cycle, which for natural quartz is extremely small. The area enclosed by the triangle 0-1-2-0 represents the electrical energy that is stored dielectrically at the peak field strength. The slope of the curve is conventionally characterized as the dielectric coefficient of the material, which is field independent for this linear material. In Figure 1b, the response of an electrostrictive material is shown. In Figure 1c, the response of a typical ferroelectric material, such as barium titanate, or lead-zirconate-titanate solid solution ceramic material, is shown for two conditions. The first, represented by the solid curve, is for a low but constant mechanical compressive stress. The second, represented by the dashed curve and the solid return curve, is for a constant high compressive stress for the dashed curve, and a constant low compressive stress for the return curve. The area enclosed by the solid curve represents the energy loss for the cycle, and the area enclosed by the dashed curve and the return curve represents the electrical energy transferred to both the mechanical work performed and the energy loss for the cycle. The area enclosed by the dotted curves represents the mechanical energy stored in the material at the maximum field strength of the cycle. The electrical energy stored dielectrically at the maximum field strength of the cycle is represented by the area enclosed by the upper solid curve and the lower dotted curve. Upon removal of the field, the stored mechanical energy adds to the dielectrically stored energy and represents the total electrical energy available at discharge, such as represented by a capacitor. The ratio of the mechanical work output to the electrical energy input measures the electromechanical effectiveness and is denoted by k^2, where k is the electromechanical coupling coefficient. This coefficient measures the capacity of the material to convert electrical energy to mechanical energy and is not a measure of efficiency. Efficiency is based on losses--not on the capacity for performing work, or for converting electrical energy into mechanical energy. Figure 1c suggests that this coefficient may depend on the cycle, as do the losses. In Figure 1d, the response of a representative transition material is shown, in which the transition from an anti-ferroelectric state to a ferroelectric state is produced by the applied field. The on-set of the field-induced transition occurs where there is an abrupt change in slope (dielectric coefficient). This transition in state continues with increasing field until the transition is complete and only the ferroelectric effect remains, as shown. The field necessary for inducing the transition is stress-dependent, as shown by the dashed curve at high compressive stress and the solid curve at low stress. The relations, such as loss, mechanical work output and dielectrically stored energy, are again represented as in the preceding D-E curves. The higher dielectrically-stored energy at the transition field relative to ferroelectric material, shown in Figure 1c, is evident and is caused by the non-linearity (squareness) of the curve for the transition material. The higher loss and the higher mechanical work output, relative to the ferroelectric material, is also shown. In Figure 1e, the response of a dielectric relaxing (slim loop material) is shown. The material shown represents a field-induced transition from the ferroelectric state to the paraelectric state which is essentially linear. The slim-loop refers to the slimness of the loss loop at a low constant mechanical stress. The high mechanical work output relative to the loss is also shown. These preceding curves show typical material responses for fields lower than those at which saturation occurs. At saturation these curves exhibit similar slopes and represent the response of a linear dielectric having essentially the same dielectric coefficient. This characteristic is similar to that exhibited by all ferromagnetic materials at saturation. Not shown is the marked increase in energy loss as the field increases toward saturation.

In Figure 1f, field-induced mechanical strain response of two materials at constant compressive stress is shown. The anti-ferroelectric-ferroelectric transition material is represented by the dashed curve, while the response of the ferroelectric material is shown by the solid curve. The bipolarity fields are sufficient to cause a polarity reversal in the ferroelectric material. Several differences in the response characteristics of these two materials are shown. Of primary interest is the response at field reversal. The FE material exhibits a bidirectional mechanical response, i.e., a positive field induces a positive mechanical strain and a negative field induces a negative strain. The transition material exhibits only a unidirectional strain. The FE material also exhibits a finite residual strain at zero field resulting from the polarity existing in the material at this condition. The transition material has zero residual strain and is unpolarized at this condition. The residual strain or polarity at zero field also accounts for another effect exhibited by the ferroelectric material, viz. the ability to generate a voltage when subjected to a mechanical compressive stress (load). This reversible electromechanical response (field-induced strain and strain-induced field) together with the bidirectional mechanical response to a bidirectional field uniquely specify the piezoelectric effect and distinguish this effect from the non-piezoelectric electromechanical response exhibited by other dielectric materials, including vacuum, gases, high dielectric coefficient non-linear materials and transition materials.

The field-induced strain response at constant mechanical stress of four commercially available materials is shown in Figure 2. The linear response of PZT-4* material is representative of "hard" ceramics such as PZT-4 and PZT-8*. The response of PZT-5H* material is representative of "soft" ceramics. The terms "hard" and "soft" refer to the modulus of elasticity of these materials. The materials PZT-4, PZT-5H and PZT-8 are piezoelectric. The non-linear response of a typical transition

---

*Trademark of Clevite Corporation, Cleveland, Ohio.

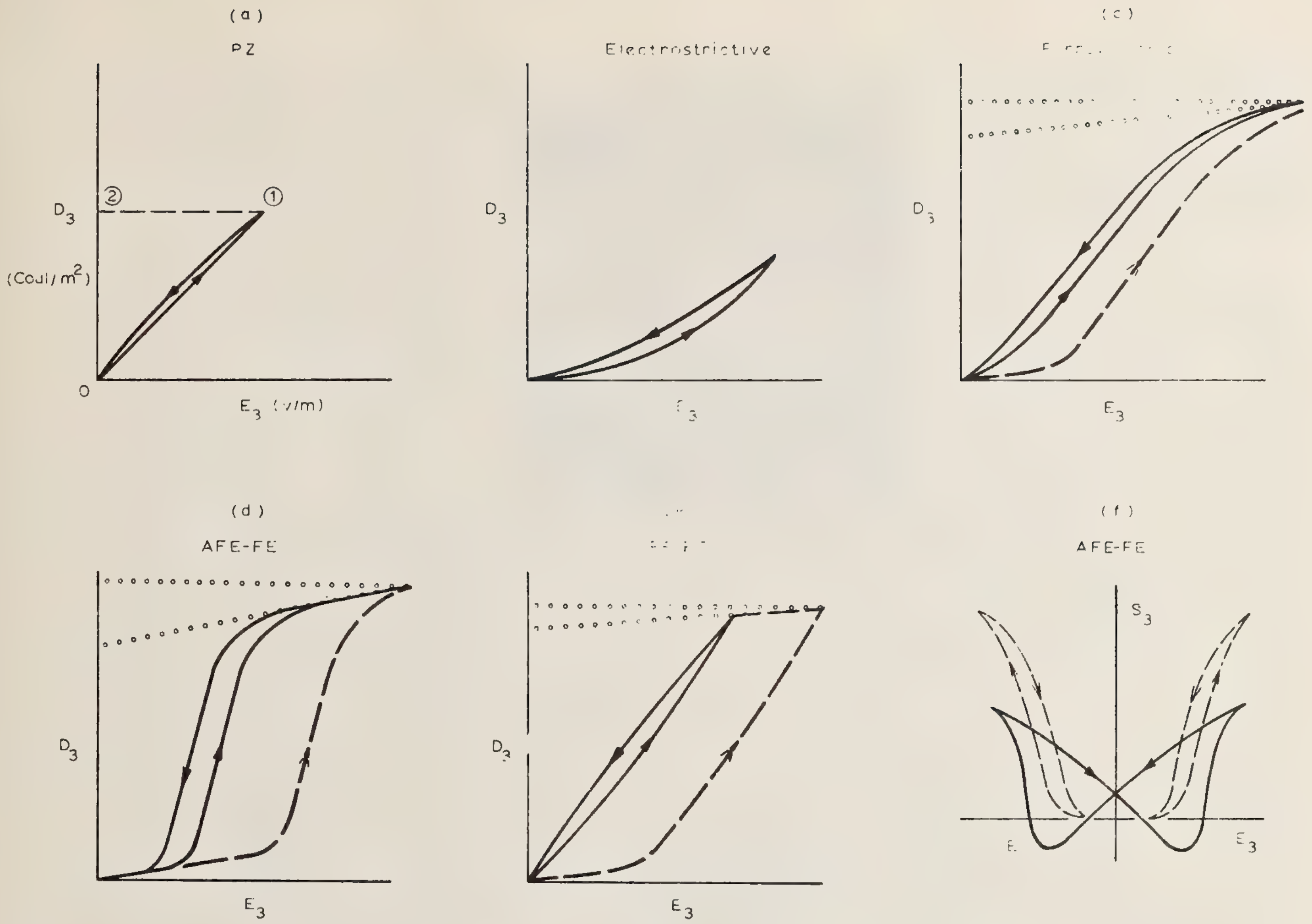

FIGURE 1. REPRESENTATIVE DISPLACEMENT CHARGE-ELECTRIC FIELD (D-E) CURVES.

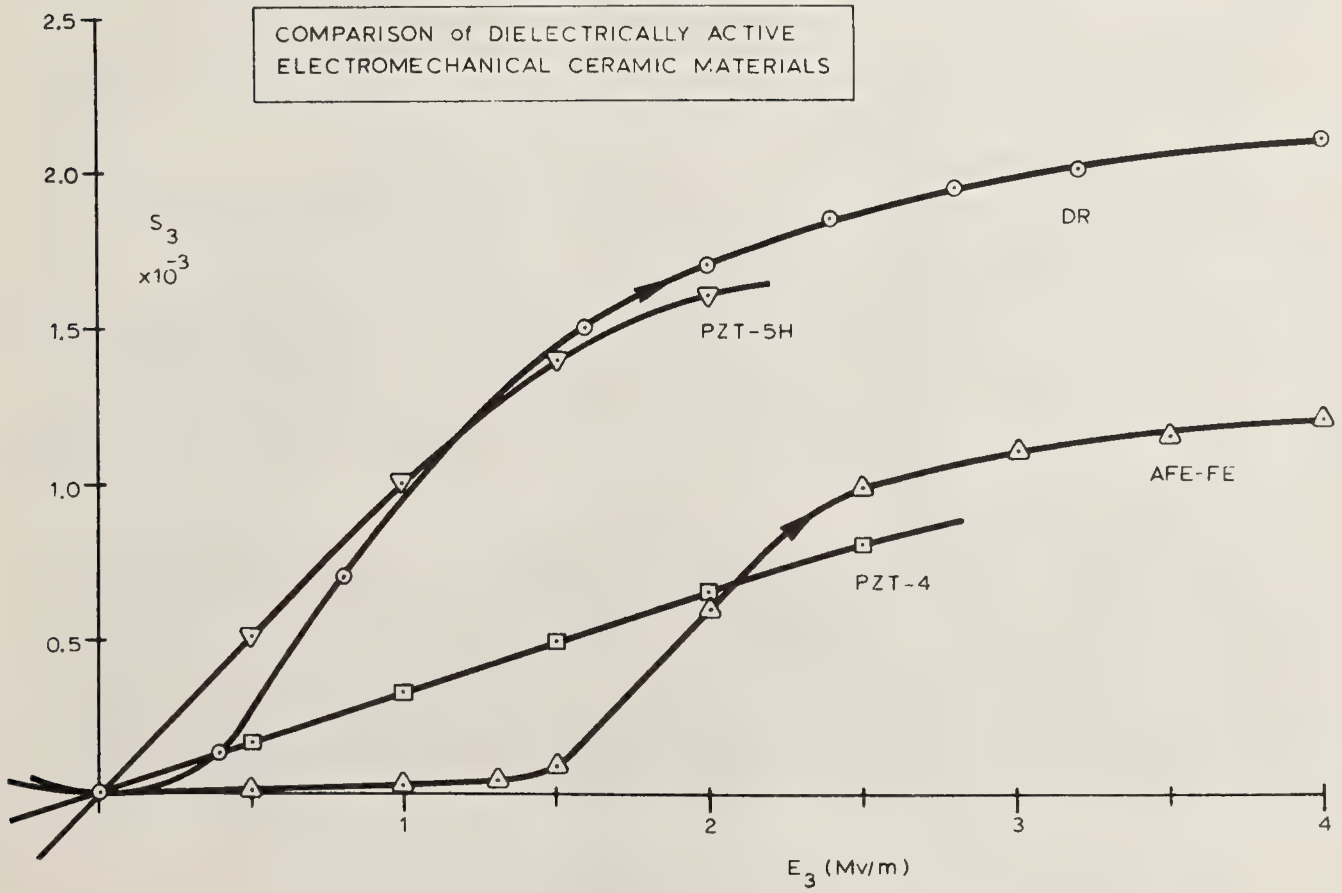

FIGURE 2.

material (AFE-FE), which undergoes a low field transition, is shown for comparison. Higher field transition materials exhibit a higher induced strain. The non-linear response of a dielectric relaxing (DR), or slim-loop material, is also shown. Of significance is the saturation field-induced strain response. At high fields all these materials appear to exhibit equal strain coefficients (slope of strain-field curve). As a result of this saturation, and that of non-linearity, the classic relationship, which specifies that the energy available and the work output are proportional to the square of the applied electric field, is invalid.

The large field-induced strains exhibited by certain materials, as shown in Figure 2, are noteworthy. Other advanced materials exist which show even greater induced strains (presently limited to about 5×10^{-3}). Exciting as these strains may be, the endurance-limited strains are much lower, particularly for soft ceramics. The endurance strain limit is a function of applied field and rate of strain, since ceramic materials exhibit inferior mechanical properties when exposed to square wave mechanical or electrical excitation. Exposure to cyclically applied electrical fields, in combination with cyclic mechanical stress loadings, further decreases the endurance strain limit. Since both movement (strain) and force (stress) are necessary for work output, and since these are generated by an applied field, the correct endurance criterion would appear to be that based on energy density (mechanical work output per unit volume of material per cycle) for low frequency applications, and power density for high frequency applications. As a result, the reliability of a material may be erroneously measured if it were determined from experiments in which a high field was cyclically applied to the material, while exposed to a constant strain or stress, or a low amplitude stress or strain level. An example of such an error is shown in Figure 3, which shows a 1/2 mm thick disc of 2 cm diameter made from PZT-5H material that was hot pressed, lapped and annealled, and then subjected to a high energy density operation. The fracture lines are evident, even though the electrical breakdown is not. Similar discs were exposed to high fields (70 volts/mil) of unipolarity and sinusoidal shape, and to a low amplitude compressive stress (2-3 kpsi) with a 2 kpsi compressive stress bias. Cycling at 10-30 Hz under mechanically non-resonant conditions produced no failures at exposures up to about 100 million cycles. However, the same fields, when applied to similar discs, operated at high amplitudes of compressive stress (1-10 kpsi) with a 1 kpsi compressive stress bias and a high strain amplitude, produced the fractures shown in less than 1,000 cycles. This failure represents a progressive failure thought to be started by micro-cracking at domain boundaries, followed by crack propagation enhanced by microscopic breakdown of the dielectrical material and terminated by complete dielectric breakdown (arcing) through the illustrated cracks. Similar results were reproducibly obtained on other soft ceramics that exhibited large field-induced strain response. Similar tests conducted on hard ceramic materials, represented by PZT-4 and PZT-8 ceramics, did not produce material failure or piezoelectric property degradation, up to approximately 5 billion cycles, even at marked increases in energy density relative to that produced by PZT-5H ceramic. As a result of these tests, conducted on both hot-pressed and cold-pressed-sintered ceramic materials, it would appear that the only materials that are suitable, based on presently available materials, are the hard ceramics. These results are confirmed by the fact that the only materials that have been successfully used on high power transducer applications, such as sonar and sonic generators, are PZT-4 and PZT-8 type of materials. In addition, the energy losses in soft ceramics are much greater than those in hard ceramics. For example, the dielectric loss exhibited by PZT-5H is compared with PZT-4 in Figure 4 at two constant stress levels. The significantly larger dielectric loss, represented as $\tan\delta_E$, for PZT-5H causes a marked decrease in electromechanical conversion efficiency for PZT-5H, relative to PZT-4. Both PZT-4 and PZT-8 ceramics exhibit linear electromechanical response up to field strengths higher than that practical (limited by loss and the resulting lower efficiency).

The electromechanical conversion characteristics of these linear materials can be analyzed by the use of displacement charge-field (D-E) curves and the corresponding strain-stress (S-T) curves for particular operating cycles. The first operating cycle for an ideal pump is shown in Figure 5. In this figure, process 1-2 corresponds to the pressurization of the pump (from pressure $P_i = 0$ to P_o) by the electric charge flowing into the PZ stack without piston movement (stack strain, $S_3 = 0$). Process 2-3 corresponds to fluid displacement caused by charge flow at increasing voltage which produces a stack strain at constant stack stress, ($T_3 = T_m$, where T_m corresponds to the maximum compressive stress of the stack). At point 3, the voltage is decreased to zero and the stack first undergoes process 3-4 wherein the stack unstresses without piston movement (stack strain, $S_3 = S_m$, where S_m corresponds to the maximum stack strain) and then unstrains at zero stress ($T_3 = 0$), corresponding to process 4-1, which completes the cycle. In the S-T plane the cycle is rectangular in shape and shows that the net work output, W_{out}, equals $S_m \cdot T_m$, which also equals the area enclosed by the parallelepiped in the D-E plane in which processes 1-2 and 3-4 occur at constant mechanical strain and processes 2-3 and 4-1 occur at constant mechanical stress.

Discrete pulse operation of an ideal piezoelectric linear motor producing mechanical output may be described by use of the electric charge-field (D-E) diagram and mechanical strain-stress (S-T) diagram shown in Figure 6. In this figure, process 1-2 corresponds to the stressing of the motor (from compressive stress $-T_o$ to $-T_m$) by the electric charge flowing into the PZ stack without rod movement (stack strain, $S_3 = 0$). Process 2-3 corresponds to a rod displacement caused by charge flow at constant voltage, which produces a stack strain at decreasing stack stress (from compressive stress $-T_m$ to $-T_o$). At point 3, the voltage is decreased to zero and the stack first undergoes process 3-4 wherein the stack unstresses at constant strain ($S_3 = S_m$ where S_m corresponds to the maximum stack strain) and then unstrains at increasing stress, corresponding to process 4-1, which completes the cycle. In the S-T plane the cycle is parallelepiped in shape and the area enclosed by the

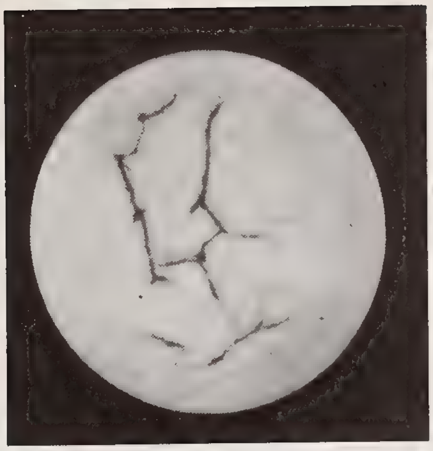

FIGURE 3. FRACTURE LINES IN DISC MADE FROM PZT-5H MATERIAL.

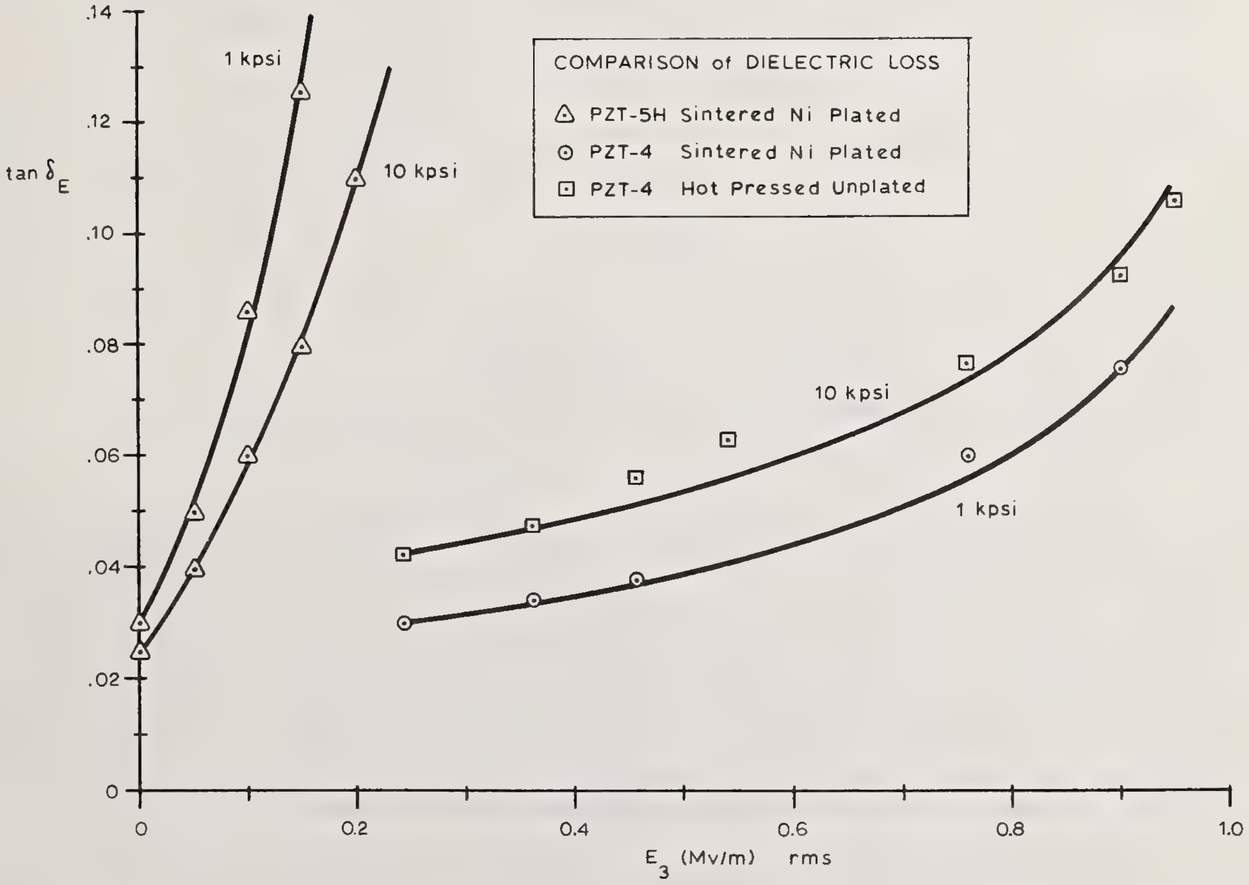

FIGURE 4.

parallelepiped equals the net work output, W_{out}, which also equals the area enclosed by the parallelepiped in the D-E plane. The processes 2-3 and 4-1 occur at constant voltage and processes 1-2 and 3-4 occur at constant strain.

Discrete pulse operation for two other loading cycles, termed III and IV, can also be obtained from Figure 6. Cycle III consists of the cycle 1-2-3-1 which corresponds to a constant-stress return process 3-1. Cycle IV consists of the cycle 1-3-4-1, which corresponds to a constant-stress expansion process 1-3.

Similarly, the electromechanical characteristics of piezoelectric materials can be obtained for sinusoidal excitation. The complete analysis for both discrete pulse and sinusoidal excitation have been reported [1]. The results are presented in Table 1.

TABLE 1

PIEZOELECTRIC PERFORMANCE VALUES

Operating Mode	Q_M *	PZT-4[a] Q_M *	PZT-4[a] P_M^b/f	PZT-4[a] η	PZT-8[a] Q_M*	PZT-8[a] P_M^b/f	PZT-8[a] η
Discrete Pulse:							
Square Wave or Arbitrary Wave Loading Cycle							
Case I	π^{-1}	0.32^c	0.011	0.52	0.32^c	0.007	0.75
Case II	$4\pi^{-1}$	1.28	0.045	0.81	1.28	0.028	0.92
Case III	$2\pi^{-1}$	0.64	0.022	0.68	0.64	0.014	0.85
Case IV	$2\pi^{-1}$	0.64	0.022	0.68	0.64	0.014	0.85
Sinusoidal:		3.94^c	0.138	0.92	5.68^c	0.122	0.98
Optimum Loading	$\left[(s_{33}^E T_{3_\ell}/d_{33}E_{3_\ell})^2 -1\right]^{-\frac{1}{2}}$	2.75^d	0.190	0.84	3.96^d	0.167	0.93
Sinusoidal:							
Bandwidth	$(1-k^2_{33})^{\frac{1}{2}}/k_{33}$	1.02^c	0.036	0.77	1.25^c	0.027	0.92
Sinusoidal:							
Nonresonant	$\frac{1}{2}$	0.50^c	0.017	0.63	0.50^c	0.011	0.83

[a] TM: Clevite Corporation, Cleveland, Ohio
[b] Energy per cycle (J/cc/cycle)
[c] Determined at $T_{3_\ell} = 7.6 \times 10^7$ n/m^2 and $E_{3_\ell} = 10^6$V/m for PZT-4
Determined at $T_{3_\ell} = 9 \times 10^7$ n/m^2 and $E_{3_\ell} = 10^6$V/m for PZT-8
[d] Determined at $T_{3_\ell} = 7.6 \times 10^7$ n/m^2 and $E_{3_\ell} = 1.4 \times 10^6$ V/m for PZT-4
Determined at $T_{3_\ell} = 9 \times 10^7$ n/m^2 and $E_{3_\ell} = 1.4 \times 10^6$V/m for PZT-8

Q_M* is defined as the equivalent mechanical Q for each operating mode. The factor p_m/f represents the net mechanical output per unit volume of piezoelectric material per unit operating frequency and has units of watts per cc per frequency. This factor is frequency independent since doubling the frequency (f) doubles the power output (p_m). The electromechanical conversion efficiency (η) represents the ratio of net mechanical output power to gross electrical input power. The four discrete-pulse operating modes, previously described, are listed as well as three sinusoidal operating modes, optimum loading, bandwidth, and nonresonant. Optimum refers to the operating mode which loads the piezoelectric material to its endurance limited stress, T_3, and its voltage limited field, E_3, under mechanical resonant conditions. Bandwidth refers to operating the piezoelectric material in a mode that maximizes the power output and efficiency throughout a frequency band centered about the mechanical resonant frequency but does not maximize these at the resonant frequency. Nonresonant refers to operating the piezoelectric material without inertial mass loading, which prevents mechanical resonance from occurring.

The high mechanical energy output densities per cycle, the low values of Q_M* and the high electromechanical efficiencies that are shown in Table 1, are noteworthy, especially for the sinusoidal, optimum-loading mode. The primary reason for this mode having the highest values is that the mechanical power output, peak stress and peak strain, generated in a given piezoelectric material driven at constant voltage field, are approximately proportional to the mechanical Q_M of the system, which, for the sinusoidal operating mode, equals the equivalent mechanical Q_M*.

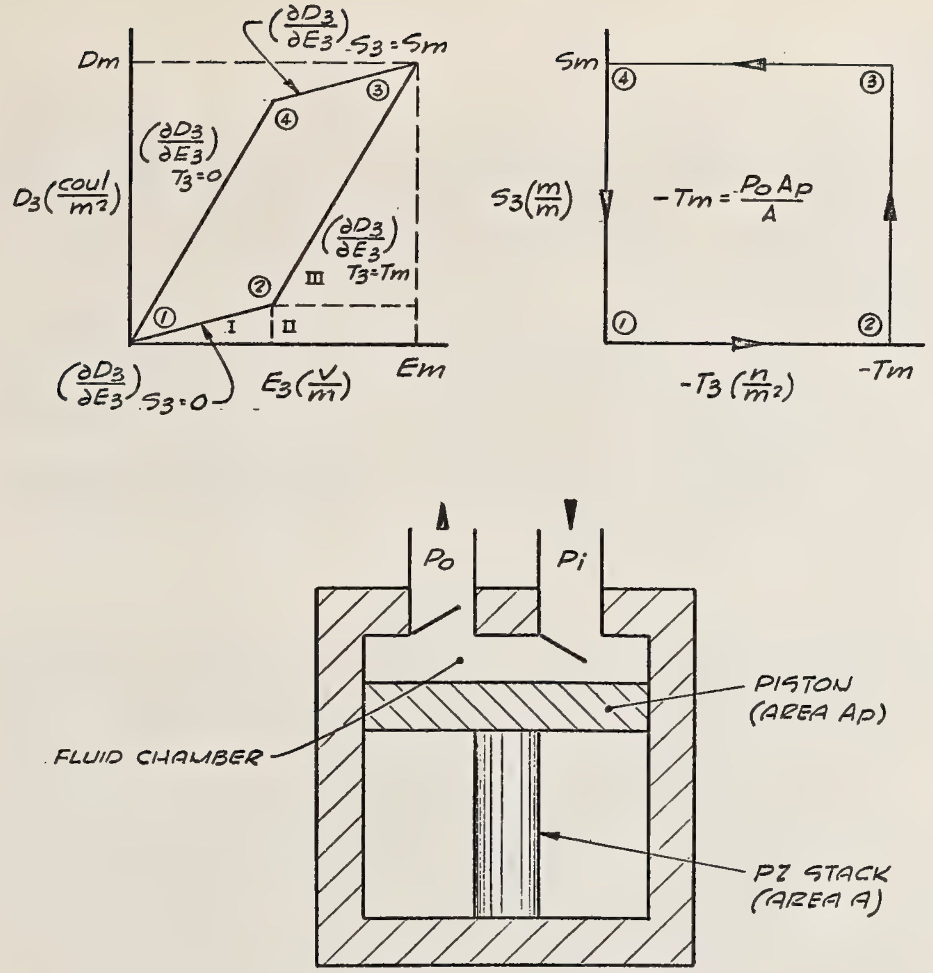
Dm
$\left(\frac{\partial D_3}{\partial E_3}\right)_{S_3=S_m}$
$\left(\frac{\partial D_3}{\partial E_3}\right)_{T_3=0}$
$D_3\left(\frac{coul}{m^2}\right)$
$\left(\frac{\partial D_3}{\partial E_3}\right)_{T_3=T_m}$
① ② ③ ④
I
II
III
$\left(\frac{\partial D_3}{\partial E_3}\right)_{S_3=0}$
$E_3\left(\frac{V}{m}\right)$
Em
Sm
$S_3\left(\frac{m}{m}\right)$
$-T_m = \frac{P_o A_p}{A}$
$-T_3\left(\frac{n}{m^2}\right)$
-Tm
Po
Pi
PISTON (AREA Ap)
FLUID CHAMBER
PZ STACK (AREA A)

FIGURE 5. IDEAL PIEZOELECTRIC PUMP CYCLE.

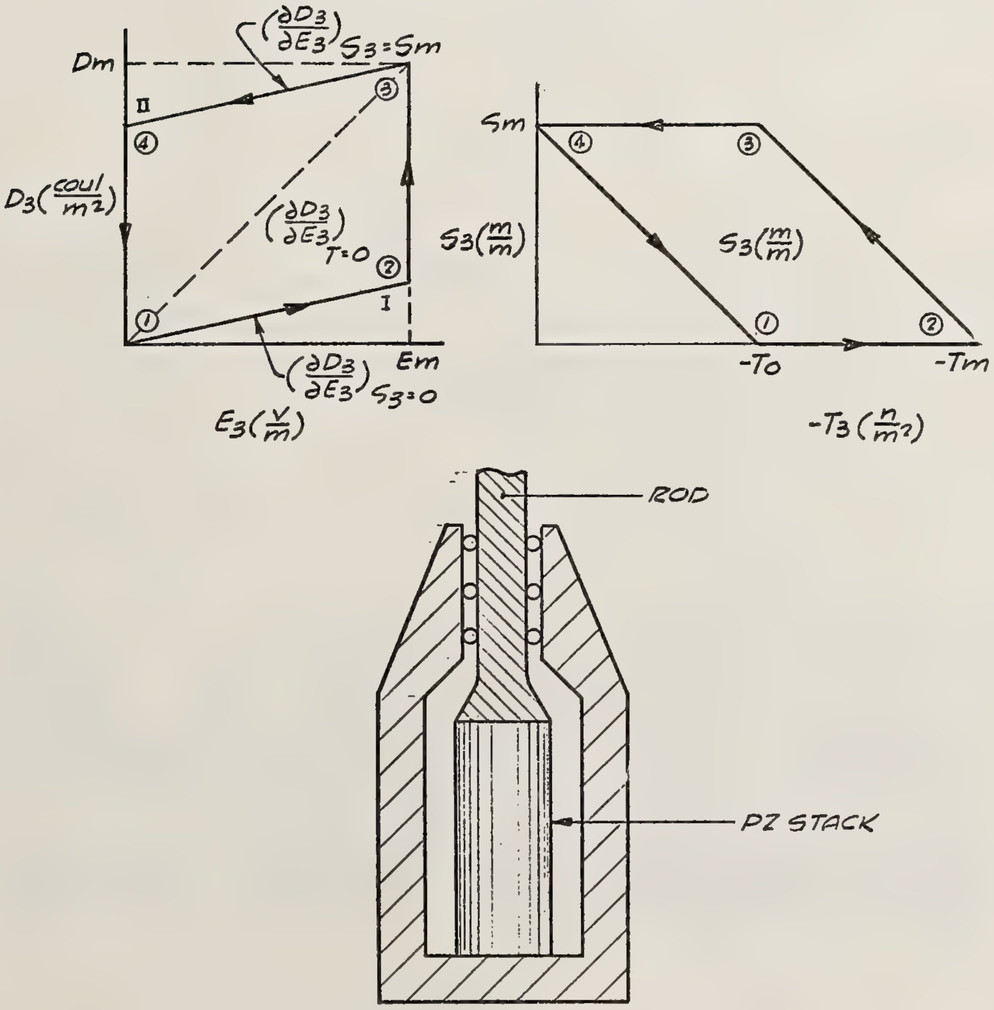
$\left(\frac{\partial D_3}{\partial E_3}\right)_{S_3=S_m}$
Dm
II
$D_3\left(\frac{coul}{m^2}\right)$
$\left(\frac{\partial D_3}{\partial E_3}\right)_{T=0}$
① ② ③ ④
I
$\left(\frac{\partial D_3}{\partial E_3}\right)_{S_3=0}$
Em
$E_3\left(\frac{V}{m}\right)$
Sm
$S_3\left(\frac{m}{m}\right)$
$S_3\left(\frac{m}{m}\right)$
-To
-Tm
$-T_3\left(\frac{n}{m^2}\right)$
ROD
PZ STACK

FIGURE 6. IDEAL PIEZOELECTRIC LINEAR MOTOR CYCLE.

The marked decrease in the power output, and in the efficiency for the discrete operating modes (non-resonant) are also noteworthy. The decrease in these values when soft ceramics are used, such as PZT-5H, is even more significant, with conversion efficiencies no higher than about 50% obtained at a power density less than half that for PZT-4. Other piezoelectric geometries, such as bimorphs, have substantially lower power density capabilities and efficiencies than those for a piezoelectric stack, as shown in the analysis presented previously[1]. As a result, only stack geometries were investigated on this program.

Experimental data for stack geometries are shown in Figure 7 for PZT-4 and PZT-8 ceramics operated sinusoidally at mechanical resonance with a mechanical Q of 3. The total loss in PZT-8 material is about 4 m J/cc/cycle for a mechanical power output of 100 m J/cc/cycle, which represents an electromechanical conversion efficiency of 100/104, or over 96%. If this material were operated at a frequency of 200 Hz then 20 watts of mechanical power would be produced per cc of piezoelectric material, at a conversion efficiency of over 96%.

Encouraging as these data may be, the piezoelectric material must be harnessed (coupled) properly to a suitable mechanical load if these performance values are to be realized. One coupling method which proved successful is described next.

ENERGY CONVERTER

The piezoelectric energy converter must effectively and efficiently convert the high-force and small-strain (stroke), developed by the piezoelectric stack into a small force and large stroke, if fluid is to be pumped at the high-flow rates and low-pressure heads required for hydraulically driving a bladder-type assist device or blood pump. One method of accomplishing this is to use a hydraulic amplifier with differential area pistons, as shown in Figure 8. The piezoelectric stack is represented mechanically by a spring at the left, having a spring constant K_1, and a force generator which generates a force, F_1. The stack is rigidly fixed at the left side and drives a large diameter piston, having a mass, M_1, through an axial displacement, X_1. The piston is sealed to a high performance metal bellows, having a spring constant, K_2, and a cross-sectional area A_1. The force generated by the stack produces a fluid pressure, P, in the bellows. This pressure is transferred to the small diameter bellows having an effective cross-sectional area, A_2, and a spring constant K_3. The small bellows is sealed to the secondary piston, having a mass, M_2 and an axial movement X_2. A bias spring, mounted at the right, has a spring constant, K_4, which compressively loads the stack and pressurizes the fluid contained within the bellows. The relationship between X_2 and X_1 depends on the compliance of the bellows and the compressibility of the fluid contained within. If the system is sufficiently compliant, no movement occurs at X_2, and no power is transferred. As a result, high performance, low compliance bellows are employed, and pure, fully deaerated mercury is used as the fluid. Under these conditions $X_2 = X_1 A_1/A_2$, and an effective transfer of mechanical power from piston 1 to piston 2 occurs. Piston 2 then converts this power to hydraulic power, since piston 2 serves as the piston for the positive displacement pump. The mass of piston 2 and the spring constants of both the bias spring and the stack provide the mechanical reactance necessary for resonant operation of the complete dynamic system. The individual components of this system are discussed next.

The first component is the PZ stack, shown in Figure 9. The stack consists of 95-1/2 mm thick discs which are arranged mechanically in series and connected electrically in parallel by two continuous electrodes, which are seen in Figure 9 as folded leaves projecting outside the stack. One electrode is at ground potential and the other is at ac supply voltage. This stack then drives a large diameter disc that is sealed by an omega-shaped metal bellows, shown in Figure 10. Mercury, contained within the chamber formed by this disc and bellows, is pressurized by the stack and axially extends the small diameter metal bellows, shown in Figure 11. The top of the bellows is electron beam welded to a threaded fitting which mates with the mercury chamber. The bottom of the bellows is electron beam welded to a pusher plate that mechanically connects to the secondary piston (hydraulic pump piston). The complete assembly is shown schematically in Figure 12. The most critical component of this assembly is the hydraulic amplifier. Measurements on the overall compliance (compressibility) of the complete amplifier, determined throughout a mercury pressure range of 1-5 kpsi, give a value that is less than four times that of the mercury contained within the amplifier, where the complete amplifier is considered to extend from the hydraulic pump piston to the bottom face of the stack and includes compliance of the housing.

The efficiency of the amplifier is a function of the load, as shown in Figure 13, where amplifier mechanical efficiency is plotted as a function of unloaded mechanical Q, with loaded Q as a parameter. The unloaded mechanical Q represents the energy loss in the amplifier due to fluid friction and hysteresis, while the loaded mechanical Q represents the energy loss plus the energy transferred by the amplifier. The unloaded Q is the more critical, since the loaded Q is determined by the hydraulic impedance impressed across the hydraulic pump, assuming a constant pump piston diameter, stroke and operating frequency. The unloaded Q of the amplifier is difficult to determine separately. However, the unloaded Q for the complete dynamic system, consisting of the PZ stack, the amplifier, the pump piston and bias spring, is easily determined by the following technique.

A variable frequency, small ac voltage is applied to the stack of the converter shown in Figure 12, which has been drained of pump fluid. The electric power at resonance frequency, f_r is measured. The frequency is then decreased until half power is reached, which determines the lower half-power frequency, f_1. The frequency is then increased beyond resonance until half power is again

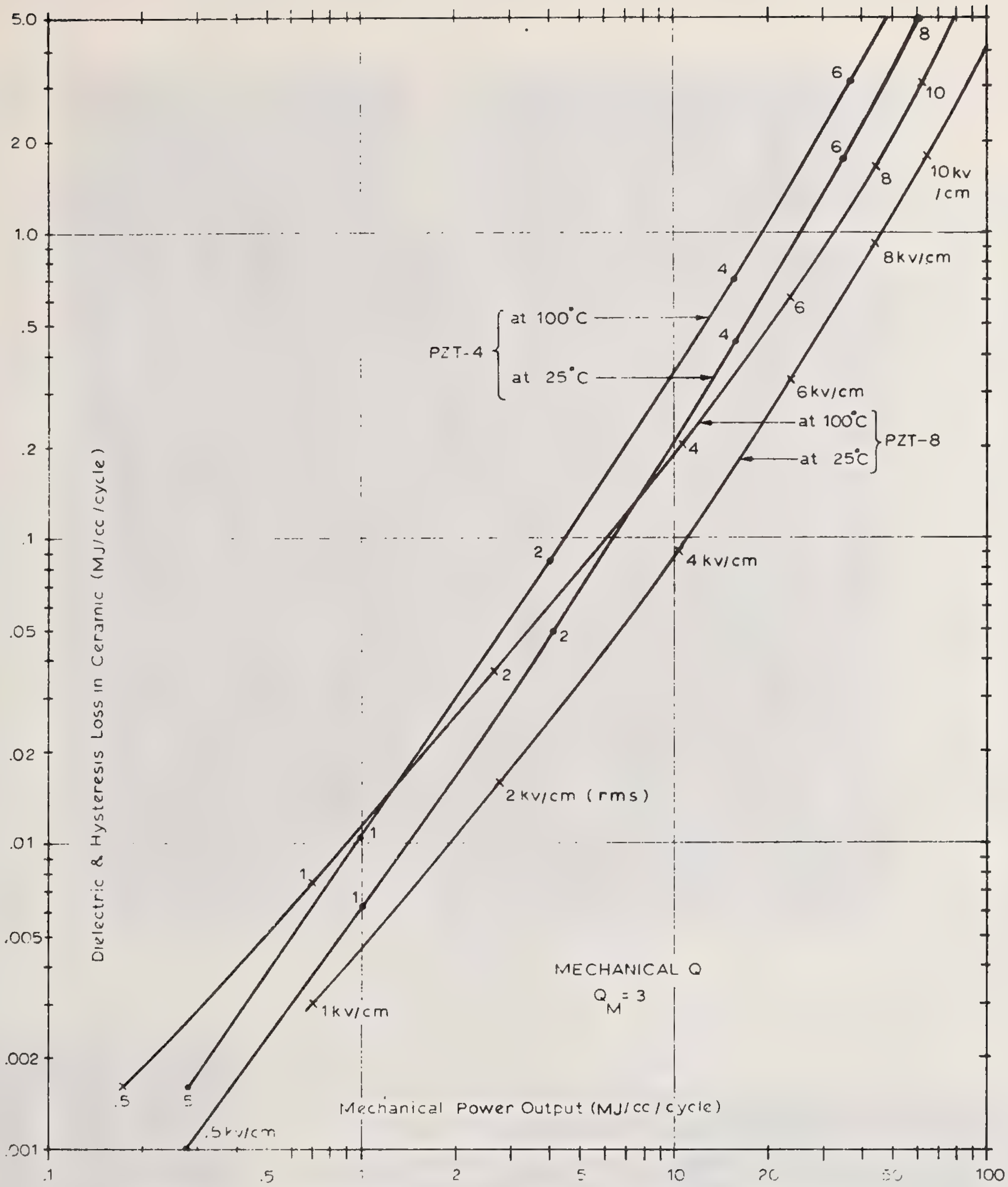

FIGURE 7. LOSS-POWER OUTPUT CHARACTERISTICS FOR PZT-4 AND PZT-8.

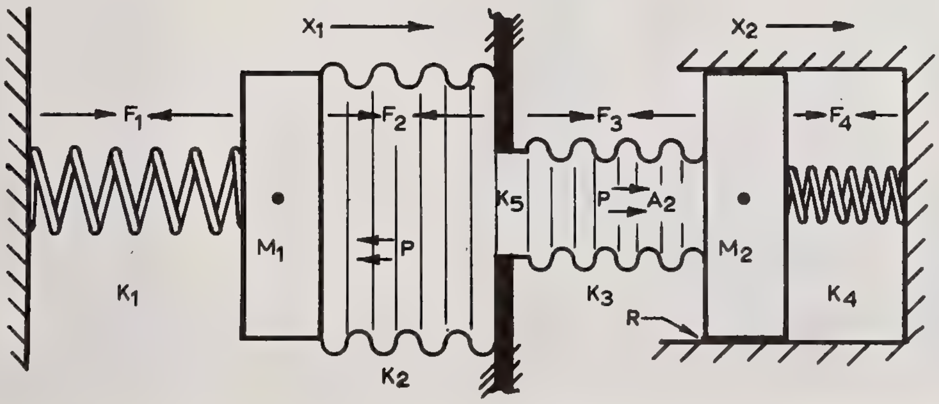

FIGURE 8. DYNAMIC MODEL OF PZ ENERGY CONVERTER.

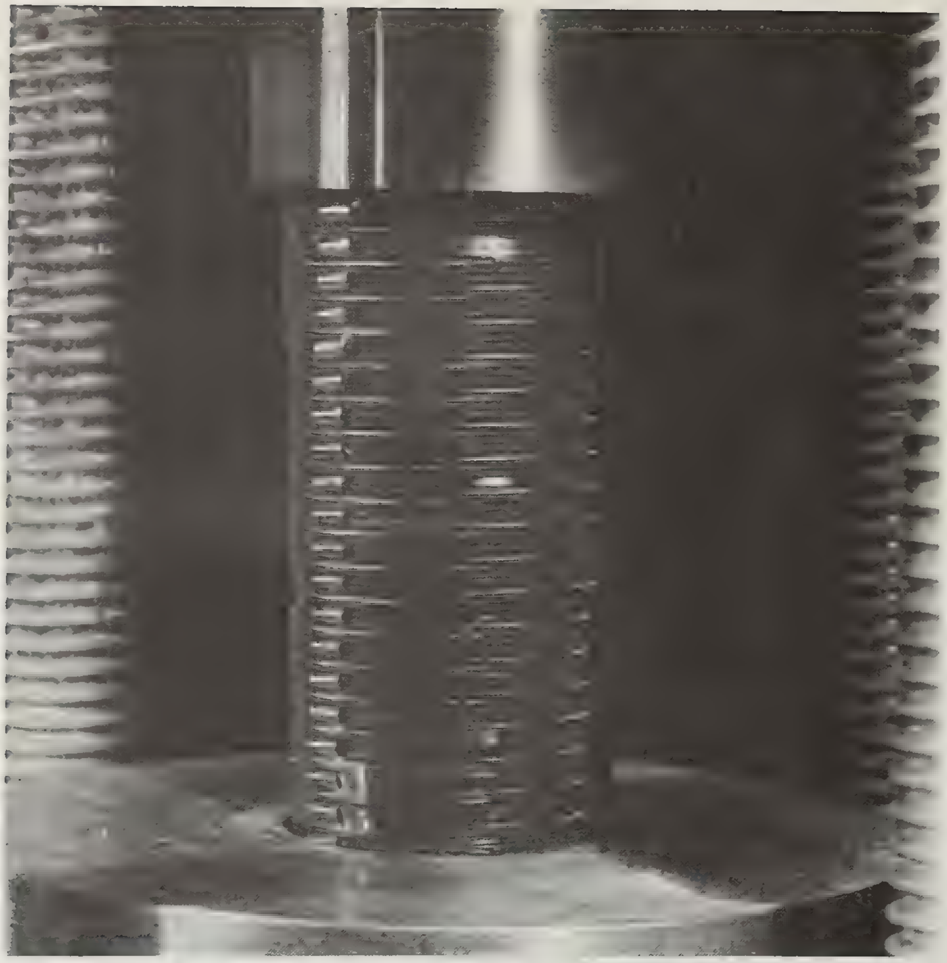

FIGURE 9. PZ STACK IN FIXTURE.

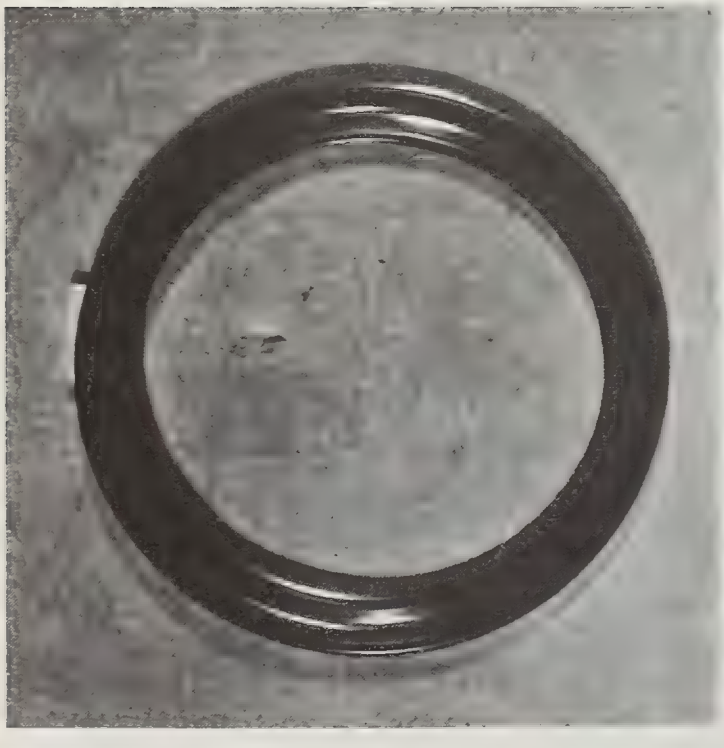

FIGURE 10. OMEGA BELLOWS.

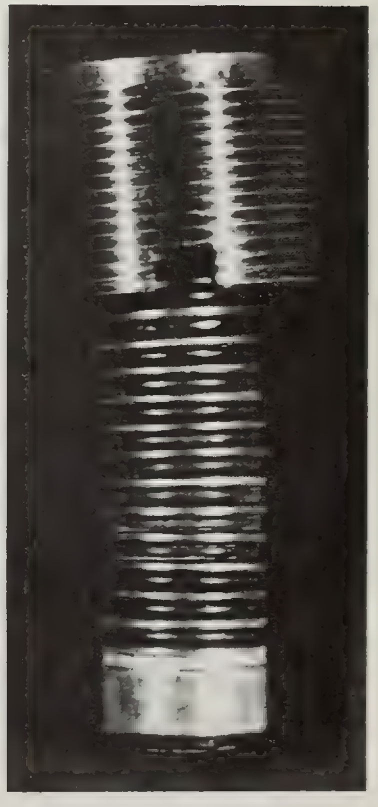

FIGURE 11. SMALL BELLOWS.

reached, which determines the upper half-power frequency, f_2. By definition the Q of the system is then:

$$Q_M^o = f_r/(f_2-f_1)$$

which represents the unloaded mechanical Q of the dynamic mechanical system. Values of Q_M^o as high as 125 have been measured for the converter shown in Figure 12 when a metal bellows has been used as the pump seal. At a loaded Q_M of 4, which is the design Q_M, an efficiency for the mechanical system of over 95% is obtained, as shown in Figure 13.

Overall electromechanical efficiencies for the system can then be determined by using Figures 7 and 13, which show that efficiencies in the 90% range are achievable throughout a wide mechanical power output range. These efficiencies correspond to shaft output efficiencies which include the mechanical friction and windage of the hydraulic pump. In addition, the low values of loaded Q provide fast response times. For example, at a loaded Q value of 4 the time required to reach 63% of full power from start is about 5 msec. As a result, these efficiency values may be compared with the overall efficiencies of high-speed rotary electric motor / centrifugal pump systems which have the capability of reaching 63% of full power from start in 5 msec. On this basis, the advantage of the resonant PZ pump system is obvious.

Performance data for the oversized PZT-4 ceramic stack, shown in Figure 12, are presented in Figures 14 and 15. Figure 14 shows the mechanical output, loss, reactive power and power factor for a loaded Q_M of 1.0. Superimposed are values furnished by Clevite Corporation for PZT-4 ceramics. Figure 15 illustrates the no-load values of loss and power factor measured on this stack. Superimposed are loss values furnished by Clevite Corporation for PZT-4 ceramics.

At loaded Q_M values higher than unity, the only increase in loss in the ceramic is that caused by mechanical hysteresis, assuming a constantly applied ac voltage. As a result, the power output and power factor increase with loaded Q_M up to the optimum loaded Q_M value, shown in Table 1.

The complete PZ converter, connected to hydraulic tubing, is shown in Figure 16. The end plug, shown at the bottom of the figure, is a retrofit bearing, which is not required in future designs.

This converter was then integrated into a complete electrical package through the combined efforts of ERG and SRI. This package, in bread board form, is shown in Figure 17. The ac/ac frequency converter, developed by SRI and shown on the left, supplies power through the transcutaneous inductive coupling, shown in front of the ac/ac converter, to the ac/dc converter, positioned to the immediate right of the ac/ac frequency converter. The ac/dc converter charges the General Electric 3-cell Ni Cd battery package, shown to the right of the ac/dc converter. The batteries supply power to the SRI dc/ac inverter, positioned to the right of the battery package. The PZ converter is shown at the far right. The two coils, positioned behind the PZ converter, balance the ac capacitive reactance of the PZ converter allowing the dc/ac inverter to deliver power at a unity power factor. The physical size of these components can be reduced considerably since no attempt was made in size reduction or packaging for these breadboard components.

A variation of the PZ converter is shown in Figure 18 in which a sleeve valve surrounds the valve galley. At pump startup, pressure is developed in the pump chambers, which rotates the sleeve valve, opening the ports to the valve galley and closing the return ports. Flow then occurs from left to right through the pump chamber. At pump shutdown, the pressure is reduced and the sleeve is rotated by the watch spring, opening the return ports and closing the ports to the valve galley. Flow then occurs from right to left through the return ports, bypassing the pump chamber. This design could be used for a passively filled assist device. However, the pressure drop through this fluid loop, consisting of the connecting tubing and converter, would be higher than that for an integral assist device and accumulator, such as represented by SRI's design described at this session and incorporated, but not shown, in the system represented in Figure 17.

Three alternate designs of a PZ converter were considered, but each have lower performance potential than the above described converter. The first alternate design is shown in Figure 19. This design represents a low-frequency valveless PZ motor with hydraulic output. The stack, hydraulic amplifier and internal housing are equivalent to that of the previous design, shown in Figure 12. A second-stage mechanical amplifier is used to achieve the necessary stroke-volume. The small bellows end-cap axially drives the end plate which in turn radially drives the pumping plates by flexing the flex strip. The pumping plates, aligned circumferentially, displace the fluid contained in the pumping chamber. The Bellofram (1) seals and the elastomer pumping plate seals (not shown) provide the flexible seals for the pumping chamber. The fluid, displaced by the pumping plates, cyclically drives a hydraulically coupled blood pump that is connected to the fluid port.

A valveless, high-frequency travelling wave pump is shown in Figure 20, consisting of circular PZ bimorph rings which are sequentially energized to produce a peristaltic action in the tubular flexible liner attached to the bimorphs. Bidirectional fluid flow is achieved by switching the electrical phasing of the bimorphs. The performance potential of the unit is comparable to other PZ bimorph pumps. The elimination of valves simplifies the design and allows higher frequency operation without the concomitant flow losses of a pulsatile output bimorph pump. However, the performance potential of PZ bimorphs is grossly less than that of PZ stacks and therefore reduces the practicality of this design.

A PZ motor with mechanical output is shown in Figure 21. This design employs a second-stage hydraulic amplifier to achieve the necessary amplification. The other components are similar to the design of the hydraulic pump shown in Figure 12. The output piston can be attached to either a bellows-sealed hydraulic transfer piston, which drives a suitable blood pump through hydraulic coupling, or to a mechanical drive that directly actuates a blood pump.

---

(1) Bellofram Seal Company.

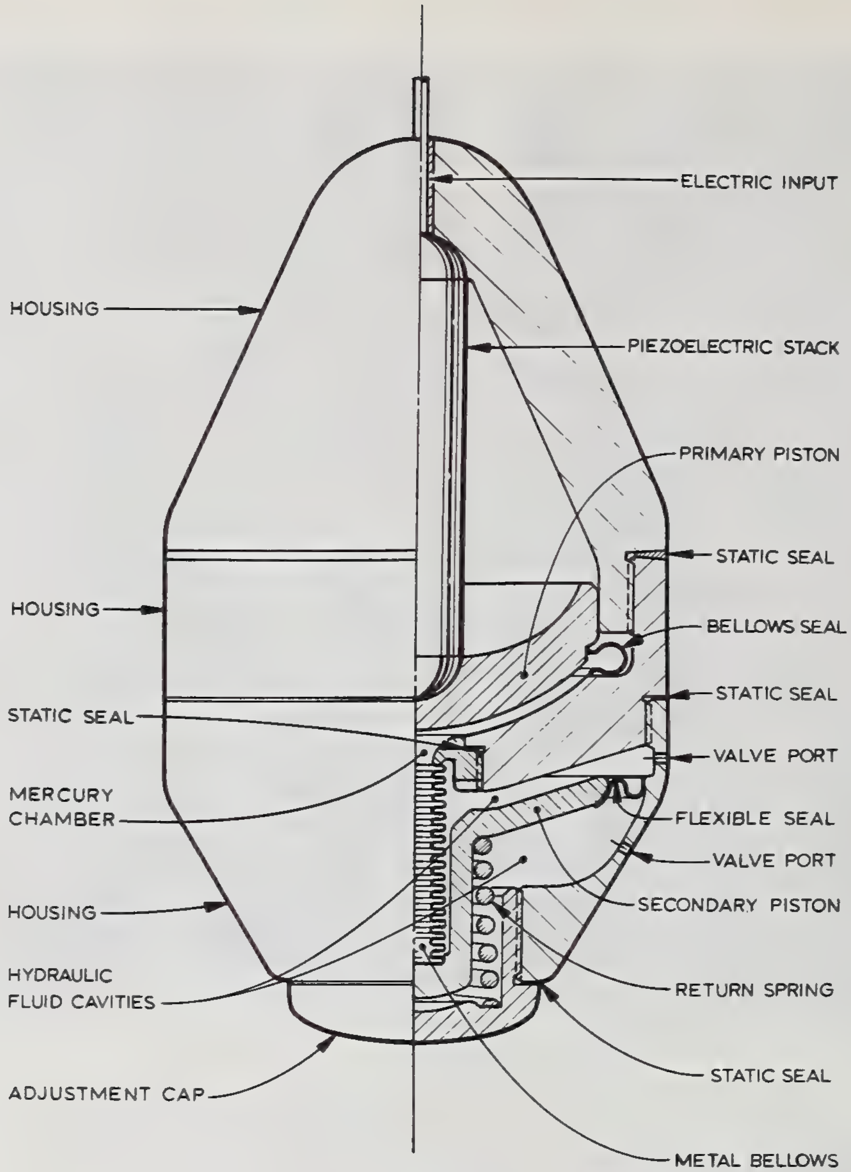

FIGURE 12. PIEZOELECTRIC MOTOR WITH DOUBLE ACTING PUMP.

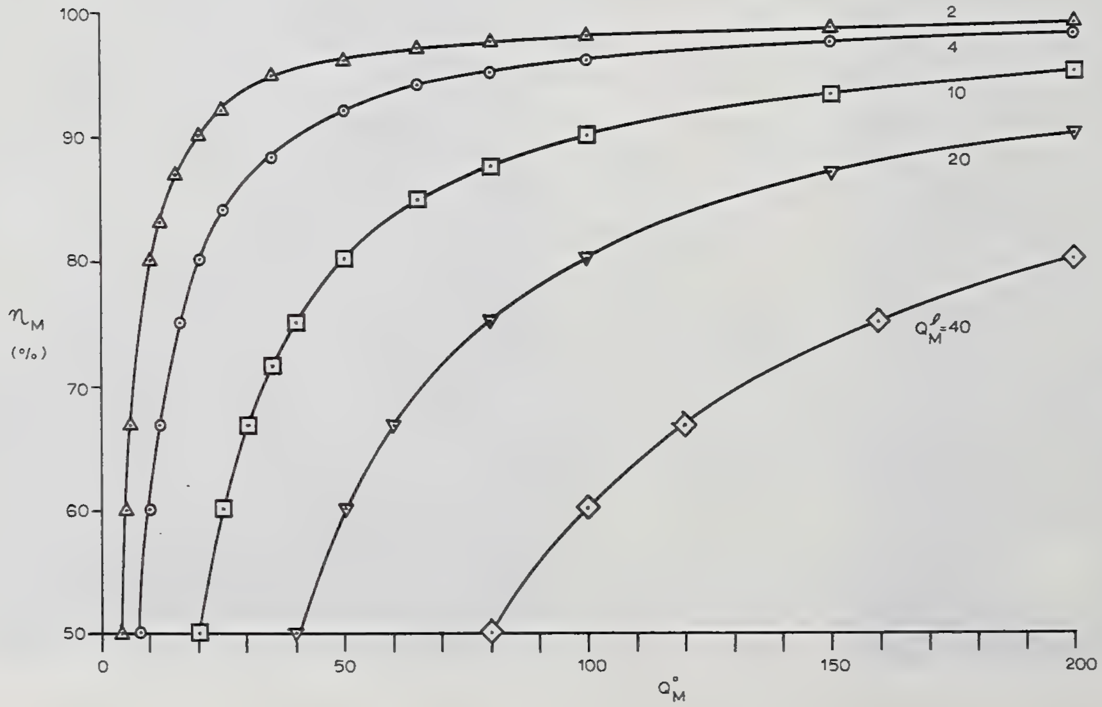

FIGURE 13. MECHANICAL TRANSFORMER EFFICIENCY.

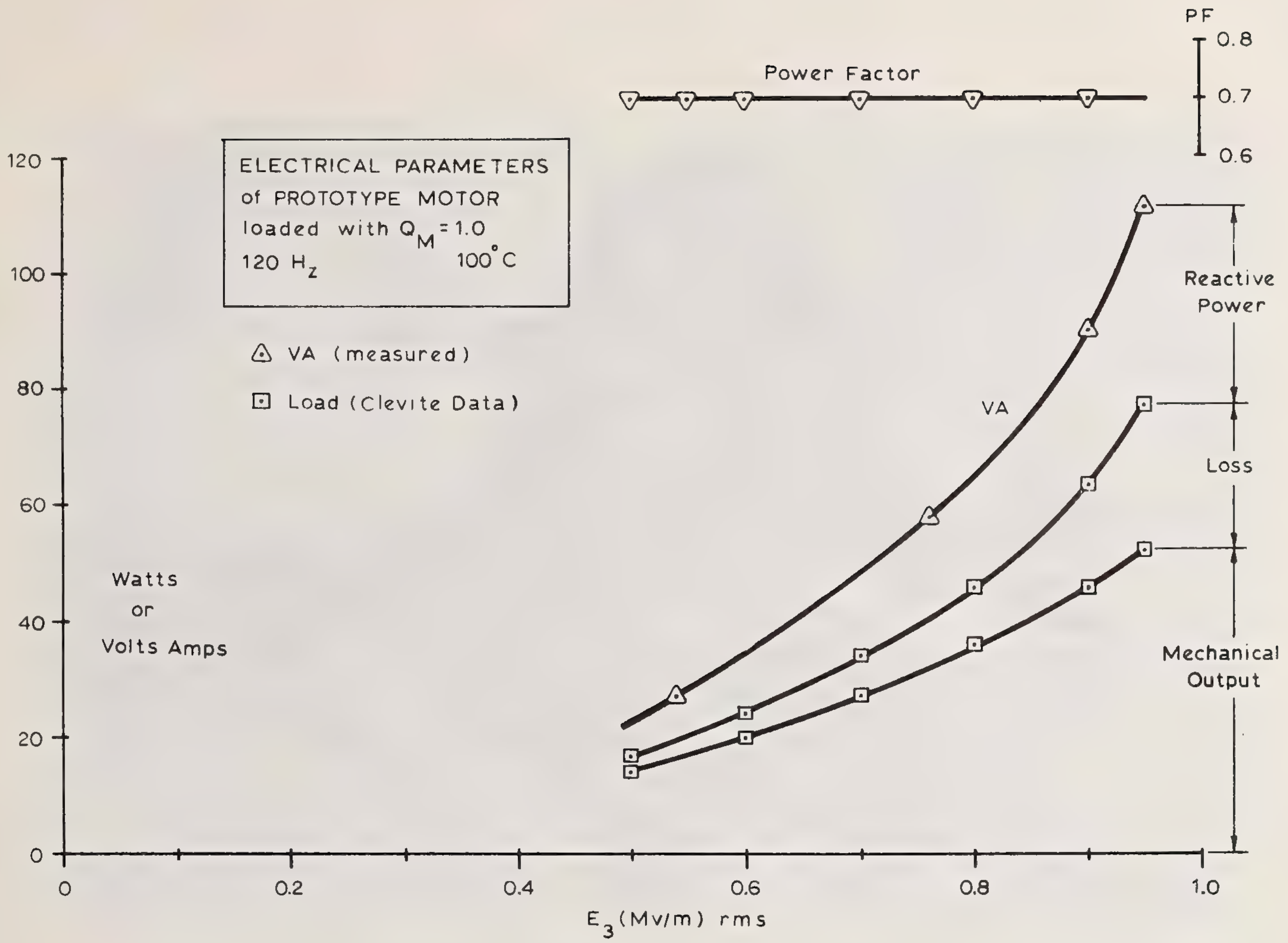

FIGURE 14.

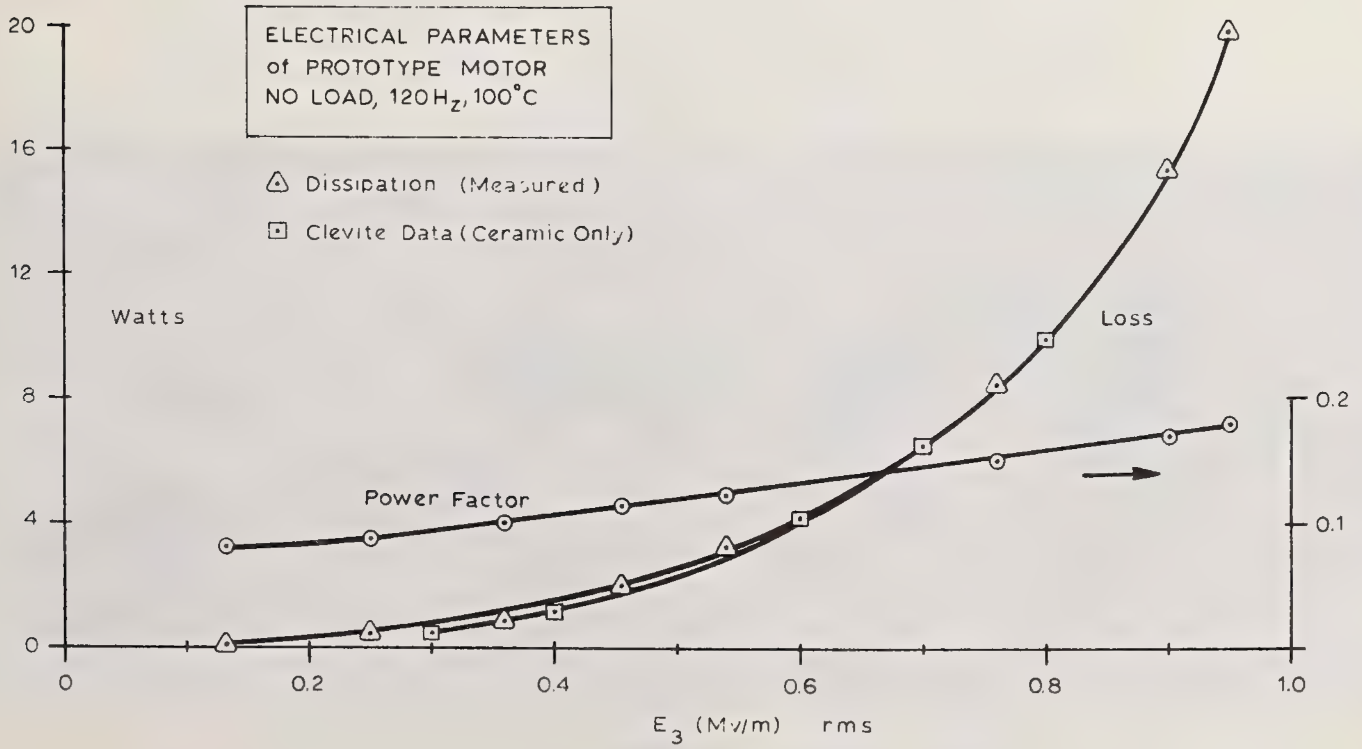

FIGURE 15.

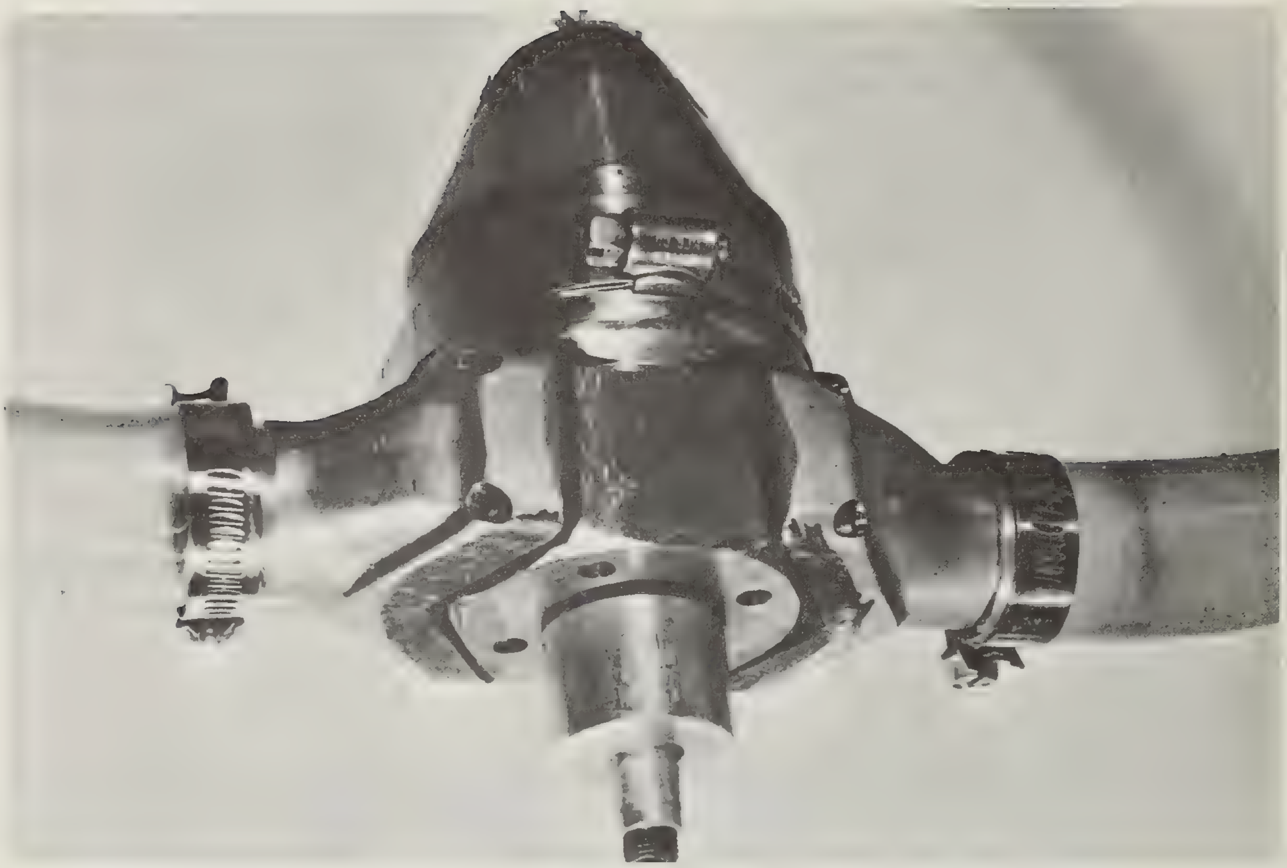

FIGURE 16. COMPLETE PZ CONVERTER, CONNECTED TO HYDRAULIC TUBING.

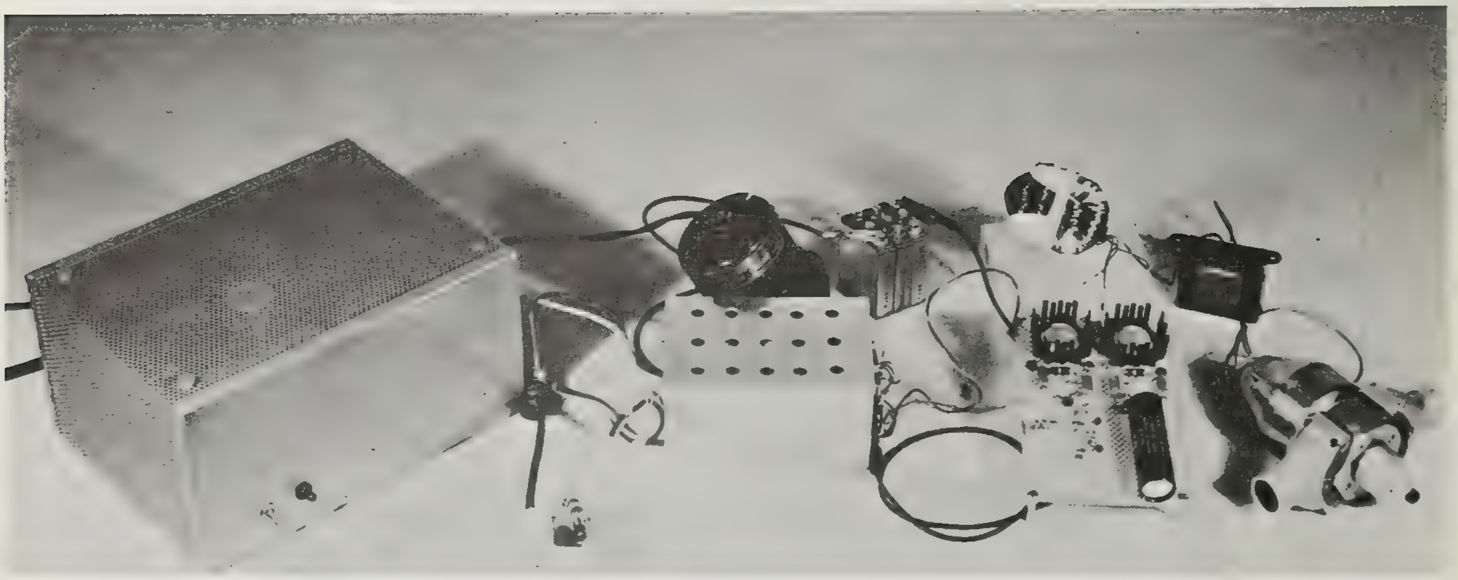

FIGURE 17. CONVERTER INTEGRATED INTO A COMPLETE ELECTRICAL PACKAGE THROUGH THE COMBINED EFFORTS OF ERG AND SRI.

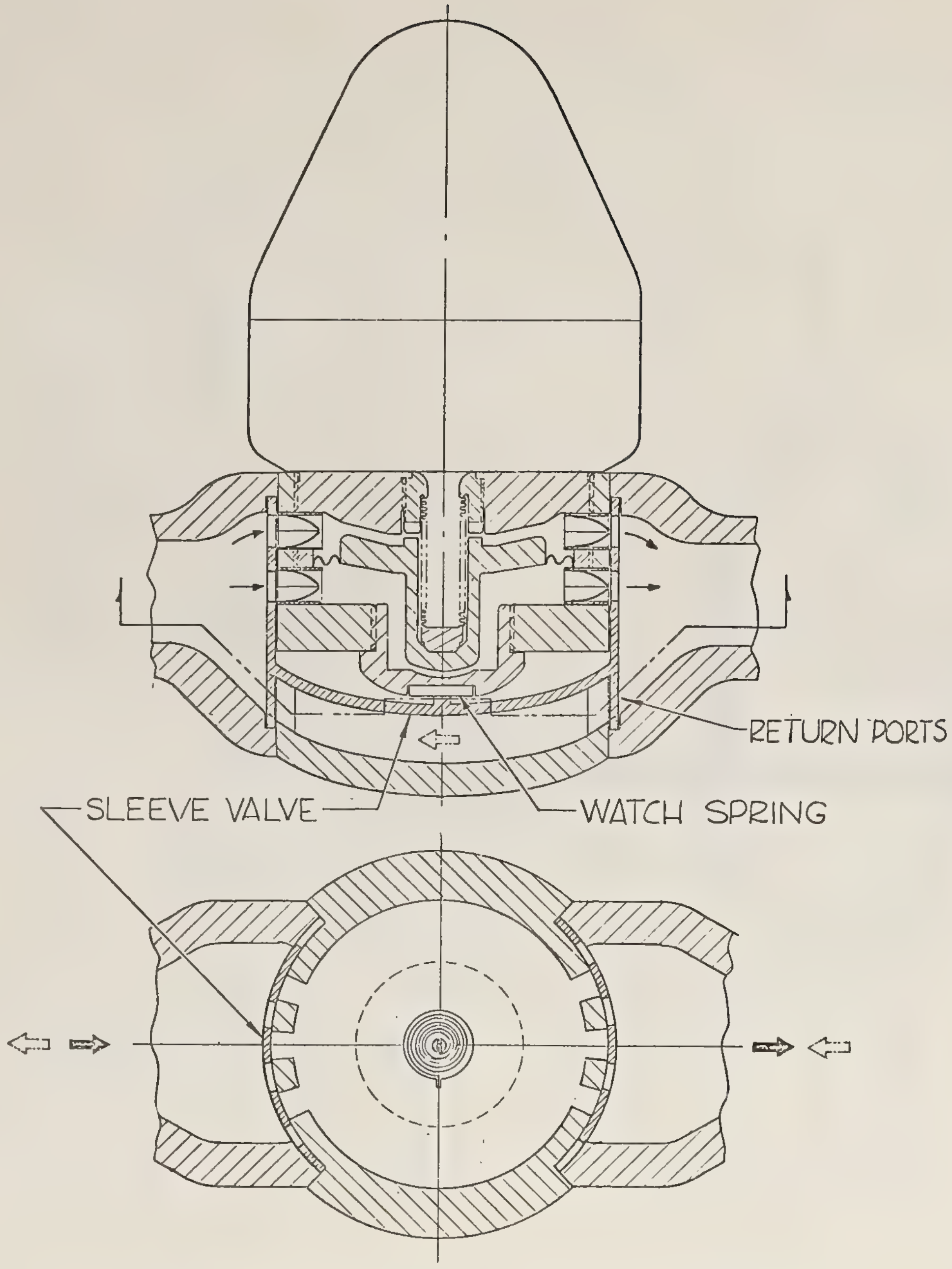

FIGURE 18. SLEEVE VALVE ON PERIPHERY OF PZ PUMP.

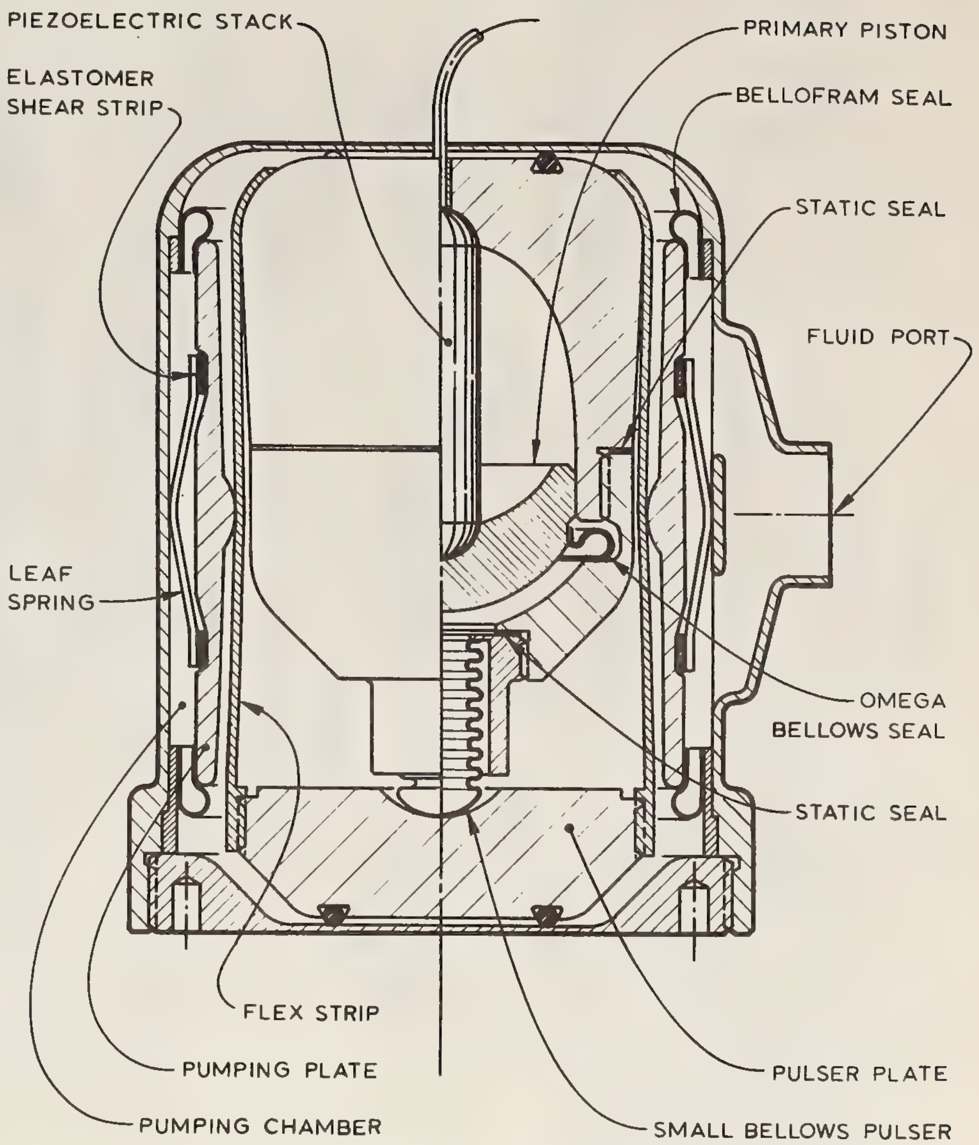

FIGURE 19. LOW FREQUENCY VALVELESS PIEZOELECTRIC MOTOR.

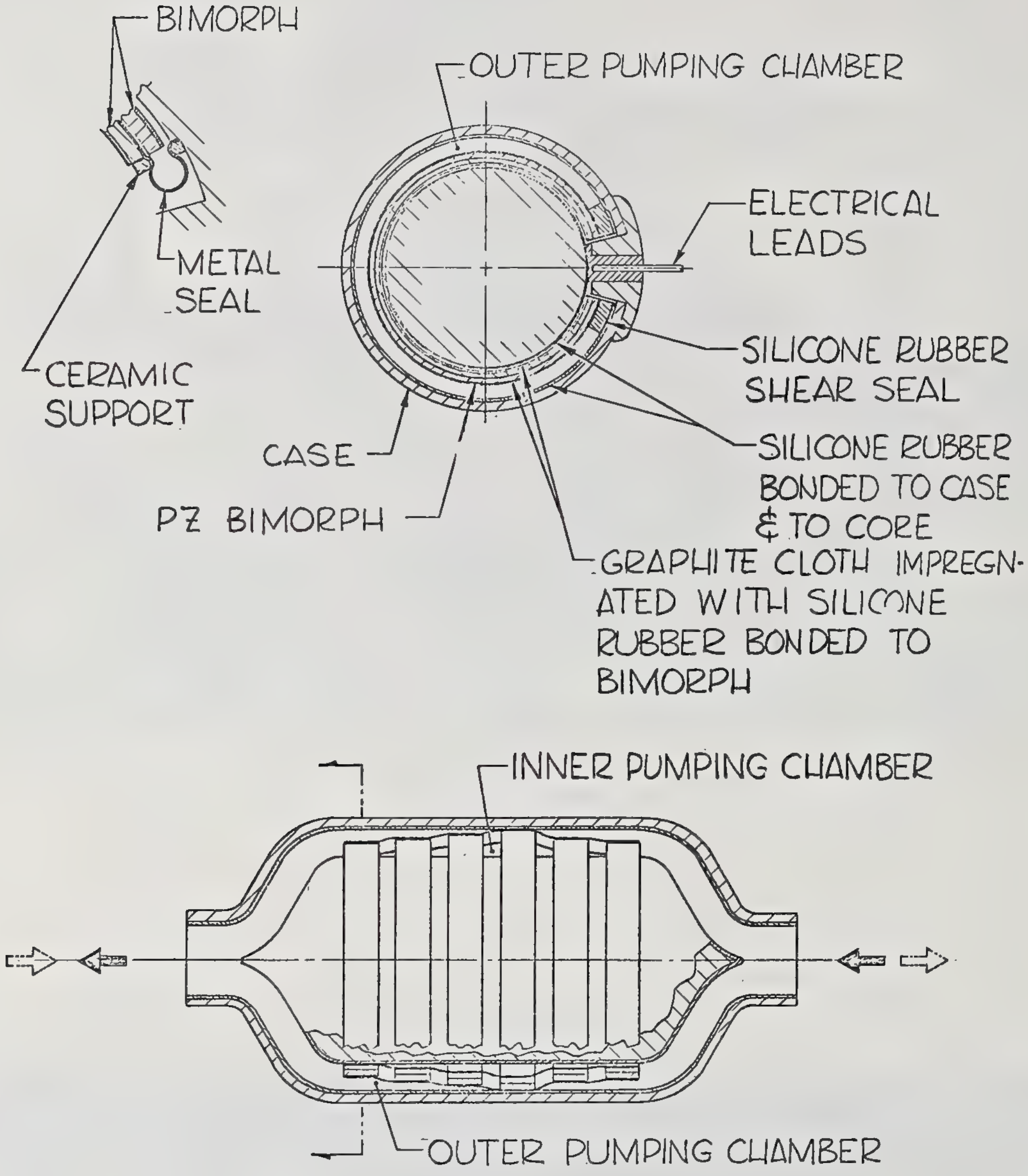
BIMORPH
OUTER PUMPING CHAMBER
ELECTRICAL LEADS
METAL SEAL
CERAMIC SUPPORT
SILICONE RUBBER SHEAR SEAL
CASE
SILICONE RUBBER BONDED TO CASE & TO CORE
PZ BIMORPH
GRAPHITE CLOTH IMPREGNATED WITH SILICONE RUBBER BONDED TO BIMORPH
INNER PUMPING CHAMBER
OUTER PUMPING CHAMBER

Fig. 20

VALVELESS
TRAVELLING WAVE PUMP

FIGURE 20. VALVELESS TRAVELLING WAVE PUMP.

CONCLUSION

Theoretical and experimental data obtained during this program demonstrate the marked performance advantage of hard ceramic piezoelectric materials, particularly PZT-8, which are arrayed in stacks formed from thin discs and connected mechanically in series and electrically in parallel, and operated in mechanical and electrical resonance at a frequency determined by the mechanical reaction of a stroke amplified piston and bias spring that are coupled by mercury filled metal bellows to the PZ stack. A PZ converter incorporating this principle was designed, tested and integrated into a breadboard artificial heart system. Performance data indicate that a high-frequency (100-200 Hz) PZ converter may be reduced in size to that of a large chicken-egg and produce low-pressure fluid power at flow rates up to 30 liters/min. at overall efficiencies of 60-90% depending on load and pump design. Alternate designs of PZ converters were presented including peristaltic pumps and mechanical drivers for blood pumps. On the basis of these results, further development appears justified and necessary before a final assessment of the applicability of PZ energy converters to the artificial heart program can be made.

REFERENCE

1. Final Report on Contract PH43-67-1409: Piezoelectric Motors as Implantable Energy Converters for Circulatory Assist Devices, Dr. Glendon Benson, February 1969. In Preparation.

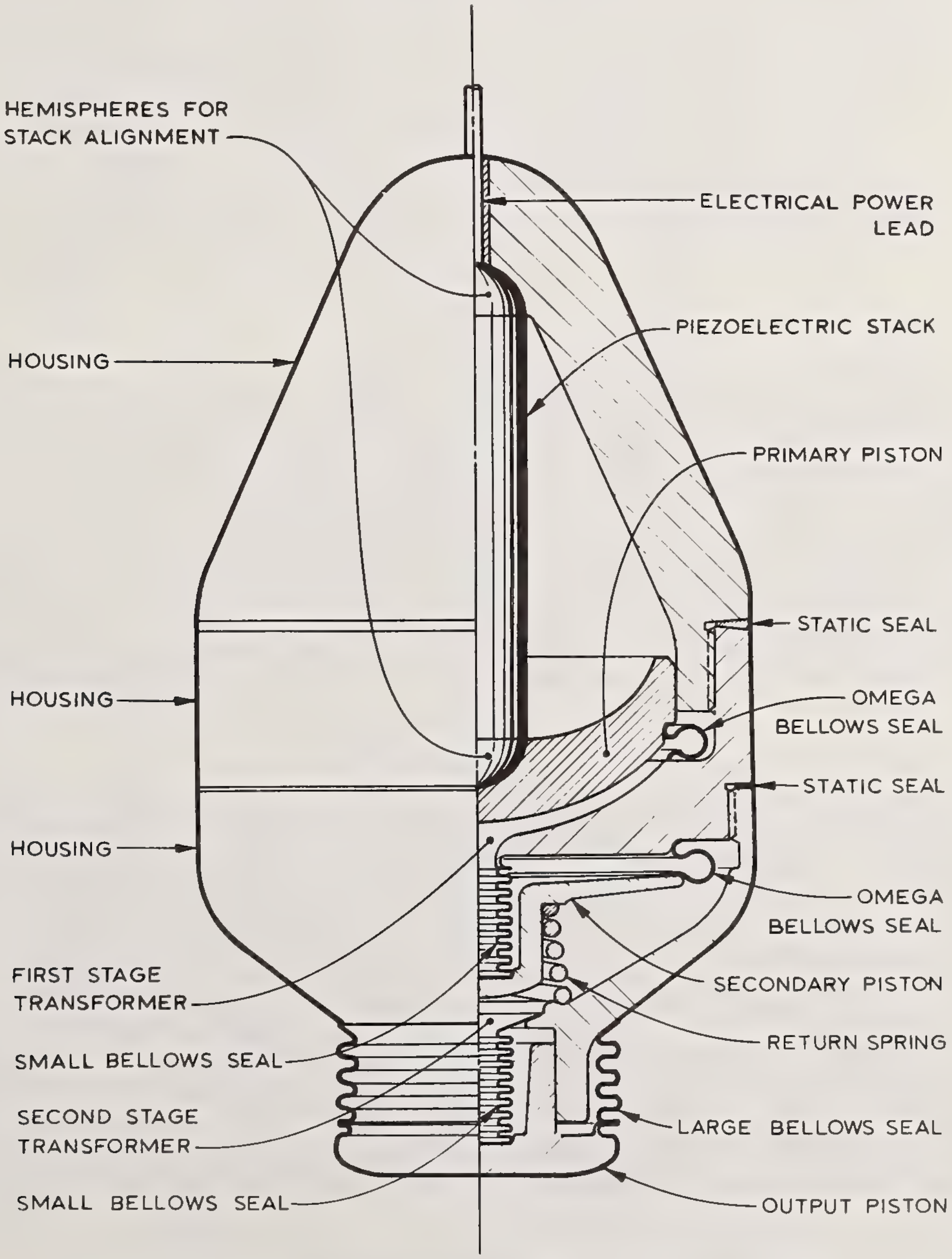

FIGURE 21. PIEZOELECTRIC MOTOR WITH MECHANICAL OUTPUT.

CHAPTER 85

HIGH FREQUENCY PIEZOELECTRIC MOTOR PUMP FOR IMPLANTED ENERGY CONVERSION

L. Heimlich, P. Knerr, B. Hanson, R. Colville and H. Chalifoux

Biomedical Systems Department
Hamilton Standard
Division of United Aircraft Corporation
Farmington, Connecticut

The high frequency piezoelectric energy conversion unit provides a unique approach to converting electrical energy into hydraulic energy suitable for use with implantable bladder-type heart assist devices. The unit derives its hydraulic output from a single piezoelectric bender which is coupled with high frequency electroviscous valves. Flow is provided by the continuous summation of the incremental volume displacements of the piezoelectric bender through "check-valve" operation. The driving element of the energy conversion unit is a single piezoelectric bender which oscillates at frequencies of 100 to 200 Hz. When an AC voltage is applied to the bender, the bender flexes, producing small spherical volume displacements. The high frequency check-valve function utilizes the electroviscous valves and fluid. Electroviscous effects can be defined as reversible changes in the apparent viscosity of a fluid when it is subjected to an externally applied electric field. The fluid is basically a dispersion of silicon dioxide in a mineral oil base. The valves are plate grid structures which are placed perpendicular to the direction of flow. Upon the application of an electrical field the fluid gels, and a "no flow" fluid condition is obtained. The development of the pump is presently being pursued at Hamilton Standard, and it is being evaluated for use as an implantable unit. The energy conversion unit will be used in conjunction with other subsystems designed to transfer electrical energy across intact skin as a total energy system.

INTRODUCTION

The intent of this report is to describe the accomplishments and the work performed on the Energy Conversion System from June 1968 up until the present. Described briefly are the program objectives followed by a description of the present system and subsystems. Following this, the accomplishments of the program and the anticipated activities are presented.

It is the purpose of the Hamilton Standard Energy Conversion System to provide conversion of electrical energy into hydraulic energy suitable for use with one or two artificial ventricles. The system uses as a pump drive a piezoelectric bender or disc, valving is accomplished by using high frequency non-mechanical electroviscous valves. These components will be discussed later.

It is the main objective of the present program to design, fabricate and develop a partially implantable energy conversion system, where the pump is implanted and the electronic controller is extracorporeal. This effort entails continued design and testing of the system's components e.g. benders, valves and housing. The goal of our present effort is to develop a partially-implantable system which can pump a peak flow of 20 liters per minute against 4 pounds per square inch, with an overall efficiency of 30%.

EXPERIMENTAL

The concept features the use of a single piezoelectric bender electrically driven at frequencies in the range of 100-300 Hz and which create displacements on the order of 0.2 ml. These small volumes are summed or captured over a given period of time by means of the high-frequency electroviscous valves. Since the bender can flex in two directions, it may be used as a double-acting pump. Figure 1 is a schematic of the system. The "LEFT" and "RIGHT" connotations refer to left and right hydraulic receivers at which point the hydraulic energy conveyed by electroviscous fluid is transferred to the blood. The interface between the blood and electroviscous fluid is a compatible collapsible member. The action of a complete pump cycle is to alternately exert positive pressures on each side so that blood is pushed through the hydraulic receiver. When the bender is deflected downward, electroviscous fluid is forced out through the bottom valve to the right hydraulic receiver. At the same time, fluid is drawn into the pump through the top left valve from the left receiver. In the next cycle, (Figure 2), the effect is to keep moving the fluid from the right receiver to the left one: the bender deflects upward, forcing fluid out through the top right valve, again to the right receiver and in through the bottom left valve again from the left ventricle. This flexing and valve switching occurs on the order of 100 times over a period of approximately 0.5 seconds. After a half a second, the controller logic changes the sequencing of the valves so that

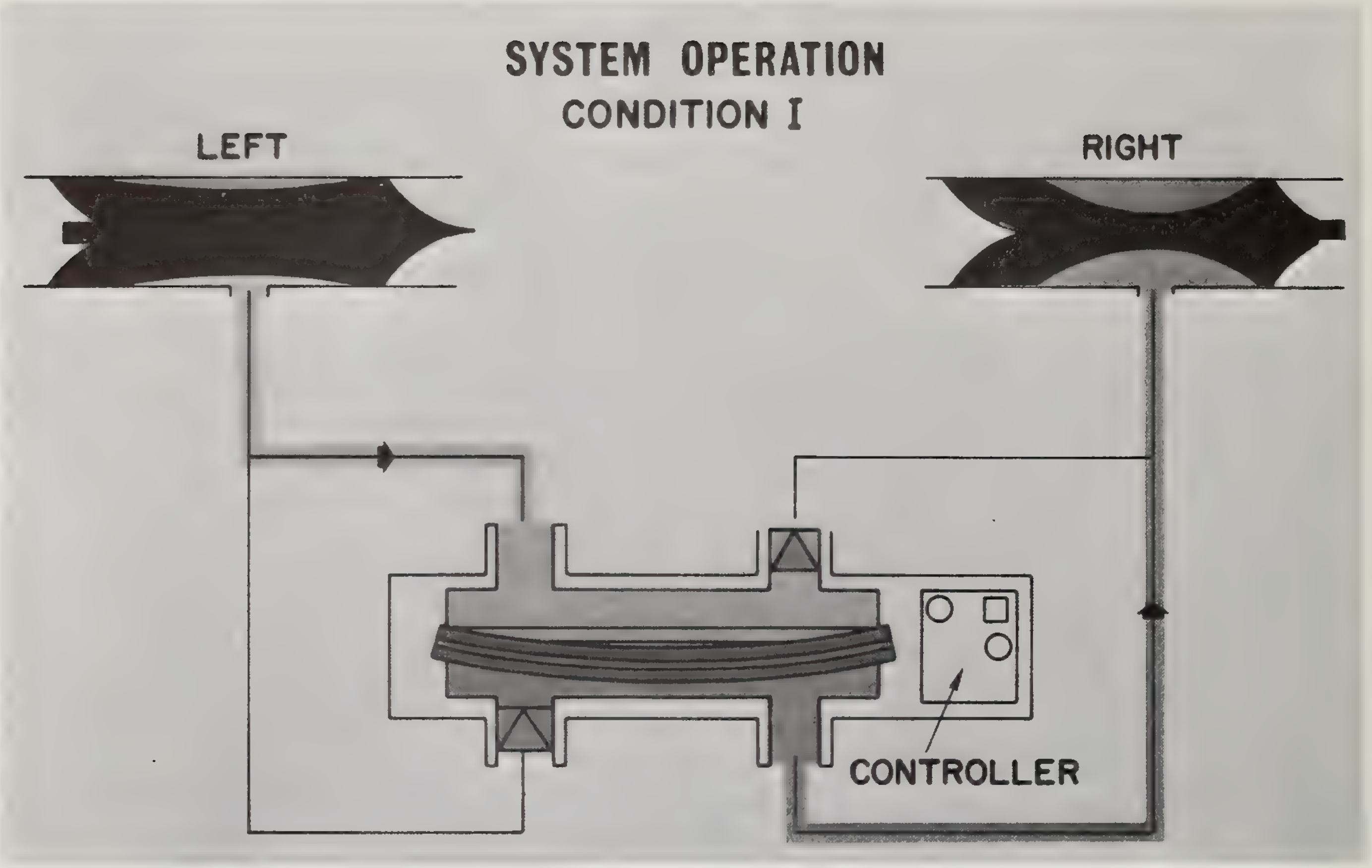

FIGURE 1.

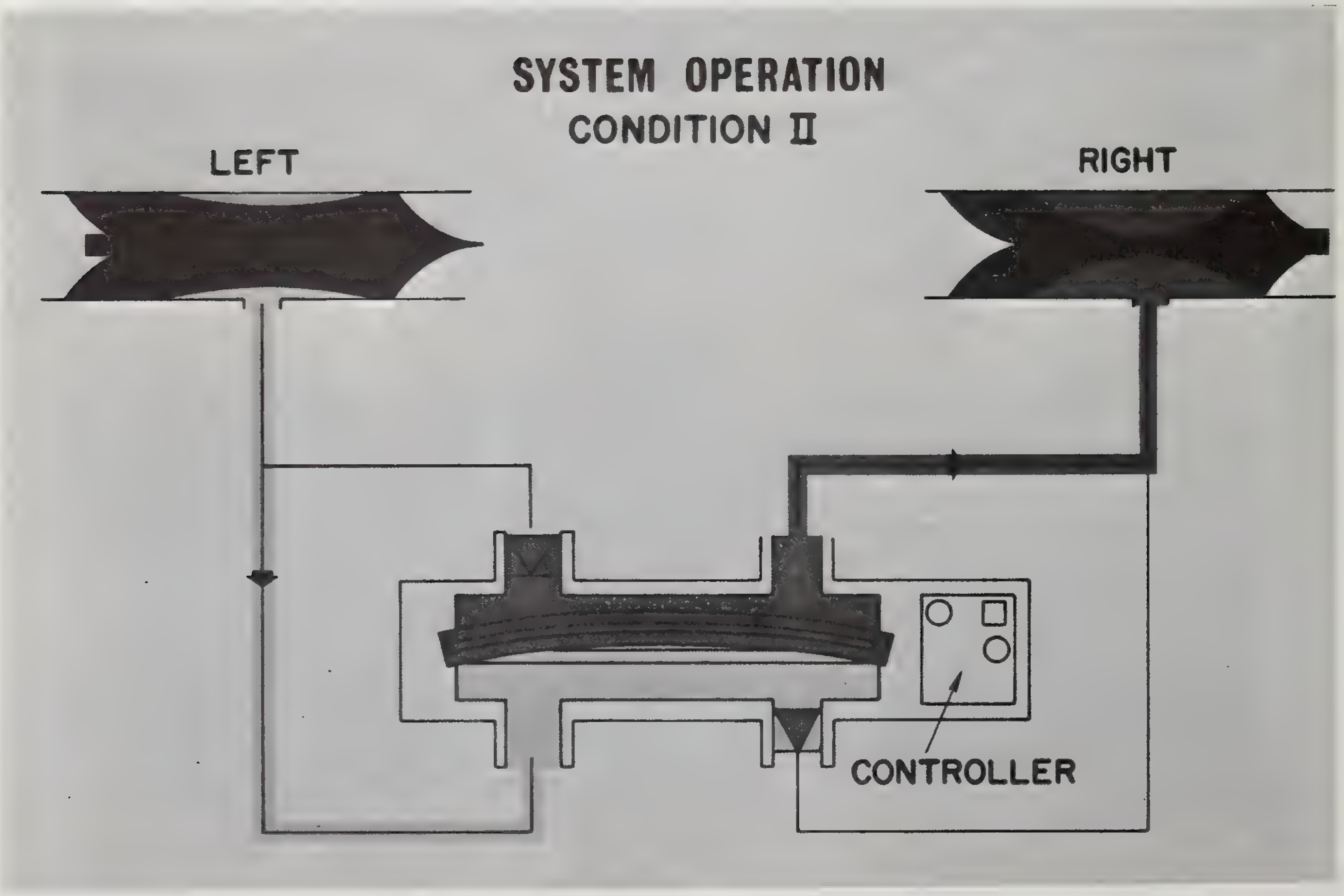

FIGURE 2.

fluid is transferred from the right side back to the left side. The bender is 3 inches in diameter and approximately 60 mils thick. The material is lead zirconate/lead titanate. The usual frequency of operation is between 100 and 300 Hz at several hundred volts.

The electroviscous fluid used with the valves consists of finely divided non-magnetic particles suspended in a high-dielectric vehicle. When a potential on the order of 2000 volts is applied across the fluid the viscosity increases, to the point where a flow of this fluid will be stopped. The first electroviscous valves (Figure 3) consisted of 3, 4.5 mil thick grids. Figure 3 actually shows 2 valves which could either be housed below or above the bender. One can be considered an outlet valve while the other is an inlet valve. Flow of the fluid is perpendicular to the plane of the valves and is parallel to the direction of the electric field between the 3 layers of grids. Although the valve which was manufactured under contract to us proved to be inefficient because of the grids' flexibility, it allowed us to gain experience and knowledge in an area in which published data was at a minimum. As a result of our experiences with this valve, we gained the capability to improve upon the design and manufacture of new valves at Hamilton Standard.

The design and operation of the system calls for a trade-off among numerous parameters such as materials, dimensions, frequencies, voltages, masses, etc. This effort consumes a significant number of man-hours. In an attempt towards simplifying the design procedures, we have computer programmed a large percentage of the system's equations which is designed to be used to predict and analyze performance.

The electroviscous fluid used throughout the program has remained a problem. The manufacturer of the fluid has stopped sales of it until they can resolve their own difficulties. In face of this, we have produced our own electroviscous fluid. The limited testing performed on it has increased the confidence that we have the capability to develop fluids in accordance with a tailored specification.

As a means of objectively testing valves, we have developed a bender simulator which is an electromagnetically driven positive displacement piston. The bender simulator was designed and built so that the electroviscous valves could be dynamically tested in an environment away from the bender. The simulator has the capability so that the amplitude and frequency of operation can be varied to realistically reflect the bender-operating parameters.

Our primary accomplishment within the past year has been to design a system capable of producing usable flows and pressures. The system which contained the grid valve was only capable of producing (single-acting, i.e. using only one-half of the pump) 0.8 lpm at 0 back pressures. The flow decreased to zero when the back pressure was increased to 0.5 psi. One of the main reasons for this marginal performance was the valve's flexibility and leakage. After a study of these problems, a new configuration was attempted. Figure 4 is a photograph of the latest electroviscous valve configuration. Its main components are the annular rings or washers. Flow comes up through the center of the valve and out through the spaces between the washers. The electrical field is between successive washers. The black rubber output ports are flexible and elastic enough to permit decoupling of the output fluid. These enabled us to operate at a higher frequency than without these decoupling devices. Before this, the more fluid within the system, the lower the resonant point and hence the lower the frequency of operation. The annular structures provided increased rigidity. The flow path was now perpendicular to the apparent direction of the field whereas in the previous valve, it was parallel. There is some argument among theorists as to what the orientation of the field to the flow should be for optimum performance. In any event, we have made significant improvements in the system's performance. The resonant frequency of the bender, the point at which we operate, was increased from approximately 100 Hz to approximately 250 Hz. Flow at zero back pressure was increased from 0.8 lpm to 1.2 lpm, and the back pressure capability was increased from 0.5 to 3.9 psi again when only 1/2 of the pump was being used. After studying the results of the testing performed on this valve, it was resolved that the flow was not greater because of the large pressure drops at the inlet and outlet ports. These large drops were caused in part by an unanticipated fluid viscosity. After studying the design parameters, it was realized that the viscosity was actually much higher than the value in the manufacturer's specification.

As a means of improving the performance of the 3-inch system, we proceeded to fabricate another valve configuration. This one combines the rigidity and field/flow orientation of the valve just discussed but will not have the large pressure drops encountered with this last valve. The valve will be a horizontal series of stainless steel slabs with the flow going between slabs and the impressed field across successive ones. It is expected that the zero back pressure flow will be increased from 1.2 lpm to approximately 4.5 lpm. The improved performance will also result from changing the valve "on" and "off" times. This will be done so that when bender begins to flex, the valve will remain closed until such time as when the fluid inertia is overcome. Secondly, it will reduce any back leakage into the area below the valve.

CONCLUSION

Up to the present we have experimented with 3-inch bender diameter systems. At the beginning of the program, this was the largest size readily available. It has been calculated that a system this small does not have the inherent capability to produce the desired flows and pressures. The 3-inch benders were useful to study the operation of the bender in our system and to gain experience in handling them. Presently under construction is a 5-inch piezoelectric bender which is also thicker. It is expected and has been realistically calculated that a double-acting system with the 5-inch bender drive will be capable of producing the desired flows and pressures. In addition, a larger valve is planned. This valve will represent the best aspects of all previous valves.

Each of the valves and benders will be component-tested to establish their objective performances. More significantly, it is being planned to develop our own fluid. This fluid will be designed to accommodate our specific needs. It is felt that knowledge of the fluids remain as the last unknown to be explored and that as a result of our present progress, this obstacle is not insurmountable.

DISCUSSION

DR. KENNEDY: What is the anticipated effect of the electroviscous valve upon the formed elements of the blood?

DR. HEIMLICH: It does remain one of the unexplored areas. The actual valve won't come in contact with the blood. The thing that has not been explored though is the field effect on the blood.

DR. ZACHARY: How do you plan to balance the flow between the two fluid circuits of the body? In your diagram the same quantity of fluid is pumped each artificial ventricle.

DR. HEIMLICH: In the actual application, there will be a hydraulic reservoir between the two sides. This would be the ideal case in which we are using the system, double acting, with two blood pumps. It is something we plan to do in the future. But it will be necessary to have a reservoir to control the flow to each ventricle.

DR. JONES: Did you say that you plan to pump the left and right sides alternately.

DR. HEIMLICH: Right, in a typical pulsatile action of total heart replacement.

DR. JONES: In the natural state the right and left ventricles contract simultaneously. How do you intend to adjust to this fact?

Clarification added in proof: The speaker referred to the two artificial chambers as "ventricles"; this confused the audience since they considered them to serve the same function as the natural ventricles, when, in fact, they are hydraulic receivers.

DR. STAPELFELDT: Would you please discuss the electrical drive requirements of the electro-viscous valve. How much energy is required for its actuation?

DR. HEIMLICH: On the first valve which I showed you, each valve required about 1.2 watts of power to operate. On the last valve that I showed you, we haven't measured the power consumption as yet.

DR. STAPELFELDT: Could you give us an idea of the electrical equivalent circuit of the valve? To what extent is it resistive and to what extent reactive?

DR. HEIMLICH: It would be capacitative.

MR. SIPIN: One of the existing problems with the electro-viscous fluid has been its high viscosity and instability. What are your plans for developing the fluid to minimize these problems?

DR. HEIMLICH: This is something that we have planned to study in the future; the problem of the silica gel settling out. The fluid we have used to date is silica dispersion in mineral oil, and we have had problems with this settling out. We do plan to develop it further in the future so that we will not have this problem.

MR. SIPIN: Do you have any idea of the approach that you will take to develop a more stable and less viscous fluid?

DR. HEIMLICH: It would be premature to speculate at this time on the method we plan to use.

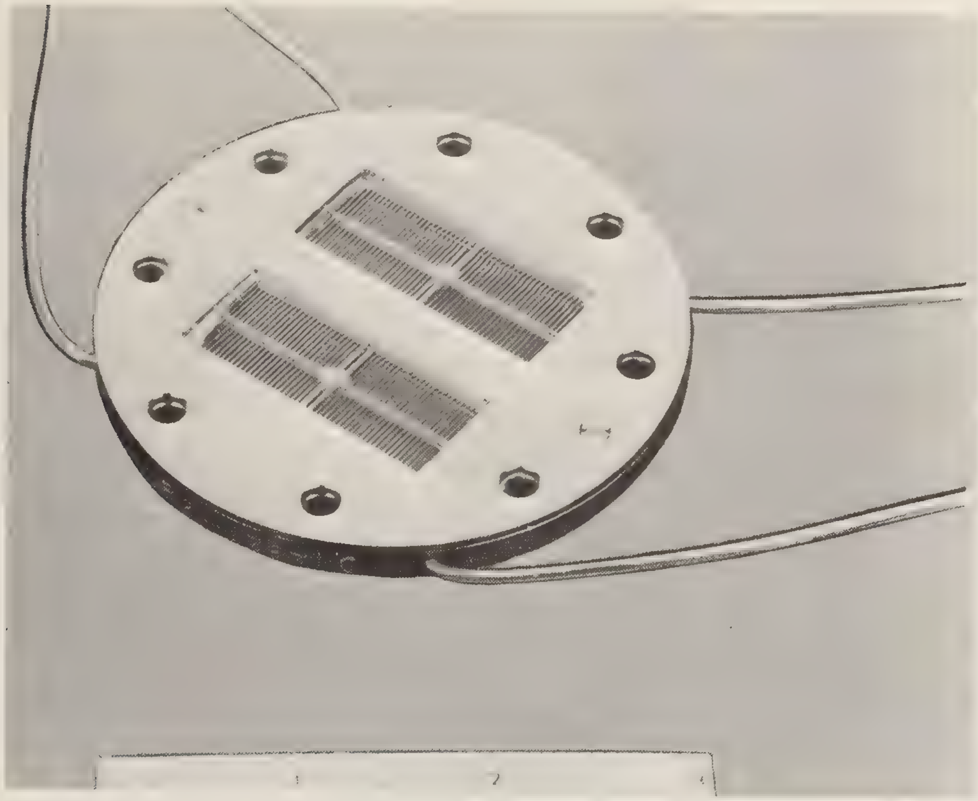

FIGURE 3. ELECTROVISCOUS VALVE.

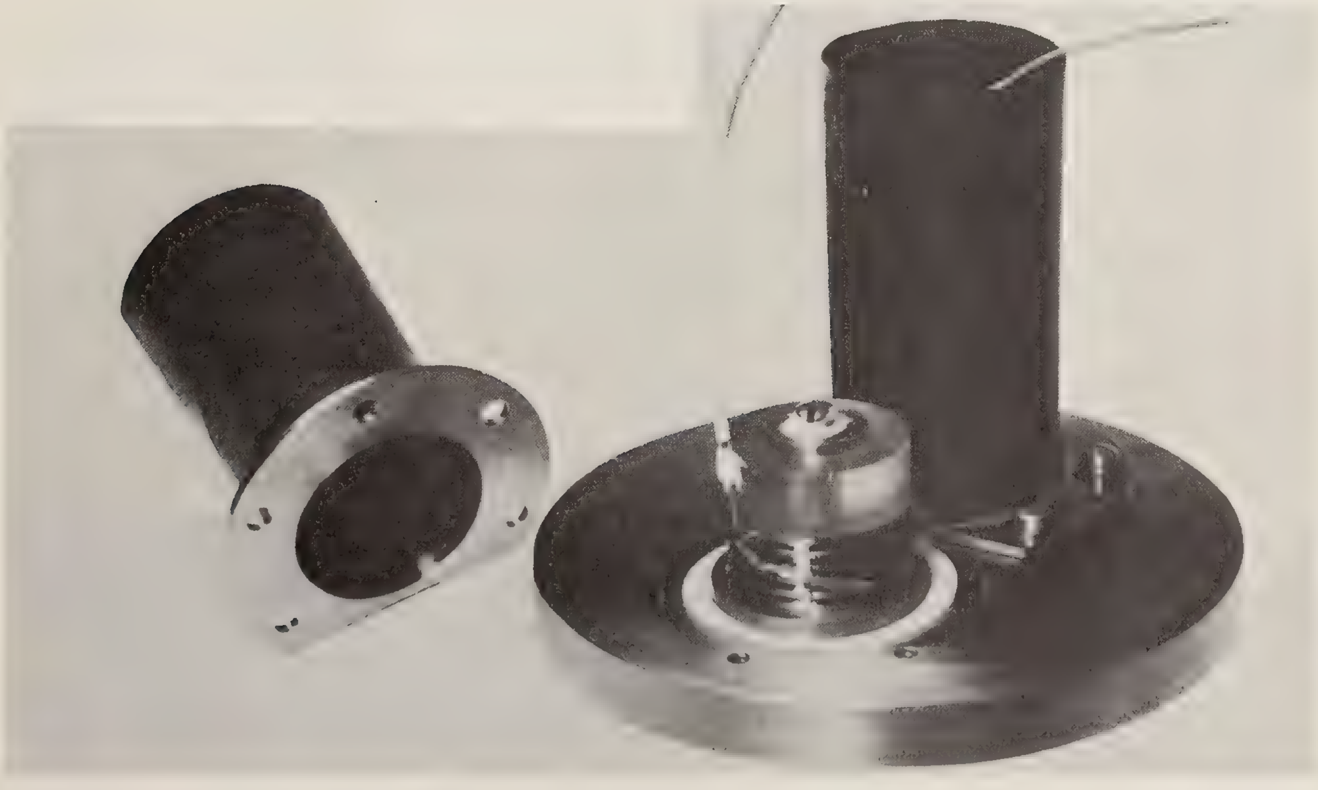

FIGURE 4. ELECTROVISCOUS TEST VALVE.

CHAPTER 86

INTERNAL ENERGY STORAGE FOR CIRCULATORY ASSIST DEVICES

R. Hamlen, E. Siwek, G. Rampel,* and L. Wechsler+

General Electric Research and Development
Schenectady, New York

Nickel-cadmium batteries offer the capability for sealed isolated operation for prolonged periods. However, at elevated temperatures, such as body temperature, their charge acceptance is reduced, decreasing electrical efficiency and increasing cell pressures. Since rapid recharge is desirable, auxiliary electrodes, along with appropriate charge control circuitry, are employed to sense internal cell pressure. Various designs have been made to improve high temperature operation. The necessary circuitry is being developed to prevent malfunction or overcharge or overdischarge. Cells are being tested at about the two-hour charge rate and the half-hour discharge rate. Three-cell batteries of two-terminal four amp-hour cells have also been cycled at body temperature at the 8-hour charge rate and the one-hour discharge rate to observe changes in capacity and in charging efficiency.

INTRODUCTION

This program was aimed at the selection and evaluation of implantable battery systems to be used in conjunction with a circulatory assist device during periods when an external power supply is disconnected. The goals aimed at in the selection of implantable batteries are shown in Table 1.

TABLE 1

GOALS FOR IMPLANTABLE BATTERIES

High Energy Density
Sealed Operation
Simple Charge Control
High Discharge Rate (2C)
Moderate to High Charge Rate (C/2)
High Cycle Life
Orientation Insensitivity

Although a high energy density is desirable, two of the major requirements are that the battery be capable of sealed operation, and that it have a high cycle life, so that it does not require frequent replacement. Table 2 shows a comparison of the energy densities and cycle lives of three battery systems[1] which are normally considered suitable for operation under isolated conditions, such as in space.

TABLE 2

COMPARISON OF SYSTEMS

	Ni-Cd	Ag-Cd	Ag-Zn
Nominal Voltage (2nd/1st step)	1.3	1.3/1.05	1.8/1.55
Watt-Hours per Pound (Practical)	12	24	20-50
Cycle Life			
(25% Discharge)	24,000	5,000	400
(50% Discharge)	9,000	2,000	150

In this comparison, the energy density of a nickel-cadmium cell is only about 1/4 the maximum energy density achievable in a rechargeable silver-zinc cell. However, the cycle life of the silver-zinc system at a 50% depth of discharge, 150 cycles, is too low to be of practical interest. The silver-cadmium system has a greater cycle life, 2000 cycles, although it is still only 1/4 that of the nickel-cadmium system. Furthermore, cells with silver electrodes on discharge show a two step discharge curve, which complicates charge control. For these reasons, as well as because of the

---

*G.E. Battery Business Section, Gainesville, Fla.
+G.E. Electronics Laboratory, Syracuse, New York

large reservoir of information existing on the application of the nickel-cadmium cell, this system was chosen as the first one for evaluation. Figure 1 is a diagram of a nickel-cadmium cell, illustrating the manner in which it is commonly operated in a sealed condition. The electrode capacities are adjusted so that at the end of charging the nickel electrode there is still an excess of charged cadmium. Under these circumstances, oxygen is evolved from the nickel electrode, and this diffuses through a porous separator to the cadmium electrode, where it recombines to form additional cadmium hydroxide. Under these conditions, the cell may be overcharged for prolonged periods without a continuous pressure increase. For most commercial cells, this maximum overcharge rate is limited to about the eight hour rate (C/8).

One of the major problems anticipated in the application of nickel-cadmium cells at body temperatures is the decrease in charge efficiency of the nickel electrode which occurs at elevated temperatures. Figure 2[2] illustrates the manner in which charge efficiency changes with temperature. The figure is a plot of the percent of the charging current resulting in electrode charging, as opposed to oxygen gassing, versus the percent of nominal capacity charged into a completely discharged cell. As the figure shows, the charging efficiency toward the end of charge decreases markedly as the temperature rises, so that a cell must be charged for a longer period in order to bring it nearly to a full charge. For example, at 96°F a battery charged to 80% of its nominal capacity accepts charge at only 65% efficiency, with the other 35% of the charging current causing oxygen evolution at the nickel electrode.

One of the immediate complications of this system is that there is little rise in voltage for the cell at the end of charge, so that cell voltage cannot be used as an indication of the end of charge. For this reason, either the maximum charge rate must be limited to that which the cell will stand on overcharge, or a means of charge control, such as by the use of auxiliary electrodes, must be employed. This will be discussed later.

CONVENTIONAL NICKEL-CADMIUM BATTERY EVALUATION

Taking into account the requirements of the artificial heart program, it was initially assumed that ten to 15 watts of power would be required for a period of about 30 minutes, and that 7.5 hours would be available for recharge. Also, considering the fact that more than a single cell would be required to allow for dc-dc conversion at a reasonably high efficiency, a battery was selected which consisted of three 4 amp-hour cells in series. The rectangular VO-4 commercial cell, shown in Figure 3, was selected for the first battery tests. This cell is classed as a sealed cell, but has a high pressure vent set for release at about 75 psig. Three of these cells were connected in series and potted in epoxy, and a pressure transducer was attached to the center cell. They were placed in a water bath at 37°C, and cycled using a 7.5 hour charge at 0.4 amps and a 0.5 hour discharge at 3.25 amps average.

Figure 4 shows the battery voltage, and the pressure and temperature of the center cell for one cycle. The pressure rises to a maximum near the end of charge, and does not rise appreciably above this on prolonged overcharge. The cell temperature decreases at the beginning of charge, as is characteristic for nickel-cadmium cells, and increases as the cell nears full charge. It rises more steeply, on the order of a few degrees centigrade, on discharge.

As a result of the relatively poor charge efficiency at this temperature, the total capacity available during one of the cycles described is lower than it would be after prolonged overcharge. This is true even though the total charge is about 50% greater than the capacity removed on each cycle. This is illustrated in Table 3, which shows the total capacity available after a prolonged overcharge, as well as the capacity obtained on complete discharge during one of the normal discharge periods. The table also shows that at the end of 365 cycles, the maximum capacity available after a prolonged overcharge is only about 60% of the initial capacity.

TABLE 3

DELIVERABLE CAPACITY AND MAXIMUM CAPACITY AFTER CYCLING, THREE CELL, VO4 FOUR AMP-HOUR BATTERY

Cycle No.	Discharge after Long Charge Amp-hours	Discharge During Cycling Amp-hours
1	4.0	
6	3.8	
58	3.7	2.8
204	3.4	
271	3.4	
365	2.4	

Table 4 summarizes the problems arising from the use of conventional nickel-cadmium two-terminal cells at body temperature. Some of these problems can be overcome by the use of an auxiliary electrode which provides a signal near the end of charge,[3] allowing for a higher charge rate and for the elimination of a constant overcharge current. This will be discussed in the following section.

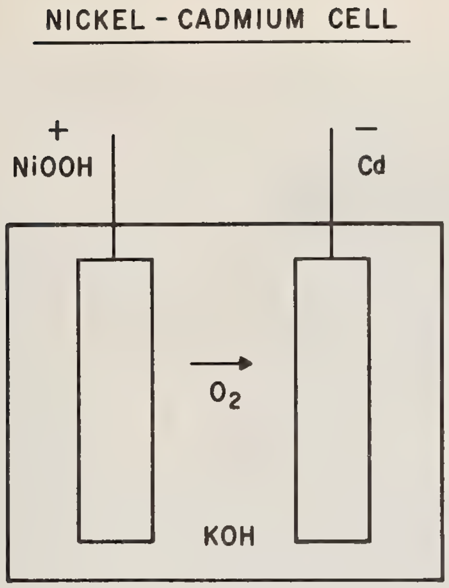

CHARGE

$Ni(OH)_2 + OH^- \rightarrow NiOOH + H_2O + e$

$Cd(OH)_2 + 2e \rightarrow Cd + 2\ OH^-$

OVERCHARGE

$2OH^- \rightarrow 1/2O_2 + H_2O + 2e$

$Cd + 1/2O_2 + H_2O \rightarrow Cd(OH)_2$

FIGURE 1. DIAGRAM OF NICKEL-CADMIUM CELL.

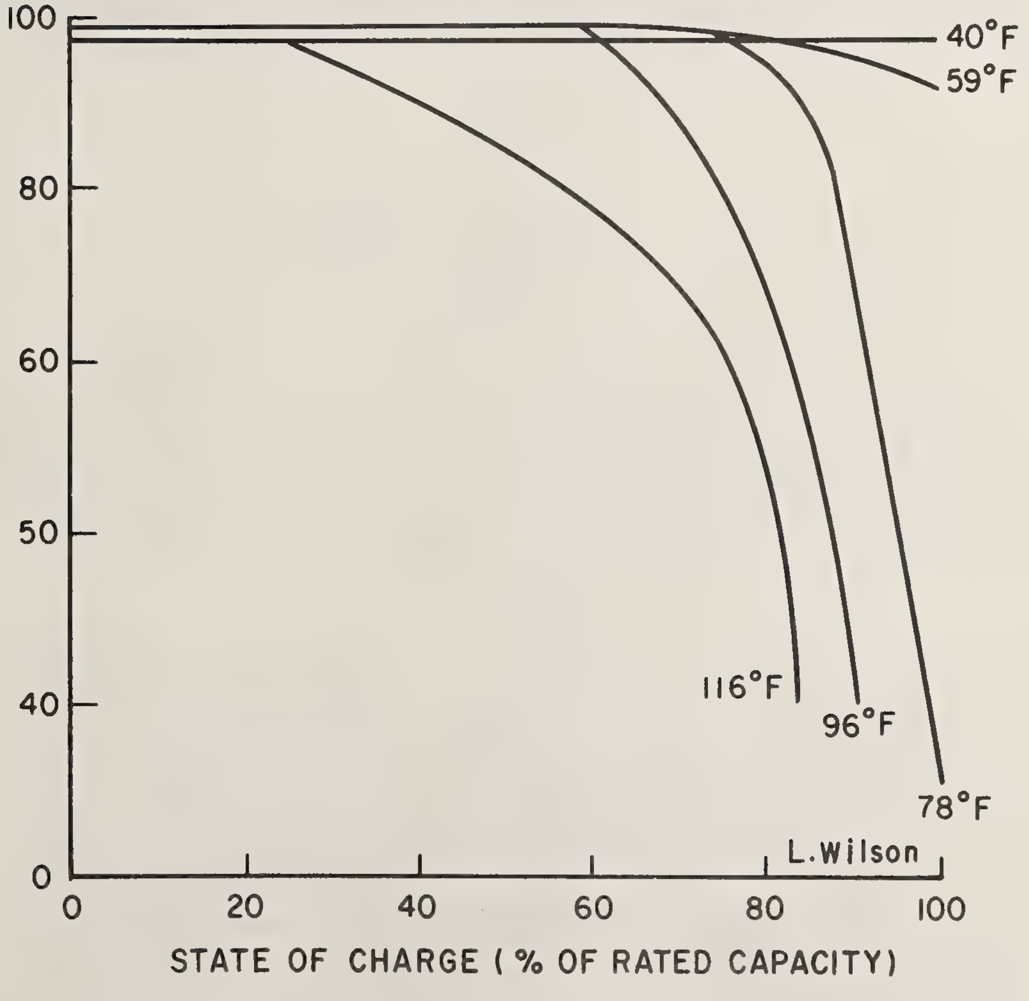

* Instantaneous value of ampere hour storage efficiency

FIGURE 2. CHARGE EFFICIENCY CHANGES WITH TEMPERATURE (FROM REFERENCE 2).

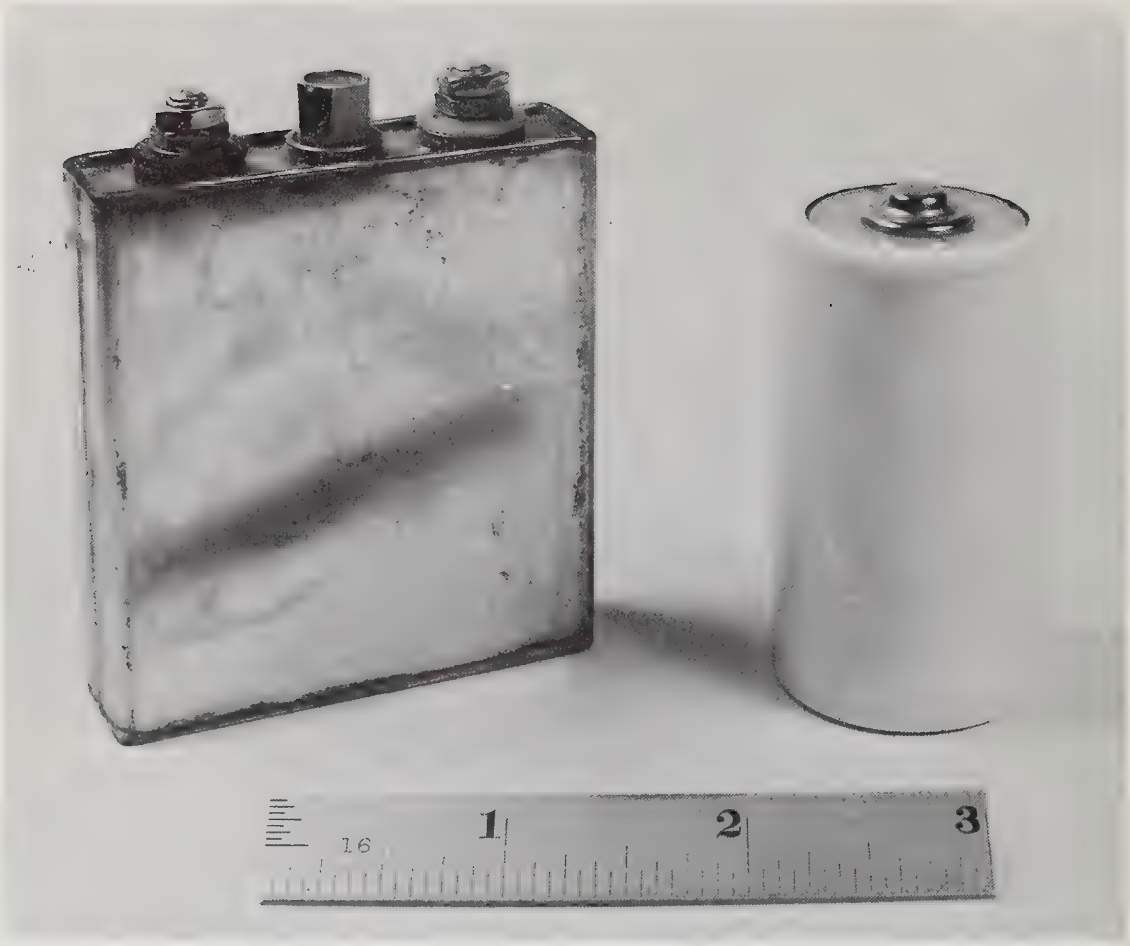

FIGURE 3. VO4 (4AMP-HR) AND D-SIZE (3.5 AMP-HR) NICKEL-CADMIUM CELLS.

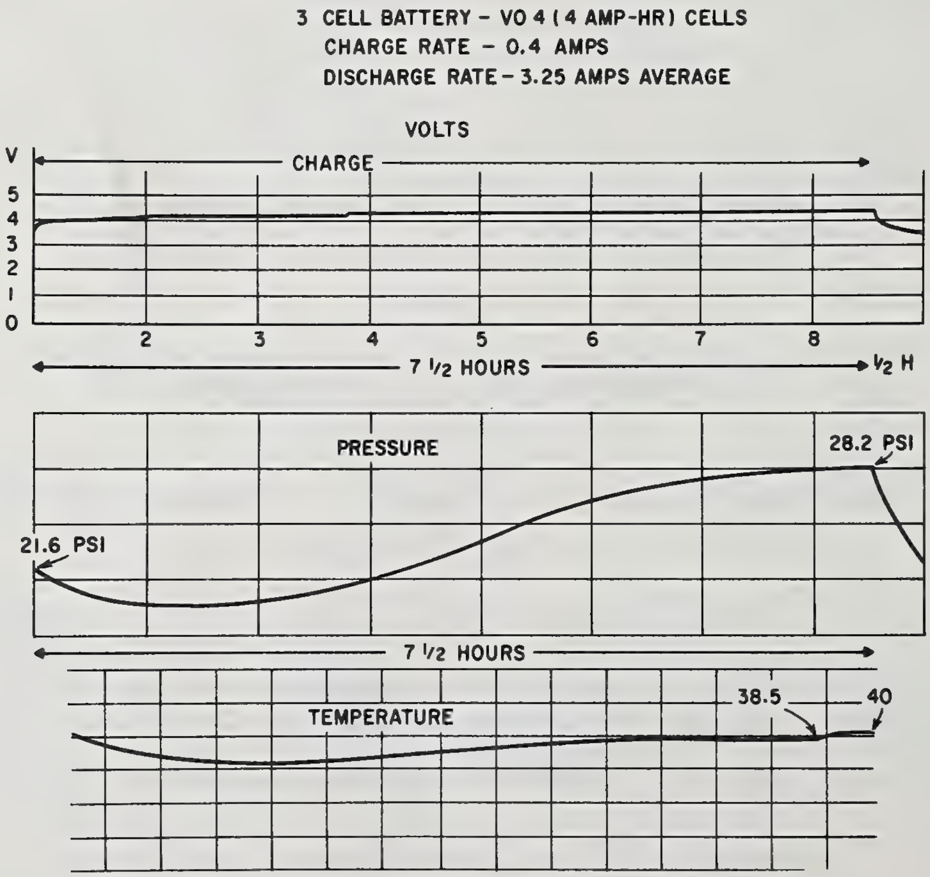

FIGURE 4. VOLTAGE, PRESSURE AND TEMPERATURE VS TIME.

TABLE 4

PROBLEMS WITH CONVENTIONAL CELLS

Little Voltage Change at End of Charge
Conventional Two Terminal Ni-Cd Cells Limited to About C/8 Overcharge Rate
Charge Acceptance Decreases with Increasing Temperature
Charge Acceptance Decreases with Decreasing Charge Rate
Cells Degrade with Increasing Numbers of Cycles

AUXILIARY ELECTRODE CELLS

Figure 5 is a schematic diagram of the arrangement of a nickel-cadmium cell employing an auxiliary electrode. The auxiliary electrode is a diffusion controlled electrode which provides a signal approximately proportional to the oxygen pressure within the cell. The oxygen generated at the nickel electrode near the end of charge or on overcharge reacts on the auxiliary electrode causing a voltage drop across the control resistor, with the accompanying discharge of a portion of the cadmium electrode. The signal generated across this resistor is used for the control of the charging current.

In order to evaluate the use of such auxiliary electrodes for a large number of cycles at elevated temperatures and relatively high charging rates, the equipment shown in Figure 6 was assembled. This is arranged so that the cells can be initially charged at the relatively high rate of 2.6 amps, and when the voltage between the auxiliary electrode and the cadmium electrode reaches a preset level, the charge can be continued at trickle rate or cut off completely. The cells are placed in an oven at body temperature. It is assumed that as a result of the high charge rate, allowable because of the charge control procedures, the charging efficiency will be greater.

Figure 7 shows the auxiliary electrode voltages for a cell (design A) which was charged and discharged at 25°C, and then again at 37°C. In each case the charge was 2.6 amps for two hours. This figure illustrates the earlier rise of the auxiliary electrode signal as a result of the poorer charge acceptance at the elevated temperature, since at 37°C the auxiliary signal reached 0.2V after only one hour, while it took two hours at 25°C. In this test, the resistance between the auxiliary electrode and the cadmium electrode was 200 ohms.

Low values of this resistance would result in a very small auxiliary electrode signal, and extremely high values would result in a large signal at the first trace of any oxygen gassing. This latter condition would cause the battery to stop charging prematurely.

This effect is illustrated in Figure 8 for a charge rate of 2.6 amps, which would normally charge a cell in less than two hours. The figure shows that if the control circuitry is set to reduce or cut off the charge rate at an auxiliary electrode voltage of 0.2 volts, an auxiliary electrode resistance of at least 100 ohms should be used in order to provide for cutoff without excessive overcharge. Figure 9 shows a plot of the auxiliary electrode voltage versus time at the same charging rate of 2.6 amps for cells of various designs. The figure shows that for one of the cells a cutoff voltage of 0.2 volts was reached when only 75% of the charge was returned to the cell. However, if a cutoff signal of 0.4 volts was selected, at least 4 amp-hours were returned to the cell in all cases. Cells displaying a delayed auxiliary electrode signal do not necessarily accept greater charge before the rise in this voltage.

Since it is desired to use more than one cell in series, and to cut off or reduce the charge rate when any one of the cells provides an auxiliary electrode signal of a predetermined value, a fairly elaborate control system is needed. It is also necessary to stop battery discharge before any of the individual cell voltages falls to zero in order to prevent a catastrophic build up of pressure in the cell. Furthermore, it is necessary to convert the low voltage dc output of the battery pack to the higher voltage dc necessary to drive the dc motor of the circulatory assist device. Figure 10 shows the schematic diagram of the circuit designed to prevent high rate overcharge.

CONCLUSIONS

In conclusion:

1. Conventional two-terminal cells cycled using a 10 hour charge rate and discharged at about the one hour rate to about the 50% depth of discharge have useful lifetimes at body temperature of at least 300 cycles.
2. Cells containing diffusion-limited type oxygen auxiliary electrodes can be employed at body temperature to allow for charging within two hours.
3. Control and conversion circuitry have been designed to allow for auxiliary charge control at high charging rates, to provide for overdischarge protection, and to provide dc/dc conversion to drive the heart pump.

Future work will be aimed at evaluating the charge efficiency for various cell designs, studying the effect of charge rate on charge efficiency at body temperature, and evaluating the best method of maintaining or increasing the capacity of the battery after the end of the normal recharge period. In closing, Figure 11 is a photograph of a three cell 3.5 volt, 4 amp-hour battery potted in an epoxy, manufactured by the H. B. Fuller Co., which is reported to be compatible with body fluids.

AUXILIARY ELECTRODE Ni-Cd CELL

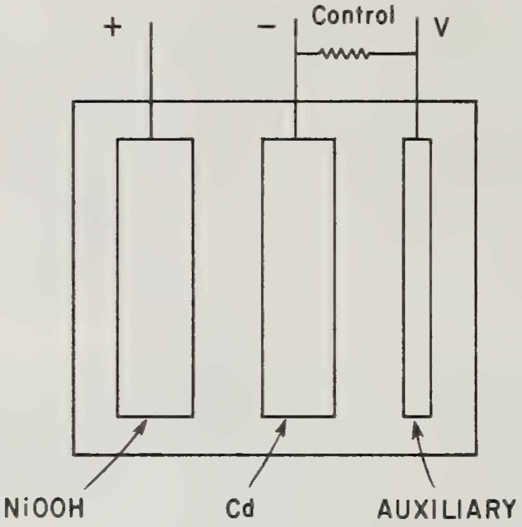

OVERCHARGE

NiOOH

$$2\,OH \longrightarrow {}^{1}/_{2}\,O_2 + H_2O + 2e$$

AUXILIARY - Cd COUPLE

$$ {}^{1}/_{2}\,O_2 + H_2O + 2e \longrightarrow 2OH^- $$

$$ Cd + 2OH^- \longrightarrow Cd(OH)_2 + 2e $$

FIGURE 5. SCHEMATIC DIAGRAM OF A NICKEL-CADMIUM CELL EMPLOYING AUXILIARY ELECTRODE.

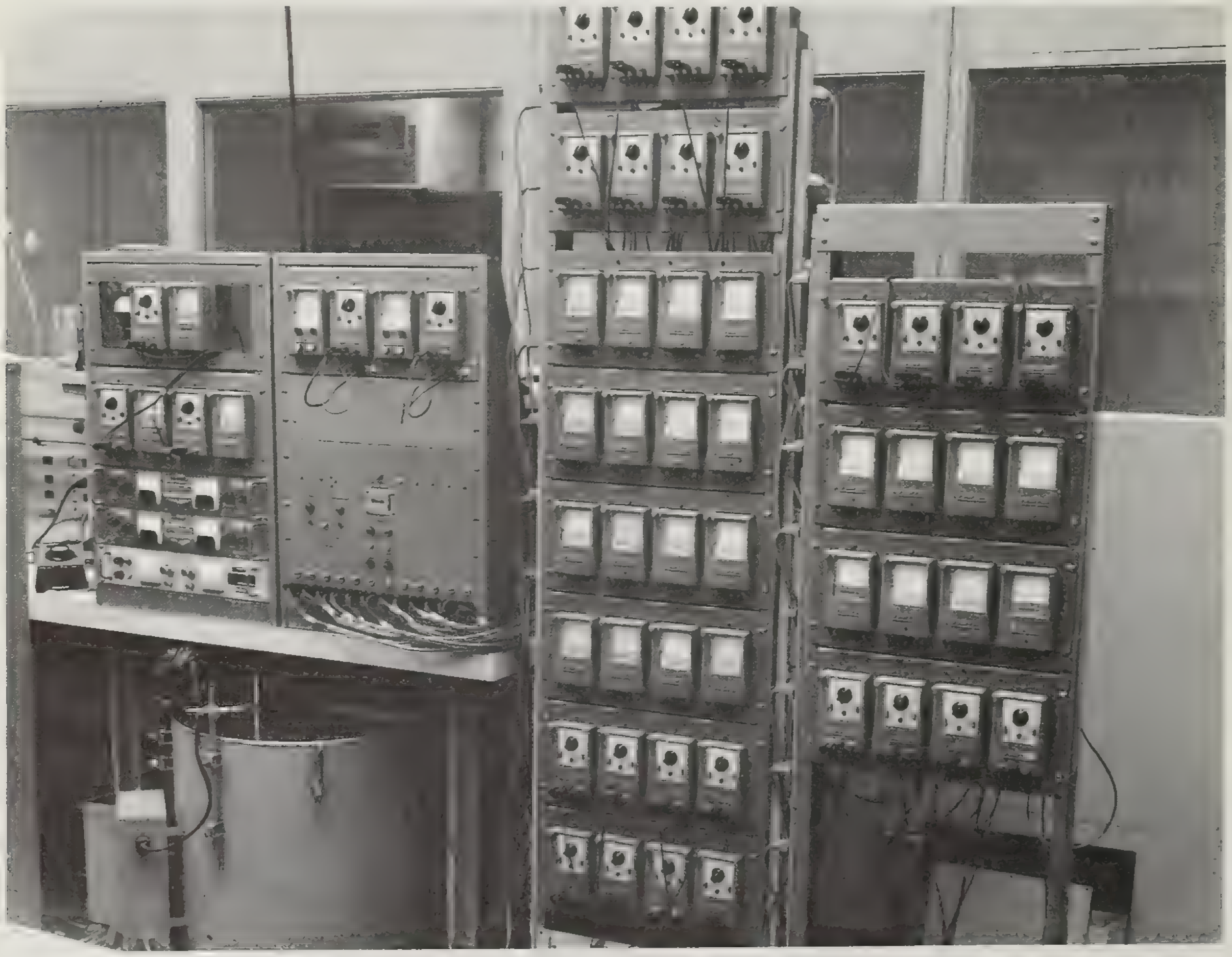

FIGURE 6. AUXILIARY ELECTRODE CELL TEST EQUIPMENT.

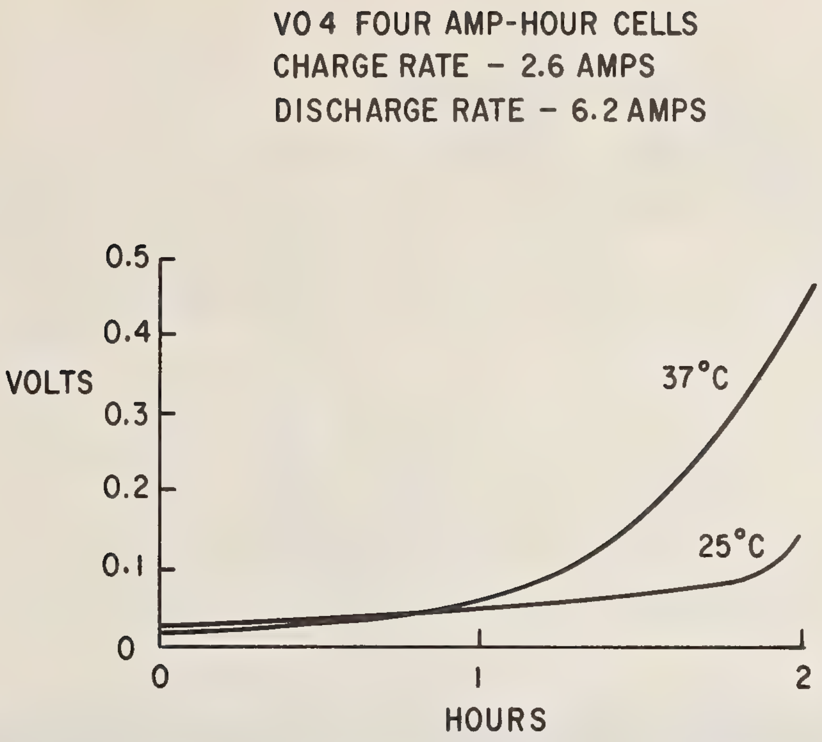

FIGURE 7. AUXILIARY ELECTRODE VOLTAGES AT 25° C and 37° C.

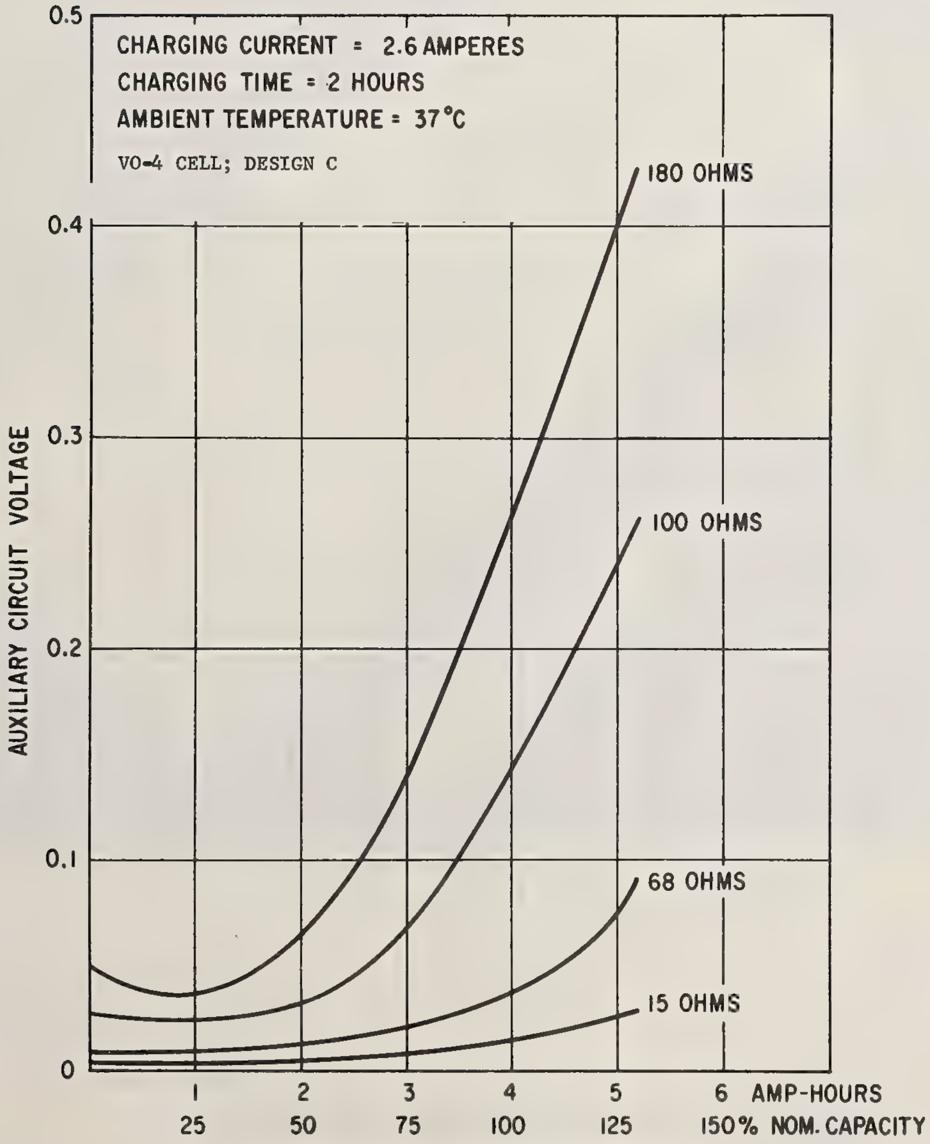

FIGURE 8. AUXILIARY ELECTRODE VOLTAGE.

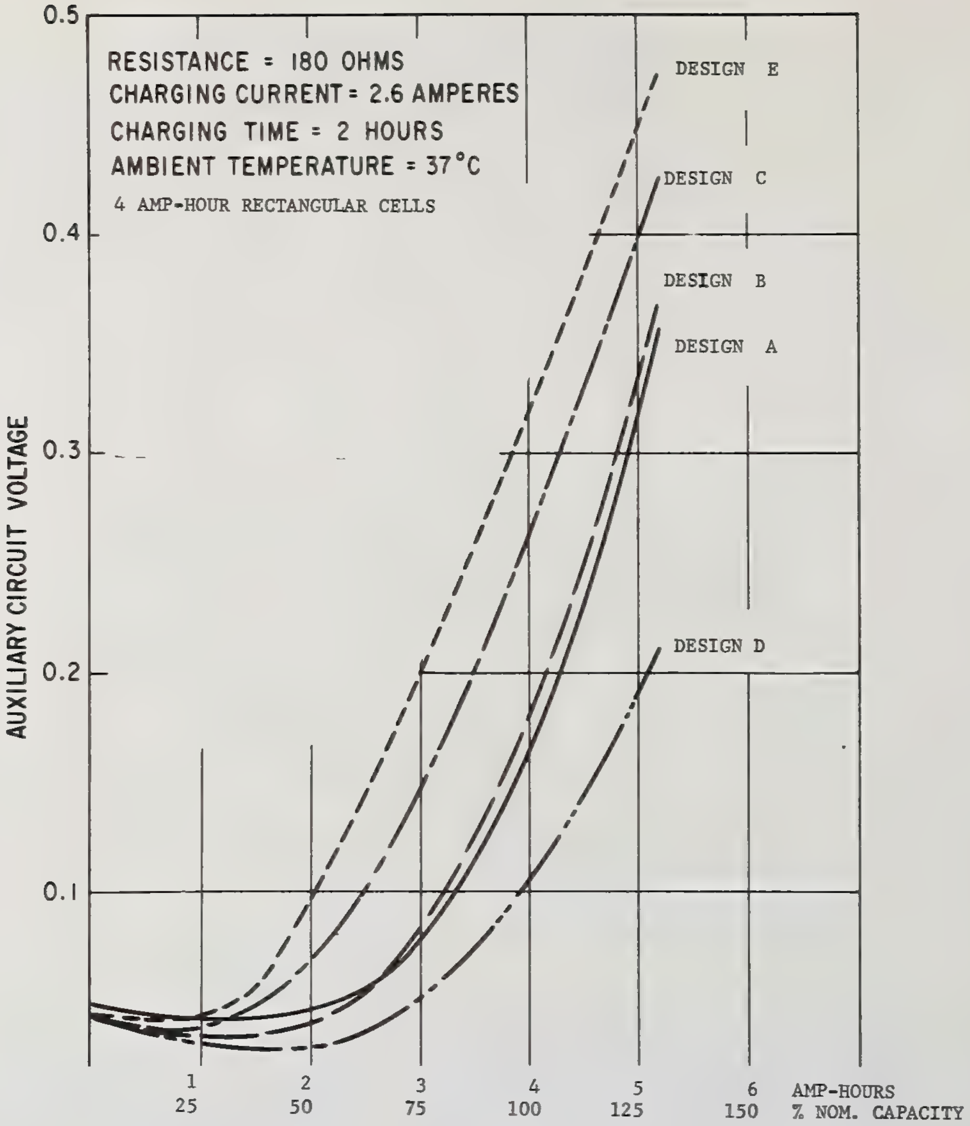

FIGURE 9. AUXILIARY ELECTRODE VOLTAGES.

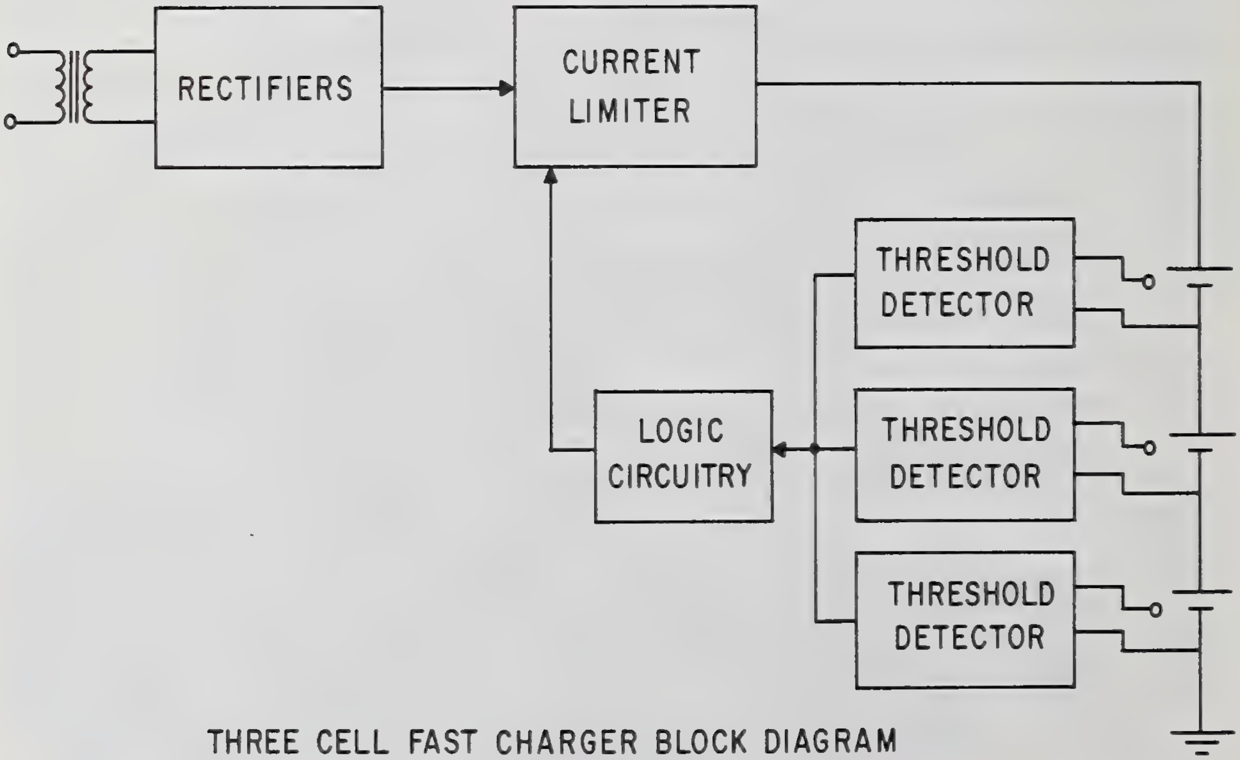

THREE CELL FAST CHARGER BLOCK DIAGRAM

FIGURE 10.

REFERENCES

1. H. T. Francis, Technology Handbook, NASA SP5004, P. J. Rappaport and A. M. Frink, "Power Systems for Space Flight," New York, 1963, p. 211, J. D. Reams, Space Power Subsystems, Vortrag DGRR (Stuttgart 1965).
2. L. Wilson, "Characteristics of Hermetically Sealed Nickel Cadmium Batteries," Johns Hopkins Applied Physics Lab., August 1967, AD 661 215.
3. W. N. Carson, Jr., G. Rampel, and I. B. Weinstock, "Characterization of Recombination and Control Electrodes for Spacecraft Nickel-Cadmium Cells," Final Report Contract, NAS 5-10261, January 1968.

DISCUSSION

MR. RYDER: Was any attempt made after 365 cycles to restore capacity to the battery by conditioning procedures.

MR. HAMLEN: No, not as yet. Part of the problem may have been leakage at the transducer connection.

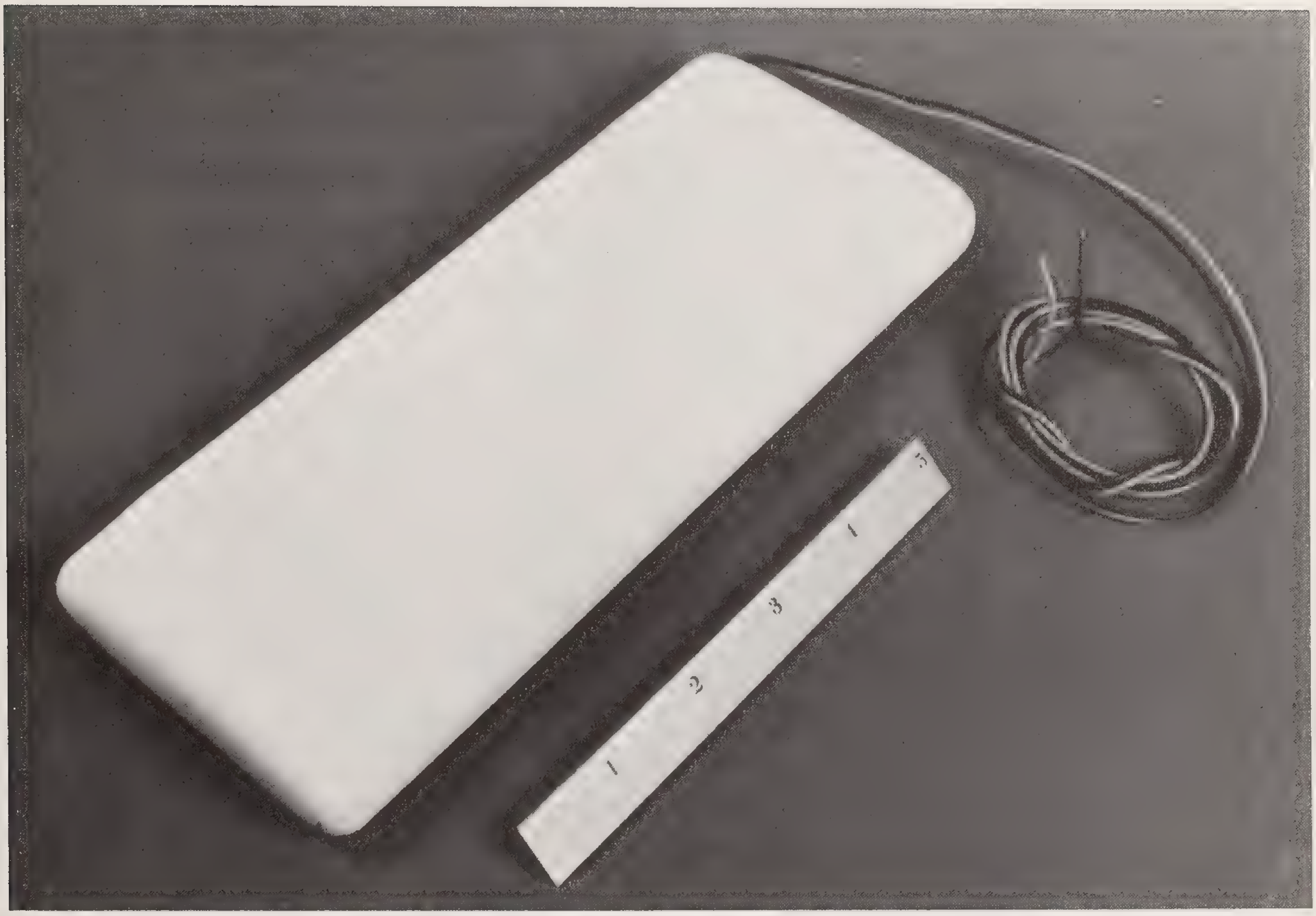

FIGURE 11. ENCAPSULATED 3-CELL 4 AMP-HOUR BATTERY.

CHAPTER 87

DEVELOPMENT OF AN ELECTRICAL ENERGY STORAGE SYSTEM FOR USE WITH A CIRCULATORY ASSIST DEVICE

R. Miller, E. Glanfield
General Electric Co.
Valley Forge Space and Technology Center
King of Prussia, Penn.

An Electrical Energy Storage System (EESS) for use with a circulatory assist device is being designed, developed and tested. The operational concept is based upon the reversible fuel cell reactions. Cells employing a Solid Polymer Electrolyte (SPE) in the form of an Ion-Exchange Membrane (IEM) and platinum black electrodes operate alternately as electrolysis cells (charge mode) and fuel cells (discharge mode). In the charge mode water contained in wicks in each cell is electrolyzed to form hydrogen and oxygen gas which are stored in separate sections of a pressure tight housing enclosing the unit. During discharge these gases are recombined to produce electrical power and form water which is again retained by the wicks. Cells are alternately charged (at 1.95 volts and 1.5 amperes) and discharged (at 0.65 volt and 1.5 amperes) for periods of 2 hours each. The present design calls for a system having nine cells, a volume of approximately 25 in^3, and a weight of approximately one pound. Energy storage capability is 18 watt hours with a continuous power output capability of approximately nine watts or one watt per cell. Overall system energy conversion efficiency is approximately 28%.

INTRODUCTION AND BACKGROUND

An operational circulatory assist device system should provide the patient with the capability to move about for limited periods of time unencumbered by an external power source. To accomplish this, it is necessary that a secondary power source be developed that can provide sufficient power to operate the circulatory assist device for a period of time sufficient to permit the user to perform a task such as traveling to or from a job. The device must be capable of being recharged or re-energized with a time equivalent to or less than the period of discharge and should be small enough and light enough so as not to encumber the user.

The Electrical Energy Storage System (EESS) approach to this problem involves the use of the reversible reactions of the fuel cell to achieve these goals. In the electrolysis or charge mode, electrical energy is supplied to the unit which electrolyzes water and produces hydrogen and oxygen gas. The gases are stored in separate sections of a pressure tight unit enclosure. During the fuel cell or discharge mode the hydrogen and oxygen are recombined to form water and electrical energy to power a circulatory assist device.

The EESS concept was originally employed under Project ELF, an Air Force program that was completed in 1962, and which centered around the same basic operational principles as the EESS although it was designed to meet a different requirement. Subsequent to ELF, the development of the fuel cell was advanced to the stage where fuel cells were used as the primary power supplies on the Gemini spacecraft flights. Water electrolysis cells were concurrently being developed for use in oxygen recovery subsystems of atmosphere control systems for extended mission manned space vehicles.

Any of the aforementioned processes can be accomplished by the same electrochemical cell configuration. In other words, the same cell can be alternated between electrolysis and fuel cell modes to function as an energy storage device or secondary battery, provided the product gases (hydrogen and oxygen) generated by the electrolysis reaction are stored for recombination during the fuel cell reaction. Conversely, fuel cell product water must be stored for dissociation by electrolysis.

Initial EESS designs were based upon the use of a "pocket cell" which employed a sulfuric acid liquid electrolyte as shown in Figure 1. The acid was retained between two ion exchange membranes (IEM) which prevented the mixing of the gases, hydrogen and oxygen, with the electrolyte and also supported the platinum black electrodes. This arrangement was basically the same as that employed in our previous IEM water electrolysis systems, but it varied from the IEM fuel cell work in that a liquid electrolyte was utilized.

The liquid electrolyte was necessary for long term operation to augment the IEM's electrolyte capabilities which degraded with time due to leaching of the electrolyte contained in the structure of the membrane material. Design goals for the pocket cell EESS unit called for a 25 in^3 package weighing one pound, capable of supplying six watts of power and having a power storage capability of twelve watt hours. Gas and liquid leakage problems hampered development testing efforts on unenclosed cell stacks. The pocket cell development effort was subsequently abandoned before successful enclosed unit operation was achieved when it was determined that impurities, principally CO_2, were being produced during the electrolysis reaction as the result of membrane degradation. The effect of these impurities on the performance of an EESS will be discussed later.

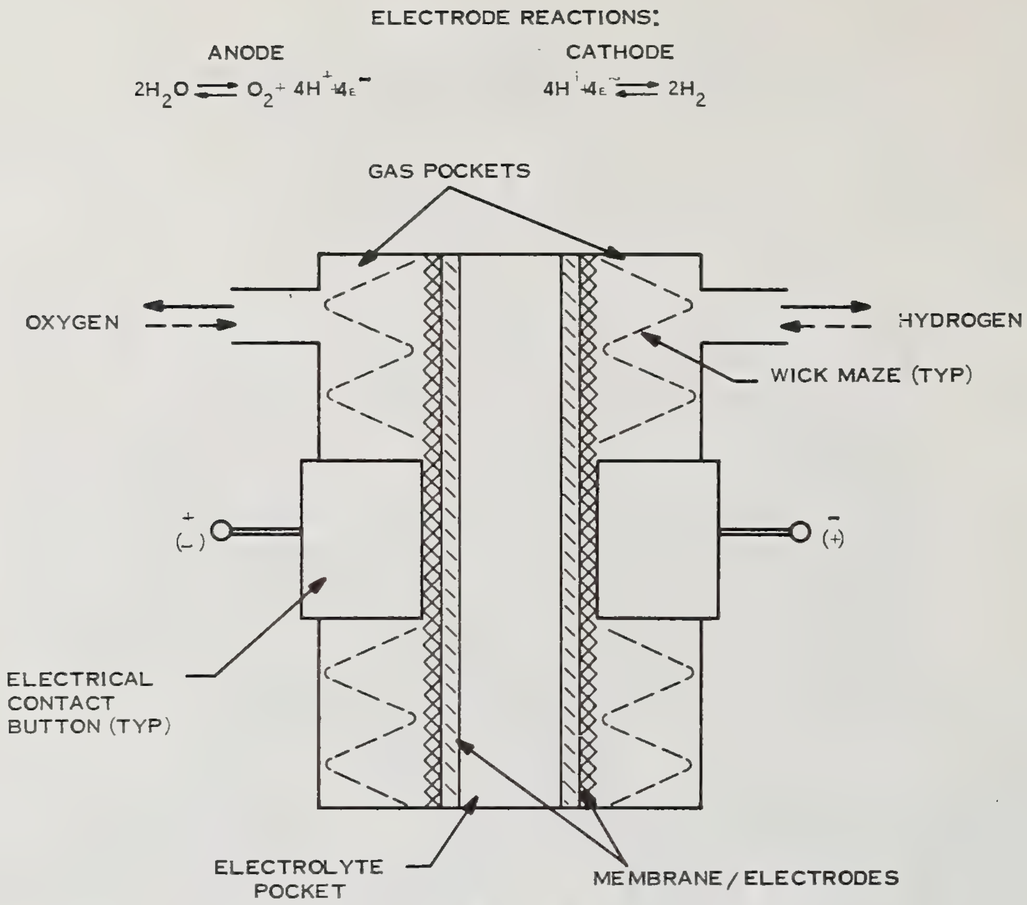
ELECTRODE REACTIONS:
ANODE
$2H_2O \rightleftharpoons O_2 + 4H^+ + 4\epsilon^-$
CATHODE
$4H^+ + 4\epsilon^- \rightleftharpoons 2H_2$
GAS POCKETS
OXYGEN
HYDROGEN
WICK MAZE (TYP)
+ (−)
− (+)
ELECTRICAL CONTACT BUTTON (TYP)
ELECTROLYTE POCKET
MEMBRANE / ELECTRODES

FIGURE 1. ION EXCHANGE MEMBRANE POCKET CELL CONCEPT.

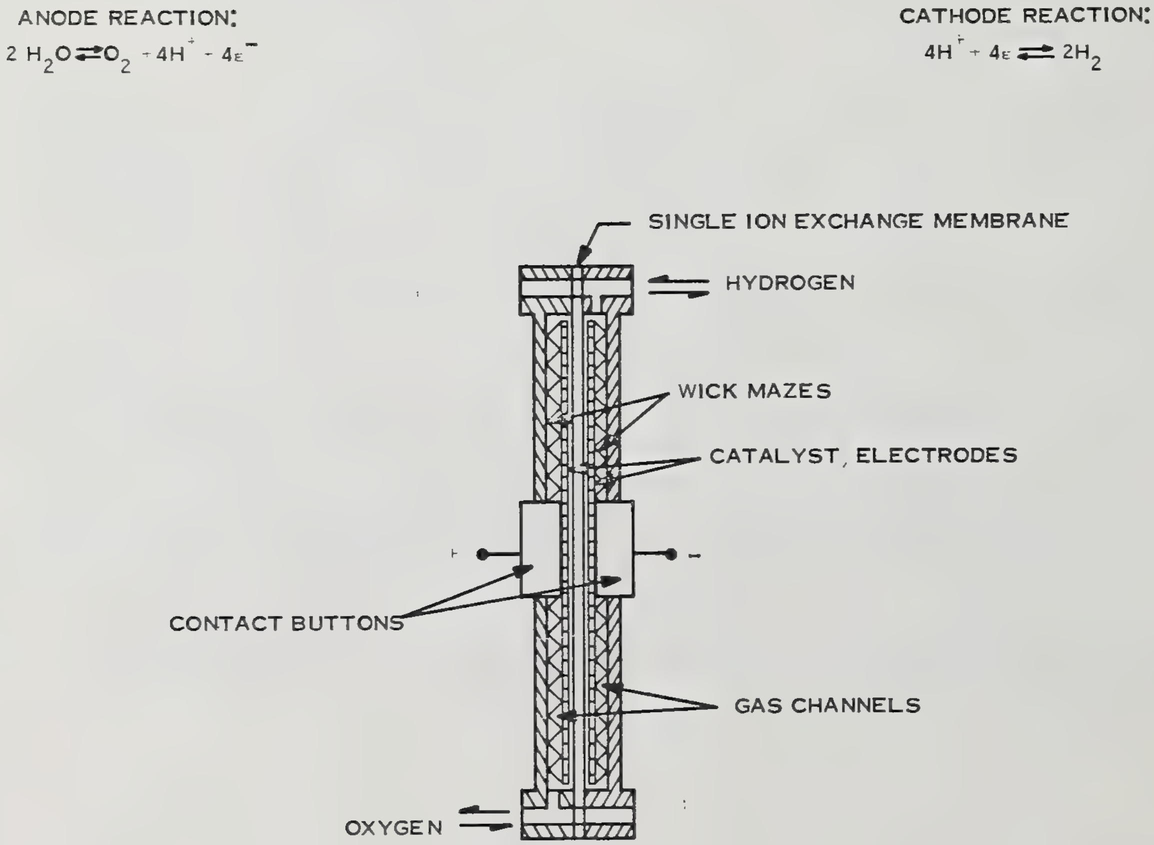
ANODE REACTION:
$2\ H_2O \rightleftharpoons O_2 + 4H^+ + 4\epsilon^-$
CATHODE REACTION:
$4H^+ + 4\epsilon \rightleftharpoons 2H_2$
SINGLE ION EXCHANGE MEMBRANE
HYDROGEN
WICK MAZES
CATALYST, ELECTRODES
+
−
CONTACT BUTTONS
GAS CHANNELS
OXYGEN

FIGURE 2. "DRY ELECTROLYTE" CELL CONCEPT.

SUMMARY OF THE PRESENT PROGRAM

Current effort on the EESS program is centered around the use of a single ion exchange membrane (SPE) cell that utilizes the IEM as a solid electrolyte. Referring to Figure 2, the SPE cell is composed of two gas pockets each containing a wick maze, which are separated by a single membrane, or solid polymer electrolyte (i.e., SPE) having a platinum black electrode on each side. The concept is made possible by utilization of a new membrane material identified as a "fully fluorinated polymer with pendant sulfonic acid ion exchange sites." This SPE membrane is much more stable than the membrane used in the pocket cells. Due to the strong chemical bond between the membrane and the sulfonic acid electrolyte within the membrane the leaching problem has been overcome, thereby obviating the need for augmentation with a liquid electrolyte.

As mentioned previously, the pocket cell design was abandoned primarily due to impurities being produced during the electrolysis reaction as a result of oxidative degradation of the membrane material. Figure 3 shows the effect of the accumulation of these impurities on the cycle time of the EESS during extended duration operation. The decrease in cycle time results from a decrease in the storage volume for hydrogen and oxygen within the unit due to the cumulative effect of the impurities generated during each cycle. It can be seen that after only 500 cycles, the cycle time would be decreased from four hours to approximately two hours.

In the pocket cell unit the oxygen produced was found to contain 0.12% carbon dioxide and 0.01% of other unidentified hydrocarbons. By implementation of the SPE membrane, the carbon dioxide production rate has been decreased to approximately 0.02%. The effect of this reduction on the operation of the unit is an increase from 500 to 3500 available cycles before the cycle time would be reduced from four hours to two hours. Assuming a use rate of two complete cycles per day, this would provide approximately 4.5 years of operation before the patient would be restricted to a one hour discharge phase.

CELL DESIGN CONSIDERATIONS

Referring to Figure 4, the SPE cell is composed of a membrane electrode assembly sandwiched between two half cell assemblies each consisting of two "Lexan" spacers bonded to a Lexan separator plate. Also bonded in place are two gold contact pads and contact pad supports. The adhesive used to bond the spacer assemblies is Flexane 85, a urethane elastomer. Flexane 85 is also used to fabricate the cell gaskets which are molded into the spacers. Ducts for the passage of gas are cut into the spacers as necessary. A wick assembly is incorporated into each pocket of the cell to remove water from the electrode during discharge and subsequently to resupply the same water to the electrode during the charge mode. A polyethylene screen is used to support the wick.

To form a stack, the individual cells are arranged in series electrically as shown in Figure 4. (The number of cells used being dependent upon the performance requirements of the unit). The stack components are retained by an external assembly bracket. End plates at either end of the stack are used as part of a clamping assembly to apply the necessary compressive load on the components.

Requirements made evident subsequent to the initiation of the EESS program call for a higher energy density (18 watt hours/pound or greater) than that for which the pocket cell unit was designed with no increase in the size of the unit. The rate at which the fuel cell reaction (discharge phase) takes place is dependent upon the load placed across the cell electrodes and the polarization characteristics of the cell. Polarization data for the cell is obtained by measuring the current produced by the cell and the potential between the electrodes (cell voltage) under varying loads. A typical dry electrolyte cell produces a polarization curve similar to Curve #1 in Figure 5, which shows the voltage to be expected in operation of a cell at various current densities (current per unit of cell area, amps/ft^2).

Power density of a cell (watts/foot^2) can also be determined by multiplying cell voltage by the current density corresponding to points on the polarization curve. A typical cell power density characteristic is represented by Curve #2 in Figure 5.

To determine the actual operating current of a cell of a particular size, the current density is multiplied by the cell electrode area. Cell power is correspondingly determined by multiplying the power density by the electrode area. In the case of the EESS, the required area was determined by selecting an operating current density of 70 amps/ft^2, which is near the maximum power capability of cells of this type. At this level a typical cell operates at a power density of approximately 47.2 watts/ft^2.

Assuming the power output of each cell is to be maintained at one watt, cell area was then determined to be:

$$\frac{1 \text{ watt}}{47.2 \text{ watts/ft}^2} = 0.0212 \text{ ft}^2$$

and the operating current was established at 70 amps/ft^2 x 0.0212 ft^2 = 1.48 amps. A circular area of 0.0212 ft^2 required an electrode diameter of 2.05 inches which was well within the volume constraints for the EESS and allowed sufficient space for the necessary ducting and seals. Several cell spacer configurations were then evaluated with attention being given to adequate sealing of the gas pockets and providing the maximum possible electrode area within the allotted envelope. The spacer configuration adopted for the first generation unit is shown in Figure 6.

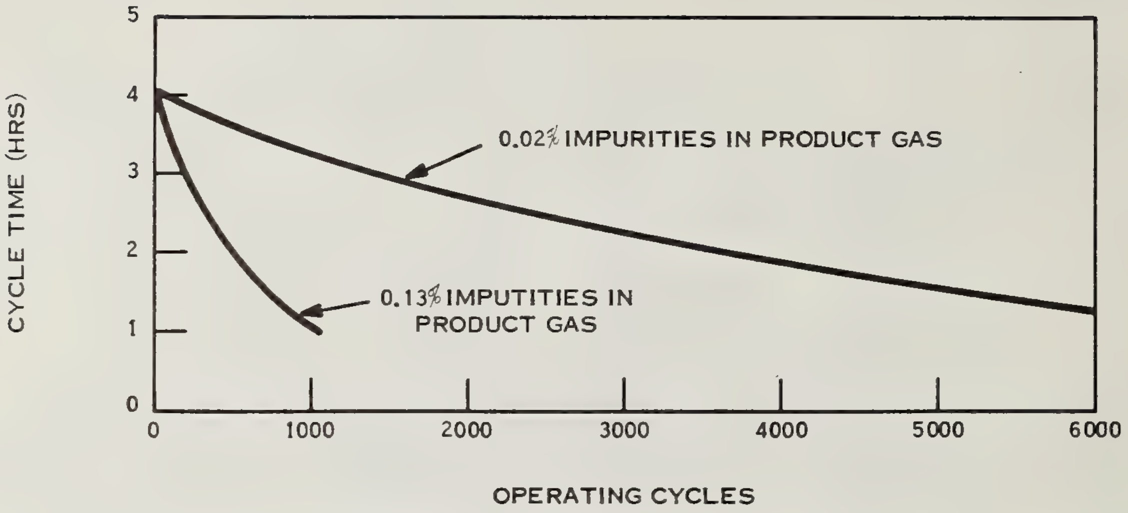

FIGURE 3. EFFECT OF IMPURITIES ON EESS OPERATION.

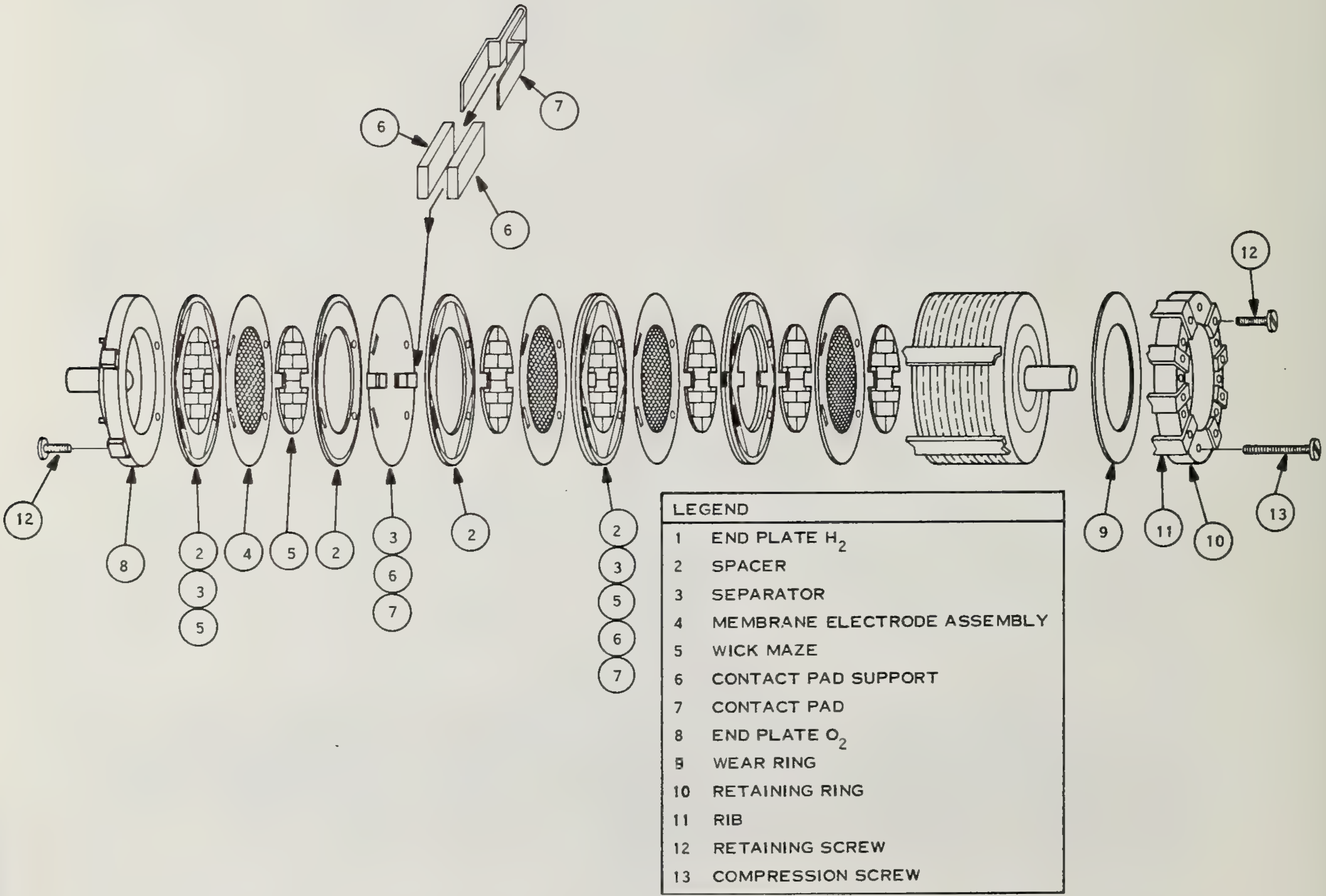

FIGURE 4. ELECTRICAL ENERGY STORAGE SYSTEM 9-CELL UNENCLOSED STACK (EXPLODED VIEW).

UNIT OPERATION AND TEST

Four units are to be fabricated and tested during the program with the first two of these being unenclosed prototypes or stacks, in which the gases (oxygen and hydrogen) generated by the unit in the charge mood will be vented from the system and the required water will be drawn from the wick maze assembly within each cell of the stack. During discharge, hydrogen and oxygen will be supplied from an external source and the water generated will be collected on the wick maze assembly for subsequent reuse. Electrical energy generated by the unit will be dissipated in a load resistor. The remaining two units are to be enclosed in a pressure-tight housing having the basic form of a prolate spheroid measuring three inches in diameter and 4.5 inches in length (Figure 7). Operation of an enclosed unit is the same as in the unenclosed configuration except that the gases produced during charge are retained within the housing and no external gas supply is provided.

During the electrolysis (charge) phase of operation the gases are generated in a 2:1 ratio of hydrogen to oxygen and are delivered to their respective storage volumes within the housing. The oxygen is stored in an inflatable bladder attached to the cell stack assembly. The bladder performs a dual function by maintaining an effective separation between the hydrogen and oxygen and by compensating for any deviation from the stoichiometric 2:1 ratio of gas production while maintaining a pressure balance between the gas sides of the cells. Thus, gas mixing problems and stresses on the membrane/electrode assemblies are minimized. The charge cycle is continued until the unit reaches a fully charged condition (i.e., maximum gas storage pressure) at which time the charging current is removed. The fuel cell, or discharge phase, may then be started.

As discharge progresses, storage gas pressures are decreased and the pressure balance between the gas cavities is maintained by the bladder as discussed above. Water produced by the discharge of the cells forms at the oxygen electrode/membrane interface and is collected by a series of wicks in contact with the electrodes for subsequent dissociation during the next electrolysis phase of the cycle.

Test Program.

The test program is centered around subjecting EESS assemblies to controlled degradation experiments. In the case of the enclosed prototype EESS units, test conditions are planned to simulate implant conditions. The unenclosed unit tests are planned to assess performance in a normal laboratory environment to facilitate obtaining detailed cell performance data and to give comparison data for determining the effects of in vitro conditions on the operation of the system.

The unenclosed unit is operated at a charge rate of approximately 1.5 amps and discharge rates of approximately 1.5 amps. The duration of both the charge cycle and the discharge phases of the cycle have been set nominally at two hours.

The sequence of operation (Figure 8) of the enclosed prototype units will be controlled by pressure switches (PSW-1, PSW-2) set to switch from charge to discharge when the housing pressure reaches 1150 psia. A timer switch (TSW-1) is used to change the rate of discharge independent of housing pressure level. Manual override switches (SW-8 and SW-9) provide the capability to switch from one mode of operation to the other at any time during a cycle.

The unenclosed units were set up to be controlled by timer switch TSW-1 set to provide equal charge and discharge times regardless of charge and/or discharge rates (Figure 9). Duration of each cycle has tentatively been set at two hours. During the charge cycle the hydrogen and oxygen produced are vented from the system. During the discharge cycle the stack is supplied with hydrogen and oxygen and the power generated is dissipated in a load resistor. A switch is provided to override the timer, thus, permitting the operating mode to be switched at any time during the cycle.

Instrumentation has been provided to permit measurement and recording of the unit current, voltage, operating temperature, housing pressure and heat sink temperature of the enclosed prototype units and the stack current and voltage, and cell voltage and temperature of the unenclosed units.

PERFORMANCE TO DATE

Initial testing was performed on a nine cell unenclosed stack which was limited somewhat in performance by three cells which failed to perform up to expectations. The remaining six cells demonstrated the capability of generating more than one watt of electrical power at a current density of approximately 70 ASF. Continued testing of the nine cell stack was cut short due to an internal leak between the hydrogen and oxygen gas pockets which resulted in a fire in the stack and damage to one of the membrane electrode assemblies. At that time it was decided to change the test program to incorporate testing two five cell units instead of the single nine cells stack to minimize the effect of a single cell failure on the test program. As of 2 June one unit has operated for more than two hundred hours while the second unit has been operated for more than one hundred hours. The longest period of continuous operation was approximately 80 hours (Figures 10 & 11). Power output capability of the five cell stacks is greater than four watts with unit efficiency (power output/power input) being approximately 35%.

During the remainder of the program period testing of the unenclosed units will be continued under gradually increasing load conditions and the two enclosed units will be fabricated and tested.

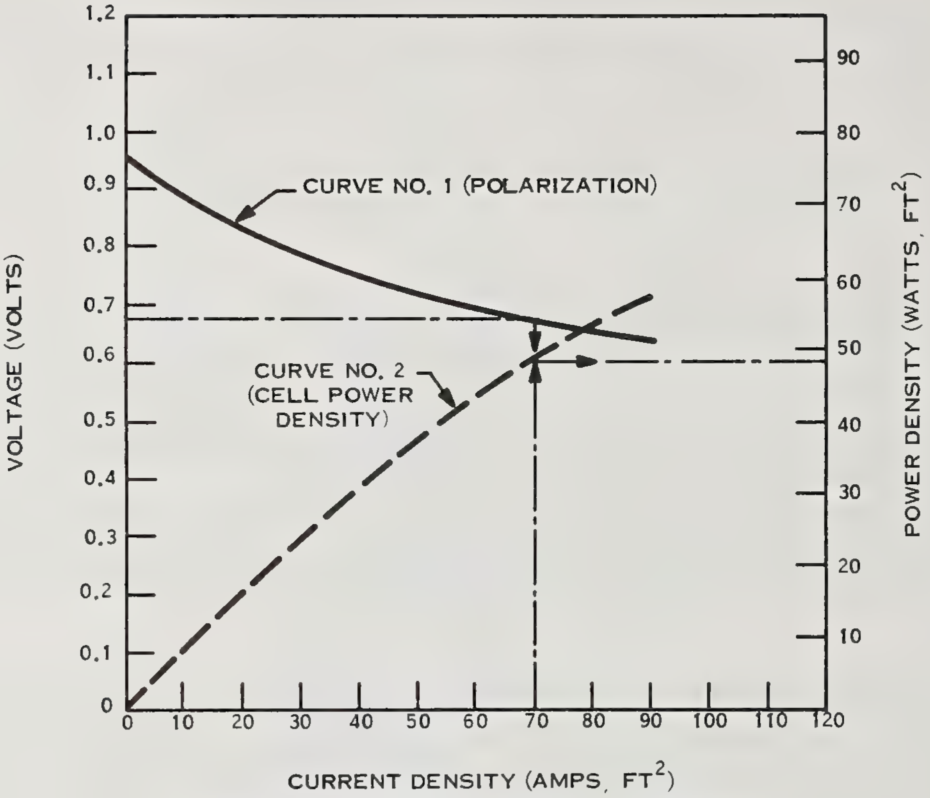

FIGURE 5. TYPICAL EESS FUEL CELL PERFORMANCE.

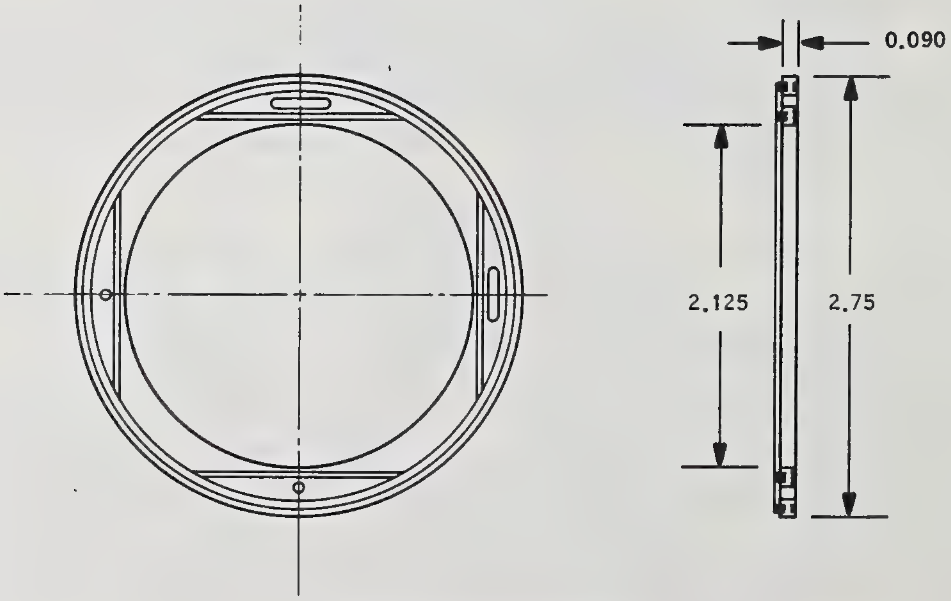

FIGURE 6. CELL SPACER.

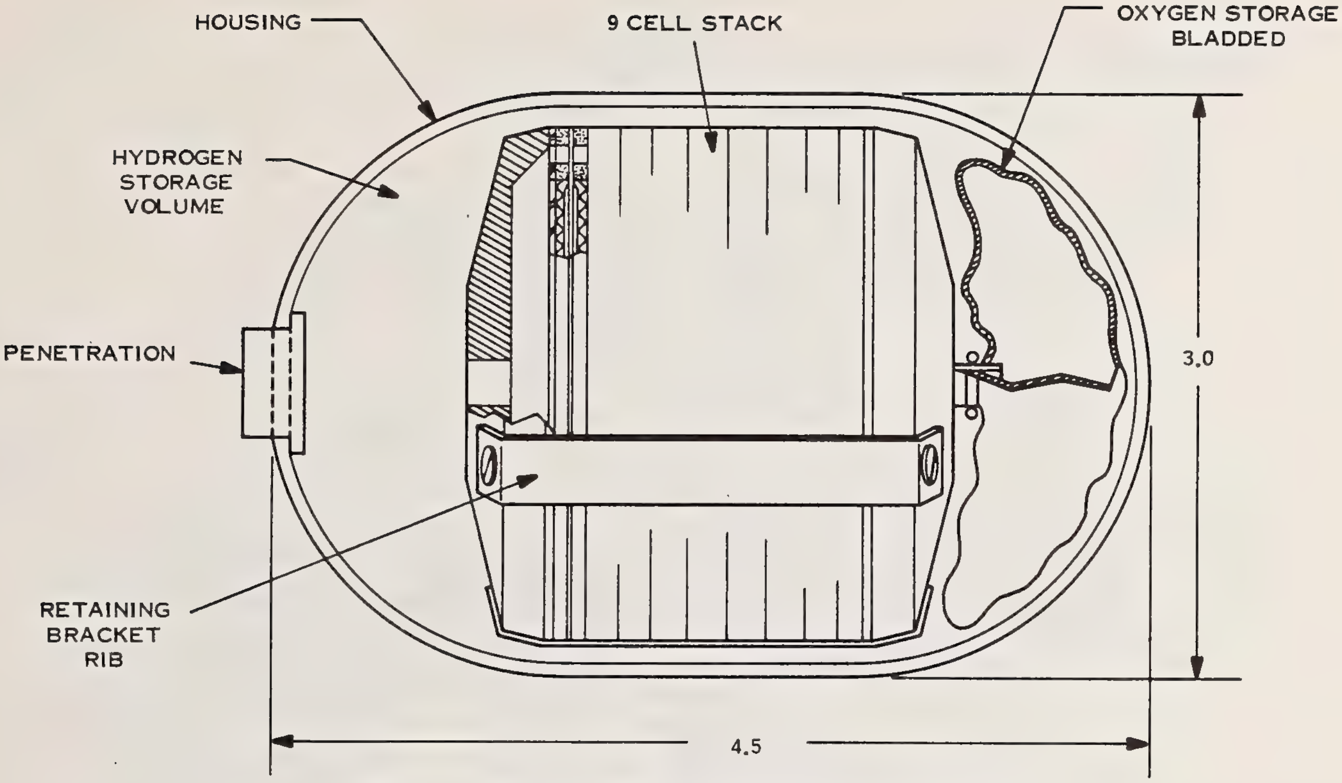

FIGURE 7. EESS CONCEPTUAL ARRANGEMENT (NOT TO SCALE).

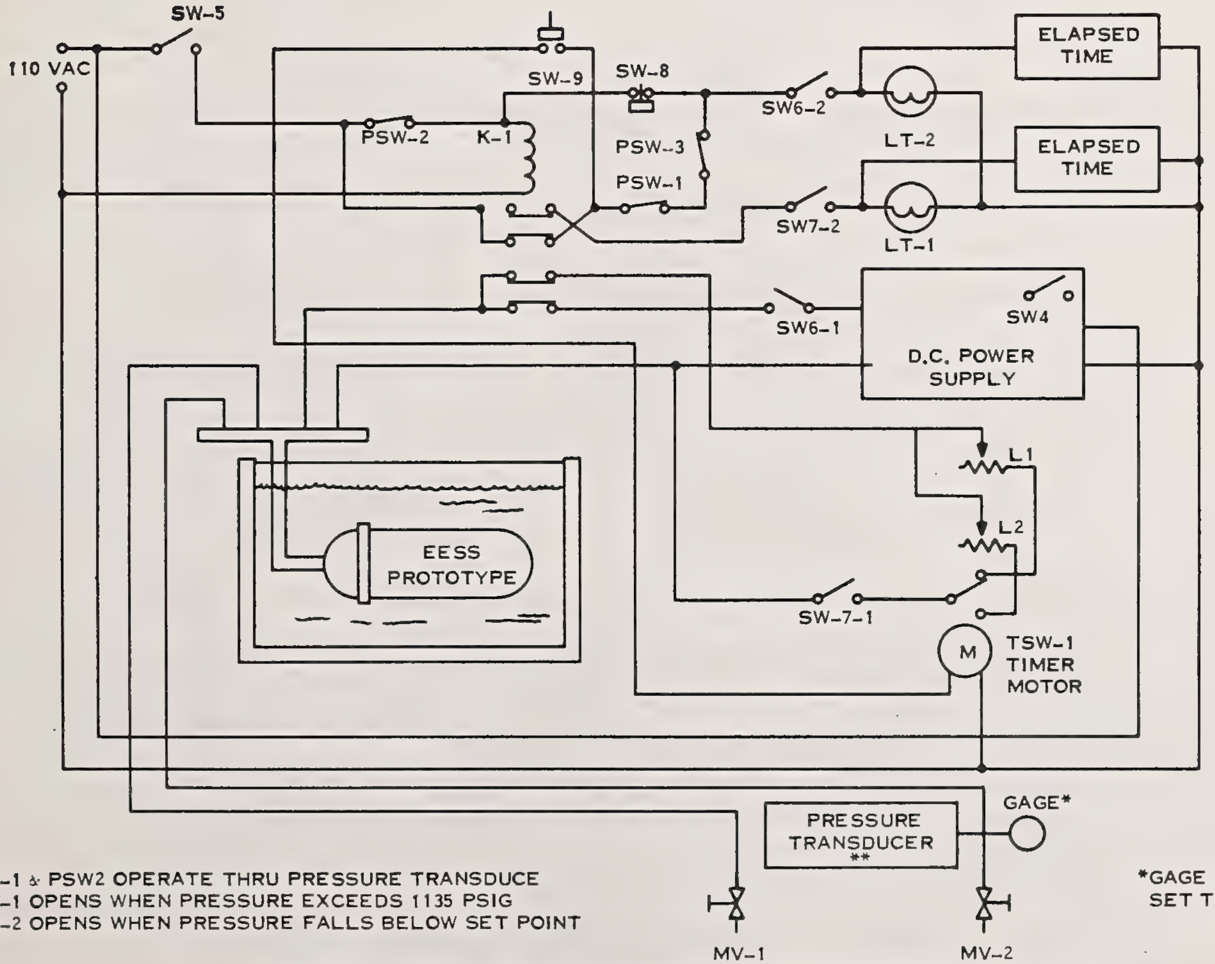

LT-1 DISCHARGE
LT-2 CHARGE

**PSW-1 & PSW2 OPERATE THRU PRESSURE TRANSDUCE
PSW-1 OPENS WHEN PRESSURE EXCEEDS 1135 PSIG
PSW-2 OPENS WHEN PRESSURE FALLS BELOW SET POINT

*GAGE CONTAINS PSW-3
SET TO OPEN AT 1200 PSIG

FIGURE 8. EESS ENCLOSED PROTOTYPE UNIT TEST SCHEMATIC (REV B 3/1).

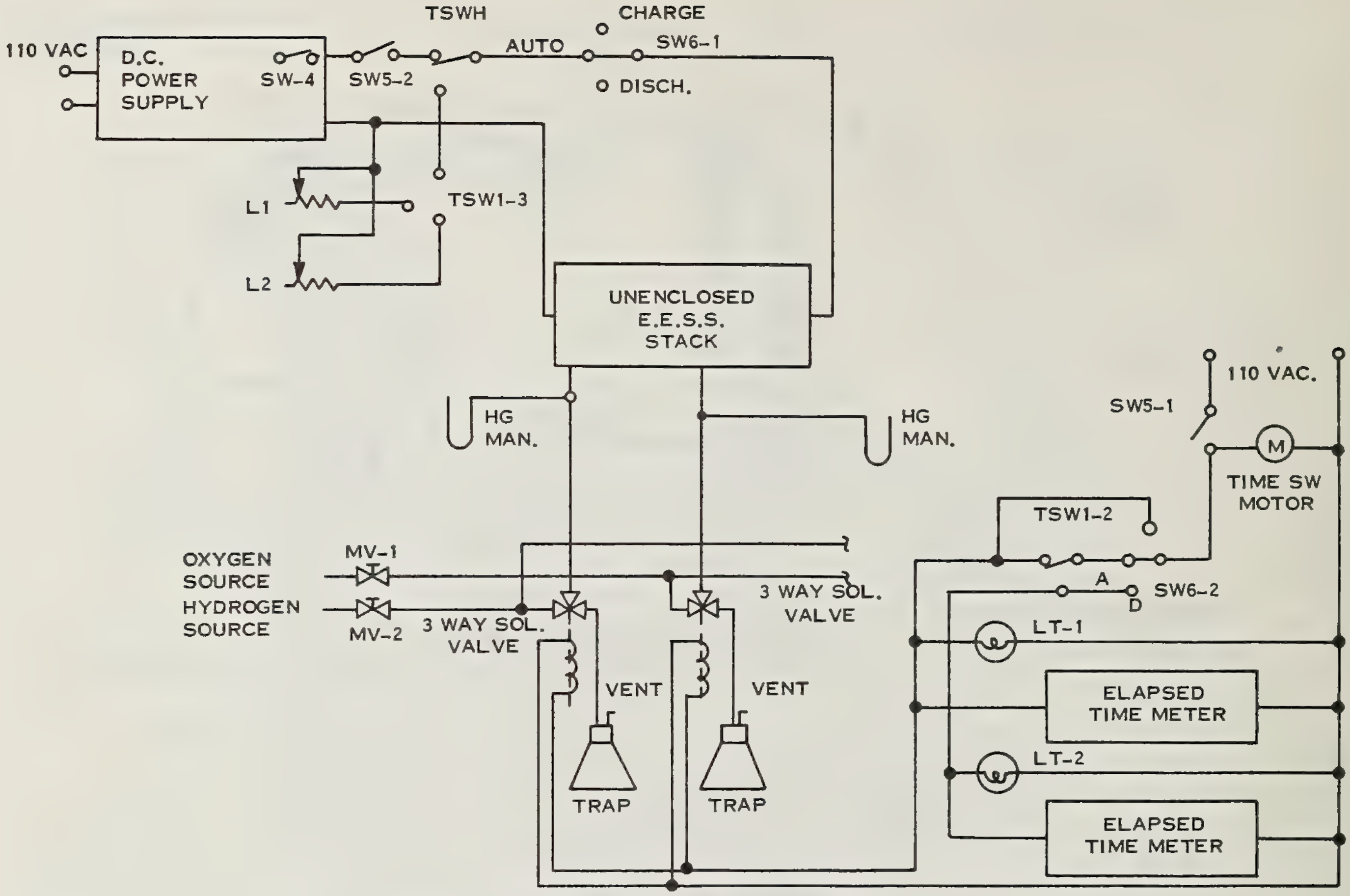

FIGURE 9. EESS UNENCLOSED UNIT TEST SCHEMATIC.

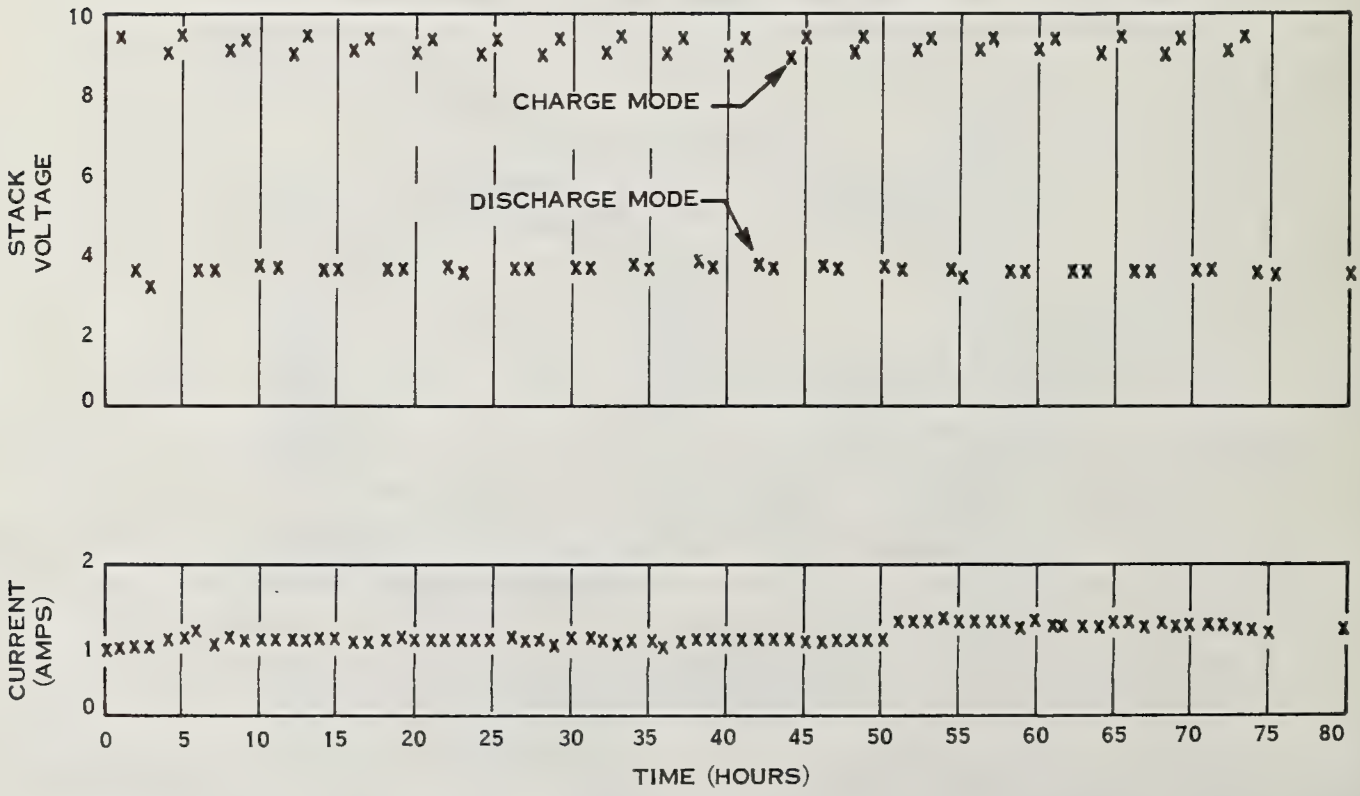

FIGURE 10. OPERATING DATA EESS 5 CELL UNIT NO. 2.

DISCUSSION

DR. CAIRNS: Have you analyzed the product water formed during discharge? What is the pH and the content of materials which might have been leached from the membranes?

MR. GLANFIELD: A detailed evaluation has not been made of the product water. The materials used, however, are the same materials that are present in fuel cells. They do tend to become acidic. Apparently, this acidity is due to some type of leaking form the membrane material. However, so far this has not affected the performance of the unit. In other words, the water that is pumped around within this unit is slightly acidic. This acidity is much less than that which was present with the 25% sulfuric acid system.

DR. MRAVA: Could you comment on the possibility of hydrogen leakage from the cell to the body in the completely enclosed, implantable version.

MR. GLANFIELD: Well, of course, that would depend upon the housing design. The housing that we are anticipating assessing is strictly pressure proof. There would be, at least with the present unit, connections and the like which would permit hydrogen leakage over a period of time. I am afraid that I could not comment too much at this time on the effect of hydrogen leakage from this unit over an extended period of time. I would expect that it would simply be a matter of the selection of the material, the method of sealing the unit, and also the electrical connections that are placed on it and how well they can be made.

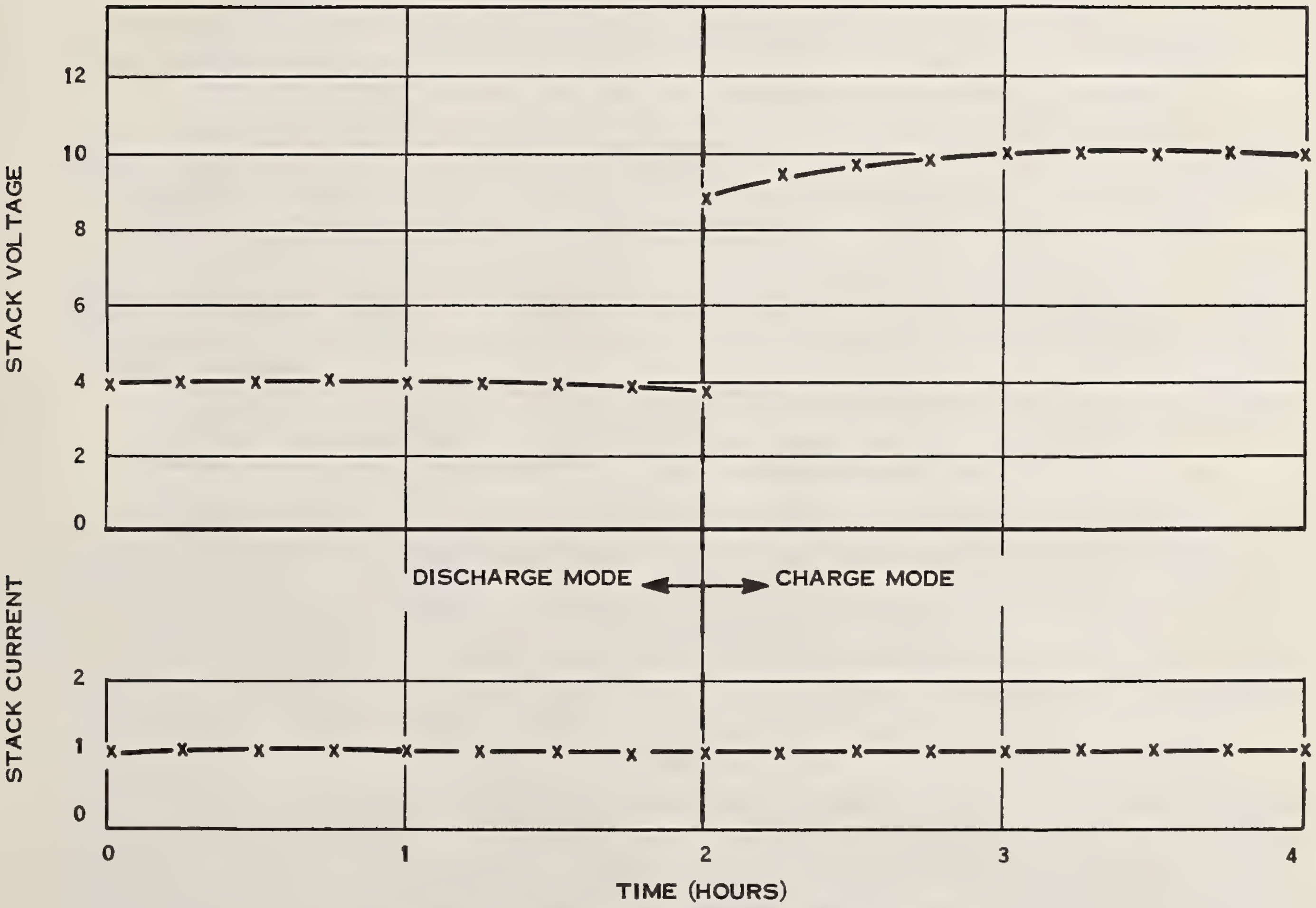

FIGURE 11. EESS 5 CELL UNIT NO. 2 SINGLE CYCLE DATA.

CHAPTER 88

DEVELOPMENT OF A HEAT SOURCE FOR AN IMPLANTABLE CIRCULATORY SUPPORT POWER SUPPLY

M. Bluestein, F. Huffman

Thermo Electron Corporation
Waltham, Mass.

An implantable power supply for circulatory support utilizing thermodynamic energy conversion requires a heat source which is thermally efficient, safe, rechargeable, and of minimum weight and volume. The objective of this effort is to develop a heat source which meets these requirements and can be coupled to a thermodynamic engine. Thermal energy is stored at 930°F in the latent heat of fusion of LiF/LiCl eutectic. Material is encapsulated in stainless steel. A monotube boiler is brazed to the TES (thermal energy storage) container. Recharging is accomplished through a resistance wire heater using transcutaneous power transmission. The TES container is surrounded by thin layers of vacuum-type multi-foil insulation. The TES container and insulation are encapsulated in a vacuum tight canister with penetrating boiler tube leads connected through thermal resistance bellows. Two heat sources have been fabricated and tested: one stores 147 watt-hours (wh) of energy; the second stores 67 wh. Heat losses at 930°F through the insulation were less than 4 watts for both units. Calorimeter tests have demonstrated removal rates up to 50 watts with thermal gradients in the TES material of less than 100°F. Tests of the eutectic in type 304 stainless steel have demonstrated the compatibility of these materials after more than one year of continuous cycled operation at 930°F. The approximate weight of a complete 67 wh heat source is two pounds.

INTRODUCTION

An attractive approach to an implantable circulatory support system is to drive the blood pump from a miniature heat engine operating off stored thermal energy. Not only are the system weight and size reasonable, but such a device could be adapted to radioisotope fuel in order to give the host a greater degree of freedom than would be possible with a rechargeable system.

One of the better ways of storing thermal energy at high temperature is to melt a solid with a high latent heat of fusion. The volume changes are small, and the heat is available at near-constant temperature as the molten material solidifies. Heat energy storage is particularly interesting for rechargeable systems, since the thermal energy storage subsystems should be capable of a practically unlimited number of recharge cycles independent of the depth and the rate of recharge.

A primary objective of the thermal energy storage (TES) program was to give hardware demonstration of the compact thermal energy storage, rechargeability, and low heat losses with a prototype TES subsystem. Such a project involves the choice of thermal storage materials, the selection of compatible container materials, the development of fabrication techniques, and the design of effective thermal insulation. The task organization of these activities to achieve the program objectives is shown in Figure 1.

Task I was a data survey of candidate thermal storage materials, containers and insulations.
Tasks 2 and 3 were devoted to thermal property measurements of lithium halide and lithium hydride. Energy storage densities, melting, and thermal expansions were surveyed.
Prototype TES units were designed, fabricated, and tested under Task 4.

A literature survey showed that selected lithium salts, with relatively high heats of fusion and suitable melting points, could serve as heat sources for miniature thermodynamic engines. Two materials were chosen for experimental evaluation. The eutectic mixture of lithium fluoride and lithium chloride was chosen as suitable for Rankine engine application. The eutectic mixture gives an isothermal melting point of 930°F. Lithium hydride was studied as a possible thermal storage material for coupling to Stirling engines; it has a melting point of about 1270°F.

A survey of container materials and containment methods showed that tungsten, stainless steel and nickel were prime candidates for containers. These materials, which can be welded by present techniques, gave promise of being compatible with the TES salts.

EXPERIMENTAL

The energy storage densities of the TES materials were measured in a test cell to verify the published data. The reported heats of fusion are 610 calories per gram for lithium hydride and 165 calories per gram for the lithium halide eutectic. A brazed electrical resistance heater of Inconel wire was used to melt the TES material. Heat was removed with a calorimeter. The test cell used to determine the heat of fusion of the materials is shown in Figure 2. This apparatus, with modified thermocouple placement, was used to investigate thermal gradients as a function of heating and cooling rates.

Figure 3 is an illustration of the test setup. The test cell, the power supply, the recorder which reads out the various temperatures from the thermocouples, and the vacuum pump with a cold trap are shown.

Figure 4 shows the placement of the thermocouples. Thermocouple No. 3 is in the center of the material and No. 4 is on a radial line one inch from the center. This container was three inches in diameter, which is a representative size for an artificial heart power supply. Thermocouple No. 2 is outside to serve as a reference. Typically, thermocouples No. 3 and 4 stay close together, indicating small thermal gradients in the TES material for the anticipated heating and cooling rates.

Figure 5 shows a test arrangement which ensures that thermocouples were not located in any void pockets inside the material. Thermocouples 3 and 5 were placed in the center and on the outer surface of the container, respectively. Temperatures were observed as a function of time for different input and output power levels. In no instance did the temperature gradient between the center and the surface exceed 100°F. It is apparent from the figure that thermal gradients in the lithium halide eutectic should not constitute a major problem.

Figures 6 and 7 summarize the tests that were performed with the different heating and cooling rates. Power input ranged from 30 watts to 250 watts; power output levels were from 50 to 120 watts. The compatibility between the lithium halide eutectic and tungsten, stainless steel, and nickel samples has been studied in long-term tests. Approximately one-inch long tabs of the candidate container materials were sealed into small-diameter stainless steel tubes with the lithium halide eutectic. The sample tubes (Figure 8) were then placed in an electric furnace with an argon atmosphere and cycled through the melting point of the eutectic.

Some results of these continuing tests are given in Table 1, which shows a spectrographic analysis of the eutectic material after an equivalent of 363 days in the furnace for the stainless steel tab and the tungsten tab and 337 for the nickel tab.

TABLE 1

SPECTROGRAPHIC RESULTS

For LiF/LiCl Eutectic

Element	Control	363 Day Stainless Steel Tab	363 Day Tungsten Tab	337 Day Nickel Tab
Li	A	A	A	A
Al	e	f	f	f
Ba	3g	ND	g	ND
Ca	3d	e	e	e
Cu	f	3f	$3f^+$	$3f^-$
Cr	f	d	e	e
Fe	e	3e	d	3d
Mg	3f	3f	3f	e
Mn	3g	e	e_+	e_+
Na	3e	e	e	e
Ni	3g	d	3f	e
Pb	f	f	ND	ND
Si	3f	e	e	e

Code:

A: 10 - 100%
b: 1 - 10%
c: 0.1 - 1%
d: 0.01-0.1%
e: 0.001 - 0.01%
f: 0.0001 - 0.001%
g: 0.00001- 0.0001%
ND: Not detected

In all cases, the furnace was cycled within a small temperature range to simulate the actual usage in a power source (that is, going from the solid end of the melting range to the liquid end and back again). The representative amount of time is one year. These are the results, in approximate parts per thousand. The control material as received from the manufacturer has never been heated. Of all the different tabs, the only metal pickups of note occurred from chromium, manganese, and nickel. These concentrations have leveled after an initial pickup of material. In addition to the spectrographic analysis of the eutectic material, photomicrographic analyses of the metals, the tabs, and the containers have been made.

Figure 9 shows a photomicrograph of the stainless steel tab in the eutectic after one year. The spots are artifacts of the etching process. There is no evidence of corrosion along the boundary. Figure 10 presents the micrograph for the container, which has a different grain size. Again, there is no evidence of corrosion at the boundaries. These tests are continuing and samples are expected to be taken after two years. They indicate that type 304 stainless steel is a suitable container material for the eutectic.

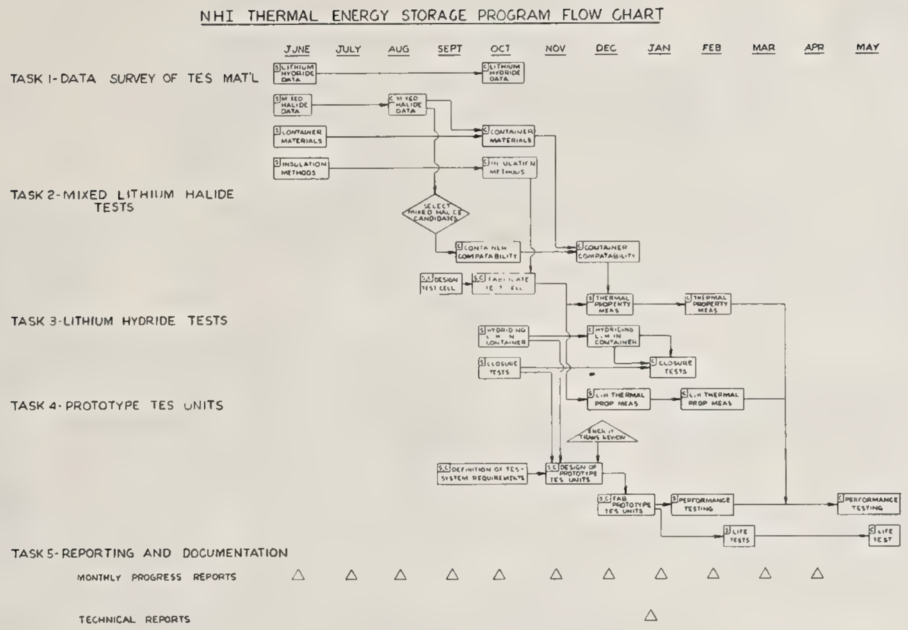

FIGURE 1. TES PROGRAM FLOW CHART.

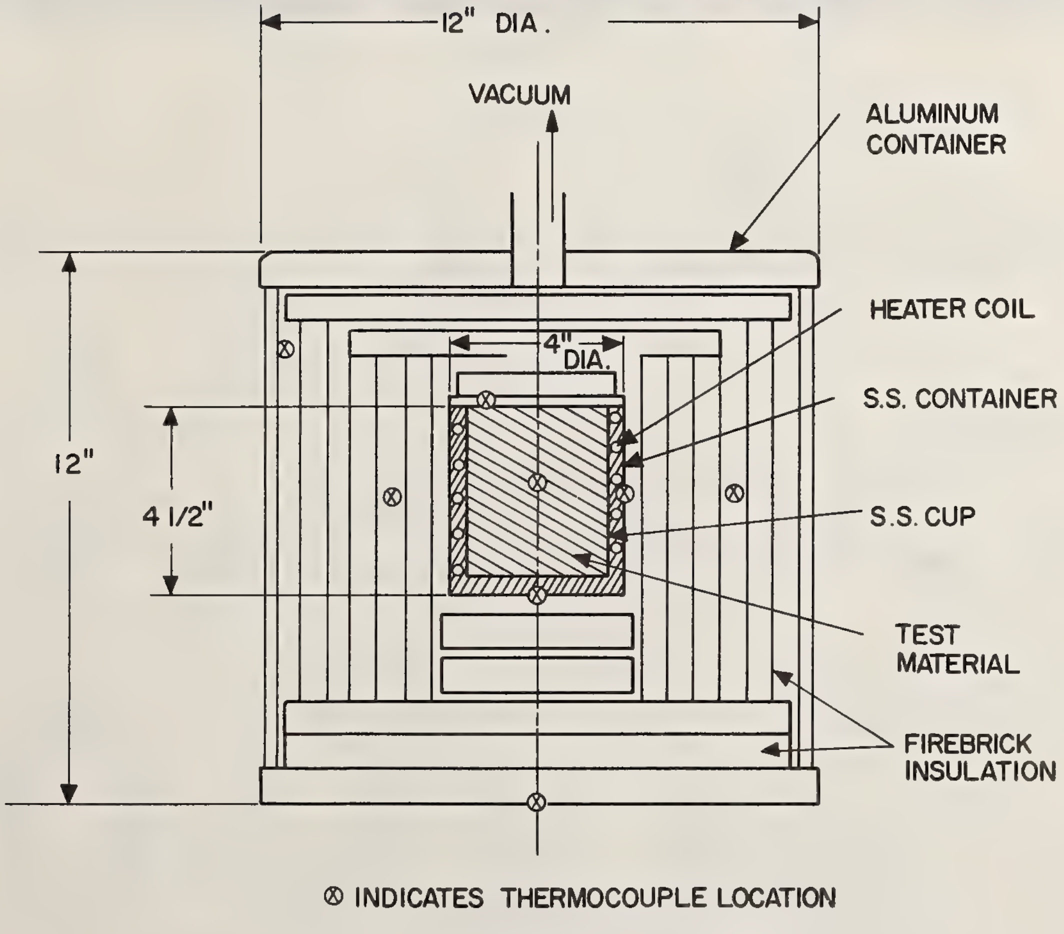

FIGURE 2. THERMAL TEST CELL (SCHEMATIC).

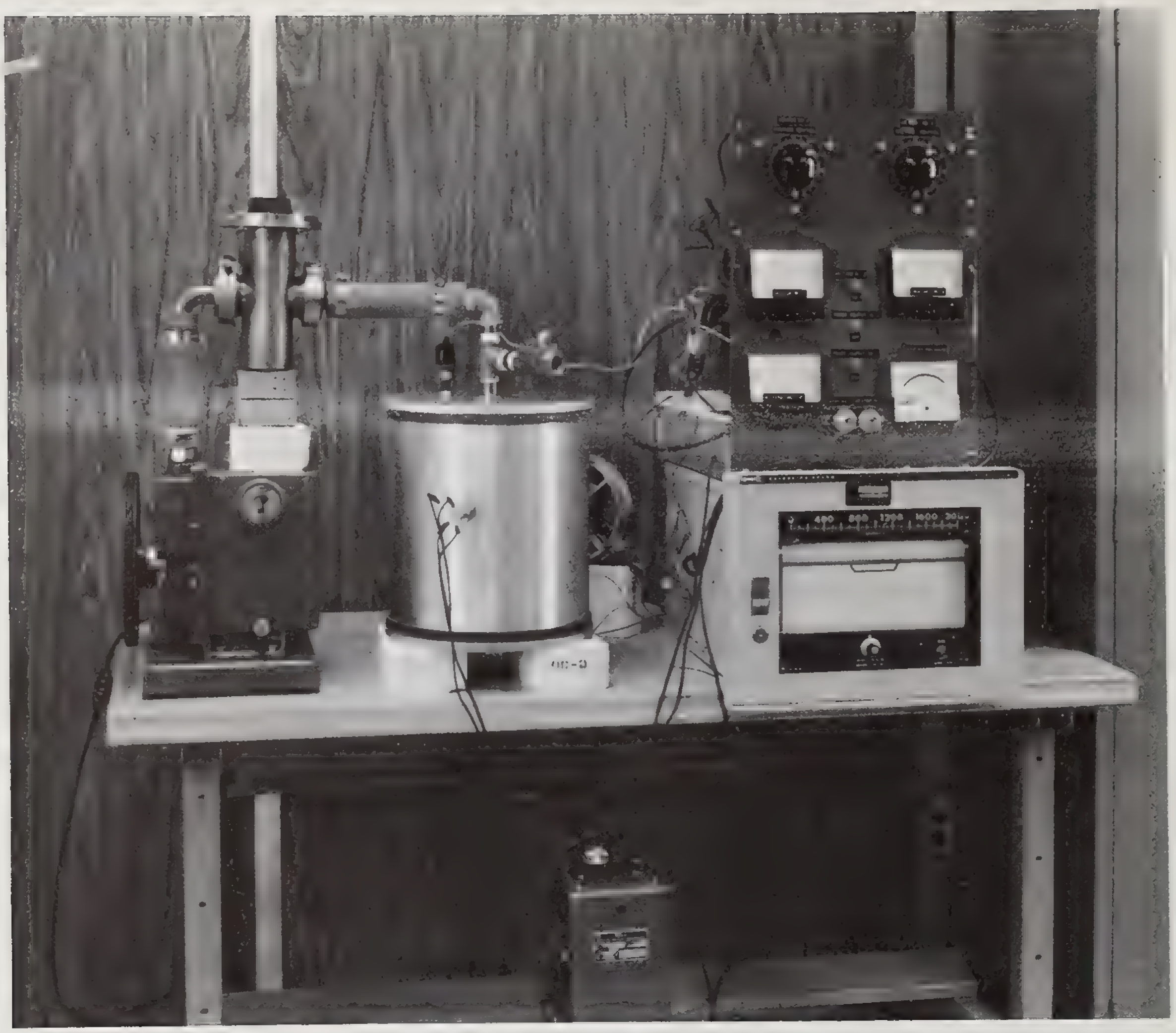

FIGURE 3. THERMAL TEST APPARATUS.

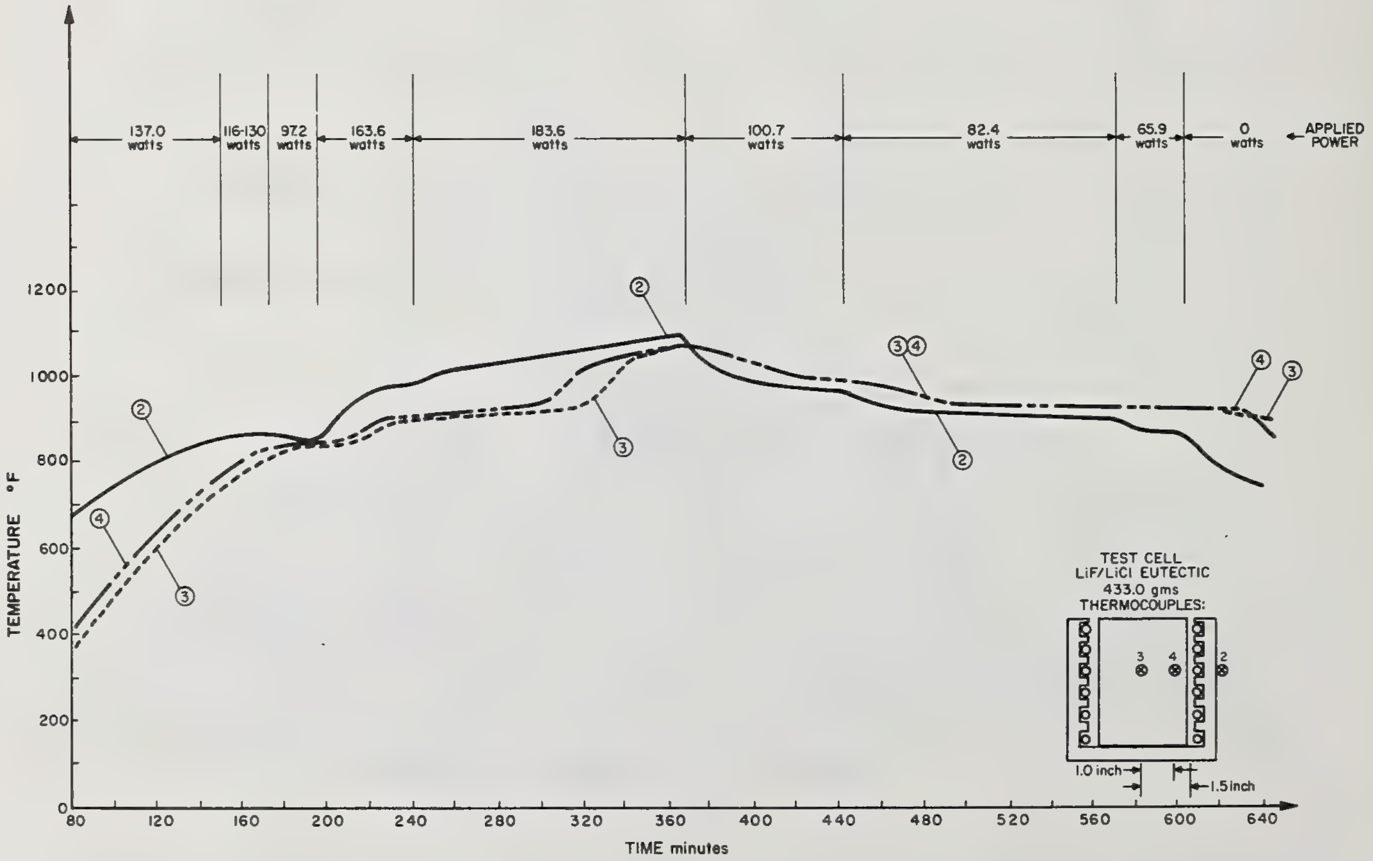

FIGURE 4. THERMAL GRADIENT TEST RESULTS.

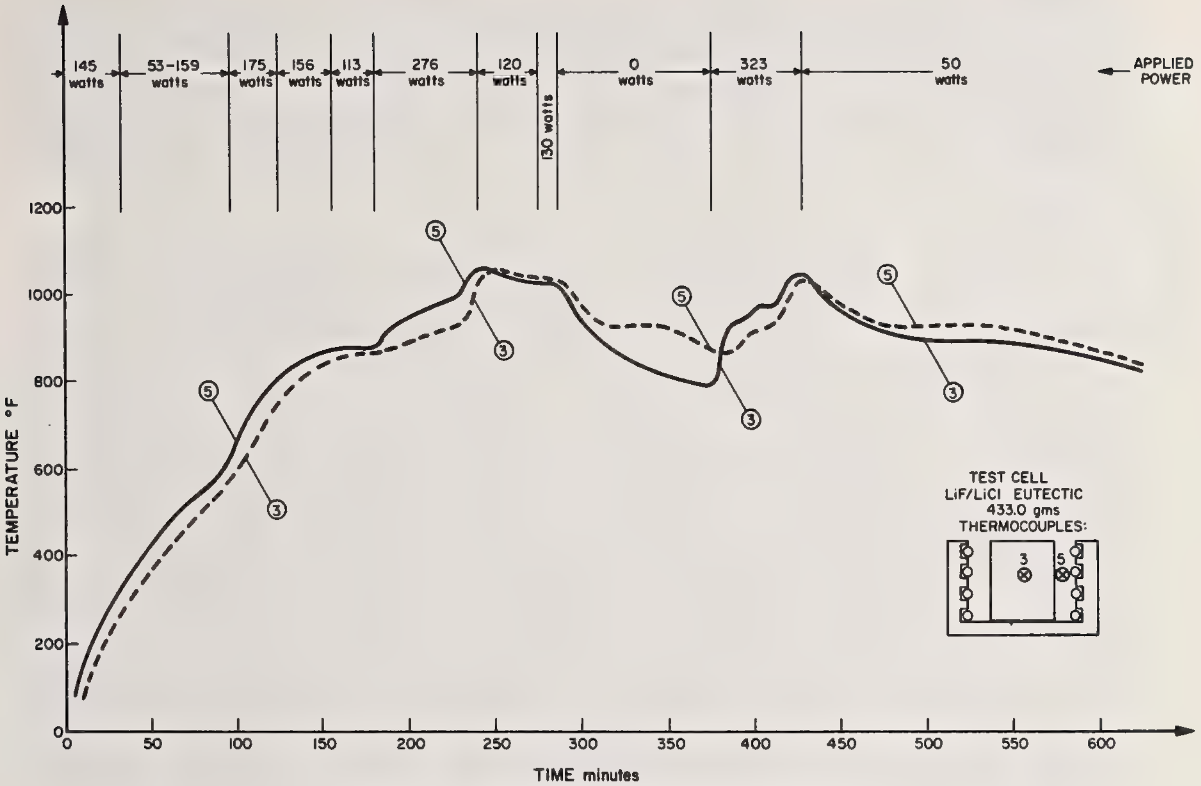

FIGURE 5. THERMAL GRADIENT TEST RESULTS.

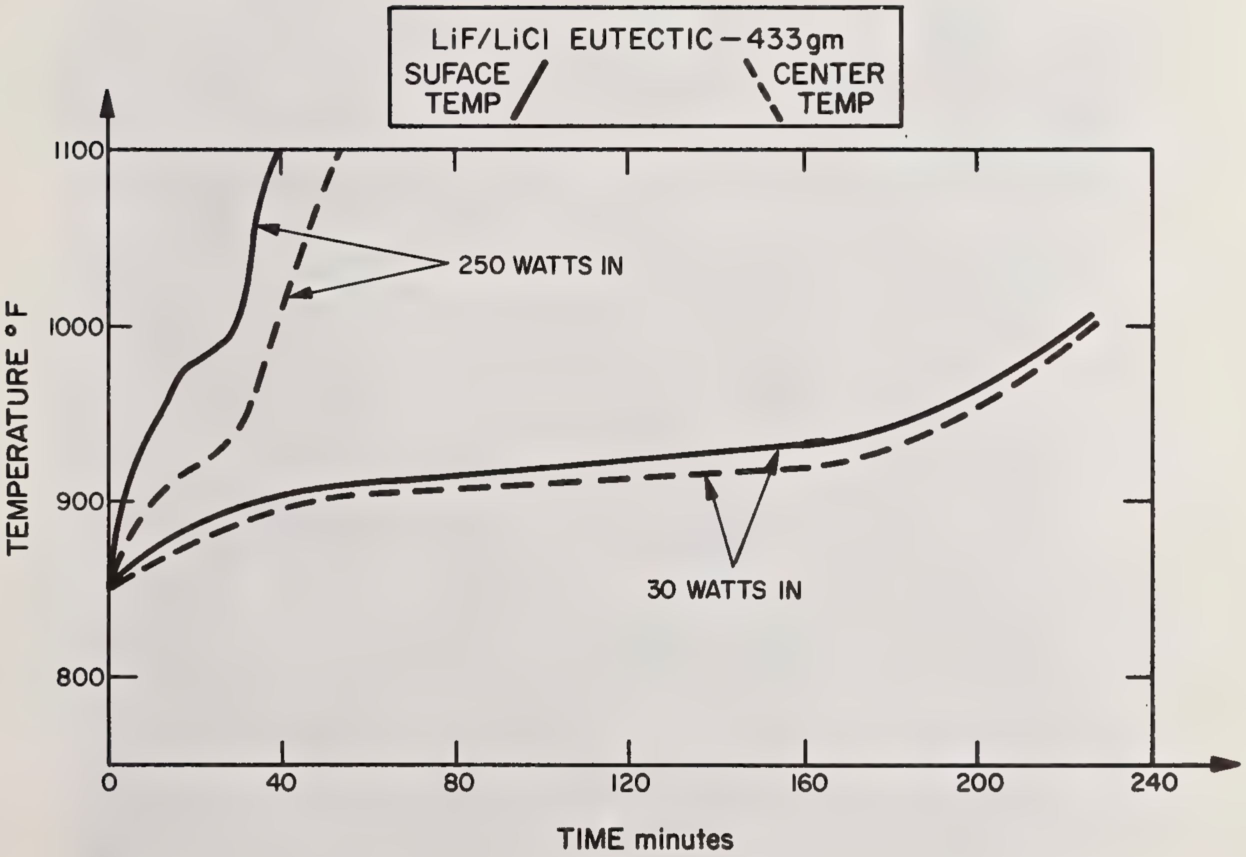

FIGURE 6. POWER INPUT TEMPERATURES VERSUS TIME.

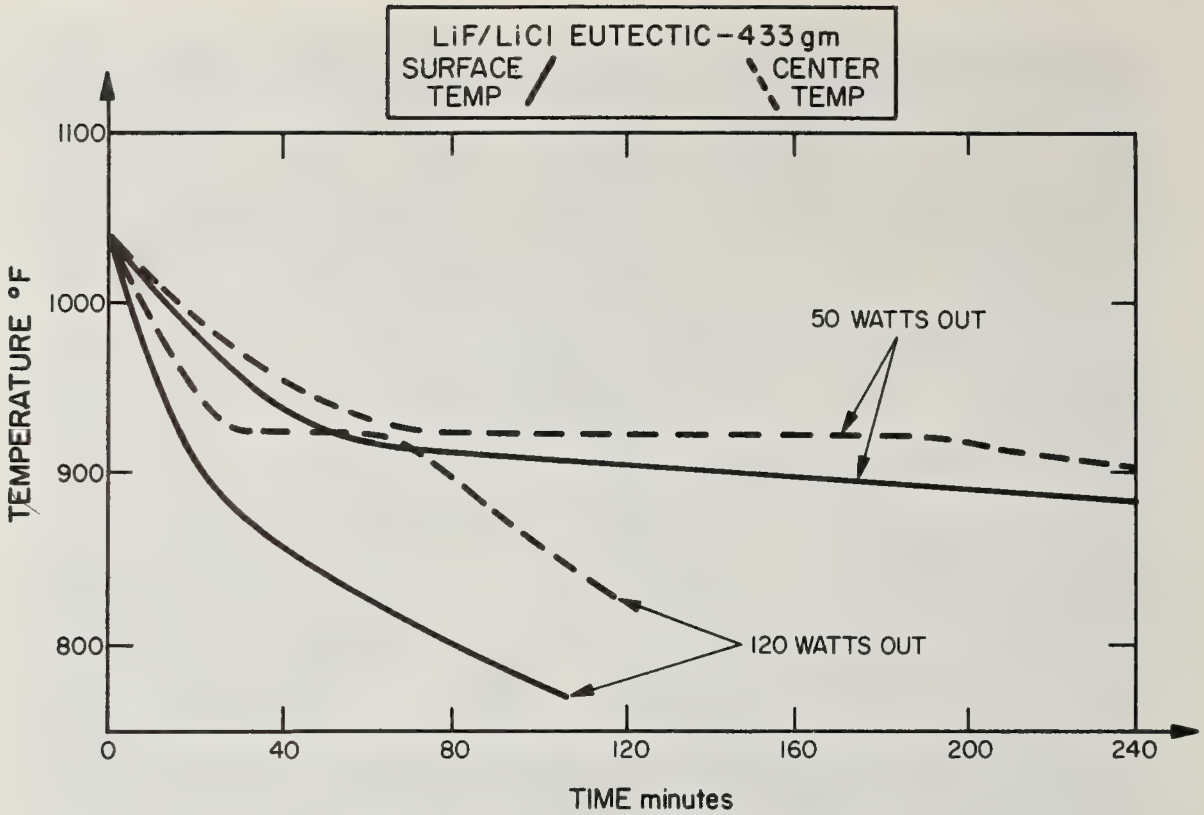

FIGURE 7. POWER OUTPUT TEMPERATURES VERSUS TIME.

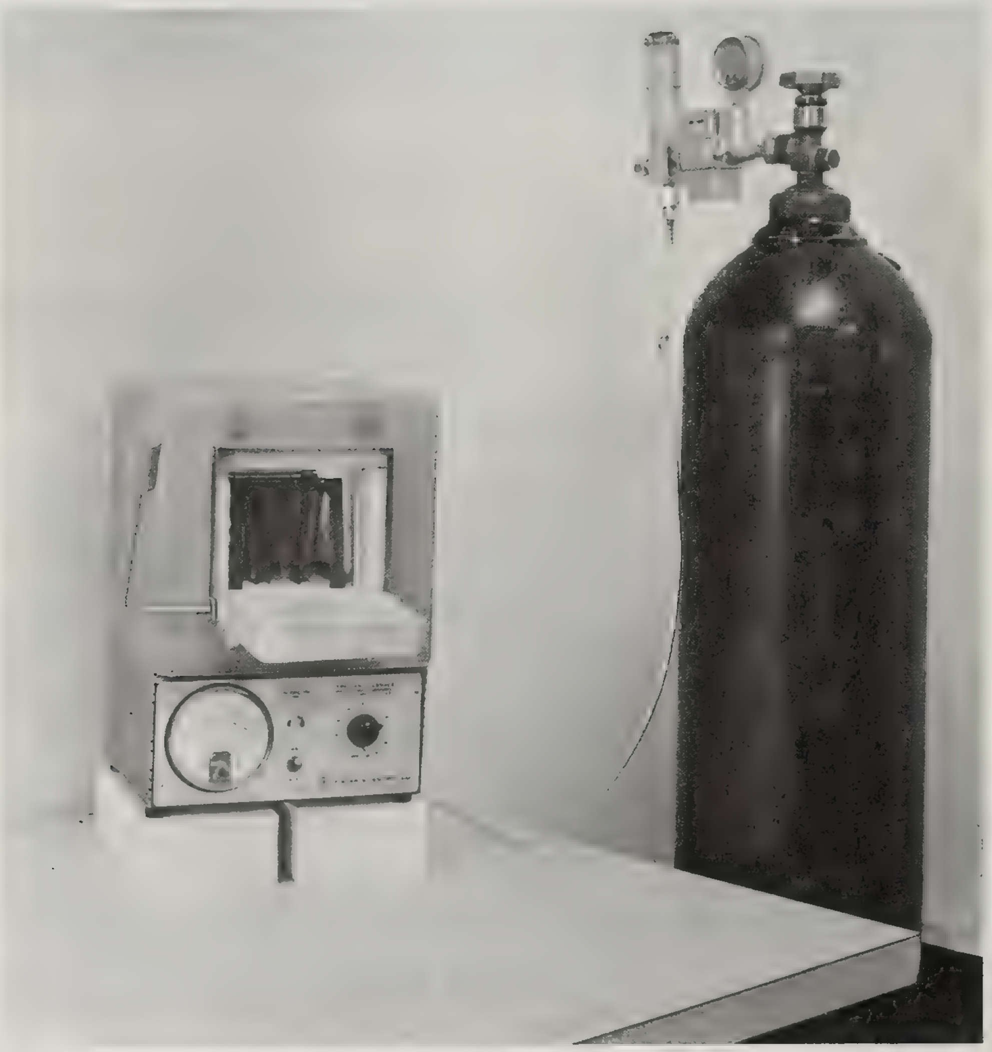

FIGURE 8. COMPATIBILITY TEST APPARATUS.

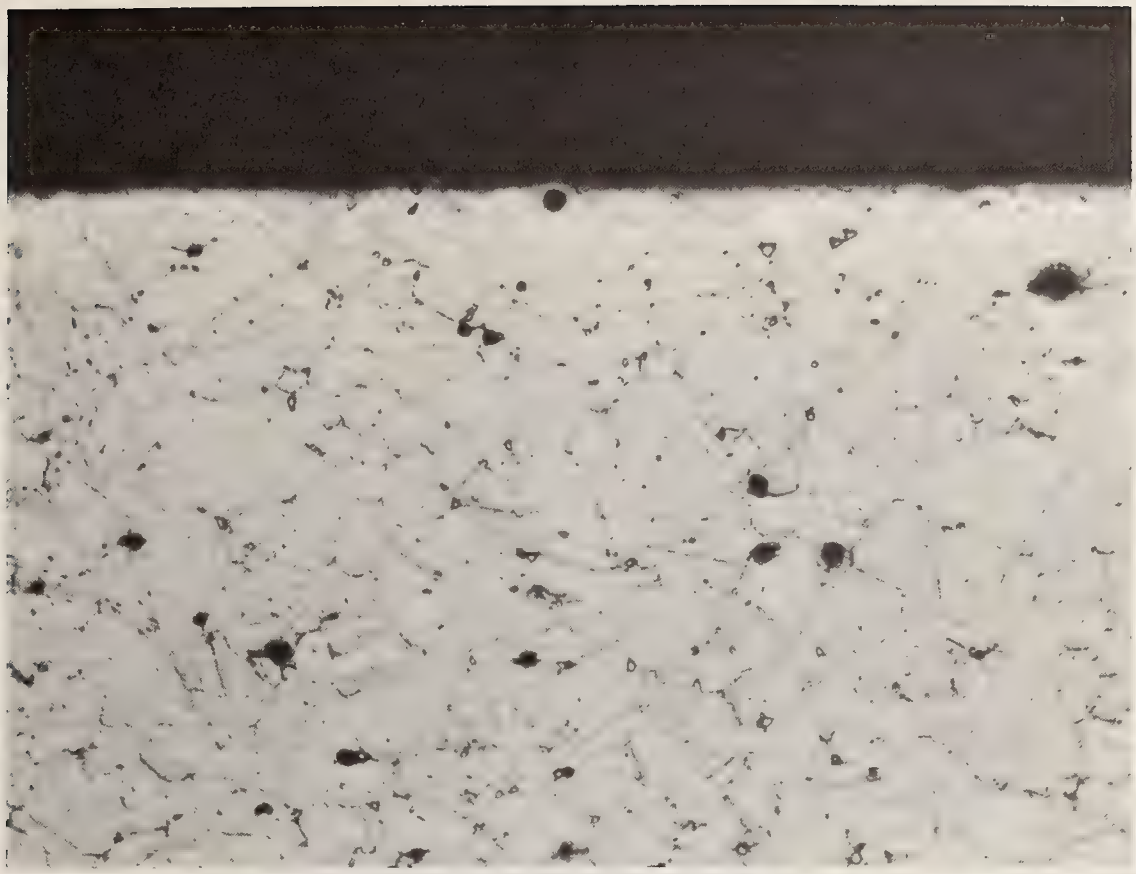

FIGURE 9. PHOTOMICROGRAPH OF STAINLESS STEEL TABS.

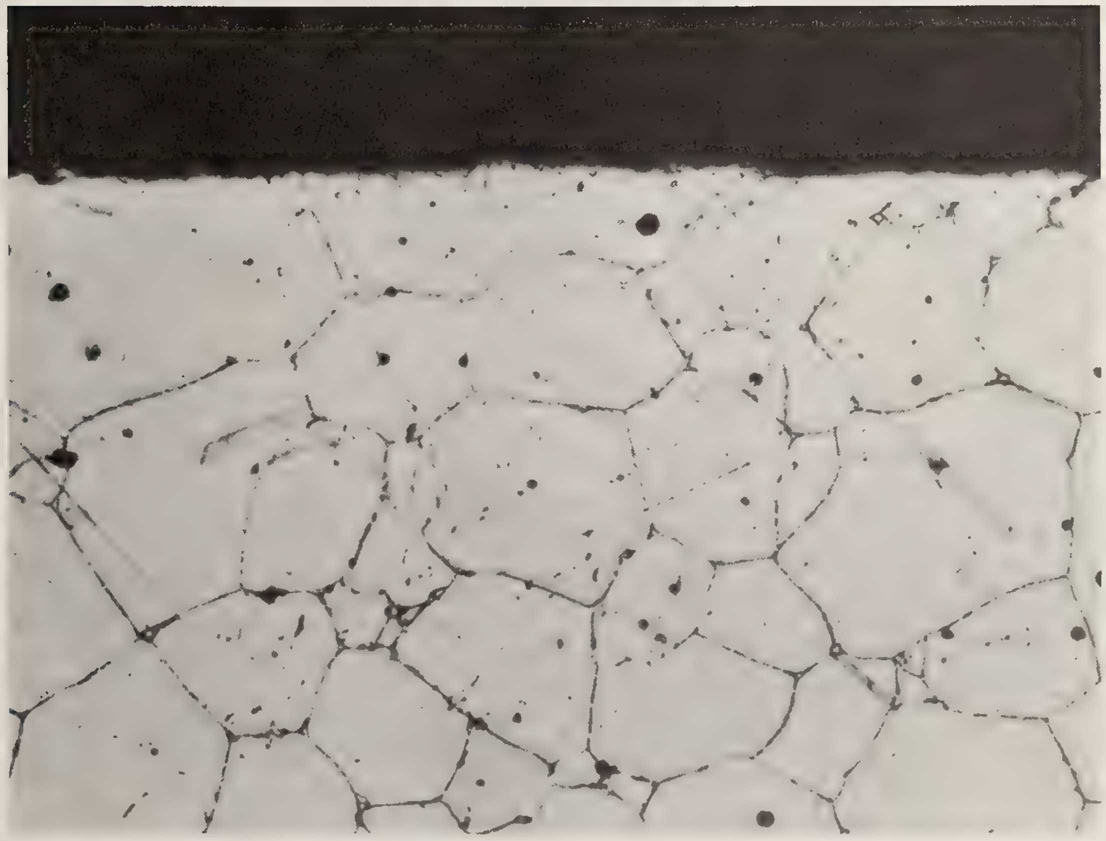

FIGURE 10. PHOTOMICROGRAPH OF STAINLESS STEEL CONTAINER.

Lithium hydride has an attractive gravimetric thermal storage capacity. However, LiH dissociates to give an equilibrium pressure of hydrogen of 30 torr at its melting point. Unfortunately, hydrogen permeates most materials rapidly at 1250°F. This problem is acute if vacuum foil thermal insulation is to be used. On the basis of available data, tungsten was chosen as the container for lithium hydride. Lithium hydride also presents a toxicity problem in addition to the problem of hydrogen diffusion out of the container.

The modified calorimeter for evaluating the TES prototype is shown in Figure 11. The second heater is used to calibrate the calorimeter. The third and lower heater is used to vary the amount of power output to the calorimeter from thermal energy storage materials. Thermo Electron foil insulation was used to reduce heat loss. Cooling coils of water were used to carry the heat away.

After calibrating the calorimeter, the thermal losses were measured at different temperatures. Heater No. 3 was adjusted to give a cooling rate of approximately 20 watts. Energy storage was measured by timing the plateau period at the melting point. Figure 12 shows the eutectic prototype unit. The stainless steel container is about four inches long by three inches in diameter. Figure 13 shows the unit in place with the foil insulation package around it on the calorimeter stand. Figure 14 shows the entire test apparatus.

The graph of the insulation heat loss versus TES surface temperature is shown in Figure 15. The insulation package consists of 40 layers of nickel foil with zirconium particle spacing. The foil assembly is evacuated to a pressure of 3×10^{-5} millimeters of mercury; this low pressure is very important for maintaining the usefulness of the insulation. At the operating point, the melting point of the eutectic is about 930°F. The insulation heat loss is less than three watts, or less than .01 watts per square centimeter of area.

Figure 16 shows a performance test of the eutectic prototype. Heater No. 3 was adjusted to give a heat flow to the calorimeter of about 20 watts, showing that the surface temperature remains at the melting point for about six hours. The mean heat flow is approximately 21 watts. These data give a thermal storage of about 125 watt-hours for a charge of 765 grams.

Two prototypes were fabricated using the lithium hydride in tungsten containers. Figure 17 will show the first prototype. An available tungsten crucible was used, and the heater was brazed into it. The calorimeter is shown post-test. Difficulty was encountered in sealing the tungsten because the lithium hydride inside would vaporize to the top as a result of the high temperatures needed to weld the tungsten. Black deposits at the top indicate lithium and the little holes indicate leaks. This unit was not suitable for any kind of data.

Figure 18 shows a somewhat larger tungsten crucible which holds 17 grams of lithium hydride. The test procedure was the same as for the eutectic. Figure 19 shows the heat losses. The operating point is 1250°F, the melting point of the hydride. These insulation losses are significantly higher than those for the eutectic, since the foil insulation was contaminated by the leakage from the original tungsten crucible. The same foil insulation package was used throughout all the tests. It is assumed that the first curve is applicable to the insulation, since that should only depend on the temperature within it. Figure 20 shows the performance curve for the lithium hydride for this second crucible, which was heated up and then cooled at approximately 25 watts for about 15 minutes. This result is consistent with the predicted watt-hours storage capacity of 17 grams of lithium hydride. These data can be extrapolated to give an idea of how such a capsule would perform for an eight-hour unit. Figure 21 presents a picture of the niobium foil, which was used as a getter to trap hydrogen. This 15-mil thick foil is placed between the insulation and the thermal energy storage capsule.

The bell jar was sealed off from the diffusion pump. The pressure went up due to the outgassing. The heat transfer through the foils was measured with the niobium in and with the niobium out; approximately an 8 percent increase in power loss through the insulation was found with the niobium removed. The test temperature of the lithium hydride was about 1000°F

SUMMARY

To summarize, both a eutectic and the hydride of lithium have been evaluated as thermal storage materials. The eutectic prototype unit has demonstrated its feasibility. The hydride system still has unresolved gettering and welding problems. The hydride certainly has attractive thermal storage capacity. However, toxicity and gettering problems make the hydride more difficult to fabricate. According to our graph of heat loss with the foil insulation, the eutectic would lose about 3 watts, the hydride about 7 watts at operating temperatures (Figure 22).

Work is continuing on fabricating a complete heat source using the eutectic. Such a unit, shown in Figure 23 includes a monotube boiler whose leads are connected to the heat source container via thermal resistance bellows. The outer container functions as the foil insulation envelope. A single heater lead is shown on top. Electron beam welding techniques were used to provide a sealed vacuum container. The storage capacity of this unit is 70 watt-hours; its total weight, including all components, is about two pounds.

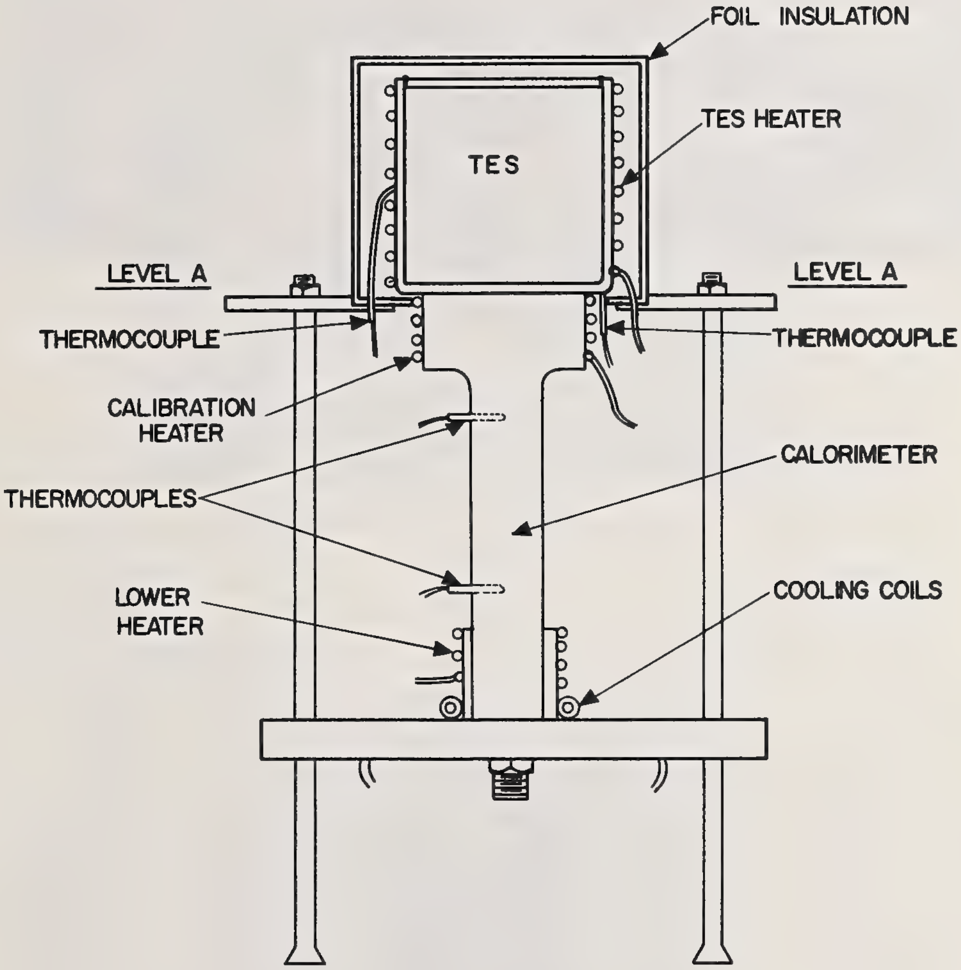

FIGURE 11. TES PERFORMANCE TEST CALORIMETER.

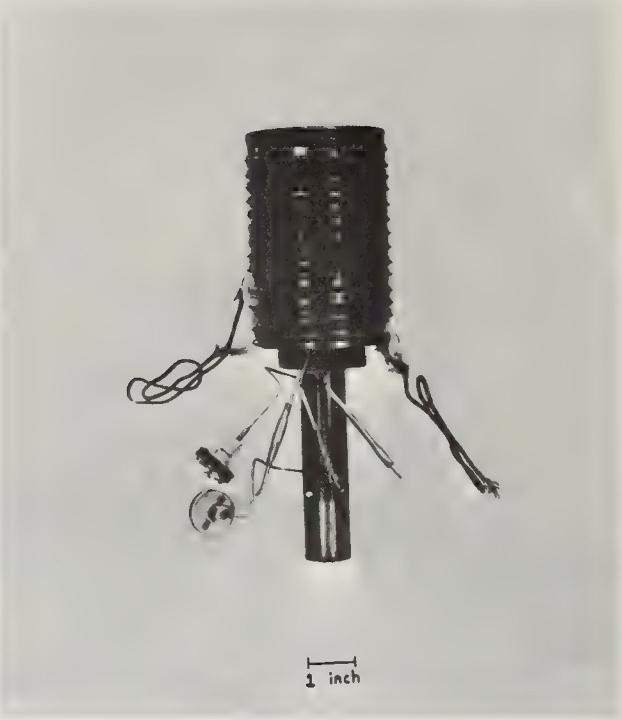

FIGURE 12. LiF/LiCl TEST PROTOTYPE.

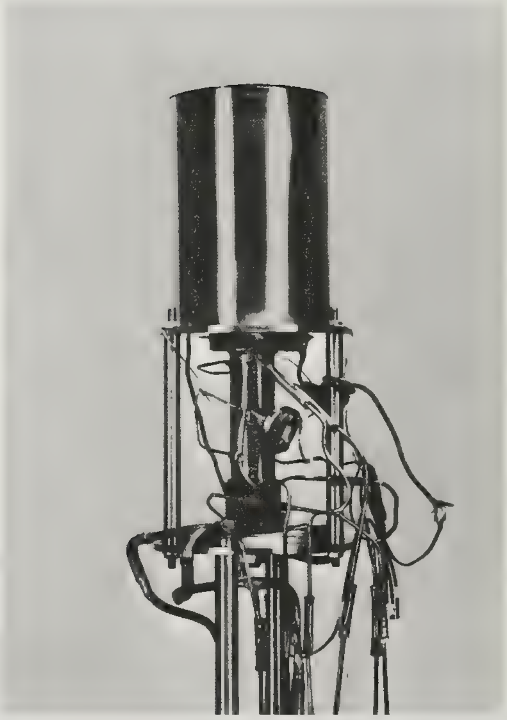

FIGURE 13. PROTOTYPE TES ASSEMBLY ON CALORIMETER.

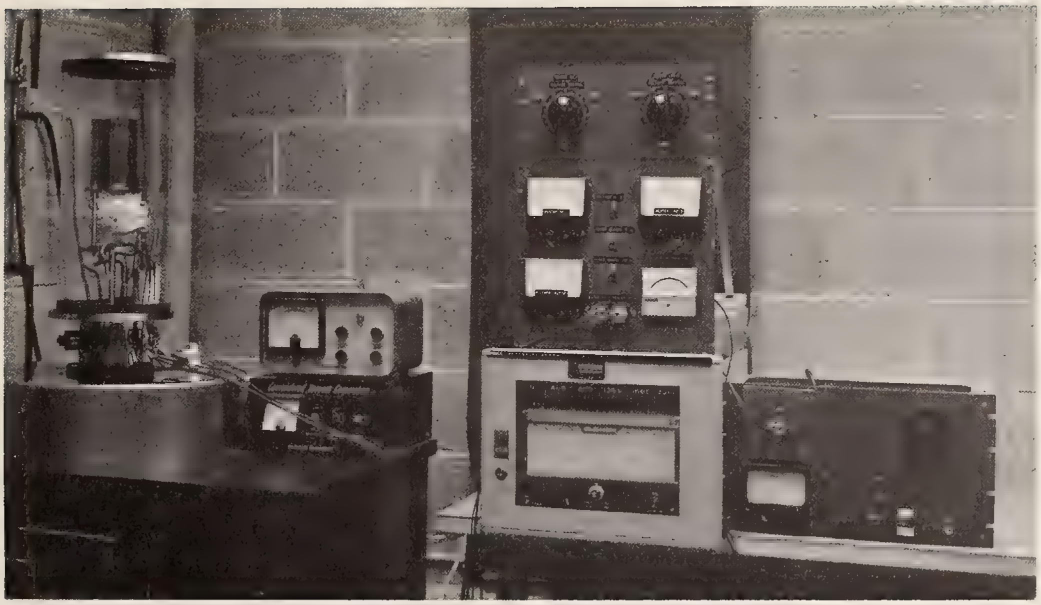

FIGURE 14. PROTOTYPE TEST APPARATUS.

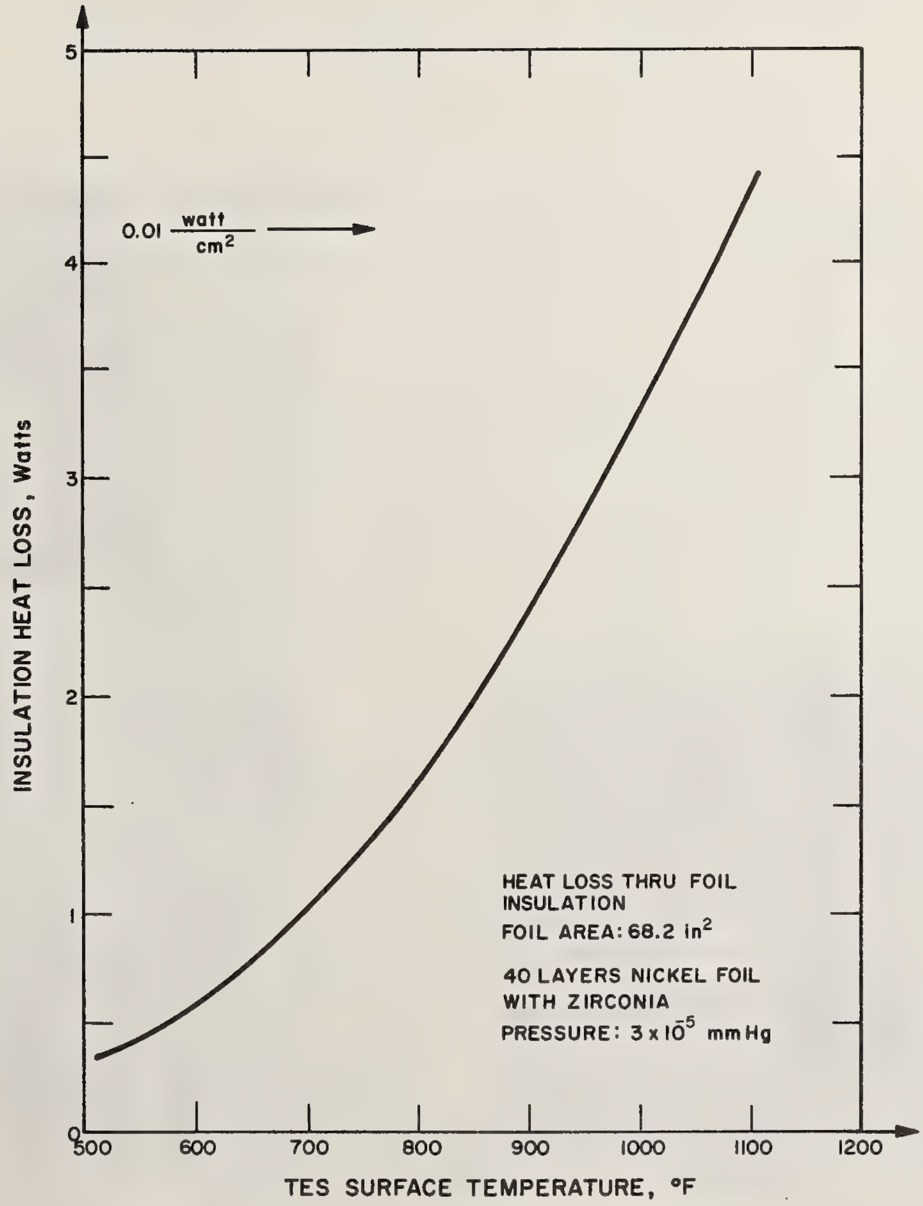

FIGURE 15. HEAT LOSS THROUGH INSULATION (LiF/LiCl).

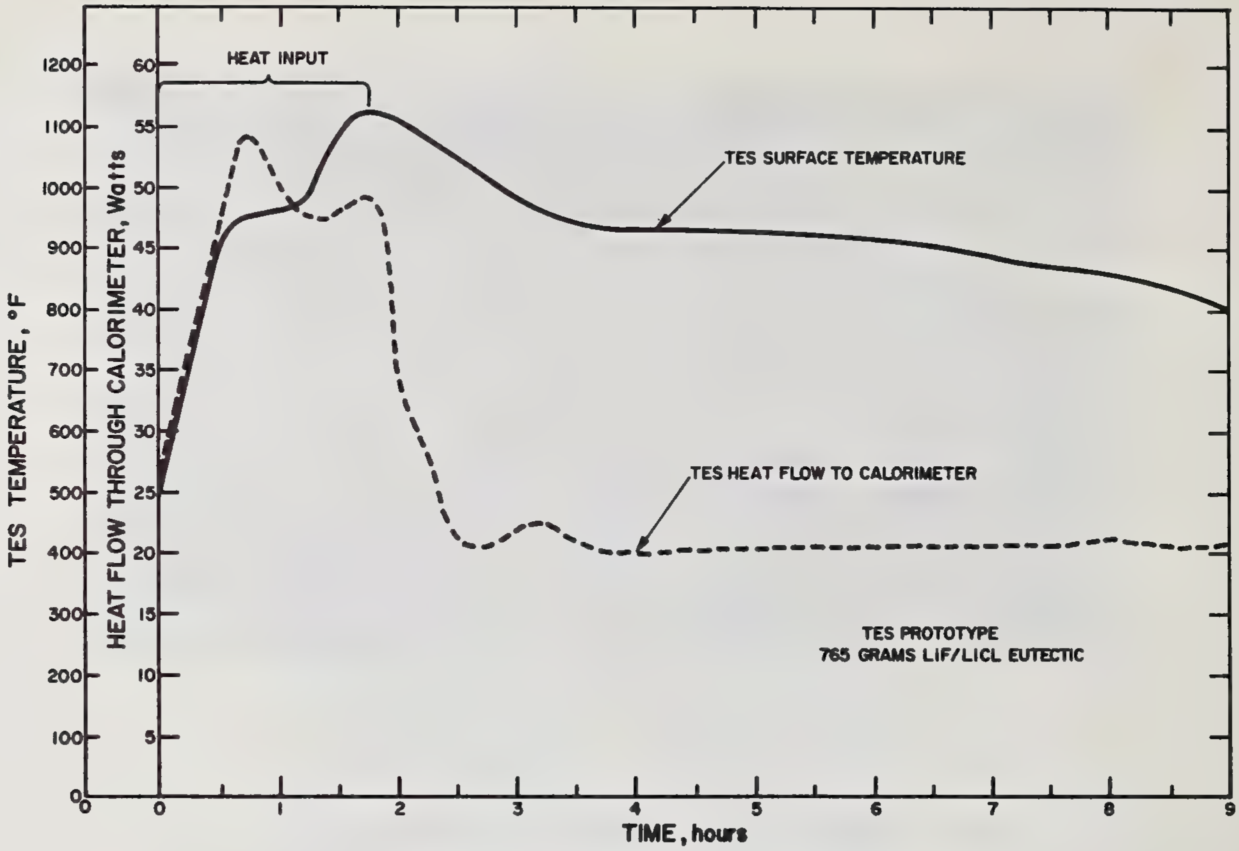

FIGURE 16. PERFORMANCE TEST RESULTS (LiF/LiCl).

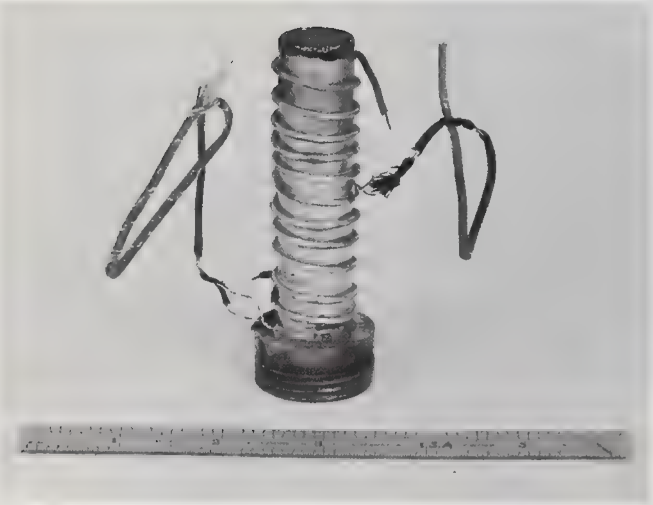

FIGURE 17. FIRST LiH PROTOTYPE.

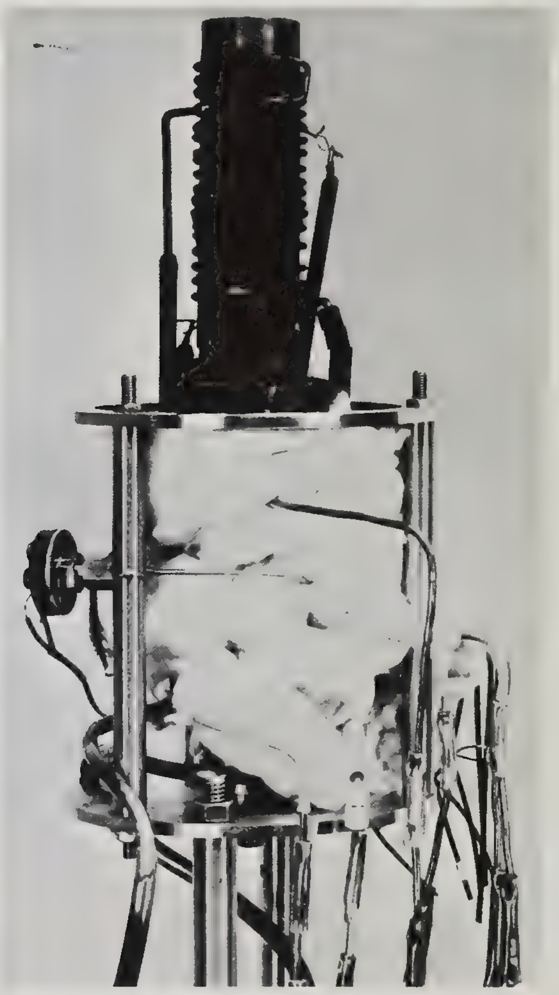

FIGURE 18. SECOND LiH PROTOTYPE.

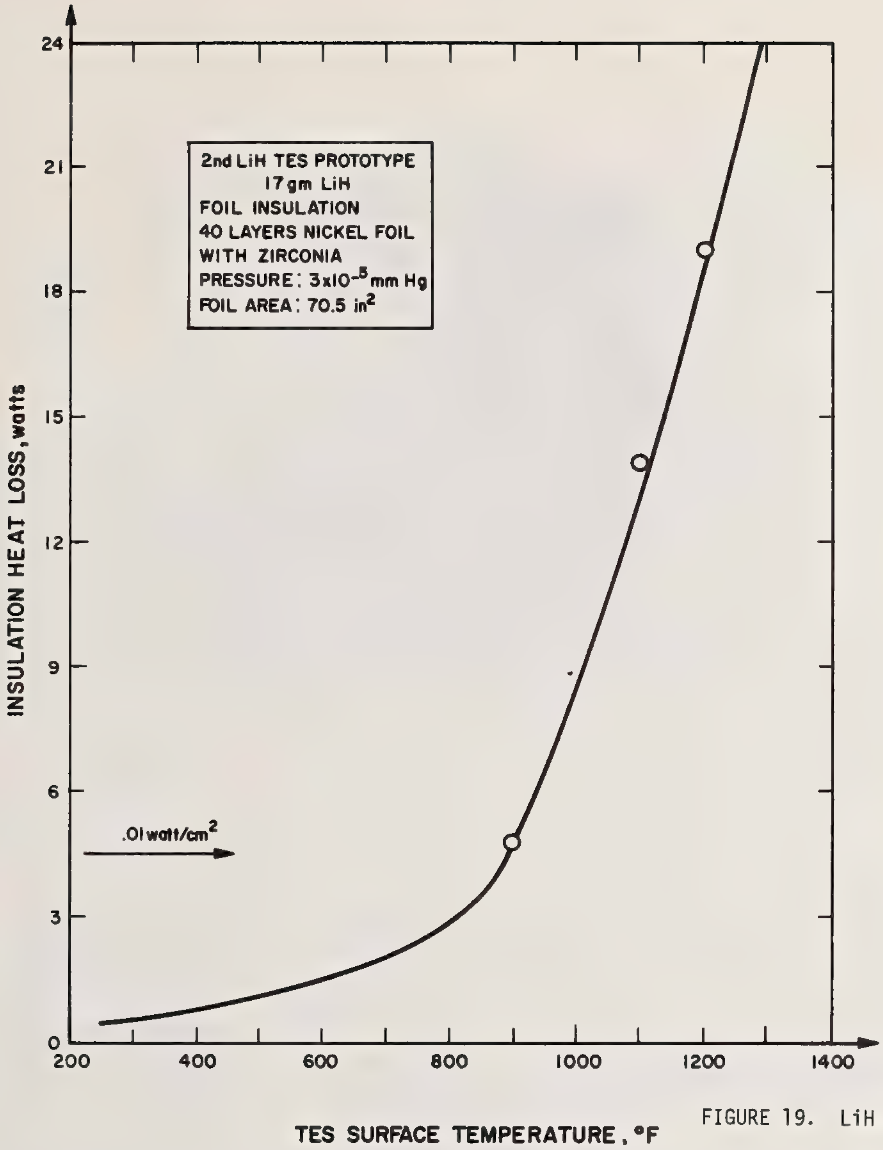

FIGURE 19. LiH PROTOTYPE HEAT LOSSES.

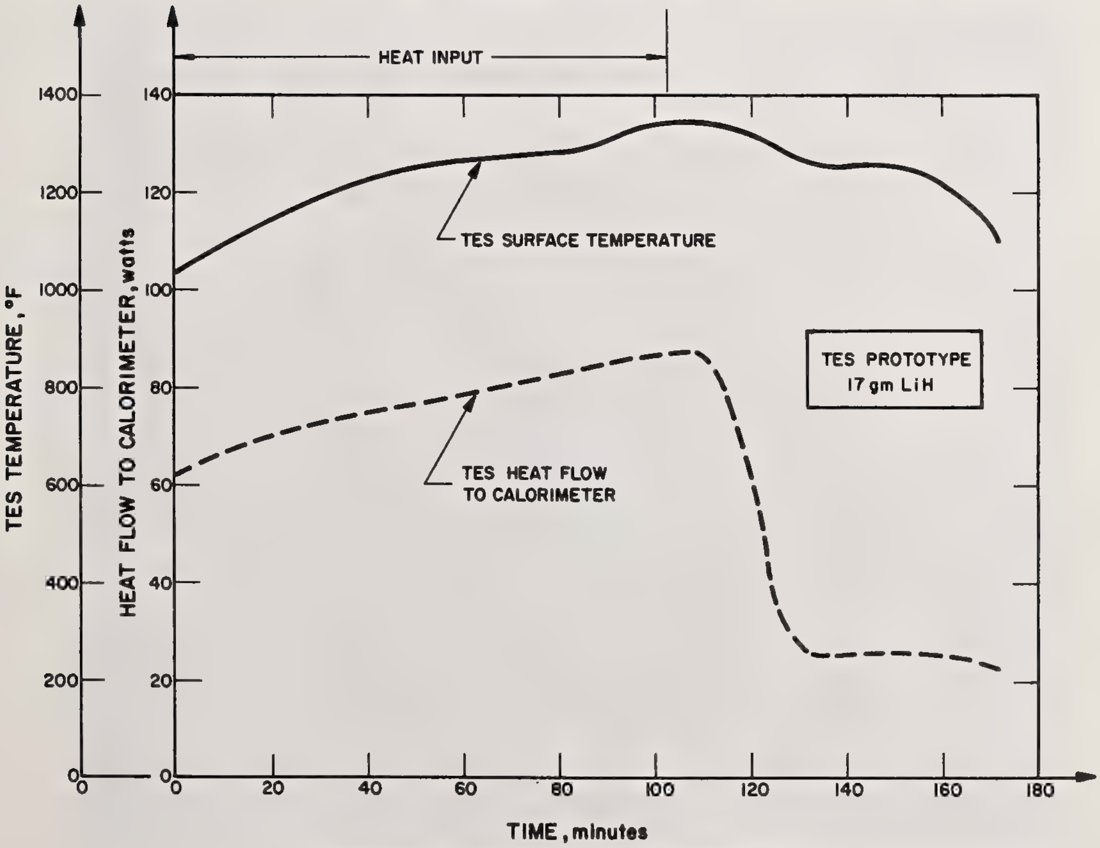

FIGURE 20. PERFORMANCE TEST RESULTS (LiH).

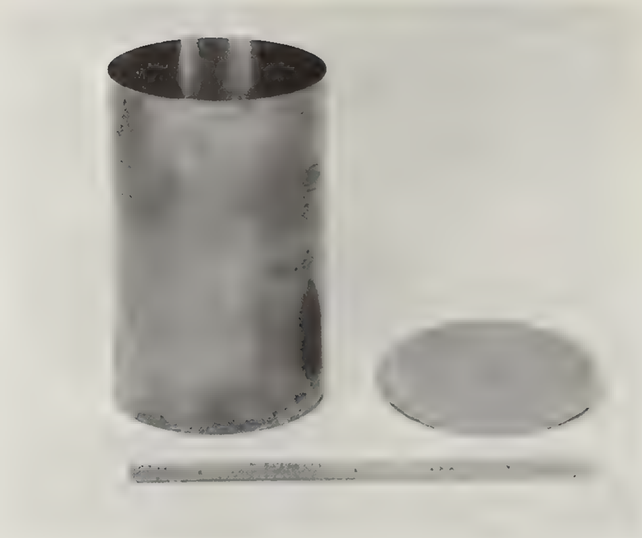

FIGURE 21. NIOBIUM FOIL GETTER.

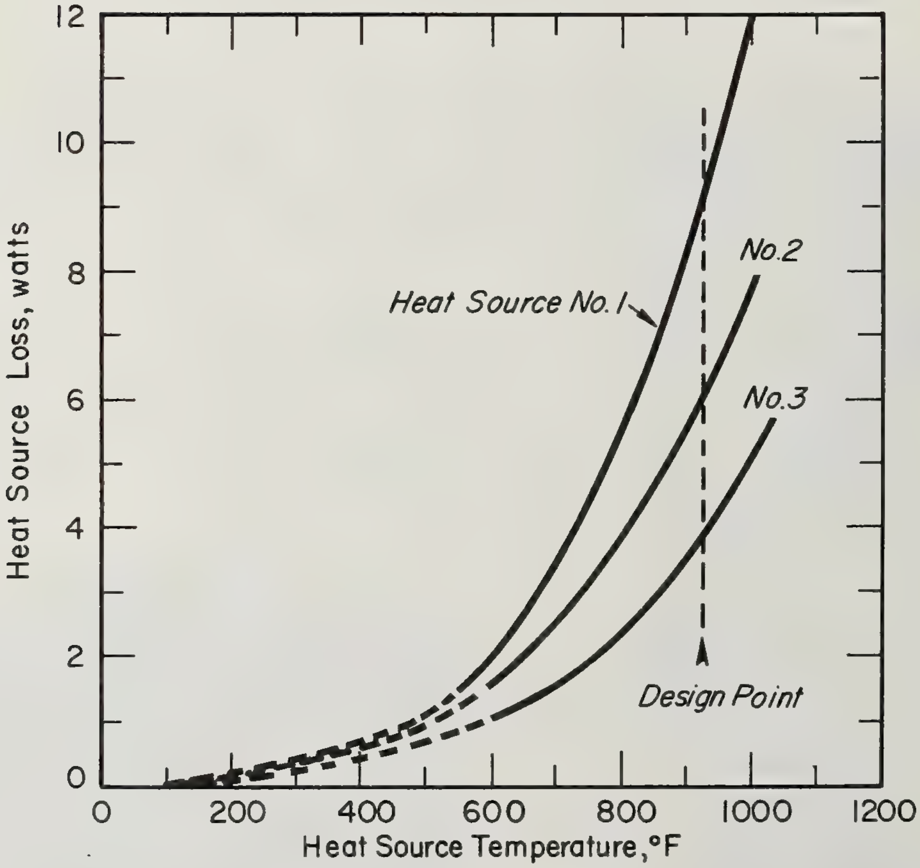

FIGURE 22. GRAPH OF HEAT LOSS.

DISCUSSION

MR. PURDY: What is expansion or contraction of the thermal storage material on freezing?

DR. HUFFMAN: It's around 20%; I don't have the number at my fingertips. If you want to see me after the session, I think I can give you the exact number.

MR. PURDY: And have you done any thermal ratchet tests to date?

DR. HUFFMAN: Some of the original data, I would say the first 60 days, were taken in this manner. The experiment was then simplified and the sample temperature held above melting point. But the ratchet test did not show anything different from our other tests.

MR. PURDY: What is the volume required for thermal storage material to power an artificial heart for about 4 hours.

DR. HUFFMAN: Probably something like 450 grams of material. It would be a unit slightly larger than Heat Source No. 3.

MR. PURDY: Your prototype design is made to power a heart for a certain amount of time?

DR. HUFFMAN: Yes , I would say for about 3-1/2 hours.

MR. PURDY: What were the dimensions of that unit.

DR. HUFFMAN: About 3-1/2 inches in diameter and about 4 inches in length.

DR. YOUNGER: How long a life do you expect for the permanent magnet switch in a variable reluctance circuit?

DR. HUFFMAN: The flux level that we are working with is really quite small, because the reed switch is chosen to be quite sensitive. From looking at published data, we would expect that this would operate for several years.

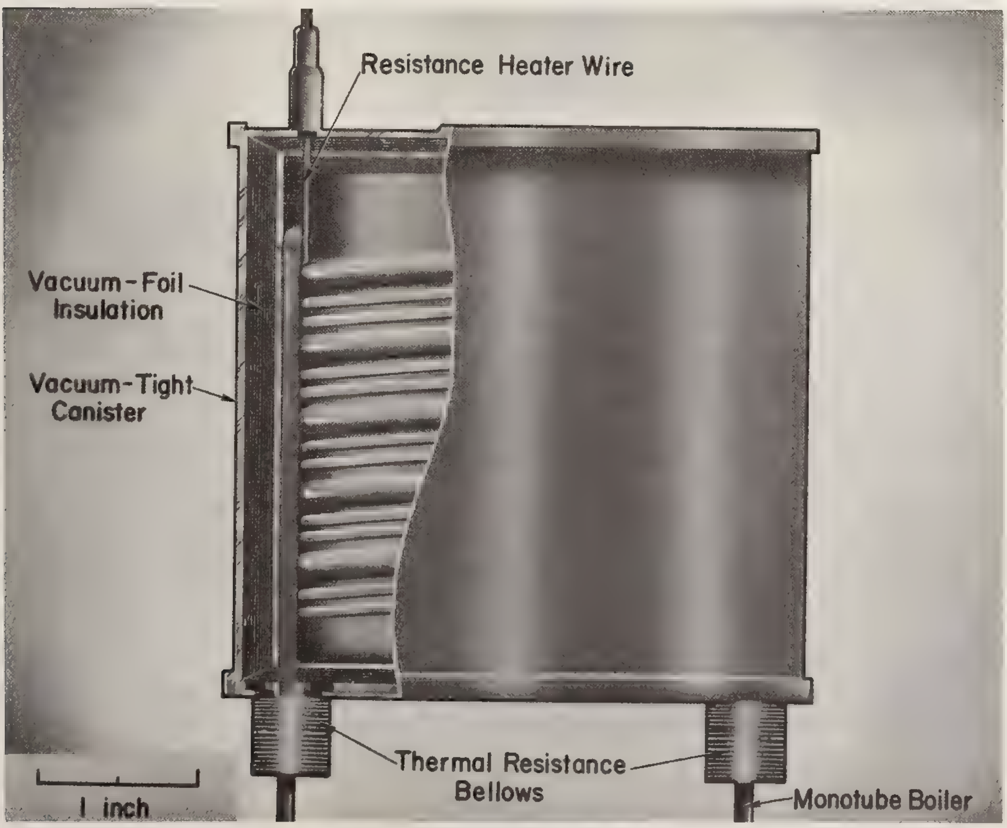

FIGURE 23. NIOBIUM FOIL GETTER.

CHAPTER 89

DEVELOPMENT OF THE THERMOCOMPRESSOR AS THE POWER SOURCE FOR AN ARTIFICIAL HEART

W. R. Martini

McDonnell Douglas Corporation
Donald W. Douglas Laboratories
Richland, Washington

The power source under development employs a thermocompressor, a heat engine to compress gas. Compressed gas under automatic control operates a pump actuator to pump blood through an intermediate drive liquid. The heat engine now being developed is a type of Stirling engine because it employs a moving thermal regenerator oscillating in a hollow cylinder between a heated and a cooled end. This regenerator serves to increase and decrease the average gas temperature almost reversibly resulting in pressure and/or volume surges. Inlet and outlet check valves in the cooled end harness these surges and compress the working gas - hence the name thermocompressor. An analysis is made of thermocompressor properties and of devices for oscillating the regenerator by the use of the engine output. Three test engines have been built with a cylinder volume of ~33 cubic inches. The best measured overall efficiency for this size engine has been 14% for an externally driven regenerator and 6% for a self-driven test. The newer implantable engine cylinder size (2 in.^{3}) has generated 12.3W at an estimated 10% efficiency. In the pump actuator the pneumatic power is stored in surge tanks, is controlled by a three-way valve, is applied to a small, bellows sealed, double acting drive piston. This small piston pumps the blood by moving a large piston which displaces the drive liquid around the blood pump bladder. The pump actuator will be tested with a blood pump acting as an assist pump to a simulated vascular system. Compressed gas under automatic control is applied to the actuator as required to maintain proper pressure and adequate synchronization with the heart. The components of the system are to be packaged for implantation inside of experimental animals. Total size of 1.1 to 1.8 liters, including blood pump, is planned.

INTRODUCTION

The long-range aim on this contract is to assemble a complete artificial heart energy system from mutually compatible components that will be compatible with the human body. The short-term goal is to develop the thermal engine and pump actuator components that are needed for the overall system, but are not available elsewhere.

This paper first treats the system as a whole and then discusses the component development that has been undertaken.

SYSTEM ANALYSIS

Figure 1 is a block diagram of the present concept. Power from the electrical utility is transformed by the electrical power supply to the proper frequency for operation of a percutaneous transformer. The implanted receiver coil of this transformer supplies an electric heater that is embedded in a thermal storage reservoir. The heater, the reservoir, and the hot part of the thermocompressor are insulated with multifoil vacuum insulation. Alternately, the heat could be supplied to the thermal storage reservoir by a radioisotope. The thermal compressor is a type of Stirling engine that converts heat to pneumatic power. This pneumatic power is stored temporarily in tanks and is applied to the pump actuator through a three-way valve that is under automatic control. The pump actuator converts high-pressure pneumatic energy from the engine to low-pressure hydraulic energy that directly operates a diaphragm or sack type blood pump, which assists the heart in a complete vascular system. This concept is for a heart assist device, but the device could be easily adapted for use as a heart replacement.

The power applied to the blood pump should be controllable from 1 to 10 watts, and the actuator should operate at from 60 to 150 beats per minute. The blood pump and associated fluid transfer lines have been measured with an efficiency of 60%. Pump actuator efficiency has not been measured; however, it has been calculated at 83% and a conservative 75% efficiency is assumed. The thermocompressor has a calculated efficiency of 18% and a measured efficiency of ~10%. The assumed efficiency for this system study is 16%. Using these efficiencies and power requirements, the energy flows shown on Figure 1 have been computed. For 4.3 watts of energy supplied to the blood, 60 watts must be supplied to the heat engine. Three hours of thermal storage appears reasonable, but no standards have been set. The waste heat that must be accepted by the human body appears to be in the reasonable range. The size of the device is the main problem.

Figure 2 is a sketch of the blood pump that would be attached between the apex of the left ventricle and the descending aorta. This blood pump is all that would need to be in the thoracic cavity. The blood pump and liquid line would require a space of 29 in.^{3} or about 1/2 liter.

Figure 3 shows the energy system that would be implanted in the abdominal cavity. This would consist of a compact and improved packaging of the present hardware. The engine cylinder is 1 in. in diameter by 2-1/2 in. long. This engine is heated by a thermal storage reservoir that has a capacity of 3 hours of full power operation. The compressed gas from the engine is fed to the pump actuator controls that are situated below the large drive piston. The compressed gas is supplied periodically to the small drive piston through the control system, which operates the large drive piston to displace low-pressure liquid through the large liquid line to the blood pump of Figure 2. The overall engine dimensions are 9 in. long by 3-1/2 in. high by about 4-1/2 in. wide, but the engine is quite irregular in shape.

Table 1 lists the volume breakdown for the complete energy system. The first column lists hardware components that are under test or construction.

TABLE 1

ESTIMATED COMPONENT VOLUMES OF COMPLETE CARDIAC ASSIST SYSTEM

Component	Present Hardware (in.^{3})	Improved Hardware (in.^{3})	With Hydrostatic Drive (in.^{3})
Transformer	--	9	9
3-hr thermal storage and heater	1.3[a]	25	19
Insulation	108.0	4	4
Engine	11.7	10	10
Pump actuator and automatic control package	58.0	32	11
Drive tube	15.0	15	1
Blood pump	14.0	14	14
TOTAL	208.0 (3.4 liters)	109 (1.8 liters)	68 (1.1 liters)

[a] Heater only.

These components are discussed in the component development section of this paper. The energy system that is described in Figures 2 and 3 is itemized in column 2 of Table 1. The total volume is about 1.8 liters, which is quite large. To reduce this volume, the large drive piston could be replaced by a much smaller high-pressure hydraulic drive called a "hydrostatic drive," which would be more efficient than the present drive and would fit inside of the bellows seal of the high-pressure pneumatic piston. As shown in column 3 of Table 1, these improvements can reduce the overall volume of the system to 1.1 liters. Although the present hardware does not include a transcutaneous transformer, the improved hardware must have one for completely implantable operation.

Figure 4 is a sketch of this improved hardware with the incorporation of the hydrostatic drive. It is much more convenient in shape and is 8 in. long by 3-1/2 in. by 1-1/2 in. thick. The same size engine is included and the hydrostatic drive liquid is made to recirculate between the drive attached to the pump actuator and the blood pump so that waste heat from the engine can be transported to the blood pump diaphragm.

Figure 5 shows a rough sketch of the blood pump that would be used. The diaphragm and the inlet and outlet valves would be the same as those that have been successful in clinical trials of blood pumps. However, the outer liquid-filled case would have movable panels actuated by a small hydraulic cylinder, which would change the volume of the case and, therefore, change the volume of the blood-filled bladder inside the case.

COMPONENT DEVELOPMENT

A number of components have been developed for the overall system. These include a simulated vascular system, a pump actuator, and a number of engine models. These components are described in the following paragraphs.

For an assist blood pump to be tested satisfactorily *in vitro* a simulated vascular system is needed to simulate the heart as well as the arteries and veins. The system that has been developed is shown in Figure 6 and has been purchased in part from Statham Instrument Company. This system includes a 50 ml pump with an apical tap and another 50 ml assist pump. This assist pump will be removed when the required blood pump and actuator system are available for test. DWDL has built an electric control for this pump actuator system. A closeup of the control panel is shown in Figure 7. Lights on the control panel show when the four solenoid valves are open. Control knobs are used to establish the length of systole, the overall pulse rate, the time delay between onset of systole in the heart and the onset of systole in the assist device, and the length of systole and diastole in the assist device.

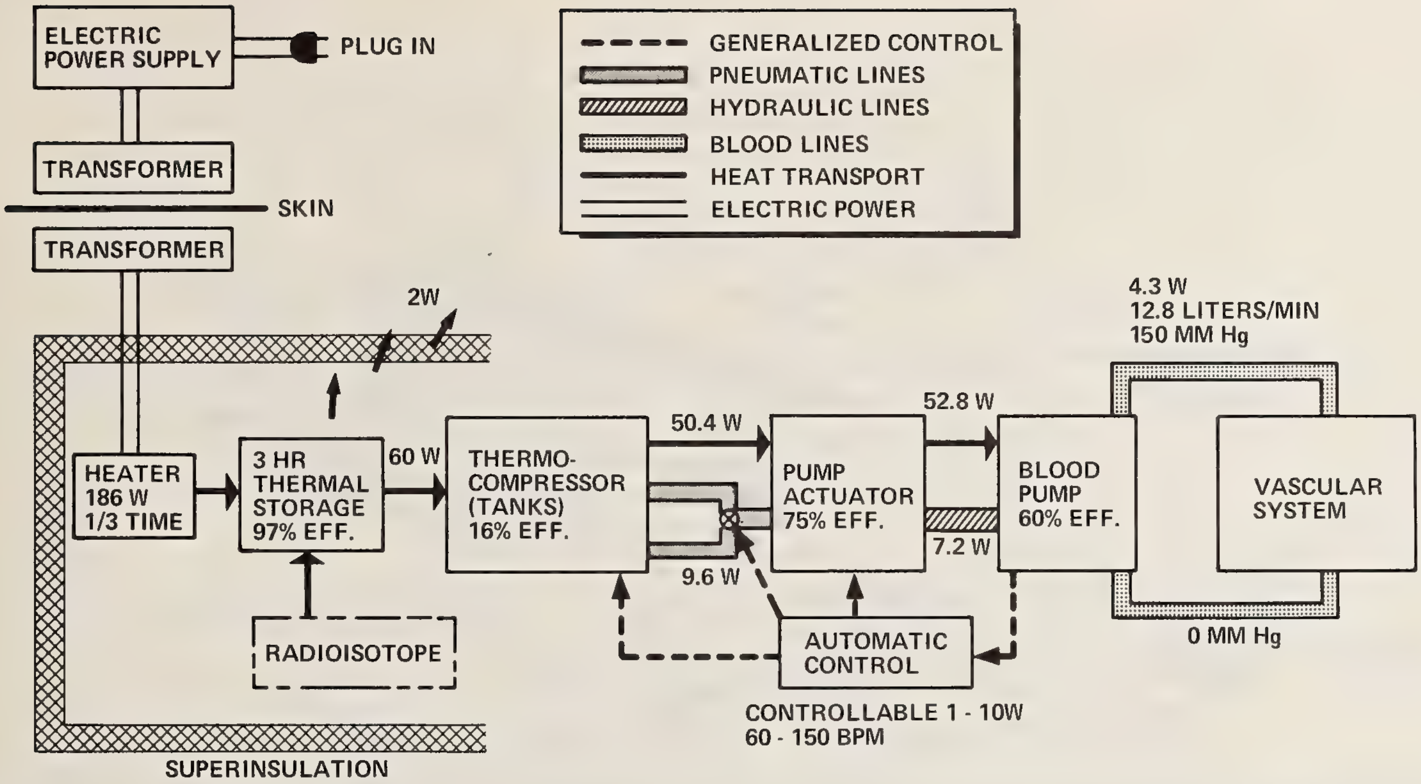

FIGURE 1. DWDL CONCEPTUAL ARTIFICIAL HEART SYSTEM.

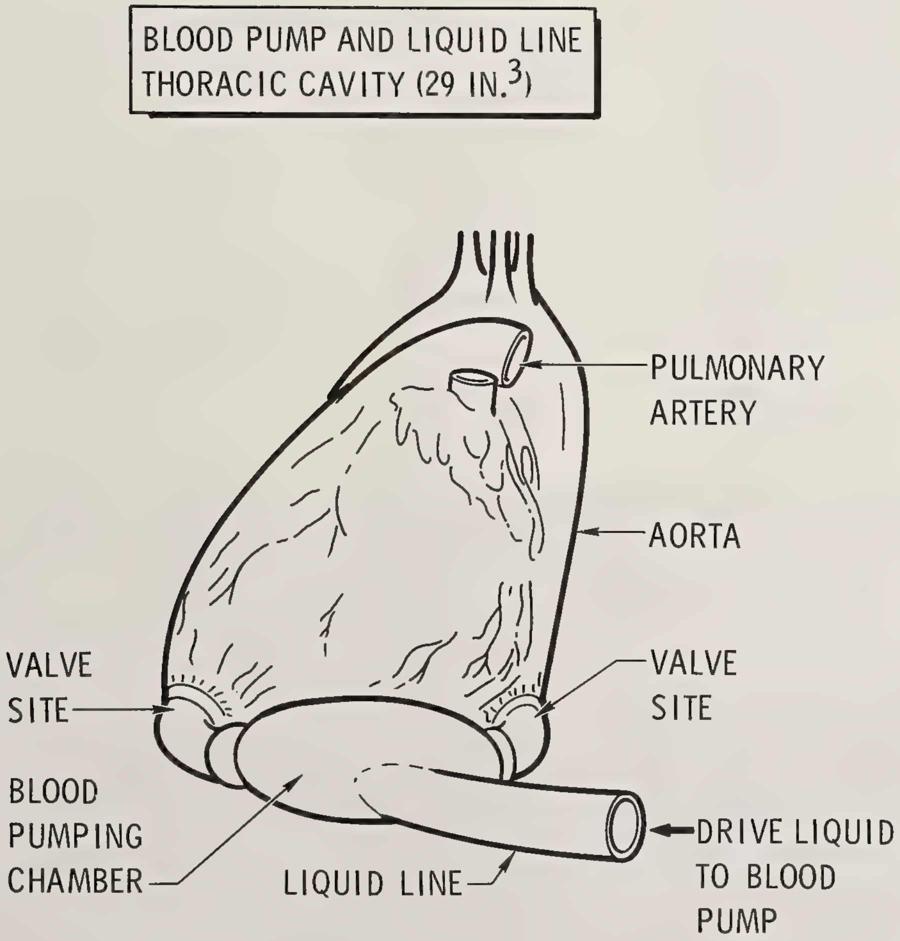
BLOOD PUMP AND LIQUID LINE
THORACIC CAVITY (29 IN.^{3})
PULMONARY ARTERY
AORTA
VALVE SITE
VALVE SITE
BLOOD PUMPING CHAMBER
LIQUID LINE
DRIVE LIQUID TO BLOOD PUMP

FIGURE 2. BLOOD PUMP ATTACHMENT.

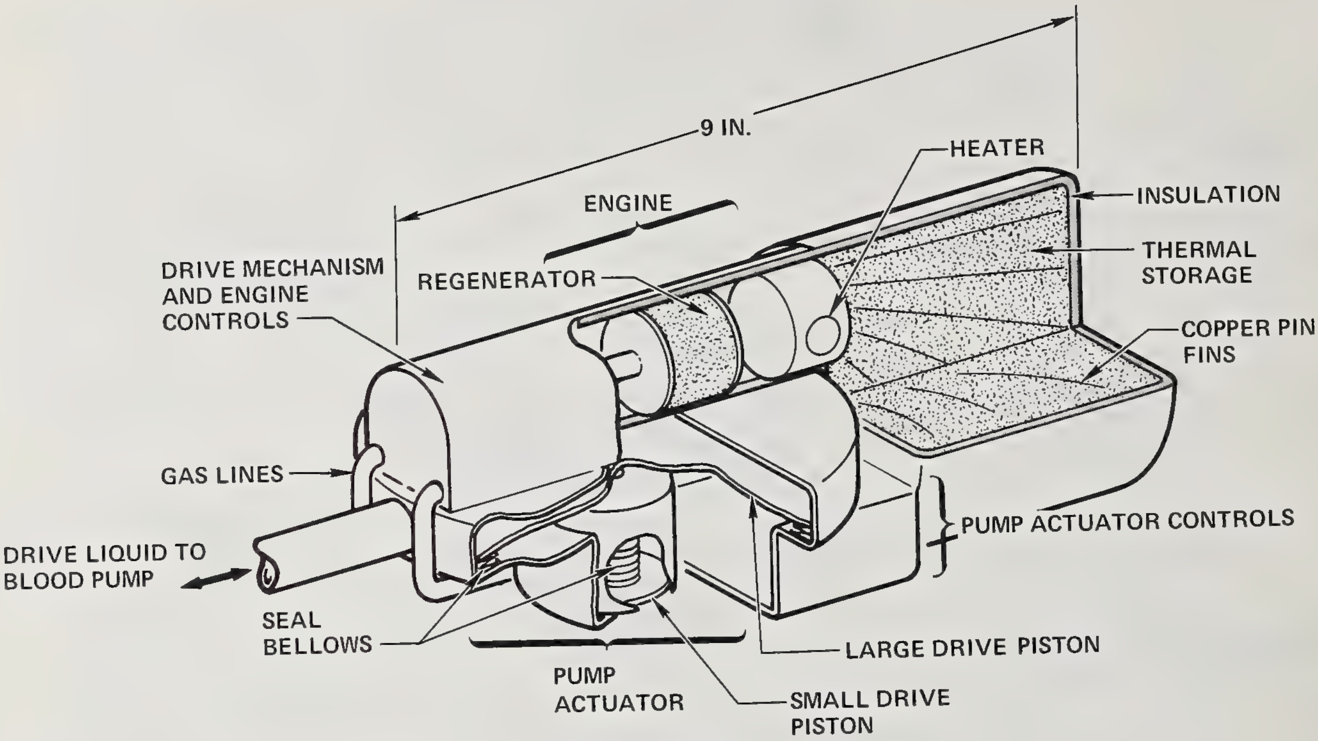

FIGURE 3. IMPROVED HARDWARE, PRESENT CONCEPT.

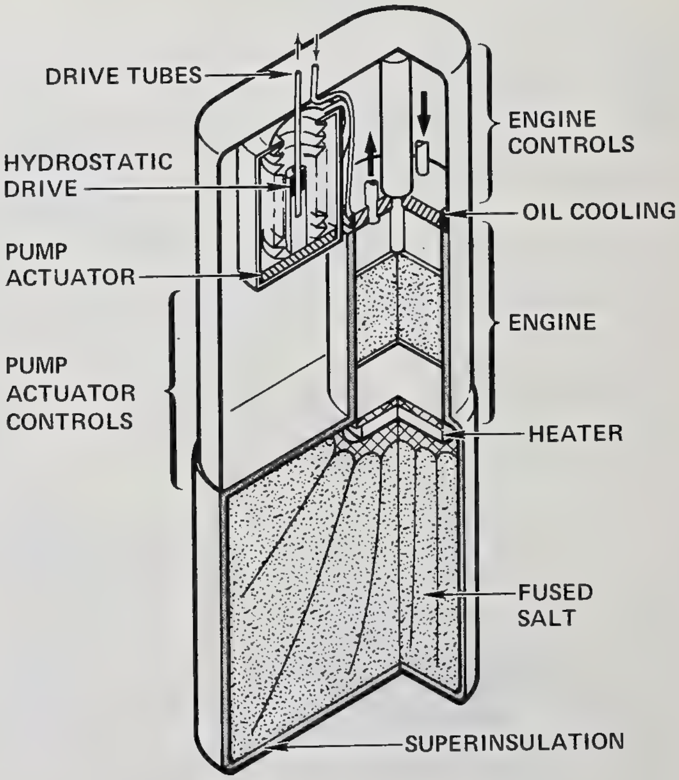

HEIGHT	8.0 IN.
WIDTH	3.5 IN.
THICKNESS	1.5 IN.

FIGURE 4. IMPROVED HARDWARE, HYDROSTATIC DRIVE.

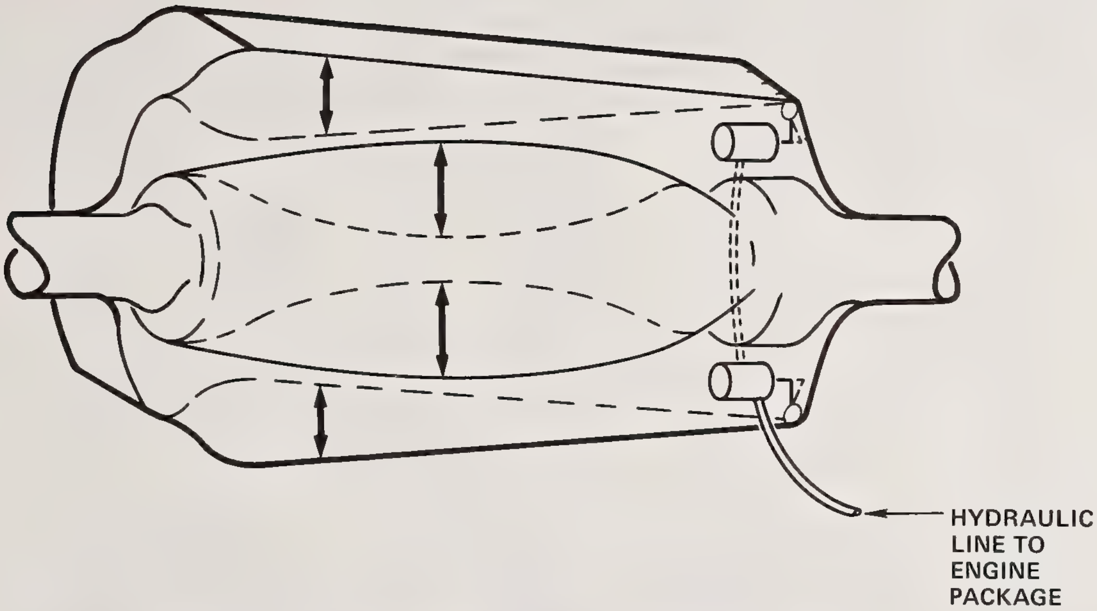

FIGURE 5. ADVANCED HYDROSTATICALLY ACTUATED BLOOD PUMP.

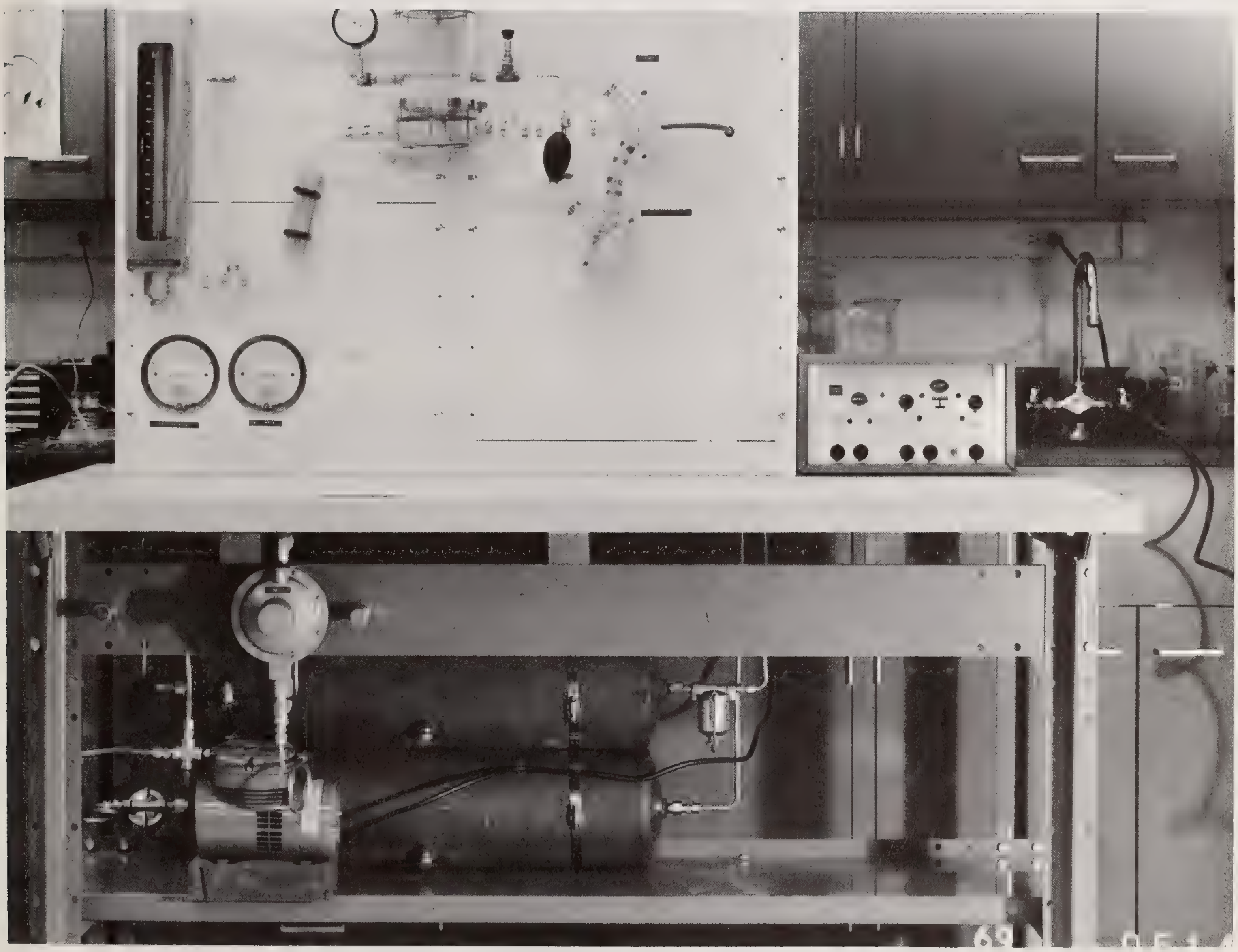

FIGURE 6. SIMULATED VASCULAR SYSTEM.

The blood pump receives its energy from a pump actuator, which is shown in simplified cross-section in Figure 8. Basically, high- and low-pressure gas through the automatic control system is applied alternately to the small piston. The motion of the small piston then moves a large amount of liquid by means of the large piston attached to it. This compact pump actuator is semi-implantable; that is, it can be disassembled to permit component changes, but still is a compact shape that may be implanted if necessary. This pump actuator is being constructed and has been designed in cooperation with Bio-Logics, Incorporated, who have been designing the automatic control for the pump actuator. Seven pneumatic valves are required, six of which are included in this case.

The chief stress has been placed on the engine development in this contract. The original DWDL concept was a Stirling engine that would produce pressure pulses usable directly in a gas-driven blood pump. A working model of this arrangement was made and operated satisfactorily; however, as analytical techniques were developed and the test program was undertaken, it was found that the engine did not follow the equations for a conventional Stirling engine. It was determined that, even with an ideal engine operating at physiological frequencies and pressures to produce the required blood pumping power, the engine would be too large for implantation. However, it is possible to reduce the size of this engine in two ways -- higher speed and higher gas pressure. The present DWDL concept uses both of these. The test program was initially conducted with a large size engine to facilitate handling during the modifications to this engine and the development of its component parts.

Figure 9 is a schematic of the test setup now used. The heat input to the hot part of the engine is measured with a wattmeter. The gas flow-out of the engine is measured with a rotameter and the pressure rise developed by the engine is measured with a manometer. The gas flow and pressure rise are converted into watts of pneumatic output by assuming isothermal expansion of the gas at 40°C. It is assumed at this scale of operation that the gas will be inevitably cooled off before it is applied to the pump actuator. More power can be obtained from the engine if the temperature of this expansion is increased; however, it does not matter what expansion temperature is used or whether the expansion is assumed to be isothermal or adiabatic, because when the combination of the pump actuator and engine is considered, this power cancels out.

Figure 10 shows the best test data that were obtained using the large 28 in.^3 engine operating with the moving regenerator actuated externally. The pertinent data are given in Figure 10. A maximum of 14.4% overall efficiency was obtained.

System considerations have dictated that a much smaller size machine operating at a much higher gas pressure be used. Engine design calculations indicate that a machine with a 1 in. in diameter by 2-1/2 in. long cylinder operating at 200 psia minimum pressure can produce 10 watts of power at greater than 16% overall efficiency. This 200 psia pressure is the highest pressure that can be handled by the available bellows that is designed for indefinite life.

Figure 11 shows a section of Engine 3, which is a bench scale prototype of an implantable size engine. In this modification, the regenerator is moved by an external drive, and the engine cylinder is surrounded by a large amount of vacuum powder insulation to allow for convenient installation of thermocouple and heater leads. Figure 12 shows the engine cylinder ready for insulation and Figure 13 shows the lower unit of this engine ready for insertion into the upper unit. (Note the small movable regenerator.) Figure 14 shows the test stand for this experiment. Temperatures and steady-state and transient pressures are recorded and gas flows and heat inputs are observed.

Figure 15 shows one of the early load curves for this externally driven engine. For 90 minutes, the pumping rate was close to the rate calculated for this engine, but performance then deteriorated to a lower level. Examination of the recorded transient pressures showed that a substantial back flow in the outlet valve was absorbing much of the power; therefore, design and construction of improved valves was started. Also, tests were undertaken with both the inlet and outlet valves shut off to determine the pressure excursion with no mass flow rate. From these pressures it is possible to compute the average gas temperatures. Table 2 shows the measured gas temperatures compared with those calculated.

TABLE 2

GAS TEMPERATURES

	Measured (°C)	Calculated (°C)
Hot Surface	750	740
Hot Gas (Average)	335-400[a]	565
Cold Gas (Average)	62[b]	70
Cold Surface	36	25

[a] Computed from pressure change data

[b] By exit gas temperature

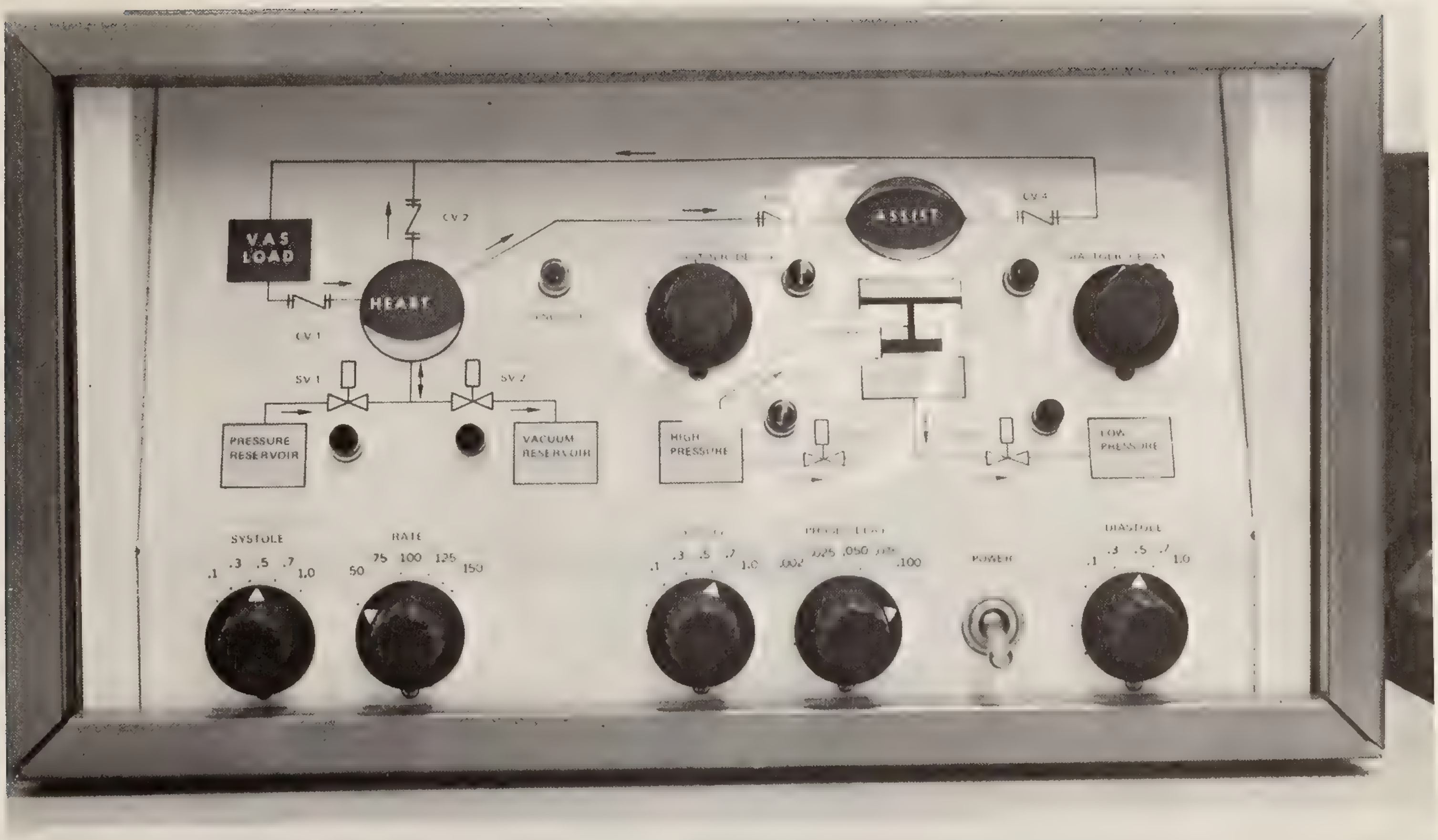

FIGURE 7. CONTROL PANEL FOR SIMULATED VASCULAR SYSTEM.

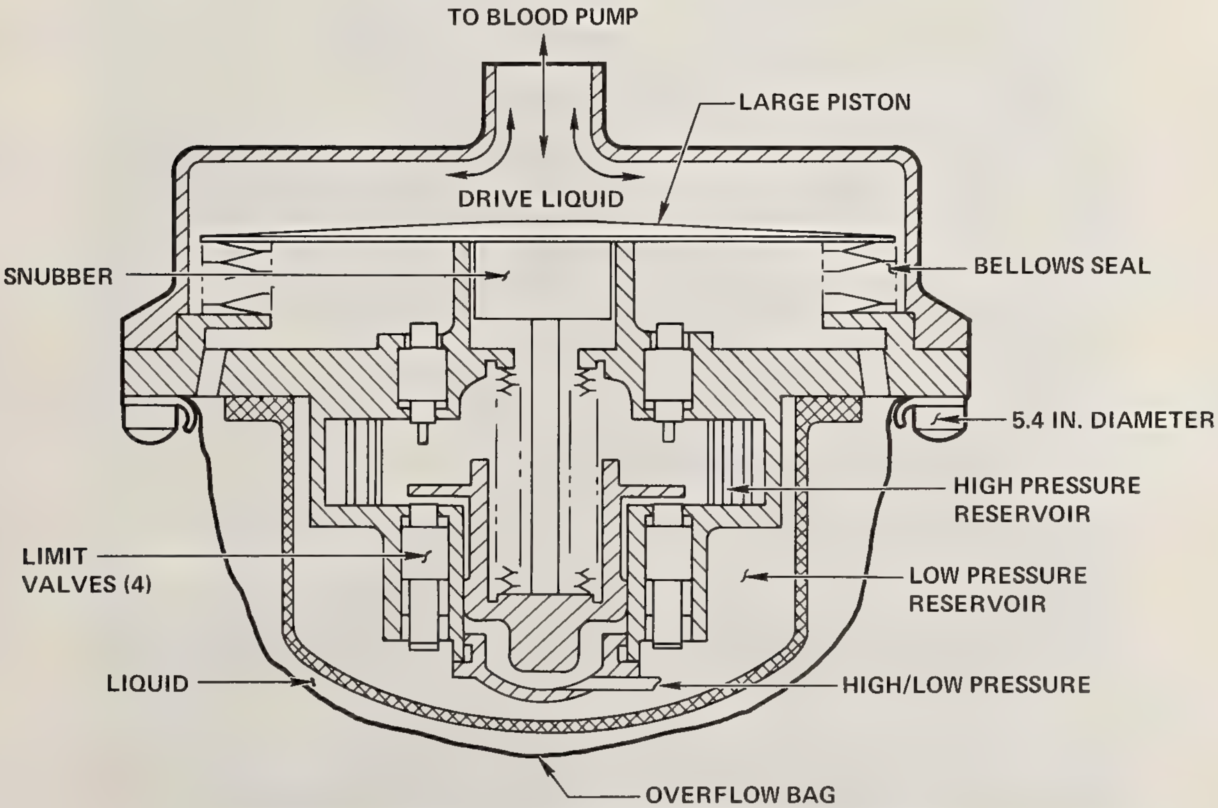

FIGURE 8. PUMP ACTUATOR DESIGNED FOR AUTOMATIC CONTROL.

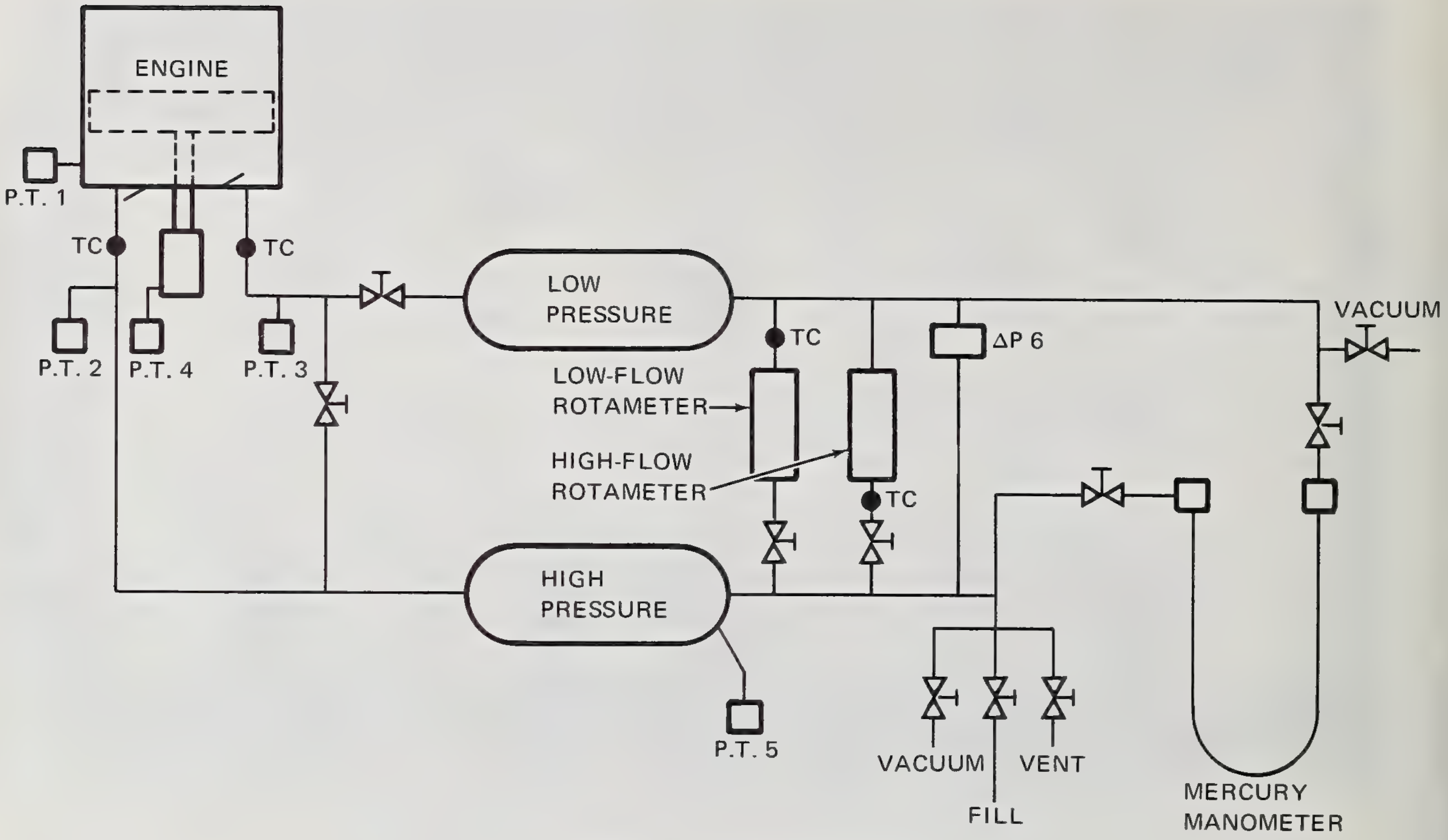

FIGURE 9. ENGINE 1B LOAD SYSTEM.

ENGINE VOLUME -- 28.4 CU IN.	HOT SURFACE -- 651^{0}C
FREQUENCY -- 10.5 HG	COLD SURFACE -- 21^{0}C
STROKE -- 1.774 IN.	MATRIX -- 5% DENSE, 0.002 IN. ROUND WIRE
AVERAGE PRESSURE -- 1900 TORR	HEAT INPUT POWER -- 206 W
GAS -- ARGON	

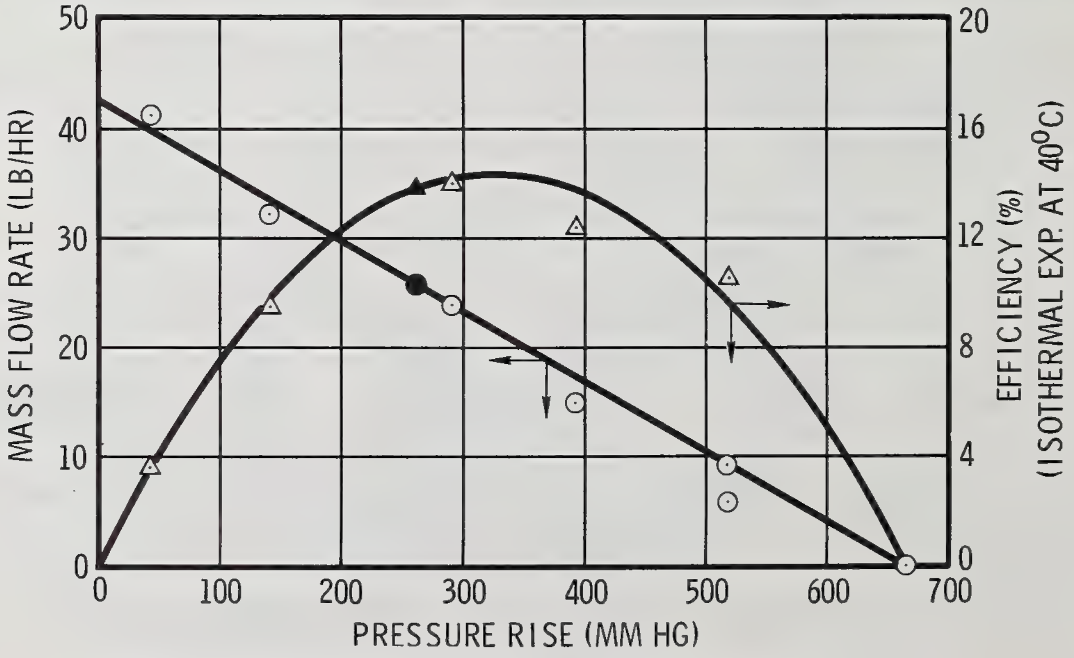

FIGURE 10. ENGINE PERFORMANCE (RUN 1B9 DATA POINTS 8 THROUGH 15) WITH EXTERNALLY DRIVEN REGENERATOR.

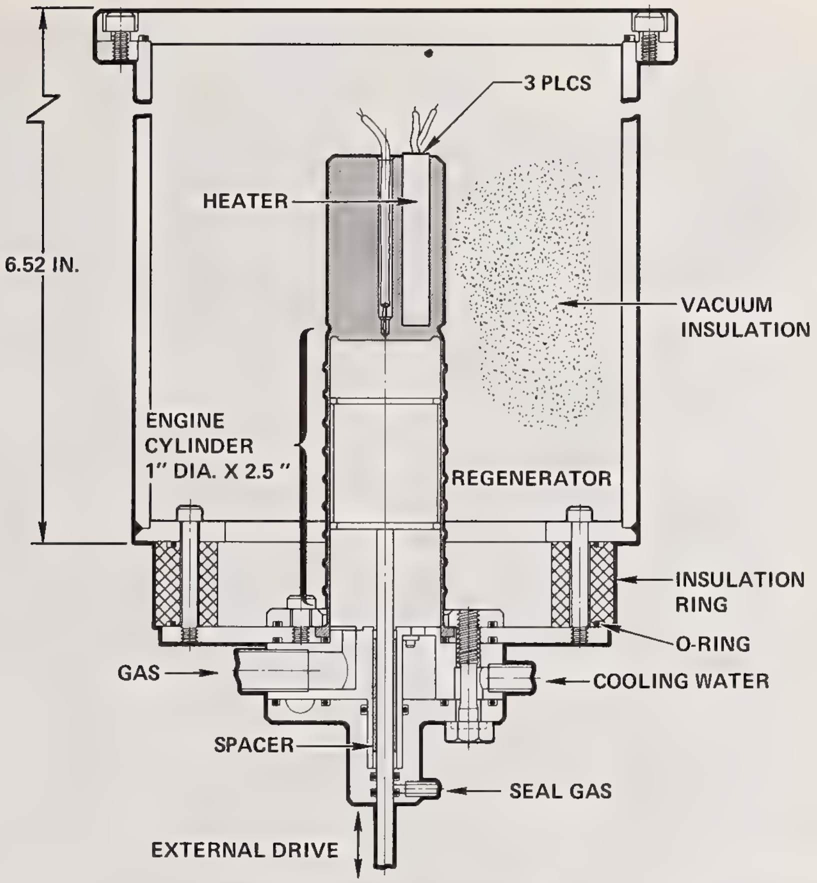

FIGURE 11. ENGINE 3 DETAILS.

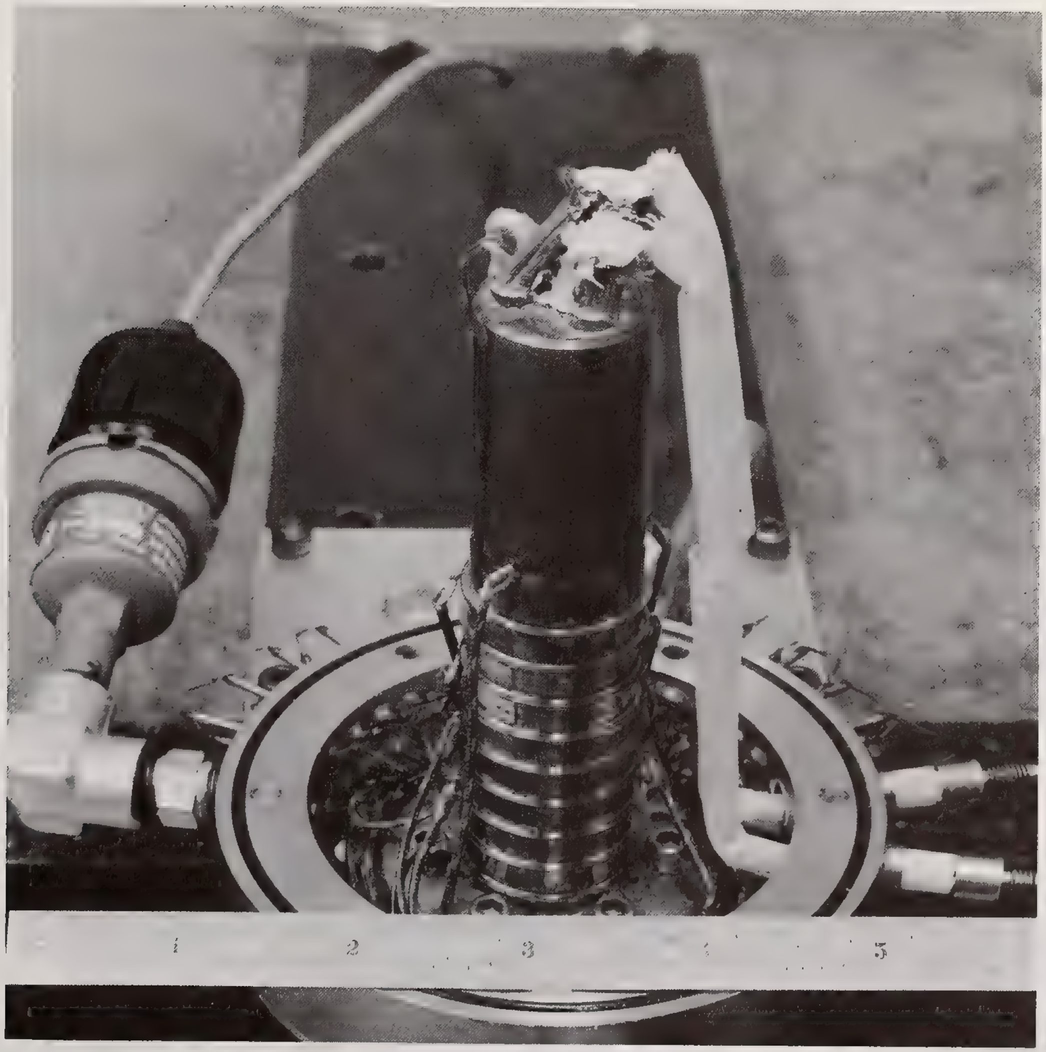

FIGURE 12. ENGINE 3 CYLINDER READY FOR INSULATION.

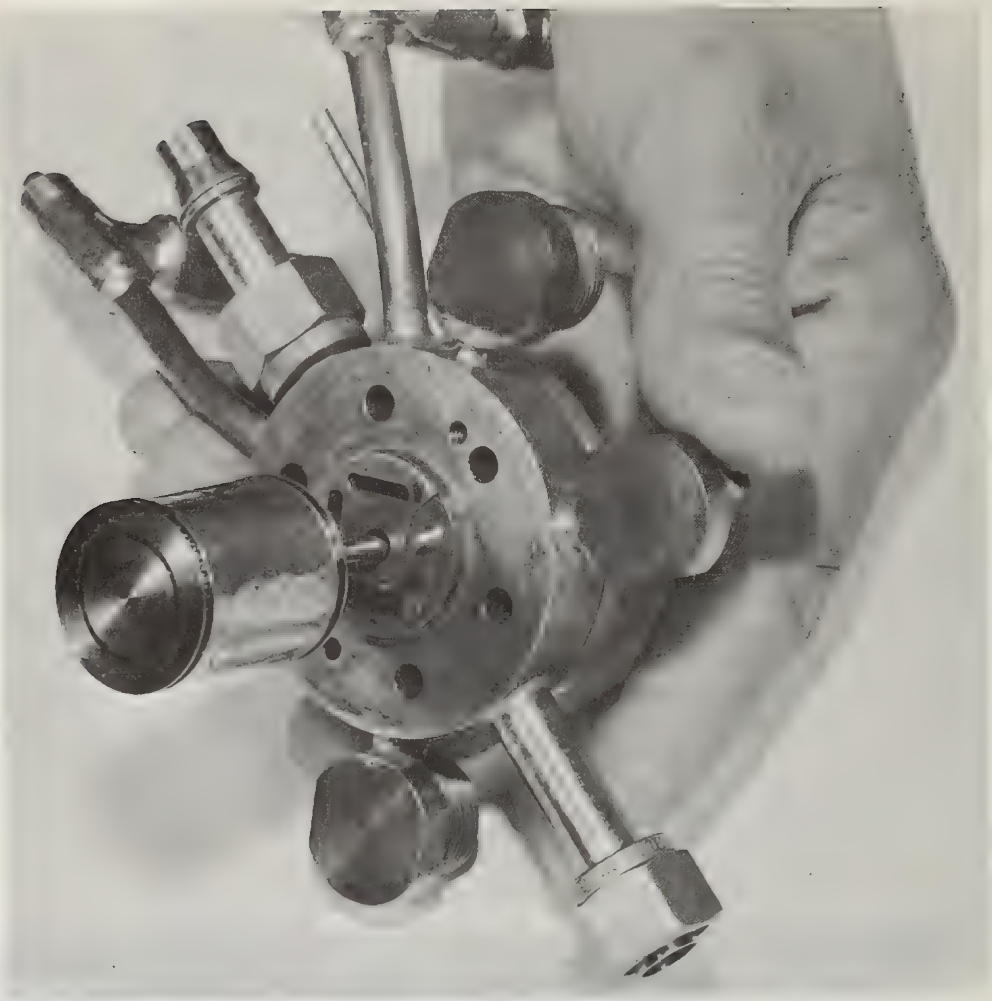

FIGURE 13. ENGINE 3 LOWER UNIT.

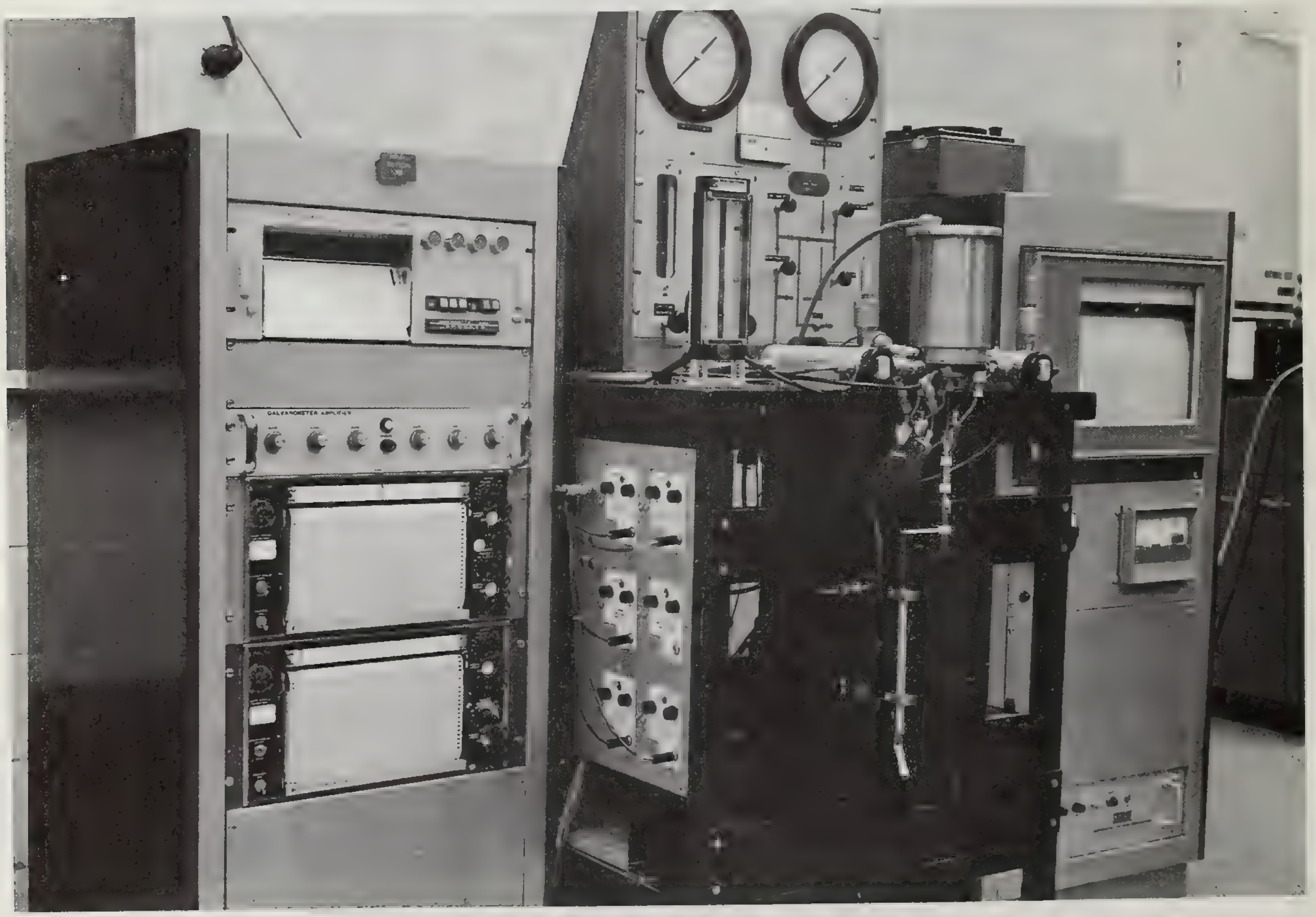

FIGURE 14. ENGINE 3 TEST STAND.

The temperature difference between the hot surface and the hot gas was approximately twice that which would have been expected from previous calculations. Apparently, the jet impingement heat transfer that had been calculated for steady flow was not applicable in this situation; therefore, an improved regenerator was designed and built to improve jet impingement heat transfer.

While the improved valves and the improved regenerator were being constructed, initial tests were started on a self-driven version of the implantable model. Figure 16 shows a simplified cross-section of this engine. The lower portion of the engine has been changed. It still has the main inlet and outlet valves, but it also has auxiliary valves that are connected from the low-pressure gas to the drive chamber and from the drive chamber to the high-pressure gas. The support shaft for the regenerator, which passes between the engine cylinder and the drive chamber, acts as a drive piston to maintain the oscillation of the regenerator. When the regenerator is moving down, the engine cylinder pressure is higher or equal to the drive chamber pressure, and when the regenerator is moving up, the drive chamber pressure is higher or equal to the engine cylinder pressure.

Figure 17 shows the lower part of the engine ready for installation. Figure 18 shows the transient pressures recorded during operation to show that the engine pressure and the drive chamber pressure behaved as desired. It is possible to change the amount of energy from the engine diverted to drive the regenerator by changing the volume of the drive chamber.

Calculated power output and efficiency for Engine 3 are presented as a function of working gas and frequency of operation in Figures 19 and 20. Note each gas has an optimum frequency of operation. The early externally driven test results also presented in Figures 19 and 20 showed the effect of inadequate valves and poor hot side heat transfer. Improvements to rectify these shortcomings were installed and results shown in Table 3 were obtained in self-drive tests.

TABLE 3

ENGINE 3A SELF-DRIVE POWER OUTPUT AND OVERALL EFFICIENCY

Data Point	Frequency Hz	Pressure - PSIA High Tank	Pressure - PSIA Low Tank	Power Output Watts[a]	Efficiency %[a]
3A4-5	17.9	316	277	12.3	(b)
3A4-17	16.8	322	281	11.7	(b)
3A4-28	15.2	232	208	8.8	8
3A5-2	16.9	300	272	11.6	7.9

[a] Isothermal expansion at 40°C.

[b] Thermal equilibrium not attained. If it were attained, an efficiency of 10% is estimated.

Higher frequencies and engine pressures were used and more than design power was attained. The best efficiency actually measured was 8%, but during tests where the electric heater was not adequate for steady state operation, an efficiency of approximately 10% has been estimated.

SUMMARY

1. A completely implantable energy system concept is described that can be assembled from available or soon to be available components. This system meets desired power and control ability requirements and is probably of implantable size. Considerable volume saving can be made with a hydrostatic drive.
2. A simulated vascular system has been constructed and checked out ready for testing.
3. A compact pump actuator and automatic control package has been designed in cooperation with Bio-Logics, Inc., and is under construction.
4. A large size engine (28 in.^{3} cylinder volume) with an externally driven regenerator has shown an overall efficiency of 14%.
5. An implantable size engine (2 in.^{3} cylinder volume) has been constructed and operated both externally and self-driven. In the self-driven mode, the power output has been measured at 12.3 watts with an estimated efficiency of 10%, assuming a 40°C isothermal expansion of the gas.

FUTURE PLANS

Donald W. Douglas Laboratories intends to continue the developments outlined in this paper under the close supervision of the Program Office. As resources are made available, an in vivo test of a complete energy system that will contain the described engine and pump actuator, combined with other components now being developed by other NIH contractors, will be demonstrated.

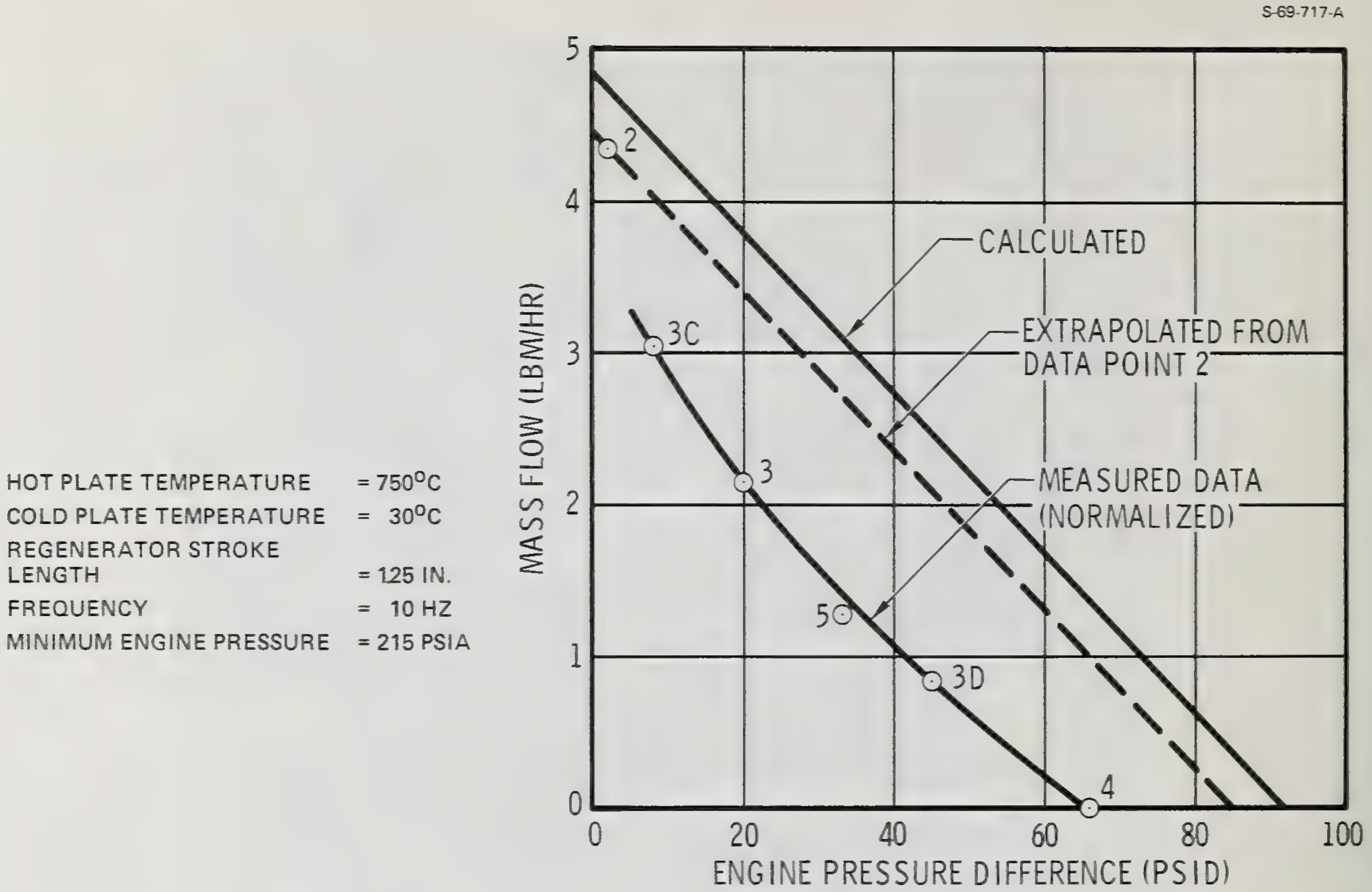

FIGURE 15. ENGINE LOAD CURVE (ENGINE 3 - RUN 3).

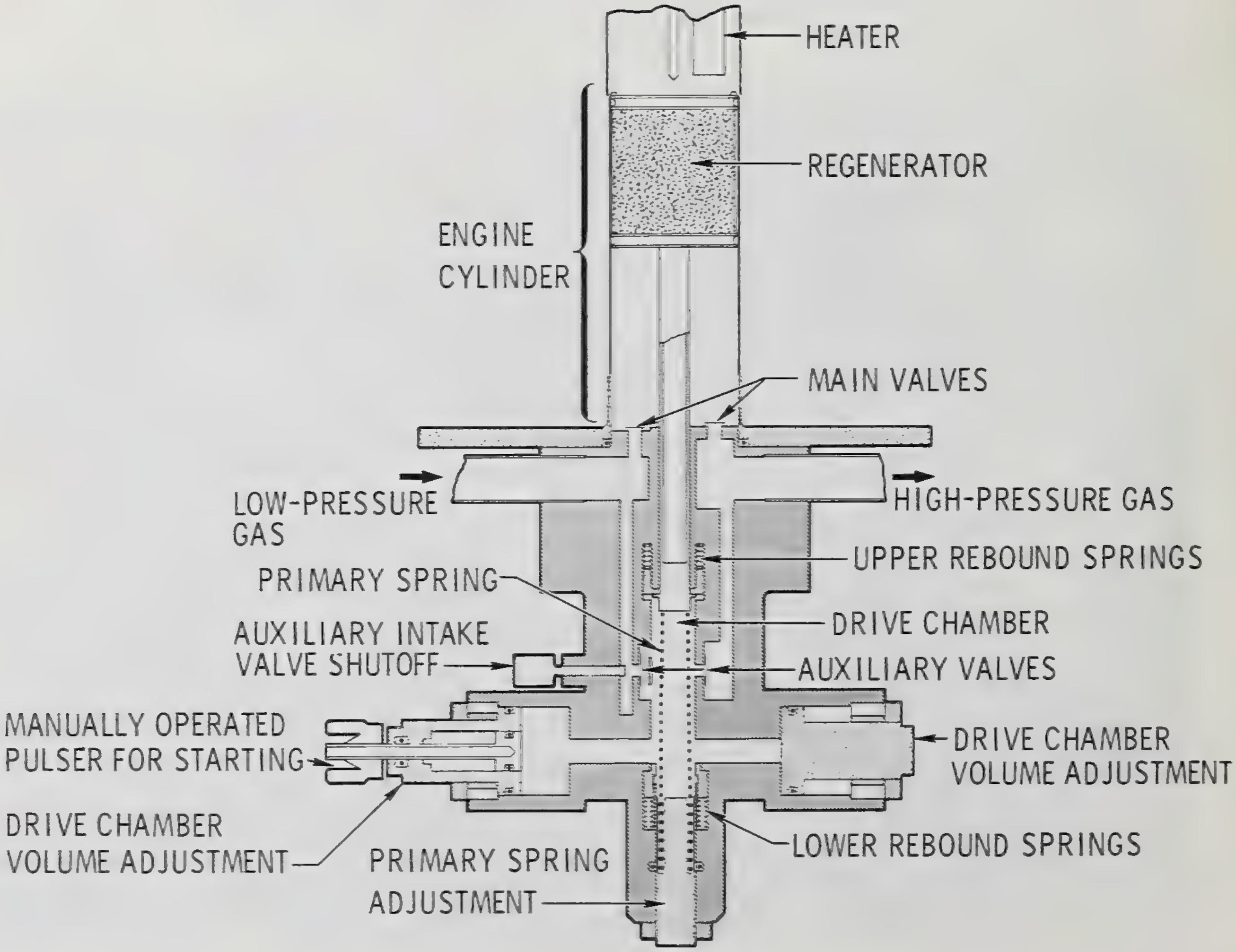

FIGURE 16. SIMPLIFIED CROSS-SECTION OF IMPLANTABLE SIZE ENGINE.

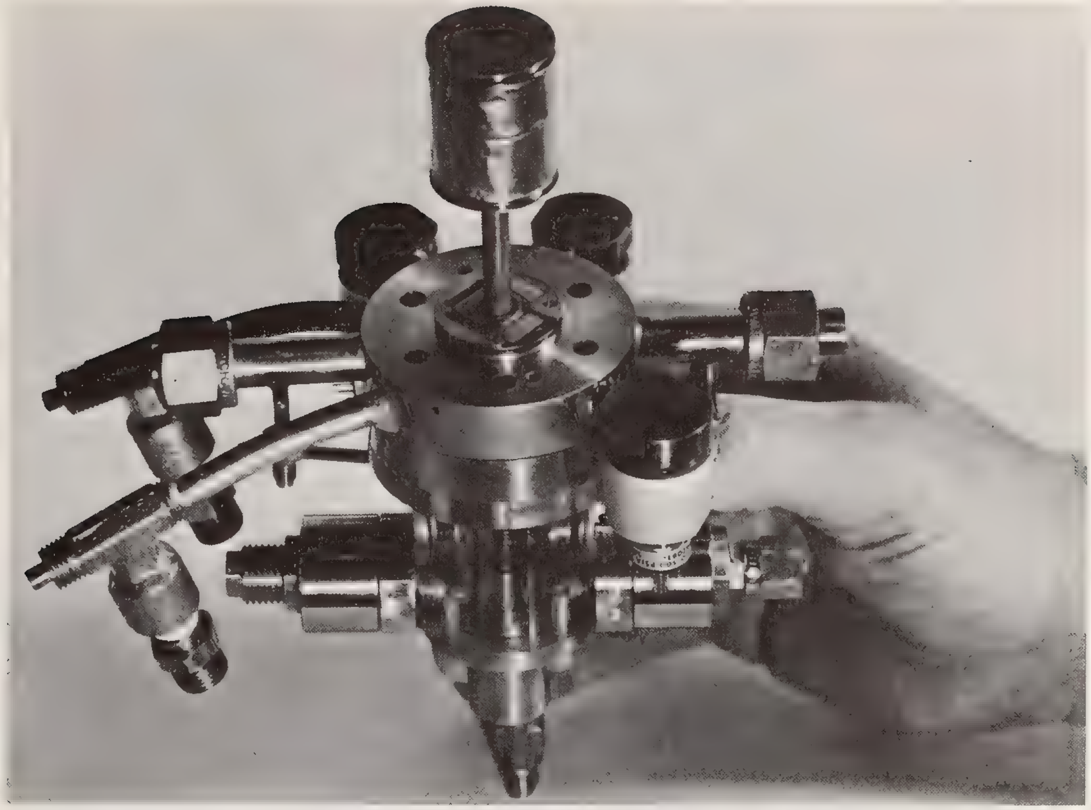

FIGURE 17. LOWER STRUCTURE ENGINE 3A.

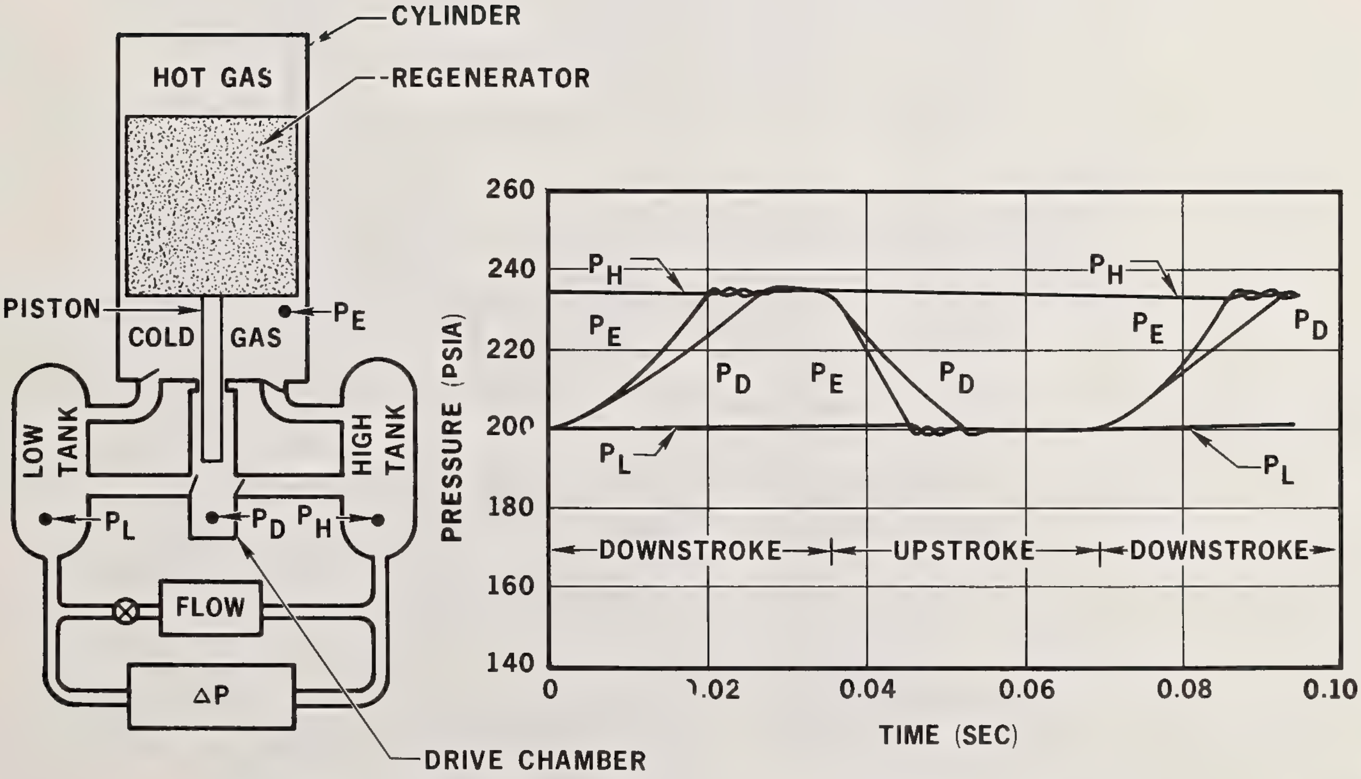

FIGURE 18. TRANSIENT PRESSURES DURING SELF DRIVE OPERATION - ENGINE 3A.

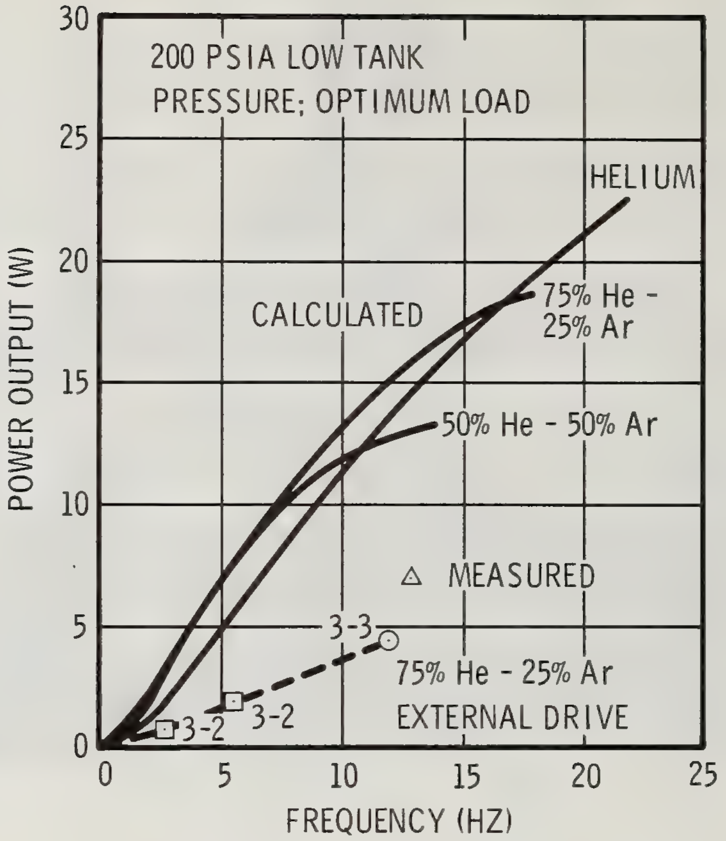

FIGURE 19. ENGINE 3 POWER OUTPUT.

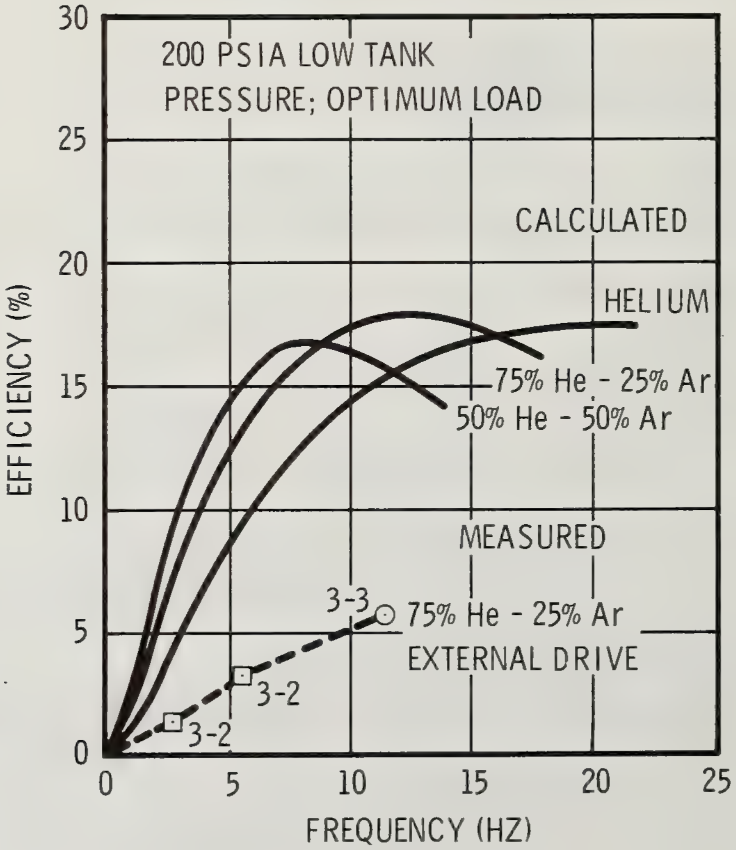

FIGURE 20. ENGINE 3 EFFICIENCY.

DISCUSSION

DR. MRAVA: Does "externally-driven" imply that the engine is being assisted or cranked from an external source?

DR. MARTINI: I didn't make that clear in the body of the talk. Many of our tests were done by moving the generator by an external electric motor. In this way we could move the generator any way we wanted to without having the motion compounded by the drive system characteristics. We did this in order to understand the engine more basically at first. Later on we found it made little difference as far as the power output and efficiency were concerned whether the engine was externally driven or not, providing the engine had the same valves and operated at the same temperature range and with the same regenerator.

DR. MRAVA: I must have misinterpreted your data then, because it appeared that the power and efficiency of the "externally-driven" unit were two to three times those achieved without an external assist.

DR. MARTINI: Well, this is a trap many people fall into by looking at the multidimensional problem superficially. Yes, there is this one difference, but it is not the important difference. Actually in our implantable size engines, Engines 3A and 3, the externally driven engine operated a a lower power output efficiency than the self driven one. So it is not the drive that is important, there are other things, the regenerator, valves or whatever else happens to be different about the engine.

DR. MRAVA: Your last figure showed a data point with an efficiency of 8%. According to your projections then, you expect to double the performance and achieve 16% efficiency. Is that correct?

DR.MARTINI: Yes, we think there is enough wrong with the engine at the present time to be able to double it still. We still believe that the analysis we do is correct and once the difficulties are corrected, the engines will work as designed.

DR. GIANNOTTI: What is the response of the system?

DR. MARTINI: When we open the load valve and allow more gas to flow, the engine immediately tries to adjust the flow. There is an optimum pressure ratio as far as the engine drive is concerned. There is another optimum pressure ratio for engine power. At extreme pressure ratios, high or low, the engine will not self operate.

DR. GIANNOTTI: Do you envision it as a constant output system or is it a variable system?

DR. MARTINI: No it will be under automatic control. We did not show this automatic control. It is controlled most efficiently by changing the volume of the drive space. By increasing the volume of the drive space you get more power and more speed, by decreasing it you get less speed, less power. We would have to control the engine to produce the pressure difference between the high pressure tank and the low pressure tank for operation of the pump.

DR. GIANNOTTI: Therefore, you think that the system would be physiologically attuned to the body from a response point of view?

DR. MARTINI: With automatic control it would follow the demands of the body by maintaining a fixed pressure difference which is fed to the pump actuator which in turn is under automatic control.

CHAPTER 90

DEVELOPMENT OF A MODIFIED STIRLING CYCLE HEART ENGINE

K. E. Buck

Aerojet-General Corp.
San Ramon, Calif.

Development of a completely implantable Stirling cycle power conversion system is described. The system is capable of converting thermal power to hydraulic power. The thermal power is received from a thermal storage unit which is periodically recharged using electric power transmitted through intact skin. The hydraulic power output is used directly to drive a circulatory assist or artificial heart device. The engine being developed is novel in two respects. Engine output is in the form of pressurized gas. This pressurized gas is used in a piston and bellows arrangement (pump actuator) to produce the required pressure pulses in the hydraulic fluid which drives the artificial heart. Only linear motion is used in the engine to convert heat to hydraulic power. Crank mechanisms, which result in high bearing loads and lateral loads on sliding surfaces, are avoided. Bearing loads are low enough to permit unlubricated operation for very long periods of time. An engine which resembles, as closely as possible, the final implantable configuration is now under test. The test engine requires only the addition of instrumentation, elimination of the thermal storage unit, and substitution of more convenient though less effective thermal insulation. Test results to date largely confirm the anticipated engine operating characteristics. Test model and implantable pump actuators are also being built and tested.

INTRODUCTION

The energy conversion system under development by Aerojet converts thermal power drawn from a thermal storage device to hydraulic power which is delivered to an artificial heart device of the flexible diaphragm type. The interface at the "input" side is with electrical power, made available inside the body to reheat the thermal storage unit. The interface at the "output" side is with the artificial heart, to which hydraulic power is delivered in pulsatile form at the required pressure, volume and pulse rate. A schematic diagram of the proposed energy conversion system is shown in Figure 1.

Thermal power is converted to mechanical power, using the Stirling cycle, by alternately heating and cooling a quantity of gas. The gas is expanded when hot and compressed when cold and mechanical work is extracted since the expansion work exceeds the compression work. The cycle is thermodynamically attractive only if a regenerator is included to limit the amount of heat that must be transferred to the gas from external sources and rejected to the environment from the gas. When a highly effective regenerator is used, the thermodynamic efficiency of the Stirling cycle is higher than that of any other practical cycle.

In the proposed system, a Stirling cycle engine operates as a compressor to compress helium from about 150 to 215 psia. This is accomplished in a single displacer chamber, with hot (about 1300^{0}F) and cold (about 250^{0}F) ends. A displacer piston moves the gas from end to end of the displacer cylinder through a regenerator and gas heater. When the displacer piston moves gas into the hot end of the cylinder, the gas is heated flowing through the regenerator and heater, and the pressure increases. When the pressure level exceeds that in the outlet reservoir, the outlet check valve opens and gas is extracted during the remainder of the stroke. As the gas is moved back through the regenerator to the cold end of the displacer cylinder, the pressure decreases until it is less than that in the inlet reservoir, at which time the inlet check valve opens and gas is drawn into the engine for the remainder of the stroke.

The proposed engine incorporates a reversing system that eliminates the requirement for the crank mechanism normally associated with Stirling engines. This, in turn, eliminates the high transverse loads between the cylinder and piston and high bearing loads resulting from acceleration force and also results in a more compact system than is possible with a crank mechanism. The reversing system allows the displacer piston to oscillate essentially as a spring-mass system. Energy must be added to the oscillating mass to compensate for energy lost as a result of mechanical and flow friction; this energy is provided directly from the displacer piston as a consequence of the unsymmetrical nature of the pressure profile in the displacer chamber. Engine speed is controlled by changing the pressure profile in the displacer chamber. The engine operates at frequencies that are high compared with the heart pulse rate (maximum speed is 1800 cpm). As a consequence, the compressed gas output is steady compared with the pulsing power requirements of the artificial heart.

The power contained in the pressurized gas is converted to pulsating hydraulic power in a pump actuator. Functionally, this component consists of a differential piston device although a bellows replaces one of the pistons. In addition to converting the essentially steady flow of high pressure gas from the engine into pulsating hydraulic power (60 to 150 cycles/min at pressures to 200 mm Hg), the pumping chambers provide a positive metallic barrier to prevent the diffusion of helium out of the engine. The pumping chamber also incorporates a system for adjusting the pressure delivered to the artificial heart for gross changes in atmospheric pressure.

Two types of control are provided: control of power delivered to the artificial heart; and control of power generated by the engine. The former is accomplished in the gas stream between engine and pumping chamber. The manner in which compressed gas is delivered to the pumping chamber is controlled to provide the proper pulse rate and fluid pressure to maintain a nearly constant atrial pressure. The engine power output is also controlled to match output power requirements by varying engine speed to maintain a constant pressure difference across the engine. The power output is varied between four and ten watts in this manner. If the required output power is less than four watts, the excess power is dissipated by throttling excess compressed gas through a pressure relief valve. In either case the output is controlled using pneumatic elements.

Waste heat from the thermodynamic cycle is removed from the engine by cooling the low pressure gas returning to the engine by transfer to the pumping fluid and, subsequently, to the blood. This two-step rejection system is employed to minimize the risk of damaging the blood by overheating. The final heat exchange from the pumping fluid to the blood can probably be accomplished through the diaphragm of the blood pump. The overall efficiency of the power conversion system, in terms of net power delivered to the artificial heart divided by the total thermal power input, is about 20% at net power output levels of eight to ten watts. At four watts, the overall efficiency is about 15.2%

A summary of work performed to date on this power system concept follows.

SUMMARY OF CURRENT WORK

Objective.

The overall objective of the program is to develop a fully qualified implantable power source, consisting of a thermal storage unit, engine, pump actuator and control system. The program was initiated in July 1968 and the specific objectives for this first phase are as follows:

Design, fabricate, test and evaluate the thermal energy conversion system at the earliest possible date. The first engine subsystem to be tested is to be of an implantable configuration and power level but is to be provided with instrumentation to permit engineering evaluation.

Redesign and modify the engine as necessary to achieve predicted or maximum obtainable overall performance.

Design and fabricate a test model pump actuator. Assist the NHI control subsystem contractor, Fluidonics Research Laboratory, in the design and development of a pump actuator control system that will provide physiologically adequate conditions at the pump actuator output.

Integrate test model engine and pump actuator and experimentally investigate dynamic characteristics of the integrated unit.

Design and fabricate an implantable model engine based on the technology level of the test engine.

Design and fabricate an implantable model pump actuator with integral control subsystem. The control subsystem is to be provided by Fluidonics Research Laboratory.

Current Status

The major effort on the program to date has been the development of the test engine and test actuator. A summary of the current status, as represented by major accomplishments, is as follows:

The test engine has been designed and fabricated and is under test. Improvements and modifications to the engine are being made as the tests progress. Test results achieved to date are very encouraging; these are discussed in more detail below.

The test model pump actuator has been designed and fabricated. The unit was given preliminary tests at Aerojet and then was delivered to Fluidonics Research Laboratory where it will be used as a test bed in the development of the control system.

Design of the implantable engine is complete. Fabrication of engine components is in process.

Design of the implantable pump actuator is complete. Fabrication of pump actuator components is in process and the purchase of long lead components has been initiated. The interface with Fluidonics is under control; control system components can be mounted within the pump actuator.

Description of Work Performed

Instrumented Test Engine (Mark II Engine). The principal criterion in the design of the Mark II engine was that it should be as close as possible to an implantable configuration but with provision for sufficient instrumentation to permit engineering evaluation of its performance. The design was also influenced by the fact that this was the first engine of this type to be built and it was to be built without benefit of a systematic component development program. These latter considerations led to a certain amount of conservatism and provision for component modification and replacement that would not be appropriate in an implantable engine.

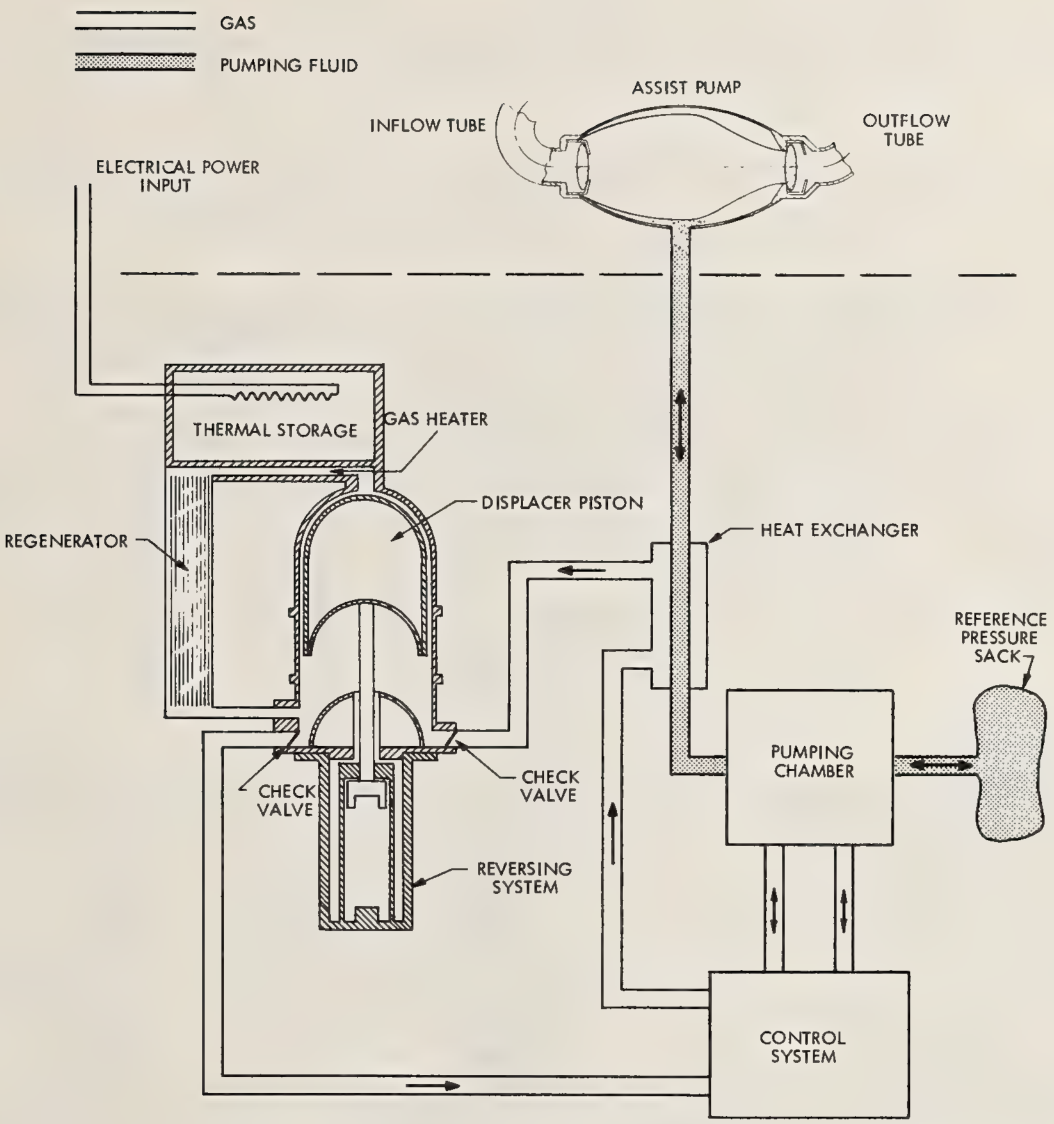

FIGURE 1. MODIFIED STIRLING CYCLE ENERGY CONVERSION SYSTEM.

A drawing of the Mark II engine is shown in Figure 2, and a photograph showing the completed engine is shown in Figure 3. A brief description of the instrumentation is presented below.

Gas temperatures are measured at the upper and lower end of the regenerator, above the piston and at the engine outlet. Gas temperatures are measured by conventional bare wire thermocouples and by platinum resistance wires. The thermocouples give a measure of average gas temperature since the time constant of the thermocouple is large in comparison with engine speed. The resistance wire temperature probes measure changes in gas temperature during each engine cycle.

Gas pressures in the engine are measured as a function of time using conventional unbonded strain gage pressure transducers (modified only to reduce gas volume). Pressures in the heater, cold chamber and reversing chamber are monitored. A separate more sensitive pressure transducer is used to measure the pressure difference across the regenerator due to gas flow resistance.

Piston position is determined using the linear displacement transducer located below the engine.

In addition to the above parameters, pressures in the inlet and outlet reservoirs, power input gas flow rate and various engine temperatures are also measured. Transient parameters are displayed on oscilloscopes and data is recorded photographically. Other data is recorded on conventional chart recorders or manually.

Mark II Engine Operating Experience. Test operation of the Mark II engine has been extremely successful, particularly in view of the novel nature of the engine and the minimum amount of component testing and development prior to engine design. The engine operated in a self-sustained mode the first time it was tested, as it has in all succeeding tests. Difficulties with instrumentation and auxilliary test equipment, common to this type of program, were encountered but few problems were attributable to the engine. The major engine problem was low speed. However, it was found that design output could be reached even at low speeds if the engine pressure level was increased. Relatively minor changes have been made to the engine bearing, reversing spring and spring keepers and the displacer piston is now vented (using a 2 mil vent hole) rather than pressurized. Further modifications to the regenerator, piston ring and check valves are planned but it appears that the engine will meet all design objectives in what is very nearly its original configuration.

Table 1 presents a brief summary of predicted and measured engine characteristics.

TABLE 1

PREDICTED VS OBSERVED ENGINE PERFORMANCE

Operating Conditions	Analytical	Experimental (Run #35A)	Analytical	Experimental (Run #28)
Maximum gas temperature, °F	1200	1215	1460	1442
Minimum gas temperature, °F	250	237	250	238
Maximum gas pressure, psia	72.0	98.7	75.0	94.7
Minimum gas pressure, psia	60.0	85.7	60.0	80.7
Engine speed, Hz	18.5	18-19	30.0	19-20
Output Power				
Gross output power, watts	5.28		13.47	12.08
Reversing power, watts	-0.54		-1.24	-1.10
Check valves, watts	-0.54		-0.76	-0.58
Net power out	4.20	7.13	11.47	10.40
Input Thermal Power				
Regenerator Conduction, watts	4.36		5.55	
Piston + cylinder wall conduction, watts	7.56		9.80	
Piston internal conduction, watts	0.40		0.45	
Insulation, watts[a]	23.0		27.5	
Instrumentation, watts	5.17		6.03	
Static power loss total	40.50	38.0	49.33	55.0
Thermodynamic power, watts	9.53		22.3	
Regenerator ineffectiveness, watts	2.73		8.01	
Mechanical pumping, watts	7.57		9.79	
Radial gap end heat, watts	1.76		5.15	
Total power in	62.09	70.0	94.63	95.0
Net Efficiency	6.7	9.2	12.2	10.9

[a] Evacuated fibrous insulation would reduce this value to one-half.

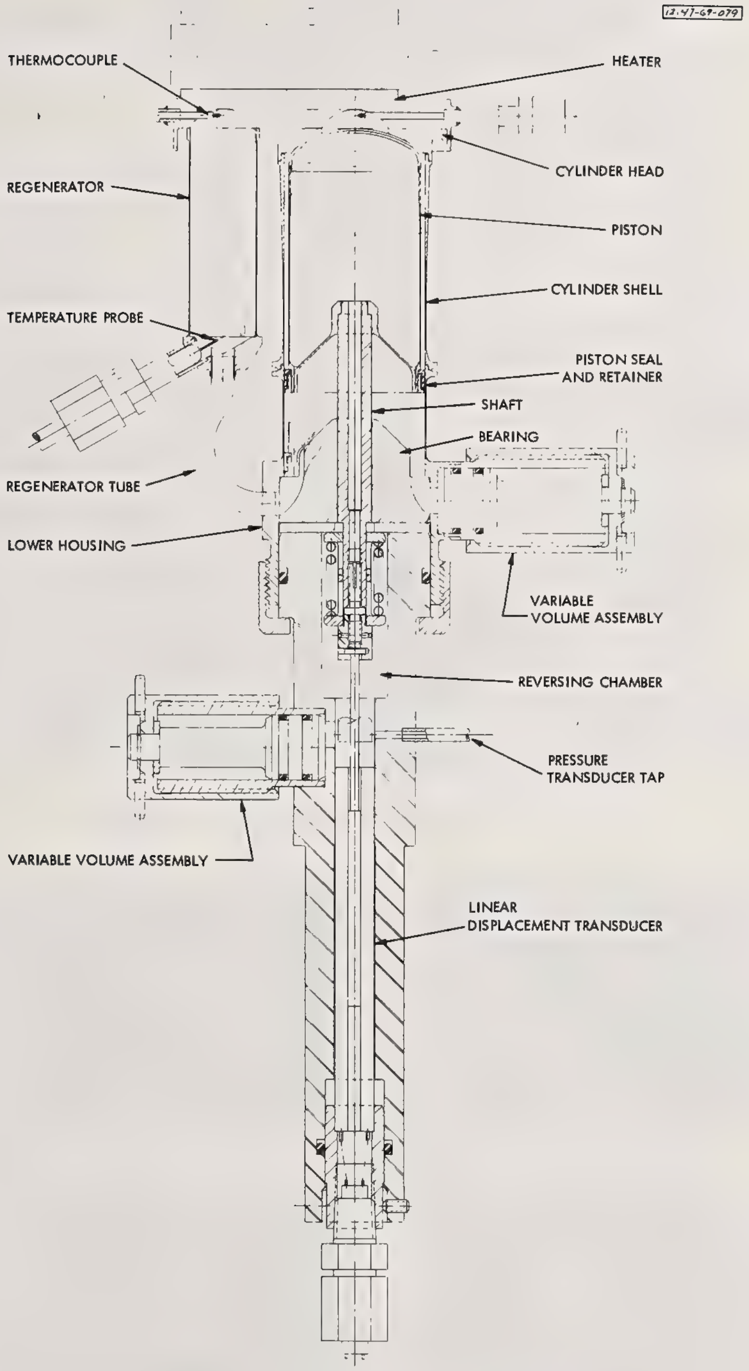

FIGURE 2. MARK II ENGINE DESIGN.

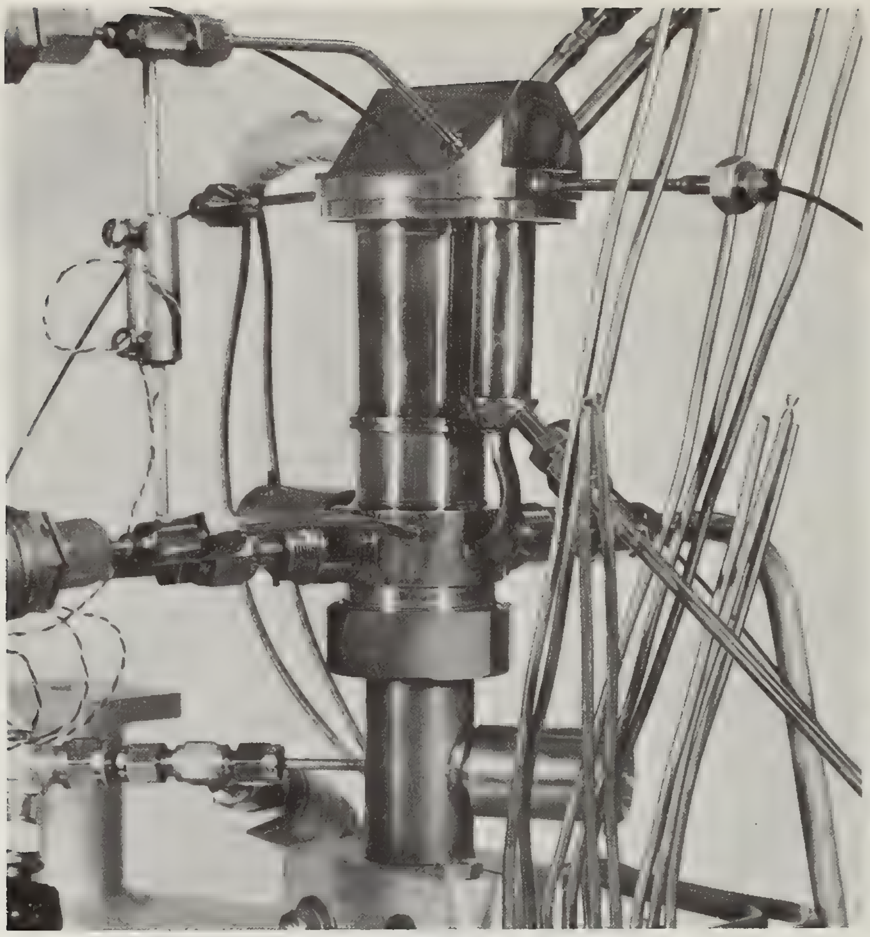

FIGURE 3. MARK II ENGINE.

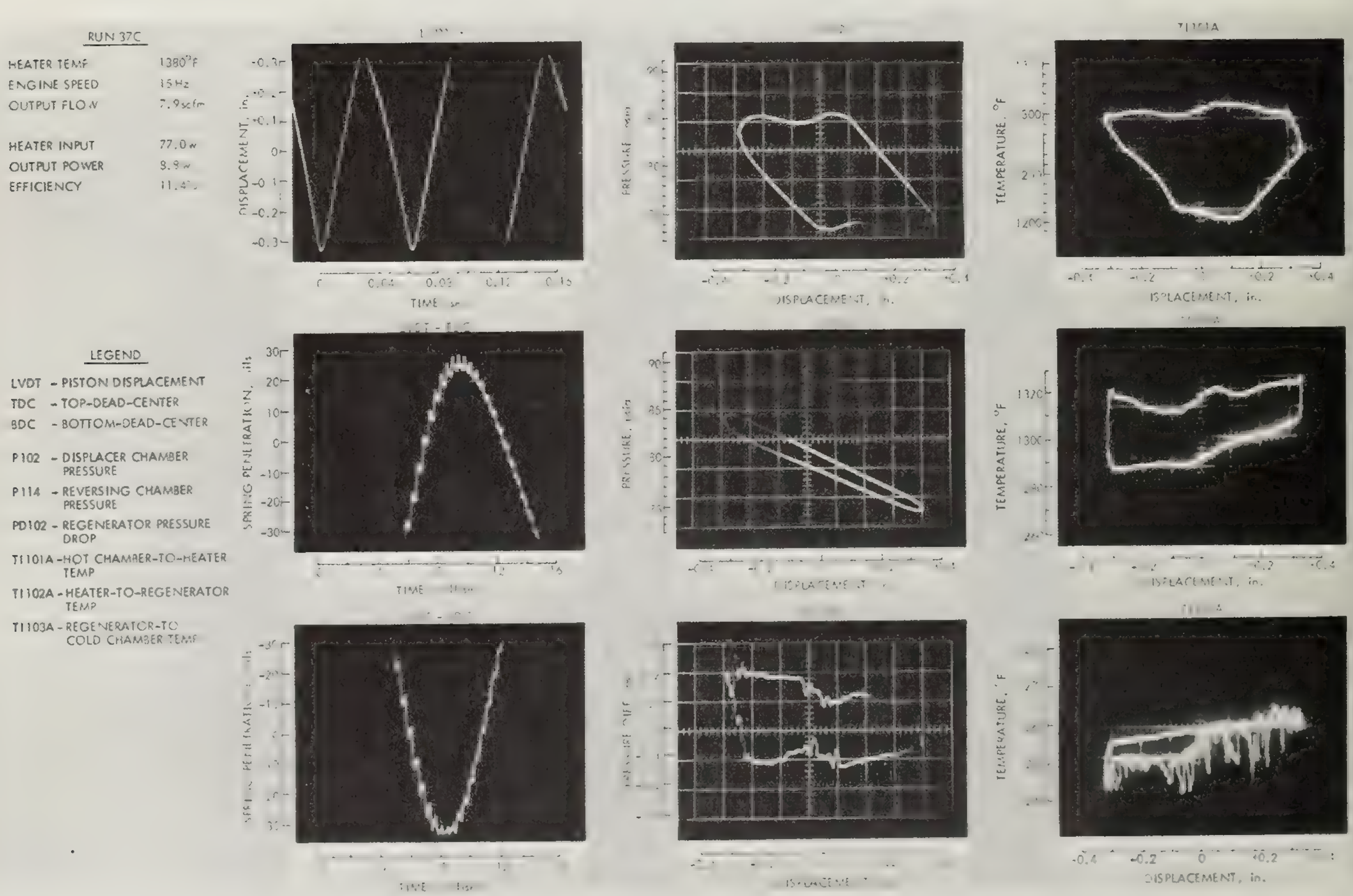

FIGURE 4. TYPICAL ENGINE PARAMETER TRACES.

The predicted performance of the Mark II engine is considerably less than that for an implantable engine due to the effect of instrumentation and non-optimum insulation. Refractory block type insulation was used to simplify the attachment of instrumentation to the engine and to simplify engine modifications but it considerably increases the amount of thermal power required to run the engine. Instrumentation also increases the required thermal power input by providing conduction paths out through the insulation, and decreases power output by increasing the unswept gas volume in the engine.

A complete set of data for an individual operating condition represents a considerable amount of information. Transient data are taken in addition to the relatively steady readings of inlet and outlet pressure, flow rate, power input, etc. Figure 4 shows a typical set of transient temperatures, pressures, piston position and regenerator pressure drop. Information on component performance can be obtained from this data. Figures 5, 6, 7, and 8 show some of the information obtained in this way. It is this type of detailed component performance information that will lead to systematic improvements in component and overall engine performance.

In summary, the Mark II engine tests have gone very smoothly, particularly when one considers the size of the technological step represented by this engine and the amount of intermediate component work that has been bypassed. The results show that the engine concept is very attractive for the planned application. Significant overall efficiency and power density have been demonstrated in the test engine configuration and these can be directly extrapolated to show that an implantable version of this engine will achieve satisfactory performance for early in vivo testing even without improvement in component performance. In addition, many design options are open for potentially large improvements in the performance of succeeding generations of this basic engine type.

Mark III Engine Design and Fabrication. The Heart Engine Program at Aerojet was recently expanded to include the design and fabrication of an uninstrumented engine (Mark III) that will closely resemble the test engine (Mark II). Changes in design will be made only to:

Eliminate all instrumentation
Modify the head to mate with the thermal storage unit
Eliminate the variable volume chambers
Provide mating surface and thermal expansion compensation for vacuum envelope around thermal insulation
Increase operating pressure level to 200 psi

A layout drawing of the Mark III engine is shown in Figure 9. A simplified layout showing integration of the Mark III engine with a thermal storage unit is shown in Figure 10. Fabrication of this engine and tests of thermal storage materials are now in progress.

Pump Actuators. A pump actuator is required to satisfy the interface requirements between the engine and blood pump. The pump actuator accepts high pressure gas from the engine at a nearly steady rate and returns the expanded gas to the engine. The energy contained in the gas is used to generate a pulsatile fluid output at the frequency, pressure and volume required by the host organism. This pump actuator function is accomplished by a device that is essentially a differential piston (with suitable bellows seals) and a control system. The use of bellows seals is an important feature of the pump actuator. It provides an essentially absolute barrier against the loss of engine gas into the body and it provides absolute control of fluid volumes in the blood pump.

Work on the pump actuator is being done at Aerojet on company funding while the control system is being provided by Fluidonics Research Laboratory.

Aerojet has built two pump actuators and is in the process of building a third. The first actuator was built to investigate the characteristics of a bellows-sealed pneumatic-to-hydraulic pressure converter, particularly the dynamic interactions between bellows spring constant and fluid inertia. During fabrication and testing of this unit it became clear that substantial size reduction would result from the substitution of a piston drive mechanism for the bellows drive of this first unit. A second test actuator incorporating a piston drive was therefore designed and built.

This second test actuator was to have two functions:

1. To serve as a load for the Mark II engine to investigate the dynamic interaction between engine and pump actuator and,
2. To assist in the development of a control system by providing a test bed that approximates the implantable pump actuator in dynamic response and spring rate.

The gas drive and fluid pumping portions of the system were physically separated to allow access to all components during testing and modification. A drawing of the drive piston portion of the test actuator is shown in Figure 11. A photograph of the completed actuator is shown in Figure 12.

Spring rate calibrations and dynamic experiments were performed on the test pump actuator assembly which was delivered to Bio-Logics for control component evaluation. Dynamic and quasi-static experimental operating characteristics were obtained by pulsing a 72 mm Hg methanol hydraulic head at helium actuator drive pressures of 20, 25, and 30 psi, and LVDT stroke settings of ±0.4, 0.3, 0.2, and 0.1 inches. Characteristics were also measured for a fixed end of discharge setting (+0.4 inches) and variable suction stroke settings ranging from 0 to -0.4 inches. A typical experimental data trace is shown in Figure 13.

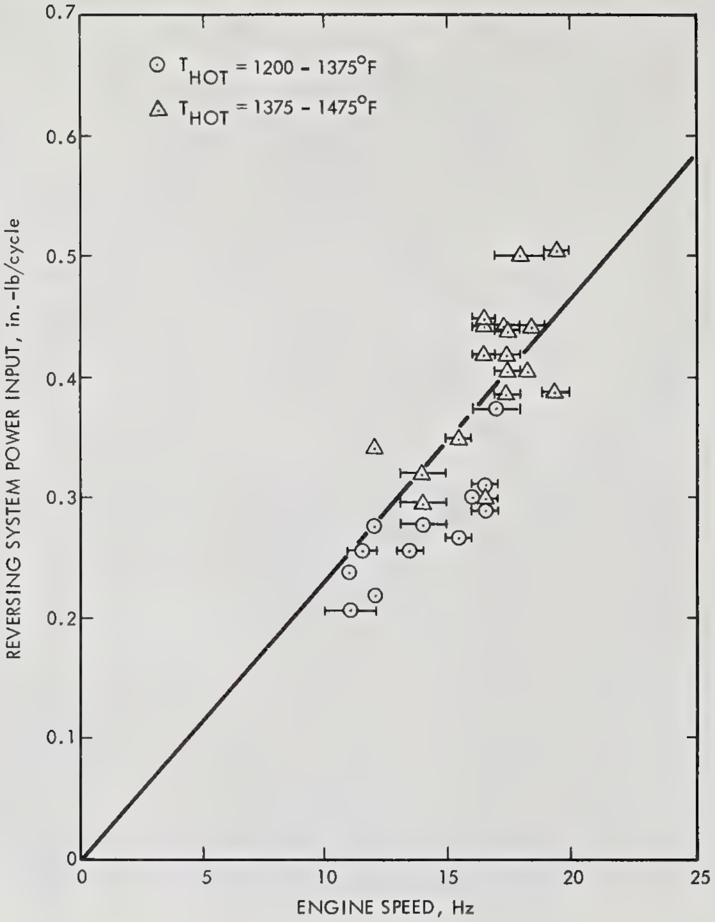

FIGURE 5. REVERSING SYSTEM POWER INPUT.

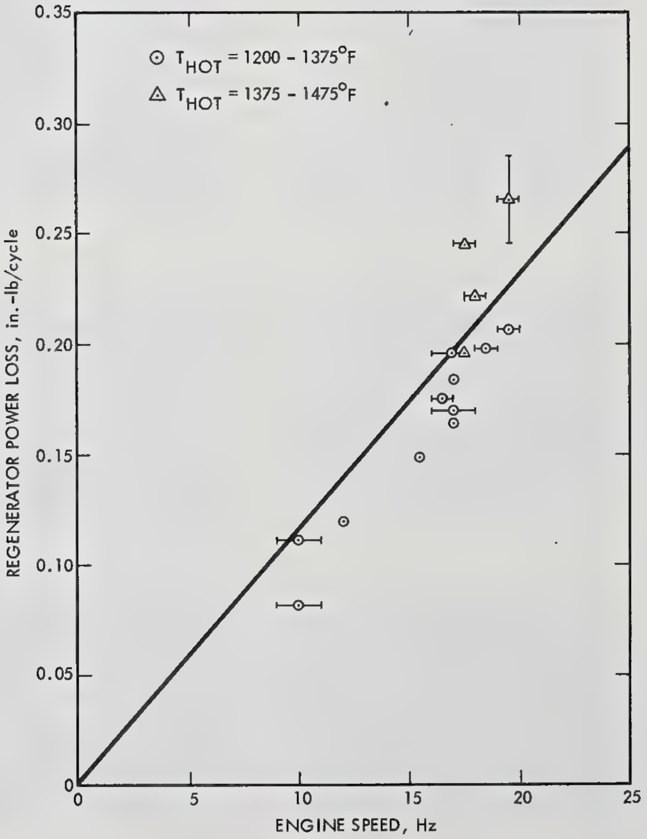

FIGURE 6. POWER LOSS DUE TO REGENERATOR PRESSURE DROP.

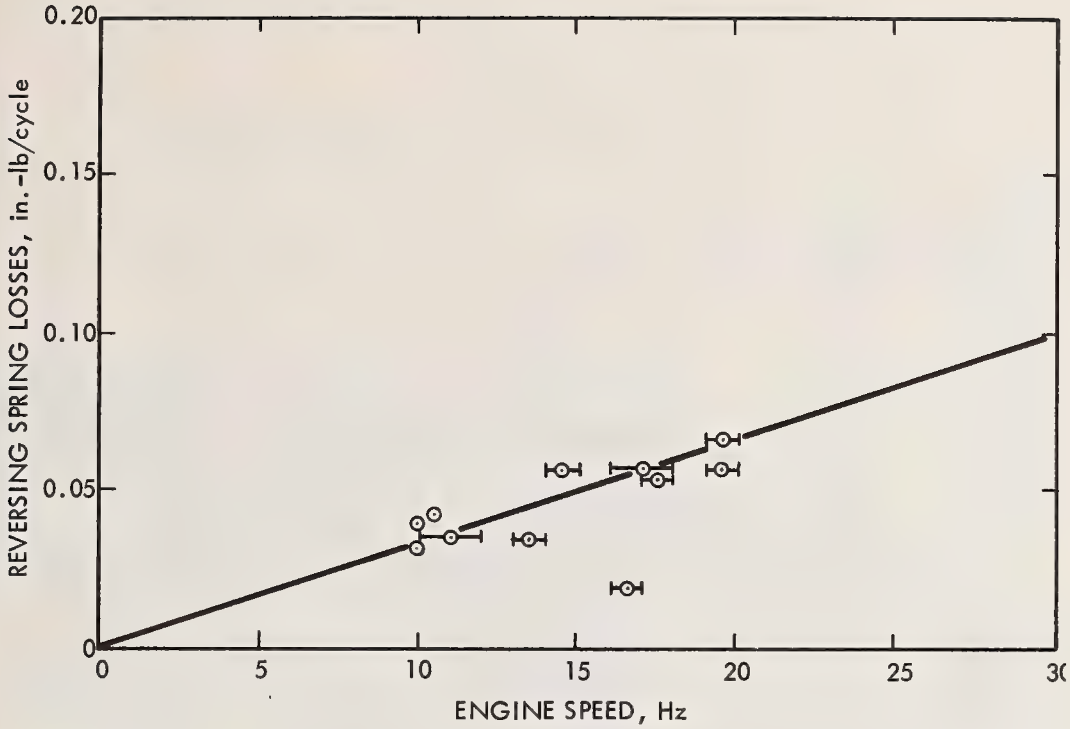

FIGURE 7. POWER LOSS IN REVERSING SPRING.

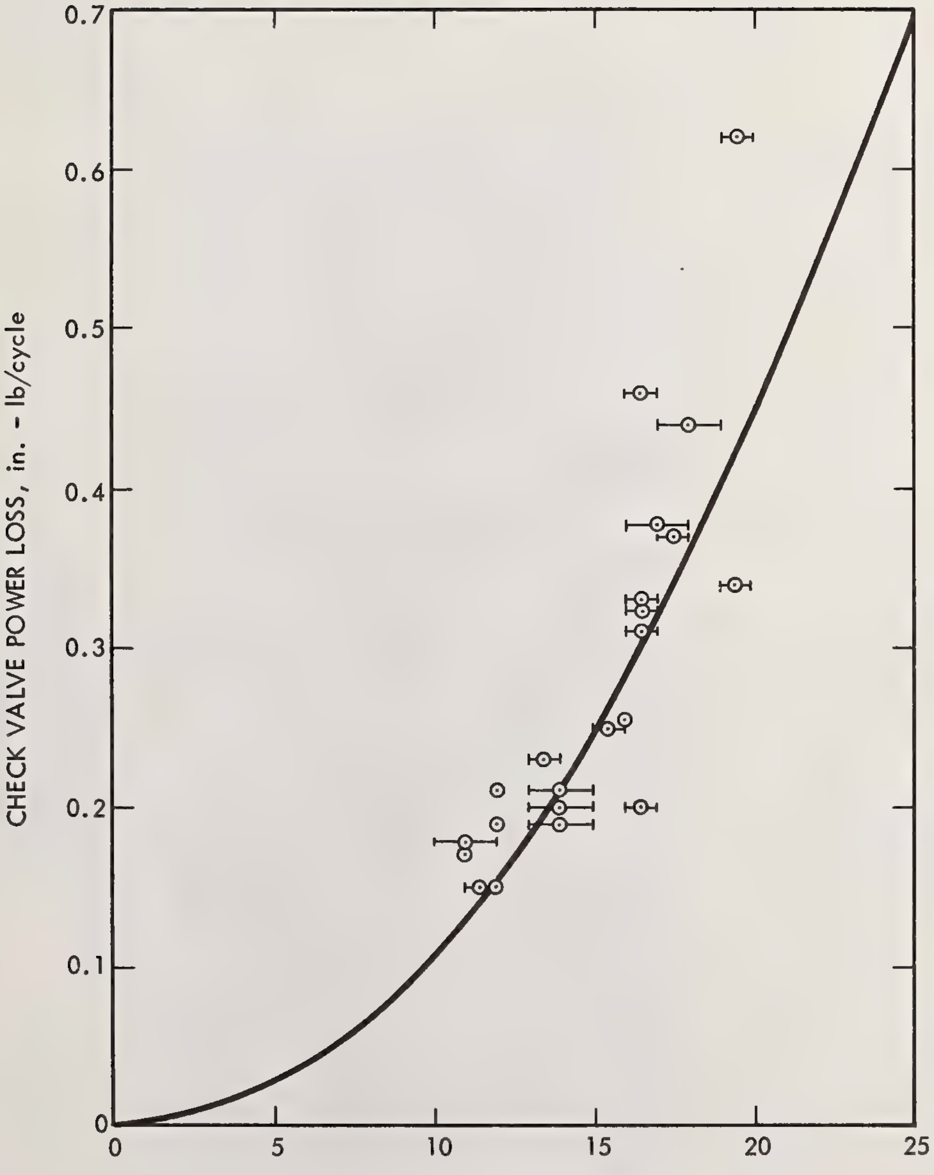

FIGURE 8. CHECK VALVE POWER LOSS.

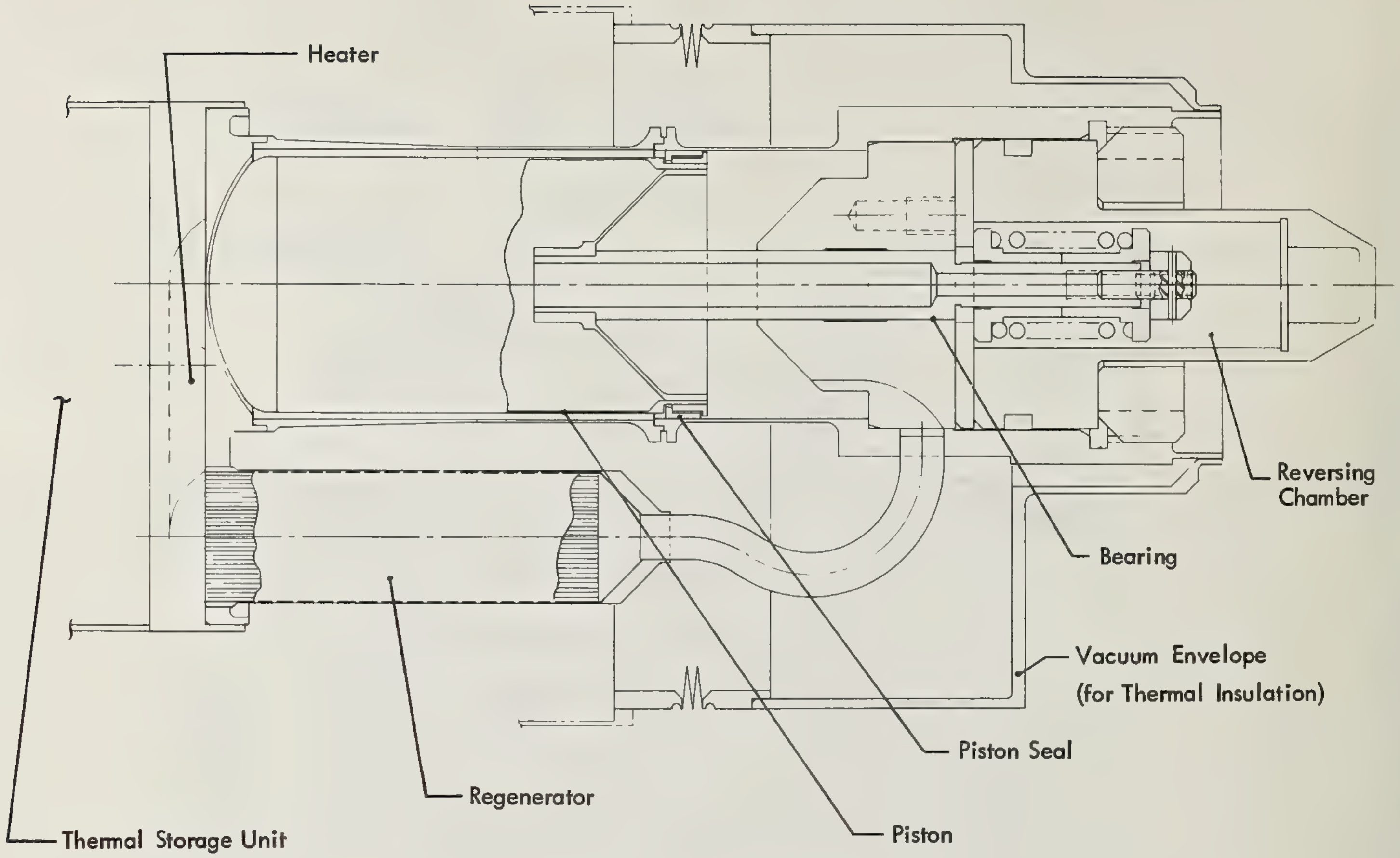

FIGURE 9. IMPLANTABLE (MARK III) ENGINE.

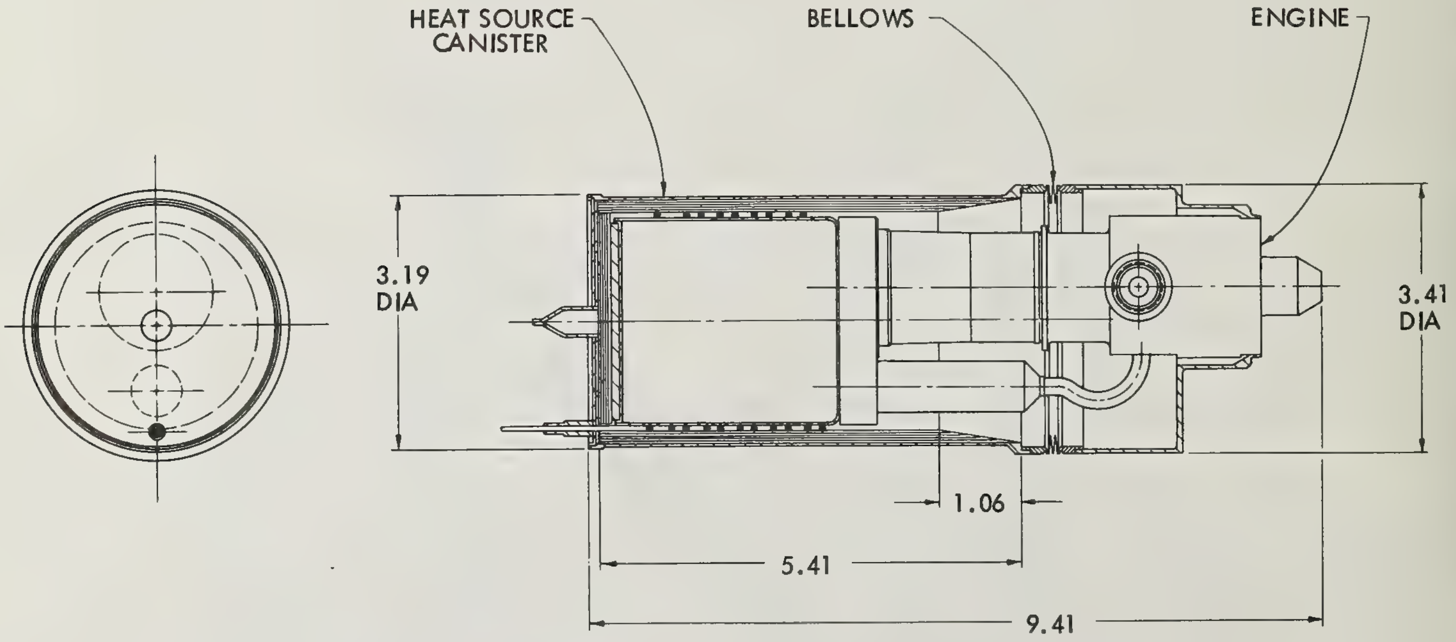

FIGURE 10. MARK III ENGINE WITH THERMAL STORAGE AND INSULATION UNIT.

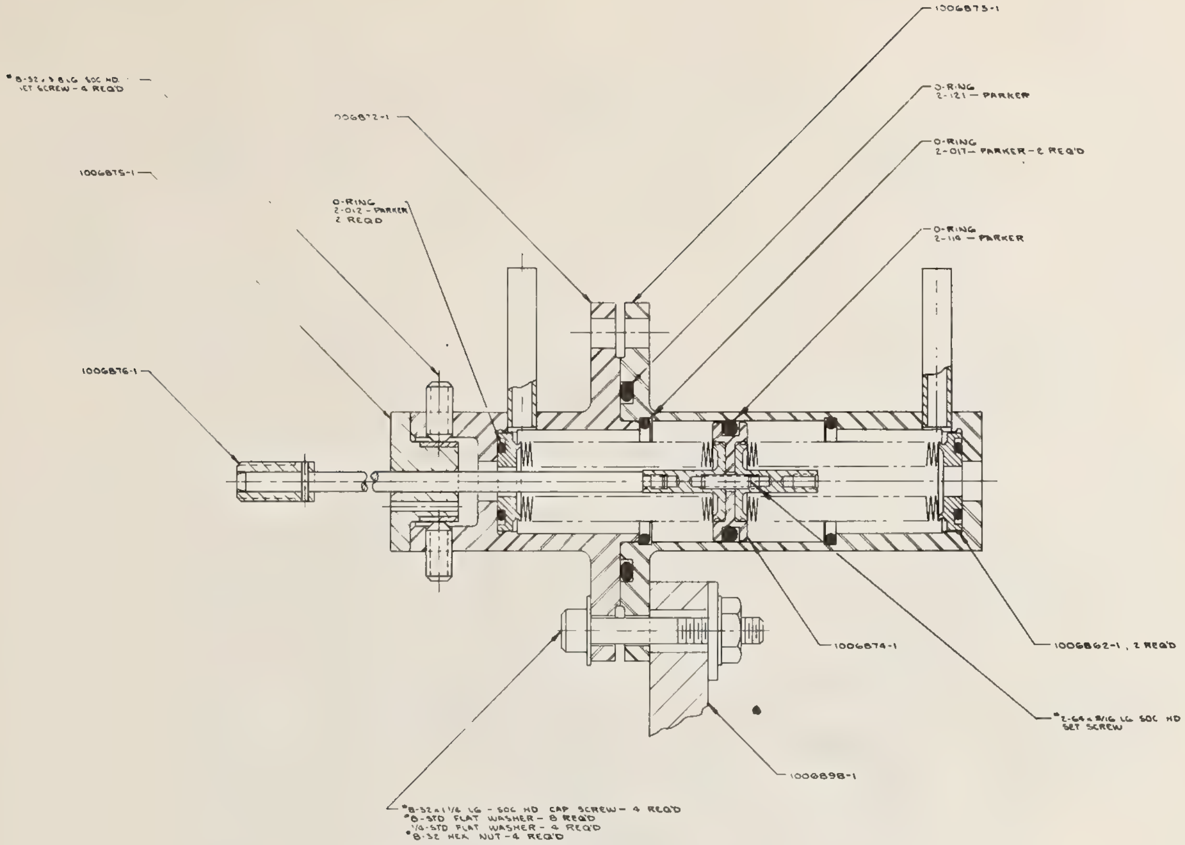

FIGURE 11. TEST PUMP ACTUATOR.

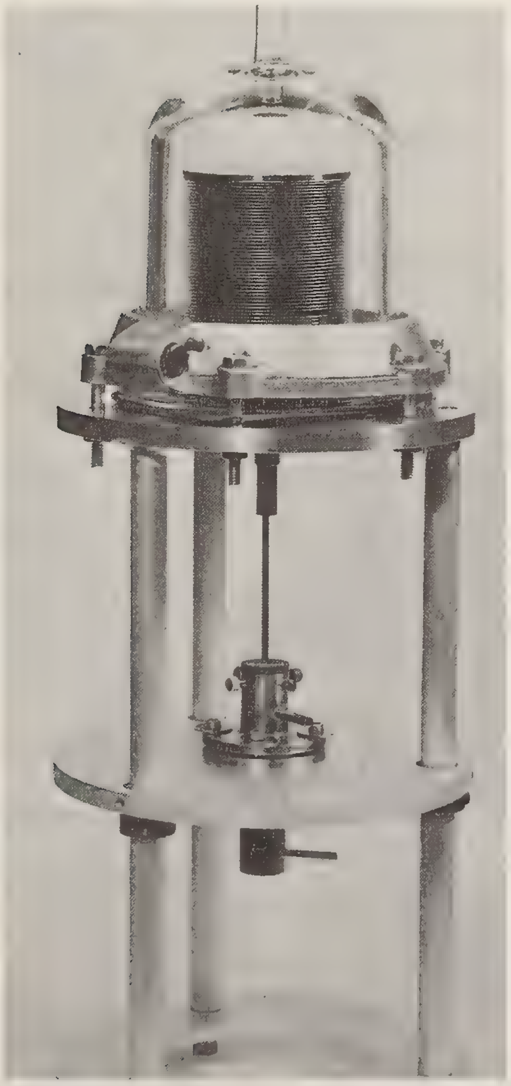

FIGURE 12. TEST MODEL PUMP ACTUATOR.

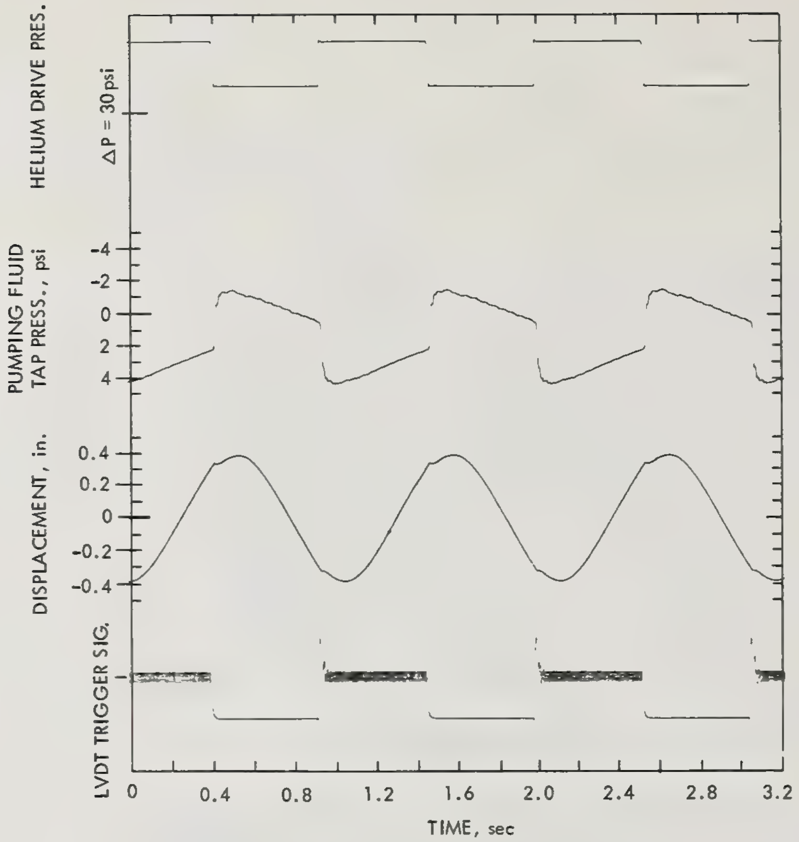

FIGURE 13. EXPERIMENTAL DATA TRACE, TEST ACTUATOR.

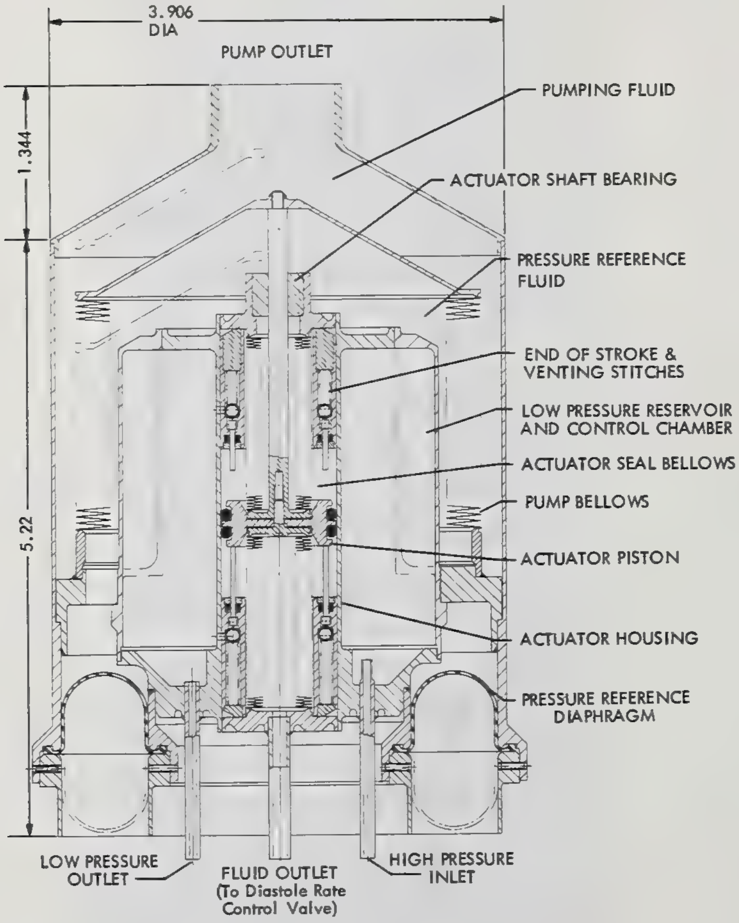

FIGURE 14. IMPLANTABLE PUMP ACTUATOR.

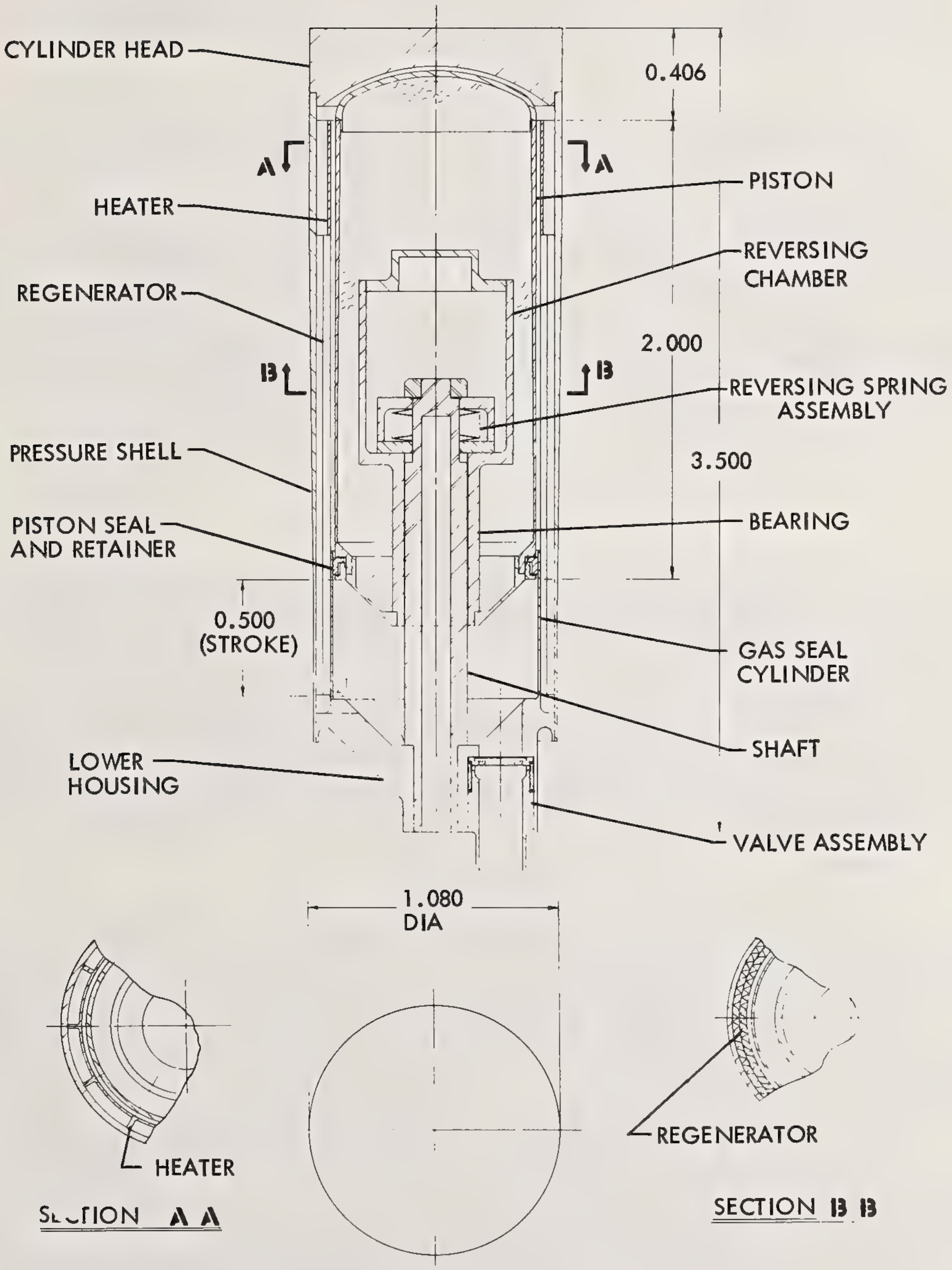

FIGURE 15. ADVANCED (MARK IV) ENGINE.

The unit has been delivered to Fluidonics where it is being used in the development of the control system. On completion of this work, it will be returned to Aerojet where the complete pump actuator and control system will be coupled with the Mark II engine for tests of the dynamic interaction between the two subsystems.

An implantable model of the pump actuator, functionally similar to the test model, has been designed and is being fabricated, again with Aerojet funding. The implantable model will be more compact than the test model and all instrumentation will be contained within the pump actuator. The fluid pulse size of the implantable model is also larger than that of the test model (100 vs 63 cm^3). A drawing of the implantable pump actuator is shown in Figure 14.

FUTURE PLANS

Next year's program will include design and fabrication of advanced engines and pump actuators. Major emphasis will be on the reduction of equipment size although increased efficiency is also anticipated.

The advanced engine concept will include major configuration modifications from the Mark II engine while retaining basic functional design. These changes will include a concentric heater inside the displacer cylinder, a concentric regenerator directly below the heater, and redesigned spring reversing system "folded" back inside the displacer piston and are shown in Figure 15.

Advanced model pump actuators will also be investigated. Promising modifications include passive falling (instead of the active filling presently used), substitution of more compliant titanium alloy bellows for the stainless steel bellows presently used, and redesign of the pressure reference diaphragm.

DISCUSSION

DR. GIANNOTTI: I would like to ask the same question on response. Do you have any information on the response of the system under a step load change?

MR. BUCK: Not really. The engine has been operating to date with fairly large reservoirs attached to it. The only thing we have done is to quickly close and open the throttle valve that connects the two reservoirs. But this has no effect on the engine, and I guess you wouldn't really expect any effect because the pressure difference between the reservoirs builds up only gradually. It is in our immediate program to look at these dynamic effects.

DR. ARP: What is the longest sustained period of operation for your engine and what is the maximum cycle rate which you have been able to obtain?

MR. BUCK: We have operated up to about 20 hertz. The longest time we have operated the engine has been some fraction of a day. We don't normally run more than a single shift, and it takes two or three hours to get the engine up to operating temperatures. So the answer to your question would be something like four hours.

DR. ARP: One other question: Have you had any problem with bellow fatigue, e.g., ruptured bellows?

MR. BUCK: We have not seen any yet.

MR. BRODD: What do you estimate would be the weight of a normal 10 watt engine.

MR. BUCK: Well, roughly a couple of pounds, the few times that we have calculated engine density, which hasn't been recently, the overall density comes out to be about one.

CHAPTER 91

DEVELOPMENT STATUS OF AN IMPLANTABLE RANKINE-CYCLE CIRCULATORY SUPPORT SYSTEM

F. Huffman, T. Robinson, S. Kitrilakis

Thermo Electron Corporation
Waltham, Massachusetts

The objective of this effort is to develop and evaluate a thermally rechargeable circulatory support system using a miniature steam engine. Electrical energy coupled across the skin is stored in the latent heat of fusion of the eutectic composition of LiF/LiCl. The stored heat produces steam which is expanded in a single cylinder, flywheel return engine to pump up a hydraulic accumulator. The accumulator is coupled to a left ventricle-to-aorta assist pump (which also functions as a blood-cooled heat exchanger and physiologic sensor) via a counterpulse, hydraulic control system which responds to changes in both heart rate and stroke volume. Transcutaneous power transmission levels of 150 watts into a 16 ohm load across a gap of 1 cm have been demonstrated using Ferroxcube cores with Litz windings. Engines of 1.2 ml displacement, miniaturized for integration into an implantable source, with both internal and external exhaust valves have been tested and an engine output of 8 watts has been measured. Extensive testing of a hydraulically actuated Model VI CHMC-TECO assist blood pump has led to an improved model with an 80% increase in effective stroke volume. Control system function has been demonstrated on a mock circulation loop. Initial in vivo tests of power transmission, component suspension, heat dissipation and diaphragm penetration have been favorable.

INTRODUCTION

The design of a thermally rechargeable Rankine-cycle implantable circulatory support system must meet a variety of complex mechanical and biological objectives. A compact blood pump which pumps efficiently and does not promote blood clots or significantly damage the blood is necessary. The thermal-to-hydraulic power conversion device required to drive the blood pump must provide thermal energy storage and a thermodynamic engine which is small, efficient, and reliable. The electromagnetic transcutaneous power transmission system must transfer and regulate power to the thermal energy storage material without dissipating excessive heat in vivo. The coupling between the blood pump and power source must be efficient and respond to the physiological requirements of the body. In addition, the reject heat from the power source must be dissipated and the entire system suspended in the body. The simultaneous satisfaction of these requirements, within severe volume and weight constraints, is the goal of this effort.

SYSTEM CONCEPT

The basic concept of the circulatory support system under development at Thermo Electron is illustrated in Figure 1. The shafts of the arrows denote fluid, thermal, mechanical, and electromagnetic flow. Electrical power is transmitted transcutaneously from an extracorporeal energy source and is used to melt a eutectic mixture of lithium halide salts. Thermal energy stored in the heat of fusion is used to produce steam by solidifying the molten salt. Mechanical energy is extracted from the steam by expansion in the heat engine and is used to pump the hydraulic fluid, water, into the high-pressure reservoir. This water is then extracted from the high-pressure reservoir to drive an actuator which reduces the drive pressure to the blood pump. Synchronization and proper phasing with the left ventricle and stroke volume control are accomplished at the actuator by the hydraulic control component.

These components are incorporated into four separate packages. The power source, which includes the thermal energy storage material, the engine and the high-pressure reservoir, will be located in the abdominal cavity and adjacent to the diaphragm. The secondary winding of the transcutaneous power transformer will be placed nearby. The blood pump control unit will be located in the abdominal cavity immediately below the diaphragm. The fourth component, the blood pump, is located in the chest. Hydraulic or electrical power lines connect these packages.

It is convenient to discuss the development status of the Rankine-cycle circulatory support system in terms of the major subsystems. The five major subsystems may be identified as: (1) transcutaneous power transmission, (2) heat storage, (3) Rankine engine and hydraulic pump, (4) blood pump controls, and (5) assist blood pump. Program status will be indicated as the design approach to the various subsystems is outlined.

TRANSCUTANEOUS POWER TRANSMISSION

The function of the transcutaneous power transformer is to recharge the heat source by melting the thermal energy storage material using a resistance heater. A plot of charging time versus recharging power, parametric in storage time, is shown in Figure 2. This graph indicates that a recharging power of 100 watts is required if the recipient of the circulatory support system is not to be unduly tethered to the recharging equipment. The heat dissipation and temperature rise of the implanted secondary from Joule heating and core losses is an important constraint on the recharge power level. After preliminary radio frequency experiments a decision was made to work at audio frequency using ferrite pot cores. The initial transformer was provided by Myers et al at New York University.

Transformer core configurations were surveyed for maximum power transfer. Calorimetric measurements demonstrated the value of Litz wire for the trifilar windings at the optimum operating frequency of 17 kHz. Transcutaneous power transmission levels of up to 185 watts into a 16-ohm load across a gap of one centimeter have been demonstrated, using modified Ferroxcube cores with Litz windings. Measured efficiencies have exceeded 80 percent.

A thermally rechargeable circulatory support system requires regulation. The regulator concept evolved by Thermo Electron is based on the variation with temperature of the permeability of a ferromagnetic material. The component arrangement is shown in Figure 3. The permeability drops rapidly as the temperature of the ferromagnetic material reaches its Curie point. Advantage may be taken of this fact by placing the ferromagnetic switch material in thermal contact with the thermal storage container, whose temperature is to be sensed as an element in a series magnetic circuit (along with a small permanent magnet and a magnetic reed switch located outside of the vacuum enclosure). With a ferromagnetic material chosen to match the melting point of the thermal energy storage material, the information required for charge control is contained in the "open" and "closed" positions of the reed switch. Below the melting point (and Curie temperature) of the storage material, the reluctance of the magnetic circuit is so low that the flux level closes the contacts of the magnetic reed switch. Above the melting point (and Curie temperature), the increased reluctance of the magnetic circuit drops the flux level and opens the contacts of the magnetic reed switch. The information contained in the switch contacts may be utilized in a variety of ways for regulating the power transmission level.

This regulator concept has the advantage of using a physical property that changes rapidly near the melting point of the thermal storage material and of requiring no moving parts other than the reed of the switch. It is physically independent of the other subsystems and requires no penetrations of the vacuum enclosure. In addition, it is attitude-insensitive, and calibration is built into the system via the Curie point of the magnetic switch material.

The response characteristics of this charge regulator are functions of the "air" gap, reed switch characteristics, magnet strength, and ferromagnetic material permeability variation with temperature. Tests have demonstrated the adequate sensitivity and stability of this control technique. Using iron-nickel alloys as the temperature sensor, the "pull in" and "drop out" of the reed switch can be adjusted to a typical range of 870 and 960°F, respectively. This is satisfactory for the LiF/LiCl eutectic storage material, which has a melting point of 930°F.

HEAT SOURCE

High-density thermal energy storage is accomplished by using the latent heat of fusion of the lithium chloride-lithium fluoride eutectic. This material (30.5 mol percent LiCl) has a high volumetric storage capacity (362 cal/cc) and a convenient melting point (930°F), and is chemically stable. Tests have demonstrated that 304 stainless steel is compatible with the molten eutectic for a period of one year and that heat may be transferred into and out of the container with modest temperature gradients.

In order to minimize extraneous heat losses, vacuum foil insulation is used around the heat source. These foils are placed perpendicular to the direction of heat flow and form radiation shields. A thin layer of oxide powder acts as the thermal conduction barrier between adjacent foils.

The thermal energy prototype vacuum insulation consists of 80 layers of titanium foil spaced with zirconia. The measured insulation loss of the prototype at the eutectic melting point (930°F) is 3.9 w. This heat source is described in more detail in the NHI paper entitled "Development of a Heat Source for an Implantable Circulatory Support Power Supply" by Bluestein and Huffman.

RANKINE ENGINE AND HYDRAULIC PUMP

The Rankine engine used is a single-expansion, single-acting positive displacement engine. Water was chosen as the working fluid for the Rankine cycle because of its good cycle efficiency, its thermal stability, and the backlog of technology involving its use in Rankine engines.

After a review of alternative engine configurations, a single-cylinder design with a flywheel was chosen. The cylinder bore is 0.5 in. and the piston stroke is 0.4 in. The engine speed ranges from a minimum of 600 rpm, while the host is at rest, to a maximum of 1800 rpm during peak activity. These speeds span a power output range from 4 to 12 w. The valving arrangement, shown in Figure 4, minimizes the work in returning the piston to top dead center. Bearing loads are reduced by rigidly connecting the steam piston to the piston of the hydraulic pump.

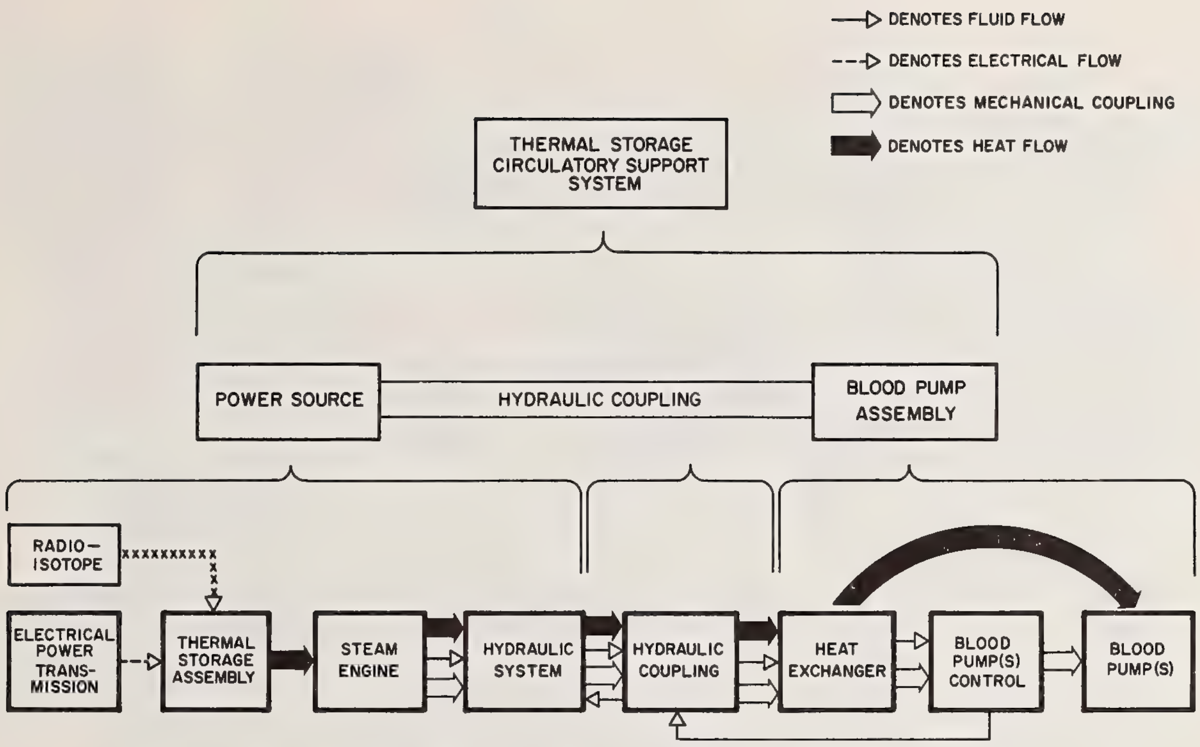

FIGURE 1. BLOCK DIAGRAM OF AN IMPLANTABLE, RANKINE-CYCLE CIRCULATORY SUPPORT SYSTEM.

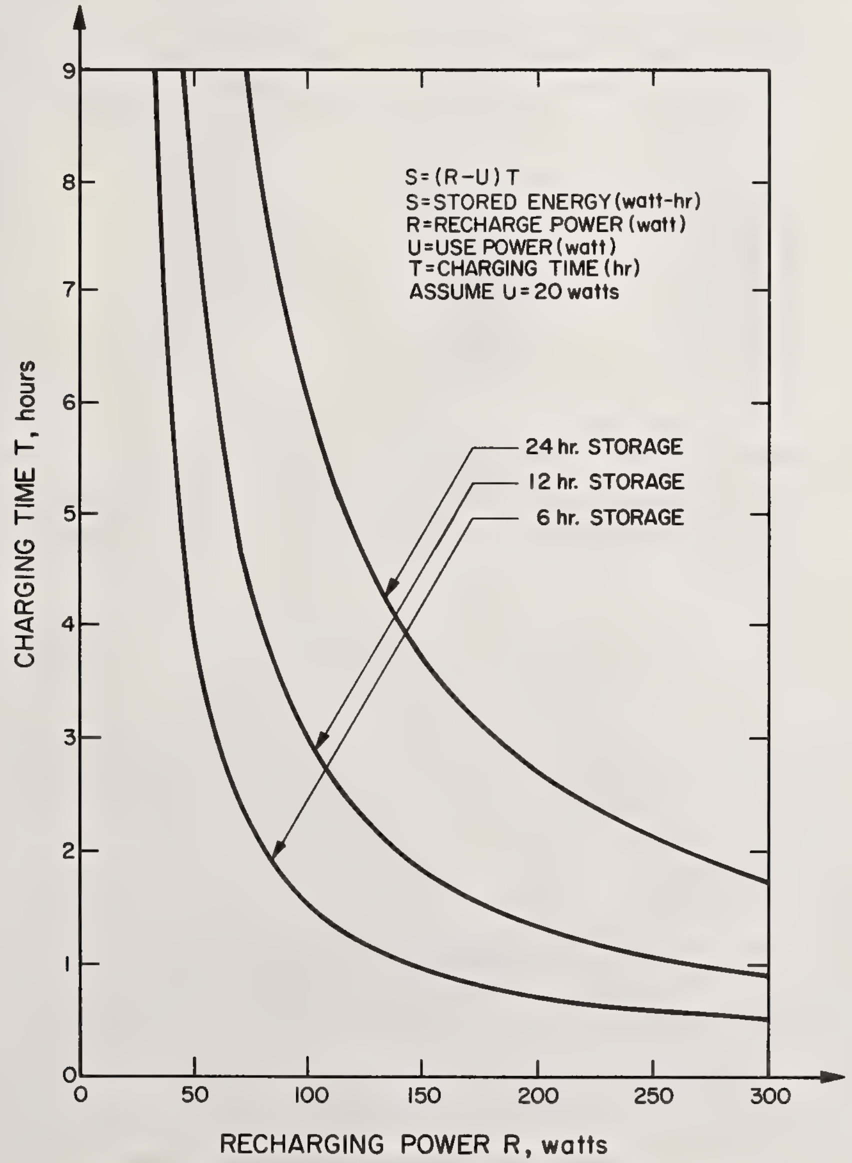

FIGURE 2. CHARGING TIME OF THE THERMAL ENERGY STORAGE.

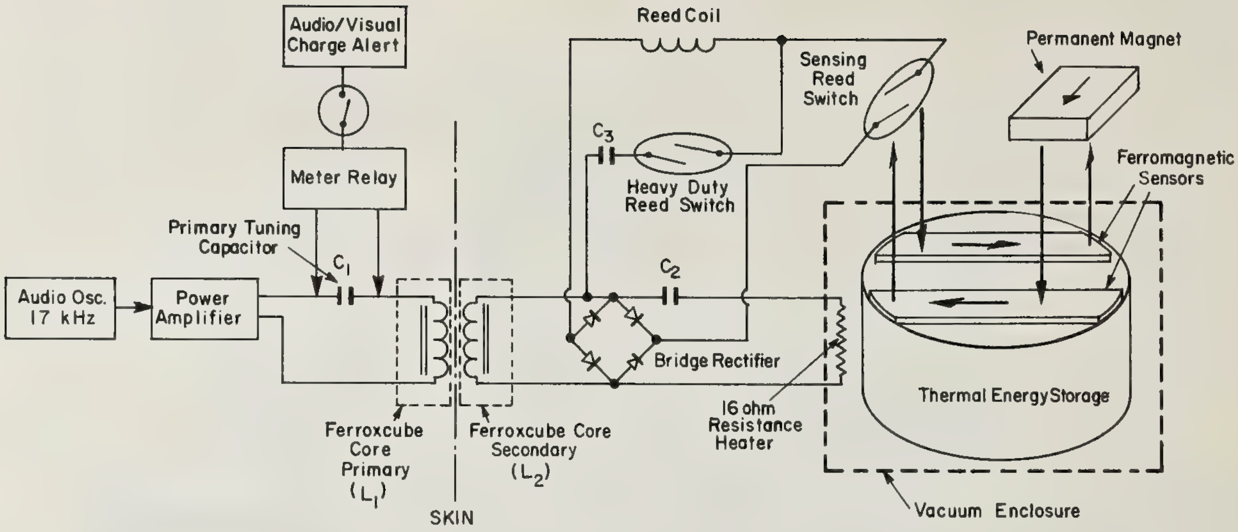

FIGURE 3. CHARGE REGULATOR FOR THERMAL ENERGY STORAGE.

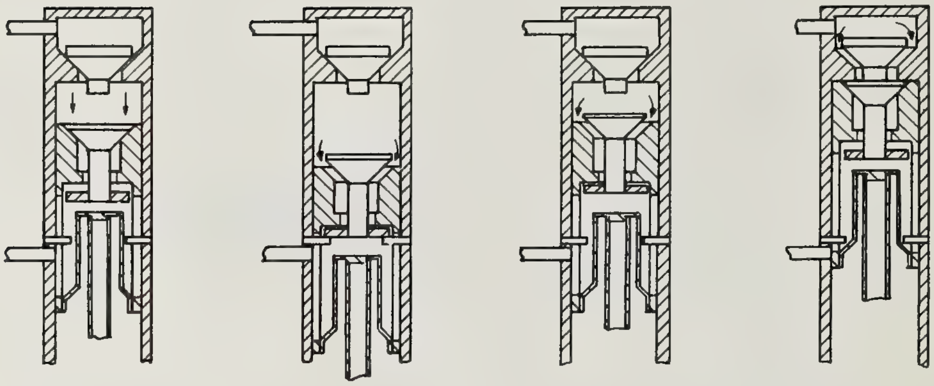

1 POWER STROKE

2 EXHAUST VALVE OPENED

3 RETURN STROKE

4 INLET VALVE OPEN

VALVE SEQUENCE FOR THERMO ELECTRON STEAM ENGINE

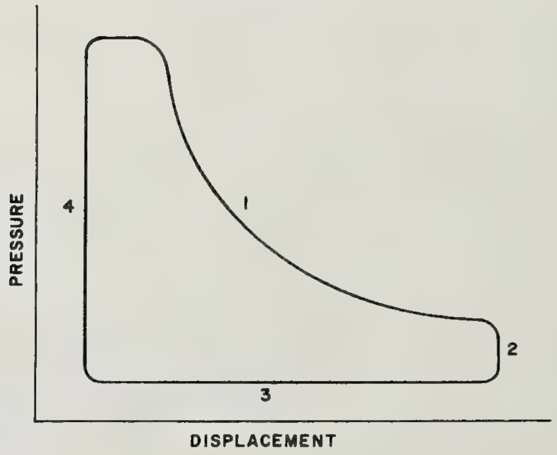

INDICATOR DIAGRAM FOR THERMO ELECTRON STEAM ENGINE

FIGURE 4. VALVE SEQUENCE AND INDICATOR DIAGRAM FOR THERMO ELECTRON STEAM ENGINE.

Several prototype steam engines have been designed, fabricated and tested. The thermodynamic and mechanical performance of both internal and external exhaust valves have been measured. Effort, to date, has been concentrated on valve action, reduction of friction, and improvements in rings and bearings. A result of this effort has been the precise and efficient valve action illustrated by the pressure-volume diagram shown in Figure 5.

A summary of the life test experience with the major power system components is given in Table 1.

TABLE 1

A SUMMARY OF THE ENDURANCE OF ALL CRITICAL RANKINE ENGINE AND HYDRAULIC PUMP COMPONENTS

			Life to Date hours	Wear Rates mils/hr	Projected Life hours
	BEARINGS				
	Sleeve	Shaft			
1.	Carbon-silver-graphite	440C	6	~.3	> 50
2.	Carbon-silver-graphite	17-4ph	14	~.15	> 50
3.	WC	440C	18	~.10	>100
4.	WC	17-4ph	123+	<.01	>500
5.	WC	WC	108+	<.01	>500
	RINGS				
	Ring	Cylinder			
1.	Carbon-silver-graphite	Titanium	7	.58	20
2.	Carbon-silver-graphite	410SS	28	.11	30
3.	Polyimide-graphite	Titanium	12	.34	15
4.	Carbon-silver-graphite	17-4ph	52	.04	>160
5.	Carbon-silver-graphite (thin)	17-4ph	88+	.02	>400
6.	Monel (Koppers)	17-4ph			
7.	Monel (Koppers)	WC			
8.	17-4ph	WC			
9.	WC	WC			
10.	WC	Carbon			
11.	17-4ph	Carbon			
12.	Koppers	Carbon			
	VALVING				
1.	External Exhaust Valve		44+		> 500
2.	Internal Exhaust Valve		287+		>1000
3.	Inlet Valve		287+		>1000
	WATER PUMP				
1.	"A" Engine		34+		> 100
2.	"B" Engine		268+		> 500

Rings: Wear ~.003 mils/hour
Valves: No wear, deformation, or change in leakage

System lifetimes in excess of 400 hours are now possible. The present performance of the engine and hydraulic pump is given in Table 2. The low overall efficiency of the engine is almost entirely due to the low mechanical efficiency of earlier bearing materials. The recent bearing materials combinations (tungsten carbide versus itself or 17-4ph stainless steel) have demonstrated both low friction and low wear rates and are expected to greatly increase the engine mechanical efficiency.

Primary control of the system is obtained by nondissipative controls. The engine speed is controlled by pressure variations in the high-pressure reservoir. Since the energy per expansion stroke is fixed, the engine must respond to fluctuations in power demand by changing its speed. Increased power demand by the blood pump drops the hydraulic reservoir pressure, which decreases the energy per stroke into the hydraulic pump. The difference between the energy of the expansion stroke and that absorbed by the hydraulic pump goes into accelerating the flywheel. Conversely, decreased power demand by the blood pump raises the hydraulic reservoir pressure and slows down the engine. A number of parameters are available for tailoring the response characteristics of the system. These include the flywheel inertia, the hydraulic accumulator pressure differential, and the accumulator volume.

TABLE 2

A SUMMARY OF RANKINE ENGINE AND HYDRAULIC PUMP PERFORMANCE

Parameter	Goal	Achieved to Date
Engine:		
Steam Pressure	250 psia	265 psia
Steam Temperature	900°F	900°F
Speed (maximum)	1500 RPM	1500 RPM
Power Output	15 watts	20.1 watts (shaft)
Engine Thermal Efficiency	82%	60-70%
Mechanical Efficiency	85%	40-50% (shaft)
Overall Efficiency	20%	7-10% (shaft)
Hydraulic Pump:		
Output Pressure	80 psia	80 psia
Volumetric Efficiency	90%	85-95%

HYDRAULIC SYSTEM

The hydraulic subsystem is made up of the following major components: hydraulic pump, hydraulic accumulator (or high-pressure reservoir), low-pressure reservoir, hydraulic lines coupling power source to the blood pump controls, and feedwater pump.

The hydraulic accumulator decouples the power source as far as possible, buffers the engine from responding to fast transients, provides the feedback for non-dissipative engine control and serves as part of the heat transfer loop carrying the reject heat from the power source to the blood pump.

The high-pressure reservoir operates at a mean pressure of about 80 psia. The low-pressure reservoir operates at 15 psia. The condenser pressure at 140°F is 2.9 psia. The hydraulic pump raises the fluid pressure from that in the low-pressure reservoir to that in the high-pressure reservoir which supplies the blood pumps. This constitutes the primary flow in the system. The flow through the feedwater pump is very much less than that through the hydraulic pump (about 1 to 5000). The feedwater pump operates between the condenser and the boiler.

ASSIST BLOOD PUMP

The blood pump must be considered an integral component of the circulatory support system, since it also acts as both a blood-cooled heat exchanger and a physiological sensor for the control system. The physiologic and *in vivo* testing of related pneumatically-driven assist pumps is described in another conference paper by Bernhard, LaFarge and Robinson. This two-valved pump removes blood from the left ventricle at low pressures and ejects blood into the descending aorta at systemic pressure. The inflow tube is introduced into the apex of the left ventricle, and the outflow tube is attached to the thoracic aorta by means of a Dacron graft.

The design of the pump is a result of extensive hydrodynamic testing. Measurement of the pressure-flow characteristics of the blood inflow, outflow, and hydraulic lines have been made. Of the hydraulic arrangements studied, the 7/8 inch I.D. single drive line entering the pump almost axially from either end proved to be the most efficient. For a range of typical flow rates the overall efficiency of pump ejection varies from 80 to 60 percent. The left ventricular pressure during filling of the pump was found to be 15 to 40 mm Hg, depending upon filling rate.

The rejected heat from the steam engine is transferred to the blood in the following sequence. First, the reject heat from the condensing steam is transferred into the high pressure hydraulic accumulator or reservoir. This heat is carried to a heat exchanger located in the control unit, where it is transferred to the trapped coupling fluid. The pump action readily mixes the coupling fluid, transferring the heat across the pump bladder. This heat rejection technique has the advantage of requiring no additional heat-dissipating prosthesis. It also simplifies the surgical implantation, and the bulk blood temperature rise is lower because the heat exchanger (i.e., blood pump) is placed in the region of greatest blood flow. The large area of the artificial ventricle reduces the heat flux into the blood and minimizes the local blood temperature rise.

BLOOD PUMP CONTROLS

The purpose of a control system for a left ventricular-aortic assist device is to achieve the goals of reduced left ventricular pressure, normal systemic blood flow, and normal aortic pressures in the presence of left ventricular failure.

Thermo Electron, in conjunction with Whiteley Hydraulics, has developed a hydraulically-driven counter pulse control which is triggered from the left ventricular or filling pulse as the pump fills. The duration of pump ejection is determined by the fixed hydraulic high reservoir pressure, the pump stroke volume, and the pump impedance.

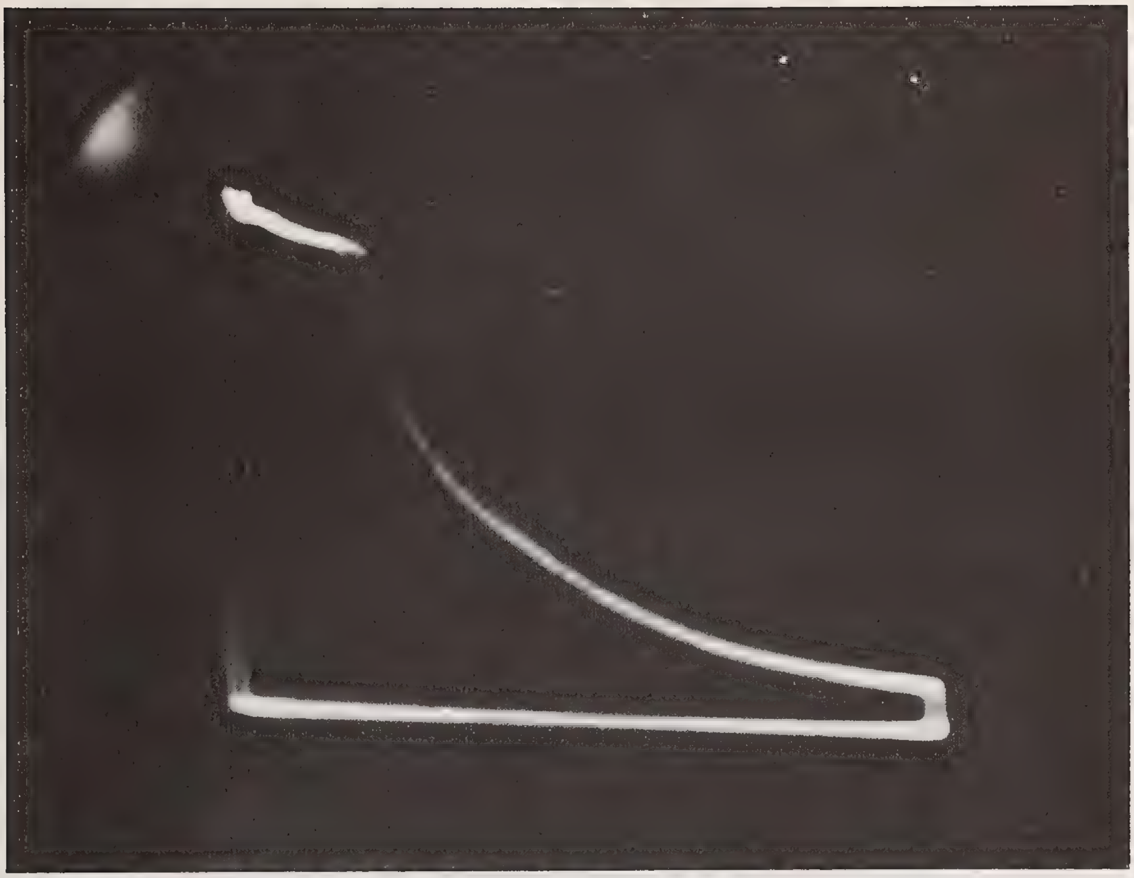

FIGURE 5. PRESSURE-VOLUME DIAGRAM OF PROTOTYPE ENGINE.

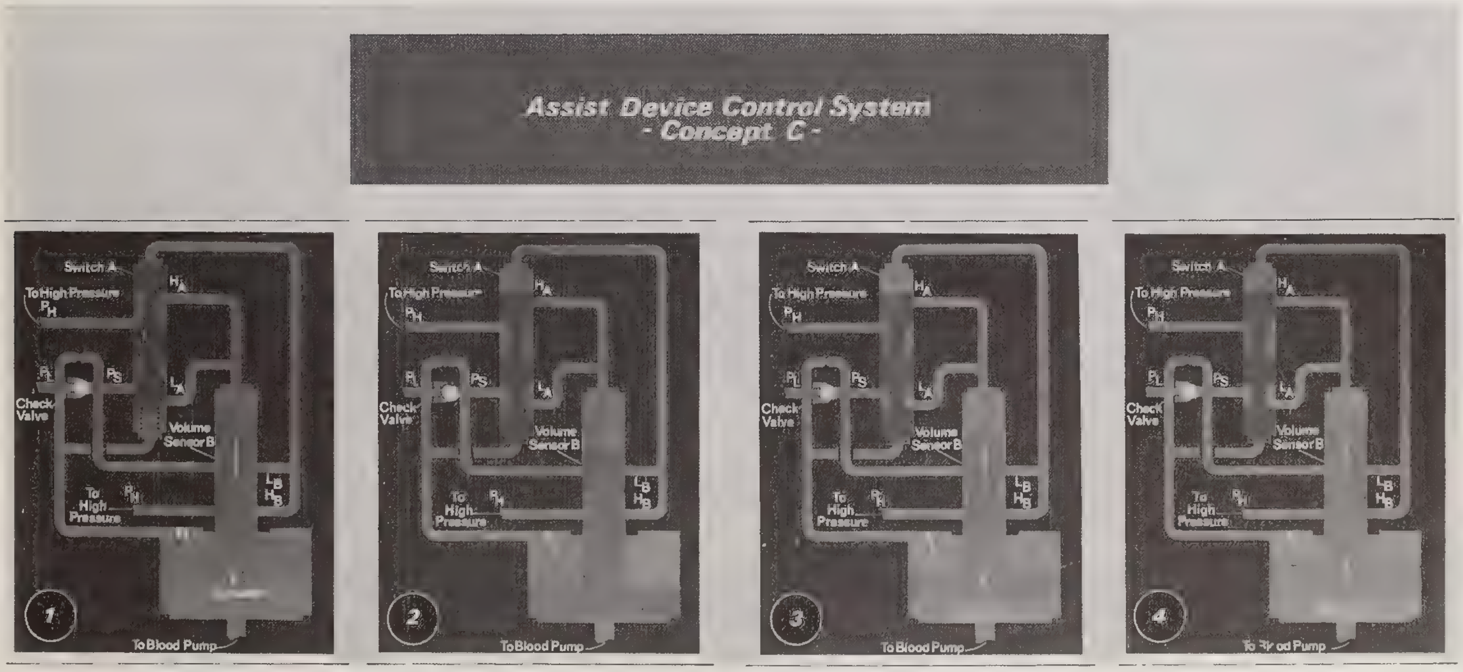

FIGURE 6. BLOOD PUMP CONTROL LOGIC SEQUENCE.

The control logic sequence is illustrated in Figure 6. The primary components are the double spool valve, the actuator piston and the relief valve. The spool valve switches the actuator piston from the high to low pressure reservoirs. Blood is ejected by the pump during high pressure reservoir phase (position 1). The spring at the bottom of this spool valve keeps the high pressure port H_A open during the mechanical systole.

Mechanical systole is determined when minimum chamber volume is reached by the groove in the actuator piston, which connects the top of the spool valve to the high pressure supply. This shuttles the spool valve, cocks the spool valve spring and switches the rear of the actuator piston from the high to the low pressure reservoir (see position 2). The actuator piston remains at bottom until the left ventricle begins to fill the blood pump (as shown in position 3 of Figure 6) and to expel the fluid behind the actuator piston into the low pressure reservoir. The spool valve remains in position due to the fluid trapped above it. The system cannot be triggered during this period. Thus the control system will ignore transient pressure fluctuations which are often present at the end of mechanical systole. If the left ventricle stroke volume is less than this minimum actuation volume, the control system will pause to trigger off the next heart beat. The control system can trigger only after port L_B is opened to the pressure behind the parallel relief valve and orifice. This pressure is sufficient to retain the spool valve in its cocked position while an appreciable flow due to passive blood pump filling continues. When blood pump filling stops, the pressure above the spool valve drops and the spring returns the spool valve to its original position. This action opens the actuator piston to high pressure and initiates mechanical systole.

Mock loop testing has demonstrated that the hardware follows the functional sequence described. Reliable triggering of the control system occurs following each ventricular pressure pulse, without overlap of systole and pump ejection. A summary of control system performance is given in Table 3.

TABLE 3

A SUMMARY OF CONTROL SYSTEM PERFORMANCE

Parameter	Goal	Achieved to Date
Stroke Volume:	0-60 ml	0-60 ml
Beat Rate:	60-180 bpm	60-120 bpm
Left Ventricular Filling Pressure:	20 mm Hg	20-60 mm Hg
Overall Efficiency:	67%	40-60%

Modifications are being made to reduce fluid leakage, reduce internal pressure drops, increase beat rate, decrease filling pressure, and increase efficiency.

A photograph of the prototype hydraulic control system is shown in Figure 7.

SUMMARY

In summary, the development of the implantable Rankine-cycle circulatory assist system has made significant progress. Feasibility demonstrations have been accomplished in the areas of power transmission, charge regulation, heat source subsystem, Rankine-cycle engine assist blood pump and blood pump control system. At this time, the effort is concentrated on improvements in performance and on the solution of problems arising from the integration of the subsystem.

DISCUSSION

MR. PURDY: Have you discontinued use of graphite piston rings?

DR. KITRILAKIS: We had rather poor experience with the graphite rings; the wear rates were excessive. We find the Monel 17-4 ph wear rates far superior to those of the graphite.

MR. PURDY: What is the percentage of loss in rings vs. other wear regions?

DR. KITRILAKIS: To give you a rough number, of the order of 15% is lost in the piston rings, the remainder is all in the crank and connecting rod bearings.

DR. KESSLER: What is the material used and tolerance involved in your spring loaded spool valve shown in the last slide?

DR. KITRILAKIS: I think I will let Dr. Huffman answer that. He is far more familiar with the details of it.

DR. HUFFMAN: The material in the spool valve is 17-4 ph hardened. In fact, the entire control system is constructed of this material. The tolerances are about .2 to .3 of a mil.

DR. GIANNOTTI: Would you please repeat the overall thermal efficiency that you have achieved and what you expect?

DR. KITRILAKIS: The maximum that we have measured is about 10%. We expect that number to end up somewhere between 15 and 17%. This is based primarily on the fact that mechanical efficiency is about half what we expect it to be.

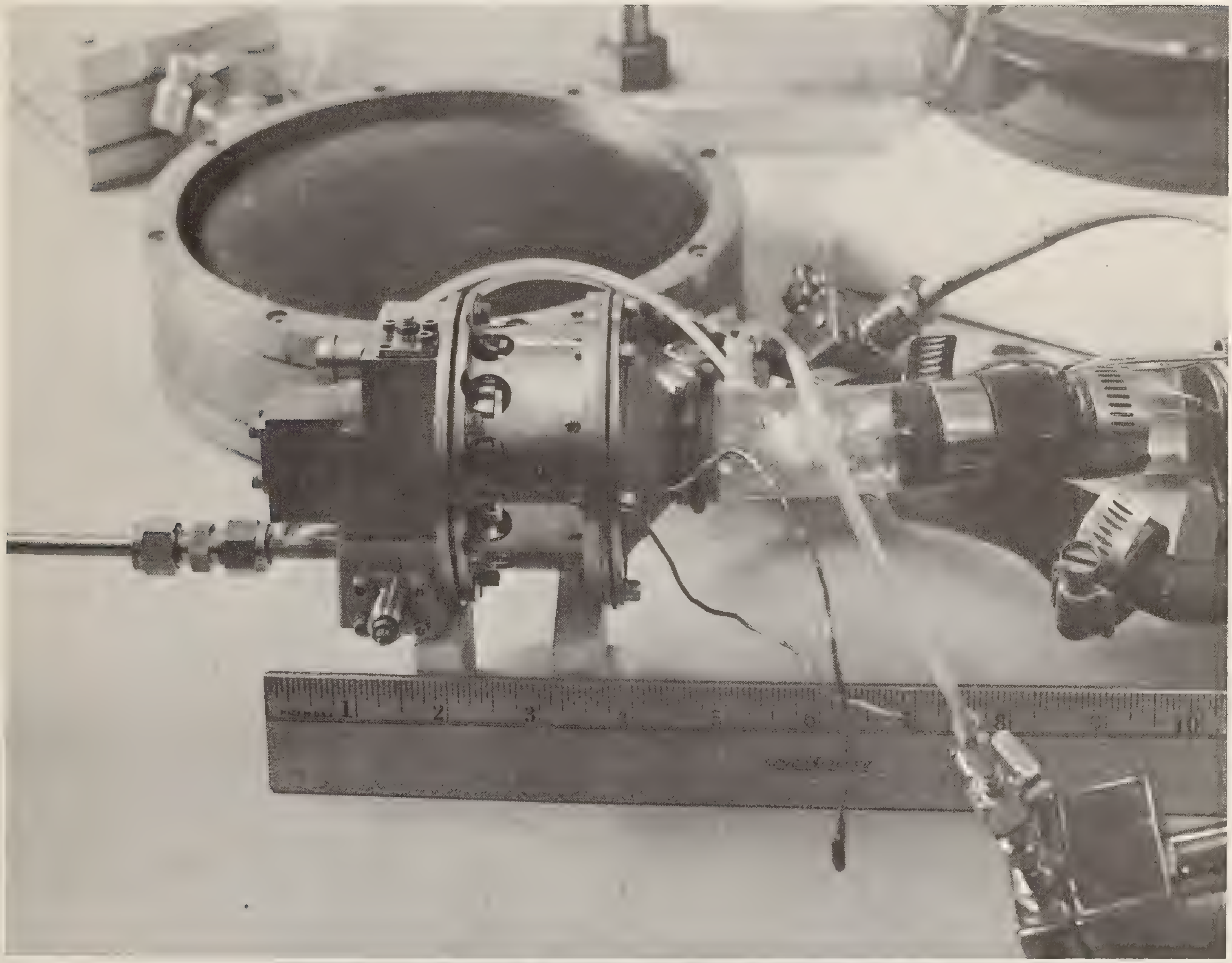

FIGURE 7. PHOTOGRAPH OF THE PROTOTYPE HYDRAULIC CONTROL SYSTEM.

CHAPTER 92

ALL FLUID CONTROL SYSTEM TO COUPLE A STIRLING ENGINE GAS COMPRESSOR TO A LEFT VENTRICULAR ASSIST DEVICE

G. Peterson, A. Kessler, G. Thorne, R. R. Clark, O. L. Wood

Bio-Logics, Incorporated
Salt Lake City, Utah

A fluid control system is under development to couple a Stirling engine gas compressor to a left ventricular assist device via a piston type pump actuator. The pump actuator is powered by the compressed gas and delivers liquid to the assist pump for actuation. The control system components developed control the actuator motion to result in variable stroke volume and variable pulse rate operation of the assist pump in response to natural heart requirements. The pump actuator is powered both during assist pump systole and diastole and therefore is an active filling system. The control system is designed to limit the minimum assist pump pressure during filling. Control components are employed in both the gas and liquid areas of the system. The present control concept developed from a study of the possible use of fluidic (no moving parts) components for both control and power delivery to the assist pump. The study was designed to identify the best fluidic components, their size, and efficiency for use in the implantable assist application. The results of this initial study demonstrated that, while fluidic devices could be used in non-implantable systems, inherent inefficiencies in all fluidic components negated their potential use in implantable assist systems.

INTRODUCTION

Bio-Logics, Incorporated, under contract to the National Heart Institute, is developing control system components for an all fluid, implantable, left ventricular assist device system. This work is being conducted in conjunction with the efforts of the Aerojet General Corporation and the Donald W. Douglas Laboratories who are developing the implantable power sources and assist pump actuators.

The Left Ventricular Assist device system as shown schematically in Figure 1 is composed of four basic subsystems:

1. Gas Compressor Power Source
2. Controls
3. Assist Pump Actuator
4. Assist Pump

The power source supplies high pressure gas to a high pressure reservoir and receives the exhaust gas from the controls and actuator in a low pressure reservoir. The control system controls the flow of gas to and from the actuator and regulates the actuator velocity during mechanical diastole in response to assist pump actuating liquid pressure. The pump actuator serves as a de-amplifier to convert the gas power at high pressure to liquid power at the required physiologic pressures. The assist pump used for this study is the TECO-CHMC left ventricular assist pump that operates in series between the left ventricle and the descending aorta.

DESIGN SPECIFICATIONS

The goal of this program is to develop a control system for a breadboard left ventricular assist device which has the following capabilities and potential:

1. All fluid - mechanical system
2. High efficiency
3. Implantable size
4. Liquid - Pump bladder interface
5. Variable stroke volume
6. Atraumatic to blood

The specification of an all fluid-mechanical system (as opposed to using electrical components) is dictated by the use of a compressed gas power source. High efficiency is an important requirement since inefficiencies manifest themselves in the form of waste heat and increased size, both of which are undesirable for an implantable system. The need for high efficiency in each subsystem is accentuated by the requirement placed on the power source to convert stored energy to pneumatic energy and at the same time limit the temperature that must be insulated from the body.

A liquid is used as the pump actuating fluid in order to eliminate the possibility of gas diffusion through the pump bladder into the blood. This is desirable not only to eliminate emboli but because the gas system is a closed system a cumulative loss of the gas working fluid would render the system inoperative. A variable stroke volume system is desirable so that the assist device will operate as does the natural heart and pump out the variable amounts of blood delivered to it by the system without sucking at its inlet. The assist device normally functions in a counter-pulse mode with the

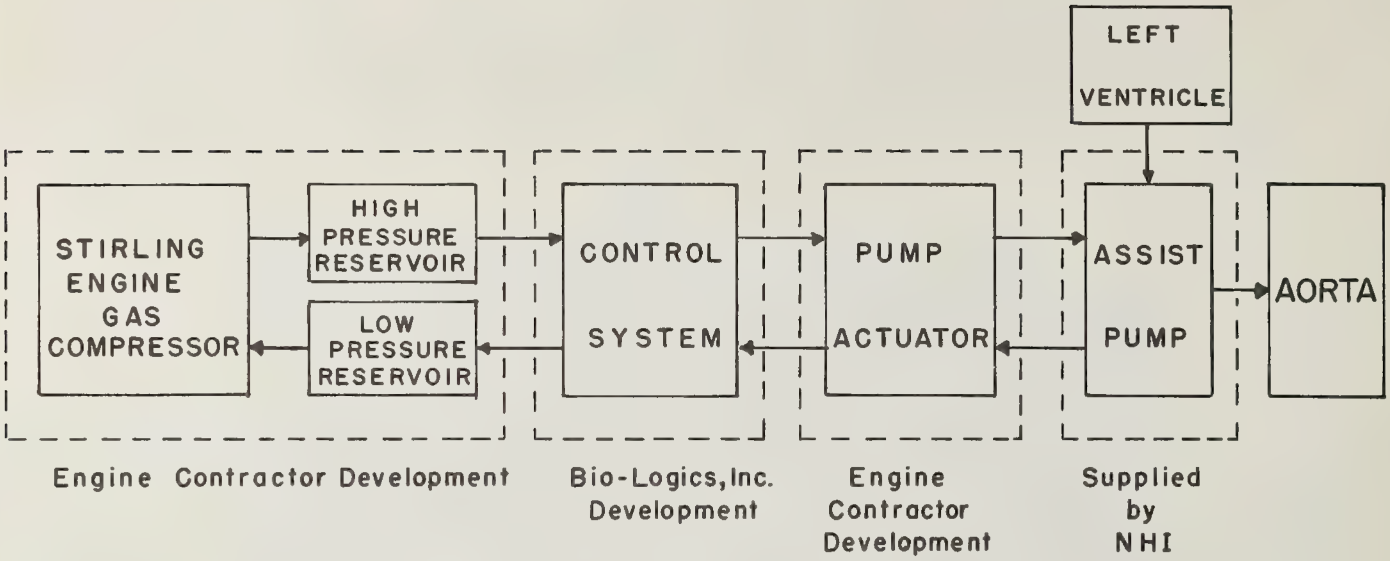

FIGURE 1. LEFT VENTRICULAR ASSIST SYSTEM.

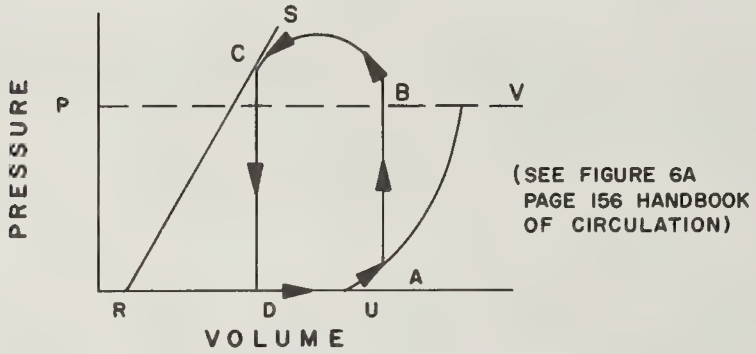

FIGURE 2. A. GENERAL PRESSURE-VOLUME CURVE.

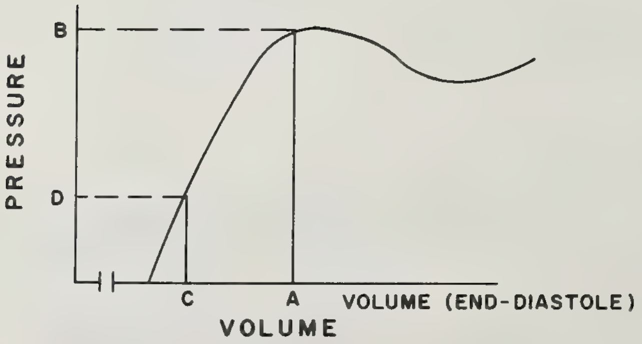

FIGURE 2. B. DIAGRAMMATIC LENGTH-TENSION CURVE.

natural heart. A description of the effect of the control system sensor natural heart operation is contained in section 3.0, Physiologic Considerations.

It is obviously necessary that the system be atraumatic to the blood being pumped. Much of this requirement is filled by the design of the assist pump itself. However, since the pump actuator is powered both during assist pump systole and assist pump diastole it is an active filling system. As such, provision is made to limit the minimum assist pump pressure during filling.

PHYSIOLOGIC CONSIDERATIONS

As well as providing a secondary pump to maintain adequate cardiac output, it is the assigned purpose of this assist system to reduce ventricular systolic pressure. Implementation of the philosophy of control for this system causes a reduction in ventricular systolic pressure by actively draining the left ventricle at all times except during ventricular assist systole (VAS), thereby minimizing ventricular end-diastolic volume.

Triggering of VAS is accomplished either the instant the pump bladder is filled or when the rate of filling from the ventricle is near zero. It is expected that the latter case will occur most commonly, synchronizing the assist pump to left ventricular systole, (LVS) and resulting in a counterpulse mode of operation. It is expected that the low rate of flow from the ventricle is indicative of a near empty ventricle.

In those circumstances where the assist stroke volume is not adequate to pump all of the blood returning to the heart during a single heart cycle, a multiple VAS may occur to provide the necessary cardiac output.

Thus, this control system attempts to reduce the systolic pressure of the ventricle by the following two means:

a. By providing a reduced outlet pressure from the ventricle during ventricular assist diastole (VAD) and,
b. By reducing left ventricular end-diastolic volume to a point where the ventricle cannot physically produce tension, resulting in a normal systolic pressure.

The effect of "a" above is demonstrated in analysis of Figure 2-a below. A "normal" pressure-volume curve is represented by ABCDA.

If pressure level "p" is the aortic pressure, systolic pressure will rise, as shown, somewhat above "p". Similarly if the threshold output pressure is determined by VAD pressure and the gradient across the assist pump input valve, the systolic pressure can be held to a lower than normal value.

In those cases where VAS and LVS occur simultaneously, the left ventricular pressure is determined by the length (volume) - tension curve shown in Figure 2-b.

Note that a high volume, represented by A in Figure 2-b results in high pressure while lowering the volume to C reduces total systolic pressure to D. Design of the assist control system should maintain the end-diastolic volume sufficiently low to significantly reduce the left ventricular pressure pulse.

Recognizing the desirability of a pulsatile system having a pumping frequency near that of the normal heart, the control system further modifies the activity of the assist pump to inhibit VAS until a minimum volumetric threshold has been reached.

To minimize hemolytic damage to the blood during assist pump filling, the negative pressure applied to the pump is controlled to a safe limit.

CONTROL APPROACHES

Given the two boundary conditions of high pressure gas at the power supply and liquid actuating fluid at physiologic pressures at the blood pump, several approaches, both from a component type and working fluid standpoint, are available to couple the power supply and blood pump. All cases require some type of de-amplification from the high pressure power source to the physiologic pressure required at the blood pump. These alternatives are summarized in Table 1.

Fluidic devices, although attractive in some applications, were not selected for use in this system because of their inherent low efficiency. However, because of the attractiveness of the no moving parts concept, an initial objective of this contract was to study their use with a liquid (water) as the working fluid to provide: (1) main power to drive a cardiac assist device and, (2) sensing and control functions to regulate the supply of pumping power.

Conceptually a control system using fluidic devices appears simple and straightforward as demonstrated by the schematic of one possible configuration in Figure 3. Four fluidic components are required with a Fluidonics Momentum Amplifier shown as the main power delivery element. The end of systole signal is obtained from a port uncovered by the pump bladder at the appropriate position as in the Woodward gas driven fluidic heart pump.[1] The end of diastole is signaled by the decay of dynamic pressure in a pickup tube installed in the diastole exhaust line.

Other implementations of fluidic circuits can be formed depending upon the main power delivery element and sensing signals. However, no fluidic circuits were reduced to the detailed design phase because of efficiency considerations.

To determine fluidic device power efficiency test data was obtained for a variety of off-the-shelf fluidic devices using water as the working fluid. Some devices considered are shown schematically to demonstrate function in Figure 4. Typical test data is shown in Figure 5. This data demonstrates the device power efficiency during the "on" condition, i.e. with no control signal

TABLE I

Component Type	Blood Pump Actuation Medium	Power Supply	Control Medium	De-Amplification
Fluidic (No Moving Parts)	Low Pressure Liquid	High Pressure Gas	High Pressure Gas	At Blood Pump
Pneumatic			High Pressure Liquid	1. At Blood Pump 2. At Power Supply Two Liquid Reservoirs
Hydraulic			Low Pressure Gas	At Power Supply
Fluidic-Pneumatic				
Fluidic-Hydraulic			Low Pressure Liquid	At Power Supply
Pneumatic-Hydraulic				

to "turn off" the device. As can be seen, the peak power efficiencies range between 20-40% except for the Pressure-Area Amplifier (PA) which continues on up to 1.0. The (PA), however, is a moving part device and is not vented as are the fluidic devices. Thus all the input flow exits through the output and the power recovery equals the pressure recovery. The actual power delivered peaks at approximately 60% pressure recovery and approaches zero as the pressure recovery approaches 1.0.

Thus fluidic devices are quite inefficient even during the "on" condition. Equally as significant as the "on" condition data is the total heart cycle efficiency data presented in Table 2.

TABLE 2

DEVICE	$\frac{P_O Q_O}{P_S Q_S}$ MAX	P_O/P_S AT MAX $\frac{P_O Q_O}{P_S Q_S}$	COMPLETE HEART CYCLE EFFICIENCY ▲▲
MA	0.24	0.6	6.4%
WA	0.24 (0.3)	0.35 (0.5)	6.4 (8.0) %
PA	0.6 ▲	0.6	60%
VA (VENTED)	0.39	0.5	19%

▲ AT CONDITION OF MAX POWER TRANSFER

▲▲ ASSUMING SYSTOLIC TIME = 0.2 SEC.
DIASTOLIC TIME = 0.55 SEC
HEART RATE = 80 BEATS / MINUTE

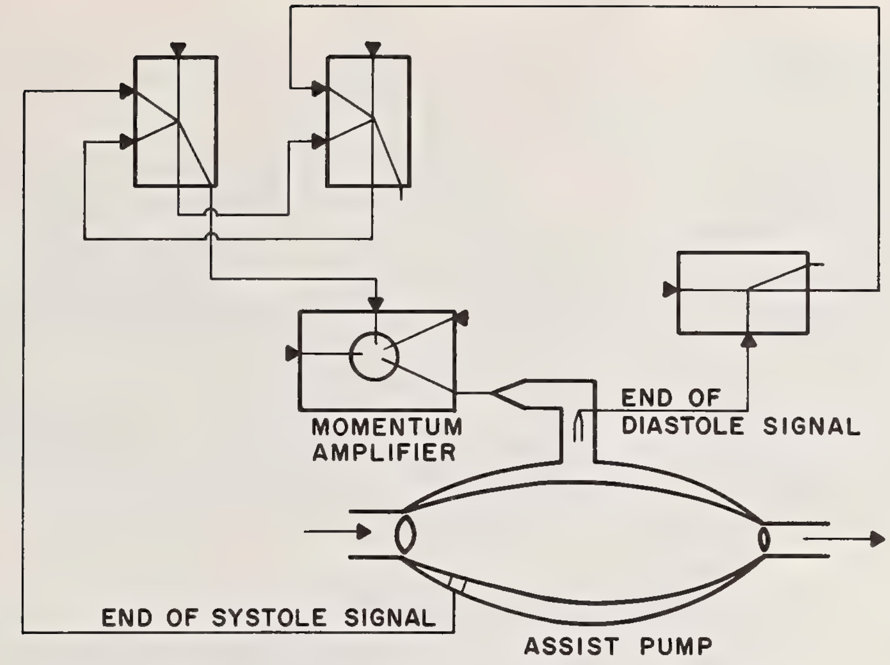

FIGURE 3. FLUIDIC CONTROL CIRCUIT.

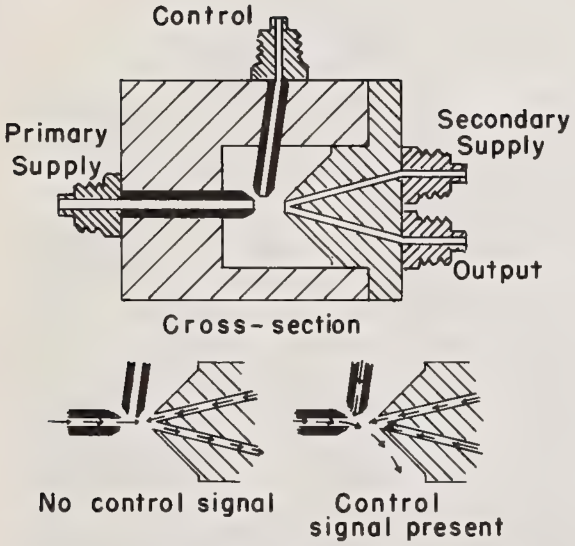

Fig. 4a MOMENTUM AMPLIFIER

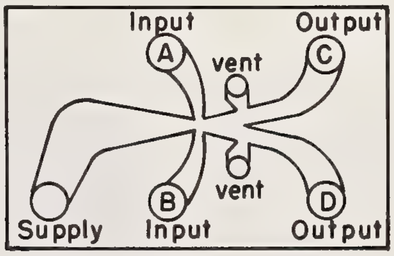

TRUTH TABLE

INPUTS		OUTPUTS	
A	B	C	D
1	0	0	1
0	0	0	1
0	1	1	0
0	0	1	0

Fig. 4b WALL ATACHMENT AMPLIFIER
Bi-stable load insensitive

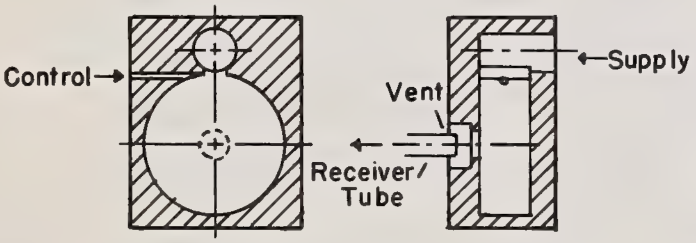

Fig. 4c VENTED VORTEX AMPLIFIER

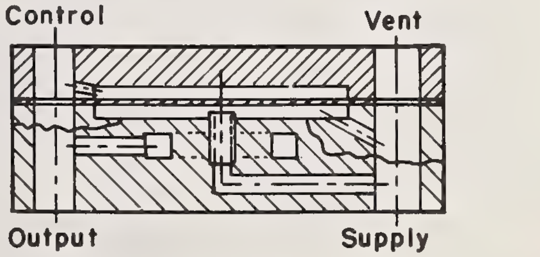

Fig. 4d PRESSURE AREA AMPLIFIER
(Semi-fluidic)

FIGURE 4. FLUIDIC DEVICES.

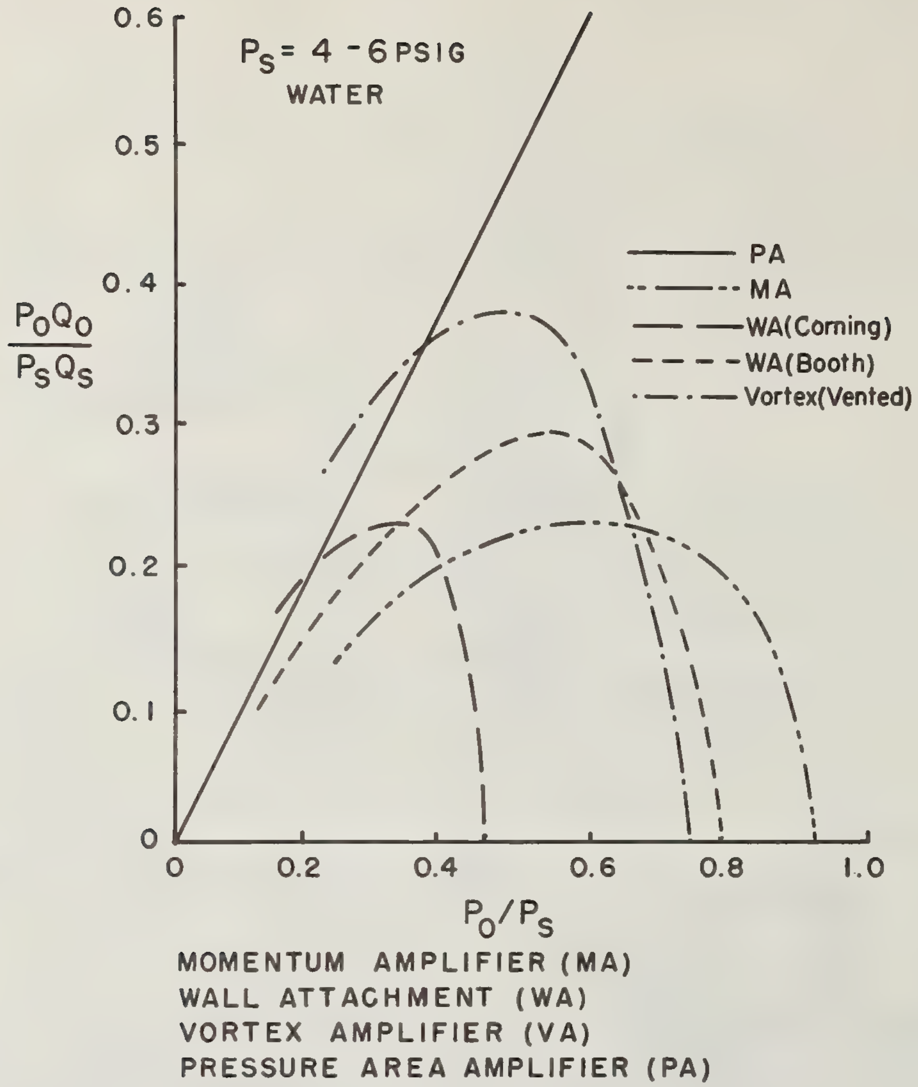

FIGURE 5. FLUIDIC DEVICE POWER RECOVERY.

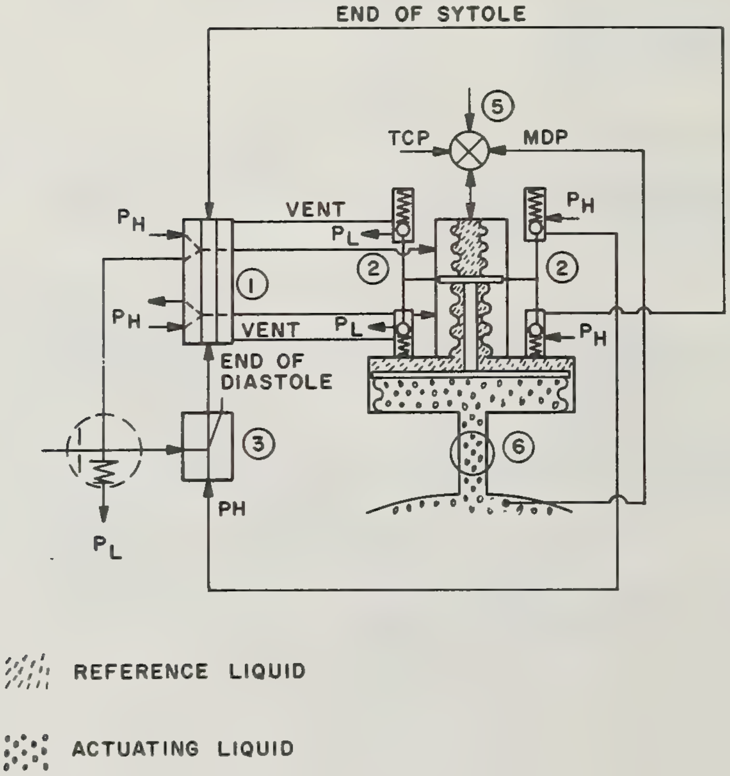

FIGURE 6. AEROJET CAD CONTROL SYSTEM.

This data which is based on each device being used as the main power delivery element to the blood pump reflects the fact that the blood pump actuating liquid is only supplied during part of the heart cycle (systole). During diastole the actuating liquid must be shut off or diverted so that the pump can fill with blood. With fluidic devices such as the (MA) and the (WA) the flow is simply diverted so that all the power supplied by the device is wasted. Hence, this leads to very low cycle efficiencies. The (VA) can be "turned down" so that the loss is not quite so great whereas the (PA) completely shuts off the flow so that there are no losses during diastole and a correspondingly higher efficiency results. This indicates the attractiveness of a mechanical valve of some sort (e.g., the (PA)) from an efficiency standpoint.

A comparison of pneumatic and hydraulic components generally results in smaller size, higher efficiency, and less inertia effects with the pneumatic devices and elimination of compressibility problems with the hydraulic devices. The hybrid fluidic-pneumatic and fluidic-hydraulic systems suffer from the low fluidic device efficiency.

The approach chosen for this development program was to employ a combination of pneumatic and hydraulic components, using each type where most advantageous. The high pressure gas is used as the primary control medium. The de-amplifier is in the form of a "pump actuator" located at the control system-blood pump interface. The pump actuator is powered by the high pressure gas and transduces this power into liquid power at higher flows and lower pressure to compress the blood pump bladder. The Aerojet General Corporation and the Donald W. Douglas Laboratories are each developing a pump actuator.

CONTROL SYSTEM DESCRIPTION

The control system under development for one pump actuator is shown schematically in Figure 6. This system can be broken down into six basic components:

1. Main control valve
2. End of stroke and venting switches
3. End of diastole switch
4. Relief valve - orifice
5. Diastole pressure control valve
6. Anti-suction device

Components (1) - (4) are pneumatic devices, i.e., they work in the high pressure gas medium, while components (5) and (6) are hydraulic devices that work in liquid.

Referring to Figure 6, during mechanical systole the high pressure gas is connected through (1) to the upper side of the actuator drive piston. The under side is vented to the low pressure gas reservoir. This differential pressure drives the actuator to produce liquid pump actuation pressure as a function of the area ratio between the drive piston and actuator piston. At the end of the mechanical systole stroke one set of components (2) is opened to supply high pressure and to vent the appropriate actuators of (1). This switches (1) to the mechanical diastole position thereby reversing the polarity on the drive pressure differential.

During mechanical diastole the gas flow exiting the drive piston cylinder exhausts in a parallel path through an orifice and relief valve (4) which maintains an approximately constant exhaust pressure. Concurrently the reference liquid inside the upper drive piston bellows exhausts through component (5). Component (5) is a valve which is opened or closed in proportion to the difference between the thoracic cavity and blood pump actuating pressure. If the actuating liquid pressure is reduced relative to the thoracic cavity reference pressure the valve tends to close. The increased exhaust restriction raises the pressure in the bellows, slows down the diastole rate, and tends to restore the actuating liquid pressure to the desired value. In this way the danger of over driving the pump during diastole with the active filling system is compensated for and damaging negative pressure on the blood is avoided. The end of diastole is signaled by the drop in exhaust flow rate through the relief valve and orifice. The reduced flow rate causes a reduced control pressure to component (3). Below the required threshold pressure component (3) switches and supplies high pressure to actuate (1) to the mechanical systole position. The reduced exhaust gas flow rate is a result of either coming to the end of the stroke or of the modulating action of valve (5). Thus, the system is a variable stroke volume system which is keyed to the reduced pressure that results if the actuator attempts to draw in more blood to the assist pump than is available from the left ventricle.

The anti-suction device (6) is a flexible tube in the hydraulic line connecting the pump actuator with the blood pump. When the liquid actuating pressure drops below the reference pressure, the tube collapses restricting the flow until the pressure rises. This action also serves to protect the blood against negative pressures and may or may not be used in conjunction with valve (5).

COMPONENT DESIGN AND PERFORMANCE

Main Control Valve, Component (1).

As previously mentioned, this valve performs the function of switching the main power flow to the actuator between the sides of the actuator drive piston and is basically a double three-way valve. The valve is shown in cross-section views in Figure 7.

The current valve design employs a sliding member that performs the switching function. The slide is actuated by high pressure gas acting on the piston actuators at either end of the valve. The slide is made from a plastic, Delrin AF, which has the dimensional stability of Delrin, but is

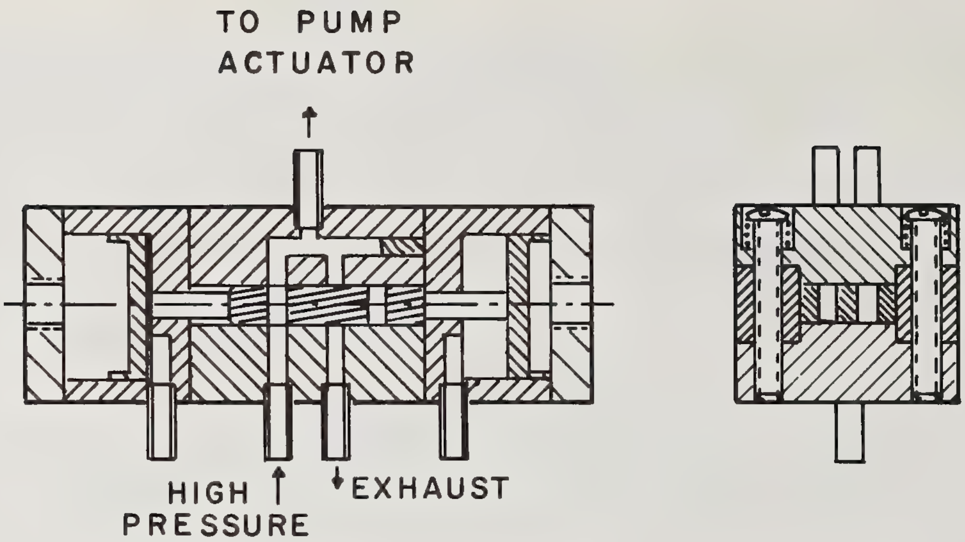

FIGURE 7. MAIN CONTROL VALVE. CROSS-SECTION VIEWS.

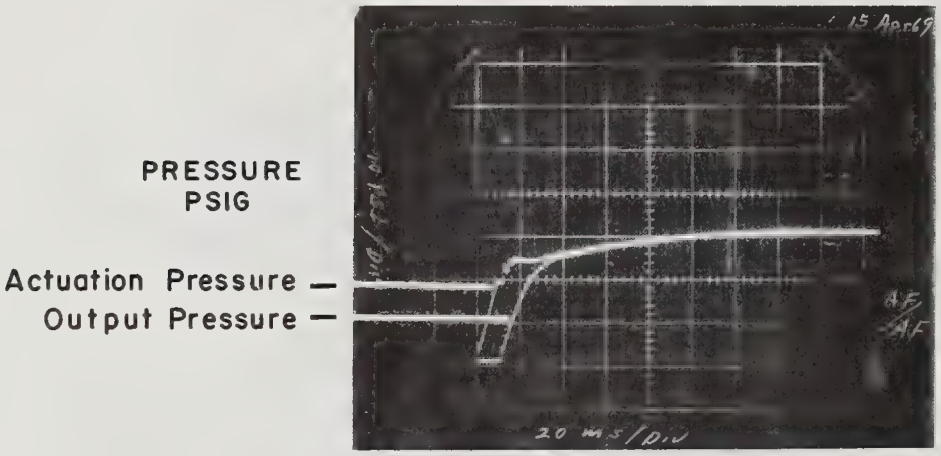

FIGURE 8. VALVE (1) PERFORMANCE. a. ACTUATION RESPONSE.

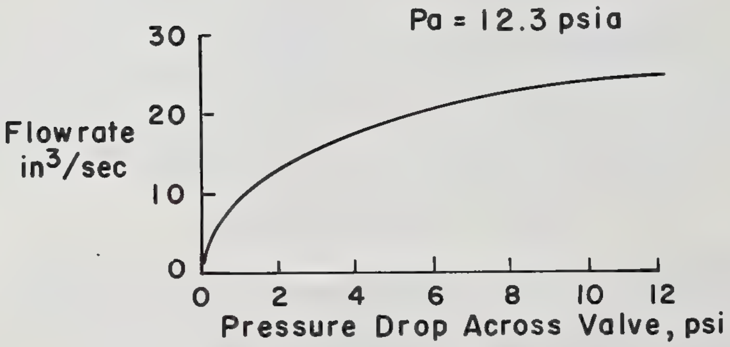

FIGURE 8. b. FLOW DELIVERY (AIR).

TFE fiber-filled to give the low sliding friction of Teflon. The actuator pistons are cup-shaped so that the high pressure actuation gas presses the cup sides against the cylinder walls for sealing during actuation. The valve slider is non-lubricated and therefore complete stoppage of leakage is impossible, since the slider must ride on a film of the working gas. The leakage is minimized by applying a force normal to the sliding surfaces by use of four compressed springs. Use of the spring forces not only serves to minimize leakage, but to compensate for valve wear and to provide memory through the friction involved.

Among other valve types considered was a spool valve configuration. However, because of the extremely tight tolerances required to minimize leakage and the desire to have built-in memory in the valve, a spool valve was not chosen.

Figure 8 presents some typical valve operating characteristics for response time and flow delivery. As is seen for this particular valve test the valve switches as soon as the actuation pressure reaches 20 psig and within 20 ms the delivered pressure has reached the supply pressure.

Switching and Venting Valves, Components (2).

These components supply switching pressures for end of stroke actuation and also perform venting functions. The two valves that act as vents for the main control valve actuators (Figure 6) could be eliminated by the use of small vent holes in the actuator piston cylinders. However, because of the desire to eliminate as much as possible all forms of continuous leakage and to balance the load of the valve acutators on the actuator piston, the two additional vent valves are included in the system. The valve design is shown in cross-section in Figure 9.

These valves are basically poppet type valves which employ precision soft rubber balls as the sealing element, to give a positive seal and eliminate leakage in the closed position. In addition, the high pressure gas is applied underneath the ball in the closed position to assist in sealing. The return springs can be soft since they need not supply a large return force. Using a spring with a spring rate of 1 lb/in. results in an actuating force relationship like that shown in Figure 10. The initial force is that required to break the seal and equalize the pressure across the ball after which the spring offers the actuating resistance.

End of Diastole Switch, Component (3).

As previously explained, this valve supplies actuation pressure to the main control valve actuator at the end of diastole in response to a drop in control pressure below a prescribed threshold level. The valve is shown in cross-section in Figure 11.

The area ratio between the control diaphragm and the pressure inlet duct diameter determine the control pressure threshold for switching. Upon switching, the supply pressure acts over a larger diaphragm area to latch the switching action and prevent oscillation.

Relief Valve, Component (4).

The action of the relief valve is to maintain the pump actuator exhaust pressure during diastole above the control pressure threshold of component (3). This action continues until the exhaust flow rate drops sufficiently that the relief valve closes, and the control threshold pressure is reached to cause switching of component (3). The relief valve is shown in cross-section in Figure 12.

The desired valve cracking pressure is determined by the diaphragm area and spring setting. The spring rate determines the control range, i.e., pressure range over which the valve is wide open to completely closed. The ratio of the diaphragm area to outlet receiver area is maintained large enough so the cracking pressure and closing pressure are essentially equivalent.

The combined operation of components (3) and (4) is illustrated in Figure 13.

The two traces represent operation with and without component (4) and show the pressure in the actuator cylinder. Note that with the relief valve functioning the exhaust pressure is held at approximately 3 psig after the initial blowdown phase and that switching occurs when the pressure has decayed to approximately 1 psig at the end of the diastole stroke.

The flow delivery capability of these components is basically equivalent to the previously described components since the basic passage sizes are the same.

Diastole Rate Control Valve - Component (5).

This valve functions to modulate the flow of liquid out of the pump actuator seal bellows as a function of the liquid actuating pressure at the assist pump bladder. The valve as initially designed is shown in cross-section in Figure 14.

With this configuration the valve is normally open and responds to negative pressure by closing beginning at a threshold determined by the diaphragm area and initial spring setting.

A spool valve design was initially chosen to avoid as much as possible the pressure feedback encountered with seating type valves.

The control action of this valve is demonstrated in Figure 15 where the two sets of pressure curves show operation without (15a) and with (15b) the control valve functioning. The four traces shown are, from top to bottom, triggering signal, pressure at the assist pump bladder, pressure in the actuator pumping chamber, and pressure in the actuator seal bellows. The pressure traces at the assist pump exhibit a considerable amount of ringing at the beginning of mechanical diastole. This is apparently associated with the dynamics of the liquid actuation, the assist pump bladder action and the assist pump valve closure. The controlling action of the control valve is seen during the

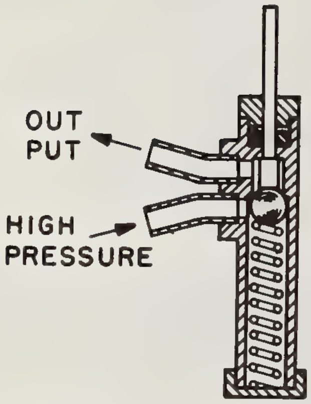

FIGURE 9. END OF STROKE AND VENTING SWITCHES. COMPONENT (2).

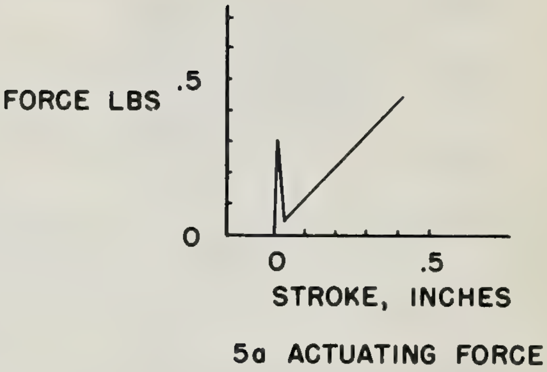

FIGURE 10. COMPONENT (2) ACTUATING FORCE.

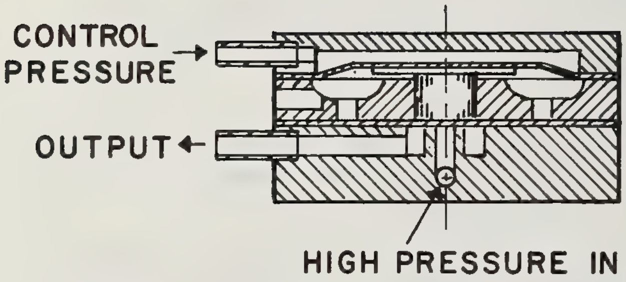

FIGURE 11. END OF DIASTOLE SWITCH. COMPONENT (3).

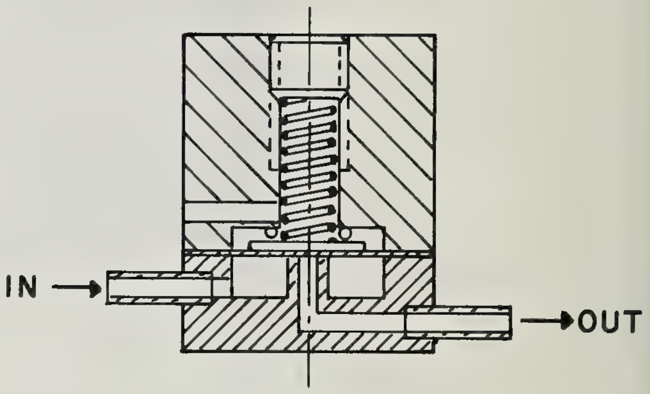

FIGURE 12. RELIEF VALVE, COMPONENT (4).

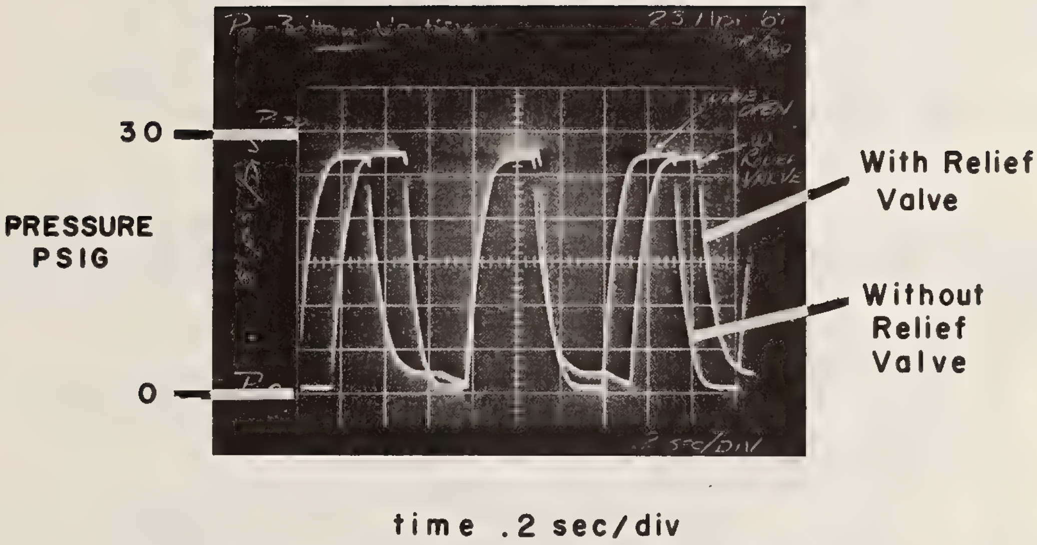

FIGURE 13. COMPONENTS (3) AND (4) PERFORMANCE.

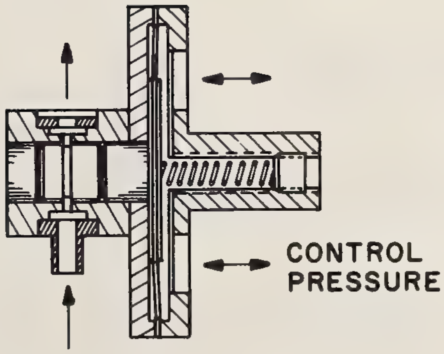

FIGURE 14. DIASTOLE RATE CONTROL VALVE. COMPONENT (5).

last part of the diastole period (Figure 15b) where the pressures at the assist pump and at the actuator pumping chamber are modulated in response to the pressure in the actuator seal bellows. The control shown results in the desired actuator action in that the actuator velocity is reduced to control the suction pressure. If the velocity is reduced sufficiently during the last half of the diastole stroke systole is triggered and a true variable stroke volume capability results.

As is apparent from the data shown, an area of future effort must be toward increasing the speed of response of the system. Since the system employs an incompressible fluid as the working medium, the potential for rapid response exists. Expansion of the seal bellows under the force of the rising control pressure and friction in the control valve are two possible causes of system performance degradation.

In summary, the basic function of this control approach has been demonstrated and has pointed the way toward system and component design refinement for increased system control performance.

SYSTEM MODELING AND ANALYSIS

Concurrent with the control system hardware design and development a mathematical characterization of the mechanical diastole pressure control loop is being developed. Digital computer solutions of the system equations will be used to aid in refining the control components for performance optimization.

The current form of this characterization is shown in block diagram form in Figure 16. There are three feedback signals in the system

(a) Unity feedback from the mechanical diastolic pressure (MDP) to component (5).
(b) Pressure feedback from the large pumping piston to the actuator piston.
(c) Feedback coupling the pressure and flowrate of the liquid exiting the actuator bellows through component (5).

Two external inputs affect the system

(a) The thoracic cavity reference pressure (TCP) plus the spring bias in component (5).
(b) Changes in blood flow (Q_B) that cause changes in MDP.

Using the state space approach, the system equations are rewritten as differential equations and difference equations.

1. $e = TCP - MDP$
2. $\frac{d^2Q}{dt^2} + \frac{b_o}{a_o}\frac{dQ}{dt} + \frac{1}{a_o} Q = -\frac{K_o}{a_o} e$
3. $Q_o = Q + K_p P_c$
4. $\frac{dP}{dt} + \frac{1}{a_1} p = -\frac{K_1}{a_1} Q_o$
5. $P_c = P + K_L P_L$
6. $\frac{d^2y}{dt^2} + \frac{b_2}{a_2}\frac{dy}{dt} + \frac{1}{a_2} y = \frac{K_2}{a_2} P_c$
7. $K_3 \frac{dy}{dt} = P_L$
8. $MDP = K_B Q_B + P_L$

State variables are assigned as follows

States: $X_1 = Q$
$X_2 = \dot{Q}$
$X_3 = P$
$X_4 = y$
$X_5 = \dot{y}$

Inputs: $u_1 = TCP$
$u_2 = Q_B$

Matrix relationships in canonical form may now be formed in terms of the state variables and the inputs.

$$\dot{X}_1 = X_2$$

$$\dot{X}_2 = -\frac{1}{a_o} X_1 - \frac{b_o}{a_o} X_2 - \frac{K_o}{a_o} (u_1 - K_B u_2 + K_3 X_5)$$

$$\dot{X}_3 = -\frac{1}{a_1} X_3 - \frac{K_1}{a_1} (X_1 + K_p X_3 + K_P K_2 K_3 X_5)$$

$$\dot{X}_4 = X_5$$

$$\dot{X}_5 = -\frac{1}{a_2} X_4 - \frac{b_2}{a_3} X_5 + \frac{K_2}{a_3} (X_3 + K_L K_3 X_5)$$

Therefore

$$\dot{X} = AX + BU$$

Where

$$X = \begin{bmatrix} X_1 \\ X_2 \\ X_3 \\ X_4 \\ X_5 \end{bmatrix} \; ; \; A = \begin{bmatrix} 0 & 1 & 0 & 0 & 0 \\ -\frac{1}{a_o} & -\frac{b}{a_o} & 0 & 0 & -\frac{K_oK_3}{a_o} \\ -\frac{K_1}{a_1} & 0 & \frac{1+K_1K_p}{-a_1} & 0 & \frac{K_1K_3K_pK_L}{-a_1} \\ 0 & 0 & 0 & 0 & 1 \\ 0 & 0 & \frac{K_2}{a_2} & -\frac{1}{a_2} & \frac{K_2K_3K_L-b_2}{a_2} \end{bmatrix}$$

$$B = \begin{bmatrix} 0 & 0 \\ -\frac{K_o}{a_o} & \frac{K_oK_B}{a_o} \\ 0 & 0 \\ 0 & 0 \\ 0 & 0 \end{bmatrix} \qquad U = \begin{bmatrix} u_1 \\ u_2 \end{bmatrix}$$

The procedure, now, is to solve the first order differential matrix equation

$$\dot{X} = AX + BU$$

for variable U and with various values of A. Then, with the time solutions of the state variables, the other parameters of interest are found.

The general procedure is as follows

Make the substitution $X = PZ$, $X_o = PZ_o$

Then $\dot{X} = P\dot{Z}$ and we have

$$P\dot{Z} = APZ + BU$$

or

$$\dot{Z} = P^{-1}APZ + P^{-1}BU$$

P is the matrix which diagonalizes A. This has a general solution

$$Z = \varepsilon^{\lambda t}Z_o + \varepsilon^{\lambda t}\int \varepsilon^{-\lambda t}p^{-1}BUd\tau$$

which becomes

$$P^{-1}X = \varepsilon^{\lambda t}P^{-1}X_o + \varepsilon^{\lambda t}\int \varepsilon^{-\lambda\tau}p^{-1}\ BUd\tau$$

or

$$X = P\varepsilon^{\lambda t}P^{-1}\ X_o + \int P\varepsilon^{\lambda t}P^{-1}\ P\varepsilon^{-\lambda\tau}P^{-1}\ BUd\tau$$

$P\varepsilon^{\lambda t}\ P^{-1}$ is called the transition matrix $\phi(t_1t_o)$.

Thus

$$X = \phi(t_1t_o)\ X_o + \int\phi(t,\tau)\ BUd\tau$$

This continuous solution has a discrete form used for digital computer solution.

$$X_{K+1} = \phi X_K + Du_K$$

where

$$D = \int_{KT}^{(K+1)T} \phi BUd\tau$$

T = sampling period
K = sampling time

The input vector, U, is assumed to be piecewise constant between sampling times.

With the discrete form of the solution equation, all of the parameters of interest may be studied as the inputs are varied and as various system constants are used.

A major objective of the study is to determine the system constants necessary to keep the MDP pressure above a specified negative value over the expected range of input values.

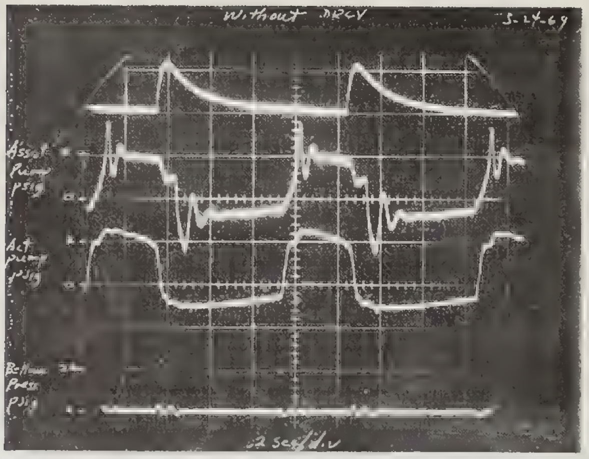

FIGURE 15. DIASTOLE RATE CONTROL VALVE OPERATION. a. WITHOUT FUNCTIONING VALVE.

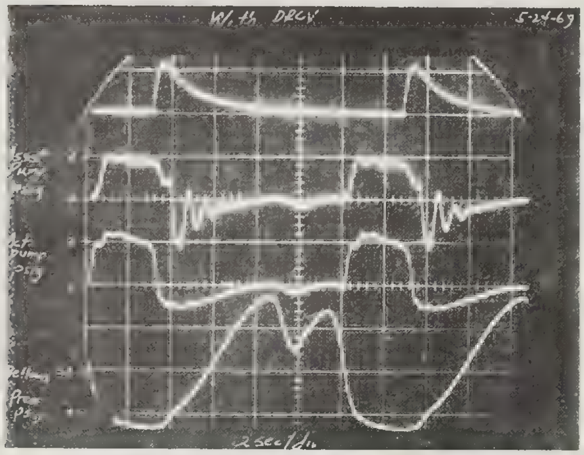

FIGURE 15. b. WITH FUNCTIONING CONTROL VALVE.

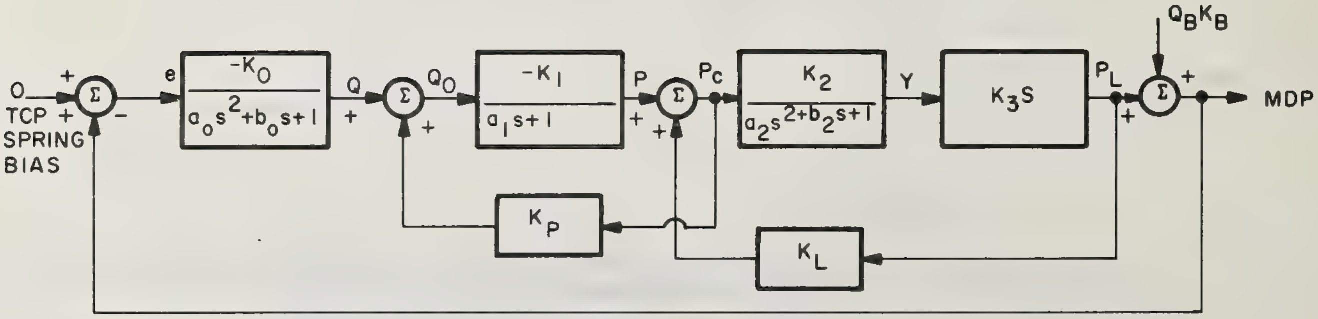

FIGURE 16. BLOCK DIAGRAM. MECHANICAL DIASTOLE PRESSURE CONTROL.

SUMMARY

The cardiac assist device control system described in this paper is in the early stages of feasibility demonstration development. Simplicity, small size and efficiency have been guiding criteria throughout this study. No great emphasis has been placed on long term-reliability as this effort will naturally follow the feasibility demonstration. The development of an integrated, all fluid-mechanical pump actuator and control system offers the potential of a completely implantable system when coupled to the implantable compressed gas power sources and assist pumps currently under development.

REFERENCE

1. Woodward, K. E., "Fluid Amplifier within an Implanted Heart," Mechanical Engineering, November 1967.

FILMS SHOWN AT CONFERENCE

THE ARP INFANT RESPIRATOR AS USED IN AN EMERGENCY AIR-GROUND TRANSPORT SYSTEM FOR NEWBORN INFANTS WITH RESPIRATORY DISTRESS SYNDROME.
L. J. Arp, Virginia Polytechnic Institute, Blacksburg, Virginia

INTRA-AORTIC BALLOON PUMPING IN HEART FAILURE
T. Dietrich, M. Feola, and J. H. Kennedy
Cleveland Metropolitan General Hospital, Case Western Reserve University, Cleveland, Ohio

INDEX OF CONTRACTORS

ABCOR, INC., Cambridge Massachusetts.
AEROJET-GENERAL CORPORATION, San Ramon, California
AMICON CORPORATION, Lexington, Massachusetts
AVCO EVERETT RESEARCH LAB., Everett, Massachusetts
BATTELLE MEMORIAL INSTITUTE, Columbus, Ohio
BATTELLE-NORTHWEST, Richland, Washington
CARNEGIE-MELLON UNIVERSITY, Pittsburgh, Pennsylvania
CASE WESTERN RESERVE UNIVERSITY, Cleveland, Ohio
CHILDREN's HOSPITAL MEDICAL CENTER, Boston, Massachusetts
COLUMBIA UNIVERSITY, New York, New York
CORBIN-FARNSWORTH, INC., Palo Alto, California
CORDIS LABORATORIES, Miami, Florida
CORNELL UNIVERSITY MEDICAL COLLEGE, New York, New York
DOW CHEMICAL COMPANY, Walnut Creek, California
DOW CORNING CORPORATION, Midland, Michigan
ENERGY RESEARCH AND GENERATION, INC., Oakland, California
EPOXYLITE CORPORATION, South El Monte, California
ESSO RESEARCH AND ENGINEERING COMPANY, Linden, New Jersey
FLUIDONICS RESEARCH LABORATORY, Salt Lake City, Utah
GENERAL ELECTRIC COMPANY, Philadelphia, Pennsylvania
GENERAL ELECTRIC COMPANY, Schenectady, New York
GENERAL ELECTRIC COMPANY, King of Prussia, Pennsylvania
GULF GENERAL ATOMIC, INC., San Diego, California
HAMILTON STANDARD, Farmington, Connecticut
HAUSER RESEARCH AND ENGINEERING COMPANY, Denver, Colorado
HITTMAN ASSOCIATES, Columbia, Maryland
HYDROSPACE RESEARCH CORPORATION, Rockville,Maryland
INDIANA UNIVERSITY MEDICAL CENTER, Indiana
INSTITUTE OF MEDICAL SCIENCES, San Francisco, California
JOHN B. PIERCE FOUNDATION LABORATORY, New Haven, Connecticut
JOHNS HOPKINS UNIVERSITY, Baltimore, Maryland
LEESONA MOOS LABORATORIES, Great Neck, New York
LITTON INDUSTRIES, Minneapolis, Minnesota
MASSACHUSETTS INSTITUTE OF TECHNOLOGY, Cambridge, Massachusetts
McDONNELL DOUGLAS CORPORATION, Richland, Washington
MEDICAL COLLEGE OF VIRGINIA, Richmond, Virginia
MELPAR, INC., Falls Church, Virginia
MONSANTO RESEARCH CORPORATION, Dayton, Ohio
MONSANTO RESEARCH CORPORATION, Everett, Massachusetts
NEW ENGLAND MEDICAL CENTER HOSPITALS, Boston, Massachusetts
NEW YORK UNIVERSITY, New York, New York
PENNSYLVANIA RESEARCH ASSOCIATES, INC., Philadelphia, Pennsylvania
PHYSICS INTERNATIONAL COMPANY, San Leandro, California
POLYSCIENCES, INCORPORATED, Warrington, Pennsylvania
SHELL DEVELOPMENT COMPANY, Emeryville, California
STANFORD RESEARCH INSTITUTE, Menlo Park, California
STANFORD UNIVERSITY MEDICAL CENTER, Stanford, California
STATE UNIVERSITY OF NEW YORK, Brooklyn, New York
STATHAM INSTRUMENTS, INC., Oxnard, California
TEXAS INSTRUMENTS, INC., Houston, Texas
THERMO ELECTRON CORPORATION, Waltham, Massachusetts
TRAVENOL LABORATORIES, INC., Morton Grove, Illinois
TYCO LABORATORIES, INC., Waltham, Massachusetts
UNION CARBIDE CORPORATION, Cleveland, Ohio
UNION CARBIDE CORPORATION, Bound Brook, New Jersey
UNIVERSITY OF CALIFORNIA, San Diego, California
UNIVERSITY OF MINNESOTA, Minneapolis, Minnesota
UNIVERSITY OF MISSISSIPPI MEDICAL CENTER, Jackson, Mississippi
UNIVERSITY OF NORTH CAROLINA, Chapel Hill, North Carolina
UNIVERSITY OF PENNSYLVANIA, Philadelphia, Pennsylvania
UNIVERSITY OF VERMONT, Burlington, Vermont
WESTERN GEAR CORPORATION, South Gate, California
WESTINGHOUSE ELECTRIC CORPORATION, Pittsburgh, Pennsylvania

NATIONAL HEART INSTITUTE

ARTIFICIAL HEART PROGRAM CONFERENCE

REGISTRANTS

Abel, Kenneth, Litton Industries, Minneapolis, Minnesota
Abroson, Frank, Epoxylite Corporation, South El Monte, California
Ackerberg, R. C., Polytechnical Institute of Brooklyn, Farmingdale, New York
Adams, Andrew P., M.D., Northwestern University, Kankakee, Illinois
Adams, Leon M., Ph.D., Southwest Research Institute, San Antonio, Texas
Adler, Ira M., Hittman Associates, Inc., Columbia, Maryland
Aisenberg, Sol, Ph.D., Space Sciences Incorporated, Waltham, Massachusetts
Akers, W. W., Ph.D., Rice University, Houston, Texas
Akutsu, Tetsuzo, M.D., University of Mississippi, Jackson, Mississippi
Almeida, Antonio M.D., Kings County Hospital, Downst. Med. Ctr., Brooklyn, New York
Amblard, M., Electronique Marcel Dassault, Paris, France
Anderson, Richard M., Abcor, Incorporated, Cambridge, Massachusetts
Anderson, Sandra, Battelle Memorial Institute, Columbus, Ohio
Anderson, Wesley D., M.D., University of Minnesota, Minneapolis, Minnesota
Andreani, S., Ph.D., Rhodia-Rhone-Poulenc, New York, New York
Anken, Milton, Cordis Corporation, N. Miami Beach, Florida
Annable, Charles R., M.D., Walter Reed General Hospital, Washington, D.C.
Anstadt, George, L., V.M.D., Johns Hopkins University, Baltimore, Maryland
Anthes, David E., IIT Research Institute, Chicago, Illinois
Argano, E.S., Ph.D., Italian National Research Council, Milan, Italy
Arp, Leon J., Ph.D., Virginia Polytechnic Institute, Blacksburg, Virginia
Asher, William J., Esso Research And Engineering Co., Fanwood, New Jersey
Astleford, William J., Southwest Research Institute, San Antonio, Texas
Atchley, F. O., M.D., National Institutes of Health, Bethesda, Maryland
Atkinson, Joe W., M.D., National Institutes of Health, Bethesda, Maryland
Atsumi, Kazuhiko, M.D., University of Tokyo, Tokyo, Japan
Austen, Gerald W., M.D., Massachusetts General Hospital, Harvard Univ., Boston, Massachusetts

Baker, R. Robinson, M.D., Johns Hopkins Hospital, Baltimore, Maryland
Baretta, Edward, Marquette School of Medicine, Milwaukee, Wisconsin
Barmat, M., Fairchild Hiller Corporation, Germantown, Maryland
Barnes, Ellen E., National Institutes of Health, Bethesda, Maryland
Barsky, Murray H., Ph.D., Argonne National Laboratory, Argonne, Illinois
Bartlett, Glenn W., M.D., American Hospital Supply Corp., Evanston, Illinois
Bartlett, Jr., R. G., Ph.D., International Business Machines, Gaithersburg, Maryland
Battista, S. P., M.D. Arthur D. Little, Cambridge, Massachusetts
Batzold, John S., M.D., Esso Research and Engineering, Linden, New Jersey
Beale, William, Ohio University, Columbus, Ohio
Beam, Benjamin H., NASA Ames Research Center, Moffett Field, California
Bean, Ross C., Ph.D., Aeronutronic Div., Philco Ford, Newport Beach, California
Bellamy, David, Travenol Laboratories, Morton Grove, Illinois
Belzer, Morton, Ph.D., Esso Research and Engineering, Linden, New Jersey
Benedict, James. S., M.D., St. Mary's Hospital, Long Beach, California
Benson, G. M., E. R. G., Incorporated, Oakland, California
Berger, Robert L., M.D., Boston University, Boston, Massachusetts
Bergling, Nils, Ph.D., Incentive A B, Stockholm, Sweden
Bernhard, William F., M.D., Children's Hospital, Boston, Massachusetts
Bernstein, E., M.D., University of Minnesota, Minneapolis, Minnesota
Bess, Michael A., University of Minnesota, Minneapolis, Minnesota
Birtwell, William C., New England Medical Center Hospitals, Boston, Massachusetts
Bishop, E. T., Shell Development Company, Emeryville, California
Bixler, H. J., M.D., Amicon Corporation, Lexington, Massachusetts
Black, Jonathan, University of Pennsylvania, Philadelphia, Pennsylvania
Black, Thomas J., Mechanical Technology, Inc., Loudonville, New York
Blackford, Virginia L., M.D., National Institutes of Health, Bethesda, Maryland
Blackshear, Jr., Perry L., M.D., University of Minnesota, Minneapolis, Minnesota
Blardinelli, Albert J., Monsanto Research Corporation, Dayton, Ohio
Blount, Don H., Melpar, Incorporated, Falls Church, Virginia
Bluestein, Maruice, M.D., Thermo Electron Corporation, Waltham, Massachusetts
Blumle, Leo J., Biomedical Systems-Hamilton Standard, Farmington, Connecticut
Bocciarelli, Carlo V., Pennsylvania Research Associates, Pennsylvania
Boies, David, IIT Research Institute, Chicago, Illinois
Bokros, Jack, M.D., Gulf General Atomic, San Diego, California
Bolduc, Lee R., Medtronic Company, Minneapolis, Minnesota
Bolooki, Hodshang, M.D., University of Miami, Miami, Florida
Boretos, John W., National Institutes of Health, Bethesda, Maryland

Borison, V. Scott, Stanford University, Stanford, California
Borsanyi, A. S., Monsanto Research Corporation, Everett, Massachusetts
Bosher, Jr., Lewis H., M.D., Medical College Hospital, Richmond, Virginia
Bosworth, J. E., American Optical Corporation, Bedford, Massachusetts
Bourget, Pierre, ORTF, Paris, France
Bourland, Hardy M., Rice University, Houston, Texas
Bowen, Robert J., Navships R & D Laboratory, Annapolis, Maryland
Boyack, James R., Ph.D., General Electric Company, West Lynn, Massachusetts
Boycks, E. E., M.D., Beckman Instruments, Inc., Santa Ana, California
Boyles, Paul W., M.D., Wyeth Labs., Berwyn, Pennsylvania
Braley, Silas, Dow Corning Center, Midland, Michigan
Brash, John L., Stanford Research Institute, Menlo Park, California
Braunwald, Nina S., M.D., University of California, San Diego, California
Brechenridge, Jr., R. Warren, Arthur D. Little, Inc., Cambridge, Massachusetts
Brender, Elliot, M.D., V.A. Hospital, Buffalo, New York
Brinkhous, K. M., M.D., University of North Carolina, Chapel Hill, North Carolina
Brobmann, Guenther F., Ph.D., University of Oklahoma, Oklahoma City, Oklahoma
Brodd, Ralph J., Union Carbide Corporation, Cleveland, Ohio
Brown, Clinton E., Hydronautics, Incorporated, Laurel, Maryland
Bruce, David W., Travenol Laboratories, Morton Grove, Illinois
Bruner, H. D., U. S. Atomic Energy Commission, Washington, D.C.
Bryant, Harold H., Huntingdon Research Center, Inc., Baltimore, Maryland
Buchanan, James W., University of Pennsylvania, Philadelphia, Pennsylvania
Buck, Keith, Aerojet General Corporation, San Ramon, California
Bull, Brian, Loma Linda University Hospital, Loma Linda, California
Burda, Charles J., Dow Corning Corporation, Midland, Michigan
Burdette, Walter J., M.D., The University of Texas M.D. Anderson Hospital, Houston, Texas
Burns, Marvin, IIT Research Institute, Chicago, Illinois
Burns, Winton, H., Indiana University, Indianapolis, Indiana
Burton, T. A., Waters Company, Rochester, Minnesota
Bussey, Phillip, State of Md., Division of Vocational Rehabilitation, Bladensburg, Maryland
Byck, Joseph S., Ph.D., Union Carbide Corporation, Bound Brook, New Jersey

Caggiano, Vincent, Biomedical Electronics, Inc., Rockville, Maryland
Cairns, Elton, J., Ph.D., Argonne National Laboratory, Argonne, Illinois
Calkins, Capt. Jerry M., Harry Diamond Laboratories, Washington, D.C.
Camac, Morton, AVCO Everett, Everett, Massachusetts
Campbell, John A., Ph.D., Presbyterian St. Luke's Hospital, Chicago, Illinois
Carey, Joseph S., M.D., V. A. Center, Artificial Heart Facility, Los Angeles, California
Carlson, Richard S., Johns Hopkins Applied Physics Laboratory, Silver Spring, Maryland
Carr, James, Children's Hospital Medical Center, Boston, Massachusetts
Cartier, Jean S., State Department, Brooklyn, New York
Chambers, Jack A., Ph.D., Statham Instruments, Ventura, California
Chang, Daniel, P. Y., California Institute of Technology, Pasadena, California
Chaptal, Paul-Andre, M.D., University Montpellier, Montpellier, France
Chardack, William M., M.D., State University of New York, Buffalo, New York
Chatterjee, S., M.D., Jewish General Hospital, Montreal, Canada
Cherry, Nancy, National Institutes of Health, Bethesda, Maryland
Child, F. W., Washington Science Industries, Minnotonka, Minnesota
Chilenskas, A., Argonne National Laboratories, Argonne, Illinois
Chiswik, H. H., Ph.D., Argonne National Laboratories, Argonne, Illinois
Cholvin, Neal R., Ph.D., Iowa State University, Ames, Iowa
Chomsky, Steven A., Newark Beth Israel Hospital, Hillside, New Jersey
Chonette, D. W., Edwards Laboratories, Inc., Santa Ana, California
Christophersen, Erling B., M.D., V. A. Hospital, Pittsburgh, Pennsylvania
Clark, Richard A., Brunswick Corporation, Muskegon, Michigan
Clark, Richard E., CDR, MC, USNR, Naval Hospital, Bethesda, Maryland
Clarke, Wm. J., M.D., Battelle Northwest Laboratory, Richland, Washington.
Cline, Robert, M.D., Duke Medical Center, Durham, North Carolina
Cobb, Carl M., Boston Globe, Boston, Massachusetts
Cohen, Lawrence S., M.D., University of Texas, Southwestern Med. Sch., Dallas, Texas
Cohn, Jay N., M.D., V. A. Hospital, Washington, D.C.
Cole, Sterling, Southern Interstate Nuclear Board, Washington, D.C.
Collins, Jr., John J., Harvard University, Boston, Massachusetts
Colwell, Gene T., Ph.D., Georgia Tech., Atlanta, Georgia
Comer, E. Wayne, Ethicon, Incorporated, Somerville, New Jersey
Constant, Jr., Paul C., Midwest Research Institute, Kansas City, Missouri
Corbin, Thomas, Corbin-Farnsworth, Incorporated, Palo Alto, California
Cortes, Luis, M.D., New York University, New York, New York
Coval, M. D., M.D., Institute of Medical Sciences, San Francisco, California
Cowin, Stephen C., Prof., Tulane University, New Orleans, Louisiana
Crim, Jr., Winfred M., U.S.A. Engineer Reactor Group, Fort Belvoir, Virginia

Cross, Robert A., Amicon Corporation, Lexington, Massachusetts
Cuello, Leo, M.D., University of Texas at San Antonio, San Antonio, Texas
Culp, Gordon W., Epoxylite Corporation, South El Monte, California
Cupples, Art, Epoxylite Corporation, South El Monte, California
Cyprus, Joel, M.D., Texas Instruments, Incorporated, Houston, Texas
Cywinski, Jozef, K., University of Pennsylvania, Philadelphia, Pennsylvania

Dahlquist, Carl, 3M Company, St. Paul, Minnesota
Dalke, John L., National Bureau of Standards, Boulder, Colorado
Dantowitz, Philip, Monsanto Research, Peabody, Massachusetts
Darby, Eleanor M. K., M.D., National Institutes of Health, Bethesda, Maryland
Davila, Julio C., M.D., Temple University, Philadelphia, Pennsylvania
Dean, James P., University of Miami, Miami, Florida
DeBakey, M. E., M.D., Baylor College of Medicine, Houston, Texas
DeBenneville, Peter L., M.D., Rohm and Hans Co., Spring House, Pennsylvania
Dedrick, R. L., M.D., National Institutes of Health, Bethesda, Maryland
DeFilippi, Richard P., Abcor, Incorporated, Cambridge, Massachusetts
Dehm, Henry C., M.D., Hercules, Inc., Magna, Utah
DeLuca, Frank G., M.D., Providence, Rhode Island
Dempler, Wayne A., Westinghouse Corp., Large, Pennsylvania
Dennis, Lewis H., M.D., Georgetown University, Washington, D.C.
Dennis, Warren H., Ph.D., University of Wisconsin, Madison, Wisconsin
Dennison, Benjamin, Melpar, Inc., Falls Church, Virginia
Detmer, Don E., M.D., National Institutes of Health, Bethesda, Maryland
DeVries, William C., University of Utah, Salt Lake City, Utah
DeWall, Richard, M.D., Cox Heart Institute, Kettering, Ohio
Diethrich, Ted., M.D., Baylor College of Medicine, Houston, Texas
Dodge, Harold T., M.D., University of Alabama Med. Ctr., Birmingham, Alabama
Dodich, N.A., University of California, Los Angeles, California
Doig, Jr., Alfred R., Monsanto Company, Everett, Massachusetts
Dolan, Alfred M., University of Alberta, Edmonton, Alberta, Canada
Donaldson, W. Lyle, Southwest Research Institute, San Antonio, Texas
Dong, Jr., Eugene, M.D., Stanford University, Stanford, California
Donnelly, Jr., Joseph C., M.D., Lankenau Hospital, Philadelphia, Pennsylvania
Dounoucos, Angelo, Environmental Technology, Inc., Latham, New York
Dragoo, John R., M.D., The Wabash Clinic, Wabash, Indiana
Drake, Roger F., Monsanto Company, Everett, Massachusetts
Driskell, Thomas D., Battelle Memorial Institute, Columbus, Ohio
Dunk, A. C., M.D., Drexel Institute of Technology, Altadena, California
Dunlavey, Edward O., Statham Instruments, Oxnard, California
Dunner, Edward, M.D., U. S. V. A. Central Office, Silver Spring, Maryland
Durfee, Robert L., Ph.D., Health and Safety Research Institute, Springfield, Virginia

Eberheart, Robert, Institute of Medical Sciences, San Francisco, California
Eby, Charles J., Ph.D., Monsanto Research Corporation, Washington, D.C.
Eden, C. Edward, M.D., Huntingdon Research Center, Baltimore, Maryland
Edmark, K. W., M.D., Providence Hospital, Seattle, Washington
Eggleton, Reginald, Interscience Research Institute, Champaign, Illinois
Eilers, George, J., M.D., Stanford Research Institute, Menlo Park, California
Elliot, Eric C., M.D., Walter Reed Army Institute of Research, Washington, D.C.
Ellis, William, M.D., Duke University, Durham, North Carolina
Ellsworth, O. T., Ph.D., Stanford University, Stanford, California
Elyash, Liberty J., Mellon Institute, Pittsburgh, Pennsylvania
Elzinga, W. E., M.D., Hittman Associates, Inc., Simpsonville, Maryland
Engdah, Richard E., Energy Research Corporation, Bethel, Connecticut
Enger, Carl C., Ph.D., Case Western Reserve University, Cleveland, Ohio
Engstrom, William R., Olson Medical Products, Inc., Boston, Massachusetts
Eriksson, Jan C., Gothenburg University, Gothenburg, Sweden
Ersek, Robert A., M.D., University of Minnesota, Minneapolis, Minnesota
Esmond, William G., M.D., University of Maryland, Baltimore, Maryland
Estes, Michael, West Virginia University, Morgantown, West Virginia
Evans, Joseph M., Ph.D., Westinghouse Electric Corporation, Pittsburgh, Pennsylvania
Everett, Milton K., Tulane University, New Orleans, Louisiana
Eyrick, T. B., Ph.D., E.G.&G., Inc., Bedford, Massachusetts
Eyster, George E., V.M.D., Michigan State University, East Lansing, Michigan

Falb, Richard D.,Ph.D., Battelle Memorial Institute, Columbus, Ohio
Farish, Charles A., University of Mississsippi, Jackson, Mississippi
Feldtman, Robert, University of Texas Medical Branch, Galveston, Texas
Felsen, Ira M., Naval Ship R & D Center, Greenbelt, Maryland
Felsenthal, Peter, Arthur D. Little, Cambridge, Massachusetts
Feola, Mario, M.D., Case Western Reserve University, Cleveland, Ohio
Ferrari, Lionel, M.D., University of Torino, Frongia, Italy
Fishman, J. H., Leesona Moos Laboratories, Long Island, New York
Fishman-Eytan, Rachel, New York, New York
Fleming, William H., M.D., Walter Reed Army Institute of Research, Washington, D.C.
Fogle, John L., West Virginia University, Morgantown, West Virginia
Foster, Eugene L., M.D., Foster-Miller Associates, Waltham, Massachusetts
Fountain, K.R., Midwest Research Institute, Kansas City, Missouri
Fourt, Lyman, Gillette Research Institute, Rockville, Maryland
Fox Gertrude W., MEDLARS, National Library of Medicine, Bethesda, Maryland
Frater, R.W.N., M.D., Altert Einstein College of Medicine, Bronx, New York
Freed, Paul S., Maimonides Medical Center, Brooklyn, New York
Freedman, Toby, North American Rockwell Corporation, El Segundo, California
Friedman, Edward, Ph.D., Amicon Corporation, Lexington, Massachusetts
Frieze, Sylvia E., Children's Hospital Medical Center, Boston, Massachusetts
Frisoli, A., M.D., National Institutes of Health, Bethesda, Maryland
Frommer, Peter L., M.D., National Institutes of Health, Bethesda, Maryland
Fuqua, Jr., John M., Melpar, Incorporated, Rockville, Maryland
Furman, Seymour, M.D., Montefiore Hospital, Bronx, New York

Gabelnick, Henry L., Ph.D., National Institutes of Health, Bethesda, Maryland
Gage, Andrew, M.D., Buffalo, New York
Gajdos, Leslie B., B. F. Goodrich Research Center, Brecksville, Ohio
Gallagher, Joseph G., University of Virginia, Charlottesville, Virginia
Galletti, Pierre M., M.D., Brown University, Providence, Rhode Island
Galysh, Fred T., Travenol Laboratories, Morton Grove, Illinois
Ganyo, Kenneth F., Westinghouse Electric Corporation, Pittsburgh, Pennsylvania
Gebben, Vernon D., NASA Lewis Research Center, Cleveland, Ohio
George, Janet B., Children's Hospital Medical Center, Boston, Massachusetts
Giannotti, Hugo, Giannotti Associates, Bellport, Long Island, New York
Gibbons, D.F., M.D., Case Western Reserve University, Cleveland, Ohio
Gilbert, Arthur C., M.D., Systems Technology Laboratory, Inc., Washington, D.C.
Gillis, M. F., M.D., Battelle-Northwest, Richland, Washington
Giner, Jose, Tyco Laboratories, Waltham, Massachusetts
Giori, Francis A., Sanders Associates, Buffalo, New York
Giron, Fabio, M.D., Tufts New England Medical Center Hospitals, Boston, Massachusetts
Gladstone, Marvin M., M.D., University of California, La Habra, California
Glanfield, Edward J., General Electric Company, Philadelphia, Pennsylvania
Glaze, Harry J., Stanford University, Palo Alto, California
Glenn, Wm., W. L., M.D., Yale University, New Haven, Connecticut
Goldberg, H.E., Ph.D., American Optical Corporation, Bedford, Massachusetts
Goldsmith, Margaret T., M.D., National Institutes of Health, Bethesda, Maryland
Gonsior, Leonard J., Union Carbide Corporation, Piscataway, New Jersey
Goodman, Lester, Ph.D., National Institutes of Health, Bethesda, Maryland
Gordon, Archer S., M.D., Statham Instruments, Oxnard, California
Gordon, Paul, Ph.D., General Electric Company, Philadelphia, Pennsylvania
Gott, Vincent, M.D., Johns Hopkins Hospital, Baltimore, Maryland
Goulder, Morton E., Sanders Associates, Nashua, New Hampshire
Gourley, Gary, M.D., University of California, Davis, California
Greenberg, Jack J., M.D., Mt. Sinai Hospital, Miami Beach, Florida
Greene, Norbert D., Rensselaer Polytechnic Institute, Troy, New York
Greenfield, L. J., M.D., University of Oklahoma Med. Ctr., Oklahoma City, Oklahoma
Gregg, Donald E., Ph.D., Walter Reed Institute of Research, Washington, D.C.
Griffen, Paul M., General Electric Research and Development Center, Schenectady, New York
Griffin, O. M., M.D., Naval Research Laboratory, Washington, D.C.
Griffith, James R., M.D., U. S. Naval Research Laboratory, Washington, D.C.
Grode, Gerald, Battelle Memorial Institute, Columbus, Ohio
Guest, M. Mason, National Institutes of Health, Univ. of Texas, Galveston, Texas
Guier, William H., M.D., Johns Hopkins University, Baltimore, Maryland
Gumnick, James C., Ph.D., Franklin Institute, Philadelphia, Pennsylvania

Haiderer, Otto, M.D., Case Western Reserve University, Cleveland, Ohio
Halbert, Seymour P., M.D., Cordis Laboratories, Miami, Florida
Hall, C. William, M.D., Southwest Research Institute, San Antonio, Texas
Halpern, B. David, Ph.D., Polysciences, Incorporated, Warrington, Pennsylvania
Hamblen, John W., Johns Hopkins University/APL, Silver Spring, Maryland
Hamlen, R. P., General Electric Research and Development Center, Schenectady, New York
Hansen, A. Tybjaerg, M.D., University of Copenhagen, Blegoamsvej 9,Copenhagen, Denmark

Kafesjian, Ralph, M.D., Monsanto Co., Wakefield, Massachusetts
Kahn, Paul, Cutter Laboratories, Berkeley, California
Kallfelz, Francis A., Ph.D., Cornell University, Ithaca, New York
Kantrowitz, Adrian, M.D., Maimonides Medical Center, Brooklyn, New York
Kantrowitz, Jean, Maimonides Medical Center, Brooklyn, New York
Kapsalis, Andreas, Travenol Laboratories, Morton Grove, Illinois
Kasanof, David, R. N., Magazine, Oradell, New Jersey
Kaszynski, Edwin, Gillette Research Institute, Rockville, Maryland
Kaufman, William M., Ph.D., Hittman Associates, Inc., Columbia, Maryland
Kayser, Kenneth L., Marquette Medical School, Inc., Milwaukee, Wisconsin
Keenan, Joseph H., Thermoelectron Corporation, Belmont, Massachusetts
Keller, Kenneth H., M.D., University of Minnesota, Minneapolis, Minnesota
Kelly, David T., M.D., National Institutes of Health, Bethesda, Maryland
Kennedy, John H., M.D., Case Western Reserve University, Cleveland, Ohio
Kessler, Alfred G., Fluidonics Research Laboratories, Salt Lake City, Utah
Keusch, Preston, RAI Research Corporation, Long Island City, New York
Khouri, Edward M., Walter Reed Army Institute of Research, Kensington, Maryland
Kihara, Kazuhiko, Minneapolis, Minnesota
Kitrilakis, S., Thermo Electron Corporation, Waltham, Massachusetts
Klein, Elias, Ph.D., Gulf South Research Institute, New Orleans, Louisiana
Kline, Jacob, Ph.D., University of Miami, Coral Gables, Florida
Kanpp, Charles E., University of Kentucky, Lexington, Kentucky
Knapp, David E., Ph.D., McDonnell Douglas Corporation, Richland, Washington
Knutti, Ralph E., Bethesda, Maryland
Kocandrle, V., M.D., University of Chicago, Chicago, Illinois
Kochwa, Shaul, Ph.D., Mount Sinai School of Medicine, New York, New York
Koffsky, Robert M., Columbia University, New York, New York
Kohn, E. T., Naval Research Laboratory, Washington, D.C.
Kolff, W., M.D., University of Utah, Salt Lake City, Utah
Konigsberg, Eph, Konigsberg Instruments, Pasadena, California
Koreski, Wm. R., Waters Co., Rochester, Minnesota
Korosi, Alexander, Monsanto Corporation, Everett, Massachusetts
Kozawa, A., Union Carbide Corporation, Parma, Ohio
Kralios, Alex, M.D., University of Utah, Salt Lake City, Utah
Kramer, Edward J., Cornell University, Ithaca, New York
Kristol, David, Ph.D., Newark College of Engineering, Newark, New Jersey
Kruglicoff, Susana R., Ph.D., Warf Institute, Inc., Madison, Wisconsin
Kubik, Paul P., Holter Company, Bridgeport, Pennsylvania
Kuchar, N. R., General Electric Company, Philadelphia, Pennyslvania
Kuhn, Leslie A., M.D., Mt. Sinai School of Medicine, New York, New York
Kulasa, Leon V., KPA Nuclear, Large, Pennsylvania
Kuo, Shen-yeh, Polysciences, Incorporated, Warrington, Pennsylvania
Kusserow, B. K., M.D., University of Vermont, Burlington, Vermont
Kwan-Gett, Clifford S., M.D., University of Utah, Salt Lake City, Utah

Laenger, Sr., Charles J., Southwest Research Institute, San Antonio, Texas
LaFarge, C. Grant, M.D., Children's Hospital Medical Center, Boston, Massachusetts
Lagergren, Hans, Karolinska Hospital, Stockholm 60, Sweden
LaGrange, Lee D., Gulf General Atomic, San Diego, California
Laird, John D., M.D., AVCO-Everett Research Lab., Everett, Massachusetts
Lance, Joseph R., KPA Nuclear, Inc., Large, Pennsylvania
Lande, Arnold J., M.D., Cornell Medical Center, New York, New York
Lang, Ronald, Hamilton Standard, Farmington, Connecticut
Lang, Ronald P., Travenol Laboratories, Morton Grove, Illinois
Langan, Linda, Georgetown University Medical Center, Washington, D.C.
Lange, Paul H., M.D., National Institutes of Health, Bethesda, Maryland
Lanham, Clifford E., Harry Diamond Laboratories, Washington, D.C.
Lasky, Midge, The Blue Sheet, Washington, D.C.
Lederman, Peter B., Ph.D., Polytechnic Institute of Brooklyn, Brooklyn, New York
Lee, Henry, Ph.D., Epoxylite Corporation, South El Monte, California
Lee, Jr., William H., M.D., Medical College of South Carolina, Charleston, South Carolina
Leeming, Michael N., Memorial Hospital, New York, New York
Lefemine, Armand A., M.D., Tufts University School of Medicine, Cambridge, Massachusetts
Leonard, E. F., Columbia University, New York, New York
Leonard, Fred, Ph.D., Walter Reed Army Medical Center, Washington, D.C.
Leonard, Ronald J., Travenol Laboratories, Morton Grove, Illinois
Leonard, R. J., Hamilton Standard, Farmington, Connecticut

Hardy, James D., M.D., University of Mississippi, Jackson, Mississippi
Harris, A. Sidney, Ph.D., Louisiana State University, New Orleans, Louisiana
Harrison Jr., Ernest, Research Triangle Institute, Research Triangle Park, North Carolina
Harth, III, George H., Battelle Memorial Institute, Columbus, Ohio
Hartnig, Quentin L., Ph.D., George Washington University, Washington, D.C.
Harvey, Douglas G., Sanders Nuclear Corporation, Nashua, New Hampshire
Harvey, H., TRW Systems Group, Redondo Beach, California
Haspert, Kent, Harry Diamond Laboratories, Silver Spring, Maryland
Hassinger, Robert J., Holter Company, Bridgeport, Pennsylvania
Hauser, Ray L., Hauser Research & Engineering Company, Boulder, Colorado
Hausner, John L., The Holter Company, Bridgeport, Pennsylvania
Haynes, Charles H., Dow Corning Corporation, Midland, Michigan
Healey, William V., M.D., Roosevelt Hospital, New York, New York
Hegyeli, Andrew F., D.V.M., Ph.D., Walter Reed Army Medical Center, Washington, D.C.
Heimlich, L. A., United Aircraft, Farmington, Connecticut
Heins, Robert, Johns Hopkins University/APL, Silver Spring, Maryland
Heisterkamp, III, Charles, M.D., U. S. Army Research and Development Command, Washington, D.C.
Helland, John R., Medtronic, Incorporated, Minneapolis, Minnesota
Hellfritzsch, A. G., Ph.D., Naval Ordnance Laboratory, Silver Spring, Maryland
Hellums, David, M.D., Rice University, Houston, Texas
Helmer, Jerry, Battelle Memorial Institute, Columbus, Ohio
Helvig, Raymond J., National Institutes of Health, Bethesda, Maryland
Henry, J.F., Leesona Moos Laboratories, Great Neck, New York
Herrold, George, Cedars Medical Research, Los Angeles, California
Hersh, Leroy,Ph.D.Corning Glass Works, Corning, New york
Hessel, II, Eugene A., M.D., University of Washington, Seattle, Washington
Heuchling, T.P., Arthur D. Little, Inc., Cambridge, Massachusetts
Hewitt, Robert L., M.D., Tulane University, New Orleans, Louisiana
Hewson, W. N., British Embassy, Washington, D.C.
Hill, Donald, M.D., Pacific Medical Center, San Francisco, California
Hill, Vivian W., National Institutes of Health, Bethesda, Maryland
Hill, Wm. J., Cardiovascular Associates, Seattle Washington
Hixson, Raymond L., University of Utah, Salt Lake City, Utah
Ho, Paul S., M.D., Cornell University, Ithaca, New York
Hochman, Ben, United Aircraft, Hamilton Standard, Farmington, Connecticut
Hoffman, John R., U. S. Army Nuclear Power, Ft. Belvoir, Virginia
Holdefer, Wilfred F., M.D., University of Alabama, Birmingham, Alabama
Holland, L. M., V.M.D., Los Alamos Scientific Laboratory, Los Alamos, New Mexico
Horenstein, Evelyn A., M.D., National Institutes of Health, Bethesda, Maryland
Horikawa, Megumi, Fuji Polymer Industries Co., Ltd., Meguro-Ku, Tokyo, Japan
Hornbeck, C. T., Air Products and Chemicals, Inc., Allentown, Pennsylvania
Hsu, S.T., Prof., University of Maryland, College Park, Maryland
Hu, Pung Nien, M.D., Space System, Inc., Waltham, Massachusetts
Hubbard, Donn B., Travenol Laboratories, Morton Grove, Illinois
Huff, James R., Ph.D., U. S. Army Research and Development Center, Ft. Belvoir, Virginia
Huffman, Fred, Ph.D., Thermo Electron Corporation, Waltham, Massachusetts
Hugo, Norman, Maj., Walter Reed General Hospital, Washington, D.C.
Hung, Tin-Kan, Ph.D., Carnegie Mellon University, Pittsburgh, Pennsylvania
Hasain, Muzaffar, M.D., Children's Hospital Medical Center, Boston, Massachusetts
Huse, Wilfred, M.D., Loma Linda University Hospital, Loma Linda, California
Hutchins, III., John R., Corning Glass Works, Corning, New York

Icenhower, David E., Navships Research and Development Lab., Annapolis, Maryland
Ikenberry, Lynn D., Ph.D., Research Triangle Institute, Research Triangle Park, North Carolina
Irving, Jack H., M.D., Aerospace Corporation, Los Angeles, California

Jacobey, John A., M.D., University of Colorado, Denver, Colorado
Jacobs, T.A., Ph.D., Aerospace Corporation, Los Angeles, California
Jacques, Maurice E., Bendix Research Laboratories, Southfield, Michigan
Jaffrin, Michel Y., M.D., Massachusetts Institute of Technology, Cambridge, Massachusetts
James, Stanley, Ph.D., Naval Ordnance Laboratory, Silver Spring, Maryland
Jaron, Dov, Ph.D., Maimonides Medical Center, Brooklyn, New York
Javier, Roger P., M.D., Mt. Sinai Hospital, Miami Beach, Florida
Johnson, Alan A., Ph.D., Polytechnic Institute of Brooklyn, Brooklyn, New York
Johnson, Eric H., M.D., National Institutes of Health, Bethesda, Maryland
Johnson, T. R., Thermo Electron Corporation, Waltham, Massachusetts
Johnson, John W., George Washington University, Washington, D.C.
Johnston, Richard P., Douglas Laboratories, Richland, Washington
Jones, Cyril J., M.D., Downstate Medical Center, SUNY, Brooklyn, New York
Jones, Richard D., Ph.D., St. Luke's Hospital, Cleveland, Ohio
Jones, T. A., Codman & Shurtleff, Incorporated, Randolph, Massachusetts
Joyce, J. W., Harry Diamond Laboratories, Washington, D.C.

Levine, Sumner, M.D., State University of New York, Stony Brook, L.I., New York
Lewis, Edward, American Optical Corporation, Framingham, Massachusetts
Lightfoot, E. N., University of Wisconsin, Madison, Wisconsin
Lilleleht, L. U., M.D., University of Virginia, Charlottesville, Virginia
Lin, Chung-Yuan, Travenol Laboratories, Morton Grove, Illinois
Lindsey, Edward S., M.D., Tulane University, New Orleans, Louisiana
Link, W. T., Ph.D., Arkon Scientific Laboratories, Berkeley, California
Lipps, Jr., Ben J., Ph.D., Dow Chemical Co, Walnut Creek, California
Littman, Fred, McDonnell-Douglas Co., Newport Beach, California
Litwak, Robert S., M.D., Mt. Sinai School of Medicine, New York, New York
Loehr, Martin L., Ph.D., Flodyne Controls, Inc., New York, New York
Long, David M., M.D., University of Illinois, Chicago, Illinois
Long, Edwin Tutt, M.D., Watson Clinic, Lakeland, Florida
Longsworth, Ralph C., Air Products and Chemicals, Inc., Allentown, Pennsylvania
Lopez, Louis, M.D., IBM Houston Scientific Center, Houston, Texas
Ludwin, Isadore, Ph.D., Newton, Massachusetts
Lundblad, Roger L., Ph.D., University of North Carolina, Chapel Hill, North Carolina
Luria, Myron H., M.D., St. Luke's Hospital, Cleveland, Ohio
Lyman, Donald J., University of Utah, Salt Lake City, Utah
Lynch, Wilfred, Medical Engineering Corporation, Racine, Wisconsin

McCormack, Michael C., University of Santa Clara, Santa Clara, California
McGinnis, Gerald E., Westinghouse Electric Corporation, Pittsburge, Pennsylvania
McIntosh, Charles, M.D., National Institutes of Health, Bethesda, Maryland
McIsaac, Jr., John M., Hamilton Standard, Farmington, Connecticut
McMahon, Thomas A., Massachusetts Institute of Technology, Cambridge, Massachusetts
McMillan, Caldwell, Maryland Div. of Vocational Rehabilitation, Bladensburg, Maryland
McMillan, G. C., M.D., National Institutes of Health, Bethesda, Maryland
Mackey, Walter J., M.D., University of Minnesota, Minneapolis, Minnesota
MacNeille, S. M., Ph.D., American Optical Corporation, Southbridge, Massachusetts
Maddy, Keith, National Institutes of Health, Bethesda, Maryland
Madurski, Joseph P., Bendix Research Laboratories, Southfield, Michigan
Magnani, Joseph, Ethicon, Inc., Somerville, New Jersey
Mahoney, Matthew, Datascope Corporation, Saddle Brook, New Jersey
Malachesky, Paul, Ph.D., Tyco Laboratories, Inc., Waltham, Massachusetts
Maloney, Jr., Thomas V., M.D., University of California, Los Angeles, California
Mark, Frank F., Applied Physics Lab/Johns Hopkins University, Silver Spring, Maryland
Marshall, David W., Amicon Corporation, North Reading, Massachusetts
Martinez, F. J., Travenol Laboratories, Morton Grove, Illinois
Martini, William R., Donald W. Douglas Laboratory, Richland, Washington
Maslan, Frank, M.D., Sanders Nuclear Corporation, Nashua, New Hampshire
Mason, R. G., M.D., University of North Carolina, Chapel Hill, North Carolina
Mathewson, W. F., General Electric Co., Schenectady, New York
Matloff, Jack M., Harvard Medical School, Los Angeles, California
Matsuyama, G., Ph.D., Beckman Instruments, Inc., Fullerton, California
Matthews, Marion, National Institutes of Health, Washington, D.C.
Mayhew, Susan H., Mellon Institute, Pittsburgh, Pennsylvania
Mayo, Kenneth E., Sanders Nuclear Corporation, New Hampshire
Mayrovitz, Harvey N., University City Science Institute, Philadelphia, Pennsylvania
Meier, Milton A., M.D., University of Illinois, Chicago, Illinois
Merchant, Suzanne, Thermo Electron Corporation, Waltham, Massachusetts
Merker, Robert L., Mellon Institute, Pittsburgh, Pennsylvania
Messinger, Stephen, Monsanto Research Corporation, Everett, Massachusetts
Metcalfe, I. J., AVCO, Everett, Lowell, Massachusetts
Metz, Howard, National Institutes of Health, Bethesda, Maryland
Middleton, Jr., William J., ILC Industries, Inc., Felton, Delaware
Millar, Huntly D., E & M Instrument Co., Houston, Texas
Miller, Don R., M.D., Kansas University Medical Center, Kansas City, Kansas
Miller, Irving F., Polytechnic Institute of Brooklyn, Brooklyn, New York
Miller, R. A., General Electric Corporation, Philadelphia, Pennsylvania
Miskimon, Robert M., M.D., Richmond, Virginia
Mitz, M. A., Ph.D. N.A.S.A., Washington, D.C.
Moacanin, J., M.D., Jet Propulsion Laboratory, Pasadena, California
Mockros, Lyle F., Northwestern University, Evanston, Illinois
Moller, Ted, National Institutes of Health, Bethesda, Maryland
Monroe, Harold C., National Institutes of Health, Bethesda, Maryland
Mosehauer, Edward, Hamilton Standard, Windsor Locks, Connecticut
Moskowitz, Gordon D., Ph.D., Drexel Institute of Technology, Philadelphia, Pennsylvania
Moskowitz, R., M. D., Ferrofluidics Corporation, Burlington, Massachusetts

Moss, Fred E., A.F.I.P., Washington, D.C.
Mrava, Gene, The Cleveland Clinic Foundation, Cleveland, Ohio
Muir, William M., Ph.D., University of Strathclyde, Glasgow, Scotland
Mulder, Don, M.D., University of California Medical Center, Los Angeles, California
Muller, William H., H.D., University of Virginia Medical Center, Charlottesville, Virginia
Murphy, Mames P., Texas Medical Instruments, Houston, Texas
Murphy, Preston, V., Ph.D., Thermo Electron, Corporation, Waltham, Massachusetts
Murthy, V. Sreedhara, M.D., Massachusetts Institute of Technology, Cambridge, Massachusetts
Musolf, Martin C., M.D., Dow Corning Corporation, Mideland, Washington
Myers, George, Ph.D., Riverside Research Institute, New York, New York

Nelsen, Lita, Amicon Corporation, Lexington, Massachusetts
Nemchin, Robert G., Ph.D., Me.par, Incorporated, Falls Church, Virginia
Newacheck, Richard L., Aerojet-General Corporation, San Ramon, California
Newby, Barbara J., National Institutes of Health, Bethesda, Maryland
Newgard, Peter, Stanford Research Institute, Menlo Park, California
Newman, Elliot Voss, M.D., National Heart Council, Nashville, Tennessee
Ng, Daniel, Y.C., M.D., Institute of Gas Technology, Chicago, Illinois
Nichols, Charles R., Ph.D., Hydrospace Research Corporation, Rockville, Maryland
Nicoloff, Demertre, M., M.D., University of Minnesota, Minneapolis, Minnesota
Nielson, C. A., U.S. Army Medical Research Lab., Walter Reed, Washington, D.C.
Nishimura, Akio, M.D., New England Medical Center Hospitals, Boston, Massachusetts
Noble, J., Richland, Washington
Norman, John C., M.D., Harvard Medical School, Boston, Massachusetts
Normann, Nils A., M.D., Case Western Reserve University, Cleveland, Ohio
Norton, Robert L., New England Medical Center Hospitals, Boston, Massachusetts
Nose, Y., M.D., The Cleveland Clinic Foundation, Cleveland, Ohio
Nuwayser, Elie, S., Ph.D., Monsanto Corporation, Peabody, Massachusetts
Nyilas, Emery, Ph.D., Avco-Everett Research Laboratory, Everett, Massachusetts

O'Bannon, William, Rice University, Houston, Texas
Ocumpaugh, David, M.D., Epoxylite Corporation, South El Monte, California
Oja, Phyllis D., Dow Chemical Company, Walnut Creek, California
Oldham, H. N., M.D., Duke University, Durham, North Carolina
O'Neill, C. G., Physics International Company, San Leandro, California
O'Neill, William P., Ph.D., Shell Development Company, Emeryville, California
Orrell, F. L., Western Gear Corporation, South Gate, California
Oser, Zale, Ethicon, Inc., Somerville, New Jersey
Ostrach, Simon, M.D., Case Western Reserve University, Cleveland, Ohio
O'Sullivan, John B., Ph.D., USAMERDC, Fort Belvoir, Virginia
Oswin, H. G., Ph.D., Energetics Science, Inc., Bronx, New York
Overcash, Michael, University of Minnesota, Minneapolis, Minnesota
Oxley, L. Thomas, Medical Engineering Corporation, Racine, Wisconsin

Page, Mark, Chemical Automation Corporation, Great Neck, New York
Page, Norbert P., D.V.M., Atomic Energy Commission, Rockville, Maryland
Palich, William E., D.V.M., Melpar, Inc., Rockville, Maryland
Pan, Coda H. T., Mechanical Technology, Inc., Latham, New York
Parker, D., University College Hospital, London, England
Patel, A. R., Ph.D., Melpar, Inc., Falls Church, Virginia
Patel, Anil S., Travenol Laboratories, Morton Grove, Illinois
Patterson, W. E., M.D., Hoffmann La Roche, Inc., Nutley, New Jersey
Paul, Milton H., M.D., Northwestern University Medical School, Chicago, Illinois
Pearson, Phillip T., M.D., Iowa State University, Ames, Iowa
Pefley, Richard K., University of Santa Clara, Santa Clara, California
Peirce, C. C., Sippican Corporation, Marion, Massachusetts
Peirce, E., Converse, II., M.D., Emory University Medical School, Atlanta, Georgia
Pennington, Carl J., Jr., Ph.D., Battelle Memorial Institute, Columbus, Ohio
Perino, Peter R., Statham Instruments, Inc., Oxnard, California
Peterson, Gerald H., Bio-Logics, Inc., Salt Lake City, Utah
Peterson, John I., Ph.D., National Institutes of Health, Bethesda, Maryland
Petrovick, Mathew, Becton-Dickinson & Company, Raleigh, North Carolina
Petschek, Harry, Avco-Everett Research Laboratory, Everett, Massachusetts
Pickup, Robert E., Holter Company, Bridgeport, Pennsylvania
Pierce, William S., M.D., University of Pennsylvania, Philadelphia, Pennsylvania
Pierpont, Gordon L., University of Wisconsin, Madison, Wisconsin
Pinkerson, Alan L., M.D., National Institutes of Health, Bethesda, Maryland
Pitzele, S., M.D., Royal Victoria Hospital, McGill University, Montreal, Canada
Pliego, Senaro, Instituto De Cardiologia, Mexico

Plzak, Louis F., Jr., M.D., Harvard Medical School, Boston, Massachusetts
Poff, G. M., Me.par, Inc., Rockville, Maryland
Polanyi, Michael L., American Optical Company, Framingham Ct., Massachusetts
Pollock, Robert, Travenol Laboratories, Morton Grove, Illinois
Pomeroy, Ronald K., West Virginia University, Morgantown, West Virginia
Porterfield, Dean C., Hamilton Standard, Farmington, Connecticut
Pouchot, Walter D., Westinghouse Electric Corporation, Pittsburgh, Pennsylvania
Powaser, Mary M., University of Wisconsin, Madison, Wisconsin
Powell, Mary S., National Institutes of Health, Bethesda, Maryland
Priddle, O. D., Jr., Data Environmental Sciences Corp., Arlington, Virginia
Prisk, Bert C., General Motors Corporation, Warren, Michigan
Proctor, Caroline E., Data Environmental Sciences Corp., Arlington, Virginia
Purdy, David L., Nuclear Materials & Equipment Corp., Apollo, Pennsylvania

Rackley, Charles E., M.D., University of Alabama Medical Center, Birmingham, Alaban
Rafferty, Edson, Litton Industries, Minneapolis, Minnesota
Rassman, William, M.D., New York Hospital, New York, New York
Rastelli, G. C., M.D., Mayo Clinic, Rochester, New York
Ratner, Buddy, Polytechnic Institute of Brooklyn, Jamaica, New York
Rawson, R. O., John B. Pierce Foundation, New Haven, Connecticut
Reed, George E., M.D., New York University, New York, New York
Regal, Timothy J., M.D., New Jersey College of Medicine, Jersey City, New Jersey
Regan, Thomas M., Ph.D., Harry Diamond Laboratories, Washington, D.C.
Regelson, William, M.D., Medical College of Virginia, Richmond, Virginia
Reger, Steven I., University of Virginia, Charlottesville, Virginia
Reich, Theobald, New York University Medical Center, New York, New York
Reichle, Frederick A., M.D., Temple University Hospital, Philadelphia, Pennslyvania
Reichner, Philip, Westinghouse Electric Corporation, Pittsburgh, Pennsylvania
Reimschuessel, Herbert K., Allied Chemical Corporation, Morristown, New Jersey
Reucroft, P. J., The Franklin Institute, Philadelphia, Pennsylvania
Reynolds, W. E., IIT Research Institute, Chicago, Illinois
Rich, Thomas R., Amicon Corporation, Lexington, Massachusetts
Richardson, Peter D., Ph.D., Brown University, Providence, Rhode Island
Ries, Robert G., Dow Corning Corporation, Midland, Michigan
Rikli, Arthur E., M.D., University of Missouri, Columbia, Missouri
Roberts, Phyllis S., Medical College of Virginia, Richmond, Virginia
Robeson, Lloyd M., Union Carbide Corporation, Bound Brook, New Jersey
Robinson, Thomas C., Thermo Electron Corporation, Waltham, Massachusetts
Rockwell, Theodore, MPR Associates, Washington, D.C.
Rodman, Nathaniel F., M.D., University of North Carolina, Chapel Hill, North Carolina
Roe, Benson B., M.D., University of California Medical Center, San Francisco,California
Rogers, Adair, Conshohocken, Pennsylvania
Rollwitz, William L., Southwest Research Institute, San Antonio, Texas
Rose, L. R., Col., U. S. Army, Washington, D.C.
Rosendahl, Thomas E., Donaldson Company, Inc., Minneapolis, Minnesota
Rosensweig, Jacob, M.D., Jewish General Hospital, Montreal, Canada
Rosenweig, R.E., Sc.D., Ferrofluidics Corporation, Burlington, Massachusetts
Roth, Wilfred, Ph.D., University of Vermont, Burlington, Vermont
Rothfusz, Ralph W., Bendix Research Laboratories, Southfield, Michigan
Rushmer, Robert, Ph.D., University of Washington, Seattle, Washington
Rutstein, David D., Harvard Medical School, Boston, Massachusetts
Ryder, William E., Gulton Industries, Inc., Metuchen, New Jersey

Saba, George P., M.D., Buffalo General Hospital, Buffalo, New York
Sabelnikov, Yelena A., Ph.D., Embassy of the U.S.S.R., Washington, D,C.
Safford, Robert E., University of Wisconsin, Madison, Wisconsin
Salisbury, Lloyd, Walter Reed Army Medical Center, Washington, D.C.
Salkin, Burton, Becton, Dickinson Research Center, Raleigh, North Carolina
Salyer, Ival O., Monsanto Research Corporation, Dayton, Ohio
Salzman, Edwin W., M.D., Harvard Medical School, Boston, Massachusetts
Sanmarco, M. E., M.D., Temple University Hospital, Philadelphia, Pennsylvania
Satinsky, Victor, M.D., Hahnemann Medical College, Philadelphia, Pennsylvania
Sato, Tomizo, M.D., Yale University, New Haven, Connecticut
Sawyer, Philip N., M.D., State University of New York, Downstate Med. Ctr., Brooklyn, New York
Scala, Sinclaire M., General Electric Company, Philadelphia, Pennsylvania
Schafer, M. E., Ph.D., Franklin Institute, Philadelphia, Pennsylvania
Scheele, Leonard A., M.D., Warner Lambert Pharmaceutical Co., Washington, D.C.
Scherrer, J. W., Jewish Hospital of Brooklyn, Brooklyn, New York

Schipper, Edgar, Ethicon, Inc., Somerville, New Jersey
Schneyer, Alvin T., TRW Systems, Washington, D. C.
Schoenfeld, Clyde D., M.D., Mount Sinai Hospital, Miami Beach, Florida
Schubert, Ronald J., Epoxylite Corporation, South El Monte, California
Schulte, Rudolf R., Heyer-Schulte Corporation, Santa Barbara, California
Schutz, Leonard, M.D., University of California, San Diego, La Jolla, California
Scott, H., Ph.D., Franklin Institute Research Labs., Philadelphia, Pennsylvania
Scott, John C., Hahnemann Medical College, Philadelphia, Pennsylvania
Seminerio, Frank J., Holter Company, Cherry Hill, New Jersey
Seremetis, Michael G., M.D., State Univ. of New York, Downstate Med. Ctr., Brooklyn, New York
Serkes, Kenneth D., M.D., Travenol Laboratories, Inc., Morton Grove, Illinois
Shacter, Bernard, National Institutes of Health, Bethesda, Maryland
Shapiro, Max, Whittaker Corporation, Beverly Hills, California
Sharpe, L. M., Ph.D., National Academy of Engineering, Bethesda, Maryland
Shea, Michael A., M.D., University of Minnesota, Minneapolis, Minnesota
Sherman, Martin, General Electric Company, Valley Forge, Pennsylvania
Shepard, Richard B., M.D., University of Alabama Medical Center, Birmingham, Alabama
Shih, Cornelius C., Ph.D., University of Alabama, Huntsville, Alabama
Short, Leland L., North American Rockwell Corporation, Anaheim, California
Sidwell, S. P., Ford Motor Company, Dearborn, Michigan
Silvay, George, M.D., Mt. Sinai School of Medicine, New York, New York
Singerman, Sol, American Cyanamid-Lederle, East Norwalk, Connecticut
Sipin, A. J., Anatole J. Sipin Company, New York, New York
Siwek, Erwin G., General Electric Company, Schenectady, New York
Skiens, W. Eugene, Ph.D., Dow Chemical Company, Walnut Creek, California
Skinner, David B., M.D., Johns Hopkins School of Medicine, Baltimore, Maryland
Sloviter, H. H., University of Pennsylvania Medical School, Philadelphia, Pennsylvania
Smiley, Parker C., Physics International Company, San Leandro, California
Smith, McKamy, M.D., Ph.D., Ochsner Foundation & Clinic, Metairie, Louisiana
Snider, M. T., Brown University, Providence, Rhode Island
Sobin, Sidney S., Univ. of Southern California School of Medicine, Los Angeles, California
Sokolov, Sergey, Embassy of the U.S.S.R., Washington, D. C.
Somers, Lewis S., 3rd, The Holter Company, Bridgeport, Pennsylvania
Soroff, Harry S., M.D., Tufts New England Medical Center Hospital, Boston, Massachusetts
Spaet, Theodore H., M.D., Montefiore Hospital, New York, New York
Speaker, David M., Melpar, Inc., Falls Church, Virginia
Sprung, John G., Western Gear Research Center, South Gate, California
Spurlock, Jack M., Health and Safety Research Institute, Springfield, Virginia
Spyker, D. A., University of Minnesota, Minneapolis, Minnesota
Spyker, Mrs. D. A., University of Minnesota, Minneapolis, Minnesota
Srinivasan, S., State University of New York, Downstate Med. Ctr., Brooklyn, New York
Stansel, H. C., Jr., Yale University, New Haven, Connecticut
Stapelfeldt, Roelif, M.D., Ph.D., Toledo Hospital, Toledo, Ohio
Starek, Peter, M.D., Cornell University, New York, New York
Steeves, H. R., III, Virginia Polytechnic Institute, Blacksburg, Virginia
Steichen, Felicien M., M.D., Albert Einstein College of Medicine, Bronx, New York
Stein, Michael, M.D., Bowman Gray Medical Center, Winston-Salem, North Carolina
Stern, Ivan J., Travenol Laboratories, Morton Grove, Illinois
Stewart, R. D., M.D., Marquette School of Medicine, Brookfield, Wisconsin
Stewart, Wolcott E., Ph.D., Hubris Heart Research, Fort Worth, Texas
Stick, John C., Jr., Perkin-Elmer Corporation, Norwalk, Connecticut
Stivala, S., Ph.D., Stevens Institute of Technology, Hoboken, New Jersey
Stoffey, Donald, Epoxylite Corporation, South El Monte, California
Stoner, Glenn E., University of Virginia, Charlottesville, Virginia
Summers, George D., Fairchild Hiller Corporation, Germantown, Maryland
Sundberg, D. R., Tulane University, New Orleans, Louisiana
Swift, Curran S., Iowa State University, Ames, Iowa
Symbas, P. N., M.D., Emory University, Atlanta, Georgia

Takagi, Hiroyuki, M.D., University of Mississippi Medical Center, Jackson, Mississippi
Talonn, Daniel, Sherwood Medical Industries, Inc., St. Louis, Missouri
Tamari, Yehuda, Westinghouse R&D, Pittsburgh, Pennsylvania
Tancredi, Robert G., M.D., Mayo Clinic, Rochester, Minnesota
Tanquary, A. C., Southern Research Institute, Birmingham, Alabama
Tarabeih, Aly, M.D., Rhode Island Hospital, Brown University, Providence, Rhode Island
Tarnay, Thomas J., M.D., West Virginia University, Morgantown, West Virginia
Tarpley, William, Franklin Institute, Philadelphia, Pennsylvania
Teeter, Charles L., WARF Institutes, Inc., Madison, Wisconsin

Tenniswood, Patricia H., Office of Naval Research, Washington, D. C.
Thomas, Randal H., Merck, Sharp & Dohme, West Point, Pennsylvania
Thorne, Gale H., Bio-Logics, Inc., Salt Lake City, Utah
Thumin, Alfred I., New York University, Bronx, New York
Tiedemann, Richard, M.D., New York Hospital, New York, New York
Timmins, Robert S., Abcor, Inc., Cambridge, Massachusetts
Tolzmann, J. A., 3 M Company, St. Paul, Minnesota
Tompkins, Frederick C., Jr., Abcor, Inc., Cambridge, Massachusetts
Topaz, Stephen R., Johns Hopkins University, Baltimore, Maryland
Topham, W. Samford, Ph.D., University of Utah, Salt Lake City, Utah
Toth, Louis S., Ohio State University, Columbus, Ohio
Tragus, Eugene T., M.D., University of Pennsylvania, Philadelphia, Pennsylvania
Triplett, William C., Sanders Nuclear Corporation, Corpus Christi, Texas
Trzeciak, M. J., Ph.D., IBM Corporation, Endicott, New York
Tsien, H. C., Esso Research & Engineering Company, Linden, New Jersey

Ulin, Alex W., M.D., Ethicon, Inc., Somerville, New Jersey
Urbach, H. B., U. S. Naval Ship R&D Laboratory, Annapolis, Maryland
Urban, John J., Walter Reed Hospital, Forest Glen, Maryland
Usdin, Vera R., Gillette Research Institute, Rockville, Maryland
Ushakoff, Alexis E., Cordis Corporation, Miami, Florida

Varco, Richard L., University of Minnesota, Minneapolis, Minnesota
Vardar, Alaattin, M.D., University of Istanbul, Bebek, Istanbul, Turkey
Vastagh, George F., University of Texas, Southwest Medical School, Dallas, Texas
Villarroel, Fernando, Harry Diamond Laboratory, Washington, D. C.
Votaw, Charles W., Naval Research Laboratory, Arlington, Virginia

Wade, Clarence W. R., Ph.D., Walter Reed Army Medical Center, Washington, D. C.
Wagner, John P., Ph.D., Johns Hopkins Applied Physics Lab., Silver Spring, Maryland
Wakabayashi, Akio, M.D., University of California, Irvine, California
Walker, Wanda Louise, University of Virginia, Charlottesville, Virginia
Wallace, Richard L., Environmental Technology, Inc., Latham, New York
Walton, Douglas M., Beckman Instruments, Inc., Fullerton, California
Warner, Hal, Emory University-Yerkes, Atlanta, Georgia
Waugh, David F., Massachusetts Institute of Technology, Cambridge, Massachusetts
Webb, John A., Jr., NASA Lewis Research Center, Cleveland, Ohio
Weber, Karl T., M.D., Temple University Hospital, Philadelphia, Pennsylvania
Wechsler, Lawrence D., General Electric Company, Syracuse, New York
Weinberg, David J., Walter Reed Army Medical Center, Washington, D. C.
Weinberger, Daniel, Hughes Aircraft, Los Angeles, California
Weir, Robert J., Hazleton Laboratories, Inc., Falls Church, Virginia
Weissman, M., Ph.D., Carnegie-Mellon University, Pittsburgh, Pennsylvania
Wheeler, Richard, State of Maryland Dept. Vocation Rehabilitation, Hyattsville, Maryland
Whiffen, James D., M.D., University of Wisconsin, Madison, Wisconsin
White, Jack, M.D., Johns Hopkins University School of Medicine, Baltimore, Maryland
Whitney, Donald R., General Motors Research, Warren, Michigan
Wiederhielm, Curt A., Ph.D., University of Washington, Seattle, Washington
Wilcox, Jane, National Institutes of Health, Bethesda, Maryland
Williams, Charles L., Hamilton Standard, Windsor Locks, Connecticut
Williams, David L., Monsanto Co., Everett, Massachusetts
Williams, T. Leigh, Medical College of Virginia, Richmond, Virginia
Willman, V. L., M.D., St. Louis University, St. Louis, Missouri
Wilson, L. S., George Washington University Medical School, Washington, D. C.
Wineman, Robert J., Monsanto Co., Everett, Massachusetts
Wingfield, Harold T., 3 M Company, St. Paul, Minnesota
Witzky, Julius E., Southwest Research Institute, San Antonio, Texas
Wolfson, Sidney K., M.D., Michael Reese Hospital & Medical Center, Chicago, Illinois
Wolzien, E. C., National Bureau of Standards, Boulder, Colorado
Wong, Patrick S. L., Massachusetts Institute of Technology, Cambridge, Massachusetts
Wooten, F. T., Research Triangle Institute, Research Triangle Park, North Carolina
Wright, William L., Memorial Hospital for Cancer & Allied Diseases, New York, New York

Yahr, William Z., M.D., USAF MC, Andrews Air Force Base, Washington, D. C.
Yao, Shang J., Ph.D., Michael Reese Hospital & Medical Center, Chicago, Illinois
Younger, Francis C., Wm. M. Brobeck & Associates, Berkeley, California

Zachary, Mary, Louisiana State University, Baton Rouge, Louisiana
Zachary, Richard E., Louisiana State University, Baton Rouge, Louisiana
Zarnstorff, William C., University of Wisconsin, Madison, Wisconsin
Zeh, Dale W., Jet Propulsion Laboratory, Pasadena, California
Zilionis, Violeta, Union Carbide Corporation, Parma, Ohio
Zivkovic, R., M.D., State University of New York, Downstate Med. Ctr., Brooklyn, New York

NATIONAL HEART INSTITUTE

ARTIFICIAL HEART PROGRAM STAFF

Frank W. Hastings, M.D., Chief

Lowell T. Harmison, Ph.D., Assistant Chief

Program Scientists

Charles E. Branch
Martin I. Broder, M.D.
Stephen D. Bruck, Ph.D.
Anthony M. Bruno, M.D.
Mahlon M. Carrington
William Ellis, M.D.
Ruth Johnsson Hegyeli, M.D.
Roger S. Powell
Allen K. Ream, M.D.
George P. Saba, II, M.D.
William P. Sears, M.D.
Karl T. Weber, Jr., M.D.

Administrative Staff

Philip Janus, Planning Officer
John A. Turlik, Contract Officer

Ann C. Bailey
Vivianne L. Baskins
Robert R. Carlsen
Ethel W. Deutsch
Alyce R. McCathran
Ellen D. Riley
Doris H. Scherbak
Rosemary F. Sheridan

CONFERENCE PRESS ROOM STAFF

William Sanders, Chief, Heart Information Center

George D. Bragaw, Jr.
Sandra L. Kamisar

OUTLINE OF RESEARCH CONTRACTS PROCEDURES

In a research contracts program, each research project must be directed toward established goals. For this reason, many of the research ideas that result in funded projects are conceived in the program office. If they come from outside the program, the decision must be made by program personnel that they fit into the over-all plan of the program before they are acted upon. Each project must be directed toward reaching established goals.

As new areas of research and development are identified, a Request for Proposal (RFP) is issued. This is a document which outlines the specifications of the project to be undertaken, as well as the legal and administrative requirements which will govern any contract which is awarded. The availability of the RFP is announced in the Commerce Business Daily, a Department of Commerce newspaper which announces daily the opportunities for contracts available in the Government. RFP's are sent to all who respond to the advertisement, to all who had previously indicated that they wished to receive RFP's issued by the Artificial Heart Program, and automatically to all Medical Schools.

Proposals received in response to the RFP are subjected to several reviews within the National Heart Institute. Consideration is given primarily to the research idea, its soundness and the course by which it will be carried out. Proposed personnel, facilities and cost are also, of course, factors which are taken into consideration. The proposals which have been approved by the institute are forwarded to the NIH Contracts Office.

The NIH Contracts Office reviews the proposal to insure that no patent or other business problems are apparent, that prior relations, if any, with the contractor have been satisfactory, that adequate competition has been solicited, and that the proposed terms are otherwise in conformance with the Federal Procurement Regulations. The Finance Analysis Branch determines whether the proposed contractor has an approved accounting system and makes an item by item analysis of the proposed budget, reviewing such matters as the established overhead rate of the contractor and wage rates.

The negotiation of the contract is carried out by a team, with a representative from the program office, the contracts office, and the Contract and Grants Finance Analysis Branch. The workscope and timing of the program proposed are worked out on a scientist to scientist basis. The business and legal matters are worked out by the contracts administrators. After agreement is reached on the workscope, amount and other terms, the contract is drawn up in final form and becomes effective only after it is signed by an authorized person representing the contractor and then by the NIH Contracting Officer. It should be emphasized that the Contract is not a legal document until the NIH Contracting Officer signs the contract.

The scientific management of the contract is provided by the Artificial Heart Program Office through a project officer and project monitors. The contractor must work within the framework which has been provided in the workscope of the contract and he must not deviate from this unless a mutually agreed upon change is effected through the amendment of the contract. The business administration of the contract (such things as assuring that the general provisions of the contract are adhered to, required prior approvals are obtained, and equipment is appropriately labeled as Government property) is carried out by the NIH Contracts Office. Audit of the charges made against the contract is provided by the Audit Section of the Financial Management Branch. If the contractor is also carrying out Department of Defense business, he must submit his vouchers through the DOD cognizant auditor who is located in his vicinity. If he does not perform DOD business, he submits them directly to the NIH Audit Section. In either case, the NIH Audit Section decides whether or not the changes being made are proper.

TECHNICAL REPORTS ON CONTRACTS OF
THE ARTIFICIAL HEART PROGRAM

The reports listed below are available from the Clearinghouse for Federal Scientific and Technical Information (CFSTI), 5285 Port Royal Road, Springfield, Virginia 22151. The reports are grouped together by technical areas; basic studies, materials for use in circulatory assist devices, mock circulatory system, blood flow through blood pumps and valves, effects of additional endogenous heat, physiological effects of assist devices in animals, circulatory assist devices, implantable energy systems, and implantable fuel cells. Each technical report is identified by its CFSTI number.

STUDIES BASIC TO CONSIDERATION OF ARTIFICIAL HEART
RESEARCH AND DEVELOPMENT

Reports resulting from National Heart Institute contracts in this area of research deal with the following tasks:

Task I	Assessment and definition of the problem
Task II	Characterization of the biomedical and technological problems
Task III	Technology survey and reference data compilation
Task IV	Estimated future extension of technology
Task V	Determination of key technical problems in artificial heart development
Task VI	Assessment of other resources for artificial heart development
Task VII	Determination of performance criteria for the artificial heart

Contractor	Report	CFSTI Number
Avco-Everett Research Laboratory	Final Report, 1966	PB 169 967
Everett Massachusetts	Task I	PB 172 411
Contract No. PH43-66-7	Task II	PB 172 412
	Tasks III, IV, & V	PB 172 413
	Task VI	PB 172 414
	Task VII	PB 172 415
General Dynamics/Convair	Final Report, January 1966	PB 169 835
San Diego, California	Task I	PB 172 426
Contract No. PH43-65-1059	Task II	PB 172 427
	Task III	PB 172 428
	Task IV	PB 172 429
	Task V	PB 172 430
	Task VI	PB 172 431
	Task VII	PB 172 432
Hamilton Standard Division, UA	Final Report, February 1966	PB 169 831
Windsor Locks, Connecticut	Bibliography & References	PB 169 966
Contract No. PH43-66-20		
Stanford Research Institute	Final Report, January 1966	PB 169 832
Menlo Park, California		
Contract No. PH43-65-1058		
Thermo Electron Engineering Corporation	Final Report, March 1966	PB 169 833
Waltham, Massachusetts	Task I	PB 172 433
Contract No. PH43-66-9	Task II Vol. I	PB 172 434
	Task II Vol. II	PB 172 435
	Task III Vol I	PB 172 436
	Task III Vol. II	PB 172 437
	Task IV - Task VII	PB 172 438
Westinghouse Electric Corporation	Final Report, January 1966	PB 169 834
Pittsburgh, Pennsylvania	Task I	PB 172 404
Contract No. PH43-65-1060	Task II Vol. A	PB 172 405
	Task II Vol. B	PB 172 406
	Task III Vol. A	PB 172 407
	Task III Vol. B	PB 172 408
	Task III Vol. C	PB 172 409
	Task IV	PB 172 418
	Task V	PB 172 417
	Task VI	PB 172 416
	Task VII	PB 172 424

Contractor	Report	CFSTI Number
Hittman Associates Inc. Baltimore, Maryland Contract No. PH43-66-90	Analytical reports on six studies listed above:	
	Vol. 1, "Assessment of Need and Characterization of the Problems" July 1966	PB 173 050
	Vol. 2, "Technology Survey for Artificial Heart Devices" July 1966	PB 173 051
	Vol. 3, "Program Recommendations" August 1966	PB 173 052
	Summary volume - Report on Six Studies	PB 173 483

STUDIES ON MATERIALS FOR USE IN CIRCULATORY ASSIST DEVICES

Contractor	Report	CFSTI Number
Amicon Corporation Lexington, Massachusetts 02173 Contract No. PH43-66-1129	"Development of Polyelectrolyte Complexes as Antithrombogenic Materials"	
	Annual Report, January 29, 1968	PB 177 694
	Annual Report, November 20, 1968	PB 183 339
Battelle Memorial Institute Columbus, Ohio Contract No. PH43-64-496	"Literature Survey on Blood-Plastic Interaction" October 20, 1964	PB 169 094
	"The Development of an Improved Hemodialysis Membrane" June 15, 1965	PB 168 936
	"Development of Blood-Compatible Polymeric Materials." June 29, 1965	PB 168 937
	"Development of Blood-Compatible Polymeric Materials" June 22, 1966	PB 173 053
	"Development of Blood-Compatible Polymeric Materials." March 30, 1967	PB 175 668
	"Development of Blood-Compatible Materials" Annual Report, January 1967 to October 1967	PB 183 317
Battelle Memorial Institute Columbus, Ohio Contract No. PH43-67-1404	"_In Vitro_ Biological Testing of Prosthetic Materials" Annual Report, July 19, 1968	PB 183 315
Carnegie-Mellon University Pittsburgh, Pennsylvania Contract No. PH43-66-977	"Studies Relative to Materials Suitable for Use in Artificial Hearts" Annual Report, October 4, 1967	PB 176 438
	"Studies Relative to Materials Suitable for Use in Artificial Hearts" Annual Report, July 22, 1968	PB 182 745
Cordis Corporation Miami, Florida Contract No. PH43-66-980	"Compatibility of Blood with Materials Useful in the Fabrication of Artificial Organs" Annual Report, July 24, 1967	PB 176 200
	"An Investigation of the Effects of Implantable Materials on Blood." Annual Report, July 15, 1968	PB 183 337
Gulf General Atomic, Inc. San Diego, California Contract No. PH43-67-1411	"The Compatibility of Carbon and Blood" Annual Report, October 1968	PB 183 393
Harris Research Laboratories Inc. Washington, D.C. Contract No. PH43-64-498	"Heparin-Bearing Surfaces and Liquid Surfaces in Relation to Blood Coagulation" 1966	Trans, Amer, Soc. Artif. Intern. Organs, XII:155-162, 1966
	"Effect of Surfaces on the Blood" Annual Report, Period concluded July 28, 1966	PB 175 678

Contractor	Report	CFSTI Number
Harris Research Laboratories Washington, D.C. 20011 Contract No. PH43-68-38	"Effect of Surfaces on Blood" Annual Report, July 1966 to July 1967	PB 178 470
	"Interaction of Surfaces and the Blood" Final Report, October 15, 1968	PB 183 316
Melpar, Inc. Falls Church, Virginia Contract No. PH43-67-1413	"Evaluation of Biopolymers as Blood Compatible Materials" Annual Report December, 1968	PB 183 340
Monsanto Research Corporation Dayton, Ohio Contract No. PH43-66-975	"Materials and Components for an Artificial Heart" Annual Technical Progress Report, June 23, 1966 to June 22, 1967	PB 176 203
	"Materials and Components for Circulatory Assist Devices" Annual Report June 1968	PB 183 338
North Carolina, Univ. of Chapel Hill, North Carolina Contract No. PH43-67-1416	"Antithrombogenic Surfaces: Platelet-Interface Reactions" Annual Report July 1968	PB 183 341
Polysciences, Inc. Rydal, Pennsylvania 19046 Contract No. PH43-66-1124	"Non-Clotting Plastic Surfaces" Annual Report, June 1966 to June 1967	PB 178 469
Stanford Research Institute Menlo Park, California Contract No. PH43-64-84	"The Effect of Polymer Surfaces on the Coagulation of Blood" November 24, 1965	PB 169 093
	"The Effect of Chemical Structure and Surface Properties of Synthetic Polymers on the Coagulation of Blood" Annual Report, April 1967 to May 1968	PB 183 314
Thermo Electron Corporation Waltham, Massachusetts 02154 Contract No. PH43-66-1126	"Studies Relative to Materials Suitable for Use in Artificial Hearts" Annual Report, January 1968	PB 178 468
	Annual Report, October 1968	PB 183 342

MOCK CIRCULATORY SYSTEM

Contractor	Report	CFSTI Number
Hydrospace Research Corporation Rockville, Maryland Contract No. PH43-64-78	Progress Report on the Mock Circulatory System, Sept. 26, 1965 to April 29, 1966	PB 172 423
	Final Report on the Mock Circulatory System, April 15, 1967	PB 175 719

BLOOD FLOW THROUGH BLOOD PUMPS AND VALVES

Contractor	Report	CFSTI Number
General Electric Company Space Sciences Laboratory Philadelphia, Pennsylvania Contract No. PH43-67-1121	"Study of Blood Flow in and Adjacent to Blood Pumps" Annual Report, June 30 1967 to June 30, 1968	PB 183 512
Avco Everett Research Laboratory Everett, Massachusetts Contract No. PH43-67-1120	"An Experimental Preparation for the Study of Thrombosis on Artificial Surfaces Under Controlled Flow Conditions" Annual Report, February 1969	PB 183 732

EFFECTS OF ADDITIONAL ENDOGENOUS HEAT

Contractor	Report	CFSTI Number
Battelle Memorial Institute Pacific Northwest Laboratories Richland, Washington Contract No. PH43-66-1130	"A Study on the Effects of Additional Endogenous Heat Relating to the Artificial Heart" Annual Report, August 10, 1967	PB 177 328
	Annual Report, December 1968	PB 180 941
Thermo Electron Corporation Waltham, Massachusetts Contract No. PH43-66-982	"Study of the Effect of Additional Endogenous Heat" Annual Report, December 1967	PB 177 753
	Annual Report, July 1968	PB 180 157
John B. Pierce Foundation New Haven, Connecticut Contract No. PH43-66-978	"The Study of the Effects of Additional Endogenous Heat" Annual Report, July 1, 1966 to June 30, 1967	PB 176 914

PHYSIOLOGICAL EFFECTS OF ASSIST DEVICES IN ANIMALS

Contractor	Report	CFSTI Number
Thermo Electron Corporation Waltham, Massachusetts 02154 Contract No. PH43-66-1123	"Study of the Physiologic Effects of Blood Pumps in Animals" Annual Report, June 1966 to June 1967	AD 671 595
Melpar, Inc. Falls Church, Virginia Contract No. PH43-67-1418	"Physiological Effects of Blood Pumps in Animals" Annual Report, October 1968	PB 182 746
Case Western Reserve University Cleveland, Ohio Contract No. PH43-67-1424	"The Physiological Effects of Circulatory Assist Devices" Annual Report, July 1967 to July 1968	PB 183 520

CIRCULATORY ASSIST DEVICES

Contractor	Report	CFSTI Number
Avco Everett Research Laboratory Everett, Massachusetts Contact No. PH43-66-1131	"Development Support to Research Teams with Circulatory Assist Devices Ready for Clinical Evaluation" Annual Report, July 1967	PB 179 724
Harry Diamond Laboratories Washington, D.C.	"Proposed Specification for an Artificial Heart to be Implanted in the Chest" January 13, 1965	AD 619 673
Westinghouse Electric Corporation Pittsburgh, Pennsylvania Contract No. PH43-67-1139	"Program to Develop Useful Artificial Heart and Ventricular Assist Devices" Annual Report, June 1968	
	Vol. I	PB 182 955
	Vol. II	PB 182 956

ENERGY SYSTEMS

Contractor	Report	CFSTI Number
Autonetics Division United Aircraft Anaheim, California Contract No. PH43-64-963	"A Pneumatic Driver for Surgically Implanted Myocardial Augmentation Devices" September 23, 1965	PB 168 862
Donald W. Douglas Laboratories Richland, Washington Contract No. PH43-67-1408	"Design and Development of the Stirling Cycle Energy Converter to Power Circulatory Support Systems" Annual Report, July 1968	PB 182 592

IMPLANTABLE FUEL CELLS

Contractor	Report	CFSTI Number
Monsanto Research Corporation Everett, Massachusetts 02149 Contract No. PH43-66-976	"Implantable Fuel Cell for an Artificial Heart" Annual Report February 15, 1968	PB 177 695
Monsanto Research Corporation Everett, Massachusetts 02149 Contract No. PH43-66-976	"Implantable Fuel Cell for an Artificial Heart" Annual Report 10 July 1968	PB 182 591

ADDENDUM

STUDIES ON MATERIALS FOR USE IN CIRCULATORY ASSIST DEVICES

Contractor	Report	CFSTI Number
Dow Corning Corporation Midland, Michigan Contract No. PH43-66-979	"Studies Relative to Materials Suitable for Use in Artificial Hearts" Annual Report, June 1968	PB 184 094

CARDIAC CONTROL PARAMETERS

Contractor	Report	CFSTI Number
Stanford University Sch. of Medicine Palo Alto, California Contract No. PH43-67-1109	"Studies in Artificial Heart Control" Annual Report August 1968	PB 183 815

PHYSIOLOGIC EFFECTS OF ASSIST DEVICES IN ANIMALS

Contractor	Report	
Travenol Laboratories, Inc. Morton Grove, Illinois Contract NO. PH43-67-1425	"Study of the Physiological Effects of Circulatory Assist Devices Annual Report, July 1968	PB 185 486

IMPLANTABLE ENERGY SYSTEMS

Contractor	Report	CFSTI Number
Kollsman Instrument Corporation Syosset, New York Contract No. PH43-67-1415	"Transmission of Energy through Intact Skin by Ultrasonic Power" Annual Report, June 1968	PB 185 482
Thermo Electron Corporation Waltham, Massachusetts Contract No. PH43-67-1423	"Thermal Energy Storage System" Annual Report July 1968	PB 185 484

☆ U. S. GOVERNMENT PRINTING OFFICE : 1969 O - 365-991

DATE DUE

~~NIH LIB MAY 26 1970~~

~~NIH LIB JUN 8 1970~~

~~NIH LIB APR 28 1971~~ 1971

~~NIH LIB AUG 20 1973~~

~~NIH LIB DEC [illegible]~~

~~NIH LIB [illegible] 1974~~

GAYLORD PRINTED IN U.S.A.

NIH LIBRARY
4 0087 0626

NIH LIBRARY
3 1496 00194 7632